2017

ANNUAL PROGRESS REPORT

DOE Hydrogen and Fuel Cells Program

ENERGY

DOE/GO-102017-5042
May 2018

U.S. Department of Energy
1000 Independence Avenue, S.W.
Washington, DC 20585-0121

FY 2017
PROGRESS REPORT FOR THE DOE HYDROGEN AND FUEL CELLS PROGRAM

May 2018

DOE/GO-102017-5042

Approved by Sunita Satyapal, Director, Hydrogen and Fuel Cells Program

NOTICE

This report was prepared as an account of work sponsored by an agency of the United States government. Neither the United States government nor any agency thereof, nor any of their employees, makes any warranty, express or implied, or assumes any legal liability or responsibility for the accuracy, completeness, or usefulness of any information, apparatus, product, or process disclosed, or represents that its use would not infringe privately owned rights. Reference herein to any specific commercial product, process, or service by trade name, trademark, manufacturer, or otherwise does not necessarily constitute or imply its endorsement, recommendation, or favoring by the United States government or any agency thereof. The views and opinions of authors expressed herein do not necessarily state or reflect those of the United States government or any agency thereof.

Available electronically at http://www.osti.gov/bridge

Available for a processing fee to U.S. Department of Energy
and its contractors, in paper, from:

U.S. Department of Energy
Office of Scientific and Technical Information
P.O. Box 62
Oak Ridge, TN 37831-0062
Phone: (865) 576-8401
Fax: (865) 576-5728
Email: mailto:reports@osti.gov

Available for sale to the public, in paper, from:

U.S. Department of Commerce
National Technical Information Service
5285 Port Royal Road
Springfield, VA 22161
Phone: (800) 553-6847
Fax: (703) 605-6900
Email: orders@ntis.fedworld.gov
Online ordering: http://www.ntis.gov/ordering.htm

Outline

I. Introduction

II. Hydrogen Production

- II.0 Hydrogen Production Sub-Program Overview
- II.A Hydrogen Production Analysis
  - II.A.1 Strategic Analysis, Inc.: Analysis of Advanced H_2 Production Pathways
- II.B Electrolysis
  - II.B.1 National Renewable Energy Laboratory: Renewable Electrolysis Integrated Systems Development and Testing
  - II.B.2 Giner, Inc.: High-Performance, Long-Lifetime Catalysts for Proton Exchange Membrane Electrolysis
  - II.B.3 Proton OnSite: High Performance Platinum Group Metal Free Membrane Electrode Assemblies through Control of Interfacial Processes
  - II.B.4 Giner, Inc.: High Temperature Alkaline Water Electrolysis
  - II.B.5 FuelCell Energy, Inc.: Solid Oxide Based Electrolysis and Stack Technology with Ultra-High Electrolysis Current Density (>3 A/cm^2) and Efficiency
  - II.B.6 Proton OnSite: Economical Production of Hydrogen through Development of Novel, High Efficiency Electrocatalysts for Alkaline Membrane Electrolysis
  - II.B.7 Tetramer Technologies, LLC: New Approaches to Improved PEM Electrolyzer Ion Exchange Membranes
  - II.B.8 Ceramatec: Multi-Scale Ordered Cell Structure for Cost Effective Production of Hydrogen by HTWS
- II.C High-Temperature Thermochemical
  - II.C.1 Sandia National Laboratories: High Efficiency Solar Thermochemical Reactor for Hydrogen Production
  - II.C.2 University of Colorado Boulder: Flowing Particle Bed Solarthermal Redox Process to Split Water
- II.D Photoelectrochemical
  - II.D.1 National Renewable Energy Laboratory: High-Efficiency Tandem Absorbers for Economical Solar Hydrogen Production
  - II.D.2 University of Hawaii: Wide Bandgap Chalcopyrite Photoelectrodes for Direct Solar Water Splitting
  - II.D.3 University of California, Irvine: Tandem Particle-Slurry Batch Reactors for Solar Water Splitting
- II.E Biological
  - II.E.1 National Renewable Energy Laboratory: Biomass to Hydrogen (B2H2)
  - II.E.2 Virginia Polytechnic Institute and State University: Sweet Hydrogen: High-Yield Production of Hydrogen from Biomass Sugars Catalyzed by in vitro Synthetic Biosystems
  - II.E.3 Oregon State University: Novel Hybrid Microbial Electrochemical System for Efficient Hydrogen Generation from Biomass
- II.F Basic Energy Sciences
  - II.F.1 University of California, Irvine: Tailoring Hydrogen Evolution Reaction (HER) Catalysts for Operation at Specific pH Values
  - II.F.2 University of Southern California: Hybrid Perovskites and Non-Adiabatic Dynamics Simulations: Catching Realistic Aspects of the Charge Recombination Process
  - II.F.3 University of Rochester: Nano-bio Systems for Light-Driven Hydrogen Production
  - II.F.4 National Renewable Energy Laboratory: Mechanistic Investigations on Hydrogen Catalysis by [FeFe]-Hydrogenase
  - II.F.5 National Renewable Energy Laboratory: Bioenergetics of Photosynthetic Energy Transduction: Control of Pathways through Redox Biochemistry
  - II.F.6 Brookhaven National Laboratory: Reversible Conversion between CO_2/H_2 and Formic Acid by Molecular Catalysts

III. Hydrogen Delivery
- III.0 Hydrogen Delivery Sub-Program Overview
- III.1 Sandia National Laboratories: Fatigue Performance of High-Strength Pipeline Steels and Their Welds in Hydrogen Gas Service
- III.2 Southwest Research Institute: Hydrogen Compression Application of the Linear Motor Reciprocating Compressor (LMRC)
- III.3 Wiretough Cylinders, LLC: Low Cost Hydrogen Storage at 875 bar Using Steel Liner and Steel Wire Wrap
- III.4 GVD Corporation: Advanced Barrier Coatings for Harsh Environments
- III.5 National Renewable Energy Laboratory: Improved Hydrogen Liquefaction through Heisenberg Vortex Separation of para- and ortho-hydrogen
- III.6 Pacific Northwest National Laboratory: Magnetocaloric Hydrogen Liquefaction
- III.7 National Renewable Energy Laboratory: 700 bar Hydrogen Dispenser Hose Reliability and Improvement
- III.8 Nanosonic, Inc.: Cryogenically Flexible, Low Permeability H_2 Delivery Hose
- III.9 Argonne National Laboratory: Hydrogen Refueling Analysis of Heavy Duty Fuel Cell Vehicle Fleets
- III.10 Lawrence Livermore National Laboratory: Liquid Hydrogen Infrastructure Analysis
- III.11 Giner, Inc.: Electrochemical Compression
- III.12 Greenway Energy, LLC: Hybrid Electrochemical Hydrogen/Metal Hydride Compressor
- III.13 Sandia National Laboratories: Metal Hydride Compression
- III.14 Ivys Energy Solutions: Advancing Hydrogen Dispenser Technologies by Using Innovative Intelligent Network
- III.15 National Renewable Energy Laboratory: H2FIRST Consolidation
- III.16 Sandia National Laboratories: Reference Station Design, Phase II

IV. Hydrogen Storage
- IV.0 Hydrogen Storage Sub-Program Overview
- IV.A Analysis
  - IV.A.1 Argonne National Laboratory: System Analysis of Physical and Materials-Based Hydrogen Storage
  - IV.A.2 Strategic Analysis, Inc.: Hydrogen Storage Cost Analysis
- IV.B System Engineering
  - IV.B.1 National Renewable Energy Laboratory: Hydrogen Storage System Modeling: Public Access, Maintenance, and Enhancements
  - IV.B.2 Savannah River National Laboratory: Investigation of Solid State Hydrides for Autonomous Fuel Cell Vehicles
- IV.C Advanced Materials
  - IV.C.1 Sandia National Laboratories: HyMARC (Core): SNL Effort
  - IV.C.2 Lawrence Livermore National Laboratory: HyMARC (Core): LLNL Effort
  - IV.C.3 Lawrence Berkeley National Laboratory: HyMARC (Core): LBNL Effort
  - IV.C.4 National Renewable Energy Laboratory: HyMARC (Support): NREL Effort
  - IV.C.5 Pacific Northwest National Laboratory: HyMARC (Support): PNNL Effort
  - IV.C.6 Lawrence Berkeley National Laboratory: HyMARC (Support): LBNL Effort
  - IV.C.7 Liox Power: HyMARC Seedling: Electrolyte Assisted Hydrogen Storage Reactions
  - IV.C.8 The Pennsylvania State University: HyMARC Seedling: Developing a Novel Hydrogen Sponge with Ideal Binding Energy and High Surface Area for Practical Hydrogen Storage
  - IV.C.9 Argonne National Laboratory: HyMARC Seedling: “Graphene-Wrapped” Complex Hydrides as High-Capacity, Regenerable Hydrogen Storage Materials
  - IV.C.10 University of Missouri–St. Louis: HyMARC Seedling: Fundamental Studies of Surface-Functionalized Mesoporous Carbons for Thermodynamic Stabilization and Reversibility of Metal Hydrides
  - IV.C.11 University of Hawaii at Manoa: HyMARC Seedling: Development of Magnesium Boride Etherates as Hydrogen Storage Materials

IV. Hydrogen Storage (Continued)

IV.C Advanced Materials (Continued)

IV.C.12 Lawrence Livermore National Laboratory: Improving the Kinetics and Thermodynamics of Mg $(BH_4)_2$ for Hydrogen Storage

IV.C.13 Ames Laboratory: High-Capacity Hydrogen Storage Systems via Mechanochemistry

IV.C.14 California Institute of Technology: Design and Synthesis of Materials with High Capacities for Hydrogen Physisorption

IV.C.15 University of Michigan: Hydrogen Adsorbents with High Volumetric Density: New Materials and System Projections

IV.C.16 Savannah River National Laboratory: Electrochemical Reversible Formation of Alane

IV.C.17 Ardica Technologies, Inc.: Low-Cost α-Alane for Hydrogen Storage

IV.D Advanced Tanks

IV.D.1 Center for Transportation and the Environment: Conformable Hydrogen Storage Coil Reservoir

IV.D.2 Materia, Inc.: Next Generation Hydrogen Storage Vessels Enabled by Carbon Fiber Infusion with a Low Viscosity, High Toughness Resin System

IV.D.3 Sandia National Laboratories: Development, Selection and Testing to Reduce Cost and Weight of Materials for BOP Components

IV.D.4 VENCORE Solutions and Services: Integrated Insulation System for Automotive Cryogenic Storage Tanks

V. Fuel Cells

V.0 Fuel Cells Sub-Program Overview

V.A Catalysts & Electrodes

V.A.1 Los Alamos National Laboratory: ElectroCat (Electrocatalysis Consortium)

V.A.2 University of New Mexico: Development of PGM-Free Catalysts for Hydrogen Oxidation Reaction in Alkaline Media

V.A.3 Northeastern University: Innovative Non-PGM Catalysts for High-Temperature PEMFCs

V.A.4 Argonne National Laboratory: Tailored High-Performance Low-PGM Alloy Cathode Catalysts

V.A.5 Brookhaven National Laboratory: Platinum Monolayer Electrocatalysts

V.A.6 National Renewable Energy Laboratory: Extended Surface Electrocatalyst Development

V.A.7 3M Company: Highly Active, Durable, and Ultra-Low PGM NSTF Thin Film ORR Catalysts and Supports

V.A.8 General Motors: Highly Accessible Catalysts for Durable High-Power Performance

V.A.9 Washington University at St. Louis: Corrosion-Resistant Non-Carbon Electrocatalyst Supports for PEFCs

V.A.10 pH Matter LLC: Regenerative Fuel Cell System (SBIR Phase II)

V.A.11 Greenway Energy, LLC: Development of Corrosion Resistant Carbon (CRC) Support for Ultra-Low Platinum Group Metal (PGM) Catalysts (SBIR Phase I)

V.A.12 Certaintech, Inc.: Mesoporous Non-Carbon Catalyst Supports of PEMFC (SBIR I)

V.A.13 Pajarito Powder: Development of Durable Active Supports for Low Platinum Group Metal Catalysts (SBIR I)

V.A.14 pH Matter LLC: Multi-Functional Catalyst Support (SBIR I)

V.A.15 Forge Nano: Highly Robust Low PGM MEAs Based upon Composite Supports (SBIR I)

V.A.16 Los Alamos National Laboratory: Advanced Electro-Catalysts through Crystallographic Enhancement

V.A.17 Ford Motor Company: Vapor Deposition Process for Engineering of Dispersed PEMFC ORR $Pt/NbO_x/C$ Catalysts

V.B Fuel Cell Performance & Durability

V.B.1 Los Alamos National Laboratory: FC-PAD: Fuel Cell Performance and Durability Consortium

V.B.2 Oak Ridge National Laboratory: FC-PAD: Components and Characterization

V.B.3 Lawrence Berkeley National Laboratory: FC-PAD: Electrode Layers and Optimization

V. Fuel Cells (Continued)

V.B Fuel Cell Performance & Durability (Continued)

V.B.4 3M Company: Novel Ionomers and Electrode Structures for Improved PEMFC Electrode Performance at Low PGM Loadings

V.B.5 General Motors: Durable High-Power Membrane Electrode Assemblies with Low Pt Loading

V.B.6 United Technologies Research Center: High Performance Polymer Electrolyte Membrane Fuel Cell Electrode Structures

V.B.7 Vanderbilt University: Fuel Cell Membrane Electrode Assemblies with Ultra-Low Pt Nanofiber Electrodes

V.C Membranes/Electrolytes

V.C.1 3M Company: New Fuel Cell Membranes with Improved Durability and Performance

V.C.2 Colorado School of Mines: Advanced Hybrid Membranes for Next Generation PEMFC Automotive Applications

V.C.3 FuelCell Energy, Inc.: Smart Matrix Development for Direct Carbonate Fuel Cell

V.C.4 Giner, Inc.: Ionomer Dispersion Impact on Fuel Cell and Electrolyzer Performance and Durability (SBIR Phase II TTO)

V.C.5 University of Delaware: Highly Stable Anion Exchange Membranes for High-Voltage Redox-Flow Batteries

V.C.6 Los Alamos National Laboratory: Advanced Materials for Fully-Integrated MEAs in AEMFCs

V.C.7 National Renewable Energy Laboratory: Advanced Ionomers and MEAs for Alkaline Membrane Fuel Cells

V.D MEAs, Cells, and Other Stack Components

V.D.1 TreadStone Technologies, Inc.: Novel Structured Metal Bipolar Plates for Low Cost Manufacturing

V.D.2 Advent Technologies, Inc.: Facilitated Direct Liquid Fuel Cells with High Temperature Membrane Electrode Assemblies

V.D.3 Giner, Inc.: Advanced Catalysts and Membrane Electrode Assemblies (MEAs) for Reversible Alkaline Membrane Fuel Cells

V.E Testing and Technical Assessment

V.E.1 National Institute of Standards and Technology: Neutron Imaging Study of the Water Transport in Operating Fuel Cells

V.E.2 Los Alamos National Laboratory: Technical Assistance to Developers

V.E.3 National Renewable Energy Laboratory: Fuel Cell Technology Status: Degradation

V.E.4 Argonne National Laboratory: Performance and Durability of Advanced Automotive Fuel Cell Stacks and Systems with Dispersed Alloy Cathode Catalyst in Membrane Electrode Assemblies

V.E.5 Strategic Analysis, Inc.: Fuel Cell Vehicle Cost Analysis

VI. Manufacturing R&D

VI.0 Manufacturing R&D Sub-Program Overview

VI.1 National Renewable Energy Laboratory: Fuel Cell Membrane Electrode Assembly Manufacturing R&D

VI.2 Ohio Fuel Cell Coalition: Clean Energy Supply Chain and Manufacturing Competitiveness Analysis for Hydrogen and Fuel Cell Technologies

VI.3 Virginia Clean Cities at James Madison University: Fuel Cell and Hydrogen Opportunity Center, www.hfcnexus.com (Hydrogen Fuel Cell Nexus)

VI.4 GLWN, Westside Industrial Retention & Expansion Network: U.S. Clean Energy Hydrogen and Fuel Cell Technologies: A Competiveness Analysis

VI.5 Automated Dynamics: Continuous Fiber Composite Electrofusion Coupler

VI.6 Mainstream Engineering: In-line Quality Control of PEM Materials

VI.7 National Renewable Energy Laboratory: Manufacturing Competitiveness Analysis for Hydrogen Refueling Stations

VII. Technology Validation

VII.0 Technology Validation Sub-Program Overview

VII.A Vehicles

VII.A.1 National Renewable Energy Laboratory: Fuel Cell Electric Vehicle Evaluation

VII.A.2 National Renewable Energy Laboratory: Technology Validation: Fuel Cell Bus Evaluations

VII.A.3 Center for Transportation and the Environment: Fuel Cell Hybrid Electric Delivery Van Project

VII.B Hydrogen Infrastructure

VII.B.1 Electricore: Innovative Advanced Hydrogen Mobile Fueler

VII.B.2 National Renewable Energy Laboratory: Hydrogen Station Data Collection and Analysis

VII.B.3 Gas Technology Institute: Performance Evaluation of Delivered Hydrogen Fueling Stations

VII.B.4 National Renewable Energy Laboratory: Hydrogen Component Validation

VII.B.5 Lawrence Livermore National Laboratory: Liquid Hydrogen Pump Performance and Durability Testing

VII.B.6 National Renewable Energy Laboratory: Hydrogen Meter Benchmark Testing

VII.C Hydrogen Energy Storage/Grid Integration

VII.C.1 National Renewable Energy Laboratory: Optimal Stationary Fuel Cell Integration and Control (Energy Dispatch Controller)

VII.C.2 Lawrence Berkeley National Laboratory: Integrated Systems Modeling of the Interactions between Stationary Hydrogen, Vehicles, and Grid Resources

VII.C.3 Idaho National Laboratory: Dynamic Modeling and Validation of Electrolyzers in Real-Time Grid Simulation

VII.C.4 FuelCell Energy, Inc.: Modular SOEC System for Efficient Hydrogen Production at High Current Density

VII.D H2@Scale

VII.D.1 National Renewable Energy Laboratory: H2@Scale Analysis

VII.D.2 Idaho National Laboratory: High-temperature Electrolysis Test Stand

VIII. Safety, Codes and Standards

VIII.0 Safety, Codes & Standards Sub-Program Overview

VIII.1 National Renewable Energy Laboratory: National Codes and Standards Development and Outreach

VIII.2 Sandia National Laboratories: R&D for Safety, Codes and Standards: Materials and Components Compatibility

VIII.3 Los Alamos National Laboratory: Hydrogen Fuel Quality

VIII.4 Sandia National Laboratories: R&D for Safety, Codes and Standards: Hydrogen Behavior

VIII.5 Sandia National Laboratories: Hydrogen Quantitative Risk Assessment

VIII.6 Pacific Northwest National Laboratory: Hydrogen Safety Panel, Safety Knowledge Tools and First Responder Training Resources

VIII.7 National Renewable Energy Laboratory: NREL Hydrogen Sensor Testing Laboratory

VIII.8 Fuel Cell & Hydrogen Energy Association: Fuel Cell & Hydrogen Energy Association Codes and Standards Support

VIII.9 Pacific Northwest National Laboratory: Compatibility of Polymeric Materials Used in the Hydrogen Infrastructure

VIII.10 Sandia National Laboratories: Enabling Hydrogen Infrastructure through Science-Based Codes and Standards

VIII.11 City and County of San Francisco: Advancing Fuel Cell Vehicles in San Francisco and Beyond

IX. Systems Analysis

IX.0 Systems Analysis Sub-Program Overview

IX.1 Argonne National Laboratory: Employment Impacts of Hydrogen and Fuel Cell Technologies

IX.2 Argonne National Laboratory: Regional Water Stress Analysis with Hydrogen Production at Scale

IX.3 Argonne National Laboratory: Cost Benefits Analysis of Technology Improvement in Light-Duty Fuel Cell Vehicles

IX. Systems Analysis (Continued)

- IX.4 Sandia National Laboratories: Hydrogen Analysis with the Sandia ParaChoice Model
- IX.5 National Renewable Energy Laboratory: Sustainability Analysis: Hydrogen Regional Sustainability (HyReS)
- IX.6 National Renewable Energy Laboratory: Hydrogen Financial Analysis Scenario Tool (H2FAST) Updates with Analysis of 101st Station
- IX.7 National Renewable Energy Laboratory: Regional Supply of Hydrogen
- IX.8 Argonne National Laboratory: Greenhouse Gas (GHG) Emissions and Petroleum Use Reduction of Medium- and Heavy-Duty Trucks
- IX.9 Argonne National Laboratory: Agent-Based Modeling of Consumer Behavior
- IX.10 Argonne National Laboratory: Life-Cycle Analysis of Air Pollutants Emission for Refinery and Hydrogen Production from SMR
- IX.11 National Renewable Energy Laboratory: Resource Availability for Hydrogen Production
- IX.12 Argonne National Laboratory: Benefits Analysis of Multi-Fuel/Vehicle Platforms with a Focus on Hydrogen Fuel Cell Electric Vehicles

X. Market Transformation

- X.0 Market Transformation Sub-Program Overview
- X.1 Hawaii Natural Energy Institute: Hydrogen Energy Systems as a Grid Management Tool
- X.2 Plug Power: Ground Support Equipment Demonstration
- X.3 Sandia National Laboratories: Maritime Fuel Cell Generator Project
- X.4 Pacific Northwest National Laboratory: Demonstration of Fuel Cell Auxiliary Power Unit (APU) to Power Truck Refrigeration Units (TRUs) in Refrigerated Trucks
- X.5 Federal Express Corporation: FedEx Express Hydrogen Fuel Cell Extended-Range Battery Electric Vehicles
- X.6 US Hybrid: Northeast Demonstration and Deployment of FCRx200

XI. Small Business Innovation Research

XII. Acronyms, Abbreviations, and Definitions

XIII. Primary Contacts Index

XIV. Hydrogen and Fuel Cells Program Contacts

XV. Project Listings by State

XVI. Project Listings by Organization

I.0 Introduction

The U.S. Department of Energy's Hydrogen and Fuel Cells Program (the Program) focuses primarily on early-stage research and development (R&D) activities and works with stakeholders to enable the widespread commercialization of hydrogen and fuel cell technologies across diverse applications. The Program is coordinated across the U.S. Department of Energy (DOE), incorporating activities in the offices of Energy Efficiency and Renewable Energy (EERE)—led through the Fuel Cell Technologies Office (FCTO)—Fossil Energy, Nuclear Energy (NE), Science, and Advanced Research Projects Agency – Energy (ARPA-E). Every year, the FCTO publishes an Annual Progress Report documenting progress, accomplishments, and technology status with respect to performance metrics. This report includes over 700 pages of accomplishments achieved by DOE-funded projects in the last year. The following summary includes only a few examples. More details can be found in the individual sub-program introductions, subsequent project reports, and in the corresponding 2017 Annual Merit Review and Peer Evaluation Report.[1]

In Fiscal Year (FY) 2017, Congress appropriated approximately $101 million for EERE's FCTO hydrogen and fuel cell activities and approximately $30 million for the Office of Fossil Energy's solid oxide fuel cell activities. In addition, funding within ARPA-E, NE, and the Office of Science relevant to hydrogen and fuel cell activities amounted to approximately $47 million, $2 million, and $22 million, respectively. This represents a total DOE budget for FY 2017 of approximately $202 million related to hydrogen and fuel cell technologies.[2] While FCTO is the primary office responsible for hydrogen and fuel cell activities, the Program coordinates across all relevant offices, and pertinent activities are identified during the year based on gap analyses and merit-reviewed project proposals that may be selected through competitive funding opportunities which vary from year to year. While the specific project summaries in this report focus on FCTO activities, examples of progress within other offices are also provided below.

In FY 2017, the Program's primary efforts focused on early-stage R&D work with three new consortia (ElectroCat [Electrocatalysis Consortium], HydroGEN [HydroGEN Advanced Water Splitting Materials consortium], and HyMARC [Hydrogen Materials—Advanced Research Consortium]), which aim to make unique, world-class expertise and capabilities of national labs more accessible and available to university and industry partners across the country. This approach creates a collaborative foundation for an innovation ecosystem that can bring in a steady influx of competitively selected projects to tackle the most pressing technical challenges in the field. Under the umbrella of DOE's Energy Materials Network, these efforts aim to use state-of-the-art computational, high-throughput/combinatorial synthesis and characterization tools; data management such as machine learning; and other approaches to accelerate progress through a multi-disciplinary team approach.

Each year, FCTO tracks U.S. patents granted specifically as a result of its funding as just one indicator of cutting-edge innovation. Cumulatively, FCTO funding has led to more than 650 hydrogen and fuel cell patents, with approximately 40% coming from the national labs, and more than 30 technologies entering today's market, with potential for another 75 to be commercialized within the next few years.[3] Some of these include catalysts for fuel cells, high-pressure hydrogen tanks, electrolyzers for hydrogen production, and fuel cell system components. DOE-funded research has also cut the cost of automotive fuel cells by 60% in the last decade,[4] quadrupled durability to over 120,000 miles,[5] and cut electrolyzer stack costs by 80% since 2002.[6]

---

[1] https://www.hydrogen.energy.gov/annual_review17_report.html

[2] Hydrogen and Fuel Cells Program budgets—https://www.hydrogen.energy.gov/budget.html, https://www.hydrogen.energy.gov/pdfs/htac_feb18_01_satyapal.pdf—and subsequent awards by ARPA-E

[3] Pathways to Commercial Success: Technologies and Innovations Enabled by the U.S. Department of Energy Fuel Cell Technologies Office, https://energy.gov/eere/fuelcells/downloads/pathways-commercial-success-technologies-and-innovations-enabled-us

[4] *Fuel Cell System Cost–2016*, Program Record (Hydrogen and Fuel Cells Program) 16020, U.S. Department of Energy, 2016. https://www.hydrogen.energy.gov/pdfs/16020_fuel_cell_system_cost_2016.pdf

[5] *On-Road Fuel Cell Stack Durability–2016*, Program Record (Hydrogen and Fuel Cell Technologies Program) 16019, U.S. Department of Energy, 2016. https://www.hydrogen.energy.gov/pdfs/16019_fuel_cell_stack_durability_2016.pdf

[6] *Hydrogen Production Cost From PEM Electrolysis*, Program Record (Hydrogen and Fuel Cells Program) 14004, U.S. Department of Energy, 2014. https://www.hydrogen.energy.gov/pdfs/14004_h2_production_cost_pem_electrolysis.pdf

PROGRESS AND ACCOMPLISHMENTS BY KEY ACTIVITY

Fuel Cells

One of the most important metrics used to guide the Fuel Cells sub-program's R&D efforts is the projected high-volume manufacturing cost for automotive fuel cells, which is tracked on an annual basis. The sub-program is targeting an interim cost of $40/kW and durability of 5,000 hours. Long-term competitiveness with alternative powertrains is expected to require further cost reduction to $30/kW and durability of 8,000 hours, which represent the sub-program's ultimate targets. This year, the preliminary cost projection for an 80-kW_{net} automotive polymer electrolyte membrane (PEM) fuel cell system based on next-generation laboratory technology and operating on direct hydrogen is $50/$kW_{net}$ when manufactured at 100,000 units/yr and $45/$kW_{net}$ when manufactured at a volume of 500,000 units/yr.[7]

In FY 2017, the core group of national laboratories in the ElectroCat consortium (led by Los Alamos National Laboratory and Argonne National Laboratory [ANL]) established a list of capabilities and evaluated their value to the community in accelerating progress towards developing completely platinum-group-metal (PGM)-free catalysts for fuel cells. Major improvements to fuel cell catalysts included an atomically dispersed (AD) Fe-N-C catalyst, developed to create single atomic Fe sites on the catalyst surface (no nanoparticles, minimal Fe clustering), as seen in microscopy images. More details and examples are provided in this report.

The Program also launched the L'Innovator (coined for "Lab Innovator") pilot program, which bundles national lab intellectual property to increase its value and mitigate risk (for example catalyst from one lab, membrane from another, and electrode fabrication intellectual property from another). This intellectual property is offered to the private sector for commercialization. In FY 2017, the first company was selected for potential licensing, contingent on industry/investor cost share.

Hydrogen Production

Significant progress was made by the Hydrogen Production sub-program on several important fronts in FY 2017. In January 2017, DOE announced SimpleFuel as the winner of the $1 million H2 Refuel H-Prize Competition. Launched in October 2014, the H2 Refuel H-Prize Competition challenged America's innovators to deploy an on-site hydrogen generation system, using electricity or natural gas, that can be used in homes, community centers, small businesses, or similar locations to fuel hydrogen vehicles. During the competition, SimpleFuel demonstrated that its home-scale refueling appliance can provide a 1-kilogram fill to vehicles in 15 minutes or less at 700 bar using hydrogen produced via electrolysis, with a cost-effective design that minimizes setback distances and reduces the physical footprint of the system.

The HydroGEN advanced water splitting materials consortium, comprised of six core national laboratories (National Renewable Energy Laboratory [NREL], Sandia National Laboratories [SNL], Lawrence Berkeley National Laboratory, Lawrence Livermore National Laboratory, Idaho National Laboratory, and Savanna River National Laboratory), launched its expanded website featuring an advanced search engine to facilitate access to the consortium's more than 80 unique world-class research capabilities.[8] HydroGEN also launched its data portal aligned with DOE's Energy Materials Network guidelines and requirements. Nineteen new projects were competitively selected in areas of advanced water splitting materials R&D, which leverage the HydroGEN Consortium's core capabilities. HydroGEN's photoelectrochemical team at NREL published three high-impact journal articles in *Nature Energy* related to the synthesis innovations, rigorous characterization, and benchmark validation of their recent world-record photoelectrochemical device. NREL's ground-breaking device incorporating an inverted metamorphic multijunction structure of III–V semiconductors has achieved photoelectrochemical solar-to-hydrogen conversion efficiencies greater than 16%, exceeding previous records closer to 10%. Besides photoelectrochemical research, the sub-program's R&D supports collaboration between FCTO and NE by enabling integrated energy systems using high- and low-temperature electrolyzers, as well as thermochemical approaches that can use high-temperature solar, nuclear, or other heat sources for hydrogen production.

[7] *Fuel Cell System Cost–2016*, Program Record (Hydrogen and Fuel Cells Program) 16020, U.S. Department of Energy, 2016. https://www.hydrogen.energy.gov/pdfs/16020_fuel_cell_system_cost_2016.pdf
[8] https://energy.gov/eere/fuelcells/hydrogen-advanced-water-splitting-materials-consortium

In addition, based on appropriations guidance, the Program allocated $3 million from FY 2017 funding for R&D on hydrogen production using new chemical synthesis methods that break apart natural gas to solid carbon and hydrogen. A report[9] was prepared on the status of these technologies, and a call for innovative concepts was issued in conjunction with the Office of Fossil Energy's National Energy Technology Laboratory. FCTO and the National Energy Technology Laboratory will report on the outcomes once projects are initiated.

Hydrogen Delivery

Hydrogen delivery, including transport, bulk storage, and dispensing, is increasingly being seen as critical to the rollout of hydrogen infrastructure. In FY 2017, ANL's innovative tube trailer consolidation approach, which is expected to lower hydrogen fueling cost by 40%, received widespread interest by industry, and a patent was issued.[10] The strategy involves using a fueling station's compressor to pressurize the hydrogen in the tube trailer during off-peak hours. As a result, the compressor has high-pressure hydrogen available during peak hours and is able to achieve higher flow rates than otherwise possible. In this way, a station can satisfy its daily demand with a compressor that costs 60% less than under normal operation.[11] The strategy is being evaluated experimentally at NREL through the Hydrogen Fueling Infrastructure Research and Station Technology (H2FIRST) project and is also being demonstrated by industry. H2FIRST is just one example of efforts aligned with appropriations guidance to engage national laboratories to pursue novel advanced demonstrations, and it provides feedback to early-stage R&D activities.

In FY 2017, materials R&D funded by DOE and the U.S. Department of Transportation was used in the modification of the ASME B31.12 Code for Hydrogen Piping and Pipelines. Evaluations of the performance of high-strength steel and fiber-reinforced polymer in high-pressure hydrogen service over the past decade have led to Code modifications that (1) allow for the use of fiber-reinforced pipeline in 170-bar hydrogen service and (2) remove thickness penalties on X70 steel used in 100-bar hydrogen service. Each of these modifications can independently lower the installation costs (material and labor) of hydrogen pipelines by 25%.[12] Such examples show how early-stage R&D can impact codes and standards, enabling industry to benefit from core capabilities at the national labs.

Hydrogen Storage

FY 2017 marked the second full year of efforts within HyMARC, the Energy Materials Network consortium on hydrogen storage. The work of the core team of national laboratory partners (SNL–lead, Lawrence Livermore National Laboratory, and Lawrence Berkeley National Laboratory) made a great deal of progress as it continued to address scientific gaps impeding the advancement of materials-based storage. For example, an experimental investigation involving several advanced characterization techniques showed that titanium is not present on the surface during hydrogen desorption from Ti-doped $NaAlH_4$, supporting the "zipper" mechanism and invalidating several other published mechanisms. This study demonstrates the power of bringing together these laboratory capabilities under the umbrella of HyMARC, as it utilized low energy ion scattering at SNL, X-ray adsorption spectroscopy at SNL, and scanning transmission X-ray microscopy as part of the Advanced Light Source project at Lawrence Berkeley National Laboratory. HyMARC researchers also continued to develop extensive theoretical modeling capabilities to complement these experimental tools. Modeling work at Lawrence Livermore National Laboratory on $Mg(BH_4)_2$, a promising material with over 14 wt.% theoretical capacity and favorable thermodynamics, and its absorption/desorption reaction pathways continues to assist other HyMARC core efforts.

In FY 2017, NREL completed the multi-laboratory round robin study on volumetric uptake in sorbents, including national laboratory, university, industrial, and international partners, and analyzed the results to identify sources of error in volumetric uptake measurements. These results are being prepared for dissemination to the hydrogen storage community.

[9] https://www.pnnl.gov/main/publications/external/technical_reports/PNNL-26726.pdf
[10] Elgowainy, A. (2017). U.S. Patent No. 9,739,418. Washington, D.C.: U.S. Patent and Trademark Office.
[11] Elgowainy, A., Reddi, K., Sutherland, E., and Joseck, F. "Tube-trailer consolidation strategy for reducing hydrogen refueling station costs." International Journal of Hydrogen Energy (2014). http://www.sciencedirect.com/science/article/pii/S036031991402833X
[12] Cost assessment for fiber-reinforced pipeline has been based on consultation with members of industry. Cost assessment for steel is published in: Fekete, J., Sowards, J.W., and Amaro, R.L. "Economic impact of applying high strength steels in hydrogen gas pipelines." International Journal of Hydrogen Energy (2015). <http://www.sciencedirect.com/science/article/pii/S036031991501575X?via%3Dihub>

Manufacturing R&D

GLWN completed an analysis of the global fuel cell and hydrogen supply chain to determine opportunities, as well as in-depth analysis of the supply chain for five key components (bipolar plates, membranes, gas diffusion layers, catalysts, and hydrogen storage vessels) at different manufacturing volumes.

The Program also continued its efforts on quality control R&D for roll-to-roll manufacturing. For example, NREL identified and tested defective samples of membrane electrode assemblies. Preliminary results indicated that defects less than 10 µm have no immediate effect on performance, but defects larger than 300 µm decrease performance. NREL also demonstrated real-time imaging of membrane thickness. Another success is the partnership of the small company, Mainstream Engineering, with NREL to develop a device to monitor defects; the device should be available in early 2019.

Technology Validation

In FY 2017, fuel cell bus durability exceeding the ultimate DOE–U.S. Department of Transportation target of 25,000 hours was validated based on one bus fuel cell power plant; seven additional fuel cell systems have surpassed the 2016 target of 18,000 hours. More R&D will be required to meet both cost and durability targets simultaneously, but these durability results through use in real-world passenger service (by AC Transit) show tremendous progress and opportunity.

The Program also continued to collect and utilize valuable data through partnership with state and industry activities. For example, using the data reported to NREL from 26 retail hydrogen stations and nine non-retail stations in FY 2017, analyses were conducted on several categories including deployment, performance, reliability, utilization, safety, energy use, and hydrogen quality. Current analysis shows that max daily utilization is beginning to approach station capacity at a few stations, which implies a need for larger and/or more stations to meet the upcoming vehicle demand. An increase in the amount of hydrogen dispensed each quarter results from more stations being built and more fuel cell electric vehicles (FCEVs) on the road. In 2016, over 107,000 kg of hydrogen were dispensed from retail stations. A further deep dive into maintenance by equipment type shows that hydrogen dispensers are now the primary items needing maintenance both in terms of number of events and labor hours. These examples show how technology validation activities help feed back information to guide future early-stage R&D within the Program.

Market Transformation

Examples of progress in market transformation activities include first-of-their-kind prototypes for airport cargo delivery, medium-duty truck parcel delivery, and maritime applications for pier-side power and ultimately ship-board auxiliary power. For airport baggage tow tractors, an initial design has been completed and units have been assembled and tested in field operations. The stacks were redesigned after a root cause failure analysis, new stacks replaced the originals, and testing in the field is underway.

The Maritime Fuel Cell Generator Project, with funding leveraged by the Maritime Administration, is testing a first-of-its-kind hydrogen fuel cell power generator. Initial operation testing at a pier-side site was completed, with results confirming substantial energy efficiency improvements compared to diesel engines. Balance-of-plant components have been redesigned and replaced.

The Fuel Cell Hybrid Electric Medium-Duty Truck Project is developing a design for a battery electric powertrain system hybridized with fuel cell power to improve drive performance and range on a medium-duty cargo truck. The project has completed a prototype design, and vehicle testing is being initiated.

Safety, Codes and Standards

This sub-program focuses on foundational R&D that enables safety and informs the development of codes and standards by industry. In FY 2017, the sub-program collaborated with the National Institute for Standards and Technology, specifically on the standard for hydrogen metering accuracy. Previously, the standard was unachievable with available technology; however, as a result of collaborations between NREL and the National Institute for Standards and Technology and through support from the State of California, a modified hydrogen metrology standard of 5% was accepted in FY 2017, which now permits hydrogen to be sold at retail stations.

Also in FY 2017, the sub-program built on results from the previous year and released the Hydrogen Risk Assessment Model (HyRAM) Version 1.1 for public use. HyRAM, developed by SNL, enables quantitative risk assessment and performance-based design while also incorporating the sub-program's hydrogen behavior models.

In addition, model development and validation began for cryogenic hydrogen releases in the newly built cryogenic laboratory to help inform separation distances for liquid hydrogen. These unique national lab capabilities provide support on key infrastructure needs such as reducing station setback distances. Finally, the use of risk assessment was applied to real-world scenarios for the use of FCEVs in tunnels. Global stakeholders across industry and relevant code organizations provided significant positive feedback on the value of such tools, and further work to support such efforts is underway.

Systems Analysis

Systems Analysis activities are foundational to the Program and help identify technology gaps, impacts, and future R&D needs. ANL's Greenhouse gases, Regulated Emissions, and Energy use in Transportation (GREET) model was expanded to assess lifecycle petroleum use and air emissions of medium- and heavy-duty vehicles compared to baseline diesel. Simulation results show that medium- and heavy-duty FCEVs generally achieve 1.7 times better fuel economy (miles per diesel gallon equivalent) compared to conventional diesel vehicles.

ANL also analyzed the lifecycle freshwater consumption associated with various transportation fuels for light-duty vehicles in the United States using the water module of the GREET model. The results show the lifecycle water consumption for FCEVs can be comparable to that of conventional gasoline vehicles for certain fuel pathways, as illustrated in Figure 1. These efforts were coordinated across FCTO, EERE's Vehicle Technologies Office, and EERE's Bioenergy Technology Office to ensure consistency in assumptions across fuel and vehicle pathways.

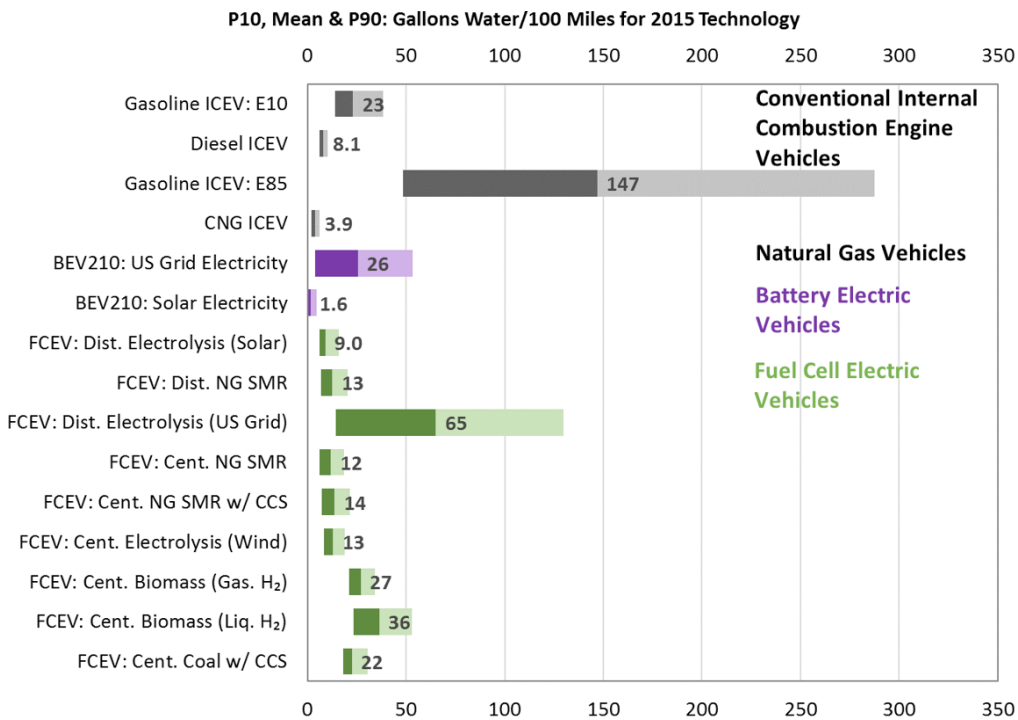

ICEV – internal combustion engine vehicle; E10 – a fuel blend consisting of 90% gasoline and 10% ethanol; E85 – a fuel blend consisting of 15% gasoline and 85% ethanol; CNG – compressed natural gas; BEV210 – battery electric vehicle with 210 miles all-electric range; NG – natural gas; Dist. – distributed; Cent. – central; SMR – steam methane reforming; CCS – carbon capture and sequestration; Gas. – gaseous; Liq. - liquid

FIGURE 1. Lifecycle water consumption per 100 miles driven (ANL). See DOE program record.[13]

Two separate projects evaluated the impacts of FCTO-funded R&D. One analysis showed that if the ultimate fuel cell and hydrogen storage R&D targets are both met, cost reduction could reach approximately $4,000 per FCEV. The second analysis concluded that successful deployment of FCTO-funded technologies in FCEVs could improve the fuel economy of the light-duty vehicle stock by 25% to 30% and reduce projected petroleum consumption by 0.3 million to approximately 1 million barrels per day.

[13] *Water Consumption for Light-Duty Vehicles' Transportation Fuels*, Program Record (EERE Offices of Fuel Cell, Vehicle, and Bioenergy Technologies) 17005, U.S. Department of Energy, 2017. https://www.hydrogen.energy.gov/pdfs/17005_water_consumption_ldv_fuels.pdf

OTHER PROGRAM ACTIVITIES AND HIGHLIGHTS FROM FY 2016–2017

ARPA-E Programs in Fuel Cells/Electrolyzers for Energy Conversion and Storage

The ARPA-E FY 2017 funding for fuel cells/electrolyzers for energy conversion and storage activities was approximately $47 million. The mission of the ARPA-E program is to develop new disruptive technologies for efficient, cost-effective electrical storage and generation systems using renewable energy and natural gas, with applications for transportation and for commercial and industrial power customers across the economy, resulting in increased energy efficiency and security, significant fuel and energy savings, and emissions reduction. The drivers are growth of intermittent renewable energy and cheap and abundant natural gas, the need for increased efficiency throughout the whole economy, an increased demand for clean/electrified transportation, and the growth of microgrids and distributed energy generation.

Renewable Energy to Fuels through Utilization of Energy-dense Liquids

The Renewable Energy to Fuels through Utilization of Energy-dense Liquids mission is to reduce transportation and storage costs of energy from remote renewable intermittent sources to consumers and to enable the use of existing infrastructure to deliver electricity or hydrogen at the end point. The budget in FY 2017 was $23 million. Specific program goals include the following.

- Develop catalytic or electrochemical fuel cracking to deliver hydrogen at 30 bar at a cost <$4.5/kg, enabling hydrogen fueling stations.
- Develop fuel cell technologies for conversion of fuels to electricity with source-to-use cost <$0.30/kWh.

Reliable Electricity Based on Electrochemical Systems

With an FY 2017 budget of approximately $3 million, the Reliable Electricity Based on Electrochemical Systems mission is to develop transformational electrochemical fuel cell technologies for distributed power generation to improve grid stability, increase energy security, and balance intermittent renewable technologies while reducing CO_2 emissions associated with current distributed generation systems. Specific accomplishments include the following.

- The Colorado School of Mines achieved 150 mW/cm^2 power density at 500°C on direct methane fuel and showed stability for thousands of hours. The project is now scaling up to larger prototypes.
- Georgia Institute of Technology achieved 200 mW/cm^2 power density at 500°C on 97% methane fuel.

Integration and Optimization of Novel Ion-Conducting Solids

Funded in FY 2016, the Integration and Optimization of Novel Ion-Conducting Solids mission is to create components for electrochemical cells using solid ion conductors to enable transformational performance and cost improvements. Specific accomplishments include the following.

- Increased the energy content of Li battery packs by >30% while reducing the cost of energy storage.
- Developed flow batteries with a fully installed cost of $150/kWh for a 5-h duration.
- Created alkaline-conducting membranes that open a path to fuel cells and electrolyzers without expensive, rare elements like Pt.

Innovative Natural-Gas Technologies for Efficiency Gain in Reliable and Affordable Thermochemical Electricity-Generation

With an FY 2017 budget of $20 million that will be expended in FY 2018, FY 2019, and FY 2020, the mission of Innovative Natural-Gas Technologies for Efficiency Gain in Reliable and Affordable Thermochemical Electricity-Generation is to reduce the cost and increase the primary energy efficiency associated with the provision of electric power to commercial and industrial customers. The approach taken is to support the development of natural-gas-fueled distributed generation systems (<1 MW) with electric efficiencies of ≥70% and installed costs of ≤$1,800/kW and to focus on engine–solid oxide fuel cell hybrid systems to leverage available thermo-economic synergies.

Office of Science, Basic Energy Sciences

The Basic Energy Sciences program within the Office of Science had a cross-cut spending level of $22 million in FY 2017. Hydrogen and fuel cells were among the topics in the Energy Frontier Research Center solicitation for which awards will be made in FY 2018. In FY 2017, Basic Energy Sciences held a basic research needs workshop on catalysis science coordinated across EERE and other programs.

Specific accomplishments include the following.

- New functional materials have been synthesized using metal-organic clusters as pore-partitioning agent inside nanoporous channels. With diverse and unprecedented compositions and functionalities, both on the framework and within the channel, these new materials have a number of potential applications such as catalysis, fuel storage, and chemical separation.
- In systems involving interfaces between catalytic surfaces and proton exchange membranes, reactive molecular dynamics, at least 1,000 times faster than ab initio molecular dynamics, has shown how the hydrophilicity of the surface affects the membrane structure, water network formation, and proton transport. Hydrophilic surfaces were found to promote robust water layer formation at the interface. Additionally, decreasing interaction between charged sulfonate groups and hydronium molecules increases diffusion.
- Post-exposure of metal organic framework materials to ethylenediamine forms a monolayer cap, which allows the trapping of small molecules, even when they are only weakly bound. The ability to create a molecular surface barrier layer on metal organic framework external surfaces constitutes an entirely new paradigm for trapping weakly adsorbing molecules within metal organic frameworks, with importance for gas storage and sequestration applications.

Office of Fossil Energy, Solid Oxide Fuel Cell Program

The Solid Oxide Fuel Cell Program within the Office of Fossil Energy had an enacted budget of $30 million in FY 2017. The Program's mission is to enable the generation of efficient, low-cost electricity from natural gas or coal. The near-term goal is to develop natural-gas-fueled distributed generation and small-scale, modular coal-fueled systems, with a long-term goal of coal and natural gas utility-scale applications with carbon capture and sequestration. Drivers include cost and efficiency benefits to coal and natural gas power systems and the development of near-term natural gas distributed generation applications. The Solid Oxide Fuel Cell Program maintains a portfolio of approximately 50 projects that focus on cell and core technology and systems development. Researchers from academia, national laboratories, research institutions, and small businesses collaborate with solid oxide fuel cell developers to address and resolve reliability issues, improve performance, and reduce the cost of solid oxide fuel cell power systems. Based on progressively larger natural-gas-fueled validation tests, MWe-class distributed generation solid oxide fuel cell power systems that are cost-competitive with existing distributed generation technologies are envisioned circa 2020.

Specific FY 2017 accomplishments include the following.

- Operated 50 kWe proof-of-concept system.
- Operated 200 kWe pressurized proof-of-concept system.
- Awarded contracts for two 250 kWe-class prototype system field tests.
- Developed multiple approaches to mitigate chromium-assisted system degradation.

Office of Nuclear Energy

NE is working with partners in EERE and industry to evaluate the potential demonstration of commercial-scale production of hydrogen using heat from a nuclear energy system. In addition to producing emissions-free electricity, some advanced nuclear reactor designs now under development by NE, which operate at very high temperatures, will be well suited for providing the low-cost heat necessary to economically produce hydrogen using promising new thermally-driven hydrogen production processes.

In FY 2017, NE provided $2 million in collaborative research funding to analyze, via advanced modeling and simulation tools, and develop the following technologies that use nuclear reactors to produce hydrogen, in collaboration with EERE's FCTO.

- High-temperature electrolysis (HTE): HTE uses electricity to produce hydrogen from steam instead of liquid water. This method promises higher efficiencies than standard electrolysis, which is employed commercially today. The new high-temperature design involves many technical challenges, including the development of high-temperature materials and membranes. FY 2017 research indicates the potential to use steam produced via current light water reactor technologies, in addition to advanced reactor designs, to support HTE.
- Reactor/hydrogen production process interface: The interface between the nuclear reactor and the hydrogen production system involves potentially long heat transfer paths at elevated temperatures, heat exchangers that are subject to both elevated temperature and corrosive chemical environments, new safety and regulatory issues, and supporting systems for chemical processes and hydrogen and oxygen storage. FY 2017 research under NE focused on developing high-fidelity, dynamic modeling and simulation tools that can be applied to determine optimal system design and operation for use of light water reactor technologies to support hydrogen production via HTE.
- Thermochemical water-splitting cycles: Previous research indicated strong potential for the use of thermochemical water splitting processes to produce hydrogen. Thermochemical cycles are a series of chemical reactions that convert water to hydrogen and oxygen using chemical catalysts at high temperatures. These processes offer the potential for high-efficiency hydrogen production at large-scale production rates, but the technology is relatively immature.

INTERNATIONAL ACTIVITIES

International Partnership for Hydrogen and Fuel Cells in the Economy (IPHE)

IPHE includes 18 member countries (Australia, Austria, Brazil, Canada, China, France, Germany, Iceland, India, Italy, Japan, the Netherlands, Norway, the Republic of Korea, the Russian Federation, South Africa, the United Kingdom, and the United States) and the European Commission. IPHE is a forum for governments to work together to advance worldwide progress in hydrogen and fuel cell technologies. IPHE also offers a mechanism for international R&D managers, researchers, and policy makers to share program strategies, early-stage R&D, and the status of demonstrations and various assessments. IPHE members embarked upon a second 10-year term in November 2013. An independent secretariat was established in 2015, and France is currently the Chair. The United States continues its strong role as Vice Chair. In FY 2017, the IPHE Steering Committee met in Gwangju, Republic of Korea (November 2016), and in Hanover, Germany (April 2017), to share progress and plans related to hydrogen and fuel cells.

International Energy Agency

The United States is also involved in international collaboration on hydrogen and fuel cell R&D through the International Energy Agency's Technology Collaboration Program on Advanced Fuel Cells. This Technology Collaboration Program provides a mechanism for member countries to share the results of pre-competitive R&D and analysis activities related to innovative fuel cell and electrolyzer technologies. In FY 2017, the Advanced Fuel Cells Technology Collaboration Program ramped up efforts. Outreach events and topical meetings will be included in future plans in addition to publication of new materials such as journal articles and books. The Executive Committee will explore standardization of measurement and reporting procedures in electrolysis to help facilitate R&D of different electrolyzer technologies.

EXTERNAL COORDINATION, INPUT, AND ASSESSMENTS

Hydrogen and Fuel Cells Technical Advisory Committee

The Hydrogen and Fuel Cells Technical Advisory Committee, a congressionally mandated committee to advise the Secretary of Energy, formally convened once in FY 2017. In July 2017, the Committee submitted its ninth annual report to DOE, which summarizes progress in hydrogen and fuel cell technologies, domestic and international R&D and demonstrations, and commercialization activities, and offers recommendations on the Department's hydrogen-related R&D activities and initiatives. Also in 2017, the Hydrogen Safety and Event Response Plan subcommittee completed its work to review and assess current resources such as safety plans; event response plans; current federal, state, and local requirements; and case studies to identify gaps and potential actions to address current and projected needs. The Committee submitted a report to the Energy Secretary summarizing the findings of the subcommittee, including recommendations to address the identified gaps.

Federal Inter-Agency Coordination

The Hydrogen and Fuel Cell Interagency Task Force, mandated by the Energy Policy Act of 2005, includes senior representatives from federal agencies supporting hydrogen and fuel cell activities, with DOE serving as the chair. One example of interagency collaboration was the development of a federal fleet strategy for early adoption of FCEVs to drive initial demand and lead by example. Four separate federal agencies—Veterans Affairs, Department of Defense, DOE, and National Aeronautics and Space Administration—each expressed interest in leasing FCEVs in California following DOE and task force input, to make use of and help grow the nascent hydrogen infrastructure there.

Another example involves DOE and the United States Postal Service. In FY 2017, the United States Postal Service installed approximately 90 fuel-cell-powered material handling equipment units at their Washington, D.C., Network Distribution Center. The Hydrogen and Fuel Cell Interagency Working Group held a webinar on the results of previous fuel cell forklift deployments within the Department of Defense and DOE, which led the United States Postal Service to move forward on its first deployment of fuel cell material handling equipment at its Capitol Heights (Maryland) Network Distribution Center. In addition, the Interagency Working Group continued to meet monthly, led by FCTO, to coordinate hydrogen and fuel cell activities across all relevant agencies.

FY 2017 Annual Merit Review and Peer Evaluation (AMR)

The Program's AMR took place June 5–9, 2017, in Washington, D.C., and provided an opportunity for the Program to obtain expert peer reviews of the projects it supports and to report its accomplishments and progress. This year, approximately 1,800 participants attended, and more than 380 experts peer-reviewed 150 of the Program's projects. The report summarizing the results and comments from these reviews is available on DOE's website.[14] The 2018 AMR will be held June 13–15 in Washington, D.C. For the first time, the AMR will include presentations from other federal agencies and state activities and will be preceded by a National Hydrogen and Fuel Cell Forum, showcasing industry progress, exhibits of technologies, and opportunities.

Funds Saved through Active Project Management

The AMR is a key part of the Program's comprehensive approach toward active management of its projects. Termination of underperforming projects—identified through the AMR as well as through go/no-go decisions (with criteria defined in the project scope of work)—helped the Program redirect approximately $3.3 million in funding in FY 2017, $2.4 million in funding in FY 2016, $1.6 million in funding in FY 2015, and over $42 million since FY 2010. In addition, the Program implements EERE's robust Active Project Management requirements to identify and resolve issues early and to mitigate risks in impactful ways, helping underperforming projects get back on track.

Hydrogen at Scale (H2@Scale) Activities

Finally, a cornerstone of the Program's activities and future plans is the H2@Scale concept. Numerous activities were conducted throughout FY 2017 in support of this effort.[15] H2@Scale is a DOE initiative to enable technology innovations that unlock revenue potential across multiple sectors. Figure 2 depicts the H2@Scale conceptual vision with hydrogen as an energy carrier, like electricity, but opening up many more value-added applications, in addition to enabling energy security, energy storage, and resilience. The premise of H2@Scale is that water-splitting technologies can be used to supply hydrogen to growing industries by leveraging low-cost sources of energy that are intermittently available throughout the year (such as solar or wind), and low-cost baseload power generation (such as nuclear), which are increasingly facing challenges as a higher proportion of renewables enter the market. R&D efforts include scalable concepts for dispatchable hydrogen production, delivery, and storage, including hydrogen carriers, liquefaction, materials development, and

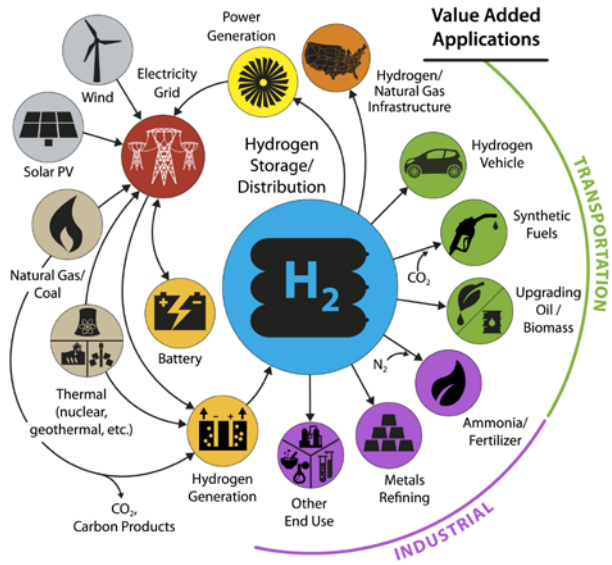

PV – photovoltaic

FIGURE 2. Schematic of H2@Scale Concept

[14] https://www.hydrogen.energy.gov/annual_review17_report.html
[15] https://energy.gov/eere/fuelcells/h2-scale

integration with diverse generation sources. To gather feedback from external stakeholders, DOE held multiple workshops and distributed a request for information. The Program also completed a report on hydrogen infrastructure, which included a discussion of the Department's coordination with other relevant agencies.

To advance H2@Scale from a strategic perspective, national labs conducted scenario analyses to determine the potential for hydrogen production using domestic resources across the nation as well as market demand potential. The next steps are to determine where hydrogen utilization could be increased from a business case perspective and to couple this increase with the potential for hydrogen generation at scale. The technical potential for hydrogen was estimated to be 60 million metric tons per year; this preliminary analysis will be updated and an estimate for the economic potential will be developed.

In FY 2017, Idaho National Laboratory developed a world-class HTE laboratory and test capability that includes a flexible test station plus infrastructure support for up to 250 kW HTE turnkey systems, in collaboration with NREL. The Program conducted R&D for modular solid oxide electrolysis systems with potential for producing hydrogen at a cost of $2/kg or less (excluding delivery, compression, storage, and dispensing). The Program also demonstrated sub-second response times and real-time simulation of the grid through a first-of-a-kind capability linking Idaho National Laboratory and NREL. These efforts demonstrate the value of hydrogen not only for energy storage, but also for grid resiliency and ancillary services such as frequency regulation, as a result of the dynamic response capabilities of electrolyzers.

A major accomplishment in FY 2017 was leveraging the private sector and state funds by offering state-of-the-art national lab capabilities to address the key challenges in enabling the H2@Scale vision. A total of 25 projects were selected as part of a Cooperative Research and Development Agreement call for proposals focused on H2@Scale. Projects selected through this process include work in hydrogen component R&D, hydrogen integration as an energy carrier, station risk analysis and safety R&D, and hydrogen production R&D. The Program will focus on these activities along with working groups to address remaining challenges in the coming year.

IN CLOSING ...

Now is an exciting time for the hydrogen and fuel cell industry. The fuel cell market has seen consistent growth in the last few years. In fact, more than 62,000 fuel cell systems and 500 MW in fuel cell power shipped in 2016, and on average, shipments of fuel cell systems are growing 30% annually worldwide.[16] More exciting yet, Toyota, Hyundai, and Honda all have commercially available fuel cell vehicle models, and growth capacity in the transportation sector nearly tripled in one year. This can be attributed to the introduction and expansion of fuel cell light-duty vehicles from Japan and Korea to new regions around the world, including the United States. In the United States, the stock of fuel cell electric vehicles has increased rapidly, especially in the past year. Research shows that there were nearly 3,500 fuel cell cars on the road, primarily in California, through the end of 2017. Automakers and hydrogen providers have made commitments for commercial deployments in the northeastern United States as well.

Another strong signal of the growing global interest in hydrogen and fuel cells is the launch of the Hydrogen Council in January 2017. The Hydrogen Council is a global initiative of chief executive officers in leading energy, transport, and industrial sectors. It includes major companies such as Toyota, General Motors, Honda, Hyundai, Shell, and others, who collectively represent total revenues of well over $1 trillion and have 1.7 million employees around the world. They have estimated the potential for over $2.5 trillion in revenues and 30 million jobs globally by 2050 as a result of hydrogen technologies worldwide across sectors.

At DOE, both Secretary of Energy Rick Perry and Daniel Simmons, Principal Deputy Assistant Secretary, were able to drive fuel cell electric vehicles that are part of the DOE fleet. Videos were created to commemorate both occasions and were posted online.[17] On loan from Toyota and Hyundai, DOE's fuel cell vehicles are used for interagency, congressional, and community outreach across the Washington, D.C., area, in addition to generating real-world fueling data that will help guide future early-stage R&D efforts.

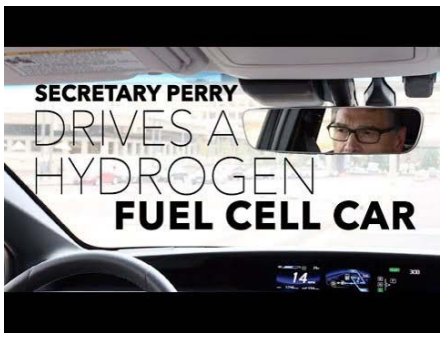

This is a critical time for fuel cells and hydrogen, particularly in addressing the challenge of hydrogen infrastructure. This introduction provides only a few examples of activities conducted within FY 2017. The hundreds of pages

[16] https://energy.gov/eere/fuelcells/downloads/fuel-cell-technologies-market-report
[17] https://energy.gov/eere/fuelcells/secretary-perry-drives-hydrogen-fuel-cell-car

that follow provide more detail from project recipients, demonstrating the value and impact of DOE funds. The DOE Hydrogen and Fuel Cells Program will continue to work in close collaboration with key stakeholders and will continue its strong commitment to effective stewardship of taxpayer dollars, fostering early-stage R&D and innovation, and enabling the success of hydrogen and fuel cell technologies as one component of an "all of the above" energy strategy for the nation.

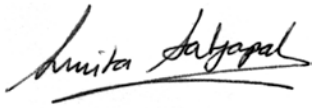

Dr. Sunita Satyapal
Director
Hydrogen and Fuel Cells Program
Fuel Cell Technologies Office
U.S. Department of Energy

II.0 Hydrogen Production Sub-Program Overview

INTRODUCTION

The Hydrogen Production sub-program supports early-stage research and development (R&D) of technologies that will enable the long-term viability of hydrogen as an energy carrier for a diverse range of end-use applications including transportation (e.g., specialty vehicles, cars, trucks, and buses), stationary power (e.g., backup power and combined heat and power systems), portable power (e.g., auxiliary power units), and chemical processing (e.g., fertilizer production, oil refining, and methanol production). In support of R&D needs identified through the U.S. Department of Energy's (DOE's) H2@Scale efforts, the Hydrogen Production sub-program is developing a portfolio of hydrogen production technology pathways utilizing a variety of sustainable domestic energy sources and feedstocks.

The Fuel Cell Technologies Office, within DOE's Office of Energy Efficiency and Renewable Energy, is developing technologies that include advanced electrochemical water splitting (including high temperature/pressure operations and novel catalysts/membranes), direct solar water splitting (including thermochemical and photoelectrochemical processes), as well as novel reforming processes of hydrocarbon and waste-stream feedstocks (including thermal, catalytic, and microbial-based processes).

Complementing the Fuel Cell Technologies Office efforts, multiple DOE offices are engaged in synergistic R&D that is relevant to hydrogen production, including:

- The Office of Science's Basic Energy Sciences program conducts research to expand the foundational understanding of processes and mechanisms relevant to hydrogen production, including interfacial phenomena, light-matter interactions, and fundamental thermodynamics and kinetics; such mechanisms are specifically relevant to photoelectrochemical and thermochemical water splitting, catalysis and electrocatalysis, membranes for gas separation, and biological and biomimetic processes.
- The Office of Nuclear Energy is currently collaborating with the Office of Energy Efficiency and Renewable Energy on the development of nuclear-renewable hybrid energy systems that are consistent with the H2@Scale vision. The systems being evaluated in this collaboration use large-scale hydrogen production as a form of energy storage or as an input to industrial processes.
- The Office of Fossil Energy is advancing the technologies for producing hydrogen from fossil fuel resources, including co-production of hydrogen and electricity and steam methane reformation. The Office of Fossil Energy also continues to develop technologies for carbon capture, utilization, and storage in fossil-based hydrogen production, including technologies for carbon-free production of hydrogen using new chemical synthesis methods that break apart natural gas to solid carbon and hydrogen.

GOAL

The goal of the Hydrogen Production sub-program is to implement early-stage applied R&D for developing low-cost, highly efficient hydrogen production technologies that utilize diverse domestic sources of energy, including sustainable and renewable resources (Office of Energy Efficiency and Renewable Energy), nuclear power (Office of Nuclear Energy), and fossil resources with carbon sequestration and utilization (Office of Fossil Energy).

OBJECTIVES

The objective of the Hydrogen Production sub-program is the development of low-cost, large-scale hydrogen production technologies that utilize diverse, domestic energy resources and feedstocks. This objective is consistent with DOE's H2@Scale vision. Analysis has established a long-term hydrogen cost target of <$4 per kilogram (kg) hydrogen, produced, delivered, and dispensed, but untaxed[1] (with <$2/kg apportioned for production only[2]); and a nearer-term, early-market target of <$7/kg dispensed hydrogen[3]. These cost targets are based on achieving cost

[1] *Hydrogen Threshold Cost Calculation*, Program Record (Office of Fuel Cell Technologies) 11007, U.S. Department of Energy, 2011. http://www.hydrogen.energy.gov/pdfs/11007_h2_threshold_costs.pdf
[2] *H_2 Production and Delivery Cost Apportionment*, Program Record (Hydrogen and Fuel Cells Program) 12001, U.S. Department of Energy, 2012. http://hydrogen.energy.gov/pdfs/12001_h2_pd_cost_apportionment.pdf
[3] *Early Market Hydrogen Cost Target Calculation—2015 Update*, Program Record (Fuel Cell Technologies Office) 15012, U.S. Department of Energy, 2015. https://www.hydrogen.energy.gov/pdfs/15012_hydrogen_early_market_cost_target_2015_update.pdf

competitiveness on a cents-per-mile basis in hydrogen fuel cell electric vehicles compared with other competing advanced vehicle technologies. Hydrogen production technologies are being developed to achieve cost goals in timeframes appropriate to their current stages of development.

FISCAL YEAR (FY) 2017 TECHNOLOGY STATUS AND ACCOMPLISHMENTS

Figure 1 shows recent and current status for the high-volume projected costs of hydrogen production for several of the near- to mid-term production pathways, highlighting the cost reductions in recent years resulting from ongoing, early-stage R&D. Although natural gas reforming (without carbon capture) already meets the DOE cost target of <$2/kg, continued early-stage R&D is needed to enable the innovations essential for reducing cost in other large-scale hydrogen production technology pathways utilizing diverse and sustainable domestic resources.

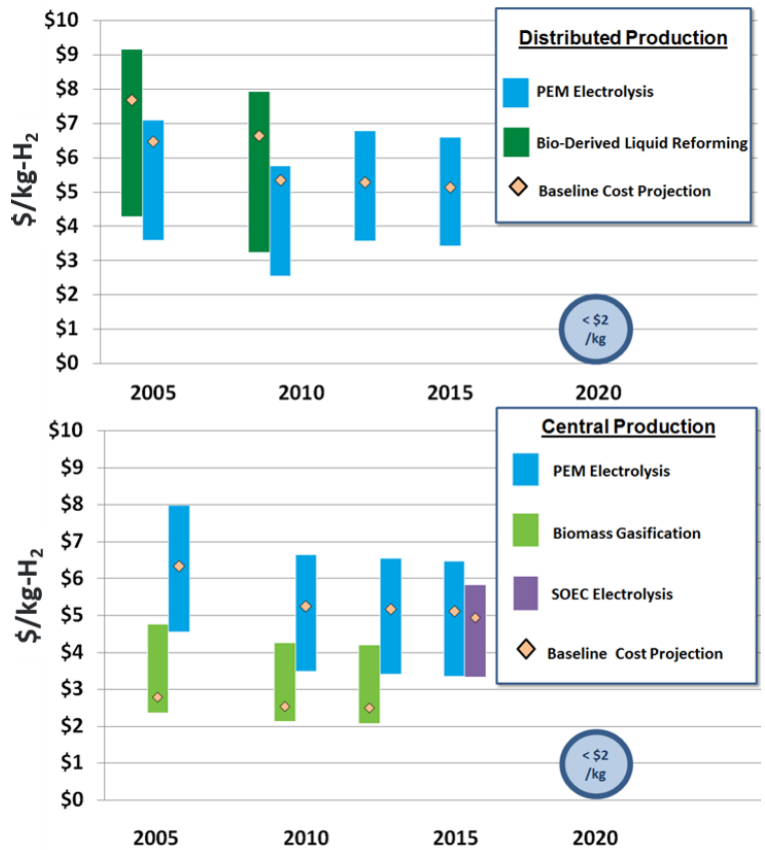

PEM – polymer electrolyte membrane; SOEC – solid oxide electrolysis cell

FIGURE 1. Range of hydrogen production costs, untaxed, for near- to mid-term distributed and centralized pathways. The high end of each bar represents a pathway-specific high feedstock cost as well as an escalation of capital cost, while the low end reflects a low end on feedstock costs and no capital escalation. Bars for different years in the same pathway represent improvements in the costs of the specific pathway, based on specific reference data for the appropriate year and pathway. Detailed information is included in the DOE Hydrogen and Fuel Cells Program Records 14005[4] and 16014[5].

Sub-Program Level Accomplishments

In FY 2017, significant progress was made by the Hydrogen Production sub-program on several important fronts. Several highlights include:

- In FY 2017, DOE announced SimpleFuel as the winner of the $1 million H2 Refuel H-Prize Competition. Launched in October 2014, the H2 Refuel H-Prize Competition challenged America's innovators to deploy

[4] *Hydrogen Production Status 2006-2013*, Program Record (Hydrogen and Fuel Cells Program) 14005, U.S. Department of Energy, 2014. https://www.hydrogen.energy.gov/pdfs/14005_hydrogen_production_status_2006-2013.pdf
[5] *Hydrogen Production Cost from Solid Oxide Electrolysis,* Program Record (Hydrogen and Fuel Cells Program) 16014, U.S. Department of Energy, 2016. https://www.hydrogen.energy.gov/pdfs/16014_h2_production_cost_solid_oxide_electrolysis.pdf

an on-site hydrogen generation system, using electricity or natural gas, to fuel hydrogen vehicles, that can be used in homes, community centers, small businesses, or similar locations. During the competition, SimpleFuel demonstrated that its home-scale refueling appliance can provide a one-kilogram fill to vehicles in 15 minutes or less at 700 bar using hydrogen produced via electrolysis, with a cost-effective design that minimizes setback distances and reduces the physical footprint of the system. SimpleFuel is a collaboration of three companies: Ivys Energy Solutions, McPhy Energy N.A., and PDC Machines.

- The HydroGEN advanced water splitting materials consortium, comprised of six core national laboratories (National Renewable Energy Laboratory, Sandia National Laboratories, Lawrence Berkeley National Laboratory, Lawrence Livermore National Laboratory, Idaho National Laboratory, and Savannah River National Laboratory), launched its expanded website featuring an advanced search engine to facilitate access to the consortium's more than 80 unique world-class research capabilities. HydroGEN also launched its data portal in compliance with DOE Energy Materials Network guidelines and requirements.
- Several important stakeholder engagement events were held, including webinars and workshops. Webinar topics included grid-integration of electrolysis as well as detailed descriptions of the Fuel Cell Technologies Office's Energy Materials Network Consortia, including the HydroGEN Consortium. A workshop co-sponsored by the Fuel Cell Technologies Office and the Advanced Manufacturing Office in the Office of Energy Efficiency and Renewable Energy was held on advanced power electronics for electrolyzer and fuel cell applications, and several workshops were held on H2@Scale.
- R&D projects in the current Hydrogen Production sub-program portfolio made significant progress, which included advances in early-stage hydrogen production pathways analysis; progress in early-stage materials research for advanced low- and high-temperature electrolysis (including catalyst and membrane innovations); advances in materials research foundational to the photoelectrochemical (PEC) and solar-thermochemical (STCH) pathways (including novel energy-conversion materials and catalysts); and progress in cutting-edge metabolic engineering for enabling early-stage biological approaches to the conversion of hydrocarbon feedstocks based on biomass and waste streams. The progress is described in further detail in the Project Level Accomplishments section below.
- Nineteen new projects were competitively selected in areas of advanced water splitting materials R&D, which leverage the HydroGEN Consortium's core capabilities. Further details are included in the following sections.

New Project Selections

In FY 2017, DOE released one funding opportunity announcement (FOA) to support R&D efforts to address critical challenges and barriers to hydrogen production via water splitting. Specifically, the FOA aimed to leverage the national laboratories' unique capabilities brought together under the HydroGEN Energy Materials Network Consortium to accelerate materials discovery and development. Advanced water splitting pathways of interest include low- and high-temperature electrolysis and PEC and STCH hydrogen production. In addition to the materials R&D topic, the FOA solicited applications for critical protocol and benchmarking development needed across all the advanced water splitting pathways to guide the materials R&D efforts resulting from the FOA, as well as the entire advanced water splitting community.

Eighteen advanced water splitting materials development projects and one benchmarking and protocol development project were selected in FY 2017 under the Production portfolio and will begin work in early FY 2018. The 19 projects are listed below:

Low-Temperature Electrolysis Materials R&D

- Proton Energy Systems, Inc. (Wallingford, Connecticut) will explore an advanced PEM electrolysis membrane electrode assembly composed of cutting-edge membrane and electrode components with optimized materials structures and interfaces, enabling cost reductions in PEM electrolyzers needed to meet long-term DOE targets.
- Los Alamos National Laboratory (Los Alamos, New Mexico) will develop a platinum-group-metal-free catalyst system for an anion exchange membrane electrolyzer allowing for efficient cell performance while substantially lowering cost.
- Northeastern University (Boston, Massachusetts) will perform a comprehensive fundamental exploration of advanced catalysts, electrodes, membranes, and membrane electrode assemblies integrating these components,

for the next generation of anion exchange membrane electrolyzers optimizing catalytic activity, conductivity, and performance.

- Argonne National Laboratory (Lemont, Illinois) will develop high-efficiency, durable platinum-group-metal-free oxygen evolution reaction catalysts for advanced PEM electrolyzers that are expected to be an order of magnitude less costly compared with current state-of-the-art catalysts.
- Los Alamos National Laboratory (Los Alamos, New Mexico) will explore advanced high-performing, durable, and economically viable elastomeric anion exchange membranes for alkaline water electrolysis under high pH conditions with lower gas permeability, greater mechanical stability, and substantially decreased production cost as compared to the state of the art.

High Temperature Electrolysis Materials R&D

- University of Connecticut (Mansfield, Connecticut) will develop novel solid oxide electrolysis cell (SOEC) technology based on proton-conducting electrolytes to enable cost-effective hydrogen production at intermediate temperatures with important operational advantages over the state of the art, resulting in reduced operational costs.
- Northwestern University (Evanston, Illinois) will utilize accelerated materials testing strategies that combine electrochemical life testing with quantitative microstructural and chemical evaluation to produce a predictive theory addressing critical degradation of SOECs and resulting in accelerated testing protocols critical for SOEC technologies.
- United Technologies Research Center (East Hartford, Connecticut) will develop a thin-film, high-efficiency, durable metal-supported SOEC based upon proton-conducting electrolyte operating at intermediate temperatures, offering an innovative electrolysis cell with the potential to meet long-term DOE targets.

Photoelectrochemical Materials R&D

- Rutgers University (New Brunswick, New Jersey) will explore the development of next-generation PEC photoelectrodes based on novel platinum-group-metal-free catalysts and new multi-junction photoabsorber materials to significantly improve durability, efficiency, and cost compared to the current state of the art.
- Stanford University (Stanford, California) aims to develop protective catalyst systems on III-V and silicon-based semiconductors for efficient and durable PEC water splitting devices made from affordable and scalable materials with the potential to meet the DOE long-term goals.
- The University of Hawaii (Honolulu, Hawaii) will utilize their advanced materials modeling/synthesis/characterization approach to design and optimize the next generation of chalcopyrite-based tandem structures as photoelectrodes for PEC water splitting with innovative surface catalysis and protection layers for enhancing device durability towards meeting long-term DOE targets.
- The University of Michigan (Ann Arbor, Michigan) will explore several novel wide-bandgap materials to develop monolithically integrated thin-film, silicon tandem photoelectrodes to enable high-efficiency and stable PEC water splitting devices.
- Los Alamos National Laboratory (Los Alamos, New Mexico) will design and develop an efficient and stable device structure for sustained PEC water splitting leveraging recent materials innovations in perovskite-based photo-absorbers and in oxygen evolution reaction and hydrogen evolution reaction catalysts.

Solar Thermochemical Materials R&D

- Colorado School of Mines (Golden, Colorado) will merge state-of-the-art combinatorial synthesis methods with combinatorial theoretical calculations to accelerate the discovery of new potential materials for use in two-step metal oxide cycles for cost-effective STCH water splitting, establishing a better understanding of fundamental links between oxide structure, chemical composition, and STCH performance and allowing for characterization of new STCH materials that can meet the long-term DOE hydrogen production targets.
- University of Colorado (Boulder, Colorado) will use a computationally accelerated and experimentally validated materials-by-design approach using advanced machine-learned models to optimize material thermodynamic and kinetic properties for solar thermochemical water splitting that meets or exceeds the long-term DOE targets for hydrogen production in terms of efficiency and cost.

- Northwestern University (Evanston, Illinois) will use a joint computational-experimental method, combined with materials design strategies and high-throughput approaches, to rapidly discover and synthesize novel thermochemical materials with properties that significantly exceed the state of the art, focusing first on novel perovskites, as well as exploring the potential of non-stoichiometric, phase-change materials for optimal thermodynamic and kinetic properties.
- Arizona State University (Tempe, Arizona) will accelerate materials discovery for improved STCH materials by developing a fundamental understanding of key thermodynamic properties of redox active, mixed ionic electronic conducting metal oxides, which can stably exist over a range of oxygen stoichiometries, utilizing intelligent, fundamental quantum mechanics investigations.
- Greenway Energy, LLC (Aiken, South Carolina) will explore the development and testing of a new catalytic material to decompose sulfuric acid, a key step of the hybrid sulfur (HyS) STCH cycle. Using a novel catalyst preparation, the project will develop lower-cost catalytic materials, with 30% higher activity and 60% lower activity degradation expected as compared to the state of the art.

Advanced Water Splitting Materials Protocol and Benchmarking Development

- Proton Energy Systems, Inc. (Wallingford, Connecticut) will establish critically needed best practices for screening, characterization, and benchmarking of the advanced water splitting materials and technologies for hydrogen production. The advanced water splitting materials technologies include advanced high-temperature electrolysis, advanced low-temperature electrolysis, and photoelectrochemical and solar thermochemical water splitting.

Project Level Accomplishments

During FY 2017, current projects in the Hydrogen Production research portfolio made important progress in several key areas, including:

Hydrogen Production Pathway Analysis

Three case studies on hydrogen production costs using the H2A v3 tool were completed: (1) the monolithic piston-type bio-oil reformation reactor, (2) the reformer-electrolyzer-purifier (REP) system, and (3) fermentation systems. In these case studies, industrial-scale systems were modeled based on input from key researchers involved in the projects developing these technologies. After the relevant, detailed information from researchers was collected, data was synthesized and amalgamated into base cases with sensitivity analyses. The baseline parameters and sensitivity limits established in each case study were vetted and peer-reviewed by appropriate industry, academic, and national laboratory stakeholders. Results from the Fermentation H2A case study were incorporated into a published, peer-reviewed Hydrogen and Fuel Cells Program Record.[6] (Strategic Analysis, Inc., National Renewable Energy Laboratory, and Argonne National Laboratory)

Electrolytic Hydrogen Production

The major emphases of the low- and high-temperature electrolysis projects were materials innovations to reduce costs and enhance efficiency and long-term durability. Technical progress included:

- Proton Onsite (Wallingford, Connecticut) demonstrated the first successful full non-platinum-group-metal low-temperature electrolyzer stack incorporating alkaline exchange membrane cells, operating for over 500 h with initial performance at <2 V/cell and 500 mA/cm^2.
- Giner Inc. (Newton, Massachusetts) successfully developed innovative approaches for scaling up low-loading (0.2–0.4 mg/cm^2) $Ir/W_xTi_{1-x}O_2$ PEM electrolyzer anode catalysts, which overcome past durability issues. These new scaled catalysts, along with low-loading 3M nanostructured thin-film anodes and baseline Ir black anodes, are being assembled into a final 36-cell, 65 kW stack for long-term durability testing.
- Ceramatec, Inc., (Salt Lake City, Utah) demonstrated cell stability of ~1% current density degradation per 1,000 h at 1.2 V in a button cell for use in a novel high-temperature water splitting technology. The project incorporated macro-features to provide mechanical support of a thin electrolyte and micro-features of the electrodes to decrease electrode losses.

[6] *Hydrogen Production Cost from Fermentation*, Program Record (Hydrogen and Fuel Cells Program) 16016, U.S. Department of Energy, 2017. https://www.hydrogen.energy.gov/pdfs/16016_h2_production_cost_fermentation.pdf

- FuelCell Energy (Danbury, Connecticut) demonstrated a 20-cell SOEC stack using novel high-power-density solid oxide electrolysis cells in an upgraded stack design for use in high-efficiency high-temperature water splitting. At a current density of 2 A/cm^2, the cell voltage was <1.4 V and the overall degradation rate was <0.60% per 1,000 h over >1,000 h of operation.

Photoelectrochemical Hydrogen Production

The main focus of projects in this area was on using state-of-the-art theory, synthesis, characterization, and benchmarking tools to develop innovative PEC materials with improved efficiency and durability. Technical progress included:

- National Renewable Energy Laboratory (Golden, Colorado) established and peer-reviewed a publication of robust protocols for accurately benchmarking PEC solar-to-hydrogen efficiency, which leverage methodologies used to certify the efficiency of multijunction solid-state solar photovoltaic cells. National Renewable Energy Laboratory applied these protocols to validate the world-record solar-to-hydrogen efficiency of 16.2% in novel III-V semiconductor-based photoelectrodes incorporating an inverted metamorphic multijunction architecture.
- University of Hawaii (Honolulu, Hawaii) demonstrated 350-hour durability in novel chalcopyrite PEC photoelectrodes based on efficient copper-gallium-selenium thin films with MoS_2/TiO_2 surface protective layers and implemented advanced electrochemical and spectroscopic characterizations of these photoelectrodes to better elucidate fundamental degradation mechanisms toward the development of improved mitigation strategies for the further durability enhancements needed in thin-film PEC approaches.
- University of California, Irvine (Irvine, California) completed the first in silico demonstration of a stacked-bed particle-based PEC reactor, sustaining indefinite operation at ~4% solar-to-hydrogen efficiency under diurnal excitation conditions using photocatalyst particles with bandgaps based on state-of-the-art materials (Rh-modified $SrTiO_3$ and $BiVO_4$); concentrations of the IO3–/I– redox shuttle within its solubility range; and membrane permeability ensuring that gas crossover poses no safety issues.

Solar Thermochemical Hydrogen Production

Efforts in these projects were directed toward performance enhancement of water splitting by novel, non-volatile metal-oxide-based reaction materials and validating materials innovations in reactor test-beds designed to optimize efficiency of the reaction cycles. Technical progress included:

- Sandia National Laboratories (Livermore, California) had the first successful demonstration of metal-oxide-based STCH hydrogen production in a cascading pressure reactor/receiver prototype system, at a demonstration scale of ~3.5 kW_{th} with a peak rate of 0.2 SLPM H_2 based on CeO_2 material; this demonstration validates a unique testing procedure that is also critical to evaluation of new complex-perovskite-based redox materials for next-generation STCH systems.
- University of Colorado Boulder (Boulder, Colorado) completed successful long-term testing of spray-dried cobalt-doped hercynite redox material for STCH hydrogen production for over 200 cycles in a stagnation flow reactor system; the active particles produced ~300 µmol/g/cycle with no loss in activity between the 100th and 200th cycles, exceeding the project's targeted performance for hercynite and supporting the viability of this material class for use in next-generation STCH systems.

Biological Conversion of Hydrocarbon Feedstocks for Hydrogen Production

The projects in this area focused on novel biological methods such as fermentation and microbial electrolysis to produce hydrogen from biomass-based hydrocarbon resources, using molecular biology and genetic engineering techniques to enhance the hydrogen production potential. Technical progress included:

- National Renewable Energy Laboratory (Golden, Colorado) successfully generated *C. thermocellum* mutants that exhibited ~30% increase in total hydrogen production with a 55% increase in specific rate of hydrogen production compared with un-mutated strains in the fermentation of biomass feedstocks; this accomplishment validates the importance of state-of-the-art metabolic engineering techniques in the ongoing development of viable fermentative approaches for hydrogen production.
- Virginia Polytechnic Institute and State University (Blacksburg, Virginia) enhanced volumetric productivity of in vitro enzymatic hydrogen production from starch, achieving a peak rate of 550 mmol H_2/L/h (compared to the previously reported 320 mmol H_2/L/h), highlighting the potential viability of this early-stage approach.

- Oregon State University (Corvallis, Oregon) demonstrated hydrogen production rates of >10 L/L/day at 40 g/L, 8 h hydraulic retention time, and 15% biomass content by immobilized fermentative cultures; this result is an important step toward enabling innovative hybrid approaches that can integrate fermentation with microbial electrolysis.

BUDGET

The FY 2017 appropriation for Hydrogen Production and Delivery projects totaled $25.4 million. With the emphasis on supporting H2@Scale and on establishing the HydroGEN Advanced Water Splitting Materials Consortium efforts, the apportionment of this funding in the Hydrogen Production portfolio was approximately $16.1 million. This funding supported (1) resource capabilities in the HydroGEN core national laboratories plus the 19 new HydroGEN projects selected in the FY 2017 funding opportunity announcement (~$9.0 million); (2) key H2@Scale initiatives, including $3 million in Congressionally-directed support for R&D in innovative technologies to split natural gas into hydrogen and value-added solid carbon byproducts; (3) ongoing legacy projects in biological approaches to converting hydrocarbons in biomass feedstocks and waste streams (~$0.9 million) and advanced electrochemical and solar water splitting technologies (~$0.97 million); and (4) ongoing analysis, technical support, and cross-cutting projects. The estimated budget breakdown for Hydrogen Production funding in FY 2017 is shown in Figure 2.

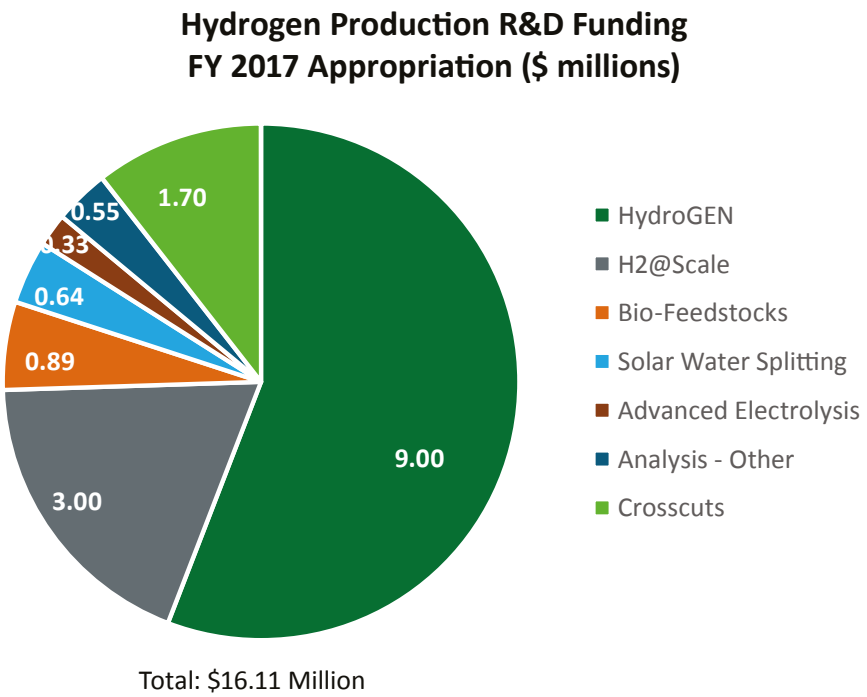

FIGURE 2. FY 2017 Appropriations

UPCOMING ACTIVITIES AND PLANS

Future plans for the Hydrogen Production sub-program include:

- Continued support of foundational research needs in hydrogen production identified through H2@Scale efforts, including a continued emphasis on research innovations for enhancing efficiency and durability and reducing costs in materials systems for all hydrogen production pathways.
- Expanded early-stage R&D through the HydroGEN Advanced Water Splitting Materials Consortium, including initiation of the 19 projects selected in the FY 2017 funding opportunity announcement and ongoing enhancement of the HydroGEN national laboratory core capabilities in advanced electrochemical, PEC, and thermochemical water splitting.

- Expanded emphasis on the development of robust materials characterization protocols and performance benchmarking standards to verify the potential of materials innovations.
- Continued leveraging of cross-office and cross-agency R&D opportunities and resources, including expanded collaboration with the National Science Foundation, the DOE Office of Basic Energy Sciences, and Advanced Research Projects Agency-Energy.

Future activities are subject to appropriations.

Eric Miller
Hydrogen Production and Delivery Program Manager
Fuel Cell Technologies Office
Office of Energy Efficiency and Renewable Energy
U.S. Department of Energy
1000 Independence Ave., SW
Washington, DC 20585-0121
Phone: (202) 586-5829
Email: Eric.Miller@ee.doe.gov

II.A.1 Analysis of Advanced H_2 Production Pathways

Brian James (Primary Contact), Daniel DeSantis, Genevieve Saur (NREL)
Strategic Analysis, Inc.
4075 Wilson Blvd.
Arlington, VA 22203
Phone: (703) 778-7114
Email: bjames@sainc.com

DOE Manager: Eric Miller
Phone: (202) 287-5829
Email: Eric.Miller@ee.doe.gov

Subcontractor:
- National Renewable Energy Laboratory (NREL), Golden, CO
- Argonne National Laboratory (ANL), Lemont, IL

Project Start Date: October 1, 2016
Project End Date: September 30, 2020

Overall Objectives

- Perform cost analysis of various hydrogen (H_2) production and delivery pathways.
- Identify key cost and performance bottlenecks of the given pathways.
- Conduct deep dive analyses and optimization studies on hydrogen delivery scenarios.
- Supply information from techno-economic studies to the U.S. Department of Energy (DOE) for life cycle analysis.
- Respond to the scope and topic areas as defined by the DOE.

Fiscal Year (FY) 2017 Objectives

- Identify a methodology for the evaluation of Hydrogen Analysis (H2A) model cases with low technology readiness level (TRL).
- Conduct a techno-economic analysis on a cascade storage pressure vessel designed by WireTough Cylinders LLC.

Technical Barriers

This project addresses the following technical barrier from the Hydrogen Delivery section of the Fuel Cell Technologies Office Multi-Year Research, Development, and Demonstration Plan.

(E) Gaseous Hydrogen Storage and Tube Trailer Delivery Costs

Technical Targets

Techno-economic analysis of a cascade storage system: The goal of this project is to conduct techno-economic analyses of DOE-supported hydrogen production and delivery projects in an effort to identify key cost drivers and process bottlenecks. Currently, the analysis work is focused on advanced designs for a steel-wire-overwrapped, Type II stationary hydrogen storage system that may lead to significantly reduced dispensing site hydrogen storage costs compared to the FY 2015 cost of high pressure cascade storage of \$2,000/kg H_2 uninstalled.

FY 2017 Accomplishments

- Developed a methodology for analyzing H2A case studies with low-TRL, emerging technologies while obtaining high-confidence cost prediction results.
- Completed a preliminary techno-economic analysis for a wire-wrapped steel vessel suitable for high pressure cascade storage of H_2.

✧ ✧ ✧ ✧ ✧

INTRODUCTION

Year 1 activities consist of two main tasks. The first task of the project was to develop a cost analysis methodology capable of providing high confidence in the accuracy of results for low-TRL H2A case studies.[1] In previous analyses, cases based on high-TRL technologies were validated by comparing modeling results with actual cost and technical assumptions from commercial units. However, with low-TRL technologies, the emerging technology being analyzed does not have a commercial product against which to compare the case study projections. As such, a "low-TRL methodology" was devised that would help to ensure accurate results for H2A cases centered on emerging technologies.

The second Year 1 task of the project is to conduct H2A or techno-economic analyses that are assigned by DOE. DOE selected a project for stationary high pressure cascade storage of H_2 at forecourt dispensing stations. The storage technology consists of a Type II steel-wire-wrapped pressure vessel that avoids use of high-cost carbon composites, as is often used in high pressure storage. A full Design for Manufacture and Assembly (DFMA®) cost analysis was used to model the wire-wrapped vessel manufacturing process. Further, the

[1] H2A is a discounted cash flow model that is used to predict the cost of production and delivery of hydrogen for a given process.

analysis was extended to incorporate the balance of system components of the full cascade storage system to identify a cost suitable for a hypothetical refueling station with the capability of refueling six vehicles simultaneously. These results may be incorporated into a full H2A cost analysis of the dispensing station and other distribution models.

APPROACH

In order to develop the low-TRL methodology, the validated process for high-TRL case studies was modified. The methodology was then reviewed by all members of the project team and submitted to DOE for review.

In order to properly analyze the hydrogen storage vessel developed by WireTough Cylinders LLC, a ground-up (DFMA®) approach was used. The DFMA® process breaks down each manufacturing process step into a material cost, a labor cost, and a utility cost. The capital cost of the equipment is amortized over the life of the equipment and combined with the material, labor, and utility costs; then, a manufacturing cost is obtained. Key process parameter values for the DFMA® analysis were provided by WireTough. These parameters were further supported by material and equipment cost quotations from various manufacturers. All process parameters and assumptions were reviewed by WireTough for accuracy and appropriateness.

RESULTS

The newly developed low-TRL methodology is comprised of four main steps. In the first step, information is gathered from a technology transfer from the product developer, extensive literature searches, and examination of similar technologies. In the second step, a system design is developed. The team determines if single design or multiple system design variants are required. The system(s) are designed, and all relevant parameters are identified. In the third step, the selected system designs are thoroughly reviewed before utilizing the system design for H2A case studies. All relevant input parameters are combined with the system design to create an H2A case. The H2A case is also run through a Monte Carlo stochastic analysis to determine the most likely hydrogen production cost given uncertainty in the input parameters. As a final step, the process is reviewed, documented, and published. Figure 1 graphically represents each step of the low-TRL H2A case study cost analysis methodology.

After the updated methodology for TRL identification was completed, DOE requested a cost analysis of WireTough's process to create Type II steel-wire-wrapped pressure vessels. The complete vessel fabrication process is illustrated in Figure 2. The wire-wrapping process begins with a 30 foot long steel liner rated for approximately 6,600 psi.[2] The liner is carried by crane to a wire-wrapping station, which combines 24 steel wires into a wire tow band

[2] For clarity within this report, the solid-metal walled pressure vessel is called a liner, while the completed, wire-wrapped product is termed a pressure vessel.

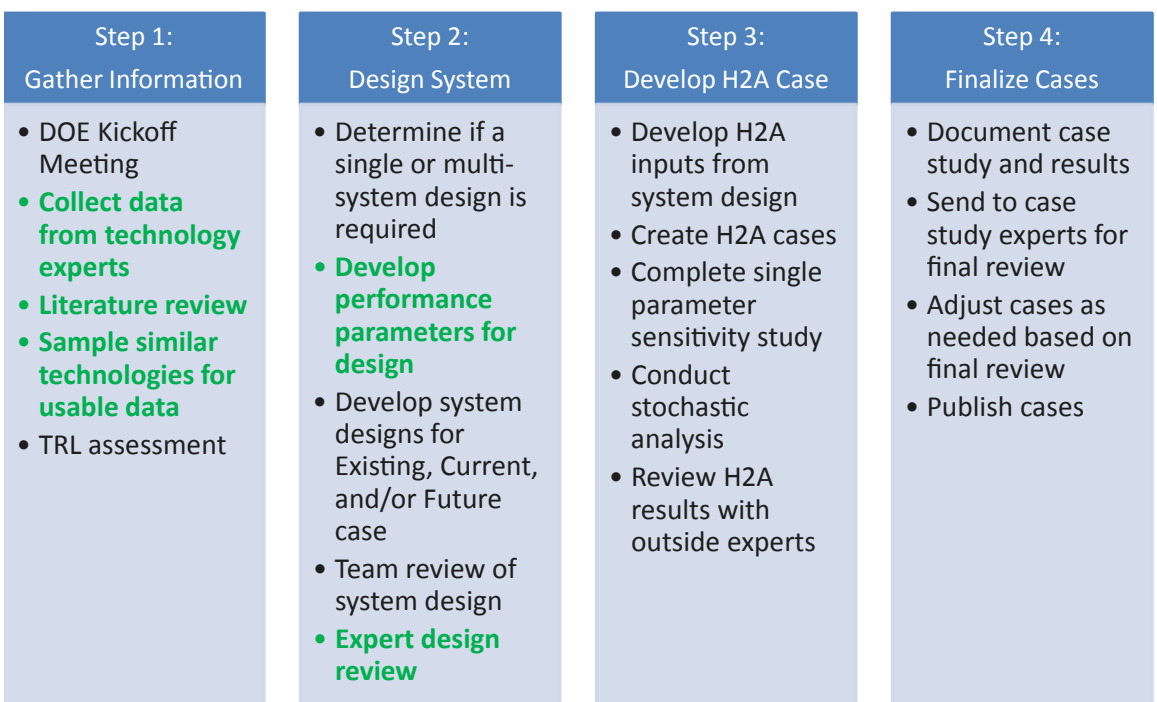

FIGURE 1. Low-TRL H2A process workflow. Steps in green are conducted for low-TRL cases but not high-TRL cases. All other steps are conducted in both high- and low-TRL cases.

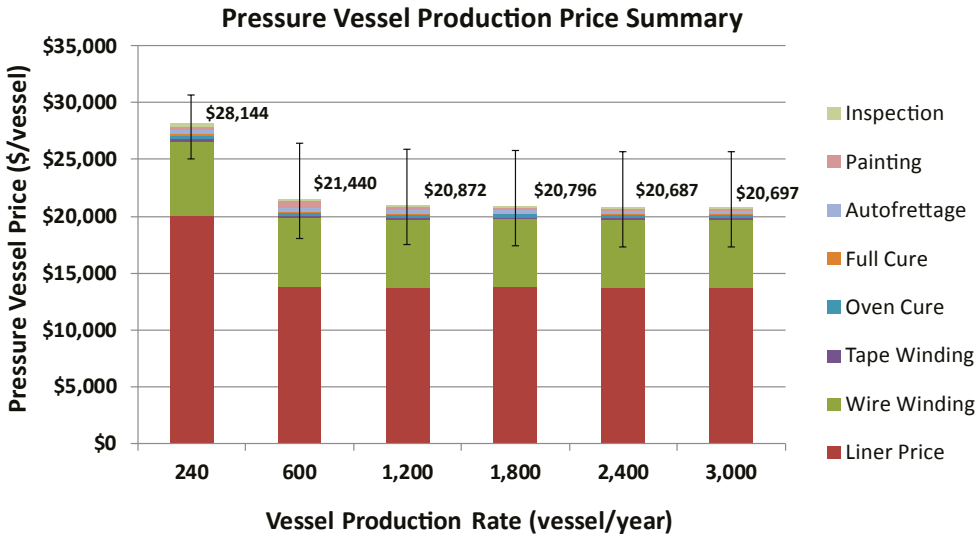

FIGURE 2. Process flow diagram for creating a wire-wound pressure vessel rated for over 1,000 bar (13,000 psi)

and then wraps the wire tow band around the cylindrical section of the liner. As the wires are wrapped around the liner, epoxy is applied to the wires. As understood, the purpose of the epoxy is to protect the wires from corrosion, provide added strength/rigidity, and prevent wire movement. Finally, the outer layer of wires is taped with non-adhesive dry wall tape and then covered with epoxy. The end-domes of the liner are not covered in the wire-wrapping process. After wrapping the liner with wire, the assembly is sent to an oven for partial epoxy curing and is then cured at room temperature to complete the process. The pressure vessel is then put through an autofrettage process. Finally, the pressure vessel is painted with an ultraviolet-resistant paint.

The projected price (after markup)[3] of the complete pressure vessel at low production volumes, as it is currently manufactured, is approximately $28,266/unit (based on a one-vessel-per-day production rate). At higher production rates and with process adjustments to account for automation, the projected price drops to under $21,000/unit. The limited variation in costs at production rates between 240 and 3,000 pressure vessels per year is a result of a constant liner cost being used at each of those production rates. With such a dominant cost being held constant at different production rates, the variation in total cost with varying production rate is minimized. When compared to DOE storage cost targets, the wire-wrapped vessels show significant improvement over the FY 2015 cost status and nearly reach the FY 2020 cost target of $600/kg (see Figure 3).[4]

The analysis was extended to develop a suitable storage cost for use in H2A cases. In order to do this, a theoretical balance of system was developed to formulate a cost for a storage system that could be used at a hydrogen forecourt station. The theoretical station would have a bank of three sets of two tanks and feed to six dispensers. When possible, the components required for the balance of system (valves, pressure relief devices, thermocouples, etc.) were quoted by various manufacturing companies. When price quotes were not available, Systems Analysis used historical data to generate prices for components. The balance of system also includes projected costs for installation, mark-up, and component assembly and testing. The combination of the storage vessel prices and the balance of system prices can then be used as a total system cost for analysis of the delivered price of hydrogen. This cost is readily used in H2A, and it may be worth updating H2A with the results of this analysis.

CONCLUSIONS AND UPCOMING ACTIVITIES

The above described methodology for analyzing low-TRL H2A cases provides a framework for developing reliable results. The new methodology is expected to provide accurate

[3] A markup rate of 25% (at all production rates) was used to translate manufacturing cost into expected sales price (inclusive of company profit, overhead, general and administrative expenses, etc.). This rate is based on information garnered from the annual report of a high-volume pressure vessel manufacturer, Hexagon, and is extrapolated from the company's publicly reported gross margin and cost of goods sold. While markup rates can vary substantially company-to-company, even within an industry, Hexagon is judged to be an industry standard in hydrogen and compressed natural gas storage vessels, and thus is thought to be an appropriate markup rate benchmark.

[4] In order to make direct comparison to the DOE targets and align with the DOE terminology for stationary gaseous hydrogen storage costs, the term "tank" is used in Figure 3 to describe the WireTough pressure vessel. Further, "price" and "cost" are used interchangeably for Figure 3, as the purchase cost to a hydrogen forecourt station for a high pressure storage tank is identical to the price WireTough would charge for its product. A table of DOE's cost targets for off-board hydrogen storage, along with descriptions of the components in question, can be found here: https://energy.gov/eere/fuelcells/doe-technical-targets-hydrogen-delivery.

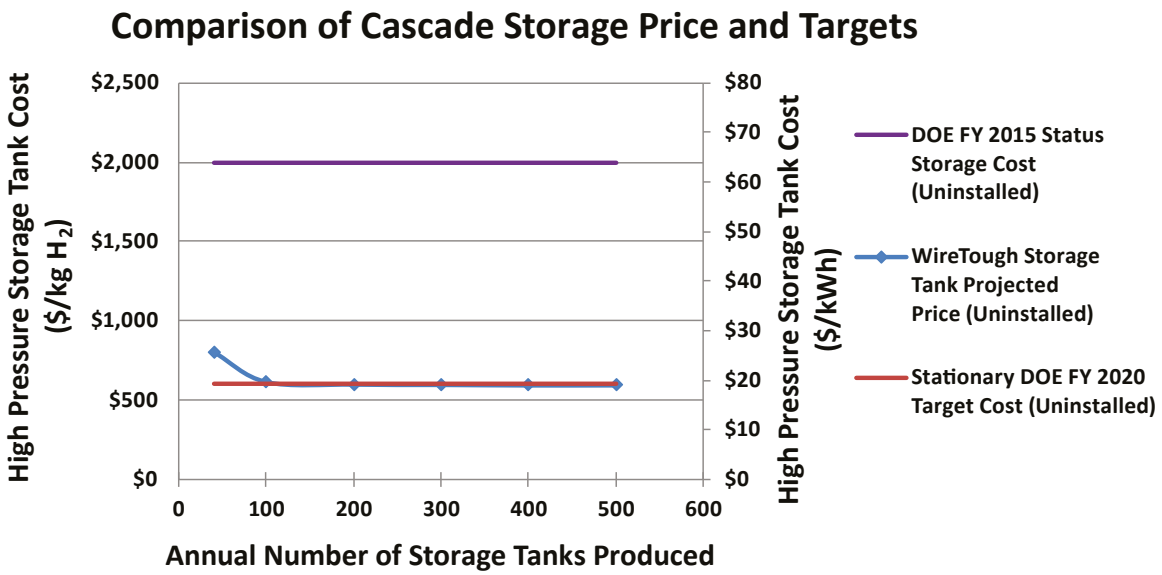

FIGURE 3. Comparison of wire-wrapped pressure vessel cost projections to various DOE targets

results because it is closely modeled on the validated high-TRL methodology and includes extensive expert review of assumptions and results.

The WireTough Cylinders LLC wire-wrapped hydrogen storage system appears to be a cost-effective alternative to metal and Type II tanks for stationary high pressure applications. Preliminary analysis projects a pressure vessel cost of ~$600/kg of stored H_2 (uninstalled), achieving the 2020 DOE target of $600/kg and surpassing the DOE 2015 status cost of $2,000/kg. The analysis for the wire-wrapped cylinders will continue into the next fiscal year. The remaining steps include external review of the results and documentation of the results. Other future analyses will be conducted once cases are assigned by DOE. Once the review is complete, the results could potentially be used in future H2A forecourt models.

FY 2017 PUBLICATIONS/PRESENTATIONS

1. Brian D. James, Cassidy Houchins, Genevieve Saur, Jennie M. Huya-Kouadio, and Daniel A. DeSantis, "Analysis of Advanced H_2 Production Pathways," presented at the Department of Energy Annual Merit Review Meeting, 7 June 2017, Washington, D.C.

II.B.1 Renewable Electrolysis Integrated Systems Development and Testing

Mike Peters (Primary Contact), Kevin Harrison, Huyen Dinh
National Renewable Energy Laboratory (NREL)
15013 Denver West Parkway
Golden, CO 80401-3305
Phone: (303) 524-0864
Email: Michael.Peters@nrel.gov

DOE Manager: David Peterson
Phone: (240) 562-1747
Email: David.Peterson@ee.doe.gov

Subcontractor:
Spectrum Automation Controls, Arvada, CO

Project Start Date: October 1, 2003
Project End Date: September 31, 2017

Overall Objectives

- Collaborate with industry to research, develop, and demonstrate optimized integration opportunities for renewable electrolysis systems for energy storage, vehicle refueling, grid support, and industrial gas end uses.
- Design, develop, and demonstrate advanced experimental and analytical methods to validate electrolyzer stack and system efficiency; including contributions of sub-systems (e.g., power conversion, drying, electrochemical compression, pumps) of advanced electrolysis systems.

Fiscal Year (FY) 2017 Objectives

- Characterize large active area stack performance by taking current-voltage (IV) curves of two state-of-the-art polymer electrolyte membrane (PEM) electrolyzer stacks.
- Develop a balance of plant (BoP) stack model that examines PEM electrolyzer system efficiency over the expected lifetime of the system.
- Explore cell performance of PEM stacks under variable power with a solid-state individual cell voltage monitoring system.

Technical Barriers

This project addresses the following technical barriers from the Fuel Cell Technologies Office 2012 Multi-Year Research, Development, and Demonstration Plan, Section 3.1.5.

(G) System Efficiency and Electricity Cost

(J) Renewable Electricity Generation Integration (for central production)

(M) Control and Safety

Technical Targets

This project is conducting research, development, and demonstration to reduce the cost of hydrogen production via renewable electrolysis for both distributed and central production pathways and to help meet the following DOE hydrogen production and delivery targets for central water electrolysis with green electricity found in the Multi-Year Research, Development, and Demonstration Plan (2011–2020, Table 3.1.5).

Stack energy efficiency

- 44 kWh/kg H_2 (76% lower heating value [LHV]) by 2015
- 43 kWh/kg H_2 (78% LHV) by 2020

System energy efficiency

- 46 kWh/kg H_2 (73% LHV) by 2015
- 44.7 kWh/kg H_2 (75% LHV) by 2020

Hydrogen Levelized Cost

- $3.00/kg H2 at plant gate by 2015
- $2.00/kg H2 at plant gate by 2020

FY 2017 Accomplishments

- NREL obtained IV polarization curves on two large active area PEM stacks.
- NREL built a BoP model to trade performance metrics like; electrolyzer system efficiency, maintenance, stack decay rate, and system output over the expected lifetime of an electrolyzer.
- NREL commissioned an individual cell voltage analyzer that is capable of reading single cell voltages on electrolyzer stacks; up to 132 cells can be measured simultaneously.

✧ ✧ ✧ ✧ ✧

INTRODUCTION

The capital cost of commercially available water electrolyzer systems, along with the high cost of electricity in many regions, limits widespread adoption of electrolysis technology to deliver low cost hydrogen. In response, PEM electrolyzer manufacturers have and continue to scale-up their systems into the multi megawatt range to improve system energy efficiency and capital cost. Along with capital cost reductions and efficiency improvements, low temperature electrolyzers are beginning to be deployed at utility scale and are capable of advanced grid integration functionality, as well as integrated into networks containing high penetration of renewable electricity sources. An integrated system with advanced sensing and communications will enable grid operators to take advantage of the controllable nature and fast response of distributed and central water electrolysis systems to help maintain grid stability. Electrolytic production of hydrogen, where fossil fuels are the primary electricity source, will not lead to significant carbon emission reduction without carbon sequestration technologies.

Renewable electrolysis is inherently distributed, but large-scale wind and solar installations exist today and take advantage of economies of scale and achieve system-level energy efficiencies less than 60 kWh/kg. Renewable electricity sources, such as wind and solar, can be closely and, in some cases, directly coupled to the hydrogen-producing stacks of electrolyzers to reduce energy conversion losses and capital costs investment of this near-zero-carbon pathway.

APPROACH

Results and insights gained from this research, development, and demonstration project aim to benefit the hydrogen-based industry and relevant stakeholders as the market for this hydrogen production equipment expands. Results from the project have demonstrated opportunities to improve efficiency and capital cost of an integrated renewably-coupled electrolysis system.

Real-world data from daily operations are demonstrating opportunities for improved system design and novel hardware configurations to advance the commercialization of this technology. The research being conducted at NREL's Energy Systems Integration Facility is advancing the integration of renewable electricity sources with state-of-the-art electrolyzer technology. Lessons learned and data-driven results provide feedback to industry and to the analytical components of this project. Finally, this project provides independent testing and verification of the technical readiness of advanced electrolyzer systems by operating them from the grid and renewable electricity sources.

RESULTS

Large Active Area Stack Testing

NREL obtained IV curves on their 120 kW and 250 kW PEM electrolyzer stacks and looked at stack efficiency (higher heating value, LHV, or kWh/kg) over the full current range of the stacks (100 A–1,160 A).

IV polarization sweeps were taken at:

- Temperature: 30°C, 40°C, and 50°C
- Pressure: 150 psig, 300 psig
- Stack Size: 120 kW, 250 kW

Stack efficiency based on the LHV ranged from 58–82% depending on the current density applied to the stacks. DOE's 2020 goal from their technical targets for distributed forecourt water electrolysis hydrogen production is a stack efficiency of 77% based on the LHV. Figure 1 is a graph of three IV sweeps that were completed. Both stacks are able to achieve the 77% target at relatively low current densities. Values **above** the 2020 DOE target line are the best efficiencies in this graph.

Balance of Plant Model

NREL built an electrolyzer model by measuring BoP component's power demand. NREL also measured stack performance values on three state-of-the-art large active area PEM stacks and monitored power on major BoP components. The system efficiency of NREL's electrolyzer stack test bed at the Energy Systems Integration Facility with the 250 kW stack operating at full power is 65.5 kWh/kg. This number is significantly higher than DOE's 2020 system efficiency of 44 kWh/kg, however the NREL system is smaller than the megawatt-scale systems needed to reach the DOE target. The components that make up the share of the overall system efficiency break down as follows (Figure 2):

- Stack: 79%
- Power Supplies: 15%
- Drying: 4%
- Main Direct Injection (DI) Pump: 1%
- Cooling: 0.5%
- Other: 0.5%

Characterizing PEM Stack Performance

NREL used data from previously tested stacks at NREL to obtain a general PEM stack performance curve. The data was used to find stack energy efficiency (kWh/kg) and was normalized to percent of full stack power for simplicity. A curve fit was applied to the combined stack data to determine stack efficiency as a function of rated power.

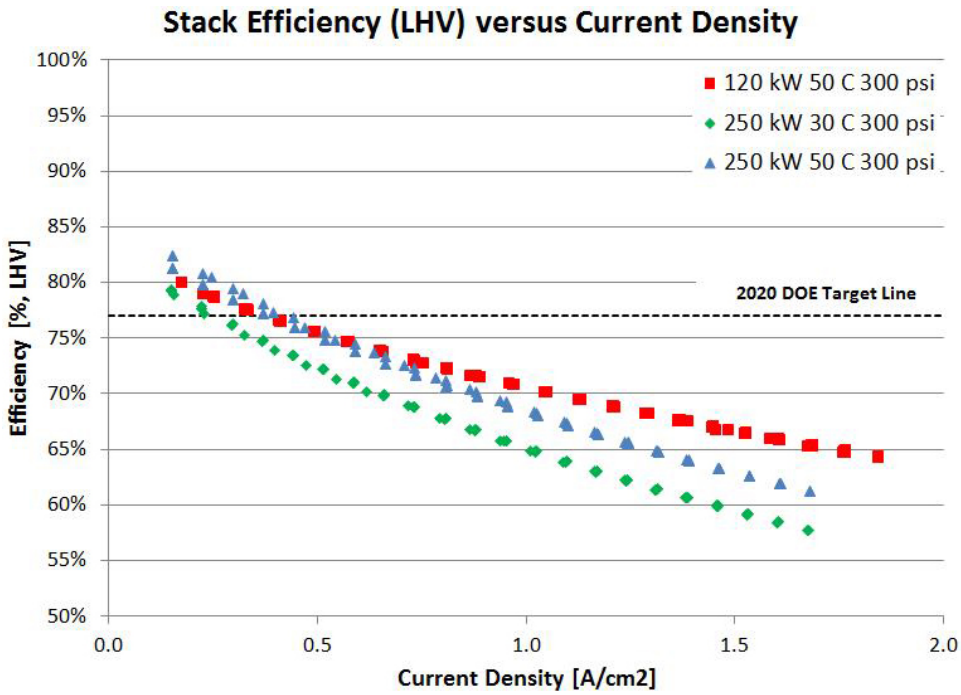

FIGURE 1. Stack efficiency (LHV) versus current density

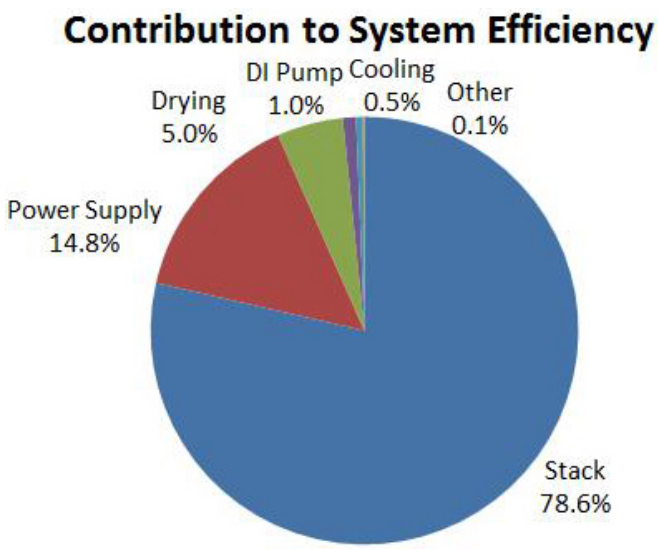

FIGURE 2. Electrolyzer system efficiency by sub-system

Power Supply Efficiency

NREL measured the efficiency on their alternating current (AC) to direct current (DC) power supplies that feed the electrolyzer stack test bed by instrumenting both the AC and DC sides of the power supply with power transducers. The power supply efficiency ranged from 85% (33% load) to 89% (100% load), which is a lower efficiency than was previously assumed. The AC power versus DC power scales linearly and allows the model to account for added AC load based on the power supply efficiency. Based on the model, for a 250 kW system operating at full power the power supply will add approximately 10 kWh/kg or ~15% to the overall system efficiency.

Time

The model is capable of looking at system performance over the lifetime of a system. The user inputs an expected stack decay rate and the model adjusts the stack and BoP loads over time to look at the system efficiency. The model assumes that stacks are replaced when they reach 20% degradation compared to their original voltage. For example, if the cell voltage of a cell at the beginning of life is 2 V, then the stack would be replaced when cell voltage reaches 2.4 V. Figure 3 is the output from the model that shows system efficiency over the lifetime of a system. The assumptions for this case are:

- 250 kW rated stack power
- 100 cells
- 80% yearly utilization
- 5 µV/(cell-h) degradation (i.e., stack decay rate)
- BoP is maintained and efficiency recovers with new stack install (in Year 10)

Figure 3 shows system efficiency at full stack power. In Year 0 (start) the system starts at 65.5 kWh/kg and slowly climbs until Year 10 when system efficiency hits 76.3 kWh/kg. At this point, the model assumes stack

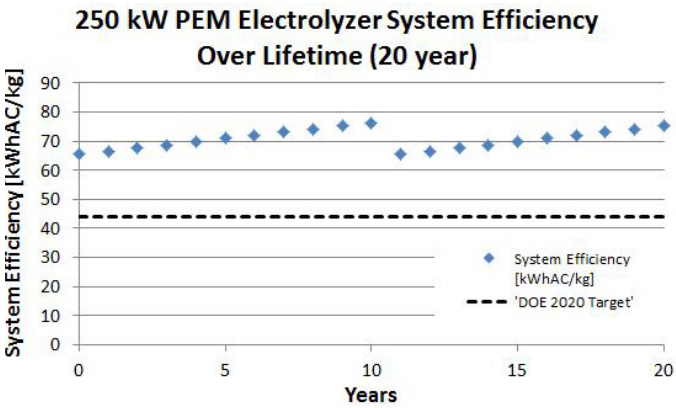

FIGURE 3. Electrolyzer system efficiency over the system lifetime

replacement and the system efficiency recovers to its original value. The model developed in this project is scalable to smaller or larger systems and is easily adjustable as more BoP or stack measurements are obtained.

Individual Cell Voltage Analyzer

NREL recently specified, procured, and implemented an individual cell voltage acquisition system that is capable of simultaneously monitoring individual cell voltages on PEM electrolyzer stacks (Figure 4). The prototype system was developed by Polyphotonics, a small business based out of Springwater, New York. The 132-channel differential voltage system utilizes a Raspberry Pi and allows for an ethernet, USB, or wireless connection to pull the data off the onboard memory.

CONCLUSIONS AND UPCOMING ACTIVITIES

- Stack and system efficiency continue to improve as systems integration and economies of scale help achieve the DOE goals.
- NREL will continue examining individual cell voltage performance under variable and constant power to inform improved integration with renewable electricity sources.
- NREL will write a final report summarizing the past 14 years as the project concludes.

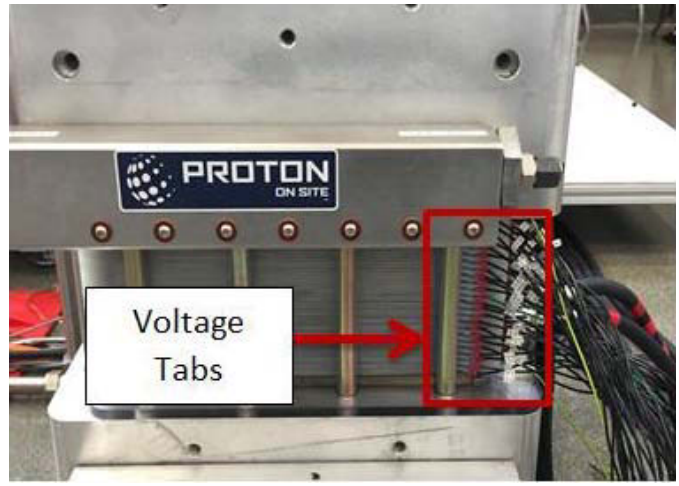

FIGURE 4. Individual cell voltage tabs for the steady-state voltage measurement device

FY 2017 PUBLICATIONS/PRESENTATIONS

1. Peters, M.; Harrison, K; Dinh, H.; Terlip, D.; Kurtz, J.; Martin, J. "Renewable Electrolysis Integrated System Development & Testing." DOE Annual Merit Review and Peer Evaluation Meeting. June, 2017. (presentation)

II.B.2 High-Performance, Long-Lifetime Catalysts for Proton Exchange Membrane Electrolysis

Hui Xu (Primary Contact), Brian Rasimick, Robert Stone, Shuai Zhao and Litao Yan
Giner, Inc.
89 Rumford Ave.
Newton, MA 02466
Phone: (781) 529-0573
Email: hxu@ginerinc.com

DOE Manager: David Peterson
Phone: (720) 356-1747
Email: David.Peterson@ee.doe.gov

Contract Number: DE-SC0007471

Subcontractor:
National Renewable Energy Laboratory, Golden, CO

Vendor:
3M Company, St. Paul, MN

Project Start Date: April 21, 2015
Project End Date: October 20, 2017

Overall Objectives

- Scale-up catalyst synthesis to short production (20 g/batch).
- Transfer the selected catalysts to membrane electrode assembly (MEA) in a large-scale fabrication platform.
- Build a sub-megawatt electrolyzer using selected catalysts with low-platinum group metal loading.
- Demonstrate sub-megawatt electrolyzer performance and durability.
- Perform economic analysis of the cost savings provided by the new catalysts at the megawatt-scale.

Fiscal Year (FY) 2017 Objectives

- Resolve the catalyst instability issue arising from catalyst scale-up.
- Scale-up catalyst synthesis to short production (>10 g/batch).
- Construct a 36-cell stack using developed catalysts and test its initial performance and durability.
- Extend catalyst durability tests to 2,000-hour testing in a short electrolyzer stack.

Technical Barriers

This project addresses the following technical barriers from the Hydrogen Production section of the Fuel Cell Technologies Office Multi-Year Research, Development, and Demonstration Plan.

(F) Capital Cost: High platinum group metal catalyst loading (Ir loading >2 mg/cm^2) due to low catalytic activity for the oxygen evolution reaction and prohibitive proton exchange membrane (PEM) electrolysis cost

(G) System Efficiency and Electricity Cost: Low system efficiency (i.e., high electricity usage) due to significant anode overpotential

Technical Targets

The target of this project is to develop high-performance and long-lifetime oxygen evolution reaction catalysts that may help meet the technical targets of DOE distributed forecourt water electrolysis as shown in Table 1. Included in this table is Giner's status as of 2013.

FY 2017 Accomplishments

- Two approaches to producing durable Ir/$W_xTi_{1-x}O_2$ catalyst for the scale-up of catalyst synthesis have been identified:
  - Heat treatment of the $W_xTi_{1-x}O_2$ supports.
  - Formation of addition layer of IrO_2 surface sites.
- Two low-Ir loading (0.4 mg/cm^2 and 0.2 mg/cm^2) cells using scale-up Ir/$W_xTi_{1-x}O_2$ catalysts demonstrate significant durability over 1,000 h.
- A 36-cell 65-kW stack using baseline Ir black, Giner Ir/$W_xTi_{1-x}O_2$ and 3M Ir–nano-structured thin film (NSTF) has been designed and is ready to be assembled.

✧ ✧ ✧ ✧ ✧

INTRODUCTION

Hydrogen production for mobility and energy storage from PEM water electrolysis is attractive due to its efficiency, ability to quickly cycle up and down, and delivery of hydrogen with high and differential pressure. However, capital costs are high due to expensive materials, especially the membrane and catalyst. Though membrane costs are predicted to decrease, precious metal catalysts costs will

TABLE 1. Technical Targets: Distributed Forecourt Water Electrolysis [1]

Characteristics		Units	2015	2020	Giner Status (2013)
Hydrogen Levelized Cost[2]		$/kg-$H_2$	3.90	<2.30	3.64[3] (5.11)[4]
Electrolyzer Cap. Cost		$/kg-$H_2$	0.50	0.50	1.30 (0.74)[5]
Efficiency	System	%LHV (kWh/kg)	72 (46)	75 (44)	65 (51)
	Stack	%LHV (kWh/kg)	76 (44)	77 (43)	74 (45)

[1] 2012 Multi-Year Research, Development, and Demonstration (MYRDD) Plan. [2] Production Only.
[3] Utilizing H2A Ver.2. [4] Utilizing H2A Ver.3 (Electric consts increased to).075/kW from 0.039$/kW). [5] Stack Only
LHV – lower heating value;

come to dominate capital costs as this technology matures. Decreasing the precious metal requirement for PEM electrolysis is therefore vital for the widespread use of this technology. The overall objective of the Phase IIB project is to commercialize the low-precious-metal-loading, high-performance catalysts for PEM water electrolysis that we have successfully developed in our Phase II project, which may significantly lower the capital cost of water electrolyzers. Both Giner's Ir/$W_xTi_{1-x}O_2$ and 3M's Ir–NSTF catalysts developed under this project have been successfully scaled-up for commercialization and are currently being tested for durability and performance.

APPROACH

In the Phase IIB project, Giner aims to transition this game-changing, innovative catalyst technology to successful commercialization. In the previous efforts, Ir/$W_xTi_{1-x}O_2$ catalyst became less stable during the catalyst scale-up. We have identified two strategies to enhance the catalyst stability upon its scale-up. One is the adoption of a precisely controlled reactor, which enables better temperature control and uniform mixing during catalyst synthesis. The other is the surface modification of the $W_xTi_{1-x}O_2$ support to form better interaction between the catalyst and its support. The scale-up catalysts have demonstrated significant durability over 1,000 hours. In addition, we have completed the design of a 36-cell stack using both Giner's Ir/$W_xTi_{1-x}O_2$ and 3M's Ir–NSTF catalysts, on the basis of Giner's 300 cm^2 commercial PEM water electrolyzer platform.

RESULTS

Figures 1a and 1b show the transmission electron microscope (TEM) images of Ir(45)/$Ti_{1-x}W_xO_2$ and IrO_2(25)/$Ti_{1-x}W_xO_2$, which represent 45 wt% and 25 wt% Ir in the catalyst, respectively. For the Ir(45)/$Ti_{1-x}W_xO_2$ sample, the iridium nanoparticles with size of 3 nm was uniformly deposited on the $Ti_{1-x}W_xO_2$ support. The observed conductive inter-connected Ir chain can enhance the electronic transfer and thus the electrolyzer performance. The distance of 0.24 nm of iridium (1 1 1) planes is confirmed by high resolution TEM image (Figure 1c), which further verify the existence of iridium. The distance of 0.35 nm of anatase $Ti_{1-x}W_xO_2$ phase (1 1 1) plane is also indexed. High-angle annual dark field–energy dispersive X-ray spectroscopy mapping (Figures 1 d–h) demonstrated the distribution of various elements including Ti, W, O and Ir. For the Ir(20)/$Ti_{1-x}W_xO_2$ sample, there was no conductive inter-connected Ir chain, indicating the significance of optimizing the Ir content on the support.

Single MEAs were prepared using the Ir/$W_xTi_{1-x}O_2$ as the anode catalyst, commercial Nafion® 115 membranes, and commercial Pt as the cathode catalyst. The electrolyzer stability was significantly enhanced by the heat treatment of the $W_xTi_{1-x}O_2$ support, which could be due to the modification of the support surface and subsequent increase in the binding between Ir nanoparticles and their support. The MEA performance of Ir/$W_xTi_{1-x}O_2$ with heat treatment was 1.76 V at a current density of 2 A/cm^2, which was close to initial performance of Ir/$W_xTi_{1-x}O_2$ without heat treatment. However, the Ir supported on heat treated $W_xTi_{1-x}O_2$ support showed little performance decay after 233 hours of operation (Figure 2a); in contrast, the performance of the catalyst that was not heat treated decayed substantially under the same operating conditions for the same operating hours (Figure 2b).

The MEAs were tested for their durability in a new test station (Figure 3) at 2 A/cm^2. The MEA loading was 0.4 mg/cm^2. The MEA is quite stable and barely without voltage increase after 1,500 h. The top line shows the average feeding water temperature (80°C) since the real temperature oscillated over the course of durability test. The figure also recorded all the incidences including power supply shutdown and heat failure, demonstrating robustness of the cell subjects to multiple incidences.

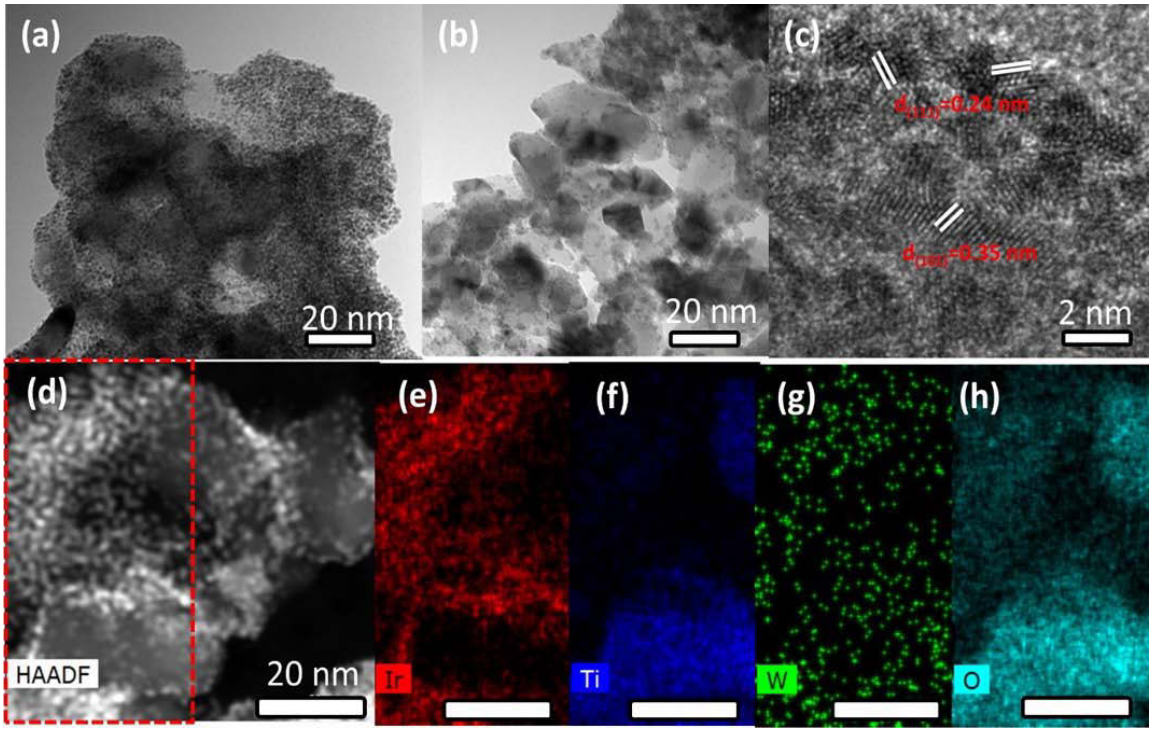

FIGURE 1. TEM images of (a) Ir(45)/$Ti_{1-x}W_xO_2$; (b) IrO_2(25)/$Ti_{1-x}W_xO_2$; (c) high resolution TEM of Ir(45)/$Ti_{1-x}W_xO_2$; (d–h) high-angle annual dark field–energy dispersive X-ray spectroscopy mapping of Ir(45)/$Ti_{1-x}W_xO_2$

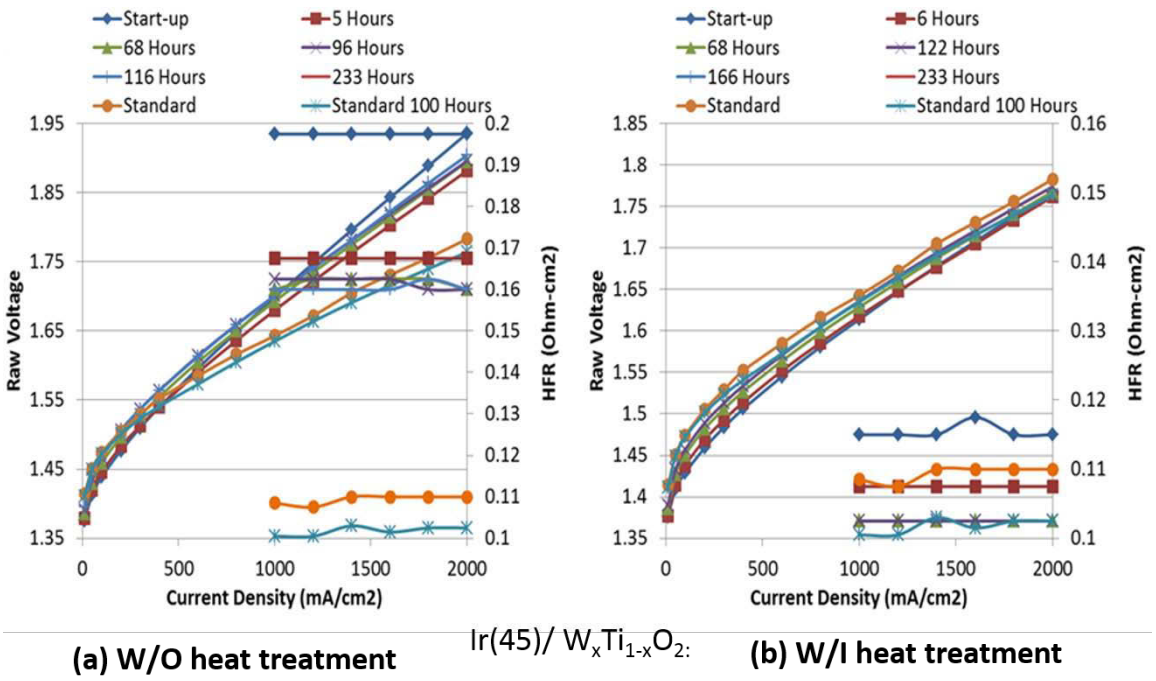

FIGURE 2. The electrolyzer performance and short durability of Ir(45)/$W_xTi_{1-x}O_2$, (a) without support heat treatment, and (b) with support heat treatment

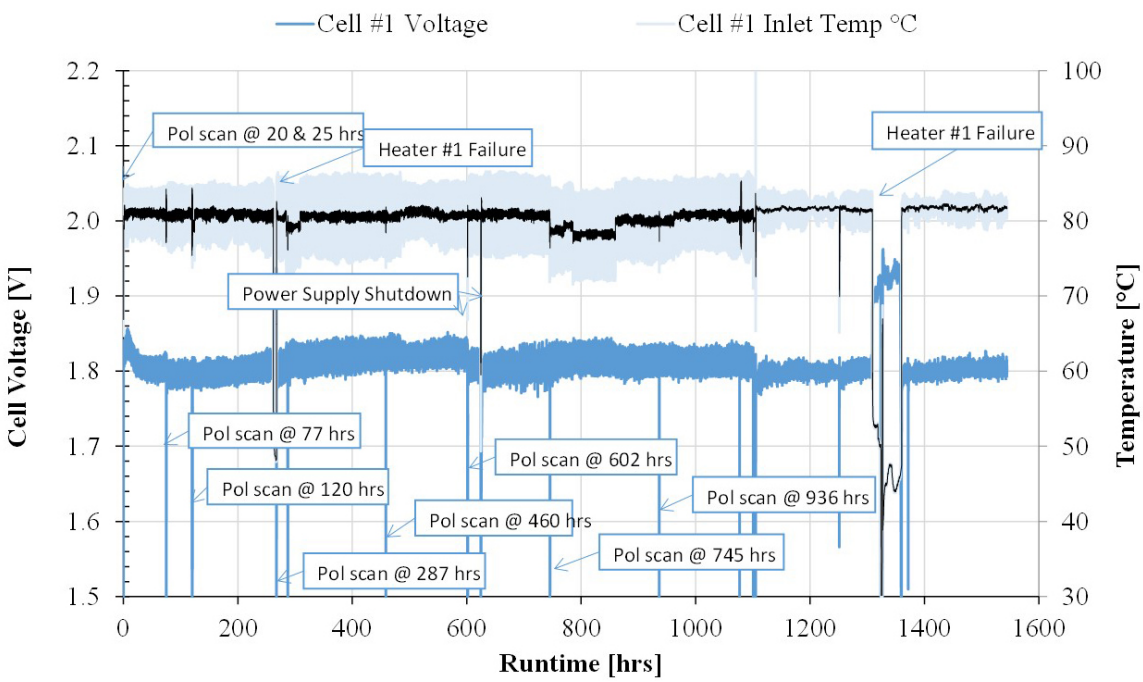

FIGURE 3. The 1,500-hour durability of Ir(45)/$W_xTi_{1-x}O_2$ catalyst with support heat treatment

Our final delivery is a 65 kW stack that consists of 36 cells with an active area of 300 cm^2 for each cell (Figure 4). These 36 cells are divided into three categories: Category 1: Cell 1 to 12 – commercial Ir black; Category 2: Cell 13 to 24 – Ir/$W_xTi_{1-x}O_2$ catalyst; Category 3: Cell 25 to 36 – 3M Ir–NSTF catalyst. The designed operating current density (CD) = 3 A/cm^2, voltage = 2.0 V, so the power = 3 (A/cm^2) x 2.0 V x 36 x (300 cm^2) = 65 kW. The stack design and hardware preparation for the 36-cell stack test has been completed.

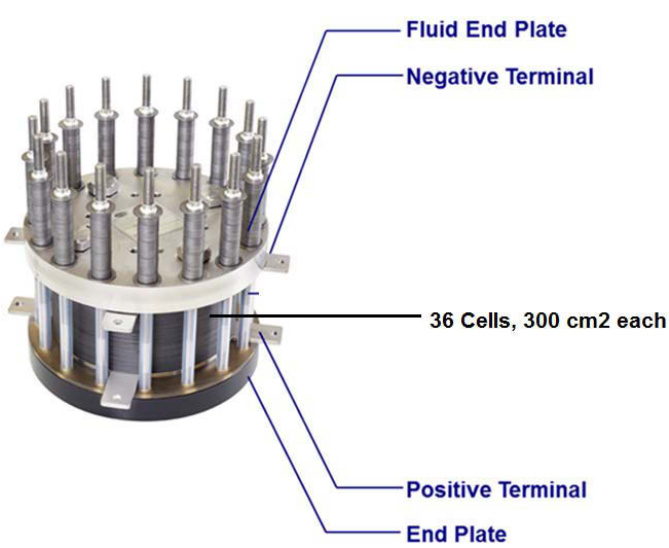

FIGURE 4. Schematic of 36-cell stack and anatomy of cell components

CONCLUSIONS AND UPCOMING ACTIVITIES

Conclusions can be drawn:

- Giner's Ir/$W_xTi_{1-x}O_2$ anode catalysts have been scaled-up and catalyst instability from scale-up in the last year has been resolved via multiple strategies.
- Giner's Ir/$W_xTi_{1-x}O_2$-based anode demonstrates superior performance up to 1,500 h, barely with any performance decay.
- A 36-cell 65-kW stack using baseline Ir black, Giner Ir/$W_xTi_{1-x}O_2$, and 3M Ir–NSTF has been designed and prepared.

Upcoming activities include:

- Complete the assembly of 36-cell 65-kW stack.
- Test the durability of the 36-cell stack over 2,000 h.
- Perform techno-economic analysis of the stack cost.

FY 2017 PUBLICATIONS/PRESENTATIONS

1. Invited Talk: "Benchmarking Catalyst Development for PEM Water Electrolysis," presented at 1st International Conference on Electrolysis (ICE), Copenhagen, June 12–15, 2017.

2. "High-Performance, Long-Lifetime Catalysts for Proton Exchange Membrane Electrolysis," Presentation at DOE Hydrogen and Fuel Cells Program Annual Merit Review meeting, Washington, D.C., June 5–8, 2017.

REFERENCES

1. Hamden, M., "PEM Electrolyzer Incorporating an Advanced Low Cost Membrane," Presentation in DOE 2012 Hydrogen and Fuel Cells Program Annual Merit Review meeting, https://www.hydrogen.energy.gov/pdfs/review12/pd030_hamdan_2012_o.pdf (2012).

II.B.3 High Performance Platinum Group Metal Free Membrane Electrode Assemblies through Control of Interfacial Processes

Katherine Ayers (Primary Contact), Chris Capuano
Proton OnSite
10 Technology Drive
Wallingford, CT 06492
Phone: (203) 678-2190
Email: KAyers@protononsite.com

DOE Manager: David Peterson
Phone: (240) 562-1747
Email: David.Peterson@ee.doe.gov

Contract Number: DE-EE0006958

Subcontractors:
- The Pennsylvania State University, College Park, PA
- University of New Mexico, Albuquerque, NM
- Northeastern University, Boston, MA

Project Start Date: May 1, 2015
Project End Date: April 30, 2017

Overall Objectives

- Evaluate non-platinum group metal (PGM) catalysts as gas diffusion electrodes (GDEs) in half cells.
- Evaluate most promising non-PGM GDEs in full-cell anion exchange membrane (AEM) water electrolysis configuration against PGM counter electrode.
- Further the fundamental understanding of non-PGM active sites and reaction mechanisms.
- Demonstrate translation from solution testing to solid electrolyte interface.
- Conduct assessment of ex situ and in situ stability comparisons to connect ex situ lab evaluation and in situ device results.
- Improve membrane and ionomer durability vs. current commercial options.
- Optimize water management through improved flow field and gas diffusion layer design.
- Fabricate full-scale membranes and ionomer solution for electrolyzer testing.
- Identify most promising non-PGM GDEs for full-cell operation and test PGM-free membrane electrode assembly (MEA) for durability (500 mA/cm^2 for up to 500 h).

Fiscal Year (FY) 2017 Objectives

- Show durability of down-selected, scale-up batch of non-PGM catalysts for >500 h.
- Further the fundamental understanding of non-PGM active sites and reaction mechanisms using synchrotron based in situ spectroscopy.
- Perform in situ operational testing of new reinforced membranes with increased chemical and mechanical degradation resilience.

Technical Barriers

This project addresses the following technical barriers from the Hydrogen Production section of the Fuel Cell Technologies Office Multi-Year Research, Development, and Demonstration Plan.

(F) Capital Cost

Technical Targets

This project is working to establish a new cost curve for water electrolysis through elimination of the highest cost materials in the cell stack, such as platinum group metals (PGMs) and valve metals such as titanium. While electrolysis still has significant needs in manufacturing in order to reach 2020 targets and beyond, the end cost will be largely dependent on raw material costs. In the long term, non-PGM catalysts for the hydrogen and oxygen evolution reactions are needed. The current program aims at meeting the following targets.

- PGM content: none
- Cell voltage: <2 V
- Cell current: 500 mA/cm^2
- Durability: 500 h of stable operation

FY 2017 Accomplishments

- Completed an evaluation of best method for supplying feed water to the stack during electrolysis operation.
- Integrated catalysts from program partners with AEM materials for a full non-PGM MEA.
- Scaled up batches of non-PGM catalysts to 15 g quantities and delivered to Proton.
- Successfully operated a full non-PGM stack at <2 V and 500 mA/cm^2.

- Initiated interfacial studies to elucidate the effects of catalyst, ionomer, and carbonate interactions.

✧ ✧ ✧ ✧ ✧

INTRODUCTION

Water electrolysis powered by wind or solar can provide a renewable source of hydrogen fuel for fuel cell vehicles. The DOE cost goals for the production of renewable hydrogen are aggressively set to compete with existing fossil fuel-based infrastructure. Fuel cells and electrolyzers based on proton exchange membranes are well-known and continue to realize reductions in cost and improvements in performance. To meet DOE goals for hydrogen production, and for growing energy markets, reductions in capital and operating costs are needed in order to justify electrolysis as a solution.

To date, the only pathway with promise to achieve platinum group metal (PGM)-free electrode formulations in membrane-based electrolysis cells is utilization of AEMs. The basic local environment of the membrane allows a range of stable transition metals and metal oxides to be utilized at high potential for catalysis. AEMs also enable the use of much less expensive flow field materials other than the titanium often used in polymer exchange membrane systems. At the same time, the solid-state electrolyte eliminates the need for corrosive liquid electrolytes such as concentrated potassium hydroxide and allows leveraging of high-performance MEA technology. Proton and team members Northeastern University and Penn State University have been exploring this technology since 2010 through an Advanced Research Projects Agency - Energy project in the GRIDS program and have made significant progress in understanding the limitations and potential of this AEM chemistry.

APPROACH

In the first year, project focus will be on catalyst synthesis and activity screening. Hydrogen evolution reaction catalysts will be based on Ni-Mo nanoparticles and other mixed oxides, while oxygen evolution reaction catalysts will focus on ternary catalysts based on Ni, Fe, Co, and Mo. A sacrificial support method will be used to synthesize novel catalyst materials in high surface area format. Electrochemical characterization will be used to down-select materials with appropriate physical parameters for in cell testing. In parallel, polymers based on polyphenylene oxide will be synthesized for use in ionomer solutions and membrane materials to look for higher membrane and ionomer stability than incumbent polymer materials. Gas diffusion layer (GDL) materials and flow field designs will be optimized for AEM electrolysis performance and incorporated into the cell stack. Materials selection, as well as application methods for coatings, will be examined for controlling the hydrophobicity and hydrophilicity of the GDL materials.

In Year 2, results from the first year will be leveraged to optimize the GDE interface, including treatments for improved water management. Additional characterization methods will be used to study the structure activity relationships of the non-PGM catalysts, to understand catalyst-ionomer interactions. The best performing catalysts based on the sacrificial support method approach will be scaled up to 10–25 g batches. On the membrane task, cation spacer polymers will be explored based on 5–10 times greater hydroxide stability vs. the side chain benzyl-linked cation materials. System architectures will be determined for optimum performance, and a test system will be built with capability for anode water feed, cathode water feed, or both. A water transport cell will also be fabricated to help understand flow characteristics as a function of membrane type, GDL, and operating conditions. Focus in cell testing will be on longer term durability testing, once initial performance targets have been met.

RESULTS

The newly commissioned AEM test stand was used to evaluate numerous operational modes to identify the system configuration that would support the most stable operation and electrical efficiency. Fixed inputs were the A201 Tokuyama membrane used, AS-4 ionomer, and baseline PGM catalysts. The cells were rebuilt for each test using new components all cut from the same sheet stock to minimize variations due to the material and manufacturing variability. Inputs that were flexed during the test focused on supplying water to either the cathode, anode, or both simultaneously. We also looked at the use of hydrophobic and hydrophilic GDEs to evaluate the water management at the electrode and membrane interface, as well as introducing carbonate into the water feed to improve conduction with the membrane and electrode structure. Polarization data from this test is included in Figure 1.

Since the alkaline water electrolysis cell consumes water at the cathode, prior to testing it was expected that the cathode fed configurations would produce the greatest stability and highest performance. Interestingly, this was not the case. Most of the configurations showed very poor performance when water was directly fed to the cathode, both with carbonate and without. Similarly, the inclusion of hydrophobic GDEs did not improve cell efficiency. The configuration that showed the lowest cell potential, while enabling operational current densities up to 1,300 mA/cm^2, was the anode fed, carbonate water feed. This mode of operation had been the predominant configuration during AEM testing under this program and will be the selected configuration for the program final durability test.

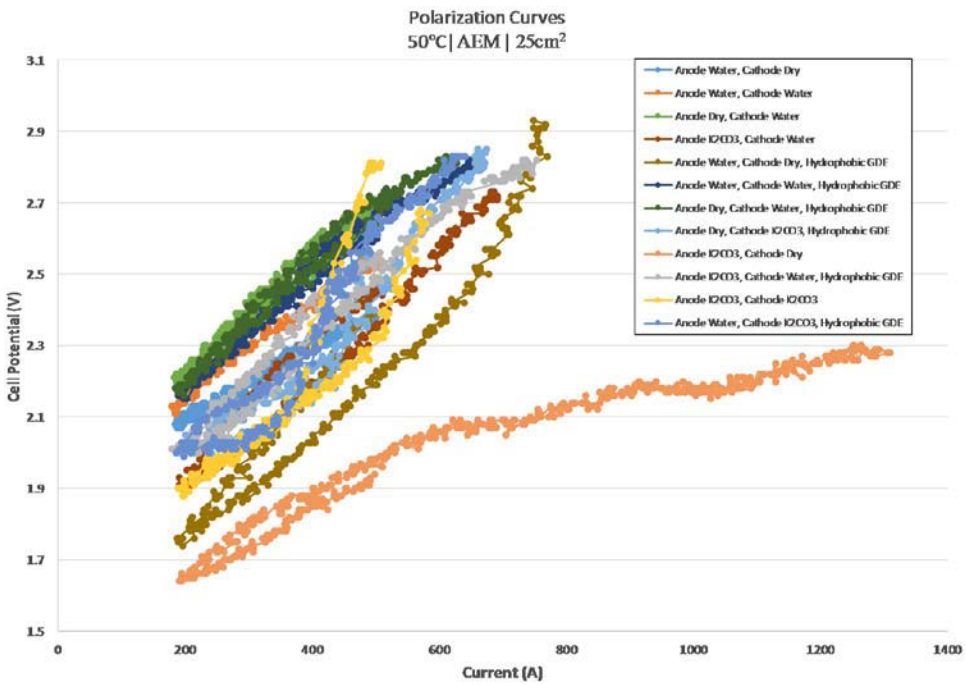

FIGURE 1. Operational mode evaluation polarization data collected at 50°C

The mechanical and electrical sections of the water transport fixture were completed and the system passed Proton's internal safety review. All components for the vessel were received and were assembled to verify against the model. All parts were made of clear polycarbonate to visualize the water flux and transport across the membrane surface during the various planned tests with alternative membrane samples and GDLs, as work continues to improve upon cell design, stability, and performance. The manufactured parts were machined, annealed, and vapor polished to produce endcaps capable of an operating pressure of 200 psi. Hydrostatic testing is conducted at 1.5x the operating point to meet industry standards for electrolysis. Hydrostatic testing was completed successfully and the vessel was installed into the system and operational verification was performed. An image of the fully built system is shown in Figure 2.

To increase membrane robustness, supported membranes were fabricated at Penn State for testing at Proton OnSite. Most samples were produced with Nylon, but polyether ether ketone and poly-tetrafluoroethylene meshes were also trialed. The addition of the mesh was intended to increase the mechanical properties of BTMA40 baseline membranes that have been tested extensively to measure degradation. In initial tests, the mechanical properties of the membranes were markedly improved with the addition of a support. Preliminary cell testing has demonstrated less cracking and mechanical degradation in the supported samples. In addition, overall life was improved under steady-state operation. Earlier non-reinforced samples tested from Penn

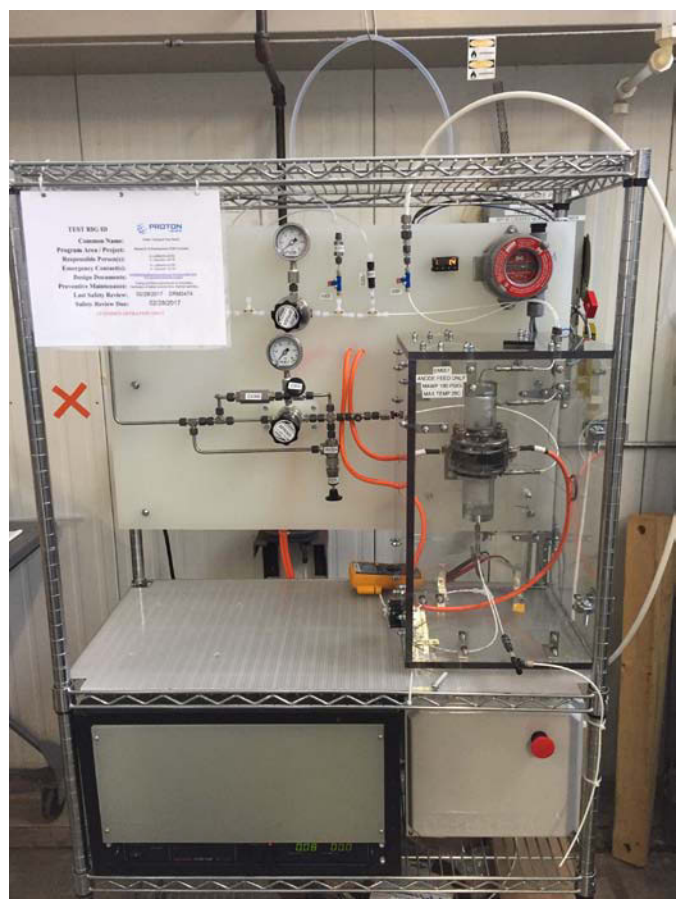

FIGURE 2. Image of water transport system and installed vessel

State had only demonstrated several hours of life before mechanical failure. Procedurally, one test was operated in deionized water and then removed for analysis and then similarly, a following test was prepared with an identical piece of the reinforced membrane and operated with the carbonate electrolyte. The samples were operated with PGM catalysts in both the cathode and anode electrodes. Both samples achieved 17 h of operation with no obvious signs of failure. The tests were halted at this point, membranes were visually inspected, and were returned to Penn State for instrumental analysis. A follow-up test was assembled and placed on test for steady-state operational testing to assess the length of time the sample would operate under in carbonate before failure. As shown in Figure 3, the cell operated for >150 h before the voltage had increased to the point where the upper shutdown limit of 2.8 V was reached. It should be noted that the cell did not fail mechanically. Upon test completion, the cell was disassembled and returned to Penn State for post operational analysis. This test represents the longest operational test at Proton of the membrane developed by Penn State demonstrating the significant improvements realized over the course of the program.

The final durability test stack was assembled as a three-cell 28 cm^2 stack; a manufacturing issue identified early in the test required removal of one of the cells and the stack was operated as a two-cell stack. The configuration leveraged improvements in cell design to manage the thinner AEM materials available. The test was operated at 50°C, 50 psi hydrogen generation pressure, 500 mA/cm^2, and with carbonate added to the anode water feed. Proton's traditional test stand was used since it provided continuous data acquisition of all operating parameters, including gas cross-over measurements to sense for membrane failure. Electrodes were fully non-PGM based. This stack uses Proton's commercial production stack to represent the most realistic operating conditions possible. The test exceeded the final milestone target of 500 h, achieving 1,000 h, doubling the program requirement. The full data set from this test is included in Figure 4.

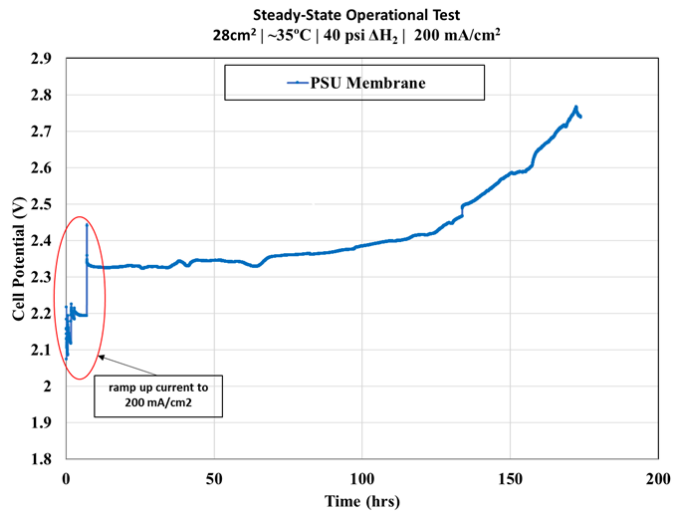

PSU – The Pennsylvania State University

FIGURE 3. Supported BTMA40 membrane with Nylon mesh operational data

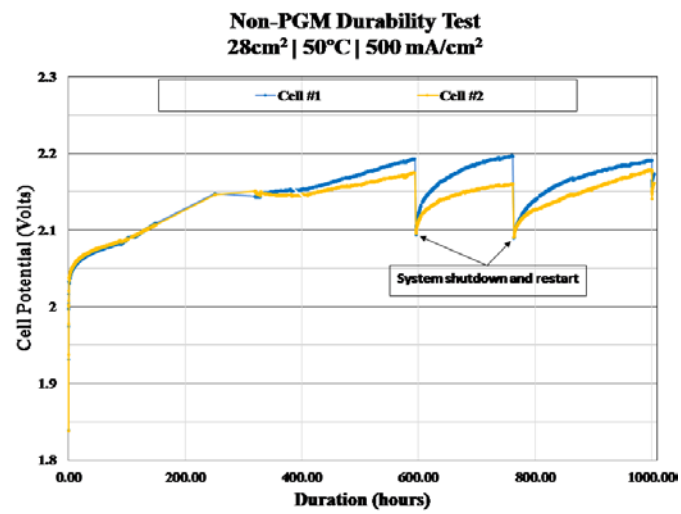

FIGURE 4. Results from final non-PGM durability test showing 1,000 h of operation

CONCLUSIONS AND UPCOMING ACTIVITIES

Non-PGM catalysts have been successfully incorporated into a full MEA and verified through in-cell operational testing. Test stand modifications helped to advance understanding of operational modes and support the final durability test. Work conducted at Penn State has continued to make improvements in membrane durability, leveraging one of Proton's commercial suppliers through the procurement and inclusion of reinforcements during casting. The final test deliverable met the final program milestone by operating for over 500 h with a full non-PGM cell.

FY 2017 PUBLICATIONS/PRESENTATIONS

1. "High Performance Platinum Group Metal Free Membrane Electrode Assemblies through Control of Interfacial Processes," Poster, DOE Merit Review, June 2017, Christopher Capuano, Proton OnSite.

2. "Catalytic and Mass Transport Effects of Carbonate Ions at an Anion Exchange Membrane Interface (PGM vs. non-PGM) for a Practical and Efficient Water Splitting Cell," ECS Conference, May 2017, Huong Doan, Northeastern University.

3. "PGM-Free OER and HER Electrocatalysts for Alkaline Electrolyzers in Alkaline Media," ECS Conference, May 2017, Alexey Serov, University of New Mexico.

II.B.4 High Temperature Alkaline Water Electrolysis

Hui Xu (Primary Contact), Kailash Patil, Winfield Greene, and Andrew Sweet
Giner, Inc.
89 Rumford Ave.
Newton, MA 02466
Phone: (781) 529-0573
Email: hxu@ginerinc.com

DOE Manager: David Peterson
Phone: (240) 562-1747
Email: David.Peterson@ee.doe.gov

Contract Number: DE-EE0007644

Project Start Date: January 1, 2017
Project End Date: December 31, 2019

Overall Objectives

The overall objective is to develop high-temperature alkaline water electrolysis using molten hydroxides in porous alumina, zirconia, or lithium aluminate. Some of our objectives are below.

- Develop alumina- and zirconia-based matrices.
- Select anode and cathode catalysts with enhanced hydrogen evolution reaction and oxygen evolution reaction activity.
- Assemble and test 25-cm^2 single electrolyzer cell and evaluate its performance and durability (at 0.5–1.0 A/cm^2 and 1,000 h).
- Construct and test 1.8 kW electrolyzer stack.

Fiscal Year (FY) 2017 Objectives

- Develop alumina- and zirconia-based matrices with optimal pore size.
- Optimize slurry formulation of the alumina and zirconia matrices using tape casting process.
- Impregnate hydroxides into porous matrices to achieve target conductivity.

Technical Barriers

This project addresses the following technical barriers from the Hydrogen Production section of the Fuel Cell Technologies Office Multi-Year Research, Development, and Demonstration Plan and contributes to the achievement of the targets shown in in Table 1.

(F) System Efficiency and Electricity Cost: associated with platinum group metals or expensive high temperature materials

(G) Operating cost: prohibitive electricity consumption for water electrolysis

Technical Targets

This project will develop high-temperature alkaline water electrolysis.

- Composite electrolyte OH- conductivity >0.1 S/cm in temperature of 350–550°C
- Per cell area-specific resistance of ≤0.2 ohm-cm^2 at 350–550°C using a membrane thickness of 200 µm
- Stack electrical efficiency >90% lower heating value (LHV) H_2 with current density at 1.2 A/cm^2

TABLE 1. Distributed Forecourt Water Electrolysis Hydrogen Production Targets

Characteristic	Units	2011 Status	2015 Target	2020 Target
Hydrogen Levelized Cost (Production Only)	$/kg H_2	4.20	3.90	2.30
Electrolyzer System Capital Cost	$/kg	0.70	0.50	0.50
	$/kW	430	300	300
System Energy Efficiency	% (LHV)	74	76	77
	kWh/kg	45	44	43
Stack Energy Efficiency	% (LHV)	74	76	77
	kWh/kg	45	44	43
Electricity Price	$/kWh	From AEO 2009	From AEO 2009	0.037

AEO – Annual Energy Outlook

FY 2017 Accomplishments

- Selected stable metal oxide matrices via investigating the stability of different metal oxides in single and binary hydroxide melts.
- Successfully fabricated and optimized lab-scale alumina- and zirconia-based matrices using a tape casting process.
- Constructed a testing facility for OH- conductivity measurement and matrix stability in molten hydroxide systems.

✧ ✧ ✧ ✧ ✧

INTRODUCTION

Hydrogen production from water electrolysis for mobile and energy storage applications is attractive due to its high efficiency, fast ramp rates, and high-pressure capability. However, current hydrogen production from electrolysis comprises only a small fraction of the global hydrogen market due to the high cost associated with expensive stack materials (membrane, catalyst, and bipolar plates) and electricity consumption of the commercially available electrolysis systems. This project aims to develop a high temperature alkaline water electrolyzer that can simultaneously reduce the electrolyzer cost (by adopting cheap material) and improve energy efficiency (due to enabling high-temperature operation).

APPROACH

The proposed project uses high-temperature alkaline electrolysis that employs lithium, sodium, potassium, or calcium hydroxide impregnated into a porous oxide matrix as the electrolyte membrane as shown in Figure 1.

The operating temperature of modal acoustic emissions can vary from 350°C–550°C, dependent on the category and ratio of each individual electrolyte. In this process, single or mixed alkali/alkaline earth hydroxides (LiOH, NaOH, and KOH) are first melted and impregnated in porous matrix of alumina or zirconia. The meticulously designed alumina or zirconia matrices can well retain molten hydroxides via capillary forces [1,2]. The alumina or zirconia containing single or mixed hydroxides is used as the electrolyte for alkaline electrolysis that can operate very flexibly in a wide temperature range, dependent on single or eutectic system. Ni- or Co-based catalysts will be used for the anode and cathode reactions.

A key factor that will influence the success of this technology is the microstructures of the porous oxide matrices. Their thickness, porosity, and pore structures largely determine whether they can successfully retain molten hydroxides in their pores, particularly over an extended period of time (DOE target, 7 years). Therefore, our overall approach is to develop the alumina- or zirconia-based matrices and design composite electrolytes with various hydroxides in order to increase the OH- conductivity. Alumina- or zirconia-based matrices will be developed and slurry formulation and tape casting process be optimized to achieve thin composite electrolyte with good mechanical strength.

RESULTS

The short-term stability of baseline powder and advanced metal oxides in single and binary hydroxide electrolyte immersion was tested at 450°C and 550°C for 10 h under air atmosphere. Shown in Figure 2a are the surface morphologies of baseline metal oxide (α-Al_2O_3) powder after exposure to LiOH and LiOH-NaOH melts in air at 450°C and 550°C for 10 h. The as-received powder consists of uniform spherical micron-size particles. Heating this baseline powder at 450°C and 550°C in both LiOH and LiOH-NaOH melts resulted in the emergence of rod-shaped Al_2O_3 particles. Significant changes in morphology of the baseline metal oxide (MO) were observed after the immersion test. Figure 2b–d shows the surface morphologies of MO-1, 2, and 3 powders after exposure to the same LiOH and LiOH-NaOH melt conditions. The microstructures of MO-1, 2, and 3 powders reveal that the particles were well

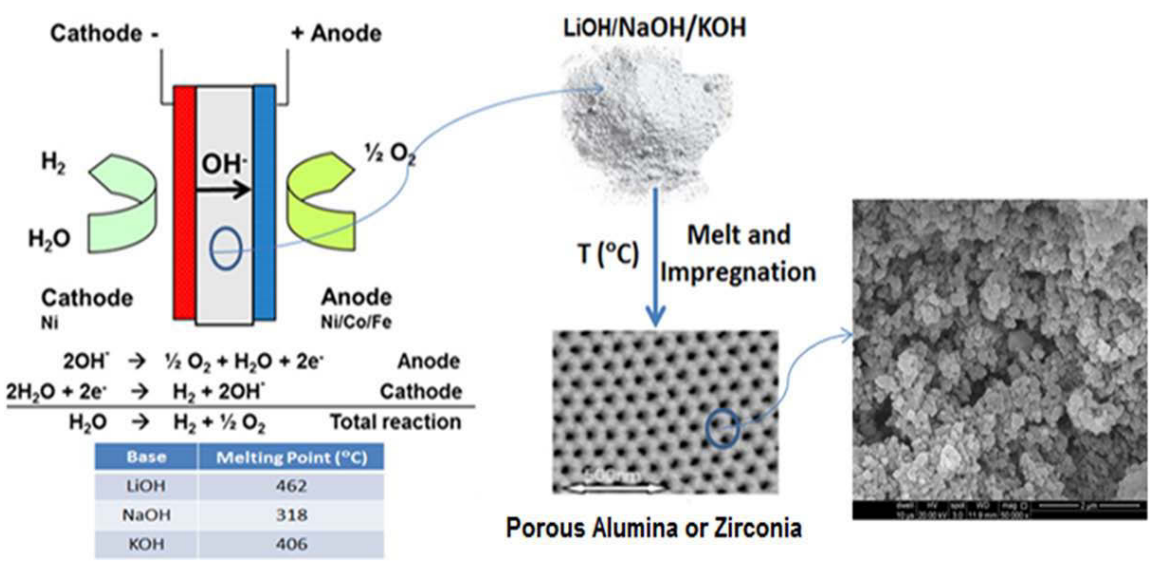

Base	Melting Point (°C)
LiOH	462
NaOH	318
KOH	406

FIGURE 1. Technical approach to achieve high temperature alkaline water electrolysis

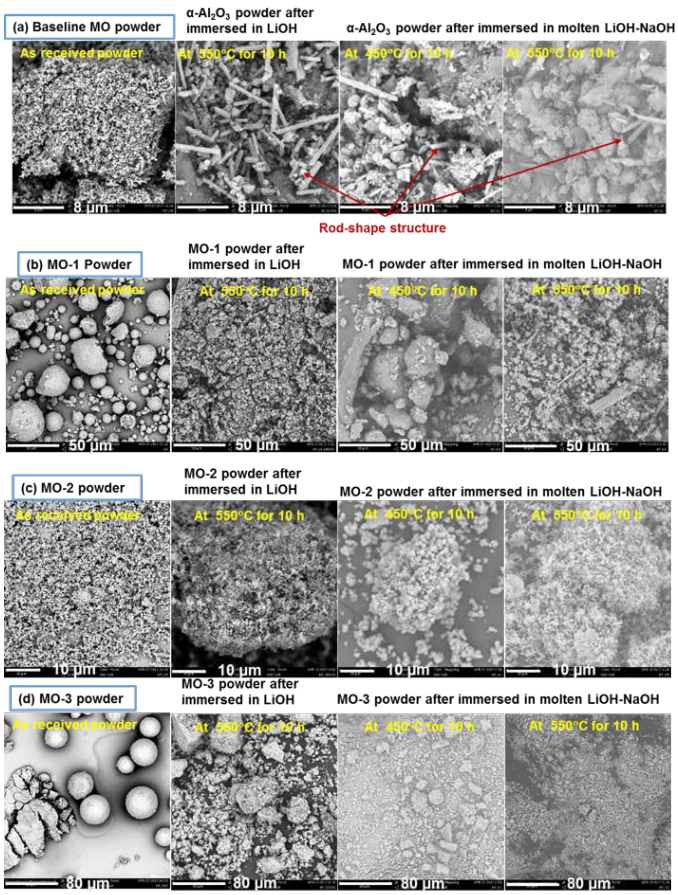

FIGURE 2. Surface morphologies of as received metal oxide powders and after immersion test of (a) baseline metal oxide, (b) MO-1, (c) MO-2, and (d) MO-3 materials, in LiOH and molten Li/Na hydroxide melts under air for 10 h

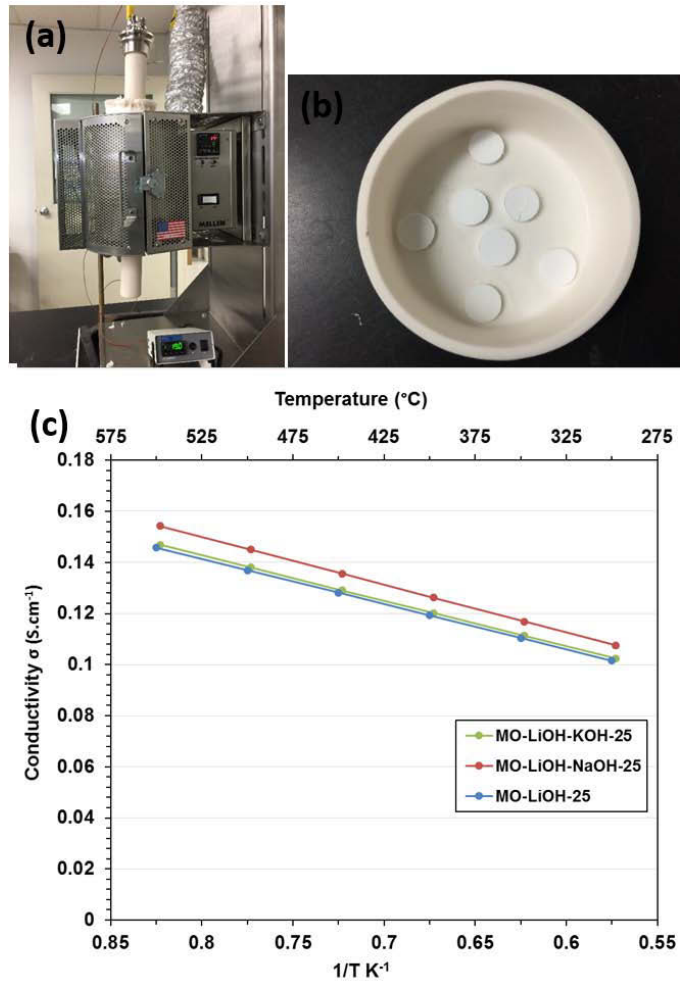

FIGURE 3. Photographs of (a) test assembly for OH- conductivity measurement and (b) sintered single/binary hydroxide pellets, and (c) temperature dependence of the OH- ion conductivity of single/binary hydroxides at 300°C–550°C in air atmosphere

defined and no significant change in the particle/grain size occurred after performing the immersion test for 10 h in both LiOH and molten LiOH-NaOH melts. Indeed, the particle size of the MO-1, 2, and 3 powders remained constant and microstructure barely changed upon immersion in both LiOH and molten LiOH-NaOH melts.

Figure 3a shows the test apparatus, including a tubular furnace, gas flow arrangement, and sample placement within the furnace to oxidizing and reducing atmosphere exposure conditions. The sintered pellets of the single or eutectic composition of initial 25% hydroxide incorporated in the metal oxides were developed to measure the OH- conductivity. Figure 3b shows the image of after-sintered pellets (13 mm diameter and thickness about 1 mm) of composite hydroxide electrolyte. The sintered pellets of mixed hydroxide and metal oxide were painted with silver paste and heated to ensure a good bond between the sample surface and silver paste. The temperature dependence of OH- ion conductivities for the pelletized composite single/binary hydroxides is shown in Figure 3c. The single and binary hydroxides showed OH- ion conductivity of 0.154 $S.cm^{-1}$ and 0.142 $S.cm^{-1}$, respectively. The binary hydroxide conductivity was higher compared to that of single hydroxide at temperatures from 300°C to 550°C in air atmosphere. The loss of single/binary hydroxide content in the pellets was observed after testing at 550°C due to evaporation of low melting point of single (~400°C) or binary hydroxide (~300°C). The conductivity can be further improved by increasing the content of electrolytes in the porous matrices.

The lab scale-up development of the matrices has been initiated to optimize slurry formulation using a tape casting process. The selected matrices have been fabricated by the tape casting method. Figure 4 shows a picture of the lab-scale tape casting machine with heating system installed in the properties of the fabricated MO-1 matrix with thickness 0.50 mm, and scanning electron spectroscopy (SEM) images showing porous MO-1 after sintering at 550°C for 2 h in air atmosphere. The attained composite electrolyte has a porosity of 65% with average pore size of 0.1 µm.

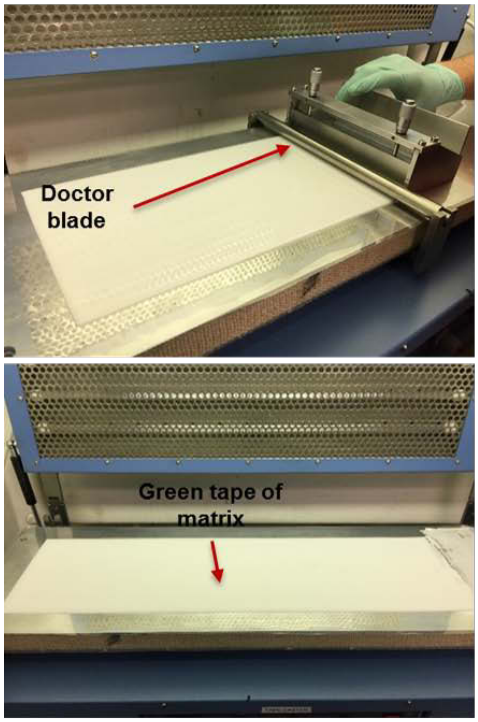

Fabrication of green tape of matrix using doctor blade

Parameters of before and after sintered green sheet matrix

Matrix	Matrix Thickness (mm)		Solid content (%)	Solid content (%)	Porosity (%)	Pore size (μm)
	Green sheet tape	After sintered	before sintered	after sintered		
MO-1	0.60	0.50	69.78	66.57	65.426	0.096

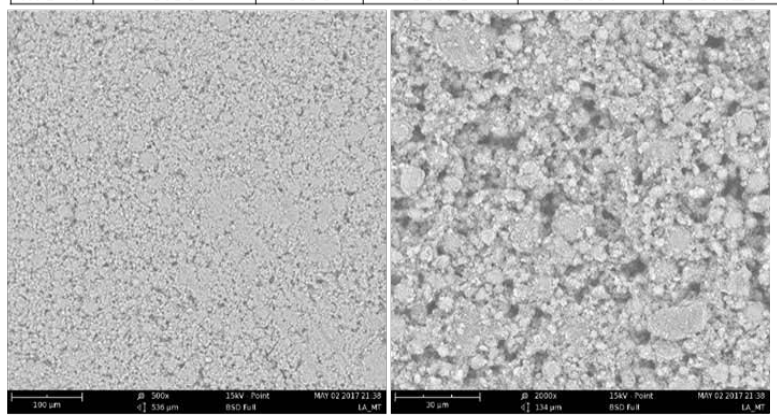

SEM images of MO-1 after sintered at 550 °C for 2 h in air

FIGURE 4. Photograph of lab-scale tape casting machine with heating system installed in the hood (left); properties (table, upper right) and morphology (lower right)

CONCLUSIONS AND UPCOMING ACTIVITIES

- The short-term stability of different metal oxides in single and binary hydroxide melts has been evaluated, and stable metal oxides have been selected.
- OH- ion conductivities of the single/binary hydroxides impregnated in metal oxide matrices have been measured. Initial conductivity is higher than 0.1 $S.cm^{-1}$ with less than 20 wt% hydroxides.
- A lab-scale tape casting machine is used for the fabrication of the electrodes and electrolyte matrix and green tape of matrix. Good porosity and pore size of green tape of matrix have been demonstrated.

Experiments will be performed to increase the OH- conductivity of the composite electrolyte by increasing the content of hydroxides. The green tape of more different metal oxide matrices will be optimized via the tape casting method and subjected to high temperature sintering (>650°C). The characterization plan for sintered matrix also consists of surface analysis, Brunauer-Emmett-Teller surface area, pore size distribution, and porosity. The anode and cathode catalysts will be selected to construct electrolyzer cells to evaluate the electrochemical performance.

FY 2017 PUBLICATIONS/PRESENTATIONS

1. Hui Xu and Kailash Patil, "High Temperature Alkaline Water Electrolysis," presented at the 2017 DOE Annual Merit Review and Peer Evaluation Meeting, Washington, DC, June 2017.

REFERENCES

1. http://www.hydrogen.energy.gov/pdfs/12001_h2_pd_cost_apportionment.pdf.

2. D. Anthony, J. Rand, and R. Dell, Hydrogen Energy Challenges and Prospects (RSC Energy Series), DOI:10.1039/9781847558022 (2008).

II.B.5 Solid Oxide Based Electrolysis and Stack Technology with Ultra-High Electrolysis Current Density (>3 A/cm^2) and Efficiency

Randy Petri (Primary Contact), Eric Tang, Tony Wood, Casey Brown, Micah Casteel, Michael Pastula, Mark Richards
FuelCell Energy, Inc. (FCE)
3 Great Pasture Rd.
Danbury, CT 06810
Phone: (303) 226-0762
Email: rpetri@fce.com

DOE Manager: David Peterson
Phone: (240) 562-1747
Email: David.Peterson@ee.doe.gov

Contract Number: DE-EE0006961

Subcontractor:
Versa Power Systems Ltd., Calgary, AB, Canada

Project Start Date: May 1, 2015
Project End Date: December 31, 2017

Overall Objective

- Develop solid oxide electrolysis cell (SOEC) technology capable of operating at ultra-high current density (>3 A/cm^2) with an operating cell voltage upper limit of 1.6 V—equivalent to 77% efficiency, lower heating value (LHV).

Fiscal Year (FY) 2017 Objectives

- Demonstrate stable solid oxide electrolysis stack operation with high current density of more than 2 A/cm^2 for 1,000 h.
- Complete a solid oxide electrolyzer process and system design that accommodates the ultra-high operating current density platform—all to meet the Department of Energy (DOE) 2020 target for advanced electrolysis technologies (2020 System Energy Efficiency Target: 75% LHV).

Technical Barriers

This project addresses the following technical barriers from the Hydrogen Production section of the Fuel Cell Technologies Office Multi-Year Research, Development, and Demonstration Plan.

(F) Capital Cost

(G) System Efficiency and Electricity Cost

(J) Renewable Electricity Generation Integration

Technical Targets

- Develop a SOEC platform capable of operating with current density up to 4 A/cm^2 at or below a voltage of 1.6 V (2020 Stack Energy Efficiency Target: 77% LHV).
- Demonstrate stable SOEC operation with high current density of 3 A/cm^2 for 1,000 h.
- Design a solid oxide electrolysis stack platform capable of operating with the high current density (>3 A/cm^2) cell technology at an upper voltage limit of 1.6 V/cell (2020 Stack Energy Efficiency Target: 77% LHV).
- Demonstrate stable solid oxide electrolysis stack operation with high current density of more than 2 A/cm^2 for 1,000 h.
- Complete a solid oxide electrolyzer process and system design that accommodates the ultra-high operating current density platform—all to meet the DOE 2020 target for advanced electrolysis technologies (2020 System Energy Efficiency Target: 75% LHV).

FY 2017 Accomplishments

- Completed 10 kW rated SOEC stack design freeze incorporating final design changes suggested by stack test results and any further modeling effort as well as final design elements that permit stacking into a 10 kW stack package.
- Completed in-depth SOEC hot module configuration design with emphasis on the detailed physical design of the module and validation of the process model in physical space.
- Coordinated this project with the stack design freeze and prototype repeat- and non-repeat-part stack development from the DOE Office of Fossil Energy (FE) innovative project for the ultra-compact, low-cost stack design platform, called the compact solid oxide fuel cell (SOFC) architecture, thus enabling a single/common stack design platform that can operate in fuel cell systems in electrolysis systems, as well as in reversible SOFC systems for energy storage applications.

✧ ✧ ✧ ✧ ✧

INTRODUCTION

Hydrogen, a valuable commodity gas, is being increasingly recognized as an important fuel and energy storage pathway of the future. Demand for hydrogen as a fuel for fuel cells, in both transport and stationary applications, will continue to grow alongside hydrogen for H2@Scale production and sales (industrial ammonia, chemicals/oil upgrades, and mobility for fuel cell electric vehicles), as well as energy storage (including power-to-gas and power-to-liquid-pathways). The renewed interest in developing electrolysis systems is driven, in part, by burgeoning solar and wind industries and the need for an energy conversion and storage technology that can serve as the vehicle for converting intermittent solar and wind energy into the production of hydrogen. Although current electrolysis systems have the potential to integrate with wind and solar energy sources, the key challenges are low system efficiency and high capital costs. This project aims to address these barriers with an innovative SOFC-based electrolysis and stack technology with ultra-high steam electrolysis current (>3 A/cm^2) for potentially ultra-low-cost, highly efficient hydrogen production from diverse renewable sources.

APPROACH

FCE (previously Versa Power Systems Inc.) has a strong solid oxide cell and stack development history through its previous Office of Energy Efficiency and Renewable Energy sponsored project and through over 15 years of cell and stack advancements from previous efforts (DOE, Solid State Energy Conversion Alliance, and Defense Advanced Research Projects Agency projects). Leveraging this experience, the project objectives will be met by executing the following scope:

- Addressing high current density electrolysis cell performance limitations by conducting multiple materials development and cell designs-of-experiment, integrating them with cell production technology development.
- Developing SOEC stack engineering modeling and process fabrication designs to address high current density operating requirements and identifying key operating parameters for the design of an integrated, SOEC-based energy conversion and storage system for renewable energy sources (wind and solar).
- Down-selecting cell technology developments and demonstrating high current density SOEC operation via single cell and stack tests.
- Investigating a high current density solid oxide electrolyzer system, including the option of integration with renewable energy sources, to meet DOE 2020 Advanced Electrolysis Technologies targets.

RESULTS

In this project, the next generation solid oxide-based high power density cells have been developed such that, when run in electrolysis mode, they are capable of operating at ultra-high electrolysis current density. These *cathode supported cells* have been developed using conventional SOFC materials comprising a nickel oxide and yttria stabilized zirconia cathode and 8 mole-% yttria stabilized zirconia electrolyte. (Note: electrolysis electrochemical nomenclature is used here. In fuel cell mode, these same cells are called *anode supported;* in electrolysis mode, it is technically accurate to refer to these cells as *cathode supported*.) The SOEC cell utilizes an all-ceramic anode with no noble metals. Electrochemical testing (current-voltage response) of the cells was performed up to 6 A/cm^2 in electrolysis mode. The steam and air are supplied in the horizontal plane, perpendicular to one another, in what is termed a cross-flow geometry. The test housing (and current collection) is made from low-cost ferritic stainless steel, and the current collection and seal materials used are the same as those used in SOFC stacks. The cell voltage includes all interfaces and the stainless steel current collection jigs and, as such, is believed to be representative of the stack-repeat-unit-cell of an FCE electrolysis stack. The cell planform dimensions are 5 x 5 x 0.03 cm with an active electrode area of 16 cm^2. This area requires a current input of 96 A to reach a current density of 6 A/cm^2 during electrolysis testing. A remarkable cell voltage of 1.67 V at 6 A/cm^2 was achieved at 800°C. Even at 750°C, the cell exceeded the project performance target of 4 A/cm^2 at 1.6 V. A long-term steady-state electrolysis test of a high power density stack-repeat-unit-cell has been operating for more than 1,000 h at 3 A/cm^2 current density with a low degradation rate of 1.8% per 1,000 h.

A 20-cell electrolysis stack was built using high power density cells and an ultra-compact, low-cost stack design platform. This stack was used to explore the boundaries of high current density electrolysis operation and achieved an incredible stack current density of 3 A/cm^2 (67 A) with an average cell voltage of only 1.493 V. The cathode test gas composition was 78% water and 22% hydrogen (20.11 SLPM water [calculated], 5.672 SLPM hydrogen) for a steam utilization of 50.0%. After load-up and tuning, a stack voltage of 29.856 V (1.493 V/cell) at stack current of 67 A (3.004 A/cm^2) was demonstrated. At this test condition, the stack produced 50.3 g/h hydrogen with a stack volume of only 200 cm^3 using 2 kW input. This equates to 2.5 kg H_2 per day for a single, 225-cell stack of this platform design. The stack was then further operated in steady-state electrolysis at 2 A/cm^2 for more than 1,000 h as shown in Figure 1. Early in the 1,000 h hold (first 300 h), three unplanned and uncontrolled test interruptions occurred which resulted in full thermal cycles. The degradation appears to have increased for a period after the first interruption, but the

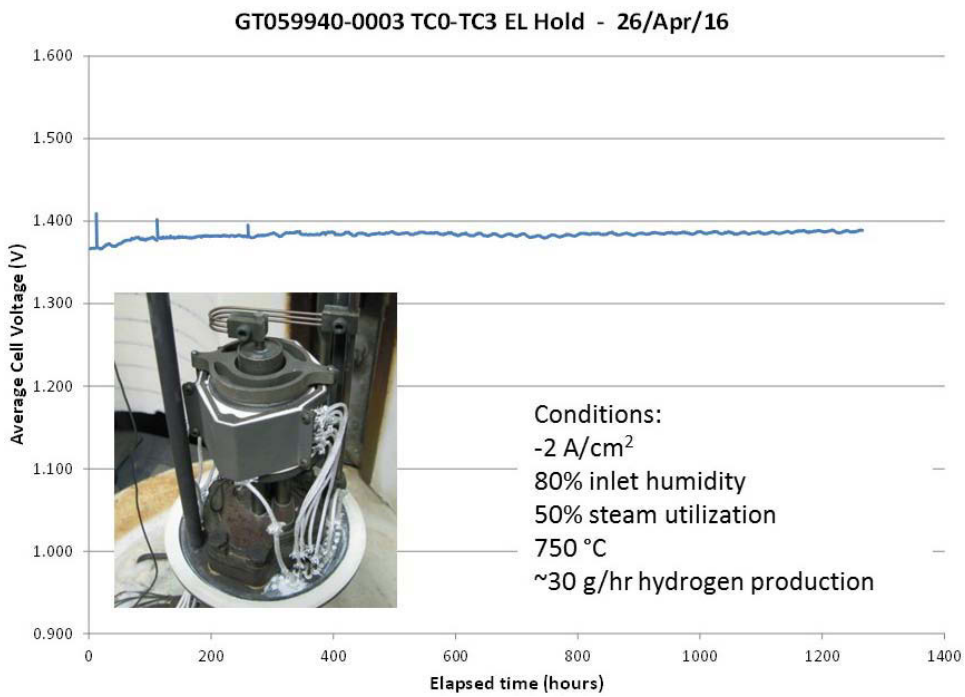

FIGURE 1. Sustained 2 A/cm^2 electrolysis test for over 1,000 h

overall degradation for the test period was relatively low, at 7.2 mV per 1,000 h per cell or 0.57% per 1,000 h.

After demonstrating stable stack operation at 2 A/cm^2 for over 1,000 h and with an improved understanding of the thermal conditions this operating point imposed on the stack, a strategic decision was made to homogenize the stack platform between this project (DE-EE006961) and an SOFC specific project (DE-FE0026093, through DOE FE). The basis for this decision was that the thermal condition at 2 A/cm^2 was not as severe as originally anticipated and therefore less compromise was required in the stack design for thermal management, thus enabling a *single/common*, ultra-compact, low-cost stack design platform called the compact SOFC architecture that can operate in fuel cell systems, in electrolysis systems, as well as in reversible SOFC systems for energy storage applications.

With that strategic shift, the main effort for stack development moved to project DE-FE0026093 (DOE FE "Innovative SOFC Stack" project). Under that project, the stack reached the point of design review and release for production, and parts and production tooling are currently on order.

Figure 2 shows the three planned compact SOFC architecture stack sizes where the commonality of design is shown. All parts through the core of the stack remain the same and are independent of stack height. The shortest stack (45 cells) is the deliverable stack for this program to meet the 10 kWe and 250 g/h program targets. Only the manifolds

FIGURE 2. Comparing the three stack sizes

and the details of the compression system hardware differ between the various stack heights. In practice, other intermediate heights would be possible if there was a specific need due to the discrete nature of the non-repeat components. By constraining development to three target stack sizes, tooling and parts can be more easily optimized.

A preliminary system design was developed by integrating the inputs from electrochemistry, cell/stack performance data, and system level implications of configuration and operational parameters. Several variations were hypothesized and modeled with the most promising design and conditions iterated several times in order to determine the best-case baseline system. The resulting system design is yet to be fully optimized; however, it provides excellent insights to the potential of a high current density, high temperature water-splitting system.

The emphasis in FY 2017 has been focused on detailed physical design of the module and validation of the process model in physical space. The general approach to develop the SOEC module was to work from the CHEMCAD process model and attempt to realize process model components, influenced and integrated with FCE's deep experience in real physical unit operations components. While this is a somewhat contrived approach, it is otherwise common to find substantial differences between the process simulation model and physical system; it served as a valuable first draft approach to creating a realistic system.

A module design was created based on a circular array of six stacks surrounded by a cool pressure vessel. Further architectural and controls philosophy impacts such as stack power control and instrumentation were determined through the development of the module. The basis of the module design included a close mechanical and thermal coupling of all aspects of the module to avoid transferring losses between components. This resulted in what is termed the Integrated Hot Module approach, shown in Figure 3. The approach integrates several heat exchangers, trim heaters, and even potentially some aspects of the vaporizer into the hot module, along with the stacks. In theory this serves to dramatically reduce nozzle or boundary temperatures in and out of the pressure vessel, thermally coupling all high temperature heat exchangers, and reduce the overall size of the plant. The six-stack circular array also naturally provides multiple physical locations for heat exchanger placement.

The basic module layout includes six stacks arrayed in a circular pattern, all around a central multi-fluid heat exchanger with radiant heat exchangers positioned between the stacks, as shown in Figure 4. The base plate performs the fluid distribution function with the exception of the air inlet flush. Following preheating in the triangular radiant heat exchangers, inlet air is flushed into the module and thoroughly mixes before entering the sides of the stack.

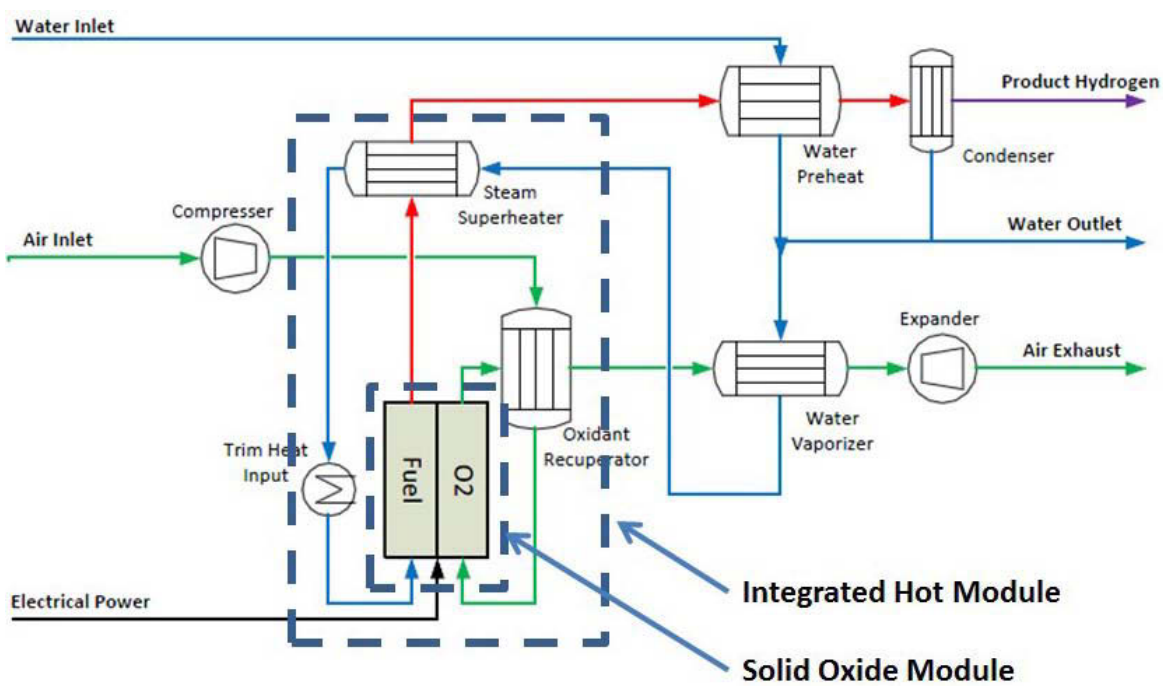

FIGURE 3. SOEC system process flow diagram

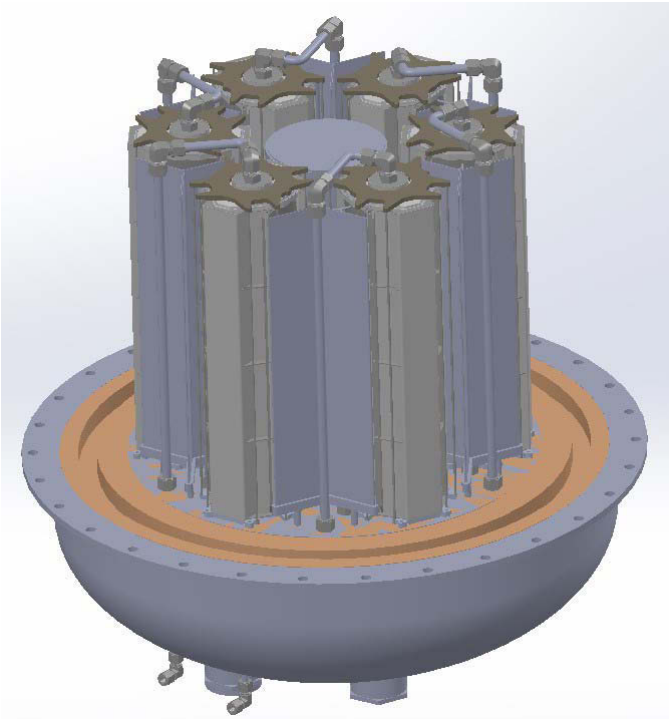

FIGURE 4. SOEC module layout

CONCLUSIONS AND UPCOMING ACTIVITIES

The project team will continue on the current development path. This includes the objectives to:

1. Demonstrate an SOEC stack with 250 g/h hydrogen production as well as demonstrating stable operation at a current density of more than 2 A/cm^2.

2. Complete a comprehensive techno-economic study of an ultra-high current density SOEC system integrated with renewable energy sources.

FY 2017 PUBLICATIONS/PRESENTATIONS

1. Oral presentation at the 2017 DOE Hydrogen and Fuel Cells Program and Vehicle Technologies Office Annual Merit Review and Peer Evaluation Meeting in June 2017.

2. Planned presentation at the 2017 Fuel Cell Seminar.

II.B.6 Economical Production of Hydrogen through Development of Novel, High Efficiency Electrocatalysts for Alkaline Membrane Electrolysis

Katherine Ayers (Primary Contact), Chris Capuano
Proton OnSite
10 Technology Drive
Wallingford, CT 06492
Phone: (203) 678-2190
Email: KAyers@protononsite.com

DOE Manager: David Peterson
Phone: (240) 562-1747
Email: David.Peterson@ee.doe.gov

Contract Number: DE-SC0007574

Subcontractors:
- Washington University, St. Louis, MO
- Georgia Institute of Technology, Atlanta, GA
- Pajarito Powder, Albuquerque, NM

Project Start Date: April 11, 2016
Project End Date: April 10, 2018

Overall Objectives

- Refine the pyrochlore synthesis technique for electrocatalysis of oxygen evolution reaction (OER).
- Replicate catalyst synthesis in the manufacturing environment and scale up.
- Compare commercial and optimized ionomers and refine formulations based on the results.
- Scale up down-selected ionomers for demonstration in electrolyzers.
- Integrate optimized catalyst, membrane, and ionomer materials into the cell stack and verify performance through durability testing.
- Develop and implement accelerated stress tests for the anionic chemistry.
- Verify a 12–14 cell stack configuration for laboratory scale hydrogen generation.
- Complete the design and build of a 12–14 cell prototype system.

Fiscal Year (FY) 2017 Objectives

- Reproduce the Washington University synthesis process at Pajarito Powder and confirm the results through physical and electrochemical characterization.
- Down-select an ionomer(s) based on stability nuclear magnetic resonance (NMR) to elevated temperature in KOH.
- Hold a concept system design review.
- Synthesize a 50-gram batch of OER catalyst at Pajarito.
- Verify sealing for a 12–14 cell 28 cm^2 cell stack.
- Complete fabrication of the prototype system.

Technical Barriers

This project addresses the following technical barriers from the Hydrogen Production section of the Fuel Cell Technologies Office Multi-Year Research, Development, and Demonstration Plan.

(F) Capital Cost

Technical Targets

The only metrics for hydrogen production at the system level are $/kW and $/kg. These high-level metrics cause difficulties in highlighting even major changes at the component level. However, the final cost will be largely dependent on raw material costs. Developing and scaling stable alkaline membrane technology is also important in establishing feasibility of the technology. The current program aims to meet the following targets.

- Scale up of catalyst synthesis to 50 g batches and show a pathway to kilogram scale
- Verify cell stack scale-up to 12–14 cells
- Durability: 500 h of stable operation

FY 2017 Accomplishments

- Operational testing of the candidate ionomers was initiated at Georgia Tech.
- Pre- and post-operated samples were shipped to Washington University where a methodology using NMR was applied to look for evidence of degradation.
- Synthesis procedure for scale-up of the high surface area pyrochlore catalysts was provided to Pajarito, as part of the tech transfer effort (milestone).
- The 14-cell stack design was completed, and a single 14-cell stack was assembled, bench-tested, and verified against Proton acceptance testing procedures.

- Operational testing of the prototype system was initiated.

✧ ✧ ✧ ✧ ✧

INTRODUCTION

As the need for renewable energy capture grows, the balance between electricity feedstock cost and capital cost shifts, due to the ability to obtain low cost electrons but at lower capacity factors. Since the electrolyzer is on for a lower percentage of the time, the capital cost has a larger impact on the overall lifecycle cost. Anion exchange membrane (AEM)-based electrolyzers offer a pathway to significantly reduce the cost of the cell stack, by enabling low cost oxygen flow fields such as nickel or stainless steel, as well as reduction or elimination of platinum group metals in the catalyst layer. The team has demonstrated the exceptional activity and stability of lead ruthenate pyrochlore electrocatalysts for the oxygen evolution reaction. While these catalysts still contain some noble metal, eliminating the titanium from the cell has a greater impact on cost and provides an initial stepping stone for product cost reduction.

In theory, AEM-based electrodes should represent a drop-in replacement to Proton's existing cell stack designs. However, the supply chain for AEMs is still developing, and membrane formats are smaller than the typical Nafion rolls produced for fuel cell and electrolyzer applications. Introduction of new materials into the cell stack that are unproven in the field also represents a large capital risk at megawatt scale. Proton's laboratory product provides an opportunity to introduce these materials to market at a lower risk entry point and gain field experience on the pathway to eventually applying AEM technology for larger energy related applications.

APPROACH

Proton will continue to work with the Ramani group at Washington University to scale up catalyst synthesis and transition to Pajarito Powder, a commercial company. Proton will also continue to incorporate the most promising membrane and ionomer combinations in order to optimize performance and stability. As one option, Proton will evaluate ionomers developed in Kohl's group at Georgia Tech, which have been used in systems at Acta.

In parallel, Proton will work to scale the stack to an appropriate capacity for the laboratory product portfolio. The planned capacity will supplement existing options rather than supplanting an existing product, to provide more value for the same investment. Proton will leverage work previously done for the U.S. Air Force on a higher capacity hydrogen generator with similar footprint to our lab line. Approaches for electrolyte management (pure water or supporting electrolyte) will be finalized and the resulting system design completed.

RESULTS

Washington University synthesized $Pb_2Ru_2O_{6.5}$ OER catalysts and provided them to Proton for operational testing. Materials provided were assembled into a single 25 cm^2 stack; results were collected and compared to the values obtained at the end of the Phase II program. This was done to show translation of the process after the Ramani group moved from their previous location at Illinois Institute of Technology. Polarization data (Figure 1) indicated comparable performance to the previous DOE Phase II target through a maximum current density of 500 mA/cm^2 at 50ºC. The method for the synthesis of $Pb_2Ru_2O_{6.5}$ OER catalysts was then transmitted to Pajarito Powder to initiate technology transfer and proceed with synthesis scale up. The selection of the material for scale up was based on OER activity and stability during electrolyzer experiments. Washington University is assuring that common synthesis protocol by opening several ways of communication (on-site visit, emails, phone calls, samples sent for analysis, and detailed reports). Washington University verified at its labs that the shared protocol produced 3.1 g of $Pb_2Ru_2O_{6.5}$ with a percentage of crystalline pyrochlore in the range of 40–60%, a Brunauer-Emmett-Teller surface area of approximately 100 m^2/g, an electronic conductivity of at least 100 S/cm, and an OER activity (measured at a potential of 1.5 V vs. reference hydrogen electrode) of 200 A/g.

The stability of the AEM binders synthesized at Georgia Tech was investigated by using NMR spectroscopy. The binders were extracted from the gas diffusion electrodes after

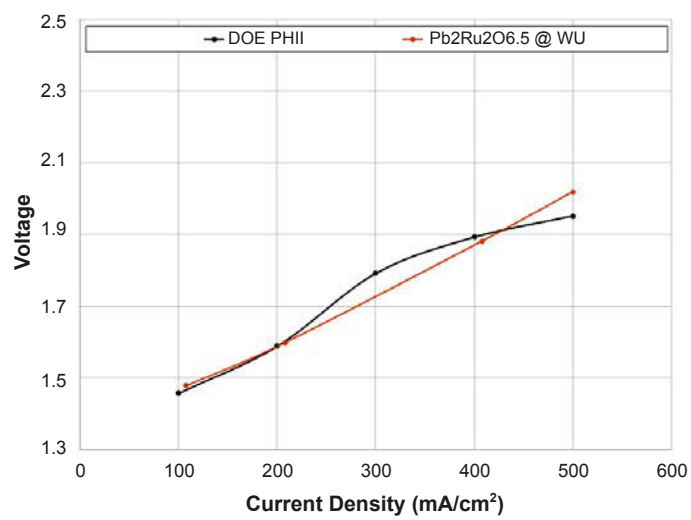

PHII – Phase II

FIGURE 1. Polarization curve comparison between Phase II end of program results and the process re-established at Washington University (WU)

several hours of operation at Georgia Tech. The intent of these experiments was to identify any signs of degradation in the binders occurring during operational testing in the AEM water electrolyzer stack. Figure 2 shows the ^{1}H NMR spectra for two of the binders tested. Evaluation of both the pristine and operated ionomer spectra revealed peaks characteristic for both ionomers, with no new peaks commonly encountered in degraded ionomers. Moreover, the peak areas were close to the expected values. All these findings suggest the binders tested do not suffer chemical degradation during electrolyzer operation. Longer term operation of the electrolyzer and postmortem analysis of the binders are required to confirm these preliminary findings. The experiments are ongoing.

Work at Proton has been conducted in parallel on the stack and system design and development. Building upon Proton's 28 cm^2 commercial cell stack, a 14-cell stack assembly drawing was created and modeled to support the build and test of the new article. After confirming the stack up configuration and procuring the components required for fabrication, build success was achieved as verified by Proton's standard acceptance text procedure, which is comprised of four assessment elements: (1) a high frequency resistance measurement conducted at ambient and full pressure conditions to ensure minimal resistive losses in each cell, (2) an electrical isolation measurement to verify the absence of potential shorting in or between cells, (3) a pressurized leak test at up to 1.5 times normal operating pressure to confirm no evidence of a cross-cell or overboard leak, and (4) an operational test at full current and pressure to confirm acceptable overall performance.

Additional efforts were focused on the design and development of the prototype system for operation of the 14-cell stack. Instrumentation has been identified for mass flow rate and dew point measurements to verify actual versus the target values for hydrogen generation and purity. The 14-cell stack was installed and operated within the system. Initial temperature profiles within the system enclosure have been collected and will be used to further understand the impact to system and stack components (instrumented stack and system shown in Figure 3). Further work has been planned to conduct a more thorough analysis, where an environmental enclosure has been developed to subject the system to elevated atmospheric temperature. As part of this, a pressure swing adsorption dryer will be tested and tuned to improve hydrogen gas purity through this range of conditions.

Proton also placed a single cell 28 cm^2 AEM water electrolysis stack on test to evaluate steady-state durability of the integrated project elements. The purpose was to combine inputs from partners at Georgia Tech, Pajarito Powder, and Washington University. Georgia Tech provided ionomer which was used at Proton in the fabrication of OER electrodes. Washington University, assisted Pajarito Powder with the synthesis details required to produce lead ruthenate powders for use as an OER catalyst. Pajarito Powder refined the synthesis steps to increase throughput and quantity. Materials were provided to Proton and processed into electrodes for the durability test. The cell stack and system used were based on the designs shown in Figure 3. Steady-state current densities were held constant at 500 mA/cm^2 and achieved >900 h of operation, showing the successful collaboration of all partners to provide robust materials

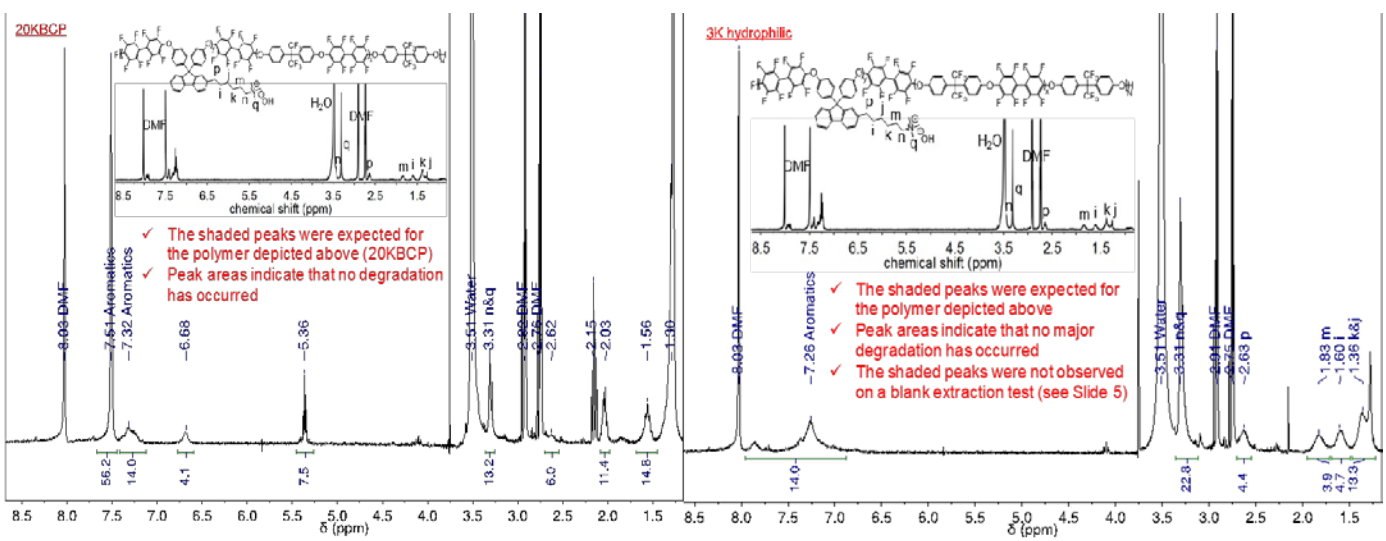

DMF – n, n-di-methyl formamide

FIGURE 2. (Left) ^{1}H-NMR of "20KBCP" AEM binder after operational testing in a water electrolyzer. The insert figure shows the spectrum of the pristine material. (Right) 1H-NMR of "3K hydrophilic" AEM binder after operational testing in a water electrolyzer. The insert figure shows the spectrum of the pristine material.

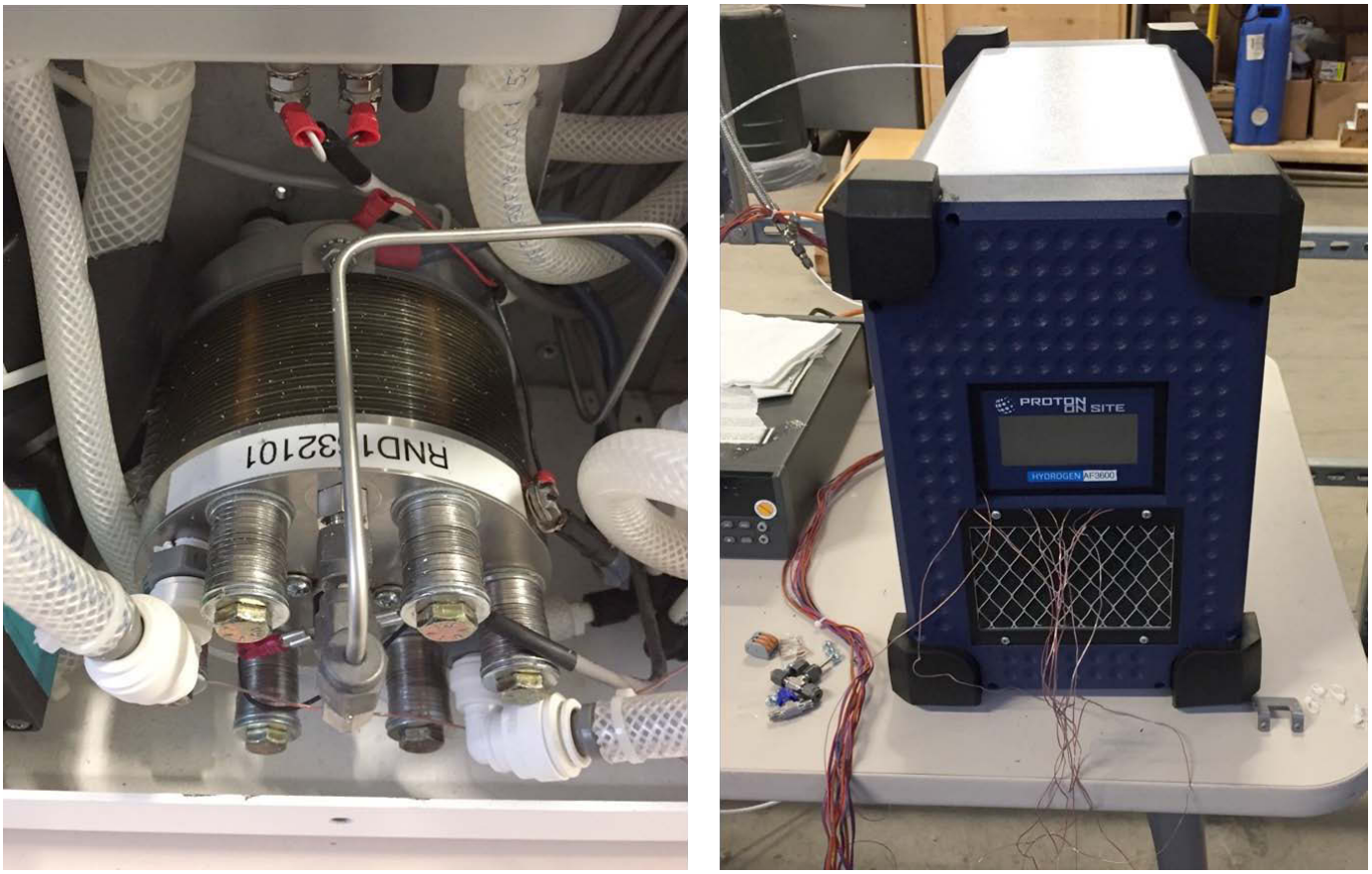

FIGURE 3. Cell stack and system instrumented for thermal measurements

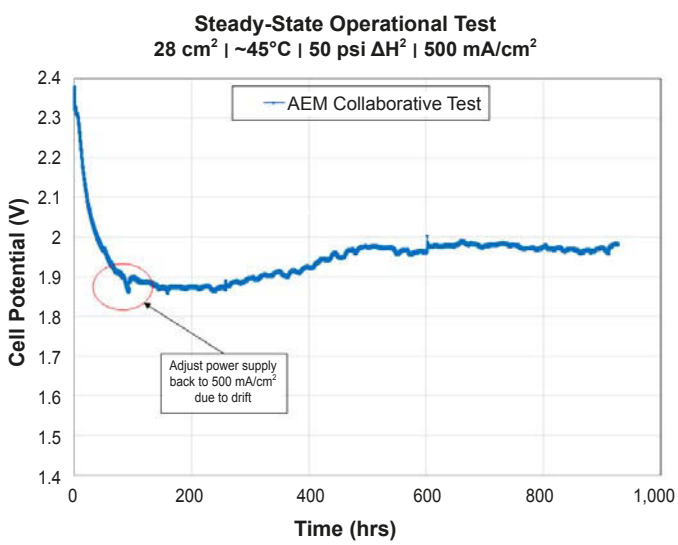

FIGURE 4. One-cell, steady-state test results collected from the durability assessment

capable of achieving stable extended operation. The results from this test are shown in Figure 4.

CONCLUSIONS AND UPCOMING ACTIVITIES

Several ionomer dispersions developed at Georgia Tech have been synthesized and show early promise in degradation studies. Longer duration tests will be used to down-select the final configuration and understand degradation effects, supported by accelerated degradation studies at Washington University. Synthesis of the lead ruthenate catalyst was recreated at the new Washington University labs and then successfully transferred to Pajarito Powder, where catalysts are in the early stages of scale-up. A 14-cell stack was assembled and functionally verified in the full-scale prototype system designed for the larger cell stack and associated hydrogen generation rates. A long-term steady-state test was conducted with inputs from all partners showing the collaborative effort and technical capability to execute the plan for scale-up and improved durability AEM water electrolysis membrane electrode assembly components.

Next steps include evaluation of advanced materials, and work to define the eventual system design, as follows:

- Compare catalysts synthesized at Washington University and Pajarito Powder.

- Scale-up to 50-gram batch size of the pyrochlore catalyst at Pajarito.
- Characterize degradation mechanisms for Georgia Tech ionomers based on post operational analysis.
- Down-select the best ionomer identified through operational and instrumental analysis.
- Hold a concept review for the proposed system.
- Create a system product requirements document, detailing the prototype system input/output criteria.
- Fix design points, procure components and fabricate a prototype system based on the on-going thermal, hydrogen flow rate, and hydrogen purity assessment.
- Integrate and test a multi-cell stack with the scaled-up catalysts and down-selected ionomers from program partners.

II.B.7 New Approaches to Improved PEM Electrolyzer Ion Exchange Membranes

Earl H. Wagener (Primary Contact), Brad P. Morgan, Chris Topping
Tetramer Technologies, LLC
657 S. Mechanic St.
Pendleton, SC 29670
Phone: (864) 646-6282
Email: earl.wagener@tetramer.com

DOE Manager: David Peterson
Phone: (720) 356-1747
Email: David.Peterson@ee.doe.gov

Contract Number: DE-SC0011305

Subcontractor:
Proton OnSite, Wallingford, CT

Project Start Date: April 6, 2015
Project End Date: April 9, 2019

Overall Objectives

- Optimize electrolyzer membrane performance.
- Refine polymer and membrane and cell architecture to maximize durability.
- Down-select materials for optimization of membrane composite configuration.
- Scale-up and confirm cost estimates.
- Build the prototype.

Fiscal Year (FY) 2017 Objectives

- Optimize down-selected ionomers and membrane configurations for performance, durability, and hydrogen permeation.
- Investigate cell design modifications for a commercial prototype.
- Demonstrate material scale-up and reproducibility and assess production costs.

Technical Barriers

This project addresses the following technical barriers from the Hydrogen Production section of the Fuel Cell Technologies Office Multi-Year Research, Development, and Demonstration Plan.

(F) Capital Cost

(G) System Efficiency and Electricity Cost

(K) Manufacturing

(L) Operations and Maintenance

Technical Targets

- Improved performance, reduced hydrogen permeation and lower costs compared with commercial perfluorosulfonic acid baseline.
- Membrane polarization loss after 500 h (200 mA/cm^2, 400 psi, 50°C) <10 mV.
- Reduction in crossover loss at 50°C and >200 psi.

FY 2017 Accomplishments

- Significant reduction in energy requirements for hydrogen production.
- 340–400 mV improvement in performance at 2 A/cm^2.
- Developed new techniques to reduce hydrogen crossover and demonstrated reduced loss at 50°C and >200 psi.
- Membrane polarization loss after 500 h (200 mA/cm^2, 400 psi, 50°C) <10 mV.
- Modified cell design for improved membrane compatibility.
- Down-selected two material configurations for further optimization.

✧ ✧ ✧ ✧ ✧

INTRODUCTION

The potential to use ion exchange membrane-based electrolyzers at much higher differential pressures than fuel cells minimizes the need for additional costly mechanical compression of the hydrogen produced. This high pressure differential requires a robust membrane that is able to prohibit hazardous back diffusion of hydrogen to the oxygen source. A common solution to both enhance mechanical durability and reduce hydrogen diffusion is to simply increase the thickness of the membrane, however this increases ionic resistance and can significantly reduce the efficiency of the system. Increasing the operating temperature can improve efficiency but this usually accelerates physical and chemical membrane degradation, especially at higher pressures. Due to the limitations of current commercial membranes, new approaches are needed

to enable efficient, cost effective proton exchange membrane (PEM)-based hydrogen generation.

Previously we demonstrated excellent performance and low hydrogen permeation at less than half the thickness of current commercial perfluorosulfonic acid membranes. During 2017 we have developed our ionomer chemistry, and investigated a number of membrane configurations in order to improve performance and durability and further reduce hydrogen crossover.

APPROACH

During this project, more than 40 different membrane configurations were produced at Tetramer and supplied to Proton OnSite for performance evaluation. Variables investigated include backbone polymer architecture and molecular weight, ion exchange capacity, membrane thickness and configuration (including the incorporation of supports and additives), and membrane casting and post treatment techniques. Membranes were evaluated for physical integrity, electrochemical performance, water uptake and swell, hydrogen permeability (crossover) and durability. Cell design and membrane treatments were also investigated to enhance performance and material compatibility.

Various analytical techniques were employed at Tetramer to assess the efficiency of each of the synthetic steps and the purity of final ionomers and their precursors. Process development was carried out throughout this project to improve yields and reduce waste with a view to scale-up for commercial production. Key processes were carried out in duplicate in order to confirm reproducibility. In addition, cost evaluations were carried out in order to compare our production costs with current commercial membranes.

RESULTS

During this 2017 period, we down-selected our leading ionomer structures based on backbone molecular architecture and ion exchange capacity. This down-selection was carried out using a wide range of performance data including electrochemical performance, hydrogen permeation, water uptake and swell, and durability collected on more than 40 different membranes. Preliminary standard operating procedures have been developed for the complete synthesis, characterization, and quality control of down-selected materials. Membranes based on two if these down-selected structures outperform current commercial Nafion® (Figure 1).

Our custom batch membrane casting conditions have also been defined, based on our current down-selected membrane configuration, and standardized in order to allow direct comparison of test samples. We have previous experience working closely with commercial coaters and expect to translate our current developments into an effective continuous membrane production process that will provide

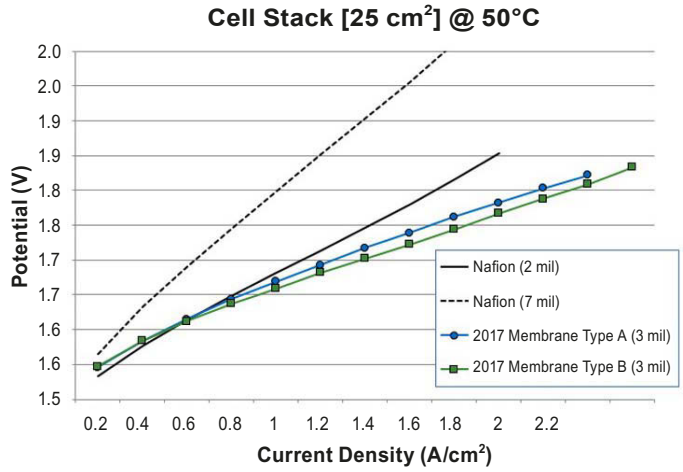

FIGURE 1. Electrochemical performance of our 2017 down-selected membranes compared with commercial perfluorosulfonic acid

membranes for an initial series of commercial electrolyzer prototypes.

The durability target of 500 h was exceeded, and stable performance and hydrogen crossover were observed for an initial down-selected membrane configuration at 50°C and 200 psi well beyond 1,000 h. We have continued efforts to further enhance durability of our down-selected materials with promising results. These durability improvements are important to allow the use of our membranes in larger capacity electrolyzer units, which operate at higher temperatures and pressures. We intend to develop these techniques to allow a further reduction in membrane thickness and thus minimize ionic resistance and reduce material costs.

A key advantage of our materials over many current commercial products is their inherently lower hydrogen permeation, which we have reduced by a factor of 2 based on our 2015 membranes (Figure 2). Additional crossover reducing techniques are under investigation to meet the requirements of larger capacity electrolyzers.

A number of cell design modifications were applied at Proton OnSite to increase the efficiency and compatibility of our membranes with their hardware. These adaptations will be continued towards prototype production in order to enhance the performance and durability of our down-selected membranes.

Initial scale-up and reproducibility studies have been successfully carried out, and standard operating procedures are in place for the individual production of our best performing membranes at a batch scale. In addition, a full production cost analysis was performed in order to assess current and future scale up production costs in comparison with current commercial membranes. Our analysis indicates that the cost of our down-selected membranes is significantly

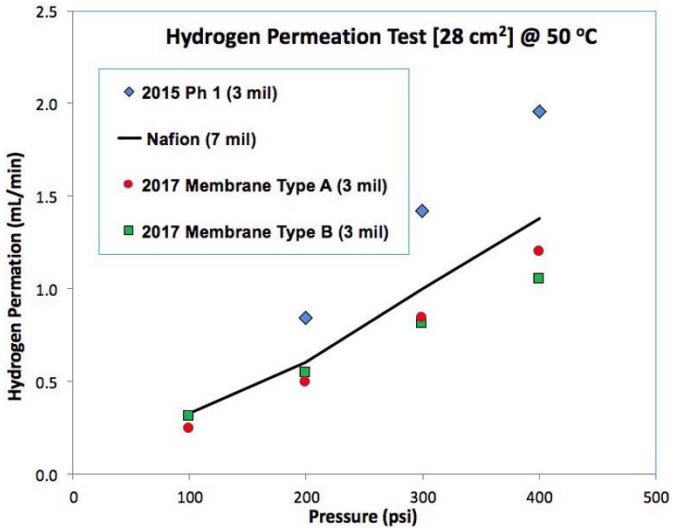

FIGURE 2. Hydrogen permeability of our 2017 down-selected membranes compared with our 2015 down-selected membrane and commercial perfluorosulfonic acid

lower than the reported cost of commercial perfluorosulfonic acid reference materials.

CONCLUSIONS AND UPCOMING ACTIVITIES

Our 2017 down-selected membranes demonstrate improved performance compared with the commercial perfluorosulfonic acid baseline (7-mil Nafion®) with lower hydrogen permeation and a potential cost reduction of >50%. The overall electrochemical performance advantages of this new lower cost technology project to a significant reduction in electricity costs.

We need additional process research for the further scale up, longer term durability and performance stability testing (beyond the 1,000 h already achieved), and further development of commercial cell prototypes, all of which will be the central focus for our ongoing commercialization efforts.

II.B.8 Multi-Scale Ordered Cell Structure for Cost Effective Production of Hydrogen by HTWS

S. (Elango) Elangovan
Ceramatec, Inc.
2425 South 900 West
Salt Lake City, UT 84119-1517
Phone: (801) 978-2162
Email: elango@ceramatec.com

DOE Manager: David Peterson
Phone: (240) 562-1747
Email: David.Peterson@ee.doe.gov

Contract Number: DE-EE0007645

Subcontractors:
- Palo Alto Research Center, Palo Alto, CA
- Gaia Energy Research Institute LLC, Arlington, VA

Project Start Date: October 1, 2016
Project End Date: September 30, 2019

Overall Objectives

- Develop and test advanced high temperature water splitting (HTWS) stacks to demonstrate pathways to hydrogen production cost goal of <$2/kg.
- Demonstrate ability to operate on intermittent renewable energy as the input.

Fiscal Year (FY) 2017 Objectives

- Fabricate structured button cells.
- Demonstrate button cell area specific resistance of ≤0.4 ohm-cm^2.

Technical Barriers

This project addresses the following technical barriers from the Hydrogen Production section of the Fuel Cell Technologies Office Multi-Year Research, Development, and Demonstration Plan.

(F) Capital Cost

(G) System Efficiency and Electricity Cost

(I) Grid Electricity Emissions

(J) Renewable Electricity Generation Integration

Technical Targets

This project is developing a novel architecture for HTWS cells. Development and testing of stacks will be conducted using cells with the structured design to meet the following DOE hydrogen production targets for HTWS.

- Area Specific Resistance ≤0.3 ohm-cm^2
- Operating Voltage 1.2 V (endothermic)
- Operating Temperature ≤800°C
- Electrical Efficiency >95% lower heating value H_2
- Degradation Rate <0.5%/1,000 h
- Levelized Cost of H_2 Production $2/kg
- H_2 Delivery Pressure Capability

FY 2017 Accomplishments

- Baseline electrolyte and electrode compositions are finalized.
- Thick electrolyte-based button cell tests show that total electrode polarization losses are within 10% to the target 0.2 ohm-cm^2.
- Button cell stability of ~1% current density degradation per 1,000 h at 1.2 V.

✧ ✧ ✧ ✧ ✧

INTRODUCTION

High temperature water splitting process efficiently produces hydrogen from steam using electric energy. In order to achieve commercial cost target for hydrogen production, the performance of the device must be improved and the hydrogen production must remain stable during the device life time. This project will demonstrate high performance and high efficiency hydrogen production by the use of a novel structured cells that increases the production capacity of the device. By judicious choice of materials, the device performance will show minimal degradation during its lifetime. The combination of these two advances will allow the device to consume less electrical energy which will favor low cost hydrogen production.

APPROACH

The project will implement approaches to address the limitations of current HTWS technology through the use of a novel cell design that introduces macro-features to provide

mechanical support of a thin electrolyte and micro-features of the electrodes to decrease electrode losses. The set of features will enable a high performance stack that is robust to handle intermittent electric load. The materials set that would be used for cell and stack fabrication will provide operational stability to decrease levelized hydrogen production cost. The approach also utilizes a combination of fabrication options that are scalable to achieve manufacturing cost objectives.

RESULTS

A novel cell structure has been designed to address the challenges of current cell design. A schematic of the structure is shown in Figure 1. The cell design incorporates a multi-scale ordered structure to improve cell performance. A thin, high conductivity electrolyte provides low electrical resistance to increase cell performance. In contrast to current state-of-the-art cell design where fuel electrode constitutes the mechanical support for the cell, a macro-featured honeycomb support is used on the oxygen electrode side. By the use of thin hydrogen electrodes, the steam diffusion limitations of fuel support are decreased. The hydrogen electrode features an ordered structure of differing materials compositions to provide a high reaction zone area where steam is reduced to produce hydrogen.

Improvements in cell lifetime is targeted through the use of thermochemically stable electrodes. For the oxygen electrode, a composition with stable dopant chemistry is selected. The composition is shown to provide stable electrode/electrolyte interface to eliminate electrode delamination on the oxygen evolution interface. A 1,000 h test of a symmetric cell tested at the target current density of 1 A/cm^2 showed no evidence of delamination as shown in Figure 2.

Electrode polarizations were studied using symmetric cells and full button cells using thick electrolyte cells in order to verify the selected compositions. Impedance measurements using reference electrodes were made to isolate contributions from anode and cathode. Typical average anode and cathode polarization values are shown in Figure 3. The combined electrode contribution averaged at about 0.2 ohm-cm^2 close to the target value for FY 2017.

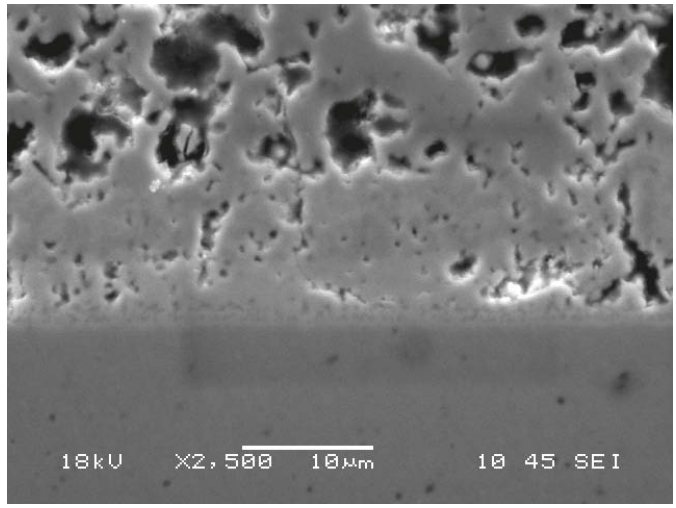

FIGURE 2. Scanning electron micrograph of delamination resistant oxygen electrode

Several button cells were tested to evaluate performance at various operating voltages (1.3 and 1.2 V) and steam conversion ranging from 10% to 60%. Cells were operated for typically 1,000 h under constant applied voltage to study the degradation. Cell performance degradation of 1% per 1,000 h is achieved at 1.2 V. The performance of a button cell is shown in Figure 4. The cell was tested for 1,000 h under varying loads and steam utilizations. The final 1,000 h performance at a specified operation is shown.

Palo Alto Research Center completed ink formulation for electrode and support structure printing evaluation. Printing trials of hydrogen electrode features and oxygen electrode support are in progress (Figure 5).

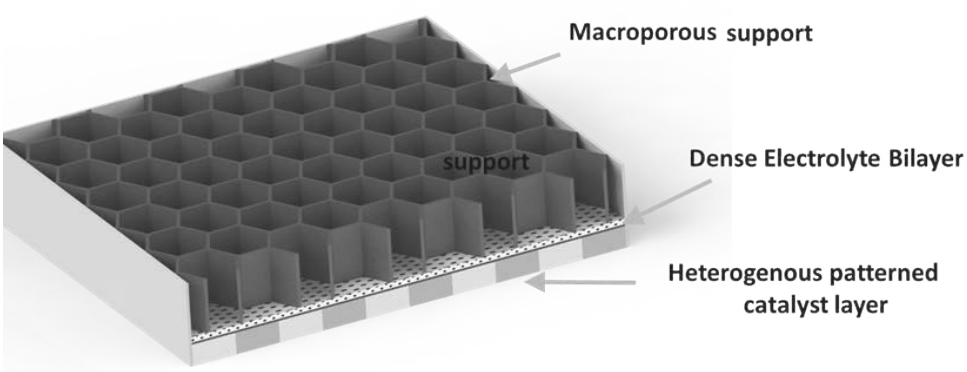

FIGURE 1. Schematic of ordered cell structure

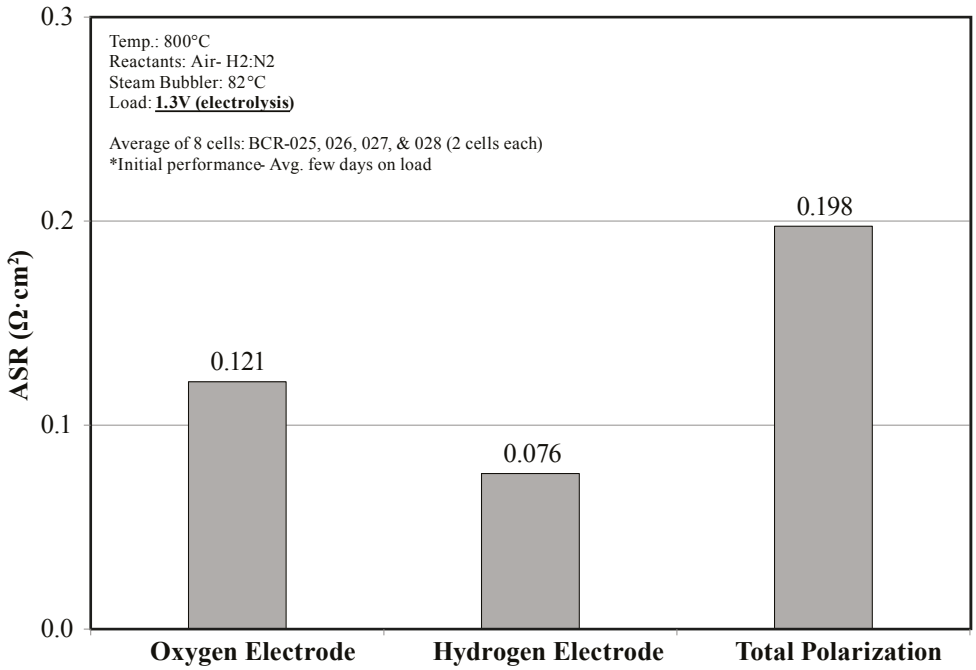

ASR – area specific resistance

FIGURE 3. Electrode polarization resistance

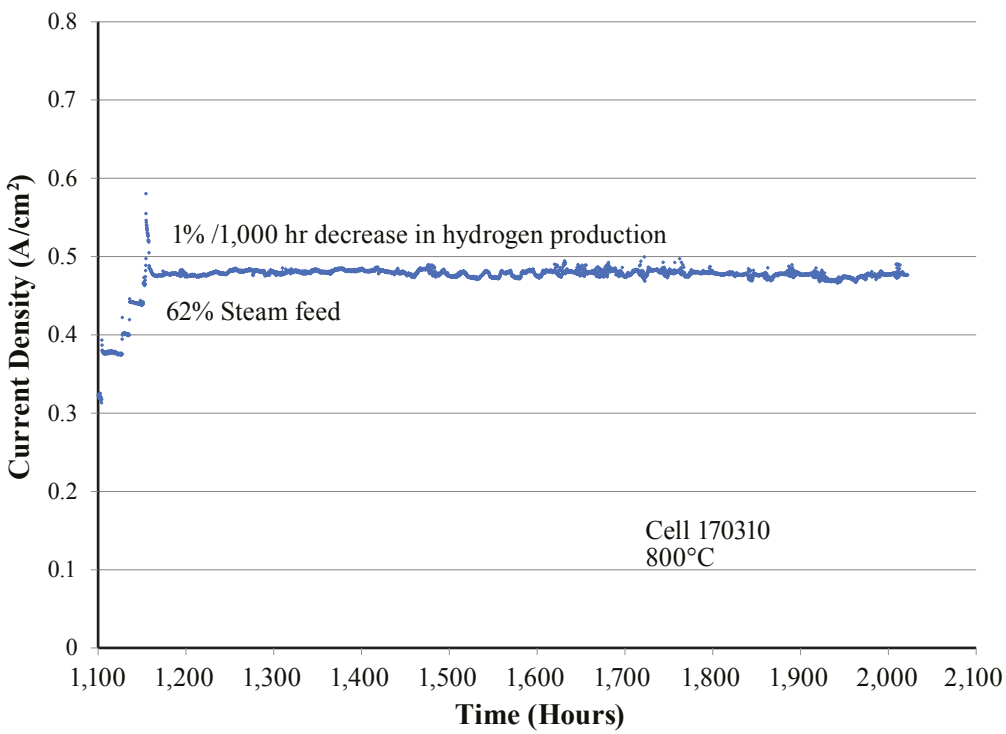

FIGURE 4. Button cell performance

(a)

(b)

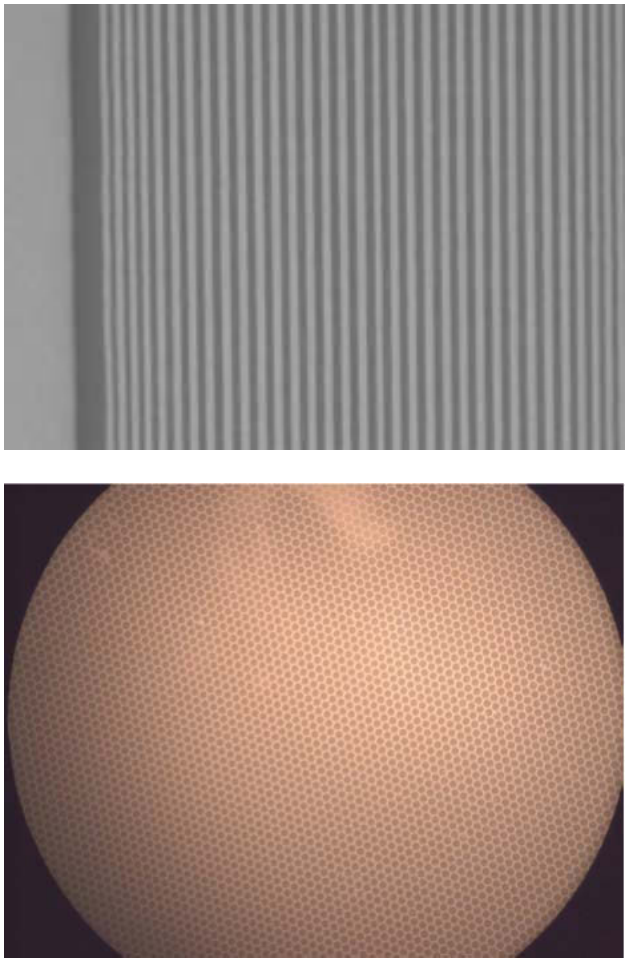

FIGURE 5. Fabrication trials of electrode features: (a) patterned fuel electrode, (b) honeycomb oxygen electrode support

CONCLUSIONS AND UPCOMING ACTIVITIES

Work conducted to date shows that the electrode compositions selected are suitable for achieving target cell performance with the structured cell. Electrode compositions also show long term stability that is indicative of their potential to meet the overall objective of levelized hydrogen production cost.

During the remainder of the project, button cells with the featured electrodes will be fabricated and tested to validate the concept to achieve high performance, robustness, and durability. Following fabrication process optimization, larger cells will be fabricated to validate stack performance to meet the end of project goal of testing a stack that is capable of 1 kg/d of hydrogen production.

FY 2017 PUBLICATIONS/PRESENTATIONS

1. Hartvigsen, Joseph J., "Sustainable Transportation Fuels as a Store of Nuclear and Renewable Energy," Johns Hopkins University, Washington D.C., November 17, 2017.

2. Colella, Whitney G., "Advanced High Temperature Water Electrolysis and Competing Hydrogen Generation Technologies," American Institute of Chemical Engineers (AICHE) 2017 Spring Meeting and 13th Global Congress on Process Safety, San Antonio, TX, March 26–30, 2017.

3. Elangovan, S., "Solid Oxide Technology: Materials and Operational Challenges," Plenary Lecture, 13th International Conference on Catalysis in Membrane Reactors, Houston, TX, July 10–13, 2017.

4. J. Hartvigsen, S. Elangovan, J. Elwell, and L. Frost, "High temperature electrolysis performance maps and extension to techno-economic analysis for hydrogen cost optimization," World Hydrogen Technology Convention, Prague, Czech Republic, July 9–12, 2017.

5. J. Hartvigsen, S. Elangovan, J. Elwell, and L. Frost, "Synthetic fuels as a store of renewable energy enabled by co-production of H2 and CO in a SOEC system," World Hydrogen Technology Convention, Prague, Czech Republic, July 9–12, 2017.

6. Colella, Whitney G., "Life Cycle and Techno-Economic Analysis of State-of-the-Art Solid Oxide Electrolyzer Systems," Fifteenth International Symposium on Solid Oxide Fuel Cells (SOFC-XV), Hollywood, FL, July 23–28, 2017.

II.C.1 High Efficiency Solar Thermochemical Reactor for Hydrogen Production

Anthony McDaniel
Sandia National Laboratories
MS9052
PO Box 969
Livermore, CA 94550
Phone: (925) 294-1440
Email: amcdani@sandia.gov

DOE Manager: Katie Randolph
Phone: (240) 562-1759
Email: Katie.Randolph@ee.doe.gov

Subcontractors:
- Profs. Ellen Stechel and Nathan Johnson, Arizona State University, Tempe, AZ
- Prof. Nathan Siegel, Bucknell University, Lewisburg, PA
- Prof. Ryan O'Hayre and Dr. Michael Sanders, Colorado School of Mines, Golden, CO
- Prof. William Chueh, Stanford University, Stanford, CA

Project Start Date: October 1, 2014
Project End Date: September 30, 2017

Overall Objectives

- Verify the potential for solar thermochemical cycles for hydrogen production to be competitive in the long term and by 2020, develop this technology to produce hydrogen with a projected cost of $3/gge at the plant gate.
- Develop a high-efficiency particle bed reactor for producing hydrogen via a thermochemical water-splitting (WS) cycle, and demonstrate continuous operation on a solar simulator producing greater than 3 L of H_2.

Fiscal Year (FY) 2017 Objectives

- Discover and characterize suitable materials for two-step, non-volatile metal oxide thermochemical water-splitting cycles. (Barriers S and T)
- Construct and demonstrate a particle receiver-reactor capable of continuous operation at greater than 3 kW thermal input. (Barrier T)

Technical Barriers

This project addresses the following technical barriers from the Hydrogen Production section of the Fuel Cell Technologies Program Multi-Year Research, Development and Demonstration Plan.

(S) High-Temperature Robust Materials

(T) Coupling Concentrated Solar Energy and Thermochemical Cycles

(X) Chemical Reactor Development and Capital Costs

Technical Targets

This project is conducting fundamental studies on materials for use in concentrated solar power applications and designing reactor concepts that, when combined, will produce hydrogen from thermochemical WS cycles. Insights gained from these studies will be applied toward the design and optimization of a large scale solar receiver and reactor that meets the following ultimate DOE hydrogen production targets.

- Hydrogen cost: <$2/kg H_2
- Material of reaction cost: ≤$11,000/yr tonne per day H_2
- Solar-to-hydrogen conversion ratio: ≥26%
- One-sun hydrogen production rate: ≥2.1 x 10^{-6} kg/s m^2

FY 2017 Accomplishments

- Discovered a novel perovskite material for solar thermochemical H_2 production. It exhibits thermodynamic cycle behavior intermediate to $Sr_xLa_{1-x}Mn_yAl_{1-y}O_3$ perovskite compositions (SLMA) and CeO_2. This is desirable because a reasonable compromise between a large reduction extent at relatively low-temperature (like SLMA), and high WS favorability in the presence of steam and hydrogen (like CeO_2), will be required for commercial viability.
- Demonstrated H_2 production through solar thermochemical water splitting in Sandia's cascading pressure receiver–reactor (CPR^2) prototype. This was accomplished at a scale of ~3.5 kW_{th} while achieving a peak rate of 0.2 SLPM H_2. The prototype validated key design objectives important to advancing the technology readiness level of this renewable WS pathway.

✧ ✧ ✧ ✧ ✧

INTRODUCTION

This research and development project is focused on the advancement of a technology that produces hydrogen at a cost that is competitive with fossil-based fuels for transportation. A two-step, solar-driven WS thermochemical

cycle is theoretically capable of achieving a solar-to-hydrogen conversion ratio that exceeds the DOE target of 26% at a scale large enough to support an industrialized economy [1]. The challenge is to transition this technology from the laboratory to the marketplace and produce hydrogen at a cost that meets or exceeds DOE targets.

Conceptually, heat derived from concentrated solar energy can be used to reduce a metal oxide at high temperature producing oxygen (Step 1). The reduced metal oxide is then taken "off sun" and re-oxidized at lower temperature by exposure to water, thus producing hydrogen (Step 2) and completing the cycle. Commercial success of solar thermochemical hydrogen production is contingent upon developing suitable redox active materials and incorporating them into an efficient reactor. There are numerous material chemistries that have attributes suitable for inclusion in a thermochemical hydrogen production system [2-4]. The challenge is to identify an optimally performing material. In addition, the development of redox material and reactor are not mutually exclusive, but must be conducted in parallel [5]. To maximize the probability of success, this project also addresses the reactor- and system-level challenges related to the design of an efficient particle-based reactor concept [6].

APPROACH

Thermochemical WS reactors are heat engines that convert concentrated solar energy (heat) to chemical work. Our approach is to discover materials to accomplish the WS chemistry and pair these with a novel CPR^2 that, when combined, can achieve an unprecedented solar-to-hydrogen conversion ratio. The material discovery work involves expanding our understanding of the underlying thermodynamics and kinetics in order to make performance improvements and/or formulate new, more redox-active compositions. Sandia's patented CPR^2 technology is based on a moving bed of packed particles that embodies key design attributes essential for achieving high efficiency operation: (1) sensible heat recovery; (2) spatial separation of pressure, temperature, and reaction products; (3) continuous on-sun operation; and (4) direct absorption of solar radiation by the redox-active material. Research efforts are focused on demonstrating this technology in a ~3 kW-scale prototype.

RESULTS

Materials Research and Development Thrust. Over the course of this project, Sandia and collaborators have synthesized and screened a large number of compounds looking for redox and WS activity. A general rule has emerged where materials that exhibit a large extent of reduction ($\delta > 0.2$) generally do not split water under commercially viable oxidation conditions [7]. Moreover, we have learned that compounds with thermodynamic redox properties that are intermediate between the SLMA perovskite and CeO_2 are desirable because they represent a reasonable compromise between a large reduction extent at relatively low-temperature (like SLMA) and high WS favorability in the presence of steam and hydrogen (like CeO_2).

Recently our group found a complex perovskite ($AB_{0.25}B'_{0.75}O_y$, where A = alkaline earth metal, B′ = rare earth metal, and B′ = transition metal) that not only exhibits thermodynamic behavior between SLMA and CeO_2, but also undergoes a very interesting reversible phase transition during redox cycling that has not been reported for perovskites capable of thermochemical water splitting. Firstly, in the course of investigating a family of compounds with $AB_xB'_{1-x}O_y$ ($0 < x < 1$) stoichiometry, we found that only the $AB_{0.25}B'_{0.75}O_y$ ($B_{25}B'_{75}$) formulation was active for WS. Evidence for this is presented in Figure 1, where the plot on the left shows a strong correlation between the amount of $B_{25}B'_{75}$ phase present in an as-synthesized sample to the total hydrogen produced during WS experiments. Samples were prepared using the sol-gel method. Various compound stoichiometries were targeted by adjusting the mass fraction of B relative to B′ in the sol-gel liquid precursors. X-ray diffraction confirmed that targeted stoichiometries ($x \neq 0.25$) having excess B or B′ were comprised of various WS inactive secondary oxide phases, mainly AB_xO_y and AB'_xO_y, along with $B_{25}B'_{75}$ suggesting that $AB_{0.25}B'_{0.75}O_y$ is a line compound.

Secondly, during an investigation of the $B_{25}B'_{75}$ oxygen redox cycle using thermogravimetric analysis, anomalies in the reduction behavior were discovered that were dependent upon the temperature profile and the oxygen partial pressure used in the experiment (data not shown). This prompted a more thorough look into the crystallography of $B_{25}B'_{75}$ during reduction using in situ high temperature X-ray diffraction; the results of which are also presented in Figure 1. The image on the right in this figure is comprised of X-ray diffraction line scans (between 23 and 32 deg. 2θ) stacked atop one another with each pixel row representing a different sample temperature (298 K→1,623 K→298 K) recorded in a low O_2-partial pressure helium atmosphere (i.e., during thermal reduction). It is clear by the manner in which the colored vertical bars at various 2θ scattering angles bend (indicating changes in lattice d-spacing due to thermal and chemical effects), disappear (crystal phases reacting away), and appear (new crystal phases forming) that there is complex solid state chemistry occurring in $B_{25}B'_{75}$ at a temperature of 1,573 K. As mentioned previously, this chemistry does not conform to that commonly observed in other solar thermochemical hydrogen perovskite materials, and could impart high reduction entropy to $B_{25}B'_{75}$ that maintains WS favorability in the presence of both steam and hydrogen (data not shown).

CPR^2 Fabrication and Demonstration Thrust. Sandia completed an intensive staged buildout and test campaign

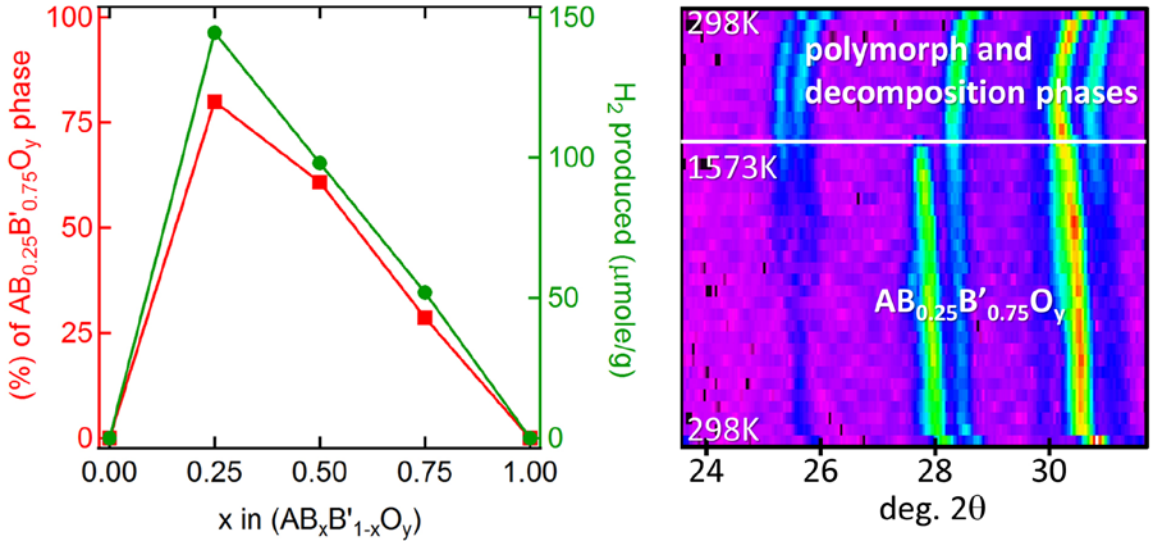

FIGURE 1. (Left) fractional amount of $AB_{0.25}B'_{0.75}O_y$ perovskite line compound contained in an as-prepared powder sample as a function of the target compound stoichiometry (x). The observed H_2 production capacity of a powder sample tested in the stagnation flow reactor is also displayed and clearly shows a strong positive correlation between $AB_{0.25}B'_{0.75}O_y$ phase fraction and total amount of H_2 produced. (Right) In situ high-temperature X-ray diffraction lines scans between 23 and 32 deg. 2θ as a function of sample temperature measured for the $AB_{0.25}B'_{0.75}O_y$ perovskite line compound during thermal reduction. Line scan intensity reveals several diffraction peaks associated with $AB_{0.25}B'_{0.75}O_y$, polymorphs of this perovskite, and decomposition products like AB_xO_y and AB'_xO_y. The abrupt phase transition at ~1,573 K is reversible, and may be responsible for maintaining WS favorability at moderate H_2O:H_2 ratios during re-oxidation.

of the CPR[2] that commenced in July 2016 and concluded in May 2017. The goal was to complete construction of Sandia's moving particle bed reactor, support structure, solar simulator, and balance of plant, and then test the complete system. The assembled CPR[2], which stands ~6 m tall, is pictured in Figure 2 and consists of several main components shown in a solid rendering on right, and in the photograph on left, in Figure 2. Key components of the CPR[2] are a particle source chamber for pre-heating and storing ~70 kg CeO_2 particles, a four-lamp, 20 kW_{ele} solar simulator array for radiant heating of particles, a receiver/reactor or thermal reduction (TR) chamber to reduce particles and produce O_2,

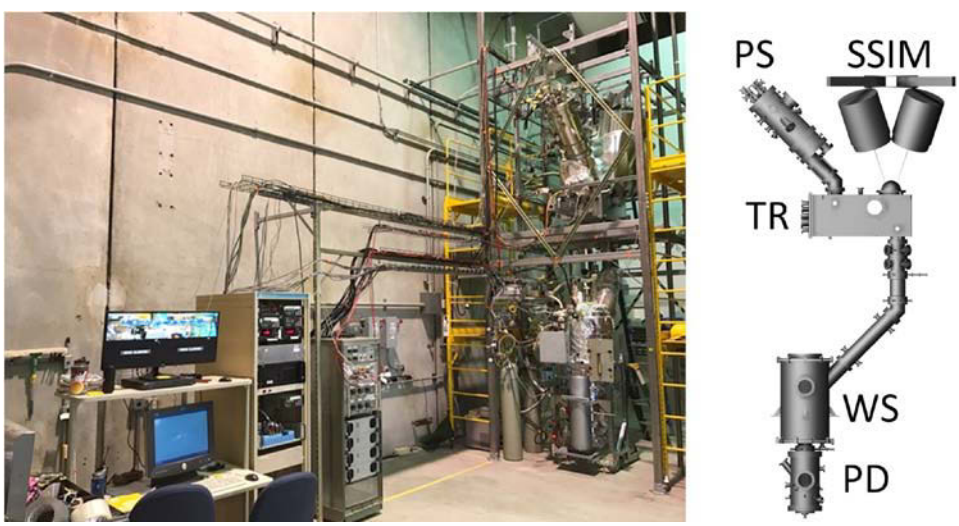

FIGURE 2. Image and schematic of Sandia's fully assembled and operational CPR[2]. PS = particle source chamber, SSIM = 4-lamp, 20 kW_{ele} solar simulator, TR = thermal reduction chamber, WS = water splitting chamber, and PD = particle drain (see text for details).

a pressure separation segment, a WS reactor to oxidize particles and produce H_2, and a particle drain chamber for collecting oxidized particles. In addition, a comprehensive balance of plant subsystem inclusive of steam generator, vacuum pumps, mass flow controllers, engineered safety components, sensors, transducers, and data acquisition and control system was assembled and integrated into the CPR^2 for the supply and control of gases and particles, power to lamp array, and signal inputs and outputs to the reactor. The fully functional CPR^2 resides at the National Solar Thermal Test Facility in Albuquerque, New Mexico.

Figure 3 consists of selected photographs and data plots that document a successful demonstration of Sandia's moving particle bed solar-driven thermochemical WS reactor technology. The demonstration was conducted in a single pass, once-through mode using CeO_2 as the redox active material. A maximum thermal reduction temperature of 1,700 K was achieved in the radiant cavity receiver, and water splitting occurred at ~970 K (see data plots of temperature and instantaneous H_2 flowrate in Figure 3). The topmost image shows the receiver cavity looking through the aperture during simulator illumination. Owing to the high-temperature incandescence and reflection from the quartz dome covering the aperture, it is difficult to observe particle flow in the receiver itself. However, the diffuse glow of incandescent particles falling from the receiver through a translucent alumina tube, and a small windowed chamber positioned beneath it, attest to hot particles falling into the WS. Two different techniques were used to measure H_2 production rate, a standard heat capacity-based mass flow meter and a Sandia patented solid state sensing device.

In summary, Sandia and collaborators designed, fabricated, and demonstrated H_2 production through thermochemical water splitting in the CPR^2 prototype. This was accomplished at a scale of ~3.5 kW_{th} (20 kW_{ele}) while achieving a peak rate of 0.2 SLPM H_2. In so doing, our prototype validated the following design objectives: (1) continuous and direct irradiation of redox material without particle shading, (2) precise control of particle flow rate and residence time in the TR, (3) pressure separation without internal mechanical components like valves, and (4) counter-flow mass exchange between steam and particles in WS (i.e., no mixing or fluidization during re-oxidation). Successful validation of these design objectives builds on knowledge needed to verify the potential for this hydrogen production technology to be cost competitive in the future, and critical to

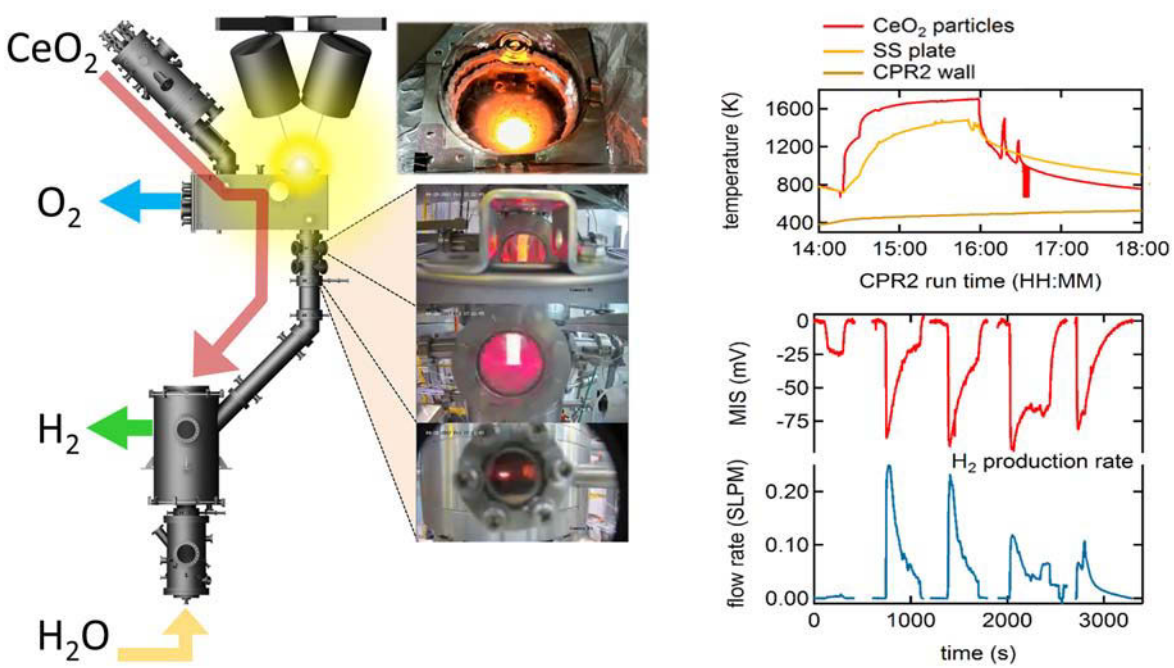

SS – stainless steel

FIGURE 3. (Left) images of the CPR^2 during operation. Starting from top to bottom, CeO_2 particles are heated by simulated solar radiation (~3.5 kW_{th} at the aperture) to ~1,700 K where O_2 is removed from the solid by vacuum pumping the TR. The radiant cavity through which CeO_2 particles flow is seen looking through the quartz dome in topmost picture. Particles then move by gravity through connecting chambers and collect in the WS. Incandescence from falling particles is clearly visible through viewports on the connecting chambers. Once a sufficient amount of reduced CeO_2 accumulates in the WS, steam is introduced causing the spontaneous re-oxidation of CeO_2 and production of H_2. (Right) selected excerpts of data streams from the CPR^2 data acquisition and control system showing temperature readings from various locations within the system and instantaneous H_2 flowrate as a function of run time during a test.

advancing the technology readiness of Sandia's concept for implementing a high-temperature, two-step thermochemical water splitting cycle.

CONCLUSIONS AND UPCOMING ACTIVITIES

- Discovering a redox material that will meet or exceed DOE cost and performance targets. We anticipate that investments made by DOE's Hydrogen Advanced Water Splitting Materials Consortium (found at http://h2awsm.org) will focus on advancing the material discovery effort.
- Establishing the CPR^2 as a "routine-use" R&D tool to support seedling projects in Hydrogen Advanced Water Splitting Materials Consortium as well as engage commercial interest and investment.
- Publish all project results in peer-reviewed journals.

Sandia National Laboratories is a multi-mission laboratory managed and operated by National Technology and Engineering Solutions of Sandia LLC, a wholly owned subsidiary of Honeywell International Inc. for the U.S. Department of Energy's National Nuclear Security Administration under contract DE-NA0003525.

FY 2017 SELECTED PUBLICATIONS/ PRESENTATIONS

1. Ermanoski et al, "Design of a particle bed reactor for solar water splitting," presented at SolarPACES 2016, October 11–14, 2016, Abu Dhabi, United Arab Emirates.

2. McDaniel et al, "A brightly-lit pathway towards decarbonizing the US energy infrastructure," presented by invitation to the Mechanical Engineering Department at University of Florida, November 15, 2016, Gainesville, FL.

3. McDaniel et al, "A novel solar thermochemical water splitting perovskite for hydrogen production," presented at 12th Pacific Rim Conference on Ceramic and Glass Technology hosted by ACS, May 21–26, 2017, Kona, HI.

4. Ermanoski, "Metal oxides in solar-thermochemical cycles: gaining breathing room through reactor design," presented at 21st International Conference on Solid State Ionics, June 18–23, 2017, Padua, Italy.

5. A.H. McDaniel, "Renewable energy carriers derived from concentrating solar power and nonstoichiometric oxides," *Current Opinion in Green and Sustainable Chemistry*, **4**, 37 (2017).

6. A. Singh, J. Lapp, J. Grobbel, S. Brendelberger, J.P. Rheinhold, L. Olivera, I. Ermanoski, N.P. Siegel, A.H. McDaniel, M. Roeb, C. Sattler, "Design of a pilot scale directly irradiated, high temperature, and low pressure moving particle cavity chamber for metal oxide reduction," accepted for publication in *Solar Energy*. (2017).

REFERENCES

1. N.P. Siegel, J.E. Miller, I. Ermanoski, R.B. Diver, and E.B. Stechel, *Ind. Eng. Chem. Res.*, **52**, 3276–3286 (2013).

2. W.C. Chueh and S.M. Haile, *Philos. Trans. R. Soc. Math. Phys. Eng. Sci.*, **368**, 3269–3294 (2010).

3. R.B. Diver, J.E. Miller, M.D. Allendorf, N.P. Siegel, and R.E. Hogan, *J. Sol. Energy Eng.*, **130**, 041001(1)–041001(8) (2008).

4. A.H. McDaniel, E.C. Miller, D. Arifin, A. Ambrosini, E.N. Coker, R. O'Hayre, W.C. Chueh, and J. Tong, *Energy Environ. Sci.*, **6**, 2424–2428 (2013).

5. J.E. Miller, A.H. McDaniel, and M.D. Allendorf, *Adv. Energy Mater.*, **4**, 1300469 (2014).

6. I. Ermanoski, N.P. Siegel, and E.B. Stechel, *J. Sol. Energy Eng.*, **135**, 031002 (2013).

7. A.H. McDaniel, *Curr. Opin. Green Sustain. Chem.*, **4**, 37–43 (2017).

II.C.2 Flowing Particle Bed Solarthermal Redox Process to Split Water

Alan W. Weimer (Primary Contact),
Charles Musgrave, Ibraheam Al-Shankiti,
Amanda Hoskins, Samantha Millican, Scott Rowe,
Ryan Trottier, Caitlin Czernik
University of Colorado Boulder
Campus Box 596
Boulder, CO 80309-0596
Phone: (303) 492-3759
Email: alan.weimer@colorado.edu

DOE Manager: Katie Randolph
Phone: (240) 562-1759
Email: Katie.Randolph@ee.doe.gov

Contract Number: DE-EE0006671

Subcontractor:
National Renewable Energy Laboratory (NREL),
Golden, CO

Project Start Date: September 1, 2014
Project End Date: November 30, 2017

Overall Objectives

The University of Colorado's overall objective is to design and test individual components of a novel flowing particle solarthermal water splitting (STWS) system by optimizing active redox materials, reactor containment materials, and reactor design, with the ultimate goal of demonstrating our technology by producing three standard liters of hydrogen in eight hours on-sun in a prototype fluidized particle reactor.

Fiscal Year (FY) 2017 Objectives

- Develop and test reactive materials with high productivity that have stable reactivity.
- Perform kinetic studies on reactive materials of interest.
- Test reactor tubes coated with specially developed containment materials for steam resistance.
- Test compatibility of containment materials with reactive materials.
- Evaluate performance of fluidized bed with high-temperature O_2 transport membrane.
- Collaborate closely with joint National Science Foundation and the Department of Energy's (DOE's) materials discovery "sister" project to screen improved active materials.
- Work with the NREL to demonstrate on-sun hydrogen production.
- Update process model and H2A to reflect experimental progress toward DOE goals.

Technical Barriers

This project addresses the following technical barriers from the Hydrogen Production section of the Fuel Cell Technologies Office Multi-Year Research, Development, and Demonstration Plan.

(S) High-Temperature Robust Materials

(W) Materials and Catalysts Development

(X) Chemical Reactor Development and Capital Costs

Technical Targets

The project's performance towards DOE's technical targets were projected using experimental results from our materials testing and thermodynamic modeling, a process model of a 50,000 kg H_2/d industrial-scale production plant, a detailed solar field model, and DOE's H2A techno-economic analysis program and are outlined in Table 1.

TABLE 1. Progress toward Technical Targets for Solar-Driven Thermochemical Hydrogen Production

Characteristics	Units	2015 Target	2020 Target	CU 2017 Status
Solar-Driven High-Temperature Thermochemical Cycle H_2 Cost	$/kg	14.80	3.70	8.79
Active Material Cost per Year	$/yr-TPD H_2	1.47M	89K	68K[a*]
STH Energy Conversion Ratio	%	10	20	13.8[*]
On-Sun Hydrogen Production Rate	kg/s per m^2	8.1×10^{-7}	1.6×10^{-6}	1.1×10^{-6}

CU – University of Colorado; STH – solar-to-hydrogen ratio; TPD – tonne per day
[a] Assuming reactive material lifetime of 1 yr
[*] Using hercynite ($FeAl_2O_4$)

FY 2017 Accomplishments

- Performed long-term stability tests of reactive materials showing no loss in reactivity between 100th and 200th cycle and 2X targeted H_2 production rate.

- Developed atomic layer deposition (ALD) barriers that improve high-temperature resistance of SiC to steam by >60%, 2X targeted impact.
- Demonstrated on-sun production of 1.91 standard liters H_2 in less than three hours.
- Assessed economic viability of thermal energy storage to provide electricity for non-intermittent STWS.
- Completed study on effects of structure and magnetic ordering for 1,343 materials.
- Continued testing of high temperature O_2 transport membrane for inert gas recycle.
- Completed construction of high-flux solar simulator to test hybrid reactor concept.

✧ ✧ ✧ ✧ ✧

INTRODUCTION

In order to meet DOE targets for economical and efficient solarthermal hydrogen production at the commercial scale, advances in active redox materials and reactor fabrication materials are needed. Ideal STWS materials have high hydrogen production capacity, relatively low thermal reduction temperatures (closer to 1,200°C than 1,500°C), fast reaction kinetics, reduction enthalpies on the order of the water splitting enthalpy, are solid in both oxidized and reduced forms, operate with small ΔT between reduction and operation, and are highly stable over hundreds of thousands of cycles. We will develop new materials that possess these properties in conjunction with project collaborators. Materials development has focused on spinel structure (Red: $AB_2O_4 \rightarrow AB_2O_{4-\delta} + \delta/2\ O_2$) and perovskite structure (Red: $ABO_3 \rightarrow ABO_{3-\delta} + \delta/2\ O_2$) materials, which have both shown promise in reaching the targets. Efficient flowing particle reactors need active materials that are robust, attrition resistant and not limited by slow heat or mass transfer properties. Therefore, we have developed particle fabrication procedures for particles that are flowable, reactive, and robust, and are currently testing their performance in fluidized bed reactors. We are also evaluating reactor containment materials to ensure stability at the high temperatures at which water splitting occurs. In the end, we will produce reactor ready materials with demonstrated hydrogen productivities to drive the field closer to meeting DOE's technical targets, as determined from our process model and techno-economic analysis.

APPROACH

A highly efficient STWS reactor must have a scalable and mechanically sound design that maximizes heat flux to the reactive materials and optimizes mass transfer. We are designing a novel reactor that maximizes heat flux, and minimizes heat and mass transfer limitations by fluidizing the active particles. The reduction step will be carried out using inert sweep gas to achieve the low oxygen partial pressures necessary for the reduction reaction. The particles are contained in fluidized bed reactors that switch between inert flow during reduction and steam flow during oxidation, and there is minimal temperature difference between oxidation and reduction, i.e., near isothermal operation. Since such high temperatures are required, the absence of moving parts greatly reduces the risk of critical reactor failure. The small ΔT between reduction and oxidation minimizes the need to reheat materials between oxidation and reduction, which leads to reduced efficiencies in other STWS designs.

In this project, we are examining the individual components of the reactor system to determine their feasibility and efficiency. These include kinetic and thermodynamic behavior of spray dried redox materials in a fluidized system, performance of coated reactor containment materials, effect of vacuum pumping vs. inert gas flow for oxygen removal following reduction, and solar concentration modeling. Using this information, we are constructing and operating a solar-powered system that can produce at least three liters of hydrogen in eight hours on-sun. By the end of the project, we will have an Aspen model that integrates the individual portions of the reactor system. We will use this in a techno-economic analysis showing that we are capable of meeting the <$2/kg H_2 at 50,000 kg H_2/d ultimate project goal.

RESULTS

A key goal of our research is to produce redox materials that can maintain high STWS activity over time. Specifically, we pursued the goal of fabricating particles that can produce at least 150 µmol H_2/g/cycle and not lose more than 10% of reactivity between the 100th and 200th redox cycles. In the past year, we have met this goal. We tested the long-term hydrogen production of a spray dried cobalt doped hercynite in a stagnation flow reactor system over 200 cycles. The active particles produced an average of 299 µmol/g/cycle over Cycles 93 through 99 and 303 µmol/g/cycle over Cycles 201 through 208, demonstrating no loss in activity between the 100th and 200th cycles. This exceeds the target of 150 µmol/g/cycle at 10% loss in reactivity. H_2 production before Cycle 100 and after Cycle 200 are shown in Figure 1. Each cycle consisted of a 15-min oxidation step at 1,350°C using 50% H_2O or CO_2 in argon at a flow rate of 300 sccm and a 30-min reduction step at 1,500°C using argon at a flow rate of 300 sccm. Control runs without the active oxide were conducted at the same reaction conditions and the average production over 10 blank cycles was subtracted from each of the experimental H_2 generation cycles to account for water splitting on the surface of the reactor. While Cycles 92–99 and 201–208 were conducted as H_2O splitting experiments to directly measure the H_2 production, CO_2 splitting experiments were conducted for the remainder of the cycles

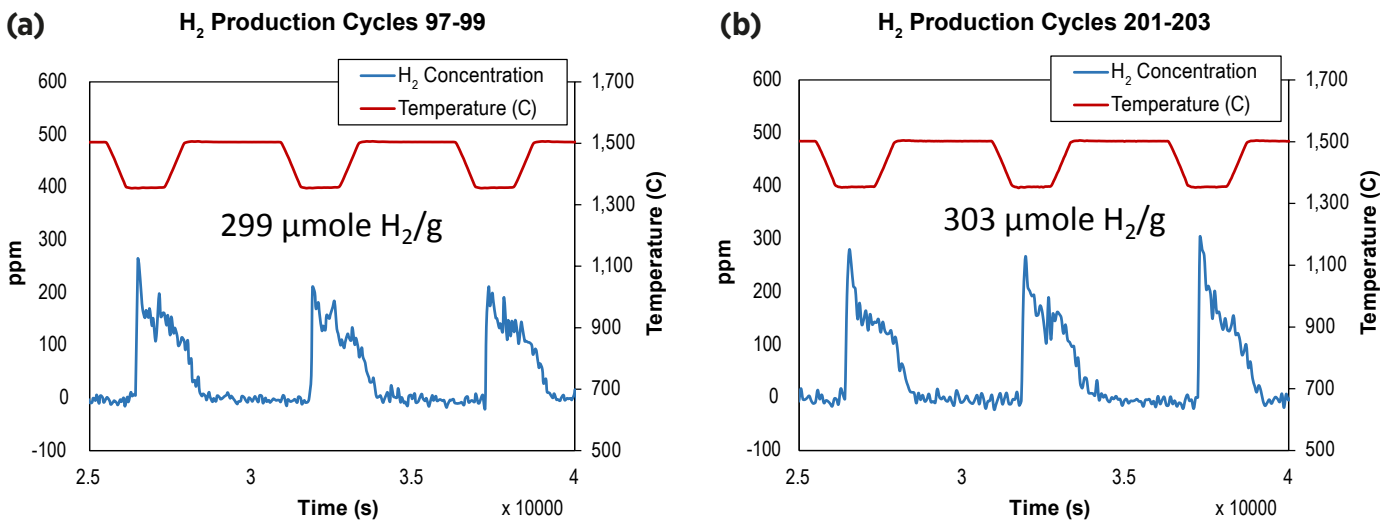

FIGURE 1. STWS activity of cobalt-doped hercynite material in long-term activity tests. (a) H_2 production for Cycles 97 through 99. (b) H_2 production for Cycles 201 through 203.

to avoid technical difficulties with long-term use of the steam generator. However, all conditions remained consistent between the H_2O and CO_2 experiments and properties between these two redox processes have been shown to be similar.

Another key challenge in the field of STWS that we wish to address is the stabilization of ceramic materials in the presence of steam. SiC has favorable mechanical and thermal properties at the temperatures required for STWS, but will react with steam to form a SiO_2 layer that eventually degrades the material and severely limits its lifetime. To address this issue, we are using particle ALD to study the stabilization effects of nanoscale diffusion barriers with atomic growth control to prevent the oxidation of SiC. Mullite ($3Al_2O_3$:$2SiO_2$) and BN have been identified as promising coating materials using density functional theory calculations. Mullite, alumina, BN and hybrid mullite/Al_2O_3 films of various thicknesses were deposited on high surface area SiC particles using ALD. All films were then annealed at 1,500°C for 20 h in order to crystallize the films.

To test the effectiveness of the films, uncoated and ALD coated SiC particles were exposed to high temperature steam at 1,000°C for 20 h in a thermal gravimetric analyzer using an evaporation rate of 3 g/h. Water vapor was introduced to the thermogravimetric analyzer furnace once the temperature had reached 1,000°C. In all of these experiments mass change of the sample over the course of the steam exposure was monitored. Mass gains during these experiments are attributed to silica growth on the surface due to oxidation. A summary of the performance of all films to date is presented in Figure 2.

The figure shows that significant improvements have been made to the oxidation resistance of SiC. Depositing a coating of only 10 nm reduced the oxidation of SiC by ~50%. Although alumina films outperformed mullite films, mullite is preferred because its thermal expansion coefficient matches well with that of SiC. Mullite films are capable of matching the performance of alumina films by increasing the thickness. This is expected based on theoretical results, even though the thicknesses of mullite films are nanometer. All but two of the films tested have met or surpassed the goal of this work, which was to improve the oxidation resistance of SiC by 25%. The highest performing film improved the oxidation resistance of SiC by 64%, far surpassing the project goal.

Hercynite is a spinel material that is highly active for STWS. Since it consists of iron and aluminum oxide, it also has the benefit of being much cheaper than most STWS materials, which often contain rare earth metals. As kinetics can have a profound effect on system efficiency, we are interested in determining the reaction rates and mechanisms of hercynite reduction.

Solid-state kinetics can be classified into two methods: model-fitting and model-free (isoconversional) methods. In the model-fitting method, different models are fit to experimental data. The model with the best statistical fit is chosen, and the pre-exponential factor and activation energy can be calculated from the fit. Isoconversional methods calculate the activation energy as a function of conversion without modelistic assumptions.

We conducted several thermogravimetric analysis experiments with different heating rates (3°C/min, 4°C/min, and 5°C/min) for materials containing aluminum oxide and iron oxide, and used isoconversional methods to analyze the data. We can see from Figure 3a that there are two distinct slopes in the mass loss signal and two O_2 peaks in the mass spectrometry signal, which indicates two different

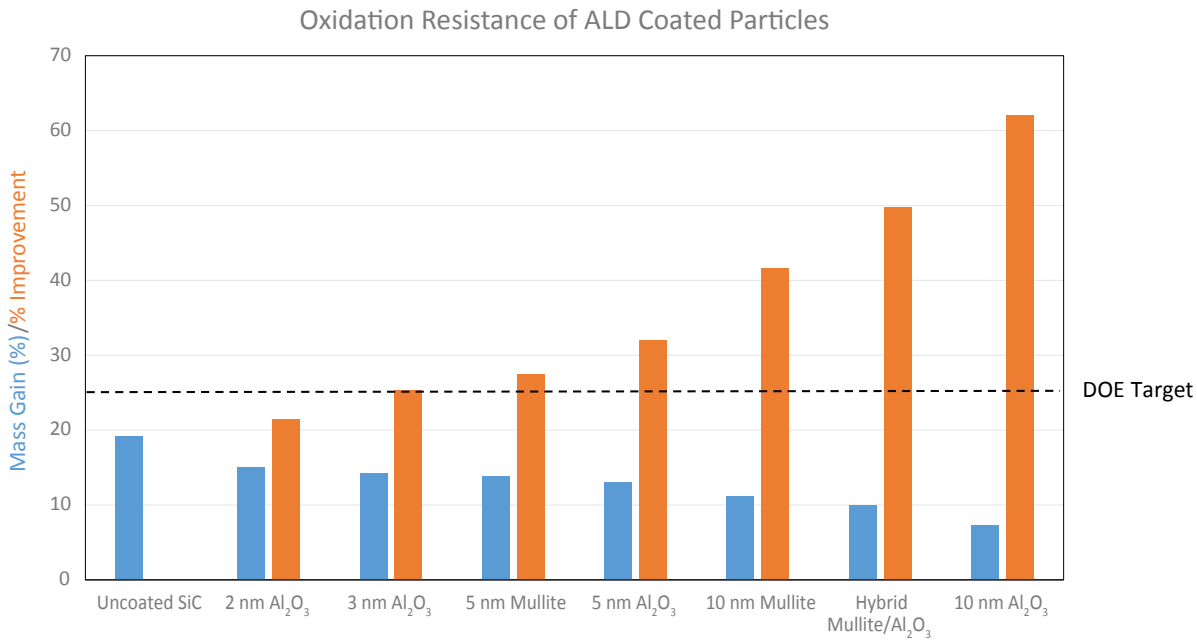

FIGURE 2. Oxidation resistance of various ALD-coated particles over 20 h of steam exposure at 1,000°C. Percent mass gain is attributed to oxidation of SiC. Most materials exceeded DOE target.

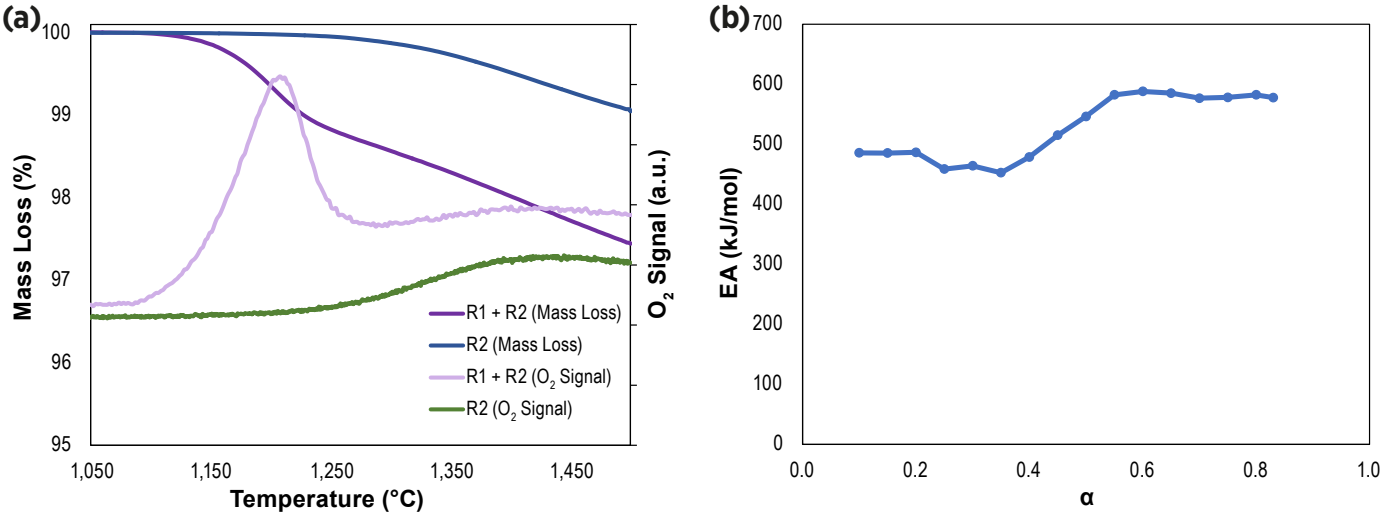

FIGURE 3. (a) Mass loss curves and O_2 mass spectrometry signals for hercynite kinetics experiments. The dark purple line shows the mass loss for the first cycle, when two reactions were occurring: the formation and reduction of hercynite. The light purple line shows the O_2 mass spectrometry signal associated with the two reactions. The blue line shows the mass loss for the reduction of hercynite. The green line shows the O_2 mass spectrometry signal for this reaction. (b) Activation energy of the formation and reduction of hercynite as a function of conversion, calculated using isoconversional methods.

rate-limiting steps. Figure 3b shows the apparent activation energies of hercynite reduction as a function of conversion (α). The formation of hercynite has an apparent activation energy of 472 kJ/mol, while the hercynite reduction reaction has an apparent activation energy of 582 kJ/mol.

The final deliverable of this research project is the production of three standard liters of H_2 in under eight hours on-sun. To achieve this goal, we are collaborating with NREL to use their High-Flux Solar Furnace to heat two fluidized bed reactors filled with hercynite. In the past year, we have made significant progress toward meeting this goal. On the best day of testing, approximately 80 g of hercynite was redox cycled two times over the course of 2 h 45 min. The hydrogen concentration and normal incident power are shown in Figure 4 as a function of time. This test included two reduction cycles and two oxidation cycles. The first

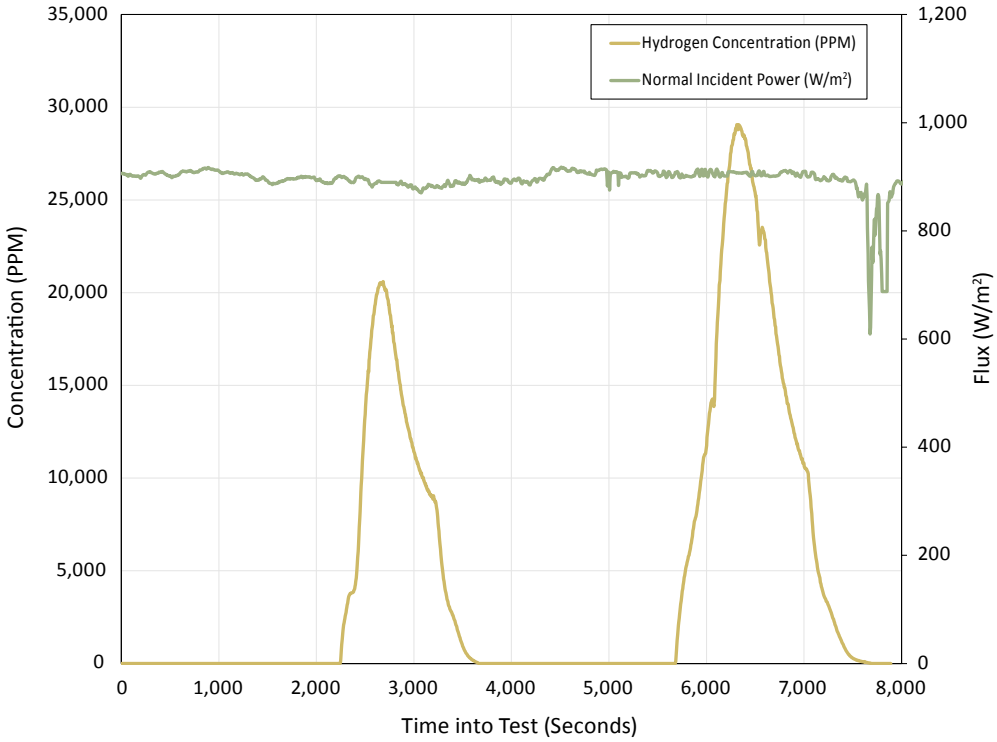

FIGURE 4. H_2 concentration and normal incident power for on-sun test at NREL's High-Flux Solar Furnace.

oxidation cycle produced 0.66 standard liters of H_2 and the second produced 1.25 standard liters of H_2, giving a total of 1.91 L. If this production rate was sustained over four cycles, the total amount of H_2 produced would be 3.81 L and the total time would be 5 h 30 min. This demonstrates that we are on target to meet our end-of-project goal.

CONCLUSIONS AND UPCOMING ACTIVITIES

After the completion of the second year of the project, several conclusions can be drawn:

- Tested redox materials can maintain high H_2 production (~300 µmol/g/cycle) over hundreds of cycles.
- ALD coatings confer substantial oxidation resistance to SiC in the presence of steam at high temperatures (1,000°C).
- Undoped hercynite undergoes an O_2 vacancy mechanism during reduction up to 1,700°C.
- Project is on target for meeting end-of-project goal of producing 3 L of H_2 in less than 8 h.

Future work will include:

- Detailed thermodynamic and kinetic studies of active materials.
- Computation work of a sister National Science Foundation project.
- Operate reduction reactor tube under vacuum and evaluate diffusional limitations.
- Develop a reactor concept for hybrid solar–electric water splitting.
- Synthesize ALD films on three SiC tubes having different thicknesses of coating material.
- Test coated tubes for stability in high temperature steam environment, and evaluate tested tubes using scanning electron microscopy, X-ray diffusion, and inductively coupled plasma optical emission spectroscopy.
- Further refine the AspenPlus model and H2A with experimental thermodynamic and kinetic results and optimal operating conditions.

FY 2017 PUBLICATIONS/PRESENTATIONS

Publications

1. A.J. Groehn, A. Lewandowski, R. Yang, A.W. Weimer. 2016. "Hybrid radiation modeling for multi-phase solar-thermal reactor systems operated at high-temperature." *Solar Energy*, *140*, 130–140.

2. C.L. Muhich, V. Poole-Aston, R.M. Trottier, A.W. Weimer, C.B. Musgrave. 2016. "A First Principles Analysis of Cation Diffusion in Mixed Metal Ferrite Spinels." *Chemistry of Materials*, 28 (1), 214–226. DOI: 10.1021/acs.chemmater.5b03911.

3. B.D. Ehrhart, C.L. Muhich, I. Al-Shankiti, A.W. Weimer. 2016. "System efficiency for two-step metal oxide solar thermochemical hydrogen production—Part 1: Thermodynamic model and impact of oxidation kinetics." *International Journal of Hydrogen Energy*, 41 (44), 19881–19893.

4. B.D. Ehrhart, C.L. Muhich, I. Al-Shankiti, A.W. Weimer. 2016. "System efficiency for two-step metal oxide solar thermochemical hydrogen production—Part 2: Impact of gas heat recuperation and separation temperatures." *International Journal of Hydrogen Energy,* 41 (44), 19894–19903.

5. B.D. Ehrhart, C.L. Muhich, I. Al-Shankiti, A.W. Weimer. 2016. "System efficiency for two-step metal oxide solar thermochemical hydrogen production—Part 3: Various methods for achieving low oxygen partial pressures in the reduction reaction." *International Journal of Hydrogen Energy,* 41 (44), 19904–19914.

6. I. Al-Shankiti, B.D. Ehrhart, A.W. Weimer. 2017. "Isothermal redox for H_2O and CO_2 splitting – A review and perspective." Solar Energy, http://dx.doi.org/10.1016/j.solener.2017.05.028.

7. "Methods and apparatus for gas-phase reduction/oxidation processing," U.S. Patent 9,399,575 (2016).

Presentations

1. Samantha L. Miller, Ryan Trottier, Kevin Sun, Alan W. Weimer, and Charles B. Musgrave, "Evaluating the Effect of Modeling Variables and Experimental Conditions on Material Development for Solar Thermochemical Water Splitting," American Institute of Chemical Engineering Annual Meeting, San Francisco, CA, November 2016.

2. Amanda Hoskins, Aidan Coffey, Charles B. Musgrave, and Alan W. Weimer, "Stabilizing SiC for Solar Thermal Water Splitting Applications," American Institute of Chemical Engineering Annual Meeting, San Francisco, CA, November 2016.

3. Amanda Hoskins, "Nano-Structured Ceramic Coatings to Stabilize SiC Against Reaction in High Temperature Steam," Paper presented at the 2017 American Ceramics Society International Conference and Expo on Advanced Ceramics and Composites, Daytona Beach, Florida, January 22–27, 2017.

4. Ibraheam Al-Shankiti, Yahya Al-Salik, Hicham Idriss, and Alan W. Weimer, "Reduction Kinetics of Iron Aluminate ($FeAl_2O_4$) for Solar Thermochemical H_2O Splitting," American Institute of Chemical Engineering Annual Meeting, San Francisco, CA, November 2016.

5. Samantha L. Miller, Kevin Sun, Charles B. Musgrave, and Alan W. Weimer, "Finite temperature modeling of metal oxides for solar thermochemical water splitting," American Chemical Society Spring Meeting, San Francisco, CA, April 2017.

6. Ryan Trottier, Samantha Millican, Christopher Bartel, Aaron Holder, Alan W. Weimer, and Charles B. Musgrave, "Rapid Computational Screening of Materials for Water Splitting Using Ab Initio and Machine Learned Models: Thermodynamic and Kinetics of Solar Thermal H_2 Generation," The 231st Electrochemical Society Meeting, New Orleans, May 2017.

7. Samantha L. Millican, Ryan Trottier, Christopher Bartel, Alan W. Weimer, and Charles B. Musgrave, "Incorporating Spin Disorder, Phase and High Temperature Free Energy into Rapid Computational Screening of Redox Materials for Water Splitting," Keynote Talk, The 21st International Conference in Solid State Ionics, Padova, Italy, June 2017.

8. Alan W. Weimer, "Solarthermal Chemistry–The Path Forward," Keynote Address - presented at the American Society of Mechanical Engineers (ASME) Power and Energy Conference, Charlotte, NC (June 30, 2016).

9. Alan W. Weimer, "Solarthermal Chemistry – The Path Forward," invited Plenary Lecture (Thermochemistry) presented at the Asia Pacific Solar Research Conference, Canberra, Australia, ACT (December 1, 2016).

10. Alan W. Weimer, "Solarthermal Chemistry – The Path Forward," University Distinguished Lecture presented at Texas A & M University at Qatar, Doha, Qatar (March 23, 2017).

II.D.1 High-Efficiency Tandem Absorbers for Economical Solar Hydrogen Production

Todd G. Deutsch (Primary Contact),
John A. Turner, James L. Young, Myles A. Steiner,
Henning Döscher, Ellis Klein
National Renewable Energy Laboratory
15013 Denver West Parkway
Golden, CO 80401
Phone: (303)275-3727
Email: Todd.Deutsch@nrel.gov

DOE Manager: David Peterson
Phone: (240) 562-1747
Email: David.Peterson@ee.doe.gov

Subcontractors:
- University of Nevada, Las Vegas, Las Vegas, NV (XGB-2-11673-01)
- University of Hawaii, Honolulu, HI (XGJ-5-52227-01)

Project Start Date: October 2014
Project End Date: September 30, 2017

Overall Objectives

- Develop a semiconductor-based, solar-driven, water-splitting photoelectrochemical (PEC) device with greater than 20% solar-to-hydrogen (STH) efficiency and several thousand hours of stability under normal operating conditions.
- Incorporate components that can be fabricated cost-effectively and are straightforward to scale up such that a plant scaled to 50,000 kg H_2 per day can achieve an estimated production cost of $1–$2/kg hydrogen using only sunlight and water as feedstocks.
- Demonstrate a prototype photoreactor that produces 3 L of standard hydrogen within an 8-hour period under moderate solar concentration (~10x).

Fiscal Year (FY) 2017 Objectives

- Push boundaries on achievable semiconductor PEC STH efficiencies.
- Benchmark STH efficiencies for multijunction (tandem) PEC devices.
- Continue to develop stabilizing surface modifications that are viable at high current densities.

Technical Barriers

This project addresses the following technical barriers from the Hydrogen Delivery section of the Fuel Cell Technologies Office Multi-Year Research, Development, and Demonstration Plan.

(AE) Materials efficiency – bulk and interface

(AF) Materials durability – bulk and interface

(AG) Integrated device configurations

(AI) Auxiliary materials

Technical Targets

This project is a materials discovery investigation to identify a single semiconductor material that meets the technical targets for efficiency and stability. The 2015 technical targets from the PEC hydrogen production goals in Table 3.1.8.A of the Fuel Cell Technologies Office Multi-Year Research, Development, and Demonstration Plan are the following.

- 15% STH conversion efficiency
- 900-hour replacement lifetime (half a year at 20% capacity factor)
- $300/m^2 PEC electrode cost

FY 2017 Accomplishments

- We tested a new III-V alloy, GaInAsP, as a candidate for the 1.7-eV bandgap top cell in a higher-efficiency tandem device, and discovered it has good intrinsic stability and photoconversion efficiency. We sent a series of GaInAsP samples to the Heske group, our surface validation team collaborators at the University of Nevada, Las Vegas to get a better understanding of the surface stabilization mechanism.
- We achieved very good durability results with the Jaramillo group at Stanford University on buried-junction pn-$GaInP_2$ capped with MoS_2. We measured 100 h with little degradation and plan to extend the testing.
- We designed a capillary mass-spectrometer-based faradaic yield system and measured trace signals of H_2 and O_2 from GaAs water-splitting microcells from Jongseung Yoon's laboratory at the University of Southern California, testing the limit of quantitative detection for this custom instrument.

- We synthesized and tested epitaxial capping layers that could potentially offer more stability and less parasitic optical absorption than the standard $GaInP_2$ cap because of an engineered wider bandgap.
- We modeled antireflective texturing of III-V surfaces with Professor Yoon at the University of Southern California and identified structures that should have reflection below 5% across the relevant wavelengths. The model was validated experimentally.
- We commenced testing of our photoreactor on a two-axis solar tracker.

✧ ✧ ✧ ✧ ✧

INTRODUCTION

Photoelectrolysis cells combine a light-harvesting system and a water-splitting system into a single, monolithic device. The catalyzed surface of a semiconductor is the light-harvesting component, as well as one part of the water-splitting system, with the balance consisting of a spatially separated counter electrode. Discovering a semiconductor system that can efficiently and sustainably collect solar energy and direct it toward the water-splitting reaction could provide renewable and economically competitive fuel for the hydrogen economy.

The goal of this work is to develop a semiconductor material set or device configuration that:

- Splits water into hydrogen and oxygen spontaneously upon illumination without an external bias.
- Has a solar-to-hydrogen efficiency of at least 15%, with a clear pathway to exceed 20%.
- Can ultimately be synthesized via high-volume manufacturing techniques with a final hydrogen production cost below $2/kg.

APPROACH

All proven zero-bias PEC devices with STH over 1% rely on two series-connected semiconductor junctions (tandem cell) to increase the majority-carrier potential at the counter electrode [1–4], providing sufficient potential difference (photovoltage) for water splitting. Tandem devices also overcome the band-alignment challenge common to PEC materials.

For maximum efficiency, the subcell currents in series-connected devices must be equal, creating the requirement of current matching. The maximum theoretical current generated by a semiconductor can be calculated by assuming unity quantum yield for every above-bandgap photon in the solar spectrum. Using the accepted lower heating-value efficiency equation [5], 20% STH corresponds to a short-circuit current density of 16.26 mA/cm^2 under air mass 1.5 global (1-sun). The largest bottom-cell bandgap that can be used and still achieve 20% STH is 1.41 eV. However, quantum yields are never 100% and semiconductors are not true step-function devices. Therefore, to realistically achieve STH values in excess of 20%, we must use lower top-cell and bottom-cell bandgap combinations, which guides our selection of candidate semiconductors.

An additional variable that can be used to match the currents is the thickness of the top cell; a thinner cell will allow more photons through to the bottom cell. This gives us some additional flexibility in the bandgaps that may be used. The lower limit of useable bandgaps is ~0.8 eV [6], dictated by the short penetration depth of lower-energy photons through water.

We will focus on III-V semiconductors, which exhibit the highest conversion efficiencies among all photoabsorber materials, and design tandem junctions to maximize the spectrally split device current, while achieving sufficient voltage to drive the maximum current through the device. We plan to initially focus on devices grown by conventional III-V metal-organic vapor-phase epitaxy to demonstrate maximum possible efficiencies. We will then port successful device structures to emerging synthesis techniques—such as spalling, epitaxial lift-off, or hydride vapor-phase epitaxy—that have the potential to meet low-cost absorber targets. We plan to improve the stability of III-V semiconductor water-splitting electrodes by a variety of surface-protecting modifications that include nitridation/sputtering, atomic layer deposition of oxides/nitrides, and thin coatings of MoS_2.

RESULTS

Solar-to-Hydrogen Efficiency Benchmarking

During the course of benchmarking over 16% STH efficiency on our inverted metamorphic multijunction (IMM) cells [7], we identified and documented two more potential sources of measurement error that were not included in our *Energy & Environmental Science* manuscript [8] that detailed ways of improving STH measurement accuracy. One systematic error we discovered is a consequence of applying light from a diverging illumination source through the multiple interfaces of an electrochemical cell. The different indices of refraction between air/glass/electrolyte cause a concentration error that can increase the light intensity on the sample by 10%, relative to the calibrated value, under commonly used experimental conditions. We recommended using a highly collimated source (i.e., sunlight with a collimating tube) to mitigate this source of error. We also made a recommendation against setting light intensity from a solar simulator with the reference diode *inside* the electrochemical cell, either with air or electrolyte inside the cell. In the case of an air-filled cell, reflection at the glass/

electrolyte interface is significantly lower than at a glass/air interface, resulting in a light intensity on the PEC sample that is about 5% greater than the calibrated value. Immersing the reference cell in electrolyte during light-intensity calibration can eliminate the reflection error at the inner electrochemical cell interface, whereas the infrared absorption of water attenuates light on a typically used Si reference cell, leading to an overcompensated simulator intensity.

To report STH water-splitting efficiency, the fraction of current going to hydrogen and oxygen generation (Faradaic efficiency) must be known. We designed and built a new Faradaic efficiency measurement system based on product gas detection by a capillary mass spectrometer. Using a mass spectrometer has several advantages over the more commonly used gas chromatograph in detecting product gases, including the following: greater sensitivity, continuous measurement, and ability to provide qualitative as well as quantitative information. We demonstrated the capability of this system by measuring the Faradaic efficiency of solar water splitting on GaAs microcells synthesized by our collaborator. We were able to quantitatively determine oxygen and hydrogen generated on 0.0025-cm^2 microcells at only 50 µA of current. The corresponding concentrations of oxygen and hydrogen under the measurement conditions were 200 ppm and 400 ppm, respectively. Confirming a near-unity Faradaic yield, we were able to use collimated sunlight to benchmark 13.1% STH efficiency from these GaAs microcells [9].

For longer-term performance assessment under more realistic conditions, i.e., those that include temporal intermittency from clouds and diurnal cycles, we designed and fabricated a photoreactor for testing on a two-axis solar tracker. The photoreactor (Figure 1) can be fitted with a Fresnel lens for measurements at low optical concentrations (~10x), and it is equipped with quantitative gas-collection capabilities, can accommodate a variety of sample dimensions, and has Nafion® membrane separators to prevent mixing of hydrogen and oxygen.

Photo credit: NREL-Dennis Schroeder

FIGURE 1. Photograph of our photoreactor mounted on a two-axis solar tracker for on-sun testing.

Durability Testing

IMM cells have advantages over upright tandems when in pursuit of higher STH efficiencies. However, the stability of the IMM cells is significantly lower than we previously observed with upright tandem water-splitting PEC cells. Corrosion on upright cells tends to be characterized by a more uniform etching from the surface toward the substrate. Degradation of IMM cells initiates locally—apparently centered around native defects in the material—leading to blistering and delamination from the Si handle, and ultimately resulting in catastrophic failure (Figure 2). It is possible that these native defects are also present in the upright cells, but their tendency to lead to catastrophic failure is tempered by the 700-µm-thick GaAs substrate. The IMM form factor of a very thin (~5 µm) absorber layer in direct contact with a gold hole-collecting back contact appears to be a less stable configuration than the upright cells that have GaAs substrate between the absorber layer and gold back contact. Similar single-crystal epitaxial III-V semiconductors are flexible when removed from their substrates—a property often highlighted as advantageous for solid-state photovoltaics—and would be expected to be susceptible to delamination should adhesion with its rigid handle become compromised. It is unclear whether the GaAs substrate provides a chemical buffer, slowing etching progression of acidic electrolyte to the gold back contact, or is merely additional mechanical support for a flimsy absorber layer.

We have attempted to passivate the IMM surfaces with epitaxial capping layers (GaInAsP and GaInAsN), which, based on experience, should have greater stability than $GaInP_2$. However, the mechanical instability of the IMM cells prevents us from evaluating their chemical stability. An example of this can be seen in Figure 3, where the GaInAsN-capped IMM structure exhibits good stability under electrochemical durability testing, but physical observation of the surface (Figure 3 inset) reveals a surface that is already deteriorating in discrete locations. Initial attempts have been unsuccessful to map native defects with optical microscopy and locally passivate them.

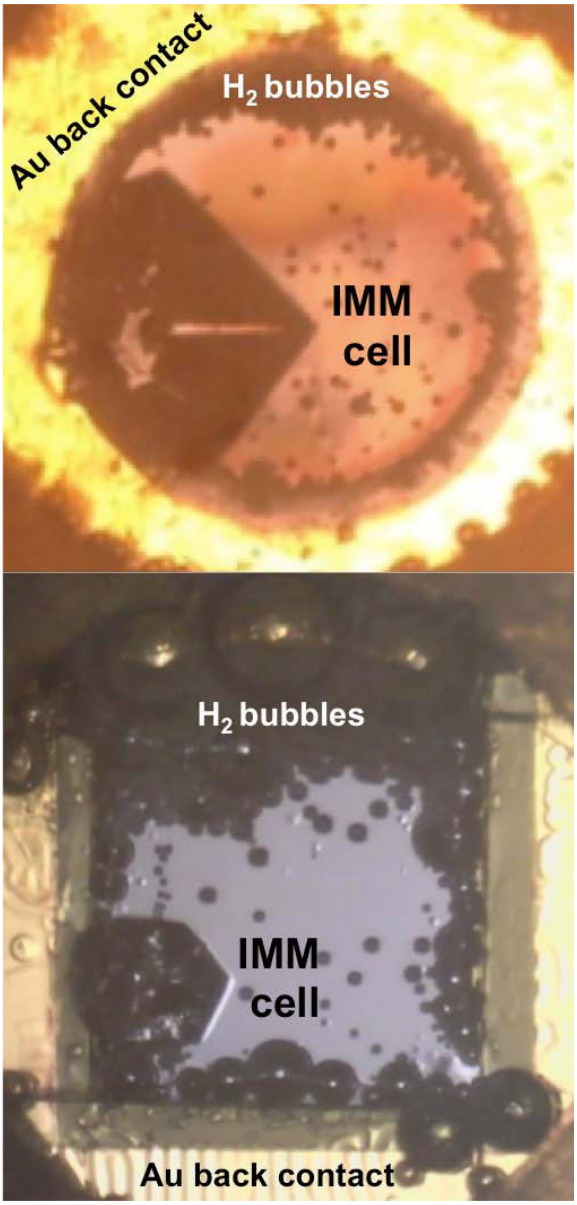

FIGURE 2. Photographs of two different IMM cell failures during durability testing in 0.5 M sulfuric acid. We tried IMMs with circular mesas (top) as well as square mesas (bottom), but most exhibited failure mechanisms similar to these. The separation of the semiconductor layer from the silicon handle can be seen to the left of the "IMM cell" label in each image. The width of the IMM cell is about 4 mm in both photos.

CONCLUSIONS AND UPCOMING ACTIVITIES

- We have established robust protocols for accurately benchmarking solar-to-hydrogen efficiency that have their foundations in the methodology used to certify the efficiency of multijunction solid-state solar photovoltaic cells.

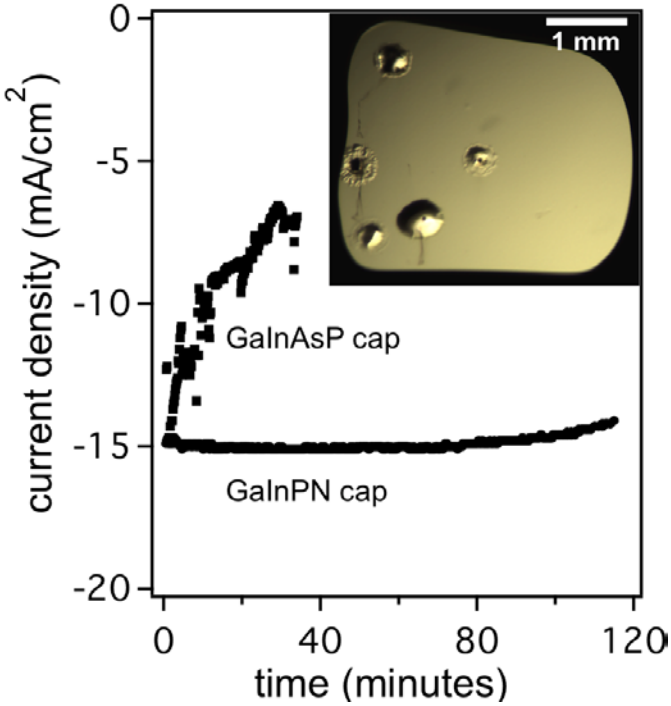

FIGURE 3. Current density vs. time plots for two IMM cells with different protective capping layers. These electrodes were tested at short circuit (0 V vs. a RuOx counter electrode) in 0.5 M sulfuric acid. A flat line indicates stability. Although the current for the GaInPN-capped electrode implies resistance to corrosion, the left side of the photograph in the inset shows that this electrode had several defects that led to blistering of the IMM layer.

- IMM cells are a good platform for meeting the STH efficiency targets established in the Fuel Cell Technologies Office Multi-Year Research, Development, and Demonstration Plan, but they are more susceptible to corrosion than upright tandems.
- Upcoming activities will focus on surface modifications that increase STH efficiency by reducing reflection at the semiconductor/electrolyte interface. We will also focus on durability by potentially developing upright metamorphic cells.

SPECIAL RECOGNITIONS & AWARDS/ PATENTS ISSUED

1. 2017 DOE Hydrogen and Fuel Cells Program R&D Award (Young, Steiner, Deutsch)

2. (Pending) Devices and methods for photoelectrochemical water splitting. Application No. 15/078,206

FY 2017 PUBLICATIONS AND PRESENTATIONS

1. "Direct solar-to-hydrogen conversion via inverted metamorphic multi-junction semiconductor architectures," James L. Young, Myles A. Steiner, Henning Döscher, Ryan M. France, John A. Turner, and Todd G. Deutsch, *Nature Energy* **2**, 17028 (2017).

2. "Employing overlayers to improve the performance of Cu_2BaSnS_4 thin Film based Photoelectrochemical Water Reduction Devices," Jie Ge, Paul J. Roland, Prakash Koirala, Weiwei Meng, James L. Young, Reese Petersen, Todd G. Deutsch, Glenn Teeter, Randy J. Ellingson, Robert W. Collins, and Yanfa Yan, *Chem. Mater.* **29**(3), 916–920 (2017).

3. "Covalent surface modification of GaAs(100) photocathodes for water splitting in highly Acidic Electrolyte," L.E. Garner, K.X. Steirer, J.L. Young, N.C Anderson, E.M. Miller, J.S. Tinkham, T.G. Deutsch, A. Sellinger, J.A. Turner, and N.R. Neale, *ChemSusChem*. **10**, 767–773 (2017).

4. "Printed assemblies of GaAs photoelectrodes with decoupled optical and reactive interfaces for unassisted solar water splitting," Dongseok Kang, James L. Young, Haneol Lim, Walter E. Klein, Huandong Chen, Yuzhou Xi, Boju Gai, Todd G. Deutsch, and Jongseung Yoon, *Nature Energy* **2**, 17043 (2017).

5. "Influence of support electrolytic in the electrodeposition of Cu-Ga-Se thin films," A.M. Fernandez, J.A. Turner, B. Lara-Lara, and T.G. Deutsch, Superlattices and Microstructures **101**, 373–383 (2017).

6. "Inverted metamorphic multijunction semiconductors for exceptionally high photoelectrolysis efficiencies: Materials development and measurement challenges," XXV International Materials Research Congress of the Materials Research Society, Cancun, Mexico. August 16, 2016. (Deutsch) *Invited*

7. "Inverted metamorphic multijunction III-V semiconductors for solar hydrogen production," Materials Research Society Fall Meeting. Boston, MA. November 30, 2016. (Deutsch)

8. "Solar-to-hydrogen efficiency – Shining light on photoelectrochemical device performance," Materials Research Society Fall Meeting. Boston, MA. November 28, 2016. (Deutsch)

9. "Inverted metamorphic multijunction semiconductors for exceptionally high photoelectrolysis efficiencies: Materials development and measurement challenges," Pacific Rim Meeting of Electrochemical and Solid State Science (PRiME), Honolulu, HI. October 6, 2016. (Deutsch)

10. "Advanced device design for photoelectrochemical water splitting derived by a detailed balance approach," Pacific Rim Meeting of Electrochemical and Solid State Science (PRiME), Honolulu, HI. October 6, 2016. (Döscher)

11. "High photoelectrochemical water splitting efficiencies: Materials development and measurement challenges" 253rd American Chemical Society National Meeting and Exposition, San Francisco, CA. April 5, 2017. (Turner) *Invited*

12. "Recent advances in III-V multijunction photo-electrochemical water splitting," Materials Research Society Spring Meeting, Phoenix, AZ. April 19, 2017. (Deutsch) *Invited*

13. "Solar-to-hydrogen efficiency: Shining light on photoelectrochemical device performance," Materials Research Society Spring Meeting, Phoenix, AZ. April 19, 2017. (Young)

14. "Photo-electrochemical hydrogen generation from inverted metamorphic multijunction III-Vs," 13th International Conference on Concentrator Photovoltaic Systems, Ottawa, Ontario. May 3, 2017. (Deutsch)

15. "Recent advances in III-V multijunction photo-electrochemical water splitting," 231st Meeting of the Electrochemical Society, New Orleans, LA. May 30, 2017. (Deutsch) *Invited*

16. "Solar-to-hydrogen efficiency: Shining light on photoelectrochemical device performance," Materials Research Society Spring Meeting, Phoenix, AZ. April 19, 2017. (Young)

17. "High-efficiency tandem absorbers for economical solar hydrogen production," DOE Hydrogen and Fuel Cells Program Annual Merit Review. Washington, DC. June 8, 2017. (Deutsch)

18. "Photo-electrochemical hydrogen generation from inverted metamorphic multijunction III-Vs," 44th IEEE Photovoltaic Specialists Conference, Washington, DC. June 26, 2017. (Deutsch)

REFERENCES

1. Fatwa F. Abdi, Lihao Han, Arno H.M. Smets, Miro Zeman, Bernard Dam, and Roel van de Krol. 2013. "Efficient solar water splitting by enhanced charge separation in a bismuth vanadate-silicon tandem photoelectrode," *Nature Communications* **4** (January). Nature Publishing Group: 2195. doi:10.1038/ncomms3195.

2. Jeremie Brillet, Jun-Ho Yum, Maurin Cornuz, Takashi Hisatomi, Renata Solarska, Jan Augustynski, Michael Graetzel, and Kevin Sivula. 2012. "Highly efficient water splitting by a dual-absorber tandem cell," *Nature Photonics* **6** (12). Nature Publishing Group: 824–28. doi:10.1038/nphoton.2012.265.

3. R.C. Kainthla, B. Zelenay, and J. O'M. Bockris. 1987. "Significant efficiency increase in self-driven photoelectrochemical cell for water photoelectrolysis," *Journal of The Electrochemical Society* **134** (4): 841. doi:10.1149/1.2100583.

4. O. Khaselev, and J. A. Turner. 1998. "A monolithic photovoltaic-photoelectrochemical device for hydrogen production via water splitting," *Science (New York, N.Y.)* **280** (5362): 425–27. http://www.ncbi.nlm.nih.gov/pubmed/9545218.

5. Chen, Zhebo, Thomas F. Jaramillo, Todd G. Deutsch, Alan Kleiman-shwarsctein, Arnold J. Forman, Nicolas Gaillard, Roxanne Garland, et al. 2010. "Accelerating materials development for photoelectrochemical hydrogen production: Standards for methods, definitions, and reporting protocols," *Journal of Materials Research* **25** (1): 3–16. doi:10.1557/jmr.2010.0020.

6. H. Döscher, J.F. Geisz, T.G. Deutsch, and J.A. Turner. 2014. "Sunlight absorption in water—Efficiency and design implications for photoelectrochemical devices." *Energy & Environmental Science* **7** (9): 2951. doi:10.1039/C4EE01753F.

7. "Direct solar-to-hydrogen conversion via inverted metamorphic multi-junction semiconductor architectures," James L. Young, Myles A. Steiner, Henning Döscher, Ryan M. France, John A. Turner, and Todd G. Deutsch, *Nature Energy* **2**, 17028 (2017).

8. "Solar to hydrogen efficiency: Shining light on photoelectrochemical device performance," H. Döscher, J.L. Young, J.F. Geisz, J.A. Turner, and T.G. Deutsch, *Energy & Environmental Science* **9**, 74–80 (2016).

9. "Printed assemblies of GaAs photoelectrodes with decoupled optical and reactive interfaces for unassisted solar water splitting,"Dongseok Kang, James L. Young, Haneol Lim, Walter E. Klein, Huandong Chen, Yuzhou Xi, Boju Gai, Todd G. Deutsch, and Jongseung Yoon, *Nature Energy* **2**, 17043 (2017).

II.D.2 Wide Bandgap Chalcopyrite Photoelectrodes for Direct Solar Water Splitting

Nicolas Gaillard
University of Hawaii / Hawaii Natural Energy Institute
2440 Campus Road, Box 368
Honolulu, HI 96822
Phone: (808) 956-2342
Email: ngaillar@hawaii.edu

DOE Manager: David Peterson
Phone: (240) 562-1747
Email: David.Peterson@ee.doe.gov

Contract Number: DE-EE0006670

Subcontractors:
- University of Nevada, Las Vegas, Las Vegas, NV
- Stanford University, Stanford, CA
- Lawrence Livermore National Laboratory, Livermore, CA
- National Renewable Energy Laboratory, Golden, CO

Project Start Date: October 1, 2014
Project End Date: September 30, 2018

Overall Objectives

In line with the Fuel Cell Technologies Office Multi-Year Research, Development, and Demonstration Plan, our project aims to identify suitable semiconducting materials for efficient and durable photoelectrochemical (PEC) hydrogen production at a cost of $2/kg or less. Specifically, our project aims to:

- Develop efficient copper chalcopyrite ($Cu(In,Ga)(S,Se)_2$) based materials with ideal optoelectronic properties for PEC water splitting.
- Identify appropriate surface treatments to prevent photo-corrosion, improve surface energetics, and enhance hydrogen evolution reaction.
- Demonstrate three liters of hydrogen produced in eight hours using a copper chalcopyrite-based standalone PEC device.

Fiscal Year (FY) 2017 Objectives

- Demonstrate copper chalcopyrite/buffer junction with open circuit voltage (Voc) over 900 mV.
- Improve chalcopyrite stability in aqueous electrolytes using MoS_2 as protection layers, with a durability goal of 1,000 hours continuous operation at 8 mA/cm^2.
- Demonstrate chalcopyrite-based PEC device with solar-to-hydrogen (STH) efficiency greater than 15%.

Technical Barriers

This project addresses the following technical barriers from the Hydrogen Production section of the Fuel Cell Technologies Office Multi-Year Research, Development, and Demonstration Plan.

(AE) Materials Efficiency – Bulk and Interface

(AF) Materials Durability – Bulk and Interface

(AG) Integrated Device Configurations

(AJ) Synthesis and Manufacturing

Technical Targets

This project aims to develop efficient and durable PEC devices using low-cost semiconducting materials. Specifically, our project aims to modify the optoelectronic properties of the photovoltaic (PV)-grade copper chalcopyrite material class for PEC water splitting. Alongside, we are engineering new surface treatments to improve chalcopyrites' surface energetics, their catalysis toward hydrogen evolution reaction, as well as their resistance against photo-corrosion. The status of this project's technical targets is documented in Table 1.

TABLE 1. Progress towards This Project's Technical Targets for FY 2017

Task #	FY 2017 Milestones	Date	% Complete
1	Photocurrent density relevant to 16–17% STH conversion efficiency with a chalcopyrite 13–14 mA/cm^2	12/2016	92%
2	Fabricate $Cu(In,Ga)S_2$ cells with Voc >900 mV	03/2017	88%
3	Durability >1,000 h at 8 mA/cm^2, with a stretch goal of 2,000 h	06/2017	33%
4	Hybrid photoelectrode PEC device with a standalone STH conversion efficiency of >15% generating at least 3 L H_2 in 8 h	09/2017	

FY 2017 Accomplishments

Accomplishments during the current project period include:

- Successful modeling of new selenide-based wide bandgap chalcopyrite candidates

- Characterization of the $CuInGaS_2$/CdS interface with spectroscopic techniques
- Voc over 850 mV achieved with 1.8 eV $CuGa_3Se_5$/CdS heterojunctions
- Photo-current density over 12 mA/cm^2 obtained with 1.8 eV $CuInGaS_2$
- Extended durability of $CuGaSe_2$ with MoS_2 protective coating, from 250 h to 350 h

✧ ✧ ✧ ✧ ✧

INTRODUCTION

The goals of this project are to demonstrate PEC hydrogen production with a dual absorber system capable of generating at least three liters of hydrogen in eight hours and to develop a standalone system with STH conversion efficiency of 15% and operational life up to 2,000 hours.

APPROACH

The chalcopyrite material class, typically identified by its most popular PV-grade alloy, $CuInGaSe_2$, provides exceptionally good candidates for PEC water splitting. A key asset of this bandgap tunable, direct absorber, thin film semiconductor material is the outstanding photon-to-electron conversion efficiency, as demonstrated with $CuInGaSe_2$-based PV cells. An STH efficiency of 4% was achieved by our team in 2012 using a 1.6 eV bandgap $CuGaSe_2$ photocathode connected in series with three a-Si PV drivers (side-by-side architecture). The use of such coplanar architecture was dictated by the bandgap of $CuGaSe_2$, which was too narrow for a "stacked" multi-junction integration. With wide bandgap chalcopyrites, we will be able to stack the PEC device over the PV driver and increase the STH efficiency.

RESULTS

Task 1. PV-grade wide bandgap absorbers: theoretical modeling. This year we continued to investigate the properties of candidate chalcopyrite alloys, focusing on the optical properties and the electronic structure as a function of composition, as well as investigations into the influence of common impurities like H. Our studies identified that H impurities can have important implications on limiting the p-type dopability of several chalcopyrite compounds, particularly those incorporating Ag. Additionally, we identified that the B-containing $CuBS_2$ and $CuBSe_2$ compounds exhibit smaller fundamental bandgaps than previously assumed from experimental measurements of the optical bandgaps, which are reported to be 3.61 and 3.13 eV, respectively. Our results on the optical spectra of these compounds identified a very weak absorption onset and that the fundamental bandgaps are actually much smaller than the optical gaps by roughly 0.8 eV. Our findings suggest that B incorporation into $CuInS_2$ or $CuInSe_2$ leads to conduction band edges that are much closer to those of the Ga-containing analogs than previously assumed.

Task 1. PV-grade wide bandgap absorbers: synthesis. During this reporting period, $CuInGaS_2$ absorbers with a current density of 12 mA/cm^2 at –1 V bias were synthesized. The absorbers were made on molybdenum substrates by co-evaporating Cu, In, and Ga to form a Cu-rich metal alloy film with a Cu/(Ga+In) ratio of 1.3 and a Ga/(Ga+In) ratio of 0.32. The alloys were sulfurized by heating them with 150 mg S in a N_2-filled capsule at 600°C for 30 minutes. The absorbers were etched in 1 M potassium cyanide solution for three minutes to remove any Cu-S compounds formed, resulting in a Cu/Ga+In ratio of 0.93. These absorbers were then completed into PV devices with a chemical-bath-deposited CdS buffer layer, radio frequency magnetron sputtered ZnO (200 nm) widow layer, and indium tin oxide (500 nm, with mask) top contact. The final device area was 0.12 cm^2. The quantum efficiency (QE) measurement of the best device at –1 V bias is shown in Figure 1, demonstrating 12 mA/cm^2 current density. The bandgap determined from the derivative of the QE cut-off is 1.8 eV. Future experiments with alkali treatments and reduced Cu excess in the metal alloy will be attempted to improve current density.

Task 2. Sub-surface energetics improvement: synthesis. We have continued material optimization to improve the properties of wide bandgap defect chalcopyrite

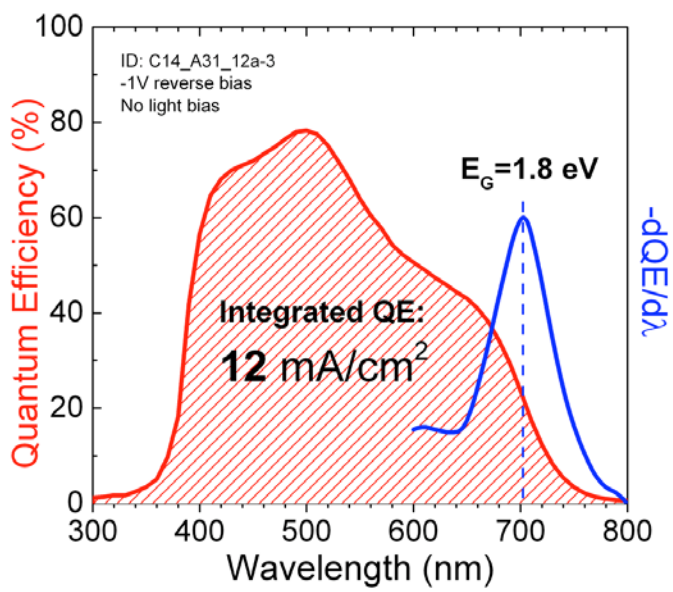

FIGURE 1. QE of best-performing $CuInGaS_2$ film made from sulfurizing a CuInGa alloy (red), and the bandgap determined from the derivative of the QE spectrum (blue)

$CuGa_3Se_5$ to achieve higher open-circuit voltage and photocurrent density. Several optimization strategies have been applied in recent material growth, including the control of sample growth temperature, bulk composition, film thickness, composition gradient, and alkaline post deposition treatments. A few device treatment strategies have also been tested to show improvement on device performance. Our results are primarily based on recent sample growth with increased growth temperature from the standard 550°C to 620°C. In general, we found that increasing the growth temperature to 620°C improves device characteristics, especially for the higher Voc. We now can regularly obtain 800–850 mV Voc using absorbers with about 1.8 eV bandgap (Eg). This is a significant accomplishment for the wide bandgap $CuGa_3Se_5$ material development, since a large voltage loss (Eg/q–Voc) represents a key energy loss associated with wide bandgap absorbers in general. For recent studies, the Cu/Ga ratio has been narrowed to about 0.33±0.03 in order to have the proper bandgap values (1.7 eV to 1.9 eV). Through our research we found that i) $CuGa_3Se_5$ may be too resistive, so thinner layers are desirable; ii) higher growth temperature works better; and iii) doping with NaF improves the fill factor of the devices.

Task 2. Sub-surface energetics improvement: advanced characterization. This project year, University of Nevada, Las Vegas's work centered on X-ray photoelectron spectroscopy (XPS) measurements and analysis of the third sample set received from the University of Hawaii, as well as first ultraviolet photoelectron spectroscopy and inverse photoemission spectroscopy measurements. Furthermore, X-ray emission spectroscopy of various samples (including those discussed below) was performed at the Advanced Light Source (Berkeley Lab). The goal of these experiments is, in particular, to determine the electronic surface and interface structure of a sample series consisting of $Cu(In,Ga)S_2$ (CIGS) absorbers with CdS buffer layers of varying thickness (deposited using chemical bath deposition). The experimental results provide valuable information about the CdS/CIGS interface, including the band alignment of the valence and conduction band, as well as the electronic surface bandgaps. Figure 2 shows the XPS survey spectra of a (sulfurized) CIGS absorber and CdS/CIGS samples with increasing buffer layer thickness. The increase in chemical bath deposition time leads to an increase in Cd intensity, in parallel to a continual attenuation of absorber-related peaks (as expected). Because the CIGS-related Cu, In, and Ga signals are still detected for the intermediate buffer layer thickness, this sample is currently being investigated to monitor the interface-induced changes in surface band bending, to be combined with the results for valence band maximum and conduction band minimum obtained with ultraviolet photoelectron spectroscopy and inverse photoemission spectroscopy, respectively. The next project steps include an ion treatment series, necessary to remove surface adsorbates for a more accurate band edge determination, followed by successive XPS, ultraviolet photoelectron spectroscopy, and inverse photoemission spectroscopy measurements.

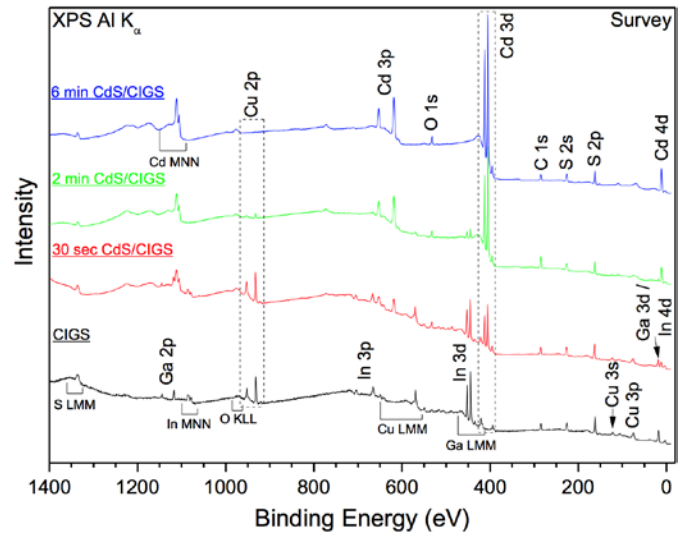

FIGURE 2. Al K_α XPS survey spectra of a $Cu(In,Ga)S_2$ absorber ("CIGS") and three additional CdS/CIGS samples with increasing buffer layer thickness (deposition times of 30 seconds, 2 minutes, and 6 minutes, respectively)

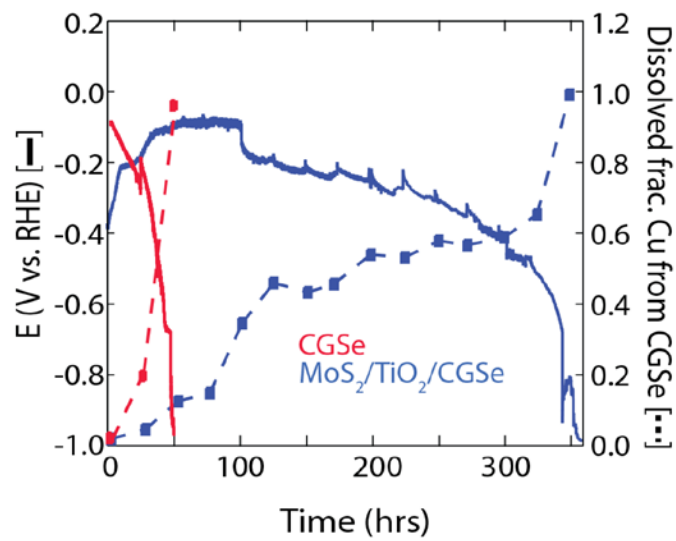

RHE – reversible hydrogen electrode

FIGURE 3. Chronopotentiometry plot of CGSe electrodes with and without catalytic and protecting schemes. On the secondary ordinate, data from inductively coupled plasma are shown, demonstrating the fraction of Cu in the film that has dissolved into the electrolyte, sampled at intervals by aliquoting.

Task 3. Surface catalysis and corrosion resistance. During the third year of our project, we worked to develop conformal MoS_2/TiO_2 coatings to protect copper gallium selenide (CGSe) electrodes and buried-junction CdS/CGSe electrodes from corrosion in sulfuric acid electrolyte

during PEC hydrogen evolution. Figure 3 shows the results of our surface protection schemes and includes durability measurements for bare CGSe electrodes and CGSe electrodes with 7.5 nm of atomic layer deposition (ALD)-deposited TiO_2 and 4.5 nm of ALD-deposited MoO_x that has been converted to MoS_2. All samples were tested by measuring the voltage required to obtain a constant current density of –8 mA cm^{-2}. The protected sample operates continuously for much longer than the bare CGSe sample, with the two electrodes failing at 350 h and 50 h, respectively. Overlaid in this figure is the fraction of the Cu atoms in the film that have dissolved into the acid electrolyte over the course of the measurement, as quantified at intervals by inductively coupled plasma analysis. The MoS_2 protecting scheme appears to provide enhanced durability to the CGSe film by slowing the rate of dissolution into the electrolyte.

CONCLUSIONS AND UPCOMING ACTIVITIES

- Achievement: Over 12 mA/cm^2 and 850 mV achieved with wide bandgap chalcopyrites. Durability improved with MoS_2 protective coating, from 250 h to 350 h.
- Achievement: Advanced modeling and characterization successfully integrated to accelerate materials and interface engineering.
- Future work: Finalize our study on CuGaSSe and CuInGaSSe to conclude on the effect of ordered vacancy compounds and re-focus effort on best candidates for final tandem PEC structure: Cu-poor $CuGaSe_2$ and $CuGa_3Se_5$.
- Future work: Continue to develop ex situ and in situ spectroscopic techniques to better understand degradation mechanisms and evaluate SiO_2 passivation layer as an alternative to TiO_2 to meet the 1,000+ h durability goal.
- Future work: Validate tandem structure using CGSe, temperature-resistant transparent conductive oxide (Mo:InO_2), and silicon or GaAs model PV drivers, and benchmark STH efficiency of best-performing tandem device.

FY 2017 PUBLICATIONS/PRESENTATIONS

1. *Novel Chalcopyrite Materials for Economical Photoelectrochemical Hydrogen Production.* N. Gaillard, A.D. DeAngelis, and K. Horsley, the 231st Electrochemical Society Meeting, Symposium I03, 1532, New Orleans (LA), 2017.

2. *First-Principle Simulations in Chalcopyrite Based Photoelectrode Development.* T. Ogitsu, J. Varley, N. Gaillard, C. Heske, and M. Blum, the 231st Electrochemical Society Meeting, Symposium I03, 1529, New Orleans (LA), 2017.

3. *Development of Wide Bandgap Copper Chalcopyrite Materials for Economical Photoelectrochemical Hydrogen Production.* N. Gaillard, A.D. DeAngelis, and K. Horsley, the 230th Electrochemical Society Meeting, Symposium L04, 3630, Honolulu (HI), 2016.

4. *Photoelectrochemical and Solid-State Properties of Wide Bandgap Copper Chalcopyrites for Renewable Hydrogen Generation.* N. Gaillard, K. Horsley, and A. Deangelis, the Materials Research Society Spring Meeting, Symposium ES7, ES7.16.02, Phoenix (AZ), 2017.

5. *Soft X-ray Spectroscopic Investigation of the CdS/Cu(In,Ga)S_2 Interface in Thin Films for Photoelectrochemical Water Splitting.* J. Carter, B. Elizan, M. Blum, K. Horsley, A. DeAngelis, W. Yang, L. Weinhardt, N. Gaillard, and C. Heske, the Materials Research Society Spring Meeting, Symposium ES7, ES7.4.04, Phoenix (AZ), 2017.

5. *Non-Precious Metal-Catalyzed Photoelectrodes for Hydrogen Production Via Solar Water Splitting.* T.R. Hellstern, A.D. DeAngelis, L.A. King, P. Chakthranont, R.J. Britto, N. Gaillard, and T.F. Jaramillo, the 230th Electrochemical Society Meeting, Symposium L04, 3718, Honolulu (HI), 2016.

6. *Solid-State Characterization of Wide-Bandgap Cuga(S,Se)$_2$ for PEC Water Splitting.* A.D. DeAngelis, K. Horsley, and N. Gaillard, the 230th Electrochemical Society Meeting, Symposium L04, 3714, Honolulu (HI), 2016.

II.D.3 Tandem Particle-Slurry Batch Reactors for Solar Water Splitting

Shane Ardo (Primary Contact), William Gaieck, Samuel Keene, Kevin Tkacz, Houman Yaghoubi
University of California, Irvine
1102 Natural Sciences II
Irvine, CA 92697
Phone: (949) 824-3796
Email: ardo@uci.edu

DOE Manager: David Peterson
Phone: (240) 562-1747
Email: David.Peterson@ee.doe.gov

Contract Number: DE-EE0006963

Subcontractors:
- Adam Z. Weber and Rohini Bala Chandran, Lawrence Berkeley National Laboratory (LBNL), Berkeley, CA
- Chengxiang Xiang, California Institute of Technology (Caltech), Pasadena, CA

Project Start Date: August 1, 2015
Project End Date: January 31, 2018 (including a 6-month no cost extension)

Overall Objectives

- Experimentally validate a benchtop-scale tandem particle-slurry batch reactor as a scalable technology for solar hydrogen production at a projected cost of ≤$20.00 per gallon of gasoline equivalent.
- Demonstrate a ~12 in x 12 in model reactor that generates H_2 at a rate of >3 L per 8 h of solar illumination.

Fiscal Year (FY) 2017 Objectives

- Incorporate into the numerical reactor model more accurate physics for electromagnetic wave propagation, thermal effects, and gas crossover.
- Experimentally demonstrate two particle materials that together exhibit a 1% solar-to-hydrogen (STH) efficiency in electrode form factor.
- Experimentally demonstrate the feasibility of a reactor that exhibits a 1% STH efficiency while using at least 80% less pipes and 80% less energy required to pump and circulate the electrolyte than modeled for similar reactors analyzed in the 2009 techno-economic analysis [1,2].

Technical Barriers

This project addresses the following technical barriers from the Hydrogen Production section of the Fuel Cell Technologies Office Multi-Year Research, Development, and Demonstration (MYRDD) Plan.

(AG) Integrated Device Configurations

(AH) Reactor Designs

(AI) Auxiliary Materials

(AJ) Synthesis and Manufacturing

Technical Targets

This project is conducting experimental studies and numerical modeling and simulations of a new tandem particle-slurry batch reactor design for solar water splitting that uses photocatalyst semiconductor particle suspensions and consists of two stacked compartments. Insights gained from these studies will be applied toward the design of plant-scale reactors to meet the following DOE hydrogen production targets for dual-bed photocatalyst reactors.

- Cost: ≤$20.00/kg H_2
- STH Energy Conversion Ratio: ≥1% and >3 L H_2 per 8 h of solar illumination

FY 2017 Accomplishments

- Performed techno-economic analyses; the results suggest that our stacked-bed reactor design can generate H_2 at a cost that meets the ultimate DOE target of <$2/kg H_2 for a ~8.5% STH efficient reactor; the side-by-side-reactor design required a ~14.5% STH efficient reactor to achieve this cost.
- Demonstrated *in silico* that a stacked-bed reactor can sustain indefinite operation at 3.8% STH efficiency under diurnal excitation conditions using photocatalyst particles with bandgaps based on state-of-the-art materials (Rh-modified $SrTiO_3$ and $BiVO_4$), concentrations of the IO_3^-/I^- redox shuttle within their solubility ranges, and membrane permeability such that gas crossover remains below the explosive limit.
- Demonstrated that several small-scale prototype reactors containing aqueous photocatalyst particle suspensions can drive H_2 evolution.

✧ ✧ ✧ ✧ ✧

INTRODUCTION

Economically, particle slurry reactors are projected to be one of the most promising technologies for clean solar photoelectrochemical hydrogen production via water splitting, according to a 2009 techno-economic analysis commissioned by the DOE and performed by Directed Technologies, Inc. [1,2]. This techno-economic analysis compared four plausible reactor designs: two panel-based reactors, which resembled typical wafer-based solar cells immersed in a liquid electrolyte, and two particle-slurry reactors. On an energy basis, the hydrogen produced from the particle-slurry reactors was projected to be by far the most cost-competitive with fossil fuels, further supporting the viability of the hydrogen economy. This project describes a new design for a particle-slurry reactor, where the main innovation is the use of a stacked-compartment arrangement, instead of the typical design where the compartments are arranged side-by-side (Figure 1a). By stacking the compartments, which results in much shorter mass transport distances and provides efficiency advantages due to the tandem light absorbers, it is projected that over five times less piping and pumps are required to circulate the electrolyte, which results in a cost that is half that of the least expensive proposed particle-slurry reactors to date (Figure 1b).

As part of the proposed work plan, the device physics of the reactor designs were numerically modeled and simulated, and it was determined that in the absence of piping and pumps, a 3.8% STH efficient reactor could operate indefinitely, for compartments that are each 1 cm tall, and including absorption by soluble state-of-the-art particles present at ideal particle concentrations and the common IO_3^-/I^- redox shuttle below its aqueous solubility limit. It was also determined that photocatalyst particles with smaller bandgap energies could drive a sustainable reactor using our design at a 10% STH efficiency. These results are significant because achieving the 3.8% STH efficiency metric would meet the 2015 MYRDD Plan targets, while demonstrating the 10% STH efficiency metric with inexpensive particle materials would meet the ultimate MYRDD Plan target. We have also fabricated and tested small-scale experimental prototypes to aid in numerical model validation and to isolate the effects of underlying physical phenomena on the overall reactor performance. By direct mass spectroscopic detection, we have observed H_2 evolution during illumination of photocatalyst particle suspensions. Eventually, we will leverage the numerical model and small-scale prototypes to experimentally evaluate a benchtop-scale (12 in x 12 in) reactor prototype. Toward this, we have synthesized several state-of-the-art semiconductor nanoparticle photocatalysts and evaluated them experimentally: Rh-modified $SrTiO_3$, $BiVO_4$, and WO_3 [3].

APPROACH

The overarching approach to achieving the objectives of the project was to combine theoretical and numerical modeling efforts with experimental measurements to design and optimize reactor performance. Simulation results were used to evaluate the feasibility of various reactor parameters, including overall design and dimensions of the reactor, properties and characteristics of the semiconductors and electrocatalysts, and concentration of redox-active electrolyte. This information was then used to synthesize state-of-the-art materials, characterize and engineer their relevant properties, and evaluate their overall efficacy in prototype reactors for solar hydrogen production. In general, the numerical and experimental data sets were in good agreement, therefore validating this choice of physical phenomena and equations used in the simulations. Discrepancies between theory and experiments were used to fine-tune each via a checks-and-balances process.

RESULTS

The numerical model was used to evaluate the reactor size and concentrations of semiconductor particle and redox shuttle that would enable at least a 1% STH efficiency,

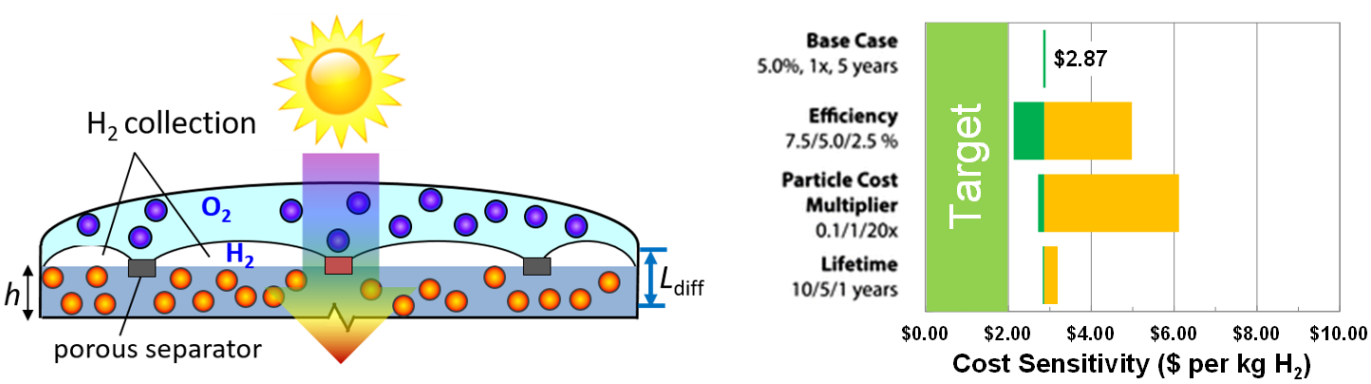

FIGURE 1. (a) Schematic of the vertically stacked particle-suspension reactor design which affords tandem light absorption for Z-scheme solar water splitting. (b) Results from a techno-economic analysis and sensitivity analyses performed using the DOE H2A tool for hydrogen production using a Type 2 reactor design (https://www.hydrogen.energy.gov/h2a_production.html) [1,2].

consistent with the prior go/no-go decision. While the go/no-go decision required modeling 10 cm tall reactor compartments, which are consistent with the heights modeled in prior techno-economic analyses of similar reactor designs [1,2], this is not a strict functional requirement for these reactors, so intermediate compartment heights down to 1 cm each were considered. The main physical processes incorporated into the model are shown in Figure 2a.

From the standpoint of designing a reactor to operate sustainably with only passive diffusion facilitating mass transport, the main factors we considered were the diffusivity and aqueous solubility of the redox shuttle and the tradeoffs in increasing the redox shuttle concentration on competitive light absorption. Based on reported data in the literature, iodine-based and iron-based redox shuttles (I_3^-/I^-, IO_3^-/I^-, and Fe^{3+}/Fe^{2+}) have been used in the most efficient tandem particle suspensions [3]. However, at the estimated minimum species concentrations needed to sustain indefinite reactor operation, i.e., 0.1–2.5 M, only the proton-coupled electron-transfer redox shuttle IO_3^-/I^- transmitted sufficient light to enable efficient operation. Model results indicated that for 1 cm tall compartments and concentrations of the redox shuttle that were less than the solubility limit (~0.4 M), a reactor operating at a 3.8% STH efficiency would reach approximate steady-periodic operating conditions in about three days (Figure 2b). *These results are important to achieving the DOE MYRDD Plan targets because they demonstrate the validity of the reactor design for a >1% STH efficient system with no physical limitations to infinitely long-term operation.*

Other physical processes that are being explored outside of the main inclusive modeling framework are effects of light scattering and thermal transport, including natural convection. In order to validate the computational approaches, model experiments using small-scale prototypes are being performed.

Figure 3 shows the overall small-scale prototype setup and gas flow diagram including mass spectrometric gas detection during photocatalytic H_2 evolution from particle suspensions. Also shown is a photograph of the small-scale reactor and data obtained using this experimental setup for Rh-modified $SrTiO_3$ particles at varying concentrations of each half of the iron aquo redox shuttle. The detection system relies on atmospheric pressure inline gas detection with an argon carrier gas and has a ~10 second detection limit. These are the first quantitative results obtained using this reactor and gas detection system and are important to achieving DOE targets because they demonstrate that a two-particle tandem particle-slurry reactor is regenerative and can evolve H_2 upon simulated solar illumination. Notably, the quantum yield for H_2 increased as the concentration of Fe(II) increased, likely because Fe(II) is required to regenerate the initial state of the photocatalyst particles during H_2 evolution. Conversely, the quantum yield for H_2 decreased as the concentration of Fe(III) increased, likely because Fe(III) competes with protons for reduction by photogenerated electrons in the photocatalyst particles.

Figure 4 shows design drawings and digital photographs of the larger-scale prototype reactor with two cubic compartments, each 1 L in volume, and a height dimension that can be easily adjusted. A slightly larger version of this reactor will be used to assess the ultimate project goal in terms of STH efficiency and long-term on-sun studies. These results are important to achieving DOE targets because they

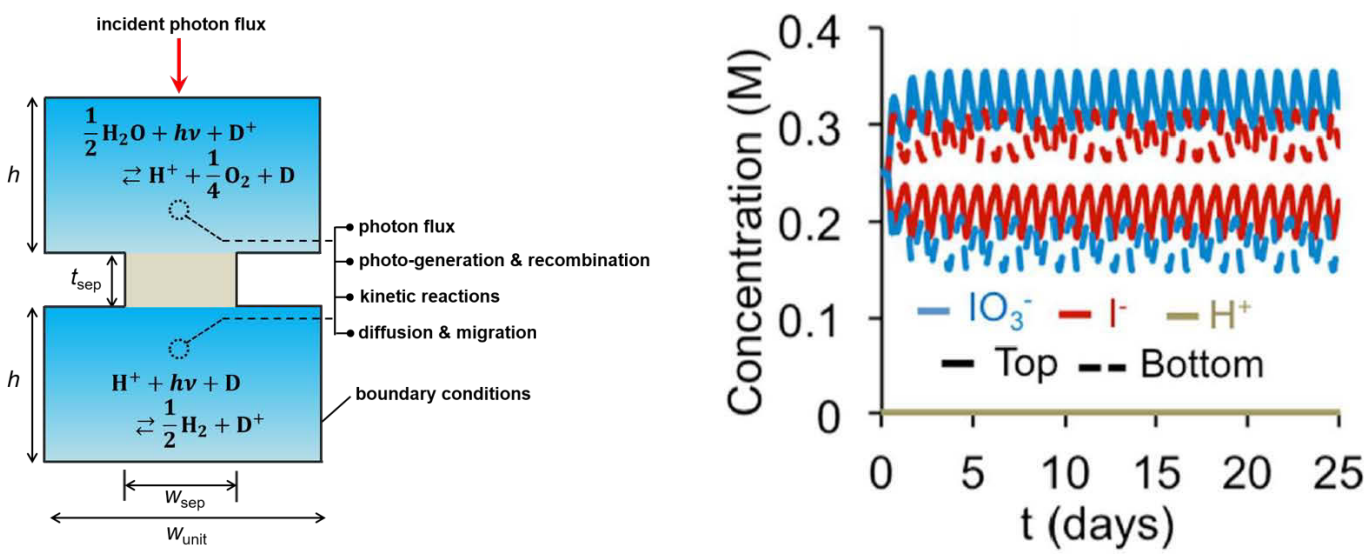

FIGURE 2. (a) Numerical device physics modeling domain for the concept shown in Figure 1a indicating the major physical processes that are incorporated into the model. (b) Average redox shuttle concentrations in each compartment as a function of time, for 1 cm tall compartments containing the IO_3^-/I^- redox shuttle (initially 0.25 M of each species) and Rh-modified $SrTiO_3$ (top, hydrogen evolution reaction [HER], 3.3×10^{-3} g L^{-1}) and $BiVO_4$ (bottom, oxygen evolution reaction [OER], 3.7×10^{-3} g L^{-1}) operating at a 3.8% STH efficiency.

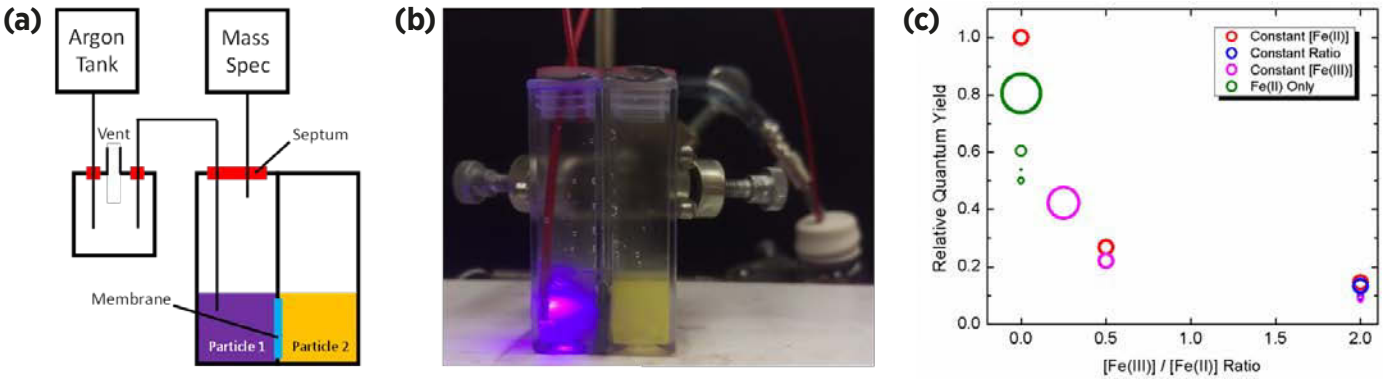

FIGURE 3. (a) Scheme and (b) digital photograph of a thin-pathlength particle suspension reactor prototype made of quartz and containing particles of Rh-modified $SrTiO_3$ in the left compartment and particles of $BiVO_4$ in the right compartment, with an intervening dialysis membrane. Optical illumination using 405 nm light was incident from the left side onto the Rh-modified $SrTiO_3$ compartment, and shown is tubing for gas flow from an Ar tank through the rapidly stirred Rh:$SrTiO_3$ compartment and to a mass spectrometer. (c) Relative quantum yield of H_2 detected by mass spectrometry during illumination of a suspension of Rh-modified $SrTiO_3$ particles with 405 nm laser light and containing a varied concentration of the Fe(II) aquo redox shuttle (ranging from 2 mM to 50 mM, denoted by marker size) and a varied Fe(III):Fe(II) ratio. Each color represents one series of experiments where only one parameter was varied. The relative size of each data point represents the concentration of Fe(II) used. Some decrease in the signal over time for the experiments containing Fe(II) only was attributed to aggregation of the particles on the sides of cuvette.

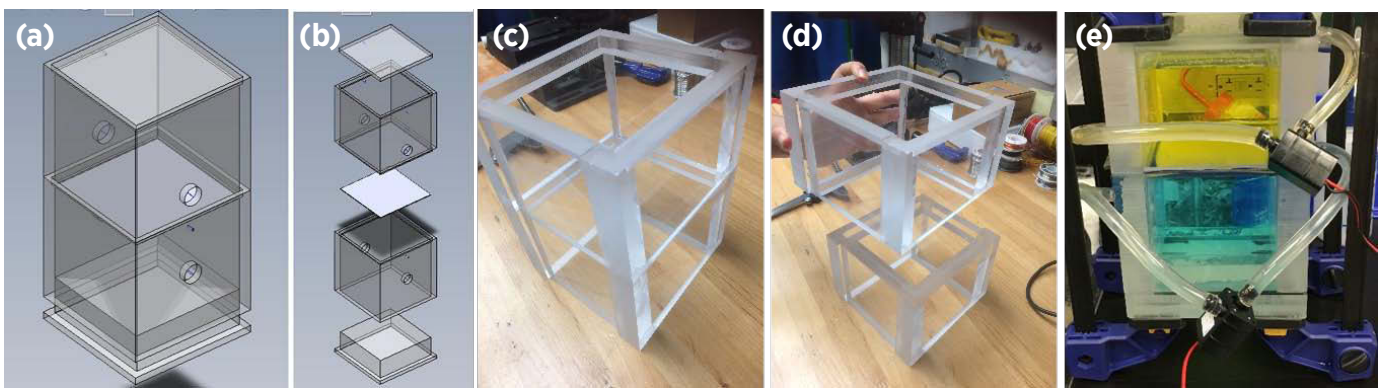

FIGURE 4. (a,b) Computer-aided design drawings and (c,d,e) digital photographs of a particle suspension reactor prototype containing dye solutions in each compartment to highlight the geometry and slow diffusive flux through a nanoporous separator. Each reactor compartment is 4 in x 4 in x 4 in, contains an adjustable borosilicate glass window on the top of the reactor, contains custom Viton seals between the top and bottom compartments to attenuate leaking, and enables forced convection through active pumping circulation of the electrolyte.

demonstrate that a reactor of near complete size exists to measure the ultimate milestone and project target of this work.

CONCLUSIONS AND UPCOMING ACTIVITIES

Numerical models, simulations, and techno-economic analyses suggest that a dual bed reactor consisting of stacked compartments and no convection can achieve at least a 1% STH efficiency and as much as a 10% STH efficiency when 1 cm tall reactor compartments and the appropriate redox shuttle are utilized. Benchtop-scale reactors have been built and H_2 has been detected from smaller-scale reactors using a new mass spectrometric detection system. Ultimately, the proposed photocatalyst particles, cocatalysts, and redox shuttles will be assessed using benchtop-scale prototypes with ~12 in x 12 in illumination areas and with a target of generating >3 L of H_2 per 8 h of solar illumination. No additional work beyond this project is likely, but open issues remain, including photocatalyst particle size effects on individual particle physics and reactivity, effects of optical scattering and thermal natural convection, optimization of photocatalyst particle performance with and without cocatalysts, and design rules for efficient photocatalyst particles.

FY 2017 PUBLICATIONS/PRESENTATIONS

1. R. Bala Chandran, S. Breen, Y. Shao, S. Ardo, A.Z. Weber, *Energy Environ. Sci*., 2017, *Advance Article,* DOI: 10.1039/C7EE01360D, "Evaluating particle-suspension reactor designs for Z-scheme solar water splitting *via* transport and kinetic modeling."

2. C. Xiang, A.Z. Weber, S. Ardo, A. Berger, Y. Chen, R. Coridan, K. Fountaine, S. Haussener, S. Hu, R. Liu, M.A. Modestino, M. Shaner, M. Singh, J. Stevens, K. Sun, K. Walczak, *Angew. Chem. Int. Ed.,* **2016**, *55*, 12974–12988, "Modeling, Simulation, and Implementation of Solar-Driven Water-Splitting Devices."

3. S. Ardo, *U.S. DOE EERE FCTO Annual Merit Review,* **June 2017**, Washington, DC, "Tandem particle-slurry batch reactors for solar water splitting."

4. W. Gaieck, K. Tkacz, C.D. Sanborn, Y. Shao, S. Breen, H. Yaghoubi, R. Bala Chandran, A.Z. Weber, S. Ardo, *231st Electrochemical Society Spring National Meeting*, **May 2017**, New Orleans, LA, *(Invited)* "Recent Progress in Fundamental Photoelectrochemical Studies Relevant to New Low-Cost Designs for Z-Scheme Solar Water Splitting Reactors."

5. R. Bala Chandran, L.-C. Weng, S. Ardo, A.T. Bell, A.Z. Weber, *231st Electrochemical Society Spring National Meeting*, **May 2017**, New Orleans, LA, *(Invited)* "Mathematical Modeling of Novel Artificial-Photosynthesis Devices."

6. R. Bala Chandran, S. Ardo, A.Z. Weber, *2016 Materials Research Society Fall National Meeting & Exhibit*, **December 2016**, Boston, MA, "Modeling Transport and Interfacial Effects in a Particle-Suspension Reactor for Solar Water Splitting."

7. W. Gaieck, K. Tkacz, C.D. Sanborn, Y. Shao, S. Breen, R. Bala Chandran, H. Yaghoubi, C. Xiang, A.Z. Weber, S. Ardo. *2016 American Institute of Chemical Engineers Fall National Meeting*, **November 2016**, San Francisco, CA, *(Invited; Plenary)* "Photocatalysis for Z-Scheme Solar Water Splitting Using New Reactor Designs."

8. W. Gaieck, K. Tkacz, C.D. Sanborn, Y. Shao, S. Breen, R. Bala Chandran, H. Yaghoubi, C. Xiang, A.Z. Weber, S. Ardo. *2016 Pacific Rim Meeting (PRiME) on Electrochemical and Solid-State Science, Joint International Meeting of the Electrochemical Society of the United States of America and Japan,* **October 2016**, Honolulu, HI, *(Invited)* "New Reactor Designs for Z-Scheme Solar Water Splitting Photocatalysis."

9. K. Tkacz, C.D. Sanborn, S. Ardo. *Pacific Rim Meeting (PRiME) on Electrochemical and Solid-State Science, Joint International Meeting of the Electrochemical Society of the United States of America and Japan*, **October 2016**, Honolulu, HI, "Photoelectrochemical Evaluation of Single Nanoparticles."

REFERENCES

1. Directed Technologies, Inc., *DOE Project Report*, **December 2009**, Contract Number: GS-10F-009J, *Technoeconomic Analysis of Photoelectrochemical (PEC) Hydrogen Production*.

2. B.A. Pinaud, J.D. Benck, L.C. Seitz, A.J. Forman, Z. Chen, T.G. Deutsch, B.D. James, K.N. Baum, G.N. Baum, S. Ardo, H. Wang, E. Miller, and T.F. Jaramillo, *Energy Environ. Sci*., **2013**, *6(7)*, 1983–2000, "Technical and economic feasibility of centralized facilities for solar hydrogen production via photocatalysis and photoelectrochemistry."

3. D.M. Fabian, S. Hu, N. Singh, F.A. Houle, T. Hisatomi, K. Domen, F.E. Osterloh, and S. Ardo, *Energy Environ. Sci*., **2015**, *8(10)*, 2825–2850, "Particle Suspension Reactors and Materials for Solar-Driven Water Splitting."

II.E.1 Biomass to Hydrogen (B2H2)

Pin-Ching Maness (Primary Contact),
Katherine Chou, Lauren Magnusson, Jonathan Lo, and Wei Xiong
National Renewable Energy Laboratory (NREL)
15013 Denver West Parkway
Golden, CO 80401
Phone: (303) 384-6114
Email: pinching.maness@nrel.gov

DOE Manager: Katie Randolph
Phone: (720) 356-1759
Email: Katie.Randolph@ee.doe.gov

Subcontractor:
Bruce Logan, Pennsylvania State University (PSU)

Start Date: July 2015
Projected End Date: Project continuation and direction determined annually by DOE

Overall Objectives

- Optimize rates and yields of hydrogen production in a sequencing fed-batch bioreactor by varying hydraulic retention time and reactor volume replacement.
- Improve biomass utilization by engineering *C. thermocellum* to co-utilize both the six-carbon (C6) sugars (cellulose) and five-carbon (C5) sugar (hemicellulose) to lower feedstock cost.
- Optimize genetic tools to transform *C. thermocellum* and obtain mutants lacking the targeted competing pathway to improve hydrogen molar yield.
- Demonstrate hydrogen production from the NREL fermentation effluent to improve overall energy efficiency in hydrogen production from cellulosic biomass using a microbial electrolysis cell (MEC) reactor.

Fiscal Year (FY) 2017 Objectives

- Optimize sequencing fed-batch parameters and ferment corn stover lignocellulose to hydrogen with a rate of 2.5 L-H_2/L/d.
- Engineer *C. thermocellum* to co-utilize both the C6 (cellulose-derived) and C5 (hemicellulose-derived) sugars to improved biomass utilization, hence lowering feedstock cost.
- Use the genetic tools developed at NREL tailored for *C. thermocellum* and delete enzymes involved in the interconversion of the various cellular redox cofactors, aimed to improve hydrogen molar yield via fermentation.
- Examine alternative materials and catalysts for the cathode and achieve H_2 production rate to 1.2 L/$L_{reactor}$/d without platinum catalyst.
- Design smaller volume of MEC reactor to further enhance the H_2 production rate to a goal of 2.4 L-H_2/L/d.

Technical Barriers

This project supports research and development on DOE Technical Task 6, subtasks "Molecular and Systems Engineering for Dark Fermentative Hydrogen Production" and "Molecular and Systems Engineering for MEC," and it addresses barriers AX, AY, and AZ.

(AX) H_2 Molar Yield

(AY) Feedstock Cost

(AZ) System Engineering

Technical Targets

See Table 1.

TABLE 1. Progress toward Meeting DOE Technical Targets in Dark Fermentation

Characteristics	Units	Current Status	2015 Target	2020 Target
Yield of H_2 from glucose	Mole H_2/mole glucose	2–3.2	6*	--
Feedstock cost	Cents/lb glucose	13.5	10	8
Duration of continuous production (fermentation)	Time	17 days	3 months	--
MEC cost of electrodes	$/m^2	$2,400	$300	$50
MEC production rate	L-H_2/L-reactor-d	1	1	---

*Yield of H_2 from glucose: DOE has a 2015 target of an H_2 molar yield of 6 (4 from fermentation and 2 from MEC) from each mole of glucose as the feedstock, derived from cellulose.
Feedstock cost: The DOE Bioenergy Technologies Office is conducting research to meet its 2015 target of 10 cents/lb biomass-derived glucose. NREL's approach is to use cellulolytic microbes to ferment cellulose and hemicellulose directly, which will result in lower feedstock costs.

FY 2017 Accomplishments

- Identified and replaced the yeast extract nutrient component with industrial waste product in the *C. thermocellum* growth media with no impact on cell fitness or H_2 production. The outcome reduced relative cost of the medium by up to 49% when the costly yeast extract was replaced with industrial corn steep liquor without impacting H_2 production.
- A *C. thermocellum* mutant was generated which can co-utilize both C6 sugar and C5 sugar simultaneously without cross inhibition. We detected twice as much hydrogen production when both sugars were present as that in either sugar alone.
- Two *C. thermocellum* mutants were generated; one lacks the enzyme catalyzing the interconversion of nicotinamide adenine dinucleotide phosphate (NADPH) and nicotinamide adenine dinucleotide (NADH) (Mutant 1) and another enzyme in the interconversion of NADH and ferredoxin (Mutant 2). Mutant 1 exhibited 29% increase in total H_2 production and 55% increase in specific rate of H_2 production. Mutant 2 produced 35% more total H_2. Findings from both mutants validate the effectiveness of metabolic engineering.
- H_2 production rate with stainless steel (SS) wool (a non-Pt based cathode) reached to 1.3±0.3 L-H_2/L/d which is comparable to the rates with Pt cathode using synthetic fermentation effluent.

✧ ✧ ✧ ✧ ✧

INTRODUCTION

Biomass-derived glucose feedstock is a major operating cost driver for economic hydrogen production via fermentation. DOE's Fuel Cells Technologies Office is taking advantage of the DOE's Bioenergy Technology Office's investment in developing less expensive glucose from biomass to meet its cost target of 10 cents/lb by 2015. One alternative and viable approach to addressing the glucose feedstock technical barrier (Barrier AZ) is to use certain cellulose-degrading microbes that can ferment biomass-derived cellulose directly for hydrogen production. One such model microbe is the cellulose-degrading bacterium *Clostridium thermocellum*, which was reported to exhibit one of the highest growth rates using crystalline cellulose [1].

Another technical barrier to fermentation is the relatively low molar yield of hydrogen from glucose (mol H_2/mol sugar; Technical Barrier AX) using existing metabolic pathways in the cells. Biological pathways maximally yield 4 mol hydrogen per 1 mol glucose (the biological maximum) [2]. However, most laboratories have reported a molar yield of 2 or less [3,4]. Molecular engineering to block competing pathways is a viable option toward improving H_2 molar yield. This strategy has resulted in improved hydrogen molar yield in *Enterobacter aerogenes* [5].

A promising parallel approach to move past the biological fermentation limit has been developed by a team of scientists led by Bruce Logan at PSU. In the absence of O_2, and by adding a slight amount of negative potential (-250 mV) to the circuit, Logan's group has produced hydrogen from acetate (a fermentation byproduct) at a molar yield of 2.9–3.8 (versus a theoretical maximum of 4) in a modified microbial fuel cell called an MEC [6]. It demonstrated for the first time a potential route for producing up to eight moles of hydrogen per mole of acetate or potentially up to 12 moles of hydrogen per mole of glucose when coupled to a dark fermentation process. Indeed, in FY 2009 the team reported a combined molar yield of 9.95 when fermentation was coupled to an MEC in an integrated system [7]. Combining fermentation with MECs could therefore address Technical Barrier AX and improve the techno-economic feasibility of hydrogen production via fermentation.

APPROACH

NREL's approach to addressing high feedstock cost is to optimize the performance of the cellulose-degrading bacterium *C. thermocellum* using corn stover lignocellulose as the feedstock. To achieve this goal, we are optimizing the various parameters in a sequencing fed-batch reactor to improve longevity, yield, and rate of H_2 production, using corn stover biomass pretreated via a de-acetylation and mechanically refined (DMR) process. We also engineer *C. thermocellum* to utilize all the sugars in biomass (both C6 and C5) aimed to lower feedstock cost. To improve hydrogen molar yield, we are selectively blocking competing metabolic pathways in this organism via genetic methods. Through a subcontract, PSU is testing the performance of an MEC using both a synthetic effluent and the real waste stream from lignocellulosic fermentation generated at NREL.

RESULTS

Lower Medium Cost for Lignocellulose Fermentation

C. thermocellum is normally cultured in a growth medium containing buffer, mineral salts, and vitamins. The addition of hydrolyzed yeast extract (0.45%, w/v at $201.5/kg) boosts cell growth due to the presence of amino acids (also serve as nitrogen nutrient), vitamins, and a few inorganic compounds. We evaluated and tested several sources of yeast extract, including Brewers yeast ($95.7/kg), corn steep liquor (CSL; $49.4/kg) (both costs cited from the Sigma Aldrich Chemical Co.), and the industrial waste corn steep liquor from Solulys ($0.61/kg). Hydrogen production with these supplements were compared with two controls where autohydrolyzed yeast extract was added (Rich) and where the cells were cultured in the absence of both yeast extract and

vitamins (Base). Data from Table 2 show that higher amount of H_2 was produced in all cases where various forms of yeast extract were added, and the outputs were comparable with that from the "Rich" medium. Industrial CSL show the most promise due to its low cost. Table 2 summarizes the amounts of H_2 produced and the medium cost per liter, with industrial CSL from Solulys realized a 49% saving in the growth medium cost, without compromising H_2 production.

TABLE 2. Amount of H2 Produced, and Overall Medium Cost when Supplemented with Comparable Concentration (0.45%, w/v) of Brewer's Yeast, Corn Steep Liquor, and Solulys Industrial CSL

	H_2 (mM)	Medium* Cost ($/L)
Rich	38.8	1.85 (1X)
BY	48.1	1.38
CSL	45.6	1.39
Industrial CSL	47.8	0.95 (0.51X)

Co-metabolism of six-carbon (cellulose-derived) and five-carbon (hemicellulose-derived) sugars to improve biomass utilization

DMR-pretreated biomass generates a solid fraction containing both cellulosic (C6) and hemicellulosic (C5) sugars. *C. thermocellum* naturally can ferment cellulose directly to H_2 without needing expensive cellulase enzyme cocktail, yet the wild-type strain lacks the ability to metabolize C5 sugar. Demonstrating co-metabolism of C6/C5 sugars hence is the goal in FY 2017 to improve the economic feasibility of fermentative H_2 production. We generated *C. thermocellum* mutant lines capable of co-metabolizing xylose (C5 hemicellulosic sugar) with either glucose or cellobiose (cellulose-derived glucose dimer) with no cross-inhibition, a seminal observation in a cellulose-degrading microbe. The mutant line yielded twice as much H_2 when both avicel (model cellulose) and xylose are present, when compared to either substrate alone. The outcomes illustrate a significant improvement in biomass conversion to H_2 with lower biomass feedstock cost.

Metabolic Engineering

The goal of this approach is to use genetic tools to inactivate genes encoding competing metabolic pathways, thus redirecting more cellular flux (i.e., electrons) to improve H_2 molar yield. We have designed a plasmid suited for genetic transformation in *C. thermocellum* strain DSM 1313 as the model cellulose-degrader. Following the protocols developed by Argyros et al. [10], we have created mutants lacking either the enzyme catalyzing the interconversion of NADPH and NADH (Mutant 1), or the interconversion of reduced ferredoxin and NADH (Mutant 2). The aim is to conserve more reduced ferredoxin and/or NADH. Mutant 1 exhibited a 29% increase in total H_2 production and 55% increase in specific rate of H_2 production. Mutant 2 produced 35% more total H_2 with a concomitant decrease in both ethanol and lactate production. Findings from both mutants validate the effectiveness of metabolic engineering in increasing H_2 output without compromising cell growth or fitness.

Hydrogen Production by MECs with 3-D SS materials (non-Pt based catalyst)

The goal of this project is to avoid using precious metal catalysts while maintaining or improving hydrogen production rates. We evaluated several different SS cathodes with different 3-D architectures (SS mesh, felt, wool and brush) in a larger-scale MEC (anode volume: 100 mL, cathode volume: 68 mL) in the absence and present of catholyte recirculation (50 mM phosphate buffer solution, 250 mL). Synthetic fermentation wastewater composed of acetate, glucose, ethanol, lactate and protein was continuously provided into the anode chamber at a hydraulic retention time of 8 h. The highest H_2 production rate (1.3±0.3 L-H_2/L/d) was observed with SS wool, and the lowest with SS mesh (0.9±0.1 L-H_2/L/d). The H_2 production rate with SS wool was comparable to the rate with Pt cathode (1.3±0.1 L-H_2/L/d) (Figure 1). The good H_2 production rates with SS wool, fiber felt and brushes compared to the SS mesh was likely due to the higher specific surface areas of these materials compared to the SS mesh which was flat and relatively non-porous. Catholyte recirculation was important for improving H_2 production rates (and current densities) as the rates decreased in MECs that did not have recirculation.

Anode Chamber Design

The goal of this project is to see if the use of flat anodes, or smaller brush anodes, could further reduce the anode chamber volume and thus result in greater hydrogen

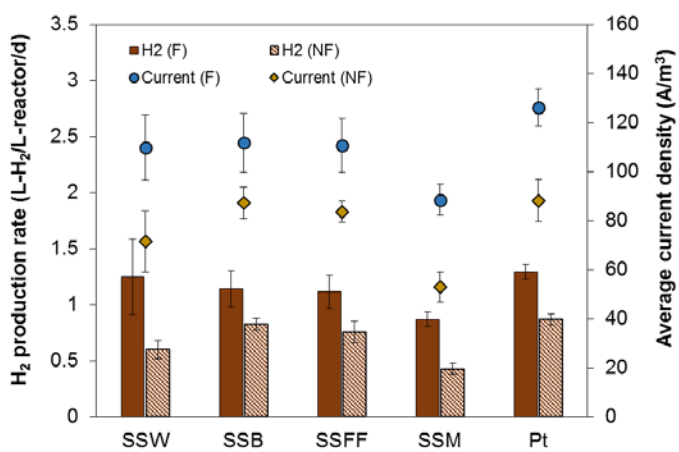

SSW – SS wool; SSM – SS mesh; SSFF – SS fiber felt; SSB – SS brushes

FIGURE 1. Hydrogen production rates (L-H_2/L-d) and current densities (A/m^3) of MECs with SS materials with a catholyte recirculation (F, 40 mL/min flow rate) or without recirculation flow (NF, 0 mL/min) (applied voltage of 0.9 V; error bars indicate ±SD, with n > 5).

production rates per volume of reactor. Two chamber reactors (14 mL anode, 28 mL cathode) with anion exchange membranes were used to examine H_2 production rates using flat carbon felt or carbon brush anodes in MECs using fed batch mode. MECs were fed sodium acetate (2 g/L) in 50 mM phosphate buffer at an applied voltage of 0.9 V. Brushes performed better, as the average current density was greater for brush anodes (3.8±0.4 A/m^2) than felt anodes (2.9±0.1 A/m^2). The average chemical oxygen demand (COD) removals were 89±2% for the brush anode and 71±2% for the felt anode. The higher current densities and greater COD removals were consistent with the higher hydrogen production rates for the brush anodes (0.38±0.06 L-H_2/L/d) compared to the felt anodes (0.32±0.02 L-H_2/L/d). The shape of the felt anode current profile (a sharp initial peak) suggested that mass transfer of acetate to the anode was limiting performance. When the anolyte was stirred, the current density and COD removals increased to 4.7±0.4 A/m^2 and 92±1%, with a hydrogen production increased to 0.41±0.04 L-H_2/L/d, confirming the mass transfer limited operation with the felt anode.

CONCLUSIONS AND UPCOMING ACTIVITIES

- We determined that the expensive yeast extract nutrient can be replaced with a commercial waste product, the CSL from Solulys, without compromising H_2 production. The replacement lowers the medium cost by 49% and is promising in scale-up H_2 production.
- We generated *C. thermocellum* mutant lines capable of using all the sugars in biomass leading to improved H_2 production with lower biomass feedstock cost.
- We deleted enzymes involved in the interconversion of NADH, NADPH, and ferredoxin, leading to conserving more reduced ferredoxin. The mutants indeed displayed higher specific rate and total H_2 production. These mutants will serve as the hosts for additional genetic engineering in future research to increase H_2 production and molar yield.
- Expensive Pt catalyst can be replaced with non-precious catalyst (e.g,. stainless steel) with larger surface area and we could obtain higher H_2 production rates by using catholyte recirculation.
- Anode volume could be further reduced using a felt electrode, but mass transfer needs to be improved to maintain performances.

In the future, we will operate the sequencing fed-batch bioreactor fermenting DMR-pretreated corn stover lignocellulose with increased solid loading to achieve a H_2 production rate of 2.5 L-H_2/L/d. We will determine what essential genes are needed to enable *C. thermocellum* mutant line to utilize xylan or hemicellulose (complex C5 sugars) directly to enhance its utilization. Deleting the ethanol-competing pathway is deemed essential to redirect more electrons toward H_2 production and will continue to be a part of this effort. Past efforts had led to unstable isolates likely due to redox imbalance. We will delete the ethanol pathway in the mutant hosts with altered balance/pools of NADH/NADPH/ferredoxin to achieve redox stability. The task using ionic liquid pretreatment was closed out in Q1, FY 2017. We will continue to examine alternative materials and catalysts for the cathode to improve reactor operation aimed at increasing H_2 production and lowering MEC cost. We will also examine a smaller reactor volume to further enhance the H_2 production rate to a goal of 2.4 L-H_2/L/d.

FY 2017 PUBLICATIONS/PRESENTATIONS

1. Xiong, W., P.P. Lin, L. Magnusson, L. Warner, J.C. Liao, and P.C. Maness. 2016. CO_2-fixing one-carbon metabolism in a cellulose-degrading bacterium *Clostridium thermocellum*. Proc. Natl. Acad. Sci. (USA). 113: 13180–13185.

2. Kim, K.-Y. and Logan, B.E. 2017. Evaluation of alternative cathode materials for hydrogen production in microbial electrolysis cells (MECs), Abstract Proceedings of the Association of Environmental Engineering and Science Professors (AEESP) 2017 Conference, University of Michigan, Ann Arber, June 20–22, 2017.

3. Maness, P.C. 2017. DOE Fuel Cell Technology Office Annual Merit Review, June 7, 2017, Washington, DC. Presentation PD038.

REFERENCES

1. Zhang, Y.P.; Lynd, L.R. (2005). "Cellulose utilization by *Clostridium thermocellum*: bioenergetics and hydrolysis product assimilation." *Proc. Natl. Acad. Sci. USA* **102**, 7321–7325.

2. Hawkes, F.R.; Dinsdale, R.; Hawkes, D.L.; Hussy, I. (2002). "Sustainable fermentative hydrogen production: Challenges for process optimisation." *Intl. J. Hydrogen Energy* **27**, 1339–1347.

3. Logan, B.E.; Oh, S.E.; Kim, I.S.; Van Ginkel, S. (2002). "Biological hydrogen production measured in batch anaerobic respirometers." *Environ. Sci. Technol.* **36**, 2530–2535.

4. Van Ginkel, S.; Sung, S. (2001). "Biohydrogen production as a function of pH and substrate concentration." *Environ. Sci. Technol.* **35**, 4726–4730.

5. Rachman, M.A.; Furutani, Y.; Nakashimada, Y.; Kakizono, T.; Nishio, N. (1997). "Enhanced hydrogen production in altered mixed acid fermentation of glucose by *Enterobacter aerogenes*." *J. Ferm. Eng.* **83**, 358–363.

6. Cheng, S.; Logan, B.E. (2007). "Sustainable and efficient biohydrogen production via electrogenesis." *Proc. Natl. Acad. Sci. USA*. **104**, 18871–18873.

7. Lalaurette, E.; Thammannagowda, S.; Mohagheghi, A.; Maness, P.C.; Logan, B.E. (2009). "Hydrogen production from cellulose in a two-stage process combining fermentation and electrohydrogenesis." *Intl. J. Hydrogen Energy* **34**, 6201–6210.

8. Guss, A.; Olson, D.G.; Caiazza, N.C.; Lynd, L.R. (2012). "Dcm methylation is detrimental to plasmid transformation in *Clostridium thermocellum*." *Biotechnol. Biofuels* **5**, 30–41.

9. Liszka, M., Kang, A., Konda, S., Tran, K., Gladden, J., Singh S., Keasling, J. D., Scown, C. D., Lee, T. S., Simmons, B., Sale, K. L. 2016. "Switchable Ionic Liquids Based on Di-Carboxylic Acids for One-Pot Conversion of Biomass to an Advanced Biofuel," *Green Chemistry*, DOI: 10.1039/C6GC00657D.

10. Argyros, D.; Tripathi, S.A.; Barrett, T.F.; Rogers, S.R.; Feinberg, L.F.; Olson, D.G.; Foden, J.M.; Miller, B.B.; Lynd, L.R.; Hogsett, D.A.; Caiazza, N.C. (2011). "High ethanol titers from cellulose by using metabolically engineered thermophilic anaerobic microbes." F *Appl. Environ. Microbiol.* **77**, 8288–8294.

II.E.2 Sweet Hydrogen: High-Yield Production of Hydrogen from Biomass Sugars Catalyzed by in vitro Synthetic Biosystems

Y-H Percival Zhang (Primary Contact)
Virginia Polytechnic Institute and State University
304 Seitz Hall, Campus mail 0303
Biological Systems Engineering Dept.
Blacksburg, VA 24061
Phone: (540) 808-8985 (cell)
Email: ypzhang@vt.edu

DOE Manager: Katie Randolph
Phone: (240) 562-1759
Email: Katie.Randolph@ee.doe.gov

Contract Number: DE-EE0006968

Subcontractor:
Mike Adams
Biochemistry and Molecular Biology Department
University of Georgia, Athens, GA

Project Start Date: June 15, 2015
Project End Date: December 31, 2017

Overall Objectives

- Decrease the production costs 1,000-fold from ~$10,000/kg (current estimated level) to ~$10/kg of hydrogen as estimated by using the H2A model by the end of the project
- Increase the volumetric productivity five-fold from current levels of ~150 mmol H_2/L/h to 750 mmol H_2/L/h
- Scale up in vitro enzymatic hydrogen production 1,000-fold from 1 mL to 1 L bioreactor.

Fiscal Year (FY) 2017 Objectives

- Decrease H_2 production costs by use of the first set of hyperthermophilic enzymes, the use of nicotinamide adenine dinucleotide (NAD), and coenzyme engineering
- Increase H_2 production rates five-fold (i.e., 750 mmol H_2/L/h)
- Scale up H_2 production volume by 1,000-fold (i.e., 1,000 mL bioreactor).
- Demonstrate 1,000-fold volume scale-up with five-fold increase in H_2 peak production rate (i.e., 750 mmol H_2/L/h) on starch

Technical Barriers

This project addresses the following technical barriers of biological hydrogen production from the Fuel Cell Technologies Office Multi-Year Research, Development, and Demonstration Plan pertaining to dark fermentation:

(AX) Hydrogen Molar Yield

(AY) Feedstock Cost

(AZ) Systems Engineering

Technical Targets

Table 1 lists the project technical targets (i.e., production cost, productivity, and reactor volume) and where our research and development efforts stand to date. The overall goals of this project are to decrease enzymatic H_2 production cost, increase its production rate, and scale up its production volume. Our goals would clear up doubts pertaining to in vitro H_2 production cost, rate, and scalability for future distributed hydrogen production from renewable liquid sugar solution.

FY 2017 Accomplishments

- Achieved the highest biological H_2 generation peak rate: 550 mmole of H_2/L/h (i.e., ~282 L H_2).
- Scaled up recombinant enzyme production by 10,000-fold from several milligrams to up to tens of grams and recombinant hydrogenase production by 100-fold from 10 mg to 1,000 mg.

TABLE 1. Virginia Polytechnic/University of Georgia Status

Targets	Units	June 2016 Project Target	December 2017 Project Target	Year 2020 Plant Gate
Production cost	$/kg H_2	1,000 (estimated)	10	10 (2020 DOE goal for advanced biological generation technologies)
Productivity	mmol H_2/L/h	550 (achieved)	750	2,000 (our goal)
Reactor volume	L of reactor	1.0 (achieved)	1.0	15,625* (our goal)

*1,500 kg H_2 per day

- Designed and validated the first NAD-based pentose phosphate pathway instead of natural nicotinamide adenine dinucleotide phosphate (NADP)-based for an ultra-high rate of biohydrogen production.
- Increased the specific activity of 6-phosphogluconate dehydrogenase (6PGDH) on a low-cost and more stable biomimetic coenzyme–nicotinamide mononucleotide (NMN), to comparable activities on NADP.
- Prolong NAD's life-time by 20-fold by linking NAD with dehydrogenases via polyethylene glycol (PEG), greatly decreasing in vitro biohydrogen production costs.

✧ ✧ ✧ ✧ ✧

INTRODUCTION

Water splitting for H_2 production is critical for sustainable, renewable H_2 production. Water electrolysis suffers from high production costs and low electrolysis efficiencies. Water splitting at high temperature requires high temperature thermal energy sources and raises serious material challenges. Water splitting at low or even ambient temperature is highly desired when considering material challenges, availability of high-temperature thermal energy sources, and distributed H_2 production systems. A few methods conducted at low temperatures are under investigation, including direct photocatalytic water splitting, photo-electrochemical water splitting, photobiological water splitting, and microbial electrolysis cells. However, they suffer from low hydrogen generation rates and/or low energy conversion efficiencies. Also, high density hydrogen storage methods are urgently needed.

Renewable H_2 production via water splitting energized by chemical energy stored in biomass (carbohydrates) is extremely attractive because biomass sugars are the most abundant renewable chemical energy and evenly distributed [1]. However, microbial anaerobic fermentation (dark fermentation) suffers from low H_2 yields, where the theoretical yield is 4 H_2 per glucose according to the reaction: $C_6H_{12}O_6 + 2\ H_2O = 4\ H_2 + 2\ CH_3COOH$ (acetate) $+ 2\ CO_2$. Although microbial electrolysis cells enable the utilization of acetate or other organic matter supplemented with an electrical input to split water to generate more H_2, this two-step conversion requires two reactors, has decreased energy efficiency compared to the theoretical H_2 yield (i.e., 12 H_2 per glucose and water) due to electricity consumption, slow H_2 generation rates, and high capital investment of microbial water electrolysis. Recently, we demonstrated in vitro synthetic enzymatic biosystems to generate theoretical yields of H_2 energized by numerous carbohydrates, such as, starch, cellodextrins, glucose, xylose, and xylooligosaccharides [2]. But some barriers to industrial scale-up potential remain, including (1) enzyme production cost, (2) enzyme stability, (3) coenzyme cost and stability, (4) (slow) reaction rates, and (5) scale-up feasibility [3]. In this project, we address these issues on the laboratory scale.

The economic viability of industrial biomanufacturing mediated by in vitro synthetic enzymatic biosystem has been in debate for nearly 10 years. This year, the first industrial example has been demonstrated for cost-competitive production of myo-inositol from starch in 20,000-L bioreactors in China [4]. Now a 5,000-ton plant is under construction.

APPROACH

The general approach for this project is to apply biochemistry and protein engineering, microbiology, molecular biology, chemistry, and chemical engineering design principles to address technical barriers pertaining to industrial needs of enzymatic hydrogen production (i.e., production costs, reaction rate, and scalability). We have multiple subtasks aiming to achieve each objective. To decrease H_2 production costs (Objective 1), we succeeded in expressing all hyperthermophilic enzymes and purify them by simple heat precipitation, replacing NADP with NAD by coenzyme engineering, and prolonging NAD lifetime (total turnover number [TTN]) by more than 20 times. To increase H_2 generation rates (Objective 2), we developed a kinetic model and identified the rate-limiting steps, constructed novel NAD-based biomimetic electron transport chains, and built enzyme complexes or conjugates featuring electron channeling. To scale up H_2 production (Objective 3), we scaled up recombinant protein production in *E. coli* and recombinant hydrogenase production, as well as demonstrated H_2 production in 1-L bioreactor.

RESULTS

The overall goal of the second phase of this project was to demonstrate 1,000-fold volume scale-up with five-fold increase in H_2 peak production rate (i.e., 750 mmol H_2/L/h) on starch. Figure 1 shows the different electron transport chains from glucose 6-phosphate to H_2 via three key enzymes: glucose 6-phosphate dehydrogenase (G6PDH), 6PGDH, and soluble NiFe-hydrogenase (SHI). The peak H_2 generation rate demonstrated was 550 mmol H_2/L/h (Figure 2) and a maximum H_2 generation rates of 530 mmol lasted for up to 3 h (Figure 3). Such biohydrogen rates are one of the highest biological H_2 production rates reported, compared to dark fermentation, photobiological means, and microbial electrolysis cells.

To decrease H_2 production costs (Objective 1), we have three subtasks: (1) decrease enzyme production and purification costs, (2) engineer the coenzyme preference of dehydrogenases from NADP to NAD to NMN, (3) stabilize

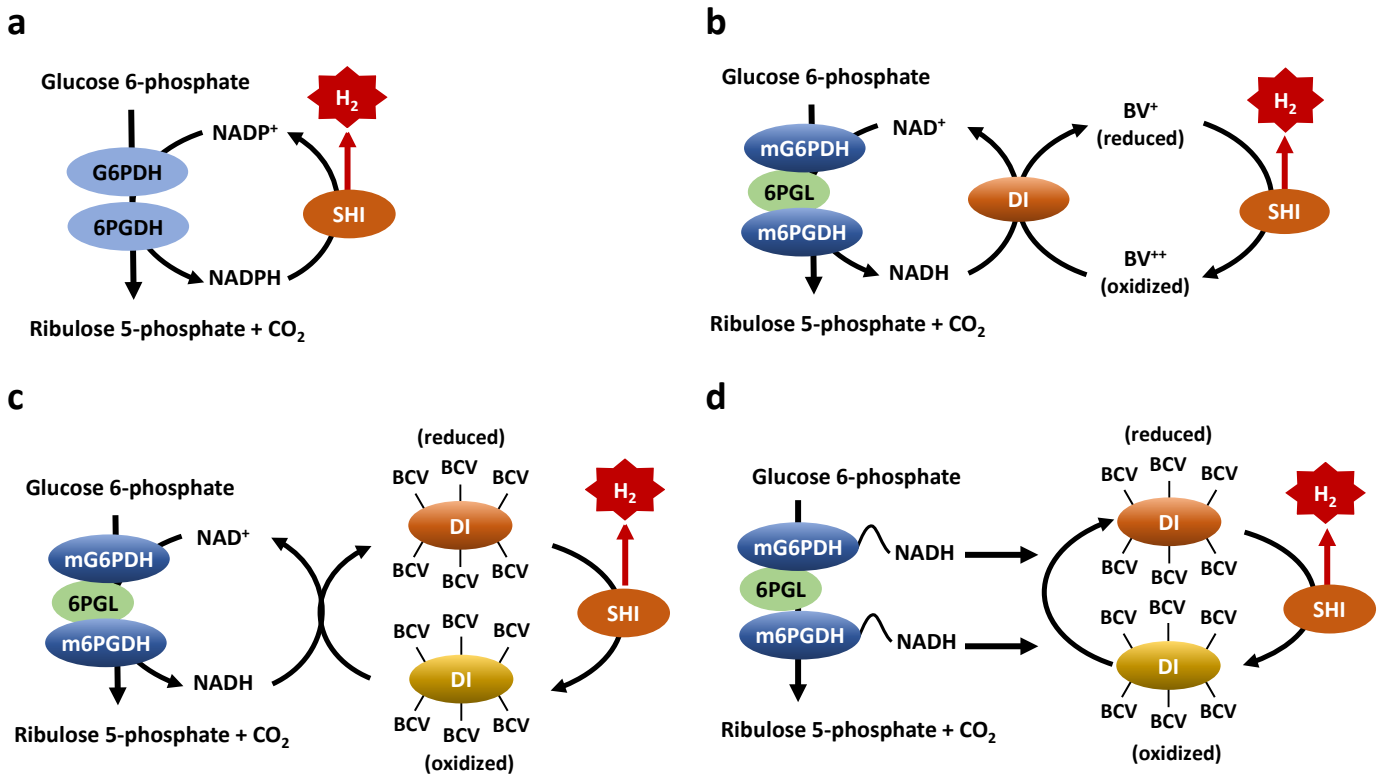

FIGURE 1. Schemes of the electron transport chain (ETC) for in vitro biohydrogen generation, where G6P regeneration via the pentose phosphate pathway is not shown. (a) direct electron transfer from NADPH to H_2 via soluble hydrogenase I (SHI); (b) indirect electron transfer via a biomimetic ETC via engineered NAD-preferred G6PDH (mG6PDH) and engineered NAD-preferred 6PGDH (m6PGDH) via an diaphorase (DI) and an electron mediator benzyl viologen (BV); (c) indirect NAD-based ETC by using a conjugate DI-BCV; and (d) indirect NAD-based ETC by using three conjugates DI-BCV, mG6PDH-NAD, mG6PPDH-NAD.

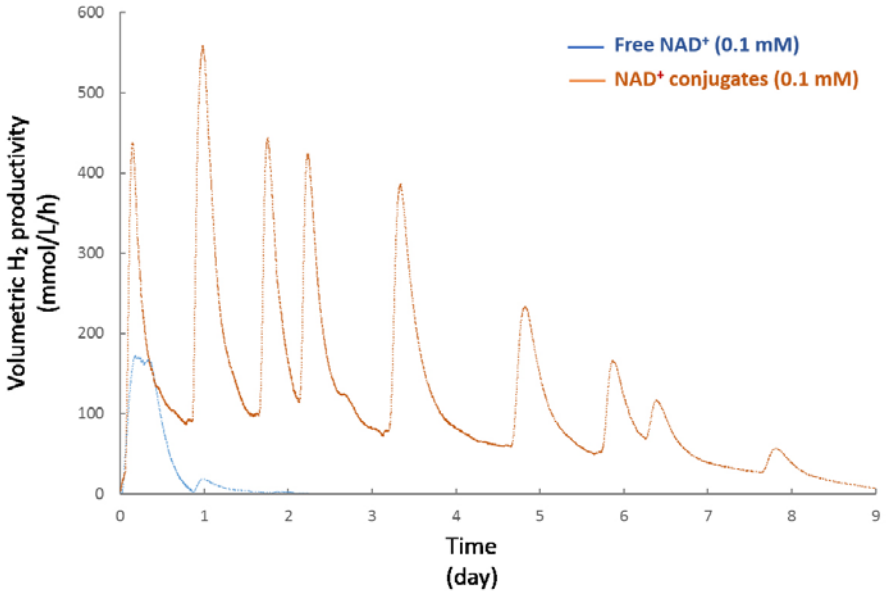

FIGURE 2. The profile of hydrogen generation from maltodextrin at a fed-batch mode via the in vitro pathway comprised of mG6PDH-NAD, mG6PPDH-NAD, DI-BCV and other 12 hyperthermophilic enzymes, in comprison of the pathway based on free NAD at 80°C.

NAD by chemical linkage with dehydrogenases, and (4) complete oxidation of all glucose units of starch.

To decrease enzyme production and purification costs, we succeeded in expressing all hyperthermophilic enzymes in *E. coli*, which are inherently stable at more than 80°C. After high-density fermentation, the cell lysate can be heated at 80°C for 20–30 min. After centrifugation to remove *E. coli* cellular proteins and ultra-filtration to concentrate target enzymes, we can make up to tens of grams of enzymes in one batch fermentation in 6-L fermenter. It is estimated that hyperthermophilic enzyme production costs could be as low as $50/kg on an industrial scale [4,5]. This suggests that enzyme costs are not a showstopper for the in vitro synthetic biology platform.

To decrease coenzyme costs in in vitro biosystems, we did coenzyme engineering, changing the coenzyme preference of two dehydrogenases (i.e., G6PDH and 6PGDH) from $NADP^+$ to NAD^+ and small-size, low-cost biomimic–NMN. The general strategy for coenzyme engineering is based on a combination of rational design and directed evolution. First, coenzyme preference of both hyper-thermophilic G6PDH and 6PGDH has been changed from NADP to NAD without significant activity discounts (manuscript submitted for publication). Therefore, we are able to construct NAD-based electron transport chains (Figure 1b). Second, we developed a novel high-throughput screening methods for rapid identification of NMN-preferred mutants by using a redox dye without influence from *E. coli* intracellular NAD(P). Three, we applied two rounds of rational design followed by four-round directed evolution. Finally, we obtained the best 6PGDH mutant exhibited the comparative activity on NMN with its wild-type enzyme on its natural coenzyme. It means that we have increased 6PDGH activity on NMN by more than 100-fold. Now we attempt to increase G6PDH activity on NMN. This result suggests a great opportunity of coenzyme engineering by using much cheaper biomimetic coenzymes. Besides its application for in vitro biohydrogen production, this breakthrough will have great impacts on biosynthesis of chiral compounds.

To decrease coenzyme costs in in vitro biosystems, we linked NAD with G6PDH and 6PGDH through chemical linkage via polyethylene glycol. Figure 2 shows the profiles of H_2 generation by using NAD-linked dehydrogenases and free NAD. Free NAD degraded rapidly, having a TTN value of 5,000 at 80°C. When NAD was linked with dehydrogenases (Figure 1d), its TTN value was increased to more than 100,000 by more than 20-fold, where maltodextrin was re-added a lot of times. Also, this in vitro synthetic systems can produce hydrogen 80°C for more than one week (Figure 3).

To increase starch utilization efficiency, we applied three supplementary enzymes (that is, isoamylase debranching amylopectin, 4-glucosyltransferase extending maltose to long-chain amylodextrin, and polyphosphate glucokinase utilizing glucose) to achieve in vitro complete oxidation of starch for the first time. As a result, starch is the best hydrogen storage compound as compared to other carbohydrates (Figure 4). Starch has a gravimetric hydrogen storage of more than 14% (wt/wt), where water is recycled from proton exchange membrane fuel cells.

To increase volumetric productivity of H_2 (Objective 2), we increased reaction temperature to 80°C by using the first set of hyperthermophilic enzymes. Furthermore, we designed a biomimetic ETC from NADH generated from glucose 6-phosphate by NAD-preferred dehydrogenases to benzyl viologen catalyzed by diaphorase (DI) to H_2 catalyzed by

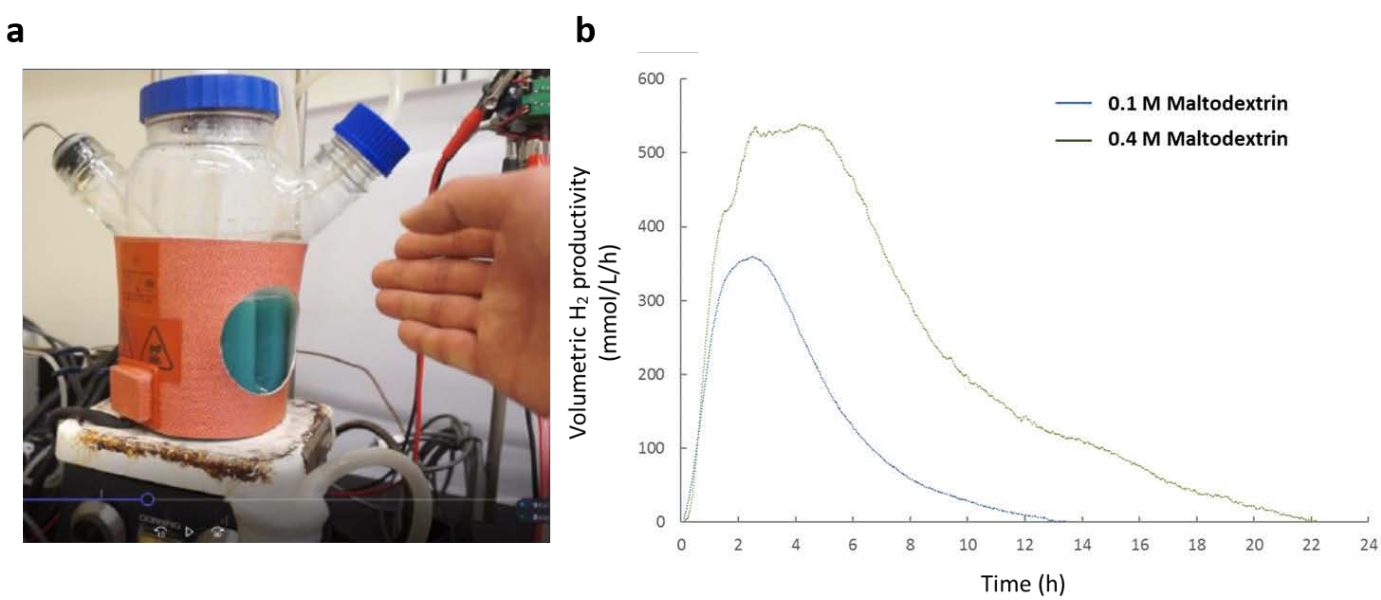

FIGURE 3. Picture of 1-L biohydrogen generation demonstration from starch (a) and the profile of hydrogen generation from starch (b).

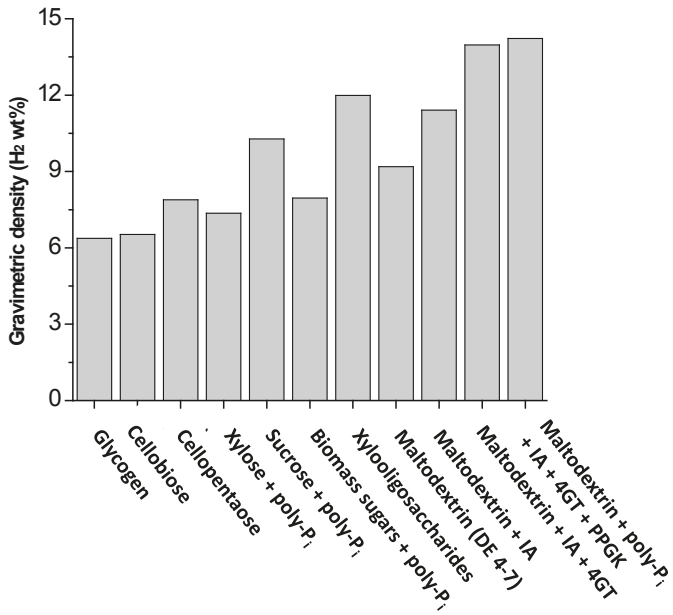

FIGURE 4. Comparison of gravimetric hydrogen storage densities (H_2% wt/wt) for different carbohydrates via different pathways.

soluble [FeNi]-hydrogenase 1 (SHI) (Figure 1b). This ETC can increase hydrogen generation rates by approximately five times relative to direct ETC from Nicotinamide adeninine dinucleotide phosphate (NADPH) to H_2 (Figure 1a). What is more, the conjugation of benzyl viologen (BV) and DI, yielding DI-BCV (Figure 1c), doubled H_2 generation rates. We also constructed enzyme complex (called metabolon) comprised of mG6PDH, DI, and SHI, which increased electron transfer rates by nearly one order of magnitude. But this metabolon was not stable at 80°C. We applied glutaraldehyde to stabilize the metabolon greatly. The combination of the use of hyperthermophilic enzymes, biomimetic ETC, and DI-BCV allows us to achieve ultra-rapid production of H_2, being 550 mmol H_2/L/h. In the past 10 years, our lab has increase in vitro biohydrogen production rates by 1,000-fold. We believe that we could increase biohydrogen production rates by another order of magnitude if we have enough funding support.

To scale up enzymatic H_2 production (Objective 3), we conducted high-cell density fermentation in 6-L fermenter and accomplished the cell density of ~50 g dry cell weight per liter. Compared to 500-mL flask, we were able to increase enzyme production capability by more than 10,000-fold. Such information suggests that bulk enzyme production costs could be as low as $50/kg [4,5]. By changing the promoter and enzyme purification tag of SHI, we increased SHI production capability by 100-fold. Consequently, we scaled up our H_2 production in 1-L reactor (Figure 3a).

CONCLUSIONS AND UPCOMING ACTIVITIES

Although sweet H_2 production is still in its early stage. Several conclusions can be made:

- The highest biological H_2 generation rates achieved suggests that these in vitro hydrogen generation rates are fast enough to produce H_2 at stationary hydrogen bioreactors.
- Successful coenzyme engineering from NADP to NAD to NMN along with NAD-linkage suggests that we are able to decrease coenzyme costs greatly, at least by a factor of 100.
- Complete oxidation of starch suggests that starch could be the best solar fuel as a high-density hydrogen carrier with a gravimetric density of up to 14% H_2 wt/wt (Figure 4).

Future work includes:

- Further increase hydrogen production rates toward the ultimate goal of on-board hydrogen generation for hydrogen fuel cell vehicles.
- Enhance activities of dehydrogenase mutants working on biomimetic coenzymes.
- Finish detailed economic analysis of enzymatic H_2 production by using the H2A model.

FY 2017 PUBLICATIONS/PRESENTATIONS

1. Huang R, Chen H, Zhang Y-HP*. 2016. High-throughput screening of coenzyme preference change of thermophilic 6-phosphogluconate dehydrogenase from $NADP^+$ to NAD^+. *Scientific Reports* 6:32644.

2. Kim E-J, Wu C-H, Adams MWW, Zhang Y-HP*. 2016. Exceptionally high rates of biohydrogen production by biomimetic in vitro synthetic enzymatic pathways. *Chemistry – A European Journal*. 22:16047–16051.

3. Chen H, Zhu ZG, Huang Rui, Zhang Y-HP*. 2016. Coenzyme engineering of a hyperthermophilic 6-phosphogluconate dehydrogenase from $NADP^+$ to NAD^+ with its application to biobatteries. *Scientific Reports*. 6:36311.

4. Moustafa HMW, Kim E-J, Zhu ZG, Wu C-H, Zaghloul TI, Adams MWW, Zhang Y-HP*. 2016. Water splitting for high-yield hydrogen production energized by biomass xylooligosaccharides catalyzed by an enzyme cocktail. *ChemCatChem*. 8: 2898–2902.

5. Kim J-E, Huang R, Chen H, You C, Zhang Y-HP*. 2016. Facile insertion of a large-size random gene mutagenesis library into *Escherichia coli* plasmid without restriction enzymes. *Biotechnology Journal*. 11:1142–1150.

6. Zhang Y-HP*. 2017. Biomanufacturing: History and Perspective. *Journal of Industrial Microbiology & Biotechnology* 44.773–784.

7. Chen H, Huang R, Zhang Y-HP*. 2017. Systematic comparison of co-expression of multiple recombinant thermophilic enzymes in *Escherichia coli* BL21(DE3). *Applied Microbiology and Biotechnology.* 101(11):4481–4493.

8. Zhang Y-HP. Constructing the electricity-carbohydrate-hydrogen cycle for a carbon-neutral future (plenary talk). SuNEC 2016, Sun New Energy Conference, Sicily, Italy. Sept. 7, 2016.

9. Biodegradable high-energy density sugar biobattery. China Bioindustry and Capital Conference, Tianjin, China. October 25, 2016.

10. Zhang Y-HP. Biomanufacturing 4.0: in vitro synthetic enzymatic biosystems beyond cells' constraints. Mitr Phol Co. Bangkok, Thailand. August 3, 2016.

11. Kim JE, Zhang Y-HP. High-yield & high-speed biohydrogen production from starch and water via in vitro synthetic enzymatic pathways. The 253rd Annual Meeting of American Chemical Society. April 2–6, 2017. San Francisco, CA.

12. Huang R, Zhang Y-HP. Coenzyme engineering of NADP-dependent hyperthermophilic dehydrogenases toward small-size biomimetic coenzymes. The 253rd Annual meeting of American Chemical Society. April 2–6, 2017. San Francisco, CA.

REFERENCES

1. Zhang, Y.-H.P. "Next Generation Biorefineries Will Solve the Food, Biofuels, and Environmental Trilemma in the Energy-Food-Water Nexus." Energy Sci. Eng. 1 (2013): 27–41.

2. Rollin, J.A., J.C. Martin, S. Myung, F. Sun, C. You, A. Bakovic, R. Castro, et al. "High-Yield Hydrogen Production from Biomass by in Vitro Metabolic Engineering: Mixed Sugars Coutilization and Kinetic Modeling." Proc. Nat. Acad. Sci. USA 112 (2015): 4964–4969.

3. Zhang, Y.-H.P. "Production of Biofuels and Biochemicals by in Vitro Synthetic Biosystems: Opportunities and Challenges." Biotechnol. Adv. 33 (2015): 1467–1483.

4. You, C., Shi, T., Li, Y., Han, P., Zhou, X., Zhang, Y.-H.P. "An in vitro synthetic biology platform for the industrial biomanufacturing of myo-inositol from starch". Biotechnol. Bioeng. 114 (2017):1855–1864.

5. Zhang, Y.-H.P., Sun, J., Ma, Y. "Biomanufacturing: history and perspective". J. Ind. Microbiol. Biotechnol. 44 (2017):773–784.

II.E.3 Novel Hybrid Microbial Electrochemical System for Efficient Hydrogen Generation from Biomass

Hong Liu (Primary Contact), Yuyan Shao, Vilayanur Viswanathan, Murthy Ganti
Oregon State University/Pacific Northwest National Laboratory
116 Gilmore Hall
Oregon State University
Corvallis, OR 97331
Phone: (541) 737-6309
Email: liuh@engr.orst.edu

DOE Manager: Katie Randolph
Phone: (240) 562-1759
Email: Katie.Randolph@ee.doe.gov

Project Start Date: February 1, 2016
Project End Date: January 31, 2019

Overall Objectives

- Design and fabricate a low-cost, robust, and highly efficient fermentation and microbial electrochemical system.
- Determine the techno-economic feasibility of the system using biomass hydrolysates and wastewater.

Fiscal Year (FY) 2017 Objectives

- Evaluate fermentative H_2 production.
- Evaluate H_2 production from liquid fermentation products in microbial electrolysis cells (MEC).
- Develop robust and low-cost cathode materials.
- Develop cost performance model.

Technical Barriers

This project addresses the following technical barriers from the Hydrogen Production section of the Fuel Cell Technologies Office Multi-Year Research, Development, and Demonstration Plan.

(AX) Hydrogen Molar Yield

(AAA) Electrode Cost

(AAB) Solution Density (Production Rate)

Technical Targets

Progress has been made in achieving the DOE targets listed in the Multi-Year Research, Development, and Demonstration Plan. Table 1 lists DOE's technical targets and where our research and development efforts stand to date.

TABLE 1. Progress towards Meeting Technical Targets for Dark Fermentative Hydrogen Production and MECs

Characteristic	Units	DOE 2015 Targets	DOE 2020 Targets	Project Status
Yield of H_2 production from glucose by integrated MEC–fermentation	mol H_2 /mol glucose	6	9	8
MEC cost of electrodes	$/m^2	300	50	120

The overall goal of this project is to develop and scale-up our novel hybrid fermentation and MEC system that can be integrated with well-developed lignocellulose pretreatment/hydrolysis or wastewater treatment processes for efficient hydrogen production at a cost less than $2/kg H_2.

FY 2017 Accomplishments

- Developed an immobilization method that can increase the fermentative bacteria density in reactors with stable H_2 production. The hydrogen production rate reached over 10 L/L-reactor/d.
- Determined the suitable design and operational conditions for MECs.
- Discovered a low-cost chemical that can effectively inhibit methanogens in MECs. The estimated chemical cost for using this inhibitor is less than 5¢/kg H_2.
- Synthesized molybdenum phosphide (MoP) hydrogen evolution reaction (HER) catalysts with high activity (comparable to Pt) and high durability. The MoP catalyst shows a stable polarization curve after 2,000 potential cycles.

✧ ✧ ✧ ✧ ✧

INTRODUCTION

The global interest in hydrogen production has been stimulated by the promise of the clean operation and high efficiencies of hydrogen fuel cells. Currently, almost all the hydrogen produced is from non-renewable fossil sources. Hydrogen can be produced from renewable biomass by biological dark fermentation. Unfortunately, the hydrogen yields using current fermentation techniques are low. Hydrogen can also be produced by MEC, which can overcome the fermentation barrier and achieve higher hydrogen yield. However, the key challenges for realizing the practical applications of MECs include (1) difficulty in utilizing biomass directly and in utilizing certain biomass

components, such as sugars; (2) low hydrogen production rate or high energy input due to inefficient reactor designs, high cathode over potential, and high solution resistance; and (3) high capital cost due to high electrode and membrane or separator costs. In this project, we will develop a hybrid system that integrates the dark fermentation and MEC processes and overcomes the challenges identified above.

APPROACH

The overall approach of this project is to develop an efficient fermentation and microbial electrolysis cell for hydrogen generation from lignocellulosic biomass hydrolysates and sugar-rich wastewater through maximizing the hydrogen production rate and yield of both processes. Since MEC cathode material is a key factor affecting both capital and operational costs of the system, robust and low-cost cathode materials with low over-potentials will also be developed. A cost-performance model will be used to supplement the H2A analysis tool throughout the project to prioritize the critical factors and demonstrate potential to meet DOE cost goals.

We had identified suitable bacterial cultures for the hybrid system in FY 2016. In FY 2017, we have been focusing on determining the optimal operational conditions using small lab reactors, developing a low-cost and low-overpotential cathode catalyst, and conducting cost and performance analysis. Based on the results, a scaled-up reactor will be designed, fabricated, and evaluated in the fiscal year of 2018.

RESULTS

Continuous hydrogen production by immobilized fermentative culture. Bacterial cell density in continuous-flow reactors can be increased significantly through immobilizing the bacterial culture with immobilization agents. Stability is a major concern when using immobilized bacterial culture. Our batch experiments demonstrated that acrylic latex silicone beads containing immobilized fermentative bacterial culture could maintain their original shapes with reliable hydrogen production over 80 days of operation. Continuous hydrogen production from mixed sugars was investigated under different hydraulic retention times, sugar concentrations, and biomass content. A hydrogen production rate of over 10 L/L/day was achieved at 40 g/L, 8 h hydraulic retention time (HRT), and 15% biomass content (Figure 1).

Identification of the limiting factors in MECs. To provide better design and operational parameters for the continuous flow reactor, we investigated the impacts of four parameters on hydrogen production, including electrode distance, buffer concentration, mixing condition, and electrode surface area ratio. The mixing condition far outweighs the effect of other parameters on current density, suggesting that MECs should be designed to facilitate mixing. The maximum current density possible for the anode is around 33 A/m^2. The cathode current density can reach 50 A/m^2 (Figure 2).

Determination of suitable inhibitor concentration and frequency for inhibiting methanogenesis in MECs. Methanogens can utilize H_2 produced and reduce hydrogen yield in MECs. We discovered that periodically adding a low-cost chemical to the reactor can effectively inhibit methane production. This discovery is critical for the operation of our continuous flow reactor, particularly using wastewater as feedstock. We have determined that the injected concentration can be as low as 1% with less than two injections per month (Figure 3), which corresponds to a few cents per kilogram H_2 produced, indicating its feasibility for practical application.

MEC cathode development. We developed a new MoP cathode catalyst, which has demonstrated comparable activity to Pt catalyst. The catalyst shows stable performance after 2,000 potential cycles (Figure 4). The MoP|P material appear as quasi-spherical nanoparticles with an average diameter of ~100 nm. High-resolution transmission electron microscopy image showed that the MoP|P nanoparticles were

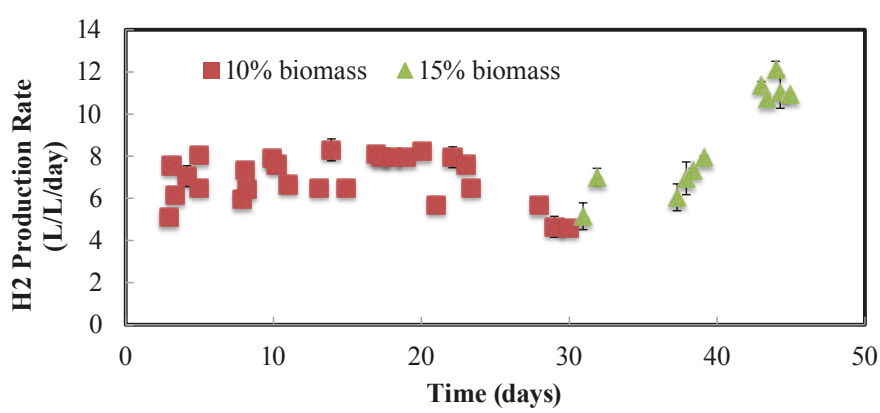

FIGURE 1. Continuous hydrogen production using immobilized fermentative culture

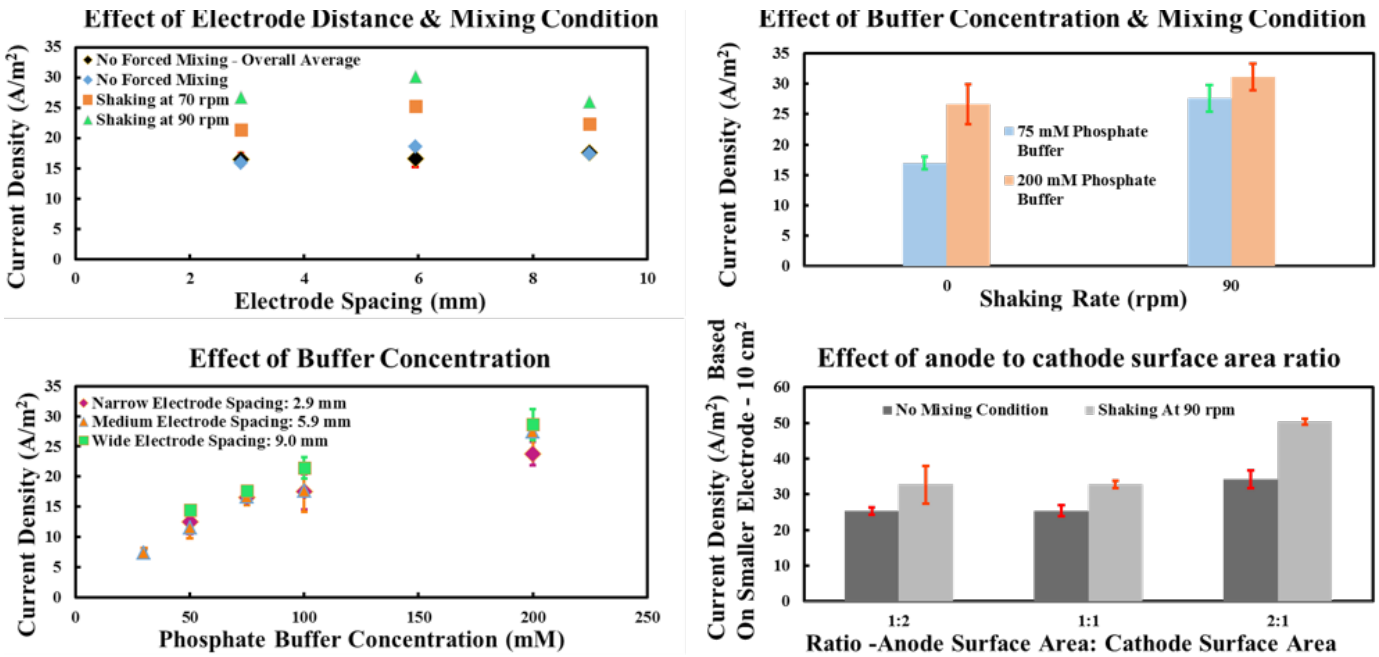

FIGURE 2. Effect of electrode spacing, buffer concentration, mixing condition, and electrode surface area ratio on current density of MECs

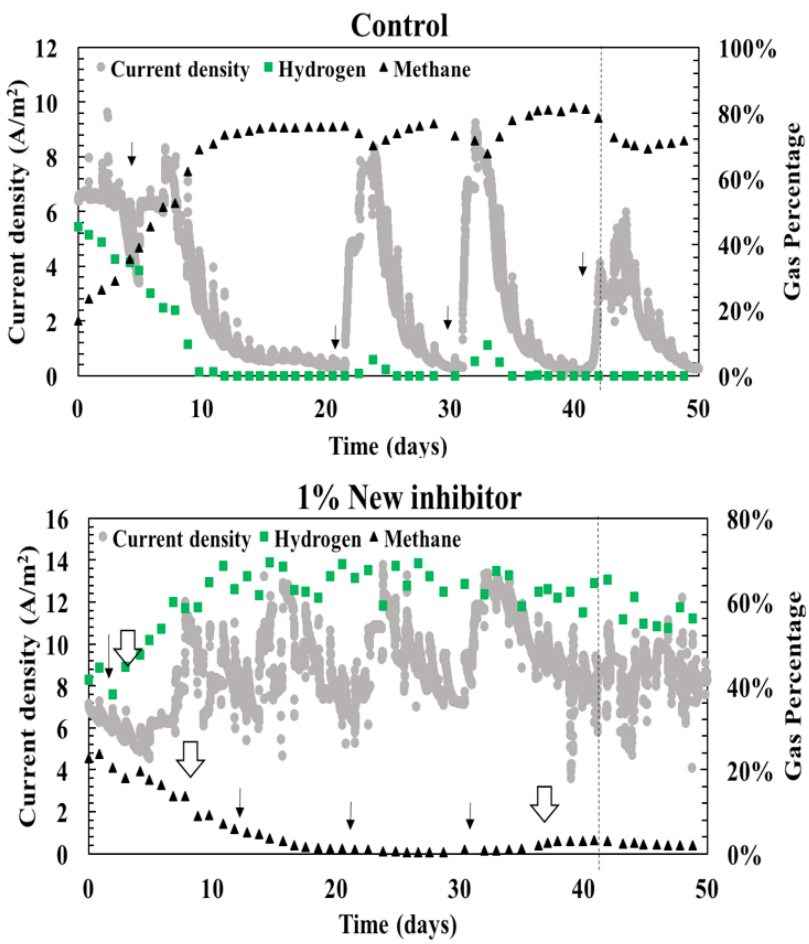

FIGURE 3. Inhibiting methane production in MECs using a low-cost chemical

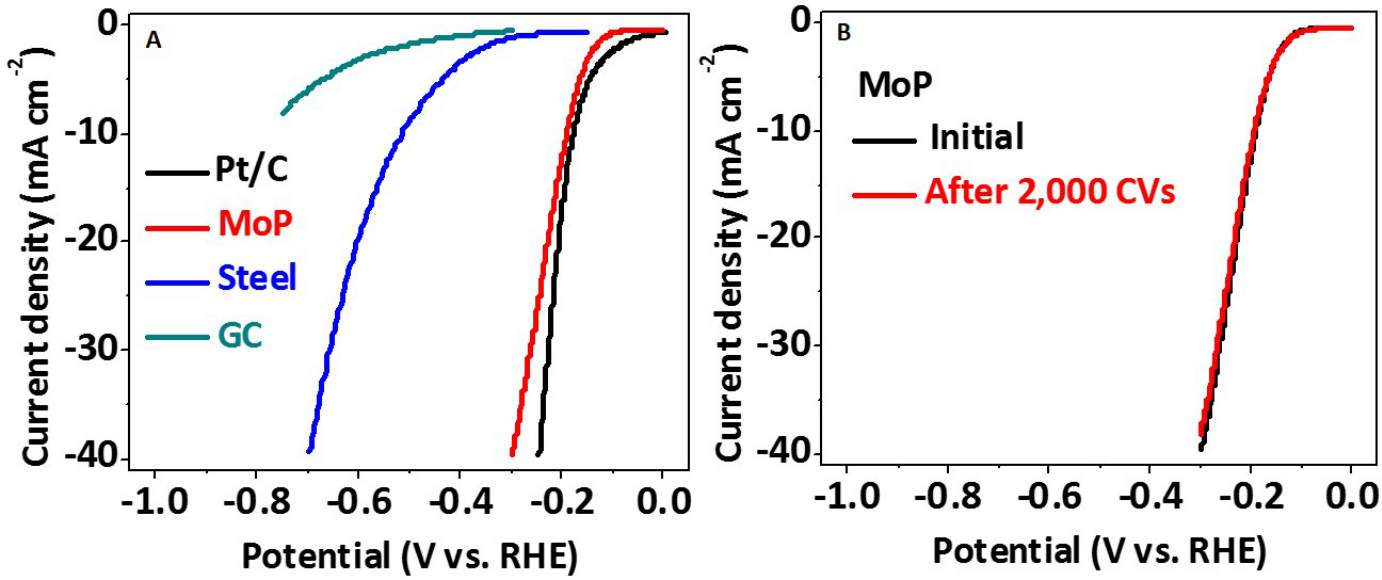

RHE – reference hydrogen electrode; GC – glass carbon; CV – cyclic voltammogram

FIGURE 4. (A) HER on MoP catalyst in comparison with other catalysts/electrode materials. MoP shows comparable activity to Pt; (B) MoP catalyst durability test.

single crystalline and faceted. The observed lattice fringes correspond to the (001) P-terminated plane of MoP, indicating that the nanoparticle surfaces exposed, among other facets, the (001) MoP|P crystal planes that have been predicted to have the highest activity for the HER.

Cost performance model. We developed an H2A model based on some of the experimental results and drew the following general conclusions: (1) increasing the overall hydrogen yield is critical when using biomass hydrolysate since the feedstock cost contributes about half of the targeted H_2 production cost; (2) increasing the current density is critical, which significantly affect the capital cost, especially for using wastewater as feedstock; (3) using wastewater as feedstock is more promising than biomass hydrolysate in term of meeting DOE's cost target even we use a more conservative cost inputs (high reactor cost, low current density).

CONCLUSIONS AND UPCOMING ACTIVITIES

We have made significant progress towards reaching our project target. We have determined the design and operational conditions for our scaled-up reactors, including the method for immobilizing the fermentative culture, the critical factors affecting fermentative and microbial electrochemical hydrogen production, the low-cost chemical for inhibiting methanogens, the low-cost and low-over potential cathode catalyst, and the anode and cathode surface area ratio. Our cost and performance analysis demonstrated that increasing current density is critical and using waste streams is more promising than biomass hydrolysate.

Future work includes:

- Stability test of the cathode catalyst
- Hybrid reactor design and fabrication
- Lab and on-site evaluation of the hybrid reactor

SPECIAL RECOGNITIONS & AWARDS/ PATENTS ISSUED

1. Filed an invention disclosure report on "A PGM-free catalyst for hydrogen evolution in neutral electrolytes," by Yuyan Shao at PNNL.

FY 2017 PUBLICATIONS/PRESENTATIONS

1. Luguang Wang, Ningshengjie Gao, Cameron Platner, Cheng Li, and Hong Liu, "Hybrid Microbial Electrochemical System for Efficient Hydrogen Generation from Lignocellulosic Hydrolysate," presented at the 2016 NA ISMET Meeting, Stanford University, CA, October 2016.

2. Hong Liu, Yuyan Shao, and Vilayanur Viswanathan, "Novel Hybrid Microbial Electrochemical System for Efficient Hydrogen Generation from Biomass," presented at the DOE Annual Merit Review and Peer Evaluation Meeting, Washington, D.C., June 2017.

3. Stephanie Trujillo, Luguang Wang, and Hong Liu, "Using Acetylene as a Low-cost and Effective Methanogenesis Inhibitor in Single Chamber Microbial Electrolysis Cells," Submitted to *International Journal of Hydrogen Energy.*

II.F.1 Tailoring Hydrogen Evolution Reaction (HER) Catalysts for Operation at Specific pH Values

Bianca Ceballos
Department of Chemistry
University of California, Irvine
Irvine, CA 92697
Phone: (949) 824-2509
Email: bceballo@uci.edu

DOE Manager: Mark Spitler
Phone: (301) 903-4568
Email: Mark.Spitler@science.doe.gov

Abstract

Electrocatalysts that can generate renewable fuels under a wide range of pH conditions in water are necessary for renewable energy applications. Metal hydrides are critical intermediates involved in bond-breaking and bond-forming steps in relevant catalytic reactions. Our group relies on thermodynamic hydricity-pH relationships to target reaction conditions for selective hydride transfer for proton reduction to H_2 or CO_2 reduction to formate (HCO_2) in water. Although metal hydricities have been measured for hundreds of transition metal complexes in organic solvents, aqueous hydricities are relatively unexplored.

We report the electrocatalytic activity of $[HNi(DHMPE)_2][BF_4]$ (DHMPE= 1,2-bis(di-(hydroxymethyl) phosphino)ethane) (1) toward hydrogen production at pH 1, with a rate of ~10^3 s^{-1}, Faradaic efficiency between 92–105%, and negligible decomposition after 18 h of electrolysis. We are currently pursuing new nickel diphosphine complexes modified to make stronger metal hydrides for the reduction of substrates such as CO_2 to other C1 fuels.

II.F.2 Hybrid Perovskites and Non-Adiabatic Dynamics Simulations: Catching Realistic Aspects of the Charge Recombination Process

Joanna Jankowska (Primary Contact)[a,b],
Oleg V. Prezhdo[a]
[a]Department of Chemistry
University of Southern California, Los Angeles
Los Angeles, CA 90095
Email: jjankows@usc.edu
[b]Institute of Physics, Polish Academy of Sciences,
Warsaw, Poland

DOE Manager: Mark Spitler
Phone: (301) 903-4568
Email: Mark.Spitler@science.doe.gov

Abstract

Dissipation of photon energy to heat and recombination of photo-generated charge carriers are among the main factors limiting the efficiency of solar-light harvesting devices. At the same time, the dynamics of excited electrons and holes depends critically on the microscopic structure of a material, including dopants, defects, grain boundaries, crystallinity and electric order. We summarize recent findings and suggest directions for improvement of hybrid organic-inorganic perovskite materials, established by means of non-adiabatic molecular dynamics (NAMD) simulations. Combined with real-time, time-dependent density functional theory, NAMD provides an ab initio description of the photo-initiated processes, including realistic aspects of material's structure and giving unique atomistic insights into the photo-active material properties.

II.F.3 Nano-Bio Systems for Light-Driven Hydrogen Production

Kara L. Bren (Primary Contact), Richard Eisenberg, Todd D. Krauss
Department of Chemistry
University of Rochester
Rochester, NY 14627-0216
Email: bren@chem.rochester.edu

DOE Manager: Mark Spitler
Phone: (301) 903-4568
Email: Mark.Spitler@science.doe.gov

Objectives

Our group is developing new approaches to storing light energy in the form of hydrogen (H_2). This collaborative project draws on synthetic chemistry, nanoscience, and biochemistry to engineer integrated systems for reducing aqueous protons to H_2. Broad goals for this work are to enhance system performance by increasing turnover number (TON) and quantum yield. We also aim to understand the fundamental reaction steps of light absorption, charge transfer, and the assembly of protons and electrons into H_2. Finally, development of externally sensitized photocathodes is being pursued as an alternative to sacrificial electron donors.

Technical Barriers

- Preparing water-soluble semiconductor nanocrystals (NCs) with improved light-induced charge separation
- Developing robust water-soluble synthetic and biomolecular catalysts for proton reduction
- Integrating NC photosensitizers and molecular catalysts for light-driven hydrogen production
- Characterizing the fundamental charge-transfer and chemical steps in hydrogen production

Abstract

Systems performing the reductive side of light-driven water splitting have been prepared using semiconductor quantum dots (QDs) or other NCs as photosensitizers and molecular catalysts for proton reduction. To improve charge separation, CdTe/CdSe/CdTe nanobarbells have been developed; pairing these NCs with nickel or cobalt catalysts yields improved TONs attributed to enhanced charge separation relative to CdSe QD-based systems. Ongoing work on new photocathodes employs layers of NCs for improved charge separation and removal of the sacrificial donor. The analysis of molecular catalysts with redox-active ligands for charge storage adds to fundamental knowledge of reaction mechanism. Biomolecular catalysts have been prepared that have high longevity in photochemical systems and yield extremely high (>100,000) TONs when paired with QDs.

Progress Report

Systems performing the reductive side of water splitting to produce H_2 require a photosensitizer and a compatible proton-reducing catalyst, as well as a source of electrons (Figure 1). Our work on semiconductor NCs is toward developing robust and tunable photosensitizers. Earlier work in our labs demonstrated that dihydrolipoic acid (DHLA)-capped CdSe QDs paired with a simple Ni(II) catalyst produce H_2 in the presence of visible light with a TON > 600,000 with respect to catalyst.

To improve the performance of these systems we are engineering QD heterostructures with enhanced internal charge separation. CdTe/CdSe/CdTe nanobarbells are promising candidates because the staggered band alignment forces spatial separation of the photoexcited electron and hole, while still allowing for facile charge transfer. Pairing a Ni-DHLA catalyst with the nanobarbell photosensitizer and ascorbic acid as the sacrificial electron donor yields H_2 from water with a TON increased ten-fold relative to QDs of similar diameter.

A second approach involves the development of photocathodes with CdSe NCs arranged in layers according to NC size on NiO deposited on ITO/NiO. Photocathodes yield H_2 from aqueous media without the need for a sacrificial donor. A system designed to improve charge separation by having the smallest NCs close to the electrode and large NCs further away shows positive results in terms of rectification and H_2 production.

Synthetic molecular catalysts in development include Ni, Co, and Fe bis(dithiolene) complexes with redox-active ligands for charge storage. When pairing these catalysts with QD photosensitizers, we found that dissociation of

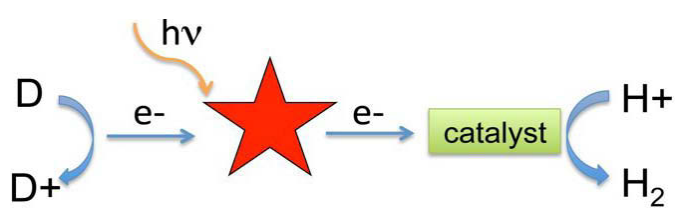

FIGURE 1. Schematic showing light-driven hydrogen generation using a photosensitizer (red star), sacrificial electron donor, and catalyst.

the water-solubilizing bidentate DHLA QD capping agent led to DHLA substitution on the catalyst. To eliminate this problem, tridentate capping agents are being employed to allow assessment of light-driven H_2 production by different coordination complexes, keeping the catalyst intact.

The development of catalysts for proton reduction has also made use of biomolecules (Figure 2). These catalysts have a number of advantages including the provision of a microenvironment for the catalytic site that can be engineered to alter second-sphere interactions. We have found that CoMP11 catalyst (left structure in Figure 2) paired with glutathione-capped CdSe QDs as electron donors yields high TON values (>100,000) for light-induced H_2 production. Unlike solid-state catalysts and molecular catalysts that are formed in situ, these catalysts are structurally defined, making this system promising for detailed mechanistic study and optimization.

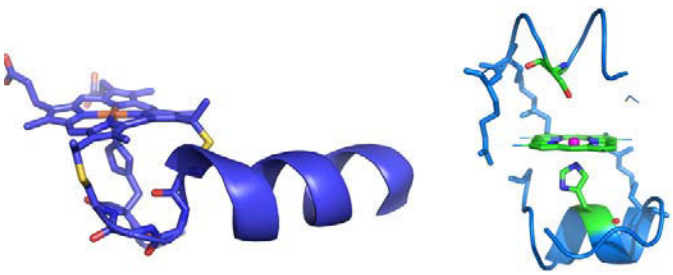

FIGURE 2. Models of biomolecular hydrogen evolution catalysts developed in this project.

Upcoming Activities

We will continue our development of systems pairing new NC photosensitizers with engineered biomolecular catalysts. In catalyst development, the polypeptide structure can be engineered to tune the level of solvent exposure and second-sphere interactions. We also will work toward the goal of eliminating sacrificial electron donors using photocathodes constructed from NC light absorbers to yield a photoelectrochemical H_2-generating assembly. Finally, we plan systematic studies of these H_2-generating systems using time-resolved spectroscopy to gain a fundamental understanding of charge transfer steps essential in catalysis.

Selected Publications

1. Kandemir, B.; Chakraborthy, S.; Guo, Yi; Bren, K.L., Semisynthetic and Biomolecular Hydrogen Evolution Catalysts. *Inorg. Chem.* **2016**, *55,* 467–477.

2. Qiu, F.; Han, Z.; Peterson, J.J.; Odoi, M.Y.; Sowers, K.L.; Krauss, T.D., Photocatalytic Hydrogen Generation by CdSe/CdS Nanoparticles, *Nano Lett.* 2016, *16*, 5347–5352.

3. Lv, H.; Ruberu, T.P.; Fleischauer, V.; Brennessel, W; Neidig, M.; Eisenberg, R., Catalytic Light-driven Generation of Hydrogen from Water By Iron Dithiolene Complexes, *JACS*, **2016**, *138*, 11654–11663.

II.F.4 Mechanistic Investigations on Hydrogen Catalysis by [FeFe]-Hydrogenase

David W. Mulder (Primary Contact),
Carolyn E. Lubner, Katherine A. Brown,
Michael W. Ratzloff, Paul W. King
National Renewable Energy Laboratory
15013 Denver West Parkway
Golden, CO 80127
Phone: (303) 384-7486
Email: david.mulder@nrel.gov

DOE Manager: Stephen Herbert
Phone: (301) 903-0383
Email: Stephen.Herbert@science.doe.gov

Objectives

The long-term objective of this project is to advance the understanding of mechanisms of redox enzymes that function in photosynthetic energy transduction networks. One of these enzymes, [FeFe]-hydrogenase, catalyzes the evolution of H_2 by coupling to the reducing potential generated by photosynthetic water oxidation as a response to dark-to-light transitions in the cell. This reaction is fundamental to microbial energy conservation, and how H_2 as a whole plays a critical role in the regulation of cellular energetics. [FeFe]-hydrogenases operate by unique proton-coupled electron transfer (PCET) chemistry, and we are investigating the composition of active site intermediates, mechanisms of proton transfer and electron transfer, thermodynamics of individual reaction steps, and electron injection from external redox networks. An overarching aim of this work is to elucidate the mechanistic principles for biological transformation of photochemical potential into chemical bonds with an emphasis on how it is accomplished by specialized protein cofactors tailored for electron transfer and catalysis.

Technical Barriers

[FeFe]-Hydrogenases couple electrochemical potential to the reversible chemical transformation of H_2 and protons; however, the reaction mechanism and composition of intermediates are not fully understood. Fast PCET and oxygen sensitivity has challenged research efforts to define the biophysical properties of the functional intermediates of catalysis, especially key iron-hydride intermediates. The aim of this project is to use the algal [FeFe]-hydrogenase from Chlamydomonas reinhardtii to determine the mechanism and role of hydride intermediates in H_2 catalysis.

Abstract

Algal H_2 production is a model pathway for coupling water oxidation to renewable production of H_2. [FeFe]-hydrogenases catalyze the reaction $2e^- + 2H^+ \rightleftarrows H_2$ by means of a unique active-site cofactor, the H-cluster. The H-cluster is carefully positioned within the protein framework to optimize proton- and electron-transfer reactions required by the reaction. Developing a unified model of H_2 catalysis is challenging due to the structural diversity of enzymes, the inherently fast exchange reaction between H_2, protons and electrons, and the complexity of redox intermediates. Using integrated spectroscopy, we have been investigating the mechanism of catalysis with the [FeFe]-hydrogenase from Chlamydomonas reinhardtii. We also have been using the CaI [FeFe]-hydrogenase from Clostridium acetobutylicum to probe the mechanisms of electron injection and electron transfer to the H-cluster. The outcome of this work will help to reveal how H_2 metabolism is controlled during adaptive transitions of photosynthetic energy transduction, to advance the understanding of PCET in H_2 activation, and to inspire the design of more efficient organometallic complexes for artificial photosynthetic systems and fuel cells.

Progress Report

Identification of an Iron-Hydride [Fefe]-Hydrogenase Intermediate

Using a variant of the [FeFe]-hydrogenase from Chlamydomonas reinhardtii (CrHydA1), we characterized a short-lived catalytic Fe-hydride H-cluster intermediate (H_{hyd}) (Figure 1). The altered proton-transfer kinetics of the CrHydA1 (C169S) variant, where the primary proton donor (Cys residue 169) to the H-cluster is changed to a Ser residue, made it possible to enrich for the otherwise fast-lived hydride intermediate. Initial hydrogen-deuterium isotope exchange experiments with Fourier transform infrared (FTIR) spectroscopy and density functional theory (DFT) analysis suggested the presence of a terminal hydride bound to the distal Fe site of the 2Fe subcluster ($[2Fe]_H$) of the H-cluster. Further analysis by infrared and Mössbauer spectroscopy, together with computational modeling, revealed details of the electronic and geometric structure of the Fe–H^- bond present in H_{hyd} formed during reversible, heterolytic H_2 activation. Redox titrations showed that the reduction potential of H_{hyd} resides at the 1-electron to 2-electron transition in the catalytic cycle leading to formation of H_2. A significant shift in the midpoint potential of the H_{ox} H-cluster state compared to the wild-type enzyme demonstrates the role of the protein environment in tuning the active site for catalytic activity.

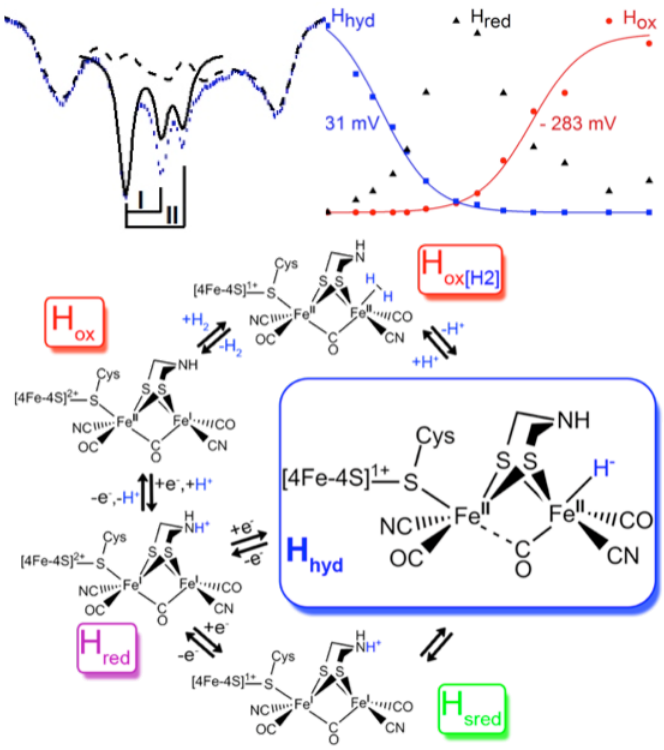

FIGURE 1. Mechanistic model, Mössbauer spectroscopic signatures, and electron paramagnetic resonance redox properties of H_{hyd}, the H-cluster hydride intermediate in the reversible H_2 activation reaction catalyzed by [FeFe]-hydrogenase

The determination of the primary properties of the H-cluster-hydride intermediate reveals the inner workings for how the H-cluster enables facile PCET through positioning of the electron rich hydride proximal to a proton-exchangeable group and an electron relay [4Fe-4S] cluster.

Thermodynamic Analysis of H-Cluster Redox Transitions using Photocatalytic Complexes

Photocatalytic complexes consisting of clostridial [FeFe]-hydrogenase Ca1and CdSe nanocrystals were used to study the mechanism of electron injection into [FeFe]-hydrogenase and the activation thermodynamics of the initial step of proton reduction (Figure 2). Compared to the algal CrHydA1 enzyme, Ca1 contains additional FeS clusters (F-clusters) that function in electron-transfer to the H-cluster. With previous collaborative studies with Professor Dukovic's group at University of Colorado Boulder, we showed evidence that nanocrystals interact with the ferredoxin binding site near the surface localized [4Fe-4S] F-cluster, the presumed entry point for electrons. Here, we combined light-driven experiments on the photocatalytic complexes with rapid-scan infrared (IR) and steady-state electron paramagnetic resonance (EPR) detection to probe both the pathway for electron-transfer and thermodynamics of active-site chemistry. The rapid scan IR made it possible to detect in

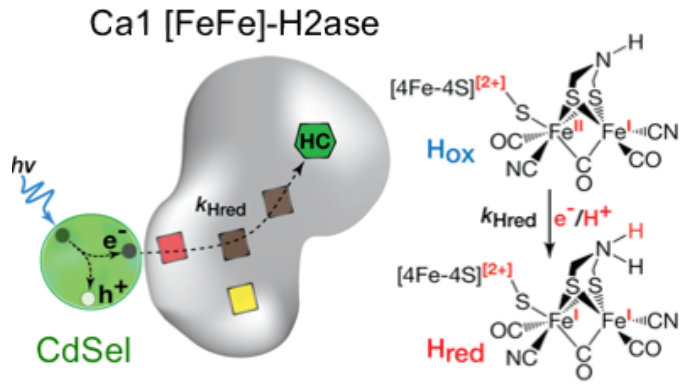

FIGURE 2. Photocatalytic CdSel:Ca1 complex and H-cluster reduction scheme for the initial proton-reduction step of H_2 catalysis

real-time the formation of H-cluster redox intermediates during catalytic proton reduction, while the EPR followed the reduction to the F-cluster conduit. Together, the results show how the F-clusters function both as a conduit and a reservoir to drive catalysis. The results also reveal that the initial transition of the H-cluster from oxidized to reduced forms and the first step of catalytic proton reduction proceeds by concerted PCET.

Upcoming Activities

- Utilize nuclear resonance vibrational spectroscopy (NRVS), in collaboration with the Cramer group at University of California, Davis, to measure the properties of the Fe-hydride H-cluster intermediate trapped in C169S CrHydA1. Hydrogen-deuterium isotope exchange will be used to identify hydride modes by the NRVS technique, and the studies will be integrated with DFT to develop structural models for reduced H-cluster intermediates.
- Develop mechanistic models that describe the individual PCET transitions and protonation states of the H-cluster. The specific order of protonation and electron-transfer steps remains largely unknown and assumed for currently catalytic models. Cryogenic IR spectroscopy, along with hydrogen-deuterium exchange and mutagenesis, will be used to identify CO and CN^- signatures that can be ascribed to different H-cluster intermediates.
- Explore the universality aspect of the enzymatic activation of H_2. It remains an open question as to whether all [FeFe]-hydrogenase operate by a similar mechanism or employ the same set of intermediates. Mössbauer spectroscopy, in collaboration with Professor Yisong Guo at Carnegie Mellon University, will be used in combination with EPR and IR spectroscopy on the CrHydA1 enzyme to examine the formation of H-cluster

intermediates at poised potentials and compared to properties of other bacterial [FeFe]-hydrogenases.

Selected Publications

1. Mulder, D.W., Guo, Y., Ratzloff, M.W., King, P.W. "Identification of a catalytic iron-hydride at the H-cluster of [FeFe]-hydrogenase." J. Am. Chem. Soc. 2017, 139: 83–86.

2. Zhao, Y., Anderson, N.C., Ratzloff, M.W., Mulder, D.W., Zhu, K., Turner, J.A., Neale, N.R., King, P.W., Branz, H.M. "Proton reduction using a hydrogenase-modified nanoporous black silicon photoelectrode." ACS App. Mater. Inter. 2016, 8: 14481–14487.

3. Morra, S., Maurelli, S., Chiesa, M., Mulder, D.W., Ratzloff, M.W., Giamello, E., King, P.W., Gilardi, G, Valetti, F. "The effect of a C298D mutation in CaHydA [FeFe]-hydrogenase: Insights into the protein-metal cluster interaction by EPR and FTIR spectroscopic investigation." BBA-Bioenerg. 2016, 1857: 98–106.

4. Swanson, K.D., Ratzloff, M.W., Mulder, D.W., Artz, J.H., Ghose, S., Hoffman, A., White, S., Zadvornyy, O.A., Broderick, J.B., Bothner, B., King, P.W., Peters, J.W. "[FeFe]-hydrogenase oxygen inactivation is initiated at the H-cluster 2Fe subcluster." J. Am. Chem. Soc. 2015, 137: 1809–1816.

5. Wilker, M.B., Shiopoulos, K., Brown, K.A., Mulder, D.W., King, P.W., Dukovic, G. "Electron transfer kinetics in CdS Nanorod-[FeFe]-hydrogenase complexes and implications for photochemical H_2 generation." J. Am. Chem. Soc. 2014, 136: 4316.

6. Mulder, D.W., Ratzloff, M.W., Bruschi, M., Greco, C., Koonce, E., Peters, J.W., King, P.W. "Investigations on the role of proton-coupled electron transfer in hydrogen activation by [FeFe]-hydrogenase." J. Am. Chem. Soc. 2014, 136: 15394.

7. Mulder, D.W., Ratzloff, M.W., Shepard, E.M., Byer, A.S., Noone, S.M., Peters, J.W., Broderick, J.B., King, P.W. "EPR and FTIR analysis on the mechanism of H_2 activation by [FeFe]-hydrogenase HydA1 from Chlamydomonas reinhardtii." J. Am. Chem. Soc. 2013, 135: 6921.

II.F.5 Bioenergetics of Photosynthetic Energy Transduction: Control of Pathways through Redox Biochemistry

David W. Mulder (Primary Contact), Melissa Cano, Sharon Smolinski, Carolyn E. Lubner, Katherine A. Brown, Michael W. Ratzloff, Jianping Yu, Maria L. Ghirardi, Paul W. King
National Renewable Energy Laboratory
15013 Denver West Parkway
Golden, CO 80127
Phone: (303) 384-7486
Email: david.mulder@nrel.gov

DOE Manager: Stephen Herbert
Phone: (301) 903-0383
Email: Stephen.Herbert@science.doe.gov

Abstract

Photosynthetic microorganisms have evolved complex metabolic networks consisting of multiple biochemical pathways that balance energy generation with utilization. Photosynthetic electron transport (PET) reactions establish the appropriate cellular adenosine triphosphate/nicotinamide adenine dinucleotide phosphate ratio, which represents the collective contributions of cyclic electron flow, linear electron flow, and alternative electron flow. One hypothesis for the function of electron flow pathways peripheral to the core PET reactions is the adaptation to differential changes in metabolic and environmental conditions. These pathways cycle photosynthate and afford enormous flexibility in cellular energy homeostasis for acclimation to fluctuations in ambient conditions and nutrient availability. Remodeling of photosynthetic complexes, and the differential regulation of biochemical pathways, redox enzymes and electron carriers implies coordinated responses among adaptive pathways, but the mechanisms for how these are controlled is not well understood. The broad goal of this project is to determine how molecular networks and enzyme mechanisms coordinate electron transfer reactions for energy balancing in model photosynthetic microbial systems. To develop a biochemical understanding of this process, we are conducting structure-function and mechanistic studies on enzymes that couple to the reductant pools, as well as optical and spectroscopic measurements of photochemical energy conversion in biohybrid complexes for solar energy conversion.

Selected Publications

1. Noone, S., Ratcliff, K., Davis, R., Subramanian, V., Meuser, J., Posewitz, M.C., King, P.W., Ghirardi, M.L. "Expression of a clostridial [FeFe]-hydrogenase in *Chlamydomonas reinhardtii* prolongs photo-production of hydrogen from water splitting." *Algal Res.* **2017**, *22*, 116–121.

2. Mulder D.W., Guo Y., Ratzloff M.W., King P.W. "Identification of a catalytic iron-hydride at the H-cluster of [FeFe]-hydrogenase." *J. Am. Chem. Soc.* **2017**, *139*, 83–86.

3. Holland, S.C., Artier, J., Miller, N.T., Cano, M., Yu, J., Ghirardi, M.L., Burnap, R.L. "Impacts of genetically engineered alterations in carbon sink pathways on photosynthetic performance." *Algal Res.* **2016**, *20*, 87–99.

4. Brown, K.A., Harris, D., Wilker, M.B., Rasmussen, A., Khadka, N., Hamby, H., Keable, S., Dukovic, G., Peters, J.W., Seefeldt, L.C., King., P.W. "Light-driven dinitrogen reduction catalyzed by a CdS:Nitrogenase MoFe protein biohybrid." *Science*. **2016**, *352*:448–450.

II.F.6 Reversible Conversion between CO_2/H_2 and Formic Acid by Molecular Catalysts

Etsuko Fujita
Chemistry Division, MS 555A
Brookhaven National Laboratory
Upton, NY 11973-5000
Phone: (631) 344-4356
Email: fujita@bnl.gov

DOE Manager: Mark Spitler
Phone: (301) 903-4568
Email: Mark.Spitler@science.doe.gov

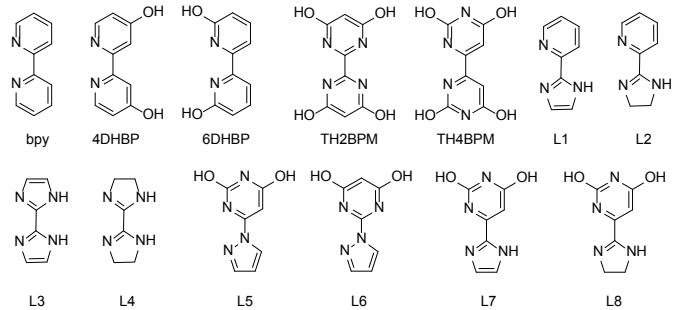

FIGURE 1. Proton responsive bidentate auxiliary ligands used in a series of Cp*Ir complexes

Abstract

The Artificial Photosynthesis Group in the Chemistry Division at Brookhaven National Laboratory (BNL) is carrying out fundamental research involving coordinated experimental and theoretical studies of factors that must be considered in designing artificial photosynthetic systems for the generation of fuels and oxygen from water. The work is aimed at unraveling kinetic and mechanistic details of various processes including (1) photo-initiated, proton-coupled, electron-transfer reactions; (2) reversible interconversion between CO_2/H_2 and formic acid using Cp*Ir complexes bearing proton responsive ligands; (3) electrochemical CO_2 reduction in organic solvents, or ionic liquids using Re, Mn, and Ru complexes as catalysts; (4) photochemical CO_2 and/or proton reduction using Ir and Co complexes as catalysts; (5) nano-structured carbide/nitride composites and oxynitrides with non-precious metals for hydrogen evolution reaction (HER) and oxygen reduction reaction/oxygen evolution reaction catalysts, respectively; and (6) water oxidation using ruthenium molecular catalysts with multifunctional ligands and at semiconductor/aqueous interfaces. At this meeting, we will report on CO_2 hydrogenation and formic acid dehydrogenation toward the use of formic acid as a sustainable H_2 storage medium.

Proton responsive ligands offer control of catalytic reactions through modulation of pH-dependent properties, second coordination sphere stabilization of transition states, or by providing a local proton source for multi-proton, multi-electron reaction pathways. Using a series of Cp*Ir complexes incorporating the proton responsive bidentate auxiliary ligands shown in Figure 1, we characterized the catalytic activity of CO_2 hydrogenation and formic acid (FA) dehydrogenation in water. Most of these complexes can act as catalysts for both reactions by simply changing the pH of the aqueous solution. For complexes with ligands possessing *ortho*-OH group(s) we found clear experimental and theoretical evidence of the involvement of a water molecule (i.e., solvent) in the rate determining H_2 heterolysis step in CO_2 hydrogenation by forming a water bridge similar to a proton channel in proteins. While complexes with hydroxyl derivatives of bipyridine and bipyrimidine ligands show maximum reaction rates for FA dehydrogenation around pH 3.8 (i.e., an equal mixture of HCOOH and $HCOO^-$), these catalysts are not stable at high temperature or low pH. However, we observed the evolution of 1 m^3 of H_2/CO_2 gases from 20 mol FA without any adjustment of the solution pH (pH ~1.6) using Cp*Ir(L2), indicating complete decomposition of FA with a turnover number of 2,000,000. This result opens future opportunities for an onboard or on-site H_2 generation system from 10 M FA or concentrated FA. We are also investigating *Earth-Abundant HER* electrocatalysts such as nano-structured Mo or W carbide/nitride composites. These catalysts are durable and efficient catalysts in water (pH 1) and can be prepared by simple, environmentally benign methods.

We thank Dr. Y. Himeda at the National Institute of Advanced Industrial Science and Technology, Tsukuba, and Drs. K. Sasaki, J. T. Muckernam and M. Z. Ertem at BNL. The work at the Japan Science and Technology Agency (JST) and at BNL was supported by JST's Advanced Catalytic Technology Transformation Program for Carbon Utilization and by the U.S. Department of Energy, Office of Science, Basic Energy Sciences program under contract DE-SC00112704, respectively.

III.0 Hydrogen Delivery Sub-Program Overview

INTRODUCTION

The Hydrogen Delivery sub-program addresses all hydrogen transmission, distribution, and dispensing activities between the point of production and the fuel cell. Research and development (R&D) activities address challenges to the cost and performance of hydrogen infrastructure, including compatibility of commonly used materials with hydrogen, efficiency of hydrogen liquefaction, development of non-mechanical station compressors, lowering the costs of hydrogen storage, and enhancing the durability and accuracy of hydrogen dispensers. Technoeconomic analysis is used by the sub-program to identify drivers of hydrogen cost and barriers to widespread growth, which inform sub-program planning and portfolio development.

GOAL

The goal of this sub-program is to enable R&D advancements that reduce the costs associated with delivering hydrogen to a point at which its use as an energy carrier in fuel cell applications is competitive with alternative transportation and power generation technologies.

OBJECTIVES

The objective of the Hydrogen Delivery sub-program is to conduct R&D that lowers the cost of hydrogen dispensed at the pump to a point at which fuel cell electric vehicles are competitive on a cents-per-mile basis with competing vehicle technologies. Based on current analysis, this translates to a hydrogen cost of <$7 per gallon gasoline equivalent (gge) (produced, delivered, and dispensed, but untaxed) by 2020.[1] In the long term, an ultimate target of <$4/gge (produced, delivered, and dispensed, but untaxed) has been set for mature markets with economies of scale.[2] This cost target has been apportioned to be <$2/gge for production and <$2/gge for delivery and dispensing.[3] The sub-program plans to meet these objectives by developing low-cost, efficient, reliable, and safe technologies to deliver hydrogen from the point of production to the point of use in both stationary fuel cells and fuel cell electric vehicles. Key objectives for specific delivery components include:

- **Station Technologies:**
  - Compression: Enhance the durability of components in conventional compressors, and develop early-stage non-mechanical technologies with potential for high-pressure hydrogen compression.
  - Storage: Develop novel designs that lower the costs of hydrogen storage vessels, guided by materials compatibility R&D.
  - Dispensers: Develop novel materials and metering technologies to improve the cost, reliability, and accuracy of 700 bar dispensers.
- **Materials Compatibility:** Identify microstructures of steel with superior resistance to hydrogen embrittlement, and develop a constitutive model of hydrogen-assisted fatigue.
- **Liquid Hydrogen Technology:** Investigate novel approaches to hydrogen liquefaction (e.g., use of superconducting magnets or vortex tubes) with potential to achieve capital and operating costs substantially lower than those of conventional liquefiers.
- **Analysis:** Conduct comprehensive analyses on near- and long-term hydrogen delivery options to identify the advantages of each and areas for potential improvement.

[1] *Early Market Hydrogen Cost Target Calculation—2015 Update*, Program Record (Fuel Cell Technologies Office) 15012, U.S. Department of Energy, 2015. https://www.hydrogen.energy.gov/pdfs/15012_hydrogen_early_market_cost_target_2015_update.pdf
[2] *Hydrogen Threshold Cost Calculation*, Program Record (Office of Fuel Cell Technologies) 11007, U.S. Department of Energy, 2011. https://www.hydrogen.energy.gov/pdfs/11007_h2_threshold_costs.pdf
[3] *H_2 Production and Delivery Cost Apportionment,* Program Record (Hydrogen and Fuel Cells Program) 12001, U.S. Department of Energy, 2012. https://www.hydrogen.energy.gov/pdfs/12001_h2_pd_cost_apportionment.pdf

FISCAL YEAR (FY) 2017 TECHNOLOGY STATUS AND ACCOMPLISHMENTS

In FY 2017, the Hydrogen Delivery sub-program kicked off seven new projects, participated in one workshop, and saw significant progress in R&D activities of existing projects.

Sub-Program Level Accomplishments

In FY 2017, significant progress was made by the Hydrogen Delivery sub-program on several important fronts. Several highlights include:

- Argonne National Laboratory was issued a patent for the tube trailer consolidation strategy[4] developed in 2013. Tube trailer consolidation can lower the capital cost of compression at a fueling station and thereby lower overall station cost by 40%. The strategy involves use of a fueling station's compressor to pressurize the hydrogen in the tube trailer during off-peak hours of a day. As a result, the station has high-pressure hydrogen available during peak hours and is able to achieve higher flow rates than otherwise possible. In this way, a station can satisfy its daily demand with a compressor that costs 60% less than under normal operation.[5] The strategy is being evaluated experimentally at the National Renewable Energy Laboratory (NREL) through the Hydrogen Fueling Infrastructure Research and Station Technology (H2FIRST) project and is also being demonstrated by FirstElement Fuel at a retail station through a Technology Commercialization Fund award.
- WireTough Cylinders developed a design for an 875 bar hydrogen storage vessel that is expected to cost >50% less than those currently on the market. The design is based on wrapping autofrettaged liners with high-strength steel wire, and its cost projections have been independently verified.
- Used materials R&D funded by the U.S. Department of Energy and the U.S. Department of Transportation in the modification of the ASME B31.12 Code for Hydrogen Piping and Pipelines. Evaluations of the performance of high-strength steel and fiber-reinforced polymer in high-pressure hydrogen service over the past decade have led to Code modifications that 1) allow for the use of fiber-reinforced polymer in 170 bar hydrogen service and 2) remove "thickness penalties" on X70 steel used in 100 bar hydrogen service. Each of these modifications can independently lower the installation costs (material and labor) of hydrogen pipelines by 25%.[6]
- Announced four new Small Business Innovation Research (SBIR) awards in the areas of metal hydride materials discovery, magnetocaloric materials development, metal-free hydrogen dispensing hoses, and evaluation of coatings for compressor seals.

Project Level Accomplishments

During FY 2017, progress was made by existing projects in several key areas, including:

Station Technologies

Sub-program efforts on station technologies improve the reliability and reduce the cost of compression, on-site storage, and dispensers.

- In FY 2017, four projects were kicked off to advance non-mechanical concepts for high-pressure hydrogen compression. These projects were all in the areas of electrochemical and metal hydride compression. Electrochemical hydrogen compression involves the use of electrochemical cells to pressurize hydrogen. A catalyst layer on the cell membrane splits hydrogen molecules into protons and electrons on one side of the cell. A voltage is applied to cell electrodes such that the electrons travel through an external circuit toward the other side of the cell (i.e., the cathode side). The resulting charge at the cathode drives diffusion of protons through the cell membrane to the cathode side as well. As a result, high-pressure hydrogen builds up on the cathode. Metal hydride compression, on the other hand, involves use of materials that reversibly absorb and desorb hydrogen at specific temperatures. The supply and removal of heat can therefore be used with metal hydride materials to enable the uptake and/or release of hydrogen at specific pressures. FY 2017 R&D accomplishments in these areas include:

[4] Elgowainy, A. (2017). *U.S. Patent No. 9,739,418*. Washington, DC: U.S. Patent and Trademark Office.
[5] http://www.sciencedirect.com/science/article/pii/S036031991402833X
[6] Cost assessment for fiber-reinforced polymer has been based on consultation with members of industry. Cost assessment for steel is published in: Fekete, J., Sowards, J.W., and Amaro, R.L. "Economic impact of applying high strength steels in hydrogen gas pipelines." International Journal of Hydrogen Energy (2015). < http://www.sciencedirect.com/science/article/pii/S036031991501575X?via%3Dihub >

- Giner is enhancing the durability and current densities of membranes that may be viable in electrochemical hydrogen compression. The project's goal is to compress 0.5 kg H_2/h in an electrochemical cell at 875 bar. In 2017, Giner achieved its target current density for an electrochemical cell (~900 mA/cm^2 at a cell voltage of 0.25 V and a hydrogen pressure of 350 bar). Optimization of the chemical compositions of cell membranes has been implemented to effectively manage water in the cell and therein prevent "flooding" and allow for high rates of hydrogen transport.
- Researchers at Sandia National Laboratories are identifying metal hydrides and modeling compressor designs for an approach to achieve metal hydride compression with an energy efficiency of <4.0 kWh/kg. The aim is to produce a two-stage system of metal hydride beds capable of compressing hydrogen from 100 bar to 875 bar on the laboratory scale, along with comprehensive cost analysis for full scale (100 kg H_2/h). Metal hydride candidates have already been identified for each compressor stage based on extensive literature research, and their physical properties have been characterized in a custom Sieverts cycling apparatus assembled specifically for compression testing.
- Greenway Energy is combining these two novel technologies, electrochemical hydrogen compression and metal hydride compression, to produce a hybrid system for hydrogen compression. The project will result in the design, fabrication, and testing of their concept at 1–5 kg/day. For the electrochemical hydrogen compression, a polybenzimidazole membrane has been experimentally shown to outperform Nafion at high temperatures and pressures. A thermodynamic model of the complete system has been completed; the metal hydride compression is driven by waste heat produced by the electrochemical hydrogen compression.
- Greenway Energy has been awarded an SBIR grant for discovery of metal hydride materials to be used in high-pressure hydrogen compression. The project team has defined key material properties that metal hydrides must exhibit for use in high-pressure compression and identified a high-throughput approach to material characterization. The characterization approach involves synthesis of a cantilever beam, upon which metal hydrides will be deposited. Motion of the beam will measure hydrogenation/dehydrogenation rates. In parallel, the team has begun development of a computational model to predict enthalpy and entropy properties of metal hydride compositions. The model is being calibrated with data in the public domain (e.g., published in the Hydrogen Storage Materials Database).

- NREL improved the reliability of hydrogen dispensers through evaluations of the impact that cycling at 875 bar and -40°C has on hose material degradation, hose composition, and overall dispenser performance. The relationship between the rate of hydrogen permeation through the hose and hose temperature was assessed, as polymer performance may change near the glass transition temperature (-50°C). With the remaining funding, dynamic mechanical analysis, scanning electron microscopy, and chemical composition testing will be performed to compare the composition and morphology of the hose pre- and post-cycling.
- Argonne National Laboratory performed technoeconomic analysis to assess cost drivers associated with filling medium- and heavy-duty fuel cell vehicle systems. The impacts of various station configurations (e.g., multiple dispensers vs. one dispenser, supply by liquid tankers vs. tube trailers) and fill parameters (e.g., flow rate) on station cost were evaluated.
- Through H2FIRST, Sandia National Laboratories and NREL published a report detailing the designs and costs of several common types of hydrogen fueling stations, including those with on-site reforming of natural gas or electrolysis and those that are delivered pre-packaged. The report is now publicly available here: https://energy.gov/sites/prod/files/2017/03/f34/fcto-h2first-reference-station-phase2-2017.pdf.
- Ivys Energy Solutions initiated a project to develop a durable, high-accuracy (at least 2% accuracy) dispenser. To date, the team has quantified the impacts that key variables (e.g., weather, transients during fueling, manufacturing tolerances) can have on meter accuracy. They have also researched dedicated short-range communications hardware for integration into their dispenser, to enable wireless communication between the dispenser and the vehicle.
- NanoSonic made progress in the development of a new metal-free hydrogen dispensing hose, expected to cost 2x less than the current state of the art and weigh 25% less. Over the past year, use of a novel ceramer has nearly doubled the burst strength of the hose to 31,000 psi. Future work will focus on development of hose fittings to increase durability, as well as iterations on fiber reinforcement.
- GVD Corporation reduced erosion of seals used in hydrogen compressors by over 70% using an innovative coating process developed at the Massachusetts Institute of Technology. Over the past year, the deposition process

of these coatings has been optimized, and testing of coating performance was conducted at PowerTech Labs. In the next year, the coatings will be tested for hydrogen permeation on compressors at NREL and will be optimized for use in dispensers as well.

Materials Compatibility

Structural steels are widely used in hydrogen infrastructure, such as in pipelines, compressors, and pressure vessels. A microstructure-based understanding of hydrogen-induced damage (i.e., hydrogen embrittlement) in steels can enhance the reliability and lower the costs of components by enabling the use of alloys that are currently assumed to be unsuitable. The Delivery sub-program's current project in this area is identifying microstructures with enhanced resilience to hydrogen effects, with the goals of (1) developing a novel steel alloy and (2) informing the development of a constitutive model of hydrogen embrittlement.

- The project team has completed triplicate measurements of fatigue crack growth in specimens of X100 base metal and welds and evaluated the impact that "residual stresses" have on specimens' resistance to fatigue; accounting for residual stresses allows for the impacts of microstructure alone to be more accurately estimated. Additionally, the team has generated samples of steel with gradient microstructures (i.e., Gleeble specimens) that will be tested in FY 2018. These specimens will allow for comparisons to be made of the performance of various microstructures in hydrogen. Finally, the data being generated experimentally is being used to calibrate a constitutive model of hydrogen embrittlement developed at Colorado School of Mines in collaboration with the U.S. Department of Transportation and the National Institute of Standards and Technology.

Liquid Hydrogen Technologies

Liquefaction represents more than 50% of the cost of hydrogen delivered to vehicles via liquid fueling stations. DOE is funding research to lower the costs of liquefaction, as well as the costs of utilizing liquid hydrogen at fueling stations.

- Pacific Northwest National Laboratory is developing a concept for hydrogen liquefaction using superconducting magnets and magnetocaloric materials, with the goal of liquefying hydrogen at twice the efficiency of conventional cycles. Magnetocaloric materials cool down in the presence of a magnetic field. In FY 2016, Pacific Northwest National Laboratory set a world record by achieving a 100-K temperature span with these materials and a 3.3-Tesla superconducting magnet. In FY 2017, researchers identified 14 alloys that can be layered and achieve the full temperature span targeted (280 K – 20 K) for hydrogen liquefaction, and they synthesized the first eight using an innovative approach known as rotating disk atomization. Models of regenerator performance were validated with experimentation on individual layers, and approaches to managing heat transfer between layers are being developed.
- At Lawrence Livermore National Laboratory, thermodynamic models of liquid hydrogen behavior (e.g., heat transfer and resulting evaporation) are being used to simulate boil-off losses from hydrogen infrastructure, such as dewars at fueling stations and/or liquid tankers. These models are meant to inform strategies to mitigate boil-off. They are additionally being used in conjunction with data on vehicle driving patterns to assess the economic viability of cryo-compressed hydrogen use in vehicles.

Workshops

The *Fifth International Workshop on Hydrogen Infrastructure and Transportation*, organized by the National Organisation Hydrogen and Fuel Cell Technology (NOW) of Germany, the New Energy and Industrial Technology Development Organization (NEDO) of Japan, the European Commission's Joint Research Center, and DOE, was held in May of 2017 in Berlin, Germany. This workshop included members of industry, academia, and government—Japan, Germany, the European Union, China, Scandinavian countries, and the United States. Key takeaways from the workshop are summarized in Table 1 below.

TABLE 1. Key Issues Discussed at the 5th International Infrastructure Workshop

Fueling	Germany, Japan, and the United States all have devices in place to collect data for validation of stations against refueling requirements. Inconsistences in station design can challenge operation of these devices. In Germany, the world's first fuel cell powered train is also being developed and will require new fueling protocols.
Hydrogen Quality	Members of government and industry in Germany, Japan, and the United States are working toward the development of inline contaminant detectors for fueling stations. Efforts are focused on identifying priority contaminants (those with greatest likelihood of occurrence, or likely to cause the greatest damage to a fuel cell).
Metering	Germany, Japan, and the United States are all currently permitting hydrogen sales at lower accuracies than the target of 2%. In the meantime, each country has ongoing R&D to develop new meters, develop meter test devices, and identify the causes of meter inaccuracies. While the accuracy of 2% is often achieved, outliers (e.g., due to vibrations from traffic or weather) can reduce the accuracy to up to 10%.
Hardware	While station availability has increased, compressors and chillers remain the primary causes of station down-time. An additional concern internationally is the ergonomics of dispensers.
Hydrogen Logistics	Innovative mechanisms of hydrogen delivery and/or uses of hydrogen fuel cells are being explored internationally. Liquid chemical carriers are being developed in Japan to allow for hydrogen imports. In the United States, non-mechanical approaches to hydrogen liquefaction are being explored to lower the costs of liquid hydrogen delivery.

Publications

NREL published the "Comparison of conventional vs. modular hydrogen refueling stations, and on-site production vs. delivery" report.[7] This report details standard designs and expected costs of hydrogen fueling stations with hydrogen production on site (in the form of steam methane reforming or electrolysis), as well as pre-assembled (i.e., modular) stations.

FY 2017 Funding

In FY 2017, DOE announced four SBIR awards and one Technology Commercialization Fund award:

- Greenway Energy was awarded an SBIR Phase I award to develop an approach to metal hydride materials discovery. It has begun machine learning, as well as high-throughput computation toward this project, as detailed above.
- General Engineering and Research LLC was awarded an SBIR Phase II award to optimize its approach to synthesizing low-cost magnetocaloric materials of interest to hydrogen liquefaction.
- GVD Corp. was awarded an SBIR Phase IIA award to modify the deposition process for its coatings, to allow for use in hydrogen dispensers. These coatings will also be tested in compressors at NREL.
- NanoSonic, Inc. was awarded an SBIR Phase IIB award to develop fittings for hydrogen dispensing hoses and optimize the design of the dispensing hose they developed in Phase II.
- Argonne National Laboratory was given a Technology Commercialization Fund award to demonstrate the tube trailer consolidation strategy at a retail hydrogen fueling station. The strategy can lower the costs of a hydrogen compressor at a fueling station by 60% and is described above under "Project Level Accomplishments."

Additional FY 2017 funding will be directed toward awards made under the H2@Scale Cooperative Research and Development Agreements Call.

BUDGET

The FY 2017 appropriation for Hydrogen Production and Delivery projects totaled $25.4 million. With the emphasis on supporting H2@Scale and on advanced technologies for fueling station, hydrogen liquefaction, and large-scale delivery options, the apportionment of this funding in the Hydrogen Delivery and Dispensing portfolio was approximately $9.3 million. The estimated budget breakdown for Hydrogen Delivery and Dispensing in FY 2017 is shown in Figure 1.

[7] https://energy.gov/sites/prod/files/2017/03/f34/fcto-h2first-reference-station-phase2-2017.pdf

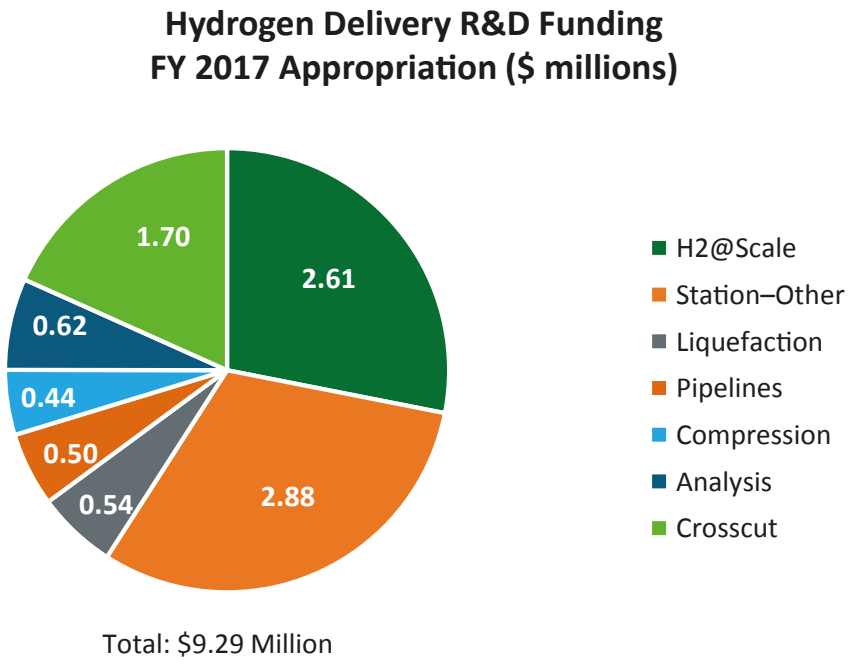

FIGURE 1. FY 2017 Appropriations

UPCOMING ACTIVITIES AND PLANS

In FY 2018, the Hydrogen Delivery sub-program will focus on several key efforts, including:

- Advancing non-mechanical magnetocaloric liquefaction concepts to enable hydrogen liquefaction with 2X efficiency, in support of H2@Scale.
- Early-stage materials development to enhance service lives and lower costs of fueling station components.
- Exploratory R&D to assess the potential of chemical carriers for high-volume hydrogen storage and delivery.

Future activities are subject to appropriations.

Neha Rustagi
Hydrogen Production and Delivery Technology Manager
Fuel Cell Technologies Office
Office of Energy Efficiency and Renewable Energy
U.S. Department of Energy
1000 Independence Ave., SW
Washington, DC 20585-0121
Phone: (202) 586-8424
Email: Neha.Rustagi@ee.doe.gov

III.1 Fatigue Performance of High-Strength Pipeline Steels and Their Welds in Hydrogen Gas Service

Joseph Ronevich (Primary Contact),
Zhili Feng (Oak Ridge National Laboratory [ORNL]),
Andrew Slifka (National Institute of Standards and Technology [NIST]), Elizabeth Drexler (NIST),
Robert Amaro (University of Alabama),
Eun Ju Song (Sandia National Laboratories)
Sandia National Laboratories (SNL)
7011 East Avenue
Livermore, CA 94550
Phone: (925) 294-3115
Email: jaronev@sandia.gov

DOE Manager: Neha Rustagi
Phone: (202) 586-8424
Email: Neha.Rustagi@ee.doe.gov

Project Start Date: October 1, 2015
Project End Date: September 30, 2018

Overall Objectives

- Enable the use of high strength steel hydrogen pipelines, as significant cost savings can result by implementing high strength steels as compared to lower strength pipes.
  - Determine whether girth welds in high-strength steel pipe exhibit fatigue performance similar to lower-strength steels in high-pressure hydrogen gas.
  - Identify pathways for developing high-strength pipeline steels by establishing the relationship between microstructure constituents and hydrogen-accelerated fatigue crack growth (HA-FCG).

Fiscal Year (FY) 2017 Objectives

- Complete fabrication of specimens from graded-microstructure high-strength steels for HA-FCG measurements. (SNL)
- Complete the draft of a peer-reviewed journal article on HA-FCG results for a current-practice arc weld in X100 steel. (SNL)
- Complete a minimum of three HA-FCG measurements on graded-microstructure high-strength steels at constant H_2 pressure, load-cycle frequency, and mean stress. (SNL)
- Incorporate a calibrated phenomenological model of X100 base metal into the framework of a physics-based model for validation of the physics-based model. (NIST)
- Analyze results of Gleeble™ tests to identify relationship between microstructure constituents and HA-FCG to inform development of lab-scale steel and NIST predictive model. (SNL, ORNL)
- Fabricate friction-stir weld in X100 steel. (ORNL)

Technical Barriers

This project addresses the following technical barriers from the Hydrogen Delivery section of the Fuel Cell Technologies Office Multi-Year Research, Development, and Demonstration Plan.

(D) High As-Installed Cost of Pipelines

(K) Safety, Codes and Standards

Technical Targets

This project impacts the following technical targets for hydrogen delivery components (Table 3.2.4 of the Fuel Cell Technologies Office Multi-Year Research, Development, and Demonstration Plan) related to pipelines for gaseous hydrogen delivery.

- Total capital investment: $695,000/mile (FY 2020)
- Transmission pressure: 100 bar (FY 2020)
- Lifetime: 50 years (FY 2020)

Design codes such as the America Society of Mechanical Engineers (ASME) B31.12 [1] contain structural integrity models which enable safety assessment of low strength steel pipelines subjected to pressure cycling. Currently there are prescribed safety factors specifically for hydrogen service (i.e., materials performance factors) to accommodate the potential for hydrogen embrittlement. These materials performance factors are a function of the specified minimum yield strength (SMYS) for the steel. Consequently, allowable stresses are significantly more restricted for high strength steel pipe compared to low strength, yet recent testing performed at both SNL and NIST [2–4] have shown similar fatigue performance of steel pipelines over a large range of SMYS. However, such conservative allowable stresses allowed in the current code nullify any cost savings that would be afforded by high strength steels. Direct reductions in capital costs would be realized if higher strength steels with thinner wall pipe thicknesses were permitted.

FY 2017 Accomplishments

- Completed triplicate fatigue crack growth rate (FCGR) tests on the base metal, weld and heat affected zone (HAZ) of a commercially available X100 girth welded pipeline steel in 21 MPa H_2 gas.
- Paper published on X52 friction stir weld: J.A. Ronevich, B.P. Somerday, Z. Feng, "Hydrogen accelerated fatigue crack growth of friction stir welded X52 steel pipe," *Int. J. of Hydrogen Energy*, Vol. 42, (7), 2017, pp. 4259–4268.
- Completed draft manuscript in collaboration with University of California, Davis entitled, "Residual stress effects on fatigue crack growth rates of X100 steel welds in high pressure hydrogen gas," to be submitted to *Engineering Fracture Mechanics.*
- Fabricated and extracted test coupons from three high strength alternative consumable welds for testing in hydrogen gas to provide comprehensive study on high strength welds.
- Determined pathway to quantify and correct for residual stresses in welds and HAZ in high strength materials to allow direct comparisons of fatigue performance of different microstructures.
- Initiated microstructure investigation and grain size distribution on X100 base materials and welds.
- Implemented calibration of plasticity-fatigue in ABAQUS framework.

✧ ✧ ✧ ✧ ✧

INTRODUCTION

Steel pipelines represent an economical means of transporting gaseous hydrogen over long distances; however, it is well known that these carbon-manganese steels are susceptible to hydrogen degradation. Current steel pipelines codes (e.g., ASME B31.12 [1]) place limitations on allowable stresses based on the SMYS of the material. These material performance factors reflect the general trend that hydrogen embrittlement can be more severe in high-strength steels. However, recent testing [2–4] of pipeline steels with a range of SMYS from 358 MPa to 689 MPa have not exhibited this trend and suggest that hydrogen assisted fatigue crack growth may not increase with strength. The conservative allowable stresses currently permitted in the code remove the cost savings that would be realized if higher strength steel pipelines were permitted. In pipeline applications without material performance factors, wall thickness is inversely proportional to steel strength; therefore, higher strength steels can reduce material and installation costs [5].

This project focuses on developing a pathway to enable the use of high-strength steel pipes. One means to accomplishing this goal is to assess the fatigue performance of high-strength steel pipelines in high pressure hydrogen gas. The fatigue crack growth rate (da/dN) versus stress-intensity factory range (ΔK) relationship is a necessary input to structural integrity models applied to steel hydrogen pipelines. One specific assessment methodology for steel hydrogen pipelines is published in ASME B31.12 code [1] which requires testing of the base metal, weld, and heat-affected zone. One of the gaps is the fatigue performance of high strength steel welds and whether the behavior will follow the same trends that the base metal exhibited over the SMYS range. As the performance of the steel base metals or welds may vary as function of microstructure, development of physics-based relationships between FCGRs and microstructure would greatly enhance the structural integrity models and drastically reduce the test burdening required to qualify materials for hydrogen use. The relationships between microstructures, contained in high-strength steels and welds, and hydrogen-assisted fatigue are evaluated in this study.

APPROACH

The objectives for this project are the following: (1) demonstrate that girth welds in high-strength steel pipe exhibit fatigue performance similar to lower-strength steels in high-pressure hydrogen gas and (2) identify pathways for development of high-strength pipeline steels by establishing the relationship between microstructure constituents and HA-FCG. Based on these project objectives, the technical tasks are designed to furnish innovative high-strength steel products for evaluation and to measure performance metrics for these high-strength steel products (i.e., fatigue crack growth rates in hydrogen gas) with high reliability. Completion of these tasks will assist in reaching the goal of this work: the deployment of steel pipe with reduced wall thickness, which can lower costs for hydrogen pipeline installation.

RESULTS

Fatigue crack growth rate testing was completed in 21 MPa H_2 gas on a commercially available X100 welded steel pipe with testing focused on the base metal, weld, and HAZ. The results from triplicate tests are shown in Figure 1a along with a test performed in air for comparison. Residual stresses were measured in collaboration with University of California, Davis to aid in decoupling the effects of residual stress from microstructural sensitivity to hydrogen degradation. The residual stresses were quantified and the FCGR curves were corrected as shown in Figure 1b. Due to the repeatability in the triplicate tests, only one curve for the weld, HAZ, and base metal were corrected. As can

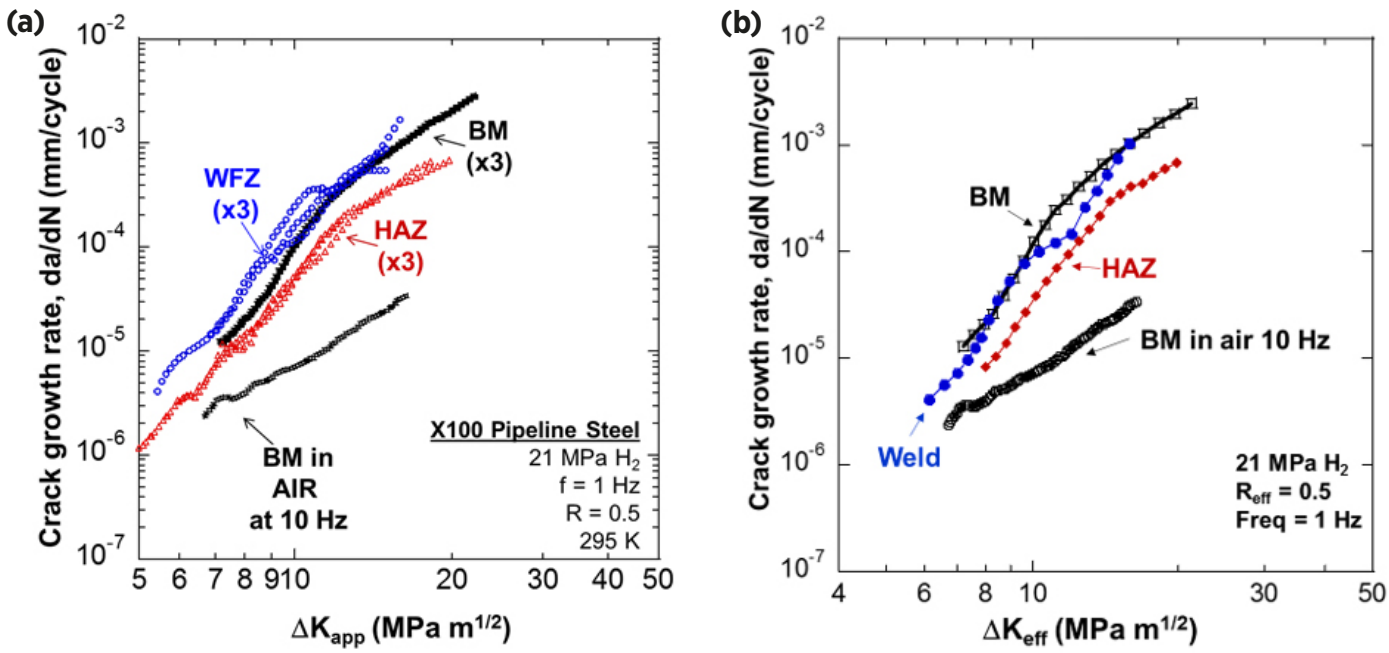

FIGURE 1. (a) Fatigue crack growth rate (da/dN versus ΔK_{app}) curves for X100A base metal (BM), weld fusion zone (WFZ), and heat affected zone (HAZ) tested in 21 MPa H_2 gas. Test performed in air at 10 Hz is shown for comparison. (b) Fatigue crack growth rates corrected for residual stress and plotted versus ΔK_{eff}.

be observed in Figures 1a and 1b, the base metal exhibits negligible difference between ΔK_{app} and ΔK_{eff}, whereas the weld and HAZ exhibit a notable difference between the ΔK_{app} and ΔK_{eff}. The removal of residual stress effects shifts the weld FCGR curve to comparable or even slightly lower FCGRs than the base metal. The HAZ data appears to have a similar shift to the right resulting in lower da/dN for a given ΔK_{eff}. This result is important as it demonstrates that residual stresses can have significant and measureable effects on fatigue crack growth rates.

In an effort to gain a more comprehensive understanding of high strength steel welds, ORNL fabricated three additional welds using different consumables from the same X100 base metal. Figures 2a, 2b, and 2c show the three welds labeled W1, W3, and W4, respectively, along with hardness maps. W1 and W3 were fabricated using commercial filler metals and W4 was fabricated with a weld wire developed by ORNL which was designed to be resistant to hydrogen embrittlement. Testing is planned of these welds in hydrogen from the fourth quarter of FY 2017 to the first quarter of FY 2018.

In order to enable a detailed study of the relationship between microstructure and hydrogen-assisted fatigue crack growth, a novel approach was developed to produce laboratory controlled microstructures using a Gleeble™ at ORNL. X80 steel coupons were subjected to non-uniform heating to produce a gradient microstructure in the axial direction. This facilitated extraction of computed tomography (CT) test coupons in which constant ΔK tests could be performed across the gradient microstructure allowing assessment of a wide range of microstructures in only a few test specimens. This is demonstrated in Figure 3a in which the CT specimen is extracted in an orientation that facilitates extension of the crack across the gradient microstructure. One challenge that was encountered during the fatigue testing was that the crack arrested due to compressive residual stresses as shown in Figure 3b. Although not directly measured, the magnitude of the residual stress in this CT test coupon convolutes a clear comparison of microstructure and da/dN. ORNL is fabricating additional Gleeble™ specimens with a less severe temperature gradient to mitigate residual stresses, thereby improving probability of comparing microstructure and fatigue crack growth rates in H_2 gas.

In collaboration with the U.S. Department of Transportation, NIST and Colorado School of Mines have derived a constitutive, phenomenological model that can predict HA-FCG in pipeline steels as a function of hydrogen pressure and specimen strain [**7**]. This model was developed through a combination of mathematical modeling and calibration with experimental results. Tensile data of X100 were used to extrapolate relationships that correlate strain (a measurable, physical parameter of steel) to applied stress (e.g. due to pressure cycling in a pipeline). Figure 4 shows some ABAQUS finite element model results of an X100 steel in which tensile experimental data were used to calibrate fully reversed loading in the model. These relationships were then incorporated into standard engineering models

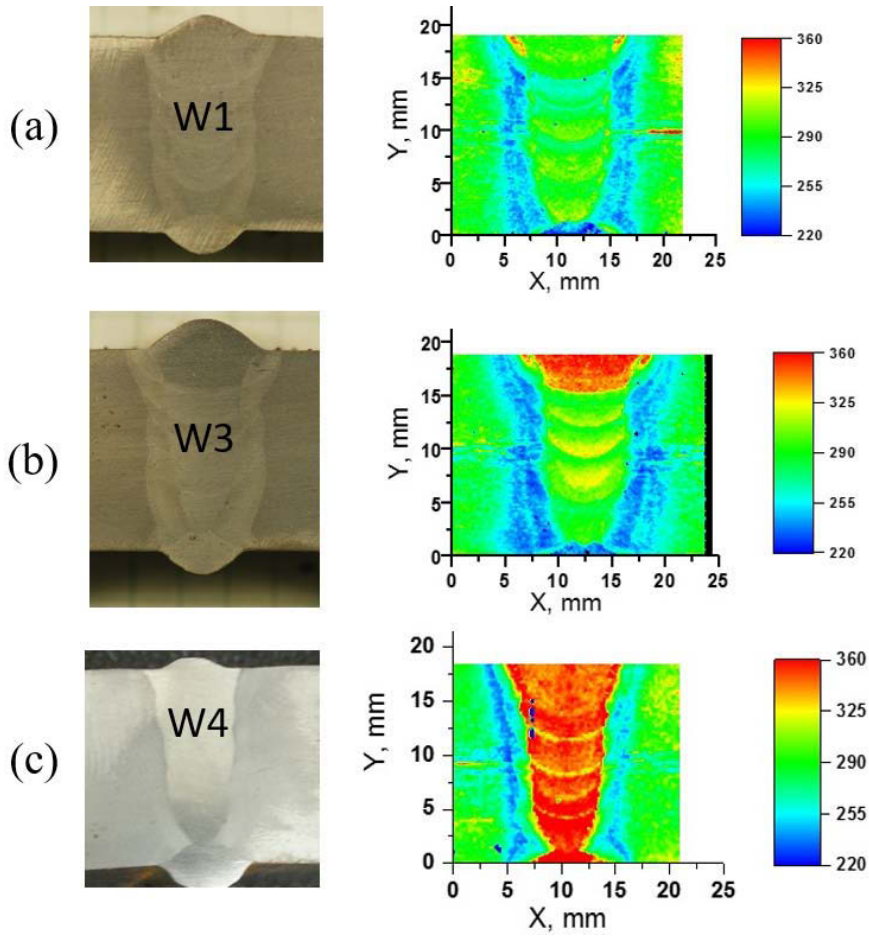

FIGURE 2. Fabricated alternative consumable welds: W1, W3, and W4, with corresponding microhardness maps.

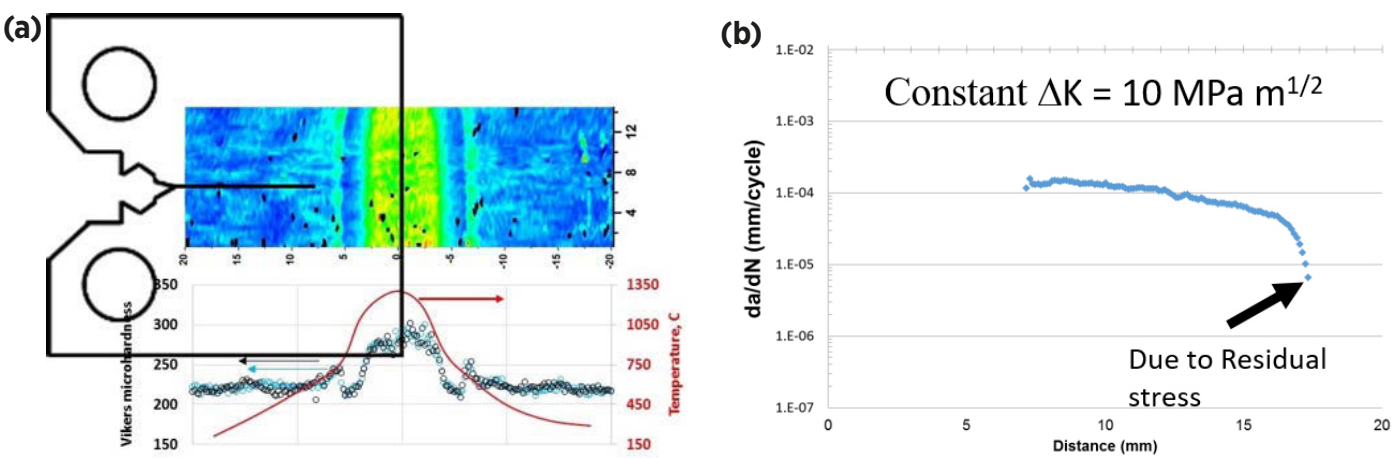

FIGURE 3. (a) CT specimen overlaid on hardness map of Gleeble™ coupon indicating gradient hardness that crack extension should encounter. (b) FCGR during a constant ΔK test as a function of position in 21 MPa H_2 gas. Fatigue crack was arrested near higher hardness area due to compressive residual stresses.

of damage from both mechanical loading and hydrogen effects to derive a constitutive model that predicts HA-FCG in CT specimens as a function of hydrogen pressure and cycle frequency [8]. The constitutive model is currently being calibrated to additional microstructures of steel used in pressure vessels, and incorporated into a finite element

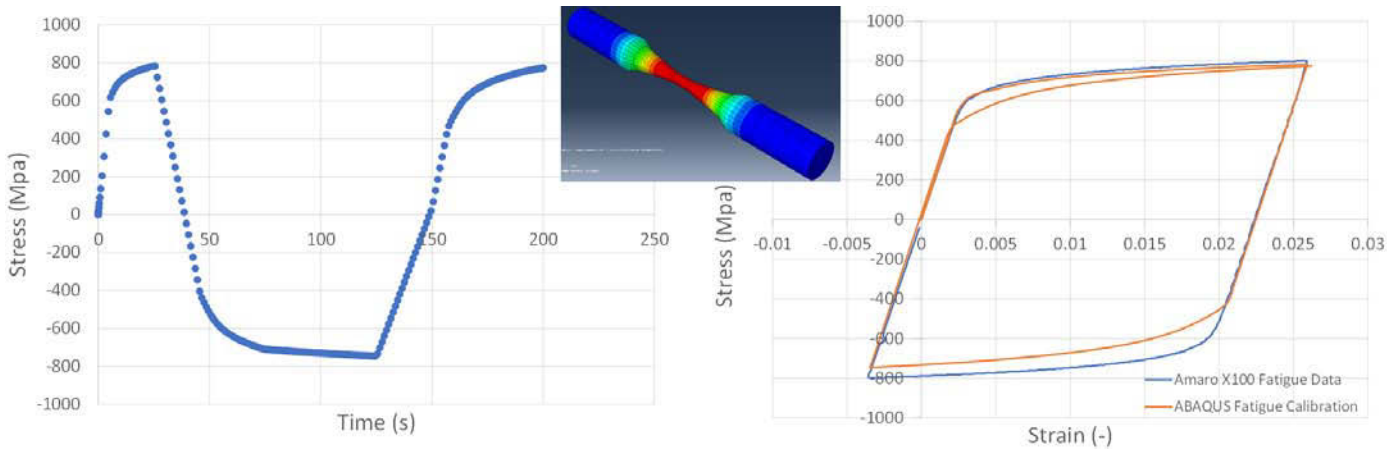

FIGURE 4. ABAQUS finite element calibration of X100 pipeline steel experiencing fully reversed load. Model predicts stress-strain response by use of Mises, kinematic work hardening, yield surface evolution.

package, ABAQUS [9]. Inclusion in ABAQUS will ultimately expand the model's applicability to a wide range of three-dimensional geometries; it is currently only applicable to coupon specimens. In parallel, NIST has been evaluating the behavior of steel specimens in hydrogen using neutron diffraction, to elucidate hydrogen diffusion behavior and interactions with microstructural features (e.g. dislocations), as well as crack tip plasticity that develops during mechanical loading. In FY 2018, the model developed will be calibrated to additional microstructures of steel that are developed by ORNL and tested at Sandia, and efforts will be made to expand it with the ability to simulate microstructure-specific phenomena such as hydrogen transport, plasticity, de-cohesion laws, and orientation specific mechanical properties at the grain level.

CONCLUSIONS AND UPCOMING ACTIVITIES

- Decoupling residual stress effects from FCGR curves facilitated direct comparison of fatigue performance of different regions of welded pipe. Once residual stress effects were removed, the base metal and weld data exhibited similar FCGR relationships in H_2 with the HAZ exhibiting the lowest FCGR.
- Fabricated three additional welds using different filler metals to provide comprehensive study on high strength welds. Additionally, fabricated gradient microstructures using Gleeble™.
- (Future) Residual stress measurements are planned for alternative weld test coupons to ensure FCGR relationships can be compared without the complications of residual stress.
- Initial testing of gradient microstructures from Gleeble™ samples was unmanageable due to significant residual stresses. (Future) Redesigned cooling profiles of Gleeble™ heat treatment were performed to mitigate residual stress to facilitate comparisons between microstructure and HA-FCG.

FY 2017 PUBLICATIONS

1. J. Ronevich, B. Somerday, Z. Feng, "Hydrogen accelerated fatigue crack growth of friction stir welded X52 steel pipe," *Int. Journal of Hydrogen Energy*, Vol. 42, Issue 7, February 2017, pp. 4259–4268.

2. J. Ronevich, B. Somerday, "Hydrogen-accelerated fatigue crack growth in arc welded X100 pipeline steel," *in proceedings of 2016 International Hydrogen Conference,* Jackson Hole, WY.

3. Amaro, R.L., Long, B.L., Slifka, A.J., Drexler, E.S., O'Connor, D.T., "Application of a Model of Hydrogen-Assisted Fatigue Crack Growth in 4130 Steel," *Proceedings of International Hydrogen Conference 2016*, Jackson Hole, WY.

4. O'Connor, D.T., Long, B.L., Slifka, A.J., Drexler, E.S., Amaro, R.L., "Computational Modeling of Hydrogen-Assisted Fatigue Crack Growth in Pipeline Steels," *Proceedings of International Hydrogen Conference 2016*, Jackson Hole, WY.

5. J. Ronevich, B. Somerday, "Hydrogen Effects on Fatigue Crack Growth Rates in Pipeline Steel Welds PVP2016-63669," *ASME 2016 Pressure Vessels & Piping Conference,* Vancouver, Canada, July 17–21, 2016.

FY 2017 PRESENTATIONS

1. J. Ronevich et al., "Fatigue Performance of High-Strength Pipeline Steels and Their Welds in Hydrogen Gas Service," 2017 FCTO Annual Merit Review, Washington D.C., June 6, 2017.

2. J. Ronevich, "Fatigue Performance of High-Strength Pipeline Steels and Their Welds in Hydrogen Gas Service," Joint Delivery-Storage Tech Team Meeting, Detroit, MI, February 15–16, 2017.

3. J. Ronevich, C. San Marchi, B. Somerday, "Hydrogen accelerated fatigue crack growth of welded steel pipelines,"

Joint HYDROGENIUS and I²CNER International Workshop on Hydrogen-Materials Interactions 2017, Fukuoka, Japan, February 3, 2017.

4. J. Ronevich, C. San Marchi, B. Somerday, "Fatigue and Fracture Performance of High Strength Pipeline Steels in High Pressure Hydrogen Gas," *ASME International Mechanical Engineering Congress & Expositions,* Phoenix, AZ, November 14–17, 2016.

5. J. Ronevich, B. Somerday, "Hydrogen Effects on Fatigue Crack Growth Rates in Pipeline Steel Welds PVP2016-63669," *ASME 2016 Pressure Vessels & Piping Conference,* Vancouver, Canada, July 17–21, 2016.

6. J. Ronevich, C. San Marchi, "Safety, R&D, and Deployment of Hydrogen Infrastructure," *International Workshop for Hydrogen Infrastructure Reliability,* Daejeon, Korea, June 27, 2016.

REFERENCES

1. ASME, "B31.12 Hydrogen Piping and Pipelines," ed. New York, NY: ASME, 2011.

2. A.J. Slifka *et al*., "Fatigue crack growth of two pipeline steels in a pressurized hydrogen environment," *Corrosion Science*, vol. 78, 2014pp. 313–321.

3. J.A. Ronevich, B.P. Somerday, C.W. San Marchi, "Effects of microstructure banding on hydrogen assisted fatigue crack growth in X65 pipline steels," *Int. J. of Fatigue,* Vol. 82, 2016, pp. 497–504.

4. C. San Marchi, B.P. Somerday, K.A. Nibur, D.G. Stalheim, T. Boggess, S. Jansto, "Fracture Resistance and Fatigue Crack Growth of X80 Pipeline Steel in Gaseous Hydrogen," in ASME Pressure Vessles & Piping Division, Baltimore, Maryland USA, 2011.

5. J.R. Fekete, J.W. Sowards, and R.L. Amaro, "Economic impact of applying high strength steels in hydrogen gas pipelines," *International Journal of Hydrogen Energy,* vol. 40, pp. 10547–10558, 2015.

6. ASTM, "E647-11 Standard Test Method for Measurement of Fatigue Crack Growth Rates," ed. West Conshohocken, PA, 2011.

7. R.L. Amaro, E.S. Drexler, and A.J. Slifka, "Fatigue crack growth modeling of pipeline steels in high pressure gaseous hydrogen," *International Journal of Fatigue,* vol. 62, pp. 249–257, 2014.

8. O'Connor, D.T., Long, B.L., Slifka, A.J., Drexler, E.S., Amaro, R.L., "Computational Modeling of Hydrogen-Assisted Fatigue Crack Growth in Pipeline Steels," *Proceedings of International Hydrogen Conference 2016*, Jackson Hole, WY.

9. Amaro, R.L., Long, B.L., Slifka, A.J., Drexler, E.S., O'Connor, D.T., "Application of a Model of Hydrogen-Assisted Fatigue Crack Growth in 4130 Steel," Proceedings of International Hydrogen Conference 2016, Jackson Hole, WY.

III.2 Hydrogen Compression Application of the Linear Motor Reciprocating Compressor (LMRC)

Eugene L. Broerman (Primary Contact), Norm Shade (ACI Services), Klaus Brun, Jeffrey Bennett, Nathan Poerner, Diana Strickland, Jerome Helffrich, Shane Coogan, Aaron Rimpel, Pablo Bueno
Southwest Research Institute® (SwRI®)
6220 Culebra Rd.
San Antonio, TX 78238
Phone: (210) 522-2555
Email: EBroerman@swri.org

DOE Manager: Neha Rustagi
Phone: (202) 586-8424
Email: Neha.Rustagi@ee.doe.gov

Contract Number: DE-EE0006666

Subcontractor:
- Norm Shade, ACI Services, Cambridge, OH

Project Start Date: September 5, 2014
Project End Date: October 4, 2018

Overall Objectives

- Demonstrate the linear motor reciprocating compressor (LMRC) by integrating individually-developed Technology Readiness Level 4 or higher components.
- Demonstrate that the compressor portion of the LMRC has improved compression efficiency and a reduced capital and maintenance cost compared to conventional reciprocating compression technology.
  - Improve isentropic efficiency above 73% by minimizing aerodynamic losses and using low-friction bearings (goal is above 95%).
  - Reduce capital costs to half those of conventional reciprocating compressors by minimizing part count.
  - Reduce required maintenance by simplifying the compressor design to eliminate common wear items.
- Meet the design requirements for all three stages of compression: compress hydrogen from 290 psia (20 bara) to 12,690 psia (875 bara) with flow rates greater than 22 lbm/h (10 kg/h) and an isentropic efficiency of compression above 73%.
- Meet the test requirements for the first stage of compression: compress hydrogen from 290 psia (20 bara) to 1,030 psia (71 bara) with flow rates greater than 22 lbm/hr (10 kg/h) and an isentropic efficiency of compression above 73%.
- Meet the fiscal year (FY) 2018 test requirements for the first stage of compression: compress hydrogen from 290 psia (20 bara) to 1,030 psia (71 bara) with flow rates greater than 22 lbm/hr (10 kg/h) and an overall system specific energy of 1.6 kWh/kg or lower.

Fiscal Year (FY) 2017 Objectives

The overall objectives for FY 2017 are final fabrication, assembly of test loop, and testing of the LMRC.

- Fabricate and assemble low pressure (LP) stage compressor parts.
- Construct the test stand and integrate the compressor.
- Commission and start up the demonstration model.
- Test the bench-scale system.
- Analyze the single stage test results.

Technical Barriers

This project addresses the following technical barriers from the Hydrogen Delivery section of the Fuel Cell Technologies Office Multi-Year Research, Development, and Demonstration (MYRDD) Plan.

(B) Reliability and Costs of Gaseous Hydrogen Compression

Technical Targets

During the proposal phase and kick-off of the project, the DOE technical targets were based on the 2012 MYRDD Plan. A 2015 MYRDD Plan was updated in August of 2015. Table 1 compares the predicted characteristics of the LMRC design with 2020 targets from both MYRDD reports.

FY 2017 Accomplishments

- Finalized plans for commissioning, safety, and operation of the test stand.
- Fabricated and assembled all of the LP stage compressor parts.
- Constructed the test stand.

TABLE 1. Progress towards Meeting Technical Targets for Hydrogen Delivery with Small Compressors: Fueling Sites (~100 kg H_2/h peak flow)

Characteristic	Units	2012 MYRDD Target for 2020	2015 MYRDD Target for 2020	LMRC 2020 Status (Predictions)
Reliability		High	NA	High
Availability	%	NA	≥85	TBD
Compressor Efficiency	Isentropic %	80%	NA	80% - all 3 stages
Compressor Specific Energy	kWh/kg	100 bar inlet: NA 500 bar inlet: NA	100 bar inlet: 1.6 500 bar inlet: 1.4	20 bar to 875 bar: 1.8 (Compressor Only) 9.2 (LMRC) 100-bar Inlet Pressure: 1.45 (Optimized LMRC)
Losses of H_2 Throughput	% of flow	<0.5%	0.5%	<0.4%
Uninstalled Capital Cost (Based on 1,000 kg/d Station, [~100 kg H_2/h Peak Compressor Flow])	$	$240,000 (1 Compressor, No Backup)	NA (1 Compressor, No Backup)	20-bar to 875-bar: $284,000 (1 Compressor, No Backup)
Uninstalled Capital Cost (Based on 750 kg/d Station, [~100 kg H_2/h Peak Compressor flow])	$	100-bar inlet: NA 500-bar inlet: NA (1 Compressor, No Backup)	100-bar inlet: 275,000 500-bar inlet: 90,000 (1 Compressor, No Backup)	100-bar to 875-bar: $195,000 500-bar inlet: $105,000 (1 Compressor, No Backup)
Annual Maintenance Cost	% of Installed Capital Cost	2.0%	4%	1.2% of Uninstalled Capital Cost
Outlet Pressure Capability	bar	860	950	875
Compression Power	kW	240 (20 bar at Inlet)	NA	170 (20 bar at Inlet) (Compressor Required Power)

NA – Not Applicable
TBD – To Be Determined
100-bar inlet – pipeline delivery of gas to the compressor
500-bar inlet – Tube Trailer Delivery of gas to the compressor

INTRODUCTION

SwRI® and ACI Services, Inc., are developing an LMRC to meet the DOE goal of increasing the efficiency and reducing the cost of forecourt hydrogen compression. The proposed advanced compression system utilizes a novel and patented concept of driving a permanent magnet piston inside a hermetically-sealed compressor cylinder through electromagnetic windings. The LMRC is an improvement over conventional reciprocating compressors as it minimizes the mechanical part count, reduces leakage paths, and is easily modularized for simple field installation (U.S. Patent 8,534,058) [1].

APPROACH

The LMRC is a novel concept compared to conventional reciprocating compression technology. The compression system replaces the functions of an electric motor drive and reciprocating compressor with an integrated, linear, electrically-actuated piston. It will have a magnetic piston within a cylinder and a gas compression chamber at each end of the piston. The compressor cylinder is comprised of an electromagnetic coil that is operable with the piston to convert an input of electrical power to a reciprocating movement of the piston. This uses the same technology seen in magnetic bearings in turbomachinery and does not require oil for lubrication. Since the driver and compressor are integrated into the same hermetically-sealed component, there is a significant reduction in the number of parts and materials needed to construct this device. In addition, the simplicity of the design reduces required maintenance, minimizes seal leakages and wear, and allows for oil-free operation.

The LMRC system minimizes parasitic losses by using reduced piston speeds, low-pressure-drop contoured valves, and inter-stage cooling manifolds. Working at low reciprocating speeds of approximately 300 cycles per minute (5 Hz), the LMRC prototype is expected to meet an isentropic efficiency goal of greater than 95% per stage [2]. That efficiency can be compared with current state-of-the-art technology that typically has an efficiency of closer to 73%. The improved isentropic efficiency and reduced mechanical losses result in an increase in overall efficiency for the LMRC system.

RESULTS

The LMRC test loop plans were finalized for testing and safety. A schematic showing the location of the LMRC test loop in relation to the existing building can be seen in Figure 1. The two chillers, electrical panel and filter, water tank, and gas cylinders rack are in place and piped together as designed. The data acquisition cabinet wiring is shown in Figure 2.

Assembly of all the machined and fabricated LMRC parts is complete. The completely assembled LMRC mounted on the test stand can be seen in Figure 3.

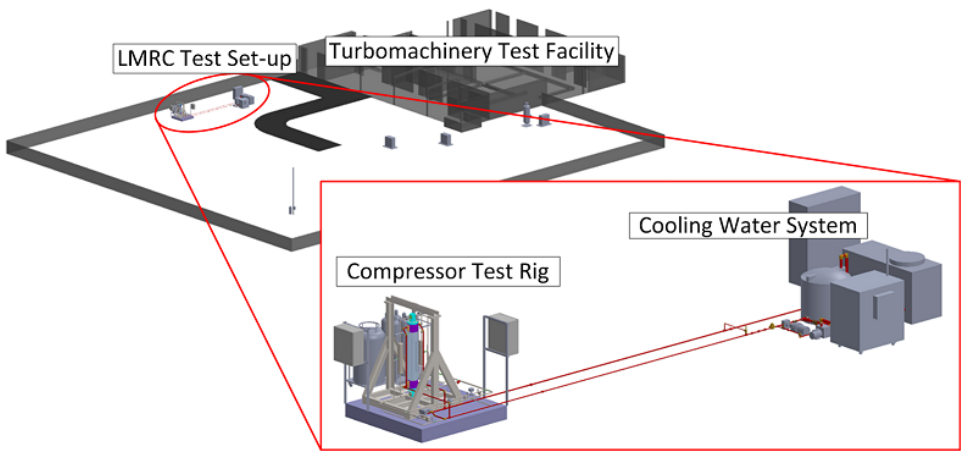

FIGURE 1. Schematic of test loop equipment and existing building

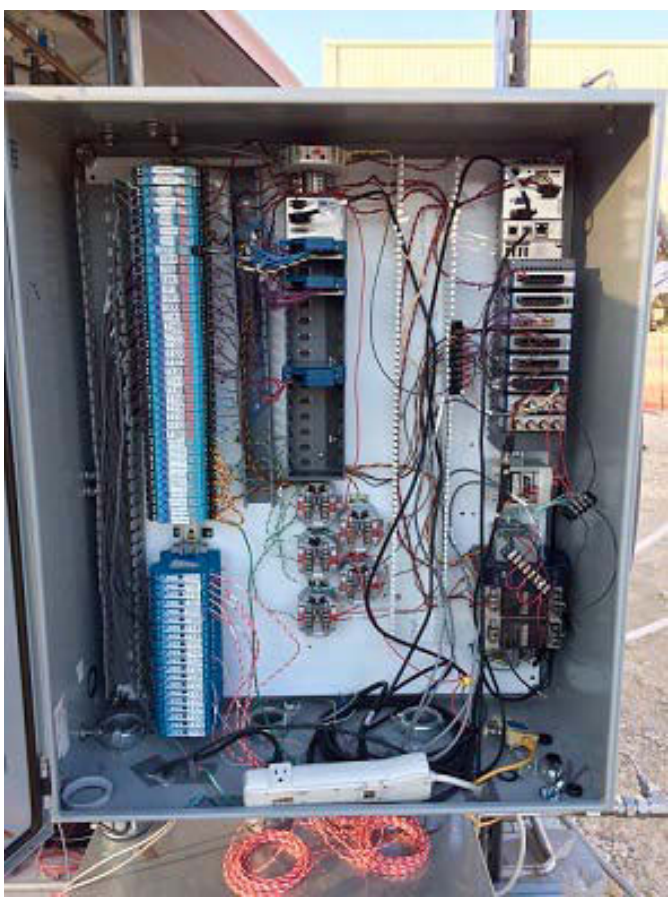

FIGURE 2. Photo of the data acquisition cabinet wiring

FIGURE 3. Photo of LMRC fully assembled and mounted on the test stand supporting structure

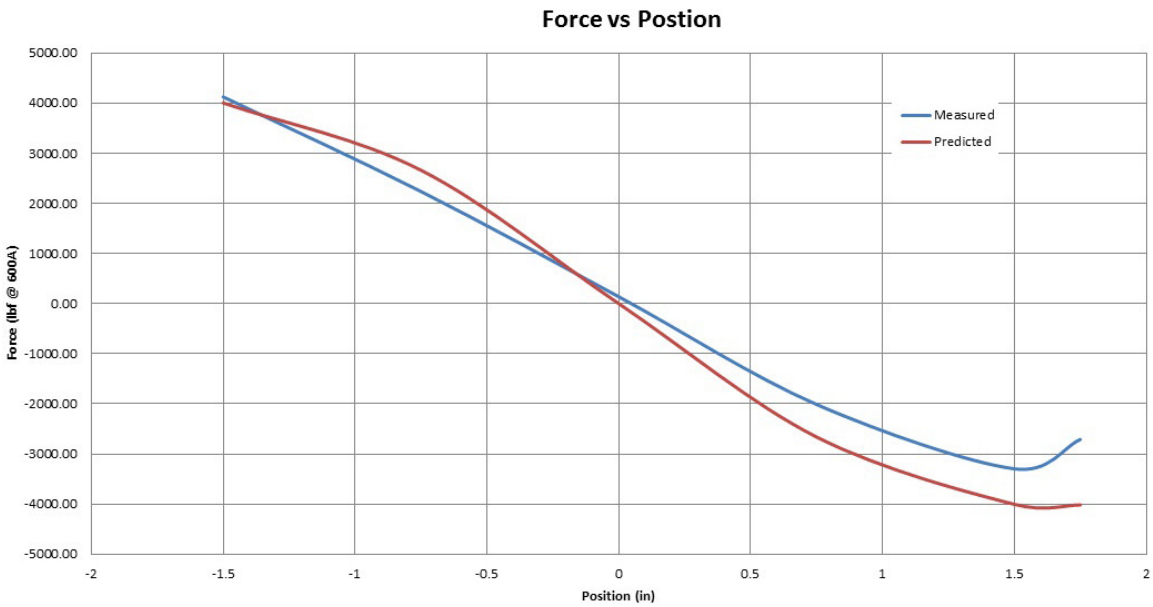

FIGURE 4. Measured and predicted motor forces plotted as a function of position

Calibration testing was performed in an effort to validate motor force predictions. It was found that there is close correlation between the predicted forces of the motor and the measured forces. Measured and predicted forces are plotted as a function of position in Figure 4.

Issues with the capabilities of the vendor-supplied electrical power controller significantly delayed testing of the LMRC. A new electrical power controller was recently received. The first stage LMRC test loop is now fully assembled. Commissioning efforts are being finalized, and testing will commence in the near future.

CONCLUSIONS AND UPCOMING ACTIVITIES

Conclusions derived from the work conducted in FY 2017 are:

- Updated predictions still indicate that highly efficient hydrogen compression is possible with an LMRC used for the compression process.
- It is concluded that the measured forces diverge from the predicted forces at the top of the LMRC (see Figure 4) as a result of the magnetic field disruption associated with the calibration fixture that was necessary for performing the measurements.

Future work in Project Year 4 (FY 2018; Budget Period 3) will include:

- Redesign the motor portion of the LP LMRC such that the overall system will have a specific energy of 1.6 kWh/kg or lower.
- Fabricate and assemble the more efficient LP LMRC.
- Commission the test bench using an inert gas and following the plan previously defined.
- Complete testing of the LMRC system according to the defined test matrix with hydrogen.
- Analyze the results from the improved LP system testing (20 bar to 71 bar pressure range, specific energy of 1.6 kWh/kg or lower).

FY 2017 PUBLICATIONS/PRESENTATIONS

1. Broerman, E.L., J. Bennett, N. Shade, "Designing, Building, and Testing a Linear Motor Reciprocating Compressor (LMRC)," presented at the 2016 GMRC Gas Machinery Conference, October 4, 2016, Denver, CO.

REFERENCES

1. U.S. Patent 8,534,058. Issued Sept. 17, 2013. "Energy Storage and Production Systems, Apparatus and Methods of Use Thereof," Patented in United States of America.

2. Deffenbaugh, D., et al., "Advanced Reciprocating Compression Technology," DOE Award No. DE-FC26-04NT42269, SwRI® Contract No. 18.11052, December 2005.

III.3 Low Cost Hydrogen Storage at 875 bar Using Steel Liner and Steel Wire Wrap

Amit Prakash (Primary Contact) and Ashok Saxena
WireTough Cylinders, LLC
14570 Industrial Park Rd., Suite C
Bristol, VA 24202
Phone: (276) 644-9120
Email: aprakash@wiretough.com; asaxena@uark.edu

DOE Manager: Neha Rustagi
Phone: (202) 586-8424
Email: Neha.Rustagi@ee.doe.gov

Contract Number: DE-EE0006668

Subcontractors:
- Oak Ridge National Laboratory, Oak Ridge, TN
- N & R Engineering, Parma Heights, OH
- C P Industries, McKeesport, PA
- Ashok Saxena, Consultant, Fayetteville, AR
- Structural Integrity Associates, Inc., San Jose, CA
- Hy-Performance Materials Testing, LLC, Bend, OR
- MVP Co, Seattle, WA

Project Start Date: September 15, 2014
Project End Date: February 28, 2018

Overall Objectives

The goal of this project is to develop a pressure vessel to safely store hydrogen at 875 bar with a safety factor of 3 or higher that also meets the DOE storage tank cost target of <$1,000/kg hydrogen ($H_2$). The objectives are:

- To wire wrap a standard American Society of Mechanical Engineers (ASME) approved, 406 mm diameter and 9.14 m long cylinder with a capacity of 765 L rated at a pressure of 460 bar to boost its operating pressure capability to 875 bar. The cylinder must meet the ASME PVP Section VIII-Division 3, KD-10 requirements for storing hydrogen.
- To keep the cost of producing the storage tanks to less than $1,000/kg of stored H_2, maintain a design life of 30 yr, and deliver hydrogen that meets the SAE J2719 hydrogen purity requirements.

Fiscal Year (FY) 2017 Objectives

- Design, build, and install the wire winding machine to wind 9.2 m long liners.
- Complete fatigue crack growth rate testing at negative load ratios in high pressure hydrogen and complete testing of steel wires in low concentrations of hydrogen.
- Conduct elastic-plastic finite element analysis for optimizing autofrettage pressures for use in manufacturing vessels.
- Seek ASME Code approval for the WireTough design of the full-size cylinder.

Technical Barriers

This project addresses the following technical barrier from the Hydrogen Delivery section of the Fuel Cell Technologies Office Multi-Year Research, Development, and Demonstration Plan.

(E) Gaseous Hydrogen Storage and Tube Trailer Delivery Costs

Technical Targets

This project's goals are to meet the 2020 targets for high-pressure hydrogen storage in the 2012 version of Fuel Cell Technoloies Office's Multi-Year Research, Development, and Demonstration Plan, as shown in Table 1.

TABLE 1. WireTough's Progress towards Meeting Technical Targets for High Pressure H_2 Ground Storage Systems

Characteristics	2020 Target	WireTough
High Pressure (860 bar) Purchased Capital Cost ($/kg of H_2 stored)	$1,000	2017 costs lower than 2020 target cost by 20%

FY 2017 Accomplishments

- The machine for winding 9.1 m long cylinders was designed, built, tested and installed.
- Analysis of fatigue crack growth data at negative load ratios was completed and the effects of hydrogen pressure and loading frequencies on the fatigue crack growth rates were quantified.
- Oak Ridge National Laboratory completed testing of wires used in WireTough's design to explore potential effects of hydrogen.
- A process for ensuring that sufficient plastic deformation occurs during autofrettage was developed.
- The ASME self-certification process for the large cylinder design, including analysis, and preparation of the necessary manufacturer's design report (MDR), was completed.

- The cyclic life of the pressure vessel was estimated to be approximately 85,000 cycles for duty cycles involving pressure fluctuations during service to range from 13,000 psi to 10,000 psi.
- The cost of producing the vessel was shown to exceed the DOE target cost.

✧ ✧ ✧ ✧ ✧

INTRODUCTION

The DOE Fuel Cell Technologies Office within the Office of Energy Efficiency and Renewable Energy is supporting research and development activities leading to the development of low cost, high pressure hydrogen storage systems for use in hydrogen refueling stations (forecourt). The goal of this project is to develop a pressure vessel to safely store 750 L of gaseous hydrogen at 875 bar that meets the ASME PVP Section VIII- Division 3, Article KD-10 design requirements and also the DOE storage tank cost target of <$1,000/kg H_2.

APPROACH

Type I metal cylinders (406 mm outer diameter) have been used for compressed natural gas and hydrogen storage for several decades but are limited to pressures of 55 MPa for various technical reasons. WireTough has a patented process to wrap these commercially available cylinders with ultra-high-strength steel wires (2 GPa or greater in strength) to approximately double the pressure capability of the cylinders, with a proven record of safely storing H_2. These wire-wrapped cylinders are further subjected to an autofrettage process in which they are subjected to pressures high enough to plastically deform the inner liner, but the wire jacket remains elastic. Upon release of the autofrettage pressure, the liner is left with high residual compressive hoop stresses. This decreases the maximum tensile hoop stress in the liner under the operating pressure and can significantly enhance the fatigue life of the vessel. In this project, this concept was first demonstrated using short, 1.9 m long cylinders and is now being extended to the full size, 9.14 m long cylinders.

RESULTS

Design and Procurement of Wire Winding Machine for 9.14 m Long Cylinders: MVP, Seattle, built a custom, wire winding machine capable of wrapping 9.2 m long liners. The machine, Figure 1, was tested in MVP facilities first and then shipped and installed in WireTough's Bristol, Virginia plant. WireTough technicians were trained in the operation of the machine and have used it to wind mock liners to assure its functionality. Two 9.14 m long liners are on order from CPI and the production of the prototype cylinders is scheduled to begin shortly.

Design Analysis and Optimization: Finite element analysis model developed in previous years was used to calculate the correct autofrettage pressure that accounts for variations in liner thickness and the yield strength that is within admissible limits of the liner specification. The purpose of autofrettage in wire-wrapped pressure vessel manufacturing is to subject the vessel during assembly to a high enough pressure resulting in the liner deforming plastically while the wire jacket remains elastic. Upon release of the autofrettage pressure, the wire jacket collapses back

FIGURE 1. Photograph of an 8-axis wire winding machine procured from MVP, Inc., capable of wire winding 9.2 m long liners now installed in WireTough's Bristol, Virginia, manufacturing facility

on the liner and places the inner diameter (ID) region of the liner in severe compression (>220 MPa). These compressive residual stresses reduce the maximum stresses in the liner walls during subsequent pressurization as part of service duty cycles resulting in enhanced fatigue life.

An analytical model was first formulated that established the relationship between applied pressure and the change in volume of the liner. The plastic deformation required in the ID region of the vessel to ensure desired levels of residual compressive stresses upon removal of the autofrettage pressure was estimated using elastic-plastic finite element analyses and was further related to the change in volumetric expansion of the vessel. A procedure based on the volumetric expansion of the vessel as measured by water volume needed to accommodate the expansion was established. This procedure ensures that desired levels of residual compressive stresses are always locked on the ID region of the pressure vessel upon completion the autofrettage process. Figure 2 shows the variations in residual stresses following the application of autofrettage pressure of various levels for a liner with a yield strength level of 724 MPa (105 ksi) and a wall thickness of 31.75 mm (1.25 in). An autofrettage pressure of 27.5 ksi was specified for this case based on these results.

Effect of Hydrogen on the Fatigue Crack Growth Rate Behavior in the Liner Material: Sandia National Laboratories data on the effect of hydrogen on the fatigue crack growth rate (FCGR) behavior of ASME SA372 Grade J Class 70 steels used as liner material show a significant acceleration of the crack growth rates relative to the rates in benign environment [1–3]. However, this data is only available for load ratios, R, between 0.1 and 0.5. WireTough's wire-wrapped and autofrettaged cylinder design places the liner wall into compression when there is no pressure. Thus, service loading conditions consist of negative R and FCGR

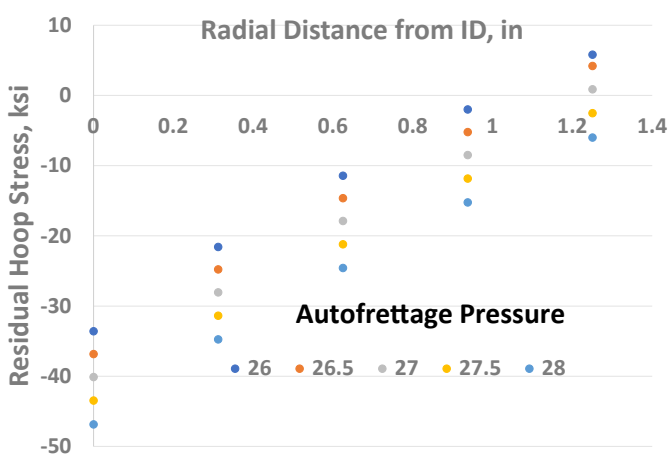

FIGURE 2. The distribution of residual compressive stresses in the liner wall as a function of autofrettage pressure estimated from the finite element analysis

data are needed for negative load ratios. WireTough, in collaboration with Hy-Performance Materials Testing, LLC designed and verified a single-edge-notch-tension geometry specimen to obtain this data. The hydrogen pressure during these tests was approximately 10 MPa and the tests were performed at room temperature in accordance with the latest version of *ASTM Standard E647: Standard Method for Fatigue Crack Growth Testing.* This testing was completed during the past year and the FCGR behavior for $-1.0 \leq R \leq 0.2$ along with the available data from Sandia National Laboratories is shown in Figure 3.

Effect of Hydrogen Environment on the Wires: The preponderance of tensile strength results in specimens exposed to hydrogen fall between 3,150 MPa and 3,350 MPa. The results show little effect of the hydrogen containing environment on the tensile properties of this wire. Extended pre-exposure of the wire under stress shows little deleterious effect on the strength of the wires.

Design Life Estimation: The FCGR data were used in a crack growth calculation to estimate design lives of wire wrapped hydrogen storage cylinders containing SA 372 Grade J steel liners that were 406 mm (16 in) outer diameter (OD) with a wall thickness of 31.75 mm (1.25 in). The initial flaw size assumed for the calculations was based on a flaw depth of 2% of the wall thickness. The initial flaw length on the surface (2c) is taken as three times the depth, a.

The cyclic life based on the following duty cycles was calculated for the pressure vessel:

- Ambient to autofrettage pressure of 190 MPa (27.5 ksi) and back to ambient pressure, one cycle during manufacturing.
- Ambient to hydrotest pressure of 131 MPa (19.5 ksi) and back to ambient pressure, one cycle during manufacturing.
- Operating pressure of 90 MPa (13.0 ksi) to ambient, 2x/yr.
- Operating pressure of 90 MPa (13.0 ksi) to 69 MPa (10 ksi), 10x/d.

Four crack paths in the liner were analyzed for estimating the design life, (a) crack starting from the thread roots on the inner surface growing toward the outer surface, (b) crack starting from the outer surface at the neck and growing toward the inner surface, (c) crack starting from the outer surface at the end of the wire wrap growing toward the inner surface, and (d) radial-axial crack on the inner surface of the vessel growing toward the outer surface. The life-limiting condition is case (d), the radial-axial crack located on the inner surface of the liner. The life was estimated as 24.0 yr that exceeded the required design life of 20 yr. Thus, the proposed design meets all the requirements of ASME Section VIII, Division 3, KD-10 requirements.

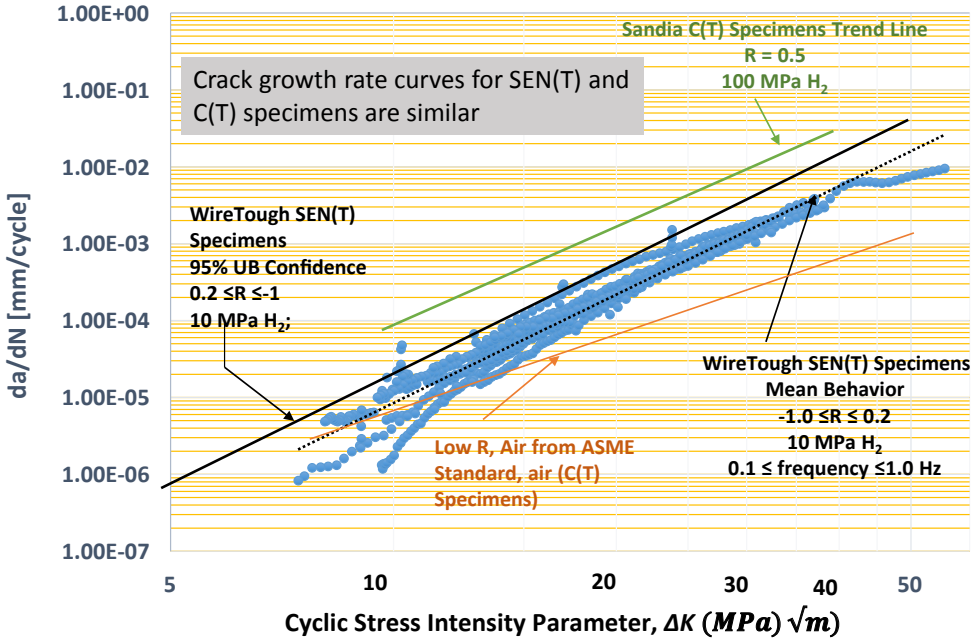

FIGURE 3. A consolidated plot of fatigue crack growth rate data in high pressure hydrogen from tests conducted by WireTough compared with literature data from Sandia National Laboratories [1–3]

ASME Certification of the WireTough Pressure Vessel Design: Structural Integrity Associates independently conducted the analysis and produced an MDR certifying WireTough's design as meeting the ASME Code.

CONCLUSIONS AND UPCOMING ACTIVITIES

- The results produced during FY 2017 on this project resulted in a successful ASME certified design of a wire wound pressure vessel for economically storing hydrogen at 875 bar.
- FCGR testing in high pressure H_2 environment at negative load ratios was completed.
- ASME KD-3 and KD-10 analysis of the 9.5 m long cylinder was completed in support of the self-certification of WireTough's design and the design is now certified.
- Testing of wires in hydrogen environment was completed by Oak Ridge National Laboratory.
- WireTough collaborated with Strategic Analysis Inc. to demonstrate that WireTough's manufacturing costs are lower than the DOE cost target for 2020.
- A machine for winding 9.5 m long (750 L) cylinders was designed, procured installed and tested. Currently the machine is undergoing preparation for producing two prototypes of our design.
- After the liners are wound, they will be shipped back to CPI for conducting the autofrettage step and the final hydrotesting as per the MDR prepared by WireTough in collaboration with Structural Integrity Associates. The interior of the vessels will be cleaned and prepared for hydrogen storage.
- WireTough expects to wrap up the project in February of 2018, meeting or exceeding all its original goals.

SPECIAL RECOGNITIONS & AWARDS/ PATENTS ISSUED

1. A. Prakash, G.R. Sharp, B.T. Deeken, W.J. Head, W.H. Thomson, "Steel Wrapped Pressure Vessel," US Patent 9,266,642B2, Issue date February 23, 2016.

FY 2017 PUBLICATIONS/PRESENTATIONS

1. A. Prakash and A. Saxena, "Low Cost Hydrogen Storage at 875 Bar Using Steel Liner and Steel Wire Wrap," DOE Annual Merit Review, Washington, DC, June 5–8, 2017.

2. A. Saxena, A. Prakash, K.A. Nibur, and I. Miller, "Considerations of the Effects of H_2 in Design of Type II Storage Vessels Built for Fatigue Resistance," Paper presented at the 2016 International Hydrogen Conference, Jackson Hole, WY, September 11–14, 2016. Paper to appear in the conference proceedings.

3. Ashok Saxena, Federico Bassi, Kevin Nibur, and James C. Newman, "On Single-Edge-Crack Tension Specimens for Tension-Compression Fatigue Crack Growth Testing," http:/dx.doi.org/10.1016/j.engfracmech.2017.03.030.

REFERENCES

1. B.P. Somerday, K.A. Nibur, C. San Marchi, "Measurement of Fatigue Crack Growth Rates for Steels in Hydrogen Containment Components," Unpublished data reproduced with permission.

2. B.P. Somerday, C. San Marchi, Kevin Nibur, "Measurement of Fatigue Crack Growth Rates for SA372-Gr J Steel in 100 MPa Hydrogen Gas Following Article KD-10," Proceedings of the ASME 2013 Pressure Vessels and Piping Conference, PVP 2013, July 14–18, 2013, Paris, France. Reproduced with permission.

3. K.A. Nibur, B.P. Somerday, C. San Marchi, J.W. Foulk, M. Dadafarnia, P. Sofronis, Met Trans., Vol. 44A, 2013, pp. 248–269; reproduced with permission.

III.4 Advanced Barrier Coatings for Harsh Environments

W. Shannan O'Shaughnessy (Primary Contact), Brett W. Guralnick, and Scott Morrison
GVD Corporation
45 Spinelli Place
Cambridge, MA 02155
Phone: (617) 661-0060 x15
Email: soshaughnessy@gvdcorp.com

DOE Manager: Neha Rustagi
Phone: (202) 586-8424
Email: Neha.Rustagi@ee.doe.gov

Contract Number: DE-SC0011339

Subcontractor:
Oak Ridge National Laboratory, Oak Ridge TN

Project Start Date: April 6, 2015
Project End Date: July 5, 2017

Overall Objectives

- Deposit a hydrogen barrier onto elastomeric materials to reduce seal failure due to hydrogen damage.
- Increase compression system seal lubricity via a reduction in friction with an application of initiated chemical vapor deposition (iCVD) poly-tetrafluorethylene (PTFE) coatings.
- Design a high-throughput, mass manufacturing system.

Fiscal Year (FY) 2017 Objectives

- Model system testing with helium and subsequent hydrogen testing.
- Lifetime gasket testing in compressors.
- Computer-aided drawing design on a tumble coater for elastomeric gaskets.

Technical Barriers

This project addresses the following technical barriers from the Hydrogen Delivery section of the Fuel Cell Technologies Office Multi-Year Research, Development, and Demonstration Plan.

(B) Reliability and Costs of Gaseous Hydrogen Compression

(I) Other Fueling Site/Terminal Operations

(J) Hydrogen Leakage and Sensors

Technical Targets

This project addresses the failure of seals in hydrogen compression, storage, and delivery operations. Large pressure and temperature variation in the hydrogen operation compromises seals and gaskets. Barrier film coatings address hydrogen ingress failure and PTFE lubricious coatings address failure due to friction wear. Results are aggregated into Table 1.

TABLE 1. Progress towards Meeting Technical Targets for Advanced Barrier Coatings for Harsh Environments

Characteristic	Units	Current Status
Average Permeation Reduction (Helium)	Percent Reduction (%)	53%
Average Permeation Reduction (Hydrogen)	Percent (%)	N/A
Compression Gasket Failure (Incumbent Benchmarking)	Pass/Fail	Pass

This project's aim is to increase the lifetime of seals and gaskets, thereby reducing failures and maintenance downtime of systems. There are no targets outlined in the Multi-Year Research, Development, and Demonstration Plan; however, current technology requires material seal changes in fueling stations every 163 fills, whereas in the United States, the average petrol fueling station fills 200–250 cars per day. Success in this project will create significant movement toward the stated DOE goal of achieving delivery and dispensing costs of <$2/gge.

FY 2017 Accomplishments

- Improved in-house measurement capabilities and achieved a reduction in helium permeability of 53%.
- Compressor seals lost 1.30 mg/h with PTFE coating, whereas uncoated seals had a reduction of 3.45 mg/h.
- Designed a tumble coater assembly for upscale manufacturing of gasket coatings.

✧ ✧ ✧ ✧ ✧

INTRODUCTION

In order to realize the full potential of zero-emissions fuel cell electric vehicles, a critical hurdle that has yet to be overcome is achieving viable cost structures for hydrogen compression, storage, and dispensing. Current hydrogen systems within fuel cell electric vehicles and the supporting

infrastructure to compress, store, and deliver hydrogen fuel are prone to systemic inefficiencies and poor reliability. Many of these reliability problems stem from plastic and elastomer seals (including O-rings, gaskets, and piston seals) employed in these hydrogen systems that leak and weaken as hydrogen molecules saturate within these materials under conditions of extreme temperature and high hydrogen pressure. The result is that these seals require frequent replacement, incurring significant labor costs and excessive equipment downtime. Thus, there is an urgent need for improved polymer seals that can withstand extreme temperature (-40°C to 200°C) and high pressure (>875 bar) hydrogen environments to enable reliable operation of hydrogen systems. This need has been emphasized in two recent meetings sponsored by DOE's Fuel Cell Technologies Office [1,2], by hydrogen compressor manufacturers, by fuel cell electric vehicle automakers, and by two leading seal manufacturers. Figure 1 shows the processes impacted by this project.

In addition, within hydrogen compressors, the wear on gaskets is a major failure point. GVD Corporation has engineered solutions to the wear problem. Increasing the lubricity of the gaskets improves the lifetime of the gaskets. This reduces downtime and equipment maintenance, one of the costliest aspects of the hydrogen fueling process.

APPROACH

This project aims to upgrade current state-of-the-art gaskets by coating a hydrogen barrier film on the outside of the gasket. This is accomplished using iCVD or plasma-enhanced chemical vapor deposition (PECVD) (Figure 2). A glass-like oxide material is coated to prevent hydrogen ingress into the sample; however, since glass is not a flexible material, it needs to be thin to prevent micro-fractures that compromise the coating. Dyads of thin glass-like oxides are alternated with polymeric layers to allow the material more flexibility and create a more tortuous path should any cracks form.

The seals that require barrier coatings come in direct contact with hydrogen at high pressures and a large temperature range. Therefore, a wide range of conditions needs to be considered. One fuel cell unit operation GVD is targeting is hydrogen compression. Since gaskets need to be replaced every 200 h of operation due to both the failure to properly seal and safety concerns, GVD is investigating coating the seals with PTFE to reduce wear. As the compressors run, they heat up due to friction. This heat causes the polymeric material to expand much faster than the metal compressor housing. This expansion leads to increased

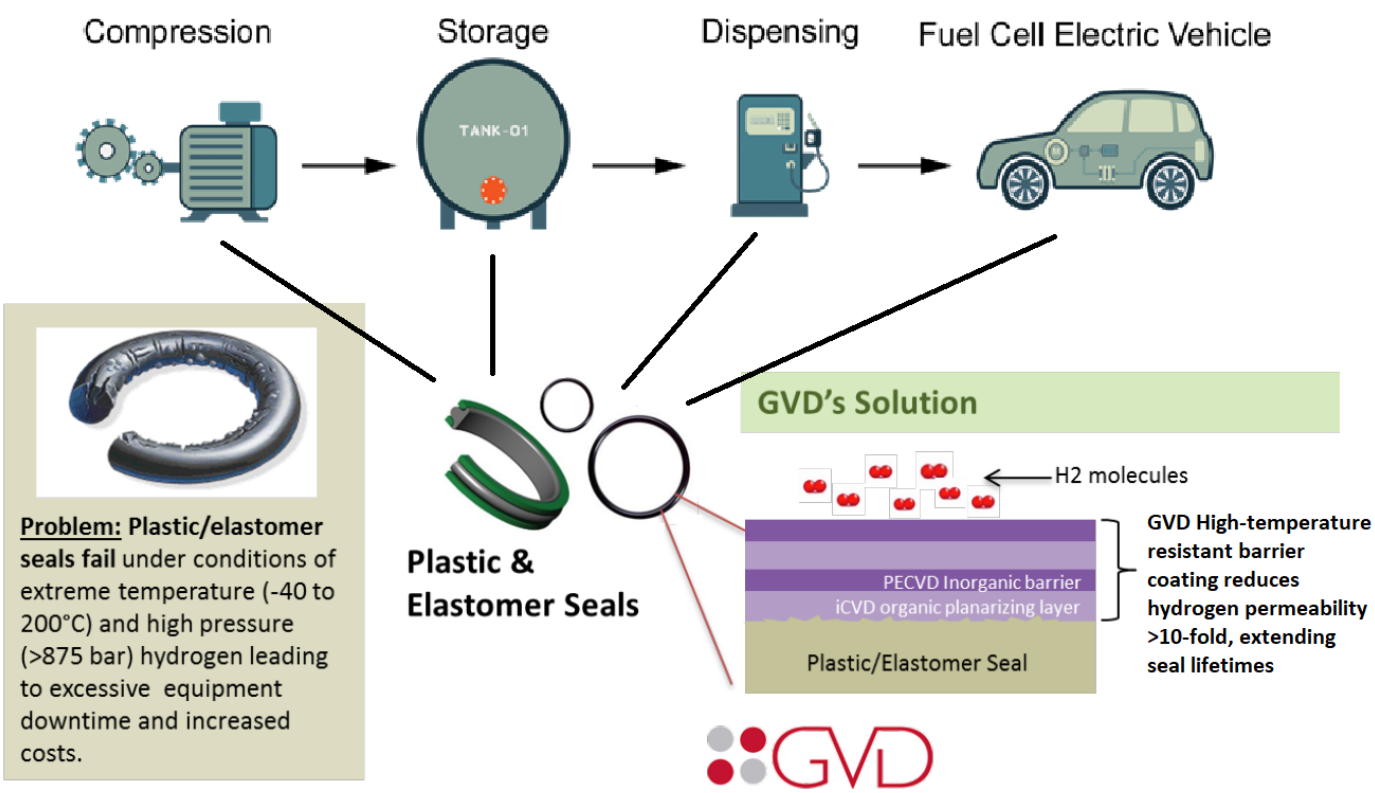

FIGURE 1. GVD's vapor-deposited, flexible, high-temperature-resistant barrier coatings are deposited on plastic and elastomer seals to prevent hydrogen permeation into the seal and thereby extend seal reliability and lifetime

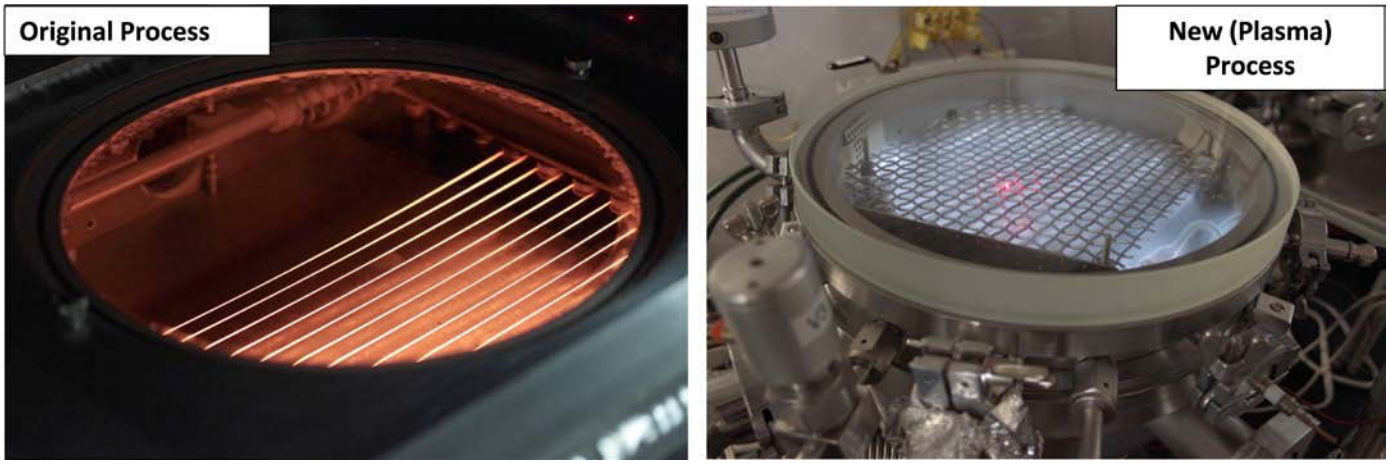

FIGURE 2. Left: iCVD process with heated filament; Right: PECVD process with radio frequency plasma

wear on the plastics. When the compressor is switched to the off state and cools, the components constrict to the room temperature size. However, the plastics lose material from abrasion while running and fail to seal at room temperature due to a size mismatch. A PTFE coating adds lubricity to the gasket, preventing friction wear leading to material loss.

RESULTS

Barrier film coatings have been shown to improve permeability of helium through a silicone gasket. A special apparatus was built for high-throughput testing prior to hydrogen testing at Oak Ridge National Laboratory (ORNL). An improvement of nearly 60% was observed on custom silicone gaskets made by a leading gasket manufacturer for this project. It was observed that reducing the oxide thickness of each layer, but keeping the total oxide thickness constant, thus increasing the number of layers, leads to a reduction in the average permeability. Oxide layer thickness changes of 65 nm lead to a 25% reduction in helium permeability. See Figure 3.

Since helium has been observed to have higher diffusivity than hydrogen, these results are positive. Samples were subsequently tested at ORNL. However, the silicone samples were shown to have the hydrogen permeability with and without the coating. It is suspected that this is due to pinholes in the oxide coatings. The surface area of the test samples at ORNL is larger than that of the samples used

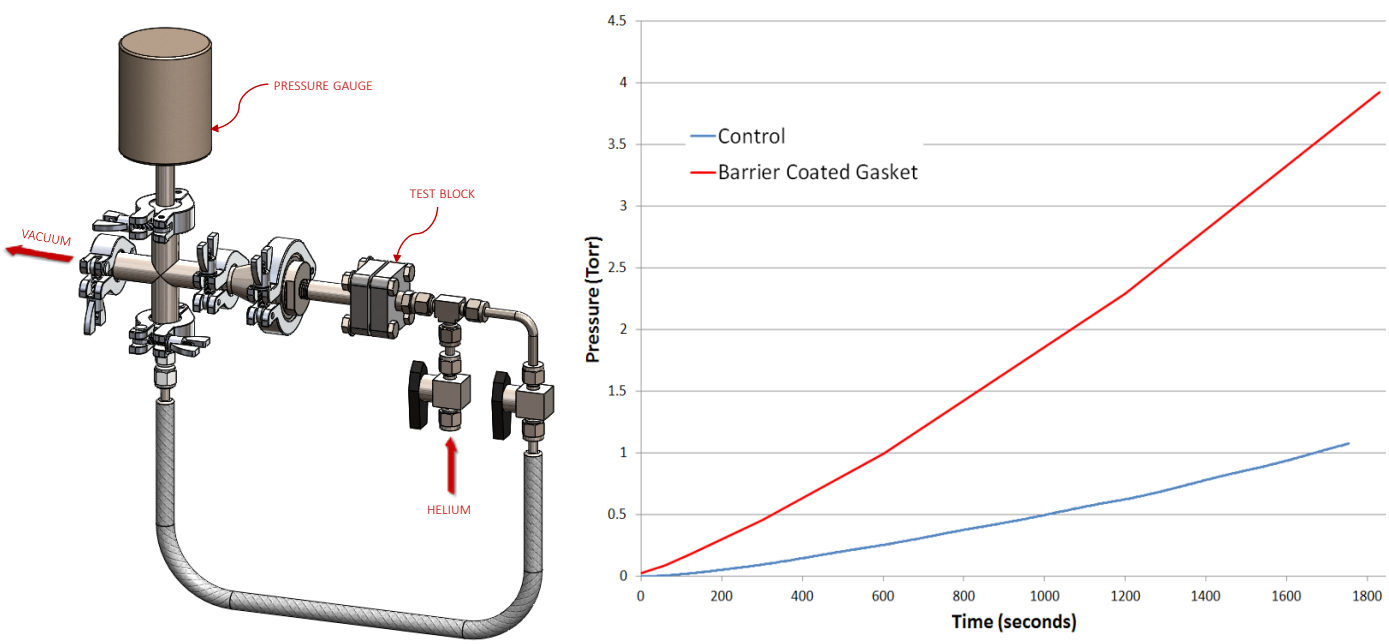

FIGURE 3. Left: Schematic of helium testing; Right: Sample graph of helium test

in the helium testing, and the increased area most likely captured more defects in the coating and negated the positive results. Efforts to coat more uniform and pinhole-free oxides layers are ongoing.

A separate effort on gaskets for compressors has promising results. The mass depletion rate of the gaskets was reduced from 3.45 mg/h to 1.30 mg/h. These gaskets passed all tests after they were removed from equipment after 177 h of run time. Unfortunately, the gaskets were removed from the compressor after a failure of another component, and while the compressor was down for maintenance, the gaskets were changed out. Therefore, a comparison of the increased running time is not available currently. A second set of gaskets has been loaded for testing. Due to the intermittent running of hydrogen compressors, a long turnaround time for results is anticipated.

Coatings are currently being done in a small research reactor. Production-level throughput would not be feasible in the current setup. A large-scale used reactor was purchased, and retrofitting has begun to transition the reactor to production-scale PECVD reactor. The design utilizes a basket that tumbles the gaskets. This allows complete 360-degree coverage of the gaskets and allows more gaskets to be coated per run. Currently, the planar systems are limited by the surface area, and samples need to be flipped to coat the back side. The tumble coater will enable reduced coating costs and increased sample throughput ultimately required to keep costs low and increase adaptation of the technology. A cross-sectional computer-aided design drawing is shown in Figure 4.

CONCLUSIONS AND UPCOMING ACTIVITIES

The project is ongoing and has been selected to be continued in a Phase IIa grant to extend this work into dispensing systems in addition to compressors and hydrogen gasketing. The oxide portion of the barrier films is undergoing ongoing improvement, and future testing with hydrogen is planned at ORNL.

Upon successful improvements to barrier properties with hydrogen, testing in dispensing systems at National Renewable Energy Laboratory will be conducted. Involvement of National Renewable Energy Laboratory is advantageous because in addition to real-world testing, GVD will also receive information on failures, which will be helpful in further designing a better coating and/or process.

Continued work with compressors will be extended in Phase IIa. Currently, coated samples are under test in compressors. A design on experiments with different PTFE densities and thicknesses has been planned to find the

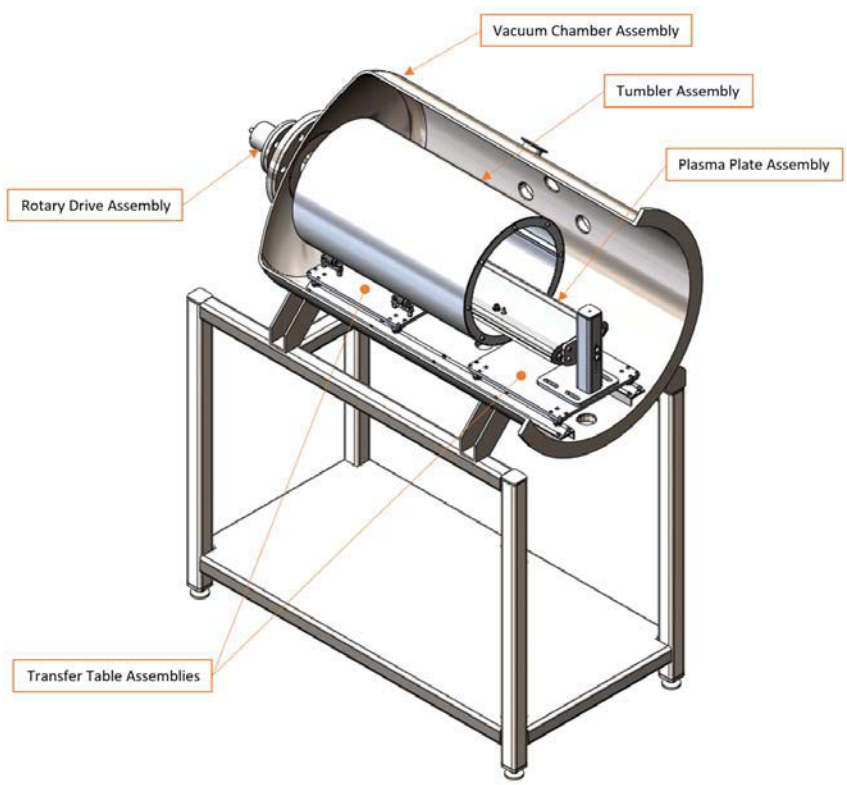

FIGURE 4. Cross sectional view of tumble coater with plasma deposition

optimal coating conditions. The first results showed that there is an improvement, but future work will quantitate and optimize the magnitude of the improvement.

FY 2017 PUBLICATIONS/PRESENTATIONS

1. Shannan O'Shaughnessy, "Advanced Barrier Coatings for Harsh Environments," Hydrogen Storage and Delivery Tech Team, Detroit, MI, February 2017.

REFERENCES

1. Polymer and Composite Materials Used in Hydrogen Service, Meeting Proceedings, October 2012. Retrieved from web on August 20, 2013. http://www1.eere.energy.gov/hydrogenandfuelcells/pdfs/poly_comp_materials_proceedings.pdf

2. S. Ahmed, E. Sutherland, 2013 Hydrogen Compression, Storage, and Dispensing Cost Reduction Workshop Final Report, April 2013. Retrieved from web on August 21, 2013. http://www1.eere.energy.gov/hydrogenandfuelcells/pdfs/2013_csd_workshop_report.pdf

III.5 Improved Hydrogen Liquefaction through Heisenberg Vortex Separation of para- and ortho-hydrogen

Christopher Ainscough (Primary Contact),
Jacob W. Leachman, Zhiwen Ma
National Renewable Energy Laboratory
15013 Denver West Parkway
Golden, CO 80401-3305
Phone: (303) 275-3781
Email: Chris.Ainscough@nrel.gov

DOE Manager: Neha Rustagi
Phone: (202) 586-8424
Email: Neha.Rustagi@ee.doe.gov

Project Start Date: October 1, 2016
Project End Date: September 30, 2018 (Project continuation and direction to be determined)

Overall Objectives

This project aims to improve three specific areas of hydrogen liquefaction.

- Improve the thermodynamic efficiency to show a path to figure of merit of 0.5 through the use of a novel separation concept.
- Reduce the delivery cost of liquid hydrogen by enabling small-scale (5–30 metric ton per day [MTPD]) liquefaction systems in optimal locations relative to markets and renewable resources.
- Reduce the installed capital cost of liquefaction plants by enabling efficient scale-down of plants to the 5–30 MTPD sizes.

Fiscal Year (FY) 2017 Objectives

This project aims to develop the vortex tube (VT) ortho/para separation concept from technology readiness level (TRL) 2 to a TRL of 4 in three years. The focuses of FY 2017 tasks are:

- Verify the VT performance experimentally and computationally to achieve the performance milestone at Washington State University.
- Small modular liquefier placement analysis for stranded renewable energy used for hydrogen production and delivery.
- Identify candidate cycles that can improve the figure of merit from 0.3 to 0.5 to achieve a work of liquefaction less than 7.92 kWh/kg.

Technical Barriers

This project addresses the following technical barriers from the Hydrogen Delivery section of the Fuel Cell Technologies Office Multi-Year Research, Development, and Demonstration Plan.

(A) Lack of Hydrogen/Carrier and Infrastructure Options Analysis

(H) High-Cost and Low Energy Efficiency of Hydrogen Liquefaction

Technical Targets

This research is in an early TRL stage. By developing and validating the performance of VT ortho/para hydrogen separation, the project team will overcome one of the major limitations and inefficiencies that exist in commercial hydrogen liquefaction plants today (i.e., ortho/para conversion).

TABLE 1. Milestones and Deliverables

Characteristic	Units	DOE 2015 Status	DOE 2020 Target
Installed Capital Cost	$-Million	70	70
Energy Required	kWh/kg of H_2	15	12

The baseline analysis on the specific energy consumption of realistic versions of these cycles shows values much higher than the Multi-Year Research, Development, and Demonstration Plan current status. The project has shown through analysis that a VT could reduce the specific energy consumption of a Linde-Hampson cycle from 36 kWh/kg to 29 kWh/kg. This is a 21% reduction. Similarly, with a pre-cooled Claude cycle, the reduction is 15%.

FY 2017 Accomplishments

- The Heisenberg vortex liquefaction project completed state measurements for combinations of binary mixtures of hydrogen, helium, and neon (H-He, H-Ne, He-Ne). The equations of state developed from these tests will be published in the National Institute of Standards and Technology Reference Fluid Thermodynamic and Transport Properties (REFPROP) database and added to the materials reference database.
- Constructed a cryogenic compatible VT and completed initial testing. A computational fluid dynamics (CFD) model was developed to simulate the VT design conditions.

- Completed a thermodynamic cycle simulation to model the advantages of adding a VT to traditional liquefaction cycles, such as Linde-Hampson and pre-cooled Claude.
- Completed a techno-economic analysis that indicates significant cost benefits from reducing the reliance on hydrogen expanders and heat exchangers, as in current cycles.
- Developed the methodology to incorporate optimization of liquefaction plant placement into existing DOE tools, including Regional Energy Deployment System and Scenario Evaluation and Regionalization Analysis, based on regional forecasts of hydrogen demand and transport network analysis.

✧ ✧ ✧ ✧ ✧

INTRODUCTION

This project explores an early-stage approach to lowering the energy requirements of hydrogen liquefaction using catalyst-coated VTs in lieu of conventional mechanical equipment (e.g., compressors, expanders, throttles). The crux of the project is the development of a cryogenic VT, which will be coated with catalysts that convert para-hydrogen to ortho-hydrogen. This endothermic reaction is expected to cause bulk cooling. During the liquefaction process, the reverse exothermic reaction (ortho-to-para conversion) typically takes place, and is a source of inefficiency; the heat of conversion between the allotropes of hydrogen is 700 kJ/kg, compared to 420 kJ/kg for the heat of vaporization. Catalysis of para-to-ortho conversion is expected to counter the heat rejection of ortho-to-para conversion at a lower cost than the use of additional heat transfer fluid. Moreover, the motion of the VT is expected to create a pressure drop in hydrogen gas, further contributing the cooling. This project targets enabling liquefaction of hydrogen at 6.0 kWh/kg, the DOE's ultimate target [3].

Liquefaction is a mainstream approach to transport of hydrogen long distances to industrial end users as well as fueling stations. Benefits of liquefaction include the high capacities of liquid tankers relative to gaseous tube trailers, the flexibility of the pathway relative to pipelines, and the high purities of liquid hydrogen relative to gaseous hydrogen. However, conventional mechanical approaches have inherent inefficiencies with little room for improvement, and are not cost-competitive at small scales; hydrogen liquefaction plants today are typically sized for 10–40 tonnes per day. The use of VTs in hydrogen liquefaction has, to the author's knowledge, only been theorized to date. This project is exploring their performance given their potential to lower the energy consumption and enhance the scalability of hydrogen liquefaction.

APPROACH

This project will address the barriers of liquefaction efficiency by developing a novel ortho/para hydrogen separation concept, and building a system around the same. This project aims to develop a vortex that separates hydrogen gas by temperature. Higher temperature molecules are expected to migrate toward the walls of the vortex. The vortex will be coated with catalyst capable of converting para-hydrogen to ortho-hydrogen. Catalysis of this endothermic reaction within the tube is expected to cause bulk cooling of the hydrogen gas being liquefied. This approach is expected to lower the energy costs of hydrogen liquefaction, and also to be viable at system sizes of 5–30 MTPD.

In FY 2017, thermodynamic modeling was performed to characterize the energy consumption of a system wherein VTs are integrated into a Claude cycle using liquid nitrogen (LN2) as a pre-coolant. For reference, Claude cycles in industry typically consume 10 kWh/kg-H_2 and 15 kWh/kg-H_2. The ideal work of liquefaction is 3.92 kWh/kg.

RESULTS

Go/No-Go Decision

The project's go/no-go milestone was to achieve 5% para/ortho-hydrogen conversion under catalyzed conditions. By the go/no-go date, the team achieved 1.44% conversion. However, the pressure ratios achieved the VTs were significantly lower than originally anticipated. As a result the team felt that achievement of the go/no-go would require more energy consumption than the project originally targeted. The project team and DOE therefore decided to discontinue the project and identify other research areas with potential to enhance the viability of the overall concept. Areas that the team is now exploring include catalyst performance in a vortical flow reactor, supercritical performance of a VT, additive manufacturing of an optimal VT, and catalyst development and characterization.

Summary of Results

Figure 1 shows a conceptual schematic of a Heisenberg Vortex Tube (HVT). Tests were performed on tubes containing internal rifling, smooth bore tubes, and those with and without an internal catalyst coating. To the author's knowledge, this was the first time that a VT has been demonstrated to cool hydrogen to cryogenic temeratures. The inset in the upper left shows a comparison of a non-catalyzed HVT to a Joule-Thompson (J-T) throttle. The throttle results in a temperature drop of 0.18 K, whereas the uncatalyzed tube has a cold end ΔT of 1.08 K, **one order of magnitude higher**. When coated with ruthenium catalyst,

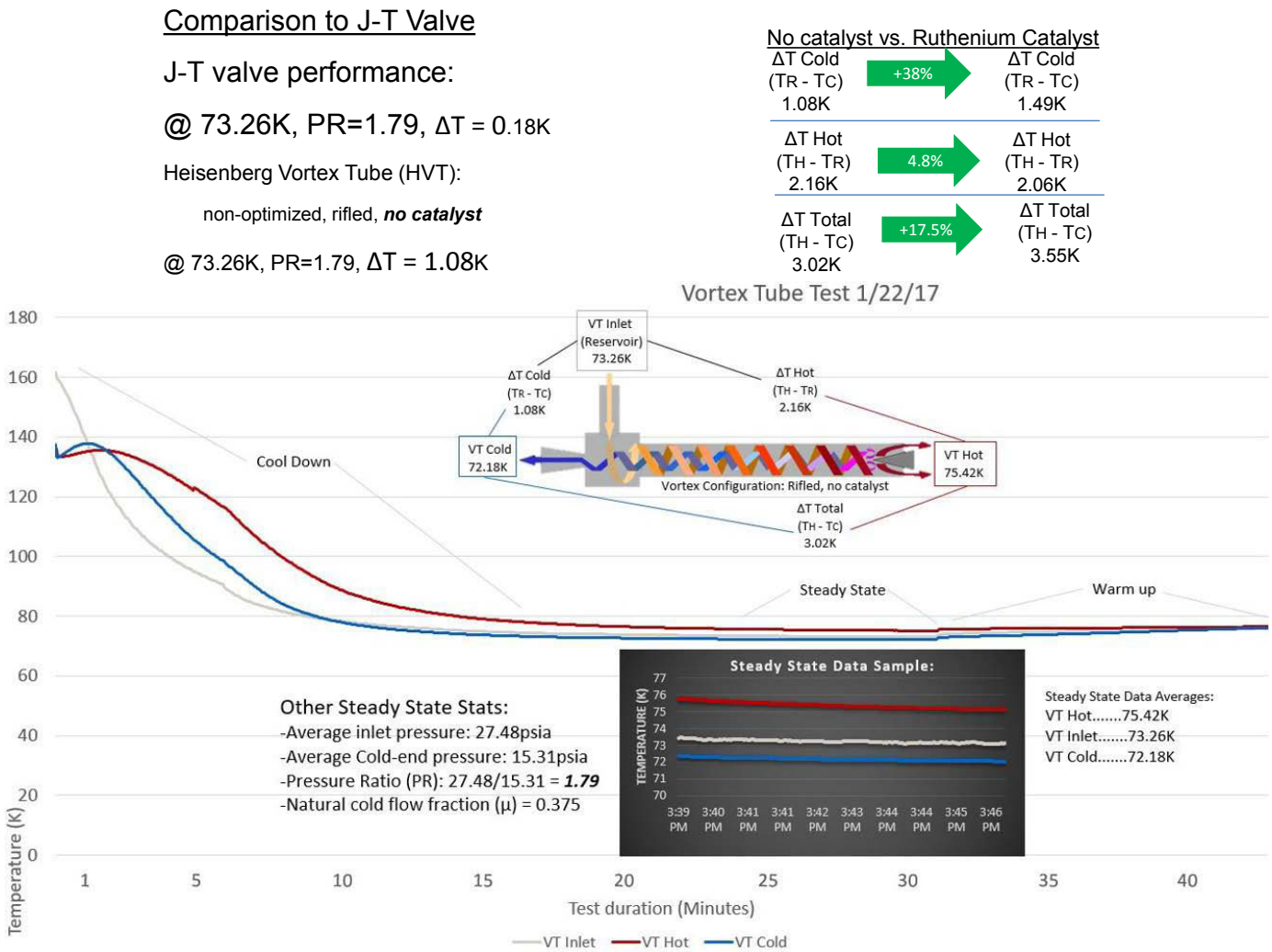

FIGURE 1. Test result on various catalyst conditions and comparison to J-T expansion

the performance increases an additional 38% to 1.49 K, as shown in the right inset in Figure 1. This increase in performance indicates that the catalyst likely caused para-to-ortho conversion, and subsequent bulk cooling.

Washington State University subsequently tested the impact of rifling in the VT on cooling power. Figure 2 shows a set of test results (details in the inset), along with expected performance based on thermodynamic models, for comparison. The temperature drop achieved by a ruthenium-coated rifled tube was 57% greater than that of a rifled tube without catalyst, and 205% greater than that of a smooth tube without catalyst.

Experimentation showed that the VT achieved 225% greater temperature drop than J-T valves conventionally used in industrial liquefaction (in Linde-Hampson and Claude cycles). This result is a substantial testament to the potential of this approach in lowering the energy consumption of liquefaction, and is supported by previous research in this space. Table 2 shows tabulated comparisons of experimental and model data from the current project and prior work in this area.

Subtask 3.2: Develop Steady State Thermodynamic Simulation of Liquefier Cycle

Using the current best estimates of VT performance at cryogenic hydrogen conditions, we estimate a 19% improvement to the standard pre-cooled, single expander, Claude cycle if the VT is used in place of a J-T valve. See Figure 3. The standard single expander cycle achieves a liquefaction work of 19.49 kWh/kg. Adding a catalyzed VT to this cycle lowers the liquefaction work to 15.44 kh/kg, or about four percentage points.

Task 4. Perform Nationwide Techno-Economic Trade Study for Optimal Vortex Liquefier Placement

National Renewable Energy Laboratory has been performing market analyses of hydrogen liquefaction to expand the Scenario Evaluation and Regionalization

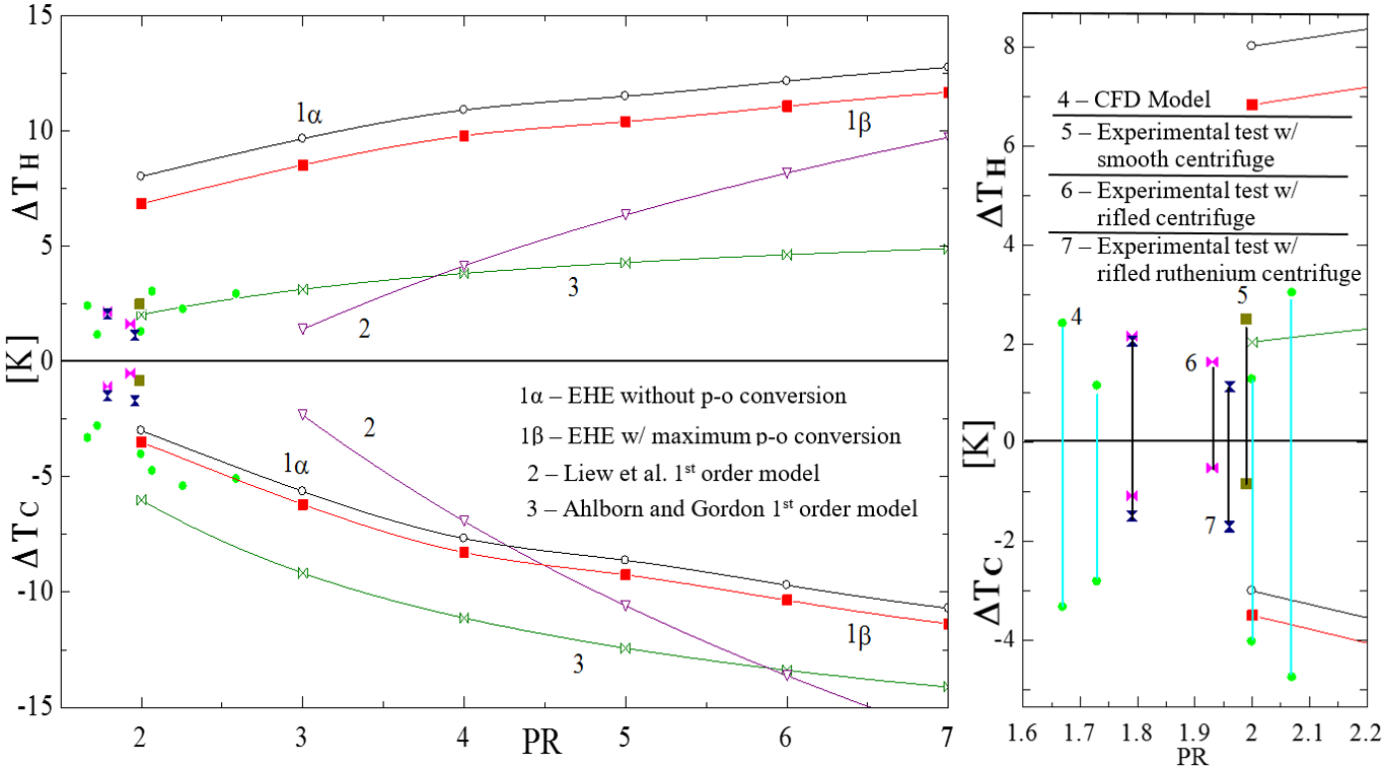

FIGURE 2. Temperature separation performance comparison of first order models, two dimensional (2D) axisymmetric CFD model, and experimental measurements with and without zoom perspectives, where 1α represents the extended heat exchanger (EHE) model without para-ortho conversion, 1β is EHE model with maximum para-ortho conversion potential, 2 represents the Liew et al. [1] model, 3 is the Ahlborn and Gordon [2] model, 4 is a 2D CFD model, 5 is an HVT experimental test with smooth centrifuge, 6 is HVT experimental test with rifled centrifuge, and 7 shows HVT experimental test with rifled ruthenium centrifuge. PR is pressure ratio of the total stagnation pressure of the upstream reservoir to total stagnation of the cold end outlet.

TABLE 2. Review of Vortex Tube Studies, and Comparison to Modelling and Experimental Work from the Current Project [4]

Report	Year	Analysis type		Results [a]					
		Fluid	Method	PR	T_R	ΔT_C	ΔT_H	ΔT_{Total}	μ
A.F. Johnson	1947	normal-H_2	Experimental	6.6	294	-15.9	-	-	-
Elser and Hoch	1951	normal-H_2	Experimental	6	285	-	-	74	0.5
T. Dutta et al.	2013	normal-H_2	FLUENT® w/REFPROP	3 3	115 115	-10 -7	25 9	35 16	0.22 0.54
Bunge et al. (this project)	2017	normal-H_2	FLUENT® w/REFPROP	1.73 2	77 75	-2.81 -6.41	1.15 0.46	3.96 6.87	0.36 0.70
Shoemake et al. (this project)	2017	para-H_2	Experimental w/o catalyst w/Ruthenium	 1.79 1.96	 73 74	 -1.08 -1.70	 2.16 1.13	 3.24 2.83	 0.37 0.42

[a] Where is temperature of the reservoir (inlet fluid) before centrifugal acceleration (*K*), ΔT_{Total} is the total differential in total temperature from hot outlet to cold outlet. Each row corresponds to the respective method.

Analysis model with the ability to optimize liquefaction plant placement. Results for this work are due at the end of FY 2017. Figure 4 illustrates the modelling plan for this task. The demand and supply mapping information and the resource locations will be the basis for a quantitative analysis of optimal liquefaction plant placement for minimum hydrogen resource and delivery cost.

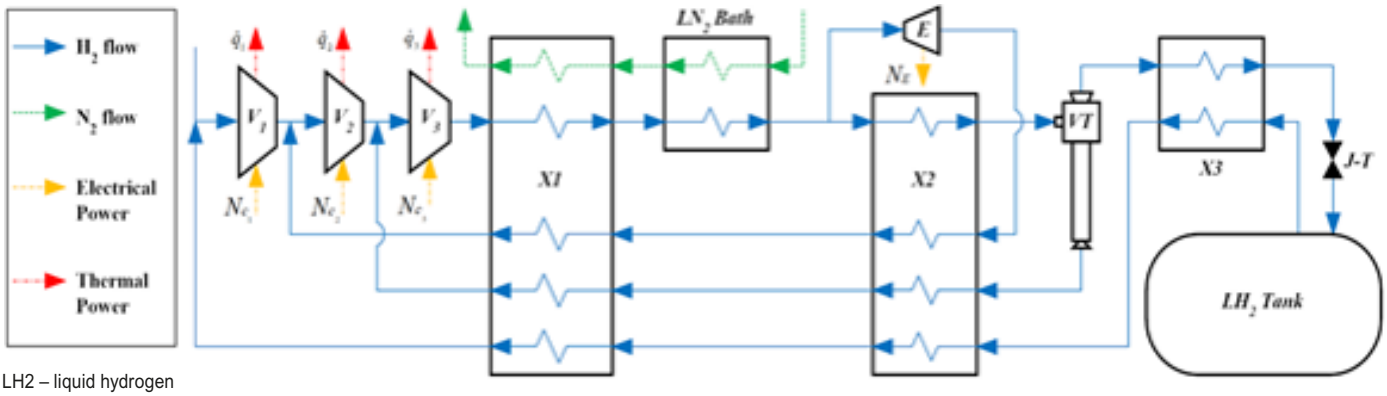

LH2 – liquid hydrogen

FIGURE 3. Diagram of pre-cooled Claude with vortex tube cycle

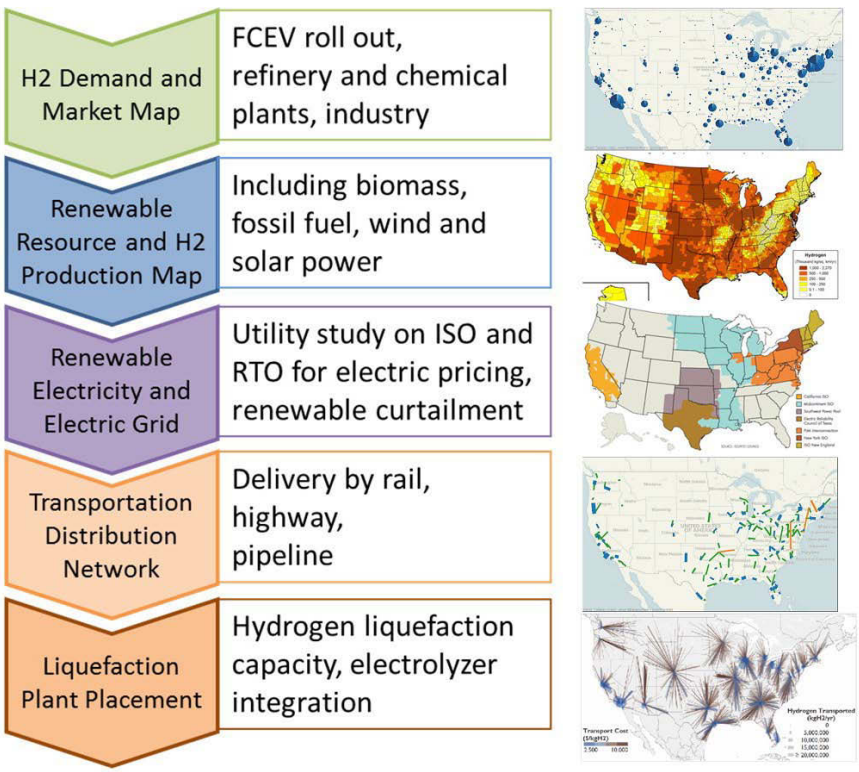

FCEV – fuel cell electric vehicle

FIGURE 4. Information and simulation flow for the liquefaction plant placement study

CONCLUSIONS AND UPCOMING ACTIVITIES

This project, represents a multi-faceted approach to improving the efficiency and capital cost of hydrogen liquefaction. The project has been stopped prior to its go/no-go milestone to re-focus future work. Areas currently being explored for future work include (1) investigation of supercritical vortex tube performance, (2) vertical flow reactor testing, (3) development of an optimal VT through three dimensional printing, and (4) and a sensitivity study of performance parameters for higher activity or surface area ortho/para conversion catalysts.

FY 2017 PUBLICATIONS/PRESENTATIONS

1. Bunge C.D., Cavender K.A., Matveev K.I., and Leachman J.W., "Analytical and numerical performance estimations of a Heisenberg Vortex Tube," In: 2017 Cryogenic Engineering Conference, (Madison, WI).

2. Presentation "Analytical and numerical performance estimations of a Heisenberg Vortex Tube," Carl Bunge, 2017 Cryogenic Engineering Conference poster presentation, July 10, 2017.

3. Presentation "Design and experimental measurements of a Heisenberg Vortex Tube for hydrogen cooling," Eli Shoemake, 2017 Cryogenic Engineering Conference poster presentation, July 10, 2017.

4. Presentation "Assessment of a Cryogenic Cycle System for Improved Hydrogen Liquefaction through Heisenberg Vortex Separation," Zhiwen Ma, Chris Ainscough, Jacob Leachman, Dustin McLarty, ASME 2017 Power & Energy Conference, June 26–29, 2017, Charlotte, NC.

5. Leachman, J., (June 2017). "Heisenberg vortex liquefaction, Delivery Tech Team Update," Presented at DOE FCTO AMR, June 7, 2017, Washington D.C.

REFERENCES

1. Liew R., Zeegers J.C.H., Kuerten J.G.M., and Michalek W.R., 2012 Maxwell's demon in the Ranque-Hilsch vortex tube *Phys. Rev. Lett.* **109.**

2. Ahlborn B. and Gordon J., 2000 The vortex tube as a classical thermodynamic refrigeration cycle *J. Appl. Phys.* **88** 3645–53.

3. U.S. Department of Energy, Office of Energy Efficiency and Renewable Energy, Fuel Cell Technologies Office Hydrogen Delivery Multi-Year Research, Development, and Demonstration Plan. https://energy.gov/sites/prod/files/2015/08/f25/fcto_myrdd_delivery.pdf

4. Dutta T., Sinhamahapatra K.P., and Bandyopadhyay S.S., 2013 CFD analysis of energy separation in Ranque-Hilsch vortex tube at cryogenic temperature, J. Fluids 2013 1–14.

III.6 Magnetocaloric Hydrogen Liquefaction

Jamie Holladay (Primary Contact),
Kerry Meinhardt, Evgueni Polikarpov, Ed Thomsen,
Reed Teyber, John Barclay (Emerald Energy NW),
Jun Cui (PNNL/Ames Laboratory),
Brandt Jensen (Ames), and Iver Anderson (Ames)
Pacific Northwest National Laboratory (PNNL)
PO Box 999, MS: K1-90
Richland, WA 99352
Phone: (509) 371-6692
Email: Jamie.Holladay@pnnl.gov

DOE Manager: Neha Rustagi
Phone: (202) 586-8424
Email: Neha.Rustagi@ee.doe.gov

Subcontractor:
Emerald Energy NW LLC, Bothell, WA

Project Start Date: October 1, 2015
Project End Date: September 30, 2018

Overall Objectives

- Quantify and incorporate novel configurations to achieve simpler, more efficient liquefier designs.
- Identify, characterize, and fabricate magnetic materials in shapes suitable for high performance active magnetic regenerators (AMRs) from 280 K to 20 K.
- Fabricate and characterize improved multi-layer magnetocaloric regenerator performance.
- Design, fabricate, test, and demonstrate a lab-scale magnetocaloric hydrogen liquefier system.
- Demonstrate a lab-scale hydrogen liquefier with a figure of merit (FOM) increase from 0.3 up to 0.5.
- Perform techno-economic analysis on a proposed full-scale (30 tons per day) system.

Fiscal Year (FY) 2017 Objectives

- Characterize eight magnetocaloric materials for use in second generation (GEN-II) design.
- Synthesize 150–250 μm particles of the magnetocaloric materials.
- Model the GEN-II regenerator using the updated materials properties.
- Adjust GEN-II design based on model results incorporating new hypothesis on layered material performance.
- Demonstrate GEN-II operation from 280 K to 120 K.

Technical Barriers

This project addresses the following technical delivery barrier from the Hydrogen Delivery section (3.2) of the Fuel Cell Technologies Office Multi-Year Research, Development, and Demonstration Plan.

(H) High-Cost and Low Efficiency of Hydrogen Liquefaction

Technical Targets

Conventional hydrogen liquefiers at any scale have a maximum FOM of ~0.35 due primarily to the intrinsic difficulty of rapid, efficient compression of either hydrogen or helium working gases (depending on the liquefier design). The novel approach of this magnetocaloric hydrogen liquefier (MCHL) project uses solid magnetic working refrigerants cycled in and out of high magnetic fields to execute an efficient active magnetic regenerative liquefaction cycle that avoids the use of gas compressors. Numerical simulation modeling of high performance MCHL designs indicates certain achievable designs have promise to simultaneously lower installed capital costs per unit capacity and to increase thermodynamic efficiency from an FOM of ~0.35 toward 0.5–0.6 (Table 1).

TABLE 1. Comparison of Magnetocaloric Hydrogen Liquefier Current Status to Targets

30 T/d (small facility)	Claude cycles (current)	PNNL's MCHL Targets	DOE Target (2017)[1]
Efficiency	<40%	***70~80%***	85%
FOM	<0.3 (small facility) 0.35~0.37 (large facility)	***~0.6 (small facility)*** ***~0.7 (large facility)***	0.5
Installed Capital Cost	$70 M[1]	***$45–70 M***	~$70 M
O&M Cost	4%	***2.8%***	--
Energy Input	10-15[1] kWh/kg H_2	***5~6 kWh/kg H_2***	12 kWh/kg H_2

O&M – operation and maintenance

FY 2017 Accomplishments

- Identified 13 ferromagnetic materials to span temperatures from 280 K to 20 K for a two-stage magnetocaloric hydrogen liquefier.
- Characterized the eight magnetic materials for use in the GEN-II system.
- Synthesized eight rare-earth alloys into 150–250 µm diameter spheres.
- Validated a new model which uses the materials properties reported by Ames.
- Modeled the GEN-II system.
- Predicted 6–10% bypass to provide optimal cooling of the process stream using the improved, validated model.
- Developed a modified GEN-II design using the model results. The GEN-II design incorporated the new layered regenerator configuration.
- Dual GEN-II regenerators constructed. In process of integrating dual regenerators with other subsystems of GEN-II and testing.
- Improved cooling to superconductive magnet sub-system which allowed its operation up to 7 T from 3.3 T.

✧ ✧ ✧ ✧ ✧

INTRODUCTION

MCHL technology promises cost effective and efficient hydrogen liquefaction because it eliminates gas compressors, the largest source of inefficiency in the traditional Claude cycle liquefiers, and the use of liquid nitrogen to precool the hydrogen. The Claude cycle liquefier is the current industrial choice for hydrogen liquefaction and uses a variety of configurations with processes where helium, hydrogen, or gas mixtures are coolants. In the case of hydrogen as the refrigerant gas and the process gas, the hydrogen feed to the process is first cooled by liquid nitrogen, and then further cooled in counter flow heat exchangers where the cooling power is provided by turbine expansion of a portion of the pre-cooled hydrogen stream. Liquefaction of the pre-cooled, high-pressure hydrogen stream is finally accomplished by throttling in a Joule-Thomson valve into a phase-separator collection vessel. Conventional liquefier technology for hydrogen is limited to an FOM of ~0.35 for a large facility, and of typically less than 0.3 for a smaller facility.

The current MCHL design is an AMR system which uses regions of high and low magnetic field and reciprocating magnetocaloric materials to transfer heat between hot and cold thermal reservoirs. In one step of the AMR cycle the magnetic material fabricated into a highly effective regenerator is adiabatically placed in a high magnetic field. The conservation of total entropy in this adiabatic process requires the magnetic refrigerants in the regenerators to increase in temperature (higher entropy) to compensate for the increased magnetic order (lower entropy) among the material's magnetic moments. The increased thermal energy is transferred to a heat sink by the cold-to-hot flow of heat transfer fluid. After the cold-to-hot heat transfer fluid flow is completed, the magnetic material is adiabatically removed from the high magnetic field resulting in an increase in entropy among the magnetic moments of the refrigerant in the regenerators so to maintain constant total entropy, the temperature of the magnetic refrigerants decreases in the magnetic regenerators. During the subsequent hot-to-cold flow of the heat transfer fluid at constant low magnetic field, the colder magnetic regenerator cools the heat transfer fluid before it exits the regenerator and accepts heat from the thermal load such as cooling the hydrogen process stream. At the end of this flow, the active magnetic regenerative cycle is repeated again at the operating frequency. To overcome the limited entropy change of magnetic refrigerants, magnetic cooling cycles typically use the active magnetic regenerator in which each differential section of the regenerator undergoes independent Brayton cycles. This allows the temperature spans required for liquefaction to be obtained. A more complete description including simplified process flow diagram and schematics is found in the FY 2016 Annual Progress Report. The AMR cycle can be highly efficient because the magnetization/demagnetization temperature changes are only a fraction of the adiabatic temperature changes of a gas compression process and the magnetic regenerators can be designed to have much higher effectiveness than a gas-to-gas counter-flow heat exchanger. In addition, the magnetization and demagnetization process are inherently reversible allowing for high efficiency. The MCHL project is developing liquefier designs that use magnetocaloric refrigeration to achieve an efficient thermodynamic liquefaction cycle. Detailed modeling of the MCHL technology coupled with experimental validation in prototypes indicate this technology has the potential to simultaneously lower liquefier installed capital costs per unit capacity, decrease delivery cost, and to increase thermodynamic efficiency from an FOM of ~0.3 toward 0.5–0.6.

APPROACH

At a high level the critical path for MCHL project can be summarized as:

- Identify, synthesize and characterize magnetocaloric materials.
- Develop an approach to understand the magnitude and utilize the second order (fero-paramagnetic) phase transaction characteristic in many magnetocaloric

materials to improve system performance while minimizing cost. Below the respective Curie temperatures of such magnetic materials have lower magnetic heat capacity in high magnetic fields compared to low magnetic field. We used the positive influence of this unique thermal characteristic on heat transfer flow in "bypass operation" described in FY 2016 Annual Progress Report as well as in the current report.

- Investigate layered material regenerator compositions, engineering and operation in an attempt to develop layering strategies and to understand how temperature changes within the layers and how different heat transfer fluid in material layers impact performance. This includes detailed models using the materials properties measured as well as experiments.
- Ortho-Para hydrogen conversion for liquefaction. This will include system research for catalyst integration into process heat exchangers or into magnetic regenerators.
- Hydrogen liquefaction by combining the research findings.

This project builds upon work first pioneered by Dr. John Barclay at Emerald Energy NW, LLC, (partner). We have modified the design and updated models previously developed. We have several major efforts occurring simultaneously to complete the critical path for this project's magnetocaloric hydrogen liquefaction research goals. (1) In house synthesized alloy ingots were used for the materials characterization using Ames's magnetic materials characterization capabilities. For use in the MCHL, the materials need to be spherical with a diameter of 150–250 µm. We are using Ames's rotating disk atomization (RDA), a low-cost material synthesis technique, to make the spheres. The RDA synthesized materials will be tested in PNNL's unique reciprocating dual regenerator research system. Details of the dual regenerator design, schematics, etc., as well as initial bypass operation are found in the FY 2016 Annual Progress Report. (2) Bypass operation was tested and identified as a key to achieving high performance operation with minimal materials. (3) The layering and system design efforts are being pursued via modeling and experimental efforts. The materials properties will be used in an advanced modeling sub-task to understand the performance and improve the system design. The models are being validated against experimental data from PNNL's research system. A second-generation device tests materials layering coupled with bypass operation. Material layering is not a new approach; however, the expected performance has not been achieved for cryogenic applications. We hypothesize that the reason for this is that each layer needs to be considered as an individual refrigerator cycle. This results in varying the amount of materials required for each layer and varying the heat transfer fluid flow for each layer. This hypothesis is tested in the second-generation system. (4) Based on the results of the previous work, integration of ortho-para catalysts to aid in hydrogen liquefaction and actual liquefaction tests will be done. This integration and research is part of the future work on this project. Finally, a techno-economic analysis will be used to measure progress against the DOE's efficiency and cost performance targets. An initial techno-economic analysis was reported in FY 2016. This analysis is currently being updated with FY 2017 results and will be completed in FY 2018.

RESULTS

Materials Synthesis and Characterization

Materials with the correct properties combined with innovation system configurations to take advantage of those properties are key to the success of this project. For materials selection, we assumed a 20 K decrease per material which results in a total of 13 materials needed in a two-stage system. Each material needs to have the appropriate Curie temperature, T_c, for operation in the desired temperature range. Molecular field theory was used to identify alloys with the desired T_c which were then synthesized as ingots to measure the properties. These materials are listed in Table 2.

TABLE 2. Materials, Their Target Operating Temperature and Associated Curie Temperatures

Material	Operating Temperature Span	Curie Temperature
	K	K
Gd	280–260	293
$Gd_{0.91}Y_{0.09}$	260–240	274
$Gd_{0.30}Tb_{0.70}$	240–220	253
$Gd_{0.69}Er_{0.31}$	220–200	232
$Gd_{0.32}Dy_{0.68}$	200–180	213
$Gd_{0.15}Dy_{0.85}$	180–160	193
$Gd_{0.27}Ho_{0.73}$	160–140	173
$Gd_{0.16}Ho_{0.84}$	140–120	153
$Gd_{0.23}Er_{0.77}$	120–100	132
$Ho_{0.90}Gd_{0.10}Co_2$	100–80	110
$Ho_{0.95}Gd_{0.05}Co_2$	80–60	90
$Gd_{0.5}Dy_{0.5}Ni_2$	60–40	70
$Dy_{0.75}Er_{0.25}Al_2$	40–20	50

In FY 2017 we have characterized and synthesized the first eight materials for use in the first stage. The RDA system, Figure 1, was used to make the spherical particles. Empirical correlations are available for pure materials to provide guidance for the alloys. Unfortunately, the alloys performed substantially different than the pure materials which caused delays in Ames being able to provide suitable

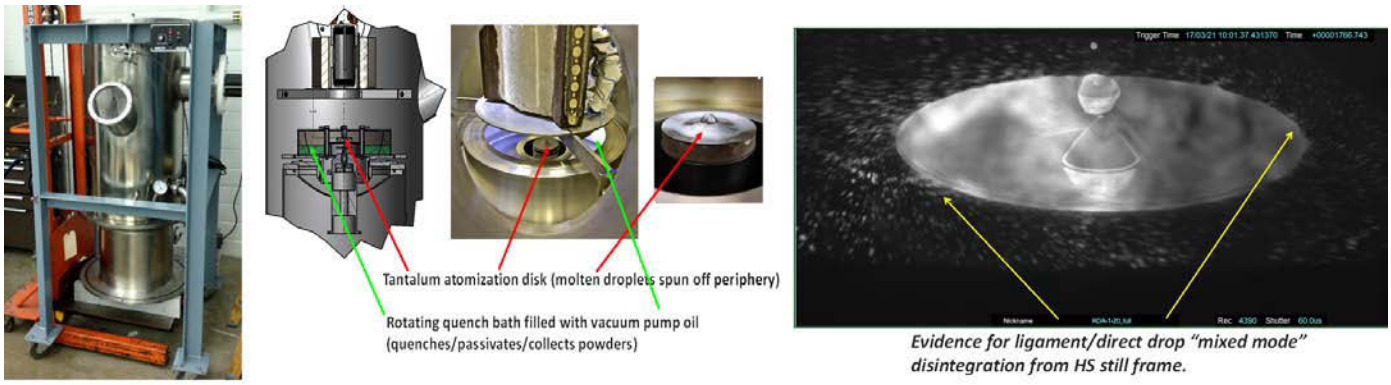

FIGURE 1. Rotating disk atomizer used to synthesize the micron scale spherical magnetocaloric materials. Picture on the far right shows atomization process of $Gd_{0.16}Ho_{0.84}$.

materials to PNNL for the regenerators. One of the major challenges was not in material size, but in achieving spheres. The MCHL system was designed for spherical particles to ensure acceptable pressure drop and uniform fluid flow through the porous regenerators. As flakes will severely limit performance, the spherical particles are needed. In order to eliminate the need to hand separate the particles, PNNL built a simple machine to quickly separate the spherical from non-spherical particles (Figure 2). Several runs were required to obtain sufficient material for each layer of the dual regenerators. The experience from these runs is helping Ames improve their RDA apparatus for rare-earth alloys.

Magnetic property characterizations included Curie temperature (T_c), magnetic moment, and heat capacity measurements from 2 K to 340 K and several magnetic fields between 0 T and 9 T. As shown in Figure 3, the heat capacity for gadolinium below its Curie temperature of 293 K varies by as much as 10% from a change in magnetic field from 0.05 T to 9 T. Similar property performance was measured in the other alloys. These properties were used in the updated model.

Bypass Operation

Bypass operation enables a system to take advantage of the fundamental properties of the second order phase transition in the materials being used. As shown in Figure 3, the magnetocaloric material had a significantly higher heat capacity at low magnetic field compared to high magnetic fields. This translates into the need for a higher heat transfer

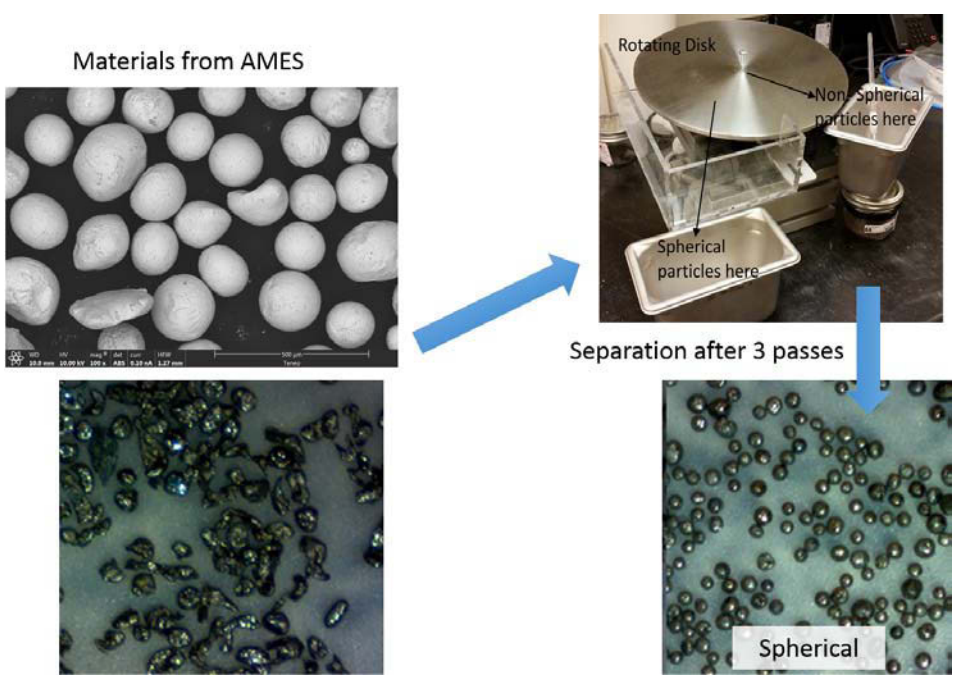

FIGURE 2. Successful separation of spherical particles from non-spherical particles using a simple apparatus

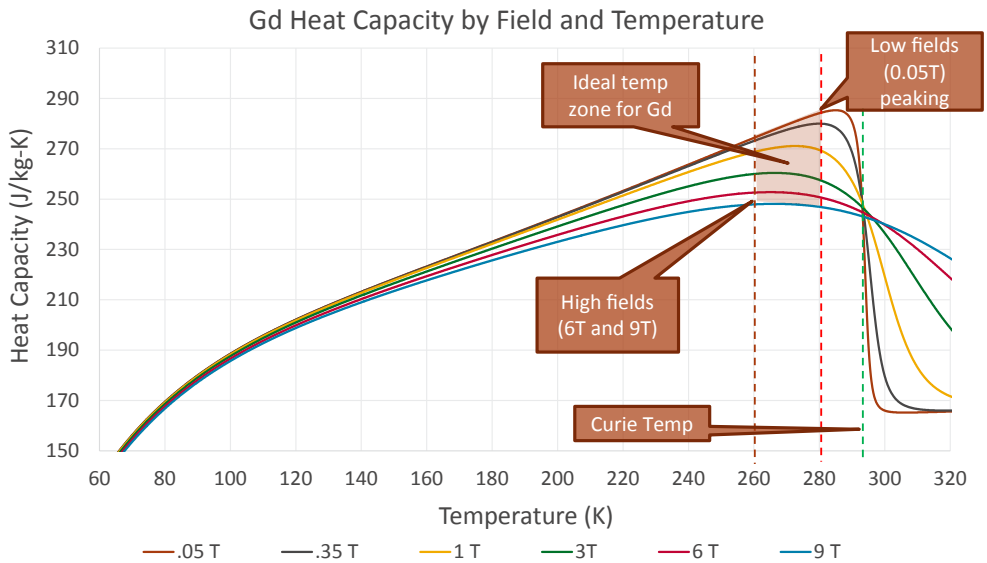

FIGURE 3. Heat capacity is magnetic field dependent

fluid flow through a regenerator located in the low magnetic field than in the high magnetic field. The excess heat transfer fluid can be redirected to bypass the regenerator in the magnetic field to not only improve the AMR performance, but it can be used to pre-cool the process stream to increase the system cooling power and continuously cool the process stream. The system modeling shows identifies 6–10% bypass operation as the optimum and Table 3 shows the impact of a 6% bypass coupled with a 6 T magnetic field change on the regenerator mass for the 280 K to 120 K stage of a 1-Hz MCHL with a 25 kg/d capacity.

Model Validation

Simulations were used to predict performance of the dual regenerators coupled with the reciprocating heat transfer gas flows. Simulations found in the literature used average material properties. For small changes in magnetic field and/or temperature average properties would be sufficient. However, the MCHL system will experience a large change in magnetic field and large temperature change so the average properties would likely result in substantial errors. Thus, large multi-property data bases created using the molecular field model and magnetic thermodynamics based on the materials properties measured by Ames were used. One of the unique features of the PNNL test apparatus is that the regenerators have thermocouples integrated into the dual regenerators which allows the axial temperature distribution in the bed to be measured. Knowing the temperature distribution allowed us to validate the model (Figure 4). The model informed us that one of the key features in the regenerators is the temperature profile and its impact on cooling power. The model showed and was consistent with the experimentally observed data that there was a dramatic change in the temperature profile between zero thermal load and a 50 W applied thermal load in the cold heat exchanger. For example, earlier assumption of regenerator performance was to assume the axial temperature profile moved up and down uniformly along the entire length of the regenerator. That is not what is observed both experimentally and numerically; the cold-end temperatures change much more rapidly than hot-end temperatures. The validated model was used to design an eight-layered regenerator.

Layered System Design and Model Simulation

The most efficient and easiest way to build a magnetocaloric system would be one where each stage is composed of a single material. However, if each stage had a separate high field magnet the capital cost of such a system would make it uneconomical. To lower the capital cost the materials are layered which decreases the balance of plant

TABLE 3. Bypass Operation Results in Significant Improvements in Performance and Reduction in Materials Required

	No Bypass	6% Bypass	% Improvement
Thermal load	4.3 kW	2.9 kW	32% reduction
Heat transfer fluid flow	31.3 L He/sec	3.8 L He/sec	87% reduction
Magnetic material required	184 kg	22.3 kg	88% reduction
Figure of Merit	0.4	>0.75	87% increase

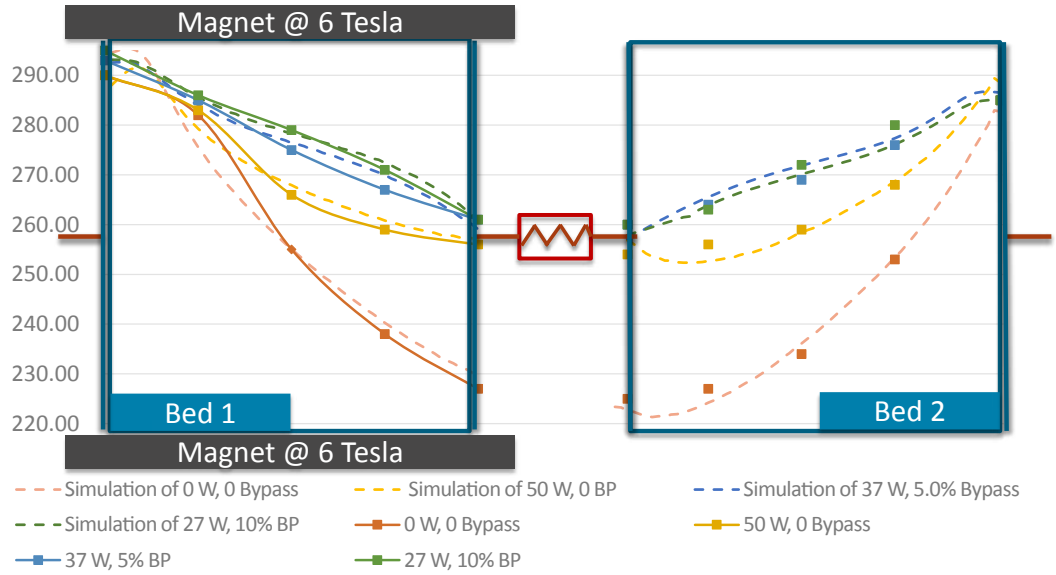

FIGURE 4. Experimental results show temperature profile changes in the regenerator and validate the numerical model

components and therefore the capital cost. In theory, multiple layers should perform equivalently as if each layer was in its own system. However, in practice this has not, to our knowledge, been achieved. We are proposing a new layering approach which we believe will overcome the limitations observed in the past. Our approach is based upon the hypothesis that each layer needs to be considered as its own refrigeration cycle. In this scenario, it results that each layer would have a different heat duty that it needs to account for. For example, layer "A" would have a heat duty of "a", layer "B" would have to reject heat from layer "A" in addition to its own heat duty, so the total heat duty for layer "B" would be "a + b". Similarly, layer "C" would need to accept the heat duty from the previous layers in addition to its own cooling heat duty, "c". Thus layer "C" would have a heat duty of "a+b+c". The implications of this hypothesis are that each layer would need to have different amounts of material and a different heat transfer fluid flow. Current designs do not vary either the material or flow. Using the validated model, we designed an eight-layer system that accounts for the varying enthalpy flow and associated differences in magnetic refrigerant material and heat transfer fluid flow as well as allowed for by-pass flow. Table 4 has the material amounts and heat duty for a device capable of pre-cooling gaseous hydrogen from 280 K to 120 K at a rate of 2.5 kg/d. Figure 5a shows the design and Figure 5b has the model results. Fluid flow was simulated using ANSYS/FLUENT and the header, footer, and packed bed design simulation showed the uniform flow. We have received the materials from Ames, assembled the dual regenerators and are in the process system testing. The results will be reported in the next report.

TABLE 4. Materials, Operating Temperature, and Heat Load for the Eight Layers in the Stage 1 System

Layer	Material	Average T_{HOT}/T_{COLD} (K)	Curie Temp (K)	Mass of Magnetic Material/Layer (grams)	Work Rate/Layer (W)	Q_{HOT} /Layer (W)
1	Gd	280/260	293	268	11.0	132
2	$Gd_{0.91}Y_{0.09}$	260/240	274	258	9.9	110
3	$Gd_{0.3}Tb_{0.7}$	240/220	253	235	8.8	90.7
4	$Gd_{0.69}Er_{0.31}$	220/200	232	202	7.6	71.9
5	$Gd_{0.32}Dy_{0.68}$	200/180	213	172	6.3	54.4
6	$Gd_{0.15}Dy_{0.85}$	180/160	193	139	4.9	38.4
7	$Gd_{0.27}Ho_{0.73}$	160/140	173	100	3.4	23.9
8	$Gd_{0.16}Ho_{0.84}$	140/120	153	57	1.8	11.0

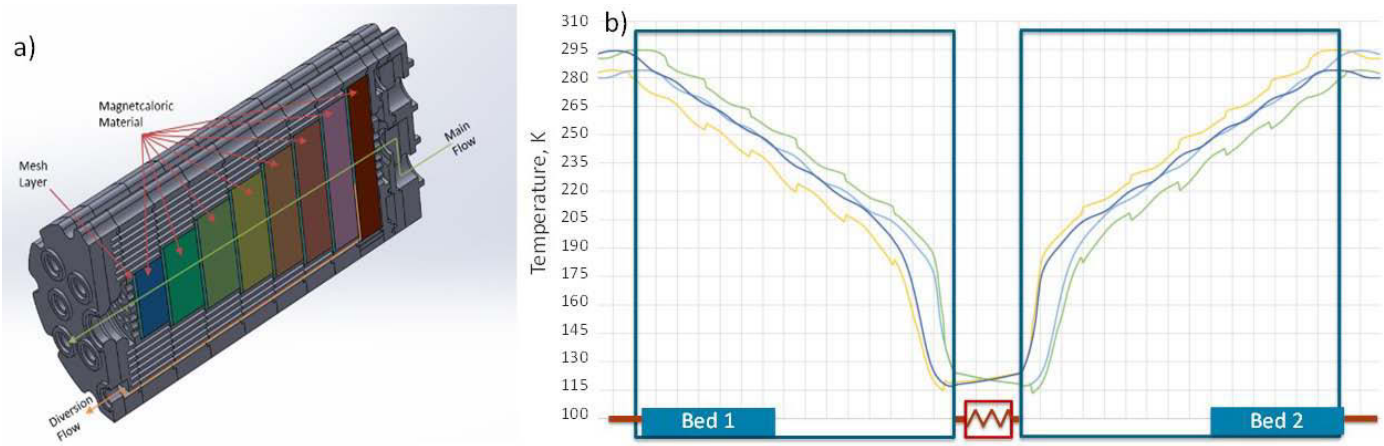

FIGURE 5. Eight-layer system design and simulation results showing the targeted temperature reduction

CONCLUSIONS AND UPCOMING ACTIVITIES

This project has made progress towards the ultimate goals of increasing the system efficiency while maintaining or decreasing the capital cost of hydrogen liquefaction technologies. In FY 2017 we have made progress along the critical path in that we have:

- Identified the 13 materials for a two-stage hydrogen liquefier.
- Characterized and synthesized the eight materials for the first stage.
- Updated the numerical simulation models with measured materials properties and validated the model against experimental data.
- Exercised the model to simulate a novel approach to multi-layered active magnetic regenerative refrigerator system.
- Assembled the fabricated components of the system.

Upcoming activities will include:

- Complete the Stage 1 testing.
- Use the lessons learned from Stage 1 to complete the design of the Stage 2 system.
- Characterize and synthesize the remaining materials for the second stage.
- Build and test the second stage.
- Complete techno-economic analysis.

SPECIAL RECOGNITIONS & AWARDS/ PATENTS ISSUED

1. Patent application: Active magnetic regenerative liquefier using process gas pre-cooling from bypass flow of heat transfer fluid (pending).

2. Patent application: Integrated fueling station (pending).

3. Patent application: Active magnetic regenerative processes and systems employing hydrogen heat transfer fluid (pending).

4. Patent application: Advanced multi-layer active magnetic regenerator systems and processes for magnetocaloric liquefaction (pending).

5. Patent application: Device for Production of Liquid Natural Gas with a 8-stage Active Magnetic Regenerative Liquefier (pending).

FY 2017 PUBLICATIONS/PRESENTATIONS

1. Holladay, J.D., K.D. Meinhardt, E. Polikarpov, E.C. Thomsen, J.A. Barclay, J. Cui, I.E. Anderson, and B. Jensen. 2017. "Magnetocaloric Hydrogen Liquefaction." Presented at Hydrogen Delivery Technical Team Review, Chicago, IL, on March 29, 2017. PNNL-SA-124817.

2. Holladay, J.D., K.D. Meinhardt, E. Polikarpov, E.C. Thomsen, J. Cui, I.E. Anderson, and J.A. Barclay. 2017. "Magnetocaloric Hydrogen Liquefaction." Presented at MRS Spring 2017, Phoenix, AZ, (Invited Speaker) on April 19, 2017. PNNL-SA-125562.

3. Holladay, J.D., J.A. Barclay, K.D. Meinhardt, J. Cui, I.E. Anderson, B. Jensen, E.C. Thomsen, and E. Polikarpov. 2017. "Magnetocaloric Hydrogen Liquefaction." Presented at Fuel Cell Technologies Annual Merit Review, Washington, DC, on June 7, 2017. PNNL-SA-125603.

4. Archipley, C.C., J.A. Barclay, J.D. Holladay, K.D. Meinhardt, E. Polikarpov, and E.C. Thomsen. 2017; "Production of LNG with an Active Magnetic Regenerative Liquefier." Poster presented at the Cryogenic Engineering Conference/International Cryogenic Materials Conference on July 11, 2017 (abstract reviewed prior to acceptance). To be published as paper in cryogenics.

5. Teyber, R., J.D. Holladay, K.D. Meinhardt, E. Polikarpov, E.C. Thomsen, J.A. Barclay, and C.C. Archipley. 2017. "Design and Experimental Analysis of a Superconducting Active Magnetic Regenerative Refrigerator." Under development for paper in cryogenics.

III.7 700 bar Hydrogen Dispenser Hose Reliability and Improvement

Kevin Harrison (Primary Contact), Owen Smith
National Renewable Energy Laboratory (NREL)
15013 Denver West Parkway
Golden, CO 80401-3305
Phone: (303) 384-7091
Email: Kevin.Harrison@nrel.gov

DOE Manager: Neha Rustagi
Phone: (202) 586-8424
Email: Neha.Rustagi@ee.doe.gov

Subcontractor:
Marc Mann, Spectrum Automation Controls, Inc., Arvada, CO

Project Start Date: July 2013
Project End Date: Project continuation and direction determined annually by DOE

Overall Objectives

- Working closely with original equipment manufacturers (OEMs) SpirStar and other groups developing advanced high pressure hydrogen hoses, NREL's hose reliability project aims to improve the reliability of 700-bar hydrogen refueling hose assemblies, and ultimately reduce the cost of dispensing hydrogen into fuel cell electric vehicles by identifying and characterizing points of failure.
- Operate a fully automated test system that unifies the four stresses of pressure, temperature, time, and bending. The test apparatus will reveal the compounding impacts of high-volume 700-bar fuel cell electric vehicle refueling that has yet to be experienced in today's low-volume market. Testing includes pre- and post-cycling chemical and physical analysis of the inner hose liner to determine any relative changes in bulk properties and degradation mechanisms due to the stress of repeated fueling events.

Fiscal Year (FY) 2017 Objectives

- Continue hose cycling towards 25,000 cycles or until failure using the test apparatus that unifies the stresses to which the hose is subjected during high volume fueling events.
- Gather and analyze data on hydrogen leakage rates, timing and sources through the use of a vacuum sampling pump system with combustible gas detectors and the deployment of chemochromic leak indication tape.
- Use data and observations to help inform preventative maintenance schedules and standards development for hydrogen stations.

Technical Barriers

This project is conducting applied research, development, and demonstration to reduce the cost of hydrogen delivery systems. This project addresses the following technical barriers from the Hydrogen Delivery section of the Fuel Cell Technologies Office Multi-Year Research, Development, and Demonstration Plan:

(I) Other Fueling Site/Terminal Operations

(J) Hydrogen Leakage and Sensors

Technical Targets

This project aims to generate data that will help OEMs and hose developers improve reliability and replacement intervals for high-pressure gaseous hydrogen dispenser hoses. This data provided by this project will ultimately reduce the cost of hydrogen delivery from the point of production to the point of use in consumer vehicles by providing robust dispenser operation with less maintenance costs and improved customer satisfaction.

- Target Hose Replacement Interval: 25,000 cycles
- Target Cost of Hydrogen Delivery: <$2.00/gge by 2020

FY 2017 Accomplishments

- Completed over 5,000 cycles on Hose Assembly #2 running various cases of SAE J2601 H70-T40 cases with excellent accuracy on pressure controls.
  - Average mass of 200 g consumed per cycle after precooling upgrade completed.
  - Selected cases of H70-T20 and H70-T30 run for comparison of leak rates as a function of hose gas temperature.
- Detected and investigated a leak pattern from crimp fittings on hose at the nozzle end.
  - Vacuum-based active sampling system detected several consistent, but small leaks from the crimp fitting on the nozzle end of the hose starting at Cycle 3033.

  - Leaks were observed through all parts of cycles and pressure holds, especially during higher pressures and during venting between cycles.
  - The leak is not isolated to the nozzle end crimp fitting, but was also observed to permeate through the hose layer for up to 25 cm from the crimp fitting, without visible damage or blistering on external surfaces. Chemochromic leak tape provides visual confirmation of this leak activity.
  - Hose continues to pass all standard leak checks, safety interlocks and pressure holds, with a calculated mass loss of up to 500 µg/s.
  - Multiple safety features implemented as part of experiment design allowing hose to be run throughout leaks without risk.
- Results and findings were shared with OEMs, field station operators, and codes and standards groups to help inform inspection requirements and standards development.

✧ ✧ ✧ ✧ ✧

INTRODUCTION

Operation and maintenance costs of dispensing are a large part of the cost of hydrogen stations. NREL has found that about 41% of maintenance hours for hydrogen fueling retail stations are associated with dispensers, with about 10% of those hours attributed to failed parts. This data can be found in NREL's infrastructure composite data products (CDPs) CDP-INFR-21 and CDP-INFR-24 [1]. These CDPs provide an early look at maintenance and reliability issues of the retail 700-bar vehicle refueling stations. Station operators have reported that they are replacing the high-pressure hoses earlier than expected in intervals of a few months. High-pressure hydrogen refueling hoses, compared with their gasoline counterparts, are significantly more expensive, and replacement intervals are much shorter. Hoses are not as high of a capital cost item ($2,000) compared with the hydrogen refueling nozzle ($7,000 for nozzles without infrared comms and $11,000 for nozzles with infrared comms) and breakaways ($3,000), however, nozzles and breakaway typically can be refurbished or serviced at a lower cost while hoses must be completely replaced. **Currently, the high frequency of hose replacement results in the high-pressure hoses being a significant operations and maintenance cost to the station operator.** Accelerating the cycle rate, monitoring the leakage patterns, and continuing past the point of typical replacement can supply valuable data on post-cycled specimens to share with OEMs and improve reliability through this project.

APPROACH

This project aims to perform long-duration accelerated life testing on commercial or prototype hose assemblies using high-pressure, low-temperature hydrogen to achieve realistic precooled fueling conditions closely following the SAE J2601-2014 fueling protocol. This work is unique and goes beyond standard OEM and certification standards agency acceptance testing in that it simultaneously stresses the hose assembly by applying mechanical bending and twisting stress to the hose and nozzle assembly to simulate people refueling vehicles. The short cycle time achieved with this system models the demand of a busy gas station where the dispensing equipment is kept cold most of the time and subjected to frequent decompression and occasional thermal cycles.

The main difference between the test plan and a high volume station is that the mass dispensed per fill is less than the 3–5 kg of a typical vehicle fill. To prevent overtaxing the production and compression capabilities of NREL's hydrogen system, the target mass dispensed per fill is 100–200 g. Back-to-back filling maintains hose temperatures under the Cold Dispenser cases of SAE J2601. Due to the low viscosity and mass of hydrogen, the additional shear stress on the hose wall from mass flow is negligible compared to the thermal stress and radial stress from pressurization cycles.

A hose reliability test stand, shown in Figure 1, was developed to support full 700-bar fueling simulation capabilities. The test stand uses a six-axis robot using pre-programmed motion paths to capture normal and realistic stresses resulting from friendly human interaction with the hose assembly while maintaining a compact footprint to safely operate in the 9.3 m^2 High Pressure Test Bay, which offers a safe and controlled environment to test components under high pressure to failure while minimizing risk to personnel or equipment. The test stand closely mirrors an actual dispenser in its design and pressure ramping capabilities. A tankless control algorithm was successfully developed using the interaction of an air-loaded pressure regulator on the dispenser side of the test apparatus and flow control valves on the vehicle side.

The leakage rate of the hose is monitored using a vacuum-pump sampling system attached to an outer protective sleeve near each flared crimp fitting to identify hydrogen leaks during the fueling cycles. The sampling flow rate is set to 400 mL/min and was calibrated to measure delayed response times. Chemochromic leak indication tape is also wrapped over the hose end assemblies to further identify exact methods of leakage, and potential inspection methods are verified at regular intervals. Data collected from the hose reliability test stand include pressure, temperature and real-time leakage rates from crimp fitting areas. These data can be used to explore dependency of leak intensity on current pressure and temperature. Permeation of hydrogen

FIGURE 1. Hose reliability test stand

through the polymer inner layers is a potential source of non-destructive leakage. Permeation activity typically follows the Arrhenius rate equation and is reduced with lower temperatures. However, temperatures that drop close to the glass transition temperature increase the brittleness of the polymer and the likelihood of internal damage to the polymer, allowing for easier permeation. Plotting the natural logarithm of the permeability rate and the inverse temperature allows correlation to the Arrhenius relationship and insights into the activation energy, or the ease of permeation of hydrogen through the polymer. Similar relationships have been tabulated for comparable polymers but a study has not been carried out for hydrogen and polyoxymethylene [2].

The project also includes analysis of the physical and chemical property changes of the inner hose liner due to long duration hydrogen cycling. Chemical tests previously identified and performed on pre-cycled inner hose specimens include scanning electron microscopy to ultimately identify blistering due to hydrogen permeation and characterization testing to identify material degradation and compositional changes such as Fourier transform infrared spectroscopy, thermogravimetric analysis, differential scanning calorimeters, X-ray spectroscopy and dynamical mechanical analysis methods. These tests will be repeated on post-cycled inner liner samples to compare any changes or degradations in the polymer properties.

RESULTS

The hydrogen detection system began sensing leaks on the nozzle-side crimp fitting at Cycle 3,033. While some leaks were also detected on the dispenser side crimp fitting earlier at Cycle 1,856, those leaks have been inconsistent. The amount of hydrogen lost per cycle is relatively small, with a mass loss rate of up to 500 µg/s, originating primarily from the nozzle-side crimp fittings. Since the leak rate is smaller than many instrumentation tolerances, pressure checks pass and these leak rates almost certainly go undetected in the field. There is only one current code and standard that has defined numerical criteria for leakage thresholds, currently set as 10 ccN/h, or 3,235 µg/s [3]. On the NREL hose test apparatus, over 1,500 cycles have been completed on the same hose assembly that exhibit signs of leakage without failure. The leak patterns can be seen in Figure 2, trending upwards with pressure and spiking during depressurization and motion back to the dispenser. This could possibly indicate leakage from the plastic to metal seat during venting, blistering of the inner layer from depressurization, or cracking of the inner liner during motion.

Typical cycles run with T20, T30, and T40 temperature profiles and longer-term (10 min) pressure holds at 82 MPa were analyzed for permeation effects. The typical cycles were observed to have leak rates that generally increased with pressure and decreased with temperature, with a notable increase in leak activity at temperatures around -40°C, close to the glass transition temperature previously measured as -50°C. Many pressure holds on the hose assembly, typically those immediately following a cold cycle, exhibit a strong exponential relationship between leak rate and temperature. Other, warmer holds performed during idle periods still leaked, but showed weaker correlations with temperature as shown in Figure 3. Activation energies of 21.9–43.8 kJ/mol were reported for the sample pressure holds shown.

Inspection methods were explored to help inform preventive maintenance requirements and codes and standards development, with a particular interest in finding out if this type of leak may be indicative of early failure of

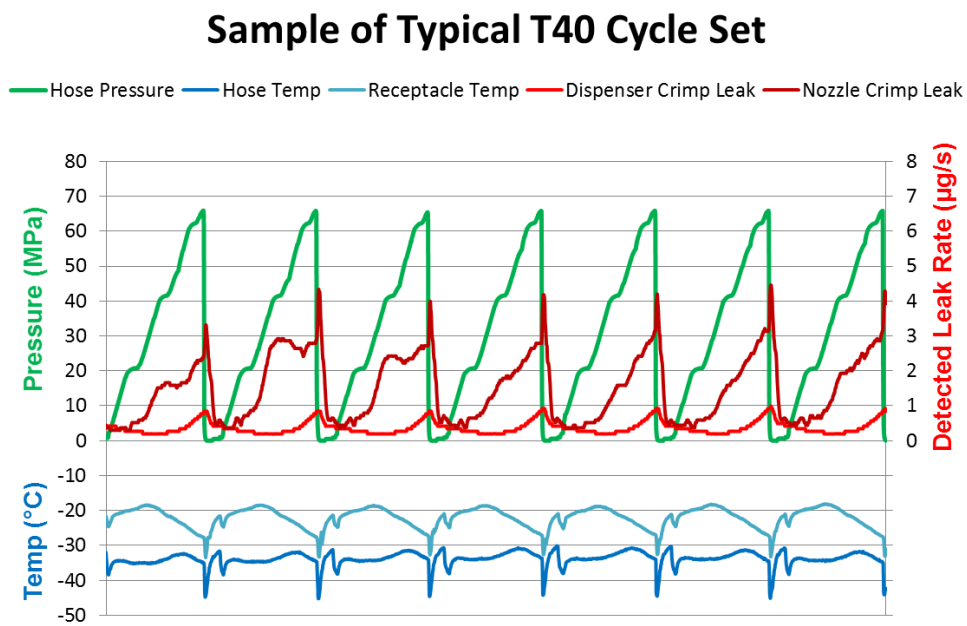

FIGURE 2. Sample of hose cycle pressure profile set, showing leak trends

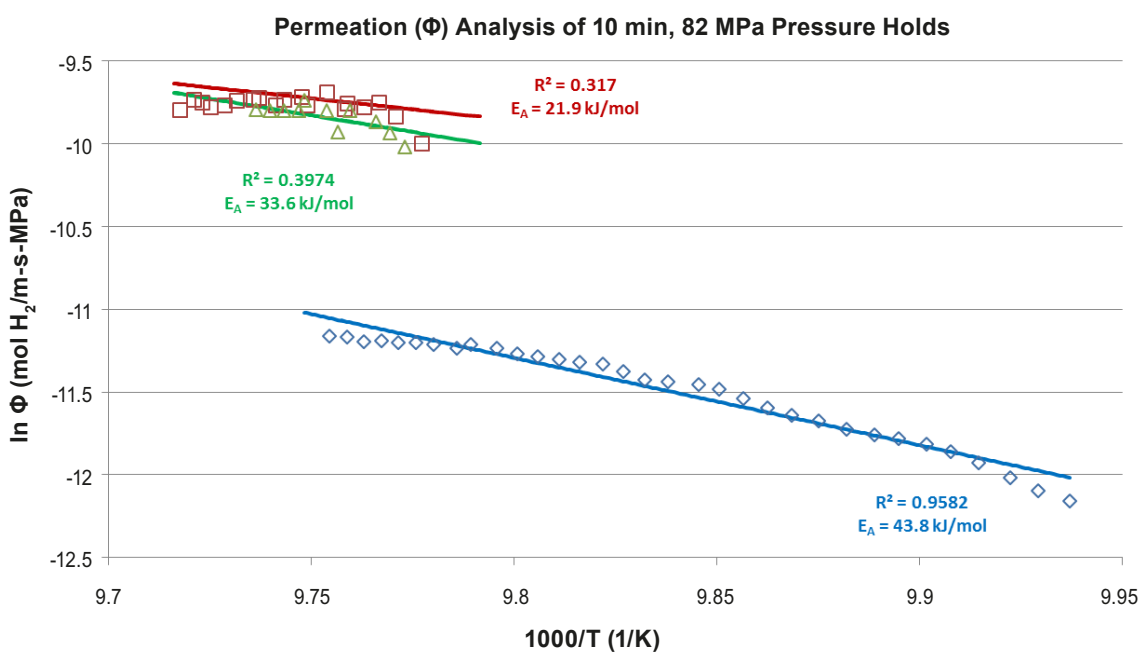

FIGURE 3. Analysis of permeation activity dependency on hose temperature

hose assemblies. This level of leak being reported is too small to be audible by operators and there is no visible damage on the outer layer. However, commonly available handheld combustible gas detectors can reliably detect leaks of this size. Hose sample #2—the one currently under test—shows stronger leak intensity near the crimp fitting, decreasing up to 25 cm from the crimp fitting. Hose Assembly #1 was burst tested at the beginning of the project to confirm the hoses from this batch were meeting the manufacturer's criteria.

A reliable inspection method may be available by using chemochromic leak indication tape that darkens upon contact with hydrogen. A sample was donated by ElementOne and deployed on both ends of Hose Sample #2, with control tapes deployed on NREL's hydrogen dispenser as well. After

1,000 cycles on the test apparatus, the tape clearly showed heavy leaking from the nozzle side crimp fitting through the pinpricks designed to relieve pressure from permeation of hydrogen, shown in Figure 4. The dispenser side crimp fitting, which had inconsistently leaked smaller amounts, showed fainter but still legible leak marks. In comparison, NREL's dispenser hose, which had filled about 150 times during the same time frame with similar mechanical stressing, had zero leak indications, confirmed with a handheld detector. Chemochromic tape may be very useful to station operators as an inspection method to identify weakened hoses before failure.

Data from these studies have been shared with the hose OEM, field station operators, and with standards groups such as ISO 19880-5 WG22 to help inform development.

FIGURE 4. Chemochromic leak indication tape on nozzle-side hose end

CONCLUSIONS AND UPCOMING ACTIVITIES

- Conclusion: Hydrogen leaks were first detected at the nozzle end of the Hose Sample #2 at Cycle 3,033, consistently leaking throughout several hundred cycles at a rate of about 500 µg/s. This leak rate does not fail standard leak checks and pressure holds, and passes current code criteria. However, it may indicate increased permeation and risk of eventual failure due to weakened inner material.
- Conclusion: Inspection methods were verified, with handheld gas detectors and chemochromic leak tape being shown as highly reliable and easy to check. Station operators may be able to use these methods to help identify hoses at risk of failure.
- Upcoming: With remaining funding, continue testing Sample #2 beyond 5,000 cycles until failure or significant degradation, and perform post-cycle scanning electron microscopic imaging, physical dynamical mechanical analysis and chemical composition testing previously identified.
- Upcoming: With future external funding, hoses from additional manufacturers could be tested and verified under similar test conditions and materials testing.

FY 2017 PUBLICATIONS/PRESENTATIONS

1. Joe Pratt, Chris Ainscough, Danny Terlip, Terry Johnson, Mike Peters, and Ethan Hecht, "H2FIRST Tasks and Impact," presented to the California Fuel Cell Partnership, December 2016.

2. Kevin Harrison and Owen Smith, "700 Bar Hydrogen Hose Reliability Project," presented to the Hydrogen Delivery Tech Team, November 2016.

REFERENCES

1. Sprik, Sam, Jennifer Kurtz, Chris Ainscough, Genevieve Saur, Michael Peters and Matthew Jeffers. "Next Generation Hydrogen Station Composite Data Products - Data through Quarter 4 of 2016." Hydrogen Fueling Infrastructure Analysis. May 2017. http://www.nrel.gov/docs/fy17osti/66555.pdf.

2. San Marchi, C., B.P. Somerday. "Technical Reference for Hydrogen Compatibility of Materials," Sandia National Laboratory Technical Report SAND2012-7321. September 2012.

3. CSA Group. "Hoses for compressed hydrogen fuel stations, dispensers and vehicle fuel systems," ANSI/CSA HGV 4.2-2013. 2013.

III.8 Cryogenically Flexible, Low Permeability H_2 Delivery Hose

Jennifer Lalli (Primary Contact), William Harrison, Keith Hill, Carleen Bowers, Tod Distler, Vince Baranauskas, and Richard Claus
NanoSonic, Inc.
158 Wheatland Drive
Pembroke, VA 24136
Phone: (540) 626-6266
Email: jhlalli@nanosonic.com

DOE Manager: Neha Rustagi
Phone: (202) 586-8424
Email: Neha.Rustagi@ee.doe.gov

Contract Number: DE-SC0010162

Subcontractors:
- National Renewable Energy Laboratory, Golden, CO
- Cardinal Rubber & Seal, Roanoke, VA
- LifeGuard Technologies, Springfield, PA

Project Start Date: April 30, 2016
Project End Date: April 29, 2017

Overall Objectives

NanoSonic's overall objectives for hydrogen dispenser technologies mirror those of the Hydrogen Delivery program within the U.S. Department of Energy's Office of Energy Efficiency and Renewable Energy Fuel Cell Technologies Office (FCTO). These technologies aim to help realize hydrogen as a safe, reliable, and cost competitive energy carrier. Outcomes of this project will include:

- A highly durable hose that can reliably perform at 875 bar (for H70 service, 70 MPa delivery) and over a temperature range of -40°C to 85°C.
- A new Class D H_2 dispensing hose, for use on station side applications, that is chemically engineered to survive 51,240 fills (70 fills/d, 2 yr) and meets the requirements of relevant industry standards outlined in American National Standards Institute (ANSI)/ Canadian Standards Association (CSA) hydrogen gas vehicle (HGV) 4.2-2013, with a dispenser compliant with SAE International Technical Information Report J2601 and National Institute of Standards and Technology Handbook 44.
- A state-of-the-art, metal-free hose based on a unique fiber reinforced, high performance, cryogenically flexible polymer to resist H_2 embrittlement, survive the Joule-Thompson effect thermal cycles, perform consistently at pressures greater than 875 bar and endure mechanical wear and fatigue at the pump.
- An alternative to the German made H_2 dispenser hose that is currently qualified for H70 service, though it does not meet the service requirement of 25,550 fills/yr, nor allow for a cost of $2–4 gallon of gas equivalent (gge).

Fiscal Year (FY) 2017 Objectives

- Demonstrate a new fitting for H70 service with NanoSonic's H_2 hose.
- Model and down-select a metal-free, fiber reinforced hose as a functions of fiber material, angle, and filament wind design.
- Quantify the burst strength of the new H_2 hose with the new fitting.
- Demonstrate durability via pressure cycle testing.
- Verify durability, purity, and consumer ease of use at dispensing stations.

Technical Barriers

This project addresses the following technical barriers from the Hydrogen Delivery section (3.2.5) of the FCTO Multi-Year Research, Development, and Demonstration Plan.

(A) Lack of Hydrogen/Carrier and Infrastructure Options Analysis

(C) Reliability and Costs of Liquid Hydrogen Pumping

(E) Gaseous Hydrogen Storage and Tube Trailer Delivery Costs

(I) Other Fueling Site/Termination Operations

Technical Targets

The goals of this project mirror those of the Office of Energy Efficiency and Renewable Energy to advance hydrogen delivery system technologies toward the FCTO Hydrogen Delivery Program's 2020 delivery targets [1]. NanoSonic has reduced the cryogenic flexibility of our H_2 hose by decreasing the glass transition temperature (T_g) to -100°C, and increasing upper thermal stability to 350°C to enable a wide service use temperature range of -50°C to 90°C. Burst strength has been increased from 9,000 psi to >31,000 psi during first quarter testing on hoses with fittings crimped in-house. The burst strength will be increased in 2018 to 51,000 psi, four times the maximum allowable working pressure (MAWP) of 12,690 psi, by modifying the fitting and the application methodology. NanoSonic modeled, produced, and down-selected a filament

wound hose that survived 50,000 cryogenic cycles at (-40°C) conducted at a working pressure of 12,000 psi. This same hose also survived nearly 2,000 cycles (at 85°C) prior to failure due to fitting slippage rather than burst. The new fitting is expected to survive 100,000 combined pressure and thermal cycles over -40°C to 85°C. A novel ceramer coupling agent with a T_g of -65°C was developed and demonstrated an increase of 25% burst strength with all fittings. Solvent and abrasion resistance are being tested per the targets outlined in ANSI/CSA HGV 4.2-2013; and evolved gas analysis and quality are being tested per the targets outlined in SAE J-2719 and International Organization for Standardization publication PDTS 14687-2. Current cost projections based on materials for 300 meters of hose are two times less than the competitor. Cost savings based on durability and normalized for lifetime, predict a 4x savings. NanoSonic can produce 16 metal-free H_2 hoses, each three meters in length, in an 8-hr work shift. NanoSonic's planned scale-up method predicts an 8x cost savings normalized for lifetime and 600 meters of hose, per targets given in Table 1.

FY 2017 Accomplishments

- Modeled, produced, and down-selected a metal-free filament wound hose.
- Demonstrated 25% weight reduction for composite H_2 hose relative to metal reinforced hose.
- Demonstrated enhanced flexibility for composite hose relative to metal reinforced hose for increased durability and an enhanced consumer experience.
- Crimped fittings onto metal-free composite hose and demonstrated burst strengths >31,000 psi; failure due to fitting slippage rather than burst.
- Demonstrated a metal-free composite hose that survives 50,000 cycles at 12,000 psi at -40°C.
- Demonstrated an additional >1,900 cycles at 12,000 psi at 85°C.
- Developed low T_g ceramer coupling agent that enhances crimp survivability by >25%.
- Ceramer coupling agent for enhanced crimp survivability and increased compression strength, exhibits compression strength >11,200 psi.
- Reduced cost to $300/m via scale-up.
- Collaborating with gas distribution original equipment manufacturers, fittings manufacturers, national laboratories, and safety standards groups to qualify the hose for H70 service.

INTRODUCTION

NanoSonic is developing and manufacturing a dispensing hose to enable cost-effective, reliable delivery of H_2 to fuel cell vehicles. This American made hose will meet FCTO's goals to enable domestic competitiveness and energy dominance through hydrogen technologies. Performance of dispensing hoses today is challenged by the operating conditions they experience during a hydrogen fill: repeated cycling at 875 bar (for H70 service, 70 MPa delivery), and over a temperature range of -50°C to +90°C. Hoses in use at stations today are, moreover, manufactured primarily outside of the United States.

NanoSonic has worked during this DOE Small Business Innovative Research program to produce a new Class D H_2 dispensing hose, for use on station side applications. NanoSonic's hose was systematically and chemically engineered to survive 51,240 fills, or 70 fills/d for a period of at least 2 yr. Our state-of-the-art hose is based on a unique fiber reinforced high performance, cryogenically flexible polymer to resist H_2 embrittlement, survive the Joule-Thompson effect of thermal cycles, perform consistently at pressures greater than 875 bar and endure mechanical wear and fatigue at the pump. Currently, there are only a couple of H_2 dispenser hoses that are qualified for H70 service. These hoses are not made in the United States, do not meet the service requirement of 25,550 fills/yr, and are not priced at a point that will allow hydrogen to cost $2–4 gge at the pump.

TABLE 1. Progress towards Meeting Technical Targets for Durable Hydrogen Hose for Fuel Cell Vehicles

Characteristic	Units	2018 Targets	NanoSonic
Tg for Cryogenic Service Temperature	° C	-50	meets
TGA 5% Weight Loss for Upper Service Temperature	° C	90	meets
Burst Strength	psi	51,000	> 31,000, failure due to fitting slippage rather than burst
Cycle Pressure Test	cycles	50,000 cycles at MAWP at -40 ° C	meets
Cycle Pressure Test	cycles	50,000 cycles at MAWP at 85 ° C	> 1900
Compression Strength	psi	12,690	meets
Hose Cost	$/m	<200	<60

TGA – thermogravimetric analysis

APPROACH

The new H_2 hose involves an all polymer material approach in contrast to the currently qualified hose that utilizes steel as its reinforcing agent. The unique polymer fiber reinforcement design shall meet the current burst strength requirements, and surpass the durability of steel based hoses which are susceptible to weakening and catastrophic failure via H_2 embrittlement. NanoSonic's state-of-the-art hose is based on a unique fiber reinforced high performance, cryogenically flexible polymer to resist hydrogen embrittlement, survive the Joule-Thompson effect of thermal cycles, perform consistently at pressures greater than 875 bar (for H70 service), and endure mechanical wear and fatigue at the pump. The polymer core is based on an ultra-low T_g backbone for cryogenic flexibility and modified for adhesion to the fiber reinforcing agents and ceramer inclusions for enhanced compression strength.

NanoSonic's manufacturing approach towards cost savings and enhanced durability is three-fold. First, a unique filament winding additive manufacturing technique allows for rapid, reproducible, and reliable production of composite hoses with tailored angular designs. Second, NanoSonic has two large scale reactors that allow for the cost effective production of 55 gal and 200 gal drum batches of our low T_g and low H_2 permeable nanocomposite resins. Finally, NanoSonic has invested in a crimper to integrate the end connection fittings directly onto our hoses, and has partnered with a hose assembly company to assist with swaged fittings. The combination of swaging and crimping allows for enhanced adhesion and mechanical fit between the fitting and the hose. Crimping in-house and with our local partners also yields a product with complete fit and finish for qualification and distribution.

RESULTS

NanoSonic's major focus during FY 2017 was on demonstrating high burst strength and pressure cycle survivability for filament wound composite hoses. Our 2017 metal-free composite hose is shown in Figure 1. NanoSonic produced hoses fitted with end connectors in-house that were 15 in. in length for hydrostatic burst strength testing, and 5 ft in length, as determined by their 9 in bend radius, as specified by the pressure cycle experiment at CSA laboratory. CSA was contracted to perform the two rounds of pressure evaluations on NanoSonic's high pressure hoses. The scheduled tests were (a) Hydrostatic Strength and (b) Pressure Cycle Test. The description of each test is described below.

Hydrostatic Strength (Section 2.4) of ANSI/CSA HGV 4.2-2013 standard for hoses for compressed hydrogen fuel stations, dispensers, and vehicle fuel systems requires a 1 min hold without burst or visible loss of fluid at a hydrostatic pressure of four times the manufacturers specified MAWP. up to a 10,000 psi MAWP hose assembly.

FIGURE 1. NanoSonic's H_2 delivery hoses demonstrating cryogenic flexibility

Two production assembly samples of each model at 12 in length are required.

Pressure Cycle Test (Section 2.17) of ANSI/CSA HGV 4.2-2013 standard for hoses for compressed hydrogen fuel stations, dispensers and vehicle fuel systems requires 50,000 cycles with MAWP (assuming 10,000 psi) at -40°C and 50,000 cycles with MAWP (assuming 10,000 PSI) at 85°C followed by compliance testing to Leakage (Section 2.2a) and Electrical Conductivity (Section 2.5). Two production assembly samples of each model hose length are required. The length of each hose is defined by:

Hose Length = π * (minimum bend radius) + 2 * (hose outer diameter)

First, NanoSonic developed a ceramer coupling agent to enhance the bond strength between the hose and the fitting. The ceramer was initially evaluated on a commercial hose and two types of commercial hose fittings. Experimentation showed that NanoSonic's ceramer increased the burst strength of each hose by 10–50% for each hose (Table 2).

NanoSonic subsequently infused their own hoses with the ceramer described above, and then tested these metal-free, carbon fiber reinforced hoses on a filament winder, wherein they exhibited hydrostatic burst strength values >31,000 psi (Table 3). Hose failure occurred for each of these hoses at the end near the fitting. The fitting crimp recipe was found to influence the burst strength. The NanoSonic hoses with highest burst strength of 31,421 psi failed due to fitting slippage (Figure 2). The commercial hoses, however, failed from burst. Also of importance; NanoSonic's hoses weigh 25% less than commercial hoses, each with fittings.

NanoSonic submitted six composites (three types, two of each) for pressure cycle testing at CSA Group (Figure 3). Each of these specimens were 5 ft in length and the architecture consisted of a low H_2 permeable core with a carbon fiber wound overwrap infused with our low T_g polymer matrix resin. Each filament wound architecture varies as a function of the overwrap angle. Pressure Cycle

TABLE 2. NanoSonic Ceramer Coupling Agent Effect on Hose Burst Strength

Hose Type	Hose ID	Fitting	Fitting OD (mm)	Ceramer	Burst Strength (psi)	Failure Mode
commercial	41A	A	16.1	yes	21,191	Burst
commercial	41B	A	16.1	no	10,096	Burst
commercial	WH208-9C20893	A	15.9	yes	58,449	Burst
commercial	WH208-9A20891	A	15.9	no	52,959	Burst
commercial	WH208-9D20894	B	15.9	yes	26,136	Burst
commercial	WH208-9B20892	B	15.9	no	9,635	Burst

ID – inner diameter; OD – outer diameter

TABLE 3. NanoSonic and Commercial H_2 Hose Crimp Recipes, Weight, and Hydrostatic Burst Strength Values

Hose Type	Hose ID	Fitting Type	Fitting OD (mm)	Ceramer	Burst Strength (psi)	Length (in)	Average Weight (g)
NanoSonic	7-1	A	14.9	yes	19,237	15	200
	7-2	A	15.3	yes	26,614	15	
	7-3	A	15.8	yes	25,380	15	
	8A-1	A	16.1	yes	31,421	15	
	8A-2	A	16.5	yes	30,475	15	
	8A-3	A	17.0	yes	16,357	15	
	8B-1	A	15.2	yes	22,591	15	
	8B-2	A	15.2	yes	30,576	15	
	8B-3	A	16.1	yes	28,063	15	
	13-1	A	15.6	yes	24,916	15	
	13-2	A	16.0	yes	24,273	15	
	13-3	A	16.4	yes	23,522	15	
Commercial	41A	A	16.1	yes	21,191	15	250
	41B	A	16.1	no	10,096	15	
	WH208-9A20891	A	15.9	yes	52,959	15	
	WH208-9B20892	B	15.9	no	9,635	15	
	WH208-9C20893	A	15.9	yes	58,449	15	
	WH208-9D20894	B	15.9	no	26,136	15	

FIGURE 2. NanoSonic hose post hydrostatic burst strength, failure due to fitting slippage

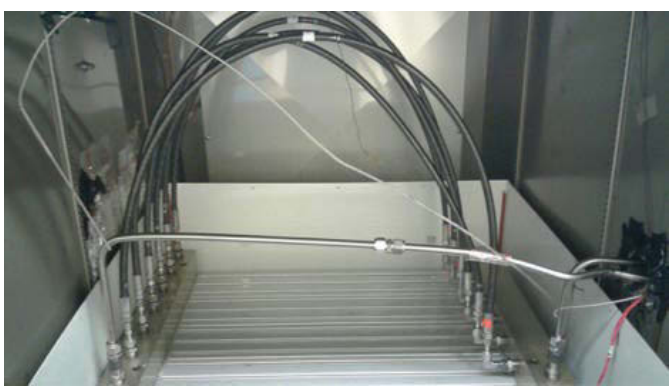

FIGURE 3. NanoSonic H_2 hoses in pressure cycle testing system

Test (Section 2.17) of ANSI/CSA HGV 4.2-2013 was conducted per the following schedule:

- 50,000 cycles at 12,000 psi (827 bar) at -40°C.
- 50,000 cycles at 12,000 psi (827 bar) at 85°C.

Our down-selected material design survived:

- 50,000 cryogenic cycles at (-40°C) conducted at 12,000 psi.
- This same specimen also survived nearly 2,000 cycles (at 85°C) prior to failure due to the fitting slipping off.
- Failure occurred at the 1,988th cycle.
- Failure mode was fitting slippage (Figure 4).

CONCLUSIONS AND UPCOMING ACTIVITIES

Conclusions derived from the work in FY 2017 are:

- NanoSonic's ceramer results in increased hydrostatic burst strength.
- Fitting crimp recipe and type influences burst strength.

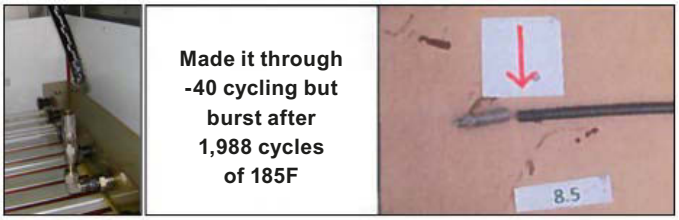

FIGURE 4. NanoSonic H_2 hose post pressure cycle testing at 12,000 psi after 50,000 cycles at -40°C and ~1,988 cycles at 85°C; failure shown due to fitting slippage

- NanoSonic's metal-free H_2 hose exhibits hydrostatic strength values >31,000 psi and fails due to fitting slippage rather than burst.
- NanoSonic's metal-free H_2 hose survives >51,900 pressure cycles at 12,000 psi per 50,000 impulses at -40°C, and >1,900 impulses at 85°C; failure due to fitting slippage rather than burst.
- NanoSonic is currently testing our hose with new fittings produced locally per internal designs with Cardinal Rubber & Seal, Shenandoah Machine, and LifeGuard Technologies.
- Benchmark testing against emerging potential commercial competitors will commence in the next quarter, such as Yokohama Rubber/Iwatani Industrial Gases, ContiTech, and Togawa Rubber. Yokohama's hose is rated for 70 MPa and the Togawa hose is rated for 35 MPa. There are few details given for ContiTech products.
- Environmental robustness and fuel quality is being established through testing with CSA and National Renewable Energy Laboratory.

III.9 Hydrogen Refueling Analysis of Heavy-Duty Fuel Cell Vehicle Fleet

Amgad Elgowainy (Primary Contact), and Krishna Reddi
Argonne National Laboratory
9700 South Cass Avenue
Argonne, IL 60439
Phone: (630) 252-3074
Email: aelgowainy@anl.gov

DOE Manager: Neha Rustagi
Phone: (202) 586-8424
Email: Neha.Rustagi@ee.doe.gov

Project Start Date: October 2007
Project End Date: Project continuation and direction determined annually by DOE

Overall Objectives

Evaluate impacts of key market, technical, and economic parameters on refueling cost of heavy-duty fuel cell vehicles.

Fiscal Year (FY) 2017 Objectives

- Evaluate the precooling requirements for various heavy-duty fuel cell vehicle (HDFCV) tank systems, characterized by the tank type and configuration, fill pressure, and fill rate.
- Develop and publish a techno-economic model to estimate the hydrogen station cost contribution for refueling HDFCV fleets.
- Evaluate the impact of market and technical parameters on the hydrogen station levelized cost ($/kg H_2).

Technical Barriers

This project directly addresses Technical Barriers A, B, C, and E in the Hydrogen Delivery section of the Fuel Cell Technologies Office Multi-Year Research, Development, and Demonstration Plan. These barriers are:

(A) Lack of Hydrogen/Carrier and Infrastructure Options Analysis

(B) Reliability and Costs of Gaseous Hydrogen Compression

(C) Reliability and Costs of Liquid Hydrogen Pumping

(E) Gaseous Hydrogen Storage and Tube Trailer Delivery Costs

(I) Other Fueling Site/Terminal Operations

Contribution to Achievement of DOE Hydrogen Delivery Milestones

This project contributes to the following DOE milestone from the Hydrogen Delivery section of the Fuel Cell Technologies Office Multi-Year Research, Development, and Demonstration Plan.

- Task 1.5: Coordinating with the H_2 Production and Storage sub-programs, identify optimized delivery pathways that meet a H_2 delivery and dispensing cost of <$2/gge for use in consumer vehicles. (4Q, 2020)
- Task 6.3: By 2020, reduce the cost of hydrogen delivery from the point of production to the point of use in consumer vehicles to <$2/gge of hydrogen for the gaseous delivery pathway. (4Q, 2020).

Accomplishments

- Developed a techno-economic model for HDFCV fleet refueling to estimate the hydrogen refueling cost.
- Studied the impact of market parameters, including fleet size, hydrogen supply state (i.e., gaseous or liquid), station utilization and market penetration, etc., as well as technical parameters, including refueling pressure, tank type, dispensed amount and fill rate, etc., on cost of hydrogen refueling of HDFCV fleets.

✧ ✧ ✧ ✧ ✧

INTRODUCTION

Medium- and heavy-duty vehicles (MHDV) constitute the second largest and fastest growing energy consumer in transportation. In the past few years, fuel cells have made significant strides in this space, with deployments in buses, drayage trucks, and military vehicles. Techno-economic models such as Argonne's Hydrogen Delivery Scenario Analysis Model and Hydrogen Refueling Station Analysis Model, which are developed to calculate the light-duty vehicle (LDV) hydrogen refueling station levelized cost, are not appropriate for the evaluation of fuel cell MHDV refueling stations due to differences in the key parameters such as fill rate, fueling pressure, fueling amount, fueling strategy, and precooling requirement. In order to inform DOE and industry stakeholders of the key parameters that impact cost of hydrogen refueling for HDFCV, we have developed a new tool that estimates the station cost for various market and technical parameters specific to HDFCV fleet fueling.

APPROACH

The Hydrogen Station Cost Optimization and Performance Evaluation Model (H2SCOPE), developed by Argonne National Laboratory, was used to examine the effect of vehicle tank configuration or properties and fueling rates (7.2 kg/min, 3.6 kg/min, and 1.8 kg/min, provided in the SAE technical information report) on the precooling requirement for fueling HDFCV. The precooling requirements for 350 bar and 700 bar, Type III and Type IV tanks have been estimated at 25°C ambient and 40°C pre-soak using the H2SCOPE model so that the tank temperature does not exceed 85°C at end of fill (Table 1).

TABLE 1. HDFCV Onboard Tank Configurations Evaluated by H2SCOPE

Bus Onboard Storage System		
	350 bar	**700 bar**
Storage System Capacity	40	40
Number of Tanks	8	16
Individual Tank Capacity [kg]	5	2.5

The developed model for HDFCV refueling is an Excel-based tool that uses a design calculation approach to estimate the contribution of individual components of refueling to levelized hydrogen cost. The tool sizes refueling components given a set of design specifications and boundary conditions, and calculates the levelized cost of hydrogen, accounting for tradeoffs among the various refueling components using basic engineering design formulas. Component cost information is obtained from vendor quotes, industry inputs, or open literature. The quality of the data and the direction of the analysis are guided and vetted through formal interaction with partners from other national laboratories and independent consultants, and via presentations to the Hydrogen Delivery Technical Team. The HDFCV refueling model is in compliance with the SAE technical information report on hydrogen fueling of HDFCVs to satisfy the fueling performance requirements (including fill rates and fill amounts, etc.). The fuel cell bus fueling has been used as a surrogate for HDFCV fleet fueling.

RESULTS

The impact of each fueling parameter has been studied by varying one parameter at a time, while keeping all other variables constant. The baseline (or default) values of fuel cell MHDV fueling variables are provided in Table 2. The precooling temperature requirements to avoid tank overheating are shown in Table 3. Type III tank system requires no precooling, while Type IV tank system requires nominal precooling for 350 bar fueling, especially at higher fill rates. For 700 bar refueling, a moderate precooling of -10°C is required at 7.2 kg/min fueling rate into Type IV tank system, as shown in Table 3.

TABLE 2. HDFCV Fleet Fueling Parameters (Baseline Values)

Market Parameters	
Fleet Size	30
Hydrogen Supply	20 bar gaseous
Market Penetration (Production Volume)	Low
Technical Parameters	
Refueling Pressure	350 bar
Tank Type	III
Dispensed Amount [kg]	35
Fill Rate [kg/min]	3.6
Fill Strategy	Back to Back (constrained by fill rate)

TABLE 3. Precooling Requirement for Fueling of HDFCV

		Precooling Temperature [°C]	
Tank Type	**Fueling Rate [kg/min]**	**350 bar**	**700 bar**
III	1.8	Not Required	N/A
	3.6	Not Required	N/A
	7.2	Not Required	N/A
IV	1.8	Not Required	15°C
	3.6	18°C	0°C
	7.2	5°C	-10°C

N/A – not applicable

Figure 1 shows the impact of fueling rate on the levelized refueling cost of hydrogen. For low fueling rates, the refueling cost is low, and is comparable for gaseous and liquid stations. Liquid stations can handle faster fills with less cost increase, primarily because the cryopumps at liquid stations have a relatively high throughput of 120 kg/h. High fueling rates increase the allowed number of back-to-back fills, which in turn increases the amount of hydrogen dispensed during each hour, thus requiring larger refueling equipment and increasing the refueling cost. With 1.8 kg/min fueling rate, the number of back-to-back fills are limited to two, requiring more dispensers due to limitation of the total hours allowed for the fleet refueling. Adding a dispenser is more favorable than doubling the fill rate for gaseous stations, while doubling the fill rate is more favorable for liquid stations than adding a dispenser. Figure 2 shows the levelized cost of hydrogen refueling for different hydrogen supply sources. The tube-trailer hydrogen supply minimizes station cost for moderate fleet sizes, but partially shifts the cost burden upstream of the station, while also suffering limited payload. For liquid station, pumping provides a lower cost option compared to compression. Figure 3 shows the impact of fleet size on the levelized cost of hydrogen

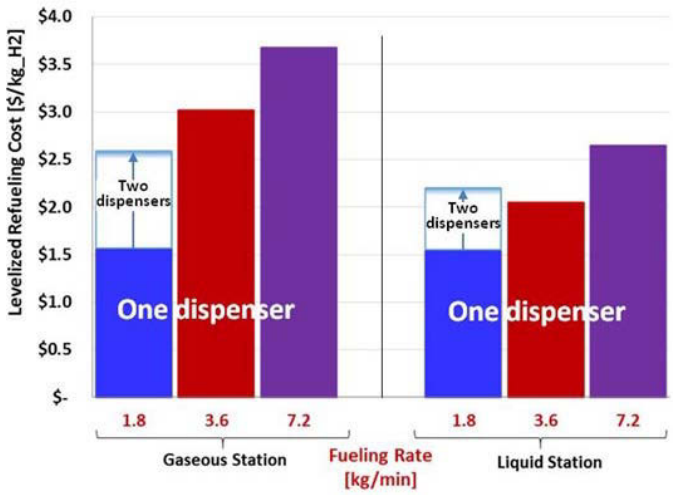

FIGURE 1. Impact of fueling rate on the levelized refueling cost of hydrogen refueling

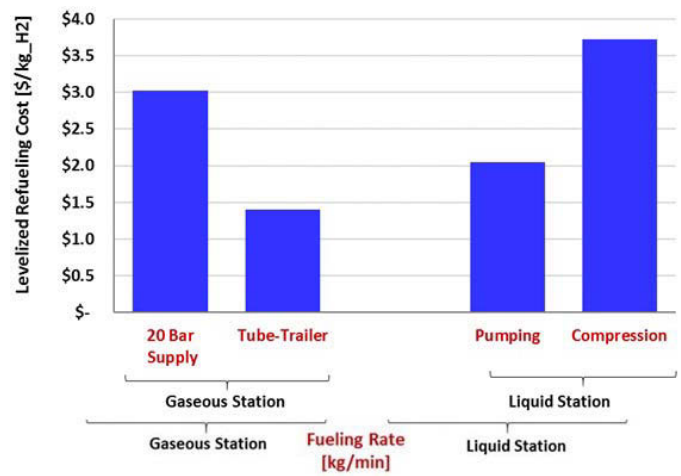

FIGURE 2. Impact of the hydrogen supply source/state on the levelized cost of hydrogen refueling

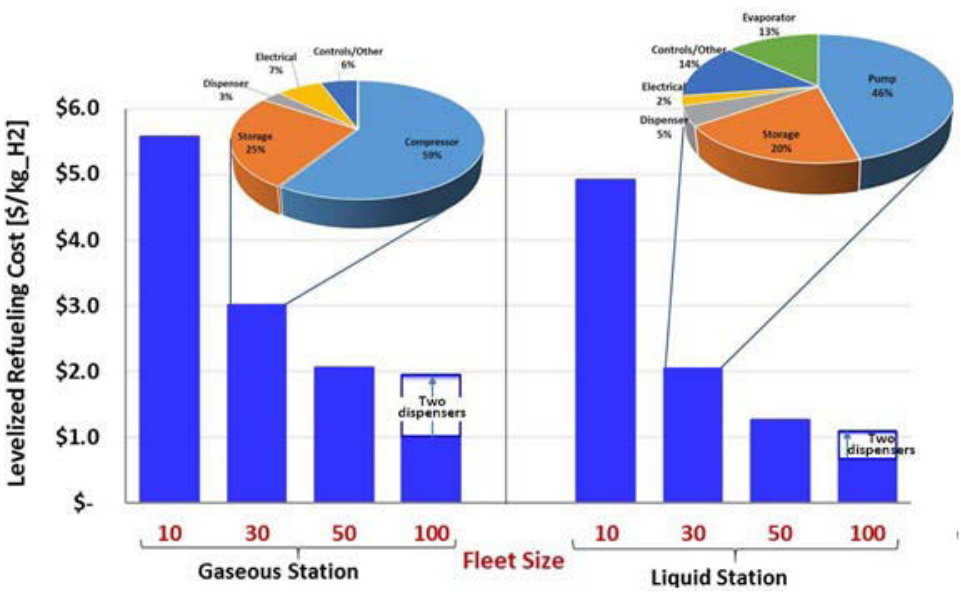

FIGURE 3. Impact of fleet size on the levelized cost of hydrogen refueling

refueling. Refueling cost can be as low as $1/kg H_2 for large fleet sizes due to the strong economies of scale. Compression and pumping dominate the refueling cost for gaseous and liquid refueling stations, respectively, as shown in the Figure 3. However, liquid stations, in general, provide lower refueling cost option compared to gaseous stations.

CONCLUSIONS AND UPCOMING ACTIVITIES

Hydrogen refueling cost for HDFCV fleet is lower when compared to LDV refueling. Strong economies of scale can be realized with fleet size and fill amount, which define the station demand or capacity. Faster fill rates require higher capacity equipment, resulting in higher refueling cost. The impact of higher fueling rate on refueling cost is lower for liquid hydrogen stations compared to gaseous stations. Compression and pumping dominate fueling cost for gaseous and liquid stations, respectively. Liquid stations provide lower refueling cost option for HDFCV fleet refueling compared to gaseous stations. Tube-trailer supply partially shifts the cost upstream and reduces the cost for small fleets in early markets, but the limited payload is not likely viable for large fleets. Refueling cost can be reduced to $1–$1.5/kg H_2 for large fleets when refueling equipment are produced at high volume. Future work may consider evaluating typical

bus service schedules and refueling profiles for commercial (non-fleet) heavy duty vehicles. The HDFCV refueling model will be peer-reviewed and posted in public domain.

SPECIAL RECOGNITIONS & AWARDS/ PATENTS ISSUED

1. Elgowainy, A., and Reddi, K., ENHANCED METHODS FOR OPERATING REFUELING STATION TUBETRAILERS TO REDUCE REFUELING COST, Docket No.: ANL-IN-13-058, submitted to United States Patent and Trademark Office on September 27, 2013 (Received Notice of Allowance on May 22, 2017).

FY 2017 PUBLICATIONS

1. Reddi, K., Elgowainy, A., & Rustagi, N., & Gupta, E., 2017, Impact of hydrogen refueling configurations and market parameters on the refueling cost of hydrogen, International Journal of Hydrogen Energy, https://doi.org/10.1016/j.ijhydene.2017.05.122

1. Reddi, K., Elgowainy, A., & Rustagi, N., & Gupta, E., 2017, Impact of hydrogen SAE J2601 fueling methods on fueling time of light-duty fuel cell electric vehicles, International Journal of Hydrogen Energy, 42(26), 16675-16685.

III.10 Liquid Hydrogen Infrastructure Analysis

Guillaume Petitpas (Primary Contact), A.J. Simon, and Julio Moreno-Blanco
Lawrence Livermore National Laboratory
7000 East Avenue
Livermore, CA 94550
Phone: (925) 423-0348
Email: petitpas1@llnl.gov

DOE Manager: Neha Rustagi
Phone: (202) 586-8424
Email: Neha.Rustagi@ee.doe.gov

Project Start Date: January 3, 2017
Project End Date: September 30, 2017

Overall Objectives

- Provide better understanding of losses along the liquid hydrogen pathway (from the liquefaction plant to the fuel cell vehicle) through thermodynamic modeling including real gas equations of state, two-phase behavior, and para–ortho conversion.
- Gather and analyze real-life driving and parking scenarios to infer typical losses for a sample population.
- Study mitigating solutions to reduce boil-off, through improved operation, hardware, upgrade or recovery.

Fiscal Year (FY) 2017 Objectives

- Build simulation platforms for both liquid hydrogen (LH2) transfer from the liquefaction plant to the dispenser (typically low pressure, low temperature) and cryogenic H_2 end-user utilization, i.e., refueling, driving, and parking onboard a fuel cell cryo-compressed vehicle (typically wider ranges of pressure and temperature, into the super-critical regime).
- Verify that the simulation results are consistent with real-life results.
- Propose mitigation strategies.

Technical Barriers

This project addresses the following technical barriers from the Hydrogen Delivery section of the Fuel Cell Technologies Office Multi-Year Research, Development, and Demonstration Plan.

(A) Lack of Hydrogen and Infrastructure Options Analysis

(C) Reliability and Costs of Liquid Hydrogen Pumping

Technical Targets

The project addresses the delivery costs targets associated with centralized H_2 production (Table 1).

TABLE 1. Delivery Targets Associated with Centralized H_2 Production

Category	FY 2011 Status	FY 2015 Status	FY 2020 Target	Ultimate Target
Aggregate cost of transport, distribution, and fueling ($/gge)	3.6–4.40	3.35–4.35	2.00	<2.00

gge – gallon gasoline equivalent

No target for H_2 losses or leakage for liquid hydrogen exists, although values <0.5% are mentioned for pipelines and tube trailer terminal truck refueling compressors.

FY 2017 Accomplishments

- Adapted MATLAB code from NASA to model heat and mass transfer phenoma in two-phase systems to simulate boil-off losses when transferring liquid H_2.
- Reviewed the available vehicle utilization scenario and selected data from the Puget Sound Regional Council (named "PSRC-2006") that consist of 298 unique driving–parking scenarios collected between March 2005 and March 2006 in the Puget Sound area, available at: https://www.nrel.gov/transportation/transportationdata/index.cfm.
- Built a refueling–parking–driving thermodynamic model for cryo-compressed vehicles in FORTRAN that includes real gas economies of scale, tank thermal mass, and para–ortho kinetics. It is capable of quantifying boil-off losses over the entire timeframe of a given utilization pattern.

✧ ✧ ✧ ✧ ✧

INTRODUCTION

Liquid hydrogen has many benefits for the hydrogen infrastructure. Its high density allows minimum costs for distribution (e.g., $167/kg H_2 for a liquid trailer vs. $783/kg H_2 for a gaseous trailer), high payload and short transfer times minimize delivery logistics, low temperature and low pressure provides very low potential burst energy, and LH2 pumps can efficiently achieve large throughputs (up to 600 kg/h) with a small footprint (low electricity consumption and compact designs). Those many benefits are the reason why many dispensing stations are using LH2 or considering using it, despite the higher cost of liquefaction.

For example, AC Transit in Oakland uses LH2, and most of the 40 fuel cell forklift refueling stations in the United States are relying on LH2.

Using LH2, however, has a few challenges. Liquefying H_2 is expensive (more than three times the energy of compression to 700 bar), setback distances are more stringent for LH2, and losses along the LH2 pathway (transfer, boil-off) may occur. LH2 losses are not well qualified nor quantified, and more analysis needs to be performed in order to evaluate their impact on the hydrogen economy.

APPROACH

Losses along the LH2 pathway are intrinsic to the utilization of a cryogenic media. They occur when the fluid is transferred between two vessels (liquefaction plant to trailer, trailer to station, station to vehicle, etc.), and when the fluid sits unused for extended periods of time. Those losses can be estimated with good accuracy using thermodynamic models based on conservation of mass and energy, providing the states of the molecules are correctly described. Indeed, the fluid undergoes various changes as it moves along the entire pathway (two-phase transition, supercritical warming, para–ortho conversion) and accurate equations of state and two-phase behavior implementations are essential. The balance of energy during the various dynamics processes then enables to quantify the losses, either through transfer or boil-off.

Two different codes are being implemented. The first simulates the losses when transferring LH2 at low pressure and temperature (<12 bar, <33 K) when the fluid is two phases, which is the condition the fluid is at from its production to its dispensing at the refueling station. The second code simulates the states of the molecules of hydrogen once the fuel is stored onboard the fuel cell vehicle, at pressures and temperatures that can vary over wide ranges (up to 700 bar and room temperature), depending on how the vehicle is refueling and used. Those conditions are generally single phase, and referred to as cryo-compressed or super-critical conditions. The first code is being written in MATLAB, the second in FORTRAN.

RESULTS

A MATLAB code previously developed by NASA to simulate rocket loading was used as the basis of the LH2 transfer model. This code implements complex physical phenomena such as the competition between condensation and evaporation, the convection vs. conduction heat transfer as a function of the relative temperatures on both sides of the saturated film. The code was modified to take into account real gas equations of state, by linking the code to a Refprop sub-routine (.dll). Some semi-empirical relationships, such as between the heat of vaporization and the critical temperature, were also replaced by a Refprop equivalent expression, assumed to be more accurate. Non-constant liquid temperature equations were added in order to simulate a sub-cooled effect. The non-linear solver was modified to enable computation of the boil-off losses during the process. Figure 1 shows an example of an LH2 transfer between a trailer and a 3,300 gal Dewar. The trailer is initially full while the Dewar is initially cold (~20 K) and 1% full. 800 kg of LH2 are transferred in about 37 min, bottom fill only. The boil-off losses from the Dewar occur during the fill and are mostly due to the changes of LH2 volume (total: 14 kg) and the losses from the trailer happen at the end of the fill, when the trailer is depressurized from ~45 psi to 20 psi (total: 14.5 kg). In that calculation, the relief device of the Dewar is set at 30 psi.

Concerning the end-user utilization, the first step consisted in finding reliable inputs for the effort, i.e., vehicle utilization patterns with sufficient resolution over a reasonable time for the simulations. A few databases were investigated, including the Institute for Transportation Studies from University of California, Davis, the Advanced Vehicles and Infrastructure department from Idaho National Laboratory, and the Secure Transportation Data Center from the National Renewable Energy Laboratory. We ended up selecting data from the Puget Sound Regional Council that consist of 298 unique driving–parking scenarios collected between March 2005 and March 2006 in the Puget Sound area. Then, a second code simulating the H_2 thermodynamic states inside the cryo-compressed fuel cell vehicle was written in Fortran. This code needed to be very flexible to accommodate various unique drive–park profiles over extended time (12 mo and over) with very different mass and energy balances depending whether the vehicle was being driven, parked, or refilled. Indeed, under driving conditions,

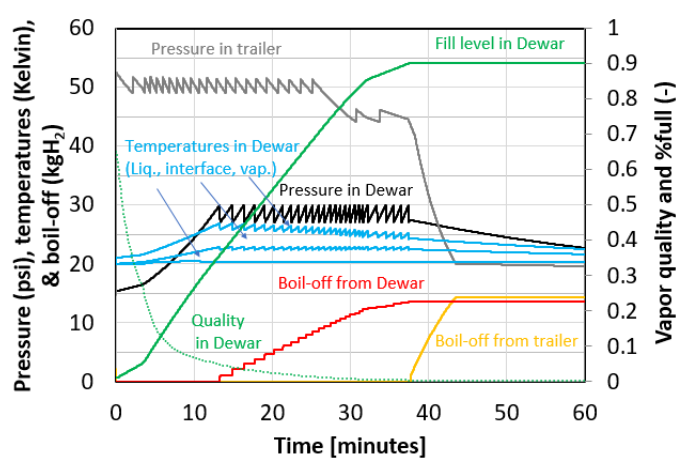

FIGURE 1. Simulation of a liquid fill from a trailer to a 3,300 gal stationary Dewar, computed using the MATLAB code. Pressures in the trailer and Dewar, temperature in the Dewar (liquid, interface, and vapor) and boil-off losses from the trailer and the Dewar are shown on the left axis; vapor quality and fill level in the Dewar are shown on the right axis. See text for details.

constant hydrogen extraction controls the temperature (quasi-adiabatic conditions), while para–ortho conversion at constant density and thermal energy absorption by the wall under external heat entry are the most important phenomena during parking, and finally pump performance (mainly, entropy) determines the final conditions after a refill. The input file was formatted as hourly data over the 12 mo period, with "0" meaning parking and non-zero meaning distance driven during that hour. A separate file was also used to specify the design and operation of the storage system: pressure rating and inner volume; length to diameter ratio; strength and density of the liner and the composite material; performance of the insulation; outside temperature; initial temperature; and pressure, fill pressure, minimum pressure in the vessel, minimum capacity before refilling, pump entropy, and pump ortho fraction. Here again, the equations of state were implemented using Refprop sub-routines. Figure 2 shows a 12-month-long simulation of a driving pattern (here, 63866-2). For those conditions, about 5 kg of losses are computed, over a total of 210 kg H_2 used (21,076 km), i.e., a 2.3% loss over one year.

CONCLUSIONS AND UPCOMING ACTIVITIES

Two separate codes were developed over the funding period, one to simulate the LH2 losses between the production and dispensing and one to simulate boil-off losses on-board a cryo-compressed fuel cell vehicle under real-life utilization patterns. The first code is undergoing verification, while the second code is fully functional, capable of screening through a lot of a vehicle's utilization scenario. The next steps under the current funding are to complete verification of the first code then run the code to identify main sources of losses, then analyze mitigation strategies.

FY 2017 PUBLICATIONS/PRESENTATIONS

1. G. Petitpas and A.J. Simon, "Liquid Hydrogen Pathway Analysis," Hydrogen Delivery Tech Team Meeting, Argonne National Laboratory, March 29, 2017.

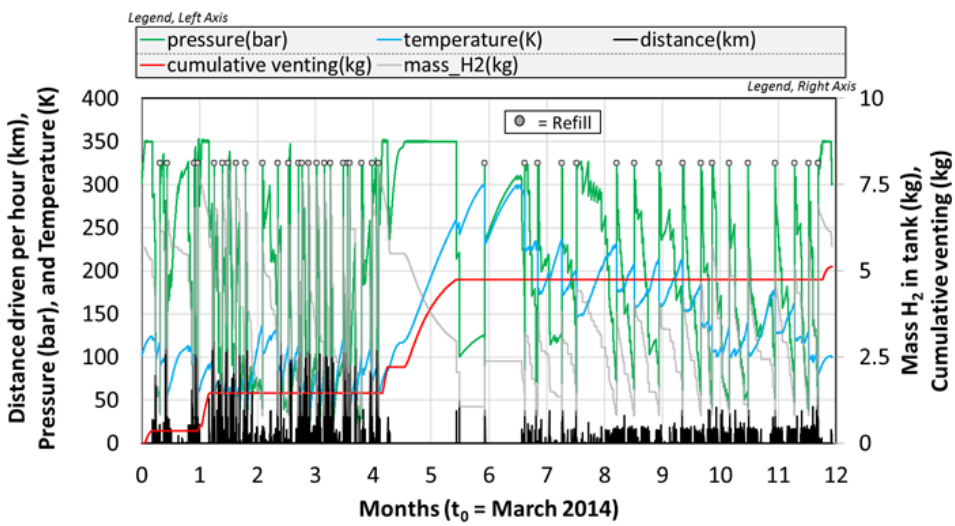

FIGURE 2. One-year-long simulation of the variations of the thermodynamic state of the fuel onboard a cryo-compressed fuel cell vehicle, for driving pattern 63866-2. Results are calculated on an hourly basis. Vehicle is refilled when less than 0.8 kg of usable H_2 is left in the tank, up to 325 bar. Most of the venting losses (see red line, right axis) occur between Months 4 and 6 (July to September) when the vehicle is seldom used (200 km in 2 mo). 210 kg H_2 is used during the 12 months (21,076 km), thus a 2.3% loss.

III.11 Electrochemical Compression

Monjid Hamdan
Giner, Inc.
89 Rumford Ave.
Newton, MA 02466
Phone: (781) 329-0306
Email: mhamdan@ginerelx.com

DOE Manager: Neha Rustagi
Phone: (202) 586-8424
Email: Neha.Rustagi@ee.doe.gov

Technical Advisor: James W. Vickers
Email: James.Vickers@ee.doe.gov

Contract Number: DE-EE0007647

Subcontractors:
- National Renewable Energy Laboratory, Golden, CO
- Rensselaer Polytechnic Institute, Troy, NY
- Gaia Energy Research Institute LLC, Arlington, VA

Project Start Date: October 1, 2016
Project End Date: September 30, 2019

Overall Objective

- Develop and demonstrate an electrochemical hydrogen compressor (EHC) to address critical needs of lower-cost, higher efficiency, and improved durability.

Fiscal Year (FY) 2017 Objectives

- Improve EHC water and thermal management .
  - Development, optimize, and demonstrate water management membranes (WaMM).
  - Engineer flow distributors for thermal management in high pressure cells.
- Optimize stack hardware and demonstrate cell performance ≤0.250 V/cell at current densities ≥1,000 mA/cm².
  - Synthesize hydrocarbon (HC) membranes for high pressure, efficient EHC operation.

Technical Barriers

This project addresses the following technical barriers from the Hydrogen Delivery section of the Fuel Cell Technologies Office Multi-Year Research, Development, and Demonstration Plan.

(B) Reliability and Costs of Gaseous Hydrogen Compression

Technical Targets

TABLE 1. Progress towards Meeting Technical Targets for Hydrogen Compressors for Fueling Sites

Characteristics	Units	2020 Target[1]	2017 Giner Status
Availability	%	85	--
Compressor Specific Energy	kWh/kg	1.6[2]	2.72[3] (<1.2)[4]
Uninstalled Cap. Cost[2]	$	275,000	<450,000
Annual Maintenance	% of Capital Cost	4	--
Lifetime	Years	10	--
Outlet Pressure Capability	bar	950	350

[1] Fuel Cell Technologies Office Multi-Year Research, Development, and Demonstration Plan/Delivery Section.
[2] 100-bar delivery/Commercial mechanical compressors are >6-8 kWh/kg (@700-bar delivery).
[3] Operation at 2-bar delivery
[4] Projected at 100-bar delivery

FY 2017 Accomplishments

Synthesized HC membranes with high ion exchange capacities (IEC), high protonic conductivity, and low electro-osmotic drag (EOD) compared to conventional perfluorosulfonic acid (PFSA) proton exchange membranes (PEM).

- Conductivity of synthesized HC membranes = 0.106 S/cm (target ≥0.100 S/cm)
- EOD: <60% of PFSA (target <50%)
- IEC: up to 2.0 mmol/g (target >1.8 mmol/g)
- Improved EHC cell voltage performance: 0.110 V/cell at 1,000 mA/cm² (target 0.25 V/cell)

- Synthesized WaMM with high water flux and high electrical conductivity.
  - Water flux: ≥0.1 g/min-cm^2 (target of ≥0.039 g/min-cm^2)
  - Conductivity: Through-plane = 1.0 S/cm, in-plane >10 S/cm (target 1.0 S/cm)
  - Demonstrated WaMM that enables passive water feed in operational EHC, that significantly improves water management, and stabilizes EHC cell voltage performance
- Successfully demonstrated >350 bar (5,000 psi) EHC operation; highest efficiency in a single-stage EHC operating at 5,000 psi.

✧ ✧ ✧ ✧ ✧

INTRODUCTION

Hydrogen compression represents a key technical challenge for the widespread commercialization of fuel cell electric vehicles. To dispense hydrogen to fuel cell electric vehicles, hydrogen must be compressed to a minimum of 875 bar. Conventional compressors account for over half of the refueling station's cost, have poor reliability, and insufficient flow rates [1–3]. In addition, the compressed hydrogen delivered by a mechanical compressor requires extensive purification to remove small amounts of contaminates that can degrade the performance of fuel cells receiving the hydrogen.

EHCs utilize direct current to electrochemically compress hydrogen to high pressures. Recent developments in membrane technology promise a new generation of very efficient low-cost EHCs. The emergence of PEM-based solid-state EHCs eliminates many of the issues associated with mechanical compression, however, current state-of-the-art EHCs are challenged by issues related to membrane sealing, and low operating current density – attributed to poor water and heat management.

Giner, Inc. (Giner) is a leading developer of PEM-based stack technology with over 40 years experience in advanced electrochemistry. Giner's technology ranges from highly-reliable high-powered electrolyzer stacks operating onboard U.S. Navy submarines to lower-cost electrolyzer systems operating at differential pressures of up to 1,000 psi for commercial applications. Giner has made significant advancements developing and demonstrating novel membrane technologies that enable zero-leakage, high-pressure, and high-efficiency for use in PEM-based electrolyzers and EHCs that operate >350 bar.

APPROACH

The work conducted in this program exploits the use of three novel technologies that include (1) dimensionally stable HC membranes engineered with low electro-osmatic drag and low hydrogen diffusivity that also exhibit high durability and sealing properties, (2) a WaMM that enables passive water feed and performance stability, and (3) an advanced high-pressure stack design optimized for safe high-pressure gas compression. Successful development and implementation of these technologies are essential to improving water and thermal management within the EHC and will enable high current density operation resulting in a low-cost hydrogen compressor.

RESULTS

Hydrocarbon Membrane Development: Water management within an EHC is significantly improved with PEMs that have a low EOD coefficient. Biphenyl based-HC membranes exhibit EOD rates as low as ~1.2 H_2O/H^+ [4]. In collaboration with Rensselaer Polytechnic Institute, high-molecular-weight, partially-fluorinated, perfluoroalkylsulfonte (BP-Ar) and bromoalkyl-tethered aromatic polymer biphenyl membranes have been synthesized. In comparison to commercially available PFSA, the biphenyl based-HC membranes have an EOD that is 60% less. Furthermore, the HC membranes have demonstrated improved EHC cell performance that is attributed to (1) higher molecular weights leading to better mechanical stability, particularly under low humidified conditions, (2) low swelling related to a hydrophobic backbone owed to partial substitutions of fluorinated moieties, and (3) higher IEC and protonic conductivity enabling higher cell performance. The achievements related to the HC membrane development are summarized below:

- Conductivity: 0.106 S/cm
- EOD of HC membrane: <1.0 H_2O/H^+
- IEC of BP-Ar: 1.45-2.0 mmol/g

WaMM Development: Water management within the EHC is significantly increased when low-EOD HC membranes are combined with a WaMM. The WaMM is a composite membrane that combines an ionomer with an electrical conductor composed primarily of carbon nanotubes. The ionomer allows water transport while the carbon completes the electrical circuit and minimizes ohmic losses. The ionomer-based WaMMs have a high affinity for water. Water fed to one side of the WaMM permeates through the membrane until it reaches the adjacent PEM. Water in the PEM is auto-replenished when a concentration gradient is created between the WaMM and the PEM. The efficacy of the WaMM to transport water is dependent on several variables including water temperature and WaMM thickness. Based on an EOD rate of ~3.5 H_2O/H^+ (in PFSA PEMs), a water flux of 0.04 g/min-cm^2 is required to satisfy operation in the EHC at a current density of 1,000 mA/cm^2. The water flux through the WaMM has been measured at >0.10 g/min-cm² which is sufficient to operate an EHC cell up to 3,000 mA/cm². In addition to high water flux, the WaMMs have been optimized for electrical conductivity. The through-plane conductivity of the WaMM has been measured at 1.0 S/cm. When assembled in a bipolar stack configuration, the WaMM introduces an insignificant cell voltage loss of <6 mV/cell at an operating current density of 1,000 mA/cm².

Membrane Performance: Membrane evaluations were conducted in low-pressure test hardware operating at a pressure of 300 psi (20.7 bar). The BP-Ar HC membranes were evaluated against commercially available PFSA

membranes. A modified flow distributor, used for water transport and thermal management within the cell was utilized. Polarization scans were conducted up to a current density range of 2,000 mA/cm². EHC cells with BP-Ar, membranes exhibit significantly lower cell voltages (higher cell efficiency) than EHC cells assembled with PFSA membranes. At an operating current density of 1,000 mA/cm², the cell voltage of the BP-Ar membrane is 0.110 V/cell; a 60-mV improvement compared to PFSA (Figure 1). In addition to polarization scans, short term duration testing was conducted on BP-Ar and PFSA membranes with and without the assistance of a WaMM. During duration testing, the EHC is held at a constant current density of 1,000 mA/cm². Results indicated that the PFSA membranes (with high EOD) tend to dry out at elevated current densities. When assisted with a WaMM, the PFSA membranes operated continuously without dehydrating. The BP-Ar membranes, however, exhibited stable performance with and without the use of a WaMM (Figure 2). The additional water contribution provided by a WaMM is not required for HC membranes with low EOD; albeit a WaMM may be required at elevated operated pressures when water losses related to hydraulic permeability have a larger effect on the water content within the PEM.

High Pressure EHC Stack Evaluation: A high-pressure EHC stack, designed with the modified flow distributors and WaMM, was used to demonstrate 5,000 psi (350 bar) EHC operation, Figure 3. Giner consumed all HC membranes in previous optimization testing; therefore, high-pressure testing was limited to PFSA membranes. During operation, the anode (inlet) of the EHC stack is fed with dry hydrogen from a cylinder tank at a pressure of 35 psi (~2 bar). The hydrogen feed is dead-ended, i.e., not recirculated and the anode is occasionally purged to remove impurities that can accumulate in the anode chamber over time. At the cathode (outlet) of the EHC stack, hydrogen flow is restricted using a back-pressure regulator to attain the desired operating pressure.

PFSA membranes were evaluated up to a pressure of 5,200 psig (~360 bar), Figure 4. During operation, the hydrogen pressure was gradually increased to 5,200 psig while monitoring cell voltage. A cell voltage of 0.25 V at a current density of ~900 mA/cm² was measured using PFSA membranes assisted with WaMM: **The highest efficiency demonstrated by a single-stage EHC operating at >5,000 psi (>350 bar)**. Future optimization of the high-pressure EHC includes the use of HC membranes with lower EODs (improved water management). Correspondingly, the EHC stack will be designed to operate at the target inlet pressure of 1,450 psi (100 bar), leading to a reduction in the Nernstian voltage penalty and a further improvement in EHC cell efficiency.

CONCLUSIONS AND UPCOMING ACTIVITIES

The developments made during this program have enabled EHC stack voltages that are in line with achieving DOE's 2020 efficiency goals. The highest efficiency in a single-stage EHC, operating at >5,000 psi (>350 bar),

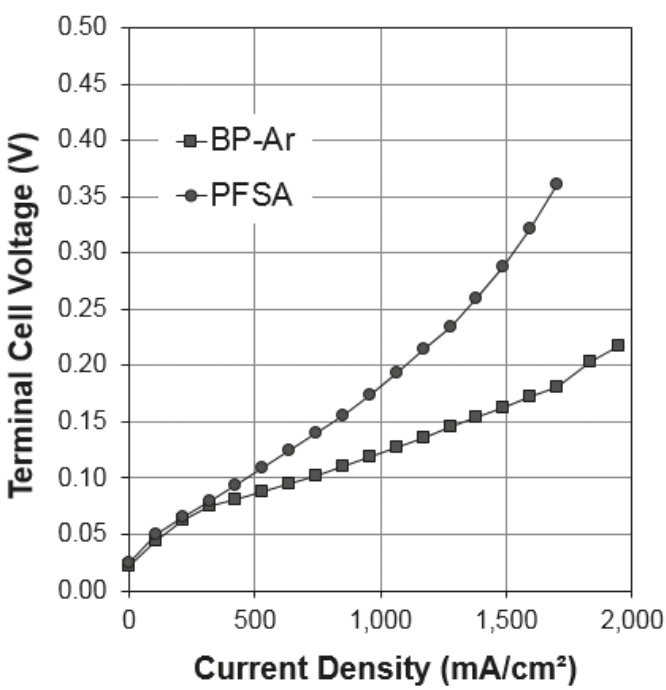

FIGURE 1. BP-Ar vs. PFSA membrane

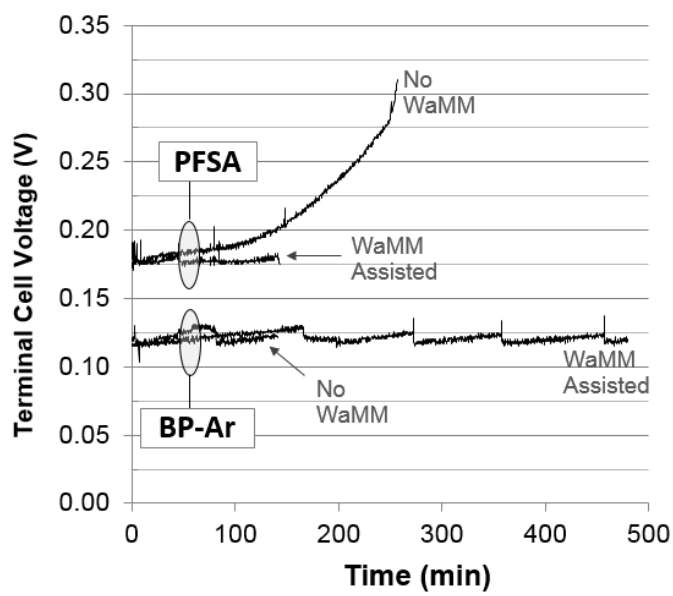

FIGURE 2. Comparison of BP-Ar and PFSA membranes held at 1,000 mA/cm²

FIGURE 3. EHC stack, 5,000 psi operation

was successfully demonstrated utilizing engineered flow distributors that eliminate thermal management issues, and the development of a WaMM that enables passive water management. In addition, significant improvements in EHC cell voltage, utilizing synthesized HC membranes with low EOD coefficients, has been demonstrated. Future work includes the design, fabrication, scale-up, and testing of a high-pressure 12,688 psi (875 bar) stack and completion of a prototype system design.

FY 2017 PUBLICATIONS/PRESENTATIONS

1. M. Hamdan, *Electrochemical Compression*. 2017 Hydrogen Annual Program Merit Review Meeting, Presentation PD136, June 6, 2017.

2. W. Colella, M. Hamdan, *Techno-economic Analysis of State-of-the-Art Electrochemical Hydrogen Compressors (EHCs)*, 6th European PEFC and Electrolyser Forum, July 4–7, 2017.

REFERENCES

1. http://energy.gov/sites/prod/files/2015/06/f22/fcto_myrdd_delivery.pdf

2. G. Parks et al., Hydrogen Station Compression, Storage, and Dispensing Technical Status and Costs (NREL Independent Review: May 2014).

3. http://www.nrel.gov/hydrogen/cdp_topic.html#infrastructure

4. Michael Anthony Hickner et al., Transport and Structure in Fuel Cell Proton Exchange Membranes (Dissertation submitted to the faculty of Virginia Polytechnic Institute, 2003).

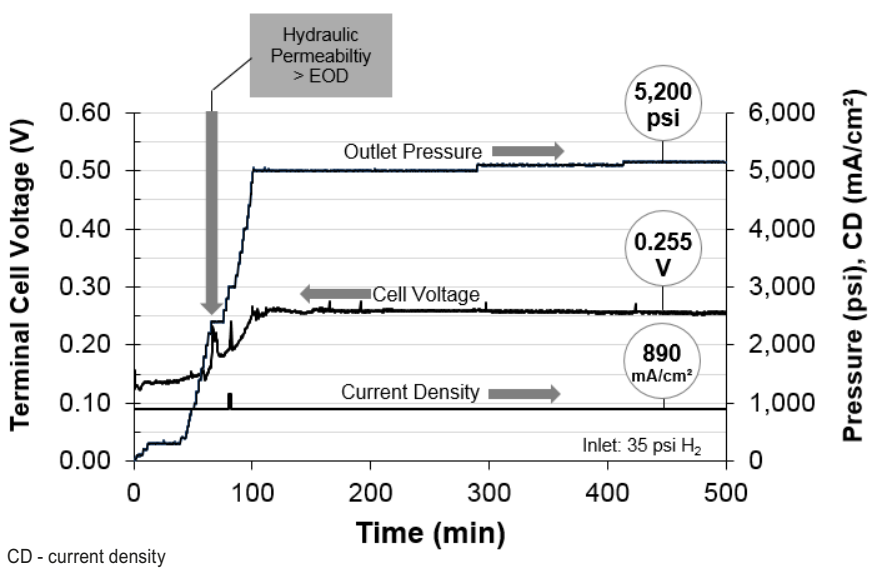

CD - current density

FIGURE 4. EHC operation at 5,000 psi with PFSA membrane

III.12 Hybrid Electrochemical Hydrogen/Metal Hydride Compressor

Scott Greenway (Primary Contact),
Theodore Motyka, Claudio Corgnale, Martin Sulic
Greenway Energy, LLC
301 Gateway Dr., Ste. 183
Aiken, SC 29803
Phone: (803) 381-1818
Email: scott@greenway-energy.com

DOE Manager: Neha Rustagi
Phone: (202) 586-8424
Email: Neha.Rustagi@ee.doe.gov

Contract Number: DE-EE-0007648

Subcontractors:
- Sustainable Innovations, LLC, East Hartford, CT: Trent Molter, Daryl Ludlow, Nancy Selma
- Savannah River National Laboratory, Aiken, SC: Bruce Hardy

Project Start Date: October 1, 2016
Project End Date: September 30, 2019

Overall Objectives

- Combine two novel technologies, electrochemical hydrogen compressor (EHC) and metal hydride compressor (MHC), into a new hybrid solid-state hydrogen compressor system.
- Evaluate the hybrid system for hydrogen refueling and other potential commercial hydrogen applications.
- Perform a techno-economic analysis against DOE cost and performance targets.
- Develop modeling tools to guide small-scale experimental testing for both the EHC and the MHC components as well as for the design and testing of a prototype hybrid compressor unit.
- Design, fabricate and test a 1–5 kg/d prototype unit and validate the models for future full-scale application of this technology.

Fiscal Year (FY) 2017 Objectives

- Develop a techno-economic modeling framework for evaluating metal hydride (MH) and electrochemical hydrogen (EH) compression stages.
- Identify at least one system, operating at large scale, based on MHC and EHC technologies, demonstrating a viable path to reach the techno-economic targets.
- Demonstrate an EHC bench-scale system, able to reach required operating conditions.
- Demonstrate the technical feasibility of the selected hybrid compressor system under partial load and transient conditions using a detailed, integrated, system model.

Technical Barriers

This project addresses the following technical barrier from the Hydrogen Delivery section of the Fuel Cell Technologies Office Multi-Year Research, Development, and Demonstration Plan.

(B) Reliability and Costs of Gaseous Hydrogen Compression

Technical Targets

Hydrogen refueling station compression systems currently have a high capital cost per unit throughput. Today's mechanical compression technology requires frequent maintenance, resulting in the need for redundancy to minimize downtime; leading to high cost. Because of this DOE is evaluating alternatives to mechanical compressors for refueling station systems up to 100 kg/h. DOE targets for hydrogen compression include achieving output pressures over 875 bar; energy consumption and efficiencies better than today's three-stage mechanical compressors and on a path to approach 1.4 kWh/kg; and a reliability of 80% with a leak rate of <0.5%. A preliminary techno-economic model developed during the first half of this fiscal year has shown a hybrid EHC/MHC configuration with good potential of meeting many of DOE's compressor targets.

FY 2017 Accomplishments

- A techno-economic modeling framework for evaluating MH and EH compression stages has been completed and a leading candidate system, operating at large scale, based on Ti-based, MH and polybenzimidazole (PBI) membrane, EHC technologies, has been identified.
- Preliminary estimates show that waste heat from a higher temperature PBI EHC system should have enough energy to drive the MHC system.
- A new MHC heat transfer design has been identified that can substantially reduce the heat transfer area, reduces required thermal, and reduces cost associated with heat transfer systems.
- EHC differential pressure tests showed that PBI membrane may be robust enough for compression applications.

- A new material type for EHC stage bipolar plates was shown to have good resistance to phosphoric acid environments.
- Small-scale MH testing and characterization systems have been designed and sample quantities of candidate MH materials have been ordered.
- The availability of larger quantities of MH materials has been identified; cost and shipping details are being pursued for Period 2.
- An integrated hybrid compressor system model is under development, the MHC system has successfully modeled and is currently being integrated with the EHC system.

✧ ✧ ✧ ✧ ✧

INTRODUCTION

Various alternatives to traditional mechanical compressor systems have been considered, including MHC and EHC. Both MHCs and EHCs are solid-state systems that have no moving parts other than valves. Both are quiet and have low maintenance requirements. However, strength and material issues as well as water and heat management issues have challenged EHCs, especially, when operated at very high pressures. Similarly, low efficiency, especially, when staging is required to attain high, pressure ratios, has challenged MHCs and has made them too complex and expensive. Material degradation, due to hydrogen impurity effects, has also created issues for MHCs.

One novel alternative evaluated here is to combine EHC and MHC technologies in a way to maximize their advantages and to minimize each of their challenges to improve the overall systems performance on a path to meet or exceed current DOE targets. A hybrid EH/MH compressor takes advantage of lower maintenance and operating costs as well as increased reliability associated with both the MHC and EHC technologies over traditional mechanical compressors. Neither the MHC nor the EHC have any moving parts other than valves. The hybrid system also takes advantage of the higher efficiency and lower cost of the EHC by operating at lower delivery pressures combined with the robust and simple operation of a single-stage, MH compressor at higher pressures. Both MHC and EHC technologies are scalable and can be used for a variety of hydrogen compression and delivery applications.

APPROACH

Greenway Energy will integrate an EHC unit with a MHC system into an overall hybrid compressor system. The hybrid compressor will be designed to compress a hydrogen flow rate of 10 kg/h (scalable to 100 kg/h) with an outlet pressure of 875 bar. A prototype hybrid unit will be designed based on the results obtained from system models and detailed models developed to simulate the overall full-scale hybrid compressor system. During Period 2, a prototype will be built and tested for a hydrogen flow rate of 1–5 kg/d and outlet pressures of 875 bar. The modeling activities (along with selected experimental tests) will represent the basis to design larger scale (10–100 kg/h) hybrid systems and assess their performance against the DOE techno-economic targets.

RESULTS

Screening Analysis of Candidate, Hybrid Compressor Systems

An initial techno-economic model has been completed. The model includes:

- EHC stack and MH vessel and materials;
- Balance of plant equipment (heat exchangers, valves, humidifiers, and dryers), with the main objective of humidify the hydrogen feeding the electrochemical compressor and dehumidify the hydrogen flow feeding the MH compressor;
- Enthalpy balance equations to assess the efficiency of the EHC system and, consequently, the available waste heat to be used to desorb hydrogen from the MH compressor system; and
- Volumetric efficiency of the MH compressor system, identifying the additional MH material to be included in the system to assure the continuity and steady state operation performance of the overall compressor.

A schematic of the two-stage compression system is shown in Figure 1. A humidifier unit is placed before the EHC stage to provide the hydrogen flow with the right water content (especially for the Nafion® membrane EHC). Two parallel EHC units compress the hydrogen up to pressures on the order of 100–200 bar. The hydrogen flow is then dehumidified in a dryer unit and the water is collected, pumped and reused in the humidifier units. The dried hydrogen feeds the MHC units (two parallel units) that compress the hydrogen up to final pressure of 875 bar.

Preliminary identification of at least one hybrid configuration that has the potential to meet DOE targets is underway. Regarding the EHC system, four membranes have been down selected as the baseline constitutive membranes: Nafion 212 membrane system, PBI film membrane system, Advent® membrane, and a Fumatech® membrane. Regarding the high-pressure MH compressor system, three baseline MH materials working at high pressures have been down-selected: HP1: $TiCr_{1.9}$; HP2: $(Ti_{0.97}Zr_{0.03})_{1.1}Cr_{1.6}Mn_{0.4}$, and HP3: $Ti_{1.1}CrMn$.

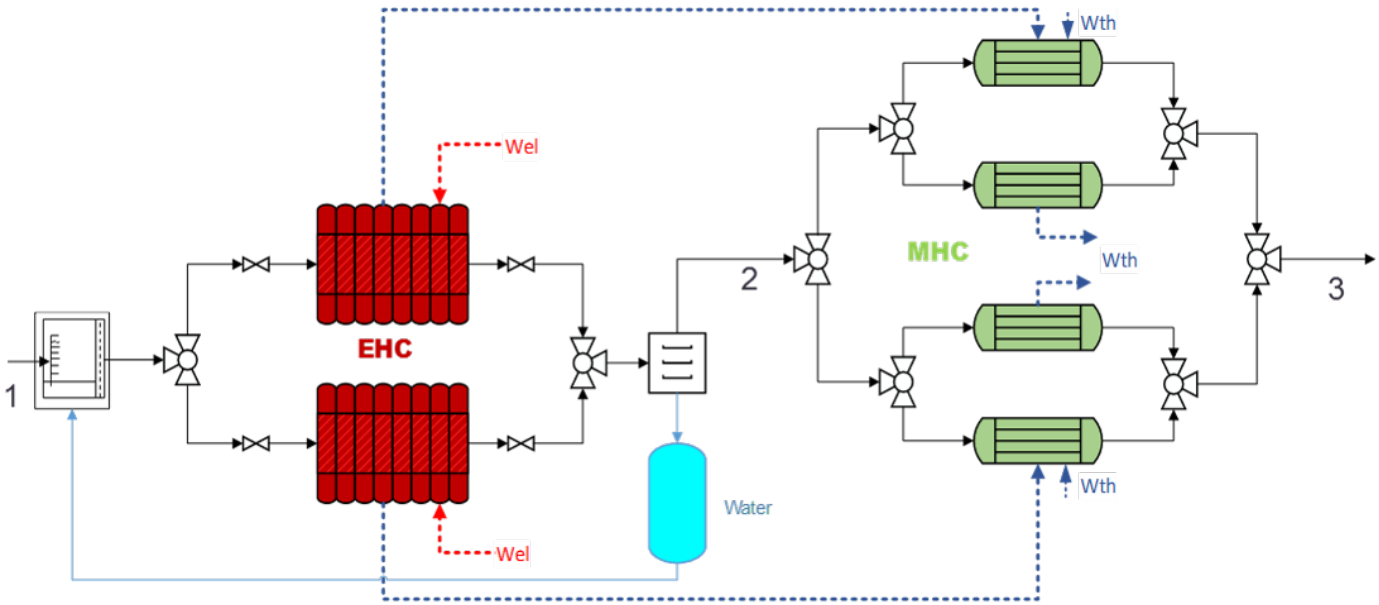

FIGURE 1. Hybrid compressor schematic (first stage: EHC; second stage: MHC)

A comparison of the Nafion 212 and PBI systems is shown in Figure 2. Figure 2 shows that the Nafion 212 EHC system has a slightly lower cell voltage than the PBI systems but it does not offer any heat recovery opportunity with the MHC, due to the low operating temperature of the Nafion system. In addition, an economic comparison between the two proposed membrane systems shows that the PBI system achieves an installed cost reduction of about 27% compared to the corresponding Nafion system.

As with the EHC system, a techno-economic analysis has been applied to the three down-selected materials for the MH system (HP1, HP2, and HP3). A new heat transfer design has been developed and modeled (an invention disclosure is being filed for the new design). Preliminary conceptual design and performance of the new vessel design for the three selected metal hydrides show that hydride materials HP2 and HP3 appear to give the best technical performance. A summary of the results from the economic analysis is shown in Figure 3. Figure 3 shows a comparison between the new conceptual design and the more traditional shell and tube (S&T) design. A less pure Ti-Fe material has been assumed for this case with a Ti cost of $3.8/kg for the HP1, HP2, and HP3 alloys highlighting the contribution of both the material cost and the vessel and heat exchanger cost. A reduction of the heat exchanger and pressure vessel cost of almost 70% has been achieved from the S&T to the new design.

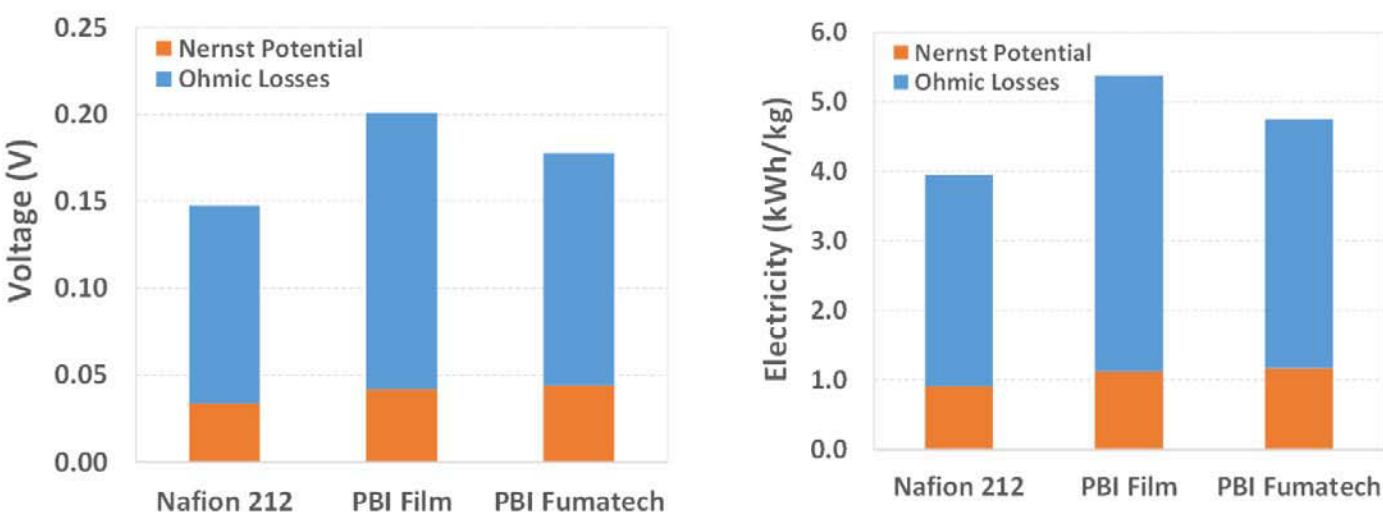

FIGURE 2. Technical performance comparison between Nafion and PBI membrane systems

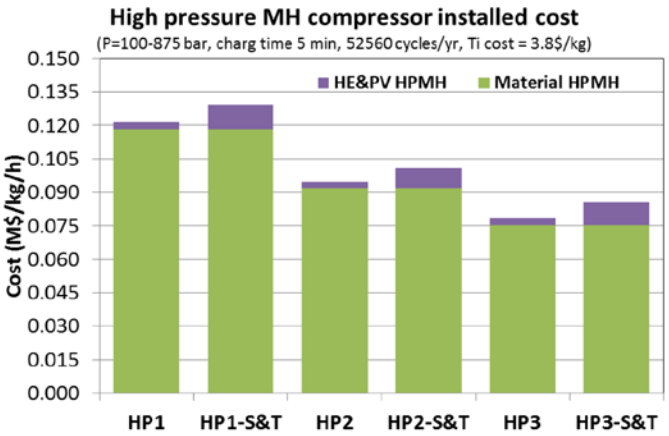

HPMH – high pressure metal hydride; HE&PV – heat exchangers and pressure vessels

FIGURE 3. Economic comparison between traditional S&T and new design with low cost Ti

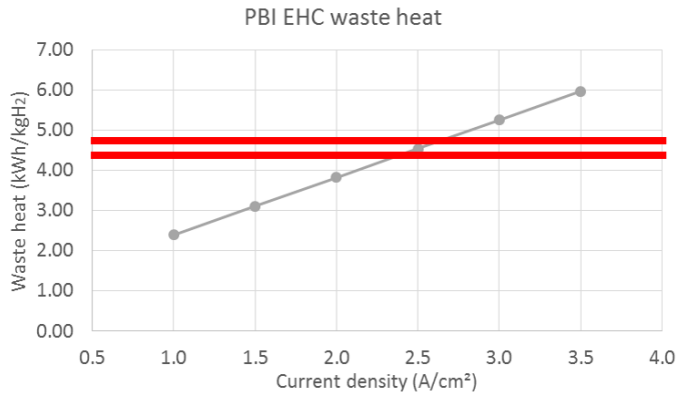

FIGURE 4. PBI EHC system waste heat (red lines represent the MHC heat required to desorb the stored hydrogen)

The techno-analysis performed took advantage of the waste heat from the EHC system to power the MHC system. It was determined that the hydrogen desorption from the MHC system requires thermal 4.3–4.9 kWh/kg at about 170°C depending on the MH alloy. The potential electrochemical system waste heat that can be recovered using a PBI membrane EHC system is shown in Figure 4. This figure shows that a high temperature PBI membrane operating at a current density of about 2.5 A/cm^2 has the required heat to desorb the hydrogen from the metal hydride system. More analyses are in progress on specific EHC and MHC configurations to arrive at an optimized hybrid compressor system taking into account not only installed costs but long-term operating cost as well as overall system performance and reliability.

EHC Bench Scale Experimental Tests

Sustainable Innovation carried out testing on a bench scale EHC system aimed at (1) developing appropriate membrane electrode assemblies for operating at high temperatures, (2) evaluation of high temperature and high-pressure membranes, and (3) identifying appropriate design modifications to the cell stack to accommodate (1) and (2).

Membrane material compatibility testing for 150–120°C operation at 90–120 bar differential pressure was begun. While Nafion and similar membranes have been demonstrated to operate at high differential pressures and with high proton conductivity, operating temperature is typically limited to less than 100°C. To date, membranes capable of higher temperature operation at 150–200°C have not demonstrated sufficient strength to withstand 90–120 bar differential pressure. Additionally, these high temperature compatible membranes utilize phosphoric acid as the electrolyte, leading to potential materials compatibility conflicts due to corrosion.

Material samples of high pressure EHC components have been exposed to phosphoric acid at operating temperature. Initial results indicate that alternate materials and or protective coatings must be employed to maximize lifetime performance. Base materials were found to completely dissolve within 24 hours. Two material options have been identified that provide corrosion resistance. Sustainable Innovation has received quotes on replacement parts for the existing compressor hardware and is purchasing samples.

Multiple PBI film options have been tested within Sustainable Innovation's high pressure EHC hardware at low and high temperature. Initial testing indicates that dry and imbibed PBI membrane can withstand 100 bar at 160°C. Properly supported PBI membrane seems to be capable of supporting high pressure differentials. Electrochemical testing of PBI membranes at pressure is scheduled for the second half of FY 2017. In addition, Nafion, which is typically limited to operation at less than 100°C, will be evaluated at higher operating ranges between 120°C and 140°C.

Hybrid Compressor System Model Development and Application

A system model for the hybrid compressor has been developed. The model includes both the ECH system as well as the MHC system. The initial results have the EHC operating at steady state providing hydrogen at 100 bar and a maximum of 100 kg/h to the MHC. The metal hydride volume is ~12 m^3 and assumes material expansion of 15% (crystal volume) on hydrogen uptake with a bed porosity of 10% when fully expanded (fully charged). Figures 5a and 5b show the operation of the metal hydride beds during four-hour cycles.

During the first three cycles, more hydrogen enters the compressor than exits. This is due to hydrogen discharge from the metal hydride during the heating phase and unavoidable re-uptake of hydrogen by the MH bed upon cooling to initial state at 314 K. This causes the amount of

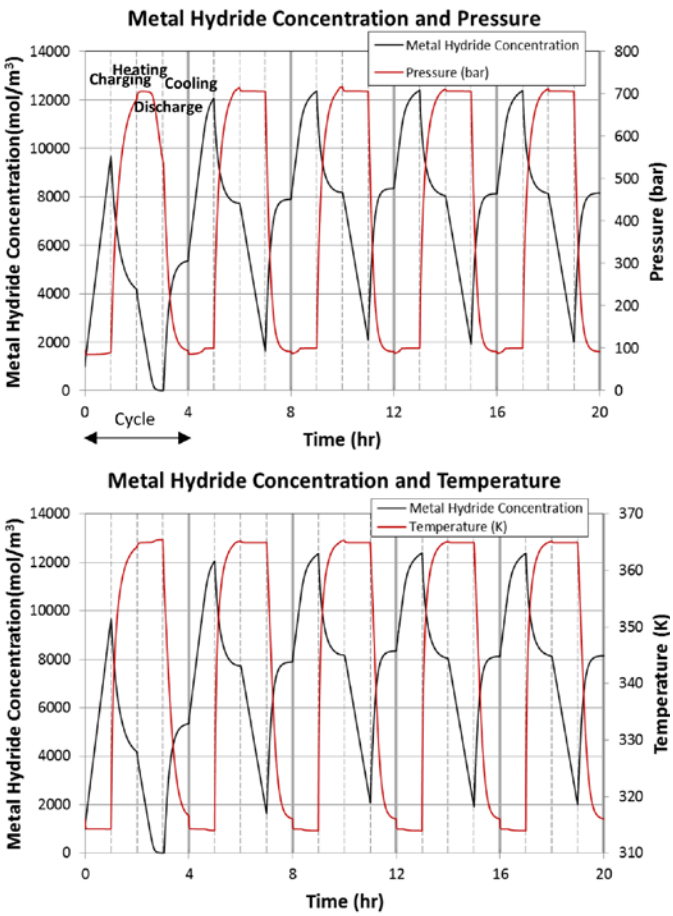

FIGURE 5. Hybrid compressor system model showing MHC performance versus pressure and temperature, respectively

hydrogen retained in solid phase, prior to charging, to rise for the first three cycles, then stabilize.

For the postulated MH properties and bed volume, delivery is ~50 kg/h at 700 bar. The current model is being updated to include the more specific information on the electrochemical and metal hydride materials obtained from the techno-economic screening analysis as well as to include other operating conditions and system configurations.

CONCLUSIONS AND UPCOMING ACTIVITIES

A techno-economic modeling framework for evaluating MHC and EHC stages has been completed and a leading candidate system, operating at large scale, based on Ti-based metal hydride and PBI membrane electrochemical technologies, has been identified. Preliminary estimates show that waste heat from a higher temperature PBI EHC system should have enough energy to drive the MHC system. A new MHC heat transfer design has been identified that can substantially reduce the heat transfer area, reduce the required thermal energy, and reduces cost associated with heat transfer systems. EHC differential pressure tests showed that PBI membrane may be robust enough for compression applications. A new material type for EHC stage bipolar plates was shown to have good resistance to phosphoric acid environments.

Upcoming Period 1 activities include fabrication and operation of a high-pressure, small-scale, MH testing and characterization system; evaluation of alternate compressor internal materials for electrochemical testing of PBI compressors; exploration of maximum temperature limitations of Nafion while under high pressure operating conditions; finalization of compressor material set (PBI or Nafion); completion of integrated hybrid compressor system; and design of an integrated hybrid EH–MH compressor prototype system by the end of Period 1 (March 31, 2018).

FY 2017 PUBLICATIONS/PRESENTATIONS

1. Greenway, S. et al., "Tech Team Project Review," National Renewable Energy Laboratory, Golden, CO, November 2, 2016.

III.13 Metal Hydride Compression

Terry Johnson (Primary Contact),
Robert Bowman (Oak Ridge National Laboratory [ORNL]), Barton Smith (ORNL),
Lawrence Anovitz (ORNL), Craig Jensen (HHC)
Sandia National Laboratories (SNL)
7011 East Avenue
Livermore, CA 94551-0969
Phone: (925) 294-2512
Email: tajohns@sandia.gov

DOE Manager: Neha Rustagi
Phone: (202) 586-8424
Email: Neha.Rustagi@ee.doe.gov

Subcontractor:
Hawaii Hydrogen Carriers LLC (HHC), Honolulu, HI

Project Start Date: October 2016
Project End Date: September 2019

Overall Objectives

- Develop a two-stage system of metal hydride beds, capable of compressing hydrogen from 100 bar to ≥875 bar at a laboratory scale.
- Complete comprehensive cost analysis of a full-scale (100 kg H_2/hr) metal hydride compressor.
- Identify an approach to achieve energy efficiency of ≤4.0 kWh/kg with metal hydride compression.

Fiscal Year (FY) 2017 Objectives

- Identify two metal hydrides for both the low pressure and high pressure stages, based on laboratory characterization of their ability to meet system level requirements.
- Down-select compressor bed designs for both stages based on trade studies.
- Develop a system-level dynamic model with realistic metal hydride properties and a baseline system design. Use model to demonstrate the capability of an energy efficiency of ≤4.0 kWh/kg.

Technical Barriers

This project addresses the following technical barriers from the Hydrogen Delivery section of the Fuel Cell Technologies Office Multi-Year Research, Development, and Demonstration Plan.

(B) Reliability and Costs of Gaseous Hydrogen Compression

Technical Targets

This project is developing metal hydride compressor technology that is currently at a technology readiness level of 2. The results of this project will address several of the DOE technical targets for small, forecourt compressors, specifically:

- Specific Energy: The 2020 target for 100 bar pipeline delivery is 1.6 kWh/kg. Our project goal is to demonstrate that a metal hydride compressor can achieve a specific energy of less than 4.0 kWh/kg as a first step towards this target.
- Uninstalled Capital Cost: The 2020 target for 100 bar pipeline delivery is $275,000. A cost analysis for a commercial system in FY 2019 will address this target.
- Outlet Pressure Capability: The 2020 and ultimate targets are 950 bar. We plan to demonstrate a prototype compressor capable of >875 bar pressure with a goal of 950 bar.

FY 2017 Accomplishments

- Developed a dynamic system-level model using MATLAB/Simulink for feasibility and design trade studies.
- Demonstrated feasibility of 50–875 bar H_2 compression and delivery at reasonably achievable temperatures through system-level analysis of a baseline design using literature data for available metal hydrides.
- Completed a parameter study using the dynamic system model to probe design space including the effects of cycle time, alloy, feed pressure, and bed geometry on hydrogen flow rate and energy efficiency.
- Identified several approaches to achieve energy efficiency and hydrogen compression cost targets including heat recuperation, waste heat utilization, and heat pump options.
- Identified five candidate alloys for each compressor stage based on extensive literature research, pared the list down to two for each stage, and engaged vendors to supply the alloys in small quantities for characterization as well as large quantities for our prototype compressor.
- Designed, assembled, and calibrated a high pressure Sieverts cycling apparatus for characterization of candidate metal hydrides.

- Completed pressure-composition-temperature (PCT) measurements of a metal hydride candidate that looks promising for the low pressure stage of the compressor.

✧ ✧ ✧ ✧ ✧

INTRODUCTION

Conventional hydrogen compressors often contribute over half of the cost of hydrogen stations, and have poor reliability. Fatigue of their moving parts contributes to failure of components, such as cracking of diaphragms and failure of seals. Furthermore, the conventional lubrication of these compressors with oil is generally unacceptable at fueling stations due to potential fuel contamination. Metal hydride (MH) technology offers a very good alternative to both conventional (mechanical) and newly developed (electrochemical, ionic liquid pistons) methods of hydrogen compression. Advantages of MH compression include simplicity in design and operation, absence of moving parts, compactness, safety and reliability, and the possibility to utilize waste industrial heat to power the compressor.

MH hydrogen compression utilizes a reversible heat-driven interaction of a hydride-forming metal alloy with hydrogen gas to form the MH phase and is a promising process for hydrogen energy applications [1,2]. To deliver hydrogen continuously, each stage of the compressor must consist of multiple MH beds with synchronized hydrogenation and dehydrogenation cycles. Multistage pressurization allows achievement of greater compression ratios using reduced temperature swings compared to single stage compressors. The objectives of this project are to investigate and demonstrate on a laboratory scale a two-stage MH H_2 gas compressor with a feed pressure of >50 bar and a delivery pressure ≥875 bar of high purity H_2 gas using the scheme shown in Figure 1. Progress to date includes the selection of two candidate metal hydrides for each compressor stage, supplier engagement and synthesis of small samples, and the beginning of in-depth characterization of their thermodynamics, kinetics, and hydrogen capacities for optimal performance with respect to energy requirements and efficiency. Additionally, bed design trade studies are underway and will be finalized in FY 2018. Subsequently, the prototype two-stage compressor will be fabricated, assembled and experimentally evaluated in FY 2019.

APPROACH

The approach for this project is split into three phases to meet the project objectives: (1) feasibility assessment and system design, (2) hydride degradation assessment and prototype fabrication, and (3) prototype performance evaluation. In the first phase, candidate hydride materials

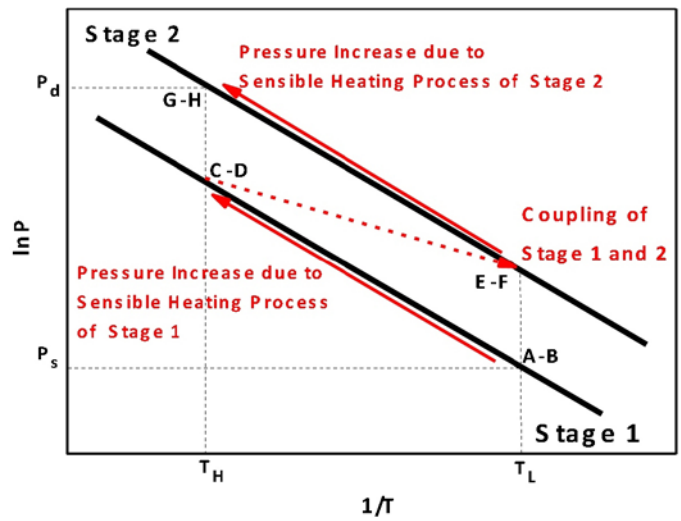

FIGURE 1. van't Hoff plots illustrating the operation of a two-stage metal hydride hydrogen compression system from the low temperature T_L to the high temperature T_H. The black lines represent the van't Hoff plot for the hydrogenation process for Stage 1 (lower black line) and for Stage 2 (upper black line). The dashed red line represents the coupling between Stage 1 and Stage 2. The compression cycle is summarized as follows: Step A, a low-pressure H_2 supply (e.g., an electrolyzer or pipeline) is attached to the first stage, at pressure P_s. The temperature of Stage 1 is maintained at T_L, during hydrogenation. Step B–C, a sensible heating process raises the bed temperature to T_H, increasing the pressure of the Stage 1 vessel. Step D–E, coupling between Stage 1 (dehydrogenation at T_H) and Stage 2 (hydrogenation at T_L) occurs. Step F–G, Stage 2 hydride bed undergoes sensible heating in order to achieve the delivery pressure of P_d. Step H, during dehydrogenation of Stage 2 high pressure hydrogen is released from the compressor at P_d.

are selected based on literature review and team experience. Absorption and desorption isotherms of selected hydrides are then measured and compared to system level requirements to demonstrate feasibility. In parallel, trade studies are performed on different design configurations for the prototype compressor beds and a down-selection made. Finally, a system-level compressor model is developed and used for feasibility assessment of the hydride materials and bed designs. In the second phase, accelerated cycling tests (~1,000 cycles) on candidate hydrides are performed to determine degradation rate, if any, and assess regeneration potential. In parallel, component fabrication and assembly drawings for compressor beds are developed based on the down-selected designs. Procurement of hydride alloys and fabrication of bed components follows. Once received, the integrated prototype compressor is assembled. In the third and final phase of the project, the prototype compressor is integrated with the test facility, and performance testing of the prototype is conducted. This testing will assess the impact of heating rates, state of charge, and temperature ranges on compressor performance as well as degradation

behavior. This will include up to 300 h of operation. Results of the prototype characterization will be documented and used for the conceptual design and cost analysis for a 100 kg H_2/h commercial system in a final report to DOE.

RESULTS

Metal Hydride Selection and Characterization

Candidate low and high pressure alloys were identified in the first quarter based on extensive literature review and design requirements. In the second quarter, these alloys were down-selected to two alloys for each stage. Seven different suppliers were then contacted to determine a reliable source for the selected hydride alloys. Of these suppliers, the list was pared down to Ames Laboratory and Japan Metals and Chemicals for their ability to produce any of the candidate alloys of interest. In addition, it was determined that SNL had possession of ~100 kg of GfE Hydralloy C5 from a previous project. In order to have representative alloys from two sources, small batches (i.e., circa 50–100 g) of four materials (i.e., two from Ames and two from Japan Metals and Chemicals were ordered of AB_2 alloys) not already in possession by the team. One objective is to assess how the manufacturing processes at each vendor impact the hydrogen absorption and desorption properties.

Characterization of these alloys is underway using PCT apparatus to provide or confirm material absorption and desorption isotherms. The low pressure alloys are being characterized at HHC using a Suzuki Shokan two-channel thermo-volumetric analyzer with medium (≥150 atm) pressure capability. Figure 2 shows isotherms of the Hydralloy C5 alloy recently measured with this system. This result is consistent with literature data for the alloy at up to 50°C, but provides higher temperature and pressure data not previously measured. The isotherms indicate that Hydralloy C5 is a viable candidate for the low pressure stage of the compressor and the measured data will be used in the system level model for confirmation.

The high pressure alloys will be characterized at ORNL using a custom designed test apparatus capable of accurate isotherm measurements up to 1,000 bar and 150°C. This high-pressure Sievert's system design was completed in early second quarter, incorporating ideas and practices from similar high-pressure cycling stations at both Jet Propulsion Laboratory and SNL (HyMARC). The design will make use of existing infrastructure at ORNL as much as possible. A safety review was completed and the design was approved in January. Assembly and system testing will be completed by the end of August. First measurements of a high-pressure hydride are set to be completed in August with full characterization of both alloys to be completed in the first quarter of FY 2018. A picture of the assembled system is shown in Figure 3.

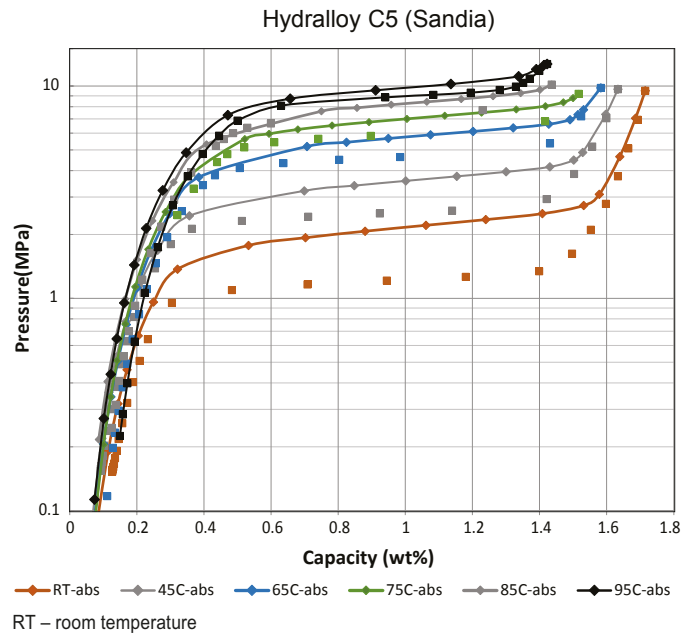

FIGURE 2. Isotherms of the low pressure candidate Hydralloy C5 measured at HHC

FIGURE 3. Picture of the high pressure Sievert's apparatus designed and assembled by ORNL

System Design

A system-level compressor model was developed using MATLAB/Simulink, as shown in Figure 4. The model includes hydride properties (thermal, thermodynamic, and kinetics) and heat and mass flow in a two-stage configuration. These properties are literature values based on experimental measurements of candidate materials. The baseline design uses two beds per stage, but the model only simulates one bed for each stage taking advantage of symmetry such that the results from the single bed pair can be used to estimate the performance of the full system. The model allows for time-dependent simulations to determine appropriate cycle

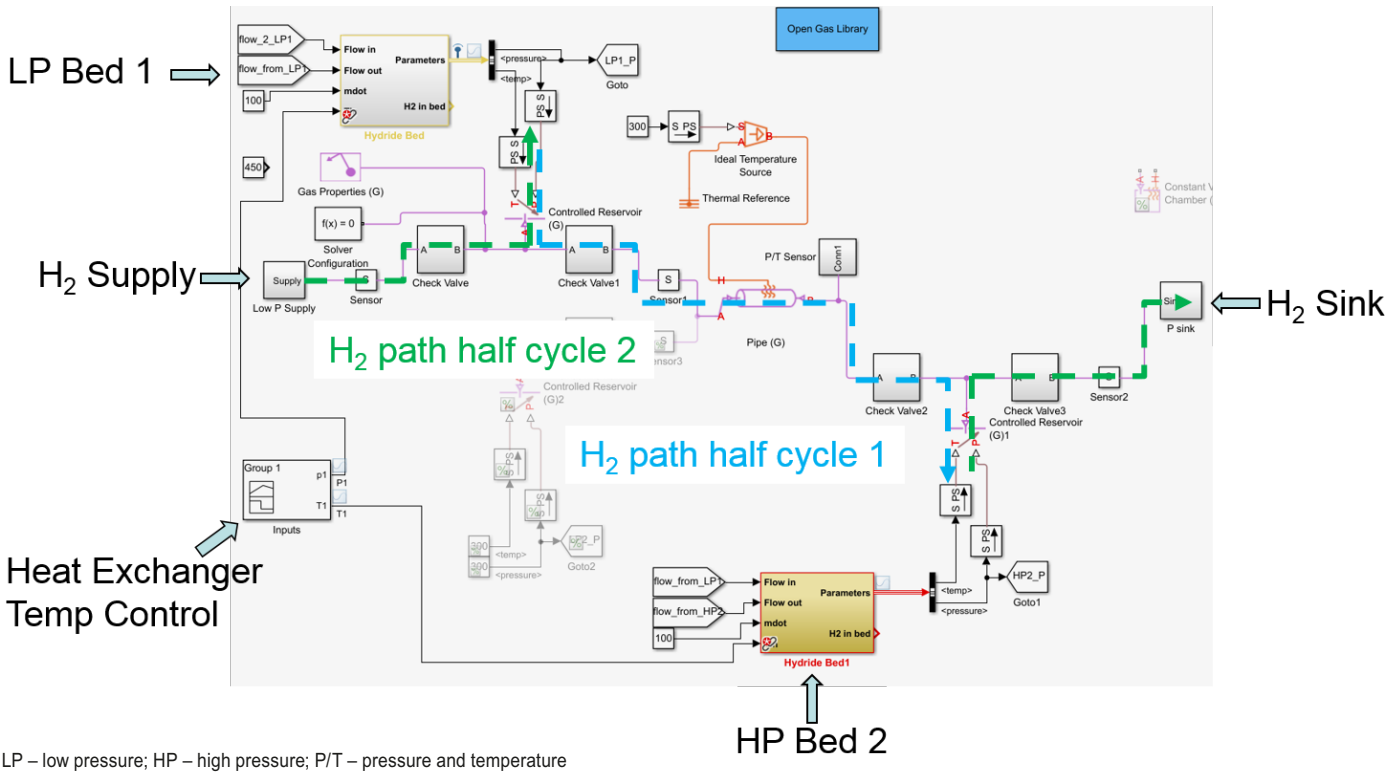

LP – low pressure; HP – high pressure; P/T – pressure and temperature

FIGURE 4. Simulink dynamic system model of the two-stage metal hydride compressor developed at SNL

times and staging to achieve quasi-continuous hydrogen compression. Simulations of a baseline compressor configuration with 12 min half cycles show the feasibility of the design. With 25 kg of metal hydride per bed, a quasi-continuous flow of hydrogen was achieved, compressed from 100 bar to 875 bar, with an average flow rate of 1.07 kg/h and a heating requirement of 12.5 kWh/kg. This flow rate is directly proportional to the size of the MH beds. A flow rate of 100 kg/h would therefore require appropriately scaled beds.

Following the baseline predictions, the model was used to simulate a number of additional configurations to look at the effect on flow rate as well as energy consumption and bed utilization. Two different low pressure alloys, three different cycle times, one different bed geometry, and a lower feed pressure were considered. A number of insights were gained from the system simulations. Firstly, energy efficiency can be improved with optimized cycle times, including the use of asymmetric cycle times (longer duration for desorption half cycles). Alloy properties can have a large impact on performance. For example, changing to a lower pressure AB_5 alloy for the low pressure stage negatively impacted performance. However, changing to smaller tube diameter to improve heat transfer and using asymmetric half cycles allowed the AB_5 performance to approach that of the AB_2 alloys. Finally, the results show that 50 bar feed pressure can be used with good performance.

Because the baseline energy use of 12.5 kWh/kg greatly exceeds the desired level, several pathways for achieving energy efficiency were pursued in second quarter. While industrial processes with sufficient waste heat to supply a metal hydride compressor (e.g., SMR plants or waste-to-energy systems) have been identified, they are not likely to exist at a fueling station. With a goal of using the compressor at hydrogen stations, other configurations have been investigated. Firstly, a heat recuperator design has been conceptually identified that could reduce the sensible heat requirement of the system by ~40% bringing required heat down to ~10 kWh/kg for the baseline system. If this heat was provided by a natural gas burner (assuming natural gas costs $0.065/mm-Btu, and burners are about 85% efficient) the operating cost would be $0.25/kg. This would be comparable to a conventional compressor using 2.3 kWh/kg at $0.11/kWh electricity cost.

Another option would be to couple the compressor to an energy efficient heat pump. Two heat pump options were considered: a vapor compression cycle and an absorption heat pump (AHP) cycle. A simple analysis of an ideal heat pump cycle shows that a vapor compression cycle with R21 operating between 25°C and 125°C has a coefficient of performance of 2.7 that would result in a compressor energy requirement 3.7 kWh/kg. A vapor compression cycle system with methanol as the refrigerant might further reduce the energy use to 3.1 kWh/kg. With compressor cooling it is

possible these coefficient of performance values could be improved somewhat. For AHP cycles there is the possibility of driving the cycle with heat rather than electricity. This is favorable because it is less expensive to provide heat than electricity. Therefore, a natural gas-fired AHP system might be advantageous. However, an AHP cycle operating over this temperature lift is not likely to produce a coefficient of performance of >1.4. At a coefficient of performance of 1.4, the heat required for the compressor would be 7.1 kWh/kg. If this heat was provided by burning natural gas, then the cost would be $0.18/kg.

CONCLUSIONS AND UPCOMING ACTIVITIES

Work in FY 2017 has demonstrated the feasibility of a two-stage metal hydride compressor to compress hydrogen from 100 bar to >875 bar over an achievable temperature range with sufficient flow rate. This has been demonstrated primarily through simulations with a dynamic system model that incorporates a baseline design for the compressor beds and literature properties for metal hydride thermodynamic and kinetic properties. The model includes a realistic representation of the heating–cooling system that would be required to drive the process as well as hydrogen flow through a manifold of connected check valves. While the hydride properties used are taken from experimental data, they have been extrapolated to higher temperature and pressure. PCT measurements of selected hydrides at actual expected operating conditions will provide further feasibility evidence.

The team has completed one such set of measurements in FY 2017 thus far. The commercial material Hydralloy C5 was cycled on a medium pressure Sievert's apparatus over six temperatures from 25°C to 95°C demonstrating desorption at over 100 bar. These results indicate that the material is suitable for the low pressure stage of the compressor. Further PCT measurements will be made on ORNL's high pressure apparatus to demonstrate performance at up to circa 150°C.

The specific energy of the baseline configuration of the MH compressor exceeds DOE's goals for this project. Simulations predict 12.5 kWh/kg H_2 for the baseline system modeled. To move this value closer to the ultimate target, several options have been investigated. Through a combination of heat recuperation and heat pump coupling, the specific energy could be reduced to 3–4 kWh/kg H_2. This level has been deemed sufficient for a low technology readiness level technology that has potential to provide reliability advantages over current technology, given sustained research and development.

Moving forward, work through FY 2017 will include down selecting bed designs and carrying out hydride PCT measurements. In FY 2018, we will perform accelerated cycling tests, complete component fabrication and assembly drawings, procure hydride alloys, fabricate bed component and assemble the prototype compressor, and configure the test facility to enable performance testing. In FY 2019, we will install the compressor in the high-pressure test facility, conduct performance testing of the prototype, and develop a conceptual design and cost analysis for a 100 kg H_2/h system.

FY 2017 PUBLICATIONS/PRESENTATIONS

1. Johnson, T., "Metal Hydride Compressor for High-Pressure (≥875 bar) Hydrogen Delivery," Presentation at the Joint HDTT-CSTT Meeting, Golden, CO, Nov. 2, 2016.

2. Bowman, R., Oral Presentation at Joint HSTT-HDTT Meeting, "Metal Hydride Compressor for High-Pressure (≥875 bar) Hydrogen Delivery," Southfield, MI, Feb. 16, 2017.

3. Bowman, R., Oral Presentation at 11th International Symposium on Hydrogen & Energy, "Status of High-Pressure Metal Hydride Compressors for Applications Exceeding 700 Bar," Waikoloa, HI, Feb. 28, 2017.

4. Johnson, T. "Metal Hydride Compression," presented at the 2017 DOE Hydrogen and Fuel Cells Program and Vehicle Technologies Office Annual Merit Review and Peer Evaluation Meeting, June 2017.

5. Bowman, R., Poster Presentation at the 2017 Gordon Research Conference on Hydrogen-Metal Systems, "Design and Development of High Pressure Metal Hydride Compressors for Vehicle Refueling," Easton, MA July 16–20, 2017.

REFERENCES

1. M.V. Lototskyy, Y.A.Yartys, B.G. Pollet, R.C. Bowman Jr., "Metal hydride hydrogen compressors: A review." Int J. Hydrogen Energy 39 (2014) 5818.

2. V.A. Yartys, M.V. Lototskyy, V. Linkov, D. Grant, A. Stuart, J. Eriksen, R. Denys, R.C. Bowman, Jr., "Metal hydride hydrogen compressors: Recent advances & future prospects," Appl. Phys. A 122 (2016) 415.

III.14 Advancing Hydrogen Dispenser Technology by Using Innovative Intelligent Networks

Darryl Pollica (Primary Contact), Bryan Gordon, and Chris O'Brien
Ivys Energy Solutions
303 Wyman St., Suite 300
Waltham, MA 02541-1208
Phone: (781) 812-6772
Email: darryl.pollica@ivysinc.com

DOE Manager: Katie Randolph
Phone: (240) 562-1759
Email: Katie.Randolph@ee.doe.gov

Contract Number: DE-EE0007273

Subcontractors:
- Air Liquide Advanced Technologies, Houston, TX
- Rheonik GmBH, Oldehausen, Germany
- National Renewable Energy Laboratory (NREL) Golden, CO

Project Start Date: June 1, 2016
Project End Date: December 14, 2018

Overall Objectives

- Improve reliability of vehicle-to-dispenser communication with the use of emerging connected-vehicle-to-infrastructure wireless communication technologies employed for Intelligent Transportation Systems, using the secure Institute of Electrical and Electronics Engineers (IEEE) 1609 vehicle communications protocol.
- Achieve consistent 2% or better metering accuracy of the dispenser system through tight design control of flow dynamics and thermal response of the meter, as well as improved thermal mass flow regulation enabled by advanced fueling event notification.
- Reduce cost and complexity of dispenser hardware, such as hydrogen pre-cooling systems, via intelligent and predictive controls incorporating individual vehicle data, and where possible, wide-area fleet data, to allow more appropriately sized equipment.

Fiscal Year (FY) 2017 Objectives

- Complete functional requirements and verification plan documents for critical components including hydrogen dispensing hardware, dedicated short-range wireless communication (DSRC) and high accuracy meter.
- Identify and procure commercially available DSRC hardware suitable for use in prototype and commercial hydrogen refueling applications.
- Develop robust multi-physics models of hydrogen dispenser system to inform component selection and hydrogen refueling control.
- Create custom software/firmware allowing DSRC to exchange all required data and commands per requirements of SAE J2799 (2014) and SAE J2601/1 (2016).
- Communicate data of multiple refueling events from a simulated dispenser to a simulated vehicle using DSRC wireless over IEEE 1609 protocols.
- Demonstrate less than or equal to 4% accuracy of flow measurement in the bench testing of a Coriolis meter, including operation at pressures up to 700 bar, fluid temperatures equal to that required in SAE J2601/1 protocols and flow rates up to at least 30 g/s hydrogen equivalent.
- Design advanced dispenser prototype system that integrates DSRC wireless communication, improved Coriolis meter hardware, and a system architecture that reduces cost while improving robustness of flow control and hydrogen cooling.

Technical Barriers

This project addresses the following technical barriers from the Hydrogen Delivery section of the Fuel Cell Technologies Office Multi-Year Research, Development, and Demonstration (MYRDD) Plan.

(I) Other Fueling Site/Terminal Operations

Technical Targets

This project will develop a SAE J2601 compliant dispenser system that aims to address reliability concerns with vehicle to dispenser communication, compliance with weights and measures standards for commercial fueling, and dispenser cost and complexity. Specifically, the project team will develop, test and demonstrate DSRC hardware for vehicle to station communication as opposed to the current infrared communication standard, as well as engineering a new high accuracy Coriolis flow meter specifically designed to maintain an accuracy of 4% or better in automotive hydrogen refueling application conditions. This meter will be integrated with the prototype dispenser in an optimized way to ensure accuracy is maintained, enabling a pathway for National Institute of Standards and Technology Handbook

44 compliance of dispenser systems. Lastly, the project will engineer and develop novel methods for hydrogen pre-cooling, flow control, and predictive control algorithms to decrease system complexity and cost. Technical targets are detailed in Table 1.

TABLE 1. Hydrogen Dispenser Targets Compared to Corresponding MYRDD Targets

Category	Project Target	MYRDD
Dispenser Capital Cost	$150,000 at low volume	$40,000 by 2020 at high volume
Communication Method	DSRC using IEEE 1609 protocols	Nozzle IR Alternative
Meter Accuracy	≤ ± 2% accuracy at temperatures between -40°C and 85°C and flow rates between 0.6 and 60 gps	≤ ± 4% Commercial Goal of ± 1.5$
Cooling System Cost	≤ $100,000 at low volume	$70,000 by 2020

IR - infrared

FY 2017 Accomplishments

- Completed functional requirements and verification plan documentation for dispenser system, mass flow meter, wireless communication and control systems.
- Research, selection and procurement of commercially available DSRC hardware for use in bench and full scale testing of wireless communication system.
- Initiated system modeling activities to understand tradeoffs of different flow control and cooling methods.
- Key factors that impact hydrogen meter accuracy were identified using empirical and computer aided engineering tools, including the following:
  - Temperature impacts on mechanical structure at variable pressure, temperature, and flow conditions were investigated using computational fluid dynamics modeling techniques.
  - Thermal shock experienced during refueling was simulated using models validated with climate chamber testing of meter hardware with chilled glycol.
  - The impact of sensor housing humidity on sensor performance was studied over multiple conditions.
- Designed, manufactured, and bench tested several prototype meters in lab and full scale settings, including the following activities:
  - Development of correction factor algorithms to compensate flow readings actively based on measured pressure and temperature of components within the device.
  - Addition of temperature sensors located throughout the meter housing to aid in measurement accuracy and sensor stability.
  - Purging of sensor housing with dry non-reactive gas to eliminate humidity/condensation.
  - Mono-block tube design to reduce turbulence and significant temperature differences between omega tube and torsion bar.
- Completed preliminary testing in a hydrogen dispensing application demonstrating that meter design is capable of obtaining <4% overall accuracy over varying flow, pressure, and temperature conditions.

✧ ✧ ✧ ✧ ✧

INTRODUCTION

This project aims to improve early adoption of fuel cell electric vehicles (FCEVs) by addressing technical obstacles and high cost associated with SAE J2601/1 compliant hydrogen dispenser systems. The team will focus on three main areas: robustness of vehicle to dispenser (SAE J2799) communication, ability to comply with National Institute of Standards and Technology Handbook 44, and complexity of system design associated with hydrogen cooling and flow control. The team intends to address these issues by improving hydrogen meter accuracy, replacing infrared communication with wireless technology used for vehicle to vehicle and vehicle to infrastructure communication, and implementing improved modeling and controls around thermal and flow management.

APPROACH

The team will design, develop and deploy an advanced hydrogen dispenser that incorporates DSRC wireless communication and improved hydrogen meter accuracy to a minimum of ≤4%. During the beginning phases of the project, demonstration of core technologies will occur at the bench level along with detailed system modeling. Testing will include wireless communication of refueling protocol messages using DSRC hardware and bench scale demonstration of hydrogen meter accuracy of at least 4% over varying temperatures, pressures, and flow conditions.

After bench validation, a prototype dispenser will be designed and manufactured for full scale simulated-environment testing at the NREL Hydrogen Infrastructure Testing and Research Facility. This phase's goals are to validate compliance with SAE J2601/1 (2016), demonstrate hydrogen meter accuracy of ≤4% when integrated in a dispenser, and show wireless communication of refueling

messages from a simulated vehicle to the dispenser control unit. Lastly, an up to six-month test of the prototype dispenser will be conducted at an Air Liquide station to validate the advanced communication, meter accuracy, and dispenser performance under real environmental operating conditions fueling FCEVs.

RESULTS

The team did extensive research on commercially available DSRC hardware suitable for use in hydrogen refueling applications and selected a hardware and software package for the prototype system. This equipment will be used to demonstrate wireless communication of refueling messages at both bench and full-scale prototype conditions. Using requirements developed for the wireless communication system, five hardware suppliers were identified and evaluated against various criteria including experience with commercial deployment, hardware cost, support capability and compliance to standards such as IEEE 1609 and IEEE 802.11p.

Requirements documents have been developed for major subsystems including wireless communication (DSRC), dispenser, mass flow meter, and control system. Additionally, detailed component specifications for pressure relief valves, heat exchanger, and solenoid valves have been created for use in component selection. Verification plans using the Design Verification Plan & Report process have been developed to define and guide testing of all critical aspects of the prototype dispenser in bench, full-scale lab, and demonstration phases. These verification plans detail specific test requirements, when to test, responsibility for testing, and pass/fail criteria.

The Rheonik team successfully completed development and preliminary testing of a high accuracy hydrogen meter. Empirical testing and computer aided engineering tools were used to study effects of pressure, temperature, and flow on current meter designs. Computational modeling was used to study turbulence and temperature effects in various parts of the meter. The team validated these models using environmental chamber testing (Figure 1).

Meter test results informed placement of additional temperature sensors, new compensation algorithms, and new manufacturing processes to improve meter accuracy (Figure 2). Several prototype meters were built and tested both at bench scale and at full scale in SAE J2601/1 compliant dispenser systems. Initial tests indicate that the meter is capable of achieving accuracies less than ±4% (Figure 3) in real application conditions. Additional testing is scheduled for August 2017 to complete validation of the new meter hardware.

The team began system modeling activities, focusing on studying feasibility and tradeoffs of variable orifice control vs. an array of fixed orifices. The model identified the range of orifice areas needed to meet flow rates between 0.6 gps and 60 gps as specified in SAE J2601/1. Sensitivity to storage pressure, vehicle initial pressure and hydrogen temperature have also been analyzed to increase model fidelity. The results show that an array of fixed orifices can be used to control of hydrogen in automotive refueling applications;

FIGURE 1. Photo of climate chamber test apparatus for meter development work

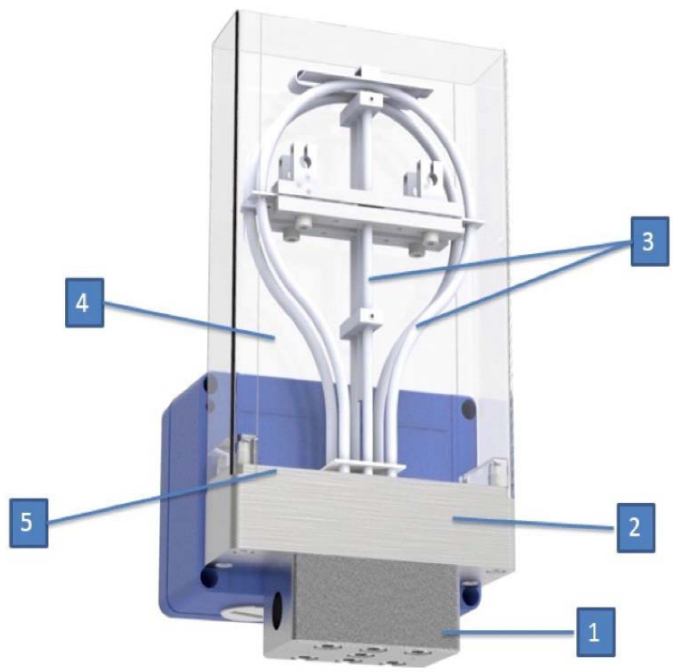

FIGURE 2. New meter design developed in the project, showing locations of various improvements: (1) Improved inlet block design; (2) and (3) Added temperature measurement locations; (4) Sealed and purged housing; (5) New seal materials

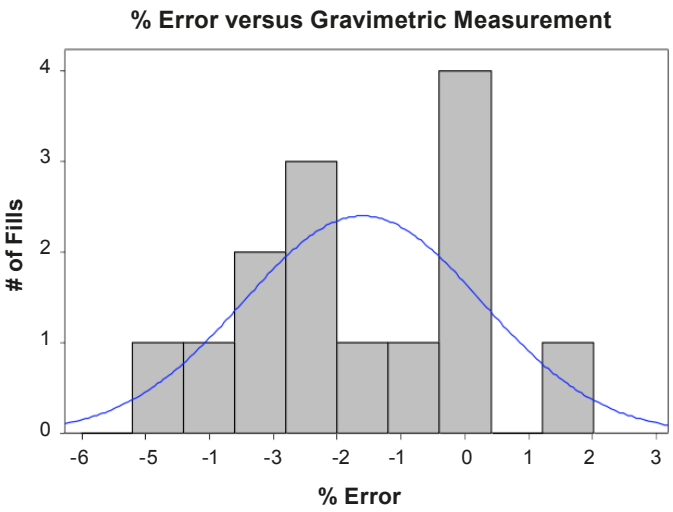

FIGURE 3. Results from initial meter testing in a hydrogen dispensing application

further cost studies and component evaluations will be involved in the final choice of flow control method and hardware.

CONCLUSIONS AND UPCOMING ACTIVITIES

In the first year of this project, significant progress has been made on bench-scale development of hydrogen meter and wireless communication technologies. Dispenser system design and modeling have been conducted to inform the design and build of the prototype dispenser system, scheduled for deployment and testing in FY 2018. Future planned activities include:

- Demonstrate successful wireless connection from a simulated dispenser to simulated vehicle and exchange of refueling event data and SAE J2601 communication filling messages over IEEE 1609 vehicle communications protocol with no messages delayed by more than 500 ms.
- Demonstrate ≤4% accuracy of flow measurement in bench testing of Coriolis meter.
- Develop first order system modeling to properly size critical dispenser components (e.g., heat exchanger, flow control valves) and to inform controls development.
- Complete detailed design, safety review and build of SAE J2601/1 prototype dispenser system that implements high accuracy meter, flow control and hydrogen cooling improvements while providing a means to demonstrate wireless communication between a vehicle and dispenser.
- Install and validate a prototype dispenser for compliance to SAE J2601/1 at the NREL's Hydrogen Infrastructure Testing and Research Facility.
  - Demonstrate ≤4% accuracy of flow measurement during simulated filling events.
  - Demonstrate ≤2.5% accuracy of flow measurement in secondary bench testing using hydrogen meter qualification equipment at NREL at pressures up to 700 bar, flow rates up to at least 30 gps and ambient hydrogen temperature.
  - Demonstrate transmission of SAE J2601/1 refueling messages from a simulated vehicle to the dispenser control unit per the requirements of SAE J2799.
- Install and validate prototype dispenser under real environmental operating conditions with FCEVs including:
  - Demonstrate ≤4% hydrogen metering accuracy with a stretch goal of ≤2% using the Hydrogen Field Standard dispenser accuracy verification.
  - Demonstrate successful wireless connection from FCEV to prototype dispenser and exchange of refueling event data using DSRC wireless communication.

FY 2017 PUBLICATIONS/PRESENTATIONS

1. Christopher O'Brien, Bryan Gordon, and Darryl Pollica, "Advancing Hydrogen Dispenser Technology by Using Innovative Intelligent Networks," presented at the 2017 DOE Annual Merit Review and Peer Evaluation Meeting, Washington, D.C., June 2017.

III.15 H2FIRST Consolidation

Chris Ainscough (NREL, Primary Contact)
Danny Terlip (NREL), Amgad Elgowainy (ANL),
Kareem Afzal (PDC), Krishna Reddi (ANL),
Josh Martin (NREL)
National Renewable Energy Laboratory (NREL)
15013 Denver West Parkway
Golden, CO 80401
Phone: (303) 827-9811
Email: chris.ainscough@nrel.gov

DOE Manager: Neha Rustagi
Phone: (202) 586-8424
Email: Neha.Rustagi@ee.doe.gov

Subcontractor:
PDC Machines, Warminster, PA

Project Start Date: October 1, 2015
Project End Date: September 30, 2017

Overall Objectives

- Decrease the contribution of station capital cost towards the levelized cost of hydrogen at fueling stations.
- Reduce the compression contribution (in terms of $\$/kg_{H2}$) by approximately 50% (current compressors for large stations ~500 kg/d can cost ~$1,000,000).
- Maximize station performance in terms of back-to-back fills.

Fiscal Year (FY) 2017 Objectives

- Operate the Hydrogen Vehicle Simulator (HyVS) capable of simulating five back-to-back fills at 70 MPa, -40°C conditions.
- Build and integrate the consolidation compressor as designed by PDC Machines.
- Integrate a new 15 hp chiller and triple block at NREL Hydrogen Infrastructure Testing and Research Facility (HITRF) to support back-to-back filling.
- Program and integrate the baseline and consolidation into the NREL HITRF supervisory control and data acquisition system.
- Perform consolidation testing and optimization at the NREL HITRF.

Technical Barriers

This project addresses the following technical barriers from the Technology Validation and Hydrogen Delivery sections of the Fuel Cell Technologies Office Multi-Year Research, Development, and Demonstration Plan.

Technology Validation

(D) Lack of Hydrogen Refueling Infrastructure Performance and Availability Data

Hydrogen Delivery

(E) Gaseous Hydrogen Storage and Tube Trailer Delivery Costs

FY 2017 Accomplishments

- HITRF station upgrades and integration successfully demonstrated.
  - Low pressure gas management panel design, build and installation.
    - Five banks
    - 189 kg total at 20 MPa
    - Pressure and combustible gas safety systems
  - Medium pressure gas management panel upgrades.
    - Upgrade existing valves and tubing to accommodate larger flow rates.
    - Installed new safety systems to support high pressure to medium pressure cross over.
  - High pressure valve and tubing installation.
    - Tubing size upgraded to 9/16 in outside diameter to accommodate larger flow rates.
    - Second process path added to each high pressure bank to allow for simultaneous filling and dispensing.
- Compressor design, build, installation, and integration.
  - PDC designed and built the compressor at their factory in Warminster, Pennsylvania, to accommodate consolidation the testing of:
    - Multiple flow paths into and out of the compressor.
    - 100 hp motor, two-stage diaphragm.

- Independent stage operation.
- Flow rate calculated to be ~1 kg/min nominal.

  – NREL and PDC integrated the compressor into the HITRF and confirmed safe operation.

- Baseline and consolidation algorithm development and implementation.

  – NREL has developed the software for control the HITRF and PDC compressor based on algorithms provided by Argonne National Laboratory (ANL).

  – NREL has tested the software and confirmed successful operation.

✧ ✧ ✧ ✧ ✧

INTRODUCTION

The project aims to decrease the contribution of hydrogen station capital cost to the levelized cost of hydrogen ($/kg) at fueling stations. The project also aims to maximize station performance in terms of back-to-back fills. These goals will be accomplished through the demonstration of ANL's tube-trailer consolidation concept and its potential to provide significant compression cost reduction at a 700 bar hydrogen refueling station. The project will demonstrate the operation and improve the optimization of refueling station design by utilizing various tube trailer consolidation schemes. The project will instrument and collect operational data to validate ANL's model predictions, identify control issues, and verify the consequent economic benefits.

The proposed concept is projected to reduce the compression contribution to hydrogen cost (in terms of $\$/kg_{H2}$) by approximately 50% (current compressors for large stations ~500 kg/d can cost ~$1,000,000). Deploying 700 bar hydrogen stations capable of multiple back-to-back

T40 vehicle fills involves high capital investment. Low utilization and reliability of installed station equipment in early fuel cell electric vehicle markets escalates the station's contribution to the cost of hydrogen even further. The compression component alone comprises about half of the refueling station installed capital cost across various refueling station capacities. ANL has developed a novel tube trailer consolidation concept and estimated that it can operate the compressor at up to 10 times its rated throughput (in terms of kg/h at supply pressure of 20 bar), and thus can reduce the compressor size dramatically. This enables efficient utilization of the tube trailer payload and compressor capital investments, which can ultimately reduce capital expenditure on stations.

APPROACH

The project takes place in three phases:

- Phase I: Demonstration Setup
- Phase II: Demonstration Preparation
- Phase III: Demonstration Testing

In order to validate the consolidation concept, the project team has upgraded the existing HITRF station at NREL in order accomplish full-scale demonstration of the consolidation concept, as the refueling components at NREL were not sized for optimum performance and cost, but rather research flexibility. Demonstrating the benefits of the consolidation concept using NREL's existing station requires careful sizing of required supplemental components and a proper design of experiment. Such sizing and design must be done with the constraints of the already existing equipment at NREL (e.g., single dispenser and pressure vessels) and the available PDC Machines compressor models, while also minimizing the overall cost of the project.

Phase I, completed January 2016, quantified the capacity of station components necessary to validate the Consolidation concept. ANL ran a matrix of simulations to determine the size requirement of high-pressure vessels required for buffer storage, as well as pressure vessels that will mimic the tube-trailer. The simulations also determined the optimum number of banks, and number of tubes in each bank, for the buffer storage and tube-trailer systems.

Prior to beginning this project, the station capacity at NREL was limited to 20 kg/d with no back-to-back fast fill capability. As noted above, the promise of the consolidation concept lies in its ability to improve the number of back-to-back fast fills, and to satisfy large station daily demands by enhancing the compressor throughput during peak demand periods. ANL sized the tube trailer vessels (considering vessels already available at NREL) to satisfy 100 kg/d demand, and also adjusted the demand profile to simulate the number back-to-back fills (during peak hours) for a 300 kg/d station.

Once the sizing and configuration of the refueling components were established, and the operation of the different operation strategies (i.e., with and without consolidation), NREL and PDC developed a process flow diagram, piping and instrumentation diagram, control strategy flow chart, and detailed bill of material.

Phase II, completed May 2017, required NREL and PDC to build out the HITRF station and compressor to meet the design specifications from Phase I. Upgrades included additional storage tanks and valves, increasing tubing diameter and valve orifice, and installation of the PDC compressor. NREL also modified the HITRF supervisory control and data acquisition system to control and log data

for all of the new components according to the algorithm provided by ANL.

The PDC compressor is a novel design that allows for operation either as two independent single stage compressors or one dual stage compressor, as show in Figure 1.

Phase III, currently active, requires NREL to perform the baseline (without consolidation) and consolidation tests according to the ANL algorithm. The HyVS will be used to create station demand according to a typical hourly filling profile (shown in FY 2016 annual report). The test results will be evaluated by NREL, PDC and ANL, and changes to optimize the station operation will be made. Additional testing will take place at the HITRF station to maximize number of back-to-back fills.

RESULTS

Phase I and Phase II are completed by NREL and ANL (see also FY 2016 annual progress report). Simulations were conducted to show expected results from consolidation and baseline testing. A process hazards analysis was also completed by NREL based on the station design.

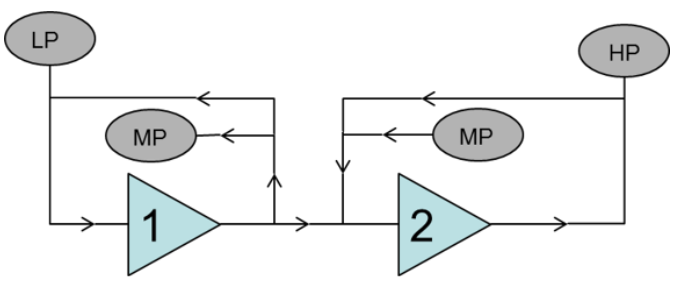

FIGURE 1. PDC compressor flow diagram. The compressor heads (1 and 2) are shown by triangles. The low, medium, and high pressure storage banks (LP, MP, and HP) are shown by the ovals.

In 2017, NREL made major modifications to the HITRF to support the consolidation testing. The images in Figure 2 show the HITRF in 2014 and today. The piping and instrumentation diagram for the station, as configured today is shown in Figure 3 with various flow paths.

NREL and PDC have tested manual operation of the compressor with the station control software, and have shown that the valves were sequenced correctly. The station will consolidate and dispense autonomously according to vehicle demand with the full implementation of the software. NREL is currently in the process of testing the baseline and consolidation algorithms. Results and analysis are expected by September 2017.

CONCLUSIONS AND UPCOMING ACTIVITIES

NREL, ANL, and PDC have worked together in FY 2017 to upgrade the HITRF to support hardware validation of the consolidation concept. This work includes installing new station equipment, programming the control software, and validating the operation. In the coming months, NREL will perform the automated baseline and consolidation tests, and will collect data for further analysis. The data will be evaluated by the team and compared to the modeling results from Phase I. The project team may make changes to the control software to optimize the algorithm.

FY 2017 PUBLICATIONS/PRESENTATIONS

1. Terlip, D., et al, "H2FIRST Tube Trailer Consolidation," Golden, CO, Hydrogen Delivery Technology Team, November 2016.

2. Terlip, D., et al, "H2FIRST Tube Trailer Consolidation," Washington D.C., DOE Annual Merit Review, June 2017.

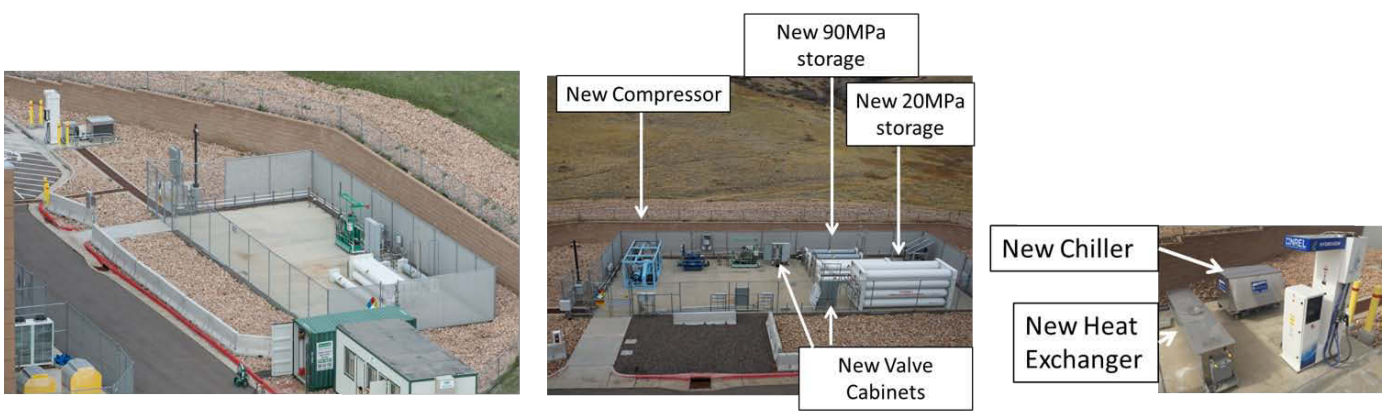

FIGURE 2. Hydrogen Infrastructure Testing and Research Facility shown before (left) and after (right) consolidation upgrades. There were eight new major station components added to the HITRF.

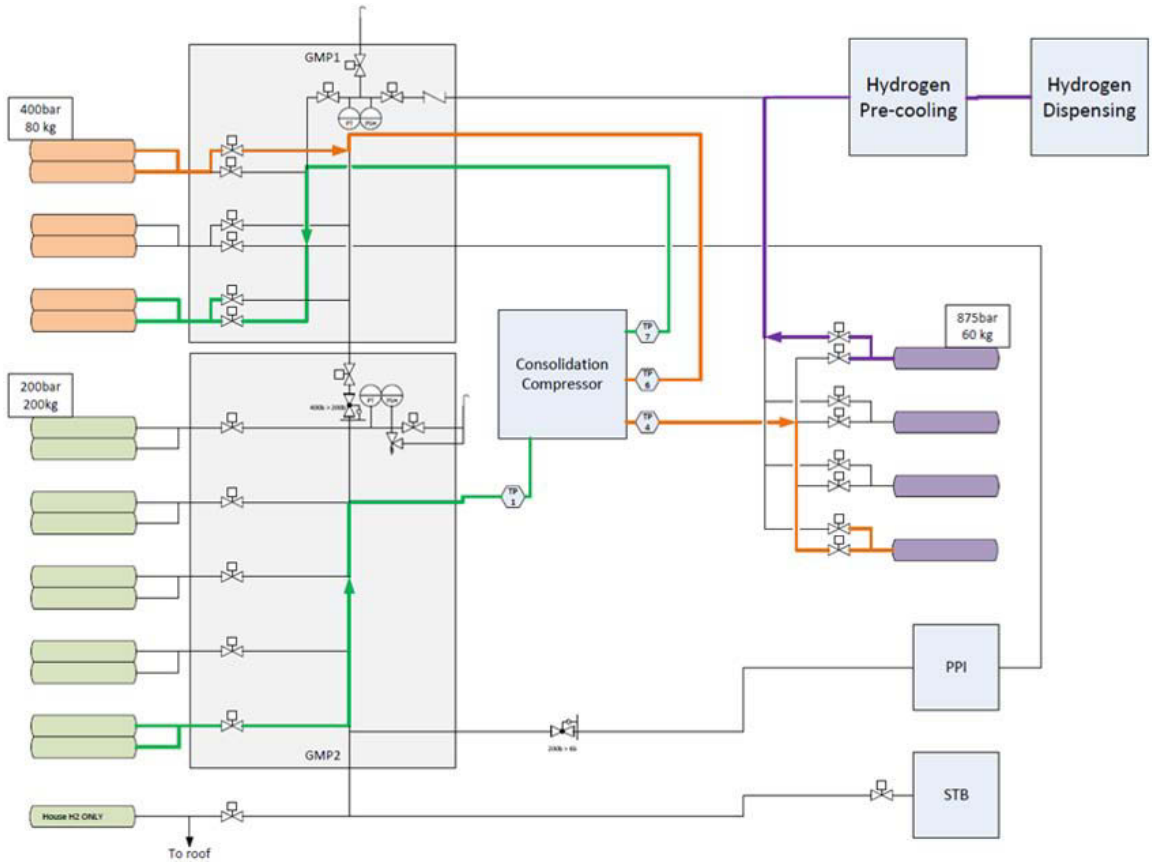

FIGURE 3. The HITRF as configured for consolidation testing. The green path shows consolidation within the tube trailer. The orange path indicates compression from the tube trailer to the station ground storage. The purple path indicates vehicle filling from the station ground storage.

III.16 Reference Station Design, Phase II

Ethan S. Hecht (Primary Contact), Joseph Pratt
Sandia National Laboratories
P.O. Box 969, MS 9052
Livermore, CA 94550
Phone: (925) 294-3741
Email: ehecht@sandia.gov

DOE Manager: Neha Rustagi
Phone: (202) 586-8424
Email: Neha.Rustagi@ee.doe.gov

Project Start Date: February 2016
Project End Date: March 2017

Overall Objectives

- Provide publicly available templates and information on representative hydrogen fueling station designs to enable quick assessment of the suitability of a particular site for a hydrogen station.
- Identify contributors to poor economics and areas of research needed for certain station designs.

Fiscal Year (FY) 2017 Objectives

- Provide near-term economic assessment of the cost of hydrogen for stations supplied by centrally produced, delivered hydrogen and those with hydrogen produced on-site.
- Illustrate the economic drivers for hydrogen delivery costs.
- Show how to reduce capital and operating costs through design decisions and operating methods.
- Demonstrate footprint reduction methods while maintaining compliance with current codes.

Technical Barriers

This project addresses the following technical barriers from the Hydrogen Delivery section of the Fuel Cell Technologies Office Multi-Year Research, Development, and Demonstration Plan.

(A) Lack of Hydrogen/Carrier and Infrastructure Options Analysis

(E) Gaseous Hydrogen Storage and Tube Trailer Delivery Costs

(I) Other Fueling Site/Terminal Operations

(K) Safety, Codes and Standards, Permitting

Contribution to Achievement of DOE Hydrogen Delivery Milestones

This project will contribute to achievement of the following DOE milestones from the Hydrogen Delivery section of the Fuel Cell Technologies Office Multi-Year Research, Development, and Demonstration Plan.

- Milestone 1.5: Coordinating with the H_2 Production and Storage sub-programs, identify optimized delivery pathways that meet a H_2 delivery and dispensing cost of <$2/gge for use in consumer vehicles. (4Q, 2020)
- Milestone 6.3: By 2020, reduce the cost of hydrogen delivery from the point of production to the point of use in consumer vehicles to <$2/gge of hydrogen for the gaseous delivery pathway. (4Q, 2020)

FY 2017 Accomplishments

- Demonstrated that for current stations, those served by centrally produced, delivered gaseous hydrogen are more economical compared to those which generate hydrogen on-site via steam methane reforming or electrolysis, and the economic drivers for this finding.
- Depicted and described how modular stations and stations with on-site production have a substantially decreased lot size requirement due to reduced equipment size, reduced truck access requirements, and reduced setback distances.
- Evaluated the economics of different station concepts and determined the lowest current hydrogen cost of $12.65/kg for a 300 kg/d modular station with delivered hydrogen at an installed cost of $1,360,000.

✧ ✧ ✧ ✧ ✧

INTRODUCTION

For the wide-spread adoption of fuel cell electric vehicles, additional fueling stations need to be constructed in the United States. A wide variety of private and public stakeholders are involved in the development of this hydrogen fueling infrastructure. Each stakeholder has particular needs to be met in the station planning, development, and operation process. A sample of stakeholders and needs is given here.

- Station developers and operators: quick evaluation of potential sites and needs, lower investment risk, general cost and return estimates.
- Local authorities: understand devices, components in a typical station.

- Code developers: understand near-term needs for code refinement.
- Other analysis groups: tools and baseline for economic studies.
- Businesses, entrepreneurs, and research and development organizations: identification of near-term business solution and technology needs.
- Local municipalities and the general public: high-level understanding of typical stations lowering acceptance risk.
- Funding and financing organizations: understanding of current technological capabilities, costs, and market needs.

Hydrogen fueling station equipment, designs, and costs vary between developers and are often treated as proprietary information. While necessary from a business standpoint, this can hinder the ability to discuss station design details in a collaborative way. Publicly available templates of representative station designs can be used to meet many of the stakeholder needs outlined above. These reference stations help reduce the cost and speed the deployment of hydrogen stations by providing a common baseline with which to start a design, enable quick assessment of the suitability of a particular site for a hydrogen station, and identify contributors to poor economics and areas of research needed for certain station designs.

APPROACH

This work presents five new reference station designs for use by the hydrogen infrastructure community. The Phase 1 Reference Station Design Task [1] examined four build-on-site stations which obtained hydrogen from compressed gas or liquid delivery trucks. The current work builds on the Phase 1 work by producing designs and economic analyses of factory built modular stations and stations utilizing on-site generation, and also brings the cost of supplied hydrogen into the analysis. It includes one traditional design from the Phase 1 work to enable equal comparisons between all station types in the two works. For all station types, three capacities were examined: 100 kg/d, 200 kg/d, and 300 kg/d. The five station types developed in this work are:

- Conventional (assemble on-site) stations with hydrogen:
  - Delivered as compressed gas from a centralized, already operational production facility (baseline).
  - Produced on-site through steam methane reforming.
  - Produced on-site through electrolysis.
- Modular fueling stations with hydrogen:
  - Delivered as compressed gas from a centralized production facility.
  - Produced on-site through electrolysis.

RESULTS

The cost components of hydrogen fueling stations consist of capital cost of equipment, installation, site acquisition and development, and operating expenses. For conventional stations, capital costs of the equipment were estimated based on updated bills of material from the Phase 1 [1] work. Capital costs for modular stations and modular hydrogen production units were based on discussions with several manufacturers. Operation costs, such as the cost of electricity and other utilities, if necessary, were estimated using data from several sources.

Revenue was assumed to be solely from the sale of hydrogen. Operating expenses and revenue calculations depend on the assumed throughput of hydrogen. The same utilization profile used in the Phase 1 work [1] was used in this project to calculate throughput, although it was delayed in the onset year. This utilization model estimates that starting in 2017, 5% of station capacity will be utilized. As the number of fuel cell vehicles on the roads continues to increase, the utilization of stations is projected to increase, up to a maximum of 80% in 2026. All costs were combined with revenue to determine the overall cost of hydrogen to the station developer/operator such that the station would break even on investments in 7 years. Station developer/operator margin and retail fuel taxes will be added to the calculated hydrogen cost to determine the final price to the consumer, but both of these aspects were outside the scope of this project.

Because the costs in this project were estimated (typically averages of costs from various situations and/or a range of manufacturers), they will likely be different than that of an actual station. To correct for differences in up-front capital or installation costs of a real-world station, a graphical tool was developed to estimate the resulting change in hydrogen cost for a given change in investment cost. This is shown in Figure 1, for a 300 kg/d station. For example, the tool can be used to show that a decrease of $300,000 in (depreciable) up-front costs from that estimated herein for a 300 kg/d station would result in a corresponding $1.00/kg decrease in hydrogen cost. When trying to meet a <$2/gge (1 gge is 1 kg of hydrogen) cost target, the capital costs must be kept low and/or the economic assumptions (such as the utilization profile or the specification of breaking even in seven years) must be changed.

Economic results of the five different station concepts showed that stations served by centrally produced, delivered gaseous hydrogen are more economical compared to those which generate hydrogen on-site via steam methane

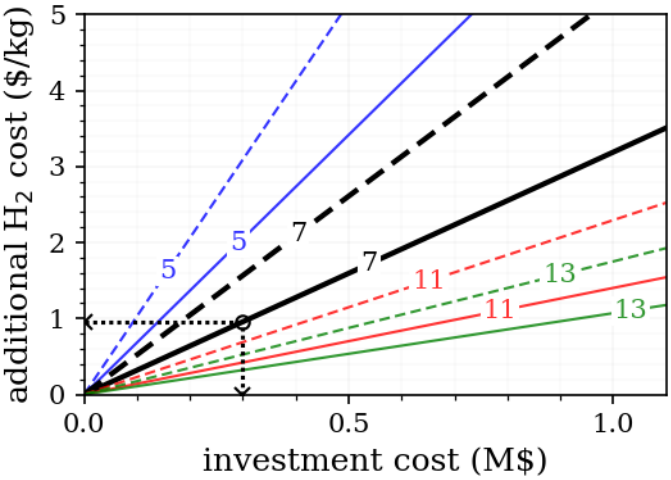

FIGURE 1. Additional cost of hydrogen as a function of the initial construction/capital investment for a 300 kg/d station. Numbers on the graph lines are the years required to break even on the investment (seven years was the baseline assumption for this project), solid lines are for a depreciable asset (on a 7-yr Modified Accelerated Cost Recovery System schedule, and dashed lines are for a non-depreciable asset).

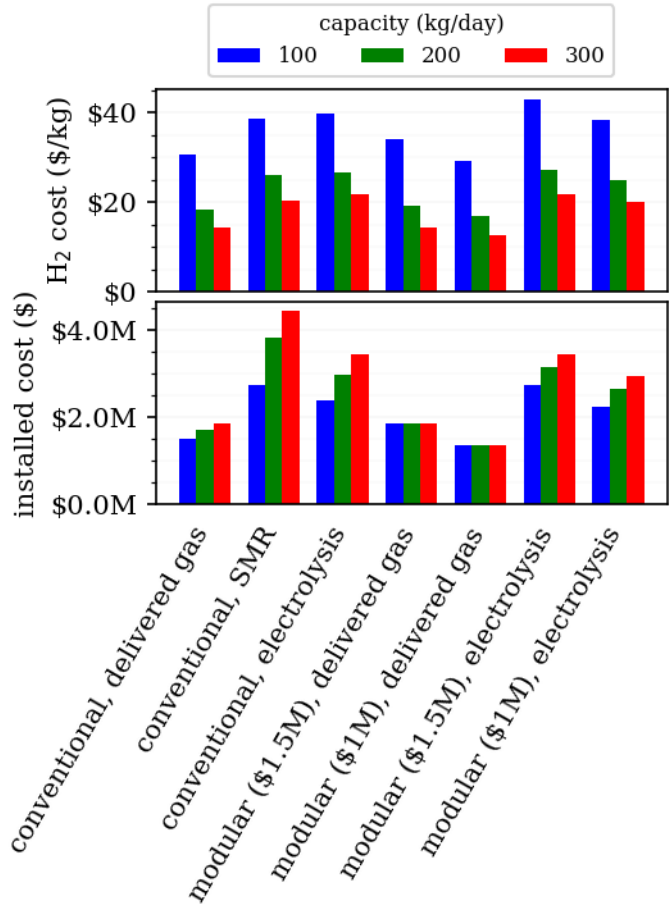

FIGURE 2. Hydrogen cost to break even at Year 7 (top), and installed cost (which includes site preparation, engineering and design, permitting, and component capital and installation costs) in 2016$ (bottom), for the stations analyzed in this work

reforming or electrolysis. Higher capacity stations were found to have a lower cost for hydrogen to break even at the same point in time compared to lower capacity stations. Use of the economic model specifying that a station would break even in Year 7 demonstrated that both 300 kg/d modular stations (at $1,500,000 for the uninstalled modular unit) and conventional stations with central hydrogen production and delivery in tube trailers, would have a hydrogen cost of $14.25/kg (a lower uninstalled modular unit price of $1,000,000 resulted in a hydrogen cost of $12.66/kg). On-site production stations, either through steam methane reforming or electrolysis, were shown to have significantly higher capital costs than delivered, centrally produced hydrogen. This increase in capital resulted in a hydrogen cost increase of $6–$10/kg, depending on the station capacity. While steam methane reforming capital costs were shown to be higher than electrolyzer costs, the electricity cost ended up making electrolyzer-supplied stations the most expensive option in terms of resulting cost per kilogram of dispensed hydrogen under the assumptions of this work. Full cost results are shown in Figure 2.

In addition to the economics, the station equipment was laid-out in typical land use arrangements, with the example of a modular station supplied by electrolysis shown in Figure 3. Modular stations and stations with on-site production were shown to substantially decrease the overall required lot size due to reduced equipment size, reduced truck access requirements, and reduced setback distances. The project report also includes piping and instrumentation diagrams of these station concepts, with system level requirements for components and instruments and an estimate of utility requirements which are intended to be useful for site screening.

CONCLUSIONS AND UPCOMING ACTIVITIES

The final report for Reference Station Design, Phase II details the economics of current hydrogen refueling stations, and includes some sketches of what these fueling stations might look like. It visually depicts the contributions to capital and operational costs of hydrogen for different station concepts, making it easy to find the largest contributors to a high cost of hydrogen to the consumer. This information can be used to devote research and development towards these high contributors. At the station, the dispenser, compressors, and chillers are expensive pieces where additional development, or higher volume production could reduce station costs. For electrolysis, the purchase of low-priced electricity could serve to make on-site production cost competitive with central production and delivery. The report

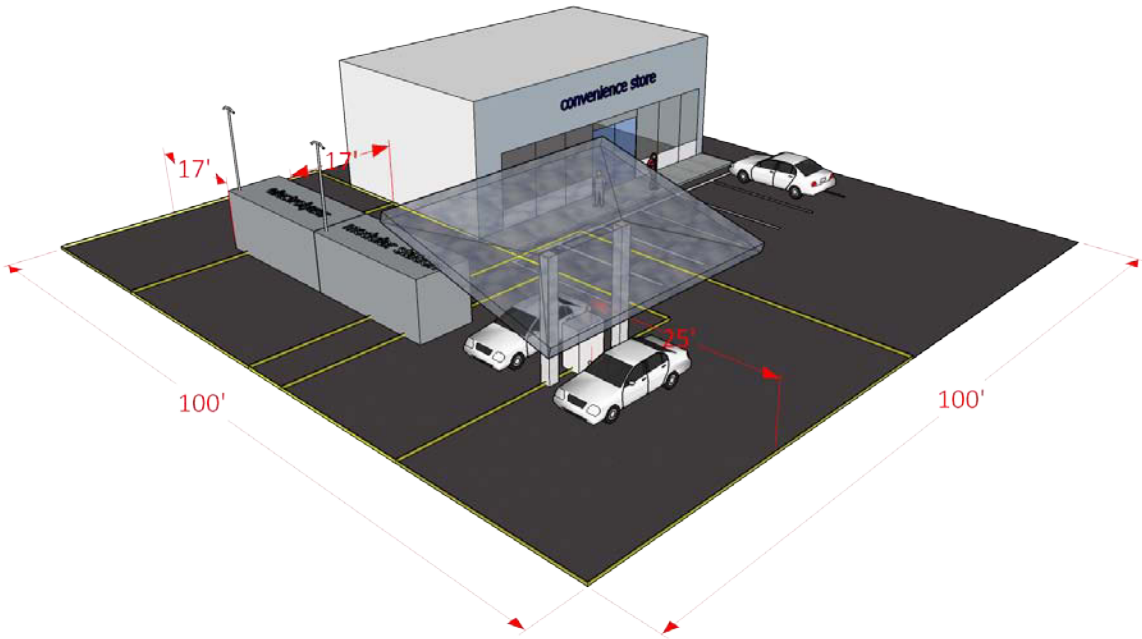

FIGURE 3. Renderings of a modular station layout with an electrolyzer for on-site production, with a small, reduced footprint

enables the comparison of different station concepts that could be implemented in various market scenarios.

As more fuel cell electric vehicles hit the roads, even larger capacity fueling stations will be needed in urban areas. Ongoing work under H2FIRST is addressing this challenge by considering unique strategies for footprint reduction of hydrogen fueling stations that could be suitable for construction in urban areas (e.g., San Francisco, Boston, New York). The work is considering new delivery concepts, potential changes to the fire code, and underground and rooftop storage concepts.

FY 2017 PUBLICATIONS/PRESENTATIONS

1. E.S. Hecht, J. Pratt. "Comparison of conventional vs. modular hydrogen refueling stations, and on-site production vs. delivery," Technical Report SAND2017-2832, Sandia National Laboratories, March 2017. (available at https://energy.gov/eere/fuelcells/h2first)

1. E.S. Hecht, J. Pratt, "Reference Station Design, Phase II: Comparison of conventional vs. modular hydrogen refueling stations, and on-site production vs. delivery," presented at the 2017 DOE Hydrogen and Fuel Cells Program Annual Merit Review, Washington D.C., June 9, 2017. (SAND2017-4928 C).

REFERENCES

1. J. Pratt, D. Terlip, C. Ainscough, J. Kurtz, and A. Elgowainy. H2FIRST reference station design task. Technical Report SAND2015-2660R, Sandia National Laboratories, April 2015. (available at http://energy.gov/eere/fuelcells/h2first)

IV.0 Hydrogen Storage Sub-Program Overview

INTRODUCTION

The Hydrogen Storage sub-program supports early-stage research and development (R&D) of materials and technologies for compact, lightweight, and inexpensive storage of hydrogen for automotive, portable, and material handling equipment applications. The Hydrogen Storage sub-program strategy is to follow two parallel paths: a near-term focus on R&D to improve the performance and lower the cost of high-pressure (700 bar) compressed hydrogen storage systems currently being used for commercial introduction of hydrogen fuel cell electric vehicles (FCEVs) and a long-term focus on developing advanced cold/cryo-compressed and materials-based hydrogen storage system technologies that have potential to meet all of the onboard hydrogen storage targets.

In Fiscal Year (FY) 2017, the first round of five early-stage R&D seedling projects under the Hydrogen Materials–Advanced Research Consortium (HyMARC) began activities aimed at discovering hydrogen storage materials with increased capacity, more favorable thermodynamics, and lower cost with the potential to meet DOE targets. Another new project was also launched, focused on an advanced cryogenic hydrogen storage insulation system to enable hydrogen to be stored at higher densities and/or lower pressures when compared to traditional high-pressure approaches. The sub-program continued supporting existing material R&D efforts for metal hydrides and sorbents, ensuring their alignment and collaboration with HyMARC's core and support functions. Late in FY 2017 the sub-program also announced selection of (1) a second round of four new seedling projects to work under HyMARC to develop advanced hydrogen storage materials and (2) three new projects focused on developing novel carbon fiber precursors with potential to significantly lower the cost of high-strength carbon fiber and high-pressure hydrogen storage systems. A major programmatic effort during FY 2017 was the revision of the DOE onboard hydrogen storage targets for light-duty FCEVs, which were last updated in 2009 and originally set in 2003. The revised targets take into account the recent advancements made in commercial fuel cell vehicles.

GOAL

The sub-program's goal is to advance early-stage, innovative hydrogen storage technologies in transportation and other niche areas, such as portable power and material handling equipment.

OBJECTIVES

The Hydrogen Storage sub-program's objective is to develop technologies that provide sufficient onboard hydrogen storage to allow fuel cell devices to meet the performance and run-time demanded for the applications. The revised 2020, 2025, and ultimate targets for light-duty vehicles allow for a progression of improved performance to be competitive with conventional and other advanced powertrains across the breadth of light-duty vehicle platforms while also meeting packaging, cost, safety, and performance requirements.

2020

- 1.5 kWh/kg system (4.5 wt%)
- 1.0 kWh/L system (0.030 kg H_2/L)
- $10/kWh ($333/kg stored hydrogen capacity)

2025

- 1.8 kWh/kg system (5.5 wt%)
- 1.3 kWh/L system (0.040 kg H_2/L)
- $9/kWh ($300/kg stored hydrogen capacity)

Ultimate

- 2.2 kWh/kg system (6.5 wt%)
- 1.7 kWh/L system (0.050 kg H_2/L)
- $8/kWh ($266/kg stored hydrogen capacity)

In addition to these high-level targets, a comprehensive set of revised targets is available on the Hydrogen Storage website at https://energy.gov/node/1315186 and a target explanation document explaining the assumptions and inputs used to develop the revised targets for light-duty vehicles is available at https://energy.gov/node/826801.

Although some commercial FCEVs are able to meet the 300-mile driving range deemed as the minimum entry point into the market, this driving range is not currently achievable across the full range of vehicle models without compromising space, performance, or cost. The high cost of high-pressure hydrogen storage systems plus the fact that the bulk of incumbent vehicles are able to provide customers with greater than 400-mile driving range make it clear that current hydrogen storage system technology must be improved in order to provide customers with the expected driving range across all vehicle platforms at a reasonable cost.

In addition to the targets for onboard hydrogen storage systems for light-duty vehicles, the sub-program also has comprehensive sets of hydrogen storage performance targets for portable power and material handling equipment applications. These targets can be found in the Hydrogen Storage section of the Multi-Year Research, Development, and Demonstration Plan at https://energy.gov/sites/prod/files/2015/05/f22/fcto_myrdd_storage.pdf.

FY 2017 TECHNOLOGY STATUS AND ACCOMPLISHMENTS

Given that 700 bar hydrogen storage system cost remains a key barrier to the commercialization of current FCEVs, the sub-program continued addressing approaches to reduce the cost of high-pressure hydrogen storage systems. The current projected high-volume cost status for 700 bar compressed hydrogen storage systems is $15/kWh, which reflects technology advancements supported by the Hydrogen Storage sub-program to reduce the cost of carbon fiber precursor and resin, balance of plant components integration, as well as changes in tank design to better reflect commercially manufactured pressure vessels.

During FY 2017 the sub-program placed a greater focus on ensuring that early-stage R&D efforts on innovative hydrogen storage materials were closely aligned with and coordinated through the HyMARC's core and support teams. The Hydrogen Storage sub-program worked to make HyMARC's full set of capabilities and expertise known and available to other hydrogen materials R&D efforts within the sub-program's portfolio, ensuring opportunities for collaboration were identified and that impact would be maximized moving forward. Figure 1 shows a screenshot of HyMARC's website and serves as an example of the HyMARC capabilities being disseminated to the hydrogen

FIGURE 1. Homepage of HyMARC website

storage community. The HyMARC lab teams are routinely providing their results to the research community through publications in high-impact, peer-reviewed science journals.

Near-Term Focus: High-Pressure Storage

The Hydrogen Storage sub-program's near-term strategy continued to focus on innovative approaches for high-pressure compressed hydrogen storage systems and remained consistent with FCEV industry trends in 2017. Automotive companies are now in their third year of commercializing FCEVs that use 700 bar compressed hydrogen storage systems onboard, and system cost remains one of the most important challenges to widespread commercialization. This year, a third FCEV model was released to the commercial market in California. Like the previous two FCEV models released in FY 2015 and FY 2016, this one is equipped with a 700 bar compressed hydrogen system onboard.

In FY 2017, projects spanning the sub-program's high-pressure storage portfolio made progress in the areas of alternative manufacturing processes, alternative fiber and resin, and conformable tank designs. For example, Materia has demonstrated improved and optimized vacuum processing for the resin impregnation of dry fiber wound tanks and demonstrated equivalent burst strength to baseline conventional tanks. Additionally, work by the Center of Transportation and the Environment and partners on conformable tank design moved the project a step closer to the development of conformable 700 bar hydrogen storage systems without use of carbon fiber composites. Finally, Sandia National Laboratories (SNL) has identified alloys for use in the balance of plant with the potential to reduce material cost and weight by over 50% compared to 316L stainless steel that has been traditionally used for balance of plant.

Three projects were selected in 2017 to develop low-cost, high-strength carbon fiber precursor materials to address the high cost of 700 bar onboard hydrogen storage systems. System cost projections indicated that high-strength carbon fiber will contribute at least 62% of the total system cost when manufactured in high annual volumes, with the precursor material contributing about half of the carbon fiber cost. The three selected projects are:

- University of Kentucky will develop hollow polyacrylonitrile (PAN) fibers using a low-cost PAN supply for conversion into high-strength carbon fiber. The project will also look to optimize the solution spinning process, especially the wash bath configuration and solvent recovery.
- The Pennsylvania State University will develop novel polyolefin precursor fibers for conversion into high-strength carbon fiber. The polyolefin fibers will not require sulfonation for conversion into carbon fiber and will provide higher mass yield of carbon fiber, reducing the mass of precursor required.
- Oak Ridge National Laboratory will investigate use of ionic liquid materials as plasticizers for reducing the melt temperature of PAN, allowing for lower-cost melt spinning of PAN precursor fibers. The ionic liquid plasticizers are also expected to facilitate the conversion into carbon fiber.

Specific accomplishment include:

- **Alternative manufacturing processes:** Materia, Inc., demonstrated improved vacuum infused composite tank processing, which reduced fabrication time from 2 h to 0.5 h for high-quality 7.5 L prototype vessels. They also achieved equivalent burst strength (1,833 bar [26,586 psi]) in static testing of small prototype vessels (Type III, 7.5 L).
- **Alternative material qualification:** SNL quantified fatigue performance for low-Ni austenitic stainless steel (21Cr-6Ni-9Mn) with nominally the same fatigue performance as the tested strain-hardened 316L stainless steel allowing potential cost saving for balance of plant components.
- **Conformable tank development:** The Center of Transportation and the Environment completed initial testing with baseline compressed natural gas vessels, including initial permeability performance measurements of the storage vessel resin, and proved test system workability.

Long-Term Focus: Cold/Cryo-Compressed and Materials-Based Storage

As shown in Figure 2, in addition to system cost challenges, compressed hydrogen storage systems are unable to meet the Program's 2020 targets for energy density. The density of hydrogen gas poses a theoretical limitation that prevents ambient compressed hydrogen systems from being able to meet the energy density targets. Given these limitations and as a longer-term strategy, the Hydrogen Storage sub-program continues to pursue less mature cold/cryo-compressed and materials-based hydrogen storage technologies that have the potential to satisfy all onboard hydrogen storage targets, including energy density.

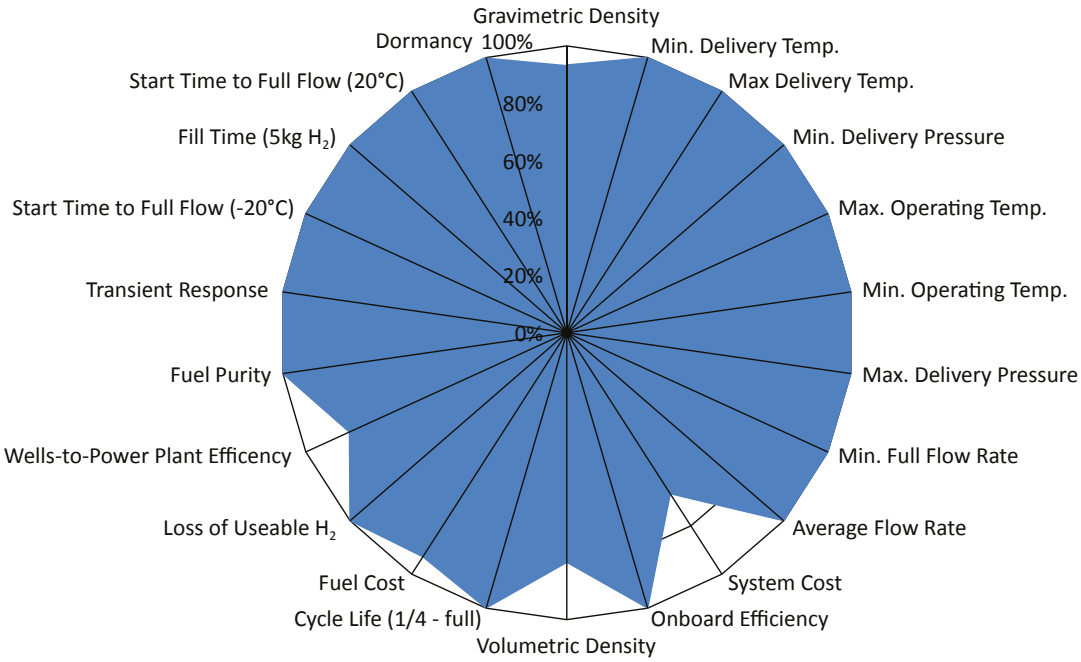

FIGURE 2. Current projected performance of a state-of-the-art 700 bar compressed hydrogen storage system with 5.6 kg usable hydrogen storage compared with the 2020 onboard automotive targets

In the area of cold-temperature operation, the sub-program selected a new project in FY 2016, led by Vencore Services and Solutions, focusing on improved thermal insulation systems for cold and cryogenic automotive tank applications, specifically to improve system dormancy (i.e., the length of time cold/cryogenic hydrogen can be stored before having to vent due to pressure build-up from warming of the hydrogen).

FY 2017 marked the second full year of efforts within HyMARC. The core team of national laboratory partners (SNL–lead, Lawrence Livermore National Laboratory, and Lawrence Berkeley National Laboratory [LBNL]) made a great deal of progress as they continue to address scientific gaps impeding the advancement of solid-state storage materials. For example, an experimental investigation involving several advanced characterization techniques showed that titanium is not present on the surface during hydrogen desorption from Ti-doped $NaAlH_4$, supporting the "zipper" mechanism and invalidating several other published mechanisms. This study demonstrates the power of bringing together these laboratory capabilities under the umbrella of HyMARC, as it utilized low energy ion scattering and X-ray adsorption spectroscopy at SNL, and scanning transmission X-ray microscopy as part of the Advanced Light Source at LBNL.

HyMARC researchers also continued to develop extensive theoretical modeling capabilities to complement these experimental tools. Modeling work at Lawrence Livermore National Laboratory on $Mg(BH_4)_2$, a promising material with over 14 wt% theoretical capacity and favorable thermodynamics, and its absorption/desorption reaction pathways continues to assist other HyMARC core efforts at SNL, HyMARC-supported efforts at Pacific Northwest National Laboratory (PNNL), and the seedling project at the University of Hawaii. In the past year, the researchers improved free energy predictions of hydrides by considering explicit thermal effects, with results tested and successfully validated on the Mg-B-H system. They also predicted stability trends of B_xH_y intermediates beyond the bulk crystalline limit to understand reaction pathways under non-equilibrium reaction conditions.

FY 2017 also marked the second full year of HyMARC's support team (also known as the Hydrogen Storage Characterization and Optimization Research Effort or HySCORE). This team, comprised of national laboratory partners (National Renewable Energy Laboratory [NREL], PNNL, LBNL) along with the U.S. Department of Commerce's National Institute for Standards and Technology Center for Neutron Research, is a subset of the overall HyMARC team and provides independent material measurement validation as well as support for the entire HyMARC consortium and seedling projects. Their function is especially focused on advanced characterization methodologies and validation of hydrogen storage concepts and mechanisms. Over the past year, NREL completed their round robin study on the hydrogen adsorption measurements of two different carbon samples, promoting improved best practices

of collecting and reporting volumetric capacity data. The study included measurements by thirteen laboratories spanning industrial, national laboratory, and academic institutions, both domestic and international. In addition, new advanced characterization techniques have been brought online for use by HyMARC partners, including variable temperature thermal conductivity measurement at NREL, diffuse reflectance infrared spectroscopy at LBNL, and variable pressure nuclear magnetic resonance at PNNL.

Four additional seedling projects were selected in FY 2017 as the second round of individual projects to collaborate with the HyMARC consortium. These projects will develop specific hydrogen storage materials with potential to meet the performance requirements for onboard FCEV hydrogen storage. The four new awards selected in FY 2017 are:

- University of Michigan will apply machine learning techniques to design and experimentally demonstrate new metal-organic frameworks (MOFs) having high usable volumetric capacities, as well as control material crystal morphology and crystallite size distribution to increase packing densities.
- NREL will synthesize and characterize a series of partially fluorinated covalent organic frameworks that are intended to exhibit improved long-range ordering and assist in tuning hydrogen binding enthalpy.
- NREL will demonstrate that atomic layer deposition processes are compatible with metal borohydrides such that nanoparticles can be encapsulated with layers to promote rapid hydrogen discharging at lower temperatures and pressures through both protective and catalytic means.
- University of California, Berkeley will utilize post-synthetic modifications to introduce a large number of open metal sites into metal-organic frameworks while retaining a favorable pore environment to achieve improved hydrogen storage properties at ambient conditions.

The existing project at the University of Michigan, with subcontractor Ford, made significant progress in FY 2017 on computational-directed MOF synthesis. They used screening methods to examine a database of nearly a half-million real and hypothetical MOF structures and identified over 2,000 materials projected to surpass the usable gravimetric and volumetric capacities of MOF-5 by over 15%. Several materials were subsequently investigated experimentally. By using the Hydrogen Adsorbent System Model developed previously through the Hydrogen Storage Engineering Center of Excellence, it was demonstrated that both IRMOF-20 and DUT-23(Co) can outperform MOF-5 on a system-level basis.

Specific accomplishments include:

- **Insulation for cryogenic tanks:** Vencore down-selected the concept technologies for an integrated advanced insulation system for vehicle applications.
- **Metal hydride dehydrogenation mechanism elucidation:** An experimental investigation using several HyMARC capabilities at SNL and LBNL demonstrated that titanium is not present on the surface during hydrogen desorption from Ti-doped $NaAlH_4$, supporting the zipper mechanism and invalidating several published mechanisms.
- **Computational method development:** Lawrence Livermore National Laboratory continued progress on several types of modeling techniques, including detailed studies on surface and interface chemistry of hydrides, enabling the development of multiscale simulations to investigate the thermodynamics and kinetics of hydrogen storage in metal hydrides.
- **Round robin testing:** NREL completed the multi-laboratory round robin study on volumetric uptake in sorbents, including national laboratory, university, industrial, and international partners, and analyzed the results to identify sources of error in volumetric uptake measurements. These results are being prepared for dissemination to the hydrogen storage community.
- **Characterization method development:** LBNL commissioned and set up the diffuse reflectance infrared spectroscopy instrument with a sample cell to enable in situ gas loading capabilities to investigate hydrogen binding in sorbent materials.
- **Enhanced kinetics and cycling via "nanoencapsulation":** Argonne National Laboratory successfully cycled sodium borohydride–graphene composite material six times with measured hydrogen capacity between 7.4 wt% and 9 wt% and improved kinetics when compared to the bulk phase material alone.

- **Material development:** For the first time, the University of Hawaii demonstrated the hydrogenation of a MgB_2 material to $Mg(BH_4)_2$ at 300°C and 700 bar.
- **High-throughput computational screening:** The University of Michigan identified multiple materials with high usable volumetric capacities by computational screening of MOF structure databases. Several MOFs were synthesized and their hydrogen adsorption properties were analyzed, experimentally confirming the predicted values.

Engineering

In FY 2017, NREL, in collaboration with Savannah River National Laboratory and PNNL, continued efforts to maintain and improve the usability and interface of the various models developed through the Hydrogen Storage Engineering Center of Excellence. The models are publicly available and continue to be a valuable tool for the hydrogen storage research community. Additionally, Savannah River National Laboratory continued leveraging the system models and system engineering expertise from the Hydrogen Storage Engineering Center of Excellence to design a materials-based storage system for use on a U.S. Navy unmanned underwater vehicle and provided a bench-scale prototype for evaluation. Preliminary analyses indicate a fuel cell system with alane (AlH_3) hydrogen storage can provide two to three times the energy storage of battery systems.

Specific accomplishments include:

- **System models development:** PNNL, NREL, and Savannah River National Laboratory completed a stand-alone isotherm data fitting routine to convert raw excess adsorption hydrogen data into its Dubinin-Astakhov parameters.
- **System models development:** NREL, Savannah River National Laboratory, and PNNL completed the executable stand-alone system design tools for both adsorbent and chemical hydrogen systems.
- **System development:** Savannah River National Laboratory refined engineering analysis to screen for the most attractive solid-state hydrogen storage material to meet Navy requirements for unmanned underwater vehicle application, performed testing to demonstrate alane storage and delivery performance against steady-state and transient operations, and prepared and delivered a bench-scale prototype system to the Naval Underwater Warfare Center for evaluation.

Testing & Analysis

In FY 2017, the Hydrogen Storage sub-program continued carrying out technoeconomic assessments of hydrogen storage technologies. Technical analysis and cost modeling of Type IV pressure vessel systems remained a critical focus during FY 2017. Analyses were performed to investigate strategies to improve carbon fiber utilization as a means of reducing cost. A focus in FY 2017 was to model performance attributes of cryo-compressed hydrogen storage systems for heavy-duty flight applications, specifically in comparison to compressed hydrogen for bus applications.

In addition, models were developed and used to analyze the onboard and off-board performance of physical and material-based automotive hydrogen storage systems. Independent systems analyses were conducted for DOE to gauge the performance of hydrogen storage systems. Interface issues and opportunities and data needs for technology development were also identified, and reverse engineering to define material properties needed to meet system-level targets was performed.

Specific accomplishments include:

- **Onboard performance of cryo-compressed systems:** Demonstrated that 2-mm stainless steel liner is preferable to aluminum liner in cryo-compressed hydrogen storage systems for buses. Showed that compared to the baseline 350-bar cryo-compressed hydrogen storage tanks currently in use, 500-bar cryo-compressed hydrogen storage tanks can achieve 66% improvement in gravimetric capacity, 132% increase in volumetric capacity, and 36% saving in carbon fiber composite. Also determined >7-day loss-free dormancy with 95% full 500-bar cryo-compressed hydrogen storage tanks.
- **Preliminary cryo-compressed hydrogen storage system cost:** Analysis showed that (1) balance of system is nearly half the total cost, (2) automated insulation wrapping is predicted to lead to insulation costs of ~$1.20/kWh at high volume, and (3) vacuum-degassing time uncertainty could lead to significant costs.

- **Preliminary savings for light-duty storage using cold compressed hydrogen:** Preliminary analysis suggests ~$2.50/kWh system savings are possible at 500 bar and 200 K.
- **Analysis of MOF-74 suggesting <$10/kg is achievable using liquid assisted grinding:** System-level cost with new MOF costs will be estimated in future work.
- **3,600 psi Type 4 compressed natural gas analysis:** The Institute for Advanced Composites Manufacturing Innovation, supported through the Office of Energy Efficiency and Renewable Energy's Advanced Manufacturing Office, provided specifications for two compressed natural gas vessels, one for potential use in light-duty vehicles and one for potential use in heavy-duty trucks. These specifications will be used to help validate the composite overwrapped pressure vessel cost models developed for compressed natural gas systems and to help establish a baseline for the Institute for Advanced Composites Manufacturing Innovation compressed gas storage efforts.

BUDGET

The FY 2017 budget request allocated $15.6 million to the Hydrogen Storage sub-program. This is consistent with the FY 2016 congressional appropriation of $15.6 million. In FY 2017, the Hydrogen Storage sub-program funds supported innovative R&D to lower the cost of high-pressure storage systems through low-cost carbon fiber precursors, demonstrate alternative fibers and resins, and identify innovative approaches to tank design. FY 2017 funds supported a variety of early-phase R&D efforts on advanced hydrogen storage materials and allowed for their coordination through the HyMARC efforts to ensure impact was maximized and resources were effectively utilized.

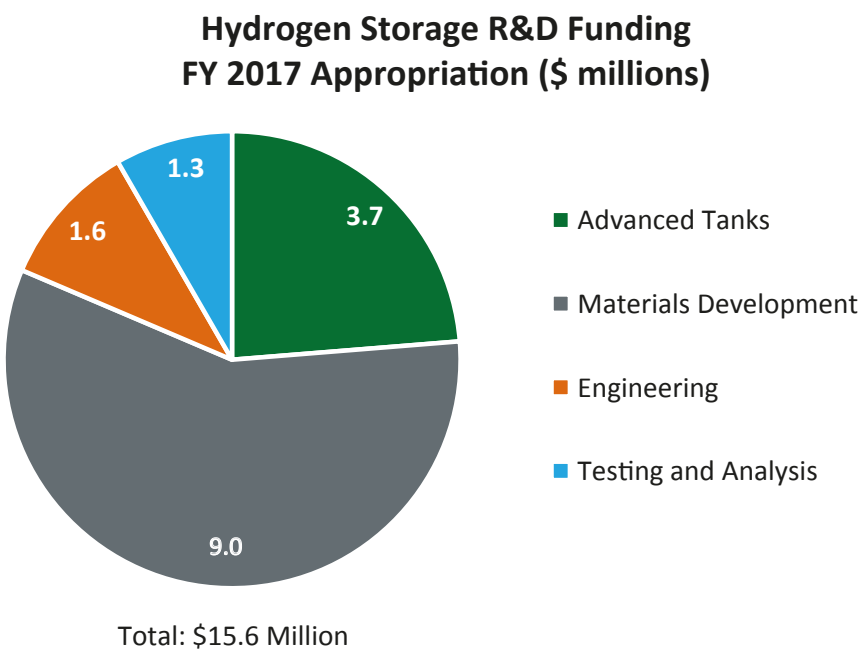

FIGURE 3. FY 2017 Appropriations

UPCOMING ACTIVITIES AND PLANS

The technology portfolio for the Hydrogen Storage sub-program will continue with a two-pronged approach focused on reducing the cost of high-pressure storage systems in the near term and increasing the capacity and overall performance of cold/cryo-compressed and material-based hydrogen storage systems for the long term to meet the Hydrogen Storage sub-program's revised 2020, 2025, and ultimate goals. The sub-program will continue early-stage R&D efforts to develop lower-cost high-pressure hydrogen storage systems in the near term with specific focus on low-cost precursors for high-strength carbon fiber. The sub-program will also coordinate with the Vehicle Technologies and Advanced Manufacturing Offices within the Office of Energy Efficiency and Renewable Energy on related carbon

fiber composite activities. Specifically, the sub-program will continue to coordinate with and leverage efforts through the Institute for Advanced Composites Manufacturing Innovation, which is led by the Advanced Manufacturing Office, to develop approaches for manufacturing low-cost compressed gas storage systems. The sub-program will also continue to utilize the capabilities established through the HyMARC lab teams for early-stage R&D of materials and technologies to meet system targets for onboard automotive and non-automotive applications in the longer term. The sub-program's R&D activities will continue to be supported and informed by system performance and cost analysis efforts performed by Argonne National Laboratory and Strategic Analysis, Inc.

Ned Stetson
Hydrogen Storage Program Manager
Fuel Cell Technologies Office
Office of Energy Efficiency and Renewable Energy
U.S. Department of Energy
1000 Independence Ave., SW
Washington, DC 20585-0121
Phone: (202) 586-9995
Email: Ned.Stetson@ee.doe.gov

IV.A.1 System Analysis of Physical and Materials-Based Hydrogen Storage

Rajesh K. Ahluwalia (Primary Contact), T.Q. Hua, J-K Peng, and Hee Seok Roh
Argonne National Laboratory
9700 South Cass Avenue
Argonne, IL 60439
Phone: (630) 252-5979
Email: walia@anl.gov

DOE Manager: Katie Randolph
Phone: (240) 562-1759
Email: Katie.Randolph@ee.doe.gov

Project Start Date: October 1, 2004
Project End Date: Project continuation and direction determined annually by DOE

Overall Objectives

- Model various developmental hydrogen storage systems.
- Provide results to DOE for assessment of performance targets and goals.
- Develop models to "reverse-engineer" particular approaches.
- Identify interface issues, opportunities, and data needs for technology development.

Fiscal Year (FY) 2017 Objectives

- Perform ABAQUS[1] and fatigue analyses to determine carbon fiber (CF) and liner thicknesses in Type III cryo-compressed tanks for light-duty and commercial fuel cell vehicles.
- Conduct system analysis of cryo-compressed hydrogen (CcH_2) storage for fuel cell buses with emphasis on dormancy, durability, and capacity.
- Update reverse engineering analysis for hydrogen storage in sorbents.
- Update 700-bar compressed hydrogen (cH_2) storage system parameters.

Technical Barriers

This project addresses the following technical barriers from the Hydrogen Storage section of the Fuel Cell Technologies Office Multi-Year Research, Development, and Demonstration Plan.

(A) System Weight and Volume

(B) System Cost

(C) Efficiency

(E) Charging/Discharging Rates

(J) Thermal Management

(K) System Life-Cycle Assessments

Technical Targets

This project is conducting system-level analyses to address the DOE technical targets for onboard hydrogen storage systems.

- System gravimetric capacity: 1.8 kWh/kg
- System volumetric capacity: 1.3 kWh/L
- Minimum H_2 delivery pressure: 5 bar
- Refueling rate: 1.5 kg/min
- Minimum full flow rate of H_2: 0.02 g/s/kW

FY 2017 Accomplishments

- Conducted autofrettage and fatigue analyses to determine the metal liner thickness for cryo-compressed Type III tanks. Demonstrated that 2-mm stainless steel liner is preferable to aluminum liner for fuel cell buses.
- Performed system analysis for cryo-compressed hydrogen storage for fuel cell buses. Showed that compared to the baseline 350-bar cH_2 tanks currently in use, 500-bar CcH_2 can achieve 66% improvement in gravimetric capacity, 132% increase in volumetric capacity, and 36% savings in carbon fiber composite. Determined >7-d loss free dormancy with 95% full 500-bar CcH_2 tanks.
- Updated analysis for 700-bar cH_2 storage. Showed that reducing the ambient temperature to 15°C and tank empty pressure to 10 bar can save ~3% CF, and the alternate tank design can save ~5% CF.
- Updated reverse engineering analysis for hydrogen storage in sorbents. Improved the heat transfer module in system analysis code to account for temperature dependence of medium thermal conductivity, and thermal resistance models in MOF-5 (metal organic framework) with random and layered enhanced natural graphite.

[1] ABAQUS is a software package for finite element analysis and computer-aided engineering.

INTRODUCTION

Several different approaches are being pursued to develop onboard hydrogen storage systems with the goal of meeting the DOE targets for light-duty vehicle applications. Each approach has unique characteristics, such as pressure and temperature, the thermal energy and temperature of charge and discharge, and kinetics of the physical and chemical process steps involved. The approaches take into account the requirements for the materials and energy interfaces between the storage system, the fuel supply system, and the fuel user. Other storage system design and operating parameters influence the projected system costs as well. Models are being developed to understand the characteristics of storage systems based on the various approaches and to evaluate their potential to meet the DOE targets for onboard applications—including the off-board targets for energy efficiency.

APPROACH

The approach is to develop thermodynamic, kinetic, and engineering models of the various hydrogen storage systems being developed under DOE sponsorship. These models are then used to identify significant component and performance issues and to assist DOE and its contractors in evaluating alternative system configurations and design and operating parameters. Performance criteria are established that may be used, for example, in developing storage system cost models. Data is refined and validated as the models become available from the various developers. An important aspect of this work is to develop overall system models that include the interfaces between hydrogen production and delivery, hydrogen storage, and the fuel cell.

RESULTS

Physical Storage – Cryo-Compressed Storage for Buses

We analyzed the cryo-compressed hydrogen storage option in buses with a particular focus on dormancy. The storage tank is a Type III tank; it consists of a stainless steel (SS) 316 or Al 6061-T6 alloy liner wrapped with T700 CF designed to withstand 225% of the nominal storage pressure with a minimum fatigue life of 15,000 cycles [1]. The storage system, shown schematically in Figure 1, consists of four tanks that hold 40 kg usable H_2. Each tank is surrounded by a vacuum gap (10^{-5} torr) filled with multi-layer vacuum superinsulation (MLVSI). A thin aluminium outer shell,

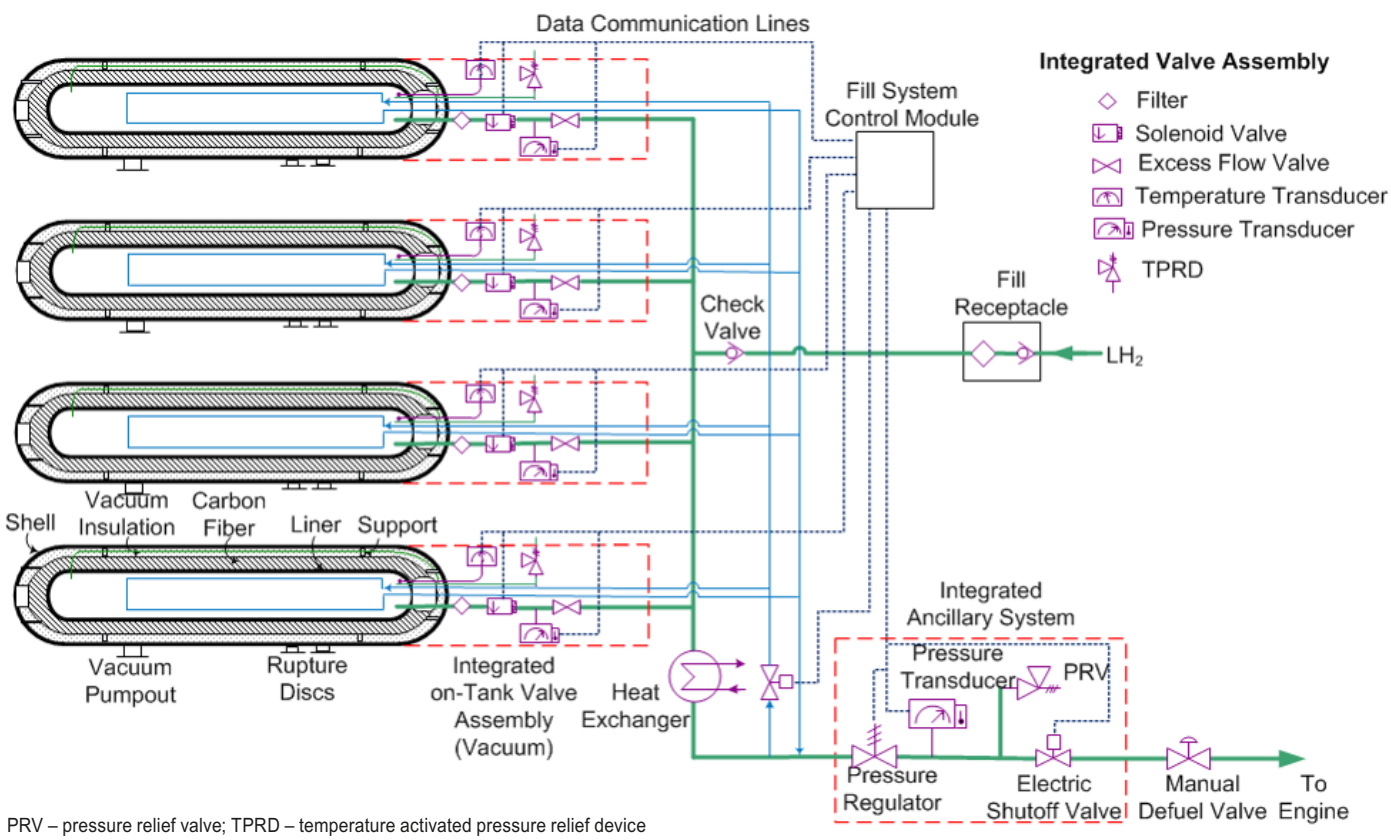

PRV – pressure relief valve; TPRD – temperature activated pressure relief device

FIGURE 1. Cryo-compressed hydrogen storage system for fuel cell buses

separated from the inner tank by two G-10 space rings, completes the main vessel. The thickness of the insulation was determined so as to limit the heat transfer rate from the ambient to 10 W.

We considered two options for extending the fatigue life of the cryo-compressed tank: AF1 – the tank is autofrettaged at room temperature, then cooled to cryogenic temperature; AF2 – the tank is first cooled to cryogenic temperature before autofrettage is carried out. Results show that in AF1 the liner is in compression following autofrettage, but thermal stress induced during cool-down causes it to be in tension. In AF2, the liner is in tension after cool-down but reverses to compression post-autofrettage, and the cylinder section has undergone plastic deformation due to thermal stress during the cool-down step. Figure 2 shows the fatigue life for tanks with a SS liner and length-to-diameter (L/D) ratio of 5, storing 10 kg usable H_2 at 84 K. Two liner thicknesses (1 mm and 2 mm) and three storage pressures (350 bar, 500 bar, and 700 bar) were analyzed. For fixed liner thickness, the fatigue life decreases with increasing storage pressure because of higher cycling stress amplitude. If autofrettage is performed at cryogenic temperature, the fatigue life improves as a result of the increase in yield stress and strain hardening behavior of metals at low temperatures. The improvement over room temperature autofrettage (AF1) is more pronounced for the thicker liner. It is noted that fatigue is not an issue with a 2-mm SS liner because its fatigue life exceeds 15,000 cycles (red dashed line in Figure 2). For storage pressure up to 50 MPa, even a 1-mm SS liner meets the fatigue life requirement. We also analyzed aluminum liner and found that the liner needs to be thicker than 15 mm to meet the required 15,000 cycles. The thick liner adds excessive amount of weight and volume to the tank. Based on these results, the choice of liner material for a cryo-compressed storage tank strongly favors stainless steel over aluminum.

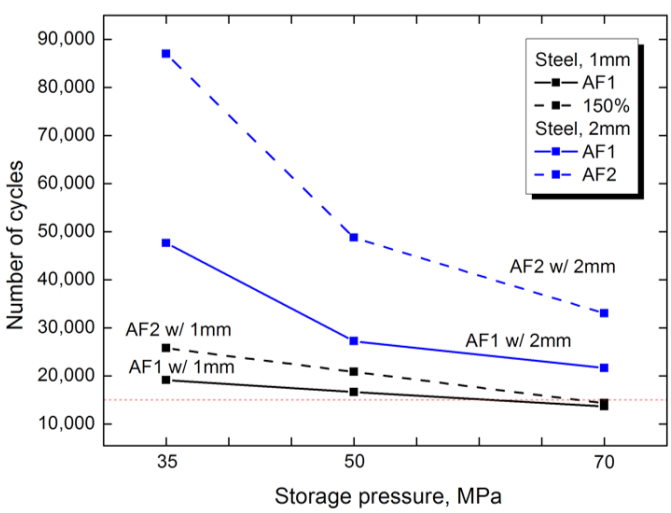

FIGURE 2. Fatigue life for Type III tanks with stainless steel liner

Table 1 shows the reference values and the range for the storage system parameters. The nominal storage pressure is 500 bar with an empty pressure of 5 bar. The storage temperature (107.9 K) and discharge temperature (47.1 K) are determined by liquid hydrogen (LH_2) refueling and the pump efficiency. In our analysis, the pump efficiency is derived from data gathered by BMW [2] on a 350-bar Linde pump as well as data gathered by Lawrence Livermore National Laboratory [3] on an 875-bar Linde pump. The pump isentropic efficiency is calculated from the flow rate, pump power, pump inlet and outlet pressure and temperature. Although LH_2 is used for refueling, hydrogen is stored in supercritical state in the tanks after being pumped to the storage pressure. In order to maintain the supercritical state at all times, a small amount of heat must be supplied to the tank during discharge to prevent liquid formation. Heat can be supplied via a small heater or an in-tank heat exchanger that recirculates a fraction of warm hydrogen back into the tank (see Figure 1). Our analysis shows that an average of 53 W is needed to maintain hydrogen in a single supercritical phase for a tank that discharges in one day, and 35 W is needed for a tank that discharges over three days.

Analysis was carried out for storage pressure ranging from 350 to 700 bar to compare the key performance metrics. For fixed empty pressure at 5 bar, the percentage of recoverable H_2 increases slightly with storage pressure. Because of pressure-volume work, the storage temperature is also higher at higher pressure; thus, the increase in storage density is not very significant. Doubling the pressure from 350 to 700 bar raises the storage density by just 16.7%. Although higher pressure results in higher storage density, it has little effect on the volumetric capacity. The improvement in storage density is negated by the increase in the amount of CF overwrap. In fact, the volumetric capacity is lower at 700 bar (42.2 g/L) than it is at 350 bar (42.4 g/L) or 500 bar (43.0 g/L). The added weight in CF reduces the gravimetric capacity from 8.4 wt% at 350 bar to 7.3 wt% at 500 bar and 6 wt% at 700 bar. CF and liner dominate the weight and account for 73% of the tank weight at 500 bar. The liner and shell thicknesses are the same for all storage pressures, so their weights vary only slightly in relation to tank size. Hydrogen has the largest share of volume. At 500 bar, the volumetric efficiency (H_2 volume divided by tank volume) is 73%. Compared to the current baseline 350-bar compressed hydrogen storage (ambient temperature) for fuel cell buses, the 500-bar cryo-compressed storage option can achieve 66% improvement in gravimetric capacity, 132% increase in volumetric capacity, and 36% savings in CF composite.

The dormancy, measured in watt-days, for the three storage pressures is shown in Figure 3a as a function of the initial amount of H_2 in the tank. Venting is initiated when the tank pressure reaches 1.25 times the nominal storage pressure. The effect of endothermic para-to-ortho conversion is included in dormancy calculations. While dormancy

TABLE 1. System Parameters for Cryo-Compressed Hydrogen Storage in Fuel Cell Buses

System Parameter	Reference Value[1]	Range[1]	Comment
Storage Pressure	500 bar	350–700 bar	Type III carbon fiber wound tank
Empty Pressure	5 bar	5–10 bar	Minimum delivery pressure set by fuel cell system
Storage Volume[2]	4 x 169 L	4 x 155–183 L	40 kg usable H_2
Storage Temperature	107.9 K	93–123 K	Determined by LH_2 refueling and LH_2 pump efficiency
Discharge Temperature	47.1 K	47.1–49.5 K	Function of duty cycle, 1–3 day discharge time
Heat Rate	4 x 53 W	4 x 52–70 W	Repeat charge-discharge cycle
Refueling Rate	1.6 kg/min	5 kg/min target	Set by LH_2 pump capacity
Tank Aspect Ratio	L/D = 5	L/D = 3-5	
Liner Thickness	2-mm SS	9.5–15.2 mm Al	SAE J2579: 11,250 duty cycles; ABAQUS FE-SAFE Model
Autofrettage Pressure	1.5 x NWP		Same as proof pressure
Carbon Fiber Amount	4 x 64.2 kg	4 x 43.2–96.2 kg	T700 CF; SAE J2579: 2.25 Safety Factor; ABAQUS-Wound Composite Modeler.
Insulation Thickness	7.4 mm	6.9–8.1 mm	10 W heat gain, MLVSI

[1] Unless noted otherwise, results are for SS liner and high-efficiency LH_2 pump
[2] Refers to gas (empty tank) volume
NWP – nominal working pressure

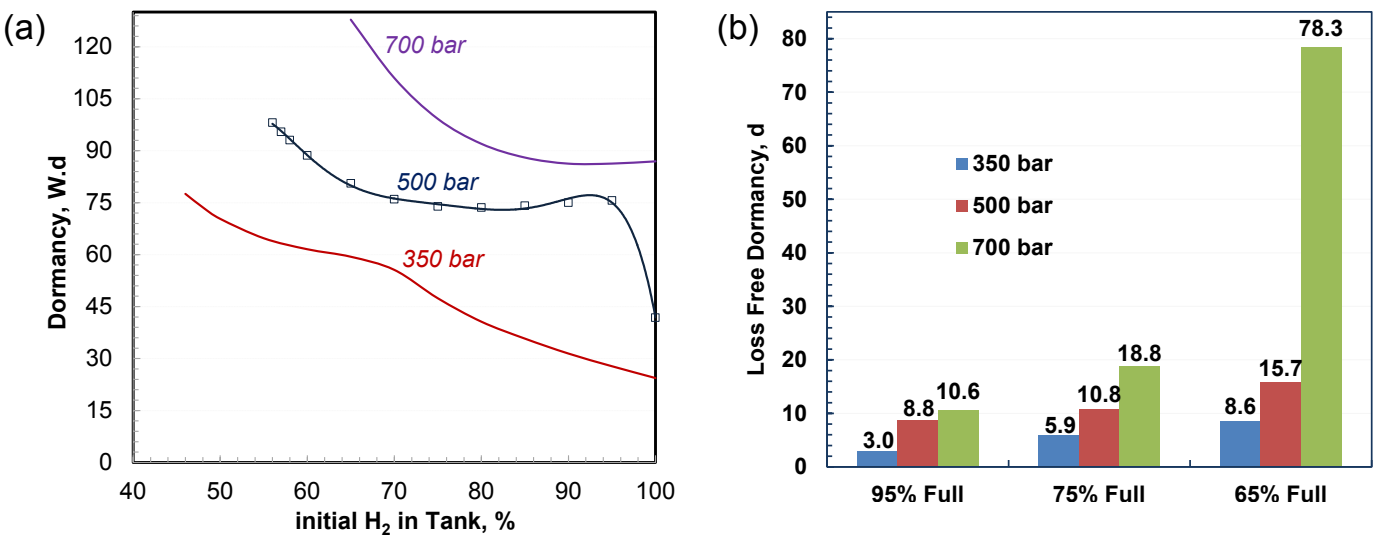

FIGURE 3. Dormancy measured in (a) watt-days and (b) days for various amounts of H_2 in tank

increases with increasing pressure, the increase also depends on the amount of H_2 stored, as shown in Figure 3b. Compared to 350-bar storage, the dormancy for a 700-bar tank is higher by a factor of 3.5 when the tank is 95% full, and by a factor of 9 if the tank is 65% full. At the reference 500-bar pressure, the dormancy for 95% full tank exceeds the 7-day target.

Physical Storage – 700 bar Compressed

We updated the key system parameters for 700-bar compressed hydrogen storage to incorporate changes in (1) ambient temperature, (2) storage tank empty pressure, and (3) tank design. The ambient temperature was changed from 20°C to 15°C to be consistent with SAE[2] regulations [1]. The tank empty pressure, previously set at 20 bar with a one-stage pressure regulator, was reduced to 15 bar and 10 bar with a two-stage pressure regulator (used on current 700-bar tanks). Finally, an alternate tank design similar to the Mirai tank [4] was adopted to take advantage of the CF savings. These changes and their impact on system gravimetric and volumetric capacities as well as CF usage are summarized in

[2] SAE International, formerly known as the Society for Automotive Engineers, is a body that sets standards to help ensure the safety, quality, and effectiveness of products and services across the mobility engineering industry.

Table 2. These changes are also expected to affect the system cost. The lower cost due to smaller tank size and less CF is partially offset by the higher cost for a two-stage pressure regulator. The CF savings are highlighted below.

- Reducing the ambient temperature from 20°C to 15°C reduces the CF amount by 1.1% because of a smaller tank size.
- Reducing the tank empty pressure increases the usable hydrogen and reduces CF usage by 1.1%–2.1%.
- The alternate tank design produces the largest savings in CF of nearly 5%.

Hydrogen Storage in Sorbents

We updated our reverse engineering analysis for hydrogen storage in sorbents. We analyzed the adsorption isotherm data for MOF-5, which was acquired and provided to us by the Hydrogen Storage Engineering Center of Excellence [5]. The data for both powder and pellets of various compact densities with and without expanded natural graphite (ENG) additives, and measured over a wide range of temperatures (77–295 K), were included in our analysis. To utilize the data for our reverse engineering study, the data were fitted to a single Langmuir equation of the form

$$N_e = \left(N_{\max} - V_a \rho_g\right)\left(\frac{K_1 P}{1+K_1 P}\right) = N_{\max}\left(1 - v_a \rho_g\right)\left(\frac{K_1 P}{1+K_1 P}\right) \quad (1)$$

$$K_1 = \frac{C_1}{\sqrt{T}} e^{\frac{E_1}{RT}} \quad (2)$$

The single-Langmuir equation is very appealing for reverse engineering since it only has four parameters (N_{max}, v_a, C_1, E_1), three of which can be related to physical material properties. N_{max} may be regarded as the sorption capacity (g-H_2/kg) of the sorbent, i.e., the maximum absolute uptake if all the active sites are occupied with H_2. Figure 4 shows the reference onboard system used in the reverse engineering analysis. Within our system performance analysis model, the heat transfer analysis was improved to incorporate (1) the temperature dependence of the medium thermal conductivity with various amounts of ENG, (2) a series-parallel thermal resistance model for MOF-5 and random ENG additives, and (3) a parallel resistance model for heat transfer in layered ENG structures. Table 3 summarizes the results of the reverse engineering analysis. Compared to our previous analysis, there is >25% smaller target uptake with improved thermal conductivity, lower ENG weight fraction, and more compact heat exchanger.

CONCLUSIONS AND UPCOMING ACTIVITIES

- The fatigue analysis shows that a 2-mm SS liner in a cryo-compressed tank for fuel cell buses meets the fatigue cycle life requirement for storage pressure up to 700 bar. Aluminum liner is not a good choice because its thickness exceeds 15 mm and it adds excessive amount of weight and volume to the tank.
- Autofrettage carried out at cryogenic temperatures (AF2) enhances the fatigue life of the liner over room temperature autofrettage (AF1). The improvement is more pronounced for thicker liners.
- Compared to the baseline 350-bar cH_2 tanks currently in use for fuel cell buses, 500-bar CcH_2 can achieve 66% improvement in gravimetric capacity, 132% increase in volumetric capacity, and 36% savings in CF composite.
- Dormancy is a function of storage pressure and the initial H_2 amount in tank. At the reference 500-bar pressure, the dormancy for 95% full tank exceeds the 7-day target.
- For 700-bar cH_2 storage, reducing the ambient temperature from 20°C to 15°C and the empty tank pressure from 20 bar to 10 bar reduces the CF amount by 3.2%.
- Compared to our previous reverse engineering analysis of hydrogen storage in sorbents, there is >25% smaller target uptake with improved thermal conductivity, lower ENG weight fraction, and more compact heat exchanger.

TABLE 2. System Parameters for Various Combinations of Ambient Temperature, Tank Empty Pressure, and Tank Design

	A	B	C	D	E	F
Empty pressure, bar	20[1]	20	15[2]	10[3]	15	10
Ambient temperature, °C	20	15	15	15	15	15
Tank design	Conv.	Conv.	Conv.	Conv.	Alt.	Alt.
CF composite, kg	97	95.9	94.9	93.9	90.3	89.3
Gravimetric capacity, wt%	4.19	4.23	4.26	4.29	4.41	4.45
Volumetric capacity, g-H_2/L	24.38	24.64	24.88	25.13	25.23	25.48

[1] Quantum two-stage pressure regulator
[2] Aerodyne Controls two-stage pressure regulator
[3] JTEKT two-stage pressure regulator used in Toyota Mirai, empty pressure unknown
Conv. – conventional; Alt. – alternative

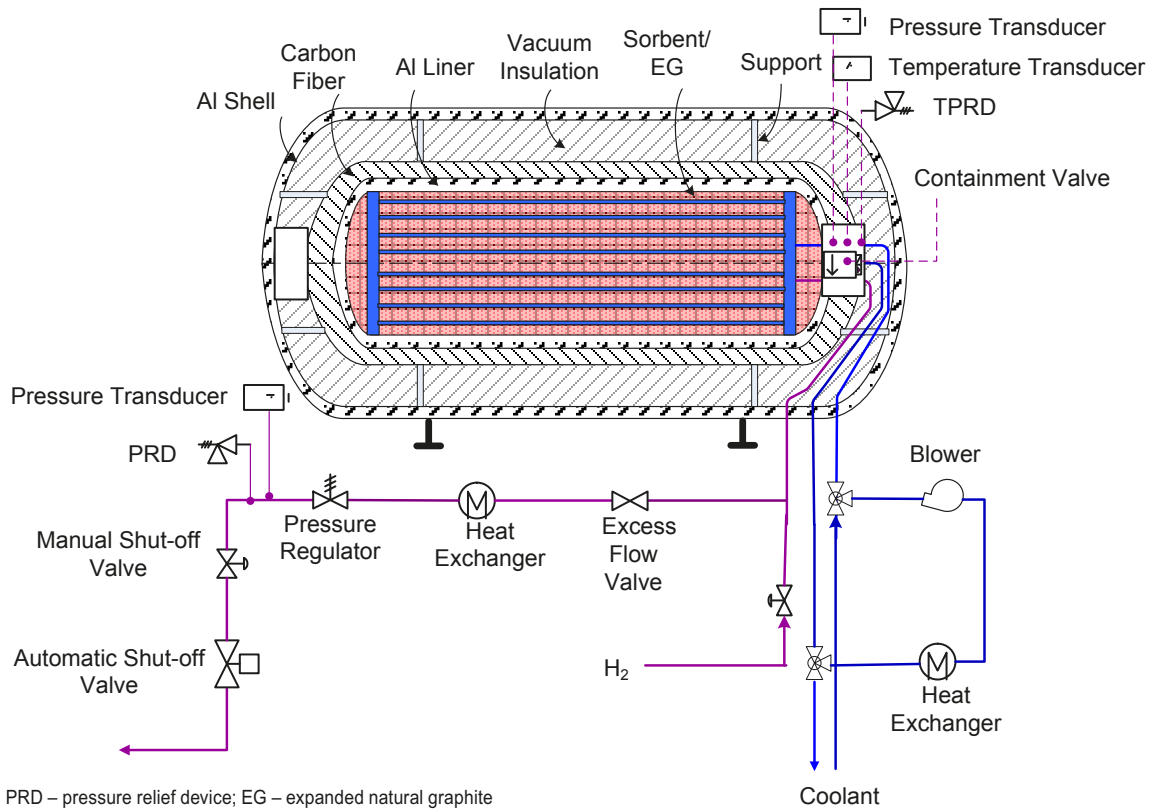

FIGURE 4. Reference onboard system for hydrogen storage in sorbents

TABLE 3. Reference Values for Meeting Onboard Targets

	Material Targets 2014	Material Targets 2017	Comments
Operating Pressures and Temperatures			
Storage Pressure (P)	100 bar	100 bar	
Storage Temperature (T)	155 K	155 K	20 K above coolant T
Discharge Pressure (P_d)	5 bar	5 bar	In addition to P swing, 60-K
Temperature Swing (DT)	60 K	60 K	DT allowed for 95% usable H_2
Off-board Coolant T (T_f)	135 K	135 K	55% well-to-tank efficiency
Material Properties			
Peak Excess Uptake at 77 K	190 g-H_2.kg^{-1}	**150 g-H_2.kg^{-1}**	5.5 wt% gravimetric capacity E_1 = 5 KJ.mol^{-1}
Excess Uptake at Storage P and T	120 g-H_2.kg^{-1}	**90 g-H_2.kg^{-1}**	V_a = 0.0125 m^3.kg^{-1} C_1 = 0.0053 atm.K$^{0.5}$
Medium Bulk Density	500 kg.m^{-3}	**530 kg.m^{-3}**	40 g.L^{-1} volumetric capacity
Bed Thermal Conductivity	1 W.m^{-1}.K^{-1}	**5.5 W.m^{-1}.K^{-1}**	
Added ENG	20-wt% Random	**5-wt% Layered**	

- In FY 2018, we will validate the impact damage model against Hexagon Lincoln test data and apply the model to determine the burst pressure after impact (degradation of tank safety factor).
- In FY 2018, we will validate the ABAQUS model against Pacific Northwest National Laboratory cryogenic burst test data for cold gas storage.

- In FY 2018, we will expand the system analysis of hydrogen storage in high-pressure, low-enthalpy metal hydrides.
- In FY 2018, we will analyze system performance with compacted sorbents using Hydrogen Storage Engineering Center of Excellence data for materials and prototypes.

FY 2017 PUBLICATIONS/PRESENTATIONS

1. R.K. Ahluwalia, J.K. Peng, and T.Q. Hua, "Cryo-Compressed Hydrogen Storage," Chapter 5 in Compendium of Hydrogen Energy, Vol. 2: Hydrogen Storage, Distribution and Infrastructure, R. Gupta, A. Basile, T.N. Veziroglu (Editors), Woodhead Publishing, 2016, 119–144.

2. N.T. Stetson, R.K. Ahluwalia, J.K. Peng, and G. Ordaz, "Characteristics of Low-Enthalpy Metal Hydrides Favorable for High-Pressure Hydrogen Storage Applications," 15th International Symposium on Metal-Hydrogen Systems, MH2016, Interlaken, Switzerland, August 7–12, 2016.

3. R.K. Ahluwalia, T.Q. Hua, J.K. Peng, and H.S. Roh, "System Level Analysis of Hydrogen Storage Options," Hydrogen Storage Tech Team Meeting, Southfield, MI, January 9, 2017.

4. T.Q. Hua, H.S. Roh, and R.K. Ahluwalia, "Performance Assessment of 700-bar Compressed Hydrogen Storage for Light Duty Fuel Cell Vehicles," Int J Hydrogen Energy 2017; 42:25121-25129.

REFERENCES

1. SAE TIR J2579. Standards for Fuel Systems in Fuel Cell and Other Hydrogen Vehicles. USA: Society of Automotive Engineers; 2016.

2. BMW, Personal Communication.

3. Salvador Aceves, Lawrence Livermore National Laboratory, Personal Communication (2016).

4. Yamashita, A., Kondo, M., Goto, S., and Ogami, N., "Development of High-Pressure Hydrogen Storage System for the Toyota "Mirai"," SAE Technical Paper 2015-01-1169, 2015, doi:10.4271/2015-01-1169.

5. M. Veenstra and J. Purewall, Ford, Personal Communication (2016).

IV.A.2 Hydrogen Storage Cost Analysis

Brian D. James (Primary Contact),
Cassidy Houchins, Daniel D. DeSantis,
Jennie M. Huya-Kouadio
Strategic Analysis, Inc.
4075 Wilson Blvd. Ste. 200
Arlington, VA 22203
Phone: (703) 778-7114
Email: bjames@sainc.com

DOE Manager: Katie Randolph
Phone: (240) 562-1759
Email: Katie.Randolph@ee.doe.gov

Contract Number: DE-EE0007601

Subcontractors:
- Argonne National Laboratory (ANL), Argonne, IL
- Pacific Northwest National Laboratory (PNNL) Richland, WA

Project Start Date: October 1, 2016
Project End Date: September 30, 2020

Overall Objectives

- Identify and/or update the configuration and performance of a variety of H_2 storage systems for both vehicular and stationary applications.
- Conduct rigorous cost estimates of multiple H_2 storage systems to reflect optimized components for the specific application and manufacturing processes at various rates of production.
- Explore cost parameter sensitivity to gain understanding of system cost drivers and pathways to lowering system cost.

Fiscal Year (FY) 2017 Objectives

- Assess the cost and performance of cryo-compressed (CcH_2) for onboard fuel cell electric bus (FCEB) H_2 storage.
- Assess the impact of alternative linker chemistries on the high-volume cost of metal organic framework (MOF) H_2 storage materials.
- Investigate potential cost savings of cold compressed H_2.
- Establish a baseline cost for Type IV compressed natural gas (CNG) storage in support of the Institute for Advanced Composite Manufacturing Innovation.

Technical Barriers

This project addresses the following technical barriers from the Hydrogen Storage section of the Fuel Cell Technologies Office Multi-Year Research, Development, and Demonstration Plan.

(B) System Cost

(H) Balance of Plant (BOP) Components

(K) System Life-Cycle Assessments

Technical Targets

This project conducts cost modeling to attain realistic, process-based system costs for a variety of H_2 storage systems, helping to inform progress towards meeting the DOE 2020 and ultimate technical targets for hydrogen system storage cost and performance.

- System storage cost: $10/kWh (2020), $8/kWh (Ultimate)
- Specific energy: 1.8 kWh/kg (2020), 2.5 kWh/kg (Ultimate)
- Energy density: 1.3 kWh/L (2020), 2.3 kWh/L (Ultimate)

FY 2017 Accomplishments

- Completed a preliminary cost analysis of CcH_2 onboard H_2 storage systems for FCEB applications (40 kg usable H_2) based on performance analysis by ANL and system design from Lawrence Livermore National Laboratory (LLNL).
- Completed an analysis of factory costs of MOF-74 based on alternative, low-cost linkers development and tested at Lawrence Berkeley National Laboratory.
- Completed an initial assessment of potential carbon fiber composite savings for Type 3 and Type 4 pressure vessels as a function of H_2 temperature and pressure.
- Completed a baseline analysis of CNG tank cost for 3,600 psi natural gas storage in Type 4 pressure vessels for light-duty and heavy-duty onboard storage.

✧ ✧ ✧ ✧ ✧

INTRODUCTION

The Fuel Cell Technologies Office has identified H_2 storage as a key enabling technology for advancing H_2 and fuel cell technologies and has established goals of developing and demonstrating viable H_2 storage technologies

for transportation and stationary applications. The cost assessment described in this report supports the overall Fuel Cell Technologies Office goals by identifying the impact of advances in components, performance levels, and manufacturing/assembly techniques on storage system cost at a variety of annual manufacturing rates. The results of this analysis enable the DOE to compare the cost impact of new components, etc., to the intermediate and ultimate DOE cost targets. The cost breakdown of the system components and manufacturing steps can then be used to guide future research and development decisions.

APPROACH

A Design for Manufacture and Assembly (DFMA®) style cost analysis methodology was used to assess the materials and manufacturing cost of hydrogen storage systems and components. Key system design parameters and engineering system diagrams describing system functionality and postulated manufacturing process flows were obtained from a combination of industry partners, ANL, PNNL, and internal analysis. This data was used to develop a mechanical design of each component, including materials, dimensions, and physical construction. Based on this design, the manufacturing process train was modeled to project the cost to manufacture each part. Cost was based on the capital cost of the manufacturing equipment, machine rate of the equipment, equipment tooling amortization, material costs, and financial assumptions. Once the cost model was complete for the system design, sensitivity data for the modeled technology was obtained by varying key parameters. Results were shared with ANL, PNNL, and industry partners to obtain feedback and further refine the model.

The analysis explicitly includes fixed factory expenses such as equipment depreciation, tooling amortization, utilities, and maintenance as well as variable direct costs such as materials and labor. However, because this analysis is intended to model manufacturing costs, a number of components that usually contribute to the original equipment manufacturer price are explicitly not included in the modeling. The following costs are excluded in this analysis: profit and markup, one-time costs for non-recurring research/design/engineering expenses, and general expenses such as general and administrative costs, warranties, advertising, and sales taxes.

RESULTS

Cryogenic H_2 storage: Cryogenic H_2 storage for FCEBs was investigated this year. A system diagram is shown in Figure 1 and system assumptions are summarized in Table 1.

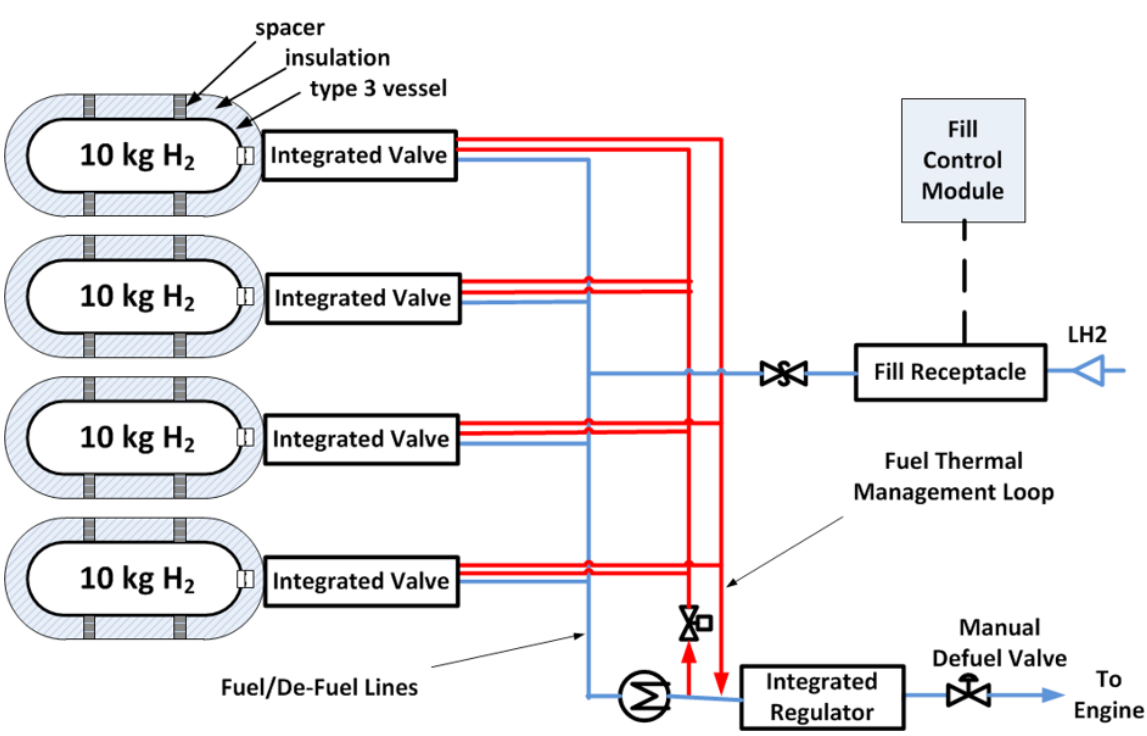

FIGURE 1. System schematic of a 40 kg $H_{2,\ usable}$ cryo-compressed storage system for FCEB applications. Integrated valves are external to the outer containment vessels and each one includes an inline filter, temperature transducer, pressure transducer, thermal pressure relief device, solenoid valve, and excess flow valve. The single integrated regulator includes a two-stage pressure regulator, pressure transducer, pressure relief valve, and an automatic shut-off valve. The fill control module has data communication lines connecting to the in-valve temperature and pressure transducers and the fill receptacle to communicate fill status to the fill station nozzle.

TABLE 1. System Parameters for CcH_2 Storage System with 40 kg Usable H_2 for FCEB Applications

Design Parameter	Base Case Value	Basis/Comment
Rated Storage Pressure	500 bar	ANL modeling assumption
Burst Pressure	1,125 bar	2.25 safety factor per SAE J2579
Minimum (Empty) Pressure	5 bar	Minimum fuel cell delivery pressure
Storage Temperature Range	93–123 K	ANL modeling assumption
Tank Volume (Water Capacity)	169.1 L	ANL modeling assumption
Usable H_2	10 kg	ANL modeling assumption
Pressure Vessel Dimension	176 cm x 35.2 cm	Internal length x diameter
Liner Thickness	2 mm	ANL modeling assumption
Carbon Fiber Type	T700S	ANL modeling assumption
Resin	Epoxy	ANL modeling assumption
Total Allowable Heat Leak	10 W	ANL modeling assumption
Insulation Thickness	7 mm	K_{eff} = 5E-5 W/m-K; $\Delta Q_{insulation} \leq 3W$
Vacuum Pressure (design)	10^{-3} Torr	LLNL feedback
Liner Material	316L	ANL modeling assumption
Vacuum Gap	8.4 mm	120% of minimum insulation thickness

Preliminary analysis of the 40 kg CcH_2 system resulted in a cost of ~$15/kWh when produced at 5,000 systems per year. A system cost breakdown at 5,000 systems per year is shown in Figure 2. The high balance of system cost (42%) reflects our current estimate that key components (regulator and valve) will be approximately twice as expensive as their ambient temperature counterparts as well as the additional complexity of thermal management associated with the cryogenic system.

Two main issues remain that lead to uncertainty in the system cost projection. First, balance of system components compatible with high pressure cryogenic H_2 are expected to be more expensive than similar components (e.g., regulator and valve) for 700 bar compressed H_2. How much more expensive these components are at high manufacturing volume is not currently well understood. Preliminary analysis of the valve at low volume suggests that the cost is similar for both the 700 bar compressed H_2 and the 500 bar CcH_2. Finally, the time to pump down the insulation gap can take up to one week for proto-type systems. We currently assume that the insulation gap can be pumped down in under 6 h.

MOF synthesis: In a paper authored by Strategic Analysis, Ford Motor Co., and Lawrence Berkeley National Laboratory, the cost of manufacturing MOFs at auto-relevant scale was estimated for traditional thermo-solvent methods, liquid assisted grinding (LAG), and aqueous solution synthesis [1]. Dramatic reductions in production cost are expected for alternative synthesis methods using little or no organic solvents (LAG and aqueous synthesis) and lead to MOF costs approaching $10/kg MOF. One limitation of the published analysis was that linker material costs were poorly understood at the volumes studied. To better understand linker costs, a full DFMA® style analysis of linker cost was conducted for two isomers of the MOF-74 linker based on recently reported results [2].

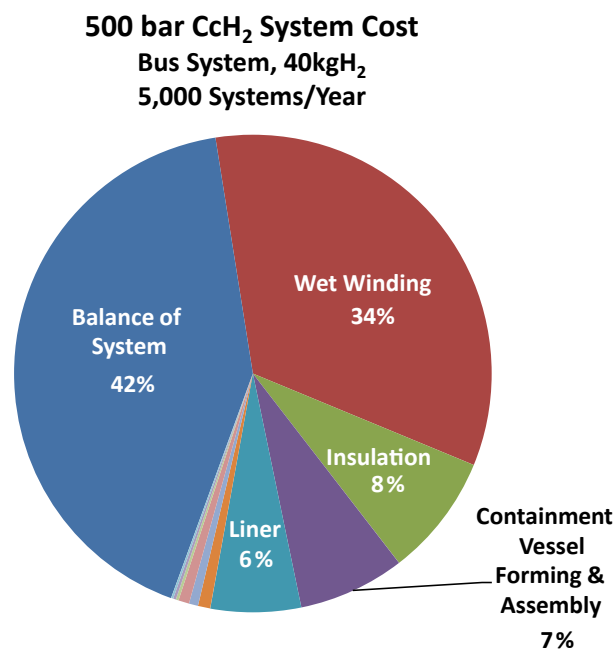

FIGURE 2. System cost breakdown for 40 kg $H_{2,\,usable}$ cryo-compressed storage system for FCEB applications manufactured at 5,000 systems per year.

The two MOF-74 linker isomers, 2,5-dioxido-1,4-benzenedicarboxylate (p-dobdc) and 4,6-dioxido-1,3-benzenedicarboxylate (m-dobdc) are prepared from different starting materials, hydroquinone and resorcinol, respectively. Linker synthesis costs were modeled based on methods described in the literature for p-dobdc [3] and for m-dobdc [4]. Figure 3 summarizes the cost to manufacture MOF-74 at 25,000 tonnes annually (sufficient for 500,000 vehicles with 50 kg MOF-74 per vehicle). MOF-74 costs are compared for the two linkers (p-dobdc and m-dobdc) prepared by solvothermal synthesis, aqueous synthesis, and LAG. This analysis suggests that MOF-74 prepared via LAG is $9.87/kg MOF using m-(dobdc) linker, and $14.57/kg MOF using p-(dobdc) linker.

Cold-compressed analysis: Finally, a computational survey of cold- and cryo-compressed H_2 storage systems was conducted to explore the cost impact of various temperature and pressure storage combinations. Figure 4 maps out regions of tank cost in hydrogen state space relative to the baseline 700 bar, 298 K Type 4 compressed H_2 storage vessel. Figure 4 shows that storage at 500 bar, 200 K has the potential to save around $3/kWh compared to the baseline pressure vessel at 700 bar and 298 K. Insulation and an outer containment vessel is estimated to add ~$0.50/kWh leading to an estimated potential $2.50/kWh savings for the pressure vessel.

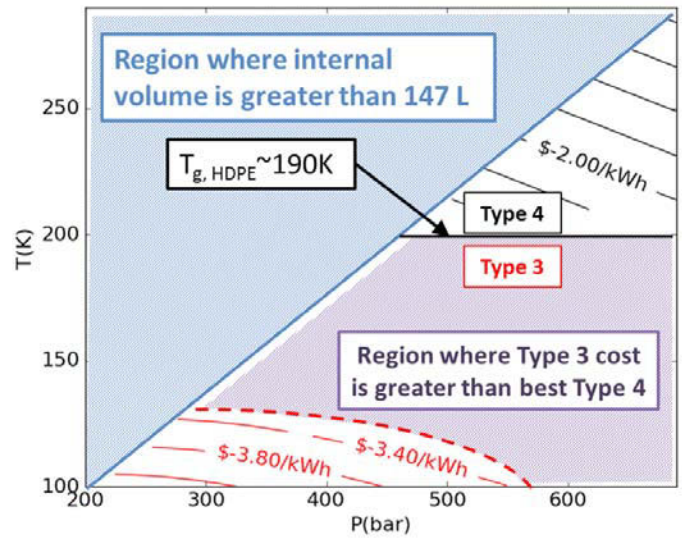

T – temperature; P – pressure

FIGURE 4. Potential cost savings for composite overwrapped pressure vessel with high-density polyethylene (HDPE) and 316 L liners. Costs are reported as relative to ambient temperature 700 bar Type 4 pressure vessels. Contour lines show constant cost savings.

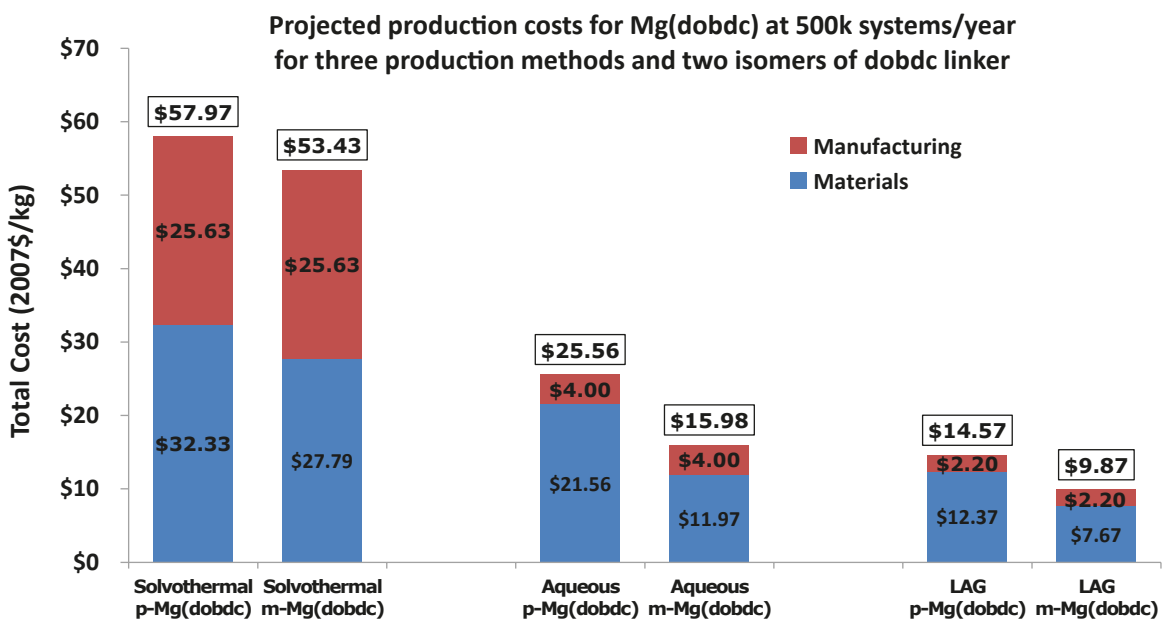

FIGURE 3. Comparison of production costs for MOF-74 (at 2,500 tonnes per year) for solvothermal, aqueous, and liquid assisted grinding using p-dobdc and m-dobdc linkers.

CONCLUSIONS AND UPCOMING ACTIVITIES

- CcH_2 storage system
  - Completed preliminary analyses for bus and light-duty vehicles.
  - In future, will finalize the analysis and publish an updated assessment of the cost and performance of CcH_2 for both bus and light-duty vehicle applications.
- MOFs can be manufactured at a cost of <$10/kg MOF using alternative linker materials and synthesis methods that minimize the use of organic solvents.
- Cold compressed H_2 (500 bar, 200 K) show promise to reduce system cost by ~$2.5/kWh; full system cost analysis will be completed to fully account for additional system costs.
- A baseline cost assessment for Type IV CNG storage was delivered to the Institute for Advanced Composite Manufacturing Innovation.

FY 2017 PUBLICATIONS/PRESENTATIONS

1. Brian D. James and Cassidy Houchins, "700 bar Type IV H_2 Pressure Vessel Cost Projections," presented at the Department of Energy Physical-Based Hydrogen Storage Workshop, Southfield, MI, 24-Aug-2016.

2. Cassidy Houchins, Daniel D. DeSantis, Jarad A. Mason, Brian D. James, Jeffrey R. Long, and Mike Veenstra, "Techno-economic analysis of metal-organic frameworks for onboard hydrogen and natural gas storage," presented at the 2016 AIChE Annual Meeting, San Francisco, CA, 16-Nov-2016.

3. D. DeSantis, J. A. Mason, B.D. James, C. Houchins, J.R. Long, and M. Veenstra, "Techno-economic analysis of metal-organic frameworks for hydrogen and natural gas storage," Energy Fuels, Jan. 2017.

4. Brian D. James and Cassidy Houchins, "Hydrogen Storage Cost Analysis," presented at the USCAR Hydrogen Storage Tech Team, Southfield, MI, 19-Jan-2017.

5. Brian D. James and Cassidy Houchins, "LDV and HDV CNG Storage System Analysis," presented at the Presentation to AMO, IACMI, and FCTO, Washington, D.C., 20-Jan-2017.

6. Brian D. James and Cassidy Houchins, "Hydrogen Storage Cost Analysis," presented at the 2017 DOE Hydrogen and Fuel Cells Program Review, Washington, D.C., 08-Jun-2017.

REFERENCES

1. DeSantis, Daniel, Jarad A. Mason, Brian D. James, Cassidy Houchins, Jeffrey R. Long, and Mike Veenstra, "Techno-Economic Analysis of Metal-Organic Frameworks for Hydrogen and Natural Gas Storage." *Energy & Fuels 31*, no. 2, January 2017.

2. M.T. Kapelewski *et al.*, "M_2(m-dobdc) (M = Mg, Mn, Fe, Co, Ni) Metal–Organic Frameworks Exhibiting Increased Charge Density and Enhanced H_2 Binding at the Open Metal Sites," *J. Am. Chem. Soc.*, vol. 136, no. 34, pp. 12119–12129, Aug. 2014.

3. Guang Dong Lei, Li Xin Li, Zhi Yun Lu, and Ming Gui Xie, "Improved One-pot Synthesis of 4,6-Dihydroxyisophthalic Acid and 2,3-Dihydroxyterephthalic Acid," *Chinese Chemical Letters*, vol. 16, no. 8, pp. 1039–1042, 2005.

4. D.J. Sikkema and A.M. Reichwein, "Process for dicarboxylating dihydric phenols," US6040478, Mar-2000.

IV.B.1 Hydrogen Storage System Modeling: Public Access, Maintenance, and Enhancements

Matthew Thornton (Primary Contact)[1],
David Tamburello[2], Kriston Brooks[3], and Sam Sprik[1]
[1]National Renewable Energy Laboratory
15013 Denver West Parkway
Golden, CO 80401
Phone: (303) 275-4273
Email: Matthew.Thornton@nrel.gov
[2]Savannah River National Laboratory (SRNL)
Savannah River Site, Bldg 999-2W
Aiken, SC 29808
Phone (803) 507-4449
Email: david.tamburello@srnl.doe.gov
[3]Pacific Northwest National Laboratory (PNNL)
P.O. Box 999
Richland, WA 99352
Phone (509) 372-4343
Email: kriston.brooks@pnnl.gov

DOE Managers:
Ned Stetson
Phone: (202) 586-9995
Email: Ned.Stetson@ee.doe.gov
Jesse Adams
Phone: (720) 356-1421
Email: Jesse.Adams@ee.doe.gov

Project Start Date: October 1, 2015
Project End Date: September 30, 2018

Overall Objectives

- Coordinate the public access of select models developed under the Hydrogen Storage Engineering Center of Excellence (HSECoE) activity, including web posting of documentation and tracking downloads and web activity.
- Maintain performance of existing storage system models and update and validate as new experimental data becomes available.
- Enhance and expand existing models to improve simulation speed and application to other uses. This will focus on expanding the parameterization of the models and their flexibility in evaluating new material candidates. This will initially include the development of pre-processor sizing routines for the adsorbent and chemical hydrogen systems followed by the metal hydride and cryo-compressed systems.

Fiscal Year (FY) 2017 Objectives

- Coordinate the public access of selected HSECoE models, including web posting of documentation and tracking downloads and web activity.
- Develop a stand-alone isotherm data fitting routine to convert raw excess adsorption hydrogen data into its Dubinin-Astakhov (D-A) parameters.
- Graphical user interface (GUI) update for user input capability and update storage system model web site documentation and manuals.
- Develop stand-alone system estimator: executable version of the sizing functions for adsorbent and chemical hydrogen (CH) storage system models to create first-order storage system estimates based on material properties.

Technical Barriers

This project addresses the following technical barriers from the Hydrogen Storage section of the Fuel Cell Technologies Office Multi-Year Research, Development, and Demonstration Plan.

(A) System Weight and Volume

(B) System Cost

(C) Efficiency

(E) Charging/Discharging Rates

(I) Dispensing Technology

(K) Systems Life-Cycle Assessments

Technical Targets

This project is conducting simulation and modeling studies of advanced onboard materials-based hydrogen storage technologies. Insights gleaned from these studies are being applied toward the hydrogen storage vessel design and materials synthesis that meet the following DOE 2020 hydrogen storage for light-duty vehicle targets.

- Storage system cost: \$333/kg $H_{2\ Stored}$
- System gravimetric capacity: 0.045 kg H_2/kg system
- System volumetric capacity: 0.030 kg H_2/L system
- Charging/discharging rates (5.6 kg H_2): 5 min
- Well to power plant efficiency: 60%

FY 2017 Accomplishments

- Completed a stand-alone isotherm data fitting routine to convert raw excess adsorption hydrogen data into its D-A parameters.
- Completed the update to the GUI for user input capabilities with documentation and updated the vehicle framework to add more user controls:
  - User can modify the chemical hydrogen material properties through the GUI in the chemical hydrogen storage system model.
- Completed the executable stand-alone system design tools for both the adsorbent and chemical hydrogen systems.
- Completed documentation updates for the posted models (including website text and downloadable user manual).
- Updated the website:
  - Added links to publications/abstracts.
  - Added relevant publications.
  - Moved vehicle framework section to the top and open by default.
- Troubleshooting of compiler and software versions.
- Tracked and monitored web activity and downloads.

✧ ✧ ✧ ✧ ✧

INTRODUCTION

Overcoming challenges associated with onboard hydrogen storage is critical to the widespread adoption of hydrogen-fueled vehicles. The overarching challenge is identifying a means to store enough hydrogen onboard to enable a driving range greater than 300 miles within vehicle-related packaging, cost, safety, and performance constraints. As new hydrogen storage materials are discovered and created, material developers must predict their full-scale vehicle performance and compare their performance with pure hydrogen storage (700 bar, cryo-compressed, and liquid H_2 storage). The goal of this work is to provide material developers with the modeling tools necessary to make these predictions based on the work done by the HSECoE.

APPROACH

The approach for FY 2017 is to complete updates, validate, enhance, troubleshoot, de-bug and document these models developed by the HSECoE so that they can be made accessible to and useful for other research within the hydrogen storage community. During subsequent years, these models will be updated with alternative storage system formulations, such as different isotherm models for adsorbents and alternative chemical reaction kinetic expressions for CHs. In addition, stand-alone system estimators that do not require special software will be developed to serve as a scoping tool for the new hydrogen storage materials that may be developed.

RESULTS

The following provides results from work completed this year with a focus on the coordination of the public access of select HSECoE models, including web posting of documentation and tracking downloads and web activity. The multi-lab team worked on the validation, refinement, GUI improvements, troubleshooting, and improving the simulation run time of the models. They also updated model documentation for selected web postings and monitored/tracked web activity and model downloads. To date there have been 164 downloads of the tank volume/cost model, 113 downloads of the framework model, 77 downloads of the metal hydride (MH) finite element model, and 47 downloads of the MH acceptability envelop.

A stand-alone isotherm data fitting routine was developed to convert raw excess adsorption hydrogen storage data into its D-A isotherm parameters. Based on the original isotherm data fitting codes developed by SRNL and the Université du Québec à Trois-Rivières, this data fitting routine takes the raw excess adsorption data along with the hydrogen properties and fits them to the D-A isotherm model. The fitting routine has a usable data range of 20 K < T < 400 K and 0.05 MPa < P < 72 MPa. The fitting routine was tested using several sets of MOF-5 and AX-21 excess adsorption data and was found to match the original HSECoE fitting routine results. These D-A parameters are used within several of the computational models, including the Simulink vehicle model framework. By allowing material developers to fit their excess adsorption data using a standard fitting routine like this one, they can more easily utilize the computational models being developed and updated through this work, including the standalone system size estimator and the full-scale vehicle framework model.

The current stand-alone isotherm data fitting routine has been completed using Mathcad®, but the team is continuing to work on the fitting routine next year with the plan of converting it into a MATLAB® script and, if possible, convert it into a stand-alone executable.

Also during this year, both PNNL and SRNL completed stand-alone executable storage system design tools for the chemical hydrogen and adsorbent material systems, respectively. These system design tools bridge the gap between the material properties as measured by hydrogen storage material developers and the information needed for the framework model to demonstrate that a material does or does not meet the DOE Technical Targets for light-duty vehicles.

Chemical Hydrogen Storage System Design Tool

The chemical hydrogen system design tool requires the reaction parameters, the hydrogen capacity, and the mass and thermal properties of a hydrogen storage material. The tool then estimates the size of the individual components that feed into the hydrogen storage model, and the control parameters required to successfully run the storage model within the framework. The total system mass and volume are also estimated and can be used to determine if a particular material is worth further consideration. If the material appears to provide reasonable gravimetric and volumetric system densities, the individual components sizes and control parameters can then be used in the framework for each of the four drive cycles and the onboard efficiency and range can be determined.

The system design tool is written in MATLAB and can be run separate from the framework or can be run as a GUI within the framework as shown in Figure 1. After the vehicle framework is opened, the GUI includes the option to change the material/design. This button opens a separate worksheet that allows the user to modify existing material properties and operating conditions and then run the system design tool to provide updated design parameters that can then replace the defaults in the framework.

This system design tool can also be run as an executable file for which the inputs are brought into the function using a user-selected Excel spreadsheet. The results of the model are then written as a separate output spreadsheet. By developing an executable file, no MATLAB license is required. Instead a free downloadable program called MATLAB Runtime is used to run the executable file and provide the results. This approach will allow materials researchers that are not familiar with and/or do not have MATLAB and Simulink to evaluate their materials and obtain estimates of system mass and volume for preliminary comparison to the DOE Technical Targets.

Chemical hydrogen storage model kinetics were originally based on an Avrami expression with either a single reaction or two independent, parallel reactions. The system design tool has been expanded to also consider n^{th} order reaction kinetics as well. In this case, the kinetics are

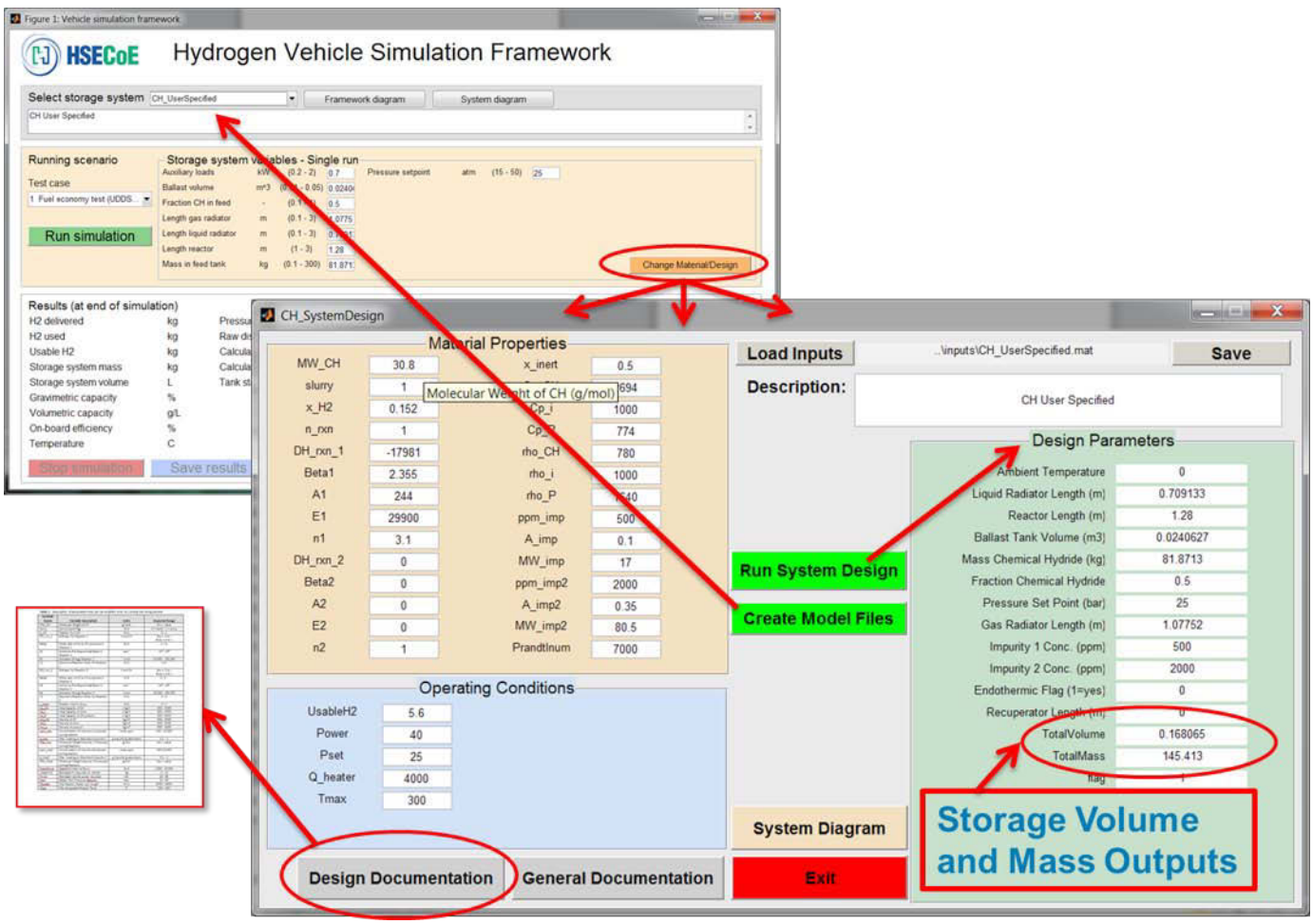

FIGURE 1. GUI format for the system design tool and its interaction with the Hydrogen Vehicle Simulation Framework

described as two series reactions of the form $A \rightarrow B + \beta_1 H_2 \rightarrow C + \beta_2 H_2$. This new analysis is described by the following kinetic expressions:

$$\left.\frac{\partial \alpha_1}{\partial t}\right|_{kinetics} = k_1\left[C_0\left(1-\alpha_1\right)\right]^{n_1} \qquad \left.\frac{\partial \alpha_2}{\partial t}\right|_{kinetics} = k_2\left[C_0\left(\alpha_1-\alpha_2\right)\right]^{n_2}$$

Two materials are included within the framework and have been used to exercise the system design tool. The first is ammonia borane, which is an example exothermic material. The second is alane, which is an example endothermic material. These are both modeled with the Avrami kinetic expression that was the initial kinetics expression within the vehicle framework. A carbon-boron-nitrogen (CBN) compound, 1,2 BN cyclohexane, is examined to evaluate the nth order kinetic model. The kinetics and thermodynamics of these materials are provided as input, while their output is shown in Table 1 below. The pure CBN material, which is a liquid, has a much smaller volume and mass than the other two materials that require 50% dilution to create a slurry. The CBN compound has an exothermic and an endothermic reaction in series.

TABLE 1. Calculated Chemical Hydrogen Parameters from the System Design Tool

Calculated System Parameter	Ammonia Borane	Alane	CBN
Total System Mass (kg)	133	188	117
Total System Volume (L)	146	161	135
System Gravimetric Capacity (kg H_2/kg system)	0.042	0.029	0.048
System Volumetric Capacity (kg H_2/L system)	0.038	0.035	0.041
Reactor Length (m)	0.64	1.28	2.3
Ballast Tank Volume (L)	14	22	32
Mass Chemical Hydride (kg)	77	128	70
Fraction Chemical Hydride	0.5	0.5	1
Liquid Radiator Length (m) (3 tubes)	2.4	1.6	0.9
Gas Radiator Length (m) (1 tube)	1.2	1.0	1.4
Recuperator Length (m) (3 tubes)	0	3.22	0.8
Startup Temperature (°C)	178	202	279
Ballast Time(s)	75	117	176

Adsorbent Hydrogen Storage System Design Tool

Similar to the chemical hydrogen design tool, the adsorbent hydrogen storage system design tool is MATLAB script that is both a part of the hydrogen vehicle simulation framework and an individual stand-alone executable design tool. It estimates the hydrogen storage system details, including the mass and volume, as well as the details of the individual components based on the material properties and the operating conditions. Note that the user cannot currently control the adsorbent materials properties within the GUI interface of the vehicle simulation framework, but this control will be included in the vehicle framework next year.

When running the stand-alone executable version of the adsorbent storage system design tool, the inputs are read into the script using a user-selected pre-formatted Excel spreadsheet, while the results are written to a separate spreadsheet. The user has full control over the operating conditions within 40 K < T < 400 K and 5.0 bar < P < 720 bar, but the user is limited to the operating conditions covered by the user's isotherm data that was used to create the materials properties. The adsorbent material's hydrogen properties must be converted into its D-A parameters, including the void volume. The user can also include the material's thermal properties and input an estimated cost. Finally, the user can choose other system-specific design parameters, such as the type of pressure vessel, the insulation thickness, and the adsorbent condition (either powder or compacted adsorbent). An example of the resulting output file for powder MOF-5, which includes the input parameters used to perform the calculation, is shown in Figure 2.

Several materials were used to test the executable stand-alone adsorption system design tool, including several forms of MOF-5 and activated carbon. Representative results of these materials are shown in Table 2. Note that the following design assumptions were used to make Table 2.

- Operating conditions: 80 K, 100 bar with swing to 160 K, 5 bar
- 5.6 kg of usable hydrogen (~5.714 kg of actual hydrogen storage)
- Type 1 aluminum pressure vessel
- LN_2 pressure vessel chiller channel thickness of 9.525 mm
- Uniform insulation thickness of 23 mm, with a 2 mm outer aluminum shell

Documentation has been completed for the stand-alone executable storage system design tools for the chemical hydrogen and adsorbent material systems, respectively. These system design tools bridge the gap between the material properties as measured by hydrogen storage material developers and the information needed for the framework model to demonstrate that a material does or does not meet the DOE Technical Targets for a light-duty vehicle. These stand-alone models, which include their documentation, are now accessible from the http://hsecoe.org website under model downloads (Table 3).

The Hydrogen Vehicle Simulation Framework model has been updated along with its documentation showing the added capability to design a storage system for the CH and adsorbent systems. Users can now access design parameters

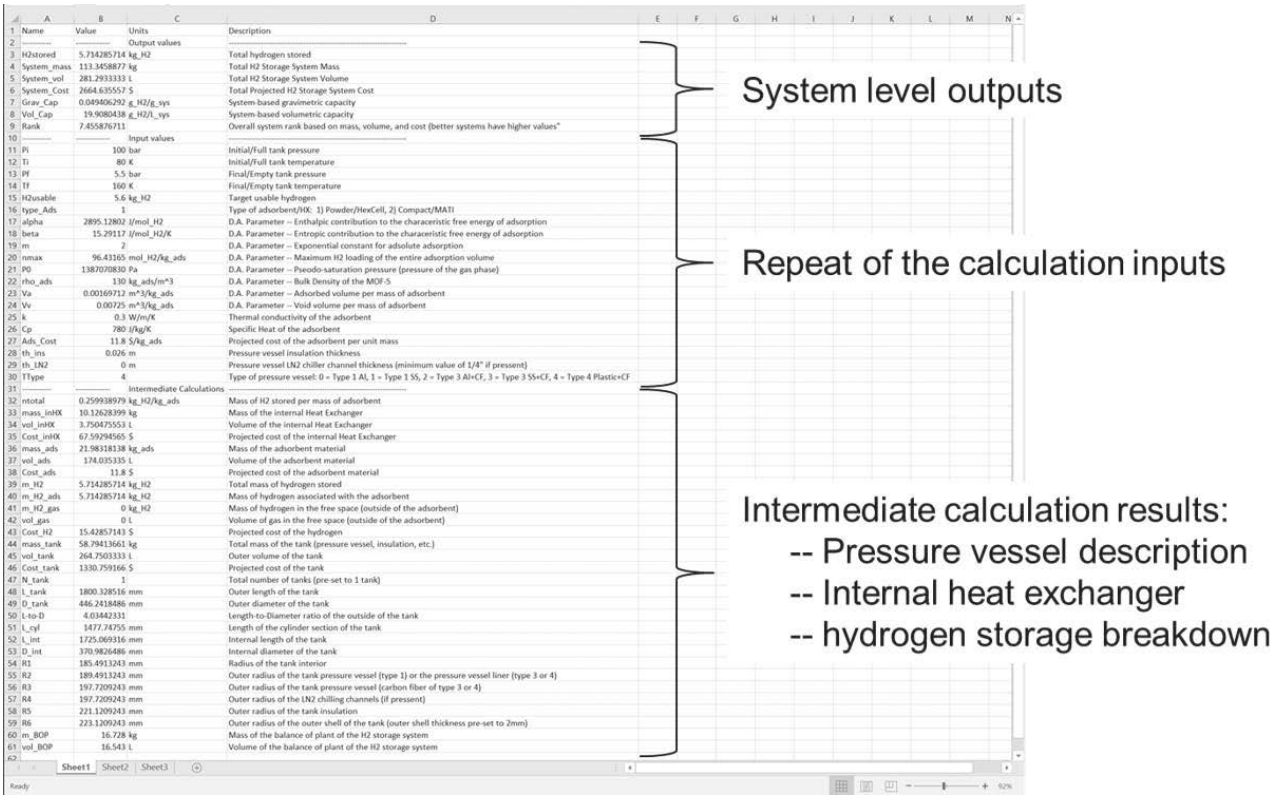

	Name	Value	Units	Description
1	Name	Value	Units	Description
2			Output values	
3	H2stored	5.714285714	kg_H2	Total hydrogen stored
4	System_mass	113.3458877	kg	Total H2 Storage System Mass
5	System_vol	281.2933333	L	Total H2 Storage System Volume
6	System_Cost	2664.635557	$	Total Projected H2 Storage System Cost
7	Grav_Cap	0.049406292	g_H2/g_sys	System-based gravimetric capacity
8	Vol_Cap	19.9080438	g_H2/L_sys	System-based volumetric capacity
9	Rank	7.455876711		Overall system rank based on mass, volume, and cost (better systems have higher values"
10			Input values	
11	Pi	100	bar	Initial/Full tank pressure
12	Ti	80	K	Initial/Full tank temperature
13	Pf	5.5	bar	Final/Empty tank pressure
14	Tf	160	K	Final/Empty tank temperature
15	H2usable	5.6	kg_H2	Target usable hydrogen
16	type_Ads	1		Type of adsorbent/HX: 1) Powder/HexCell, 2) Compact/MATI
17	alpha	2895.12802	J/mol_H2	D.A. Parameter -- Enthalpic contribution to the characeristic free energy of adsorption
18	beta	15.29117	J/mol_H2/K	D.A. Parameter -- Entropic contribution to the characeristic free energy of adsorption
19	m	2		D.A. Parameter -- Exponential constant for adsolute adsorption
20	nmax	96.43165	mol_H2/kg_ads	D.A. Parameter -- Maximum H2 loading of the entire adsorption volume
21	P0	1387070830	Pa	D.A. Parameter -- Pseudo-saturation pressure (pressure of the gas phase)
22	rho_ads	130	kg_ads/m^3	D.A. Parameter -- Bulk Density of the MOF-5
23	Va	0.00169712	m^3/kg_ads	D.A. Parameter -- Adsorbed volume per mass of adsorbent
24	Vv	0.00725	m^3/kg_ads	D.A. Parameter -- Void volume per mass of adsorbent
25	k	0.3	W/m/K	Thermal conductivity of the adsorbent
26	Cp	780	J/kg/K	Specific Heat of the adsorbent
27	Ads_Cost	11.8	$/kg_ads	Projected cost of the adsorbent per unit mass
28	th_ins	0.026	m	Pressure vessel insulation thickness
29	th_LN2	0	m	Pressure vessel LN2 chiller channel thickness (minimum value of 1/4" if pressent)
30	TType	4		Type of pressure vessel: 0 = Type 1 Al, 1 = Type 1 SS, 2 = Type 3 Al+CF, 3 = Type 3 SS+CF, 4 = Type 4 Plastic+CF
31			Intermediate Calculations	
32	ntotal	0.259938979	kg_H2/kg_ads	Mass of H2 stored per mass of adsorbent
33	mass_inHX	10.12628399	kg	Mass of the internal Heat Exchanger
34	vol_inHX	3.750475553	L	Volume of the internal Heat Exchanger
35	Cost_inHX	67.59294565	$	Projected cost of the internal Heat Exchanger
36	mass_ads	21.98318138	kg_ads	Mass of the adsorbent material
37	vol_ads	174.035335	L	Volume of the adsorbent material
38	Cost_ads	11.8	$	Projected cost of the adsorbent material
39	m_H2	5.714285714	kg_H2	Total mass of hydrogen stored
40	m_H2_ads	5.714285714	kg_H2	Mass of hydrogen associated with the adsorbent
41	m_H2_gas	0	kg_H2	Mass of hydrogen in the free space (outside of the adsorbent)
42	vol_gas	0	L	Volume of gas in the free space (outside of the adsorbent)
43	Cost_H2	15.42857143	$	Projected cost of the hydrogen
44	mass_tank	58.79413661	kg	Total mass of the tank (pressure vessel, insulation, etc.)
45	vol_tank	264.7503333	L	Outer volume of the tank
46	Cost_tank	1330.759166	$	Projected cost of the tank
47	N_tank	1		Total number of tanks (pre-set to 1 tank)
48	L_tank	1800.328516	mm	Outer length of the tank
49	D_tank	446.2418486	mm	Outer diameter of the tank
50	L-to-D	4.03442331		Length-to-Diameter ratio of the outside of the tank
51	L_cyl	1477.74755	mm	Length of the cylinder section of the tank
52	L_int	1725.069316	mm	Internal length of the tank
53	D_int	370.9826486	mm	Internal diameter of the tank
54	R1	185.4913243	mm	Radius of the tank interior
55	R2	189.4913243	mm	Outer radius of the tank pressure vessel (type 1) or the pressure vessel liner (type 3 or 4)
56	R3	197.7209243	mm	Outer radius of the tank pressure vessel (carbon fiber of type 3 or 4)
57	R4	197.7209243	mm	Outer radius of the LN2 chilling channels (if pressent)
58	R5	221.1209243	mm	Outer radius of the tank insulation
59	R6	223.1209243	mm	Outer radius of the outer shell of the tank (outer shell thickness pre-set to 2mm)
60	m_BOP	16.728	kg	Mass of the balance of plant of the H2 storage system
61	vol_BOP	16.543	L	Volume of the balance of plant of the H2 storage system

FIGURE 2. Executable stand-alone adsorbent system design tool output for powder MOF-5

TABLE 2. Representative Results from the Adsorbent Hydrogen System Design Tool

	Gravimetric Capacity [g_{H2}/g_{sys}]	Volumetric Capacity [g_{H2}/L_{sys}]	Source
MOF-5 Powder [130 kg/m^3]	0.0339 g/g	18.6 g/L	HSECoE
MOF-5 Compact [406 kg/m^3]	0.0314 g/g	21.4 g/L	HSECoE
DUT-23 (Co) Powder* [200 kg/m^3]	0.0348 g/g	20.7 g/L	Ford/Univ. of Michigan
IRMOF-20 Powder* [200 kg/m^3]	0.0341 g/g	20.3 g/L	Ford/Univ. of Michigan
MOF-5 Powder [200 kg/m^3]	0.0332 g/g	19.6 g/L	HSECoE

*Special thanks to Ford and the University of Michigan for sharing their data.

and material properties to input their own storage systems from the main GUI of the framework or work with the stand-alone models mentioned previously.

The models are available publicly through the HSECoE web page, where web site activity and model down loads are tracked. Figure 3 shows the latest web site activity over the three month period from April to June, 2017. The site received over 200 visitors during this time, with roughly 50% of those being new visitors. The bounce rate is 18%, indicating that 82% of the visitors browse further than the landing page, and have an average stay of over 5 min. Figures 4 and 5 provide the user flows for the site and user origin cities, respectively.

TABLE 3. HSECoE Models Available on Web Portal and Model Posting Status

Model Name	Lead	Status
MH Acceptability Envelop	SRNL	Complete
MH Finite Element Model	SRNL	Complete
Tank Volume/Cost Model	PNNL	Complete
MH Framework Model	SRNL	Complete
CH Framework Model	PNNL	Complete
Adsorption Data (AD) Framework Model	SRNL	Complete
AD Finite Element Model	SRNL	Model Complete*
Adsorption Data Fitting Routine	SRNL	Model Complete*
AD Stand-alone System Design Tool	SRNL	Complete
CH Stand-alone System Design Tool	PNNL	Complete

*Awaiting user's manual completion before the model is released to the public.

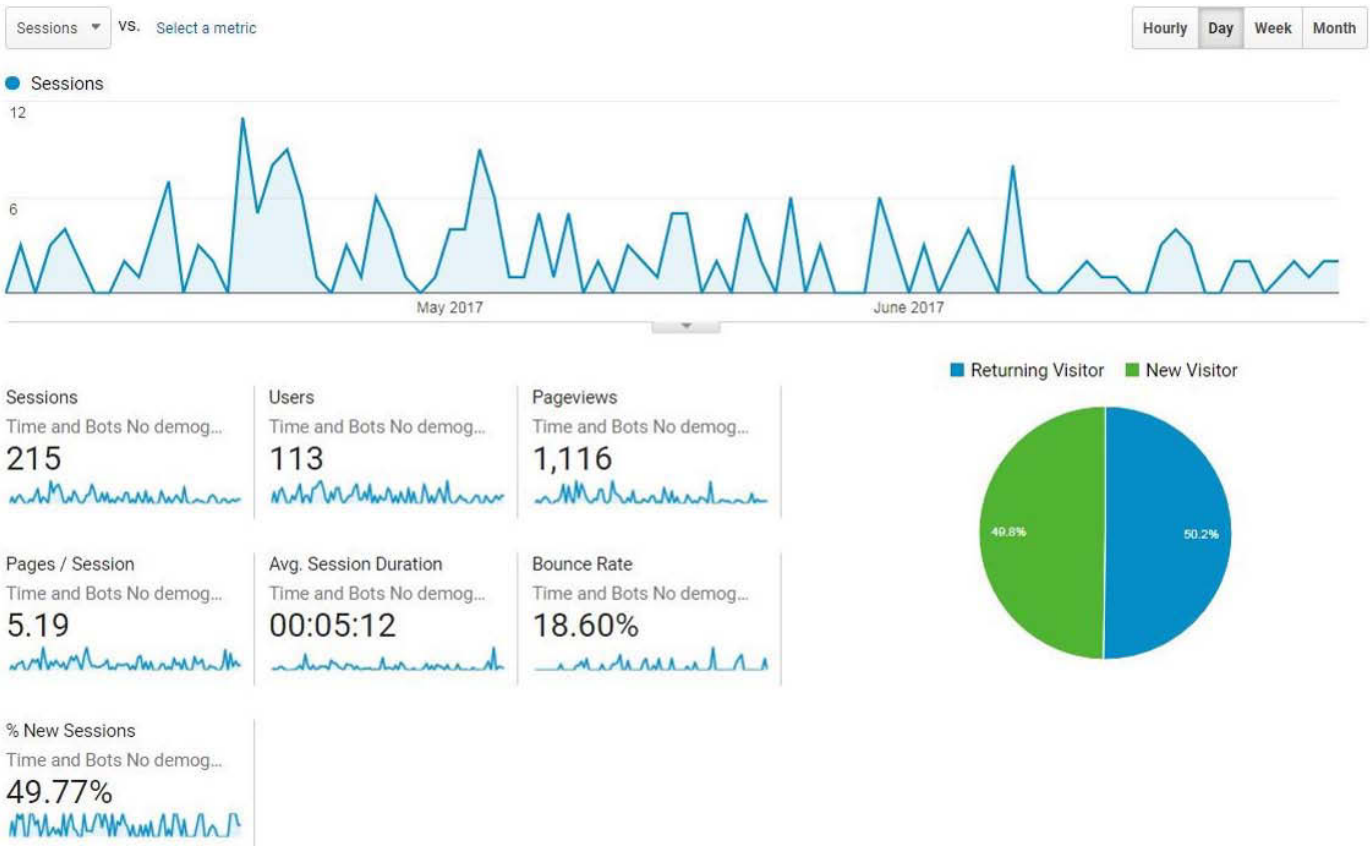

FIGURE 3. HSECoE web analytics: three month site activity metrics

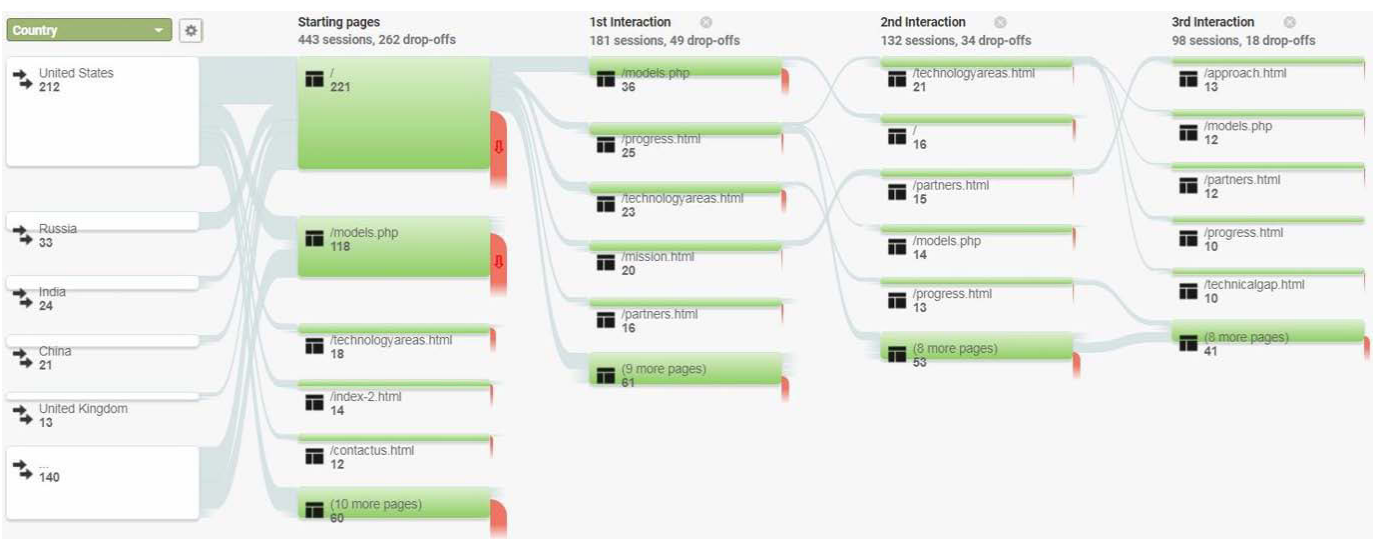

FIGURE 4. HSECoE web analytics: user flows

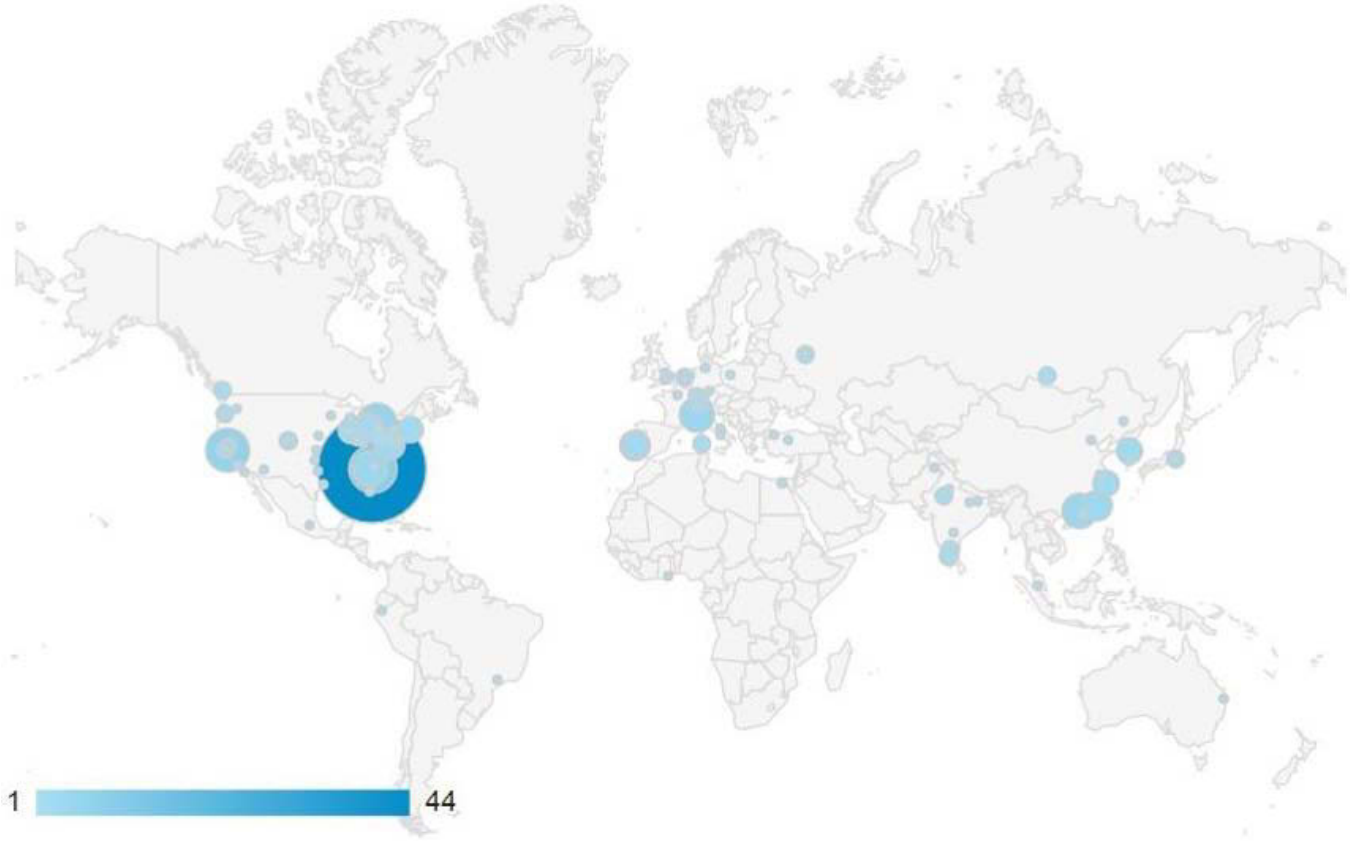

FIGURE 5. HSECoE web analytics: user origin countries

CONCLUSIONS AND UPCOMING ACTIVITIES

- Work with HSECoE partners to continue to update and improve center developed models. Make these models available and accessible to the broader research and academic community through a controlled web based access portal and track downloads and web site activity.
- Create stand-alone executable versions of the HSECoE developed material storage models to provide first-order storage system estimates based on material property information.
- Update the hydrogen storage equations with additional, alternative theoretical storage system formulations to allow users to choose the most appropriate theory for their material.

FY 2017 PUBLICATIONS/PRESENTATIONS

1. Thornton, M., D. Tamburello, K. Brooks, S. Sprik, "Hydrogen Storage System Modeling: Public Access, Maintenance, and Enhancements," U.S. Department of Energy Hydrogen and Fuel Cells Program Annual Merit Review and Peer Evaluation Meeting, June 8, 2017.

2. Thornton, M., D. Tamburello, K. Brooks, S. Sprik, "HSECoE Models on the WEB," Hydrogen Storage Technical Team Review, January 19, 2017.

IV.B.2 Investigation of Solid State Hydrides for Autonomous Fuel Cell Vehicles

Ragaiy Zidan (Primary Contact), Patrick Ward, Bruce Hardy, and Scott McWhorter
Savannah River National Laboratory (SRNL)
Bldg. 999-2W
Aiken, SC 29808
Phone: (803) 646-6358
Email: ragaiy.zidan@srnl.doe.gov

DOE Manager: Ned Stetson
Phone: (202) 586-9995
Email: Ned.Stetson@ee.doe.gov

Subcontractor:
Joseph Teprovich, Theodore Motyka, and Claudio Corgnale, Savannah River Consulting, Aiken, SC

Project Start Date: March 1, 2015
Project End Date: Project continuation and direction determined annually by DOE

Overall Objectives

- Develop a methodology that incorporates engineering modeling and analysis tools to screen and down-select storage materials and material systems against cost and performance targets (initially developed and applied by SRNL to light-duty vehicle in the Hydrogen Storage Engineering Center of Excellence [HSECoE]).
- Apply this methodology to an initial system design for an unmanned underwater vehicle (UUV) application for the Navy to reduce design time and lead to a more cost effective and better performing final product.
- Maintain hydrogen storage system capabilities and expertise at DOE and SRNL to support a variety of hydrogen and energy initiatives.
- Extends the long-term partnership between DOE and the Department of Defense in hydrogen and renewable energy systems.

Fiscal Year (FY) 2017 Objectives

- Develop a preliminary design of an integrated H_2-fuel cell UUV system design with a solid hydrogen storage system.
- Obtain and generate engineering material property data for alane to be use with prototype system and detailed models.
- Complete detailed design of a hydrogen storage system.
- Design and build a prototype, alane-based, hydrogen storage vessel.
- Perform preliminary testing on the prototype, storage system.
- Package and ship prototype vessel and alane material to the Navy.
- Provide technical support to Navy's Naval Underwater Warfare Center for their further testing and evaluation.

Technical Barriers

This project addresses the following technical barriers from the Hydrogen Storage section of the Fuel Cell Technologies Office Multi-Year Research, Development, and Demonstration Plan.

(A) System Weight and Volume

(B) System Cost

(C) Efficiency

(D) Durability

(E) Charging/Discharging Rates

(G) Materials of Construction

(H) Balance-of-Plant (BOP) Components

(J) Thermal Management

Technical Targets

SRNL has worked with the Navy to modify the DOE hydrogen storage targets [1] developed for light-duty vehicles to Navy UUV requirements. The proposed hydrogen storage and performance targets for Navy UUV systems include both near-term and longer-term requirements. The main difference between near- and long-term UUV targets are higher hydrogen storage densities and capacities and higher associated fuel cell average and peak power requirements. While many of the proposed Navy UUV targets are similar to DOE hydrogen storage targets some areas where they differ substantially are in initial material cost and material durability since most Department of Defense applications can withstand higher costs and shorter operating lifetimes than consumer passenger vehicles.

FY 2017 Accomplishments

- Testing was performed to demonstrate alane hydrogen storage properties and delivery performance including steady-state and transient operations.
- Delivered alane material and test module to Naval Underwater Warfare Center for further Navy testing.
- Ongoing systems and detailed modeling for UUV platforms are in progress.
- Key engineering material properties for alane have been generated.
- Preliminary analyses indicate two to three times the energy storage compared to battery systems.
- End of year objective is to develop a preliminary prototype alane-based UUV system design and system model for potential Navy applications.

✧ ✧ ✧ ✧ ✧

INTRODUCTION

This project builds upon the core capabilities of DOE and SRNL and leverages their collective experiences to support new roles in other hydrogen applications, which includes the rapidly growing fuel cell areas for portable power and material handling equipment. Current battery technology is not able to meet the growing gravimetric and volumetric energy density demand for small portable power applications.

One solution that is actively being evaluated is to use fuel cells. Fuel cells offer efficient and high-quality power but require safe, efficient and cost-effective hydrogen storage systems to make them practical. An attractive means for storing hydrogen is the use of solid-state materials that have demonstrated the ability to increase the density of hydrogen by a factor of more than twice that of liquid hydrogen and more than five times that of compressed gas at 70 MPa [2]. Several materials exist that appear to be suitable for hydrogen storage for Department of Defense UUV applications. However, the viability of storage systems based on these materials for UUV operating conditions has never been demonstrated.

APPROACH

The overall approach of this research is to develop a methodology that incorporates engineering modeling and analyses to efficiently screen, design, and select storage materials and material systems against cost and performance targets leading to an initial system design for a UUV application. This methodology, which was initially developed by SRNL and applied to light-duty vehicles in the HSECoE, requires updates and modifications for it to be useful for other hydrogen and fuel cell applications. More specifically in this research, this methodology will be applied to UUVs to reduce design time and lead to a more cost effective and better performing final product. The modeling analysis, applied to this project, integrates various hydrogen storage system options with other system components, including fuel cell and balance of plant models to evaluate and compare the overall performance of the onboard hydrogen storage system.

RESULTS

Previous year's activities, involved performing an engineering screening analyses on a variety of metal hydrides and chemical hydrogen storage candidate materials using a modified version of the acceptability envelope tool [3] developed for light-duty vehicles in the HSECoE. The acceptability envelope tool was used to apply the Navy's UUV targets and requirements to several standard hydrogen storage system designs and configurations. Based on the results from the study and discussions with Navy personnel, aluminum hydride or alane (AlH_3) was selected as the leading candidate material.

Following selection of alane as the preliminary candidate hydrogen storage material for this project, a demonstration reactor was designed and fabricated utilizing commercially available parts and connectors. The purpose of the reactor was to provide the Navy with a simple system to evaluate the characteristics of an alane storage system to better understand its operation and performance under a variety of temperature conditions. Figure 1 shows the SRNL alane reactor (Alane Rx) undergoing testing by the Navy. The tubular reactor is located in an annular shell that provides hot and cold oil to control the discharge of hydrogen from the alane material. Preliminary test results of the demonstration reactor are shown in Figure 2. The results show the ability of the desorbed alane in the system to be controlled by cooling and heating the reactor. This is a key requirement for the UUV system which was verified by the Navy testing.

Engineering material property data was collected for similar alane material that is to be used for future bench and pilot scale studies with the Navy. The data collected included thermal conductivity measurements after various amounts of hydrogen release as shown in Table 1. Results indicate that while the thermal conductivity increases as alane is decomposed into aluminum, additives such as expanded natural graphite (ENG) may be required to enhance the thermal conductivity of the starting alane. Preliminary results from the incorporation of ENG have shown mild improvements of the thermal conductivity at room temperature. Further studies into the degree of volume change during desorption, which will also effect thermal transport, are currently underway. Another key engineering material property measured was desorption and kinetic data. The isothermal desorption of hydrogen from the material was measured between 110–140°C with 1 bar of hydrogen back pressure on the sample initially. The isothermal desorption

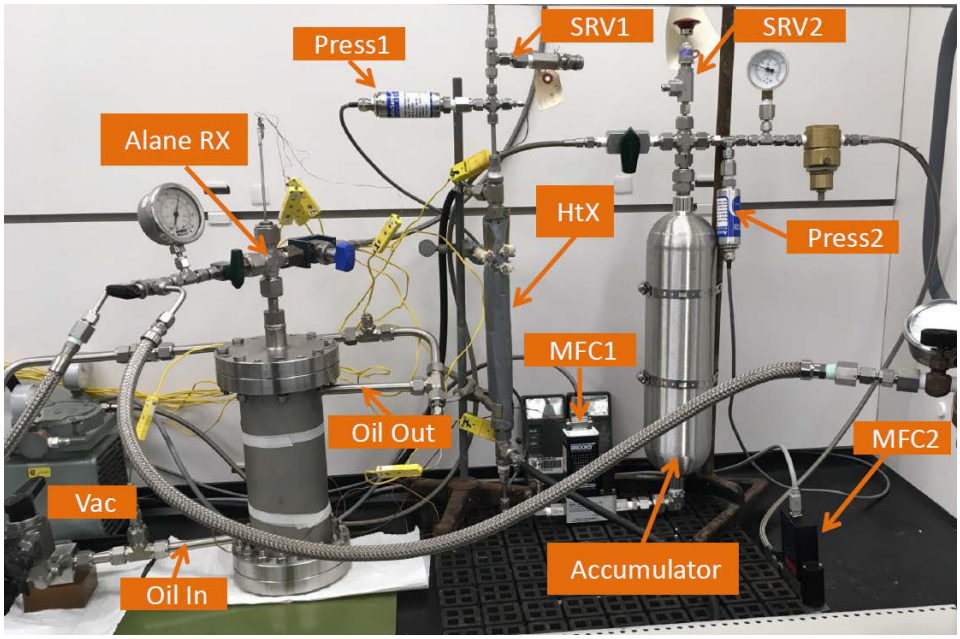

MFC – mass flow controller; SRV – safety release valve; RX – reaction vessel; Vac – vacuum pump; HtX – heated transfer fluid line

FIGURE 1. Demonstration alane reactor and testing apparatus

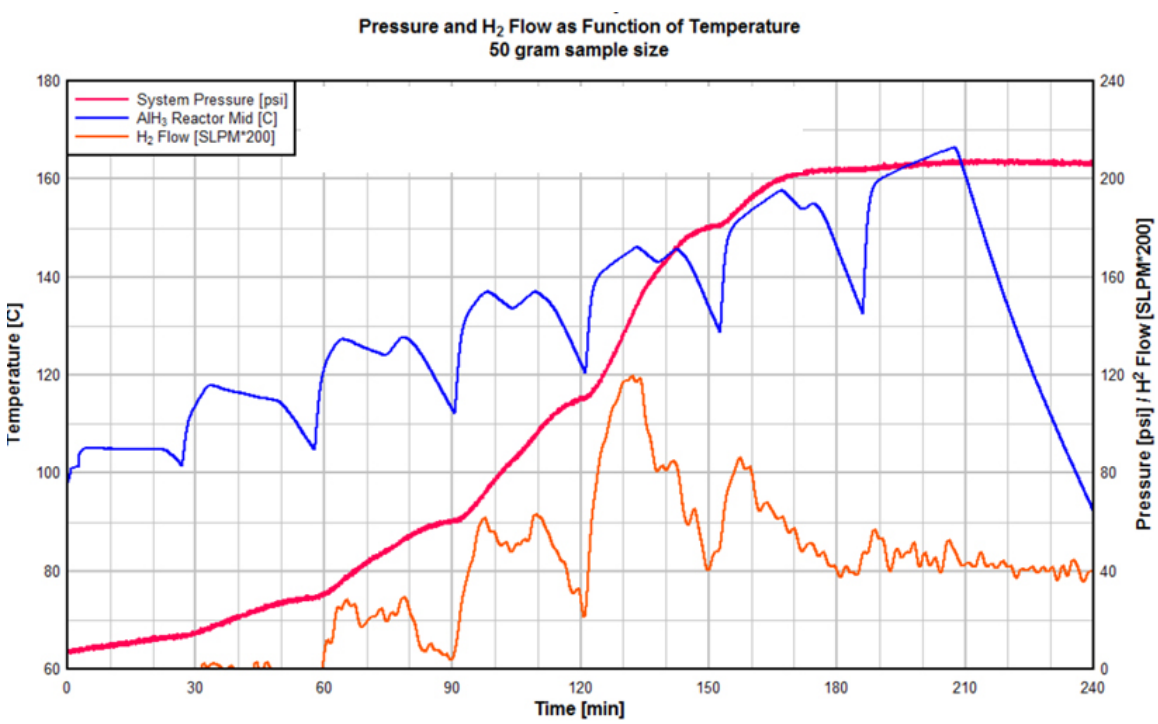

FIGURE 2. Alane decomposition testing and verification results

TABLE 1. Thermal Conductivity of Alane at Various Stages of Decomposition

Sample (wt% ratio)	Thermal Conductivity (W/m*K)
AlH_3:Al (0:100)	18.2
AlH_3:Al (25:75)	13.9
AlH_3:Al (50:50)	9.54
AlH_3:Al (75:25)	5.23
AlH_3:Al (100:0)	0.915

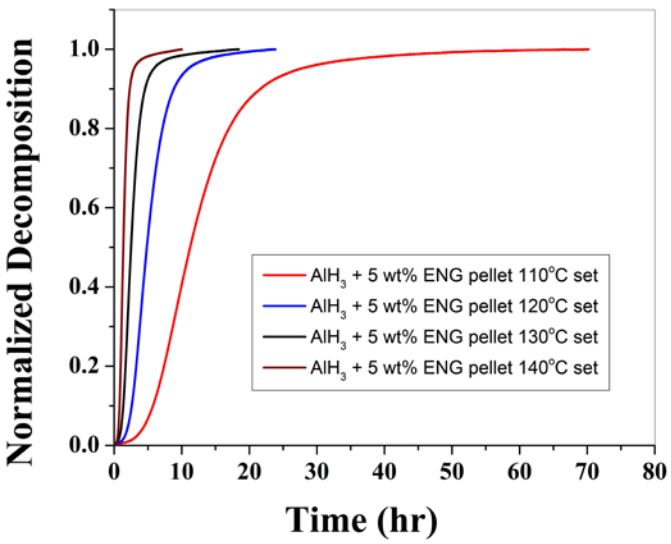

FIGURE 3. Isothermal desorption data from alane with 5 wt% ENG from 110°C to 140°C

plots, shown in Figure 3, demonstrate consistent hydrogen desorption behavior in which the rate of hydrogen release increases as a function of the experiment temperature. The addition of ENG and utilizing a pelletized form of the sample did not have a noticeable effect on the kinetic profiles of hydrogen release.

During the previous year, an alane-based hydrogen storage system model was developed using Comsol™ Multiphysics software. The model was general and was readily applicable to a wide range of conceptual designs. The model solves the governing equations for mass, momentum, and energy conservation that are coupled to expressions for chemical kinetics and thermodynamics. The detailed model was applied to the bench-scale demonstration unit and now is being modified to support the design of the prototype hydrogen storage system for the Navy. As part of this effort, a preliminary high level conceptual design of the alane reactor was performed. This includes the assumptions and restraints described in Tables 2 and 3 for the sizing and heat transfer system in the alane bed and material properties for the alane, respectively.

TABLE 2. Assumptions and Constraints for the Alane Vessel Design

Startup/shut down	10 min
Max diameter	0.254 m
Length	0.229–0.33 m
Thermal power heat transfer fluid	Pressurized water
Inlet/Outlet Temperature	150/130°C
Pressure	10 bar

TABLE 3. Alane Properties

Mass of hydrogen	1.13 kg
Hydrogen flow rate	0.2 g/min for about 96 h
DH, heat of desorption	7.6 kJ/mol H_2
Cp, heat capacity	1340 J/kg K
k. thermal conductivity	7 W/m K
wf, weight fraction	10%
Bulk density	1000 kg/m^3

FIGURE 4. Complete power system design

A high-level model, including mass and energy balance of the reactive system and the heat transfer system, has been developed. A shell and tube heat exchanger concept has been assumed. The cooling power to shut down the reactor in 10 minutes has been included in the preliminary heat exchanger design model. The results from the model indicate that the assumptions and constraints made for the vessel design and alane properties (Tables 2 and 3, respectively) will allow the alane vessel to fit in the designated area allotted inside of the UUV. Figure 4 illustrates the conceptual design of the power system. This model accounts for the space occupied by the shell and tube heat exchanger with additional space to allow for additional balance of plant components.

CONCLUSIONS AND UPCOMING ACTIVITIES

Alane was selected as the most promising candidate material due to the potential to meet and exceed many of the Navy UUV requirements, with the potential to provide twice the energy storage of current battery systems. Navy testing of a SRNL supplied demonstration unit was performed to validate the hydrogen delivery and performance of an alane-based hydrogen storage system. Key engineering and material property data for alane were generated for ongoing prototype model and design efforts. Preliminary modeling activities indicated that alane-based power systems can double the range of current battery-based UUVs. System and detailed modeling for a prototype UUV design are currently underway this fiscal year with plans to fabricate and deliver a prototype storage system to the Navy in early 2018.

2017 PUBLICATIONS/PRESENTATIONS

1. Teprovich J. et al, "ONR Undersea Power and Energy Program Review," Arlington, VA, March 28–30, 2017.

2. Teprovich J. et al., "Investigation of Solid State Hydrides for Autonomous Fuel Cell Vehicles," Annual Merit Review, Washington D.C., June 8, 2017.

REFERENCES

1. US DOE Targets for Onboard Hydrogen Storage Systems for Light-Duty Vehicles; http://www1.eere.energy.gov/hydrogenandfuelcells/storage/pdfs/targets_onboard_hydro_stor age.pdf.

2. Klebanoff, L., Keller, J., 5-Year Review of Metal Hydride Center of Excellence. Int. J. Hydrogen Energy 38 (2013) 4533–4576. In Proceedings of the 2010 U.S. DOE Hydrogen Program Annual Merit Review, Washington, DC, USA, 7–11 June 2010; Available online: http://www.hydrogen.energy.gov/pdfs/review10/st029_klebanoff_ 2010_o_web.pdf.

3. Corgnale C, Hardy B.J., Tamburello D.A., Garrison S.L., Anton D.L., Acceptability envelope for metal hydride-based hydrogen storage systems. Int J Hydrogen Energy 2012;37:2812e24 http://dx.doi.org/10.1016/j.ijhydene.2011.07.037.

IV.C.1 HyMARC (Core): SNL Effort

Mark D. Allendorf (Primary Contact),
Vitalie Stavila, Lennie Klebanoff, Rob Kolasinski,
Farid El Gabaly, Xiaowang Zhao, James White
Sandia National Laboratories (SNL)
7011 East Avenue
Livermore, CA 94551
Phone: (925) 294-3059
Email: mdallen@sandia.gov

DOE Manager: Ned Stetson
Phone: (202) 586-9995
Email: Ned.Stetson@ee.doe.gov

Project Start Date: September 17, 2015
Project End Date: September 30, 2018

Overall Objectives

- Accelerate discovery of breakthrough storage materials by developing foundational understanding of phenomena governing the thermodynamics and kinetics limiting the development of solid-state hydrogen storage materials.
- Develop community tools and capabilities to enable materials discovery, including computational models and databases, new characterization tools and methods, and tailorable synthetic platforms.
- Provide technical direction to HyMARC via leadership of Task 1 (Thermodynamics), Task 3 (Gas Surface Interactions) and Task 5 (Additives).
- Provide gas sorption and other property data required to develop and validate thermodynamic models of sorbents and metal hydrides, including the effects of ultrahigh hydrogen pressure.
- Identify the structure, composition, and reactivity of gas-surface and solid-solid hydride surfaces contributing to rate-limiting desorption and uptake.
- Synthesize metal hydrides and sorbents in a variety of formats (e.g., bulk powders, thin films, nanostructures) and develop in situ techniques for their characterization.
- Apply SNL multiscale codes to discover new materials and new mechanisms of storing hydrogen, and provide input for database development.
- Elucidate the role of additives in improving H_2 storage adsorption and desorption reactions.

Fiscal Year (FY) 2017 Objectives

- Demonstrate in situ soft X-ray ambient pressure X-ray photoelectron spectroscopy (AP-XPS), X-ray absorption spectroscopy (XAS), and X-ray emission spectroscopy tools, with sample heating.
- Synthesize and characterize library of nanoparticles for one hydride with diameters in the ranges of 1–5 nm, 5–10 nm, >10 nm.
- Sensitivity analysis of local binding and second-sphere effects.
- Rank improvement strategies for sorbents per decision criterion: select the two with the greatest potential for increasing $\Delta H°$.
- Modify low-energy ion scattering (LEIS) to enable laser-induced thermal desorption.
- Evaluate additive/composite strategies for improving effective ΔE.
- Assess bulk additives (TiF_3, $TiCl_3$) for their reactivity towards hydrogen.
- Develop prototype hydride surface and interface chemistry kinetic models.

Technical Barriers

This project addresses the following technical barriers from the Hydrogen Storage section of the Fuel Cell Technologies Office Multi-Year Research, Development, and Demonstration Plan.

(O) Lack of Understanding of Hydrogen Physisorption and Chemisorption

(A) System Weight & Volume

(E) Charging/Discharging Rates

(F) Cost, Efficiency, Durability

Technical Targets

The goal of this project is to develop foundational understanding of phenomena governing thermodynamics and kinetics of hydrogen release and uptake in all classes of hydrogen storage materials. Insights gained from these studies will be applied toward the design and synthesis of hydrogen storage materials that meet the following DOE 2020 hydrogen storage targets.

- Cost: $10/kWh net; Specific energy: 1.8 kWh/kg; Energy density: 1.3 kWh/L

FY 2017 Accomplishments

- The HyMARC website was brought online to enhance external communications.
- An extensive suite of modeling capabilities was developed, many of which are ready for use through internal and external collaborations.
- The ultrahigh-pressure reactor (up to 1,000 bar H_2 and 400ºC) is now online and available for use by Seedling projects and other collaborators.
- An approved program was granted at the Advanced Light Source (ALS) at Lawrence Berkeley National Laboratory, providing dedicated access to beam lines for X-ray spectroscopy and scanning transmission X-ray microscopy (STXM) for three years.
- Substantial interactions with all five Seedling projects currently in operation, including visits to Sandia by members of Seedling project teams, and exchange of samples for measurements using HyMARC capabilities.
- Extensive collaborations among all three laboratories in the HyMARC Core Team occurred, leading to several joint publications.
- A go/no-go decision point was reached in which improvement strategies for sorbents were ranged according to their potential for increasing the heat of adsorption. Of the six strategies assessed, the two predicted to have the greatest potential are the incorporation of open metal sites into metal-organic frameworks (MOFs) and related framework materials, and the addition of Lewis-acid sites into porous carbons. A detailed report in the form of a peer-reviewed journal article will be submitted that describes the perspective of the HyMARC team on a wide range of sorbent improvement strategies.
- An experimental investigation using Sandia and ALS capabilities shows that titanium is not present on the surface during H_2 desorption from Ti-doped $NaAlH_4$, supporting the "zipper" mechanism and invalidating several published mechanisms.
- Extensive high-pressure hydrogen cycling data for several MOFs show that H_2 uptake is not always fully reversible.
- A series of MOFs was synthesized, characterized at SNL, and sent to HySCORE/National Renewable Energy Laboratory for high-accuracy gas sorption measurements to enable model validation and testing of the Chahine rule.
- Several strategies for altering metal hydride uptake and release were evaluated; results indicate that thermodynamics in the Li-M-N-H system can be modified and kinetics of intermediate formation in borohydrides can be altered.

✧ ✧ ✧ ✧ ✧

INTRODUCTION

Storage of hydrogen on board vehicles is one of the critical technologies needed to create hydrogen-fueled transportation systems that can improve energy efficiency, resiliency, and energy independence and reduce oil dependency. Stakeholders in developing hydrogen infrastructure (e.g., state governments, automotive original equipment manufacturers, station providers, and industrial gas suppliers) are currently focused on high-pressure storage at 350 bar and 700 bar, in part because no viable solid-phase storage material has emerged. Early-state research to develop a foundational understanding of solid-state storage materials, including novel sorbents and high-density hydrides, is of high importance because of their unique potential to meet all DOE Fuel Cell Technologies Office targets and deliver hydrogen with lower storage pressures and higher onboard densities. However, existing materials suffer from thermodynamic and kinetic limitations that prevent their application as practical H_2 storage media.

Sandia's objectives and responsibilities within HyMARC are to (1) provide technical leadership to the Consortium at the Director level, as well as through leadership of Task 1 (Thermodynamics), Task 3 (Gas Surface Interactions), and Task 5 (Additives); (2) provide gas sorption and other property data required to develop and validate thermodynamic models of sorbents and metal hydride storage materials, including the effects of 350 bar and 700 bar H_2 delivery pressures, serving as a resource for the Consortium; (3) identify the structure, composition, and reactivity of gas surface and solid-solid hydride surfaces contributing to rate-limiting desorption and uptake; (4) provide metal hydrides and MOFs in a variety of formats tailored for specific consortium tasks; (5) develop sample preparation methods and experimental protocols to enable facile use of the new characterization probes employed by the Consortium; (6) apply SNL multiscale codes to discover diffusion pathways and mechanisms of storage materials; (7) elucidate the role of additives in promoting hydrogen storage reactions; and (8) determine if LEIS can be used as a unique tool to measure H atom diffusion on thermally sensitive materials.

APPROACH

HyMARC seeks to address critical gaps in the science of hydrogen storage by leveraging recent advances in predictive multiscale modeling, high-resolution in situ characterization, and novel material synthesis techniques. By focusing on the underlying thermodynamic and kinetic limitations of storage

materials, we will generate foundational understanding that will accelerate the development of all types of advanced storage materials, including sorbents, metal hydrides, and liquid carriers.

RESULTS

Substantial progress was made on each of the five tasks being performed at SNL, with all of the quarterly goals met on time. Sandia principal investigators led the organization of task groups, helping to guide the science in collaboration with our partners, and scheduling and coordinating task team meetings involving all three HyMARC laboratory partners. Technical results include the following:

Task 1: Thermodynamics

Sandia's effort to elucidate the factors contributing to the thermodynamics of hydrogen uptake and release by sorbents and metal hydrides provided new data and contributed to the foundational understanding of these materials.

Key results for sorbents: protocols for the reproducible synthesis of MOFs were developed. The H_2 isotherms at 77 K for a library of these materials were measured to provide data for comparison with quantum Monte Carlo calculations of the heats of adsorption and grand canonical Monte Carlo (GCMC) predictions of gas sorption isotherms. Simulations and experiment are in agreement within a 10–20% band of uncertainty; this uncertainty is primarily the result of different equations of state and variations in the H_2 potential used in the force field. A detailed analysis of these effects is underway (Figure 1). As part of these experiments extensive high-pressure cycling tests (up to 700 bar) were done for several MOFs; these showed, surprisingly, that in some cases the surface area and capacity degraded after as few as 100 cycles. The reasons for this are unclear but X-ray diffraction suggests that it is not due to structural degradation.

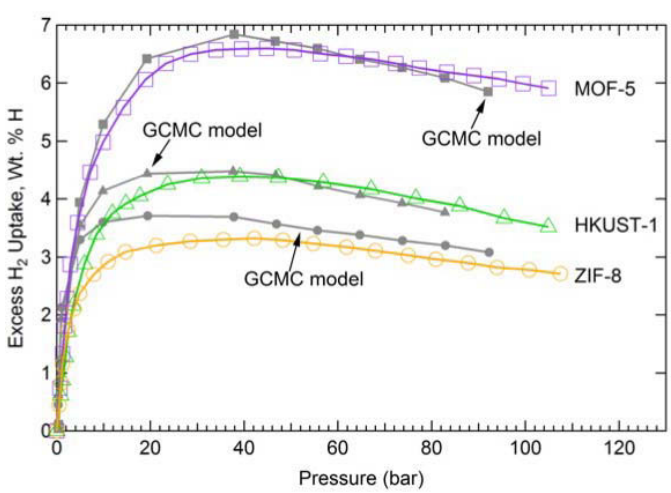

ZIF – zeolitic imidazolate framework

FIGURE 1. Comparison of measured H_2 uptake with GCMC predictions. The best combination of H_2 potential and equation of state identified from an evaluation of several common ones in the literature were used for the GCMC calculations.

Key results for metal hydrides: The effect for potassium hydride doping on the thermodynamics of H_2 release from hydrides in the Li-Mg-N-H system were conducted. The results show that the equilibrium H_2 pressure increases when small amounts (0.14–10 mol%) of KH were added (Figure 2). We also showed the reactivity of alkali metal $B_{12}H_{12}$ intermediates, which form during decomposition of borohydrides, can be increased, either by applying ultrahigh-pressure hydrogen (700 bar) to shift the equilibrium toward reformation of the parent borohydride, or by heating the $B_{12}H_{12}$ samples in the presence of binary metal hydrides, such as MgH_2, to further dehydrogenate the intermediates to yield the corresponding metal borides.This is significant because it suggests strategies for avoiding kinetic dead ends that prevent materials with attractive thermodynamics, such as $Mg(BH_4)_2$, from being practical storage materials.

In a second major effort, we advanced our understanding of nanoscale effects on the thermodynamics and kinetics of metal hydrides. First, we demonstrated that the kinetics of H_2 uptake by Li_3N can be dramatically improved by confining the material within porous carbons. A new one step synthetic route involving liquid NH_3 infiltration achieves high Li_3N loadings (>50 wt%) into pores <12 nm. Five weight percent reversible H_2 cycling and suppression of the detrimental Li_2NH species were shown to occur using Li_3N within 6-nm porous carbon (Figure 3). Second, we performed in-pore synthesis of nanoscale $Mg(BH_4)_2$ inside MOFs and graphene aerogels. Scanning electron microscopy and energy dispersive X-ray spectroscopy mapping shows Mg and B are evenly distributed within the sample, confirming $Mg(BH_4)_2$ is inside the pores. The new synthetic method enables efficient infiltration of high-capacity metal borohydrides, which is critical to minimize the weight penalty associated with the dead volume associated with a host material.

Finally, the Sandia ultra-high-pressure hydrogen reaction station (UHPR) is now fully operational (Figure 4), creating an additional unique HyMARC capability. The reactor achieves H_2 pressures up to 1,000 bar at temperatures up to 400ºC, allowing HyMARC to access the highest pressures currently used by new hydrogen fueling stations that are coming online. From a research perspective, the UHPR enables, for example, synthesis of metal hydrides that are unattainable by conventional routes and the probing of the destabilization of *closo*-borane intermediates.

Task 2: Kinetics of Mass Transport

This year we continued our development of validated models of hydrogen diffusion, which are used in models to determine whether mass transport is a rate-limiting factor in the desorption or release of H_2 from metal hydrides.

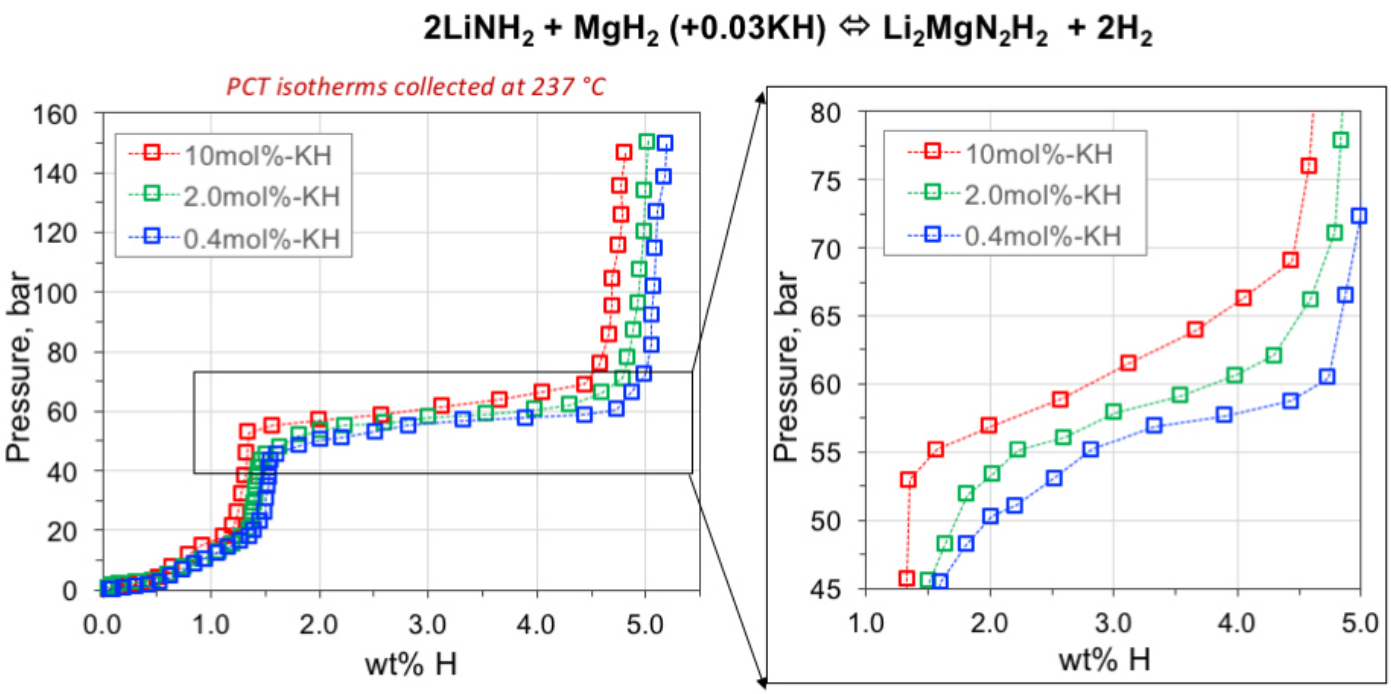

FIGURE 2. Pressure-composition-temperature curves showing that KH doping increases the equilibrium H_2 pressure of the Li-Mg-N-H metal hydride system.

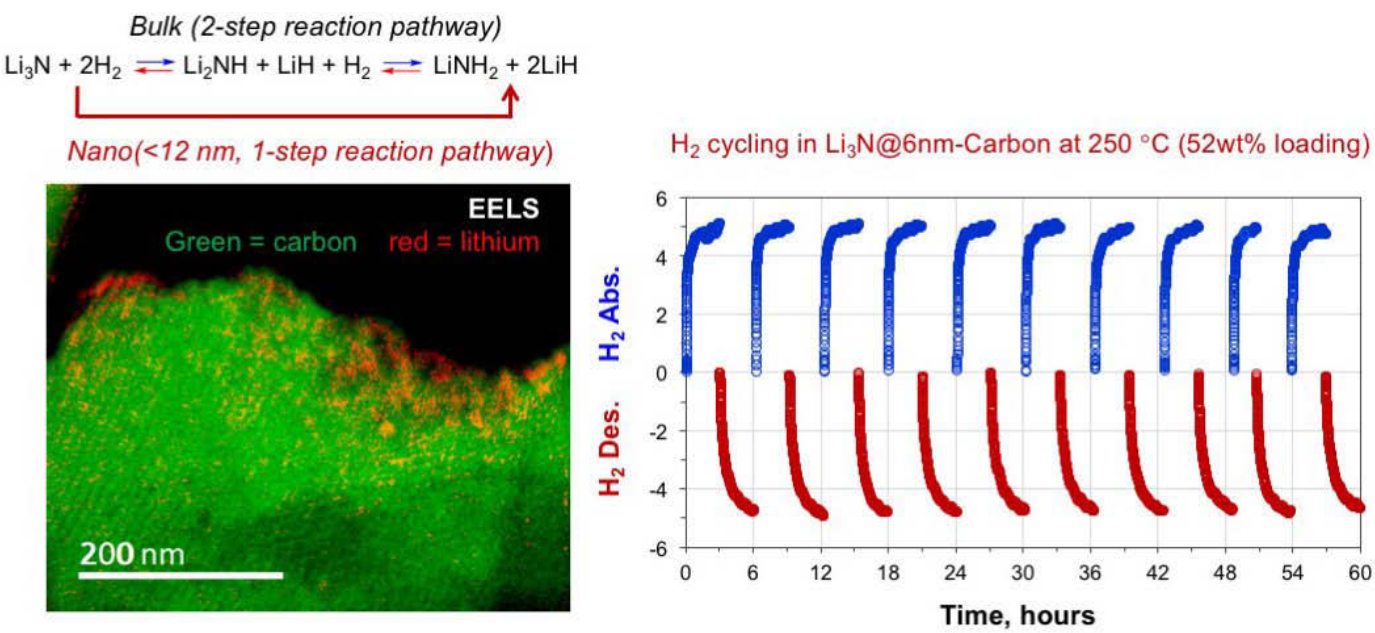

FIGURE 3. Nanoscale Li_3N formed within 6-nm porous carbon and the reproducible cycling of H_2 release at high gravimetric loading.

Our approach begins with model systems of progressively higher complexity so that we can validate individual aspects of model performance. Initially, we considered PdH_x, an interstitial hydride with well-understood properties that undergoes no phase transition upon hydrogen uptake. We validated the diffusion rate of H in bulk Pd by comparison with experimental data in the literature; in particular, our model is consistent with experiments showing that H segregates on Pd(111) surfaces. Next, which applied our modeling approach to diffusion of hydrogen in MgH_2, a material with covalent Mg-H bonds that undergoes a phase transition and large change in unit cell volume upon uptake of hydrogen.

FIGURE 4. New UHPR station now available for use at Sandia.

As part of this effort, we developed new methods to accelerate force field optimization, which is typically a very time-consuming process. A new capability to fit forces for any atom in any specified phase was added to our existing force field parameterization tools, which can fit energy, lattice constant, and elastic constants of a variety of phases. This new capability was used to apply further constraints to the Mg-H bond order potential parameterization, resulting in much more robust parameterization. We also developed new analysis tools that require only a few seconds of labor to launch a job to analyze molecular dynamics data and 30 minutes of computing time to obtain the final results using standard institutional cluster machines. Our previous automated tools could submit hundreds of MD jobs. However, analysis of the results became a labor-limiting factor. For example, our bulk diffusion analysis alone is done at 10 compositions and 13 temperatures for any hydride. Data reduction for these 130 simulations could easily take several days of labor time. These new analytical tools are a unique HyMARC capability that will be extended to more complex hydrides in the coming year.

Task 3: Surface Science

Development of HyMARC's comprehensive suite of diagnostics to probe chemical phenomena at all relevant length scales continued this year, with the development of a method to measure surface diffusion using LEIS. The new LEIS diffusion capability uses the ion beam to clear the surface area of H, then uses ion scattering to monitor diffusion from the periphery (Figure 5). The approach can detect surface H and ~ 0.1 monolayer levels, avoids thermal damage to sensitive samples, and can detect the refilling of the clear space by H within seconds. With this new method we can now probe chemical composition at the first monolayer (<1 nm) using LEIS, near-surface region (<10 nm) using XPS or AP-XPS, and the bulk using STXM or XAS. We applied all of these tools to understand the desorption of hydrogen from Ti-doped $NaAlH_4$ (see additional details under Task 5) and are now applying them to complex hydrides that are much more poorly understood, such as $Mg(BH_4)_2$.

Task 4: Solid-Solid Interfaces

The primary contribution of the Sandia team to this task was the development of sample preparation techniques for STXM measurements at the ALS. As part of the HyMARC ALS approved program, which provides dedicated beam time for three years, we conducted STXM measurements during 15 eight-hour shifts using Ti-doped $NaAlH_4$, Li_3N, and Mg nanoparticles as test cases for method development. Sandia also contributed XAS data to a collaborative effort involving HyMARC investigators at Pacific Northwest National Laboratory, the National Institute of Standards and Technology, and Lawrence Berkeley National Laboratory

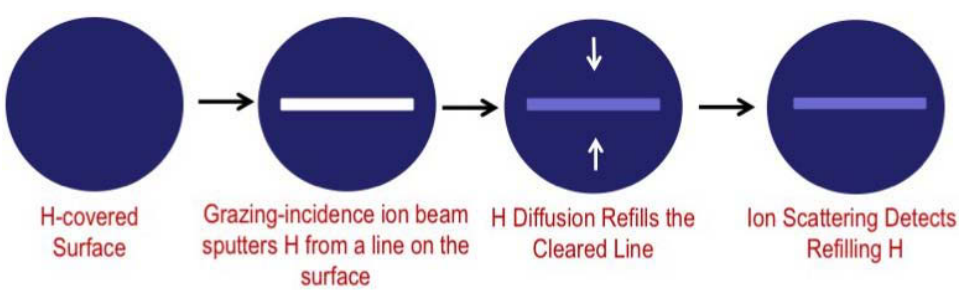

FIGURE 5. New methodology for probing surface diffusion using LEIS.

to generate a library of spectroscopic standards to facilitate understanding of novel storage materials.

Task 5: Additives

New understanding concerning the role of titanium in accelerating desorption of H_2 from complex metal hydrides was obtained using HyMARC's suite of surface diagnostics and soft X-ray spectroscopies. Among the most heavily studied and yet least understood systems is titanium-doped $NaAlH_4$ (Ti@$NaAlH_4$), for which there exist more than 2,000 papers in the literature. Many of the proposed mechanisms involve surface titanium in some form. Using samples ball-milled for long times and cycled to simulate a material used in a fuel tank, we employed a suite of diagnostic tools that probe all relevant length scales in the reaction (probe depth given in parentheses): LEIS (1 monolayer), AP-XPS (5 nm; ~15 atomic layers), STXM (bulk), and Fourier transform infrared (bulk). Together, the data obtained from these diagnostics indicate that no Ti-containing surface or near-surface species exist during H_2 desorption from Ti@$NaAlH_4$. The Ti is located in the bulk and reemerges upon exposure to H_2 during the regeneration phase. These results contradict several proposed mechanisms and support the so-called zipper model, in which Ti-containing surface species are destabilized when sodium diffuses to the surface during desorption. Moreover, it is clear from these investigations that bulk titanium halides themselves do not promote H_2 dissociation, showing that Ti-containing additives must be chemically altered to have a catalytic effect. A final important conclusion of this investigation is the critical need for reliable assignments of XAS and XPS spectroscopic features, for which there is disagreement in the hydrogen storage literature. The spectroscopic standards effort under Task 4 coupled with computational spectroscopy performed by HyMARC investigators at the Molecular Foundry, are addressing this issue.

Interactions with Seedling projects and collaborations: HyMARC expertise and capabilities have been accessed extensively by several of the current Seedling projects. Researchers from three of the projects were hosted for periods of up to a month. Capabilities used include the UHPR, XPS, LEIS, X-ray diffraction, Fourier transform infrared spectroscopy, and high- and low-pressure porosimetry. Due to the exceptional complexity of metal borohydride hydrogen chemistry, HyMARC core lab investigators are collaborating with HySCORE researchers at National Institute of Standards and Technology and Pacific Northwest National Laboratory to perform a detailed mechanistic investigation of hydrogen release and uptake by $Mg(BH_4)_2$.

CONCLUSIONS AND UPCOMING ACTIVITIES

The Sandia HyMARC team continued its development of new synthetic, modeling, and diagnostic tools that are providing new insights into all major classes of storage materials, ranging from relatively simple systems such as PdH_x and MgH_2, to exceptionally complex ones, such as the metal borohydrides, as well as materials thought to be very well-understood, such as Ti-doped $NaAlH_4$. This unprecedented suite of capabilities, capable of probing all relevant length scales within storage materials, is already having a significant impact, as they are now being used by both Seedling projects and collaborators at other laboratories within HyMARC. We expect this impact to grow as new Seedling projects begin and through collaborations with other scientists outside HyMARC. In the coming year, Sandia efforts will focus on the highest impact problems, in coordination with the other HyMARC National Laboratory partners, to provide the foundational science necessary to accelerate the discovery of new hydrogen storage materials.

SPECIAL RECOGNITIONS & AWARDS/ PATENTS ISSUED

1. V. Stavila, L. Klebanoff. "Nanostructured metal amides and nitrides for hydrogen storage," US Patent Application 62/235,930, November 2016.

2. V. Stavila. "Solid state synthesis of alkali metal borohydrides," US Patent Application 63/237,752, March 2017.

FY 2017 PUBLICATIONS/PRESENTATIONS

Publications

1. B.C. Wood, V. Stavila, N. Poonyayant, T.-W. Heo, K. Ray, L.E. Klebanoff, T.J. Udovic, J.R.I. Lee, N. Angboonpong, J.D. Sugar, P. Pakawatpanurut "Nanointerface-Driven Reversible Hydrogen Storage in the Nanoconfined Li–N–H System," cover feature *Adv. Mater. Interfaces*, 2017*, 4,* 1600803.

2. M. Dimitrievska, J.L. White, W. Zhou, V. Stavila, L.E. Klebanoff, T.J. Udovic, "Structure-dependent vibrational dynamics of $Mg(BH_4)_2$ polymorphs probed with neutron vibrational spectroscopy and first-principles calculations," *Phys. Chem. Chem. Phys.*, 2016, *18*, 25546.

3. X.W. Zhou, et al. "Molecular Dynamics Simulations of Hydrogen Diffusion in Aluminum," *J. Phys. Chem. C*, 120, 7500 (2016).

4. E.S. Cho, et al., "Graphene Oxide/Metal Nanocrystal Multilaminates as the Atomic Limit for Safe and Selective Hydrogen Storage," *Nature Commun.*, 2016, 7, 10804.

Presentations

1. Nine presentations (one keynote and four invited) were delivered at national and international conferences and symposia over the past 12 months.

IV.C.2 HyMARC (Core): LLNL Effort

Brandon Wood (Primary Contact), Tae Wook Heo, ShinYoung Kang, Jonathan Lee, Keith Ray, Stanimir Bonev, Tadashi Ogitsu, Patrick Shea, Theodore Baumann, Patrick Campbell
Lawrence Livermore National Laboratory (LLNL)
7000 East Ave., L-413
Livermore, CA 94550
Phone: (925) 422-8391
Email: brandonwood@llnl.gov

DOE Manager: Ned Stetson
Phone: (202) 586-9995
Email: Ned.Stetson@ee.doe.gov

Project Start Date: September 17, 2015
Project End Date: September 30, 2018 (Phase I End)

Overall Objectives

- Accelerate discovery of breakthrough storage materials by developing foundational understanding of phenomena governing the thermodynamics and kinetics limiting the development of solid-state hydrogen storage materials.
- Develop community tools and capabilities to enable materials discovery, including computational models and databases, new characterization tools and methods, and tailorable synthetic platforms.
- Provide technical direction to HyMARC via leadership of Task 2 (Mass Transport) and coordination of theory efforts.
- Provide new computational models for hydrogen interactions in hydrides and sorbents.
- Provide tailored porous aerogel materials for sorbents and encapsulants.
- Provide characterization of hydrides and sorbents using soft X-ray absorption and emission spectroscopy.

Fiscal Year (FY) 2017 Objectives

- Develop computational methods for more accurate thermodynamics of hydrides and their interfaces.
- Investigate mass transport in complex microstructures in metal hydrides.
- Establish computational framework for solid mechanics and confinement effects on reaction enthalpies.
- Understand H_2 interactions with model sorbents and catalysts.
- Establish synthetic protocols for incorporating dopants into graphene aerogels.

Technical Barriers

This project addresses the following technical barriers from the Hydrogen Storage section of the Fuel Cell Technologies Office Multi-Year Research, Development, and Demonstration Plan.

(O) Lack of Understanding of Hydrogen Physisorption and Chemisorption

(A) System Weight and Volume

(E) Charging/Discharging Rates

Technical Targets

This project will develop foundational understanding and new capabilities that will enable accelerated discovery of breakthrough materials in all classes of storage materials, in particular metal hydrides and sorbents. It is anticipated that the insights gained from this research, coupled with new synthetic, characterization, modeling, and database tools that will be made available to the hydrogen storage research community, will lead to materials that meet DOE system targets such as gravimetric and volumetric capacity, system fill time, delivery temperature, and cost.

FY 2017 Accomplishments

- Established synthetic protocols for B/N doping of graphene aerogels for hydride infusion and direct sorption testing.
- Improved free energy predictions of hydrides by considering explicit thermal effects, with results tested and successfully validated on a Mg-B-H system.
- Predicted stability trends of B_xH_y intermediates beyond the bulk crystalline limit to understand reaction pathways under non-equilibrium reaction conditions.
- Developed new theory capability to quantify the destabilizing effect of internal and external stress on reaction enthalpy due to volume expansion upon hydrogenation.
- Demonstrated new computational methods for non-equilibrium mass transport in complex microstructures.
- Performed reactive ab initio molecular dynamics simulations of MgB_2/H_2 and MgB_2/etherate interfaces to elucidate local reaction mechanisms and coordination complexes.

- Examined thermodynamic, kinetic, and electronic effects of TiF_3 catalysts via first-principles calculations.

✧ ✧ ✧ ✧ ✧

INTRODUCTION

Storage of hydrogen onboard vehicles is one of the critical enabling technologies for creating hydrogen-fueled transportation systems that can improve efficiency, enhance resiliency, and encourage independence of the national energy infrastructure. Stakeholders in developing hydrogen infrastructure (e.g., state governments, automotive original equipment manufacturers, station providers, and industrial gas suppliers) are currently focused on high-pressure storage at 350 bar and 700 bar, in part because no viable solid-phase storage material has emerged. Nevertheless, solid-state materials, including novel sorbents and high-density hydrides, remain of interest because of their unique potential to meet all DOE Fuel Cell Technologies Office targets and deliver hydrogen with lower storage pressures and higher onboard densities. However, the existing materials suffer from thermodynamic and kinetic limitations that are often poorly understood, which prevent their application as practical H_2 storage media.

APPROACH

HyMARC seeks to address these gaps by leveraging recent advances in predictive multiscale modeling, high-resolution in situ characterization, and novel material synthesis techniques. By focusing on the underlying thermodynamic and kinetic limitations of storage materials, we will generate foundational understanding that will accelerate the development of all types of advanced storage materials, including sorbents, metal hydrides, and liquid carriers. LLNL objectives and responsibilities within HyMARC include (1) providing technical leadership for Task 2 (Mass Transport) and coordinating all theory efforts; (2) providing computational methods for more accurate prediction of sorbent and hydride thermodynamics; (3) developing tools for multiscale modeling of hydride kinetics, including mass transport, chemical kinetics, and phase kinetics; (4) synthesizing carbon frameworks and sorbents with tailored porosity and chemistry; and (5) support HyMARC characterization efforts surrounding soft X-ray spectroscopy.

RESULTS

Sorbent synthesis: A key goal of our synthesis efforts is the development of protocols for making tailored graphene aerogels that can be chemically optimized via B and N doping. We prepared B-doped and N-doped graphene aerogels by thermal treatment of graphene aerogels in the presence of a B or N precursor. Graphene aerogels were immersed in a solution of the precursor and freeze dried, then the composite was thermally annealed at elevated temperatures ranging from 1,000–2,000°C. The annealed samples were then submitted for compositional analysis by X-ray photoelectron spectroscopy. B and N lattice incorporation was confirmed at levels of up to 2.7 at% for B and 2.0 at% for N. We have found success using two approaches, boron oxide incorporation plus annealing for B doping and melamine incorporation plus annealing for N doping. However, we are still trying to increase the overall doping levels, as well as to increase chemical purity. For instance, B doping tends to also introduce N, possibly due to the conditions for the carbonization process. This suggests the need to investigate different gel formation precursors for B and N doping that may be able to introduce higher dopant concentrations.

Free energies of complex metal hydrides: We have implemented improved ab initio thermodynamics computations of hydrides, focusing on the use of ab initio molecular dynamics as a tool for obtaining more accurate free energies of the complex metal hydride systems as a function of temperature and composition. Our improved ab initio thermodynamics *captures* full dynamical contributions from both quasi-harmonic and anharmonic vibrations, and we applied our strategy to the Mg-B-H system as an example and evaluated the significance of anharmonicity.

As shown in Figure 1a, the differences between the standard enthalpy (zero-K intercepts, including zero-point energy contributions), the free energy within the harmonic approximation (dashed lines), and fully dynamical free energy descriptions (solid lines) are rather dramatic, particularly at high temperatures. The origin of this difference can be traced to the molecular reorientations and soft vibrations of the complex anions, which have significant anharmonic contributions that are not captured by conventional treatments. This fundamentally alters the predicted thermodynamics under the extreme conditions of dehydrogenation, having a large stabilizing influence on intermediates like $MgB_{12}H_{12}$ and $Mg(B_3H_8)_2$ that have major anharmonic molecular contributions. Notably, these results suggest the need to revisit earlier thermodynamic computations of all complex metal hydrides, which differ from conventional simple and interstitial metal hydrides in the relevance of the complex anion dynamics. Although ab initio molecular dynamics carries significant computational expense, the more accurate free energies obtained by these computations will serve as a far more reliable basis to investigate potential engineering strategies, such as changes in particle size or the introduction of mechanical stress induced by a confinement medium.

Stability of B_xH_y intermediates in metal borohydrides: In the Mg-B-H system, our thermodynamic free energy predictions in Figure 1a qualitatively agree with those of Zhang et al. [1] in that they do not predict stable formation

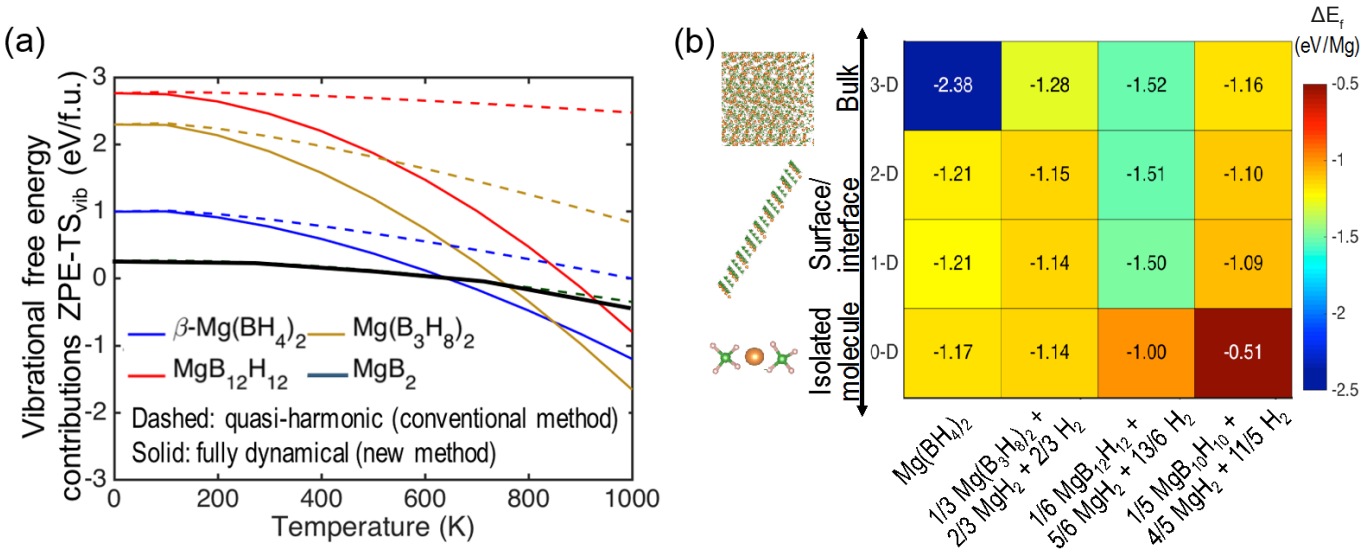

FIGURE 1. (a) Calculated thermal energy contributions from the quasi-harmonic approximation (dashed lines) and full ab initio molecular dynamics including anharmonicity (solid lines) for various compounds in the Mg-B-H system. (b) Mass-balanced formation energies of MgB_xH_y compounds as isolated molecules (0-dimensional), lines and planes of molecules that are more representative of surfaces and interfaces (1-D and 2-D), and bulk materials (3-D).

of MgB_xH_y intermediates other than $MgB_{12}H_{12}$. However, several other chemical intermediates have been observed experimentally, most commonly via ^{11}B nuclear magnetic resonance [2–4]. Assuming moderate accuracy of density functional theory (DFT) as a computational tool, we are left to conclude one of four possibilities: (1) another as-yet-undiscovered structure exists, causing us to mispredict the thermodynamics; (2) the intermediates are kinetically stabilized; (3) the intermediates exist not as solid phases but as chemical species whose energetics depend on their solid-state environment; or (4) the amorphous nature of the intermediates alters their relative thermodynamics. In the effort to address the last two possibilities and gain qualitative insights into how intermediate stability might change in an amorphous state or as a molecular or polymeric species at a solid-solid interface, we modeled the morphology-dependent stability of Mg-B-H compounds by considering the chemical bond properties more explicitly.

Specifically, the stability of molecular complexes at interfaces were estimated by considering the formation energies as a function of *dimensionality*. These values are shown in Figure 1b. The 0-dimensional case represents the isolated molecular complexes of the proper stoichiometry in the gas phase, for example an $Mg(BH_4)_2$ molecule, whereas the 3-dimensional (3-D) reference case is for the crystalline bulk material. In 1-dimensional (1-D) and 2-dimensional (2-D), the MgB_xH_y molecules are arranged in a chain and in a plane, respectively. These 1-D and 2-D configurations are broadly representative of how the molecules might coalesce in interfacial or surface layers. The results in Figure 1b show that $Mg(BH_4)_2$ is significantly more stable (>1 eV) when condensed in the 3-D crystal, as expected. However, $Mg(B_3H_8)_2$, $MgB_{12}H_{12}$, and $MgB_{10}H_{10}$ become competitive with $Mg(BH_4)_2$ when coordinated in lower dimensions. Particularly, for $MgB_{12}H_{12}$ the energy penalty incurred to form 1-D chains or 2-D sheets from 3-D bulk is negligible, since most of its energy stabilization lies in the chemical stability of the closoborane $B_{12}H_{12}^{2-}$ unit and in its ionic interaction with Mg^{2+}, which do not depend on the dimensionality. In fact, the formation energy of $MgB_{12}H_{12}$ in 1-D and 2-D is even lower that that of $Mg(BH_4)_2$, suggesting it could be the preferred species at a solid-state interface and could nucleate easily in this environment. This new dimension-dependent energy analysis could be a powerful tool for understanding the stability of borohydride intermediates, as well as devising strategies for relative destabilization of competing products.

Mass transport at surfaces and through complex hydride microstructures: Our theory effort to model the mass transport within a realistic material microstructure with structural inhomogeneities has focused on two activities. First, we established a computational framework to model full 2-D hydrogen transport on a surface (e.g., during a spillover hydrogenation process). This multiscale capability simulates the long-range and long-time mass transport behavior by coupling the atomistic jumping mechanism to a continuum diffusion model.

We applied this extended simulation capability to the hydrogen refilling and redistribution process within a cleared region on Mg(0001) surface, which emulates the low-energy ion scattering experiments being performed by HyMARC partners. The relevant surface diffusivity tensor

were derived from kinetic Monte Carlo based on barriers from DFT combined with geometric analysis of diffusion pathways. Using the derived surface diffusivity tensor, we next numerically solved the contiuum diffusion equation for hydrogen refilling via surface diffusion into pre-cleared regions. Resulting refiilling rates for pre-cleared areas with different initial geometries (but identical areas) are compared in Figure 2a. Monitoring the hydrogen concentration at the center of the cleared region, the simulation results verify that the refilling kinetics depends strongly on the geometry. By coupling upcoming low-energy ion scattering experiments with corresponding surface diffusion simulations, we can more precisely determine the hydrogen surface diffusion coefficients and mechanisms. With proper parameterization, the method may also be extended to model the chemically reactive structural diffusion in complex hydrides.

Second, we established an efficient mesoscale computational method for extracting the effective diffusivity of an inhomogeneous microstructure containing multiple grains and phases. Synthesized hydrides for hydrogen storage are typically highly polygranular, and a complex variety of additional intermediate phases appears during (de) hydrogenation. As a result, metal hydrides exhibit complex microstructures under operating conditions. Obviously, the diffusion properties of such microstructures with multiple grains in different orientations, multiple phases in different crystal structures, and a complex grain and phase boundaries network would deviate from those of a pristine single crystal. To address this challenge, we integrated the atomistically dervied bulk and surface diffusivity tensors with an established computational method for extracting the effective diffusivity of an inhomogeneous and complex microstructure containing mulitple grains and grain boundaries.

Using hydrogen diffusivity tensors of bulk and surface Mg derived from the kinetic Monte Carlo approach mentioned above, we extracted the effective diffusivities of a polycrystalline grain structure (see the inset of Figure 2b) for several temperatures. Figure 2b shows the computed results along with the bulk and surface diffusivities for comparison. The results show that the effective diffusivities have activation barriers that are dominated by bulk behavior at higher temperatures and surface behavior at lower temperatures. Encouraged by this successful demonstration, we can now systematically investigate the relationship between diffusion properties and microstructural features and topology.

Mechanical stress effects on hydride enthalpy: Mechanical stresses, whether induced intrinsically from the growth of a product phase with significant associated volume change or else extrinsically imposed by an confining medium, can play a significant role in determining the thermodynamics and kinetics of phase transformations of hydrides. Residual stresses upon cycling are also closely related to the material fatigue and fracture, and can limit cycle life of a hydride. To predict the mechanical stress effects arising from crystallographic structural changes and/or volume expansion during solid-state phase transformations of metal hydrides with or without an confining medium, we have begun with the Mg-H system as a model of a simple hydride.

Our methods are based on a multiscale approach borrowed from the metallic alloy phase transformation community [5,6], which integrates microelasticity theory in continuum mechanics with first principles-derived materials parameters. First, we derived the associated transformation strain matrix, which connects the crystallographic planes of the product and reactant phases. Due to the crystallographic symmetry changes associated with the Mg (*hcp*)-to-MgH_2 (*bct*) phase transformation, the system exhibits "multi-variant" characteristics, meaning it has multiple symmetry-

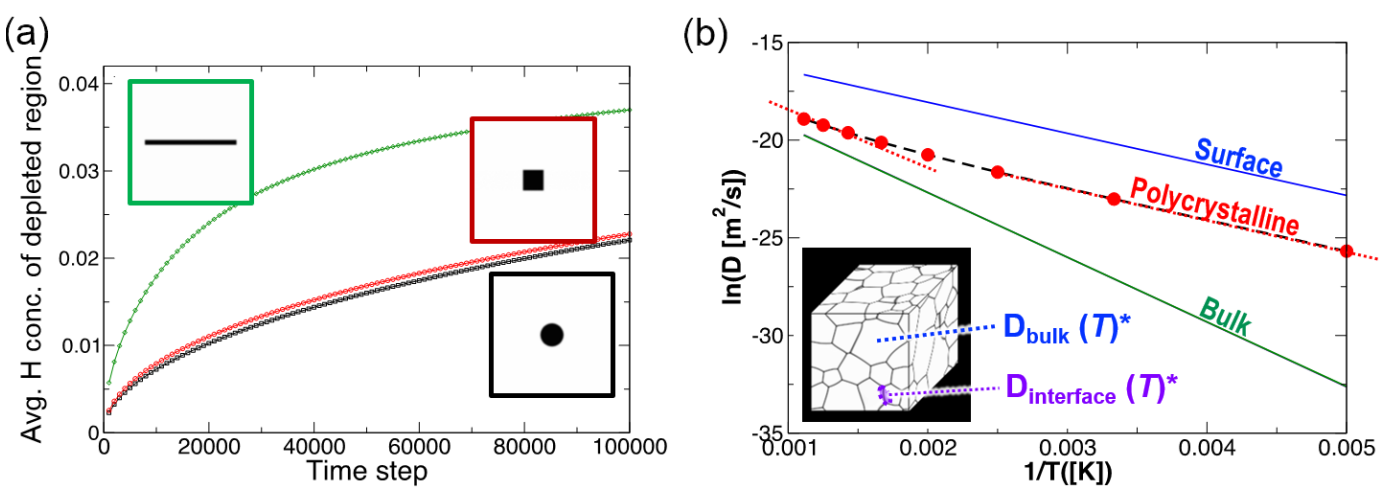

FIGURE 2. Multiscale computational modeling approach for (a) simulating surface diffusion of H on Mg(0001) surface after local depletion in regions with different geometries and (b) extracting effective diffusivities of H in polycrystalline Mg.

equivalent possible distortion orientations. Using the lattice parameters and elastic moduli for each phase as computed with DFT, deformation matrices and lattice mismatches between the two phases were derived.

The Mg to MgH_2 phase transformation involves a significantly large (~30%) volume change. If we consider the formation of MgH_2 created within an Mg matrix under volumetric constraint, this volume mismatch is predicted to have an unrealistically large value of elastic energy (~35 GPa). We can therefore safely assume that the system will introduce interfacial dislocations and other defects at the Mg/MgH_2 boundary. This phenomenon, known as "coherency loss," relaxes the elastic energy. In complex hydrides, the volume change upon hydrogenation is often far greater than in the Mg/MgH_2 system; thus, it is reasonable to assume that this same coherency loss condition is universal to non-interstitial metal hydrides. Following a method we recently developed and published [7], we explored the possibility of coherency loss by introducing factors (m, n) that describe the density of dislocations incurred along each of the two lattice-unique crystallographic directions in Mg and MgH_2. Then, the characteristic strain energy variations for possible coherency states were computed and confirmed that the strain energy magnitude is highly sensitive to the interfacial coherency state (i.e., dislocation density) as expected. For instance, the elastic strain energy is reduced from 35 GPa in the fully coherent case to 1.5 GPa for a dislocation density of ~40%. This strongly implies that the interfaces exhibit significant coherency loss in the Mg/MgH_2 system, and gives a better picture of the actual disordered structure of the interface.

The same approach was also used to calculate the characteristic internal strain energy in confined Mg associated with external stress imposed by the confining medium. To do so, a (de)hydrogenating Mg particle in a confining medium was constructed and modeled as assembled segments with bi-axially compressed thin film geometries in different crystallographic orientations (assuming a core-shell geometry; see Figure 3a). As shown in Figure 3b, the resulting computed elastic strain energy arising from the external volumetric confinement depends on the crystallographic orientation, as expected from the symmetries of the parent phases. If we average over all orientations to obtain the average strain energy for the entire particle, we predict that volumetric constraint can destabilize MgH_2 with respect to Mg by ~8.2 kJ/mol H_2. This agrees extremely well with a relative destabilization of 8.1 kJ/mol H_2 measured by our HyMARC partners via pressure-composition-temperature analysis of Mg/MgH_2 confined in reduced graphene oxide [8]. The excellent agreement suggests that mechanical stress effects may largely account for the observed changes the reaction thermodynamics for confining media with different stiffness and pore geometry, thereby altering the stabilities of hydrides during (de) hydrogenation.

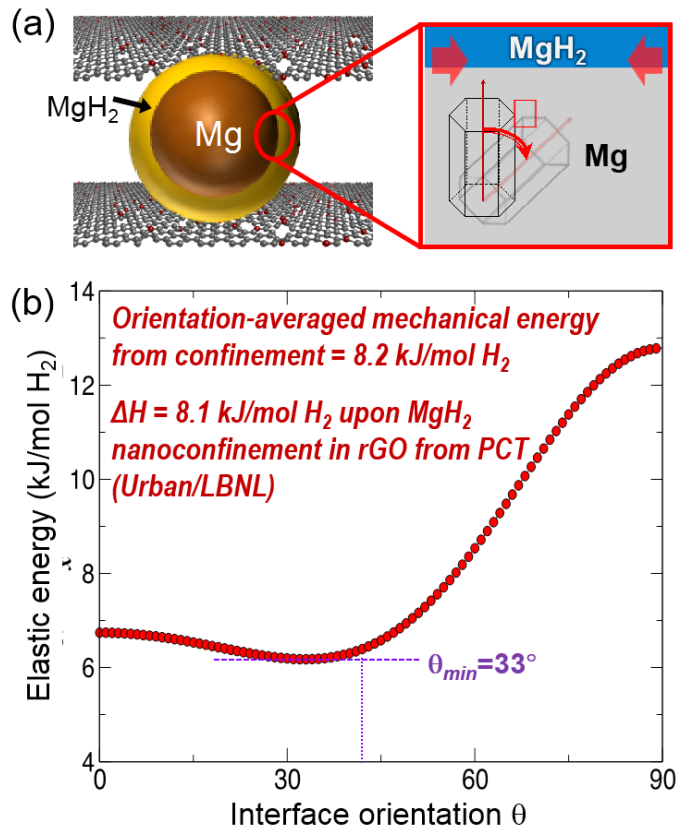

FIGURE 3. (a) Schematic of the orientation-dependent mechanical stress effect at Mg/MgH_2 interfaces in our multiscale micromechanical approach. (b) The calculated orientation-dependent elastic energy affecting the reaction enthalpy of an Mg-H particle in a confining medium.

Surface interaction of H_2 with model catalyst additives: Although TiF_3 and $TiCl_3$ are often added as catalysts in a wide variety of metal hydrides, their activity mechanism has not been well understood. A first step is to understand whether the additives themselves are inert to hydrogen, which would verify that their activity instead relies on incorporation into other reaction materials. This would also establish whether Ti can act as a dissociation catalyst in these materials—one of its many proposed roles. X-ray absorption spectroscopy performed by HyMARC partners recently established that pure TiF_3 and $TiCl_3$ phases without metal hydrides are not intrinsically reactive to H_2, but only become so upon interaction with the active material. To better understand the origin of these results, we performed additional DFT-based theoretical investigations of catalytic reactivity of TiF_3 by computing hydrogen dissociation energetics and barriers on TiF_3 surfaces.

If we assume the presence of surface fluorine vacancies to form binding sites for H_2, then dissociative adsorption on TiF_3 is found to be energetically favorable (e.g., by -0.18 eV/H_2 for the reaction shown in Figure 4). However,

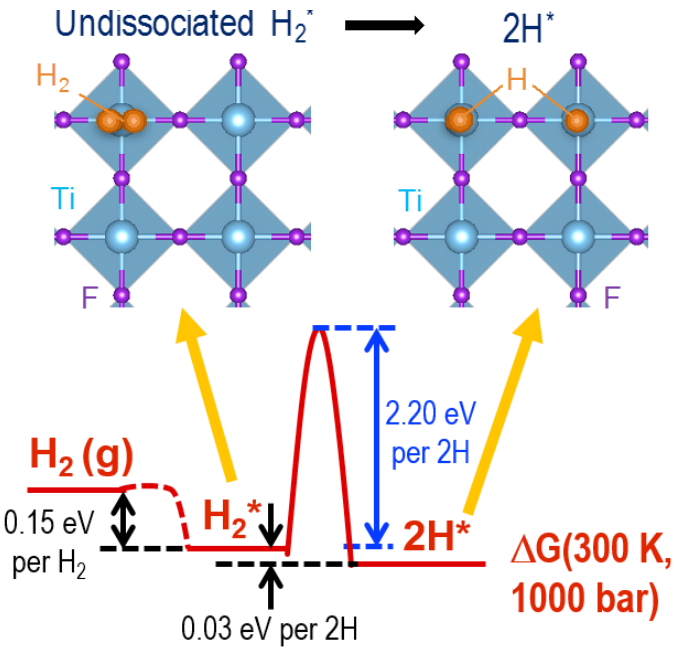

FIGURE 4. Illustration and full energy landscape for one possible H_2 dissociative adsorption reaction on the surface of TiF_3 when outermost surface F atom sites are vacant.

the dissociation energy barriers computed in DFT nudged elastic band calculations were found as high as 2.18–2.21 eV, leading us to conclude that TiF_3 is intrinsically inactive as a catalyst towards H_2. It is worth noting that these thermodynamic driving forces and kinetic energy barriers are highly influenced by the local environment of surface Ti, most notably, by the number and arrangement of surrounding F atoms. By systematic computation of the driving forces and energy barriers as a function of the coordination number of F around surface Ti, we found that the catalytic reactivity observed in experiments when TiF_3 is ball milled with hydrogen storage systems can be understood by one or more of following possibilities. First, different phases, phase morphologies, or chemical species that are reactive towards H_2 may form when TiF_3 is dissociated upon mixing and incorporates directly into the active material. This possibility is widely assumed in the literature. Second, some Ti may remain as TiF_3, but they become highly under-coordinated as F atoms are stripped due to mechanical erosion during ball-milling. Such highly under-coordinated Ti (e.g., Ti with two neighboring F vacancies in TiF_3) could in principle be reactive towards H_2. Third, Ti coordination in TiF_3 may be significantly altered at interfaces by placing it in direct contact with the active material. In this case, H_2 (or atomic H) may simultaneously interact with the TiF_3 catalyst material and the active material, possibly lowering the energy barrier for dissociating H_2.

CONCLUSIONS AND UPCOMING ACTIVITIES

Our team has interacted closely with the other HyMARC partners and new seedling projects to build foundational understanding of thermodynamics and kinetics in solid-state hydrogen storage materials. This year, our synthetic efforts on porous carbon sorbents have mostly focused on boron and nitrogen incorporation. On the characterization side, we have continued our investigations into materials changes upon hydrogenation using soft X-ray probes in collaboration with the other HyMARC labs. On the theory side, we have prioritized development of new computational frameworks for improving the accuracy and realism of complex materials simulations for hydrogen storage. For instance, we showed that the accuracy of hydride thermodynamics computations could be improved using explicit thermal effects taken from ab initio molecular dynamics, suggesting previous first-principles calculations of hydride thermodynamics should be revisited. We also developed a formalism for introducing solid mechanics and interfacial effects in thermodynamic computations, and showed excellent agreement with measured data on the reaction enthalpies of nanoconfined Mg/MgH_2. Furthermore, we performed detailed studies examining the interaction of hydrogen with surfaces in catalysts and sorbents that provide additional insights into the functionality of these materials in (de)hydrogenation reactions. In the coming months, we will:

- Continue our computations of entropy effects and free energies of the remaining borohydride systems.
- Investigate confinement effects in the Mg-B-H and Na-B-H systems using first-principles computations and solid mechanics.
- Use theory to investigate the surface chemistry of complex hydrides in the presence of oxide contamination.

SPECIAL RECOGNITIONS & AWARDS/ PATENTS ISSUED

1. Urban, J.J., Ruminski, A.M., Cho, E.S., Bardhan, R., Brand, A., Wood, B.C., Heo, T.W., Shea, P.T., Kang, S., and Zhou, X., "Hierarchically Controlled Inside-Out Doping of Mg Nanocomposites for Moderate Temperature Hydrogen Storage," U.S. Provisional Patent #62/445,610 (2017).

FY 2017 PUBLICATIONS/PRESENTATIONS

1. Wood, B.C., Stavila, V., Poonyayant, N., Heo, T.W., Ray, K.G., Klebanoff, L.E., Udovic, T.J., Lee, J.R.I., Angboonpong, N., and Pakawatpanurut, P., "Nanointerface-driven reversible hydrogen storage in the nanoconfined Li-N-H system," *Adv. Mater. Interfaces* **4**, 1600803 (2017) [cover feature].

2. Ray, K.G., Klebanoff, L.E., Lee, J.R.I., Stavila, V., Kang, S., Heo, T.W., Bagge-Hansen, M., White, J.L., Shea, P., Baker, A.A., Liu, Y.S., and Wood, B.C., "Elucidating the mechanisms of MgB_2 initial hydrogenation via a combined experiment-theory study," *Phys. Chem. Chem. Phys*., 19(34), 22646–22658 (2017).

3. Kang, S., Ogitsu, T., Bonev, S.A., Heo, T.W., Allndorf, M.D., and Wood, B.C., "Understanding charge transfer at Mg/MgH_2 interfaces for hydrogen storage," *ECS Trans*. 77(10), 81–90 (2017).

4. Zhou, X.W., Heo, T.W., Wood, B.C., Stavila, V., Kang, S., and Allendorf, M.D., "Finite-Temperature Behavior of PdH_x Elastic Constants Computed by Direct Molecular Dynamics," *MRS Adv.*, 2, 3341 (2017).

5. Zhou, X.W., Heo, T.W., Wood, B.C., Stavila, V., Kang, S., Allendorf, M.D., "Fundamental Properties of Palladium Hydrides upon Hydrogenation / Dehydrogenation from Molecular Dynamics: Part I: Bulk Thermodynamic and Kinetic Properties," submitted (2017).

6. Cho, E.S., Ruminski, A.M., Liu, Y.-S., Shea, P., Kang, S., Zaia, E.W., Chuang, Y.-D., Zhou, X.W., Heo, T.W., Guo, J., Wood, B.C. and Urban, J.J., "Hierarchically controlled inside-out doping of Mg nanocomposites for moderate temperature hydrogen storage," Adv. Funct. Mater., in press (2017).

7. K.G. Ray, "X-ray absorption and emission spectroscopy of the initial hydrogenation of MgB_2," Advanced Light Source User Meeting, Berkeley, CA, October 2016 [invited].

8. S. Kang, "Beyond-ideal modeling of (de)hydrogenation in complex metal hydrides," International Symposium on Hydrogen Energy, Waikoloa, HI, February 2017 [invited].

9. S. Kang, "Thermodynamics and Kinetics at Interfaces of Metal Hydrides for Hydrogen Storage," American Chemical Society Meeting, San Francisco, CA, March 2017.

10. T.W. Heo, "Multiscale modeling of solid-state phase transformations in metal hydrides for hydrogen storage," Materials Research Society Spring Meeting, Phoenix, AZ, April 2017.

11. T.W. Heo, "Mesoscale modeling approaches for hydrogen generation and storage," Electrochemical Society Meeting, New Orleans, LA, May 2017 [invited].

12. S. Kang, "Challenges and opportunities for interface modeling in metal hydrides for hydrogen storage," Electrochemical Society Meeting, New Orleans, LA, May 2017.

13. B. Wood, "Predicting properties of complex interfaces for hydrogen production and storage: Challenges and strategies," Electrochemical Society Meeting, New Orleans, LA, May 2017 [invited].

14. B.C. Wood, "Complex dynamics in metal borohydrides: From hydrogen storage to solid-state batteries," Gordon Research Conference on Hydrogen-Metal Systems, Easton, MA, July 2017 [invited].

15. S. Kang, "Multiscale modeling of interfaces in metal hydrides," Gordon Research Seminar on Hydrogen-Metal Systems, Easton, MA, July 2017.

REFERENCES

1. Zhang, Y., Majzoub, E., Ozoliņš, V., and Wolverton. C., "Theoretical Prediction of Metastable Intermediates in the Decomposition of $Mg(BH_4)_2$." *J. Phys. Chem. C* 116 (2012): 10522–10528.

2. Chong, M., Karkamkar, A., Autrey, T., Orimo, S., Jalisatgid, S., and Jensen, C.M., "Reversible Dehydrogenation of Magnesium Borohydride to Magnesium Triborane in the Solid State under Moderate Conditions." *Chem. Commun.* 47 (2011): 1330–1332.

3. Chong, M., Matsuo, M., Orimo, S., Autrey, T., and Jensen, C.M., "Selective Reversible Hydrogenation of $Mg(B_3H_8)_2/MgH_2$ to $Mg(BH_4)_2$: Pathway to Reversible Borane-Based Hydrogen Storage?" *Inorg. Chem.* 54 (8) (2015): 4120–4125.

4. Yan, Y., Remhof, A., Rentsch, D., and Züttel, A., "The role of $MgB_{12}H_{12}$ in the hydrogen desorption process of $Mg(BH_4)_2$." *Chem. Commun.* 51 (2015): 700–702.

5. Ji, Y.Z., Issa, A., Heo, T.W., Saal, J.E., Wolverton, C., and Chen, L.-Q., "Predicting *b¢* Precipitate Morphology and Evolution in Mg–RE Alloys Using a Combination of First-Principles Calculations and Phase-Field Modeling." *Acta Mat.* 76 (2014): 259–271.

6. Heo, T.W., Wang, Y., and Chen, L.-Q., **"**Spinodal Twinning of a Deformed Crystal." *Phil. Mag.* 94 (2014): 888–897.

7. Heo, T.W., Tang, M., Chen, L.-Q., and Wood, B.C., "Defects, Entropy, and the Stabilization of Alternative Phase Boundary Orientations in Battery Electrode Particles." *Adv. Energy Mater.* 6 (2016): 1501759.

8. Cho, E.S., Ruminski, A.M., Liu, Y.-S., Shea, P., Kang, S., Zaia, E.W., Chuang, Y.-D., Zhou, X.W., Heo, T.W., Guo, J., Wood, B.C., and Urban, J.J., "Hierarchically controlled inside-out doping of Mg nanocomposites for moderate temperature hydrogen storage," Adv. Funct. Mater., in press (2017).

IV.C.3 HyMARC (Core): LBNL Effort

Jeffrey J. Urban
Lawrence Berkeley National Laboratory (LBNL)
1 Cyclotron Road, Mail Stop 67R4110
Berkeley, CA 94720
Phone: (510) 486-4526
Email: jjurban@lbl.gov

DOE Manager: Ned Stetson
Phone: (202) 586-9995
Email: Ned.Stetson@ee.doe.gov

Project Start Date: September 17, 2015
Phase I End Date: September 30, 2018

Overall Objectives

- Facilitate community discovery of light, high-capacity hydrogen storage materials and new materials strategies with fine control of nanoscale dimensions to meet weight and volume requirements via modalities such as encapsulation and confinement.
- Develop in situ and in operando soft X-ray characterization capabilities in combination with first-principles simulations to extract atomic and molecular details of functional materials and interfaces.
- Develop community tools and capabilities to enable materials discovery, including computational models and databases, new characterization tools and methods, and tailorable synthetic platforms.

Fiscal Year (FY) 2017 Objectives

- Develop graphene-encapsulated metal borohydride nanocrystal hydrides with control over material phase (alpha, beta, gamma) to produce environmentally-stable, high performance hydrogen storage materials. (This work is projected to aid the seedling project led by D.J. Liu from Argonne National Laboratory [ANL]).
- Control the size of metal hydride nanocrystals from 3–12 nm to provide model systems for hydriding/dehydriding phenomena for ongoing modeling efforts.
- Fabrication of an in situ X-ray spectroscopic gas flow cell to provide a new HyMARC capability able to be used to examine internal hydride interfaces dynamically during hydriding/dehydriding.
- Application of ex-situ X-ray absorption spectroscopy (XAS) to magnesium borohydride ($Mg(BH_4)_2$) to monitor changes in the local electronic structure indicative of kinetically limiting intermediates.
- Preparation of graphene nanoribbons featuring 1,10-phenanthroline ligands to test the hypothesis that functionalized carbons bearing binding sites for discrete metal complexes can catalyze hydrogen dissociation/association at the surface of the metal/metal hydride.
- Simulation and modeling of metal-graphene solid-solid interfaces to understand prototype metal hydride interfaces under oxidative and reductive environments.
- Identified the mechanistic role of functionalized graphene nanoribbons (GNRs) towards H_2 adsorption and dissociation in GNRs encapsulated Mg nanoparticles.
- Use first-principles modeling tools to deepen understanding of the surface structures of γ-$Mg(BH_4)_2$, which is thought to play a significant role in determining its practical performance.
- Deepen modeling efforts on hydride-graphene interfaces, in particular the interaction between graphene and cubic $NaBH_4$ (this work is in projected to aid the seedling project led by D.J. Liu from ANL).

Technical Barriers

This project addresses the following technical barriers from the Hydrogen Storage section of the Fuel Cell Technologies Office Multi-Year Research, Development, and Demonstration Plan.

(O) Lack of Understanding of Hydrogen Physisorption and Chemisorption

(A) System Weight and Volume

(E) Charge/Discharge Rate

Technical Targets

This project does not have specific technical targets. However, some storage metrics are presented below after the discussion of HyMARC objectives.

Technical goal of HyMARC: This project will develop foundational understanding and new capabilities that will enable accelerated discovery of breakthrough materials in all classes of storage materials, in particular metal hydrides and sorbents. It is anticipated that the insights gained from this research, coupled with new synthetic, characterization, modeling, and database tools that will be made available to the hydrogen storage research community, will lead to materials that meet DOE targets such as system gravimetric and volumetric capacity, system fill time, and delivery temperature.

As mentioned, for context, Table 1 shows relevant storage metrics and how they stand in relation to some of the development of materials developed through this effort.

TABLE 1. Technical System Targets for Hydrogen Storage for Fuel Cell Vehicles

Storage Parameter	Units	DOE 2020	Ultimate
System Gravimetric Capacity	kWh/kg (kg H_2/kg System)	1.5 (0.045)	2.2 (0.065)
System Volumetric Capacity	kWh/L (kg H_2/L System)	1.0 (0.030)	1.7 (0.050)
Min/Max Delivery Temperature	°C	-40/85	-40/85
System Fill Time (5 kg)	minutes	3-5	3-5
Min/Max Delivery Pressure from Storage System	bar	5/12	5/12

This project is conducting studies on Mg nanocrystals encapsulated by reduced graphene oxide (rGO) layers. DOE hydrogen storage targets are quantified based on the system, while material-based numbers are presented.

- Gravimetric Capacity (based on the total material): 0.065 kg H_2/kg material
- Volumetric Capacity (based on the total material): 0.105 kg H_2/L material

FY 2017 Accomplishments

- Designed a graphene-encapsulation for different phases (γ, β, α) of magnesium borohydride ($Mg(BH_4)_2$) nanocrystals with a solution-based synthetic approach (Figure 1). This is based upon prior Mg/rGO work in the Urban group.
- Prepared $Mg(BH_4)_2$ nanocrystals encapsulated by rGO layers which releases 10.2 wt% H_2 in terms of the total material weight. Investigated the effect of different rGO loading on the hydrogen desorption properties (Figure 2).
- Established the role of thin interfacial oxide layer in contributing stronger binding between reduced graphene oxide and the Mg nanoparticle, thus improving the mechanical and chemical stability of the functioning nanocomposite without hindering the overall hydrogenation-dehydrogenation process.
- Developed instrumentation: The new soft X-ray in situ gas flow cell is now under commissioning at the Advanced Light Source (ALS). It gives better temperature control on the sample surface (room temperature to 300°C). In addition, this new gas cell has better gas sealing for evacuating the sample environment. Figure 3 shows the design drawing of the new version of the in situ X-ray spectroscopic gas flow cell. The gas cell has been fabricated and is currently under testing in order to examine its working temperature range, vacuum/gas sealing and safety.
- Studied pristine and hydrogenated $LiBH_4$ by ex situ XAS at B K-edge with possible intermediate products such as $Li_2B_{12}H_{12}$ (Figure 4). Furthermore, a series of reference samples, including Li_3N, $LiNH_2$ and $LiNH_3$, were studied at N K-edge XAS for future XAS spectra database use.
- Discovered that the improvement of H_2 uptake processes (both H_2 adsorption and dissociation) in nitrogen-functionalized GNR (4N-GNR)/Mg nanocomposite is due to interfacial interactions that create a number of undercoordinated, slightly oxidized Mg (Figure 5).
- Studied various surface terminations of γ-$Mg(BH_4)_2$ (001) surface. The thermodynamically most stable surface was found to be the BH_4^- terminated surface with low BH_4^- coverage. When the BH_4^- coverage increases, it spontaneously transforms into a $B_2H_7^-$ terminated surface by releasing H_2 gas.

✧ ✧ ✧ ✧ ✧

INTRODUCTION

Storage of hydrogen onboard vehicles is one of the critical enabling technologies for creating hydrogen-fueled transportation systems that can provide U.S. energy independence and abate air pollution. Stakeholders in developing hydrogen infrastructure (e.g., state governments, automotive original equipment manufacturers, station providers and industrial gas suppliers) are currently focused on high-pressure storage at 350 bar and 700 bar, in part because no viable solid-phase storage material has emerged. Nevertheless, solid-state materials, including novel sorbents and high-density hydrides, remain of interest because of their unique potential to meet all Fuel Cell Technologies Office targets and deliver hydrogen at lower pressures and higher onboard densities. A successful solution would significantly reduce costs and ensure the economic viability of a U.S. hydrogen infrastructure.

LBNL's effort within HyMARC is to provide leadership to the LBNL effort of HyMARC as well as Task 4 (solid-solid interfaces). The LBNL effort also seeks to develop (via multidisciplinary and multi-lab collaborations) novel materials platforms and cutting-edge, in situ characterization to reveal key functional aspects of various materials components in enhancing the efficiency and stability of hydrogen storage. By focusing on encapsulation, protection, or confinement of active materials within lightweight, selectively permeable, functional media, we have realized advances in the performance of model systems, specifically

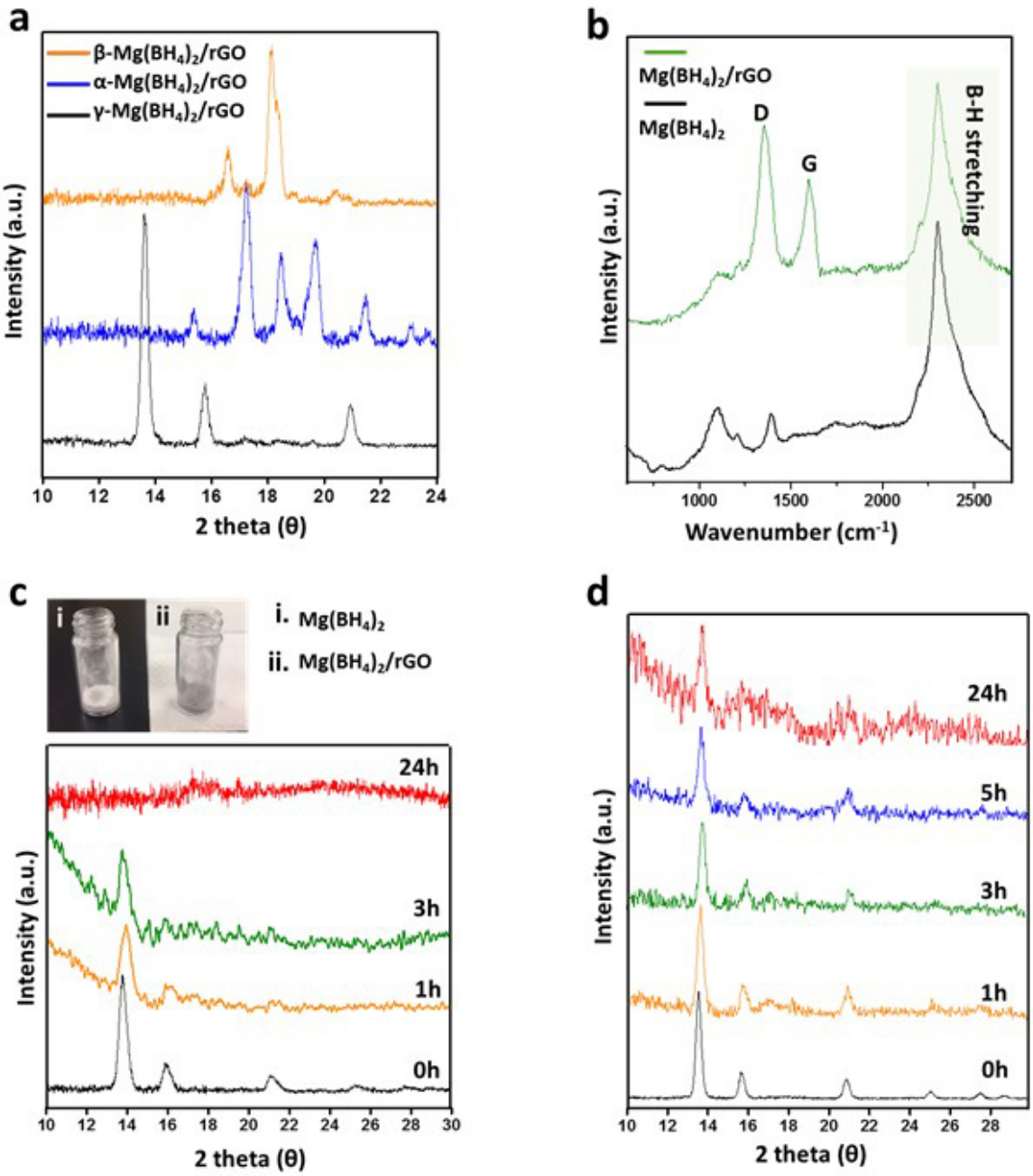

FIGURE 1. (a) X-ray diffraction patterns of β-, α-, γ-$Mg(BH_4)_2$/rGO heterostructures. (b) Raman spectra of $Mg(BH_4)_2$ and $Mg(BH_4)_2$/rGO heterostructures. The Raman spectrum of $Mg(BH_4)_2$/rGO displays B-H stretching of $Mg(BH_4)_2$ which is well matched with bulk $Mg(BH_4)_2$ and the D and G band of rGO at between at 1,300 cm^{-1} and 1,700 cm^{-1}. Air stability of $Mg(BH_4)_2$ without (c) and with (d) rGO. $Mg(BH_4)_2$/rGO composites show better air stability compared to $Mg(BH_4)_2$ without rGO. Photograph of white powder of $Mg(BH_4)_2$ (c inset, i) and grey powder of $Mg(BH_4)_2$/rGO (c inset, ii).

magnesium wrapped in rGO, and are seeing similar gains in complex borohydrides (Tasks 1 and 2). The same systems are being analyzed using unique in situ X-ray spectroscopic probes, such as XAS, that reveal depth-dependent and interfacial chemical composition at various stages of loading with hydrogen and throughout the history of cycled materials (Tasks 3 and 4). Furthermore, such systems can be understood in atomic and electronic detail using first-principles calculations, consistent with characterization, that reveal the important role of materials interfaces in controlling the kinetics and stability of thermodynamically well-defined storage systems (Task 2), or perhaps alter

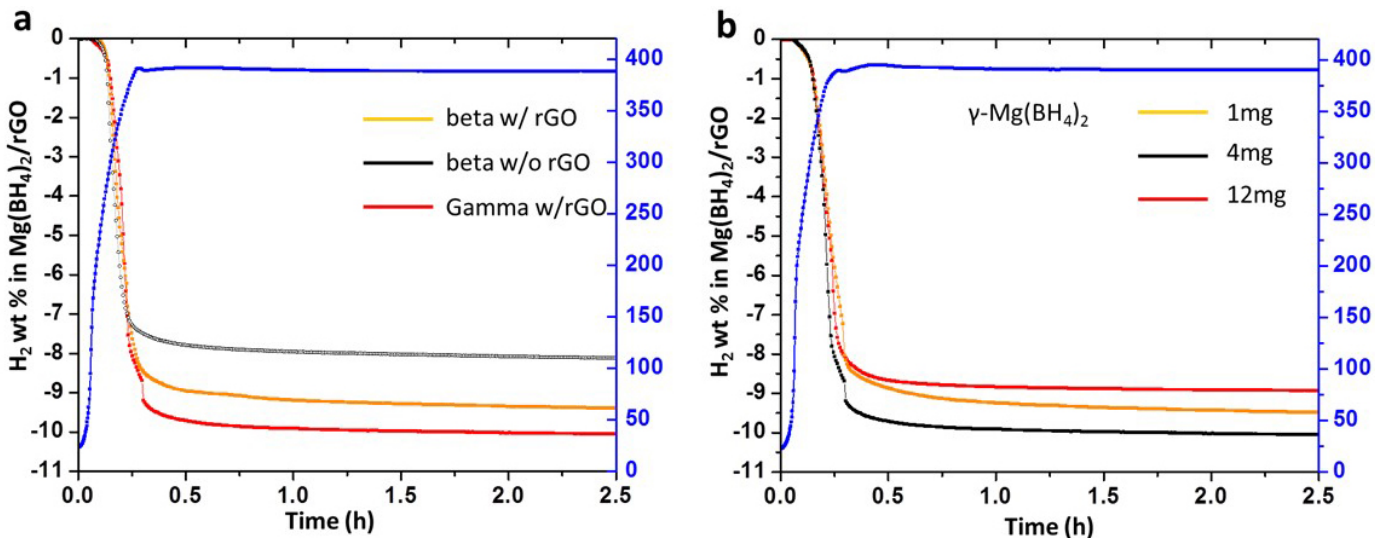

FIGURE 2. Hydrogen desorption (at 390°C and 0 bar) for the as-synthesized $Mg(BH_4)_2$/rGO. (a) γ-$Mg(BH_4)_2$/rGO releases a large amount of hydrogen (10.2 wt%). In addition $Mg(BH_4)_2$ without rGO less released hydrogen (8.1 wt%) compared to $Mg(BH_4)_2$ with rGO. (b) γ-$Mg(BH_4)_2$ with rGO loading of 4 mg shows the best hydrogen desorption performance.

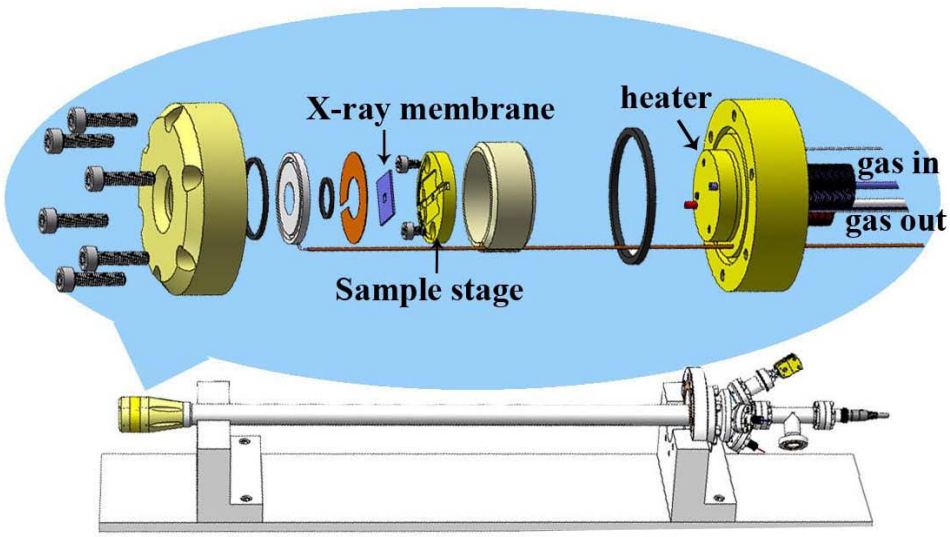

FIGURE 3. The in situ X-ray spectroscopic gas flow cell design drawing. The design specification for the cell are; provide higher accuracy and stability in temperature on sample surface to 300°C, improve better gas and vacuum sealing ideal for hydrogen dehydronation process.

the thermodynamics by defining interphases with distinct energetics, such as the interfacial suboxide in rGO-encapsulated magnesium (Task 1). Incorporation of additives (transition metals in magnesium) or chemical functional groups within confining media (N and O functionalization of GNRs) to enhance activity is being explored synthetically and theoretically (Task 5). Finally, we are engaged in large scale investigations of sorbent databases using empirical modeling to derive descriptors for hydrogen storage that can guide materials development (Task 6). The expertise gained in each of these efforts is available to seedling projects and already being utilized by efforts related to graphene encapsulation of complex hydrides (Liu, ANL) and etherate additives in the $MgB_2/Mg(BH_4)_2$ system (Severa, University of Hawaii).

APPROACH

HyMARC seeks to overcome the lack of foundational understanding that is key to materials systems advances in increasing efficiency and stability of hydrogen storage through our integrated studies of model systems and

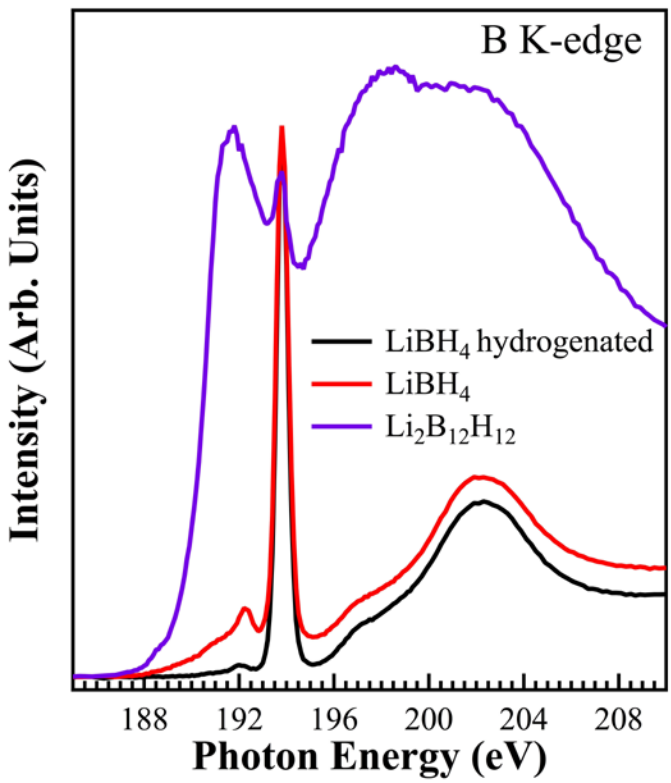

FIGURE 4. Boron K-edge XAS spectra of $LiBH_4$ (pristine and hydrogenated $LiBH_4$ under 70 bar at 400°C) with reference sample $Li_2B_{12}H_{12}$ are presented. A very small portion of $Li_2B_{12}H_{12}$ may present in $LiBH_4$, which recently been observed by NMR experiment from Stavila. The presence of $(BH_4)^{2-}$ ion is considered responsible to the degradation of reversibility. Therefore, possible intermediate $Li_2B_{12}H_{12}$ could form in hydrogenated process.

promising materials classes using synthesis, characterization, and theory and modeling. The LBNL component of the HyMARC team leverages expertise in chemical and materials synthesis, X-ray spectroscopic characterization, first-principles theory and modeling and force-field based exploration of materials databases.

RESULTS

Substantial results on all tasks were made, and nearly all quarterly goals were met on time. LBNL principal investigators led or co-led task groups and helped coordinate and participate in meetings. In addition to managerial output, the key technical results were as follows:

Complex hydride synthesis: This is a key result, translating the approaches developed on model Mg hydride materials to higher capacity borohydrides. A rGO-encapsulation strategy was developed to provide phase control for different phases (γ, β, α) of $Mg(BH_4)_2$ nanocrystals with a solution-based synthetic approach (Figure 1). Because $Mg(BH_4)_2$ is one of the highest-capacity hydrogen storage materials (14.9 wt%) known, this is a key step toward robust high-capacity systems. This nano-hybrid system is important for understanding how solid-solid interfaces impact absorption/desorption kinetics and provide a reaction pathway to improved kinetics.

The stability and performance of these materials were studied as well. The air stability of γ-$Mg(BH_4)_2$ with and without rGO was studied to prove that rGO is able to show the high gas selectivity that is sufficient to discriminate between H_2 and other molecules (H_2O, O_2) (Figure 1c and 1d). The performance of prepared $Mg(BH_4)_2$ nanocrystals encapsulated by rGO layers was performed in collaboration with Stavila (SNL), demonstrating the release of 10.2 wt% H_2 in terms of the total material weight (Figure 2a). This system is now approaching the theoretical capacity value (14.9%) of $Mg(BH_4)_2$. Further, the effect of different rGO loadings on the hydrogen desorption properties was investigated to learn how the amount of rGO impacts desorption kinetics and thermodynamics (Figure 2b).

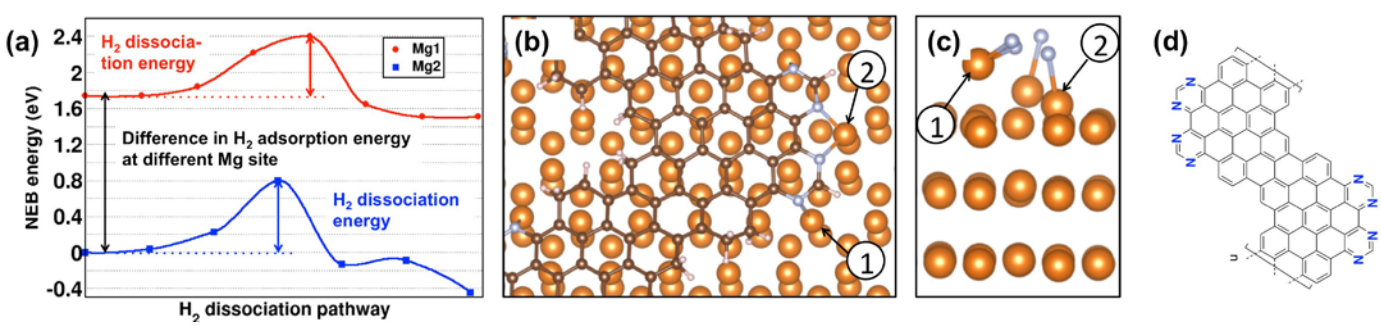

FIGURE 5. (a) H_2 dissociation energy at different Mg sites in 4N-GNR/Mg nanocomposite. (b) The structure of 4N-GNR/Mg (top view). The Mg atoms, marked as 1 and 2, are moving outward to directly bond with N from the 4N-GNR and the H_2 dissociation energy on these Mg atoms is calculated using the climbed imaging nudged elastic band (NEB) methods in (a). (c) Side view of the 4N-GNR/Mg structure. (d) The structure of 4N-GNR. In these structure representations, Mg, C, N and H are shown as orange, brown, light blue, and pink spheres, respectively.

Results in sorbents–modeling and synthesis: Efficient and accurate determination of the volumetric and gravimetric capacity of nanoporous adsorbents at hydrogen fueling (100 bar) and delivery (5 bar) pressures is key to materials selection and development for onboard hydrogen storage applications. We have analyzed the variance in simulated hydrogen isotherms in nearly 500 metal-organic frameworks (MOFs) due to model inputs such as classical H_2 potentials, equations of state for H_2, and density functional theory-based optimization of experimentally-derived MOF structures. Our high-throughput analysis revealed a strong correlation between total H_2 adsorption at 100 bar and MOF void volume that outperforms a well-known correlation between H_2 adsorption and surface area.

Furthermore, it was determined that the coverage of hydrogen is the same for the neutral MCF-17 mesoporous silica as for the acidified MCF-17 (Al-MCF-17) with two different concentrations of acidic sites (Al-MCF-17 with Si:Al ratio of 11:1 and 57:1) (Figure 6). Nevertheless, the concentration of acidic sites (Brønsted and Lewis) was found to affect the heat of adsorption determined from low temperature adsorption studies (-50°C to -90°C) as presented in Table 2. The primary goal of this work was to understand how charges or acidic protons affect the heat of hydrogen adsorption.

Application of X-ray spectroscopic capabilities: Advancing the performance of these capabilities is essential to understanding the role that internal solid-solid interfaces and transient intermediates play in hydrogen storage. Soft X-ray spectroscopy and imaging characterization measurements were carried out with Jinghua Guo at the ALS working closely with the HyMARC teams of Tasks 1, 3, 4, 5. We have characterized air-stable γ-$Mg(BH_4)_2$ nanocomposites and several solid-state metal hydrides ($Mg(BH_4)_2$, Li_3N, Li_2NH, and $LiNH_2$, $LiBH_4$, LiH, $Li_2B_{12}H_{12}$, $LiAlH_4$, LiOH, and $LiBH_4$). These efforts assist the foundational understanding of the relevant physical and chemical interactions occurring on the spatial scale of atoms and molecules with solid-state metal hydrides.

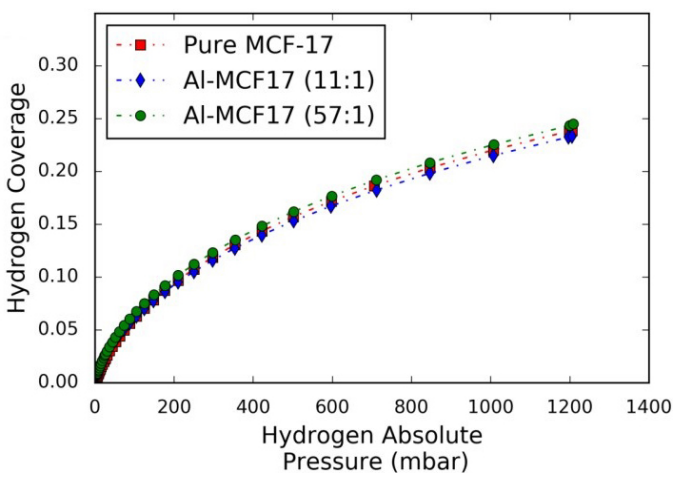

FIGURE 6. Normalized hydrogen adsorption in terms of coverage on neutral (MCF-17) and acidified (Al-MCF-17) mesoporous silica with different concentration of aluminum (or acidic) sites. The measurements were carried out at 77 K.

TABLE 2. Heat of Adsorption for Neutral and Acidified Mesoporous Silica and for Carbon as a Standard Sample

Samples	Surface area (m^2/g)	Heat of Adsorption (kJ/mol of H_2)
Carbon	930.0	8.4
MCF-17		4.5
Al-MCF-17 (57:1)	322.8	2.9
Al-MCF-17 (11:1)	498.5	4.9

Specific highlights include the ex situ XAS characterization of α-, β-, and γ-$Mg(BH_4)_2$, both with and without rGO encapsulation, including both the pristine and dehydrogenated γ-phase. Mg K-edge spectra of γ-$Mg(BH_4)_2$ with and without rGO capsulation is shown in Figure 7. We studied pristine and hydrogenated $LiBH_4$ by ex situ XAS at B K-edge with possible intermediate products such as $Li_2B_{12}H_{12}$ (Figure 4). The access to the soft X-ray region of B K-edge is more critical now owing to results from the previous year. Furthermore, a series of reference samples were studied at N K-edge XAS, including Li_3N, $LiNH_2$ and $LiNH_3$, for future XAS spectra database use.

Development of new X-ray in-situ instrumentation: The new soft X-ray in situ gas flow cell is now under commissioning at the ALS. It provides better temperature control on the sample surface (room temperature to 300°C). In addition, this new gas cell has better gas sealing for evacuating the sample environment. Figure 3 shows the design drawing of the new version of the in situ X-ray spectroscopic gas flow cell. The gas cell has been fabricated and is currently under testing in order to examine its working temperature range, vacuum/gas sealing and safety.

Accomplishments in additives: In an effort to lower the activation temperature for H_2 adsorption and desorption in metal hydrides we developed a stabilizing GNR matrix that is functionalized with molecularly defined hydrogen dissociation catalysts (Task 5). The close proximity of these catalysts to the metal surface (the site of hydrogen uptake) increases the local concentration of hydrogen atoms during the uptake process. The principle of microscopic reversibility allows the same catalyst to lower the barrier for hydrogen atom recombination during the H_2 release. These study of these catalytic GNRs will allow us to decouple the kinetic contribution from diffusion/effusion in the solid from the H_2 dissociation reaction at the surface of different metals. We successfully introduced transition metal complexes along the edges of 1,10-phenanthroline functionalized GNRs (Figure 8). In an initial effort to optimize the reaction conditions and monitor the progress, the coordination

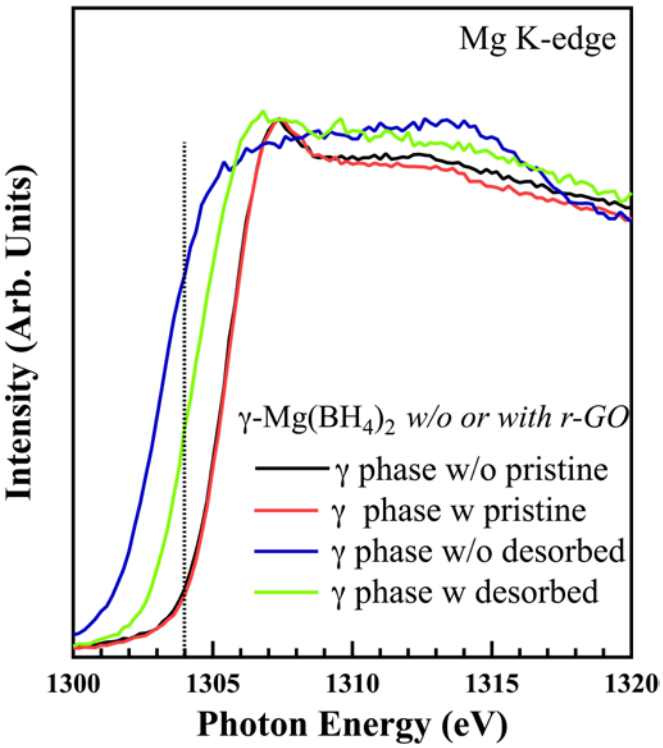

FIGURE 7. Mg K-edge XAS spectra of pristine and hydrogen desorbed $Mg(BH_4)_2$ without or with rGO capsulation. The dotted line indicates the lower onset in energy upon hydrogen desorption, i.e., black and blue curves. The earlier onset is also observed in MgB_2, which is not shown in this figure. Hence, the different onset in spectra between without and with rGO $Mg(BH_4)_2$ are indicating that the rGO layer plays an important role in kinetics. In addition, it is also clear evidence that $MgB_{12}H_{12}$ is not present after hydrogen desorption since the early onset is absent in the spectrum. The XAS results indicate that $MgB_{12}H_{12}$ is not present which is harmful to reversibility during hydrogen desorption/absorption process.

of $Re(CO)_5Cl$ (a known catalyst capable of activating dihydrogen) to the 1,10-phenanthroline decorated GNRs was studied. The resulting complex, a $Re(CO)_3Cl$(phenanthroline), features three carbonyl groups that were used as characteristic markers in infrared spectroscopy. Thermogravimetric analysis and elemental analysis indicate that under the optimized reaction conditions, the yield of metallated 1,10-phenanthroline groups in GNRs exceeds 99%. Current work is dedicated to expanding the variety of transition metal based hydrogenation catalysts (Pt, Pd, Ni, Rh, Ir) that can be coordinated to the functionalized GNRs. The process of developing a standard reaction protocol to benchmark the activity of the respective GNR heterostructure hydrogenation complexes is underway in collaboration with Lennie Klebanoff of Sandia National Laboratories.

Results in theory and simulation of solid-solid interfaces: Within the context of graphene or rGO encapsulation as a means to protect nanoparticles of active materials from oxidizing environmental agents (e.g., oxygen, water) and provide a selectively permeable membrane for H_2, we noted the presence of some oxidation in model Mg nanoparticle systems based on XAS measured at the ALS. Using first-principles calculations of both atomistic models and associated simulated spectra (a capability available within HyMARC) we established the role of an atomically thin interfacial oxide layer in contributing stronger binding between rGO and the Mg nanoparticle, thus improving the mechanical and chemical stability of the functioning nanocomposite without hindering the overall hydrogenation-dehydrogenation process.

First-principles calculations revealed improvements in H_2 uptake (both H_2 adsorption and dissociation) in 4N-GNRs encapsulating Mg, synthesized by Fischer. There is a strong interfacial interaction that creates a number of undercoordinated, slightly oxidized Mg atoms at the metal nanoparticle surface, which are active sites of H_2 uptake (Figure 5). Moving towards higher capacity complex hydrides, we used first-principle calculations to study various surface terminations of the γ-$Mg(BH_4)_2$ (001) surface, finding the thermodynamically most stable surface to be the BH_4^- termination with low BH_4^- coverage. When the BH_4^- coverage increases, it spontaneously transforms into the $B_2H_7^-$ terminated surface by releasing H_2 gas indicating intrinsic activity of this surface. In relation to the Liu (ANL) HyMARC seedling project, we determined using first-principles calculations that weak graphene/$NaBH_4$ interactions are generally found at different $NaBH_4$ surfaces, except for the Na-terminated $NaBH_4$ (111) surface.

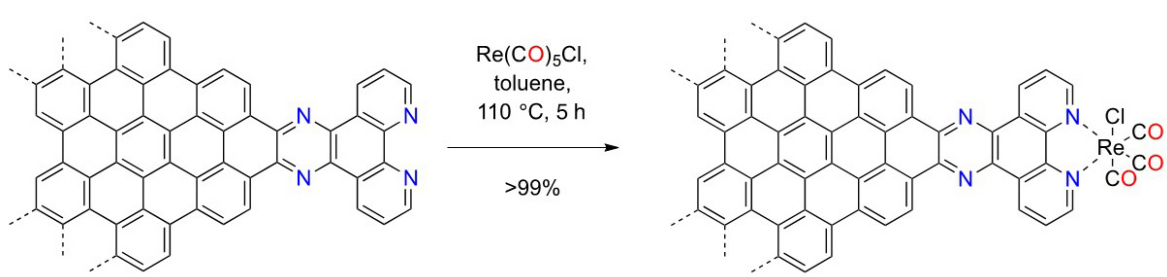

FIGURE 8. Synthetic scheme detailing the integration of molecularly defined transition metal complexes along the edges of functional GNRs.

CONCLUSIONS AND UPCOMING ACTIVITIES

Our team has interacted closely with the other HyMARC partners and new seedling projects to build foundational understanding of thermodynamics and kinetics in solid-state hydrogen storage materials. This year we met a key goal, transitioning our synthetic activities from model Mg hydrides to more complex and higher capacity Mg borohydrides. Other synthetic work aims to use functionalized carbon materials to protect hydrides from degradation while also providing catalytic enhancement of kinetics via targeted placement of transition metal species. On the characterization side, our investigations into hydride interfaces using soft X-ray probes continue, with development of in situ cells being a substantial advance. On the theory side, we discovered that sub-oxide interfacial chemistry plays a surprisingly beneficial role in metal hydride kinetics and reversibility. Further, the modeling work on the MOF database has expanded and will soon be ready to make testable predictions of the thermodynamics and capacity of new porous materials. In the coming months, we aim to:

- Optimize the thermodynamics and kinetics of the dehydrogenation and hydrogenation processes of encapsulated $Mg(BH_4)_2$/rGO hybrid nanomaterials (collaboration with the seedling project at ANL).
- Extend our study of the chemical stability of γ-$Mg(BH_4)_2$ towards oxidation and water contamination and more fully explore the interfacial interaction between γ-$Mg(BH_4)_2$ and graphene, based on the surprising beneficial role of limited oxidation in model Mg NP/rGO composites and initial studies of pristine stable surface terminations.
- Use first-principles molecular dynamics to examine the thermodynamics and kinetics of the dehydrogenation process in etherated $Mg(BH_4)_2$ (collaboration with the seedling project at the University of Hawaii).
- Continue to develop multivariate linear models to correlate MOF pore descriptors (pore volumes, cavity diameters, cavity curvature) to H_2 adsorption at other temperature and pressure conditions (5 bar, near-ambient temperatures). These models will enable rapid characterization of H_2 storage performance at both storage and delivery conditions. This effort will place particular emphasis on MOFs with coordinately unsaturated ("open") metal sites, supporting the University of California, Berkeley seedling project.
- Utilize the new Advanced Materials Beamline for Energy Research (AMBER 6.0.1) at the ALS, in use starting April 2018, which will offer a new capability for the entire HyMARC effort.
- Continue building on the demonstration that molecularly defined hydrogen dissociation catalysts can be seamlessly integrated into a functional GNR/metal nanoparticle composite material. This technology will enable us to decouple the H_2 dissociation kinetics from the diffusion dynamics that dominate uptake and release kinetics in metal hydrides. Our next steps will establish the benchmark kinetics for catalyst modified GNRs (Task 5 in collaboration with Lennie Klebanoff, Sandia National Laboratories) and study the change in the uptake/release kinetics for metal hydride composites (initial experiments will rely on the MgH_2 and AlH_3 system established through our work in Task 4).

SPECIAL RECOGNITIONS & AWARDS/ PATENTS ISSUED

1. (Urban) SBIR awarded for H_2 storage work with Agiltron, Inc. (scale up of metal hydrides).

2. (Urban) New PCT filed on H_2 work partially supported by HyMARC: 2015-089-02 H_2 storage laminates.

3. (Urban) New provisional patent filed on H_2 work partially supported by HyMARC: 2013-065-01 doped nanostructures for H_2 storage.

FY 2017 PUBLICATIONS/PRESENTATIONS

Publications

1. "Atomically-thin interfacial suboxide key to hydrogen storage performance enhancements of magnesium nanoparticles encapsulated in reduced graphene oxide," Liwen F. Wan, Yi-Sheng Liu, Eun Seon Cho, Jason D. Forster, Sohee Jeong, Hsiao-Tsu Wang, Jeffrey J. Urban, Jinghua Guo, and David Prendergast, *accepted*, *Nano Letters*.

2. "Tailoring polymer configuration for nanocrystal growth: the role of chain length and solvent," Eun Seon Cho, Fen Qiu, and Jeffrey J. Urban, *Small,* **13(3)**, (2017). DOI: 10.1002/smll.201602572. This article is featured on the frontispiece (inside cover) of *Small,* 13(3), (2017).

3. "Graphene ribbon nanobelted Mg crystals for high capacity hydrogen storage," Eun Seon Chô, Tomas Marangonî, Yi-Sheng Liu, Cameron Rogers, Edmond W. Zaia, Ryan R. Cloke, Patrick T. Shea, Yi-De Chuang, Jinghua Guo, Brandon C. Wood, Felix R. Fischer*, and Jeffrey J. Urban*, *submitted* (2017).

4. "Hierarchically controlled inside-out doping of Mg Nanocomposites for moderate temperature hydrogen storage," Eun Seon Chô, Anne M. Ruminski, Yi-Sheng Liu, Patrick T. Shea, ShinYoung Kang, Edmond W. Zaia, Yi-De Chuang, Xiaowang Zhou, Tae Wook Heo, Jinghua Guo, Brandon C. Wood, and Jeffrey J. Urban, *under revision, Advanced Functional Materials* (2017).

Presentations

Jeffrey J. Urban:

1. May 2017 – ECS National Meeting, New Orleans, LA (Invited keynote).

2. January 2017 – Invited talk at ALS-U workshop, Berkeley, CA.

3. October 2016 – ECS National Meeting, Honolulu, HI (Invited).

4. September 2016 – Department of Civil Engineering, Berkeley, CA.

Felix R. Fischer:

1. Max Planck Gesellschaft – Conference on Molecular Nanostructures, Ascona, Switzerland, February 6–10, 2017.

2. Polymers Gordon Research Conference, Mt. Holyoke College, U.S.A., June 11–16, 2017.

3. Physical Organic Chemistry Gordon Research Conference, Holderness School, U.S.A., June 25–30, 2017.

4. International Conference on Novel Aromatics, Stoney Brook, U.S.A., July 23–28, 2017.

Jinghua Guo:

1. "In-Situ/Operando Soft X-Ray Spectroscopy of Catalytic and Electrochemical Reactions," The 252nd ACS National Meeting, symposium: Advanced Nanoscale Chemical Imaging of Catalyst Materials, Philadelphia, PA (August 21–25, 2016).

2. "In-Situ/Operando Soft X-Ray Spectroscopy of Catalytic and Electrochemical Reactions," SPIE 2016 Optics + Photonics for Sustainable Energy, symposium: Solar Hydrogen and Nanotechnology XI, San Diego, CA (August 28–September 1, 2016).

3. "In-Situ/Operando Resonant Inelastic Soft X-ray Scattering Characterization of Chemical and Catalytic Reactions," Department of Chemistry, Materials Science & Engineering, University of California, Berkeley, CA (September 23, 2016).

4. "Synchrotron Radiation Based Soft X-ray Characterization of Energy Materials," invited lecture, Tokyo University of Science, Japan (December 22, 2016).

IV.C.4 HyMARC (Support): NREL Effort

Thomas Gennett[1] (Primary Contact),
Craig Brown[2] (Principal Investigator),
Phillip Parilla[1], Terry Udovic[2], Michele Olsen[1],
Katherine Hurst[1], Jeff Blackburn[1], Jacob Tarver[1,2],
Mirjana Dimitrievska[1,2], Noemi Leick[1],
Steven Christensen[1], W. Ellis Klein[1],
Wade Braunecker[1]

[1]National Renewable Energy Laboratory (NREL)
15313 Denver West Parkway
Golden, CO 80401
Phone: (303) 384-6628
Email: thomas.gennett@nrel.gov

[2]National Institute of Standards and Technology (NIST)
100 Bureau Drive
Gaithersburg, MD 20899

DOE Manager: Jesse Adams
Phone: (720) 356-1421
Email: Jesse.Adams@ee.doe.gov

Subcontractor:
Justin Lee, Thesis Corporation, Westminster, CO

Project Start Date: October 1, 2015
Project End Date: Project continuation and direction determined annually by DOE

Overall Objectives

- Develop a series of advanced characterization tools that allow for rapid advancement and in-depth understanding of next-generation hydrogen storage materials.
- Develop a hydrogen storage material with a total material-based capacity of greater than 45 g/L, at a temperature above 150 K and less than 100 bar, and reversible for multiple cycles.
- Develop a consensus protocol for the measurement and reporting of hydrogen gravimetric and volumetric capacities.
- Validate the performance of various hydrogen storage materials as requested by DOE.

Fiscal Year (FY) 2017 Objectives

- Develop new characterization tools (specifically: thermal conductivity and cryostat temperature control of pressure-concentration-temperature [PCT] apparatus).
- Demonstrate the ability to increase the binding energy and/or hydrogen desorption temperature in a sorbent material.
- Develop computational program to control the advanced cryostat controlled PCT apparatus.
- Determine the viability of boron and nitrogen doped materials for increased binding energy and capacities that could approach the 2020 DOE onboard hydrogen storage targets.
- Conduct a multi-laboratory PCT round-robin investigation to determine the volumetric and gravimetric capacities of two standard sorbent materials.
- Assist the DOE Hydrogen Materials – Advanced Research Consortium (HyMARC) seedling projects.

Technical Barriers

This project addresses the following technical barriers from the Hydrogen Storage section of the Fuel Cell Technologies Office (FCTO) Multi-Year Research, Development, and Demonstration Plan.

(A) System Weight and Volume

(B) System Cost

(C) Efficiency

(E) Charging/Discharging Rates

(O) Lack of Understanding of Hydrogen Physisorption and Chemisorption

(P) Reproducibility of Performance

Technical Targets

Hydrogen Storage Materials: This project is conducting validation studies of various framework materials, sorbents, hydrides and model compounds. Concurrently, the team also is developing new characterization tools for the rapid enhancement of materials development. Insights gained from these studies will be applied toward the design and synthesis of hydrogen storage materials that meet the following DOE onboard 2020 automotive usable hydrogen storage targets.

- 1.5 kWh/kg system (4.5 wt% H_2)
- 1.0 kWh/L system (0.030 kg H_2/L)
- Cost of \$10/kWh (\$333/kg H_2 stored)
- Operating at ambient temperatures (-40°C to 60°C)
- Onboard efficiency of 90% and minimum hydrogen delivery pressure of 5 bar
- Total refuel time of 5 min

FY 2017 Key Accomplishments

- Completed an NREL-led round robin study on the hydrogen adsorption measurements of two different carbon samples. The study included 13 laboratories, plus two DOE FCTO program participants.
- Established the ability to control the desorption temperature of hydrogen in pore-restricted sorbents with a resultant range from 80 K to 300 K.
- Modified carbon sorbents for introduction of metal sites with resultant high surface areas while increasing hydrogen desorption temperature.
- Utilized the thermal conductivity apparatus that can operate from 50 K to 380 K with gas overpressures up to 100 bar for preliminary experiments on MOF-5 (metal organic framework).
- Validated the adsorption capacities of multiple external laboratory materials under investigation for DOE.
- Initiated the protocols for reporting volumetric capacity of sorbent materials through DOE, U.S. DRIVE Tech Team, and international partner interactions.
- Established multiple experimental and modeling partnerships and collaborations with the HyMARC team.
- Correlated the theoretical and experimental binding energies for a series of boron substituted carbon-based sorbents (in collaboration with Pacific Northwest National Laboratory [PNNL]).
- Designed, constructed, and utilized the cryostat temperature controlled PCT apparatus for experiments from 50 K to 300 K under pressures up to 180 bar hydrogen.

✧ ✧ ✧ ✧ ✧

INTRODUCTION

The Hydrogen Storage program supports research and development of technologies to lower the cost of near-term physical storage options and longer-term material-based hydrogen storage approaches. The program conducts research and development of low-pressure, materials-based technologies and innovative approaches to increase storage potential and broaden the range of commercial applications for hydrogen. These advanced-materials activities focus on development of core capabilities designed to enable the development of novel materials with the potential to store hydrogen near room temperature, at low-to-moderate pressures, and at energy densities greater than either liquid or compressed hydrogen. Key activities include improving the energetics, temperature, and rates of hydrogen release. Advanced concepts include high-capacity metal hydrides, chemical hydrogen storage materials, and hydrogen sorbent materials, as well as novel material synthesis processes. The overarching goal of the FCTO Hydrogen Storage program is to develop and demonstrate viable hydrogen storage technologies for transportation, stationary, portable power, and specialty vehicle applications (e.g., material handling equipment, airport ground support equipment, etc.), with a key goal of enabling >300-mile driving range across all light-duty vehicle platforms, without reducing vehicle performance or passenger cargo space.

APPROACH

This national laboratory collaboration brings together internationally recognized leaders in hydrogen storage materials characterization and development at NREL, PNNL, Lawrence Berkeley National Laboratory, and NIST, as the HyMARC support team (also known as the Hydrogen Storage Characterization and Optimization Research Effort [HySCORE]). This collaboration is based on a synergistic approach to further validate hydrogen storage concepts and develop the key core capabilities necessary for accurate evaluation of hydrogen storage materials capacity, kinetics, and sorption/desorption physio-chemical processes. The overall approach involves parallel experimental and modeling efforts to utilize the core capabilities developed to rapidly define, model, synthesize, and characterize the appropriate materials necessary for achieving the 2020 Hydrogen Storage goals set forth by DOE. The approach is multifaceted to mitigate risk and ensure success as we bridge the gap between physisorption and chemisorption to provide the basis for a new generation of hydrogen storage materials technologies.

Our approach in FY 2017 (specifically NREL and NIST in this report) included efforts to develop state-of-the-art characterization techniques for hydrogen storage materials including advanced thermal conductivity, PCT, and neutron-based spectroscopic techniques. Through theoretical–experimental iterations, we focused on addressing questions and validating recent concepts and mechanisms related to materials-based hydrogen storage community including:

- Can multiple hydrogen molecules be adsorbed on an unsaturated metal center within a sorbent?
- Is it possible to enhance the kinetics of hydride formation with additives?
- Does the incorporation of boron sites improve the binding energy of carbon-based sorbents?
- How can one alter/increase the hydrogen binding energies for physisorption in non-crystalline and crystalline sorbents?

Our team directly interacts with and supports the entire HyMARC core team, as well as the HyMARC seedling projects.

KEY RESULTS

Volumetric Round Robin Study

The NREL-led round robin study involved the hydrogen adsorption measurements of two different carbon samples. Participants were asked to measure and calculate capacities at ambient temperature and liquid nitrogen temperatures. Detailed instructions and protocols were provided. The data comes from 13 different laboratories: one industry, eight government, and four academic institutions. The participants included four international laboratories and nine laboratories within the United States. Due to the large amount of data, we have decided to write two manuscripts: (1) presentation of the data with comparative analysis, and (2) in-depth analysis of the data including modeling to adjust data based on possible errors. Our current focus is to publish the first manuscript, which is in draft form.

To highlight some of the analysis and data, Figures 1–3 show the final compilation of the data taken at ambient temperature for Sample 1. This includes excess gravimetric capacity (Figure 1), excess volumetric capacity (Figure 2), and total volumetric capacity (Figure 3). The data shown in Figure 1 includes 16 different volumetric measurements and one gravimetric measurement. The data in Figures 2 and 3 are all based on volumetric measurements. The data were corrected by the participants for any obvious calculation errors that were discovered. One set of data was removed because of system contamination issues. The full manuscript will present all data for Sample 1 and 2 at both temperatures.

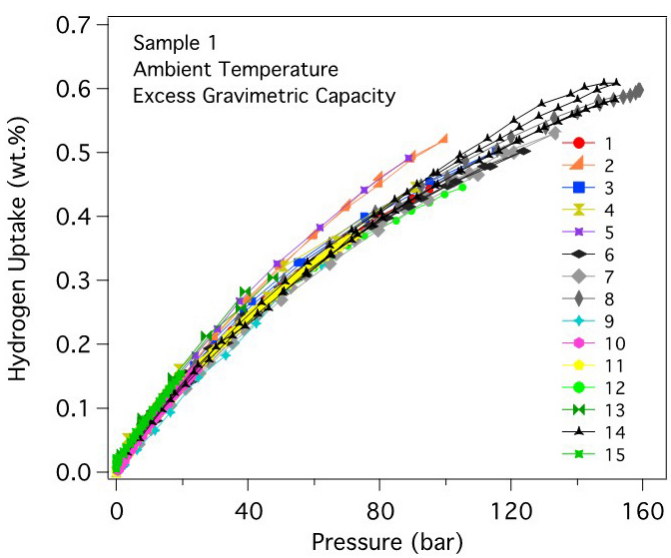

FIGURE 1. Excess gravimetric capacity at ambient temperature for sorbent Sample 1

We are currently utilizing multiple statistical approaches to analyze the variability in the data. One approach is displayed in Figure 4, where each data set is interpolated to a common pressure in order to calculate statistics and evaluate the range of error. The error bars shown in Figure 4a are larger for Sample 2 than Sample 1. This is expected because Sample 2 is a powder while Sample 1 is pelletized. Experimentally, it is more difficult to determine sample mass, packing density, etc., in a powder sample than a pelletized sample. The error bars associated with the total volumetric capacity in Figure 4b are larger at higher pressures for

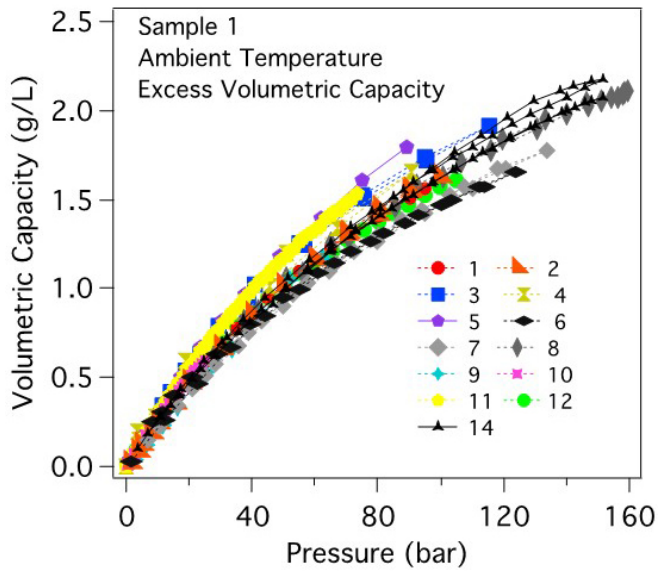

FIGURE 2. Excess volumetric capacity at ambient temperature for sorbent Sample 1

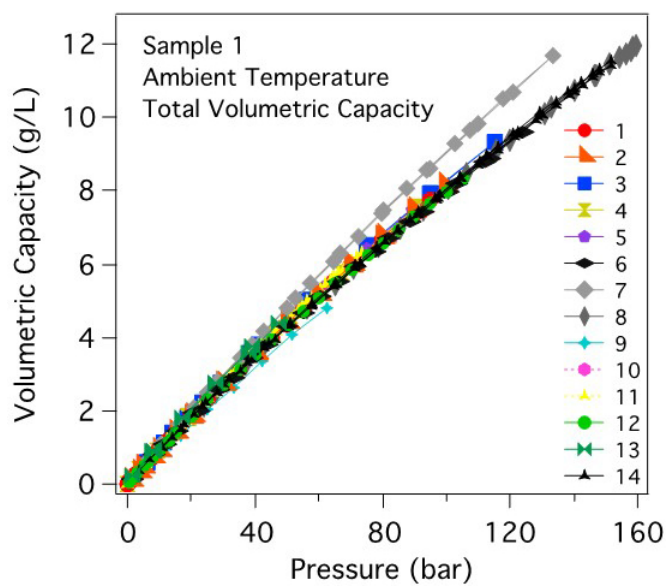

FIGURE 3. Total volumetric capacity at ambient temperature for sorbent Sample 1

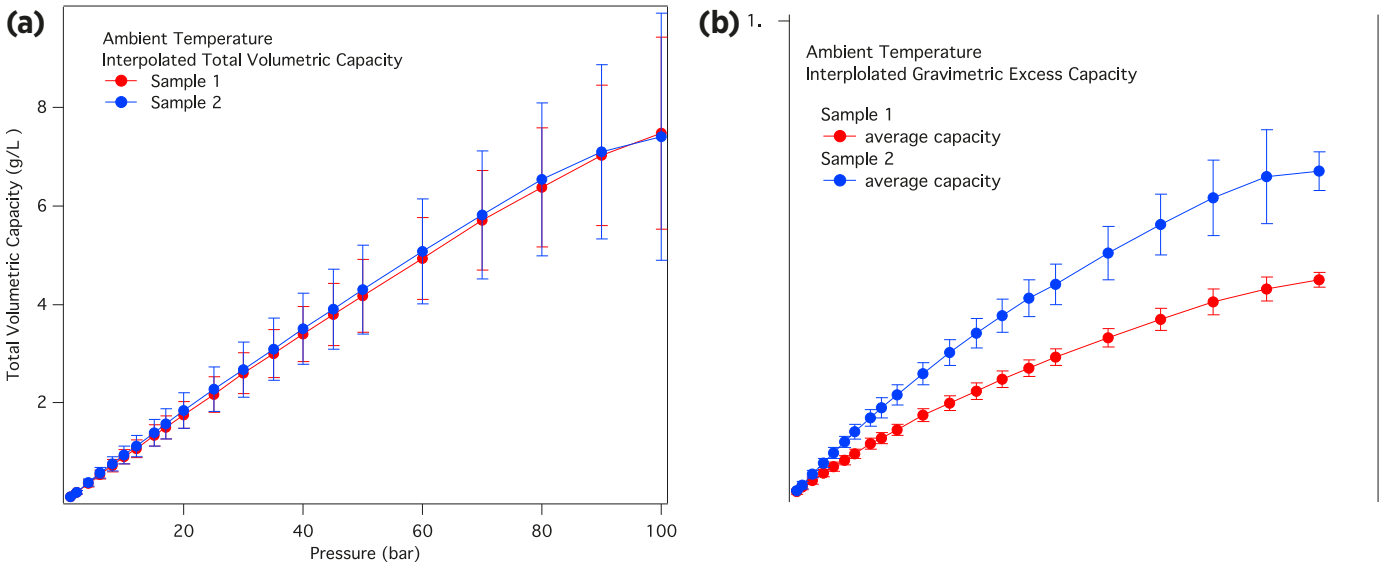

FIGURE 4. The average of interpolated data for the excess gravimetric capacity (a), and the total volumetric capacity (b) at ambient temperature for sorbent Sample 1 and Sample 2

both samples. This can be attributed to the variation in the packing density measured by different laboratories. We continue to analyze the data and work closely with the study participants to make sure all details are reported and conveyed in the coming manuscripts. In summary, it appears that the community at large has improved in the reporting of viable hydrogen adsorption data, especially with gravimetric capacities. There still needs to be improvement in developing a standard protocol for the determination of excess volumetric capacity of less dense powder samples to reduce the relative range in results observed in this study.

Control of Hydrogen Desorption Temperature

In our attempts to control the desorption temperature of the hydrogen from sorbents in FY 2016, we investigated a series of oxo-carbon species with different metal centers. The most interesting of these materials turned out to be calcium oxalate, which exhibited a highly unusual hydrogen adsorption behavior (Figure 5). While the Brunauer–Emmett–Teller surface area was only 4 m^2/g, the material still adsorbed 1.2 wt.% hydrogen at 200 K, but only <0.01 wt.% at 77 K. As shown in Figure 5, the reversible desorption peak of the hydrogen appears at 180 K with a binding energy of ~19 kJ/mol as determined by variable heating rate temperature programmed desorption. To better understand this odd behavior, Lawrence Berkeley National Laboratory modeled the hydrogen binding in calcium oxalate, and computationally identified the binding site and computed the interaction energy. It was predicted that within the oxalate framework there were non-specific interactions that were dispersion dominated in the ultramicroporous structure. The calculated binding energy was 24 kJ/mol, which was very close to the experimental value. This work

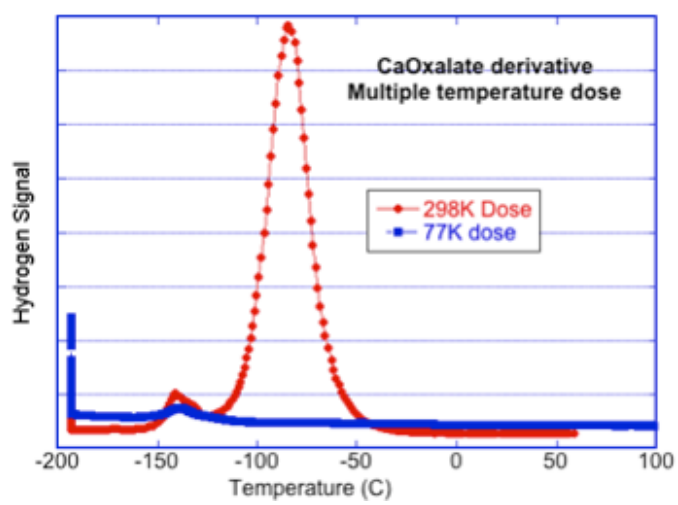

FIGURE 5. Temperature programmed desorption spectra of calcium oxalate hydrogen sorption experiments. In the red curve the material was dosed for 10 minutes with 1.4 bar hydrogen at 298 K and then quenched to 77 K, while the blue curve was dosed at 77 K. The heating rate was 15 K/min.

is the first demonstration of how small pores can control both the thermodynamics and kinetics of hydrogen sorption mechanisms. We are planning to submit a full part on this result and further investigate other materials with higher capacity but similar dispersion interactions.

Variable Temperature PCT Apparatus

NREL has developed a variable temperature PCT apparatus to facilitate hydrogen capacity measurements at pressures up to 200 bar over a wide temperature range (50 K to 350 K). It consists of a modified PCTPro 2000 integrated

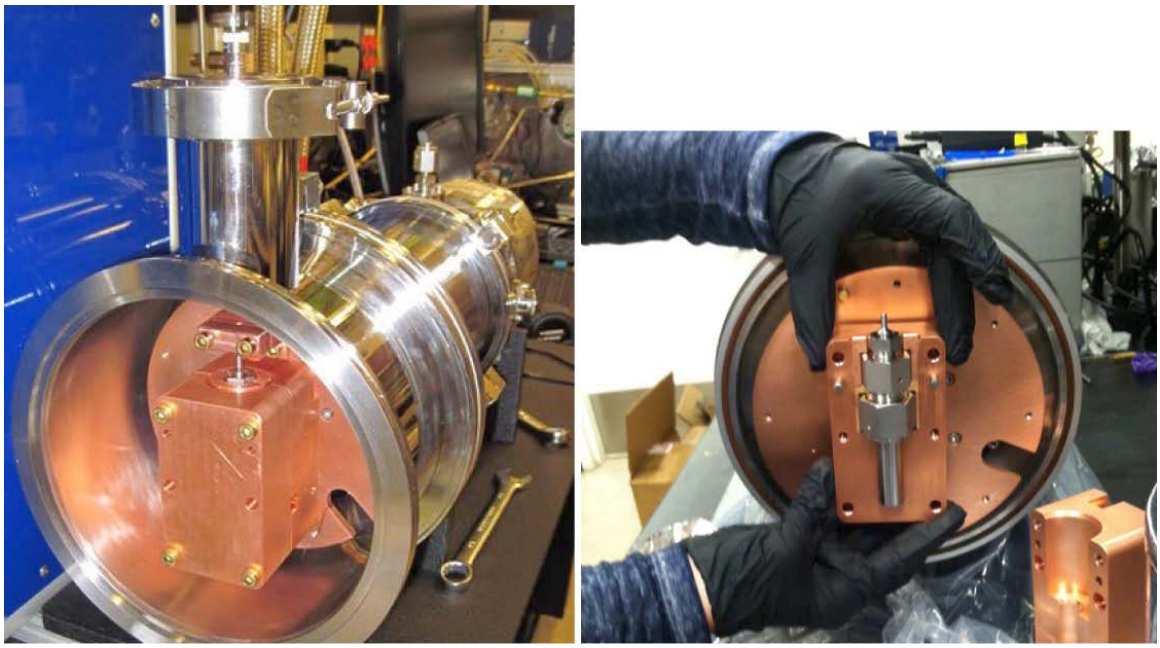

FIGURE 6. Cryostat attached to the NREL PCT system. Left: complete isothermal copper jacket; right: the sample cell within the copper jacket.

with a heavy-duty cryocooler used for the temperature control and a custom made isothermal sample holder that was designed to minimize temperature gradients at the sample (Figure 6). At the time of this report, verification of its operation is in progress and will show that this new apparatus will produce accurate and reliable measurements. Initial verification efforts consist of null measurements to show acceptable results at all temperatures and pressures and indeed, these initial results are acceptable. Future efforts will integrate new data acquisition software into the instrument and validate isosteric heat of adsorption measurements.

Boron-Doped Materials

The goal of this work is to incorporate B functionalities into carbon materials for enhanced hydrogen binding using vapor phase synthesis and/or modification. The boron incorporation (BC_x) has been predicted to enhance the hydrogen binding energy (to the range of 10–15 kJ/mol) through strain-induced distortion of the sp^2 network to produce sp^3-like boron. This is termed "graphitic puckering" and is depicted in Figure 7. Increased puckering is expected to promote H_2–BC_X interactions with higher binding energy.

Near edge X-ray absorption fine structure (NEXAFS) measurements conducted at end station 10-1 at the Stanford Synchrotron Radiation Lightsouce (SLAC) National Accelerator Laboratory confirm the presence of non-planar boron consistent with the puckered sp^2-sp^3 structure. Figure 7 shows boron 1*s* NEXAFS data for a BC_X material compared to hexagonal boron nitride (*h*-BN). The BC_x NEXAFS data shows three peaks in the π* region labeled 1, 2, 3. Peaks 1 and 2 are consistent with non-planar boron that is attributed to a puckering structure. The π* Peak 3 aligns to the π* peak of *h*-BN which is consistent with the sp^2 structure for boron. No boron–oxygen species could be detected by NEXAFS

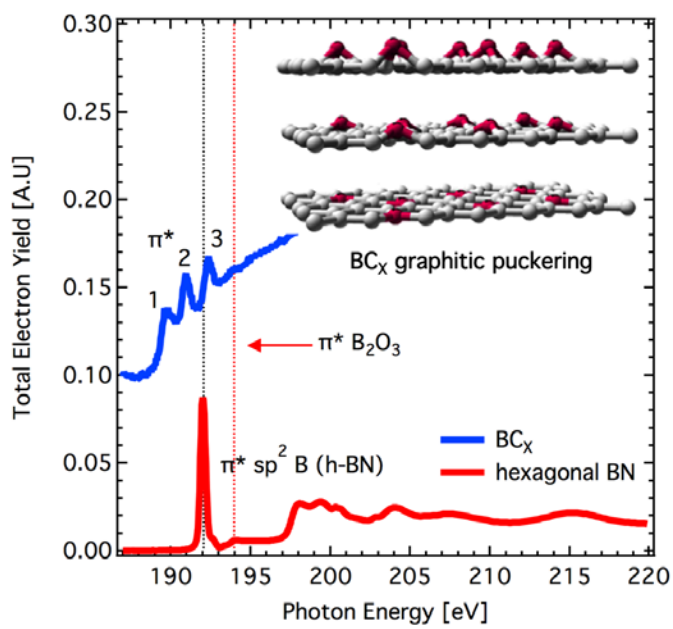

FIGURE 7. Boron 1*s* NEXAFS data for BC_X carbon and schematic of BC_X graphitic puckering. π* Peaks 1 and 2 at denote BC_X species with non-planar structure indicative of puckering. π* Peak 3 is consistent with sp^2 B within hexagonal boron nitride. The red dashed line denotes the position of boron–oxygen species.

where the red dashed line denotes the position of the B_2O_3 π* peak. Neutron prompt gamma analysis performed on BC_X seeds and BC+PECVD materials yielded a 0.47 mol% B and 2.2 wt% B, respectively. The results are a promising indication that sp^3 boron is being incorporated.

PNNL has conducted a new series of theoretical predictions of the binding energies for hydrogen after the incorporation of boron, and found that a binding energy of 7–8 kJ/mol is predicted. For the materials described above, variable temperature programmed desorption found a binding energy of ~7 kJ/mol. We have recently conducted a second synthetic approach to incorporate more boron throughout the sample; the analysis will be complete by the end of the fiscal year.

Thermal Conductivity

In collaboration with Troy Semelsberger (LANL), we discovered unusual behavior while measuring the thermal conductivity of MOF-5 under a variety of temperatures and pressures. We conducted measurements on two sets of MOF-5 samples under helium pressures ranging from 0.03 bar to 100 bar, and at temperatures ranging from 40 K to 400 K.

Figure 8 shows the measured thermal conductivity and diffusivity of MOF-5 at various temperatures and pressures. Two different MOF-5 sample sets (a set consists of two pucks) were measured. In Figure 8, the two sets are called "NREL MOF" and "LANL MOF," with the name indicating the laboratory where each was first measured. Both sets were provided by Mike Veenstra at Ford and are expected to have the same thermal properties. The "@ NREL" and "@ LANL" in the legend indicate where the measurements were made. Note that the LANL MOF has been measured at 77 K by both LANL and NREL, and the results show good agreement between the two instruments.

At sub-ambient temperatures, both the thermal conductivity and diffusivity show a pronounced peak, which shifts to lower pressure as the temperature decreases. For all investigated temperatures, the peak in thermal diffusivity occurs at lower pressure than the peak in the thermal conductivity. Though the room temperature and elevated temperature conductivity data do not roll over in the range of pressures measured, they may follow the trend if the pressure were further increased.

To understand the source of the non-monotonic behavior observed in the MOF-5+He system, we will be measuring the thermal conductivity of MOF-5 in the presence of other gases at different pressures and temperature. Troy Semelsberger at LANL has measured MOF-5 in hydrogen at both room temperature and at 77 K, and did not observe a peak in the thermal conductivity as a function of pressure at either temperature. In the coming weeks, we will measure MOF-5 samples in the presence of hydrogen to confirm this result and in the presence of argon at a variety of temperatures.

CONCLUSIONS AND UPCOMING ACTIVITIES

We have validated several key aspects of hydrogen storage materials that were first reported in FY 2016. These include:

- Conducting an international round robin to establish the validity of the proposed protocol for hydrogen sorption measurement.
- Binding two hydrogen molecules to a metal center in a framework material.
- Controlling the binding energy by changing metal centers in several sorbent species.
- Increasing the binding energy in carbon sorbents by the introduction of catecholates and metal centers.
- Validating several models/predictions of materials' performance.

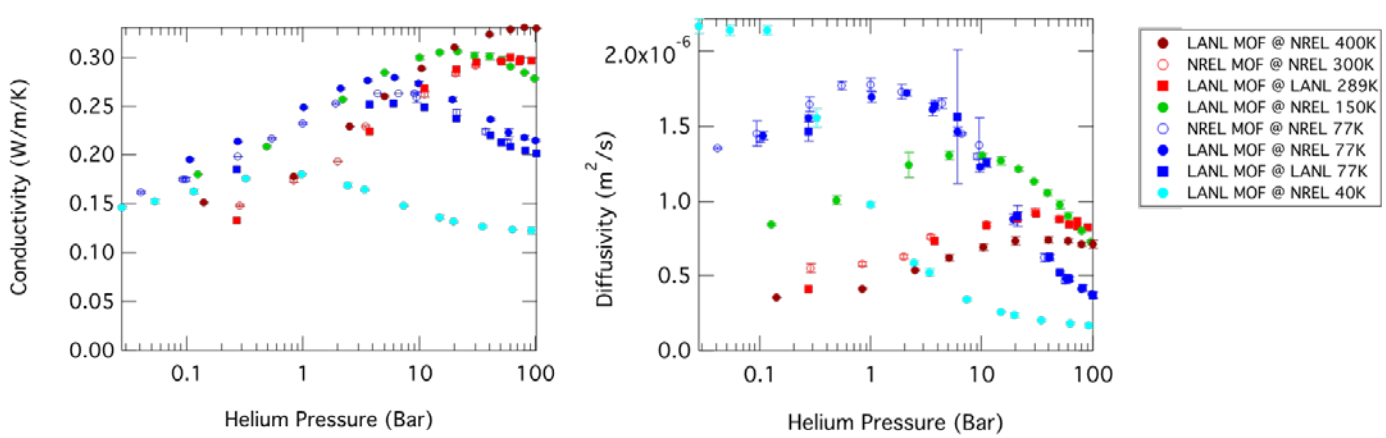

FIGURE 8. Thermal conductivity of MOF-5 in helium as a function of pressure at different temperatures

- Developed advanced characterization techniques that have already had a significant impact in the community and established the effect of systematic error on the reported capacities of standard carbon materials.

Taken together these results have established a multitude of possible solutions for advanced hydrogen storage materials—both sorbents and hydrides. Our upcoming activities will be to continue our development of the PCT cryostat system that will be essential to the DOE FCTO hydrogen storage programs. We will finish our validation of the concepts associated with the claims that boron doped sorbents are materials with the potential to display increased binding energies of physisorption. Finally, we will continue to interact with the theoreticians on various materials' matrix possibilities as we strive to increase the capacity of a new genre of hydrogen sorbents and improve the reversibility kinetics of possible hydrides. These iterative interactions will help to answer the following questions.

- Does the insertion of calcium into framework materials increase binding energy as predicted?
- Is it possible to bind more than two hydrogen molecules per open metal site?
- Through the control of pore size and chemistry, can we manipulate binding energies?
- Can we manipulate the binding energy with improved capacity?
- Can heterolytic cleavage of hydrogen be utilized as a possible mechanism to reach the 2020 targets?

SPECIAL RECOGNITIONS & AWARDS/ PATENTS ISSUED

1. Katherine Hurst (NREL) attended the International Symposium Hydrogen & Energy in Hawaii, March 2017 and won the award for best poster.

2. Mira Dimitrievska (NIST/NREL), "Neutron scattering applications in materials for hydrogen energy storage," 23rd Annual Sigma Xi Postdoctoral Poster Presentation, Gaithersburg, USA, February 2017 received the most outstanding poster award.

3. Thomas Gennett, Steve Christensen, "*Nanostructured Composite Metal Hydrides,"* U.S. provisional patent application was filed on May 17, 2017 at the United States Patent & Trademark Office and has received Application No. 62/507,354.

FY 2017 PUBLICATIONS

1. M. Dimitrievska, J.L. White, W. Zhou, V. Stavila, L.E. Klebanoff and T.J. Udovic, **Phys. Chem. Chem Phys.,** 18, 25546 (2016).

2. W.S. Tang, M. Dimitrievska, J.-N. Chotard, W. Zhou, R. Janot, A.V. Skripov, and T.J. Udovic, **J. Phys. Chem. C**, 120, 21218 (2016).

3. V. Soloninin, M. Dimitrievska, R.V. Skoryunov, O.A. Babanova, A.V. Skripov, W.S. Tang, V. Stavila, S. Orimo, and T.J. Udovic, **J. Phys. Chem. C**, 121, 1000 (2017).

4. W.S. Tang, K. Yoshida, A.V. Soloninin, R.V. Skoryunov, O.A. Babanova, A.V. Skripov, M. Dimitrievska, V. Stavila, S. Orimo, and T.J. Udovic, **ACS Energy Lett.**, 1, 659 (2016).

5. H. Wu, W.S. Tang, W. Zhou, J.D. Tarver, V. Stavila, C.M. Brown, T.J. Udovic, **Journal of Solid State Chemistry**, 243, 2016, 162–167.

6. Y. Tulchinsky, C.H. Hendon, K.A. Lomachenko, E. Borfecchia, B.C. Melot, M.R. Hudson, J.D. Tarver, M.D. Korzynski, A.W. Stubbs, J.J. Kagan, C. Lamberti, C.M. Brown, M. Dinca, **Journal of the American Chemical Society**, 139, 2017, 5992–5997.

7. K.E. Hurst, T. Gennett, and P.A. Parilla, "A Multi-Laboratory Measurement Comparison Study of Hydrogen Sorption," in preparation, 2017.

8. K.E. Hurst, T. Gennett, and P.A. Parilla, "Lessons Learned based on Analysis of a Multi-Laboratory Measurement Study of Hydrogen Sorbent Materials," in preparation, 2017.

9. P.A. Parilla, T. Gennett, and K.E. Hurst, "Systematic Error from Using a Popular but Flawed Model for Manometric Instruments," in preparation, 2017.

FY 2017 PRESENTATIONS

1. Jacob Tarver and Craig Brown (NREL/NIST), "Using Neutrons to Probe Hydrogen Storage in Metal-Organic Frameworks," presented at 11th Intl Symp Hydrogen and Energy (Febuary 2017).

2. Jacob Tarver and Craig Brown (NREL/NIST), "Using Neutrons to Probe Hydrogen Storage in Metal-Organic Frameworks," presented at Gordon Research Conference, Metal Hydrogen Systems (July 2017).

3. Katherine Hurst, Philip Parilla, and Thomas Gennett, "A Multi-laboratory Comparison Study of Volumetric Hydrogen Adsorption Measurements on Sorbents," International Hydrogen and Energy Symposium, Waikoloa Village, HI, March 1, 2017.

4. Katherine Hurst, Philip Parilla, and Thomas Gennett, "HYSCORE/NREL Opportunities for Collaboration," IEA Task 32 Experts Meeting, Waikoloa Village, HI, March 3, 2017.

5. Katherine Hurst, Thomas Gennett, and Philip Parilla, "Update on NREL's Validation Efforts: Inter-Laboratory Comparison," Hydrogen Storage Tech Team Meeting, Southfield, MI, March 16, 2017.

6. Katherine Hurst, Steven Christensen, Noemi Leick, and Thomas Gennett, "Modification of Hydride Materials for Hydrogen Storage by ALD," ALD2017, Denver, CO, July 15–18, 2017.

7. Mirjana Dimitrievska and Terrence Udovic, "Anion Dynamical Behaviors and Their Possible Relationship to Superionic Conductivities in Hydro-Closo-Borate Salts of Lithium and Sodium," MRS Fall meeting, Boston, USA, December 2016.

8. Mirjana Dimitrievska and Terrence Udovic, "Neutron scattering applications in materials for hydrogen energy storage," 23rd Annual Sigma Xi Postdoctoral Poster Presentation, Gaithersburg, USA, February 2017.

9. Philip Parilla, Katherine Hurst, and Thomas Gennett, "Update on the Inter-Laboratory Comparison on Volumetric Capacity Determination," Task 32 IEA HIA Expert Meeting, December 2016, Berlin, Germany.

10. Thomas Gennett, "HySCORE, an Overview," International Hydrogen and Energy Symposium, Waikoloa Village, HI, March 1, 2017.

11. Thomas Gennett, "HySCORE, an Overview," ECS International Meeting, New Orleans, LA, May 31, 2017.

12. Philip Parilla, Katherine Hurst, and Thomas Gennett, "Hydrogen Sorbent Measurement Qualification and Characterization," AMR, Washington, D.C., June 2017.

13. Mirjana Dimitrievska, Jacob Tarver, Thomas Gennett, Terrence Udovic, and Craig Brown, "HySCORE: Technical Activities at NIST," AMR, Washington, D.C., June 2017.

IV.C.5 HyMARC (Support): PNNL Effort

Tom Autrey (Primary Contact), Mark Bowden, Abhi Karkamkar, Bojana Ginovska, Marina Chong, Iffat Nayyar, Adrian Houghton
Graduate students (University of Hawaii): Phuong Nguyen, Sunil Shrestha
Pacific Northwest National Laboratory (PNNL)
902 Battelle Blvd.
Richland, WA 99354
Phone: (509) 375-3792
Email: tom.autrey@pnnl.gov

DOE Manager: Jesse Adams
Phone: (720) 356-1421
Email: Jesse.Adams@ee.doe.gov

Subcontractor:
Prof Craig Jensen, University of Hawaii at Mānoa
Honolulu, HI

Project Start Date: October 1, 2015
Project End Date: Project continuation and direction determined annually by DOE

Overall Objectives

- Develop a series of advanced characterization tools that allows for rapid advancement and in-depth understanding of next-generation hydrogen storage materials.
- Develop a hydrogen storage material with a total materials-based capacity of >45 g/L above 150 K, that is possible with hydrogen overpressures <100 bar and reversible for multiple cycles.
- Optimize thermal management in hydrogen storage systems by the incorporation of unique phase-change materials.
- Demonstrate the importance of computational methods in developing and understanding of next generation hydrogen storage materials.
- Assist the DOE Hydrogen Materials – Advanced Research Consortium (HyMARC) seedling projects.

Fiscal Year (FY) 2017 Objectives

- Validate concept of enhanced reactivity and selectivity for hydrogen release from tetrahydrofuran (THF) adduct of magnesium borohydride, $Mg(BH_4)_2$.
- Calculate thermodynamic properties of solvated and unsolvated $Mg(BH_4)_2$.
- Resolve the discrepancy for the enthalpy of hydrogen uptake by liquid organic hydrogen carrier (LOHC) triazine.
- Determine the best computational methods required to calculate the binding energy of hydrogen to boron doped carbon.

Technical Barriers

This project addresses the following technical barriers from the Hydrogen Storage section of the Fuel Cell Technologies Office Multi-Year Research, Development, and Demonstration Plan.

(A) System Weight and Volume

(B) System Cost

(C) Efficiency

(E) Charging/Discharging Rates

(O) Lack of Understanding of Hydrogen Physisorption and Chemisorption

(P) Reproducibility of Performance

Technical Targets

Hydrogen Storage Materials: This project is conducting validation studies of various framework materials, sorbents, hydrides and model compounds. Concurrently, the team also is developing new characterization tools for the rapid enhancement of materials development. Insights gained from these studies will be applied toward the design and synthesis of hydrogen storage materials that meet the following DOE onboard 2020 automotive hydrogen storage targets.

- 1.5 kWh/kg system (4.5 wt% H_2)
- 1.0 kWh/L system (0.030 kg H_2/L)
- Cost of $10/kWh ($333/kg H_2 stored)
- Operating at ambient temperatures (-40 to 60ºC)
- Onboard efficiency of 90% and minimum hydrogen delivery pressure of 5 bar
- Total refuel time of 5 minutes

FY 2017 Accomplishments

- Validated the concept that Lewis base adducts of $Mg(BH_4)_2$ enhance reactivity and selectivity.
- Calculated thermodynamics (entropy, enthalpy, and free energy) and ^{11}B nuclear magnetic resonance (NMR) chemical shifts of key intermediates and products

resulting from hydrogen release from $Mg(BH_4)_2$ and THF adducts of $Mg(BH_4)_2$.

- Determined the enthalpy of hydrogenation of triazine $C_3N_3H_3 + 3H_2 \Leftrightarrow C_3N_3H_9$ (ca. 69 g H_2/L) to resolve the apparent literature discrepancy for hydrogen release from the LOHC.
- Demonstrated capability of time-resolved reaction calorimetry to measure thermodynamics and kinetics for hydrogen uptake by LOHCs. Kinetic measurements are critical for catalyst screening.
- Benchmarked density functional theory (DFT) methods against experiment to determine most promising approach to determine binding energy of hydrogen to boron doped graphene.

✧ ✧ ✧ ✧ ✧

INTRODUCTION

The Hydrogen Storage program supports research and development of technologies to lower the cost of near-term physical storage options and longer-term material-based hydrogen storage approaches. The program conducts R&D of low-pressure, materials-based technologies and innovative approaches to increase the hydrogen storage capacity, reduce cost, and broaden the range of commercial applications for hydrogen. These advanced-material activities focus on development of core capabilities designed to enable the development of novel materials with the potential to store hydrogen near room temperature, at low-to-moderate pressures, and at energy densities greater than either liquid or compressed hydrogen on a systems basis. Key activities include improving the energetics, temperature, and rates of hydrogen release. Advanced concepts include high-capacity metal hydrides, chemical hydrogen storage materials, and hydrogen sorbent materials, as well as novel material synthesis processes. The overarching goal of the Fuel Cell Technologies Office Hydrogen Storage program is to develop and demonstrate viable hydrogen storage technologies for transportation, stationary, portable power, and specialty vehicle applications (e.g., material handling equipment, airport ground support equipment), with a key goal of enabling >300-mile driving range across all light-duty vehicle platforms, without reducing vehicle performance or passenger cargo space.

APPROACH

This national laboratory collaboration brings together internationally recognized leaders in hydrogen storage materials characterization and development at National Renewable Energy Laboratory, PNNL, Lawrence Berkeley National Laboratory, and the National Institute of Standards and Technology, as the HyMARC support team (also known as the Hydrogen Storage Characterization and Optimization Research Effort [HySCORE]). This collaboration is predicated on a synergistic approach to further validate hydrogen storage concepts and develop the key core capabilities necessary for accurate evaluation of hydrogen storage materials capacity, kinetics, and sorption/desorption physio-chemical processes. The overall approach involves collaborative experimental and modeling efforts. We are validating concepts and utilizing core capabilities to rapidly define, model, synthesize, and characterize the appropriate materials necessary for achieving the 2020 Hydrogen Storage goals set forth by DOE. The approach is multifaceted to mitigate risk and ensure success as we bridge the gap between physisorption and chemisorption to provide the basis for a new generation of hydrogen storage materials technologies.

Specifically in this project, PNNL is developing advanced characterization capabilities to provide critical approaches to validate theories and test concepts proposed in the development of new details into the chemical and physical properties of hydrogen storage materials. Variable pressure (1–200 bar) and temperature (298–473 K) in situ multi-nuclear solid state magic angle spinning NMR is being developed to identify key intermediates in the release and uptake of hydrogen in complex metal hydrides to validate claims that additives control selectivity and enhance reversibility. Low temperature (down to 5 K) solid state ^1H NMR is being developed to measure the enthalpy of adsorption of hydrogen in high surface area adsorbent materials and to assist in the validation of the concept that more than one hydrogen molecule can bind to a metal site on a high surface amorphous material. Variable pressure (1–100 bar) and temperature (250–350 K) multi-nuclear liquid NMR is available to measure key intermediates. Variable pressure (1–20 bar) and temperature (298–353 K) reaction calorimetry is available to measure kinetics and enthalpies of hydrogen uptake in liquid and solid stores to benchmark and validate computational predictions of binding enthalpies in liquid carriers.

Our work in FY 2017 included efforts to develop state-of-the-art characterization techniques for hydrogen storage materials including calorimetry and in situ NMR spectroscopy. Through a theoretical and experimental interaction, we focused on (i) the validation of key intermediates formed during release of hydrogen from solid state complex hydrides (i.e., magnesium borohydride, $Mg(BH_4)_2$); (ii) determination of the thermodynamics of H_2 uptake and release from liquid carriers (i.e., triazine and diazine); and (iii) characterization of computational approaches to gain insight into the binding energies of hydrogen in boron and nitrogen doped carbons. In addition, we were able to assist a number of HyMARC seedling projects in their characterization efforts using NMR, X-ray diffraction, and transmission electron microscopy.

RESULTS

I. Validation of Key Intermediates Formed during Release of H_2 from Solid State Complex Hydrides. Using Lewis basic adducts complexed to alkali and alkaline metal borohydrides has the potential to open new dimensions in chemical materials space to be explored by the research community. Sub-stoichiometric quantities of THF to $Mg(BH_4)_2$, e.g., $Mg(BH_4)_2 \cdot 0.67$ THF (5.6 wt% hydrogen) enhances the rate of H_2 release and selectively yields products that fall in the desirable thermodynamic range for reversible storage.

We used NMR spectroscopy to compare and contrast the products formed upon hydrogen release from a series of Lewis base adducts of $Mg(BH_4)_2$. This work validated the claim that THF enhances reactivity and selectivity for $MgB_{10}H_{10}$ formation. Additives that drive the reaction towards $B_{10}H_{10}$ are highly desired as regeneration of $Mg(BH_4)_2$ from the closoborane $MgB_{10}H_{10}$ is thermodynamically more favorable than regeneration from $MgB_{12}H_{12}$. The experimental studies suggest that a low temperature phase change to make a more mobile phase of borohydride enhances kinetics while thermodynamics, i.e., destabilization of the closoborane products, drive the reaction selectivity (Figure 1).

Computational studies were undertaken to gain insight into the enhanced selectivity. Solid-state DFT calculations were performed to determine thermodynamics of complex borohydride species that may be observed on the reversible reaction pathway during the release of hydrogen from $Mg(BH_4)_2$. We calculated the thermodynamic energies, ΔH and ΔG (at 300 K), for the conversion of $Mg(BH_4)_2$ to $Mg(B_3H_8)_2$, $Mg_3(B_3H_6)_2$, $MgB_{10}H_{10}$, $Mg(B_{11}H_{14})_2$, MgB_2H_6, MgB_2 and $MgB_{12}H_{12}$ to gain insight into the reaction pathways leading to the release of H_2. Using combination of experiment and theory, we have used a combination of vibrational spectroscopy (infrared and Raman) and NMR chemical shift calculations for these borohydride clusters in order to predict unknown observable intermediates in release of H_2 from $Mg(BH_4)_2$. Figure 1 shows the structure of $MgB_{12}H_{12} \cdot 3$ THF determined from PXRD that was used to calculate the destabilization of the closoborane.

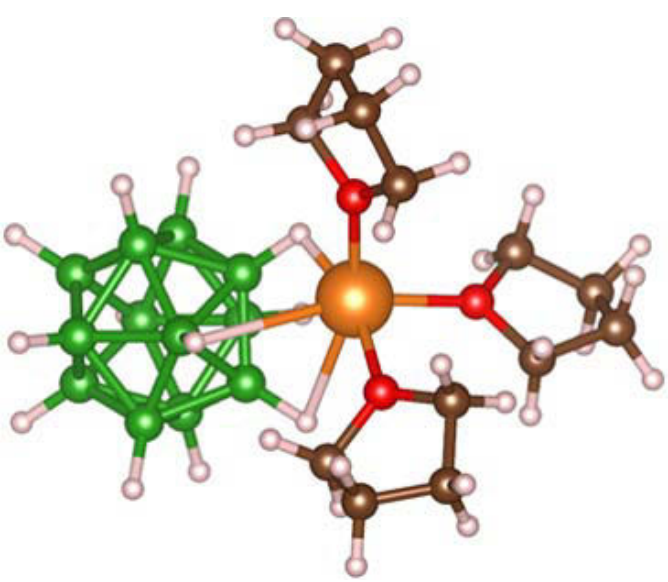

FIGURE 1. Structure of THF adduct of $MgB_{12}H_{12}$ showing the attachment of THF molecules to the magnesium cation.

II. Determination of the Thermodynamics of H_2 Uptake and Release from Liquid Organic Hydrogen Carriers. Our work focused on calculating the reaction energy for addition of three H_2 molecules to $C_3N_3H_3$ (ca. 69 g H_2/L). The work suggested four different configurations for the product state $C_3N_3H_9$, differing in the orientation of the hydrogen atoms attached to nitrogen atoms, relative to the plane of the ring. The structures of the four product states are denoted in Figure 2 as ip0 to ip3. All stable structures were confirmed by absence of imaginary frequencies in the vibrational analysis of the hessian, calculated in the framework of the rigid rotor-harmonic oscillator approximation. Table 1 compares the enthalpy of H_2 addition of a stable isomer with a calculated enthalpy of 43 kJ/mol H_2 in agreement with the low end of reported enthalpies, whereas ip2 and ip3 are

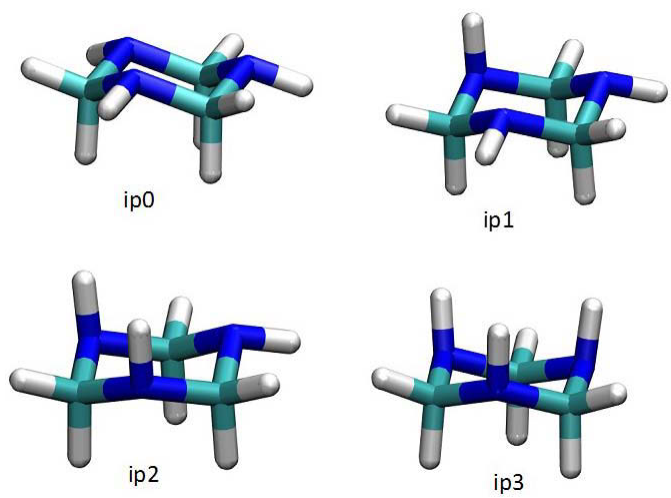

FIGURE 2. Structural isomers of reduced triazine. Absolute energies are shown in Table 1.

TABLE 1. Thermodynamics for the reaction $C_3N_3H_3 + 3H_2 \rightarrow C_3N_3H_9$ (in kJ/mol per H_2)

	ΔE	E+zpc	ΔH	TΔS	ΔG
ip0	-70.7	-35.1	-43.1	-35.6	-7.5
ip1	-79.5	-43.5	-51.0	-35.6	-15.5
ip2	-84.5	-48.1	-55.6	-35.6	-20.1
ip3	-85.8	-49.0	-56.9	-36.4	-20.5

the most stable isomers with a calculated enthalpy of ca. 56 kJ/mol H_2 in agreement with the high end of reported enthalpies.

The least stable isomer, ip0, could be formed at the surface of a heterogeneous catalyst if all the H_2 was added to one side. If the barrier for inversion of the ring at the nitrogen center is sufficiently high it could be possible to form the unstable isomer and then release the H_2 in a cyclic reaction at temperatures less than 80°C. To gain insight into the inversion barrier we calculated the transition state energy for inversion of one isomer to another. These studies showed that the barrier for inversion is sufficiently low that the most thermodynamically stable isomer will form even at room temperature.

We demonstrated the utility of reaction calorimetry to measure the enthalpy of H_2 uptake by LOHCs. This approach provides an opportunity to benchmark computational methods to determine the optimum approach to predict the enthalpies of hydrogen release from new LOHCs. In addition, the time-dependence of the heat release provides critical insight into kinetics and the ability to compare different catalyst materials to optimize efficiency in LOHCs.

For triazine, with a T_c of 110°C and 69 g H_2/L, additional catalyst work is warranted. The product perhydrotriazine is not stable with Pd/C but further catalysis development work was outside the scope of funded project. NMR is valuable to monitor stability and products formed while reaction calorimetry is valuable to compare rates of H_2 uptake and release for both heterogeneous and homogeneous catalysis.

III. Evaluation of Computational Approaches to Predict Binding Energies of H_2 to Boron and Nitrogen Doped Carbons. Our research focused on the evaluation of different DFT methods to gain insight into the effects of boron and nitrogen doping on the H_2 interaction (physisorption) with carbon (graphene). We used two models as representative classes of molecular systems (coronene) and extended systems (graphene) (Figure 3). Evaluation of molecular systems allows us to rapidly and systematically study the electronic and steric effects of heteroatoms (boron or nitrogen). The accuracy of theoretical calculations, as determined by agreement with experimental benchmarks, depends on the various functionals used in performing DFT calculations. We also compared correlations between molecular and extended systems. Our key findings are summarized below:

- The B3LYP functional with DFT-D3 Grimme's dispersion correction provides the best agreement with experiment for known published values.
- Calculations show an enhancement of H_2 physisorption by ca. 22%, i.e., 6.2–7.6 kJ/mol H_2 for sp2 hybridized B in $BC_{23}H_{13}$ (around 2.7% of B doping).
- Non-planarity of the coronene surface results in increase in the binding energy of H_2 physisorption.

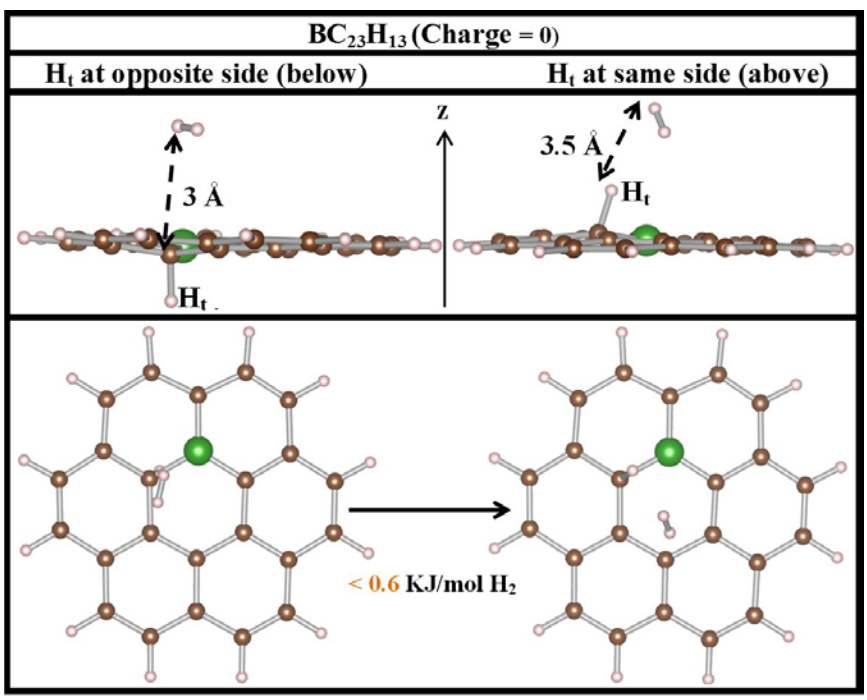

FIGURE 3. H_2 is stabilized near the defect created by insertion of boron into coronene $BC_{23}H_{12}$; however, there is little difference in the binding energy of H_2 approaching from above or below the plane of the coronene ring.

- The steric hindrance pushes the H_2 molecule towards the C atoms with ≤0 charge.
- Site of physisorption is a function of non-planarity, steric hindrances and charge distribution.
- Binding energies are dependent on site of physisorption and charge delocalization which in turn is governed by atomic arrangements of dopants and the corresponding defects.

CONCLUSIONS AND UPCOMING ACTIVITIES

We have validated the claim that THF adducts of $Mg(BH_4)_2$ enhance reactivity and selectivity for hydrogen release to yield closodecaborane as the major hydrogen release product. Experimental studies suggest the enhanced reactivity, i.e., hydrogen release at temperature below 180°C, is due in part to a phase change to a mobile complex. Calculations support that the THF adduct destabilizes the products in greater magnitude than the starting materials. This is a positive result that leads to new materials classes of complex hydrides that can reversibly store hydrogen with greater efficiency. Going forward we will test the hypothesis that solvates enable regeneration of $Mg(BH_4)_2$ from the closoboranes.

SPECIAL RECOGNITIONS & AWARDS/ PATENTS ISSUED

1. Excellent Poster award for Marina Chong. 11th International Symposium on Hydrogen Energy.

FY 2017 PUBLICATIONS/PRESENTATIONS

1. Solvent-coordinated Compounds Formed from Magnesium Hydroborates and Tetrahydrofuran. Mark Bowden, Marina Chong, Phuong Nguyen, Sunil Shrestha, Bojana Ginovska, Iffat Nayyar, Abhi Karkamkar, Craig Jensen, and Tom Autrey. 11th International Symposium on Hydrogen Energy.

2. Hydrogen storage characterization and optimization research effort. 11th International Symposium on Hydrogen Energy. HyScore. Iffat Nayyar, Marina Chong, Abhi Karkamkar, Mark Bowden, Bojana Ginovska, Adrian Houghton, Phuong Nguyen, Sunil Shrestha, Craig Jensen, Tom Gennett, and Tom Autrey. 11th International Symposium on Hydrogen Energy.

3. A New Role for Solvents: from Undesirable Residue to Useful Additive (at least, in the dehydrogenation of $Mg(BH_4)_2$). Marina Chong, Phuong Nguyen, Sunil Shrestha, Mark Bowden, Abhi Karkamkar, Tom Autrey, and Craig Jensen. 11th International Symposium on Hydrogen Energy.

4. High Capacity Hydrogen Cycling between Magnesium Borohydride and Magnesium Boranes under Moderate Conditions. Marina Chong, Junzhi Wang, Phuong Nguyen, Motoaki Matsuo, Mark Bowden, Tom Autrey, Shin-ichi Orimo, and Craig M. Jensen. MH 2016.

IV.C.6 HyMARC (Support): LBNL Effort

Jeffrey R. Long, Martin Head-Gordon
Lawrence Berkeley National Laboratory (LBNL)
1 Cyclotron Rd.
Berkeley, CA 94720
Phone: (510) 642-0860
Email: jrlong@lbl.gov

DOE Manager: Jesse Adams
Phone: (720) 356-1421
Email: Jesse.Adams@ee.doe.gov

Project Start Date: October 1, 2015
Project End Date: Project continuation and direction determined annually by DOE.

Overall Objectives

- Develop in situ infrared spectroscopy as a tool for characterizing emerging H_2 storage materials that may allow for a driving range greater than 300 miles.
- Materials sought with the potential for meeting the DOE targets of reversible uptake.
- Validate new concepts for H_2 storage mechanisms in adsorbents.
- Provide accurate computational modeling for H_2 adsorbed in porous materials.

Fiscal Year (FY) 2017 Objectives

- Research and development of metal–organic framework materials with high volumetric and gravimetric H_2 capacities (Barrier A, B, C).
- Diffuse reflectance infrared Fourier transform spectroscopy (DRIFTS) characterization (Barrier N, O).
- Assist the DOE Hydrogen Materials – Advanced Research Consortium (HyMARC) seedling projects.

Technical Barriers

This project addresses the following technical barriers from the Hydrogen Storage section of the Fuel Cell Technologies Office Multi-Year Research, Development, and Demonstration Plan.

(A) System Weight and Volume

(B) System Cost

(E) Charging/Discharging Rates

(O) Lack of Understanding of Hydrogen Physisorption and Chemisorption

(P) Reproducibility of Performance

Technical Targets

This project is conducting validation studies of various framework materials, sorbents, hydrides, and model compounds. Concurrently, the team also is developing new characterization tools for the rapid enhancement of materials development. Insights gained from these studies will be applied toward the design and synthesis of hydrogen storage materials that meet the following DOE onboard 2020 automotive hydrogen storage targets.

- 1.5 kWh/kg system (4.5 wt% H_2)
- 1.0 kWh/L system (0.030 kg H_2/L)
- Cost of $10/kWh ($333/kg H_2 stored)
- Operating at ambient temperatures (-40ºC to 60ºC)
- Onboard efficiency of 90% and minimum hydrogen delivery pressure of 5 bar
- Total refuel time of 5 minutes

FY 2017 Accomplishments

- Received and set up infrared spectrometer with in situ gas dosing capabilities.
  - Designed and built optical sample cell with in situ gas loading capabilities for DRIFTS measurements.
  - Validated the performance of the instrument at a resolution of 4 cm^{-1} by observing an infrared (IR)-active gas dosed into the sample cell and known reference materials.
  - Validated the high-pressure performance of the instrument at a resolution of 4 cm^{-1} by observing hydrogen adsorption on Ni_2(*m*-dobdc) at 100 bar.
- Targeted the synthesis of a room-temperature hydrogen adsorbent with a high density of unsaturated metal sites.
  - Synthesized several frameworks featuring protected catechol groups with high crystallinity and high surface area.
  - Extensively investigated deprotection protocol for these materials, yielding frameworks with complete incorporation of catechol functionalities with high crystallinity and high surface area.

- Performed theory calculations to understand both the desolvation process of metals bound to catechols and the binding of H_2 in calcium oxalate.
  - Used computational methods to understand the mode of H_2 binding in calcium oxalate.
  - Calculated the binding energies of additional H_2 to the metal-catecholate system and the influence of bound solvent.

✧ ✧ ✧ ✧ ✧

INTRODUCTION

Efficient onboard storage of molecular hydrogen remains a key challenge faced by the hydrogen economy. The development of new hydrogen storage materials is a promising route towards replacing conventional compression methods requiring both high pressures and low temperatures, thereby overcoming one of the key limitations of the hydrogen economy. New materials will need to be validated and compared; therefore the development of world-class measurement methods and standards is crucial in ensuring that new materials may be validated and compared.

This national laboratory collaboration brings together internationally recognized leaders in hydrogen storage materials characterization and development at National Renewable Energy Laboratory, Pacific Northwest National Laboratory, LBNL, and the National Institute of Standards and Technology, as the HyMARC support team (also known as the Hydrogen Storage Characterization and Optimization Research Effort [HySCORE]). This collaboration is predicated on a synergistic approach to further validate hydrogen storage concepts and develop the key core capabilities necessary for accurate evaluation of hydrogen storage materials capacity, kinetics, and sorption/desorption physio-chemical processes. The overall approach involves collaborative experimental and modeling efforts. We are validating concepts and utilizing core capabilities to rapidly define, model, synthesize, and characterize the appropriate materials necessary for achieving the 2020 Hydrogen Storage goals set forth by DOE. The approach is multifaceted to mitigate risk and ensure success as we bridge the gap between physisorption and chemisorption to provide the basis for a new generation of hydrogen storage materials technologies.

Specific to this project, LBNL is constructing a state-of-the-art variable temperature DRIFTS instrument with high-pressure in situ gas dosing as a new core capability. Installation and validation of the IR spectrometer, optical array, gas dosing, and high-pressure capabilities have been completed, demonstrating accurate measurements of materials at up to 100 bar of H_2 pressure at room temperature. Cryogenic variable-temperature capabilities are currently under installation. Concurrently, novel adsorbent materials with strong binding sites are being developed computationally and synthetically, focusing on a strategy which will lead to enhanced storage properties at temperatures relevant to onboard applications.

APPROACH

IR spectroscopy is a powerful technique which can be used to gain site-specific adsorption information through the spectroscopic observation of vibrational modes associated with adsorbed hydrogen. As the vibrational modes of background gas-phase hydrogen molecule are not IR active, this technique is particularly suited for in situ gas dosing measurements examining sorbent–sorbate interactions. Different H_2–sorbent interactions give rise to discrete signals in the IR, allowing identification and quantification of specific adsorption sites and the extraction of thermodynamic parameters. The DRIFTS geometry is particularly suitable due to both enhancement of weak adsorbate signals and lenient sample morphology requirements, allowing this core capability to measure and compare a wide range of samples.

Physisorption of hydrogen into porous materials is a promising route towards achieving reversible storage with fast recharge times, however due to the weak interactions, capacity at ambient temperatures is low. Computational efforts have determined that metal–catecholate motifs are able to bind strongly to multiple H_2 molecules. As such, we are concurrently pursing frameworks incorporating these motifs in order to synthesize advanced hydrogen storage materials.

RESULTS

Characterization Techniques

The DRIFTS setup consists of a Bruker Vertex 70 Fourier transform infrared spectrometer, an Oxford Instruments top-loading optical cryostat, and a custom designed optical array allowing DRIFTS measurements to be taken in the cryostat chamber. A high-pressure sample cell and dosing manifold was designed and constructed in-house, and the system was coupled to a Micromeritics ASAP2020 Plus instrument. Control of the atmosphere inside the sample cell was demonstrated by dosing of CO_2, an IR-active gas, into the cell at varying pressures, and the DRIFTS measurement mode was validated by ex situ measurement of a known material. These measurements confirmed the working state of the spectrometer and the gas dosing apparatus.

Gas dosing measurements were performed on Ni_2(*m*-dobdc) (*m*-dobdc^{4-} = 4,6-dioxido-1,3-benzenedicarboxylate), a material previously synthesized by our lab which demonstrates strong physisorption of H_2. Peaks corresponding to different H_2 binding sites in the material were observed in good agreement to previous measurements.

Difference spectra were collected up to a pressure of 100 bar at approximately 10 bar intervals, and an increase of the signal originating from adsorbed H_2 was observed as expected (Figure 1).

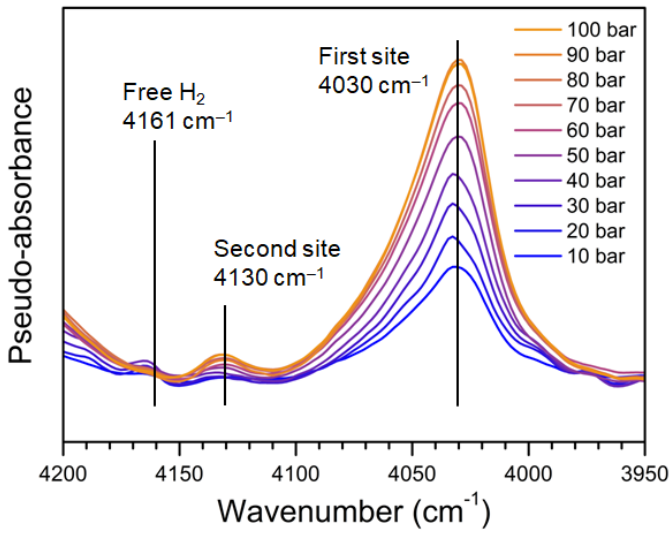

FIGURE 1. Room-temperature in situ DRIFTS spectra showing H_2 adsorbed in Ni_2(*m*-dobdc) at H_2 pressures of 10–100 bar. The peak position of H_2 bound to the first (4,030 cm^{-1}) and second (4,130 cm^{-1}) sites are in good agreement with literature.

Materials Discovery

Computations predict the binding of multiple hydrogen molecules to a metal-catecholate fragment with high binding energies. We have developed a synthetic route towards incorporating these fragments into a porous material in order to improve H_2 uptake under relevant conditions. A protection—framework assembly—deprotection strategy was successfully employed to functionalize two different framework morphologies with catechol groups which could not be incorporated into the framework via direct synthesis. We are able to synthesize highly crystalline frameworks with high surface areas and full incorporation of the catechol ligand by employing this strategy (Figure 2), and metalation trials are forthcoming.

Furthermore, extensive computational modeling has been performed on a range of materials. In a collaboration with the National Renewable Energy Laboratory, H_2 binding in calcium oxalate has been modeled and compared with experiment. H_2 was found to bind in a non-specific manner which was dominated by dispersion interactions (Figure 3). The effect of binding multiple H_2 molecules as well as the effect of residual solvent on the metal–catecholate system has been further studied (Figure 4). Usable capacities for a potential framework incorporating this system has been estimated, with a Ca–catecholate fragment contributing around 30 g/L H_2 to the capacity.

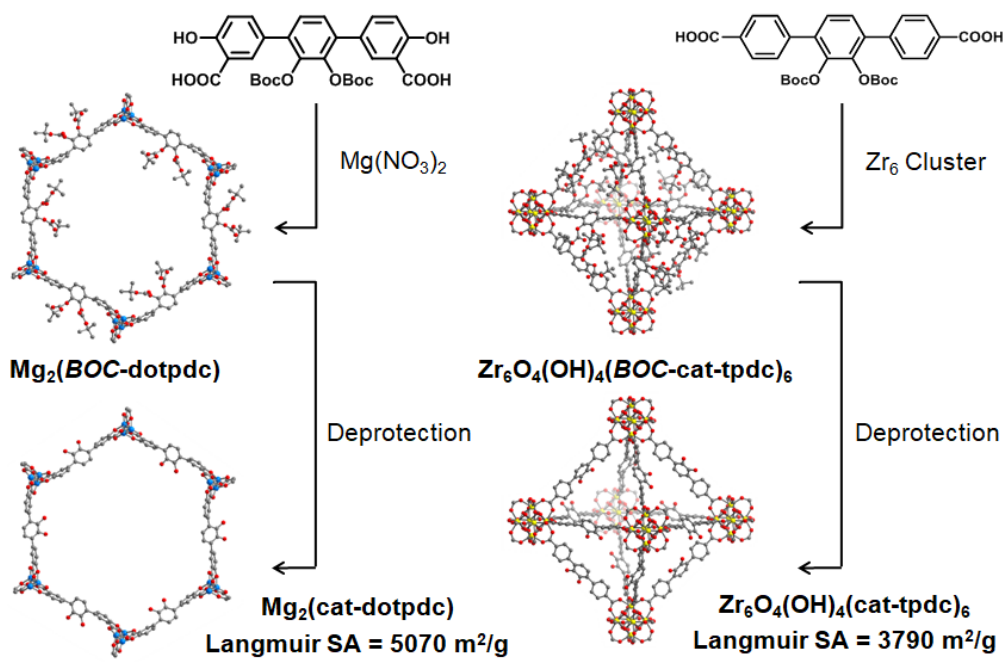

FIGURE 2. Catechol-functionalized frameworks with high crystallinity and surface area (SA) prepared from a protection—framework assembly—deprotection method. The organic linker is protected with a thermolabile group, solvothermal synthesis is performed to assemble the framework, and the resulting material is deprotected post-synthetically to yield free catechol groups in the framework. Structural models were generated using *Materials Studio* software. Atom colors: C, gray; O, red; Mg, blue; Zr, yellow. H atoms are omitted for clarity.

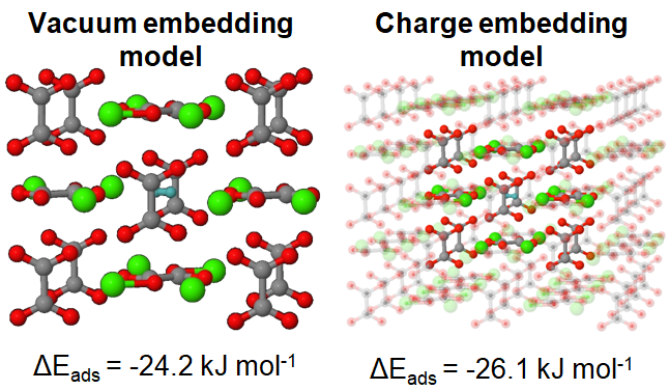

FIGURE 3. H_2 molecules adsorbed in calcium oxalate. H_2 does not interact with exposed metals, but instead is held in small pores by dispersion forces.

TABLE 1. Differential Adsorption Energies for Various Metal–Catecholate Systems (Figure 4) upon Adsorption of the *n-th* H_2 (kJ/mol)

n	Mg–catecholate	Ca–catecholate	Mg–thiocatecholate
1	–23.8	–15.9	–18.7
2	–22.2	–15.5	–12.8
3	–15.4	–15.1	–7.4
4		–14.7	–8.4

CONCLUSIONS AND UPCOMING ACTIVITIES

The successful installation and validation of the DRIFTS instrument with in situ high pressure gas loading capabilities has been demonstrated, and will be a core capability for the measurement and validation of a wide variety of internal and external samples. Following previous computational efforts, a catechol linker has been successfully incorporated into a metal–organic framework with high crystallinity and high surface area. Computational efforts have further investigated multiple H_2 binding in the metal–catecholate system, demonstrating high usable capacities resulting from our strategy of utilizing metals with multiple unsaturated sites. Future work will validate the low-temperature performance of the DRIFTS instrument, and develop synthetic routes towards metalation of the catechol frameworks.

FY 2017 PUBLICATIONS

1. Teo, J.M.; Coghlan, C.J.; Evans, J.D.; Tsivion, E.; Head-Gordon, M.; Sumby, C.J.; Doonan, C.J. "Hetero-bimetallic Metal–Organic Polyhedra," *Chem. Commun.* **2016**, *52*, 276.

2. DeSantis, D.; Mason, J.A.; James, B.D.; Houchins, C.; Long, J.R.; Veenstra, M. "Techno-economic Analysis of Metal–Organic Frameworks for Hydrogen and Natural Gas Storage," *Energy Fuels* **2017**, *31*, 2024.

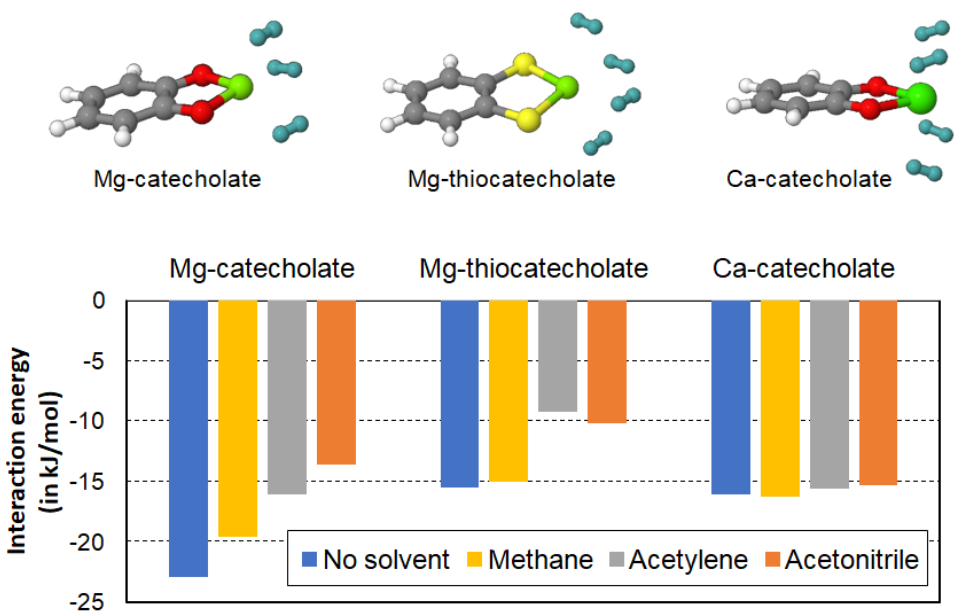

FIGURE 4. Top: H_2 molecules adsorbed on metalated catechols. Bottom: Differential adsorption energies of H_2 in metal-catecholate systems (blue) pre-adsorbed with methane (yellow), acetylene (grey) and acetonitrile (orange).

3. Tsivion E.; Veccham, S.P.; Head-Gordon, M. "High Temperature Hydrogen Storage of Multiple molecules: Theoretical Insights from Metalated Catechols," *ChemPhysChem* **2017**, *18*, 184.

4. Tsivion, E.; Head-Gordon, M. "Methane Storage: Molecular Mechanisms Underlying Room-Temperature Adsorption in $Zn_4O(BDC)_3$ (MOF-5)," *Submitted.*

5. Kapelewski, M.T.; Runčevski, T.; Tarver, J.D.; Jiang, H.Z.H.; Ayala, A.; Gennett, T.; FitzGerald, S.A.; Brown, C.M.; Long, J.R. "Evaluating Metal−Organic Frameworks for High-Pressure H_2 Storage: Record High Volumetric Capacity in Ni_2(*m*-dobdc)," *Submitted*.

FY 2017 PRESENTATIONS

1. Kapelewski, M.T.; Runčevski, T.; Jiang, H.Z.; Hurst, K.E.; Gennett, T.; FitzGerald, S.A.; Brown, C.M.; Long, J.R. "H_2 Storage on Open Metal Coordination Sites — Best Performance in Ni_2(*m*-dobdc) and Two H_2 Molecules on One Metal in Mn_2(dsbdc)," 5th International Conference on Metal-Organic Frameworks, Long Beach, CA (September 15, 2016).

2. Kapelewski, M.T.; Head-Gordon, M. "Hydrogen Storage in Metal−Organic Frameworks," DOE H_2 Tech Team Meeting, Southfield, MI (March 16, 2017).

3. Runčevski, T.; Long, J.R. "*In Situ* Diffraction and Spectroscopic Studies of Metal−Organic Frameworks under Variable Temperature and Gas Pressure," 253rd ACS National Meeting & Exposition, San Francisco, CA (April 2, 2017).

IV.C.7 HyMARC Seedling: Electrolyte Assisted Hydrogen Storage Reactions

Channing Ahn (Primary Contact), Dan Addison, John Vajo and Jason Graetz (HRL)
Liox Power, Inc.
129 N. Hill Ave.
Pasadena, CA 91106
Phone: (626) 395-2174
Email: cca@caltech.edu

DOE Manager: Katie Randolph
Phone: (240) 562-1759
Email: Katie.Randolph@ee.doe.gov

Contract Number: DE-EE0007849

Subcontractor:
HRL Laboratories, LLC, Malibu, CA

Project Start Date: January 20, 2017
Project End Date: June 19, 2018 for Phase 1

Overall Objectives

- Address critical deficiencies of hydrogen storage systems design based on hydride materials, as determined by the Hydrogen Storage Engineering Center of Excellence (HSECoE).
- Obviate the need for high temperature release of hydrogen in complex hydride and destabilization reactions through electrolyte use.
- Demonstrate an improvement in dehydrogenation kinetics by 10X.

Fiscal Year (FY) 2017 Objectives

- Survey of electrolytes to determine thermal and electrochemical stability, ionic conductivity, solubility (salt and H_2), and vapor pressure.
- Demonstrate electrolyte assisted hydrogen evolution based on Li^+ and/or Mg^{2+} cations (or other) storage materials.
- Demonstrate electrolyte assisted reversible hydrogen uptake based on Li^+ and/or Mg^{2+} cations with endothermic H_2 evolution.

Technical Barriers

This project addresses the following technical barriers from the 2015 Hydrogen Storage section (3.3) of the Fuel Cell Technologies Office Multi-Year Research, Development, and Demonstration Plan with sub listings from the Technical Task Description Table 3.3.8.

(O) Lack of Understanding of Hydrogen Physisorption and Chemisorption.

- Decomposition pathways and products of materials to better understand their mechanisms and kinetics.
- H_2 storage capacity of potential storage materials and demonstrate reproducibility of their synthesis and capacity measurements.
- Develop reversible metal hydrides that improve kinetics while maintaining high gravimetric capacity at relevant release temperatures and pressures.

Technical Targets

TABLE 1. Technical System Targets: Onboard Hydrogen Storage for Light-Duty Fuel Cell Vehicles

Storage Parameter	Units	DOE 2020	Project Status
System Gravimetric Capacity Usable, specific-energy from H_2 (net useful energy/max system mass)	kWh/kg (kg H_2/kg system)	1.8 0.055	TBD
System Volumetric Capacity Usable energy density from H_2 (net useful energy/max system volume)	kWh/L (kg H_2/L) system	1.3 (0.040)	TBD
Charging/Discharging Rates System fill time (5 kg)	min	3.3	TBD

TBD – to be determined

While we note the system targets listed above from the DOE 2015 Multi-Year Research, Development, and Demonstration Plan hydrogen storage section, this project is conducting fundamental studies on the role of enhanced kinetics through the use of electrolyte assisted hydrogenation/dehydrogenation on complex hydride and destabilization hydride reactions. While the systems being studied, at least on a materials basis, show capacities in excess of system targets for volumetric and gravimetric densities, the kinetics required for hydrogenation/dehydrogenation are too slow under technologically relevant temperatures. Our effort explores the improvement in kinetics with the aim of nearing thermodynamic temperatures for relevant materials systems.

FY 2017 Accomplishments

- Analysis of di-, tri- and tetraglyme solvent stability for use with $Mg(BH_4)_2$ using gas chromatography-mass

spectrometry at ambient and 80°C temperatures. This technique for solvent decomposition analysis is more sensitive than nuclear magnetic resonance.

- Residual gas analysis (RGA) from ambient to 200°C at modestly high Ar pressures (to suppress solvent boiling) of the same systems in order to evaluate specific decomposition products showing dimethyl ether product.
- 10X enhanced kinetics of the MgH_2+Si destabilization reaction using a eutectic molten iodide salt of Li-K-CsI that has a 210°C melting temperature for equimolar composition.

✧ ✧ ✧ ✧ ✧

INTRODUCTION

State-of-the-art hydrogen storage material studies supported by DOE funded projects have included complex hydrides and destabilized systems, both of which typically involve multiple solid phases [1]. While these materials can exhibit high hydrogen densities and tunable thermodynamic properties, the rates of hydrogen exchange (i.e., the rates of dehydrogenation and rehydrogenation) are too kinetically limited for relevant applications. These limitations occur in part, because multiple component materials are typically formulated as solid-state powder mixtures where reaction between the phases can only take place across solid-solid interfaces where particles are in direct atomic-scale contact. Nanoscale engineering, using mechanical milling or templates, and additives or catalysts have been employed to increase reaction rates by decreasing diffusion distances and increasing interfacial contact area and mobility. While significant kinetic improvements have been achieved, and are still undergoing refinement, they have thus far been insufficient for practical applications.

APPROACH

Given the interface-controlled processes of solid-state destabilization reactions that normally require thermal activation, we have defined a free energy difference that needs to be overcome before any relevant transformation or reaction can take place. Noting the difference between the effective empirically determined temperature required to promote a reaction in comparison to what might be expected on a purely thermodynamic basis, we note that the free energy barrier is typically >20 kJ. However, in so-called electrochemical conversion battery reactions that involve diffusing species in an electrolyte, the activation barrier has been observed to be as low as 4 kJ. Given the similarity of compounds used in both electrochemical and hydrogen storage reactions, the expectation is that the use of electrolytes will help lower the free energy barrier height by promoting solubilization of the diffusing species so that reactions are no longer controlled by limited interfacial areas.

Electrolytes under consideration for this effort will ultimately require redox stability, low vapor pressure, high hydrogen permeability and relatively low mass and volume with respect to the reacting species. Our effort is aimed at evaluating and testing electrolyte suitability to enhance hydrogen storage materials reaction kinetics.

RESULTS

Solvent Stability Results with $Mg(BH_4)_2$

Initial results from HRL on the use of diglyme with $Mg(BH_4)_2$ showed evidence of gas release but with some uncertainty over the relative level of hydrogen with possible solvent decomposition products. With the official start of this effort and Liox's several unique analytical capabilities for gas analysis that were developed as part of its electrolyte studies since 2009, both gas chromatography-mass spectrometry and RGA analyses were used to re-examine glyme–$Mg(BH_4)_2$ reactions.

To obviate the possibility of water reactions, di-, tri and tetraglyme solvents were initially analyzed using a Karl Fischer titration, to assess and reduce the quantity of water to below the 10 ppm level. These solvents were then used to determine the extent of reactivity or decomposition.

Cell pressure and RGA data for tetraglyme with $Mg(BH_4)_2$ are presented in Figures 1 and 2 and were evaluated due to the higher boiling point of this solvent, with the anticipation that it might show a higher level of stability against decomposition. Using the unique RGA

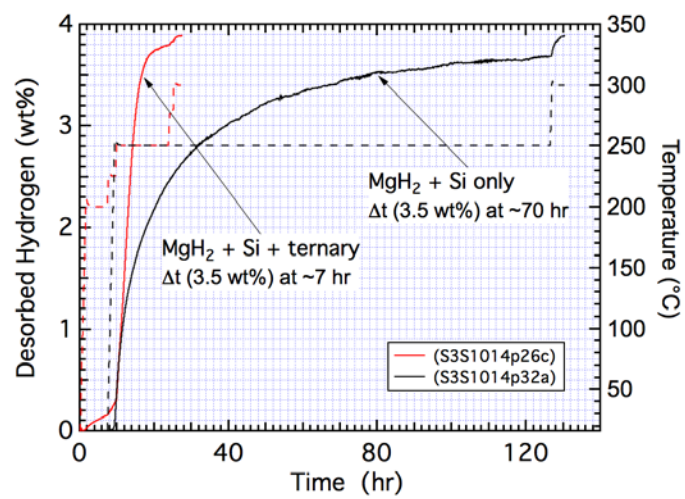

FIGURE 1. Cell pressure vs time for a cell containing $Mg(BH_4)_2$ with tetraglyme. Gas was extracted at dips and points indicated by the arrows and gas analysis data from these points is presented in Figure 2.

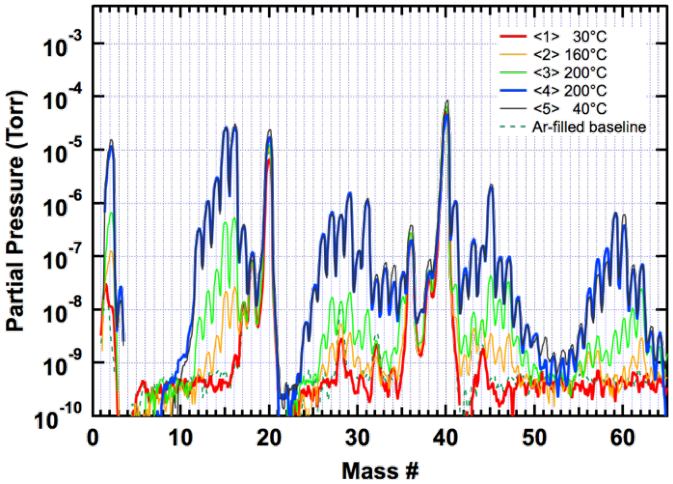

FIGURE 2. RGA data for points indicated from the gas extraction points shown in Figure 1. Decomposition to dimethyl ether (RGA peaks at mass numbers 13–15, 29–31, 45–46) is indicated, in addition to hydrogen evolution when tetraglyme is added to $Mg(BH_4)_2$. These peaks do not appear in the RGA in the absence of $Mg(BH_4)_2$.

instrumentation at Liox for determining gas compositions we determined that solvent decomposition does occur in the presence of $Mg(BH_4)_2$. Dips in the pressure data of Figure 1 indicated points where gas was extracted for the RGA analysis. Figure 2 shows the RGA plot for gas extraction times and temperatures from Figure 1. We note that the dimethyl ether reaction product peaks do not appear in the RGA in the absence of $Mg(BH_4)_2$. Similar results for di- and triglyme and hexamethylphosphoramide were presented in the ST137 Annual Merit Review 2017 presentation for this project.

Eutectic Molten Salt Analyses

Inorganic molten salts have a high level of thermal stability over a wide temperature range for dehydrogenation and can be formulated with components that are chemically inert to hydrogen storage compounds.

We have used iodide salts of Li, K and Cs in an attempt to find a low temperature eutectic (melting) point composition to probe for the effectiveness of these salts in improving the kinetics of dehydrogenation. Binary phase diagram data for these iodides are available for the most part from computed values so an initial identification of an equimolar ternary melting point was determined by calorimetry and is shown in Figure 3.

To test for the effectiveness of this mixture in promoting kinetics, an equimolar salt ternary was combined with the MgH_2+Si destabilization reaction system and a comparison of this reaction with and without the ternary is shown in Figure 4.

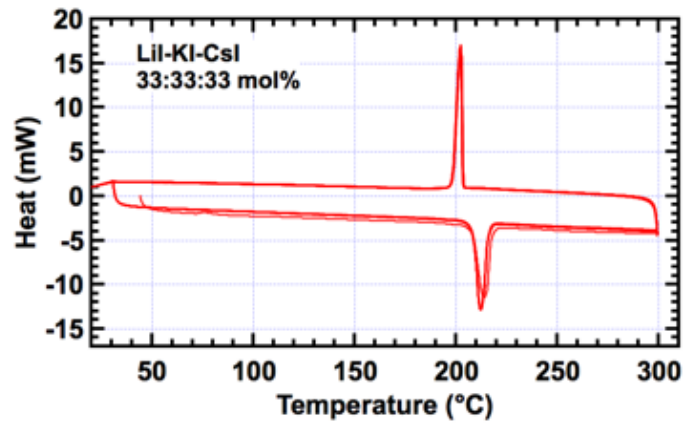

FIGURE 3. Differential scanning calorimetry trace of the ternary mixture of LiI, KI and CsI salts indicating a melting point of ~210°C. A different composition based on tie-line analysis of the binary phase diagrams was performed but yielded the same melting temperature.

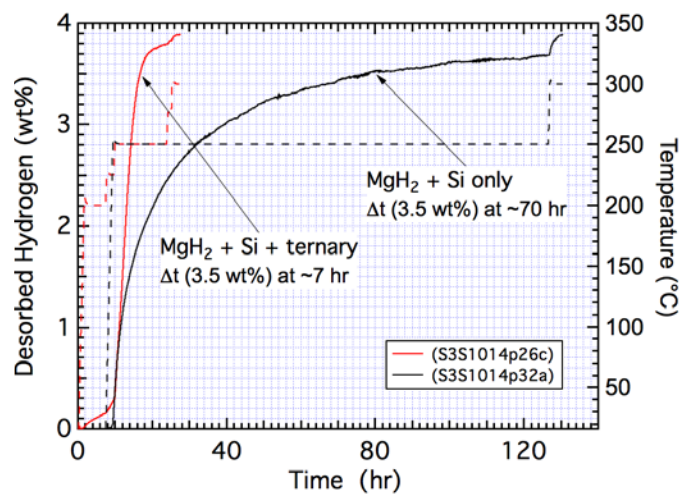

FIGURE 4. 10X improvement in dehydrogenation kinetics of MgH_2+Si in the presence of a ternary LiI:NaI:KI eutectic compared to no eutectic is shown for the neat reaction shown in the black trace in comparison to the reaction in the presence of the ternary shown in the red trace.

The fall-off in the "neat" reaction shown in the black trace of Figure 4 is typical for destabilization reactions. The nearly straight-line dehydrogenation shown in the presence of the ternary salt has not been observed before and gives evidence for enhanced solubility of the reactants. The ~10-fold increase in kinetics demonstrated here in the presence of the ternary under these conditions points to the effectiveness of the iodide ternary in promoting the dehydrogenation of this system.

We have also examined the possibility of a $LiBH_4$-KBH_4 binary eutectic that has a melting point of ~105°C and anticipate other low temperature eutectic systems suitable

for fulfilling all of the electrolyte requirements that include (a) redox stability, (b) low vapor pressure, (c) suitable hydrogen gas exchange and transport, and (d) minimal weight and volume.

CONCLUSIONS AND UPCOMING ACTIVITIES FOR PHASE 1

Given our success in achieving a 10X kinetic improvement with the MgH_2+Si destabilization reaction through the use of an iodide salt ternary electrolyte, it appears that the electrolyte has provided the means necessary to solubilize the reactant phases.

- While the melting temperatures for the iodide ternary are still too high for applications, the observation of kinetic improvement suggests that our approach of electrolyte use provides a pathway for practical implementation.
- With existing funding, we plan to evaluate other systems using electrolytes that have lower melting temperatures that fall within the range of values where reactions are expected on the basis of equilibrium thermodynamic values.
- While the ternary iodide salt had a melting point of ~210°C, we have already determined other systems with melting temperatures <110°C and are poised to use these in systems where the kinetics under thermodynamic equilibrium conditions will benefit from electrolyte use.

SPECIAL RECOGNITIONS & AWARDS/ PATENTS ISSUED

1. Patent Invention Disclosure: Title: Hydrogen storage material formulations containing electrolytes, filed June 1, 2017.

FY 2017 PUBLICATIONS/PRESENTATIONS

1. Channing Ahn, "HyMARC Seedling: Electrolyte Assisted Hydrogen Storage Reactions," ST137, presented at the 2017 DOE Hydrogen and Fuel Cells Annual Merit Review, Washington DC, June 7, 2017.

REFERENCES

1. Lennie E. Klebanoff and Jay O. Keller, 5 Years of hydrogen storage research in the U.S. DOE Metal Hydride Center of Excellence (MHCoE), International Journal of Hydrogen Energy, 38 (2013), 4533–76.

IV.C.8 HyMARC Seedling: Developing a Novel Hydrogen Sponge with Ideal Binding Energy and High Surface Area for Practical Hydrogen Storage

T.C. Mike Chung
The Pennsylvania State University
302 Steidle Building
University Park, PA 16802
Phone: (814) 863-1394
Email: chung@ems.psu.edu

DOE Manager: Jesse Adams
Phone: (720) 356-1421
Email: Jesse.Adams@ee.doe.gov

Contract Number: DE-EE0007655

Project Start Date: October 1, 2016
Project End Date: September 30, 2019

Overall Objectives

- Within 18 months of the project starting, develop at least one B-polymer network structures with a surface area of at least 3,000 m^2/g with average hydrogen binding energy (ΔH) of at least 15 kJ/mol and hydrogen adsorption capacity in the range of 5 wt% excess on a material basis.
- Ultimately design, synthesis, and evaluation of a new class of B-containing polymer networks that can simultaneously exhibit a ΔH of 15–25 kJ/mol, a specific surface area (SSA) >4,000 m^2/g, and a material density >650 g/L on a material basis.
- Ultimate goals also include achieving the 2025 DOE targets, with a gravimetric capacity of 1.8 kWh/kg (5.5 wt% H_2) and volumetric capacity of 1.3 kWh/L (40g H_2/L) at ambient temperature and mild pressure on a system basis.
- Molecular simulation and advanced structural characterization to support scientific understanding and polymer materials development.
- Collaboration with HyMARC core team for H_2 adsorption isotherm measurements and understanding the structure-property relationship.

Fiscal Year (FY) 2017 Objectives

- Developing chemical routes for the preparation of two proposed nanoporous π-electron conjugated B-containing polymer networks.
- Structural characterization of the resulting B-polymer networks by the combination of Fourier transform infrared spectroscopy (FTIR), ^{1}H, ^{11}B, and ^{13}C nuclear magnetic resonance (NMR) spectroscopic techniques.
- Applying volumetric gas adsorption techniques, with CO_2, N_2, and H_2 gases under various temperatures and pressures, to understand the nanoporous textures, specific surface areas, and H_2 adsorption profiles of the synthesized polymers.
- Collaboration with HyMARC core team for H_2 adsorption isotherm measurements.

Technical Barriers

This project addresses the following technical barriers from the Hydrogen Storage section of the Fuel Cell Technologies Office Multi-Year Research, Development, and Demonstration Plan.

(A) System Weight and Volume

(B) System Cost

(C) Efficiency

(E) Charging/Discharging Rates

(O) Lack of Understanding of Hydrogen Physisorption and Chemisorption

Technical Targets

Design and synthesis of hydrogen storage materials that meet the following DOE onboard 2020 automotive usable hydrogen storage targets.

- 1.5 kWh/kg system (4.5 wt% H_2)
- 1.0 kWh/L system (0.030 kg H_2/L)
- Cost of \$10/kWh (\$333/kg H_2 stored)
- Operating at ambient temperatures (-40ºC to 60ºC)
- Onboard efficiency of 90% and minimum hydrogen delivery pressure of 5 bar
- Total refuel time of 5 minutes

FY 2017 Accomplishments

- Synthesis and characterization of two proposed nanoporous π-electron conjugated B-containing polymer networks, with a combination of spectroscopic techniques to determine the molecular structure and volumetric gas adsorption technique to understand

their nanoporous textures, specific surface area, and H_2 adsorption profiles.

- Discovery of a π-electron conjugated B-moiety in a B-containing polymer network with enhanced H_2 binding energy (exact value to be validated in FY 2018).
- Collaboration with HyMARC core team for H_2 adsorption isotherm measurements.

✧ ✧ ✧ ✧ ✧

INTRODUCTION

A practical hydrogen storage technology is essential in realizing the H_2 economy, especially for onboard applications. Current H_2 storage methods, including compressed gas, cryogenic liquid, metal hydrides, chemical hydrides, and adsorbents, all show significant deficiencies and limitations. Among them, adsorbents would be ideal materials for practical applications if the adsorbent could show a sufficient gravimetric capacity (>5 wt%) at moderate operational temperatures (-20°C to 40°C) and pressures (20–100 bar). The primary barrier is the H_2 binding energy on traditional high SSA adsorbents (i.e., metal-organic frameworks, carbons) is too weak (in the range of 4–7 kJ/mol). Thus, the physisorption of H_2 requires very low temperatures (liquid N_2 temperature).

APPROACH

The primary objective of this research project is to develop a specific polymer network with surfaces that can display H_2 binding energies in the range of 15–25 kJ/mol. In addition, the targeted polymers will also exhibit a nanoporous morphology with high surface areas greater than 4,000 m^2/g and mass densities >0.65 g/cm^3. In general, the adsorption capacity is proportional to the SSA accessible to H_2, ~1 wt% per 500 m^2/g as predicted by the Chahine rule. We propose to develop a new class of H_2 adsorbing polymer frameworks (H_2 sponges) that can automatically form free volume with continuous nanoporous channels (~1 nm in diameter) to achieve the specific surface area and mass density targets. These thermoplastic-based materials can be produced in large-scale with robotic properties and have the potential to achieve the 2025 DOE targets, with a gravimetric capacity of 1.8 kWh/kg (5.5 wt% H_2) and volumetric capacity of 1.3 kWh/L (40 g H_2/L) at ambient temperature and mild pressure.

In the first phase of this research project, we focus on the synthesis and characterization of two proposed B-containing polymer networks (A) and (B), with an objective to study the correlation between B-moiety and H_2 binding energy. After the discovery of a suitable B-moiety with the potential to meet the specific metrics and a go/no-go decision scheduled in December 2017, we will fine-tune the network morphology (polymer free volume) with the assistance of molecular simulation and a good understanding of structure-property relationships by collaborating with the HyMARC core team. The objective is to identify the most suitable H_2 sponge that meets all DOE metrics, including thermodynamic and kinetic properties. Since the proposed H_2 sponge is a polymer-based material with spontaneously formed open morphology, the adsorbent shall exhibit strong, reliable, and easy handling as many plastic materials do.

RESULTS

Synthesis and Molecular Structure Characterization

We have synthesized both B-polymer networks (A) and (B). The B-polymer network (A) was prepared by 2,6-divinyl-9,10-dimethoxyboraanthracene monomer that contains two pairs of active sites, including two B-OCH_3 groups and two styrenic groups, which can engage in two independent polycondensation reactions. Several B-polymer network (A) samples were prepared and showed the spontaneous formation of nanoporous morphology with pore sizes less than 1 nm. However, the specific surface area is quite small (<500 m^2/g), which may be due to the structural inhomogeneity in the network (A). It is somewhat difficult to control the sequential polycondensation reactions in this reaction scheme. Thus, we have been focusing on B-polymer network (B) that can be formed by two consecutive reactions with good control in each step. As shown in Figure 1, the chemistry involves butyenyl styrene monomer (I) with two reaction steps. First is the metallocene-mediated polymerization of butyenyl styrene (I) that contains two asymmetric olefinic units (styrene and α-olefin). We select a suitable homogeneous syndio-specific metallocene catalyst that can selectively initiate styrene polymerization to form syndiotactic poly(butyenyl styrene) (II) with high polymer molecular weight, high syndiotacticity, and high yield. The stereo-selectivity results in an alternating arrangement of butyenylphenyl side chains, located along the polymer backbone. This stereo-arrangement is essential to create free volume and nanopores. The second reaction step involves facile hydroboration reaction of the pending olefinic groups with tri-valent BH_3 to form highly cross-linked boron-containing poly(butyenyl styrene) network (B-PBS) (III). During the slow titration of BH_3/tetrahydrofuran (THF) reagent into polymer solution, the hydroboration reaction was very effective at room temperature to form an insoluble B-PBS network (III) which automatically precipitated out from the solution. The resulting B-PBS network (III) was further heat-treated at 200–300°C to form the objective π-electron conjugated B-polymer network (B). The acidic B-moieties, connecting the conjugated side chains, serve as in situ p-type dopants to increase the surface energy around the nanopores (automatically created by free volume). It is interesting to note that this low temperature (<300°C)

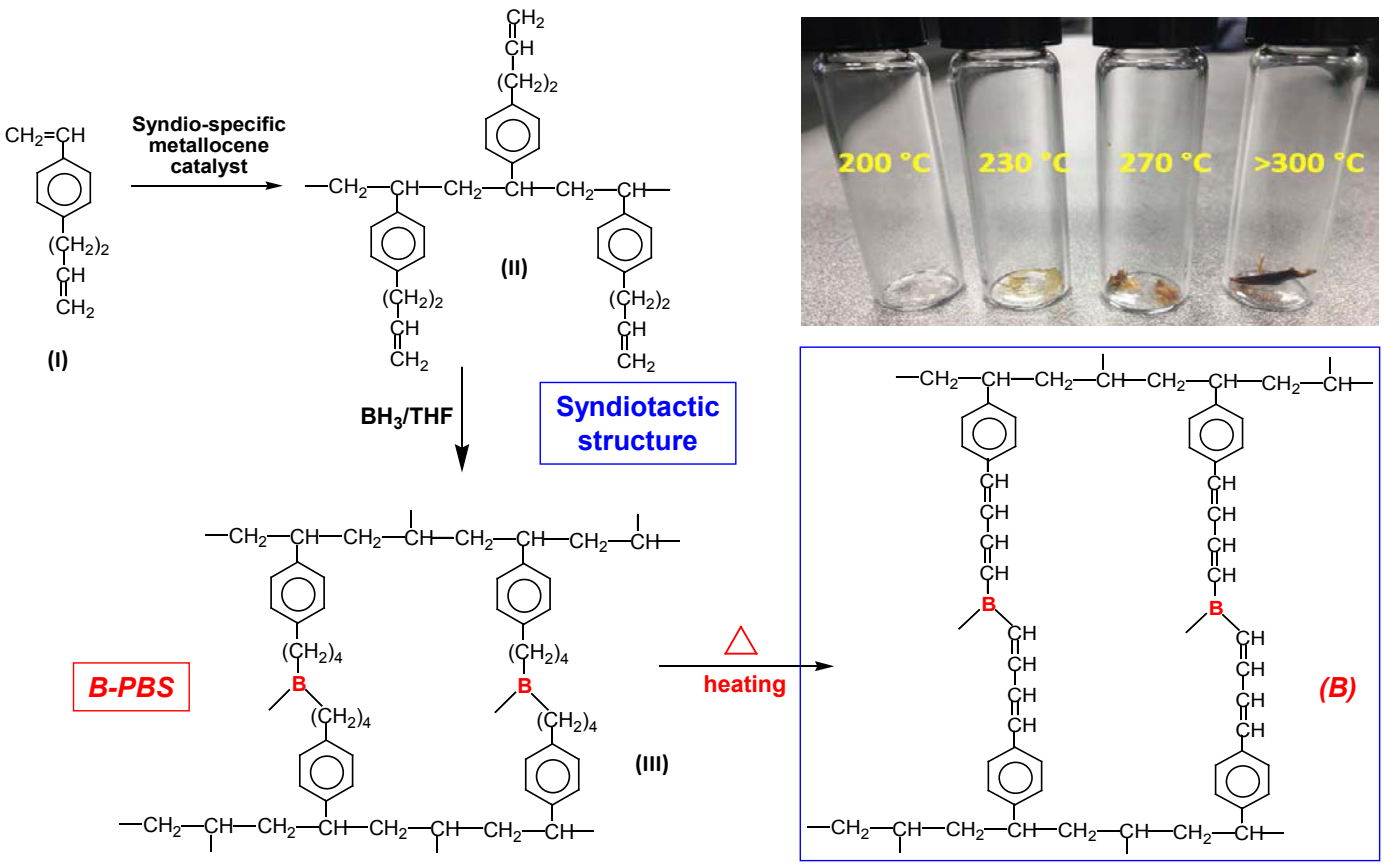

FIGURE 1. Synthesis of boron-containing poly(butyenyl styrene) polymer network (III) and the subsequent heat-treatment to form the π-electrons conjugated B-polymer network (B), and the picture of samples after heat-treating for one hour at various temperatures

thermal-induced dehydrogenation reaction was also observed in our previous study [1–7] in the preparation of boron-substituted carbon materials by using boron-containing precursors. As shown in the pictures, the transparent and colorless polymer film of B-PBS (III) gradually increases its color with heating. At 300°C for 1 h, the polymer becomes very dark, indicating long conjugated sequences that absorb all visible light.

Figure 2 (left) shows FTIR spectra of three thermal-treated B-PBS samples at 200°C, 230°C, and 270°C for 1 h, respectively. Upon heating, a new broad band with two absorption peaks at 1,017 cm^{-1} and 1,090 cm^{-1}, corresponding to C=C-B vibrational modes, appear at 200°C and sharply increases intensity at 230°C. These peak intensities then level off at 270°C. Evidently, the FTIR results show the thermal transformation of organoborane moieties into the π-electrons conjugation sequences, centered around the acidic (electron-deficient) boron species. Based on the peak intensity, it only requires a low temperature (230°C) to achieve a highly π-conjugated B-polymer framework (B). It is interesting to identify the resulting B moieties and determine their acidities (electron deficiency) in this π-electron conjugated B-polymer network (B), which shall be directly relative to their H_2 binding energy. Figure 2 (right) shows a magic angle spinning ^{11}B solid state NMR spectrum of B-PBS-230 network, formed after heating the corresponding B-PBS (III) at 230°C for 1 hr. Three chemical shift bands, peaked at 50 ppm, 25 ppm, and 17–10 ppm, imply multiple acidic boron moieties. Since the sample only contains B, C, and H elements, without exposure to air, the chemical shifts imply the boron moieties with various π-conjugated structures. The most acidic B species peaked at 50 ppm may only have two π-conjugated ligands as indicated by the structure in Figure 2 (right). The other high field chemical shifts (between 30 ppm and 10 ppm) may be associated with tri-valence π-conjugated ligands having different conjugation lengths. In other words, there are significant inhomogeneity of π-electron conjugated B-moieties in this B-polymer network (B) sample, which may exhibit several H_2 binding energy sites on the surfaces. The most acidic B-moiety (peaked at 50 ppm) with about 50% content (based on the peak intensity) shall offer the highest H_2 binding energy.

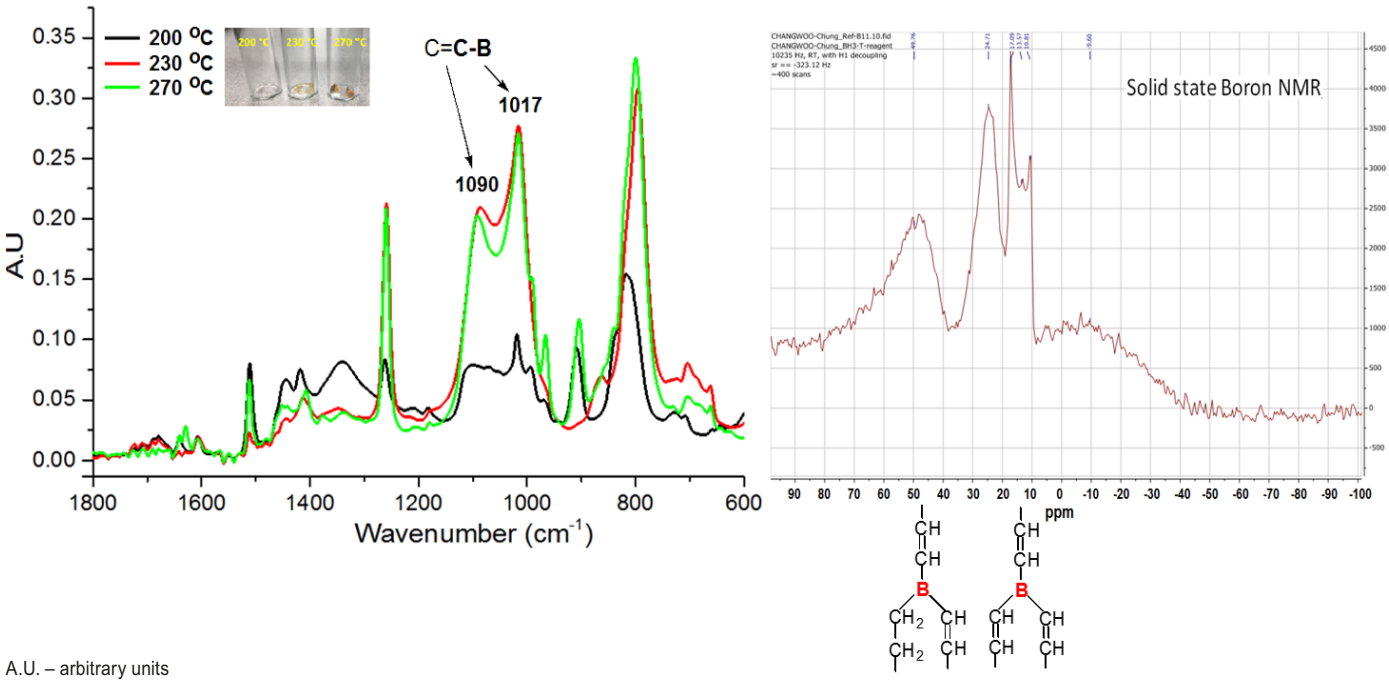

A.U. – arbitrary units

FIGURE 2. (left) FTIR spectra of three B-PBS polymer networks after heat treatment at 200°C, 230°C, and 270°C; (right) magic angle spinning ^{11}B solid state NMR spectrum of B-PBS-230 polymer network

Pore Size Distribution and Hydrogen Adsorption Isotherm

All the resulting B-polymer network (A) and (B) samples were examined by volumetric gas adsorption technique, using CO_2, N_2, and H_2 gases under various temperatures and pressures, to understand their nanoporous textures and adsorption capacities. The mass density of samples were also determined by a pycnometer. Figure 3 shows pore size distribution curves of two representative B-polymer network (B) samples, including B-PBS-230 and B-PBS-300, respectively, with their surface areas and mass density information. The pore size distribution was determined from adsorption isotherms of N_2 (77 K) and CO_2 (273 K) measurements at low pressure (<1 bar) with BJH (Barrett, Joyner, and Halenda) and D–R (Dubinin-Radushkevich) calculation methods, respectively. It is interesting to note that the surface areas measured by CO_2 adsorption consistently show high values, but almost no N_2 adsorption in both samples. Since the CO_2 measurement is capable of covering the extremely small nanopores (size <12 Å), all B-polymer network samples with free volume only contain nanopores with relatively low nanopore volumes. In fact, all samples also show mass density at about 1 g/cm^3, which is only about 10–20% below many typical hydrocarbon polymers with dense morphologies.

In the B-PBS-230 sample, the pore sizes are in the range of 5–8 Å with a surface area of 1,150 m^2/g (so far, the highest SSA in this B-polymer network system). The pore size slightly increases to the range of 8–11 Å in B-PBS-300 sample, after increasing the heat-treatment temperature to 300°C. However, the surface area reduces somewhat to 800 m^2/g. We were somewhat surprised with the relatively small surface area for the material that has a molecule-level controlled free volume morphology. The possibility of underestimated the surface area does exist as some sub-nano size pores may be difficult to form the continuous open pore channels required for gas access under low pressure conditions, especially the accessibility to H_2 molecules.

We measured H_2 adsorption isotherms by volumetric measurement under various temperature and pressure conditions. Figure 4 shows the H_2 adsorption isotherms of B-PBS-230 at 298, 273, and 77 K, respectively. Under 70 bar H_2 pressure, the absorption capacity of B-PBS-230 sample reaches to 1 wt% and 0.7 wt% at 0°C and 25°C, respectively. The linear H_2 absorption isotherm profiles indicate the adsorption capacity well below the saturation level. Thus, we measured the isotherm at 77 K with the attempt to observe the saturation level. A typical Type I isotherm was observed with the saturation level at above 2 wt%, which is quite in consistent with the adsorbent with SSA about 1,150 m^2/g, based on the Chahine's rule. Comparing with the known adsorbents with similar surface areas, this B-PBS-230 sample shows a significantly higher H_2 uptake at ambient temperature, implying a high H_2 binding energy. We are currently arranging the validation experiment with the National Renewable Energy Laboratory group to confirm the isotherm results and estimate the H_2 binding energy.

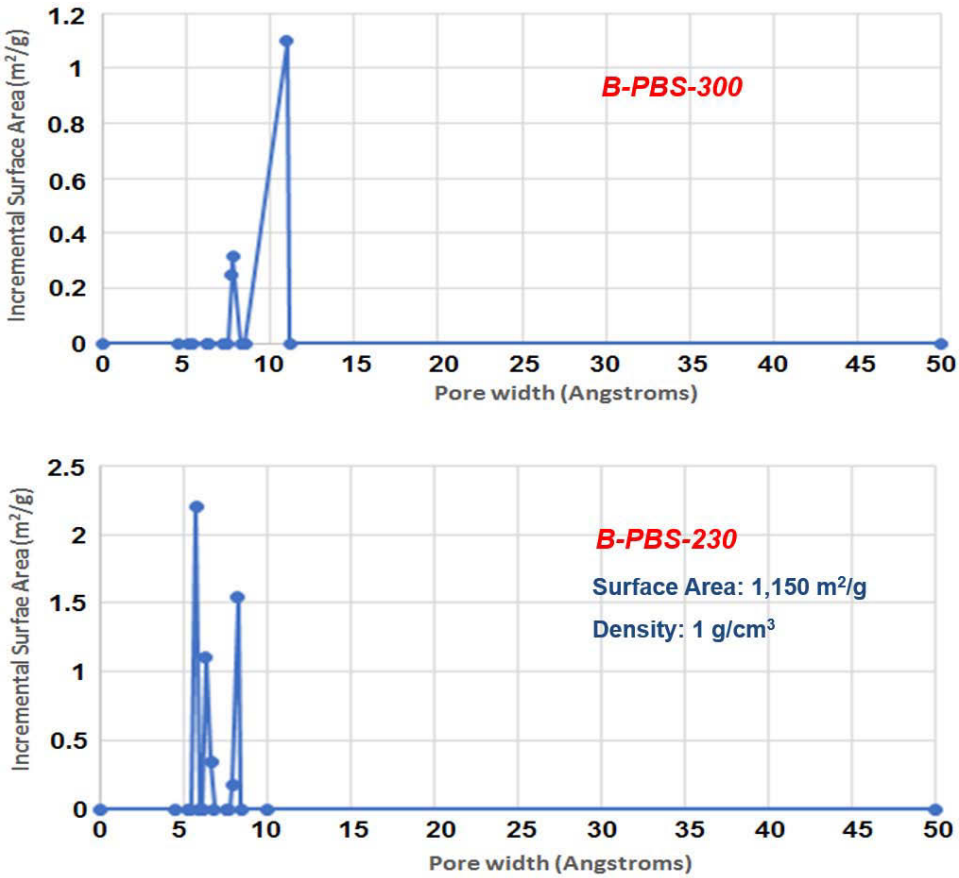

FIGURE 3. Pore size distribution (with specific surface area and mass density) of two B-PBS polymer networks after the heat-treatment at 230°C (bottom) and 300°C (top) for 1 h

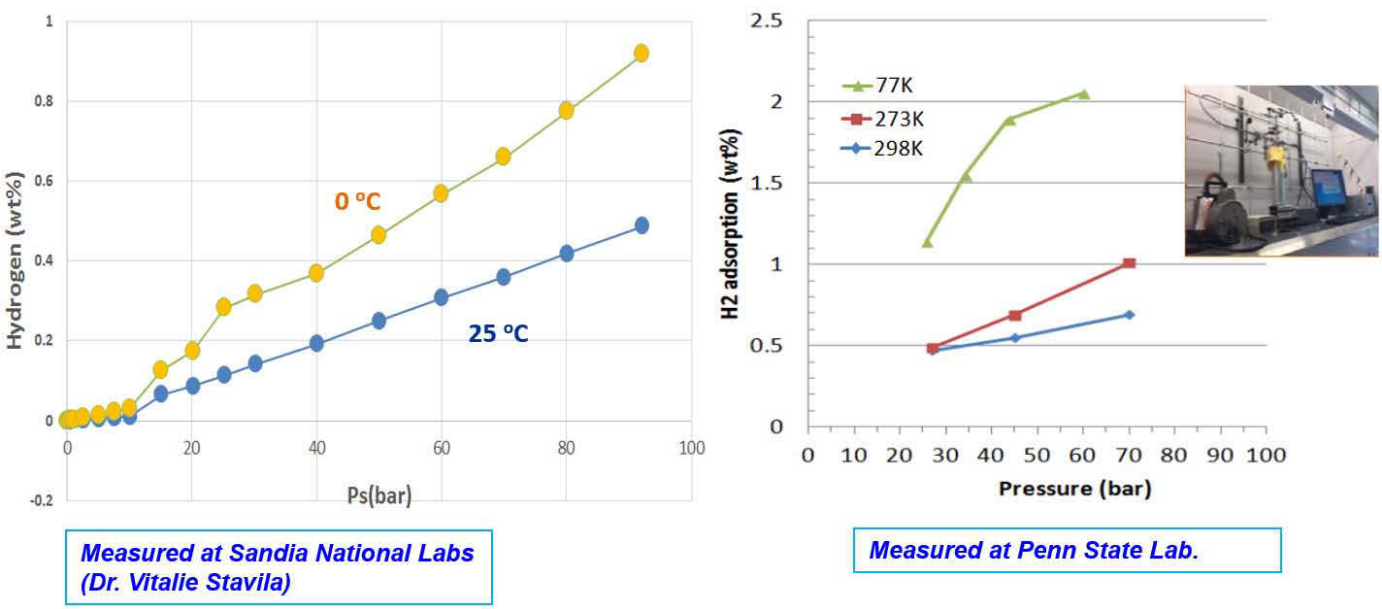

FIGURE 4. H_2 adsorption isotherm of B-PBS-230 at 77 K, 273 K, and 298 K

CONCLUSIONS AND UPCOMING ACTIVITIES

This research project proposes the investigation of two B-polymer networks with the objective to simultaneously show three essential properties, including high H_2 binding energy 15–25 kJ/mol, high surface area >4,000 m^2/g, and mass density >0.65 g/cm^3. If successful, the new sorbent material should achieve the 2020 DOE hydrogen storage targets with a material gravimetric capacity of 4.5 wt% H_2 and volumetric capacity of 30 g H_2/L under mild condition. Among three key properties, the surface binding energy is the most challenging one. So far, there is no known adsorbent material that exhibits a H_2 binding energy in the range of 15–25 kJ/mol (most of them showing less than a half). Thus, in our research strategy, the initial priority is to tackle the specific surface functionality that can show the desirable H_2 binding energy. If successful, we will adopt the known network material design principles to prepare the B-polymer network with desirable nanoporous morphology that can offer high surface area and suitable mass density.

In the past three quarters of this Phase I period, we have developed the chemical routes to prepare two proposed B-polymer network structures (A) and (B). Several B-polymer network (B) samples were systematically synthesized by using boron-containing poly(butyenyl styrene) (B-PBS) precursor and the subsequent heat-treatment procedure to achieve the B-polymer network (B) with a π-electrons conjugated framework containing B-moieties. Some resulting B-polymer network (B) samples were carefully examined to understand their molecular structures, nanopores morphology based on automatically formed free volume, and H_2 adsorption isotherms under various temperatures and pressures to know their H_2 sorption capacities and profiles, as well as the structure-property relationship. The resulting π-electrons conjugated B-moieties in the B-polymer framework (B) show strong acidity, which may offer high H_2 binding energy. However, it requires further confirmation.

The other immediate research activity is to modify the reaction condition to prepare B-polymer network (B) with only a well-defined π-electrons conjugated B-moiety that shows the desirable H_2 adsorption profile. At the same time, we will expand the molecular structure design to increase the specific surface area. Following the known network design principles for high surface areas, we hope to prepare the next generation of B-polymer frameworks with a uniform nanoporous morphology (pore size about 1 nm), which shall offer both high surface area and high mass density. During the entire research period, we will continue the collaboration with Sandia core team and understand the structure-property relationship.

FY 2017 PUBLICATIONS/PRESENTATIONS

1. T.C. Mike Chung, "Developing a Novel Hydrogen Sorbent for Practical Hydrogen Storage and Achieving DOE 2020 Targets," presented at the Kickoff Meeting for new EERE/FCTO Hydrogen Storage Projects, Sandia National Laboratories, California, October 2016.

2. T.C. Mike Chung, "Developing a Novel Hydrogen Sorbent for Practical Hydrogen Storage and Achieving DOE 2020 Targets," presented at the 2017 DOE Annual Merit Review and Peer Evaluation Meeting, Washington, D.C., June 2017.

3. Changwoo Nam, Houxiang Li, and T.C. Mike Chung, "Transportation Big Data: Unbiased Analysis and Tools to Inform Sustainable Transportation Decisions," Gordon Research Conference on Hydrogen-Metal Systems, (GRC-HMS), Easton, MA, July 2017.

REFERENCES

1. R. Hu and T.C. Chung, *Carbon* **1996**, 34, 595.

2. R. Hu and T.C. Chung, *Carbon* **1996**, 34, 1181.

3. R. Hu and T.C. Chung, *Carbon* **1997**, 35, 1101.

4. R. Hu and T.C. Chung, *Carbon* **1997**, 35, 1101.

5. Youmi Jeong, Alfred Kleinhammes, Yue Wu, and T.C. Mike Chung, *J. Am. Chem. Soc*. **2008**, 130, 6668.

6. Youmi Jeong and T.C. Mike Chung, *Carbon* **2011**, 49, 140.

7. A. Kleinhammes, R.J. Anderson, Q. Chen, Y. Jeong, T.C. Mike Chung, Y. Wu, J. *Phys. Chem. C* **2010**, 114, 13705.

IV.C.9 HyMARC Seedling: "Graphene-Wrapped" Complex Hydrides as High-Capacity, Regenerable Hydrogen Storage Materials

Di-Jia Liu (Primary Contact) and Lina Chong
Argonne National Laboratory
9700 South Cass Avenue
Lemont, IL 60439
Phone: (630) 252-4511
Email: djliu@anl.gov

DOE Manager: Jesse Adams
Phone: (720) 356-1421
Email: Jesse.Adams@ee.doe.gov

Subcontractor:
Qingfeng Ge, Southern Illinois University, Carbondale, IL

Project Start Date: October 1, 2016
Project End Date: September 30, 2019

Overall Objectives

- Produce one or more hydride@graphene composites with regenerable hydrogen storage gravimetric density >10 wt% and volumetric density >0.055 kg H_2/L.
- Develop a scale-up plan of manufacturing the new composite at the cost <$333/kg H_2.
- Establish fundamental understanding on the improved dehydrogenation and rehydrogenation kinetics promoted by graphene.

Fiscal Year (FY) 2017 Objectives

- Deliver a hydride@graphene system with reversible >8 wt% total gravimetric and >0.03 kg H_2/L total volumetric hydrogen storage capacities at temperatures <400°C over at least five dehydrogenation (DH)–rehydrogenation (RH) cycles.
- Understand the structural changes in $NaBH_4$@graphene during DH and RH cycles.
- Improve $NaBH_4$@graphene dehydrogenation kinetics by exploring structural or chemical approaches.

Technical Barriers

This project addresses the following technical barriers from the Hydrogen Storage section of the Fuel Cell Technologies Office Multi-Year Research, Development, and Demonstration Plan.

(A) System Weight and Volume

(B) System Cost

(C) Efficiency

(D) Durability/Operability

(E) Charging/Discharging Rates

(O) Lack of Understanding of Hydrogen Physisorption and Chemisorption

Technical Targets

This project is to design and synthesize "graphene wrapped" complex hydride composites as the next generation hydrogen storage materials that meet the following DOE hydrogen storage targets.

- Excess gravimetric hydrogen storage capacity:
  - DOE 2025 Target: 5.5 wt% system basis
  - Project Target: 10 wt% on material basis
- Volumetric H_2 storage capacity:
  - DOE 2025 Target: 0.040 kg H_2/L of system
  - Project Target: 0.055 kg H_2/L of material total

FY 2017 Accomplishments

- Successfully synthesized a $NaBH_4$@graphene composite and demonstrated six DH and RH cycles with measured capacity between 7.4 wt% and 9 wt%.
- Successfully demonstrated the improvement in hydrogen release kinetics at lower temperature in $NaBH_4$@graphene over the bulk phase $NaBH_4$.
- Successfully demonstrated the regeneration of sodium borohydride in $NaBH_4$@graphene at 350°C and 40 bar by X-ray diffraction and other characterization techniques.

✧ ✧ ✧ ✧ ✧

INTRODUCTION

This project is focused on the development of a new class of hydrogen storage material, hydride@graphene, for next-generation hydrogen-powered fuel cell vehicles. The new approach is based on a recent breakthrough through the collaboration between Shanghai Jiao Tong University and Argonne National Laboratory [1]. Using a simple solvent-based method, we successfully synthesized a "nanoencapsulated" sodium borohydride–graphene composite, $NaBH_4$@graphene, in which $NaBH_4$

nanocrystallites are individually wrapped by single layer graphene. The new composite offers regenerable high hydrogen storage capacity in multiple DH and RH cycles. The graphene sheet tightly envelops the hydride nanoparticles like a candy wrapper and restricts the solid hydride phase from segregation and agglomeration. It also prevents the leakage of any harmful byproduct other than hydrogen, which is the only molecule permeable through the graphene layer. The hydride crystallites are encapsulated at nanometer size by graphene and can release/recharge hydrogen more readily than the bulk phase hydride.

Under this project, we will expand the method to prepare a broader range of hydride@graphene composites using the complex hydrides of higher intrinsic gravimetric and volumetric densities. We will explore various morphological and chemical approaches to improve the DH–RH kinetics, guided by computational modeling. We will collaborate with Hydrogen Materials–Advanced Research Consortium (HyMARC) in modeling, synthesis, measurement, and characterization.

APPROACH

The new approach we will apply in this project will focus on improving the hydrogen storage capacity of the hydride–graphene composites by reducing the amount of graphene while maintaining the nano-encapsulation. Phase I focuses on improving the synthesis of the $NaBH_4$@graphene system and initiating the investigation of Mg-based hydride@graphene systems. The $NaBH_4$@graphene composite in which sodium borohydride nanocrystallites are individually wrapped by single layer graphene, can be prepared from a solvent-based method (Figure 1). The new composite offers regenerable hydrogen storage capacity in multiple DH and RH cycles. The improved $NaBH_4$@graphene will be evaluated by a DOE designated lab for validation. Throughout the project, the new hydride composites will be characterized using various conventional and advanced characterization tools. The DH–RH capacities will be first evaluated in-house before delivering to other labs. Computational modeling and simulation will be carried out to provide insights for DH–RH kinetics improvement. We will also leverage the existing capabilities at HyMARC in computational modeling, structural characterization, and capacity measurement to facilitate the material development.

RESULTS

The project was initiated at the beginning of FY 2017. During this period, we accomplished the following tasks.

We prepared several batches of $NaBH_4$@graphene with theoretical gravimetrical capacities ranging from 7 wt% to 9 wt% on the composite basis. These samples were tested under multiple DH and RH cycles. The DH tests were completed through temperature-programmed discharge while the RH cycles in between were achieved by recharging the composite at elevated pressure (40 bar) and temperature (350°C). Figure 2a shows the hydrogen releases in six consecutive cycles measured by a Sievert apparatus over an $NaBH_4$@graphene composite composed of 86 wt% of sodium borohydride and 14 wt% of graphene. The theoretical hydrogen storage capacity for this composite was 9.13 wt%. For DH, a gravimetric capacity of 9 wt% was reached at the end of the first discharge. After the regeneration, the gravimetric capacity was reduced but maintained above 7.3 wt% during the following five cycles, shown by Figure 2b,

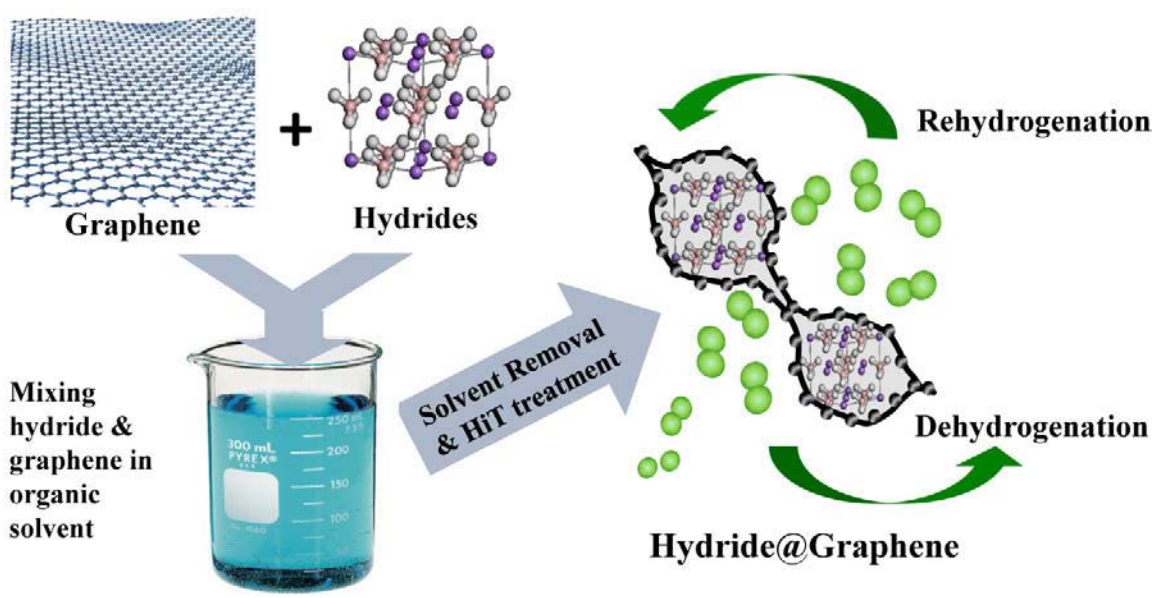

FIGURE 1. Schematics of solution-based synthesis of hydride wrapped by graphene

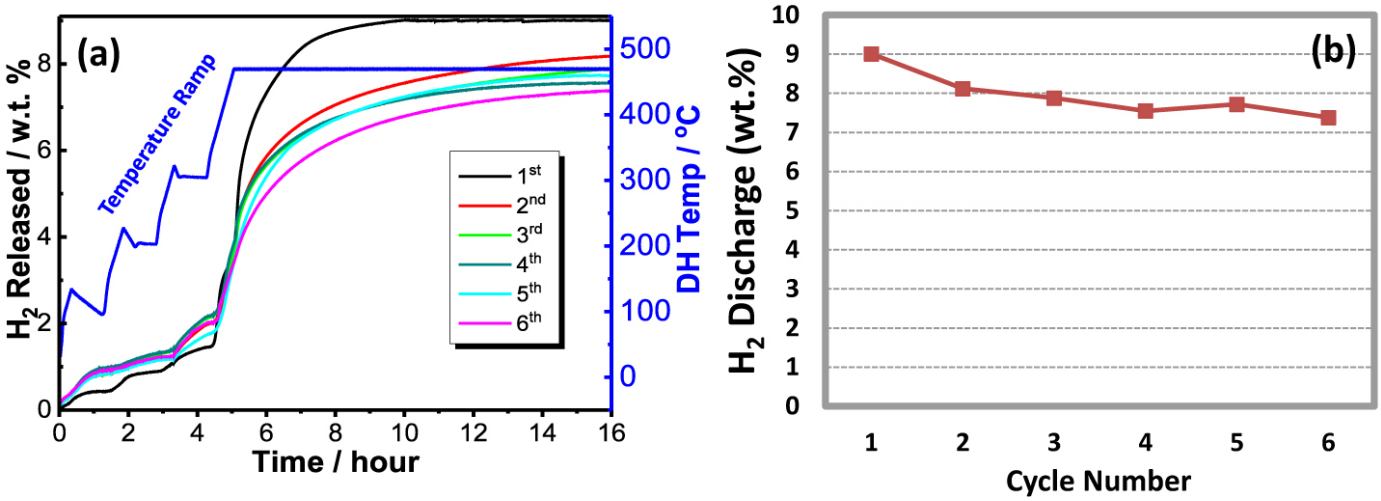

FIGURE 2. (a) Temperature-programmed hydrogen release from $NaBH_4$@graphene; (b) the hydrogen discharge gravimetric capacity as a function of cycle number

representing the retention of >81% of the theoretical value. These values are also listed in Table 1. Compared to previous studies on bulk or nano-confined complex hydrides, the graphene encapsulated hydride developed by our approach show significant improvements in capacity, cyclability, and reversibility [2].

TABLE 1. Gravimetric Capacities and Their Percentage against Theoretical Value During DH Cycles for $NaBH_4$@Graphene

Cycle #	1	2	3	4	5	6
H_2 Discharge (wt%)	9.01	8.12	7.88	7.55	7.72	7.38
% to Theoretical Value	99%	89%	86%	83%	85%	81%

We also investigated the reactivity and structural changes of $NaBH_4$@graphene during hydrogen discharge and through the DH–RH cycle. To demonstrate the chemistry and kinetics affected by graphene, the investigations generally included bulk $NaBH_4$ for comparison. Figure 3 shows a side-by-side study on the hydrogen release as the function of DH temperature between NaBH4@graphene and bulk $NaBH_4$ using a thermogravimetric analysis method. In this study, discharged hydrogen was detected by mass spectrometer in tandem of thermogravimetric analysis while the sample weight loss was measured by the gravimetric balance. For bulk $NaBH_4$, no decipherable amount of hydrogen release was found until the temperature nearly reached 500°C. The $NaBH_4$@graphene, on the other hand, started to release a significant amount of hydrogen at a temperature as low as 330°C. Two peaks near temperatures of 340°C and 435°C represent the hydrogen detachment from two different intermediate species during hydride decomposition. Clearly,

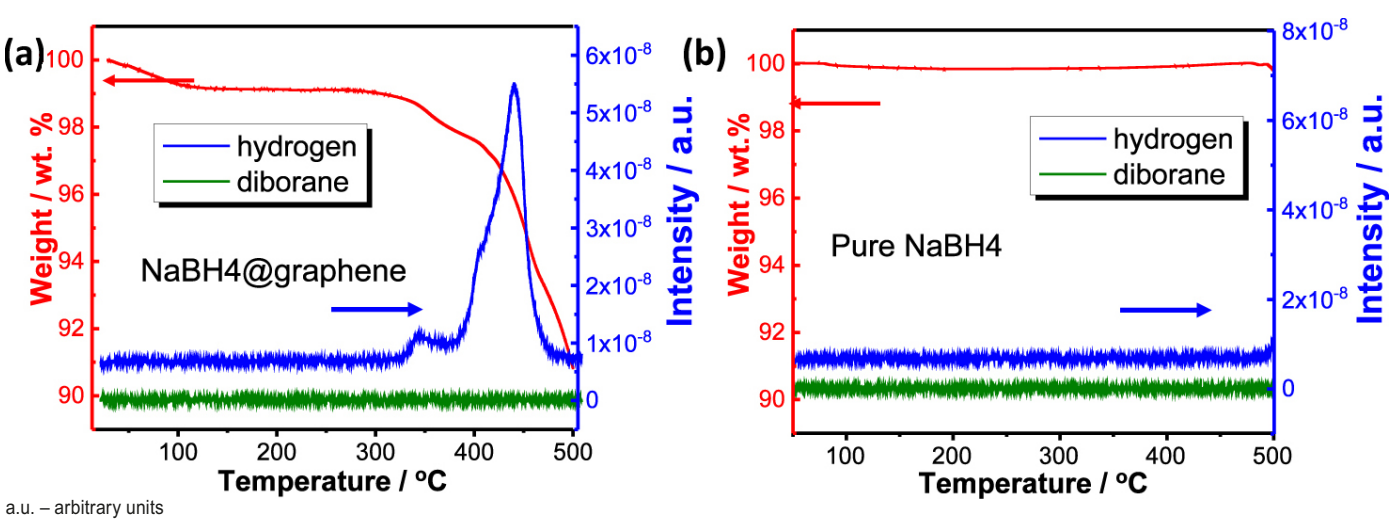

a.u. – arbitrary units

FIGURE 3. Thermogravimetric analysis study on dehydrogenation from (a) $NaBH_4$@graphene and (b) bulk $NaBH_4$ as a function of temperature

the interaction between graphene and $NaBH_4$ has facilitated the hydrogen release from the NaBH4@graphene composite. We also investigated the hydride structural reversibility in $NaBH_4$@graphene during a DH and RH cycle using X-ray diffraction (XRD). Three samples, including fresh composite, dehydrogenated and rehydrogenated $NaBH_4$@graphene, and bulk $NaBH_4$ were studied. Their XRD spectra are shown in Figure 4. The pattern of fresh $NaBH_4$@graphene matches well with that of bulk $NaBH_4$, suggesting that sodium borohydride retained its crystal structure after being encapsulated inside of graphene. After the DH reaction, the peaks associated with $NaBH_4$ all disappeared, as was anticipated due to the loss of hydrogen and therefore the crystal structure. The XRD peaks reappeared after the RH reaction, indicating the recovery of hydride crystallites. We calculated the hydride crystallite size using the Scherrer equation and found that the average hydride particle size in $NaBH_4$@graphene is about 32 nm for both fresh and RH samples, which is about two-thirds of that found in bulk $NaBH_4$ (48 nm).

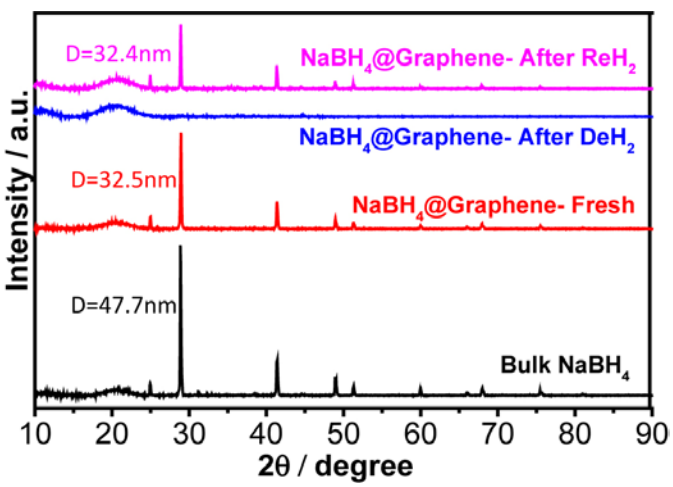

FIGURE 4. Comparison of XRD pattern and particle size for fresh, dehydrogenated and rehydrogenated $NaBH_4$@graphene samples using bulk $NaBH_4$ material as reference

CONCLUSIONS AND UPCOMING ACTIVITIES

We successfully demonstrated hydride cyclability in $NaBH_4$@graphene during multiple DH–RH cycles, measured by temperature-programmed desorption/isotherm regeneration and characterized by a variety of analytic tools. The kinetics of DH was clearly improved for the hydride wrapped by graphene in comparison to its bulk phase. We will continue to improve $NaBH_4$@graphene preparation and testing to reach the capacity and cyclability goals during the reminder of Phase I.

FY 2017 PUBLICATIONS/PRESENTATIONS

1. "Research on novel reversible hydride-graphene based hydrogen storage materials," Lina Chong and Di-Jia Liu, poster presentation at 2017 Gordon Research Conference in "Hydrogen-Metal Systems," July 16–21, 2017, Stonehill College, Easton, MA, USA.

REFERENCES

1. $NaBH_4$ in "Graphene Wrapper": Significantly Enhanced Hydrogen Storage Capacity and Regenerability through Nano-encapsulation, L. Chong, X. Zeng, W. Ding, D.-J. Liu, and J. Zou, *Advanced Materials*, **2015,** *27*, 5070–5074.

2. Recent progress in metal borohydrides for hydrogen storage, H.-W. Li, Y. Yan, S. Orimo, A. Züttel, and C.M. Jensen, *Energies,* **2011**, *4*, 185–214.

IV.C.10 HyMARC Seedling: Fundamental Studies of Surface-Functionalized Mesoporous Carbons for Thermodynamic Stabilization and Reversibility of Metal Hydrides

E.H. Majzoub
University of Missouri–St. Louis
One University Blvd
St. Louis, MO 63121
Phone: (314) 516-5779
Email: majzoube@umsl.edu

DOE Manager: Katie Randolph
Phone: (240) 562-1759
Email: Katie.Randolph@ee.doe.gov

Subcontractors:
- Saint Louis University, St. Louis, MO
- Washington University, St. Louis, MO

Project Start Date: October 1, 2017
Project End Date: March 30, 2018

Overall Objectives

- Reach the DOE hydrogen storage targets of 70 g/L H_2 using a reversible metal hydride.
- Render alane (AlH_3) reversible at temperatures around 100°C and pressures accessible at compressed gas filling stations.

Fiscal Year (FY) 2017 Objectives

- Prepare nitrogen-doped nanoporous carbon frameworks and quantify the N/C ratio and the amount of nitrogen that is pyridinic (able to form Lewis-acid/base complexes).
- Incorporate alane into N-doped carbon frameworks in solution using base exchange with dimethylethylamine-alane (DMEAA).
- Incorporate alane into N-doped carbon frameworks via melt-infiltration using alanates with cations that may intercalate into the carbon (e.g., Li, Na) leaving alane to complex with pyridinic nitrogens in the framework.
- Demonstrate Lewis-acid/base complex of alane via solid-state nuclear magnetic resonance (NMR) on 15N-doped carbon frameworks infiltrated with alane via solution base-exchange.

Technical Barriers

This project addresses the following technical barriers from the Hydrogen Storage section of the Fuel Cell Technologies Office Multi-Year Research, Development, and Demonstration Plan.

(A) System Weight and Volume

(E) Charging/Discharging Rates

Technical Targets

Surface-Functionalized Nanoporous Carbons for Complex Hydride Confinement and Reversibility

This project is conducting fundamental studies of nitrogen-doped, ordered nanoporous carbons with specific surface functionality. Pyridinic nitrogen atoms contained in the carbon structure have "lone pair" electrons capable of acting as a Lewis base and coordinating with alane (AlH_3), forming a Lewis-acid/base complex. Information about the interactions between alane and these pyridinic nitrogens in a nanoframework environment will be used to tune the synthesis and structure of these frameworks to optimize their storage characteristics and meet the following DOE 2020 hydrogen storage system targets.

- System Gravimetric Capacity: 4.5 wt%
- System Volumetric Capacity: 30 g H_2/L

FY 2017 Accomplishments

- Preparation of nitrogen-doped nanoporous (10–20% N) frameworks with pyridinic nitrogen.
- Characterization of N-doped carbons with N_2 adsorption porosimetry, X-ray photoelectron spectroscopy (XPS), NMR, and X-ray diffraction (XRD).
- Infiltration of alane via base-exchange from DMEAA.
- Infiltration of alanate via the melt from sodium alanate.
- In situ ^1H solution NMR of alane-infiltration experiments with DMEAA and carbon frameworks in dichloromethane solution.
- Characterization of alane-infiltrated carbons using XRD, and magic angle spinning (MAS) NMR for the nuclei ^1H, ^{27}Al, and ^{23}Na.

✧ ✧ ✧ ✧ ✧

INTRODUCTION

Metal hydrides used for applications today have a low hydrogen weight percent, e.g., 1.1 wt% H_2 for $LaNi_5H_6$, due to the much heavier transition metal elements. The light metal hydrides, including sodium alanate ($NaAlH_4$), have a much larger weight percentage of hydrogen but suffer from poor kinetics and reversibility because of phase separation of the components—aluminum metal in the case of sodium alanate. Although many light metal hydrides such as pure alane (AlH_3) and many complex light metal hydrides are known, most are either too stable, requiring high temperatures to drive the hydrogen off, or too unstable and difficult to rehydride under safe hydrogen pressures at reasonable temperatures. In order to reach the DOE volumetric and gravimetric targets the light metals must be utilized and these problems must be overcome. The goal of this project is to render light metal hydrides like AlH_3 reversible under moderate conditions.

APPROACH

Our approach is to perform fundamental studies on functionalized porous carbons (FPC) doped with nitrogen heteroatoms to understand the mechanisms of thermodynamically stabilized high-capacity metal hydrides (MH). Ultimately, our goal will be to stabilize alane (AlH_3) in a nanoporous carbon framework through Lewis-acid/base interactions provided by pyridinic nitrogen on the interior wall of the carbon framework. This capping layer should provide the kinetic stabilization analogous to that of the oxide layer on bulk alane that allows it to be stable in air for many years despite the relative instability of the compound. More importantly, in very small pores this interaction is expected to solvate and increase the enthalpy change of alane dehydriding. This approach is plausible for two reasons. (1) Ligand-stabilized alane chemistry is well known and understood (e.g., triethylenediamine-stabilized alane, and other amine-stabilized alanes) and the pyridinic nitrogen in the pore walls of the carbon may effectively solvate the surface of alane infiltrated in the pores of the framework. (2) The quantity of pyridinic and pyrrolic nitrogen is quantifiable in hard carbon templates using XPS. The proposed concept capitalizes on recently discovered nanoporous hosts capable of binding metal hydride particles and altering the kinetics and thermodynamics of H_2 release and absorption. Computational guidance of synthetic activities by a suite of validated modeling tools will be used to efficiently converge on the best hydride and doped carbon materials. This approach allows for a systematic variation in the MH-FPC interactions, enabling the thermodynamics to be tuned to achieve materials with greater than 70 g H_2/L. Our preliminary experimental results show that nanostructured MH materials are stabilized in N-doped carbons, with activation energies of desorption increased over 30 kJ/mol compared to undoped carbons. This will pave the way for practical applications of binary and complex metal hydrides that are not practically reversible in bulk, but can be fully cycled under mild conditions when confined inside nanoporous frameworks displaying strong surface interactions with MH nanoparticles.

RESULTS

Preparation of nitrogen-doped nanoporous carbons: Two types of nanoporous carbons (NPC) have been prepared for investigation. (1) NPC-type carbons have open cylindrical pores resulting in steep N_2 adsorption profiles. These carbons are prepared from phenolic resins that are the carbon precursor, and block co-polymer templates that give the resulting pore morphology [1]. (2) CMK3-type carbons are prepared from a carbon precursor such as sucrose (no ring structure in the precursor) and use SBA-15 nanoporous silica as the template that is etched out with HF after calcination [2]. Figure 1a shows nitrogen adsorption data for these carbons. Prepared carbon frameworks that contain nitrogen precursors are designated with an "N" before the type or morphology of the carbon, i.e., CMK3-type carbons containing nitrogen are designated NCMK3.

It is important in the N-doped carbons that the electronic structure of the nitrogen contains a lone pair of electrons like that in the molecule pyridine. This nitrogen is called pyridinic and may be quantified with XPS. XPS results are shown in Figure 1b and indicate the presence of pyridinic nitrogen (about 1/3 of the all of the nitrogen in the sample).

Infiltration of NNPC and NCMK3 with alane via base exchange: In order to incorporate alane into the N-doped carbons, we attempted a base exchange using dimethylethylamine (DMEA). The basic concept is that pyridinic nitrogen in the pore wall will provide stronger binding to alane than will the DMEA, and the alane will switch bases. A solution of DMEAA in dichloromethane was introduced to N-doped carbons as shown in Figure 2a.

If alane exchange to the framework occurs during exposure of the carbons to the DMEAA in solution, there will be free DMEA in solution that may be quantified with solution ^{1}H NMR. In our results, shown in Figure 2b, the shift observed in the NMR spectra for DMEA indicated not only that the alane exchanged with the framework, but that the newly free DMEA was becoming protonated. The shifts in the ^{1}H spectra were confirmed by comparing the DMEAA-exposed carbons with a control sample of DMEA protonated with HBF_4.

Figure 3 shows the ^{1}H proton peak from alane for both non-N-doped carbons (NPC, CMK3) and N-doped carbons (NNPC, NCMK3). It is clear from the NPC and NNPC panels that the alane peak diminishes in intensity and disappears around 6 h, while in the CMK3-type carbons the alane peak persists and may even become narrowed. The narrow nature of the peaks in solution NMR is due to

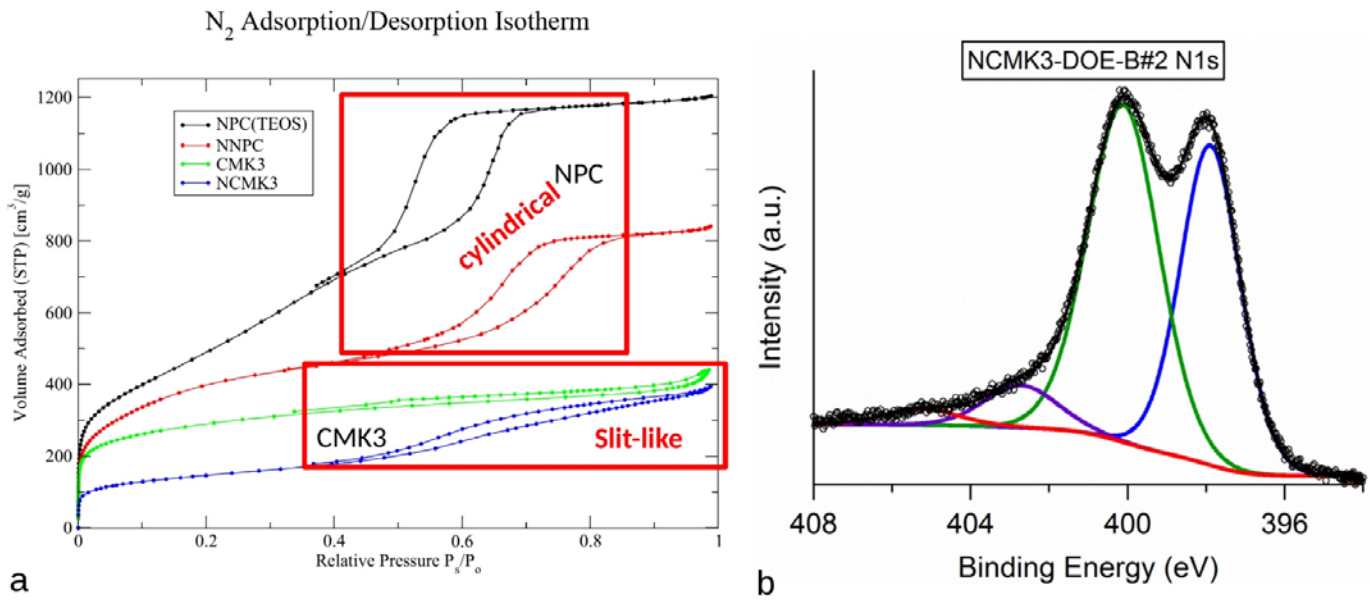

STP – Standard temperature and pressure

FIGURE 1. (a) Nitrogen adsorption porosimetry of bare and N-doped carbons showing both slit like and cylindrical pore structures. (b) N 1s spectra of the NCMK3-type carbon. Four different bonding environments pyridinic (blue), pyrrolic (green), graphitic (violet) and oxidized (red) are shown in the figures. Data taken at Sandia National Laboratories, California, by Jim White.

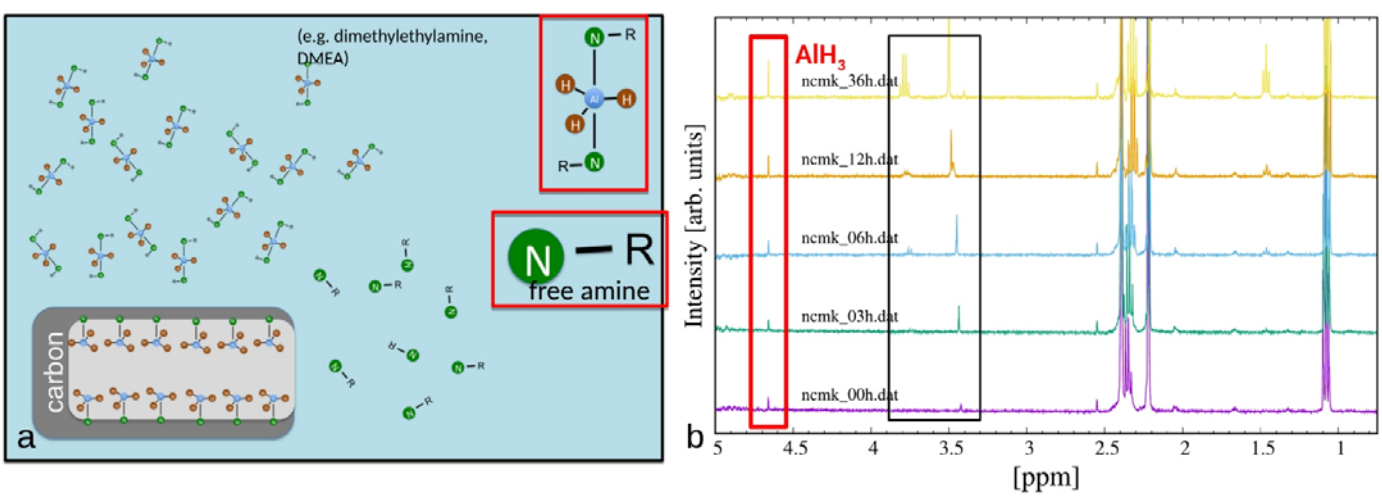

FIGURE 2. (a) Cartoon showing the exchange of alane from DMEA to the carbon, leaving free DMEA in solution. (b) In situ ^{1}H solution NMR spectra of NCMK3-type carbon exposed to DMEAA in solution.

rapid molecular tumbling. Their absence suggests that in the NPC-type carbons the alane is no longer in solution; it has either decomposed and is gone, or has attached to some larger structure such that the ^{1}H peak is no longer visible. In contrast, the CMK3-type carbons show a persistent alane peak that does not diminish, except for late times in the CMK3 spectra, suggesting that the alane remains in solution and may not exchange with the CMK3 framework.

It is important to determine whether infiltration attempts result in material internal or external to the nanopores. In wide-angle XRD one looks for Bragg peaks with a width corresponding to a coherence length larger or smaller than the pore size determined from N_2 porosimetry measurements. XRD spectra following solvent evaporation of alane-exposed samples at a ratio of AlH_3:N of 4:1 are shown in Figure 4a. The narrow peaks from the trace in green indicate that the NCMK3 sample contains material outside the pores. These peaks do not match any known phases containing any combination of {Al,O,N,C,H}. They do, however, have some correspondence with a reported phase of alane (α') [3,4], and may indicate a new polymorph of alane. One possibility may be that the surface interaction of the alane coming

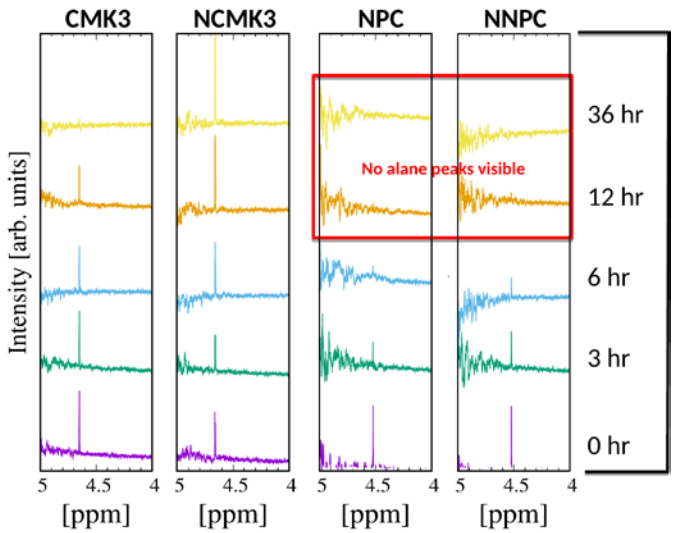

FIGURE 3. In situ ^{1}H solution NMR spectra of bare and N-doped carbons exposed to DMEAA in solution. NPC-type carbons indicate likely uptake of alane.

out of solution nucleates a metastable phase of alane that is visible in the XRD. Neither NPC nor NNPC samples show any Bragg peaks, indicating any alane in the sample is either amorphous or inside the pores if it did not decompose.

Figure 4b shows ^{27}Al MAS NMR spectra of the samples in panel (a). The triplet of peaks in the NCMK3 spectra is indicative of Al-oxide species [5], but no Al-oxide was found in the XRD spectra, suggesting some oxidation took place during sample transfer before NMR measurements. The spectra from the CMK3, NPC, and NNPC samples are not conclusive, but suggests possible α-alane at 4.6 ppm, γ-alane at 35.8 ppm and an unknown phase at 66.4 ppm.

Preliminary computational results not shown here indicate that base-exchange of AlH_3 should occur from DMEAA to the N-doped carbon substrates, as well as some hydrogen-terminated non-N-doped carbon substrates.

Work not included in this report is the infiltration of the nanoporous carbons using alanates whose cation may intercalate into the carbon itself, delivering a large amount of alane to the pores. These experiments include both $NaAlH_4$ and $LiAlH_4$. Melt-infiltration with sodium alanate indicates that a large amount of alanate is incoporated into the carbons, and is reversible. While MAS ^{27}Al NMR measurements indicate alanate in the pores, there is no indication of alane in the pores. MAS ^{23}Na NMR is inconclusive on the presence of any intercalated Na due to the width of the resonance. Additional experiments using lithium alanate will be attempted due to the clear preference of Li over Na to intercalate into carbon.

CONCLUSIONS AND UPCOMING ACTIVITIES

The project has demonstrated that nitrogen-doped porous carbons with differing types of pore structure interact very differently with base-stabilized alane depending on the synthesis method and resulting pore structure of the carbon. Our preliminary results indicate that CMK3-type carbons may not infiltrate via base-exchange with DMEAA, while NPC-type carbons appear to do so. We have prepared isotopically-labeled ^{15}N-doped carbons for the critical MAS NMR measurements that will investigate the nature of the Al-N interaction and determine whether the Lewis-acid/base complex is forming. In addition to these experiments, we are beginning to investigate the hydrogen release from the N-doped carbons infiltrated with alane using our residual

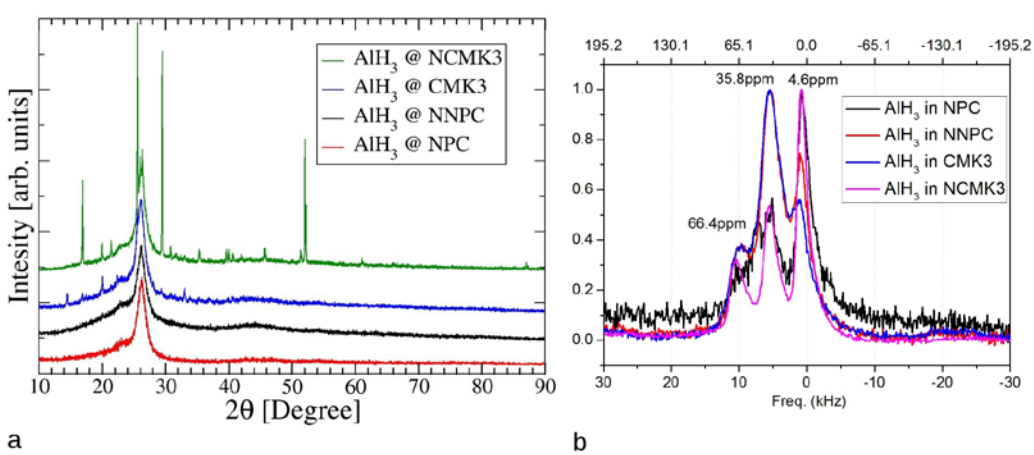

FIGURE 4. (a) XRD spectra of alane-infiltrated carbons showing external material in the CMK3-type carbons indicating a possible new polymorph of alane, but external to the pores, while the NPC-type carbons show no Bragg peaks, suggesting uptake of the alane. The wide peak at 26 degrees is from a mylar film used to minimize air exposure to the samples during measurement. (b) MAS ^{27}Al NMR of the carbons in panel (a) with peak positions showing possible alane with some oxidized Al in the samples.

gas mass spectrometer system at University of Missouri–St. Louis. The sensitivity of this instrument will allow us to examine the reversibility of small samples if those samples are desorbed and rehydrided.

FY 2017 PUBLICATIONS/PRESENTATIONS

1. "$LiBH_4$ in Aerogel: Ionic Motions by NMR," Hongyang Zou, Anton Gradišek, Samuel B. Emery, John J. Vajo, and Mark S. Conradi, Hydrogen-Metal Systems (GRS), Gordon Research Seminar, July 15–16, 2017.

2. "Surface Functionalized Nanoporous Carbons for Kinetically Stabilized Complex Hydrides through Lewis acid-Lewis base Chemistry," Christopher L. Carr, Eric H. Majzoub, TMS 2017 Annual Meeting and Exhibition, February 2017.

3. "Influence of Functionalized Nanoporous Carbons on the Properties of Confined $NaAlH_4$," Christopher L. Carr, Waruni Jayawardana, University of Missouri St. Louis Graduate Research Fair, April 2017.

4. "Surface-functionalized Mesoporous Carbons for Electrochemical and Hydrogen Storage Applications," Gordon Research Conference on Metal-Hydrogen Systems, Stonehill College, MA, July 16–21, 2017.

5. "The Chemistry and Physics of Energy Storage Materials at the Nanoscale," E.H. Majzoub, Science in St. Louis Series, Academy of Science of St. Louis, St. Louis, MO, November 15, 2016.

6. "Influence of Functionalized Nanoporous Carbons on the Properties of Confined $NaAlH_4$," Christopher Carr, Waruni Jayawardana, Eric Majzoub, Missouri Inorganic Day, May 15, 2017.

7. "Influence of Functionalized Nanoporous Carbons on the Properties of Confined $NaAlH_4$," Christopher Carr, Waruni Jayawardana, Eric Majzoub, Graduate Research Fair- University of Missouri St Louis, April 28, 2017.

REFERENCES

1. Meng, Y.; Gu, D.; Zhang, F.; Shi, Y.; Cheng, L.; Feng, D.; Wu, Z.; Chen, Z.; Wan, Y.; Stein, A.; Zhao, D. Chem. Mater.,18, 4447, (2006).

2. Carr, C.L., Majzoub, E.H., J. Phys. Chem. C, 120, 11426–11432, (2016).

3. M. Paskevicius, D.A. Sheppard, C.E. Buckley, J. Alloy. Comp., 487, 370–376, (2009).

4. H.W. Brinks, A. Istad-Lem, B.C. Hauback, J. Phys. Chem. B, 110, 25833–25837, (2006).

5. E.H. Majzoub, J.L. Herberg, R. Stumpf, S. Spangler, R.S. Maxwell, J. Al. Comp., 394, 265-270, (2005).

IV.C.11 HyMARC Seedling: Development of Magnesium Boride Etherates as Hydrogen Storage Materials

Godwin Severa (Primary Contact), Cody Sugai, Stephen Kim, and Craig Jensen
University of Hawaii at Manoa
1680 East West Rd., POST 109
Honolulu, HI 96822
Phone: (808) 956-3723
Email: severa@hawaii.edu

DOE Manager: Katie Randolph
Phone: (240) 562-1759
Email: Katie.Randolph@ee.doe.gov

Contract Number: DE-EE0007654

Project Start Date: October 1, 2016
Project End Date: September 30, 2019

Overall Objectives

- Improve the hydrogen cycling kinetics and cycling capacity of the magnesium boride/magnesium borohydride system to meet Department of Energy (DOE) hydrogen storage targets.
- Synthesize and characterize novel magnesium boride (MgB_2) etherate materials with improved hydrogen cycling kinetics and hydrogen storage capacities.
- Determine if the reversible hydrogenation of novel boride etherates show vastly improved hydrogen cycling kinetics and cycling capacities to levels that are practically viable.
- Demonstrate capability of MgB_2 ether materials to meet the DOE 2020 hydrogen storage targets.

Fiscal Year (FY) 2017 Objectives

- Synthesize and characterize novel magnesium boride etherates.
- Demonstrate uptake of ≥7 wt% H_2 at ≤300°C, 700 bar, and 48 h.
- Demonstrate reversible release of ≥2 wt% H_2 by at least one MgB_2 etherate.

Technical Barriers

This project addresses the following technical barriers from the Hydrogen Storage section of the Fuel Cell Technologies Office Multi-Year Research, Development, and Demonstration Plan [1].

(A) System Weight and Volume

(D) Durability/Operability

(E) Charging/Discharging Rates

(O) Lack of Understanding of Hydrogen Physisorption and Chemisorption

Technical Targets

This project will determine if the reversible hydrogenation of magnesium boride etherates show vastly improved hydrogen cycling kinetics while extending the cycling capacities to levels that are practically viable. Improvement in kinetics has been demonstrated by the decrease in both hydrogenation pressure and hydrogenation temperature to 300°C and 700 bar of a magnesium boride material. Insights gained from this project will be applied toward the development of boride hydrogen storage materials that meet the DOE hydrogen storage targets.

- System Gravimetric Capacity of 0.055 kg H_2/kg system
- System Volumetric Capacity of 0.040 kg H_2/L system
- Durability/Operability (max H_2 delivery temperature) 85°C
- Charging/Discharging Rates (system fill times for 5 kg of H_2) 1.5 kg H_2/min

FY 2017 Accomplishments

- Formation of novel MgB_2 materials from direct reactions with ethers.
- Demonstrated for the first time hydrogenation of a MgB_2 material to $Mg(BH_4)_2$ at 300°C.
- Demonstrated for the first time hydrogenation of a MgB_2 material to $Mg(BH_4)_2$ at 700 bar.
- Demonstrated significant weight loss of ~4.9 wt% from MgB_2-tetrahydrofuran hydrogenated at 300°C and 1,000 bar.
- ^{11}B nuclear magnetic resonance (NMR) analyses of a hydrogenated MgB_2-tetrahydrofuran, confirmed $Mg(BH_4)_2$ formation at 300°C and 700 bar.
- Completed preliminary design of a medium pressure system (350 bar H_2, 350°C).
- Theoretical studies indicate plausibility of tetrahydrofuran (THF) coordination to MgB_2.

✧ ✧ ✧ ✧ ✧

INTRODUCTION

Magnesium borohydride, $Mg(BH_4)_2$, is one of the few materials that has a demonstrated gravimetric hydrogen storage capacity greater than 11 wt%, and thus a demonstrated potential to be utilized in a hydrogen storage system capable of meeting DOE hydrogen storage targets. However, due to very slow kinetics, cycling between $Mg(BH_4)_2$ and MgB_2 has been accomplished only at high temperature (~400°C) and under high charging pressure (~900 bar). Previous work has shown rapid kinetics at moderate temperatures for the reversible dehydrogenation of magnesium borohydride etherates, $Mg(BH_4)_2$•$(ether)_x$ to magnesium triborane etherates, $Mg(B_3H_8)_2(ether)_x$. These type of materials have much lower hydrogen cycling capacities as a consequence of the weight contribution of the coordinated ethers. However, extending the dehydrogenation to MgB_2•$(ether)_x$ would result in the H_2 wt% of the system potentially meeting DOE targets. If successful the solid-state MgB_2 etherate would be safer and cheaper than the high pressure compressed H_2 (700 bar) or liquid H_2 alternative onboard storage systems on the market.

APPROACH

The project explores the effect of different types of ether ligands and ether stoichiometries on the hydrogen storage properties of the MgB_2. In addition to the electronic perturbation caused by the interaction of ethers with the magnesium which may alter the thermodynamics of the reversible hydrogenation of MgB_2, the presence of the ethers also results in a kinetic enhancement of phase changes in the $Mg(BH_4)_2/MgB_2$ system. Since significant hydrogenation of magnesium boride to magnesium borohydride has only been achieved at very high pressure (~900 bar), a high-pressure system will be initially utilized for hydrogenation of the borides to magnesium borohydride etherate. We therefore intend to team with HyMARC in order to utilize their high pressure capabilities in the hydrogenation of the magnesium boride etherates as well as their surface characterization equipment. We will determine if the ether-magnesium bonding remains intact during the reversible hydrogenation of boride to borohydrides and if so, what influence it has on the reaction kinetics and thermodynamics. Of foremost interest will be the reduction of the temperatures and pressures required for the hydrogenation and subsequent dehydrogenation of the boride materials. The ratio of ether ligand to the MgB_2 will be optimized to allow for the maximum attainable gravimetric and volumetric density without sacrificing hydrogen cycling kinetics at moderate conditions. We will determine whether the MgB_2 etherate can access new polyborane reaction pathways which prevent formation of $MgB_{12}H_{12}$ during hydrogen cycling. An inherent endeavor of the project will be to understand the mechanisms of kinetic enhancement and intermediates formed during the hydrogenation and dehydrogenation process in order to optimize the hydrogen storage performance of the $MgB_2/Mg(BH_4)_2$ ether materials. A thorough correlation of experiments with theory will be utilized in this effort using HyMARC's multiscale modeling approaches (kinetic Monte Carlo simulation and phase field modeling) to help elucidate the kinetic constraints on hydrogen cycling resulting at both particle surface interfaces and within the bulk of the materials. The results of these studies will provide us with adequate insight to conceivably identify a magnesium boride species whose hydrogen cycling kinetics are adequate to meet the DOE target.

RESULTS

The majority of the work in the first year of this project was geared towards synthesis, characterization and hydrogenation of novel magnesium borides with sub-stoichiometric ether content. We considered syntheses of the MgB_2 etherates from direct reactions of MgB_2 with various ethers (triglyme, tetraglyme, 1,4-dioxane and 1,3-dioxolane and tetrahydrofuran) and from dehydrogenation of magnesium triborane tetrahydrofuran in accordance to Equations 1 and 2.

$$MgB_2 + x(ether) \rightarrow MgB_2(ether)_x \quad (1)$$

$$Mg(B_3H_8)_2(THF)_x + 2MgH_2 \rightarrow 3MgB_2(THF)_x + 10H_2 \quad (2)$$

The direct syntheses of MgB_2 etherates involved the direct reaction of MgB_2 with ethers using mechanochemistry and heat treatment approaches. The breaking of the MgB_2 bonds during the high energy mechanical milling was anticipated to create electron deficient reactive sites in the MgB_2 structure, allowing for the instantaneous reaction and/or binding of sub-stoichiometric amounts of ether. The incorporation of sub-stoichiometric amounts of ether species into the MgB_2 is key to the maintenance of high gravimetric and volumetric hydrogen densities.

The products of MgB_2 etherate synthesis from MgB_2 were characterized by a variety of techniques including solid state and solution ^{11}B and ^{1}H NMR, X-ray diffraction (XRD), infrared vibrational spectroscopy (Fourier transform-attenuated total reflection), thermogravimetric analyses, and differential scanning calorimetry (DSC). Mechanical milling with the ethers reduced crystallinity of the MgB_2 as evidenced by a reduction of MgB_2 peak intensity in X-ray diffraction patterns. As expected, no new phases attributable to the minute quantities of coordinated ether were observed in the diffraction pattern. Furthermore, negligible chemical shifts were observed in the ^{11}B solid state NMR spectra of materials synthesized by mechanical milling process. A similar trend was observed for products from reaction of MgB_2 and ethers under heat treatment at <300°C. The only exception was MgB_2-tetraglyme samples which showed new

infrared vibrations and an amorphous broad peak at 20° *2θ* in XRD spectra. Thermogravimetric analyses (Figure 1) indicated significant mass loss of >15 wt% for the MgB_2-tetraglyme material.

The dehydrogenation of $Mg(B_3H_8)_2(THF)_2/MgH_2$ to form MgB_2-THF was also performed at 390°C for 24 h followed by a second low temperature heat treatment in presence of THF. ^{11}B solution NMR of the dehydrogenated material in D_2O indicated no soluble boron species confirming absence of water soluble magnesium borane species (e.g., $MgB_{12}H_{12}$). Fourier transform-attenuated total reflection spectra showed no B-H stretches in 2,100–2,800 cm^{-1} region. The surprising absence of $MgB_{12}H_{12}$ below 400°C points towards plausibility of pathways for forming MgB_2 at lower temperatures. Further investigations are underway to optimize the dehydrogenation reactions of $Mg(B_3H_8)_2(THF)_2$.

The syntheses and characterization work was subsequently followed by high pressure hydrogenations of the products of MgB_2 etherate synthesis. The preliminary high pressure hydrogenations were performed to determine the magnesium boride etherate materials with the best potential pathway to meeting DOE hydrogen storage targets. The magnesium boride etherates were hydrogenated at HyMARC-Sandia National Laboratories facility at ≤1,000 bar, ≤400°C and ≤72 h, with the assistance of Dr. Stavila, Dr. White, and Dr. Allendorf. Pure, as received MgB_2 and ball milled pure MgB_2 were also hydrogenated and used as controls for comparison with the synthesized MgB_2 etherates. Prior to hydrogenation experiments, all the samples were vacuumed for at least 12 h in the Sandia National Laboratories glovebox antechamber to ensure removal of any residual weakly coordinated ethers on the MgB_2 etherates and hence reduce contamination of the hydrogenation reactor system. Subsequent characterizations of the hydrogenated samples were performed using XRD, NMR, thermogravimetric analyses-DSC and Fourier transform-attenuated total reflection. The MgB_2-THF synthesized by mechanochemistry was determined to have the best hydrogenation performance. Significant hydrogenation of an MgB_2 material at 300°C and 1,000 bar was demonstrated for the first time using this material. Thermogravimetric analyses (Figure 2) indicated about 4.9% weight loss from the MgB_2-THF hydrogenated at 300°C and 1,000 bar. The XRD of the MgB_2-THF showed new patterns around 20° 2θ attributed to $Mg(BH_4)_2$ (Figure 3). ^{11}B and ^{1}H solution NMR spectra confirmed the presence of $Mg(BH_4)_2$ as major borohydride product in sample.

Following the initial hydrogenations, more effort was placed on direct syntheses of the boride etherates using a mechanochemistry approach with special emphasis on

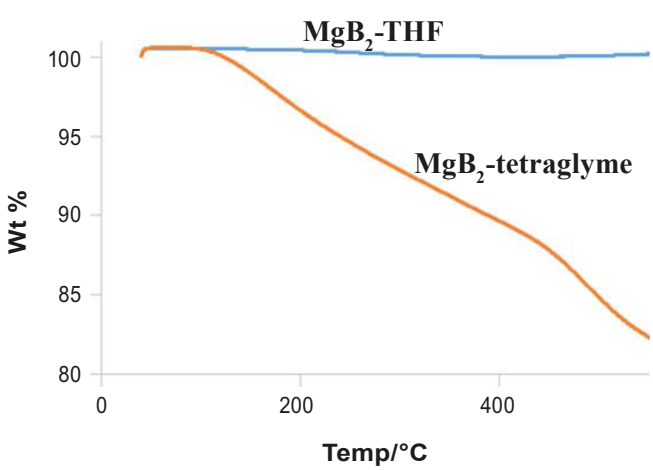

FIGURE 1. Thermogravimetric analysis of heat treated MgB_2-tetraglyme and MgB_2-THF samples at 5°C/min in Ar

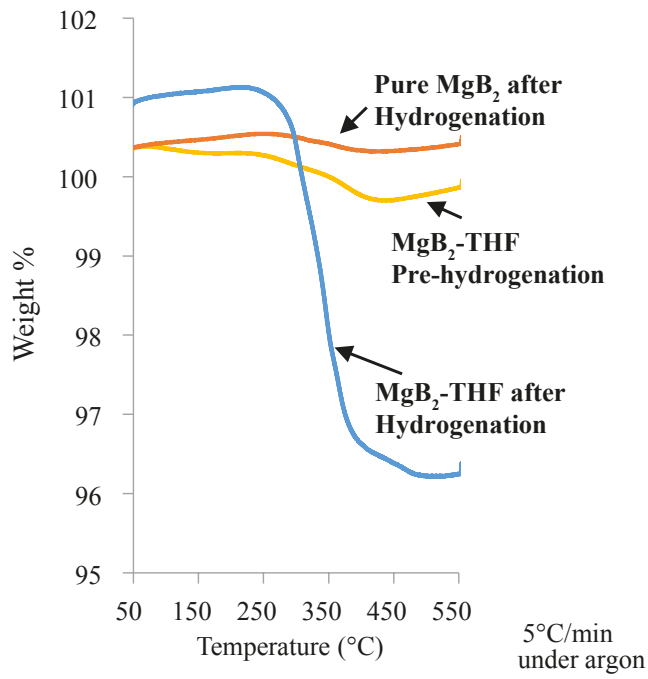

FIGURE 2. Thermogravimetric analysis of hydrogenated 9 h ball milled MgB_2-THF indicating significant weight loss (~4.9 wt%) at 300°C and 1,000 bar

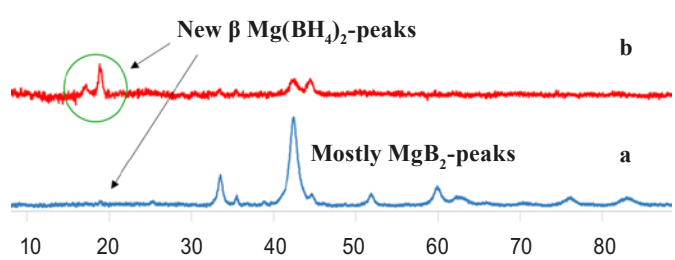

FIGURE 3. XRD of hydrogenated ball milled samples of pure MgB_2 and MgB_2-THF, confirming $Mg(BH_4)_2$ formation at 300°C and 1,000 bar

THF. Hydrogenation of this next set of MgB_2-THF materials demonstrated for the first time hydrogen uptake by an MgB_2 material at 300°C and 700 bar. ^{11}B solution NMR confirmed presence of $Mg(BH_4)_2$ in the MgB_2-THF hydrogenated material (Figure 4). No hydrogenation was observed in pure ball milled MgB_2 as evidenced by absence of boron species in ^{11}B solution NMR spectra. This result points towards the THF greatly perturbing the MgB_2 structure hence allowing for the increased kinetics of hydrogenation of MgB_2. Efforts to determine the weight percent hydrogen uptake and complete characterization of the boride materials are underway. We are also collaborating with Dr. Gennett at National Renewable Energy Laboratory on performing temperature programmed desorption studies coupled with mass spectroscopy analyses to attempt to detect the tightly bound ether or ether derived species in the novel MgB_2 materials. This is necessitated by the current lack of conclusive, direct evidence of the strongly bound ether in most magnesium boride etherates from techniques such as NMR. Theoretical modelling work on the project is concurrently being led and performed by HyMARC groups of Dr. Wood at Lawrence Livermore National and Dr. Prendergarst at Lawrence Berkeley National Laboratory. The molecular dynamics simulations of magnesium boride etherates indicate plausibility of THF coordination to MgB_2. The THF is observed to bond to both the Mg and B atoms on edge and basal planes of MgB_2 sheets. The safe design of a medium pressure (350 bar, 350°C) hydrogenation reactor system was performed in consultation with HyMARC-Sandia National Laboratories personnel. When built this reactor system will assist in the efficient hydrogenation of samples at high and medium pressures.

CONCLUSIONS AND UPCOMING ACTIVITIES

In this first year of the project we have demonstrated that our novel MgB_2 materials have better performance than state-of-the-art pure MgB_2. Through this work we have shown for the first time that the MgB_2 system can be hydrogenated at temperatures as low as 300°C and at pressures as low as 700 bar. Significant hydrogenation (up to 4.9 wt%) of an MgB_2 material was demonstrated at 300°C and 1,000 bar for the first time, using the mechanochemically synthesized MgB_2-THF. The improved hydrogenation performance of MgB_2-THF indicates the effective interaction of MgB_2 and THF allowing the MgB_2 material to be hydrogenated at lower temperature and pressure than pure MgB_2. Molecular Dynamics Simulations support the plausibility of strong coordination between THF and MgB_2. Our work proves it is possible to continuously lower the H_2 uptake temperature and pressure of MgB_2 hydrogenation to $Mg(BH_4)_2$.

Future work guided by the quest to attain DOE onboard targets include:

- Complete characterization of products of boride etherate synthesis.
- Understanding mechanism of hydrogenation enhancement by ethers.

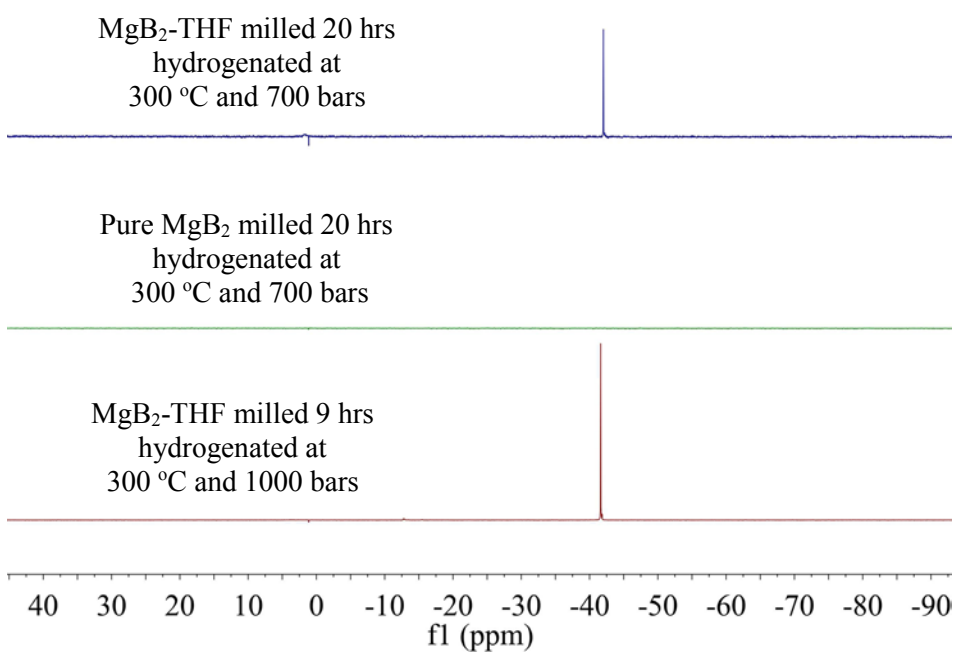

FIGURE 4. ^{11}B solution NMR of ball milled MgB_2-THF samples hydrogenated at 300°C, confirming formation of $Mg(BH_4)_2$ at 1,000 bar and 700 bar

- Variable hydrogenation time studies at 700 bar and 300°C.
- Demonstration of hydrogen uptake ≥7 wt% at 700 bar and 300°C.
- Hydrogen cycling studies and determining the factors that limit H_2 cycling kinetics.
- Size-dependent stability and morphology of MgB_2 clusters + particles.
- Coordination analysis of solutions and solvent-dependence of stability.

FY 2017 PUBLICATIONS/PRESENTATIONS

1. "Development of Magnesium Boride Etherates as Hydrogen Storage Materials," presented at the 2017 DOE Annual Merit Review and Peer Evaluation Meeting, Washington, D.C., June 2017.

REFERENCES

1. "Fuel Cell Technologies Office Multi-Year Research, Development and Demonstration Plan," https://energy.gov/eere/fuelcells/downloads/fuel-cell-technologies-office-multi-year-research-development-and-22

IV.C.12 Improving the Kinetics and Thermodynamics of $Mg(BH_4)_2$ for Hydrogen Storage

Brandon Wood (Primary Contact),
Lennie Klebanoff, Vitalie Stavila, Tae Wook Heo,
Keith Ray, Jonathan Lee, Alex Baker,
ShinYoung Kang, Hui-Chia Yu, Katsuyo Thornton
Lawrence Livermore National Laboratory
7000 East Ave., L-413
Livermore, CA 94550
Phone: (925) 422-8391
Email: brandonwood@llnl.gov

DOE Manager: Jesse Adams
Phone: (720) 356-1421
Email: Jesse.Adams@ee.doe.gov

Subcontractors:
- Sandia National Laboratories (SNL), Livermore, CA
- University of Michigan, Ann Arbor, MI

Project Start Date: August 1, 2014
Project End Date: September 30, 2017

Overall Objectives

- Combine theory, synthesis, and characterization across multiple scales to understand the intrinsic kinetic and thermodynamic limitations in $MgB_2/Mg(BH_4)_2$.
- Construct and apply a flexible, validated, multiscale theoretical framework for modeling (de)hydrogenation kinetics of the Mg-B-H system and related metal hydrides.
- Devise strategies for improving kinetics and thermodynamics through nanostructuring and doping.

Fiscal Year (FY) 2017 Objectives

- Synthesize and test hydrogenation in unconfined MgB_2 nanoparticles.
- Compute free energies and validated phase diagram for the Mg-B-H system.
- Investigate mechanisms of initial and deeper MgB_2 hydrogenation.

Technical Barriers

This project addresses the following technical barriers from the Hydrogen Storage section of the Fuel Cell Technologies Office Multi-Year Research, Development, and Demonstration Plan.

(O) Lack of Understanding of Hydrogen Physisorption and Chemisorption

(A) System Weight and Volume

(E) Charging/Discharging Rates

Technical Targets

This project is conducting fundamental studies of hydrogenation and dehydrogenation of nanoscale $Mg(BH_4)_2$-based materials using a combined theory and experiment approach. Insights will be applied toward the design and synthesis of hydrogen storage materials that meet the following DOE hydrogen storage targets.

- Specific energy: 1.8 kWh/kg
- Energy density: 1.3 kWh/L
- Minimum delivery pressure: 5 bar
- Minimum delivery temperature: 85°C
- System fill time: 1.5 kg H_2/min

FY 2017 Accomplishments

- Computed and validated reference phase diagram of Mg-B-H including explicit thermal effects.
- Predicted that nanosizing/confinement affects reaction stability and pathway.
- Refined synthesis procedure for clean and pure unconfined MgB_2 nanoparticles.
- Demonstrated ~3x lower barriers in the initial uptake kinetics of unconfined MgB_2 nanoparticles with respect to bulk.
- Determined energy landscape for a two-step mechanism of initial hydrogen uptake in MgB_2 determined from X-ray and vibrational spectroscopy.
- Devised and applied a kinetic model for validation of the proposed two-step MgB_2 hydrogen uptake mechanism.
- Performed first full phase-field kinetics simulation of cycling between $MgB_{12}H_{12}$ and MgB_2, suggesting the possibility of different pathways for rehydrogenation and dehydrogenation in the hydrogen-poor domain.

✧ ✧ ✧ ✧ ✧

INTRODUCTION

$Mg(BH_4)_2$ is one of very few metal hydride candidates that lie close to the "viability window" of capacity (14.9 wt% H) and desorption enthalpy (ΔH_{des}) required to satisfy the 2020 and ultimate DOE hydrogen storage targets [1–2]. However, $Mg(BH_4)_2$ suffers from extremely poor kinetics whose origin is not well understood. If the kinetic limitations could be removed and the effective ΔH_{des} slightly improved, then facile hydrogen uptake and release could be attained, and a complex metal hydride-based system could achieve long-term targets. Prior work points to particle size reduction and doping with additives as viable and cost-effective improvement strategies [3]. However, it is difficult to fully leverage these without comprehending how, why, and under what conditions these improvements are observed. This project applies multiscale theoretical and experimental tools to develop a fundamental understanding of kinetic and thermodynamic limitations in the Mg-B-H hydrogen storage system, and to devise specific strategies for optimizing its performance under cycling conditions.

APPROACH

This project aims to establish a closely coupled theory–characterization–synthesis approach to understand the roles of nanostructuring and doping in the Mg-B-H system, and apply it to devise possible strategies for improving kinetics and thermodynamics. We focus on three objectives: (1) identifying chemical, phase nucleation, or transport processes and determining which are rate limiting, (2) understanding the origin of the kinetic and thermodynamic changes upon nanosizing and doping, and (3) devising and implementing rational modifications for improvement of H_2 storage properties. Our modeling effort relies on the application of a multiscale framework that combines atomistic density functional theory (DFT) for predictive chemistry and thermodynamics with continuum phase-field modeling for describing phase nucleation and growth and non-equilibrium transport kinetics. The predictions are informed and validated by controlled synthesis of size-selected nanoparticles free from binders and nanoscaffolds that may otherwise burden the system with unacceptably high gravimetric penalties. To better understand the kinetic pathways and processes, we apply gravimetric and thermochemical analysis, and utilize in situ and ex situ microscopy and spectroscopy aided by computational interpretations to derive chemical and phase compositions. Particular emphasis is placed on understanding kinetic factors governing the rehydrogenation of MgB_2, which is generally less well understood than dehydrogenation.

RESULTS

MgB_2 Nanoparticle Synthesis & Characterization

To isolate mechanisms associated with nanosizing independently of confinement, we need doped and undoped nanoparticles of MgB_2 that are freestanding without a confining medium. This year, effort was directed to establishing a set procedure that allows the production of nanoparticles via surfactant ball milling without contamination from the milling hardware, surfactants, or solvents. We ball milled commercial MgB_2 using tungsten carbide milling hardware for 20 h in the presence of oleic acid and oleyl amine surfactant (stainless steel balls were previously found to introduce significant iron contamination). We found that tungsten carbide contamination could be minimized by interrupting the milling after 10 h, removing and replacing the balls under the glove bag, and continuing to mill for another 10 h. Next, we performed centrifugal separation of the product taken up in heptane (at 5,000 rpm for 25 min), with no supernatant observed. This material was washed three times with ethanol, consisting of adding ethanol to the deposit, ultrasonicating for 10 min, and centrifuging at 5,000 rpm for 25 min with decanting of the ethanol/surfactant solution. The deposit was dried overnight, then taken up in heptane and driven through a 100 nm Teflon filter. Transmission electron microscopy images confirmed that most of the particles we produced were <50 nm in diameter.

We used a combination of Fourier transform infrared spectroscopy (FTIR) and X-ray absorption spectroscopy (XAS) to confirm the purity of the particles. Figure 1 shows these tests for a particle using a 200 nm filter. In Figure 1a, FTIR was used to verify that the material is free of the surfactants (oleic acid, oleyl amine), the solvents used in the nanoparticle dispersal (heptane) and collection (ethanol), and oxidation. No signatures of the any of the dominant infrared-active frequencies are visible in the MgB_2 nanoparticles. The lack of significant oxide or nitride contaminants (MgO, Mg_3N_2) from air or moisture exposure was also confirmed by comparing against standards using Mg K-edge XAS, confirming the suitability of our sample handling procedures. Additional elemental analysis confirmed a lack of N or significant amounts of H. Some residual ~5 mole% carbon contamination was observed, but the carbon was unaffected by hydrogenating the MgB_2 sample at 140 bar H_2 and 365°C for 120 h.

Figure 1b shows the Sieverts uptake isotherm for hydrogenation of our unconfined nano-MgB_2 samples at 365°C and 140 bar H_2 pressure. The improvement in uptake kinetics is immediately visible. (Note that the decrease in total sample wt% H in the Sieverts data is likely due to the presence of residual surfactant, as these samples were extracted and tested prior to our refinement of the cleaning procedure described above.) A better idea of the kinetics can

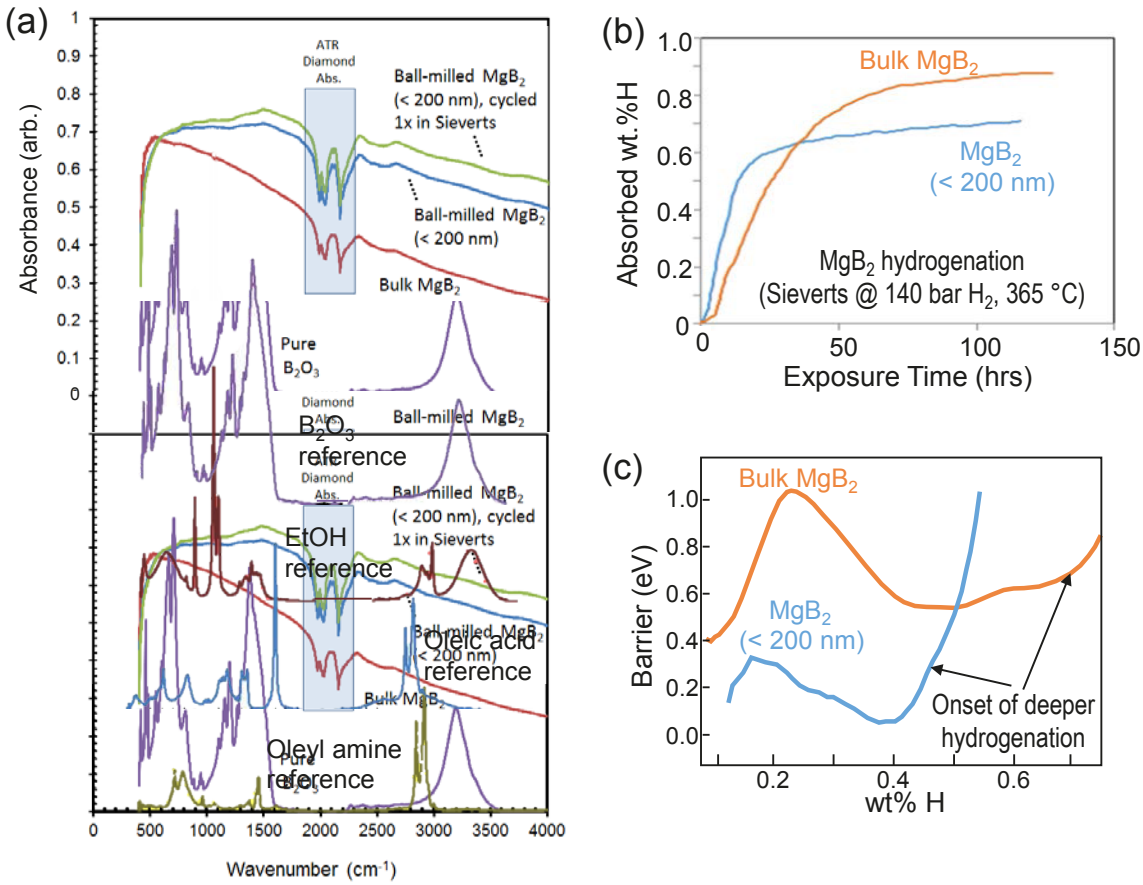

FIGURE 1. (a) FTIR spectra of nano-MgB_2 prepared according to the procedure described in the text (as-prepared and cycled). Spectra for bulk MgB_2 and possible contaminants from solvents or exposure to air are shown for comparison. (b) Sieverts initial hydrogen uptake in bulk MgB_2 and nano-MgB_2. (c) Evolution of the effective barrier during hydrogenation from Arrhenius analysis of the data in (b).

be gained by performing an Arrhenius analysis as a function of degree of hydrogenation. Following the procedure used in our recent work on understanding initial hydrogenation in bulk MgB_2 [4], we performed hydrogenation of nano-MgB_2 at two additional temperatures (378°C, 391°C) at 140 bar H_2 pressure. The resulting Arrhenius analysis is shown in Figure 1c. Similar to the bulk case, two barriers are observed in the initial hydrogenation regime. As described further in the sections below, the first corresponds to surface dissociation of H_2, whereas the second involves diffusion and binding to a lower-energy site. However, both barriers are dramatically reduced by ~3x upon nanosizing. Although these results clearly demonstrate the kinetic benefits of nanosizing, it should be emphasized that the Sieverts results can probe only the initial hydrogenation (<1 wt% H); the effect on the kinetics of the entire decomposition reaction has not yet been determined.

Free Energy Predictions for Mg-B-H

We computed free energies of the Mg-B-H compounds as a function of temperature (T) and H_2 partial pressure (pH_2), explicitly accounting for full finite-temperature dynamical contributions. Specifically, the solid vibrational density of states is computed from ab initio quantum molecular dynamics (based on DFT within the generalized gradient) and decomposed into (quasi)harmonic and anharmonic contributions. For these calculations, we have used the predicted structures in Zhang et al. [5] for $MgB_{12}H_{12}$. In principle, the predicted free energies can be used to construct a phase diagram for the conversion of $Mg(BH_4)_2$ to MgB_2 through the $MgB_{12}H_{12}$ solid-state intermediate. In doing so, we use the experimental entropy for hydrogen gas, as is standard practice in ab initio thermodynamics.

However, because DFT within standard approximations can mispredict reaction enthalpies, we first calibrated the temperature against pressure-composition-temperature (PCT) data in the literature from Li et al [6]. Although poor kinetics in the Mg-B-H system reduces the accuracy of PCT-derived thermodynamic data, the extracted values are nonetheless useful for approximate calibration. We found that a shift to higher temperatures by 280 K put the computations in good agreement with the PCT data. Note that this shift assumes that DFT errors in enthalpies are systematic, which is often the case. The calibrated $Mg(BH_4)_2$-$MgB_{12}H_{12}$-MgB_2

phase diagram based on ab initio molecular dynamics is shown in Figure 2a. By combining PCT measurement with transmission electron microscopy and selected area diffraction pattern, Li et al. observed the formation of MgH_2 at (360°C, 85 bar) and (285°C, 15 bar). [6] These points were used for temperature calibration of our phase boundary for the $Mg(BH_4)_2 \leftrightarrow 1/6\ MgB_{12}H_{12} + 5/6\ MgH_2 + 13/6\ H_2$ reaction. In addition, their X-ray diffraction analysis identified Mg metal at (360°C, 4.8 bar) formed from decomposition of MgH_2. This point resides close to our phase boundary between $1/6\ MgB_{12}H_{12} + 5/6\ MgH_2 + 13/6\ H_2$ and $1/6\ MgB_{12}H_{12} + 5/6\ Mg + 3\ H_2$, offering validation of our calibration choice.

To further validate our computed phase diagram, we have also been collaborating with the Hydrogen Materials—Advanced Research Consortium (HyMARC) to obtain the fraction of non-crystalline intermediate phases experimentally for $Mg(BH_4)_2$ and MgB_2 at different (pH_2,T) conditions. We have concentrated our validation efforts on the high-pressure end of the phase diagram, where the phase behavior is predicted to have higher sensitivity and where less data is generally available. ^{11}B nuclear magnetic resonance (NMR) is then used to estimate the fractions of MgB_2, $Mg(BH_4)_2$, and MgB_xH_y intermediates (mostly $MgB_{12}H_{12}$). These fractions can be compared against the predicted phase fractions from the free energy analysis.

NMR and X-ray diffraction (XRD) were used to obtain additional data points for samples obtained and hydrogenated through SNL/HyMARC and Pacific Northwest National Laboratory/HySCORE, as well as data published by Severa et al [7]. These analyses were performed around 400~550°C at various pressures up to 1,000 bar (marked with black, red, blue, and green circles in Figure 2a and identified in Figure 2c). Since the NMR and XRD data provide information about phase fractions, we also calculated the equilibrium phase fractions between $MgB_{12}H_{12}$ (as a broader stand-in for MgB_xH_y intermediates) and $Mg(BH_4)_2$ at 400–700°C close to the experimental conditions based on the phase coexistence approach we demonstrated previously [8]. While NMR and XRD data include kinetic effects, our phase diagram is solely based on thermodynamics. Therefore, direct comparison between the NMR/XRD-analyzed and our predicted phase fractions should be performed with caution. Nevertheless, the phase evolution trend found in NMR and XRD matches well with the trend in our predicted phase fractions, with higher levels of intermediates (or MgH_2 as a proxy for intermediates in XRD) appearing in regions near predicted phase boundaries, supporting our phase diagram prediction especially at higher (pH_2,T) conditions where the effect of anharmonic dynamics becomes dominant.

Kinetic Modeling of Initial MgB_2 Hydrogenation

As part of our ongoing investigation into the initial hydrogenation of MgB_2, we previously used a combination of

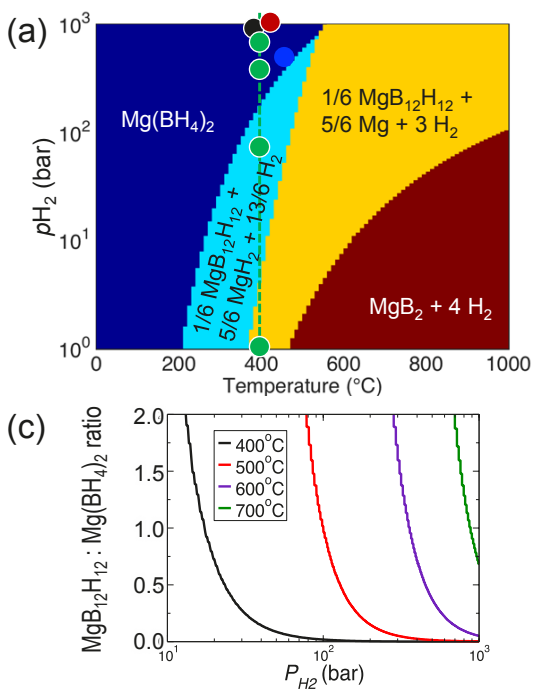

(b) **Experimental validation at high *P***

Sample	Method	T (°C)	pH_2 (bar)	Relative mole fractions of products (%)		
				MgB_xH_y	$Mg(BH_4)_2$	
Severa (2010)[1]	^{11}B NMR	390	900	7	93	
SNL #1	^{11}B NMR	420	1000	13	87	
SNL #2	^{11}B NMR	450	500	53	47	
				$Mg(BH_4)_2$	MgB_2	MgH_2
SNL/HyMARC #3 (White/Stavila)	XRD	400	1	75	25	0
		400	70	0	10	90
		400	350	66	34	0
		400	700	84	16	0

[1]Severa *et al.*, *Chem. Commun.* **46**, 421 (2010)

FIGURE 2. (a) Predicted and calibrated Mg-B-H phase diagram. (b) Details of experimental phase fractions measured under different conditions using ^{11}B NMR and XRD. The corresponding reaction conditions are shown as symbols in (a). (c) Calculated equilibrium phase ratio between $MgB_{12}H_{12}$ and $Mg(BH_4)_2$ for comparison with the experimental data in (b).

DFT calculations, FTIR, and XAS to suggest a two-barrier mechanism that is compatible with the barriers in Figure 1c. Ultimately, our proposed mechanism (shown in Figure 3a) leads to hydrogen segregation at high-energy B-B bonds of grain boundaries or interfaces and "etching" of the boron from these edge binding sites inward. In particular, this process involves successive chemical processes including H_2 molecule dissociation and adsorption of dissociated atomic H mediated by surface diffusion ("diffusive adsorption," hereafter) from the dissociation sites to the edge binding sites.

To verify and systematically analyze the proposed mechanism in Figure 3a, we devised a kinetic model that combines relevant non-equilibrium chemcial processes. We first constructed an energy diagram for the process in Figure 3a. The energetics of the proposed intermediates and products were computed from DFT, whereas the Arrhenius kinetic analysis of the experimental data in Figure 1c were used to parameterize the energy barriers of the corresponding chemical processes. The DFT calculations considered the coverage-dependent energy associated with binding hydrogen to exposed boron edge sites (the sites compatible with the XAS and FTIR results), as well as the dissociation energy of H_2 on Mg-rich planes of MgB_2(0001). The resulting energy landscape is shown in Figure 3b.

Using the constructed energy diagram, a simple reaction rate law, and a well established isotherm model, we derived a mathematical model of reaction equations for the successive dissociation/association and diffusive adsorption/desorption processes. Our model couples differential equations for each of these two processes as follows. The overall reaction may be written as $H_2\,(g) \leftrightarrow 2H^* \leftrightarrow 2H_{ads}$, where H* represents hydrogen at the initial dissociation site and H_{ads} represents hydrogen bound to the edges of hexagonal boron in MgB_2. The set of differential equations can be written as:

$$\frac{\partial c_{H^*}}{\partial t} = k_1 \cdot P_{H_2} - \tilde{k}_1 \cdot c_{H^*}^2 - \frac{\partial c_H^{ads}}{\partial t}$$

$$\frac{\partial c_H^{ads}}{\partial t} = k_2 \cdot c_{H^*}^2 \cdot c_s^3 \cdot (1-\theta)^2 - \tilde{k}_2 \cdot c_s^3 \cdot \theta^2$$

Here, c_{H^*}, c_H^{ads} are concentrations of H^*, H_{ads}, respectively, in wt.% H, P_{H_2} is the pressure of H_2 gas, and θ is the edge binding site (adsorption site) coverage by adsorbed hydrogen. Note that c_H^{ads} and θ are related by $c_H^{ads} = f_{cv} N_s \theta$, where N_s ($= N_s^0 \cdot \exp(-E^{acc}/k_B T)$) is the number

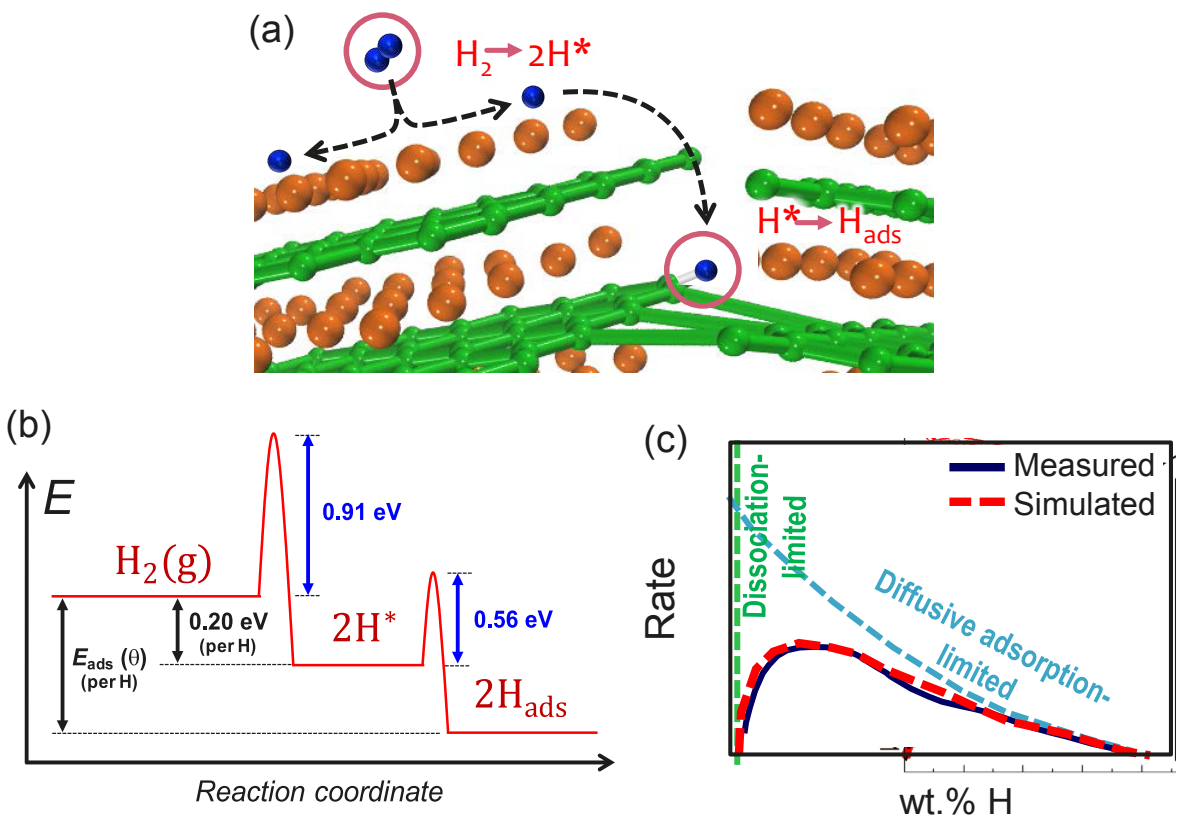

FIGURE 3. (a) Proposed mechanism of initial hydrogenation of MgB_2, involving dissociation ($H_2 \rightarrow 2H^*$) and diffusive adsorption ($H^* \rightarrow H_{ads}$) steps. (b) Corresponding energy diagram for the mechanism in (a). (c) Experimental and simulated uptake rate curves; results in the limit of a single-barrier rate limitation are also shown.

of accessible edge binding sites participating in adsorption and f_{cy} is the unit conversion factor to *wt.%* H. We define $c_s = c_s^0 \exp(-E^{acc}/k_B T)$ as the *effective* concentration parameter of the accessible edge binding sites, where c_s^0 is the corresponding prefactor and E_{acc} is the associated activation energy. The kinetic coefficients k_1, $\tilde{k}_1$, k_2, and $\tilde{k}_2$ correspond to dissociation, association, adsorption, and desorption, respectively. These kinetic coefficients are expressed in the form $k_0 \exp(-E^{acc}/k_B T)$, where k_0 is the prefactor, E is the activation energy, and k_B is the Boltzmann constant, and T is the temperature.

The above equations are numerically solved simultaneously to capture the interactions between the two processes. Note that this model contains some elements that are computed (e.g., DFT-derived energetics for different coverages), some that are measured (e.g., experimentally derived activation energies), and some that are purely descriptive (e.g., prefactors for the kinetic rate constants fitted to match simulated and experimental uptake curves). Our kinetic model can capture the significant mechanistic features, which allows us to verify our proposed initial hydrogenation mechanism. Figure 3c shows the simulated isotherm uptake curve versus the experimentally measured result, from which it is clear that the two-step mechanism reproduces the major kinetic features of the experimentally observed uptake. For more detailed analysis, we conducted controlled simulations for a particular temperature (T = 391°C) by manipulating the relative rates of the two operating reactions (dissociation/association and diffusive adsorption). Simulated rate curves for reactions limited entirely by dissocation/association (green dashed line) and entirely by diffusive adsorption (blue dashed line) are shown in Figure 3c. As expected, the blue line exhibits a monotonous decreasing trend with the increasing extent of hydrogenation due to the site saturation. In addition, it converges to the later stage of the fully relaxed simulation and experimental result (represented by red curves in Figure 3c). This manifests our above argument that the later-stage behavior of the rate curve is determined by the diffusive adsorption and site saturation processes. In contrast, the green line exhibits a monotonous increasing trend with the increasing the extent of hydrogenation. From this observation, we may further confirm that the very initial behavior of the uptake is determined by the dissociation/association reaction.

Phase-Field Kinetic Modeling

The kinetics of deeper rehydrogenation (>1 wt% H) in the hydrogen-poor region of the phase diagram are more difficult to probe, since they require higher temperatures that are inaccessible to our Sieverts apparatus. Instead, we performed phase-field kinetics simulations to qualitatively understand the relationship between diffusion, phase formation, and reaction pathways in the transformation between $MgB_{12}H_{12}$ and MgB_2. $MgB_{12}H_{12}$, MgB_4, MgB_2, and Mg were selected as the stoichiometric compounds for the hydrogen-poor region of the phase diagram (denoted Phase Triangle 3, the yellow region in Figures 4a and 4b). These compounds were proposed as possible intermediates by H.-W. Li et al [9]. The underlying free energy landscape was constructed based on our DFT-computed free energies at 350°C, with intermediate compositions interpolated using a mathematical smoothing function.

Multiphase phase field simulations were performed to examine the reaction pathways for rehydrogenation of MgB_2. In the simulations, a boundary condition corresponding to a high H chemical potential (i.e., high H_2 pressure) outside the particle is imposed to trigger the initial rehydrogenation. This allows the large nucleation barrier associated with

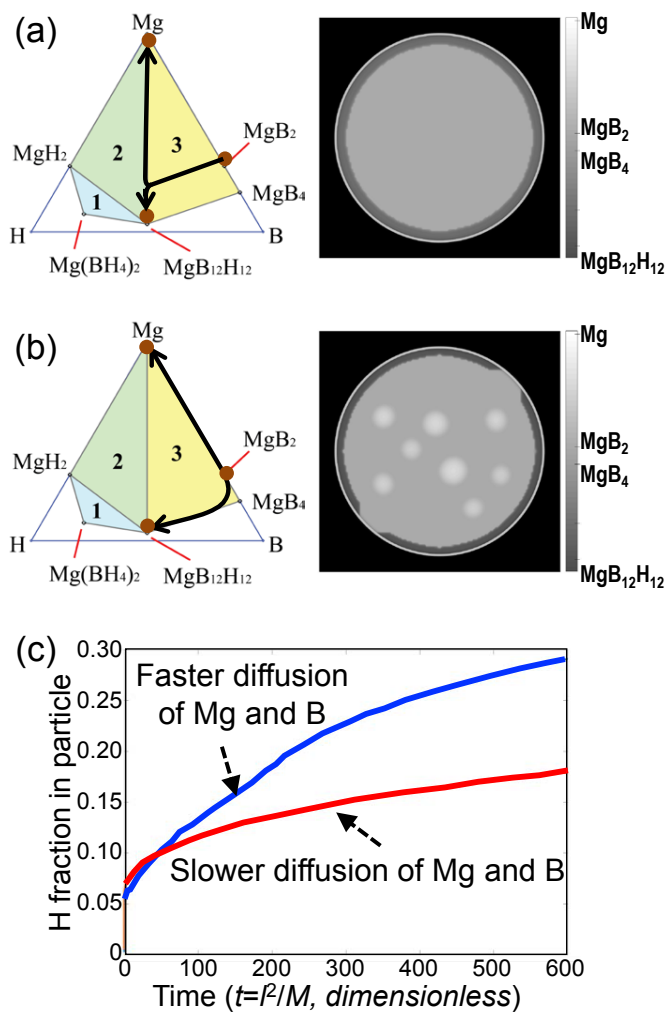

FIGURE 4. Simulated kinetic pathways and microstructure evolution during rehydrogenation of MgB_2 in the cases where (a) B and Mg mobilities are much smaller than H mobility (unitless mobilities: M_H = 0.01, M_B = M_{Mg} = 0.0001); and where (b) B and Mg mobilities are larger than H mobility (unitless mobilities M_H = 0.01, M_B = 1, M_{Mg} = 0.2). (c) Comparison of overall hydrogen uptake kinetics for the cases described in (b) and (b).

the initial insertion of H into MgB_2 to be overcome. Note that this barrier is associated with the steep gradient of the energy landscape near MgB_2 and suggests additives are necessary to catalyze B-B bond cleavage, as has been proposed. Figure 4a shows rehydrogenation simulation results if B and Mg mobilities are assumed to be sluggish compared to H mobility. As H is inserted into the particle, a core-shell morphology forms with a non-stoichiometric shell (the composition of which is approximately MgB_4H_4) and a core of MgB_2. The reaction pathway follows the pathway indicated in the left panel of Figure 4a; the low B and Mg mobilities hinder separation between these two species to form stoichiometric compounds and metallic Mg.

Another simulation was performed to examine the case when B and Mg mobilities are higher than H mobility (Figure 4b). Although this condition is unrealistic for bulk MgB_2, it represents a case for which B-B bond cleavage and Mg extraction are catalyzed. The result shows a very different morphological evolution from the previous one. As shown in Figure 4b, a $MgB_{12}H_{12}$ layer forms near the particle surface as H is inserted into the particle. As rehydrogenation proceeds, phases with high Mg concentration emerge from the MgB_2 region. Next, MgB_4 phases form and grow from the MgB_2 region. Meanwhile, the MgB_4 phases transform to $MgB_{12}H_{12}$, which grows with Mg inclusions. This composition evolution is indicated in the left panel of Figure 4b. The overall kinetics of hydrogen uptake from the two rehydrogenation simulations in Figures 4a and 4b are shown in Figure 4c. It is clear that faster Mg and B diffusion (as in Figure 4b) improves reaction kinetics, presumably because the composition evolution is allowed to occur via the low-energy pathways, i.e., from MgB_2 via MgB_4 to $MgB_{12}H_{12}$. Overall, the results in Figures 4 point to a close coupling between microstructure evolution, phase pathway, and (de) hydrogenation kinetics that merits further exploration.

CONCLUSIONS AND UPCOMING ACTIVITIES

This year, we refined our MgB_2 nanoparticle synthesis procedure and demonstrated the capability to make unconfined nanoparticles (MgB_2) without significant levels of contamination. The first tests of these materials were successfully made, showing significant kinetic enhancement for initial hydrogenation. The lack of a confining medium means the enhancement can be attributed exclusively to size effects. We also completed and validated a calibrated free energy-derived phase diagram for the transformation of $Mg(BH_4)_2$ to MgB_2 via a $MgB_{12}H_{12}$ intermediate. We further elucidated and verified a two-step kinetic mechanism for the initial hydrogenation of MgB_2, demonstrating the importance of interface reactions in determining the initial uptake kinetics of that material. Notably, the results suggest that introducing interfaces and/or defects will create additional reaction sites that should aid kinetics. Finally, we introduced the first phase-field kinetic model for probing the relative effect of Mg and B diffusion kinetics on the $MgB_{12}H_{12} \leftrightarrow MgB_2$ reaction pathway and rate. In the remaining months of the project, we will:

- Perform a more detailed analysis of the products and phase fractions of unconfined nano-MgB_2 in further detail, as well as of Ti-catalyzed samples of nano-MgB_2;
- Extend the phase-field model to the remaining region of the phase diagram (hydrogen-rich domain) and refine the energy landscape used as an input to the model.

FY 2017 PUBLICATIONS/PRESENTATIONS

1. B.C. Wood, V. Stavila, N. Poonyayant, T.W. Heo, K.G. Ray, L.E. Klebanoff, T.J. Udovic, J.R.I. Lee, N. Angboonpong, and P. Pakawatpanurut, "Nanointerface-driven reversible hydrogen storage in the nanoconfined Li-N-H system," *Adv. Mater. Interfaces* **4**, 1600803 (2017).

2. K.G. Ray, L.E. Klebanoff, J.R.I. Lee, V. Stavila, S. Kang, T.W. Heo, M. Bagge-Hansen, J. White, P. Shea, Y.-S. Liu, and B.C. Wood, "Elucidating the mechanisms of MgB_2 initial hydrogenation via a combined experiment-theory study," *Phys. Chem. Chem. Phys*., in press (2017).

3. B.C. Wood, "Complex dynamics in metal borohydrides: From hydrogen storage to solid-state batteries," Hydrogen Metal Systems Gordon Research Conference, Easton, MA, July 2017 [invited].

4. S. Kang, "Thermodynamics and Kinetics at Interfaces of Metal Hydrides for Hydrogen Storage," American Chemical Society Meeting, San Francisco, CA, March 2017.

5. S. Kang, "Beyond-ideal modeling of (de)hydrogenation in complex metal hydrides," International Symposium on Hydrogen Energy, Waikoloa, HI, February 2017 [invited].

6. K.G. Ray, "X-ray absorption and emission spectroscopy of the initial hydrogenation of MgB_2," Advanced Light Source User Meeting, Berkeley, CA, October 2016 [invited].

REFERENCES

1. Klebanoff, L.E., and J.O. Keller. "5 Years of Hydrogen Storage Research in the US DOE Metal Hydride Center of Excellence (MHCoE)." *Int. J. Hydr. Energy* 38 (2013): 4533–4576.

2. Pasini, J.M., C. Corgnale, B.A. van Hassel, T. Motyka, S. Kumar, and K.L. Simmons. "Metal hydride material requirements for automotive hydrogen storage systems." *Int. J. Hydr. Energy* 38 (2013): 9755–9765.

3. Fichtner, M., Z. Zhao-Karger, J. Hu, A. Roth, and P. Weidler. "The kinetic properties of $Mg(BH_4)_2$ in ltrated in activated carbon." *Nanotechnology* 20 (2009): 204029.

4. Ray, K.G., Klebanoff, L.E., Lee, J.R.I., Stavila, V., Kang, S., Heo, T.W., Bagge-Hansen, M., White, J., Shea, P., Liu, Y.-S., and Wood, B.C., "Elucidating the mechanisms of MgB_2 initial hydrogenation via a combined experiment-theory study," *Phys. Chem. Chem. Phys*., in press (2017).

5. Zhang, Y., Majzoub, E., Ozolins, V., and Wolverton, C., "Theoretical Prediction of Metastable Intermediates in the Decomposition of $Mg(BH_4)_2$." *J. Phys. Chem. C* 116 (2012): 10522.

6. Li, H.-W., Miwa, K., Ohba, N., Fujita, T., Sato, T., Yan, Y., Towata, S., Chen, M. W., and Orimo, S., "Formation of an intermediate compound with a $B_{12}H_{12}$ cluster: experimental and theoretical studies on magnesium borohydride $Mg(BH_4)_2$." *Nanotechnology* 20 (2009): 204013.

7. Severa, G., Rönnebro, E., and Jensen, C.M., "Direct hydrogenation of magnesium boride to magnesium borohydride: demonstration of >11 weight percent reversible hydrogen storage." *Chem. Commun.* 46 (2010): 421.

8. Wood, B.C., Stavila, V., Poonyayant, N., Heo, T.W., Ray, K.G., Klebanoff, L.E., Udovic, T.J., Lee, J.R.I., Angboonpong, N., and Pakawatpanurut, P., "Nanointerface-driven reversible hydrogen storage in the nanoconfined Li-N-H system," *Adv. Mater. Interfaces* 4 (2017): 1600803.

9. Li, H.-W., Yan, Y., Orimo, S., Züttel, A., and Jensen, C.M., "Recent Progress in Metal Borohydrides for Hydrogen Storage." *Energies* 4 (2011): 185–214.

IV.C.13 High-Capacity Hydrogen Storage Systems via Mechanochemistry

Vitalij K. Pecharsky (Primary Contact),
Duane D. Johnson, Marek Pruski, Shalabh Gupta,
Viktor Balema
Ames Laboratory
Iowa State University
253 Spedding Hall
Ames, IA 50011-3020
Phone: (515) 294-8220
Email: vitkp@ameslab.gov

DOE Manager: Ned Stetson
Phone: (202) 586-9995
Email: Ned.Stetson@ee.doe.gov

Subcontractor:
Eric Majzoub, University of Missouri, St. Louis, MO

Project Start Date: August 1, 2015
Project End Date: July 30, 2018

Overall Objectives

The overarching goal of the project is to discover and develop hydrogen storage materials that are constituted largely from earth abundant, benign and low cost elements, such as silicon and boron. Specifically, the goal is to identify computationally and synthesize hitherto unknown high H-capacity Si-based borohydrides (Si-BHs) with useable gravimetric density of over 10 wt% H_2, and decomposition enthalpies in range of 25–35 kJ/mol-H_2, such that H_2 desorption occurs at the operating temperature (~80–100°C) of the proton exchange membrane fuel cells.

Fiscal Year (FY) 2017 Objectives

- Establish composition and structure of a new Si-BH hypersalt discovered in the $LiBH_4$–SiS_2 system, and demonstrate H_2 reversibility in this system.
- Explore synthesis of analogous Si-BH compounds in related systems including $NaBH_4$–SiS_2, KBH_4–SiS_2 and $Mg(BH_4)_2$–SiS_2 using mechanochemical processes, and characterize their structure, composition, and hydrogen sorption properties. Demonstrate feasibility of synthesis of Si-BHs from elemental and pre-reacted components via mechanochemistry under high H_2 pressure (delayed due to equipment availability).

Technical Barriers

This project addresses the following technical barriers from the Hydrogen Storage section (3.3) of the Fuel Cell Technologies Office Multi-Year Research, Development, and Demonstration Plan.

(A) System Weight and Volume

(B) System Cost

(D) Durability/Operability

(O) Lack of Understanding of Hydrogen Physisorption and Chemisorption

Technical Targets

The project addresses lack of suitable materials impeding implementation of materials-based onboard H-storage systems. Successful completion would provide an H-storage material with high gravimetric and volumetric capacity, and kinetics and thermodynamics suitable to supply high-purity hydrogen to a proton exchange membrane fuel cell. The new materials identified and synthesized as an outcome of this project will achieve or exceed the DOE targets, see Table 1.

TABLE 1. H-Storage Parameters of Si-based Borohydrides in Comparison with the DOE Targets

Storage Parameters	DOE Technical Targets*	Our Targets**
Gravimetric capacity (kg H_2/kg)	0.065	>0.100
Volumetric capacity (kg H_2/L)	0.050	>0.130

*Ultimate system level targets, **material basis

FY 2017 Accomplishments

- A detailed structural characterization of the novel Si-BH compound synthesized in the $LiBH_4$–SiS_2 system was achieved by solid-state nuclear magnetic resonance (SSNMR) and Fourier transform infrared (FT-IR) analyses, establishing the role of sulfide anions in formation of mixed silicon borohydrides.
- A thorough investigation of other $M_x(BH_4)_y$–SiS_2 systems (M = Na, K, Mg) shows formation of Si-BHs likely analogous to the $LiBH_4$–SiS_2 system. Among the systems investigated, hydrogen cycling in $Mg(BH_4)_2$–SiS_2 was found to be the most promising.
- Decomposition onset temperatures and amounts of H_2 released from the new Si-BHs meet the DOE targets; high purity H_2 (>99.8%) is released and diborane release, if any, is below the detection limits.

- In conjunction with experimental results in the $LiBH_4$–$SiBr_4$ system, the multi-gas canonical linear programming (MGCLP) calculations [1], revealed that halogenated silanes have relatively low formation energies among silicon-borohydride species, leading to the possibility to engineer the reaction pathway for stabilizing Si-BHs.
- Experimental evidence indicates that complexes such as $\{PhSiCl_{3-x}(BH_4)_x\}$ (Ph = phenyl) are likely to form during the reaction between $LiBH_4$ and $PhSiCl_3$. Suitable substituents at the Si atom can (de)stabilize Si-BHs structures and alter their chemical behavior.
- A series of "4Li:Si:xB" compounds prepared mechanochemically shows promising hydrogen sorption behavior, and could potentially meet DOE targets.

✧ ✧ ✧ ✧ ✧

INTRODUCTION

Because of the practical barriers and safety concerns associated with the H-storage in liquid and gaseous forms, hydrogen storage in solids continues to be a promising alternative storage technology for fuel cell applications. A material that can fully satisfy demands must store a large amount of hydrogen in a light and compact form, can be rapidly refueled, and be affordable for safe, easy and inexpensive production in large quantities. Despite the discovery and synthesis of numerous hydrogen rich compounds, their utility for H-storage and delivery remains limited by unfavorable thermodynamics or/and kinetics of hydrogen release and uptake [2]. The U.S. Department of Energy, in collaboration with the automotive industry defined the criteria for onboard H-system, which requires 1–10 bar H_2 equilibrium pressure at the working temperature of a proton exchange membrane fuel cell. Only a few candidates hold promise to achieve this with required gravimetric density and enthalpies of dehydrogenation in the range of -25 to -30 kJ/mol-H_2.

Guided by validated computational tools, this project seeks to discover hitherto unknown silicon-based borohydrides (Si-BHs) and optimize their low cost synthesis in powder form. Materials will be experimentally accessed via mechanochemistry, a sustainable, green, energy-efficient process that potentially offers a cost-effective solution for large-scale production of functional materials.

APPROACH

Guided by computations and known chemistry of metal borohydride solids, numerous systems covering a broad compositional landscape of potential Si-BH hypersalts have been identified. After a preliminary screening, an exploratory, primarily mechanochemical, synthesis is conducted in the most promising systems. The computational crystal structure search is performed by the prototype electrostatic ground state approach [3] followed by structure relaxation using density functional theory. Thermodynamic properties and reaction pathways involving gas-phase precursors are determined using the MGCLP method. Structure and phase characterization is performed using powder X-ray diffraction, FT-IR, and SSNMR spectroscopies, and hydrogen de/absorption properties are evaluated using volumetric methods.

RESULTS

Silicon-based borohydrides via hypersalt stabilization: Mechanochemical synthesis targeting Si-BHs in the $LiBH_4$–$SiBr_4$ system led to the formation of a mixed anion borohydride compound and release of gaseous SiH_4 and B_2H_6 as shown in Equation 1.

$$8LiBH_4 + SiBr_4 \rightarrow 8Li(BH_4)_{0.5}Br_{0.5} + 2B_2H_6\uparrow + SiH_4\uparrow \qquad (1)$$

These results are in line with MGCLP calculations that indicate that Si-BHs are unstable toward decomposition to SiH_4 and B_2H_6. Trends in MGCLP-derived reaction energies, however, indicate that the formation of SiH_4 and B_2H_6 may be prevented in reactions under elevated pressure.

In another approach to stabilize Si-BHs, large electron-withdrawing groups were introduced in place of similarly electronegative halide anions. For example, trichloro(phenyl)silane ($PhSiCl_3$) was used instead of $SiHal_4$ (Hal = Cl or Br) to carry out the exchange reaction with $LiBH_4$. Thermogravimetric analysis-differential scanning calorimetry, FT-IR and ^1H nuclear magnetic resonance (NMR) data indicate possible formation of $\{PhSiCl_{3-x}(BH_4)_x\}$-like complex(s) in the $PhSiCl_3$–$LiBH_4$ system. In contrast to $PhSiCl_3$, $PhSiH_2Cl$ reacts with $LiBH_4$ yielding $PhSiH_3$, B_2H_6, and H_2. Although the reasons for the difference in products from $PhSiH_2Cl$ and $PhSiCl_3$ is yet unclear, it is likely that an appropriate choice of substituents at the silicon center can stabilize/destabilize Si-BH-like structures and alter chemical behavior of silicon derivatives. This conclusion is indirectly supported by results obtained in the $LiBH_4$–SiS_2 system.

Mechanochemical reactions in the $LiBH_4$–SiS_2 system were studied at length by FT-IR and SSNMR. Based on the observed build-up curves in the cross-polarization experiments, Si atoms are within ~4 Å of H atoms and most likely belong to the same compound (Figure 1a). This Si–H distance is consistent with the formation of $Si\text{-}S^{(-)}\text{-}Li^{(+)}$ motifs [4], where $[BH_4]^-$ coordinates the Li atoms as shown in Figure 1b. The increased E^1 intensity in the cross polarization magic angle spinning (CPMAS) spectra suggests that more E^1 sites have $Si\text{-}S^{(-)}\text{-}Li^{(+)}$ structure than the others. The ^{11}B direct polarization magic angle spinning (DPMAS) spectra of the ball milled samples showed the presence of BH_4^- anion in both 2:1 and 6:1 compositions. The following mechanism

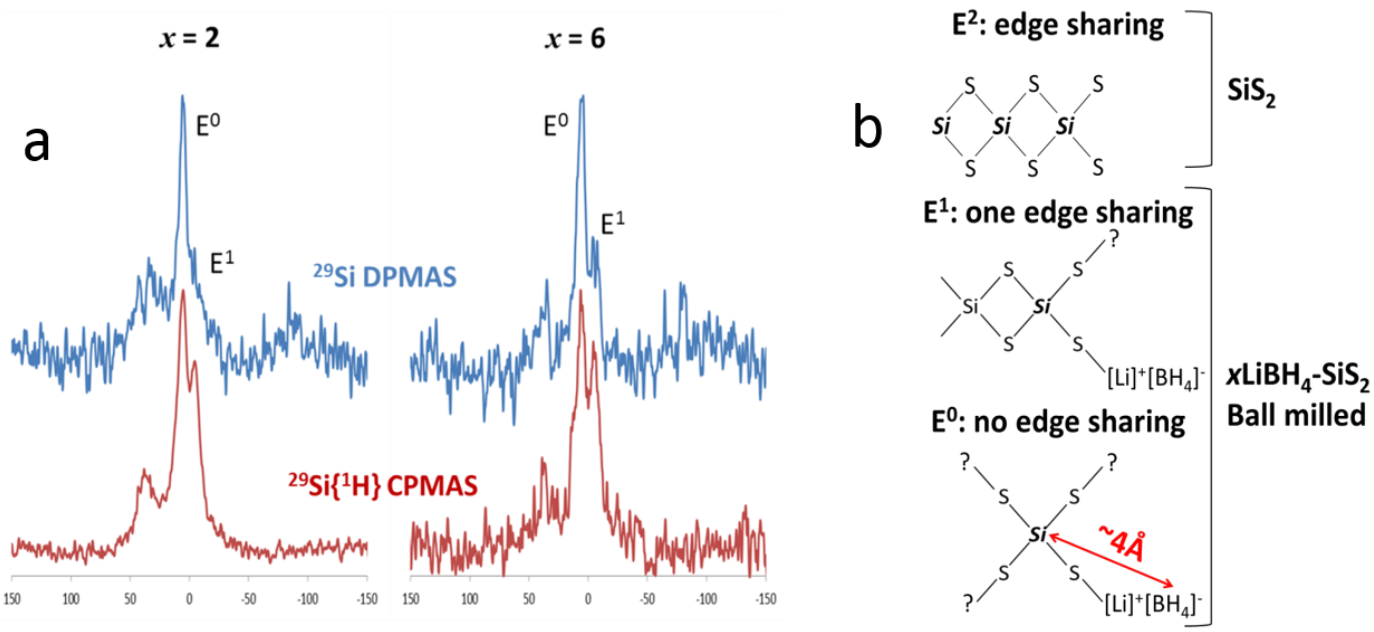

FIGURE 1. (a) ^{29}Si DP/CP MAS NMR spectra of ball milled $xLiBH_4$–SiS_2 (x = 2, 6) mixtures and (b) proposed peak assignments to Si-co-ordinations in the complex (question marks represent bonds of S to Si or Li)

(sequence of events) leading to the Si-BH complex may be proposed:

- Edge-shared SiS_2 (E^2) transforms into a mixture of one (E^1) and no-edge shared (E^0) forms.
- The formation E^1 and E^0 proceeds through appearance of "free bonds" with S^- in the structure.
- The proximity of a positively charged Li^+ leads to S^-–Li^+ bonds. The Li atoms expectedly remains coordinated to the BH_4^- anion.

Hence, complex structures containing both Si^{4+} and BH_4^- are possible through their coordination with S (for Si^{4+}) and Li (for BH_4^-).

Amorphous products of mechanochemical transformations in the $Mg(BH_4)_2$–SiS_2 system were characterized by FT-IR. Broad peaks corresponding to B-H stretching in $Mg(BH_4)_2$ indicate that BH_4^- anions in the product remain in configurations similar to pristine $Mg(BH_4)_2$.

Considering similarities in the chemistry of $LiBH_4$ and $Mg(BH_4)_2$, it is likely that the Mg-analogue is closely related to that described for $LiBH_4$ - SiS_2 system. SSNMR experiments to establish the local structures of the amorphous products in this system are in progress.

Reversibility of sulfur stabilized Si-BHs: Hydrogen (de)absorption properties of $M_x(BH_4)_y$–SiS_2 systems (M = Li, Na, K and Mg) are summarized in Table 2. As also shown in Figure 2, nearly 4 wt% of H_2 is released during the second

TABLE 2. TPD Results of $M_x(BH_4)_y$–SiS_2 Systems (M = Li, Na, K and Mg). Numbers in parentheses represent data from the second desorption cycle after hydrogen absorption.

System, ratio	wt% H_2	T_{ons}, °C	wt% of total H_2
$LiBH_4$–SiS_2			
2:1	4.3(1.5)	88(230)	73(35)
4:1	7.1	113	81
5:1	7.5	116	76
6:1	8.2(2.4)	92(199)	77(30)
8:1	6.2	96	52
$LiBH_4$ (B.M. 3h)	2.9	276	16
$NaBH_4$–SiS_2			
2:1	3.3(1.0)	124(270)	69(30)
5:1	2.1	134	29.6
6:1	2.4	159	32
$Mg(BH_4)_2$–SiS_2			
2:1	5.6	101	70
3:1	5.9(1.8)	99(246)	62.8(30.5)
6:1	8.94	104	77.7
6:1 (B.M.)	10.12(4.0)	117(249)	88(40)
10:1	8.5(3.77)	112(243)	67.5(44.3)
$Mg(BH_4)_2$ (pure)	10.7	150	72.3
KBH_4–SiS_2			
6:1 (B.M. 3h)	1.3	165	17.6

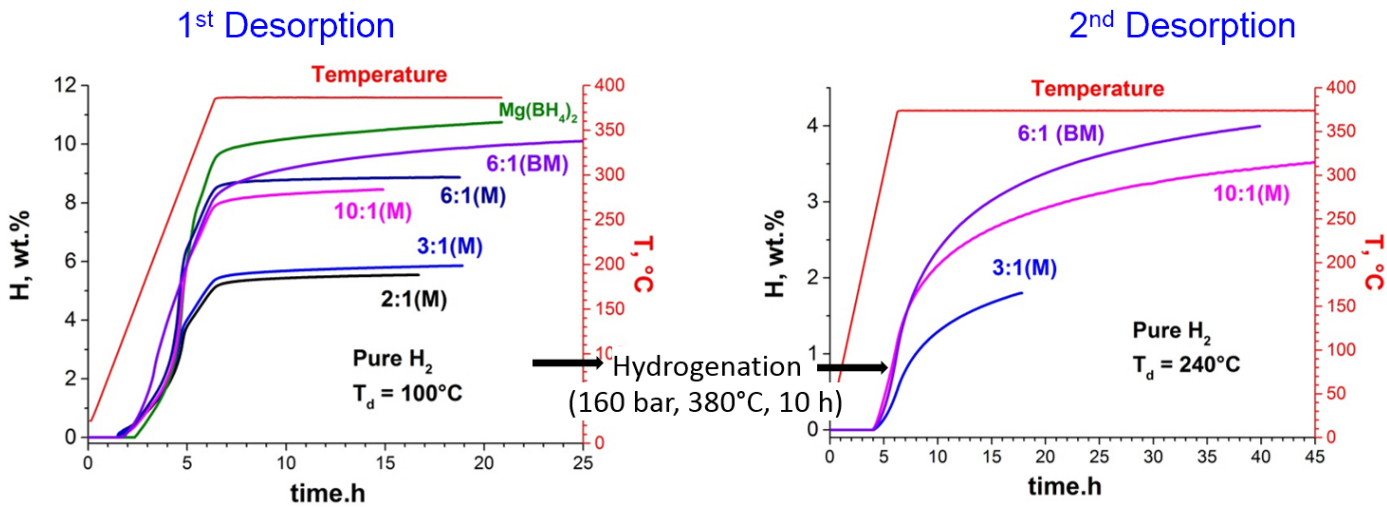

FIGURE 2. Temperature programmed desorption plots of the pristine mixtures (M) and ball-milled samples (BM) of the $Mg(BH_4)_2$–SiS_2 system taken in different molar ratios, (left) first decomposition and (right) decomposition after rehydrogenation

desorption cycle in the $6Mg(BH_4)_2$–SiS_2 mixture, accounting for ~40% reversible gravimetric capacity. This system has the potential to achieve Phase 2 targets, i.e., 2.5 wt% (at 200°C) and 5 wt% (at 300°C).

Si-BHs by high-pressure ball-milling: Density functional theory calculations carried out during Phase 1 revealed higher relative stabilities for Si^{2+} in Si-based borohydrides. Notwithstanding these findings, no stable compounds with Si^{2+} are known that may serve as a suitable precursor. To get around the problem, elemental Si was combined/alloyed with B and other alkali and alkaline earth metals, e.g. as in $M_xSi_yB_z$ (M = Li, Na, Mg, Ca) that were further reacted with hydrogen to yield borohydrides of the type $M_xSi_y(BH_4)_z$. Hydrogenation of such metal borosilicides can be performed either by milling under pressurized H_2 similar to conversion of MgB_2 to $Mg(BH_4)_2$ [5] or by high temperature hydrogenation [6].

Hydrogenation of one such system based on Li-Si-B was found to be very promising. A compound with composition Li_4Si and structure similar to $Li_{4.25}Si$ (also known as $Li_{17}Si_4$), forms upon liquid-assisted ball milling of the 4:1 molar mixture of Li and Si in heptane. Addition of elemental B into the reaction mixture leads to products with nominal compositions of "4Li:Si:xB" (x = 1 – 4) and structures, where boron is incorporated into the Li_4Si structure. Preliminary hydrogenation study of the "4Li:Si:2B" sample shows ~1.2 wt% reversible H_2 storage with T_{onset} at 146°C (Figure 3). It was also observed that T_{onset} of hydrogen release from hydrogenated samples is lowered when boron is present in the mixture compared to pure Li_4Si. More importantly, the amount of reversible hydrogen nearly doubles (to 2.4 wt%) when the composition is changed from "4Li:Si:2B" to "4Li:Si:4B". The FT-IR analysis of the hydrogenated products shows absorption bands with frequencies that correspond to

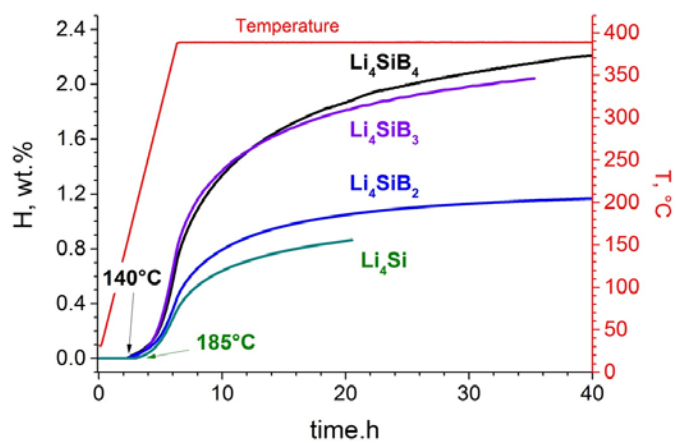

FIGURE 3. Temperature programmed desorption plots of the Li-Si-B mixtures prepared by high-energy ball milling of different compositions followed by their hydrogenation

B–H bonds; their intensity is highest for the hydrogenated "4Li:Si:4B". The coordination of Si and Li in this compound will be subject of future investigation by SSNMR. The formation of B-H bonds upon hydrogenation of the Li-Si-B system under hydrogen pressure provides support for possibility of increased hydrogen uptake during milling under hydrogen pressure.

CONCLUSIONS AND UPCOMING ACTIVITIES

As evidenced by experimental results in the $LiBH_4$–SiS_2 system, mechanochemical reactions are suitable for stabilization of Si-based borohydride complexes, particularly with sulfur. The newly synthesized complex shows low

desorption onset temperatures that meets DOE requirements and releases pure hydrogen. Therefore, studies on this system will continue to further improve the cycling properties. Such investigations will be extended to other metals and mixed metal borohydrides $M_xM'_y(BH_4)_z$–SiS_2 (M or M' = Li, Na, K, Al, Ca, Mg). The project will also continue to focus on other sulfur based systems using precursors like Al_2S_3 and B_2S_3.

The Si-BH complex(es) may be stabilized by relatively bulky electron-withdrawing phenyl groups, therefore investigation of different $RSiX_3$ carbosilanes (X = F, Cl, Br) with increased hydrogen content is considered.

Based on the computational results it was concluded that elevated pressure may stabilize Si-BHs. Therefore, synthesis of Si-BHs via ball milling under high pressures and in a cryo-mill is planned in the next phase. The M-Si-B systems (M = Li, Na, Ca, Mg), prepared mechanochemically from metals shows promising preliminary results, and opens up a possibility of formation Si-BH complexes by hydrogenation at elevated temperatures or mechanical milling under high pressure. The high-pressure milling capabilities are expected to be fully functional by the end of September 2017, and the latter investigations will be given highest priority.

FY 2017 PUBLICATIONS/PRESENTATIONS

1. T. Kobayashi, O. Dolotko, S. Gupta, V.K. Pecharsky, M. Pruski, "Insights into the role of composition for purity of released hydrogen from the $LiBH_4$-$AlCl_3$ system," *manuscript in preparation*.

2. O. Dolotko, T. Kobayashi, S. Gupta, M. Pruski, E. Majzoub, V.K. Pecharsky, "Novel hydride and destabilization of the lithium borohydride by SiS_2," *manuscript in preparation*.

3. T. Kobayashi, O. Dolotko, S. Gupta, Y. Fillinchuk, V.K. Pecharsky, M. Pruski, "Solid-State NMR studies of hydrogen storage materials; mechanochemically induced reaction of $LiBH_4$ and $AlCl_3$," 58th ENC, Asilomar, USA, March 26–31, 2017.

4. O. Dolotko, S. Gupta, T. Kobayashi, E. Majzoub, V.P. Balema, M. Pruski, V.K. Pecharsky, "Novel hydrides and destabilization of the alkali-metal borohydrides by SiS_2," GRC Hydrogen-Metals Interactions: Making the Hydrogen Economy Work - New Developments and Recent Applications, Stonehill College, Easton, MA, July 16–21, 2017.

REFERENCES

1. N. Poonyayant et. al., J. Phys. Chem. C., 2014, 118, 14759.

2. L.E. Klebanoff, et. al., Int. J. Hydrogen Energy, 2013, 38, 4533.

3. E.H. Majzoub, et. al., Phys. Rev. B., 2008, 77, 104115.

4. H. Eckert et. al., J. Non-Crystalline Solids, 1989, 113, 287.

5. S. Gupta et. al., Chem. Comm., 2013, 49, 828.

6. G. Severa et. al., Chem. Comm., 2010, 46, 421.

IV.C.14 Design and Synthesis of Materials with High Capacities for Hydrogen Physisorption

Brent Fultz (Primary Contact), Channing Ahn, David Boyd, Hillary Smith, Nick Weadock
California Institute of Technology (Caltech)
1200 E. California Blvd.
Pasadena, CA 91125
Phone: (626) 395-2170
Email: btf@caltech.edu

DOE Manager: Jesse Adams
Phone: (720) 356-1421
Email: Jesse.Adams@ee.doe.gov

Contract Number: DE-EE0007048

Project Start Date: August 1, 2015
Project End Date: July 31, 2018

Overall Objectives

- Develop a carbon-based, functionalized material prepared by new methods (graphene) or old (exfoliated graphite) with a capacity for hydrogen storage by physisorption of 11 wt% excess and 40 g/L total (near 77 K and <100 bar), a near-constant isosteric heat of adsorption, excellent kinetics, and long cycle life. Understand how far hydrogen physisorption capacity can be extended beyond the present rules of thumb for carbon materials (e.g., 1 wt% excess per every 500 m^2/gram). The goal is achieving >1.5 wt% excess per every 500 m^2/g.
- Demonstrate a near-constant isosteric heat of adsorption, excellent kinetics, and long cycle lives.

Fiscal Year (FY) 2017 Objectives

- Achieve at least 1.3 wt% excess H_2/500 m^2/g in graphene based material with >3,000 m^2/g specific surface area and 45 g/L total volumetric capacity at pressures less than 100 bar and 77 K.
- Etch 1–2 nm pores in graphene sheet structures and determine if pores contribute <10% to Brunauer–Emmett–Teller (BET) surface area and to hydrogen sorption characteristics.
- Produce 300 mg quantities of material with demonstrated gravimetric and volumetric capacities within 5% of smaller scale material performance.
- Deposit sub-nanometer clusters of metal atoms on surfaces of two carbon materials and demonstrate a reduction in surface area of <10%.
- Demonstrate an improvement in average isosteric heat, an isosteric heat of adsorption in the Henry's law regime of >10 kJ/mole H_2.

Technical Barriers

This project addresses the following technical barriers from the Hydrogen Storage section of the Fuel Cell Technologies Office Multi-Year Research, Development, and Demonstration Plan.

(A) System Weight and Volume

(O) Lack of Understanding of Hydrogen Physisorption and Chemisorption

Technical Targets

This project is developing functionalized graphene materials to maximize hydrogen uptake and increase temperatures of operation. These materials are intended to meet the 2020 DOE hydrogen storage targets for high hydrogen gravimetric and volumetric capacity.

- System gravimetric capacity: 1.5 kWh/kg (4.5 wt% H_2)
- System volumetric capacity: 1.0 kWh/L (30 g H_2/L)

FY 2017 Accomplishments

- Used direct and indirect oxygen and nitrogen plasma as well as focused ion beam exposure to produce holes in monolayer graphene, vertical graphene, graphene nanoflakes, and activated carbon, resulting in holes observed with Raman spectroscopy, scanning electron microscopy (SEM), and transmission electron microscopy (TEM).
- Synthesized and characterized graphene-based carbon in gram quantities. Received initial batches of large-scale plasma grown graphene from a start-up company using Caltech-licensed technology.
- Functionalized materials with varying amounts of copper clusters, achieving surface area reduction of <5% for low copper concentration.
- Demonstrated an improvement in isosteric heat of adsorption in Henry's law regime for copper-functionalized materials at 300 K.

✧ ✧ ✧ ✧ ✧

INTRODUCTION

One of the advantages of adsorbents as a storage medium is that dihydrogen retains its molecular form throughout the adsorption/desorption cycle, and the cycle requires minimal activation energy. The primary disadvantage of sorbents is that typical adsorption enthalpies are relatively weak, compared to bond formation with chemical hydrogen, or to interstitial atomic hydrogen in metal hydrides. Additionally, the van der Waals dimension of molecular hydrogen is large in comparison to atomic hydrogen, putting limits on the overall volumetric density that systems based on dihydrogen can achieve.

Graphene-based materials offer an excellent starting platform for hydrogen sorption owing to their high surface area for dihydrogen adsorption. The key step is to optimize functional groups on the graphene for maximizing the volumetric density of dihydrogen adsorption. Part of the effort at Caltech is directed toward this optimization. While prior work on physisorbents has illustrated the importance of high surface area in achieving gravimetric uptakes of relevance to the program, volumetric densities have recently been recognized as a critical metric. Under many conditions, the nature of the adsorption process can still offer volumetric density advantages over the use of compressed gas storage, although not as high as intermetallic hydride densities. For dihydrogen that adsorbs onto a substrate, the London dispersion forces that can be regarded as transient dipoles in polarizable substances are a major contributor to physisorption processes. We are designing metal functionalizations for carbon surfaces that should optimize these attractive forces, enabling higher heats of adsorption, higher temperatures of operation, and higher capacities per surface area of material.

APPROACH

Previous work at Caltech has shown that alkali metal-intercalated graphites, which have pore dimensions similar to the graphene geometries we seek, can result in constant isosteric enthalpies of adsorption. These specialized structures had the advantage of electron back donation from the alkali metal to the graphitic planes, but these observations motivate the addition of metal atoms substitutionally in the graphene or on graphene surfaces. These local centers could increase both the isosteric heat of adsorption and the number of active sites for dihydrogen adsorption. We also note that for H_2 on metal surfaces, adsorption and desorption typically occurs above room temperature.

This project aims to promote high surface packing density of hydrogen and high constant isosteric enthalpy in graphene and graphene-based materials. Specific key goals are to attain a high volumetric density of hydrogen, a near-constant heat of adsorption, rapid kinetics for adsorption and desorption, and long cycle life. We have altered the carbon surfaces by incorporating metal centers to increase the strength of the dispersion forces. The incorporation of these metal centers will continue to be optimized to gain better understanding of hydrogen physisorption and to reach technical targets for system gravimetric and volumetric capacity.

RESULTS

Efforts for the second phase of this project occurred in three primary areas: (1) synthesis of graphene and graphene materials, (2) modification of graphene via pore formation and metal functionalization, and (3) hydrogen adsorption measurements.

Two pathways have been employed to synthesize graphene-based carbon in reasonable quantities. Caltech has licensed its technology for plasma grown graphene to Cealtech AS, a Norwegian-based start-up [1,2]. Caltech has assembled a large-scale plasma system for continuous graphene growth. Figure 1a shows team member David Boyd standing next to the plasma chamber during assembly in Germany. A TEM micrograph in Figure 1b and corresponding selected area diffraction plot in Figure 1c indicate that this plasma approach for graphene synthesis yields high quality graphene. Raman spectroscopy confirms a large defect band at 1,350 cm^{-1} and indicates that the graphene planes stack turbostratically. Parallel efforts have used a traditional synthesis and activation route to produce graphene-based carbon from reaction of graphene oxide with biomass including sucrose and lignin. These materials can be easily obtained in large quantities (5–10 g per reaction), and show an increase in surface area of over 1,000% after activation.

Modification of graphene and graphene-based carbons is at the core of our plan to reach DOE hydrogen storage targets for high volumetric density of hydrogen. The second phase of the project has focused on the modification of materials by introduction of pores and functionalization with metals. The rationale for etching of pores in graphene is to improve surface area and create active edge sites for functionalization. Plasma etching was employed to modify monolayer and bulk materials. SEM, TEM, Raman spectroscopy, and BET surface area measurements indicate the successful introduction of nanometer-scale holes. Figure 2a shows an SEM image of a graphene monolayer suspended over a copper grid with a large triangular hole resulting from focused ion beam exposure. Nanometer-sized pores were observed near the large triangular hole by TEM, as shown in Figure 2b.

Functionalization with metals is central to our approach of increasing surface packing density of hydrogen. In the first phase of the project, we demonstrated the deposition of Au and Cu metal nanoclusters <1 nm by both chemical and plasma deposition routes. In the second phase of the

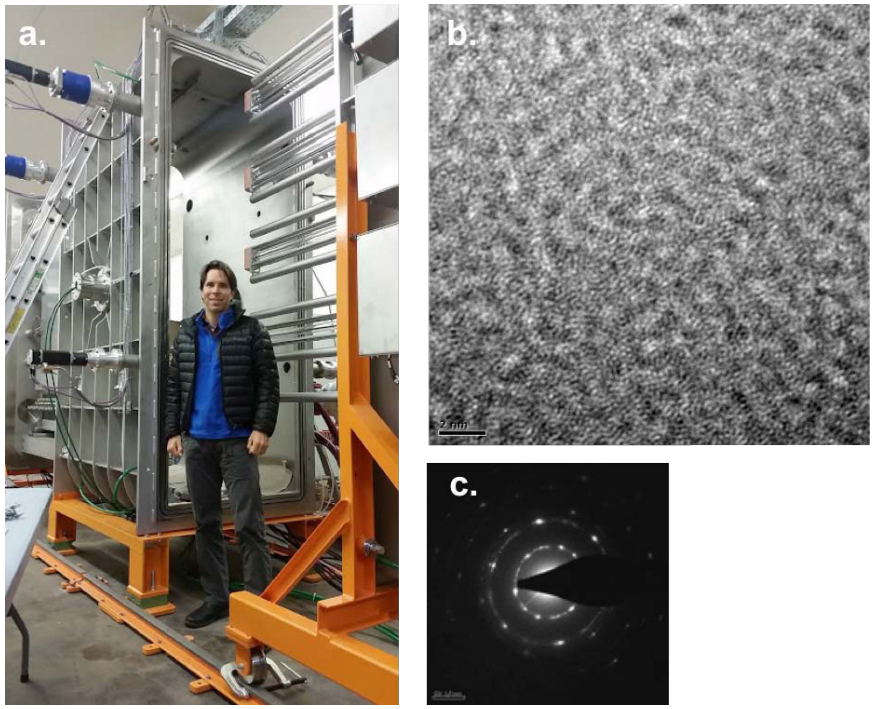

FIGURE 1. (a) Caltech team member David Boyd standing next to the plasma reactor for large-scale graphene synthesis, (b) TEM image of plasma-grown graphene, and (c) Selected area diffraction indicating that this plasma approach for graphene synthesis yields high quality graphene.

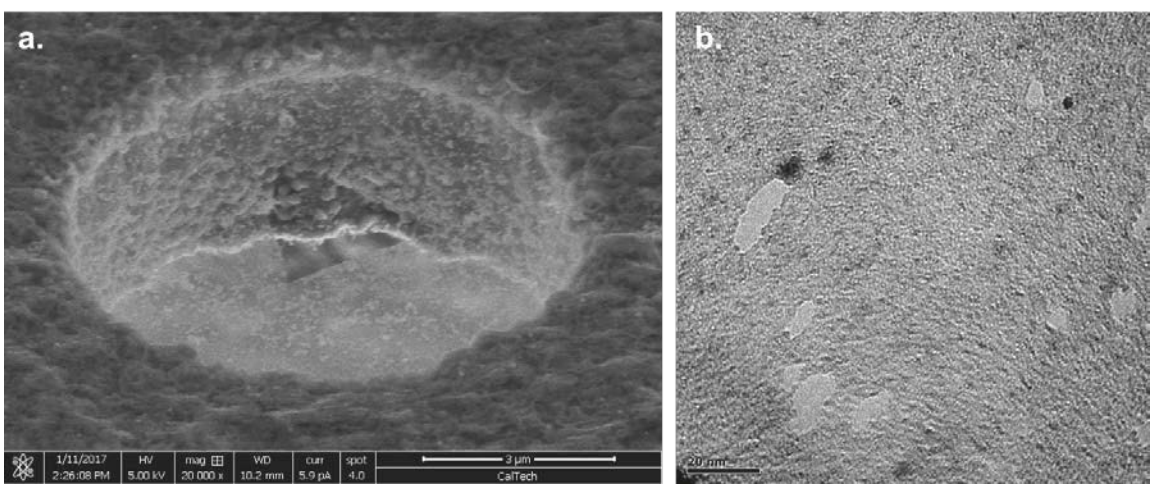

FIGURE 2. (a) SEM image of a graphene monolayer suspended over a copper grid with a large triangular hole resulting from focused ion beam exposure, and (b) nanometer-sized holes near the large hole observed with TEM.

project, these functionalization efforts were scaled-up to produce sample quantities sufficient for hydrogen adsorption testing. Figure 3 shows a high angle annular dark field TEM images of Cu atoms and Cu nanoclusters, as evidenced from the small white dots. Images were obtained by Hydrogen Storage Characterization and Optimization Research Effort (HySCORE) collaborators at Pacific Northwest National Laboratory. This material, with a surface area of 3,006 m^2/g, was functionalized from $CuCl_2 \cdot 2H_2O$ salt and annealed under hydrogen gas at 125°C. This material is one example of more than a dozen large-batch samples prepared from various metal salts that resulted in materials with varying metal concentrations, metal cluster sizes, and surface areas. Functionalization results in a decrease in surface

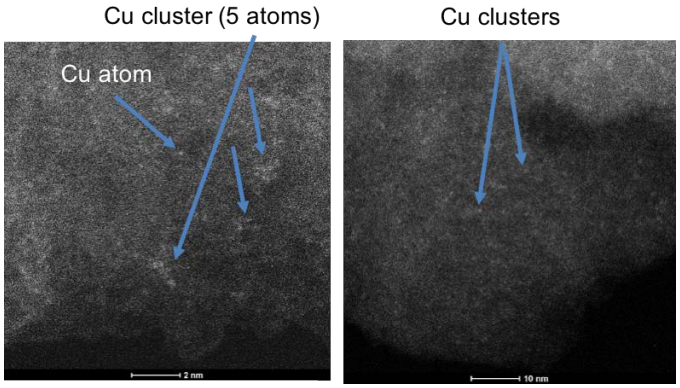

FIGURE 3. TEM high angle annular dark field image of graphene functionalized with Cu nanoclusters (appearing in bright white regions).

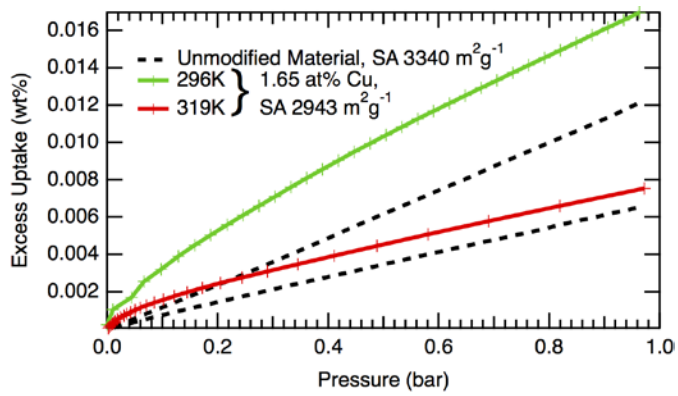

FIGURE 4. Isotherm data for functionalized material indicating an enhancement in uptake (colored curves) over pristine material (black lines) at 296 K and 319 K.

area ranging from 0.5– 40% compared to pristine material, however this may be overcome by increased hydrogen packing density on the surface, as discussed below.

Hydrogen adsorption measurements using the Sieverts method are critical to characterization of the materials we develop. In the first phase of the project, a second Sieverts apparatus was commissioned to mitigate data acquisition constraints, and a "Rapid Sieverts" screen method to assess materials using a single data point at 77 K and 20 bar. In the second phase of the project, the screening of materials has been further streamlined by adaptation of the BET system used for surface area measurements to also obtain hydrogen isotherms (<1 bar) at 77 K, 242 K, 300 K, and 322 K. Initial ambient temperature low pressure isotherm data indicate an enhancement with Cu modification, an example of which is shown in Figure 4. This figure compares pristine material (black dashed lines) with its functionalized counterpart at 296 K and 319 K. The functionalized material, containing 1.65 at% Cu, has a surface area of 2,943 m^2/g. This represents a reduction in surface area of 12% from the pristine material. However, at 296 K and 1 bar, the uptake of hydrogen by the functionalized material is 131% of the pristine material. This is a positive indication of how metal centers increase the enthalpy of adsorption, indicating a promising pathway for the practical use of adsorbents.

CONCLUSIONS AND UPCOMING ACTIVITIES

As this project reaches the end of its second phase, several conclusions can be drawn:

- Relatively large quantities of graphene-based materials can be produced and functionalized with metals.
- Chemical functionalization of materials with metals can produce varying sizes and concentrations of metal clusters.
- Ambient temperature low pressure isotherm data show an enhancement of hydrogen adsorption with Cu modification, indicating an increased enthalpy of adsorption in metal-functionalized materials.

Goals for work in the third phase of the project are:

- Identification of the role of low dimensional structure, and validation of >40 g/L total adsorption; multi temperature analyses over 77 K to 160 K for isosteric heat validation >10 kJ/mole.
- Achieve ≥1.5 wt% excess H_2/500 m^2/g in material with >3,000 m^2/g specific surface area at pressures <100 bar and 77 K.
- Achieve net adsorption of ≥6 wt% H_2 at any temperature or pressure. Achieve net adsorption of ≥1 wt% H_2 at 30 bar and 300 K.
- High gravimetric and volumetric density analysis. Gravimetric density meeting or exceeding 11 wt% H_2 and volumetric capacities exceeding 40 g/L total at 77 K and 40 bar pressure.

REFERENCES

1. Boyd, D.A., et al. (2015). Single-step deposition of high-mobility graphene at reduced temperatures. *Nature Communications*, *6*. http://doi.org/10.1038/ncomms7620

2. Issued US patent 9,150,418.

IV.C.15 Hydrogen Adsorbents with High Volumetric Density: New Materials and System Projections

Donald J. Siegel (Primary Contact, UM), Alauddin Ahmed (UM), Yiyang Liu (UM), Adam Matzger (UM), Justin Purewal (Ford), Saona Seth (UM), Mike Veenstra (Ford), and Antek Wong-Foy (UM)
University of Michigan (UM)
Ann Arbor, MI 48109
Phone: (734) 764-4808
Email: djsiege@umich.edu

DOE Manager: Jesse Adams
Phone: (720) 356-1421
Email: Jesse.Adams@ee.doe.gov

Contract Number: DE-EE0007046

Subcontractor:
Ford Motor Company, Dearborn, MI

Project Start Date: August 1, 2015
Project End Date: July 31, 2018

Overall Objectives

- Demonstrate metal-organic frameworks (MOFs) that exhibit high volumetric and gravimetric hydrogen densities simultaneously, and that exceed the performance of the benchmark adsorbent, MOF-5, at cryogenic conditions.
- Project the performance of most promising compounds to the system level by parameterizing models developed by the Hydrogen Storage Engineering Center of Excellence (HSECoE).

Fiscal Year (FY) 2017 Objectives

- Estimate system level performance of selected high-capacity MOFs using HSECoE system models parameterized from isotherm measurements.
- Demonstrate at least one MOF with hydrogen capacities exceeding baseline MOF-5 by 15%.

Technical Barriers

This project addresses the following technical barriers from the Hydrogen Storage section of the Fuel Cell Technologies Office Multi-Year Research, Development, and Demonstration Plan.

(A) System Weight and Volume

(B) System Cost

(C) Efficiency

Technical Targets

The outcomes of this project contribute to the optimization and assessment of hydrogen storage materials, and also provide input to models that project the performance of these materials at the system level. Insights gained from this study can be applied towards the development of materials that attempt to meet the DOE 2020 and ultimate hydrogen storage targets, which are summarized in Table 1. The ultimate success of this project rests upon developing MOFs that out-perform the baseline MOF-5 adsorbent. Therefore, Table 1 also summarizes the materials-level hydrogen capacity of MOF-5 and compares against the best adsorbents identified by this project to-date, IRMOF-20 and SNU-70.

FY 2017 Accomplishments

- Demonstrated that IRMOF-20 surpasses the usable capacity of MOF-5 and therefore meets the project's first go/no-go milestone.
- Nearly 500,000 MOFs were assessed computationally; more than 2,000 compounds identified that can surpass MOF-5 by 15%.
- Several promising MOFs were synthesized and evaluated with respect to their H_2 uptake; demonstrated that the

TABLE 1. System-level technical targets compared to materials-level performance of the baseline MOF-5 adsorbent and the highest-performing MOFs identified by this project to date, IRMOF-20 and SNU-70. Total capacities are reported at 77 K and 100 bar. Usable capacities are determined assuming an isothermal pressure swing at 77 K between 100 bar and 5 bar. All materials-level capacities are based on single-crystal densities.

Storage Parameter	Units	DOE 2020 Target (system level, usable)	DOE Ultimate Target (system level, usable)	MOF-5 Baseline (materials level, total/usable)	Project Status: IRMOF-20 (materials level, total/usable)	Project Status: SNU-70 (materials level, total/usable)
Gravimetric Capacity	wt%	4.5	6.5	8.0 / 4.5	9.3 / 5.7	10.7 / 7.3
Volumetric Capacity	$g{\cdot}H_2/L$	30	50	53 / 31	52 / 33	49 / 34

usable volumetric capacity of SNU-70 exceed that of IRMOF-20.

- Estimated system level performance of IRMOF-20 and DUT-23(Co) using HSECoE system models parameterized from isotherm measurements.

✧ ✧ ✧ ✧ ✧

INTRODUCTION

A high-capacity, low-cost method for storing hydrogen remains one of the primary barriers to the widespread commercialization of fuel cell vehicles. Although many storage technologies have been proposed, storage via adsorption remains one of the more promising approaches due to its fast kinetics, facile reversibility, and high gravimetric densities. Adsorbents struggle, however, in two key measures: volumetric density and operating temperature. For example, it is well known that high surface area adsorbents such as MOFs can achieve high gravimetric densities. Nevertheless, high volumetric densities are uncommon in these materials, and it has recently been suggested that total volumetric density and gravimetric density are inversely related beyond a threshold surface area [1]. In the case of operating temperatures, the relatively weak enthalpy of H_2 adsorption implies that high hydrogen densities are possible only at cryogenic temperatures.

Although an ideal adsorbent would overcome both of these shortcomings, it is important to recognize that volumetric density and operating temperature are controlled by different factors: the former depends upon the adsorbent's *structure*, whereas the latter depends on the *chemistry* of the H_2-adsorbent interaction. Therefore, distinct approaches are needed to address these independent issues. While some effort has previously been devoted to increasing ΔH (e.g., MOFs with open metal sites), attempts to increase volumetric densities have received much less attention. This is unfortunate, as analysis by the HSECoE has indicated that vehicle range is highly sensitive to volumetric density. Consequently, the development of adsorbents that simultaneously achieve high volumetric and gravimetric hydrogen densities—while maintaining reversibility and fast kinetics—would constitute a significant advance. Moreover, these materials would serve as logical starting points for follow-on efforts aimed at increasing the operating temperature.

APPROACH

This project aims to circumvent the tradeoff between total volumetric and gravimetric hydrogen densities typical of most hydrogen adsorbents. This will be accomplished by combining computational screening for promising compounds with experimental synthesis and measurement of hydrogen storage densities within those compounds. The ultimate goal is to demonstrate materials having balanced gravimetric and volumetric performance that can surpass the storage density of the benchmark compound, MOF-5. The performance of the most promising compounds will be projected to the system level by parameterizing system models developed by the HSECoE.

RESULTS

As described above, a major focus of this effort is to demonstrate MOFs whose hydrogen density surpass that of MOF-5 in its optimal or "pristine" form (i.e., MOF-5 which has not been exposed to air, and from which all solvent/reactants have been removed). Toward this goal, our FY 2016 effort demonstrated IRMOF-20, a MOF whose capacities slightly surpassed that of MOF-5 (see Table 1). In FY 2017 we aimed to improve performance further, by identifying and demonstrating MOFs that surpass the usable capacity of MOF-5 by 15%.

The first step in this search involved an expansion of our computational screening protocol. In FY 2016 approximately 2,000 known MOFs were screened for their usable H_2 capacities. In FY 2017 we dramatically enlarged our catalogue of screened compounds to include 5,109 known MOFs and approximately 464,600 hypothetical compounds. In total, 469,741 MOFs were examined from seven databases. A summary of this screening effort is provided in Table 2. Importantly, more than 2,000 MOFs were identified whose capacities can theoretically surpass that of MOF-5 by 15%.

Based on these computational predictions, several MOFs were examined experimentally. A partial list of compounds evaluated includes: ZJU-32 [8], MOF-143 [9], DUT-12 [10], DUT-10(Co) [10], MOF-177-NH_2 [11], DUT-23(Co) [12], DUT-23(Cu) [12], ZELROZ [13], EDUVOO [14], GAGZEV [15,16], and SNU-70. Hydrogen uptake isotherms for a subset of these compounds is shown in Figure 1 (based on single crystal densities). Based on these calculations and measurements, it was demonstrated that SNU-70 can out-perform both MOF-5 and IRMOF-20 (last year's top-performing compound). A list of the total and usable capacities of SNU-70 is shown in Table 1, and compared against the performance of MOF-5 and IRMOF-20.

Another accomplishment of FY 2017 was the demonstration of the Hydrogen Adsorbent System Model to project system level performance of two promising MOFs identified in the present program, IRMOF-20 and DUT-23(Co). The system model was developed by the Hydrogen Storage Engineering Center of Excellence, and previously applied to model MOF-5 based systems. Figure 2 illustrates the projected performance of these systems, demonstrating that a 3% improvement in gravimetric performance and 11% improvement in volumetric performance can be achieved using a DUT-23(Co)-based storage system.

TABLE 2. Summary of Screening of MOFs for Usable H_2 Capacities

Database	Number of MOFs				Calc. Usable Capacity	
	Available in database	Zero surface area	H_2 capacity evaluated empirically	H_2 capacity evaluated w/GCMC	Al least equals MOF-5	Exceeds MOF-5 by 15%
Real MOFs [1,2]	**5,109**	**1,978**	**3,131**	**3,131**	**90**	**20**
Mail-Order MOFs [3]	112	4	108	112	32	15
In Silico MOFs [4]	2,816	154	2,662	466	21	1
NW Hypothetical MOFs [5]	137,000	30,160	106,840	12,374	4,437	768
Zr-MOFs [6]	204	0	204	204	126	35
UO Hypothetical MOFs [7]	324,500	32,993	291,507	16,372	7,768	1,209
Total	**469,741**	**65,289**	**404,452**	**32,659**	**12,474**	**2,048**

GCMC – Grand Canonical Monte Carlo

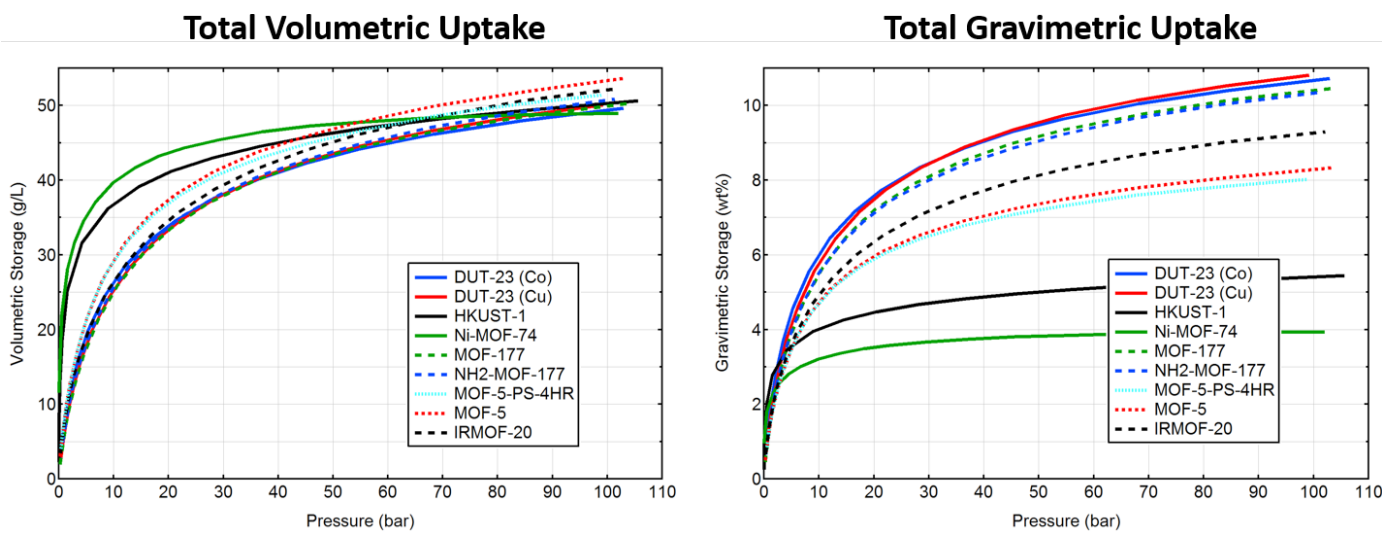

FIGURE 1. H_2 isotherms of several promising MOFs measured at T = 77 K

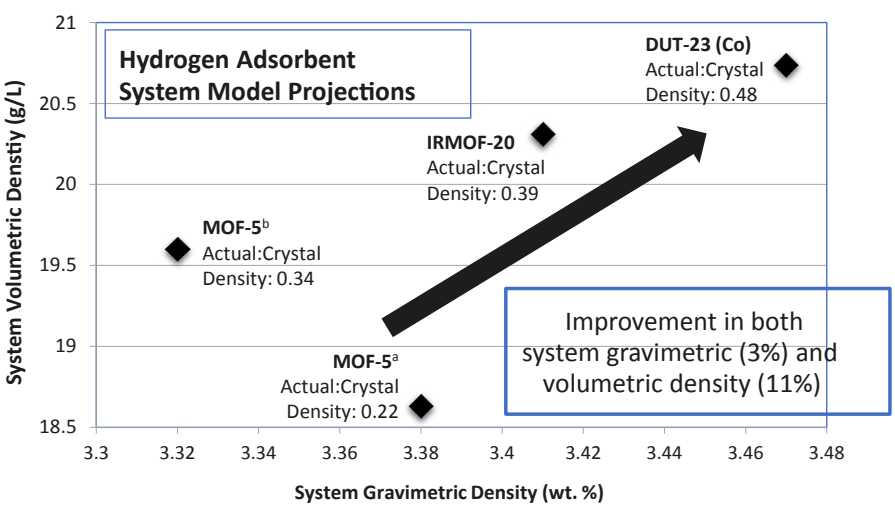

System Assumptions

Initial/Full Pressure:	100 bar
Initial/Full Temp:	80 K
Final/Empty Pressure:	5.5 bar
Final/Empty Temp:	160 K
Useable Hydrogen:	5.6 kg
Heat Exchanger:	HexCell
MOF Density:	Powder (see table)
Pressure Vessel:	Type 1 Al
Insulation Thickness:	23 mm
Outer Shell Thickness:	2 mm

FIGURE 2. Application of the HSECoE System Model to project the performance of IRMOF-20 and DUT-23(Co)-based systems

CONCLUSIONS AND UPCOMING ACTIVITIES

Computational screening and experimental synthesis/characterization revealed SNU-70 as a hydrogen adsorbent which can surpass the usable capacity of the benchmark compounds MOF-5 and IRMOF-20 under cryogenic conditions. Upcoming activities will focus on evaluating additional compounds with the goal of identifying MOFs that can surpass the performance of MOF-5 by 15%.

FY 2017 PUBLICATIONS/PRESENTATIONS

1. D.J. Siegel, "Hydrogen Adsorbents with High Volumetric Density: New Materials and System Projections," 2017 DOE Hydrogen Program Annual Merit Review Meeting, Washington, June 8, 2017.

2. D.J. Siegel, "Metal-Organic Frameworks for Gas Capture and Storage: Computational Discovery and Experimental Validation," TMS 2017 Annual Meeting & Exhibition, Symposium on "Computational Materials Discovery and Optimization–From Bulk to Materials Interfaces and 2D Materials," San Diego, CA, February 26–March 2, 2017.

REFERENCES

1. Goldsmith, J., A.G. Wong-Foy, M.J. Cafarella, and D.J. Siegel, Chem. Mater., 2013. **25**: p. 3373–3382.

2. Chung, Y.G., J. Camp, M. Haranczyk, B.J. Sikora, et al., Chem. Mater., 2014. **26**: 6185–6192.

3. Martin, R.L., L.-C. Lin, K. Jariwala, B. Smit, and M. Haranczyk, J. Phys. Chem C, 2013. **117**: p. 12159–12167.

4. Bao, Y., R.L. Martin, C.M. Simon, M. Haranczyk, B. Smit, et al., J. Phys. Chem. C, 2015. **119**: 186–195.

5. Wilmer, C.E., M. Leaf, C.Y. Lee, O.K. Farha, B.G. Hauser, et al., Nat. Chem., 2012. **4**: 83–89.

6. Gomez-Gualdron, D.A., O.V. Gutov, V. Krungleviciute, et al., Chem. Mater., 2014. **26**: p. 5632–5639.

7. Aghaji, M.Z., M. Fernandez, P.G. Boyd, T.D. Daff, and T.K. Woo, Eur. J. In. Chem., 2016. **2016**: 4505–4511.

8. Cai, J. et al., *Chem. Commun.* **2014***, 50,* 1552.

9. Furukawa, H. et al., *Inorg. Chem.* **2011,** *50*, 9147.

10. Grünker, R. et al., *Eur. J. Inorg. Chem.* **2010,** 3835.

11. Dutta, A. et al., *Angew. Chem. Int. Ed.* **2015**, *54*, 3983.

12. Klein, N. et al., Chem. *Eur. J. Chem.* **2011**, *17*, 13007.

13. Rankine, D. et al., *Chem. Commun.* **2012**, *48*, 10328.

14. Eddaoudi, M. et al., *Science* **2002**, *295*, 469.

15. Yuan, D. et al., *Angew. Chem. Int. Ed.* **2010**, *49*, 5357.

16. Farha, O.K. *Nat. Chem.* **2010**, *2*, 944.

IV.C.16 Electrochemical Reversible Formation of Alane

Ragaiy Zidan (Primary Contact), Patrick Ward, Joseph Teprovich, Scott McWhorter, Scott Greenway
Savannah River National Laboratory (SRNL)
Bldg. 999-2W
Aiken, SC 29808
Phone: (803) 646-8876
Email: ragaiy.zidan@srnl.doe.gov

DOE Manager: Ned Stetson
Phone: (202) 586-9995
Email: Ned.Stetson@ee.doe.gov

Subcontractor:
Savannah River Consulting, Aiken, SC

Project Start Date: October 1, 2006
Project End Date: September 30, 2017

Overall Objectives

- Develop novel methods to reduce production costs of alane.
- Demonstrate scalable low-cost alane etherate production methods which can be translated into a suitable crystallization process.
- Develop a crystallization process to produce high quality α-alane.
- Develop passivation methods to produce alane which is stable over time.
- Demonstrate a process to regenerate α-AlH_3 from spent alane.

Fiscal Year (FY) 2017 Objectives

- Develop methods to utilize lower cost precursor $NaAlH_4$ in order to significantly reduce the overall cost of alane production.
- Improve operational conditions of electrochemical alane production with a primary focus on the conductivity of the solvent.
- Utilize density functional theory (DFT) calculations to gain deeper insight into the potential crystallization of alane from alternative adducts.
- Determine ligands which can exchange with the AlH_3•THF (tetrahydrofuran) adduct, so THF can be used in the electrochemical cell to improve electrical conductivity.
- Demonstrate crystallization of alane from alternative adducts.

Technical Barriers

This project addresses the following technical barriers from the Hydrogen Storage section of the Fuel Cell Technologies Office Multi-Year Research, Development, and Demonstration Plan.

(A) System Weight and Volume

(B) System Cost

(C) Efficiency

(Q) Regeneration Processes

Technical Targets

- Acquire DFT data on various alane adducts to gain insight into the parameters which influence the production of alane from these adducts.
- Develop methods to produce alane from lower cost precursors.
- Demonstrate a lower cost crystallization method for the production of high quality α-alane.
- Demonstrate ligand exchange with AlH_3•THF to produce alternative adducts.
- Demonstrate the crystallization of alternative adducts of alane.

FY 2017 Accomplishments

- Crystallization method developed which significantly lowers the cost of production of high quality α-alane.
- DFT calculationswere performed on a series of alane adducts to gain a deeper understanding of the variables which affect the production of alane.
- Novel method for the production of alane from $NaAlH_4$ was developed.

✧ ✧ ✧ ✧ ✧

INTRODUCTION

The main objective at SRNL is to develop a low-cost hydrogen storage material with favorable thermodynamics and kinetics capable of fulfilling various portable power applications. Our specific goal is to develop an economical method to regenerate aluminum hydride (alane - AlH_3) from aluminum metal, since aluminum hydride has a gravimetric capacity of 10 wt%, volumetric capacity of 149 g/L H_2, and a desorption temperature range of ~60°C to 175°C (depending on particle size and the addition of catalysts). Direct synthesis of alane from hydrogen and aluminum is

unfeasible due to the enormously high pressure of hydrogen required thermodynamically to drive direct hydrogenation. Conventional chemical methods for alane synthesis react alkaline metal or alkali-earth metal hydrides or alanates with aluminum chloride to produce an alane adduct using significant quantities of polar aprotic solvents such as THF or ether that form complexes with the alane product. The high energy required for significant solvent separation, product purification, and the large energy required to recycle reaction byproducts (primarily LiCl) makes production of alane prohibitively expensive for hydrogen storage applications. It is currently estimated that production of alane by the conventional chemical route costs between $3,000/kg and $5,000/kg. Electrochemical alane production methods have promise for significant cost reduction for the synthesis of alane. This method has been developed and demonstrated by SRNL to have the potential to reduce alane production costs by over 100 times, which would make alane cost effective for various applications. However, technical challenges still remain to improve and optimize these methods.

APPROACH

The electrochemical generation of α-alane has been shown by Zidan et al. [1,2] to be capable of generating high purity material using methods that can be developed into a fueling cycle for hydrogen vehicles, portable power systems, or other applications. This research has demonstrated methods to enhance the practicality of utilizing the electrochemical method for the large scale production of alane etherate as well as the crystallization of the etherate to produce stable crystals of α-alane. By reinvestigating the traditional DOW method for alane crystallization, conditions required to produce large crystals of pure α-alane have been demonstrated in an enhanced process intensified chemical method. The understanding of this process has provided direction in a path to utilizing cheaper and less hazardous crystallizing solvents under more industrially viable conditions. Improvements to the electrochemical cell voltage patterns have also resulted in a method to nearly eliminate the dendrite formation which limits the time that an electrochemical process can run continuously without interruptions. Another opportunity for enhancement of the electrochemical process lies in the poor ionic conductivity of diethyl ether. The ionic conductivity of $LiAlH_4$ in diethyl ether is significantly lower than the ionic conductivity of alanates in THF. Furthermore, the lack of solubility of $NaAlH_4$ in diethyl ether restricts the use of $NaAlH_4$ in an electrochemical method to directly produce the alane diethyl etherate adduct. Unfortunately, attempts to crystallize the AlH_3•THF adduct have not been successful in producing pure α-alane. Therefore, investigation into ligands which can exchange with the AlH_3•THF adduct and produce an adduct capable of being crystallized to high purity α-alane would bypass the conductivity and higher expense issue associated with operation of the electrochemical cell with diethyl ether.

RESULTS

Previously, we reported a method to eliminate the issue related to dendrite formation in the electrochemical process which limits continuous operational time of the process on an industrial scale [3]. The other primary roadblock in this electrochemical method is the limited ionic conductivity in diethyl ether. To circumvent this limitation, the electrochemical cell can be operated in THF, but a ligand exchange process would be required afterwards. In order to gain insight into the capability to exchange ligands in the AlH_3•THF adduct, bond dissociation energies were calculated for 18 various alane adducts using the hybrid DFT functional B3LPY and the triple zeta Pople basis set G6-311 with polarization functions on all atoms. Predicted bond dissociation enthalpies of various adducts are given in Table 1. There are two definitive trends apparent from the computational results. The first trend is that asymmetry of the ligand around the bonded atom tends to result in lower bond dissociation enthalpies than a symmetric adducting ligand. The second trend noticed is that steric hindrance plays a role in destabilizing the adduct bond as graphically illustrated in Figure 1. These calculations give insight into the adduct exchange reaction because ligands which form a stronger bond with alane will undergo the exchange reaction more rapidly and with a higher yield. Unfortunately, the bond dissociation energy calculated here does not provide a full picture for alane crystallization (adduct removal). This is because many of these adducts form an intermediate species before crystallizing into α-alane. This is known for the diethyl ether adduct and we recently determined intermediate adduct species (AlH_3•$L_{x<1}$) to be present during the crystallization of the triethyl amine and dimethyl ethyl amine adducts. Since there is an intermediate adduct species, the bond dissociation energy is actually the sum of energy required to go from the initial adduct to the intermediate adduct and then to alane. Because these intermediate adducts were only recently discovered in the less common adducts

TABLE 1. Bond Dissociation Enthalpies for Various Alane Adducts Calculated at the B3LYP Level of Theory

Adduct	Bond Dissociation Enthalpy (kJ/mol)	Bond Dissociation Enthalpy (kcal/mol)
AlH_3•Me_2EtN	110.27	26.36
AlH_3•Me_2O	85.40	20.41
AlH_3•Et_2MeN	73.13	17.48
AlH_3•IsoproMe2N	92.35	22.07
AlH_3•Et3N	98.23	23.48
AlH_3•DiisoproMeN	87.51	20.92
AlH3•MeButylO	77.70	18.57
AlH3•MTBE	73.16	17.49
AlH3•MeProO	81.18	19.40
AlH3•MeEtO	81.00	19.36

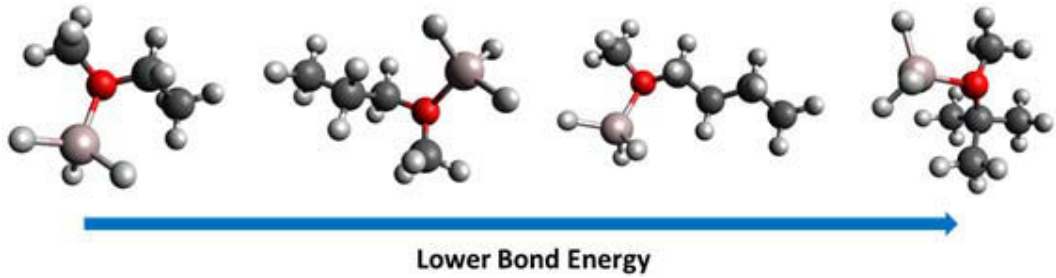

FIGURE 1. Effect of steric hindrance on adducts bond energy

of alane, the crystal structure is unknown and the bond dissociation energies cannot be modeled without first solving the crystal structures for each intermediate adduct species. Nonetheless, this set of calculations still provides valuable insight into the influences associated with the alane-ligand bond.

Another alternative to the electrochemical process, which is capable of utilizing the lower cost $NaAlH_4$ precursor, was recently developed by SRNL and a patent was filed. This process involves the production of alane diethyl etherate from the milling of $NaAlH_4$ and $AlCl_3$ in diethyl ether under particular temperature and pressure conditions. The presence of alane diethyl ether adduct was confirmed by thermal-gravimetric analysis (TGA)/residual gas analysis (RGA), as shown in Figure 2, and then a dry method crystallization was carried out to convert the material to α-alane. This milling process significantly reduces the cost of alane production by avoiding the use of $LiAlH_4$, which costs nearly an order of magnitude greater. The advantage of producing the diethyl ether adduct of alane lies in the known crystallization methods to produce pure α-alane. While other adducts can produce α-alane, the control of particles size, purity, and morphology is difficult. Previously reported alane production methods from alane diethyl ether adduct required the use of the more expensive $LiAlH_4$ precursor. The production of alane can be compartmentalized into three primary steps: front end adduct production, crystallization, and passivation. While the electrochemical process and newly patented process address the production of the alane adduct, crystallization of this adduct is still the critical step of the production of stable and high purity α-alane. Recently, SRNL has developed a process intensified chemical process to crystallize the diethyl ether adduct of alane which significantly reduces solvent requirements under less energy intensive conditions. This increases the production capacity and reduces the cost of the material. The newly developed crystallization process produces stable high purity α-alane as determined by X-ray diffraction shown in Figure 3. The importance of the production of α-alane without the presence of other phases lies in the significantly higher stability of the α-phase, but even α-phase alane can decompose over time if not properly passivated. The alane produced via the new crystallization process was passivated and demonstrated to have no loss in capacity (Figure 4) over 6 months of storage in air.

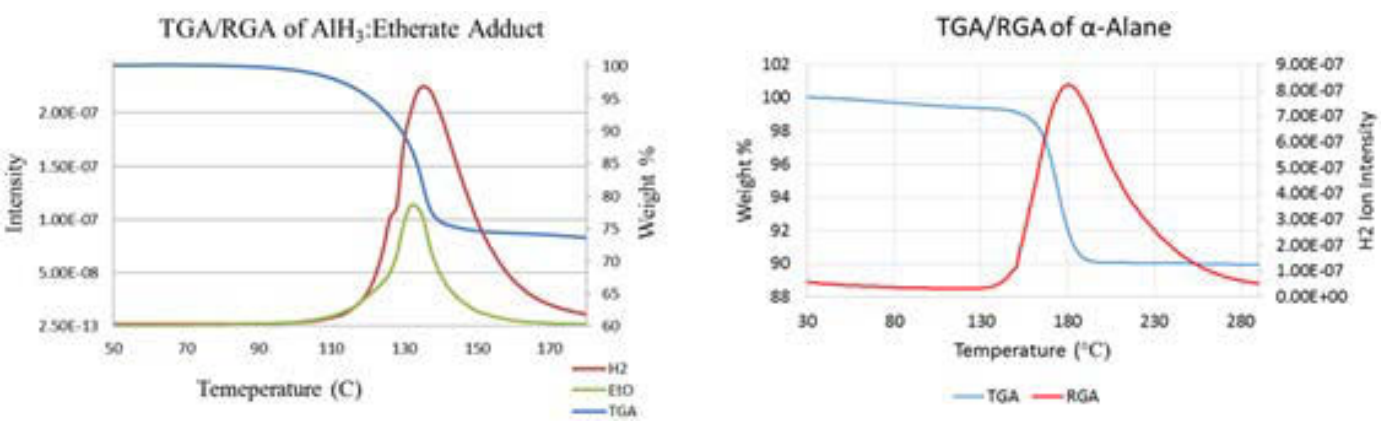

FIGURE 2. TGA/RGA of alane diethyl ether adduct produced by milling process (left) and TGA/RGA of alane adduct converted to α-alane via the dry method (right)

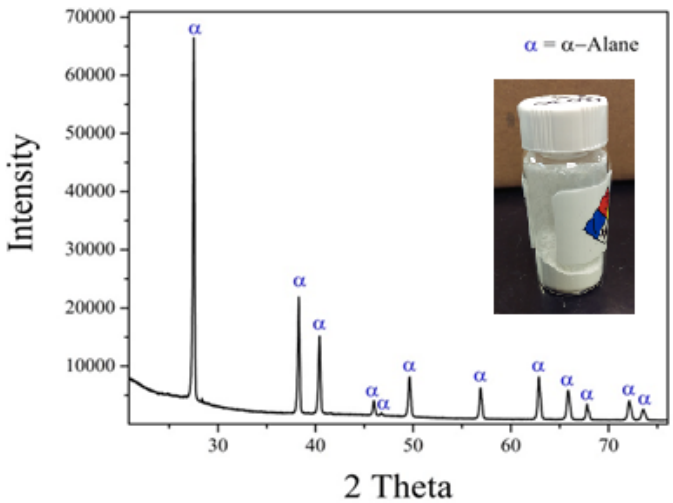

FIGURE 3. X-ray diffraction pattern of alane obtained from the process intensified crystallization process

CONCLUSIONS AND UPCOMING ACTIVITIES

Advancements in the low-cost production of alane were achieved with respect to both the etherate production process and the alane crystallization process. A novel ball milling method to produce alane etherate from $NaAlH_4$ was developed which reduces the cost of chemical precursors required. Furthermore, a process intensified method to crystallize alane etherate under ambient pressure in toluene was developed which is capable of producing more than seven times more alane per unit volume than the previously reported DOW method. The newly developed crystallization method produced high purity α-alane, reduced the required solvent (by nearly an order of magnitude), and was found to produce α-alane which was stable in air and demonstrated no observable degradation over 6 mo. To evaluate alternative adducts for the electrochemical process, a large number of amine and ether adducts of alane were evaluated by DFT methods to determine the viability of adduct exchange from the AlH_3•THF ligand to an adduct more suitable for crystallization. It was determined that the bond dissociation energy of the adduct is affected by both symmetry and steric hindrance contributions from the binding ligand. The improvements for alane production techniques demonstrated during the course of the project have defined a feasible path forward for the low-cost production of high quality α-alane.

SPECIAL RECOGNITIONS & AWARDS/ PATENTS ISSUED

1. Zidan, Ragaiy; Ward, Patrick A. MECHANOCHEMICAL SOLID/LIQUID REACTION IN FORMATION OF ALANE Patent: U.S. Application No.: 15/482,913.

REFERENCES

1. Zidan, R., et al., Chemical Communications, 2009(25): p. 3717–3719.

2. Martinez-Rodriguez, M.J., et al., Appl. Phys. A-Mater. Sci. Process., 2012. 106(3): p. 545–550.

3. Zidan, R. et al. SRNL FY 2016 Report.

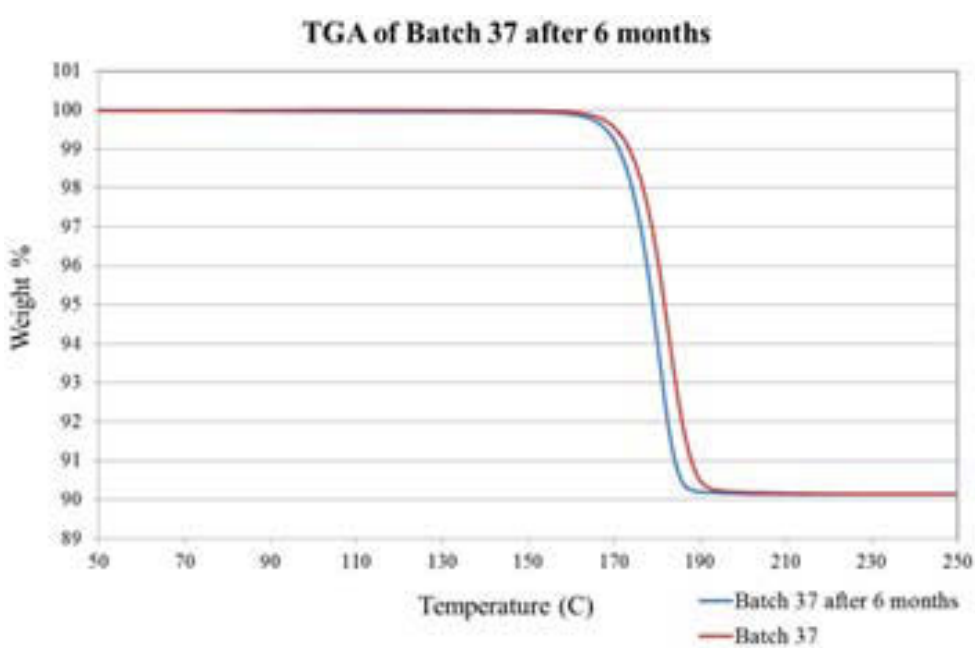

FIGURE 4. TGA of alane obtained from the process intensified crystallization process after production (red) and after being stored six months in air (blue)

IV.C.17 Low-Cost α-Alane for Hydrogen Storage

Tibor Fabian
Ardica Technologies, Inc.
2325 3rd Street, Suite 424
San Francisco, CA 94107
Phone: (412) 358 1922
Email: tibor@ardica.com

DOE Manager: Katie Randolph
Phone: (240) 562-1759
Email: Katie.Randolph@ee.doe.gov

Technical Advisor: Mark Petrie
Phone: (650) 859-4574
Email: mark.petrie@sri.com

Contract Number: DE-EE0006629

Subcontractor:
SRI International, Menlo Park, CA

Project Start Date: July 15, 2014
Project End Date: July 14, 2017

Overall Objective

Reduce production cost of α-alane (AlH_3) to meet the DOE 2015 and 2020 hydrogen storage system cost targets for portable low- and medium-power applications. This will enable broader applications in consumer electronics (i.e., smart phones, tablets, laptops), back-up power, unmanned aerial vehicle, forklifts, and vehicles.

Fiscal Year (FY) 2017 Objectives

- Demonstrate electrochemical alane adduct generation at high current density and product yield.
- Identify alane adducts suitable for trans-ligation from alane-tetrahydrofuran (THF) adduct. Characterize trans-ligation yields and yields of alane adduct conversion into alpha alane.
- Demonstrate high yield regeneration of $NaAlH_4$ from the reaction of recovered cell cathode product, aluminum and hydrogen.
- Update process and economic models.

Technical Barriers

This project addresses the following technical barriers from the Hydrogen Storage section of the Fuel Cell Technologies Office Multi-Year Research, Development, and Demonstration Plan.

(A) System Weight and Volume

(B) System Cost

(C) Efficiency

(J) Thermal Management

(K) System Life-Cycle Assessments

(Q) Regeneration Processes

Technical Targets

The following was the progress made towards the DOE technical targets (Table 1).

FY 2017 Accomplishments

- Cost modeling. Using lab results, updated the cost model showing the cost of alane produced by the electrochemical route (Table 1) translates to a storage system costs of <$1/g H_2, achieving the DOE hydrogen storage system metrics for 2015 and 2020.
- Electrochemical alane adduct generation. Implemented a sodium-ion conducting, non-porous membrane as the electric cell separator raising alane-THF adduct formation to 71% with a cathode product formation yield of 99%.
- Alane adduct conversion. Determined that for trans-ligation of THF for another Lewis base (in which the resulting AlH_3-L adduct can be converted to α-AlH_3) the N-ethylmorpholine (NEM) and N,N-dimethylisopropyllamine (N^iPrMe_2) had the highest overall conversion yield, 97% trans-ligation and 20–30% α-alane conversion yield for NEM and 70% trans-ligation and 20–40% α-alane conversion yield for N^iPrMe_2.
- Electrolyte regeneration. Showed that electrochemically generated, recovered cathode product could be converted to electrolyte salt with additional aluminum derived from de-hydrided alane under elevated H_2 pressure and temperature. The regeneration yield was 92% after only 18 h.
- Hydrogen storage system performance. The alane fuel storage system energy densities based on the H_2 produced were:
  - 0.98 kWh/kg (target was 1.0 kWh/kg)
  - 1.26 kWh/L (target was 1.3 kWh/kg)

✧ ✧ ✧ ✧ ✧

TABLE 1. Progress towards Meeting Technical Targets for Hydrogen Storage

Storage System Costs			Chemical Route [1,2]	Electrochemical Route [3]	
				Baseline [1,4]	Cathode Recycle [1]
			Commercial Scale	(80% AlH_3 from R1)	(80% AlH_3 from R1, 80% $LiAlH_4$ regenerated)
Alane Fuel Costs		$/kg alane	112	82	50
Cartridge Cost		$/kg alane	53	53	53
Total		$/kg alane	165	135	103
Storage System Cost		**$/g H_2**	**1.79**	**1.47**	**1.12**
DOE Metrics		**$/g H_2**	**Target Met?**	-	-
Low Power	**2015**	3	Y	Y	Y
	2020	1	N	N	N
Medium Power	**2015**	6.7	Y	Y	Y
	2020	3.3	Y	Y	Y

[1] Chemical and electrochemical route productions costs are for a 320 MT/y process.
[2] Commercial scale estimate provided by industrial partner.
[3] Assumes 90% electrochemical utilization of NaAlH4 and 90% adduct conversion.
[4] Baseline (Anode Reactions): (**R1-80%**) $3\ LiAlH_4 + Al_{metal} \rightarrow 4\ AlH_3 + 3\ Li^+ + 3\ e^-$, (**R2-20%**) $LiAlH_4 \rightarrow AlH_3 + 1/2H_2 + Li^+ + e^-$

INTRODUCTION

This project is developing improvements to the Savannah River National Laboratory lab-scale electrochemical synthesis of alane and Ardica-SRI chemical downstream processes that are necessary to meet DOE cost metrics and transition alane synthesis to large scale production. These modifications are focused on critical cost-saving design improvements.

APPROACH

To develop synthesis technology to reduce the cost of α-alane to <$5/kg, the approach is to transition a bench-scale electrochemical route to alane to an electrochemical process that will be more conducive and economical for large-scale alane production. Specifically, we focus on a continuous synthesis/regeneration reactor and process design that ideally only requires low-cost elemental aluminum (preferably spent alane) and hydrogen as input. This approach could greatly reduce fuel costs and accelerate the commercial acceptance of the alane-based fuel-cell technology. The cost of alane produced by the electrochemical route (Table 1) translates to a storage system costs of <$1/g H_2, achieving the DOE H_2 storage system metrics for 2015 and 2020 for both low and medium portable power. The longer-term goal of the project is to reduce the cost of the initial alane charge to $4/kg and the recycling cost to $2/kg. This will result in hydrogen costs that are competitive with the cost of gasoline.

RESULTS

During Phase 3, updates were made to the process and economic models for the electrochemical route for the synthesis of α-alane. The costing included detailed estimates for material and utilities requirements and capital and manufacturing costs. The updated cost table above shows alane fuel costs associated with the chemical route (pilot plant and 320 MT/yr scale) and different developmental stages of the electrochemical process. The electrochemical alane production cost is estimated to be <$82/kg alane at 320 MT/year and an estimated storage system cost of <$1.47/g H_2 for the worst-case scenario.

Alane Manufacturing Cost: Process Yield Sensitivity

A major thrust of the current phase of this project was a determination of the likely yields of the various steps involved in the electrochemical process for alane. We have modeled process yield sensitivities for production at the 320 MT/y scale. At the outset, we have focused on the yields of three key elements of electrochemical alane production: $NaAlH_4$ utilization, adduct conversion, and $NaAlH_4$ regeneration.

Figure 1 shows our estimates of the cost-yield sensitivities for the three processes. In each case, a single sensitivity is plotted at the constant, nominal values of the remaining quantities. For reference, if nominal value of these quantities is chosen to be 90%, 90%, and 80%, respectively, the alane cost is predicted to be approximately $50/kg at scale.

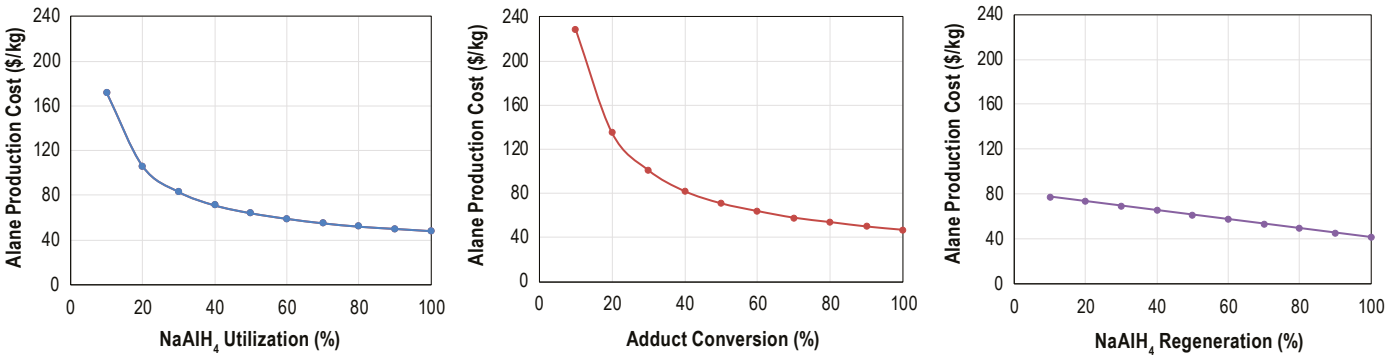

FIGURE 1. Cost-yield sensitivities for three aspects of alane production

High Current Density Electrochemical Alane Adduct Generation

Thermodynamically, the soluble alane adduct formed at the anode in the electrochemical cell design is predicted to react with any electrically-disconnected, solid Na_3AlH_6 or NaH present on the cathode which it encounters to regenerate the adduct-stabilized, soluble $NaAlH_4$ electrolyte.

Cells of the following general design: (-) Al (1 cm^2)/1.3 M $NaAlH_4$ in THF/separator/1.3 M $NaAlH_4$ in THF/Al (approx. 24 cm^2) (+) were operated at 100 mA cm^{-2} referred to the anode area with a variety of porous separators. The highest yield of recovered alane-THF adduct, 61% referred to the total charge passed, was obtained with a 1–1.6 µm pore diameter, porous silica separator. Cells with less restricted anolyte/catholyte separations resulted in lower adduct yields. In recent work, a sodium-ion conducting, non-porous membrane was used as the separator. In this case, the adduct formation yield rose to 71% with a cathode product formation yield of 99%.

Conversion

The conversion of Lewis acid-base adducts of alane (AlH_3-L) into α-AlH3 is determined in part by the strength of the Al-L interaction. A strong Al-L interaction requires forcing conditions for the conversion and can lead to AlH_3 decomposition, whereas weak binding leads to instability of the AlH_3-L adduct. Our studies found that the $MAlH_4$/THF (M = Li or Na) electrolyte is better suited for the electrochemical synthesis of AlH_3-L due to its greater electrical conductivity compared to $LiAlH_4/Et_2O$. However, the use of the $MAlH_4$/THF electrolyte generates AlH_3-THF, which is not known to convert to α-AlH_3.

We reasoned that post-electrosynthetic trans-ligation of THF for another Lewis base may be a promising synthetic strategy. We have characterized trans-ligation yields from alane-THF adduct and yields of adduct conversion to α-AlH_3 for several promising ligands. Our studies were performed in collaboration with Savannah River National Laboratory, which has been calculating the Al-L interaction free energy using density functional theory methods on the national laboratory's computing resources. Among the tested ligands NEM and N^iPrMe_2 had the highest overall conversion yields, 97% trans-ligation and 20–30% alpha alane conversion yield for NEM and 70% trans-ligation and 20–40% alpha alane conversion yield for N^iPrMe_2.

Electrolyte Regeneration

In addition to electrochemical alane-adduct isolation and subsequent conversion efficiencies, the efficiency of electrolyte salt ($MAlH_4$, where M = Li or Na) regeneration from the electrochemical cathode product, and supplemental aluminum and hydrogen, is an important component of the overall alane production cost reduction strategy. Using a high-pressure Parr reactor we have evaluated $NaAlH_4$ regeneration yields from aluminum and cathode reaction products generated at 100 mA/cm^2 current density.

In the most promising experiment, we have shown that electrochemically generated, recovered cathode product could be converted to electrolyte salt with additional aluminum derived from de-hydrided alane under elevated H_2 pressure and temperature. The regeneration yield was 92% after only 18 h. This result clearly indicates that cost-effective electrolyte regeneration may be achievable on a commercial scale.

CONCLUSIONS AND UPCOMING ACTIVITIES

- Design, fabricate, and test a scalable electrochemical cell that builds on our experience with the H-cell that optimizes electrode kinetics, enables high-current, and hence high-throughput operation.
- Optimize solvent swap methods for complete separation of alane adduct from the concentrated $NaAlH_4$ based electrolyte. Optimize thermal conversion to α-alane from amine adducts using crystallization aides and heating profiles.

SPECIAL RECOGNITIONS & AWARDS/ PATENTS ISSUED

The following patents or inventions were reported to DOE:

1. 7260US, Use of Fluidized-Bed Electrode Reactors for Alane Production.

2. 7369PRV, Alane Production in an Electrochemical Process Utilizing Li Battery Cathode.

3. Invention-Capillary Flow Cell for Use with Resistive Electrolyte for Alane Production.

IV.D.1 Conformable Hydrogen Storage Coil Reservoir

Erik Bigelow
Center for Transportation and the Environment
730 Peachtree Street, Suite 760
Atlanta, GA 30308
Phone: (404) 376-5390
Email: erik@cte.tv

DOE Manager: Katie Randolph
Phone: (240) 562-1759
Email: Katie.Randolph@ee.doe.gov

Contract Number: DE-EE0006967

Subcontractors:
- High Energy Coil Reservoirs, LLC (HECR) Fort Wayne, IN
- The University of Texas at Austin Center for Electromechanics, Austin, TX
- Stan Sanders, Technical Expert, Fort Wayne, IN

Project Start Date: September 1, 2015
Project End Date: December 31, 2017

Overall Objectives

- To develop and demonstrate a conformable, lightweight, 700 bar gaseous hydrogen storage system with nominal capacity of approximately 1 kg.

Fiscal Year (FY) 2017 Objectives

- Identify suitable resins for the pressure vessel.
- Build and test pressure vessel prototypes.

Technical Barriers

- Resin selection that offers low permeability, flexibility, durability, impact resistance and thermoplastic (extrusion) performance.

This project addresses the following technical barriers from the Hydrogen Storage section of the Fuel Cell Technologies Office Multi-Year Research, Development, and Demonstration Plan.

(A) System Weight and Volume

(B) System Cost

Technical Targets

This project seeks to address the high cost of conventional gaseous 700 bar hydrogen storage, as well as the overall weight of the hydrogen storage system. Although this project will not improve the volumetric efficiency of gaseous storage, the pressure vessel design should allow a more flexible on-vehicle packaging than a conventional rigid cylinder. Possible tank layouts could optimize the use of areas in the same way that current gasoline tanks are molded to best use available space. Using HECR's pressure vessel technology for hydrogen storage promises to provide breakthroughs in commercially available pressure vessel costs, conformability, and weight.

There are additional project requirements for system selection:

- Low hydrogen leakage (<0.05 g/h-kg H_2 stored at 700 bar)
- Operational temperature limit (-40°C ≤ T ≤ 85°C)
- Corrugation process compatibility (i.e., needs to be process compatible, range of viscosity, melt temperature, and durometer)
- Burst pressure exceeding 2,170 bar

FY 2017 Accomplishments

- Revised braid design led to vessels that met a 10,000 psi burst pressure.
- A single high pressure burst test was conducted, with the burst occurring at over 33,000 psi, which meets Department of Transportation pressure vessel

TABLE 1. Progress towards Meeting Technical Targets for Hydrogen Storage

	DOE Projections for Type IV 700 bar Storage at 500,000 units/yr	DOE 2017 Target	DOE Ultimate Target	Proposed Project Vessel	Current Project Vessel
Gravimetric Capacity	1.5 kWh/kg (4.5 wt% H_2)	1.8 kWh/kg (5.5 wt% H_2)	2.5 kWh/kg (7.5 wt% H_2)	3.7 kWh/kg (10.0 wt% H_2)	Testing not complete
Volumetric Capacity	0.8 kWh/L (24 g H_2/L)	1.3 kWh/L (40 g H_2/L)	2.3 kWh/L (70 g H_2/L)	0.7 kWh/L (20 g H_2/L)	Testing not complete
Cost	$17/kWh ($570/kg H_2 stored)	$12/kWh ($400/kg H_2 stored)	$8/kWh ($267/kg H_2 stored)	$8.40/kWh ($280/kg H_2 stored)	Testing not complete

requirements for 700 bar (10,000 psi) nominal working pressure.

- Confirmed performance of leak test equipment with agreement between pressure lost from test sample to pressure rise in containment chamber using preliminary test vessels.

✧ ✧ ✧ ✧ ✧

INTRODUCTION

This project consists of four project partners: Center for Transportation and the Environment, project prime recipient responsible for project management; HECR, intellectual property owner; The University of Texas Center for Electromechanics, responsible for permeability testing and resin technical information; and Stan Sanders, technical expert.

The overall goal of this research and development project is to develop an approach for compressed hydrogen gas storage that will provide a cost-effective and conformable storage solution for hydrogen. The team will develop and demonstrate a conformable, lightweight 700 bar gaseous hydrogen storage system with a nominal capacity of approximately 1 kg. The nature of the HECR's technology allows for a higher capacity pressure vessel to be constructed simply by creating a longer vessel through the same process.

APPROACH

The hydrogen storage system development will occur over two budget periods beginning with an initial design, including candidate resin down selection and over-braid final development. The design includes overwrapping an extruded thermoplastic elastomeric resin liner with high performance Kevlar™. The team will then build test vessels and perform key testing to validate the suitability for hydrogen containment. This testing will include hydrostatic burst testing, hydrostatic pressure cyclic testing, and hydrogen permeability testing conducted on a number of resin liners.

RESULTS

Since the 2016 annual report, multiple hydrogen pressure vessels have been tested. Several vessels were built using an ethylene vinyl alcohol (EVOH) resin provided by the resin manufacturer Kuraray. The resin was able to adequately bend for manufacturing (Figure 1) using hot water to form the vessels. Using this hot water forming, HECR was able to build and test a hand-wrapped Kuraray cores with a proprietary tensile fiber for high pressure testing. The original end fittings split and burst at 34,000 psi, which exceeded the burst pressure requirement of 31,000 psi. This test indicates that there is a good likelihood that a conformable pressure vessel that meets Department of Transportation burst specifications at half the weight of a conventional hoop wound cylinder can be built.

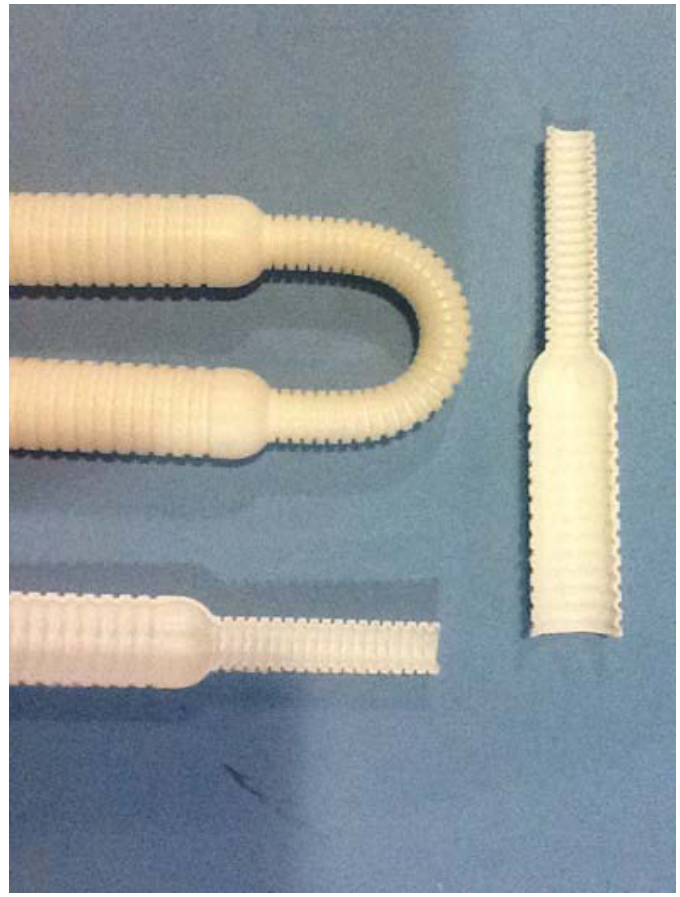

FIGURE 1. Initial EVOH cores and core section

Center for Electromechanics tested several iterations of the hydrogen storage vessels with a Hytrel resin material for the core liner. The initial tests were found to have high leak rates due to inadequate end fittings. Once the end fittings were improved and determined to be leak-free, Center for Electromechanics conducted two leak tests: one at 1,000 psi and one at 1,800 psi (Figure 2). In both cases, the leak rate did not meet the goals of the program. The 1,000 psi test leaked over 100 psi in less than 21 h, resulting in a 0.6 g/h-kg H_2 leak rate, while the 1,800 psi test leaked 200 psi in 23 h, resulting in a 0.6 g/h-kgH_2 leak rate. This was expected as the initially tested resin, Dupont Hytrel, was selected for process compatibility and to confirm the testing process while the material selection was on going.

The project team explored additional resins to examine if there were other possibilities that were both manufacturing-process compatible, and compatible with the flexibility requirements of the conformable vessel. This is a challenge because the least permeable resins are typically stiff and brittle, with a high crystallinity. For this prototype to work,

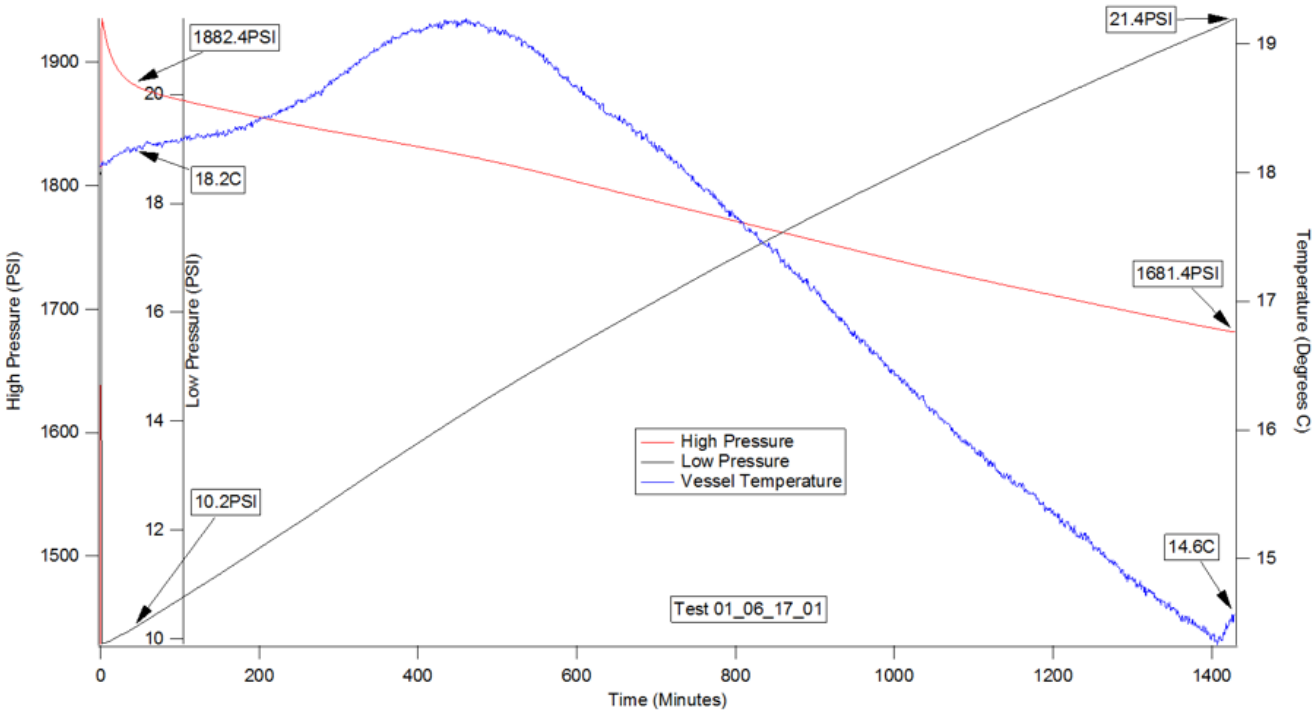

FIGURE 2. Example permeability data results

the vessel requires the highest permeability resistance to hydrogen available. Even with these high performance resins, a wall thickness of 20–40 thousandths may be required. This is at odds with the assembly flexibility required, where the vessel must bend 180° at the narrow body section, as well as undergo repeated expansion and contraction cycles during filling.

The team also planned to create hydrogen storage vessels with Kuraray-based resin cores, but the initial core production tests with the Kuraray resin have not been compatible with the manufacturing process. Kuraray provided a stiff and flexible EVOH formulation for testing, hoping one would be compatible with the manufacturing process. The stiff resin was too brittle, shattering easily, and the flexible resin had little to no resiliency, and tore easily. During Spring 2017, the manufacturing subcontractor was able to blend the two resins together, and arrive at core samples which meet the minimum flexibility requirements of the internal cores, which allows the cores to be bent 180° to allow a tight packing of vessels once the over-braiding is complete. These flexible cores are shown in Figure 3.

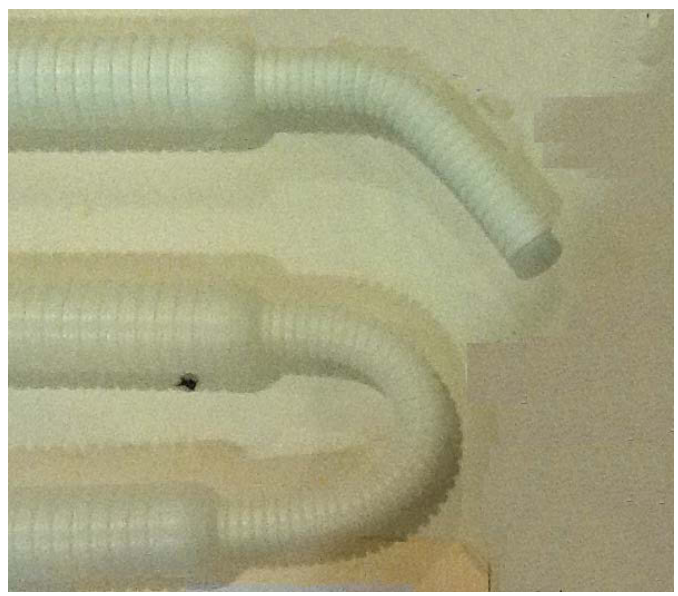

FIGURE 3. Blended EVOH core with greater flexibility

CONCLUSIONS AND UPCOMING ACTIVITIES

The project team currently has the new, more flexible, vessels in hand and is preparing to complete the over-braiding with a proprietary tensile fiber. When this is complete, the vessels will be sent to Center for Electromechanics for permeability testing. Additional burst testing to determine if the 31,000 psi burst pressure requirement can be met with a machine over-wrapped pressure vessel will be conducted. Meeting the project permeability goal, as well as the 31,000 psi pressure are the two key targets for the go/no-go determination to progress to Budget Period 2.

IV.D.2 Next Generation Hydrogen Storage Vessels Enabled by Carbon Fiber Infusion with a Low Viscosity, High Toughness Resin System

Brian Edgecombe
Materia, Inc.
60 N. San Gabriel Blvd.
Pasadena, CA 91107
Phone: (626) 584-8400, Ext. 210
Email: bedgecombe@materia-inc.com

DOE Manager: Jesse Adams
Phone: (720) 356-1421
Email: Jesse.Adams@ee.doe.gov

Contract Number: DE-EE0006625

Subcontractors:
- Montana State University, Bozeman, MT
- Spencer Composites Corporation, Sacramento, CA

Project Start Date: August 1, 2014
Project End Date: November 30, 2017

Overall Objectives

The project is focused on supporting the key DOE metrics for a 700-bar, Type IV tank by meeting the following objectives:

- Reduce the carbon-fiber (CF) composite volume by 35%.
- Demonstrate cost of composite materials of $6.5/kWh. This component cost is an important element of the DOE 2020 system cost target of $10/kWh.
- Demonstrate industry-standard performance (burst strength of 1,575 bar and 45,000 cycle life).

Fiscal Year (FY) 2017 Objectives

- Manufacture large tanks with more efficient usage of CF and an overall reduction in CF.
- Optimize new process technique for larger (>30 L) tanks to demonstrate scalability.
- Conduct key tests related to burst strength and drop testing to confirm performance meets current standards.

Technical Barriers

This project addresses the following technical barriers from the Hydrogen Storage section of the Fuel Cell Technologies Office Multi-Year Research, Development, and Demonstration Plan.

(A) System Weight and Volume

(B) System Cost

(D) Durability/Operability

(G) Materials of Construction

Technical Targets

The project is focused on the technical targets highlighted in Table 1 related to the gravimetric and cost metrics of onboard automotive hydrogen storage systems. Since a significant portion of the cost is directly from the CF composite overwrap, the project aims to reduce the amount of composite necessary to meet the tank specifications. During FY 2016 and 2017, the project has met some key milestones to provide an updated estimates on the progress towards the technical targets in Table 1.

TABLE 1. Progress towards Technical Targets for Onboard Automotive Hydrogen Storage System

Characteristic	Units	2020 Target	Current Project Estimates
Gravimetric	kWh/kg sys	1.5	1.6 to 1.8 Estimated*
System Cost	$/kWh at 500,000 units/yr	10	9 to 10.5 Estimated*

*Estimates based on assumptions of 30% and 15% CF reduction

FY 2017 Accomplishments

- Designed and installed processing vessel and associated systems for material transfer and heating.
- Demonstrated improvements in total processing time including preparation, infusion, oven-curing, and clean-up for high-quality 7.5 L prototype vessels.
- Demonstrated ability to prepare 37 L tanks (11-in diameter) and larger tanks.

✧ ✧ ✧ ✧ ✧

INTRODUCTION

DOE Office of Energy Efficiency and Renewable Energy has established aggressive performance targets for Type IV hydrogen storage vessels for Year 2020. Current designs

and materials of construction for composite-overwrapped pressure vessels (COPVs) within the industry do not reach the performance targets, as shown by the base-case published by Ahluwalia et al. from Argonne National Laboratory. The specialty chemical producer, Materia, has developed a novel composite resin system, Proxima®, with ultra-low viscosity (5 cP to 10 cP) that enables vacuum infusion processing for thick CF composite components. The use of this process with Proxima circumvents some challenges inherent with traditional wet filament winding, such as the presence of voids and dry spots. The use of vacuum infusion processing, also known as vacuum-assisted resin transfer molding, for fiberglass composite parts is commonplace in several large-scale industries (marine, wind blades), but the feasibility of vacuum-assisted resin transfer molding for compressed gas vessels is not clear. While the concept of infusing dry-filament wound structures has been mentioned in the open literature, the small inter-fiber gaps associated with high-performance CF composites potentially presents significant processing difficulties. Therefore, the commercial application of this approach appears to be limited, which may be related to traditional resins possessing viscosities >200 cP.

In addition to reducing void content, Proxima-based composites also have significantly improved fracture toughness (>3x higher interlaminar fracture toughness) and fatigue performance over currently employed composites for hydrogen storage tanks. The project seeks to leverage this combination of tough resin and new processing to produce CF composite overwrap with better performance, especially in fatigue and damage-tolerance testing. These high performing composites will enable the reduction of the quantity of CF composite overwrap, which alone can account for over 75% of the storage tank system cost. The processing-related costs for this new approach are expected to be similar to current processing costs with wet winding. By reducing the CF composite content in COPVs by 35%, the project aims to reduce the cost and weight of COPVs and contribute to meeting the DOE 2020 cost target of $10/kWh.

APPROACH

Since the project requires an expertise in a variety of fields, the project team includes Spencer Composites Corporation and Hypercomp Engineering to provide the specialized filament-winding activities. Montana State University in Bozeman will experimentally characterize composite materials and also use finite element analysis models to anticipate problem areas in tanks designs. Materia is leveraging its experience in infusion process optimization with low-viscosity resin (<10 cP) to demonstrate a series of prototype parts, including tanks and model flat plates of filament wound composites. In order to manage the risks associated with a new resin and a new process for COPVs, the project activities have been divided into stages and the objectives (1) process optimization, (2) COPV design, (3) design optimization, and (4) scale-up of process for vessel testing.

RESULTS

During FY 2017 the team focused on the design and implementation of a simpler, scalable process technique which takes advantage of resin infusion without the use of traditional vacuum bagging film. Also, during this period the emphasis was placed on producing larger tanks for testing. For the new process technique, the team had previously demonstrated the process in proof of concept experiments by making a few high quality dry-wound parts including a 7.5 L vessel, all from dry-wound forms. The new process is similar to a commercially practiced technique called vacuum pressure infusion.

The schematic in Figure 1 outlines the basic elements of the new process equipment which has similarities to a simple autoclave design used for some aerospace composite parts. First, the dry-wound COPV is secured inside a resin confinement vessel which is sized slightly larger than COPV diameter. Next, the resin-confinement vessel is placed into the pressure vessel to make the final assembled pressure vessel with nested COPV/resin confinement vessel. The schematic in Figure 2 outlines the basic steps of the new process. After the resin/curative mixture is prepared, the resin is vacuum transferred into the center vessel for infusion of the COPV. After complete infusion, excess resin is removed and hot air is introduced to cause preliminary curing to achieve ~70% degree of cure. After this is achieved, the tank can be removed easily and placed in the oven for complete curing.

The equipment has been commissioned using a 7.5 L tank and then a 37 L tank. Currently, tanks are being produced for testing of burst strength and drop testing. For the remaining period of the project, the focus will remain on the continued production and testing of larger Type IV tanks (37 L and 133 L) with lower levels of CF in the tanks. In parallel to the process development activities, the use of an alternative CF (Mitsubishi Grafil tow with 800 ksi strength) was studied in 7.5 L tanks but the Grafil fiber appears to require further optimization to avoid damage during processing.

CONCLUSIONS AND UPCOMING ACTIVITIES

From the current results of the project, the team has derived the following conclusions:

- Preparation of small COPV (Type III, 7.5 L) and larger 37 L COPV can achieve complete resin infusion within 30 min.

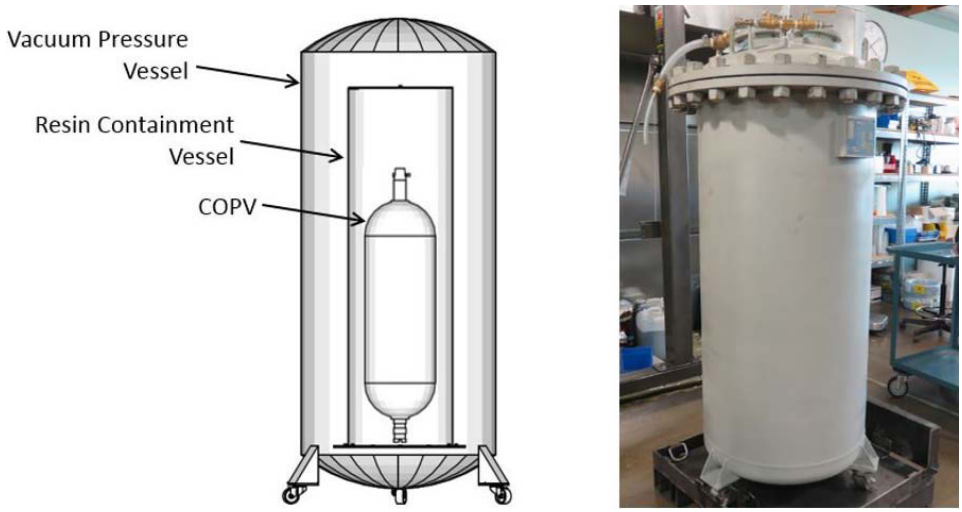

FIGURE 1. Nested arrangement of dry-wound COPV inside a resin containment vessel which is inside a vacuum pressure vessel. Photo of processing pressure vessel positioned under the gantry crane during preliminary test trials.

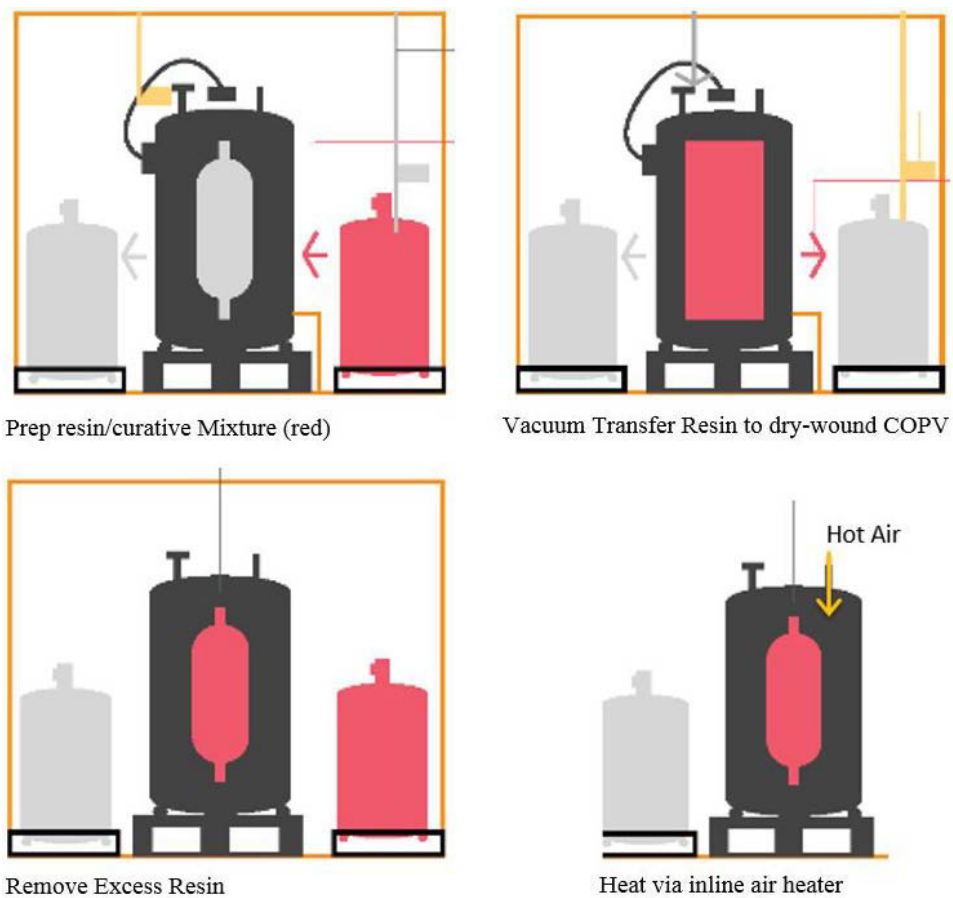

FIGURE 2. Schematic of the process steps for vacuum pressure infusion processing followed by heat curing using forced hot air.

- Demonstration of new process technique suitable for tank series manufacturing.

The following activities will be the area of focus in the future:

- Produce larger COPVs for testing purposes and as a demonstration of the compatibility for series manufacturing.
- Update current cost model of tanks based on design and processes (Figure 3).
- Generate key performance data including drop-testing larger vessels with lower CF content.

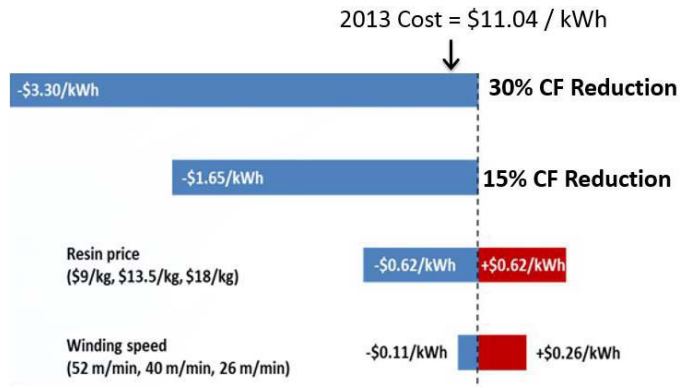

FIGURE 3. Updated sensitivity analysis of COPV cost based on preliminary processing and design estimates. The arrow denotes a 2013 baseline cost of $11.03/kWh before any CF reductions. (Analysis performed by Strategic Analysis, Inc.).

IV.D.3 Development, Selection and Testing to Reduce Cost and Weight of Materials for BOP Components

Chris San Marchi (Primary Contact),
Jonathan Zimmerman
Sandia National Laboratories
7011 East Avenue – MS 9161
Livermore, CA 94550
Phone: (925) 294-4880
Email: cwsanma@sandia.gov

DOE Manager: Ned Stetson
Phone: (202) 586-9995
Email: Ned.Stetson@ee.doe.gov

Subcontractor:
Hy-Performance Materials Testing LLC, Bend, OR

Project Start Date: July 15, 2014
Project End Date: March 31, 2018

Overall Objectives

- Reduce weight of structural stainless steels for balance of plant (BOP) components by 50%.
- Reduce cost of structural stainless steels for BOP components by 35%.
- Expand the technical basis for selecting a diverse set of austenitic stainless steels for materials of construction in BOP components.
- Identify simplified testing procedures to enable materials qualification.

Fiscal Year (FY) 2017 Objectives

- Assess fatigue strength, material weight and cost of several engineering alloys in a representative hydrogen environment, including a technologically relevant gall resistance austenitic stainless steel and a low-Ni, high-strength austenitic stainless steel.
- Evaluate consistency of reduced-order model of stacking fault energy with first-principles calculations.
- Develop publicly accessible framework for visualization of computation output (both reduced order models and results from first principles calculations) and other relevant metrics such as cost and nickel equivalent.
- Document the technical basis for selection of materials that satisfy the targets of this program in the context of fatigue performance, as well as a user manual for the web-based design tool.

Technical Barriers

This project addresses the following technical barriers from the Hydrogen Storage section of the Fuel Cell Technologies Office Multi-Year Research, Development, and Demonstration Plan:

(A) System Weight and Volume

(B) System Cost

(H) Balance-of-Plant (BOP) Components

Technical Targets

No specific technical targets have been set. This project is a basic study of materials of construction for BOP with the goals of identifying lower-cost alternatives to the baseline of annealed Type 316L that can be implemented in lighter-weight designs. The project targets are:

- Reduce weight of structural stainless steels for BOP components by 50%.
- Reduce cost of structural stainless steels for BOP components by 35%.

FY 2017 Accomplishments

- Several low-nickel alloys have been shown to have similar fatigue performance in gaseous hydrogen as the benchmark material, Type 316/316L austenitic stainless steel, for relevant allowable design stresses.
- Several high-strength alloys have been shown to display similar fatigue performance in gaseous hydrogen as the benchmark material, Type 316/316L austenitic stainless steel, but at higher applied stress.
- Estimated component weight and cost savings from alloys with the combination of low nickel composition and high strength can be greater than 50% and 40% respectively, and could be as high as 70% and 60% in some cases.
- A web-based, user-friendly (and expandable) design tool has been developed for visualization and multi-variable optimization of compositionally-derived materials characteristics, such stacking fault energy, martensite transformation temperature, nickel equivalent and cost. The tool allows calculation of materials characteristics from reduced order models, or interpolation from databases of first principles calculation results.
- More than 4,000 alloy compositions have been screened for stacking fault energy and incorporated into the alloy design tool.

✧ ✧ ✧ ✧ ✧

INTRODUCTION

The primary objective of this effort is to identify alloys to replace Type 316/316L in hydrogen service for BOP applications onboard fuel cell electric vehicles. Type 316/316L austenitic stainless steels are used extensively in hydrogen systems for their resistance to hydrogen embrittlement, which is attributed to the relatively high nickel content of Type 316/316L alloys. Nickel content, however, drives the cost of austenitic stainless steels, thus Type 316/316L alloys impose a cost premium compared to similar alloys with lower nickel content. Since the cost of BOP components is a large fraction of the cost of hydrogen fuel systems (even dominating the cost at low production volumes [1]), alternative materials are desired. In addition, Type 316/316L alloys are relatively low strength, thus high-pressure components tend to be heavy to accommodate the stresses associated with the pressure loads. Higher-strength materials enable reduction of weight of BOP components and contribute to lower cost since less material is needed. However, engineering data to justify selection of lower cost and higher strength alloys for high-pressure hydrogen service are currently unavailable.

Additionally, high-throughput computational materials science has evolved to a level of sophistication that large databases of composition can be screened based on knowledge of sensitive performance metrics. While first-principles prediction of fatigue performance is still beyond the capability of computational materials science, many intrinsic behaviors of alloys can be predicted from first principles. This effort uses stacking fault energy, which can be calculated, as an indicator of resistance to hydrogen embrittlement to screen large compositional space. Databases of these calculations are combined into an interactive tool where a user can assess multiple compositionally-sensitive attributes to design new alloy compositions. In this case, alloy compositions that optimize cost and hydrogen resistance (through the stacking fault energy indicator).

APPROACH

The objective of this project is addressed from two perspectives: (1) experimental evaluation of commercial alloys and (2) computational materials discovery of new alloys. In the first case, fatigue properties in hydrogen environments are evaluated for low-cost, high-strength alloys and compared to the benchmark of annealed Type 316/316L. The test program seeks appropriate trade-offs between materials cost and performance, such that hydrogen embrittlement can be effectively managed in design for BOP components onboard fuel cell vehicles where the anticipated number of refuelings is significantly less than 10^4 pressure (fatigue) cycles. Performance includes fatigue at low temperature associated with refueling protocols at -40°C; the effect of hydrogen on fatigue as a function of temperature has not been previously reported. An additional goal of the experimental activity is to demonstrate a straightforward, simplified methodology by which materials may be qualified for safe hydrogen service, including the use of internal hydrogen (saturation of the material with hydrogen by thermal precharging) as a robust substitute for testing in gaseous hydrogen.

The goal of the computational discovery activity, like the experimental activity, is to identify low-Ni content (and thus lower cost) stainless steel alloys for use in BOP components. To achieve this goal from a computational perspective, a framework has been developed to screen compositionally-derived characteristics of austenitic stainless steels in relevant trade spaces. Screening can be performed based on optimization of cost and performance metrics and can be expanded to include additional materials characteristics. The evaluation framework uses databases of performance metrics based on stacking fault energy (an indicator of resistance to hydrogen) derived by either a reduced-order thermodynamic model or ab initio calculations. This effort represents a new initiative in the DOE Fuel Cell Technologies Office research portfolio to use computational materials science coupled with high-performance computing to aid materials development. This innovative approach will provide the DOE and U.S. industry with a framework and computational tools to efficiently and effectively explore the design space for next-generation materials used in fuel cell technologies.

RESULTS

Materials Selection and Fatigue Characterization

The fatigue behavior of a diverse range of austenitic stainless steels have been characterized in several hydrogen environments. The tested alloys include high-strength conditions of common 304L and 316L austenitic stainless steels; a high-strength, low-nickel austenitic stainless steel used for heat exchanger tubes (XM-11); a gall-resistant austenitic stainless steel in a high-strength condition (Nitronic 60); and a nitrogen-strengthened, low-nickel austenitic stainless steel for resistance to rotating fatigue (SCF-260). Table 1 provides the strength and major alloying elements for the tested alloys.

Weight and cost savings of the tested alloys were estimated by considering a cylindrical shell using the minimum required wall thickness according to the ASME code for Hydrogen Piping and Pipelines (ASME B31.12). The maximum allowable stress in the wall thickness calculation is 1/3 of the minimum specified tensile strength (or 2/3 of the yield strength, whichever is lower) from relevant materials specifications. The weight reduction of a given alloy represents the difference between the alloy and the annealed 316L benchmark. The cost reduction is realized by using less material (proportional to weight) and by assuming the

material cost per kilogram is proportional to the sum of the nickel content and half of the manganese content. As shown in Table 1, the upper bound weight and cost savings are projected to be greater than 50%.

The projected cost and weight savings are substantial, but the simple analysis assumes that the fatigue limit in hydrogen is greater than the allowable stress; in other words, the design stress is limited by the characteristic strength of the alloy and not by the fatigue performance. Prior to this study, there was no available fatigue life data for high-strength austenitic stainless steels in gaseous hydrogen. Additionally, the effects of hydrogen on fatigue at low temperature was largely unknown. In general, the fatigue life of austenitic stainless steels at room temperature is relatively insensitive to pressure (Figure 1). Moreover, the fatigue life in gaseous hydrogen at pressure of 10 MPa at low temperature was found to be greater than the fatigue life at room temperature (for the same applied stress; Figure 2). Nitronic 60 is the only exception to these trends, but still displays a fatigue life similar to the other alloys for allowable stresses greater than 300 MPa. While the combination of high-pressure hydrogen and low temperature remains to be tested, these data suggest that fatigue testing at low temperature may not be necessary to qualify austenitic stainless steels for vehicle applications (if pressure insensitivity is maintained at low temperature). It is important to recognize that all of the data in Figures 1 and 2 represents notched specimens and are conservative relative to conventional smooth test specimens; however, in all cases, fatigue life of more than 10^5 cycles can be achieved for allowable stresses less than 200 MPa, demonstrating infinite life in the vehicle context that is superior to the benchmark of an allowable stress of 115 MPa (i.e., superior to annealed 316L).

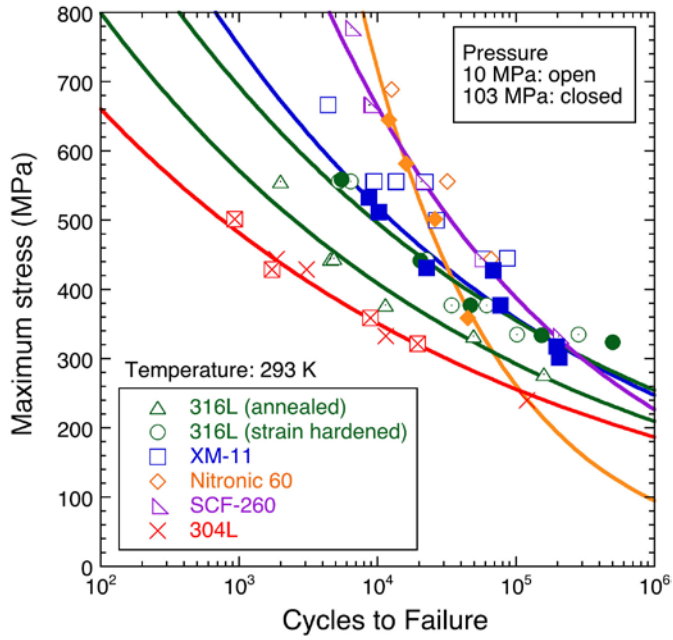

FIGURE 1. Fatigue life curves of notched specimens (K_t ~ 3.9) at room temperature for hydrogen pressure of 10 MPa and 103 MPa show little effect of pressure. Load ratio and frequency are 0.1 and 1 Hz, respectively.

Computational Materials Discovery

While stacking fault energy has been shown to be a first-order screening metric for assessing hydrogen effects on tensile ductility, stacking fault energy is not predictive of tensile properties and does not correlate with fatigue behavior. Stacking fault energy, however, remains an important characteristic of the deformation character of austenitic alloys. The stacking fault energy of more than 4,000 alloy compositions, consisting of Fe, Ni, Cr, Mn, Mo and Si, have been calculated using the coherent potential approximation with density functional theory. The data revealed several alloys with low Ni content and relatively large stacking fault energy. We are currently in the process of expanding the data set to include alloys containing Al and Cu. The general utility of high-throughput calculations, however, is limited without methods to analyze and visualize these data.

To address this limitation, a user-friendly, web-based, materials-screening tool has been developed with the goal of providing an expandable and flexible platform to visualize large data sets and explore empirical metrics (or reduced order models) over large parameter spaces.

TABLE 1. Characteristics of Tested Austenitic Stainless Steels as Well as Projected Weight and Cost Savings (CW = Strain-Hardened to High Strength).

Alloy	Cr (wt%)	Ni (wt%)	Mn (wt%)	N (wt%)	Sy (MPa)	Su (MPa)	Allowable stress (MPa)	Weight savings (%)	Cost savings (%)
316L	17.5	12	1.2	0.04	280	562	115	–	–
CW 316L	17.5	12	1.2	0.04	573	731	218	72	58
CW 304L	18.3	8.2	1.8	0.056	497	721	195	66	65
XM-11	20.4	6.2	9.6	0.26	539	881	207	69	59
Nitronic 60	16.6	8.3	8.0	0.16	880	1,018	218	72	60
SCF-260	19.1	3.3	17.4	0.64	1,083	1,175	333	85	77

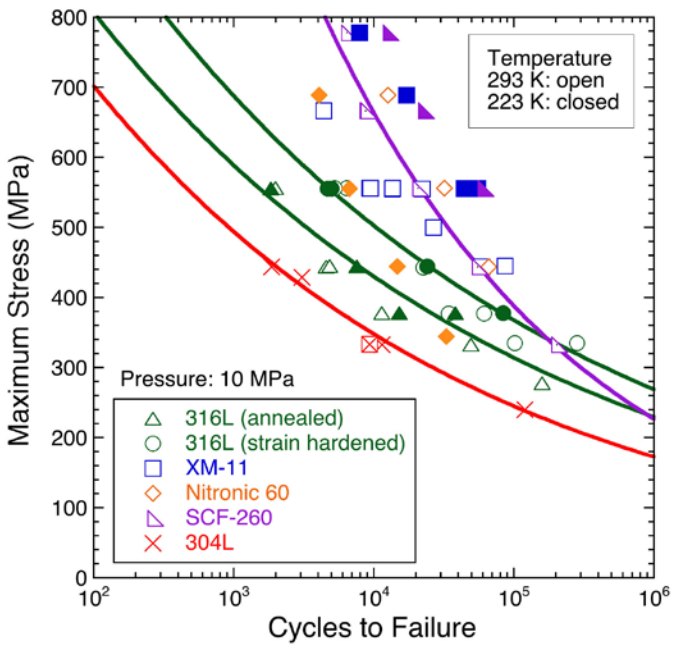

FIGURE 2. Fatigue life curves of notched specimens (K_t ~ 3.9) at hydrogen pressure of 10 MPa and temperature of 223 K and 293 K generally show room temperature represents limiting fatigue performance; Nitronic 60 appears to be a notable exception. Load ratio and frequency are 0.1 and 1 Hz, respectively.

Example output from the tool is shown in Figure 3: a color-contour plot of stacking fault energy in nickel manganese compositional space. In this case, the stacking fault energy is calculated with a reduced-order thermodynamic model. Each of the parameters can be filtered to further screen the parameter space displayed; for example, the plotted data can be restricted to a user-defined compositional range of chromium and/or other elements. The tool is also capable of visualizing other databases of information in the same manner, such as the density functional theory/coherent potential approximation output or any tabular data that exists in a comma-separated values file. In addition to empirical relationships for martensite transformation temperature and nickel equivalent, the tool currently includes also a framework for estimating cost based on the elemental composition. Visualization in this manner enables alloy optimization for parameters of interest as well as parametric studies of variance due to the allowable variation in composition; austenitic stainless steels have large specified compositional ranges (e.g., nickel content in type 316L can vary between 10 wt% and 14 wt% in most public materials specifications).

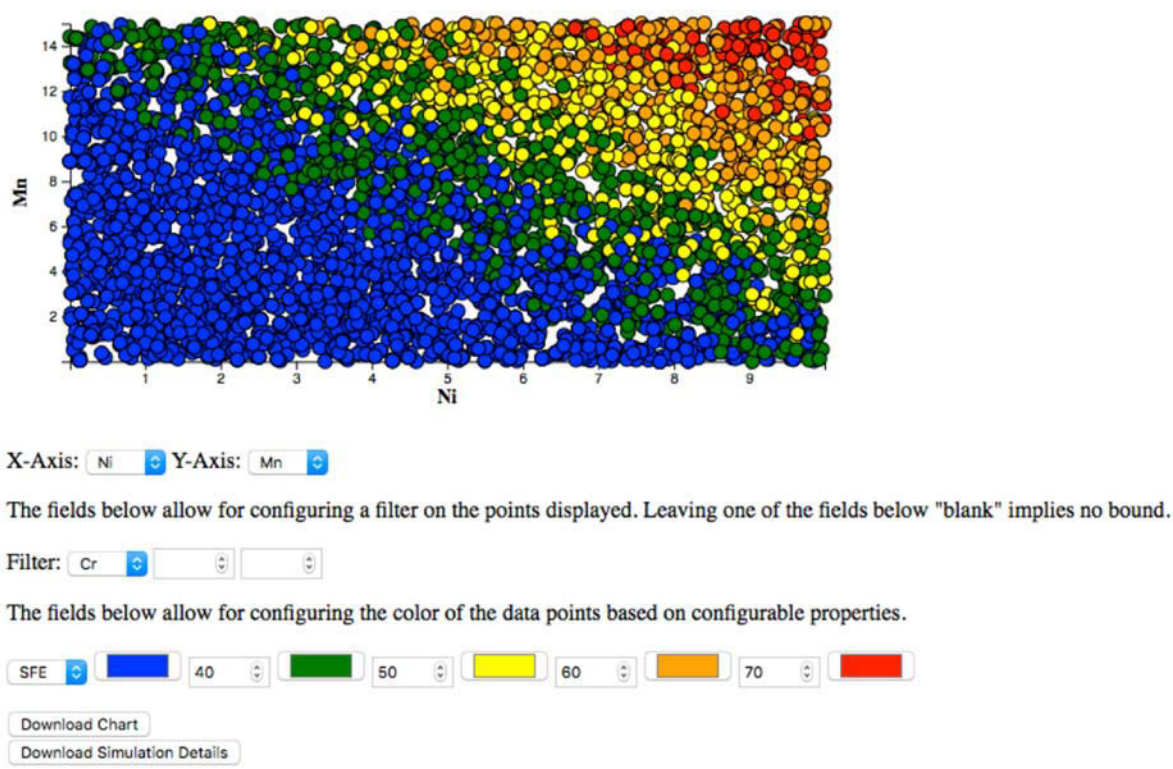

FIGURE 3. Screen-shot of the web-based, materials-screening tool shows color contours representing stacking fault energy plotted in nickel-manganese compositional space.

CONCLUSIONS AND UPCOMING ACTIVITIES

- A diverse range of austenitic stainless steels show acceptable fatigue performance for allowable stresses greater than the benchmark of annealed 316L; in other words, the fatigue life is greater than 10^5 cycles for maximum fatigue stress of 1/3 of the tensile strength (for load ratio of 0.1 and frequency of 1 Hz).
- Potential significant weight savings of more than 60% can theoretically be achieved for a range of alternatives to annealed 316L in BOP components. These weight savings translate to cost savings of more than 50% and potentially in excess of 60% for optimized designs.
- A user-friendly analysis tool has been developed to compare materials metrics based on composition. A database of stacking fault energy from more than 4,000 alloy density functional theory calculations can be probed, or the reduced-order thermodynamic calculation of stacking fault energy can be used as a comparison metric. Other comparison metrics (such as cost, nickel equivalent and martensite transformation temperature) can also be evaluated and other metrics can be added to the flexible alloy comparison tool.
- Testing capability for the combination of high pressure and low temperature is needed to confirm the hypotheses that (i) the limiting fatigue behavior can be established at room temperature (rather than at low temperature) and (ii) limiting behavior can be potentially established at pressure lower than the design pressure.
- Further weight and cost reductions can be achieved in less-conservative, finite-life designs (i.e., designing for higher fatigue stresses). To enable finite-life designs, the foundational mechanisms of hydrogen-assisted fatigue must be better understood and a design framework must be established to quantitatively capture the mechanical behavior of short cracks in hydrogen environments.

FY 2017 PUBLICATIONS/PRESENTATIONS

1. K.A. Nibur, P.J. Gibbs, J.W. Foulk, C. San Marchi: "Notched fatigue of austenitic alloys in gaseous hydrogen," (PVP2017-65978), Proceedings of the 2017 ASME Pressure Vessels & Piping Conference, 16–20 July 2017, Waikoloa, HI.

2. P.J. Gibbs (presenter), P.D. Hough, K. Thuermer, B.P. Somerday, C. San March, J.A. Zimmerman: "Stacking fault energy based alloy identification for hydrogen compatibility," presented at TMS 2017, 26 February–2 March 2017, San Diego, CA.

3. P.J. Gibbs, K.A. Nibur, C. San Marchi: "Plastic ratcheting and fatigue crack formation in austenitic steels with hydrogen," 2016 International Hydrogen Conference, 11–14 September 2016, Moran, WY, paper accepted for publication in proceedings, ASME 2017.

IV.D.4 Integrated Insulation System for Automotive Cryogenic Storage Tanks

Barry Meneghelli (Primary Contact),
David Tamburello, James Fesmire, Adam Swanger
VENCORE Solutions and Services
Kennedy Space Center, FL 32899
Phone: (321) 867-2567
Email: barry.j.meneghelli@nasa.gov

DOE Manager: Jesse Adams
Phone: (720) 356-1421
Email: Jesse.Adams@ee.doe.gov

Contract Number: DE-EE0007649

Subcontractors:
- Aspen Aerogels, Northborough, MA
- Energy Florida, Cape Canaveral, FL
- Hexagon Lincoln, Lincoln, NE
- ITB Inc, Merritt Island, FL
- NASA, Kennedy Space Center, FL
- Savannah River National Laboratory, Savannah River Site, Aiken, SC

Project Start Date: October 1, 2016
Projected End Date: September 30, 2019 – Project continuation/direction determined annually by DOE

Overall Objectives

- Develop integrated insulation system concepts for cold/cryo-compressed hydrogen storage systems.
- Complete preliminary component testing and thermal models.
- Validate system concepts and design a sub-scale prototype.
- Fabricate and test a prototype system.
- Develop a market commercialization plan.

Fiscal Year (FY) 2017 Objectives

- Complete preliminary design for full-scale storage system.
- Down-select potential concept technologies based on system requirements.
- Complete initial component testing.
- Update system concept based on costs.

Technical Barriers

This project addresses the following technical barriers from the Hydrogen Storage section of the Fuel Cell Technologies Office Multi-Year Research, Development, and Demonstration Plan.

(A) System Weight and Volume

(D) Durability/Operability

(G) Materials of Construction

(H) Balance of Plant Components

(J) Thermal Management

(N) Hydrogen Venting

Technical Targets

This project is developing an integrated insulation system for cryogenic automotive tank applications that is designed to meet the following 2020 DOE technical targets.

- Demonstrate a dormancy target time of 7 d (minimum time until first release of hydrogen from initial 95% usable capacity)
- Demonstrate a boil-off loss target of 10% (max reduction in stored hydrogen from initial 95% usable capacity after 30 days)

Project specific targets also include:

- Utilize a full-scale 100 L tank with geometries from 3:1 to 6:1 length-to-diameter
- Demonstrate a heat leak for the overall integrated system ≤7 W under a reduced vacuum of 0.1 torr, assuming an insulation thickness of ≤2.5 cm

FY 2017 Accomplishments

- Identified several potential thermal insulation systems/materials for evaluation as part of the thermal analysis model.
- Completed the initial version of the thermal analysis model.
- Initiated the evaluation of potential aerogel-based insulation materials.
- Identified and obtained potential tanks for evaluation of vacuum retention/stability, permeation, outgassing, and structural–mechanical properties
- Completed the initial cost estimate for a cryo-compressed hydrogen storage system with an insulated

4:1 Type 3 pressure vessel, including the necessary balance of plant components for integration with a light-duty fuel cell vehicle.

✧ ✧ ✧ ✧ ✧

INTRODUCTION

Cryo-compressed and cryo-adsorption are two leading candidate technologies for storing hydrogen onboard light-duty vehicles. The technical hurdles hindering the application of these technologies are simultaneously achieving high volumetric density, high gravimetric density, and low loss of useable hydrogen while the vehicle is not in use. The primary cause of loss of useable hydrogen in cryogenic systems is through heat ingress and the resultant rise in hydrogen pressure requiring activation of a pressure relief device. While multi-layer vacuum insulation (MLI) may be able to achieve the ≤7 W heat leak required for these systems, the maintenance of very high vacuum levels would require frequent evacuation, a cost element which may not be supportable by the commercial automobile industry. The objective of this effort is to develop an integrated insulation system that would utilize low maintenance, lightweight, inexpensive insulation.

APPROACH

The initial approach to this project involves data mining of the cryostat libraries at the Cryogenics Test Laboratory (CTL) to identify potential insulation systems that can meet or exceed the project's target heat leak of ≤7 W and evaluation of commercially available insulation material. Part of the evaluation process for these insulation systems/materials will be to narrow the search to those candidates that are best suited to work in the soft to medium vacuum range (1 mTorr to 1,000 mTorr). This range provides a distinct advantage over traditional MLI in requiring minimal or no periodic maintenance.

The development of an integrated insulation system will rely heavily on modeling of cryogenic tank and insulation material properties along with balance of plant component test data to facilitate the choice of the final system. To this end, discrete elements of heat transmission have been identified for the insulated tank to aid in modeling the overall heat leak. This heat leak is part of the overall hydrogen system model that represents a full-scale cryo-compressed hydrogen storage system and includes full balance of plant hardware.

RESULTS

Screening of the test results contained in the data libraries of the CTL were initiated using the following criteria:

- *Effective thermal conductivity* (k_e) < 2 mW/m-K at 100 mTorr cold vapor pressure (CVP) with any thickness up to 23 mm
- *Heat flux (q)* < 20 W/m^2 at 100 mTorr CVP; based on approximately 23 mm thickness.

The results of this screening were compared to the iCAT target parameters of:

- *Heat Leak (Q)* <7 W for 100-L tank with boundary temperatures of 300 K (warm) and 78 K (cold);
- q < 5 W/m^2
- A system thermal conductivity (k_s) < 0.5 mW/m-K

To date, approximately 50% of over 700 materials and systems have been analyzed. The results of screening the CTL data libraries are shown in Figure 1. The shaded area of the graph represents the "moderate cryogenic vapor pressure" region that holds the greatest potential for applicability in an integrated insulation system. The use of a system that runs at a lower overall pressure will require less maintenance. Note that this graph shows a sample of the representative data materials that have been tested at the CTL and is not intended to encapsulate the "best" or "final" materials being considered.

The modeling of heat transmission for an integrated tank includes considering elements such as penetrations, structural supports, facing surfaces, and all thermal insulation to approximate the overall heat leak. Table 1 identifies each of these elements, while Figure 2 provides a schematic of the pressure vessels elements. The materials that comprise the integrated insulation system are chosen to minimize heat loss through each element and, thus, minimize the full heat load.

A full-scale cryo-compressed hydrogen (CcH_2) storage system (Figure 3) includes a full balance of plant hardware with the following characteristics:

1. Operating Temperature Range: 40 K to 80 K
2. Operating Tank Pressure: 300 bar (designed to vent at 350 bar)
3. Tank Characteristics: Type 3 aluminum-carbon fiber tank
4. Tank Shell: 2-mm outer aluminum shell
5. Insulation thickness: 23-mm thick with supports

Each of the elements shown in Figure 3 can have multiple materials within an element, or use extremely different materials from element to element, to minimize the thermal load of each element as well as the total system heat load. The balance of plant, which has been minimized to match the needs of a cryo-compressed system, can be easily changed to match any hydrogen storage system. The pressure

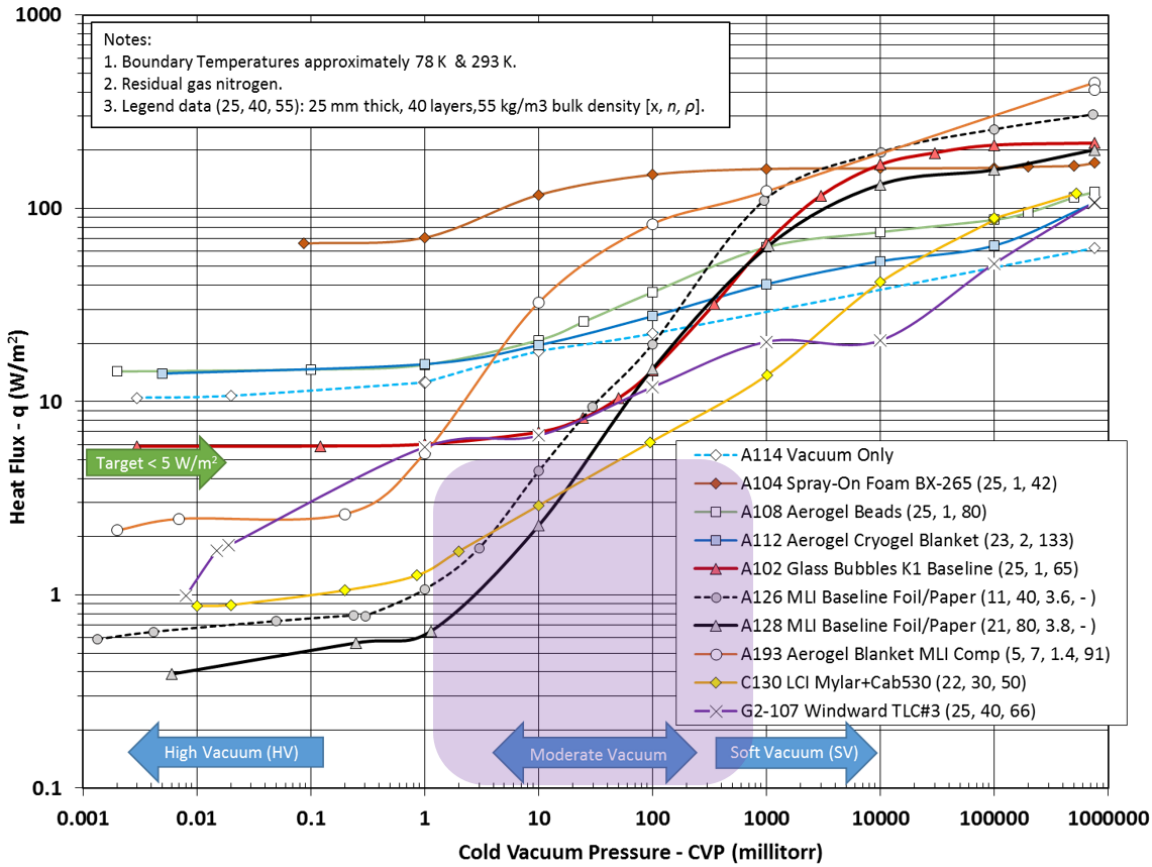

FIGURE 1. Selected cryostat data: insulation system heat flux (q)

TABLE 1. Integrated Tank Heat Transmission Elements

Heat Transmission Element	Designator	Description
Penetration	F	Fill Line [End-A]
	V	Evacuation/Service [End-B]
	A	Auxiliary/Instrumentation
Structural Supports	S_A	Support, End A
	S_B	Support, End B
	S_C	Support, Side (Cylinder)
Facing Surfaces	R_1	Reflective Surface One, Outer of Inner Vessel (zero for e = 0)
	R_2	Reflective Surface Two, Inner of Outer Jacket (zero for e = 0)
Thermal Insulation	Z_{1A}	Insulation Zone 1A, End-A support area
	Z_{1B}	Insulation Zone 1B, End-B support area
	Z_{2A}	Insulation Zone 2A, End-A support area
	Z_{2B}	Insulation Zone 2A, End-B support area
	Z_3	Insulation Zone 3, Side (Cylinder)
Insulation Quality Factor (IQF) [degradation; one for each zone]	Q_{1A}	
	Q_{1B}	
	Q_{2A}	
	Q_{2B}	
	Q_3	

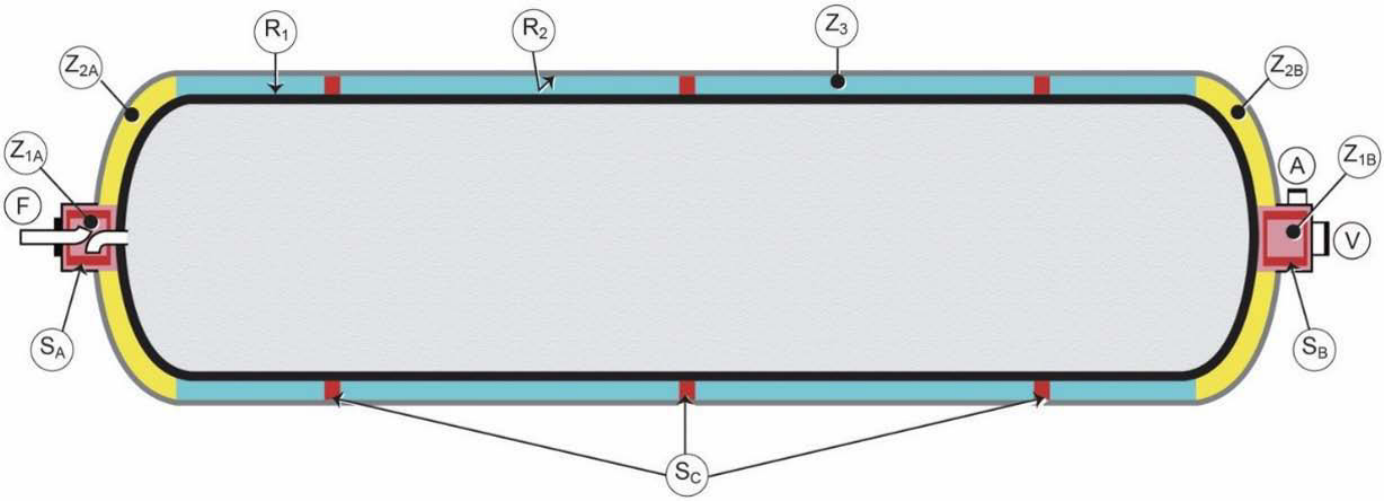

FIGURE 2. Cryogenic tank and heat transfer elements

vessel type, volume, and length-to-diameter relationship can also be changed as necessary.

Several cryo-compressed hydrogen storage systems have been designed as a basis for the thermal analysis model. These systems each use a 100-L internal volume Type 3 aluminum-carbon fiber pressure vessel with length-to-diameter ratios of 3:1, 4:1, and 6:1. The vacuum insulation thickness around the pressure vessel has been set to 23 mm with a 2 mm outer aluminum shell. The pressure vessel's boss/plug (penetrations) and support rings are pre-defined based on the designs used by the Hydrogen Storage Engineering Center of Excellence (HSECoE), but with updates based on the current design decisions. Because the pipe/tube penetration is part of the tank pressure boundary, the total heat load to the tank heat will depend, in part, on the design pressure of the vessel. Therefore, new approaches to the design of the pipe/tube penetration must be considered for a given pressure(s) as part of the complete thermal insulation system.

Estimates for the cost of the integrated insulation system were developed that integrated the components illustrated in Figure 3 along with previously published analysis for similar systems [1]. Some balance of plant components were also taken from the cryo-adsorbent designs originating in the HSECoE. The Type 3 pressure vessel cost is based on the material costs plus a 56% addition for manufacturing. Working with Hexagon Lincoln, these manufacturing costs will be updated in future iterations. In addition, the cost and manufacturing of insulation system components has been considered in updating the current design selections as well as the current working costs. The following assumptions were used in the cost model and analysis:

- A linear process for development: prototypes (quantity 3); beta test units (quantity 100); first production run (quantity 1,000); mass production quantities (quantity 10,000).
- A standard model for economies of scale for this type of manufacturing.
- A reduction of labor cost at the mass production scale due to automation.
- The cost of the insulation and its' application do not realize economies of scale in this model.
- No vacuum pump was included in this model. Maintaining a quality vacuum in the systems was determined to be a service and an operational cost and not assumed in this model.
- Standard manufacturing overhead cost structures were applied to this model.

Table 2 illustrates the methodology used in estimating the overall system cost (NOTE: For clarity, only a subset of the total system components is shown). The preliminary working total cost estimate for the current design, utilizing all components, is $2,732.45 as of June 30, 2017.

Progress has been made in identifying a potential wrapping technique for insulation material used in the integrated system. Some of the wrapping techniques employed when using aerogel-type insulation materials are illustrated in Figure 4. These techniques are called "cigarette wrapping" and may be applicable to facilitate the wrapping of balance of plant components. The benefit of using this technique is the prevention of direct heat leak through insulation seams. Aerogel material (5–10 mm thick) is easy to cut using a razor blade or scissors and is flexible so installation by wrapping is simple and fast. The use of these wrapping techniques will lower the heat leak and improve the thermal performance of the insulated system.

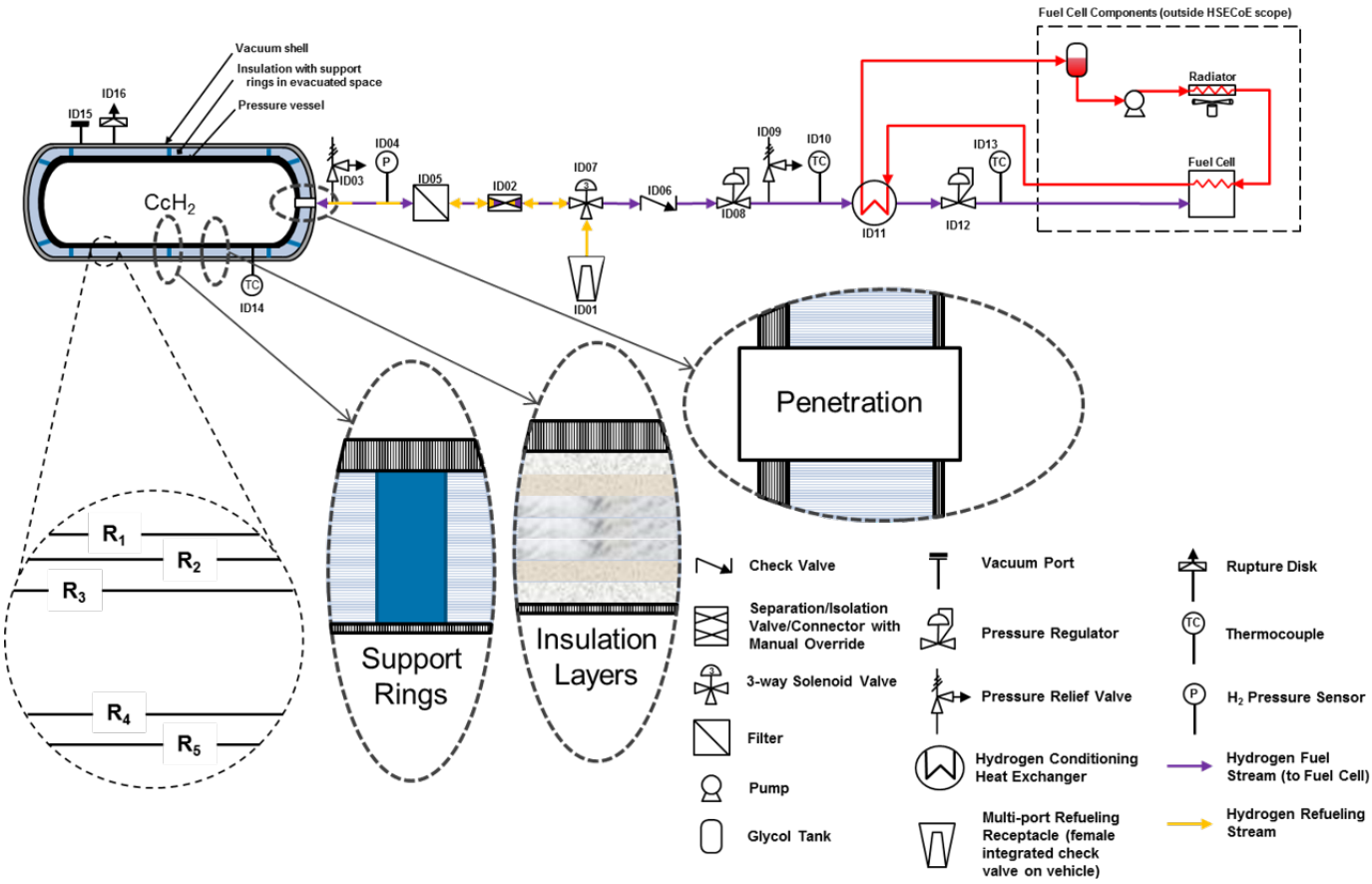

FIGURE 3. Hydrogen system model diagram

TABLE 2. Cost Estimate for Integrated Hydrogen Storage System

Component	Estimate Cost	Comments
Tank – PV Liner	$199.50	Aluminum liner
Tank – CF Wrap	$1,397.28	Carbon fiber wrap
Tank – Insulation and Vacuum Vhamber	$100.09*	Integrated insulation system (place holder)
Tank – Al Shell	$66.07	2 mm thick outer aluminum shell
Balance of Plant	$969.52	Full BOP connecting the CcH2 tank and the vehicle's fuel cell
Total System Estimate	$2,732.45	Total cost estimate as of 6/30/2017

*Note that this value will change with each iteration of the integrated insulation system throughout the project.
PV – pressure vessel ; CF – carbon fiber; BOP – balance of plant

CONCLUSIONS AND UPCOMING ACTIVITIES

The work completed this past year has identified potential insulation materials, initiated modeling for cryogenic tank heat leak elements, identified leading candidate material options for each element of heat transmission and developed a general model for the overall hydrogen integrated system. Upcoming activities include the following:

- Complete data mining of cryostat data libraries for material data relevant to development of the integrated cryogenic hydrogen storage system.
- Complete the thermal analysis model and perform a parametric study of the leading hydrogen storage designs.
- Initiate component testing of insulation material and tanks.
- Continue development of vacuum stability protocol for component testing.

FIGURE 4. Potential wrapping schemes for aerogel-type material

- Update the system concept based on the parametric study results, the component thermal testing, and the integrated insulation system cost analysis.

REFERENCES

1. https://www.hydrogen.energy.gov/pdfs/15013_onboard_storage_performance_cost.pdf

V.0 Fuel Cells Sub-Program Overview

INTRODUCTION

The Fuel Cells sub-program supports applied, early-stage research and development (R&D) of fuel cell technologies for transportation applications, as well as stationary and early market applications, with a primary focus on reducing cost and improving durability. Efforts predominantly concentrate on R&D of fuel cell stack materials and components but also include system balance-of-plant components to achieve low-cost, high-performance fuel cell systems. The sub-program seeks a balanced, comprehensive approach to fuel cells for near-, mid-, and longer-term applications. The development of fuel cells for transportation applications is a primary focus due to the nation's goal of significantly reducing its energy and petroleum needs and due to the benefits inherent in fuel cell electric vehicles (FCEVs) (e.g., high efficiency, long driving range, zero emissions). One stationary application for fuel cells is distributed power generation, including combined heat and power (CHP) for residential and commercial applications. Existing early markets and near-term markets generating traction for adoption of FCEVs include backup power, auxiliary power units, and specialty applications such as material handling equipment. The sub-program's R&D portfolio is primarily focused on polymer electrolyte membrane (PEM) fuel cells but also includes longer-term technologies, such as alkaline membrane fuel cells, and higher-temperature fuel cells like molten carbonate fuel cells for stationary applications.

Durability and cost are the primary challenges to fuel cell commercialization. Improvements in multiple components are required to concurrently meet these challenges. The sub-program's fuel cell tasks are delineated in the Fuel Cell Technologies Office (FCTO) *Multi-Year Research, Development, and Demonstration Plan*, with R&D focused in the key areas of fuel cell components and materials, as well as fuel cell performance and durability.

GOAL

The sub-program's goal is to advance fuel cell technologies for transportation, stationary, and early market applications.

OBJECTIVES[1]

The sub-program's key objectives include:

- Developing a 65% peak-efficient, direct hydrogen fuel cell power system for transportation that can achieve 5,000-h durability (ultimate 8,000 h) and be mass produced at a cost of $40/kW by 2020 (ultimate $30/kW).
- Developing distributed generation and micro-CHP fuel cell systems (5 kW) operating on natural gas that achieve 45% electrical efficiency and 60,000-h durability at an equipment cost of $1,500/kW by 2020.
- Developing medium-scale CHP systems (100 kW–3 MW) by 2020 that achieve 50% electrical efficiency, 90% CHP efficiency, and 80,000-h durability at a cost of $1,500/kW for operation on natural gas and $2,100/kW when configured for operation on biogas.

FISCAL YEAR (FY) 2017 TECHNOLOGY STATUS AND ACCOMPLISHMENTS

Reducing cost and improving durability while maintaining performance continues to be the key challenge facing fuel cell technology R&D. For platinum group metal (PGM)-based catalysts, both a reduction in PGM loading and an increase in membrane electrode assembly (MEA) area power density are required to reduce material costs. Current state-of-the-art MEAs with very low cathode PGM loadings experience a higher-than-expected reduction in performance when operating at high power (e.g., near the rated power point), but FY 2017 saw continued progress towards addressing this performance loss. Commercial fuel cells are expected to use PGM-based catalysts in the near term; however, reaching cost competitiveness with conventional automobiles in the long term will require a transition from PGM-based catalysts to PGM-free catalysts. Two low-PGM catalyst projects produced catalysts exceeding the 2020 technical target for specific power output (8.0 kW/g_{PGM}). The sub-program's consortia (Fuel Cell Performance and Durability [FC-PAD] and the Electrocatalysis Consortium [ElectroCat]) made great strides in materials innovation

[1] Note: Targets and milestones were recently revised; therefore, individual project progress reports may reference prior targets.

and phenomenological understanding of fuel cell catalysts and electrode components through increased cooperative application of national laboratory capabilities.

One of the most important metrics used to guide the sub-program's R&D efforts is the projected high-volume manufacturing cost for automotive fuel cells, which is tracked on an annual basis. The sub-program is targeting a cost reduction to $40/kW by 2020. Long-term competitiveness with alternative powertrains is expected to require further cost reduction to $30/kW, which represents the sub-program's ultimate cost target. This year, the preliminary cost projection for an 80-kW_{net} automotive PEM fuel cell system based on next-generation laboratory technology and operating on direct hydrogen is $50/$kW_{net}$ when manufactured at 100,000 units/yr and $45/$kW_{net}$ when manufactured at a volume of 500,000 units/yr. For comparison, the estimated cost of automotive PEM fuel cell systems that are based on currently deployed commercial technology in 2017 is approximately $230/$kW_{net}$ when manufactured at a volume of 1,000 units/yr. The expected cost for an analogous system based on state-of-the-art materials (lower platinum loading catalyst, coated stainless steel bipolar plates) is $180/$kW_{net}$.

The 2017 projected system cost is significantly less than that of the previous year (the cost decreased from $53/$kW_{net}$ to $45/$kW_{net}$ at 500,000 systems/yr or from $60/$kW_{net}$ to $50/$kW_{net}$ at 100,000 systems/yr). The main change that reduced the system cost compared to the 2016 analysis is an increase in power density (749 mW/cm^2 to 1,095 mW/cm^2) with a concomitant decrease in total platinum (Pt) loading on the cathode (0.134 mg/cm^2 to 0.125 mg/cm^2). This reflects a change in the catalyst basis from a de-alloyed PtNi/C catalyst in 2016 to a PtCo/HSC (high surface area carbon) catalyst developed by General Motors (GM). The proprietary HSC support led to increased performance, which surpassed that of the PtNi/C catalyst; hence, PtCo was used as the 2017 baseline. In 2016, Argonne National Laboratory (ANL) modeled the de-alloyed PtNi/C catalyst under optimized conditions, and although PtCo/C had not been modeled for optimized conditions, there was a consensus between ANL and GM that de-alloyed PtNi/C would have similar performance to PtCo/C if both catalysts were supported by GM's proprietary HSC support. The similarity in performance is due to the expectation of similar cathodic kinetic reaction rates whether using PtNi or PtCo. The catalyst synthesis cost was based on PtNi. The synthesis method of PtCo is proprietary to GM; however, GM has said that the synthesis costs of the two catalysts would be equivalent. Additional changes that reduced cost compared to 2016 included improved bipolar plate stamping process assumptions and the removal of the hydrogen sensors from the fuel cell system design (but not from within the vehicle). The decreased system cost is shown in Figure 1.

To enable vehicle commercialization, fuel cell systems must also meet the sub-program's durability targets. These targets vary by application; for automotive systems, DOE has set a 2020 target of 8,000 h, which is meant to represent the durability requirement in terms of miles driven (150,000 mi) for a larger range of drivers. An independent assessment of the current fuel cell durability test data from leading fuel cell developers found that the current average state-of-the-art laboratory durability status, defined as average hours to 10% voltage degradation, is approximately 3,700 h.

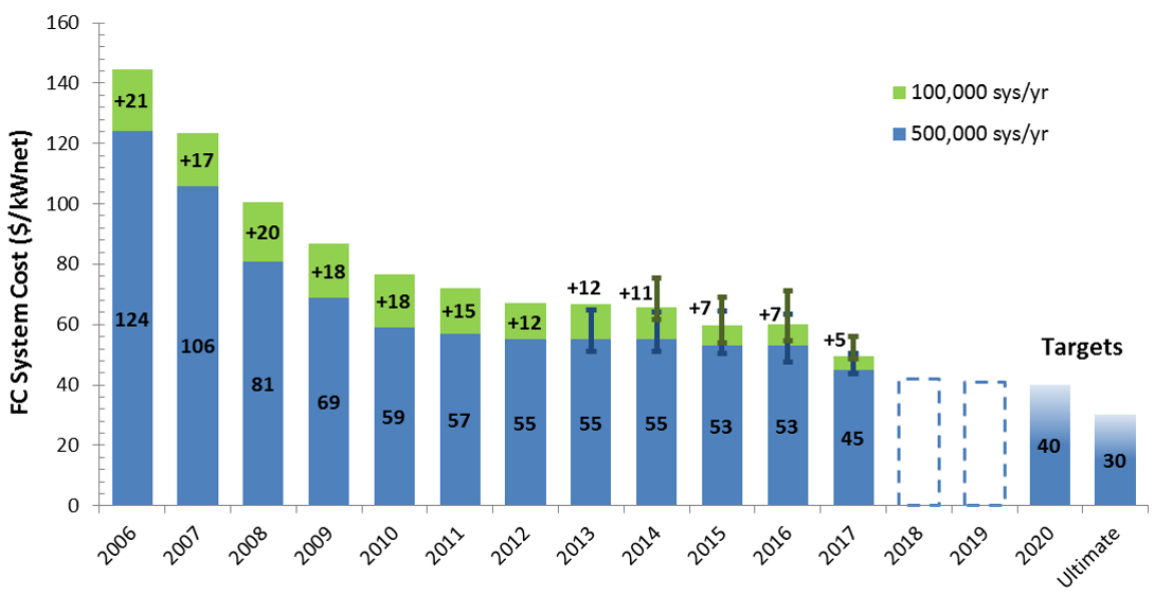

FIGURE 1. Modeled cost of an 80-kW_{net} PEM fuel cell (FC) system based on projection to high-volume manufacturing

Meanwhile, DOE independent validation of on-road FCEVs showed a more than four-fold increase in the maximum projected durability of fuel cell systems, increasing from 950 h in 2006 to over 4,100 h in 2017. Additionally, the maximum operating hours recorded for a single FCEV has remained at 5,600 h. The durability of fuel cell electric buses has also been evaluated since 2000 in transit agency demonstrations and has continued to increase after having surpassed the 2016 interim target of 18,000 h in 2015. The current bus maximum lifetime is over 25,300 h and was attained by a bus that continues to operate, surpassing the 2020 target of 25,000 h. High operational hours have been demonstrated by several other buses as well: nine have surpassed the 18,000-h interim target, with six demonstrating over 20,000 h in operation.

Consortia

Fuel Cell Performance and Durability (FC-PAD)

The FC-PAD consortium was formed to advance performance and durability of PEM fuel cells to further enable their commercialization. This R&D consortium is led by a team of national laboratories and began operations in FY 2016. Overall objectives of the consortium include building a knowledge base and optimizing transport and structures for highly performing, durable PEM fuel cell components; improving high current density performance at low PGM loadings; improving component stability and durability; and developing new diagnostics, characterization tools, and models. In FY 2017 work continued at the national laboratories in three main areas: cerium migration and cation interaction with membranes and ionomers; modeling and testing of ionomers, interfaces, and diffusion media; and characterization and testing of low-PGM alloy catalysts. The FC-PAD team evaluated a series of state-of-the-art PtCo catalysts from various sources (GM, Umicore, EWii) in terms of size, composition, and morphology using microscopy, inductively coupled plasma-mass spectrometry, and X-ray scattering methods, in beginning of life (BoL) and end of life (EoL) conditions (following several different accelerated stress test [AST] protocols). The Co leaching during AST was quantified (Figure 2), and it was determined that regardless of the starting structure and composition, all the alloy catalysts behaved similarly in terms of compositional stability, e.g., all catalysts lost greater than 50% of the Co, which resulted in (1) the electrocatalysts becoming more Pt-like and (2) Co migration into the membrane.

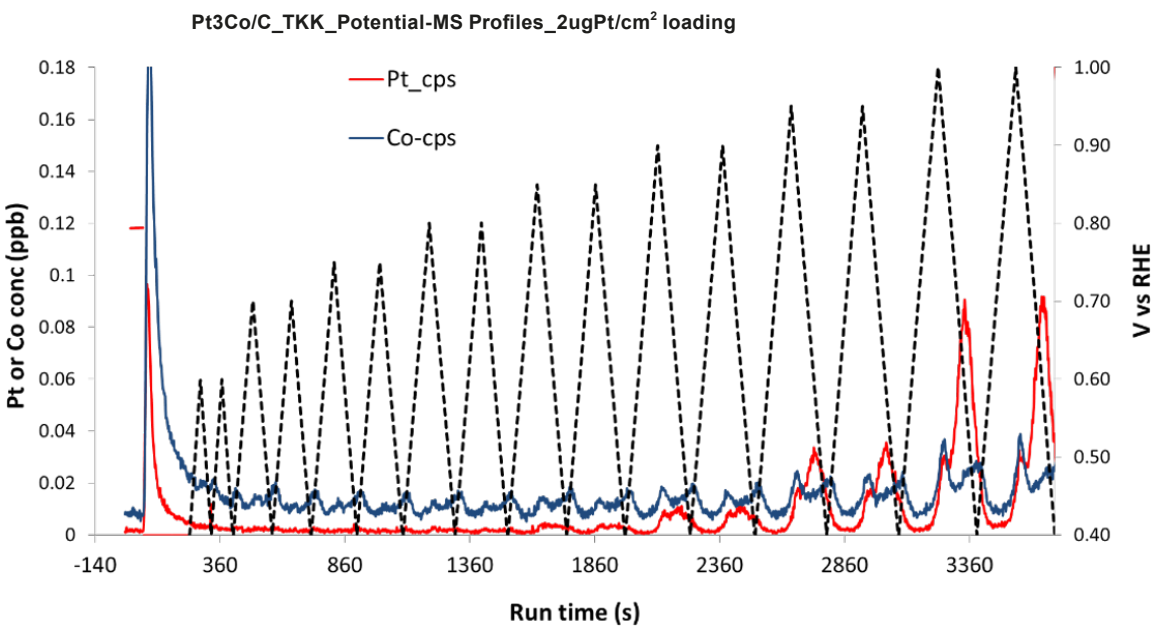

RHE – reference hydrogen electrode; TKK – Tanaka Kikinzoku Kogyo

FIGURE 2. Inductively coupled plasma-mass spectrometry quantification of Pt and Co leaching from a Pt_3Co/C TKK catalyst during potential cycling demonstrates the constant baseline leaching of Co with increased loss during cathodic sweep, and peaks due to Pt leaching during anodic sweeps at high potential (>0.95 V)

Significant progress also was made in other materials necessary for the function of electrodes, including ionomers, membranes, and electrode structures. The effect of cerium migration through ionomer and membrane polymers is important to increasing fuel cell durability by optimizing its incorporation into electrodes. Migration and diffusion coefficients were quantified at low (50%) and high (100%) relative humidity. Cerium zirconium oxide (CZO) was demonstrated to enhance membrane durability much better than the increased addition of cerium cations. Work also demonstrated advances in modeling of membrane structures and detailing water uptake with various cationic species. Combined modeling and experiments to understand interfaces demonstrated the importance of water droplets at the gas diffusion layer/flowfield boundary as well as the possible increase in performance through catalyst layer architecture optimization. Limiting-current diagnostics across a systematic study of different catalyst layers demonstrated the importance of accurate, effective active area measurements as well as the apparent dominance of diffusion-like transport at the local ionomer scale.

FC-PAD's approach couples national lab capabilities with funding opportunity announcements (FOAs) for an influx of innovative ideas and research. This year marked the beginning of the cooperation of the FC-PAD consortium with FOA projects led by 3M, GM, United Technologies Research Center, and Vanderbilt University.

ElectroCat (Electrocatalysis Consortium)

The sub-program also established a second consortium in FY 2016 under the umbrella of DOE's Energy Materials Network to address the materials problem of developing high-performance, low-cost, PGM-free catalysts for automotive fuel cells. The ElectroCat consortium aims to accelerate PGM-free catalyst and electrode development by coordinating relevant expertise and tools at the national labs to provide easy access to external researchers. ElectroCat's capabilities consist of high-throughput combinatorial methodologies, computational tools, and PGM-free catalyst expertise. In FY 2017, the core group of national laboratories established a list of capabilities and evaluated their value to the community by performing state-of-the-art experiments. Major improvements to fuel cell catalysts included an atomically dispersed (AD)Fe-N-C catalyst, developed to create single atomic Fe sites on the catalyst surface (no nanoparticles, minimal Fe clustering), as seen in high-angle annular dark field scanning transmission electron microscopy images (Figure 3a). The catalyst (AD)Fe-N-C comprises leaf-shaped structures with hierarchical pore structure, the result of Zn evaporation during pre-treatment. The oxygen reduction reaction (ORR) activity of this catalyst (half-wave potential, $E_{1/2}$) was increased by 20 mV (Figure 3b). This catalyst is the same one chosen for high-throughput synthesis at ANL and for which direct microscopic and spectroscopic evidence was found for a majority of Fe sites being on the surface. These Fe sites were shown to be more stable than those in another state-of-the-art catalyst that incorporates cyanamide and polyaniline, (CM+PANI)-Fe-C.

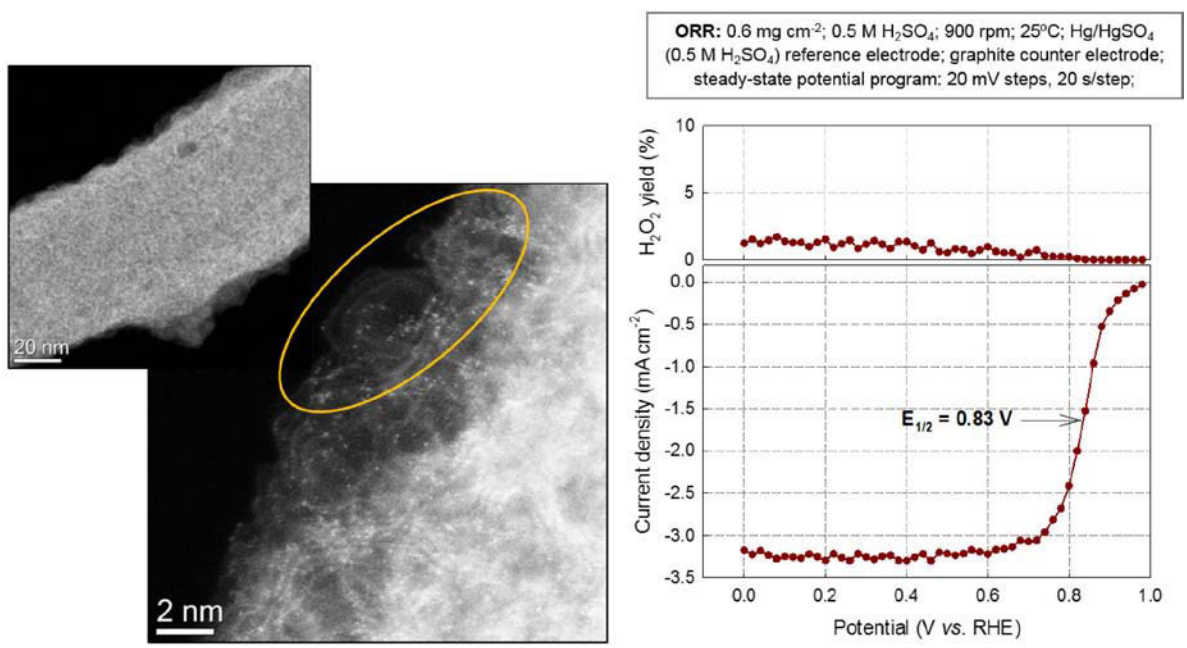

FIGURE 3. Characterization and testing of (AD)Fe-N-C catalyst: (a) high-angle annular dark field scanning transmission electron microscopy images (left); (b) H_2O_2 yield and ORR activity determined by rotating ring disc electrode testing (right)

The performance of the (CM+PANI)-Fe-C catalyst was improved by using Zn salts during preparation as pore-forming agents, by using magnetic separation to remove Fe clusters and nanoparticles, and by eliminating the hot-pressing step of MEA fabrication. These changes increase the H_2-air cathode performance by 25% over previous versions of the catalyst, up to 0.83 mA/cm^2 at 0.8 V (120 mA/cm^2 at 0.8 $V_{IR\text{-}free}$) (Figure 4).

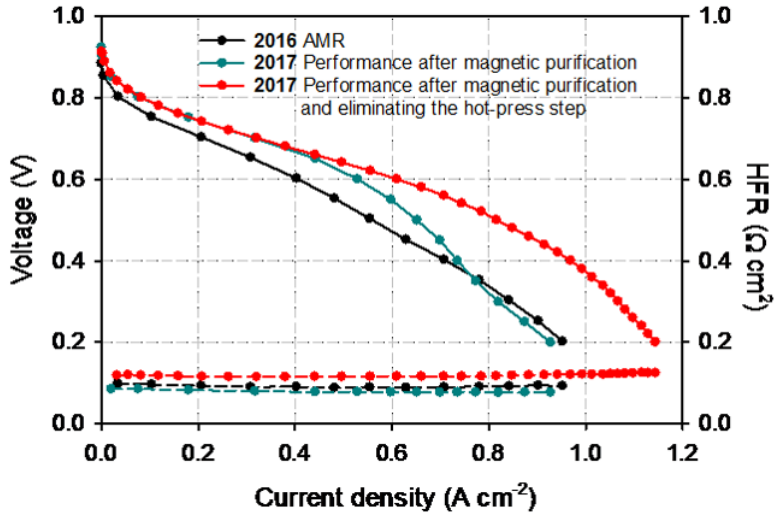

FIGURE 4. Polarization curve and high frequency resistance (HFR) measurements of (CM+PANI)-Fe-C(Zn) catalyst developed by LANL displaying improvement in performance over catalyst featured in 2016 Annual Merit Review status

High-throughput, combinatorial methods for PGM-free catalyst R&D are among the core competencies of ElectroCat. The high-throughput robotic catalyst synthesis system at ANL enhances foundational understanding of promising materials and expedites materials optimization by efficient, automated exploration of the relevant variable space. The rapid characterization of these catalysts is key to understanding structure-function relationships, which will inform further advances in catalyst development. In FY 2017, the utility of the system was demonstrated by the preparation of 40 samples of the (AD)Fe-N-C catalyst developed at Los Alamos National Laboratory (LANL) with varying composition, precursor, and pyrolysis temperature. These catalysts were then examined by high-throughput structural characterization (X-ray diffraction and X-ray absorption fine-structure spectroscopy) and ORR activity testing via rotating disk electrode. Analysis of the metadata collected from these systems is ongoing.

Pioneering results in the area of computational approaches to PGM-free catalysts were also demonstrated. At LANL, a durability descriptor calculation, based on an electron beam damage model, was applied to all atoms in 30 putative M_xN_y active sites. By examining the elastic collision energy of a potential-accelerated electron required to eject atoms from each site, and compiling these knock-on displacement threshold energies (E_{KODTE}) into a database, relative stabilities of these sites could be elucidated. These results suggest that nitrogen atoms are the most susceptible to damage for all of the structures and that edge sites, particularly those in an "armchair" configuration, were least stable. These calculations are amenable to high-throughput screening of possible active sites and fit with the consortium's goal of increasing foundational understanding of PGM-free catalysts through advanced computational capabilities at the national laboratories. Late in FY 2017, DOE organized a PGM-free modeling workshop to discuss ongoing challenges and capability needs in the area and to increase collaboration among computation experts and experimentalists. A report will be prepared based on the proceedings and released in FY 2018.

In FY 2017, the first group of FOA projects were announced, and their goals address the preeminent challenges in PGM-free catalyst development mentioned above. The first of these projects is led by Giner, Inc., and proposes to develop Mn-based, PGM-free catalysts that will not suffer from the durability issues of Fe-containing catalysts due to the Fenton activity of Fe. A Carnegie Mellon University-led project focuses on increasing power density and durability through control of electrode microstructure. Pacific Northwest National Laboratory is leading an effort to increase ORR electrocatalyst durability through synergetic active sites to decrease selectivity to peroxide formation. The fourth project, led by GreenWay Energy, LLC, will attempt rational design of PGM-free, ORR framework nano-structure catalysts.

Low-PGM Catalysts

In FY 2017, two catalysts were developed that surpassed the FCTO 2020 technical target for specific power output of 8.0 kW/g_{PGM} at the stipulated Q/ΔT of 1.45 kW/°C.

The first of these catalysts was developed by GM as part of a project that focuses on the need to develop catalysts with high performance and durability at both low and high current densities. The project aims to understand and overcome oxygen and proton transport limitations at high current density with low Pt loadings (<0.100 mg_{Pt}/cm^2). The highest specific activity to date was achieved using PtCo alloy particles supported on HSC. A PtCo/HSC catalyst (-f in

Figure 5) with a Pt loading of 0.063 mg_{Pt}/cm^2 showed the highest PGM utilization of any catalyst to date: 10.6 kW/g_{PGM} at 150 kPa and 94°C (14.1 kW/g_{PGM} at 250 kPa and 94°C), meeting the Q/ΔT requirement imposed by DOE targets. The two HSC catalysts developed in 2017 (PtCo/HSC-e and -f) show similar high activity at low current density compared to the 2016 PtCo/HSC-a catalyst, but with decreased transport losses at high current density. This improvement in performance is attributed to improved understanding of Pt and Co dissolution and to the selection of the carbon support based on improved understanding of support degradation and resistance to mass transport in nanopores.

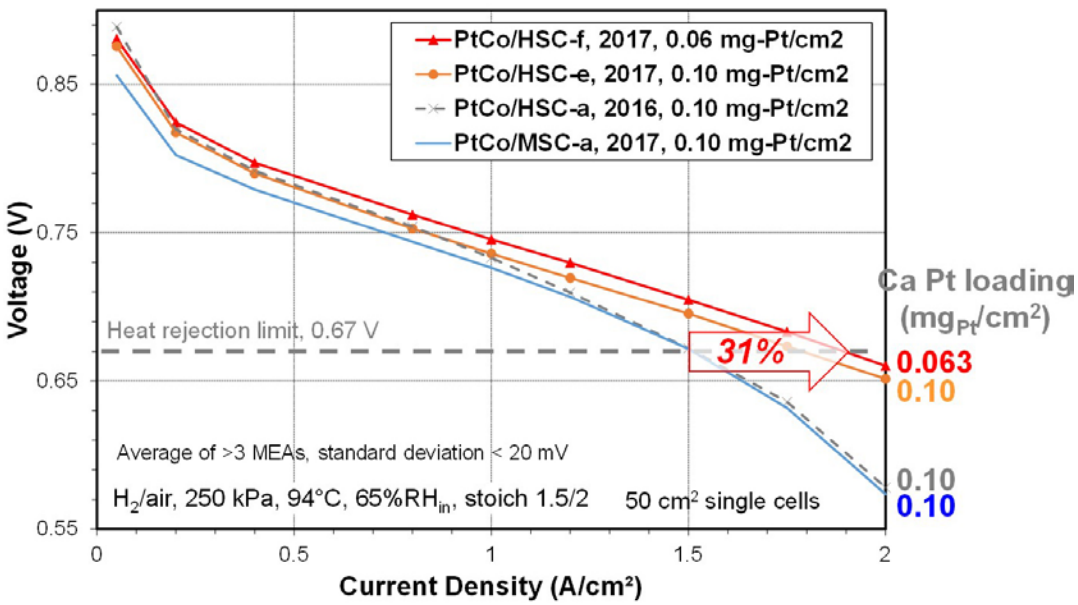

FIGURE 5. Fuel cell polarization curves of PtCo/C catalyst at different cathode Pt loadings showing improved high current density performance in recently developed catalysts over medium surface area carbon catalyst and the highest-performing HSC catalyst from 2016

The FCTO 2020 technical target for specific power output was also surpassed by a catalyst developed by 3M. The 3M project focuses on a thin film catalyst layer approach using Pt alloy (PtNi, PtNiIr) nanoporous thin film and ultra-thin film (UTF) catalysts, two distinct catalyst layer morphologies based on 3M technology. The catalysts have been improved in the last year by modifying film preparation methods, including annealing and leaching steps to control composition and morphology. Several catalysts with a total PGM loading of 0.077 mg_{PGM}/cm^2 exceed the mass activity target of 0.044 A/mg_{Pt}. One of these catalysts, PtNi UTF-f, achieves a specific power output of 8.1 kW/g_{PGM}. The improvement in high current density performance is demonstrated in Figure 6. The addition of a relatively small amount of Ir to these catalysts was found to improve their durability.

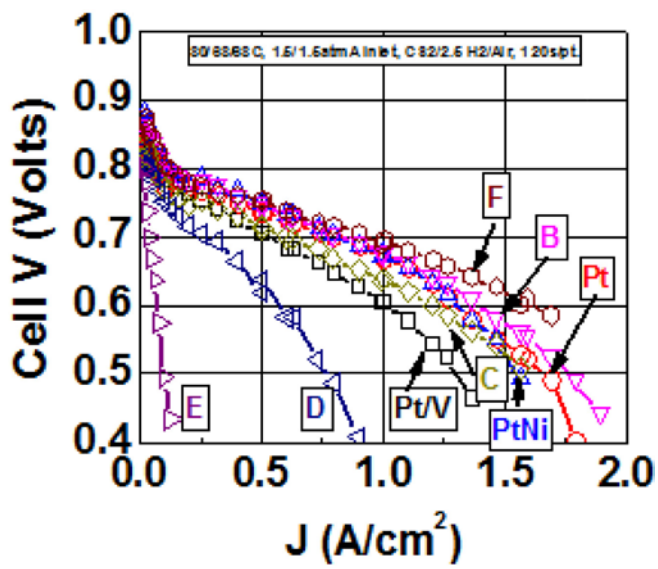

FIGURE 6. Fuel cell polarization curves of PtNi and PtNilr nanoporous thin film and ultra-thin film catalysts demonstrating the improvement in performance at high current density

Electrolytes

Alkaline Membranes

Significant improvements in the performance and durability of alkaline electrolyte membranes (AEMs) were demonstrated in FY 2017. Two areas in particular are highlighted: perfluoro-based and hydrocarbon-based alkaline membranes.

The performance of functionalized polyphenylene membrane AEMs at LANL was improved significantly this year. The hexamethyl ammonium side chains were down-selected on the basis of low area specific resistance (~0.05 Ω cm^2) and improved chemical stability. The achieved area specific resistance meets the FCTO technical target for AEM area specific resistance of <0.1 Ω cm^2. These membranes exhibited no chemical degradation at 80°C during 3,600 h in 0.5 M NaOH (1,800 h in 4 M NaOH) in ex situ testing and >300 h in in situ testing. A large increase in power density was also made possible by further exploration of the anode (hydrogen oxidation reaction) catalyst deactivation mechanism first cited in FY 2016 in which phenyl rings within the ionomer adsorb strongly on Pt catalyst surfaces. Using a commercially available PtRu catalyst, which does not adsorb these groups as strongly, and switching to an electron-withdrawing fluorene-based polymer made an increase in power from 0.4 W/cm^2 to ~1 W/cm^2 possible (Figure 7). Furthermore, the low HFR (0.07 cm^2) of this catalyst is commensurate with sufficient hydroxide conductivity for high-performing AEM fuel cells.

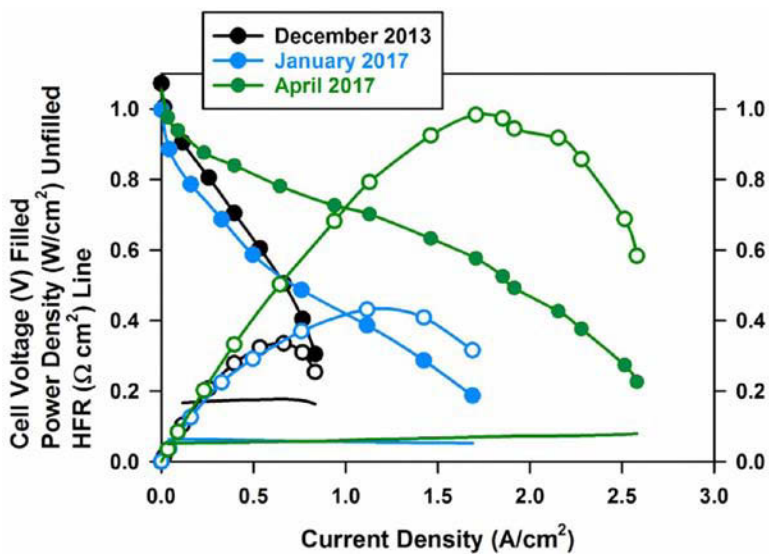

FIGURE 7. Polarization curve (closed symbols), power density (open symbols), and HFR (no symbols) demonstrating recent progress performance in hydrocarbon-based alkaline membranes

Advances in perfluoro-based AEMs at the National Renewable Energy Laboratory were demonstrated through MEA testing using Pt/C cathode and PtRu/C anode catalysts (Figure 8). The sulfonamide-linked chemistry was further optimized, achieving hydroxide ion conductivity of to up to 52 mS/cm and up to 90% of theoretical ion exchange capacity. Improved processing has enabled the synthesis of over 200 g, which was distributed to 10 other laboratories. A University of Connecticut (UConn)-prepared gas diffusion electrode (GDE) applied to the perfluoro AEM demonstrated enhanced performance at 60°C, meeting the FCTO FY 2017 area specific resistance target of <0.1 Ω cm^2. Unlike the perfluoro AEM catalyst-coated membrane (PFAEM CCM), which lost all performance within 15 h, the UConn GDE retained reasonable performance after 500 h of testing at 600 mA/cm^2.

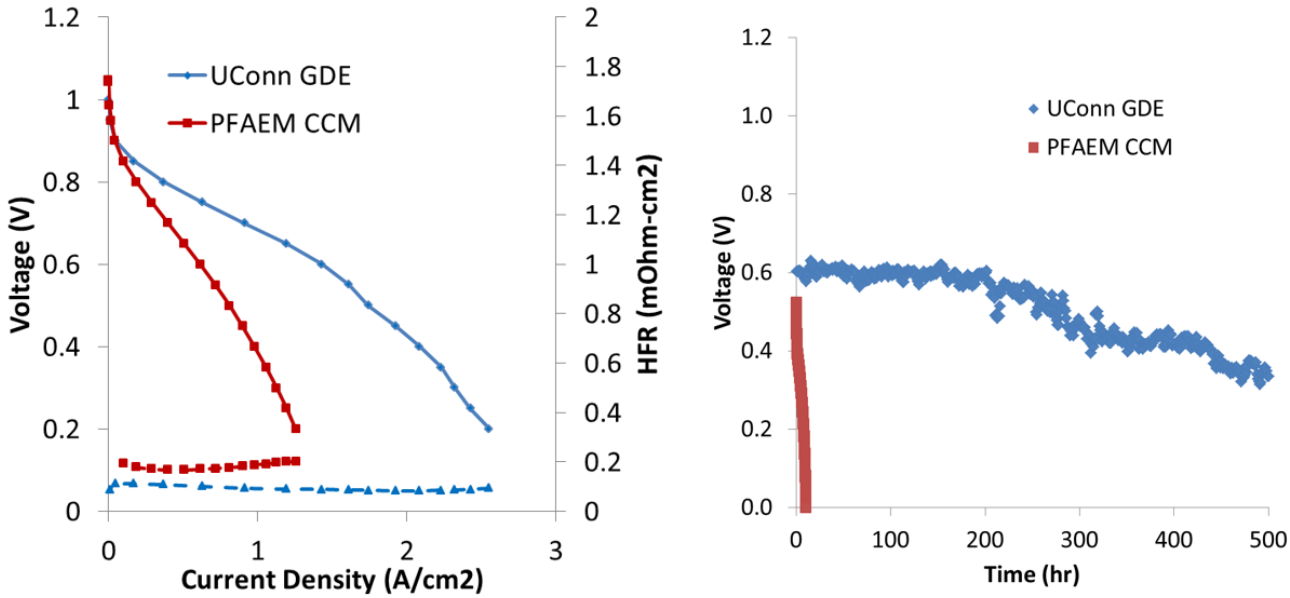

FIGURE 8. Polarization curves at 95°C and 50% inlet humidity for perfluoroimide-acid-based membranes (red lines) and a perfluorosulfonic acid control (blue lines). Voltage versus current density data are shown by lines with symbols, HFR is shown with solid lines, and HFR corrected data are shown with dashed lines.

Rotating Disc Electrode (RDE) Testing Protocols and Best Practices Disseminated

Accurate benchmarking of baseline Pt/C catalysts is necessary to expedite the ultra-low PGM catalyst development crucial for commercialization of FCEVs. It has been shown that measured ORR activity and reproducibility are correlated with system cleanliness, evaluation protocol, operating conditions, and the RDE catalyst film thickness and uniformity resulting from ink formulation, composition, and film drying. In order to establish baseline performance, a best practices and common protocol for RDE testing was developed by three independent laboratories and used to test three commercially available Pt/C catalysts (from Umicore, Johnson Matthey, and TKK). The performance of these catalysts and the reliability of the protocols for RDE testing used at the three laboratories were verified, and these results and best practices were published this year in a journal article[2]. This publication provides the standard test protocol and best practices to assist the scientific community by enabling procedural consistency and less variability.

L'Innovator

The L'Innovator (for "Lab innovator") aims to accelerate the commercialization of innovative hydrogen and fuel cell technologies developed at national labs and enable a robust domestic industry and supply base in the emerging area of hydrogen and fuel cells. In FY 2017, FCTO successfully launched the first L'Innovator pilot, building upon the due diligence carried out in FY 2016 to develop the concept. The national laboratories involved in the pilot, LANL and Brookhaven National Laboratory, executed an interlab agreement and successfully completed a cooperative research and development agreement call for a commercialization partner, run by LANL. In FY 2018, the commercial partner will work with LANL and Brookhaven National Laboratory to develop a pathway towards buildout of a working prototype MEA that can be made via a roll-to-roll process by the end of the year. Specifically, LANL's MEA technology will be optimized to integrate core-shell catalyst technology developed at Brookhaven National Laboratory, and National Renewable Energy Laboratory will be involved in developing and applying roll-to-roll processing methods to demonstrate manufacturability.

[2] S.S. Kocha, K. Shinozaki, J.W. Zack, D.J. Myers, N.N. Kariuki, T. Nowicki, V. Stamenkovic, Y. Kang, D. Li, D. Papageorgopoulos. Electrocatalysis. 8 (2017) 366.

BUDGET

The FY 2017 appropriation is $32.0 million for the Fuel Cells sub-program. In FY 2017 the sub-program funded early-stage R&D efforts focused on fuel cell stack components to increase performance and durability while reducing cost, broken down into the four key areas shown in Figure 9. FY 2017 funding was primarily directed towards improving catalysts and electrodes in order to increase performance and reduce catalyst cost by developing ultra-low PGM or PGM-free catalysts for oxygen reduction; ElectroCat and the four newly awarded FOA projects are included in this area. Slightly more than a quarter of the funding total was dedicated to the FC-PAD consortium, including the core national lab membership and its four associated industry/university-led projects. The sub-program also continued to fund innovative projects for resilient, lower-cost membrane materials, with approximately $3.2 million in funding.

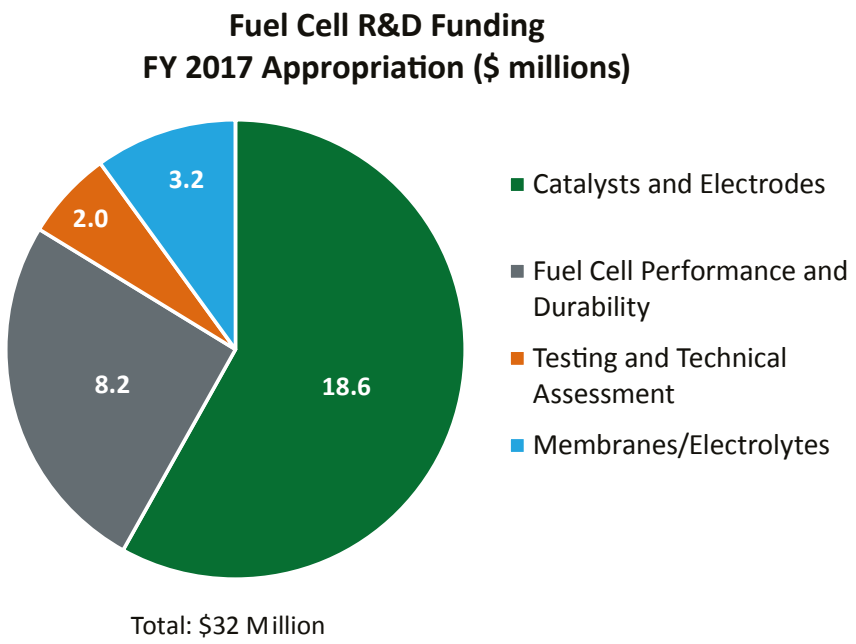

FIGURE 9. FY 2017 Appropriations

UPCOMING ACTIVITIES AND PLANS

In FY 2018, the Fuel Cells sub-program will continue early-stage applied fuel cell R&D for diverse applications that employ a variety of technologies (including PEM and AEM fuel cells) and a range of fuels (including hydrogen, natural gas, and liquid fuels). Fuel Cells R&D will focus on the key areas of fuel cell components and materials, such as catalysts, alkaline and non-water-dependent membranes, electrodes, and component innovations (such as components for reversible fuel cells), with an emphasis on cost reduction and durability improvement. The sub-program's consortia will continue fostering national lab capabilities and collaborations with stakeholders and the research community. The sub-program will place particular emphasis on expediting the development of PGM-free catalysts and electrodes through ElectroCat, utilizing unique experimental and advanced computing capabilities at the national labs. Fuel Cells R&D will also continue efforts to advance fuel cell performance and durability through FC-PAD. Both consortia are now working with their first set of FOA projects, which will further increase the cooperativity and effectiveness of the respective communities. Ongoing support of modeling will guide component R&D, benchmarking complete systems before they are built and enabling exploration of alternate system components and configurations. The sub-program will also continue to pursue efforts to expand L'Innovator to increase adoption of the groundbreaking early-stage fuel cell technologies being developed by the national labs.

Future activities are subject to appropriations.

Dimitrios Papageorgopoulos
Fuel Cells Program Manager
Fuel Cell Technologies Office
Office of Energy Efficiency and Renewable Energy
U.S. Department of Energy
1000 Independence Ave., SW
Washington, DC 20585-0121
Phone: (202) 586-5463
Email: Dimitrios.Papageorgopoulos@ee.doe.gov

V.A.1 ElectroCat (Electrocatalysis Consortium)

Steering Committee Members:
Piotr Zelenay[1] (Primary Contact), Deborah J. Myers[2], Huyen N. Dinh (National Renewable Energy Laboratory), Karren L. More (Oak Ridge National Laboratory [ORNL])
[1]Los Alamos National Laboratory (LANL)
Los Alamos, NM 87545
Phone: (505) 667-0197
Email: zelenay@lanl.gov
[2]Argonne National Laboratory (ANL)
Lemont, IL 60439
Phone: (630) 252-4261
Email: dmyers@anl.gov

DOE Managers:
Dimitrios Papageorgopoulos
Phone: (202) 586-5463
Email: Dimitrios.Papageorgopoulos@ee.doe.gov
Adria Wilson
Phone: (240) 479-0198
Email: Adria.Wilson@ee.doe.gov

Project Start Date: February 1, 2016
Project End Date: September 30, 2020

Consortium Objectives

- Expedite the development of platinum group metal (PGM)-free catalysts, electrodes, and membrane electrode assemblies (MEAs) for fuel cell applications by facilitating collaboration between national laboratories.
- Foster the development of necessary capabilities.
- Create an interface for making those capabilities available to industry and academic partners.

Fiscal Year (FY) 2017 Objectives

Los Alamos National Laboratory

- Develop draft technology transfer and agreements (TT/A) plan for ElectroCat and receive feedback from member national laboratories.
- Synthesize and, in collaboration with other ElectroCat partner laboratories, characterize and evaluate oxygen reduction reaction (ORR) activity of PGM-free catalysts based on di-iron complexes.
- Synthesize and demonstrate atomic dispersion of Fe sites in (Zn, Fe)-PSIE-metal organic framework-derived catalyst; provide samples to ANL for further development of high-throughput screening techniques.
- Demonstrate 20 mA cm^{-2} at 0.90 V (*iR*[1]-corrected) in an H_2-O_2 fuel cell and 100 mA cm^{-2} at 0.80 V in an H_2-air fuel cell (measured); maintain partial pressure of $O_2 + N_2$ at 1.0 bar (cell temperature 80°C).

Argonne National Laboratory

- Achieve half-wave potential agreement of < 20 mV between rotating disk electrode (RDE) and multi-electrode channel flow double electrode ORR measurements for a benchmark PGM-free catalyst.
- Select and prepare six PGM-free electrode specimens and obtain three-dimensional (3D) micro-structures using synchrotron X-ray computed tomography.
- Demonstrate current densities in the combinatorial MEA for all 25 electrodes within 10% of those in a standard 5 cm^2 test cell using identical PGM-free electrode compositions in both cells.
- Construct microstructure models of six PGM-free electrodes from LANL by combining X-ray computed tomography data with information from porosimetry, electron microscopy, and other characterization techniques.

National Renewable Energy Laboratory

- Demonstrate F-doping onto LANL's PGM-free catalyst (e.g., Fe-CM-PANI-C catalyst) with either CF_4 or F_2.
- Demonstrate the synthesis of the M-C-N model catalyst with the chemical composition comparable to the state-of-the-art literature, and study its structural properties. The first target moiety is a nitrogen coordinated transition metal center in a carbon matrix, e.g., FeN_4 in graphene matrix.
- Demonstrate improved feasibility of segmented cell system for combinatorial PGM-free samples (e.g., Fe-CM-PANI-C catalyst) to minimize crosstalk of a one electrode layer with gradient composition and allow for a sufficient resolution and data interpretation; based on availability, demonstration performed either with standard (i.e., non-combinatorial) PGM-free samples or first generation combinatorial PGM-free samples.
- Extract values for the reaction order with respect to oxygen partial pressure and activation energy as a function of PGM-free catalyst type and/or electrode design. Utilize these extracted values to help determine the reaction mechanism for said PGM-free electrocatalyst (e.g., Fe-CM-PANI-C catalyst).

[1] *iR* is internal resistance

Oak Ridge National Laboratory

- Characterize at least three new candidate PGM-free catalysts using scanning transmission electron microcoscopy (STEM) imaging and analysis and X-ray photoelectron spectroscopy (XPS).
- Coordinate characterization effort at ORNL with high-throughput combinatorial results from ANL towards down-selecting potential catalysts for in-depth structural and chemical analyses.
- Coordinate 3D electron tomography effort at ORNL with 3D X-ray tomography efforts from both ANL and LANL.
- Initiate in situ microscopy studies after coordinating experimental variables with national laboratory and potential external partners.

ElectroCat Annual Milestone

- Demonstrate 20 mA cm^{-2} at 0.90 V (*iR*-corrected) in an H_2-O_2 fuel cell and 100 mA cm^{-2} at 0.80 V in an H_2-air fuel cell (measured); maintain partial pressure of $O_2 + N_2$ at 1.0 bar (cell temperature 80°C).

Technical Barriers

This project addresses the following technical barriers from the Fuel Cells section of the Fuel Cell Technologies Office Multi-Year Research, Development, and Demonstration Plan [1].

(A) Durability (catalyst, MEA)

(B) Cost (catalyst)

(C) Performance (catalyst, MEA)

Technical Targets

This project focuses on the development and implementation of high-performing and durable PGM-free cathode catalysts for polymer electrolyte fuel cells, following DOE technical targets outlined in Table 3.4.7 in Section 3.4.4 (Technical Challenges) of the Multi-Year Research, Development, and Demonstration Plan [1]. The overall goal is durable PGM-free oxygen reduction reaction catalysts that achieve an activity of 0.044 A/cm^2 at 0.90 V in a polymer electrolyte fuel cells MEA by 2020 (Table 1).

FY 2017 Accomplishments

Consortium Development

- Established a steering committee and selected unique national laboratory capabilities relevant to PGM-free catalyst development and implementation.
- Inaugurated a public ElectroCat website in February 2016 and posted the network of national laboratory capabilities (www.ElectroCat.org).
- Established a data management plan based on Comprehensive Knowledge Archive Network and leveraging the Materials Data Facility data publication capabilities.
- Completed and approved a streamlined cooperative research and development agreement (CRADA) template and non-disclosure agreement (NDA), available for use.

Performance Improvement

- Demonstrated 83 mA/cm^2 at 0.80 V (120 mA/cm^2 at 0.8 $V_{iR\text{-free}}$) in H_2-air fuel cell.
- Achieved half-wave potential ($E_{1/2}$) of 0.83 V with atomically dispersed (AD) Fe-N-C in RDE testing, an increase of 0.02 V over the 2016 status.
- Improved PGM-free catalyst activity in an MEA: 16 mA/cm^2 at 0.90 $V_{iR\text{-free}}$ and 0.044 A/cm^2 at 0.87 V (H_2-O_2 fuel cell).

Characterization and Capability Development

- Determined >10× lower Fe dissolution rate with (AD) Fe-N-C than (CM+PANI)-Fe-C(Zn).
- Obtained direct evidence of a majority of Fe sites being atomically dispersed and on the (AD)Fe-N-C catalyst surface using STEM, a molecular probe and X-ray spectroscopies.
- Using STEM and nano-computed tomography, elucidated the source of performance limitations and identified pathways to improving (AD)Fe-N-C fuel cell performance.
- Synthesized 40 variations of (AD)Fe-N-C catalyst and characterized atomic structure using high-throughput X-ray diffraction and spectroscopy.

TABLE 1. Progress towards Meeting Technical Targets for PGM-free Electrocatalysts and MEAs for Transportation Applications

Characteristic	Units	DOE 2020 Electrocatalyst and MEA Targets	Current ElectroCat Status
H_2-air fuel cell performance	mA/cm^2 @ 800 mV (measured)	300	100
PGM-free catalyst activity	mA/cm^2 @ 900 $mV_{iR\text{-free}}$	≥44	16

- Synthesized and characterized the composition of model thin-film FeN/C catalyst.
- Obtained 9 mV ORR half-wave potential agreement for Pt/C and <30 mV agreement for PGM-free catalyst between RDE and multi-channel flow double electrode measurements.
- Developed and utilized the capability to characterize by X-ray absorption fine structure (XAFS) the atomic structure of catalysts during heat treatment.
- Developed a PGM-free cathode performance model considering the effects of flooding, mass, and charge transfer and applied it to the (CM+PANI)-Fe-C cathode.

ORR Active-Site Activity and Durability Modeling

- Completed install, test, and linking of Vienna ab initio Simulation Package on dedicated computational cluster high-throughput software (Materials Simulation Toolkit and durability descriptor calculation automation [DDCA]) for structural relaxation calculation of ORR activity descriptor, and calculation of durability descriptor with output structure determined for input into ElectroCat data portal.
- Developed DDCA approach to determine the values of knock-on displacement threshold energy (KODTE), a proposed durability descriptor.
- Successfully completed initial set of library calculations for bulk-C, zig-zag edge-C, armchair edge-C structures (FeN_4, MnN_4, CoN_4, Fe_2N_5, $MnCoN_5$ with and without *OH ligand) including calculated ORR activities and KODTEs.
- Calculated NH and F ligand effects on OH binding energy, a proposed ORR activity descriptor.
- Generated additional Python scripts to aid in automation of computational cell set up (including addition of ligands to atoms in a given structure) and visualization (including 3D movies with tight integration between simulation output and 3D rendering software).

✧ ✧ ✧ ✧ ✧

INTRODUCTION

The Energy Materials Network collates national laboratory capabilities into consortia accessible to industry and academia. The Electrocatalysis Consortium (ElectroCat) targets increasing U.S. competitiveness in manufacturing fuel cell electric vehicles and other fuel cell-based devices by addressing one of the greatest remaining challenges on the path to fuel cell electric vehicle commercialization: the high cost and limited availability of PGM catalysts for polymer electrolyte fuel cells. In particular, the cost of noble metal catalysts restricts the ability to develop fuel cells that are cost-competitive with traditional hydrocarbon-based power sources. For that reason, electrocatalysts, especially for the cathode, represent the most pressing material barrier for fuel cell development and deployment. In response to the catalyst cost challenge, ElectroCat focuses on accelerating the deployment of PGM-free catalysts in fuel cells for fuel cell electric vehicles and other applications.

APPROACH

Developing effective PGM-free catalysts using cheaper, more abundant materials at an accelerated pace requires a systematic approach, by which potential catalysts are synthesized and analyzed rapidly and comprehensively using high-throughput, combinatorial methods that are in turn guided by computational studies and a fundamental knowledge of electrocatalysis. The effort is expected to benefit in a major way from the close collaboration of four national laboratories (ANL, LANL, National Renewable Energy Laboratory, and ORNL) with core competencies in PGM-free fuel cell catalyst development, including high-throughput synthesis and analysis. A consortium approach involving industry and university players provides rapid access to the unique capabilities housed at the national laboratories that make up ElectroCat, furthering meaningful progress towards the deployment of PGM-free catalysts, electrodes, and MEAs. Ultimately, the capabilities developed as part of ElectroCat could be applied to the broader advancement of electrocatalyst research, accelerating the discovery of interim solutions to the barriers posed by high PGM-content catalysts in other fields of use. As one of the first Energy Materials Network members, ElectroCat provides input on best practices and organizational support to the Energy Materials Network, thus facilitating the development of future consortia.

In addition to the development of PGM-free catalysts, ElectroCat focuses on creating the tools and catalyst information database critical to industrial deployment of PGM-free catalyst in fuel cells. ElectroCat national laboratory members use their combined expertise to refine and streamline the hardware and software tools necessary to model, analyze, and optimize PGM-free catalysts, electrode structures, and performance for a broad range of systems. These tools are expected to become enduring capabilities within the national laboratory system and to simultaneously grow the publicly-available data set as a resource. ElectroCat engages industry and university partners through funding opportunity announcements, providing an opportunity to further strengthen capabilities and advance innovative catalyst concepts. External partners also have the opportunity to approach the consortium and partner with laboratory experts through it by way of a CRADA.

RESULTS

Consortium Development

ElectroCat infrastructure support. LANL, with support from ANL, has been leading the coordination of TT/A for ElectroCat. The ElectroCat TT/A coordinator facilitates rapid and uniform contractual agreements between the laboratories themselves, as well as between the consortium and external users (e.g., agreements around intellectual property, indemnification, and/or payments to access laboratory resources). Current status of these agreements is:

a. *ElectroCat Industry Engagement Plan and Intellectual Property Management Plan.* ElectroCat Industry Engagement Plan, laying out guiding principles to be incorporated into a future Intellectual Property Management Plan, was sent to each of the ElectroCat member labs and has been finalized and agreed upon. We will begin circulating the Intellectual Property Management Plan for concurrence by each of the ElectroCat labs.

b. *Multi-Lab ElectroCat Non-Disclosure Agreement (NDA-17-0073).* The ElectroCat Multi-Lab NDA, modeled after the Fuel Cell Performance and Durability (FC-PAD) NDA, was sent to all of the ElectroCat member labs for execution of the multi-lab base NDA.

c. *ElectroCat CRADA Template.* A copy of the ElectroCat CRADA template was sent to each of the ElectroCat member labs for their review and concurrence. The template is based upon the LightMat Multi-Lab CRADA template, which all of the ElectroCat member labs have previously agreed upon. The template is available for use for any ElectroCat project award in which a CRADA may be necessary.

d. *Coordination Conference Call with TT/A Representatives.* A call with the TT/A representatives for each of the participating labs was held in March 2017 to ensure that all of the labs are aligned regarding the status of the various agreements and the consortia TT/A deliverables and timelines.

PGM-Free Catalyst Development

Catalysts with improved microporosity. Highly porous PGM-free catalysts, developed from a simple synthesis process using Zn salts ($ZnCl_2$) instead of Zn-metal organic frameworks, were further improved by removing spectator magnetic Fe species (magnetic purification). The combination of magnetic purification and removal of the hot-pressing step led to improved fuel cell performance in both kinetic and mass transport regions reaching a current density of 83 mA/cm^2 (120 mA/cm^2 at 0.80 $V_{iR\text{-}free}$). The kinetic region improvement is being attributed to an increased micropore surface area, c*a.* 1,100 m^2/g, from Zn evaporation at an elevated heat-treatment temperature of 1,000°C (Figure 1).

Catalysts with atomically dispersed transition-metal sites. Nitrogen-doped PGM-free catalysts containing atomically dispersed Fe, (AD)Fe-N-C, were successfully synthesized using a Zn-derived metal organic framework as the parent structure (Figure 2a). The synthesized (AD)Fe-N-C catalyst is composed of plate-shaped carbon structures, 30–50 nm in diameter and ca. 100–200 nm long. The carbon plates have a hierarchical micropore structure, critical for active site accessibility, formed from Zn evaporation during the high-temperature heat treatment. Characterization of (AD)Fe-N-C catalyst via high-angle annular dark-field STEM show well dispersed Fe atoms with minimal clustering. ORR activity measured in an electrochemical cell achieved a high half-wave potential ($E_{½}$) of 0.83 V vs. reference hydrogen electrode (RHE) (Figure 2b).

Direct detection of Fe sites. Nuclear resonance vibrational spectroscopy (NRVS) has been used to monitor structural perturbations of O_2-accessible Fe sites via an O_2-analogue gaseous probe molecule, nitric oxide (NO). This technique has provided new insight into the nature of Fe sites in PGM-free catalysts responsible for O_2 reduction. Isotope specificity of NRVS requires the use of ^{57}Fe to maximize signal intensity during data acquisition. ^{57}Fe-enriched (AD)^{57}Fe-N-C catalyst was synthesized with atomically dispersed ^{57}Fe, with a minimal ^{57}Fe-clustering (Figure 3a). The (AD)^{57}Fe-N-C was electrochemically reduced to change Fe^{3+} in the catalyst to Fe^{2+} for NO adsorption. The NRVS data of reduced and $NO_{(g)}$-treated (AD)^{57}Fe-N-C catalyst are shown in Figure 3b. A new vibrational feature with

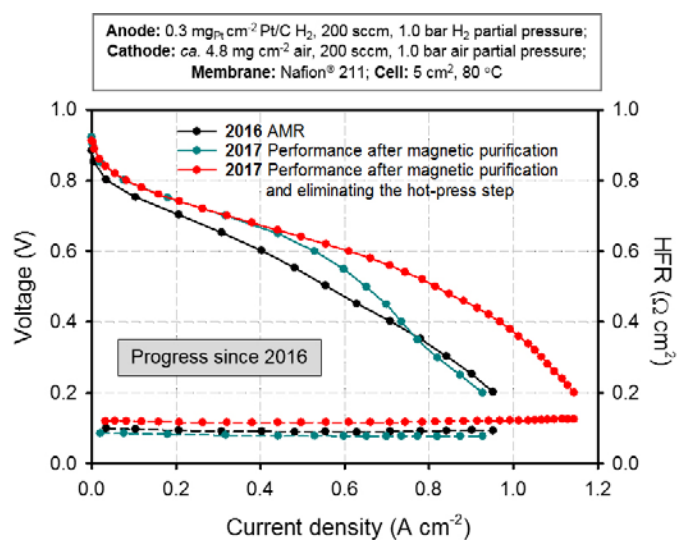

HFR – high frequency resistance

FIGURE 1. Improved H_2-air fuel cell performance of Zn-derived (CM+PANI)-Fe-C(Zn) PGM-free catalyst (red curve) compared to 2016 performance reported at Annual Merit Review (AMR).

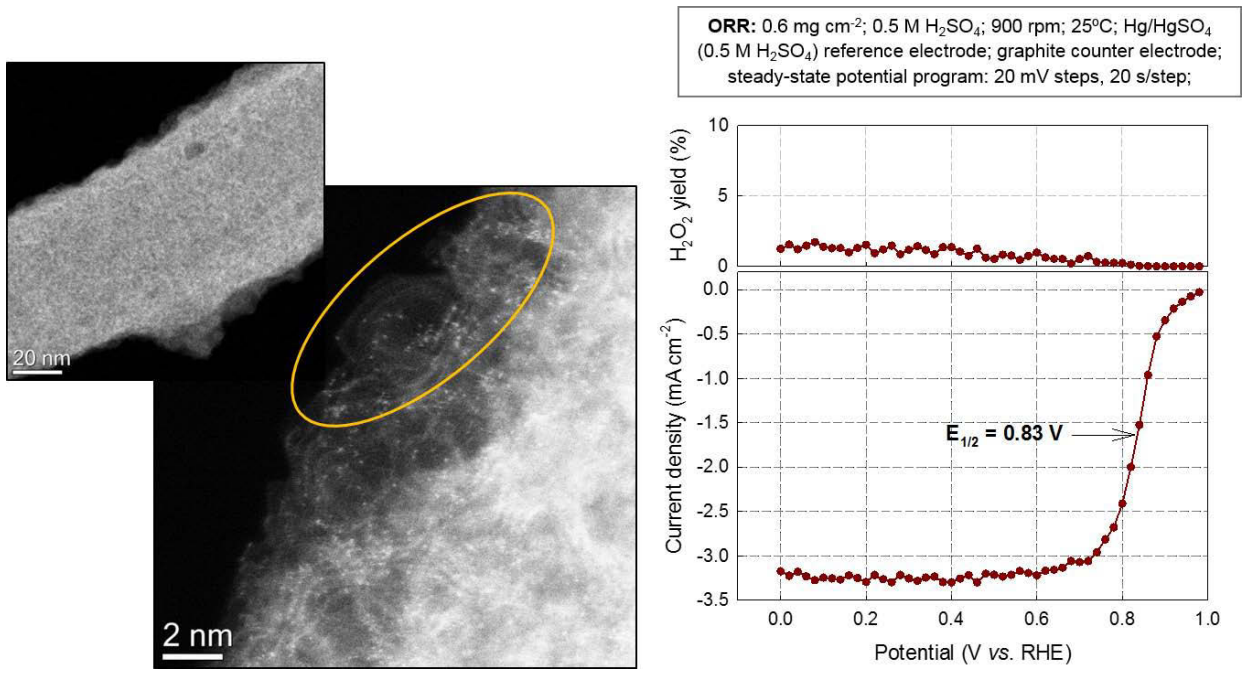

FIGURE 2. (a) High-angle annular dark-field STEM images of (AD)Fe-N-C catalyst showing a typical plate-shaped carbon structure (ca. 50 nm in diameter), as well as atomically dispersed iron over the carbon support with minimal Fe clustering (dark yellow); (b) ORR activity measured in an electrochemical cell demonstrating high ORR activity, $E_{½}$ = 0.83 V vs. RHE.

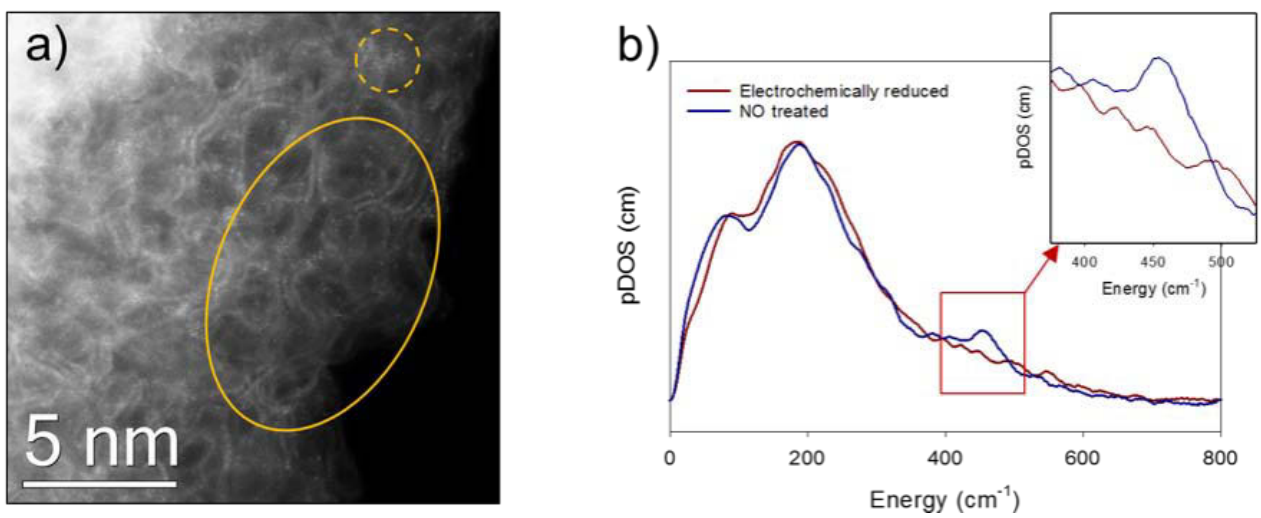

pDOS – partial density of state

FIGURE 3. (a) High-angle annular dark-field STEM images of (AD)^{57}Fe-N-C catalyst showing atomically dispersed iron (solid yellow line), with some Fe-clustering (dashed yellow line); (b) NRVS data for reduced (AD)^{57}Fe-N-C (red) and $NO_{(g)}$-treated (AD)^{57}Fe-N-C (blue). Vibrational feature for NO-treated catalyst at a frequency of 450 cm^{-1} likely corresponding to the Fe-NO bond stretch.

the $NO_{(g)}$-treated (AD)^{57}Fe-N-C catalyst is clearly seen at a frequency of 450 cm^{-1}. This vibrational feature is likely due to a Fe-NO bonding. This is a direct, surface-specific, evidence indicating that atomic Fe on the surface of the catalyst can act as an adsorption site for O_2. Fe K-edge XAFS measurements before and during NO exposure also indicate that the majority of Fe in the catalyst is able to coordinate with NO.

ORR Active-Site Activity and Durability Modeling

Density functional theory relaxation calculations of all bulk-C, zig-zag edge-C, and armchair edge-C structures, as well as structures with ORR intermediates/adsorbates (OO, OOH, O, and OH) were completed using the Materials Simulation Toolkit. These calculations were then used for the determination of the thermodynamic limiting potential, U_l, which serves as the ORR activity descriptor for a specific atomic-scale structure. DDCA scripts were created enabling high-throughput calculation of KODTE for arbitrary input atoms over a relevant range of energies. These scripts were integrated with the Atomic Simulation Environment and Python Materials Genomics (pymatgen) codes. KODTEs, the proposed durability descriptors that incorporate kinetics of bond breaking and atomic detachment, were calculated for all structures using the developed software. These calculations confirmed that the DDCA-based descriptor methodology fits well with the high-throughput high pressure cell paradigm and, that this descriptor is able to distinguish changes in durability descriptor with changes in atomic scale structure. Particularly, multi-metal atom structures ($M_1M_2N_5$) were found to be less durable than their single-metal atom (MN_4) counterparts. Additionally, it was determined that N atoms, particularly those at edges, defined the lowest KODTE for all explored structures, independent of metal speciation and structure.

High-Throughput Techniques for Synthesis and Characterization of PGM-Free Catalysts

A high-throughput and, where possible, combinatorial approach to synthesis, characterization, ORR-activity measurement, electrode fabrication, and fuel cell performance testing is being utilized to expedite progress toward achieving the ElectroCat goals (Figure 4). The previously mentioned LANL (AD)Fe-N-C catalyst was chosen as the first catalyst system for this approach. This system was selected due to the observed high ORR activity in RDE testing ($E_{½}$ = 0.83 V vs. RHE) and because only a small fraction of the possible composition and synthesis parameters have been explored using batch synthesis methods. The parameters varied in the high-throughput synthesis were the Fe-to-Zn ratio in the precursors, the identity of the Fe salt, and the heat-treatment temperature. The robotic system at ANL was utilized to rapidly synthesize forty precursors in which these three parameters were varied. After combinatorial heat treatment, the structural properties of the forty powders were determined using X-ray diffraction (XRD) and X-ray absorption spectroscopy (XAS). For a subset of these precursors, a capability was developed and utilized to determine the atomic structure of six samples simultaneously during heat treatment using Fe K-edge XAS. These experiments showed that the predominant Fe species

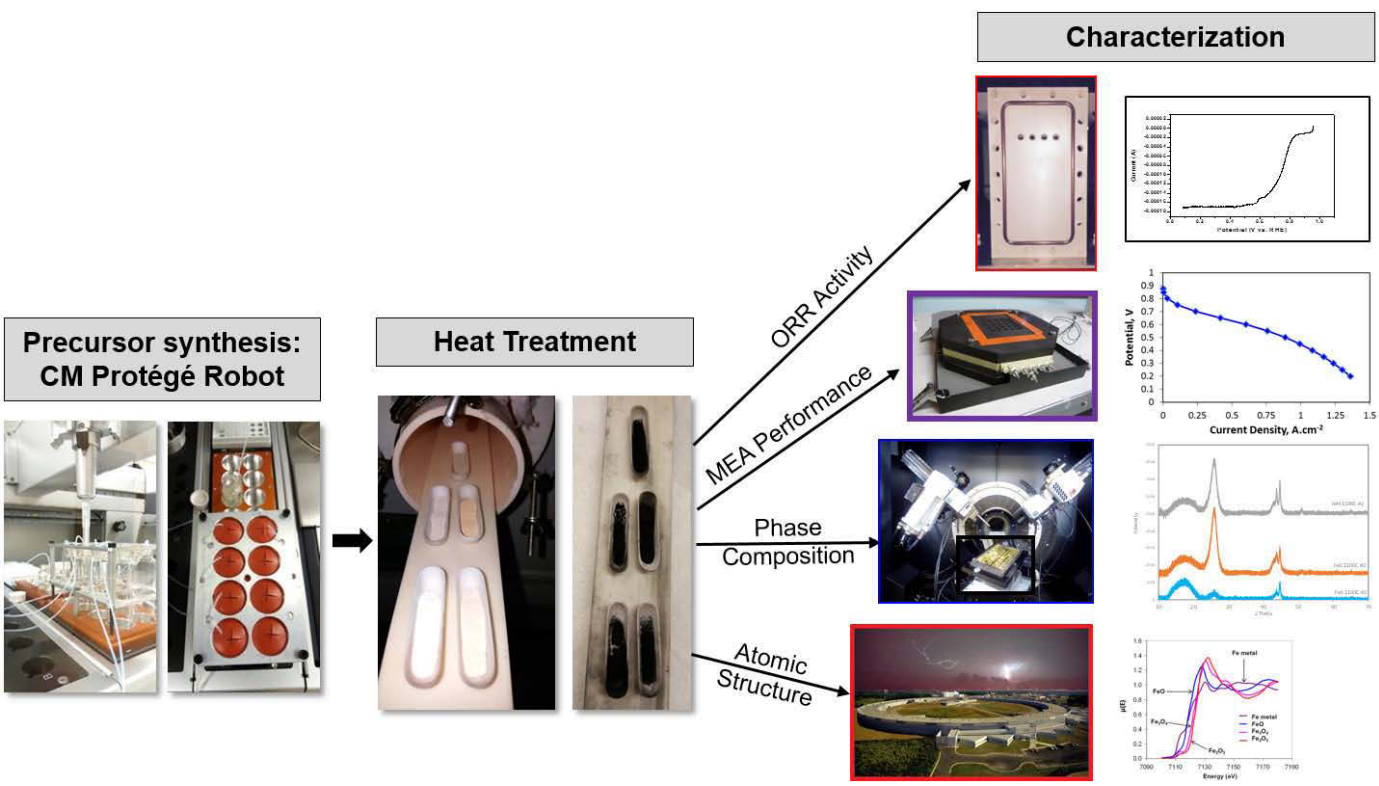

FIGURE 4. ANL high-throughput synthesis and characterization system: robotic system, simultaneous heat treatment, high-throughput structural characterization using X-ray diffraction and XAFS, and multi-channel flow double electrode cell for ORR activity characterization.

present in the active catalyst is formed in the 620–700°C temperature range during the increasing temperature heat-treatment step (Figure 5). Trends in the phase composition and atomic structure were discerned as a function of Fe precursor, Fe content, and heat treatment temperature. Examples of these trends were that the Fe nitrate precursor resulted in Fe species with a lower oxidation state than those derived from Fe sulfate and Fe acetate precursors and that higher heat-treatment temperature and iron content result in larger amounts of crystalline iron carbide. The ORR activity is currently being characterized using a multi-channel flow double electrode cell, which allows the aqueous hydrodynamic measurement of ORR activity of four samples simultaneously. The goal is to correlate ORR activity and structural composition of the catalysts.

Capability Development

ElectroCat is developing several capabilities that show potential to impact PGM-free electrocatalyst development. One such capability is the fabrication and characterization of model systems, such as thin films deposited on planar substrates. The purpose of this activity is to elucidate the nature of the active site and to potentially discover material compositions with enhanced ORR activity. National Renewable Energy Laboratory has developed the capability to deposit films of uniform or gradient composition or thickness (5–100 nm) of Fe and N on a planar substrate using physical vapor deposition (Figure 6). Characterization of these films shows that Fe-N bonds are formed in the film and C-N bonds are formed at the interface with the glassy carbon substrate, with the likely formation of the proposed active moiety, FeN_4, in the carbon matrix. Further spectroscopic and electrochemical characterization are underway.

Another capability being developed and demonstrated in ElectroCat is combinatorial fuel cell performance testing. The purpose of this activity is to accelerate the optimization of the electrode composition and structure for PGM-free catalysts by developing methods for the high-throughput synthesis and deposition of catalyst-ionomer-solvent inks, and measuring ORR activity and fuel cell performance. Two test fixtures are being evaluated for this purpose: a combinatorial 25-electrode setup with segmented flow field, gas diffusion layer, and electrode (NuVant) and a segmented current collector/flow field, with 121 individually-addressable segments, with a common/continuous gas diffusion layer and electrode. The 25-electrode setup shows identical *iR*-corrected hydrogen-air polarization curves for the 25 electrodes and measures are underway to improve the electrode-to-electrode resistance uniformity. The latter set-up showed significant cross-talk between the 121 segments and cell redesign is underway to address the cross-talk issue.

CONCLUSIONS AND UPCOMING ACTIVITIES

The following are highlighted conclusions from the ElectroCat activities thus far:

- An Fe-N-C catalyst, (AD)Fe-N-C, has been developed in which the majority of Fe sites are atomically-dispersed and on the catalyst surface, as determined by low-voltage, atomic-scale STEM imaging, and X-ray absorption and vibrational spectroscopies with probe molecules.
- The Fe sites within the atomically dispersed catalyst are more stable against dissolution than catalysts made via

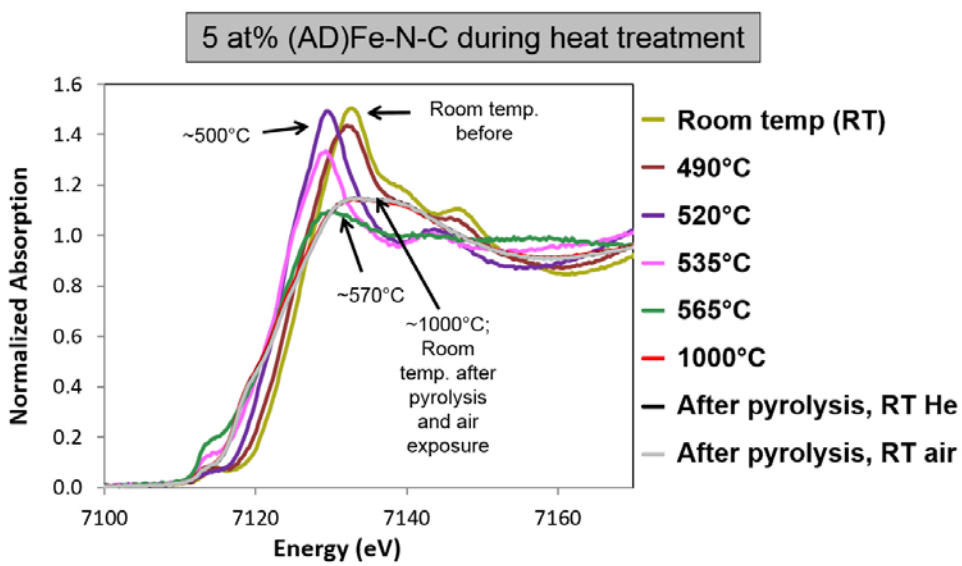

FIGURE 5. In situ XAFS during heat treatment showing Fe species found in ORR active catalysts forming at ~620–700°C.

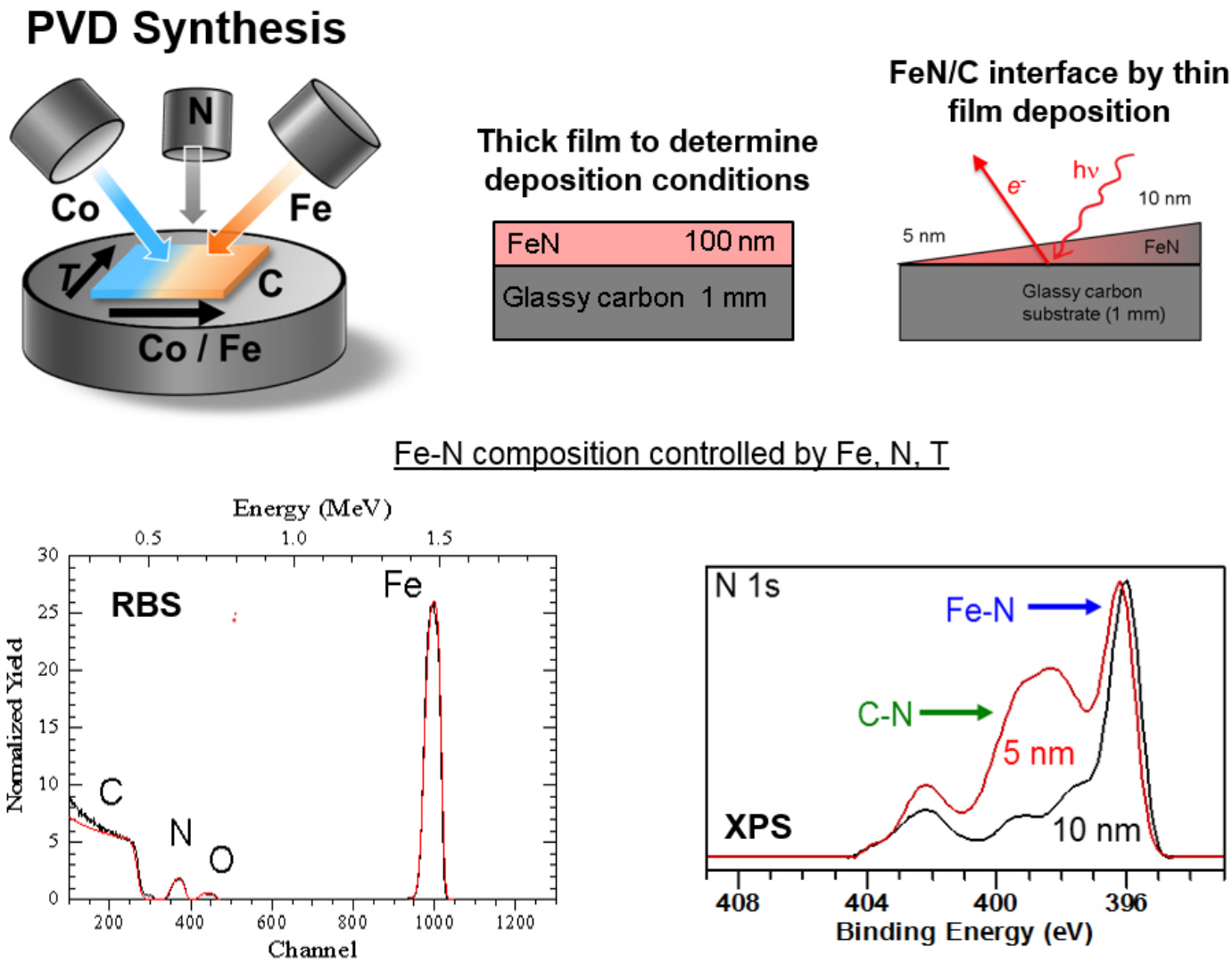

PVD – physical vapor deposition; RBS – Rutherford back scattering

FIGURE 6. Synthesis of model systems via physical vapor deposition on a glassy carbon substrate. XPS characterization of these films (bottom right) show presence of Fe-N and C-N bonds.

heat treatment of Fe-polyaniline-cyanamide, with over an order of magnitude lower Fe dissolution rates.

- A computation durability descriptor was identified and applied to various proposed active site configurations, showing that edge atoms in an "armchair" configuration are the least stable and that the nitrogen in the structures is the most susceptible to damage.
- An H_2-air fuel cell performance with a PGM-free cathode, 83 mA/cm² at 0.80 V (120 mA/cm^2 at 0.8 $V_{iR\text{-free}}$), was obtained by increasing the micropore surface area, removing spectator magnetic Fe species, and eliminating the hot-pressing step in cell fabrication.

The following are the remaining challenges and barriers in developing and implementing PGM-free ORR catalysts:

- Need for improvement in ORR activity to reduce cathode thickness and lower cost of other stack components.
- Insufficient long-term stability and performance durability under steady-state and load-cycling conditions.
- Limited understanding of the ORR mechanism, nature of the ORR active site and mechanism of catalyst degradation preventing rational design of next-generation PGM-free catalysts.
- Low volumetric density of active sites.

- Electrode design and component integration to provide adequate ionic, electronic, and mass transport to and from active sites.
- Replacement of Fe in catalyst with another PGM-free transition metal not catalyzing hydroperoxyl radical formation and ionomer degradation.
- Integration with existing automotive fuel cell stack and system technology.

The focus of future work to address these challenges includes the following.

Consortium Development

- Incorporate collaborators from DE-FOA-0001647 into ElectroCat and coordinate activities of all ElectroCat partners.
- Update ElectroCat website with information from funding opportunity announcement projects, status of capabilities, publications.
- Implement capabilities to mint digital object identifiers and other identifiers with persistent landing pages for datasets and to support automated data capture and publication.
- Document ElectroCat data sources: (i) formats, (ii) associated metadata, (iii) sharing needs, and (iv) dataset comparison or integration needs.
- Execute intellectual property management plan and material transfer agreements.

Performance and Durability Improvement

- Advance activity of atomically dispersed catalysts by maximizing concentration and accessibility of active centers through (i) the development of novel synthesis approaches, (ii) optimization of hierarchical pore-size and ionomer distribution, and (iii) decreasing electrode tortuosity.
- Explore (AD)Fe-N-C parameter space for improved performance and durability using high-throughput activity, durability, and performance testing of 40 materials synthesized to date.
- Determine primary factors governing the durability of PGM-free catalysts, concentrating predominantly on homogenous and thus easier to study materials.
- Further develop surface-specific methods for the ORR active-site determination.

Characterization and Capability Development

- Active-site identification, influence of Fe-to-N-to-C ratio on ORR activity, and influence of synthesis parameters on active-site formation: (i) thin-film model systems; (ii) ex situ, in situ, and operando X-ray spectroscopies and electron microscopy; (iii) high-throughput catalyst synthesis, characterization, and activity testing.
- ORR kinetics, mechanisms, and reactant/product transport: (i) in-cell polarization and impedance measurements as a function of oxygen partial pressure, temperature, cell voltage, etc., with systematic extraction of ORR kinetic and transport parameters, including oxygen/water transport in gas channel, diffusion media and electrodes; (ii) electrochemical techniques in aqueous electrolytes.
- Degradation mechanisms/durability: (i) online ICP-MS-RDE to correlate activity with catalyst component loss; (ii) ex situ and in situ tomography, spectroscopy, and microscopy; (iii) voltage-loss analysis using polarization curves and impedance spectroscopy.
- Electrode optimization: (i) segmented cell combinatorial studies of electrode performance coupled with high-throughput catalyst-ink synthesis and deposition; (ii) tomography and electron microscopy/energy dispersive X-ray visualization of solid, pore, and ionomer distribution coupled with electrode transport modeling.

ORR Active-Site Activity and Durability Modeling, Including High-Throughput

- Further analysis of ligand modification effects.
- Improved, automated analysis and structure generation scripts to determine limiting potential and allow for initial rotation of ligand via input Euler angles.
- Application to other proposed structures and ligands, particularly those from industry, national labs, and academia, including non-covalently bonded edge Fe structure and NO and CO ligands.

SPECIAL RECOGNITIONS & AWARDS/ PATENTS ISSUED

1. Argonne Director's Award, Theodore Krause, Sheldon Lee, and Deborah Myers, Argonne National Laboratory, June 2017.

2. "ORNL Mentor of Early Career Researcher Award," Karren More, November 2016.

FY 2017 PUBLICATIONS/PRESENTATIONS

Publications

1. "Resolving Electrode Morphology's Impact on Platinum Group Metal Free Cathode Performance using Nano-CT of 3D Hierarchical Pore and Ionomer Distributions;" S. Komini Babu, H.T. Chung, P. Zelenay, S. Litster, *ACS Appl. Mater. Interfaces*, 8 (48), 32764–3277, 2016.

2. "Direct Simulations of Coupled Transport and Reaction on Nano-Scale X-Ray Computed Tomography Images of Platinum Group Metal-Free Catalyst Cathodes;" S. Ogawa, S. Komini Babu, H.T. Chung, P. Zelenay, and S. Litster, *ECS Trans*, 75 (14), 139–146, 2016.

3. "Linking Structure to Function: The Search for Active Sites in Non-Platinum Group Metal Oxygen Reduction Reaction Catalysts;" E.F. Holby and P. Zelenay, *Nano Energy*, 29, 54–64 (2016).

4. "Heat-Treated Non-Precious Metal Catalysts for Oxygen Reduction;" H. Chung, G. Wu, D. Higgins, P. Zamani, Z. Chen, and P. Zelenay, in Electrochemistry of N4 Macrocyclic Metal Complexes, Volume 1: Energy, J. H. Zagal and F. Bedioui (eds.), pp. 41–68, Springer, 2016.

5. "Non-Precious Metal Fuel Cell Cathodes: Catalyst Development and Electrode Structure Design;" P. Zelenay, H. Chung, U. Martinez, E. Holby, X. Yin, G. Purdy, L. Ling, J. Ziegelbauer, M. Odgaard, J.H. Brewster, D. Schlueter, S. Litster, S.K. Babu, M. Neidig, J. Kehl, J. Kneebone, Z. Chen, P. Zamani, X. Fu, J.-Y. Choi, K.L. More, and D. Cullen; US Department of Energy, Hydrogen and Fuel Cells Program; 2016 Annual Progress Report; https://www.hydrogen.energy.gov/pdfs/progress16/v_a_1_zelenay_2016.pdf

Patent Applications

1. H.T. Chung, L. Lin, and P. Zelenay; "Zinc-derived Microporous Structure in Non-Precious Catalysts for Polymer Electrolyte Fuel Cell Cathodes;" filed November 14, 2016.

2. G. Wu and P. Zelenay; "Non-precious Fuel Cell Catalysts Comprising Polyaniline" (divisional of U.S. Application No. 13/267,579); filed October 17, 2016.

Presentations

1. Department of Chemical and Biomolecular Engineering, University of Tennessee, Knoxville, Tennessee, March 27, 2017. Title: "Platinum Group Metal-free Electrocatalysts for Oxygen Reduction in Fuel Cells;" P. Zelenay (*invited lecture*).

2. Technische Universität Darmstadt, Graduate School of Energy Science and Engineering, Darmstadt, Germany, February 7, 2017. Title: "PGM-free Electrocatalysis Research at Los Alamos;" P. Zelenay (*invited lecture*).

3. 7th International Conference on Fundamentals and Development of Fuel Cells (FDFC 2017), Stuttgart, Germany, January 31–February 2, 2017. Title: "Oxygen Reduction on PGM-free Electrocatalysts;" P. Zelenay*, H.T. Chung, U. Martinez, L. Lin, X. Yin, G.M. Purdy, and E. F. Holby (*invited lecture*).

4. Beijing Forum 2016 on Electrochemical Frontier, Wuhan, China, December 6–8, 2016. Title: "Recent Progress in ORR Electrocatalysis on Me-N-C Catalysts;" U. Martinez, J. Dumont, L. Lin, X. Yin, G.M. Purdy, E.F. Holby, H.T. Chung, and P Zelenay* (*invited lecture*).

5. School of Materials Science and Engineering, Huazhong University of Science and Technology, Wuhan, China, December 6, 2016. Title: "Oxygen Reduction Reaction at Platinum Group Metal-free Fuel Cell Electrocatalysts;" P. Zelenay (*invited lecture*).

6. DGIST Global Innovation Festival (DGIF), Daegu, South Korea, December 1–2, 2016. Title: "Fuel Cell Electrocatalysis: Accomplishments and Challenges;" P. Zelenay (*invited lecture*).

7. Department of Energy Systems Engineering, Daegu Gyeongbuk Institute of Science Technology (DGIST), Daegu, South Korea, November 30, 2016. Title: "A Few Highlights from PGM-free ORR Catalysis Research at Los Alamos National Laboratory;" P. Zelenay (*invited lecture*).

8. Department of Chemistry and Chemical Engineering, Chalmers University of Technology, Gothenburg, Sweden, November 24, 2016. Title: "Platinum Group Metal-free ORR Catalysts for Fuel Cells Applications;" P. Zelenay (*invited lecture*).

9. DOE Energy Efficiency and Renewable Energy Office, Fuel Cell Technologies Office, November 8, 2016. Title: "FCTO Lab Consortia Overview: ElectroCat and HyMARC;" D. Myers, M. Allendorf, and P. Zelenay, (*invited webinar*). http://energy.gov/sites/prod/files/2016/11/f34/fcto_webinarslides_electrocat_hymarc_consortia_overview_110816.pdf

10. Fuel Choices Summit, Tel Aviv, Israel, November 2–3, 2016. Title: "Panel 2: A Global Fuel Cell Technology Roadmap;" P. Zelenay, D. Stelten, L. Elbaz (S. Satyapal – moderator), (*invited webinar*).

11. Fuel Cells Workshop, Bar-Ilan University, Ramat Gan, Israel, November 1, 2016. Title: "PGM-free ORR Catalysts for Fuel Cell Applications;" P. Zelenay* (*invited lecture*).

12. Pacific Rim Meeting on Electrochemical and Solid-State Science (PRiME), Honolulu, Hawaii, October 2–7, 2016. Title: "Graphene Oxide-Based Non Precious Metal Catalysts for Oxygen Reduction Reaction with Improved Selectivity and Performance;" J.H. Dumont*, U. Martinez, G.M. Purdy, A M. Dattelbaum, P. Zelenay, P. Atanassov, A. Mohite, and G. Gupta.

13. Pacific Rim Meeting on Electrochemical and Solid-State Science (PRiME), Honolulu, Hawaii, October 2–7, 2016. Title: "Binary Fe-Free Transition Metal Catalysts for the Oxygen Reduction Reaction;" U. Martinez*, E.F. Holby, J.H. Dumont, and P. Zelenay.

14. Pacific Rim Meeting on Electrochemical and Solid-State Science (PRiME), Honolulu, Hawaii, October 2-7, 2016. Title: "Zinc-Derived Microporous Structure in Non-Precious Metal Catalysts for Polymer Electrolyte Fuel Cell Cathodes; L. Lin*, H.T. Chung, X. Yin, U. Martinez, and P. Zelenay.

15. Pacific Rim Meeting on Electrochemical and Solid-State Science (PRiME), Honolulu, Hawaii, October 2–7, 2016. Title: "High-Temperature Synthesized PGM-Free Oxygen Reduction Reaction Catalyst;" H.T. Chung*, D.A. Cullen, B. Sneed, L. Lin, X. Yin, U. Martinez, G.M. Purdy, K.L. More, and P. Zelenay.

16. Pacific Rim Meeting on Electrochemical and Solid-State Science (PRiME), Honolulu, Hawaii, October 2–7, 2016. Title: "Resolving Active Sites and Porosity in PGM-Free Catalysts by Electron Microscopy;" D.A. Cullen*, B. Sneed, K.L. More, J.H. Brewster, M. Odgaard, H.T. Chung, and P. Zelenay.

17. Pacific Rim Meeting on Electrochemical and Solid-State Science (PRiME), Honolulu, Hawaii, October 2–7, 2016. Title: "Modeling PGM-Free Active Site Structures: Activity and Durability;" E.F. Holby*, U. Martinez, H.T. Chung, and P. Zelenay.

18. Pacific Rim Meeting on Electrochemical and Solid-State Science (PRiME), Honolulu, Hawaii, October 2–7, 2016. Title: "Magnetic Purification of PGM-Free Catalysts;" X. Yin*, U. Martinez, H.T. Chung, L. Lin, and P. Zelenay (poster presentation).

19. Pacific Rim Meeting on Electrochemical and Solid-State Science (PRiME), Honolulu, Hawaii, October 2–7, 2016. Title: "Imaging Fuel Cell Components: From Flow Field Channels to Catalyst Layers;" D. Spernjak, R. L. Borup, D. S. Hussey, P. Zelenay, and R. Mukundan (*invited lecture*).

20. Pacific Rim Meeting on Electrochemical and Solid-State Science (PRiME), Honolulu, Hawaii, October 2–7, 2016. Title: "Direct Simulations of Coupled Transport and Reaction on Nano-Scale X-Ray Computed Tomography Images of Platinum Group Metal-Free Catalyst Cathodes;" S. Ogawa*, S. Komini Babu, H.T. Chung, P. Zelenay, and S. Litster.

21. Workshop on Material Challenges for Fuel Cell & Hydrogen Technologies, Grenoble, France, September 19–21, 2016. Title: "PGM-free ORR Catalysts: State of the Art and Recent Progress;" P. Zelenay*, H.T. Chung, U. Martinez, L. Lin, Xi Yin, G. M. Purdy, and E.F. Holby (*invited plenary lecture*).

22. 67th Annual Meeting of the International Society of Electrochemistry, The Hague, Netherlands, August 21–26, 2016. Title: "Recent Progress in the Development of Non-Precious Metal ORR Catalysts for Fuel Cells;" P. Zelenay*, H.T. Chung, U. Martinez, L. Lin, X. Yin, G.M. Purdy, and E.F. Holby (*invited lecture*).

23. ElectroCat Workshop, Argonne National Laboratory, Lemont, Illinois, July 26, 2017, Title: "Overview of high-throughput techniques as applied to fuel cell catalysts and electrodes", D. Myers.

24. ElectroCat Workshop, Argonne National Laboratory, Lemont, Illinois, July 26, 2017, Title: "Summary of ElectroCat experimental capabilities", P. Zelenay, D. Myers, K. More, and H. Dinh.

25. ElectroCat Workshop, Argonne National Laboratory, Lemont, Illinois, July 26, 2016, Title: "DFT modeling of PGM-free catalyst activity and durability", E.F. Holby.

26. ElectroCat Workshop, Argonne National Laboratory, Lemont, Illinois, July 26, 2016, Title: "Electrode microstructure and transport modeling", F. Cetinbas.

27. ElectroCat Workshop, Argonne National Laboratory, Lemont, Illinois, July 26, 2016, Title: "Data management and technology transfer/agreement approaches", I. Foster and L. Barber.

28. ElectroCat Workshop, Argonne National Laboratory, Lemont, Illinois, July 26, 2016. Title: "State of the art of PGM-free catalyst activity and durability;" P. Zelenay.

29. U.S. Department of Energy, Energy Efficiency and Renewable Energy, Fuel Cell Technologies Program, 2016 Merit Review and Peer Evaluation Meeting, Washington, D.C., June 6–10, 2016. Title: "Non-Precious Metal Fuel Cell Cathodes: Catalyst Development and Electrode Structure Design;" P. Zelenay (*DOE invited lecture*). https://www.hydrogen.energy.gov/pdfs/review16/fc107_zelenay_2016_o.pdf

REFERENCES

1. "Fuel Cell Technologies Office Multi-Year Research, Development, and Demonstration Plan," updated May 2017, https://energy.gov/eere/fuelcells/downloads/fuel-cell-technologies-office-multi-year-research-development-and-22.

V.A.2 Development of PGM-Free Catalysts for Hydrogen Oxidation Reaction in Alkaline Media

Alexey Serov
Department of Chemical and Biological Engineering
University of New Mexico (UNM)
MSC01 1120 1 University of New Mexico
Albuquerque, NM 87131-0001
Phone: (505) 238-9837
Email: serov@unm.edu

DOE Manager: Nancy L. Garland
Phone: (202) 586-5673
Email: Nancy.Garland@ee.doe.gov

Contract Number: DE-EE0006962

Subcontractors:
- Los Alamos National Laboratory, Los Alamos, NM
- EWII Fuel Cells LLC, Albuquerque, NM
- Pajarito Powder LLC, Albuquerque, NM

Project Start Date: June 1, 2015
Project End Date: May 31, 2017

Overall Objectives

- Develop and scale up platinum group metal (PGM)-free electrocatalyst for hydrogen oxidation in alkaline media.
- Develop novel alkaline exchange ionomer.
- Integrate PGM-free catalysts and novel ionomers into high performance alkaline exchange membrane fuel cell.
- Demonstrate peak power density of the membrane electrode assembly (MEA) of 250 mW cm^{-2}.

Fiscal Year (FY) 2017 Objectives

- Screen possible candidates for hydrogen electro-oxidation.
- Scale up best performing material.
- Synthesize ionomers for integration of materials into MEA.
- Achieve performance in MEA of 250 mW cm^{-2} using completely PGM-free anode.

Technical Barriers

This project addresses the following technical barriers from the Fuel Cells section of the Fuel Cell Technologies Office Multi-Year Research, Development, and Demonstration Plan.

(B) Cost
- (Task 1.B) Reduce/eliminate PGM loading of catalysts
- (Task 1.B) Design and demonstrate small-scale production of newly developed and promising catalysts (minimum viable product)

(C) Performance
- (Task 2.C) Improve electrolyte conductivity, for both proton and alkaline systems, over the entire temperature and humidity operating range
- (Task 3.C) Integrate catalysts with membranes and GDLs (gas diffusion layers) into MEAs

Technical Targets

The goal of this project is an integration of PGM-free anodic electrocatalysts with novel anion exchange ionomer in high performance MEAs. The project is in an early stage of development compared with well-established polymer electrolyte membrane fuel cell technology; however, achieving the goals of the project will allow us to reach DOE fuel cell targets (Table 1).

- Cost: $14/kW net
- Start-up/shutdown durability: >5,000 cycles
- Performance @ 0.8 V: 300 mA/cm^2

FY 2017 Accomplishments

- Two classes of electrocatalysts were found to be most active in hydrogen oxidation reaction (alkaline): NiMo/KetjenBlack and NiCu/KetjenBlack. These catalysts

TABLE 1. Progress towards Meeting Technical Targets for Electrocatalysts and MEAs for Transportation Applications

Characteristic	Units	DOE 2020 Electrocatalyst and MEA Targets	Project Status (5 cm^2 cell, H_2/O_2)
PGM total loading	mg-PGM/cm^2_{geo}	≤0.125	0.1, cathode
PGM-free catalyst activity	A/cm^2 @ 900 $mV_{IR\text{-}free}$	0.044	0.005
MEA performance	mW/cm^2_{geo} @ 675 mV	≥1,000	~10

were synthesized at UNM by a thermal reduction method. Technology was transferred to Pajarito Powder and scaled up to 25 g per batch.

- The Los Alamos team screened several alkaline exchange ionomers with different cationic groups and studied their interaction with catalyst. Ionomer was supplied to UNM and EWII for integration of PGM-free catalysts in the amount of 50 mL.
- EWII Fuel Cells optimized the automatic ink deposition system to manufacture MEAs by catalyst-coated membrane and catalyst-coated substrate methods. Several MEAs with areas of 5 and 25 cm^2 were fabricated and tested.
- The overall goal of the project was achieved by successful accomplishment of all milestones and two go/no-go design points.

✧ ✧ ✧ ✧ ✧

INTRODUCTION

Alkaline membrane fuel cells have been drawing attention because they have the potential to convert hydrogen fuel to electricity without using precious metal catalysts in the electrodes. Unlike polymer electrolyte membrane fuel cells that require substantial amounts of expensive Pt catalyst to catalyze the inherently sluggish oxygen reduction reaction, alkaline membrane fuel cells are able to operate using inexpensive and earth-abundant PGM-free oxygen reduction reaction catalysts. One of the most significant reasons for the substitution of anode materials from Pt to other catalysts is much slower hydrogen oxygen reduction kinetics of electrocatalyst under high pH conditions. Gasteiger et al. reported that the hydrogen oxidation reaction (HOR) of platinum electrocatalysts is several orders of magnitude slower in alkaline electrolytes compared to acidic electrolytes [1].

This project has an enabling impact on the DOE alkaline membrane fuel cell portfolio for two major reasons: first, this is the first project on PGM-free catalysts for electro-oxidation of hydrogen in alkaline media; second, catalyst and ionomer developers have teamed up in this project for industrial scale-up and MEA fabrication. This project directly ties to the mission, goals, and targets of DOE's Fuel Cell Technologies Office, both by addressing the capital cost targets for fuel cells and by advancing materials applicable for electro-oxidation of different liquid fuels.

APPROACH

In general, the approach towards successful achievement of project goals can be described through the roles of team members. UNM focuses on the development of several synthetic approaches for synthesis of Ni-based electrocatalysts for hydrogen oxidation in alkaline media: sacrificial support method, thermal reduction, and chemical reduction. These methods will allow preparation of Ni-based materials with controlled properties. Los Alamos National Laboratory's role is the preparation of perfluorinated anion exchange ionomers having selected cationic groups and electrochemical characterization at the catalyst-ionomer interface. The sacrificial support method and other synthetic approaches for Ni-based materials developed at UNM will be transferred to Pajarito Powder, where direct scale-up using identical equipment as UNM and using down-selected formulations will be conducted. Pajarito Powder will scale up the sacrificial support method/thermal reduction approaches and manufacture batches of the best performing formulations developed by UNM. EWII Fuel Cells will integrate the HOR catalyst and anion exchange ionomers to an MEA with a peak power density >250 mW cm^{-2} (2nd Generation) and will develop and manufacture alkaline exchange MEAs based on scalable processes with MEA areas of 5 and 25 cm^2.

RESULTS

The overall goals of the second phase as well as of the whole project were: (1) down-selection of the most active PGM-free electrocatalysts for HOR in alkaline media, (2) ranking and synthesis of novel anion exchange membrane ionomer, (3) establishment of MEA fabrication protocols using completely PGM-free electrocatalyst, and (4) demonstration of peak power density in MEA of 250 mW cm^{-2}.

More than 15 different Ni-based catalysts were synthesized. The variable parameters were co-catalytic elements to nickel, the ratio between elements, and synthetic parameters (temperature, duration, reducing atmosphere, etc.). Among studied systems, NiMo and NiCu supported on high-surface-area carbons (KetjenBlack [KB] and Denka) were selected as the most promising, and additional experiments were performed using nickel, molybdenum, and copper as a main catalytic matrix. The synthesized materials were characterized by rotating disk electrode, and performance (in alkaline HOR) of both NiMo/KB and NiCu/KB was higher than previously reported in literature. Materials were comprehensively characterized by X-ray diffraction, scanning electron microscopy, transmission electron microscopy, Brunauer–Emmett–Teller, and X-ray photoelectron spectroscopy, which allow the further optimization of synthesis and improvement of electrocatalytic activity of Ni-based materials.

After full optimization of synthetic parameters and choice of metal precursors, the UNM team decided to use NiMo/KB and NiCu/KB as the main materials for the anode in a fuel cell. The optimization of synthesis allows us to substantially suppress formation of the NiO phase.

Rotating disk electrode method was used for screening electrocatalytic activity of NiMo/KB and NiCu/KB electrocatalyst. Figure 1 demonstrates electrochemical performance of NiMo/KB material in HOR. It can be clearly seen that the material possesses high activity, reaching 1 mA cm^{-2} with increased loading on the working electrode. Based on the results of the rotating disk electrode HOR experiments, the preparation method of Ni-rich unsupported and supported on carbon catalyst was transferred to scale-up subcontractor Pajarito Powder. The method was successfully adopted and scaled up to the level of 25 g of catalyst per single batch. The performance of scaled material was ±10% by limiting current compared to NiMo/KB and NiCu/KB synthesis at UNM.

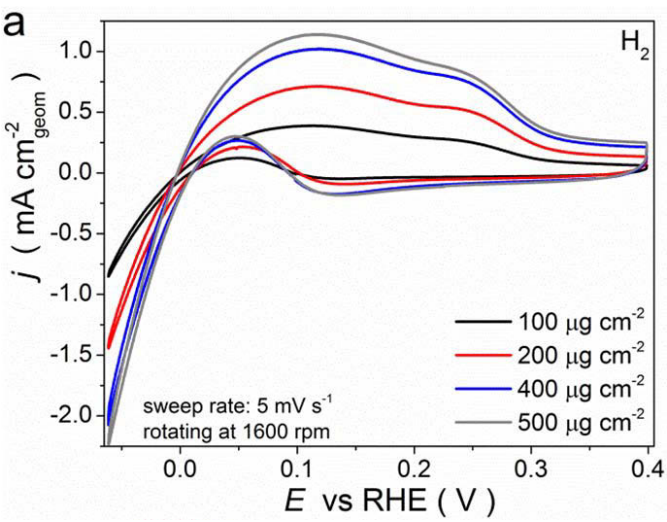

RHE – reference hydrogen electrode

FIGURE 1. Rotating disk electrode data of NiMo/KB material in HOR in dependence of catalyst loading on working electrode. Conditions: 0.1 M NaOH, 1,600 revolutions per minute.

Los Alamos National Laboratory synthesized two ionomers: methyl ammonium poly(phenylene) (ATMPP) and ethyl ammonium poly(styrene) (QASOH). Comparison of the HOR activity of PGM-free anodes with Pt/C shows that platinum strongly interacts with anion exchange ionomers, which leads to decrease in activity. NiMo/KB and NiCu/KB are substantially less prone to poisoning by alkaline exchange ionomers (Figure 2). The activity of NiMo/KB electrocatalyst integrated with ATMPP ionomer was similar to that of Pt/C (Figure 2a). Los Alamos National Laboratory optimized synthesis of ionomer on the level of 100 ml, which allows integration of PGM-free electrocatalysts into MEAs by EWII Fuel Cells.

The high performance NiMo/KB and NiCu/KB electrocatalysts were tested in fuel cell tests performed at UNM and EWII Fuel Cells. UNM prepared MEAs by hand spraying, while EWII used proprietary digital printing techniques to manufacture MEAs. The performance of NiMo/KB in the fuel cell test is illustrated in Figure 3. It was found that an increase in temperature from 60°C to 80°C resulted in a substantial increase in peak power density up to 120 mW cm^{-2}. The highest performance in MEA tests with NiMo/KB catalyst was ~175 mW cm^{-2} (Figure 4). A similar trend was observed in the case of NiCu/KB material, where peak power density was demonstrated on the level of 350 mW cm^{-2}. Such results allow our team to successfully

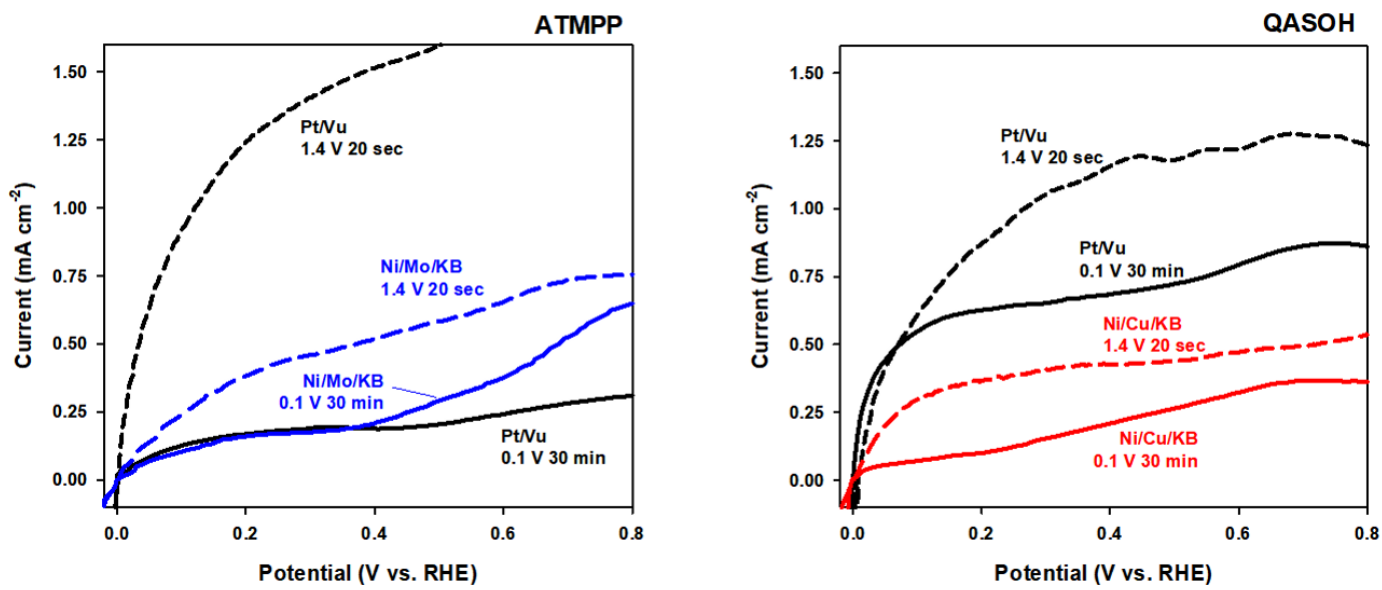

FIGURE 2. Interaction of anion exchange ionomers with Pt/C and PGM-free HOR catalysts (NiMo/KB and NiCu/KB) studied in micro electrode studies. Conditions: electrode with 100 µm diameter at 100% relative humidity, at room temperature and ambient pressure, saturated with H_2. Catalyst loading: 0.1 mg_{metal}/cm^2.

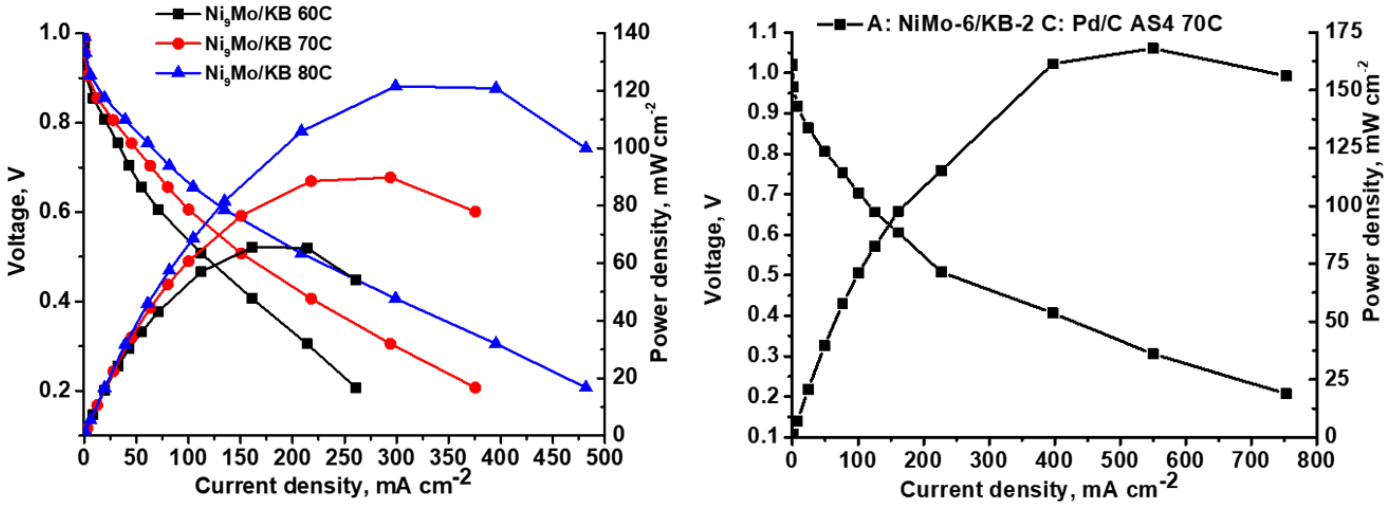

FIGURE 3. Fuel cell performance of MEA prepared with NiMo/KB electrocatalyst. Conditions: NiMo/KB (anode, 4 mg cm^{-2}); Pt/C (cathode, 0.4 mg cm^{-2}); Tokuyama AS4 ionomer (anode and cathode); catalyst coated membrane; T_{cell}= 60, 70, and 80°C; 100% relative humidity; 20 psi_g backpressure.

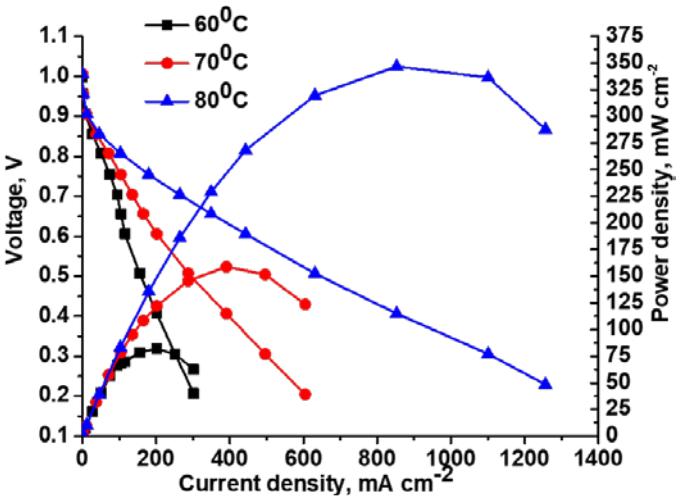

FIGURE 4. Fuel cell performance of MEA prepared with NiCu/KB electrocatalyst. Conditions: NiCu/KB (anode, 4 mg cm^{-2}); Pt/C (cathode, 0.4 mg cm^{-2}); Tokuyama AS4 ionomer (anode and cathode); catalyst coated membrane; T_{cell}= 60, 70, and 80°C; 100% relative humidity; 20 psi_g backpressure.

accomplish the final goal of the project: peak power density of 250 mW cm^{-2}.

CONCLUSIONS AND UPCOMING ACTIVITIES

The conclusions from the second and final year of the project can be summarized as follows:

- Materials were synthesized and all milestones were met: particle size, phase purity, surface area. Two rotating disk electrode protocols were developed. Milestones on performance were met.
- Ionomer developed by Los Alamos National Laboratory was supplied to UNM and EWII for integration of PGM-free catalysts into MEAs.
- EWII Fuel Cells optimized the automatic ink deposition system to manufacture MEAs by catalyst coated membrane and catalyst coated substrate methods. Several MEAs with areas of 5 and 25 cm^2 were fabricated and tested.
- The final goal of project was achieved with MEA performance of 350 mW cm^{-2}.

FY 2017 PUBLICATIONS/PRESENTATIONS

1. A. Serov, Y.S. Kim, M. Odgaard, B. Halevi, P. Atanassov, "Novel Electrocatalyst for Hydrogen Oxidation in Alkaline Media," ECS PRiME (2016).

2. A. Serov, S. Kabir, K. Lemire, K. Artyushkova, A. Roy, M. Odgaard, D. Schlueter, A. Oshchepkov, A. Bonnefont, E. Savinova, D.C. Sabarirajan, P. Mandal, I.V. Zenyuk, P. Atanassov, "NiMo Electrocatalysts for Hydrogen Oxidation Reaction for Alkaline Exchange Membrane Fuel Cells," to be submitted (2017).

3. T. Reshetenko, M. Odgaard, D. Schlueter, A. Serov, "Analysis of alkaline membrane fuel cells performance at different operating conditions using steady-state DC and AC methods," under review (2017).

4. H.T. Chung, U. Martinez, I. Matanovic, Y.S. Kim, "Cation-Hydroxide-Water Coadsorption Inhibits the Alkaline Hydrogen Oxidation Reaction," J. Phys. Chem. 7, 22, 4464–4469 (2016).

5. H.T. Chung, Y.-K. Choe, U. Martinez, J.H. Dumont, A. Mohanty, C. Bae, I. Matanovic, Y.S. Kim, "Effect of Organic Cations on Hydrogen Oxidation Reaction of Carbon Supported Platinum," J. Electrochem. Soc. 163, 14, F1503–F1509 (2016).

REFERENCES

1. W. Sheng, H.A. Gasteiger, Y. Shao-Horn, J. Electrochem. Soc. 157, (2010), B1529–B1536.

V.A.3 Innovative Non-PGM Catalysts for High-Temperature PEMFCs

Sanjeev Mukerjee
Department of Chemistry and Chemical Biology
Northeastern University (NEU)
Boston, MA 02115
Phone: (617) 373-2382
Email: S.mukerjee@neu.edu

DOE Manager: David Peterson
Phone: (720) 356-1747
Email: David.Peterson@go.doe.gov

Contract Number: DE-EE0006965

Subcontractors:
- Prof. Plamen Atanassov, University of New Mexico, Albuquerque, NM (UNM)
- Dr. Barr Halevi, Pajarito Powder, LLC, Albuquerque, NM

Other Partners:
- Dr. Emory De Castro, Advent Technologies Inc., Cambridge, MA, Industry, Special Materials Supplier
- Dr. Ludwig Lipp, eT2M, Danbury, CT, Industry, T2M Research Vendor

Project Start Date: October 1, 2015
Project End Date: December 31, 2017

Overall Objectives

This objective of this project is to revolutionize high-temperature proton exchange membrane fuel cell (PEMFC) technology based on polymer membranes imbibed with phosphoric acid through development of stable, high-performance non-precious cathode catalysts. High-temperature PEMFCs operate in a range of 150–220°C, making them ideal candidates for combined heat and power applications. This incubator effort is however exclusively focused on catalyst development for H_3PO_4-imbibed PEMFCs.

The principle objectives of this effort are:

- Develop non-platinum group metal (PGM) catalysts based on a metal-organic framework (MOF) with unique iron–nitrogen–carbon active sites that are immune to anion poisoning. Elimination of Pt from the cathode would lower total Pt loading from the current state of the art of 3 mg/cm^2 to less than 1.5 mg/cm^2, thereby halving the cost of the catalyst in the membrane electrode assembly (MEA). These catalysts will be scaled up from the ~1 g laboratory level to 100 g batch size.
- Develop unique corrosion resistant support structures for enhanced corrosion resistance as compared to conventional carbon-based supports.
- Provide enhanced mass transport within the reaction layer and gas diffusion layer using a combination of modeling and experiments for obtaining mass transport parameters designed to enable systematic formulation of the gas diffusion and reaction layers.
- Prepare MEAs and perform fuel cell testing using test conditions designed to experimentally obtain mass transport parameters. Perform durability testing relevant to stationary fuel cells. This project aims to meet and exceed the current PGM-based high temperature polymer electrolyte membrane MEA metrics of 200 mA/cm^2 in H_2/air, 0.65 V with 2.5 bar total pressure at 180°C.
- Perform economic analysis of the fuel cell system to determine market segments for deployment.

Technical Barriers

Cost is the primary barrier preventing membrane imbibed phosphoric acid (PA) fuel cells and similar systems from reaching commercial reality, with noble metal loading representing a significant cost component. Cost of noble metals in current state-of-the-art membrane-based PA systems is approximately $800–1,000/kW. Our goal is to bring this cost to below $500/kW. Durability limitations due to carbon corrosion also represent a major barrier to commercialization. This project will address both of these issues, thereby enabling commercialization of membrane imbibed PA fuel cells on an accelerated schedule.

Technical Targets

The technical targets for the second year of this project are listed in Table 1 with status towards these milestones given below.

- Fifth quarter (Q5) target: demonstration of chronopotentiometric durability testing @ 650mV (air, 2.5 bar) showing less than 5% losses in activity for 24–48 h.
  - Target Achieved at NEU using both NEU MOF and Pajarito PMF-2010 catalyst. PMF-2010 data shown later in this report.
- Sixth quarter (Q6) target: demonstration of corrosion resistance durability at OCP (air, 2.5 bar), showing less than 3% losses in activity for 3 h.

TABLE 1. Milestone Summary Table

Task Title	Milestone Description (Go/No-Go Decision Criteria)	Milestone Verification Process	Anticipated Quarter
Durability Studies	Durability testing on scaled up samples based on reactive ball milling (30–50 g batch). The sequence will include reactive ball-milled materials.	MEA performance of 200 mA/cm^2 at 0.6 V, H_2/air, 180°C, 2.5 bar total pressure. Chronoamperometric testing at 0.8 V (H_2/air) 2.5 bar total pressure (180°C) with 5% loss in activity for 24 h and 48 h.	Q5
Durability Studies	Corrosion testing of SSM-based materials.	Open circuit test on SSM-based materials at 180°C, H_2/air	Q6
Final Down Select	Down select of scaled up integrated material containing FE-MOF-based active site, SSM-based microporous layer incorporated on GDL structures.	Achieving H_2/air performance target of 200 mA/cm^2 at 0.65 V, 180°C, 2.5 bar pressure.	Q7
Fuel Cell Test Validation	Fuel cell test validation with 100 cm^2 MEA using PA-imbibed membrane and non-PGM cathode catalyst.	Achieving H_2/air performance target of 200 mA/cm^2 at 0.65 V, 180°C, 2.5 bar total pressure	Q8

SSM – sacrificial support method

  - Target Achieved at NEU using both NEU MOF and Pajarito PMF-2010 catalyst. PMF-2010 data shown later in this report.
- Seventh quarter (Q7) target: (July–September 2017): catalyst downselect, showing performance of 200 mA/cm^2 at 650 mV (air, 2 bar).
  - Currently 25 mV shy of target (data shown in this report). However, PMF-2010 material is currently being sieved for particle size uniformity, which should allow for enhanced transport and higher subsequent performance.
- Eighth quarter (Q8) target: (October–December 2017): scale-up to larger MEAs, tested at NEU (45 cm^2) while maintaining Q7 performance. Preliminary testing (shown in this report) demonstrates no performance losses as electrodes are increased from 5 cm^2 to 45 cm^2.
  - Currently 25 mV shy of target (data shown in this report).

✧ ✧ ✧ ✧ ✧

INTRODUCTION

New materials tested at NEU have demonstrated higher performance than acquired during the first year of the project leading up to a successful go/no-go decision point. Additionally, these materials have shown themselves to be very stable under multiple durability protocols. This includes both chronopotentiometric measurements as well as a protocol designed to facilitate carbon corrosion. Subsequently, the catalyst in question (described later) has been chosen to be the material of choice going forward (catalyst downselect), and variants on it will be the focus of the remaining portion of the project.

APPROACH

All of the data in this report focuses on a new catalyst from Pajarito Powder, hereon referred to as PMF-2010 (referred to in previous reports as NPC-2010). It demonstrated higher single-cell performance than the MOF-based materials (both the NEU solution reaction as well as the Pajarito Powder solid state reaction) and the other UNM materials tested throughout this project, and therefore has been chosen as the material going forward, as was directed in the Q7 target metric (catalyst downselect).

In general, it is a catalyst based off of the technology that was used for the development of an earlier catalyst. More specifically, the PMF-2010 is a precious metal free oxidiation reduction reaction catalyst designed for stability and is made using Pajarito's VariPore process. The VariPore process is based on a combination of licensed (UNM) and internally developed intellectual property and allows for intrinsic control of pore size, a critical catalyst characteristic for improved performance. The catalyst was developed out of a UNM/automotive original equipment manufacturer project, using know-how evolved over four years of PGM-free development, and further developed by Pajarito for high-temperature polymer electrolye membrane operations in consultation with Advent Technologies.

RESULTS

At the time of the last annual report, NEU testing on the MOF catalyst was roughly 50 mV shy of the air performance metric (200 mA/cm^2 at 650 mV in air, 2.5 bar). Additionally, a UNM IMID catalyst had been tested offsite at the University of South Carolina and had achieved the necessary performance metrics. Since then, Pajarito Powder has a newly developed catalyst prepared through their silica support method that has far outperformed the other materials in this project to date. Single-cell 5 cm^2 MEA performance in oxygen is shown below in Figure 1a (associated Tafel plot in

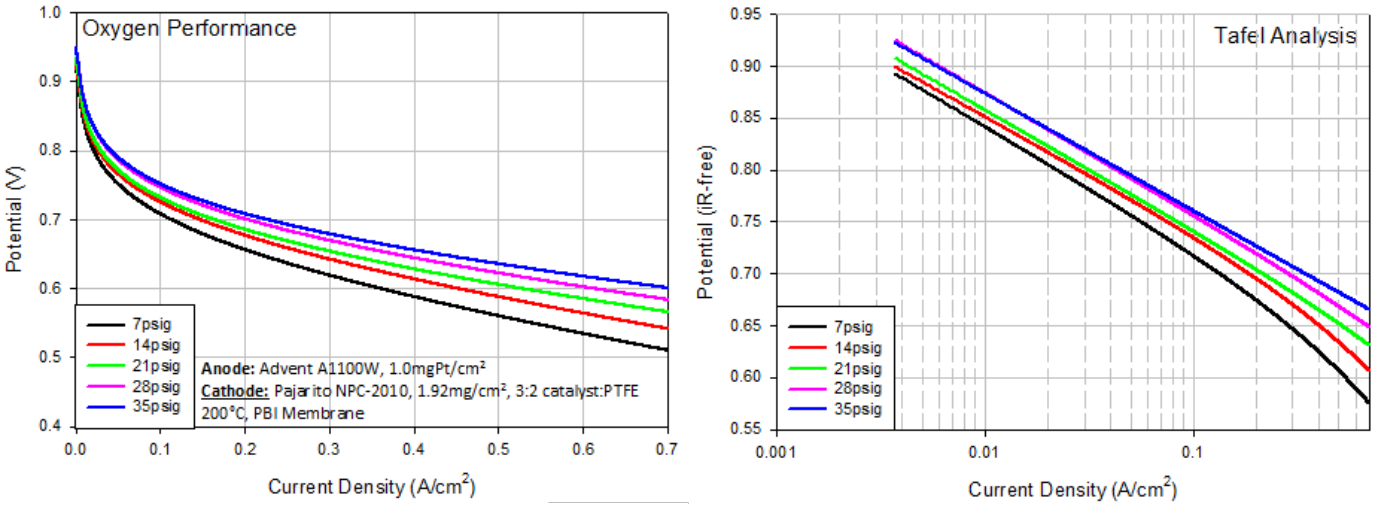

FIGURE 1. (a) Oxygen performance of Pajarito PMF-2010 as a function of applied backpressure, 5 cm^2, (b) oxygen performance of Pajarito PMF-2010 as a function of applied backpressure, 5 cm^2, Tafel analysis

Figure 1b), while performance in air is shown in Figure 2, all figures as a function of applied backpressure.

As can be seen in Figure 1a, the oxygen performance reached 710 mV at 100 mA/cm^2 at 7 psig (1.5 bara), well exceeding the target of 100 mA/cm^2 at 700mV. In addition, in air, the performance achieves 200 mA/cm^2 at 625 mV at 21 psig (2.5 bara), far elapsing the established target of 200 mA/cm^2 at 600 mV. This represents the best single-cell performance to date of any material tested over the course of this project. While this initial performance is very good, it is also key to demonstrate stability over the numerous metrics established for this work. The first of two methods that were previously established was chronopotentiometric measurements in air at 2.5 bar, where less than 5% losses in activity need to be observed over the course of 24–48 h. The second metric is to show less than 3% losses during a protocol meant to accelerate the effects of carbon corrosion. Therefore, the cell is held at its open circuit potential for 3 h in air at 2.5 bar. Figures 3 and 4 demonstrate the results of these experiments.

As is evident in Figures 3 and 4, regardless of which of the testing protocols was implemented, the catalyst performance was not altered, demonstrating that the PMF-2010 catalyst was incredibly stable. Additional durability protocols will be used in future experiments, including a temperature cycling procedure that would simulate a startup/shutdown protocol typical of a stationary power generation unit. Also, experiments are in progress to more intricately study the performance of this particular catalyst as a function of operating temperature, which could potentially allow for the operating temperature to be reduced from the current 200°C. It is expected that the higher temperature would generally correspond to a higher performance. However, the higher temperature should theoretically result in less long-

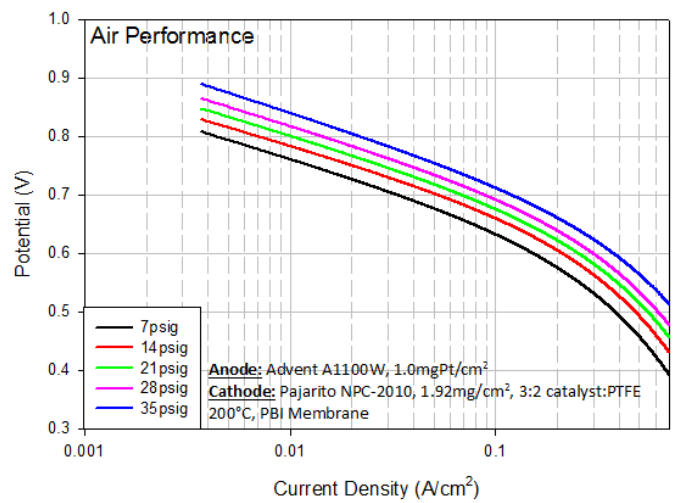

FIGURE 2. Air performance of Pajarito PMF-2010 as a function of applied backpressure, 5 cm^2, Tafel analysis

term stability, as the operating temperature of 200°C is close (<10°C) from a temperature at which the PBI membrane will start to degrade. Additionally, the higher temperature should further increase the carbon corrosion. This was largely the reasoning behind the initial target cell temperature of 160°C. Given that the catalyst is not showing any signs of degradation during the implemented protocol, it is reasonable to run the cell at a higher temperature in order to take advantage of the higher cell performance.

Often, scaling up in the electrode will cause a small drop in performance. Therefore, in an effort to predict the losses that might occur while achieving the Q8 metric (200 mA/cm^2 at 650 mV), preliminary studies were done to scale the electrode size from the above-used 5 cm^2 single-cells to

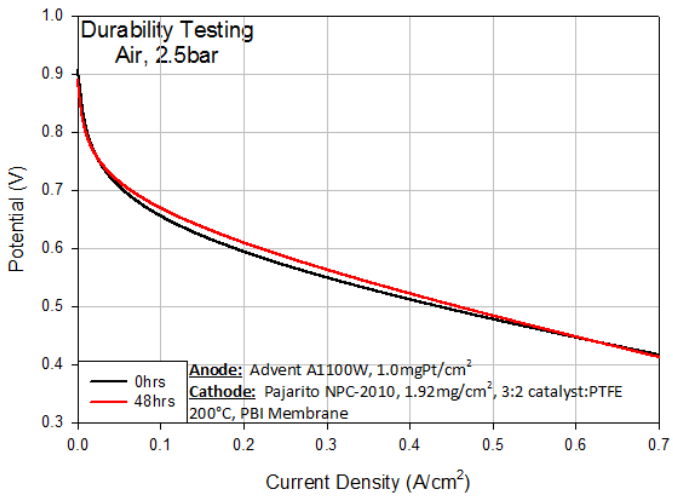

FIGURE 3. Chronopotentiometric durability in air at 2.5 bar, 48 h, 5 cm^2

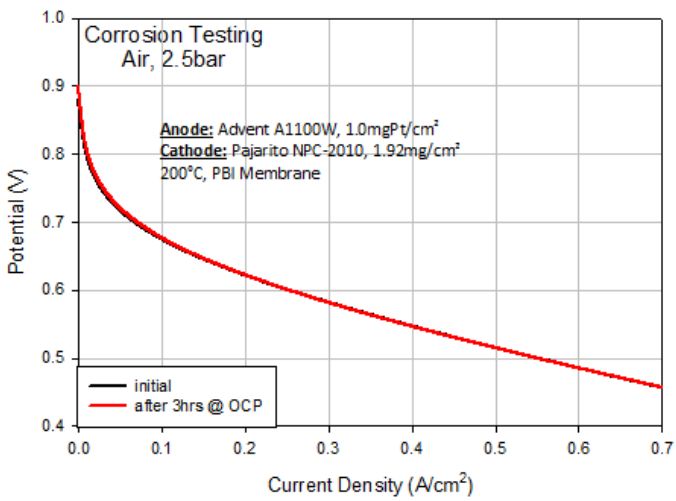

FIGURE 4. Corrosion Resistance durability in air at 2.5 bar, 3 h, 5 cm^2

45 cm^2 single-cells. Figure 5 demonstrates the results of these experiments.

From Figure 5, it is clear that the 5 cm^2 and 45 cm^2 MEAs performed at the same level. This is encouraging in that it is no longer anticipated that there will be performance losses when trying to reach the Q8 target from the Q7 metric. Therefore, in addition to the single-cell 5 cm^2 performance only being 25 mV from the Q7 target, the single-cell 45cm^2 performance is also only 25 mV from the Q8 target.

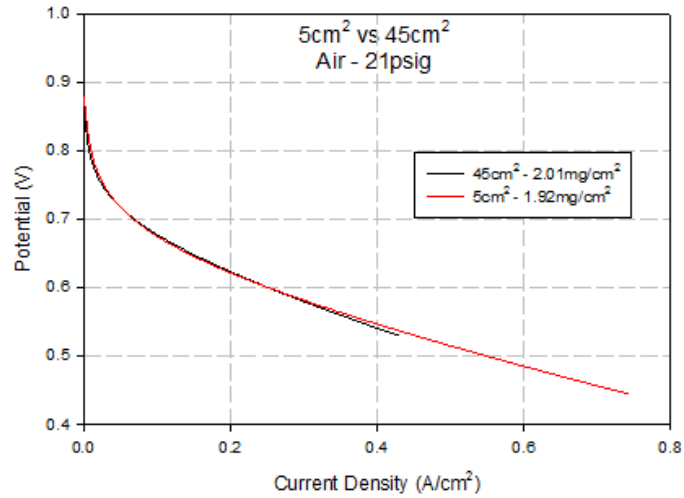

FIGURE 5. Comparison of 5 cm^2 and 45 cm^2 single-cell performance, air, 2.5 bar

CONCLUSIONS AND UPCOMING ACTIVITIES

The data shown demonstrates that the PMF-2010 catalyst from Pajarito Powder has achieved all single-cell performance metrics that were established for the first year of the project, including surpassing the go/no-go target. Additionally, it satisfies both durability metrics set forth as the Q5 and Q6 targets. It stands 25 mV shy of achieving both the Q7 target (end of September, catalyst downselect) as well as the Q8 target (end of December, 45 cm^2 scale-up).

At this time, the pathway by which the remaining 25 mV can be gained is through electrode modifications in order to optimize the gas transport through the gas diffusion electrode. Along these lines, two processes are currently being investigated. First, sieving of the catalyst is being done. Previously, Advent Technologies determined on its platinum-based systems that catalyst powders should be sieved in order to achieve particular particle size distributions, which allows for optimal gas and mass transport. All of the work shown above was done with an unsieved catalyst material. Therefore, Pajarito Powder is currently sieving an identical material, and this material will be tested at NEU. The second method that is being undertaken is to alter the particle size distribution of the initial catalyst itself. Pajarito has already prepared a variant on the PMF-2010 that incorporates a smaller particle size, which will be tested at NEU once provided. They are also working on a larger particle size material, which will also subsequently be tested at NEU. It is anticipated that between particle size optimization of the catalyst and optimization of the particle size distribution through sieving, that the final 25 mV could be gained to successfully meet the Q7 and subsequently the Q8 final metrics.

FY 2017 PUBLICATIONS/PRESENTATIONS

1. Use of Hybrid Cathodes to Reduce Platinum Content in High Temperature PEMFCs (Ryan Pavlicek, Kara Strickland, Sanjeev Mukerjee), presentation at the 229th Meeting of the Electrochemical Society (June 1, 2016; San Diego, CA).

2. Evaluation of the Durability of a Metal-Organic Framework Catalyst in High-Temperature Proton Exchange Membrane Fuel Cells (HT-PEMFCs) (Todd Miller, Ryan Pavlicek, Sanjeev Mukerjee), presentation at the 231st Meeting of the Electrochemical Society (May 31, 2017; New Orleans, LA).

V.A.4 Tailored High-Performance Low-PGM Alloy Cathode Catalysts

Vojislav R. Stamenkovic and Nenad M. Markovic
Argonne National Laboratory (ANL)
9700 Cass Ave.
Argonne, IL 60439
Phone: (630) 252-8946
Email: vrstamenkovic@anl.gov

DOE Manager: Nancy L. Garland
Phone: (202) 586-5673
Email: Nancy.Garland@ee.doe.gov

Subcontractors:
- Karren More, Oak Ridge National Laboratory (ORNL), Oak Ridge, TN
- Rod Borup, Los Alamos National Laboratory, Los Alamos, NM
- Peidong Yang, Lawrence Berkeley National Laboratory (LBNL), Berkeley, CA

Project Start Date: October 2015
Project End Date: September 2018

Overall Objectives

- Develop and deliver advanced low-PGM (platinum group metal) cathode catalysts for use in polymer electrolyte membrane fuel cells (PEMFCs) with increased mass activity at high electrode potentials, enhance performance at high current density.
- Improve durability while reducing the total loading of PGM and cost.
- Reduce PGM loading in the catalyst through alloying of Pt with other transition metals.
- The low-PGM materials will be in form of nanomaterials deployed on high surface area supports.
- Rational development and evaluation of durable high surface area supports for tailored nanomaterials.
- Development and implementation of scalable chemistry that would allow synthesis of tailored nanomaterials at the gram scale.
- Insight on the differences and similarities between the rotating disk electrode (RDE) and membrane electrode assembly (MEA) performance.
- Ionomer catalyst interaction and optimization of catalyst layers.
- The MEA will have a total PGM loading of <0.125 mg PGM/cm^2 and 0.125 g PGM/kW with mass activity higher than 0.44 A/mg PGM.
- Total loss of electrochemically mass activity will be less than 40% after 30,000 voltage cycles.

Fiscal Year (FY) 2017 Objectives

- Development of active and durable catalysts for fuel cell cathodic reaction.
- Synthesis, structural, and electrochemical evaluation of Pt-alloy nanoparticles with controlled physical parameters such as size, compositional profile and topmost surface.
- Development of scalable process to produce larger quantities of catalysts.
- Integration and evaluation of novel carbon supports with tailored Pt-alloy nanoparticles.
- Reproducibility of performance measured in MEA for tailored Pt-alloy catalysts with total PGM loading of <0.125 mg PGM/cm^2 and mass activity >0.44 A/mg PGM.

Technical Barriers

This project addresses the following technical barriers from the Fuel Cells (3.4.5 Technical Barriers) section of the Fuel Cell Technologies Office Multi-Year Research, Development, and Demonstration Plan:

(A) Durability

Develop improved catalysts:

- Reduce precious metal loading of catalysts.
- Increase the specific and mass activities of catalysts.
- Increase the durability and stability of catalysts with cycling.
- Test and characterize catalysts.

Technical Targets

The project is aimed at developing nanoparticles with tailored architectures and composition based on Pt-alloys with transition metals PtM (M = Ni, Co, Cr, V, Ti, etc.), including alloys with Au, to improve performance for the fuel cell cathodic oxygen reduction reaction. The design principles will be focused to produce systems with low content of PGMs while exhibiting highly active and durable electrochemical properties evaluated in MEAs that will meet and/or exceed the DOE 2020 targets (Table 1).

TABLE 1. Progress towards Meeting DOE 2020 Technical Targets for Electrocatalysts

	Unit	2020 DOE Targets	Project Status
PGM Total Loading	mg $_{PGM}$/cm^2	0.125	0.120
Mass Activity	A/mg $_{PGM}$ @ 900 mV	0.44	0.60
Mass Activity Loss	%	<40	<20

FY 2017 Accomplishments

- Established relationship between surface morphology and dissolution rates for Pt surfaces by implementing RDE-inductively coupled plasma with mass spectrometer (ICP/MS).
- Established relationship between the thickness of Pt overlayer and dissolution rates for Pt-based thin films by implementing RDE-ICP/MS.
- Established relationship between the particle size and dissolution rates for Pt/C catalysts by implementing RDE-ICP/MS.
- Improved durability and established stabilization mechanism for Pt thin films and nanoparticles by different metal subsurfaces.
- Established optimal, highly active and durable Pt:Ni ratio to be 1:1.
- Discovered and synthesized novel Pt-alloy nanoscale architectures that are highly active and durable: nanopinwheels, nanocages, nanoframes with radial joists and excavated nanoframes.
- Established scalable chemistry to produce 3 g and 5 g amount of PtNi catalyst with multilayered Pt-skin surfaces in a single batch.
- Exceeded mass activity 2020 DOE technical targets for PtNi catalyst in MEA; mass activity = 0.5 A/mg $_{PGM}$.
- Delivered gram-scale quantities of Pt-alloy catalysts to collaborators and stakeholders and performed electrochemical evaluations of the catalysts in MEA.

✧ ✧ ✧ ✧ ✧

INTRODUCTION

The major obstacle for broad utilization of PEMFCs in transportation is cost, performance, and durability of Pt catalysts that are employed in each individual cell of a fuel cell stack. Considering that Pt is the best known catalyst for both hydrogen oxidation and oxygen reduction reaction (ORR), it is of paramount importance to develop practical catalysts that will exhibit optimal performance through high specific activity (current per electrochemical surface area of catalyst), with minimal content of PGMs that will ensure high mass activity (current per mass unit of PGM). The cathode in PEMFCs suffers from substantial kinetic limitations and degradation of catalyst for the ORR, and for that reason the main focus in catalyst development is to create a highly efficient, durable cathode with low content of PGM. Therefore, this project will aim to develop and deliver advanced low-PGM cathode catalysts for PEMFCs that will increase mass activity at high electrode potentials, enhance performance at high current density, and improve durability while decreasing the cost. The decrease of the total loading of PGM in the fuel cell will be accomplished by improving activity and durability of Pt-based catalysts through alloying with other transition metals [1]. These PGMs in the form of nanomaterials will be deployed on high surface area supports in the cathode of the MEA with total PGM loading less than the DOE 2020 target of 0.125 mg $_{PGM}$/cm^2 and 0.125 mg $_{PGM}$/kW with mass activity higher than 0.44 A/mg $_{PGM}$.

APPROACH

This is a multi-performer project led by ANL and supported by inter-lab collaborations with LBNL, Los Alamos National Laboratory, and ORNL. ANL leads and coordinates this applied research effort with other national laboratories, defines project scope, topics, milestones, and is responsible for deliverables as well as quarterly and annual reports to the Fuel Cell Technologies Office. LBNL is involved in chemical synthesis of advanced nanoscale structures and development of scaling-up protocols of the most promising catalytic systems. Los Alamos National Laboratory fabricates and tests the MEAs and provides alternative carbon-based supports to conventional high surface area carbon. ORNL characterizes synthesized materials and catalysts deployed in an MEA before and after testing protocols by electron microscopy. The approach of this project is based on the knowledge obtained from well-defined systems that will be used to tailor functional properties of corresponding nanoscale materials, with desired shape, size, structure and compositional profile. Integration of engineered nanomaterials in electrochemical systems requires integration of a broad range of scientific disciplines such as solid state physics, surface science, physical chemistry and electrochemistry. This effort also includes a combination of highly diverse experimental tools supported by state-of-the-art synthesis and characterization strategies, together with the fabrication and testing capabilities. The project is executed simultaneously in five tasks throughout duration of the project: Task 1 – Well-Defined Systems, Task 2 – Synthesis of Nanoscale Materials, Task 3 – Electrochemical and Structural Characterization of Catalyst, Task 4 – Advanced Supports for Novel Catalysts, and Task 5 – Scaling Up of Catalysts.

RESULTS

Pt Dissolution Rates and the Mechanism of Catalyst Degradation

In the development of superior low-PGM catalysts it is of paramount importance to address the stability of Pt-based catalysts by establishing stability range dissolution rates and mechanism. In the previous period, we combined efforts between Tasks 1, 2, and 3 to reveal trends in dissolution of Pt surfaces. As reported last year [2], dissolution trends from Pt single crystals are clearly indicating that the topmost surface atoms with the highest coordination number are less sensitive to dissolution processes. For that reason, the most stable surface was found to be Pt(111). Linking the properties between well-defined single crystalline surfaces and a real world catalyst would ultimately lead towards design of advanced systems with high durability. The most recent efforts aimed at exploring different Pt thin film surfaces and nanoparticles. In all cases, a glassy carbon electrode was used as a substrate either to deposit a thin metal film or thin catalyst layer. In each case, the experiments were executed in ultra clean environments to ensure high purity of electrochemically active constituents. Depositions of thin metal films were done in a magnetron sputtering chamber with the ability to vary the thickness from 1 ML (monolayer) to multilayers of Pt. These films were transferred either to an electrochemical cell for evaluation or to an ex situ scanning tunneling microscope (STM) to determine the surface morphology. Figure 1a depicts a STM image of 4 ML Pt film over glassy carbon. From the STM image, it is obvious that the surface has highly corrugated morphology with well-defined average cluster size distribution, which was found to be 5 nm in diameter. On the other electrode, monodisperse 5 nm Pt/C catalyst was deposited and characterized by high transmission electron microscopy. Each sample was characterized by cyclic voltammetry in RDE, which was followed by on line ICP/MS. It is important to note that thin film clusters and the 5 nm Pt/C catalyst have identical cluster-particle size. However, the main difference

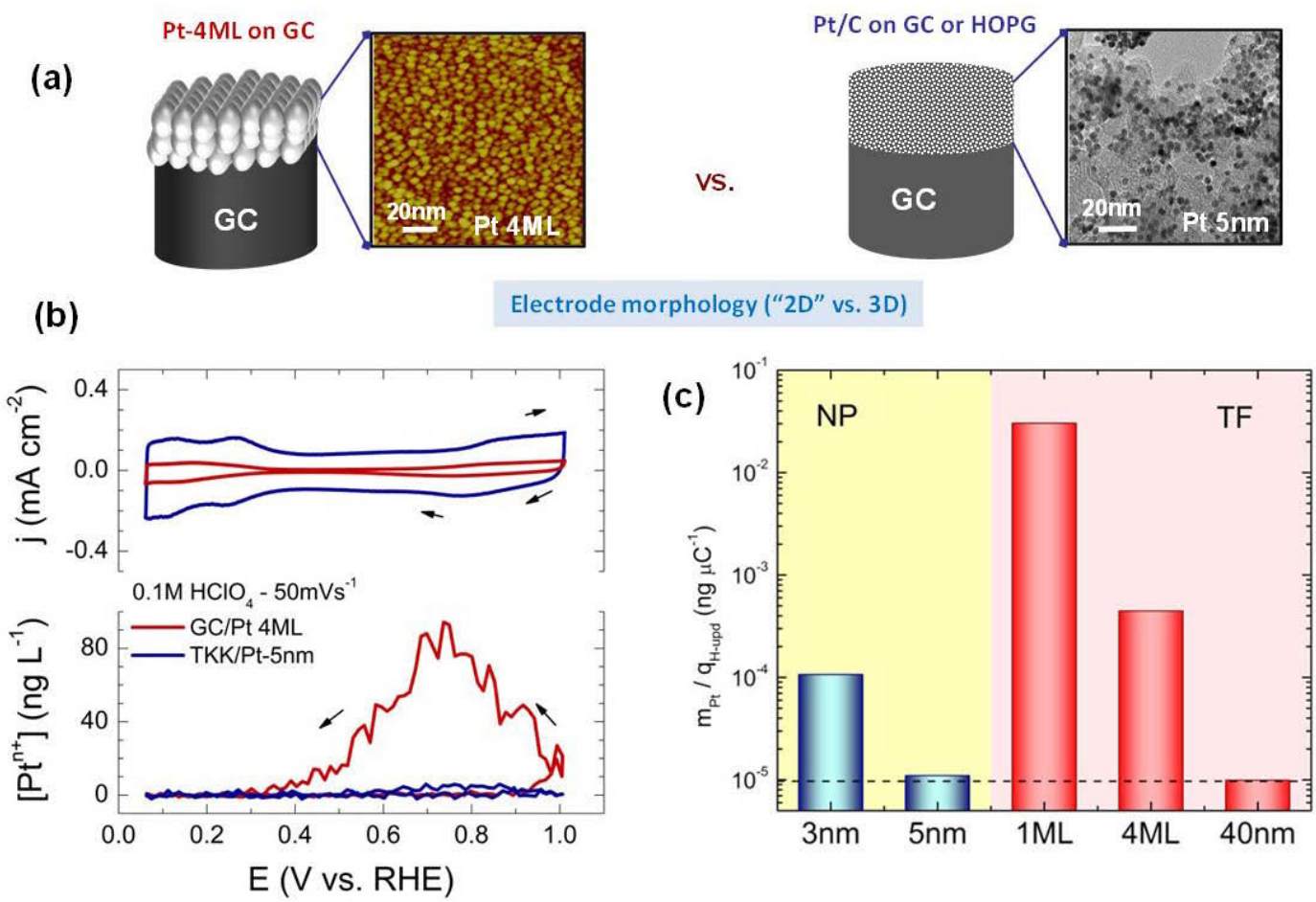

GC – glassy carbon; HOPG – highly oriented pyrolytic graphite; RHE – reference hydrogen electrode; NP – nanoparticle; TF – thin film

FIGURE 1. Structural and electrochemical characterization of Pt thin film surfaces and Pt nanoparticles deposited over the glassy carbon electrode by (a) STM and high resolution transmission electron microscope, (b) RDE-ICP/MS, and (c) dissolution rates from during single potential cycle between 0.6 V and 1.0 V from different Pt nanoparticles and Pt thin films with various thicknesses.

between them is due to the two-dimensional (2D) nature of the thin film surface versus a three-dimensional (3D) catalyst overlayer. Accordingly, dissolution rates measured from these samples exhibit remarkably different values. Pt dissolution from thin film surfaces is higher by more than one order of magnitude compared to the Pt/C catalyst. The main reason is due to the 3D nature of the catalyst layer where high surface area carbon matrix acts as a scavenger of dissolved Pt atoms. Based on this finding, thin metal films can be used to magnify the real dissolution effect in order to resolve the dissolution mechanism and propose more stable systems. Along those lines, a subsurface made of different metals including Au was used to evaluate influence on the topmost Pt dissolution. Thin metal films of various precious metals (Pd, Re, Au, Ir, Ag, etc.) were deposited over a glassy carbon electrode and then 4 ML of Pt has been added to the topmost surface layer (not shown here). It was confirmed that subsurface Au has the most beneficial properties for preventing Pt dissolution. As reported before [3], a rather high dissolution rate of 4 ML Pt on glassy carbon can be completely suppressed by Au subsurface. This has been used [4,5] and will be implemented in novel nanoscale systems.

Novel Nanoscale Architectures of Pt-Alloy Catalysts

A series of monodispersed nanoparticles with novel architectures have been synthesized and characterized to determine particle size, composition, morphology, and electrochemical performance in RDE. The most promising systems are summarized in Figure 2 together with high-angle annular dark-field and elemental mapping images. Nanopinwheels depict highly porous morphology, rather large particle size (~50 nm) and homogeneous elemental distribution between Pt and Ni. The synthesis protocol allows formation of highly dealloyed structures with high roughness factor that creates sufficient number of active sites and hence,

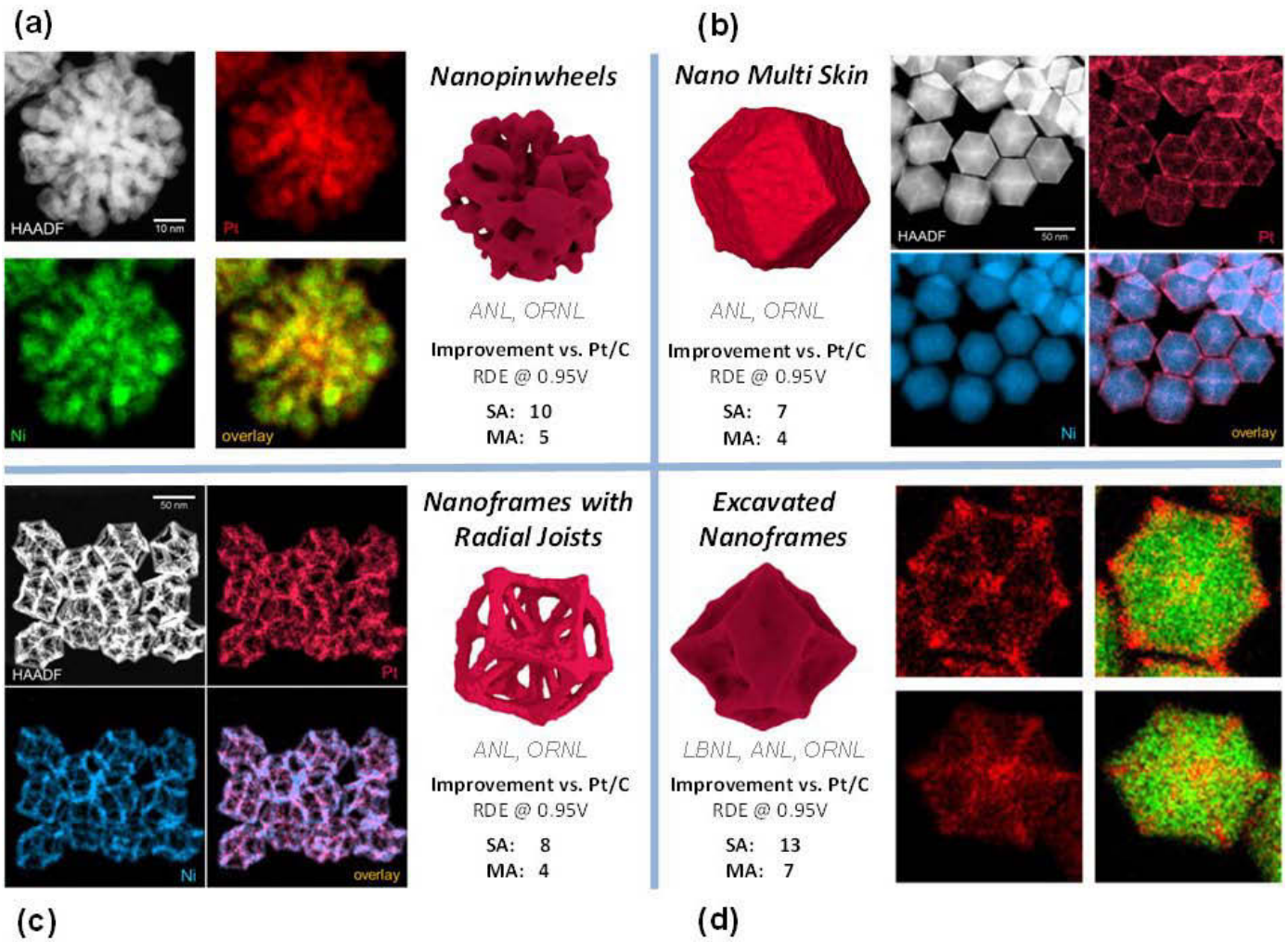

SA – specific activity; MA – mass activity

FIGURE 2. High-angle annular dark-field micrographs and elemental distribution of synthesized monodisperse PtNi NPs with novel architecture along with their performance for the ORR measured in 0.1 M $HClO_4$ by RDE: (a) nanopinwheels, (b) octahedrons with multilayered Pt-skin surfaces, (c) nanoframes with radial joists, and (d) excavated nanoframes.

high specific and mass activities. Figure 2b shows PtNi alloy particles that are highly monodisperse cuboctahedrons with multilayered Pt-skin surfaces with well-defined compositional profile. In addition to previously reported PtNi nanoframes [6], we report here two novel architectures: nanoframes with radial joists as additional active sites within the nanoframe structure and excavated nanoframes. Based on the RDE screening of these catalysts dispersed in high surface area carbon, the increase in specific activity is up 13-fold, and mass activity up 7-fold when compared to Pt/C. Each of these nanoarchitectures will be evaluated for scale-up protocol.

Scaling the Amounts Synthesized Pt-Alloy Catalysts to Gram Levels

A new procedure which is capable of making 5 g catalyst per batch with similar or higher RDE activity was developed by modifying several steps of the original small batch synthesis process (Figure 3).

In the original procedure [7], Pt precursor dissolved in 1,2-dichlorobenzene (boiling point 180°C) was preheated to 80°C and injected into Ni precursor solution at 200°C. This process is not operationally practical and may not be safe for large-scale synthesis because of the pressure change and possibility of introducing oxygen during injection.

The new scale-up procedure utilizes one-pot synthesis that avoids the injection of the hot Pt precursor. This makes the scale-up of the monodispersed PtNi nanoparticles feasible at least to a gram-scale. In the loading PtNi nanoparticles onto carbon step of the original procedure, nanoparticles were dispersed in hexane or chloroform solvent and then mixed with carbon black (Tanaka, KK), which was followed by evaporation of the solvent. Evaporation of the large amount of flammable and/or toxic solvents is both prohibited by regulations and not operationally safe. In addition, loading of the significant amount of nanoparticles in hexane, usually results in non-uniform dispersion of nanoparticles on carbon support. Although the loading of nanoparticles on carbon in chloroform is uniform, some particles will come off the carbon support if a centrifuge is used to separate them from the solvent.

In the new procedure, PtNi nanoparticles are dispersed in chloroform and then mixed with carbon black which was already dispersed in chloroform. After mixing, hexane is

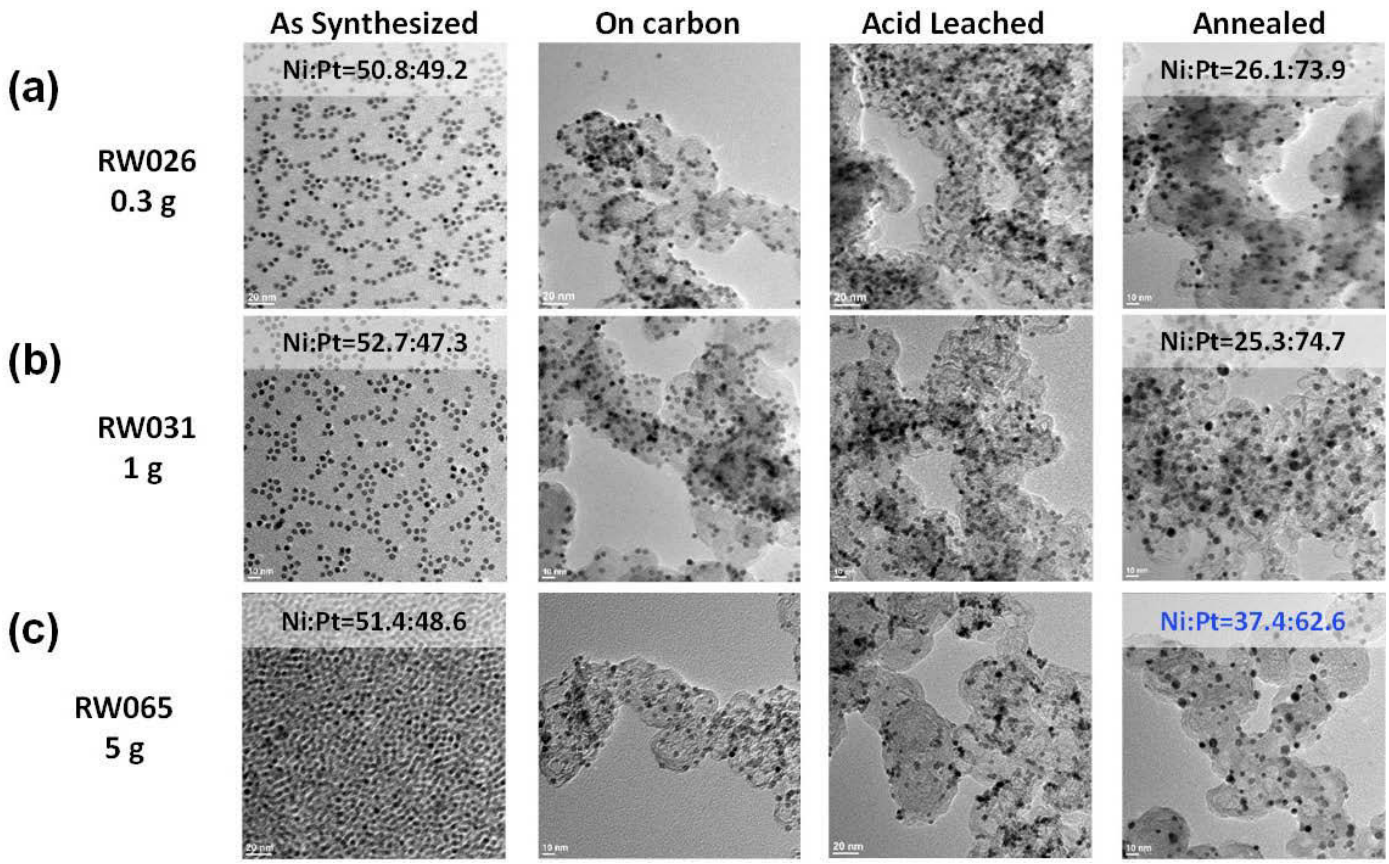

SA – specific activity; MA – mass activity

FIGURE 3. Progress and evolution of the scaling-up synthesis protocol for PtNi/C nanoparticles with multilayered Pt-skin surfaces. (a) Initial synthesis batch of about 0.3 g and was successfully scaled to (b) 1 g and (c) 5 g of catalyst, while particles maintained the same composition, particles size distribution, and multilayered Pt-skin surfaces.

introduced to precipitate PtNi/C from the solvent. Finally, PtNi/C could be separated from the solvent by filtration. In the acid leaching step of the original procedure, PtNi/C was assumed to be mixed with 0.1 M $HClO_4$ by brief sonication and further soaking in this solution was allowed. This process works well for a small amount of catalyst (typically milligram-scale). However, to disperse a large amount of PtNi/C, prolonged sonication is needed which results in severe loss of Ni from the nanoparticles. In the new procedure, PtNi/C was dispersed in water before mixing with 0.1 M $HClO_4$, and the leaching process was systematically investigated to give the best RDE activity. With all the modifications, the new procedure is capable of making 5 g catalyst per batch. Mass activity of the catalyst prepared with this procedure is 8–9 times higher than commercial Pt/C. The reproducibility of the process was confirmed with a second batch synthesis. Transmission electron microscopy tomography confirms that all the PtNi particles are located on the surface of carbon which results in higher catalyst utilization at different humidification conditions in the MEA.

MEA Evaluation of Scaled Up Catalyst with Multilayered Pt-Skin Surfaces

The nanoparticle evaluations were made in RDE and 5 cm^2 MEA at ANL. The MEAs were made by the decal method with the ionomer and membrane in the proton form and hot-pressing of the decals to the membrane at 130°C. The ionomer to carbon ratio was 0.8. The summary of the MEA test results is given in Figure 4. The MEAs were tested at temperatures ranging from room temperature to 80°C, with 150 kPa(abs) humidified hydrogen on the anode at 1 L/min, and with 150 kPa(abs) humidified oxygen and/or air on the cathode, with a relative humidity of 100%. The

(a)

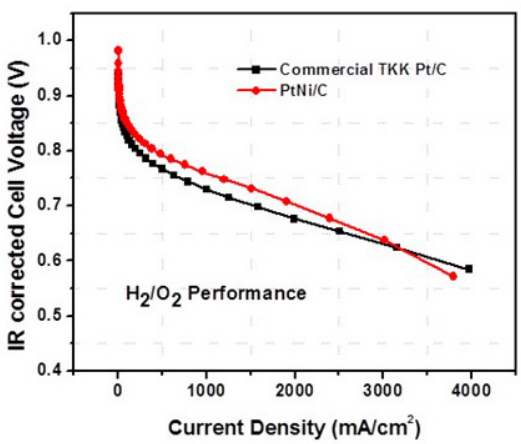

(b)

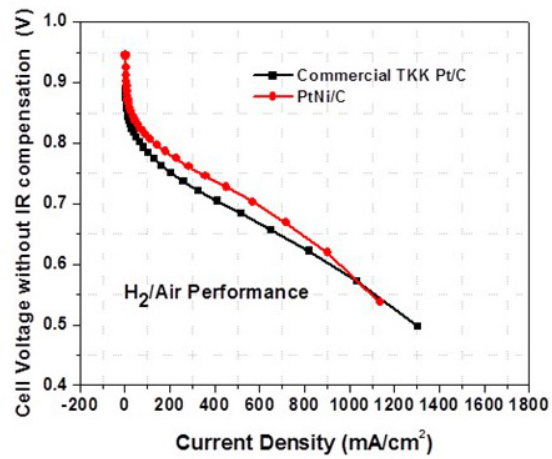

(c)

	Units	PtNi Cathode	TKK Pt Cathode
Pt total loading	mg_{Pt}/cm^2_{geo}	~0.04	~0.04
Mass activity (H2-O2)	A/mg_{PGM} @0.9 $V_{iR\text{-}free}$	0.5	0.22
Specific activity (H2-O2)	mA/cm^2_{PGM} @0.9 V	1.01	0.39
MEA performance (H2-Air)	mA/cm^2 @0.8 V	131.34	64.3
ECSA	m^2/g_{PGM}	50	52.5

IR – internal resistance; ECSA – electrochemically active surface area

FIGURE 4. MEA characterization of scaled 20 wt% PtNi/C catalyst with multilayered Pt-skin surfaces (red) and Pt/C TKK (black) obtained in 5 cm^2 cell: (a) hydrogen–oxygen polarization curves, (b) hydrogen–air polarization curves. The cathode Pt loading is 0.04 mg_{Pt}/cm^2, ionomer to carbon ratio = 0.8, 80°C, 150 kPa, 100% relative humidity. (c) Performance parameters of PtNi/C retrieved from MEA hydrogen–oxygen polarization curves.

mass activities are shown in the table in Figure 4c. High performance PtNi/multilayered–Pt-skin nanoparticles have been evaluated by MEA and it has been confirmed that high durability originates from the protective multilayered Pt-skin surface that encapsulates the core that is Ni rich, as mentioned before. The multilayered Pt-skin catalyst was prepared by scaled-up protocol developed at ANL and its performance measured in MEA has achieved the DOE 2020 technical target. The Pt loading on the cathode was 0.04 mg $_{PGM}$/cm^2 and measured mass activity was found to be 0.50 A/mg $_{PGM}$ at 0.9 V. In addition to MEA evaluation at ANL, the same catalyst was distributed to our collaborators at Los Alamos National Laboratory, as well as to stakeholders. These characterizations are still undergoing.

CONCLUSIONS AND UPCOMING ACTIVITIES

New insights into dissolution mechanism of Pt have been obtained and it was confirmed that subsurface Au can indeed suppress dissolution of Pt. This will be further evolved and applied to nanoscale systems in the next phase of the project. Dissolution will continue to be strictly monitored for all promising nanoscale systems. A series of Pt-alloy nanoparticles with unique architectures were synthesized and have been employed in harvesting high catalytic performance. The next step will be to evaluate these systems for a scale-up protocol which would enable distribution of the catalyst among the network of collaborators and stakeholders. A number of carbon supports have been evaluated for the support that would lead to better utilization of Pt-alloy nanoparticles, however, most of these systems did not reach the performance of currently used carbon black. This effort will continue to be integral part of this project. MEA evaluation will be performed in 5 cm^2 to 50 cm^2 cells. The project will continue to explore novel architectures of Pt-alloy nanoparticles that would allow implementation of the scale-up protocol. All of these efforts are expected to generate new patents that would be readily available for licensing.

FY 2017 PUBLICATIONS/PRESENTATIONS

1. V.R. Stamenkovic, P.P. Lopes, D. Strmcnik, and N.M. Markovic, *Energy and Fuels from Electrochemical Interface,* Nature Materials*,* 16 (2017) 57–69.

2. Y. Kang, P. Yang, N.M. Markovic, and V.R. Stamenkovic, *Shaping Electrocatalysis through Tailored Nanomaterials,* Nano Today*,* 11 (2016) 587–600.

3. H. Lv, D. Li, P.P. Lopes, D. Strmcnik, R. Wang, N. Markovic, and V. Stamenkovic*, From Fundamentals to PEMFC Systems*, 231st Electrochemical Society Meeting, May 2017, New Orleans, LA.

4. D. Strmcnik, D. Li, P.P. Lopes, E. Coleman, H. Lv, N.M. Markovic, and V. Stamenkovic*, Advanced Carbon Structures for PEMFC,* 231st Electrochemical Society Meeting, May 2017, New Orleans, LA.

5. D. Li, H. Lv, D. Strmcnik, N. Markovic, and V. Stamenkovic*, From Well-Defined Electrochemical Interfaces to Functional Nanoscale Materials,* 253rd American Chemical Society National Meeting, April 2017, San Francisco, CA.

6. D. Li, D. Strmcnik, N. Markovic, and V. Stamenkovic*, Design and Synthesis of Nanomaterials for Energy Applications,* Gordon Research Conference, February 2017, Ventura, CA.

7. V. Stamenkovic, *Tailored Electrocatalysts with Advanced Properties,* Fuel Cells Workshop, Bar Ilan University, November 2016, Tel Aviv, Israel.

8. P.P. Lopes, D. Li, D. Strmcnik, N. Markovic, and V. Stamenkovic*, Tuning of the ORR Performance-Durability for Pt-Based Electrocatalysts,* 230th Electrochemical Society Meeting, October 2016, Honolulu, HI.

9. D. Li, D. Strmcnik, N. Markovic, and V. Stamenkovic*, Novel High-Performance Low-PGM Catalysts*, Gordon Research Conference, August 2016, Easton, MA.

10. N. Markovic and V. Stamenkovic, *State of the Art and Challenges Facing Low-Temperature Fuel Cell Electrocatalysis*, DOE-EERE Catalysis Working Group Meeting, July 2016, Argonne, IL.

REFERENCES

1. V. Stamenkovic, B. Fowler, B.S. Mun, G. Wang, P.N. Ross, C. Lucas, and N.M. Markovic, "Improved Oxygen Reduction Activity on Pt_3Ni(111) via Increased Surface Site Availability," *Science*, 315 (2007) 493–497.

2. P.P. Lopes, D. Strmcnik, J. Connell, V.R. Stamenkovic, and N.M. Markovic, "Relationships between Atomic Level Surface Structure and Stability/Activity of Platinum Surface Atoms in Aqueous Environments", *ACS Catalysis*, 6 (4), 2536–2544, 2016.

3. V.R. Stamenkovic and N.M. Markovic, "Tailored High-Performance Low-PGM Alloy Cathode Catalysts," FY 2016 Annual Progress Report*, DOE Hydrogen and Fuel Cells Program*.

4. C. Wang, D. van derVliet, K.L. More, N.J. Zaluzec, S. Peng, S. Sun, H. Daimon, G. Wang, J. Greeley, J. Pearson, A.P. Paulikas, G. Karapetrov, D. Strmcnik, N.M. Markovic, and V.R. Stamenkovic, "MultimetallicAu/$FePt_3$ Nanoparticles as Highly Durable Electrocatalysts," *Nano Letters*, 11 (2011) 919–928.

5. Y. Kang, J. Snyder, D. Li, K. More, N.M. Markovic, and V.R. Stamenkovic, "Multimetallic Core/Interlayer/Shell Nanostructures as Advanced Electrocatalysts," *Nano Letters*, 14 (2014) 6361–6367.

6. C. Chen, Y. Kang, J. Snyder, M. Mavrikakis, Y. Li, N.M. Markovic, G. Somorjai, Peidong Yang, V.R. Stamenkovic "Highly Crystalline Multimetallic Nanoframes with Three-Dimensional Electrocatalytic Surfaces," *Science*, 343 (2014) 1339–1343.

7. C. Wang, M. Chi, D. Li, D. Strmcnik, D. van derVliet, G. Wang, V. Komanicky, K.-C. Chang, A.P. Paulikas, D. Tripkovic, J. Pearson, K.L. More, N.M. Markovic and V.R. Stamenkovic, "Design and Synthesis of Bimetallic Electrocatalyst with Multilayered Pt-Skin Surfaces," *Journal of American Chemical Society*, 133 (2011) 14396.

V.A.5 Platinum Monolayer Electrocatalysts

Radoslav Adzic (Primary Contact), Jia Wang, Miomir Vukmirovic, Kotaro Sasaki
Brookhaven National Laboratory, Bldg. 555
Upton, NY 11973-5000
Phone: (631) 344-4522
Email: adzic@bnl.gov

DOE Manager: Nancy L. Garland
Phone: (202) 586-5673
Email: Nancy.Garland@ee.doe.gov

Collaborator:
Piotr Zelenay, Los Alamos National Laboratory, Los Alamos, NM

Project Start Date: July 1, 2015
Project End Date: July 2018

Overall Objectives

- Synthesizing high performance Pt monolayer (ML) electrocatalysts for the oxygen reduction reaction (ORR) consisting of a Pt ML shell on stable, inexpensive metal, alloy, metal oxide, nitride or carbide nanoparticle cores.
- Increasing activity and stability of Pt ML shells and stability of supporting cores while reducing noble metal contents.

Fiscal Year (FY) 2017 Objectives

Further improvement of performance of Pt monolayer catalysts while reducing their platinum group metal (PGM) contents by the following studies and strategies:

- Membrane electrode assembly (MEA) testing of Pt ML catalysts with high rotating disk electrode (RDE) performance.
- Modifying non-noble metal core components by nitriding, alloying, doping.
- Modifying Pt ML shell by doping with a very small amount of Au.
- Metal aerogels as support.
- Doping carbon by NbO_2 oxide for stabilization.

Technical Barriers

This project addresses the following technical barriers from the Fuel Cells section of the Fuel Cell Technologies Office Multi-Year Research, Development, and Demonstration Plan:

(A) Durability

(B) Cost

(C) Performance

Technical Targets

We are focusing on simplifying the synthetic processes to obtain better catalyst activity, higher Pt utilization, lower content of PGM, and simpler MEA fabrication (see Table 1).

FY 2017 Accomplishments

- Developed catalysts with non-noble metal core components stabilized by nitriding.
- Developed catalysts with cores that have own core-shell structure with a refractory metal core (inner core) and thin noble metal shell (outer core).
- Nitriding at high pressure and high temperature of non-noble metal core components.
- Improved Pt ML shell by doping it by negligible amount of Au; improvements obtained also by doping core by small amount of Ir.

TABLE 1. Progress toward Meeting DOE Fuel Cell Electrocatalysts Technical Targets

	DOE 2017 Targets	$Pt/NbO_2/C$	$Pt/Pd_4IrNi/C$	$Pd_{20}Au$ Aerogels
Pt loading mg/cm^2			C 71%, Pd 18%, Ni 3%, Ir 7%	30 ug/cm^2
PGM total loading, mg_{PGM}/cm^2	<0.125			
Loss in performance @ 0.8 A/cm^2 after 30,000 AST	<30 mV	No loss after 5,000 cycles to 1.5 V		
Mass activity @ 900 $mV_{iR\ free,}$ A/mg_{Pt}			1.59	5 A/mgPt
Mass activity @ 900 $mV_{iR\ free,}$ A/mg_{PGM}	>0.44	0.5 A/mg_{PGM} after 5,000 cycles to 1.5 V	0.155	0.75 A/mg_{PGM}

AST – accelerated stress test

- Improved stability of the Pt/C catalysts by doping C by NbO_2.
- Demonstrated that metal aerogels have properties of very promising supports.
- Improved catalyst response at high current densities.

✧ ✧ ✧ ✧ ✧

INTRODUCTION

Further improvements of oxygen reduction electrocatalysts are necessary to overcome the remaining technological difficulties that cause slow automotive applications of fuel cells. To address these problems our research was focused on reducing Pt and PGM contents in our electrocatalysts while increasing their stability and activity. The improvements were obtained by optimizing the properties of supporting cores by varying their composition; size and shape for high activity and high stability of Pt monolayer shells have been studied.

APPROACH

Our approach to improving Pt ML catalysts is based on synthetic methods that facilitate stabilizing cores, controllable deposition of refractory metal core components from aqueous and ionic liquids solutions, doping cores and Pt monolayer shell for increased activity and stability. Cores in this approach have their own core-shell structure: a refractory metal inner core and noble metal thin outer cores.

Cores containing non-noble metals were stabilized by nitrating at high pressure, high temperature, or doping by negligible amounts of noble metals. Additional promising approaches for improving Pt monolayer catalysts include (i) doping Pt ML shells by negligible amount of Au, (ii) improving stability of the Pt/C catalysts by doping C by NbO_2, and (iii) use of metal aerogels as support to enhance stability activity and catalysts.

RESULTS

Improvement of MEA Performance of Nitride-Stabilized Pt/PdNiN/C

Nitride-stabilized Pt-M core-shell electrocatalysts (1 h, in NH_3 at 500°C) for the ORR in acid media showed high activity ($E_{1/2}$ = 0.9 V), and stability (30,000 potential cycles) in the RDE measurements. Pd content is reduced by 50% in comparison with the Pt/Pd/C catalyst. Figure 1a shows comparison of the results of the MEA tests having cathodes Pt/PdNiN/C, Pt/Pd/C, and reference Pt/C. Composition of catalysts is indicated in the graph. Hysteresis in polarization curves was observed at low voltage due to possible flooding. Decreased relative humidity (RH) from 100% to 60% caused a significant performance increase (Figure 1b). The current density at 0.3 V increased from 1 A/cm^2 to 1.4 A/cm^2. Optimization of the MEA structure, and of ionomer to catalyst ratio, is expected to further increase performance.

Preliminary results with high pressure nitriding showed formation of PtV_3N intermetallic compound which has a high activity and durability for the ORR (not shown). MA of

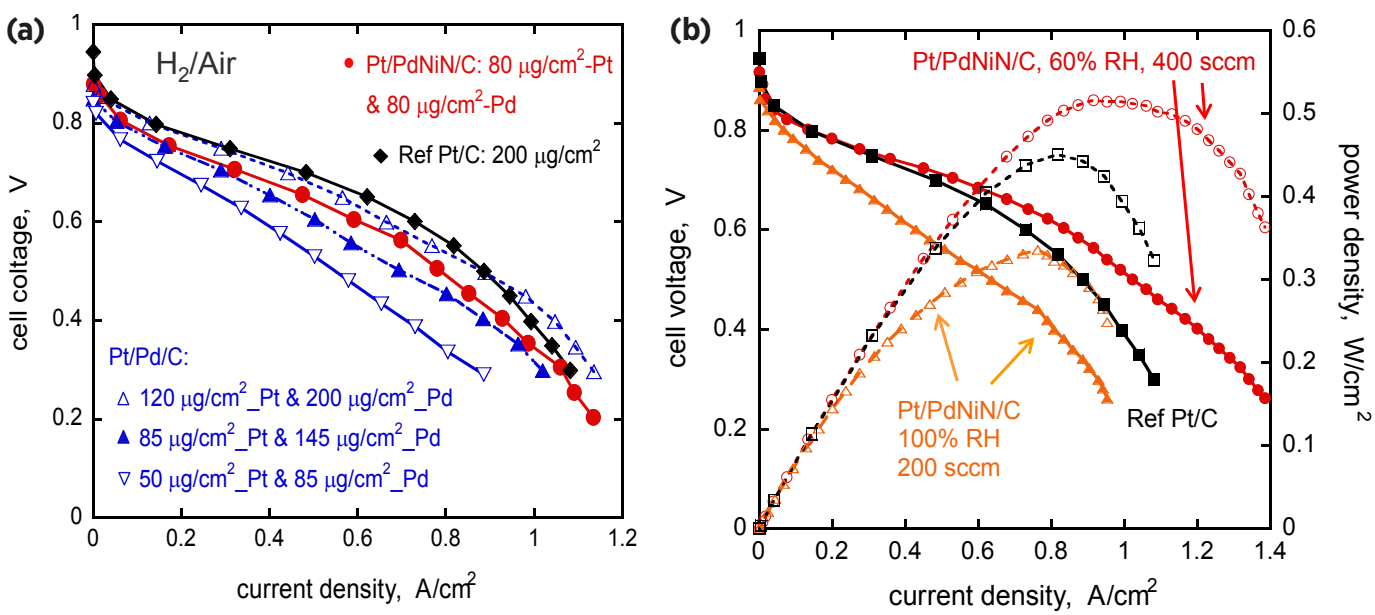

FIGURE 1. (a) MEA polarization curve with H_2–air feed at three different Pt/Pd/C loadings and nitrided Pt/Pd/NiN/C compared with the standard reference catalyst. (b) The effect of relative humidity on the MEA performance of the PtPdNiN/C catalyst. Cathode: Pt/PdNiN/C 120 $\mu g_{Pt} cm^{-2}$, 70 $\mu g_{Pd} cm^{-2}$, air, 1.0 bar air partial pressure.

PtV_3N is comparable to Pt/C; its SA is much higher, stability is significant.

Au-Doped Pt_{ML}/Pd/C and Au Outer Core on Metallic Tungsten Nanoparticle Inner Cores

Alloying or doping cores, or decorating Pt surface by Au can improve catalysts activity and stability for the ORR, as we demonstrated earlier [1]. Here we show that negligible amounts of Au ions can interact with Pd through pinholes in a Pt monolayer. Au replaces galvanically some Pd and "plugs" the holes. Au atoms in a Pt ML, by its size, can cause some contraction in the surrounding Pt atoms and increase activity and stability. A large increase of the response at high current density, 1.1–1.5 A/cm^2, is observed after placing a small amount of Au (it cannot be detected by energy dispersive X-ray spectroscopy) (Figure 2a). This simple procedure is a very efficient last step in improving core-shell catalysts.

Tungsten nanoparticles were prepared via decomposition of tungsten nitrides obtained from WCl_6 annealed in NH_3 at 600°C that decomposes at 800°C. Propylene carbonate as solvent was used to galvanically displace some W by Pd. Core-shell structure is indicated by a lack of W oxidation.

Interlayer of another metal to form a shell is necessary since the half-filled d-band has large electronic effect on adlayers. The best catalysts contained the following cores: Pd_6W_9 and Au_3Pd_2W. Pt/Pd_6W_9/C has mass activity 1.04 A/mg Pt or 0.1 A/mg PGM. Increasing activity, as a function of core composition, indicates a possibility for further improvements.

Pt on NbO_2: A Solution for ORR Performance Decay in Start-Stop Cycles to 1.5 V

The voltage transients of up to 1.5 V at the cathode accelerate the carbon degradation causing agglomeration of Pt particles and a loss of electrochemical surface area of Pt catalysts. This, and worsened transport properties of the porous catalyst layer, result in PEMFC performance decay. We developed a unique procedure to stabilize carbon support (Ketjen black) by oxide nanoparticles (NbO), which also stabilizes Pt against agglomeration. Niobium oxides are embedded into the porous surface of carbon blacks, by sonication and decomposing Nb(V) ethoxide and reducing dried Nb(V) precursor to small particles of NbO or NbO_2 or Nb_2O_5, controllable via hydrogen partial pressure, temperature, and time. Pt is deposited by galvanic reaction of NbO and $PtCl_4^{-2}$ giving Pt and NbO_2 with ethanol as solvent and additional reductant. Half-sphere Pt (bright dots) on NbOx (gray area on left) indicates that is confined in carbon. (Figure 3a). The Pt mass activity of Pt-NbO_2-C catalysts reaches 0.5 A/mg $_{Pt}$ having excellent durability against 0.6–1 V and 1–1.5 V potential cycles. (Figures 3b and 3c). The high degree dispersion and uniformity of NbO_x particles over the entire carbon surface achieved by utilizing the surface pores on carbon are unprecedented. Controlling particle size and distribution by size and density of surface pores allow a wide temperature range to be used in synthesis for fabricating small and well dispersed particles. The concept may be applied for making other metal, alloy, and oxide particles. All these unique and desirable features

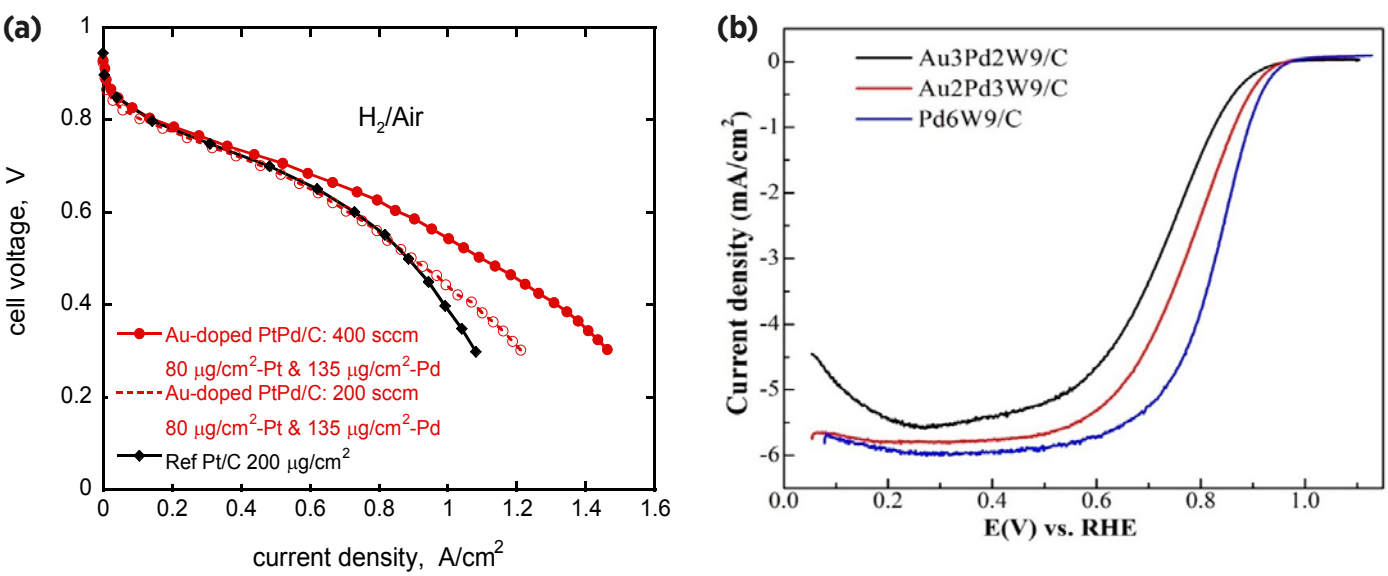

RHE – reference hydrogen electrode

FIGURE 2. (a) MEA test of Au-doped Pt_{ML}/Pd/C. Cathode: BNL Au-doped Pt/Pd/C, air 200/400 sccm, 1.0 bar partial pressure 80 μg/cm^2-Pt, 135 μg/cm^2-Pd. The Au content is very small, difficult to measure. (b) Metallic tungsten nanoparticles as inner cores. Effect of interlayers on RDE polarization curves. Pt/Pd6W9/C Pt mass activity 1 A/mg; PGM mass activity 0.1 A/mg; 28% Pd, 72% W.

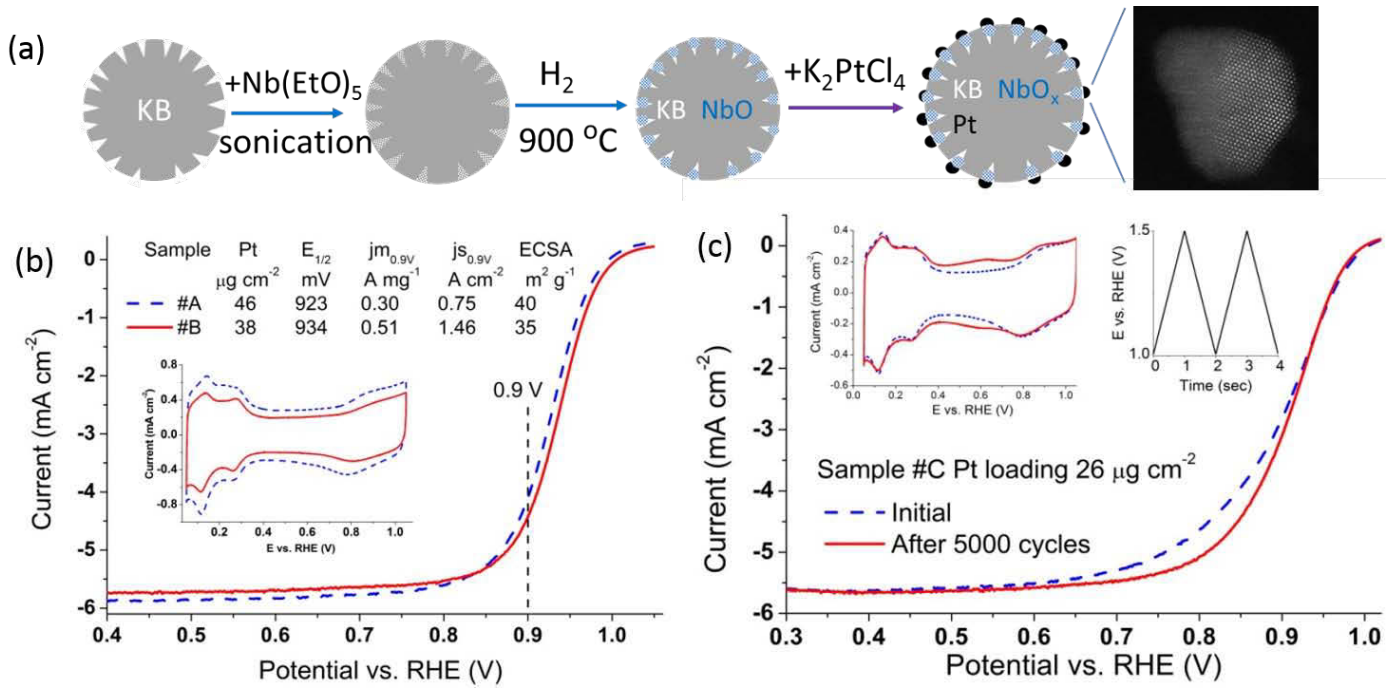

ECSA – electrochemical surface area

FIGURE 3. (a) Schematic illustration of ~4-nm pores on the surface of a ~30 nm carbon particle, filled by Nb ethoxide in ethanol, NbO-embedded carbon after thermal decomposition and reduction of Nb precursor, and semi-spherical Pt particles formed on top of NbO_x far right. Transmission electron microscopy image of Pt particle shows Pt atoms (bright dots) tightly bound with NbO_2 (gray area). The carbon surrounding NbO_2 is invisible due to its low electron density in the Z-contrast image. (b) ORR activities of two Pt-NbO_2-C samples prepared using different Pt precursors measured in O_2-saturated 0.1 M $HClO_4$ solutions. (c) Polarization curves of a Pt-NbO_2-C sample before and after 5,000 potential cycles between 1 V and 1.5 V. Voltammetry curves shown in the inserts were measured at 50 mV s^{-1}.

contributed to the high ORR activity and exceptional durability against potential cycles up to 1.5 V.

Aerogels PdAu as Cores

We demonstrate the use of metallic aerogels as cores in high activity core shell catalysts. The core-shell aerogel catalysts have several advantages: (i) rapid electron transfer, (ii) large surface area, high porosity (90%), (iii) accelerated mass transfer, (iii) no support corrosion. Core-shell aerogels amplify the enhancement factors of core-shell and aerogel structures, which integrate several catalysis enhancement factors. Here we demonstrate the synthesis of Pd_xAu-Pt core-shell aerogels comprised of an ultrathin Pt shell and a composition-tunable Pd_xAu alloyed core. Their activities for oxygen reduction exhibit a volcano-type relationship as a function of the lattice parameter of the core substrate. The maximum mass and specific activities are 5.25 A mg^{-1}_{Pt} and 2.53 mA cm^{-2}, which are 18.7 and 4.1 times higher than those of Pt/C, respectively, demonstrating the superiority of the core-shell metallic aerogels. Noble metal mass activity is 0.69 A/mg. Figure 4a shows the energy dispersive X-ray spectroscopy element maps for the $Pd_{10}Au$-Pt core-shell aerogel. Pt and noble-metal mass activities are given in Figure 4b. The proposed core-based activity descriptor provides a new possible strategy for the design of future core-shell electrocatalysts. This work highlights the great potential of pure metallic core-shell aerogels as highly efficient electrocatalysts through structural engineering.

CONCLUSIONS AND UPCOMING ACTIVITIES

New results show the possibility of developing high-performance, low cost Pt ML catalysts with non-noble metal cores. MEA tests were carried out with promising Pt ML catalysts including Pt/Pd/C, Au-doped Pt/Pd/C, aerogel Pt/PdAu, and nitride stabilized Pt/PdNiN/C. Pt/PdNiN/C has a similar performance as the control catalyst with higher Pt loading, but below expectations based on the RDE data. Decreased humidification improved its activity to better than that of the control. Au-doped Pt ML catalyst showed outstanding activity, with considerably better response in the high current density region (40%) than the control. Aerogel Pt/PdAu performed poorly in the first MEA test, possibly because a low Pt content of 30 μg/cm^2, or damaged structure in making MEA. The aerogel supports will have a strong impact on future electrocatalyst applications.

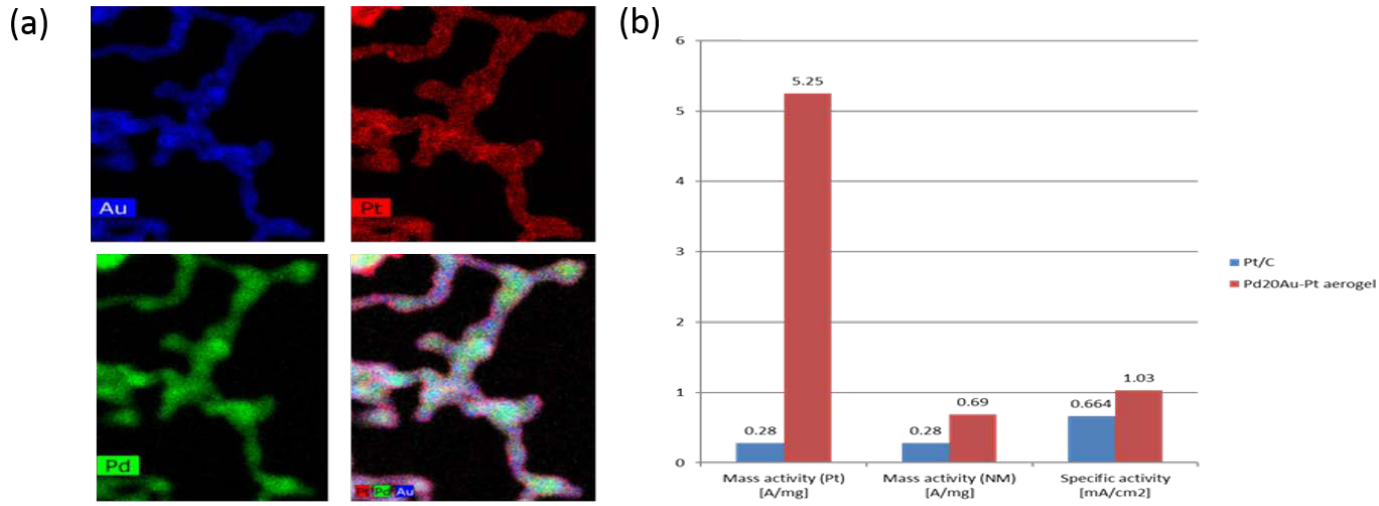

FIGURE 4. (a) Energy dispersive X-ray spectroscopy element maps for the $Pd_{10}Au$-Pt core-shell aerogel catalyst. (b) Pt mass, noble metal mass, and specific activity of $Pd_{10}Au$-Pt aerogel catalyst compared with commercial Pt/C catalyst.

Future work will focus on MEA studies of selected catalysts to optimize catalyst properties, MEA structure and composition, and to determine catalysts' stability in MEAs. These include:

- Pt/Pd/C with a Pt ML doped with small amount of Au atoms, $Pt/Pd_9Au_1/C$ catalysts, and Pt/PbW-Ni/C catalyst obtained by electrodeposition and by chemical route.
- W, WC, and WN nanoparticles of 4 nm particle size, will be used as an inner core with a Pd or PdAu thin layer outer core as a support for a Pt ML.
- High pressure nitridation (1,100°C in an NH_3 gas at 10 MPa) to generate various types of nitride nanoparticles with refractory metals to enhance the stability and activity of Pt shells.
- Further improvement of stabilizing carbon and Pt deposit to potential cycles of 1.5 V by NbO_2 in 4 nm pores.
- MEA tests of a new core-PdAu aerogel as support for a Pt ML.

SPECIAL RECOGNITIONS & AWARDS/ PATENTS ISSUED

1. Radoslav Adzic, Thomson Reuters Web of Science: Highly Cited Researcher, 2016.

FY 2017 PUBLICATIONS/PRESENTATIONS

1. K.A. Kuttiyiel, Y.M. Choi, K. Sasaki, D. Su, S.M. Hwang, S.D. Yim, T.H. Yang, G.G. Park, R.R. Adzic, "Tuning electrocatalytic activity of Pt monolayer shell by bimetallic Ir-M (M = Fe, Co, Ni or Cu) cores for the oxygen reduction reaction," *Nano Energy*, **29** (2016) 261–267.

2. G.Y. Chen, K.A. Kuttiyiel, D. Su, M. Li, C.H. Wang, D. Buceta, C.Y. Du, Y.Z. Gao, G.P. Yin, K. Sasaki, M.B. Vukmirovic, R.R. Adzic, "Oxygen Reduction Kinetics on Pt Monolayer Shell Highly Affected by the Structure of Bimetallic AuNi Cores," *Chemistry of Materials*, **28** (2016) 5274–5281.

3. M.B. Vukmirovic, K.A. Kuttiyiel, H. Meng, R.R. Adzic, "Controllable Deposition of Platinum Layers on Oxide Surfaces for the Synthesis of Fuel Cell Catalysts," *ChemElectroChem*, **3** (2016) 1635–1640.

4. X.L. Tian, J.M. Luo, H.X. Nan, H.B. Zou, R. Chen, T. Shu, X.H. Li, Y.W. Li, H.Y. Song, S.J. Liao, R.R. Adzic, "Transition Metal Nitride Coated with Atomic Layers of Pt as a Low-Cost, Highly Stable Electrocatalyst for the Oxygen Reduction Reaction," *Journal of the American Chemical Society*, **138** (2016) 1575–1583.

5. Y. Li, K.A. Kuttiyiel, L. Wu, Y.M. Zhu, E. Fujita, R.R. Adzic, K. Sasaki, "Enhancing Electrocatalytic Performance of Bifunctional Cobalt-Manganese-Oxynitride Nanocatalysts on Graphene," *ChemSusChem*, **10** (2017) 68–73.

6. K.E. Ayers, J.N. Renner, N. Danilovic, J.X. Wang, Y. Zhang, R. Maric, H. Yu, "Pathways to Ultra-Low Platinum Group Metal Catalyst Loading in Proton Exchange Membrane Electrolyzers," *Catalysis Today*, **262** (2016) 121–132.

7. M.E. Scofield, Y.C. Zhou, S.Y. Yue, L. Wang, D. Su, X. Tong, M.B. Vukmirovic, R.R. Adzic, S.S. Wong, "Role of Chemical Composition in the Enhanced Catalytic Activity of Pt-Based Alloyed Ultrathin Nanowires for the Hydrogen Oxidation Reaction under Alkaline Conditions," *ACS Catalysis*, **6** (2016) 3895–3908.

8. M.E. Scofield, C. Koenigsmann, D. Bobb-Semple, J. Tao, X. Tong, L. Wang, C.S. Lewis, M.B. Vukmirovic, Y.M. Zhu, R.R. Adzic, S.S. Wong, "Correlating the Chemical Composition and Size of Various Metal Oxide Substrates with the Catalytic Activity and Stability of As-Deposited Pt Nanoparticles for the Methanol Oxidation Reaction," *Catalysis Science & Technology*, **6** (2016) 2435–2450.

REFERENCES

1. *Stabilization of platinum oxygen reduction electrocatalysts using gold clusters*, J. Zhang, K. Sasaki, E. Sutter, R.R. Adzic, *Science*, 315 (2007) 220.

V.A.6 Extended Surface Electrocatalyst Development

Bryan Pivovar (Primary Contact), Shaun Alia, K.C. Neyerlin, Katie Hurst, Jason Zack, Scott Mauger, Shyam Kocha, Ahmad Mayyas
National Renewable Energy Laboratory
15013 Denver West Parkway
Golden, CO 80401
Phone: (303) 275-3809
Email: Bryan.Pivovar@nrel.gov

DOE Manager: David Peterson
Phone: (240) 562-1747
Email: David.Peterson@ee.doe.gov

Subcontractors:
- Yushan Yan (PI), Brian Setzler, University of Delaware, Newark, DE
- Svitlana Pylypenko, Sarah Shulda, Chilan Ngo, Colorado School of Mines, Golden, CO
- Al Weimer, Will Medlin, Wilson McNeary, University of Colorado, Boulder, CO
- Karen Buechler, Joe Spencer, ALD Nanosolutions, Broomfield, CO

Project Start Date: December 10, 2015
Project End Date: September 30, 2018

Overall Objectives

- Increasing mass activity and durability of Pt-based electrocatalysts through the synthesis and implementation of high surface area extended surface electrocatalysts.
- Optimize fuel cell performance of extended surface electrocatalysts.
- Demonstrate DOE 2020 target performance and durability in fuel cell tests.

Fiscal Year (FY) 2017 Objectives

- Determine (using experimental measurements and developed models) and report overpotential losses associated with unique features of extended surface electrodes include protonic and electronic resistances of electrodes, and mass transfer losses including $R_{O2,local}$.
- Quantify and report increase in catalytic performance (both specific activity and mass activity at 0.9 V iR corrected) for shape and surface controlled nanostructures relative to standard Ni nanowires (NWs).
- Demonstrate a mass activity of >440 mA/mgPt at 0.9 V (DOE 2020 target) in fuel cell tests while also meeting at least one of Fuel Cell Technologies Office's membrane electrode assembly (MEA) durability targets.

Technical Barriers

This project addresses the following technical barriers from the Fuel Cells section (3.4) of the Fuel Cell Technologies Office Multi-Year Research, Development, and Demonstration Plan.

(A) Durability (of catalysts and MEAs)

(B) Cost (of catalysts and MEAs)

(C) Performance (of catalysts and MEAs)

- Start-up and Shut-down Time and Energy/Transient Operation

Technical Targets

This project synthesizes novel extended thin film electrocatalyst structures (ETFECS) and incorporates these catalysts into electrodes for further study. The project has targets outlined in the Multi-Year Research, Development, and Demonstration Plan for both electrocatalysts for transportation applications (Table 3.4.7) and MEAs (Table 3.4.5). The specific targets and status of highest relevance are presented in Table 1.

TABLE 1. Technical Targets for Electrocatalysts for Transportation Applications

Characteristic	Units	2020 Target	Status
Mass Activity (150 kPa H_2/O_2 80°C 100% RH)	A/mg-Pt @ 900 mV	0.44	>0.5
Electro catalyst support stability	% mass activity loss	<40	41
Loss in initial catalytic activity	% mass activity loss	<40	66

RH – relative humidity

FY 2017 Accomplishments

- The project has demonstrated the ability to achieve high performance of atomic layer deposition (ALD) synthesized PtNi NWs in reasonable scale and reproducibility.
- Performance and durability have been significantly improved with annealing and pre-leaching of as-synthesized PtNi NWs.
- Limiting current measurements show very low $R_{O2,local}$ for ETFECS MEAs.

- MEAs with pre-leached ETFECS (spontaneous galvanic displacement [SGD] and ALD) demonstrate mass activity Pt ~240 mA/mgPt with low ionomer content.

✧ ✧ ✧ ✧ ✧

INTRODUCTION

Conventional nanoparticle Pt/C electrocatalysts (2–5 nm) used in automotive fuel cells appear to have plateaued in terms of electrochemical area and catalytic activity. ETFECS offer the possibility of higher specific activities, comparable to that of bulk poly-Pt. ETFECS materials formed by galvanic displacement have shown promising performance and durability in rotating disk electrode tests, but have shown limitations in compositional control, reproducibility and batch size (scale-up). We are focusing on Pt and Ni ALD in order to address the limitations found with galvanic displacement. The materials are then explored for optimum electrode structures through cell diagnostics that isolate and target mitigation strategies for loss mechanisms.

APPROACH

Our overall approach is towards developing extended surface Pt catalysts synthesized by ALD with high mass activity and durability, and incorporating these structures into robust, high efficiency MEAs. This approach focuses on the synthesis of novel ETFECS formed by ALD, specifically with the co-deposition of Ni and Pt. We are targeting high surface areas as this has been a specific challenge for extended surface Pt catalysts (3M [1], others [2]). Our multi-tiered approach involves the synthesis of novel template nanostructures, the synthesis and characterization of ALD-synthesized ETFECS, and the optimization of these materials in fuel cells.

RESULTS

In the area of novel template nanostructure development we made a no-go decision on the University of Delaware efforts that were focused on the synthesis of facet controlled extended surface Ni nanoparticles. This effort has been refocused to the area of MEA fabrication and fuel cell testing. In the area of nano-templates, we have worked with a commercial supplier of Ni NWs to determine the materials that offer the best performance once platinized and processed. This has allowed us to focus on larger scale Ni NW batches (100 g) and increase the material availability and performance of novel PtNi NWs.

Our efforts in the area of Pt deposition by ALD have allowed us to routinely generate high performance materials at the 0.5 g scale. We identified oxidation as a key concern and optimized our reaction conditions to work at lower oxygen partial pressure allowing for improved processing characteristics and higher performance. We have also scaled up reaction batch size to 2 g. Initial results suggest we have succeeded in reaching target Pt compositions and that this approach is scalable to much higher batch sizes. Post-processing results have shown significant increases in activity after H_2 annealing, as shown in Figure 1. This increase in performance is attributed to improved alloying of the Pt phase and a shift in the Pt lattice X-ray diffraction spectra. Acid leaching has also been a major focus of our post-processing studies, and we have demonstrated the ability to achieve active catalysts with most of the metallic Ni content removed by acid leaching, see Figure 2, without sacrificing electrochemical surface area. This has allowed for significantly more MEA testing of PtNi NWs.

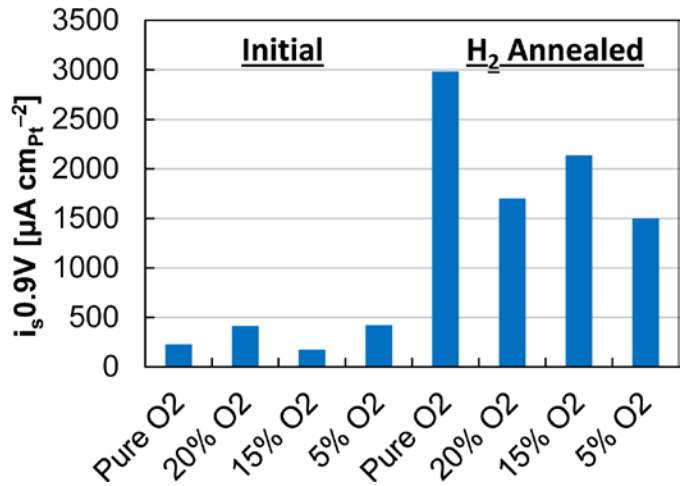

FIGURE 1. Specific activity of PtNi NWs as a function of oxygen partial pressure before and after hydrogen annealing

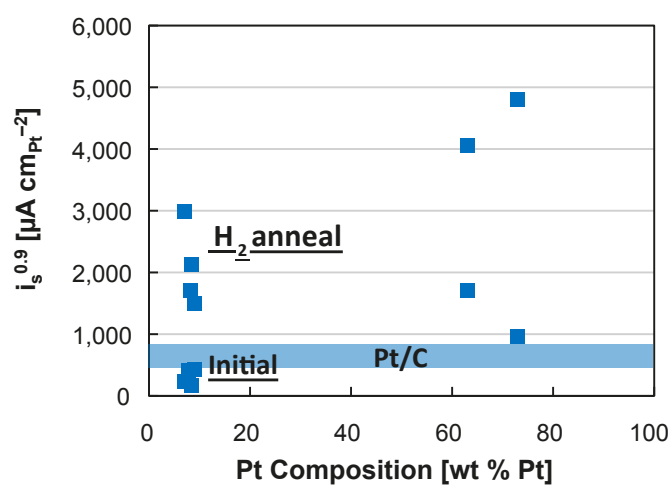

FIGURE 2. Specific activity of PtNi NWs as a function of processing condition: as-synthesized, H_2 annealed, and acid leached

MEA tests of PtNi NWs have been conducted on a number of samples. Scanning electron microscopy cross-section and top down views of the pre-leached PtNi NWs are shown in Figure 3. These catalyst layers are thin, ~1 µ, show short, hollow tubes as the predominant structure within the catalyst layer. Figure 4 shows that we were able to match the fuel cell performance of PtNi NWs synthesized by SGD with PtNi NWs synthesized by ALD. Both of these MEAs were synthesized with pre-leached nanowires and reached mass activity of 280 mA/mg$_{Pt}$ at 0.9 V. We have performed optimization and diagnostic studies on these systems that includes AC impedance and diffusion-limited current measurements. From these and related experiments we have found the highest performance at traditionally low ionomer content (~10 % relative to leached PtNi NW weight). We have found through impedance that low RH performance of these electrodes starts to exhibit alternate behavior to traditional Pt/carbon electrodes. And from limiting current measurements, we have found that local transport resistance of these electrodes is less than that of traditional Pt/carbon electrodes.

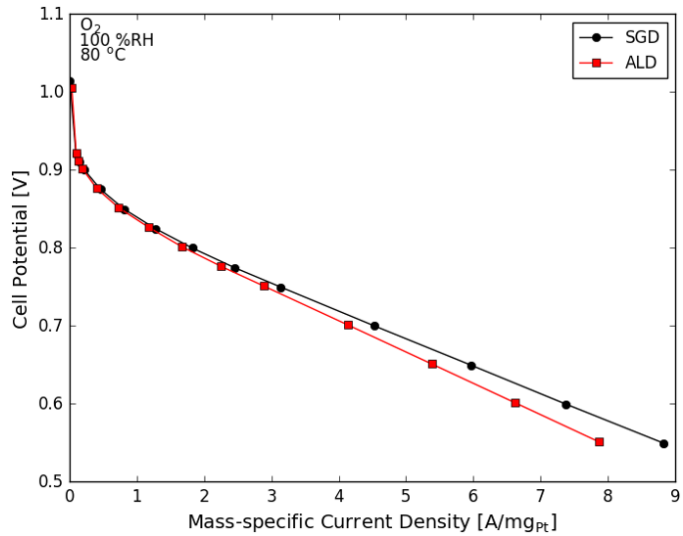

FIGURE 4. Fuel cell polarization curves of PtNi NWs of preleached samples comparing SGD and ALD synthesized materials

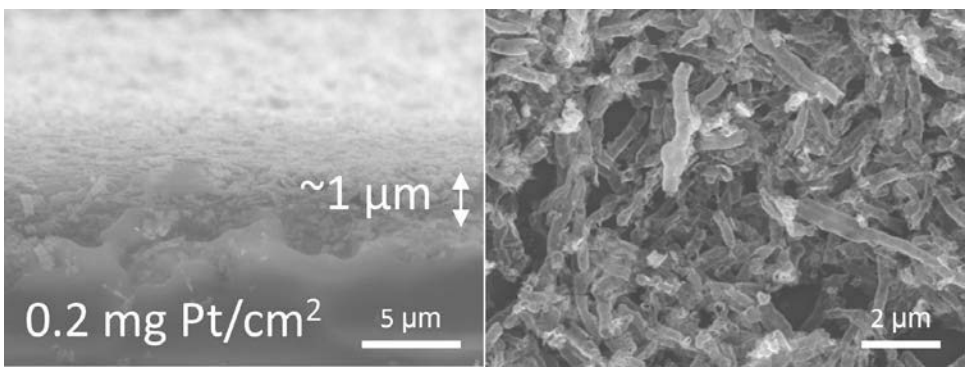

FIGURE 3. Scanning electron microscopy cross-section (left) and top-down (right) micrographs of PtNiNW electrodes using acid leached samples

CONCLUSIONS AND UPCOMING ACTIVITIES

The project has demonstrated the ability to achieve high performance of ALD synthesized PtNi NWs in reasonable scale and reproducibility. Performance and durability have been significantly improved with annealing and pre-leaching. MEAs with pre-leached ETFECS (SGD and ALD) demonstrate mass activity Pt ~240 mA/mgPt with low ionomer content. Limiting current measurements show very low $R_{O2,local}$ for ETFECS MEAs. Future work includes:

- Nano-template synthesis:
  - Validation of targeted performance from commercial supplier.
- Electrocatalysts:
  - ALD scale-up to 10 g batch size. Further increase of electrochemical surface area and specific activity. Co-deposition of Pt and Ni/Co.
  - Post-processing optimization of resultant catalysts (annealing and acid leaching).
  - Characterization and optimization (electrochemical and structural studies).
- Fuel cell testing:
  - Optimization of electrode structure/performance using ALD materials.
  - Isolation and minimization of overpotential losses in MEA electrodes (separation of mass transfer, ohmic, and kinetic losses).
  - Durability studies to quantify and minimize performance losses.

FY 2017 PUBLICATIONS/PRESENTATIONS

1. S.M. Alia, C. Ngo, S. Shulda, M.-A. Ha, A.A. Dameron, J. Nelson Weker, K.C. Neyerlin, S.S. Kocha, S. Pylypenko, and B.S. Pivovar, "Exceptional Oxygen Reduction Reaction Activity and Durability of Platinum-Nickel Nanowires Through Synthesis and Post-Treatment Optimization," ACS Omega, 2, 1408–1418, 2017. DOI: 10.1021/acsomega.7b00054.

2. Kazuma Shinozaki, Yu Morimoto, Bryan S. Pivovar, and Shyam S. Kocha, "Suppression of oxygen reduction reaction activity on Pt-based electrocatalysts from ionomer incorporation," Journal of Power Sources 325 (2016): 745–751.

3. Shaun Alia, Svitlana Pylypenko, Arrelaine Dameron, K.C. Neyerlin, Shyam Kocha, and Bryan Pivovar, "Oxidation of Platinum Nickel Nanowires to Improve Durability of Oxygen-Reducing Electrocatalysts," J. Electrochem. Soc. 2016 163(3): F296–F301. doi:10.1149/2.0081605jes.

4. Scott A. Mauger, Shaun M. Alia, Siddharth Komini-Babu, Shyam S. Kocha, Chilan Ngo, Katherine E. Hurst, Svitlana Pylypenko, Shawn Litster, Bryan S. Pivovar, and K.C. Neyerlin, "Platinum-Nickel Nanowire Extended Surface Catalysts in PEMFC: Challenges and Lessons Learned," PRiME 2016/230th ECS Meeting, October 4, 2016, Honolulu, HI.

5. William W. McNeary, Katherine M. Hurst, Shaun M. Alia, James W. Medlin, Alan W. Weimer, Karen J. Buechler, and Bryan S. Pivovar, "Atomic Layer Deposition for Extended Surface Electrocatalyst Development," North American Catalysis Society Meeting, Denver, CO, June 4–9, 2017.

6. B. Pivovar, "Development and Implementation of Catalysts and Membrane Electrode Assemblies based on Extended Thin Film Electrocatalysts," CARISMA, Newcastle, UK, April 12, 2017.

REFERENCES

1. http://www.hydrogen.energy.gov/pdfs/review08/fc_1_debe.pdf.

2. Z. Chen, W. Li, M. Waje, Y.S. Yan, *Angew. Chem. Int. Ed.* 2007, 46:4060–4063.

V.A.7 Highly Active, Durable, and Ultra-Low PGM NSTF Thin Film ORR Catalysts and Supports

Andrew Steinbach (Primary Contact), Isaac Davy, Cemal Duru, Andrew Haug, Amy Hester, Monika Kuznia, Krzysztof Lewinski, Sean Luopa, Jason Petrin, and Grant Thoma
3M Company, Corporate Research Materials Laboratory
3M Center, Building 201-2N-19
St. Paul, MN 55144-1000
Phone: (651) 737-0103
Email: ajsteinbach2@mmm.com

DOE Manager: David Peterson
Phone: (240) 562-1747
Email: David.Peterson@ee.doe.gov

Contract Number: DE-EE0007270

Subcontractors:
- J. Erlebacher, Johns Hopkins University, Baltimore, MD
- J. Greeley and Z. Zeng, Purdue University, West LaFayette, IN
- D. Cullen, Oak Ridge National Laboratory, Oak Ridge, TN
- D. Myers and A.J. Kropf, Argonne National Laboratory, Lemont, IL

Project Start Date: January 1, 2016
Project End Date: March 31, 2019

Overall Objectives

The overall objective is development of improved thin film oxygen reduction reaction (ORR) catalysts on nanostructured thin film (NSTF) supports for proton exchange membrane fuel cells (PEMFCs) which achieve:

- Mass activity of 0.80 A/mg_{PGM} or higher.
- Platinum group metal (PGM) total content (both electrodes) of ≤0.1 g/kW at 0.70 V.
- PGM total loading (both electrodes) <0.1 mg_{PGM}/cm^2.
- Mass activity durability of <20% loss.
- Loss of performance <20 mV at 0.8 A/cm^2 and 1.5 A/cm^2.

Fiscal Year (FY) 2017 Objectives

- Develop new ultra-thin film (UTF) and nanoporous thin film (NPTF) electrocatalysts, towards achievement of activity, durability, and cost objectives.
- Employ advanced composition and structural analysis to guide electrocatalyst development, including transmission electron microscopy, energy dispersive X-ray spectroscopy (EDS), and X-ray adsorption fine structure spectroscopy (XAFS).
- Validate density functional theory (DFT) and kinetic Monte Carlo (kMC) models, and utilize models to predict novel electrocatalyst concepts with improved activity and durability.
- Validate high throughput electrocatalyst fabrication and characterization methods, towards acceleration of project electrocatalyst development.

Technical Barriers

This project addresses the following technical barriers from the Fuel Cells section of the Fuel Cell Technologies Office Multi-Year Research, Development, and Demonstration Plan.

(A) Durability

(B) Cost

(C) Performance

Technical Targets

Table 1 summarizes 2017 project status against the relevant 2020 DOE targets and project targets. All reported status values are measurements made in 50 cm^2 active area membrane electrode assemblies (MEAs). PGM total content and PGM total loading are reported for two MEAs, containing either UTF PtNi or NPTF PtNiIr catalysts. MEAs were evaluated with an anode gas diffusion layer and a cathode interlayer optimized to improve NSTF MEA operational robustness [1]. The cathode interlayer contains 16 $\mu g_{Pt}/cm^2$. Both MEAs had less PGM total loading than the DOE target (0.125 mg/cm^2) and the UTF catalyst MEA also exceeded the DOE PGM total content target (0.125 g/kW) while simultaneously meeting the DOE Q/ΔT target of 1.45 kW/°C.

Beginning of life (BOL) mass activity values were 0.38 A/mg_{PGM} and 0.44 A/mg_{PGM} (vs. 0.44 A/mg target) for NPTF PtNiIr and UTF PtNiIr catalysts, respectively. A new UTF catalyst was developed which achieved mass activity of 0.56 A/mg_{PGM}, significantly exceeding the DOE target. After evaluation under the DOE electrocatalyst accelerated stress test (AST), both UTF and NPTF PtNiIr catalysts demonstrated a loss in catalytic (mass) activity of 45% (vs. 40% DOE target) and a loss in performance at 0.8 A/cm^2 of less than 25 mV (vs. DOE target of 30 mV loss).

TABLE 1. Status against Technical Targets

Characteristic	2020 Target and Units	Project Target	2017 Status	
			UTF	NPTF
PGM total content (both electrodes)	0.125 g/kW ($Q/\Delta T \leq 1.45$)	0.1 ($Q/\Delta T = 1.41$)	0.13[2](1.41) 0.12[2](1.45)	0.15[1](1.41) 0.14[1](1.45)
PGM total loading (both electrodes)	0.125 mg/cm^2	0.10	0.077[2]	0.122[1]
Loss in catalytic (mass) activity	40%	20	45[4]	45[3]
Loss in performance at 0.8 A/cm^2	30 mV	20	23[4]	21[3]
Loss in performance at 1.5 A/cm^2	30 mV	20	NA	NA
Mass activity @ 900 mV$_{iR\text{-}free}$	0.44 A/mg	0.80 (in MEA)	0.44[4] 0.56[5]	0.38[3]

[1]2017 (Jan.) NPTF best of class (BOC) MEA. 0.016 mg$_{Pt}$/cm^2 NSTF anode, 0.090 mg$_{PGM}$/cm^2 NPTF PtNiIr cathode, 0.016 mg$_{Pt}$/cm^2 cathode interlayer.
[2]2017 (Jan.) UTF BOC MEA. 0.015mg$_{Pt}$/cm^2 NSTF anode, 0.046 mg$_{PGM}$/cm^2 UTF PtNi cathode, 0.016 mg$_{Pt}$/cm^2 cathode interlayer.
[3]NPTF PtNiIr/NSTF cathode from 2017 (Jan.) NPTF BOC MEA, 0.09mg$_{PGM}$/cm^2.
BOL and/or after 30,000 electrocatalyst AST cycles.
[4]UTF PtNiIr. BOL and/or after 30,000 electrocatalyst AST cycles.
[5]UTF catalyst, 26 μg$_{PGM}$/cm^2.
PGM total content values at 90°C cell, 1.5 atmA H_2/air, and 0.692 V and 0.700 V cell voltages.

FY 2017 Accomplishments

- Developed four distinct electrocatalysts which met or exceeded the DOE 2020 mass activity target of 0.44 A/mg$_{PGM}$, including one electrocatalyst with 0.56 A/mg$_{PGM}$. Electrocatalysts were evaluated in MEA format with cathode electrode loadings below those required to achieve DOE 2020 PGM total loading (both electrodes) target. Three of the electrocatalysts were based on the UTF morphology, and the highest mass activity electrocatalyst demonstrated a specific activity of 3 mA/cm$^2_{Pt}$, 2.5x higher than UTF pure Pt catalyst and 7.5x higher than pure Pt nanoparticle catalyst.
- Established quantitative relationships between fabrication processes, physical properties, and resultant catalyst performance with three UTF PtNi catalyst characteristic variables. Catalyst activity correlated with bulk Pt-Pt strain after fuel cell testing, which was influenced by the pre-test electrocatalyst composition, grain size, and electrocatalyst film thickness. Through this work, an optimized UTF PtNi catalyst was developed and achieved PGM total content of 0.12 g/kW, exceeding the DOE target of ≤0.125 g/kW, and PGM total loading (both electrodes) of 0.077 mg$_{PGM}$/cm^2, exceeding the DOE target of ≤0.125 mg$_{PGM}$/cm^2.
- Electrocatalyst models were successfully validated against the experiment. The kMC model was validated for predictive capability towards nanoporosity formation, specific area development, and compositional evolution of NPTF Pt_xNi_{1-x}. Model predictions agreed with experiment, both in terms of compositional sensitivity and relative magnitude of nanoporosity development for catalysts with seven initial Pt mole fractions. The DFT modeling of activity and stress predictions of Pt skins (various thicknesses, pseudomorphic and strain-relaxed) on Pt_xNi_{1-x} bulk films has been completed. Model predictions of activity variation with Pt-Pt bond distances agree in trend with experiment. Validated DFT and kMC models are now used to predict new electrocatalyst candidates with improved activity and durability.
- Developed new UTF and NPTF catalysts based on PtNi with Ir-modified surfaces, leading to improved activity, durability, and/or performance. We identified that addition of Ir to UTF Pt and PtNi surfaces can result up to a 46% increase in PGM mass activity over Ir-free catalysts. Optimal NPTF PtNiIr achieved 0.38 A/mg$_{PGM}$ (vs. 0.44 A/mg$_{PGM}$ target), durability of 45% mass activity loss (vs. 40% loss target) and 21 mV loss at 0.8A/cm^2 (vs. 30 mV loss target), and specific power of 7.3 kW/g (vs. 8.0 kW/g target). The to-date optimal UTF PtNiIr catalyst met the DOE mass activity target and exceeded the loss in performance at 0.80 A/cm^2 durability target and achieved 45% mass activity loss, which approached the 40% loss target.
- Modeling and advanced characterization were utilized to determine the role of Ir towards the observed activity and durability enhancement imparted by the addition of Ir to the surface of NPTF and UTF PtNi. Transmission electron microscopy and EDS analyses indicated that Ir increased Ni retention in NPTF PtNi after accelerated durability testing, and Ir content was stable. XAFS analysis indicates that surface Ir is generally minimally coordinated with other elements, but may reduce formation of Ni oxide. DFT modeling indicated that it is energetically favorable for Ir to move below the Pt surface, enabling ORR activity on the exposed Pt. kMC

modeling was utilized to evaluate the evolution and stability of nanoporosity in NPTF PtNi with a Ir surface layer, and determined that Ir preferentially forms a shell over the nanoporous PtNi structure which keeps the porous structure from coarsening and collapsing onto itself via capillary wetting.

- Progress was made towards validation and implementation of high throughput (HT) electrocatalyst development methods. This year, HT XAFS characterization has been developed and validated, successfully characterizing the atomic scale structure of NSTF catalysts with gradient composition with spatial position. Additionally, HT electrochemical characterization of catalyst activity and surface area has been established as reproducible.

✧ ✧ ✧ ✧ ✧

INTRODUCTION

State-of-the-art membrane electrode assemblies utilized in today's prototype automotive traction fuel cell systems continue to suffer from key technical and economical limitations of high cost, insufficient durability, and low robustness to off-nominal operating conditions. Many state-of-the art MEAs based on conventional carbon-supported Pt nanoparticle catalysts currently incorporate precious metal loadings which are significantly above those needed to achieve MEA cost targets. As electrode catalyst loading is lowered to reduce cost, performance and durability typically decrease significantly. New catalysts and electrodes are needed which simultaneously achieve the cost, performance, and durability targets to enable the possibility of wide-spread commercialization of automotive fuel cells.

This project focuses on development of novel thin-film electrocatalysts based on 3M's NSTF catalyst technology platform. NSTF electrocatalysts and electrodes are a unique approach towards addressing key technical commercialization challenges. The thin film electrocatalyst structure imparts substantially high ORR specific activities and high resistance to electrocatalyst dissolution and sintering induced by electrochemical cycling [2]. The NSTF support is based on an oriented, sub-micron scale crystalline organic pigment whisker, not carbon particles, which enables exceptional resistance to corrosion in fuel cell and water electrolysis applications [3]. Traditional NSTF electrodes, which are a single layer of NSTF electrocatalyst particles partially embedded into an ion-conducting membrane, are ultrathin (<1 µm) and do not require ionomer for proton conduction [4]. When integrated into state-of-the-art operationally robust MEAs, the NSTF electrode structure enables high absolute and specific power densities [1].

APPROACH

The project approach is to establish relationships between electrocatalyst functional response (activity, durability), physical properties (bulk and surface structure and composition), and fabrication processes (deposition, annealing, dealloying) via systematic investigation. Once established, these relationships will be utilized towards development of electrocatalysts with further improved properties. Electrocatalysts will be generated in one of two distinct morphologies, nanoporous thin film and ultrathin film, each with distinct pathways towards achieving project targets. Additionally, this project utilizes high throughput material fabrication and characterization, electrocatalyst modeling, and advanced physical characterization to guide and accelerate development.

RESULTS

We previously reported initial results from a new UTF PtNi electrocatalyst system, with systematic studies of the impacts of composition and structure on activity and performance [5]. Mass activity was found to depend strongly on annealing conditions, ranging from 0.15 A/mg (unannealed) to as high as 0.39 A/$mg_{PGM.}$ Additional analysis was conducted this year towards understanding the underlying causes of the activity sensitivity towards annealing. UTF PtNi catalysts with 0.027 mg/cm^2 were prepared and characterized with a range of annealing times at either one of two annealing temperatures (T1 < T2), summarized in Figure 1.

Specific activity generally increased as annealing time and temperature decreased through the process condition ranges evaluated (Figure 1A). After fuel cell testing, some of the electrocatalysts were analyzed for composition by EDS, and the bulk Pt-Pt strain of the catalyst, relative to bulk pure Pt, was calculated based on the measured composition and Vegard's law. Figure 1B shows that as the annealing time and temperature increased, the calculated bulk strain increased, and the trends in bulk strain were qualitatively similar to the observed variation in specific activity from Figure 1A. Figure 1C directly compares the relationship between the calculated bulk strain and the catalyst specific activity, and a very good correlation is observed over nearly a 2.5x range of specific activity. Figure 1D summarizes DFT model predictions of catalyst activity for pseudomorphic Pt skins of various thicknesses on Pt_xNi_{1-x} substrates of varying strain (composition). The DFT model predicts a peak in activity near 2.5% strain for Pt skins between 2–4 monolayers, and the peak activity is approximately 20x higher than unstrained Pt(111). The DFT prediction of activity vs. strain agrees well with the experimental data in trend but not in magnitude. The cause for the discrepancy in magnitude between model and experiment is not known and is currently under investigation.

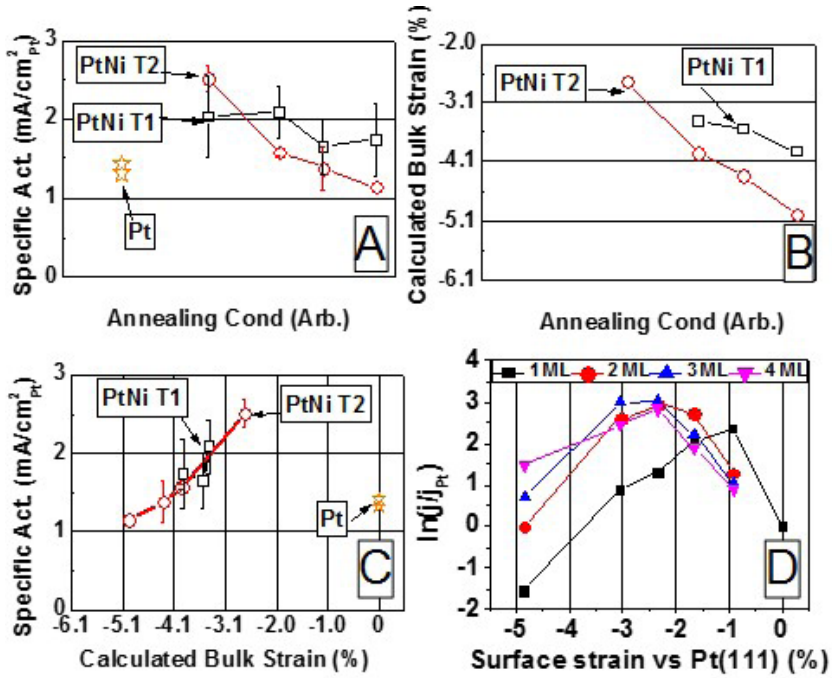

Act. – activity; Arb. – arbitrary

FIGURE 1. UTF PtNi activity dependence on bulk and surface strain. (A) Activity vs. annealing conditions. (B) Calculated bulk strain vs. annealing conditions. (C) Correlation of specific activity to calculated bulk strain. (D) DFT model prediction of activity vs. strain (note logarithmic scale).

Based on the understanding developed with the UTF PtNi system and previous studies with NPTF PtNi, development expanded into the fabrication and characterization of several new alloy candidates. Five new Pt binary alloy candidate systems were fabricated and characterized in MEA for beginning of life activity and H_2/air performance. Each alloy system was evaluated with a range of Pt mole fractions and annealing conditions and one of two Pt loadings (25–30 $\mu g_{Pt}/cm^2$ for UTF catalysts, 80–90 $\mu g_{Pt}/cm^2$ for NPTF catalysts). Additionally, NPTF catalysts were dealloyed prior to MEA fabrication to minimize leachable alloying element content and potentially inducing nanoporosity. Figure 2 summarizes the mass activities and H_2/air performances from the highest performing UTF and NPTF catalysts identified in each binary alloy system (PtNi and new alloys "B," "C," "D," "E," and "F"). Additionally, data for NSTF Pt catalyst and Pt nanoparticle catalysts on Vulcan carbon (Pt/V) in dispersed electrodes is included for reference. Figures 2A and 2B summarize BOL mass activity for the NPTF and UTF alloys, respectively. Four catalysts overall were identified with mass activity of 0.39 A/mg_{PGM} or higher, NPTF PtNi, UTF PtNi, UTF B and UTF E. The highest overall activity of 0.47 A/mg_{PGM} was obtained with NPTF PtNi, which exceeded the DOE target of 0.44 A/mg_{PGM}. Figures 2C and 2D summarize the H_2/air performances obtained at 1.5 atmA H_2/air reactant pressures for the NPTF and UTF catalysts, respectively. For NPTF catalysts, PtNi, B, C, and F had improved performance at high current density over Pt/V electrodes with 0.10 mg_{Pt}/cm^2 electrode loading. The best overall high current density performance was obtained with NPTF "F," which yielded a ca. 100 mV improvement over Pt/V at 1.0 A/cm^2 current density. UTF PtNi, B, D, and F catalysts with 25–30 $\mu g_{Pt}/cm^2$ had higher H_2/air performance than the reference Pt/V catalyst containing 50 $\mu g_{Pt}/cm^2$ electrode loading. UTF PtNi and F yielded the highest overall high current density performance, as much as 69 mV higher than Pt/V at 0.50 A/cm^2 current density.

Several electrocatalyst candidates were also evaluated for durability with the DOE electrocatalyst AST [6], consisting of 30,000 triangle wave cycles between 0.60 V and 1.0 V at 50 mV/s. Last year, we reported that the integration of an additive substantially improved the durability of NPTF PtNi catalyst. Mass activity losses decreased from about 65–70% without the additive to 42% with the additive, close to the DOE target of 40%. While effective at improving the durability, BOL mass activity and H_2/air performance were suppressed relative to additive-free NPTF PtNi catalysts [5]. This year, new electrocatalyst development was conducted towards improving the mass activity, performance, and durability of NPTF PtNi and UTF PtNi via integration of small amounts of Ir. Figure 3A summarizes beginning of life mass activity of NPTF PtNiIr catalysts as a function

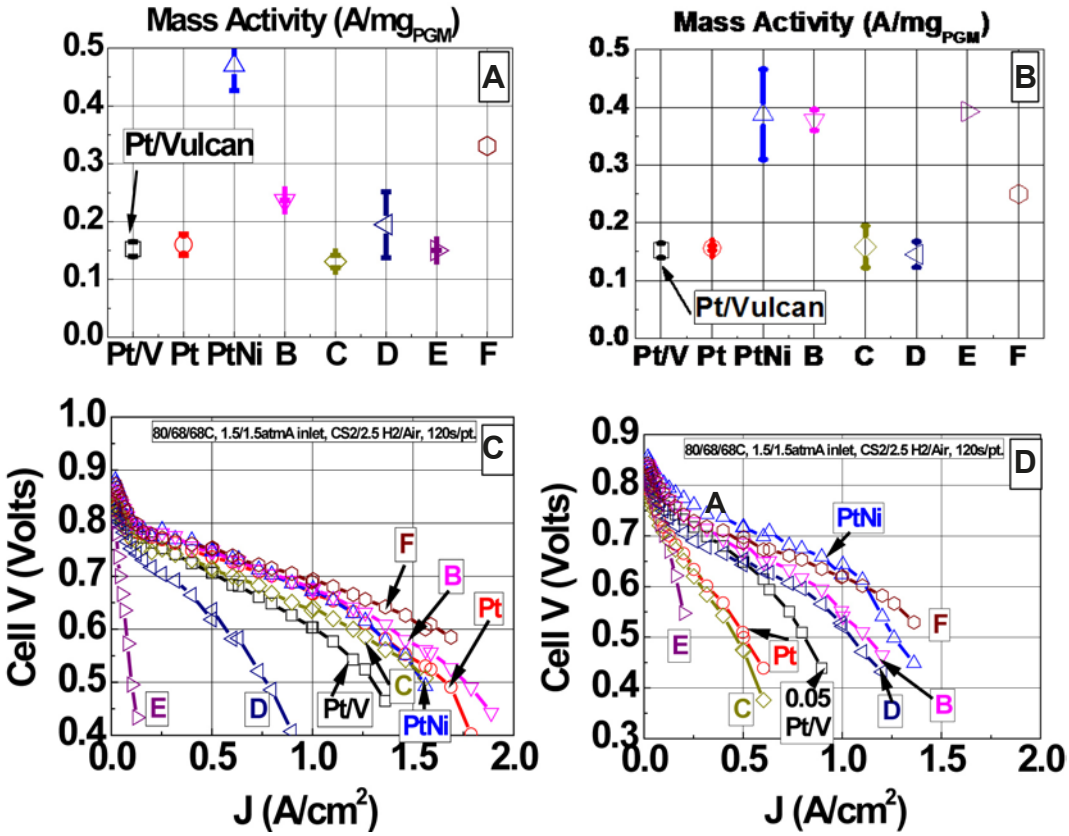

FIGURE 2. Mass activity and H_2/Air performance of Pt on Vulcan, Pt/NSTF, PtNi/NSTF, and NSTF Pt binary alloys "B," "C," "D," "E," and "F." (A) NPTF catalyst mass activity. (B) UTF catalyst mass activity. (C) NPTF catalyst H_2/Air performance at 80°C, 1.5 atmA H_2/air. (D) UTF catalyst H_2/air performance.

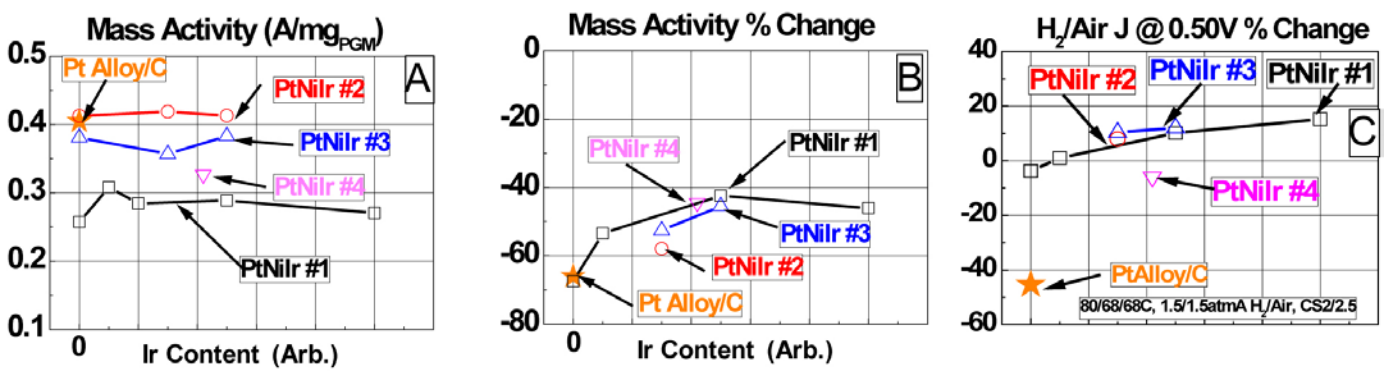

FIGURE 3. Mass activity and durability of several NPTF PtNiIr catalysts as a function of Ir content. (A) Mass activity at beginning of life. (B) Change in mass activity after accelerated durability testing. (C) Change in H_2/air current density at 0.50 V cell voltage after durability testing.

of Ir content and Ir integration method (#1, #2, #3, and #4). Reference data for a high activity Pt alloy nanoparticle on carbon catalyst with an electrode loading of 0.09 mg_{PGM}/cm^2 is included for reference. The mass activity of NPTF PtNiIr varied from ca. 0.25 A/mg_{PGM} to 0.41 A/mg_{PGM} and depended primarily on Ir integration method, not on Ir content through the range evaluated. Figure 3B shows that with integration method #1 and #3, mass activity losses after accelerated durability testing were as low as 42% and 45%, respectively, and appeared to decrease as Ir content increased to a relatively moderate level. Figure 3C summarizes the changes in H_2/air current density at 0.50 V cell voltage after the durability testing, and for most NPTF PtNiIr catalysts the performance at 0.50 V was either unchanged or slightly

improved after the test. With PtNiIr#1, performance improvement after the durability test appeared to increase monotonically with Ir content. For reference, the Pt alloy on carbon catalyst lost 70% mass activity and 50% of the H_2/air current density at 0.50 V after the durability test.

Ir integration studies were also conducted with UTF Pt and PtNi to determine the impact of Ir on activity, performance, and durability. Figure 4A summarizes beginning of life mass activities for UTF PtIr and three UTF PtNiIr catalysts as a function of Ir content. The PtIr catalyst contained 30 $\mu g_{Pt}/cm^2$ loading in the electrode and the three PtNiIr catalysts' loadings were 9 $\mu g_{Pt}/cm^2$, 26 $\mu g_{Pt}/cm^2$, and 50 $\mu g_{Pt}/cm^2$, respectively. The PGM mass activity of all four catalysts depended strongly on Ir content, with evidence of an activity peak through a narrow Ir content range which may be specific to each catalyst. Peak PtIr mass activity was 45% higher than comparable Ir-free Pt, and peak PtNiIr #1 activity was 46% higher than comparable Ir-free PtNi #1. Peak mass activities for the 9 $\mu g_{Pt}/cm^2$, 26 $\mu g_{Pt}/cm^2$, and 50 ug_{Pt}/cm^2 UTF PtNi catalysts were 0.36 A/mg_{PGM}, 0.41 A/mg_{PGM}, and 0.44 A/mg_{PGM}. The increased mass activity observed within the narrow and low Ir content range was primarily due to increased specific activity. Figure 4B shows that mass activity losses of the PtIr and PtNiIr after accelerated durability ranged from 35% to 65% vs. the 40% DOE target. The UTF PtNiIr catalyst with the highest beginning of life mass activity of 0.44 A/mg_{PGM} lost 45% mass activity after accelerated durability testing, which exceeded the project go/no-go criteria for Budget Period 1. The data suggests that the mass activity durability of the highest activity PtNiIr catalysts with optimal Ir content is comparable to or lower than Ir-free catalyst, but at higher Ir contents the mass activity durability may be moderately improved over Ir-free. While the impact of Ir on mass activity durability of UTF Pt and PtNi was moderate, Ir did significantly improve the durability of specific surface area and H_2/air performance at high current density. Figure 4C shows that the specific area losses after the accelerated durability test decreased monotonically with increasing Ir content for all four Ir-containing catalysts. Figure 4D shows that the loss in H_2/air current density at 0.50 V cell voltage also generally improved with increasing Ir content for the UTF PtIr and the two higher Pt content PtNiIr catalysts. With the highest Pt-content UTF PtNiIr catalyst, performance change at 0.50 V ranged from essentially no change to a modest improvement, and loss in performance at 0.80 V was 21 mV, exceeding the DOE target of 30 mV loss.

Modeling and advanced characterization were utilized to determine the role of surface Ir towards the observed activity and durability enhancements with NPTF and UTF PtNiIr catalysts. Catalysts were evaluated for atomic-scale structure by scanning transmission electron microscopy (STEM) imaging and for bulk composition by EDS. Figure 5 summarizes the analysis of a particular UTF PtNiIr catalyst, evaluated after fuel cell conditioning. Ir content was relatively stable through fuel cell conditioning and after the electrocatalyst AST, and Ir deposited on the catalyst surface largely remains at the surface. DFT modeling was conducted

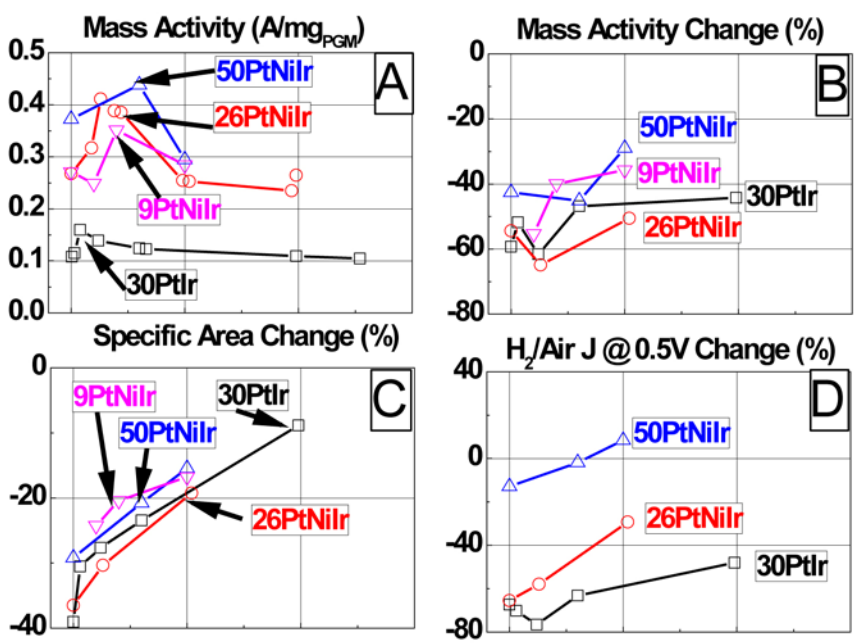

FIGURE 4. Mass activity and durability as a function of Ir content for UTF PtIr and three PtNiIr catalysts with electrode Pt loadings ranging from 9 $\mu g/cm^2$ to 50 $\mu g/cm^2$. (A) PGM mass activity at beginning of life. (B–D) Changes in PGM mass activity, PGM specific area, and current density at 0.50 V after the DOE electrocatalyst AST.

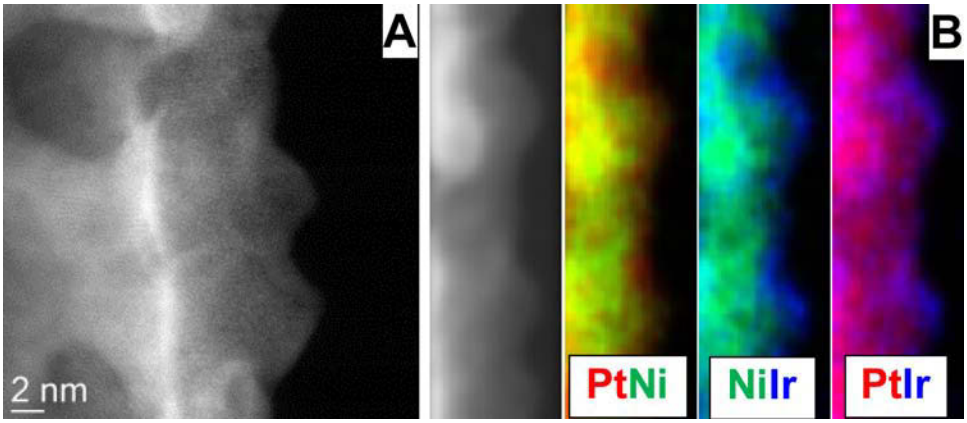

FIGURE 5. STEM-EDS analysis of UTF PtNiIr catalysts. (A) High-angle annular dark field STEM. (B) EDS composition maps.

to assess the thermodynamic stability of Ir-modified Pt(332) surfaces with varying surface coverages of Ir (Figure 6). The model determined that the formation energy for Ir deposition on the surface of Pt(332) is not energetically favorable, and that this formation energy is significantly reduced upon surface rearrangement where Ir is covered by a monolayer of Pt. kMC modeling was conducted to assess the impact of surface Ir content on the nanoporosity formation in PtNi. The model appeared to accurately capture the nanoporous structure obtained experimentally, as shown in Figure 7. The kMC model predicted that Ir deposited on the surface is relatively immobile with potential cycling, consistent with experimental observations. Additionally, the model suggests that Ir may enhance the nanoporous surface area durability via promotion of capillary wetting of Pt and Ni onto the stable Ir shell.

In additional catalyst development work, two new UTF Ir-free catalysts have been identified with further improved mass and specific activities over UTF PtNi (Figure 8). Average mass activities for the two new catalysts were 0.47 A/mg$_{PGM}$ and 0.56 A/mg$_{PGM}$ as measured in MEA, both exceeding the DOE 2020 target of 0.44 A/mg$_{PGM}$. The new catalysts have markedly higher specific activity than UTF Pt and PtNi, as much as 50% higher than UTF PtNi, 2.5x higher than UTF Pt, and 7.5x higher than Pt nanoparticle catalyst.

Select NPTF PtNiIr, UTF PtNi, and UTF PtNiIr catalysts from above were evaluated for rated and specific power density. The catalysts were integrated into MEAs with previously-identified components which enable improved operational robustness of NSTF MEAs, including an optimized anode gas diffusion layer and cathode interlayer, which contains 16 μg$_{Pt}$/cm^2 [1]. Figure 9 summarizes the measured H_2/air polarization curves for the three 2017 catalysts, as compared to the pre-project baseline. Polarization curves were obtained with 90°C cell temperature and 1.5 atmA H_2/air reactant pressures, conditions relevant for assessment of rated and specific power densities at the DOE MEA Q/ΔT heat rejection target of 1.45 kW/°C. Status against relevant DOE targets is summarized in Table 2. The absolute performance of the 2017 NPTF PtNiIr catalyst overlaps the performance obtained with the baseline NPTF PtNi (no Ir) catalyst. Overall catalyst loading of the 2017

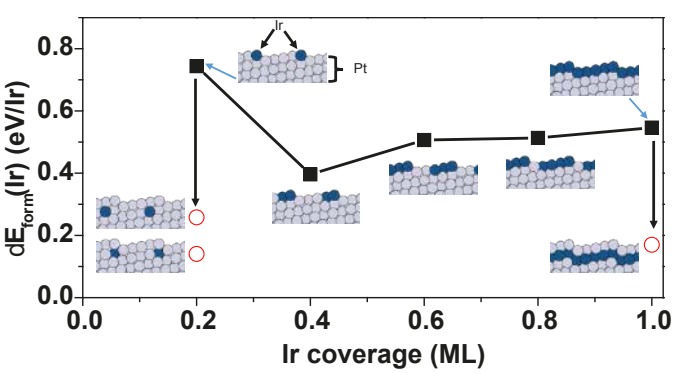

FIGURE 6. DFT predicted formation energies of Ir-modified Pt(332) surfaces.

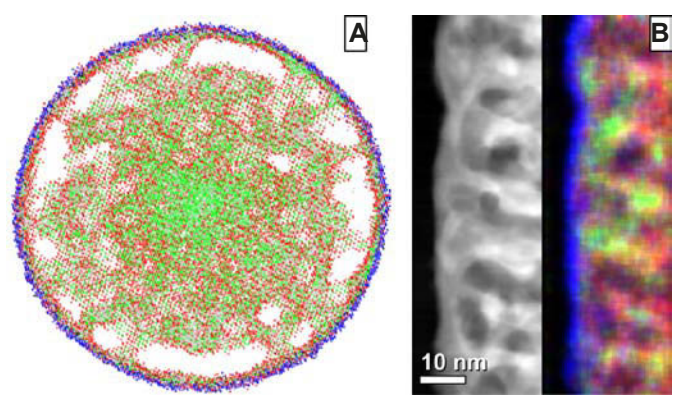

FIGURE 7. Structure of modeled and experimental dealloyed NPTF PtNiIr. (A) kMC model. (B) STEM-EDS analysis.

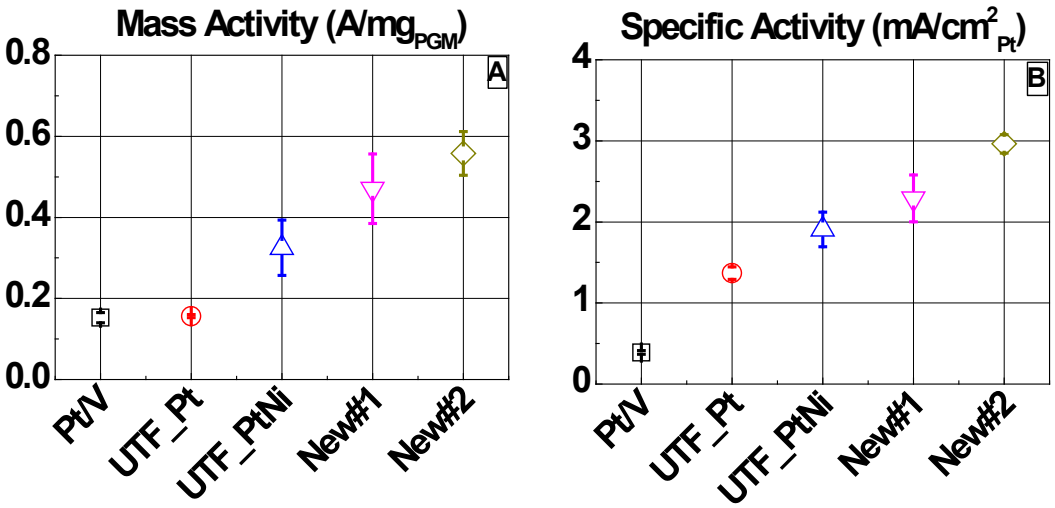

FIGURE 8. Mass activity of UTF Pt, PtNi, and new catalysts.

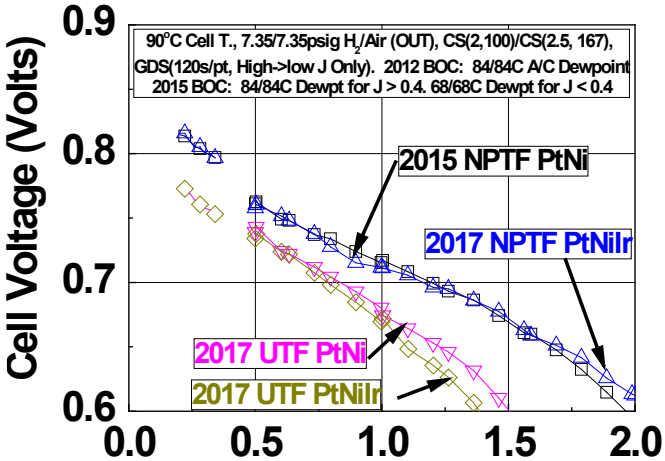

GDS – galvanodynamic scan

FIGURE 9. Performance of UTF and NPTF PtNi and PtNiIr catalysts.

NPTF PtNiIr MEA was reduced slightly vs. baseline to just below the DOE target, yielding modestly improved specific power which was 91% of the DOE target. Both the 2015 and 2017 MEAs slightly exceeded the DOE ¼ power target of 0.30 A/cm^2 at 0.80 V. Along with the improved MEA loading and specific power density, the 2017 NPTF PtNiIr cathode has improved mass activity durability vs. the baseline (45% vs. 65% loss for the NSTF cathode) and exceeded the DOE performance loss at 0.8 A/cm^2 target. The UTF PtNi and PtNiIr MEAs' absolute performances were substantially lower than those obtained with the NPTF PtNi and PtNiIr MEAs. Rated power densities of the UTF PtNi and PtNiIr MEAs were 0.63 W/cm^2 and 0.58 W/cm^2, respectively, which are substantially below the DOE target of 1 W/cm^2. The primary reason for the relatively lower absolute performance of the UTF MEAs than the comparative NPTF MEAs is because the UTF catalysts had ca. 50% lower absolute PGM loading in the NSTF cathode electrodes. The UTF PtNi MEA achieved the DOE specific power target of 8.1 kW/g_{PGM} while meeting the DOE Q/ΔT heat rejection target, and had 38% lower PGM total loading (both electrodes) than the DOE target. The UTF PtNiIr MEA absolute power density was slightly lower than the UTF PtNi MEA, but met the total loading and performance loss at 0.8 A/cm^2 targets.

Work has continued towards establishment of reproducible methods for HT electrocatalyst development. Last year, we reported that we had developed a method of fabricating Pt_xNi_{1-x} catalyst with a range of spatially-varying compositions, and that spatial variation in the catalyst's composition and bulk crystalline structure could be reproducibly characterized via HT-compatible methodologies. This year, we have validated a method for conducting HT XAFS towards characterizing the atomic scale catalyst structure with two gradient composition Pt_xNi_{1-x} catalysts. Full spectral analysis and fitting conducted on Pt-rich and Ni-rich ends of the gradient catalyst substrates showed excellent reproducibility of coordination numbers and bond lengths within the three annealed and unannealed sets. The spectra of intermediate compositions were determined via linear combinations of the Pt-rich and Ni-rich endpoint spectra, allowing rapid extraction of the atomic structure information at intermediate compositions. An example of this analysis is shown in Figure 10A, which shows the Pt-Pt, Pt-Ni, and Ni-Ni bond distances determined from a gradient composition PtNi catalyst. Additionally, work has continued towards establishment of reproducible electrochemical characterization of HT-fabricated catalysts with a segmented cell. Reproducibility of catalyst activity has been established with a homogenous catalyst, yielding a 3.2% relative standard deviation across three separate replicate MEA measurements and across all 121 individual segments, exceeding the project

TABLE 2. Best of Class MEAs Loading, Specific Power, Rated Power, and ¼ Power Performances

MEA Construction	Total MEA Loading (mg/cm^2)	Spec. Power @ Q/ΔT =1.45 (kW/g_{PGM})	Rated Power @ Q/ΔT=1.45 (W/cm^2)	1/4 Power J @ 0.80V (A/cm^2)	Electrocatalyst AST Durability (NSTF catalyst only)	
					Mass Act. Loss (%)	Loss @ 0.8A/cm^2 (mV)
DOE 2020 Target	0.125	8.0	1.000	0.300	40	30
Baseline 2015 NPTF PtNi	0.131	6.8	0.891	0.310	~65	NA
2017 NPTF PtNiIr	0.122	7.3	0.897	0.308	45	21
2017 UTF PtNi	0.077	8.1	0.626	NA	43	50
2017 UTF PtNiIr	≤0.089	≥6.6	0.584	<0.200	45	23

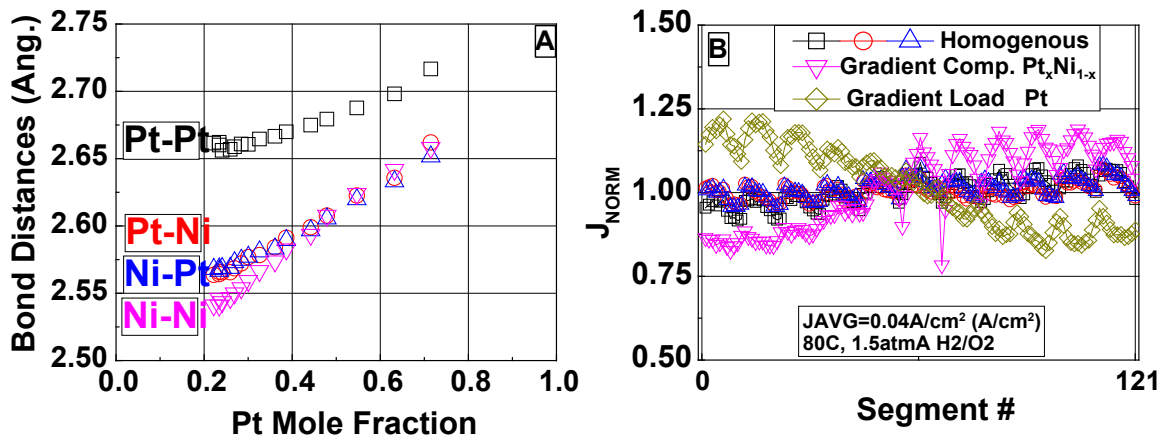

FIGURE 10. High Throughput Electrocatalyst Method Development. (A) HT XAFS of gradient composition PtNi catalyst. (B) HT-segmented fuel cell characterization of catalyst activity.

milestone of less than 20% relative standard deviation (Figure 10B). Two electrocatalysts with spatially-varying activity were assessed, where the activity variation was due to either a spatial variation in catalyst loading or catalyst composition. Significant spatial variations in activity were observed, consistent with expectation. However, the magnitude of activity variation appeared to be limited to a factor of 1.5 vs. the expected 2.5x and 3–4x variations for the gradient loading and gradient composition catalysts, respectively. The root-cause of this sensitivity limitation has been identified and the necessary hardware modification to resolve it is being planned.

CONCLUSIONS AND UPCOMING ACTIVITIES

Over the past year, UTF catalysts with ultra-low PGM content have been demonstrated which meet or exceed the DOE 2020 catalyst targets for mass activity, PGM total content, PGM total loading, loss in performance at 0.8 A/cm^2, and the MEA Q/ΔT heat rejection target. Three compositionally-distinct UTF catalysts have met or achieved the mass activity target, with one exceeding the target of 0.44A/mg_{PGM} by 27% due to an enhanced specific activity of 3 mA/cm^2_{Pt}. A UTF PtNi catalyst has met the platinum group metal total content (both electrodes) target of 0.125 g/kW and the DOE heat rejection Q/ΔT target of 1.45 kW/°C, with a PGM total loading (both electrodes) of 0.077 mg_{PGM}/cm^2, 40% below the target loading level. A UTF PtNiIr catalyst has exceeded the loss in performance at 0.8 A/cm^2 target after the electrocatalyst AST, and nearly achieves the loss in catalytic (mass) activity target. While active and durable, UTF catalyst rated power is only ca. 60% of the DOE target of 1 W/cm^2, due in part to the ultra-low PGM areal loadings used with current UTF catalysts. Paths to improve the rated power of UTF catalyst MEAs have been identified.

Systematic studies have revealed that the activity of UTF PtNi catalysts correlates with the catalyst Pt-Pt bulk strain after fuel cell conditioning, measured both directly (Pt-Pt bond distances via XAFS) and indirectly (composition via EDS). The post-test composition systematically depends upon the as-fabricated catalyst composition and also the catalyst grain size, which is determined by fabrication conditions. DFT modeling of monolayer-scale Pt skins on Pt_xNi_{1-x} alloys confirmed the catalyst activity dependence on bulk composition and agreed well with experiment in terms of the activity trends with composition. However, the model predicted activity enhancement with optimal strain

exceeded the experimentally-observed activity enhancement by a factor of 20. The causes for the discrepancy are under investigation, but may be due to non-optimal skin structures on highly-strained substrates.

Extensive studies have been conducted towards improving the durability of project electrocatalysts. One promising approach investigated was incorporation of relatively small amounts of Ir onto the surface of PtNi catalysts. Ir imparted stabilization against specific activity and specific area losses of NPTF and UTF PtNi catalysts, respectively, and generally resulted in improved performance retention at high current density. Additionally, addition of Ir to the surface of UTF Pt and PtNi within a narrow composition range increased the PGM mass activity by up to 46% vs. Ir-free. Microscopy characterization indicates that Ir is substantially stable, and electrocatalyst modeling has provided insight into the activity and durability mechanisms.

In future work, the project will continue development efforts towards achieving the overall project Budget Period 2 milestone, reflecting demonstration of a single catalyst which simultaneously exceeds the DOE 2020 targets for mass activity, mass activity durability, and specific power in an MEA. This will be accomplished by several development pathways occurring in parallel. Experiments and modeling efforts are already underway towards development of new UTF electrocatalysts with significantly further improved specific surface area and specific activity via Pt skin optimization. An additional modeling and experimental focus is identification of electrocatalyst compositions and structures which can achieve the aggressive project durability targets. Absolute performance and rated power of UTF electrocatalysts will be increased by integration of the high specific activity electrocatalyst onto NSTF supports with higher absolute surface area while maintaining the mass-specific activity and area. In addition, work has been initiated to evaluate down-selected catalysts for their impact on two key challenges for NSTF MEAs, rated power durability and break-in conditioning.

FY 2017 PUBLICATIONS/PRESENTATIONS

1. A.J. Steinbach et al., "3M NSTF Electrocatalysts for PEM Fuel Cells and Water Electrolyzers," 20th International Symposium on Batteries, Fuel Cells, and Capacitors, Chiba, Japan, November 29, 2016. *Invited*.

2. J. Greeley, "First Principles Analysis of Interfacial Electrocatalysis," McKetta Department of Chemical Engineering at the University of Texas at Austin, Austin, TX, January 24, 2017.

3. D.A. Cullen et al, "Understanding the Origins of Activity through in situ Annealing and Dealloying of Fuel Cell Catalysts," 2017 Spring Materials Research Society Meeting, Phoenix, AZ, April 2017.

4. A.J. Steinbach, "Highly Active, Durable, and Ultra-low PGM NSTF Thin Film ORR Catalysts and Supports," USCAR Fuel Cell Tech Team, Detroit, MI, April 19, 2017.

5. J. Greeley, "Ab-initio Studies of Heterogeneous Catalysis and Electrocatalysis at Metal-Liquid Interfaces," Department of Chemical and Petroleum Engineering, University of Pittsburgh, Pittsburgh, PA, April 20, 2017.

6. Z. Zeng and J. Greeley, "DFT Studies of Electrochemical Oxygen Reduction Reactions on Pt Skin Alloys," 231st Meeting of the Electrochemical Society, New Orleans, LA, May 30, 2017.

7. A.J. Steinbach, 2017 Annual Merit Review, DOE Hydrogen and Fuel Cell Vehicles Technology Programs, Presentation FC143, Washington DC, June 2017.

8. A.J. Steinbach et al., "Ultrathin Film NSTF ORR Electrocatalysts for PEM Fuel Cells," *ECS Trans.,* submitted.

REFERENCES

1. A.J. Steinbach, Presentation FC104, 2016 Annual Merit Review, DOE Hydrogen and Fuel Cell Vehicles Technology Programs, June 2016, Washington DC.

2. M.K. Debe et al., "Stop-Start and High-Current Durability Testing of Nanostructured Thin Film Catalysts for PEM Fuel Cells," *ECS Trans.* **3**(1) 835–853 (2006).

3. M.K. Debe et al., "Initial Performance and Durability of Ultra-Low Loaded NSTF Electrodes for PEM Electrolyzers," *J. Electrochem. Soc.* **159**(6) K165–K176 (2012).

4. M.K. Debe, "Tutorial on the Fundamental Characteristics and Practical Properties of Nanostructured Thin Film (NSTF) Catalysts," *J. Electrochem. Soc.* **160**(6) F522–F534 (2013).

5. A.J. Steinbach et al., "Highly Active, Durable, and Ultra-low PGM NSTF Thin Film ORR Catalysts and Supports," 2016 Annual Project Progress Report to DOE.

6. U.S. Department of Energy, Office of Energy Efficiency & Renewable Energy, "Fuel Cell Technologies Office Multi-Year Research, Development, and Demonstration Plan," retrieved April 6, 2015.

V.A.8 Highly Accessible Catalysts for Durable High-Power Performance

Anusorn Kongkanand (Primary Contact), Venkata Yarlagadda, Michael K. Carpenter, Yun Cai, Thomas E. Moylan, Joseph M. Ziegelbauer, Srikanth Arisetty, and Wenbin Gu
General Motors
850 Glenwood Ave.
Pontiac, MI 48340-2920
Phone: (585) 953-5538
Email: anusorn.kongkanand@gm.com

DOE Manager: Gregory Kleen
Phone: (240) 562-1672
Email: Gregory.Kleen@ee.doe.gov

Contract Number: DE-EE0007271

Subcontractors:
- Dr. Andrew Haug, Matthew Lindell, Tyler Matthews, 3M Company (3M), St. Paul, MN
- Prof. Shawn Litster, Shohei Ogawa, Jonathan Braaten, Carnegie Mellon University, Pittsburgh, PA
- Prof. David Muller, Prof. Héctor Abruña, Elliot Padgett, Barnaby Levin, Yin Xiong, Yao Yang, Cornell University (Cornell), Ithaca, NY
- Prof. Joshua Snyder, Yawei Li, Drexel University (Drexel), Philadelphia, PA
- Dr. K.C. Neyerlin, Jason Christ, Shaun Alia, Jason Zack, Shyam Kocha, National Renewable Energy Laboratory, Golden, CO

Project Start Date: April 1, 2016
Project End Date: June 30, 2019

Overall Objectives

- Lower overall stack cost by improving high current density (HCD) performance in H_2/air fuel cells appropriate to meet DOE heat rejection and Pt-loading targets.
- Maintain long term high electrocatalytic mass activities.
- Mitigate catalyst HCD degradation.

Fiscal Year (FY) 2017 Objectives

- Identify and quantify performance loss terms observed on state-of-the-art cathode catalyst and membrane-electrode assembly (MEA).
- Identify pathways to improve the fuel cell performance toward DOE targets.
- Evaluate effects of carbon supports on fuel cell performance.

Technical Barriers

This project addresses the following technical barriers from the Fuel Cells section of the Fuel Cell Technologies Office Multi-Year Research, Development, and Demonstration Plan.

(A) Durability

(B) Cost

(C) Performance

Technical Targets

See Table 1 on next page.

FY 2017 Accomplishments

- Met DOE high-power target by developing a carbon support with low transport resistance while maintaining high oxygen reduction reaction (ORR) activity.
- Obtained early promising results with intermetallic PtCo electrocatalysts and ionic liquids.
- Improved understanding of the degradation of PtCo electrocatalysts and its impact.

✧ ✧ ✧ ✧ ✧

INTRODUCTION

The amount of platinum used in the ORR catalyst in fuel cells must be lowered by at least four-fold to enable proton exchange membrane fuel cells (PEMFCs) cost-competitiveness with other power sources. In our previous DOE-funded project, we demonstrated that carbon-supported Pt-alloy catalysts (PtNi/HSC and PtCo/HSC) exhibited very high ORR electrocatalytic activity and impressive durability, exceeding the DOE targets [1]. However, their high-power performance fell short of the target.

As the Pt content is lowered in the cathode, approaching <0.1 mg_{Pt}/cm^2, large oxygen and proton fluxes must be supplied to the Pt surface, causing a performance loss due to a relatively high local transport resistance in the state-of-the-art electrode. In addition, the non-precious transition metal in the catalyst, such as Ni or Co, can dissolve and migrate

TABLE 1. Progress towards Meeting Technical Targets for Electrocatalysts and MEAs for Transportation Applications

Metric	Units	PtCo/HSC-a	PtCo/HSC-e	PtCo/HSC-f	DOE 2020 Target
		2016	2017-1	2017-2	
PGM total loading (both electrodes)	mg/cm^2	0.125	0.125	0.088	<0.125
Mass activity @ 900 $mV_{iR\text{-}free}$	A/mg_{PGM}	0.6-0.7	0.6	0.7	>0.44
Loss in catalytic (mass) activity	% loss	0-40%	40%	TBD	<40%
Performance at 0.8 V (150 kPa, 80°C)	A/cm^2	0.304	0.306	**0.382**	>0.3
Power at rated power (150 kPa, 94°C)	W/cm^2	0.80	0.89	0.93	>1.0
Power at rated power (250 kPa, 94°C)	W/cm^2	1.01	**1.19**	**1.26**	-
PGM utilization (150 kPa, 94°C)	kW/g_{PGM}	6.4	7.1	**10.6**	>8
PGM utilization (250 kPa, 94°C)	kW/g_{PGM}	8.1	**9.5**	**14.3**	-
Catalyst AST (0.6–1.0 V)	mV loss at $0.8A/cm^2$	30	20	TBD	<30
Support AST (1.0–1.5 V)	mV loss at $1.5\ A/cm^2$	>500	>500	TBD	<30

Green: meets target; Red: does not meet target
HSC – high surface area carbon; PGM – platinum group metal; AST – DOE's accelerated stability test; TBD – to be determined

into the ionomer phase, replacing protons and consequently lowering the ionomer proton conductivity and causing hydrodynamic performance loss. As a result, although these Pt-alloy catalysts exhibit excellent durable high-activity at low power, the target performance at high power has not been realized, limiting its cost reduction benefit.

APPROACH

The general approach for this project is to identify and select a carbon support and an electrolyte that have favorable transport properties, and subsequently develop a high performance Pt-alloy electrode using these subcomponents. The efforts can be divided into four thrusts: (1) development of carbon support, (2) selection of electrolyte (ionomer or ionic liquid), (3) development of stable highly-dispersed Pt alloy nanoparticles, and (4) understanding the effects of the transition metal on performance.

RESULTS

As Pt loading and the available Pt area for the ORR are lowered, higher oxygen and proton fluxes must be delivered to the Pt surface, leading to noticeable performance losses. A detailed analysis showed that this performance loss was predominantly attributable to oxygen transport resistance, with the resistance showing a strong dependency on available Pt area and ionomer-Pt interface [2]. As a result, particularly on low-Pt content electrodes, the Pt surface area and the ionomer type become very important factors in determining the performance at high power. Moreover, state-of-the-art Pt alloy catalysts are commonly deposited on HSC, whose particles are porous in nature. A majority of the deposited Pt particles are embedded in the carbon, making it difficult for proton and O_2 to access.

The PtCo/HSC, developed in the previous project, showed a relatively high local oxygen resistance of 25 s/cm. According to previous analysis, we would achieve the DOE target if the resistance could be reduced to 10 s/cm. We found that by changing the carbon support to a non-porous "solid" type carbon, such resistance could be reduced to 10 s/cm. However, the ORR activity also decreased by 2–3 fold. It is believed that the direct contact of the ionomer with the Pt surface poisons the ORR activity of Pt, and that a porous carbon support could help prevent such direct contact for Pt located inside the pores. Figure 1 shows the fuel cell polarization curves of Pt catalysts supported on different carbons. In the low current density region,

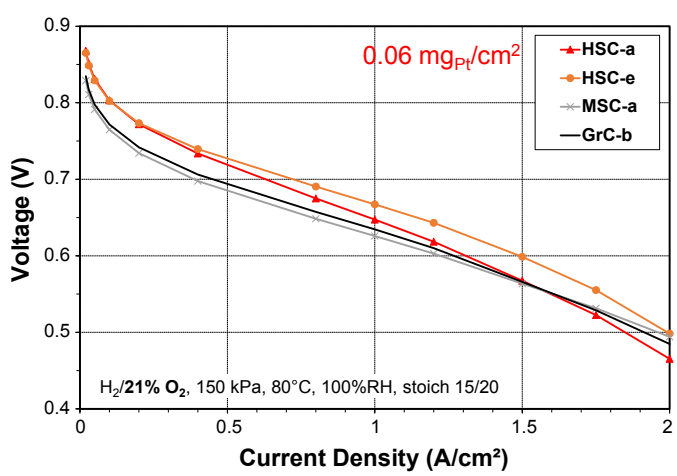

MSC – medium surface area carbon; GrC – graphitized carbon

FIGURE 1. Fuel cell polarization curves under differential operating condition with cathode Pt loadings of 0.06 mg_{Pt}/cm^2. H_2/air, 80°C, 100% relative humidity (RH), 150 kPa_{abs}, stoichiometry of 15/20. 5 cm^2 active area.

where ORR activity dominates, porous carbons (HSC) show higher voltage. In the HCD region, where transport losses become noticeable, solid carbons (medium surface area carbons and graphitized carbon) perform better. By selecting the appropriate carbon support, we were able to develop a catalyst with both good ORR activity and transport properties (HSC-e).

Further development of the PtCo catalysts on these new carbon supports yielded very high ORR mass activity of about 0.6–0.7 A/mg_{PGM}, comparable to the best PtNi and PtCo developed in the previous project [1]. The fuel cell performance, particularly at HCD, is significantly improved as shown in Figure 2. Under fuel cell operating conditions, relevant to DOE's heat rejection criteria (relatively high temperature and pressure), no noticeable transport-related voltage loss was observed on the new carbon supports operating at HCD. This results in a substantial improvement in high-power performance and PGM utilization as summarized in Table 1. Using the performance of PtCo/HSC-e, our second best electrocatalyst, the DOE-funded cost analysis team estimated that it would reduce the cost of the fuel cell system by about 14% or $7.5/kW [3,4].

Electrochemical evaluation of the catalyst with various carbon supports after DOE ASTs showed that porous carbons generally better retained Pt surface area and ORR activity under normal fuel cell operation, but did poorly under highly abusive testing. Evaluation of the electrode after the catalyst AST, using a range of advanced characterization techniques at Cornell, Carnegie Mellon University, and Argonne National Laboratory indicated that, regardless of the carbon type employed, the degradation was very similar at a macroscopic scale (Figure 3). This confirms that Pt dissolution/redeposition and migration dominate degradation. On the other hand, at the microscopic scale, as identified by high-resolution transmission electron microscopy with electron energy loss microscopy, Pt and PtCo nanoparticles in HSC catalysts show a lesser degree of particle coalescence after the stability test. The HSC advantage in mitigating particle coalescence is also manifested in a higher retention of Pt electrochemical surface area and ORR activity. These results illustrate the advantages of using porous carbon support on both initial performance and durability of the catalyst.

At the metal catalyst level, Cornell has been developing high loading (40%) ordered intermetallic Pt_3Co nanoparticle catalysts on HSC supports. A procedure for upscaling and preventing trace halide contamination was developed. Promising ORR activity was observed in rotating disk electrode, and MEA evaluation is underway. On the other hand, previous studies showed that interactions of the electrolyte (ionomer) and the Pt surface poison ORR activity and contribute to the local transport losses [2]. 3M and Drexel have been evaluating alternative ionomers and ionic liquids to mitigate these losses.

Cobalt and platinum dissolution is a major cause of catalyst degradation. National Renewable Energy Laboratory has performed extensive ex situ dissolution tests to determine the rate of Pt and Co dissolution and redeposition under various conditions. A cell level degradation model is being developed to incorporate these findings. Figure 4 presents one example, showing the effects of the potential on the Pt equilibrium concentration in solution and a comparison

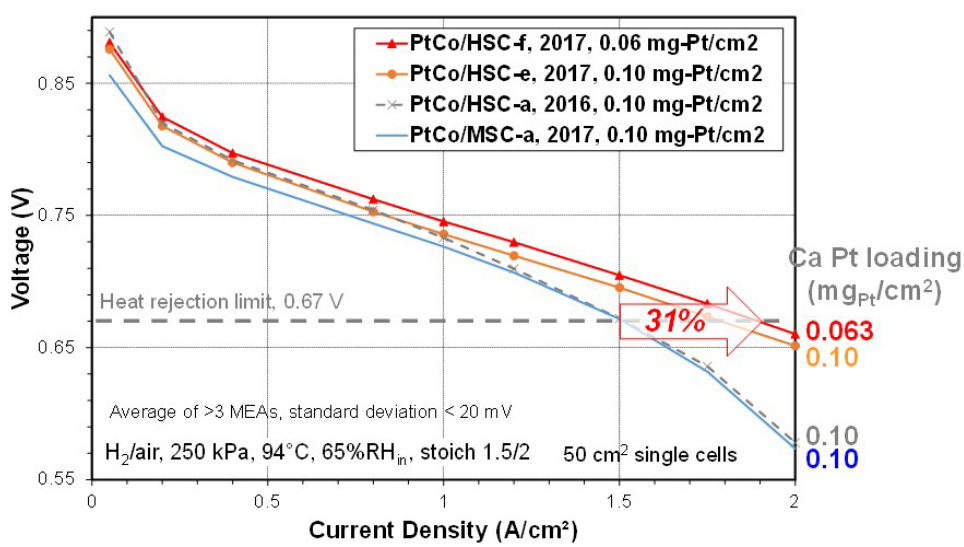

FIGURE 2. 50 cm^2 fuel cell polarization curves of PtCo catalysts deposited on different carbon supports. Cathode Pt loadings were 0.06 mg_{Pt}/cm^2 or 0.10 mg_{Pt}/cm^2 as indicated in the legend. Operating conditions in the order of anode/cathode: H_2/air, 94°C, 65/65% RH, 250/250 $kPa_{abs,outlet}$, stoichiometries of 1.5/2. Horizontal dash line indicates heat reject target (Q/ΔT of 1.45) recommended by DOE.

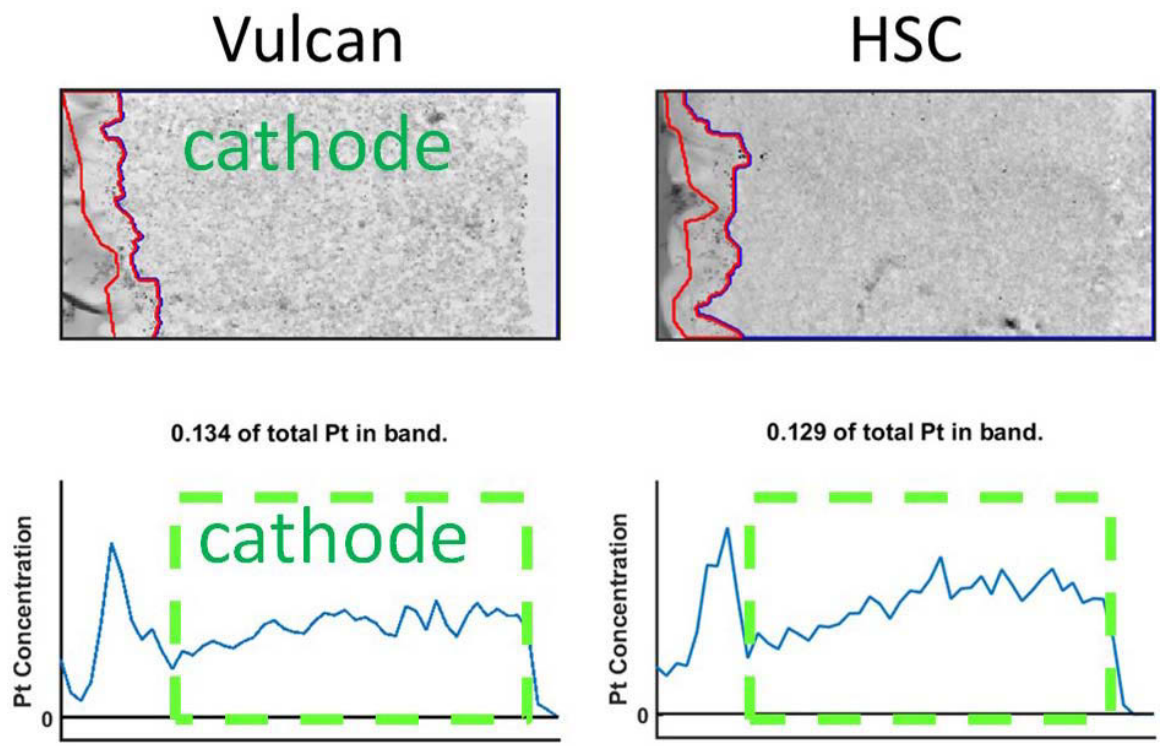

FIGURE 3. Quantification using transmission electron microscopy with energy-dispersive X-ray spectroscopy of Pt distribution in the cathode and cathode/membrane interface after AST (30,000 cycles between 0.6 V and 0.95 V, trapezoidal wave)

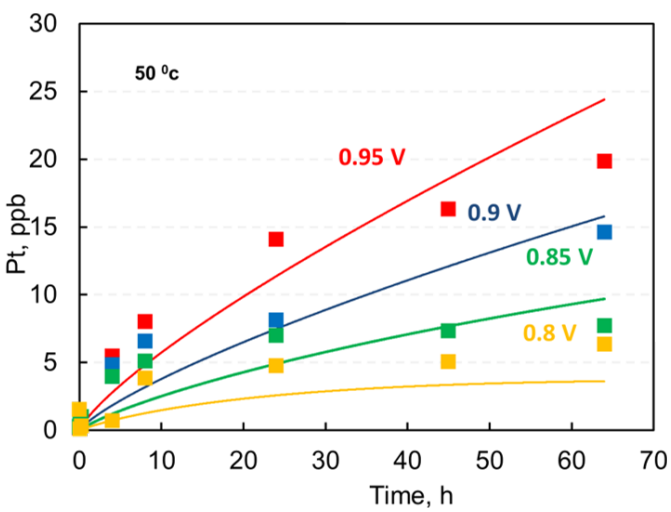

FIGURE 4. Equilibrium concentration of dissolved Pt in the electrolyte solution during a potential hold experiment

between the experiment and model. Experimental and modeling efforts at Carnegie Mellon University and General Motors are focused on understanding the effects of dissolved Co on the proton and oxygen transport properties of the ionomer. These results provide critical information, useful for determining the operating condition of a fuel cell so as to mitigate catalyst degradation.

Last, several new techniques and capabilities have been developed to accelerate the development of low-PGM electrodes. These include: (1) MEA preparation from small amounts of catalyst powder, (2) CO displacement in an MEA to quantify Pt-ionomer interactions, (3) CO stripping in an MEA to quantify Pt accessibility, (4) mathematical modeling to predict fuel cell performance with dissolved cobalt, and (5) mathematical modeling with nano/meso morphology determined from X-ray computed tomography and transmission electron microscopy tomography.

CONCLUSIONS AND UPCOMING ACTIVITIES

- Exceeded DOE 2020 target on PGM utilization with new carbon supports. This was largely done by lowering the resistance in carbon micropores while maintaining the ORR activity advantage gained in porous carbons.
- Improved the understanding of catalyst degradation due to (a) the effects of the carbon support and (b) Pt and Co dissolution/redeposition.
- Improved understanding of the performance tolerance to dissolved cobalt.

- Several new techniques and capabilities have been developed to accelerate the development of low-PGM electrodes.
- Upcoming activities include:
  - Optimizing PtCo deposition on selected carbons.
  - Continuing development of intermetallic alloys, alternative ionomers, and ionic liquids for improved ORR activity/stability and transport.
  - Experimental and modeling studies to understand the proton and oxygen transport in carbon micropores.
  - Visualization of dissolved cobalt during operation.

SPECIAL RECOGNITIONS & AWARDS/ PATENTS ISSUED

1. R&D Award by the DOE Hydrogen and Fuel Cells Program. "For outstanding achievements in developing low platinum group metal catalysts for PEMFC." June 2017.

2. Editors' Choice recognition by the *J. Electrochem. Soc.* for excellent publication.

FY 2017 PUBLICATIONS/PRESENTATIONS

1. "Electrochemical Diagnostics and Modeling in Developing the PEMFC Cathode," Anusorn Kongkanand, Venkata Yarlagadda, Taylor Garrick, Thomas E. Moylan, Wenbin Gu, *ECS Transactions* (2016) 75, 25.

2. *[Editors' Choice]* "Electrochemically Active Surface Area Measurement of Aged Pt Alloy Catalysts in PEM Fuel Cells by CO Stripping," Taylor Garrick, Thomas E. Moylan, Michael K. Carpenter, Anusorn Kongkanand, *J. Electrochem. Soc.* (2017) 164, F55.

3. "Characterizing Electrolyte and Platinum Interface in PEM Fuel Cells Using CO Displacement," Taylor Garrick, Thomas E. Moylan, Venkata Yarlagadda, Anusorn Kongkanand, *J. Electrochem. Soc.* (2017) 164, F60.

4. "Preparation of PEMFC Electrodes from Milligram-Amount Catalyst Powder," Venkata Yarlagadda, Samuel E. McKinney, Cristin L. Keary, Levi Thompson, Barr Zulevi, and Anusorn Kongkanand, *J. Electrochem. Soc.* (2017) 164, F845.

5. "High-Loading Intermetallic Pt_3Co/C Core-shell Nanoparticles as an Enhanced Catalyst toward the Oxygen Reduction Reaction," Yin Xiong, Yao Yang, Li Xiao, Héctor D. Abruña. (submitted).

REFERENCES

1. B. Han, et al., *Record Activity and Stability of Dealloyed Bimetallic Catalysts for Proton Exchange Membrane Fuel Cells.* Energy Environ. Sci. 2015, 8(1): p. 258–266.

2. A. Kongkanand and M. Mathias, *The Priority and Challenge of High-Power Performance of Low-Platinum Proton-Exchange Membrane Fuel Cells*. J. Phys. Chem. Lett. 2016, 7: p. 1127–1137.

3. S. Satyapal, Annual Merit Review DOE Hydrogen and Fuel Cells and Vehicle Technologies Programs, Washington, DC, June 2017. https://www.hydrogen.energy.gov/pdfs/review17/01_satyapal_plenary_2017_amr.pdf

4. B. James, Annual Merit Review DOE Hydrogen and Fuel Cells and Vehicle Technologies Programs, Washington, DC, June 2017. https://www.hydrogen.energy.gov/pdfs/review17/fc163_james_2017_o.pdf

V.A.9 Corrosion-Resistant Non-Carbon Electrocatalyst Supports for PEFCs

Vijay K. Ramani
Washington University in St. Louis
One Brooking Drive
St. Louis, MO 63130
Phone: (312)259-0801
Email: ramani@wustl.edu

DOE Manager: Gregory Kleen
Phone: (240) 562-1672
Email: Gregory.Kleen@ee.doe.gov

Contract Number: DE-EE-0007272

Subcontractors:
- Nissan Technical Center, North America, Farmington Hills, MI (Dr. Nilesh Dale)
- University of New Mexico, Albuquerque, NM (Prof. Plamen Atanassov)

Project Start Date: March 1, 2016
Project End Date: August 31, 2019 (six month no-cost extension secured from DOE)

Overall Objectives

- Design, develop and demonstrate high-surface-area (>70 m^2g^{-1}), high conductivity (>0.2 S/cm) and corrosion-resistant (as per funding opportunity announcement requirements), non-carbon supports based on doped/mixed metal oxides (that do not contain platinum group metals [PGMs]).
- Derivatize said supports to yield functional supported platinum (Pt) electrocatalysts that leverage strong metal-support interactions (SMSI).
- Demonstrate stability, activity, and performance approaching the Department of Energy's (DOE) 2020 targets using DOE-prescribed accelerated protocols in rotating disk electrode (RDE) and membrane electrode assembly polymer electrolyte fuel cell (PEFC) experiments by optimizing the structure of the support and the structure of the electrode.
- Provide DOE with at least six 50-cm^2 membrane electrode assemblies prepared using the best down-selected formulations that (a) meet all the stability metrics and (b) provide a clear pathway to meeting DOE 2020 targets for Pt loading and mass activity metrics.

Fiscal Year (FY) 2017 Objectives

- Density functional theory (DFT) calculations to evaluate Pt dissolution and SMSI of relevant doped metal oxides.
- Synthesis and characterization of tantalum (Ta)-doped-TiO_2 and other doped metal oxides (MO).
- High surface area support synthesis by employing sacrificial support method.
- Characterization of the doped metal oxides and the derived Pt catalysts.
- Electrochemical evaluation of the stability of supports and Pt/MO electrocatalysts.
- Investigation of SMSI in Pt/doped-metal-oxide systems using X-ray photon spectroscopy and DFT.
- Measurement of beginning of life (BoL) oxygen reduction reaction activity and electrochemically active surface area (ECSA) of selected catalysts in RDE experiments.
- Electrode optimization: RDE and membrane electrode assembly.
- Evaluation of selected catalysts in a PEFC: BoL oxygen reduction reaction activity and ECSA, and fuel cell performance.

Technical Barriers

This project addresses the following technical barriers from the Fuel Cells section of the Fuel Cell Technologies Office Multi-Year Research, Development, and Demonstration Plan.

(A) Durability

(B) Cost

(C) Performance

Technical Targets

Table 1 shows current status (with commercial Pt/C and with the Pt/ruthenium dioxide-titanium dioxide [RTO] catalyst developed in our previous DOE EERE project) and the proposed targets for the current project. The preliminary data obtained with our proposed approach (see Table 1, Pt/TiO_2-Ta) was obtained without any optimization of the support, the catalyst deposition process, or the electrode preparation process. Clearly, there is much room for improvement in performance and baseline mass activity, which is precisely our goal in this project. These

improvements, in conjunction with the enhancement in durability, will allow us to advance towards the DOE 2020 targets. The advantages of our approach over the incumbent technology and any alternate approach (and to even our prior success with RTO) are that we eliminate the noble metal in the support (cost reduction), we ensure 100% tolerance towards start-stop cycling, and we promote SMSI between the support and Pt, providing a pathway to enhance BoL mass activity and stability under load cycling conditions. Hence, the proposed approach addresses the remaining challenges and technical issues and provides a pathway to advance the state of the art and meet the DOE 2020 targets.

FY 2017 Accomplishments

- DFT calculations have been performed by University of New Mexico to examine the electronic structure of platinum supported on rutile TiO_2(110) surface doped with 4% Ta, Nb, W and Mo. Based on the DFT calculated interaction energy between Pt and the doped metal oxide, the most stable Pt catalyst was on TiO_2 doped with Ta followed by TiO_2 doped with W, Mo and Nb. Preliminary DFT work on antimony-doped tin oxide have also been conducted.
- Antimony doped tin oxide was synthesized and characterized at Washington University in St. Louis using a xerogel method. The antimony doped tin oxide had an electron conductivity of 2.2 S/cm (well above the project target) and a surface area of 74 m^2/g (just exceeding the project target).
- Atomic layer deposition was used to produce a catalyst with smaller Pt particle size and a better dispersion of the Pt onto the antimony doped tin oxide. The BoL ECSA of this catalyst was 75 m^2/g_{Pt} (similar to the benchmark Pt/C; Tanaka TEC10E50E, which was about 85 m^2/g). No decrease in the ECSA of the catalyst was observed during start/stop cycling tests (performed in a RDE). A decrease of 21% in the ECSA was observed for the same catalyst when it was subjected to the load cycling protocol (RDE).

INTRODUCTION

Carbon black is the commonly used catalyst support for PEFC electrocatalysts due to its high surface area and high conductivity. However, under certain automotive fuel cell operation conditions (start-stop), carbon can corrode rapidly [1], resulting in significant and irrecoverable loss in performance. To address this issue, it is desirable to explore non-carbon supports with high conductivity, high surface area, and high corrosion resistance under fuel cell operating conditions. In this project, we will design, develop and evaluate electrochemically stable, high-surface-area, metal-oxide and doped-metal-oxide supports and supported Pt electrocatalysts therein. The Pt/MO catalysts should meet the DOE 2020 targets for stability and approach DOE 2020 targets for the BoL mass activity and Pt loading (as per DOE testing protocols).

APPROACH

DFT simulations will be performed to understand the electronic structure of the oxide upon doping, and to examine SMSI between Pt clusters and the support. The DFT results will guide dopant choice and doping levels. Once suitable combinations are identified and evaluated, we will employ the sacrificial support method pioneered by University of New Mexico as well as other methods suitable for the purpose, to prepare the supports with high surface area.

The evaluation of the electrochemical stability will be performed following the start-stop DOE protocol, by sweeping (linear ramp) the working electrode potential from 1 V to 1.5 V (vs. reference hydrogen electrode [RHE]). The experiment will be performed for 10,000 cycles (at 500 mV/s). Cyclic voltammograms will be recorded at periodic intervals (at a scan rate of 20 mV/s) to investigate any changes in the pseudo-capacitance or the appearance any new oxidation or reduction peaks (sign of changes in the oxide surface). The Pt catalysts (Pt deposited onto the MO) will be evaluated by

TABLE 1. Technical Targets

Metric	Units	SOA (Pt/C)*	SOA (Pt/RTO)	Proposed approach status (Pt/TiO_2-Ta)	End target	DOE 2020 target
Total PGM content	g kW^{-1}	0.55	0.55	N/A	0.25	<0.125
Total PGM loading	mg cm^{-2}	0.4	0.4	0.6	0.25	<0.125
Voltage at 1.5 A cm^{-2} (air)	mV	0.45	0.48	0.3	0.55	N/A
Loss in mass activity	% loss	32	33	<10%	<5%	<40
Voltage loss at 0.8 A cm^{-2}	mV	81	9	<15	<10	30
Voltage loss at 1.5 A cm^{-2}	mV	182+	20	N/A; 20 mV at 1 Acm^{-2}	<20	30
Mass activity @ 900 $mV_{iR\text{-}free}$	A mg^{-1}_{PGM}	0.07	0.07	ca. 0.05	0.3	0.44

SOA – state of the art; N/A – not available

using the start-stop and the load-cycling stability protocols. During the load-cycling protocol the electrode containing the Pt/MO catalyst will be cycled between 0.6 V and 0.95 V (vs. RHE) for 10,000 cycles employing a square wave. Cyclic voltammetry will be performed periodically to estimate the ECSA. Linear polarization experiments will be performed to estimate mass- and area-specific activities.

RESULTS

DFT with Perdew-Burke-Ernzerhof exchange correlation functional revised for solids and full Heyd-Scuseria-Ernzerhof hybrid functional was used to further study the structural, electronic, and stability properties of TiO_2 doped with 4% Ta, Nb, Mo, and W. The order of the stability of the doped TiO_2 structures was determined to be: Ta > W > Nb > Mo (Figure 1). Moreover, defect thermodynamics calculations showed that only *doping TiO_2 with Ta will create a thermodynamically stable doped structure starting from atomic/ionic Ta*. DFT with Perdew-Burke-Ernzerhof exchange correlation functional was also used to study the electronic structure of platinum supported on TiO_2 doped with 4% Ta, Nb, Mo, or W. It is known that platinum binds to oxygen strongly, which implies that its *d*-band center is too high. Our analysis of the DFT calculated partial density of states showed that depositing Pt on doped TiO_2 lowers the *d*-band center of platinum by altering its electronic structure and Pt(111) surface on TiO_2 is expected to bind oxygen more weakly than unsupported platinum. The *d*-band center (ε_d) relative to the Fermi level (E_F) was determined to be -2.02 eV for unsupported Pt(111), -2.34 eV for Pt(111) on Ta-TiO_2, -2.32 eV for Pt(111) on Nb-TiO_2, -2.28 eV for Pt(111) on Mo-TiO_2, and -2.30 eV for Pt(111) on W-TiO_2.

Ta-TiO_2 was synthesized using the sacrificial support method and significant changes in the both surface area and conductivity was observed following the second heat treatment post etching the sacrificial support (silica) with KOH, see Table 2. The large decrease in surface area was due to sintering and grain growth, which was expected at the synthesis temperature of 950°C. However, the increase in conductivity, by approximately three orders of magnitude, measured after the second heat treatment was attributed to the effect of n-type doping of tantalum into the TiO_2 lattice and to the reduction of TiO_2 during the second heat resulting in the formation of oxygen vacancies.

TABLE 2. Physical Properties of Step 1, High Surface Area Ta-TiO_2 Following KOH Etch, and Step 2, TiO_2 Doped with ~5 wt% Ta after Second Heat Treatment

Step	S_{BET}, m^2/g	Conductivity, S/cm	Temperature, °C
$1_{(post\ KOH)}$	220	1.00E-03	950
2	60	0.9	950

In parallel, $Sb_{0.05}Sn_{0.95}O_2$ (antimony-doped tin oxide [ATO], Sb-doped-SnO_2) was synthesized using the xerogel method. The resulting material had a conductivity of 2.2 S/cm and a Brunauer-Emmett-Teller surface area of 74 m^2/g. Transmission electron microscopy (TEM) pictures (Figures 2a and 2b) showed that the particle size of this metal oxide was 10±2 nm. $Sb_{0.05}Sn_{0.95}O_2$ exhibited very high

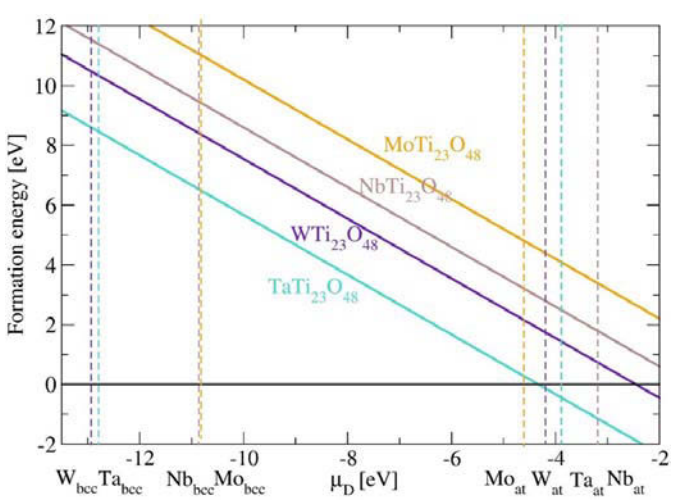

FIGURE 1. Formation energy (in eV) of the TiO_2 doped with Ta, Nb, Mo, or W as a function of the chemical potential of the dopant. Intercept of a dashed and a solid line of the same color denotes the energy required to replace 4% Ti atom in TiO_2 rutile with dopant (D), starting with a dopant in an atomic or metallic form.

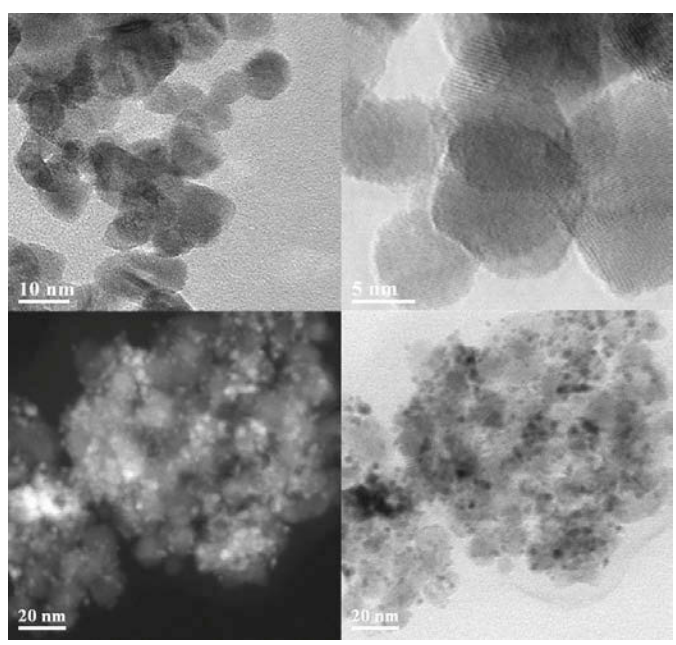

FIGURE 2. TEM and scanning TEM of ATO and Pt deposited onto ATO

electrochemical stability under the start-stop protocol, with only 1.5% change in pseudo-capacitance after 10,000 cycles, in contrast to carbon (Figure 3a). Pt supported on ATO catalyst was synthesized using the atomic layer deposition method, amongst other methods. The resultant catalyst had an ECSA of 75 m^2/g_{Pt} (Figure 4), very close to the benchmark Pt/C catalyst (85 m^2/g_{Pt}). TEM images (Figures 2c and 2d) showed approximately 2.5 nm Pt particles homogeneously dispersed onto the ATO support. Electrochemical testing (in RDE) showed good electrochemical stability under start-stop cycling protocol, with no loss in the ECSA over 10,000 start-stop potential cycles, and a loss of 21% of the initial ECSA after 10,000 cycles under the load cycling protocol (Figure 3b).

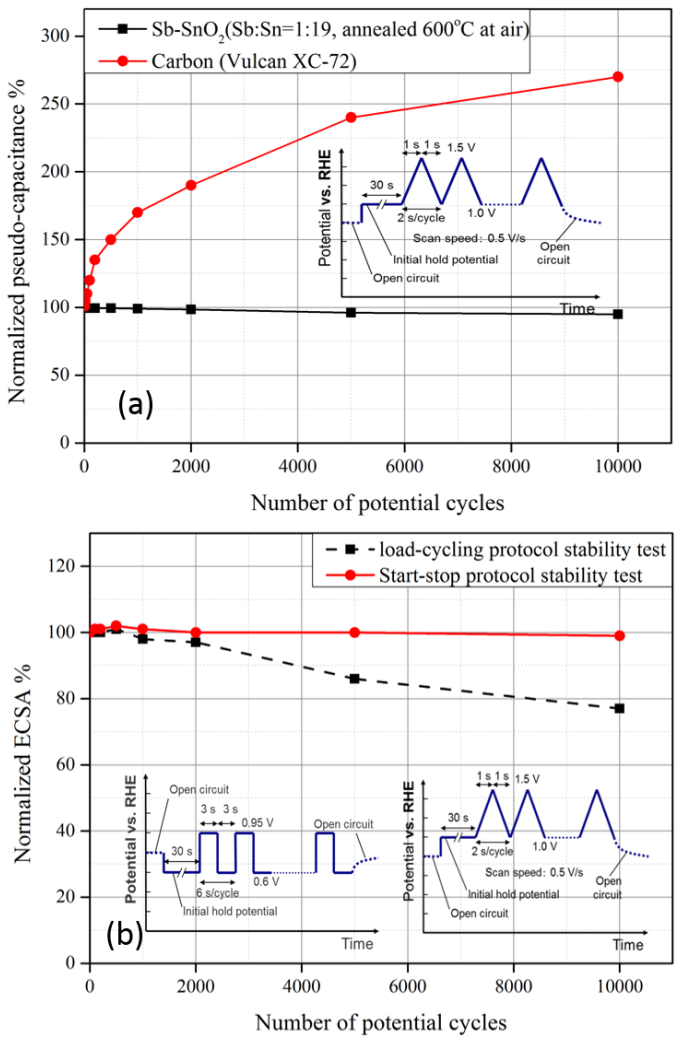

FIGURE 3. (a) Normalized pseudo-capacitance of carbon and ATO under start-stop potential cycling. (b) Loss of ECSA for Pt deposited onto antimony doped tin oxide under start-stop (support protocol) and load cycling protocols (catalyst protocol).

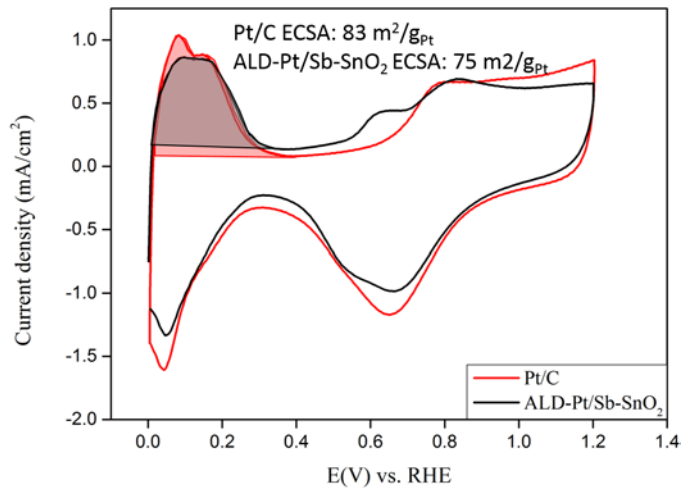

FIGURE 4. Cyclic voltammagrams for Pt/C and Pt deposited onto ATO in N_2-saturated 0.1 M $HClO_4$; sweep rate: 50 mV/s; room temperature

CONCLUSIONS AND UPCOMING ACTIVITIES

We have used DFT to identify several plausible doped-metal-oxide formulations that will provide both high conductivity and provide SMSI. In parallel, we have synthesized high surface area (74 m^2/g) and high conductivity (2.2 S/cm) ATO as a support, and successfully deposited Pt on this support to obtain a catalyst with an ECSA of 75 m^2/g_{Pt}. This catalyst only lost 21% of its original ECSA under the load cycling protocol after 10,000 cycles showing its potential to be stable catalyst under fuel cell operation. Over the next year, we will continue with the synthesis and optimization of ATO support and Pt/ATO catalyst, and its evaluation during PEM fuel cell operation. We will also in parallel prepare Ta-doped-TiO_2 supports and supported catalysts (using the sacrificial support method) and study SMSI in this and other variants suggested by our DTF calculations.

REFERENCES

1. N. Takeuchi; T.F. Fuller, J. Electrochemical Society, 155 (2008) B770–B775.

V.A.10 Regenerative Fuel Cell System (SBIR Phase II)

Paul Matter (Primary Contact), Minette Ocampo, Michael Beachy, Chris Holt, Nora Shaheen, Monica Chan, and Jimmy Gaydos
pH Matter LLC
1275 Kinnear Rd.
Columbus, OH 43212
Phone: (614) 396-7820
Email: info@phmatter.com

DOE Manager: Donna Ho
Phone: (202) 586-8000
Email: Donna.Ho@ee.doe.gov

Contract Number: DE-SC0013111 Small Business Innovation Research (SBIR) Phase II

Subcontractors:
- Hui Xu and Shuai Zhao, Giner, Inc., Newton, MA
- Bryan Pivovar, Shaun Alia, and Andrew Park, National Renewable Energy Laboratory (NREL), Golden, CO

Project Start Date: April 12, 2016
Project End Date: April 11, 2018

Overall Objectives

- Demonstrate a reversible 25-cm^2 anion exchange membrane fuel cell (AEMFC) for 1,000 cycles (42% round-trip efficiency; >250 mA/cm^2 power generation; >50 mA/cm^2 energy storage).
- Incorporate membrane electrode assemblies into a regenerative stack.
- Perform economic analysis on reversible AEMFC system following established DOE guidelines for candidate grid load leveling technologies.

Fiscal Year (FY) 2017 Objectives

- Demonstrate a reversible 25-cm^2 AEMFC that achieves performance targets (42% round-trip efficiency; >250 mA/cm^2 power generation; >50 mA/cm^2 energy storage) with <10% degradation over 200 cycles.
- Perform economic analysis on the AEMFC system following a previous DOE analysis [1] for candidate grid energy storage technologies.

Technical Barriers

This project addresses the following technical barriers from the Fuel Cell section of the Fuel Cell Technologies Office Multi-Year Research, Development, and Demonstration Plan, with respect to alkaline fuel cells for energy storage:

(A) Durability: increase the durability of reversible fuel cell electrodes for stationary load cycles

(B) Cost: develop low-PGM and PGM-free catalysts and electrodes for reversible anion-exchange membrane fuel cells (oxygen and hydrogen electrodes)

(C) Performance: optimize reversible anion-exchange membrane fuel cell and stack performance while maintaining cost and durability.

Technical Targets

This Phase II SBIR project is developing new catalyst materials and membrane electrode assemblies for a regenerative alkaline fuel cell stack. The materials being developed address the following technical targets for energy storage applications:

- 1,000 cycles at target current density and above the efficiency targets
- 42% efficiency; >250 mA/cm^2 power generation; >50 mA/cm^2 energy storage

FY 2017 Accomplishments

The following work related to the technical objectives has been accomplished on this SBIR Phase II project:

- Developed low-cost Pt-free hydrogen electrode catalyst; demonstrated 25-cm^2 cell that simultaneously achieves performance and the economic model cost targets.
- In 25-cm^2 reversible cell testing, demonstrated 360 cycles between target fuel cell and electrolysis current density at 50°C with cell that achieves performance and economic model cost targets.
- Refined an economic model based on the assumptions developed by Steward et al. [1] and the Phase II targets. The model includes a sensitivity analysis for key cell parameters being developed, i.e., current density, efficiency, lifetime, and fuel cell cost.

✧ ✧ ✧ ✧ ✧

INTRODUCTION

Low temperature fuel cells, such as proton exchange membrane (PEM) and alkaline fuel cells, offer an efficient and clean means of energy conversion of hydrogen to electricity. However, PEM fuel cells typically require platinum in the cathode to operate at high power density

and high efficiency, which hurts the economics for this technology. Platinum is used as an electrocatalyst for the oxygen reduction reaction (ORR), the cathode side half reaction is shown below for acidic and alkaline electrolytes, respectively:

(1) Oxygen Reduction Reaction (acid)
$O_2 + 4\ H^+ + 4\ e^- \rightarrow 2\ H_2O$

(2) Oxygen Reduction Reaction (alkaline)
$O_2 + 2\ H_2O + 4\ e^- \rightarrow 4\ OH^-$

The slow kinetics in the cathode is one of the largest sources of inefficiency in fuel cells, thus high platinum catalyst loadings are needed to prevent even more voltage losses (or overpotential). At commercial scale, precious metals in the cathodes of PEM fuel cells would comprise a significant portion of the entire stack cost [1,2]. Additionally, Pt-based ORR catalysts can degrade quickly under fuel cell operating conditions, such as frequent load cycling.

More recently, there has been renewed interest in alkaline fuel cells for stationary applications. Development of commercial anion exchange membranes (AEMs) is helping to alleviate system-level problems with alkaline fuel cells, such as pressure balance. Further, recent published results at Los Alamos National Laboratory have shown that alkaline fuel cells could potentially operate at high efficiency with non-platinum ORR catalysts [3]. Alkaline fuel cells are of particular interest for energy storage applications that do not have volume limitations, such as grid load leveling. In an alkaline fuel cell, oxygen is reduced by Reaction 2, and hydrogen is oxidized by Reaction 3.

(3) Hydrogen Oxidation Reaction (alkaline)
$H_2 + 2\ OH^- \rightarrow 2\ H_2O + 2\ e^-$

Alkaline fuel cells could potentially be operated in a reversible manner, allowing renewable energy to be stored in the form of hydrogen. This would be particularly valuable when coupled with renewable energy generation (wind or solar) to provide energy storage and load leveling. However, when operating in regeneration mode, cathode degradation is even more pronounced for conventional ORR catalysts because of the high voltages required for the oxygen evolution reaction (OER), the reverse of Reaction 2. Consequently, in existing reversible systems, separate cell stacks for fuel cell and electrolysis operation are used, adding to the already high system cost. If a low-cost regenerative stack could be developed, it would be a key breakthrough in the commercial viability of energy storage systems [4]. In this project, pH Matter LLC is partnering with Giner, Inc., and NREL to develop and demonstrate a low-cost regenerative alkaline fuel cell.

APPROACH

The overall objective of the project is to develop and demonstrate a regenerative fuel cell stack technology that is economically viable in stationary energy storage. Researchers at pH Matter will synthesize a matrix of platinum group metal (PGM)-free hydrogen oxidation reaction–hydrogen evolution reaction catalysts, and gas diffusion electrodes (GDEs) based on these materials. Researchers at NREL will synthesize a matrix of low-PGM hydrogen electrode materials. The hydrogen oxidation reaction–hydrogen evolution reaction materials and GDEs will be fully characterized and tested under cycling conditions to determine performance and stability. Additionally, pH Matter will further optimize ORR/OER electrodes previously developed in Phase I for improved performance and durability at higher temperatures and pressures. The hydrogen and oxygen electrodes will then be demonstrated in 25-cm^2 single cells for over 1,000 cycles. Cells that degrade during cycling will be characterized by pH Matter and NREL to determine degradation mechanisms. This information will be used to iteratively prepare more optimized cells. Engineers at Giner will test cells in conjunction with Giner's water-management membrane technology. Down-selected cells will then be incorporated into a regenerative fuel cell stack and demonstrated in simulated application testing at Giner. The project will establish a foundation for future work, where the technology will be incorporated into a prototype regenerative fuel cell system. Additionally, a design and economic model of the regenerative fuel cell system will be built to verify advantages of the approach compared to available energy storage technologies. The successful result of this Phase II work will demonstrate the feasibility of a regenerative fuel cell system with economic advantages compared to existing technologies.

RESULTS

In Phase I of this project, PGM-free catalysts for ORR and OER based on nitrogen- and phosphorus-doped graphitic carbon (CN_xP_y) were synthesized and tested in a half-cell GDE test stand. GDEs were made using a screen-printing method. Various catalyst formulations, catalyst loadings, ionomers and/or binders, ink compositions, and electrode substrates were examined. Testing was conducted with commercial AEMs in an in-house constructed stainless steel half-cell set-up. This testing demonstrated the durability of the down-selected CN_xP_y catalyst for over 100 h in either fuel cell or electrolysis operation and for over 300 cycles between fuel cell and electrolysis operation.

In the most recent year, work has focused on development of novel PGM-free and low-PGM hydrogen electrode catalysts, and optimization of the electrodes for regenerative cell operation. Fuel cell I-V curves for down-selected hydrogen electrode catalysts are shown in Figure 1. NREL has

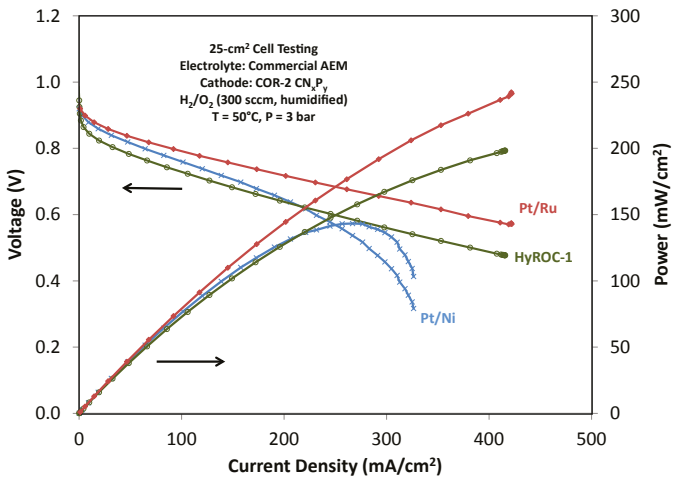

FIGURE 1. 25-cm^2 fuel cell performance curves at 50°C for cells containing down-selected hydrogen electrodes and optimized PGM-free oxygen-electrode; Pt/Ru is the commercial standard catalyst with 3.2 mg/cm^2 Pt loading, Pt/Ni is NREL's down-selected nano-wire catalyst with 1.0 mg/cm^2 Pt loading, and HyROC-1 is pH Matter's down-selected proprietary catalyst with no Pt.

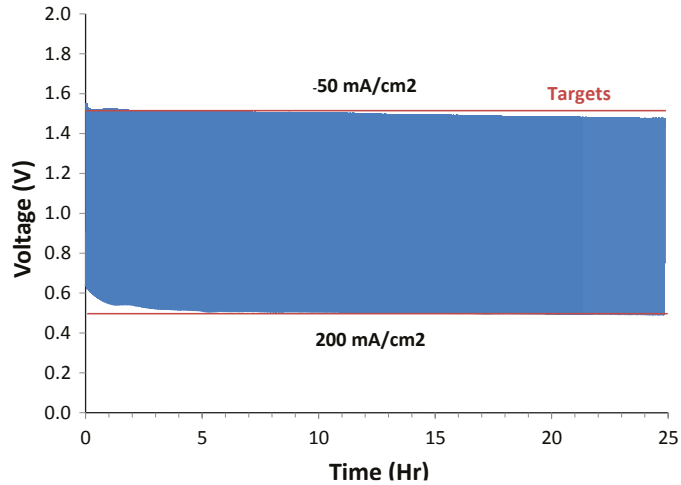

FIGURE 2. 25-cm^2 fuel cell/electrolysis cycling at 50°C with CN_xP_y oxygen electrode and Pt-free hydrogen electrode; cycles were run for 1 min in fuel cell operation at 200 mA/cm^2 and 1 min electrolysis operation at 50 mA/cm^2, with 1 min relaxation at open circuit voltage (OCV); go/no-go targets for end of life are 1.5 V (~82% efficiency) for electrolysis and 0.5 V (~41% efficiency) for fuel cell operation.

developed Pt/Ni nano-wires with low-Pt loading that show kinetic activity that matches the commercial Pt/Ru standard; however, further electrode optimization is required to match performance at high current density. pH Matter developed a low-cost Pt-free composition (HyROC-1) that has slightly higher overpotential, but performs well at high current density. Further, pH Matter and Giner optimized the oxygen electrode composition and membrane/electrolyte interface. All of the cells in Figure 1 were tested with the same optimized PGM-free oxygen electrode in a 25-cm^2 test stand.

For the grid load-leveling application, it is expected that current density will be highest (by a factor of 5–6) during periodic cell discharges (ORR operation) compared to OER operation. Cell testing examined cycling between fuel cell and electrolysis conditions. For these tests at 50°C and 3 bar, cycles were conducted at 50 mA/cm^2 for electrolysis, and 200 mA/cm^2 for ORR with the direction of the current being reversed every 2 min (1 min of current, 1 min of rest). The regenerative cell showed excellent stability for cycling during these tests in up to 360 cycles above the go/no-go target performance. Figure 2 shows the cycle test for pH Matter's Pt-free cell with a commercial AEM, and operating in pure hydrogen and oxygen. The results demonstrate the ability of this cell technology to undergo a number of cycles without rapid degradation.

Finally, an economic model was updated to project electricity costs for energy stored with a reversible alkaline fuel cell system based on the recent test results. The guidelines for the model and assumptions generally followed those used by Steward et al. [1], but assumed a reversible alkaline fuel cell stack that could operate for 1,000 cycles at the demonstrated performance. The projected delivered electricity would cost less than $0.18/kWh if technical targets can be achieved at the stack scale. At this cost a reversible alkaline membrane fuel cell would be cost-competitive with compressed air energy storage and pumped hydro energy storage approaches; however, unlike these approaches, a fuel cell system is not subject to geologic restrictions. The model was also used to run sensitivity of the electricity cost to a number of factors. The sensitivity analysis found that competitive economic performance will be dependent on stack life-time greater than four years.

CONCLUSIONS AND UPCOMING ACTIVITIES

The following conclusions can be drawn from work completed to this point:

- The novel PGM-free oxygen electrode developed on this project shows performance comparable to precious metal catalysts, good stability during cycling from ORR to OER voltages, and excellent stability during long-term electrolysis or fuel cell operation.
- The novel PGM-free hydrogen electrodes developed on this project shows higher over potential than commercial Pt/Ru, but excellent stability. The novel low-PGM hydrogen electrodes developed on this project show similar over-potential as commercial Pt/Ru and excellent stability, but require further optimization for high current density operation.

- Full 25-cm^2 cells that meet the project cost and performance targets have been demonstrated for 360 cycles above the go/no-go operating conditions.
- Economic modeling suggests that the reversible AEMFC concept would be an excellent energy storage option for grid load leveling if performance targets can be achieved at the system level.

Future work in the remainder of the Phase II project will include:

- Further optimization of hydrogen electrodes for improved performance.
- Characterization of the electrodes before and after cycling to better understand any degradation mechanisms.
- Demonstration of single cell durability over 1,000 cycles.
- Demonstration of a regenerative stack.
- Design of a prototype energy storage system that incorporates the stack.
- Update economic analysis of a reversible AEMFC system for a specific energy storage application.

FY 2017 PUBLICATIONS/PRESENTATIONS

1. S.M. Alia, C. Ngo, S. Shulda, S. Pylypenko, B.S. Pivovar, *Platinum-Nickel Nanowires as Electrocatalysts in Alkaline Hydrogen Oxidation and Evolution*, 230th ECS Meeting 2016 (Honolulu, HI) 2787.

2. S.M. Alia, C. Ngo, S. Shulda, S. Pylypenko, B.S. Pivovar, *Platinum-Nickel Nanowires as Electrocatalysts in Alkaline Hydrogen Oxidation and Evolution*, AIChE Annual Meeting 2016 (San Francisco, CA) 474452.

3. P. Matter, M. Ocampo, C. Holt, M. Beachy, N. Shaheen, M. Chan, and J. Gaydos, *Reversible Fuel Cell System for Energy Storage*, 2017 TechConnect World Innovation Conference, May 17, 2017, Washington, D.C.

4. P. Matter, M. Ocampo, M. Beachy, C. Holt, N. Shaheen, M. Chan, and J. Gaydos, *Regenerative Fuel Cell System*, 2017 DOE Hydrogen and Fuel Cells Program Annual Merit Review and Peer Evaluation, June 8, 2017, Washington, DC.

REFERENCES

1. Steward, D., G. Saur, M. Penev, and T. Ramsden, "Lifecycle Cost Analysis of Hydrogen Versus Other Technologies for Electrical Energy Storage." NREL Report NREL/TP-560-46719 (2009). Accessed July 23, 2015. http://www.nrel.gov/docs/fy10osti/46719.pdf

2. James, Brian D., Jennie M. Moton, and Whitney G. Colella, "Mass Production Cost Estimation of Direct H_2 PEM Fuel Cell Systems for Transportation Applications: 2013 Update." Accessed July 23, 2015. http://energy.gov/sites/prod/files/2014/11/f19/fcto_sa_2013_pemfc_transportation_cost_analysis.pdf

3. Chung, H.T., J.H. Won, and P. Zelenay, "Active and stable carbon nanotube/nanoparticle composite electrocatalyst for oxygen reduction." *Nature Communications* 4 (2013). Accessed July 23, 2015. doi: 10.1038/ncomms2944.

4. Remick, R.J., and D. Wheeler, "Reversible Fuel Cells Workshop Summary Report." Accessed July 23, 2015. http://www1.eere.energy.gov/hydrogenandfuelcells/pdfs/rev_fc_wkshp_report.pdf

V.A.11 Development of Corrosion Resistant Carbon (CRC) Support for Ultra-Low Platinum Group Metal (PGM) Catalysts (SBIR Phase I)

Prabhu Ganesan
Greenway Energy, LLC
301 Gateway Dr.
Aiken, SC 29803
Phone: (803) 447-8319
Email: prabhu.ganesan@greenway-energy.com

DOE Manager: Donna Ho
Phone: (202) 586-8000
Email: Donna.Ho@ee.doe.gov

Contract Number: DE-SC0017106

Subcontractor:
Savannah River National Laboratory, Aiken, SC

Project Start Date: February 21, 2017
Project End Date: November 20, 2017

Overall Objectives

- Demonstrate corrosion resistant carbon (CRC) support stability in the presence of Pt and Pt-alloy nanoparticles under 1.0–1.5 V potential cycling condition.
- Optimize support surface area, pore-size-distribution, and hydrophilic/hydrophobic properties.
- Enhance catalyst-support interaction through functionalization with an inexpensive additive.
- Synthesize Pt and Pt-alloy catalysts deposited on the CRC support.
- Evaluate catalyst activity (at 0.9 $V_{iR\text{-}free}$) through rotating disc electrode studies.
- Evaluate high power density performance under H-air in 25-cm^2 membrane electrode assemblies (MEAs).

Fiscal Year (FY) 2017 Objectives

- Optimize support surface area, pore-size-distribution, and hydrophilic/hydrophobic properties.
- Synthesize Pt and Pt-alloy catalysts deposited on the CRC support.
- Evaluate catalyst activity (at 0.9 $V_{iR\text{-}free}$) through rotating disc electrode studies.

Technical Barriers

This project addresses the following technical barriers from Fuel Cells section of the Fuel Cell Technologies Office Multi-Year Research, Development, and Demonstration Plan.

(A) Durability

(B) Cost

(C) Performance

Technical Targets

The technical target for the Small Business Innovative Research (SBIR) Phase I project is the demonstration of CRC support stability in the presence of Pt and Pt-alloy nanoparticles under 1.0–1.5 V potential cycling conditions to meet the following 2020 DOE technical targets for catalyst support: (i) <40% loss of electrochemical surface area (ECSA) after 5,000 cycles for Pt/CRC catalysts and (ii) initial mass activity of 0.35–0.44 A/mg_{PGM} at 0.9 $V_{iR\text{-}free}$ and mass activity and ECSA losses of <40% after 5,000 cycles for Pt-alloy catalysts.

FY 2017 Accomplishments

- Optimized the parameters to prepare reproducible CRC support.
- Optimized a surface functionalization process.
- Deposited Pt uniformly on the CRC support.

✧ ✧ ✧ ✧ ✧

INTRODUCTION

CRC support with excellent support stability was developed at Greenway Energy, LLC. The CRC support showed ~10% ECSA loss in the presence of platinum when tested under 1.0–1.6 V potential cycling condition in a rotating disk electrode study when compared to the commercial Pt/C catalyst (56% ECSA loss) (Figure 1).

APPROACH

A commercial carbon was selected and its properties such as pore size, pore volume, and Brunauer–Emmett–Teller surface area were modified by optimizing the heat treatment temperature, time, and atmosphere to prepare the CRC support. A surface functionalization procedure was used to achieve an optimum hydrophilic/hydrophobic property to

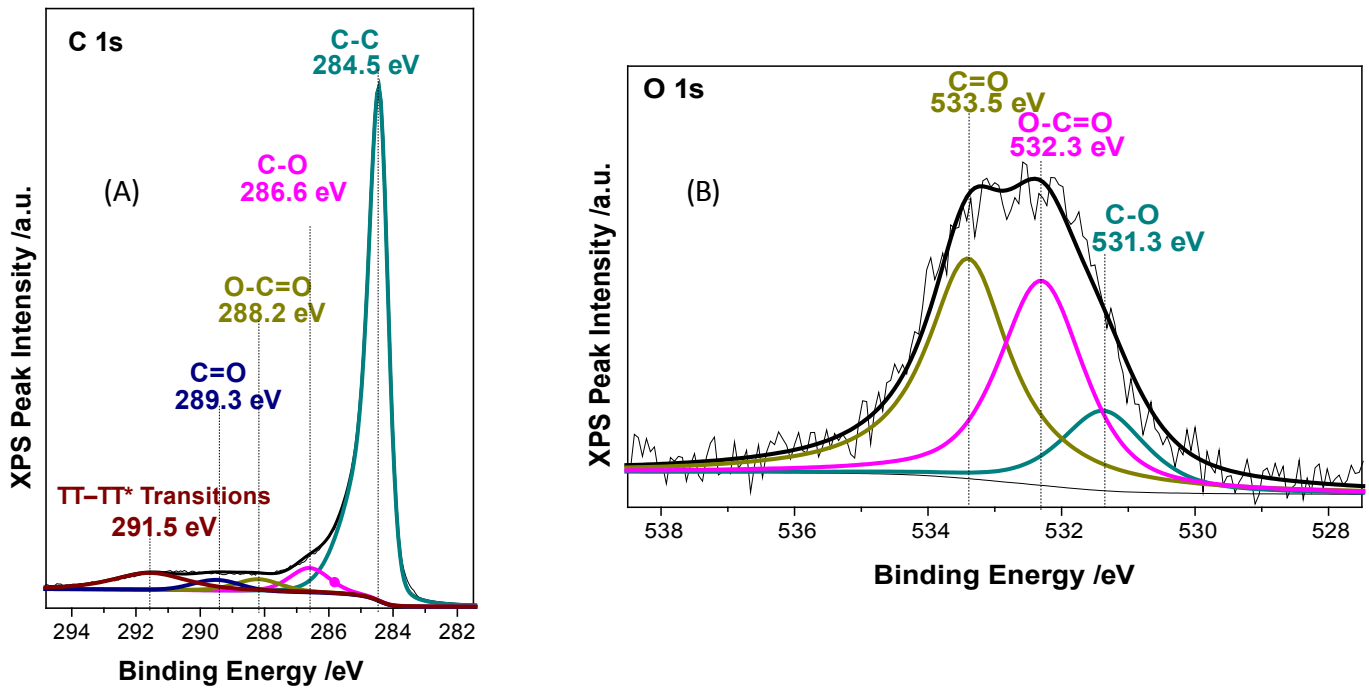

a.u. – arbitrary units

FIGURE 1. XPS analysis of CRC support. (A) C1s peak and (B) O1s peak.

enable uniform platinum deposition and distribution on the CRC support.

RESULTS

During the reporting period, parameters were optimized to prepare CRC supports in 5 g batches and surface functionalization of CRC supports in 1.5 g batch sizes. X-ray photoelectron spectroscopy (XPS) analysis showed the presence of highly oriented pyrolytic graphite having carbonyl (C = O) and carboxylate (O – C = O) functional groups on the surface (Figure 1A and Figure 1B).

Barrett-Joyner-Halenda pore volume analysis of CRC support indicated a significant increase in pore volume when the fresh carbon precursor was subjected to surface modification Processes 1 and 2 (Figure 2).

The surface functionalization of CRC support resulted in an average Pt particle size of 3–4 nm as measured by the high-resolution transmission electron microscopy (Figure 3).

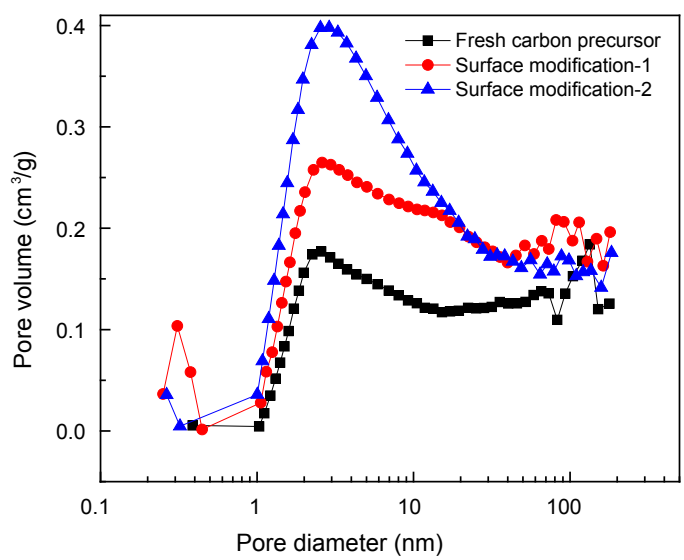

FIGURE 2. Barrett-Joyner-Halenda pore volume analysis of CRC support

CONCLUSIONS AND UPCOMING ACTIVITIES

Conclusions

- Optimized the parameters to prepare reproducible 5 g batches of CRC support (10X increase since project start).
- Optimized a surface functionalization process to prepare 1.5 g batches (15X increase since project start).
- Deposited 3–5 nm Pt particles uniformly on the CRC support.

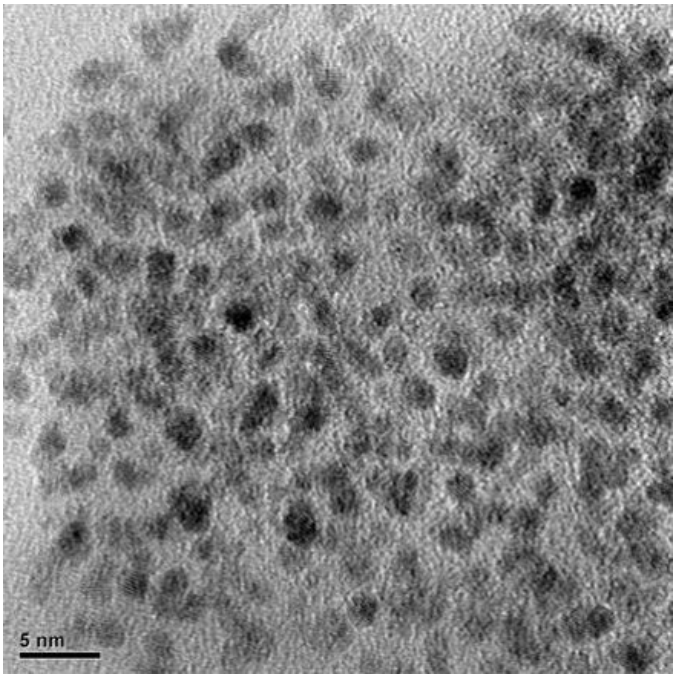

FIGURE 3. High-resolution transmission electron microscopy image of Pt/CRC catalyst

Upcoming Activities

Phase I

- Scale-up synthesis of CRC support; process optimization for 10g batch size.
- Synthesis and performance evaluation of Pt-alloy/CRC catalysts.
  - Evaluation of initial mass activities of PtCo/CRC catalyst in rotating ring disk electrode and fuel cell MEAs.
  - Support stability studies under accelerated stress test conditions in rotating ring disk electrode (1.0–1.6 V) and MEAs (1.0–1.5 V).
- Support preparation for industrial partner for Pt and Pt-alloy catalyst synthesis.
  - Agreed to provide 100 g CRC support and 10 g functionalized CRC support (25 g support shipped to Johnson Matthey Fuel Cell; 75 g CRC support and 10 g functionalized CRC support preparation is in progress).

Phase II

- Scale-up synthesis of CRC support; process optimization for 10–100 g batch size.
- Negotiation for trial runs using a rotary tube furnace at a leading furnace manufacturer's facility has been initiated. 50 g and 100 g batch sizes are planned to optimize the process parameters.
- Continuous process to produce CRC support has also been planned after acquiring the rotary tube furnace.
- Scale-up surface functionalization process for CRC support.
- Scale-up synthesis of Pt/CRC and Pt-alloy/CRC catalysts (in collaboration with Johnson Matthey Fuel Cell).
- Uniform Pt deposition process (3–5 nm particles) optimization for 1 g, 5 g, 10 g, 50 g, and 100 g batches.
- Process optimization for Pt-alloy/CRC with enhanced activity and catalyst-support interaction.
- Support stability studies using 25/50 cm^2 MEAs (1.0–1.5 V cycling).
  - Initial mass activity ≥0.44 A/mg_{PGM}.
  - Mass activity and ECSA losses ≤40% after 5,000 cycles.
  - 30 mV loss at 1.5 A/cm^2 after 5,000 cycles.
- Catalyst stability studies using 25/50 cm^2MEAs (0.6-1.0 V cycling).
  - Initial mass activity ≥0.44 A/mg_{PGM}.
  - Mass activity and ECSA losses ≤40% after 30,000 cycles.
  - 30 mV loss at 0.8 A/cm^2 after 30,000 cycles.
- MEA optimization studies (in collaboration with General Motors).
  - Performance evaluation of optimized catalyst in single cells (50 cm^2) and short stacks.
- Commercialization strategy.
- Intellectual property.
- Technology transfer.

FY 2017 PUBLICATIONS/PRESENTATIONS

1. Development of Corrosion Resistant Carbon (CRC) Support for Ultra-low PGM Catalysts (Phase I). Poster presented at 2017 U.S. DOE Hydrogen and Fuel Cells Program and Vehicle Technologies Office Annual Merit Review and Peer Evaluation Meeting, June 5–9, 2017, Washington, DC.

V.A.12 Mesoporous Non-Carbon Catalyst Supports of PEMFC (SBIR I)

Jacob Coppage-Gross
CertainTech Inc.
20695 Settlers Point Pl.
Sterling, VA 20165
Phone: (703)-584-5721
Email: jcoppagegross@gmail.com

DOE Manager: Bahman Habibzadeh
Phone: (202)-287-1657
Email: Bahman.Habibzadeh@ee.doe.gov

Contract Number: DE-SC0017112

Project Start Date: February 21, 2017
Project End Date: November 21, 2017

Overall Objectives

- Produce high surface area platinum–metal carbide (Pt-MC) mesoporous powders by a nanocasting route.
- Determine morphology of Pt-MC material.
- Evaluate electrochemical performance of Pt-MC as an alternative catalyst support material for use in proton exchange membrane fuel cells (PEMFCs).

Fiscal Year (FY) 2017 Objectives

- Demonstrate minimal loss in electrocatalytic activity in Pt-MC catalyst and membrane electrode assembly.
- Reduce required loading level of platinum.
- Evaluate alternate precursor materials to determine feasibility of producing mesostructured support material.

Technical Barriers

This project addresses the following technical barriers from the Fuel Cells section of the Fuel Cell Technologies Office Multi-Year Research, Development, and Demonstration Plan.

(A) Durability

(B) Cost

Technical Targets

This project is addressing the following (Table 1) technical targets related to the durability of catalyst supports in PEMFCs.

TABLE 1. Technical Targets: Electrocatalysts for Transport Applications

Characteristic	Unit	2015 Status	2020 Target
PGM total content	g/kW @ 150 kPA	0.16	0.125
PGM loading	mg PGM/cm^2	0.13	0.125
Mass activity	A/mg PGM @ 900 mV	>0.5	0.44
Loss in initial catalytic activity	% mass activity loss	66	<40
Loss in performance at 0.8 A/cm^2	mV	13	<30
Electrocatalyst support stability	% mass activity loss	41	<40
Loss in performance at 1.5 A/cm^2	mV	65	<30
PGM-free catalyst activity	A/cm^2 @ 900 mV	0.024	<0.044

PGM – platinum group metal

FY 2017 Accomplishments

- Evaluated several fabrication routes to a durable, mesoporous metal carbide powder using new precursors.
- Achieved fabrication of a high surface area metal catalyst product to be used as a support material (565 m^2/g).

✧ ✧ ✧ ✧ ✧

INTRODUCTION

PEMFCs are promising energy conversion systems that harness energy from hydrogen and air with clean emissions. A big obstacle preventing the commercialization of PEMFCs is the significant decrease in performance over long-term operation. Lack of durability of catalyst supports has been attributed as a major source of overall fuel cell performance deterioration. Metal carbides are promising alternative materials to carbon black, the most commonly used catalyst support. A mesoporous metal carbide in particular is attractive because of its high active surface area and favorable transport properties.

Although metal carbides are fabricated commercially for a variety of applications, no process exists to produce a mesoporous material with such a high surface area. In this project, the development of such a process was investigated

through the use of a series of unique precursor polymers integrated with a templating method to achieve mesoporosity.

APPROACH

The focus of this research effort is to evaluate the feasibility of using a non-carbon support material in PEMFCs and to establish a method of producing the alternative support that is cost effective. With respect to utilizing a metal carbide support as the substitute material, the overall approach is defined in two stages: investigation of synthesis routes to a mesoporous metal carbide and electrochemical analysis of the metal carbide with platinum functionalization. Although research is ongoing to replace platinum with a cheaper catalyst, this is not within the scope of this project.

Four types of precursor materials were synthesized and converted into the associated metal carbide products, utilizing a silica template and a developed heating process. The morphologies of the resulting products were analyzed to determine the best fabrication route. Once the ideal process is established, electrochemical activity of a Pt-MC catalyst will be assessed by functionalizing the surface of the metal carbide with Pt and performing basic testing including rotating disk and lab-scale membrane electrode assembly cyclic voltammetry. From this data, we will establish the proof of concept of the Pt-MC catalyst support in terms of both production and performance.

RESULTS

Three polymeric and one molecular precursor were synthesized according to prior literature. These precursors had been used to prepare metal carbide products, but not with a mesoporous structure. The difficulty in fabrication of mesoporous metal carbides is that often high temperatures are required for the reaction of the precursor to complete, but high temperatures will cause the mesoporous structure of a template material to degrade. The precursor must be successfully infiltrated into a mesoporous template, heated to an appropriate temperature, and then the product must be etched to remove the template. This unique process is outlined in Figure 1.

It was found that the MCM-41 (silica) was the best candidate for use as a template because of its stability and high surface area (931 m^2/g). Figure 2 shows X-ray diffraction patterns of this material at 600°C and 1,150°C. The relative stability of the low angle peaks (indicative of mesopores) and the retention of the broad amorphous peaks at higher angles suggest good stability for use in heat treatment procedures.

In addition to the method of silica template, one alternative procedure was explored, utilizing a cotton T-shirt as both a carbon source and a template to produce metal carbide nanowires. When combined with a nickel catalyst, this process produced a partially crystalline metal carbide product (Figure 3) with moderately high surface area (Table 2). Surface area analysis was conducted on the metal carbide products prepared using the silica or fiber template and a moderate temperature heat treatment (<1,200°C).

A high surface area of 565.5m^2/g was obtained for one sample type using the MCM-41 template, which should give good electrochemical activity as it is comparable to typical carbon based supports. The effect of different types of infiltration is clearly shown in Table 2, resulting in significantly different surface areas. It is vital to ensure proper filling of the template pores to produce a high surface area product.

CONCLUSIONS

Preparation of a high surface area metal carbide was demonstrated, establishing the groundwork of a process for making a mesoporous Pt-MC catalyst material. Once these high surface area carbides are functionalized with platinum, electrochemical testing will be conducted to determine the performance and durability of the supports.

FY 2017 PUBLICATIONS/PRESENTATIONS

1. Jacob Coppage-Gross "Mesoporous Non-Carbon Catalyst Supports of PEMFC." Department of Energy Annual Merit Review, July 2017.

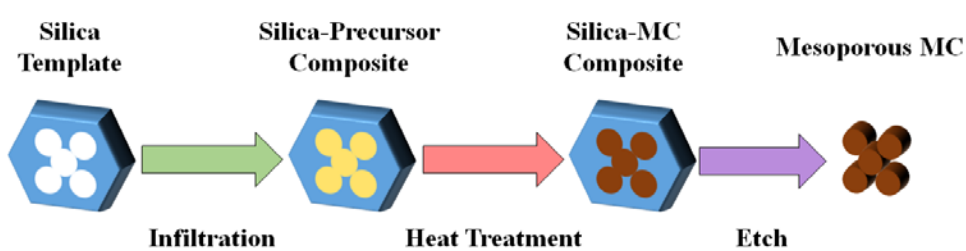

FIGURE 1. Schematic of templating process for producing mesoporous MC

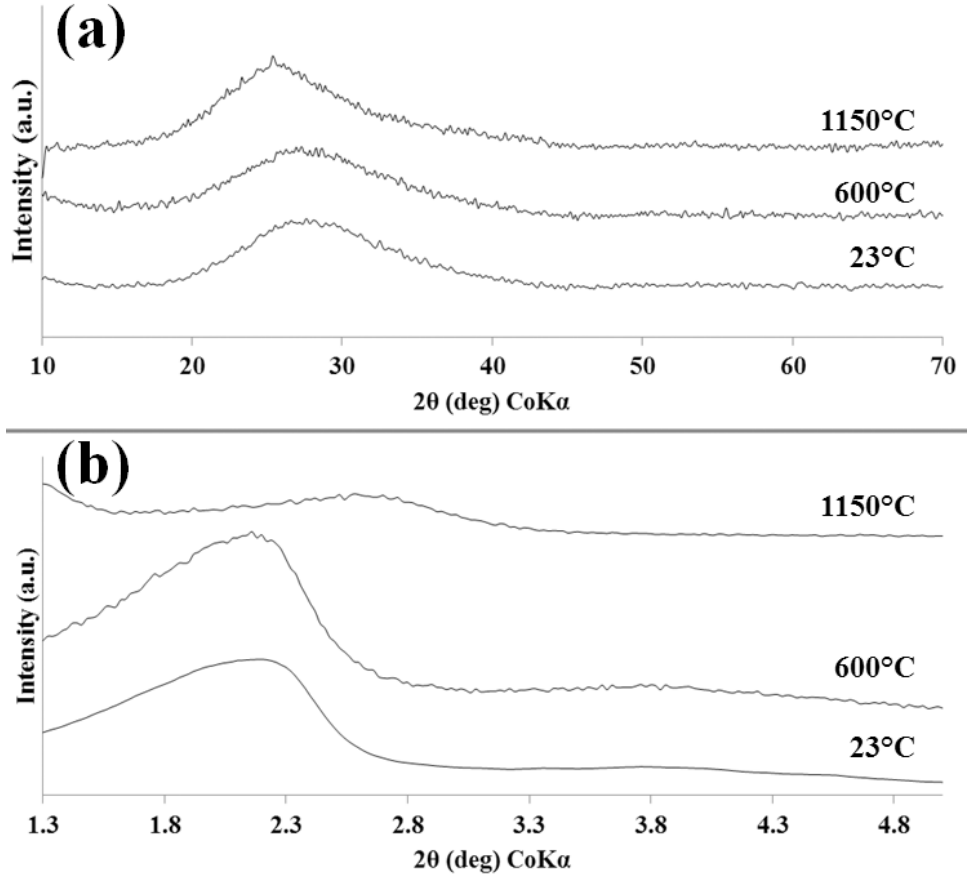

FIGURE 2. X-ray diffraction patterns of MCM-41 at (a) high angles and (b) low angles

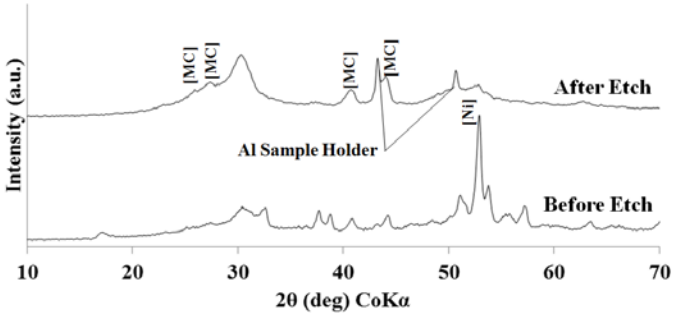

FIGURE 3. X-ray diffraction pattern of MC nanowire product before and after etching

TABLE 2. Calculated Surface Areas of Metal Carbide Products

Precursor	Infiltration Method	BET Surface Area
Type 1	No template	47.66 m^2/g
Type 1	Type 1	17.3 m^2/g
Type 1	Type 2	31.49 m^2/g
Type 1	Type 3 (SBA-15 template)	352.7±19.2 m^2/g
Type 1	Type 3 (MCM-41 template)	565.5 m^2/g
Type 2	Solution Infiltration	156.4 m^2/g
Type 3	T-Shirt	91.3±13.1 m^2/g

BET – Brunauer–Emmett–Teller

V.A.13 Development of Durable Active Supports for Low Platinum Group Metal Catalysts (SBIR I)

Barr Zulevi (Primary Contact), Alexey Serov
Pajarito Powder, LLC (PPC)
3600 Osuna Road NE, Suite 309
Albuquerque, NM 87109-4427
Phone: (215) 687-2290
Email: bhalevi@pajaritopowder.com

DOE Manager: Gregory Kleen
Phone: (240) 562-1672
Email: Gregory.Kleen@ee.doe.gov

Contract Number: DE-SC0017250

Subcontractor:
Advent Technologies Inc., Cambridge, MA

Project Start Date: February 21, 2017
Project End Date: November 20, 2017

Overall Objectives

To develop novel active carbon supports (cathode side of membrane electrode assembly [MEA]) with engineered morphology which allows platinum to be uniformly dispersed in 3-dimensional mesoporous structure and increase the graphitization of the engineered carbon support (ECS) in order to improve durability of Pt/ECS.

- Synthesize engineered active carbon-based supports.
- Optimize supports characteristics to improve platinum dispersion, platinum-carbon interaction, and level of ECS graphitization.
- Demonstrate durability of electrocatalysts in accelerated stress protocol.

Fiscal Year (FY) 2017 Objectives

- Synthesize active ECS with controlled morphology and high graphitization level.
- Optimize platinum dispersion on ECS.
- Demonstrate improved durability of optimized Pt/ECS in accelerated stress protocol.

Technical Barriers

This project addresses the following technical barriers from the Fuel Cells section of the Fuel Cell Technologies Office Multi-Year Research, Development, and Demonstration Plan.

(A) Durability: Low durability of carbon supported commercial Pt/C catalysts

(B) Cost: High cost of commercial Pt/C catalysts

(C) Performance: Low performance of low Pt content MEA

Technical Targets

The project main target is engineering an active carbon support with controlled morphology and chemical speciation to allow platinum to be dispersed inside of three-dimensional matrix. The final Pt/ECS catalyst will approach DOE 2020 design point in catalyst activity and durability (Table 1).

FY 2017 Accomplishments

Pajarito Powder synthesized several active ECS materials with variation of pore former agents, organic precursors, and transition metals. The main accomplishments of the project up to this date can be summarized as follows:

- Preliminary data on screening of different transition metals for formation of active ECS showed that cobalt produced highly graphitized carbon supports with high surface area and well dispersed Pt.
- A proprietary method of platinum deposition was optimized to deposit platinum on active ECS controlling Pt particle size in the range of 2.1–7 nm.
- Methods of integration of novel Pt/ECS into the MEA was developed and several MEAs were evaluated by fuel cell tests.

TABLE 1. MEAs for Transportation Applications

Characteristic	Units	DOE 2020 Electrocatalyst and MEA Targets	Project Status (5 cm^2 cell, differential conditions)
Mass activity	A/mg_{PGM} @ 0.9 $mV_{iR\text{-}free}$	≥0.44	0.29
PGM total loading	$mg\text{-}PGM/cm^2_{geo}$	≤0.125	0.100 cathode
Support cycling (1.0–1.5 V, 5,000 cycles)	Support cycling (1.0–1.5 V, 5,000 cycles)	mV loss at 1.5 A cm^{-2}	NA

PGM – platinum group metal

- Initial data shows that the developed Pt/ECS has a lower degradation rate in start-stop protocol compared to commercial Pt/C catalyst (Figure 1).

✧ ✧ ✧ ✧ ✧

INTRODUCTION

Commercially available carbon materials are designed for multiple applications, such as conductive additives, solar cells, and supercapacitors [1]. Some of these generic carbon materials were adopted for development projects optimizing the synthesis of supported PGM catalysts and MEAs in fuel cell applications [2]. Research groups are evaluating several classes of carbon-based materials to be used as PGM supports in low temperature fuel cells [3]. However, these materials are either not commercially available or are cost prohibitive to be utilized by PGM catalysts manufacturers.

The main degradation routes in MEA performance are platinum poisoning (anode), platinum dissolution (cathode), and carbon corrosion (cathode). In this proposal, PPC will develop durable, carbon-based supports based on the concept of active co-catalysis in oxygen reduction reaction (ORR). The PGM nano-particles will be loaded on the support which consists of (1) atomically dispersed electrocatalytically active centers with intrinsic ORR activity, (2) optimized morphology for PGM deposition and triple phase interface, and (3) an increased level of graphitization.

APPROACH

The synthetic approach on making active ORR carbon-based catalyst is based on University of New Mexico technology licensed by PPC. Pajarito Powder modified and improved this method, which is trademarked as VariPore™ (Figure 2). The synthesis of active support includes formation of 3-dimensional porous structure by using pore forming agents. Hard templates (MgO, Al_2O_3 and SiO_2) are used in the synthesis and support characteristics will be optimized. The support characteristics to be controlled include pore size, pore modality, and surface area.

In order to create active carbon supports such structure as Fe-N-C will be formed by high temperature treatment of mixture of transition metal (Fe, Co, Mn, and Cr), organic precursor, and pore forming engines. After synthesis catalysts will be extensively washed with $HNO_{3(diluted)}$ to remove unreacted transition metals and then both evaluated on their own in fuel cell tests and once Pt is added.

UPCOMING ACTIVITIES

Additional experiments with active support derived from cobalt are needed. We will optimize them by tuning the amount and type of pore formers, heat treatment temperature, and duration of heat treatment. Platinum will be deposited by PPC in order to evaluate the activity of Pt/ECS by MEA tests and the best candidate will be down-selected for evaluation by team member Advent.

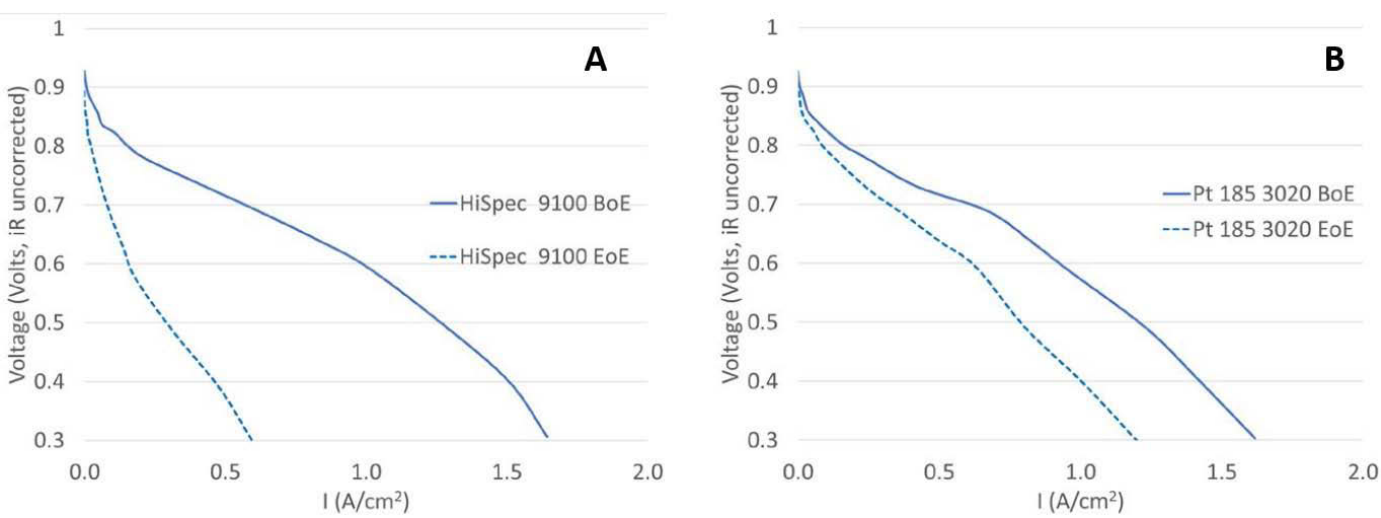

BoE – beginning of everything; EoE – end of everything; iR – internal resistance

FIGURE 1. MEA performance of (A) commercial Pt/C cathode and (B) PPC developed Pt/ECS catalyst in beginning of life (BoE) and after accelerated stress protocol support corrosion test. Conditions: (A) Anode Pt/C (0.05 mg cm^{-2}), Cathode: Pt/C (0.1 mg cm^{-2}); (B) Anode: Pt/C (0.05 mg cm^{-2}), Cathode: Pt/ECS (0.1 mg cm^{-2}). T_{cell} = 80ºC, 100% relative humidity, 26 psig back pressure.

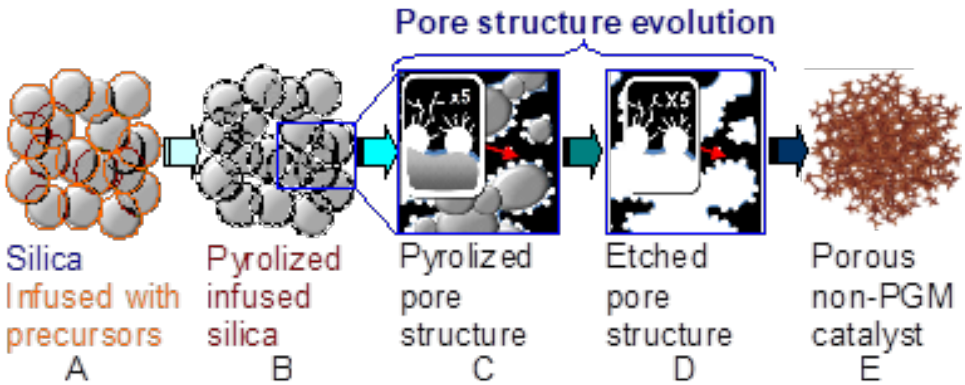

FIGURE 2. The approach on making durable active support

FY 2017 PUBLICATIONS/PRESENTATIONS

1. B. Halevi, A. Lubers, G. McCool, S. McKinney, and H. Romero, *"Durable Engineered Carbon Supports*," 231st ECS Meeting, New Orleans, 2017.

REFERENCES

1. H.O. Pierson *Handbook of carbon, graphite, diamonds and fullerenes: processing, properties and applications*. William Andrew, 2012.

2. S. Sharma, B.G. Pollet, *Support materials for PEMFC and DMFC electrocatalysts—a review*, J. of Power Sources 208 (2012) 96–119.

3. E. Antolini, *Carbon supports for low-temperature fuel cell catalysts*, Appl. Catal. B: Environmental (88) (2009) 1–24.

V.A.14 Multi-Functional Catalyst Support (SBIR I)

Minette Ocampo (Primary Contact), Paul Matter, Chris Holt, Julia Mueller, Michael Beachy, Mary Cramer, and Monica Chan
pH Matter LLC
6655 Singletree Dr.
Columbus, OH 43229
Phone: (614) 396-7820
Email: mcocampo@phmatter.com

DOE Manager: Donna Ho
Phone: (202) 586-8000
Email: Donna.Ho@ee.doe.gov

Contract Number: DE-SC0017144 Small Business Innovation Research (SBIR) Phase I

Project Start Date: February 21, 2017
Project End Date: November 20, 2017

Overall Objectives

- Develop a multi-functional carbon support, based on doped carbon nano-structures (i.e., CNxPy), that is engineered to perform better than conventional proton exchange membrane (PEM) fuel cell pure carbon supports.
- Improve the catalyst stability, durability and current density with lower platinum group metal (PGM) loadings.
- Demonstrate DOE 2020 targets for catalyst durability and support corrosion resistance in a membrane electrode assembly (MEA).

Fiscal Year (FY) 2017 Objectives

- Prepare a matrix of candidate CNxPy-based supports to examine the effects of synthesis parameters on important properties.
- Demonstrate catalyst activity and durability in rotating disk electrode (RDE) testing and down-select catalyst for further MEA testing.
- Transfer RDE results to gas diffusion electrodes (GDE) for MEA testing and optimize GDE synthesis parameters to demonstrate DOE 2020 targets for catalyst durability and support corrosion resistance in an MEA.
- Demonstrate the potential of tuning the GDE hydrophobicity for improved current density.

Technical Barriers

This project addresses the following technical barriers from the Fuel Cells section of the Fuel Cell Technologies Office Multi-Year Research, Development, and Demonstration Plan.

(A) Durability
  - Optimize the interaction between the catalyst and the support material to improve chemical and thermal stability.

(B) Cost
  - Enhancement of the Pt catalyst activity to reduce its loading levels.

(C) Performance
  - Demonstrate improved performance with the multi-functional supports in an MEA.

Technical Targets

This project aims to develop a multi-functional carbon support that will demonstrate the following 2020 DOE targets for low-PGM loading [1].

- PGM loading (both electrodes): 0.125 mg/cm^2
- Catalyst durability in an MEA
  - <40% loss in initial mass activity
  - <30 mV loss at 0.8 A/cm^2
  - <40% loss in initial area
- Support corrosion resistance in an MEA
  - <40% loss in initial mass activity
  - <40% loss in initial area

FY 2017 Accomplishments

- Prepared CNxPy support samples and examined different variables on the catalytic activity (Table 1).

TABLE 1. Matrix of Variables Examined for the Prepared Carbon Supports Samples

Variable	Ranges
Carbon Support Synthesis	
Metal Precursor	None, Various Transition Metals
Hydrophobicity Treatment	None, Partial, Full
Metal Deposition	
Pt Loading	5–20 wt%
Metal	Pt and Pt/Ni Alloy

- Explored two platinum deposition procedures for each CNxPy carbon support and RDE tested. Down-selected a procedure that gave a more uniform and homogenous platinum deposition onto the carbon support (Figure 1) and higher oxygen reduction reaction (ORR) activity.
- RDE tested Pt/CNxPy samples for intrinsic activity and durability. Down-selected Pt/CNxPy samples for further MEA testing (Figure 2).
- Prepared MEAs for testing.

✧ ✧ ✧ ✧ ✧

INTRODUCTION

PEM fuel cells offer the capability to provide a more efficient and cleaner route for energy conversion in numerous applications, including automotive power. Unfortunately, wide-scale PEM fuel cell adoption is limited by the high cost of the fuel cell stacks. PEM fuel cells currently use Pt as the catalyst both at the cathode and at the anode. Current challenges with the electrodes are the high cost of the PGM electrode materials and the relatively fast degradation of the electrodes, specifically the cathode. To lower PEM fuel cell cathode costs, a reduction in PGM loading level with an increase in catalyst activity to maintain power output, would be needed. One way of improving low-PGM catalyst performance and durability is by optimizing the interaction between the catalyst and the support material.

pH Matter is developing a multi-functional carbon support for PEM fuel cell cathodes that is optimized to perform better than conventional PEM fuel cell pure carbon supports by enhancing the catalyst stability, durability, and electrode current density with lower PGM loadings. Nitrogen and phosphorus doped carbon nano-fibers have been reported to enhance dispersion and provide better binding of Pt nano-particles when used as a support for PEM fuel cell catalysts and can also contribute to the ORR activity. This doped-carbon support showed improved metal-support adhesion which reduces the mobility of the platinum during long-term operation. It also showed improved resistance to oxidation, a major source of cathode degradation. The hydrophobicity of the electrodes can also be tuned to minimize cathode flooding.

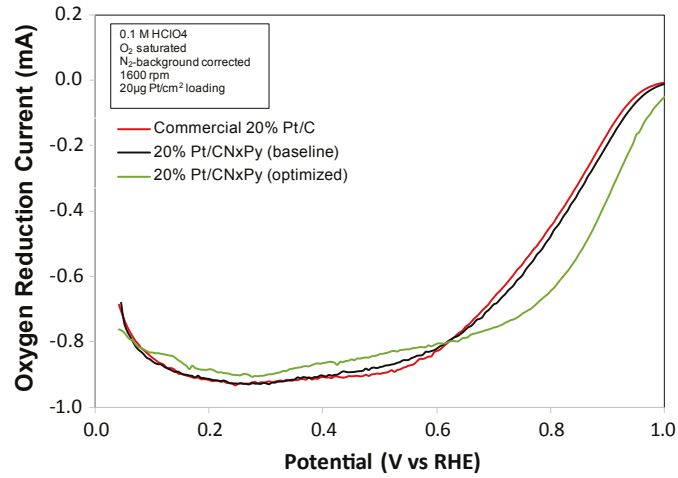

rpm – revolutions per minute; RHE – reference hydrogen electrode

FIGURE 2. Down-selected Pt/CNxPy catalyst samples that showed good ORR activity in RDE testing

APPROACH

A matrix of doped-carbon supports are prepared wherein different variables are examined to evaluate the effects on ORR activity and porosity. Synthesis variables

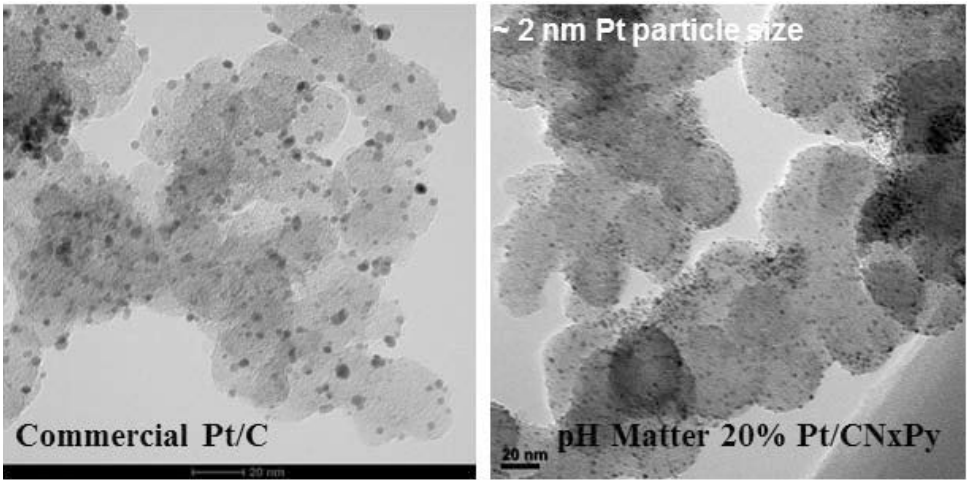

FIGURE 1. Transmission electron microscopy imaging showed good dispersion of Pt on CNxPy carbon support using the developed deposition method

include precursors for carbon formation, including metal and non-metal options (to address the issue of ionomer and membrane poisoning), after-treatment of the carbon material and hydrophobicity treatment prior to platinization. The prepared catalysts are then screened for their intrinsic ORR performance and acceptable support oxidation resistance in RDE testing. High-performing catalyst in RDE testing are then down-selected for MEA testing to meet DOE's automotive fuel cell targets for performance and durability.

UPCOMING ACTIVITIES

RDE and MEA testing will continue and include:

- RDE high-voltage cycling (start-stop simulation) on down-selected supports.
- Testing MEAs of down-selected supports to meet DOE targets on MEA performance.
  - Demonstrate DOE 2020 targets for catalyst durability (<40% loss in activity, <30 mV loss at 0.8 A/cm^2 and <40% area loss after 30,000 cycles) in an MEA with a target Pt loading in the cathode and anode of 0.125 mg/cm^2.
  - Demonstrate DOE 2020 targets for support corrosion resistance (<40% loss in activity, <30 mV loss at 1.5 A/cm^2 and <40% area loss after 5,000 cycles) in an MEA with a target Pt loading in the cathode and anode of 0.125 mg/cm^2.
  - Show potential for high current density by tuning hydrophobicity.
- Connect with MEA developers to establish partnerships for future work.
- Partner with future customers to demonstrate catalyst.

FY 2017 PUBLICATIONS/PRESENTATIONS

1. Minette Ocampo, Paul Matter, Chris Holt, Julia Mueller, Michael Beachy, Mary Cramer, and Monica Chan, "Multi-Functional Catalyst Support," presented at the 2017 DOE Annual Merit Review and Peer Evaluation Meeting, Washington, D.C., June 2017.

REFERENCES

1. "Fuel Cell Technologies Office (FCTO) Multi-Year Research, Development, and Demonstration (MYRDD) Plan," Office of Efficiency and Renewable Energy, https://energy.gov/eere/fuelcells/downloads/fuel-cell-technologies-office-multi-year-research-development-and-22

V.A.15 Highly Robust Low PGM MEAs Based upon Composite Supports (SBIR I)

Arrelaine Dameron
Forge Nano
1172 Century Dr., #240
Louisville CO 80027
Phone: (720) 259-8579
Email: adameron@forgenano.com

DOE Manager: Bahman Habibzadeh
Phone: (202) 287-1657
Email: Bahman.Habibzadeh@ee.doe.gov

Contract Number: DE-SC0017192

Subcontractors:
Ugur Pasaogullari and Aman Uddin, Center for Clean Energy Engineering, Storrs, CT

Project Start Date: February 21, 2017
Project End Date: November 20, 2017

Overall and Fiscal Year (FY) 2017 Objectives

- Demonstrate a successful overcoat method on commercial low platinum group metal Pt/C catalysts, specifically targeting uniform coverage of the carbon support with gas phase access to the Pt catalysts.
- Evaluate the activity, ohmic resistance and cycling stability of overcoated catalyst materials by rotating disk electrode (RDE) and membrane electrode assembly (MEA) testing.
- Demonstrate improved cycling durability with MEA testing of optimized encapsulated catalysts without significant loss in activity.
- Down-select to a viable encapsulated Pt/C catalyst material based on performance, process scalability and techno-economic considerations.

Technical Barriers

This project addresses the following technical barrier from the Fuel Cell section of the Fuel Cell Technologies Office Multi-Year Research, Development, and Demonstration Plan.

(A) Durability

Technical Targets

Achieve the 2020 MEA targets:

- $40/kW at the system level, $14/kW at the MEA level.
- Greater than 5,000 start–stop cycles with less than 5% loss in voltage.
- Less than 10% loss in power after 5,000 hours of normal operation and less than 40% loss in mass activity under start–stop conditions at the electrocatalyst level.

FY 2017 Accomplishments

- Demonstrated a variety of atomic layer deposition (ALD) overcoats onto commercial Pt/C catalysts with 1–10 wt% coating added.
- Preliminary RDE measurements indicate an unoptimized durability retention of >70% for both mass activity and specific activity after 5,000 electrochemical cycles (1–1.5 V at 500 mV/s, compared to ~25% for the baseline).

✧ ✧ ✧ ✧ ✧

INTRODUCTION

The proton exchange membrane fuel cell platinum catalyst is deposited at the nanoscale on high surface area carbon, with a goal of achieving very high catalytic surface area and dispersion. However, well documented aging processes tend to increase catalyst particle size, with corresponding decrease in available surface area and catalytic activity. Aging appears to be the result of the combined effects of catalyst migration, Ostwald ripening (particle dissolution followed by redepositing on larger particles), and significant corrosion of the high surface area carbon catalyst support. Cell durability is degraded by corrosion of the carbon support through carbon oxidation that occurs through the electrochemical formation of CO_2 and/or through the water gas shift reaction, producing CO. As carbon is consumed via these reactions, the sites which accommodate the platinum electrocatalyst are eliminated, thereby decreasing the surface area for electrochemical reaction, and which in turn decreases the performance of the fuel cell, becoming a dominant durability limiting mechanism.

Approaches that promise to eliminate catalyst substrate corrosion will improve fuel cell durability dramatically, but must do so without negatively effecting other attributes of the substrate and current cell construct. These include the conductivity and low cost of the catalyst support, catalytic

activity, and the ability to achieve catalyst dispersion and substrate adhesion. The Forge Nano approach achieves protection of the carbon via nanolayer coatings which will not significantly impact conductivity and which can be tailored to ensure catalyst application. ALD coatings are very thin, yet can be tailored in thickness, can change composition and materials through the depth of the coating (by applying coating layers), are uniform in thickness and are defect free. In addition, the high-throughput ALD technology developed by Forge Nano is very low cost, and may even lower the cost of the electrode by enabling further reductions in catalyst loading. These attributes promise to facilitate use of the current inexpensive carbon material, yet solving the durability issues experienced today.

APPROACH

The ideal catalyst system will promote Pt stability, reduce Pt mobility, increase Pt dispersion with ideal-sized nanoparticles, and reduce Pt induced carbon corrosion. Several studies have focused on increasing Pt-carbon support interactions and developing Pt alloys to reduce Pt mobility and reduce Pt dissolution. However, the successful strategies to increase Pt stability are largely ineffective at reducing carbon corrosion. This is because the presence of the Pt near the C–H_2O interface likely catalyzes the oxidation of the carbon support under start–stop conditions. In contrast, ceramic catalyst supports have demonstrated fantastic cycling durability. However ceramic supports generally have lower specific activities because of mass differences relative to carbon, lower surface areas of the supports, less dispersion and larger Pt size that combined lead to reduced electrochemical surface area, and because the supports are not inherently conductive so binders or conductive additives are implemented. To mitigate the carbon corrosion reaction, we have demonstrated an overcoat on the Pt/C catalyst materials with an ultrathin ceramic ALD encapsulation layer. The ideal encapsulation layer will provide a barrier to water and oxygen at the carbon interface, without impeding electron flow in the electrode or gas diffusion to the Pt particles. As such, our Phase I technical approach also includes implementing ALD over-coating layers with high conductivity through the incorporation of dopants to explore the impacts of and mitigate added electrical resistance from the coating.

The ALD coatings were found to uniformly coat the commercial catalyst, and through process design the total surface area (as measured by Brunauer–Emmet–Teller [BET]) could also be refined by filling progressively larger pores in the underlying substrate (see Figure 1). Preliminary RDE measurements targeting carbon corrosion (1–1.5 V cycling) show improved durability of the ALD overcoated samples compared to the baseline (uncoated) catalyst (Figures 2 and 3).

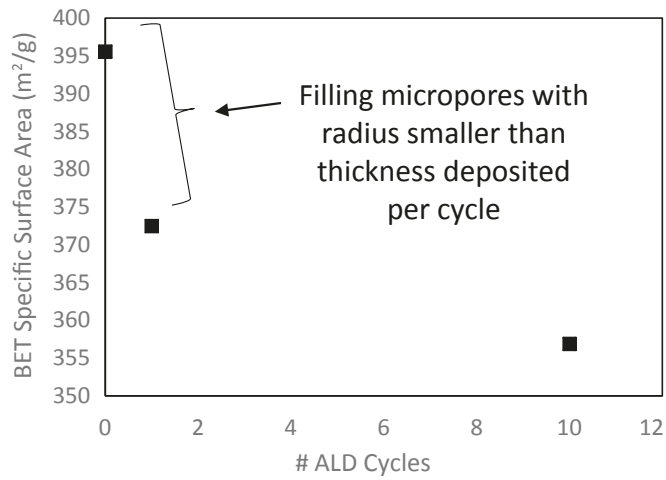

FIGURE 1. Physical surface area (BET) modification as a function of the number of ALD cycles

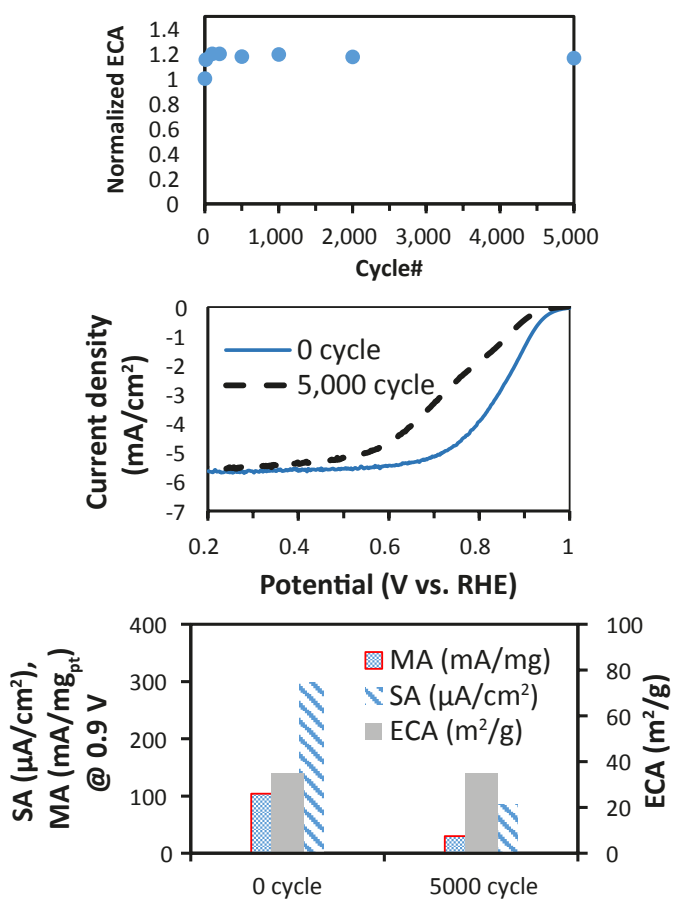

FIGURE 2. Normalized electrochemical surface area, current density, and activities for the unmodified catalysts before and after electrochemical cycling (17 ugPt/cm^2; 1–1.5 V at 500 mV/s)

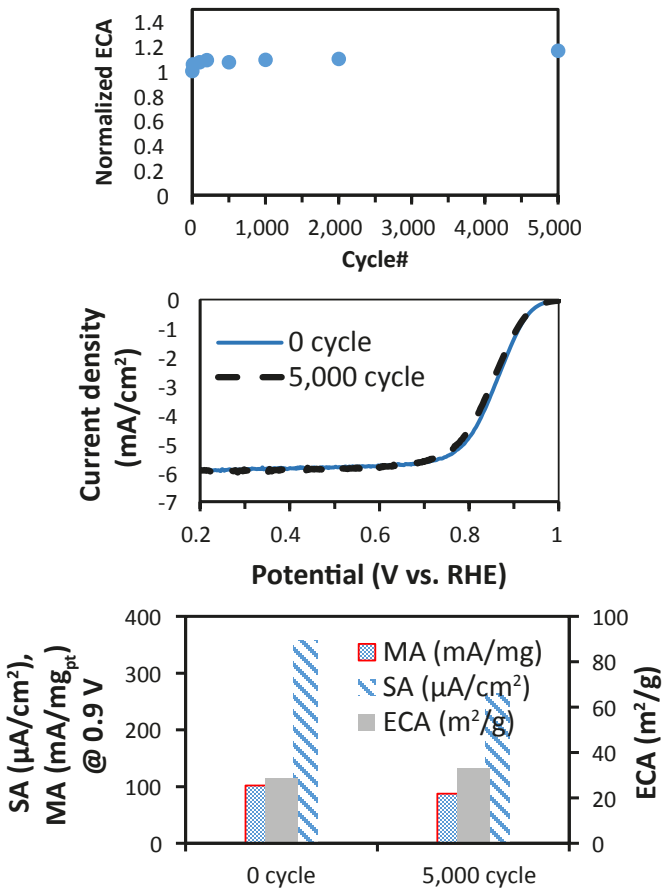

FIGURE 3. Normalized electrochemical surface area, current density, and activities for the ALD overcoated catalysts before and after electrochemical cycling (17 ugPt/cm^2; 1–1.5 V at 500 mV/s)

CONCLUSIONS AND UPCOMING ACTIVITIES

MEA testing of the ALD overcoated catalysts will be performed, specifically investigating activities, mass transport and conductance changes as a function of the coating parameters. Additional RDE measurements will be made to understand the impacts of process parameters during the coatings process. Ex situ analysis of catalysts and cast catalyst films will be performed to understand coating quality and crystallinity of the ALD films and any porosity changes as a result of the ALD. Finally, technoeconomic analysis will be performed to determine the cost of ALD overcoats for the best coatings with respect to the savings from their implementation.

V.A.16 Advanced Electro-Catalysts through Crystallographic Enhancement

Jacob S. Spendelow (Primary Contact),
Yung-Tin Pan, and Yu Seung Kim
Los Alamos National Laboratory
PO Box 1663
Los Alamos, NM 87545
Phone: (505) 667-9434
Email: spendelow@lanl.gov

DOE Manager: Nancy L. Garland
Phone: (202) 586-5673
Email: Nancy.Garland@ee.doe.gov

Subcontractors:
- Shouheng Sun and Andrew Peterson, Brown University, Providence, RI
- Christopher Murray, University of Pennsylvania, Philadelphia, PA
- Gang Wu, State University of New York at Buffalo, Buffalo, NY
- Madeleine Odgaard, EWII Fuel Cells, Albuquerque, NM

Project Start Date: October 1, 2016
Project End Date: September 30, 2019

Overall Objectives

- Design and synthesize fully ordered intermetallic MPt (M represents non-precious metals other than Fe) nanoparticles.
- Optimize the Pt-support interaction to maximize the catalyst activity and durability.
- Establish effective material interfaces in membrane electrode assemblies (MEAs).
- Scale up to 50 cm^2 MEAs and synthesize up to a 100 g batch of carbon-supported alloy nanoparticles.

Fiscal Year (FY) 2017 Objectives

- Synthesize fully ordered face-centered tetragonal (fct)-FePt nanoparticles from FePt-Fe_3O_4 precursors and perform initial electrochemical characterization.
- Incorporate at least two distinct ordered intermetallic catalysts into MEAs and perform fuel cell testing including mass activity and high-current performance.
- Perform initial durability testing using square-wave accelerated stress test (AST) on ordered intermetallic catalysts in MEA.
- Demonstrate 5–7 nm fct-MPt with durability in electrocatalyst AST superior to baseline Pt/C.

Technical Barriers

This project addresses the following technical barriers from the Fuel Cells section of the Fuel Cell Technologies Office Multi-Year Research, Development, and Demonstration Plan.

(A) Durability

(B) Cost

(C) Performance

Technical Targets

The technical targets and status for this project are listed in Table 1.

FY 2017 Accomplishments

- fct-FePt and fct-CoPt nanoparticles were synthesized and tested.
- Mass activity of 0.46 A/mg_{PGM} and 0.43 A/mg_{PGM} demonstrated for fct-FePt and fct-CoPt, respectively.

TABLE 1. Progress towards Meeting Technical Targets for Electrocatalysts and MEAs for Transportation Applications

Characteristic	Units	DOE 2020 Electrocatalyst and MEA Targets	Project Status (5 cm^2 cell, differential conditions)
Mass activity	A/mg_{PGM} @ 0.9 $mV_{iR\text{-}free}$	≥0.44	0.46
Mass activity loss after catalyst AST	%	<40	65
Loss at 0.8 A/cm^2 after catalyst AST	mV	30	52
MEA performance	mA/cm^2 @ 800 mV	≥300	240
MEA performance	mW/cm^2 @ rated power (663 mV)	≥1,000	557

PGM – platinum group metal, iR – internal resistance

INTRODUCTION

Platinum intermetallic nanoparticles have recently been demonstrated as promising catalytic materials for fuel cells and other electrochemical energy technologies [1–3], with initial results suggesting that these intermetallic structures can have higher performance and durability than disordered alloys in electrochemical applications such as fuel cells. However, most work to date has used partially-ordered nanoparticles. Scalable synthesis of fully-ordered intermetallics with high surface-to-volume ratio is a key challenge preventing advancement of this field. The goal of this project is to develop novel synthetic routes to prepare monodisperse, highly-ordered, high surface area intermetallics in large quantities with high quality control.

APPROACH

The overall approach is to synthesize advanced fuel cell catalysts based on intermetallic alloys and subject them to performance and durability testing in MEAs. The targeted catalysts consist of fully-ordered intermetallic alloy nanoparticles, and are being developed at Los Alamos National Laboratory as well as at subcontractors Brown University and University of Pennsylvania. The advanced catalyst nanoparticles are being supported on high-performance, nitrogen-doped carbon supports as developed by subcontractor State University of New York at Buffalo, as well as on commercially-available carbon supports. Catalysts examined include PtFe, PtNi, and PtCo, with subsequent examination of ternary catalyst systems. While PtFe is being examined as a model catalyst, the project team is working to remove all Fe from the catalyst system to alleviate durability concerns.

By forming fully-ordered intermetallic compounds with face centered tetragonal structure, the project team seeks to produce catalysts that retain high activity during durability testing with reduced leaching of base metal components when compared with conventional non-ordered alloys. Theory-based design principles based on a machine-learning technique developed at Brown University are being used to guide the catalyst development.

RESULTS

Several fct catalysts were successfully synthesized in FY 2017, including fct-FePt and fct-CoPt supported on high surface area carbon. Initial fct-FePt catalysts had mass activity lower than the target, but they exhibited good stability during catalyst durability testing using the 0.6–0.95 V square wave AST, with very little change in polarization behavior (Figure 1).

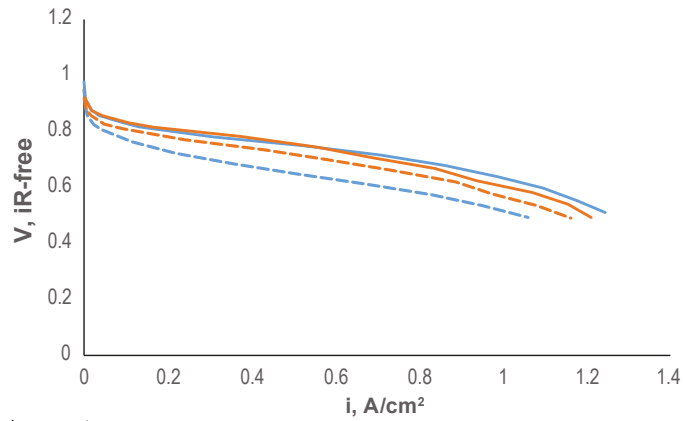

i – current

FIGURE 1. Polarization behavior of fct-FePt catalyst (orange) compared with commercial Pt/C (TKK TEC10E50, blue). Test conditions: 150 kPa_{abs}, 100% relative humidity, 500/1,000 sccm anode/cathode, 0.1/0.1 mg_{Pt}/cm^2 anode/cathode, NR212 membrane. Solid lines represent initial performance, while dashed lines represent performance after the 30,000 cycle AST.

Characterization including X-ray absorption spectroscopy, wide-angle X-ray scattering, and small angle X-ray scattering was performed at the Advanced Photon Source on fresh catalyst, catalyst on as-prepared MEAs, and catalyst after 30,000 cycle AST MEA testing. Little change in catalyst structure was observed. Wide-angle X-ray scattering results showed negligible change in particle size, while small-angle X-ray scattering results showed that the fct structure remains even after the AST (Figure 2). Similarly, X-ray absorption fine structure results indicated little change in bond distance. The catalysts also showed very little change in electrochemical surface area during the AST (Figure 3).

While the initial catalysts had high durability, they did not have sufficient mass activity. Synthesis of smaller fct-FePt particles (approximately 5 nm) enabled mass activity values as high as 0.46 A/mg_{PGM}, but these particles exhibited lower durability. Similarly, approximately 5 nm fct-CoPt nanoparticles with mass activity values as high as 0.43 A/mg_{PGM} were synthesized, but without sufficient durability. The small particles exhibited a lower degree of ordering, which may account for the lower durability. Work is underway to try to increase the degree of ordering of these small fct particles.

Several novel supports based on nitrogen-doped graphitic carbon were synthesized and used as supports for Pt nanoparticles. These catalysts exhibited good activity and stability in rotating disk electrode testing, but efforts to match this performance in MEA testing are still underway.

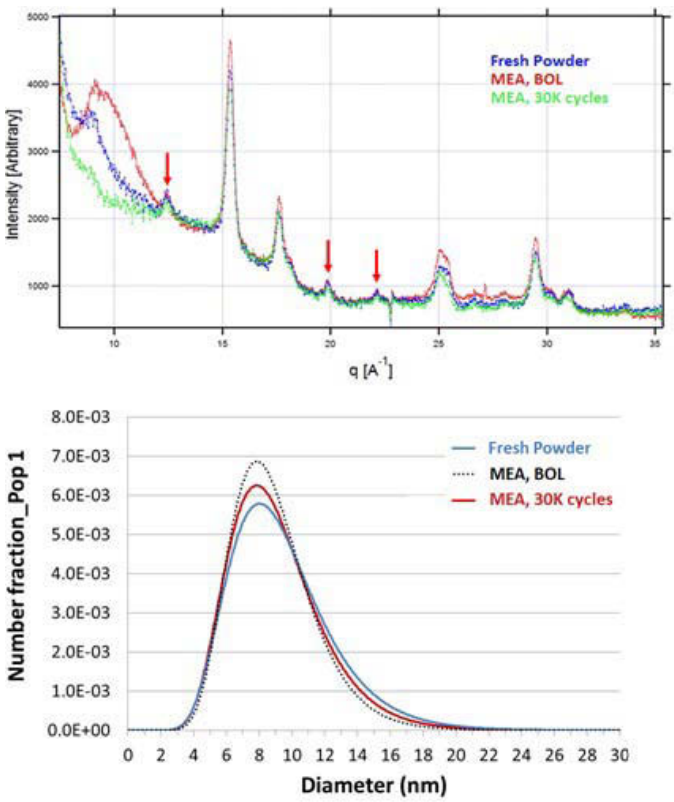

BOL – beginning of life

FIGURE 2. Top: Wide-angle X-ray scattering analysis demonstrates that superlattice peaks (marked with red arrows) remain after 30,000 cycles, indicating that the fct structure survives the AST. Bottom: Small-angle X-ray scattering demonstrates negligible change in particle size due to AST.

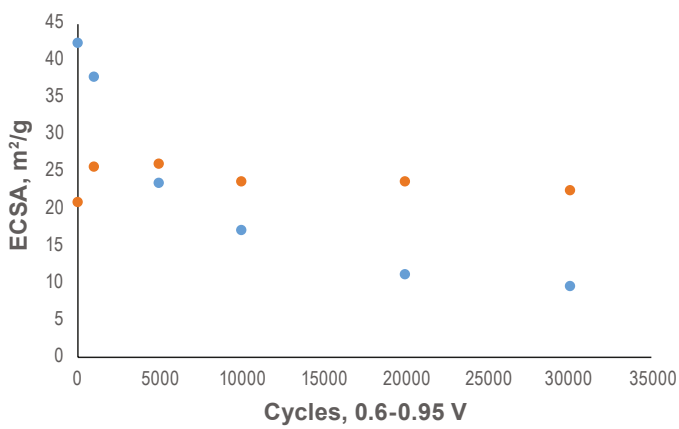

FIGURE 3. Electrochemical surface area (ECSA) change of fct-FePt (orange) during the 30,000 cycle AST is much smaller than the electrochemical surface area change of commercial Pt/C (TKK TEC10E50, blue).

CONCLUSIONS AND UPCOMING ACTIVITIES

Results from the first year of the project indicate that high durability can be achieved through formation of ordered fct-FePt nanoparticles, and that this ordering can survive even during extended durability testing. However, the relatively large particles that exhibit good ordering and high durability have a relatively low surface area and do not yet meet the mass activity target. Formation of smaller particles (around 5 nm) has been demonstrated, and these smaller particles are capable of meeting the mass activity target, but improved ordering is required to increase durability.

Upcoming activities include efforts to increase the degree of ordering through improved annealing procedures, and efforts to replace Fe content with Co or Ni. Work is also underway to improve the incorporation of these fct catalysts into high-performance MEAs. Further efforts on synthesis of nitrogen-doped graphitic carbon supports are planned to produce structures that can be more readily incorporated into MEAs. Once these structures are demonstrated as supports for Pt catalysts, they will be further developed and demonstrated as supports for the novel fct catalysts being developed in this project.

FY 2017 PUBLICATIONS/PRESENTATIONS

1. Jacob S. Spendelow and Yu Seung Kim, "Advanced Electro-Catalysts through Crystallographic Enhancement," presentation to the Fuel Cell Tech Team, Southfield, MI, February 15, 2017.

2. Jacob S. Spendelow, "Advanced Electro-Catalysts through Crystallographic Enhancement," presentation at the 2017 DOE Annual Merit Review and Peer Evaluation Meeting, Washington, D.C., June 7, 2017.

REFERENCES

1. M. Nguyen et al., "Synthesis of carbon supported ordered tetragonal pseudo-ternary $Pt_2M'M''$ (M = Fe, Co, Ni) nanoparticles and their activity for oxygen reduction reaction," J. Power Sources 2015, 280, 459–466.

2. D. Chung et al., "Highly Durable and Active PtFe Nanocatalyst for Electrochemical Oxygen Reduction Reaction," J. Am. Chem. Soc. 2015, 137, 15478–15485.

3. Q. Li et al., "New Approach to Fully Ordered fct-FePt Nanoparticles for Much Enhanced Electrocatalysis in Acid," Nano Lett. 2015, 15, 2468–2473.

V.A.17 Vapor Deposition Process for Engineering of Dispersed PEMFC ORR Pt/NbO_x/C Catalysts

James Waldecker (Primary Contact) and Jun Yang
Ford Motor Company
2101 Village Road
Dearborn, MI 48121
Phone: (313) 575-7561
Email: jwaldeck@ford.com

DOE Manager: Adria Wilson
Phone: (240) 479-0198
Email: Adria.Wilson@ee.doe.gov

Contract Number: DE-EE0007675

Subcontractors:
- Exothermics, Inc., Amherst, NH
- EWII Fuel Cells, LLC, Albuquerque, NM
- Northeastern University, Boston, MA
- University of Michigan, Ann Arbor, MI

Project Start Date: January 1, 2017
Project End Date: March 31, 2020

Overall Objectives

- Develop a new cathode catalyst powder.
- Improve the catalyst powder manufacturing process.
- Demonstrate the physical vapor deposition (PVD) process is scalable in a cost effective manner.
- Show ease of integration of catalyst into a membrane electrode assembly.

Fiscal Year (FY) 2017 Objectives

- Execute subcontracts.
- Demonstrate metal particle distribution from PVD process between 2 nm and 10 nm.
- Demonstrate consistency of Pt and NbO_x loadings from PVD processes.

Technical Barriers

This project addresses the following technical barriers from the Fuel Cells section of the Fuel Cell Technologies Office Multi-Year Research, Development, and Demonstration Plan.

(A) Durability

(B) Cost

(C) Performance

Technical Targets

The project seeks to develop an electrocatalyst for oxygen reduction, as well as membrane electrode assemblies (MEAs) containing the electrocatalyst, that meet targets relating to the durability, cost, and performance technical barriers. Targets associated with reducing platinum group metal (PGM) content relate to cost.

Most project work so far has focused on fabricating new catalyst powders using PVD systems at Oak Ridge National Laboratory (ORNL). The 5 cm^2 cell status shown in Table 1 is from samples produced with arc plasma deposition prior to the project award.

FY 2017 Accomplishments

- PVD processes at ORNL were able to produce carbon-supported platinum catalyst (Pt/C) with mass activities measured by rotating disk electrode (RDE) that ranged from 0.3 A/mg_{PGM} to 0.5 A/mg_{PGM}.

TABLE 1. Progress towards Meeting Technical Targets for Electrocatalysts and MEAs for Transportation Applications

Characteristic	Units	DOE 2020 Electrocatalyst and MEA Targets	Project Status (5 cm^2 cell)
Mass activity	A/mg_{PGM} @ 0.9 $mV_{iR\text{-}free}$	≥0.44	0.078
PGM total loading	mg_{PGM}/cm^2_{geo}	≤0.125	0.087, cathode
PGM content at rated power	g_{PGM}/kW_{gross}	≤0.125	0.620, cathode
MEA performance	mW/cm^2_{geo} @ V, T where Q/ΔT = 1.45 kW/K	≥1.000	140
Electrocatalyst stability (0.6 V ↔ 0.95 V)	% mass activity loss after 30,000 cycles	<40	N/A
Loss at 0.8 A/cm^2 (0.6 V ↔ 0.95 V)	mV loss after 30,000 cycles	<30	N/A
Support stability (1.0 V ↔ 1.5 V)	% mass activity loss after 5,000 cycles	<40	N/A
Loss at 1.5 A/cm^2 (1.0 V ↔ 1.5 V)	mV after 5,000 cycles	<30	N/A

N/A – not available

- PVD process Pt/C samples from ORNL showed platinum particle sizes that ranged from 2 nm to 11 nm.

✧ ✧ ✧ ✧ ✧

INTRODUCTION

The Department of Energy has set targets for higher performing catalysts that will address the two major vehicle-related barriers to the commercialization of automotive fuel cell systems: cost and durability. This project seeks to generate new catalysts that meet these targets by (1) applying vapor deposition processes to fabricate catalyst powders and (2) incorporating amorphous niobium oxide as a secondary support in the powders. The project aims to produce powders, as opposed to a structured catalyst layer, in order to enhance roughness factor and allow ease of integration into established ink processes at catalyst coated membrane suppliers.

Vapor deposition provides numerous advantages. With a well-controlled, high volume sputtering process, reproducibility of the catalyst powders should be enhanced compared to the conventional wet chemistry process. Targets made for vapor deposition are very pure, limiting the possibility of impurities (e.g., chlorides, iron) being incorporated into the final powder and compromising performance or durability. Furthermore, a vapor deposition process may be able to limit the amount of aqueous or solvent waste generated in catalyst powder fabrication, although some estimation of precious metal reclamation processes still needs to be considered. Specifically, with regard to niobium oxide, vapor deposition processes yield an amorphous niobium oxide, which has not been shown to convert to the electrically insulating, crystalline Nb_2O_5 phase. The niobium oxide should also provide benefit; numerous studies have shown that the presence of niobium oxide can enhance either mass-normalized or area-normalized activity by 2–3X [1–3]. Furthermore, this project will explore whether depositions of niobium oxide on the surface of porous carbon have the capability to eliminate routes toward platinum surface coalescence.

APPROACH

The project approach centers on two sources for the production of $Pt/NbO_x/C$ catalysts, beginning with small batch (1–2 g) production at ORNL and scaling up to much larger batch (20–40 g) production at Exothermics. ORNL will establish the procedure needed to make $Pt/NbO_x/C$ catalysts by varying parameters such as carbon type, deposition time, pressure, power applied to the metal targets, and, in the case of reactive sputtering, inert/oxidant ratio in the chamber. Samples will then be evaluated for repeatability in terms of platinum and niobium weight percentages by X-ray fluorescence (XRF), as well as for particle size by transmission electron microscopy (TEM). RDE will be used to screen which catalyst samples are most active, and X-ray absorption spectroscopy will be used to understand why catalysts are active or durable in the contexts of adsorbates, Pt-Pt and Pt-Nb interatomic distances, and Pt-Pt and Pt-Nb coordination numbers.

Fuel cell testing will also be conducted using the $Pt/NbO_x/C$ catalyst powders according to the protocols and metrics outlined by the Department of Energy. Tests will include polarization curves, performance checks at rated power conditions, electrocatalyst cycling at voltages between 0.6 V and 0.95 V, and catalyst support cycling between 1.0 V and 1.5 V. The project team expects that the use of niobium oxide will prompt adjustments in ink formulations, and will reveal performance losses at high current density that will need to be improved. To address these concerns, the project will make use of limiting current techniques to diagnose non-Fickian mass transport resistances, as well as pressure-dependent mass transport resistances. Other diagnostics covering gas crossover, roughness factor, proton conductivity in the catalyst layer, and catalyst activity will also be used in testing.

RESULTS

The project has begun with preparation of samples at ORNL. Before depositing niobium oxide, ORNL prepared Pt/C samples using PVD. The PVD process involved the rotation of a carbon powder—either XC-72 or an acetylene black—upon which platinum was sputtered from a pure platinum metal target at room temperature. Table 2 summarizes the results. Sample gmv-080 showed an amazingly high specific activity (2,418 $\mu A/cm^2$), which more closely resembled the activity of platinum bulk phase, as opposed to platinum nanoparticles. However, the surface area measurement of 21 m^2/g indicated that nanoparticles were in existence, and the TEM image generated at the University of Michigan confirmed the presence of nanoparticles (Figure 1).

While the high activity of the gmv-080 sample was impressive, the lower platinum weight percent measured by XRF (11.4%) was indication that a catalyst layer made from this catalyst would be relatively thick, even at lower mg/cm^2 loading. Therefore, other samples were made in hopes of increasing platinum weight percent. Samples gmv-081, -082, and -083 showed low platinum weight percent, although high specific activities were still seen for gmv-081 and gmv-082. Samples gmv-084 and gmv-085 showed that higher platinum weight percent could be achieved using acetylene black carbon. Like with gmv-084 and gmv-085, higher specific activities were obtained than expected. Given the relatively conventional surface areas, the higher specific activities also translated into higher mass activities. Figure 2 shows that while mass activity might be expected to decrease at

TABLE 2. Results of Pt/C Fabrication at ORNL

Sample:	gmv-080	gmv-081	gmv-082	gmv-083	gmv-084	gmv-085
Carbon	XC-72	XC-72	XC-72	XC-72	acetylene black	acetylene black
Pt wt% (XRF at Ford)	11.4	3.9	5.9	0.5	15.1	23.3
Deposition time (h:mm)	1:00	2:16	2:55	3:00	3:00	2:28
Pressure (mtorr)	10	20	10	10	10	10
Stir bars?	No	Yes	Yes	No	No	Yes
Temperature	Room	Room	Room	Room	Room	Room
Average mass activity (A/g_{Pt}, RDE)	492	520	462		372	405
Average specific activity ($\mu A/cm^2$, RDE)	2,418	1,079	1,325		1,473	726
Average surface area (m^2/g, RDE)	21	48	35		25	58
Calculated Pt particle size (nm)	13	6	8		11	5

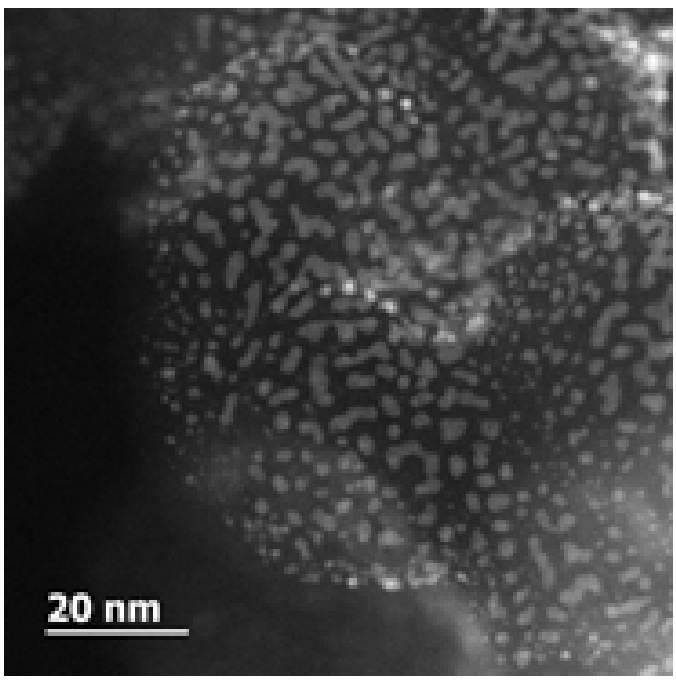

FIGURE 1. TEM image of sample gmv-080: Pt deposited on XC-72 carbon

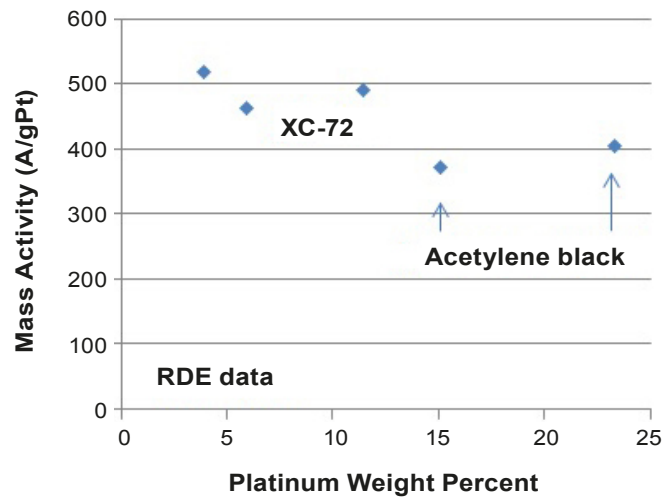

FIGURE 2. Mass activity versus Pt weight percent for ORNL PVD Pt/C samples

higher and more desirable Pt weight percentages, the higher Pt weight percentage samples still show high mass activity. Figure 3 shows that based on RDE data, most samples are between 0.3 A/mg_{PGM} and 0.5 A/mg_{PGM} mass activity, although in some cases higher surface area compensates for lower specific activity.

CONCLUSIONS AND UPCOMING ACTIVITIES

The project has demonstrated particularly high mass activity Pt/C samples made from PVD, at Pt weight percentages up to 23%. In the immediate future, efforts will be undertaken with X-ray absorption spectroscopy to understand why the activity is high. At the very least, X-ray absorption spectroscopy should be able to show whether coordination, Pt-Pt interatomic distances and oxygen-containing adsorbates are similar to Pt bulk phase. ORNL PVD deposition will move on to making $Pt/NbO_x/C$ samples after having achieved high activity with Pt/C. Characterization such as TEM and XRF will be used to iterate ORNL deposition conditions toward targeted weight percentages of Pt and Nb, and toward high activity and durability of the catalysts.

FY 2017 PUBLICATIONS/PRESENTATIONS

1. James Waldecker, "Vapor Deposition Process for Engineering of Dispersed PEMFC ORR $Pt/NbO_x/C$ Catalysts," presented at the 2017 Department of Energy New Project Kick-Off Meeting, Washington, D.C., February 2017.

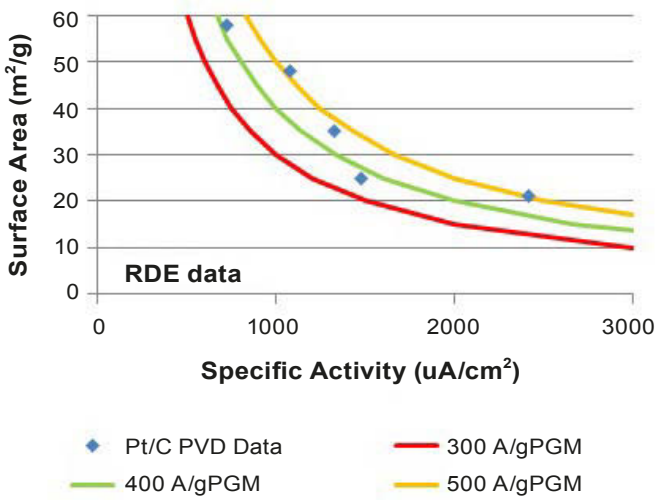

FIGURE 3. Surface area versus specific activity plots with constant mass activity curves for ORNL PVD Pt/C samples

2. James Waldecker, "Vapor Deposition Process for Engineering of Dispersed PEMFC ORR Pt/NbO_x/C Catalysts," presented at the 2017 Department of Energy Annual Merit Review and Peer Evaluation Meeting, Washington, D.C., June 2017.

REFERENCES

1. K. Sasaki, L. Zhang, and R.R. Adzic, "Niobium Oxide-Supported Platinum Ultra-Low Amount Electrocatalysts for Oxygen Reduction," *Phys. Chem. Chem. Phys.* **10** (2008) 159–167.

2. T. Trefz, N. Kremliakova, D. Susac, and J. Jankovic, "Sol-Gel Syntheses of Durable Metal-Oxide Hybrid Platinum Catalysts for PEFC," 224th ECS Meeting, Abstract 1501 (2013)

3. L. Zhang, L. Wang, C.M.B. Holt, T. Navessin, K. Malek, M.H. Eikerling, and D. Mitlin, "Oxygen Reduction Reaction Activity and Electrochemical Stability of Thin-Film Bilayer Systems of Platinum on Niobium Oxide," *J. Phys. Chem. C* **114** (2010) 16463–16474.

V.B.1 FC-PAD: Fuel Cell Performance and Durability Consortium

Rod Borup[1] (Primary Contact), Andrew Baker[1], Ahmet Kusoglu[2], Rangachary Mukundan[1], Joseph Dumont[1], David Langlois[1], Adam Weber[2], Rajesh Ahluwalia[3], Deborah Myers[3], Shyam Kocha[4], Karren More[5]

[1] Los Alamos National Laboratory
MS D429, P.O. Box 1663
Los Alamos, NM 87545
Phone: (505) 667-2823
Email: Borup@lanl.gov

[2] Lawrence Berkeley National Laboratory, Berkeley, CA

[3] Argonne National Laboratory, Argonne, IL

[4] National Renewable Energy Laboratory, Golden, CO

[5] Oak Ridge National Laboratory, Oak Ridge, TN

DOE Managers:

Dimitrios Papageorgopoulos
Phone: (202) 586-5463
Email: Dimitrios.Papageorgopoulos@ee.doe.gov

Gregory Kleen
Phone: (720) 356-1672
Email: Gregory.Kleen@ee.doe.gov

Additional no-cost partners:

- Ion Power, New Castle, DE, Steve Grot
- University of Delaware, Newark, DE, Suresh G. Advani and Ajay K. Prasad

Project Start Date: October 1, 2015
Project End Date: September 30, 2021

Overall Objectives

- Advance performance and durability of polymer electrolyte membrane fuel cells (PEMFCs) primarily at a pre-competitive level.
- Develop the knowledge base and optimize structures for more durable and high-performance PEMFC components.
- Improve high current density performance at low Pt loadings.
  - Loading: 0.125 mg Pt/cm^2 total
  - Performance @ 0.8 V: 300 mA/cm^2
  - Performance @ rated power: 1,000 mW/cm^2
- Improve component durability (e.g., membrane stabilization, self-healing, electrode-layer stabilization).
- Provide support to industrial and academic developers.
- Develop new diagnostics, characterization tools, and models.
- Each thrust area has a sub-set of objectives which lead to the overall performance and durability objectives.

Fiscal Year (FY) 2017 Objectives

- Quantify cerium migration and diffusion within the membrane under both applied potential and applied current, including modeling of the migration.
- Demonstrate methods to stabilize cerium migration, improving membrane durability.
- Measure cation effects on membrane conductivity and water uptake.
- Measure effect of ionomer-cations on the oxygen reduction reaction (ORR).
- Establish database of Ce/ceria, carbon corrosion effects, and ionomer distribution observations as input data for model development.

Technical Barriers

This project addresses the following technical barriers from the Fuel Cells section of the Fuel Cell Technologies Office Multi-Year Research, Development, and Demonstration Plan.

(A) Durability

(B) Cost

(C) Performance

Technical Targets

This project develops membrane electrode assemblies (MEAs) that meet the targets in Table 1.

TABLE 1. Technical Targets: MEAs for Transportation Applications

Characteristic	Units	2020 Targets
Cost	$ / KW_{net}	14
Durability with cycling	Hours	5,500
Start-up/shutdown durability	Cycles	5,000
Performance @ 0.8 V	mA/cm^2	300
Performance @ rated power (150 kPa_{abs})	m /cm^2	1,000

FY 2017 Accomplishments

- Measured cerium migration in-plane, through-plane, and in in situ hydrogen pump mode.
- Analyzed cerium data to quantify migration and diffusion coefficients (at 100% relative humidity [RH]).
- Measured cation effect on conductivity and ORR in microelectrodes.
  - Measured reductions in microelectrode current due to cation content in ionomer.
- Identified Ce/carbon interactions as a likely cause for Ce stabilization in the catalyst layers.
- Measured a large improvement in membrane durability by incorporating Ce as CZO (cerium-zirconia) over similar concentrations of ion-exchange cerium.
- Measured perfluorinated sulfonic acid (PFSA) conductivity as a function of cation and water content.
  - Large/heavy cations → disrupt domains → lower uptake
  - Multi-valent cations → ionic crosslinks → restricted mobility
  - Conductivity *scales with water per charge*, not per poly(anion).
- Conducted a comparison study of perfluoroimide acid versus PFSA water uptake and conductivity.

✧ ✧ ✧ ✧ ✧

INTRODUCTION

Although fuel cells are being deployed in cars with limited commercialization, they still fall short of the DOE targets for this technology, which are required for widespread consumer acceptance. The FC-PAD consortium was formed to advance performance and durability of PEMFCs at a pre-competitive level to further enable their commercialization. This consortium coordinates national laboratory activities related to fuel-cell performance and durability, provides technical expertise, and harmonizes activities with industrial developers. The consortium serves as a resource that amplifies the Office of Energy Efficiency and Renewable Energy impact by leveraging the core capabilities of several labs.

The major challenge to be addressed by this consortium is to develop the knowledge base and optimize structures for more durable, high-performing PEMFC component technologies, while simultaneously reducing cost. Current research is focused on achieving high performance and durability in low-Pt-loaded PEMFCs.

For FY 2017, FC-PAD is represented by three annual merit review presentations and annual progress reports:

- FC135 FC-PAD: Fuel Cell Performance and Durability Consortium (this report)
- FC136 FC-PAD: Components and Characterization (primary contact: Karren More)
- FC137 FC-PAD: Electrode Layers and Optimization (primary contact: Adam Weber)

FC-PAD is an integrated consortia of five national laboratories with a large number of contributing staff scientists, research technicians, post-docs, and students. For FY 2017, FC-PAD contributors were:

- **Argonne National Laboratory:** Debbie Myers, Rajesh Ahluwalia, Nancy Kariuki, Dennis Papadias, C. Firat Cetinbas, J-K Peng, Xiaohua Wang;
- **Lawrence Berkeley National Laboratory:** Adam Weber, Ahmet Kusoglu, Kelsey Hatzell, Lalit Pant, Huai-Suen Shiau, Anna Freiburg, Meron Tesfaye, Anamika Chowdhury, Sarah Berlinger, Andrew Crothers, Grace Lau, Michael Tucker, Clayton Radke, Thomas Chan;
- **Los Alamos National Laboratory:** Rangachary Mukundan, Rod Borup, Natalia Macauley, Mahlon Wilson, Yu Seung Kim, Sarah Stariha, David Langlois, Roger Lujan, Siddharth Komini Babu, Andrew Baker, Joseph Dumont, Jacob Spendelow;
- **National Renewable Energy Laboratory:** Shyam Kocha, KC Neyerlin, Nihal Shah, Jason Zack, Jason Christ, Huyen Dinh, Guido Bender, Jocelyn Mackay, Lawrence Anderson;
- **Oak Ridge National Laboratory:** Karren More, David Cullen, Brian Sneed, Shawn Reeves.

APPROACH

This consortium incorporates national laboratory investigators with proven experience (developed in prior projects) related to durability, transport, and performance, and combines them into one highly coordinated effort. The consortium formalizes already existing and effective collaborations among the national laboratories that have established leadership in PEMFC performance and durability research and development. Three thrust areas are related to components: (1) electrocatalysts and supports; (2) electrode layers; (3) ionomers, gas diffusion layers, bipolar plates, interfaces; three additional thrust areas are cross-cutting in nature; (4) modeling and validation; (5) operando evaluation–benchmarking, accelerated stress tests (ASTs), and contaminants; and (6) component characterization and diagnostics.

Four FC-PAD projects from DE-FOA-0001412 were announced by DOE during FY 2017. Those projects are led by 3M Company, General Motors, United Technologies Research Center, and Vanderbilt University. The core national lab team is working to support those four projects with an equal level of effort utilizing national lab capabilities. A national lab primary point of contact was assigned for each project, with a statement of work negotiated for FY 2017. National lab work for those projects is represented in those project reports.

RESULTS

The results in this FC-PAD report are limited to our work related to membrane durability and understanding the membrane structure and performance.

Cerium is an additive used to improve the durability of fuel cell polymer electrolyte membranes (PEMs); however, migration of cerium (Ce) can be an issue. Cerium ions enhance the durability of PEM fuel cell components by rapidly and reversibly scavenging degrading radical species, which can be generated during operation. However, Ce migrates between the membrane and the catalyst layers (CLs). The migration of cerium is demonstrated in Figure 1, where a fresh MEA has a large concentration of cerium in the membrane (Figure 1a); however, after testing either by AST holding the cell at open circuit potential (Figure 1b) or operating the U.S. Drive Cycle Protocol (Figure 1c), little cerium remains in the membrane, with the majority residing in the catalyst layers, both anode (aCL) and cathode (cCL).

Hydrogen pump experiments were utilized in FY 2017 to understand the effects of potential gradients and proton/water flux on Ce migration. Figure 2 shows two-dimensional Ce maps during hydrogen pump experiments performed at 2 V and 100% RH for different amounts of charge transfer. The cerium concentration profiles show a progression of cerium migration to the counter electrode with time and charge transfer. After complete migration of the cerium, potential was removed and the corresponding time-dependent diffusion measured to define a cerium diffusion coefficient. With this cerium diffusion coefficient, a migration coefficient was modeled by the Nernst-Plank equation (Equation 1):

$$\frac{\delta c}{\delta t} + V.\,(-DVc - zu_m FcV\varphi_{ionic}) = 0 \qquad (1)$$

The coefficients determined and used in the modeling (solid lines) were:

- Diffusion Coefficient 0.686 [$x10^{-10}$ m^2 s^{-1}]
- Mobility 7.2±0.8 [$x10^{-15}$ s mol kg^{-1}]

To improve membrane durability to alleviate issues with migration, we have employed more effective radical scavengers in the cathode CL, nearest to the location of peroxide and reactive hydroxyl radical generation, based on CZO (cerium-zirconia) [1]. CZO addition to the cathode CL at a loading of 10 µg/cm^2 improved the durability of Nafion XL PEMs, which is demonstrated by reduced electrochemical gas crossover, open circuit voltage decay, and fluoride emission rates (shown in Figure 3) during PEM chemical stability ASTs. Additionally, this improvement in durability counteracts undesirable Ce migration due to ionomer degradation. The overall degradation rate, indicated by average fluoride emission rate (FER) over the test duration, also correlates well to the final Ce content in the PEM after ASTs. This result is consistent with our hypothesis that during aggressive ASTs, Ce movement from the PEM into the CLs is affected by degradation of the Ce-containing ionomer, itself. Therefore, employing a highly effective radical scavenger, such as CZO, dramatically mitigates PEM degradation, which negates the effects of Ce migration due to side chain scission. MEAs with improved chemical stability, which do not compromise cell performance, as shown here, directly address barriers of lifetime and cost which currently hinder PEM fuel cell commercialization.

A large effect of cations such as cerium is the reduction of water uptake and loss of conductivity. A series of cations

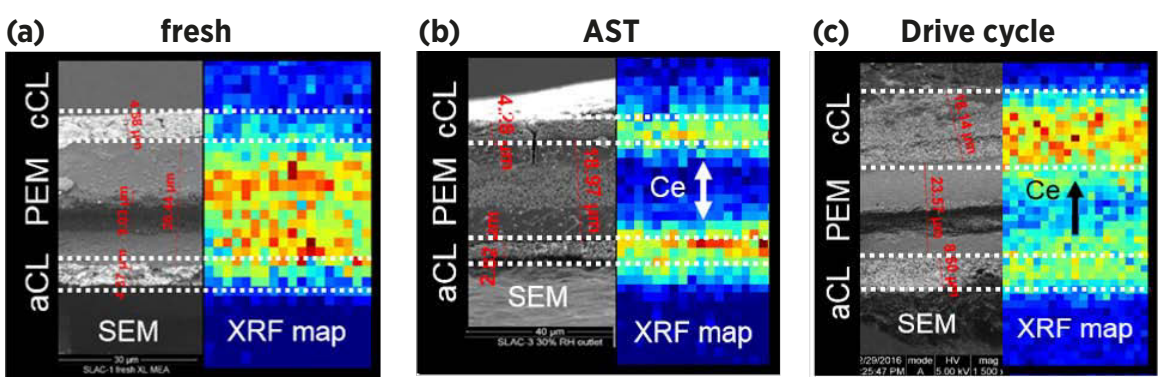

FIGURE 1. Cross-section images by scanning electron microscopy (SEM) and cerium mapping by X-ray fluorescence (XRF) of (a) fresh MEA, (b) an MEA after the membrane open circuit potential AST, and (c) an MEA after the U.S. Drive Cycle test

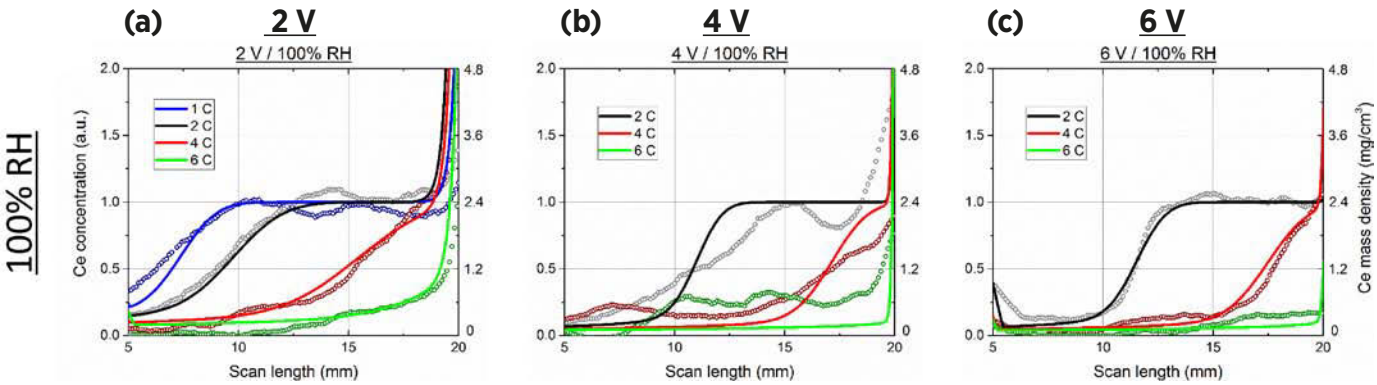

a.u. – arbitrary units

FIGURE 2. Cerium profiles by XRF measurement and modeled post hydrogen pump operation after 1 coulomb (blue), 2 coulombs (black), 4 coulombs (red), and 6 coulombs of charge transfer at (a) 2 V, (b) 4 V, and (c) 6 V at 100% RH

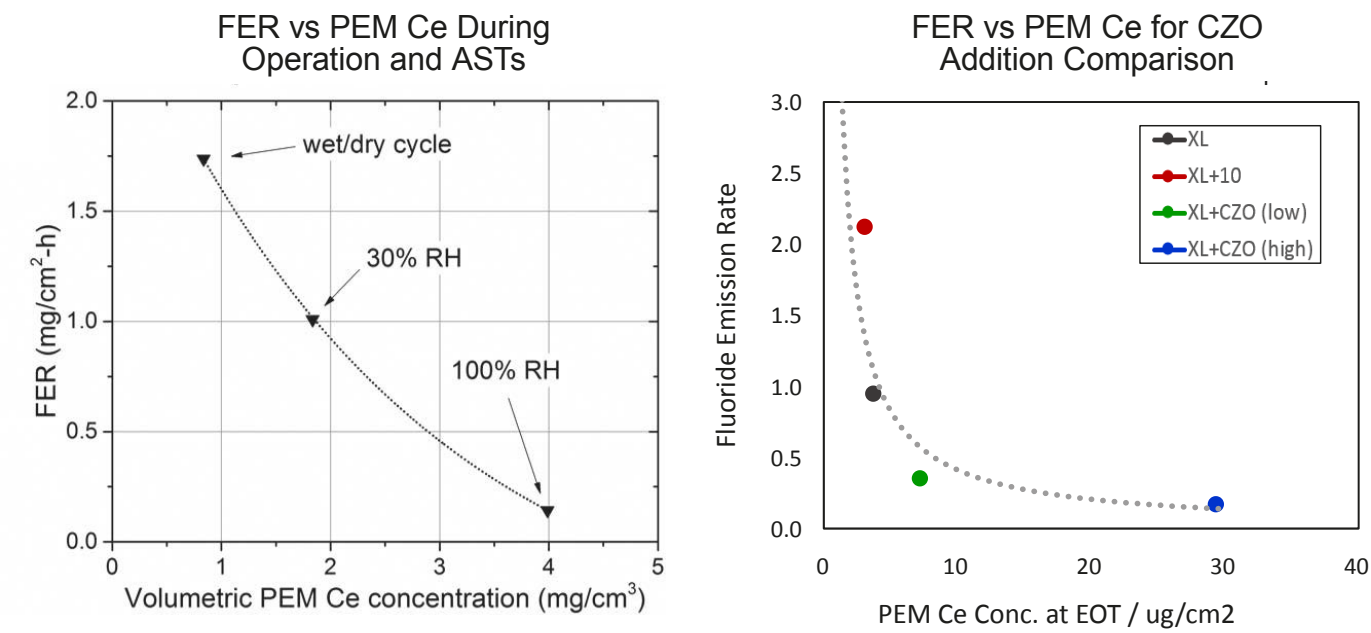

FIGURE 3. Relationship between fluoride emission rate and the residual amount of Ce in the PEM after ASTs at EOT (end of test)

was examined to correlate the membrane conductivity to cation concentration and water content. The membrane conductivity versus water content is shown in Figure 4 for this series of cations. From this, we can determine that conductivity *scales with water per charge*, not per poly(anion). Overall, the cationic-interaction-dependent properties are strongly affected by hydration/RH to which the system is exposed, with the effect of the different cations being:

Large/heavy cations → disrupt domains → lower uptake

Multi-valent cations → ionic crosslinks → restricted mobility

Interestingly, cerium has an exceptionally high conductivity, higher than it expected from similar sized or valance cations. This is a fortuitous result as cerium is a cation of choice for radical scavenging, and these properties may limit deleterious effects of the cation on membrane and ionomer conductivity.

CONCLUSIONS AND UPCOMING ACTIVITIES

Significant progress is reported in this report related to understanding cerium migration in membranes and its potential effects on durability. Migration and diffusion coefficients were quantified at 50% and 100% RH. CZO is shown to enhance the membrane durability much better than adding cerium cations. Work also demonstrates advances in

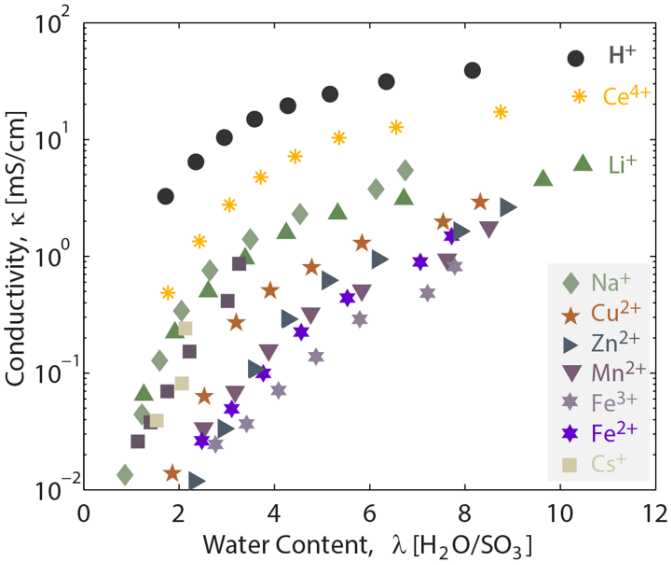

FIGURE 4. Membrane conductivity versus water content for a series of cations

modeling of membrane structures and detailing water uptake with various cationic species.

As a consortium, the future work planned is broad, but concentrates on developing the foundational science understanding of the MEA components:

- MEA/catalyst layer structure
  - Binary interactions that govern structure in an ink (polymer/solvent, Pt/C and solvent, Pt/C and ionomer, etc.).
  - Effect of interactions on catalyst layer morphology.
    - Microporosity, ionomer/carbon, and ionomer/Pt structure.
  - Catalyst layer restructuring during conditioning.
  - Cation effect on CL and ionomer structure (Ce, Co, Ni, etc.).
- Micro-continuum model for domain-scale physics
  - Nanoscale interactions: electrostatics, solvation, finite size, image charge, dispersion forces.
  - Effect of elected cations relevant to leaching, for thin film ionomers.
  - Isolation of nanoscale and mesoscale resistances.
- Durability: low catalyst loading and catalyst type effect
  - Comparative H_2O_2 and radical formation at lower loadings ($2e^-$ versus $4e^-$).
  - Ionomer degradation in catalyst layer; ionomer degradation versus structural change.
  - Local conditions effects on performance and durability (e.g., dissolution).
  - Alloy-type/support/ionomer effect on catalyst layer durability.

Specifically related to this report, future work related to membrane durability includes:

- Membrane, membrane additives, and cation effects
  - In situ fuel cell operation with measurement of Ce concentration profiles.
  - Surface analysis of Ce/C catalyst supports to identify Ce bonding/stabilization.
  - Correlation or demonstration of no correlation of R_{CL} with Ce ionomer concentrations.
  - Better stabilization of Ce in localized areas of the membrane (CZO, Ce stabilized within fibers or capsules).
  - 2D (or 3D) modeling of the cation migration.
  - Model prediction of durability with Ce content and migration.

SPECIAL RECOGNITIONS & AWARDS/ PATENTS ISSUED

- Ahmet Kusoglu received the Supramaniam Srinivasan, Early Career Award from the Energy Technology Division of the Electrochemical Society.
- Ahmet Kusoglu received a Toyota Young Investigator Award from the Electrochemical Society.
- Andrew Baker received the Bill Baron Fellowship in recognition of his contributions related to the renewable energy field from the University of Delaware.
- Rangachary (Mukund) Mukundan has been selected as a 2017 recipient as a fellow of the Electrochemical Society.

REFERENCES

1. S.M. Stewart, R.L. Borup, M.S. Wilson, A. Datye, and F.H. Garzon, *ECS Trans.*, 2014, **64**, 403–411.

FY 2017 PUBLICATIONS/PRESENTATIONS

1. Publications and presentations listed here represent the three FC-PAD annual merit review presentations and annual progress reports: FC135 (V.B.1), FC136 (V.B.2), and FC137 (V.B.3).

Publications Relevant to FC-PAD from Consortium Members

1. Iryna V. Zenyuk, Prodip K. Das, and Adam Z. Weber, 'Understanding Impacts of Catalyst-Layer Thickness on Fuel-Cell Performance via Mathematical Modeling,' *Journal of the Electrochemical Society*, 163 (7), F691–F703 (2016). doi: 10.1149/2.1161607jes.

2. Ahmet Kusoglu, Thomas J. Dursch, and Adam Z. Weber, 'Nanostructure/Swelling Relationships of Bulk and Thin-Film PFSA Ionomers,' *Advanced Functional Materials*, 26, 4961–4975 (2016). doi: 10.1002/adfm.201600861.

3. Shouwen Shi, Adam Z. Weber, and Ahmet Kusoglu, 'Structure/property relationship of Nafion XL composite membranes,' *Journal of Membrane Science*, 516, 123–134 (2016). doi: 10.1016/j.memsci.2016.06.004.

4. Iryna Zenyuk, Dilworth Y. Parkinson, Liam G. Connolly, and Adam Z. Weber, 'Gas-Diffusion-Layer Structural Properties under Compression via X-Ray Tomography,' *Journal of Power Sources*, 328, 364–376 (2016). doi: 10.1016/j.jpowsour.2016.08.020.

5. Shouwen Shi, Adam Z. Weber, and Ahmet Kusoglu, 'Structure-Transport Relationship of Perfluorosulfonic-Acid Membranes in Different Cationic Forms,' *Electrochimica Acta*, 220, 517–528 (2016). doi: 10.1016/j.electacta.2016.10.096.

6. Iryna Zenyuk, Adrien Lamibrac, Jens Eller, Dilworth Parkinson, Federica Marone, Felix Büchi, and Adam Z. Weber, 'Investigating Evaporation in Gas Diffusion Layers for Fuel Cells with X-ray Computed Tomography,' *Journal of Physical Chemistry C*, 120(50), 28701–28711 (2016). doi: 10.1021/acs.jpcc.6b10658.

7. Ahmet Kusoglu and Adam Z. Weber, 'New Insights into Perfluorinated Sulfonic-Acid (PFSA) Ionomers,' *Chemical Reviews*, 117 (3), 987–1104 (2017). doi: 10.1021/acs.chemrev.6b00159.

8. Franz B. Spingler, Adam Phillips, Tobias Schuler, Michael C. Tucker, Adam Z. Weber, 'Investigating Fuel-Cell Transport Limitations using Hydrogen Limiting Current,' *International Journal of Hydrogen Energy* (2017). doi: 10.1016/j.ijhydene.2017.01.036.

9. S. Shukla, S. Bhattacharjee, A.Z. Weber, M. Secanell, 'Experimental and Theoretical Analysis of Ink Dispersion Stability for Polymer Electrolyte Fuel Cell Applications,' *Journal of the Electrochemical Society*, 164 (6), F600–F609 (2017). doi: 10.1149/2.0961706jes.

10. Lalit M. Pant and Adam Z. Weber, 'Modeling Transport in PEFC Cathode Agglomerates with Double Trap Kinetics,' *Journal of the Electrochemical Society*, 164 (11), E3081–E3091 (2017). doi: 10.1149/2.0081711jes.

11. Anna T.S. Freiberg, Michael C. Tucker, and Adam Z. Weber, 'Polarization Loss Correction Derived from Hydrogen Local-Resistance Measurement in Low Pt-Loaded Polymer-Electrolyte Fuel Cells,' *Electrochemical Communications* (2017). doi: 10.1016/j.elecom.2017.04.008.

12. N. Macauley, R. Mukundan, D.A. Langlois, K.C. Neyerlin, S.S. Kocha, K.L. More, Madeleine Odgaard, and Rod L. Borup, 'Durability of PtCo/C Cathode Catalyst Layers Subjected to Accelerated Stress Testing,' *ECS Transactions*, 75 (14), 281–287.

13. A.M. Baker, R. Mukundan, D. Spernjak, S.G. Advani, A.K. Prasad, and R.L. Borup, 'Cerium Migration in Polymer Electrolyte Membranes,' *ECS Transactions*, 75 (14), 707–714.

14. K. Shinozaki, Y. Morimoto, B.S. Pivovar, and S.S. Kocha, 'Suppression of oxygen reduction reaction activity on Pt-based electrocatalysts from ionomer incorporation,' *Journal of Power Sources*, 325, 745–751 (2016).

15. K. Shinozaki, Y. Morimoto, B.S. Pivovar, and S.S. Kocha, 'Re-examination of the Pt Particle Size Effect on the Oxygen Reduction Reaction for Ultrathin Uniform Pt/C Catalyst Layers without Influence from Nafion,' *Electrochimica Acta*, 213, 783–790 (2016).

16. C. Firat Cetinbas, Rajesh K. Ahluwalia, Nancy Kariuki, Vincent De Andrade, Dash Fongalland, Linda Smith, Jonathan Sharman, Paulo Ferreira, Somaye Rasouli, and Deborah J. Myers, 'Hybrid approach combining multiple characterization techniques and simulations for microstructural analysis of proton exchange membrane fuel cell electrodes,' *Journal of Power Sources*, 344, 62–73 (2017).

17. Andrew M. Baker, Rangachary Mukundan, Dusan Spernjak, Elizabeth J. Judge, Suresh G. Advani, Ajay K. Prasad, and Rod L. Borup, 'Cerium migration during PEM fuel cell accelerated stress testing,' *Journal of The Electrochemical Society*, 163 (9), F1023–F1031.

18. B.T. Sneed, D.A. Cullen, K.S. Reeves, O.E. Dyck, D.A. Langlois, R. Mukundan, R.L. Borup, and K.L. More, '3D Analysis of Fuel Cell Electrocatalyst Degradation on Alternate Carbon Supports,' submitted to *ACS Catalysis* (under review).

19. Natalia Macauley, Joseph Fairweather, Rangachary Mukundan, D.D. Papadias, Dusan Spernjak, David Langlois, R. Ahluwalia, Karren More, and Rodney L. Borup, 'Accelerated testing of carbon corrosion in PEM fuel cells,' submitted.

20. Natalia Macauley, Roger W. Lujan, Dusan Spernjak, Daniel S. Hussey, David L. Jacobson, Karren More, Rodney L. Borup, and Rangachary Mukundan, 'Durability of Polymer Electrolyte Membrane Fuel Cells Operated at Subfreezing Temperatures,' *J. Electrochem. Soc.*, 163 (13), F1317–F1329 (2016).

Presentations Relevant to FC-PAD from Consortium Members

1. A. Kusoglu, "State of Understanding of PFSA Ionomers and Thin Films," Gordon Research Conference (GRC) Fuel Cells, Easton, MA, August 2016.

2. A. Kusoglu, "New Insights into PFSA Ionomers: From Membranes to Thin Films," 3M Company, February 2017.

3. A.Z. Weber, (Keynote) "Multiscale Modeling of Polymer-Electrolyte-Fuel-Cell Components," Meeting Abstracts, MA2016-01 (2016) 2211.

4. A. Shum, K.B. Hatzell, L.G. Connolly, O.S. Burheim, D.Y. Parkinson, A.Z. Weber, and I.V. Zenyuk, "Exploring Phase-Change-Induced Flow in Fuel Cells through X-Ray Computed Tomography," ECS Meeting, 2016.

5. T. Schuler, M.C. Tucker, and A.Z. Weber, "Gas-Transport Resistances in Fuel-Cell Catalyst Layers," ECS Meeting, 2016.

6. Adam Z. Weber, Lalit Pant, Tobias Schuler, Haui-Suen Shiau, Anna Freiberg, Michael C. Tucker, Anamika Chowdhury, K.C. Neyerlin, Shyam Kocha, and Iryna Zenyuk, "Elucidating and Understanding Transport Phenomena in Polymer-Electrolyte Fuel Cells," CARISMA, Newcastle upon Tyne, United Kingdom, April 2017.

7. Adam Z. Weber, Tobias Schuler, Franz Spingler, Anna Freiberg, Michael C. Tucker, Anamika Chowdhury, K.C. Neyerlin, and Ahmet Kusoglu, "Ionomer-Associated Transport Resistances in Fuel Cell Electrodes," 21st International Conference on Solid State Ionics, Padua, Italy, June 2017.

8. Andrew R. Crothers, Shouwen Shi, Peter Dudenas, Ahmet Kusoglu, and Adam Z. Weber, "Structure-Transport Relationships of Perfluorinated-Sulfonic-Acid Membrane Interfaces," Polymer-Electrolyte Fuel Cell Components, Asilomar, 2017.

9. Andrew R. Crothers, Clayton Radker, and Adam Z. Weber, "Elucidating Multiscale, Multiphysics Coupled Transport Phenomena in Polymer-Electrolyte Membranes Structure-Transport Relationships of Perfluorinated-Sulfonic-Acid Membrane Interfaces," Coupled Problems, Rhodes, Greece, 2017.

10. Pablo A. García-Salaberri, Jeff T. Gostick, Gisuk Hwang, Marcos Vera, Iryna Zenyuk, and Adam Z. Weber, "Multiphysics, Multiphase and Multiscale Modeling of Polymer Electrolyte Fuel Cells: With a Focus on the Gas Diffusion Layers," Coupled Problems, Rhodes, Greece, 2017.

11. Andrew Shum, Liam Connolly, Kelsey B. Hatzell, Xianghui Xiao, Dilworth Y. Parkinson, Odne Burheim, Adam Z. Weber, and Iryna V. Zenyuk, "In-Situ Examination of Phase-Change-Induced Flow in Gas Diffusion Layers and Water Distribution in Microporous Layers using X-Ray Computed Tomography," MRS Fall Meeting, 2016.

12. Adam Z. Weber, "Understanding Transport in Polymer-Electrolyte-Fuel-Cell Ionomers," Mechanical Engineering Seminar, UC Merced, 2016.

13. Ahmet Kusoglu, "Ion-Conductive Polymer for Energy Conversion Devices," Mechanical Engineering Department Seminar, UC Berkeley, February 2017.

14. Ahmet Kusoglu, "Structural Characterization of Ionomers using X-rays," Advanced Light Source, Chemical Sciences Seminar Series, Berkeley Lab, Berkeley, CA, July 2016.

15. Ahmet Kusoglu, "New Insights into PFSA Ionomers," National Renewable Energy Lab, Golden, CO, 2017.

16. A. Kusoglu, S. Shi, and A. Weber, "Impact of Cation Form on Structure/Function Relationships of Perflurosulfonic Acid Ionomers," APS Meeting, New Orleans, LA, March 2017.

17. A. Kusoglu, S. Shi, and A. Weber, "Impact of Equivalent Weight and Side-Chain on Structure/Functionality of PFSA Ionomers," ECS Meeting, Hawaii, 2016.

18. Iryna V. Zenyuk, Adrien Lamibrac, Jens Eller, Felix N. Büchi, and Adam Z. Weber, "Understanding Evaporation in Fuel-Cell Gas-Diffusion Layers with X-ray Computed Tomography," Interpore, 2016.

19. Meron Tesfaye, Bryan D. McCloskey, and Adam. Z. Weber, "Gas Permeation Study in Thin and Ultra-thin Ionomer Films," ECS Fall Meeting, Hawaii, 2016.

20. A.R. Crothers, S. Shi, C.J. Radke, and A.Z. Weber, "Decoupling the influences of molecular- and mesoscales on macroscopic transport properties in perfluorosulfonic-acid membranes," Fall ECS Meeting, Hawaii, 2016.

21. I.A. Cordova, C. Wang, A.Z. Weber, R.A. Segalman, M.A. Brady, and G.M. Su, "Operando Resonant Soft X-Ray Scattering As a Spatio-Chemical Characterization Technique for Electrochemistry," Fall ECS Meeting, Hawaii, 2016.

22. Kelsey Hatzell, Ahmet Kusoglu, Pete Dudenas, Nancy Kariuki, Deborah Myers, and Adam Weber, "Indirect and direct observation of ionomer colloidal systems with applications to membrane electrode assemblies for energy conversion systems," Fall ECS Meeting, Hawaii, 2016.

23. Anna Freiberg, Tobias Schuler, Franz Spingler, Michael C. Tucker, and Adam Z. Weber, "Determination and Origin of Local Resistances in PEFC Catalyst Layers," ISE Annual Meeting, Hague, Netherlands, 2016.

24. Andrew Shum, Kelsey B. Hatzell, Liam Connely, Odne Burheim, Dilworth Y. Parkinson, Adam Z. Weber, and Iryna V. Zenyuk, "Understanding Phase-Change-Induced Flow in PEFCs Through *In-situ* X-ray Computed Tomography," ISE Annual Meeting, Hague, Netherlands, 2016.

25. A. Kusoglu, "Morphology of PFSA ionomers and thin films," 21st International Conference on Solid State Ionics, Padua, Italy, June 2017.

26. R.L. Borup (Invited), "Material Degradation in PEM Fuel Cell Electrodes," 231st ECS Meeting, May 2017.

27. R.L. Borup (Invited), "The FC-PAD Consortium: Advancing Fuel Cell Performance and Durability," 231st ECS Meeting, May 2017.

28. R.L. Borup (Invited), R. Mukundan, T. Rockward, M. Brady, J. Thomson, D. Papadias, et al., "(Metal) Bipolar Plate Testing," DOE Bipolar Plate Workshop, Detroit, February 2018.

29. R.L. Borup (Invited), Rangachary Mukundan, Andrew Baker, Dusan Spernjak, David Langlois, Sarah Stariha, Natalia Macauley, Karren More, Shyam Kocha, Adam Z. Weber, Debbie Myers and R. Ahluwalia, "Material Degradation in PEM Fuel Cell Electrodes," CARISMA, Newcastle upon Tyne, United Kingdom, April 2017.

30. R.L. Borup (Invited), Adam Z. Weber, Deborah Myers, Shyam Kocha, Rajesh Ahluwalia, Rangachary Mukundan, and Karren More, "The FC-PAD Consortium: Material Degradation in PEM Fuel Cell Electrodes," EMN Meeting on Fuel Cells 2017, Prague, Czech Republic, June 2017.

31. R.L. Borup (Invited), A.M. Baker, R. Mukundan, D. Spernjak, E.J. Judge, S.G. Advani, and A.K. Prasad, "Membrane Degradation in PEM Fuel Cells: Antioxidant Migration and Recoverable Degradation Losses," 21st International Conference on Solid State Ionics, Padua, Italy, June 2017.

32. D. Myers (Invited), "Structural Characterization of Polymer Electrolyte Fuel Cell Cathode Catalyst Layers," NCNR/LENS Workshop, National Institute of Science and Technology, September 29, 2016.

33. Firat Cetinbas, Rajesh Ahluwalia, Nancy Kariuki, Karren More, David Cullen, Brian Sneed, Robert Winarski, Jan Ilavsky, Vincent De Andrade, and Debbie Myers, "Structural

Characterization and Transport Modeling of Pt and Pt Alloy Polymer Electrolyte Fuel Cell Cathode Catalyst Layers," PRIME 2016, Electrochemical Society Meeting, October 5, 2016.

34. N.N. Kariuki, D.J. Myers, D. Fongalland, A. Martinez, and J. Sharman, "Microstructure Analysis of Polymer Electrolyte Membrane Fuel Cell Catalyst-Ionomer Inks and Cathode Catalyst Layers by Small Angle X-ray Scattering," 229th Electrochemical Society Meeting, San Diego, California, June 1, 2016.

35. R.L. Borup (Invited), "FC-PAD: PEM Fuel Cell Durability," Workshop on Recent Advances in PEMFC, CEA, Grenoble, France, September 2016.

36. K.C. Neyerlin, Jason W. Zack, Natalia Macauley, Rangachary Mukundan, Rod L. Borup, Karren L. More, and Shyam S. Kocha, "Investigation of the Performance of PtCo/C Cathode Catalyst Layers for ORR Activity and Rated Power for Automotive PEMFCs," In *Meeting Abstracts*, no. 38, pp. 2488–2488. The Electrochemical Society, 2016.

37. K.C. Neyerlin, Jason M. Christ, Jason W. Zack, Wenbin Gu, Swami Kumaraguru, Anusorn Kongkanand, and Shyam S. Kocha, "New Insights from Electrochemical Diagnostics Pertaining to the High Current Density Performance of Pt-Based Catalysts," In *Meeting Abstracts*, no. 38, pp. 2492–2492. The Electrochemical Society, 2016.

38. Shyam Kocha, "Investigation of the Performance of PtCo/C Cathode Catalyst Layers for ORR Activity and Rated Power for Automotive PEMFCs," In *PRiME 2016/230th ECS Meeting (October 2–7, 2016).* The Electrochemical Society, 2016.

39. K.C. Neyerlin (Invited Talk), "Low Pt Resistances," DOE Transport Modeling and Durability Working Group, Lawrence Berkeley National Lab, May 11–12, 2016.

40. K.C. Neyerlin (Invited Talk), "Examinations of Kinetic and Transport Losses in Low Pt Electrodes," DOE Catalysis Working Group, Argonne National Lab, July 27, 2016.

41. K.C. Neyerlin (Invited Talk), "Examinations of Kinetic and Transport Losses in Low Pt Electrodes," Gordon Research Conference on Fuel Cells, Stonehill College, Easton, MA, August 7–12, 2016.

42. Rod Borup, "On track for a clean, hydrogen-powered future," Santa Fe New Mexican, October 9, 2016.

43. Rod Borup, "Forget jetpacks. Where are our hydrogen-powered cars?" The Huffington Post, December 13, 2016.

44. R. Borup, Video: Science in 60–A Clean, Renewable Power Source, Los Alamos National Laboratory, Los Alamos, NM.

45. Natalia Macauley, Rod L. Borup, Rangachary Mukundan, Mahlon S. Wilson, Dusan Spernjak, K.C. Neyerlin, Shyam S. Kocha, and Stephen Grot, "Performance of Stratified Fuel Cell Catalyst Layer," Meeting Abstracts, pp. 2490–2490. The Electrochemical Society, 2016.

46. Dusan Spernjak (Invited), Rod L. Borup, Daniel S. Hussey, Piotr Zelenay, and Rangachary Mukundan, "Imaging Fuel Cell Components: From Flow Field Channels to Catalyst Layers," Meeting Abstracts, pp. 2493–2493. The Electrochemical Society, 2016.

47. D.A. Cullen (Invited), B.T. Sneed, and K.L. More, "Fuel Cell Electrode Optimization through Multi-Scale Analytical Microscopy," Microscopy & Microanalysis 2016, Columbus, OH, July 24–28, 2016.

48. D.A. Cullen, B.T. Sneed, and K.L. More, "Fuel Cell Electrode Optimization through Multi-Scale Analytical Microscopy," Gordon Research Conference, Easton, MA, August 7–12, 2016.

49. K.L. More (Invited), "Correlating Structure and Chemistry of PEM Fuel Cell Materials with Performance and Durability using Advanced Microscopy Methods," PRiME 2016, Honolulu, HI, October 3–7, 2016.

50. K.L. More (Invited), "Correlating Structure and Chemistry of PEM Fuel Cell Materials with Performance and Durability using Advanced Microscopy Methods," University of Illinois – Chicago, November 15, 2016.

51. B.T. Sneed, D.A. Cullen, K.S. Reeves, and K.L. More, "3D STEM Analysis of Ionomer Dispersion and Pore Structures within PEM Fuel Cell Catalyst Layers," MRS Fall Meeting, Boston, MA, November 28 – December 1, 2016.

52. B.T. Sneed, D.A. Cullen, K.S. Reeves, and K.L. More, "Structural and Chemical Study of the Stability of Pt-Based Fuel Cell Electrocatalysts in 3D via Electron Tomography," Pacific Rim Symposium on Surfaces, Coatings, and Interfaces (PAC-SURF), Kohala Coast, HI, December 12–15, 2016.

53. K.L. More (Invited), B.T. Sneed, and D.A. Cullen, "Understanding Fuel Cell Materials Degradation Through the Use of Advanced Microscopy Methods," 231st Meeting of the Electrochemical Society, New Orleans, LA, May 29 – June 2, 2017.

54. K.L. More (Invited), B.T. Sneed, and D.A. Cullen, "Critical Interfaces in PEM Fuel Cells: Understanding Behavior Through Advanced Microscopy Studies," 21st International Conference on Solid State Ionics, Padua, Italy, June 18–23, 2017.

55. Rangachary Mukundan, Dusan Spernjak, Daniel Hussey, David L. Jacobson, and Rod Borup, "Application of high resolution neutron imaging to polymer electrolyte fuel cells," Abstracts of Papers, 253rd ACS National Meeting & Exposition, San Francisco, CA, April 2–6, 2017.

56. R. Mukundan, D.A. Langlois, K.C. Neyerlin, S.S. Kocha, K.L. More, M. Odgaard, and R.L. Borup, "Durability of PtCo/C Cathode Catalyst Layers Subjected to Accelerated Stress Testing," 230th Meeting of the Electrochemical Society.

57. R.L. Borup, R. Mukundan, D. Spernjak, D.A. Langlois, N. Macauley, and Y.S. Kim, "Recoverable Degradation Losses in PEM Fuel Cells," 230th Meeting of the Electrochemical Society.

58. A.M. Baker, D. Spernjak, E.J. Judge, S.G. Advani, and A.K. Prasad, "Cerium Migration in PEM Fuel Cells," 230th Meeting of the Electrochemical Society.

59. D.S. Hussey, J.M. LaManna, D.L. Jacobson, S.W. Lee, J. Kim, B. Khaykovich, M.V. Gubarev, D. Spernjak, R. Mukundan, and R.L. Borup, "Neutron Imaging of the MEA Water Content of Pemfcs in Operando," 230th Meeting of the Electrochemical Society.

60. K.L. More, D.A. Cullen, B. Sneed, D.J. Myers, R.L. Borup, and R. Mukundan, "Correlating Structure and Chemistry of PEM Fuel Cell Materials with Durability and Performance Using Advanced

Microscopy Methods," 230th Meeting of the Electrochemical Society.

61. J.S. Spendelow, L. Castanheira, G. Hinds, T. Rockward, D.A. Langlois, R. Mukundan, and R.L. Borup, "Measurement of Local Electrode Potentials in an Operating PEMFC Exposed to Contaminants," 230th Meeting of the Electrochemical Society.

V.B.2 FC-PAD: Components and Characterization

Karren L. More (Primary Contact),[1]
David A. Cullen,[1] Brian T. Sneed,[1]
Deborah J. Myers,[2] Rajesh Ahluwalia,[2]
Nancy Kariuki,[2] Rangachary Mukundan,[3]
Rod Borup,[3] Shyam Kocha,[4] K.C. Neyerlin,[4]
Adam Weber,[5] and Ahmet Kusoglu[5]

[1] Oak Ridge National Laboratory (ORNL)
1 Bethel Valley Road
Oak Ridge, TN 37831
Phone: (865) 574-7788
Email: morekl1@ornl.gov

[2] Argonne National Laboratory (ANL), Argonne, IL

[3] Los Alamos National Laboratory (LANL), Los Alamos, NM

[4] National Renewable Energy Laboratory, Golden, CO

[5] Lawrence Berkeley National Laboratory (LBNL), Berkeley, CA

DOE Managers:

Dimitrios Papageorgopolous
Phone: (202) 586-5463
Email: Dimitrios.Papageorgopolous@ee.doe.gov

Greg Kleen
Phone: (720) 356-1672
Email: Gregory.Kleen@ee.doe.gov

Additional No-Cost Partners:

- Umicore – Sascha Toelle
- General Motors (GM) – Anu Konkanand
- EWii Fuel Cells – Madeleine Odgaard
- Ion Power – Steve Grot

Project Start Date: October 1, 2015
Project End Date: September 30, 2021

Overall Objectives

- Develop the knowledge base and optimize structures for more durable and high-performance polymer electrolyte membrane fuel cells (PEMFCs).
- Understand and elucidate specific structural and chemical factors and/or mechanisms that contribute to and control material constituent stability (e.g., electrocatalyst, catalyst support, ionomer, membrane) within electrode layers and membrane electrode assemblies (MEAs) during fuel cell operation.
- Define and measure specific degradation mechanisms through extensive characterization and diagnostics, such as electron microscopy, time-resolved on-line inductively coupled plasma mass spectrometry (ICP-MS), Synchrotron-based X-ray methods, etc.
- Coordinate characterization efforts and methods with materials development (e.g., new state-of-the-art [SOA] materials) and accelerated stress testing (AST) activities.
- Develop and/or optimize novel techniques towards PEMFC materials characterization.

Fiscal Year (FY) 2017 Objectives

- Evaluate and quantify transition metal (TM) dissolution (e.g., Co) from a series of SOA PtCo catalysts (supplied by IRD Fuel Cells (now EWii Fuel Cells), Umicore, and GM) during ASTs.
- Optimize and integrate multiple characterization methods to fully understand and correlate TM and Pt dissolution behavior to describe observations following ASTs; these methods include analytical scanning transmission electron microscopy (STEM) at ORNL, time-resolved on-line ICP-MS at ANL, thin film characterization at LBNL, Synchrotron X-ray techniques performed using the Advanced Photon Source at ANL (e.g., X-ray nano computed tomography, wide-angle X-ray scattering (WAXS), and small-angle X-ray scattering, microelectrode studies, electrical impedance spectroscopy, and other diagnostic tools at LANL.
- Initiate support for industrial and academic FC-PAD partners awarded new projects as part of Funding Opportunity Announcement 1412.

Technical Barriers

This project addresses the following technical barriers from the Fuel Cells section (3.4) of the Fuel Cell Technologies Office Multi-Year Research, Development, and Demonstration Plan.

(A) Durability

(B) Cost

(C) Performance

Technical Targets

This project develops MEAs that incorporate SOA Pt-alloy catalysts that meet the technical targets summarized in Table 1.

TABLE 1. Technical Targets for MEAs for Transportation Applications

Characteristic	Units	2020 Targets
Cost	$/kW$_{net}$	14
Durability with cycling	Hours	5,500
Start-up/shutdown durability	Cycles	5,000
Performance @ 0.8 V	mA/cm^2	300
Performance @ rated power (150 kPa$_{abs}$)	mW/cm^2	1,000

FY 2017 Accomplishments

- Introduced new catalyst durability AST (30,000 cycles; 5s square wave (0.6–0.95 V) cycles) that is 5X faster than old catalyst durability AST (30,000 cycles; 15s triangle wave (0.6–1.0 V) cycles), that reduces test time from 133 h (old triangle wave) to ~50 h (new square wave).
- Time-resolved on-line ICP-MS measurements were developed and used to perform real time measurements of Pt and Co dissolution from PtCo alloy catalysts under cyclic potentials and to resolve anodic vs. cathodic dissolution by applying staircase potential cycling. In general, Co dissolution occurred at all potentials whereas Pt dissolution occurred above 0.9 V.
- Several SOA PtCo catalysts were provided to FC-PAD for extensive characterization after incorporation into cathode catalyst layers (CCLs) in MEAs, and were evaluated before and after catalyst durability ASTs as well as after testing under Fuel Cell Tech Team (FCTT) wet-dry drive cycle protocols (wet-portion only). A combination of three-dimensional electron tomography, high-resolution STEM-based imaging and energy dispersive X-ray spectroscopy, and WAXS were used to study catalyst degradation (e.g., coarsening) and compositional changes due to TM dissolution.
- The amount of Co loss from CCL into membrane during ASTs was quantified for each of the catalysts studied (GM, Umicore, and EWii) using STEM-based energy dispersive X-ray spectroscopy; it was shown that 50% of the Co initially present in the catalyst nanoparticles in the CCL dissolved into the ionomer and migrated/diffused from the CCL into the membrane during ASTs.

✧ ✧ ✧ ✧ ✧

INTRODUCTION

The FC-PAD consortium was formed to advance performance and durability of PEMFCs at a pre-competitive level to meet DOE targets and further enable their commercialization. This will be accomplished by developing a comprehensive knowledge base regarding materials durability and by using this knowledge to optimize structures for more durable and high-performance PEMFC components, while simultaneously reducing cost.

As part of the component and characterization effort, which coordinates activities across most of FC-PAD's thrust areas, we will actively study SOA materials provided by the fuel cell community, including novel electrocatalysts, catalyst supports, ionomers, and membranes. Materials will be fabricated into MEAs and examined/studied at the beginning-of-life (BoL) and after exposure to specific ASTs (end-of-life [EoL]) using a comprehensive suite of characterization and diagnostic tools, which are located at the different FC-PAD partner national laboratories (ANL, ORNL, LANL, National Renewable Energy Laboratory, LBNL). The staff expertise and unique capabilities available at the five national laboratories will also be incorporated in the research of the four new funding opportunity announcement projects with Vanderbilt University, GM, 3M, and United Technologies Research Center in the future.

APPROACH

The FC-PAD consortium is comprised of five national laboratories, with investigators at each lab having proven expertise in specific research areas developed during the course of prior DOE fuel cell projects related to durability, transport, and performance. The FC-PAD consortium combines expertise and cutting-edge capabilities into a single, highly coordinated effort that is broken down into six thrust areas (see the annual progress report for project FC135 [1] for additional details regarding FC-PAD organization). This report (summary for project FC136) highlights work that was coordinated primarily across five thrust areas: Thrust 1: Electrocatalysts and Supports; Thrust 2: Electrode Layers; Thrust 3: Ionomers; Thrust 4: Operando Evaluation; and Thrust 6: Component Characterization. The thrust areas and activities within FC-PAD are highly integrated and comprise three reports (FC135 [1], FC136, FC137 [2]), each of which incorporates many thrust areas, albeit with a different material/component focus.

This report focuses on the evaluation of several SOA PtCo electrocatalysts incorporated into the CCL of MEAs, which were studied at BoL and EoL to elucidate the mechanisms of Co and Pt dissolution and subsequent effect on performance loss. Multiple characterization tools (involving most of the thrust areas and unique tools available at the national laboratories) were used to interrogate the stability of several highly active PtCo alloy catalysts, and to understand the degradation issues specific to morphology and chemistry of these alloy catalysts. New tools were optimized (e.g., time-resolved on-line ICP-MS and micro-electrodes) and successfully used by FC-PAD researchers, and will be available for use by the new FC-PAD funding opportunity announcement partners.

RESULTS

A major focus of FC-PAD is understanding CCL degradation, most notable CCLs incorporating Pt-alloy catalysts, and the impact of the catalyst composition, physicochemical properties, and cell operating conditions on catalyst degradation. ANL developed a system for studying the real-time dissolution rates of TM alloying elements and Pt under cyclic potentials using ICP-MS coupled with a thin-layer, flow electrochemical cell. For the initial studies reported here, two types of PtCo catalysts, TKK (TEC36-E52 Pt_3Co) and Umicore (Elyst Pt30 0670 Pt_3Co), were deposited as a catalyst + ionomer thin film on a glassy carbon electrode. The time delay between generation of the dissolved species in the film and detection at the ICP-MS was calibrated using Au nanoparticles. Initial results were demonstrated using triangle-wave stair-case potential cycling between 0.4–1.0 V (black dashed line in Figure 1a) using the TKK catalyst. The plot in Figure 1a clearly shows the correlation between potential and dissolution, indicating that Co dissolution occurred at all potentials (blue line) and that there were distinct peaks for anodic and cathodic dissolution of Pt (red line) at potentials greater than 0.9 V.

It was determined from the initial triangle-wave experiment (Figure 1a) that improved resolution of anodic and cathodic dissolution could be achieved using square-wave potential cycling (Figure 1b); this protocol also more closely matched the new square-wave catalyst durability AST. Pt will dissolve via several anodic reactions below 0.9 V (e.g., $Pt = Pt^{2+} + 2e^-$), which is evidenced in the stepping

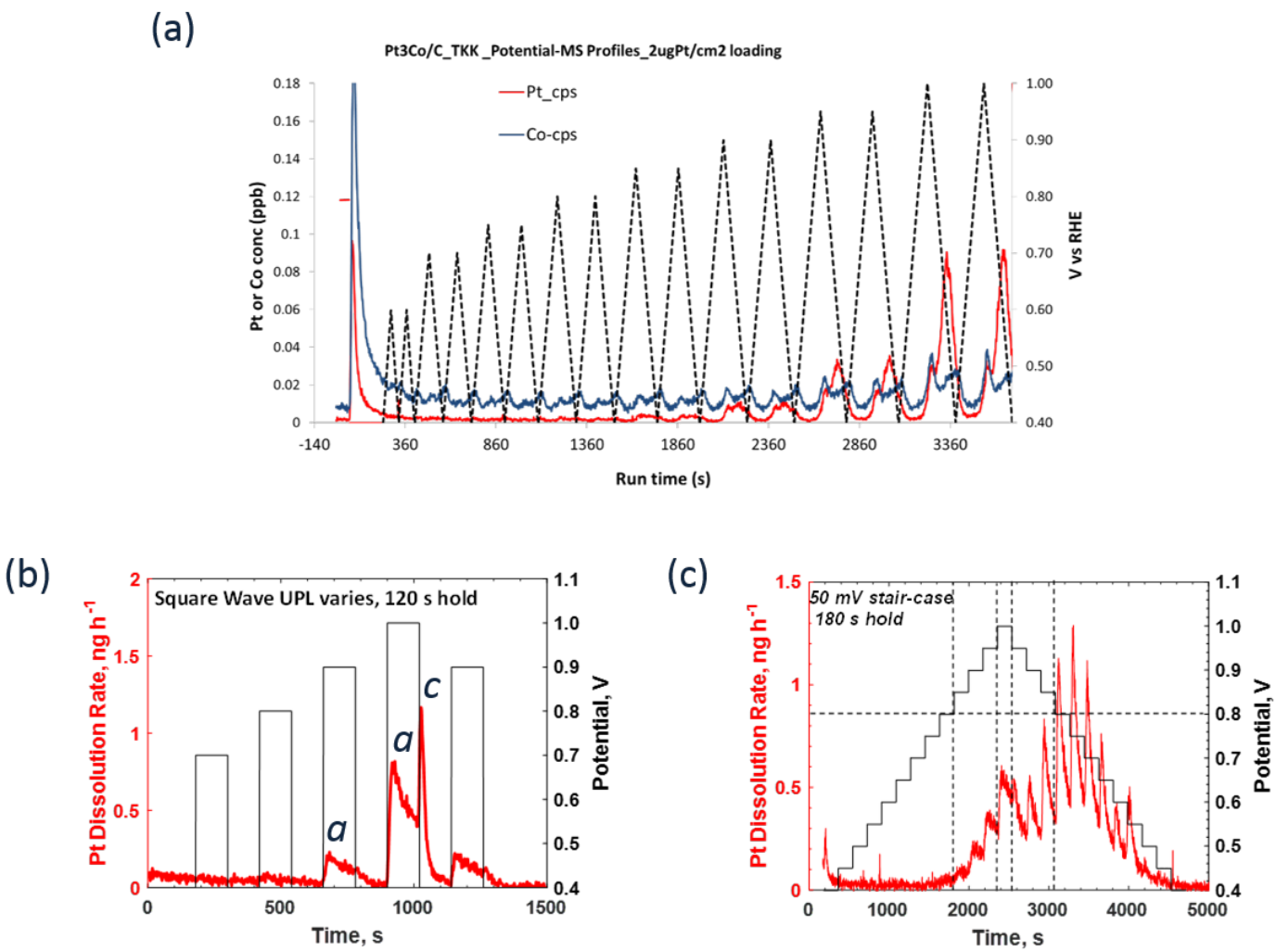

RHE – reference hydrogen electrode

FIGURE 1. (a) Initial triangle-wave stair-case potential cycling between 0.4–1.0 V (dashed line) for TKK Pt_3Co catalyst indicates that Co dissolution occurred at all potentials (blue line) and distinct anodic and cathodic dissolution of Pt at potentials greater than 0.9 V (red line). (b) Square-wave stair-case potential cycling between 0.4–1.0 V shows anodic Pt dissolution below 0.9 V (labeled a) and cathodic Pt dissolution above 0.9 V (labeled c). (c) 50 mV stair-case potential cycles with a UPL of 1.0 V shows that the Pt dissolution rate during cathodic steps is ~3X higher than during anodic steps.

up of the potential from 0.4 V to 0.9 V, labeled *a* in Figure 1b. Higher oxides of Pt will dissolve by multiple cathodic reactions above 0.9 V, as evidenced by the appearance of a large dissolution peak when the potential is stepped down, labeled *c* in Figure 1b. Thus, during square-wave stair-case potential cycling, the anodic peaks increase in magnitude as the potential is stepped up and the cathodic peak is highest during step down from 0.9 V to 0.85 V. For 50 mV stair-case potential cycles with an upper potential limit (UPL) of 1.0 V (Figure 1c), the Pt dissolution rate during cathodic steps is ~3X higher than during anodic steps, indicating the formation and dissolution of Pt oxides. The anodic peaks are higher at higher potentials and both anodic and cathodic Pt dissolution rates increase at higher potential steps.

Unlike observations for Pt, Co is unstable and dissolves at all potentials above 0.4 V (Figure 1a). As shown in Figure 2a, a break-in protocol of ~1 h conditioning using a 0.4–1.0 V square-wave cycling is required to reach a constant Co dissolution rate. Figure 2b is higher resolution of the square-wave stair-case potential cycling showing that the Co dissolution rate is nearly constant for potentials stepping up to 0.8 V, with prominent anodic peaks above 0.8 V (labeled *a* in Figure 2b) and the highest cathodic peak at the potential step down from 0.8 V to 0.6 V (labeled *c* in Figure 2b). The Co dissolution rate slows during potential holds, suggesting that Co may form oxides. The cathodic dissolution peaks suggest possible coordination of formed Co-oxides with Pt-oxides. Unlike Pt dissolution, the Co dissolution rates during anodic and cathodic steps are comparable.

While multiple PtCo catalysts have been evaluated by the FC-PAD team, this report will focus on the GM SOA PtCo catalyst incorporated into the CCL of an MEA (catalyst loading 0.1 mg_{Pt}/cm^2 and electrochemically active surface area [ECSA] of 43 m^2_{Pt}/g_{Pt}; MEA prepared with a DuPont XL-100 membrane and Pt supported on high surface area carbon [HSAC] anode), which had a BoL PtCo average particle size of 4.5 nm and a Pt:Co composition of 85:15 in the bulk CCL. This MEA was subjected to several AST protocols to evaluate alloy catalyst durability; the old triangle-wave (30,000 [0.6–1.0 V] cycles) AST, the new square-wave (30,000 [0.6–0.95 V] cycles) AST, and the wet-portion of the FCTT drive cycle protocol for 1,200 h (the most aggressive test). Results for the final alloy particle size distributions (PSD) determined by STEM imaging in the CCL after each test are compared to the BoL PSD in Figure 3a, where the resulting particle sizes are labeled according to the specific test (5.0 nm for triangle-wave AST, 5.1 nm for square-wave AST, and 7.4 nm for 1,200 h wet-drive cycle test). More significant is the accompanying change in the individual catalyst nanoparticle compositions shown in Figure 3b as determined from STEM-based energy dispersive X-ray spectroscopy, which exhibit a very distinct particle size vs. composition profile that degrades with the different tests. It is noted that the smaller particles are consistently Pt-rich, whereas the larger particles are Co-rich for the BoL condition, with the average composition in the CCL of 1,000s of particles of 85Pt:15Co. This trend is exacerbated after the various testing protocols (EoL), with the smallest nanoparticles losing nearly all their Co through dissolution, with several of the larger particles showing very high Co levels (note results for most aggressive test, FCTT wet-drive cycle test). This size vs. composition relationship should not be ignored for SOA alloy catalysts; it was observed for all the PtCo catalysts analyzed by FC-PAD to date, and is especially prominent for catalysts exhibiting a wide PSD. After both the square-wave and triangle wave catalyst durability ASTs, the bulk CCL composition changed from 85Pt:15Co at BoL to 90Pt:10Co at EoL, representing a significant loss of Co out of the catalyst nanoparticles into the XL-100 membrane. More

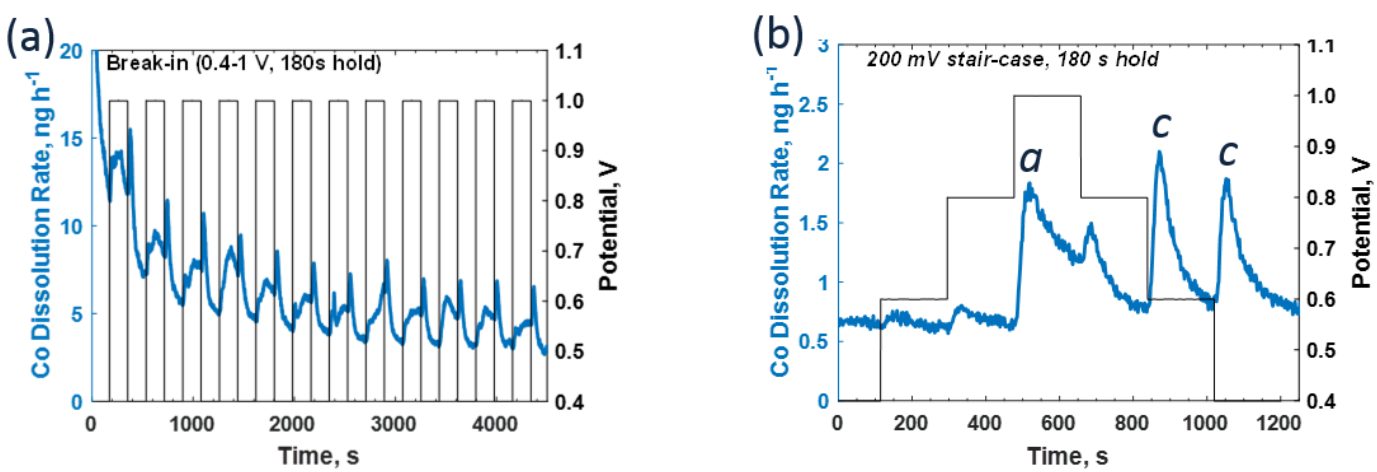

FIGURE 2. (a) Break-in protocol of ~1 h conditioning using a 0.4–1.0 V square-wave cycling is required to reach a constant Co dissolution rate. (b) High resolution square-wave stair-case potential cycling between 0.4–1.0 V shows Co dissolution rate is constant for potential stepping up to 0.8 V with anodic peaks above 0.8 V (labeled a) and the highest cathodic peak (labeled c) at the potential step down from 0.8 V to 0.6 V.

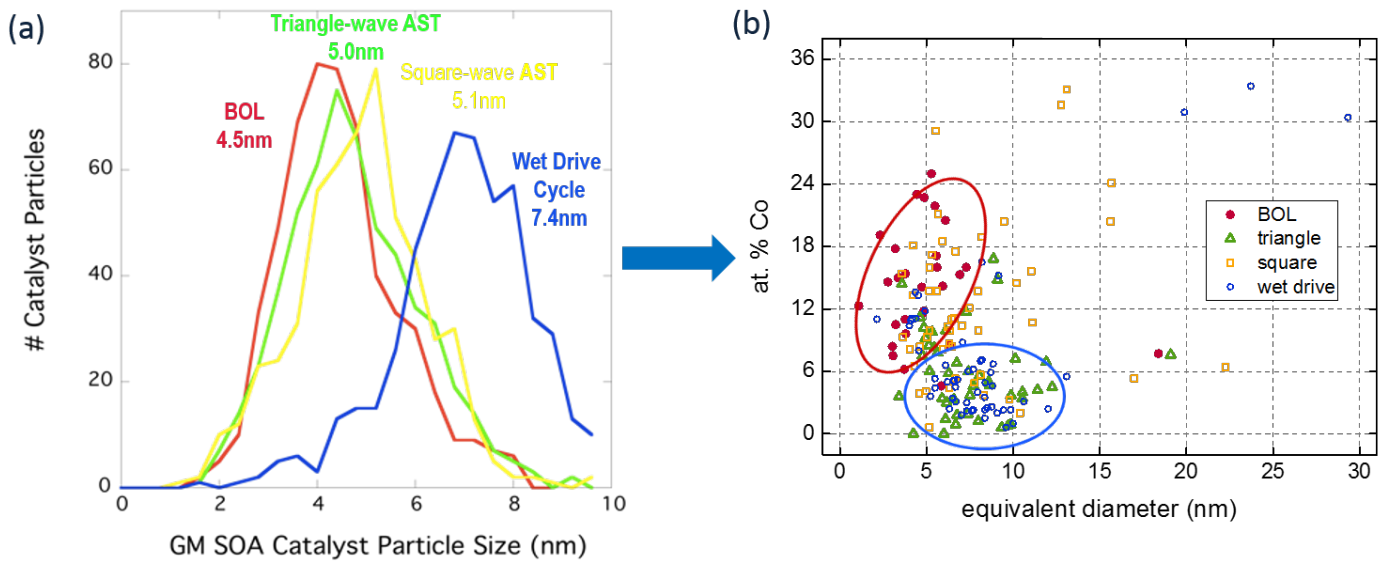

FIGURE 3. (a) GM PtCo catalyst PSDs comparing BoL (red) and EoL conditions (triangle-wave AST, green; square-wave AST, yellow; wet-drive cycle, blue). (b) Particle size vs. composition scatter plot for GM PtCo catalysts in BoL (red) and EoL conditions (triangle-wave AST, green; square-wave AST, yellow; wet-drive cycle, blue).

significantly, after the FCTT wet-drive cycle test for 1,200 h, the composition of the CCL further degraded to 95Pt:5Co, representing a Co loss of greater than 50% out of the CCL and into the XL-100 membrane.

WAXS data collected from the GM CCL at BoL and the three EoL conditions are summarized in Figure 4a. The PSDs determined by small-angle X-ray scattering are consistent with the STEM–based measurements of PSDs for the GM catalyst. The WAXS data is certainly more informative than simple PSDs since these data provide the average change in the (111) *d*-spacing as a function of testing protocol. Interestingly, as the GM PtCo catalyst is subjected to more aggressive testing (compare GM BoL to GM square-wave EoL and GM wet-drive EoL), the (111) *d*-spacing values become larger indicating that as more Co is lost (dissolves/leaches) out of the catalyst nanoparticles, the PtCo electrocatalysts become more "Pt-like."

Figure 4b shows polarization curves comparing all the PtCo catalysts evaluated by FC-PAD to date (SOA GM, Umicore, EWii catalysts) with Pt-only (ECSA vs. number of potential cycles); each of these PtCo catalysts are supported on HSAC and exhibit differences in initial particle size, morphology, and composition. While the initial characteristics of the various PtCo catalysts are different, it is interesting to note that after square-wave catalyst durability AST, the EoL ECSAs converge to the same value after 30,000 0.6–0.95 V cycles, matching the EoL ECSA of Pt-only catalysts.

CONCLUSIONS AND UPCOMING ACTIVITIES

Work conducted during the previous year has been highly focused on understanding the durability and performance of Pt-alloy catalysts. The FC-PAD team evaluated a series of SOA PtCo catalysts from various sources (GM, Umicore, EWii) in terms of size, composition, and morphology using microscopy, ICP-MS, and X-ray scattering methods, in the BoL and EoL (following several different ASTs) conditions. The Co leaching during AST was quantified, and it was determined that regardless of the starting structure and composition, all the alloy catalysts behaved similarly in terms of compositionally stability, e.g., all catalysts lost greater than 50% of the Co, which resulted in the electrocatalysts becoming more Pt-like and Co migration into the membrane.

Future work will continue to focus on alloy catalyst durability, with a specific emphasis on assessing catalysts with different morphologies and compositions (for example, core-shell catalysts and ordered structures). The FC-PAD team will continue to develop, optimize, and apply unique methods towards understanding alloy cathode catalyst durability and performance. The work will be highly focused on fundamental dissolution studies of selected alloy catalysts; for example, particle size and morphological effects. These data, in combination with microscopy and X-ray scattering, will provide input for catalyst (and catalyst layer) degradation models. In addition, the FC-PAD team will improve methods to interrogate ionomer thin films (layers) within the electrodes to further our understanding of dissolution effects on ionomer transport properties, which will be coordinated

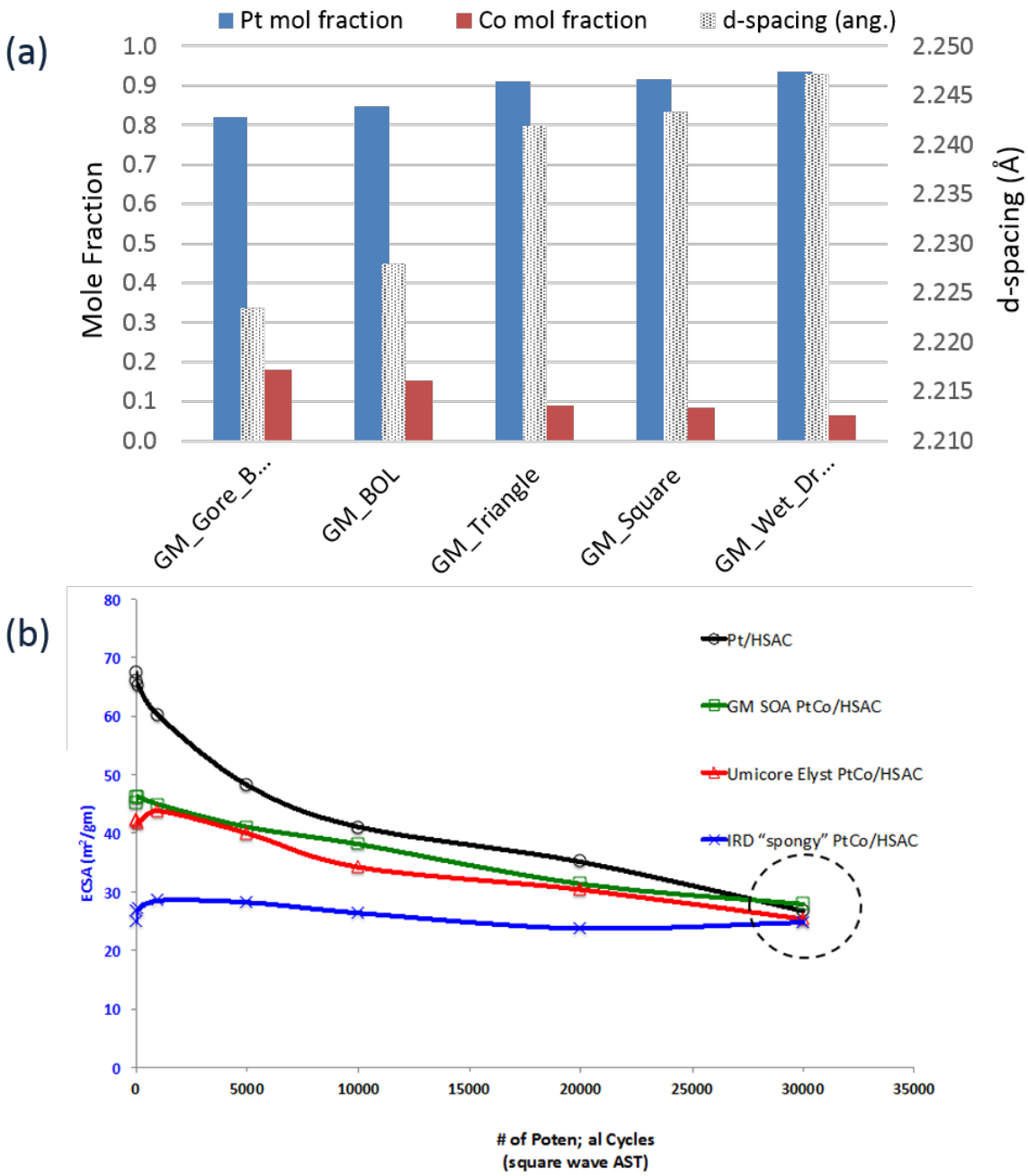

FIGURE 4. (a) WAXS data comparing PtCo catalysts for BoL and EoL conditions showing that PtCo catalysts become more Pt-like with more aggressive testing. (b) Polarization curves comparing all PtCo catalysts evaluated by FC-PAD team showing that regardless of initial nanoparticle size, morphology, and ECSA, after square-wave AST (30,000 [0.6–0.95 V] cycles) the EoL ECSAs converge to values consistent with Pt-only catalyst.

with model studies of ionomer thin films. These fundamental studies will be coupled with refinement of ASTs to study specific materials components within catalyst layers, most notably related to catalyst and ionomer stability towards improving performance and durability.

SPECIAL RECOGNITIONS & AWARDS/ PATENTS ISSUED

1. Ahmet Kusoglu received the Supramaniam Srinivasan Early Career Award from the Energy Technology Division of the Electrochemical Society.

2. Ahmet Kusoglu received a Toyota Young Investigator Award from Electrochemical Society (ECS).

3. Andrew Baker received the Bill Baron Fellowship in recognition of his contributions related to the renewable energy field from the University of Delaware.

4. Rangachary (Mukund) Mukundan was named a 2017 Fellow of the Electrochemical Society.

5. Karren More was named ORNL's "Mentor of Early Career Researchers," November 2016.

REFERENCES

1. R. Borup, A. Baker, A. Kusoglu, Rangachary Mukundan, J. Dumont, D. Langlois, A. Weber, R. Ahluwalia, D. Myers, S. Kocha, K. More. *FC-PAD: Fuel Cell Performance and Durability Consortium*. U.S. DOE Annual Progress Report 2017.

2. A. Weber, A. Kusoglu, T. Schuler, S.Berlinger, L. Pant, A. Freiberg, M. Tesfaye, R. Mukundan, S. Babu, N. Macauley, J. Spendelow, M. Wilson, R. Borup, K. More, B. Sneed, S. Kocha, K.C. Neyerlin, D. Myers, F. Cetinbas, R. Ahluwalia. *FC-PAD: Electrode Layers and Optimization*. U.S. DOE Annual Progress Report 2017.

FY 2017 PUBLICATIONS/PRESENTATIONS

The list below includes all publications and presentations relevant to FC-PAD from consortium members representing the three FC-PAD annual merit presentations and reports: FC135 (V.B.1), FC136 (V.B.2), and FC137 (V.B.3).

Publications Relevant to FC-PAD from Consortium Members

1. I.V. Zenyuk, P.K. Das, and A.Z. Weber, "Understanding Impacts of Catalyst-Layer Thickness on Fuel-Cell Performance via Mathematical Modeling," *Journal of the Electrochemical Society* **163**[7] F691–F703 (2016).

2. A. Kusoglu, T.J. Dursch, and A.Z. Weber, "Nanostructure/Swelling Relationships of Bulk and Thin-Film PFSA Ionomers," *Advanced Functional Materials* **26** 4961–4975 (2016).

3. S. Shi, A.Z. Weber, and A. Kusoglu, "Structure/property Relationship of Nafion XL Composite Membranes," *Journal of Membrane Science* **516** 123-134 (2016).

4. I. Zenyuk, D.Y. Parkinson, L.G. Connolly, and A.Z. Weber, "Gas-Diffusion-Layer Structural Properties under Compression via X-Ray Tomography," *Journal of Power Sources* **328** 364–376 (2016).

5. S. Shi, A.Z. Weber, and A. Kusoglu, "Structure-Transport Relationship of Perfluorosulfonic-Acid Membranes in Different Cationic Forms," *Electrochimica Acta* **220** 517–528 (2016).

6. I. Zenyuk, A. Lamibrac, J. Eller, D. Parkinson, F. Marone, F. Büchi, and A.Z. Weber, "Investigating Evaporation in Gas Diffusion Layers for Fuel Cells with X-ray Computed Tomography," *Journal of Physical Chemistry C* **120**[50] 28701–28711 (2016).

7. N. Macauley, R. Mukundan, D.A. Langlois, K.C. Neyerlin, S.S. Kocha, K.L. More, M. Odgaard, and R.L. Borup, "Durability of PtCo/C Cathode Catalyst Layers Subjected to Accelerated Stress Testing," ECS Transactions **75**[14] 281–287 (2016).

8. A.M. Baker, R. Mukundan, D. Spernjak, S.G. Advani, A.K. Prasad, and R.L. Borup, "Cerium Migration in Polymer Electrolyte Membranes," ECS Transactions **75**[14] 707–714 (2016).

9. K. Shinozaki, Y. Morimoto, B.S. Pivovar, and S.S. Kocha, "Suppression of Oxygen Reduction Reaction Activity on Pt-based Electrocatalysts from Ionomer Incorporation," *Journal of Power Sources* **325** 745–751 (2016).

10. K. Shinozaki, Y. Morimoto, B.S. Pivovar, and S.S. Kocha, "Re-examination of the Pt Particle Size Effect on the Oxygen Reduction Reaction for Ultrathin Uniform Pt/C Catalyst Layers without Influence from Nafion," *Electrochimica Acta* **213** 783–790 (2016).

11. N. Macauley, R.W. Lujan, D. Spernjak, D.S. Hussey, D.L. Jacobson, K.L. More, R.L. Borup, and R.Mukundan, "Durability of Polymer Electrolyte Membrane Fuel Cells Operated at Subfreezing Temperatures," *Journal of The Electrochemical Society* **163**[13] F1317–F1329 (2016).

12. A.M. Baker, R. Mukundan, D. Spernjak, E.J. Judge, S.G. Advani, A.K. Prasad, and R.L. Borup, "Cerium Migration during PEM Fuel Cell Accelerated Stress Testing," *Journal of The Electrochemical Society* **163**[9] F1023–F1031(2016).

13. C.F. Cetinbas, R.K. Ahluwalia, N. Kariuki, V. De Andrade, D. Fongalland, L. Smith, J. Sharman, P. Ferreira, S. Rasouli, and D.J. Myers, "Hybrid Approach Combining Multiple Characterization Techniques and Simulations for Microstructural Analysis of Proton Exchange Membrane Fuel Cell Electrodes," *Journal of Power Sources* **344** 62–73 (2017).

14. A. Kusoglu and Adam Z. Weber, "New Insights into Perfluorinated Sulfonic-Acid (PFSA) Ionomers," *Chemical Reviews* **117**[3] 987–1104 (2017).

15. S. Shukla, S. Bhattacharjee, A.Z. Weber, and M. Secanell, "Experimental and Theoretical Analysis of Ink Dispersion Stability for Polymer Electrolyte Fuel Cell Applications," *Journal of the Electrochemical Society* **164**[6] F600–F609 (2017).

16. L.M. Pant and A.Z. Weber, "Modeling Transport in PEFC Cathode Agglomerates with Double Trap Kinetics," *Journal of the Electrochemical Society* **164**[11] E3081–E3091 (2017).

17. F.B. Spingler, A. Phillips, T. Schuler, M.C. Tucker, and A.Z. Weber, "Investigating Fuel-Cell Transport Limitations using Hydrogen Limiting Current," *International Journal of Hydrogen Energy* **42**[19] 13960–13969 (2017).

18. A.T.S. Freiberg, M.C. Tucker, and A.Z. Weber, "Polarization Loss Correction Derived from Hydrogen Local-Resistance Measurement in Low Pt-Loaded Polymer-Electrolyte Fuel Cells," *Electrochemistry Communications* **79** 14-17 (2017).

19. B.T. Sneed, D.A. Cullen, K.S. Reeves, O.E. Dyck, D.A. Langlois, R. Mukundan, R.L. Borup, and K.L. More "3D Analysis of Fuel Cell Electrocatalyst Degradation on Alternate Carbon Supports," accepted for publication in *ACS Applied Materials & Interfaces*.

Presentations Relevant to FC-PAD from Consortium Members

1. A. Kusoglu, "State of Understanding of PFSA Ionomers and Thin Films," Gordon Research Conference (GRC) Fuel Cells, Easton, MA (2016).

2. A. Kusoglu, "New Insights into PFSA Ionomers: From Membranes to Thin Films," 3M Company, Minneapolis, MN (2017).

3. A.Z. Weber (Keynote), "Multiscale Modeling of Polymer-Electrolyte-Fuel-Cell Components," Meeting Abstracts, MA2016-01 (2016) 2211.

4. A. Shum, K.B. Hatzell, L.G. Connolly, O.S. Burheim, D.Y. Parkinson, A.Z. Weber, and I.V. Zenyuk, "Exploring Phase-Change-Induced Flow in Fuel Cells through X-Ray Computed Tomography," PRiME 2016 - 230th ECS Meeting, Honolulu, HI (2016).

5. T. Schuler, M.C. Tucker, and A.Z. Weber, "Gas-Transport Resistances in Fuel-Cell Catalyst Layers," PRiME 2016 - 230th ECS Meeting, Honolulu, HI (2016).

6. A.Z Weber, L. Pant, T. Schuler, H. Shiau, A. Freiberg, M.C. Tucker, A. Chowdhury, K.C. Neyerlin, S. Kocha, and I. Zenyuk, "Elucidating and Understanding Transport Phenomena in Polymer-Electrolyte Fuel Cells," CARISMA, Newcastle upon Tyne, UK (2017).

7. A.Z. Weber (Invited), T. Schuler, F. Spingler, A. Freiberg, M.C. Tucker, A. Chowdhury, K.C. Neyerlin, and A. Kusoglu, "Ionomer-Associated Transport Resistances in Fuel Cell Electrodes," 21st International Conference on Solid State Ionics, Padua, Italy (2017).

8. A.R. Crothers, S. Shi, P. Dudenas, A. Kusoglu, and A.Z. Weber, "Structure-Transport Relationships of Perfluorinated-Sulfonic-Acid Membrane Interfaces," Polymer-Electrolyte Fuel Cell Components, Asilomar, CA (2017).

9. A.R. Crothers, C. Radker, and A.Z. Weber, "Elucidating Multiscale, Multiphysics Coupled Transport Phenomena in Polymer-Electrolyte Membranes Structure-Transport Relationships of Perfluorinated-Sulfonic-Acid Membrane Interfaces," Coupled Problems, Rhodes, Greece (2017).

10. P.A. García-Salaberri, J.T. Gostick, G.Hwang, M. Vera, I. Zenyuk, and A.Z. Weber, "Multiphysics, Multiphase and Multiscale Modeling of Polymer Electrolyte Fuel Cells: With a Focus on the Gas Diffusion Layers," Coupled Problems, Rhodes, Greece (2017).

11. A. Shum, L. Connolly, K.B. Hatzell, X. Xiao, D.Y. Parkinson, O. Burheim, A.Z. Weber, and I.V. Zenyuk, "In-Situ Examination of Phase-Change-Induced Flow in Gas Diffusion Layers and Water Distribution in Microporous Layers using X-Ray Computed Tomography," MRS Fall Meeting, Boston, MA (2016).

12. A.Z. Weber (Invited), "Understanding Transport in Polymer-Electrolyte-Fuel-Cell Ionomers," Mechanical Engineering Seminar, UC Merced, CA (2016).

13. A. Kusoglu (Invited), "Ion-Conductive Polymer for Energy Conversion Devices," Mechanical Engineering Department Seminar, UC Berkeley, CA (2017).

14. A. Kusoglu, "Structural Characterization of Ionomers using X-rays," Advanced Light Source, Chemical Sciences Seminar Series, LBNL, Berkeley, CA (2016).

15. A. Kusoglu, "New Insights into PFSA Ionomers," National Renewable Energy Laboratory, Golden, CO (2017).

16. A. Kusoglu, S. Shi, and A.Z. Weber, "Impact of Cation Form on Structure/Function Relationships of Perflurosulfonic Acid Ionomers," APS Meeting, New Orleans, LA (2017).

17. A. Kusoglu, S. Shi, and A.Z. Weber, "Impact of Equivalent Weight and Side-Chain on Structure/Functionality of PFSA Ionomers," PRiME 2016 – 230th ECS Meeting, Honolulu, HI (2016).

18. I.V. Zenyuk, A. Lamibrac, J. Eller, F.N. Büchi, and A.Z. Weber, "Understanding Evaporation in Fuel-Cell Gas-Diffusion Layers with X-ray Computed Tomography," 8th International Conference on Porous Media, Cincinatti, OH (2016).

19. M. Tesfaye, B.D. McCloskey, and A.Z. Weber, "Gas Permeation Study in Thin and Ultra-thin Ionomer Films," PRiME 2016 – 230th ECS Fall Meeting, Honolulu, HI (2016).

20. A.R. Crothers, S. Shi, C.J. Radke, and A.Z. Weber, "Decoupling the Influences of Molecular- and Mesoscales on Macroscopic Transport Properties in Perfluorosulfonic-acid Membranes," PRiME 2016 – 230th ECS Meeting, Honolulu, HI (2016).

21. I.A. Cordova, C. Wang, A.Z. Weber, R.A. Segalman, M.A. Brady, and G.M. Su, "Operando Resonant Soft X-Ray Scattering As a Spatio-Chemical Characterization Technique for Electrochemistry," PRiME 2016 – 230th ECS Meeting, Honolulu, HI (2016).

22. K. Hatzell, A. Kusoglu, P. Dudenas, N. Kariuki, D. Myers, and A. Weber, "Indirect and Direct Observation of Ionomer Colloidal Systems with Applications to Membrane Electrode Assemblies for Energy Conversion Systems," PRiME 2016 – 230th ECS Meeting, Honolulu, HI (2016).

23. A. Freiberg, T. Schuler, F. Spingler, M.C. Tucker, and A.Z. Weber, "Determination and Origin of Local Resistances in PEFC Catalyst Layers," ISE Annual Meeting, Hague, The Netherlands (2016).

24. A. Shum, K.B. Hatzell, L. Connely, O. Burheim, D.Y. Parkinson, A.Z. Weber, and I.V. Zenyuk, "Understanding Phase-Change-Induced Flow in PEFCs Through In-situ X-ray Computed Tomography," ISE Annual Meeting, Hague, The Netherlands (2016).

25. A. Kusoglu, "Morphology of PFSA Ionomers and Thin Films," 21st International Conference on Solid State Ionics, Padua, Italy (2017).

26. R.L. Borup (Invited), "Material Degradation in PEM Fuel Cell Electrodes," 231st ECS Meeting, New Orleans, LA (2017).

27. R.L. Borup (Invited), "The FC-PAD Consortium: Advancing Fuel Cell Performance and Durability," 231st ECS Meeting, New Orleans, LA (2017).

28. R.L. Borup (Invited), R. Mukundan, A. Baker, D. Spernjak, D. Langlois, S. Stariha, N. Macauley, K. More, S. Kocha, A.Z. Weber, D. Myers, and R. Ahluwalia, "Material Degradation in PEM Fuel Cell Electrodes," CARISMA, Newcastle upon Tyne, United Kingdom (2017).

29. R.L. Borup (Invited), A.Z. Weber, D. Myers, S. Kocha, R. Ahluwalia, R. Mukundan, and K. More, "The FC-PAD Consortium: Material Degradation in PEM Fuel Cell Electrodes," EMN Meeting on Fuel Cells 2017, Prague, Czech Republic (2017).

30. R.L. Borup (Invited), A.M. Baker, R. Mukundan, D. Spernjak, E.J. Judge, S.G. Advani, and A.K. Prasad, "Membrane Degradation in PEM Fuel Cells: Antioxidant Migration and Recoverable Degradation Losses," 21st International Conference on Solid State Ionics, Padua, Italy (2017).

31. D. Myers (Invited), "Structural Characterization of Polymer Electrolyte Fuel Cell Cathode Catalyst Layers," NCNR/LENS Workshop, National Institute of Science and Technology (2016).

32. F. Cetinbas, R. Ahluwalia, N. Kariuki, K. More, D. Cullen, B. Sneed, R. Winarski, J. Ilavsky, V. De Andrade, and D. Myers, "Structural Characterization and Transport Modeling of Pt and Pt Alloy Polymer Electrolyte Fuel Cell Cathode Catalyst Layers," PRiME 2016 – 230th ECS Meeting, Honolulu, HI (2016).

33. R.L. Borup (Invited), "FC-PAD: PEM Fuel Cell Durability," Workshop on Recent Advances in PEMFCs, CEA, Grenoble, France (2016).

34. S.S. Kocha, "Investigation of the Performance of PtCo/C Cathode Catalyst Layers for ORR Activity and Rated Power for Automotive PEMFCs," PRIME 2016 – 230th ECS Meeting Honolulu, HI (2016).

35. K.C. Neyerlin (Invited), "Low Pt Resistances," DOE Transport Modeling and Durability Working Group, Lawrence Berkeley National Laboratory, Berkeley, CA (2016).

36. K.C. Neyerlin (Invited), "Examinations of Kinetic and Transport Losses in Low Pt Electrodes," DOE Catalysis Working Group, Argonne National Laboratory, Argonne, IL (2016).

37. K.C. Neyerlin (Invited), "Examinations of Kinetic and Transport Losses in Low Pt Electrodes," GRC on Fuel Cells, Easton, MA (2016).

38. R. Borup, "On Track for a Clean, Hydrogen-powered Future," Santa Fe, NM (2016).

39. R. Borup, "Forget Jetpacks. Where are our Hydrogen-powered Cars?" The Huffington Post (2016).

40. R. Borup, Video: Science in 60–A Clean, Renewable Power Source, LANL, Los Alamos, NM (2016).

41. N. Macauley, R.L. Borup, R. Mukundan, M.S. Wilson, D. Spernjak, K.C. Neyerlin, S.S. Kocha, and S. Grot, "Performance of Stratified Fuel Cell Catalyst Layers," 231st ECS Meeting, New Orleans, LA (2017).

42. D. Spernjak (Invited), R.L Borup, D.S. Hussey, P. Zelenay, and R. Mukundan, "Imaging Fuel Cell Components: From Flow Field Channels to Catalyst Layers," 231st ECS Meeting, New Orleans, LA (2017).

43. D.A. Cullen (Invited), B.T. Sneed, and K.L. More, "Fuel Cell Electrode Optimization through Multi-Scale Analytical Microscopy," Microscopy & Microanalysis 2016, Columbus, OH (2016).

44. D.A. Cullen, B.T. Sneed, and K.L. More, "Fuel Cell Electrode Optimization through Multi-Scale Analytical Microscopy," GRC on Fuel Cells, Easton, MA (2016).

45. K.L. More (Invited Plenary), "Correlating Structure and Chemistry of PEM Fuel Cell Materials with Performance and Durability using Advanced Microscopy Methods," PRiME 2016 – 230th ECS Meeting, Honolulu, HI (2016).

46. K.L. More (Invited), "Correlating Structure and Chemistry of PEM Fuel Cell Materials with Performance and Durability using Advanced Microscopy Methods," University of Illinois – Chicago, Departmental Seminar, Chicago, IL (2016).

47. B.T. Sneed, D.A. Cullen, K.S. Reeves, and K.L. More, "3D STEM Analysis of Ionomer Dispersion and Pore Structures within PEM Fuel Cell Catalyst Layers," MRS Fall Meeting, Boston, MA (2016).

48. B.T. Sneed, D.A. Cullen, K.S. Reeves, and K.L. More, "Structural and Chemical Study of the Stability of Pt-Based Fuel Cell Electrocatalysts in 3D via Electron Tomography," Pacific Rim Symposium on Surfaces, Coatings, and Interfaces (PAC-SURF), Kohala Coast, HI (2016).

49. K.L. More (Invited), B.T. Sneed, and D.A. Cullen, "Understanding Fuel Cell Materials Degradation Through the Use of Advanced Microscopy Methods," 231st ECS Meeting, New Orleans, LA (2017).

50. K.L. More (Invited), B.T. Sneed, and D.A. Cullen, "Critical interfaces in PEM Fuel Cells: Understanding Behavior through Advanced Microscopy Studies," 21st International Conference on Solid State Ionics, Padua, Italy (2017).

51. R. Mukundan, D. Spernjak, D. Hussey, D. Jacobson, and R.L. Borup, "Applications of High Resolution Neutron Imaging to Polymenr Electrolyte Fuel Cells," 253rd ACS National Meeting, San Francisco, CA (2017).

52. R. Mukundan, D.A. Langlois, K.C. Neyerlin, S.S. Kocha, K.L. More, M. Odgaard, and R.L. Borup, "Durability of PtCo/C Cathode Catalyst Layers Subjected to Accelerated Stress Testing," PRiME 2016 – 230th ECS Meeting, Honolulu, HI (2016).

53. R.L. Borup, R. Mukundan, D. Spernjak, D.A. Langlois, N. Macauley, and Y.S. Kim, "Recoverable Degradation Losses in PEM Fuel Cells," PRiME 2016 – 230th ECS Meeting, Honolulu, HI (2016).

54. A.M. Baker, D. Spernjak, E.J. Judge, S.G. Advani, and A.K. Prasad, "Cerium Migration in PEM Fuel Cells," PRiME 2016 – 230th ECS Meeting, Honolulu, HI (2016).

55. D.S. Hussey, J.M. LaManna, D.L. Jacobson, S.W. Lee, J. Kim, B. Khaykovich, M.V. Gubarev, D. Spernjak, R. Mukundan, and R.L. Borup, "Neutron Imaging of the MEA Water Content of PEMFCs in Operando," PRiME 2016 – 230th ECS Meeting, Honolulu, HI (2016).

56. J.S. Spendelow, L. Castanheira, G. Hinds, T. Rockward, D.A. Langlois, R. Mukundan, and R.L. Borup, "Measurement of Local Electrode Potentials in an Operating PEMFC Exposed to Contaminants," PRiME 2016 – 230th ECS Meeting, Honolulu, HI (2016).

V.B.3 FC-PAD: Electrode Layers and Optimization

Adam Weber[1] (Primary Contact), Ahmet Kusoglu[1], Tobias Schuler[1], Sarah Berlinger[1], Lalit Pant[1], Anna Freiberg[1], Meron Tesfaye[1], Rangachary Mukundan[2], Siddharth Babu[2], Natalie Macauley[2], Jacob Spendelow[2], Mahlon Wilson[2], Rod Borup[2], Karren More[3], Brian Sneed[3], Shyam Kocha[4], K. C. Neyerlin[4], Debbie Myers[5], Firat Cetinbas[5], Rajesh Ahluwalia[5]

[1]Lawrence Berkeley National Laboratory
1 Cyclotron Rd, MS70-108B
Berkeley, CA 94720
Phone: (510) 486-6308
Email: AZWeber@lbl.gov

[2]Los Alamos National Laboratory, Los Alamos, NM

[3]Oak Ridge National Laboratory, Oak Ridge, TN

[4]National Renewable Energy Laboratory, Golden, CO

[5]Argonne National Laboratory, Argonne, IL

DOE Manager: Dimitrios Papageorgopolous
Phone: (202) 586-5463
Email: Dimitrios.Papageorgopoulos@ee.doe.gov

Additional No-Cost Partners:

- Iryna Zenyuk, Tufts University, Medford, MA
- Odne Burheim, Norwegian University of Science and Technology, Trondheim, Norway
- David Jacobson and Dan Hussey, National Institute of Standards and Technology, Gaithersburg, MD
- Marc Secanell, University of Alberta, Edmonton, AB, Canada
- Mike Perry, United Technologies Research Center, East Hartford, CT

Project Start Date: October 1, 2015
Project End Date: September 30, 2021

Overall Objectives

- Demonstrate improved performance and durability of fuel cells.
- Develop and implement characterization techniques for gas diffusion layers (GDLs), membranes, and ionomers.
- Characterize and understand interfaces and interfacial properties on fuel cell performance and durability.
- Elucidate and mitigate ionomer film resistances in the catalyst layer through model studies to better evaluate performance and durability of fuel cells.
- Explore and optimize transport phenomena related to liquid water.

Fiscal Year (FY) 2017 Objectives

- Develop and examine new catalyst layer structures.
- Investigate origin of local resistance at low Pt loadings.
- Initiate catalyst layer ink studies.
- Conduct multimodal determination of catalyst layer microstructure.
- Explore multiphase flow and interactions within the GDLs using advanced diagnostics and imaging.

Technical Barriers

This project addresses the following technical barriers from the Fuel Cells section (3.4) of the Fuel Cell Technologies Office Multi-Year Research, Development, and Demonstration Plan.

(A) Durability

(B) Cost

(C) Performance

FY 2017 Accomplishments

- Initiated studies on catalyst layer inks, including investigation of aggregation and stability as a function of solvent dielectric constant.
- Examined water transport throughout the membrane electrode assembly (MEA), including X-ray imaging of phase-change-induced flow in the GDLs.
- Investigated novel microporous layers with hydrophilic additives that demonstrate improved water management and performance.
- Examined local resistance measurements with hydrogen and oxygen limiting current, including delineation of interfacial resistance and carbon structure.
- Developed several novel catalyst layer architectures, including stratified and array ones as well as specific Pt deposition concepts.
- Utilized model and advanced diagnostics to determine catalyst layer microstructure.
- Conducted experiments and developed model of droplet formation and shedding from GDL to flow channel.
- Modeled and validated delta-V and polarization curve analysis utilizing oxygen gain.

✧ ✧ ✧ ✧ ✧

INTRODUCTION

The FC-PAD consortium was formed to advance performance and durability of polymer electrolyte membrane fuel cells to meet DOE targets and further enable the commercialization of fuel cells. The major challenge to be addressed by this consortium is to develop the knowledge base and optimize structures for more durable, high-performing polymer electrolyte membrane fuel cell component technologies, while simultaneously reducing cost. Specifically, we will develop validated models and advanced in situ and ex situ characterization techniques to further improve the performance and durability of fuel cells. We will also evaluate polymer electrolyte membrane fuel cell component issues from low to operating temperatures of interest, including the impact of liquid water. We will characterize and understand components from the membrane to the porous media and their interfaces, with a focus on the ionomer within the catalyst layers.

APPROACH

The FC-PAD consortium incorporates national laboratory investigators with proven experience (developed in prior projects) related to durability, transport, and performance, and combines them into one highly coordinated effort. The effort is sub-divided into six thrust areas, including three materials-related thrusts and three cross-cutting thrusts. This report summarizes some of the work performed in the three cross-cutting thrust areas: (1) Modeling and Validation; (2) Operando Evaluation: Benchmarking, Accelerated Stress Tests, and Contaminants; and (6) Component Characterization and Diagnostics. The thrust areas of the consortium are highly integrated, and the work performed related to the various specific components is presented in the reports of the three materials thrust areas. The project will also benchmark the performance and durability of state-of-the-art MEAs provided by original equipment manufacturers and materials suppliers. Finally, the project will apply in situ and ex situ characterization techniques to reveal the performance losses and degradation mechanisms operational in fuel cells and propose strategies to improve performance and durability.

This report focuses on the analysis of electrode layers and their subsequent optimization. Included in this area are integration efforts for both existing and novel catalyst layer structures that improve performance. In addition, work related towards understanding water and thermal management in various components and demonstrating improved performance is also mentioned, including both modeling and experimental diagnostics. Finally, examining the origin of the observed local resistances for low platinum group metal catalyst layers is discussed.

RESULTS

It is well accepted that low-Pt-loaded electrodes suffer from a local resistance that is due in part to mass transport [1,2]. It is believed that such resistance could be due to the ionomer films covering the reaction site, and we have been investigating this using limiting-current techniques. A key issue is that using established methods [3] requires knowledge of the electrochemically active surface area (ECSA). However, this area is not measured under limiting-current conditions. Furthermore, as shown in Figure 1, for high-surface-area carbons (HSC), this is a strong function of relative humidity (RH) due to the fact that over 70% of the platinum particles are within the primary pores of the carbon agglomerates. This is not the case for low-surface-area supports such as Vulcan, where the majority of platinum particles are on the surface. Thus, it makes sense for studies that examine local resistances to use effective ECSAs as well as Vulcan-type supports to probe resistances due to transport through the ionomer thin-films. In addition, the effective ECSA is expected to be even smaller at limiting current since only the surface platinum is active due to limiting-current conditions wherein kinetic overpotentials are not limiting. This is seen when one compares the ECSA slope method utilizing multiple MEAs with that of a single MEA measurement using stacked GDLs. Using Vulcan supports, the resistance in the latter is about 70% of the former, suggesting that not all platinum is active under limiting current and care must be taken when analyzing the data. Finally, comparison between oxygen and hydrogen methods suggests that the bulk of the transport resistance is due to traditional diffusional-type mass transport losses.

In analyzing local resistances and understanding transport through the catalyst layer, there is a need to be able to probe the catalyst layer structure. We have shown that advanced transmission electron microscopy can determine some ionomer distributions in the catalyst layer, including preferential agglomeration towards Pt compared to carbon, yet the finest structure on the 10 nm or so scale remains elusive. To overcome this bottleneck, we have utilized a combined approach of stochastic modeling and realizations with advanced X-ray and electron microscopy studies. As shown in Figure 2, we utilize measured distributions for solids and catalyst with a random carbon nucleation and growth to reconstruct the catalyst layer. By subtracting the carbon distribution from the measured solid distribution, we can determine the ionomer film thickness and its subsequent coverage. As shown, various realizations demonstrate that the majority of the carbon surface is covered by ionomer films less than 10 nm in thickness.

While knowing the catalyst layer structure is one thing, there is a need to optimize it, especially for performance. To do so, we investigated several approaches, including catalyst layer architectures based on more rational design and fabrication of ionomer and even platinum nanoparticles.

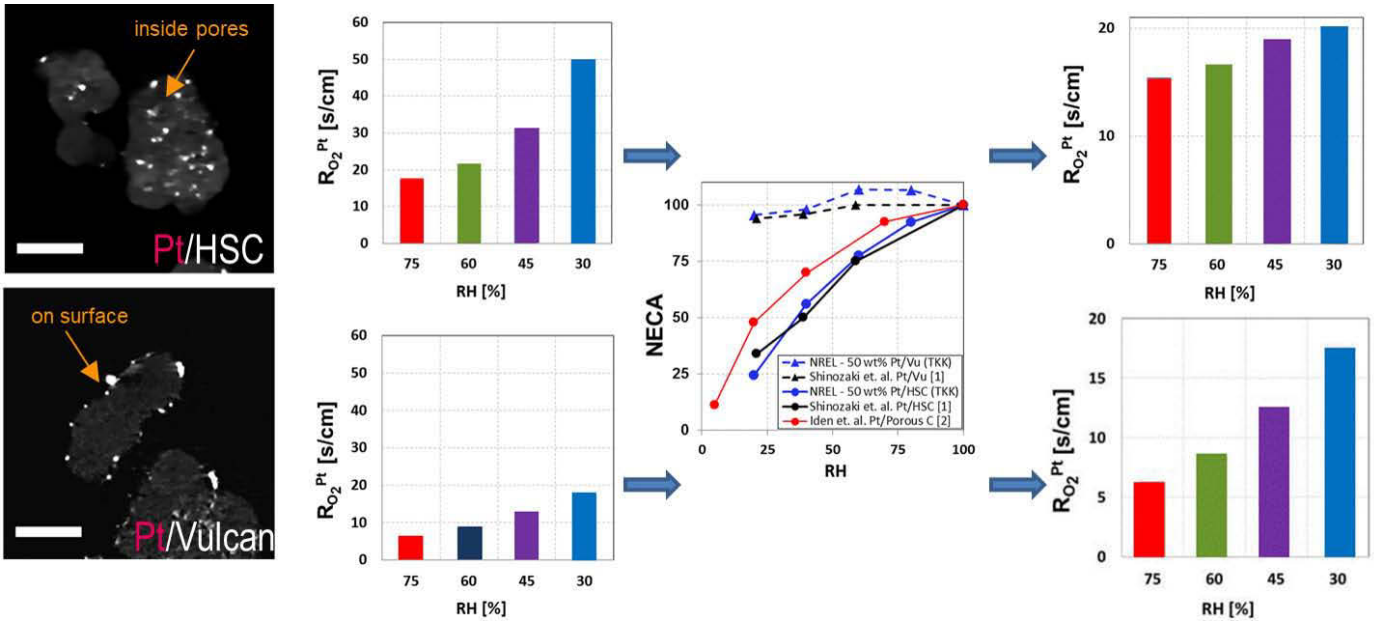

FIGURE 1. Transmission electron microscope micrographs showing platinum on higher-surface-area carbon and low-surface-area carbon that results in different effective ECSA values (net electrochemical activity [NECA]). Local resistances when corrected for NECA result in less humidity dependence and similar values for the two different supports.

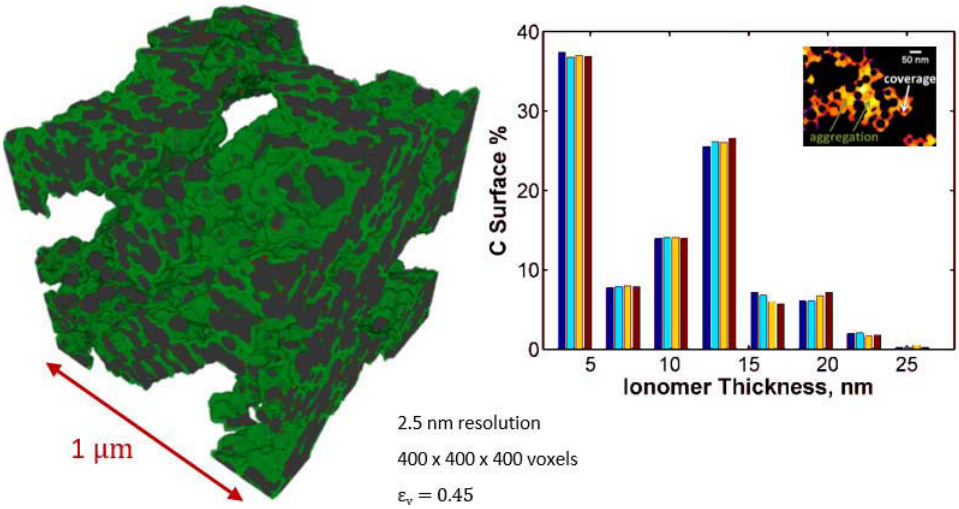

FIGURE 2. Catalyst layer reconstruction from nano X-ray tomography and stochastic nucleation modeling resulting in shown ionomer film distribution.

One such approach is shown in Figure 3, where modeling and subsequent experiments were conducted and demonstrated that placing the platinum-containing catalyst layers in a stratified manner can increase overall performance, especially in the mass transfer (MT) regime, without requiring an increase in loading. Placing the active catalyst layer (CL) under the channels more so than the lands provided for more efficient water management and higher performance compared to baseline samples. It was also observed that there is a need to still have blank carbon in the nonactive catalyst layer regions to ensure adequate water removal pathways as well as to mitigate possible durability concerns.

For exploring multiphase water interactions, both modeling and experimental studies were conducted. It was shown how analysis of oxygen gain and polarization curves can be used as a diagnostic to determine the key limiting phenomena. In addition, the often suspected phase-change-induced flow, where water moves down a temperature gradient, was quantified using X-ray microtomography. Also,

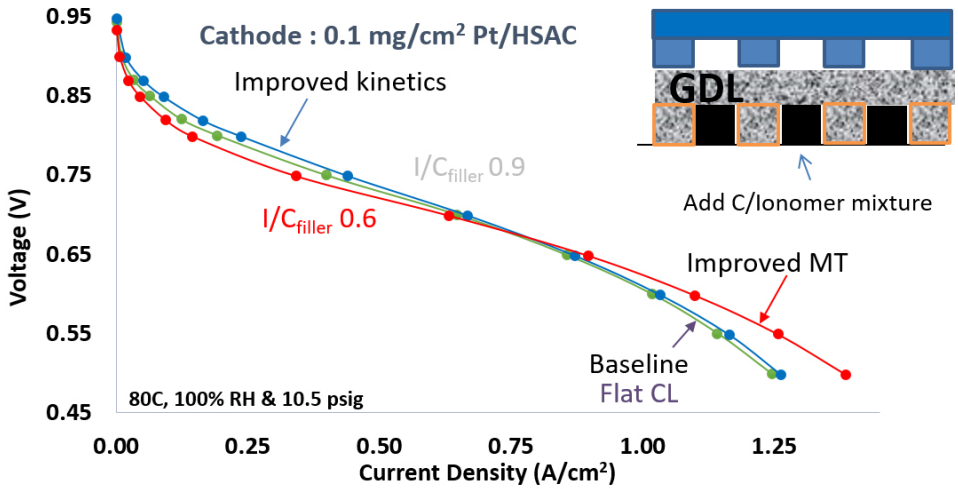

HSAC – high surface area cathode

FIGURE 3. Polarization curves with stratified catalyst layers. Inset shows the stratification structure.

the impact of water dynamics and droplet shedding from the GDL to the flow channel was visualized and modeled. Finally, to improve water management and in agreement with mathematical predictions [4], microporous layers with hydrophilic additives were explored. As shown in Figure 4, such structures provide for better performance due to their ability to remove liquid water from the catalyst layer, which agreed with X-ray tomographic observations of liquid water in the microporous layers. In particular, the addition of carbon nanotubes demonstrated the best performance. This performance gain was not only quantified in terms of lower water content, especially in the cathode, but also a decreased adhesion force at the GDL boundary with the flowfield that enables more efficient water movement. This more efficient water management not only resulted in better performance, but also increased durability during wet drive cycle testing.

CONCLUSIONS AND UPCOMING ACTIVITIES

To optimize performance and durability of fuel cell components including ionomers, interfaces, and diffusion media in this thrust of FC-PAD, we have enacted a synergistic combination of the crosscutting thrusts to explore component properties, behavior, and phenomena. Combined modeling and experiments to understand interfaces demonstrated the importance of water droplets at the GDL/flowfield boundary as well as the possible increase in

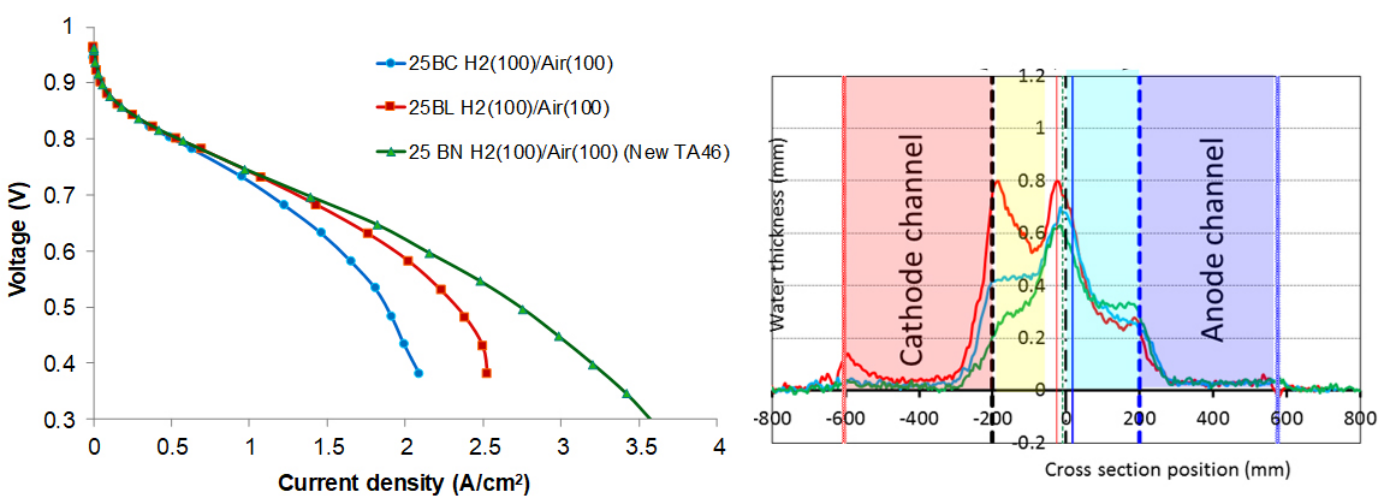

FIGURE 4. Polarization curves at 80°C, 100% relative humidity and neutron imaging demonstrating that microporous layers with hydrophilic additives (either carbon nanotube [BN] or aluminasilicate [BL] fibers) demonstrate better performance and differences in cell water content.

performance through catalyst layer architecture optimization. Limiting-current diagnostics across a systematic study of different catalyst layers demonstrated the importance of accurate effective active area measurements as well as the apparent dominance of diffusion-like transport at the local ionomer scale.

For upcoming activities, we plan to focus on elucidating critical bottlenecks for performance and durability from ink to formation to conditioning to testing. We will continue work on optimizing catalyst layer structure for high performance at low loadings. This includes exploration of different architectures, including stratified, array, electrospun, HSC/Vulcan-layered, and specific Pt deposition. Along with this will be microstructural modeling of both catalyst-layer structure as well as transport through the layer. This modeling will work in tandem with the multiscale modeling of cell and components to understand water and thermal management and their impact on durability and performance. The models will also be validated by comparison with various differential, integral, and segmented cell data. Finally, we will explore the genesis of membranes and thin films and their associated properties. This includes both ex situ studies of thin-film morphology with various cations and under electrochemical potential as well as in situ limiting-current interrogations under a variety of conditions, techniques, ionomers, gases, temperature, and humidity.

FY 2017 PUBLICATIONS/ PRESENTATIONS/HONORS

1. Please see the FC-PAD: Overview annual report for the complete list of 61 presentations, 20 publications, 2 invention disclosures, and 4 awards.

REFERENCES

1. A.Z. Weber, A. Kusoglu, J. Mat. Chem. A, 2014, 2, 17207.

2. A. Kongkanand, M.F. Mathias, J. Phys. Chem. Lett., 2016, 7 (7), 1127–1137.

3. T.A. Greszler, D. Caulk, P. Sinha, J. Electrochem. Soc., 2013, 159, F831–F840.

4. A.Z. Weber, J. Power Sources, 2010, 195, 5292–5304.

V.B.4 Novel Ionomers and Electrode Structures for Improved PEMFC Electrode Performance at Low PGM Loadings

Andrew Haug (Primary Contact), M. Lindell, T. Matthews, J. Abulu, M. Yandrasits, A. Steinbach, M. Kurkowski, G. Weatherman, G. Thoma, I. Khan
3M Company, 3M Center, Building 0201-02-N-14
St. Paul, MN 55144-1000
Email: Athaug@mmm.com

Iryna V. Zenyuk, D. Sabarirajan, S. Normile
Tufts University, Medford, MA (Subcontractor)

J. Allen, K. Tajiri, E. Medici, and team
Michigan Technological University, Houghton, MI (Subcontractor)

A. Weber, A. Kusoglu
Lawrence Berkeley National Laboratory (FC-PAD), Berkeley, CA

KC Neyerlin
National Renewable Energy Laboratory (FC-PAD), Golden, CO

K. More
Oak Ridge National Laboratory (FC-PAD), Oak Ridge, TN

R. Borup
Los Alamos National Laboratory (FC-PAD), Los Alamos, NM

D. Myers
Argonne National Laboratory (FC-PAD), Argonne, IL

DOE Manager: David Peterson
Phone: (240) 562-1747
Email: David.Peterson@ee.doe.gov

Contract Number: DE-EE0007650

Project Start Date: October 1, 2016
Project End Date: September 30, 2019

Overall Objectives

- Achieve DOE 2020 targets for platinum group metals (PGM) total loading, mass activity, startup-shutdown accelerated stress tests (ASTs), catalyst support ASTs, electrocatalyst ASTs, and membrane electrode assembly (MEA) robustness.
- Develop novel, electrode-focused ionomers, focusing on combining conductivity with improved oxygen transport.
- Integrate nanostructured thin film (NSTF) catalyst powder into a dispersed electrode structure.
- Integrate novel ionomers with state of the art NSTF powder electrocatalyst to develop an advanced cathode of high activity, performance, and durability.
- Investigate electrode transport at bulk, intermediate and local levels for limiting effects including ionomer gas and proton transport, and impacts of hydrophilicity and the transition metal.
- Guide development with state of the art and novel characterization and modeling techniques, including in-operando nano-computed tomography (CT) and electrode pore network models.

Fiscal Year (FY) 2017 Objectives

- Generate
  - Initial imide and multi-acid side chain (MASC) ionomers (at least three over Budget Period [BP] 1).
  - Initial NSTF powders (more than 25 g).
  - Baseline catalyst coated membranes (CCMs) and electrodes, novel CCMs and electrodes.
  - Set up and validate DOE ASTs, local O_2 transport test, O_2 permeability test; test and characterize baseline CCMs.
  - Characterize novel ionomers using rotating disk electrode (RDE), grazing-incidence small-angle X-ray spectroscopy (GISAXS), four-point conductivity, and O_2 permeability.
  - Characterize baseline electrodes and dispersed NSTF electrodes using nano-CT, water imbibition and capillary pressure testing, scanning electron microscopy with energy dispersive spectrum (SEM-EDS), and transmission electron microscopy (TEM).
  - NSTF powder electrode achieves mass activities ≥0.30 A/mg Pt, electrochemical surface area (ECSA) ≥15 m^2/g, surface enhancement factor (SEF) >40 m^2/m^2, and 0.7 robustness factor.
  - Ionomer material developed exceeds the bulk O_2 permeability of the baseline 3M825 ionomer, with similar or better proton conductivity to 3M825.

Technical Barriers

This project addresses the following technical barriers from the Fuel Cells section of the Fuel Cell Technologies Office Multi-Year Research, Development, and Demonstration Plan.

(B) Cost

(A) Durability

(C) Performance: operational robustness

Technical Targets

Relevant DOE technical targets and progress as of May 1, 2017, are listed in Table 1.

FY 2017 Accomplishments

- Engaged subs and the Fuel Cell Consortium for Performance and Durability (FC-PAD), finalized statements of project objectives (SOPOs), completed all non-disclosure agreements (NDAs), and commenced research.
- Generated electrode and CCM baselines utilizing 3M825 ionomer, TKK 10V50E catalyst, and an ionomer to carbon ratio of 0.9.
- Generated dispersed NSTF powder exceeding 50 total grams and generated baseline dispersed NSTF cathodes with different ionomers, supports, and whisker metal loadings.
- Generated more than seven novel ionomers for electrode development, including materials containing amides and MASC.
- Generated more than fifty electrode types (different ionomers from 520–1100 equivalent weight [EW], ionomer to catalyst [I/C] ratios from 0.3 to 1.2, loadings from 0.03 mg Pt/cm^2 to 0.35 mg Pt/cm^2).
- Developed a bulk membrane O_2 permeability test process based on General Motors method.
- Achieved 30 m^2/g dispersed NSTF ECSA in cell, exceeding Budget Period 1 (BP1) and Budget Period 2 (BP2) second quarter (Q6) targets; and dispersed NSTF surface roughness up to 90 cm^2/cm^2, also exceeding BP1 targets.
- Achieved dispersed NSTF activities >0.26 A/mg Pt utilizing PtCoMn and PtNi NSTF powders.
- Achieved fourth quarter BP2 power target of 5.7 kW/gPt with initial best in class dispersed NSTF down-select.
- Exceeded DOE electrode support stability project targets utilizing dispersed NSTF, achieving 20,000 cycles.
- Analyzed dispersed NSTF materials with nano-CT.
- Evaluated perfluoroimide acide (PFIA) ionomer utilizing GISAXS, demonstrating potential transport benefits.
- Began development of more novel ionomer types with initial prospects targeted for fourth quarter 2017 (Q4) delivery.

✧ ✧ ✧ ✧ ✧

INTRODUCTION

Among the various recommendations for fuel cell performance enhancement at low precious metal loadings are increasing ionomer and electrode O_2 transport, and

TABLE 1. Progress towards Meeting Technical Targets for Electrocatalysts and MEAs for Transportation Applications

METRIC	2020[1] Target	Integrated Cathode	PROGRESS
PGM total loading, mg/cm^2	0.125	0.125	0.102[2]
PGM total loading, g/kW [150 kPa abs]	0.125	0.125	0.172[2]
Mass activity @ 900 mV iR-free, A/mg	0.44	0.44+	0.28
SUSD AST, % ECSA loss	<20 %	<20	N/A
SUSD AST, % mV loss @ 1.2 A/cm^2	<5%	<5%	N/A
Support AST, % mass activity loss	<30	<30	28% (Pt)
Electrocatalyst AST, mV loss @ 1.5 A/cm^2	<30	<30	NA
Electrocatalyst AST, % mass activity loss	<40	<40	45% (Pt)
MEA robustness (cold/hot/cold transient)	0.7/0.7/0.7	>0.7/>0.7/>0.7	0.6/NA/0.6[3]

[1]All metrics and DOE 2020 targets are taken from DE-FOA-0001412
[2]Assume using 0.025 mgPt/cm^2 anode
[3]3M transient protocols used for NSTF testing
abs – absolute; iR – internal resistance; SUSD – startup-shutdown; NA – not available

increasing ionomer hydrophobicity. Further proposed limitations include local (near catalyst) water generation and flooding and transport losses due to alloying (non-Pt) metal dissolution. Additionally, catalysts and electrodes with increased activity and durability are required to meet automotive performance and lifetime targets. The focus of this project is to develop electrode ionomers with improved O_2 transport, integrate these into electrodes containing durable, active NSTF powder, and achieve DOE 2020 power and durability targets.

In BP1, several electrode-focused ionomers were generated and evaluated. Increased ionomer conductivity has led to improved electrode performance while lower ionomer content has shown some activity increases. For the first time, NSTF as a powder is being integrated into a more classic electrode structure. Most of its industry leading activity and durability has been maintained; DOE electrode support stability targets have been exceeded. Advanced NSTF alloys are showing promising activities and initial characterization of these electrodes by nano-CT, SEM and TEM, and mathematical models are underway. Integration efforts of these novel ionomers with dispersed NSTF has begun and will continue into BP2 and BP3 with the goal of meeting DOE performance and durability targets. The expected outcome is a cathode electrode and integrated CCM with increased activity, performance, and operational robustness over current state of the art, and which is suitable for stationary and automotive applications.

APPROACH

The approach will be to develop novel electrode-specific ionomers aimed at increasing O_2 permeability, conductivity, and cathode performance. Ionomer development will proceed along three paths: developing and evaluating MASC materials, imide-only materials (BP1, BP2), and more novel O_2 permeable ionomer structures (BP2, BP3). NSTF will then be integrated into this ionomer containing electrode framework. The best high activity, durable ***ultra thin film (UTF) alloy powder*** having a minimal number of monolayers (i.e., maximum ECSA) will potentially achieve areas approaching 70 cm^2_{PGM}/cm^2_{planar} with specific activities as high as 4 mA/cm^2 with 0.105 mg PGM/cm^2. This is a ***theoretical mass activity entitlement of 2.5 A/mg$_{PGM}$***, a 5X increase beyond the exceeding the DOE 2020 0.44 A/mg PGM mass activity target. Activity losses stabilizing UTF powder against cyclic decay and integrating UTF powder into an ionomer containing electrode are expected, but such UTF's can lose over 80% activity and still achieve DOE 2020 targets. Finally, optimization of the electrode framework, containing novel ionomers and optimal NSTF, will be completed to achieve the above targets. Guiding this development at every stage will be state-of-the-art characterization and modeling including nano-CT imaging, GISAXS, TEM, water imbibition, and pore hydrophobicity/philicity measurements.

The proposed work is broken down into five tasks: electrode ionomer development and characterization (Task 1), advanced NSTF electrode development and characterization (Task 2), integration of novel ionomers and NSTF into electrodes (Task 3), model development (Task 4), and project management (Task 5). The project contains three 12-month budget periods. NSTF development will focus mainly on the integration of state-of-the-art NSTF catalyst powder into an ionomer-containing electrode architecture.

RESULTS

More than seven new ionomers and 25 g of NSTF powder have been generated, along with electrodes and CCMs of these under Tasks 1.1, 2.1, 2.3. Ionomers as low as 520 EW have been built into CCMs and evaluated. Additional carbon-ionomer electrodes (free-standing) of various types have been provided for evaluation. A procedure for measuring oxygen permeability of ionomer membranes has been developed in 3M based on the paper by Zhang et al [1]. Local oxygen transport techniques were adapted based on the work by Baker et al [2].

Initial conductivity and oxygen permeability tests were run on the new ionomers. As shown in Figure 1, Imide 2 is demonstrating oxygen permeability slightly above the baseline while Imide 1 is approaching baseline 3M825 perfluorinated sulfonic acid (PFSA) conductivity. As expected, MASC ionomers are showing exceptional conductivities. These results demonstrate that ionomer work is leading toward a BP1 ionomer goal of exceeding baseline ionomer conductivity and permeability simultaneously. Newer ionomers are expected to exceed both targets.

The initial baseline electrode for this project is the TKK 10V50E, 3M825 PFSA ionomer, and an ionomer to carbon ratio of 0.9 at 0.2 mg Pt/cm^2. A future, lower loading baseline will use 10V20E. All new ionomers are initially tested with 10V50E at various I/C ratios and loadings. As shown in Figure 2, MASC 1 performance under DOE conditions has significantly improved upon the baseline. A combination of high inherent conductivity and lower ionomer content likely leads to reduced bulk and local transport losses. Testing at 6% O_2 at 1 A/cm^2 leads to 100 mV gain over the baseline, while local transport testing is showing significant reductions in O_2 resistance losses (less than 10 S/m for total resistance). This result is further enhanced by GISAXS results from Lawrence Berkeley National Laboratory showing that PFIA ionomer (a MASC ionomer) produces a more random thin film structure, thereby becoming less of a barrier to oxygen permeation. Exceptionally low I/C ratios are demonstrating good promise for lowering local gas transport and improving performance. Further, lowering ionomer contact does seem to offer modest (10–15%) activity gains, especially with

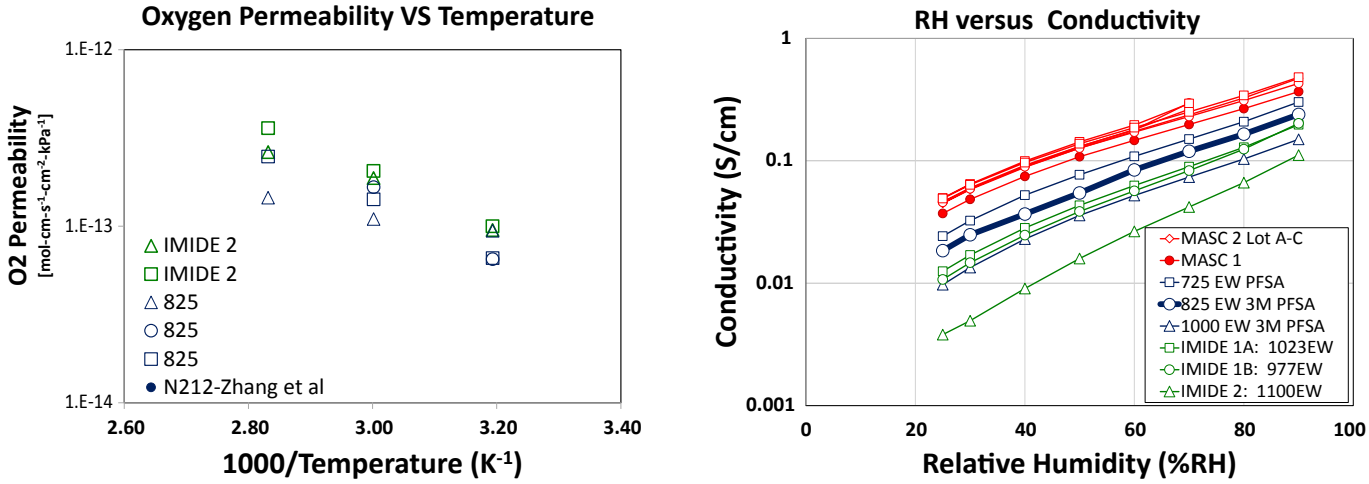

RH – relative humidity

FIGURE 1. Conductivity (right) and oxygen permeability (left) of baseline PFSA and novel imide ionomers

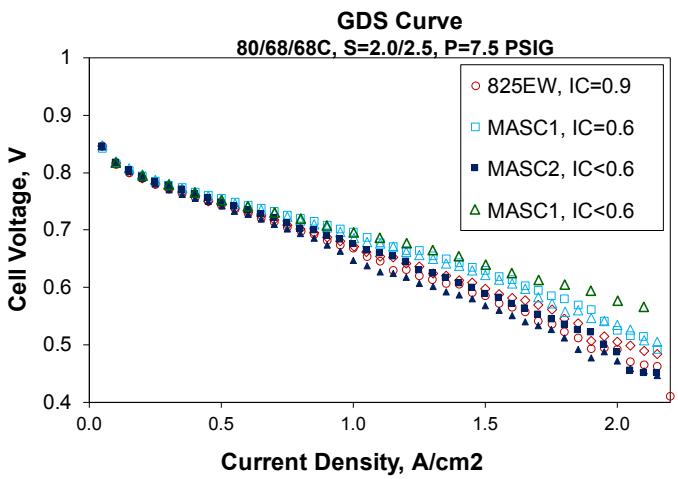

GDS – galvanodynamic scan

FIGURE 2. Performance curves for 10V50E at 0.2 mgPt/cm^2 with various ionomers and ionomer to carbon (IC) ratios

PFSA ionomers (725 EW and 825 EW). These down-selected materials will be further evaluated by transport testing and other means.

More conductive ionomers are showing some reduction in low temperature (40°C) performance. Baseline values at 0.4 V, 40°C are 1.6 A/cm^2, while MASC 1 at I/C = 0.9 is 0.9 A/cm^2. However, lowering I/C ratios are bringing these values up to >1.2 A/cm^2. An important part of upcoming work will be optimizing potentially more hydrophilic ionomers with wettable NSTF powder.

Initial work integrating powdered NSTF 2–25 µg/cm^2 Pt (geometric on liner) into an electrode resulted in cathodes that exceeded the initial surface area (ECSA) BP1 go/no-go of 15 m^2/g Pt. The ECSA of 15 ug/cm^2 Pt (geometric on liner) exceeded 25 m^2/g in fuel cell testing. It is clear that lowering the PGM on the whisker will increase the specific area to the point where Pt-only whiskers can achieve Milestone Q6 target of 25 m^2/g. Of greater significance is that the initial PtNi #1 sample down-selected from FC143 (A. Steinbach, Principal Investigator) [4] (28 ug/cm^2 Pt on liner as Pt38Ni62) shows 26-28 m^2/g ECSAs at relatively high Pt loadings on the whisker. Based on current data, a path to >35 m^2/g PGM seems probable. Down-selects from FC143 [4] show promise of further specific area increases. Further, surface roughness up to 90 cm^2/cm$^2_{GEO}$ have been achieved for powdered NSTF cathodes, well exceeding BP1 goals.

Electrodes containing powdered NSTF, support and ionomer have significantly improved operational robustness, especially at low temperatures, approaching the target of 70% peak power. Of more significance is that activity and durability, NSTF differentiators, can largely be maintained. Figure 3 shows roughly 33% mass activity is lost for NSTF electrodes containing ionomer. This is unexpected considering the ionomer has good opportunity to poison the NSTF surface, and encouraging for achieving project activity targets. Thus, mass activities of 0.28 A/mg Pt have been achieved with dispersed NSTF to date. Initial performance results with PtNi #1 are very promising. For a loading of 0.077 mg PGM/cm^2, and assuming and anode of 0.025 mg Pt/cm^2, a power output of 0.171 g/kW has been achieved. This exceeds the Milestone Q6 and BP2 go/no-go points. What is more significant about this result is that the dispersed package seems to handle the transition metals in the electrode.

Additionally, NSTF powdered electrodes have achieved support durability targets of 5,000 AST cycles with 5% activity loss. More than 20,000 cycles have been run without

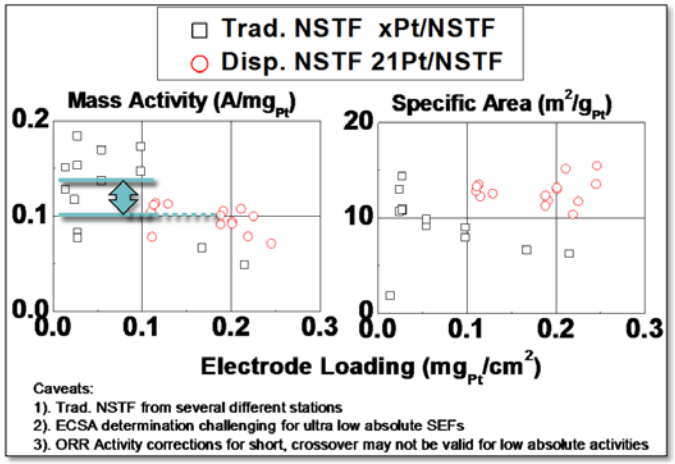

ORR – oxygen reduction reaction

FIGURE 3. Mass and specific area comparisons for traditional NSTF and powdered NSTF electrodes. The left plot shows the mean differences in mass activity for comparable whiskers showing ~33% activity loss for the powdered NSTF electrode.

failure. NSTF powdered electrodes are also showing promise for achieving electrocatalyst durability targets, currently showing 50% metal area loss vs. 90% for 10V50E in the electrocatalyst AST.

Further, with new ionomers, and more knowledge about how to improve the dispersed NSTF cathode electrode package, it is likely that both performance, activity and power density will improve. Fundamental characterization of NSTF electrodes are underway as well, as shown in Figure 4. TEM and nano-CT can isolate NSTF materials. Imagery and data will be used to diagram ionomer, pore and solid structure of these electrodes. Resulting structures, performance differences, and the impacts of decay will be used in pore network model development.

In summary, ionomers novel ionomers are showing some promise for oxygen permeability, performance, and activity improvements. Dispersed NSTF is showing results for activity and durability above what was expected for the early stages of this project. Much of the NSTF electrode emphasis of this project will be to improve the power output of the NSTF material as a dispersed catalyst. Here is where the combination of 3M materials generation with Tufts, Michigan Technical University, and FCPAD's analysis will focus ionomer development, provide insight on electrode local transport, and integration.

CONCLUSIONS AND UPCOMING ACTIVITIES

Conclusions

- Initial dispersed NSTF electrode testing shows good operational stability. Low temperature performance issues of classic NSTF are eliminated as increasing support is added.
- Initial dispersed NSTF testing shows very little activity loss (0–25%) versus conventional NSTF. This is critical to the project's success and differentiation. Other unsupported catalysts show up to 95% activity loss.
- Initial dispersed NSTF alloy testing resulted in mass activities close to year one targets (0.28 A/mg Pt achieved with target of 0.30 A/mg Pt).
- Initial results show NSTF with support can exceed DOE support AST targets. Up to 20,000 cycles were achieved.
- Initial electrocatalyst durability cycling with low (25 ug/cm^2) whisker loading (0.1–0.2 mg Pt/cm^2 electrode loading) shows good catalyst stability. Down-selected samples from A. Steinbach [3] will likely improve upon this.
- Initial imide ionomers achieve good activity and performance. MASC ionomers show paths to improved performance and lower transport losses. Imide materials are showing good performance and moderate O_2 permeability improvements.

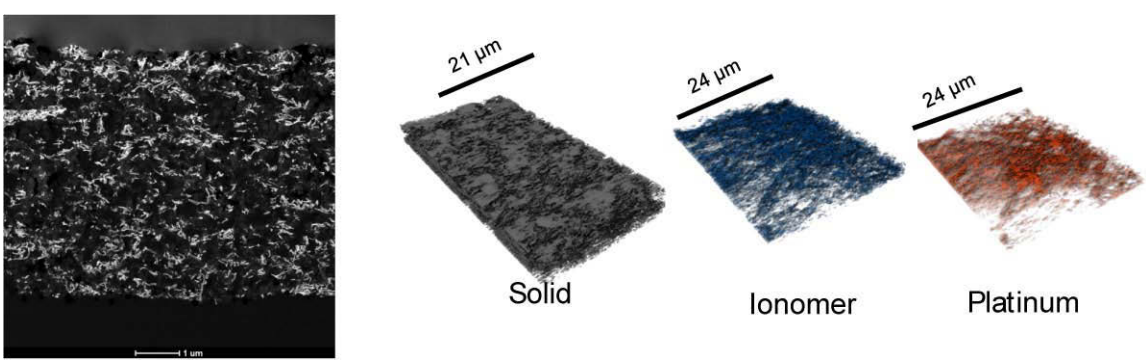

FIGURE 4. Characterization of powdered NSTF electrodes by TEM (Oak Ridge National Laboratory), and nano-CT (Tufts)

Upcoming Activities (BP2)

- Additional new ionomers with increasingly novel oxygen permeability-focused structures will be generated and evaluated.
- Transition metal impact of NSTF alloys on dispersed electrode performance will be evaluated and minimized.
- Quarterly testing of best-in-class NSTF down-selects from FC143 [4].
- Integration of dispersed NSTF with novel ionomers will commence.
- The pore network model is operational and and will begin its first predictions.
- An electrode water imbibition/capillary pressure diagram will be developed.
- In-operando nano-CT will continue to be developed.
- Additional new ionomers will be evaluated through GISAXS, including imide-only materials.
- Additional cathode baselines will be developed to better evaluate in-cell ionomer poisoning and lower loaded operation.
- RDE evaluation of novel ionomers for Pt poisoning will be conducted.
- Powdered NSTF electrodes will be evaluated with TEM for performance and decay characteristics.

FY 2017 PUBLICATIONS/PRESENTATIONS

1. FC155 at DOE's Annual Merit Review in Washington, D.C., on June 6, 2017.

REFERENCES

1. Zhang et al., J. Electrochem. Soc., 160, F616 (2013).

2. D.R. Baker, J. Electrochem. Soc., 156, B991 (2009).

3. A. Steinbach, GM DOE project FC144 entitled "Highly-Accessible Catalysts for Durable High-Power Performance." Award# DE-EE0007271.

4. A. Steinbach, 3M DOE project FC143 entitled "Highly Active, Durable, and Ultra-low PGM NSTF Thin Film ORR Catalysts and Supports." Award# DE-EE0007270.

V.B.5 Durable High-Power Membrane Electrode Assemblies with Low Pt Loading

Swami Kumaraguru
General Motors (GM)
850 N. Glenwood Avenue
Pontiac, MI 48340-2920
Phone: (585) 683-8413
Email: swami.kumaraguru@gm.com

DOE Manager: Gregory Kleen
Phone: (240) 562-1672
Email: Gregory.Kleen@ee.doe.gov

Contract Number: DE-EE0007651

Subcontractors:
- Prof. Paulo Ferreira, University of Texas, Austin, TX
- Dr. Cortney Mittelsteadt, Giner, Inc., Newton, MA

Project Start Date: April 1, 2017
Project End Date: March 31, 2020

Overall Objectives

- Identify best in class materials and generate state-of-the-art (SOA) membrane electrode assembly (MEA) that meets DOE 2020 performance and cost target.
- Study impact of operating condition on durability of SOA MEAs in differential cell conditions supported with advanced electrochemical and analytical characterization.
- Develop predictive model for electrode and membrane degradation and recommend implementable benign operating conditions to prolong MEA durability to >5,000 h.

Fiscal Year (FY) 2017 Objectives

- Down-select best in class catalyst, ionomer, and membranes to generate SOA MEAs that will meet DOE 2020 performance and cost targets.
- Systematic study to correlate catalyst layer structure formation from ink properties to its impact on measured polarization curve.
- Deliver 5 cm^2 and 50 cm^2 SOA MEAs to Fuel Cell Performance and Durability consortium (FC-PAD) partners for durability studies.

Technical Barriers

This project addresses the following technical barriers from the Fuel Cells section of the Fuel Cell Technologies Office Multi-Year Research, Development, and Demonstration Plan.

(A) Durability

(B) Cost

(C) Performance

Technical Targets

See Table 1.

FY 2017 Accomplishments

- Several best in class catalysts, ionomers and membranes identified for evaluation.
- Initial activity measurement on several best in class catalyst exceeds DOE mass activity target of 440 mA/mg_{Pt}.

TABLE 1. Progress towards Meeting Technical Targets for Electrocatalysts and MEAs for Transportation Applications

Characteristic	Units	DOE 2020 Electrocatalyst and MEA Targets	Project Status (5 cm^2 cell, differential conditions)
Mass activity (MA)	A/mg_{PGM} @ 0.9 $mV_{iR\text{-}free}$	≥0.44	0.60
Specific activity	$\mu A/cm^2_{PGM}$ @ 0.9 $mV_{iR\text{-}free}$	≥720	1,477
PGM total loading	mg-PGM/cm^2_{geo}	≤0.125	≤0.125
MEA performance	mW/cm^2_{geo} @ 675 mV	≥1,000	≥900
Electrocatalyst durability	% loss after 30,000 V-cycles	<40% loss in ECSA <40% loss in MA <30 mV loss @ 0.8 A/cm^2	*In progress*
Durability with cycling	Hours @ <10% V loss	5,000	*TBD*

TBD – to be determined; PGM – platinum group metals; ECSA – electrochemical surface area

- MEA performance of >900 mW/cm^2_{geo} at 675 mV achieved for best in class catalyst materials. Identified gaps to meet >1,000 mW/cm^2_{geo}.
- PtCo alloy catalysts on porous high surface area carbon supports exhibit a distinct advantage in both activity and H_2-air performance over solid carbons.

✧ ✧ ✧ ✧ ✧

INTRODUCTION

PtCo-alloy catalysts have achieved mainstream application approximately 20 years after they were first reported. Thanks to the recent high activity of these alloy catalysts [1], GM and other automotive MEA developers have achieved very impressive beginning of life performance using low-Pt (0.05–0.1 mg_{Pt}/cm^2) loading cathodes and thin (10–15 µm) membranes. Unfortunately, these MEAs are subject to life-limiting degradation during operation, and developers add twice the Pt and increase membrane thickness by 5–10 µm, substantially sacrificing cost, in order to achieve durability requirements.

These high performing MEAs suffer especially at peak power, because of complex degradation mechanisms that are highly sensitive to the materials, MEA design, and fuel cell operating strategy. Specifically, power degradation of the cathode occurs via Pt and Co dissolution as well as deterioration of O_2 transport properties. Additionally, thin membranes are subject to failure due to manufacturing defects in the adjacent gas diffusion media and electrodes and the formation of membrane-attacking radical species caused by high gas crossover. This project is designed to systematically study these degradation phenomena in an SOA MEA, applying and extending diagnostic and modeling tools available at GM, its partners, and FC-PAD.

APPROACH

The project approach is based on our understanding that there is substantial opportunity to select operating conditions and voltage waveforms to reduce life-limiting electrode and membrane degradation rates. In this project, we intend to map the impact of operating conditions on SOA MEA durability for proton exchange membrane fuel cells. This will be achieved by systematic durability studies relying on advanced characterization tools, degradation mechanism model development and validation. The framework for the studies envisioned in the project is shown in Figure 1. Specifically, the project approach is to improve MEA performance and durability by executing the following work elements: (1) integrating the best in class materials to generate an SOA MEA, (2) incorporating systematic durability studies to assess the impact of operating conditions on MEA life, (3) conducting extensive post mortem characterization of MEAs to provide mechanistic understanding of MEA degradation along with developing and validating models to predict electrode and membrane degradation, and (4) recommending benign, yet realistic operating conditions to extend durability of MEA past 5,000 h of the DOE 2020 durability target.

The output of the project will be a detailed understanding of operating condition sensitivity on cathode and membrane failure, critical for defining operating conditions and hybridization strategies that can guide system controls to maximize low-Pt MEA life. The project will utilize the expertise of GM, its partners, and FC-PAD to achieve project objectives.

RESULTS

First year objective of the project is to procure best in class materials that can be optimized and integrated to generate an SOA MEA. In the first two quarters, few best in class catalyst candidates, like PtCo alloy from various suppliers and in house synthesis, have been studied for activity and performance. A few other high activity categories, such as faceted catalysts or core shell catalysts, are still early in development to be considered for this study. Location of the Pt particle (inside the pore vs. outside the pore) has been shown to have an impact on both activity and performance in the DOE project DE-EE0007271 (FC144 – Highly Accessible Catalyst). Recent scanning transmission electron microscopic tomography studies indicate the majority of particles are embedded inside carbon on high surface area carbon (HSC) supports, making them inaccessible during dry operation. Alternatively, solid carbon such as Vulcan or acetylene black would provide a majority of particles on the exterior surface of carbon, making them more accessible even during dry operation [2,3].

To address drawbacks and opportunities from this learning, high active PtCo catalysts on both porous HSC carbon and solid carbons like Vulcan were tested for activity and H_2-air performance. The catalysts were tested in MEAs fabricated as catalyst coated membrane with 0.1 mg_{Pt}/cm^2 on cathode electrode and 0.025 mg_{Pt}/cm^2 anode electrode laminated on 18 µm membrane. Initial test results (Figure 2 and Figure 3) indicate most of the PtCo alloy catalysts on various high surface area carbon supports exceeds DOE mass activity requirements of 440 mA/mg_{Pt}. Also, there are significant differences in activity for PtCo alloy catalysts on porous HSC like carbon supports compared with solid carbon like Vulcan. Activity of PtCo alloy catalysts on porous HSC catalysts are 3X higher (600 mA/mg_{Pt} vs. 175 mA/mg_{Pt}) compared to solid carbon. Activity variations can be found even among several high surface area carbon supports. In the next few quarters, we will continue both electrochemical and analytical characterization of the MEAs to down-

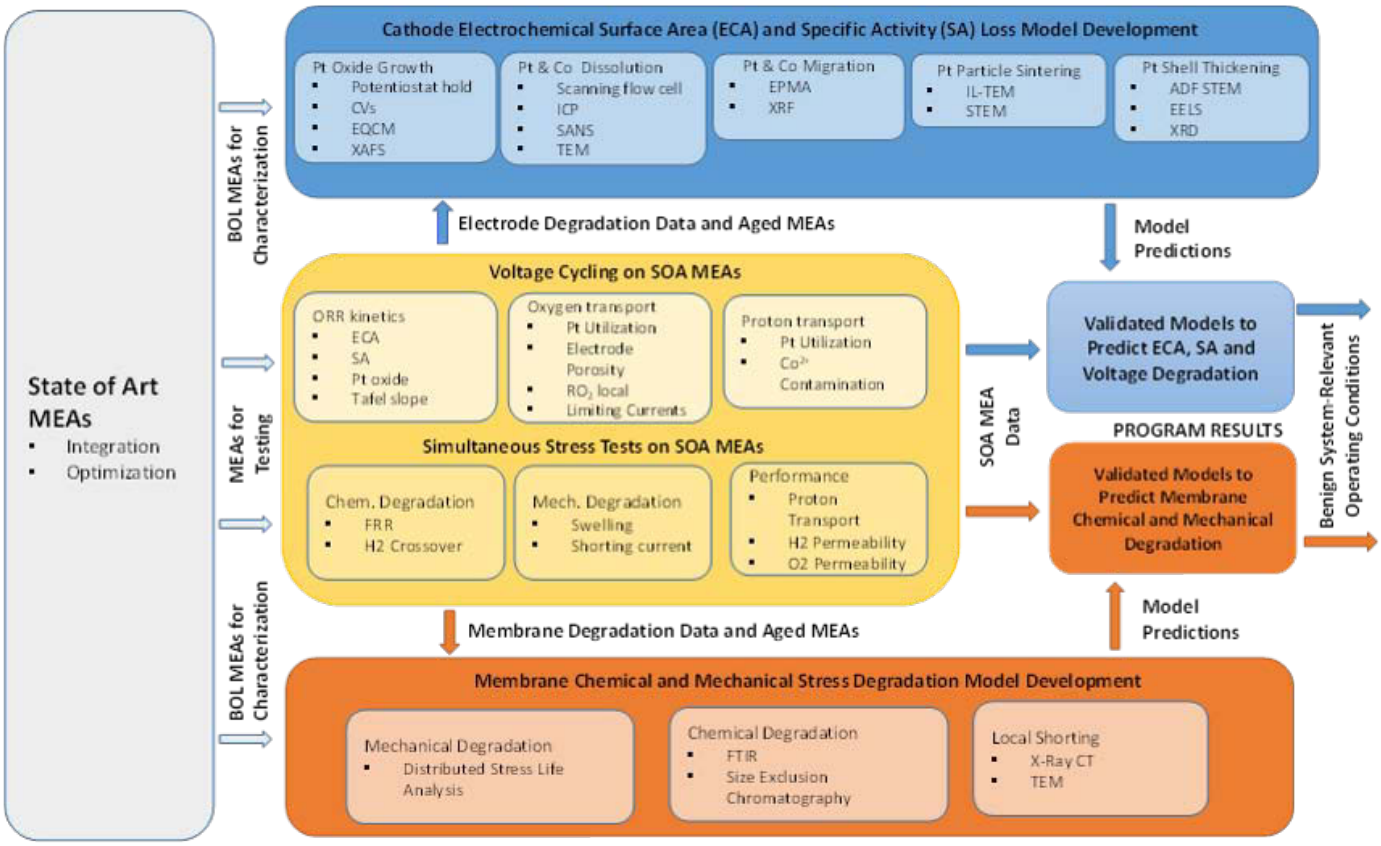

CV – cyclic voltammetry; EQCM – electrochemical quartz crystal microbalance; XAFS – X-ray absorption fine structure; ICP – inductively coupled plasma; SANS – small angle neutron scattering; TEM – transmission electron microscopy; EPMA – electron probe micro analyzer; XRF – X-ray fluorescence; IL-TEM – identical location-TEM; ADF – annular dark-field imaging; EELS – electron energy loss spectroscopy; XRD – X-ray diffraction; FTIR – Fourier transform infrared; CT – computed tomography; STEM – scanning transmission electron microscopy

FIGURE 1. Project framework for electrode and membrane degradation studies

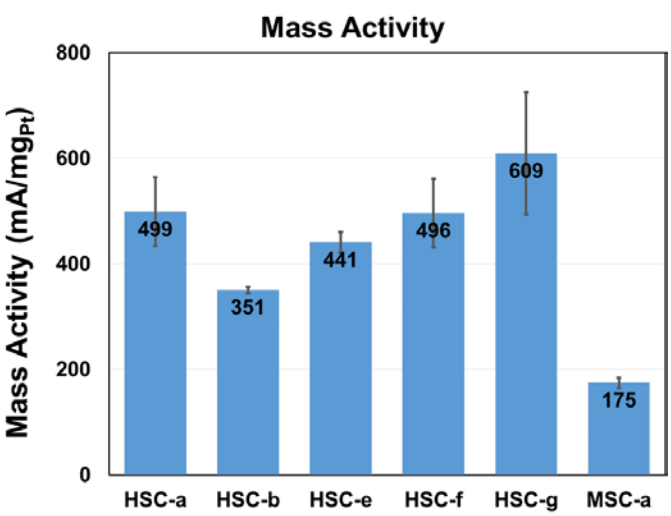

MSC – medium surface area carbon

FIGURE 2. Oxygen reduction reaction mass activity measurements at 0.9 V, 80°C, 100% relative humidity, H_2/O_2

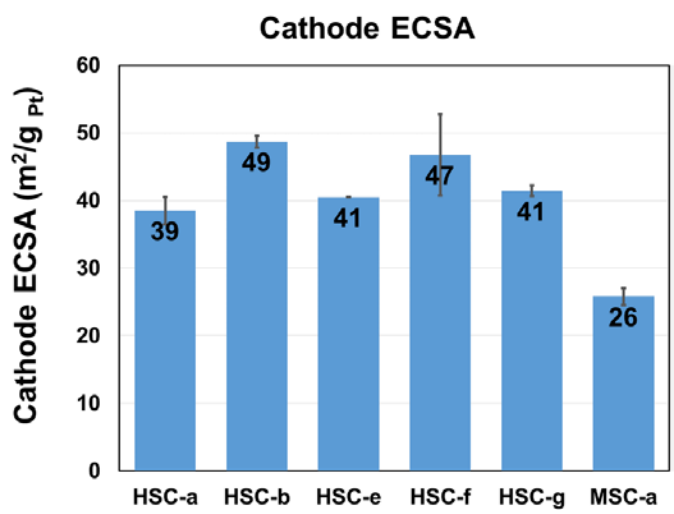

FIGURE 3. ECSA measurements at 25°C

select catalyst and other components such as ionomer and membrane for SOA MEA.

UPCOMING ACTIVITIES

For the remainder of the first year, the project will focus on generating the state-of-the-art MEA and deliver 5 cm^2 and 50 cm^2 MEA to FC-PAD. Key activities will be conducted in collaboration with FC-PAD partners to generate the SOA, including:

- Identifying catalyst, ionomers and membranes for improved performance and durability (GM) and MEA characterization (University of Texas at Austin).
- Electrochemical diagnostics including limiting current, etc., to quantify voltage loss terms of the MEA (National Renewable Energy Laboratory).
- Study ink properties using X-ray scattering methods (Argonne National Laboratory) and correlate with catalyst layer structure and ionomer interaction using advanced microscopy tools (Oak Ridge National Laboratory).
- Develop combined chemical and mechanical degradation test (GM and Giner) and explore use of advanced characterization method like X-ray micro CT (Lawrence Berkeley National Laboratory) to study membrane degradation.

The second and third years of the project will focus on electrode and membrane durability studies and MEA degradation model development.

REFERENCES

1. A. Kongkanand and M. Mathias, *The Priority and Challenge of High-Power Performance of Low-Platinum Proton-Exchange Membrane Fuel Cells*. J. Phys. Chem. Lett. 2016, 7: p. 1127–1137.

2. E. Padgett, N. Andrejevic, Z. Liu, A. Kongkanand, K. Moriyama, S. Kumaraguru, Y. Jiang, D. Mueller, *Connecting Nanostructure with the Utilization of Hydrogen Fuel Cell Catalysts using Quantitative Cryo-STEM Tomography*, Nano Lett. 2017, (submitted).

3. K.L. More, *FC-PAD: Components and Characterization*, DOE Annual Merit Review Proceedings, 2017.

V.B.6 High Performance Polymer Electrolyte Membrane Fuel Cell Electrode Structures

Mike L. Perry
United Technologies Research Center (UTRC)
411 Silver Lane
East Hartford, CT 06118
Phone: (860) 610-7339
Email: perryml@utrc.utc.com

DOE Manager: David Peterson
Phone: (240) 562-1747
Email: David.Peterson@ee.doe.gov

Contract Number: DE-EE-0007652

Subcontractors:
- Ion Power Inc., New Castle, DE
- University of Arkansas at Little Rock (UALR) Little Rock, AR

Project Start Date: October 1, 2016
Project End Date: December 31, 2019

Overall Objectives

- Develop improved understanding of the various transport losses in polymer electrolyte fuel cell (PEFC) cathode catalyst layers with state-of-the-art ultra-low platinum group metal (PGM) catalyst loadings.
- Obtain this fundamental understanding by developing and validating a detailed microstructural cathode-catalyst layer model.
- Utilize this validated cathode-catalyst layer model to develop and demonstrate membrane-electrode assemblies (MEAs) that can potentially meet all of DOE's 2020 Technical Targets for MEAs.

Fiscal Year (FY) 2017 Objectives

- Finalize multi-party non-disclosure agreement with all partners, including FC-PAD Consortia members.
- Demonstrate MEA with state-of-the-art performance with ultra-low PGM loadings.
- Complete framework of microstructural cathode-catalyst layer model.

Technical Barriers

This project addresses the following technical barriers from the Fuel Cells section of the Fuel Cell Technologies Office Multi-Year Research, Development, and Demonstration Plan.

(A) Durability (Improved understanding of initial transport losses is required to mitigate degradation)

(B) Cost (MEAs with ultra-low PGM loadings have relatively large transport losses)

(C) Performance (Reduced transport losses are required to meet high power density targets)

Technical Targets

- This project is ultimately focused on developing high performance MEAs with ultra-low PGM catalyst loadings. However, to date, the team has focused on MEAs with Pt-only catalysts (i.e., not Pt-alloy catalysts that have higher activities) since these MEAs are less complex.

TABLE 1. Progress towards Meeting MEA Technical Targets for Transportation

Characteristic	Units	DOE 2020 Targets	Project Status (differential operating conditions)
PGM total loading	mg-PGM/cm$^2_{geo}$	≤0.125	0.2 total (0.1 each electrode)
MEA performance	mA/cm$^2_{geo}$ @ 0.8 V	≥300	222 (Pt-only catalyst)
MEA performance	mW/cm$^2_{geo}$ @ rated power (~0.65 V)	≥1,000	722 (Pt-only catalyst)

FY 2017 Accomplishments

- Developed and demonstrated MEAs with improved performance, even with reduced catalyst loadings (i.e., MEAs with 0.2 mg-Pt/cm² exhibited superior performance to initial MEAs with 0.3 mg-Pt/cm²).
- Demonstrated that MEAs with low loadings of Pt-only catalysts exhibit similar transport losses as MEAs with Pt-alloy catalysts, as long as total catalyst surface area is comparable.
- Developed PEFC-electrode model that includes basic framework for microstructural features in state-of-the-art MEAs.
- Have begun fabricating novel thin-film catalysts with varying catalyst densities.

✧ ✧ ✧ ✧ ✧

INTRODUCTION

MEAs with ultra-low loadings of highly active Pt-alloy catalysts have already been demonstrated to exceed DOE's 2020 high-efficiency target of >0.3 A/cm^2 at 0.8 V [1]; however, the rated-power target of 1 W/cm^2 cannot be met with these MEAs due to transport losses unique to MEAs with ultra-low catalyst loadings. Therefore, what is primarily needed to fully realize DOE's 2020 targets is mitigation of these transport losses, which is the focus of this project. The initial focus of this project is to improve the fundamental understanding of transport losses in PEFC cathode catalyst layers since the sources of these losses are not sufficiently understood. Subsequently, this improved understanding will be used to design advanced MEAs that have significantly reduced transport losses. This should ultimately enable the simultaneous requirements of high mass activity, low PGM loading, and high power density to be achieved.

APPROACH

The project objective will be realized by first developing and validating a detailed microstructural cathode-catalyst layer (CCL) model. CCLs are complex structures and there are many constituents and mechanisms within this critical layer that may make significant contributions to the observed transport losses. Furthermore, the relative importance of processes may vary with operating conditions. One needs to be able to differentiate between the wide variety of possible microstructures and phases within the electrodes with sufficient geometric detail in order to discern the transport-loss mechanisms. UTRC has begun to develop a detailed geometric model of the CCL that can be used to uniquely determine what components and mechanisms are major contributors to transport losses in this critical layer. A wide variety of CCL-characterization methods are being used to validate the model's geometric details and testing of a variety of MEAs under various operating conditions will enable validation of the model's performance-prediction capabilities.

The core project team has the capability to fabricate state-of-the-art MEAs using conventional carbon-support catalysts. In addition, UALR has unique capabilities to fabricate thin-film catalysts architectures, which shall eventually be used to develop CCLs with alternative electrocatalyst structures. Therefore, the team has ability to make both state-of-the-art MEAs and novel catalyst materials, and these capabilities will be used to design innovative catalyst-layer morphologies in order to achieve high performance at both high and low power densities. Discerning the sources and magnitudes of the various losses requires testing a matrix of CCLs that provide sufficient variations in the underlying parameters to highlight the different losses. Furthermore, each CCL variant needs to be subjected to a battery of diagnostic tests that help to quantify the different overpotentials. The iterative process to develop these high-performance MEAs is depicted in Figure 1, which includes utilizing the world-class capabilities of the FC-PAD Consortium.

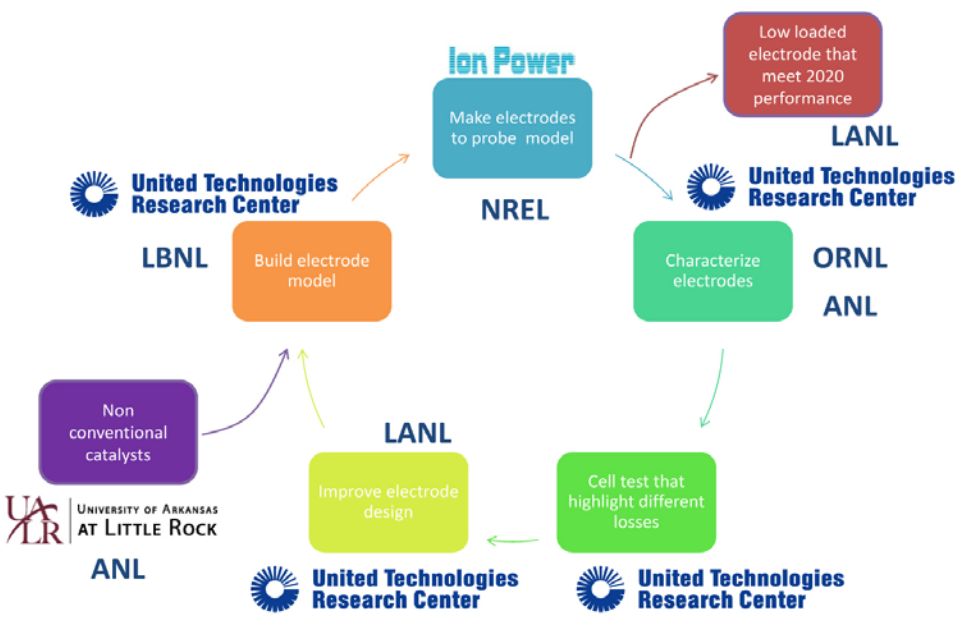

LBNL – Lawrence Berkeley National Laboratory; NREL – National Renewable Energy Laboratory; LANL – Los Alamos National Laboratory; ORNL – Oak Ridge National Laboratory; ANL – Argonne National Laboratory

FIGURE 1. Simple graphical summary of the team's approach to achieving the project's objectives

RESULTS

UTRC has developed a framework of a microstructural geometric model of the CCL that can be used to determine what components and mechanisms are major contributors to transport losses in this critical layer. The general structure is similar to film-plus-core models of agglomerates like those reviewed by Weber [2]. In the case of conventional Pt alloy on carbon catalysts, emphasis is placed on the contents and structure of the agglomerate. Figure 2 shows calculated values for the number of carbon particles per agglomerate (n_c/n_a) and ionomer film thickness assuming that the ionomer forms a spherical shell around the C particles. The number of C particles per agglomerate and the thickness of the ionomer film increases with agglomerate diameter and both of these effects tend to decrease oxygen transport to catalyst sites. Packing more C particles in an agglomerate increases the flux through the ionomer film, while increasing the film thickness increases transport resistance. Most of the C particles should contact the ionomer shell when the number of carbon particles per agglomerate is small. Pt located on C that is disconnected from the ionomer may be underutilized when the fuel cell is operated. Understanding the distributions of catalyst and ionomer on carbon are essential to the unlocking of the microstructure of the CCL.

Limiting current densities for oxygen transport in the CCL can be derived for different geometries. Examination of limiting cases is instructive as it shows how to construct test electrodes that may help to discriminate the best approximation to the true electrode structure. For example, Figure 3 shows four interesting limiting cases for oxygen diffusion in the CCL that have already been included in the UTRC model. Each of the four limiting cases depicted in Figure 3 have different limiting current densities, which have unique dependencies on key CCL geometric parameters. Therefore, these limiting cases provide a useful starting point for the process of understanding the structure-performance relationships of the CCL. The various unique dependencies on CCL parameters can also be organized and used to guide the preparation of MEAs that highlight the differences between these limiting cases. Additional limiting cases are also possible and will be included in the model.

UALR has been working on density-modulated platinum thin film (Pt-TF) catalysts produced by high-pressure sputtering deposition. Change of working gas pressure of the sputtering system from low to high values during film growth can result in denser film bottoms and more porous tops. It is hypothesized that low-density film tops can provide effective transportation of oxygen and water, which could enhance catalyst utilization and result in reduced Pt-loading and enhanced activity. Porous, yet interconnected, networks of Pt atoms in the low-density Pt-TF surface can also potentially mitigate agglomeration and dissolution problems. In addition, high-density film bottom is expected to provide a strong adhesion to the substrate, potentially leading to enhanced physical and electrochemical stability of the Pt-TF. Stronger bonds, along with self-protection against the acidic environment due to the dense-packing of Pt atoms at the interface with the substrate, can hinder leaching of Pt and avoid the detachment of large regions of Pt-TF from the substrate as a whole. Additionally, high-density layer can reduce contact resistance and enhance the electronic conductivity. UALR has fabricated Pt-TFs with different

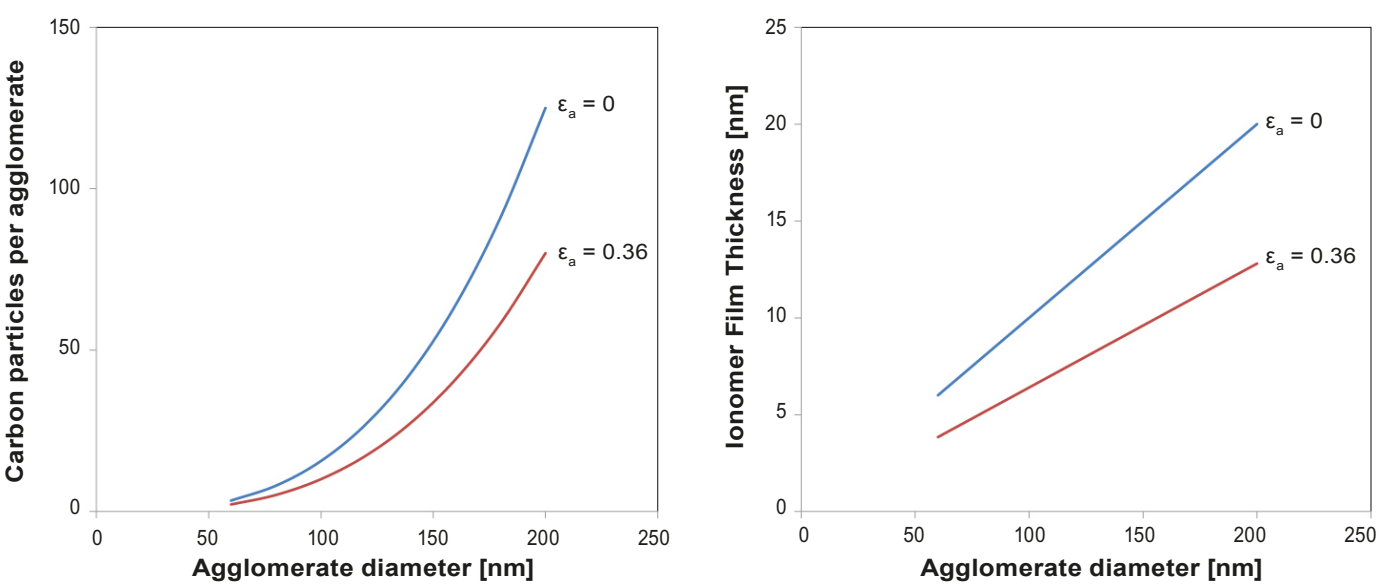

FIGURE 2. Carbon particles per agglomerate and ionomer-film thickness as a function of agglomerate diameter. The C particles are assumed to be 40 nm in diameter and the ionomer-to-C ratio is assumed to be 0.6. Two values of the intra-agglomerate porosity are assumed: $\varepsilon_a = 0$ and $\varepsilon_a = 0.36$, which is the porosity of a bed of randomly close packed spheres.

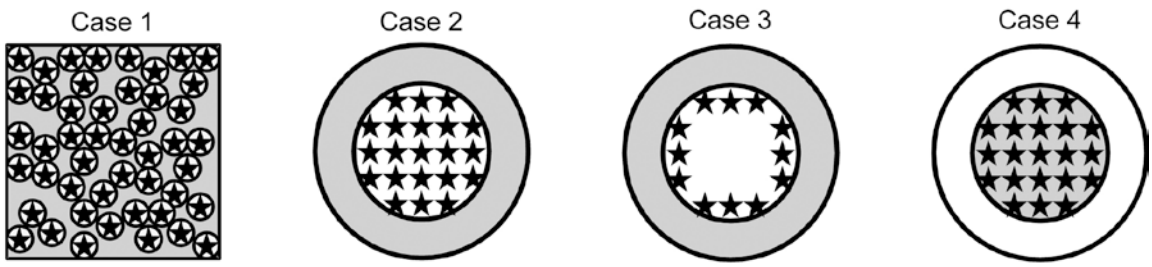

FIGURE 3. Schematic illustration of four limiting cases for O_2 transport in the CCL. Grey represents regions of hindered transport in all cases, while white denotes regions where transport is facile. O_2 reduction occurs at the black stars. Case 1 treats diffusion through the thickness of the electrode. Case 2 treats diffusion through an ionomer film surrounding spherical agglomerates where all interior catalyst sites are fully utilized. Case 3 is similar to Case 2, but only those catalyst sites in contact with the ionomer are active. Case 4 treats transport limitations inside the agglomerates; O_2 transport in the core of the agglomerates could occur in (a) gas with Knudsen effects, (b) ionomer, or (c) liquid water.

densities/porosities and performed cyclic voltammetry and rotating disk electrode measurements in aqueous perchloric-acid electrolyte to study their electrochemical activity and stability. Specific activity values showed that porous films have higher catalytic activity compared to that of denser films with rotating disk electrode measurements. This data will be used to design the density-modulated Pt-TF by optimizing the thickness and the density of the bottom and top layers of the film.

CONCLUSIONS AND UPCOMING ACTIVITIES

The primary focus of this project, to date, has been on developing both the advanced methods and materials required to develop the next-generation of MEAs. It is projected that these MEAs shall have significantly different CCL structures than conventional MEAs. These advanced MEAs may utilize both conventional catalyst materials (e.g., PGMs supported on carbon), as well as novel catalysts (e.g., Pt-TFs). The complete theoretical models and the fundamental understanding derived from the combination of modeling and testing of advanced MEAs with various electrode structures in this project shall eventually be published in the open literature, and this should help the entire PEFC community understand the key transport mechanisms in ultra-low-loaded MEAs, which should lead to the development of improved PEFCs that meet both the cost and performance targets established by DOE for transportation applications.

FY 2017 PUBLICATIONS/PRESENTATIONS

1. M.L. Perry, "Polymer Electrolyte Fuel Cell Diagnostics," presented at the 2017 Spring *Electrochemical Society* Meeting (invited talk), New Orleans, LA, May 2017.

2. M.L. Perry, "High Performance PEFC electrode structures," presented at the 2017 FCTO Annual Merit Review (AMR) meeting, Project ID# FC157, Washington DC, June 2017.

REFERENCES

1. D. Myers, et. al., Rationally designed catalyst layers for PEMFC performance optimization," presented at the 2016 FCTO AMR meeting, Project ID# FC157, Washington DC, June 2016.

2. A. Weber, et al., "A Critical Review of Modeling Transport Phenomena in Polymer-Electrolyte Fuel Cells, J. Electrochem. Soc., **161**, F1254 (2014).

V.B.7 Fuel Cell Membrane Electrode Assemblies with Ultra-Low Pt Nanofiber Electrodes

Peter N. Pintauro
Vanderbilt University
PMB 351604
3201 Vanderbilt Place
Nashville, TN 37235
Phone: (615) 343-3878
Email: pn.pintauro@vanderbilt.edu

DOE Manager: Donna Ho
Phone: (202) 586-8000
Email: Donna.Ho@ee.doe.gov

Technical Advisor: John Kopasz
Phone: (630) 252-7531
Email: kopasz@anl.gov

Contract Number: DE-EE0007653 (FC-PAD)

Subcontractors:
- Nilesh Dale, Nissan Technical Center North America, Farmington Hills, MI
- Younan Xia, Georgia Institute of Technology, Atlanta, GA
- Mike Yandrasits, 3M Company, St. Paul, MN

Project Start Date: January 1, 2017
Project End Date: December 31, 2020

Overall Objectives

- Improve performance and local transport properties in fuel cell electrodes through development of elctrospun electrode structures.
- Fabricate, characterize, and evaluate membrane electrode assemblies (MEAs) with nanofiber mat cathodes containing highly active oxygen reduction reaction catalysts for hydrogen–air fuel cells.
- Generate useful correlations and insightful understandings regarding nanofiber electrode electrospinning.
- Develop collaborations with The Fuel Cell Consortium for Performance and Durability researchers at national laboratories.

Fiscal Year (FY) 2017 Objectives

- Synthesize PtNi/C shape-controlled catalyst (at Georgia Tech).
- Identify and optimize conditions for electrospinning particle/polymer nanofiber mats with TKK (Tanaka Kikinzoku Kogyo) PtCo/C and PtNi/C catalysts and with Georgia Tech PtNi/C catalyst, where the catalyst binder is a perfluorsulfonic acid or perfluoroimide acid ionomer.
- Fabricate and evaluate the performance of nanofiber and sprayed cathode MEAs.

Technical Barriers

This project addresses the following technical barriers from the Fuel Cells section of the Fuel Cell Technologies Office Multi-Year Research, Development, and Demonstration Plan.

(A) Durability (ageing and degradation of fuel cell electrodes)

(B) Cost (lowering the material and manufacturing costs of high performance electrodes and MEAs)

(C) Performance (fabricating MEAs that generate higher power at lower precious metal loading, with special emphasis on the cathode)

Table 1 shows the progress towards meeting the technical targets for electrocatalysts and MEAs for transportation applications.

FY 2017 Accomplishments

- Electrospun particle/polymer nanofiber mat cathodes were prepared at 0.1 mg_{Pt}/cm^2 with commercial PtCo/C and PtNi/C catalysts, where the binder was a mixture of Nafion and PAA.
- A 5 cm^2 MEA with a PtNi/C nanofiber cathode (0.1 mg_{Pt}/cm^2) produced 68% more power at 0.65 V, 80°C, 100% relative humidity, and 200 kPa_{abs} vs. a conventional sprayed cathode MEA at the same conditions.
- In 5 cm^2 MEAs with a Nafion 211 membrane, PtCo/C nanofiber cathodes performed very well, with a rated power of 784 mW/cm^2 at 95°C and 150 kPa_{abs} (which is approaching the DOE 2020 target of 1 W/cm^2).
- Nanofiber cathode MEAs exhibited excellent durability in a load cycling accelerated stress test, with a power loss of 30% at 0.65 V after 30,000 voltage cycles from 0.60 V to 0.95 V. This power loss is significantly less than that in a conventional slurry electrode MEA.
- Batches of shape-controlled PtNi/C catalyst were prepared at Georgia Tech and sent to Vanderbilt for initial electrospinning studies.

TABLE 1. Progress towards Meeting Technical Targets for Electrocatalysts and MEAs for Transportation Applications

Characteristic	Units	DOE 2020 Electrocatalyst and MEA Targets	Project Status[a]
Mass activity	A/mg_{PGM}@0.90 $mV_{iR\text{-}free}$	0.44	0.29[b]
PGM total loading (both electrodes)	$mg\text{-}PGM/cm^2_{geo}$	0.125	0.20
Loss in performance at 0.80 A/cm^2 after a load cycling AST (30,000 voltage cycles)	mV	<30	59
Loss in performance at 1.5 A/cm^2 after a load cycling AST (30,000 voltage cycles)	mV	<30	95
MEA performance @ 0.80 V	mA/cm^2_{geo}	300	347
MEA performance @ rated power (150 kPa_{abs})	mW/cm^2_{geo}	1,000	784

[a] 5 cm^2 MEA, TKK PtCo/C cathode catalyst, Pt/C anode catalyst, Nafion® + poly(acrylic acid) (PAA) binder, Nafion 211 membrane, temperature = 80°C, 200 $kPa_{abs,}$ 100% relative humidity.
[b] measured at 150 kPa_{abs}
PGM – platinum group metal; AST – accelerated stress test

- 5 cm^2 nanofiber cathode MEAs were prepared and sent to Los Alamos National Laboratory for preliminary testing.

✧ ✧ ✧ ✧ ✧

INTRODUCTION

Despite widespread literature demonstration of excellent oxygen reduction reaction activity of some new catalysts in rotating disk electrode experiments, almost none of them have shown promising performance in fuel cell MEAs. This is because MEA fabrication remains centered on decal, catalyst coated membrane, and/or catalyst coated gas diffusion electrode methodologies, with little or no control over the macro-scale organization of catalyst particles and polymer binder. Features such as electrode macroporosity, microporosity, and particle and binder interconnectivity become more critical when high-performance nanomaterials are used in electrodes. Consequently, new electrode fabrication techniques are needed for next-generation MEAs, which accommodate and control the multi-scale arrangement of catalyst and binder for improved power output and durability.

Building from strong initial data showing electrospinning as a viable approach to the design and fabrication of fuel cell electrodes [1-3], the present project seeks to fabricate MEAs containing nanostructured Pt-alloy catalyst powders and selected perfluorosulfonic acid ionomer and blended polymer binders with the capability of meeting the DOE 2020 performance and durability targets for MEAs and catalyst layers.

APPROACH

The research approach for this project directly addresses three critical issues: (1) the use of new high activity PtNi/C and PtCo/C catalysts in hydrogen–air fuel cell MEA cathodes; (2) the organization of Pt-alloy catalytic nanoparticles into intelligently designed nanofiber mat electrodes via particle/polymer electrospinning, where the fiber volume fraction, nanoparticle loading, binder type, fiber diameter, and mat thickness are independently controlled; and (3) the identification of the optimum composition and structure of nanofiber electrode MEAs which meet the DOE 2020 performance, Pt loading, and durability targets.

The project has five major tasks: (1) prepare and compare nanofiber and sprayed electrode MEAs with commercial Pt-alloy cathodes at ultra-low Pt loading with various perfluorinated ionomer-based binders; (2) synthesize Pt-Ni octahedra catalysts with high oxygen reduction activity; (3) incorporate the octahedra Pt-Ni catalysts into nanofiber and sprayed electrode MEAs; (4) optimize the nanofiber cathode mat composition and mat morphology to maximize fuel cell performance and durability at high and low relative humidity conditions; and (5) provide catalyst powder, electrospun cathode mats, MEAs, experimental skills, and the team's electrospinning knowledge base to our Fuel Cell Consortium for Performance and Durability collaborators.

RESULTS

Figure 1 shows a top-down scanning electron microscope image of an electrospun mat composed of commercial TKK PtCo/C catalyst powder with a binder of Nafion perfluorosulfonic acid and PAA. The catalyst/Nafion/PAA weight ratio of the fibers is 55/30/15 and the average fiber diameter is approximately 600 nm. Representative examples of hydrogen–air fuel cell polarization data from nanofiber and slurry PtCo/C cathode MEAs (both made at Vanderbilt University) are shown in Figure 2. The nanofiber MEA power density at 0.65 V was 40% higher than that for the slurry electrode MEA (where the latter utilized a neat Nafion binder), i.e., 784 mW/cm^2 vs 559 mW/cm^2. At

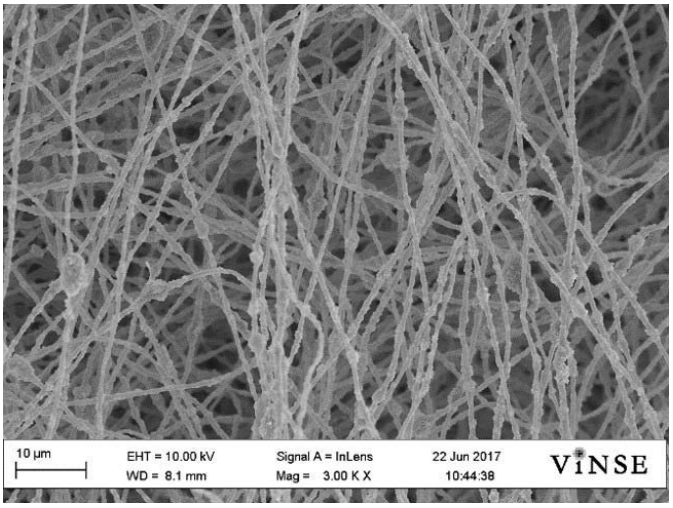

FIGURE 1. Scanning electron microscope image of a nanofiber mat with TKK PtCo/C catalyst and a binder of Nafion and PAA

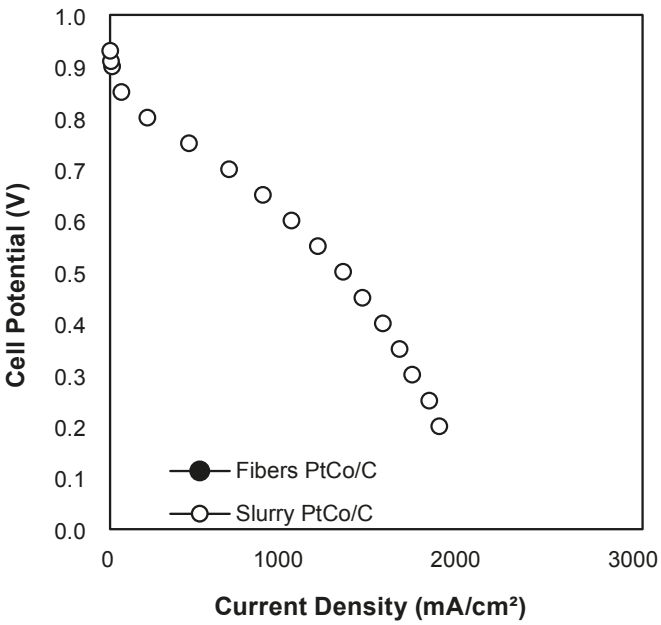

FIGURE 2. Hydrogen–air fuel cell polarization data for a nanofiber cathode MEA vs. a slurry cathode MEA using PtCo/C at 80°C and 200 kPa_{abs} pressure

maximum power, the improvement was 32%. Higher power densities are attributed to (1) a more uniform distribution of binder and catalyst particles throughout the fiber, resulting in a significantly higher electrochemically active surface area for the nanofiber cathode (60 vs. 34 m^2/g) and (2) rapid removal of product water due to inter- and intra-fiber porosity, which is particularly important at maximum power where the current density is high.

Rated power was found from fuel cell polarization data, at a voltage given by Equation 1, where the stack power was selected to be 90 kW, Q/ΔT was fixed at 1.4 kW/°C, the fuel cell operating temperature was set at 95°C, the pressure was 150 kPa_{abs}, and the ambient temperature was 40°C. At rated power (0.674 V, according to Equation 1), the power density of a PtCo/C nanofiber cathode MEA at 0.1 mg_{Pt}/cm^2 was 784 mW/cm^2, which is approaching the DOE 2020 target of 1,000 mW/cm^2.

Catalyst support (carbon corrosion) and electrocatalyst (metal dissolution) voltage cycling ASTs were performed with nanofiber electrode and painted slurry electrode MEAs, where the nanofiber cathode had a binder of Nafion + PAA and where the slurry MEA used a neat Nafion binder. The catalyst support AST protocol involved triangular wave potential cycling from 1.0 V to 1.5 V for 1,000 cycles. For the electrocatalyst AST, the voltage was cycled 30,000 times from 0.6 V to 0.95 V. The fuel cell operating pressure during collection of polarization data was 200 kPa_{abs}, the feed gas flow rates were 500 cm^3/min for hydrogen and 2,000 cm^3/min for air, the temperature was 80°C, and the relative humidity was fixed at 100%. Both the anode and cathode Pt loadings were 0.1 mg/cm^2. Beginning of life and end of life fuel cell polarization curves for the catalyst support AST are shown in Figure 3. The slurry electrode lost 41% of its maximum power during the test, as compared to a 27% power loss for the nanofiber cathode (where the latter is closely approaching the 2020 DOE target). The results of the electrocatalyst AST are shown in Figure 4. As was the case for the catalyst support AST, the durability of the nanofiber electrode MEA in the electrocatalyst AST is excellent (only a 32% power loss at 0.65 V), with an end of life polarization curve that is at or above the beginning of life curve for the slurry electrode.

CONCLUSIONS AND UPCOMING ACTIVITIES

The use of nanofiber electrode MEAs significantly improved the fuel cell performance with a commercial TKK PtCo/C catalyst at 0.10 mg_{Pt}/cm^2, with a 32% boost in the maximum power and 40% higher power at 0.65 V vs. a slurry cathode MEA. The rated power at 95°C and 150 kPa_{abs} pressure was promising at 784 mW/cm^2. The nanofiber MEA also exhibited improved durability vs. a non-optimized slurry cathode MEA, with higher power densities at end of life, after catalyst support and electrocatalyst ASTs.

$$\frac{Q}{\Delta T} = \frac{\left[Stack\ Power\ (kW) \times (1.25 - V\ @\ rated\ \ power) / V\ @\ rated\ \ power)\right]}{Cell\ Operating\ \ Temperature\ (^{o}C) - Ambient\ \ Temperature\ (^{o}C)} \quad (1)$$

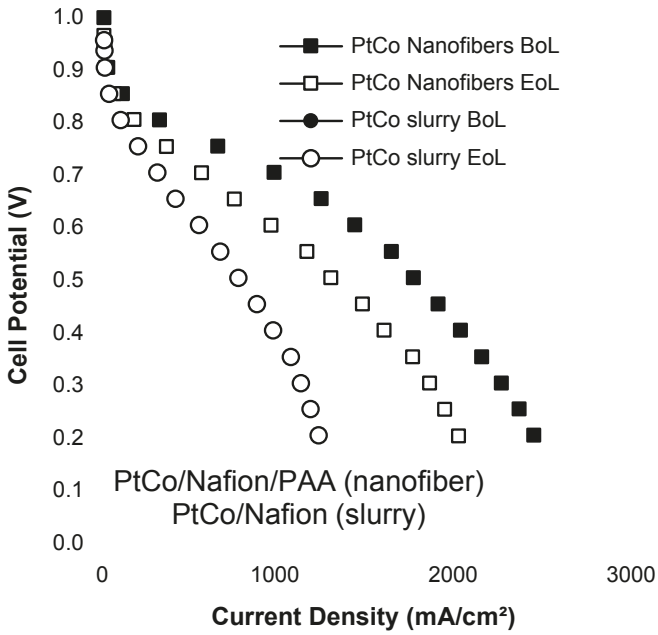

FIGURE 3. Carbon corrosion AST (1,000 voltage cycles at end of life) results for nanofiber and slurry cathode MEAs with PtCo/C and a binder of Nafion + PAA

Upcoming activities will focus on:

- Preparing, characterizing, and testing nanofiber mat cathodes with (1) TKK PtCo/C catalyst and different binders, (2) TKK PtNi/C catalyst and Nafion/PAA binder, and (3) Georgia Tech shape-controlled PtNi/C catalyst and Nafion/PAA binder.
- Measuring oxygen limiting current in nanofiber cathode MEAs.
- Preparing 5 cm^2 and 25 cm^2 nanofiber MEAs for initial performance assessment and durability testing at Nissan Technical Center North America and at Los Alamos National Laboratory.

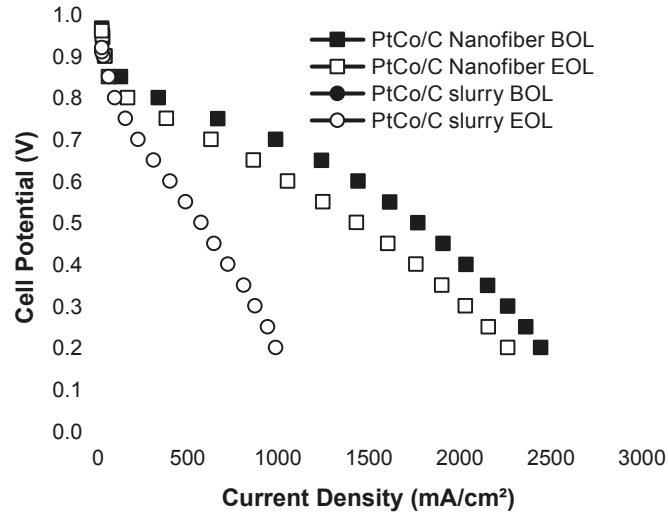

FIGURE 4. Fuel cell polarization results before and after a metal dissolution AST (end of life after 30,000 voltage cycles, 0.6 V to 0.95 V) for nanofiber and slurry cathode MEAs with PtCo/C and a binder of Nafion + PAA

FY 2017 PUBLICATIONS/PRESENTATIONS

1. J.J. Slack, R. Wycisk, N. Dale, A. Kumar, and P.N. Pintauro, "Electrospun Nanofiber Fuel Cell MEA Cathodes with PtCo/C Catalyst" *ECS Transactions* (2017).

REFERENCES

1. W. Zhang and P.N. Pintauro, "High Performance Nanofiber Fuel Cell Electrodes", *ChemSusChem*, **4**, 1753–1757 (2011).

2. M. Brodt, R. Wycisk, and P.N. Pintauro, "Nanofiber Electrodes with Low Platinum Loading for High Power Hydrogen/Air PEM Fuel Cells", *J. Electrochem. Soc*, **160**, F744–F749 (2013).

3. M. Brodt, T. Han, N. Dale, E. Niangar, R. Wycisk, and P. Pintauro, "Fabrication, In-Situ Performance, and Durability of Nanofiber Fuel Cell Electrodes", *J. Electrochem. Soc.*, **162**, F84–F91 (2015).

V.C.1 New Fuel Cell Membranes with Improved Durability and Performance

Michael Yandrasits
3M Company
3M Center, Building 201-1W-28
St. Paul, MN 55144
Phone: (651) 736-5719
Email: mayandrasits@mmm.com

DOE Manager: Gregory Kleen
Phone: (240) 562-1672
Email: Gregory.Kleen@ee.doe.gov

Contract Number: DE-EE0006362

Subcontractors:
- General Motors (GM) Fuel Cell Activities, Pontiac, MI, Craig Gittleman
- Vanderbilt University, Nashville, TN, Peter Pintauro

Project Start Date: October 1, 2013
Project End Date: September 30, 2017

Overall Objectives

- All of the DOE Fuel Cell Technologies Office Multi-Year Research, Development, and Demonstration (MYRDD) Plan membrane performance, durability, and cost targets will be met simultaneously with a single membrane.
- Membranes will be based on multi-acid side chain (MASC) ionomers.
- Electrospun nanofiber structures will be developed to reinforce membranes.
- Peroxide scavenging additives will be used to enhance chemical stability.
- New membranes will have improved mechanical properties, low area specific resistance, and excellent chemical stability compared to the current state of the art.
- Experimental membranes will be integrated into membrane electrode assemblies (MEAs) and evaluated in single fuel cells and finally in fuel cell stacks.

Fiscal Year (FY) 2017 Objectives

- Begin stack test at General Motors, demonstrate 2,000 h durability with membranes developed in this project.
- Postmortem analysis on MEA cells from stack test.
- Investigate origin of performance decay observed in the open circuit voltage (OCV) accelerated stress test.

Technical Barriers

This project addresses the following technical barriers from the Fuel Cells section of the Fuel Cell Technologies Office MYRDD Plan.

(A) Durability

(B) Cost

(C) Performance

Technical Targets

The DOE 2020 technical targets for membrane are shown in Table 1 along with the data for the membrane developed in this project (Milestone #8). This membrane consists of ionomer and nanofiber developed in this project and optimized peroxide stabilizing additives.

FY 2017 Accomplishments

- Stack testing completed at General Motors. Testing terminated at about 800 h due to several cell failures.
- Postmortem analysis of cells from stack test were completed at GM. Cross section images on failed membranes showed membrane degradation and debris in some locations.
- Degradation mechanism for perfluoroimide acid (PFIA) ionomer investigated at 3M using multi-layer membrane technique.

✧ ✧ ✧ ✧ ✧

INTRODUCTION

Fuel cell membranes with low resistance are highly desirable in order to maximize system power and efficiency. This objective is especially difficult under low humidity conditions where the proton resistance of the membrane is the highest. Increasing the number of charge carriers and decreasing the thickness can both be effective in reducing resistance, however, they can compromise the membrane durability if not designed properly. Proton conductivity can be increased by simply adding charge carriers, such as sulfonic acid groups, to a polymer backbone; however, it will ultimately become a water-soluble polymer and not be effective as a membrane. Likewise, reducing the thickness of a membrane can result in poor durability in both accelerated testing and actual use conditions. Because of these reasons, a membrane is needed that has increased

TABLE 1. Fuel Cell Membrane Targets from DOE Fuel Cell Technologies Office MYRDD Plan and Results for Project Milestone #8 Membrane

Characteristic	Units	2017 & 2020 Targets	MS#8 PFIA-S (10 µm)
Maximum oxygen cross-over	mA/cm^2	2	0.6[a], 3.5[b]
Maximum hydrogen cross-over	mA/cm^2	2	1.9[c]
Area specific proton resistance at:			
120°C, P_{H2O} 40 kPa	Ohm cm^2	0.02	0.054
120°C P_{H2O} 80 kPa	Ohm cm^2	0.02	0.019
80°C P_{H2O} 25 kPa	Ohm cm^2	0.02	0.020
80°C P_{H2O} 45 kPa	Ohm cm^2	0.02	0.008
30°C P_{H2O} up to 4 kPa	Ohm cm^2	0.03	0.018
-20°C	Ohm cm^2	0.2	0.2[d]
Minimum electrical resistance	Ohm cm^2	1,000	1,635[e]
Cost	$/$m^2$	20	Not available
Durability			
Mechanical	Cycles with <10 sccm crossover	20,000	>24,000
Chemical	h	>500	614

[a] O_2 crossover based on DOE Table 3.4.12 indicating measurement at 0.5 V
[b] Calculated from GM O_2 permeability data at 80°C, 100% relative humidity (RH), 1 atm.
[c] In cell measurements at 3M 70°C, 100% RH, 1 atm.
[d] Calculated from in-plane data
[e] Data provided by GM

conductivity, is water insoluble, and is stable to chemical and mechanical degradation. This project aims to develop a new membrane based on a perfluorinated ion conducting polymer and nanofiber support that can meet the DOE targets for membrane performance, durability, and cost.

APPROACH

The approach for this project is to develop a new ionomer based on a perfluorinated polymer that contains MASC in order to provide improved conductivity at dry conditions. This strategy has the advantage of creating a polymer with a large number of charge carriers, in other words high ion exchange capacity, while maintaining a polytetrafluoroethylene backbone that prevents the polymer from dissolving in water. Both perfluoro sulfonic acid and perfluoro bis(sulfonyl)imides are strong acids and have excellent conductivity characteristics. The bis(sulfonyl) imide functionality also serves as a chain extender, allowing for multiple acid groups per side chain (Figure 1). When the side chain contains one imide and one sulfonic acid group it is designated as a PFIA ionomer. In the case where multiple imides are used per side chain, the ionomer is considered perfluoro ionene chain extended.

In combination with the new ionomer, mechanical support will be provided by electrospun nanofibers. Work at both 3M and Vanderbilt University will determine an optimum architecture for the fiber supported membrane based on filling an existing nanofiber mat with ionomer

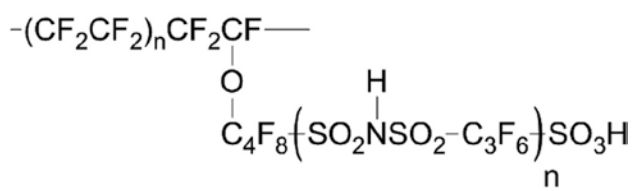

FIGURE 1. Structure for perfluoro ionene chain extended ionomers. Where n=1 the ionomer is designated PFIA.

(3M) or spinning both ionomer fibers and support fiber simultaneously followed by consolidating the ionomer fibers into a continuous matrix (Vanderbilt).

Membranes developed in this project are evaluated against the DOE 2020 targets using a variety methods with the ultimate program objective of demonstrating 2,000 h of durability in a small stack, tested at GM. Additional information regarding the failure modes and insight into improved durability will be obtained by postmortem analysis at the end of this test.

RESULTS

Throughout the course of this project we have demonstrated exceptional membrane performance and durability in accelerated stress tests as shown in Table 1. In almost all cases we have been able to meet the DOE 2020 targets for automotive membranes. This year, as a

final demonstration, we initiated a stack test at GM using experimental membranes developed in this project. This stack test represents the first long term performance test that was run under non-accelerated conditions such as OCV hold or humidity cycling. Unfortunately, the experimental samples did not meet the 2,000 h target and the test was terminated at about 800 h. Failed MEAs were cross sectioned as part of the postmortem analysis. Regions of thin and missing membrane were observed in areas where leaks were detected. Images from other areas of the MEA show cracks in the membrane layer on the anode side that were arrested by the nanofiber support material. An unexpected level of debris was also observed in many of the images. Complete understanding of the origins of the premature stack failure are currently under investigation.

Accelerated stress testing such as the OCV hold has been used throughout this project as a means of comparing the stability of new membranes to those of established controls. While membranes made with the PFIA ionomer have routinely exceeded the 500 h DOE target, these samples exhibit two new behaviors. Figure 2 shows representative OCV hold data for membranes made with PFIA ionomer and a perfluorosulfanic acid (PFSA) control. Early in the test, the PFIA membrane shows a decay in the OCV potential in the first 200 h. In addition, the membrane resistance increases over the time of the test. The role of chemical stability is under investigation as a potential cause of these observations.

To better understand the chemical stability of the PFIA ionomer, we devised an experiment using three layers of membrane where, at the end of an OCV test, the center layer could be removed from the catalyst containing outer layers and analyzed for conductivity and chemical composition. Several MEAs were run in this configuration and large pieces of the center membrane were removed and analyzed. The conductivity of the PFIA membrane was lower than that for the membrane at the beginning of life (data not shown) where the traditional PFSA-based membrane showed little to no change. In addition, ^{19}F nuclear magnetic resonance (NMR) was run on the aged PFIA membrane and showed the appearance of a sulfonamide functionality during the OCV test. Figure 3 shows the ^{19}F NMR curves for the PFIA sample prior to testing (top), a sample with a known sulfonamide content of 10% (center) and the PFIA membrane after OCV testing (bottom). The aged membrane clearly shows the appearance of the sulfonamide functionality and the sulfonic acid associated with the PFSA side chain. The appearance of the sulfonic acid may be a result of decomposition or simply transfer of PFSA from the outer membrane layers, however, the amide functionality suggests the degradation of the PFIA side chain follows a somewhat more complicated pathway than that of the simpler PFSA ionomer.

A complete understanding of the degradation mechanism and kinetics is not known at this time; however, it appears as if the oxidative degradation of the PFIA polymer may

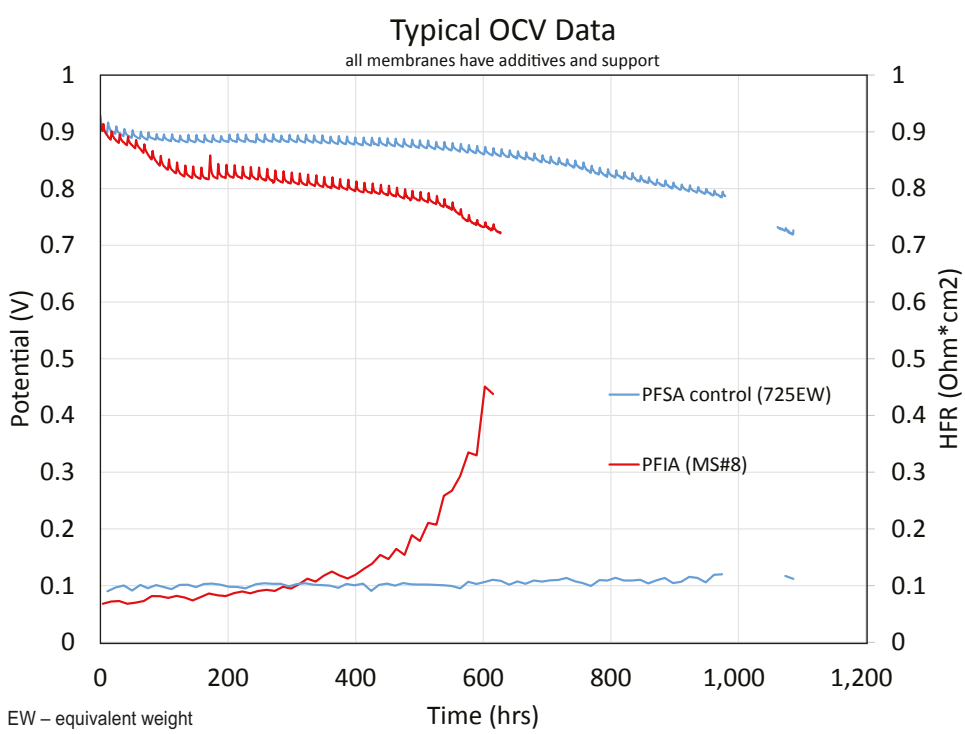

FIGURE 2. Representative accelerated stress testing at OCV. Cell potential and high frequency resistance (HFR) as shown for membranes made using a traditional PFSA ionomer (blue data) and PFIA ionomer (red data).

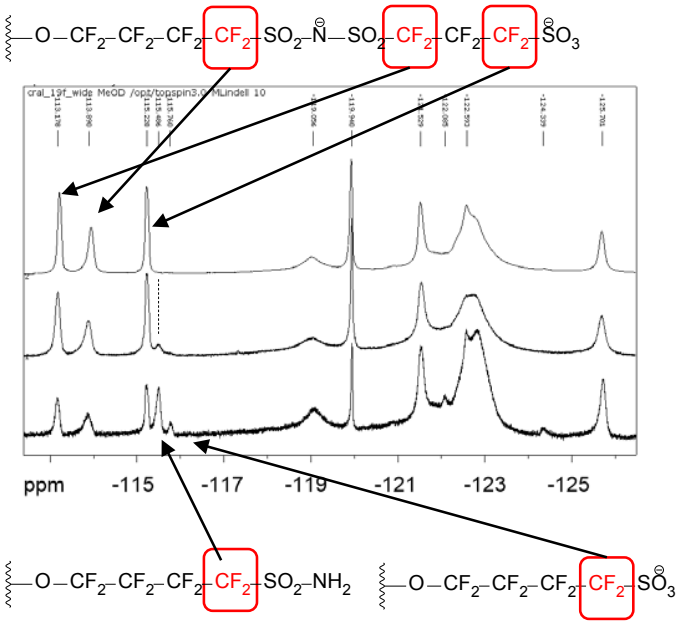

FIGURE 3. ^{19}F NMR spectra with associated peak assignments for a new PFIA ionomer (top), a sample with known sulfonamide content (center), and a PFIA based membrane after OCV testing (bottom).

be similar to that of the more well-known PFSA systems [1]. The key difference between these two ionomers is the number of protoengic groups on the side chain. In the case of PFSA ionomers, oxidative attack on the sulfonic acid result in degradation of the sidechain and, ultimately, backbone cleavage. In the PFIA case attack at the terminal sulfonic acid or the sulfonamide group may result in the degradation of the side chain resulting in a sulfonamide structure. Or, attack at the sulfonimide may also result in the degradation of the side chain leading to backbone chain cleavage and fragments of the side chain. While the specifics are not known, the possible decomposition pathways for the PFIA structure are shown in Figure 4. At this time, there is no evidence that the imide linkage is more subject to degradation than the sulfonic acid group, however, it appears that the consequences of this degradation may be different.

The benefits of the MASC approach with a nanofiber mechanical support and peroxide scavenging additives have been demonstrated throughout the course of this project. Understanding the degradation consequences of these new ionomers and membranes will be the remaining focus of the project.

CONCLUSIONS AND UPCOMING ACTIVITIES

- Membrane based on 3M's PFIA ionomer and nanofiber support materials have meet nearly all the DOE 2020 targets for performance and accelerated durability.
- Stack testing at GM was terminated after 800 h of run time on four experimental membranes developed in this project.
- Conductivity and ^{19}F NMR data shows that the PFIA degradation results in new functional groups.
- Additional investigation into PFIA stability is planned through the use of model compounds.
- Rotating disk electrode studies are planned to study the effect of ionomer decomposition products on catalyst activity.

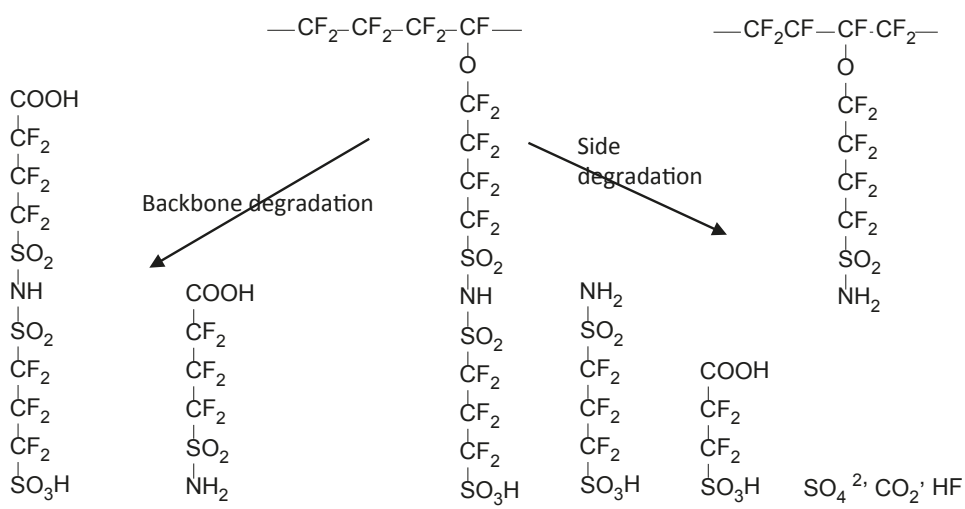

FIGURE 4. Possible degradation pathways and associated fragments for a PFIA ionomer.

FY 2017 PUBLICATIONS/PRESENTATIONS

1. FC109 at DOE's Annual Merit Review in Washington, D,C., on June 8, 2017.

2. USCAR Fuel Cell Tech Team Presentation, "New Fuel Cell Membranes with Improved Durability and Performance," November 16, 2016, Southfield, MI.

3. "V.C.1 New Fuel Cell Membranes with Improved Durability and Performance," 2016 DOE Hydrogen and Fuel Cells Annual Progress Report.

4. M. Yandrasits, M. Lindell, M. Kurkowski, M. Schaberg, "Ultra-Low EW Ionomers and Membranes for Fuel Cells," PRiME 2016, Fall ECS Conference, Honolulu, HI, October 5, 2016.

5. M. Yandrasits, "Perfluoro Imide Acid (PFIA) Ionomers for Fuel Cell Membranes," Gordon Research Conference Stonehill College, Easton, MA, August 8, 2016.

6. M. Yandrasits, M. Lindell, M. Kurkowski, M. Schaberg, "Increasing Fuel Cell Efficiency by Using Ultra-Low Equivalent Weight Ionomers," The Electrochemical Society Interface, Spring 2017.

V.C.2 Advanced Hybrid Membranes for Next Generation PEMFC Automotive Applications

Andrew M. Herring (Primary Contact), Mei-Chen Kuo, James L. Horan, and Andrew R. Motz
Colorado School of Mines (CSM)
1500 Illinois St.
Golden, CO 80401
Phone: (303) 384-2082
Email: aherring@mines.edu

DOE Manager: Gregory Kleen
Phone: (240) 562-1672
Email: Gregory.Kleen@ee.doe.gov

Contract Number: DE-EE0006363TDD

Subcontractors:
- Bryan Pivovar, National Renewable Energy Laboratory, Golden, CO
- Nilesh Dale and Ramesh Yadav, Nissan Technical Center North America (NTCNA), Farmington Hills, MI
- Michael Yandrasits, 3M Fuel Cell Components Group, St. Paul, MN
- Steven Hamrock, Independent Consultant, St. Paul, MN

Project Start Date: October 1, 2013
Project End Date: July 31, 2017

Overall Objectives

- Fabricate a low cost, high performance proton exchange membrane to operate at the temperature of an automotive fuel cell stack, with excursions to 120°C and requiring no system inlet humidification.
- Optimize the membrane to meet durability, cross-over, and electrical resistance targets.
- Incorporate the membrane into a 50 cm^2 membrane electrode assembly (MEA).

Fiscal Year (FY) 2017 Objectives

- Achieve a membrane that meets all the DOE membrane targets simultaneously in the same film.
- Incorporate the material into a sub-scale MEA, 5–10 cm^2, and test the materials using DOE and NTCNA protocols for chemical and mechanical durability, hydrogen or oxygen crossover, and performance.
- Fabricate a 50 cm^2 MEA for evaluation by the DOE or their designated third party.

Technical Barriers

This project addresses the following technical barriers from the Fuel Cells section of the Fuel Cell Technologies Office Multi-Year Research, Development, and Demonstration Plan.

(A) Durability

(B) Cost

(C) Performance

Technical Targets

The technical targets are shown in Table 1.

FY 2017 Accomplishments

- Detailed processing study that resulted in reproducible 20 μm thin films that were of suitable mechanical robustness for MEA fabrication.
- Showed that in thicker films, 80 mm, that the DOE chemical or mechanical durability targets where easily met.
- Began work towards the fabrication of a 50 cm^2 MEA that meets all the DOE membrane targets simultaneously.

✧ ✧ ✧ ✧ ✧

INTRODUCTION

The objective of this project was to fabricate a low cost, high performance hybrid inorganic–polymer membrane that had a proton area specific resistance (ASR) <0.02 ohm cm^2 at the operating temperature of an automotive fuel cell stack (95–120°C) at water partial pressures from 40–80 kPa with good mechanical and chemical durability. Additionally, the membrane was optimized for low hydrogen and oxygen crossover with high electrical ASR at all temperatures and adequate proton ASR at lower temperatures. We also gained valuable insights into rapid proton transport at the limit of proton hydration. Additional research was performed to incorporate the membrane into a 50 cm^2 MEA.

The materials at the start of this project were at a technology readiness level of 2, as we had shown that they had proton conductivity under high and dry conditions, but we had not yet consistently shown that they will function in an operational fuel cell. At the project's end the materials are at a technology readiness level of 4 and have been integrated into an MEA, demonstrating that they can function with

TABLE 1. Progress towards Meeting Technical Targets for Membranes for Transportation Applications

Characteristic/units	2020 Target	Status June 2017	Film Thickness µm	Measured Conditions
120°C and water partial pressures from 40–80 kPa/Ω cm^2	0.02	0.015	10	110°C and 50% RH
80°C and water partial pressures from 25–45 kPa/Ω cm^2	0.02	<0.01	20	80°C and 95% RH
30°C and water partial pressures up to 4 kPa/Ω cm^2	0.03	0.01	20	30°C and 95% RH
H_2 cross-over, mA/cm^2	2	2.7	20	
Chemical durability, h	<20% OCV loss 500 h	<4% 500+ h	80	90°C/30% RH/O_2 More severe than DOE test
Mechanical durability 20,000 cycles	H_2 Cross-over <15 mA/cm^2	H_2 Cross-over <1 mA/cm^2	80	20,000 wet/dry 80°C

RH – relative humidity; OCV – open circuit voltage

electrodes as a single fuel cell. This work will enable hydrogen-powered fuel cells as it will negate the need for costly and bulky external humidification unit operations in the fuel cell system. Additionally, excess water will not be an issue for freeze or fuel cell reactant supply. The project addressed the 2020 DOE technical targets for membranes for transportation applications.

APPROACH

In past funding from the Department of Energy/National Science Foundation, we have developed completely new ionomer systems based on incorporation of inorganic super acids into polymer systems, which have high proton conductivity under conditions of low humidity, higher temperature operation, high oxidative stability, and little swelling when wet. This project will perform the work to optimize the proton conductivity and mechanical properties in these materials to produce a robust thin film for proton exchange membrane fuel cells in automotive applications. The technical concept is to use functionalized inorganic super acids that utilize little water for high proton conductivity, as the protogenic group covalently attached to a polymer backbone optimized for all other functions of the membrane.

Many composite inorganic–polymer films have been fabricated, but unless the particles have dimensions on the nano-scale there is no advantage as the improvement to film properties occurs at the particle polymer interface. The limit of this approach is to use molecules with high acidity as the highly activating functionalities, but to do this we must immobilize them, control the morphology of the proton conducting channel, and fabricate an amorphous material. The two moieties that have received the most attention and appear to greatly enhance proton transport are heteropoly acids (HPAs) and zirconyl phosphonates. In previous work, we demonstrated these materials as composite membranes [1–3] but the inorganic super acid in the membrane was not immobilized. Here, we continue our work to fabricate true hybrid materials where the inorganic super acid is incorporated as a functionalized monomer [4–6]. At the beginning of the project these materials were not yet fuel cell ready, as the syntheses were inefficient and there were no methods of processing the polymers into thin proton conductive films. In this project, we have overcome all of these disadvantages with one down selected materials involving HPAs covalently attached to a commercial perfuorinated elastomer in an innovative approach to amorphous materials to produce high proton conductivity and all other properties desired of a proton exchange membrane.

RESULTS

At this stage in the project we have finished improving the chemical synthesis of the HPA material. At the beginning of the year, the material showed very promising ASR as a thin film but was not mechanically strong enough to meet the other DOE targets for fuel cell membranes. We achieved our first polarization curves by casting a thin film, 10 µm, on a gas diffusion electrode that was used as a support to obtain an MEA for testing. While this gas diffusion electrode supported MEA gave very encouraging results at 70% RH and 80°C, we were still required to produce a free standing film. We therefore cast 80 µm films for testing. The materials were fabricated into MEAs and was tested at the National Renewable Energy Laboratory in a mechanical durability test with 20,000 wet and dry cycles. The film easily met the end of test hydrogen cross-over target, with <1 mA of hydrogen cross-over current, Figure 1 (left), although the performance was not impressive at end of life as the membranes were too thick and the ASR was too high Figure 1 (right). These membranes were also sent to NTCNA for testing in the OCV chemical durability test under dry conditions at 90°C under oxygen. Usually, the incumbent perfluorosufonic acid membranes, such as Nafion® without radical scavenges as additives, in these tests have poor chemical durability and

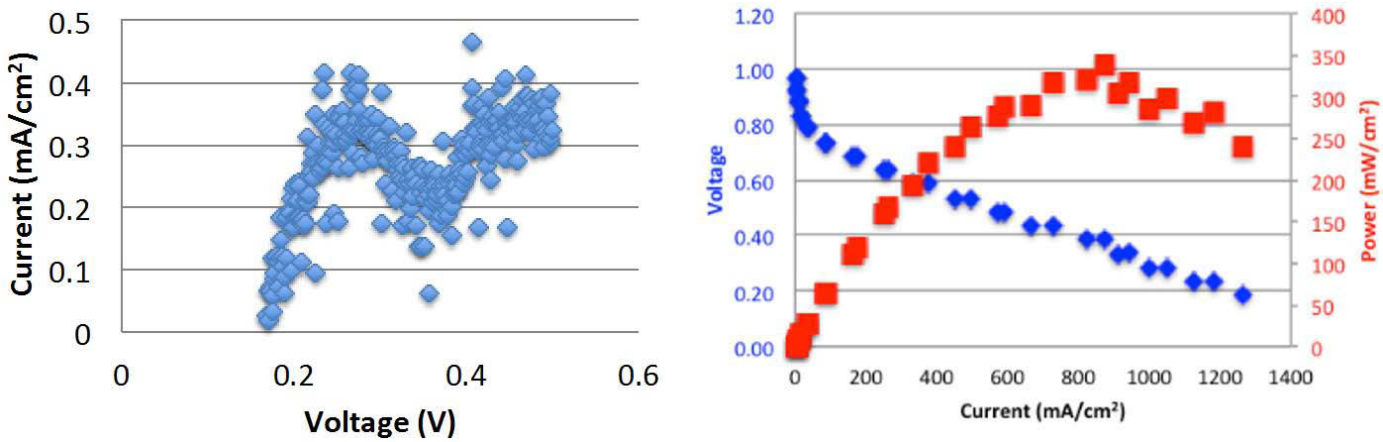

FIGURE 1. Hydrogen cross-over current (left) and polarization curve, 80°C, 100% RH, at end of test (right) for the 70 wt% HPA 80 µm film after the accelerated mechanical durability test, 20,000 wet/dry cycles

fail in the OCV hold evaluation. As shown in Figure 2, the benchmark perfluorosufonic acid NR-211 membrane fails in the OCV hold test and lasts only 90 hours. In contrast, the CSM HPA 70 wt% 80 µm membrane clearly demonstrates a very strong chemical durability of >500 h without losing <5% of the initial voltage. This durability is remarkable and goes a long way in addressing one of the key challenges of fuel cell membranes. This exceptional durability behavior of the CSM membrane is partly due to its low gas cross-over and partly due to the hydrocarbon–inorganic nature of membrane materials. It is expected that a thinner CSM membrane will continue to exhibit such exceptional chemical durability.

We spent considerable time learning how to process the materials into thin films. The conductivity and ASR for a 20 µm and a 30 µm film at 80°C, 95% RH are shown in Figure 3 (left), and we were even able to fabricate a 10 µm film, Figure 3 (right). Unfortunately, the 10 µm film proved to not be suitable for MEA development and so a series of 20 µm films were sent to NTCNA. Polarization curves with NTCNA MEAs are shown in Figure 4. The data in Figure 4 (left) using oxygen shows that the HPA membrane outperforms the incumbent perfluorosufonic acid material. Unfortunately, the data in Figure 4 (right) using air shows that the MEA has severe mass transport limitations. This highlights that the next step in the development of these membranes for vehicular MEAs will need to focus on ionomer electrode development.

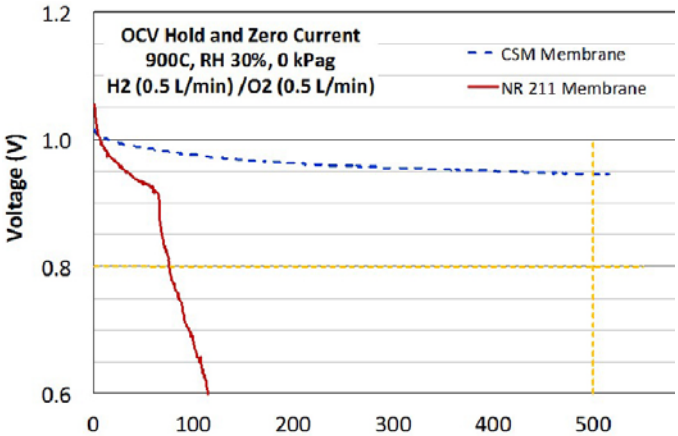

FIGURE 2. Accelerated chemical durability test for the 70 wt% HPA 80 µm film

CONCLUSIONS AND UPCOMING ACTIVITIES

- 80 µm films of the HPA materials demonstrated that the mechanical and chemical durability tests were easily passed, with the material showing exceptional durability in an OCV test under hot and dry conditions.
- 20 µm films were produced and demonstrated excellent performance in fuel cell testing under humid conditions.
- To achieve materials that will fully function under hot and dry conditions, further innovations will be needed in film processing.
- The full potential of these films will not be realized in fuel cell applications until a comprehensive study of ionomer formulation and electrode design is initiated and completed. The team is now looking for further sponsorship of these efforts.

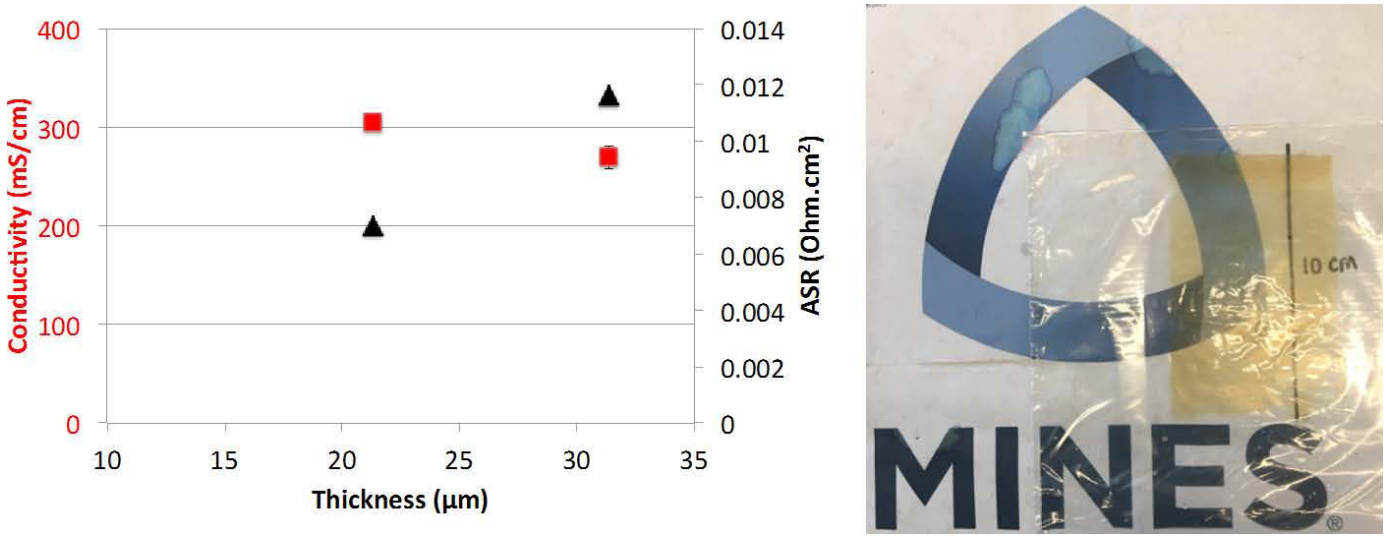

FIGURE 3. Conductivity (red) and ASR (blue) for 70 wt% HPA thin films at 80°C, 95% RH (left) and a large area 10 µm film (right)

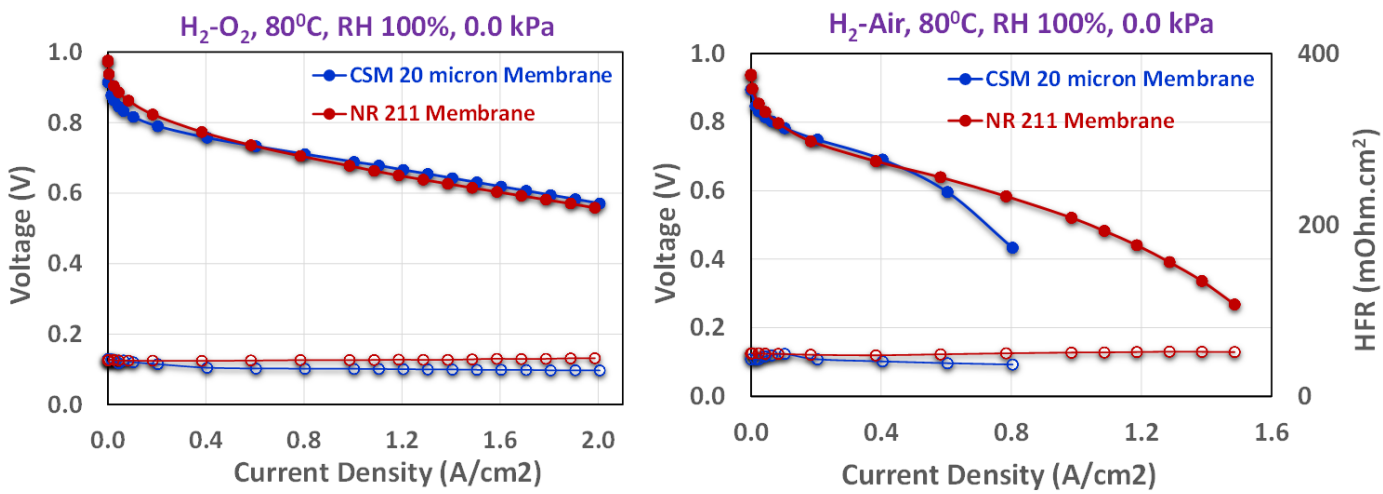

FIGURE 4. Polarization curves for 70 wt% HPA 20 µm film at 80°C, 100% RH, using oxygen (right) and air (left)

FY 2017 PUBLICATIONS/PRESENTATIONS

1. "Developing New Polymer Electrolyte Membranes to Enable Electrochemical Energy Conversion." A.M. Herring, invited oral presentation presented at Columbia University, New York, NY, April 2017.

2. "Developing New Polymer Electrolyte Membranes to Enable Electrochemical Energy Conversion." A.M. Herring, invited oral presentation presented at University of New Mexico, Albuquerque, NM, May 2017.

3. "Developing New Polymer Electrolyte Membranes to Enable Electrochemical Energy Conversion." A.M. Herring, invited oral presentation presented at Sandia National Laboratory, Albuquerque, NM, May 2017.

4. "Using Heteropoly Acids As a Proton Conductor in High Temperature Proton Exchange Membrane Fuel Cells." A.M. Herring, A. Motz, and M.-C. Kuo, invited oral presentation presented at the 231st meeting of the Electrochemical Society, New Orleans, LA, May 2017.

5. "Advanced Hybrid Membranes for Next Generation PEMFC Automotive Applications." A.M. Herring, invited oral presentation presented at the Annual Merit Review and Peer Evaluation Meeting (AMR) for the Hydrogen and Fuel Cells Program, Washington, D.C., June 2017.

6. "Membranes for Hotter and Drier Proton Exchange Membrane Fuel Cell Operation Based on the Heteropoly Acids." A.M. Herring, Andrew R. Motz, Tara P. Pandey, and Mei-Chen Kuo, oral presentation, presented at Solid State Ionics – 21, Padova, Italy, June 2017.

REFERENCES

1. Haugen, G.; Meng, F.; Aieta, N.; Horan, J.; Kuo, M.; Frey, M.; Hamrock, S.; Herring, A. *Electrochemical and Solid State Letters* **2007**, *10*, B51.

2. Malers, J.; Sweikart, M.; Horan, J.; Turner, J.; Herring, A. *Journal of Power Sources* **2007**, *172*, 83.

3. Meng, F.; Aieta, N.; Dec, S.; Horan, J.; Williamson, D.; Frey, M.; Pham, P.; Turner, J.; Yandrasits, M.; Hamrock, S.; Herring, A. *Electrochimica Acta* **2007**, *53*, 1372.

4. Horan, J.; Genupur, A.; Ren, H.; Sikora, B.; Kuo, M.; Meng, F.; Dec, S.; Haugen, G.; Yandrasits, M.; Hamrock, S.; Frey, M.; Herring, A. *ChemSusChem* **2009**, *2*, 226.

5. Schlichting, G.J.; Horan, J.L.; Jessop, J.D.; Nelson, S.E.; Seifert, S.; Yang, Y.; Herring, A.M. *Macromolecules* **2012**, *45*, 3874.

6. Horan, J.L.; Lingutla, A.; Ren, H.; Kuo, M.-C.; Sachdeva, S.; Yang, Y.; Seifert, S.; Greenlee, L.F.; Yandrasits, M.A.; Hamrock, S.J.; Frey, M.H.; Herring, A.M. *The Journal of Physical Chemistry C* **2014**, *118*, 135.

V.C.3 Smart Matrix Development for Direct Carbonate Fuel Cell

Chao-Yi Yuh (Primary Contact), Abdelkader Hilmi, Arun Surendranath
FuelCell Energy (FCE), Inc.
3 Great Pasture Road
Danbury, CT 06813
Phone: (203) 825-6112
Email: cyuh@fce.com

DOE Manager: David Peterson
Phone: (240) 562-1747
Email: David.Peterson@ee.doe.gov

Technical Advisor: Thomas Benjamin
Phone: (630) 252-1632
Email: benjamin@anl.gov

Contract Number: DE-EE0006606

Subcontractor:
University of Connecticut, Storrs, CT

Project Start Date: September 22, 2014
Project End Date: October 31, 2017

Overall Objectives

Develop an innovative durable DFC® (Direct Fuel Cell) electrolyte matrix (smart matrix) to enable >420 kW rated stack power and 10-year (80,000 h) stack service life (current generation: 350 kW rated stack power and 5-year stack service life).

- Increase market penetration for stationary fuel cells.
- Enable domestic clean energy job growth.
- Enable technology for hydrogen infrastructure and CO_2 capture.

Fiscal Year (FY) 2017 Objectives

- Continue refining matrix degradation mechanistic understanding.
- Confirm smart matrix meeting all technical targets in >5,000 h accelerated cell tests.
- Verify production-ready full-area smart matrix meeting beginning of life (BOL) cell performance, sealing efficiency and resistance stability targets in >5,000 h 30 kW endurance technology stack test.

Technical Barriers

This project addresses the following technical barriers from the Fuel Cells section of the Fuel Cell Technologies Office Multi-Year Research, Development, and Demonstration Plan [1].

(A) Durability: incomplete understanding of degradation mechanism and lack of clear long-term degradation mitigation schemes

(B) Cost: cost-effective matrix degradation–mitigation schemes

Technical Targets

This project aims to develop an innovative smart matrix to enable combined heat and power (CHP) distributed generation fuel cell systems to meet DOE 2020 research, development, and demonstration technical targets [1] (Table 1).

TABLE 1. FCE Progress towards Meeting DOE Research, Development, and Demonstration Technical Targets for 100 kW–3 MW CHP Distributed Generation Fuel Cell Systems Operating on Natural Gas

Characteristic	Units	2020 Targets	DFC Baseline
Electrical Efficiency at Rated Power	%	>50	47
CHP Energy Efficiency	%	90	90
Operating Lifetime	Hours	80,000	>44,000

Specific technical targets for the smart matrix are established based on multi-year DFC field operation experience:

- >25% BOL mechanical strength increase, >20% porosity increase and improved fine-pore microstructure (>30% reduction on pores larger than 0.2 μm) compared to the baseline.
- Stable fine-pore microstructure (<50% pores larger than 0.2 μm at end of life [EOL]) for enhanced capillary electrolyte retention, projected from >5,000 h accelerated cell and 30 kW technology stack tests.
- Verify smart matrix stack performance (BOL electrochemical performance: >760 mV at 185 mA/cm^2 at 71% fuel utilization), sealing performance (<0.4% nitrogen crossover) and resistance stability (<30 mΩcm^2 increase per year) in >5,000 h 30 kW technology stack.
- Understand matrix material degradation mechanism.
- Scale-up production of smart matrix for 1 m^2 full-area 30 kW technology stack validation.

FY 2017 Accomplishments

- Verified selected smart matrix meeting (by projection) EOL targets in >5,000 h accelerated single-cell tests.
- Achieved high-yield production of 1 m^2 full-area smart matrix.
- Met targeted electrochemical performance and seal efficiency in >5,000 h 30 kW technology stack test.

✧ ✧ ✧ ✧ ✧

INTRODUCTION

FCE's DFC products based on high-temperature internal-reforming carbonate fuel cell technology are striving to meet growing worldwide demand for high-efficiency ultra-clean power generation. The electrolyte membrane (matrix), a porous microstructure consisting mainly of ultra-fine sub-micron α-$LiAlO_2$ powders sandwiched between two electrodes, immobilizes liquid electrolyte, isolates fuel from oxidant, and facilitates ionic transport [2]. However, α-$LiAlO_2$, although phase stable in DFC operation, slowly coarsens lowering capillary force leading to matrix drying and electrolyte redistribution, which contributes to gas crossover and performance loss. This program aims to develop a high-yield production-ready smart matrix with robust and stable fine-pore microstructure to enable DFC meeting DOE 2020 targets for CHP distributed generation fuel cell systems.

APPROACH

The approaches to achieve the technical targets are listed below in Table 2. The targets will be validated in long-term >5,000 h accelerated cell and full-area 30 kW technology stack tests. Full-scale production trials will be conducted to fabricate full-area smart matrices for the technology stack tests and to assure the manufacturing process ready for product implementation.

RESULTS

Baseline α-$LiAlO_2$ powders dissolve slightly in liquid carbonate and are expected to coarsen gradually via Ostwald ripening. However, the coarsening was found much accelerated at the reducing anode side at higher temperatures. The mechanism of such accelerated coarsening was not well understood. The as-made powders already exhibited some surface Li deficiency and cationic disorder. Exposure to high-temperature reducing environments, even in the absence of liquid electrolyte, enhanced not only such disorders but also aluminum metallic nature. The as-made powders also contained metastable hydrated impurities that were found transformed to less stable γ-$LiAlO_2$ under high-temperature reducing atmosphere.

Long-term (500–1,100 h) α-$LiAlO_2$ immersion tests at 650°C under oxidizing (PO_2 ~0.15 atm) and reducing (PO_2 ~10^{-23} atm) atmospheres with various PCO_2 (0–0.3 atm) were conducted to understand if the Ostwald ripening rate was controlled by equilibrium solubility (Table 3). The experiments confirmed that, under the H_2-containing reducing atmosphere, increasing PCO_2 from 0.005 atm to 0.3 atm suppressed the equilibrium solubility as well as coarsening, agreeing with the basic dissolution mechanism suggested in the literature. However, increasing PO_2 to 0.15 atm (oxidizing atmosphere), while maintaining PCO_2 at 0.3 atm reduced the equilibrium solubility by approximately one order of magnitude. The coarsening rate was also reduced. Under extremely basic CO_2-free reducing atmosphere (not a typical DFC condition), rapid α→γ phase transformation and coarsening occurred. Apparently already highly coarsened and faceted (low surface area) γ-$LiAlO_2$ exhibited a lower solubility probably due to Gibbs–Thomson effect. This test result suggests α→γ transformation may participate in the α-$LiAlO_2$ coarsening process.

The measured higher α-$LiAlO_2$ solubility under the CO_2-containing reducing atmosphere could be caused by the enhanced surface non-stoichiometry/disorder as well as aluminum metallic nature, as mentioned above. Density functional theory calculation performed by University

TABLE 2. Approaches to Achieve Smart Matrix Technical Targets

Technical Targets	Approaches
BOL: >25% mechanical strength increase, >20% porosity increase and improved fine-pore microstructure (>30% reduction on pores larger than 0.2 μm) than baseline	Nano-pore former for increased porosity Reinforcement additives to increase mechanical strength
	Optimize slurry formulation and processing for improved particle size distribution, particle packing and production yield
EOL: Stable fine-pore microstructure for maintaining capillary electrolyte retention (<50% pores larger than 0.2 μm)	Stabilized $LiAlO_2$ or additives to slow down coarsening to maintain capillary electrolyte retention
Coarsening mechanistic understanding	Investigate effects of temperature, gas atmosphere, and electrolyte composition on matrix microstructure evolution, $LiAlO_2$ stability, wettability, and solubility in single-cells/stacks and controlled out-of-cell tests

TABLE 3. α-$LiAlO_2$ Immersion Tests at 650°C in Carbonate Electrolyte under Atmospheric Pressure

Atmosphere	Test time, h	Phase (X-Ray diffraction)	Specific surface area, relative	$LiAlO_2$ solubility, ppm
70% air–30% CO_2	800	α-$LiAlO_2$	1	2.7
4% H_2–3% H_2O–N_2	500	Major γ-$LiAlO_2$ Minor α-$LiAlO_2$	0.06	1.5
4% H_2–0.5% CO_2–3% H_2O–N_2	1,100	Major α-$LiAlO_2$ Minor γ-$LiAlO_2$	0.75	28.2
4% H_2–30% CO_2–3% H_2O–N_2	1,100	α-$LiAlO_2$	0.93	21.3

of Connecticut suggested that the thermodynamically equilibrated and coarsened α-$LiAlO_2$ crystal shapes (observed by transmission electron microscopy) could be predicted by minimizing the surface energy levels of several preferred oxygen-terminating crystallographic planes. Therefore, the exposure conditions (temperature, gas composition, etc.) could have affected the surface energy levels of the crystallographic planes and hence stable atomic termination in the crystal, thereby influence the solubility, crystallographic plane stability, and coarsening rate.

The coarsening could also be contributed by the presence of metastable contaminants and intermediates and/or surface defects, enhanced under the reducing anode side atmospheres. Adding LiOH to the molten carbonate in the immersion tests was found to cause the formation of ultra-fine metastable intermediates such as α-Li_5AlO_4 and $LiAl_2(OH)_7{\cdot}2H_2O$, as well as accelerating coarsening and $\alpha \rightarrow \gamma$ transformation. [OH^-] may increase at the triple-phase boundary near the anode–matrix interface due to hydrogen oxidation reaction [3]. In summary, the reducing anode side atmosphere increases $LiAlO_2$ solubility as well as destabilizes the crystal surface (by creating surface defects and disorders and metastable intermediates and by promoting the growth of certain crystallographic planes), all could contribute to the accelerated α-$LiAlO_2$ coarsening.

FCE has developed a smart matrix design that disrupted the above underlying accelerating coarsening mechanisms. The consistency of BOL and EOL pore structure was verified in numerous accelerated single-cells. Short-term (<1,000 h) and long-term (>5,000 h) accelerated cell tests demonstrated finer and more stable pore structure compared to the baseline. Figure 1 showed essentially little pore structure change for up to ~6,000 hours (>50% reduction of pores larger than >0.2 µm at fuel inlet), meeting the targeted requirements.

The scale up optimization of the smart matrix formulation was continuing by fine-tuning the tape casting parameters such as slurry delivery system, drying conditions, and the lamination process in full-size production-scale (~90 gallons) trials. Results so far already show >15% improved process yield over the baseline. The BOL physical properties were all consistent with the lab-scale matrix results, confirming the reproducibility and robustness of the scaled-up process. Short- and long-term accelerated single-

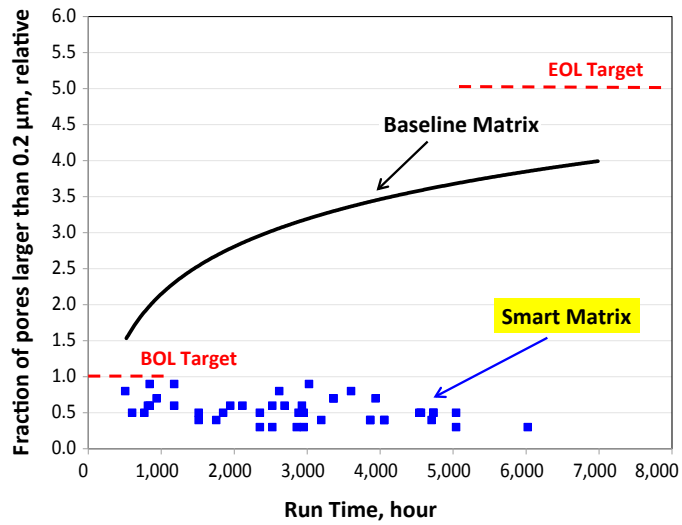

FIGURE 1. Excellent pore structure stability of smart matrix has been demonstrated in accelerated single-cells meeting EOL target by projection.

cell tests of these production trial matrices also validated excellent gas sealing efficiency (~0% crossover) and pore structure stability. The full area (~1 m^2) smart matrices had been evaluated in a 30-cell 30 kW technology stack (Figure 2). The stack, utilizing FCE's baseline commercial DFC active cell design, also incorporated baseline matrices for comparison. Initial operating results showed that the smart matrix cells exhibited consistent higher open circuit voltage than the baseline, indicating enhanced gas sealing. Anode gain testing (increasing hydrogen concentration in fuel at open circuit voltage to assess sealing efficiency) also showed that the smart matrix cells exhibit faster and higher voltage gain, further confirming the enhanced matrix sealing efficiency. The initial BOL electrochemical performance at 185 mA/cm^2 demonstrated excellent electrochemical performance (~763 mV) at 71% fuel utilization (Figure 3), meeting the BOL target. Crossover target of <0.4% was successfully met during the 6,000 h test. The resistance stability of the smart matrix also met the target of <30 mΩcm^2 increase per year, further confirming the improved electrolyte retention capability. The stack has been terminated for post-test validating pore structure stability and electrolyte retention capability.

FIGURE 2. A full-area 30 kW technology stack was built for validating selected smart matrix design. The stack was successfully operated for ~6,000 h.

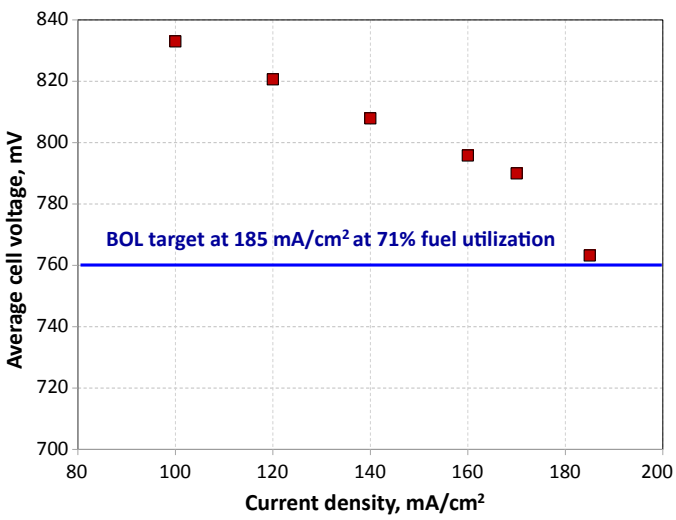

FIGURE 3. Smart matrix cells achieved BOL electrochemical performance target in a 30 kW technology stack.

CONCLUSIONS AND UPCOMING ACTIVITIES

Mechanistic investigation has shown that reducing anode side atmosphere increases $LiAlO_2$ solubility, crystal defects, and metastable intermediate formation all likely contributing to the accelerated coarsening. Lab-scale and production trial smart matrices have successfully met all BOL and EOL pore structure technical targets in accelerated single-cell tests operated for up to ~6,000 hours. The high-yield production trial smart matrix (~1 m^2) consistently reproduced all targeted physical and mechanical properties. A 6,000 h, 30 kW technology stack test had validated the smart matrix electrochemical performance, resistance stability, and sealing efficiency.

The remainder of the project will focus on further refining mechanistic understanding, developing an Ostwald ripening model, and validating the pore structure stability of the production smart matrix in the technology stack test.

FY 2017 PUBLICATIONS/PRESENTATIONS

1. S. Heo, et al., "Stability of Lithium Aluminate in Reducing and Oxidizing Atmospheres at 700ºC," International Journal of Hydrogen Energy, 41, 18884 (2016).

2. C. Yuh, et al., "Molten carbonate electrolyte matrix progress review," 6th International Congress on Ceramics (ICC6), August 21–25, 2016, Dresden, Germany.

3. Program Go/No Go decision presentation to DOE-EERE, September 14, 2016.

4. A. Surendranath, et al., "Mechanistic understanding of molten carbonate matrix coarsening in endurance operation," Materials Science & Technology 2016 Conference, October 23–27, 2016, Salt Lake City, UT.

5. A. Hilmi, et al., "Smart electrolyte matrix for enhanced carbonate fuel cell life," Abstract #1641, 231st ECS meeting, May 28–June 2, 2017, New Orleans, LA.

6. S. Heo, et al. "Role of Exposure Atmospheres on Particle Coarsening and Phase Transformation of $LiAlO_2$," J. Electrochem. Soc., 168(4), H5086 (2017).

7. C. Yuh and A. Hilmi, "Smart Matrix Development for Direct Carbonate Fuel Cell," 2017 DOE Hydrogen and Fuel Cells Program and Vehicle Technologies Office Annual Merit Review and Peer Evaluation Meeting, Washington D.C., June 8, 2017.

REFERENCES

1. DOE Office of Energy Efficiency and Renewable Energy (EERE) Fuel Cell Technologies Offices Multi-Year Research, Development and Demonstration (MYRD&D) Plan, Section 3.4 "Fuel Cells", Updated June 2016, http://energy.gov/sites/prod/files/2016/06/f32/fcto_myrdd_fuel_cells_0.pdf

2. C. Yuh and M. Farooque, "Materials and Life Considerations," in *Fuel Cells-Molten Carbonate Fuel Cells, Encyclopedia of Electrochemical Power Sources,* 497–507, Elsevier Science, 2009.

3. P. Ang and A. Sammells, "Influence of Electrolyte Composition on Electrode Kinetics in the Molten Carbonate Fuel Cell," J. Electrochem. Soc., 127(6), 1287(1980).

V.C.4 Ionomer Dispersion Impact on Fuel Cell and Electrolyzer Performance and Durability (SBIR Phase II TTO)

Hui Xu (Primary Contact), Chao Lei, Zachary Green, Tom McCallum
Giner, Inc.
89 Rumford Ave.
Newton, MA 02466
Phone: (781) 529-0573
Email: hxu@ginerinc.com

DOE Manager: Donna Ho
Phone: (202) 586-8000
Email: Donna.Ho@ee.doe.gov

Technical Advisor: John Kopasz
Phone: (630) 252-7531
Email: kopasz@anl.gov

Contract Number: DE-SC0011307 (SBIR Phase II TTO)

Collaborators:

- Yu-Seung Kim, Los Alamos National Laboratory (LANL), Los Alamos, NM
- Karren More, Oak Ridge National Laboratory, Oak Ridge, TN

Project Start Date: July 28, 2015
Project End Date: February 27, 2018

Overall Objectives

- Further develop and commercialize LANL's non-aqueous solvent-based ionomer dispersion technology.
- Scale-up ionomer and dimensionally-stable membrane (DSM™) production to allow for continuous roll-to-roll production of low platinum-group metals (PGM) membrane electrode assemblies (MEAs) for fuel cells and electrolyzers.
- Demonstrate the durability of polymer electrolyte membrane (PEM) fuel cell and electrolyzer MEAs at more extensive cycling and operating conditions.

Fiscal Year (FY) 2017 Objectives

- Characterize the influence of non-aqueous solvents on ionomer particle morphology and electrode layer structure.
- Fabricate MEAs using various non-aqueous ionomer dispersions from LANL and investigate the influence of the solvent on fuel cell performance.
- Demonstrate the durability advantages of using non-aqueous ionomers in the electrode.

Technical Barriers

This project addresses the following technical barriers from the Fuel Cells section of the Fuel Cell Technologies Office Multi-Year Research, Development, and Demonstration Plan.

(A) Durability

(B) Cost

Technical Targets

The targets of this project are to apply ionomer dispersion technology to make durable fuel cell and electrolyzer MEAs. DOE targets for PEM fuel cells are listed in Table 1.

TABLE 1. MEA Durability Targets

Characteristic	Units	DOE 2020 Target
Platinum group metal (PGM) total content (both electrodes)	g/kW	<0.125
PGM total loading (both electrodes)	mg-PGM/cm²$_{geo}$	<0.125
Loss in catalytic (mass) activity	% Loss	<40
Loss in performance at 0.8 A/cm^2	mV	<30
Loss in performance at 1.5 A/cm^2	mV	<30
Mass activity @ 900 mV$_{iR\text{-}free}$	A/mg$_{PGM}$	0.44

For PGM electrolyzers, DOE has not set a target. Giner's targets are:

- Low PGM loading electrolyzer MEA demonstrates less than 20 mV loss (at 1.5 mA/cm^2) after 50,000 cycles from 1.4 V to 1.9 V.
- Low PGM loading electrolyzer MEA demonstrates less than 20 mV performance loss after 1,000 hour test at 1.5 A/cm².

FY 2017 Accomplishments

- Upgraded electrode layer manufacturing from batch spraying to an ink-casting process. DSM-based MEAs were fabricated from selected ionomer dispersions.
- Characterized the non-aqueous solvent influence on ionomer particle morphology via small-angle neutron scattering measurements and electrode layer structure by high resolution transmission electron microscopy.

- Fabricated MEAs using various non-aqueous ionomer dispersions and established the ranking of the solvent influence on fuel cell performance.
- Demonstrated the durability advantages of using ethylene glycol (EG)-based ionomer in the electrode, with only 20 mV voltage loss at 1 A/cm^2 after 30,000 cycles in the accelerated stress test (AST).

✧ ✧ ✧ ✧ ✧

INTRODUCTION

LANL has developed a revolutionary method of building an MEA for PEM fuel cells that can significantly reduce manufacturing costs and extend MEA lifetimes. This method incorporates unique polymer dispersions in non-aqueous liquids to produce superior electrode performance, stability, and durability during harsh fuel cell operating conditions [1–7]. The LANL-produced MEA has been evaluated and certified using an AST developed by DOE in conjunction with car manufacturers; the voltage loss of LANL's MEA remained below 30 mV even after 70,000 cycles.

The ionomer dispersion work at LANL has great potential to significantly improve the lifetime of PEM fuel cells [2–4]. However, the ionomer dispersion used was Nafion® 1100 equivalent weight; there has been a strong push in the industry towards lower equivalent weight membranes that can increase proton conductivity. Low equivalent weight ionomers are less dimensionally stable and could benefit more from Giner's well-established DSM™ technology. Also, the work at LANL has been done with dispersions of ionomer in the salt form, rather than in the proton form. This requires additional processing after membrane production to put the membrane in the acid form. Using dispersions from LANL in the acid form and utilizing Giner's DSM technology, this Phase II program will validate these technologies towards viable commercial applications in advanced fuel cell and electrolyzer systems.

APPROACH

Conventional PEM fuel cell and membrane-based water electrolyzer technology suffers from a lack of durability, high manufacturing costs, and rapid performance degradation. In this project, Giner, in collaboration with LANL, investigates a revolutionary method of building membrane electrode assemblies for PEM fuel cells and water electrolyzers in order to reduce manufacturing costs and extend the lifetime of the electrochemical devices. In FY 2017, we focused on improving beginning of life (BOL) fuel cell performance using a single-dispersion-agent-processed electrode. This work is motivated by the fact that these electrodes showed good durability but limited BOL performance compared to the conventional water/isopropyl alcohol (IPA/H_2O) processed electrodes. Our approach to obtain good BOL fuel cell performance is to (i) understand ionomer particle morphology in dispersion; (ii) investigate the electrode morphology, catalyst, and ionomer binder distributions in the electrodes; (iii) evaluate the electrode performance using various electrodes prepared from different dispersing agents. Giner and LANL prepared several perfluorosulfonic acid dispersions (proton form) from various single dispersion systems. Electrodes were made from different dispersions and tested both at Giner and LANL. Oak Ridge National Laboratory characterized the electrode morphology including polymer electrolyte and catalyst distribution to correlate the BOL performance with electrode morphology. Giner performed MEA durability tests following the DOE AST protocols.

RESULTS

First, laser diffraction particle size analysis was used to understand the various solvents' impacts on catalyst ink structure (see Figure 1). It can be seen that n-propyl alcohol (nPA)/H_2O and EG solvent systems provide better ink structure, implied by much smaller agglomeration sizes. IPA/H_2O and pentanediol-based solvent systems exhibit large agglomerations in the ink, which may account for their poor quality. The laser diffraction particle size will be correlated with electrode structure and fuel cell performance later.

The electrode morphology and structures were characterized. Most of the electrodes demonstrate smooth coating surfaces and good quality (see Figure 2a), except that the cathode layer made from IPA/H_2O-based ink exhibits large "mud cracks." Low magnification transmission electron microscopy element mapping was then used to characterize the ionomer distribution in these cathode layers, as shown in Figure 2b. The best ionomer distribution was found in the ethylene glycol-based sample, with ionomer aggregates <50 nm. On the other hand, the 3M ionomer/pentanediol

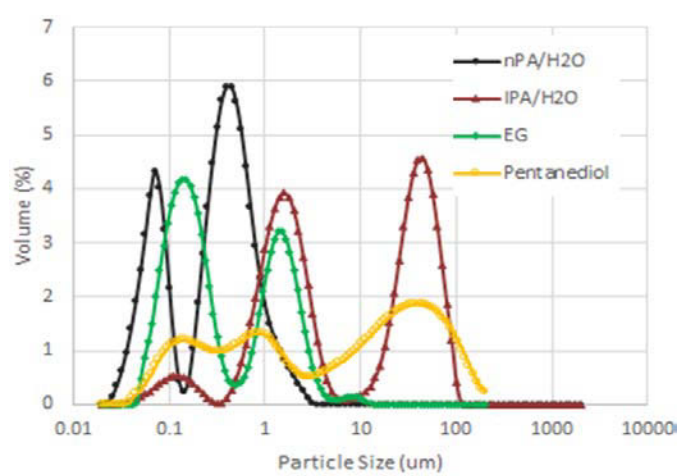

FIGURE 1. Particle size distribution in various solvents

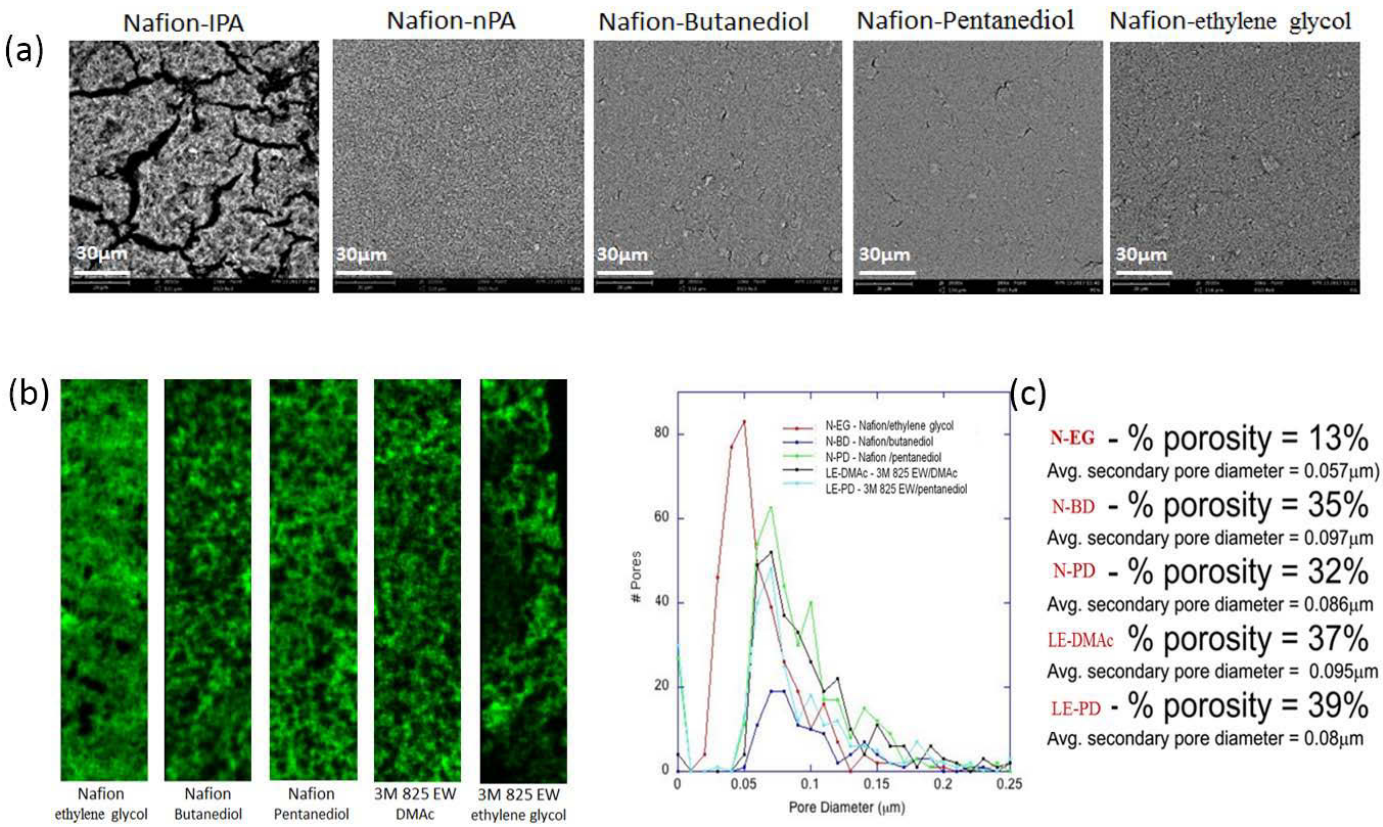

EW – equivalent weight; N-EG – Nafion in ethylene glycol; N-BD – Nafion in butanediol; N-PD – Nafion in pentanediol; DMAc – dimethylacetamide; LE-DMAc – 3M 825 EW in dimethylacetamide; LE-PD – 3M 825 EW in pentanediol

FIGURE 2. (a) Scanning electron microscopy images of catalyst layers prepared from different solvents. (b) Ionomer distribution in catalyst layers prepared from different ionomer dispersions. (c) Pore size distribution of the electrode layers.

sample showed the worst ionomer distribution, which was consistent with its poor coating quality. The porosity and pore size distribution of the electrode layers were also obtained from transmission electron microscopy image analysis, as shown in Figure 2c. The EG-based electrode shows the lowest porosity (i.e., 13%), indicating its high density. It also contains the smallest pore sizes and the highest number of pores. All the other samples have similar porosity, i.e., ranging from 32% to 39%. Among these electrodes, the 3M ionomer/pentanediol-based sample has the highest porosity.

The effect of the dispersing agents on initial fuel cell performance was investigated. In this experiment, four ionomer dispersions were used and compared with nPA/H_2O and IPA/H_2O. All MEAs had a Pt loading of ~0.20 mg_{Pt}/cm^2. The initial fuel cell performance is shown in Figure 3. The IPA/H_2O baseline shows very low performance especially in the mass transport region, which is probably attributed to its poor coating quality. The ionomer dispersions have shown significant influence on the fuel cell performance, with a general ranking as: nPA/H_2O > ethylene glycol > butanediol > pentanediol > pentanediol (3M). The ethylene glycol-based sample displays the best performance of all the non-aqueous samples, and its performance is very comparable to the nPA/H_2O baseline. The cathode processed from butanediol showed relatively lower mass transfer performance than the ethylene glycol-based sample.

Based on the initial fuel cell performance, the ethylene glycol-based sample was selected for durability testing according to the DOE AST voltage cycling protocol: voltage cycles between 0.6 V and 1.0 V; at 80°C, 100% relative humidity (RH), and 0.2 standard liters per minute (SLPM) H_2/0.075 SLPM N_2 (shown in Figure 4). The voltage loss at 1 A/cm^2 from BOL to end of test is about 20 mV. Further in situ electrochemical characterization, including hydrogen crossover, cycling voltammetry, electrochemical impedance spectroscopy and high frequency resistance (HFR), etc., was carried out to understand the degradation mechanism in this sample. The cycling voltammetry plots show that electrochemical surface area (ECSA) gradually decreases during durability test, which is very common in the AST and related to catalyst particle degradation. HFR stays nearly the same after the AST. It is indicated that the main losses during the AST are in the ECSA and enhanced charge transfer resistance.

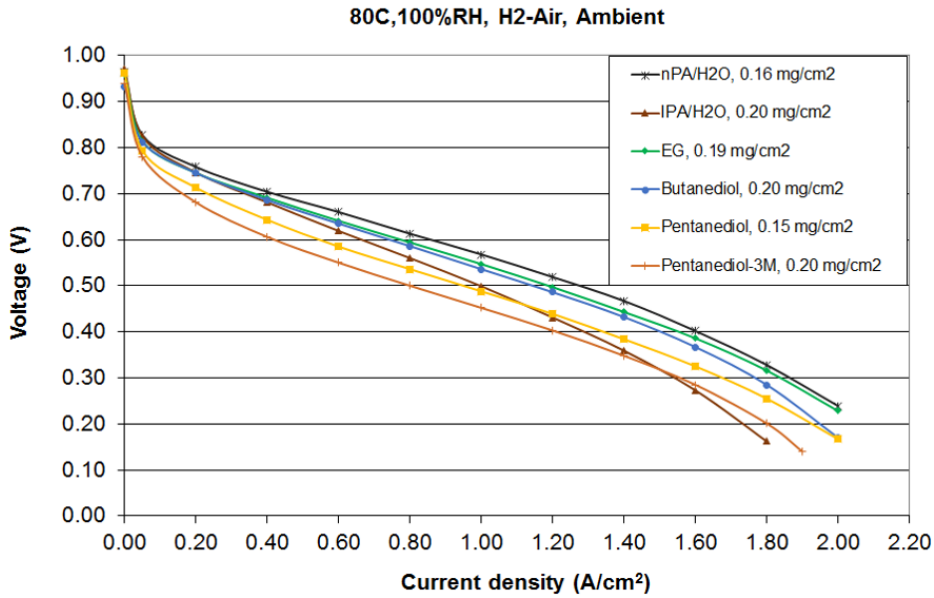

FIGURE 3. Solvent effect of the ionomer dispersion in cathode layer on H_2-air fuel cell performance: 80°C, 100% RH, ambient, H_2: 1.5 SLMP, air: 3 SLMP

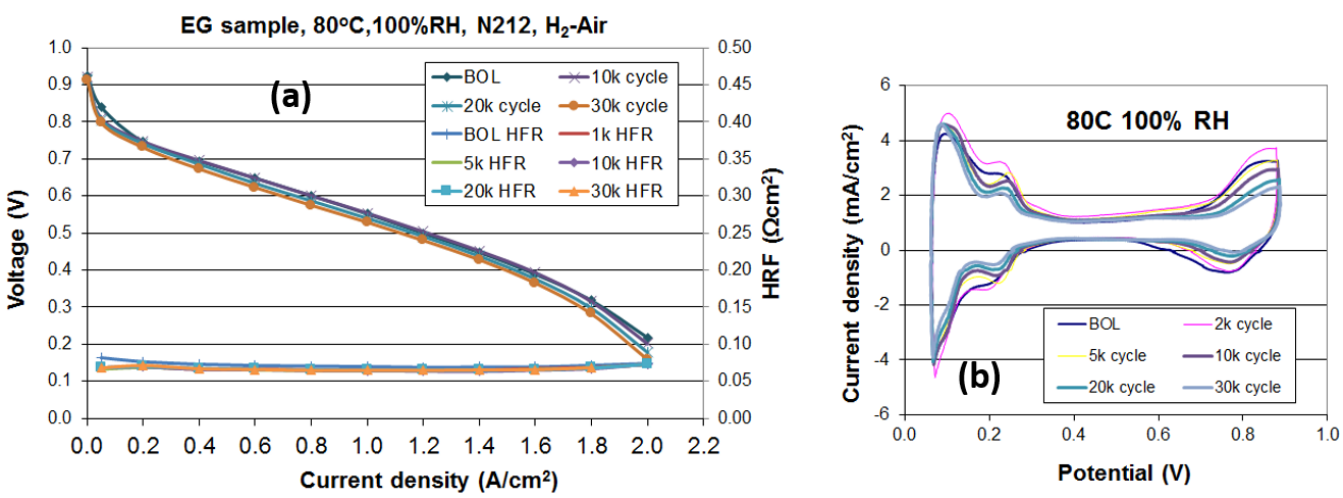

FIGURE 4. Durability test of EG-based sample for up to 30,000 voltage cycling: voltage cycles between 0.6 V and 1.0 V, at 80°C, 100% RH, 0.2 SLPM H_2 / 0.075 SLPM N_2. (a) H_2-air fuel cell performance as a function of voltage cycling. (b) Cycling voltammetry as a function of voltage cycling.

CONCLUSIONS AND UPCOMING ACTIVITIES

Conclusions

- LANL's non-aqueous solvent-based ionomer dispersion technology in a variety of solvents has been investigated; the solvent affects ionomer morphology and ink particle size distribution.
- Ionomer dispersions impact the electrode structures by affecting the ionomer distribution and pore size distribution. Ionomer distribution seems to be improved with hydrophilicity of the solvent.
- Ionomer dispersions influence fuel cell electrode performance. nPA- and EG-dispersed Nafion ionomers demonstrate the best fuel cell performance.

Upcoming Activities

- Further investigate the mechanism of solvent influence on fuel cell performance and durability via in situ and ex situ characterizations.

- Further investigate interactions between non-aqueous ionomer dispersions and catalysts to develop scalable MEA manufacturing for Giner's water electrolyzer business.
- Develop large-scale DSM/non-aqueous ionomer dispersion based fuel cell MEA manufacturing processes and perform techno-economic analysis.

FY 2017 PUBLICATIONS/PRESENTATIONS

1. Xu, H., "Ionomer Dispersion Impact on Advanced PEM Fuel Cell Performance and Durability," Oral Presentation. DOE Hydrogen and Fuel Cell Annual Merit Review Meeting, Washington, DC. June 2017.

REFERENCES

1. Brosha, E., F. Garzon, C. Johnston, A. Labourieau, Y.S. Kim, K.-S. Lee, B. Orler, B. Pivovar, D. Torraco, C. Welch, and H. Xu., "Studies Towards Optimizing Fuel Cell Electrode Structure and Composition," Canada to USA Fuel Cell and Hydrogen Cluster Connection Workshop, Vancouver, BC, Canada, February 16–17, 2009.

2. Kim, Y.S.; Lee, K.S.; Rockward T. U.S. Patent 7981319 B2, 2011.

3. Kim, Y.S.; Lee, K.S.; Rockward T. U.S. Patent 8236207 B2, 2012.

4. Welch, C., A. Labouriau, R. Hjelm, B. Orler, C. Johnston, and Y.S. Kim, "Nafion in Dilute Solvent Systems: Dispersion or Solution?" ACS Macro Lett., 1, 1403–1407 (2012).

5. Y.S. Kim, C.F. Welch, R.P Hjelm, N.H. Mack, A. Labouriau, E.B. Orler, *Macromolecules*, 48 (7), 2161–2172 (2015).

6. Y.S. Kim, C.F. Welch, N.H. Mack, R.P. Hjelm, E.B. Orler, M.E. Hawley, K.S. Lee, S.-D. Yim, C.M. Johnston, *Phys. Chem. Chem. Phys.* 16 (13) 5927-5932 (2014).

7. B. Choi, D.A. Langlois, N.H. Mack, C.M. Johnston, Y.S. Kim, *J. Electrochem. Soc.* 161 (12), F1154–F1162 (2014).

V.C.5 Highly Stable Anion Exchange Membranes for High-Voltage Redox-Flow Batteries

Yushan Yan (Primary Contact), Shuang Gu, Bingjun Xu
University of Delaware
150 Academy Street
Newark, DE 19716
Phone: (302) 831-2552
Email: yanys@udel.edu

DOE Manager: Donna Ho
Phone: (202) 586-8000
Email: Donna.Ho@ee.doe.gov

Technical Advisor: John Kopasz
Phone: (630) 252-7531
Email: kopasz@anl.gov

Contract Number: DE-EE0006964 (Incubator)

Subcontractor:
Bryan Pivovar, National Renewable Energy Laboratory, Golden, CO

Project Start Date: June 1, 2015
Project End Date: August 31, 2017

Overall Objectives

- Develop a new class of anion-exchange membranes (AEMs) with very high oxidation resistance for high-voltage cerium redox-flow batteries (RFBs), and other alkaline membrane-based electrochemical devices such as fuel cells and electrolyzers.

Fiscal Year (FY) 2017 Objectives

- Test poly-tetrafluoroethylene (PTFE) reinforced tris(2,4,6-trimethoxyphenyl) phosphonium ($9MeOTTP^+$)–hexafluoro polybenzimidazole (F_6PBI) membrane with oxidation stability in 0.5 M Ce(IV) $(ClO_4)_4$ at 55°C for 100 h (this condition is equivalent to 40°C for 1,000 h).

Technical Barriers

This project addresses the following technical barriers from the Fuel Cells section of the Fuel Cell Technologies Office Multi-Year Research, Development, and Demonstration Plan:

(A) Durability

(B) Cost

(C) Performance

Technical Targets

This project aims to develop new AEMs with high oxidation stability. These AEMs are targeted for applications in high-voltage cerium RFBs, and other alkaline membrane-based electrochemical devices such as fuel cells and electrolyzers.

FY 2017 Accomplishments

- Synthesized $9MeTTP^+$-F_6PBI polymer without crosslinking and prepared its membranes with 0.52 mmol/g titration ion-exchange capacity and only 3.58% water uptake.
- $9MeTTP^+$-F_6PBI membranes had less than 1 mS/cm OH^- conductivity in water at 20°C possibly due to the hydrophobic $9MeTTP^+$ cation.
- Tethered hydrophilic $9MeOTTP^+$ cation to F_6PBI backbone, and prepared $9MeOTTP^+$-F_6PBI PTFE reinforced membrane with 17.4% water uptake to increase the mechanical strength and durability in cerium (IV) solution.
- Demonstrated that cerium (IV) had a 27-fold lower permeability through the cationic $9MeOTTP^+$-F_6PBI PTFE reinforced membrane than Nafion 212.
- Demonstrated that $9MeOTTP^+$-F_6PBI PTFE reinforced membrane had less than 20% conductivity loss during accelerated oxidation stability test in 0.5 M cerium (IV) and 1.3 M $HClO_4$ at 55°C for 100 h.
- Demonstrated that $9MeOTTP^+$-F_6PBI PTFE reinforced membrane had more than doubled lifetime during accelerated oxidation stability test in 0.5 M cerium (IV) and 1.3 M $HClO_4$ at 55°C than commercial FAS-30 and FAB-PK-130 anion exchange membranes.

✧ ✧ ✧ ✧ ✧

INTRODUCTION

As a reversible fuel cell, RFBs are one of the most promising electrochemical technologies with the scalability and durability (e.g., 15–20 years) required for intermittent renewable energy storage. In particular, cerium redox pair [Ce(IV)/Ce(III)]-based RFBs are appealing because of their unprecedented high cell voltages (up to 3.08 V) in aqueous

systems. High cell voltage is a key factor in achieving high energy and power densities, which lead to low storage cost. An AEM is needed as a key component in cerium RFBs to achieve stable cell voltage and high coulombic efficiency. However, existing commercial ammonium cation-based AEMs have very limited stability when working with Ce(IV) electrolytes (e.g., less than 200 h of durability). The lack of stable AEMs causes cerium RFBs to suffer from either high self-discharge rate or low coulombic efficiency. The development of highly stable and conductive AEMs has become one of the most urgent challenges for cerium RFBs to become a viable electricity storage solution. Herein, we propose to develop highly stable AEMs based on the $9MeOTTP^+$ cation and F_6PBI backbone.

APPROACH

Our approach is to explore the chemistry of grafting $9MeTTP^+$ and $9MeOTTP^+$ to the thermo-oxidatively stable F_6PBI backbone and then examine the performance and stability of membranes made from these materials in a cerium (IV) environment.

RESULTS

After several attempts that could not tether $9MeTTP^+$ to the polymer backbone using approaches of direct quarternization and use of $7MeTTP^+$ synthesized from Grignard reaction and so on, we were finally able to obtain $9MeTTP^+$-F_6PBI polymer by quarternization using diiodobutane at 150°C with copper powder to inhibit diiodobutane degradation. The $9MeTTP^+$-F_6PBI polymer showed excellent ion-exchange capacity retention (less than 0.59% loss) during accelerated oxidative stability tests in cerium (IV) (presented in FY 2016 annual progress report). However, its membrane had less than 1 mS/cm OH^- conductivity in water at 20°C, which is possibly due to the hydrophobic nature of $9MeTTP^+$ cation. In order to solve the problem, a hydrophilic $9MeOTTP^+$ cation was tethered to F_6PBI backbone, and $9MeOTTP^+$-F_6PBI PTFE reinforced membrane (picture shown in Figure 1) with 17.4% water uptake was successfully prepared to increase the mechanical strength and durability in cerium (IV) solution.

Considering the strong acidic environment of the permeation test (0.1 M cerium (IV) and 1 M H_2SO_4), the F_6PBI backbone is also positively charged due to the formation of hydrogen bonds between the acid and nitrogen groups. The repulsion the cerium cations have with the $9MeOTTP^+$ cations and the positively charged basic heterocyclic groups on the polymer backbone creates a high selectivity based on Donnan exclusion. In our test, cerium (IV) had a 27-fold lower permeability through $9MeOTTP^+$-F_6PBI PTFE reinforced membrane than through Nafion 212 (Table 1).

FIGURE 1. Prepared $9MeOTTP^+$-F_6PBI PTFE reinforced membrane with thickness 20 µm

TABLE 1. Cerium (IV) Permeability Results

Membrane	Thickness (µm)	Cerium Permeability (m^2s^{-1})
Nafion 212	50±2	$3.64*10^{-13}$
$9MeOTTP^+$-F_6PBI PTFE Reinforced Membrane	20±2	$1.36*10^{-14}$

After the accelerated oxidation stability test in 0.5 M Ce(IV) and 1.3 M $HClO_4$ at 55°C for 100 h, $9MeOTTP^+$-F_6PBI PTFE reinforced membrane showed 13% to 19% conductivity loss across 20°C to 70°C (results in Figure 2). This membrane met the milestone Q8/7 (i.e., less than 20% loss of initial anion conductivity). In addition, commercial anion exchange membranes FAS-30 and FAB-PK-130 from Fumasep® were also tested in the same procedure, and all failed the test in the first 100 hours. As shown in Figure 3 and Table 2, FAB-PK-130 membrane suffered significant loss of polymer, while $9MeOTTP^+$-F_6PBI PTFE reinforced membrane has no breakages or holes. (Note that in 3b and 3b', the color difference is due to the different background brightness.)

CONCLUSIONS AND UPCOMING ACTIVITIES

The project has achieved all milestones scheduled within the reporting period:

- $9MeTTP^+$-F_6PBI membrane was prepared and tested, but has insufficient conductivity likely due to the hydrophobic $9MeTTP^+$ cation.

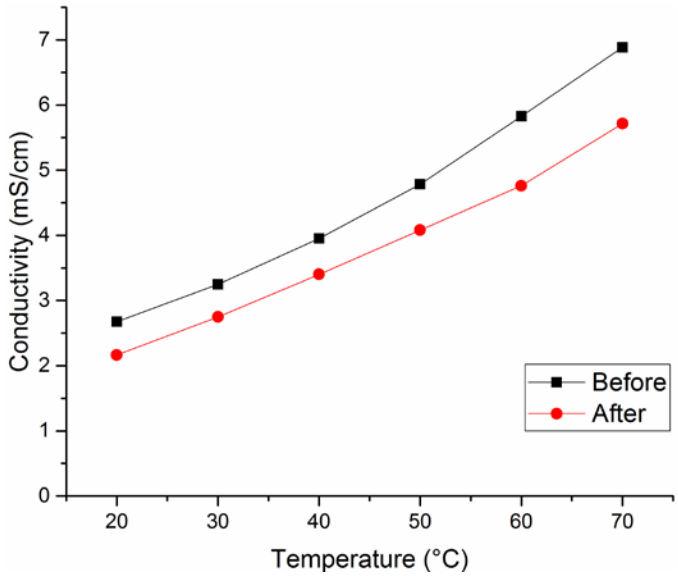

FIGURE 2. Conductivity (ClO_4^- form) of 9MeOTTP$^+$-F_6PBI PTFE reinforced membrane measured at different temperatures before and after accelerated oxidation stability test in cerium (IV)

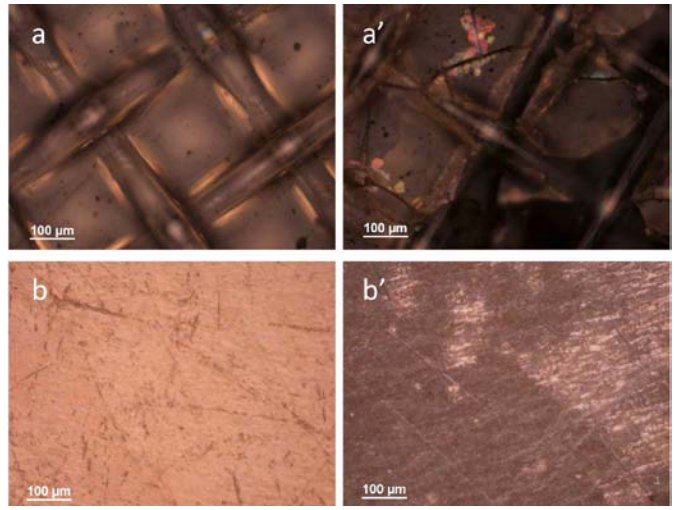

FIGURE 3. Microscopy image of FAB-PK-130 and 9MeOTTP$^+$-F_6PBI PTFE reinforced membrane before and after accelerated oxidation stability test in 0.5 M cerium (IV) and 1.3 M $HClO_4$ at 55°C for 100 h (a and a': FAB-PK-130 before and after; b and b': 9MeOTTP$^+$-F_6PBI PTFE reinforced membrane before and after)

TABLE 2. Accelerated Stability Test Results in 0.5 M Cerium (IV) and 1.3 M $HClO_4$ at 55°C

Membrane	Thickness (µm)	24 h	100 h	200 h
FAS-30	30	Break into pieces		
FAB-PK-130	130		Loss of polymer	
9MeOTTP$^+$-F_6PBI PTFE reinforced membrane	20			No appreciable morphological change

- 9MeOTTP$^+$-F_6PBI PTFE reinforced membrane showed excellent oxidative resistance against cerium (IV) solution.

Upcoming activities include:

- Membranes and ionomers shipped to the National Renewable Energy Laboratory for membrane electrode assembly preparation and tests.
- Collaborate with Xergy to prepare reinforced membranes.
- Collaborate with Giner to prepare reinforced membranes using their dimensionally stable membrane technology.

V.C.6 Advanced Materials for Fully-Integrated MEAs in AEMFCs

Yu Seung Kim (Primary Contact), Sandip Maurya, Joseph Dumont, Eun Joo Park
Los Alamos National Laboratory (LANL)
MPA-11: Materials Synthesis and Integrated Devices
Los Alamos, NM 87545
Phone: (505) 667-5782
Email: yskim@lanl.gov

DOE Manager: David Peterson
Phone: (720) 562-1747
Email: David.Peterson@ee.doe.gov

Subcontractors:
- Cy Fujimoto and Michael Hibbs, Sandia National Laboratory, Albuquerque, NM
- Vojislav Stamenkovic, Argonne National Laboratory, Lemont, IL
- Chulsung Bae and Woo Hyung Lee, Rensselaer Polytechnic Institute, Troy, NY

Project Start Date: November 2, 2015
Project End Date: November 1, 2018

Overall Objectives

- Synthesize highly conductive and stable hydrocarbon-based anion exchange membranes (AEMs).
- Prepare ionomeric electrode binders for the fabrication of fuel cell electrodes.
- Integrate non-precious or low-Pt-metal-loading electrocatalysts into membrane electrode assemblies (MEAs).
- Demonstrate the high performance of anion exchange membrane fuel cells (AEMFCs).
- Demonstrate AEMFC durability under steady and accelerated stress conditions.

Fiscal Year (FY) 2017 Objectives

- Obtain AEM area specific resistance (ASR) ≤ 0.1 Ω cm^2, maintained for 500 h at 600 mA/cm^2 at T > 60°C.
- Achieve stable AEM resistance in both ex situ and in situ measurements.
- Obtain AEMFC peak power density > 0.6 W/cm^2.

Technical Barriers

This project addresses the following technical barriers from the Fuel Cells section (3.4) of the Fuel Cell Technologies Office Multi-Year Research, Development, and Demonstration Plan [1].

(A) Durability (polymer electrolytes)

(B) Cost (non-precious metal catalysts)

(C) Performance (AEMFCs)

Technical Targets

This project is developing advanced materials for AEMFCs for practical use in power applications. Insights gained from this project will be applied towards the next-stage AEMFC systems. The technical targets for AEMFCs in the Multi-Year Research, Development, and Demonstration Plan [1] are listed below.

- Q2, 2017: AEM ASR ≤ 0.1 Ω cm^2, maintained for 500 h at 600 mA/cm^2 at T > 60°C
- Q4, 2017: AEMFC power density > 600 mW/cm^2

FY 2017 Accomplishments

- Demonstrated alkaline stability of down-selected hexamethyl trimethyl ammonium functionalized Diels-Alder poly(phenylene) polymers.
  - Alkaline stability: no structural change after 3,600 h in 0.5 M NaOH at 80°C.
- Demonstrated alkaline stability of resonance-stabilized guanidinium functionalized Diels-Alder poly(phenylene) polymers.
  - Alkaline stability: no structural change after 10,000 h in 0.5 M NaOH at 80°C.
- Discovered new inhibition mechanism for alkaline hydrogen oxidation reaction (HOR).
- Achieved 1 W/cm^2 peak power density of AEMFC using AEM and ionomers made by the LANL team with commercial electrocatalysts.

✧ ✧ ✧ ✧ ✧

INTRODUCTION

In the previous research (2008–2013), we identified that aryl-ether linkage of the polymer backbone is not chemically stable under high pH conditions [2, 3]. Based on this result, we have developed several aryl-ether-free AEMs over the last three years [4–6]. In FY 2016, we down-selected hexamethyl ammonium functionalized Diels-Alder poly(phenylene)s (TMAC6PP) and poly(phenyl alkylene)s as AEMs. Also, we started to develop advanced hydrocarbon ionomeric binding

materials for AEMFC electrodes. Electrochemical and spectroscopic analyses were initiated in order to elucidate major HOR inhibition mechanisms, which helps to design advanced ionomeric binders for AEMFC anode. In FY 2017, we focused on alkaline stability of the down-selected AEMs in both ex situ and in situ measurements. We also measured ex situ alkaline stability of resonance-stabilized hydrocarbon binders. For electrode works, we found a new alkaline HOR inhibition mechanism and improved the AEMFC performance.

APPROACH

Our general approach to prepare stable and highly conductive AEMs is to synthesize cationic group functionalized aryl-ether-free polymers. Our strategy also includes changing the most popular benzyl trimethyl ammonium group to more stable alkylammonium. There are several viable synthetic pathways to accomplish synthesizing such polymer structure. First, alkyl ammonium functionalized poly(phenylene)s can be prepared using Diels-Alder poly(phenylene) precursor developed by Fujimoto et al. [7] (Sandia National Laboratories) or acid-catalyzed Friedel-Crafts polycondensations [4] (Rensselaer Polytechnic Institute). Second, alkyl ammonium functionalized poly(styrene-ethylene-butylene-styrene) block copolymers can be prepared via transition-metal-catalyzed C-H borylation and Suzuki coupling reaction. Third, resonance-stabilized cationic group containing polymers can be prepared by Diels-Alder poly(phenylene) frameworks (LANL and Sandia National Laboratories).

Our general approach to prepare advanced high-performing ionomeric binders for AEMFCs is to develop different cationic groups for anode and cathode catalyst layers. For this, we evaluated the catalytic activities of Pt using various electrolytes and screened the candidate functional groups (LANL). Then, the selected candidate functional groups were employed into a polymeric structure and further structural optimization was made (LANL). Advanced catalysts will be provided from Argonne National Laboratory and other no-cost collaborators.

RESULTS

Alkaline stability of anion exchange membranes: Figure 1a compares the hydroxide conductivity change of benzylammonium functionalized Diels-Alder poly(phenylene) (ATM-PP control) and hexamethylammonium functionalized Diels-Alder poly(phenylene) (TMAC6PP) during ex situ stability test at 0.5 M and 4 M NaOH at 80°C. Note that the conductivity of ATM-PP quickly deteriorated within 200 h, but the conductivity of TMAC6PP was stable to 3,600 h in 0.5 M NaOH conditions and to 1,800 h in 4 M NaOH conditions. Figure 1b shows the Fourier transform infrared spectroscopy spectrum change of TMAC6PP after 3,600 h, 0.5 M NaOH treatment. No changes on the C–N stretching peaks at 910 cm^{-1} and 970 cm^{-1} were observed, indicating that significant improvement of alkaline stability was obtained with the TMAC6PP AEM.

The alkaline stability of the TMAC6PP was evaluated during AEMFC operating conditions. Figure 2 shows the

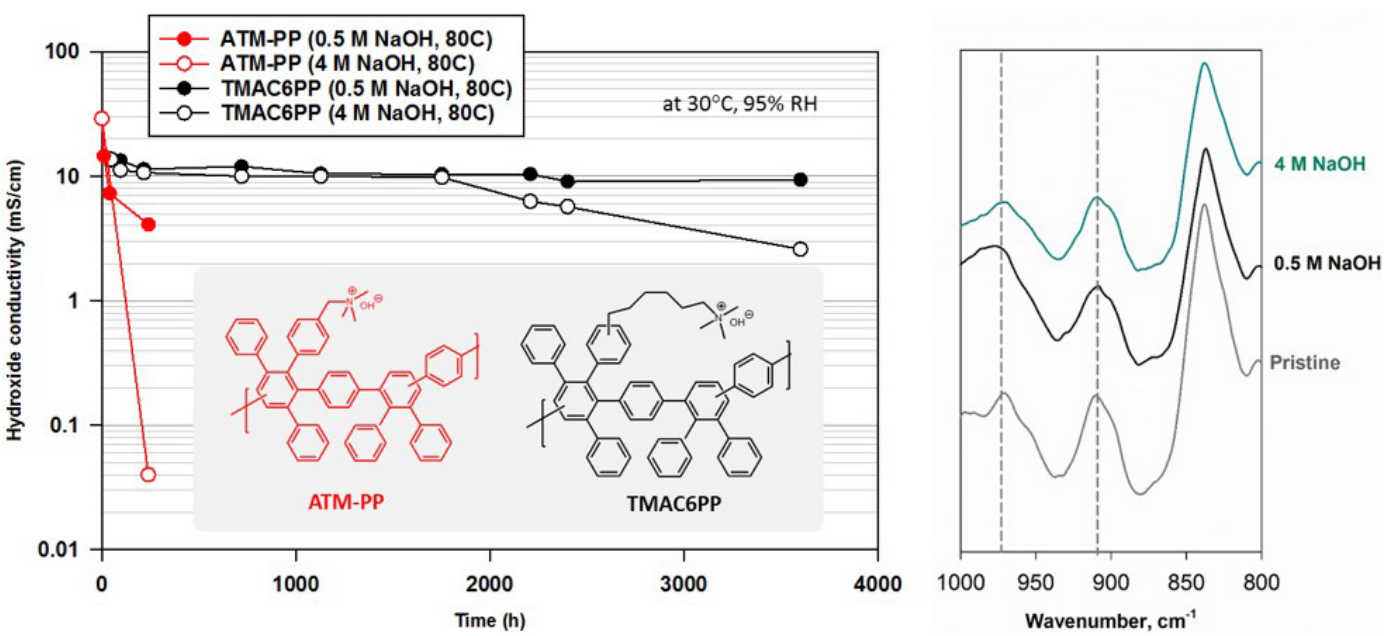

FIGURE 1. (a) Hydroxide conductivity change of TMAC6PP during ex situ alkaline stability test at 80°C; (b) Fourier transform infrared spectroscopy spectrum change after 3,600 h (0.5 M NaOH) and 1,800 h (4 M NaOH)

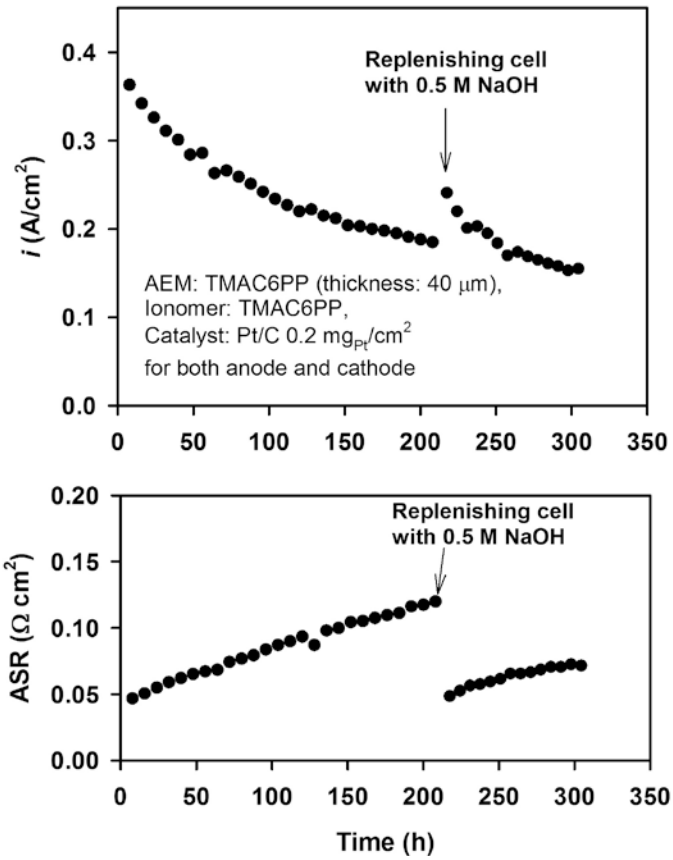

FIGURE 2. AEMFC life test for 300 h with replenishing cell with 0.5 M NaOH at 210 h

cell current density change and AEM ASR during AEMFC operation at 80°C and constant voltage of 0.3 V. The AEM ASR was obtained from cell high-frequency resistance and measured cell electronic resistance [8]. The initial ASR of TMAC6PP was 0.05 Ω cm^2, which met the DOE milestone for AEM ASR (<0.1 Ω cm^2). The cell current density slowly decreased from 0.37 A/cm^2 – 0.19 A/cm^2, and the AEM ASR increased from 0.05 to 0.12 Ω cm^2 after ~200 h life test. A separate study indicated that the ASR increase is due to the carbonation issue. So we took out the MEAs and replenished the cell with 0.5 M NaOH followed by thorough rinsing with deionized water. After resuming the life test, the AEM ASR recovered to 0.05 Ω cm^2, indicating that the ASR increase during the life test was not due to the AEM degradation but due to the carbonation build-up possibly from water humidification. The current density of the cell, however, did not fully recover to the initial value after replenishing the cell, indicating that the AEMFC performance loss may be related to other degradation mechanisms. After 300 h, we stopped the life test. The alkaline stability of the extended-resonance structure was also evaluated. The extended-resonance structure was obtained by a series of connections of phenyl group–ketone–phenyl group–methyl guanidinium via LANL-developed activated fluoro-amine reaction [9]. The extended-resonance group functionalized Diels-Alder poly(phenylene) is a potential candidate for anode ionomeric binder. During in situ 0.5 M NaOH stability test at 80°C, the resonance stabilized Diels-Alder poly(phenylene)s exhibited unprecedented alkaline stability: no degradation after 10,000 h treatment.

HOR inhibition mechanisms and H_2/O_2 AEMFC performance: Rotating disk electrode investigation on alkaline HOR indicated that the HOR activity of Pt-based catalysts is greatly hindered by the benzene adsorption parallel to the Pt surface [10]. We found that this is a major issue for our AEMFC performance as our polymer electrolyte binders have benzene groups in the polymer backbone and side chain. In order to minimize benzene adsorption on the HOR catalyst surface, we further investigated the effect on Pt bimetallic catalysts. The result indicated that Pt–Ru bimetallic catalyst efficiently prevents the benzene adsorption and can improve the HOR activity. Based on this result, Argonne National Laboratory started to synthesize Pt–Ru catalysts. In order to prevent the benzene adsorption, we synthesized new ionomeric binders based on fluorene moiety [11]. Figure 3 shows the AEMFC performance improvement achieved in FY 2017. When the project started, the peak power density of AEMFC using Diels-Alder poly(phenylene)s was only a little over 300 mW/cm^2. Until January 2017, the AEMFC performance improvement was marginal: peak power density ≈400 mW/cm^2. When we changed the HOR catalyst to commercially available Pt–Ru/C catalysts and used new fluorene-based ionomers, the AEMFC performance jumped to 1 W/cm^2 peak power density. The low high-frequency resistance of ~0.07 Ω cm^2 confirms that the AEMs developed by the LANL team have high enough hydroxide conductivity for high-performing AEMFCs.

A major achievement for alkaline electrode study during FY 2016 was the HOR inhibition by cation–hydroxide–water co-adsorption [12]. In FY 2017, we completed the elucidation of the inhibition mechanism by electrochemical impedance study. We measured the faradaic impedance of the Pt electrode at 0.01 V, 0.05 V, and 0.1 V vs. reverse hydrogen electrode at two different electrode rotating speeds, ca. 900 rpm and 2500 rpm. The smaller semi-circle with the higher rotating disk electrode rotating speed indicated that the second low-frequency circle was likely originated from a diffusion-controlled process rather than kinetic process. The H_2 diffusion-related HOR inhibition mechanism looks counterintuitive because H_2 is a small molecule and the diffusion of H_2 is fast. A possible explanation is the extremely low solubility and diffusivity of H_2 through the co-adsorbed layer, which has a very high hydroxide population. We are trying to measure the thickness of the co-adsorbed layer and the composition by neutron reflectometry experiments [13]. Further study with different cationic groups indicates that longer alkyl chain tethered ammonium groups tend to adsorb less [14].

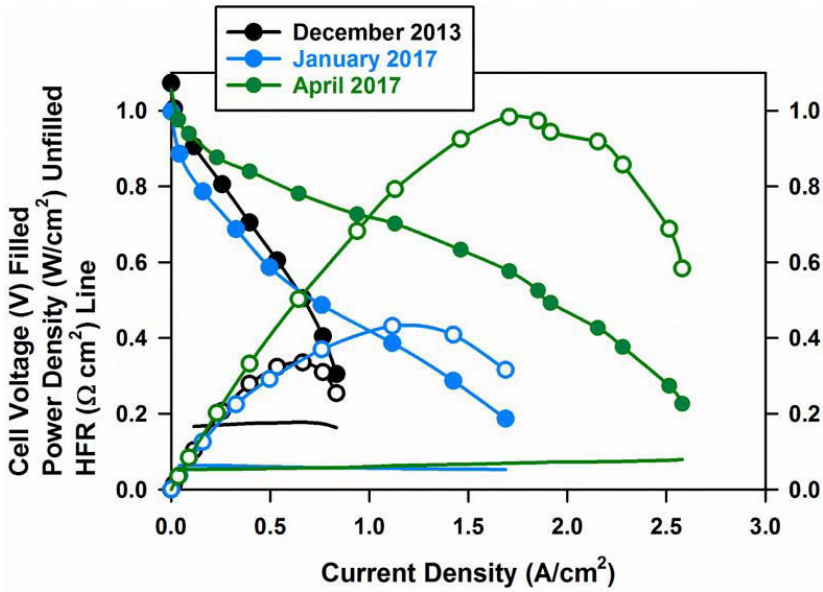

FIGURE 3. Progress of AEMFC performance improvement; AEMFC performance was measured under H_2/O_2 conditions at 30 psig backpressure at 80°C. December 2013 cell, AEM: ATM-PP (80 μm thick), ionomeric binder: ATM-PP, catalyst: Pt black (3 mg_{Pt}/cm^2) for both anode and cathode. January 2017 cell, AEM: Poly(terphenyl alkylene) (30 μm), ionomeric binder: AS 4 (Tokuyama), catalyst: Pt/C (0.6 mg_{Pt}/cm^2) for both anode and cathode. April 2017 cell, AEM: Poly(terphenyl alkylene) (30 μm), ionomeric binder: poly fluorene based, catalyst: Pt–Ru/C (0.5 mg_{Pt}/cm^2) for anode, Pt/C (0.6 mg_{Pt}/cm^2) for cathode.

CONCLUSIONS AND UPCOMING ACTIVITIES

- Down-selected hexamethyl-ammonium functionalized AEM showed low ASR (~0.05 Ω cm^2) and no chemical degradation during 3,600 h ex situ test, >300 h in situ test.
- New HOR inhibition mechanism was explored and based on the study, high AEMFC performance (up to 1 W/cm^2 peak power density) was obtained.
- Time-dependent cation–hydroxide–water co-adsorption behavior was further examined. New ionomeric binders are being synthesized based on this result.
- In FY 2018, further improved fuel cell performance and durability will be demonstrated from the developing AEMs and ionomers.

SPECIAL RECOGNITIONS & AWARDS/ PATENTS ISSUED

1. Yu Seung Kim, Kwan-Soo Lee, Cy Fujimoto, "Poly(phenylene)-based Anion Exchange Polymers and Methods Thereof," U.S. Patent Application Publication, US 2017/0190831, July 6, 2017.

FY 2017 PUBLICATIONS/PRESENTATIONS

1. Poly(terphenylene) Anion Exchange Membrane with Molecular Ordered Structure, Woo-Hyung Lee, Eun Joo Park, Dong Won Shin, Yu Seung Kim, Chulsung Bae, *ACS Macro Lett.6, 5,* 566–570 (2017).

2. Effect of Organic Cations on Hydrogen Oxidation Reaction of Carbon Supported Platinum, Hoon Taek Chung, Yoong-Kee Choe, Ulises Martinez, Joseph H. Dumont, Angela Mohanty, Chulsung Bae, Ivana Matanovic, Yu Seung Kim, *J. Electrochem. Soc.* 163 (14) F1503–F1509 (2016).

3. Cation-Hydroxide-Water Coadsorption Inhibits the Alkaline Hydrogen Oxidation Reaction, Hoon Taek Chung, Ulises Martinez, Ivana Matanovic, Yu Seung Kim, *J. Phys. Chem. Lett.* 7, 4464–4469 (2016).

4. Design Aspect of Ionomeric Binder for Alkaline Membrane Fuel Cells, Yu Seung Kim, Workshop on Ion Exchange Membranes for Energy Applications, EMEA2017, June 26–28, Bad Zwischenahn, Germany.

5. Impact of Cation-Hydroxide-Water Co-adsorption on Alkaline Hydrogen Oxidation Reaction, Yu Seung Kim, 21st Solid State Ionics Meeting, June 18–24, 2017, Padua, Italy.

REFERENCES

1. Fuel Cell Technologies Office Multi-Year Research, Development, and Demonstration Plan, 2014. http://energy.gov/sites/prod/files/2014/12/f19/fcto_myrdd_fuel_cells.pdf.

2. Cy Fujimoto, Dae-Sik Kim, Michael Hibbs, Debra Wrobleski, Yu Seung Kim, "Backbone Stability of Quaternized Polyaromatics for Alkaline Membrane Fuel Cells," *J. Memb. Sci.* 423–424 (2012): 438.

3. Yoong-Kee Choe, Cy Fujimoto, Kwan-Soo Lee, Luke T. Dalton, Kathy Ayers, Neil J. Henson, Yu Seung Kim, "Alkaline Stability of Benzyl Trimethyl Ammonium Functionalized Polyaromatics: A Computational and Experimental Study," *Chem. Mater.* 26 (2014): 5675.

4. Woo-Hyung Lee, Yu Seung Kim, Chulsung Bae, "Robust Hydroxide Ion Conducting Poly(biphenyl alkylene)s for Alkaline Fuel Cell Membranes," *ACS Macro Letters* 4 (2015): 814.

5. Angela D. Mohanty, Chang Y. Ryu, Yu Seung Kim, Chulsung Bae, "Stable Elastomeric Anion Exchange Membranes Based on Quaternary Ammonium-Tethered Polystyrene-b-poly (ethylene-co-butylene)-b-polystyrene Triblock Copolymers," *Macromolecules* 48 (2015): 7085.

6. Woo-Hyung Lee, Eun Joo Park, Dong Won Shin, Yu Seung Kim, Chulsung Bae, "Poly(terphenylene) Anion Exchange Membrane with Molecular Ordered Structure, *ACS Macro Lett.6, 5,* 566–570 (2017)."

7. Cy Fujimoto, Michel Hickner, Christopher Cornelius, Douglas Loy, "Ionomeric Poly(phenylene) prepared by Diels-Alder Polymerization: Synthesis and Physical Properties of a Novel Polyelectrolyte," *Macromolecules* 38 (2005): 5010.

8. Bryan Pivovar, Yu Seung Kim, "The Membrane-Electrode Interface in PEFCs I. A Method for Quantifying Membrane-Electrode Interfacial Resistance," *Journal of the Electrochemical Society*, 154 (2007): B739.

9. Dae Sik Kim, Andrea Labouriau, Michael Guiver, Yu Seung Kim, "Guanidinium-functionalized Anion Exchange Polymer Electrolytes via Activated Fluorophenyl-amine Reaction," *Chemistry of Materials*, 23 (2011): 3795.

10. Ivana Matanovic, Hoon Taek Chung, Yu Seung Kim, "Benzene Adsorption - A Significant Inhibitor for the Hydrogen Oxidation Reaction in Alkaline Conditions," *J. Phys. Chem. Lett.* (2017) accepted.

11. Woo-Hyung Lee, Angela, D. Mohanty, Chulsung Bae, "Fluorene-Based Hydroxide Ion Conducting Polymers for Chemically Stable Anion Exchange Membrane Fuel Cells," *ACS Macro. Let.* 4 (2015), 453.

12. Hoon T. Chung, Ulises Martinez, Ivana Matanovic, Yu Seung Kim, "Cation-hydroxide-water coadsorption Inhibits the Alkaline Hydrogen Oxidation Reaction," *The Journal of Physical Chemistry Letters*, 7, (2016): 4464.

13. Joseph Dumont, Rex Hjelm, Erik Watkins, Yu Seung Kim, Manuscript in preparation (2017).

14. Hoon T. Chung, Yoong-Kee Choe, Ulises Martinez, Joseph Dumont, Angela Mohanty, Chulsung Bae, Yu Seung Kim, "Impact of Organic Cation Adsorption on the Hydrogen Oxidation Reaction of Pt in Alkaline Fuel Cells," *Journal of the Electrochemical Society*, 163, (2015) F1503–F1509.

V.C.7 Advanced Ionomers & MEAs for Alkaline Membrane Fuel Cells

Bryan Pivovar (Primary Contact), Andrew Park, Ami Neyerlin, K.C. Neyerlin, Shaun Alia, Hai Long, Zbyslaw Owczarczyk
National Renewable Energy Laboratory (NREL)
15013 Denver West Parkway
Golden, CO 80401
Phone: (303) 275-3809
Email: Bryan.Pivovar@nrel.gov

DOE Manager: David Peterson
Phone: (720) 356-1747
Email: David.Peterson@ee.doe.gov

Subcontractors:
- Adam Weber (principal investigator [PI]), Huai-Suen Shiau, Lawrence Berkeley National Laboratory, Berkeley, CA
- Tom Zawodzinski (PI), Ramez Elgammel, Zhijiang Tang, Oak Ridge National Laboratory/University of Tennessee, Oak Ridge, TN
- Andy Herring (PI), Ashutosh Divekar, Colorado School of Mines, Golden, CO
- (in-kind) Mike Yandrasits (PI), Steve Hamrock, 3M Company, St. Paul, MN

Project Start Date: October 1, 2015
Project End Date: September 30, 2018

Overall Objectives

- Improve novel perfluoro (PF) anion exchange membrane (AEM) properties and stability.
- Employ high performance PF AEM materials in electrodes and as membranes in alkaline membrane fuel cells (AMFCs). Apply models and diagnostics to AMFCs to determine and minimize losses (water management, electrocatalysis, and carbonate related).

Technical Barriers

This project addresses the following technical barriers from the Fuel Cells section (3.4.4) of the Fuel Cell Technologies Office Multi-Year Research, Development, and Demonstration Plan.

(A) Durability (of membranes and membrane electrode assemblies)

(B) Cost (of membranes and membrane electrode assemblies)

(C) Performance (of membranes and membrane electrode assemblies)

Technical Targets

This project will synthesize novel PF AEMs and ionomers and incorporate these into membrane electrode assemblies (MEAs) for fuel cell testing. The project generally supports targets outlined in the Multi-Year Research, Development, and Demonstration Plan in application specific areas (portable, stationary, transportation). However, as AMFCs are at an earlier stage of development, specific target tables have not yet been developed. There are four tasks presented by Dimitrios Papageorgopoulos at the AMFC Workshop, April 1, 2016 [1].

TABLE 1. Targets for AMFCs Presented at the April 2016 AMFC Workshop

	Task
Q2, 2017	Develop anion-exchange membranes with an area specific resistance ≤0.1 ohm cm^2, maintained for 500 hours during testing at 600 mA/cm^2 at T >60°C.
Q4, 2017	Demonstrate AMFC peak power performance >600 mW/cm^2 on H_2/O_2 (maximum pressure of 1.5 atm_a) in MEA with a total loading of ≤0.125 mg_{PGM}/cm^2.
Q2, 2019	Demonstrate AMFC initial performance of 0.6 V at 600 mA/cm^2 on H_2/air (maximum pressure of 1.5 atm_a) in MEA a total loading of <0.1 mg_{PGM}/cm^2, and less than 10% voltage degradation over 2,000-hour hold test at 600 mA/cm^2 at T > 60°C. Cell may be reconditioned during test to remove recoverable performance losses.
Q2, 2020	Develop non-PGM catalysts demonstrating AMFC peak power performance >600 mW/cm^2 under H_2/air (maximum pressure of 1.5 atm_a) in PGM-free MEA.

T – temperature; PGM – platinum group metal

FY 2017 Accomplishments

- The project has successfully improved performance, durability, and processing of Generation (Gen) 2 PF AEMs.
- Implementing PF AEMs into devices plus University of Connecticut gas diffusion electrodes (GDEs) has allowed us to demonstrate performance ~1 W/cm^2 and durability beyond 500 hours (demonstrating a 2017 second quarter DOE milestone).
- Model development is providing insight into the role of water and carbon dioxide in these systems, allowing the performance potential and limitations of AMFCs to be better understood.

✧ ✧ ✧ ✧ ✧

INTRODUCTION

AMFCs are of interest primarily because they enable the use of non-Pt catalysts, the main cost/supply limitation of proton exchange membrane fuel cells. AMFCs, therefore, offer the potential of greatly decreased polymer electrolyte fuel cell cost. Operating AMFCs under ambient conditions where carbon dioxide is present remains a challenge due to carbonate formation. An approach that has shown promise for carbon dioxide tolerance is increased operating temperature. Unfortunately, the stability of the cation side chains on the membrane polymer and water management within the membrane both become more difficult as temperature rises.

The use of perfluorinated ionomers, similar to those used in proton exchange membrane systems, with tethered cation head groups that allow hydroxide conduction should help improve water transport properties and offer exceptional chemical durability of the backbone. The significant advances demonstrated in AMFC systems have been accomplished primarily through improving water management and the bonding between membrane and electrode. Both issues can be tackled much more effectively when employing PF AEMs and ionomers. The project consists of three sub-tasks: synthesis of novel perfluorinated alkaline ionomers (NREL); characterization of PF AEMs (NREL, Oak Ridge National Laboratory/University of Tennessee, Colorado School of Mines); and fuel cell performance and modeling optimization (NREL, Lawrence Berkeley National Laboratory).

APPROACH

The team has focused on achieving higher-temperature, higher-power-density AMFC operation through implementation of novel alkaline PF membranes and ionomeric dispersions. PF materials are expected to enhance water transport capabilities and electrode performance and durability significantly, thereby enabling higher temperature and power density operation. The combination of high current density and operating temperature will improve the ability of these devices to tolerate ambient CO_2 and potentially enabling tolerance to these conditions. Starting with the sulfonyl fluoride form of current perfluoro ionomers we have identified, and in several cases verified, the ability to convert commercially available precursors into anion exchange polymers and membranes. The synthesized PF ionomers have been cast into membranes, made into polymeric dispersions, and characterized in fuel cell tests. Modeling efforts have been made in parallel to better understand cell performance, loss mechanisms, and mitigation approaches.

RESULTS

While PF chemistry improves PF sulfonic acid acidity, the strongly electron withdrawing PF backbone creates challenges for anion exchange membranes. From the readily available perfluoro sulfonyl fluoride precursor, different strategies can be employed to tether cations to the polymer backbone. We have focused on an amide linkage as shown in Figure 1 for our Gen 1 and Gen 2 PF AEMs. We have improved our processing of Gen 2 PF AEM and have demonstrated 90% of theoretical ion exchange capacity with hydroxide conductivity as high as 52 mS/cm (liquid equilibrated at room temperature). These materials have demonstrated reasonable water uptake and conductivity as a function of relative humidity (RH). They behave essentially as PF AEM analogues to perfluorosulfonic acids with many of the envisioned benefits of a perfluorinated system (high conductivity and water mobility) being maintained. While our Gen 1 materials have shown greater than 90% loss of ion exchange capacity (IEC) after two days in 2 M KOH at 80°C, our Gen 2 materials have shown >50x improvement in chemical stability and have allowed us to significantly increase our fuel cell durability testing, as shown in Figure 2. Following optimization of reaction and processing conditions, tough, ductile films and ionomeric solutions and dispersions have been obtained. We have synthesized over 200 g of Gen 2 PF AEM and have shared this material with more than 10 collaborating institutions.

Our Gen 2 PF AEM materials have been tested in AMFCs under a range of conditions. When used as an ionomer solution in electrode inks, performance has achieved up to 300 mw/cm^2 on H_2/O_2. Through collaboration with the Prof. Bill Mustain (University of Connecticut [UConn]) we also tested electrodes (UConn GDE) based on ionomer supplied by Prof. John Varcoe (University of Surrey). These electrodes were applied to our PF AEM materials and demonstrated performance approaching 1 W/cm^2. These two PF AEM AMFCs tests show significantly different performance and durability, as shown in Figure 3. The performance benefits of the UConn GDE are significant and cannot be fully explained by the improved high frequency resistance. Additionally, the UConn GDE was found to have a lower catalyst surface area (29 m^2/g Pt vs. 71 m^2/g Pt) in spite of its higher performance. The UConn GDE also showed a high sensitivity to water balance, achieving stable, high

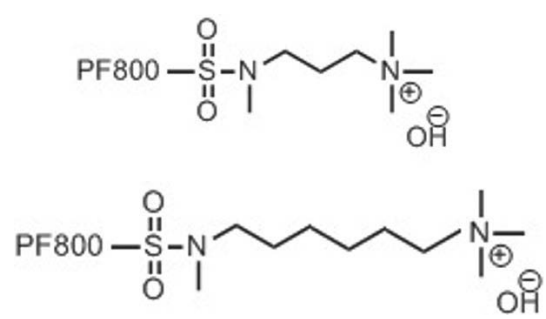

FIGURE 1. Chemical structures of Gen 1 and Gen 2 PF AEMs

current density within a narrow range of anode and cathode humidification. This AMFC also showed significantly improved durability compared to the PF AEM catalyst coated membrane. Unlike the PF AEM catalyst coated membrane which lost all performance within 15 h, the UConn GDE retained reasonable performance after 500 h of testing at 600 mA/cm^2 at 60°C. The high frequency resistance of this cell showed a slight increase over time, but demonstrated the ability to meet the DOE second quarter 2017 milestone of an area specific resistance ≤0.1 ohm cm^2, maintained for 500 h during testing at 600 mA/cm^2 at temperature >60°C.

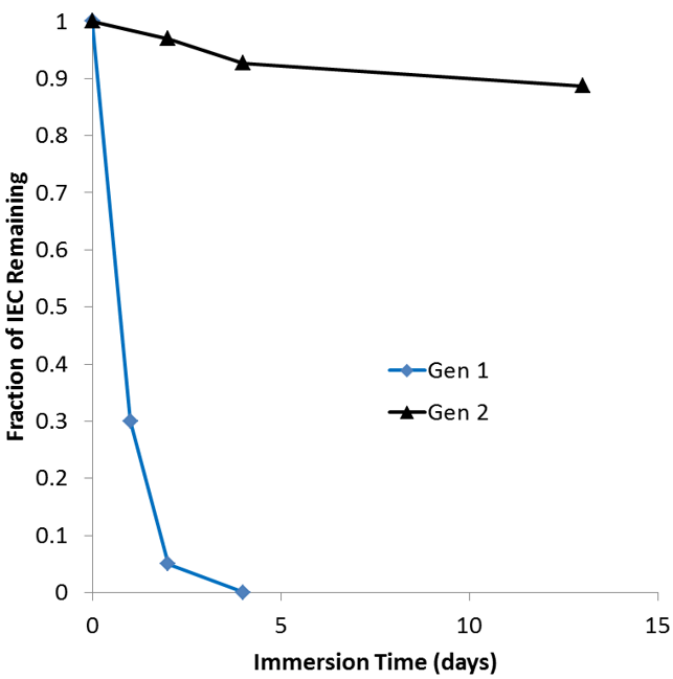

FIGURE 2. Chemical durability of Gen 1 and Gen 2 PF AEMs

The areas of modeling and advanced diagnostics have both been lacking in the AMFC area, and we have been addressing these aspects in this project. In last year's report we highlighted efforts to develop AMFC models. This year we expanded our use of models to study additional aspects of AMFC performance. Shown in Figure 4 are model results that investigate the impact of RH and oxygen content. These studies highlight the tremendous impact that RH has on AMFC performance. Additionally, we have been investigating carbonate formation due to the presence of carbon dioxide through models and experimental studies. In order to enable widespread commercialization of AMFCs, tolerance to atmospheric CO_2 levels will likely be required.

CONCLUSIONS AND UPCOMING ACTIVITIES

The project has successfully synthesized PF AEM sulfonamide-linked chemistries for highly OH-conductive AEMs. Extensive characterization has been performed on the polymer. Implementing this polymer into devices yields reasonable AMFC power densities. Modeling and diagnostic techniques are being performed to advance/optimize AMFC architecture. Upcoming activities focus on:

- Polymer synthesis:

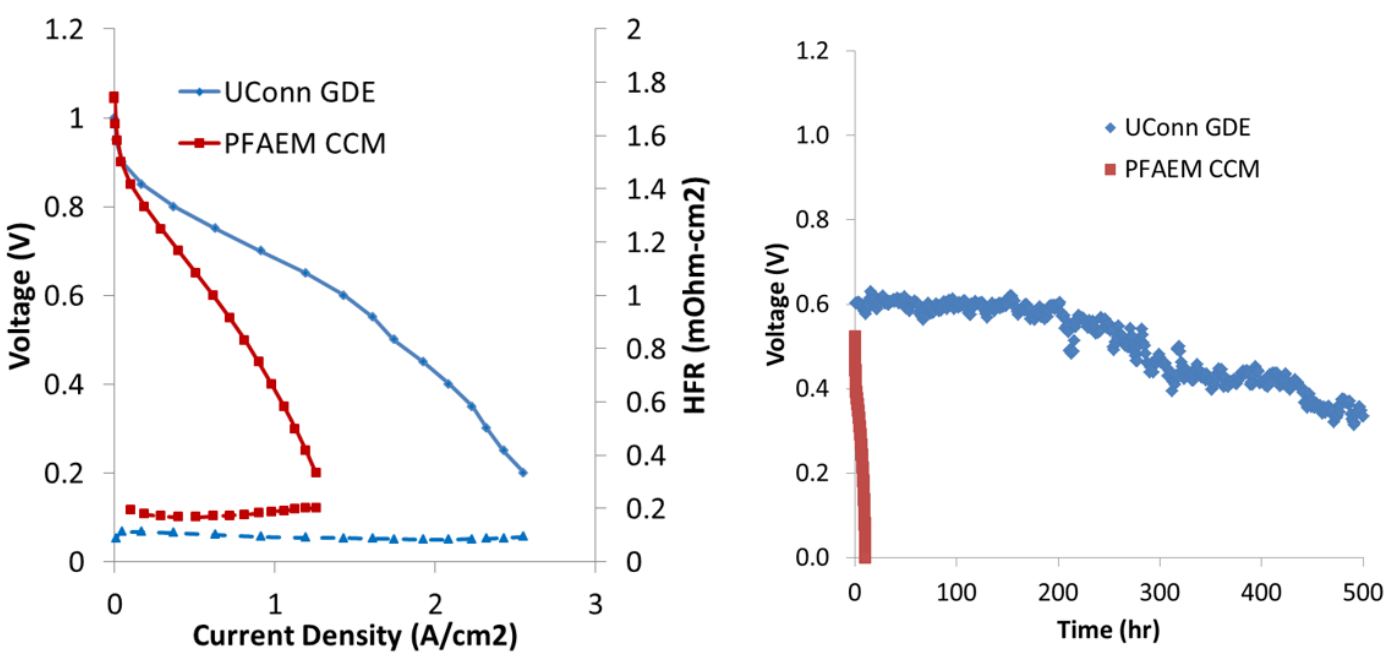

FIGURE 3. AMFC performance and durability of PF AEM membranes with standard PF AEM ink electrodes and UConn GDEs

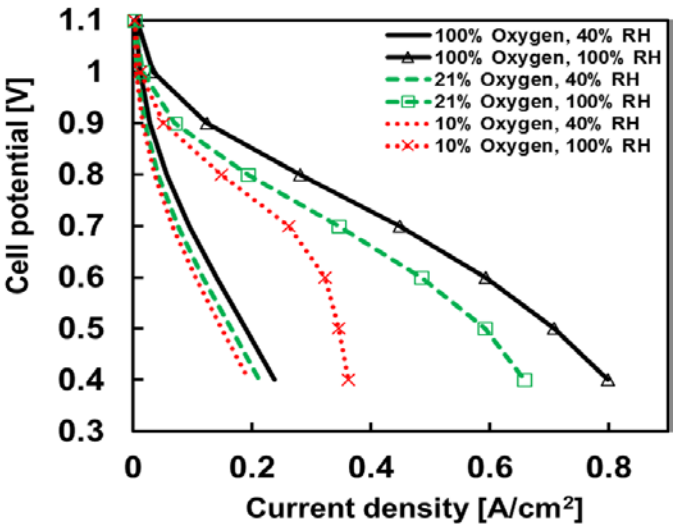

FIGURE 4. Modeling of AMFC performance as a function of oxygen concentration and RH

- Avoid sulfonamide linkage.
- Focus on Gen 3 polymer development.

- Characterization:
  - Conductivity, stability, water transport, carbonate formation and resulting effects.
- AMFC implementation, modeling, and diagnostics:
  - Electrode optimization and diagnostic studies focused on further characterization of electrodes and elucidating performance loss and durability.
    - In situ: limiting current, RH studies, cyclic voltammetry, and impedance (and water management).
    - Ex situ: microscopic, electrochemical, and spectroscopic analysis.
  - Integration of modeling efforts with cell testing.
    - Further elucidation of the impact of operating conditions (temperature, RH, current density, CO_2 concentration).

FY 2017 PUBLICATIONS/PRESENTATIONS

1. Adam Z. Weber, Lalit Pant, Tobias Schuler, Haui-Suen Shiau, Anna Freiberg, Michael C. Tucker, Anamika Chowdhury, K.C. Neyerlin, Shyam Kocha, Iryna Zenyuk, "Elucidating and Understanding Transport Phenomena in Polymer-Electrolyte Fuel Cells," CARISMA, Newcastle, UK, April 11, 2017.

2. B. Pivovar, "Status of AMFC Technology and Advances in NREL's Perfluorinated Anion Exchange Membranes (PFAEM)," Ion Exchange Membranes for Energy Applications, Bad Zwischenahn, Germany, June 26, 2017.

3. B. Pivovar, "Development and Implementation of Perfluoro Anion Exchange Membranes (PF AEMs)," 21st International Solid State Ionics Meeting, June 21, 2017, Padua, Italy.

4. A.M. Park, Z.R. Owczarczyk, L.E. Garner, A.C. Yang-Neyerlin, H. Long, C.M. Antunes, M.R. Sturgeon, M. Lindell, S.J. Hamrock, M.A. Yandrasits, B.S. Pivovar, "Synthesis and Characterization of Perfluorinated Anion Exchange Membranes," submitted to ECS Transactions.

5. H-S. Shiau, I.V. Zenyuk, and A.Z. Weber, J. Electrochem. Soc., submitted (2017).

REFERENCES

1. D. Papageorgopoulos presentation AMFC Workshop, Phoenix, AZ, April 1, 2016.

V.D.1 Novel Structured Metal Bipolar Plates for Low Cost Manufacturing

Conghua "CH" Wang
TreadStone Technologies, Inc.
201 Washington Road
Princeton, NJ 08543
Phone: (609) 734-3071
Email: cwang@TreadStone-Technologies.com

DOE Manager: Bahman Habibzadeh
Phone: (202) 287-1657
Email: Bahman.Habibzadeh@ee.doe.gov

Contract Number: DE-EE0007732

Subcontractor:
Hawaii Natural Energy Institute, University of Hawaii, Honolulu, HI

Project Start Date: January 15, 2017
Project End Date: January 14, 2018

Overall Objectives

- Develop the physical vapor deposition (PVD) process for the doped titanium oxide (TiO_x) coating.
- Characterize the doped TiO_x coated metal plates, including the chemical composition and thickness of the doped TiO_x surface layer, electrical contact resistance and the corrosion resistance of the coating for proton exchange membrane (PEM) fuel cell applications.
- Evaluate the coating on low cost stainless steel (SS) and post-coating stamping.
- Analyze the manufacturing cost of the technology.

Fiscal Year (FY) 2017 Objectives

- Develop the PVD process for the doped TiO_x coating.
- Characterize the doped TiO_x coated metal plates, including the chemical composition and thickness of the doped TiO_x surface layer, electrical contact resistance and the corrosion resistance of the coating for PEM fuel cell applications.
- Analyze the manufacturing cost of the technology.

Technical Barriers

This project addresses the following technical barriers from the Fuel Cells section of the Fuel Cell Technologies Office Multi-Year Research, Development, and Demonstration Plan.

(A) Durability (improve the durability of bipolar plates in fuel cell operation conditions)

(B) Cost (reduce the cost of the bipolar plate production)

(C) Performance (improve the performance of the bipolar plates)

Technical Targets

The technical objective of the project is to further develop the manufacturing process of the doped TiO_x coating for PEM fuel cell applications that meet the following targets.

- Low electrical contact resistance with gas diffusion layer (<5 $m\Omega.cm^2$)
- Low corrosion resistance: <1 $\mu A/cm^2$
- Low cost: $3/kW by 2020
- Capable of roll-to-roll coating and post-coating stamping

FY 2017 Accomplishments

- Finished the manufacture cost analysis indicating the proposed technology has the lowest cost comparing with other competing technologies.
- Designed the sputtering target material.
- Determined the TiO_x coating microscopic characterization methods.
- Developed the process to minimize the coating surface composition segregation.

✧ ✧ ✧ ✧ ✧

INTRODUCTION

The components of the transportation fuel cell system and stack play an important role in the cost reduction and performance improvement of the fuel cell system. The metal bipolar plate is an important component in fuel cell stack. For example, the automobile industry has confirmed that metal bipolar plates are essential to ensure rapid start of fuel cell vehicles in cold weather (-40°C). The metal plate cost is a significant part of the fuel cell stack cost. Figure 1 shows results of the PEM stack cost analysis recently (December 2015) conducted by our team partner Strategic Analysis, Inc. It shows that bipolar plates account for 14–27% of the

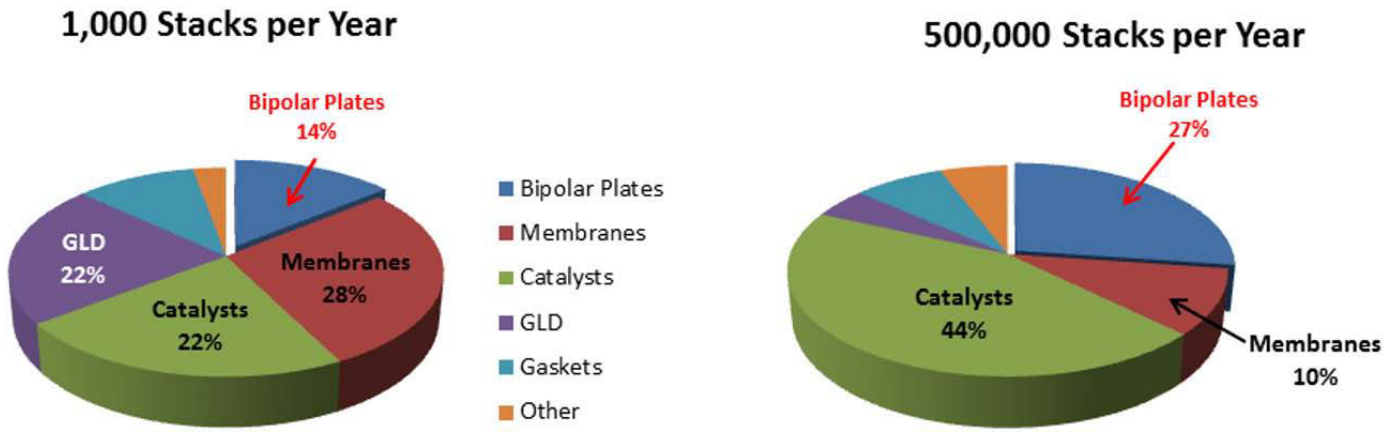

FIGURE 1. Cost breakdown of PEM fuel cell stacks [1]

overall stack cost (1,000–500,000 stacks/yr using 2015 technology) [1]. Therefore, any reduction in plate costs will have significant impact on the overall stack cost.

APPROACH

The technical approach of this project is to develop a precious metal free coating technology for PEM fuel cell applications. The schematic drawing of the technology is shown in Figure 2. The SS foil substrate surface is covered with a thin (~100-nm thick) titanium alloy sub-layer and an ultrathin (several nanometers) electrically conductive doped TiO_x surface layer. This surface oxide layer is grown on the titanium alloy sub-layer surface. The titanium alloy contains the alloy element that is the dopant in the doped TiO_x.

TreadStone's approach overcomes the key technical barriers of using doped titanium oxide semiconductive material [2,3] as the coating material, which are (1) the thickness control of the oxide coating layer and (2) the adhesion of the oxide layer with the metal substrate. The technology utilizes the inherent characteristics of titanium alloys to overcome these barriers and makes it reliable at large volume fabrication and low cost.

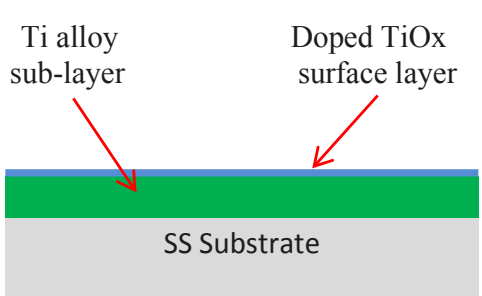

FIGURE 2. Schematic drawing of TreadStone's doped TiO_x coating on SS foil

RESULTS

The manufacture cost analysis of the corrosion resistant coating using the proposed technology was conducted by our team partner, Strategic Analysis, Inc. The analysis is based on stacks using 377 pieces of bipolar plates with the power density of 1,095 mW/cm^2. The coating is conducted on the stamped and welded plates, using a post-forming coating process. Figure 3 is the coating cost at different production volumes. It shows that the major cost item is the capital cost for PVD equipment. The production cost is related with the production volume. At 500,000 systems/yr volume, the coating cost is $0.14/plate. The total coating cost is $0.85/kW which can meet DOE's requirement.

In previous Small Business Innovation Research projects, it was found that there is composition segregation of the titanium alloy coating in the surface layer. The dopant element Nb or Ta is separated from the surface layer of the alloy coating, which results in a pure titanium surface layer. The pure titanium surface layer can only grow titanium oxide that is not as conductive as doped titanium oxide. In this project we have adjusted the processing condition in the sputtering deposition process to reduce the kinetic energy of doping element to minimize the dopant element penetration into the coating surface. Figure 4 shows X-ray photoelectron spectroscopy core level spectra of a deposited Ti–2Ta alloy coating. It was found that surface layer contains 0.5 at% of Ta. Although this concentration is still lower than the target, it shows the feasibility of control composition segregation of the dopant element using deposition energy control to obtain the doped titanium oxide on the coating surface.

A challenge for the proposed project in the manufacturing process development is high manufacturing cost and long lead time of the PVD target. The project's limited time and budget make it challenging to optimize the process and the composition of the coating. In this project, we have developed a new method to overcome the cost and

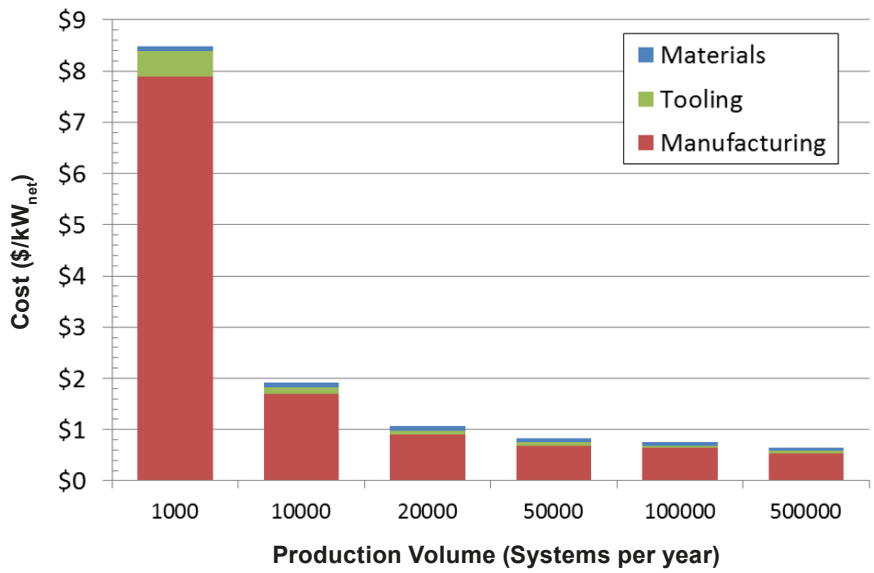

FIGURE 3. The coating manufacture cost of bipolar plates at different production volumes

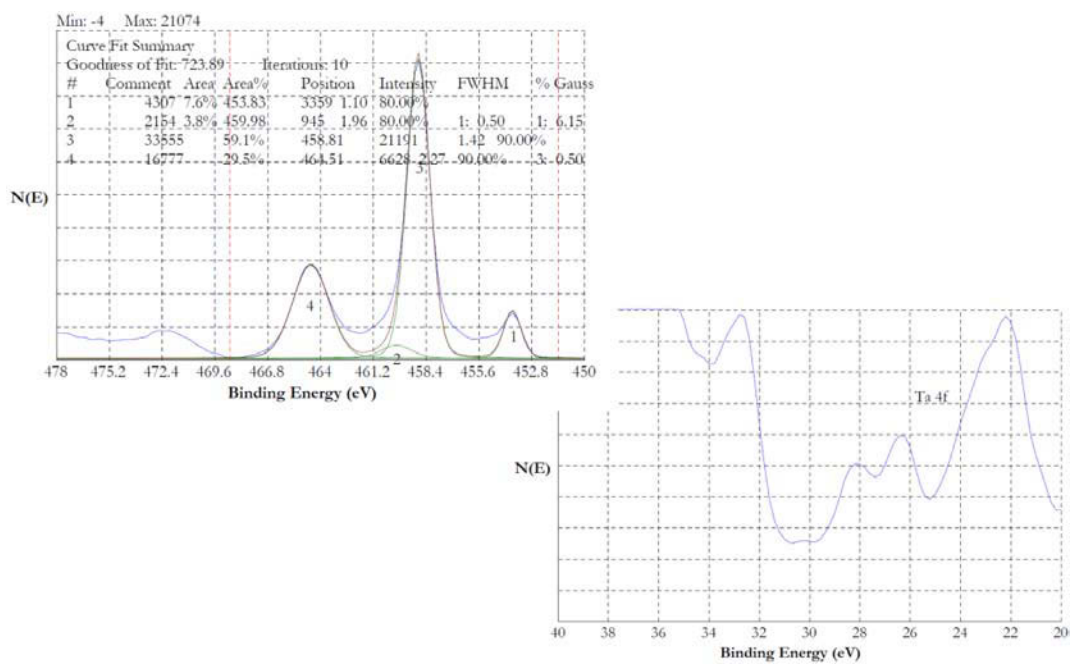

FIGURE 4. The X-ray photoelectron spectroscopy core level spectra of as deposited Ti–Ta coating, showing the existence of Ta in the coating surface layer

lead time barriers. We will use a mosaic-type of target for the deposition. The target is made of strips of target material that are placed in a titanium tray. The coating composition is determined by the width ratio (in combination with the sputtering rate) of each element. For example, the Ti–Nb coating can be obtained with the Nb and Ti strips in the titanium tray, and the ratio of Nb and Ti in the coating can be adjusted using the width of Nb and Ti strips. We have identified a partner PVD coating company whose PVD systems can meet the requirement of the process. We are in the process of developing the manufacturing technology for the doped titanium oxide coating.

CONCLUSIONS AND UPCOMING ACTIVITIES

The project is focused on the manufacture technology development of the novel precious metal free coating technology for PEM fuel cell applications. The manufacture cost analysis indicates the technology will have the lowest production cost, compared with other competing technologies. The project has developed technical solutions to overcome key technical barriers.

The project will continue the development of the manufacture process based on PVD technology. The characterization process of the coating will be developed for the manufacture process quality control method development. The coated SS plates will be evaluated in ex situ corrosion tests and post-coating stamping tests. The substrate material will include 316L SS and lower cost 304 SS. The performance of the coating on both substrates will be compared.

REFERENCES

1. Mass Production Cost Estimation of Direct H_2 PEM Fuel Cell Systems for Transportation Applications, 2015 Update, B.D. James, J.M. Huya-Kouadio, and C. Houchins, Strategic Analysis, Inc. December 2015.

2. M. Casarin, C. Maccato, and A. Vittadini, *Phys. Chem. Chem. Phys.*, **1**, 3793–3799 (1999).

3. L.R. Shepard, T. Bak, and J. Norwotny, *J. Physical Chemistry C.,* **112**, 611–617 (2008).

V.D.2 Facilitated Direct Liquid Fuel Cells with High Temperature Membrane Electrode Assemblies

Emory S. De Castro
Advent Technologies Inc.
One Mifflin Place, Suite 400
Cambridge, MA 02138
Phone: (857) 264-7035
Email: EmoryDeCastro@Advent-Energy.com

DOE Manager: Gregory Kleen
Phone: (240) 562-1672
Email: Gregory.Kleen@ee.doe.gov

Contract Number: DE-EE0006959

Subcontractors:
Piotr Zelenay (Principal Investigator), Hoon T. Chung and Xi Yin; Los Alamos National Laboratory, Los Alamos, NM

Project Start Date: October 1, 2015
Project End Date: September 30, 2017

Overall Objectives

- Demonstrate direct dimethyl ether (DME) oxidation with a high temperature membrane electrode assembly (MEA) that achieves significantly better performance than direct methanol fuel cells (DMFC).
- Leverage a highly active ternary catalyst for high temperature DME fuel cells.

Fiscal Year (FY) 2017 Objectives

- Establish enhanced kinetics for DME oxidation at the higher temperatures.
- Demonstrate DME oxidation anode specific current (A/g_{PGM}) equivalent or better than that obtained for the state-of-the-art DMFC.
- Evaluate DME crossover, compare to methanol crossover in DMFC.

Technical Barriers

This project addresses the following technical barriers from Section 3.4.5 Fuel Cells of the Fuel Cell Technologies Program Multi-Year Research, Development, and Demonstration Plan [1], using DMFC systems as a reference fuel cell system.

(A) Durability (catalyst, membrane)

(B) Cost (catalyst, system)

(C) Performance (catalyst, electrodes, MEAs)

Technical Targets

This project falls under DOE's incubator initiative, which explores high impact research in new areas. Thus, the technical targets for this project were created relative to the state-of-the-art DMFC system, the only other viable direct fuel oxidation system at this time (see Table 1).

TABLE 1. Progress towards Meeting Technical Targets for Direct DME Oxidation

Key Performance Indicator (this period)	Current DMFC	Target	Project Status
Total precious metal loading	5 mg_{PGM}/cm^2	3 mg_{PGM}/cm^2	4.1 mg_{PGM}/cm^2
Anode mass-specific activity	50 A/g at 0.5 V	75 A/g at 0.5 V	50 A/g at 0.5 V
Crossover current	60–120 mA/cm^2 (*)	<60 mA/cm^2	6 mA/cm^2

(*) 60 mA/cm^2 with 0.5 M methanol, 80°C, Nafion® 117; 120 mA/cm^2 with 1.0 M methanol
PGM – platinum group metal

FY 2017 Accomplishments

- Identified cathode catalyst loading impeding anode activity.
- Demonstrated anode mass-specific activity for direct DME oxidation at high temperature (180°C) equivalent with benchmark PtRu catalyst equivalent to state-of-the-art DMFC (80°C).
- Demonstrated very low crossover currents for DME at high temperature compared to DMFC, at least an order of magnitude improvement.

✧ ✧ ✧ ✧ ✧

INTRODUCTION

In searching for an exemplary carbon-neutral fuel, DME may be one of the most appealing candidates. This simplest of the ethers can be readily produced from renewably sourced hydrogen and CO_2, making it an effective hydrogen carrier. Being both nontoxic and easy to be liquefied under moderate pressure, DME closely matches diesel and has been run in trucks. Recently, Los Alamos National Laboratory (LANL) demonstrated the potential for direct oxidation of DME in a fuel cell [2]. Thus, DME could bridge both internal combustion and fuel cell technologies, while remaining carbon neutral with low or no ancillary emissions.

LANL has identified a highly active catalyst for direct oxidation of DME that already in the early phase of development allows for matching performance of the DMFC when using typical low-temperature perflurosulfonic acid membranes. However, the output is not sufficient to approach commercial acceptance targets for higher power applications with considerable precious metal cost. More importantly, the LANL work has noted an acute sensitivity of the DME oxidation rate to temperature increase. High-temperature MEAs, based on phosphoric acid-imbibed membranes, operate at 160°C to 180°C without additional water and are highly tolerant to carbon monoxide—an intermediate of DME oxidation. This work is to exploit a novel ternary LANL anode catalyst with the features of high-temperature operation to produce high-power, low-cost direct DME MEAs. We envision the use of such systems as auxiliary electrical power for transport applications.

APPROACH

The project consists of three phases. In the first phase, we demonstrated direct oxidation of DME at a small-scale (5 cm^2) MEA without the advanced catalyst. The second phase focused on the development of a small-scale gas diffusion electrode matched for the advanced LANL catalyst; however, we first used a binary catalyst that has good activity for DME oxidation. In the last phase, we will scale up MEA to a 50 cm^2 size and optimize the gas diffusion electrode structure for the use in practical devices. We initially employed two kinds of high-temperature membranes. One is polybenzimidazole (PBI) and is characterized as a high-acid, low-solids material. The other is referred to by a generic Advent trademark TPS®, and, relative to PBI, is low-acid, high-solids material based on pyridine and polysulfone. Throughout the three experimental phases, key performance indicators, such as power output, amount of precious metal employed, and durability, will be compared to the state-of-the-art DMFC and incorporated as project milestones. We are currently in the second phase.

RESULTS

Cathode catalyst loading impeding anode reaction. The objective of this project has been to demonstrate superior anode activity for direct oxidation of a high energy content fuel. In actual test systems, this objective can be impeded if the cathode reaction (reduction of oxygen in air) limits whole fuel cell performance. Additionally, the project has defined a total PGM loading limit in order to be competitive with state-of-the-art DMFC, yet one method to increase current when limited by slow reactions is to increase the amount of PGM employed. Thus, initially we kept the cathode PGM loading fixed at a reasonable level and experimented with changing only the anode loading. However, as Figure 1 shows, our initial loading on the cathode limited the full

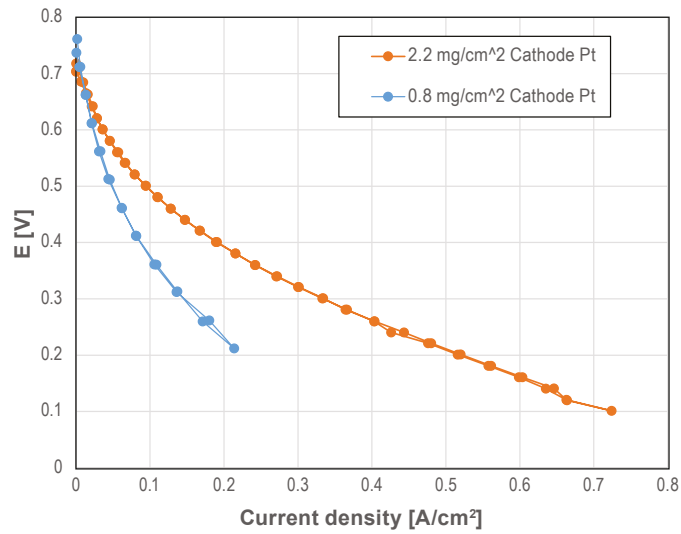

FIGURE 1. Impact of increasing cathode PGM loading for PBI-based MEA DME fuel cell performance at 180°C. Cathode: Pt-alloy/C as indicated; air 500 sccm, backpressure 3.5 psig. Anode: HiSPEC® 12100 PtRu/C 1.9 mg/cm^2; DME 125 sccm, humidified at backpressure 3.5 psig.

reaction and fuel cell performance. Figure 1 demonstrated a substantial improvement in DME oxidation current by increasing the *cathode* platinum loading from 0.8 mg Pt/cm^2 to 2.2 mg Pt/cm^2.

Improvement in anode mass specific activity. Having established an improved cathode configuration, we were able to incorporate the benchmark PtRu anode catalyst in various configurations with the objective of maximizing activity and minimizing mass transport resistance. The general approach is to use the benchmark catalyst to develop well-performing architectures, and then use that configuration as the first trial for the LANL PtRuPd catalyst. The process of developing architectures for new catalysts involves a materials approach whereby a key performance indicator, anode mass specific activity in this case, is gauged as a function of electrode layer porosity, hydrophobicity, and phosphoric acid loading. Citing the results of Figure 2, we note several salient observations. First, with a combination of higher cathode catalyst loading and improved electrode structure, we have almost doubled the anode specific current from 32 A/g_{PGM} in 2016 to 50 A/g_{PGM} at 0.5 V. Second, when comparing direct DME oxidation at a lower temperature MEA (green squares), we obtain more than double the anode specific current but employed half the total PGM loading and nearly tenfold less pressure on the DME gas feed (26 psig *vs.* 3.5 psig), whereby higher pressures typically increase current. While not at our final goal of 75 A/g_{PGM}, these results confirm the potential for a direct DME fuel cell exceeding the state-of-the-art DMFC.

Crossover current. For any fuel cell employing a membrane as electrolyte, the diffusion of fuel (for example, hydrogen, methanol, or DME) from the anode to the cathode

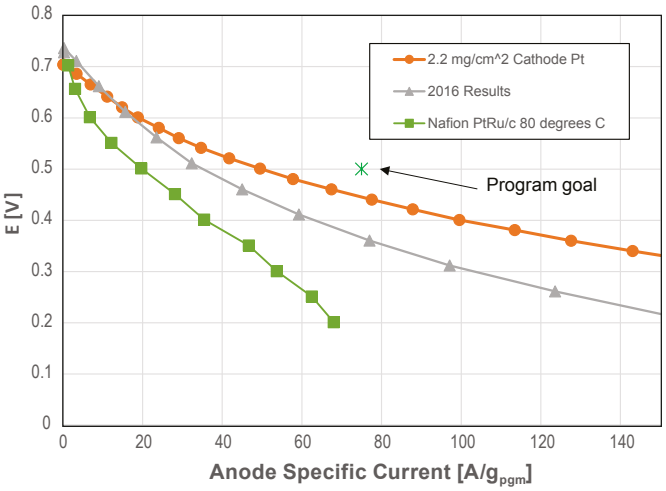

FIGURE 2. Anode-specific current for PBI-based MEA DME fuel cell performance at 180°C. Orange circles: replotted data from Figure 1 as anode-specific current; gray triangles: 2016 Results, HiSPEC® 12100 PtRu/C 1.9 mg PGM/cm^2, Pt/C 0.8 mg Pt/cm^2; green squares: LANL data from prior project, DME at PtRu, 80°C, total 8 mg/cm^2 PGM, 26 psig *vs.* 3.5 psig of this project.

represents a loss in performance not only from efficiency, but also potential losses in operating voltage. One metric for fuel crossover is to measure the effective current obtained by oxidizing the fuel that diffuses through the membrane, and ultimately, relating this current to a molar flux once the reaction mechanism is understood. However, using only the current is a good approximation of loss of fuel through the membrane.

A typical crossover experiment configures the single cell MEA as a detector, that is, a voltage is applied across the anode and cathode and current is measured. For our studies, we used a high temperature MEA and introduced nitrogen to the anode compartment, and DME to the cathode. By applying a voltage bias to the MEA, DME that diffuses through the PBI membrane to the anode compartment is oxidized. Figure 3 illustrates the results of such a test. One sees that once the bias voltage is high enough to oxidize DME, current flows. In the absence of DME, no current is generated. What makes these results remarkable is that we obtain roughly 6 mA/cm^2 of crossover current (oxidation of DME that diffuses through the membrane), which compares

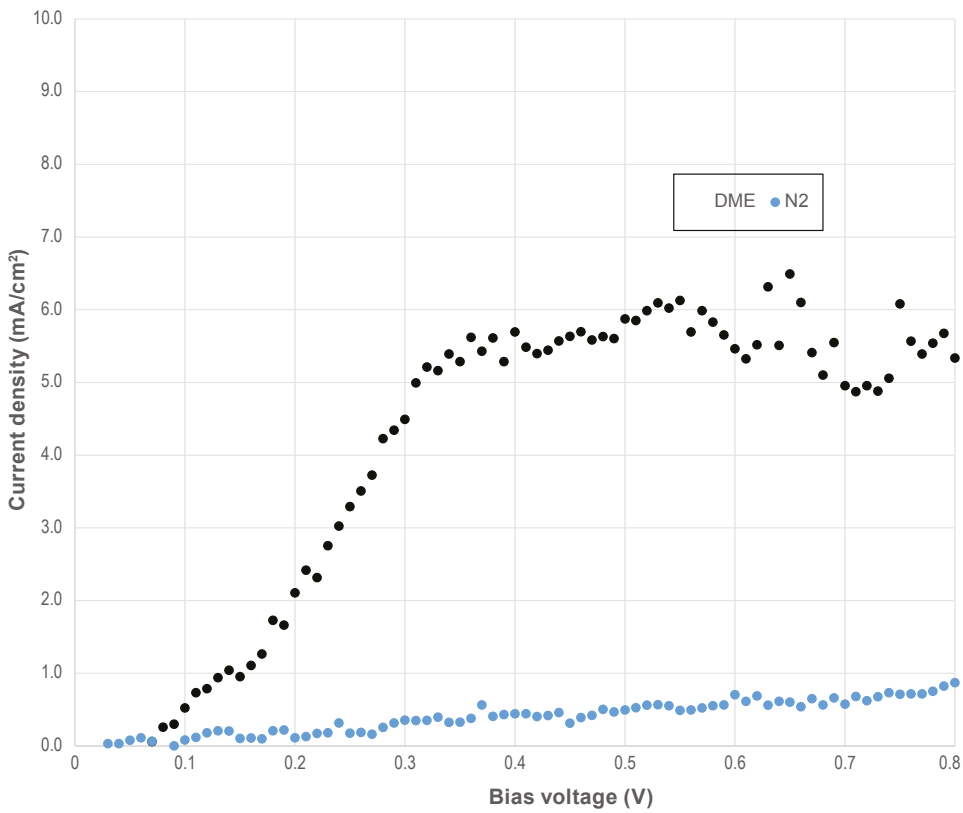

FIGURE 3. Crossover current for DME in high-temperature polymer electrolyte membrane. Anode: PtRu 2.52 mg/cm^2; N_2 3.5 psig backpressure; 100 sccm; cathode: Pt alloy; 3.5 psig DME/H_2O backpressure; DME : water = 1 : 3; DME 125 sccm; water 0.3 mL/min; membrane: PBI; 180°C. Cell size: 5 cm^2.

favorably to standard currents of 60–120 mA/cm^2 for DMFC cells operating with either 0.5 M or 1.0 M methanol.

CONCLUSIONS AND UPCOMING ACTIVITIES

Based on the improved anode specific current and very low crossover currents, direct DME fuel cells offer great potential to exceed the performance of the state-of-the-art DMFC. While we have started to evaluate assembles with the LANL ternary catalyst, the morphology of this material is significantly different than that of our benchmark PtRu, and we do not get the immediate improvement expected. Upcoming efforts are focused on revising electrode processing conditions to fully realize the expected activity of the LANL catalyst.

FY 2017 PUBLICATIONS/PRESENTATIONS

1. "Facilitated Direct Dimethyl Ether Fuel Cells through High Temperature Membrane Electrode Assemblies," Emory S. De Castro, Andrew Van Dyke, Xi Yin, Hoon Taek Chung, and Piotr Zelenay, 230th Electrochemical Society Meeting, Oahu, HI, USA, October 2–7, 2016; Abstract 2396.

2. "High Temperature Membrane Electrode Assemblies for Intermediate Temperature Fuel Cells: Past, Present, and Future," Emory S. De Castro, Brian Benicewicz, Xi Yin, Hoon Taek Chung, and Piotr Zelenay, 231st Electrochemical Society Meeting, New Orleans, MS, USA, October 2–7, 2016; Abstract 97024.

REFERENCES

1. Multi-Year Research, Development, and Demonstration Plan: Section 3.4 Fuel Cells, Fuel Cell Technologies Office, 2016. http://energy.gov/sites/prod/files/2016/06/f32/fcto_myrdd_fuel_cells_0.pdf

2. Li, Q., Wen, X., Wu, G., Chung, H.T., and Zelenay, P., "High-Activity PtRuPd/C Catalyst for Direct Dimethyl Ether Fuel Cell," *Angew. Chem. Int. Ed.*, **54**, 1–6, 2015.

V.D.3 Advanced Catalysts and Membrane Electrode Assemblies (MEAs) for Reversible Alkaline Membrane Fuel Cells

Hui Xu (Primary Contact), Shuai Zhao
Giner, Inc.
89 Rumford Ave.
Newton, MA 02466
Phone: (781) 529-0573
Email: hxu@ginerinc.com

DOE Manager: David Peterson
Phone: (240) 562-1747
Email: David.Peterson@ee.doe.gov

Contract Number: DE-EE0006960

Subcontractors:
- Gang Wu, State University of New York at Buffalo (SUNY Buffalo), Buffalo, NY
- Bryan Pivovar, National Renewable Energy Laboratory, Golden, CO

Project Start Date: June 1, 2015
Project End Date: December 31, 2017

Fiscal Year (FY) 2017 Objectives

- To develop highly efficient bifunctional electrocatalysts related to the heteroatom doped carbon/graphene nanotubes.
- To optimize regenerative fuel cell MEAs using developed bifunctional catalysts and selected alkaline membranes.
- To test the fabricated MEAs in a reversible fuel cell system under both fuel cell and electrolyzer modes to demonstrate their performance and to meet the reversible fuel cell targets.

Technical Barriers

This project addresses the following technical barriers from the Fuel Cells section of the Fuel Cell Technologies Office Multi-Year Research, Development, and Demonstration Plan.

(A) Durability (catalysts, electrode layers)

(B) Cost (catalyst, MEAs)

(C) Performance (catalysts, electrodes, MEAs)

Technical Targets

This project is developing novel bifunctional oxygen reduction reaction (ORR) and oxygen evolution reaction (OER) cathodes for reversible alkaline fuel cells. The new materials will achieve the following targets at the end of the project for viable applications.

- In a rotating disk electrode, demonstrate ORR activity >1 mA/mg at internal resistance (IR)-free 0.9 V; and OER activity >15 mA/mg at IR-free 1.6 V.
- Achieve reversible current density of 600 mA/cm^2 at 0.55 V for fuel cell and 2.0 V for electrolyzer.
- Achieve fuel cell and electrolyzer life of 500 h with less than 10% performance decay.

FY 2017 Accomplishments

During this period, we have achieved the following accomplishments.

- Bifunctional ORR and OER catalysts with various compositions have been successfully synthesized at Giner and SUNY Buffalo.
- MEA fabrication and operation have been optimized by varying bifunctional catalysts, ionomer dispersion content, and introduction of diluted liquid electrolyte.
- Fuel cell and electrolyzer performance have been improved simultaneously, reaching 700 mA/cm^2 at 0.55 V in fuel cell mode and 850 mA/cm^2 at 2.0 V in electrolyzer mode, which exceeded the milestone targets.

✧ ✧ ✧ ✧ ✧

INTRODUCTION

The primary goal of this project is to design advanced bifunctional non-platinum group metal catalyst-based MEAs for a reversible alkaline membrane fuel cell. Water is split into H_2 and O_2 to be stored in electrolyzer mode, and reversibly, the gases can be utilized in fuel cell mode to produce electricity. The performance of the innovative reversible alkaline membrane fuel cell technologies greatly relies on a bifunctional oxygen electrode capable of high activity for the ORR and the OER. The development of highly efficient bifunctional cathode catalysts derived from earth-abundant elements faces two grand challenges. The first is that the optimal active sites for the ORR differ from those for the OER. The second is stability during the high potential/voltage (>1.6 V) of the OER. As a result, most of the studied traditional carbon catalysts likely suffer from significant performance loss during ORR–OER dual-

operation modes. In FY 2016, Giner and SUNY Buffalo developed transition metal-based oxide nanocomposites and heteroatom doped graphene tube catalysts with high ORR and OER activities and limited durability. In the past year, the stability of nano-carbon catalysts has been tremendously enhanced by doping Mn into the nanocarbon. The newly developed catalysts were integrated with selected anion-exchange ionomers and membranes. The MEAs were tested under both fuel cell and electrolyzer operating modes.

APPROACH

The stability of nano-carbon composite catalysts was further enhanced via Mn doping into the graphene tubes. The graphitic feature and thickness influences on the catalyst stability were analyzed. The best-performing ORR–OER bifunctional catalysts, which include transition metal oxide–carbon composites (cobalt oxide supported on carbon nanotubes, Co_3O_4/CNT, Giner), binary transitional metal oxides (nickel cobalt oxide, MOx, SUNY Buffalo), and metal nanocarbon composites (FeCoNiMn-derived N-doped graphene tube, NC-FeCoNiMn$_4$, SUNY Buffalo), were screened using rotating disk electrode experiments. These catalysts were incorporated into MEAs for cell performance tests. Ionomer and membrane materials, ionomer and catalyst ratios, electrode configurations, and testing protocols were optimized to maximize the cell performance. The synthesis of Co_3O_4/CNT and MOx catalysts are illustrated in Figure 1**.** Both catalysts were derived from metal precursors and

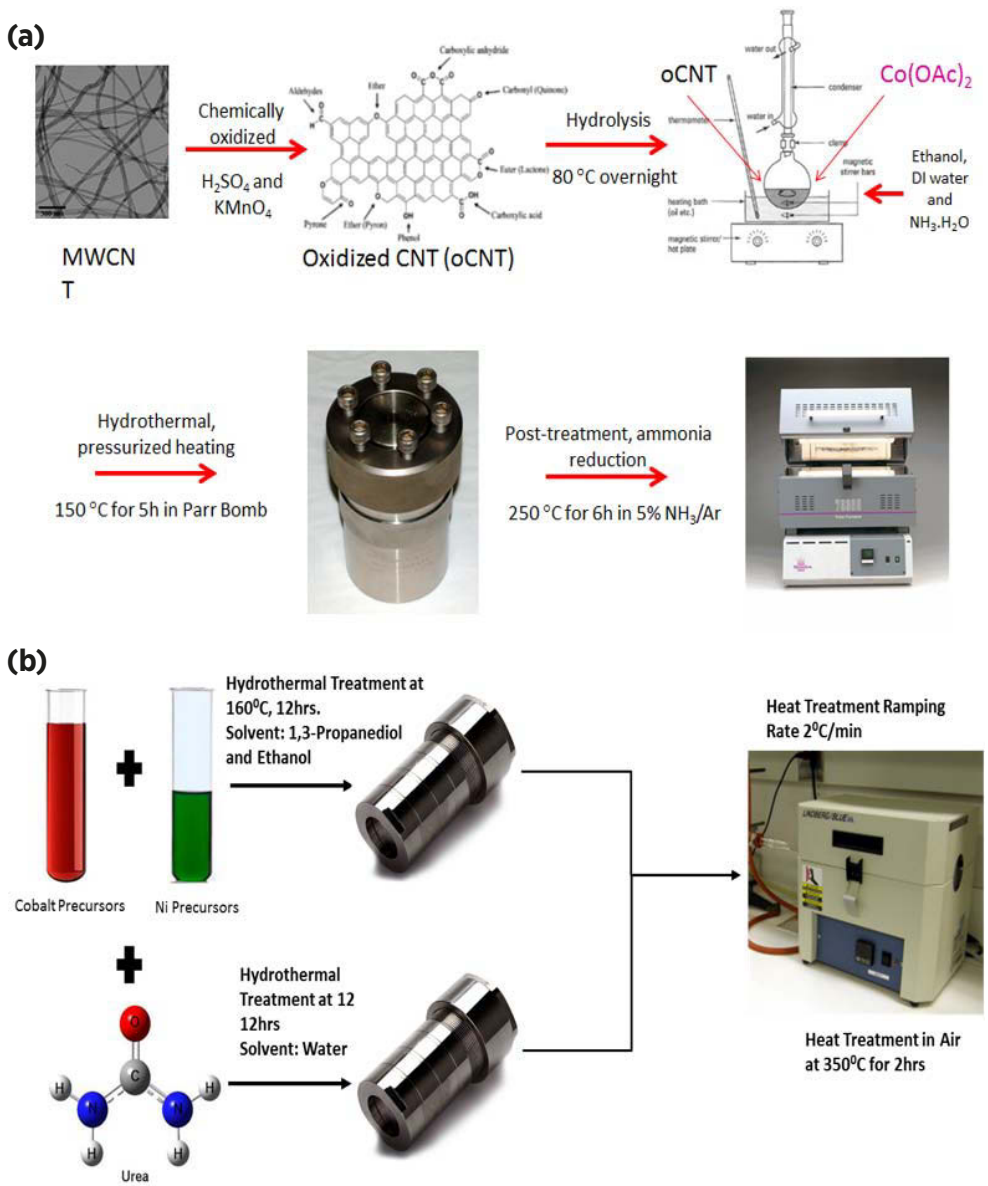

FIGURE 1. The synthesis routes for Giner Co_3O_4/CNT and SUNY Buffalo MOx catalysts

synthesized using a scalable and cost-effective hydrothermal approach.

RESULTS

The above catalysts were incorporated into MEAs that were tested in both fuel cell and electrolyzer operating modes. Figure 2 demonstrates the steady progress that was made towards improved cell performance. The initial fuel cell and electrolyzer performances were very poor as the maximum current density was less than 60 mA/cm^2. However, the current densities were significantly increased to above 1,000 mA/cm^2 with reasonably low overpotentials. The performance improvements were due to electrode configuration changes (from catalyst-coated membrane [CCMs] to gas diffusion electrodes [GDEs]), ionomer category and content optimization, and introduction of diluted liquid electrolyte.

The optimization of electrode design and operation using Giner Co_3O_4/CNT catalysts is elaborated in Figure 3. Figures 3a and 3b show that the electrode fabrication approach impacts electrolyzer performance more noticeably than fuel cell performance. For fuel cell operation, the GDE achieved slightly better performance at high current density, but both the GDE and the CCM met the milestone 0.55 V at 600 mA/cm^2. For electrolyzer operation, the GDE achieved significantly better performance than the CCM. Therefore, all the following tests were conducted using the GDEs. The ionomer content was varied to find the optimal amount in the electrode (Figure 3c); the electrode with a lower ionomer content (20 wt%) exhibited a much better performance due in part to a lower high frequency resistance and mass transport resistance. The same cell was tested when flowing 0.1 M KOH solution into both the anode and cathode to improve the membrane conductivity and to enable intimate contact between the catalyst and OH^- ions. The performance with the addition of diluted KOH solution improved significantly, reaching 850 mA/cm^2 at 2 V, which exceeded the milestone: 600 mA/cm^2 at 2 V (Figure 3d).

For the SUNY Buffalo MOx catalysts, focus was placed on optimizaiton of the MO_x-based O_2 electrode at a fixed 3 mg/cm^2 catalyst loading, ionomer percentages were varied from 18 wt% to 22 wt% (Figure 4). As shown in Figure 4a, the electrolyzer performance improved with decreasing ionomer content; the electrodes containing 18 wt% ionomer performed much better than that with 22 wt% ionomer. The influence of feeding diluted KOH was also investigated and again the performance was tremedously boosted with the addition of dilute KOH solution. A short durability test (up to 7 h) is shown in Figure 4b; the voltage at a constant current

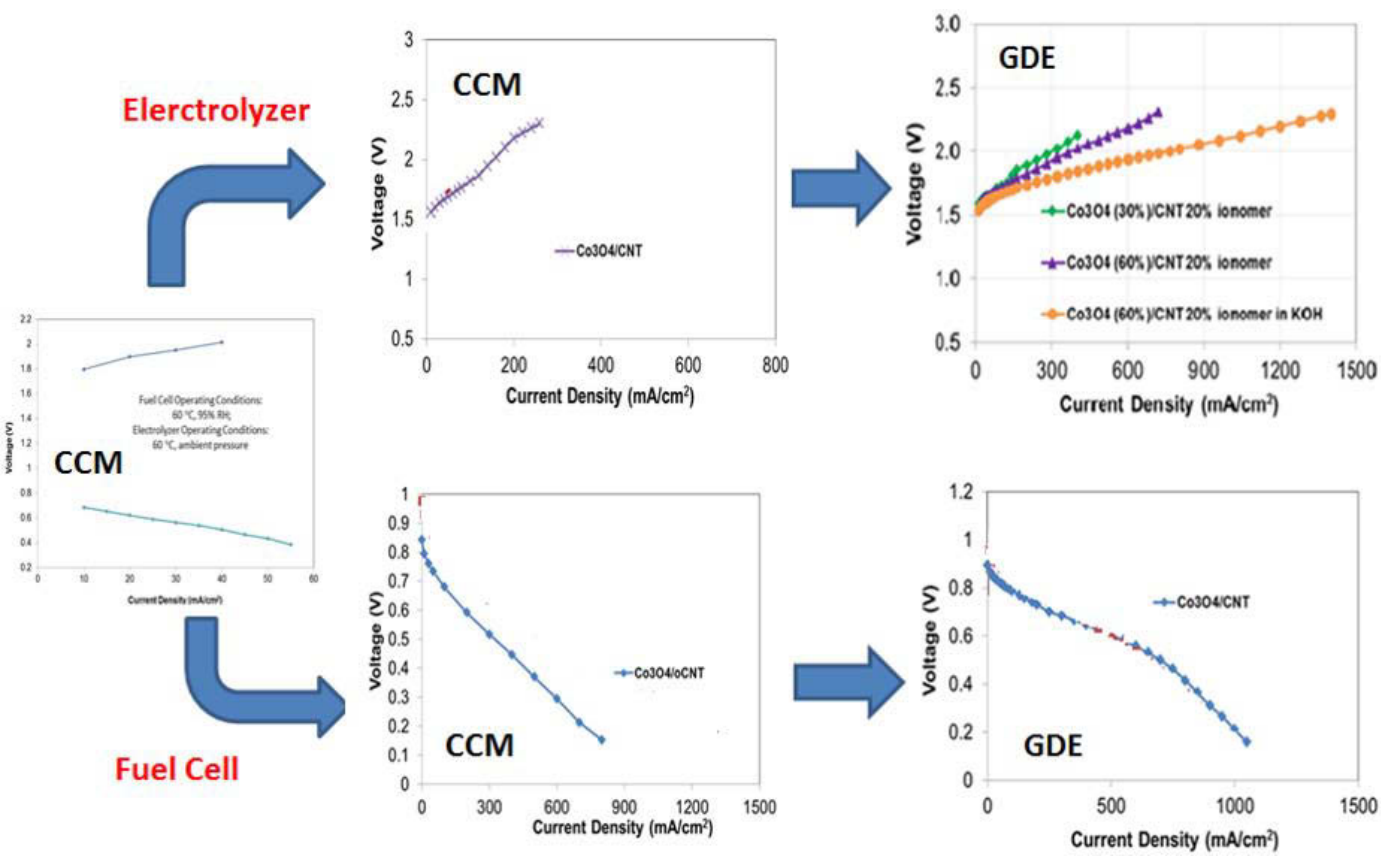

FIGURE 2. Cell performance progress for both fuel cell and electrolyzer operations

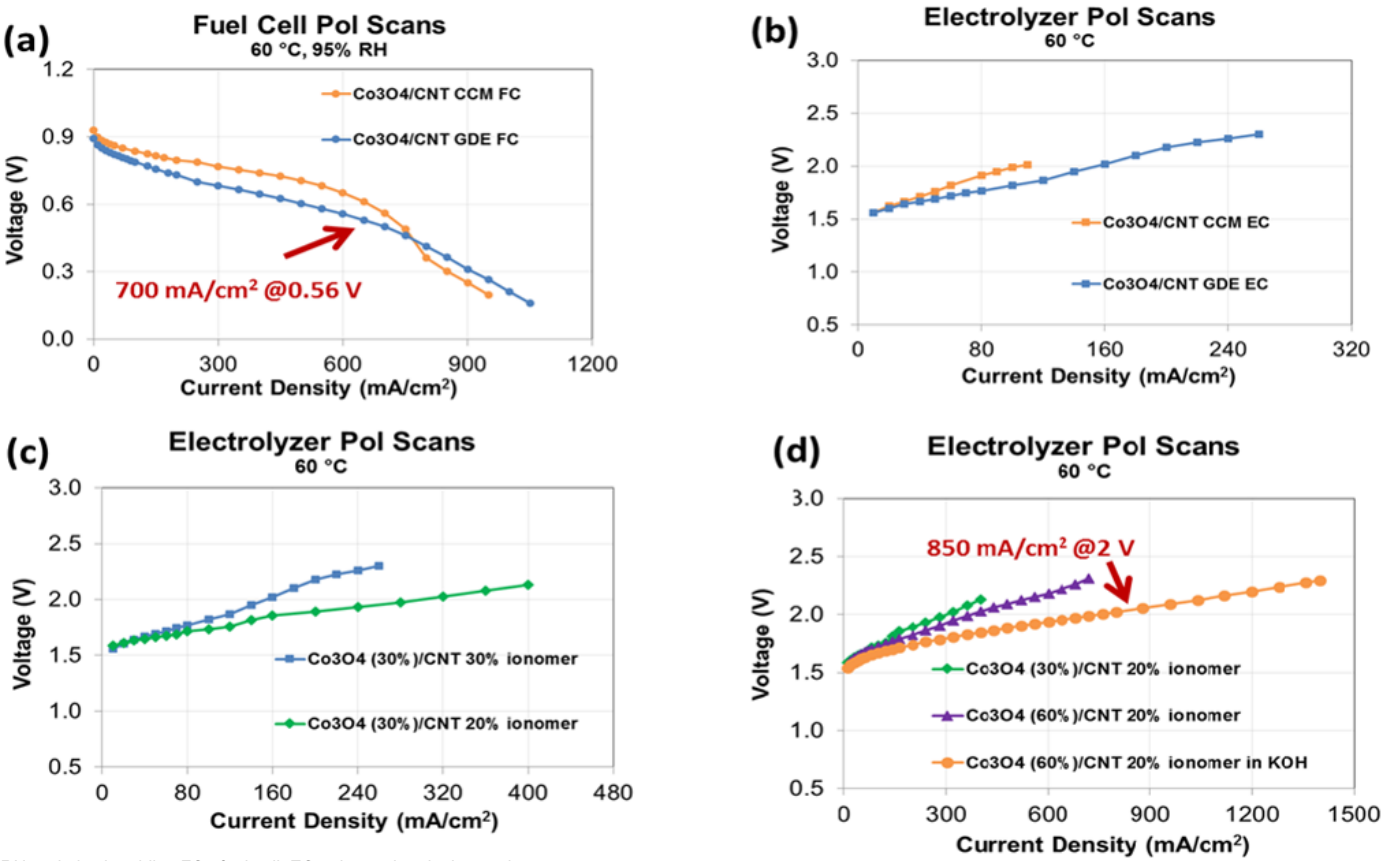

RH - relative humidity; FC - fuel cell; EC - electrochemical capacitance

FIGURE 3. Fuel cell and electrolyzer performance using Giner Co_3O_4/CNT catalysts: (a) and (b) impact of electrode fabrication; (c) ionomer concentration influence; (d) introduction of diluted KOH solution. Fuel Cell Test conditions: H_2/O_2 flow rate 1,000 ccm/min, temperature 60°C. The membrane was Tokuyama A201 and ionomer was National Renewable Energy Laboratory Gen 2. The H_2 electrode for all the following non-platinum group metal catalyst MEA tests are identical: PtRu/C (0.7 mg_{PtRu}/cm^2, ionomer to catalyst ratio = 0.8).

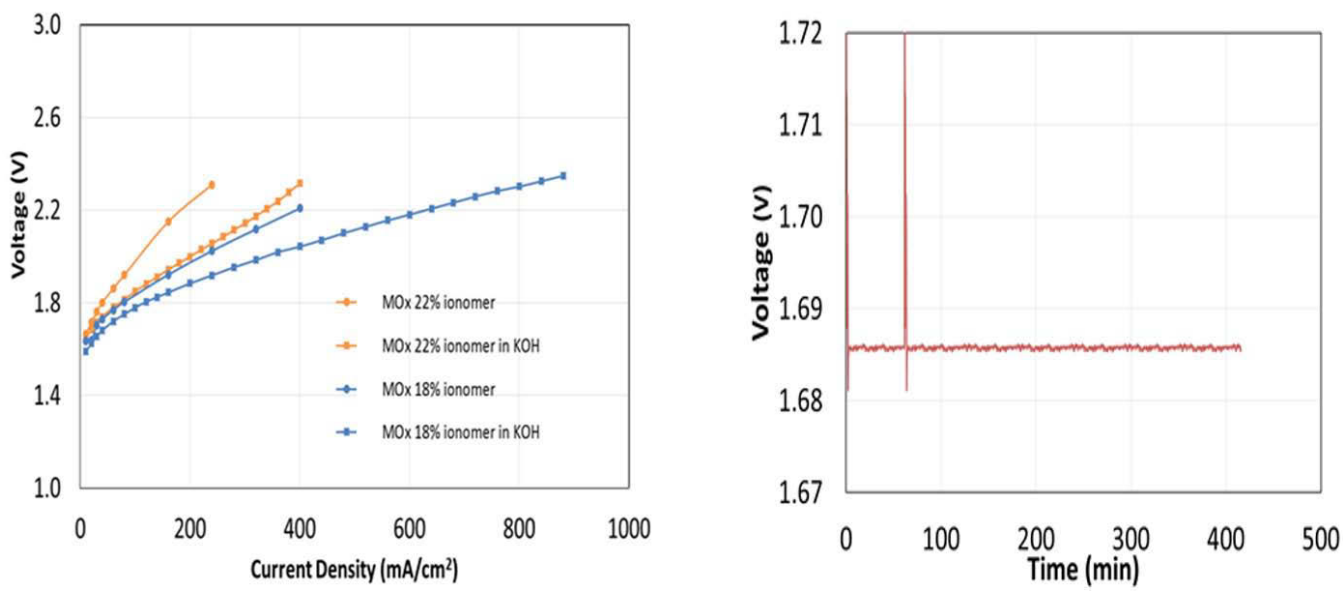

FIGURE 4. Electrolyzer performance and durability using SUNY Buffalo MOx catalysts. (a) Impact of ionomer concentration and introduction of diluted KOH solution; (b) 7-hour durability test. Test conditions: H_2/O_2 flow rate 1,000 ccm/min, temperature 60°C. The membrane was Tokuyama A201 and ionomer was National Renewable Energy Laboratory Gen 2. The H_2 electrode for all the following non-platinum group metal catalyst MEA tests are identical: PtRu/C (0.7 mg_{PtRu}/cm^2, I/C = 0.8).

density of 100 mA/cm^2 remained very stable over the course of the durability test. Operation with lower concentrations of KOH will be investigated later.

CONCLUSIONS AND UPCOMING ACTIVITIES

Conclusions

- A variety of bifunctional OER–ORR catalysts (Giner Co_3O_4/CNTs and SUNY Buffalo NC-FeCoNiMn/$NiCo_2O_4$) have been synthesized with improved activity and durability in the MEA.
- The factors contributing to improved cell performance have been identified:
  - Electrode fabrication (CCM vs. GDE).
  - Ionomer content optimization.
  - Introduction of diluted liquid electrolyte.
- Both fuel cell and electrolyzer MEAs using Co_3O_4/CNT surpassed the milestones of 0.55 V at 600 mA/cm^2 and 2.0 V at 600 mA/cm^2.

Upcoming Activities

- Test the reversible alkaline membrane fuel cell at elevated temperature (>90°C) using a more advanced membrane and ionomer from a selected collaborator.
- Complete dual-operation durability test up to 500 h after integration of the fuel cell and electrolyzer test station.

FY 2017 PUBLICATIONS/PRESENTATIONS

1. Xu, H, "High-Performance, Long-Lifetime Catalysts for Proton Exchange Membrane Electrolysis," Presentation in DOE Hydrogen and Fuel Cell merit review meeting, Washington, D.C., June 5–8, 2017

2. Zhao, S., Rasimick, B., Mustain, W., & Xu, H. "Highly durable and active Co_3O_4 nanocrystals supported on carbon nanotubes as bifunctional electrocatalysts in alkaline media." *Applied Catalysis B: Environmental*, 2017 *203*, 138–145.

3. Gupta, S.; Zhao, S.; Ogoke, O.; Lin, Y.; Xu, H.; Wu, G., "Engineering Favorable Morphology and Structure of Fe-N-C Oxygen-reduction Catalysts via Tuning Nitrogen/Carbon Precursors." *ChemSusChem* 2017, *10* (4), 774–785.

4. Osgood, H.; Devaguptapu, S.V.; Xu, H.; Cho, J.P.; Wu, G., "Transition Metal (Fe, Co, Ni, and Mn) Oxides for Oxygen Reduction and Evolution Bifunctional Catalysts in Alkaline Media." *Nano Today* 2016, *11*, 601–625.

5. Gupta, S.; Qiao, L.; Zhao, S.; Lin, Y.; Vamsi, D.S.; Xu, H.; Wang, X.; Swihart, M.; Wu, G., "Highly active and stable graphene tubes decorated with FeCoNi alloy nanoparticles via a template-free graphitization for bifunctional oxygen reduction and evolution." *Advanced Energy Materials* 2016, *6* (22), 1601198.

6. Gupta, S.; Kellogg, W.; Xu, H.; Liu, X.; Cho, J.; Wu, G., "Bifunctional Perovskite Oxide Catalysts for Oxygen Reduction and Evolution in Alkaline Media." *Chemistry - An Asian Journal* 2016, *11* (1), 10–21.

V.E.1 Neutron Imaging Study of the Water Transport in Operating Fuel Cells

David L. Jacobson (Primary Contact),
Daniel S. Hussey, Jacob M. LaManna, Elias Baltic, Muhammad Arif
National Institute of Standards and Technology (NIST)
100 Bureau Drive
Gaithersburg, MD 20899
Phone: (301) 975-6303
Email: arif@nist.gov

DOE Manager: Nancy L. Garland
Phone: (202) 586-5673
Email: Nancy.Garland@ee.doe.gov

Contract Number: DE-AI-01-01EE50660

Project Start Date: Fiscal Year (FY) 2001
Project End Date: Project continuation and direction determined annually by DOE

Overall Objectives

- Provide state-of-the-art research and testing infrastructure to enable the fuel cell industry to design, test, and optimize prototype to commercial grade fuel cells using in situ neutron imaging techniques.
- Provide a secure facility for proprietary research by industry. Provide beam time at no cost to non-proprietary research through a competitive proposal process. Make open research data available for beneficial use by the general fuel cell community.
- Continually improve and develop methods and technology to accommodate rapidly changing industry and academia needs.

FY 2017 Objectives

- Collaborate and support groups from the DOE Hydrogen and Fuel Cells Program performing water transport measurements with neutron imaging at NIST.
- Install fuel cell and support infrastructure at the new cold imaging facility.
- Explore and develop high resolution neutron imaging methods to enable water transport studies of catalyst and membrane electrode assemblies (MEAs).
- Employ a high resolution imaging method to achieve resolution approaching 1 µm to resolve water concentration in fuel cell electrodes.
- Develop in situ X-ray imaging for fuel cells at the neutron imaging facility.

Technical Barriers

This project addresses the following technical barriers from the Fuel Cells section of the Fuel Cell Technologies Program Multi-Year Research, Development, and Demonstration Plan.

(A) Durability

(B) Cost

(C) Performance

Technical Targets

NIST is conducting fundamental studies of water transport in the fuel cell. Insights gained from these studies will be applied toward the design of components and operation strategies of polymer electrolyte membrane fuel cells that meet the following 2020 DOE fuel cell targets.

- Durability with cycling at operating temperature of ≤80°C: 5,000 h
- System energy density: 650 W/L
- System specific power: 850 W/kg
- Energy efficiency: 60% at 25% rated power
- Cost: $40/kW$_e$
- Start-up time to 50% power: 30 s from -20°C, 5 s from 20°C
- Assisted start from low temperatures: -40°C

FY 2017 Accomplishments

- First 4 µm resolution fuel cell images using slits.
- Installation of a new, second neutron imaging instrument.
- Installation of micro-focus X-ray source for simultaneous neutron/X-ray imaging.
- Components for new high resolution imaging detector systems acquired.

✧ ✧ ✧ ✧ ✧

INTRODUCTION

At NIST, we maintain the premier fuel cell neutron imaging facility in the world and continually seek to

improve its capabilities to meet the changing needs of the fuel cell community. This facility provides researchers with a powerful and effective tool to visualize and quantify water transport inside operating fuel cells. Imaging the water dynamics of a fuel cell is carried out in real time with the required spatial resolution needed for fuel cells that are being developed today. From these images, with freely available NIST-developed image analysis routines, fuel cell industry personnel and researchers can obtain in situ, non-destructive, quantitative measurements of the water content of an operating fuel cell. Neutron imaging is the only *non-destructive, in operando* method for visualizing the water distribution in a "real-world" fuel cell. Unlike X-rays, whose interaction with materials increases with the number density of electrons, neutrons interact via the nuclear force, which varies somewhat randomly across the periodic table, and is isotopically sensitive. For instance, a neutron's interaction with hydrogen is approximately 100 times greater than that with aluminum, and 10 times greater than that with deuterium. It is this sensitivity to hydrogen (and insensitivity to many other materials) that is exploited in neutron imaging studies of water transport in operating fuel cells.

APPROACH

The typical length scales of interest in a fuel cell are: channels approximately 1 mm wide and 1 mm deep, the diffusion media are 0.1 mm to 0.3 mm thick, the membrane is 0.01 mm to 0.02 mm thick, and the active area of test sections can range from 2 cm^2 to 500 cm^2. Though the study of water transport within these length scales is technically very challenging, the unique capabilities of neutron imaging have already successfully addressed many questions. Thus, as fuel cell research matures, the water transport questions become increasingly more demanding, requiring for instance resolving the water content in catalyst layers. To meet these demands, based on fuel cell community feedback and need, we continue to develop new facilities and improve existing capabilities for obtaining higher spatial and temporal resolution neutron images. These improvements will enable users to perform even more detailed, nondestructive, and in situ studies of the water and hydrogen transport in fuel cells to meet DOE goals. In addition, employing mathematical models of neutron scattering, we will develop a software suite that enables users to obtain reliable, accurate, quantitative measurements of the water content in an operating fuel cell. Due to the complexity of fuel cells and the large number of remaining open questions regarding water transport within the membrane electrode assembly, we will develop partnerships with industry, academia, national laboratories, and the DOE Fuel Cell Technologies Office consortia to train them in the use of the facility, seek their feedback, and collaborate with them on research projects, to seek measurement breakthroughs that will facilitate the rapid, efficient, and robust development of fuel cells.

RESULTS

The NIST Neutron Imaging Facility provides year-to-year support for DOE Hydrogen and Fuel Cell Program projects through beam time and by collaboration with users on a variety of related neutron imaging projects that support the DOE mission. For FY 2017, General Motors, Rochester Institute of Technology, Los Alamos National Laboratory, University of Toronto, University of Connecticut, Colorado School of Mines, and the University of Hawaii have received project support for experiments at the facility. The results published during FY 2017 from these experiments are reflected in the publication list attached to this report.

In consultation with the fuel cell community, one of the leading issues this project has been asked to address is fuel cell flooding and degradation due to liquid water in the catalyst layers. To study commercial grade platinum-based catalysts requires at least a factor of 10 improvement in spatial resolution over the current state of the art, about 15 µm. The limiting factor in spatial resolution for current detector systems stems from the range of charged particles (3.5 µm to 70 µm) that are used to detect neutrons. To overcome this limit, we have been exploring several methods. The first method (slit method) uses nanofabricated neutron absorbing gratings with an opening of ~1 µm or less in width to define the neutron illuminated area of the fuel cell with high spatial resolution in one dimension. By translating the grating across the through-plane direction of the fuel cell, one obtains a high resolution image of the water content from anode to cathode, overcoming the resolution limit of the detector. This method was described as well in FY 2016 annual report and has since been improved to achieve 2 µm spatial resolution. The second method (centroiding method) previously described in the FY 2016 annual report has been significantly improved as of this FY 2017 report. The centroiding method works by capturing images quickly (0.005 s exposures), making it possible to capture individual neutron scintillation events and find the center of mass of each event [1]. During FY 2017 we have realized 1.5 µm spatial resolution through improvements to the center of mass calculation. The centroiding method currently suffers an 83% dead time due to delays in the file saving speed of the computer system and a field of view of about 3 mm × 4 mm. However, there is strong interest in the fuel cell community to use this method, evidence by a rise in users proposals (five new) aimed at using the new method. In the future, the centroiding method can be enhanced using hardware-based designs to run optimally with near zero deadtime and a field of view of about 1 cm diameter. For this reason, the centroiding method has been selected over the slit scanning method described earlier. A comparison of the uncertainty versus exposure time of the various methods is shown in Figure 1.

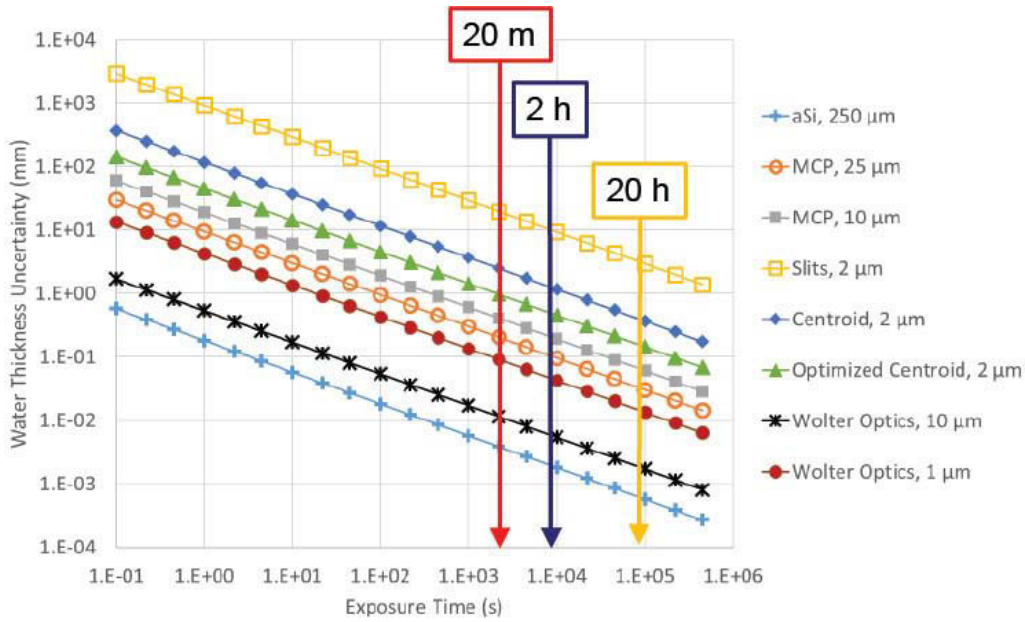

MCP – microchannel plate

FIGURE 1. Liquid water uncertainty for various methods/detectors. Comparison exposure times are noted for 20 m (ideal), 2 h (centroiding time) and 20 h (slit scan time).

The centroiding method has been used by Los Alamos to look at MEAs with two different ionomer to carbon ratios of 1.1 and 0.9. The results shown in Figure 2 show a clear difference in the shape of the water distribution for the two MEAs. For a ratio of 1.1 we see a more symmetric water distribution for the different operating voltages. For the ratio of 0.9 the distribution is no longer symmetric and is peaked near the cathode [2].

Ultimately resolution of 1 µm is expected to be efficiently and practically achieved using a neutron magnifying lens. By using a neutron lens, it could be possible to increase the neutron intensity by 50–100 times than that currently available. Previously, practical lenses for neutrons have not been available due to the low neutron refractive power of all materials. However, a new X-ray telescope lens technology using thin nickel foil mirrors developed by NASA has shown great promise to provide a practical lens for neutron imaging. By nesting several mirrors, the flux can be increased up to a factor of 100 over that achievable at Beam Tube 2 at the NIST Center for Neutron Research.

An engineering optic (Figure 3) was tested during FY 2016 and showed good figure. To achieve 1 µm spatial resolution, a lens that has an angular resolution of 1 arcsec is necessary. The current fabrication method provides an overall lens figure that achieves this resolution. The tested optic did not achieve this resolution due to surface roughness. However, the surface roughness can be corrected using differential deposition. With 10 mirrors, an increase of 70x can be achieved over previous measurements made at Beam Tube 2 at the NIST Center for Neutron Research (1 s vs. 120 s). Now that the mandrel fabrication method has been established, NIST and NASA will proceed to create nine remaining mandrels starting in September of 2017. NIST will create the basic mandrels and provide these to our partners at NASA for final polishing. Progress has been unavoidably delayed due to an upcoming launch. Future program achievements are expected to have a 1:1 lens by 2020 and a 1 µm magnifying optic by 2021.

In addition to improvements to spatial resolution we have also improved the in situ X-ray method as well. Here we use an X-ray source oriented at 90° to the neutron beam to acquire simultaneous in situ X-ray images during tomography of a fuel cell [3]. Using X-rays to image the cell in situ could allow for better characterization of the interfaces in the MEA that are nearly transparent to neutrons. This would allow for better determination of the MEA boundaries to improve the quantification of the water distribution in the MEA, including the new effort with ~1 µm spatial resolution. The results of 3-dimensional (3D) images taken with 10 µm resolution are shown in Figure 4. We have written a new software tool written using Matlab which incorporates all of the necessary image processing steps to create these 3D images from both neutrons and X-rays into one analysis package available to all facility users.

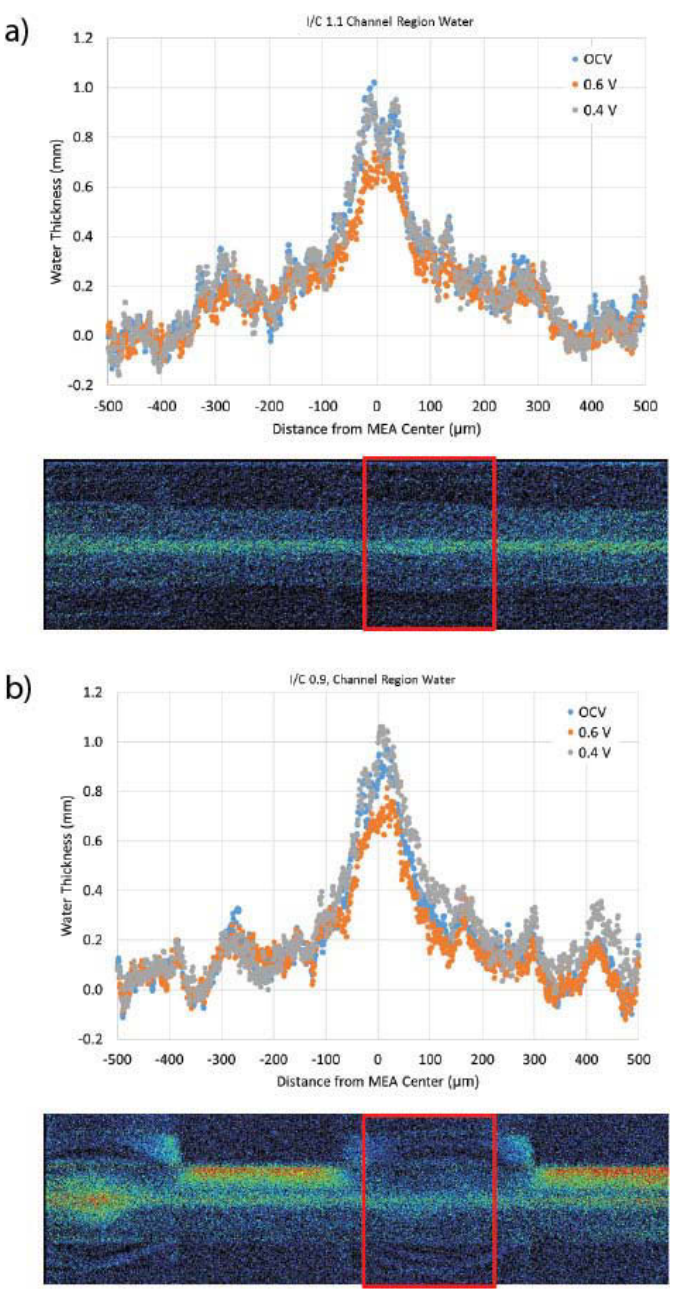

FIGURE 2. Water content comparison for two different ionomer/carbon (I/C) ratio catalysts: (a) 1.1 I/C and (b) 0.9 I/C. Cell conditions: temperature 80°C with constant voltage operation, open circuit voltage (OCV), 0.4 V 100 % relative humidity, 0.6 V, 75% relative humidity. Images are at 0.4 V with cathode on top; plots cathode positive distance from MEA center.

CONCLUSIONS AND UPCOMING ACTIVITIES

- The NIST Neutron Imaging Facility continues to maintain a robust fuel cell user program.

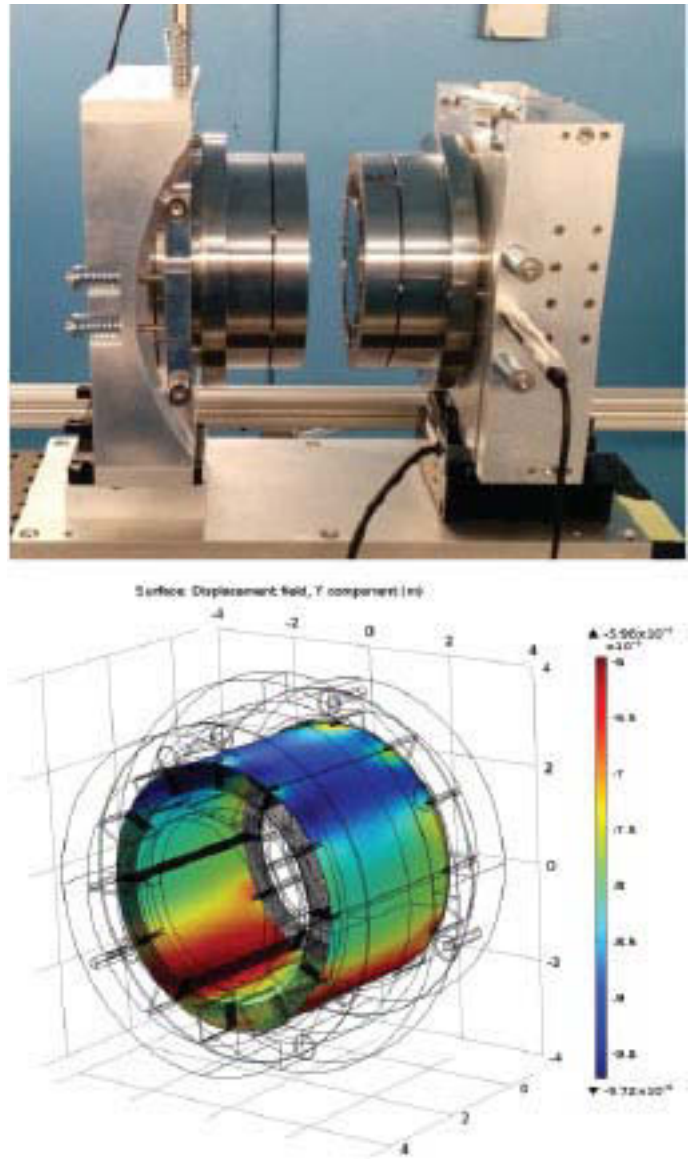

FIGURE 3. Test engineering optic in (a) verifying good figure, surface roughness to be improved with differential deposition. Finite element modeling in (b) shows gravity causes ~80 nm sag of mirrors, which contributes 0.1 arcsec error to resolution or 10% of targeted resolution of 1.0 arcsec needed to achieve 1 µm spatial resolution.

- Good progress has been made towards developing the method to measure liquid saturation values in the catalyst and membrane.
  - Slit scanning:
    - 2 µm spatial resolution was demonstrated.
    - Acquisition time is 17 h, but could be improved to less than 8 h with a smaller grating period.

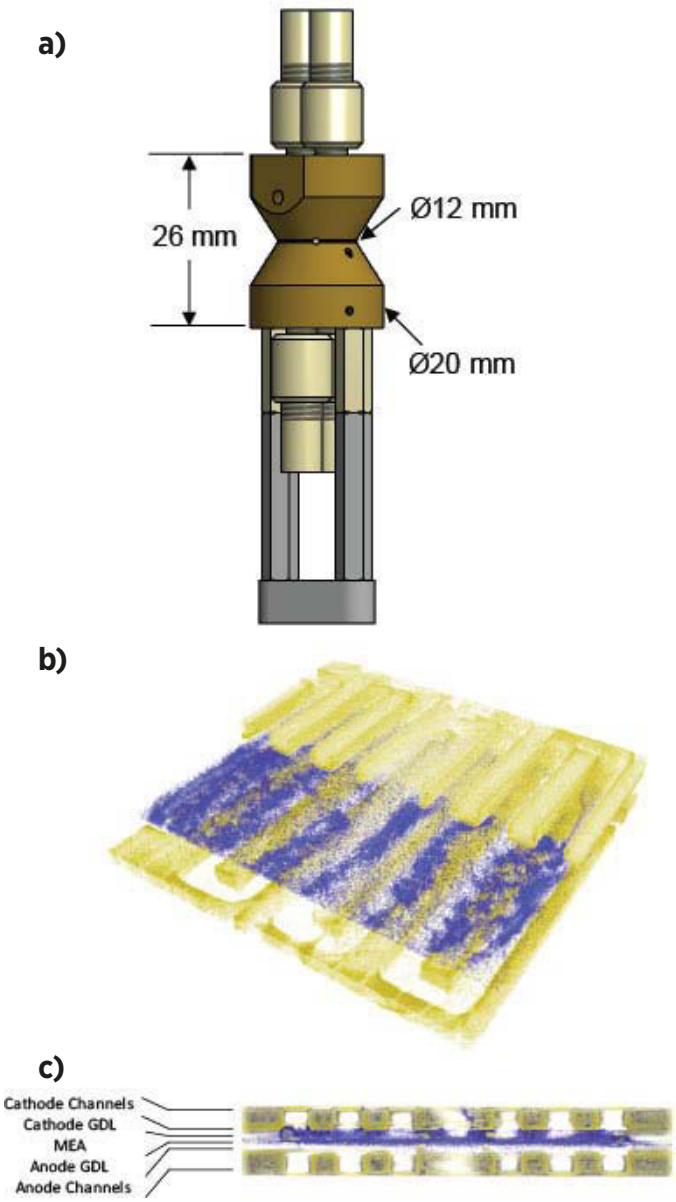

GDL – gas diffusion layer

FIGURE 4. Fuel cell (a) designed for both X-ray and neutron tomography. The 3D water distribution is shown in (b) and (c) measured with neutrons overlayed with the X-ray image of the hardware and electrode interfaces. Cell active area 0.36 cm^2 active area, ambient temperature, flow both sides 200 sccm, exhaust pressure 150 kPa_a, dew point 25°C, scan time 18 h, 200 mV shown (1.9 A cm^{-2}).

- Centroiding has shown that 1.5 µm resolution has been achieved.
  - Future: Pursue detector package optimization that reduces light losses and incorporates hardware-based centroiding to:
    - Reduce deadtime to near zero.
    - Provide images in real time.
    - Increases field of view to 1 cm diameter.
  - Future: Fabricate planar test section.
- Wolter optics:
  - Flagship method to achieve spatial resolution of 1 µm.
  - Future 2020: high speed 20 µm optics, 2021: 1 µm optics.

- Progress has been made to develop an in situ X-ray method.
  - Developments are scalable to higher spatial resolution.
  - Allows clear distinction of interfaces that are not visible to neutrons.
  - Neutron imaging provides complementary picture of the water distribution.
  - Future: Using X-rays inline will allow for radiographic distinction of interfaces with high spatial resolution.
- User program:
  - New user proposals due to availability of 1.5 µm spatial resolution through the centroiding method.
  - Future: Cold imaging facility is currently being upgraded to include full support.
  - Future: Including electrochemical impedance spectroscopy into the scripting of the test stand would be a great benefit to the users.

REFERENCES

1. D.S. Hussey, J.M. LaManna, E. Baltic, and D.L. Jacobson, Neutron imaging detector with 2 µm spatial resolution based on event reconstruction of neutron capture in gadolinium oxysulfide scintillators, NIMA 866 (2017) 9–12.

2. D.S. Hussey, J.M. LaManna, E. Baltic, D.L. Jacobson, S. Stariha, D. Spernjak, R. Mukundan, and R.L. Borup, "Membrane/Electrode Assembly Water Content Measured with 2 µm Spatial Resolution Neutron Imaging," accepted, ECS Transactions 80 (2017).

3. J.M. LaManna, D.S. Hussey, E. Baltic, D.L. Jacobson, "Neutron and X-ray Tomography (NeXT) system for simultaneous, dual modality tomography," submitted Review of Scientific Instruments (2017).

FY 2017 PUBLICATIONS/PRESENTATIONS

1. F. Nandjou, J.-P. Poirot-Couvezier, M. Chandesris, S. Rosini, D.S. Hussey, D.L. Jacobson, J.M. LaManna, A. Morin, Y. Bultel, "A pseudo-3D model to investigate heat and water transport in large area PEM fuel cells – Part 2: Application on an automotive driving cycle," Int. J. Hydrogen Energy, Volume 41, Issue 34, pgs. 15573–15584 (2016).

2. N. Macauley, R.W. Lujan, D.S. Hussey, D.L. Jacobson, K. More, D. Spernjak, R L. Borup, and R. Mukundan, "Durability of Polymer Electrolyte Membrane Fuel Cells Operated at Subfreezing Temperatures," J. Electrochem. Soc., volume 163, issue 13, F1317-F1329, doi: 10.1149/2.0191613jes (2016).

3. Spernjak, D., G. Wu, J. Fairweather, D. Hussey, R. Mukundan, R. Borup, and P. Zelenay, In situ measurement of flooding in thick Pt and PANI-derived catalyst layers in PEM fuel cells. Journal of the Electrochemical Society, in preparation (2017).

4. D.S. Hussey, J.M. LaManna, E. Baltic, D.L. Jacobson, "Neutron Imaging Detector with Scintillation Light Magnification and Amplification," ECS Transactions, 75 (14) 245–250 (2016).

5. D.S. Hussey, J.M. LaManna, E. Baltic, D.L. Jacobson, "High spatial resolution neutron detector based on event reconstruction of neutron capture in gadolinium oxysulfide scintillators," submitted, Nuclear Instruments and Methods-A (2017).

6. J.M. LaManna, D.S. Hussey, E. Baltic, D.L. Jacobson, "Neutron and X-ray Tomography (NeXT) system for simultaneous, dual modality tomography," submitted, Review of Scientific Instruments (2017).

7. Jacob LaManna, Matthew Mench, "Channel-land configuration control of temperature driven water transport in polymer electrolyte fuel cells," in preparation (2017).

8. J. LaManna, J. Owejan, M. Mench, "Anode water content control using high tortuosity anode diffusion media," in preparation (2017).

9. J. LaManna, A. Pezeshki, G. Veith, M. Mench, "Changes to water balance and material properties with operational age in polymer electrolyte fuel cells," in preparation (2017).

10. J. LaManna, M. Mench, "Thermally driven water transport in PEFCs: A parametric design guide," in preparation (2017).

11. Mukundan, R.; Spernjak, D.; Hussey, D.S.; Jacobson, D.L.; Borup, R., "(Invited) Application of high resolution neutron imaging to polymer electrolyte fuel cells", 253rd American Chemical Society National Meeting, Applications of X-Ray & Neutron Scattering Techniques in Energy Technologies: Fuel Cells, ENFL 366 (2017).

12. Jacobson, D.L.; Hussey, D.S.; Lamanna, J.; Baltic, E.; "(Invited) Using neutron imaging to understand transport phenomenon in fuel cell and batteries", 253rd American Chemical Society National Meeting, Applications of X-Ray & Neutron Scattering Techniques in Energy Technologies: Fuel Cells, ENFL 362 (2017).

13. De Beer, F. "PEM Water Electrolysis: Preliminary Investigations Using Neutron Radiography," ITMNR-8, Beijing, China, September 5, 2016.

14. Arif, M. "NIST's capabilities for materials science research using neutron imaging," ITMNR-8, Beijing, China, September 5, 2016.

15. Lamanna, J. "Simultaneous Neutron and X-ray Tomography for Quantitative Composition and Structure Analysis," ITMNR-8, Beijing, China, September 6, 2016.

16. D. Muirhead, R. Banerjee, S. Chevalier, N. Ge, M.G. George, J. Hinebaugh, J. Lee, H. Liu, P. Shrestha, and A. Bazylak, "Impact of Liquid Water on Oxygen Transport Resistance in a PEMFC Cathode Via Limiting Current Methods and Concurrent Synchrotron X-Ray Radiography," PRiME, Honolulu, HI, October 6, 2016.

17. D.S. Hussey, J.M. LaManna, E. Baltic, and D.L. Jacobson, "Imaging Detector with Scintillation Light Magnification and Amplification," PRiME, Honolulu, HI, October 4, 2016.

18. D. Spernjak, R.L. Borup, D.S. Hussey, P. Zelenay, and R.Mukundan, "Imaging Fuel Cell Components: From Flow Field Channels to Catalyst Layers," PRiME, Honolulu, HI, October 4, 2016.

19. J.M. LaManna, D.S. Hussey, E. Baltic, and D.L. Jacobson, "Neutron and X-Ray Imaging Techniques for Enhanced Water Management Diagnostics," PRiME, Honolulu, HI, October 4, 2016.

V.E.2 Technical Assistance to Developers

Tommy Rockward and Rod Borup (Primary Contacts), LANL Fuel Cell Team
Los Alamos National Laboratory (LANL)
P.O. Box 1663
Los Alamos, NM 87545
Phone: (505) 667-9587, (505) 667-2823
Email: trock@lanl.gov, borup@lanl.gov

DOE Manager: Nancy L. Garland
Phone: (202) 586-5673
Email: Nancy.Garland@ee.doe.gov

Project Start Date: October 2006
Project End Date: Project being discontinued at end of current funds

Overall Objectives

This task supports Los Alamos technical assistance to fuel-cell component and system developers as directed by the DOE. This task includes:

- Testing and validation of materials.
- Participation in the further development and validation of single cell test protocols.
- Assistance to Durability Working Groups, the U.S. Council for Automotive Research (USCAR), and the USCAR/DOE Driving Research and Innovation for Vehicle efficiency and Energy sustainability (U.S. DRIVE) Fuel Cell Technical Team.
- Providing technical experts available to DOE and the Fuel Cell Technical Team.

Fiscal Year (FY) 2017 Objectives

- Perform quantitative comparison of oxygen reduction reaction (ORR) activity and cyclic voltammogram redox peaks of different platinum group metal (PGM)-free catalysts defining what correlation exists from minimum two sets of externally provided PGM-free catalysts.
- Provide Ford a sufficient quantity (200 mg) of reactively sputter-deposited niobium oxide layers onto Ford-provided substrates for catalyst support synthesis for Ford electrochemical evaluation of NbO_x intermediate layer.
- Participate with Fuel Cell Tech Team with a minimum of six tech team meetings in person and reports on results of tech assistance to developers.
- Hold annual fuel cell training workshop for industrial and academic participants; give reports on results of tech assistance to developers.
- Test University of California, Los Angeles' (UCLA's) Mo-doped Pt_3Ni octahedra catalysts for performance and durability.
- Characterize and test industry catalyst for performance and durability and investigate the stability of a different support.

Technical Barriers

This project addresses the following technical barriers from the Technology Validation section of the Fuel Cell Technologies Office Multi-Year Research, Development, and Demonstration Plan.

(A) Durability

(B) Cost

(C) Electrode Performance

FY 2017 Accomplishments

- Ford Motor Co.
  - Provided eight catalyst samples
  - Performed approximately 134 depositions for multi-layering metal plates
- UCLA Catalysts
  - Performed initial testing of Mo-doped Pt_3Ni octahedra catalysts (10,000 cycles)
- Blue-O Technology, Inc.
  - Prepared catalyst inks and membrane electrode assemblies (MEAs)
  - Conducted initial performance tests in fuel cell: pressure and temperature dependence
  - Air vs oxygen polarization curves
  - X-ray diffraction showed well defined catalyst structures
- Savannah River National Laboratory (SRNL)
  - Independent tests results did correlate: redox potentials vs. ORR activity
- National Institute of Standards and Technology (NIST), University of Hawaii, University of Tennessee-Knoxville
  - Provided neutron imaging hardware and guidance on its usage

- Participate on the DOE/USCAR U.S. DRIVE Fuel Cell Tech Team
- Continue to support DOE working groups (WG)
  - Durability WG
  - Mass Transport WG
- Provide technical assistance to developers as requested by DOE and report on the results to DOE and the U.S. DRIVE Tech Team
- Provided input on refined fuel cell targets and multi-year program plan

✧ ✧ ✧ ✧ ✧

INTRODUCTION

This task provides technical support to fuel cell component and system developers free of cost to the developer, by experts within the LANL fuel cell team. In addition, it also includes the participation in the further development and validation of single cell test protocols, interacting with durability working groups, the USCAR and the U.S. DRIVE Fuel Cell Technical Team, and making technical experts available to DOE and the Fuel Cell Tech Team.

The work performed this fiscal year, approved by the DOE included customers and collaborators from industry, national laboratories, and various universities. In FY 2017, technical assistance included requests from Ford Motor Company, SRNL, Argonne National Laboratory, Lawrence Berkeley National Laboratory, NIST, National Physical Laboratory, Blue-O Technology, Inc., and several universities and colleges.

APPROACH

Our approach for this effort is governed by our customers' requests and the DOE's interest. Support is generally provided using available in-house equipment such as scanning electron microscopy or energy dispersive X-ray analysis, X-ray fluorescence spectroscopy, differential scanning calorimetry, Fourier transform infrared spectroscopy, tapered element oscillating microbalance, thermogravimetric analysis, simultaneous thermogravimetric analysis/differential scanning calorimetry, differential thermal analysis, solid-phase and liquid-phase nuclear magnetic resonance, gas chromatography, mass spectroscopy, X-ray diffraction, solid-state diffuse reflectance infrared Fourier transform spectroscopy, Raman spectrometer, electron beam evaporation, radio frequency magnetron sputtering, alternating current impedance spectroscopy, and Brunauer-Emmett-Teller surface area measurements. LANL also has 38 test stands equipped with automated data acquisition and computer-controlling features that are available for this project. In FY 2017, customers and their requests included:

- SRNL
  - Testing and validation of PGM-free
- NIST
  - Neutron imaging hardware
- University of Tennessee
  - Neutron imaging hardware
- University of Hawaii
  - Neutron imaging hardware
- Ford Motor Co.
  - Bipolar plate
  - Catalyst development
- Blue-O Technology
  - Catalyst testing of Pt, PtM, and Pt/TiO_2
  - Catalyst performance and durability
  - Investigate novel support materials
- UCLA
  - Catalyst testing of Mo-doped Pt_3Ni
  - MEA performance and durability using accelerated stress tests

RESULTS

In this section, we highlight some results from this year's accomplishments. These results and discussions are concise due to a length constraint of this document.

We continued working with Ford Motor Co. on novel catalyst support coating and metal bipolar plates. They were provided eight catalysts samples for their catalyst support request and 20 samples with approximately 134 depositions performed for multi-layering metal plates utilizing four different customizable sputtering systems to achieve desired thickness of titanium and gold, which acts as corrosion barrier on stainless steel substrates for metal bipolar plates. These materials were tested at their facilities and the results presented at the Electrochemical Society Meeting.

In 2015, UCLA reported high catalytic activity with rotating disk electrode activity with Mo-doped Pt_3Ni octahedral catalysts. In FY 2017, LANL received catalysts to test for performance and durability in a fuel cell for comparison against DOE targets. Catalyst inks and MEAs were prepared and tested. Polarization curves were measured as a function of voltage cycles to gauge both performance and durability. The voltage cycling followed a DOE accelerated stress test that cycled the voltage in a square

wave pattern between 0.6 V to 0.95 V. We also measured the electrochemical surface area and mass activity of the catalyst. Polarization curves showed 20 mV in losses after 10,000 V-cycles measured at 0.8 A/cm^2. The electrochemical surface area lowered by 12% while the mass activity reduced by 18%. These losses are below the DOE targets, but testing is not complete considering the DOE protocols call for 30,000 cycles.

Blue-O Technology requested independent verification of performance and durability of their novel catalyst which utilizes a different support. LANL performed electrochemical characterization using rotating disk electrode to test the durability of the catalyst support, prepared catalyst inks, and made MEAs for fuel cell testing as well as performed X-ray diffraction on catalyst samples (Figure 1). Initial test results were performed on MEAs with un-optimized ionomer to catalyst ratios (total Pt loading <0.1 mg/cm^2). Performance at these ultra-low Pt loadings show promise and rotating disk electrode tests demonstrated a durable catalyst support.

LANL along with SRNL conducted independent experiments to investigate the electrochemistry of Fe-N-C catalyst. They focused on the redox couple in the cyclic voltammogram and whether or not it correlates to ORR performance. Both labs utilized different mixtures of H_2SO_4 and $HClO_4$ to perform their measurements. As a result, different redox potentials of the Fe-based catalyst were observed as the electrolyte ratios varied. The ORR of the catalyst was for each mixture and finding directly contradicts the literature. Both labs' results agreed and found no correlation between redox peaks and ORR performance (Figure 2).

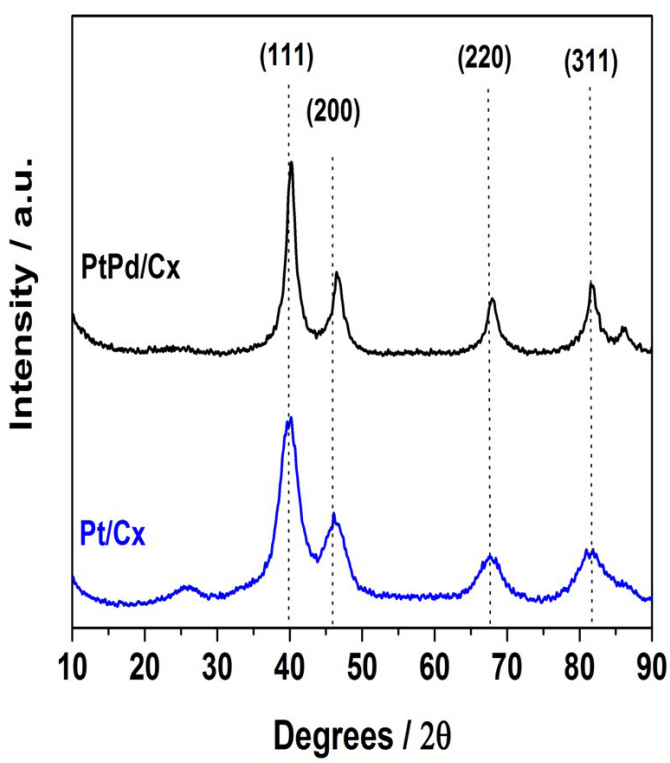

FIGURE 1. X-ray diffraction results of Blue-O Technology catalyst samples

UPCOMING ACTIVITIES

The Fuel Cell Technologies Office has decided to discontinue this project; as a result, the completion of any ongoing and or future work is uncertain. Below we still list the details of the anticipated work:

- UCLA catalysts
  - Continue to perform testing of Mo-doped Pt_3Ni octahedra catalysts
- Blue-O Technology
  - Complete catalyst testing of Pt, Pt, and Pt TiO_2
  - Catalyst performance and durability
  - Investigate novel support materials
  - ElectroChem, Inc.
  - Stack testing and validation (awaiting stack)
- SRNL
  - Compete results with PGM-free testing to solidify finding: redox potentials vs. ORR activity
- NIST, University of Hawaii, University of Tennessee-Knoxville
  - Provide neutron imaging hardware and guidance on its usage
- Participate on the DOE/USCAR U.S. DRIVE Fuel Cell Tech Team
- Continue to support DOE working groups
  - Durability WG
  - Mass Transport WG
- Provide technical assistance to developers as requested by DOE and report on the results to DOE and the U.S. DRIVE Tech Team

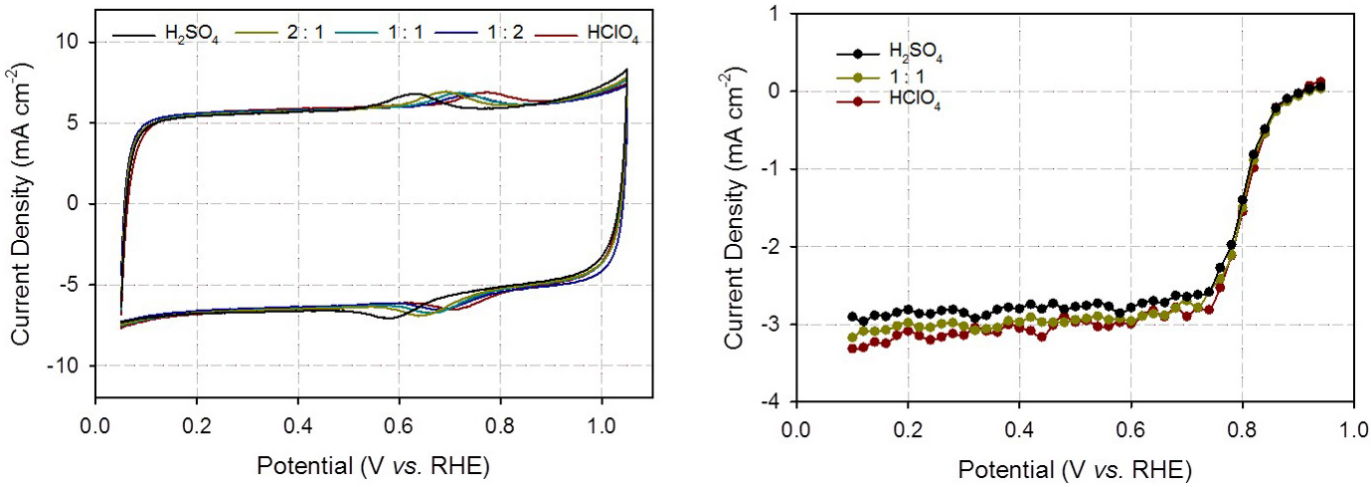

RHE – reference hydrogen electrode

FIGURE 2. Left graph shows cyclic voltammograms for different mixtures of H_2SO_4 and $HClO_4$; right graph compares ORR for H_2SO_4, $HClO_4$, and a 50% mixture of the two

FY 2017 PUBLICATIONS/PRESENTATIONS

A significant portion of this effort often goes unpublished at the customer's request.

1. Le Xin, Yu Kang, Fan Yang, Aytekin Uzunoglu, Tommy Rockward, Paulo Jorge Ferreira, Rod L. Borup, Jan Ilavsky, Lia Stanciu, Jian Xie, Novel Catalyst-Layer Structures with Rationally Designed Catalyst/Ionomer Interfaces and Pore Structures Aided By Catalyst Functionalization, 2016/9/1, Meeting Abstracts, The Electrochemical Society.

2. Le Xin, Fan Yang, Aytekin Uzunoglu, Tommy Rockward, Rod L. Borup, Lia Stanciu, Jian Xie, Highly Stable Hierarchical Polybenzimidazole (PBI) Grafted Graphene/Nanographene Hybrids As Catalyst Supports for Polymer Electrolyte Membrane Fuel Cells, 2016/9/1, Meeting Abstracts, The Electrochemical Society.

3. Jacob S. Spendelow, Luis Castanheira, Gareth Hinds, Tommy Rockward, David A. Langlois, Rangachary Mukundan, Rod L. Borup, Measurement of Local Electrode Potentials in an Operating PEMFC Exposed to Contaminants, 2016/9/1, Meeting Abstracts, The Electrochemical Society.

4. Xin, Le; Yang, Fan; Qiu, Yang; Uzunoglu, Aytekin; Rockward, Tommy; Borup, Rodney L.; Stanciu, Lia A.; Li, Wenzhen; Xie, Jian, Polybenzimidazole (PBI) Functionalized Nanographene as Highly Stable Catalyst Support for Polymer Electrolyte Membrane Fuel Cells (PEMFCs), Journal of the Electrochemical Society (2016), 163(10), F1228–F1236.

5. Kerrie K. Gath, Mark Ricketts, Jun Yang, Chunchuan Xu, and Shinichi Hirano, Multi-Layer Thin Film Coatings on Bipolar Metal Plates for PEMFC, 2016/9/1, Meeting Abstracts, The Electrochemical Society.

V.E.3 Fuel Cell Technology Status: Degradation

Jennifer Kurtz (Primary Contact), Huyen Dinh, Genevieve Saur
National Renewable Energy Laboratory (NREL)
15013 Denver West Parkway
Golden, CO 80401-3305
Phone: (303) 275-4061
Email: Jennifer.Kurtz@nrel.gov

DOE Manager: Adria Wilson
Phone: (202) 586-5782
Email: Adria.Wilson@ee.doe.gov

Project Start Date: July 1, 2009
Project End Date: Project continuation and direction determined annually by DOE

Overall Objectives

- Conduct an independent assessment to benchmark current fuel cell system cost and price in a non-proprietary method.
- Leverage National Fuel Cell Technology Evaluation Center (NFCTEC) activities.
- Collaborate with key fuel cell developers on the voluntary data share and NFCTEC analysis.

Fiscal Year (FY) 2017 Objectives

- Receive and analyze new laboratory durability data.
- Publish aggregated, current fuel cell voltage durability status.
- Include electrolysis and updated price data.

Technical Barriers

This project addresses the following technical barriers from the Fuel Cells section of the Fuel Cell Technologies Office Multi-Year Research, Development, and Demonstration Plan.

(A) Durability (Lack of data for current fuel cell durability status per targets)

(B) Cost (Lack of data for current fuel cell costs and status per targets)

Technical Targets

This project is conducting an independent assessment of the current fuel cell durability test data from leading fuel cell developers. All results are aggregated to protect proprietary information and are reported on by the system application. Table 1 shows the durability targets.

TABLE 1. Fuel Cell Durability Target and Status Table

Application	2020 Durability Target	Lab Status – Average Hours to 10% Voltage Degradation
Light-Duty Automotive	5,000 h	3,700 h
Public Transit	25,000 h	6,200 h
Forklift	20,000 h Target Under Review	13,500 h
Backup	10,000 h	2,600 h
Stationary 1–10 kW	0.3%/1,000 h	11,900 h
Stationary 100 kW–3 MW	80,000 h	

Per the Fuel Cells section of the Fuel Cell Technologies Office Multi-Year Research, Development, and Demonstration Plan, the cost targets are as follows:

- The 2020 transportation fuel cell system cost target is $40/kW with an ultimate target of $30/kW.
- The 2016 fuel cell transit bus cost target is $1,000,000 with a 2020 target of $600,000.
- The 2020 micro-combined heat and power (5 kW) fuel cell system cost target is $1,500/kW.
- The 2020 medium combined heat and power (100 kW–3 MW) fuel cell system cost target is $1,000/kW for natural gas and $1,400/kW for biogas.

FY 2017 Accomplishments

- Collected new fuel cell voltage degradation data sets from fuel cell developers (including data on proton exchange membrane, direct methanol, and solid oxide fuel cell of full active area short stacks and full stacks with systems).
- Analyzed, aggregated, and published current status of platinum loading over time.
- Analyzed, aggregated, and published current status of fuel cell voltage degradation versus DOE targets.
- Published 22 composite data products (CDPs) [1] with data from 23 domestic and international fuel cell and electrolysis developers.

✧ ✧ ✧ ✧ ✧

INTRODUCTION

DOE has funded significant research and development activity with universities, national laboratories, and the fuel cell industry to improve the market competitiveness of fuel cells. Most of the validation tests to confirm improved fuel cell stack performance and durability (indicators of market competitiveness) are completed by the research organizations themselves. Although this allows the tests to be conducted by the developers most familiar with their specific technology, it also presents a number of challenges in sharing progress publicly because test conditions and data analysis take many forms and data collected during testing are often considered proprietary.

NREL is benchmarking the state-of-the-art fuel cell performance, specifically focusing on durability, through independent assessment of current laboratory data sets. NREL's data processing, analysis, and reporting capitalize on capabilities developed in DOE's Fuel Cell Electric Vehicle Learning Demonstration. Fuel cell stack durability status is reported annually and includes a breakdown of status for different applications. A key component of this project is the collaborative effort with key fuel cell developers to understand what is being tested in the laboratory, study analysis results, and expand the included data sets.

APPROACH

The project involves voluntary submission of data from relevant fuel cell developers. NREL is contacting fuel cell developers for fuel cell voltage degradation, cost, and price data for multiple fuel cell types to either continue or begin a data sharing collaboration. A continuing effort is to include more data sets, types of fuel cells, quantity of units sold, and developers. The fuel cell voltage degradation data are sent from fuel cell developers performing testing and studied over time against DOE's voltage degradation targets.

Raw and processed data are stored in NREL's NFCTEC. The NFCTEC is an off-network room with access provided to a small set of approved users. Processing capabilities are developed or modified for new data sets and then included in the analytical processing of NREL's Fleet Analysis Toolkit, an internally developed tool for data processing and analysis structured for flexibility, growth, and simple addition of new applications. Analyses are created for general performance studies as well as application- or technology-specific studies. The incoming raw data may be new or a continuation of data that have already been supplied to NREL. An internal analysis of all available data is completed annually and a set of technical CDPs is published every year. Publications are uploaded to NREL's technology validation website [1] and presented at industry-relevant conferences. The CDPs present aggregated data across multiple systems, sites, and teams to protect proprietary data and summarize the performance of hundreds of fuel cell systems and thousands of data records. A review cycle is completed before the CDPs are published. This review cycle includes providing detailed data products of individual system- and site-performance results to the specific data provider. Detailed data products also identify the individual contribution to the CDPs.

RESULTS

Results published in May 2017 were the seventh update for this analysis effort. The annual voltage degradation analysis of state-of-the-art laboratory durability was completed in advance of the milestone to provide an update that could be presented at DOE's Annual Merit Review and Peer Evaluation Meeting. In the current published data set, seven applications were covered and 23 fuel cell and electrolyzer developers supplied data (more than one data set in many cases). The data sets covered proton exchange membrane, direct methanol, and solid oxide fuel cell stack testing as well as electrolyzer testing. A total of 224 data sets have been analyzed with 50 new additions from the previous year. Note that a data set may represent test data from a short stack, full stack, or system. Of the total data sets, 84% have been retired, meaning the system or stack is not accumulating any new operation hours either because of test completion, technology upgrades, or failures. The published data results include 22 CDPs, including a new CDP looking at platinum loading over time as well as a new degradation CDP showing results of only recent data sets (excluding pre-2013). The power capability illustrates the range of fuel cell power for the data sets by application from less than 2 kW to more than 50 kW. Most of the analyzed data sets are laboratory systems at less than 14 kW power.

The analyzed data sets are from laboratory testing of full active area short stacks (e.g., stacks with fewer cells than the expected full power stack) and test systems with full power stacks. The data sets also vary from one to the other in how the stack or system was tested. Data were generated between 2004 and late 2016 from different testing methods that included constant load, transient load, and accelerated testing. The variability in test conditions and test setups creates a group of data that can be difficult to compare.

Fuel cell durability is studied at a design-specific current point and measured against a target of 10% voltage drop from beginning of life. The 10% voltage drop metric is used for assessing voltage degradation with a common measurement, but the metric may not be the same as end-of-life criteria and does not address catastrophic failure modes. Figure 1 and Figure 2 are aggregated set of results separated by application; Figure 1 includes all data sets received to date, while Figure 2 includes only data sets from 2013 and after. Not all application categories have enough data sets to be included in Figure 2. For both the automotive and prime application categories, data from 2013 and on have higher durability projections than the durability projections for all

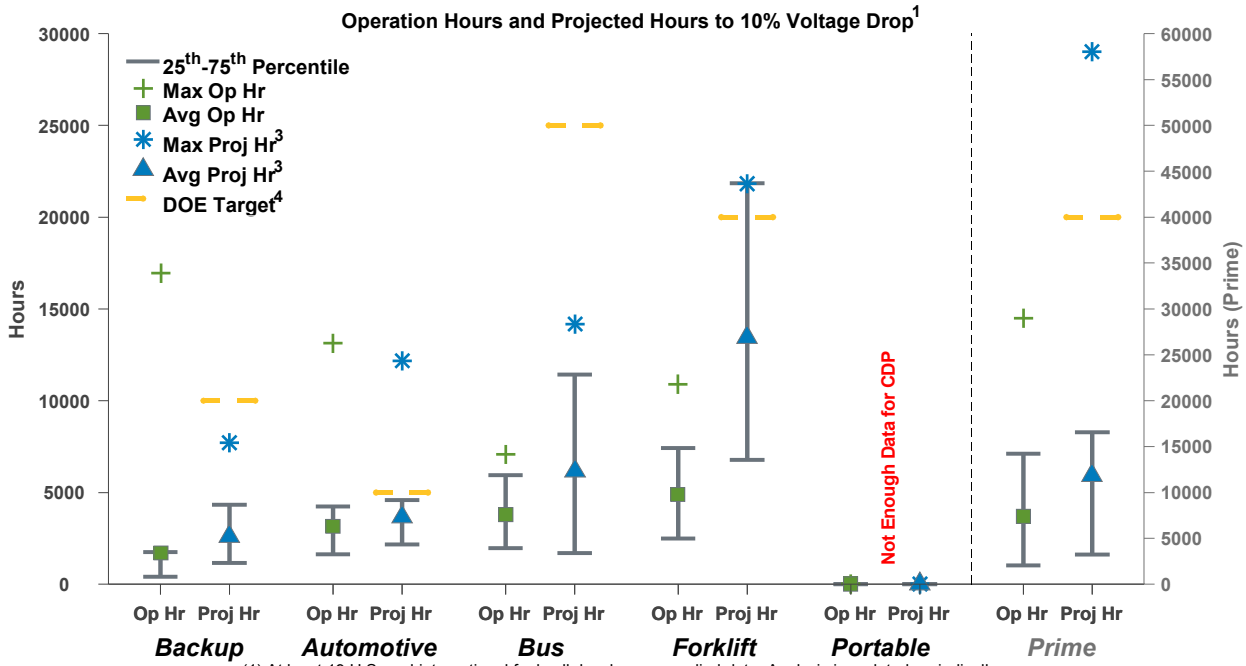

NREL cdp_lab_01
Created: May-08-17 12:06 PM | Data Range: 2004Q1-2016Q4

(1) At least 19 U.S. and international fuel cell developers supplied data. Analysis is updated periodically.
(2) PEMFC, DMFC & SOFC data from lab tested, full active area short stacks and systems with full stacks. Data generated from constant load transient load, and accelerated testing between 2004 and 2016.
(3) The DOE 10% voltage degradation metric is used for assessing voltage degradation; it may not be the same as end-of-life criteria and does not address catastrophic failure modes.
(4) DOE targets are for real-world applications; refer to Hydrogen, Fuel Cells, & Infrastructure Technologies Program Plan.

FIGURE 1. Voltage degradation results by application

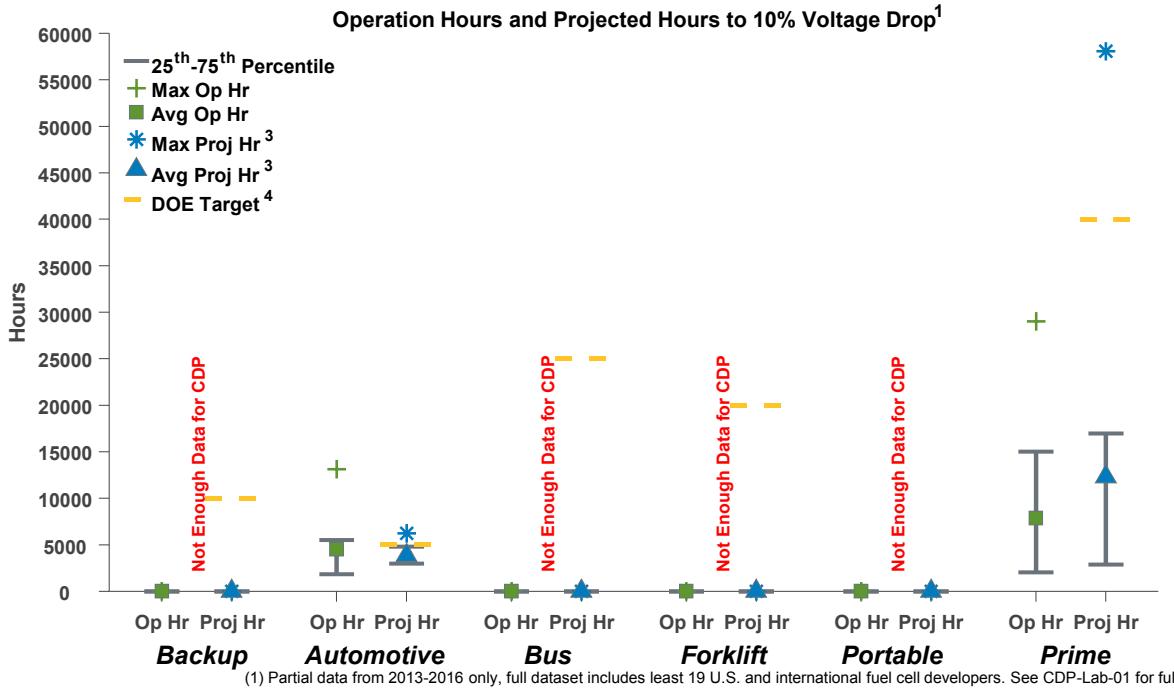

NREL cdp_lab_21
Created: Apr-20-17 11:49 AM | Data Range: 2009Q1-2016Q4

(1) Partial data from 2013-2016 only, full dataset includes least 19 U.S. and international fuel cell developers. See CDP-Lab-01 for full data set.
(2) PEMFC, DMFC & SOFC data from lab tested, full active area short stacks and systems with full stacks. Data generated from constant load, transient load, and accelerated testing between 2004 and early 2012.
(3) The DOE 10% voltage degradation metric is used for assessing voltage degradation; it may not be the same as end-of-life criteria and does not address catastrophic failure modes.
(4) DOE targets are for real-world applications; refer to Hydrogen, Fuel Cells, & Infrastructure Technologies Program Plan.

FIGURE 2. Voltage degradation, recent results (2013+)

data starting before 2009. The automotive category is 200 hours higher and the prime category is 400 hours higher. For each application, the average, maximum, and 25th and 75th percentile values are identified for the operation hours and the projected hours to 10% voltage drop. Current density variation (Figure 3) is dependent on developer-selected test protocols and objectives. NREL updated this CDP in 2017 to include several higher density bins to accommodate the variations in data. The automotive data sets are primarily in the higher current density bins because of vehicle packaging constraints for power density. More than 60% of automotive data sets were studied at ≥1.2 A/cm^2 in the 2017 results (<50% in the 2016 analysis results). A future comparison could be the study of voltage degradation at one chosen current density for all data sets within a category or type. The current density points used for the aggregated durability results are based on individual designs, and data may not be available at multiple current densities. The most variety in current density is seen in the prime and automotive categories.

The 10% voltage drop level is not necessarily a measurement for end of life or even a significant reduction in performance. Many data sets have not passed (or did not pass) the metric of 10% voltage degradation. The reason data sets operated beyond 10% voltage degradation could be because end-of-life criteria may be greater than 10% voltage degradation or because the test was designed to operate until a failure occurred. The stack configuration and test conditions can have a significant impact on the projected time to 10% voltage degradation within an application. In general, the average projection decreases with more aggressive test conditions and full systems. Not all applications have data sets in each configuration or test condition group. The test condition groups include:

- Steady—little or no change to load profile.
- Duty Cycle—load profile mimics real-world operating conditions.
- Accelerated—test profile is more aggressive than real-world operating conditions.

In a new analysis in FY 2017 NREL added a request for platinum loading based on range categories from fuel cell loading research and targets. The project team also went through all old data sets to retroactively ask for the platinum data where possible. Platinum loading is highly correlated to cost for some types of fuel cells, and a new CDP (Figure 4) looks at the trends of platinum loading over time. The platinum loading per square centimeter is decreasing on the data sets analyzed, per the trend for the mode in both 2015 and 2016. In the future NREL hopes to combine this with the degradation analysis in order to study how or if the platinum loading has affected degradation projections over time. In the automotive category, voltage durability projections are relatively stable over the years of analysis, but additional data are needed in order to look at this further.

In the automotive category, voltage durability projections are relatively stable over the years of analysis. This may

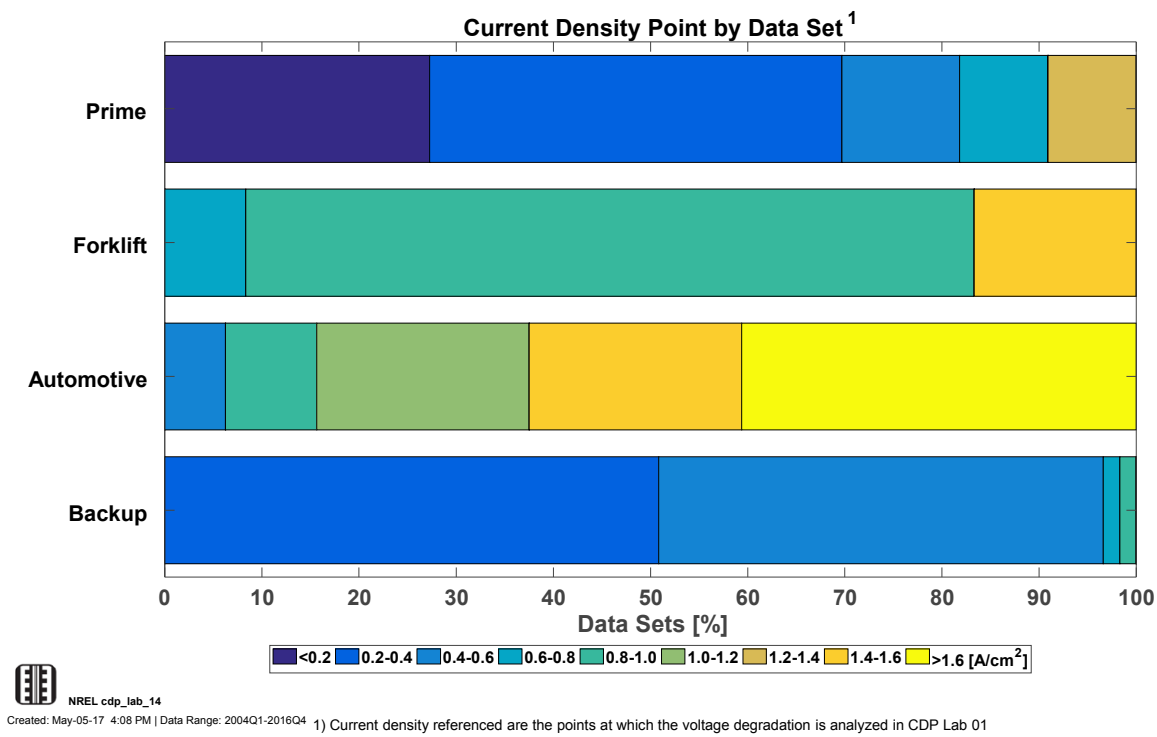

FIGURE 3. Current density variation between data sets

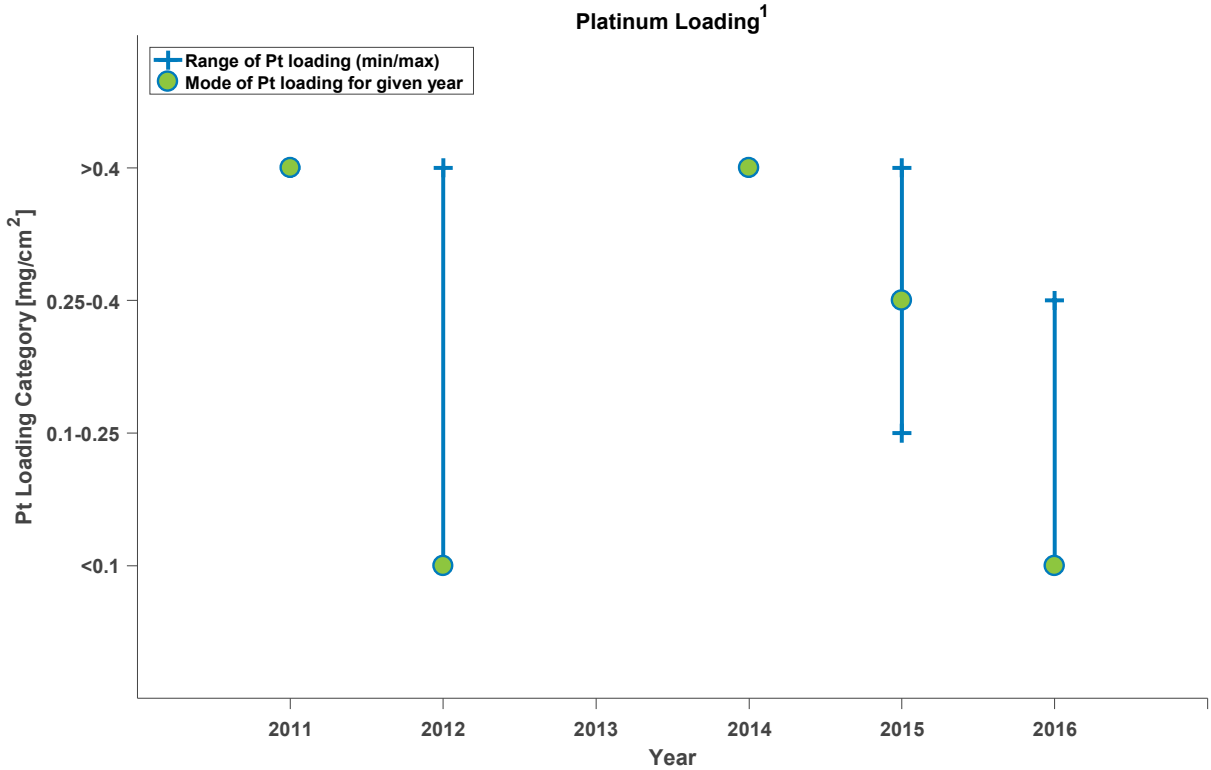

NREL cdp_lab_20
Created: May-05-17 4:12 PM | Data Range: 2004Q1-2016Q4

1. Platinum loading is plotted in the year when lab operation started and aggregates all applications, configurations and test conditions for data sets that provided loading data.

FIGURE 4. Platinum loading trend

be due in part to a shift in focus from durability to cost reduction while maintaining an acceptable degradation rate, as seen in Figure 4. There is an interdependence between cost and durability, and, depending on the economics, durability may not be the driving technical parameter at this time.

CONCLUSIONS AND UPCOMING ACTIVITIES

This project has leveraged other technology validation projects and existing industry relationships to steadily increase the quantity and depth of reporting on the state-of-the-art fuel cell durability status with a relatively low level of investment from DOE. Both U.S.-based and international developers have voluntarily supplied at least one data set, and it is an ongoing effort to include new data sets, update data sets already included (if applicable), and include new fuel cell developers, applications, and types. The voluntary participation of leading fuel cell and electrolyzer developers provides an overall technology benchmark (with the published aggregated data) and an individual developer benchmark (with the detailed data products). Additional breakdown of the data sets is an important aspect of future work and is dependent on the accumulation of more data sets to not reveal an individual data supplier's contribution to the results or proprietary data. Future work, following the path of degradation and cost/price status updates every other year, includes the following activities:

- Continue cultivating existing collaborations and developing new collaborations with fuel cell and electrolyzer developers.
- Gather, process, and report on current fuel cell product cost and/or price.
- Add analyses around accelerated testing comparisons.
- Address legacy data in several of the analyses.

FY 2017 PUBLICATIONS/PRESENTATIONS

1. Jennifer Kurtz, Huyen Dinh, Genevieve Saur, and Chris Ainscough, "Fuel Cell Technology Status – Degradation," presented at the 2017 DOE Annual Merit Review and Peer Evaluation Meeting, Washington, D.C., June 2017.

2. Genevieve Saur, Jennifer Kurtz and Huyen Dinh, "Fuel Cell Technology Status – Degradation: FC Tech Team," presented to the Fuel Cell Tech Team, May 2017.

3. Jennifer Kurtz, Huyen Dinh, Chris Ainscough, and Genevieve Saur, "State-of-the-Art Fuel Cell Voltage Durability Status: 2017 Composite Data," NREL/PR-5400-68621, Golden, CO: National Renewable Energy Laboratory, May 2017.

4. "Fuel Cell Technology Status Analysis Project: Partnership Opportunities," NREL/FS-5400-67899, Golden, CO: National Renewable Energy Laboratory, March 2017.

5. Jennifer Kurtz, Huyen Dinh, and Genevieve Saur, "Fuel Cell Technology Status – Degradation," excerpt from the 2016 DOE Hydrogen and Fuel Cells Program Annual Progress Report, February 2017.

REFERENCES

1. "Fuel Cell Technology Status Analysis," National Renewable Energy Laboratory, https://www.nrel.gov/hydrogen/fuel-cell-technology-status.html.

V.E.4 Performance and Durability of Advanced Automotive Fuel Cell Stacks and Systems with Dispersed Alloy Cathode Catalyst in Membrane Electrode Assemblies

Rajesh K. Ahluwalia (Primary Contact),
Xiaohua Wang, and J-K Peng
Argonne National Laboratory
9700 South Cass Avenue
Argonne, IL 60439
Phone: (630) 252-5979
Email: walia@anl.gov

DOE Manager: Nancy L. Garland
Phone: (202) 586-5673
Email: Nancy.Garland@ee.doe.gov

Project Start Date: October 1, 2003
Project End Date: Project continuation and direction determined annually by DOE

Overall Objectives

- Develop a validated model for automotive fuel cell systems, and use it to assess the status of the technology.
- Conduct studies to improve performance and packaging, to reduce cost, and to identify key research and development issues.
- Compare and assess alternative configurations and systems for transportation and stationary applications.
- Support DOE/U.S. DRIVE automotive fuel cell development efforts.

Fiscal Year (FY) 2017 Objectives

- Quantify the impact of low-platinum group metal (PGM) alloy catalysts and alternate catalyst supports on the performance of automotive stacks and fuel cell systems.
- Understand the durability of low-PGM alloy catalysts under cyclic potentials.
- Extend system analysis to non-nanostructured thin film (NSTF) membrane electrode assemblies (MEAs) with conventional Pt/C and advanced Pt alloy/C cathode catalysts.
- Incorporate durability considerations in system analysis.
- Provide modeling support to Strategic Analysis, Inc., in annual update of progress in meeting technical targets including fuel cell system (FCS) cost.

Technical Barriers

This project addresses the following technical barriers from the Fuel Cells section of the Fuel Cell Technologies Office Multi-Year Research, Development, and Demonstration Plan.

(A) Durability

(B) Cost

(C) Performance

Technical Targets

This project is conducting system level analyses to address the following DOE 2020 technical targets for automotive fuel cell power systems operating on direct hydrogen.

- Energy efficiency: 60% at 25% of rated power
- Q/ΔT: 1.45 kW/°C
- Power density: 850 W/L for system, 2,500 W/L for stack
- Specific power: 850 W/kg for system, 2,000 W/kg for stack
- Transient response: 1 s from 10% to 90% of maximum flow
- Start-up time: 30 s from –20°C and 5 s from +20°C ambient temperature
- Precious metal content: 0.125 g/kW$_e$ rated gross power

Accomplishments

- Projected \$44.9/kW$_e$ FCS cost at high volume manufacturing and 0.126 g/kW$_e$ Pt content with high performance d-PtNi/C cathode catalyst, reinforced 14-µm 850 equivalent weight (EW) membrane, and Q/ΔT = 1.45 kW/°C constraint.
- Estimated 10% degradation in net FCS power with 40% decrease in d-PtNi/C cathode catalyst electrochemical surface area (ECSA) (0.05–0.15 mg/cm^2 Pt loading) due to cyclic potentials.

- Showed the possibility of removing cathode humidifier if MEA membrane is <14-µm thick, and stack inlet pressure is 2.5 atm or higher.
- Demonstrated through a computational fluid dynamic model that H_2 recirculation blower can be eliminated by using a pulse ejector and maintaining <20% N_2 mole fraction to avoid fuel starvation.
- Evaluated extreme conditions (cell voltage, manufacturing volume, Q/ΔT constraint) where high stack inlet pressures (4 atm) may offer advantages.

✧ ✧ ✧ ✧ ✧

INTRODUCTION

While different developers are addressing improvements in individual components and subsystems in automotive fuel cell propulsion systems (i.e., cells, stacks, balance-of-plant components), we are using modeling and analysis to address issues of thermal and water management, design-point and part-load operation, and component-, system-, and vehicle-level efficiencies and fuel economies. Such analyses are essential for effective system integration.

APPROACH

Two sets of models are being developed. The GCtool software is a stand-alone code with capabilities for design, off-design, steady state, transient, and constrained optimization analyses of FCS. A companion code, GCtool-ENG, has an alternative set of models with a built-in procedure for translation to the MATLAB/SIMULINK platform commonly used in vehicle simulation codes, such as Autonomie.

RESULTS

We implemented a formal methodology for developing an integral cell model using differential cell data [1]. As outlined in Figure 1a, it consists of taking polarization data at different operating conditions, and determining the cathode catalyst layer (CCL) ionic conductivity (σ_c) and high-frequency resistance (R_Ω^m) from the impedance (EIS) data in H_2/N_2 and Pt oxide formation (θ) and kinetics from the cyclic voltammetry data. Knowing σ_c and θ, a model for distributed oxygen reduction reaction (ORR) kinetic (η_s^c) and ionic overpotentials (iR_Ω^c) is constructed using the low current density (i) polarization data at different pressures (P), temperatures (T), O_2 mole fraction (X_{O2}) and relative humidity (RH). Next, the complete set of polarizations is analyzed to determine the mass transfer overpotentials (η_m) at high current densities and to correlate η_m in terms of limiting current density (i_L). Together with ORR kinetic model, η_m correlation can be used in a finite difference model to predict the performance of large integral cells operating non-isothermally at finite stoichiometry with co- or counter-current anode, cathode and coolant flows. Alternatively, η_m correlation can be used to distinguish the individual contributions of gas channel (R_g), gas diffusion layer (R_d), and CCL (R_{cf}) to the overall O_2 mass transport resistance (R_m).

We used the above methodology to determine the mass activity and kinetics of different Pt and Pt alloy catalyst systems for ORR. All the dispersed catalysts in this study used the same high surface-area carbon support, i.e., Ketjen black. Table 1 summarizes the measured mass activities for ORR in H_2/O_2 at 0.9 V (internal resistance [IR]-free), 1-atm O_2 partial pressure, 80°C and 100% RH. It also includes the modeled activities derived from the polarization data at low current densities in H_2/air and H_2/O_2. The important results from this study are briefly discussed below.

- Annealing (a) highly dispersed Pt/C catalyst grows the median size of the nanoparticles from 2–3 nm to 4–5 nm, and reduces ECSA by ~47% [2]. The resulting ~28% decrease in mass activity is less than the reduction in ECSA because the specific activity is higher for larger nanoparticles.
- De-alloyed (d) $PtNi_3$/C catalyst has undergone the same thermal treatment as a-Pt/C catalyst, has nearly the same particle size, but has 40–100% higher mass activity [2]. The wide disparity in mass activity data is due to variability in samples with different ionomer EW and I/C ratio.
- PtCo/C alloy catalysts have mass activities comparable to d-PtNi/C. The three PtCo/C catalyst systems listed in Table 1 had similar mass activities even though they had different electrode microstructures and the Co contents varied over a wide range [3]. Transmission electron microscopy analysis of the high-Co content (H) catalyst electrode, 0.2 mg/cm^2 Pt loading, showed a "spongy" porous (hollow) catalyst nanoparticle morphology with ~6.7 nm median Pt-Co particle size after conditioning. The medium-Co content (M) catalyst electrode, 0.1 mg/cm^2 Pt loading, showed a crystalline fully alloyed catalyst nanoparticle morphology with ~4.4 nm particle size after conditioning. The low-Co content (L) catalyst electrode, 0.1 mg/cm^2 Pt loading, also showed catalysts with a fully alloyed crystalline morphology with ~4.5 nm median particle size.
- Binary d-Pt_3Ni_7/NSTF catalyst has 80–100% higher mass activity than the baseline $Pt_{68}(CoMn)_{32}$/NSTF catalyst [4,5]. Higher ECSA and improved specific activity contribute almost equally to the increase in mass activity of the binary NSTF catalyst over the baseline ternary catalyst. Addition of the dispersed Pt/C cathode interlayer increases ECSA but does not improve the mass activity.

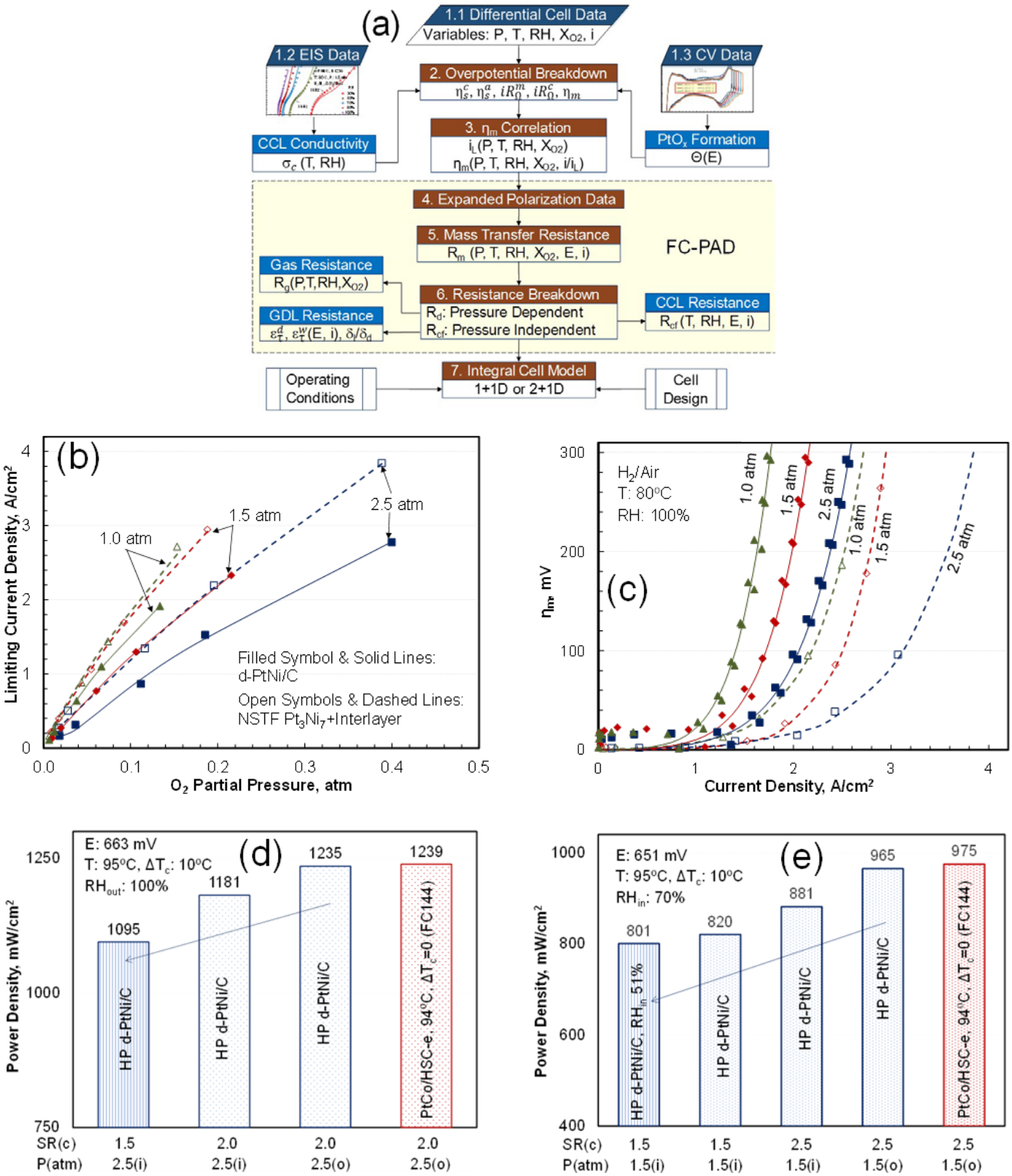

GDL – gas diffusion layer

FIGURE 1. Stack model development methodology and calibration: (a) methodology for development of integral cell model using differential cell data; (b) dispersed and NSTF electrodes: i_L; (c) dispersed and NSTF electrodes: η_m; (d) calibration of d-PtNi/C cathode model at 2.5 atm; (e) calibration of d-PtNi/C cathode model at 1.5 atm

TABLE 1. Mass Activities of Pt and Pt Alloy Catalyst Systems [2–5]

Cathode Catalyst	Ionomer EW (I/C)	L_{Pt}(c)	Cathode ECSA	Mass Activity Data	Mass Activity Model
		mg/cm^2	m^2/g	A/g$_{Pt}$	A/g$_{Pt}$
Dispersed De-alloyed Catalyst (FC106, 12.25-cm^2 cell)					
d-$PtNi_3$/C	850 (1.0)	0.1	64±11	500±100	650±120
Baseline Annealed Pt Catalysts (FC106, 12.25-cm^2 cell)					
a-Pt/C	1100 (0.8, 1.2)	0.104	48±4	312±24	319±30
Baseline Dispersed Pt Catalysts (FC106, 12.25-cm^2 cell)					
Pt/C	1100 (0.8)	0.092	90±8	432±22	456
Dispersed PtCo Catalysts (FC-PAD, 50-cm^2 cell)					
$Pt_{60}Co_{40}$/C	(0.34)	0.21	42.4	745	763
$Pt_{70}Co_{30}$/C	(0.9)	0.1	42.4±0.7	659	623
$Pt_{85}Co_{15}$/C	(0.9)	0.1	42.4	760	661
NSTF Catalysts (FC104, 50-cm^2 cells, 5-cm^2 for binary catalyst with CI)					
$Pt_{68}(CoMn)_{32}$/NSTF	None	0.1	9.8	180	190
d-Pt_3Ni_7/NSTF	None	0.125	14.5±0.7	330±30	392
d-Pt_3Ni_7/NSTF + Cathode Interlayer (CI)	None	0.096 + 0.016 (CI)	22±3	380±60	334

- The modeled mass activity can be different than the measured values, up to 50% for d-$PtNi_3$/C. However, the calculated polarization curves for H_2/air in the kinetic region using the modeled mass activity and other kinetic constants are in good agreement with the experimental data.

We also used the above methodology to determine the limiting current densities (i_L) and mass transfer overpotentials (η_m) for the alloy catalyst systems listed in Table 1. Figures 1b and 1c compare i_L and η_m for the dispersed d-$PtNi_3$/C and binary d-Pt_3Ni_7/NSTF electrodes in differentials cells. At 80°C, i_L are considerably higher and η_m are significantly lower in the thin NSTF electrode (<1 µm thick) than the thick dispersed catalyst electrode (~7–10 µm thick).

We calibrated the performance model for d-PtNi/C cathode catalyst with 50-cm^2 cell data for d-PtCo/C catalyst, finite cathode/anode stoichiometry and operating temperature needed to satisfy the Q/ΔT constraint [6]. Figure 1c shows the measured power densities for PtCo/C alloy catalysts at 95°C and 100% outlet RH for two combinations of outlet pressures and cathode stoichiometry (SR), 1239 mW/cm^2 at 663 mV, 2.5 atm and SR(c) = 2.0, and 975 mW/cm^2 at 652 mV, 1.5 atm and SR(c) = 2.5. Also shown are modeled results for PtNi/C alloy catalyst that has similar ECSA, mass activity and Pt loadings, 0.025/0.1 mg/cm^2 on anode/cathode, and 10°C rise in coolant temperature (ΔT_c). The chemically-stabilized reinforced membrane (14-µm dry thickness, 850 EW) was chosen to have similar high frequency resistance, ~42 mΩ.cm^2. The model was aligned with the experimental data by increasing the limiting current density by 20% to reflect more accessible pores in the high surface-area carbon support for the PtCo/C alloy catalyst. The modeled electrode sheet resistance compares well with the measured value, 47 mΩ.cm^2 at 100% RH. System analysis results are generally quoted at specified stack inlet rather than outlet pressures in which case the model indicates 4.4% decrease in power density at 2.5 atm and 8.7% decrease at 1.5 atm. System analysis shows lower FCS cost at SR(c) = 1.5 for which SR(c) the modeled power density further decreases by 7.3% to 1,095 mW/cm^2 at 2.5 atm and by 6.9% to 820 mW/cm^2 at 1.5 atm. System analysis also shows lower FCS cost under drier conditions (70% outlet RH) for 1.5 atm stack inlet pressure in which case the power density further decreases by 2.3% to 801 mW/cm^2.

Figure 2 summarizes the projected cost ($/kW$_e$) and performance (g$_{Pt}$/kW$_e$) of 80-kW$_e$ FCS with d-PtNi alloy catalyst supported on high surface area carbon with accessible pores as in Figure 1c. At 2.5 atm stack inlet

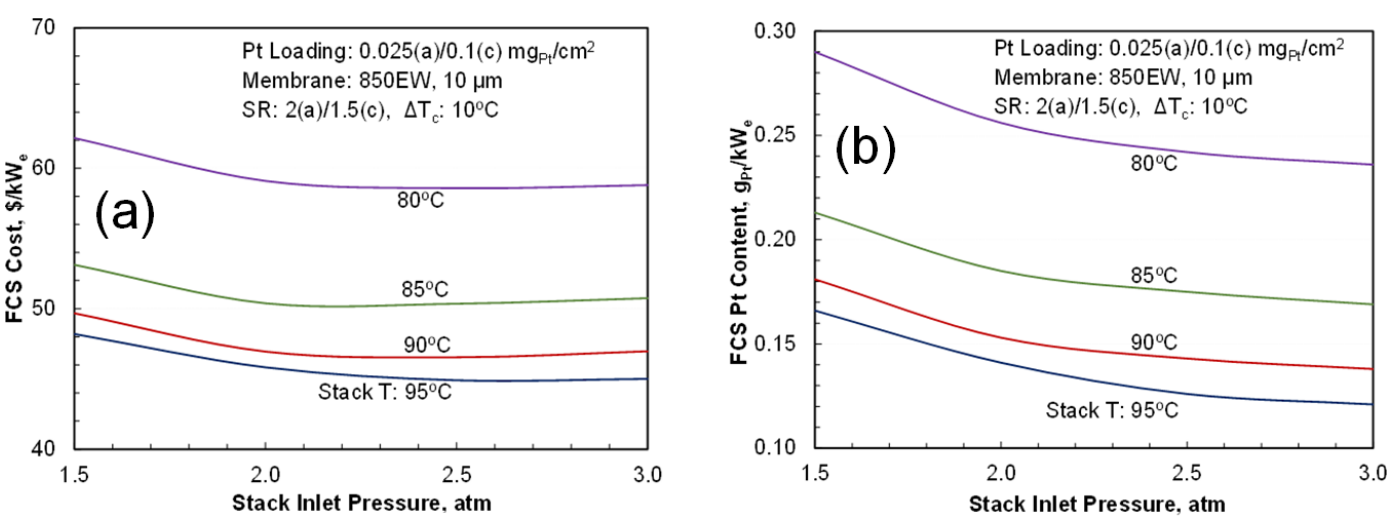

FIGURE 2. Projected cost and performance of automotive fuel cell systems with de-alloyed cathode catalyst: (a) projected cost of FCS with d-PtNi/C cathode; (b) projected Pt content with d-PtNi/C cathode

pressure, the projected cost at high volume manufacturing (500,000 units/yr) is less than \$45/kW$_e$ [7] and the stack Pt content exceeds the 2020 target of 0.125 g_{Pt}/kW_e (see Table 2). Pending demonstration in full-size stacks, these results are considered landmark accomplishments for automotive fuel cell systems.

TABLE 2. Projected Performance of Air Management Subsystem, Stack, and FCS

T: 95°C		Stack Gross				FCS Net	
P	CEM Power	Current Density	Cell Voltage	Power Density	Stack Pt Content	Pt Cost	Stack Cost
atm	kW$_e$	A/cm^2	mV	mW/cm^2	g$_{Pt}$/kW$_e$	\$/kW$_e$	\$/kW$_e$
3.0	8.8	1.735	670	1162	0.108	5.8	18.6
2.5	7.0	1.651	663	1095	0.114	6.1	19.2
2.0	5.5	1.457	657	956	0.131	6.8	21.1
1.5	4.1	1.231	651	801	0.156	8.0	24.2

CEM – compressor-expander-motor

Figure 3 summarizes results of a study to determine the optimum Pt loading in d-PtNi/C cathode. With Q/ΔT= 1.45 kW/°C constraint and bipolar plate temperature restricted to 95°C, the cell voltage is mainly a function of the operating pressure, 663 mV at 2.5 atm and 651 mV at 1.5 atm, and the total overpotential is nearly independent of Pt loading. Figures 3a and 3b show that the current density adjusts such that the mass transfer overpotentials (η_m) are similar, but the higher cathode overpotentials ($\eta_c = \eta_s^c + iR_\Omega^c$) at lower Pt loadings are compensated by the corresponding lower Ohmic overpotentials (iR_Ω^m). Figures 3c and 3d show that the resulting power density is about 33% lower at 0.05 mg/cm^2 than at 0.15 mg/cm^2 Pt loading but the overall cost differences are small. Thus, even though the overall FCS cost is smallest for 0.10 mg/cm^2 Pt loading in cathode, other factors such as packaging and durability may favor higher Pt loadings.

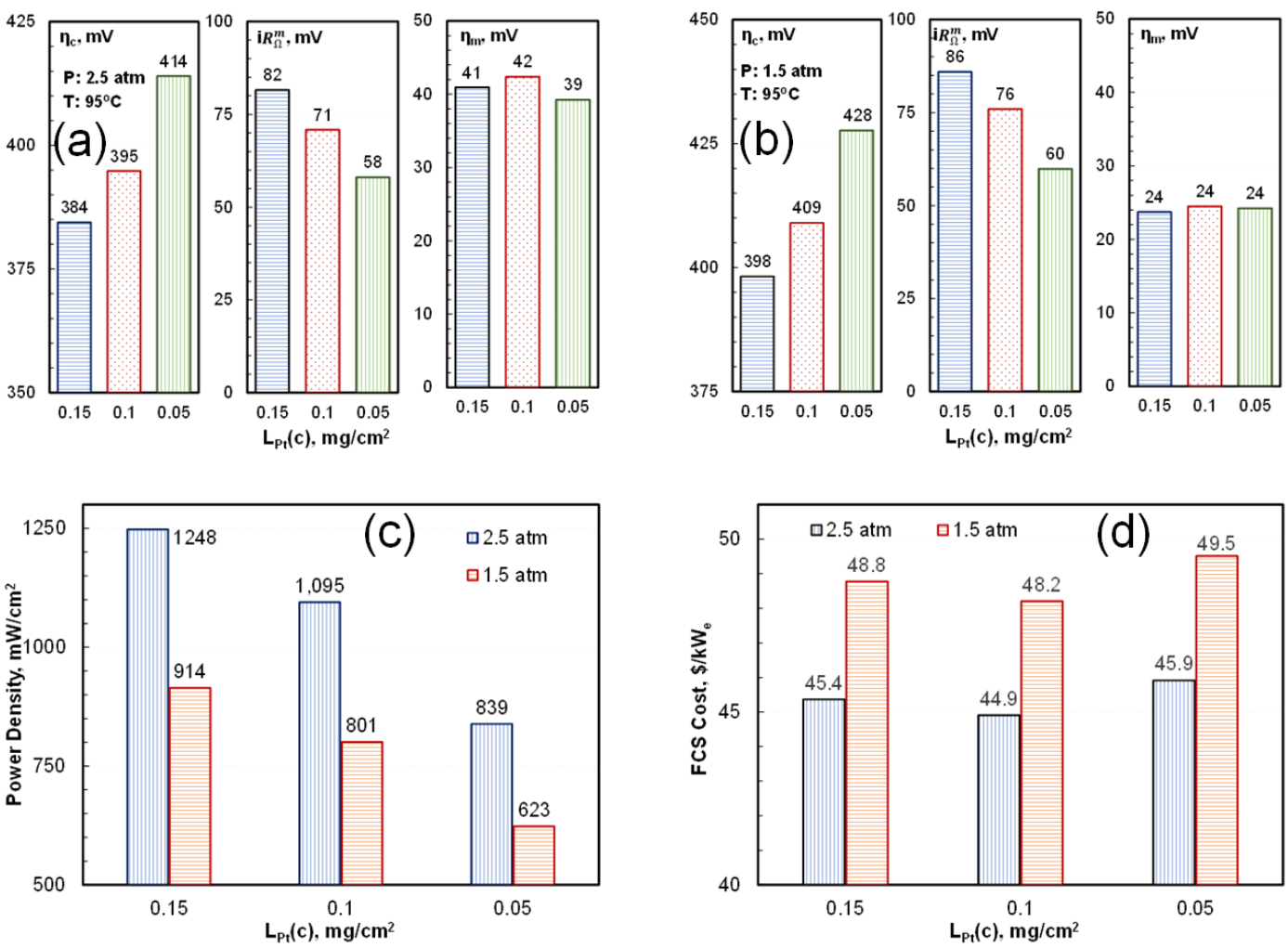

FIGURE 3. Optimum Pt loading (L_{Pt}) in d-PtNi/C cathode electrode: (a) cell overpotentials, 2.5 atm inlet pressure; (b) cell overpotentials, 1.5 atm inlet pressure; (c) stack power density; (d) projected FCS cost

Durability of MEAs with d-PtNi/C Catalysts

We investigated the durability of d-PtNi/C electrodes by analyzing the data acquired in FC-106 project [2] using differential cells subjected to 30,000 trapezoid (0.6–0.95 V, 700 mV/s) and triangle (0.6–0.925 V, 50 mV/s) cycles in H_2/N_2. The trapezoid cycle mimics the new catalyst durability protocol: 0.6 V lower potential limit, 0.95 V upper potential limit, and 700 mV/s scan rate. The triangle cycle shares many features of the old catalyst durability protocol: 0.6 V lower potential limit, 0.925 V upper potential limit, and 50 mV/s scan rate. Figure 4a shows that catalyst durability, as characterized by transition metal and ECSA retention, is worse under the trapezoid cycle that has higher upper potential limit and scan rate than the triangle cycle. Extensive intra-cycle diagnostics also has adverse impact on catalyst durability.

Wide angle X-ray scattering measurements indicate extensive leaching of the transition metal (Ni) that depends on the duty cycle in much the same way as ECSA loss, although the mechanisms are entirely different. Even with >90% Ni loss from the alloy catalyst, Figure 4b indicates <10% degradation in catalyst specific activity (SA), suggesting that only a small amount of Ni may be needed in alloy to enhance the ORR activity of Pt catalysts. Besides Ni loss, degradation in SA should also depend on growth of catalyst particle size with cycling. Lacking sufficient data and recognizing that ECSA loss (ΔA_{Pt}) is related to Ni loss and particle size growth, we find it convenient to correlate the degradation in SA with ΔA_{Pt}.

Figure 4c shows the correlation in mass activity degradation with ECSA loss. The degradation in mass activity (product of SA and A_{Pt}) is more than linear with ΔA_{Pt} because, as noted above, SA also decreases with ECSA loss.

Employing procedures developed earlier, we determined the limiting current densities (i_L) and mass transfer overpotentials (η_m) for d-PtNi/C electrodes using the polarization curves obtained at beginning of test and after 30,000 potential cycles. Figure 4d shows that the effect of potential cycling on limiting current density can be captured by correlating with catalyst roughness (S_{Pt}) which is the product of ECSA and Pt loading.

Using the data in Figures 4b–4d, we conducted system analysis to determine the acceptable loss in ECSA to satisfy the target of limiting net FCS power loss to less than 10% after 5,000 h. Figure 4e presents FCS net power, 80 kW_e at beginning of life, as a function of ΔA_{Pt} for three Pt loadings in d-PtNi/C cathodes. We conclude that the target of 10% derating in net FCS power over lifetime can be met by limiting ECSA loss to <40% for 0.1 mg/cm^2 Pt loading in cathode. There is only a small dependence of acceptable ECSA loss on Pt loading although Pt loading may affect ECSA loss over cyclic potentials and during startup/shutdown. Regardless of Pt loading, Figure 4f shows that increase in kinetic and mass transfer overpotentials contribute equally to voltage loss. Future work will consider additional degradation mechanisms involving other components (membrane, catalyst support) and fuel/air impurities.

CONCLUSIONS AND UPCOMING ACTIVITIES

- We have formalized a methodology for developing an integral cell model using differential cell data. It provides a consistent basis for determining ORR kinetic parameters, mass transfer overpotentials, and distinguishing O_2 mass transfer resistances in the gas channel, diffusion medium and cathode catalyst layer.
- We demonstrated that a low-PGM alloy catalyst (0.125 mg/cm^2 total Pt loading in anode and cathode) supported on an advanced high surface area carbon support with tailored pore size distribution can achieve power densities exceeding the 2020 target of 1,000 mW/cm^2 at lower than 0.125 g/kW_e PGM content under operating conditions (95°C, <100% outlet RH, SR(c) = 1.5, 2.5 atm stack inlet pressure) required to meet the heat rejection constraint (Q/ΔT: 1.45 kW/°C).
- Analysis of the complete fuel cell system with the above alloy catalyst and carbon support and passive anode gas recirculation leads us to project \$45/kW_e FCS cost at high volume manufacturing. Pending demonstration in full-size stacks, these results are considered landmark accomplishments for automotive fuel cell systems.
- We developed a model for alloy catalyst durability under cyclic potentials and used it to determine the acceptable loss in ECSA to satisfy the target of limiting net FCS power loss to less than 10% after 5,000 h. We concluded that the target of 10% derating in net FCS power over lifetime can be met by limiting ECSA loss to <40% for 0.1 mg/cm^2 Pt loading in cathode. There is only a small dependence of acceptable ECSA loss on Pt loading although Pt loading may affect ECSA loss over cyclic potentials and during startup/shutdown.
- Our future work will focus on verifying the above conclusions by obtaining differential cell data with d-PtCo/C catalyst supported on surface area carbon with tailored pore size distribution. We will also analyze the durability of this catalyst system under cyclic potentials.

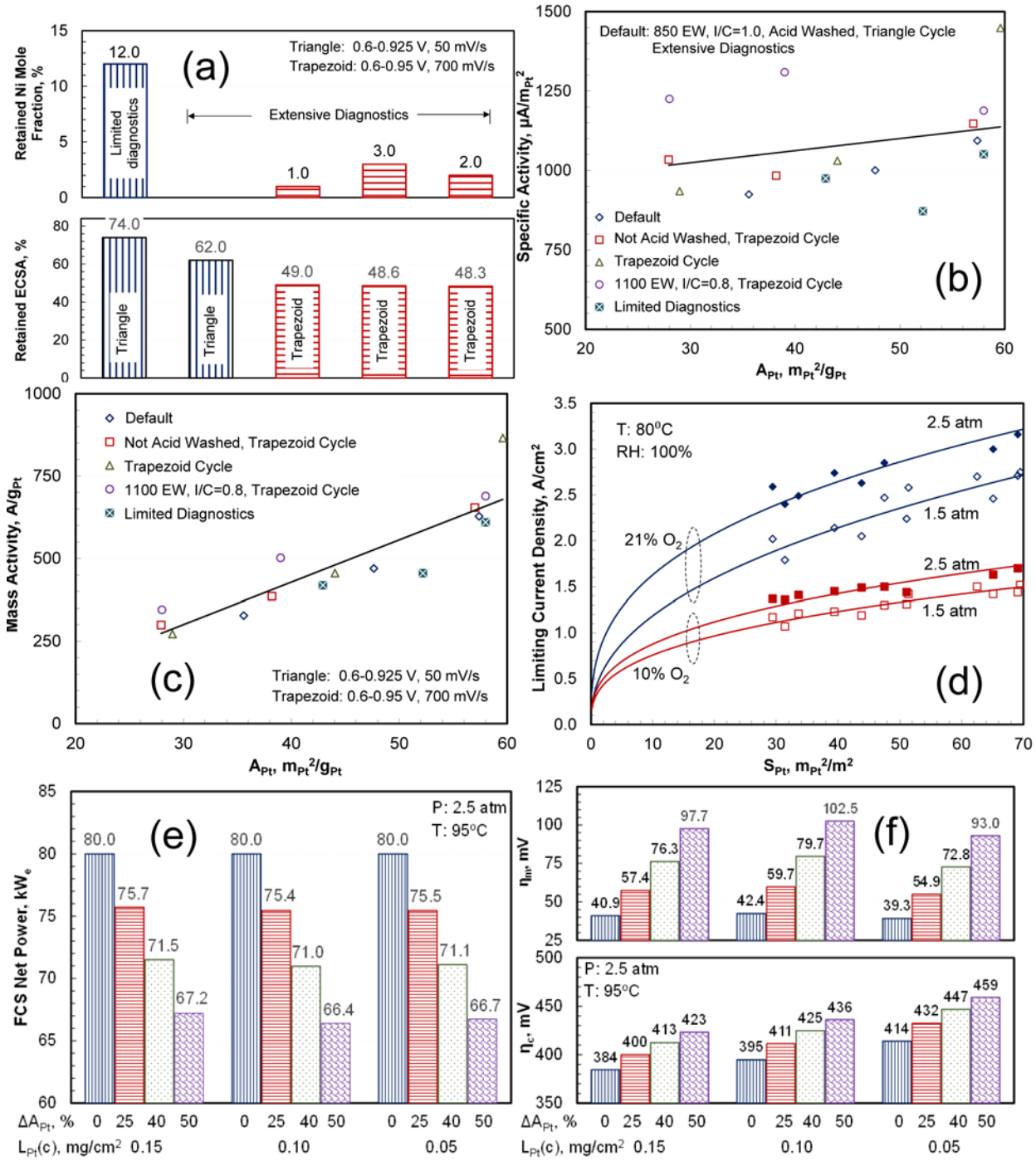

FIGURE 4. Stability of alloy catalysts and projected FCS performance degradation: (a) retention of transition metal and ECSA under cyclic potentials; (b) specific activity degradation; (c) mass activity degradation; (d) limiting current density degradation; (e) performance degradation; (f) increase of overpotentials with aging

FY 2017 PUBLICATIONS/PRESENTATIONS

1. R.K. Ahluwalia, X. Wang, and A.J. Steinbach, "Performance of Advanced Automotive Fuel Cell Systems with Heat Rejection Constraint," Journal of Power Sources, Vol. 309, pp. 178–191, 2016.

2. R.K. Ahluwalia, J.-K. Peng, X. Wang, D.A. Cullen, and A.J. Steinbach, "Long-Term Stability of Nanostructured Thin Film Electrodes at Operating Potentials," Journal of the Electrochemical Society, Vol. 164(4), pp. F306–F320, 2017.

3. F.C. Cetinbas, R.K. Ahluwalia, N. Kariuki, et al., "Hybrid Approach Combining Multiple Characterization Techniques and

Simulations for Microstructural Analysis of Proton Exchange Membrane Fuel Cell Electrodes," Journal of Power Sources, Vol. 344, pp. 62–73, 2017.

4. R.K. Ahluwalia, X. Wang, J-K Peng, and C.F. Cetinbas, "Fuel Cells Systems Analysis," U.S. DRIVE Fuel Cell Tech Team Meeting, Southfield, MI, May 18, 2016.

5. C.F. Cetinbas, R.K. Ahluwalia, N. Kariuki, D.J. Myers, V.J. De Andrade, "Hybrid Approach for PEM Fuel Cell Electrode Microstructural Analysis," ElectroCat Workshop, Argonne National Laboratory, Argonne, IL, July 26, 2016.

6. D. Myers, N. Kariuki, R. Ahluwalia, X. Wang, C.F. Cetinbas, and J.-K. Peng, "Performance and Stability of MEA for PEMFC with Pt Alloy Cathode Catalyst," IEA Annex 34 Meeting, Beijing, China, November 9, 2016.

7. R.K. Ahluwalia, V. Weissbecker, C. Wang, S. Hirano, H. Bramfeldt, and H. Ljungcrantz, "Bipolar Plates for Automotive Fuel Cells: Annex 34 Summary Report," IEA Annex 34 Meeting, Beijing, China, November 9, 2016.

8. R.K. Ahluwalia and N.L. Garland, "Reports from the Annexes: Annex 34," IEA AFC ExCo 53rd Meeting, Beijing, China, November 10–11, 2016.

9. R.K. Ahluwalia, D.D. Papadias, X. Wang, R. Borup, R. Mukundan, M. Brady, J. Thompson, H. Wang, and J. Turner, "Modeling Performance and Stability of Bipolar Plates for Automotive Fuel Cells," DOE 2017 Bipolar Plates Workshop, Southfield, MI, February 14, 2017.

10. R. Borup, R. Mukundan, T. Rockward, M. Brady, J. Thompson, D.D. Papadias, R.K. Ahluwalia, H. Wang, and J. Turner, "Metal Bipolar Plate Testing," DOE 2017 Bipolar Plates Workshop, Southfield, MI, February 14, 2017.

11. R.K. Ahluwalia, "IEA Advanced Fuel Cells Annex 34: Fuel Cells for Transportation," Beijing, China, November 9, 2016.

REFERENCES

1. R.K. Ahluwalia, X. Wang, and A.J. Steinbach, "Performance of Advanced Automotive Fuel Cell Systems with Heat Rejection Constraint," J. Power Sources 309 (2016) 178–191.

2. D.J. Myers, N. Kariuki, R.K. Ahluwalia, X. Wang, C.F. Cetinbas, and J-K Peng, "Rationally Designed Catalyst Layers for PEMFC Performance Optimization," DOE Hydrogen and Fuel Cells Program, FY 2016 Annual Progress Report, DOE/Go-102017-4891, V.D.3, 1–5.

3. S.S. Kocha, J. Christ, et al., "FC-PAD: Electrode Layer Integration," DOE Hydrogen and Fuel Cells Program, FY 2016 Annual Progress Report DOE/Go-102017-4891, V.D.1, 1–6.

4. A.J. Steinbach, A. Hester, et al., "High Performance, Durable, Low Cost Membrane Electrode Assemblies for Transportation Applications," DOE Hydrogen and Fuel Cells Program, FY 2016 Annual Progress Report, DOE/Go-102017-4891, V.B.3, 1–6.

5. R.K. Ahluwalia, X. Wang, and J-K Peng, "Performance and Durability of Advanced Automotive Fuel Cell Stacks and Systems with Nanostructured Thin Film Catalyst Based Membrane Electrode Assemblies," DOE Hydrogen and Fuel Cells Program, FY 2016 Annual Progress Report, DOE/Go-102017-4891, V.F.5, 1–8.

6. A. Kongkanand, "Highly Accessible Catalysts for Durable High-Power Performance," DOE Hydrogen and Fuel Cells Program, 2017 Annual Merit Review and Evaluation Meeting, FC144, Washington, DC, June 5–9, (2017).

7. B.D. James, J.M. Huya-Kouadio, C. Houchins, and D.A. DeSantis, "Fuel Cell Vehicle and Bus Cost Analysis," DOE Hydrogen and Fuel Cells Program, FY 2016 Annual Progress Report, DOE/Go-102017-4891, V.F.6, 1–5.

V.E.5 Fuel Cell Vehicle Cost Analysis

Brian D. James (Primary Contact),
Jennie M. Huya-Kouadio, Cassidy Houchins,
Daniel A. DeSantis
Strategic Analysis, Inc. (SA)
4075 Wilson Blvd., Suite 200
Arlington, VA 22203
Phone: (703) 778-1114
Email: bjames@sainc.com

DOE Manager: Adria Wilson
Phone: (202) 586-5782
Email: Adria.Wilson@ee.doe.gov

Contract Number: DE-EE0007600

Subcontractors:
- Argonne National Laboratory (ANL), Argonne, IL
- National Renewable Energy Laboratory, Golden, CO

Project Start Date: October 1, 2016
Project End Date: September 30, 2021

Overall Objectives

- Provide thorough, annually updated assessment of the technical status of current on-road and advanced (2020 and 2025) proton exchange membrane (PEM) fuel cell (FC) power systems for light-duty vehicles (LDVs), medium and heavy-duty vehicles (MDVs/HDVs), and buses, detailed to the extent necessary to track system performance and manufacturability.
- Report cost estimates of the fuel cell systems (FCSs) described above to reflect optimized components and manufacturing processes at various rates of production, and to update these on an annual basis.
- Conduct sensitivity analyses of FCS cost and identify key system cost parameters with the goal of fully understanding the cost drivers.
- Identify most promising pathways to system/lifecycle cost reduction.
- Perform review of all components of the analysis, both internally and with the help of perspectives external to the project, and document analysis assumptions and results through various media (presentations and a complete, comprehensive report).

Fiscal Year (FY) 2017 Objectives

- Conduct model validation of currently manufactured, representative, industry accepted hydrogen FCSs, subsystems, or components for production passenger vehicles.
- Update 2016 automotive FCS cost projections to reflect the latest performance data and system design information.
- Extend automotive cost projections to 2020 and 2025 future year analyses.
- Conduct an MDV/HDV fuel cell electric truck (FCET) scoping study to identify the system(s) for study in subsequent years (e.g., issues, power level, architecture, level of hybridization).

Technical Barriers

This project addresses the following technical barriers from the Fuel Cells section of the Fuel Cell Technologies Office Multi-Year Research, Development, and Demonstration Plan.

(B) Cost

Technical Targets

TABLE 1. DOE Technical Targets for 80-kW_{net} Integrated Transportation Fuel Cell Power Systems Operating on Direct Hydrogen

Characteristic	Units	Project Status	DOE 2020 Targets	DOE Ultimate Target
Cost of Transportation FC Power Systems[1]	$/$kW_{net}$	45	40	30
Cost of Transportation FC Stacks[1]	$/$kW_{net}$	19	20	15
Cost of Bipolar Plates[1]	$/$kW_{net}$	5	3	NA

[1]Based on high production volume of 500,000 vehicles per year.
NA - not applicable

FY 2017 Accomplishments

- Projected the FCS cost for an 80 kW_{net} LDV application using a Design for Manufacture and Assembly (DFMA®) methodology at annual production rates of 1,000 to 500,000 FCSs per year.
- Projected a cost reduction (~$7.50/$kW_{net}$) from improved electrochemical performance (749 mW/cm^2 to 1,095 mW/cm^2) made possible by use of a General Motors (GM) high surface area carbon (HSC) support in conjunction with a platinum cobalt on carbon (PtCo/C) cathode catalyst.
- Estimated the automotive FCS cost to be $45/$kW_{net}$ for 2017, $43/$kW_{net}$ for 2020, and $36/$kW_{net}$ for 2025 at 500,000 vehicles produced per year.

- Cost modeled the Toyota Mirai FCS (88.5 kW_{net}, 114 kW_{gross}), estimating FCS materials and manufacturing cost at \$183/kW_{net} and a total projected sales price of \$56,965 at 3,000 systems per year (sys/yr) (compared to Toyota's manufacturer's suggested retail price (MSRP) of \$57,500).

✧ ✧ ✧ ✧ ✧

INTRODUCTION

This project assesses the cost and performance impact of research advancements on FCs for transportation applications using a DFMA®-style [1] cost analysis methodology. Results from this analysis provides assistance to the Fuel Cell Technologies Office in assessing the impact of current project portfolios and in identifying areas where R&D is still needed to address shortfalls in meeting cost targets. Low temperature PEM FCSs operating on hydrogen with peak electrical capacities of current (2017) and future (2020 and 2025) 80 kW_{net} for LDV, and MDV/HDV applications are analyzed. Onboard compressed hydrogen storage, battery energy storage, and traction drive motor subsystems are not included in this cost assessment. The impact of annual production rates on the cost of the automotive and truck systems is examined to assess the difference between a nascent and a mature product manufacturing base. LDV FCSs are analyzed at six annual production rates: 1,000, 10,000, 20,000, 50,000, 100,000, and 500,000 FCSs per year. DFMA® analysis of MDV/HDV systems will be conducted in 2018 at annual production rates between 1,000 and 250,000 FCSs per year.

This 2017 work focused primarily on a continuation of a previous DOE award (DE-EE0005236 between 2011 and 2016). Existing FCS DFMA® cost models for current and future year LDV system designs were analyzed, and a scoping study of the system design parameters for MDV/HDV FCSs was conducted. Stack and balance of plant designs and performance parameters are discussed, and the methods of modeling each are explained. New technologies, materials data, and optimization modeling are incorporated to provide updated system cost. Cost trends are evaluated in terms of the capital costs per unit of installed electrical capacity (\$/kW_{net}) and system annual production rate.

APPROACH

A DFMA®-style analysis is conducted to estimate the manufacturing cost of PEM FCSs for 80 kW_{net} LDVs at various manufacturing production rates. The optimum stack operating conditions and operating point are selected in collaboration with ANL and the Fuel Cell Tech Team. ANL first principles models of FC stack operating conditions [2] and SA DFMA® cost models are used to identify cost and performance optimized conditions, which are vetted by the Fuel Cell Tech Team. Output from the ANL model provides insight into cell voltage, stack pressure, cathode catalyst loading, air stoichiometry, and stack outlet coolant temperature while the DFMA® cost model provides insight into cost and performance tradeoffs. The FCS is sized to provide 80 kW_{net} based on rated power operating parameters. System performance is based on performance estimates of individual components, built up into an overall system energy budget.

DFMA® process-based cost estimation techniques are applied to the major system components (and other specialty components) such as the FC stack, membrane humidifier, air compressor/expander/motor unit, and hydrogen recirculation ejectors. For each of these, a manufacturing process train details the specific manufacturing and assembly machinery, and processing conditions are identified and used to assess component cost.

RESULTS

A blend of the final 2016 system cost results (reported for the first time) and 2017 system cost results are described in this report.

2016 and 2017 Automotive System Cost

The operating conditions and assumptions used to project costs for the 2016, 2017, 2020, and 2025 auto systems are summarized in Table 2. A significant reduction in projected system cost occurred between 2016 and 2017 (from \$53/kW_{net} to \$45/kW_{net} at 500,000 sys/yr) primarily due to an increase in power density from 749 mW/cm^2 to 1,095 mW/cm^2 with a simultaneous decrease in total Pt loading (0.134 mg/cm^2 to 0.125 mg/cm^2). The difference in performance and Pt loading is based on a recent GM study [3] where a proprietary HSC was used for the support of a PtCo/C cathode catalyst. In 2016, ANL modeled de-alloyed PtNi/C catalyst performance for optimized conditions. In 2017, PtCo/C cathode catalyst was used for the baseline. Although ANL had not modeled PtCo/C for optimized conditions, there was a consensus between ANL and GM that de-alloyed PtNi/C (used as the 2016 catalyst) would have similar performance to a PtCo/C (used for the 2017 and 2020 catalysts) if both catalysts were supported by GM's proprietary HSC support. The similarity in performance is due to the expectation of similar cathodic kinetic reaction rates whether using PtNi or PtCo. The PtCo synthesis process was not conveyed in detail to SA, but GM states that it would be very similar to that of PtNi. Consequently, the 2017 and 2020 catalyst synthesis cost is based on de-alloyed PtNi/C.

2020 and 2025 Future Automotive system Cost

The system parameters chosen for the 2020 year analysis assume reasonable and attainable performance

TABLE 2. PEM FC Auto Systems Operating Conditions and Assumptions

Auto System Year	2016	2017	2020	2025
System Gross Power (kW_{net})	87.68	87.90	87.90	87.90
System Net Power (kW_{net})	80	80	80	80
Power Density (mW/cm^2)	749	1,095	1,165	1,500
Cell Voltage (mV)	659	663	663	663
Stack Temp (Coolant Exit Temp) (°C)	94	94	94	94
Pressure (atm)	2.5	2.5	2.5	2.5
Pt Loading (mg/cm^2)	0.134	0.125	0.125	0.088
Platinum Group Metal Total Content (g/ kW_{gross})	0.191	0.124	0.116	0.064
Air stoichiometry	1.4	1.5	1.5	1.5
Cathode Catalyst System*	Disp. d-PtNi/C	Disp. PtCo/ HSC-e	Disp. PtCo/ HSC-f	Disp. Adv. High Perf. Catalyst
Cells per System	379	377	377	377
Total System Cost ($/$kW_{net}$) (100,000 sys/yr)	$59	$50	$47	$40
Total System Cost ($/$kW_{net}$) (500,000 sys/yr)	$53	$45	$43	$36

* Disp. = Dispersed. All years assume dispersed Pt/C on the anode.

and manufacturing methods that have been demonstrated at the lab scale. In contrast, the system parameters for the 2025 year system are based on aggressive or optimistic technology advances, i.e., advances that might be possible in approximately 2025 if there was a focused and well-funded effort (or possibly in a later year if development efforts are not focused or well-funded). Figure 1 shows the key system assumptions and resulting cost for each system evaluated.

Between the current and future year studies, performance is assumed to increase while simultaneously reducing Pt loading. The system designs are very similar with the exception of the hydrogen recirculation system changing. The 2016 and 2017 systems include two fixed geometry ejectors to supply recirculation of H_2 while the 2020 and 2025 systems assume a pulsed ejector (injector upstream of the ejector) that is able to achieve the targeted H_2 recirculation even at the low flow conditions of FC part power operation (rather than using a battery at very low power). Even with multiple improvements in the performance and simplified system, the 2020 auto system cost ($43/$kW_{net}$ at 500,000 sys/yr) does not meet the 2020 DOE target of $40/$kW_{net}$. It is also noted that achievement of the power density specified for 2025 (1,500 mW/cm^2) may require a new, as yet undeveloped, catalyst.

MDV/HDV Fuel Cell Electric Truck Scoping Study

A scoping study was conducted to define the MDV/HDV FCSs to be cost analyzed in the next year of the project. To determine representative system(s) for MDV/HDV FCETs, information was gathered on current demonstrations of FCETs and to assess their similarities to bus FCSs. ANL provided data from their recent FCET study [4] regarding the power levels required by both MDV/HDV trucks. The

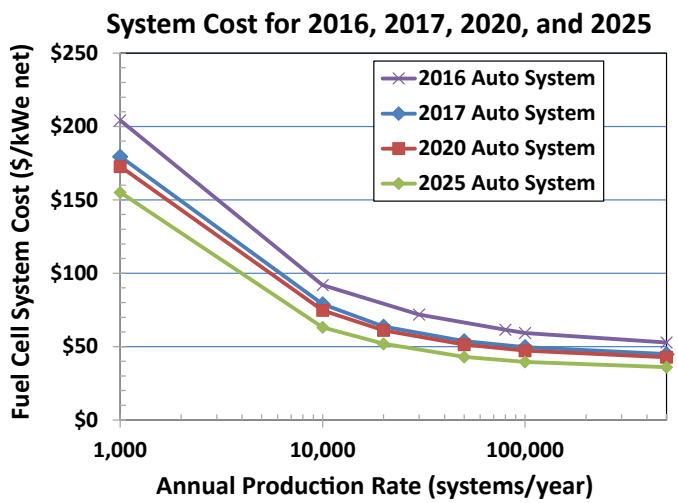

FIGURE 1. System cost for 2016, 2017, 2020, and 2025 analyses at all production rates

ANL study was based on commercial fleet vehicle operation data for 12 different applications and weight classes of trucks (seen in Figure 2). All of these trucks, with the exception of the Nikola One truck, are based on a FC dominant system with a battery for peak acceleration events. Although most upcoming demonstrations size the FC for range extension, where the FC charges the battery and the battery is sized for peak power, SA chose FC dominant systems as the baseline type of truck in which to perform a detailed DFMA® cost estimate. In FC dominant systems, the FC is sized for the peak sustained power and the battery is only for power augmentation. Future work may incorporate a comparison for a FC dominant versus a battery dominant system. As

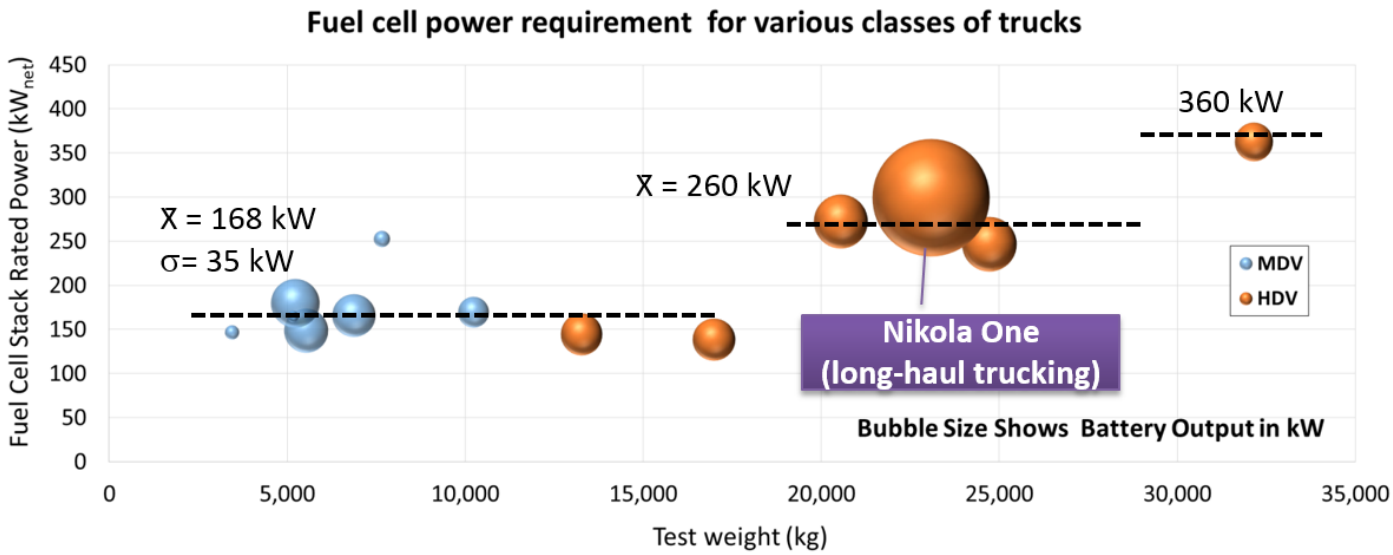

FIGURE 2. FC power requirements for different FCET applications based on vehicle weight

can be seen in Figure 2, three power levels (168 kW, 260 kW, and 360 kW) capture the majority of MDV/HDV FCET applications. Coincidentally, these sizes are approximate multiples of 80–90 kW stacks and thus offer synergies with LDV stacks. Feedback from bus FCS manufacturers suggests that the FCSs in buses, with minor adjustments, could be used in FCETs. Based on this scoping study, the preliminary parameters contained in Table 3 are proposed for possible systems to analyze for the 2018 DFMA® cost study of FC dominant MDV/HDV FCETs. The number and types of systems analyzed will be determined based on additional feedback from system integrators and input from DOE. The remaining FCS parameters will be selected as part of the 2018 analysis.

Model Validation Study

Since Toyota Motor Co. has published numerous open literature reports on the Mirai FC vehicle, the Mirai FCS was selected for a validation study. All data was derived from open sources and Toyota did not provide input specifications or comment on the cost results. Two areas of SA cost model validation are of interest: (1) validation of the system design and (2) validation of the projected system cost. For the validation of system design, SA researched and modeled, to some degree, every component listed by Toyota in publically available documentation. Comparisons were made between SA's baseline automotive system and the Mirai system. Key differences include a projected higher Pt loading, use of titanium bipolar plates (instead of stainless

TABLE 3. PEM FC Bus and MDV/HDV FCET Systems Operating Conditions and Assumptions

	2016 Bus System	2017 MDV System	2017 HDV System
Annual Production (sys/year)	200–1,000	Up to 150,000 (total market) [5]	Up to 250,000 (total market) [5]
Target Stack Durability (hours)	25,000 [6]	25,000 [6] / 5,000 [7]	25,000 [6]
Total Pt loading (mgPt/cm$^2_{total\ area}$)	0.5	0.5	0.5
Pt Group Metal (PGM) Total Content (g/kW$_{gross}$)	0.719	0.719	0.719
Power Density (mW/cm^2)	739	TBD	TBD
Cell Voltage (V/cell)	0.659	prelim. 0.659 (subject to time-at-power analysis)	prelim. 0.659 (subject to time-at-power analysis)
Net Power (kW$_{net}$)	160	~160	240/360
Gross Power (kW$_{gross}$)	195	TBD	TBD
Operating Pressure (atm)	1.9	prelim. 1.9 (to be cost optimized)	prelim. 1.9 (to be cost optimized)
Stack Temp. (Coolant Exit Temp) (°C)	72	72*	72*

*Lower temperature selected for durability
TBD – to be determined; prelim. – preliminary

steel), use of hydrogen recirculation pump, removal of an external humidifier, and other minor differences as discussed in SA's 2016 Annual Progress Report [8]. Since Toyota-supplied cost data was not available, SA validated its cost model projections against the Toyota Mirai's MSRP. To convert DFMA® projected costs into a corresponding sales price, the following assumptions were made: 17% markup for production overhead on the FCS and hydrogen storage system [9], $17,600 for other auto component costs (including battery; electric traction motor; inverter; gear box; glider; regenerative braking system; and heating, ventiliation, and cooling system) [10], 20% markup for marketing and warranty [9], and 9% markup for corporate overhead and profit [9].

As seen in Figure 3, SA examined cost at both 1,000 sys/yr and 3,000 sys/yr production rates, with price projections effectively bracketing Toyota's MSRP of $57,500 for 2017. At 3,000 vehicles per year, SA estimates the FC manufacturing cost to be ~$183/kW$_{net}$ ($16,204 per system) for the 114 kW$_{gross}$ (88.5 kW$_{net}$) Mirai FCS and $6,168 per system for the H_2 storage system. With the markup and overhead rates mentioned previously, this equates to ~$56,965 per system in total projected vehicle price and is an excellent match with Toyota's MSRP of $57,500.

CONCLUSIONS AND UPCOMING ACTIVITIES

- The use of GM's high performing PtCo catalyst on HSC catalyst support lowers automotive FCS projected cost by $7.50/kW$_{net}$ (a 14% reduction from $53 in 2016 to $45/kW$_{net}$ in 2017 at 500,000 sys/yr).
- Future projections for automotive FCS cost are $43/kW$_{net}$ for 2020 and $36/kW$_{net}$ for 2025 at 500,000 sys/yr.
- FCSs for MDV/HDV trucks are expected to be very similar to buses. When designed for FC dominant operation, FCET would utilize multiple 80–90 kW FC stacks. Three possible system sizes of FCSs may be analyzed in 2018 (160 kW$_{net}$, 240 kW$_{net}$, 360 kW$_{net}$) and possible comparison to FC range extenders.
- The SA cost model has been validated against the Toyota Mirai FCS in design and estimated vehicle price ($56,965 compared to Toyota's $57,500 MSRP).
- Future work includes evaluation of an electrospun membrane support material, and ionomer material such as perfluoro imide acid as an alternative to perfluorosulfonic acid.

FY 2017 PUBLICATIONS/PRESENTATIONS

1. James, B.D., Huya-Kouadio, J. M., Houchins, C., "Mass Production Cost Estimation of Direct H2 PEM Fuel Cell Systems for Transportation Applications: 2016 Update," Strategic Analysis report for DOE FCTO, September 30, 2016.

2. James, B.D., Huya-Kouadio, J.M., Houchins, C., "Bipolar Plate Cost and Issues at High Production Rate," presented at the DOE Workshop on Research and Development Needs for Bipolar Plates for PEM Fuel Cell Technologies, Southfield, MI, February 14, 2017.

3. James, B.D., Huya-Kouadio, J.M., Houchins, C., "Fuel Cell Vehicle Cost Analysis," presented to the Fuel Cell Technical Team, Southfield, MI, May 17, 2017.

4. James, B.D., Huya-Kouadio, J.M., Houchins, C., DeSantis, D.A., "2017 [redacted] Review: Fuel Cell Systems Analysis," presented at the 2017 DOE FCTO Annual Merit Review Meeting, Washington, DC, June 8, 2017.

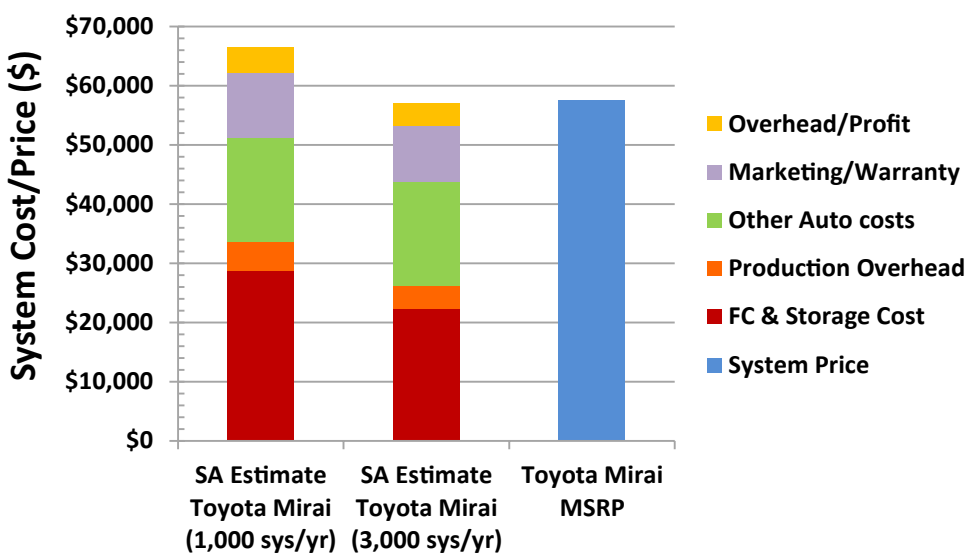

FIGURE 3. Validation of SA's DFMA® model of the Toyota Mirai FC vehicle

REFERENCES

1. Boothroyd, Geoffrey, Peter Dewhurst, and Winston A. Knight. *Product Design for Manufacture and Assembly, Third Edition*. Boca Raton: CRC Press, Taylor & Francis Group, 2011.

2. Ahluwalia, Rajesh, "Fuel Cell Systems Analysis," presented at the DOE Fuel Cell Tech Team, Southfield, MI, July 17, 2017.

3. Anusorn Kongkanand and Mark F. Mathias, "The Priority and Challenge of High-Power Performance of Low Platinum Proton-Exchange Membrane Fuel Cells," *Physical Chemistry Letters* 7 (2016): 1127–1137.

4. Vijayagopal, Ram, "Fuel Cell Electric Truck (FCET) Component Sizing," presented at the 2016 DOE FCTO Annual Merit Review Meeting, Washington, DC, June 7, 2016.

5. Davis, Stacy C., Williams, Susan E., Boundy, Robert G., and Moore, Sheila, "Chapter 4: Heavy Trucks," in *2016 Vehicle Technologies Market Report,* written by Oakridge National Laboratory for the DOE Vehicle Technologies Office, 113–131, 2016. Accessed July 17, 2017. http://cta.ornl.gov/vtmarketreport/pdf/2016_vtmarketreport_full_doc.pdf

6. Spendelow, Jacob and Papageorgopoulos, Dimitrios, "Fuel Cell Bus Targets Record #12012," in DOE FCTO 2012 Fuel Cell Technologies Program Record, September 12, 2012. Accessed July 17, 2017. https://www.hydrogen.energy.gov/pdfs/12012_fuel_cell_bus_targets.pdf

7. "Medium- & Heavy-Duty Fuel Cell Electric Truck: Action Plan for California," report written by the California Fuel Cell Partnership (CAFCP), October 2016. Accessed July 7, 2017. http://cafcp.org/sites/default/files/MDHD-action-plan-2016.pdf

8. James, Brian D., Huya-Kouadio, Jennie M., Houchins, Cassidy, and DeSantis, Daniel A., "Fuel Cell Vehicle and Bus Cost Analysis," Annual Progress Report written by Strategic Analysis Inc. for DOE FCTO, 2016.

9. Vyas, Anant, Santini, Dan, and Cuenca, Roy, "Comparison of Indirect Cost Multipliers for Vehicle Manufacturing," report by Center for Transportation Research, Energy Systems Division, Argonne National Laboratory for DOE Office of Transportation Technologies, April 2000.

10. Greene, David, "Status and Prospects of the Global Automotive Fuel Cell Industry and Plans for Deployment of Fuel Cell Vehicles and Hydrogen Refueling Infrastructure," report by Oak Ridge National Laboratory for the DOE FCTO, July 2013.

VI.0 Manufacturing R&D Sub-Program Overview

INTRODUCTION

The Manufacturing Research and Development (R&D) sub-program supports activities needed to reduce the cost of manufacturing hydrogen and fuel cell systems and components. Manufacturing R&D will enable the mass production of components in parallel with technology development and will foster a strong domestic supplier base. The sub-program's R&D activities address the challenges of moving today's technologies from the laboratory to high-volume, pre-commercial manufacturing to drive down the cost of hydrogen and fuel cell systems. The sub-program focuses on early-stage commercialization needs for the manufacturing of hydrogen and fuel cells, along with necessary components and systems. Reducing cost for components being used now and in the future remains the research investment focus, as well as reducing overall processing times. Progress toward targets is measured in terms of reductions in the cost of producing fuel cells, increased manufacturing processing rates, and growth of manufacturing capacity.

In Fiscal Year (FY) 2017, manufacturing projects continued in the use of rolled goods quality control to detect defects in membrane electrode assembly materials and modeling of the effect of defects on fuel cell material performance. In addition, the sub-program significantly expanded hfcnexus.com, the U.S. Hydrogen and Fuel Cell Directory, showcasing commercial hydrogen and fuel cell products.

GOAL

The sub-program's goal is to reduce the cost of manufacturing hydrogen production, delivery, storage, and fuel cell component systems through research, development, and demonstration.

OBJECTIVES[1]

Key objectives for Manufacturing R&D include:

- Develop manufacturing techniques to reduce the cost of automotive fuel cell stacks at high volume (500,000 units/yr) from the 2008 value of $38/kW[2] to $20/kW by 2020.
- Develop fabrication and assembly processes to produce compressed hydrogen pressure vessels to enable a total onboard storage system cost of $10/kWh for widespread commercialization of hydrogen fuel cell vehicles across most light-duty platforms by 2020, with an ultimate target of $8/kWh.
- Support efforts to reduce the cost of manufacturing components and systems to produce hydrogen at <$4/gge (2007 dollars) (untaxed, delivered, and dispensed) by 2020, compared with the baseline[3] cost estimates for producing, delivering, and dispensing (untaxed) hydrogen in the near-term market of $13/kg–$16/kg (i.e., $13/gge–$16/gge) without incentives.

FY 2017 TECHNOLOGY STATUS AND ACCOMPLISHMENTS

Presently, fuel cell systems are fabricated in small quantities. The cost of a 10-kW, low-temperature polymer electrolyte membrane (PEM) fuel cell system for combined heat and power (CHP) is projected to be ~$1,170/kW at a volume of 50,000 systems/yr.[4] For automotive applications, the cost of an 80-kW PEM fuel cell system is projected to be $50/kW for low-volume manufacturing (100,000 systems/yr) and $45/kW for high-volume manufacturing (500,000 systems/yr). Projected costs include labor, materials, and related expenditures, but do not account for manufacturing R&D investment.

[1] Note: Targets and milestones were recently revised; therefore, individual project progress reports may reference prior targets.
[2] *Mass Production Cost Estimation for Direct H2 PEM Fuel Cell Systems for Automotive Applications: 2008 Update*, Brian D. James and Jeffrey A. Kalinoski, 2009. http://www1.eere.energy.gov/hydrogenandfuelcells/pdfs/mass_production_cost_estimation_report.pdf
[3] *Low Volume Production and Delivery Cost*, Program Record (Hydrogen and Fuel Cells Program) 15011, U.S. Department of Energy, 2015. https://www.hydrogen.energy.gov/pdfs/15011_low_volume_production_delivery_cost.pdf
[4] *A Total Cost of Ownership Model for Design and Manufacturing Optimization of Fuel Cells in Stationary and Emerging Market Applications*, Max Wei, 2016. https://www.hydrogen.energy.gov/pdfs/review16/fc098_wei_2016_o.pdf

Accomplishments in the manufacture of fuel cells and hydrogen storage systems in FY 2017 include the following:

- The Ohio Fuel Cell Coalition held a series of fuel cell supply chain exchanges in conjunction with workshops to facilitate socializing of U.S. fuel cell supply chain companies through regional technical exchange centers and began efforts to organize national standardization efforts.
- Virginia Clean Cities completed significant expansion of the www.hfcnexus.com website (Figure 1), adding a total of 352 companies with a variety of hydrogen and fuel cell components and products to provide supplier information for hydrogen and fuel cell technologies, as well as matchmaking capabilities to introduce suppliers and integrators to each other and advertising capabilities to create a self-sustaining site.

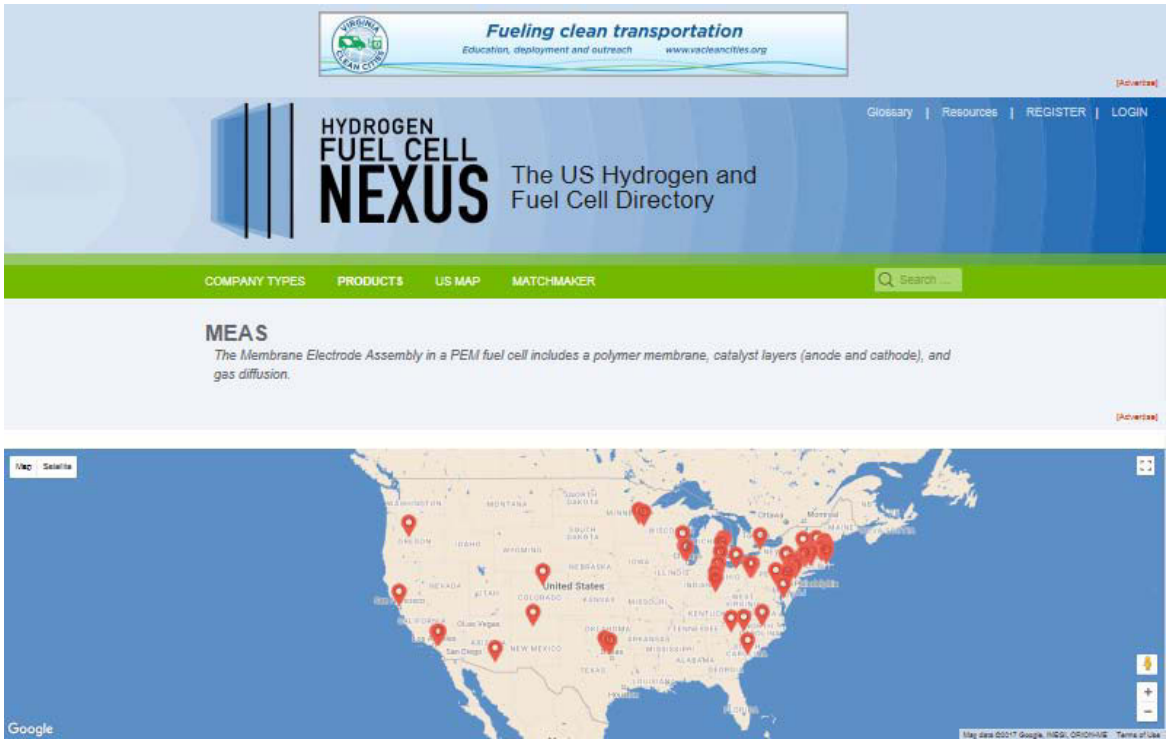

FIGURE 1. www.hfcnexus.com homepage

- GLWN developed a final report and in-depth analysis for five key components (bipolar plates, membranes, gas diffusion layers, catalysts, and hydrogen storage vessels). The drawings were sent to suppliers to obtain price quotations at four vehicle volume levels (1,000; 10,000; 100,000; and 500,000 units/yr). GLWN also completed an analysis of the global fuel cell and hydrogen supply chain to determine opportunities for U.S. competition and expansion.
- Automated Dynamics developed an innovative metal/polymer composite hydrogen pipeline coupler and is now developing and refining the design specification with some metal parts to reduce the possibility of hydrogen embrittlement. The design included mechanical loading, environmental effects, and leak rates. It is passing pressure and leak rate tests and will be subject to testing and analysis to pass fatigue requirements.
- Mainstream developed a small-scale (6-in web width) winder/unwinder to run at 100 ft/min for quality control in roll-to-roll processing of fuel cell membranes. Mainstream also demonstrated an optical system that detected 40 out of 40 100-µm pinhole defects in real time on National Renewable Energy Laboratory's continuous roll-to-roll web line with Nafion211 membrane material at speeds of up to 30 ft/min. With post processing, all defects were successfully identified at web line speeds up to 100 ft/min.
- National Renewable Energy Laboratory identified and tested defective samples, and preliminary results indicated that defects less than 10 µm have no immediate effect on performance, and defects larger than 300 µm decrease performance. National Renewable Energy Laboratory also demonstrated real-time imaging of membrane

thickness as seen in Figure 2, which shows the thickness map of a nominally 25-µm membrane taken at a scanning speed of 5 ft/min.

- The Manufacturing R&D sub-program joined the DOE Office of Energy Efficiency and Renewable Energy's Roll-to-Roll Consortium (R2R) focused on batteries, fuel cells, and membranes for water purification and issued a cooperative research and development agreement (CRADA) call soliciting projects.

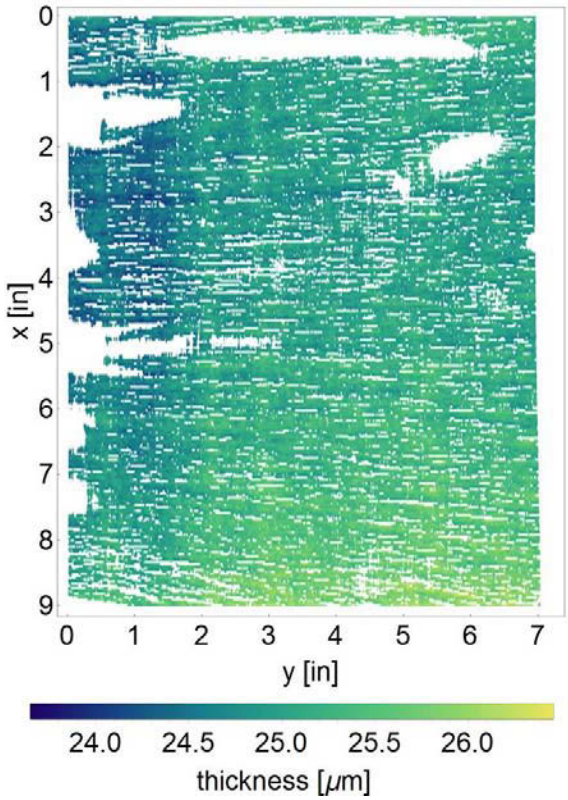

FIGURE 2. Thickness image of 25-µm membrane taken at 5 ft/min

BUDGET

The FY 2017 budget allocated $1 million to the Manufacturing R&D sub-program (Figure 3).

UPCOMING ACTIVITIES AND PLANS

Using funding from prior year appropriations, in FY 2018, the Manufacturing R&D sub-program will:

- Continue projects on supply chain development, report on fuel cell shipments and revenues, and conduct global manufacturing competitive analysis.
- Use the four-laboratory consortium to solicit projects for a CRADA call on fuel cell roll-to-roll processing in collaboration with, and leveraging investment by, the Advanced Manufacturing Office in the Office of Energy Efficiency and Renewable Energy.
- Complete the project to manufacture reliable joints (with very low leak rates) that connect fiber-reinforced pipeline for hydrogen delivery at 100 bar with a final design and physical fatigue tests.

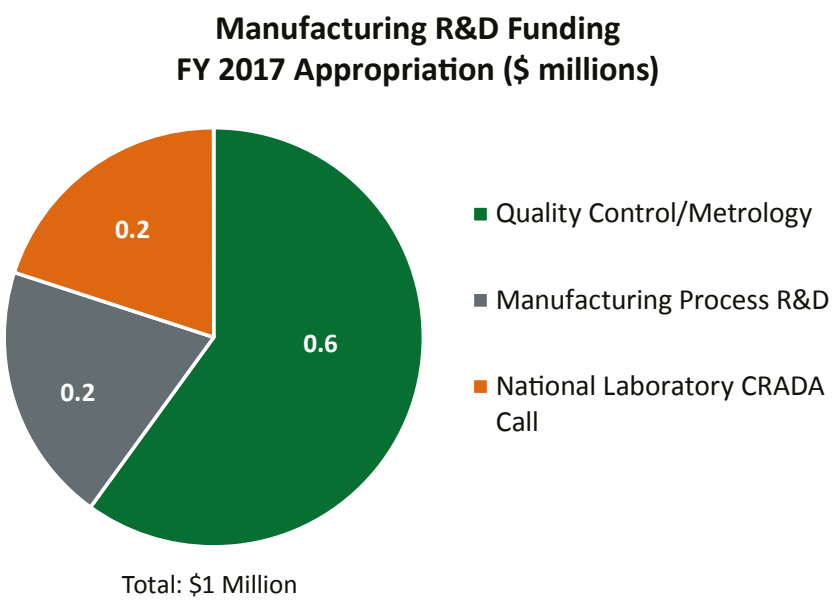

FIGURE 3. FY 2017 Appropriations

- Correlate size of defects generated during membrane, membrane electrode assembly, and gas diffusion electrode fabrication to loss in fuel cell performance.
- Continue to use predictive modeling and single and segmented cell test methods to assist diagnostic development.
- Expand implementation of defect diagnostic techniques on industry production lines to original equipment manufacturers.

The Fuel Cell Technologies Office will continue to coordinate with other agencies (including the National Institute of Standards and Technology and the U.S. Department of Defense) and with other technology offices within DOE's Office of Energy Efficiency and Renewable Energy to identify synergies and leverage efforts.

Future activities are subject to appropriations.

Nancy L. Garland
Manufacturing R&D Project Manager
Fuel Cell Technologies Office
Office of Energy Efficiency and Renewable Energy
U.S. Department of Energy
1000 Independence Ave., SW
Washington, D.C. 20585-0121
Phone: (202) 586-5673
Email: Nancy.Garland@ee.doe.gov

VI.1 Fuel Cell Membrane Electrode Assembly Manufacturing R&D

Michael Ulsh (Primary Contact), Guido Bender, Peter Rupnowski, Scott Mauger
National Renewable Energy Laboratory (NREL)
15013 Denver West Parkway
Golden, CO 80401
Phone: (303) 275-3842; Fax: (303) 275-3840
Email: michael.ulsh@nrel.gov

DOE Managers:
Nancy L. Garland
Phone: (202) 586-5673
Email: Nancy.Garland@ee.doe.gov
Jesse Adams
Phone: (720) 356-1421
Email: Jesse.Adams@ee.doe.gov

Partners:
- Lawrence Berkeley National Laboratory (LBNL), Berkeley, CA
- Colorado School of Mines, Golden, CO
- Georgia Institute of Technology (Georgia Tech) Atlanta, GA
- Tufts University, Medford, MA
- General Motors, Pontiac, MI
- W.L. Gore & Associates, Elkton, MD
- Mainstream Engineering, Rockledge, FL
- Altergy, Folsom, CA

Project Start Date: July 16, 2007
Project End Date: Project continuation and direction determined annually by DOE

Overall Objectives

- Perform early-stage development of real-time characterization techniques relevant to membrane electrode assembly (MEA) component critical material properties, and validate these techniques under relevant fabrication conditions.
- Study the effects of MEA component fabrication variations on MEA performance and lifetime to understand the required characteristics of real-time characterization systems.
- Develop and utilize models to predict the effects of local variations in MEA component properties and to improve our understanding of material-excitation interactions during real-time characterization.
- Study material-process-performance relationships for MEA materials in scalable processes, providing guidance for new process development to lab and academic partners via the Energy Materials Network consortia, including exploration of particle-polymer interactions between ionomers, catalysts, supports, and solvents to better understand their influence on ink structure and stability.
- Our specific development activities have been and will continue to be fully informed by direct input from industry. As new technologies emerge and as the needs of the industry change, the directions of this project will be adjusted.

Fiscal Year 2017 Objectives

- Evaluate thermal scanning as a technique for thickness and/or property measurement.
- Generate spatially resolved initial performance data for cells with membranes having as-cast irregularities fabricated at Georgia Tech.
- Fabricate and characterize baseline slot-die and micro-gravure roll coated electrodes, at least one of which is to meet the following criteria: (1) achieving a target catalyst loading in the range of 0.05 to 0.2 mg Pt/cm^2, (2) achieving the target loading at a line speed of at least 1 m/min, and (3) achieving at least 70% of the average mass activity (900 mV_IR-free) of MEAs containing spray-coated gas diffusion electrodes (GDEs).
- Generate in situ MEA failure data for cells with electrode irregularities.
- Demonstrate a moving-substrate configuration for the through-plane reactive excitation technique.

Technical Barriers

This project addresses the following technical barriers from the Manufacturing R&D section (3.5) of the Fuel Cell Technologies Office Multi-Year Research, Development, and Demonstration Plan.

(E) Lack of Improved Methods of Final Inspection of MEAs

(H) Low Levels of Quality Control

Contribution to Achievement of DOE Manufacturing Milestones

This project contributes to the achievement of the following DOE milestones from the Manufacturing R&D section (3.5) of the Fuel Cell Technologies Office Multi-Year Research, Development, and Demonstration Plan.

- Milestone 5.3: Validate and extend models to predict the effect of manufacturing variations on MEA performance. (1Q, 2017)

- Milestone 5.4: Design and commercialize an in-line quality control (QC) device for polymer electrolyte membrane fuel cell (PEMFC) MEA materials based on NREL's optical reflectance technology. (4Q, 2017)
- Milestone 1.3: Develop continuous MEA manufacturing processes that increase throughput and efficiency and decrease complexity and waste. (4Q, 2017)
- Milestone 5.5: Develop correlations between manufacturing parameters and manufacturing variability, and performance and durability of MEAs. (4Q, 2018)
- Milestone 5.6: Demonstrate methods to inspect full MEAs and cells for defects prior to assembly into stacks in a production environment. (4Q, 2018)

FY 2017 Accomplishments

- Demonstrated the feasibility of thermal scanning for measuring the thickness of membranes already attached/laminated to GDEs.
- Demonstrated the feasibility of imaging to fully map reinforced and non-reinforced membrane thickness in real time, while the membrane is still attached to one or two liners.
- Evaluated process improvements for the reactive impinging flow technique.
- Performed in situ studies of the impacts of electrode and membrane irregularities on the initial performance, performance over time, and failure of MEAs.
- Demonstrated gravure-coated GDEs with performance comparable to lab-standard fabrication methods.
- Performed extensive studies of the rheology and formulation of electrode inks.
- Increased the throughput of ultrasonically sprayed electrodes by two orders of magnitude while maintaining acceptable MEA performance.
- Expanded multi-physics modeling of the through-plane reactive excitation technique to further assist in the development of an in-line configuration for the technique.
- Continued collaboration with our industry partners in accordance with our project charter.

✧ ✧ ✧ ✧ ✧

INTRODUCTION

In FY 2005–2007, NREL provided technical support to DOE in developing a new key program activity: manufacturing R&D for hydrogen and fuel cell technologies. This work included a workshop on manufacturing R&D, which gathered inputs on technical challenges and barriers from the fuel cell industry, and subsequent development of a roadmap for manufacturing R&D. In late FY 2007, NREL initiated a project to assist the fuel cell industry in addressing these barriers, initially focusing on in-line quality control of MEA components.

APPROACH

NREL and its partners are addressing the DOE manufacturing milestones listed above by performing early-stage R&D in the areas of real-time characterization, understanding the impacts of irregularities in MEA materials originating during fabrication and handling, and elucidating how material and fabrication parameters impact MEA performance. We utilize industry relationships to understand MEA material, structure, and processing directions and challenges. We then develop real-time characterization techniques, using computational modeling to (a) assist in the development and optimization of unique measurement techniques and to (b) predict the effects of material irregularities on performance. These techniques are validated under simulated processing conditions. In parallel, we use in situ testing to perform detailed parametric studies of the effects of material irregularities on performance and lifetime. As a new element to the project, we explore material-process-performance relationships in the scalable fabrication of MEA materials. Finally, we publish results in the public domain.

RESULTS

We continued to have a major focus on in situ testing to understand the effects of variations in electrode and membrane materials that originate during the fabrication process. In coordination with Georgia Tech, we performed spatial initial performance studies of MEAs with membranes cast on Georgia Tech's processing line. These membranes had a variety of irregularities that resulted from purposefully casting under conditions on the edge of the process window. Local performance effects were observed using the segmented cell, and increased hydrogen crossover was detected in the cells at the locations of the membrane irregularities using our novel infrared imaging in situ hardware. In an effort coordinated with the segmented cell work, LBNL performed modeling to validate and help explain our findings of locally increased performance at the bends of the serpentine flow-field. This behavior was shown to occur as a result of increased local gas convection in the flow-field channel bend. In electrode studies, we continued to utilize accelerated stress testing (AST) and our infrared hardware to explore the impact of electrode irregularities on failure. Figure 1 shows an example, in this case of a pristine MEA, where cross-over current density was continuously monitored throughout the accelerated aging. Stable values were obtained until approximately 114.7 hours of the test, where an exponential increase in crossover began. By 123.8 hours of the test, the

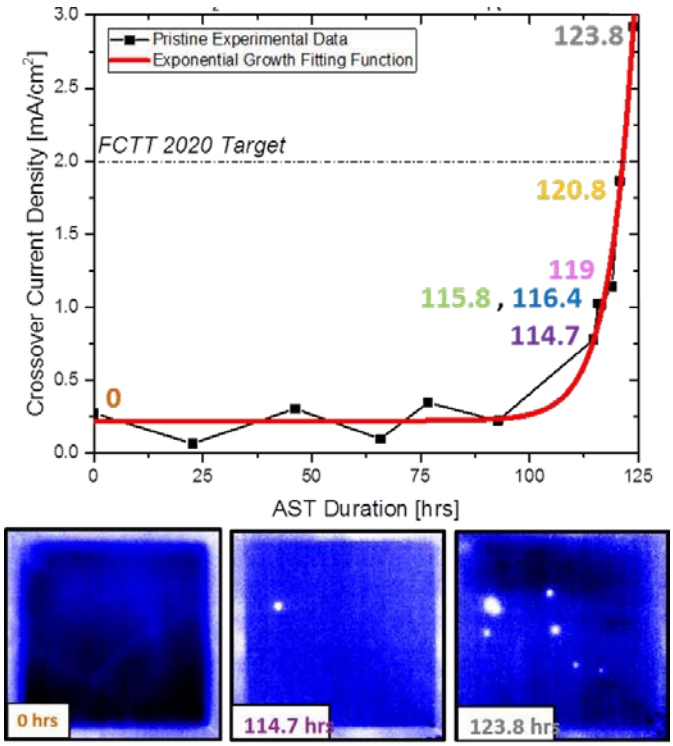

FIGURE 1. Crossover current density data for a pristine MEA aged using a combined chemical-mechanical AST (top); infrared spatial crossover images of the MEA (cathode side) at different times during the AST testing showing the development of multiple failure points (bottom)

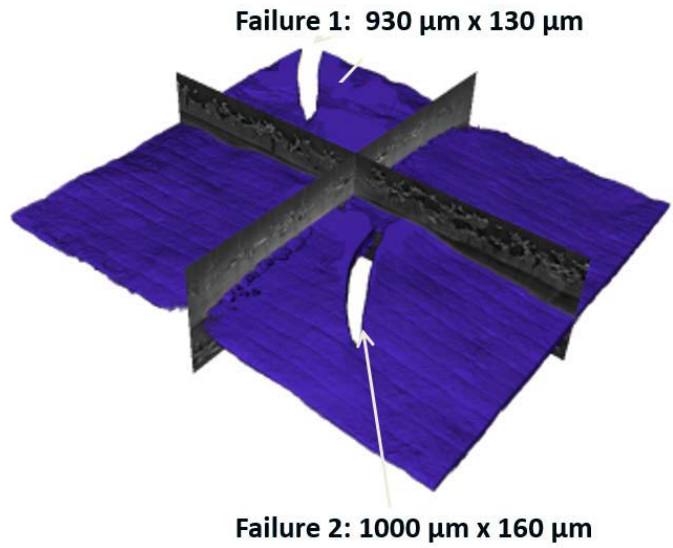

FIGURE 2. X-ray computed tomography data of a failed MEA showing two breaches in the integrity of the membrane

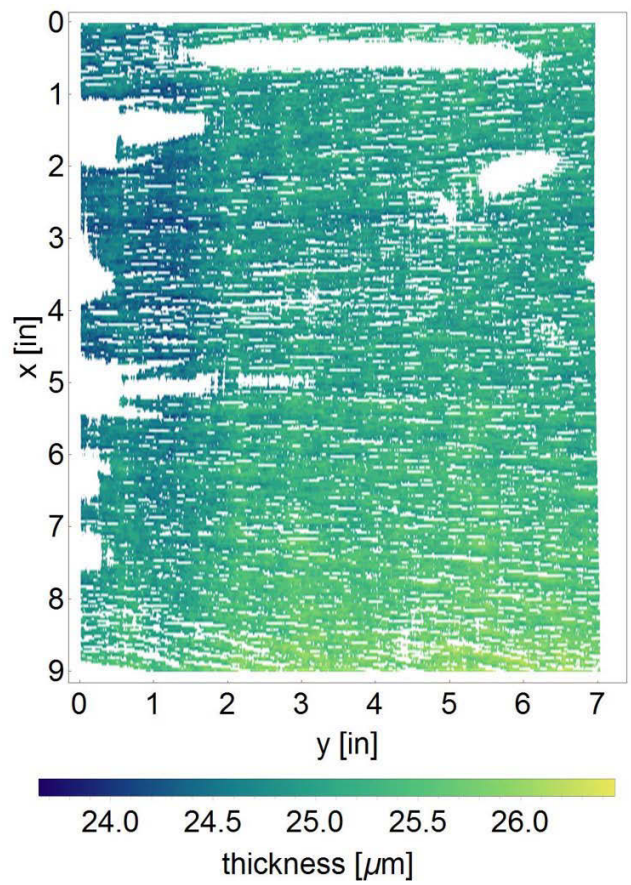

FIGURE 3. Real-time thickness imaging of a nominally 25 µm membrane taken at 5 foot per minute sample speed

MEA had exceeded our failure criteria, the 2020 Fuel Cell Tech Team (FCTT) crossover target for membranes. The infrared spatial crossover images at the bottom of Figure 1 show: on the left at time zero, full membrane integrity; in the center at time 114.7 hours, the development of a single failure point; and on the right at 123.8 hours, the growth of the initial failure point and the development of several other failure points. In coordination with the failure studies, our partners at LBNL and Tufts University performed X-ray computed tomography imaging of MEAs observed to have failed during AST testing. With the spatial crossover imaging as a guide to the location of the failures, X-ray computed tomography was performed and captured in three dimensions the nature and extent of the failure. Figure 2 shows X-ray computed tomography imaging of a location at which two tears in the membrane formed during the AST.

As we mentioned in our report last year, a key area of study recently has been demonstrating real-time membrane thickness imaging. In that report, we showed successful single-point thickness measurements as an initial feasibility step. We have now demonstrated actual real-time imaging of membrane thickness. The method uses a unique areal detector, where the well-known thin-film interference fringe effect is used with fast Fourier transform. The image in Figure 3 shows the thickness map of a nominally 25 µm membrane taken at a scanning speed of 5 feet per minute. The sensitivity in the z (thickness) direction is significantly

less than a micrometer. Critically, we have shown that this technique works for membranes both with and without a reinforcing layer, as well as for membranes still attached to one or two casting/protective liners. In additional exploratory work, we have demonstrated the feasibility of a thermal imaging technique to measure the thickness of membranes that are already attached to a GDE. Generically, we provide a focused thermal excitation to the membrane and measure the peak and/or decay of that excitation, real-time. This measurement is then correlated to a thermal model of the material to back out a physical property, such as porosity or thickness. In an example study of three half-cell samples of membrane thickness zero (bare GDE), 1/3A, and A, we observe a monotonic response of the measurement to the membrane thickness.

In a new element of the project, we have initiated material-process-performance studies of electrode fabrication. In this first year, the focus was on understanding the material, ink, and process modifications needed to transition from a baseline lab-scale process, ultrasonic spray, to scalable processes such as gravure and slot-die coating. Extensive exploration of electrode ink rheology was performed to understand the properties of individual ink constituent (carbon, platinum, and ionomer) solutions as well as combined solutions. Process parameters were also explored. Figure 4 shows the macro-scale uniformity of gravure-coated electrodes fabricated under different roll speeds and different roll patterns. Ultimately, the milestone noted above was achieved, having fabricated gravure-coated electrodes with comparable performance to baseline ultrasonically sprayed electrodes. Slot-die coating studies were also initiated.

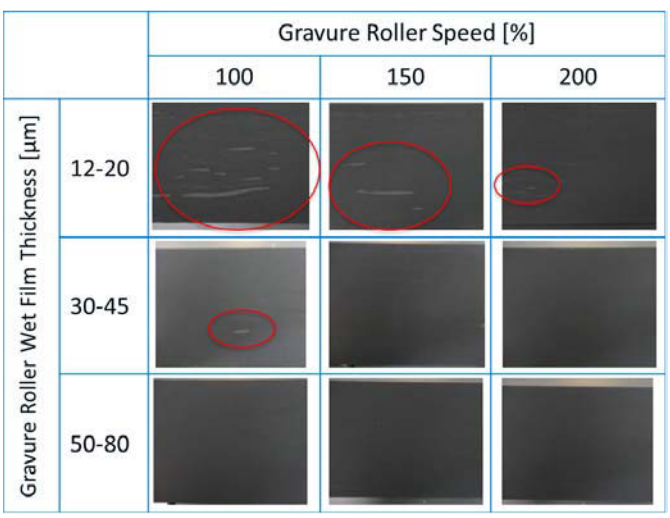

FIGURE 4. Optical imaging of gravure-coated GDE material showing macro-scale uniformity at different roll speeds and with different roll patterns

UPCOMING ACTIVITIES

- Continue to use predictive modeling and single and segmented cell test methods to study the effects of as-fabricated irregularities on MEA performance and lifetime.
- Advance our understanding of the intrinsic detection and excitation physics for novel inspection techniques including membrane thickness imaging, platinum loading imaging, and thermal scanning.
- Advance our understanding of electrode ink rheology and particle-polymer interactions.
- Advance our understanding of scalable fabrication methods for electrodes and membranes, including novel structure and morphology.
- Demonstrate in-line detection of membrane pinholes using through-plane reactive excitation.

FY 2017 PUBLICATIONS/PRESENTATIONS

1. I.V. Zenyuk, N. Englund, G. Bender, A.Z. Weber, M. Ulsh, "Reactive impinging-flow technique for polymer-electrolyte-fuel-cell electrode-defect detection," *J. Power Sources* (332), 2016; p. 372–382.

2. G. Bender, A. Phillips, J. Mackay, J. Porter, M. Ulsh, "The Effect of Catalyst Layer Coating Irregularities on Initial Fuel Cell Performance," presented at the ECS Fall meeting, Honolulu, HI; October, 2016.

3. A. Phillips, G. Bender, J. Mackay, J. Porter, M. Ulsh, "Failure Point Analysis of Defected PEMFC MEAs," presented at the ECS Fall meeting, Honolulu, HI; October, 2016.

4. A. Phillips, M. Ulsh, J. Porter, G. Bender, "Utilizing a Segmented Fuel Cell to Study the Effects of Electrode Coating Irregularities in PEM Fuel Cell Initial Performance," *Fuel Cells*, DOI: 10.1002/fuce.201600214, 2017.

5. M. Ulsh, "Fuel Cell MEA Manufacturing R&D," presented at the Hydrogen and Fuel Cells Program Annual Merit Review; June 2017.

6. M. Ulsh, S. Mauger, K.C. Neyerlin, "Material-Process-Performance Relationships for Roll-to-Roll Coated PEM Electrodes," presented at the Hydrogen and Fuel Cells Program Annual Merit Review; June 2017.

7. U.S. Provisional Patent Application, "Thickness mapping using multispectral imaging."

VI.2 Clean Energy Supply Chain and Manufacturing Competitiveness Analysis for Hydrogen and Fuel Cell Technologies

Patrick Valente
Ohio Fuel Cell Coalition (OFCC)
151 Innovation Drive, Suite 240D
Elyria, OH 44035
Phone: (614) 542-7308
Email: pat.valente@fuelcellcorridor.com

DOE Managers:
Nancy L. Garland
Phone: (202) 586-5673
Email: Nancy.Garland@ee.doe.gov
Greg Kleen
Phone: (240) 562-1672
Email: Gregory.Kleen@ee.doe.gov

Contract Number: DE-EE0006931

Subcontractors:
- Connecticut Center for Advanced Technology East Hartford, CT
- DJW Technology, LLC, Dublin, OH
- National Renewable Energy Laboratory, Golden, CO
- National Fuel Cell Research Center, Irvine, CA

Project Start Date: September 1, 2015
Project End Date: August 30, 2018

Overall Objectives

- Objective 1. Establish Regional Technical Exchange Centers (Centers) to increase communication between original equipment manufacturers (OEMs) and hydrogen and fuel cell component and subsystem suppliers.
- Objective 2. Establish a readily web-accessible database containing inputs from suppliers and OEMs along with a supplier contact lists.
- Objective 3. Standardize component and subsystem component specifications.
- Objective 4. Develop strategies for lowering cost, increasing performance, and improving durability of components and subsystem components.

Fiscal Year (FY) 2017 Objectives

- Operation of the four Centers and host supply chain exchanges to facilitate one-to-one communication between suppliers and OEMs.
- Working groups will assist with the projections of cost reduction and initiation of component fabrication based on standardization of specifications.
- Expansion of number of suppliers and OEMs relevant for inclusion into the regional databases, with the ultimate goal of adding to the national database.
- Conduct national supply chain exchange at the Fuel Cell Seminar.

Technical Barriers

This project addresses the following technical barriers from the 3.4 Fuel Cells section of the Fuel Cell Technologies Office Multi-Year Research, Development, and Demonstration Plan.

(A) Durability

(B) Cost

(C) Performance

This project also addresses the following technical barrier from the 3.5 Manufacturing R&D section of the Fuel Cell Technologies Office Multi-Year Research, Development, and Demonstration Plan.

(I) Lack of Standardized Balance-of-Plant Components

Contribution to Achievement of DOE Manufacturing R&D Milestones

Due to the nature of this project, this section is not applicable.

FY 2017 Accomplishments

- Four Centers continue operations to collect and categorize hydrogen and fuel cell information that will be included in a national web-centered database. Identification of states and regions per Center was made to prevent duplication of efforts. An application program interface was developed to link regional supply chain database to national database.
- The OFCC, in conjunction with DOE, executed two Ohio events (September 2016 and March 2017): a Fuel Cell Supply Chain Stakeholder Session and a Balance of Plant Workshop. Successful supply chain exchanges were held, which included fifty percent new participants.
- Connecticut Center for Advanced Technology, with DOE, executed the Hydrogen and Fuel Cell Forum in Connecticut (November 2016). The first live DOE

request for information for hydrogen and fuel cell components for manufacturing standardization was held.

- National Renewable Energy Laboratory is currently working in collaboration with several regional manufacturing organizations to present the Cleantech Manufacturing Forum (August 2017), with a supply chain exchange event following.
- We received approval from DOE to proceed with the standardization working group. Working group invitation letters were finalized and sent to a selected listing of OEMs, integrators, and suppliers. Some OEMs have agreed, but not all. Components for standardization have been suggested and identified.
- The OFCC attended the Hannover Messe Industrial Trade show in Germany (April 2017), the DOE Annual Merit Review in Washington D.C., (June 2017), and the Renewable Hydrogen Fuel Cell Collaborative Public Transit Workshop (June 2017).

✧ ✧ ✧ ✧ ✧

INTRODUCTION

The project goal is to facilitate the development of a robust supply chain for fuel cell and hydrogen systems that will benefit manufacturing and the supply chain with accelerated mass production, cost reduction, and improved performance and durability of these systems. OFCC will identify and address the critical gaps in the needs and capabilities of the fuel cell supply chain. This will contribute to the United States maintaining a competitive advantage and global leadership in the industry.

This project builds on existing manufacturing infrastructure to help reverse the decline in and/or create new manufacturing jobs, as well as acts as an economic lever for additional technology development. The benefits that will be gained from addressing the manufacturing barriers (cost, performance, and mass production) and product standardization, will facilitate commercialization of hydrogen and fuel cell technologies, and promote energy efficiency and renewable energy.

APPROACH

The Centers are now operational. These centers will continue to research, collect and catalog non-proprietary company and product information from their assigned regions for ultimate inclusion in the national web-centered database. The regional Centers are promoting communication between fuel cell component and subsystem suppliers and OEMs. This is done through facilitated one-on-one interactions, relevant industry events, and addressing the needs and capabilities of the fuel cell supply chain.

Identification and invitations to participants in the OEM and supplier working groups are underway. The working groups will investigate and address pathways to standardization of component and subsystems, with the focus on functionality and cost reduction. The project focus is a two-way technology transfer between OEMs and suppliers.

RESULTS

The four Centers continue to be the catalyst for this project. One of the main components of this project is to increase communication between fuel cell OEMs and fuel cell component and subsystem suppliers. Through promotion of regional events, and in partnership with DOE and other regional entities, we were able to attract participants from 18 states and two Canadian provinces, for a combined attendance of over 500. The first DOE live request for information for manufacturing standardization was held in conjunction with our event.

In conjunction with the Centers' collaboration on industry events, Supply Chain Exchanges were held. Partnering with larger, relevant events encourages attendance and participation for the supply chain portion of the event as well. Supply Chain Exchanges are more personal face-to-face introductions for OEMs to meet suppliers and share their wants and needs. Prior to the event, participants are asked to complete a grid of their needs and/or capabilities. From this information, the companies and organizations are matched accordingly to be sure the introductions are relevant. There was a 50% increase in new supplier participants, and many renewed past contacts. These exchanges facilitated over 300 individual OEM and supplier interactions.

Another facet of the Centers is the research, collection, and inclusion of information into regional databases, with ultimately becoming part of the national database, housed at John Madison University. This work is an ongoing task. Approximately 750 potential supply chain companies have been identified and were added to the Connecticut Center for Advanced Technology supply chain database, and the mountain region database has begun and continues to grow. The application program interface was developed to link one regional supply chain database to the national database. Expansion of the database and the information gained will contribute to our domestic manufacturing supply chain, business-to-business interaction, and promote the industry as a whole.

Establishment of supplier and OEM working groups focused on supply chain requirements and standardization of fuel cell components and subsystems has progressed slower than anticipated. Invitations to participate have been issued, and consideration and acceptance to participate in

the working group has not been as forthcoming as we had hoped. It has required multiple individual interactions and dissemination of additional information, which has slowed the process. We have been given the DOE go-ahead to continue with the standardization effort and are encouraged that the working groups will be an important part of this. We are working with DOE and information gained from the live request for information to assist in developing a plan for the standardization effort.

The work detailed above is a necessary stepping stone to help the United States and our fuel cell industry to be a competitive and global leader in the fuel cell market. The formation of resources, such as the regional and national databases, and communication between fuel cell component and subsystem suppliers, both individually and within working groups, is a must to achieve the goal of developing a robust supply chain, standardize and improve functionality and performance, and maintain competitive pricing.

CONCLUSIONS AND UPCOMING ACTIVITIES

We continue to utilize our partnerships and collaborations in expanding our contacts and promotion of communication with the industry. While we see the industry growing stronger, there is still much hesitation among the "industry players" to be forthcoming with their efforts and the sharing of information that would be beneficial to our goals of standardization and building a robust fuel cell supply chain. We have confirmed that there are definite gaps between what OEMs need and the suppliers' capabilities to provide for those needs. As we continue to move the project forward in the next year, our databases will be refined and contacts increased as we work together with the national database initiatives. We will be hosting several additional regional supply chain exchanges, as well as one on the national level, to promote further interactions. The working group and standardization components of this project should gain momentum and move the project towards our final goals of component specifications, cost efficiency, and improve durability and performance of the fuel cell components and subsystems.

FY 2017 PUBLICATIONS/PRESENTATIONS

1. Presentation at the DOE Annual Merit Review in Washington, D.C. on June 6, 2017.

VI.3 Fuel Cell and Hydrogen Opportunity Center, www.hfcnexus.com (Hydrogen Fuel Cell Nexus)

Alleyn Harned (Primary Contact) and
Matthew Wade
Virginia Clean Cities (VCC) at James Madison University
1401 Technology Drive MSC 4115
Harrisonburg, VA 22807
Phone: (540) 568-8896
Email: aharned@vacleancities.org

DOE Managers:
Nancy L. Garland
Phone: (202) 586-5673
Email: Nancy.Garland@ee.doe.gov
Greg Kleen
Phone: (240) 562-1672
Email: Gregory.Kleen@ee.doe.gov

Contract Number: DE-EE0006932

Subcontractors:
- Birch Studio, Charlottesville, VA
- Breakthrough Technologies Institute, Woodbridge, VA

Project Start Date: July 1, 2015
Project End Date: May 31, 2018

Overall Objectives

- To expand the domestic supply chain of hydrogen components and systems.
- Scale-up of the fuel cell and hydrogen supply chain by building and populating a comprehensive communications database.
- Drive U.S. companies to the free website via an engaging outreach campaign.
- Advance hydrogen fuel cell suppliers in the transportation, utility, industrial, commercial, and residential sectors, with a focus on the transportation sector in fuel and infrastructure supply chain systems.
- Reduce greenhouse gas emissions and air pollution and contribute to a more diverse and efficient energy balance by facilitating the widespread commercialization of hydrogen and fuel cell technologies.

Fiscal Year (FY) 2017 Objectives

- Develop interface to allow fuel cell and hydrogen companies to post their needs and specifications, and allow potential supply chain companies to post their capabilities. The idea is to stimulate a dialogue and encourage supplier-to-end-manufacturer connections.
- Update the opportunity center continuously and technical specifications quarterly and if necessary, revise and update the interface based on user experience. The number of suppliers/components added during each quarter will be included in the quarterly reports.
- Mine the traffic on the website, compile information gained during outreach efforts, and discuss with DOE and fuel cell industry leaders to identify critical gaps in the supply chain and develop a response plan.
- Identify the fuel cell system gaps and cater the opportunity center to narrow the gaps identified. Deliver a preliminary and final assessment.
- Seek information bi-annually from additional suppliers not previously captured.
- Collect data and research suppliers. Currently there are multiple thousands of suppliers in the U.S. alone and the existing BTI database consists of only 1,000 suppliers. When we reach a critical mass of users, suppliers will hear about the database and be able to sign up on their own initiative, long after our outreach campaign has ended. Rich content will allow for new ways to search and for companies to connect, and also allow organic scaled growth of fuel cell industry sectors.
- Open a dialogue with potential partners through dissemination of the developed materials. The project team will track the materials distribution by using actual numbers of printouts distributed, website hits, webinars participants, and video views.
- Seek opportunities for information placement in trade journals, which often make space available for nonprofits. The team will use free sources and a limited budget to purchase internet-based advertising through Google AdWords and Facebook in order to reach people as they search for words or phrases and browse websites with themes related to fuel cells.
- Create and advance a sustainability program for long-term continued life of the website and database and for continued upkeep and enhancement of data. This will include exploring collaboration with industry, federal agencies, and national laboratories.

Technical Barriers

This project addresses the crosscutting technical barriers of supply chain transparency and business and

product information of the Manufacturing R&D section. The project also addresses the following specific barrier from the Education and Outreach section of the Fuel Cell Technologies Office Multi-Year Research, Development, and Demonstration Plan.

(A) Lack of Readily Available, Objective, and Technically Accurate Information

Contribution to Achievement of DOE Manufacturing R&D Milestones

This project will directly contribute to achievement of DOE milestones of the Fuel Cell Technologies Office Multi-Year Research, Development, and Demonstration Plan. The project is a cross-cutting effort to publish available supply chain business content and connect industry partners. As such, milestones associated with development and demonstration in the Manufacturing R&D section are supported, and this project takes those milestones to deployment.

FY 2017 Accomplishments

- HFCnexus launched on July 11, 2016.
- The HFCnexus has 350 fuel cell and hydrogen companies.
- The HFCnexus has 74 active user accounts.
- HFCnexus.com Matchmaker function launched in October 2016.
- Using Google Analytics to track the website traffic, VCC can report that the directory saw 6,100 users, 8,000 sessions, and an average of eight daily active users from July 1, 2016, through June 30, 2017. Daily use has increased with 38 daily users in recent months compared with lower use at launch. A daily active user is a unique user who had at least one session within a 30-day period. Each daily active user equals one unique user.
- Instructional video created for how to create an account and posted to YouTube and included in every registration confirmation email.
- Instructional video created for how to create a company profile and posted to YouTube and included in every registration confirmation email was created on October 3, 2016. It has 23 views as of December 31, 2016. Another instructional video for how to set up a Matchmaker account was created on October 12, 2016.

✧ ✧ ✧ ✧ ✧

INTRODUCTION

The Fuel Cell and Hydrogen Opportunity Center, renamed the Hydrogen Fuel Cell Nexus (and live at www.hfcnexus.com and www.hfcnexus.org, Figure 1) will expand the domestic supply chain of components and systems necessary for the manufacture and distribution of the hydrogen and fuel cell equipment. The supply chain will benefit through the development of a comprehensive online database. This effort will advance hydrogen fuel cell suppliers in the transportation, utility, industrial, commercial, and residential sectors, with a focus on the transportation sector in fuel and infrastructure supply chain systems.

APPROACH

VCC and project partners addressed the main objective of the Fuel Cell and Hydrogen Opportunity Center project by collaboratively identifying gaps and developing elements of interest for a comprehensive supplier tool, gathering national supplier information to fill the database, identifying and encouraging new suppliers to become engaged in the hydrogen industry, and releasing and maintaining a public directory tool for interaction with the data. Birch Studio developed the user interface for the website. VCC populated the database with U.S. companies from the FuelCells2000 directory. After the website was launched, VCC began an aggressive outreach campaign using trade association outreach, webinars, social media, and personal contact to drive companies to this resource.

FIGURE 1. www.HFCnexus homepage

RESULTS

The FY 2017 efforts of the Fuel Cell and Hydrogen Opportunity Center project team culminated in the release of a live and interactive website directory on July 11, 2016. The website directory has grown from an initial population of 220 companies to 350 companies (Figure 2). These companies were verified that they are active in the hydrogen or fuel cell industries. Phone numbers, email addresses, and mailing information for employees at each company was uploaded for each company to provide a method for website users to contact the company (Figure 3). The website has grown from zero user accounts to 74 active user accounts.

FIGURE 2. Example of category page

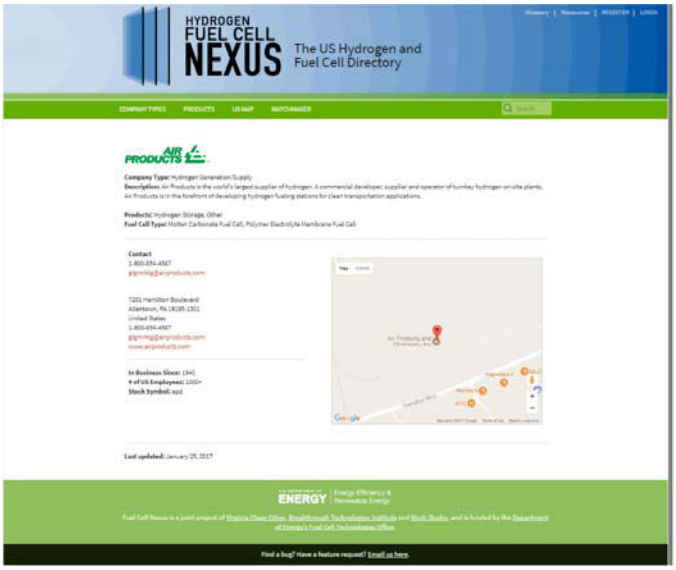

FIGURE 3. Example of company page

During the fourth quarter of 2016 (July to September), the project team was active in several areas of the project related to improving the website and adding companies. The project team continued verifying data and company information and revising as needed. The project team began direct marketing and outreach to hydrogen and fuel cell companies. During this period VCC developed and disseminated marketing and outreach materials that described the website and how to utilize it. Birch Studio developed the Matchmaker interface for companies to connect with one another. Birch Studio began a maintenance and iteration phase to continue improving the website interface. VCC staff continued promoting the database at events and collected data on hydrogen and fuel cell companies to include in the database. Project staff developed website branding with DOE guidance.

Throughout the rest of the year and moving through to June 30, 2017, the project team entered a supply chain growth phase. Throughout the second budget year, the team engaged in an outreach campaign to drive appropriate suppliers to the site, by initiating friendly partnerships with business-to-business marketing associations and other business associations in areas of critical need.

The database and website tools have three main areas for public access, supplier secure access, and system administrator's access. The content will be accessible 24 hours per day, seven days per week.

For FY 2018, the project team will continue maintenance and iteration of the website, approve new users, add new companies, and begin a campaign to secure outside funding from advertisers. This funding will ensure the website is fully funded and operational into the future.

FY 2017 PUBLICATIONS/PRESENTATIONS

1. Alleyn Harned presented "Session Remarks and Supply Chain Analysis: Hydrogen Fuel Cell Nexus" at Fuel Cell Supply Chain Stakeholder Session in North Canton, OH on September 27, 2016.

2. Virginia Clean Cities at James Madison University's Deputy Director Matthew Wade attended the Invest! Design! Make! Use! Hydrogen Fuel Cell Industry Forum in Hartford, CT to present an update on the Hydrogen Opportunity Center on November 17, 2016. The presentation was entitled "Hydrogen Fuel Cell Nexus."

3. Principal Investigator Alleyn Harned presented the website to the Hydrogen Technical Advisory Committee in Washington, D.C., on December 7, 2016. The presentation was entitled "Hydrogen Fuel Cell Nexus."

4. Alleyn Harned also presented the project at the Annual Merit Review, Washington, D.C. June 6, 2017. The presentation was entitled "Fuel Cell and Hydrogen Opportunity Center."

5. Chris Mueller of Virginia Clean Cities moderated a panel discussion the hydrogen summit at the ACT Expo from May 2–4, 2017. VCC did not present a slide deck but provided a summary of the website and distributed informational brochures about the website.

VI.4 U.S. Clean Energy Hydrogen and Fuel Cell Technologies: A Competiveness Analysis

Patrick Fullenkamp
GLWN, Westside Industrial Retention & Expansion Network
4855 West 130th Street, Suite 1
Cleveland OH 44135-5137
Phone: (216) 920-1956
Email: pfullenkamp@glwn.org

DOE Managers:
Nancy L. Garland
Phone: (202) 586-5673
Email: Nancy.Garland@ee.doe.gov
Jesse Adams
Phone: (720) 356-1421
Email: Jesse.Adams@ee.doe.gov

Contract Number: DE-0006935

Subcontractors:
- Strategic Analysis, Inc, Arlington, VA
- DJW Technologies, Dublin, OH
- E4tech, Lausanne, Switzerland
- Bowen Liu, Newmarket, Ontario, Canada
- Brent Fourman, New Paris, OH

Project Start Date: June 1, 2015
Project End Date: May 31, 2019

Overall Objectives

- Global competitiveness analysis of hydrogen and fuel cell systems and components manufactured, including 700 bar compressed hydrogen storage systems in the United States, Europe, and Asia, to determine the global cost leaders, the best current manufacturing processes, the key factors determining competitiveness, and the potential means of cost reductions.
- Analysis to assess the status of global hydrogen and fuel cell markets for four years, 2014 to 2017. The analysis of units, megawatts by country and by application, will focus on polymer electrolyte membrane fuel cell (PEMFC) systems (automotive and stationary).

Fiscal Year (FY) 2017 Objectives

- Map automotive fuel cell system supply chain evolution.
- Develop detailed questionnaire with current DOE cost target and process assumptions baseline shared, and conduct 30 interviews.
- Gather shareholder data on the current DOE cost model provided by Strategic Analysis.
- Generate drawings and specifications for five key components and send out to suppliers to get price quotes/guidance at 1,000 and 100,000 vehicle annual volume.
- Complete cost breakdown analysis and value stream mapping based upon quotes.
- Gather and deliver fuel cell systems shipment data for 2016.

Technical Barriers

This project addresses the following technical barriers from the Manufacturing R&D section of the Fuel Cell Technologies Office Multi-Year Research, Development, and Demonstration Plan.

(A) Lack of High Volume MEA [membrane electrode assembly] Processes (includes catalyst, membrane, gas diffusion layer)

(B) Lack of High Speed Bipolar Plate Manufacturing Processes

(K) Lack of Low Cost Fabrication Techniques for Storage Tanks

(I) Lack of Standardized Balance-of-Plant Components

Contribution to Achievement of DOE Manufacturing R&D Milestones

This project will contribute to achievement of the following DOE milestones from the (Manufacturing R&D) section of the Fuel Cell Technologies Office Multi-Year Research, Development, and Demonstration Plan.

- Milestone 1.6: Develop fabrication and assembly processes for PEMFC MEA components leading to an automotive fuel cell stack that costs $20/kW. (4Q, 2020)
- Milestone 2.1: Develop manufacturing processes for PEMFC bipolar plates that cost <$3/kW while meeting all other technical targets. (1Q, 2017)
- Milestone 3.3: Develop fabrication and assembly processes for automotive PEMFC stacks that meet the cost of $20/kW. (4Q, 2020)
- Milestone 6.1: Develop fabrication and assembly processes for high-pressure hydrogen storage technologies that cost $12/kW for Type IV, 700 bar tanks. (4Q, 2017)

FY 2017 Accomplishments

- Mapped automotive fuel cell system supply chain evolution.
- Detailed questionnaire developed with current DOE cost target and process assumptions with baseline shared and input gathered at four annual volume levels: 1,000; 10,000; 100,000; 500,000. Seven original equipment manufacturers (OEMs) interviewed, three OEMs visited, 28 suppliers interviewed, 21 suppliers visited.
- Updated the current DOE cost model as provided by Strategic Analysis from interview input.
- Generated drawings and specifications for five key components (bipolar plate, membrane, gas diffusion layer [GDL], catalyst, hydrogen storage vessel) and sent out to suppliers to get actual price quotes/guidance at 1,000 and 100,000 vehicle annual volume.
- Completed Design For Manufacturing and Assembly®/ discounted cash flow, cost breakdown analysis and value stream mapping of five key components in three global regions.
- Gathered and delivered fuel cell systems shipment data for 2015 and preliminary 2016 data in June 2017.

✧ ✧ ✧ ✧ ✧

INTRODUCTION

A healthy component supply chain is needed to support global OEMs as they launch hydrogen fuel cell vehicles into the market. OEMs need suppliers that can meet performance, quality, and cost targets. This project will provide a global analysis of the current supply chain technology and manufacturing readiness levels and cost levels through updated cost modeling and actual quotations and recommendations. The outcome of this project will aid DOE/Clean Energy Manufacturing Initiative in identifying strategic investments, lay out prospective future supply chain per feedback, and identify technology areas for R&D investment.

This study will also provide a four-year analysis of units, megawatts by country and by application of PEMFC systems (automotive and stationary).

APPROACH

First GLWN developed a historical perspective on the automotive supply chain evolution. GLWN then utilized cost analysis to show components contributing most to the final automotive fuel cell system. A questionnaire was developed for OEMs and suppliers which reflected the DOE cost model of five key components at four production levels to serve as the baseline for discussion. A structured interview process was conducted to gather data on the status of development of different components. Interviews and plant visits were conducted in the most important regions to allow visualization and in-depth discussion on relevant development needs. Detailed data on the fuel cell industry were gathered, including annual shipment numbers and different regional support. Value stream mapping was conducted to identify the flows within the relevant manufacturing processes. Implications for the United States were identified.

RESULTS

A comprehensive questionnaire was developed to gather key industry information in an information sharing manner that enabled OEMs and suppliers to provide directional and discrete information on the DOE cost model, technical and manufacturing readiness, current and future manufacturing process assumptions, and future development to meet the high volume needs of this industry at >100,000 vehicles per year. A large quantity of data has been gathered from the questionnaire interview with seven OEMs and 28 suppliers, with actual visits at three OEMs and 21 suppliers. The following are the findings and themes:

- Global OEMs have a focus on performance and cost through design and manufacturing process development to build a positive business case for hydrogen fuel cell vehicles with a targeted sales price of $50,000. The leading OEMs are reporting 30–40% incremental cost reduction as they introduce next-generation models. OEMs are in the initial phases of growing the supply chain. Most have a lead supplier for each of the key components, with a goal of at least two per component in maturity.
- Suppliers have a focus on component design and process development with no OEM or supplier capable of producing 100,000 units. Most are comfortable with 1,000 to 5,000 units per year. Suppliers are very cautious about investing in new manufacturing facilities with the limited book of business and the concern for potential major design changes which could obsolete the current manufacturing process.
- Bipolar Plate: Europe and Asia hold the lead in bipolar plate technology. The United States is behind in forming and coating; U.S. prospects are high in far term.
- Catalyst: Europe (Umicore, Johnson Matthey) and Asia (Tanaka) are currently the world leaders in fuel cell catalyst technology. U.S. prospects are low to moderate in far term.
- GDL: Four main competitors predominate and are divided among Europe (SGL, Freudenberg), Asia (Toray), and the United States (Avcarb). Overall, the

Accomplishments: Industry Scorecard Technology and Manufacturing Readiness by Region

Global industry ready for 10k systems per year. High volume capabilities need further development

Technology Readiness	Bipolar Plate				Catalyst				Gas Diffusion layer				Membrane				H2 Vessel			
	US	EU	Asia		US	EU	Asia		US	EU	Asia		US	EU	Asia		US	EU	Asia	
			Japan	China			Japan	China			Japan	China			Japan	China			Japan	China
1-10k	HIGH	HIGH	HIGH	HIGH	HIGH	HIGH	HIGH	HIGH	HIGH	HIGH	HIGH	HIGH	HIGH	HIGH	HIGH	HIGH	HIGH	HIGH	HIGH	HIGH
100k	M-L	MOD	MOD	LOW	MOD	H-M	H-M	MOD	MOD	MOD	MOD	LOW	H-M	H-M	H-M	H-M	H-M	H-M	H-M	H-M

Manufacturing Readiness	Bipolar Plate				Catalyst				Gas Diffusion layer				Membrane				H2 Vessel			
	US	EU	Asia		US	EU	Asia		US	EU	Asia		US	EU	Asia		US	EU	Asia	
			Japan	China			Japan	China			Japan	China			Japan	China			Japan	China
1-10k	H-M	HIGH	HIGH	HIGH	H-M	HIGH	HIGH	HIGH	H-M	HIGH	HIGH	HIGH	H-M	HIGH	HIGH	HIGH	HIGH	HIGH	HIGH	HIGH
100k	M-L	MOD	MOD	LOW	MOD	H-M	H-M	LOW	M-L	MOD	MOD	LOW	LOW	MOD	M-L	LOW	M-L	M-L	M-L	M-L

Readiness Legend:

HIGH	Currently sufficient to produce to stated demand
HIGH TO MODERATE	Capability and capacity exist, although no current production demonstrated at stated demand
MODERATE	Requires some advancements or capital investment to produce to stated demand
MODERATE TO LOW	Requires some advancements capital investment, and no current production demonstrated at stated demand
LOW	Requires major advancements or major capital investments to produced to stated demand

FIGURE 1. Industry scorecard of technology and manufacturing readiness by region

Accomp: Value Stream Map (bipolar plate example)

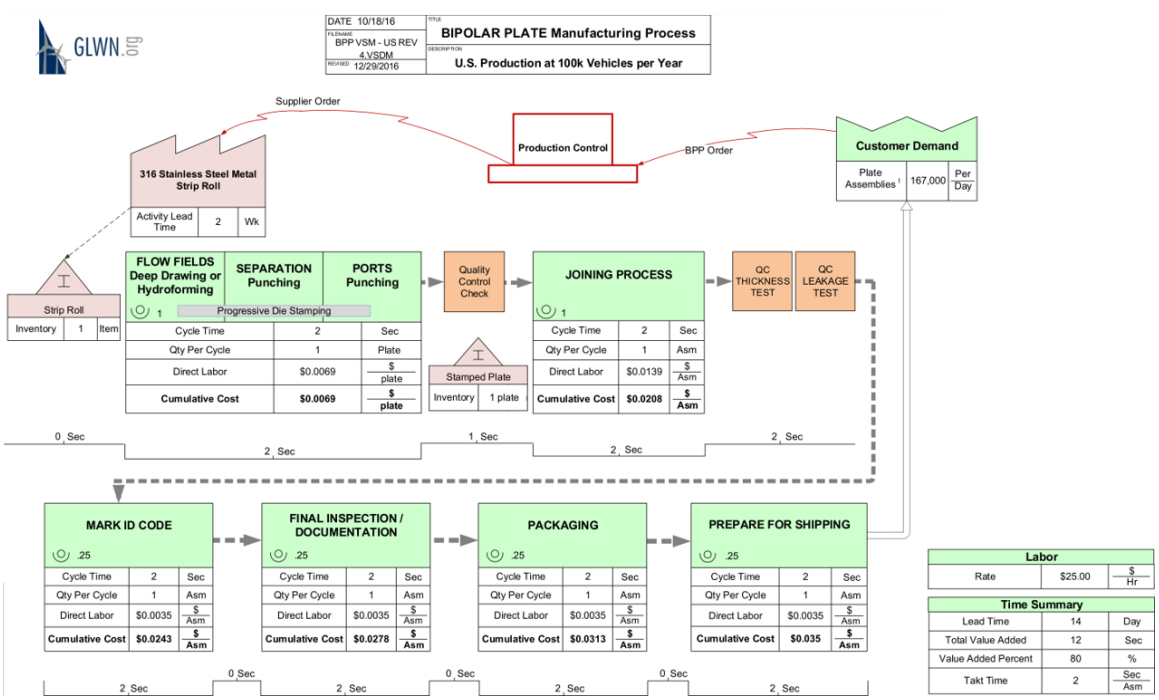

Value Stream Map is a hybrid of process flow used in DFMA and inputs from suppliers and OEMs VSM outputs are used for cost breakdown analysis and as a cost reduction tool

QC – quality control; Qty – quantity

FIGURE 2. Value stream map (VSM) of bipolar plate manufacturing

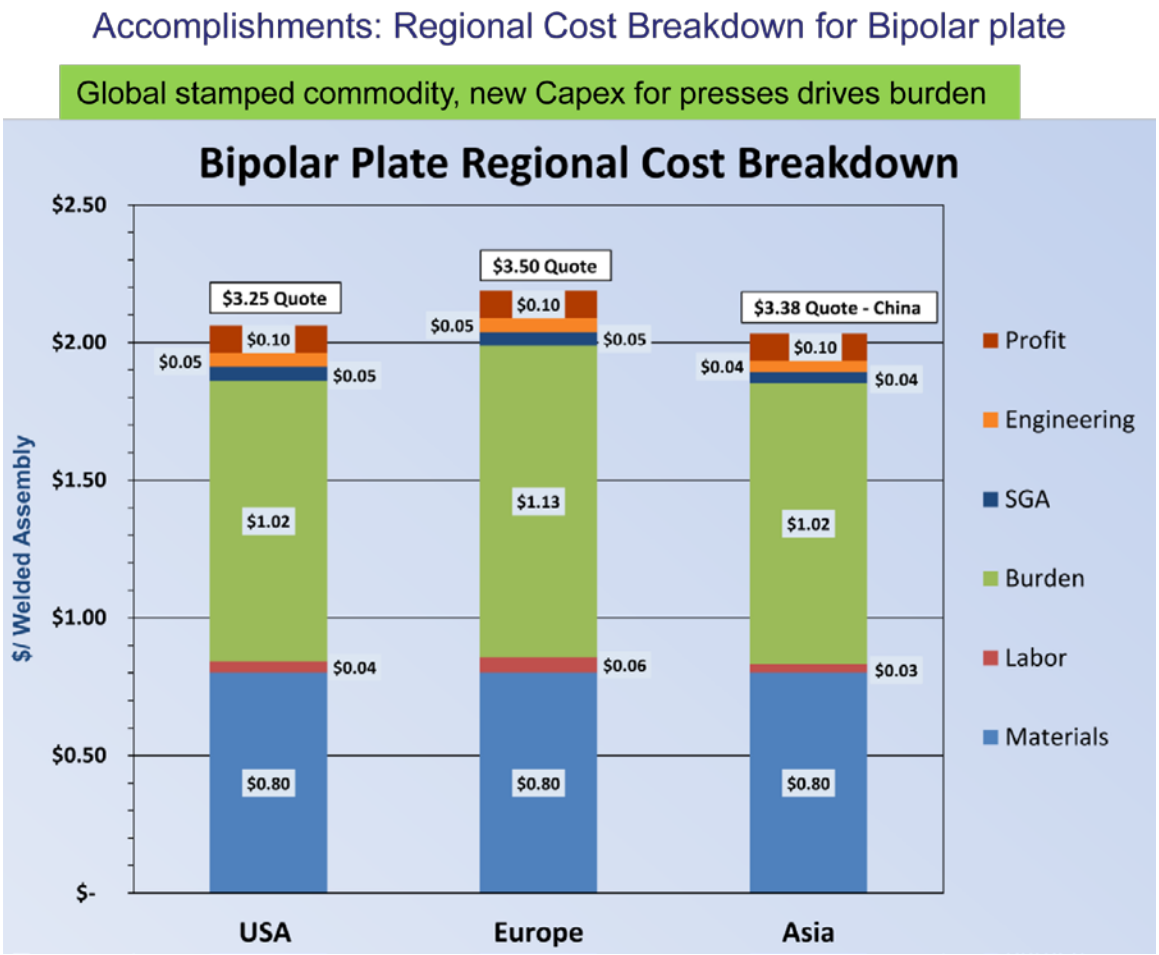

SGA – selling, general, and administrative expenses

FIGURE 3. Regional cost breakdown for bipolar plates

outlook for U.S. GDL production and innovation competitiveness is rated moderate.

- Membrane: The United States currently holds the global lead in membrane technology.
- Pressure Vessel: Pressure vessel competitiveness is divided into carbon fiber production and vessel fabrication. Both areas are ripe for technology advancement; the United States is active in both areas. The prospect for U.S. production and innovation competitiveness is rated high.
- In Japan, strongly shaped by its lack of natural energy resources and diversification from fossil fuels, fuel cells and hydrogen energy are seen as an opportunity for industry. Serial production of fuel cell systems is being demonstrated by Toyota (Mirai) and Honda (Clarity), and a nascent supply chain exists.
- China's motivations are (1) to reduce reliance on overseas technology and expertise, (2) to increase potential for high-value jobs, (3) cleaner and better-performing industry, and (4) high-value exports.
- In the United States, many states support fuel cell technology, 30 include fuel cells or hydrogen as eligible renewable portfolio standards, 32 permit net metering, and 25 offer funding including rebates, grants, loans, and bonds.
- Germany's priorities include industrial and innovation policy (automotive industry strong), air quality, and climate change.

CONCLUSIONS AND UPCOMING ACTIVITIES

No single nation is clearly dominant regarding prospects for the long-term fuel cell market, but U.S. OEMs and manufacturers have fallen behind Japan and Europe in bipolar plates, membranes, GDLs, and catalysts (on par in hydrogen vessels). The U.S. potential is broadly moderate to high, though with weaknesses in bipolar plate manufacturing and ionomers in the near term.

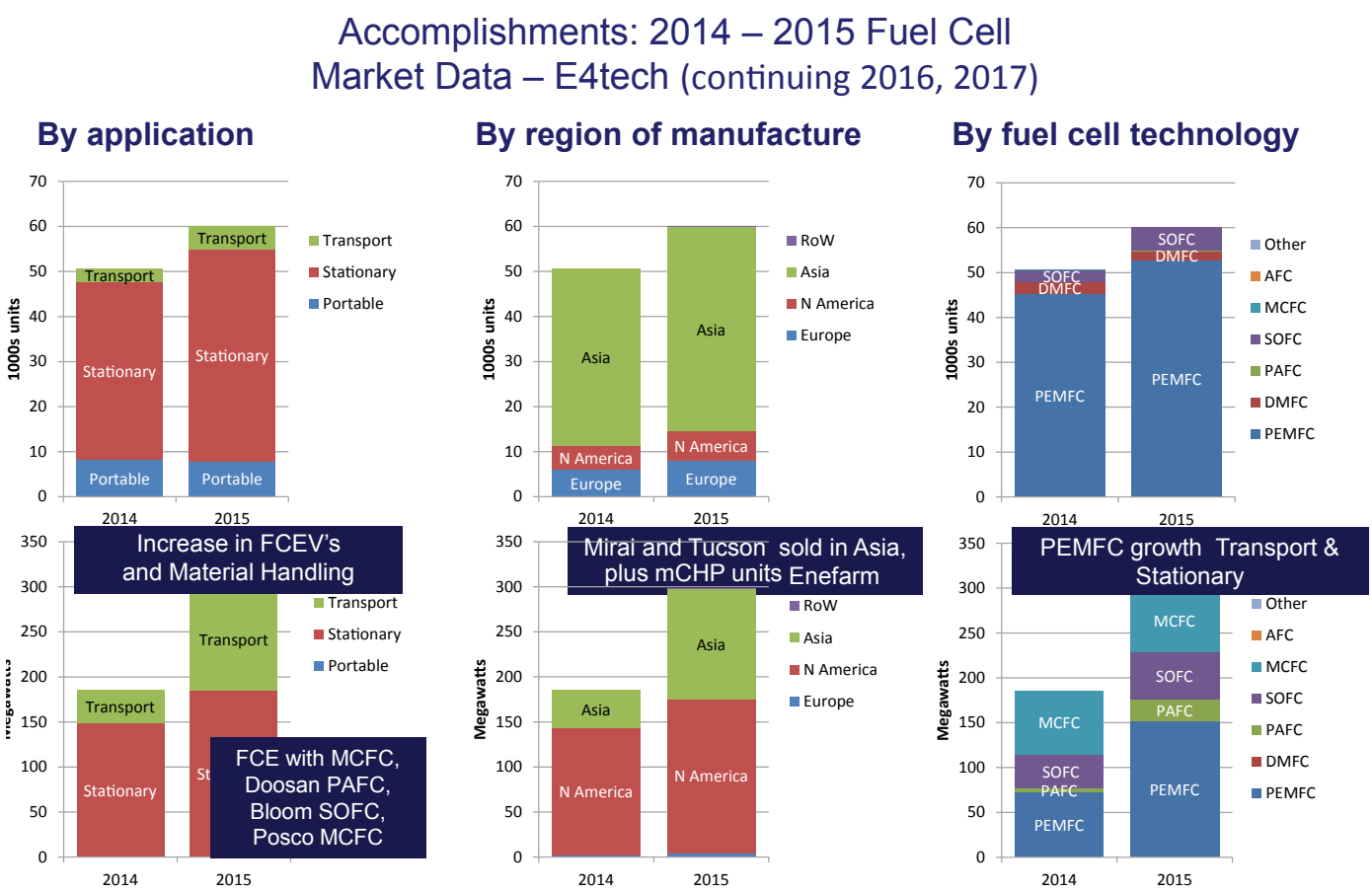

RoW – region of world; SOFC – solid oxide fuel cell; DMFC – direct methanol fuel cell; PEMFC – polymer electrolyte membrane fuel cell; PAFC – phosphoric acid fuel cell; AFC – alkaline fuel cell; MCFC – molten carbonate fuel cell; FCEV – fuel cell electric vehicle; FCE – FuelCell Energy; mCHP – micro combined heat and power

FIGURE 4. E4tech 2014 and 2015 market data

- The United States has great depth in the science and technology of fuel cells and high quality in existing automotive industry and supply chain capability. California, in particular, has been a global driver of the fuel cell industry for two to three decades.
- The industry is only just beginning, and judicious investment now could reap benefits for many years to come.
- Increasing domestic fuel cell demand is viewed as a critical enabler of domestic fuel cell system production.
- U.S. OEMs and manufacturers need to restart local development as they have fallen behind Japan and Europe in bipolar plates, membranes, GDLs, and catalysts (on par in hydrogen vessels).

SPECIAL RECOGNITIONS & AWARDS

1. Patrick Fullenkamp, 2017 DOE Hydrogen and Fuel Cells Program R&D Award

FY 2017 PUBLICATIONS/PRESENTATIONS

1. Patrick Fullenkamp, "U.S. Clean Energy Hydrogen and Fuel Cell Technologies: A Competitiveness Analysis," Presentation at Hydrogen and Fuel Cells Technical Advisory Committee meeting, December 7, 2016.

2. Patrick Fullenkamp, "U.S. Clean Energy Hydrogen and Fuel Cell Technologies: A Competitiveness Analysis," Presentation at Annual Merit Review meeting, June 8, 2016.

3. Patrick Fullenkamp, "U.S. Clean Energy Hydrogen and Fuel Cell Technologies: A Competitiveness Analysis," Presentation at WIRE-Net Board of Directors, June 15, 2016.

REFERENCES

1. Pikes Research Report, Executive Summary at http://www.navigantresearch.com/wp-content/uploads/2012/02/FCSC-12-Executive-Summary.pdf

VI.5 Continuous Fiber Composite Electrofusion Coupler

Brett Kimball
Automated Dynamics
2 Commerce Park Dr.
Niskayuna, NY 12211
Phone: (518) 377-6471 x239
Email: bkimball@automateddynamics.com

DOE Managers:
Nancy L. Garland
Phone: (202) 586-5673
Email: Nancy.Garland@ee.doe.gov
Jesse Adams
Phone: (720) 356-1421
Email: Jesse.Adams@ee.doe.gov

Contract Number: DE-EE0007274

Subcontractors:
- NOV Fiberglass Systems, Houston, TX
- Savannah River National Laboratory, Aiken, SC

Project Start Date: December 1, 2015
Project End Date: December 30, 2018

Overall Objectives

- Quantify
  - Various mechanical characteristics of coupler: burst strength, axial strength, leak rates, fatigue characteristics.
  - Manufacturing costs of coupler.
- Optimize
  - Mechanical design of composite coupler: maximize strength characteristics while constraining costs.
- Demonstrate
  - Coupler without mechanical components, which would require underground maintenance.
  - Manufacturability of a robust coupler that reduces cost and complexity of hydrogen pipeline installation.
  - Advanced electrofusion coupler meets mechanical requirements for pipeline designed to transport hydrogen at 100 bar (and pass test at 350 bar)

Fiscal Year (FY) 2017 Objectives

- Demonstrate a functioning coupler that passes required burst, leak, and fatigue tests consistently through testing.
- Optimize the electrofusion process to melt-bond components sufficiently but without overheating given variation in both coupler's componentry and fusion equipment.
- Analyze the coupler's fatigue life and failure modes by finite element modeling of the multi-material coupler.

Technical Barriers

This project addresses the following technical barriers from the Hydrogen Delivery section of the Fuel Cell Technologies Office Multi-Year Research, Development, and Demonstration Plan.

(D) High As-Installed Cost of Pipelines

Contribution to Achievement of DOE Hydrogen Delivery Milestones

This project will contribute to achievement of the following DOE milestones from the Hydrogen Delivery section of the Fuel Cell Technologies Office Multi-Year Research, Development, and Demonstration Plan.

- Milestone 1.5: Coordinating with the H_2 Production and Storage sub-programs, identify optimized delivery pathways that meet a H_2 delivery and dispensing cost of <$2/gge for use in consumer vehicles. (4Q, 2020)
- Milestone 6.3: By 2020, reduce the cost of hydrogen delivery from the point of production to the point of use in consumer vehicles to <$2/gge of hydrogen for the gaseous delivery pathway (4Q, 2020)

FY 2017 Accomplishments

- Identified near-final design configuration. Testing to date has met requirements set forth for hydrogen pipelines:
  - Passed multiple burst tests at 350 bar with water.
  - Passed leak rate tests by an order of magnitude greater than that required (5×10^{-4} cm^3 He/s required).
  - Passed tensile load requirements of 10,000 lb tension.

- Selected and implemented a singular electrofusion machine and process allowing consistent fusion parameters to be used.
- Shown through finite element analysis that the coupler should survive fatigue loading required of 28,500 cycles at R = 0.5, at 350 bar maximum pressure.

✧ ✧ ✧ ✧ ✧

INTRODUCTION

Traditional pipe couplers considered for a nonmetallic buried hydrogen pipeline employ elastomeric sealing components, such as O-rings. The American Society of Mechanical Engineers code committee responsible for hydrogen piping and pipelines has expressed concerns that such underground maintenance would be problematic and unsatisfactory.

The proposed coupler design under this project will eliminate need for such elastomeric seals. This coupler seals adjacent nonmetallic composite pipes by the electrofusion of two adjacent cylindrical plastic surfaces (applying heat via electrical current). State of the art electrofusion couplers are rated at too low of a pressure for the hydrogen pipeline proposed. Therefore, a new design is required.

APPROACH

This research draws from existing electrofusion pipe coupling technology, but extends to be suitable for use on a variety of materials available for composite pipelines. Automated Dynamics' technology is well-suited to couple thermoplastic bonded pipes (where each of the pipe's radial adjacent layers are bonded to each other) by our fiber placement technology that bonds continuous media (fiber reinforced composite, plastic coated wire) on the fly without need for post-curing. The coupler designed in this program shall be available for such pipes and for non-bonded pipes. Existing electrofusion couplers do not allow continuous fiber composite reinforcement necessary to achieve high pressures sought by the DOE. Our coupler will employ this continuous fiber thermoplastic composite as a structural layer for high pressures and high induced axial loads.

RESULTS

The project has been focused on achieving the following results:

- Passed tensile test requirements, failing pipe before failing coupler on average at 11,000 lb.
- Passed burst test requirements, failing pipe before failing coupler on average at 5,400 psig.
- Passed leak-rate test requirements, achieving 10×10^{-5} cm^3 He/s leak rate.
- Demonstrated through analysis that coupler will pass fatigue requirements (28,500 cycles at minimum/maximum stress, R = 0.5). Actual tests slated for later this year.

Further progress of the past fiscal year includes finalizing the design of most of the components and the associated manufacturing and machining processes to produce the custom components. While the first year was spent optimizing some manufacturing processes such as wire placement and fiber placement of the custom electrofusion coupler, this past fiscal year has focused on refining design and geometric tolerances and refining the electrofusion and assembly process, both of which are nearly final.

CONCLUSIONS AND UPCOMING ACTIVITIES

We expect to pass the last of the three milestones in 2017 (fatigue testing) to proceed into the last year of this active project. Then a final design will be chosen and fatigue testing will be performed to yield statistically significant results. Additionally, the manufacturing and quality plans will become more detailed, which will aid in the evolving commercialization plan.

Further funding in 2017 and 2018 will be spent on final fatigue testing and design of procedures for in-field assembly, such as machining the pipe-ends in preparation for fusion.

Lastly, commercialization preparation remains a challenge and focus for this hydrogen line infrastructure. With less than 2,000 miles of currently installed hydrogen pipeline in the United States, the existing market for this infrastructure pales compared to natural gas pipeline infrastructure which is three orders of magnitudes greater.

VI.6 In-line Quality Control of PEM Materials

Paul Yelvington (Primary Contact), Andrew Wagner
Mainstream Engineering
200 Yellow Place
Rockledge, FL 32955
Phone: (321) 631-3550
Email: pyelvington@mainstream-engr.com

DOE Managers:
Nancy L. Garland
Phone: (202) 586-5673
Email: Nancy.Garland@ee.doe.gov
Jesse Adams
Phone: (720) 356-1421
Email: Jesse.Adams@ee.doe.gov

Contract Number: DE-SC0013774

Subcontractors:
- National Renewable Energy Laboratory, Golden, CO
- Professor Tequila Harris, Georgia Institute of Technology Atlanta, GA

Project Start Date: Phase I: June 8, 2015, Phase II: August 1, 2016
Project End Date: Phase I: March 7, 2016, Phase II: July 31, 2018

Overall Objectives

- Identify membrane defect size that leads to cell failure.
- Create a production-intent prototype automated vision system to perform quality control and demonstrate it on a full-speed membrane web line.
- Detect defects down to 4 µm at 100 ft/min.
- Determine membrane thickness to 0.5 µm resolution.
- Achieve a 5σ false-positive and false-negative rate.

Fiscal Year (FY) 2017 Objectives

- Create defective membrane and identify defect size that leads to cell failure.
- Create calibration samples to identify the smallest detectable defect.
- Bring new hardware online and fully automate software for membrane thickness mapping and defect identification.
- Scan the membrane with 100% coverage, marking and logging defective regions.

Technical Barriers

This project addresses the following technical barriers from the Manufacturing R&D section of the Fuel Cell Technologies Office Multi-Year Research, Development, and Demonstration Plan.

(E) Lack of Improved Methods of Final Inspection of Membrane Electrode Assemblies (MEAs)

(H) Low Levels of Quality Control

Contribution to Achievement of DOE Manufacturing R&D Milestones

This project will contribute to achievement of the following DOE milestones from the Manufacturing R&D section of the Fuel Cell Technologies Office Multi-Year Research, Development, and Demonstration Plan.

- Milestone 1.3: Develop continuous MEA manufacturing processes that increase throughput and efficiency and decrease complexity and waste. (4Q, 2017)
- Milestone 1.6: Develop fabrication and assembly processes for PEMFC MEA components leading to an automotive fuel cell stack that costs $20/kW. (4Q, 2020)
- Milestone 5.2: Demonstrate improved sensitivity, resolution, and/or detection rate for MEA inspection methods. (4Q, 2016)
- Milestone 5.4: Design and commercialize an in-line quality control device for PEMFC MEA materials based on National Renewable Energy Laboratory's (NREL) optical reflectance technology. (4Q, 2017)
- Milestone 5.6: Demonstrate methods to inspect full MEAs and cells for defects prior to assembly into stacks in a production environment. (4Q, 2018)
- Milestone 5.8: Implement demonstrated in-line quality-control techniques on pilot or production lines at PEMFC MEA material manufacturers. (4Q, 2020)

FY 2017 Accomplishments

- Defective membranes have been made for testing and calibration that include bubbles and 5 µm, 10 µm, and 25 µm pinholes.
- NREL and Georgia Tech have tested defective samples and preliminary results indicate that defects less than

10 µm have no immediate effect on performance, while larger than 300 µm cause decreased performance.

- Software development is complete, hardware has been selected, and packaging has begun.
- A static membrane test station was made for repeatable measurements of membrane sheets.
- Mainstream's small-scale (6-inch web width) winder/unwinder was improved to run at 100 ft/min.

✧ ✧ ✧ ✧ ✧

INTRODUCTION

Fuel cells stand on the cusp of commercialization for large-scale applications such as zero-pollution automotive systems. They are held back by high manufacturing costs and expensive catalysts. The membrane alone accounts for as much as 45% of the total material cost of a commercial fuel cell system [1]. Moreover, manufacturing defects in the membrane not only lead to wasted expensive materials but they also cause cell failures that can cascade into complete stack failure. This requires additional labor to rework the stack as well as results in the loss of expensive catalyst and gas diffusion electrode materials. Current inspection methods look for defects after batch production of the membrane, leading to delayed correction of issues with the membrane and membrane electrode fabrication process. Reaching the quality targets for fuel cell system manufacturing requires a new, high-efficiency, real-time quality control system. Mainstream Engineering is developing a real-time optical quality control system that provides significant benefits with increased resolution, improved accuracy, and increased detection speeds for the examination of fuel cell and other membranes.

APPROACH

Mainstream's overall approach to create a prototype automated vision system for quality control was to rigorously prove out the patent-pending optical technique with a wide-range of commercially available membranes, select upgraded hardware for Nafion®, prove out the defect detection abilities of the hardware, automate the software, and build the prototype. A wide range of typical defects were induced and examined in the Nafion® membranes and characterized with Mainstream's machine vision system. Pinholes down to 5 µm were the focus during the first year and the limits of the upgraded hardware were determined. Then the software used for defect detection was fully automated to image the membrane, detect defects, log the defects, track the defect location, and print an identifying marker beside the defect. The software and hardware were validated on Mainstream's 6-inch web-line at speeds up to 100 ft/min. During this time, NREL and Georgia Tech created defective membrane samples and tested them to determine the smallest defect that impacts cell performance. These results are guiding our determination of an appropriate limit of detection for detect size.

RESULTS

Created Controlled Membrane Defects

Mainstream obtained a variety of Nafion® samples with controlled defects of varying sizes, including bubbles and pinholes, for equipment optimization and validation. Georgia Tech produced membrane sheet materials with a range of thicknesses and a variety of as-cast defects. These membranes were created under several off-design coating conditions that represent real, non-reinforced, polymer electrolyte membrane (PEM) membrane materials. In general, the as-cast defects produced were on the order of several hundred microns in size and were mainly bubbles and color defects. In addition, Georgia Tech created Nafion® samples with pinhole defects of 10, 50, and 100 microns using electron-beam lithography. Mainstream also created calibration samples using laser drilling to make a set of membrane sheets consisting of Nafion-115®, Nafion-211®, and Nafion-HP® that were laser drilled to create a 12 in × 12 in array of 5 µm, 10 µm, and 25 µm holes. A schematic of the sheet and microscope image of a nominally 5 mm laser machined hole are shown in Figure 1.

Analyzed Membrane Defects for Impact on Cell Performance

The pinhole and bubble defect samples were characterized, and in situ performance testing was conducted. The defective membranes were characterized with optical microscopy, assembled in cells, tested in NREL's segmented cell system for spatially resolved initial performance, and then tested for spatial hydrogen crossover with NREL's infrared cell hardware. Two examples of this series of testing are given in Figure 2 for a pinhole and a surface cut, in which the local performance impact (center images) correlates with the known location of the defect in the cell and with increased hydrogen crossover (right images). Samples with very small pinholes were also tested, but the cells did not show any local or total cell initial performance impact or increased hydrogen crossover. These preliminary results indicate that defects smaller than 10 µm have no immediate impact on cell performance, while defects larger than 300 µm immediately degrade cell performance.

Developed and Tested Upgraded Hardware and Fully Automated Software

Mainstream conducted a trade study of performance and cost (e.g., line speed, limits of detection) of over 30 cameras, 50 lenses, 10 polarizers, 10 machine vision lights, three software platforms, and four data transfer protocols alone and

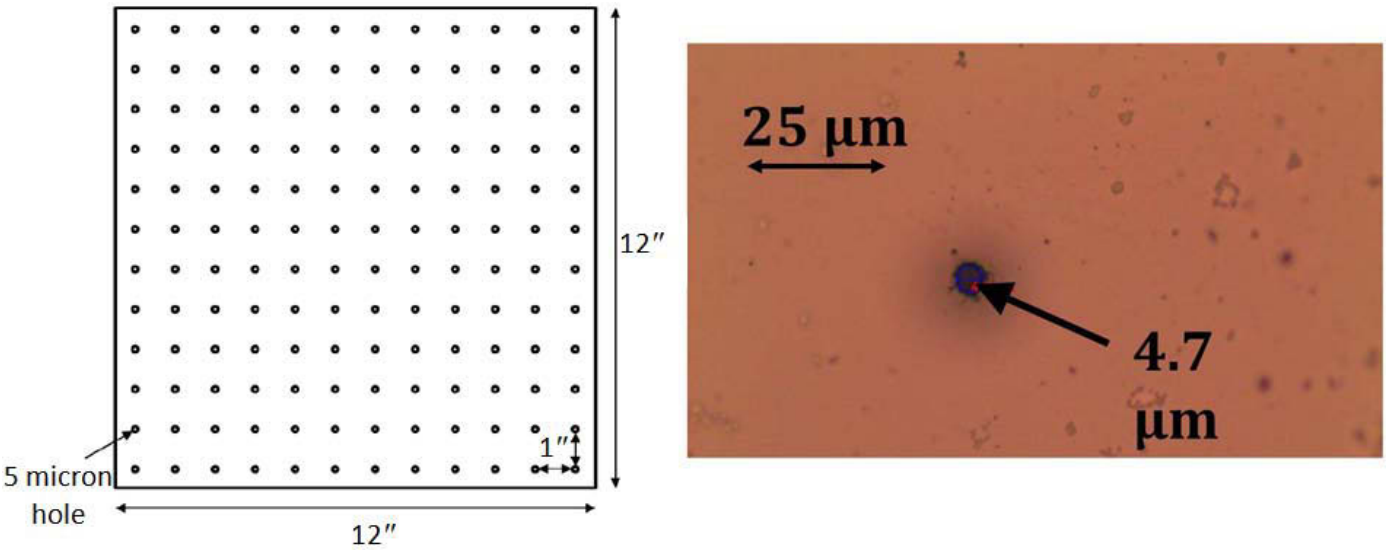

FIGURE 1. Schematic of a membrane calibration sheet and a microscope image of a laser machined hole

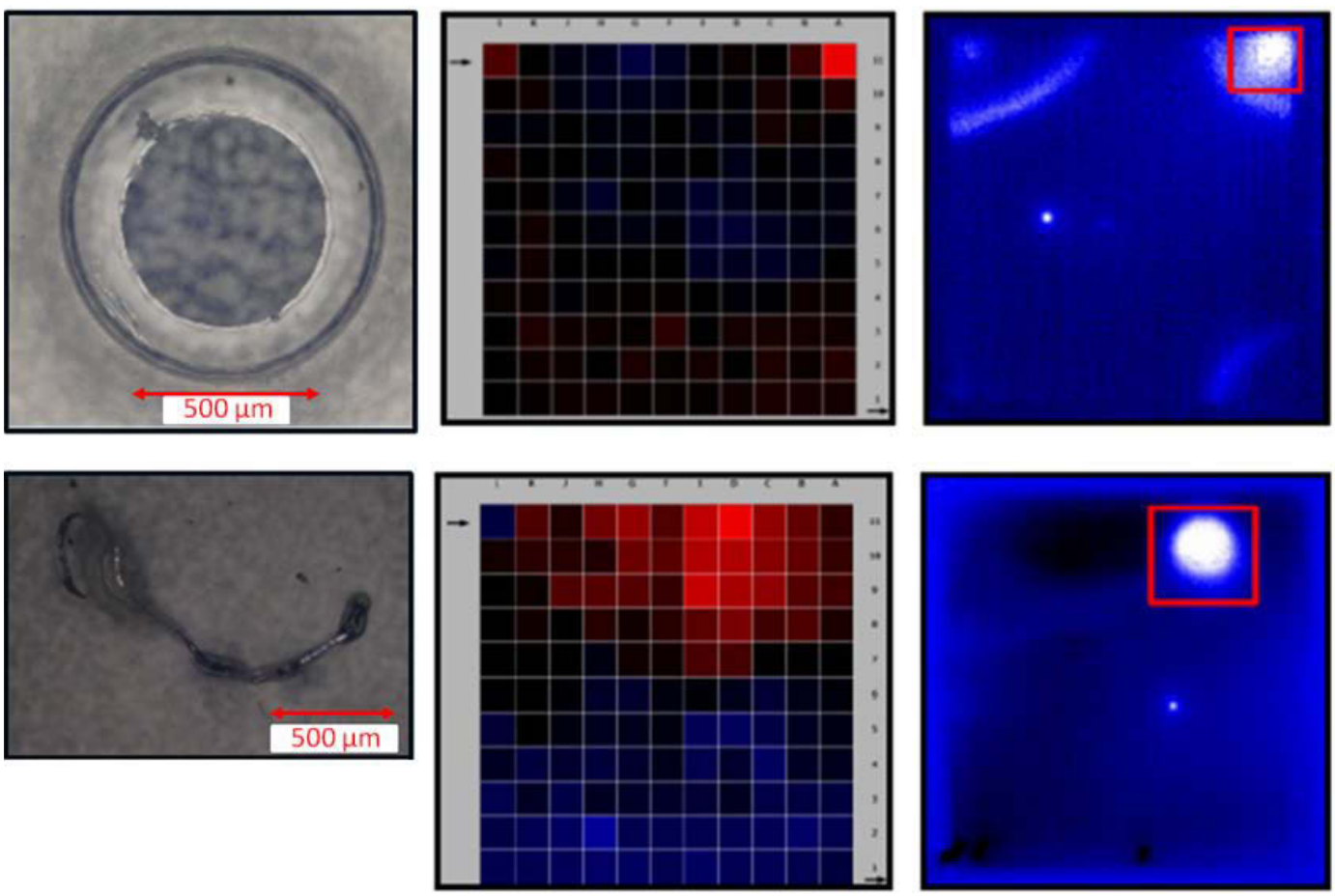

FIGURE 2. Optical microscopy, spatial performance, and spatial hydrogen crossover imaging of two as-cast membrane defects

working as a system. The best equipment within initial cost targets was procured and assembled into an upgraded Phase II system shown in Figure 3. An alpha release of a LabVIEW program for detecting defects in fuel cell membranes was then completed.

The LabVIEW program contains three basic loops, each of which perform different functions and run with different priority levels. The basic architecture is shown in Figure 4. Images are acquired by the camera and pre-processed in the Acquisition Loop. The images are then placed in a buffer. The Field-Programmable Gate Array (FPGA) Loop performs additional processing on the images as well as interfaces with the encoder and printer. The image is sent back to the controller central processing unit, and the machine vision algorithms are performed in the Processing Loop. This loop also performs all image saving and data recording functions, as well as graphical user interface updates. The Acquisition Loop provides an interface between the camera and the software program. Images are acquired at speeds up to 16 frames/s and are pre-processed before being sent to the buffer. The user can select many different camera settings such as scaling, frame rate, image size, exposure time, and gain. The Acquisition Loop also performs adjustments to the brightness, contrast, and gamma of the image, as well as selecting the region of interest. After the image is sent to the buffer, the FPGA Loop reads the oldest image in the buffer. Typically, the buffer never has more than two images at steady-state operation since the Acquisition Loop is acquiring and storing a new image while the previous image is being processed. On the FPGA, the image is deconstructed into a pixel stream, and up to eight pixels are processed at a time via parallel loops. Most of the machine vision algorithm is implemented on the FPGA. The FPGA Loop also interfaces with the encoder and printer. The Image Processing Loop receives the image from the FPGA and performs all the image analysis and recording functions. Once processing of an image is complete, the Image Processing Loop records all relevant data. The combined software and hardware was tested on Mainstream's 6-in web line and operated successfully up to the maximum line speed of 100 ft/min.

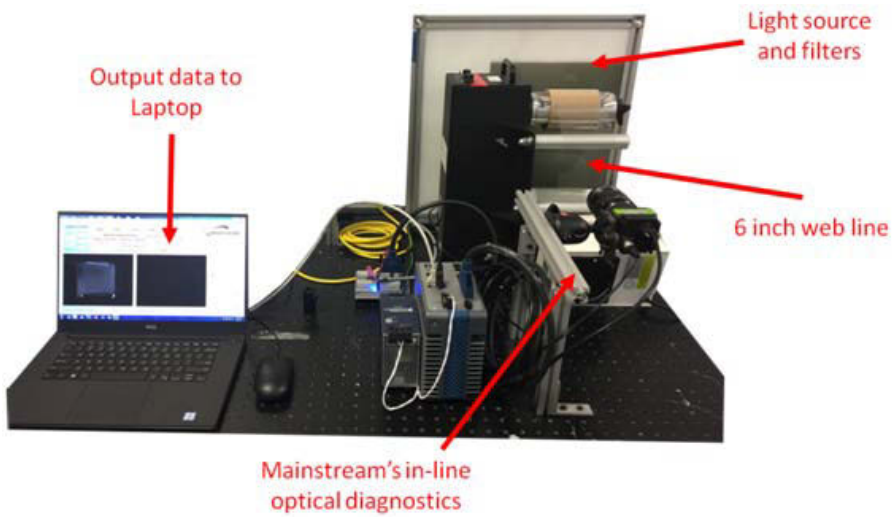

FIGURE 3. Small-scale winder/unwinder inspection station with photosynthetic electron transport film

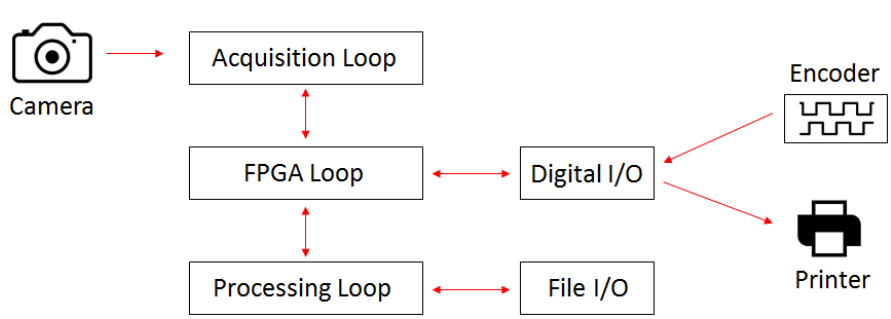

I/O - input and output

FIGURE 4. Image processing software architecture

CONCLUSIONS AND UPCOMING ACTIVITIES

The overall goal of the Phase II program is to research, develop, and commercialize an in-line quality control system for roll-to-roll membrane manufacturing. Mainstream Engineering developed a low-cost, real-time optical detector for quality control using continuous analysis of membranes for polymer electrolyte membrane fuel cell MEAs. The inspection system samples, logs, and marks every location on the roll of material such that defects in MEA materials can be removed prior to assembly into complete cells. An upgraded prototype system was built, and an initial version of the fully automated software was developed. The system was tested on Mainstream's 6-in web line at speeds up to 100 ft/min. The device will identify and mark defects as well as monitor membrane thickness in real time to improve line efficiency and to reduce waste. For FY 2018, the main goals will be to produce new defective membranes for use in determining defect size that leads to cell failure, to package a prototype system for a 24-in web, to validate the system, and to demonstrate it on multiple web lines including on-site manufacturing demonstrations.

SPECIAL RECOGNITIONS & AWARDS/ PATENTS ISSUED

1. Invention Disclosure Attorney Docket No. 62988US titled, "Apparatus and Method for Cross-polarized, Optical Detection of Polymer Film Thickness and Defects Using Polarimetric Thickness Mapping."

FY 2017 PUBLICATIONS/PRESENTATIONS

1. Wagner, A., Lasko, T., Yelvington, P.E., "In-line Quality Control of PEM Materials," presented, DOE 2017 Annual Merit Review, Washington, D.C., June 2017.

REFERENCES

1. Kleen, G.J., "Membrane Development in the U. S. DOE Fuel Cell Technologies Program," Fuel Cell Seminar and Exhibition, Orlando, FL, 2011.

VI.7 Manufacturing Competitiveness Analysis for Hydrogen Refueling Stations

Ahmad Mayyas (Primary Contact), Margaret Mann
National Renewable Energy Laboratory
15013 Denver West Parkway
Golden, CO 80401
Phone: (303) 384-7446
Email: Ahmad.Mayyas@nrel.gov

DOE Managers:
Nancy L. Garland
Phone: (202) 586-5673
Email: Nancy.Garland@ee.doe.gov
Jesse Adams
Phone: (720) 356-1421
Email: Jesse.Adams@ee.doe.gov

Project Start Date: April 6, 2015
Project End Date: March 31, 2018

Overall Objectives

- Develop manufacturing cost models for major components in the hydrogen refueling stations such as the compressors, storage system, dispenser, chiller, and heat exchanger.
- Identify cost drivers associated with manufacturing of the hydrogen station parts and systems and highlight potential cost reduction through economies of scale and standardization.

Fiscal Year (FY) 2017 Objectives

- Provide a platform for manufacturing cost analysis for major hydrogen refueling station (HRS) systems and components.
- Identify potential cost reductions in the manufacturing of dispensers, pressure vessels, chillers, and heat exchangers.
- Study international markets and global trade flows to examine potential competiveness using number of installed HRSs in each country and number of HRSs shipped from/to certain countries.

Technical Barriers

This project addresses the following technical barriers from the Hydrogen Delivery section of the Fuel Cell Technologies Office Multi-Year Research, Development, and Demonstration Plan.

(A) Lack of Hydrogen/Carrier and Infrastructure Options Analysis

(B) Reliability and Costs of Gaseous Hydrogen Compression

(E) Gaseous Hydrogen Storage and Tube Trailer Delivery Costs

Contribution to Achievement of DOE Hydrogen Delivery Milestones

This project will contribute to achievement of the following DOE milestones from the Hydrogen Delivery section of the Fuel Cell Technologies Office Multi-Year Research, Development, and Demonstration Plan.

- Milestone 6.3: By 2020, reduce the cost of hydrogen delivery from the point of production to the point of use in consumer vehicles to <$2/gge of hydrogen for the gaseous delivery pathway. (4Q, 2020)

FY 2017 Accomplishments

- Manufacturing cost models were developed for hydrogen dispensers, pressure vessels, chillers, and heat exchangers.
- New set of updated maps were developed to assess global HRS supply chain and international trade flows for the period (2005–2017).
- Manufacturing cost model was developed for proton exchange membrane electrolyzers using different hydrogen production capacities (kilogram H_2 per day) and different annual production rates (electrolyzers/yr).

✧ ✧ ✧ ✧ ✧

INTRODUCTION

This study is one of a few studies that discuss cost of hydrogen infrastructure. While other studies focus on the big picture by assessing the effect of capital cost reductions on the hydrogen prices, this study provides a complete bottom-up manufacturing cost analysis for major systems in the hydrogen refueling stations (compressors, pressure vessels, chillers, heat exchangers, and dispensers). Manufacturing competitiveness analysis was performed to study the effect of cost components (e.g., labor, facilities and energy costs) in different countries on the final product cost. Besides the manufacturing competiveness analysis, this study also aims at developing detailed supply chain and international trade

flow maps, which may help decision makers in visualizing main trade flows in the international markets and spot main markets for hydrogen station components from manufacturing countries to final installation locations.

APPROACH

This study is centered around three main analyses: manufacturing competiveness analysis, supply chain analysis, and effect of qualitative factors on the selection of the manufacturing facility locations for manufacturing of the systems and parts used in the hydrogen refueling stations.

Manufacturing competiveness analysis is used to evaluate relative manufacturing cost in selected countries in North America, Europe, and Asia, on manufacturing of main components in the hydrogen stations such as compressors, storage vessels, chillers, heat exchangers, and dispensers. Supply chain analysis was conducted with the aid of trade flow maps which show main trade flows between international markets from country of production to the final installation locations. Besides these two mentioned analyses, this study is also trying to address major factors that play a role in selecting manufacturing locations in the United States and other countries and the method of translating these factors into competitiveness metrics. Examples of these qualitative factors include manufacturing experience, product quality, skilled labor requirements and availability, tax policy, currency fluctuations, etc.

RESULTS

Manufacturing Competitiveness Analysis

The goal of this analysis is to dive deeper to study cost drivers associated with the manufacturing of some systems and major parts in the hydrogen refueling stations such as hydrogen compressors, Type I storage tanks, dispensers, chillers, and heat exchangers. The following example discusses the manufacturing cost model for two types of dispensers: H35 (35 MPa) single-hose dispenser and dual-hose dispenser H35/H70 (35 MPa and 70 MPa). Generally speaking, most of the dispenser manufacturers acquire major parts in the dispensers from reliable part vendors and then assemble these parts in-house. The main manufacturing processes involved in the production of the hydrogen dispenser include a sequence of manual and semi-automatic assembly processes followed by a pressure testing. If it passes the final pressure testing, then the end product can be shipped to the installation location.

After collecting the parts cost (Figures 1a and 1b), we plugged these numbers in the standard CEMAC cost model to estimate the final manufacturing cost with six cost components (parts, labor, capital, variable, energy, and building costs). Another cost component was estimated using the weighted average cost of capital method to account for the profit margin. Compiling these cost components in one chart gives the final manufacturing cost curve represented by the minimum sustainable price (MSP) curve. MSP can be defined as the minimum price that sustains a manufacturer's

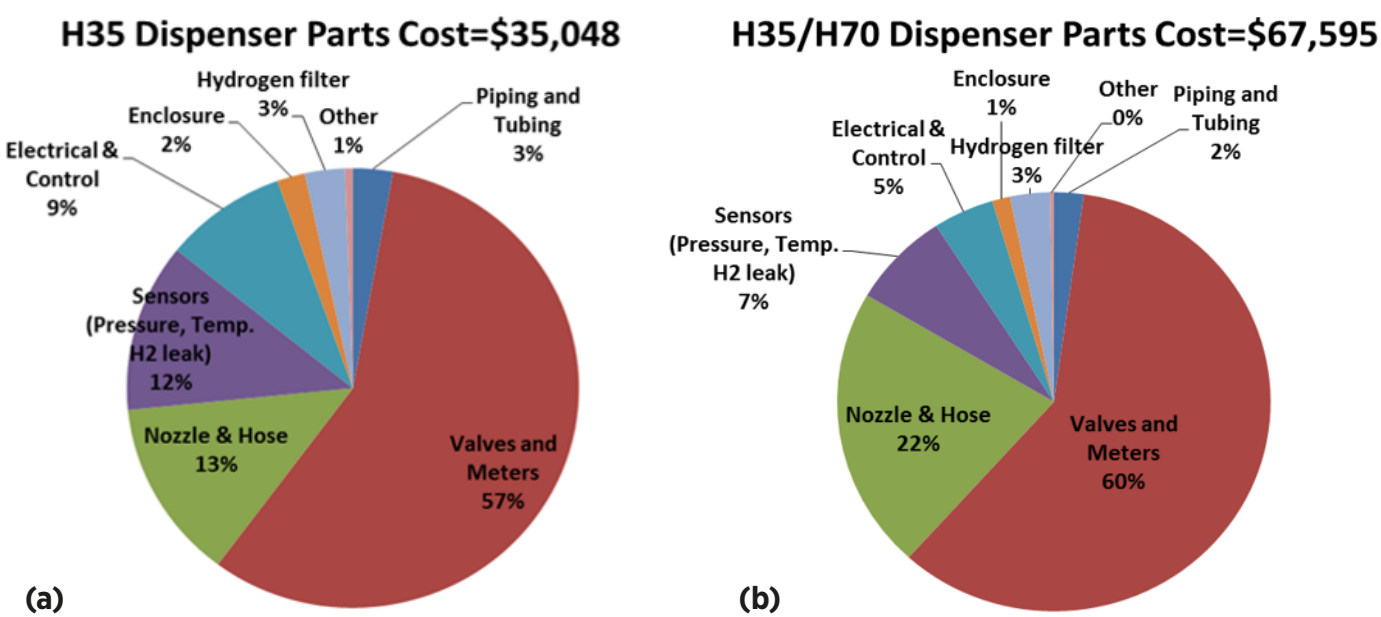

FIGURE 1. Part cost breakdown for (a) H35 single-hose dispenser and (b) H35/H70 dual-hose dispenser

business in a good financial state with no losses and no gains other than the manufacturing cost and internal rate of return required to cover the loan principal and interest (if presented) (see Figures 2a and 2b for H35 and H35/H70 dispensers, respectively). The MSP curve indicates significant cost reductions upon producing more units in the manufacturing facility as a direct result of better resource utilization, i.e., lower capital and building cost per unit produced.

A comparative cost analysis using minimum sustainable prices was performed for hydrogen dispensers in selected countries (Figure 3). It can be seen clearly that Chinese- and Mexican-based manufacturers have advantages of lower labor

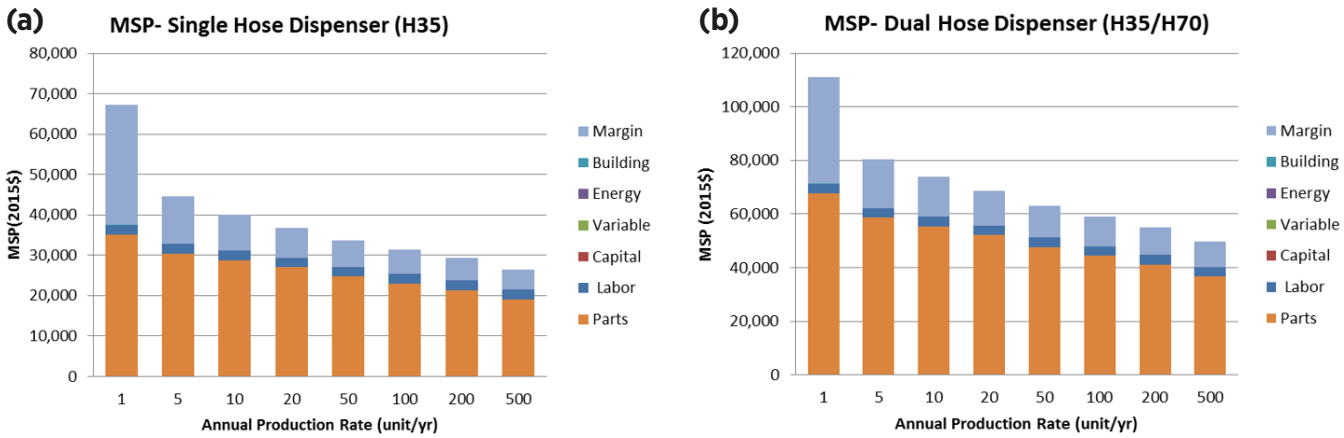

FIGURE 2. MSP curve for hydrogen dispensers manufactured in the United States for (a) H35 single-hose dispenser and (b) H35/H70 dual hose dispenser

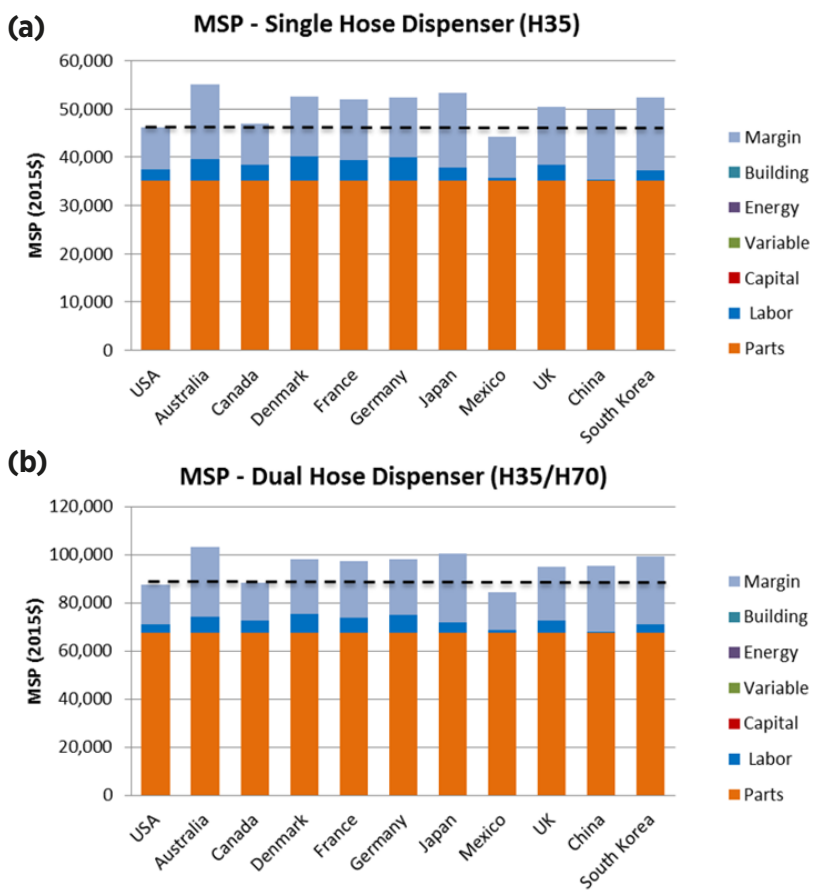

FIGURE 3. Comparative manufacturing cost analysis using MSP for hydrogen dispensers manufactured in selected countries: (a) H35 single-hose dispenser and (b) H35/H70 dual-hose dispenser

cost, lower building cost, lower materials cost, and lower energy cost (China only).

Supply Chain and Trade Flow Maps

This analysis is used as a qualitative measure to assess manufacturing competiveness in selected countries and investigate level of specialization in manufacturing certain components used in hydrogen refueling stations. Figure 4 shows the location of major international manufacturers of hydrogen refueling station systems and HRS developers. Two main clusters can be seen in North America and Western Europe. Unsurprisingly, these two regions also see the highest level HRS activities represented by the number of HRS installations in the past few years (Figure 5). We can say that the United States and Germany are the leading countries in number of manufactured HRSs and number of installations followed by Canada and Japan.

CONCLUSIONS AND UPCOMING ACTIVITIES

This project discusses manufacturing competitiveness and supply chain analyses for the hydrogen refueling stations and can help in understanding cost associated with manufacturing major components and systems in HRSs. Bottom-up cost analysis was used to develop manufacturing cost models for major systems in the HRS. Minimum sustainable price curves for hydrogen dispensers suggest that significant cost reductions (up to 40% or more) can be

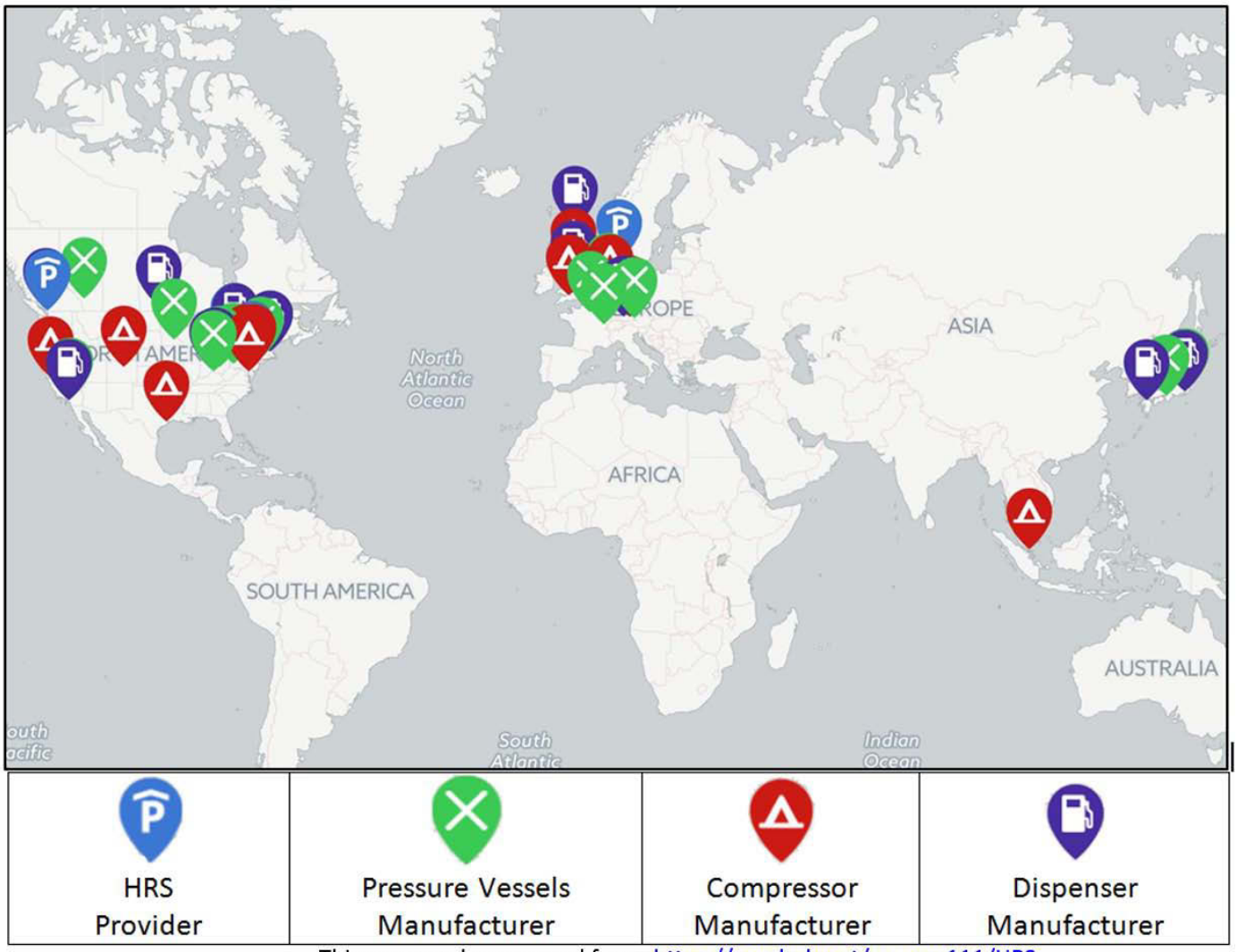

This map can be accessed from: https://maphub.net/mayyas111/HRS

FIGURE 4. Major international manufacturers of hydrogen refueling station systems

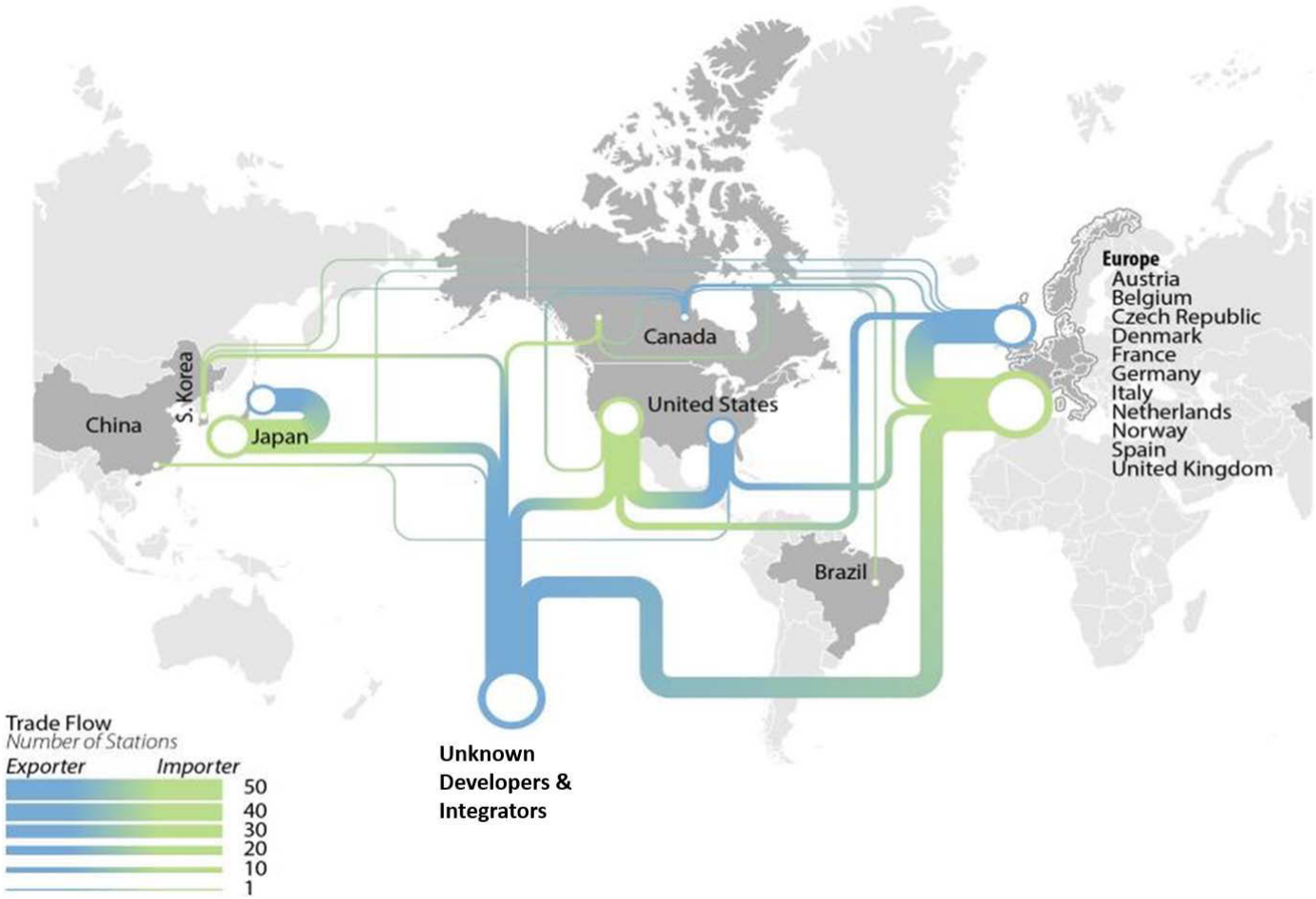

FIGURE 5. International trade flow map showing number of HRS shipped globally between 2005–2017 [1–4]

achieved if 100 units/yr are manufactured relative to the dispenser cost at 5 units/yr. International trade flow maps showed that the United States and Germany are leading countries in terms of number of produced units and number of installed hydrogen stations.

For FY 2018, manufacturing cost models and minimum sustainable price curves will be developed for onsite hydrogen production systems (proton exchange membrane and alkaline electrolyzers and small size steam methane reformers). After that the estimated MSP values will be summed up to estimate the capital cost of HRSs in different regions. These estimates will be then used to study the effect of capital cost reductions on the hydrogen prices.

FY 2017 PUBLICATIONS/PRESENTATIONS

1. Ahmad Mayyas, "Manufacturing Competitiveness and Supply Chain Analyses for Hydrogen Refueling Stations." FCTO monthly webinar. May 11, 2017.

2. Ahmad Mayyas, "Manufacturing Competitiveness Analysis for Hydrogen Refueling Stations." Presentation at the Annual Merit Review, June 6, 2017. Washington, D.C.

REFERENCES

1. California Energy Commission (CEC). Joint Agency Staff Report on Assembly Bill 8: Assessment of Time and Cost Needed to Attain 100 Hydrogen Refueling Stations in California. December 2015. http://www.energy.ca.gov/2015publications/CEC-600-2015-016/CEC-600-2015-016.pdf

2. PNNL (Pacific Northwest National Laboratory). Hydrogen Analysis Resource Center. International Hydrogen fueling stations. http://hydrogen.pnl.gov/hydrogen-data/international-hydrogen-fueling-stations

3. A. Iborra, E. Gupta, L. Seissler. 4th International Workshop on Hydrogen Infrastructure and Transportation. 24–25 May 2016, Egmond aan Zee, The Netherlands. http://publications.jrc.ec.europa.eu/repository/bitstream/JRC103586/4%20int%20workshop%20on%20h2%20infra%20final%20pdfonline.pdf. Last accessed 08/09/2017.

4. www.H2Stations.org

VII.0 Technology Validation Sub-Program Overview

INTRODUCTION

The Technology Validation sub-program demonstrates, tests, and validates hydrogen and fuel cell technologies and uses the results to provide feedback to the Fuel Cell Technologies Office's research and development (R&D) activities. Continuing efforts include real-world evaluation and data collection associated with fuel cells operating in transportation applications (e.g., light-duty vehicles, medium- and heavy-duty trucks, and buses) and with hydrogen stations. The sub-program is also implementing projects that support the advancement of hydrogen infrastructure by developing and validating a prototype device to measure hydrogen dispenser performance; validating infrastructure components; implementing and validating advanced hydrogen storage, delivery, and dispensing technologies; and creating tools to enhance access to hydrogen station status information. Activities of the sub-program have expanded into examining hydrogen-based energy storage, where electrolyzers may be used as a controllable electrical load that can provide real-time grid services.

GOAL

The goal of the Technology Validation sub-program is to validate the state-of-the-art of fuel cell systems in transportation and stationary applications, as well as hydrogen production, delivery, and storage systems, and assess technology status and progress to determine when technologies should be moved to the market transformation phase.

OBJECTIVES

The objectives of the Technology Validation sub-program are to:

- Validate a hydrogen fueling station capable of producing and dispensing 200 kg H_2/d (at 5 kg/3 min; 700 bar) to fuel cell electric vehicles (FCEVs) by 2019.
- Validate large-scale systems for grid energy storage that integrate renewable hydrogen generation and storage by operating for more than 10,000 hours with an electrolysis system efficiency of 60% lower heating value by 2021.
- Validate hydrogen FCEVs with fuel cell system efficiency of 65% lower heating value and 5,000 h fuel cell durability.

FISCAL YEAR (FY) 2017 TECHNOLOGY STATUS AND ACCOMPLISHMENTS

Vehicles

Fuel Cell Electric Vehicle Evaluation

Over the last 10 years, the National Renewable Energy Laboratory (NREL) has completed analysis of 227 on-road vehicles that have accumulated more than seven million miles. Current data are supplied by three original equipment manufacturers for 42 vehicles, with model years spanning 2008 to 2016.

Fuel cell durability has steadily and significantly improved over the last decade, and on-road fuel economy and driving range between fills have also increased over the last 10 years. The maximum vehicle odometer reading is 296,300 mi (approximately 10% of the vehicles have surpassed 100,000 mi), and the maximum fuel cell operation is 5,648 hours. NREL is seeing the FCEVs operated in similar ways to traditional gasoline vehicles for driving and fueling. Analysis results show progress against key U.S. Department of Energy (DOE) metrics of voltage durability, system gravimetric and volumetric capacity, specific power, and power density. Future plans for this project include evaluating the interdependence between FCEV and hydrogen station performance, continuing to benchmark fuel cell durability and FCEV range, and developing and validating a predictive FCEV fueling demand model. (NREL)

Fuel Cell Electric Bus Evaluation

Fuel cell propulsion systems in buses have continued to show progress in increasing the durability and reliability of fuel cell electric buses and their primary components. Table 1 shows that the current technology meets the ultimate reliability target for road call frequency for both the overall bus and the fuel cell system. The fuel cell system on one

bus is nearing the ultimate target for power plant lifetime, and seven additional fuel cell systems have surpassed the 2016 target. Table 1 also summarizes the current status compared to the DOE and U.S. Department of Transportation Federal Transit Administration performance targets. Transit agencies have made major progress over the last two years to transition maintenance to transit agency staff. (NREL)

TABLE 1. FY 2017 Summary of Progress toward Meeting DOE and Federal Transit Administration Targets

	Units	2017 Status	2016 Target	Ultimate Target
Bus lifetime	Years/miles	5.6/150,000[a]	12/500,000	12/500,000
Power plant lifetime	Hours	3,061–24,800[a]	18,000	25,000
Bus availability	%	75	85	90
Road call frequency (bus/fuel cell system)	Miles between road call	4,500/20,700	3,500/15,000	4,000/20,000
Operation time	Hours per day/days per week	19/7	20/7	20/7
Maintenance cost	$/mile	0.46–2.28	0.75	0.40
Fuel economy	Miles per diesel gallon equivalent	5.8–6.6	8	8
Range	Miles	220–270	300	300

[a] Accumulation of miles and hours to date—not end of life.

Fuel Cell Hybrid Electric Delivery Van Development and Deployment

This project aims to develop and demonstrate a hydrogen fuel cell hybrid electric van with a 125-mi operational range and validate the vehicle through in-service deployment in a California United Parcel Service fleet. In FY 2017, the vehicle design was finalized, including component layout and packaging details, after completing a hazard analysis with support from DOE's Hydrogen Safety Panel. Long lead time components were procured, and primary components of the fuel cell hybrid electric powertrain were integrated into the vehicle. The fueling requirements were reviewed with Linde, while fueling tests and fuel purchase strategies were discussed in preparation for the demonstration. The next step will be to validate a prototype van through a six-month demonstration in parcel delivery service, while also collecting and evaluating operating data during deployment. (Center for Transportation and the Environment)

Infrastructure and H2FIRST

Innovative Advanced Hydrogen Mobile Fueler

The design of the mobile hydrogen fueling system proposed by this project has been completed, and the team is ready to begin construction. The team solicited input from selected automotive companies and DOE to determine crucial design specifications and parameters for the mobile fueler. Air Liquide's C100 station design was selected as the base design. A safety plan was also developed. Major and long lead components are currently being purchased, including two Hydrogen Technology & Energy Corporation Power Cubes, a compressor, and the heat exchanger. In addition, the team is actively pursuing vendor quotes and purchase order agreements for the remaining equipment items. During the design process, the team identified barriers and challenges associated with the operation and site selection and developed a plan with DOE and other stakeholders to reduce risk and address the barriers identified. Planned activities include assembly, testing of sub-systems and full system, and site selection. (Electricore)

Hydrogen Station Data Collection and Analysis

Using the data reported to NREL by 26 retail hydrogen stations and 9 non-retail stations, analyses were conducted on several categories including deployment, performance, reliability, utilization, safety, energy use, and hydrogen quality. Current analysis shows that maximum daily utilization is beginning to approach station capacity at a few stations, which implies a need for larger and/or more stations to meet the upcoming vehicle demand. An increase in the amount of hydrogen dispensed each quarter results from more stations being built and more FCEVs on the road. In 2016, over 107,000 kg of hydrogen was dispensed from retail stations. A look at maintenance by equipment type shows that hydrogen dispensers are now the primary items needing maintenance both in terms of number of events and labor hours. Fueling rates average 0.83 kg/min, fueling amounts average 2.86 kg, and fueling time averages 3.6 min. Compressors use 3.65 kWh/kg and electrolyzers use 62 kWh/kg on average. There are 23 hours of maintenance at a station on average per month. (NREL)

Performance Evaluation of Delivered Hydrogen Fueling Stations

This project aims to assess the readiness level of current and state-of-the-art infrastructure technologies by collecting and reporting on operational, transactional, safety, and reliability data for five hydrogen fueling stations located in California. Two key technologies that are part of this project are a Gas Technology Institute (GTI) data acquisition system and a Linde ionic compressor. Two of the five sites are operational (West Sacramento and San Juan Capistrano), and data collection has commenced. The GTI data acquisition system was installed and commissioned at the San Ramon station, and the site will open for public use in the near future. Construction began at the Mountain View station in June 2017, with expected installation of the GTI panel likely occurring in September or October of 2017. Progress continues to be made on the installation of the final station; a site has been proposed and the major equipment have been built and are awaiting final site selection. (GTI and Linde)

Hydrogen Component Validation

This project addresses two challenges facing forecourt hydrogen stations today: particulate contamination and station components' energy consumption. The particulate contamination project was developed to collect field samples of particulate matter, determine the origin, and identify major issues impacting a high percentage of stations. Currently, 11 stations are participating and NREL is reaching out to more stations as they become operational. NREL identified metal particulates as a significant portion of particulate contamination. Using in-line filters, NREL examined the impact of three cleaning methods to remove metal particulates after tube cutting, beveling, and threading. The filters from tubing cleaned with the air and rag method showed the most contamination with the greatest filter mass change and the highest number of particles on the filter. Filters from tubing cleaned with the sonication method had the lowest filter mass change, and filters from the systems cleaned by tube brush had the lowest number of particles. Plans are to develop an outreach program for station fabricators on tube cleaning techniques.

Power and energy consumption of major station components impacts operating costs at hydrogen stations. To better understand the contribution of major station components, NREL monitored the power requirements for two hydrogen compressors and the hydrogen pre-cooling system at the NREL Hydrogen Infrastructure Testing and Research Facility (HITRF) and compared the results to data from commercial fueling stations. The HITRF compressor data matched well with the retail data while the pre-cooling data comparison was found to be highly variable between HITRF and the retail stations. The primary parameters causing the variability were the ambient temperature and the mass of hydrogen chilled per unit of time. Figure 1 shows one instance of performance data, with a cost per component for each kilogram of hydrogen assuming a typical electricity rate for Los Angeles, $0.184/kWh. (NREL)

Performance and Durability Testing of Volumetrically Efficient Cryogenic Vessels and High Pressure Liquid Hydrogen Pump

An experimental vessel was cycle tested 456 times to 700 bar with cryogenic pressurized hydrogen (before failing by developing a crack through the liner), while simultaneously measuring system performance. The liquid hydrogen pump delivered 1.65 tonnes of hydrogen to the experimental vessel during the cycle testing. The pump consistently demonstrated high hydrogen throughput (96 kg/h average and 100+ kg/h peak hydrogen flow rate). Throughput is a key parameter for reducing refueling cost per vehicle. The experimental vessel was consistently refueled in under 3 min at ~3.7 kg hydrogen per refuel. While the prototype vessel is small (65 L), these results show promise for future practical refueling times (<5 min) in larger vessels with 5–8 kg of hydrogen capacity. The pump showed low electricity consumption at an average of 1.1 kWh/kg hydrogen active power during the fill, which is considerably lower than for available alternatives. Several sources of boil-off were identified, and results indicate that the station lost 430 kg of hydrogen (25.9% of dispensed hydrogen) to boil-off during the 19-day experiment. Lower boil-off losses (16%) were measured for a typical day of operation where 300 kg of hydrogen were dispensed. Substantial reductions in boil-off to as little as 3.6% are projected for an improved delivery system where the liquid hydrogen truck is not depressurized after dewar refueling and the liquid hydrogen pump is in close proximity to the station dewar. (Lawrence Livermore National Laboratory)

Hydrogen Meter Benchmark Testing

This project aimed to design and build a laboratory-grade gravimetric standard for measurement of hydrogen flow and to evaluate the performance of three commercially available hydrogen flow meters using the gravimetric standard. High-pressure testing of commercially available flow meters (two Coriolis; one Turbine) was conducted over a range of simulated SAE J2601 fueling protocols. For the best meter, the probability that a single fill will be within 2% was found to be 82.2% for all cases, 64.6% for high flow, and 88.1% for typical flow. The probability that a single fill would fall within the 2% or 10% accuracy classes for all the data, and for high flow cases (≥2 kg/min), is shown in Table 2. (NREL)

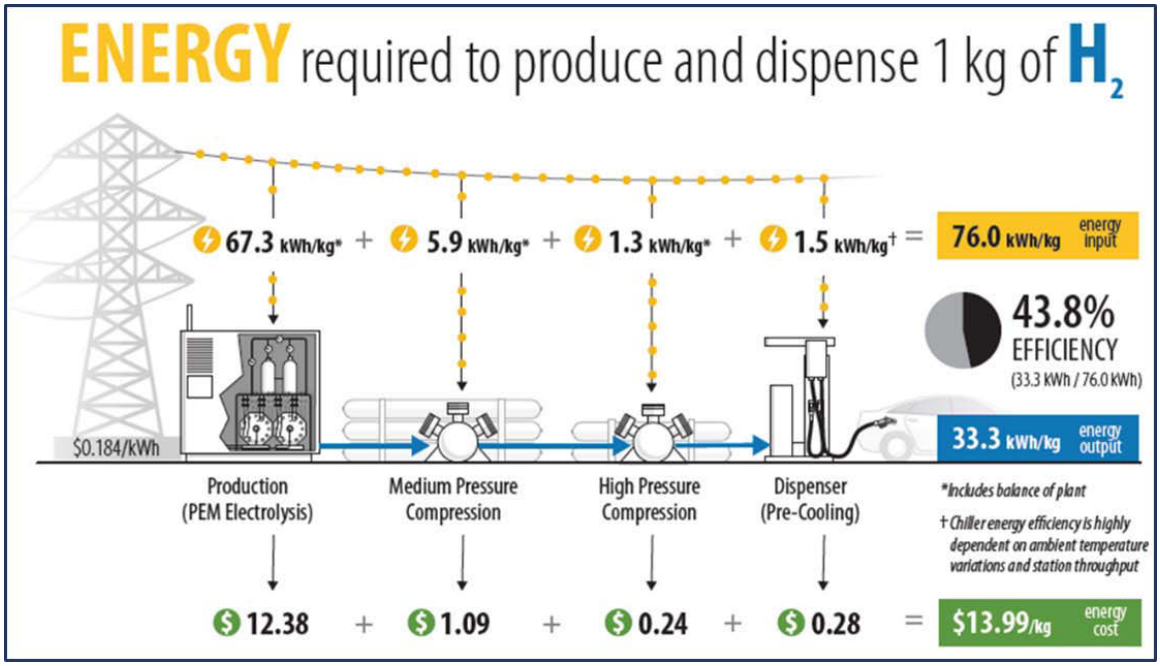

PEM – polymer electrolyte membrane

FIGURE 1. Energy consumption for major components at the HITRF. An electricity price of $0.184/kWh, typical of Los Angeles, is assumed to show the cost of producing 1 kg of hydrogen at 700 bar and -40°C.

TABLE 2. Single Fill Performance Data

Probability a Single Fill Falls Within an Accuracy Class	All Data		High Flow Data (2+ kg/min)	
Accuracy Class	2%	10%	2%	10%
C1	46.5%	99.8%	34.1%	97.3%
C2	82.2%	100%	64.6%	100%
T1	12.6%	58.7%	35.0%	98.5%

C1 and C2 are the two Coriolis flow meters; T1 is the Turbine flow meter.

Hydrogen Energy Storage/Grid Integration

Optimal Stationary Fuel Cell Integration and Control (Energy Dispatch Controller [EDC])

This project aims to create a tool set to foster growth in fuel cell-integrated buildings by implementing an open source tool (EDC) for optimized dispatch of building components and a planning tool for optimal component selection and sizing that uses the chosen dispatch control strategy. The EDC optimization framework was demonstrated to show how varying inputs would drive different behaviors for controlling building components. Four different methods for building load forecasting (for uncontrollable loads, as input to the EDC optimization) are being evaluated. A co-simulation environment is also being established for the EDC and EnergyPlus (DOE's whole-building energy simulation engine). This co-simulation will allow the EDC to run against a building simulation, which will provide a feedback loop to which the EDC can react. The EDC and the EnergyPlus simulation are currently running separately, and the project team is working towards a functioning co-simulation environment. (NREL)

Integrated Systems Modeling of the Interactions between Stationary Hydrogen, Vehicle, and Grid Resources

This project aims to establish the available capacity, value, and impacts of interconnecting hydrogen infrastructure and fuel cell electric vehicles to the electric grid. A hydrogen–vehicle–grid integration (H2VGI) toolset is being developed to quantify and optimize the complex interactions between these energy systems. Progress has been made on developing several sub-models for the H2VGI tool set, looking at vehicle deployment scenarios, FCEV drivetrains,

fueling demand from large vehicle populations, and fueling station components that demand electricity. The potential benefit to California's net load shaping from a large population of FCEVs fueled by electrolytic production of hydrogen has been modeled for the first time. Increasing overall electrolyzer capacity in megawatts (or equivalently, successively lower capacity factors) may provide some valley-filling of the net load shape. Electrolytic hydrogen production also was found to provide net load ramping mitigation. Ramp rates can be significantly reduced when the electrolyzer is slightly oversized (capacity factor reduced from 1 to 0.9), with a ramping rate reduction of about 2.85 GW/h, or about 26% from the maximum ramp rate, without hydrogen production. (Lawrence Berkeley National Laboratory)

Dynamic Modeling and Validation of Electrolyzers in Real-Time Grid Simulation

This project aims to quantify the value of electrolyzers at hydrogen refueling stations from a grid integration perspective. The anticipated value of electrolyzers stems from the fact that they are a controllable load with fast response. The test set-up involves real-time simulations of power systems at Idaho National Laboratory (INL) with hardware-in-the-loop of a 250 kW electrolyzer at NREL. In FY 2017, INL and NREL performed an aggregate of over 500 hours of testing of the 250 kW electrolyzer stack, primarily for stack characterization and front end controller (FEC) functionality. Test results demonstrated capability of the electrolyzer to provide local grid services and the ability of the FEC as hardware to control the electrolyzer. Economic optimization of the FEC also has been developed and implemented, allowing the FEC to make optimal decisions under different market rates and structures to generate hydrogen at a low cost. (INL and NREL)

Modular Solid Oxide Electrolysis Cell System for Efficient Hydrogen Production at High Current Density

This project aims to demonstrate the potential of solid oxide electrolysis cell systems to produce hydrogen at a cost of \$2.00/kg H_2 or less (excluding delivery, compression, storage, and dispensing). An additional objective involves enhancing stack endurance and imparting subsystem robustness for operation on load profiles compatible with intermittent renewable energy sources. During FY 2017, work was initiated on cell-, stack-, and system-level technology development and verification. Steady-state degradation tests of the electrolysis cells were completed over 4,500 hours of operation at 1 A/cm^2 and 2 A/cm^2, showing degradation rates of 1.3%/1,000 h and 2.6%/1,000 h, respectively, well below the 4% value as the upper limit target. A new generation of the cell design has been developed to reduce degradation rates further and is currently undergoing degradation testing. System-level investigations have focused specifically on the effects of system operating parameters and system architecture on overall system efficiency and economic feasibility. The baseline system process model has been completed and tradeoff analysis is ongoing to determine optimal system architecture and operating conditions. Future work will focus on further improvements in cell and stack endurance, forecourt system optimization, and detailed system design for the >4 kg H_2/d demonstration system. (FuelCell Energy)

H2@Scale

H2@Scale Analysis

The H2@Scale concept was presented by the national laboratory-led team during the FY 2016 Big Idea Summit and is based on utilizing hydrogen's unique ability to both support the electric grid and provide clean energy to a variety of demands. This project is focused on improving initial analysis estimates by analyzing both the technical and economic potential for hydrogen markets. The technical potential demand for hydrogen under the H2@Scale concept was estimated to be 60 million metric tonnes per year. Analyses revealed that sufficient domestic fossil and nuclear resources are available to meet the potential hydrogen demand. Assuming that hydrogen demand is supplied by water electrolysis using renewably generated electricity, the analyses indicated that fossil energy use would decrease by 15%. During the remainder of FY 2017, the team will analyze the economic potential of H2@Scale by using supply and demand curves to estimate hydrogen demand at market equilibrium. Possible work in later years could extend the analysis to consider regional analysis, storage and infrastructure development challenges, and macroeconomic impacts. (NREL)

High-Temperature Electrolysis (HTE) Test Stand

INL developed a world-class HTE laboratory and test capability that includes both a 25 kW flexible test station plus infrastructure support for up to 250 kW HTE turnkey systems. A three-dimensional computer aided design model of the 25 kW HTE system layout has been prepared, and operating specifications have been determined. Assembly of the 25 kW HTE demonstration facility will be completed during the first and second quarters of FY 2018, and full-scale testing is planned for later in FY 2018 (third and fourth quarters). (INL)

BUDGET

The Technology Validation sub-program was allocated $18 million in FY 2017 (Figure 2). This funding enabled it to continue to collect and analyze data from fuel cells operating in transportation applications (e.g., light-duty vehicles, medium- and heavy-duty trucks, and buses), while validating and evaluating hydrogen infrastructure (e.g., fueling stations, components, and delivery/dispensing). In coordination with the Office of Electricity and other offices in the Office of Energy Efficiency and Renewable Energy, major focus areas in FY 2017 were hydrogen-based energy storage and grid integration activities, including H2@Scale.

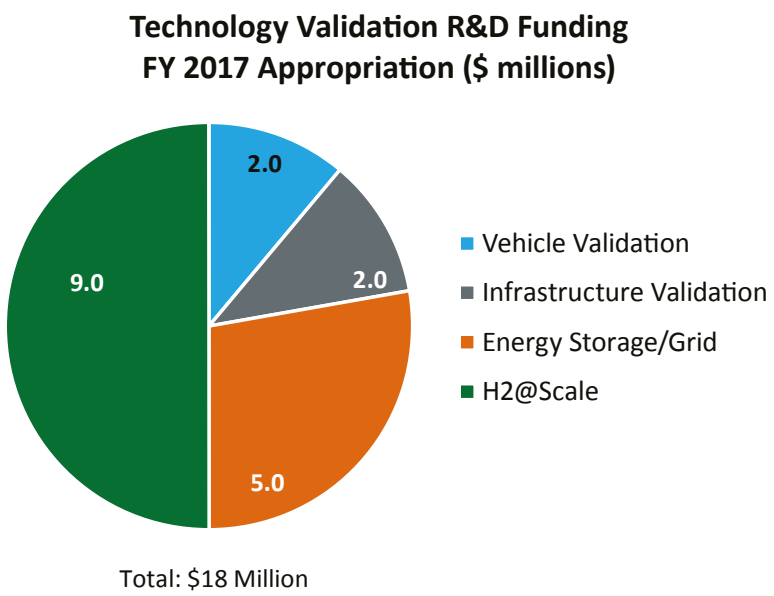

FIGURE 2. FY 2017 Appropriations

UPCOMING ACTIVITIES AND PLANS

With funding remaining from previous fiscal year appropriations, the Technology Validation sub-program will continue the following activities in FY 2018:

- Collection of performance and maintenance data from hydrogen fueling stations.
- Collection of performance data from fleets of FCEVs and fuel cell systems.
- Performance testing of high-pressure liquid hydrogen pump to 300 bar.
- Modeling and validation of electrolyzers in real-time grid simulation scenarios.
- Prototype testing and demonstration of medium-duty parcel delivery truck using a fuel cell solution for increased range.
- Construction and testing of a J2601-compliant mobile hydrogen fueler for FCEVs.
- Detailed design of a 4 kg/d modular solid oxide electrolysis cell hydrogen production system.
- Establishment of co-simulation environment for an EDC.
- Quantification of the scale of the opportunity for hydrogen–vehicle–grid integration.
- Assembly of 25 kW high temperature electrolysis test stand.

Future activities are subject to appropriations.

Jason Marcinkoski
Technology Validation Project Manager
Fuel Cell Technologies Office
Office of Energy Efficiency and Renewable Energy
U.S. Department of Energy
1000 Independence Ave., SW
Washington, DC 20585-0121
Phone: (202) 586-7466
Email: Jason.Marcinkoski@ee.doe.gov

VII.A.1 Fuel Cell Electric Vehicle Evaluation

Jennifer Kurtz (Primary Contact), Sam Sprik, Chris Ainscough, and Genevieve Saur
National Renewable Energy Laboratory (NREL)
15013 Denver West Parkway
Golden, CO 80401-3305
Phone: (303) 275-4061
Email: Jennifer.Kurtz@nrel.gov

DOE Manager: James Alkire
Phone: (720) 356-1426
Email: James.Alkire@ee.doe.gov

Project Start Date: October 1, 2012
Project End Date: Project continuation and direction determined annually by DOE

Overall Objectives

- Validate hydrogen fuel cell electric vehicles (FCEVs) in a real-world setting.
- Identify current status and evolution of the technology.

Fiscal Year (FY) 2017 Objectives

- Analyze FCEV fueling events and driving range between fueling.
- Make results available through online publications, highlights, and presentations.
- Complete one publication cycle (Spring 2017).

Technical Barriers

This project addresses the following technical barrier from the Technology Validation section of the Fuel Cell Technologies Office Multi-Year Research, Development, and Demonstration Plan.

(A) Lack of Fuel Cell Electric Vehicle and Fuel Cell Bus Performance and Durability Data

Contribution to Achievement of DOE Technology Validation Milestones

This project contributes to the achievement of the following DOE milestone from the Technology Validation section of the Fuel Cell Technologies Office Multi-Year Research, Development, and Demonstration Plan.

- Milestone 2.3: Validate fuel cell electric vehicles achieving 5,000-hour durability (service life of vehicle) and a driving range of 300 miles between fuelings (4Q, 2019).

FY 2017 Accomplishments

- Completed one publication cycle of real-world FCEV operation data. The data analyzed have come from 42 vehicles, with model years spanning 2008 to 2016.
- While the 42 vehicles analyzed do not represent all FCEVs on the road today, it is a statistically significant set of data for evaluation with 2,377,000 total miles traveled and 72,780 total fuel cell operation hours. The maximum vehicle odometer is 296,300 mi (approximately 10% of vehicles have passed 100,000 mi) and the maximum fuel cell operation is 5,648 h.
- Since 2006, driving and fueling data from 227 FCEVs over 7 million miles have been analyzed.

✧ ✧ ✧ ✧ ✧

INTRODUCTION

Under Funding Opportunity Announcement DE-FOA-0000625, the U.S. Department of Energy has funded projects for the collection and delivery of FCEV data to NREL for analysis, aggregation, and reporting. Multiple real-world sites and customers are included in this FCEV demonstration project. This activity addresses the lack of on-road FCEV data and seeks to validate improved performance and longer durability from comprehensive sets of early FCEVs, including first-production vehicles. NREL's objective in this project is to support DOE in the technical validation of hydrogen FCEVs under real-world conditions. This is accomplished through evaluating and analyzing data from the FCEVs to identify the current status of the technology, comparing that status to DOE program targets, and assisting in evaluating progress between multiple generations of technology, some of which will include commercial FCEVs for the first time.

The project includes six original equipment manufacturers (OEMs): General Motors, Mercedes-Benz, Hyundai, Nissan, Toyota, and Honda. The latter three OEMs are part of one DOE project with Electricore, which has been completed as scheduled. Up to 90 vehicles are expected to supply data over potentially two phases, with particular attention on fuel cell stack durability and efficiency, vehicle range and fuel economy, driving behavior, maintenance, on-board storage, refueling, and safety. Previous technology validation work on FCEVs and hydrogen infrastructure was performed through the FCEV learning

TABLE 1. Current Status Against DOE 2020 Targets

Vehicle Performance Metrics	DOE Target (Year 2020)[a]	LD3[b]	LD2+[c]	LD2[c]	LD1[c]
Durability					
Max fuel cell durability projection (hours)	5,000	4,130	--	2,521	1,807
Average fuel cell durability projection (hours)		2,442	1,748	1,062	821
Max fuel cell operation (hours)		5,648	1,582	1,261	2,375
Efficiency					
Adjusted dyno range (miles) (window sticker)		200–320	--	196–254	103–190
Median on-road distance between fuelings (miles)		122 miles	98	81	56
Fuel economy (mi/kg) (window sticker)		52 (median)	--	43–58	42–57
Fuel cell efficiency at ¼ power	60%	57% (average)	--	53%–59% (max)	51%–58%
Fuel cell efficiency at full power		43% (average)	--	42%–53%	30%–54%
Specs					
Specific power (W/kg)	650	240–563	--	306–406	183–323
Power density (W/L)	850	278–619	--	300–400	300–400
Storage					
System gravimetric capacity (kg H2/kg system)	5.5%	2.5%–3.7%	--	--	2.5%–4.4%
System volumetric capacity (kg H2/L system)	0.04	0.018–0.054	--	--	0.017–0.025

[a] Fuel Cell Technologies Office Multi-Year Research, Development, and Demonstration Plan [1]
[b] Current results are available online [3] (updated May 2017) from Learning Demonstration 3 (LD3)
[c] National Fuel Cell Vehicle Learning Demonstration (LD) Final Report [2] which included two more phases Learning Demonstration 2 (LD2) and Learning Demonstration 2+ (LD2+) that had different generation vehicles and number of participating OEMs

demonstration [2], also known as the Controlled Hydrogen Fleet and Infrastructure Demonstration and Validation Project. Some of the current partners were also part of the learning demonstration. Those vehicles and technologies are not necessarily the same as the vehicles currently under evaluation even though some of the platforms are the same. Except where referenced or labeled, all of the data reported here are for the current project.

APPROACH

The project's data collection plan builds on other technology validation activities. Operation, maintenance, and safety data for fuel cell system(s) and accompanying infrastructure are collected on site by project partners. NREL receives the data quarterly and stores, processes, and analyzes the data in NREL's National Fuel Cell Technology Evaluation Center (NFCTEC). The NFCTEC is an off-network room with access provided to a small set of approved users. An internal analysis of all available data is completed quarterly and a set of technical composite data products (CDPs) is published annually. Publications are uploaded to NREL's technology validation website [3] and presented at industry-relevant conferences. The CDPs present aggregated data across multiple systems, sites, and teams in order to protect proprietary data and summarize the performance of hundreds of fuel cell systems and thousands of data records. A review cycle is completed before the CDPs are published. This review cycle includes providing detailed data products of individual system- and site-performance results to the specific data provider. Detailed data products also identify the individual contribution to the CDPs. The NREL Fleet Analysis Toolkit is an internally developed tool for data processing and analysis structured for flexibility, growth, and simple addition of new applications. Analyses are created for general performance studies as well as application- or technology-specific studies.

RESULTS

The current FCEV evaluation analyses include the following categories: durability, deployment (e.g., number of vehicles included), system specifications, range, fuel economy, efficiency, fill performance, reliability, drive and fill behaviors, power and energy management, fuel cell transients (e.g., frequency of rapid increases or decreases

in fuel cell power), emissions, and benchmarking against technical targets and typical gasoline vehicle operation. All of the public results are available on the NFCTEC website.

The current evaluation includes 42 vehicles with more than 2.3 million miles traveled and more than 72,000 fuel cell operation hours. As of December 2016, seven vehicles were retired. Many of the OEMs are retiring legacy vehicles because commercial product vehicles are on the road or are soon to be on the road. The durability target for fuel cell systems is 5,000 h (equivalent to 150,000 mi), which is on par with light-duty vehicle customer expectations and conventional technologies. In FY 2017 the number of OEMs supplying data from on-road FCEVs for analysis decreased to three (Honda, Hyundai, and Mercedes-Benz). The vehicles are a mixture of pre-commercial and commercial vehicles, operated within fleets and by individual drivers. The reduction in data sharing partners was a combination of award completion and vehicle production phases. Some data are voluntarily supplied and not consistent across all OEMs, therefore not all analysis results were published. Our analysis in 2017 has focused on tracking progress and fueling performance that helps to inform capabilities, needs, and gaps at the interface between the FCEV and hydrogen station.

Newer-generation vehicles have been added to the current set of FCEVs analyzed, where the most recent model year included is 2016. More than 7 million miles of vehicle travel by 227 FCEVs have been analyzed at NFCTEC. Figure 1 presents results that demonstrate the trend over time for six key DOE metrics. The FCEV performance and specifications have made good progress since NREL started studying the technology in 2006, without sacrificing efficiency and capability. Figure 1 also depicts gaps with the targets. For instance, the voltage durability projections have increased by more than 160% since 2006, when durability results were initially published (the first generation of the learning demonstration project). The durability results were not published in May 2017 because there was not sufficient data to aggregate per the CDP process.

The fueling time of day, day of week, and amounts follow the trends that NREL's results have shown in the past and have a similar trend to the Chevron profile from the "Hydrogen Delivery Infrastructure Options Analysis" published in 2008. There are a few gaps in this comparison. For instance, fueling times peak around 9 a.m. and 4 p.m. for FCEV fills in NREL's analysis, but they only peak around 4 p.m. in the Friday Chevron profile (Figure 2). And there are fewer FCEV fills on the weekend than in the sample gasoline station profile. This may be driven in part by fleet operation instead of individual drivers. More than 16,000 fills have been analyzed and can be used for the development of data-

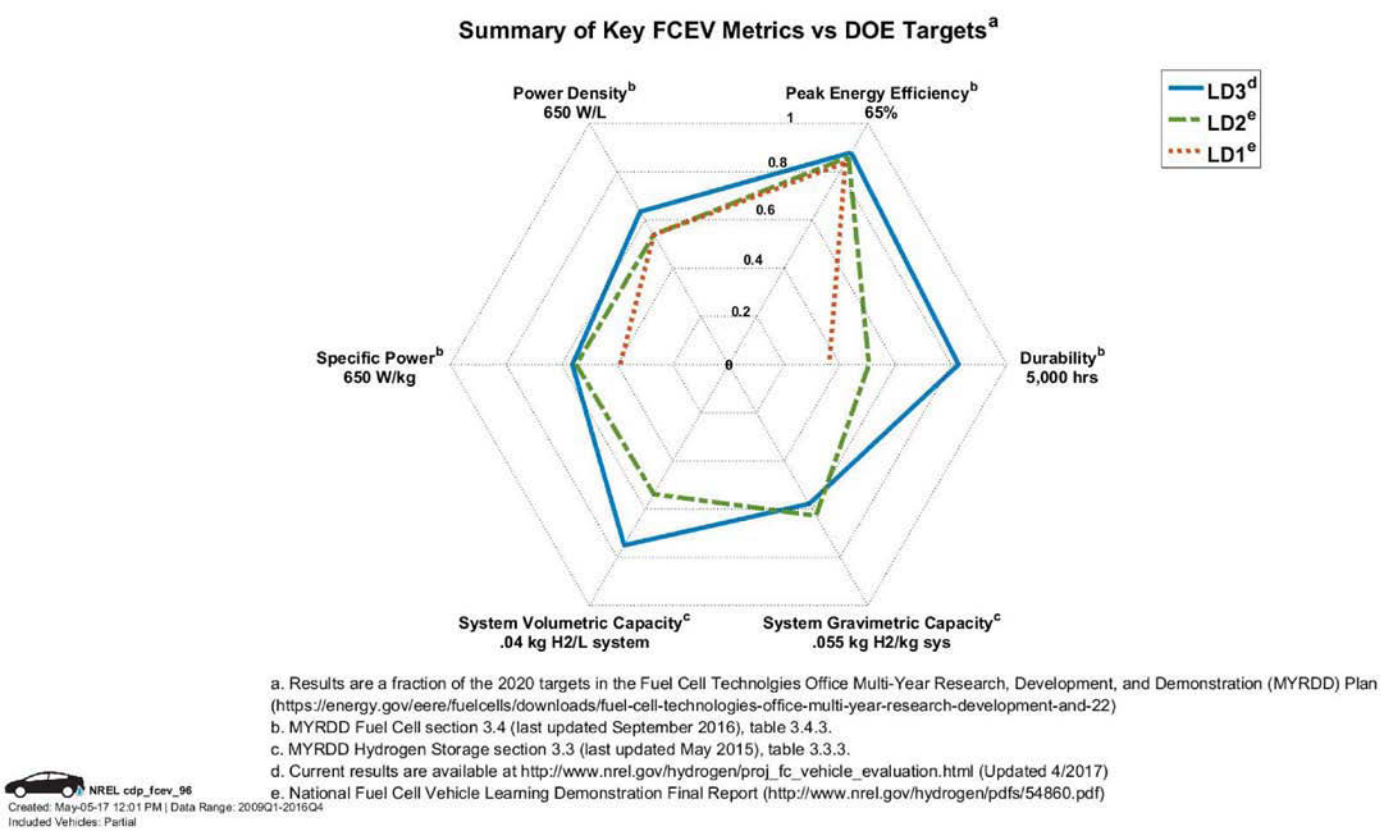

FIGURE 1. FCEV progress toward targets

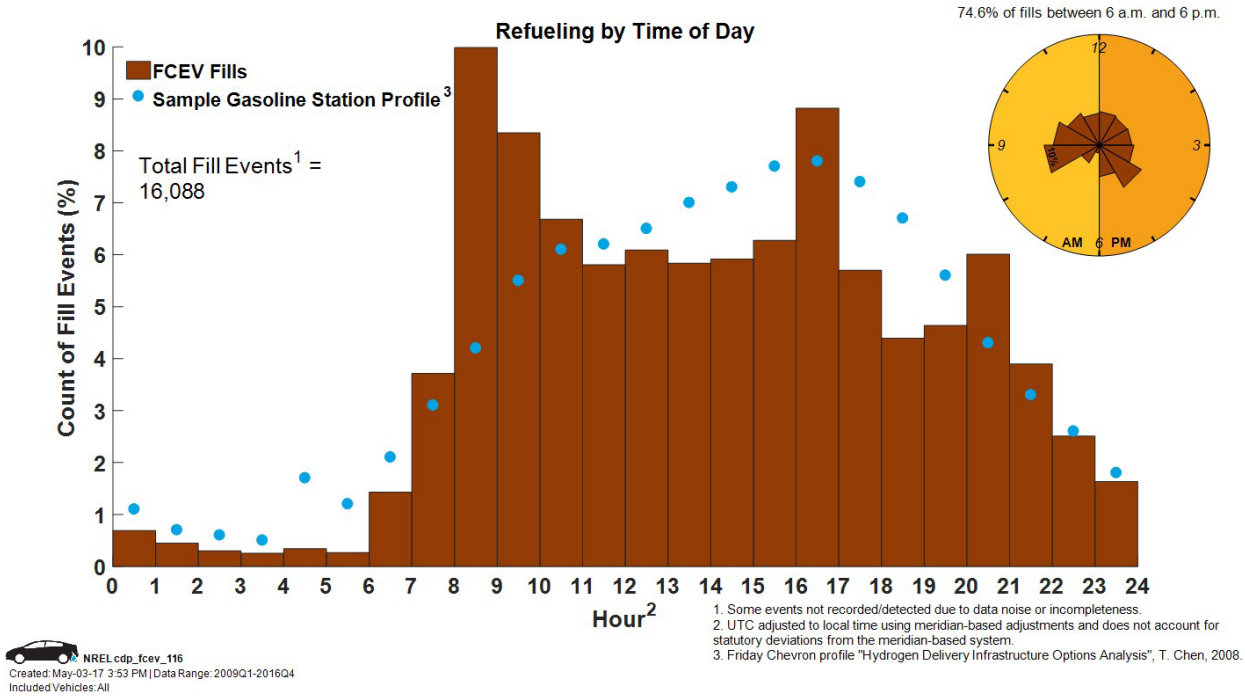

FIGURE 2. FCEV refueling by time of day

based fueling demand profiles. NREL is using the driving behavior to inform fueling behavior. For instance, the driving time of day closely follows the driving time according the National Household Transportation Survey results (Figure 3). These data can be used as a quality control of predictive hourly fueling demand profiles, just as driving range between fueling can be used to check demand profiles. The median, actual driving range of the FCEVs is ~120 mi, which is much less than the window sticker range. Fill frequency and amounts will likely change as the number and availability of hydrogen stations changes.

This predictive fueling demand model (built on both FCEV and hydrogen station fill data) can be integrated with hydrogen station operation for optimized controls. An example of the station operation control optimization based on fueling demand is storage level management and when to operate high-energy-consuming equipment such as compressors and chillers. A predictive fueling demand profile, which should improve as new fueling data are used to update the model, may also inform the best times for maintenance with the least amount of impact on the revenue-providing fills.

Figure 4 depicts the final temperature and pressure limits of more than 16,000 35-MPa and 70-MPa hydrogen fills. The highest concentration of fills was in the preferred (that is, fastest fills within acceptable safety limits) region (shown in green), and the SAE J2601 pressure and temperature limits were not exceeded for any fills. The temperature and pressure measurements were all taken from the vehicles' on-board storage systems.

CONCLUSIONS AND UPCOMING ACTIVITIES

Over the last 10 yr, NREL's NFCTEC has completed analysis of 227 on-road vehicles that have accumulated more than 7 million miles. The current data analyzed come from 42 vehicles and three OEMs, with model years spanning 2008 to 2016. Fuel cell durability has steadily and significantly improved over the last decade, and on-road fuel economy and actual driving range between fills have also increased over the last 10 yr. NREL is seeing the FCEVs operated in similar ways to traditional gasoline vehicles for driving and fueling, yet there are some behaviors that are more representative of fleet FCEV operation instead of use by individual drivers. Analysis results show progress against key DOE metrics of voltage durability, system gravimetric and volumetric capacity, specific power, and power density. The future work includes the following:

- Study the interdependence between FCEV and hydrogen station performance.
- Continue benchmarking fuel cell durability and FCEV range.
- Develop and validate a predictive FCEV fueling demand model.

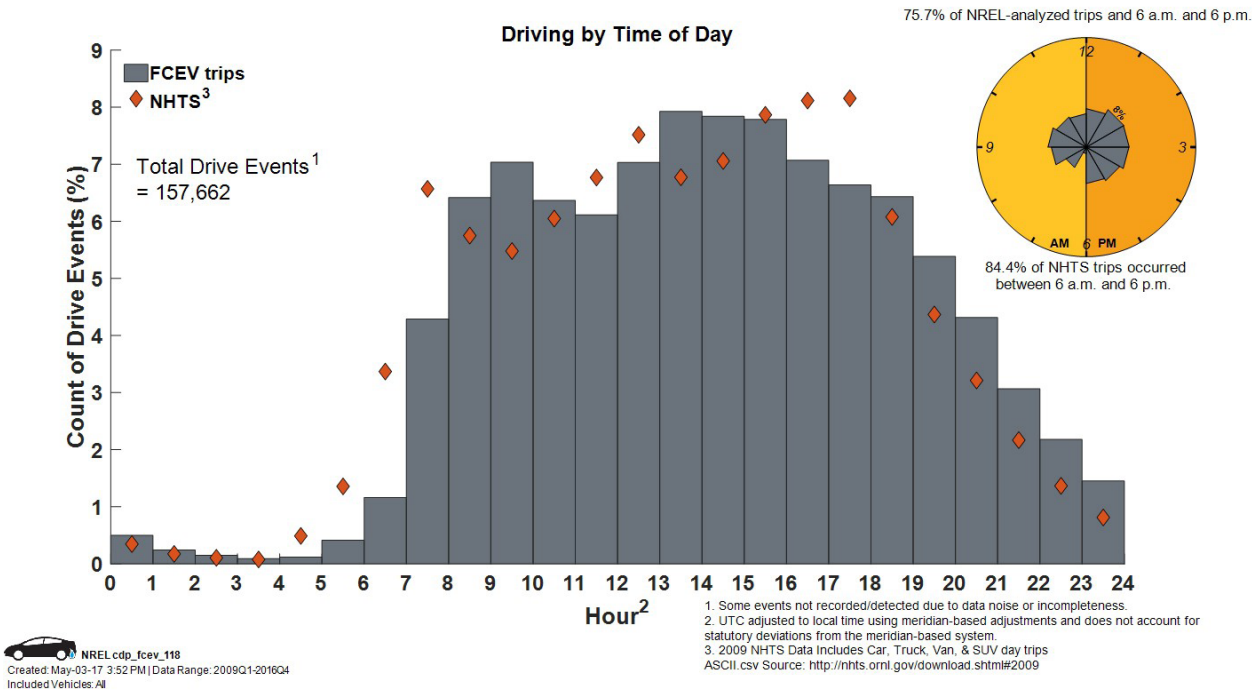

FIGURE 3. FCEV driving time of day

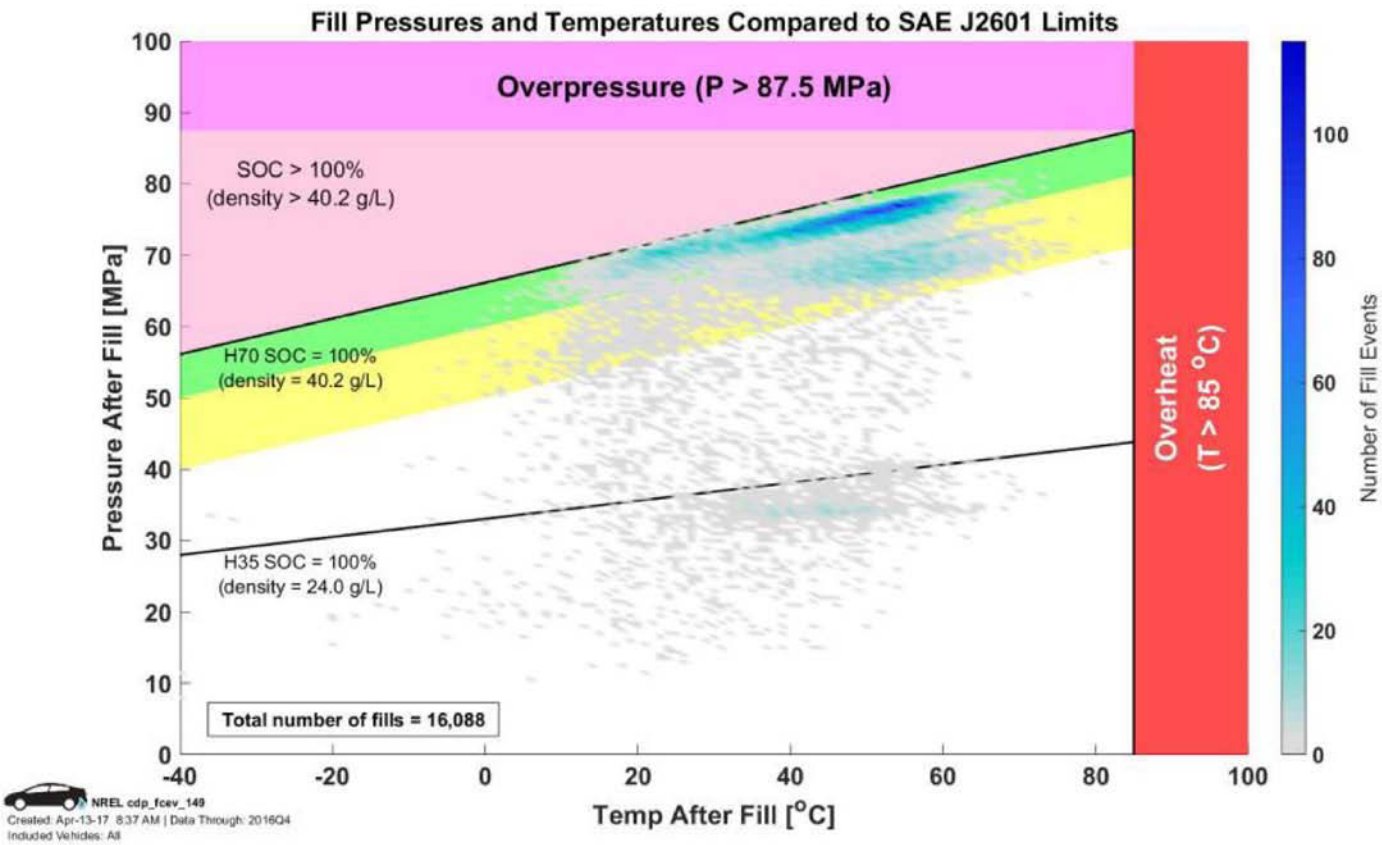

FIGURE 4. FCEV fill comparison to SAE J2601 temperature and pressure limits

FY 2017 PUBLICATIONS/PRESENTATIONS

1. J. Kurtz, S. Sprik, C. Ainscough, and G. Saur, "Fuel Cell Electric Vehicle Evaluation," Presented at the 2017 DOE Annual Merit Review Meeting, June 2017.

2. J. Kurtz, S. Sprik, C. Ainscough, and G. Saur, "Fuel Cell Electric Vehicle (FCEV) Performance Composite Data Products: Spring 2017," NREL/PR-5400-68647, May 2017.

REFERENCES

1. *Fuel Cell Technologies Office Multi-Year Research, Development, and Demonstration Plan*, Fuel Cells chapter, Table 3.4.3 Technical targets for automotive application, Washington, D.C.: U.S. Department of Energy, 2012, accessed October 13, 2014, http://energy.gov/eere/fuelcells/downloads/fuel-cell-technologies-office-multi-year-research-development-and-22.

2. K. Wipke, S. Sprik, J. Kurtz, T. Ramsden, C. Ainscough, and G. Saur, *National Fuel Cell Electric Vehicle Learning Demonstration Final Report*, NREL/TP-5600-54860. Golden, CO: National Renewable Energy Laboratory, July 2012, http://www.nrel.gov/hydrogen/pdfs/54860.pdf.

3. "Fuel Cell and Hydrogen Technology Validation," National Renewable Energy Laboratory, https://www.nrel.gov/hydrogen/technology-validation.html.

4. T. Chen, *Hydrogen Delivery Infrastructure Options Analysis*, Nexant, June 2008, https://energy.gov/sites/prod/files/2014/03/f11/delivery_infrastructure_analysis.pdf.

VII.A.2 Technology Validation: Fuel Cell Bus Evaluations

Leslie Eudy (Primary Contact), Matthew Post, Matthew Jeffers
National Renewable Energy Laboratory (NREL)
15013 Denver West Parkway
Golden, CO 80401
Phone: (303) 275-4412
Email: Leslie.Eudy@nrel.gov

DOE Manager: James Alkire
Phone: (720) 356-1426
Email: James.Alkire@ee.doe.gov

Project Start Date: March 2001
Project End Date: Project continuation and direction determined annually by DOE

Overall Objectives

- Validate fuel cell electric bus (FCEB) performance and cost compared to DOE and U.S. Department of Transportation targets and conventional technologies.
- Coordinate with the U.S. Department of Transportation Federal Transit Administration (FTA) on the data collection for the National Fuel Cell Bus Program and with international work groups to harmonize data collection methods and enable the comparison of a wider set of vehicles.

Fiscal Year (FY) 2017 Objectives

- Document performance results from each current FCEB demonstration site.
- Complete an annual status report comparing results from the different demonstrations.

Technical Barriers

This project addresses the following technical barriers from the Technology Validation section of the Fuel Cell Technologies Office Multi-Year Research, Development, and Demonstration Plan.

(A) Lack of Fuel Cell Electric Vehicle and Fuel Cell Bus Performance and Durability Data

(D) Lack of Hydrogen Fueling Infrastructure Performance and Availability Data

Contribution to Achievement of DOE Technology Validation Milestones

This project has contributed to achievement of the following DOE milestone from the Technology Validation section of the Fuel Cell Technologies Office Multi-Year Research, Development and Demonstration Plan.

- *Milestone 2.3: Validate fuel cell electric vehicles achieving 5,000-hour durability (service life of vehicle) and a driving range of 300 miles between fuelings. (4Q, 2019)* Through FY 2017, NREL collected data on 18 FCEBs. NREL documented 12 fuel cell power plants (FCPP) with operation hours in excess of 16,000 h. One of these systems has logged more than 24,800 h in service and five additional systems have surpassed 20,000 h. Bus fuel economy is dependent on duty cycle. Based on in-service fuel economies of 6.5 mi/kg, the hybrid FCEBs currently in service can achieve a range of approximately 245 mi per fill.

FY 2017 Accomplishments

- Published reports on performance and operational data covering 17 full-size FCEBs in revenue service in the United States.
- Documented more than 24,800 h on a single FCPP.

✧ ✧ ✧ ✧ ✧

INTRODUCTION

Transit agencies continue to aid the FCEB industry in developing and optimizing fuel cells for buses. These in-service demonstration programs are vital to validate the performance of fuel cell systems in buses and to determine issues that require resolution. Using fuel cells in a transit application can help accelerate the learning curve for the technology because of the high mileage accumulated in short periods of time. During the last year, the project teams have made progress in transitioning training to transit staff and improving the ability to troubleshoot issues. More work is still needed to improve reliability, lower capital and operating costs, and improve parts availability.

APPROACH

NREL uses a standard evaluation protocol to provide:

- Comprehensive, unbiased evaluation results of advanced technology vehicle development and operations.

- Evaluations of hydrogen infrastructure development and operation.
- Descriptions of facility modifications required for the safe operation of FCEBs.
- Detailed FCEB performance and durability results to validate status against technical targets, educate key stakeholders, and further DOE goals.

The evaluation protocol includes collecting operation and maintenance data on the bus and infrastructure. The analysis, which consists of economic, technical, and safety factors, focuses on performance and use, including progress over time and experience with vehicle systems and supporting infrastructure. The data are compared to DOE and FTA technical targets and to conventional baseline buses in similar service.

RESULTS

During FY 2017, NREL collected and analyzed data on the following FCEB demonstrations at two U.S. transit agencies and one university transit system.

- Zero Emission Bay Area (ZEBA) Demonstration—Five Bay Area transit agencies led by AC Transit (Oakland, California) are demonstrating thirteen 40-ft Van Hool buses with 120 kW fuel cells in a Siemens hybrid system. The hybrid system was integrated by Van Hool and uses lithium ion batteries from EnerDel.
- American Fuel Cell Bus (AFCB) Project—SunLine Transit Agency (Thousand Palms, California) is operating four ElDorado National 40-ft buses with a BAE Systems hybrid propulsion system using Ballard Power Systems fuel cells and lithium batteries.
- University of California, Irvine (UCI)—UCI operates one AFCB in its fleet that is the same design as the SunLine buses.

NREL kicked off two additional evaluations during FY 2017 funded by FTA. Once there are enough data from these evaluations, they will be included in future reports. The evaluations are:

- Massachusetts AFCB—Massachusetts Bay Transportation Authority is operating another AFCB, adding data on the bus design in a cold climate.
- Orange County Transportation Authority AFCB—Orange County Transportation Authority is operating an AFCB in southern California.

These projects involve fuel-cell-dominant hybrid buses. A summary of selected results is included in this report. NREL completed reports on operational and performance data from the FCEBs and from conventional baseline buses at each agency. The results are also compared to technical targets for FCEB performance established by DOE and FTA and published in a Fuel Cell Technologies Program Record in September 2012 [1]. Tables 1, 2, and 3 provide a summary of the reported results from the operation at each agency, including data from the baseline buses.

TABLE 1. FY 2017 Summary Data Results for ZEBA FCEBs

Vehicle data	FCEB	Diesel
Number of buses	13	10
Data period (month, year)	Sep 2011 – Mar 2017	Jul 2013 – Mar 2017
Number of months	59	45
Total fleet miles	1,773,305	2,029,503
Average miles per month	2,456	4,510
Total FC hours	204,639	–
Fuel economy (mi/kg)	5.81	–
Fuel economy (mi/diesel gal equivalent)	6.56	4.29
Average speed (mph)	8.8	–
Availability (%)	77	89

FC – fuel cell; gal – gallon

TABLE 2. FY 2017 Summary Data Results for SunLine FCEBs

Vehicle data	AFCB	CNG
Number of buses	4	5
Data period (month, year)	Mar 2012 – May 2017	Mar 2012 – Dec 2016
Number of months	63	58
Total fleet miles	374,104	1,369,822
Average miles per month	2,539	4,724
Total FC hours	27,341	–
Fuel economy (mi/kg)	5.67	–
Fuel economy (mi/diesel gal equivalent)	6.41	3.21
Average speed (mph)	13.7	16.3
Availability (%)	78	87

CNG – compressed natural gas

TABLE 3. FY 2017 Summary Data Results for UCI FCEB

Vehicle data	AFCB
Number of buses	1
Data period (month, year)	Jan 2016 – May 2017
Number of months	17
Total fleet miles	40,725
Average miles per month	2,407
Total FC hours	4,676
Fuel economy (mi/kg)	5.13
Fuel economy (mi/diesel gal equivalent)	5.79
Average speed (mph)	10.2
Availability (%)	90

One performance target set by DOE and FTA is for an FCPP durability of 4–6 yr (or 25,000 h), which would be approximately half the life of the bus. The FCPP would be rebuilt or replaced at that time, similar to what transit agencies typically do for diesel engines. Over the last year, NREL collected data on 18 FCPPs. Figure 1 shows the total hours accumulated on individual FCPPs for the current projects tracked by NREL. The average of 16,149 h is shown on the graph as a dashed line. The 2016 and ultimate targets are included on the graph. As of May 2017, the highest-hour FCPP had reached 24,800 h, nearing the ultimate target of 25,000 h. Eight FCPPs have surpassed the 2016 target of 18,000 h. Of the 18 total FCPPs included in the graph, 67% (12) have surpassed 16,000 h of operation. (The FCPPs with the lowest hours accumulated are newer buses.) This shows significant improvement in durability toward meeting the 25,000-h target.

The transit industry measures reliability as mean distance between failures, also known as miles between roadcall (MBRC). Figure 2 tracks the MBRC over time for the ZEBA, SunLine, and UCI FCEB demonstrations and includes the MBRC for the bus as a whole and MBRC for the fuel cell system. The targets for each category are included on the chart. Table 4 provides the MBRC by year since 2012. Reliability has shown a marked increase over time, reaching the ultimate targets for both bus MBRC and fuel cell system MBRC. Roadcalls due to bus-related issues, such as problems with doors and air conditioning, made up 41% of the total failures. Although still over the ultimate target, the fuel cell system MBRC dropped over the last year as a result of several fuel cell system roadcalls. Fuel-cell-related issues made up approximately 22% of the roadcalls during the period.

TABLE 4. MBRC by Year through April 2017

	Bus MBRC	FC System MBRC
April 2012	2,230	12,215
April 2013	2,644	14,884
April 2014	3,510	17,714
April 2015	3,910	20,082
April 2016	4,210	21,482
April 2017	4,531	20,737
% improvement from 2012 to 2017	103	70

CONCLUSIONS AND UPCOMING ACTIVITIES

Fuel cell propulsion systems in buses have continued to show progress in increasing the durability and reliability of FCEBs and the primary components. The current technology meets the ultimate reliability target for roadcall frequency of both the overall bus and the fuel cell system. The fuel cell system on one bus is nearing the ultimate target for power plant lifetime and seven additional fuel cell systems have surpassed the 2016 target. Table 5 summarizes the current status compared to the DOE and FTA performance targets. Transit agencies have made major progress over the last two years toward transitioning maintenance to staff. There are still challenges to overcome before fuel cell buses can match the current performance standard of diesel buses. These include:

- Continuing operation to validate durability and reliability of the fuel cell systems and other components to match transit needs.

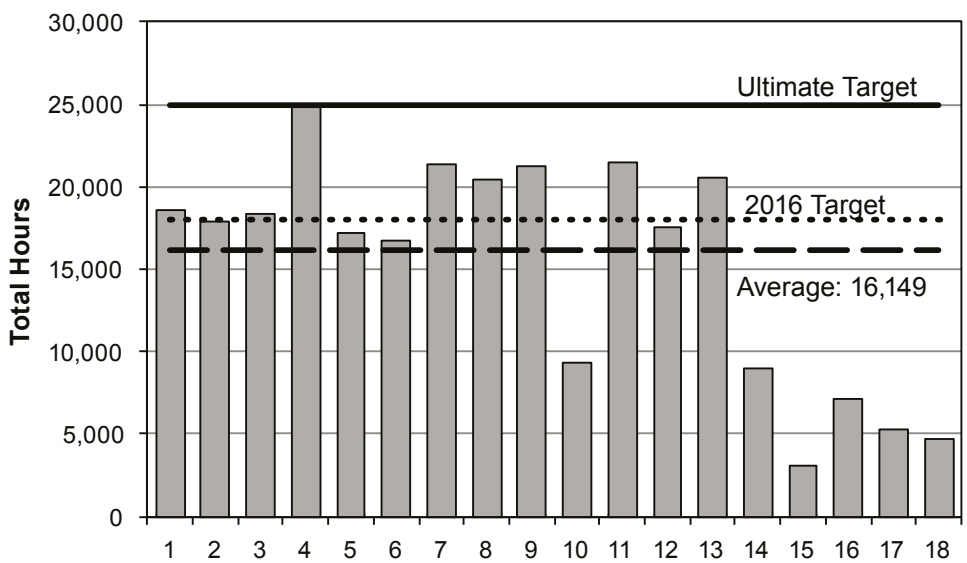

FIGURE 1. Total fuel cell hours accumulated on each FCPP

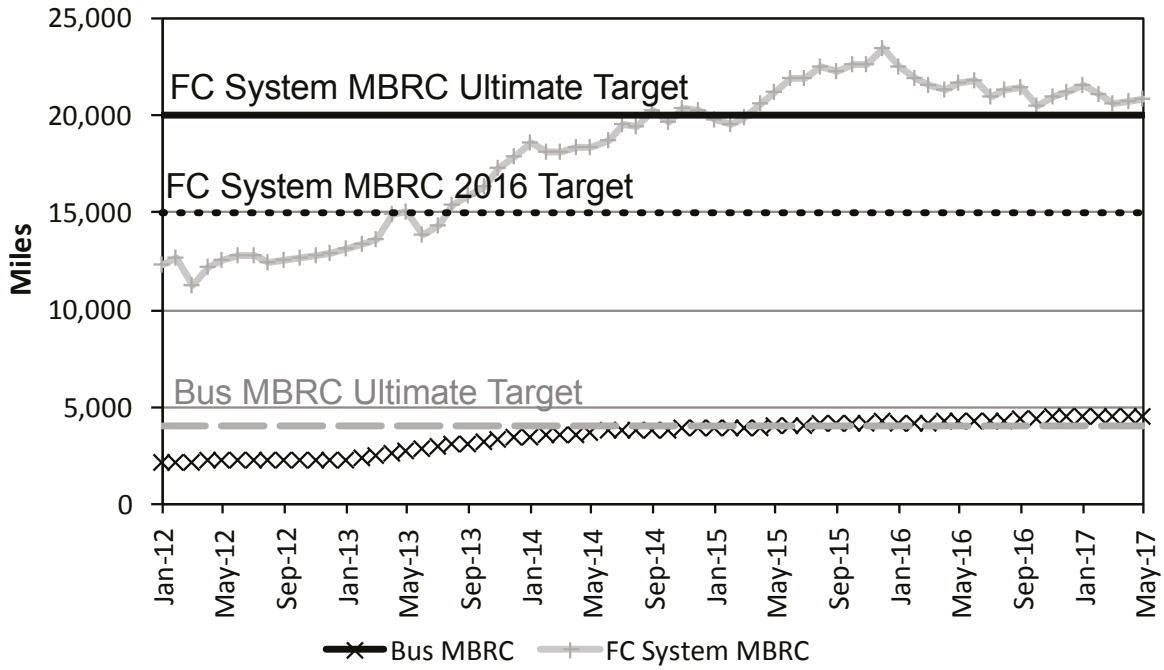

FIGURE 2. Miles between roadcall

- Completing the transfer of all maintenance work to transit personnel.
- Lowering the costs of purchasing, operating, and maintaining buses and infrastructure.
- Scaling up the introduction and operation of larger numbers of FCEBs.

Future work by NREL includes:

- Continuing data collection, analysis, and reporting on performance data for FCEBs in service at the following sites:
  - ZEBA FCEB demonstration led by AC Transit
  - SunLine
  - UCI
  - Additional sites as funding allows
- Investigating reliability, durability, and lifecycle of FCEBs as a part of ongoing evaluations.
- Coordinating with FTA to collect data on the demonstrations funded under the National Fuel Cell Bus Program.
- Coordinating with national and international FCEB demonstration sites.

TABLE 5. FY 2017 Summary of Progress Toward Meeting DOE and FTA Targets

	Units	2017 Status	2016 Target	Ultimate Target
Bus lifetime	Years/miles	5.6/150,000[a]	12/500,000	12/500,000
Power plant lifetime	Hours	3,061–24,800[a]	18,000	25,000
Bus availability	%	75	85	90
Roadcall frequency (bus/FC system)	Miles between roadcall	4,500/20,700	3,500/15,000	4,000/20,000
Operation time	Hours per day/days per week	19/7	20/7	20/7
Maintenance cost	$/mile	0.46–2.28	0.75	0.40
Fuel economy	Miles per diesel gallon equivalent	5.8–6.6	8	8
Range	Miles	220–270	300	300

[a] Accumulation of miles and hours to date—not end of life.

FY 2017 PUBLICATIONS/PRESENTATIONS

1. L. Eudy, "Technology Validation: Fuel Cell Bus Evaluations," Presentation at the DOE Hydrogen and Fuel Cells Program Annual Merit Review, Washington, D.C., June 2017.

2. L. Eudy, M. Post, M. Jeffers, *American Fuel Cell Bus Project Evaluation: Third Report*, National Renewable Energy Laboratory, Golden, CO, NREL/TP-5400-67209, May 2017.

3. M. Post, "Fuel Cell Electric Bus Evaluation Results," Presentation at the American Public Transit Association Annual Bus and Paratransit Conference, May 2017.

4. L. Eudy, "Guideline for Assessing Readiness Levels for Maintenance of ZEBs," Presentation at the American Public Transit Association Annual Bus and Paratransit Conference, May 2017.

5. L. Eudy, "U.S. Fuel Cell Electric Bus Evaluation Results," Presentation at the 10th International Fuel Cell Bus Workshop, December 2016.

6. L. Eudy, M. Post, M. Jeffers, *Fuel Cell Buses in U.S. Transit Fleets: Current Status 2016*, National Renewable Energy Laboratory, Golden, CO, NREL/TP-5400-67097, December 2016.

REFERENCES

1. Fuel Cell Technologies Program Record #12012, September 2012, www.hydrogen.energy.gov/pdfs/12012_fuel_cell_bus_targets.pdf.

VII.A.3 Fuel Cell Hybrid Electric Delivery Van Project

Jason Hanlin
Center for Transportation and the Environment
730 Peachtree Street, Suite 760
Atlanta, GA 30308-1209
Phone: (404) 808-6489
Email: Jason@cte.tv

DOE Manager: James Alkire
Phone: (720) 356-1426
Email: James.Alkire@ee.doe.gov

Contract Number: DE-EE0006523

Subcontractors:
- Hydrogenics USA, San Diego, CA
- United Parcel Service (UPS), Sandy Springs, GA
- Unique Electric Solutions, Stony Brook, NY
- University of Texas at Austin - Center for Electromechanics, Austin, TX
- Valence Technology, Austin, TX

Project Start Date: July 15, 2014
Project End Date: November 30, 2020

Overall Objectives

- Increase the zero-emission driving range and commercial viability of medium-duty electric drive trucks.
- Phase 1 – develop a fuel cell hybrid electric delivery van and validate its design and construction through in-service operation.
- Phase 2 – build the Phase 1 delivery van at pre-commercial volume (up to 16 vehicles) and perform at least 5,000 operation hours of in-service demonstration.
- Develop an economic/market opportunity assessment for medium-duty fuel cell hybrid electric trucks.

Fiscal Year (FY) 2017 Objectives

- Conduct hazard analysis and update system safety plan.
- Complete vehicle design, component procurement, and build.
- Coordinate fueling availability at West Sacramento, California demonstration site.
- Train end-user fleet operations and maintenance personnel.
- Begin demonstrating the prototype van in regular parcel service delivery. Collect and evaluate operating data during the demonstration period.

Technical Barriers

This project addresses the following technical barriers from the following sections of the Fuel Cell Technologies Office Multi-Year Research, Development, and Demonstration Plan.

Technology Validation

(A) Lack of Fuel Cell Electric Vehicle and Fuel Cell Bus Performance and Durability Data

Market Transformation

(D) Market uncertainty around the need for hydrogen infrastructure versus timeframe and volume of commercial fuel cell applications

(F) Inadequate user experience for many hydrogen and fuel cell applications

Technical Targets

This project directly addresses Market Transformation Section 3.9.4 Sub-Program Targets. It provides a pathway for the introduction of fuel cell technologies into the medium-duty vehicle market. The project has a technology validation phase and a follow-on deployment of a pre-commercial volume of the vehicles in parcel delivery service. The project is built upon the initial structure that DOE prescribed in the funding opportunity announcement and is augmented by the active participation and guidance of a major commercial fleet operator, UPS. UPS operates 46,000 medium-duty vehicles worldwide. Furthermore, the vehicles will be deployed in California to take advantage of that state's focused growth of fueling infrastructure and desire to deploy zero-emission vehicles. The Center for Transportation and the Environment has coordinated with station providers early in the project in order to identify and overcome fueling station barriers for this emerging application of fuel cell technologies, such as the limitation of J2601 fueling protocol described below. This project further leverages the resources and support of the State of California. The project team has also focused on upfront design to ensure that (1) selection of the fuel cell size will take advantage of volume growth from other applications and markets, and (2) the design will meet the needs of our commercial fleet operator by matching the performance of incumbent technologies, while meeting the range requirements for over 97% of delivery van duty cycles.

FY 2017 Accomplishments

- Completed a hazard analysis with support from DOE's Hydrogen Safety Panel.
- Finalized vehicle design. Procured long lead-time components and integrated primary components of the fuel cell hybrid electric powertrain into the vehicle.
- Displayed the vehicle chassis with primary fuel cell and electric powertrain components installed at the 2017 ACT Expo in Long Beach, California.
- Reviewed project fueling requirements with Linde, the hydrogen fueling station operator in West Sacramento, California. Discussed fueling tests and fuel purchase strategies in preparation for the demonstration.
- Outlined training plans, demonstration support plans, and an operator's manual.

✧ ✧ ✧ ✧ ✧

INTRODUCTION

Parcel delivery van fleets are currently dominated by diesel and compressed natural gas-powered Class 3–6 trucks. In recent years, some parcel delivery services have integrated battery-electric trucks into their fleet; however, these battery-electric vehicles have been unable to match the performance of existing delivery vans and their limited range significantly impacts deployment strategy. The intent of this project is to develop a hydrogen fuel cell hybrid electric van that provides fleet operators with a zero-emission vehicle capable of meeting route range requirements while matching the performance characteristics of its existing fleet vehicles. According to Fleet DNA Project Data compiled by the National Renewable Energy Laboratory, a vehicle with a 125-mile range will meet 97% of Class 3–6 daily delivery driving distances [1]. Meeting this 125-mile range threshold will increase the attractiveness of zero-emission trucks to fleet operators and increase their commercial viability.

APPROACH

This project aims to develop and demonstrate a hydrogen fuel cell hybrid electric van with a 125-mile operational range and validate the vehicle through in-service deployment in a California UPS fleet. This project has two phases:

- Develop a fuel cell hybrid electric delivery van and validate its design and construction through in-service operation.
- Build the Phase 1 delivery van at pre-commercial volume (up to 15 additional vehicles) and perform at least 5,000 operation hours of in-service demonstration.

During Phase 1, real-world delivery van route data is collected to define the expected duty cycle requirements. All potential fuel cell hybrid electric van powertrain configurations are then modeled and simulated on the duty cycles to assess vehicle performance and aid final design. Trade studies (including cost and projected costs at high volumes) are accomplished and vehicle components are then downselected and the physical layout is completed. The first delivery van can then be built and validated through in-service operation. If the delivery van meets Phase 1 performance requirements, the project team will build and deploy up to 15 additional vans in Phase 2. All of the vans will be demonstrated in California. Vehicle performance data during the demonstration periods will be collected and provided to the National Renewable Energy Laboratory's National Fuel Cell Technology Evaluation Center for analysis.

The project team benefits from having members with extensive hydrogen fuel cell experience, including the University of Texas and Hydrogenics, and one of the largest medium-duty truck fleet operations in the world, UPS. UPS has deployment experience with delivery vans powered by various fuels, including gasoline, diesel, compressed natural gas, and battery-electric. This experience gives them a unique perspective on the commercial viability of alternative fueled vehicles and their project contributions are invaluable. Project funding is provided by the DOE, the California Energy Commission, and the South Coast Air Quality Management District. UPS is providing cost share during the demonstration periods by supplying operation, maintenance, and fueling costs.

RESULTS

Vehicle design was finalized, including component layout and packaging details. The fuel cell module and balance of plant are positioned in the engine compartment area, where the internal combustion engine is located in traditional trucks. This is a retrofit project, and the project team overcame significant design challenges related to the limited space inside the existing engine compartment area. The fuel cell system is mounted to a removable skid to simplify future maintenance for the end-user. Hydrogen tank cylinders are mounted to the outside face of the chassis frame rails and the mounting hardware was designed to mimic the tank mounting strategy that UPS currently uses for their compressed natural gas fleet vehicles. The vehicle's high-voltage battery system is positioned between the frame rails in four individual enclosures. An illustration of the vehicle chassis that shows the physical layout and component packaging is shown in Figure 1. Notice that no components are positioned behind the rear axle or in the cargo area above the chassis frame.

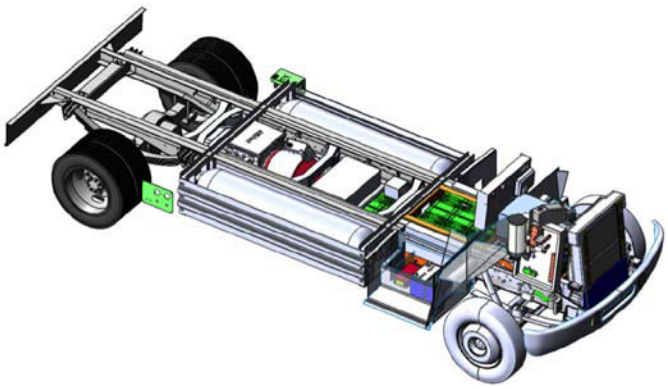

FIGURE 1. Illustration of the vehicle chassis with energy storage and fuel cell hybrid electric powertrain components

Project stakeholders, including members of DOE's Hydrogen Safety Panel, conducted a hazard analysis of the vehicle based on traditional failure mode and effect analysis practices. The analysis focused on the systems that are unique to fuel cell hybrid configuration, such as hydrogen system, high voltage system, and the electric drive train. Strategies for design and operations to mitigate high-risk hazards during daily delivery, hydrogen fueling, and maintenance were identified and incorporated into the vehicle design.

Long-lead time components were procured and vehicle build activities began. Primary components of the fuel cell hybrid electric powertrain were integrated and the vehicle chassis was displayed at the 2017 ACT Expo in Long Beach, California. Figures 2 and 3 show the vehicle chassis and project team members at the Expo.

CONCLUSIONS AND UPCOMING ACTIVITIES

The Fuel Cell Hybrid Electric Delivery Van project is utilizing team member experience with hydrogen fuel cell technologies, alternate fuel vehicle fleet familiarity, and stakeholder feedback to develop commercially viable zero-emission medium-duty trucks. The team has developed:

- Vehicle and component specifications to promote commercial acceptance.
- Component selection to ensure performance on real-world delivery duty cycles.
- Solid models of major components within vehicle body.
- Strategy to ease UPS fleet acceptance and fueling procedures.

Upcoming activities includes:

FIGURE 2. The vehicle chassis on the ACT Expo display floor, with primary powertrain components installed

FIGURE 3. Project team members around the vehicle chassis on the ACT Expo display floor, May 2017

- Finish building, commission, and deliver prototype van.
- Validating prototype van through a 6-month demonstration in parcel delivery service.
- Building final van design at pre-commercial volume (minimum six additional vehicles).
- Training end-user fleet operations and maintenance personnel.
- Coordinating fueling availability at other deployment sites and continue coordinating the development of medium-duty hydrogen fueling protocol.
- Deploying and supporting vans in UPS California fleets.

- Collecting and evaluating operating data during deployment in parcel delivery service.
- Developing an economic/market opportunity assessment for the vehicles.
- Continuing to pursue additional funding from outside sources to build and demonstrate more Phase 2 vehicles.

FY 2017 PUBLICATIONS/PRESENTATIONS

1. J. Hanlin, "Fuel Cell Hybrid Electric Delivery Van Project," presented at the DOE Annual Merit Review, Washington, D.C., June 2017.

2. M. Lewis, et al. "Design and Modeling for Hydrogen Fuel Cell Conversion of Parcel Delivery Trucks." Paper presented at the 2017 IEEE Transportation Electrification Conference and Expo (iTEC), June 2017.

REFERENCES

1. Walkowicz, K.; Kelly, K.; Duran, A.; Burton, E. (2014). *Fleet DNA Project Data*. National Renewable Energy Laboratory. http://www.nrel.gov/fleetdna

VII.B.1 Innovative Advanced Hydrogen Mobile Fueler

Sara Odom (Primary Contact), Spencer Quong
Electricore, Inc.
27943 Smyth Drive, Suite 108
Valencia, CA 91355
Phone: (661) 607-0260
Email: sara@electricore.org

DOE Manager: James Alkire
Phone: (720) 356-1426
Email: James.Alkire@ee.doe.gov

Contract Number: DE-EE0007275

Subcontractors:
- Air Liquide, Houston, TX
- Hydrogen Technology & Energy Corporation, Vancouver, BC, Canada
- Quong & Associates, Inc., San Francisco, CA
- Manta Consulting, Carmel, CA

Project Start Date: July 1, 2016
Project End Date: December 31, 2019

Overall Objectives

- Design and build an Advanced Hydrogen Mobile Fueler (AHMF).
- Deploy AHMF to support a network of hydrogen stations and vehicles in the United States.
- Gather and analyze fueling data for the National Renewable Energy Laboratory Technology Validation Team.

Fiscal Year (FY) 2017 Objectives

- Completion of the final design of the AHMF including the selection of applicable components and key vehicle parameters.

Technical Barriers

This project addresses the following technical barriers from the Technology Validation section of the Fuel Cell Technologies Office Multi-Year Research, Development, and Demonstration Plan.

(C) Hydrogen Storage

(D) Lack of Hydrogen Refueling Infrastructure Performance and Availability Data

(E) Codes and Standards

Contribution to Achievement of DOE Technology Validation, Safety, Codes & Standards, and Hydrogen Delivery Milestones

This project will contribute to achievement of the following DOE milestones from the Technology Validation, Hydrogen Delivery, and Hydrogen Safety, Codes and Standards sections of the Fuel Cell Technologies Office Multi-Year Research, Development, and Demonstration Plan.

Technology Validation

- Milestone 2.3: Validate fuel cell electric vehicles achieving 5,000-hour durability (service life of vehicle) and a driving range of 300 miles between fuelings. (4Q, 2019)
- Milestone 3.4: Validate station compression technology provided by delivery team. (4Q, 2018)
- Milestone 3.8: Validate reduction of cost of transporting hydrogen from central production to refueling sites to <$0.90/gge. (4Q, 2019)

Hydrogen Delivery

- Milestone 2.1 and 6.2: By 2015, reduce the cost of hydrogen delivery from the point of production to the point of use for emerging regional consumer and fleet vehicle markets to <$4/gge. (4Q, 2015)
- Milestone 2.4 and 6.3: By 2020, reduce the cost of hydrogen delivery from the point of production to the point of use in consumer vehicles to <$2/gge. (4Q, 2020)

Hydrogen Safety, Codes and Standards

- Milestone 2.19: Validate inherently safe design for hydrogen fueling infrastructure. (4Q, 2019)
- Milestone 3.4: Develop hydrogen material qualification guidelines including composite materials. (4Q, 2017)

FY 2017 Accomplishments

- Determined crucial design specifications (Table 1) and parameters for the AHMF and its components. The final design reflects target specifications identified for storage, fueling, performance, usage, etc.
- Selected and approved major components and subsystems for the AHMF design, such as the dispenser, storage, compressor, and cooling system, as well as initiated purchases of long lead items.
- Completed the final design package of the AHMF, including the following design documents: piping and

TABLE 1. AHMF Specifications

Specification	Description
Pressure Class	H70 (70 MPa) after compressing high bank storage
Pre-cooling	T30 (-30°C) or T40 (-40°C)
Performance	Up to 15 kg/h, 100-120 kg in 8-10 hours
Fueling Protocol	SAE J2601-2014 table based for 2-7 kg tanks SAE J2799-2014
Setup	One hour for limited performance, 8 hours for full performance
Storage	Up to 170 kg H_2 at 45 MPa with ability to connect to external storage
Power	On-board 480 VAC, low noise, low emissions diesel generator with option of using external power
Usage	Dispenser human machine interface allows fueling by minimally trained users

instrumentation diagrams; process flow diagrams; component layouts; three-dimensional conceptual modeling (Figure 1); and bill of materials. A final design report was provided to DOE on February 27, 2017.

- Conducted a design and safety review session with selected members of the DOE program office and Hydrogen Safety Panel. Initial hazard analysis completed.

✧ ✧ ✧ ✧ ✧

INTRODUCTION

This project will design, develop, deploy, and analyze the economic viability of a mobile fueling system for hydrogen. The project team proposed use of the AHMF to support a network of stations in the United States. As part of the design activity the project team was to define, in collaboration with an automaker, the preferred network of stations. The team has selected a northeast United States network. Automaker(s) will support the project by providing specifications based upon vehicle requirements, and support the evaluation of the AHMF with respect to compliance with specific fueling performance criteria. The AHMF will have the capacity to fuel approximately 10–20 fuel cell vehicles per day consistent with the requirements of the H70 fueling category. The AHMF will operate without remote power connections, be modular for easy transport and deployment, and have the ability to provide expanded daily capacity and multi-day operations through the use of delivered gaseous hydrogen.

APPROACH

The project consists of two primary phases each consisting of several key tasks and milestones.

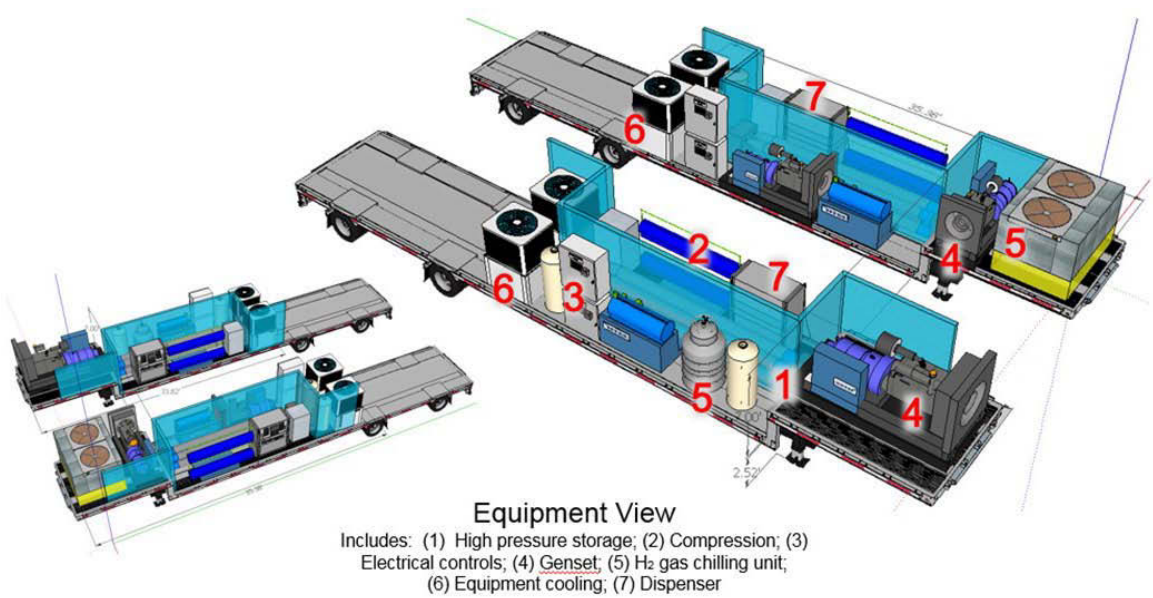

FIGURE 1. AHMF equipment view

The first phase will involve the design, development, and construction of the AHMF, moving from the conceptual design through to completion of assembly and testing so the AHMF is ready to deploy. The first phase will contain two key decision points: the final design review and construction and testing of the AHMF.

The second phase will demonstrate the AHMF over 18 months at multiple site locations and gather key data in collaboration with participating automotive companies. Fueling data will be provided to the National Renewable Energy Laboratory quarterly for review and analysis; economic data will be included in the project's final report.

RESULTS

The AHMF project has completed the design stage and is ready to begin construction. The team solicited input from selected automotive companies (potential users of the AHMF) and DOE to determine crucial design specifications and parameters for the AHMF and its components. The team decided to use Air Liquide's C100 station design as the base design for this project. The design utilizes several components from the C100, with appropriate modifications to accommodate the AHMF specifications and mobile approach. The AHMF will be a self-contained, full performance mobile hydrogen station.

In addition to the design specification, the team developed a project safety plan that addresses potential threats and impacts to personnel, equipment, and the environment. By utilizing the Air Liquide C100 station design, the team has efficiently reduced project risks and saved time by using components that have already been tested and approved by Air Liquide.

The team has started to acquire major and long lead components including the purchase of two Hydrogen Technology & Energy Corporation Power Cubes, compressor, and heat exchanger. In addition, the team is actively pursuing vendor quotes and purchase order agreements for the remaining equipment items.

During the design process the team identified barriers and challenges associated with the operation and site selection of the AHMF including high pressure storage, retail sale of hydrogen, and unattended fueling. The team has developed a plan with DOE and other stakeholders to reduce risk and address the barriers identified.

The Final Design Report submitted to DOE specifically addresses the selected components to be installed, and a comparison with DOE's cost targets for compression, storage, and dispensing.

CONCLUSIONS AND UPCOMING ACTIVITIES

Upon approval of Budget Period 2 funding the team will begin construction on the AHMF. Planned activities include assembly, testing of sub-systems and full system, and site selection.

FY 2017 PUBLICATIONS/PRESENTATIONS

1. 2017 DOE Annual Merit Review Presentation.

VII.B.2 Hydrogen Station Data Collection and Analysis

Sam Sprik (Primary Contact), Jennifer Kurtz, Chris Ainscough, Genevieve Saur, and Mike Peters
National Renewable Energy Laboratory (NREL)
15013 Denver West Parkway
Golden, CO 80401-3305
Phone: (303) 275-4431
Email: Sam.Sprik@nrel.gov

DOE Manager: James Alkire
Phone: (720) 356-1426
Email: James.Alkire@ee.doe.gov

Project Start Date: October 1, 2011
Project End Date: Project continuation and direction determined annually by DOE

Overall Objectives

- Analyze current state-of-the-art hydrogen infrastructure using several metrics including efficiency, performance, cost, and reliability of station components and systems.
- Perform an independent assessment of technology in real-world operating conditions, focusing on hydrogen infrastructure for on-road vehicles.
- Leverage the data processing and analysis capabilities at the National Fuel Cell Technology Evaluation Center (NFCTEC), originally developed under the Fuel Cell Vehicle Learning Demonstration, as well as from forklift, backup power, and bus projects.
- Publish aggregated results for existing hydrogen stations in the form of composite data products (CDPs).

Fiscal Year (FY) 2017 Objectives

- Obtain and collect data from state-of-the-art hydrogen fueling facilities that receive funding through DOE Funding Opportunity Announcement DE-FOA-0000626 awards, California Energy Commission (CEC) awards, and others, to enrich the analyses and the set of publicly available CDPs on hydrogen fueling infrastructure.
- Work with codes and standards activities and fueling facility owners and operators to benchmark performance of the fueling events relative to current SAE procedures.
- Perform analysis and provide feedback on sensitive data from hydrogen infrastructure for industry and DOE. Aggregate these results for publication.
- Participate in technical review meetings and site visits with industry partners to discuss results from NREL's analysis.
- Provide input to the Alternative Fuels Data Center (AFDC) station locator for accurate and up to date hydrogen station information through close partnership with CEC, California Fuel Cell Partnership (CaFCP), and station providers including efforts in the Northeastern United States.
- Publish a set of aggregated results for all stations including stations that are not considered retail and another set for just the retail stations which are open to all original equipment manufacturer fuel cell electric vehicle (FCEV) customers.

Technical Barriers

This project addresses the following technical barrier from the Technology Validation section of the Fuel Cell Technologies Office Multi-Year Research, Development, and Demonstration Plan.

(D) Lack of Hydrogen Refueling Infrastructure Performance and Availability Data

Contribution to Achievement of DOE Technology Validation Milestones

This project will contribute to achievement of the following DOE milestone from the Technology Validation section of the Fuel Cell Technologies Office Multi-Year Research, Development, and Demonstration Plan.

- Milestone 4.4: Complete evaluation of 700-bar fast fill fueling stations and compare to SAE J2601 specifications and DOE fueling targets. (3Q, 2016)

FY 2017 Accomplishments

- Created and published Winter 2016 and Spring 2017 CDPs based on available station data.
- Provided input to the AFDC to keep the hydrogen station information up to date through close partnership with CaFCP, CEC, station providers, and the northeastern United States stations.
- Participated in the CaFCP working group meetings and H2USA hydrogen fueling station working group.
- Internally processed and analyzed quarterly infrastructure data in the NFCTEC for inclusion in the two sets of published CDPs and the Detailed Data Products shared with those providing data.

- Kept the infrastructure data collection templates up to date and reviewed with external partners including new station providers.
- Gathered and provided updates on stations under the DOE Funding Opportunity Announcement DE-FOA-0000626-funded projects.
- Analyzed data from the CEC on their awarded retail stations.
- Updated NREL Fleet Analysis Toolkit code to accept and analyze data in multiple formats from stations.
- Presented results at the 2017 Annual Merit Review.

✧ ✧ ✧ ✧ ✧

INTRODUCTION

In the past, approximately 60 hydrogen fueling stations supported a few hundred FCEVs in the United States. Of these stations, 25 supported the 183 DOE Learning Demonstration vehicles. As we moved out of a learning demonstration environment into a commercialization environment, manufacturers carefully ramped up FCEV production to match the infrastructure effort. This effort moved from demonstration type stations, of which most have been decommissioned, to a network of consumer-friendly retail stations, focusing on a few clusters of stations to cover strategic areas where vehicles are introduced.

California has been a leader in supporting hydrogen infrastructure with a goal of 100 stations within a carefully planned network. Early efforts in California focus on clusters of stations near population centers in the Los Angeles and San Francisco Bay areas along with connector stations and destination stations. Through past funding efforts, 28 retail stations are in place in California supporting over 1,000 FCEVs with 14 more in near-term development. The most recent notice of proposed awards from the CEC through GFO-15-605, announced in February of 2017, proposes $33 million for 16 additional retail stations. California State funding of hydrogen stations comes through the CEC's Alternative and Renewable Fuel and Vehicle Technology Program. The retail stations that are open in California are currently providing data to this project. Besides California, there are efforts in the northeastern states to build 12 retail stations, with several already under construction, which will establish hydrogen infrastructure for the upcoming FCEVs and will also contribute data to this project.

Keys to success for improving hydrogen fueling availability are selecting the fueling location, ensuring customer-friendly public access, and providing adequate and reliable output to support the vehicles. Hydrogen output from existing and upcoming facilities varies from 50 kg/d to 350 kg/d, with most new fueling facilities being more than 100 kg/d. Although it is currently most economical to make hydrogen from natural gas, there are efforts and requirements to make hydrogen from renewable sources. Using available hydrogen energy from landfills and wastewater treatment plants is one way to make use of a renewable feedstock and to lower greenhouse gas emissions. Another renewable pathway is to make hydrogen through electrolysis with the electrical energy coming from a renewable source such as wind or solar. As more vehicles come online, these fueling facilities will need to have higher uptimes/availability and be more cost effective to operate and maintain. The continued data collection and analysis will show the progress being made in these areas and determine future technology development needs.

APPROACH

The emphasis of this project is documenting the innovations in hydrogen fueling and how well they meet customer needs. This includes analysis that captures the technology capability (such as back-to-back filling capability, impact of pre-cooling temperature, and radio frequency identification of vehicles to allow unique fueling profiles) as well as the customer perspective (such as fueling times and rates, safety, and availability). Individual components, such as compressors, will be evaluated with the available data to establish current status and research needs. Station locations will be evaluated within the context of both available vehicles and future vehicles and their fueling patterns. NREL will also use the analysis results to support DOE in identifying trends from the data that will help guide DOE's research and development activities.

Data analysis will be performed on sensitive industry hydrogen fueling data in the NFCTEC and recommendations will be provided to DOE on opportunities to refocus or supplement research and development activities. Aggregation of the analyzed data allows for creation of composite results for public dissemination and presentation. Some existing CDPs from the previous learning demonstration will be updated with new data, as appropriate. All this involves working with industry partners to create and publish CDPs that show the current technology status without revealing proprietary data. Feedback to industry takes form in detailed data products (protected results) and provides direct benefit to them from the NREL analysis performed on their data. We will continue exercising the fueling analysis functionality of the NREL Fleet Analysis Toolkit to preserve and archive a snapshot of the analysis results from each quarter. This allows a deeper level of results to be stored in an easy-to-access form within the NFCTEC.

Using unique analysis capabilities and tools developed at NREL, researchers are providing valuable technical recommendations to DOE based on real-world experiences with the technology. NREL will continue to provide multiple outputs in the form of CDPs and presentations and papers at technical conferences.

RESULTS

As stations are built or retired, the publicly viewable AFDC station database is updated by this project, through California updates, and by station providers. Currently, there are 37 public stations (28 are considered retail) in the United States with 19 more planned in the near future. The newer stations are being built to be accessible to the public in a retail environment and most are located in California with several also under construction in the Northeast United States this year. Using the data reported to NREL by 26 of these retail stations and nine non-retail stations over 80 CDPs were developed for the retail group of stations and over 80 CDPs were created for all the stations combined. Additionally, Detailed Data Products were created for each station showing their data relative to the aggregated data. The public results were presented at the DOE Annual Merit Review. Results were also published to NREL's website and cover several analysis categories including deployment, performance, reliability, utilization, safety, energy use, and hydrogen quality.

The goals of the early stations included covering geographic areas to prevent range anxiety by FCEV customers. This goal is partially achieved, but the current analysis (Figure 1) shows that max daily utilization is beginning to approach station capacity at a few stations. This implies a need for larger and/or more stations to meet the upcoming vehicle demand beyond just having a single station in the area. An increase in the amount of hydrogen dispensed each quarter (Figure 2) results from both more stations being built and more FCEVs on the road. For 2016, over 107,000 kg of hydrogen were dispensed from retail stations. A look at maintenance by equipment type (Figure 3) shows that hydrogen dispenser equipment is now the primary item needing maintenance both in terms of number of events and labor hours. Entire system, compressor, chiller, and safety system (e.g., false alarms and sensors), are the next highest items in terms of number of maintenance events. Many of the maintenance items, especially for the chiller and the dispenser are due to temperature variations resulting from chilling the hydrogen down to -40°C at the stations. Several new CDPs show cause and effects for maintenance items for the different components. For the dispenser, most of the effects are alarms followed by hydrogen leaks but causes are mostly undetermined. Causes do include operator error, failed parts, communications errors, and environmental factors. As more detail comes in for maintenance items these cause and effect plots should help identify common issues with the stations. Through processing of data from the HyStEP device to measure performance at the stations, we see that most fills are not meeting the temperature requirements within the 30 s after start of fill that is required from the SAE J2601 standard (Figure 4). Second by second data has been requested from the stations that would help compare the target pressures and average pressure ramp rates that the standard specifies. This detailed data will hopefully be available next year as it would prove very useful. Other CDPs show results including levels of contaminants in

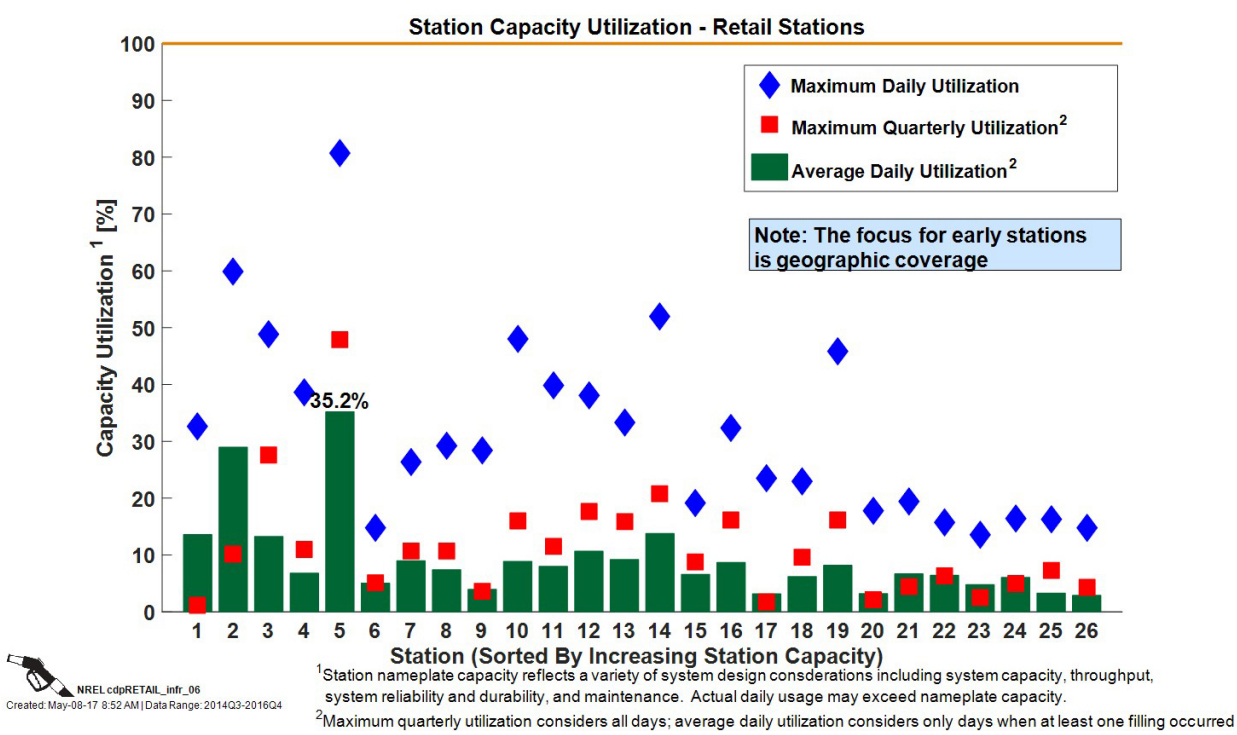

FIGURE 1. Station capacity utilization

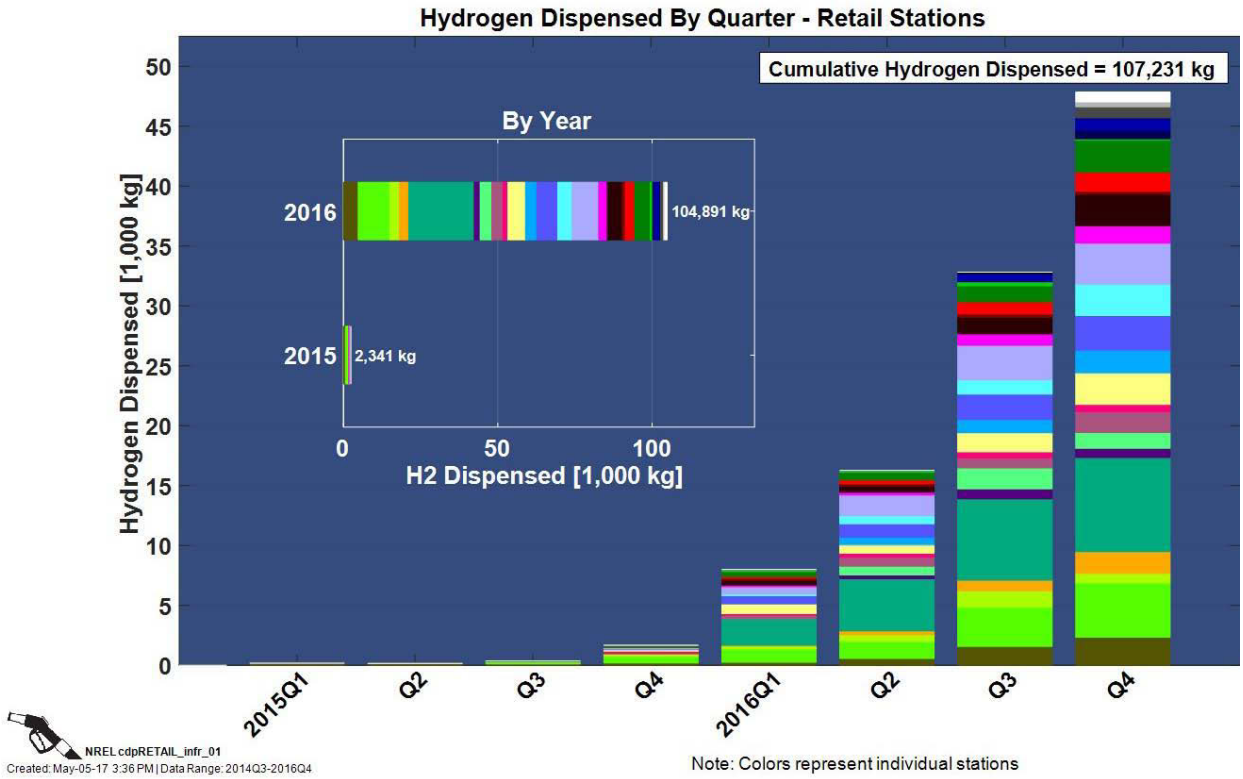

FIGURE 2. Amount of hydrogen dispensed

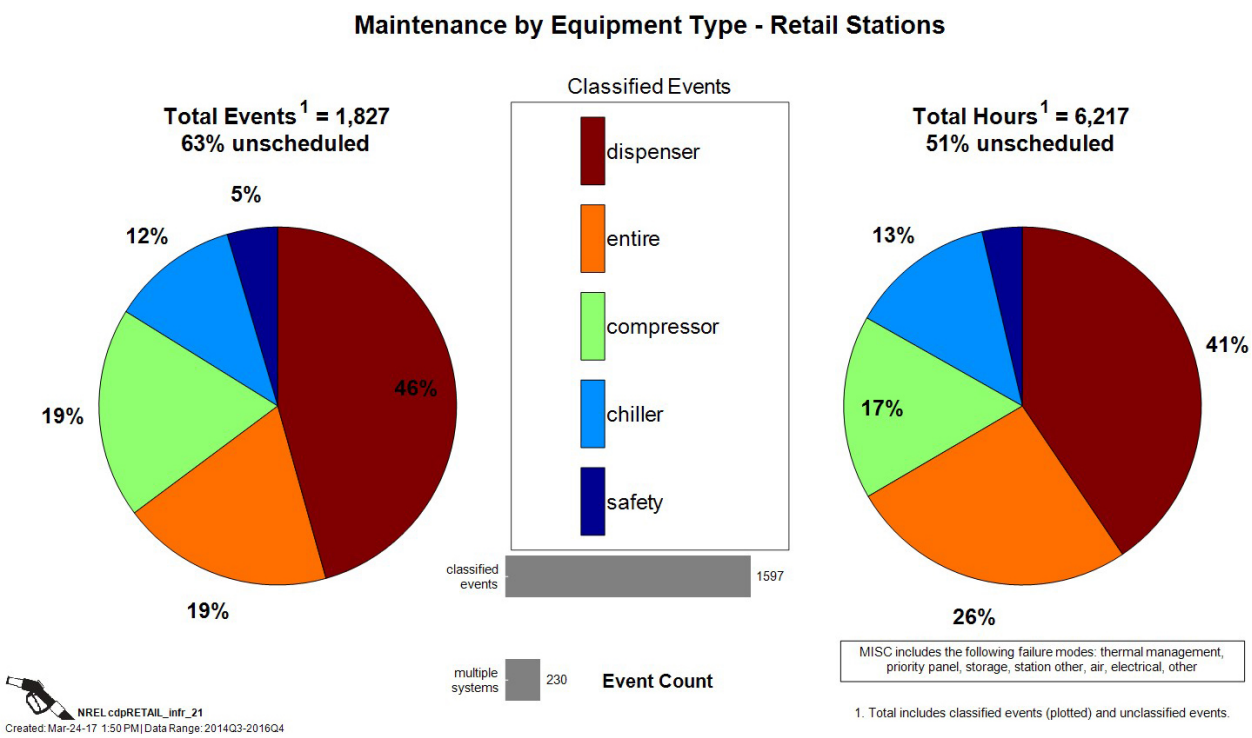

FIGURE 3. Maintenance by equipment type

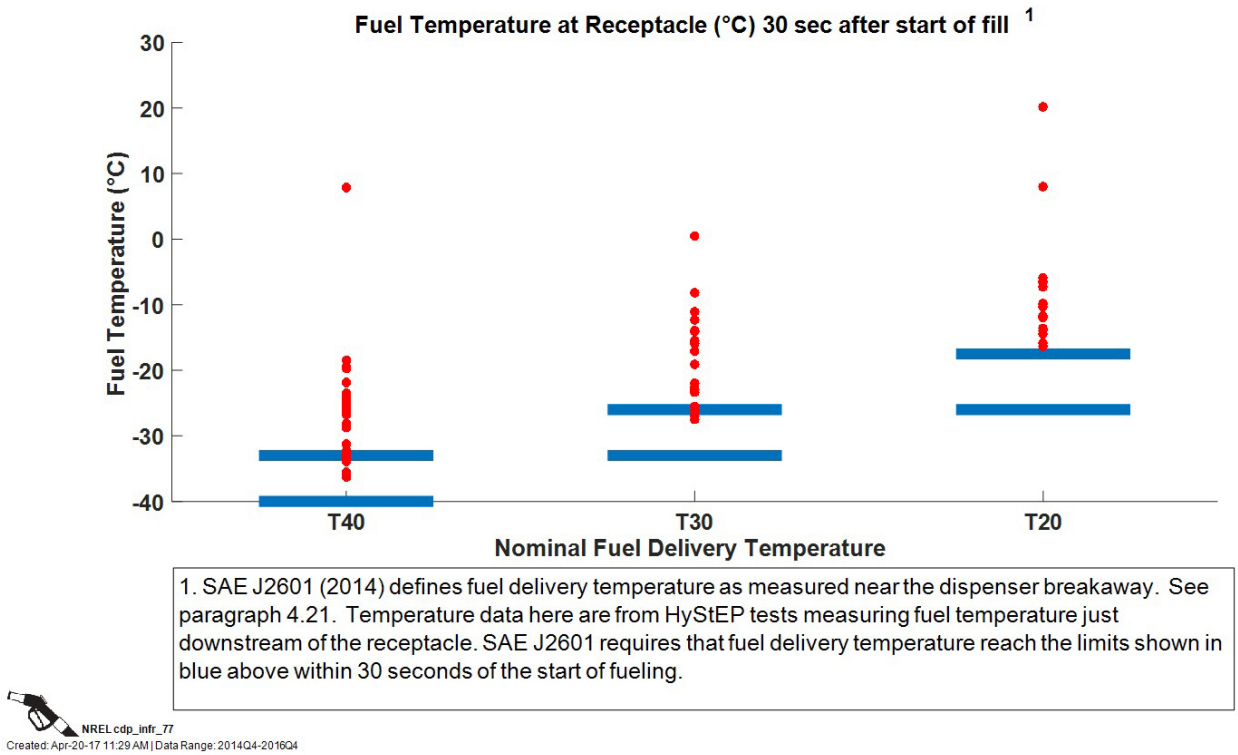

FIGURE 4. Fuel temperature at receptacle after 30 s

the hydrogen, energy used per kilogram dispensed and energy cost per kilogram dispensed. Fueling rates average 0.83 kg/min, fueling amounts average 2.86 kg and fueling time averages 3.6 min. Compressors use 3.65 kWh per kg and electrolyzers use 62 kWh per kg on average. There are 23 h of maintenance at a station on average per month and there are 289 fills per hydrogen leak reported. These results and all the other CDPs are published on NREL's website.

CONCLUSIONS AND UPCOMING ACTIVITIES

As new stations come online or are updated, their performance and availability will affect how successfully they support the current and upcoming fleet of fuel cell vehicles. Continual data collection, analysis, and feedback will provide DOE and the hydrogen and fuel cell community with awareness of the technology readiness and identify areas for improvement that could be research topics. Many new stations are coming online and will be included in the data set as they report data. Their data will be aggregated and published in CDPs without revealing individual station identity and will help identify general trends for the latest stations. As more data become available from newer stations and as more FCEVs enter the market, there will be an increase in data analysis possibilities to validate the technology for hydrogen infrastructure including focusing on trends over time for usage, reliability, and performance of the stations.

FY 2017 PUBLICATIONS/PRESENTATIONS

1. Sam Sprik, Jennifer Kurtz, Chris Ainscough, Genevieve Saur, and Mike Peters, "TV017: Hydrogen Station Data Collection and Analysis" (presented at the 2017 DOE Annual Merit Review and Peer Evaluation Meeting, Washington, DC, June 2017).

2. Next Generation Hydrogen Station Composite Data Products: All Stations (Retail and Non-Retail Combined), Data through Quarter 4 of 2016, Sam Sprik, Jennifer Kurtz, Chris Ainscough, Genevieve Saur, and Michael Peters (May 2017) http://www.nrel.gov/hydrogen/proj_infrastructure_analysis.html.

3. Next Generation Hydrogen Station Composite Data Products: Retail Stations , Data through Quarter 4 of 2016, Sam Sprik, Jennifer Kurtz, Chris Ainscough, Genevieve Saur, and Michael Peters (May 2017) http://www.nrel.gov/hydrogen/proj_infrastructure_analysis.html.

4. Next Generation Hydrogen Station Composite Data Products: All Stations (Retail and Non-Retail Combined)PDF, Data through Quarter 3 of 2016, Sam Sprik, Jennifer Kurtz, Chris Ainscough, Genevieve Saur, Michael Peters, and Matthew Jeffers (January 2017) http://www.nrel.gov/hydrogen/proj_infrastructure_analysis.html.

5. Next Generation Hydrogen Station Composite Data Products: Retail StationsPDF, Data through Quarter 3 of 2016, Sam Sprik, Jennifer Kurtz, Chris Ainscough, Genevieve Saur, Michael Peters, and Matthew Jeffers (January 2017) http://www.nrel.gov/hydrogen/proj_infrastructure_analysis.html.

VII.B.3 Performance Evaluation of Delivered Hydrogen Fueling Stations

Ted Barnes (Primary Contact) and Devin Halliday
Gas Technology Institute (GTI)
1700 S Mt. Prospect Rd.
Des Plaines, IL 60018
Phone: (847) 544-3405
Email: ted.barnes@gastechnology.org

DOE Manager: James Alkire
Phone: (720) 356-1426
Email: James.Alkire@ee.doe.gov

Contract Number: DE-EE0005886

Subcontractor:
Linde LLC (Linde), Hayward, CA

Project Start Date: March 1, 2013
Project End Date: April 30, 2018

Overall Objectives

- Integrate non-intrusive data collection systems at five 100 kg/d delivered liquid hydrogen fueling stations located in California for a 24-month performance period.
- Submit complete sets of the National Renewable Energy Laboratory (NREL) Hydrogen Station Data Templates to National Fuel Cell Technology Evaluation Center.
- Provide useful data to accurately benchmark and characterize station capacity, utilization, maintenance, and safety.

Fiscal Year (FY) 2017 Objectives

- Installation and commissioning of the third and fourth systems in new Linde hydrogen fueling stations in San Ramon, California, and Mountain View, California.
- Produce the complete sets of data for the all active sites at the end of each quarter after startup and commissioning is completed.
- Monitor progress on final (fifth) planned hydrogen fueling station to ensure data acquisition systems are prepared for installation.

Technical Barriers

This project addresses the following technical barriers from the Technology Validation section of the Fuel Cell Technologies Office Multi-Year Research, Development, and Demonstration Plan.

(A) Lack of Fuel Cell Electric Vehicle and Fuel Cell Bus Performance and Durability Data

(D) Lack of Hydrogen Refueling Infrastructure Performance and Availability Data

Contribution to Achievement of DOE Technology Validation Milestones

This project will contribute to the achievement of the following DOE milestones from the Technology Validation section of the Fuel Cell Technologies Program Multi-Year Research, Development, and Demonstration Plan.

- Milestone 3.2: Validate novel hydrogen compression technologies or systems capable of >200 kg/d that could lead to more cost-effective and scalable (up to 500 kg/d) fueling station solutions for motive applications. The stations currently being constructed will incorporate Linde's patented ionic fluid compressor. This technology utilizes a liquid piston to compress gas rather than a diaphragm or metal piston used in conventional compressor technologies. Linde is optimistic that this technology can be cost effectively scaled to larger capacity stations in the future.
- Milestone 3.4: Validate station compression technology provided by the delivery team. See Milestone 3.2
- Milestone 3.8: Validate reduction of cost of transporting hydrogen from central production to refueling sites to <$0.90/gge. This project will yield data directly aiding to develop baseline benchmarking and measure improved cost of delivery of liquid hydrogen to fueling stations in California.
- Milestone 4.4: Complete evaluation of 700-bar fast fill fueling stations and compare to SAE J2601 specifications and DOE fueling targets. This project will supply data to the National Fuel Cell Technology Evaluation Center that aid the program in the characterization of the stations' storage and delivery capacities, compression performance, fueling transactional data, operational cost, maintenance, and safety. Data supplied will provide points of direct comparison to SAE fueling standards and DOE fueling targets.

FY 2017 Accomplishments

- Completed installation of the GTI-designed data acquisition system at the San Ramon station. Station

opening is imminent; data collection to begin once open to public.

- Data submitted to NREL each quarter for West Sacramento and San Juan Capistrano stations.
- All equipment ordered and assembled for installation at the fourth station, Mountain View. The Mountain View station began construction in June 2017 and plans on commissioning by end of the year.

✧ ✧ ✧ ✧ ✧

INTRODUCTION

The objective of this project is to collect, organize, and report on operational, transactional, safety, and reliability data for five hydrogen fueling stations located in California. Goals of the project are as follows. (1) The data collected will be statistically meaningful and the stations will have sufficient throughput and vehicle fueling frequency to minimize data aberrations. (2) The data collected will be accurate. (3) The data collected will be comprehensive and timely.

This project will directly assist DOE in assessing the readiness level of current infrastructure and state-of-the-art technologies utilized to support planned fuel cell vehicle deployment within the next five years. The data and observations collected during the performance period of this project will provide NREL with information detailing the operational costs, efficiencies, and reliability of the delivered hydrogen fueling station design. Furthermore, the Linde design utilizes the patented IC90 ionic fluid compressor package; through this project GTI will provide the performance data which will enable DOE and original equipment manufacturer to evaluate real world efficiencies further gauging the technology's adequacy in this application. This system is a first of its kind utilized for hydrogen fueling applications in the United States.

APPROACH

Hydrogen station data will be submitted quarterly to the National Fuel Cell Technology Evaluation Center at NREL using the appropriate Hydrogen Station Data Templates. GTI's project partner, Linde, is currently developing delivered hydrogen fueling stations under programs sponsored by the California Energy Commission. The sites will be accessible to the public for fueling consumer fuel cell vehicles, commercial vehicles, or government-owned vehicles. All five of the sites will be developed at existing or at new sites along with conventional gasoline stations operated by major, branded fuel providers. This provides the project with vehicle fueling data from a broad cross-section of real world vehicle applications. The station sites were selected to provide convenient, consumer-friendly vehicle fueling for drivers of fuel cell vehicles. Development of each of these stations has the support of vehicle original equipment manufacturers and each site has passed stringent location selection requirements of the California Energy Commission to ensure the stations will be utilized by a high volume of fuel cell vehicle operators.

The data collection system will utilize a variety of methods in order to provide the entire data requirements set forth by NREL. This system will utilize the existing control architecture of the compressor and dispenser equipment as well as monitor and record signals from a set of installed instrumentation that will supplement information required that is not already captured inherently by the stations' operating system. There are multiple descriptive (opposed to measured data) deliverables that will be taken manually and submitted to GTI for processing and formatting prior to delivery to NREL. Manually collected data templates include:

- NREL Site Log: recording safety drills, training, or public meetings
- Storage and Delivery: compiling liquid hydrogen supplies delivery quantities and cost
- Fuel Log: transferring transactional data from monthly reports emanating from fuel management system
- Maintenance: station maintenance and operations reporting
- Hydrogen Cost: Collection of utility bills
- Safety: station environmental, health, and safety reporting
- Hydrogen Quality: SAE quality analysis completed annually and submitted

GTI will collaborate with Linde and create a reporting/submittal process to collect this type of data required to populate the NREL templates.

RESULTS

Installation of the San Ramon station was slow this year, partly due to the station being a green-field site, and not an addition to an existing gasoline station like other sites. The GTI data acquisition system has been installed and commissioned at the station. The San Ramon site will open for public use in the very near future and data collection will begin as soon as the station is open. Data collection continues for the two operational sites in West Sacramento and San Juan Capistrano. Figures 1 and 2 show the quarterly (Q) dispensed hydrogen data collected from these sites. The utilization of both of these sites has increased substantially over the past year. This is just a small subset of the large amount of data that is being reported to NREL each quarter. Other data collected includes the energy used in compression

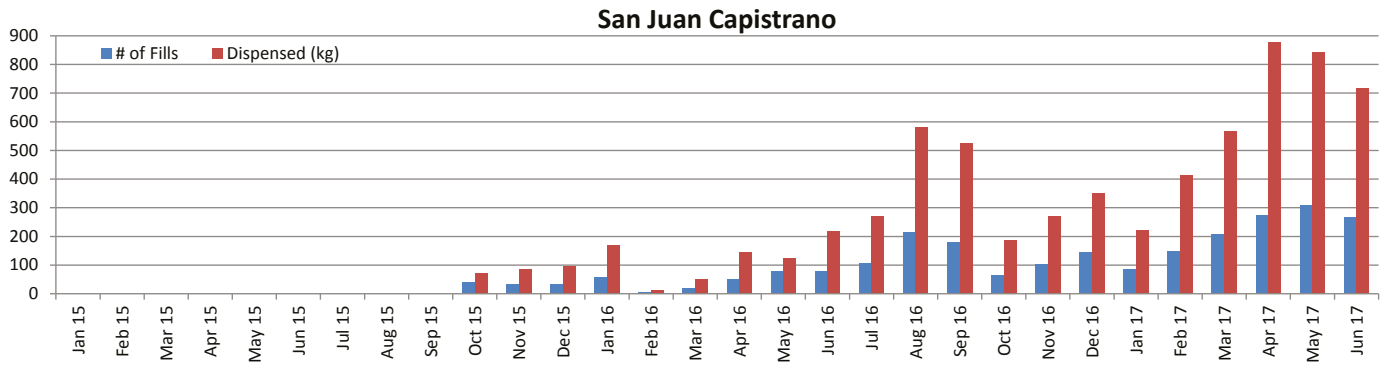

FIGURE 1. West Sacramento usage data

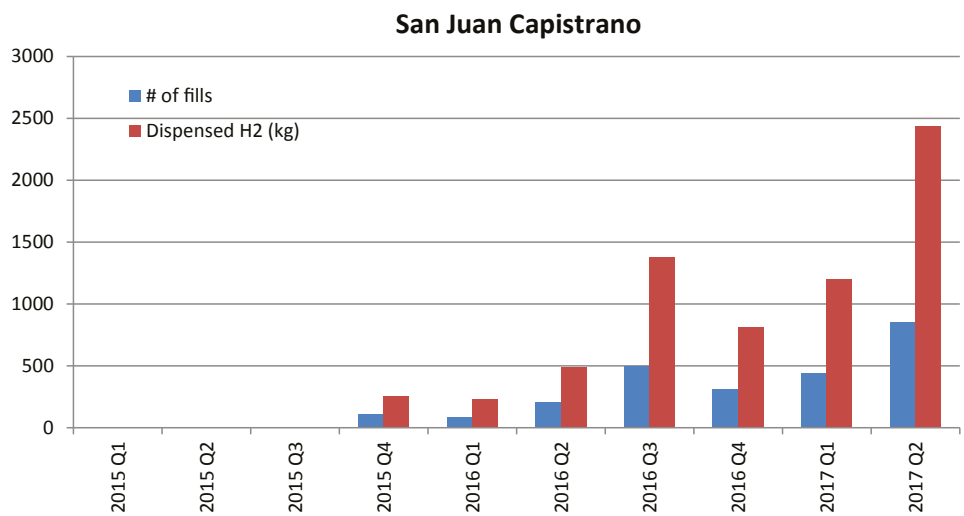

FIGURE 2. San Juan Capistrano usage data

and precooling of the hydrogen, maintenance and safety logs, and hydrogen control quality results.

The West Sacramento station was completed and commissioned in December 2014. The data collection portion of this project has continued and ten quarters of data have been collected from the site and submitted to NREL. The San Juan Capistrano station was completed and commissioned in September 2015. The data collection portion of this project has continued and seven quarters of data have been collected from the site and submitted to NREL. The Mountain View station began construction June 2017. Installation of the GTI panel will likely occur in September or October of this year. The GTI-supplied hydrogen gas flow meter for the system (longest lead item) has been delivered to the Linde staging area for integration into the compressor skid prior to the skid being installed at the site. The GTI data logger panel was assembled in early 2017 and is ready for installation whenever site construction progress allows. Lastly, progress continues to be made on the installation of the final station. A site has been proposed and is expected to be confirmed very shortly. The major equipment for each site has already been built and is awaiting installation.

CONCLUSIONS AND UPCOMING ACTIVITIES

- Begin data collection at San Ramon station.
- Complete panel installation and commissioning at Mountain View site.
- Produce the complete sets of data for all active sites at the end of each quarter.
- Continue monitoring progress on final station site. Begin engineering review of site once documents are available.

FY 2017 PUBLICATIONS/PRESENTATIONS

1. "tv025_barnes_2017_p.pptx" – Poster Presentation 2017 AMR.

VII.B.4 Hydrogen Component Validation

Danny Terlip
National Renewable Energy Laboratory (NREL)
15013 Denver West Parkway
Golden, CO 80401
Phone: (303) 275-4180
Email: danny.terlip@nrel.gov

DOE Manager: Jason Marcinkoski
Phone: (202) 586-7466
Email: Jason.Marcinkoski@ee.doe.gov

Subcontractors:
- Smart Chemistry, Sacramento, CA
- Spectrum Automation, Arvada, CO

Project Start Date: October 2012
Project End Date: Project continuation and direction determined annually by DOE

Overall Objectives

- Reduce fuel contamination introduced by forecourt station components.
- Improve station reliability and uptime.
- Increase the publicly available energy and performance data of major station components.

Fiscal Year (FY) 2017 Objectives

- Understand common failures at hydrogen stations.
- Understand the source of particulate contamination in hydrogen stations.
- Quantify the costs incurred when operating a hydrogen station.

Technical Barriers

This project addresses the following technical barrier from the Technology Validation section of the Fuel Cell Technologies Office Multi-Year Research, Development, and Demonstration Plan.

(D) Lack of Hydrogen Refueling Infrastructure Performance and Availability Data (detailed compressor reliability data and analysis)

Contribution to Achievement of DOE Technology Validation Milestones

This project will contribute to achievement of the following DOE milestone from the Technology Validation program section of the Fuel Cell Technologies Office Multi-Year Research, Development, and Demonstration Plan.

- Milestone 3.4: Validate Station Compression technology provided by delivery team (4Q, 2018).

FY 2017 Accomplishments

- Quantified the energy consumption of major components of the Hydrogen Infrastructure Testing and Research Facility (HITRF).
- Mapped the chiller energy usage based on the amount of hydrogen dispensed and the ambient temperature.
- Designed and performed an experiment that quantified the impact of cleaning methods on removing metal particulates from hydrogen tubing after it is cut and conditioned for installation.

✧ ✧ ✧ ✧ ✧

INTRODUCTION

The Hydrogen Component Validation task is focused on addressing three challenges currently facing forecourt hydrogen stations today. These challenges were prioritized from an H2USA Fueling Stations Working Group brainstorming session: fuel contamination introduced by forecourt station components, station reliability and uptime, and lack of publicly available energy and performance data of major station components. Improvement in each one of these topic areas is critical for successful station operation, positive fuel cell driver experience, and a robust hydrogen economy.

APPROACH

NREL is working to better understand particulate contamination in the hydrogen process stream by distributing contaminant collection packets to forecourt station operators. When a maintenance event occurs, the participating station operators collect samples from hydrogen tubing or components and send the samples to NREL to be analyzed. NREL noticed macroscopic metal particulates in samples taken from many of the failed parts. The metal particulates were analyzed and shown to be similar to 300 series stainless steel. Most wetted metal in a typical hydrogen station is 300 series stainless. One of the most likely sources of particulates is debris from the cutting, beveling, and threading process of tubing. This process often utilizes a sulfur based lubricant that can remain on the tubing if not cleaned properly (sulfur irreversibly degrades fuel cell performance). NREL designed an experiment with 18 tube samples that considered two different sizes of tubing, 3/8 in

outside diameter (OD) and 9/16 in OD and three different cleaning methods: (1) compressed air and rag, the most common method; (2) tube brush and rag; and (3) sonication, which is not feasible for hydrogen station tubing. The tube samples were installed in a filling system with a 0.2 micron filter behind it. Two kilograms of hydrogen were passed through each tube. Filters were weighed for mass change and examined with a microscope.

NREL installed power meters on two hydrogen compressors and the hydrogen pre-cooling system at the HITRF. The HITRF supervisory control and data acquisition (SCADA) system is collecting power and energy data as each of these components operates to support the HITRF. NREL engineers are analyzing the data and collaborating with other DOE researchers to better understand operating costs of forecourt hydrogen stations and possible precursors to equipment failures that can be used to indicate the need for pre-emptive maintenance.

RESULTS

Many of the contaminant samples NREL collected from both retail hydrogen stations and the HITRF contained metal shards. Figure 1 shows examples of metal particulate contaminants that were collected. The image on the left shows metal shards embedded in a valve seat. The image in the middle shows metal impregnated in a compressor rider band. The image on the right shows metal shards magnetically attracted to a compressor check valve (austenitic stainless steels are typically nonmagnetic, yet heat treating and physical deformation, as may take place in a compressor environment, have been shown to magnetize austenitic steels and may be responsible for magnetizing the metal particulates here).

NREL compared the mass change of filters, the number of particles, and the size of particles across cleaning methods and tubing size. The filters from tubing cleaned with the air and rag method had the highest mass change and highest number of particles, indicating the most contamination. Filters from tubing cleaned with the sonication method had the lowest mass change, indicating the least amount of particles by mass. Filters from the samples cleaned by tube brush had the lowest number of particles. The largest particles were found in the filters from tubing cleaned by the air and rag method. Filters from the 3/8 in OD tubing had a higher mass change than filters from the 9/16 in OD tubing did. The results were inconclusive for the number of particles collected on filters between 3/8 in OD tubing and 9/16 in OD tubing. Results for two samples (6 and 8) were thrown out due to an operator error in the testing procedure. Figure 2 and Figure 3 show the mass change and the number of particulates for each of the tests.

NREL engineers installed power meters on two hydrogen compressors and one pre-cooling system compressor. The HITRF SCADA system is collecting the amount of power and energy consumed by each component at one second intervals. NREL engineers perform detailed analysis on the data resulting in quantitative performance information. Figure 4 shows one instance of performance data for the NREL HITRF station. The metric is electric energy consumption (including balance of plant) per kilogram of hydrogen produced, compressed, or dispensed. The graphic shows a cost per component for each kilogram of hydrogen assuming a typical electricity rate for Los Angeles, $0.184/kWh. The performance metric and subsequent cost reported for the dispenser includes the pre-cooling system and assumes one vehicle fill per hour.

As noted in Figure 4, the performance metric for the dispenser (including pre-cooling) is highly variable. The two factors affecting the variability are the ambient temperature and the mass of hydrogen chilled per unit of time. NREL collected this data for the single heat exchanger block (27 cu ft) and 6.75 kW chiller that circulates R404a. The results are shown in Figure 5.

FIGURE 1. Three contaminant samples collected as part of Hydrogen Component Validation task

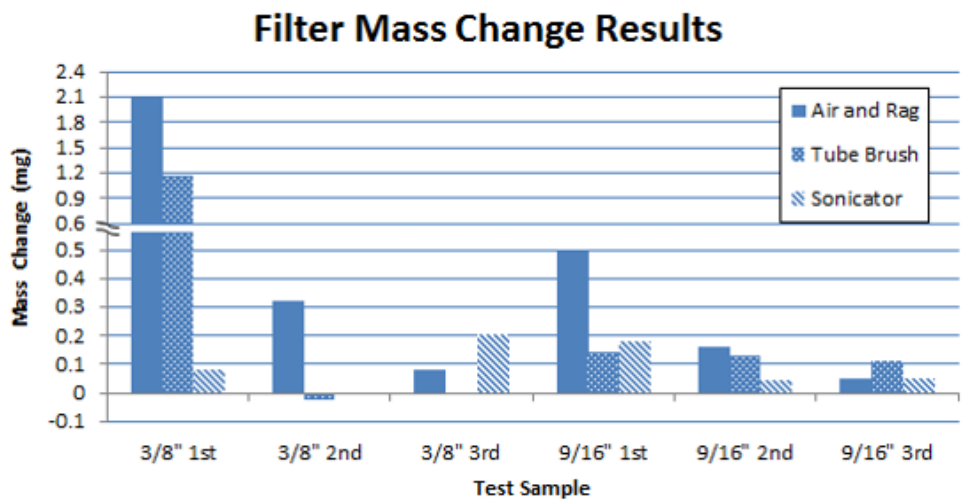

FIGURE 2. Mass change for filters of the 18 tubes. The 3/8 in air and rag tubes were tested first, then the 3/8 in tube brush, then the 3/8 in sonicator. The same order was then followed for the 9/16 in tubes.

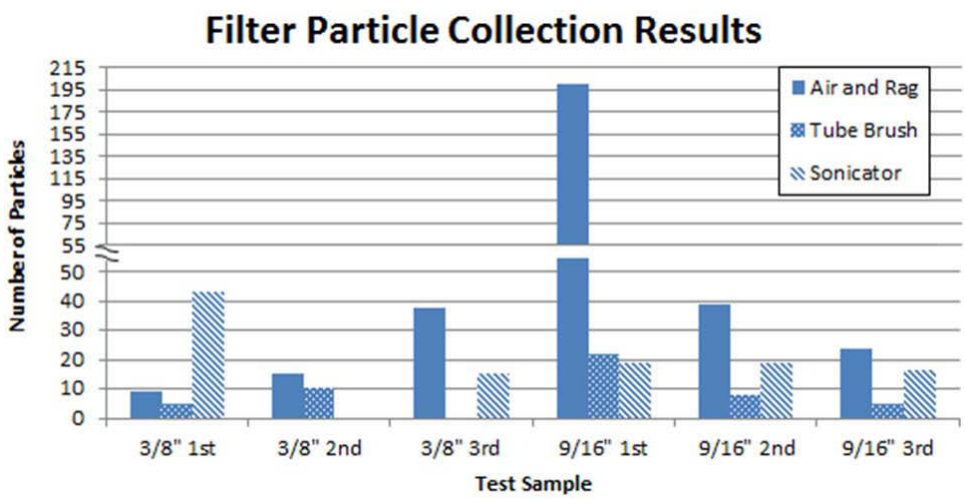

FIGURE 3. Particle count for filters of the 18 tubes. The 3/8 in air and rag tubes were tested first, then the 3/8 in tube brush, then the 3/8 in sonicator. The same order was then followed for the 9/16 in tubes.

CONCLUSIONS AND UPCOMING ACTIVITIES

The Hydrogen Component Validation project addresses two challenges facing forecourt hydrogen stations today: particulate contamination from various sources and energy consumption of major station components. Both tasks involve collecting data from forecourt hydrogen stations and the NREL HITRF. Data and conclusions from these activities are communicated through presentations and research publications.

The particulate contamination project was developed to collect field samples of particulate matter, determine the origin, and publish the results to identify major issues impacting a high percentage of stations. Currently 11 stations are participating and NREL is reaching out to more stations as they become operational. NREL identified metal particulates as a significant portion of particulate contamination, and performed a study to determine the impacts of cleaning methods to remove metal particulates after tube cutting, beveling, and threading.

Regardless of the tubing size or cleaning method, any metal particulate can cause a problem in hydrogen stations or fuel cell electric vehicles, where they may be accelerated to high velocity and destroy filters or prevent a valve from operating properly. The specification for cleanliness of

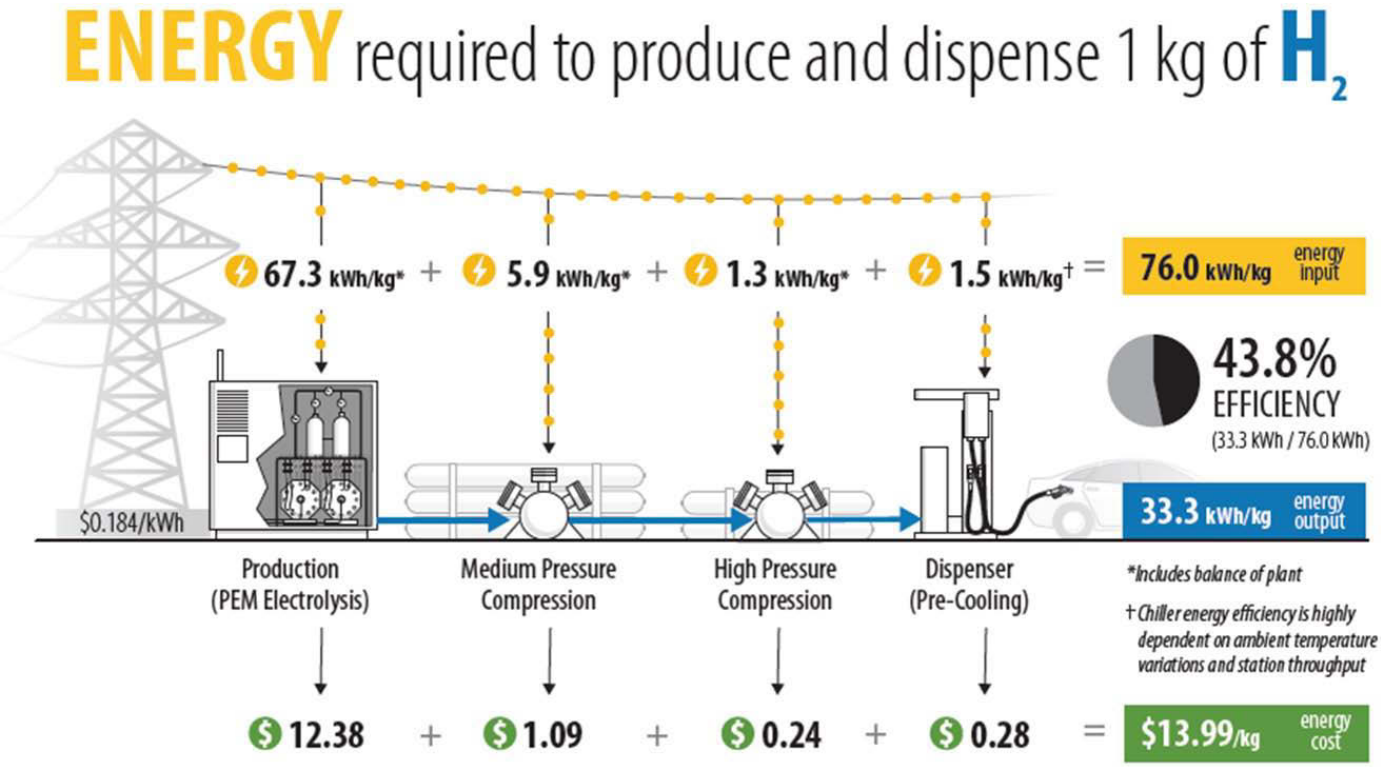

FIGURE 4. Energy consumption for major components at the HITRF. An electricity price of $0.184/kWh, typical of Los Angeles, is taken to show the cost of producing 1 kg of hydrogen at 700 bar and -40°C.

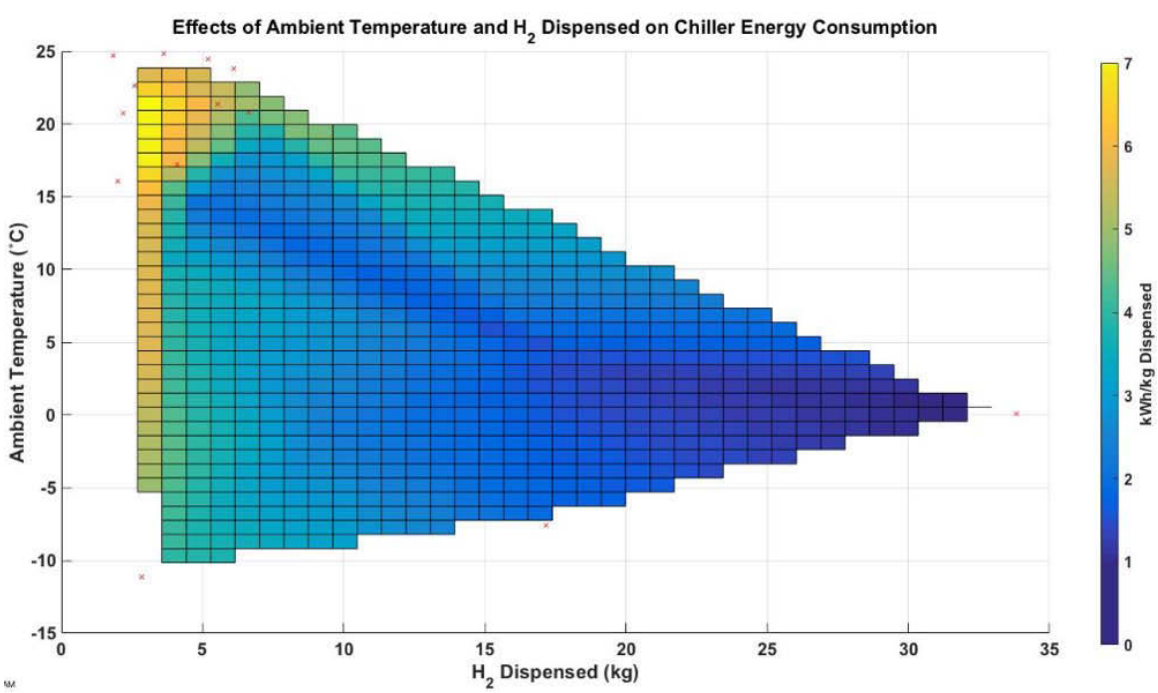

FIGURE 5. Chiller performance data showing electrical energy consumption per mass of hydrogen chilled (or dispensed). The vertical axis shows that pre-cooling becomes more costly with increasing ambient temperature, while the horizontal axis shows that pre-cooling becomes less costly with the amount of hydrogen dispensed.

hydrogen dispensed to fuel cell electric vehicles (SAE J2719) allows a maximum of 1 mg of particulate matter per 1 kg of hydrogen. Hydrogen stations could contain 100 or more of these tubes with cuts and conditioning on both sides. Thus it can be seen that particulate contamination from tube cutting and conditioning can result not only in station reliability problems but also can result in a station dispensing hydrogen that is outside of specification. Future work will determine the impact of other likely sources of particulate contamination.

As the number of stations and fuel cell electric vehicles change, retail hydrogen stations are currently experiencing variable utilization. It is critical for station operators to understand the cost of operation under low and high utilization to ensure financially sustainable operations. Power and energy consumption of major station components impacts operating costs at hydrogen stations. NREL has installed power meters on two hydrogen compressors and the hydrogen pre-cooling system. The HITRF SCADA system continually records data during operation and NREL engineers analyze the data. The analysis is used to inform modeling efforts of hydrogen stations. Future work will involve analyzing the data for possible precursors to failure and impacts for reducing operating costs at hydrogen stations.

FY 2017 PUBLICATIONS/PRESENTATIONS

1. "Hydrogen Component Validation," Terlip, Danny. Annual Merit Review 2017. Washington D.C., 7 June 2016.

2. "Adapted Tube Cleaning Practices to Reduce Particulate Contamination at Hydrogen Fueling Stations," Terlip, Danny; Martin, Joshua; Hartmann, Kevin; accepted for publication at ICHS Conference, September 2017.

VII.B.5 Liquid Hydrogen Pump Performance and Durability Testing

Salvador M. Aceves (Primary Contact),
Guillaume Petitpas, Julio Moreno-Blanco,
Juan Manuel Garcia-Guendulain
Lawrence Livermore National Laboratory (LLNL)
7000 East Avenue
Livermore, CA 94550
Phone: (925) 422-0864
Email: aceves6@llnl.gov

DOE Manager: Jason Marcinkoski
Phone: (202) 586-7466
Email: Jason.Marcinkoski@ee.doe.gov

Subcontractors:
- Spencer Composites Corporation, Sacramento, CA
- Linde LLC, Hayward, CA

Project Start Date: January 2014
Project End Date: December 2017

Overall Objectives

- Measure liquid hydrogen (LH_2) pump performance parameters including: hydrogen flow rate, refuel density, electricity consumption, boil-off, hydrogen temperature and pressure during fill, pump degradation, maintenance requirements, and incidents.

Fiscal Year (FY) 2017 Objectives

- Complete construction of LLNL's hydrogen test facility by installing and commissioning a heat exchanger manufactured by Linde.
- Demonstrate durability (1,000 thermomechanical cycles) of cryogenic vessel prototype manufactured by BMW.

Technical Barriers

This project addresses the following technical barriers from the Technology Validation section of the Fuel Cell Technologies Office Multi-Year Research, Development, and Demonstration Plan.

(C) Hydrogen Storage

(D) Lack of Hydrogen Infrastructure Performance and Availability Data

Contribution to Achievement of DOE Technology Validation Milestones

This project will contribute to achievement of the following DOE milestones from the Technology Validation section of the Fuel Cell Technologies Office Multi-Year Research, Development, and Demonstration Plan.

- Milestone 3.4: Validate station compression technology provided by delivery team (4Q, 2018).

FY 2017 Accomplishments

- Cycle tested experimental vessel prototype 456 times with cryogenic hydrogen to 700 bar.
- Measured pump performance while delivering 1.65 tonnes of cryogenic pressurized hydrogen.
- Installed heat exchanger in test facility enabling ambient temperature hydrogen refueling.
- Initiated testing of cryogenic vessel supplied by BMW by conducting 100 cycles with cryogenic hydrogen to 300 bar.

✧ ✧ ✧ ✧ ✧

INTRODUCTION

An experimental vessel was cycle tested 456 times to 700 bar with cryogenic pressurized hydrogen while simultaneously measuring pump performance: flow rate, refuel density, electricity consumption, boil-off, hydrogen temperature and pressure during fill, pump degradation, maintenance requirements, and incidents. In this 19-day experiment, the LH_2 pump delivered 1.65 tonnes of hydrogen to the experimental vessel over eight days of cycle testing. This report focuses on pump performance during the 456 fill cycles conducted in the experiment. Vessel test results have been reported elsewhere [1].

APPROACH

Experiments were conducted at LLNL's Hydrogen Test Facility (Figure 1) [2]. Built over the last four years at the south end of the LLNL campus, the Hydrogen Test Facility includes an 875 bar LH_2 pump manufactured by Linde, a liquid hydrogen dewar with 12.5 m^3 capacity, a 40 kW heat exchanger for delivery of ambient temperature hydrogen, a 2.8 m^3 containment vessel rated for 60 bar maximum pressure, two vent stacks (for high-pressure and low-pressure hydrogen discharges), a control room for remote operation, connecting high-pressure cryogenic lines,

FIGURE 1. Hydrogen Test Facility at LLNL showing the main components

and instrumentation (for measuring temperature, pressure, hydrogen level, electricity consumption, and vacuum).

The experimental pressure vessel was built for maximum volumetric and gravimetric storage performance (project targets 50 g H_2/L, 9% H_2 by weight). Vessel characteristics include 65 L capacity, 700 bar maximum operating pressure, 32 kg total weight, and high volumetric efficiency (81% vs. 70% typical of today's 700 bar vessels). The prototype vessel was wrapped in multilayer insulation, instrumented, and cycle tested inside the containment vessel (Figure 2).

RESULTS

Key results from the 19-day experiment include the following:

- The experimental vessel was cycled 456 times before failing by developing a crack through the liner. During these cycles, the pump delivered 1,658 kg of hydrogen into the experimental vessel. The 456 cycles were completed over eight days of operation and four dewar refuels.
- The pump consistently demonstrated high hydrogen throughput (96 kg/h average and 100+ kg/h peak hydrogen flow rate). This is a key parameter for reducing refueling cost per vehicle, as pump capital cost can be amortized over many vehicles served.
- The experimental vessel was consistently refueled in under 3 min at ~3.7 kg hydrogen per refuel. While the prototype vessel is small (65 L), these results show promise for future practical refueling times (<5 min) in larger vessels with 5–8 kg of hydrogen capacity.
- The pump shows low electricity consumption at an average of 1.1 kWh/kg H_2 active power during the fill. This is considerably lower than for available alternatives (on-site gas compression), minimizing station electricity consumption. Apparent electricity consumption is higher, at 1.5 kVAh/kg H_2.
- We identified several sources of boil-off: (1) LH_2 delivery to station dewar, (2) heat transfer into the station dewar, (3) pump cool-down and warm-up, (4) pump losses, and (5) LH_2 run-off from pump dewar. We measured boil-off originating from Mechanisms 1–4 by instrumenting the vent stack with a mass flow meter. Run-off from the pump dewar (Mechanism 5) does not vent through the main stack and therefore was not measured. Instead, it was estimated with assistance from Linde.
- The results indicate that the station lost 430 kg of hydrogen (25.9% of dispensed hydrogen) to boil-off during the 19-day experiment. This, however, is not a reliable indication of LH_2 pump performance when integrated into a commercial fueling station, since the pump was only operated eight days for vessel cycling, pre-cooled three days for testing without any vessel fills, and remained idle for eight days. Lower boil-off losses (16%) are measured for a typical day of operation where 300 kg of hydrogen were dispensed. Substantial reductions in boil-off to as little as 3.6% are projected for an improved delivery system where the LH_2 truck is not depressurized after dewar refueling, and the LH_2 pump is in close proximity to the station dewar.
- We evaluated pump performance degradation by comparing initial (Cycle 1) and final (Cycle 456) values of electricity consumption and pump outlet temperature, considering that increases in either of these would

FIGURE 2. Prototype thin-lined experimental pressure vessel (left), and multilayer insulation-wrapped and instrumented prototype vessel being introduced into containment vessel for cycle testing (right)

indicate degraded pump performance. Initial and final cycles showed comparable pump operation, leading to the conclusion that no performance degradation was identified during the experiment.

- Incidents identified during the experiment include (1) two occasions of excessive boil-off upon station dewar fill, (2) overheating of LH_2 pump oil after two hours of operation, (3) a data acquisition error, (4) loose bolts on the flange connecting the hydraulic piston and the LH_2 pump, (5) temperature sensor failure, and (6) experimental prototype vessel failure. All these incidents were quickly resolved, and none of them resulted in unsafe operating conditions. In general, the pump demonstrated excellent reliability, consistently performing as expected with minimum supervision or maintenance.

CONCLUSIONS AND UPCOMING ACTIVITIES

Upcoming activities include durability testing of a cryogenic pressure vessel provided by BMW (1,000 cycles; 100 completed to date) while simultaneously determining LH_2 pump performance to 300 bar. These objectives will be met by (1) establishing a protocol for accelerated testing of cryogenic pressure vessels and (2) running the cryogenic vessel through the test protocol while measuring all relevant LH_2 pump experimental parameters. These parameters are critical for a full characterization of cryogenic vessel technology, and will be reported and shared with other institutions for determining costs and benefits.

SPECIAL RECOGNITIONS & AWARDS/ PATENTS ISSUED

1. Salvador M. Aceves, Elias Rigoberto Ledesma-Orozco, Francisco Espinosa-Loza, Guillaume Petitpas, Vernon A Switzer, "Compact insert design for cryogenic pressure vessels," US Patent 9,677,713, 2017.

REFERENCES

1. Salvador M. Aceves, Guillaume Petitpas, "Thermomechanical Cycling of Thin Liner High Fiber Fraction Cryogenic Pressure Vessels Rapidly Refueled by Liquid Hydrogen Pump to 700 Bar," DOE Hydrogen and Fuel Cells Program Annual Progress Report, 2016, https://www.hydrogen.energy.gov/pdfs/progress16/iv_d_2_aceves_2016.pdf

2. Salvador M. Aceves, Guillaume Petitpas, "Performance and Durability Testing of Volumetrically Efficient Cryogenic Vessels and High-Pressure Liquid Hydrogen Pump," DOE Hydrogen and Fuel Cells Program Annual Progress Report, 2016, https://www.hydrogen.energy.gov/pdfs/progress16/vii_c_4_aceves_2016.pdf

VII.B.6 Hydrogen Meter Benchmark Testing

Michael Peters (Primary Contact), Robert Burgess, Matt Post, Josh Martin, Jeff Tomerlin, Chris Ainscough
National Renewable Energy Laboratory (NREL)
15013 Denver West Parkway
Golden, CO 80401-3305
Phone: (303) 275-3712
Email: Michael.Peters@nrel.gov

DOE Manager: Jason Marcinkoski
Phone: (202) 586-7466
Email: Jason.Marcinkoski@ee.doe.gov

Subcontractor:
Spectrum Automation, Arvada, CO

Project Start Date: September 1, 2015
Project End Date: December 31, 2017

Overall Objectives

- Design and build a laboratory grade gravimetric standard for measurement of hydrogen flow. The gravimetric standard will be capable of verifying compliance with National Institute of Standards and Technology Handbook 44 requirements for ±1.5% accuracy for the dispensing of motor vehicle fuel (gravimetric standard capability of one-third the required level or ±0.5%).
- Measure flow meter performance of three commercially available meters using the gravimetric standard. Testing will be conducted in high-pressure hydrogen at flow conditions simulating the range of dispenser operation.
- Disseminate results through communications and reporting to provide data on current flow meter performance, identifying the shortfalls to meeting regulations.

Fiscal Year (FY) 2017 Objectives

- Design, build, and conduct flow meter performance testing on three hydrogen flow meters.

Technical Barriers

This project addresses the following technical barriers from the Technology Validation and Safety, Codes and Standards sections of the Fuel Cell Technologies Office Multi-Year Research, Development, and Demonstration Plan.

Technology Validation

(D) Lack of Hydrogen Refueling Infrastructure Performance and Availability Data

Safety, Codes and Standards

(F) Enabling National and International Markets Requires Consistent RCS

(G) Insufficient Technical Data to Revise Standards

(J) Limited Participation of Business in the Code Development Process

Contribution to Achievement of DOE Technology Validation and Safety, Codes & Standards Milestones

This project will contributes to achievement of the following DOE milestones from the Technology Validation and Safety, Codes and Standards sections of the Fuel Cell Technologies Office Multi-Year Research, Development, and Demonstration Plan.

- Technology Validation Milestone 4.4: Complete evaluation of 700-bar fast fill fueling stations and compare to SAE J2601 specifications and DOE fueling targets (3Q, 2016).
- Safety, Codes and Standards Milestone 3.1: Develop, validate, and harmonize test measurement protocols (4Q, 2014).

FY 2017 Accomplishments

- Completed fill testing on three hydrogen flow meters: two Coriolis, one turbine.
  - C1 – Coriolis, commercially available, designed specifically for hydrogen
  - C2 – Coriolis, in development, designed specifically for hydrogen
  - T1 – Turbine, commercially available, not designed specifically for hydrogen
- Used statistical analysis to determine significant difference in flow meter performance based on different conditions (e.g., meter position, flow rate, and pressure range).

✧ ✧ ✧ ✧ ✧

INTRODUCTION

The hydrogen meter benchmarking project is being supported under the DOE Technology Validation program and is part of the DOE–NREL–Sandia National Laboratories–H2FIRST (Hydrogen Fueling Infrastructure Research and Station Technology) project. The H2FIRST objective is to ensure that fuel cell electric vehicle customers have a positive fueling experience similar to conventional gasoline and diesel stations as vehicles are introduced (2015–2017) and transition to advanced fueling technology beyond 2017. The H2FIRST activities are expected to positively impact the cost, reliability, safety, and consumer experience of fuel cell electric vehicle stations.

APPROACH

The meter benchmark (Figure 1) project collected baseline performance data on three different hydrogen flow meters with the following approach:

- Design and build a laboratory-grade gravimetric hydrogen standard.
- Conduct high-pressure hydrogen testing at a range of typical flow rates.
- Report on flow meter performance.

RESULTS

A hydrogen flow meter's purpose in a hydrogen dispenser is to accurately and precisely measure the amount of hydrogen a station sells to a customer. Accordingly, NREL considered the percent error of the meter from the start to the end of a fill as the ultimate performance metric, since this will account for all hydrogen that flows through the meter. NREL labeled this measurement as the peak pulse error.

FIGURE 1. A picture of the hydrogen metering test apparatus

There are many other performance metrics that need to be taken into consideration by the industry when considering a meter's applicability to the hydrogen dispenser application, for instance: instantaneous error, pressure differential, temperature differential across the meter, external vibration effects, and the delay in meter readout after the cessation of flow. As part of this project, NREL tracked all of these metrics.

NREL used the percent error equation below to calculate the peak pulse error. When the peak pulse error was positive, the meter over predicted the amount of hydrogen dispensed and the customer would be burdened with the extra cost. When the percent error was negative the meter under predicted the amount of hydrogen dispensed and the station operator would bear the cost burden.

$$Peak\ Pulse\ Error = \left(\frac{\Delta Scale - \Delta Meter}{\Delta Scale}\right) * 100$$

$$\Delta Scale = Scale(kg)_{end\ of\ fill} - Scale(kg)_{start\ of\ fill}$$

$$\Delta Meter = Meter(kg)_{end\ of\ fill} - Meter(kg)_{start\ of\ fill}$$

With each meter, NREL split the data into the identified factors and calculated the peak pulse error. The probability a single fill would be within a specified error range is the ultimate way that a meter would be tested by weights and measures agencies. This probability was calculated by using the mean, standard deviation, and confirming the normality of the data and analyzing with Minitab. The normality of the data was checked using the Anderson–Darling test and when confirmed, the mean and standard deviation were input into a distribution plot to obtain the single fill probability.

The results of the data suggested that on average, a sum total of fills would meet the 2% maintenance requirement; however, this does not necessarily mean that a single fill would fall into that category. Looking solely at the mean of a data set can be deceiving. For instance, over every test, the C2 meter had a mean error of 0.5% and the C1 meter had a mean error of -0.1% which gives the perception that the C1 meter performed better than the C2 meter. However, both are within the 2% maintenance tolerance. Upon further inspection, it was discovered that the C1 meter had a much higher standard deviation than the C2 meter (Figure 2). This means that one fill could be -4% and the next could be +4%, which is undesirable when comparing to a 2% accuracy requirement. For this reason, the data sets were sorted into probabilities based on a single fill being within the specified range.

The C2 flow meter performed consistently better than the C1 and the T1 meters in every category associated with meter error. The C1 meter performed slightly better than the T1 meter under most categories except for at high flow rates where the meters were nearly identical with regard to overall performance. The probability that a single fill would fall

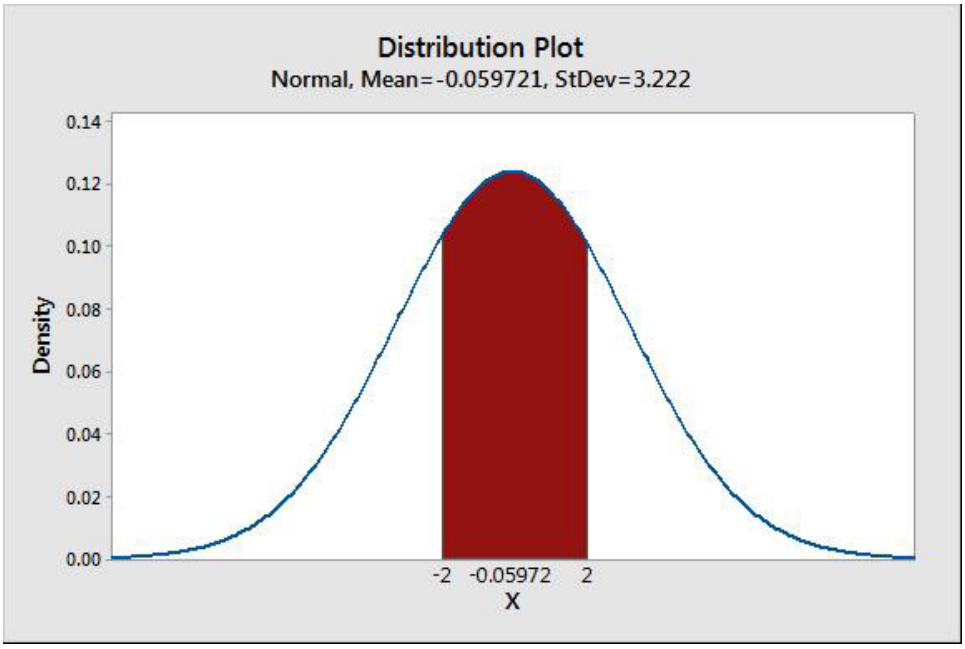

FIGURE 2. Distribution plot for 2% accuracy class, meter C1 – all data

within the 2% or 10% accuracy classes for all the data, and for high flow cases (≥2 kg/min), is shown in Table 1.

TABLE 1. Single Fill Performance Data

Probability a Single Fill Falls Within an Accuracy Class	All Data		High Flow Data (2+ kg/min)	
Accuracy Class	2%	10%	2%	10%
C1	46.5%	99.8%	34.1%	97.3%
C2	82.2%	100%	64.6%	100%
T1	12.6%	58.7%	35.0%	98.5%

CONCLUSIONS AND UPCOMING ACTIVITIES

This project has reached its conclusion. NREL plans to publish a report on the findings from the project so that the information is available to the public.

Potential future work could include an advanced dispenser control scheme that would adjust predicted kilograms dispensed based on meter accuracy data, developing a next generation mobile metrology device, testing meters under pre-chilled conditions, and working with meter manufacturers to develop next-generation metering technologies that have the potential to meet market requirements for cost and accuracy.

FY 2017 PUBLICATIONS/PRESENTATIONS

1. "Hydrogen Meter Benchmark Testing," 2017 DOE Hydrogen and Fuel Cells Program, Annual Merit Review, June 2016 (presentation).

2. "Hydrogen Meter Benchmark Testing Interim Report," NREL Report, January 2016.

VII.C.1 Optimal Stationary Fuel Cell Integration and Control (Energy Dispatch Controller)

Genevieve Saur
National Renewable Energy Laboratory
15013 Denver West Parkway
Golden, CO 80401-3305
Phone: (303) 275-3783
Email: genevieve.saur@nrel.gov

DOE Manager: Jason Marcinkoski
Phone: (202) 586-7466
Email: Jason.Marcinkoski@ee.doe.gov

Subcontractors:
- Washington State University, Pullman, WA
- University of Colorado Boulder, Boulder, CO

Project Start Date: June 2016
Project End Date: May 2019

Overall Objectives

Create an open source tool set to foster growth in fuel cell integrated buildings with emphasis on optimal dispatch control.

- Objective 1: Energy Dispatch Controller (EDC) – Implement an open source tool for optimized dispatch of building components, to be used in building management systems in communicating and transacting with a fuel cell integrated building system and the grid.
- Objective 2: System Planning Tool – Implement a planning tool for optimal component selection and sizing for distributed energy systems and smart building components, using location-specific energy markets, building energy modeling, and chosen dispatch control strategy.

Fiscal Year (FY) 2017 Objectives

- Initial formulation of the EDC optimization using model predictive control.
- Develop initial graphical user interface screens to provide interface for testing and feedback.
- Create interface for providing building specification and design.
- Create a functioning co-simulation environment for testing EDC.

Technical Barriers

This project addresses the following technical barriers from the Grid Modernization Initiative Multi-Year Program Plan.

- 4.2.3 Utilizing open standards and middleware software approaches to enable integration of energy management systems, distribution management systems, and building management systems. [1]
- 4.3.3 Develop efficient linear, mixed-integer, and nonlinear mixed-integer optimization solution techniques customized for stochastic power system models, novel bounding schemes to use in branch and bound, and structure exploiting algorithms. Demonstrate the cost-benefit achieved by these techniques relative to existing ones. [1]

Contribution to Achievement of DOE Technology Validation Milestones

This project provides program-specific support from the Fuel Cell Technologies Office to DOE's Grid Modernization Initiative. There are no specific milestones set for this multi-program effort [1], but this project provides support that aligns fuel cell integration and grid modernization efforts. Beneficial impacts include:

- Enhanced energy management and added benefits of an integrated building system.
- Expansion of grid supportive features of buildings as distributed energy resources.
- Support for fuel cell market development.

FY 2017 Accomplishments

- Completed initial formulation of the optimization for building controls and demonstrated the EDC optimization framework with a number of simplified cases to show how varying inputs would drive different behaviors for controlling building components.
- Developed and coded initial modules of the graphical user interface with several reviews and improvements.
- Collected foundational material on combined heat and power (CHP) design for inclusion as an option in the building design module.
- Initiated evaluation of building load forecasting for the uncontrollable loads for use as an input to the EDC optimization. Evaluating four different methods for load

forecasting: corrected naïve, autoregressive integrated moving average, neural network, and surface fit.

- Developing a co-simulation environment using EnergyPlus [2] in order to evaluate the EDC with a feedback loop using simulated buildings.

✧ ✧ ✧ ✧ ✧

INTRODUCTION

Current building control strategies can rely on arbitrary assignment of value to assets and be simplistic, needing prior analysis for set control strategies. This project is creating open source tools for dynamic building energy management: an energy dispatch controller capable of supervisory control, and a planning tool for component sizing of distributed generation and storage components using simulated dispatch. The controllable components within a building can be equipment such as fuel cell, chiller, or water heater, or the thermal mass of the building envelope as controlled through the temperature. Constraints to the energy management can be thermal comfort or required operations of specific equipment.

The project aims to modernize building energy management by holistically integrating control of building elements for optimal operation, including maximizing benefit of distributed generation and storage. The project also aids grid modernization by characterizing the potential of buildings to participate in ancillary grid services and positioning building operators to participate in ancillary grid service markets as they are available.

APPROACH

The project is using a cross-functional approach with team members who have expertise in fuel cells, power systems, commercial buildings, and building communication networks, leveraging prior knowledge with tools and research from the different areas to create a novel controller and planning tool.

The EDC optimization utilizes a model predictive control strategy. This approach allows forecasting of building loads and operation, which facilitates participations in grid ancillary service markets. The planning tool then uses simulated optimal dispatch to size added components into the system.

RESULTS

The first year of the project involved initial formulations of the EDC and foundational work on the different modules needed to run the tool (Figure 1). A graphical user interface has been developed to aid visualization of the different modules. Common methods of integrating CHP were catalogued and described, in order to portray current methods of integration and to have a basis for providing novel designs that may offer additional benefits. Initial evaluation of several load forecasting methods was also performed; insights gained will be used as input to the EDC.

The model predictive control strategy for building dispatch control allows prediction of the building operation, which facilitates participation in ancillary grid services. The forecast provides knowledge of expected capacity for providing services at different times. Factors such as current temperature, equipment states, utility costs, weather prediction, and load forecasting are used as inputs. The EDC optimization then determines an optimal operation over the next 24-hour period and implements set-points for the next one hour. The optimization runs again each hour over a rolling 24-hour period. Variation between scheduled and actual operation occur due to building feedback and variability in actual building loads versus the forecast.

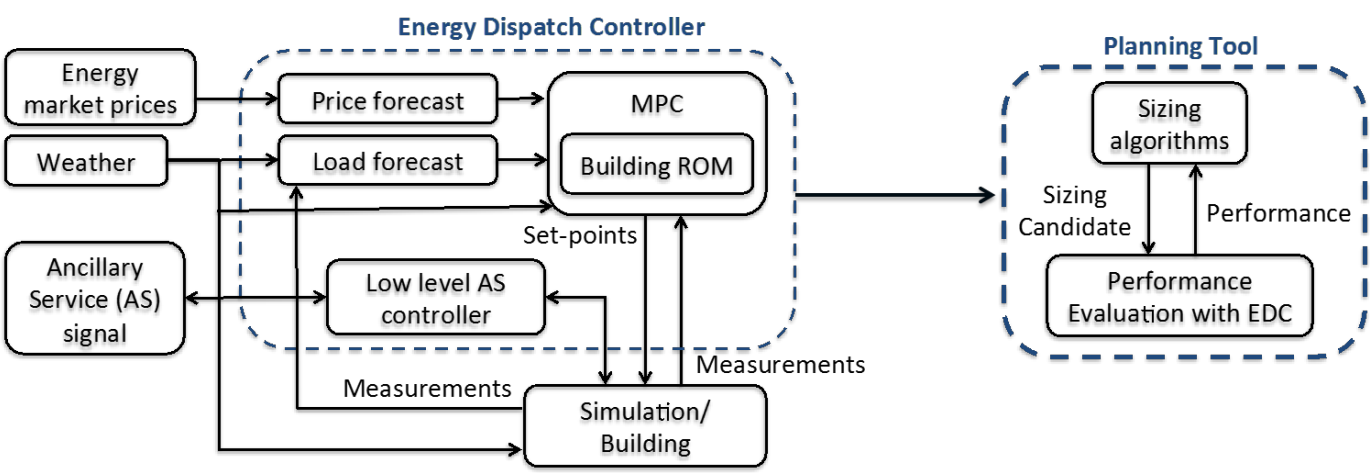

FIGURE 1. EDC and planning tool modules and flow

The EDC takes into account the cost of providing energy to the buildings as well as payment for any potential grid services. Using load and operation prediction, distributed generation and storage can be dispatched in optimal ways. Several simplified demonstration cases were done to show how different inputs would influence the controller and change operation. Figure 2 is a case in which cooling is required and the electricity price will increase during peak hours. One can see from the figure that the temperature of the building is allowed to increase in small increments up to near the thermal comfort constraint in order to minimize the cooling requirements. Additionally, the battery is charged during times of low electricity price and discharged during high electricity cost in order to reduce electricity costs. Figure 3 shows a heating case in which the fuel cell provides excess heat. One can see that to reduce the heating load, the building temperature is allowed to incrementally decrease. The fuel cell exceeds the heating demand, but during times of low natural gas cost it is still economic to provide only electricity. When there are high natural gas prices, it is not

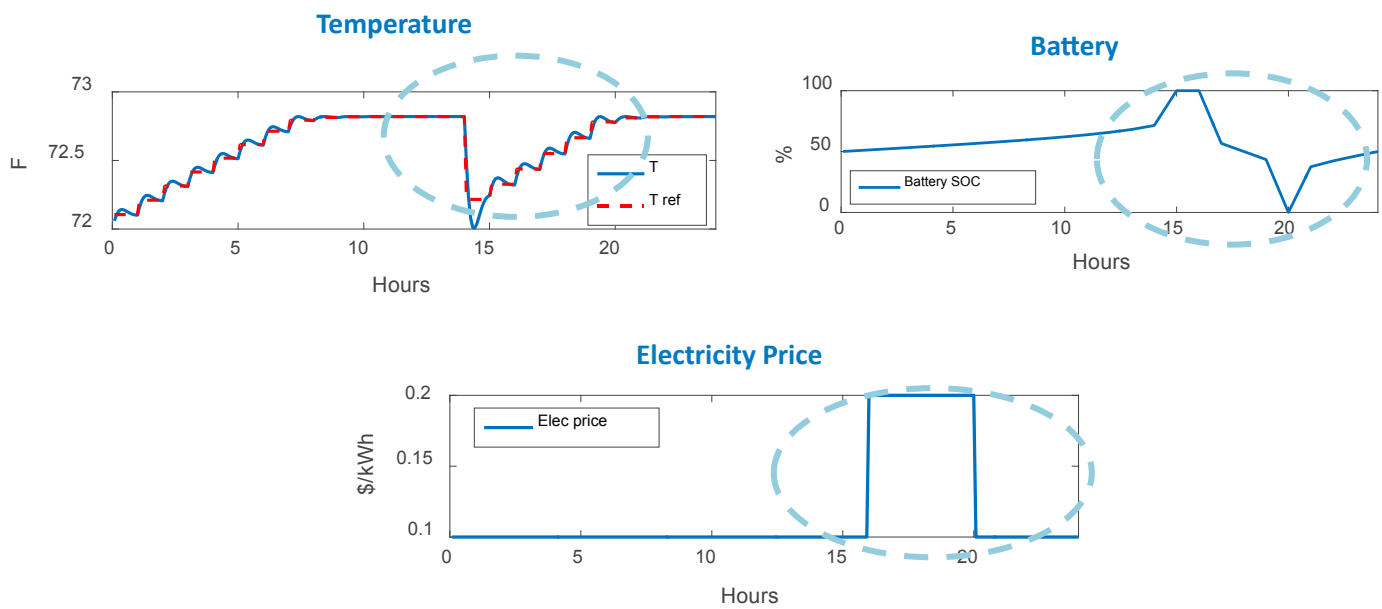

FIGURE 2. EDC demonstration results, cooling case

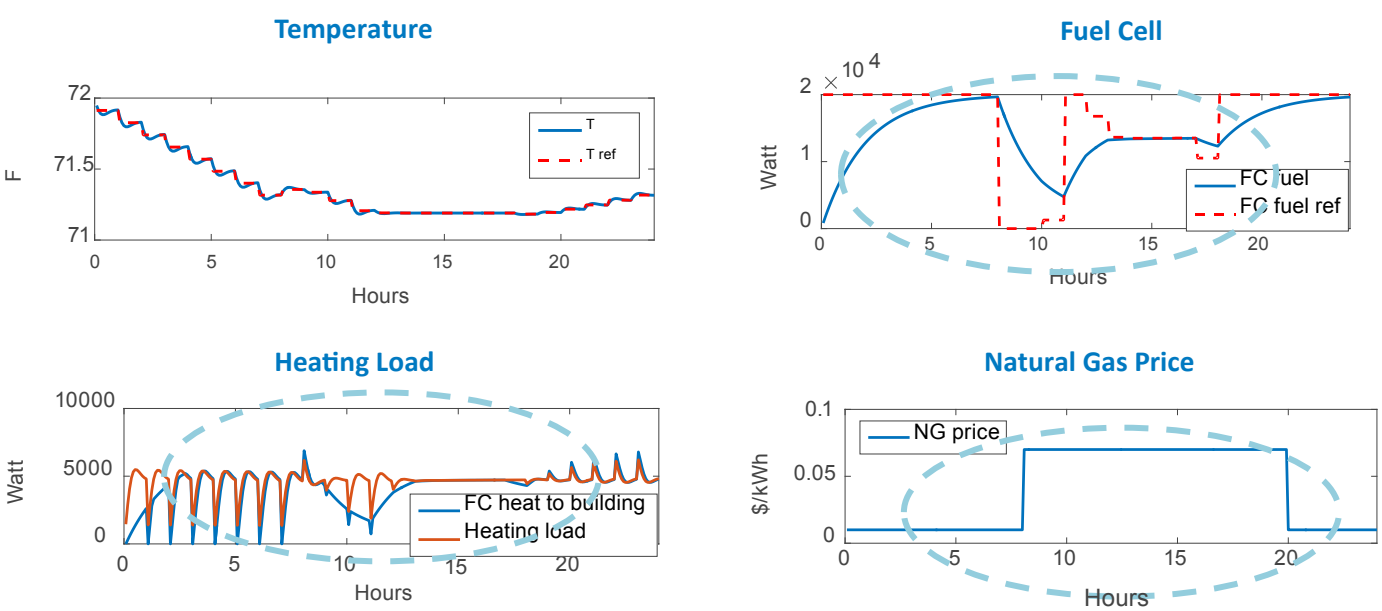

FIGURE 3. EDC demonstration results, excess heat

economic for the fuel cell to generate only electricity so the fuel cell operates at part load as determined by the thermal demand.

Load forecasting is an important module for the EDC. Several methods for forecasting uncontrollable loads have been identified and are being evaluated:

- Corrected Naïve: A simple exponential smoothing using a single calibration constant.
- ARIMA: Autoregressive integrated moving average with multiple calibration points.
- Neural Network: Trained by previous week's data and compatible with machine learning.
- Surface Fit: Best guess from historical data, e.g., time and weather.

Figure 4 shows the four test methods compared to test data. Initial evaluations suggest that a combination of methods may be best as determined by the quantity and type of historical data available.

Building design work has been ongoing. This includes researching current common methods for CHP integration and developing a design framework which can accommodate both current and novel CHP designs. The building design framework is required for specifying the building and its components and for developing reduced order model representations which will be used in the EDC optimization.

A co-simulation environment is being set-up using EnergyPlus. This will allow the EDC to run against a building simulation which will provide a feedback loop to which the EDC can react to. The EDC and the EnergyPlus simulation are currently running separately and the project team is working towards a functioning co-simulation environment by the end of FY 2017.

CONCLUSIONS AND UPCOMING ACTIVITIES

The first year of this project has been instrumental in laying the foundational groundwork for creating a suite of novel tools for building energy management and component sizing. The initial formulation of the EDC has been completed and testing has been started. The testing and evaluation of the EDC in co-simulation will be used for iterative improvements to the methods and implementation of the approach.

Second year activities include:

- Continued and more extensive testing of the EDC in co-simulation.
- Evaluation of the commercial solver, Gurobi, versus open source solvers (ultimate goal).
- Evaluation and refinement of forecasting modules for both load forecasting and ancillary service pricing.
- Continued development and refinement of the building design framework, which will be used to specify CHP designs. This will also be used for the extraction of reduced order models that will be used in the EDC.
- Continued development of the graphical user interface to meet the needs of building operators and testing environments.
- Development work on a communications backbone for allowing communication between the EDC and building equipment, providing the EDC supervisory control.
- Development of the component sizing optimization algorithms for use in the planning tool.

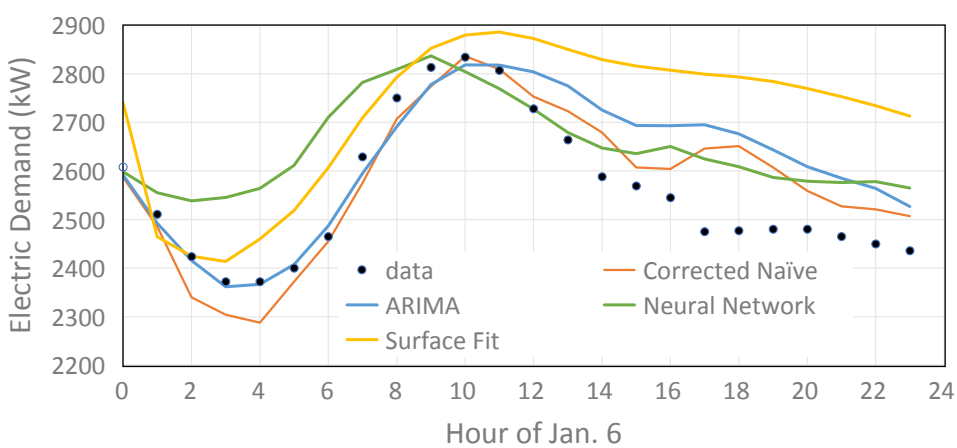

FIGURE 4. Comparison of four load forecasting methods

FY 2017 PUBLICATIONS/PRESENTATIONS

- Genevieve Saur, "Optimal Stationary Fuel Cell Integration and Control," presented at the 2017 DOE Annual Merit Review and Peer Evaluation Meeting, Washington, D.C., June 2017.
- Genevieve Saur, Zhiwen Ma, Annabelle Pratt, Yashen Lin, Bill Livingood, Luigi Gentile Polese, Brian Ball, Jereme Haack, Dustin McLarty, "NREL Energy Dispatch Controller Project: Stakeholders Review," presented for identified stakeholders in a webinar, Golden, CO, June 2017.
- Genevieve Saur, Zhiwen Ma, Annabelle Pratt, Yashen Lin, Dustin McLarty, William Livingood, Luigi Gentile Polese, Brian Ball, Jereme Haack, Gregor Henze, "Optimal Stationary Fuel Cell Integration and Control (Energy Dispatch Controller)," presented as a poster at the 2017 DOE Grid Modernization Initiative Peer Review, Washington, D.C., April 2017.
- Genevieve Saur, "NREL Energy Dispatch Controller Project: GUI Review for Stakeholders," presented for identified stakeholders in a webinar, Golden, CO, December 2016.

REFERENCES

1. Grid Modernization Initiative Multi-Year Program Plan, November 2015, https://energy.gov/sites/prod/files/2016/01/f28/Grid%20Modernization%20Multi-Year%20Program%20Plan.pdf

2. EnergyPlus is a whole building energy simulation program that engineers, architects, and researchers use to model both energy consumption—for heating, cooling, ventilation, lighting and plug and process loads—and water use in buildings. https://energyplus.net/

VII.C.2 Integrated Systems Modeling of the Interactions between Stationary Hydrogen, Vehicles, and Grid Resources

Sam Saxena (Primary Contact), Dai Wang,
Max Wei, Giulia Gallo, Josh Eichman[a],
Matteo Muratori[a], Fernando Dias[b], Stevic Svetomir[b]
Lawrence Berkeley National Laboratory (LBNL)
1 Cyclotron Road
Mailstop 90R1121
Berkeley, CA 94720
Phone: (510) 269-7260
Email: SSaxena@lbl.gov
[a]National Renewable Energy Laboratory (NREL)
[b]Idaho National Laboratory

DOE Manager: Jason Marcinkoski
Phone: (202) 586-7466
Email: Jason.Marcinkoski@ee.doe.gov

Project Start Date: June 1, 2016
Project End Date: May 31, 2019

Overall Objectives

- Provide an integrated modeling capability (hydrogen–vehicle–grid integration [H2VGI] model) to quantify the interactions between stationary hydrogen generation, fuel cell vehicles, and grid support resources.
- Quantify potential grid support and balancing resources from flexible hydrogen systems (e.g., dispatchable production of hydrogen by electrolysis).
- Develop methods to optimize the systems configuration and operating strategy for grid-integrated hydrogen systems.

Fiscal Year (FY) 2017 Objectives

- Survey prior studies on hydrogen–vehicle–grid integration and existing simulation tools.
- Develop H2VGI model structure and code development, including sub-model data exchange formats.
- Demonstrate sub-models for vehicle activity initializer, and individual vehicle models ready for integration into overall H2VGI model.
- Integrate fuel cell electric vehicle (FCEV) hydrogen consumption sub-models with hydrogen station models developed by NREL.
- Define case studies for hydrogen vehicle–station–grid integration.
- Quantify the value of hydrogen production for FCEVs in California to support renewable supply integration.
- Show input–output validation of fully integrated hydrogen sub-models within H2VGI model to confirm that the directions of model results change as expected with inputs that have well understood sensitivities.
- Demonstrate that the H2VGI model produces results that are directionally correct based on input–output validation.

Technical Barriers

This project addresses the following technical barriers from the Systems Analysis section of the Fuel Cell Technologies Office Multi-Year Research, Development, and Demonstration Plan.

(A) Future Market Behavior

(B) Stove-piped/Silod Analytical Capability

(D) Insufficient Suite of Models and Tools

Contribution to Achievement of DOE Systems Analysis Milestones

This project contributes to the achievement of the following DOE milestones from the Systems Analysis section of the Fuel Cell Technologies Office Multi-Year Research, Development, and Demonstration Plan.

- Milestone 1.5: Complete evaluation of hydrogen for energy storage and as an energy carrier to supplement energy and electrical infrastructure (4Q, 2012).
- Milestone 1.16: Complete analysis of program performance, cost status, and potential use of fuel cells for a portfolio of commercial applications (4Q, 2018).
- Milestone 1.19: Complete analysis of the potential for hydrogen, stationary fuel cells, fuel cell vehicles, and other fuel cell applications such as material handling equipment including resources, infrastructure, and system effects resulting from the growth in hydrogen market shares in various economic sectors (4Q, 2020).
- Milestone 3.3: Complete review of status and outlook of non-automotive fuel cell industry (biennially from 4Q, 2011 through 4Q, 2019).

FY 2017 Accomplishments

- Formulated and calibrated fuel cell vehicle models for use within the H2VGI framework, allowing FCEV hydrogen consumption to be predicted for any trip when given speed and terrain versus time profiles for the trip.
- Developed preliminary hydrogen demand sub-models for H2VGI to predict fueling station hydrogen demand from large collections of vehicles.
- Generated self-consistent FCEV adoption and hydrogen demand scenarios relevant to early market transition, considering geospatially- and temporally-resolved vehicle adoption in each urban area in California using the Scenario, Evaluation, Regionalization, and Analysis model [1].
- Integrated several vehicle deployment scenarios from NREL into hydrogen consumption sub-models from LBNL to estimate net load peak shaving and ramp mitigation from flexible hydrogen generation for the California net load "duck curve" [2] for 2016 and 2025.
- Produced preliminary results from the hydrogen station model developed at NREL (e.g., electricity consumption by component and component pressures).
- Incorporated national Utility Rate Database information into the RODeO (Revenue Operation and Device Optimization Model) model previously developed at NREL for the optimization of various equipment [3].

✧ ✧ ✧ ✧ ✧

INTRODUCTION

The goal of this multi-year project is to establish the available capacity, value, and impacts of interconnecting hydrogen infrastructure and fuel cell electric vehicles to the electric grid. The first objective is to quantify the opportunity of utilizing flexibility from hydrogen systems to support the grid. This includes provision for vehicle and station controllable loads. Additionally, the methodology and results of this project can support understanding of available grid services and their optimal implementation as it relates to hydrogen systems.

The second objective is to develop and implement methods to assess optimal system configuration and operating strategy for grid-integrated hydrogen systems. This involves developing a modeling framework that can analyze the value of optimally dispatching resources based on grid needs, while respecting hydrogen production and vehicle travel requirements. There are a number of emerging use cases for hydrogen systems that this work will expand upon. Delineating these use cases is of particular importance since hydrogen production spans a variety of energy sectors. Success of this project after three years is measured by the development and integration of a set of models to assess the opportunity for hydrogen grid integration. This includes development of new models and controllers and leveraging existing models to understand the capacity of available hydrogen infrastructure to provide grid support and to understand the value stemming from that support.

APPROACH

This project will develop an H2VGI toolset to quantify and optimize the complex interactions between these energy systems. The toolset will consider the needs, technical capabilities, value streams, and costs for drivers, vehicles, hydrogen stations, utilities, system operators, and other stakeholders. The H2VGI toolset will be applied in several case studies to both quantify the opportunity for hydrogen to simultaneously support mobility and the grid and to develop implementation approaches that provide the best value proposition. One key question to be explored is to what extent can grid support from hydrogen generation provide sufficient value to justify near-term investment in fueling infrastructure prior to widespread deployment of FCEVs?

Figure 1 shows the model components and interactions. First, vehicle and station rollout scenarios will be developed using the Scenario, Evaluation, Regionalization, and Analysis model. Individual vehicle models, energy demands from large numbers of FCEVs, and backup power capacity for grid services will be developed using the LBNL V2G-Sim modeling framework [4]. NREL will lead the development of individual hydrogen generation and station models and aggregate hydrogen generation capacity allocation for grid services. Finally, vehicle and hydrogen generation data will be integrated into external grid models (e.g., vehicle operating characteristics and historical market prices) to quantify the impacts of flexible hydrogen resources on grid operation. Case studies will focus on specific regions and balancing authorities in the United States such as California Independent System Operator (CAISO) and New England ISO and will explore outcomes as a function of deployment scenarios, performance assumptions, and timescales.

RESULTS

Fuel cell vehicle models have been formulated and calibrated for use with V2G-Sim [4], which has been extended to include FCEVs. The FCEV models allow hydrogen consumption to be predicted for any trip given speed and terrain versus time profiles for the trip and the prediction of hydrogen demand from large collections of vehicles based on travel itinerary data from national household travel surveys [5]. The coupled sub-models include calibrated fuel cell vehicle models and a preliminary refueling sub-model, which governs when individual vehicles are refueled within their travel itineraries.

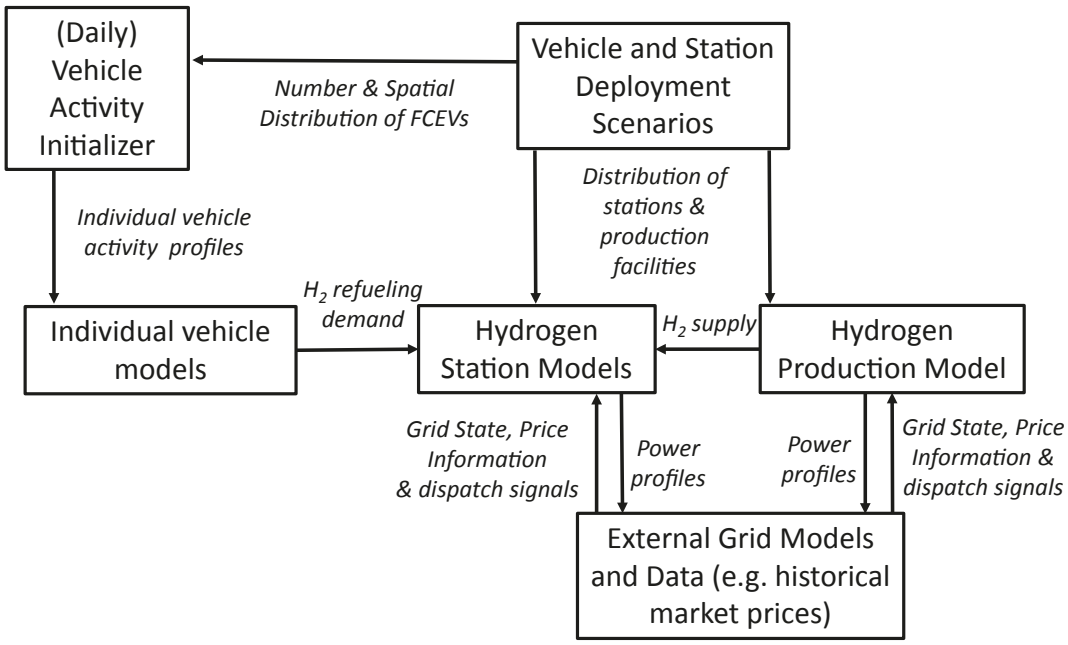

FIGURE 1. Modeling approach – H2VGI model structure

Using the hydrogen FCEV demand sub-models, preliminary results have been found for hydrogen demand, electrolyzer cycling profiles, and grid power demand at the hydrogen fueling station for nearly 3,000 vehicles driving and refueling over 40 days. This capability to predict and aggregate FCEV hydrogen demand is a key building block for determining temporally- and spatially-resolved hydrogen fueling demand as a function of adoption scenario.

The potential benefit to California's net load shaping from a large population of FCEVs fueled by electrolytic production of hydrogen has been modeled for the first time. Increasing overall electrolyzer capacity in megawatts (or equivalently, successively lower capacity factors) is seen to provide some valley-filling of the net load shape (Figure 2a). Figure 2b shows the potential that electrolytic hydrogen production can provide to net load ramping mitigation. Key results are that ramp rates can be significantly reduced when the electrolyzer is slightly oversized (capacity factor reduced from 1 to 0.9) with a ramping rate reduction of about 2.85 GW/h or about 26% from the maximum ramp rate without hydrogen production. The direction of these results are as expected when viewing the electrolyzer generation as a controllable load.

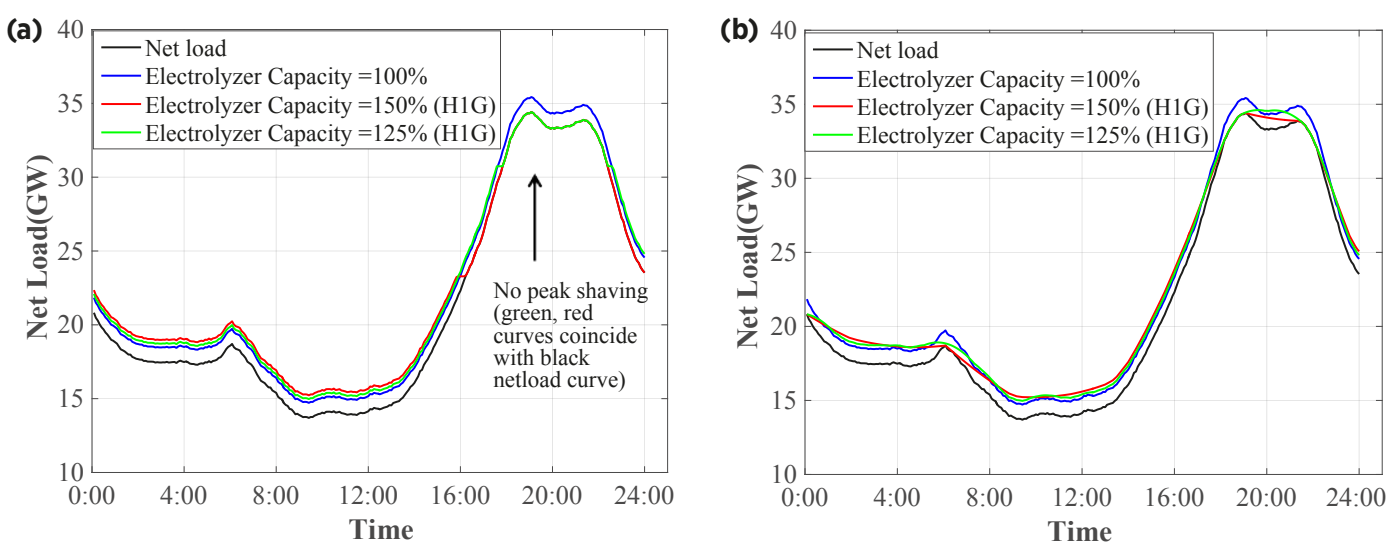

FIGURE 2. Illustration of grid support in California for 2025 net load, 1.5 million FCEVs and controllable electrolytic production of hydrogen for (a) peak shaving and valley filling, and (b) ramping mitigation

Preliminary results from the hydrogen station model developed at NREL (e.g., electricity consumption by component and component pressures) will be used to compare various station configurations for grid support (Figure 3). Electricity consumption is from compression, cooling, and other plant components. National Utility Rate Database information [6] has also been incorporated into the RODeO modeling tool previously developed at NREL. This model uses mixed-integer linear programming to determine best operation of hydrogen station and generation equipment, and this inclusion of utility rate structures allows RODeO to determine the ideal operation strategy and resulting cost for a specific utility. An example of electrolyzer operation for several Pacific Gas and Electric Company (PG&E) utility rates is shown in Figure 4, assuming that the electrolyzer produces 90% of its maximum yearly rated capacity. Comparing with the yearly cost patterns of PG&E tariff sheets shows that this behavior avoids high price hours and focuses on low price hours to minimize both demand and energy charges [7].

CONCLUSIONS AND UPCOMING ACTIVITIES

The team has made progress on developing several sub-models for the H2VGI tool set, looking at: vehicle deployment scenarios, FCEV drivetrains, fueling demand from large vehicle populations, and fueling station components that demand electricity. An initial case study has also been developed, where the potential grid support that hydrogen produced from electrolysis can provide to California's net load curve is depicted.

Upcoming activities include publishing initial results on first case study to quantify the scale of opportunity for hydrogen–vehicle–grid integration; developing material for second case study to address the benefits and shortcomings, from an electrical perspective, between different hydrogen system configurations (e.g., on-site vs. centralized production); and incorporating hydrogen resource modules (e.g., electrolytic hydrogen generation, fuel cells, etc.) into the PLEXOS production cost model for preliminary assessment of the impacts and benefits that flexible hydrogen resources can provide to the electricity grid.

FY 2017 PUBLICATIONS/PRESENTATIONS

1. Sam Saxena, Dai Wang, Max Wei, Giulia Gallo, Josh Eichmana, Matteo Muratoria, Fernando Dias, Stevic Svetomir, "Integrated Systems Modeling of the Interactions between Stationary Hydrogen, Vehicles, and Grid Resources," presented at the 2016 DOE Annual Merit Review and Peer Evaluation Meeting, Washington, D.C., June 2017.

REFERENCES

1. B. Bush, M. Melaina, M. Penev, and W Daniel, "SERA Scenarios of Early Market Fuel Cell Electric Vehicle Introductions: Modeling Framework, Regional Markets, and Station Clustering," National Renewable Energy Laboratory, Colden, CO, United States, NREL/TP-5400-56588, 2013.

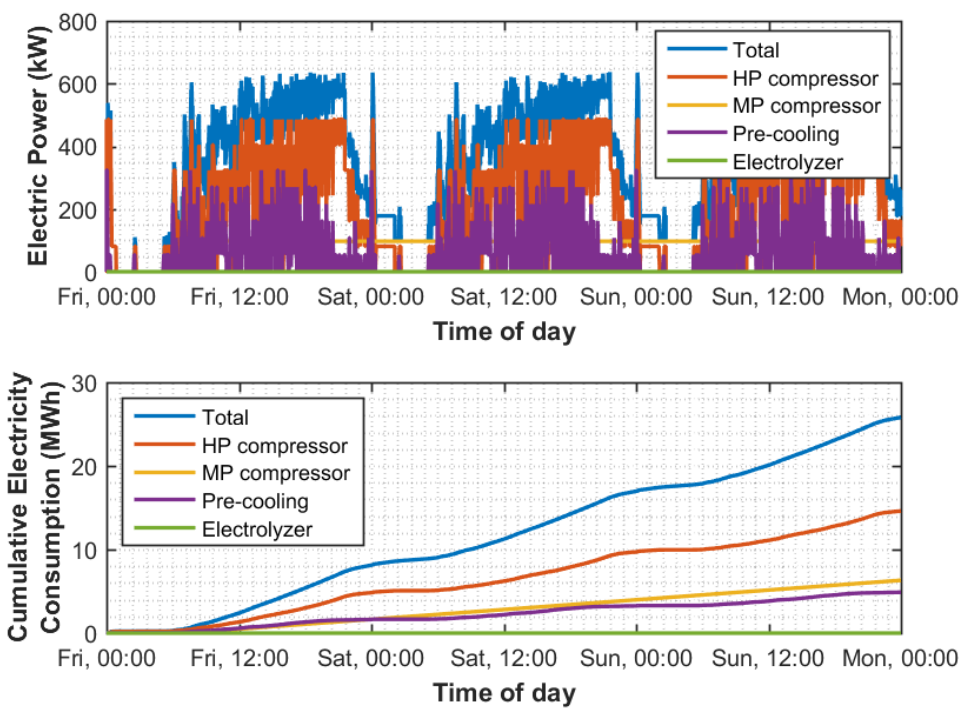

FIGURE 3. Example output from hydrogen station electricity consumption and grid support model

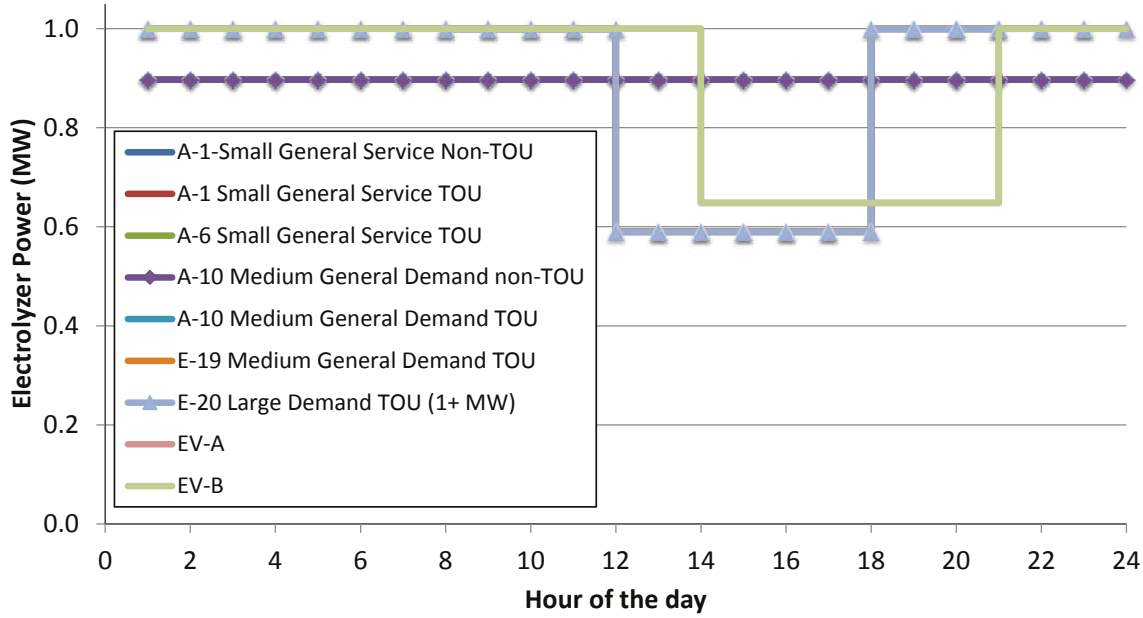

TOU – time of use

FIGURE 4. Example electrolyzer optimal operation from RODeO for several Pacific Gas and Electric retail utility rates

2. California ISO 2016, "What the duck curve tells us about managing a green grid," https://www.caiso.com/Documents/FlexibleResourcesHelpRenewables_FastFacts.pdf.

3. J. Eichman and F. Flores-Espino "California Power-to-Gas and Power-to-Hydrogen Near-Term Business Case Evaluation," National Renewable Energy Laboratory Technical Report NREL/TP-5400-67384 December 2016.

4. LBNL 2017, V2G-Sim model, http://v2gsim.lbl.gov/.

5. National Household Travel Survey, "National Household Travel Survey," 2009.

6. OpenEI Utility Rate Database, http://en.openei.org/wiki/Utility_Rate_Database.

7. Rate information for PG&E E20 can be found here: http://en.openei.org/apps/USURDB/rate/view/574dbcac5457a3d3795e629f.

VII.C.3 Dynamic Modeling and Validation of Electrolyzers in Real-Time Grid Simulation

Rob Hovsapian (Primary Contact),
Manish Mohanpurkar, Yusheng Luo, Fernando Dias,
Anudeep Medam, Rahul Kadavil
Idaho National Laboratory (INL)
750 University Blvd.
Idaho Falls, ID 83406
Phone: (208) 526-8217
Email: rob.hovsapian@inl.gov

Jennifer Kurtz, Kevin Harrison, Danny Terlip,
Joshua Eichman
National Renewable Energy Laboratory (NREL)
15013 Denver West Parkway
Golden, CO 80401

DOE Manager: Jason Marcinkoski
Phone: (202) 586-7466
Email: Jason.Marcinkoski@ee.doe.gov

Subcontractors:
- Florida State University, Tallahassee, FL
- Humboldt State University, Arcata, CA

Project Start Date: June 29, 2015
Project End Date: September 30, 2017

Overall Objectives

- Validate the benefits of hydrogen electrolyzers through grid services and hydrogen sale to fuel cell vehicles in full-scale deployment.
- Characterize potential and highest economic value based on the needs of multiple stakeholders for specific grid regions.
- Demonstrate reliable, fast-reacting performance of hydrogen-producing electrolyzers as at-scale energy storage devices.
- Verify communications and controls needed for successful participation in electricity markets and Demand Response (DR) programs.

Fiscal Year (FY) 2017 Objectives

- Expand the utility network (Pacific Gas and Electric [PG&E]) in the digital real-time simulation platform, to accommodate futuristic hydrogen refueling stations. This platform will be used to assess the value of electrolyzers under existing and futuristic DR programs and any other grid services using historic energy and ancillary service prices.
- Implement the front end controller (FEC), which interprets sample utility signals and safely controls the operation of the hydrogen refueling station. Test the control signals generated by the FEC for the lower level controller to respond to different utility signals, hence participate in DR and ancillary service programs.
- Perform real-time simulation within which a future hydrogen refueling station is controlled by the FEC to provide local fast loop support and macro grid level slow loop support.
- Test and validate the performance of single and multiple electrolyzers in providing local voltage and frequency support when integrated with the FEC.
- Test the performance of FEC in driving electrolyzer participation in demand response operated by multiple utility companies.

Technical Barriers

This project addresses the following technical barriers from Technology Validation section of the Fuel Cell Technologies Office Multi-Year Research, Development, and Demonstration Plan.

(B) Lack of Data on Stationary Fuel Cells in Real-World Operation

(G) Hydrogen from Renewable Resources

(H) Hydrogen and Electricity Co-Production

Contribution to Achievement of DOE Technology Validation Milestones

This project will contribute to achievement of the following DOE milestone from the Technology Validation section of the Fuel Cell Technologies Office Multi-Year Research, Development, and Demonstration Plan.

- Milestone 3.9: Validate large-scale system for grid energy storage that integrates renewable hydrogen generation and storage with fuel cell power generation by operating for more than 10,000 hours with a round-trip efficiency of 40% (4Q, 2020).

FY 2017 Accomplishments

- Demonstrated real-time connectivity between the simulators and electrolyzer at the two labs.

- Implemented first version of the FEC as a hardware at INL.
- Multiple utility demand response signal profiles were tested. Test results showed that the FEC can rapidly and precisely drive the electrolyzer set points to follow the command.
- Completed the baseline assessment (without hydrogen refueling stations) of the notional PG&E network, based on typical faults and the disturbances due to them.
- Performed wider range of scenarios on the expanded PG&E network that included hydrogen refueling stations, based on typical faults and the disturbances due to them.
- Compared real-time simulations to the baseline results, to assess the local voltage and frequency benefits due to hydrogen refueling stations integrated with FECs.

✧ ✧ ✧ ✧ ✧

INTRODUCTION

This project aims to quantify the value of hydrogen refueling stations (electrolyzers) from a grid integration perspective. The anticipated value of electrolyzers stems from the fact that they are a controllable load with fast response. They are typically coupled with hydrogen energy storage, dispensers, and compressor units to form the hydrogen refueling stations. They provide the flexibility to meet hydrogen demand with stored hydrogen when responding to the grid demand, and store more hydrogen when the grid power demand is low. The input resource for electrolyzers is electricity and hence allows flexible co-placement of electrolyzers with other distributed energy sources in a power system network, leading to an optimal value of the objective function.

The test set-up involves real-time simulations of power systems at INL with hardware-in-the-loop (HIL) of a 250 kW electrolyzer, along with the supplementary systems representing the hydrogen refueling station. This project leverages the existing work at both INL and NREL in the areas of power systems, electrolyzers, power markets, and control systems. The FEC developed in this research helps integrate the operations of the electrolyzer with the grid management systems and adds flexibility. This flexibility can be utilized to assimilate renewable energy, manage distribution loads, and provide grid support. The adoption of the FEC developed and tested in this project will drive down the cost of generating hydrogen, while maintaining requisite reserves for demands.

APPROACH

In FY 2017, INL and NREL performed an aggregate of over 500 hours of testing of the 250 kW electrolyzer stack. The tests primarily included stack characterization and FEC functionality tests. Stack characterization was repeated for the newly upgraded electrolyzer stack rated at 250 kW, which was 120 kW for the FY 2016 tasks. This re-characterization was essential as the project direction hinged on the basic controllability of the electrolyzer stack. The FEC controlling the operation of the electrolyzer in response to utility demand was experimentally verified and the optimal location and sizing of the electrolyzer was analyzed. Several other grid scenarios related to grid dynamics and transients were also simulated in real-time to assess the coordinated operation of FEC and electrolyzers. For these cases, the FEC and electrolyzer were observed to demonstrate voltage and frequency support to the grid. Being capable of participating in demand response programs is key for electrolyzers providing support to the macro-level transmission grid. This functionality was rigorously tested under several utility conditions across the United States. Eleven different utility-based demand response profiles utilizing diverse tariffs, with both baseloads and flexible operation, were tested based on varying conditions. The key takeaway is that the optimal location and sizing of the electrolyzer can greatly affect the performance of the electrolyzer in providing local support.

RESULTS

Distributed real-time simulations and power HIL were performed, utilizing the 250 kW electrolyzer stack and a hardware implementation of the FEC. The functionalities of the electrolyzer stack responding to control signals from the FEC was verified for applications including grid services within required time resolutions. Representation of the PG&E network in real-time environment was created to understand and assess the performance of the integrated FEC and electrolyzer stack, as shown in Figure 1. Figure 2 shows the functional role of a FEC in a typical grid management related infrastructure. The FEC has two major functional modules represented by two control loops – slow and fast loops. The slow loop is associated with primarily the cost optimization of hydrogen, whereas the fast loop deals with the provision of grid services by the stack. Both these loops and their respective functionalities were verified through 500 hours of testing. Figures 3 and 4 show the performance of the electrolyzers integrated with the FEC that were tested in real-time simulations to confirm voltage and frequency regulations.

The distributed real-time simulations between INL and NREL initially involved controlling the electrolyzer hardware stack using the FEC implemented on the PI-card (a processor card), in order to verify the communication between them. The data transmission for controlling the stack power

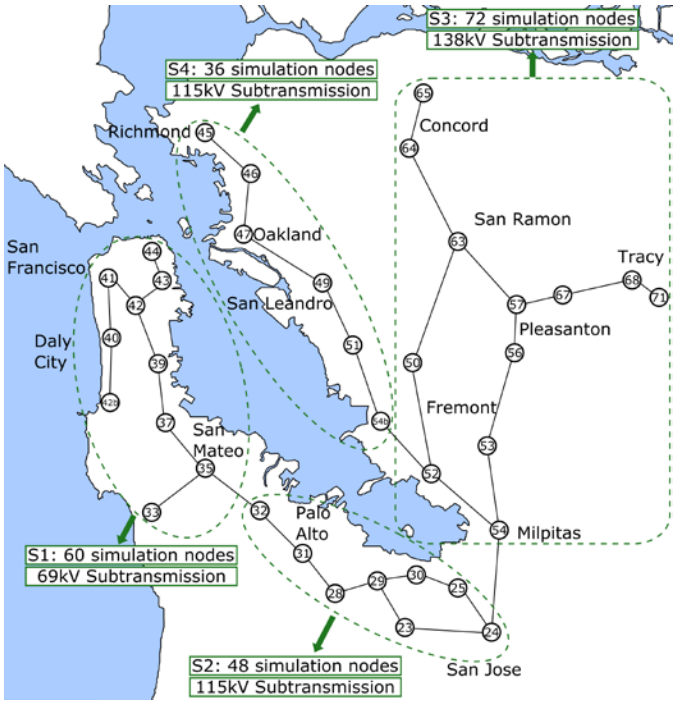

FIGURE 1. Real-time model of the PG&E electric grid to study response of hydrogen refueling stations

consumption was 100 Hz. The next phase of testing involved integrating the controller-HIL of the FEC on the PI-card, PG&E sub-transmission real-time model, grid simulator, and the electrolyzer stack. This integrated platform was utilized to test the controllability of electrolyzer stacks based on the functionalities defined in the FEC under dynamic grid conditions. The electrolyzer stack controlled via the FEC on the PI-card demonstrated voltage and frequency support to the PG&E grid based on varying grid conditions.

Test results demonstrated capability of the electrolyzer to provide local grid services and the ability of the FEC as hardware to control the electrolyzer. Economic optimization of the FEC has also been developed and implemented. This allows the FEC to make optimal decisions under different market rates and structures to generate hydrogen at a low cost. The optimization developed for the electrolyzer and implemented in the FEC hardware serves the purpose of striking a balance between providing support to grid operations and increasing the profit of the hydrogen producer.

CONCLUSIONS AND UPCOMING ACTIVITIES

Capabilities of an electrolyzer as a controllable load and in providing grid services was realized to be significant and was experimentally verified in a real-time environment. The controllability of the electrolyzer was enabled by a vendor-neutral approach termed as the FEC. The FEC ensures an optimal response of the electrolyzer to provide essential grid support in the form of voltage and frequency support. The FEC is a generic controls topology that can be integrated with existing controllers of electrolyzers that are available in the market. The objective of the development of the FECs is demonstration of the immense flexibility that electrolyzers can add to supporting power grid operations and lowerig hydrogen costs. Integrated FEC configurations were tested in both centralized, large electrolyzer plants and smaller distributed ones. Both configurations were observed to perform and provide essential flexibility to the grid under dynamic grid conditions. Additionally, the FEC can drive the hydrogen production cost lower by considering different utility rate structures, participating in DR programs, and interfacing with market signals. A utility-scale network (PG&E distribution network) was modeled in real-time to accommodate the future refueling stations as planned in the San Francisco Bay Area served by PG&E and also assessing the performance of electrolyzers with and without the FEC integration. A cumulative 500-hour test of distributed HIL was performed in FY 2017 and was a significant accomplishment as it was a one of a kind real-

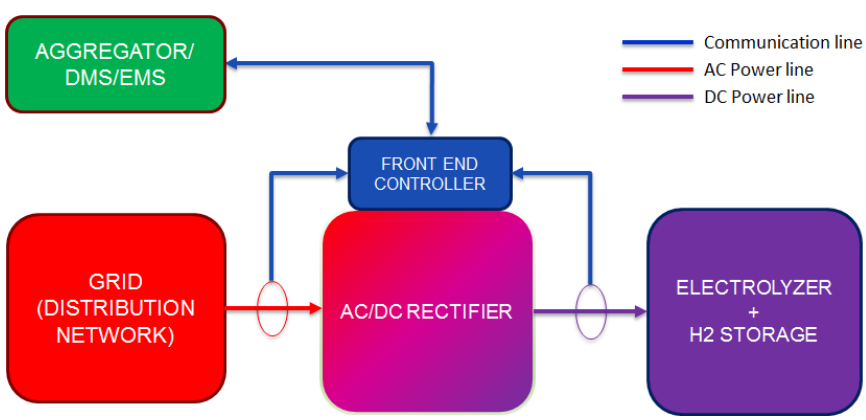

FIGURE 2. FEC interfaces hydrogen refueling stations with the grid management systems for providing grid services

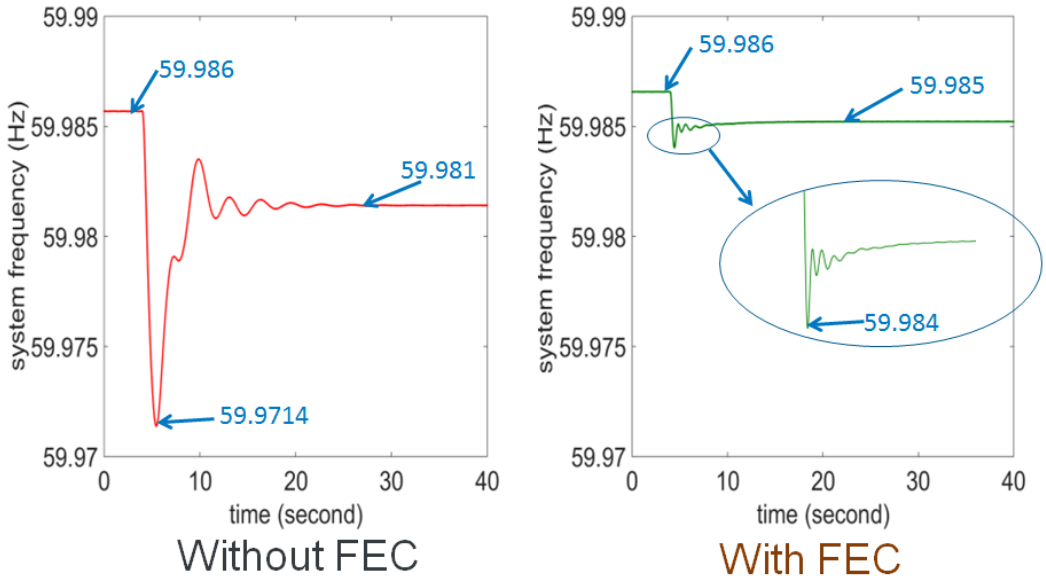

FIGURE 3. Frequency response by the integrated FEC and electrolyzers for a grid disturbance

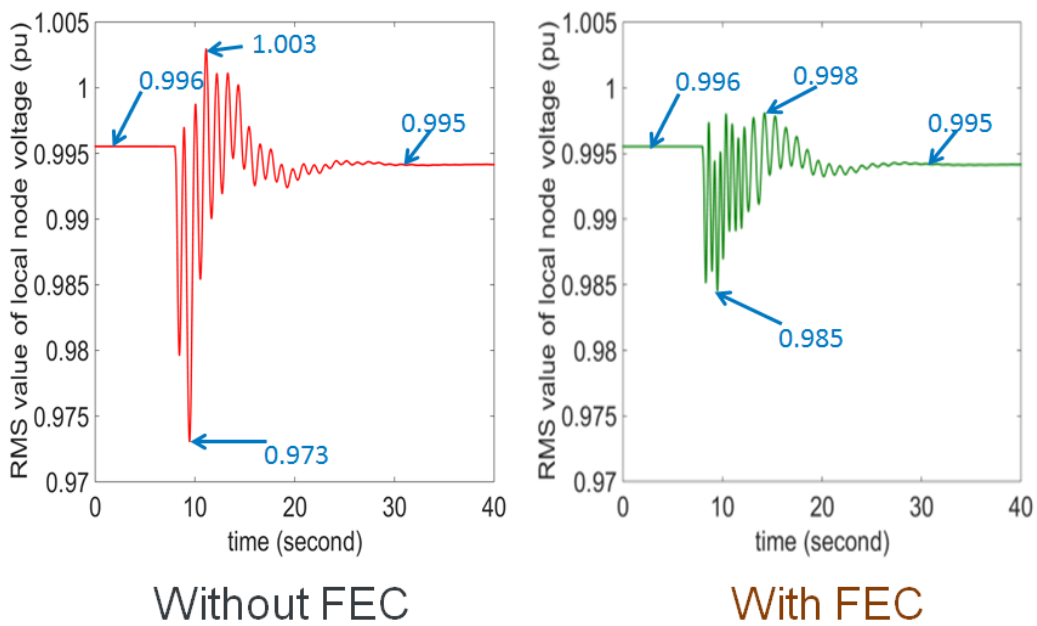

FIGURE 4. Voltage response by the integrated FEC and electrolyzers for a grid disturbance

time simulation that yielded accurate results and leveraged laboratory assets. Hardware-based testing in real-time was used to infer and augment the understanding of the role electrolyzers can play in markets for additional revenue. The FEC is now implemented on a hardware controller card and its functionality testing with the electrolyzer stack (250 kW) has also been completed. Performance metrics and acceptable ranges for the FEC with the electrolyzer were established. The final deliverable of the project at the end of FY 2017 is the deployment of this FEC hardware at NREL as an integral part of the existing 250 kW electrolyzer stack.

VII.C.4 Modular SOEC System for Efficient Hydrogen Production at High Current Density

Hossein Ghezel-Ayagh (Primary Contact), Stephen Jolly, Eric Tang, Micah Casteel
FuelCell Energy, Inc.
3 Great Pasture Rd.
Danbury, CT 06813
Phone: (203) 825-6048
Email: hghezel@fce.com

DOE Manager: David Peterson
Phone: (240) 562-1747
Email: David.Peterson@ee.doe.gov

Contract Number: DE-EE0007646

Subcontractor:
Versa Power Systems, Ltd., Calgary, AB, Canada

Project Start Date: October 1, 2016
Project End Date: September 30, 2019

Overall Objectives

- Demonstrate the potential of solid oxide electrolysis cell (SOEC) systems to produce hydrogen at a cost of less than \$2.00/kg H_2, exclusive of delivery, compression, storage, and dispensing.
- Improve SOEC stack performance to achieve >95% stack electrical efficiency based on the lower heating value of hydrogen (>90% system electrical efficiency), resulting in significant reduction in cost of electricity usage for electrolysis.
- Enhance cell and stack durability to enable dynamic load profiles associated with intermittent renewable integration.
- Design, fabricate, and test a >4 kg H_2/d SOEC proof-of-concept system validating the technical and economic objectives.

Fiscal Year (FY) 2017 Objectives

- Validate electrolysis cell degradation rate of ≤4%/1,000 hours in tests of a single cell for greater than 1,000 hours.
- Develop electrolysis performance characteristic maps of system operating parameters to be used for optimization.
- Identify system design improvements by testing of a stack across a matrix of ≥5 operating points for >500 hours.
- Develop SOEC system design configuration to achieve >75% overall (thermal + electric) efficiency.

Technical Barriers

This project addresses the following technical barriers from the Hydrogen Production section of the Fuel Cell Technologies Office Multi-Year Research, Development, and Demonstration Plan, subsection Hydrogen Generation by Water Electrolysis.

(F) Capital Cost

(G) System Efficiency and Electricity Cost

(J) Renewable Electricity Generation Integration (for central)

Contribution to Achievement of DOE Hydrogen Production Milestones

This project will contribute to achievement of the following DOE milestones from the Hydrogen Production - Advanced Electrolysis Technologies section of the Fuel Cell Technologies Office Multi-Year Research, Development, and Demonstration Plan.

- Milestone 2.9: Verify the BOP's ability to meet the 2020 system efficiency targets. (Q1, 2018)
- Milestone 2.10: Create modularized designs for optimized central electrolysis systems projected to meet 2020 capital and hydrogen production cost targets. (Q3, 2018)
- Milestone 2.11: Verify the stack and system efficiencies against the 2020 targets. (Q1, 2020)

FY 2017 Accomplishments

- Baseline degradation testing of High Power Density (HiPoD) solid oxide electrolysis cell was completed over 4,500 h of continuous operation at 1 A/cm^2 and 2 A/cm^2 with degradation rates of 1.3%/1,000 h and 2.6%/1,000 h, respectively, after the initial stabilization period.
- Parametric tests of an electrolysis cell were performed, generating nearly 600 distinct voltage–current curves to determine optimal system operating conditions.
- Stack baseline parametric testing was completed for a range of nine separate operating conditions examined over a total of 1,750 h.

- The second iteration of the HiPoD cells, identified as Low Temperature Firing, were developed, manufactured, and have completed over 1,200 h of continuous long-term degradation testing.
- Baseline system design was developed and a system flowsheet was incorporated in a computer simulation program.
- Preliminary system simulation runs including heat and materials balances were completed.
- System parametric tradeoff analysis was initiated to investigate the impact of operating conditions and balance of plant (BOP) equipment on the system performance.

✧ ✧ ✧ ✧ ✧

INTRODUCTION

The overall objective of the project is to demonstrate the potential of SOEC systems to produce hydrogen at a cost of \$2.00/kg H_2 or less (excluding delivery, compression, storage, and dispensing). An additional objective of the project is to enhance stack endurance and impart subsystem robustness for operation on load profiles compatible with intermittent renewable energy sources. Advanced high temperature electrolysis systems are able to vary the composition of energy input between thermal and electrical energy which offers the possibility of upgrading low value waste heat into high value hydrogen. This feature enables an SOEC system with extremely high electricity-to-hydrogen conversion efficiency, which is not feasible by conventional low temperature electrolysis.

The project work plan, focused on achieving the techno-economic targets, includes research and development in a wide range of disciplines covering from cell performance and stability improvements through system design, modeling, optimization, and performance verification. Cell and stack endurance are planned to be improved by reducing cell degradation rates to <1%/kh and stack degradation to <2%/kh. These reduced degradation rates will be achieved at current densities greater than 1 A/cm^2 to meet capital cost targets. System efficiencies will exceed 95% stack electrical efficiency, 90% system electrical efficiency and 75% total (electric + thermal) efficiency. This corresponds to less than 37 kWh electricity consumed per kilogram of hydrogen produced, with the remainder of energy supplied thermally. A modular system architecture will reduce system cost, increase scalability, and impart the required flexibility and robustness to operate on dynamic load profiles such as those supplied by intermittent energy sources.

APPROACH

The approach to meeting the objectives of the project consists of both cell and stack technology development as well as system design and verification.

Cell development activities include materials development, single-cell testing, and post-test microstructural analysis. In particular, the optimal intersection between system operational parameters, cell performance, and degradation will be thoroughly investigated. This includes the effect of inlet steam concentration and utilization, operating temperature, current density, system pressure, flush gas composition, and load cycling effects. Stack development efforts will focus on manufacturability and thermal management. A novel stack architecture will be utilized for electrolysis operation at moderate current density (1–2 A/cm^2). Stack manufacturing, testing, and validation will seek to demonstrate a 4 kg H_2/d production rate at greater than 95% electrical efficiency with less than 2%/1,000 h degradation.

System development and techno-economic analysis will focus on system architecture, operational parameter selection, and tradeoff analyses to determine an optimal system layout and operating regime. Due to the broad range of potential operating conditions, a baseline system will be developed for comparison purposes in the examination of potential system architectures. Quantitative comparative metrics will be developed to determine the relative effects of different operating conditions on the overall system performance, cost, and flexibility. A breadboard demonstration system (>4 kg H_2/d) will be designed, manufactured, and tested to validate the system performance. Finally, techno-economic analyses will be performed throughout the system development process to investigate the cost and performance impact of system operation parameters and layout.

RESULTS

Work was focused on characterizing the performance and degradation behavior of the HiPoD cell across a broad spectrum of system relevant conditions. Steady-state degradation tests of the electrolysis cells completed over 4,500 hours of operation at 1 A/cm^2 and 2 A/cm^2, showing degradation rates of 1.3%/1,000 h and 2.6%/1,000 h, respectively, well below the 4% value as the upper limit target. The microstructure of the HiPoD cells, shown in Figure 1, is based on FuelCell Energy's recent cell technology using optimized porosity [1] which had demonstrated an unprecedented hydrogen production rate at 6 A/cm^2 and 78% electrical efficiency. A new generation of the cell design has been developed to reduce degradation rates further and is currently undergoing degradation testing with nearly 1,200 h of operation completed to date.

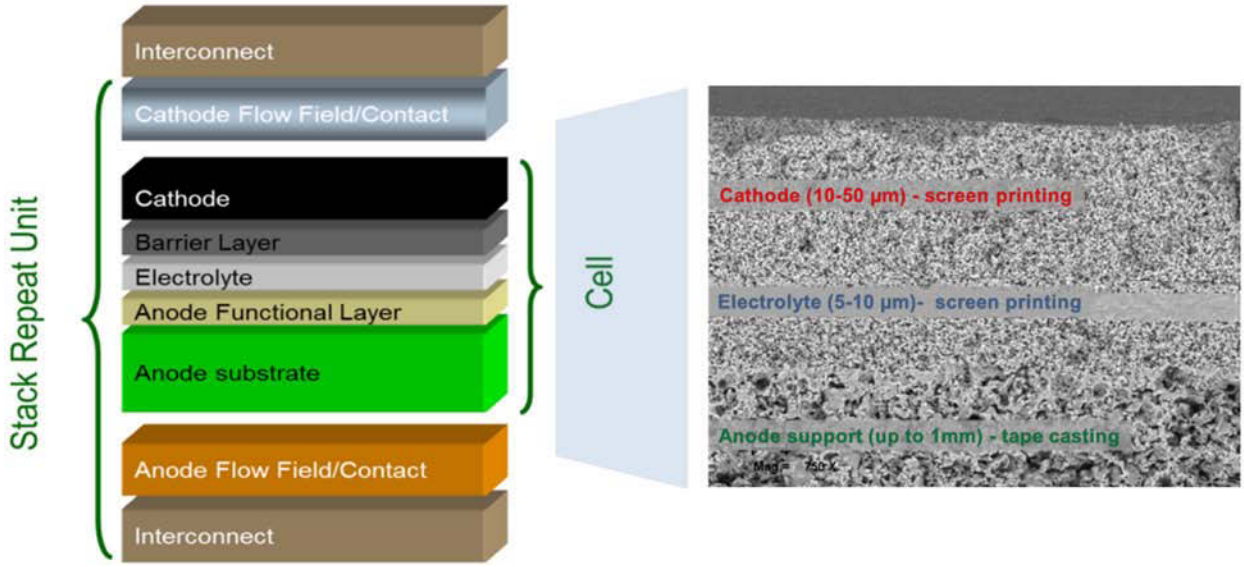

FIGURE 1. HiPod cell materials and architecture are based on FuelCell Energy's conventional tape cast/screen printed cell with nearly identical materials and proportions. A novel approach to optimization of the support layer porosity has demonstrated substantial performance improvements.

Parametric cell testing has generated nearly 600 distinct polarization curves across a wide spectrum of system operating conditions including pressure, inlet humidity, temperature, steam utilization, current density, and flush gas composition. The bulk effects of these independent parameters are summarized in Table 1, with a specific example of pressure dependence shown in Figure 2. A similar parametric testing effort was completed at the stack level with 1,750 h of testing across nine operating points, in order to establish a desirable and efficient operating window for the system design. Additionally, stack manufacturing validation of the hardware components for the Compact Stack Architecture stack [2], shown in Figure 3, has been initiated.

System level investigations have focused specifically on the effects of system operating parameters and system architecture on overall system efficiency and economic feasibility. Initial work was focused on first principles analysis of high temperature electrolysis and on the development of complete system process models. The

TABLE 1. Parametric Cell Testing Results

Operating Parameter	Range	System Impacts at Higher End of Range
Current	1–2 A/cm^2 (Target 1.1–1.32 V/cell)	1- Reduced Stack Cost 2- Higher Stack Exit Temperature for Heat Recovery 3- Lower Stack Efficiency 4- Life Impact
Steam Utilization (Stack)	50%–95%	1- Simpler H_2 Purification 2- Lower Stack Efficiency
Steam Inlet Concentration	40%–100%	1- Higher Stack Efficiency 2- Less Recycle (Reduced BOP Cost) 3- Harder H_2 Purification 4- Potential Life Impact
Cell Pressure	1–10 bara	1- Higher Stack Efficiency (First ~4 bar) 2- Simpler H_2 Purification 3- Lower Stack Efficiency (Above ~5 bar) 4- Potential Life Impact
Anode O_2 Concentration (outlet)	40%–100%	1- Less Air Flow to Anode (Less BOP Cost) 2- Simpler for Pressurized Operation (Less BOP Cost) 3- Higher Voltage (Less Efficient)
Operating Temperature	650°C to 800°C	1- Higher Stack Efficiency 2- Potential Life Impact

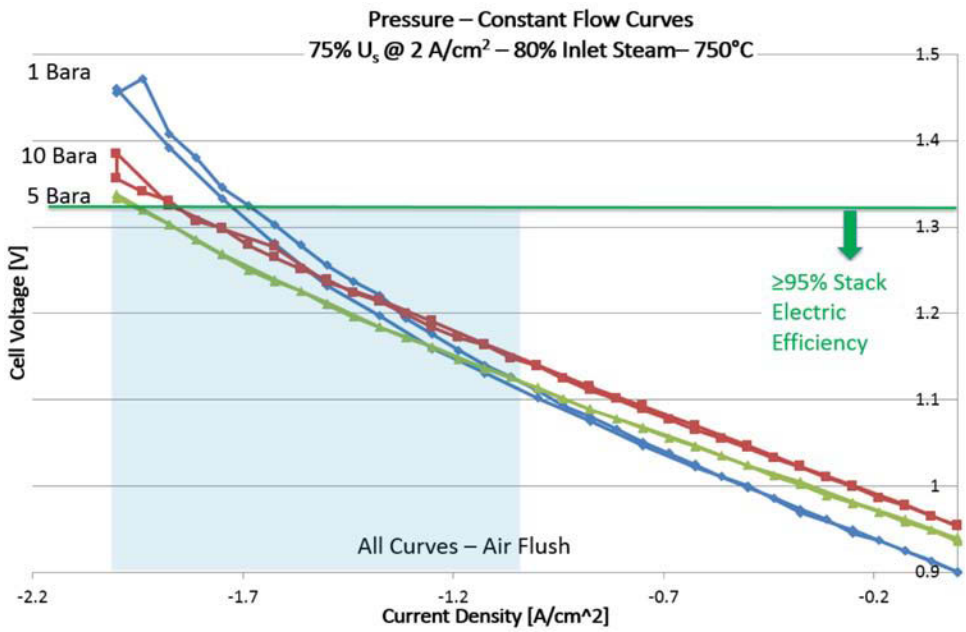

FIGURE 2. The impact of pressurization on cell performance in electrolysis operation. The higher pressure operation results in reduced cell voltage at low current densities (due to lower Nernst potential), whereas, yields higher voltage at increased current densities due to the decrease in activation and concentration losses.

FIGURE 3. The Compact Stack Architecture capitalizes on an automated manufacturing approach that enables high cell density and low material usage resulting in high volumetric and gravimetric power density while reducing cost.

baseline system process model, utilizing the process flow diagram shown in Figure 4, was completed. Work was also initiated on alternative system architectures and operating conditions in comparison with the baseline system to allow a quantitative tradeoff analyses to be performed.

CONCLUSIONS AND UPCOMING ACTIVITIES

During FY 2017 work was initiated on cell, stack, and system level technology development and verification. Initial degradation measurements were performed and data collected was utilized for improvement of the cell technology for its durability. Cell and stack parametric testing across a wide range of potential operating conditions was completed and the resulting data is being utilized in the system design process. Finally the baseline system process model has been completed and tradeoff analysis is ongoing to determine optimal system architecture and operating conditions. Future work will focus on further improvements in cell and stack endurance, forecourt system optimization, and detailed system design for the >4 kg H_2/d breadboard demonstration system.

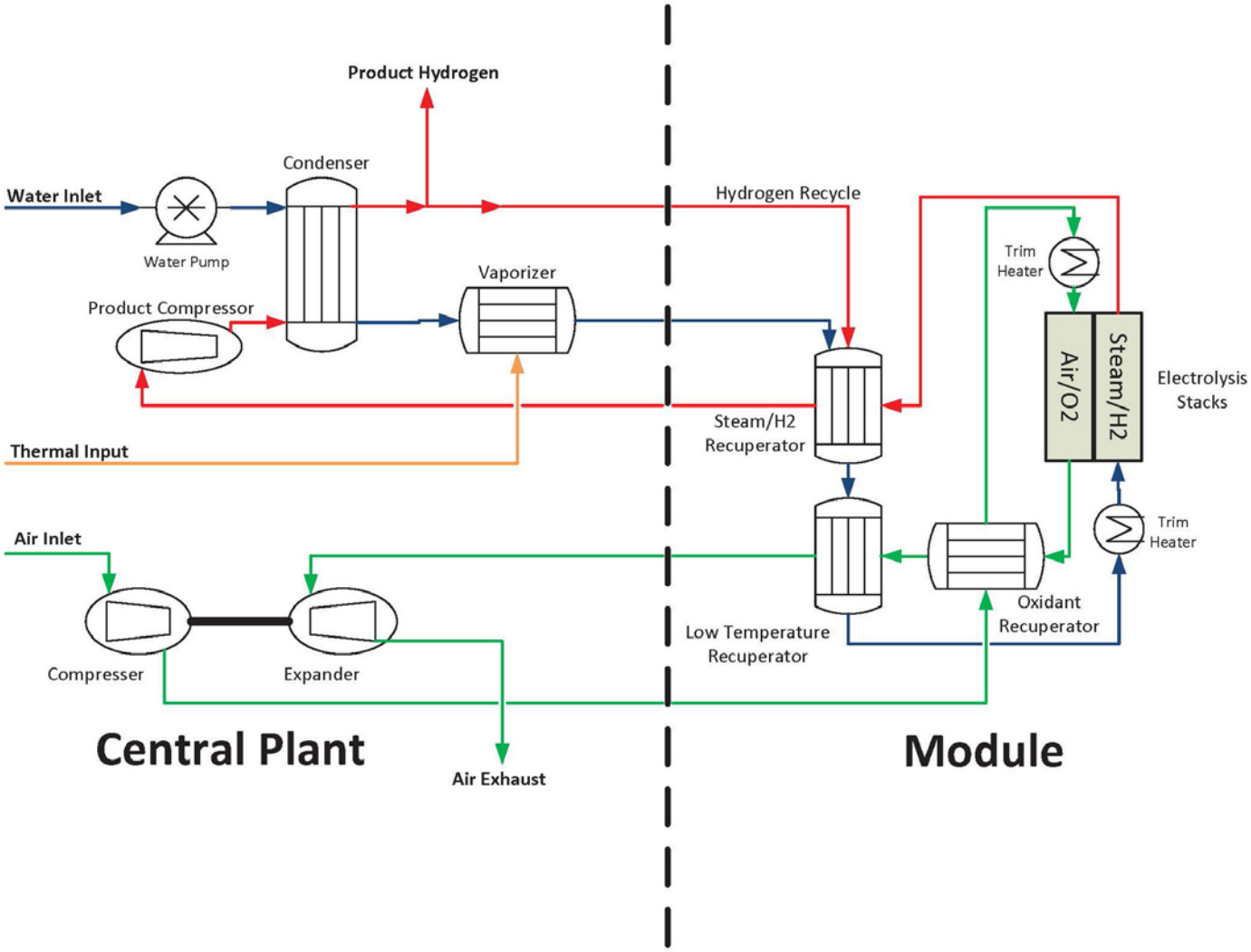

FIGURE 4. The modular system approach segregates system functions between "plant side" and "module side" to provide the optimal integration of unit operations while allow for system size scalability and operational flexibility. The baseline system utilizes a simple steam condensation approach for hydrogen separation.

REFERENCES

1. A. Wood, H. He, T. Joia, M. Krivy, D. Steedman; "Communication—Electrolysis at High Efficiency with Remarkable Hydrogen Production Rates," Journal of Electrochemical Society, 2016 volume 163, issue 5, F327–F329.

2. H. Ghezel-Ayagh, "Advances in SOFC Power System Development," 17th Annual Solid Oxide Fuel Cell (SOFC) Project Review Meeting, Pittsburgh, PA, July 19–21, 2016, https://www.netl.doe.gov/File%20Library/Events/2016/sofc/Ghezel-Ayagh.pdf

VII.D.1 H2@Scale Analysis

Mark F. Ruth (Primary Contact), Nicholas Gilroy, Elizabeth Connelly, Josh Eichman, Paige Jadun, Amgad Elgowainy*, Max Wei†, Karen Studarus§
National Renewable Energy Laboratory (NREL)
15013 Denver West Parkway
Golden, CO 80401-3305
Phone: (303) 384-6874
Email: mark.ruth@nrel.gov
* Argonne National Laboratory
† Lawrence Berkeley National Laboratory
§ Pacific Northwest National Laboratory

DOE Manager: Fred Joseck
Phone: (202) 586-7932
Email: Fred.Joseck@ee.doe.gov

Project Start Date: January 2, 2017
Project End Date: Project continuation and direction determined annually by DOE

Overall Objectives

- Improve fidelity of the value proposition of H2@Scale.
- Provide results that are supported by in-depth analysis of market potential and economics.
- Quantify potential impacts on economic, resource use, and emissions metrics.
- Identify regional opportunities and challenges.

Fiscal Year (FY) 2017 Objectives

- Quantify the technical potential of hydrogen demands and hydrogen production technologies.
- Identify potential regional issues that would be challenges for the H2@Scale concept.
- Quantify the national economic potential of the H2@Scale concept under several scenarios.

Technical Barriers

This project addresses the following technical barriers from the Systems Analysis section of the Fuel Cell Technologies Office Multi-Year Research, Development, and Demonstration Plan.

(A) Future Market Behavior − Potential market for low value energy and potential hydrogen markets beyond transportation

(D) Insufficient Suite of Models and Tools − Tools integrating hydrogen as an energy carrier into the overall energy system and quantifying the value hydrogen provides

(E) Unplanned Studies and Analysis − H2@Scale is a new concept and requires analysis of its potential impacts for input in prioritizing research and development

It also addresses the following technical barriers from the Technology Validation section of the Fuel Cell Technologies Office Multi-Year Research, Development, and Demonstration Plan.

(F) Centralized Hydrogen Production from Fossil Resources – Investigating potential value stacks for hydrogen production from various resources

(G) Hydrogen Production from Renewable Resources – Investigating the potential for hydrogen to be produced from renewable electricity and support higher penetrations of renewable electricity generation

Contribution to Achievement of DOE Milestones

This project will contribute to achievement of the following DOE milestone from the Systems Analysis section of the Fuel Cell Technologies Office Multi-Year Research, Development, and Demonstration Plan.

- Milestone 1.19: Complete analysis of the potential for hydrogen, stationary fuel cells, fuel cell vehicles, and other fuel cell applications such as material handling equipment including resources, infrastructure and system effects resulting from the growth in hydrogen market shares in various economic sectors (4Q, 2020).

In addition, this project will contribute to achievement of the following DOE milestone from the Technology Validation section of the Fuel Cell Technologies Office Multi-Year Research, Development, and Demonstration Plan.

- Milestone 3.9: Validate large-scale system for grid energy storage that integrates renewable hydrogen generation and storage with fuel cell power generation by operating for more than 10,000 hours with a round-trip efficiency of 40%. (4Q, 2020).

FY 2017 Accomplishments

- Estimated the current technical potential demand for hydrogen at 60 million metric tonne (MMT) annually, including demands from refineries and the chemical processing industry, metals refining, ammonia production, direct injection into the nation's natural gas system, light-duty fuel cell electric vehicles (FCEVs),

and other transportation including medium-duty trucks and buses.

- Quantified the impact on renewable resources' technical potential if each resource is used to produce 60 MMT/yr hydrogen in addition to its current demand. Current demand for each resource plus production of 60 MMT/yr hydrogen is satisfied by less than 1% of the technical potential of solar energy, about 6% of the technical potential of wind, and about 100% of the technical potential of solid biomass.
- Quantified the impact on fossil and nuclear resources if each resource is used to produce 60 MMT/yr hydrogen in addition to its current demand. The domestic natural gas resource has 70 years to depletion at its current usage plus the additional requirement to meet the technical potential demand for hydrogen. The domestic coal resource has over 300 years to depletion. The domestic uranium resource has over 400 years to depletion.
- Estimated the impacts if 60 MMT/yr hydrogen is produced via water electrolysis using renewable electricity and that hydrogen is used for the markets listed in the first bullet. Based on analysis assumptions and without considered secondary benefits such as increasing generation of renewable electricity, hydrogen has the potential to reduce total national greenhouse gas (GHG) emissions and fossil energy use by approximately 15%.

INTRODUCTION

The H2@Scale concept was presented by the national laboratory-led team during the FY 2016 Big Idea Summit because it has the potential to enable large reductions in national GHG emissions, both by increasing the profitability of low-carbon electricity generators via providing value for otherwise potentially curtailed electricity, and by supplying a clean energy source for industry and transportation. The concept is graphically portrayed in Figure 1. It is based on utilizing hydrogen's unique ability to both support the electric grid and provide clean energy to a variety of demands. Hydrogen can support an electric power grid with high penetrations of fixed generation (i.e., constant generation from nuclear reactors) and variable renewable generation (i.e., from photovoltaic (PV) solar and wind) by being generated by low-cost electrolyzers that can be used as a controllable load. The hydrogen that is produced in that way can be stored for months without degradation and then

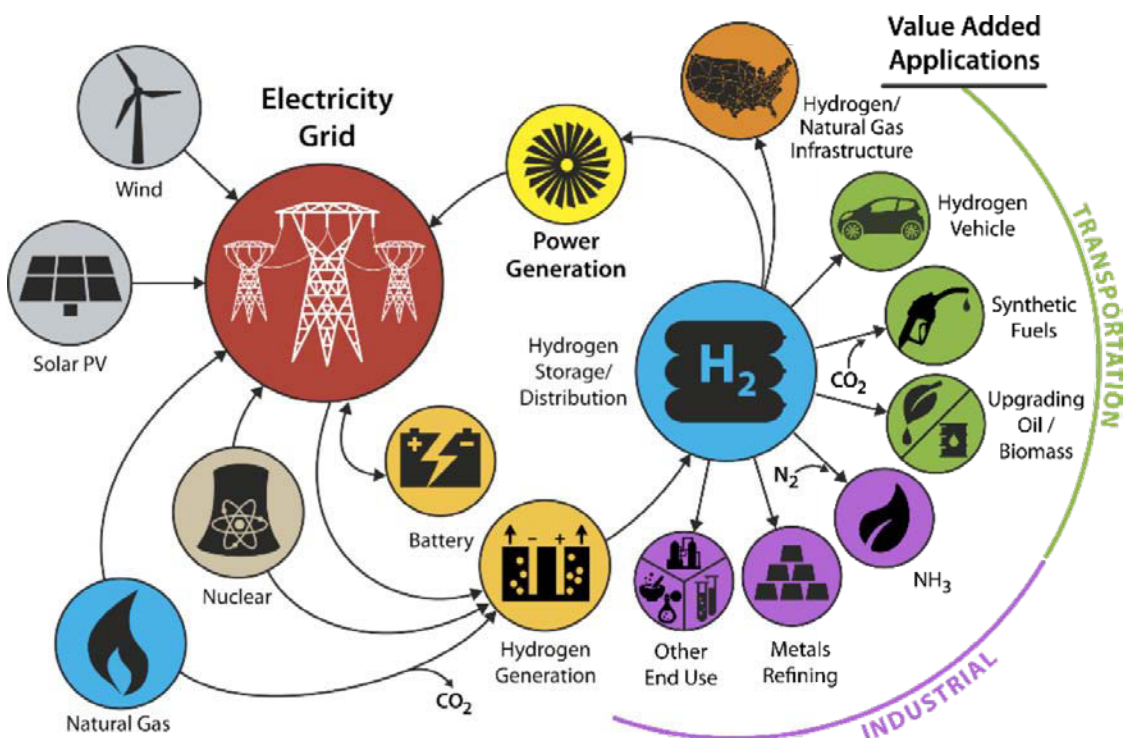

FIGURE 1. Graphical depiction of the H2@Scale concept, showing the use of otherwise curtailed electricity and other hydrogen generation resources and potential uses of hydrogen, including on-demand electricity, transportation, and industrial uses, in addition to injection into the natural gas infrastructure.

used to provide electricity back to the grid or for a number of alternative purposes shown in Figure 1, including as fuel for FCEVs, as a chemical feedstock for refining and ammonia production, and as a clean energy supplement in the natural gas system.

When the H2@Scale concept was originally proposed, only preliminary analysis had been performed. Thus, market size and impact estimates were not precise and the analysis results and methods had not been reviewed sufficiently. This project is focused on improving those estimates by analyzing both the technical and economic potential for hydrogen markets during FY 2017. Proposed work in later years extends the analysis to consider regional issues, storage and infrastructure development challenges, and macroeconomic impacts.

APPROACH

This project is composed of three stages with the first two being performed in FY 2017. The first two are estimating (1) the technical potential for the H2@Scale concept and (2) the economic potential of the H2@Scale concept. The third stage, including additional analysis related to topics such as regional needs and constraints, transport and storage, and macroeconomic issues, is proposed for future years.

To estimate the technical potential of hydrogen demands, the team reviewed literature and worked with experts to determine the potential market size for hydrogen in seven markets [1–5]. To estimate production technical potential, the team used the methodology previously developed (when possible [6]) to estimate resources. To estimate the wind, utility-scale PV, and biomass technical potential, the team used resource data developed at NREL [6–8] and calculated the potential annual hydrogen production using an efficiency of 46 kWh/kg hydrogen as used in Melaina et al. [6]. The team calculated impacts on fossil energy resources and GHG emissions using the GREET® model developed by Argonne National Laboratory [9].

RESULTS

The technical potential demand for hydrogen under the H2@Scale concept is 60 MMT/yr. It is comprised of the following categories:

- 8 MMT/yr for refineries and the chemical processing industry
- 5 MMT/yr for metals refining (primarily for steel production)
- 5 MMT/yr for ammonia production
- 7 MMT/yr for direct injection into the nation's natural gas system
- 4 MMT/yr for hydrotreating biofuels
- 28 MMT/yr for light-duty FCEVs
- 3 MMT/yr for other transportation including medium-duty trucks and buses

The domestic technical potential of electricity supply from utility-scale solar power is 1,360 quadrillion Btu (quads) per year. Of that supply, only 9 quads would be necessary to produce 60 MMT/yr hydrogen, and thus the utilization of the solar potential would be less than 1%. The domestic potential for land-based wind power in the United States is 170 quads per year, so the 9 quads of electricity necessary to produce 60 MMT/yr hydrogen is only 6% of that total. The biomass technical potential in the United States is 20 quads per year and its conversion efficiency is lower than electrolysis, so 75% of that resource would be needed to produce 60 MMT/yr hydrogen. Since 25% is currently used for wood products, pulp and paper and other demands, the full biomass resource

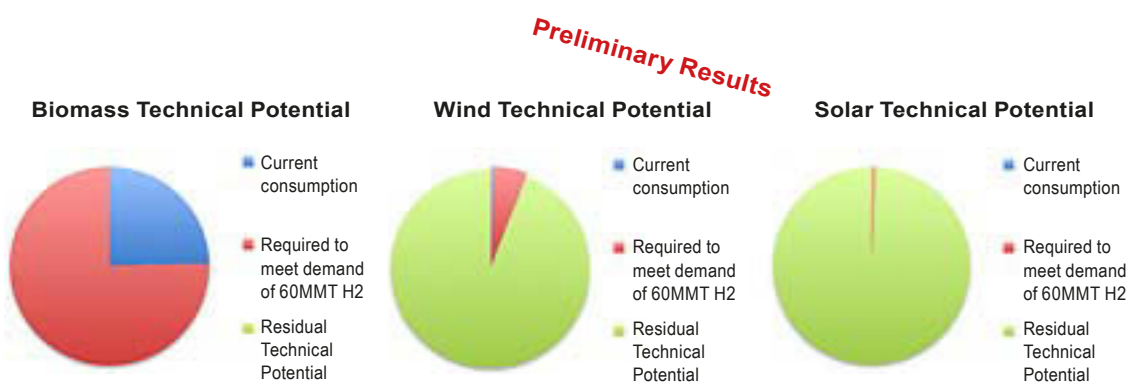

FIGURE 2. Fractions of the technical potential of three renewable resources that are utilized today and required to produce 60 MMT/yr hydrogen. Current demand for each resource plus production of 60 MMT/yr hydrogen is satisfied by less than 1% of the technical potential of solar energy, about 6% of the technical potential of wind, and about 100% of the technical potential of solid biomass. Results are in the process of being finalized.

would be necessary to meet the demand. Figure 2 shows those fractions.

Sufficient domestic fossil and nuclear resources are also available to meet the technical potential hydrogen demand. The domestic natural gas resource (proven and unproven reserves) has 70 years to depletion at its current usage plus the additional requirement to meet the technical potential demand for hydrogen. The domestic coal resource has over 300 years to depletion. The domestic uranium resource has over 400 years to depletion based on reasonably assured reserves at <$260/kg uranium and the use of both once-through and breeder reactors.

Figure 3 shows the difference between technical potential hydrogen production from wind and utility-scale PV, and technical potential hydrogen demand by counties (overlaid with locations of nuclear power plants). Only the counties colored red have less potential generation from those two sources than the potential demand. Note that many of those counties are urban areas with high demand for transportation energy use. However, all the counties with less wind and solar resource than potential demand are close to counties with sufficient resources or to nuclear plants (noted by the green, black, and purple dots).

Producing 60 MMT/yr hydrogen via water electrolysis using renewable electricity and using that hydrogen in markets identified by the technical potential demand analysis has the potential to reduce GHG emissions and fossil energy use by approximately 15%. Consideration of secondary benefits such as from increasing generation of renewable electricity would increase that potential reduction.

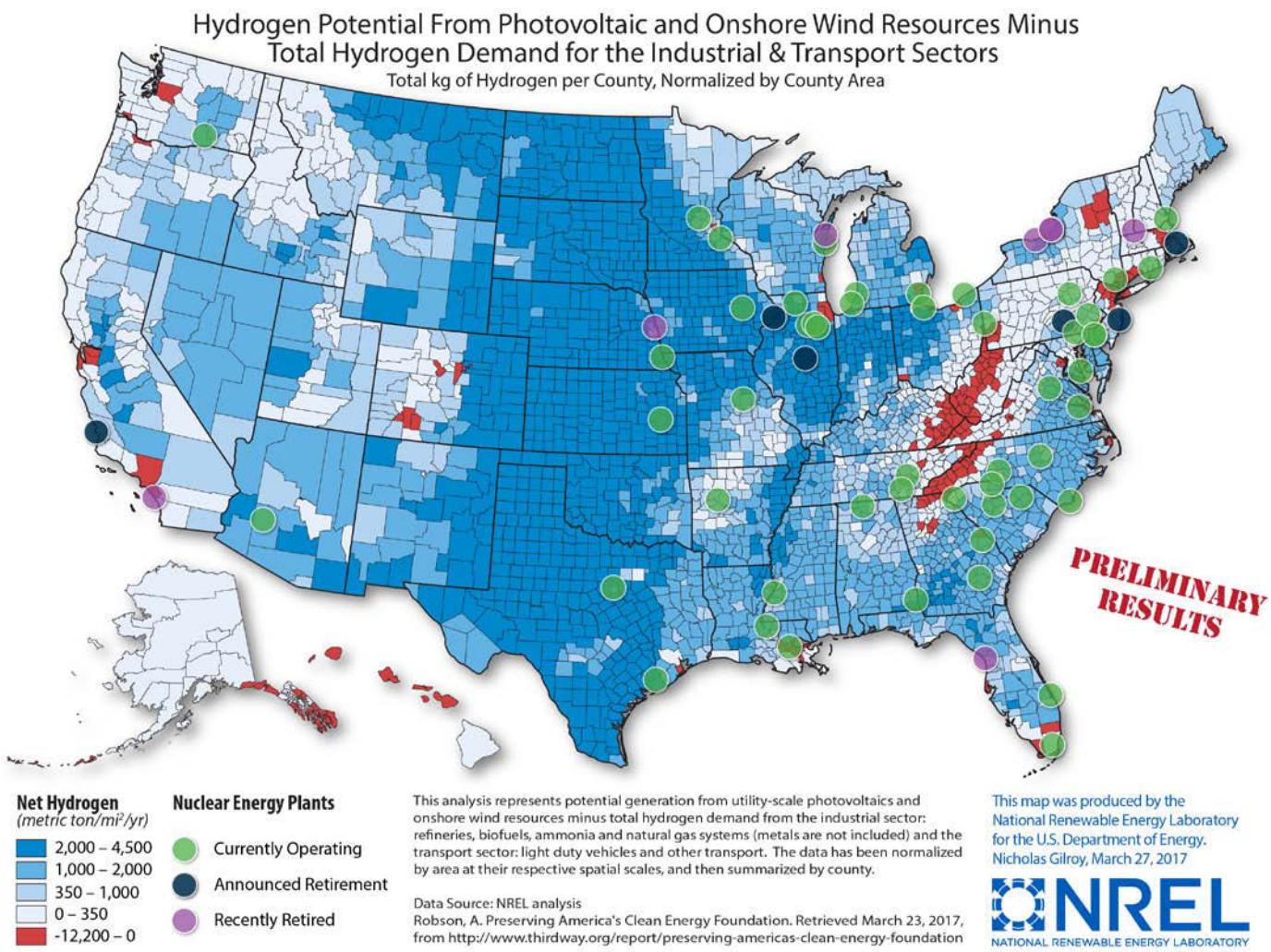

FIGURE 3. Difference between technical potential hydrogen production from wind and utility-scale PV and technical potential demand by counties overlaid with locations of nuclear power plants. Counties colored blue have more wind and PV resource than potential demand. Counties colored red have more potential demand than production. Results are in the process of being finalized.

CONCLUSIONS AND UPCOMING ACTIVITIES

Technical potential analysis estimates a potential market for 60 MMT of hydrogen per year. If that hydrogen is produced via water electrolysis using renewably generated electricity, it would directly reduce national GHG emissions and fossil energy use by 15%. Additional indirect reductions are possible if providing a value for curtailed electricity improves the economics of solar, wind, and nuclear generation, resulting in higher penetration of those resources.

During the remainder of FY 2017, the team will analyze the economic potential of H2@Scale by using supply and demand curves to estimate hydrogen demand at market equilibrium. Supply curves will consist of national hydrogen production estimates at prices from $0.50/kg to $3.00/kg. Production estimates will be developed for hydrogen produced from otherwise curtailed electricity, steam methane reforming of natural gas, and nuclear energy. Demand curves will consist of national demand estimates for each of the seven hydrogen markets that were identified in the technical potential analysis. The intersection of the supply and demand curves will indicate the hydrogen price and quantity, which will be used to estimate the resulting economic and environmental impacts. The need for and the type of additional analyses will be identified as well. Possible work in later years extends the analysis to consider regional analysis, storage and infrastructure development challenges, and macroeconomic impacts.

FY 2017 PUBLICATIONS/PRESENTATIONS

1. Mark Ruth "H2@Scale Resource and Market Analysis" (presentation to the Hydrogen Technical Advisory Committee, May 4, 2017).

2. Mark Ruth "H2@Scale: Concept Overview and Preliminary Analysis" (presentation at the U.S. Department of Energy H2@Scale Workshop, May 23, 2017).

REFERENCES

1. IHS Chemical Economics Handbook "Hydrogen Report" (June 2015).

2. IHS Chemical Economics Handbook "Ammonia Report" (February 2014).

3. Energy Information Agency, "Annual Energy Outlook 2017. Energy Consumption by Sector and Source" (December 2016).

4. A. Lopez, B. Roberts, D. Heimiller, N. Blair, G. Porro, "U.S. Renewable Energy Technical Potentials: A GIS-Based Analysis." NREL/TP-6A20-51946. Golden, CO: National Renewable Energy Laboratory (2012).

5. Cities-LEAP, "Highway Performance Monitoring System (HPMS) VMT on a county basis" (2013).

6. M. Melaina, M. Penev, and D. Heimiller, "Resource Assessment for Hydrogen Production: Hydrogen Production Potential from Fossil and Renewable Energy Resources." National Renewable Energy Laboratory NREL/TP-5400-55626 (2013).

7. NREL Renewable Energy Potential (reV) model (2017).

8. U.S. Department of Energy, "Billion-Ton Report: Advancing Domestic Resources for a Thriving Bioeconomy" (2016).

9. Argonne National Laboratory, "The Greenhouse gases, Regulated Emissions, and Energy Use in Transportation Model," https://greet.es.anl.gov/ (2017).

VII.D.2 High Temperature Electrolysis Test Stand

James O'Brien (Primary Contact),
Richard Boardman
Idaho National Laboratory (INL)
MS 3870
2525 Fremont Ave.
Idaho Falls, ID 83415
Phone: (208) 526-9096
Email: james.obrien@inl.gov

DOE Manager: Jason Macinkoski
Phone: (202) 586-7466
Email: Jason.Marcinkoski@ee.doe.gov

Project Start Date: August 1, 2016
Project End Date: Project continuation and direction determined annually by DOE

Overall Objectives

- Deploy a 25 kW high temperature electrolysis (HTE) flexible test facility at the INL Energy Systems Laboratory.
- Integrate the HTE system with co-located thermal energy systems, including a high-temperature, high-pressure water flow loop and a thermal energy storage system.
- Integrate the HTE test station with co-located digital real-time simulators for dynamic performance evaluation and hardware-in-the-loop simulations.
- Perform HTE stack testing using hardware obtained from industry partners; focus on flexible intermittent and reversible operation and the effects of flexible operation on long-term performance.
- Deploy infrastructure for up to 250 kW HTE turnkey systems.
- Work with HTE industry partners to demonstrate performance of flexible intermittent operation of large HTE systems.

Fiscal Year (FY) 2017 Objectives

- Complete design of 25 kW HTE system, including operating and design specifications, piping and instrumentation diagram, system layout, and laboratory infrastructure requirements.
- Identify and procure system components and vendors.
- Begin installation and assembly of HTE experimental system (to be completed in FY 2018).
- Prepare research documentation, including Quality Level Determination and Laboratory Instruction.

Technical Barriers

This project addresses the following technical barriers from the Technology Validation section of the Fuel Cell Technologies Office Multi-Year Research, Development, and Demonstration Plan.

(G) Hydrogen from Renewable Resources

(H) Hydrogen and Electricity Co-Production

Contribution to Achievement of DOE Technology Validation Milestones

This project will contribute to achievement of the following DOE milestones from the Technology Validation section of the Fuel Cell Technologies Office Multi-Year Research, Development, and Demonstration Plan.

- Milestone 3.5: Validate distributed production of hydrogen from renewable liquids at a projected cost of $5.00/gge and from electrolysis at a projected cost of $3.70 with an added delivery cost of <$4/gge (4Q, 2018).
- Milestone 3.9: Validate large-scale system for grid energy storage that integrates renewable hydrogen generation and storage with fuel cell power generation by operating for more than 10,000 hours with a round-trip efficiency of 40% (4Q, 2020).

FY 2017 Accomplishments

- Completed research plan, documenting overall objectives, technical and commercial barriers, HTE test objectives, summary of previous HTE research at INL, test stand design requirements, installation and operational requirements, and system integration plan.
- Completed system design, including functional and operational requirements documentation, piping and instrumentation diagram, identification and specification of components and vendors, procurement of components, design and fabrication of test skid, and design of supporting laboratory infrastructure (ventilation, power, water, drain, etc.).
- Engaged INL engineering group on laboratory infrastructure requirements and design.

- Contacted HTE industry representatives concerning HTE stack specifications and procurement options.
- Completed research documentation including Quality Level Determination and Laboratory Instruction.

✧ ✧ ✧ ✧ ✧

INTRODUCTION

High-temperature electrolysis of steam for hydrogen production is an advanced water splitting technology that exhibits high electric-to-hydrogen efficiency, especially when coupled to integrated high-temperature process heat sources. INL developed a world-class HTE laboratory and test capability under the DOE Office of Nuclear Energy Nuclear Hydrogen Initiative during the 2002–2012 time period. The focus of this project is to establish a new HTE demonstration facility at INL to enhance the existing INL core capability in HTE and to support systems integration, systems operation, HTE model validation, and technical performance characterization of advanced hydrogen production by high-temperature water splitting. The initial thrust of this project is the development of a 25 kW flexible test station for demonstration of state-of-the-art HTE stack technologies from multiple industry partners. Establishment of the 25 kW HTE system will be followed by deployment of a test skid with infrastructure support for up to 250 kW HTE turnkey systems.

The new HTE test capability will be designed for integrated operation with the INL Power Systems Test Bed (comprised of Real-Time Digital/Real-Time Simulation units and a renewable power microgrid) and the forthcoming Dynamic Energy Transport and Integration Laboratory (DETAIL). The HTE system will be co-located with a high-temperature high-pressure water flow loop, which is the first leg of the Advanced Reactor Technology Integral System Test Facility that will be installed under an Office of Nuclear Energy Hybrid Energy Systems project. System integration will enable assessment and characterization of dynamic HTE operation to simulate load leveling capability with intermittent power from renewables and a fluctuating demand profile. Thermal integration with co-located thermal energy sources including a high-temperature flow loop and thermal energy storage systems can also be demonstrated. This project leverages emerging and demonstrated high-temperature water splitting by HTE and high-temperature solid oxide fuel cell technology which may include reversible HTE/solid oxide fuel cell operation.

APPROACH

The new HTE Technology Validation demonstration capability under development at INL will include both a 25 kW flexible test station plus infrastructure support for up to 250 kW HTE turnkey systems. At the 25 kW scale, this approach will enable demonstration of thermal integration with co-located thermal energy sources as well as integrated operation with the INL Power Systems Test Bed. The 25 kW system will be flexible, allowing HTE operation from the 5 kW to the 25 kW scale, with support for intermittent and reversible operation. INL will work with various industrial partners to supply the HTE stacks and to design the test matrices. The 250 kW infrastructure installation will support demonstration and testing of industry-supplied pilot-scale turnkey systems with grid integration and variable operation.

RESULTS

This is a new experimental project. Progress to date is represented by the system design and supporting analyses.

A schematic of the 25 kW HTE testbed is provided in Figure 1. The system has been designed to be as simple as possible, with all major components obtained commercially, rather than custom-designed and fabricated. The steam generator is an inductively heated unit that provides high-temperature superheated steam directly from liquid water. The system will also include a heat exchanger option for process-heat-based steam generation when the DETAIL thermal network is complete. The electrolysis stacks are positioned within the hot zone for testing at 800°C. The inlet flow will include steam plus hydrogen. Hydrogen must be included on the inlet side in order to maintain reducing conditions on the electrolysis cell cathodes. During startup, hydrogen will be supplied from a gas cylinder, but for long-term operation, a fraction of the produced hydrogen will be recycled from the outlet flow back to the inlet after steam is removed by a combination of condensation, compression, and desiccant drying. Nitrogen is included as an inert carrier gas and a purge gas.

A three dimensional computer aided design model of the 25 kW HTE system layout has been prepared, as shown in Figure 2. Major components include a large lift-top furnace, steam generator/superheater, air compressor, chiller, hydrogen compressor, air-cooled hydrogen outlet finned tube array, water-cooled condensers, hydrogen storage tank, and a desiccant dryer. In terms of safety, since this system will be deployed in a large, high-bay laboratory, all hydrogen-related components are positioned inside of a ventilated enclosure (12 ft x 14 ft x 10 ft) which includes a gas monitoring system. The gas monitoring system is interlocked to the hydrogen gas supply (see solenoid valve in Figure 1) and electrolyzer power supplies such that hydrogen gas inlet flows and hydrogen production in the electrolyzer are both stopped in the case of a hydrogen gas alarm situation.

Operating specifications for 25 kW testing are listed in Table 1. The values listed in Table 1 are based on four 50-cell electrolysis stacks with active area of 144 cm^2. The cell area specific resistance value is assumed to be 0.6 $\Omega\ cm^2$ and the

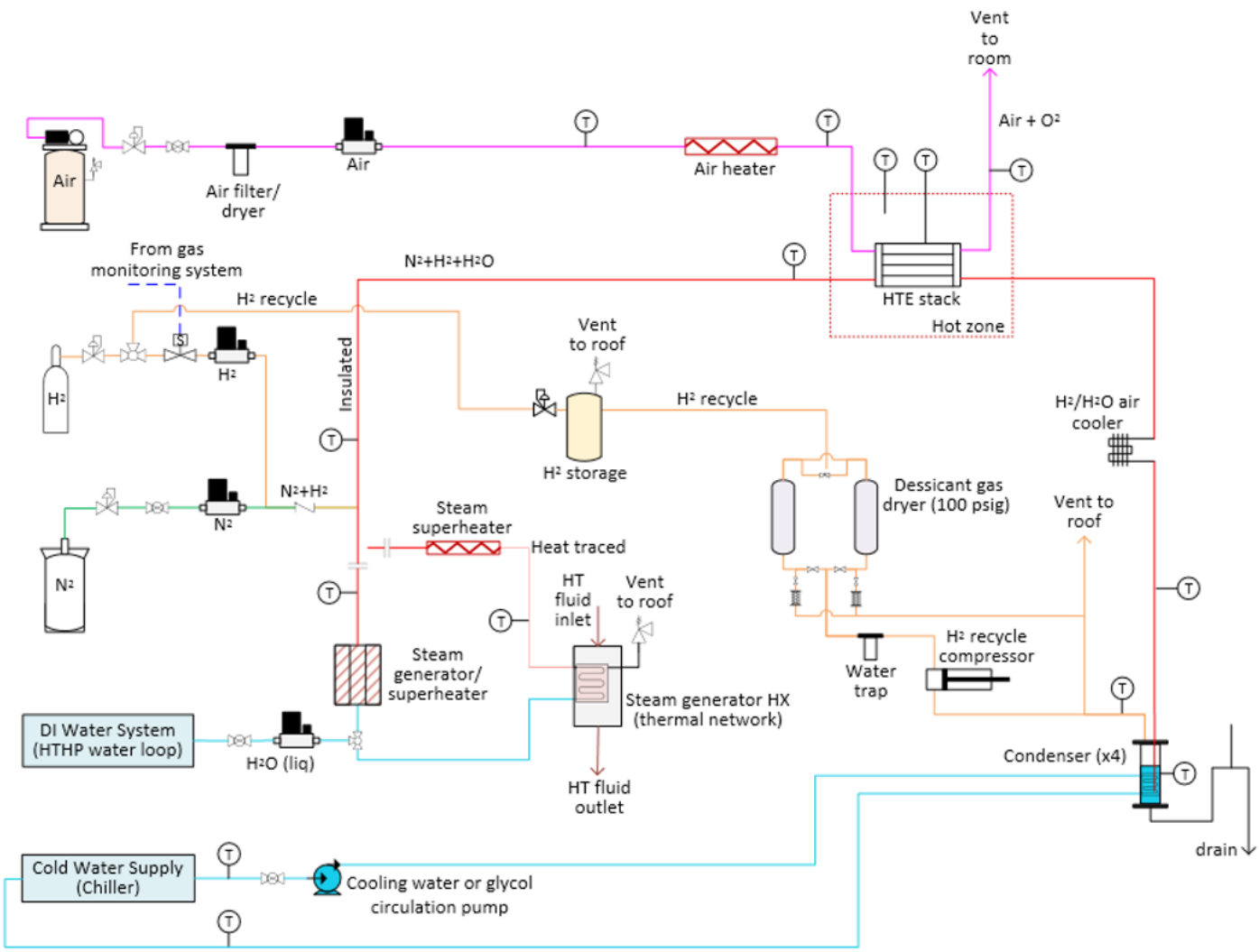

HT – high temperature; HTHP – high temperature high pressure

FIGURE 1. Schematic of 25 kW high-temperature test stand

current density is 0.67 A/cm^2 (these are conservative values). Steam utilization of 0.6 and a hydrogen inlet mole fraction of 0.1 are assumed. Instrumentation such as gas mass flow controllers have been specified based on these operating conditions. In addition, tubing sizing has been based on these flow rates.

CONCLUSIONS AND UPCOMING ACTIVITIES

Assembly of the 25 kW HTE demonstration facility will be completed during the first and second quarters of FY 2018. This will include shakedown testing and initial stack testing at the 5 kW scale. Procurement of stacks for support of 25 kW testing will also occur in the second quarter of FY 2018. Full-scale testing is planned for later in third and fourth quarters of FY 2018. Thermal integration of the HTE test stand with the high-temperature water loop will be implemented during FY 2018. This integration will require procurement of a heat exchanger to support boiling of the liquid water feedstock, plus a separate steam superheater.

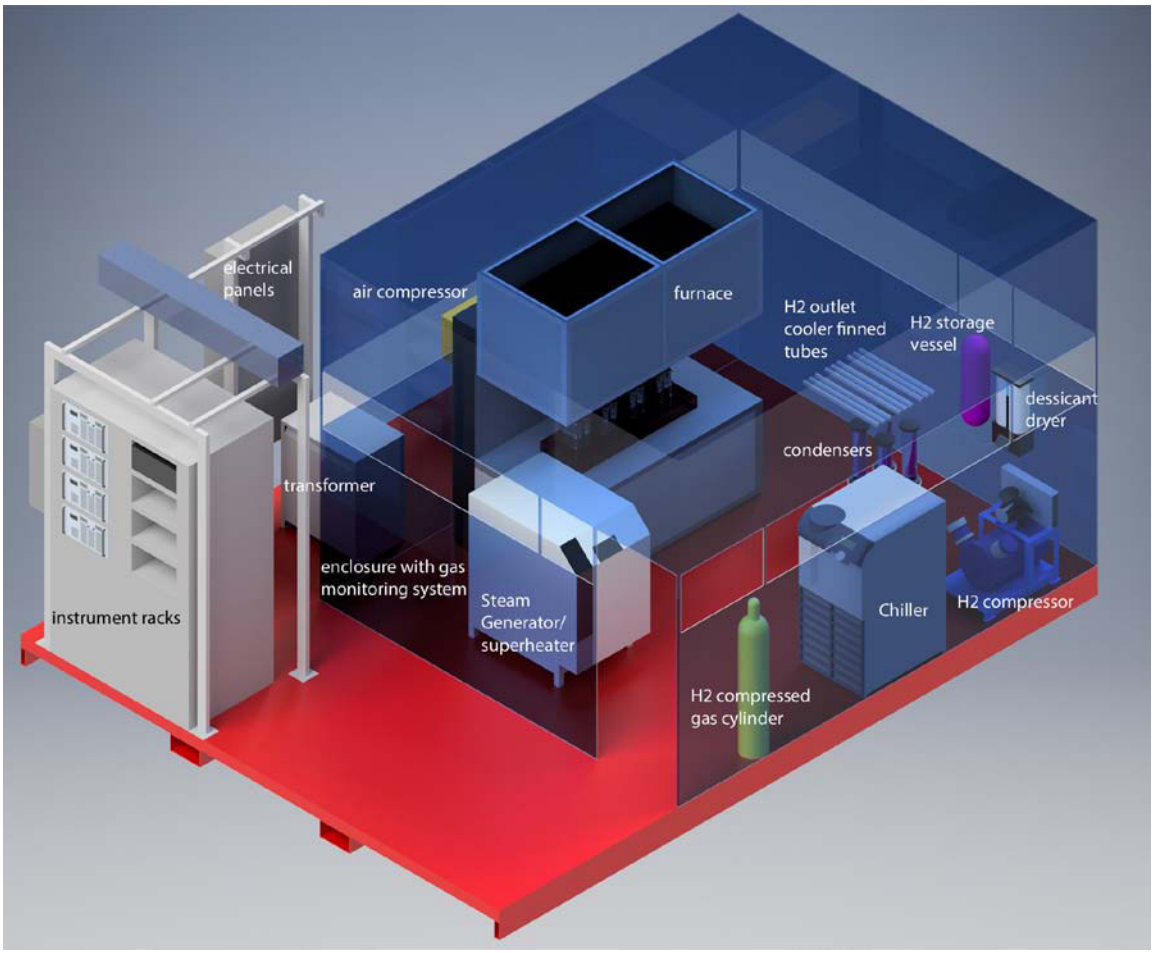

FIGURE 2. Layout for 25 kW HTE test facility

TABLE 1. Electrolyzer Operating Specification for 25 kW Operation

Flow Rates		Units
H_2 in	24.9	SLPM
	0.879	SCFM
H_2 production rate	134.5	SLPM
H2 out	159	SLPM
H_2O in (liq)	180	gm/min
H_2O in (liq)	10.8	kg/h
H_2O in (steam)	224	SLPM
H_2O out (steam)	89.6	SLPM
N_2 in	0	SLPM
Total cathode gas flow in	249	SLPM
	8.79	SCFM
Air in	160	SLPM
	5.65	SCFM
O_2 production rate	67.2	SLPM
Air+O_2 out	227	SLPM
	8.03	SCFM
Recycle Flow Rates		
H_2 through beds (avg)	0.879	SCFM
H_2O into beds (avg)	0.014	SCFM
Recycle compressor flow	5.8	SCFM
N_2 through beds (avg)	0	
N_2 added after recycle	0	
H_2 compressor run time	29.9	s
H_2 compressor idle time	162	s
Stack Electric		
Cell voltage	1.302	V
Stack voltage	65.1	V
Stack current	96.5	A
Module current	385.9	A
Module power	25.1	kW
Hot Zone		
Top	800	°C
Heater Power		
Steam generator (H_2O from 20°C to 150°C)	8.1	kW
Superheater (H_2 +N_2 from 20°C to 800°C + steam from 150°C to 800°C)	4.15	kW
Air heater/superheater	2.85	kW

SLPM – standard liters per minute; SCFM – standard cubic feet per minute;
liq – liquid; avg – average

VIII.0 Safety, Codes & Standards Sub-Program Overview

INTRODUCTION

The Safety, Codes and Standards sub-program identifies and performs high priority research and development (R&D) that provides an experimentally validated, fundamental understanding of the relevant physics, critical data, and safety information needed to define the requirements for technically sound and defensible codes and standards. This information is used to facilitate and enable the widespread deployment and commercialization of hydrogen and fuel cell technologies. In Fiscal Year (FY) 2017, the sub-program continued to identify and evaluate safety and risk management measures that can be used to define the requirements and close the gaps in codes and standards in a timely manner.

The sub-program promotes collaboration among government, industry, codes and standards development organizations, universities, and national laboratories in an effort to harmonize regulations, codes, and standards (RCS) both internationally and domestically. Communication and collaboration among codes and standards stakeholders, the Federal government, industry, national labs, and trade associations is emphasized in order to maximize the impact of the sub-program's efforts and activities in international RCS development. To support these efforts, in FY 2017 the Inter-Laboratory Research Integration Group was created to identify research needs across the national laboratories, which can be integrated into science-based revisions of NFPA 2 (National Fire Protection Association's hydrogen technologies code) and other hydrogen RCS.

GOALS

The sub-program's key goals are to provide the validated scientific and technical basis required for the development of codes and standards, to promulgate safety practices and procedures to allow for the safe deployment of hydrogen and fuel cell technologies, and to ensure that best safety practices are followed in Hydrogen and Fuel Cells Program activities.

OBJECTIVES

The sub-program's objectives are to:

- Support and facilitate development and promulgation of essential codes and standards to enable widespread deployment and market entry of hydrogen and fuel cell technologies and completion of all essential domestic and international RCS.
- Conduct R&D to provide critical data and information needed to define requirements in developing codes and standards.
- Ensure that best safety practices underlie research, technology development, and market deployment activities supported through DOE-funded projects.
- Develop and enable widespread sharing of safety-related information resources and lessons learned with first responders, authorities having jurisdiction, and other key stakeholders.

FY 2017 TECHNOLOGY STATUS AND ACCOMPLISHMENTS

The sub-program continues to support R&D to provide the scientific basis for codes and standards development, with projects in a wide range of areas, including fuel specification, separation distances, materials and components compatibility, and hydrogen sensor technologies. Utilizing the results from these R&D activities, the sub-program continues to actively participate in discussions with standards development organizations such as the National Fire Protection Association (NFPA), the International Code Council, SAE International, the CSA Group, and the International Organization for Standardization to promote domestic and international collaboration and harmonization of RCS. The sub-program has also collaborated with the National Institute for Standards and Technology, specifically on the standard for hydrogen metering accuracy. Previously, the standard was unachievable with current technology; however, as a result of collaborations between the National Renewable Energy Laboratory and the National Institute for Standards and Technology and through support by the State of California, a modified hydrogen metrology standard

of 5% was accepted in FY 2017, which will incrementally decrease to allow for technology improvements over the next several years.

In FY 2017, the sub-program built on results from the previous year, specifically by releasing the Hydrogen Risk Assessment Model (HyRAM) version 1.1 for public use. HyRAM enables quantitative risk assessment and performance-based design, while also incorporating hydrogen behavior models that were developed through the sub-program. Version 1.1 has improved capabilities including reductions in processing time and expanded models. In addition, model development and validation was begun for cryogenic hydrogen releases in the newly built cryogenic laboratory to help inform separation distances for liquid hydrogen. Finally, risk assessment was applied to real-world scenarios for the use of fuel cell electric vehicles in tunnels, and a risk analysis framework was developed and scenarios of concern identified.

The sub-program continues to advance its materials R&D for both metallic and non-metallic hydrogen compatibility. For metallic materials, the testing burden for qualification in high-pressure service was reduced through a performance-based fatigue metric proposed to the SAE Fuel Cell Safety Task Force. Last year's stakeholder feedback on non-metallic materials helped to identify polymers and elastomers of interest, leading to tribology testing to evaluate performance in high-pressure hydrogen. In the area of fuel quality assurance, the prototype in-line fuel quality analyzer developed at Los Alamos National Laboratory demonstrated its capability of detecting low carbon monoxide concentrations (<50 ppm) in dry hydrogen.

The sub-program continues to utilize the expertise of the Hydrogen Safety Panel to disseminate relevant information and implement safe practices pertaining to the operation, handling, and use of hydrogen and fuel cell technologies. The Safety Panel, with over 400 years of experience in the hydrogen industry, provides recommendations on the safe conduct of DOE-funded project work and non-DOE efforts, as well as lessons learned and best practices that can be of broad benefit to the sub-program. Furthermore, the State of California has leveraged the Safety Panel as a resource in their 2017 Grant Funding Opportunity. The sub-program continues to share current safety information and knowledge with the community through the continued development of resources for the Hydrogen Tools Portal (http://h2tools.org) which serves as a centralized resource for hydrogen safety information, news, and user-specific content. In FY 2017, the Hydrogen Equipment Certification Guide was made available for public download, and the Hydrogen Tools Portal expanded its resources, adding the Hydrogen Analysis Resource Center, as well as presentations and papers from the International Conference on Hydrogen Safety.

The sub-program continued to make progress in several key areas, including the following.

Hydrogen Behavior, Risk Assessment (Sandia National Laboratories)

- Publically released the HyRAM 1.1 software for risk analysis of hydrogen infrastructure systems, which benefits from improved capabilities such as reduced computing time. HyRAM capabilities were expanded by adding new models, such as three-dimensional positioning for flame targets, improved flame modeling, updated heat flux radiation modeling, and a TNT Mass Equivalence[1] calculator.
- Developed a new analytical technique to simultaneously measure cryogenic hydrogen concentration and mixture temperature, providing high-quality data for model validation. This project also initiated the validation process by comparing the data to an existing model of cold hydrogen dispersion that will be used for risk assessment and to provide the scientific basis for risk-informed safety distances.

Materials Compatibility (Sandia National Laboratories, Pacific Northwest National Laboratory, Oak Ridge National Laboratory)

- Documented fracture and fatigue performance of high hardenability pressure vessel steels in high-pressure hydrogen, showing that these alloys perform similarly to the pressure vessel steels currently used for stationary storage. Also proposed a performance-based fatigue metric for qualifying materials for high-pressure service to the SAE Fuel Cell Safety Task Force, significantly reducing the testing burden for materials qualification, as well as supporting the Global Technical Regulation 13 Phase II effort. Identified four polymers and elastomers of interest (Viton™, ethylene propylene diene monomer, nitrile, polytetrafluoroethylene), temperature and pressure of interest, and tests of interest through feedback from 25 stakeholders.

[1] TNT equivalent is a convention for expressing energy, which defines a "ton of TNT" as being equivalent to 4.184 gigajoules, which is the approximate energy released in the detonation of a metric ton of trinitrotoluene (TNT).

Hydrogen Quality (Los Alamos National Laboratory)

- Continued a parametric study of impurities to quantify carbon monoxide (CO) and hydrogen sulfide tolerance levels of low-loaded membrane electrode assemblies (0.15 mg Pt/cm^2), in order to establish data sets to assist in the advancement of developing predicative mechanistic models.
- Developed an in-line fuel quality analyzer prototype (patent applied for) and demonstrated its capability of detecting low CO concentrations (<50 ppm) in dry hydrogen. Additional performance capabilities include demonstrated CO sensitivity of less than 50 ppm, a demonstrated response time of less than 10 min, and demonstrated sustained operation under dry hydrogen for over one month.

Coordination of Codes and Standards Development, Domestic and International, and Codes and Standards Outreach (Sandia National Laboratories, National Renewable Energy Laboratory, Fuel Cells and Hydrogen Energy Association)

- Performed calculations and risk analysis for revised bulk gaseous separation distances using revised risk criteria for adoption by the NFPA 2/55 technical committees, which will enable more sites to readily accept hydrogen infrastructure.
- Developed risk analysis framework and identified scenarios of concern for tunnel access for hydrogen fuel cell electric vehicles. Completed computational fluid dynamics and heat transfer models to evaluate hydrogen fire impact on steel structure and concrete in passenger vehicle tunnels. Submitted proposal to NFPA 52 technical committee on characterizing hydrogen releases in tunnels.
- Created the Inter-Laboratory Research Integration Group to integrate research across the DOE laboratories into NFPA 2 and other hydrogen codes and standards. Submitted key proposals through the Inter-Laboratory Research Integration Group to NFPA 2 on adding flexibility to the bulk liquid hydrogen storage requirements.
- Supported the Telecommunications Industry Association publication of its Reference Guide to Regulations, Codes, and Standards for the Deployment of Stationary Fuel Cells.

Hydrogen Safety Panel, Databases, Props, and First Responders (Pacific Northwest National Laboratory)

- The Hydrogen Safety Panel conducted 33 project reviews (including safety plans and project designs) from July 2016 to July 2017.
- Provided four first responder training classes at three locations in the northeastern United States with approximately 250 attendees.
- Published the completed Hydrogen Equipment Certification Guide for public download in January 2017. Expanded available resources on the Hydrogen Tools Portal (http://h2tools.org), adding the Hydrogen Analysis Resource Center and presentations and papers from the International Conference on Hydrogen Safety.

Hydrogen Sensors (National Renewable Energy Laboratory)

- Co-organized a Hydrogen Sensor Workshop entitled "Hydrogen Safety Sensors and Their Use in Applications with Hydrogen as an Alternative Fuel," in collaboration with the European Joint Research Centre and the Fuel Cell and Hydrogen Joint Undertaking. In this workshop, critical gaps in hydrogen safety sensor performance were identified, and the resulting gap analysis is to be presented at the 7th International Conference on Hydrogen Safety.
- Developed a prototype analyzer to verify that hydrogen levels in fuel cell electric vehicle exhaust are within the regulated levels as prescribed by the Global Technical Regulation No. 13. The exhaust analyzer will ultimately be used by the U.S. Department of Transportation's National Highway Traffic Safety Administration for compliance verification.

BUDGET

The sub-program received an appropriation of $7 million in FY 2017. FY 2017 funding has allowed for continued support of codes and standards related R&D and of the domestic and international collaboration and harmonization efforts for codes and standards that are needed to support the commercialization of hydrogen and fuel cell technologies. The Safety Research and Development category includes such activities as hydrogen behavior, risk assessment and mitigation, materials compatibility, hydrogen fuel quality, metering, sensors, and component testing. The Safety Resources and Support category includes the Hydrogen Safety Panel, databases, training, and props. The Codes and Standards Support and Harmonization category includes codes and standards and permitting activities, continuous codes and standards improvement, and resource dissemination.

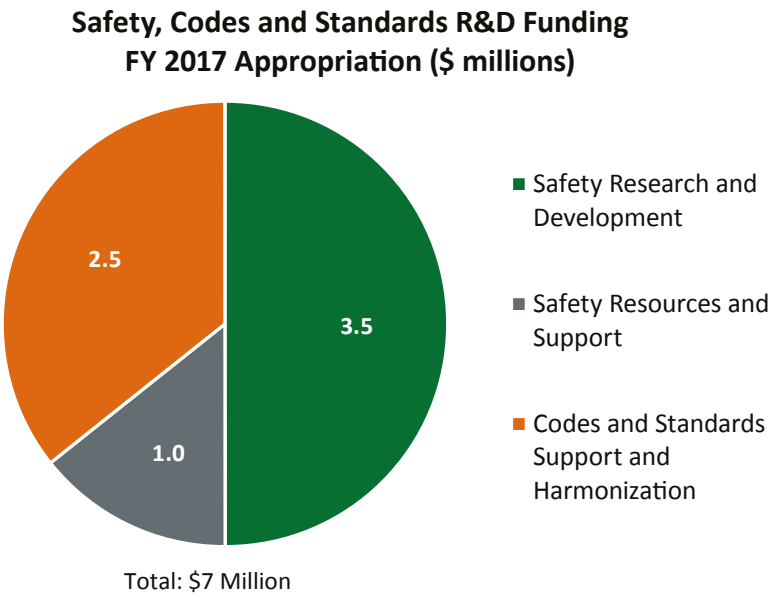

FIGURE 1. FY 2017 Appropriations

UPCOMING ACTIVITIES AND PLANS

The Safety, Codes and Standards sub-program will continue to support rigorous technical R&D—including assessment of materials compatibility for component designs and high-pressure tank cycle testing—and continue to promote a performance-based quantitative risk assessment approach to analyze risks and establish protocols to identify and mitigate risk. The sub-program will continue to work with codes and standards development organizations to ensure that the R&D performed enables science-based hydrogen-specific codes and standards.

The sub-program will also continue to perform the R&D necessary to promote the domestic and international harmonization of test protocols for qualification and certification as well as the harmonization of RCS for hydrogen fuel quality and other key international standards. This harmonization will be enabled by providing R&D results to the appropriate domestic and international organizations such as the NFPA, the International Code Council, SAE International, the CSA Group, and the International Organization for Standardization. Future activities are subject to appropriations.

Charles "Will" James
Safety, Codes & Standards Project Manager
Fuel Cell Technologies Office
Office of Energy Efficiency and Renewable Energy
U.S. Department of Energy
1000 Independence Ave., SW
Washington, DC 20585-0121
Phone: (202) 287-6223
Email: Charles.James@ee.doe.gov

VIII.1 National Codes and Standards Development and Outreach

Carl Rivkin (Primary Contact), Robert Burgess, and William Buttner
National Renewable Energy Laboratory (NREL)
15013 Denver West Parkway
Golden, CO 80401
Phone: (303) 275-3839
Email: Carl.Rivkin@nrel.gov

DOE Manager: Will James
Phone: (202) 287-6223
Email: Charles.James@ee.doe.gov

Subcontractor:
A.V. Tchouvelev & Associates, Inc.,
Mississauga, ON, Canada

Project Start Date: October 1, 2002
Project End Date: Project continuation and direction determined annually by DOE

Overall Objectives

- Support the deployment of hydrogen technologies for hydrogen fuel cell vehicles and associated infrastructure, industrial trucks, and stationary fuel cell applications.
- Integrate safety research into codes and standards.
- Make critical safety information readily available through webinars, training sessions, safety reports, online training, and technical presentations.
- Inform key stakeholders of the safety, codes, and standards requirements for the safe use of hydrogen technologies.
- Work with potential infrastructure developers to accelerate the deployment of hydrogen fueling stations and other key infrastructure.
- Identify and resolve safety issues associated with hydrogen technologies infrastructure.
- Support the continuous improvement of codes and standards through incorporating research and field data into the code development process.

Fiscal Year (FY) 2017 Objectives

- Publish papers on the large scale hydrogen systems and multi-fuel alternative fuel stations.
- Support the deployment efforts through participation in the H2USA's Market Support and Acceleration Working Group.
- Support the development of the next edition of the National Fire Protection Association (NFPA) 2 Hydrogen Technologies Code by chairing the Technical Committee on Hydrogen Technology, leading the NFPA Hydrogen Storage Task Group, and acting as principal committee member of the NFPA Technical Committee on Industrial and Medical Gases. Additionally, support NFPA 502 Standard for Road Tunnels, Bridges, and other Limited Access Roadways by incorporating fire safety analysis into document annex.
- Develop outreach products for permitting hydrogen technologies including an updated Code Official Training Course and Guide for Siting Stationary Fuel Cells.
- Implement Continuous Codes and Standard Improvement (CCSI) process by evaluating field data to determine codes and standards development priorities through a NREL technical report on safety research needs.
- Provide codes and standards information to critical stakeholders such as code officials through in-person training, updated on-line training, NREL technical reports posted on DOE websites, and development of relevant videos.
- Support the coordination of international and domestic hydrogen standards such as participating in International Organization for Standardization/Technical Committee 197 hydrogen technologies, hydrogen component development working groups, and domestic standards organizations such as the CSA Group.

Technical Barriers

This project addresses the following technical barriers from the Hydrogen Safety, Codes, and Standards section of the Fuel Cell Technologies Office Multi-Year Research, Development, and Demonstration Plan:

(A) Safety Data and Information: Limited Access and Availability

(D) Lack of Hydrogen Knowledge by AHJs

(F) Enabling National and International Markets Requires Consistent RCS

(G) Insufficient Technical Data to Revise Standards

(H) Insufficient Synchronization of National Codes and Standards

(I) Lack of Consistency in Training of Officials

(K) No Consistent Codification Plan and Process for Synchronization of R&D and Code Development

(L) Usage and Access Restrictions

Contribution to Achievement of DOE Safety, Codes & Standards Milestones

This project will contribute to achievement of the following DOE milestones from the Hydrogen Safety, Codes, and Standards section of the Fuel Cell Technologies Office Multi-Year Research, Development, and Demonstration Plan:

- Milestone 4.6: Completion of standards for critical infrastructure components and systems. (4Q, 2014)
- Milestone 4.7: Complete risk mitigation analysis for advanced transportation infrastructure systems. (1Q, 2015)
- Milestone 4.8: Revision of NFPA 2 to incorporate advanced fueling and storage systems and specific requirements for infrastructure elements such as garages and vehicle maintenance facilities. (3Q, 2016)
- Milestone 4.9: Completion of GTR Phase 2. (1Q, 2017)

FY 2017 Accomplishments

- Created the Inter-Laboratory Research Integration Group (IRIG) to integrate research across the DOE laboratories into NFPA 2 and other hydrogen codes and standards.
  - Submitted key proposals through IRIG to NFPA 2 on adding flexibility to the bulk liquid hydrogen storage requirements, and NFPA 502 on characterizing hydrogen releases in tunnels.
- Lead The NFPA Hydrogen Technologies Technical Committee as committee chair in producing the 2020 edition of NFPA 2 Hydrogen Technologies Code.
  - Leading the NFPA Hydrogen Storage Task Group to develop technical basis for setback distances and safety mitigation measures in NFPA 55 and NFPA 2 and submitting the revised bulk gaseous setback distances to the Technical Committee on Industrial and Medical Gases and the proposal to add flexibility to siting bulk liquid systems to NFPA 55 and NFPA 2.
- Developed new permitting and codes and standards training tools to support hydrogen technologies deployment, including an updated Code Official Training Course and publishing the Telecommunications Industry Guide to Siting Stationary Fuel Cells.
- Released a training video titled "Permitting Hydrogen Fueling Stations" in collaboration with the Orange County Fire Authority, an authority having jurisdiction (AHJ) with experience permitting several hydrogen fueling stations. This video should reduce the time and cost of both preparing and processing hydrogen fueling station permit applications by quickly orienting people to both the basics of the fueling technology and the code requirements.

✧ ✧ ✧ ✧ ✧

INTRODUCTION

The fundamental purpose of this work is to support the safe deployment of hydrogen technologies. To achieve this objective, codes and standards must be in place to protect public safety and any significant safety issues must be resolved before deployment proceeds. The primary focus of this project is to identify research needs to support codes and standards development and integrating that research into the appropriate documents.

The work under this project has helped develop a national set of codes and standards to safely deploy hydrogen technologies. Additionally, key safety issues have been identified and are in the process of being resolved. Safety, codes, and standards information has been distributed to interested parties using a variety of techniques including webinars, NREL technical reports, workshops, in-person presentations, videos, online training tools, and web-based products.

APPROACH

The project approach involves integrating the efforts from as many key stakeholders as possible in codes and standards development and coordination and outreach activities to achieve maximum impact. These stakeholders include industry partners, standards development organizations, research organizations including other national laboratories, AHJs, local government in locations where projects will be deployed, and trade organizations involved in technology development and deployment.

RESULTS

NREL, at the direction of DOE, has helped develop a baseline set of codes and standards for the deployment of hydrogen technologies. This accomplishment helps meet several DOE milestones, including 4.4 and 4.8.

The next step in this codes and standards development process after the promulgation of the baseline set of codes and standards is monitoring the field performance of these documents, determining where modifications are required (including the research required to support these modifications), and supporting the implementation of those modifications. Examples of these modifications include the revised setback distances for bulk gaseous hydrogen storage, development of requirements of fuel cell electric vehicles in

repair garages, and material supporting the use of fuel cell electric vehicles in tunnels in NFPA 502. This helps DOE meet Milestone 4.5.

This modification process is illustrated in Figure 1. The process consists of evaluating field deployment of hydrogen technologies through use of NREL data and site visits, determining whether there are issues with codes and standards based on this information, and developing modified codes and standards requirements to resolve these issues. This process also integrates NREL (and other DOE laboratories) laboratory research activities involving hydrogen technologies safety by using this research to address codes and standards issues.

The CCSI process has already begun to produce results in the following areas:

- The NFPA Hydrogen Storage Task Group submitted proposals to revise the bulk gaseous hydrogen setback distances and provide additional flexibility in siting bulk liquid hydrogen systems in the 2020 edition of NFPA 55/2. This plan produced proposals to NFPA 55/2 that were submitted in June 2016 and in NFPA 2.
- The NFPA Enclosures Task Group has submitted an extensive set of proposals to the 2020 edition of NFPA 2 to address modular hydrogen fueling stations.

NREL completed codes and standards and permitting training tools such as the "Permitting Hydrogen Fueling Stations" video done in collaboration with the Orange County Fire Authority. As an extension of this permitting support work, NREL introduced the concept of standard permits for hydrogen fueling stations and other infrastructure projects with the intent of developing this concept in FY 2018.

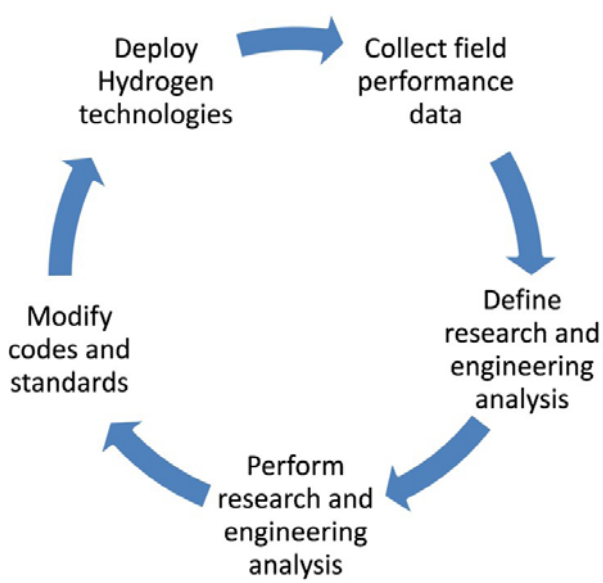

FIGURE 1. CCSI process

NREL supported the work of H2USA by participating as a member of the Market Support and Acceleration Working Group.

NREL supported testing required to develop Federal Motor Vehicle Safety Standards required to implement Global Technical Regulation in the United States. This supports DOE Milestone 4.9.

NREL has acted as Task Group Leader for the NFPA Hydrogen Storage Task Group that will develop new requirements for bulk gaseous and liquefied hydrogen and associated safety mitigation measures for the next edition of NFPA 55/2. This supports DOE Milestone 4.9.

CONCLUSIONS AND UPCOMING ACTIVITIES

Conclusions

- Codes and standards
  - The CCSI process is effective at modifying key codes to incorporate research results and define required research, such as characterization of liquid hydrogen releases.
  - Integration of DOE (and other) research into hydrogen codes and standards is a priority to ensure DOE safety research achieves the greatest possible impact on public safety by integration in widely used safety documents.
  - Ongoing coordination of the fire and building codes and key hydrogen codes and standards is a priority.
  - Field deployment information will help set codes and standards development priorities and improve the quality and relevance of codes as this information is incorporated through the American National Standards Institute-proscribed revision process.
- Outreach
  - Outreach deployment support will be reduced to focus limited resources on IRIG (research integration) efforts.
  - Deployment support focused on infrastructure at locations with project activity and concrete deployment plans, for example jurisdictions in California and the Northeast can be effective at moving projects forward but this is a labor intensive effort.
  - These goals can only be accomplished through collaborations with key stakeholders at all levels.

  - NREL supports the deployment of hydrogen and fuel cell technologies through programs such as technical reports, webinars, safety reviews, and the web-based information compendium. NREL has developed permitting tools that address the different needs of stakeholders and are readily accessible through various DOE websites. These internet accessible tools have provided permitting support for all types of users from the infrequent user to more knowledgeable users.

Upcoming Activities

- Codes and standards
  - NREL will focus on the IRIG project of integrating safety research into codes and standards. Key project areas will be station siting requirements, high-risk component safety, critical infrastructure such as tunnels and garages, and codes and standards streamlining to reflect higher levels of infrastructure deployment.
  - Support H2@Scale work by identifying gaps in safety knowledge and research required to fill these gaps.
  - Continue work to coordinate codes and standards with special focus on taking information from deployment projects back to code development committees.
  - Resolve infrastructure codes and standards issues such as hydrogen setback distances in NFPA codes.
  - Continue coordination between National Fire Codes and International Code Council codes, as well as International Organization for Standardization hydrogen component standards and domestic hydrogen component standards.
  - Support efforts to adopt NFPA 2 Hydrogen Technologies Codes (and other key codes), such as the work done by the California's Office of the State Fire Marshal to adopt NFPA 2 earlier than adoption of the International Fire Code would dictate.
  - Continue to incorporate research into the codes through the CCSI process using the IRIG as the primary mechanism to achieve these incorporations.
  - Support efforts to develop standard permits for hydrogen infrastructure projects to streamline project permitting efforts.
- Outreach
  - Outreach activities will likely be reduced in FY 2018. If they continue work would be performed in the following project areas with a special focus on H2@Scale.
  - Continue to publish NREL technical reports, deliver webinars, and provide web-based information on key safety issues required to support hydrogen technologies deployment.
  - Assist code officials, project developers, and other interested parties in use of new codes and standards and safety information through outreach activities, with special focus on key jurisdictions such as California and the Northeast.
  - Utilize NREL hydrogen fueling station for training purposes such as videos on hydrogen fueling operations and maintenance.
  - Work with interested parties to provide information to assist in infrastructure deployment.
  - Provide in-person codes and standards training or consultation in key locations such as California, New York, Massachusetts, and other zero-emission vehicle states.

FY 2017 PUBLICATIONS/PRESENTATIONS

1. Rivkin, C., R. Burgess, and W. Buttner. 2017. *Regulations Codes and Standards (RCS) for Multi-Fuel Stations.* International Conference for Hydrogen Safety.

2. Rivkin, C., R. Burgess, and W. Buttner. 2017. *Regulations Codes and Standards (RCS) for Large Scale Hydrogen Installations*. International Conference for Hydrogen Safety.

3. *Guide for Compliance with Regulations, Codes and Standards for the Deployment of Stationary Fuel Cells*. 2017. Telecommunications Industry Association.

VIII.2 R&D for Safety, Codes and Standards: Materials and Components Compatibility

Chris San Marchi
Sandia National Laboratories
7011 East Ave
Livermore, CA 94550
Phone: (925) 294-4880
Email: cwsanma@sandia.gov

DOE Manager: Will James
Phone: (202) 287-6223
Email: Charles.James@ee.doe.gov

Project Start Date: October 1, 2003
Project End Date: Project continuation and direction determined annually by DOE

Overall Objectives

- Optimize the reliability and efficiency of test methods for structural materials and components in hydrogen gas.
- Generate critical hydrogen compatibility data for structural materials to enable technology deployment.
- Create and maintain information resources such as the "Technical Reference for Hydrogen Compatibility of Materials" and the "Database for Hydrogen Compatibility of Materials."
- Demonstrate leadership in the international harmonization of standards for qualifying materials and components for high-pressure hydrogen service.

Fiscal Year (FY) 2017 Objectives

- Perform fatigue and fracture tests on high-hardenability pressure vessel steels in high-pressure gaseous hydrogen, evaluating multiple alloys representing a range of strength.
- Demonstrate fatigue and fracture testing in high-pressure hydrogen at low temperature in the context of vehicle applications.
- Develop performance-based materials qualification metric for vehicle applications, emphasizing austenitic stainless steels.
- Major revision of Database on Hydrogen Compatibility of Materials to include recent fatigue and fracture data from the literature.

Technical Barriers

This project addresses the following technical barriers from the Hydrogen Safety, Codes and Standards section of the Fuel Cell Technologies Office Multi-Year Research, Development, and Demonstration Plan.

(A) Safety Data and Information: Limited Access and Availability

(F) Enabling National and International Markets Requires Consistent RCS

(G) Insufficient Technical Data to Revise Standards

Contribution to Achievement of DOE Safety, Codes & Standards Milestones

This project will contribute to achievement of the following DOE milestones from the Hydrogen Safety, Codes and Standards section of the Fuel Cell Technologies Office Multi-Year Research, Development, and Demonstration Plan.

- Milestone 2.9: Publish technical basis for optimized design methodologies of hydrogen containment vessels to account appropriately for hydrogen attack. (4Q, 2014)
- Milestone 2.16: Demonstrate the use of new high-performance materials for hydrogen applications that are cost-competitive with aluminum alloys. (4Q, 2017)
- Milestone 2.18: Implement validated mechanism-based models for hydrogen attack in materials. (4Q, 2018)
- Milestone 3.3: Reduce the time required to qualify materials, components, and systems by 50% relative to 2011 with optimized test method development. (1Q, 2017)
- Milestone 3.4: Develop hydrogen material qualification guidelines including composite materials. (Q4, 2017)
- Milestone 4.9: Completion of the GTR Phase 2. (1Q, 2017)
- Milestone 5.2: Update materials compatibility technical reference. (4Q, 2011 – 2020)
- Milestone 5.4: Develop and publish database for properties of structural materials in hydrogen gas. (2Q, 2013)

FY 2017 Accomplishments

- Documented fracture and fatigue performance of high hardenability pressure vessel steels in high-pressure hydrogen, showing that these alloys perform similarly

to the pressure vessel steels currently used for stationary storage.

- Proposed a performance-based fatigue metric for qualifying materials for high-pressure service to the SAE Fuel Cell Safety Task Force, which significantly reduces the testing burden for materials qualification.
- Provided leadership to international partnership to develop low-temperature hydrogen testing capabilities in the United States, Europe, and Asia and to harmonize materials qualification methods for proposal to Global Technical Regulation (GTR) No. 13 Phase 2; draft proposal has general consensus.
- Developed schema for public access of hydrogen compatibility of materials database and greatly expanded available data records; database has substantial global visibility with hundreds of visitors, and nearly 8,000 page views, significantly extending the dissemination of data on hydrogen compatibility of materials.

✧ ✧ ✧ ✧ ✧

INTRODUCTION

A principal challenge to the widespread adoption of hydrogen infrastructure is the lack of quantifiable data to define safety margins and to mitigate potential hazards. To convince regulatory officials, local fire marshals, fuel suppliers, and the public at-large that hydrogen refueling is safe for consumer use, the risk to personnel and bystanders must be quantified and minimized to an acceptable level. Such a task requires strong confidence in the safety performance of high-pressure hydrogen systems. Developing meaningful materials characterization and qualification methodologies in addition to enhancing understanding of the performance of materials is critical to eliminating barriers to the development of safe, low-cost, high-performance, high-pressure hydrogen systems for the consumer environment. This activity develops scientifically defensible, accelerated testing strategies and critically evaluates test methodologies for quantifying hydrogen effects on materials. Additionally, the program engages the international scientific community to harmonize test methods, provide guidance on materials selection for hydrogen service and disseminate the latest scientific knowledge on the hydrogen compatibility of materials and suitability of components.

APPROACH

The Materials and Components Compatibility program element leverages decades of experience in high-pressure hydrogen systems, well-developed industry partnerships, and a core capability in hydrogen–materials interactions anchored by the Hydrogen Effects on Materials Laboratory to focus on three critical activities: (1) optimize materials characterization methodologies, (2) generate critical hydrogen compatibility data for materials to enable technology deployment, and (3) provide international leadership by assembling and maintaining a technical reference and database that compile technical data relevant to understanding the effects of hydrogen on materials. To achieve these goals, the Hydrogen Effects on Materials Laboratory develops and maintains unique hardware and test methods for measuring fracture and fatigue behavior of materials in high-pressure gaseous hydrogen environments over a range of temperature. This program element also leverages state-of-the-art materials science characterization tools to advance the understanding of hydrogen–materials interactions in both structural and functional materials.

RESULTS

High-Hardenability Pressure Vessel Steels

Manufacturers of stationary hydrogen storage solutions have demonstrated interest in high hardenability pressure vessel steels, which enables larger storage systems to serve larger refueling stations. A memorandum of understanding with several pressure vessel manufacturers documents the common interest in high-hardenability (Ni-Cr-Mo) pressure vessel steels and includes Fiba Technologies (North America/United States), Tenaris-Dalmine (Europe/Italy), and Japan Steel Works (Asia/Japan). Three heats of Ni-Cr-Mo steels have been tested, including one of these steels in both a low-strength and high-strength condition (four steels with tensile strength in the range from 860 MPa to 1,150 MPa). Fracture results (Figure 1) demonstrate the basic trend of significantly lower fracture resistance for steels with tensile strength greater than 950 MPa [1]. While the fracture resistance is sensitive to the strength of the steel, fatigue results are decidedly different.

Fatigue crack growth rates for the tested steels are insensitive to composition and strength at low stress intensity factor range (ΔK). Testing was conducted primarily at 1 Hz with load ratio in the range of 0.1 to 0.7 in gaseous hydrogen at pressure of 106 MPa. An example of the measured fatigue crack growth rates (load ratio = 0.5) is shown in Figure 2, representing data for four Ni-Cr-Mo steels as well as two heats of Cr-Mo pressure vessel steel. These results are consistent for all steels, suggesting that a simple fatigue crack growth relationship can represent the performance of all Cr-Mo and Ni-Cr-Mo steels within this strength range; moreover, Ni-Cr-Mo steels perform similarly to the Cr-Mo steels, which are commonly employed in existing infrastructure. The high-strength steels transition to higher crack growth rates than the basic trend at higher ΔK as the maximum stress intensity factor approaches the fracture resistance – this is referred to as Stage III fatigue crack growth. This trend emphasizes the challenge of designing hydrogen pressure vessels with high strength steels.

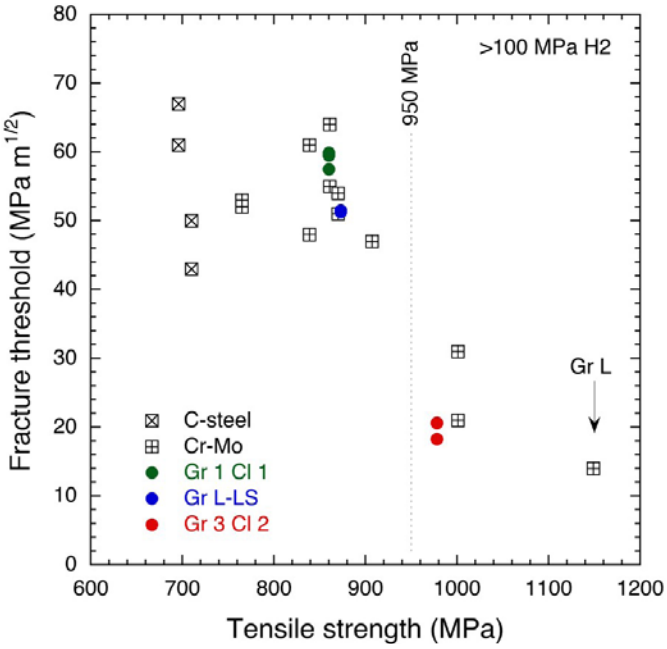

FIGURE 1. Fracture threshold determined from elastic–plastic fracture toughness measurements in gaseous hydrogen at pressure of 106 MPa. Carbon steel [2,3] and Cr-Mo steel [4,5] data from previous studies in hydrogen at pressure of 103 MPa and displacement rate of 1.5 and 3 mm/h, respectively. Each data point represents an individual test.

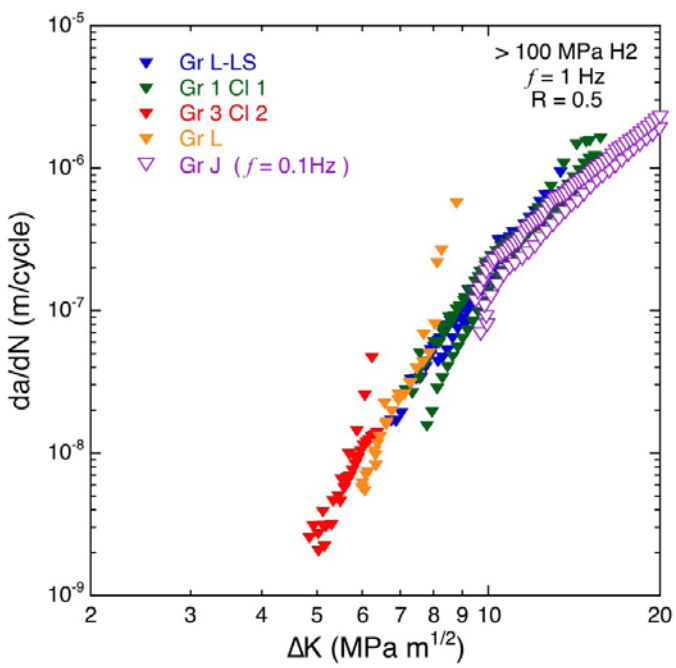

FIGURE 2. Comparison of fatigue crack growth rates for Ni-Cr-Mo pressure vessel steels and Ni-Cr pressure steels in high-pressure gaseous hydrogen at load ratio of 0.5. The Ni-Cr-Mo data (Gr L-LS, Gr 1 Cl 1, Gr 3 Cl 2, Gr L) was generated at a frequency of 1 Hz in hydrogen at pressure of 106 MPa [1], while the data for Cr-Mo steel (two heats of Gr J) was generated at a frequency of 0.1 Hz in hydrogen at pressure of 103 MPa from Refs. [6,7].

Additional testing may focus on developing a simplified testing strategy to verify consistency of other steel classes over an extended load ratio range using these results as a benchmark. With this benchmark data, the number of specimens and the time for testing other steels can, in principle, be substantially reduced while ensuring performance in hydrogen. It should also be noted that the fracture tests in gaseous hydrogen were performed at the conclusion of fatigue testing (rather than using separate specimens for evaluating fracture resistance), which also reduces the number of test specimens needed to characterize the steels.

Performance Methods for Materials Qualification

Establishing robust performance metrics for materials qualification is challenging because materials are often selected for multiple characteristics, which depend on the specifics of the design. However, when properties can be bounded by general performance requirements, criteria can often be established. The H2 Compatibility Expert Team from the SAE Fuel Cell Safety Task Force has been engaged in conversation to develop internationally harmonized materials performance metrics for several years. Previously, progress on this discussion had been inhibited by lack of relevant fatigue data; however, active research programs (such as funded by the hydrogen storage subprogram, but also internationally) have recently made data available for assessment and these data are actively being discussed to inform performance metrics for in the SAE Fuel Cell Safety Task Force. The Safety, Codes and Standards subprogram, which developed the tension-tension notched fatigue test method for hydrogen, has proposed a performance metric of $\geq 10^5$ cycles at a maximum fatigue stress of one-third of the tensile strength, as shown in Figure 3. This simple performance metric can be applied to fatigue testing in gaseous hydrogen for either the smooth fatigue specimen (load ratio of -1) or the notched fatigue specimen (load ratio of 0.1). In both test methods, the target is to verify that the maximum allowable stress in the material is less than the fatigue limit (implying infinite life design) using a relatively small number of tests and avoiding extensive fatigue life testing. While not yet formally adopted, the proposed criterion is the first step toward a performance-based materials qualification metric and has been discussed as a possible proposal for discussion at the GTR no. 13 Phase 2 negotiations.

The H2 Compatibility Expert Team at SAE has also been engaged in information sharing toward developing testing capability for fatigue testing in high pressure gaseous hydrogen at low temperature, in addition to developing the test methods for materials qualification. Three international institutes (namely Kyushu University, MPA Stuttgart and Sandia National Laboratories) are independently developing new capability for testing in the combination of high-pressure and low-temperature, and sharing their experience toward

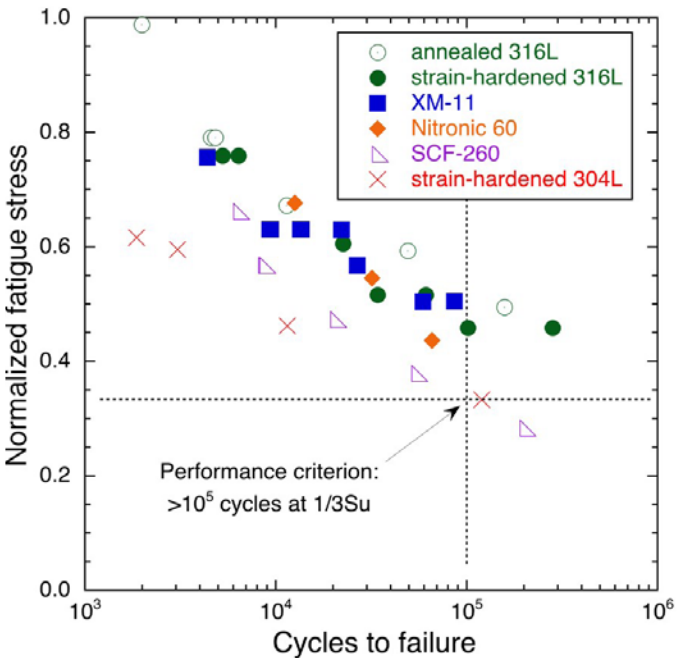

FIGURE 3. Fatigue life curves for several austenitic steels measured in gaseous hydrogen at pressure of 10 MPa (tension-tension notched fatigue: stress concentration factor of 3.9, frequency of 1 Hz, and load ratio of 0.1), plotted for maximum fatigue stress normalized by the tensile strength (Su). The proposed materials qualification metric is indicated on the plot: $>10^5$ cycles to failure at maximum fatigue stress representing one-third of the tensile strength of the material.

coordinated testing to verify test methods for qualification of materials for vehicle components. The H2 Compatibility Expert Team meets quarterly at the SAE Fuel Cell Safety Task Force meetings, but these meetings are supplemented by technical exchanges almost monthly via teleconference. The technical institutes seek to complete a testing campaign by the end of 2017 to compare equivalent tests from each institute. These results will aid test method development and will also help establish the limiting conditions for fatigue performance in gaseous hydrogen.

Information Resources

The Database for Hydrogen Compatibility of Materials uses the Granta database tool software. It is currently publicly accessible through a web-based interface at https://granta-mi.sandia.gov. Public access to this database is made available by special agreement with Granta and hosted by Sandia National Laboratories. The database has experienced over 20,000 hits, and nearly 8,000 page views by hundreds of unique visitors. The database is undergoing a major revision for release at the end of Summer 2017. Recently published data is being integrated into the database by soliciting authors to aid the incorporation of their data into this state-of-the-art tool. The database enables comparison of data from different sources, verification of materials and testing pedigrees, and may eventually be the basis for prescriptive design data. While the database enables quantitative access to materials properties measured in gaseous hydrogen by institutes throughout the world, the Technical Reference provides interpretation of the data and specific guidance on materials selection for hydrogen service for nonexperts. The updated database content will greatly facilitate the revision of the Technical Reference by providing the authors with advanced comparison tools and wider range of data from which to establish concrete recommendations and confirm broadly applicable trends where appropriate.

CONCLUSIONS AND UPCOMING ACTIVITIES

- Testing of high-hardenability pressure vessels steels with a range of strength show that hydrogen-accelerated fatigue crack growth is similar to the pressure vessel steels currently in service, while fracture resistance of pressure vessels steels displays a steep reduction when tensile strength exceeds 950 MPa.
- A simple method for evaluating fatigue performance in hydrogen has been proposed. The method consists of tension-tension fatigue life testing of notched specimens and a conservative performance-based metric of $>10^5$ cycles to failure at maximum fatigue stress of one-third of the tensile strength.
- The Database on Hydrogen Compatibility of Materials is receiving a major upgrade, which will be transitioned to public access at the end of summer.
- Low-temperature testing in high-pressure gaseous hydrogen will be the focus of the next method development campaign, allowing for evaluation of the limiting conditions for fatigue behavior of austenitic stainless steels for vehicle and vehicle refueling applications. This testing represents a significant advancement of capabilities for hydrogen testing within the United States and is being coordinated with an international team of experts developing similar testing capability to support GTR no. 13 Phase 2 discussions.

FY 2017 PUBLICATIONS/PRESENTATIONS

1. C. San Marchi, E.S. Hecht, I.W. Ekoto, K.M. Groth, C. LaFleur, B.P. Somerday, R. Mukundan, T. Rockward, J. Keller, C.W. James: "Overview of the DOE hydrogen safety, codes and standards program, part 3: Advances in research and development to enhance the scientific basis for hydrogen regulations, codes and standards." *Intern J Hydrogen Energy* 42 (2017) 7263–74.

2. B.P. Somerday, J.A. Campbell, K.L. Lee, J.A. Ronevich, C. San Marchi: "Enhancing safety of hydrogen containment components through materials testing under in-service conditions." *Intern J Hydrogen Energy* 42 (2017) 7314–7321.

3. B. An, Z. Hua, T. Iijima, C. Gu, J. Zheng, C. San Marchi: "Scanning Kelvin probe force microscopy study of hydrogen distribution and evolution in duplex stainless steel" (PVP2017-66121), Proceedings of the 2017 ASME Pressure Vessels & Piping Conference, 16–20 July 2017, Waikoloa, HI.

REFERENCES

1. C. San Marchi, P. Bortot, J. Felbaum, Y. Wada, J.A. Ronevich: "Fatigue and fracture of high-hardenability steels for thick-walled hydrogen pressure vessels," International Conference on Hydrogen Safety, Hamburg, Germany, 11–13 September 2017.

2. C. San Marchi, B.P. Somerday, K.A. Nibur, D.G. Stalheim, T. Boggess, and S. Jansto: "Fracture and fatigue of commercial grade pipeline steels in gaseous hydrogen" (PVP2010- 25825), ASME Pressure Vessels and Piping Division Conference, American Society of Mechanical Engineers, 18–22 July 2010, Bellevue WA.

3. C. San Marchi, B.P. Somerday, K.A. Nibur, D.G. Stalheim, T. Boggess, and S. Jansto: "Fracture resistance and fatigue crack growth of X80 pipeline steel in gaseous hydrogen" (PVP2011-57684), ASME Pressure Vessels and Piping Division Conference American Society of Mechanical Engineers, July 2011, Baltimore, MD.

4. K.A. Nibur, B.P. Somerday, C. San Marchi, J.W. Foulk III, M. Dadfarnia, P. Sofronis, G.A. Hayden: "Measurement and interpretation of threshold stress intensity factors for steels in high-pressure hydrogen gas," SAND2010-4633, Sandia National Laboratories, Livermore, CA.

5. K.A. Nibur, B.P. Somerday, C. San Marchi, J.W. Foulk, M. Dadfarnia, P. Sofronis: "The relationship between crack-tip strain and subcritical cracking thresholds for steels in high-pressure hydrogen gas." *Metall Mater Trans* 44A (2013) 248–269.

6. B.P. Somerday, K.A. Nibur, and C. San Marchi: "Measurement of fatigue crack growth rates for steels in hydrogen containment components," 3rd International Conference on Hydrogen Safety (ICHS3), September 2009, San Sebastian, Spain.

7. B.P. Somerday, C. San Marchi, and K.A. Nibur: "Measurement of fatigue crack growth rates for SA-372 Gr. J steel in 100 MPa hydrogen gas following Article KD-10" (PVP2013-97455), ASME Pressure Vessels and Piping Division Conference, American Society of Mechanical Engineers, 14–18 July 2013, Paris, France.

VIII.3 Hydrogen Fuel Quality

Tommy Rockward (Primary Contact),
Chris Romero, Stefan Williams, Eric Brosha,
Mahlon Wilson, and Rangachary Mukundan
Los Alamos National Laboratory (LANL)
P.O. Box 1663
Los Alamos, NM 87545
Phone: (505) 667-9587
Email: trock@lanl.gov

DOE Managers:
Will James
Phone: (202) 287-6223
Email: Charles.James@ee.doe.gov
Laura Hill
Phone: (202) 586-8384
Email: Laura.Hill@ee.doe.gov

Collaborators/Partners:
- Japan Automotive Research Institute
- SAE International, Warrendale, PA
- Smart Chemistry, Sacramento, CA
- CEA-Liten, Grenoble, France
- VTT, Helsinki, Finland
- International Organization for Standardization (ISO)/ Technical Committee (TC) 197/Working Groups (WG) 27 and 28

Project Start Date: October 2006
Project End Date: Project continuation and direction determined annually by DOE

Overall Objectives

- Support the Hydrogen Safety, Codes and Standards subprogram through:
  - Providing leadership to hydrogen fuel quality efforts.
  - Performing the research and development (R&D) needed to develop science-based codes and standards.
  - Developing tools that can remove safety and hydrogen fuel quality barriers to the commercialization of fuel cells.
  - Participation in working groups.

Fiscal Year 2017 Objectives

- Evaluate the effect of critical fuel impurities on the performance of membrane electrode assemblies (MEAs) with low loadings (A/C: 0.05/0.10 mg Pt/cm^2).
  - Test MEAs in two modes (hydrogen single pass and re-circulation).
  - Test the impact of fuel contaminants at the SAE J2719/ISO 14687-2 levels.
  - Disseminate results.
- Demonstrate a prototype fuel quality analyzer capable of detecting fuel impurities in dry hydrogen at the SAE J2719 specification levels.
  - Test the prototype for a fuel quality analyzer.
  - Optimize sensitivity to CO.
  - Operate analyzer under dry conditions.
  - Investigate clean-up strategies.

Technical Barriers

This project addresses the following technical barriers from Section 3.7.5 Hydrogen Safety, Codes & Standards of the Fuel Cell Technologies Office Multi-Year Research, Development, and Demonstration Plan.

(F) Enabling National and International Markets Requires Consistent RCS

(G) Insufficient Technical Data to Revise Standards

(H) Insufficient Synchronization of National Codes and Standards

(K) No Consistent Codification Plan and Process for Synchronization of R&D and Code Development

FY 2017 Accomplishments

- Performed R&D to demonstrate that low-loaded MEAs are not tolerant to SAE J2719 level of impurities (both CO and H_2S), especially when operated in re-circulation mode.
- Continued a parametric study of impurities to quantify CO and H_2S tolerance levels of low-loaded MEAs to establish data sets to assist in the advancement of developing predicative mechanistic models. This study is critical in determining the impurity tolerance levels of low-loaded MEAs under various operating conditions.
- Developed an in-line fuel quality analyzer and demonstrated its capability of detecting low CO concentrations in dry hydrogen. Additional performance capabilities include:
  - Demonstrated CO sensitivity of <200 ppm.
  - Demonstrated response time <10 min.

- Demonstrated sustained operation under dry H_2 for >1 mo.
- Developed prototype (patent application filed).
- Demonstrated the ability to reset analyzer after poisoning.

✧ ✧ ✧ ✧ ✧

INTRODUCTION

The FY 2017 work performed in this project has two distinct tasks: (1) R&D for fuel quality standards including international interactions and (2) in-line fuel quality analyzer development.

While steam reforming natural gas will make hydrogen affordable and available, it will produce trace amounts of CO and H_2S. The international team (ISO TC197 WG-12) for "development of hydrogen fuel product specifications for use in proton exchange membrane fuel cell applications for road vehicles" (developed standards ISO 14687-2:2012) [1] and SAE J2719 [2], which indicate acceptance levels of several contaminants. Although these contaminants are at sub-ppm levels, their effect on fuel cell performance is uncertain, especially since the total platinum content in the fuel cell MEA has been continuously lowered. Previously conducted fuel cell tests with the fuel specification indicated that ammonia, carbon monoxide, and hydrogen sulfide were the critical constituents most harmful to proton exchange membrane fuel cell performance and/or its durability. LANL conducted fuel quality testing to evaluate the impact of these critical constituents on current fuel cell MEAs and has continued to engage the international community to incorporate the research results into future updates to these standards.

Although science-based standards for fuel quality have been established, there is still a need to provide the tools necessary to implement this standard. For example, the ISO and SAE standards have a maximum allowance of 0.2 ppm for CO and 4 ppb for H_2S [1,2]. LANL has demonstrated proof-of-concept for an in-line fuel quality analyzer using various concentrations of CO at or below the levels in the aforementioned standard. We optimized the MEA response time to <10 min (approximate time for two fuel refills) and have finalized a design for a prototype in-line fuel quality analyzer. Our goal is to provide a quick and cheap method of detection at various points in the supply chain. The successful commercialization of this product will have a positive impact on the safety of filling stations and the reliability of fuel cell vehicles. This work directly addresses the targets set in Table 3.7.6 of the Safety, Codes and Standards technical plan.

APPROACH

R&D for Fuel Quality Standards

In our fuel impurity testing, we are continuing to use MEAs produced by Ion Power. Here we report fuel cell results for fuel impurity studies that were conducted on 25 cm^2 cells. In this report we summarize the results obtained with both high (0.4 mg Pt/cm^2) and low (0.15 mg Pt/cm^2) platinum loaded MEAs. Our overall objective was to test MEAs with total platinum loadings equivalent to the 2015 DOE target loading, 0.15 mg Pt/cm^2 total. X-ray fluorescence results of the original set of MEAs provided by the manufacturer indicated a total platinum loading range from 0.4 mg Pt/cm^2 to–0.44 mg Pt/cm^2 for the high-loading MEAs. LANL obtained the lower-loading MEAs during the third quarter of FY 2017, and the X-ray fluoresence results showed the total platinum loadings were near the DOE targets (approximately 0.143 mg Pt/cm^2 total). These two results will be used to evaluate the effect of Pt loading using the SAE J2719 fuel specification for contaminant levels: hydrogen sulfide, carbon monoxide, and ammonia.

In-line Fuel Quality Analyzer

Over the past two years, we focused on electrode materials optimization utilizing a relatively thick membrane. LANL has experimentally shown using the ISO 14687-2/SAE J2719 contaminant levels of 200 ppb CO and 4 ppb H_2S in hydrogen gas that it is possible to obtain responses within minutes using ultra-low-loaded electrodes made by sputtering relatively larger particle-size platinum directly on a gas diffusion media. This working electrode is coupled with a platinum-ruthenium reference electrode on a 7 mil thick membrane. Tests on these materials were performed with humidified hydrogen fuel at both electrodes in hydrogen pump mode using a standard 5 cm^2 fuel cell hardware made by Fuel Cell Technologies (Albuquerque, New Mexico). In the last fiscal year, we demonstrated a humidification scheme that would keep the membrane wet when exposed to dry H_2. In this fiscal year, we built a prototype analyzer using this humidification scheme and designed flow fields and MEAs to maximize response to CO impurity in hydrogen fuel.

RESULTS

Hydrogen Fuel Quality

Table 1 provides a summary of the decay in fuel cell voltage under various conditions over a 100 h test. It is seen that at 32% relative humidity, the high-loaded MEAs are tolerant to all the CO concentrations at all the pressures tested. However, at the higher relative humidity, the MEA is tolerant to 200 ppb CO (which is the SAE J2719 level) only at the higher pressures. Since fuel cell systems are expected to operate at pressures greater than 150 kPa, the

TABLE 1. Voltage Loss Measured at 1 A/cm^2 Under Various Impurity Testing Conditions

T: 80°C		Tolerance of [CO] in PEM Fuel Cells								
Pressure (kPa)		80	150		80	150		80	150	
[CO] (ppm)		1	1		0.5	0.5		0.2	0.2	
RH (%)	32	0	0		0	0		0	0	
	50	51 mV	42 mV		25 mV	9 mV		2 mV	0	
	100	51 mV	51 mV		29 mV	10 mV		13 mV	0	

MEA can be deemed tolerant to CO at the SAE J2719 levels. Currently this matrix is being populated with data obtained from a 0.05 mg Pt/cm^2 loaded anode. This data will be used as input to models that can predict the CO tolerance of these lower-loaded MEAs under various operating conditions. Furthermore, a drive cycle test will be performed in addition to these constant current holds to understand the effect of potential cycling on improving CO tolerance. Fuel cell test results for 0.143 mg Pt/cm^2 (total Pt loading) in the presence of 200 ppb CO showed 30 mV losses after 100 h of exposure, while the losses due to 4 ppb H_2S were approximately 19 mV for the same exposure time.

LANL has been conducting tests using a recirculating system over the past year, and this has been shown previously to enhance impurity losses compared to a single pass system. During this fiscal year, we continued this testing to evaluate the effect of the simultaneous presence of CO and H_2S. In one experiment, the MEA was pre-dosed with either 4 ppb or 10 ppb of H_2S for 5 min. During this pre-dosing step, there was no loss in performance. However, when 200 ppb of CO was then subsequently added, the losses were amplified significantly for the higher sulfur pre-dosed sample (red line versus green line in Figure 1). This data is consistent with the fact that the H_2S pre-dosing does poison some of the Pt surface sites in proportion to the total dosage of H_2S. Although this dosage is not sufficiently high to result in performance loss, these poisoned Pt sites remain poisoned during the CO portion of the test and result in the enhanced losses that are seen. These tests are indicative of the additive effects of impurities and show that small upsets in H_2 impurity concentration can accumulate over time and result in fuel cell losses.

In-line Analyzer

In FY 2017 we were able to design a prototype analyzer capable of detecting impurities in dry H_2. LANL has applied for a patent for this novel analyzer design. We also demonstrated a way to reproducibly return the analyzer to its

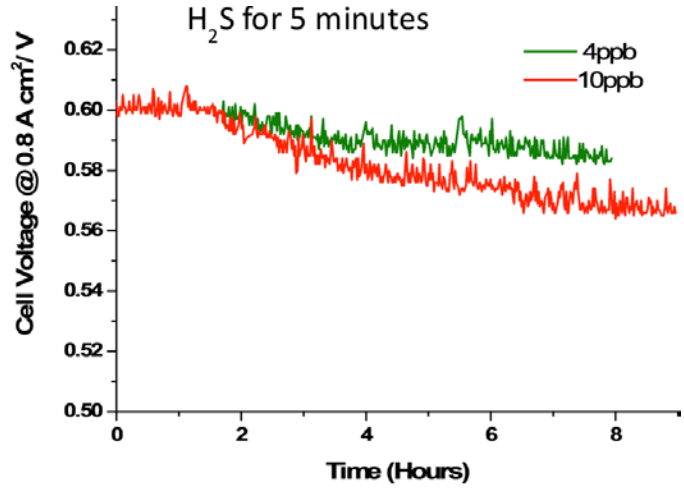

FIGURE 1. Effect of 200 ppb CO on fuel cells pre-dosed with either 4 ppb or 10 ppb H_2S for 5 min

baseline, and to improve the response characteristics in the presence of CO. We demonstrated that a 0.75 V, 10 min clean-up step resulted in almost complete recovery of the baseline current. However, the analyzer did require a long break-in period, which was thought to be the result of excessive ionomer content. Varying the ionomer content of the working electrode resulted in an improved analyzer response.

The analyzer had an electrode with 0.035 mg Pt/cm^2 sputtered onto a 30 AA gas diffusion layer with 2.3 mg of ionomer painted on top. While this dramatically increased the active area of Pt and helped improve the baseline current signal (3x improvement in baseline current over previous design without ionomer), the sensor was sluggish and the break-in time excessive (>1 wk). This is illustrated in Figure 2. We reduced the ionomer loading from 2.3 mg to 0.2 mg, an order of magnitude decrease, and kept the Pt loading nearly constant at 0.041 mg Pt/cm^2. This analyzer exhibited a very short break-in time; essentially on the order of a couple of hours were required to stabilize temperature and test with CO. The new analyzer with the lower ionomer content showed a stable baseline during the very first run, before any conditioning, and the exposure to high concentration of CO was the only conditioning performed. From the very second run, the analyzer showed sensitivity to even trace contaminants in base H_2. Longer-term tests are needed to quantify this baseline and develop a calibration curve that would quantify the dosage of CO that has gone through the analyzer. We also showed that the analyzer does not saturate even at 50 ppm CO and can be easily cleaned up with the application of 0.75 V. This is illustrated in Figure 3, where the impedance responses after clean-up are identical for all three CO exposures. The increase in the electrode resistance (the arc in the impedance data) is attributable to the CO poisoning and is proportional to the CO dosage.

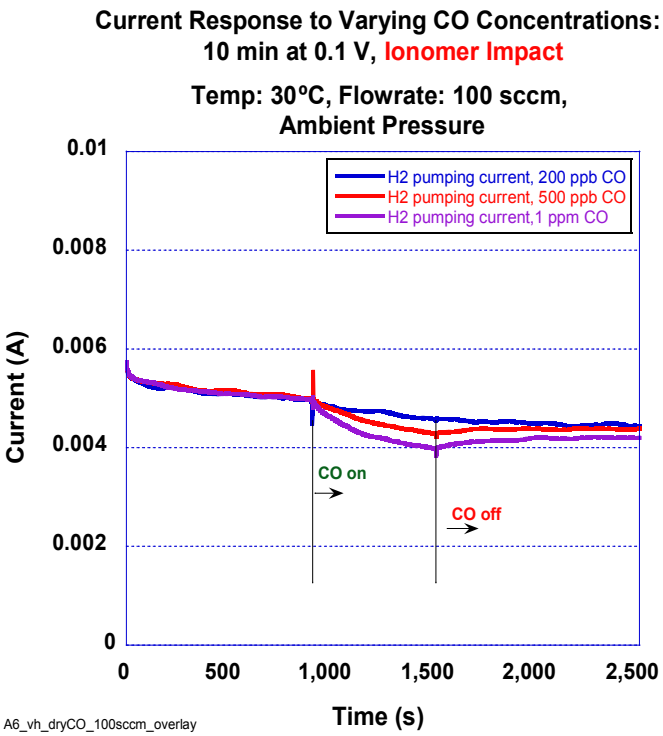

FIGURE 2. Current response to varying CO concentrations using analyzer (with membrane wicking system) in a dry gas stream

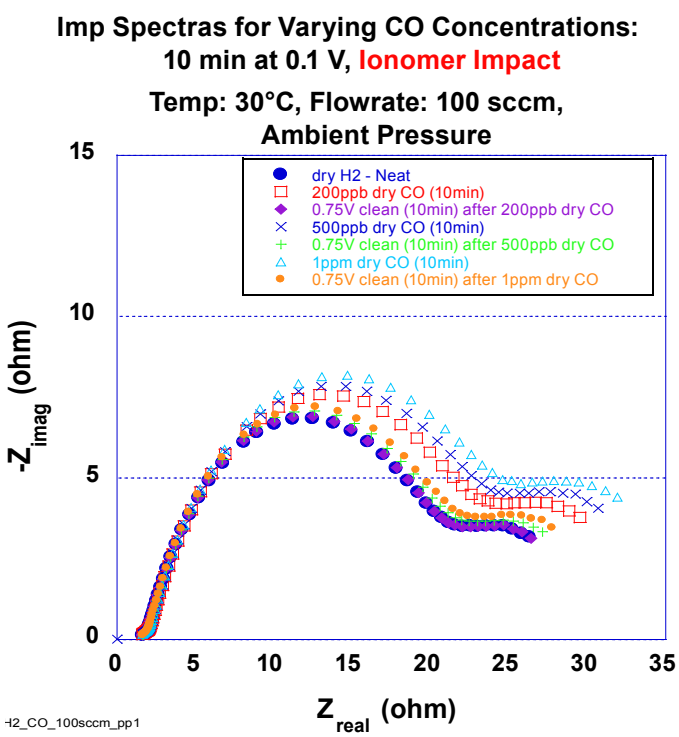

FIGURE 3. Impedance spectra for varying CO concentrations before and after applying 0.75 V for clean-up

CONCLUSIONS AND UPCOMING ACTIVITIES

In FY 2017, LANL has made significant progress in both focus areas: fuel quality and analyzer development. MEAs with the DOE 2015 target loadings (0.15 mg Pt/cm^2) were evaluated at various conditions in the presence of impurities at the SAE J2719 levels. Unlike the higher-loaded MEAs, the low-loaded MEAs are not tolerant to these levels of impurities and show performance losses. The exact amount of performance loss is dependent on the operating conditions and can vary from a few millivolts to hundreds of millivolts. A new fuel quality analyzer prototype was designed, constructed, and built. The analyzer was sensitive to approximately <200 ppb of CO and responded in <10 min. The analyzer baseline was reset by the application of 0.75 V, even after exposure to 250 times the allowable CO limit. LANL will evaluate this analyzer in the field in FY 2018 and use the learning to modify key components and parameters to advance the analyzer design to improve sensitivity, response time, and stability.

REFERENCES

1. Organization, I.S., *Hydrogen fuel — Product specification — Part 2: Proton exchange membrane (PEM) fuel cell applications for road vehicles*, in *ISO TC 197*2012, ISO copyright office: Case postale 56 • CH-1211 Geneva 20.

2. SAE J2719: Hydrogen Fuel Quality for Fuel Cell Vehicles, www.sae.org

VIII.4 R&D for Safety, Codes and Standards: Hydrogen Behavior

Ethan S. Hecht (Primary Contact), Pratikash Panda, Anthony McDaniel, Radoslav Bosinoski
Sandia National Laboratories
P.O. Box 969, MS 9052
Livermore, CA 94550
Phone: (925) 294-3741
Email: ehecht@sandia.gov

DOE Manager: Will James
Phone: (202) 287-6223
Email: Charles.James@ee.doe.gov

Project Start Date: October 1, 2003
Project End Date: Project continuation and direction determined annually by DOE

Overall Objectives

- Develop a science and engineering basis for the release, ignition, and combustion behavior of hydrogen across its range of use (including high pressure and cryogenic).
- Create models and engineering tools that enable the assessment of the safety (risk) of hydrogen systems, the revision of regulations, codes, and standards, and the permitting hydrogen fueling stations.

Fiscal Year (FY) 2017 Objectives

- Measure cryogenic hydrogen dispersion (hydrogen at <50 K) in lab-scale experiments with precise control of boundary conditions using high-fidelity imaging diagnostics. Use this data to validate the COLDPlume model for cryogenic hydrogen dispersion that will be used to provide scientific basis for safety distances for liquefied hydrogen systems.
- Design large-scale experiments to enable validated modeling of pooling and vaporization of liquid hydrogen.

Technical Barriers

This project addresses the following technical barriers from the Hydrogen Safety, Codes and Standards section of the Fuel Cell Technologies Office Multi-Year Research, Development, and Demonstration Plan.

(A) Safety Data and Information: Limited Access and Availability

(G) Insufficient Technical Data to Revise Standards

Contribution to Achievement of DOE Safety, Codes & Standards Milestones

This project will contribute to achievement of the following DOE milestones from the Hydrogen Safety Codes and Standards section of the Fuel Cell Technologies Office Multi-Year Research, Development, and Demonstration Plan.

- Milestone 2.13: Develop and validate simplified predictive engineering models of hydrogen dispersion and ignition. (4Q, 2015)
- Milestone 2.19: Validate inherently safe design for hydrogen fueling infrastructure. (4Q, 2019)
- Milestone 4.8: Revision of NFPA 2 to incorporate advanced fueling and storage systems and specific requirements for infrastructure elements such as garages and vehicle maintenance facilities. (3Q, 2016)

FY 2017 Accomplishments

- Developed a novel diagnostic to simultaneously measure cryogenic hydrogen concentration and mixture temperature in two dimensions, providing high-quality data for model validation.
- Measured the dispersion and warming characteristics for a range of hydrogen releases, including some with a source temperature below 50 K, extending the hydrogen dispersion validation data set to cryogenic sources.
- Initiated the validation process by comparing the concentration and temperature data to an existing model of cold hydrogen dispersion that will be used for risk assessment and to provide the scientific basis for risk-informed safety distances, with initial results showing reasonable agreement between the experimental results and the model simulations.

✧ ✧ ✧ ✧ ✧

INTRODUCTION

Fire codes govern the required distances between hydrogen sources (e.g., a liquid hydrogen tank at a fueling station) and hazards (e.g., ignition sources). Revisions to the fire code distances require justification, which is facilitated by models. These models must be validated with carefully controlled experiments, under relevant conditions, which can include high pressures (10,000 psi) or cryogenic temperatures (20 K). Over the course of this project, experiments have been designed and run to provide validation data for models. Models have been developed and exercised to inform the fire codes. This work has enabled quantitative risk assessments

of hydrogen systems, and subsequent reduction of setback distances from high pressure hydrogen sources. Currently, we are focusing on developing a scientific basis for modeling dispersion and flames from cryogenic (liquid) hydrogen sources. Validated models from this project will be exercised to provide a technical basis for the revision of fire codes related to liquid hydrogen.

APPROACH

The goals of this work are to develop and validate scientific models to accurately predict hazards and harm from unintentional hydrogen releases. In this project, we previously developed one-dimensional and engineering models of hydrogen dispersion and flames that can run quickly on a personal computer. While these models are one-dimensional, they include enough physics (e.g., the effect of buoyancy) to be accurate under a wide range of scenarios. These models are able to characterize the hazards from hydrogen releases and flames and are fast enough that they can be run multiple times and incorporated into a quantitative risk assessment framework. While the models we used to inform fire codes have been validated, carefully controlled experiments are required to validate and develop new models for cryogenic hydrogen to have an impact on liquid hydrogen separation distances. Advanced optical and laser diagnostics are used, along with more conventional diagnostics (e.g., thermocouples) to characterize the dispersion and flame properties of releases, at a lab scale. The temperature, pressure, and orifice of the unignited releases and flames are controlled while characteristics are measured (e.g., concentration, flame temperature, radiative heat flux).

RESULTS

The cryogenic hydrogen release laboratory was constructed and commissioned last fiscal year. This fiscal year, the laboratory was used to measure the concentration and temperature fields of a range of cryogenic hydrogen releases. We have performed a comparison of this data to a previously developed model for the dispersion of cryogenic hydrogen. We are planning to gather more data through the end of the fiscal year. By the end of the fiscal year, we will conclude the required development and validation of this model.

One accomplishment this fiscal year was developing and implementing the diagnostic that could be used to measure the concentration and temperature in two dimensions. Previous work in the laboratory with room temperature releases of hydrogen used planar laser Rayleigh scattering to measure the concentration of hydrogen. However, cryogenic hydrogen entrains humid air and the water vapor from the air condenses in the ultra-cold flow. The scattered light from the water vapor scatters light much more intensely than the Rayleigh scatter from the gas molecules, saturating the cameras and precluding this method as a diagnostic. After unsuccessful attempts to implement filtered Rayleigh scattering to reduce the light scattered off of the water vapor, we were successful at imaging planar laser Raman scattered light with the experimental setup shown in Figure 1. This technique takes advantage of the known large Raman wavelength shift of light scattered off of different gas molecules. In the laboratory setup, we measure Raman scattering off of both hydrogen and nitrogen. The 532-nm wavelength laser light is shifted to 607 nm when the light scatters off of nitrogen molecules, and 683 nm when it scatters off of hydrogen molecules. We use two scientific cameras, each with several bandpass filters and a notch filter at 532 nm to suppress the light by a factor of 18 at the laser wavelength (532 nm), and a factor of at least 12 for all wavelengths except for a 10-nm wide passband near the wavelength of interest (the passband for nitrogen is centered at 610 nm and the passband for hydrogen is centered at 685 nm). By simultaneously measuring light scattered off of nitrogen and hydrogen, we are able to determine the instantaneous mole fraction of hydrogen, mole fraction of nitrogen, and temperature in the two-dimensional plane of the laser sheet. Much like previous experiments in this laboratory, we keep the laser and cameras fixed and move the release point to gather statistics on how cryogenic hydrogen disperses and warms at different distances from the release point.

A model, known as ColdPLUME, that was developed at Sandia [1,2], has shown reasonable agreement with some limited centerline concentration measurements of hydrogen cooled to liquid nitrogen temperatures (80 K). ColdPLUME includes equations to describe accelerating flow through the leak, the expansion of an under-expanded jet, initial

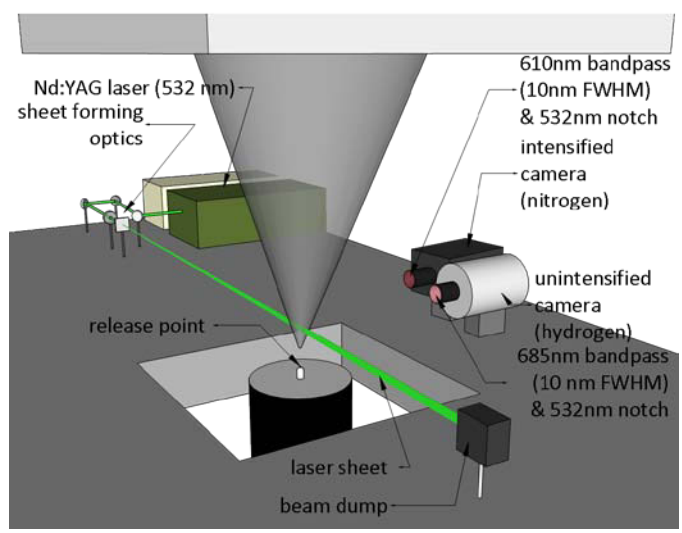

FIGURE 1. Diagnostic setup of experiment. A frequency doubled neodymium-doped yttrium aluminum garnet laser is formed into a sheet, and Raman signals at two specific wavelengths are collected simultaneously by two cameras.

entrainment and heating, establishment into a turbulent plume, followed by a one-dimensional set of ordinary differential equations that conserve mass, momentum and energy along the streamline of that turbulent plume. Although the model is one-dimensional along the streamline, buoyancy is taken into account, and the plume can rise or fall, depending on the density of the plume along the streamline relative to the surrounding air. The model relies on the assumption that within the established flow, the mean velocity and density profiles (looking radially) are Gaussian shaped, as has been shown previously for turbulent plumes. That these profiles are Gaussian for cryogenic hydrogen has been confirmed by the experiments performed this fiscal year. This can be seen in Figure 2, where the normalized distribution of mass fraction and temperature both align well with a Gaussian curve at all distances downstream. In addition to the experimental data points, Figure 2 shows two Gaussian distributions: a curve fit to the data by the thick red line, and the previously measured distribution of mass fraction of room temperature hydrogen and other gases by the thin black line [3,4]. The fit of the mass fraction data for this particular release is quite close to the literature fit for room temperature gases, although the fit to the data for all nine of the releases performed thus far of cryogenic hydrogen is a little further from this particular fit. This may be due to experimental noise, or could suggest that some of the empirical parameters in the model, such as the entrainment rate of air, may need to be modified for these cryogenic hydrogen releases as compared to room temperature hydrogen releases. The data also shows that the normalized temperature distribution is Gaussian, for which there is no literature data, due to the fact that previous measurements were all on room temperature releases and there was no variation in temperature across the plume. The temperature data is noisier than the mass fraction data, but the data suggests that the distribution is wider for temperature than for mass fraction.

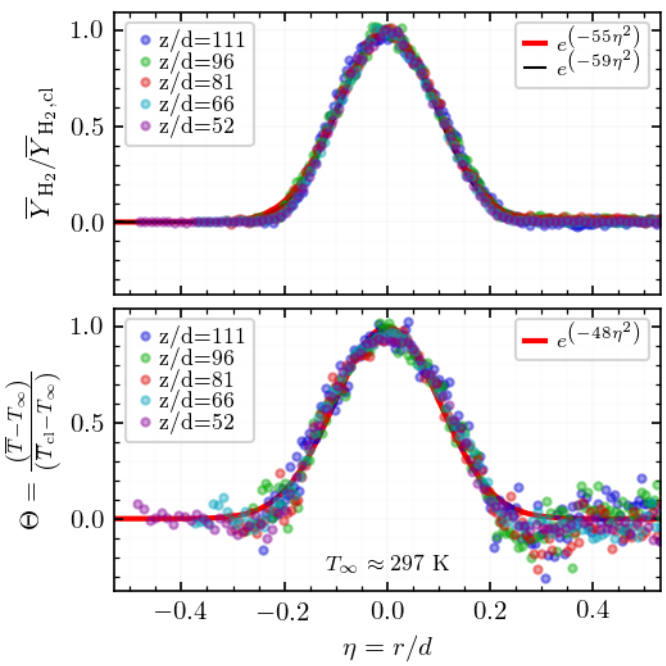

FIGURE 2. Radial mass fractions at selected distances, normalized by the centerline mass fraction (top) and radial temperatures at selected distances, normalized by the temperature excursion from the atmosphere (bottom). Data is shown by the points; the red line shows the fit to the data, and the black line shows the expected distribution for atmospheric temperature gases [3,4].

Figure 3 shows the mean mole fraction and temperature fields observed experimentally by the thick dashed lines and shading, and those predicted by ColdPLUME by the thin solid lines for one of the release experiments. The model is doing a good job of predicting the mole fraction contours for this data set. In terms of temperature, the model seems to be a bit further off, predicting cold temperatures along the centerline that penetrate further downstream than the data would suggest, although the data is noisier in this case. This figure demonstrates the amount of data generated by the planar laser Raman imaging—two-dimensional measurements of concentration and temperature—is ideal for validating a model that is generating two-dimensional predictions of concentration and temperature. This data is superior to sparse centerline measurements of concentration or temperature only. We extracted the centerline inverse mass fraction from our experiments and found that the decay rate scaled linearly with the normalized (by the effective diameter) distance from the release, and was quite close to the inverse mass fraction decay rate of room temperature hydrogen and other gases.

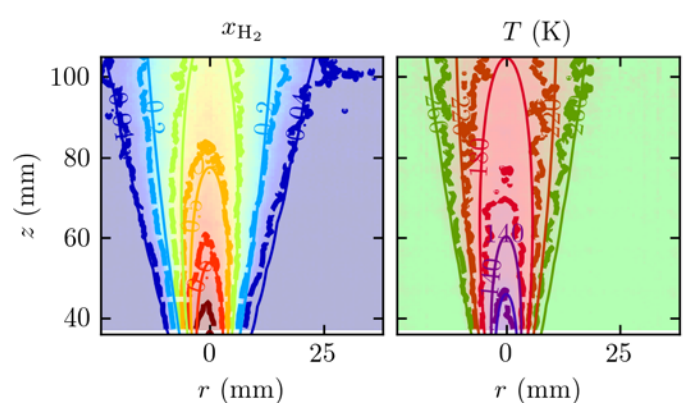

FIGURE 3. Comparison of the model predictions shown by the solid, thin lines, to the experimental data, shown by the thick, dashed lines and shading for mole fraction (left) and temperature (right).

CONCLUSIONS AND UPCOMING ACTIVITIES

We have successfully measured the concentration and temperature fields for a range of cryogenic hydrogen releases. This data is being compared to a previously developed model, which will be subsequently validated, or modified to be valid to predict the flow field of cryogenic hydrogen. Through the end of this fiscal year, we will be performing more experiments to increase the range of known model validity and conclude model development and validation activities.

Other fundamental aspects of liquid hydrogen releases, such as the pooling and evaporation from liquid hydrogen pools are poorly understood and modeling capabilities are limited or nonexistent. This fiscal year, we are also planning additional research and development looking at these aspects of liquid hydrogen. Developing a diagnostic that can be used on a larger release that would actually pool and evaporate is one thrust of the work this fiscal year. Developing the experimental platform on which to use the diagnostic will occur next fiscal year.

FY 2017 PUBLICATIONS/PRESENTATIONS

1. C. San Marchi, E.S. Hecht, I.W. Ekoto, K.M. Groth, C. LaFleur, B.P. Somerday, R. Mukundan, T. Rockward, J. Keller & C.W. James, "Overview of the DOE hydrogen safety, codes and standards program, part 3: Advances in Research and Development to Enhance the Scientific Basis for Hydrogen regulations, Codes and Standards," *International Journal of Hydrogen Energy* 42 (2017): 7263–7274.

2. K.M. Groth & E.S. Hecht, "HyRAM: A methodology and toolkit for Quantitative Risk Assessment of hydrogen systems," *International Journal of Hydrogen Energy* 42 (2017): 7485–7493.

3. P.P. Panda & E.S. Hecht, "Ignition and flame characteristics of cryogenic hydrogen releases," *International Journal of Hydrogen Energy* 62 (2017): 775–785.

4. E.S. Hecht & P. Panda. "Liquid Hydrogen Behavior Studies," Presented to the LH2 Separation Distance Technical Panel, June 2016, (SAND2016-6149 PE).

5. E.S. Hecht. "Cryogenic Hydrogen Plume Behavior," Prepared for the HySAFE Research Priorites Workshop, Petten, The Netherlands, September 2016, (SAND2016-9482 C).

6. E.S. Hecht. "Accidental Hydrogen Ignition," Prepared for the HySAFE Research Priorites Workshop, Petten, The Netherlands, September 2016, (SAND2016-9481 C).

7. E.S. Hecht. "Non-Premixed Hydrogen Combustion," Prepared for the HySAFE Research Priorites Workshop, Petten, The Netherlands, September 2016, (SAND2016-9480 C).

8. E.S. Hecht, P. Panda. "Validation data for cryogenic hydrogen releases and flames." Presented to the Hydrogen Codes and Standards Tech Team, October 2016, (SAND2016-10307 PE).

9. E.S. Hecht, P. Panda. "Validation data for cryogenic hydrogen releases and flames," Presented to the LH2 Separation Distance Stakeholders, November 2016, (SAND2016-11548 PE).

10. E.S. Hecht. "Validation data for cryogenic hydrogen releases and flames," Presented to the NFPA 2 task group, February 2017, SAND2017-2308 PE.

11. E.S. Hecht, P. Panda "Mixing and Warming of Cryogenic Hydrogen Releases," Accepted for the International Conference on Hydrogen Safety, Hamburg, Germany, September 2017. (SAND2017-7481 C).

REFERENCES

1. W.S. Winters and W.G. Houf, "Simulation of small-scale releases from liquid hydrogen storage systems," *International Journal of Hydrogen Energy* 36 (2011): 3913-3921.

2. W.G. Houf and W.S. Winters, "Simulation of high-pressure liquid hydrogen releases," *International Journal of Hydrogen Energy* 38 (2013): 8092–8099.

3. C.D. Richards, W.M. Pitts, "Global density effects on the self-preservation behavior of turbulent free jets," *Journal of Fluid Mechanics* 254 (1993): 417–435.

4. A.J. Ruggles, "Statistically advanced, self-similar, radial probability density functions of atmospheric and under-expanded hydrogen jets," *Experiments in Fluids* 56 (2015): 202.

VIII.5 Hydrogen Quantitative Risk Assessment

Alice Muna (Primary Contact), Ethan Hecht, John Reynolds (SAIC), Myra Blaylock, Chris LaFleur, Brian Ehrhart
Sandia National Laboratories (SNL)
P.O. Box 5800 MS 0849
Albuquerque, NM 87185
Phone: (505) 844-2580
Email: amuna@sandia.gov

DOE Manager: Will James
Phone: (202) 287-6223
Email: Charles.James@ee.doe.gov

Project Start Date: October 1, 2003
Project End Date: Project continuation and direction determined annually by DOE

Overall Objectives

- Develop algorithms, models, and data to enable industry-led codes and standards revisions to be based on a strong, traceable science and engineering basis.
- Develop hydrogen-specific quantitative risk assessment (QRA) and consequence models and methods to support regulations, codes, and standards decisions and to enable alternate means of code compliance, such as performance-based design.
- Develop the Hydrogen Risk Assessment Model (HyRAM) toolkit to provide a rigorous, documented basis for analyzing hydrogen infrastructure safety with QRA and consequence modeling.

Fiscal Year (FY) 2017 Objectives

- Review/update HyRAM to include overpressure, layer, gas plume models and Engineering Toolkit in version releasable to the public.
- Develop a research plan to address the next phase of the risk task that will include the intersection of materials research and QRA to address an industry barrier.

Technical Barriers

This project addresses the following technical barriers from the Hydrogen Safety, Codes, and Standards section of the Fuel Cell Technologies Office Multi-Year Research, Development, and Demonstration Plan.

(A) Safety Data and Information: Limited Access and Availability

(F) Enabling national and international markets requiring consistent RCS

(G) Insufficient technical data to revise standards

Contribution to Achievement of DOE Safety, Codes & Standards Milestones

This project will contribute to achievement of the following DOE milestones from the Safety, Codes, and Standards section of the Fuel Cell Technologies Office Multi-Year Research, Development, and Demonstration Plan.

- Milestone 2.4: Publish a methodology for estimating accident likelihood. (2Q, 2013)
- Milestone 2.8: Publish risk mitigation strategies. (2Q, 2014)
- Milestone 2.11: Publish a draft protocol for identifying potential failure modes and risk mitigation. (4Q, 2014)
- Milestone 2.13: Develop and validate simplified predictive engineering models of hydrogen dispersion and ignition. (4Q 2015)
- Milestone 2.19: Validate inherently safe design for hydrogen fueling infrastructure. (4Q, 2019)
- Milestone 4.7: Complete risk mitigation analysis for advanced transportation infrastructure systems. (1Q, 2015)
- Milestone 4.8: Revision of NFPA 2 to incorporate advanced fueling storage systems and specific requirements for infrastructure elements such as garages and vehicle maintenance facilities. (3Q, 2016)

FY 2017 Accomplishments

- Publically released the HyRAM 1.1 software for risk analysis of hydrogen infrastructure systems.
- Improved existing HyRAM capabilities to include reduced computing time, and fixed critical issues, in addition to quality assurance testing.
- Expanded HyRAM capabilities by adding new models, such as three-dimensional positioning for flame targets, improved flame model, updated heat flux radiation model, and a TNT Mass Equivalence calculator.
- Published a SAND Report which identifies and evaluates research areas in hydrogen materials where QRA could be used to address a barrier to the progress of the hydrogen fuel cell industry. The areas with the most promise were stress rupture of composite pressure vessel, polymer failure modes and mechanisms in high

pressure hydrogen, and initial crack distribution in metallic pressure vessels.

✧ ✧ ✧ ✧ ✧

INTRODUCTION

DOE has identified consistent safety, codes, and standards as a critical need for the deployment of hydrogen technologies, with key barriers related to the availability and implementation of technical information in the development of regulations, codes, and standards. Advances in codes and standards have been enabled by risk-informed approaches to create and implement revisions to codes, such as National Fire Protection Association (NFPA) 2, NFPA 55, and International Organization for Standardization (ISO) Technical Specification (TS)-19880-1. This project provides the technical basis for these revisions, enabling the assessment of the safety of hydrogen fuel cell systems and infrastructure using QRA and physics-based models of hydrogen behavior. The risk and behavior tools that are developed in this project are motivated by, shared directly with, and used by the committees revising relevant codes and standards, thus forming the scientific basis to ensure that code requirements are consistent, logical, and defensible.

APPROACH

This work leverages Sandia's unique experimental and modeling capabilities and combines these efforts with stakeholder engagement and international leadership. Sandia develops the algorithms and methods for performing QRA, including scenario development, likelihood and consequence analysis, and risk quantification. Sandia's Turbulent Combustion Laboratory develops and validates predictive engineering models for flame initiation, flame sustainment, radiative heat flux, and overpressures. The resulting QRA and hydrogen behavior models are integrated into the HyRAM toolkit to enable consistent, traceable, and rigorous risk and consequence assessment. HyRAM's hydrogen behavior and QRA models are then applied to relevant technologies and systems to provide insight into the risk level and risk mitigation strategies with the aim of enabling the deployment of fuel cell technologies through revision of hydrogen safety, codes, and standards.

RESULTS

HyRAM 1.1 Updates

Code committees and industry are both interested in using QRA and behavior modeling to enable code development and code compliance for hydrogen systems. Gaps and limited availability of data, models and tools relevant to hydrogen infrastructure systems form a barrier to this goal. This core research activity addresses this gap by developing and releasing HyRAM, an innovative software tool that integrates QRA and physical models of hydrogen behavior and consequences. HyRAM reduces industry burden and allows hydrogen safety experts to focus on obtaining safety insights rather than creating, validating, and documenting risk assessment algorithms and physical models.

The HyRAM package will enable installation designers and code and standards development organizations to conduct consequence modeling and QRA with state-of-the-art, validated science and engineering models. HyRAM formalizes the tools and methods which have been developed by Sandia through multiple Fuel Cell Technologies Office projects. HyRAM development began in FY 2014. In FY 2015 we issued a prototype HyRAM (V1.0alpha) to selected stakeholders with limitations on its use. During FY 2016 we revised the HyRAM copyright to make HyRAM 1.0 available for free download.

In February 2017, we released HyRAM 1.1 via http://hyram.sandia.gov, which reflects multiple new modules, significant testing and quality assurance activities. HyRAM 1.1 includes fixes to 10 major and several minor code defects as well as improved code readability and international compatibility. Issues with workspace load/save feature across versions, jet flame plot truncation and fonts issue, stability/proper execution issue in Engineering Toolkit, Windows 10 compatibility issue were also corrected. Features such as extended workspace save/load functionality, user-selectable Python language, 3-dimensional positioning input to H2-Flame input, improved flame model, updated XRad model, and TNT Mass Equivalence calculation were added. The updated version achieves a 67% reduction in computing time, with QRA mode now running in approximately 2.5 min with the curved flame model. We communicated the availability of HyRAM 1.1 to current users. Along with this release, we also published a revised SAND report documenting the algorithms of HyRAM 1.1.

We continue to see a steady number of downloads of HyRAM due to the many stakeholder interactions and external presentations. The comparison between October 2016 (first six months of HyRAM 1.0) and the second six months of HyRAM release is shown in Table 1. Users come from a wide range of stakeholder types, including multiple users from U.S. and international national labs, regulators, and universities, small businesses, and large multi-national gas suppliers, manufacturers, and consultants. In FY 2017 we added users from Greenlight Innovation (CA), Tongji University (CH), Telemark University and Safety & Risk Management Group (Denmark), VTT (FI), Ineris and Neodyme (FR), HPS Gmbh, Indian Oil R&D, Kawasaki Heavy Indsutries (JP), SynergenOG (Malaysia), KGS (KA), HNTB, Air Liquide, Hornblower, International Energy Association, National Renewable Energy Laboratory, Plug

Power, Pacific Northwest National Laboratory, and SNL (USA) and other users from Saudi Arabia and China. The increasing number of users provides evidence of direct value to the community.

TABLE 1. HyRAM Download and User Tracking Metrics

	March–October 2016	October 2016–March 2017
	HyRAM 1.0	HyRAM 1.1
Countries	20	20
Downloads	100 +	137
Licensed Users	55	77

During FY 2017, the commercialization of HyRAM was evaluated. It was concluded that the licensing of HyRAM 1.1 in its current form is limited and would not achieve the goal of generating sufficient funds to support maintenance and further development in the next FY. Currently, the fault trees feeding the QRA calculations in HyRAM are based on retail hydrogen refueling stations. Many of the users for whom this application is of interest already took advantage of the free download of HyRAM. However, HyRAM could be marketed to a broader customer base with the following two capabilities. First, the integration of risk software (targeting IRIS which was developed previously for the Federal Aviation Administration at University of Maryland) would enable the user to edit the fault trees so the QRA calculation can be adapted to a broader range of applications, including grid-scale applications. Initial efforts regarding the feasibility of integrating IRIS into HyRAM were explored in FY 2017. Second, adapting HyRAM to other alternate fuels, namely compressed natural gas and propane, would also increase the number of potential customers. This feature could be completed through a cooperative research and development agreement with South Korea researchers who have already been awarded funding for this effort.

QRA and Material Risk

Sandia possesses core capabilities in hydrogen research, including hydrogen QRA, hydrogen behavior, and hydrogen materials. These interrelated activities are enabled by a set of differentiating capabilities, including the HyRAM software tool for QRA and consequence modeling, and the Turbulent Combustion Laboratory, which enables lab-scale experiments into the behavior of hydrogen under a wide range of controlled conditions. The objective of this research is to capitalize on SNL's capabilities in hydrogen materials and QRA to address a barrier to the progress of the hydrogen fuel cell industry. In particular, this research plans to quantify the risk of materials for pressure vessel failure and identify a path forward to characterizing the calculation of this risk. This research will provide a better understanding of pressure vessel failure to cylinder manufacturers, the hydrogen fuel cell safety community and other applications.

Hydrogen storage technologies are a key part of hydrogen infrastructure for transportation and have implications for large scale problems. A key scientific question is determining how to account for material properties with a QRA framework. Sandia has developed a framework for predicting overall risk of the system from knowledge of reliability of various components such as storage tanks. However, we have little data to predict reliability of components, such as composite storage vessels. Without data it is necessary to use knowledge of material properties, defects, and design elements to predict the reliability and risk. There is currently little understanding of how the distribution of defects affects the ultimate performance of components, like storage tanks.

Progress was made on the new tasking focused on developing a vision for leveraging the fundamental research of SNL's core competencies in QRA and materials science to identify and address a barrier, such as pressure vessel reliability. Multiple issues were identified where materials research could potentially benefit from QRA. Each of these issues were researched further and documented into a SAND report. The SAND report will be completed in FY 2017 and includes a suggested path forward for future research activities in materials risk.

CONCLUSIONS AND UPCOMING ACTIVITIES

The HyRAM toolkit provides a platform with state-of-the-art hydrogen models for assessing the risk of hydrogen systems and the consequences of hydrogen releases and fires, to enable industry-led analyses. However, additional challenges remain within codes and standards, including the development of defensible separation distances for liquid hydrogen stations and need for additional data for QRA. We plan to add modules for consequence modeling, including the ability to calculate the physical effects of liquid hydrogen releases, cold plumes, and subsequent ignitions, pending the results from SNL's liquid hydrogen experiments and modeling. Existing HyRAM models (e.g., the gas plume model) will be kept current as scientific consensus changes. We plan to expand the capabilities of the QRA algorithm to support modeling of additional scenarios as well as features to enable more detailed insight into system reliability.

Applying QRA concepts to pressure vessel reliability analysis can ideally create a framework that can be broadened beyond cylinders. Similarly, using these approaches will create new pressure vessel data that can be used within a QRA framework as part of system-level safety assessment. Addressing the root causes of hydrogen release will impact every application of hydrogen as an energy solution. Any system that uses hydrogen, from large grid scale application such as those proposed in H2@Scale to an individual hydrogen vehicle refueling station require hydrogen storage

of various sizes. Our work in determining how to account for material properties within a QRA framework will provide a better understanding of pressure vessel failure and support the hydrogen fuel cell safety community.

FY 2017 PUBLICATIONS/PRESENTATIONS

1. Software: HyRAM 1.1. Issued February 2017. Software available at http://hyram.sandia.gov.

2. K.M. Groth, E.S. Hecht, J.T. Reynolds, M.L. Blaylock, E.E. Carrier. Methodology for assessing the safety of Hydrogen Systems: HyRAM 1.1 technical reference manual. SAND2017-2998.

3. K. Groth. "SCS011: Hydrogen Quantitative Risk Assessment" at DOE FCTO Hydrogen Program Annual Merit Review, Washington DC, June 6, 2017.

4. K. Groth. "Hydrogen QRA & HyRAM: 2016 in review." US DRIVE H2 Codes & Standards Tech Team Meeting, October 13, 2016.

5. K. Groth (invited presentation). "Enabling hydrogen safety, codes, and standards through Quantitative Risk Assessment." George Mason University Physics Colloquium, Fairfax, VA, November 4, 2016.

6. K. Groth. "Hydrogen QRA & HyRAM: Status and next directions." Presented at the IEA HIA Hydrogen Safety Task 37 Meeting, Bethesda, MD, November 28, 2016.

7. K. Groth (invited panelist). "Managing safety risk in new energy technologies." Reliability & Maintainability Symposium (RAMS) in Orlando, FL. January 24, 2017. SAND2017-0260 C.

VIII.6 Hydrogen Safety Panel, Safety Knowledge Tools and First Responder Training Resources

Nick Barilo
Pacific Northwest National Laboratory (PNNL)
P.O. Box 999
Richland, WA 99352
Phone: (509) 371-7894
Email: nick.barilo@pnnl.gov

DOE Manager: Laura Hill
Phone: (202) 586-8384
Email: Laura.Hill@ee.doe.gov

Subcontractors:
- Eric Binder, Santa Monica Fire Department, Santa Monica, CA
- Ken Boyce, UL, Northbrook, IL
- David J. Farese, Air Products and Chemicals, Inc., Allentown, PA
- Don Frikken, Becht Engineering, St. Louis, MO
- Livio Gambone, CSA Group, Langley, BC, Canada
- Richard A. Kallman, City of Santa Fe Springs, CA
- Larry Moulthrop, Proton OnSite, Wallingford, CT
- Glenn W. Scheffler, GWS Solutions of Tolland, LLC, Tolland, CT
- Tom Witte, Witte Engineered Gases, Seminole, FL
- Robert G. Zalosh, Firexplo, Wellesley, MA

Project Start Date: 2004
Project End Date: Project continuation and direction determined annually by DOE

Overall Objectives

- Enable the safe and timely transition to hydrogen and fuel cell technologies.
- Provide expertise and recommendations to help identify safety-related technical data gaps, best practices, and lessons learned.
- Help integrate safety planning into funded projects to ensure that projects address and incorporate hydrogen safety practices.
- Collect information and share lessons learned from hydrogen incidents and near misses to help prevent similar safety events in the future.
- Capture vast and growing knowledge base of hydrogen experience and make it publicly available to the hydrogen community and stakeholders.
- Support implementation of hydrogen and fuel cell technologies by providing technically accurate hydrogen safety and emergency response information to first responders.

Fiscal Year (FY) 2017 Objectives

- Complete a third party hydrogen certification guide to facilitate timely project permitting and approval by code officials.
- Meet with code officials, project proponents, and stakeholders from recently completed fuel station projects to discuss and document safety learnings and needs.
- Provide classroom training for first responders at a minimum of three locations in the Northeast U.S. to support the deployment of fueling stations and rollout of fuel cell electric vehicles.
- Participate in outreach events on hydrogen safety aimed at a variety of stakeholder groups to emphasize available tools and resources.

Technical Barriers

This project addresses the following technical barriers from the DOE Fuel Cell Technologies Office (FCTO) Multi-Year Research, Development and Demonstration Plan [1].

Safety, Codes and Standards

(A) Safety Data and Information: Limited Access and Availability

(C) Safety is Not Always Treated as a Continuous Process

(D) Lack of Hydrogen Knowledge by AHJs

(E) Lack of Hydrogen Training Materials and Facilities for Emergency Responders

(F) Insufficient Technical Data to Revise Standards

Education and Outreach

(A) Lack of Readily Available, Objective, and Technically Accurate Information

(D) Lack of Educated Trainers and Training Opportunities

Contribution to Achievement of DOE Milestones

This project contributes to achievement of the following DOE tasks and milestones from the FCTO Multi-Year Research, Development, and Demonstration Plan:

Safety, Codes, and Standards

- Task 1: Address Safety of DOE R&D Projects (ongoing)
- Task 5: Dissemination of Data, Safety Knowledge, and Information (ongoing)
- Milestone 5.1: Update safety bibliography and incidents databases. (4Q, 2011 – 2020)

Education and Outreach

- Task 1: Educate Safety and Code Officials (ongoing)
- Milestone 1.1: Update "Introduction to Hydrogen Safety for First Responders" Course for First Responders. (Biannually)

FY 2017 Accomplishments

- Conducted 33 project reviews (including safety plans and project designs) from July 15, 2016 to July 1, 2017.
- Evaluated 12 applicant safety plans in support of the California Energy Commission (CEC) general funding opportunity for new light-duty vehicle hydrogen fueling stations.
- Provided four first responder training classes at three locations in the Northeast United States, November 6–10, 2016, with approximately 250 attendees.
- Held the 23rd Hydrogen Safety Panel (HSP) meeting in Washington, D.C., November 15–17, 2016, enabling consideration of timely and relevant safety issues and the engagement of key hydrogen infrastructure stakeholders.
- Published the completed Hydrogen Equipment Certification Guide for public download in January 2017.
- Expanded available resources on the Hydrogen Tools Portal (http://h2tools.org), adding the Hydrogen Analysis Resource Center and presentations and papers from the International Conference on Hydrogen Safety (ICHS).
- Provided outreach and educational sessions for a variety of audiences including the National Fire Protection Association, Boston Tunnel Authorities, and Hydrogen South Africa.

INTRODUCTION

Safety is essential for realizing the "hydrogen economy," safe operation in all of its aspects from hydrogen production through storage, distribution, and use; from research, development, and demonstration to deployment and commercialization. As such, safety is given paramount importance in all facets of the research, development, demonstration, and deployment work of the DOE FCTO. This annual report summarizes activities associated with three project tasks: the HSP, Safety Knowledge Tools, and First Responder Training Resources.

Recognizing the nature of the DOE FCTO program and the importance of safety planning, the HSP was formed in December 2003 to assemble a broad cross-section of expertise from the industrial, government, and academic sectors to help ensure the success of the program as a whole. The panel's experience resides in industrial hydrogen production and supply, hydrogen research and development and applications, process safety and engineering, materials technology, risk analysis, accident investigation, and fire protection. The panel provides expertise and recommendations on safety-related issues and technical data gaps, reviews individual hydrogen projects and their safety plans, and explores ways to develop and disseminate best practices and lessons learned, all broadly benefiting industry and the FCTO program. The panel currently has 15 members with a total of over 400 years of industry and related experience (see Table 1 for FY 2017 panel membership).

TABLE 1. Current Hydrogen Safety Panel Membership

Nick Barilo, Program Manager	PNNL
Richard Kallman, Chair	City of Santa Fe Springs, CA
Eric Binder*	Santa Monica Fire Department
Ken Boyce*	UL
David Farese	Air Products and Chemicals
Don Frikken	Becht Engineering
Livio Gambone	CSA Group
Aaron Harris	Air Liquide
Chris LaFleur	Sandia National Laboratories
Miguel Maes	NASA White Sands Test Facility
Steve Mathison	Honda Motor Company
Larry Moulthrop	Proton OnSite
Glenn Scheffler	GWS Solutions of Tolland, LLC
Tom Witte	Witte Engineered Gases
Robert Zalosh	Firexplo

* New panel members

Widespread availability and communication of safety-related information are crucial to ensuring the safe operation of future hydrogen and fuel cell technology systems. The entire hydrogen community benefits if hydrogen-safety-related knowledge is openly and broadly shared. To that end, PNNL continues to improve the safety knowledge software tools and develop new techniques for disseminating this information. This report covers the Hydrogen Tools Portal (http://h2tools.org), the Hydrogen Lessons Learned database (http://h2tools.org/lessons/), and the Hydrogen Safety Best Practices online manual (https://h2tools.org/bestpractices). These resources are key to reaching, informing, and educating users and stakeholders whose contributions will help enable the deployment of new hydrogen and fuel cell technologies.

Suitably trained emergency response personnel are essential to a viable infrastructure. The FCTO has placed a priority on training emergency response personnel, not only because these personnel need to understand how to respond to a hydrogen incident, but also because firefighters and other emergency responders are influential in their communities and can be a positive force in the introduction of hydrogen and fuel cells into local markets. This report covers hazardous materials emergency response training to provide a tiered hydrogen safety education program for emergency responders. The effort started with development and distribution of the awareness-level online course in FY 2006–2007. An operations-level classroom curriculum was developed in FY 2008–2009, including design, construction, and operation of a fuel cell vehicle prop for hands-on training. PNNL and the California Fuel Cell Partnership (CaFCP) collaborated to develop a national hydrogen safety training resource for emergency responders, which was made publicly available in September 2014.

APPROACH

The HSP strives to raise safety consciousness most directly at the project level through organizational policies and procedures, safety culture, and priorities. Project safety plans and design documents are reviewed to encourage thorough and continuous attention to safety aspects of the specific work being conducted. Panel safety reviews focus on engagement, learning, knowledge sharing, and active discussion of safety practices and lessons learned, rather than performing audits or regulatory exercises. Through this approach, the HSP is trying to achieve safe operation, handling, and use of hydrogen and hydrogen systems for all projects.

The approach for disseminating safety knowledge in FY 2017 focused on adding resources to the existing Hydrogen Tools Portal and participating in impactful outreach activities. The portal brings together and enhances the utility of a variety of tools and web-based content on the safety aspects of hydrogen and fuel cell technologies. It is intended to help inform those tasked with designing, approving, or using systems and facilities, as well as those responding to incidents. Additional discussion is provided in the Results section of this report.

PNNL collaborates with subject matter experts in hydrogen safety and first responder training to develop, review, and revise training materials as needed. The PNNL project team works with DOE to inform stakeholder groups of training opportunities and to provide live training when appropriate. The online awareness-level course provides the student with a basic understanding of hydrogen properties, uses, and appropriate emergency response actions. The operations-level classroom and hands-on prop-based course has been presented at the Volpentest Hazardous Material Management and Materials Response Federal Training Center in Richland, Washington, and at several fire training centers in California, Hawaii, and the Northeastern United States to reach larger audiences in areas where hydrogen and fuel cell technologies are being deployed. The National Hydrogen and Fuel Cell Emergency Response Training Resource provides a consistent source of accurate information and current knowledge to ensure that training organizations have the information needed to develop or supplement their own courses. As part of this resource, a training template has been developed to guide the delivery of a variety of training regimens to various audiences.

RESULTS

The 23rd HSP meeting was held in Washington, D.C., November 15–17, 2016. The meeting provided opportunities to consider timely and relevant safety issues and provide direct input to the FCTO. The topics discussed and outcomes achieved at the meeting are detailed in the meeting minutes [2]. Significant activities during the panel meeting included interaction with representatives from the Department of Transportation on hydrogen safety issues associated with vehicles and tank testing, and a panel review of a Department of Defense project.

During the past year, the HSP has provided safety reviews and support to the 31 projects identified in Table 2. Since 2004, the panel has participated in 474 project reviews (including safety plans, site visit reviews, follow-up phone interviews, and design review work). In addition to reviewing safety plans for DOE, the HSP provided crucial support to the CEC in support of the California general funding opportunity for fueling stations through formal evaluation of applicant safety plans. The feedback provided by the HSP assisted the CEC in evaluating applicants and determining awardees. Future support will be provided in the form of a site visit and teleconferences with awardees to ensure that the final station configurations have addressed the necessary safety considerations. The HSP is also contracted to provide expertise to the CEC should a hydrogen incident occur.

TABLE 2. HSP Project Safety Work July 15, 2016 to July 1, 2017

Work	Project Title	Contractor
Safety Plan Review	High Performance PEFC Electrode Structures	UTRC
Safety Plan Review	Advancing Hydrogen Dispenser Technology by Using Innovative Intelligent Networks	Ivys, Inc.
Safety Plan Review	Modular SOEC System for Efficient H2 Production at High Current Density	FuelCell Energy
Safety Plan Review	High Temperature Alkaline Water Electrolysis	Giner, Inc.
Safety Plan Review	Solid Oxide Based Electrolysis and Stack Technology with Ultra-High Electrolysis Current Density (>3 A/cm2) and Efficiency	FuelCell Energy
Safety Plan Review	Hybrid Electrochemical Hydrogen/Metal Hydride Compressor	Greenway Energy, LLC
Safety Plan Review	Novel Ionomers and Electrode Structures for Improved PEMFC Electrode Performance at Low PGM Loadings	3M
Safety Plan Review	Integrated Insulation System for Cryogenic Automotive Tanks (iCAT)	Vencore Services and Solutions, Inc.
Safety Plan Review	Metal Hydride Compressor for High Pressure Hydrogen Delivery	HHC
Safety Plan Review	Advanced Electrochemical Hydrogen Compressor	Giner, Inc.
Safety Plan Review	Development of Magnesium Boride Etherates as Hydrogen Storage Materials	University of Hawaii
Safety Plan Review	Multi-Scale Ordered Cell Structure for Cost Effective Production of Hydrogen by HTWS	Ceramatec
Design Review	Advanced Hydrogen Mobile Fueler	Electricore, Inc.
Design Review	Fuel Cell Hybrid Electric Delivery Van	Center for Transportation and the Environment
Safety Plan Review	CHEF HAZOP/Safety Plan	Washington State University
Safety Plan Review	Light Duty Hydrogen Vehicle Fueling Station	CEC/Everfuel
Safety Plan Review	Light Duty Hydrogen Vehicle Fueling Station	CEC/Shell
Safety Plan Review	Light Duty Hydrogen Vehicle Fueling Station	CEC/ITM Power (#4)
Safety Plan Review	Light Duty Hydrogen Vehicle Fueling Station	CEC/ITM Power (#5)
Safety Plan Review	Light Duty Hydrogen Vehicle Fueling Station	CEC/Jensen-Linde
Safety Plan Review	Light Duty Hydrogen Vehicle Fueling Station	CEC/Hydrogen-XT
Safety Plan Review	Light Duty Hydrogen Vehicle Fueling Station	CEC/Air Liquide
Safety Plan Review	Light Duty Hydrogen Vehicle Fueling Station	CEC/FirstElement
Safety Plan Review	Light Duty Hydrogen Vehicle Fueling Station	CEC/HTEC
Safety Plan Review	Light Duty Hydrogen Vehicle Fueling Station	CEC/Air Products
Safety Plan Review	Light Duty Hydrogen Vehicle Fueling Station	CEC/A3L-Next Hydrogen
Safety Plan Review	Light Duty Hydrogen Vehicle Fueling Station	CEC/StratosFuel
Safety Plan Review	Highly Active, Durable, and Ultra-Low PGM NSTF Thin Film ORR Catalysts and Supports	3M
Site Visit	H-Prize	Ivys, McPhy and PDC
Site Visit	Hydrogen Incident Fact Finding - Simple.Fuel	Washington State University
Safety Plan Review	Linear Motor Reciprocating Compressor (LMRC) for Forecourt Hydrogen Compression (Updated Safety Plan)	Southwest Research Institute

PEFC – proton exchange fuel cell; SOEC – solid oxide fuel cell; PEMFC – proton exchange membrane fuel cell; PGM – precious group metal

In March 2017, members of the HSP met with code officials, project proponents, and stakeholders from recently completed hydrogen fueling station projects to discuss participant experiences and what has been learned from these activities. This activity, combined with the HSP's review of previously mentioned general funding opportunity safety plan reviews, provided a unique opportunity to consider safety learnings from early light duty hydrogen fueling infrastructure deployments. Feedback from the meetings was captured, analyzed, and categorized, and the resulting items were further evaluated and ranked by HSP members. The results of this activity were presented to industry stakeholders at the CaFCP working group meeting in June 2017. Additional presentations of the HSP learnings are expected to be shared at the ICHS in Hamburg, Germany, in September 2017, and the Fuel Cell Seminar and Energy Exposition in Long Beach, CA, in November 2017. It is hoped that this information will be beneficial to:

- DOE and stakeholders, in planning and funding impactful research activities focused on new innovative approaches to station implementation.
- Code development organizations, in further considering storage system configuration and its safety, including separation distance requirements.
- Station providers, in considering and implementing safe and cost-effective design features.
- First responder training organizations, to ensure that first responders are prepared to respond appropriately to vehicle and station incidents.

A significant HSP accomplishment during FY 2017 was the public release of the completed Hydrogen Equipment Certification Guide. The purpose of the guide is to enable designers, users, and code officials to better apply the requirements in cases where the use of listed, labeled, certified, or approved equipment or methods are required, and to increase awareness and understanding of what the equipment is expected to do. The challenge with equipment certification is that the listing process for rapidly changing products, consistent with developing technologies, tends to be cost-prohibitive for equipment providers (each change to the equipment requires recertification). The circumstance of new technologies under development and low demand for early market applications results in few components and systems being currently listed. The scarcity of listed equipment places an extraordinary burden on code officials to ensure (and approve) that products include the appropriate inherent or automatic safety measures. The guide identified listing requirements in the International Code Council codes and National Fire Protection Association 2 (Hydrogen Technologies Code) for hydrogen equipment, and suggests criteria for approval when listed equipment is not available.

The Hydrogen Tools Portal was made publicly available in June 2015 and continues to grow in popularity. Based on current Google Analytics, the portal is becoming an international resource, as approximately half of all user sessions are from outside of the United States. Additional resources added to the portal in FY 2017 included the Hydrogen Analysis Resource Center – data, calculators and analytical tools for use in evaluating hydrogen-related technologies; and papers and presentations from all ICHS events, including all six conferences from 2005–2015 and 633 presentations. HSP reports from the aforementioned CEC safety plan reviews have also been added to the portal for public dissemination.

Disseminating safety information continues to be an important aspect of this project. FY 2017 activities focused on two areas: reaching new audiences and supporting efforts to remove barriers to deployment. For the former, PNNL presented at the National Fire Protection Association Conference and Expo in Boston, Massachusetts, in June 2017. The event was attended by a national and international audience of designers, consultants, contractors, service companies, end-users, and public safety authorities. PNNL also participated in outreach to personnel that construct, operate, and maintain energy-efficient and cost-effective federal facilities and fleets in the United States. Working with the Federal Energy Management Program, PNNL participated in an outreach at the 2017 Energy Exchange Training and Trade Show in Tampa, Florida, in August 2017. The 90-minute presentation on fuel cell technologies was professionally recorded and produced into training material that can be deployed on Federal Energy Management Program's website and the Hydrogen Tools Portal.

PNNL assisted in removing barriers to technology deployment by participating in outreach events and discussions with stakeholders in Boston, Massachusetts, and Baltimore, Maryland. Presentations made at these events help addressed safety concerns and identify future activities to address allowing fuel cell vehicles to travel through tunnels.

PNNL's leadership in hydrogen safety is reinforced through its international collaborations. PNNL worked with Hydrogen South Africa, the International Association for Hydrogen Safety, and the United Kingdom's Health and Safety Laboratory to provide an online hydrogen safety awareness webinar/panel discussion for code officials and stakeholders in South Africa in October 2016. PNNL also presented on hydrogen safety to Korean and Japanese Delegations in January 2017.

First responder outreach activities for FY 2017 focused on classroom training conducted in Hempstead, New York, Stow, Massachusetts, and Hartford, Connecticut, November 6–10, 2016. More than 250 people attended the training sessions. The events provided an opportunity to reevaluate material contained in the National Hydrogen and Fuel Cell Emergency Response Training Resource (https://h2tools.org/fr/nt) (referred to as "national template") in support of future updates. Additionally, PNNL purchased virtual

reality software to enhance the national template focusing on more impactful information through new video, slides, and scenario development (see Figure 1 for an example). It is anticipated that new material will be incorporated in late FY 2017 or early FY 2018.

CONCLUSIONS AND UPCOMING ACTIVITIES

The HSP will continue to focus on how safety knowledge, best practices, and lessons learned can promote the safe conduct of project work and the deployment of hydrogen technologies and systems in applications of interest and priority in the DOE FCTO. The HSP can also be used more broadly as an asset for safe commercialization by reaching out to new stakeholders and users involved in early deployment, as shown by the success of activities in California.

HSP initiatives over the next year will include the following:

- Continue to support the CEC's rollout of California's hydrogen fueling station infrastructure.
- Engage non-DOE entities to identify opportunities to use the panel to review hydrogen and fuel cell initiatives and promote safety.
- Continue to evaluate the panel membership to maintain its leadership role in hydrogen safety through an appropriate mix of safety expertise and perspective to perform safety reviews and address relevant issues.

Hydrogen safety knowledge tools help remove barriers to the deployment and commercialization of hydrogen and fuel cell technologies. The introduction of the Hydrogen Tools Portal opens opportunities for sharing new information and reaching broader audiences. Based on the president's budget request and direction toward early stage research and development, the primary focus in FY 2018 will be to maintain the portal in an operating state with minimal change.

The project's First Responder Training Resources can help ensure a safe transition to fuel cell vehicles and a hydrogen infrastructure, and pave the way for broader public acceptance. Based on the president's budget request and direction toward early stage research and development, only minor changes to the available training resources and support of industry led first responder training are anticipated in FY 2018.

REFERENCES

1. U.S. Department of Energy, "Fuel Cell Technologies Office Multi-Year Research, Development, and Demonstration Plan," http://energy.gov/eere/fuelcells/downloads/fuel-cell-technologies-office-multi-year-research-development-and-22.

2. Barilo, N.F. to Farese, D. et al., "Minutes from the 23rd Hydrogen Safety Panel Meeting," January 23, 2017.

FY 2017 PUBLICATIONS/PRESENTATIONS

1. Barilo N.F. 2017. "Learnings from Hydrogen Fueling Station Projects." Presented by Nick F. Barilo at California Fuel Cell Partnership (CaFCP) In-Person Working Group Meeting, Sacramento, CA, on June 21, 2017. PNNL-SA-127046.

2. Barilo N.F. 2017. "Hydrogen Safety Panel, Safety Knowledge Tools and First Responder Training Resources." Presented by Nick F. Barilo at 2017 DOE Hydrogen Program Annual Merit Review and Peer Evaluation Meeting, Washington, D.C., on June 6, 2017. PNNL-SA-125384.

3. Barilo, N.F, "Hydrogen and Fuel Cells -- Emerging Technology and Safety-Related Issues," NFPA Conference & Expo, Boston, MA, June 5, 2017.

Barilo N.F. 2017. "Hydrogen Safety Panel Strategic Plan?" Presented at Hydrogen Technical Advisory Committee meeting, Washington, D.C., on May 5, 2017. PNNL-SA-125602.

Barilo N.F., "Hydrogen Equipment Certification Guide Listing, Labeling and Approval Considerations." Pacific Northwest National Laboratory, Richland, WA. PNNL-25053, January 2017.

FIGURE 1. Examples of virtual reality software use for first responder training resources

VIII.7 NREL Hydrogen Sensor Testing Laboratory

William Buttner (Primary Contact), Carl Rivkin, Robert Burgess
National Renewable Energy Laboratory
15013 Denver West Parkway
Golden, CO 80401
Phone: (303) 275-3903
Email: Willaim.Buttner@nrel.gov

DOE Manager: Will James
Phone: (202) 287-6223
Email: Charles.James@ee.doe.gov

Subcontractors:
- Element One, Boulder, CO
- Bloomfield Automation, Denver, CO
- A.V. Tchouvelev & Associates, Inc. (AVT), Mississauga, ON, Canada

Project Start Date: October 1, 2010
Project End Date: Project continuation and direction determined annually by DOE

Overall Objectives

- Support the safe implementation of hydrogen as an alternative fuel by assuring the availability of gas detection technology.
- Quantify performance of commercial hydrogen sensors relative to DOE metrics.
- Support development and assess performance of advanced sensor technologies.
- Support development and updating of hydrogen sensor codes and standards.
- Support infrastructure and vehicle deployment by providing expert guidance on the use of hydrogen sensors and analyzers.
- Educate the hydrogen community on the proper use of hydrogen sensors.

Fiscal Year (FY) 2017 Objectives

- Support infrastructure deployment by providing sensor testing capability and guidance to stakeholders in the hydrogen energy field.
- Quantify performance metrics of commercial and developmental sensor technologies from both the private sector and government laboratories.
- Validate hydrogen safety sensors for specific infrastructure and vehicle applications.
- Support Department of Transportation (DOT) National Highway Transportation Safety Administration on the development of the Federal Motor Vehicle Safety Standard (FMVSS) for hydrogen fuel cell electric vehicles (FCEVs), especially with regards to hydrogen detection requirements identified in the Global Technical Regulation (GTR) 13 [1].
- Facilitate safe deployment of FCEVs by participation on SAE Fuel Cell Standards committees, and to lead the development of the SAE Technical Information Report J3089 "Characterization of On-board Vehicular Hydrogen Sensors."
- Support the science of hydrogen safety by integrated theoretical-empirical profiling of hydrogen releases (indoor and outdoor).
- Support hydrogen safety code and standard development by active participation with standard and code development organizations.
- Support the deployment and implementation of hydrogen sensors and monitoring technology for safety and fuel quality.

Technical Barriers

This project addresses the following technical barriers identified in the Hydrogen Safety, Codes and Standards section of the Fuel Cell Technologies Office Multi-Year Research, Development, and Demonstration Plan.

(A) Safety Data and Information: Limited Access and Availability

(C) Safety is Not Always Treated as a Continuous Process

(D) Lack of Hydrogen Knowledge by AHJs

(F) Enabling National and International Markets Requires Consistent RCS

(G) Insufficient Technical Data to Revise Standards

(H) Insufficient Synchronization of National Codes and Standards

(K) No Consistent Codification Plan and Process for Synchronization of R&D and Code Development

Contribution to Achievement of DOE Safety, Codes & Standards Milestones

This project will contribute to the achievement of the following DOE milestones from the Hydrogen Safety, Codes and Standards section of the Fuel Cell Technologies Office Multi-Year Research, Development, and Demonstration Plan.

- Milestone 2.15: Develop holistic design strategies. (4Q, 2017)
- Milestone 2.19: Validate inherently safe design for hydrogen fueling infrastructure. (4Q, 2019)
- Milestone 3.1: Develop, validate, and harmonize test measurement protocols. (4Q, 2014)
- Milestone 4.9: Completion of GTR Phase 2. (1Q, 2017)
- Milestone 5.1: Update safety bibliography and incidents databases. (4Q, 2011 – 2020)

FY 2017 Accomplishments

- *Hydrogen Safety Sensor Gap Analysis*: Co-organized a Hydrogen Sensor Workshop entitled "Hydrogen Safety Sensors and Their Use in Applications with Hydrogen as an Alternative Fuel," in collaboration with the European Joint Research Centre (JRC) and the Fuel Cell and Hydrogen Joint Undertaking (FCH JU), which identified critical gaps in hydrogen safety sensor performance. The resulting gap analysis is to be presented at the 7th International Conference on Hydrogen Safety (ICHS) [2].
- *FCEV Exhaust Gas Measurement Technology*: Developed a prototype analyzer for verifying that hydrogen levels in FCEV exhaust is within the regulated levels as prescribed by GTR-13 [1]. The exhaust analyzer will ultimately be used by the DOT National Highway Transportation Safety Administration for compliance verification.
- *Characterization of Outdoor Liquid Hydrogren (LH2) Releases*: Developed the Cold Hydrogen Plume Analyzer, which was designed to empirically profile hydrogen plumes generated during LH2 venting; field measurements with the analyzer supported the recommendation proposed for the upcoming edition of National Fire Protection Agency (NFPA) 2 that the hydrogen vent stacks ought to be directed up and away from ground level.
- *Characterization of Indoor Hydrogen Releases*: Profiled indoor hydrogen releases through the development of empirically verified theoretical models, in collaboration with AVT, which will be incorporated into NFPA 2 as a guidance document on sensor placement.
- *Expedited Sensor Test Methods*: Developed and verified expedited sensor test methods, in collaboration with the JRC, using an apparatus based on a flow-through design which provides results in a fraction of the time of previous designs.
- *Obtained National Renewable Energy Laboratory Record of Invention (NREL ROI 17-94)* "In-Situ, Low-Cost, Low-Pressure Interface to a Fuel Contaminant Analyzer within a High Pressure Hydrogen Dispenser." The ROI will be the basis for a provisional patent.
- *SAE Technical Information Report (TIR) J3089*: Completed the formal draft of SAE TIR J3089 "Characterization of On-board Vehicular Hydrogen Sensors," which was developed for the SAE Fuel Cell Standards Committee. The TIR will be submitted for ballot in the fall of 2017.
- *Recognition of the Sensor Laboratory Publications*: The significance of an NREL Sensor Laboratory publication was recognized in the International Association for Hydrogen Energy Newsletter, which identified the paper (An Overview of Hydrogen Sensors and Requirements, W. Buttner, et al., IJHE, 36, (2011) 2462-2470) as the fifth most cited article in the International Journal for Hydrogen Energy over the past five years.

✧ ✧ ✧ ✧ ✧

INTRODUCTION

Hydrogen sensors are an enabling technology to assure the safe use of hydrogen as an alternative, renewable fuel. Sensors facilitate the safe implementation of FCEVs and the supporting infrastructure. To assure the availability of reliable safety sensors and their proper use, the DOE Fuel Cell Technology Office established the NREL Safety Sensor Testing Laboratory. The NREL Sensor Test Laboratory provides stakeholders (e.g., sensor developers and manufacturers, end users, and code officials) a resource for an independent, unbiased evaluation of hydrogen sensor performance. Sensor evaluations are performed using test protocols that were guided by the requirements in national [3] and international sensor standards [4], as well as by the sensor performance targets established by DOE [5]. In some cases, performance testing is also guided by the specific requirements of the application. In addition to laboratory assessment of sensor performance, a critical mission of the NREL Safety Sensor Testing Laboratory is to assure the proper use of hydrogen sensors. This is achieved, in part, through topical studies designed to illustrate fundamental properties and limitations of various hydrogen sensor technologies, and through outreach activity such as participation on code and standards development organizations (CDOs/SDOs), safety committees, workshops, conferences, and webinars. Furthermore, in collaboration with an international team of hydrogen sensor experts, the director of the NREL sensor laboratory (William Buttner) co-authored a book on hydrogen sensor technology, which covers a variety of sensor related topics ranging from a detailed description of the fundamentals of sensor design to practical applications and selection criteria [6]; this book represents an invaluable resource to the hydrogen community as a single source for understanding and using hydrogen

sensors. The NREL sensor laboratory further facilitates deployment by partnering directly with end users to assist in the design and implementation of their sensor system.

APPROACH

The NREL sensor laboratory RD&D effort is guided by the needs of the hydrogen community. Unbiased and confidential performance evaluation of hydrogen sensors has been and remains a core activity within the NREL sensor laboratory. In this function, the Sensor Laboratory supports sensor developers, end users, as well as permitting officials and standard and code developers. Sensor evaluations are performed using a custom-built sensor test apparatus (Figure 1), which was designed with advanced capabilities, including parallel testing of multiple hydrogen sensors, sub-ambient to elevated temperature, sub-ambient to elevated pressure, active humidity control, and accurate control of gas parameters with multiple precision digital mass flow meters operating in parallel. In addition, other test fixtures have been developed for lifetests and chemical poison studies, as well as for specialized applications. The test apparatus are fully automated for control and monitoring of test parameters and for data acquisition with around-the-clock operation capability. Selected sensors are subjected to an array of tests to quantify the impact of variation of environmental parameters and chemical matrix on performance. Although standard test protocols have been developed [7], these can be adapted for specialized requirements. Results are reported back to the client to support their future development work. NREL sensor testing also supports end users by qualifying sensor technology for their application [8] and by educating the hydrogen community on the proper use of hydrogen sensors.

FIGURE 1. The NREL Hydrogen Sensor Test Apparatus

The NREL sensor laboratory maximizes its impact by direct collaborations with stakeholders in the hydrogen community; this is achieved in part through numerous formal agreements with industrial partners. The NREL Sensor Laboratory was a recipient of two projects under the DOE Small Business Voucher Pilot Program [9] which facilitates access to the DOE national labs for American small businesses. Strategic partnerships have also been maintained with other government organizations, most notably with the Sensor Testing Facility at the JRC in Petten, Netherlands, under which the respective sensor test facilities collaborate on hydrogen sensor research projects of common interests. Currently, this collaboration is formalized under a DOE-JRC agreement [10]. The NREL–JRC collaboration provides a platform for the international distribution of the NREL sensor research and development.

In addition to sensor performance characterization, the scope of the NREL Safety Sensor Testing Laboratory has expanded its active participation on a variety of national and international codes and standards development organizations, including NFPA 2, International Organization for Standardization (ISO) Technical Committee 197, SAE, UL, ASTM International, and the GTR. The type of support provided by the NREL Sensor Laboratory to safety development organizations and code development organizations include (i) pre-normative research to support code and standard requirements, (ii) document development, (iii) development and deployment of verification technology, and (iv) expert guidance and recommendations. Increasingly, the NREL sensor laboratory uses its expertise to develop sensor-based tools for the hydrogen community; currently this includes tools for hydrogen plume profiling to support NFPA 2 and a hydrogen analyzer to verify compliance of FCEV exhaust requirements as prescribed in the GTR.

Dissemination of results is through a variety of venues, including participation on international hydrogen safety committees, presentations at international conferences and workshops, publications in the open literature, and direct outreach to the hydrogen community.

Finally, it is noted that the NREL Sensor Laboratory has an on-going commitment for training young scientists and engineers in the field of renewable energy. Accordingly, the Sensor Laboratory has for several years provided internship opportunities to undergraduate engineering majors. While supervised by the Director of the NREL Sensor Laboratory, interns are assigned and thus responsible for a specific project (or several projects). Responsibilities include experimental design and data analysis, as well as interaction (under supervision) with clients. Interns have made significant contributions to numerous projects within the NREL Sensor Laboratory, including several described in this report. Accordingly they have been included as co-authors on

numerous presentations and papers. Upon graduation, several interns have remained at NREL as entry-level engineers or consultants.

RESULTS

Hydrogen Sensor Workshop—Sensor Gap Analysis: A workshop on hydrogen sensors was held on May 10, 2017, at the headquarters of the European FCH JU in Brussels, Belgium (*Hydrogen Safety Sensors and Their Use in Applications with Hydrogen as an Alternative Fuel*). A primary purpose of the workshop was to get input from a cross-section of stakeholders on hydrogen sensor needs and experiences. The workshop was jointly organized by the JRC and NREL sensor laboratories and the FCH JU. The focus was on the ability of existing hydrogen sensor technology to meet end-user needs in applications pertaining to hydrogen as alternative fuel. With over twenty participants that included program administrators, sensor manufacturers, end-users, facility managers, and experts from sensor test laboratories, the workshop identified critical gaps in hydrogen safety sensor performance. Critical metrological gaps include sensor lifetime and stability, the need for capital and maintenance cost reduction, and improved response time, especially for specialized applications such as the FCEV exhaust gas analyzer. There also exists a need for the reduction in complexity of Regulations, Codes and Standards, especially with regards to international acceptance and harmonization because many countries or regions require their own national standards. A thorough gap analysis is being prepared and will be presented at the ICHS [2].

FCEV Exhaust Gas Measurement Technology and support of the GTR and FMVSS: GTR 13 [1] is the defining document regulating hydrogen vehicle safety requirements. GTR-13 has been formally implemented, and accordingly, national authorities overseeing development and enforcement of vehicle regulations are to endeavor to harmonize their national regulations with the GTR. Within the United States, the national authority for vehicle safety is the DOT and the prevailing regulatory code is the FMVSS. Included within the GTR are safety requirements on allowable hydrogen emission levels in FCEVs. The NREL Safety Sensor Testing Laboratory, in cooperation with DOT, has been developing an off-vehicle exhaust gas analyzer and analytical methods for compliance verification to the hydrogen emission requirements specified in the GTR. The analyzer has been developed for use by regulatory agencies such as DOT to verify compliance to this GTR specification, although vehicle manufacturers have also expressed a need and interest in the technology. A laboratory bench top prototype analyzer was previously demonstrated [11]. The prototype analyzer with gas collection probe was field tested on an FCEV to measure hydrogen in the exhaust gas stream. Figure 2 shows a series of hydrogen pulses that were discharged from the FCEV during operation, all of which were within compliance to the GTR regulations. Based upon the field results, a modified gas collection system for the probe has been developed.

Characterization of Outdoor LH2 Releases: Cold hydrogen plumes formed during LH2 releases are currently not well understood because field data is essentially non-existent. This lack of understanding leads to overly

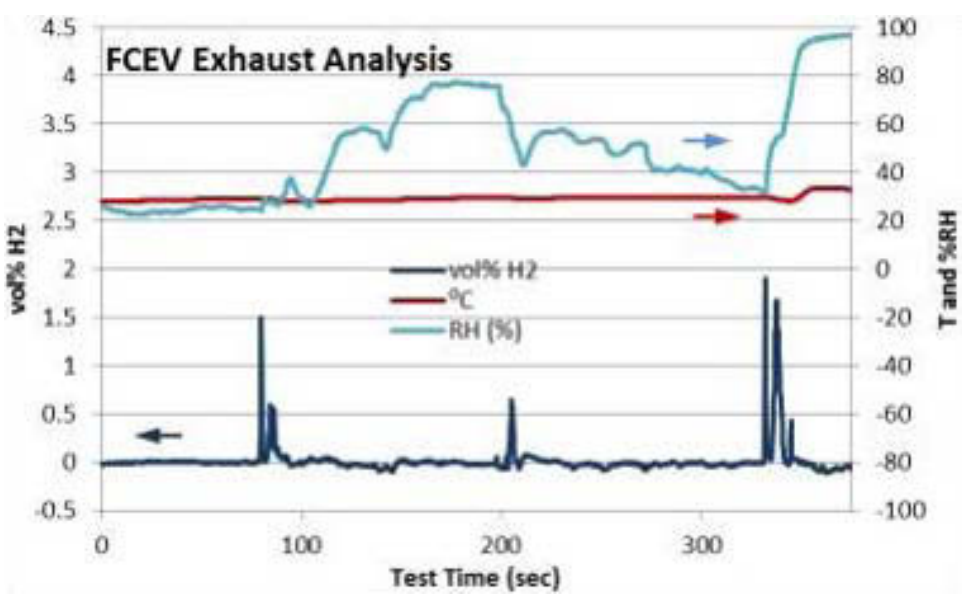

RH – relative humidity

FIGURE 2. Hydrogen concentrations as measured from an actual FCEV using the NREL Exhaust Gas Analyzer. Physical parameters (temperature and humidity) are plotted relative to the right ordinate.

conservative safety distances at LH2 facilities. To address this need, the NREL sensor laboratory, in collaboration with NFPA 2 hydrogen storage task group, developed the prototype Cold Hydrogen Plume Analyzer to empirically monitor LH2 storage tank venting. The prototype Analyzer, which consisted of multiple sampling points for gas (e.g., hydrogen and oxygen) and environmental (e.g., temperature and humidity) sensors, was deployed during an actual LH2 venting operation. Critical findings included the detection of hydrogen above the lower flammable limit more than two meters below the horizontal release point. The venting process is shown in Figure 3, which clearly shows the downward momentum of the vapor cloud (formed from chilled water vapor) during the LH2 venting. Although the measured hydrogen concentration did not correlate to the vapor cloud, the field measurements did verify that hydrogen would be observed below the horizontal release point, an observation that was not predicted by models existing at the time. Thus, hydrogen buoyancy would not necessarily dominate the dispersion process. The demonstration that the hydrogen plume would be observed below the horizontal release point contributed significantly to the ready acceptance by the NFPA Hydrogen Storage Task Group to support incorporation into the upcoming edition of NFPA 2 the proposal that the hydrogen vent stacks ought to be directed up and away from ground level. The outcome of this study and proposed future applications will be presented at the ICHS [12].

Although developed for LH2 facilities, the Analyzer is amenable to gaseous hydrogen as well. The Analyzer has been upgraded for enhanced metrological capabilities including improved spatial and temporal profiling of hydrogen plumes and tracking of prevailing weather conditions. The system can be readily adapted for hydrogen wide area monitoring of small to large-scale gaseous hydrogen and LH2 facilities.

Characterization of Indoor Hydrogen Releases: Sensors are mandated by both the International Fire Code and NFPA 2 for numerous indoor hydrogen infrastructure applications. However, no guidance is provided on the selection or use of sensor technology. The NREL Sensor Laboratory and AVT (Mississauga, Ontario, Canada) collaborated to profile indoor hydrogen releases. As a model system, AVT performed computational fluid dynamics modeling of a leak scenario associated with an electrolyzer system housed within a 20 foot ISO container. Figure 4 illustrates the hydrogen dispersion following a release. In this modelling, a leak scenario was identified that would otherwise be undetected by other methods, such as the inability of a small leak to be detector by a pressure loss within a flowing pneumatic line. The theoretical dispersion profile is to be validated by NREL using the hydrogen wide area monitoring Analyzer developed for the LH2 release and consists of an array of hydrogen and physical sensors to temporally and spatially profile hydrogen releases. The outcome of this work will be incorporated into NFPA 2 as a guidance document on sensor placement.

Expedited Sensor Performance Test Protocols: In collaboration with the JRC, expedited sensor test methods were developed and verified using an apparatus based on a flow-through design that provides results similar to chamber methods, such as those prescribed in performance standards (e.g., UL 2075 [3], ISO 26142 [4]), but in only a fraction of the time. This work was performed under an international collaborative agreement between DOE and the JRC [10].

FIGURE 3. The NREL Hydrogen Plume Analyzer deployed during a planned LH2 venting process. The observation of hydrogen below the horizontal release point facilitated the recommendation proposed for future editions of NFPA 2 that the vent stack be designed to direct the release up away from ground level.

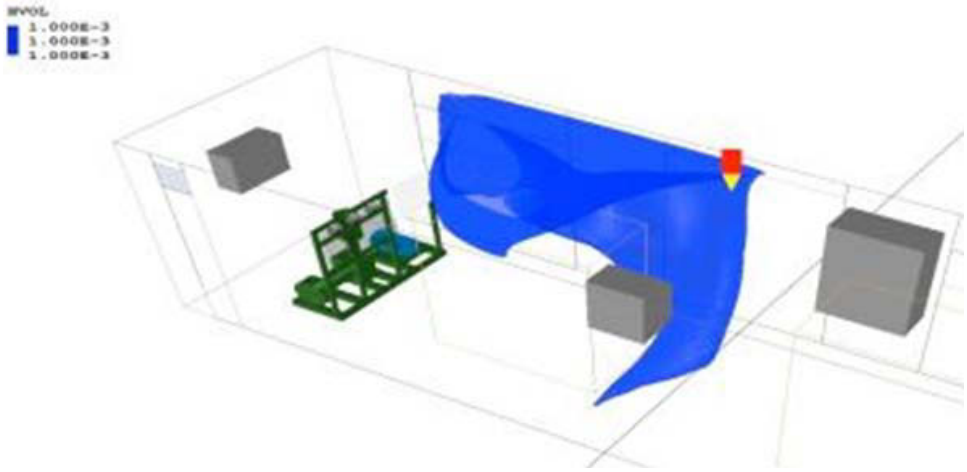

FIGURE 4. Hydrogen concentration contour as predicted from computational fluid dynamics modeling formed following an indoor release

The outcome of this study on the use of the expedited test methods will be presented at the ICHS [13].

Record of Invention (NREL ROI 17-94): There are two aspects necessary for practical on-site chemical analysis for verification of hydrogen fuel purity, the availability of the appropriate analytical technology (e.g., the hydrogen contaminant detector) and an interface to allow transfer of hydrogen from the high pressure dispenser to the (low pressure) analytical instrument. The NREL Sensor Laboratory recently submitted an ROI "In-Situ, Low-Cost, Low-Pressure Interface to a Fuel Contaminant Analyzer within a High Pressure Hydrogen Dispenser." This invention provides an automated interface to support the onsite analysis of hydrogen at commercial fueling facilities and is compatible with almost any existing or proposed field deployable gas detection technology. A bench-scale model has been developed for prototype testing of hydrogen contaminant detector technology. The bench-scale model will also serve as the design guideline for the in-dispenser system, which will be used for real-world deployment of hydrogen contaminant detectors at hydrogen fueling facilities. A provisional patent on this concept is to be filed.

SAE Technical Information Report J3089: SAE TIR J3089 "Characterization of On-board Vehicular Hydrogen Sensors" was prepared under the auspices of SAE Fuel Cell Standards Committee. The purpose of the TIR was to provide a uniform performance assessment guide for FCEV manufacturers and their sensor suppliers. The finish draft of TIR will be submitted for ballot in the fall of 2017.

CONCLUSIONS AND UPCOMING ACTIVITIES

The Hydrogen Plume Analyzer (Cold Hydrogen Plume Analyzer) was developed for outdoor empirical measurements during LH2 releases. The initial deployment demonstrated that hydrogen buoyancy will not always dominate the dispersion process, and that hydrogen will often be observed below the horizontal release point. The analyzer is amenable to both LH2 and gaseous hydrogen and can form the basis of a hydrogen wide area monitor. Although future direction of this work is pending appropriations the sensor laboratory is in discussion with industrial partners to support further characterizations of hydrogen releases which will provide empirical correlations of environmental and physical parameters to hydrogen dispersions. These empirical studies will ultimately integrate with theoretical dispersions models to provide predictive capabilities.

The analytical performance of the NREL FCEV Exhaust Analyzer has been demonstrated. Currently a probe design that integrates to the analyzer is being developed to provide better measurement integrity. The DOT has provided support to the NREL FCEV to perform real-world measurements on an FCEV. This testing is in support of DOT mission to demonstrate vehicle safety, in part by developing test protocols per regulatory requirements. Currently the proposed requirements are those prescribed in GTR 13, which may be directly incorporated into the FMVSS.

While funding for continued sensor performance testing is pending appropriations, the NREL Sensor Laboratory will endeavor to continue to support FCEV and infrastructure implementation. This will be through addressing the gaps identified in the workshop [2]. In addition to sensor testing, this support will be in the form of expert guidance provided by, for example, topical Webinars. Presently, the NREL Sensor Laboratory is soliciting topics from members of the SAE Fuel Cell Standards Committee.

FY 2017 PUBLICATIONS/PRESENTATIONS

Talks and Presentations

1. "Sensor Testing Overview (The NREL Hydrogen Sensor Test Laboratory)," W. Buttner, R. Burgess, C. Rivkin, K. Schmitt, H. Wright, K. Hartmann, Joint CSTT-HDTT Meeting Agenda, National Renewable Energy Laboratory, Golden, CO, November 1–2, 2016.

2. "NREL and JRC Sensor Testing Laboratory Programs-H2 Safety Sensor Gap Analysis-Support of Safety Codes and Standards," W. Buttner, E. Weidner, R. Burgess, C. Rivkin, R. Ortiz Cebolla, C. Bonato, P. Moretto, K. Schmidt, H. Wright, K. Hartmann, IEA-HIA Task 37 Experts Meeting, Bethesda, MD, November 28–29, 2016.

3. "The NREL Analyzer For Profiling Cold Hydrogen Plume Release," W. Buttner, C. Rivkin, K. Schmitt, H. Wright, K. Hartmann, NFPA 2 Hydrogen Storage Task Group, Sandia National Laboratories, Livermore, CA, March 1, 2017.

4. "Empirical Profiling of Cold Hydrogen Plumes formed from Venting of LH2 Storage Vessels," W. Buttner, C. Rivkin, K. Schmidt, K. Hartmann, H. Schmidt, E. Weidner, 7th International Conference on Hydrogen Safety, Hamburg, Germany, September 11–13, 2017.

5. "Flow-through method validation for hydrogen sensors testing," R. Ortiz-Cebolla, E. Weidner, C. Bonato, W. Buttner, K. Hartmann, K. Schmidt, 7th International Conference on Hydrogen Safety, Hamburg, Germany, September 11–13, 2017.

Publications

1. "Hydrogen monitoring requirements in the global technical regulation on hydrogen and fuel cell vehicles," W. Buttner, C. Rivkin, R. Burgess, K. Hartmann, I. Bloomfield, M. Bubar, M. Post, L. Boon-Brett, E. Weidner, P. Moretto, *International Journal of Hydrogen Energy* (http://doi.org/10.1016/j.ijhydene.2016.06.053).

2. "Empirical Profiling of Cold Hydrogen Plumes formed from Venting of LH2 Storage Vessels," W. Buttner, C. Rivkin, K. Schmidt, K. Hartmann, H. Schmidt, E. Weidner, To be published in the proceedings of the 7th International Conference on Hydrogen Safety, Hamburg, Germany, September 11–17, 2017.

3. "Flow-through method validation for hydrogen sensors testing," R. Ortiz-Cebolla, E. Weidner, C. Bonato, W. Buttner, K. Hartmann, K. Schmidt, To be published in the proceedings of the 7th International Conference on Hydrogen Safety, Hamburg, Germany, September 11–17, 2017.

4. "Hydrogen Safety Sensor Performance and Use Gap Analysis," W. Buttner, R. Burgess, K. Schmidt, K. Hartmann, H. Schmidt, E. Weidner, R. Ortiz Cebolla, C. Bonato, P. Moretto, To be published in the proceedings of the 7th International Conference on Hydrogen Safety, Hamburg, Germany, September 11–17, 2017.

5. High Pressure Hydrogen Pressure Relief Devices: Accelerated Life Testing and Application Best Practices, R. Burgess, M. Post, W. Buttner, C. Rivkin, NREL Technical Report, in press.

6. *FY 2016 DOE Hydrogen and Fuel Cells Program Annual Report*, "VIII.7 NREL Hydrogen Sensor Testing Laboratory," W. Buttner, R. Burgess, C. Rivkin.

REFERENCES

1. Addendum 13: Global technical regulation No. 13 Global technical regulation on hydrogen and fuel cell vehicles ECE/TRANS/180/Add.13, July 19, 2013). (see http://www.unece.org/fileadmin/DAM/trans/main/wp29/wp29wgs/wp29gen/wp29registry/ECE-TRANS-180a13e.pdf, accessed July 22, 2015)

2. "Hydrogen Safety Sensor Performance and Use Gap Analysis," W. Buttner, R. Burgess, K. Schmidt, K. Hartmann, H. Schmidt, E. Weidner, R. Ortiz Cebolla, C. Bonato, P. Moretto, To be published in the proceedings of the 7th International Conference on Hydrogen Safety, Hamburg, Germany, September 11–17, 2017).

3. "UL 2075 Gas and Vapor Detectors and Sensors."

4. "ISO 26142 Hydrogen Detector for Stationary Apparatus."

5. Hydrogen, Fuel Cells & Infrastructure Technologies Program Multi-Year Research, Development and Demonstration Plan, Planned program activities for 2005–2015, U.S. DOE Office of Renewable Energy and Efficiency (EERE), 2005. http://www.nrel. gov/docs/fy08osti/39146.pdf

6. "Sensors for Safety and Process Control in Hydrogen Technologies", Thomas Hűbert, Lois Boon-Brett, William Buttner, CRC Press ISBN 9781466596542 (2015).

7. "Standard Hydrogen Test Protocols for the NREL Sensor Testing Laboratory," NREL Brochure (see http://www.nrel.gov/hydrogen/pdf=s/53079.pdf, accessed July 22, 2016).

8. "Hydrogen-Powered Vehicles–A Safe Alternative to Traditional Gasoline Internal Combustion Engines" William Buttner (March 2017). (see https://www.kpaonline.com/ehs/hydrogen-powered-vehicles-safe-alternative-traditional-gasoline-internal-combustion-engines/)

9. DOE Small Business Voucher Pilot (see https://www.sbv.org/).

10. Collaboration Arrangement for Research and Development in Energy-Related Fields DOE-JRC signed June 2, 2016. (see: https://eeas.europa.eu/headquarters/headquarters-homepage/2817/node/2817_nl).

11. "Hydrogen monitoring requirements in the global technical regulation on hydrogen and fuel cell vehicles," W. Buttner, C. Rivkin, R. Burgess, K. Hartmann, I. Bloomfield, M. Bubar, M. Post, L. Boon-Brett, E. Weidner, P. Moretto, *International Journal of Hydrogen Energy* (http://doi.org/10.1016/j.ijhydene.2016.06.053).

12. "Empirical Profiling of Cold Hydrogen Plumes formed from Venting of LH2 Storage Vessels," W. Buttner, C. Rivkin, K. Schmidt, K. Hartmann, H. Schmidt, E. Weidner, To be published in the proceedings of the 7th International Conference on Hydrogen Safety, Hamburg, Germany, September 11–17, 2017.

13. "Flow-through method validation for hydrogen sensors testing," R. Ortiz-Cebolla, E. Weidner, C. Bonato, W. Buttner, K. Hartmann, K. Schmidt, To be published in the proceedings of the 7th International Conference on Hydrogen Safety, Hamburg, Germany, September 11–17, 2017.

VIII.8 Fuel Cell & Hydrogen Energy Association Codes and Standards Support

Karen Quackenbush (Primary Contact),
Morry Markowitz, Connor Dolan
Fuel Cell and Hydrogen Energy Association (FCHEA)
1211 Connecticut Ave. NW, Suite 650
Washington, DC 20036
Phone: (202) 261-1331
Email: khall@fchea.org

DOE Manager: Will James
Phone: (202) 287-6223
Email: Charles.James@ee.doe.gov

Project Start Date: November 16, 2011
Project End Date: June 30, 2017; Project continuation and direction determined annually by DOE

Overall Objectives

Enhance and sustain industry participation to enable:

- Timely development of regulations, codes, and standards (RCS) deemed critical by industry for the commercial deployment of hydrogen and fuel cell technologies and the infrastructure needed to support them.
- Timely and coordinated industry participation in key forums for safety and RCS development for hydrogen energy and fuel cell technologies.
- Efficient, productive, and timely information exchange between the hydrogen and fuel cell industry, regulatory officials, codes and standards development organizations, and other interested parties by providing a common, current, and factual information base.

Fiscal Year (FY) 2017 Objectives

- Enhance and sustain industry participation to enable:
  - Timely development of RCS deemed critical by company with input from seller and industry for the commercial deployment of hydrogen and fuel cell technologies and the infrastructure needed to support them.
  - Timely and coordinated industry participation in key forums for safety and RCS development for hydrogen energy and fuel cell technologies.
  - Efficient, productive, and timely information exchange between the hydrogen and fuel cell industry, regulatory officials, codes and standards development organizations, and other interested parties by providing a common, current, and factual information base.

Technical Barriers

This project addresses the following barriers identified in the DOE Fuel Cell Technologies Office Multi-Year Research, Development, and Demonstration (MYRDD) Plan, Section 3.7: Hydrogen Safety, Codes and Standards.

(F) Enabling National and International Markets Requires Consistent RCS

(H) Insufficient Synchronization of National Codes and Standards

(J) Limited Participation of Business in the Code Development Process

Contribution to Achievement of DOE Safety, Codes & Standards Milestones

This project will contribute to achievement of the following DOE milestones from the Safety, Codes & Standards section of the Fuel Cell Technologies Office MYRDD Plan.

- Milestone 2.17: Publication of updated international fuel quality standard to reflect fuel cell technology advancement. (3Q, 2018)
- Milestone 2.19: Validate inherently safe design for hydrogen fueling infrastructure. (4Q, 2019)
- Milestone 4.6: Completion of standards for critical infrastructure components and systems. (4Q, 2014)
- Milestone 4.8: Revision of NFPA 2 to incorporate advanced fueling and storage systems and specific requirements for infrastructure elements such as garages and vehicle maintenance facilities. (3Q, 2016)

FY 2017 Accomplishments

- Supported over 300 draft public inputs to National Fire Protection Agency's NFPA 2, NFPA 55, and the International Fire Code developed by FCHEA in 2016 to address key industry needs for fuel cell electric vehicle repair booths and harmonized requirements for defueling, and addressing inconsistencies or lack of clarity between model codes.
- Made progress on technical gaps for micro fuel cell power systems to facilitate national and international harmonization of shipping regulations. Working to

ensure international standards are inclusive of all fuel types. IEC 62282-6-101 Edition 2, and associated fuel specific Part 2 documents. Took on convenorship of international working group (WG), International Electrochemical Commission Technical Committee (IEC/TC) 105 WG#8 to advance this effort.

- Managed the development of industry comments to draft international standards for hydrogen fueling components to support harmonization of national and international requirements, and supported these comments in the U.S. technical advisory group and International Organization for Standardization (ISO) Working Groups.
- Supported the Telecommunications Industry Association (TIA) publication of its *Reference Guide to Regulations, Codes, and Standards for the Deployment of Stationary Fuel Cells*. FCHEA contributed to the development of this guide in previous years. A PDF of the document is available online (http://www.tiaonline.org/resources/tia-fuel-cell-reference-guide).

✧ ✧ ✧ ✧ ✧

INTRODUCTION

As the premiere trade association for the fuel cell and hydrogen energy industry, FCHEA utilizes a working group structure to facilitate focused effort in each of the three following applications: portable power, stationary power, and transportation, which includes vehicles and the infrastructure to support them.

FCHEA's project contributes directly to achievement of four of the seven objectives outlined in the Fuel Cell Technologies Office MYRDD Plan, Chapter 3.7, Hydrogen Safety, Codes, and Standards by engaging industry to develop consistent technical requirements and harmonized national and international safety codes and standards.

APPROACH

FCHEA working groups and monthly facilitation of the National Hydrogen & Fuel Cells Codes & Standards Coordinating Committee (NHFCCSCC) provide regular opportunities to engage industry in developing RCS through discussion of priorities, opportunities to participate in technical committees and WGs directly, and opportunities to comment on draft standards. Industry priorities in codes and standards development are captured and tracked in FCHEA's regulatory matrix, which is updated regularly and published quarterly (see Figure 1).

Our bi-monthly Hydrogen and Fuel Cell Safety Report, available online at www.hydrogenandfuelcellsafety.info (Figure 2), provides timely information on the progress of developing codes, standards, and regulations to stakeholders including authorities having jurisdiction (AHJs), emergency responders, industry, researchers, and other interested parties.

RESULTS

Our Portable Power WG authorized staff to take on convenorship of international working group IEC/TC 105 WG #8 to ensure international standards are inclusive of all fuel types. WG #8 is leading the development of IEC 62282-6-101 Edition 2, and associated fuel specific Part 2 documents. This effort supports the following objective from MYRDD Plan: "enabling national and international markets requires consistent RCS," by ensuring national and international standards for micro fuel cell applications are harmonized, then adopted by international regulations.

Our Transportation Working Group Hydrogen Codes Task Group continues to support harmonized public inputs for the next development cycles of key model codes. In 2016, over 300 public inputs on NFPA 2, NFPA 55, and the International Fire Code were solicited from business and experts with operational experience, and focus on harmonizing requirements with other industry-accepted standards and codes. This effort supports the following objective from MYRDD Plan: "Provides consistent RCS and synchronization of national codes and standards."

Our Stationary Power WG worked with TIA to publish its *Reference Guide to Regulations, Codes, and Standards for the Deployment of Stationary Fuel Cells*. FCHEA contributed to the development of this guide in previous years. A PDF of the document is available online: http://www.tiaonline.org/resources/tia-fuel-cell-reference-guide. This effort supports the following objective from MYRDD Plan: "Develop and enable widespread sharing of safety-related information resources and lessons learned with first responders, authorities having jurisdiction (AHJs), and other key stakeholders." Working closely with related industries provides consistency in requirements and reduces duplication of effort.

Publication of our Regulatory Matrix and the Hydrogen & Fuel Cell Safety Report keep stakeholders informed of the progress and issues encountered in the development of RCS. It has introduced industry to the many new working groups in ISO Technical Committee (TC) 197 and the call for participation in U.S. standards committees. The integrated calendar of events aids in scheduling meetings. Facilitation of the monthly web-based meetings of the NHFCSCC provides a regular forum to coordinate and align efforts in standards activities and harmonize requirements. This effort contributes to the DOE goal to develop and enable widespread sharing of safety-related information resources and lessons learned with first responders, AHJs, and other key stakeholders. These activities also increase participation of stakeholders in development of harmonized RCS.

Significance to Commercialization
⇦ More Critical
Highest Effort

A. Essential To or Enables Commercialization	B. Important to Commercialization	C. Supports Commercialization	
~~IEC 62282-4-102: Fuel cell systems for forklift applications – Performance requirements and test procedures: Approved for FDIS circulation.~~			VEHICLES
ISO 19880-1 Gaseous Hydrogen Filling Stations. TS published in June. Development of IS continues. Glenn Scheffler has been appointed as co-convenor. **CSA Group HPIT 2: Compressed Hydrogen Station and Components for Fueling Industrial Trucks:** ~~In publication~~ Published – to be removed in next update of matrix. **Hydrogen Dispenser Metrology:** The July 2016 National Conference on Weights and Measures (NCWM) Meeting agreed to (1) recognize that a Category 3 device may make the required information from the event logger available electronically and (2) expanding the current hydrogen code acceptance tolerance of 1.5 % to 5.0 % and the current maintenance tolerance of 2.0 % to 7.0 %. The code will have only one accuracy class designated as Accuracy Class 7.0 in NIST Handbook 44 Section 3.39 Hydrogen Gas-Measuring Devices-Tentative Code. ~~The National Conference on Weights and Measures (NCWM) approved hydrogen gas measuring devices and 5% increase in specification clause, with no sunset clause. Enables dispenser designers to apply for certificates.~~	**ISO 19880-2: Gaseous hydrogen filling station dispensers** DIS is scheduled for early 2017. **HGV 4.3 Fueling Parameters** Work on the next edition will commence in the first quarter of 2017 to align with SAE J2601. **ISO 17268 Gaseous Hydrogen Land Vehicle Refuelling Connection Devices** is developing a revised standard. The DIS is anticipated ~~in a few weeks~~shortly, pending resolution of pressure definitions and relevant requirements.	**ISO/CD 19880-3 Gaseous hydrogen -- Fueling stations -- Valves** Covers the safety performance of valves over 1MPa for gaseous hydrogen fueling stations. Revised CD passed; however DIS 2 will be circulated in March 2017. **CSA HPRD1Work on the next revision of Pressure Relief Devices** is pending. **NFPA 55: Compressed Gases and Cryogenic Fluids Code:** Reopened First Draft. Agreed to act on Public Inputs submitted to NFPA 2 on extract text from NFPA 55. Revision cycle has officially been changed from Annual 2018 to Annual 2019, and will remain in-cycle with NFPA 2.	INFRASTRUCTURE
			RESEARCH

FIGURE 1. Sample page from FCHEA's Regulatory Matrix, showing progress in developing codes, standards, and regulations during the first half of 2017.

CONCLUSIONS AND UPCOMING ACTIVITIES

The DOE objectives supported by this project are ongoing and on target to be reached between now and 2020.

- This project has produces further advances on U.S. model codes. This includes reference to available harmonized standards.
- Working along with H2USA, FCHEA has facilitated easy access to technical papers to aid adoption of NFPA 2 and withdrawal of regional restrictions (such as fuel cell electric vehicles in tunnels, over bridges, in parking garages, etc.).

International standards need to develop in a coordinated fashion to ensure they reflect the needs of industry and consistency with accepted practices.

- Significant progress: ISO/TC 197 WGs on hydrogen fueling stations and components.
- Progress: published standards being updated to reflect advances and learnings.
- CSA Group seed document on hydrogen fueling components to be brought back to CSA following ISO publication.

Significant work remaining: Work with stakeholders to update the national and international RCS templates to determine gaps and areas where harmonization efforts are needed. CSA has begun this effort for the national template. FCHEA to ensure industry priorities are reflected in updated templates, and provide technical experts to any resulting new efforts. Work closely with H2USA to provide expertise or data required to remove any regional restrictions for deployment of fuel cell electric vehicles and hydrogen infrastructure.

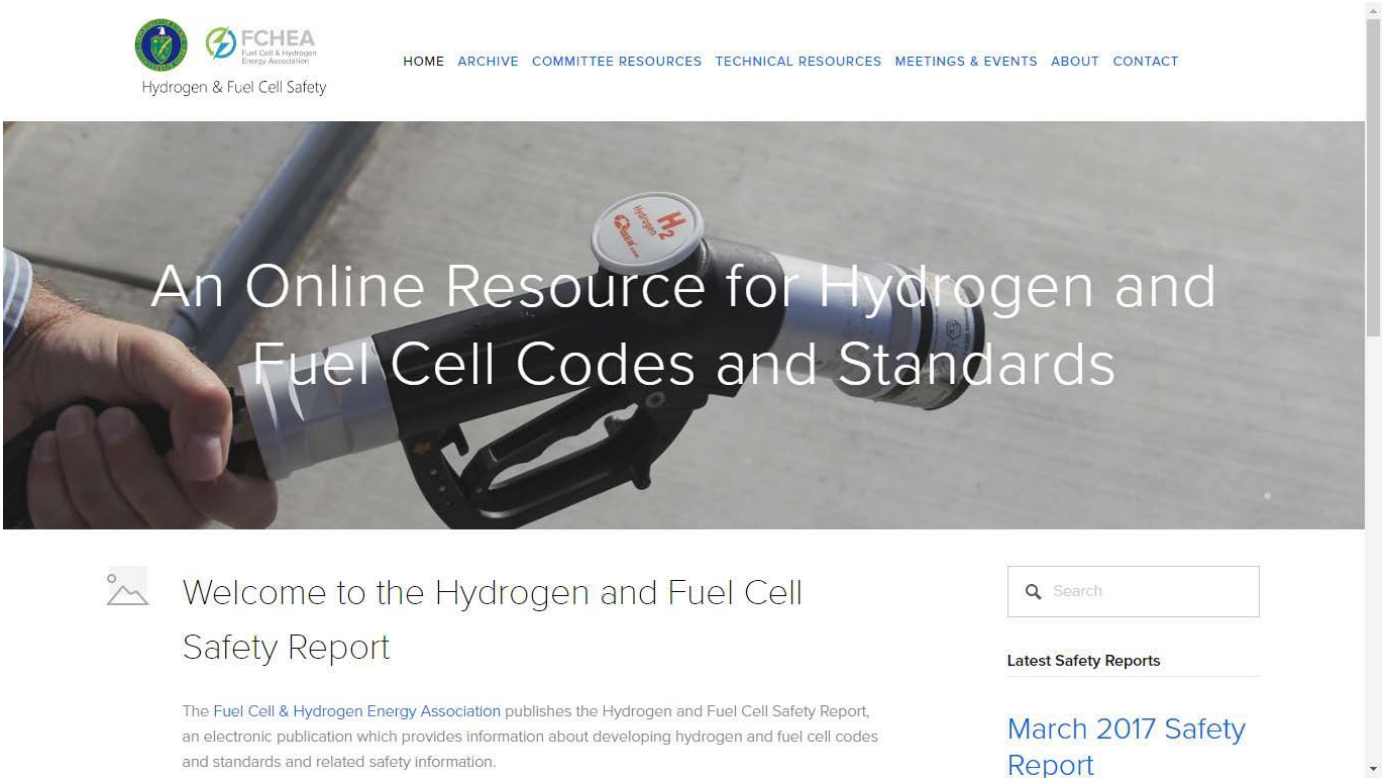

FIGURE 2. Hydrogen and Fuel Cell Safety Report

Portable Power WG: through IEC/TC 105, revise micro fuel cell and cartridges documents to ensure harmonization with international standards for fuel cells as carry on and checked baggage. Department of Transportation continues to not be harmonized with inclusion of Divisions 2.1 and 4.3 fuel cartridges for checked baggage (micro fuel cell applications).

Transportation WG: contribute to updating national and international RCS templates to ensure U.S. industry interests and priorities are reflected. Continue dialog with component manufacturers to resolve issues in advance of infrastructure roll-out.

Stationary Power WG: continue to review international standards and United States as well as state regulations to ensure consistency with accepted U.S. requirements and best practices.

Continue to administer the NHFCCSCC and publish the Safety Report.

Technology Transfer Activities: we develop consensus and information rather than technologies. These are shared openly at www.hydrogenandfuelcellsafety.info. We also hold regular working group meetings, monthly coordination webinars, and web-based workshops/webinars to reach beyond our membership.

FCHEA will continue to administer the NHFCCSCC, including identify key issues, and document discussions and outcomes. Provide industry feedback to the DOE Safety, Codes and Standards subprogram on RCS development needs and priorities; outreach needs and priorities; and R&D needs and priorities to support RSC development activities.

FCHEA will continue to produce the Hydrogen and Fuel Cell Safety Report to report on the developing RCS to increase awareness of published and developing requirements, improve coordination of activities, and improve information transfer.

FY 2017 PUBLICATIONS/PRESENTATIONS

1. Markowitz, Quackenbush, and Dolan; "Fuel Cell & Hydrogen Energy Association Codes and Standards Support;" (project presented at the DOE Annual Merit Review; June 5–9, 2017, Washington, DC).

VIII.9 Compatibility of Polymeric Materials Used in the Hydrogen Infrastructure

Kevin L Simmons (Primary Contact), Kyle Alvine (Pacific Northwest National Laboratory),
Nalini Menon (Sandia National Laboratories),
Barton Smith (Oak Ridge National Laboratory),
Amit Naskar (Oak Ridge National Laboratory),
Mike Veenstra (Ford)
Pacific Northwest National Laboratory
PO Box 999
Richland, WA 99352
Phone: (509) 375-3651
Email: kl.simmons@pnnl.gov

DOE Manager: Will James
Phone: (202) 287-6223
Email: Charles.James@ee.doe.gov

Subcontractor:
Ford Motor Company, Detroit, MI

Project Start Date: October 1, 2015
Project End Date: September 30, 2018

Overall Objectives

- Provide scientific and technical basis to enable full deployment of hydrogen and fuel cell technologies by filling the critical knowledge gap for polymer performance in hydrogen environments.
- Identify applications, conditions, and materials of interest to the polymer community by interfacing with stakeholders.
- Develop experimental test methodologies that are relevant to the stakeholder's needs.
- Evaluate relevant materials with these test methodologies and disseminate the results through literature, databases, or codes and standards organizations to support the deployment of the hydrogen infrastructure.

Fiscal Year (FY) 2017 Objectives

- Complete analysis of stakeholder feedback utilizing failure mode and effects analysis (FMEA).
- Develop preliminary test methodology for in situ high pressure hydrogen testing of friction and wear of polymers.
- Complete high-pressure hydrogen cycling design and installation for testing polymers.
- Disseminate information to the hydrogen community by participating in committees, journal articles, and conferences.

Technical Barriers

This project addresses the following technical barriers from the Hydrogen Safety, Codes and Standards section of the Fuel Cell Technologies Office Multi-Year Research, Development, and Demonstration Plan.

(A) Safety Data and Information: Limited Access and Availability

(G) Insufficient Technical Data to Revise Standards

(J) Limited Participation of Business in the Code Development Process

(K) No Consistent Codification Plan and Process for Synchronization of R&D and Code Development

Contribution to Achievement of DOE Safety, Codes & Standards Milestones

This project will contribute to achievement of the following DOE milestones from the Hydrogen Safety, Codes and Standards section of the Fuel Cell Technologies Office Multi-Year Research, Development, and Demonstration Plan.

- Milestone 5.2: Update materials compatibility technical reference. (4Q, 2011 – 2020)

FY 2017 Accomplishments

- Identified four polymers and elastomers of interest (Viton™, EPDM, NBR, PTFE), temperature and pressure of interest (-40°C to +85°C, 0–20,000 psi), and tests of interest (pressure transients, wear and abrasion, pressure cycling) through feedback from 25 stakeholders.
- Performed tribology testing on three materials (nitrile butyl rubber [NBR], ethylene propylenediamene [EPDM], and polytetrafluoroethylene [PTFE]) that show an increase in coefficient of friction between 40–80% and an increase in wear by 40% on NBR in high-pressure hydrogen.
- Completed initial study on high-pressure purge and leak test gas to identify influences of gases on startup. Helium identified as the preferred choice of startup gas for purge and leak testing with reduced impact on material.
- Completed FMEA to provide prioritization and future research and development activity focus.

- Disseminated information to the hydrogen community through eight presentations, four publications, and one invention disclosure, including a keynote presentation at International Hydrogen Energy Development Forum in Japan and an invited presentation at the Hydrogenius Research Symposium in Japan.

✧ ✧ ✧ ✧ ✧

INTRODUCTION

Polymers are critical to hydrogen infrastructure applications to reduce cost and eliminate the design constraints of metallic components. However, unlike metals that have been studied extensively in high-pressure hydrogen, there is a significant knowledge gap in understanding polymer performance under these conditions. Standardized qualification methodologies and databases of acceptable conditions and polymers are not available to the hydrogen design community to guide material selection. The overall goal of this project is to fill this knowledge gap and support stakeholders in the safe selection of polymers for use in the wide range of required applications and conditions.

This will be done by developing a technical foundation to understand the effects of hydrogen on polymers and composites to enable the development of appropriate test protocols for evaluating materials for hydrogen service. The information generated from these tests of target polymeric materials will be disseminated to hydrogen users and standard and code development organizations.

APPROACH

The project consists of four main tasks: (1) gather information from stakeholder, (2) develop test methodologies, (3) characterize polymers, and (4) disseminate the information generated. The information gathered from stakeholders will be used to ensure that the materials being evaluated, the range of conditions of study, and the testing protocols being developed as part of this project will benefit stakeholders from polymer, component, and system manufacturers. The aim of the test methodologies being developed is to mimic the conditions of interest and accelerate the process to produce meaningful results in a reasonable timeframe. Because properties differ widely for a single polymeric material based on its additives and processing approach, testing results would be meaningless unless key polymer characteristics are understood. The project will fully characterize the polymers to allow others to compare their materials to those that were tested. Finally, the information generated, both the test protocol and the compatibility results will be disseminated through material databases, standards organizations, and peer-reviewed journals.

RESULTS

The project has engaged over 25 stakeholders from the hydrogen community to provide feedback in how the test and evaluate materials for use in hydrogen, and what are the most important test conditions to evaluate the material in a hydrogen environment. The data from the feedback was developed into 27 failure criteria and used in a FMEA tool to document the risk and to and help prioritize the key actions to reduce failures. The applications include compressors, valves, seals, refueling stations, liners, and others. The failure modes were based on three primary functions/applications, static seals, dynamic seals, and barriers. The team completed the FMEA and the results were presented at the Annual Merit Review and with the Canadian Standards Association committee for developing the new Compressed Hydrogen Materials Compatibility 2 standard for hydrogen compatibility in polymers. The FMEA risk priority number (RPN) value is calculated based on a ranked severity rating, an occurrence rating, and a detection rating that was agreed on prior to ranking. The rankings were based on available information and current test methods developed for hydrogen. The average of the 27 identified failure modes had an average of 300. Table 1 illustrates the top six results that are above the average of the calculated RPN and are in line with our current research. The FMEA is dynamic and is adjusted as new information is learned thereby changing the ranking of priority.

The project developed a preliminary test methodology for in situ high-pressure hydrogen testing of friction and wear and delivered a report to DOE. The test methodology was an adaptation of ASTM G-133 and has demonstrated differences in hydrogen, argon, and ambient air. This fiscal year three materials were tested following newly developed test method, NBR, EPDM, and PTFE. Initial control parameters are load, speed, track length, pin diameter, pin roughness, and pin material. Results of the test demonstrate the effect that hydrogen has on NBR, EPDM, and PTFE which show an increase in coefficient of friction in 4,000 psi hydrogen by factors of 1.4, 1.8, and 1.5, respectively as compared to ambient air as shown in Figure 1. Ex situ optical profilometry (interference) shows a clear increase in wear in high-pressure hydrogen over ambient air, over high-pressure argon for NBR. The ex situ wear track depths are 100 microns, 60 microns, and 7 microns, respectively for high-pressure hydrogen, ambient air, high pressure argon. Figure 2 clearly indicates the difference in wear between the gases and testing condition. Future work for heating and cooling is shown in Figure 3.

The project also assessed the impact of purge and leak test gases on the material being tested. It is important to separate out the effects of other gases used as part to the test method so that the hydrogen effect can be evaluated. Figure 4 illustrates the damage in elastomer seal materials related

TABLE 1. Top Four RPN Items Based on the Initial FMEA Assessment (>300)

Potential Cause	Failure Mode (RPN)	Function
#17 Polymer seal (dynamic) material experiences a change in properties (strength, modulus, shear, hardness, etc.) due to hydrogen exposure	Seal exceeds allowable dynamic performance when exposed to hydrogen (initially, after pressure cycles, after temperature cycles, or over extended time). (490)	Contain hydrogen with dynamic seal at all operating pressures (5 bar to 875 bar) and temperatures (-40°C to 85°C) until end of life • Maintain seal dynamic performance
#24 Polymer barrier material degrades from rapid high-pressure differentials (explosive decompression) due to hydrogen exposure • Material extrudes, cracks, or fragments	Liner exceeds allowable external leak rate limit when exposed to hydrogen (initially, after pressure cycles, after temperature cycles, or over extended time). (420)	Contain hydrogen with barrier liner at all operating pressures (5 bar to 875 bar) and temperatures (-40°C to 85°C) until end of life • Lower than acceptable external leakage rate of 10 Nml/h
#1 & #9 Polymer seal (static & dynamic) material selected exceeds hydrogen permeation rate • Unable to contain hydrogen through the material	Seal exceeds allowable external and/or external leak rate limit when exposed to hydrogen (initially, after pressure cycles, after temperature cycles, or over extended time). (400)	Contain hydrogen with static seal and dynamic seal at all operating pressures (5 bar to 875 bar) and temperatures (-40°C to 85°C) until end of life • Lower than acceptable external and internal leakage rate of 10 Nml/h
#6 & #14 Polymer seal (static & dynamic) material geometry changes and volume swells or reduction due to hydrogen exposure • Unable to maintain seal design and compression (compression set occurs) • Material extrudes, cracks, or fragments	Seal exceeds allowable external and/or external leak rate limit when exposed to hydrogen (initially, after pressure cycles, after temperature cycles, or over extended time). (350)	Contain hydrogen with static seal and dynamic seal at all operating pressures (5 bar to 875 bar) and temperatures (-40°C to 85°C) until end of life • Lower than acceptable external and internal leakage rate of 10 Nml/h

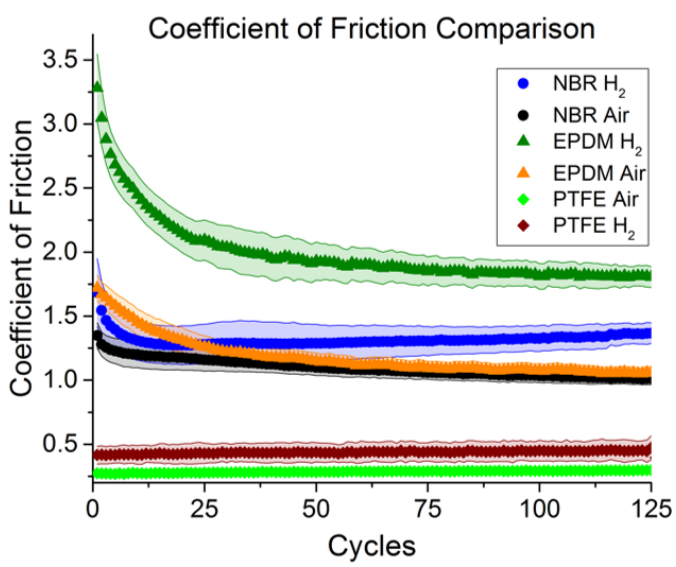

FIGURE 1. Comparing coefficient of friction

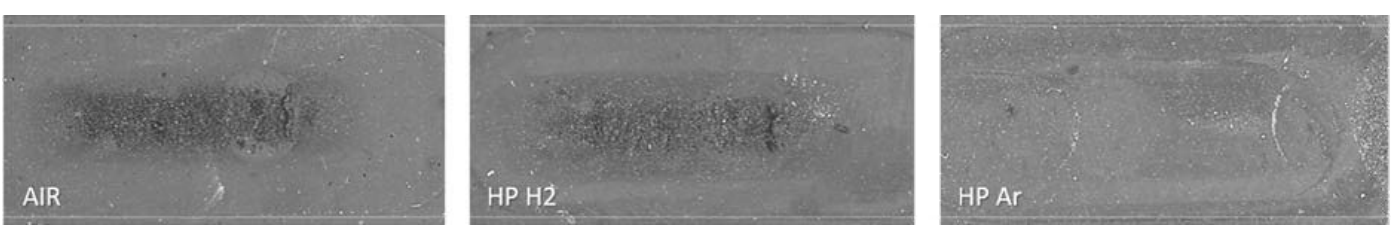

FIGURE 2. Ex situ wear tracks in NBR

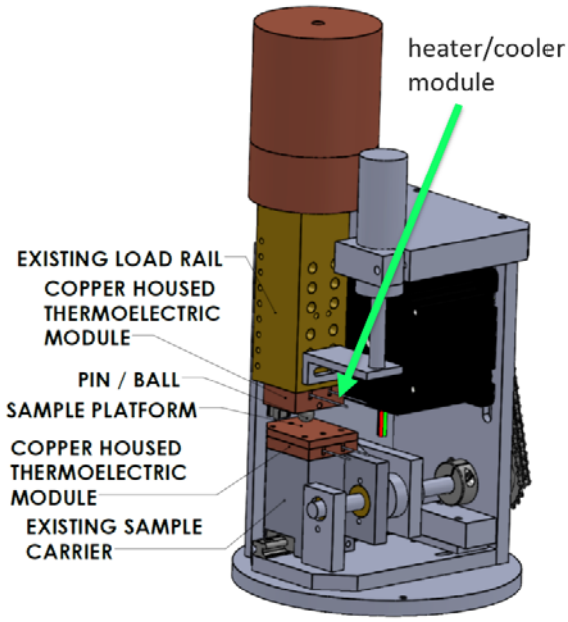

FIGURE 3. Novel high pressure hydrogen in situ tribometer

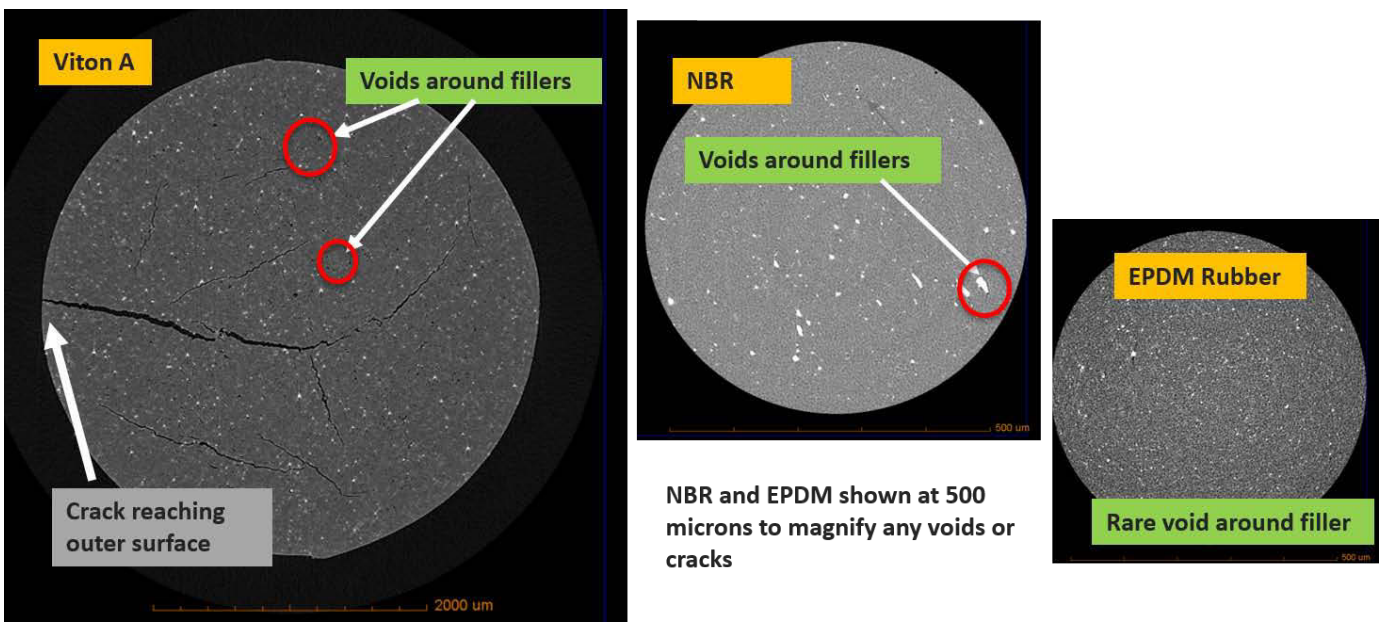

FIGURE 4. Damage in elastomer seal materials related to their purge/leak test gas study

to their purge and leak test gas study. Viton A shows the most damage and influence from argon and argon/hydrogen, whereas helium has a small to negligible effect. It does seem to be polymer/elastomer dependent. Table 2 illustrates the influence of the material properties associated with the gas used. It was also found that compression set can have increased effect based on the gas.

CONCLUSIONS AND UPCOMING ACTIVITIES

The project has prioritized the most important attributes based on the FMEA results and the feedback provided by the stakeholders. Tribology work resulted in delivering an initial test methodology for novel in situ friction and wear testing. The tribology results show hydrogen significantly influence

TABLE 2. Damage or Influence in Elastomer Seal Materials Related Purge and Leak Gas

Polymer properties (characterization methods)	Maximum effects seen in various gas environments		
	Argon/Hydrogen**	Helium/Hydrogen***	Helium
Swelling (Density measurements)	73% with 100% recovery seen with NBR	36% with 100% recovery seen with Viton A	14% with 100% recovery seen with NBR
Storage modulus changes (DMTA)	41% decrease for Viton A	20% decrease with Buna N	No change observed
Compression set (elastomers only)	5 times increase seen for Viton A	1.6 times increase with Viton A	2.0 times increase with Viton A
Mass loss (TGA) indicating gas diffusion out of polymer after 48 h after removal from test	Highest mass loss	Mass loss is lower than unexposed	Lowest
Explosive decompression (micro CT)	Viton A shows severe damage; much less effects on NBR and EPDM	Viton A shows voids around specific fillers; NBR and EPDM unaffected	All polymers are unaffected

Micro CT – micro computed tomography; TGA – thermogravimetric analysis; DMTA – dynamic mechanical thermal analysis

the coefficient of friction in EPDM, NBR, and PTFE. Likewise, the gas species can also influence the friction and the wear. Purge and leak test gases have also shown to have an impact on the material. Viton A was severely impacted with argon gas in several attributes as well as severe cracking. Helium gas shows the least impact, but is also polymer/elastomer dependent on the influence.

The future work includes the following:

- Study heating and cooling impacts on friction and wear.
- Study the influence of material additives in elastomers in both friction and wear, and decompression.
- Complete the cyclic testing experiment build and functional tests.

FY 2017 PUBLICATIONS/PRESENTATIONS

1. N.C. Menon, A.M. Kruizenga, A. Nissen, C. San Marchi, K.J. Alvine, K. Brooks, D.B. Smith, and A.K. Naskar, "Polymer Behavior in High Pressure Hydrogen environments with relevance to the Hydrogen Infrastructure," submitted to International Hydrogen Conference, Moran, WY, September 2016.

2. Alvine K., Brooks K., Duranty E., Menon N., Kruizenga A., San Marchi C., Smith B., Naskar A.,"Hydrogen Compatibility of Polymers for Infrastructure Applications: Friction and Wear." Submitted to the 2016 International Hydrogen Conference, Moran, WY, September 2016.

3. Duranty E., Roosendaal T., Pitman S., Tucker J., Owsley Jr. S., Suter J., Alvine K., "An In Situ Tribometer for Measuring Friction and Wear of Polymers in a High Pressure Hydrogen Environment." Submitted to Review of Scientific Instruments, April 2017.

4. Alvine, Brooks, et al., "Hydrogen Compatibility of Polymers for Infrastructure Applications," submitted to International Hydrogen Conference, Moran, WY, September 2016.

5. Simmons et al., "Hydrogen Compatibility of Polymers Program Overview," International Hydrogen Energy Development Forum,Fukuoka, Japan, February 2017 Invited Keynote Speaker.

6. Alvine et al., "In Situ Friction and Wear of Polymers in High Pressure Hydrogen." HYDROGENIUS Research Symposium, Fukuoka, Japan, February 2017 Invited Speaker.

7. Menon et al., "High Pressure Cycling and Tribology Effects on Polymers in Hydrogen Environments," MSRF Workshop, Livermore, CA, March 2017.

VIII.10 Enabling Hydrogen Infrastructure Through Science-Based Codes and Standards

Chris LaFleur (Primary Contact), Alice Muna, Myra Blaylock, Gaby Bran-Anleu, Ethan Hecht
Sandia National Laboratories
P.O. Box 5800 MS 0748
Albuquerque, NM 87185
Phone: (505) 844-5425
Email: aclafle@sandia.gov

DOE Manager: Will James
Phone: (202) 287-6223
Email: Charles.James@ee.doe.gov

Project Start Date: October 1, 2003
Project End Date: Project continuation and direction determined annually by DOE

Overall Objectives

- Utilize fundamental science and engineering to enable the growth of hydrogen infrastructure and improve the basis of codes and standards.
- Enable industry-led codes and standards revision and safety analyses by providing a strong science and engineering basis for code improvements.
- Eliminate barriers to deployment of hydrogen fuel cell technologies through scientific leadership in codes and standards development efforts.

Fiscal Year (FY) 2017 Objectives

- Revise/update codes and standards that address critical limitations to station implementation.
- Streamline cost and time for station permitting by demonstration of alternative approaches to code compliance.

Technical Barriers

This project addresses the following technical barriers from the Hydrogen Safety, Codes and Standards section of the Fuel Cell Technologies Office Multi-Year Research, Development, and Demonstration Plan.

(H) Insufficient technical data to revise standards

(A) Insufficient Synchronization of National Codes and Standards

(K) No Consistent Codification Plan and Process for Synchronization of R&D and Code Development

(A) Usage and Access Restrictions

Contribution to Achievement of DOE Safety, Codes and Standards Milestones

This project will contribute to achievement of the following DOE milestones from the Safety, Codes and Standards section of the Fuel Cell Technologies Office Multi-Year Research, Development, and Demonstration Plan.

- Milestone 2.19: Validate inherently safe design for hydrogen fueling infrastructure. (4Q, 2019)
- Milestone 4.7: Complete risk mitigation analysis for advanced transportation infrastructure systems. (1Q, 2015)
- Milestone 4.8: Revision of NFPA 2 to incorporate advanced fueling and storage systems and specific requirements for infrastructure elements such as garages and vehicle maintenance facilities. (3Q, 2016)

FY 2017 Accomplishments

- Performed calculations and risk analysis for revised bulk gaseous separation distances using revised risk criteria for adoption by the National Fire Protection Association (NFPA) 2/55 technical committees, which will enable more sites to readily accept hydrogen infrastructure.
- Developed risk analysis framework and identified scenarios of concern for tunnel access for hydrogen fuel cell electric vehicles.
- Completed computational fluid dynamics (CFD) and heat transfer models to evaluate hydrogen fire impact on steel structure and concrete in passenger vehicle tunnels.

✧ ✧ ✧ ✧ ✧

INTRODUCTION

The DOE Fuel Cell Technologies Office has identified safety, codes, and standards as a critical barrier to the deployment of hydrogen, with key barriers related to the availability and implementation of technical information in the development of regulations, codes, and standards. This project provides the technical basis for assessing the safety of hydrogen fuel cell systems and infrastructure using quantitative risk assessment and physics-based models of

hydrogen behavior. The risk and behavior tools are used to support alternate methods of code-compliant hydrogen infrastructure and directly support code committees in incorporating science-based revisions that address critical limitations to refueling station implementation. This project provides the scientific basis to ensure that code requirements are consistent, logical, and defensible.

APPROACH

State-of-the-art integrated hydrogen behavior and quantitative risk assessment models are applied to relevant technologies and systems to provide insight into the risk level and risk mitigation strategies with the aim of enabling the deployment of fuel cell technologies through revision of hydrogen safety codes and standards. In the short-term focus of providing alternative methods for code compliance, this effort will enable hydrogen refueling stations that are unable to explicitly meet prescription code requirements to utilize alternate means allowed by the current code. Implementing the template at a real-world hydrogen station planned in California will provide precedence for a performance-based design and will allow the cost and schedule for developing this type of station design to be optimized.

Towards the longer-term goal of achieving science-based revisions of codes and standards, a review and revision of the risk-informed code requirements for bulk gaseous hydrogen storage will enable behavior models and technology not available during the 2009 revision to be incorporated into the risk criteria used to determine these requirements. The bulk liquid hydrogen storage code requirements will also be revised following a similar review. For northeastern United States tunnel access, a risk framework and scenarios of concern will be developed and analyzed to address the concerns of local authorities having jurisdiction.

RESULTS

Science-based Hydrogen Storage Code Improvements

The bulk hydrogen storage separation distances in NFPA 2/55 are categorized into three groups depending on the hazard scenario and harm criteria used to determine the separation distances. The revised distances for bulk gaseous storage, based on Sandia's risk calculations for the revised risk and harm criteria, were proposed in the first draft stage of the 2020 NFPA code revision cycle. The resulting reductions in the 2016 separation distances are shown in Table 1. The Technical Committee approved these revisions for adoption in the 2020 edition of NFPA 2/55.

The NFPA task group also worked to apply the risk-informed process to the bulk liquefied hydrogen storage separation distances using the same process as the gaseous storage. The prioritized hydrogen release scenarios include those that occur during liquid hydrogen transfer operations from a tanker truck to the bulk liquid hydrogen storage tank as well as during normal system operations. These scenarios will be modeled with Sandia's hydrogen release model to help revise the distances in the next code cycle so that they are risk-informed and based on sound science and physics for the behavior of released hydrogen.

Evaluation of Existing Tunnel for Fuel Cell Electric Vehicle Safety

Several authorities in the Northeast expressed concerns about allowing fuel cell electric vehicle access to important tunnels in their metro areas (New York City, Baltimore, and Boston). Our goal is to provide the scientific modeling and risk analysis for these authorities having jurisdiction and emergency responders to address their concerns regarding fuel cell electric vehicles. We participated in several face-to-face meetings with the authorities having jurisdiction in order to collect information about the nature of their concerns. We developed a risk framework in the form of an event sequence diagram to capture the possible scenarios and analyzed data to assign probabilities, based on frequencies of tunnel incidents, for each branch line. We conducted an initial analysis to compare anticipated hydrogen release scenarios with the NFPA 502 (National Fire Protection Association, 2016) [1] requirements for tunnel fires. We subsequently performed a computational fluid dynamics modeling analysis to address concerns for a specific incident where an overturned vehicle releases hydrogen through its thermal

TABLE 1. Technical Committee Approved Updated Values to NFPA 2 and NFPA 55 Separation Distance Tables

Exposures >0.10 to 1.7 MPa (>15 to 250 psig)		Separation Distance			
		>1.7 to 20.7 MPa (>250 to 3,000 psig)	>20.7 to 51.7 MPa (>3,000 to 7,500 psig)	51.7 to 103.4 MPa (7,500 to 15,000 psig)	
Group 1	Existing	12 m (40 ft)	14 m (46 ft)	9 m (29 ft)	10 m (34 ft)
	Approved New	**5 m (16 ft)**	**6 m (20 ft)**	**4 m (13 ft)**	**5 m (16 ft)**
Group 2	Existing	6 m (20 ft)	7 m (24 ft)	4 m (13 ft)	5 m (16 ft)
	Approved New	**5 m (16 ft)**	**6 m (20 ft)**	**3 m (10 ft)**	**4 m (13 ft)**
Group 3	Existing	5 m (17 ft)	6 m (19 ft)	4 m (12 ft)	4 m (14 ft)
	Approved New	**4 m (13 ft)**	**5 m (16 ft)**	**3 m (10 ft)**	**4 m (13 ft)**

pressure relief device (TPRD). This modeling was intended to address concerns regarding explosive spalling conditions in the concrete tunnel structures, impact of hydrogen jet fire on bolt/epoxy assemblies that support the load of concrete ceiling panels, and the impact of the fire environment on the steel support structures via a strain analysis.

Figure 1 shows the results of the heat release rate comparison to the RijksWaterStaat (RWS) fire curve, and Figure 2 shows the same comparison to the RWS curve for the temperature in a tunnel fire. Figure 3 provides a screen capture of the steady state temperature at the ceiling resulting from the hydrogen jet fire with tunnel ventilation.

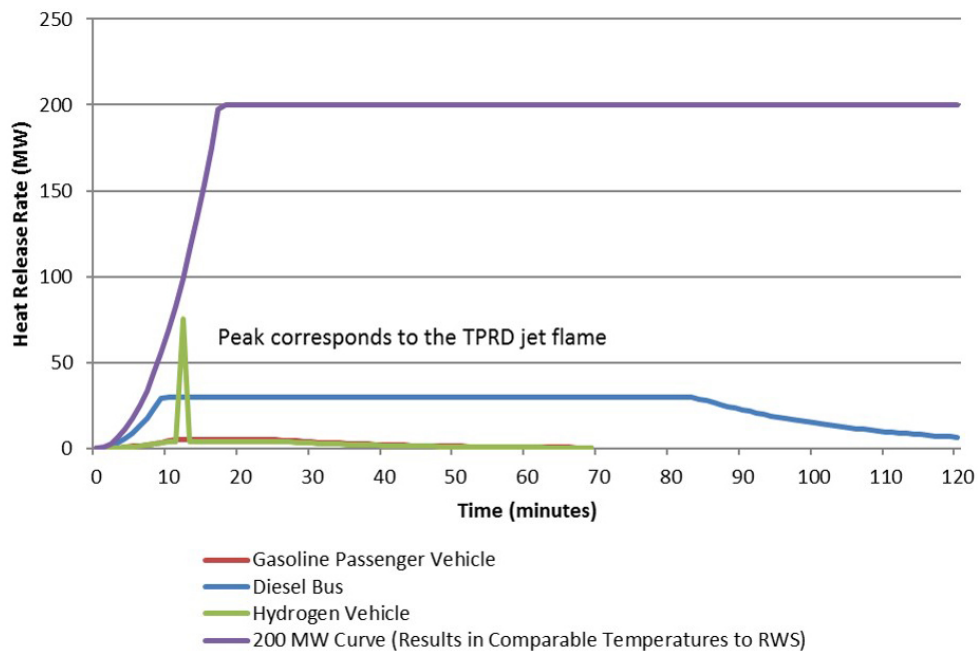

FIGURE 1. Heat release rate comparison to the RWS fire curve

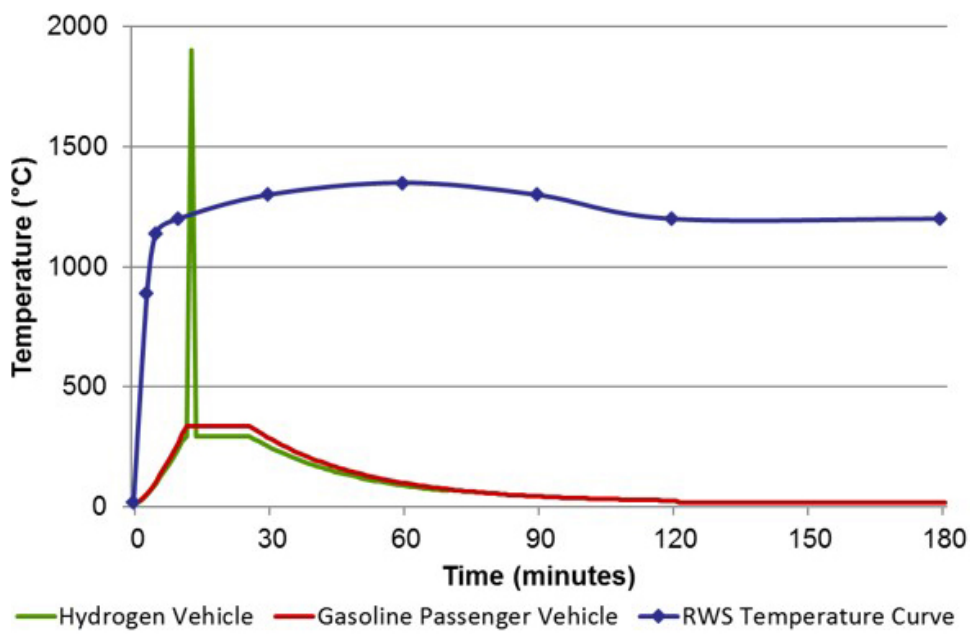

FIGURE 2. Temperature comparison to the RWS fire curve

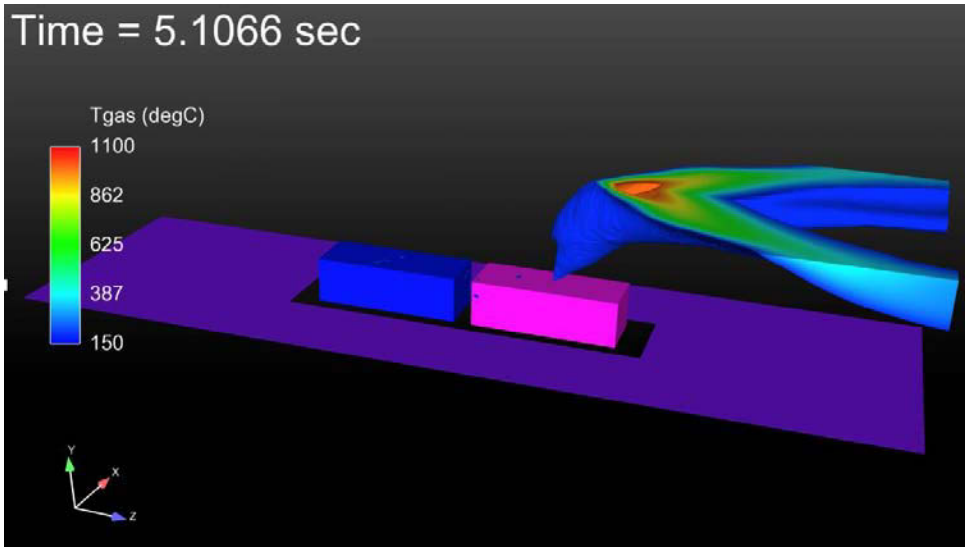

FIGURE 3. Steady-state temperature at the ceiling resulting from the hydrogen jet fire with tunnel ventilation

The results indicated that the conditions may be present for localized spalling of the concrete—but it is a very limited area (<1 m diameter) and shallow into the concrete (<1 in). The temperature in the steel hangers and the bolts/epoxy assemblies never rises above ambient temperature, so the epoxy is not compromised. The portion of the steel structure supporting the concrete panels has a temperature gradient, and the analysis of the strain impacts on the steel is nearing completion.

Demonstration of Performance-based Design for a Real-World Station

NFPA 2, Hydrogen Technologies Code, allows for the use of alternate means of code compliance, including performance-based design, for hydrogen facilities as a means of complying with the code without strict adherence to the prescriptive code requirements. While the Hydrogen Risk Assessment Models software can be used as a means of evaluating the risk of alternate designs, it can also be used to quantitatively evaluate risks associated with alternate means of code compliance. The establishment and demonstration of alternate means will directly increase the availability of locations for hydrogen fueling stations, reduce the effort required by industry to use alternate approaches, and lay the groundwork for similar quantitative-risk-assessment-backed design processes for other alternative fuels. Efforts focused on identifying a refueling station to demonstrate alternate means of compliance in a real-world permitting situation.

CONCLUSIONS AND UPCOMING ACTIVITIES

The scientific analysis of the risks, hazards, and consequences associated with hydrogen applications is important as it informs the codes and standards governing the use of hydrogen and addresses barriers to technology advancement while addressing safety concerns. This work will continue in the future; however, the work will be assimilated under the associated program capabilities at Sandia National Laboratories, including hydrogen behavior studies, materials compatibility research, and quantitative risk analyses.

SPECIAL RECOGNITIONS & AWARDS/ PATENTS ISSUED

A 2017 Hydrogen and Fuel Cells Program R&D Award was awarded to Chris LaFleur at the 2017 Annual Merit Review and Peer Evaluation Meeting for her outstanding technical leadership in hydrogen behavior and risk assessment to enable the safe deployment of hydrogen fuel cell technologies worldwide.

FY 2017 PUBLICATIONS/PRESENTATIONS

1. C. San Marchi, E.S. Hecht, I.W. Ekoto, K.M. Groth, C. LaFleur, B.P. Somerday, R. Mukundan, T. Rockward, J. Keller, C.W. James: "Overview of the DOE hydrogen safety, codes and standards program, part 3: Advances in research and development to enhance the scientific basis for hydrogen regulations, codes and standards." Intern J Hydrogen Energy (proof online).

2. E.S. Hecht, P. Panda (presentation), "Validation data for cryogenic hydrogen releases and flames." Presented to Liquid

Hydrogen Separation Distance project stakeholders (web meeting), November 9, 2016. SAND2016-11548 PE.

3. C.B. LaFleur (presentation), "Hydrogen Vehicle Tunnel Safety." Presented to personnel from Massachusetts Department of Transportation, Boston Fire Department, and Massachusetts State Fire Marshal's Office, October 20, 2016. SAND2016-10789 PE.

4. C.B. LaFleur (presentation), "Hydrogen Vehicle Tunnel Safety." Presented to personnel from Maryland Department of Transportation, February 7, 2017. SAND2016-10789 PE.

5. C.B. LaFleur (presentation), "Enabling Hydrogen Infrastructure Through Science-based Codes and Standards." Presented at the 2017 Hydrogen and Fuel Cells Program Annual Merit Review and Peer Evaluation meeting, June 6, 2017. SAND2017-5264 PE.

REFERENCES

1. NFPA 55 *Compressed Gases and Cryogenic Fluids Code*, 2016 NFPA, Quincy, MA.

2. NFPA 2 *Hydrogen Technologies Code*, 2016 NFPA, Quincy, MA.

VIII.11 Advancing Fuel Cell Electric Vehicles in San Francisco and Beyond

Jessie Denver (Primary Contact), Suzanne Loosen
City and County of San Francisco
Department of the Environment
1455 Market Street, Suite 1200
San Francisco, CA 94103
Phone: (415) 355-3720
Email: Jessie.Denver@sfgov.org

DOE Manager: Gregory Kleen
Phone: (240) 562-1672
Email: Gregory.Kleen@ee.doe.gov

Contract Number: DE-EE0007599

Subcontractors:
- Frontier Energy (formerly known as BKi), West Sacramento, CA
- Newcomb Anderson McCormick, San Francisco, CA
- Business Council on Climate Change, San Francisco, CA

Project Start Date: October 1, 2017
Project End Date: September 30, 2018

Overall Objectives

- Update and harmonize best practices in permitting and inspection of hydrogen fueling stations among Bay Area authorities having jurisdiction (AHJs).
- Deliver hydrogen safety and best practice education to elected officials and planning, building inspection, and public safety professionals across the Bay Area.
- Increase community awareness of the availability and value of hydrogen and fuel cell electric vehicles (FCEVs).
- Drive market demand for FCEVs through an established, public-facing group procurement program.

Fiscal Year (FY) 2017 Objectives

- Identify and address training needs for AHJs.
- Deliver permitting technical assistance to station developers and AHJs.
- Promote hydrogen and FCEVs via outreach events.
- Implement SunShares 2017 group procurement program.

Technical Barriers

This project addresses the following technical barriers from the Fuel Cell Technologies Office Multi-Year Research, Development, and Demonstration Plan, Section 3.8, Education and Outreach.

(A) Lack of Readily Available, Objective, and Technically Accurate Information

(D) Lack of Educated Trainers and Training Opportunities

Contribution to Achievement of DOE Education and Outreach Milestones

This project will contribute to achievement of the following DOE milestones from the Fuel Cell Technologies Office Multi-Year Research, Development, and Demonstration Plan, Section 3.8, Education and Outreach.

- Task 1: Educate Safety and Code Officials
- Task 2: Educate Local Communities
- Task 3: Educate State and Local Government Representatives
- Task 4: Educate Potential End-Users

FY 2017 Accomplishments

- Organized pre-application meetings with station developers and AHJs.
- Conducted outreach and community awareness events, including ride-and-drive events.
- Developed and implemented training plan.
- Launched "Clean Cities Hydrogen and Fuel Cell Electric Vehicle" newsletter.
- Distributed Request for Proposals to FCEV makers for the 2017 SunShares program.

✧ ✧ ✧ ✧ ✧

INTRODUCTION

This program supports the introduction of FCEVs and retail hydrogen fueling stations in San Francisco and the nine-county Bay Area. The California Energy Commission is investing in a network of 100 hydrogen fueling stations in California by 2022 to support the broader introduction of FCEVs. By applying lessons learned from the build-out of the solar and electric vehicles industries, we are working

on reducing soft costs tied to two primary barriers. The first is the cost and complexity of permitting and inspection processes among multiple AHJs, and the second is a lack of consumer awareness of hydrogen and FCEVs.

APPROACH

To address the cost and complexity of permitting, we provide training and technical assistance to AHJs and station developers in proposed development areas. This includes organizing and facilitating pre-application meetings, documenting permitting and inspection processes among AHJs, publishing a newsletter, and developing specialized trainings, such as webinars. As stations near completion, we will organize local community awareness events in partnership with the AHJs and station developers.

To address the lack of consumer awareness, we use the SunShares group procurement program to provide discounts on FCEVs coupled with consumer workshops for municipalities and major Bay Area employers. We have also incorporated FCEVs in our annual Clean Cities workshops and local ride-and-drive events.

RESULTS

Our work will support hydrogen station development in San Francisco and the nine-county Bay Area. Figure 1 shows stations that are open, in development, or recommended for funding as of Spring 2017. Three of those stations received funding approval on June 14, 2017. The balance will be considered at the California Energy Commission's August 2017 business meeting.

Permitting best practice recommends organizing pre-application meetings with AHJs to review local permitting requirements and timelines in advance of submittal. The California Energy Commission requires that station developers include basic California Environmental Quality Act information in their proposals for funding, which requires at least minimal contact with the AHJ. In partnership with the Center for Transportation and Environment, we organized such a meeting for a station applicant, Equilon Enterprises (a Shell/Toyota partnership). We suggested that the applicant might strengthen their California Energy Commission application with a commitment to procure 100% renewable energy for their operations. This is possible through CleanPowerSF, a community choice aggregation program administered by the San Francisco Public Utilities Commission. Equilon Enterprises did include procurement of 100% renewable energy in their application, which prevailed over two other applications. Funding is anticipated in August 2017.

Our outreach to AHJs and station developers has led us to design a webinar for code officials, in partnership with Frontier Energy's California Fuel Cell Partnership and the Governor's Office of Business and Economic Development. The webinar will be delivered in July 2017 and be available online. Invitations were sent to over 400 Bay Area AHJ contacts, as well as stakeholders and Clean Cities Coordinators in Southern California and the Northeast Hydrogen Station Network. In addition, we have developed

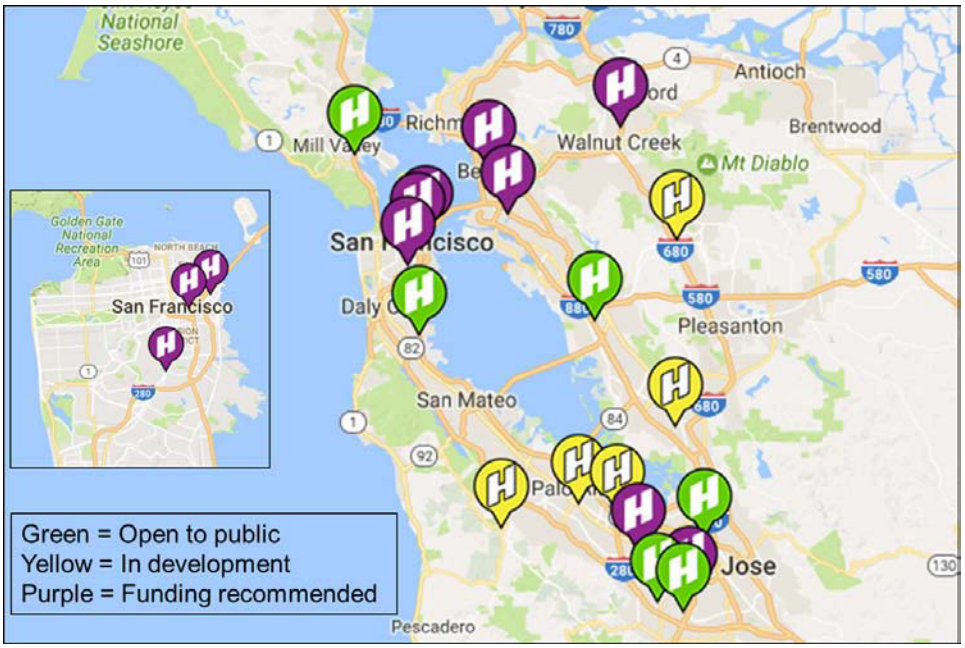

FIGURE 1. Map of San Francisco Bay Area hydrogen stations, Spring 2017

a technical training schedule, which will coincide with anticipated development of the eight proposed Bay Area hydrogen stations (Table 1).

The 2016 SunShares group procurement program for residential solar and zero emission vehicles resulted in over 1,800 registrations in a three-month period. Participants engaged in 30 workshops conducted across the Bay Area, where they learned more about technology product options (e.g., solar photovoltaics, battery electric vehicles, FCEVs) available through the program and available incentives/financing. In the 2016 round of SunShares, we invited Toyota to include the newly introduced Mirai FCEV, which resulted in four program participant vehicle purchases. SunShares originally began in 2011, providing bulk discounts on residential solar. In 2015 the program evolved to include battery electric vehicles. The program is successful in reducing soft costs and complexity for participants by leveraging the existing communication channels of affinity groups such as employers and municipalities to reach participants, and pre-negotiating bulk pricing through a competitive process.

The *SF Clean Cities Hydrogen and Fuel Cell Electric Vehicle Newsletter* was launched in March 2017 (Figure 2) and distributed to about 100 Clean Cities stakeholders and through the California Fuel Cell Partnership's contact list of over 11,000 individuals. The content includes hydrogen/FCEV 101, along with videos and links to news articles.

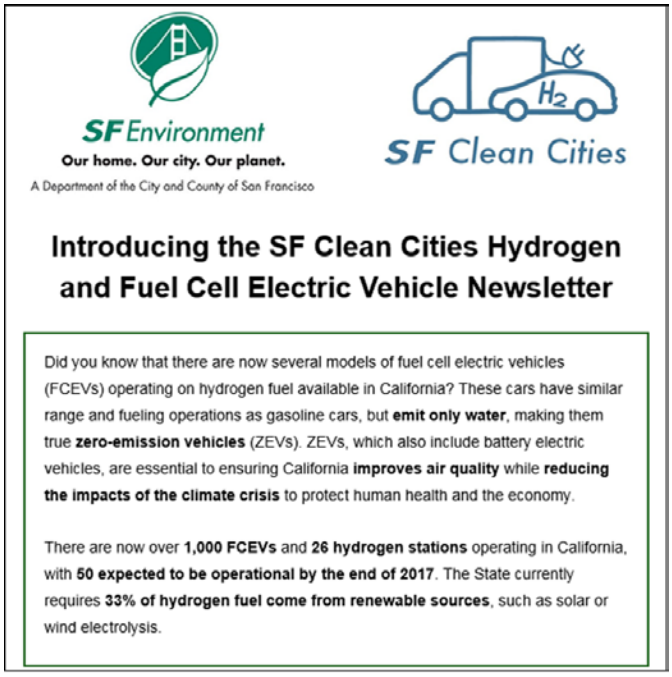

FIGURE 2. SF Clean Cities Hydrogen and Fuel Cell Electric Vehicle Newsletter

CONCLUSIONS AND UPCOMING ACTIVITIES

Our work is having the anticipated impact of reducing the complexity of permitting processes by providing technical assistance and coordination to developers and AHJs. We have incorporated FCEVs into our community awareness events, ride-and-drives, and the SunShares program, thereby expanding the promotion of FCEVs to the public.

The second year of our program builds upon the first with additional training, community awareness events, and the 2017 SunShares program. Our biggest consumer awareness event in Calendar Year 2017 will be EV Week, held in conjunction with San Francisco Fleet Week, which attracts approximately one million people to the city each October. Nearly 600 people participated in ride-and-drives at last year's event. Planning has begun for this year's event, and it appears that all FCEV manufacturers will participate.

TABLE 1. Outreach and Training Schedule

Topic	Audience	Begins	Frequency
Hydrogen Safety for Permitting Authorities	Building officials; planning, safety and fire, sustainability staff	Summer 2017	Multiple sessions at AHJs, Webinars
Hydrogen and FCEVs for Decision Makers	Elected officials, department/division leaders, general public	Fall 2017	Two sessions North Bay and South Bay
Community Engagement	Community members in vicinity of stations	Fall 2017	As needed
Hydrogen/FCEV Safety for First Responders	First responders	Summer 2018	Multiple sessions at AHJs

IX.0 Systems Analysis Sub-Program Overview

INTRODUCTION

Systems Analysis supports the decision-making of the Fuel Cell Technologies Office (FCTO) by providing a greater understanding of technology gaps, options, and risks. The Systems Analysis sub-program analyzes the contribution of individual technology components and systems to overall pathways. For example, the team provides techno-economic analysis of fuel production on a lifecycle basis for light-, medium-, and heavy-duty fuel cell electric vehicles (FCEVs). Analysis is also conducted to assess cross-cutting issues, such as integration of hydrogen and fuel cells with the electric grid for energy storage and grid services.

Systems Analysis made several significant contributions to the Hydrogen and Fuel Cells Program in Fiscal Year (FY) 2017. The hydrogen financial analysis scenario tool (H2FAST) was expanded to provide in-depth financial and stochastic analysis of hydrogen refueling stations. The sub-program also studied how increasing fuel cell efficiency would impact the costs of fuel cells and hydrogen storage systems and the performance of FCEVs. The Greenhouse gases, Regulated Emissions, and Energy use in Transportation (GREET®) model continues to be enhanced for the analysis of petroleum use, greenhouse gas (GHG) emissions, criteria pollutants, and water consumption for multiple hydrogen pathways for light-, medium-, and heavy-duty vehicles on a lifecycle basis.

GOAL

The goal of the Systems Analysis sub-program is to provide system-level analysis to support hydrogen and fuel cell technology development and technology readiness by evaluating technologies and pathways, including resource requirements, to guide the selection of research and development (R&D) projects and estimate the potential value of specific R&D efforts.

OBJECTIVES

- By 2018, complete an assessment of fuel cell cost and power requirements for multiple medium- and heavy-duty truck applications.
- By 2018, update the risk analysis process for FCTO-supported technologies, prepare a risk analysis plan for FCTO, and apply the process to at least one FCTO sub-program.
- By 2018, complete a preliminary resource analysis supporting the H2@Scale initiative and identify excess hydrogen generation capacity available for hydrogen fueling or other applications.
- By 2019, complete a sustainability analysis of FCTO metrics and develop a method of incorporating metrics in sub-program targets.
- By 2019, complete an analysis of the potential for hydrogen, stationary fuel cells, FCEVs, and other fuel cell applications such as grid services. The analysis will address necessary resources, hydrogen production, and performance of stationary fuel cells and vehicles.
- Provide milestone-based analysis, including risk analysis and independent reviews, to support the fuel cell technologies' needs prior to technology readiness.
- Periodically update the lifecycle energy and petroleum use analysis for technologies and pathways for fuel cell technologies to include technological advances or changes.

FY 2017 TECHNOLOGY STATUS AND ACCOMPLISHMENTS

The Systems Analysis sub-program focuses on examining the economics, benefits, opportunities, and impacts of fuel cells and renewable fuels with a consistent, comprehensive analytical framework. Analysis conducted in FY 2017 included analysis of socio-economic impacts such as employment impacts from the penetration of hydrogen and FCEVs, enhancement of the H2FAST tool, analysis of the reduction of fuel cell and storage system costs as a result of improved fuel cell efficiency, lifecycle analysis of petroleum use and GHG emissions for medium- and heavy-duty trucks, and lifecycle analysis of water use and criteria emissions for multiple hydrogen and conventional light-

duty fuel/vehicle pathways. Systems Analysis leverages the key models shown in Figure 1. These models have been developed in prior years for critical sub-program analyses.

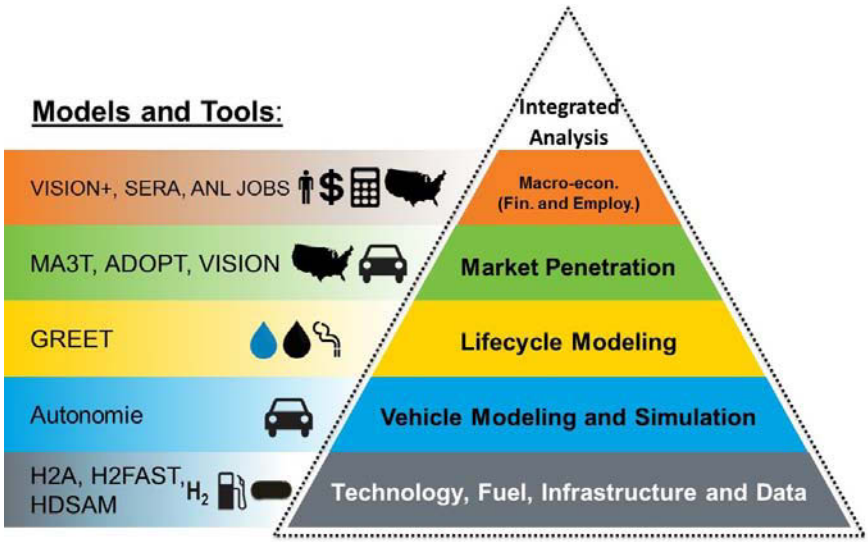

Model Description Fact Sheets: http://www.energy.gov/eere/fuelcells/systems-analysis

FIGURE 1. Systems Analysis Models and Tools

Develop and Maintain Models and Systems Integration

Lifecycle Analysis of Air Pollutants for Hydrogen Production from Steam Methane Reforming (SMR)

The GREET model has been updated to assess the lifecycle emissions impact of FCEVs relative to baseline petroleum fuels usage in internal combustion engine vehicles (ICEVs). The model update methodology included developing criteria air pollutants emission factors for hydrogen production via SMR process. These factors were calibrated to air pollutant emissions from U.S. standalone SMR units and aggregated to the national level. The model simulations show that use of SMR hydrogen in FCEVs can reduce most criteria pollutant emissions from 35%–97% when compared to gasoline ICEVs.

The comparison of criteria pollutants emissions for various fuel-vehicle technologies is provided in Table 1 on grams per million British thermal units (g/mmBtu) and grams per mile bases. As shown, the hydrogen FCEV has significantly lower per-mile well-to-wheel (WTW) emissions than ICEVs for most pollutants, but SOx emissions are an exception. The higher WTW SOx emissions are attributed to the emissions associated with electricity generation for hydrogen compression, which is required for both hydrogen delivery and FCEV refueling. As the future grid electricity generation mix is projected to have a reduced share of coal-based generation, the WTW SOx emissions for FCEVs is expected to be proportionally reduced.

Lifecycle Analysis of Fuel Cell Applications for Medium- and Heavy-Duty Trucks

Medium- and heavy-duty vehicles (MHDVs), particularly trucks, are the second-largest and fastest-growing petroleum consumers and GHG emitters in the U.S. transportation sector. The significance of MHDVs is even greater for local air quality management in some areas. FCEVs can play an important role, as they create zero tailpipe emissions and do not consume petroleum fuels. The main goal of this project is to quantify and examine the WTW petroleum energy use and emissions of hydrogen fuel cell MHDVs in comparison with conventional diesel ICEVs by expanding the GREET model by adding FCEVs to the existing MHDV technology portfolio.

Simulation results show that medium- and heavy-duty FCEVs generally achieve 1.7 times better fuel economy (miles per diesel gallon equivalent) compared to conventional diesel vehicles, resulting in a significant reduction in petroleum use and GHG emissions. An example of the potential GHG emissions reduction for a Class 6 FCEV compared to a conventional medium-duty truck is provided in Figure 2.

TABLE 1. Lifecycle Emissions for Various Fuel–Vehicle Technologies

(g/mmBtu basis)	VOC	CO	NOx	SOx	PM10	PM2.5
Gasoline ICEV	84.7	645	65.3	21.3	8.89	4.58
Diesel ICEV	42.3	796	67.0	14.4	8.58	4.42
LPG ICEV	59.2	645	56.4	21.5	6.82	3.36
H_2 FCEV	13.7	33.6	51.8	61.0	13.2	6.35
(g/mile basis)						
Gasoline ICEV	0.364	2.78	0.281	0.091	0.038	0.020
Diesel ICEV	0.152	2.86	0.240	0.051	0.031	0.016
LPG ICEV	0.255	2.77	0.243	0.092	0.029	0.014
H_2 FCEV	0.028	0.069	0.106	0.125	0.027	0.013

Source: Argonne National Laboratory (ANL)
LPG – liquefied petroleum gas; VOC – volatile organic compound; CO – carbon monoxide; NOx – oxides of nitrogen; SOx – sulfur oxides; PM10 – particulate matter with diameter 10 mm or smaller; PM2.5 – particulate matter with diameter 2.5 mm or smaller

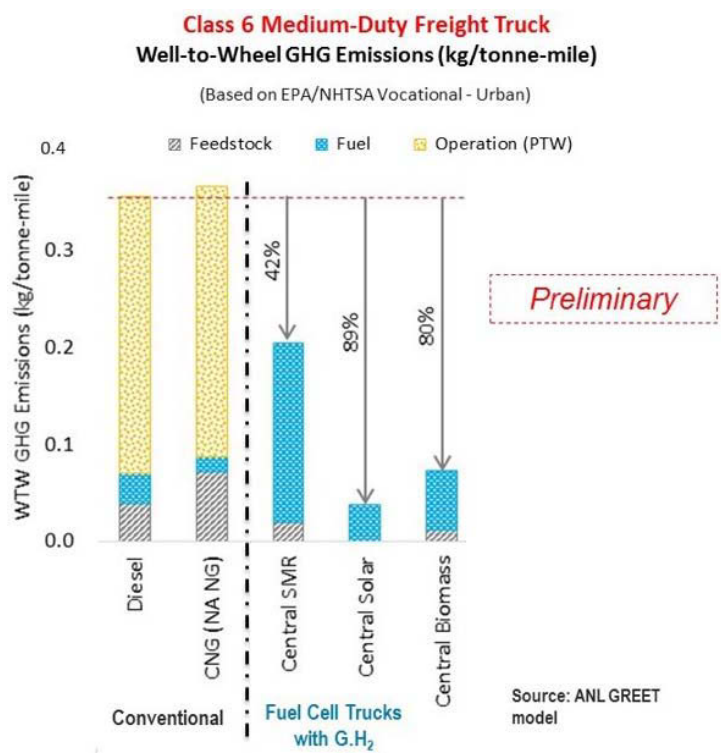

EPA – U.S. Environmental Protection Agency; NHTSA –National Highway Traffic Safety Administration of the U.S. Department of Transportation; PTW – pump-to-wheel; CNG – compressed natural gas; NA NG – North American natural gas; $G.H_2$ – gaseous hydrogen

FIGURE 2. Well-to-Wheel GHG emissions of hydrogen fuel cell truck pathway

The Hydrogen Financial Analysis Scenario Tool (H2FAST)

The H2FAST tool has been enhanced to provide in-depth financial analysis for hydrogen fueling stations to facilitate investments in hydrogen stations, improve policy design decisions to support early station and FCEV deployment, and examine the associated financial risks. Features added to the model include additional fixed operating costs (e.g., electrical demand charges), more detailed hydrogen demand ramp-up, and the ability to provide custom feedstock and retail price profiles. The expanded version also enables risk analysis for input parameters; assessment

of incentives and policies, take-or-pay contract implications, and additional feedstocks for hydrogen production; and analysis of scenarios with a number of larger stations.

The tool was thoroughly peer-reviewed and issued to the public through the following website: http://www.nrel.gov/hydrogen/h2fast.

Studies and Analysis

Impact of Fuel Cell System Peak Efficiency on Fuel Consumption and Cost

The impact of different fuel cell targets on vehicle energy consumption and cost was studied using the Autonomie model to evaluate the incremental impacts and benefits of improving onboard hydrogen fuel storage and fuel cell technologies through FCTO-supported R&D. Figure 3 exhibits fuel and vehicle cost savings as a result of improvements in hydrogen storage and fuel cell technologies. These improvements include hydrogen storage changes to reduce tank costs and design changes for increased fuel cell efficiency. The largest savings for the individual technologies is achieved when the fuel cell targets are achieved; if the ultimate fuel cell and storage targets are both met, cost reduction could reach approximately $4,000 per vehicle. The results of this work will be published in an ANL report. Future work will continue to focus on examining the marginal benefits of improved fuel cell efficiency and onboard storage versus the marginal cost.

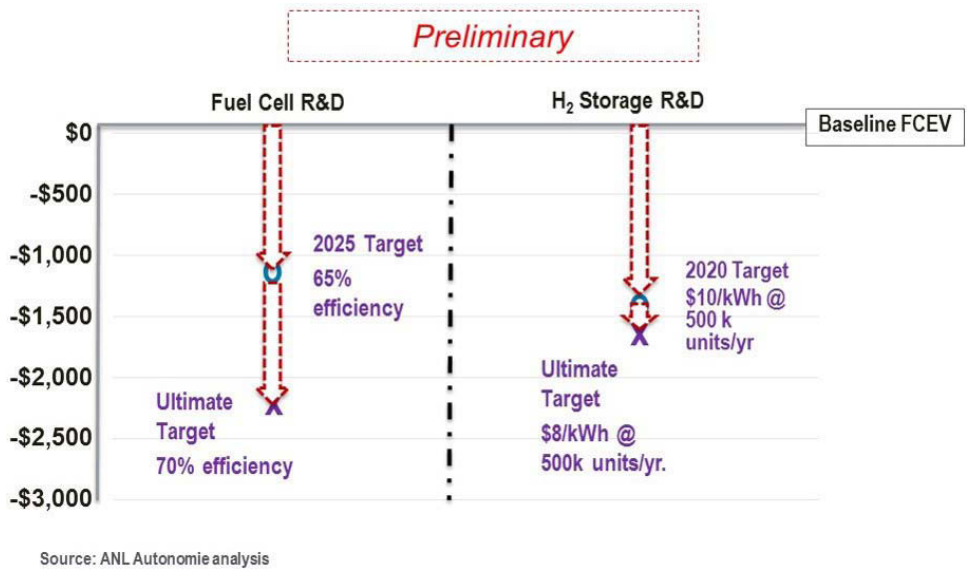

FIGURE 3. Impact of FCTO targets on fuel savings and vehicle cost reduction

Analysis of Sub-Program Benefits

Scenarios were developed and analyzed to estimate petroleum use reduction benefits as a result of the successful deployment of FCEVs. The successful development of hydrogen and fuel cell technologies as a result of DOE-funded R&D was compared to a base case without government-funded R&D. As shown in Figure 4, these advances could improve the fuel economy of the light-duty vehicle stock by 25% to 30% and reduce projected petroleum consumption by 0.3 million to ~1 million barrels per day. The results of this analysis will be published in an ANL report.

Employment Study

ANL, with assistance from RCF Economic and Financial Consulting, is analyzing the economic impacts associated with the development of FCEV technology and the associated hydrogen infrastructure technology achieved through DOE R&D funding. Scenario analysis will be used to identify fuel cell markets and regions that are most likely to experience employment and economic gains from the technology advancement. A reference ("core multi market") scenario of FCEV deployment in five U.S. regions was developed, and initial estimates of gross employment under two manufacturing assumptions were generated. Under this scenario, approximately 260,000 jobs (100,000 associated with manufacturing and 160,000 associated with distribution and sale of 3.7 million FCEV cars and light trucks) were estimated nationally in 2050, as shown in Figure 5. This work builds on the 2008 DOE Report to

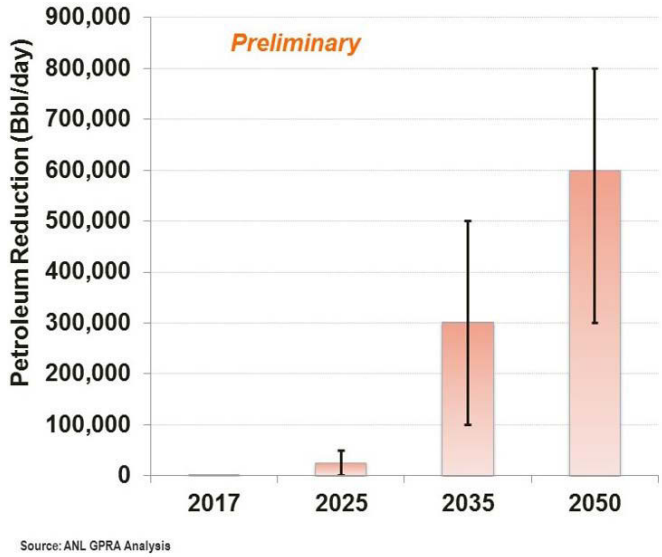

FIGURE 4. Energy security benefit – petroleum reduction attributed to FCEV market penetration

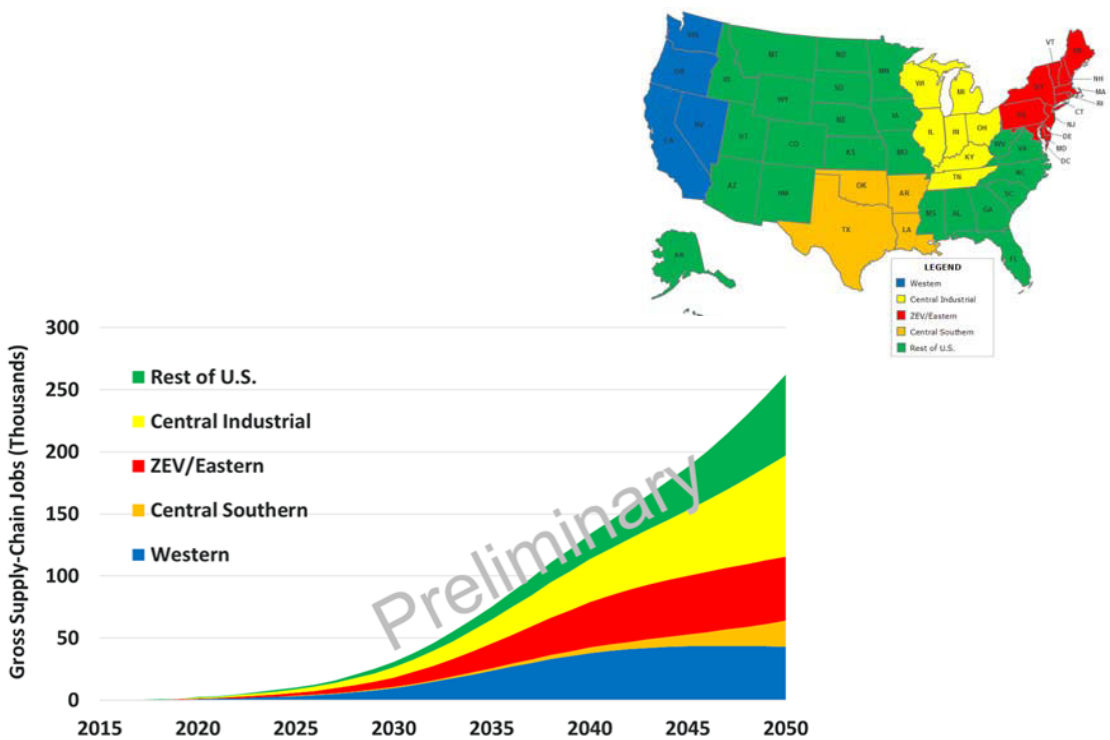

ZEV – zero emission vehicle; NE – Northeast

FIGURE 5. Employment impacts from FCEV penetration

Congress (*Effects of a Transition to a Hydrogen Economy on Employment in the United States*), estimating job creation and expanding that analysis to include insights gained from FCTO R&D and market developments. An ANL report will be issued on the study results.

Future work may include expanding the "core" scenario to include heavy-duty trucks and buses; analyzing hydrogen production, distribution, and sale to all FCEVs (light- and heavy-duty); and analyzing sensitivities and workforce development needs.

Water Lifecycle Analysis

The lifecycle freshwater consumption associated with various transportation fuels for light-duty vehicles in the United States was analyzed by ANL using the water module of the GREET model. The results of the analysis show that lifecycle water consumption for FCEVs can be comparable to that for conventional gasoline vehicles for certain fuel pathways, as illustrated in Figure 6. The values range from roughly 9 to 65 gal of water per 100 mi driven depending on the pathway for hydrogen production, delivery, storage, and dispensing. The baseline lifecycle water consumption for conventional gasoline vehicles (with 10% ethanol) is roughly 23 gal per 100 mi driven. The results of the analysis will be documented in a DOE Hydrogen and Fuel Cells Program record.

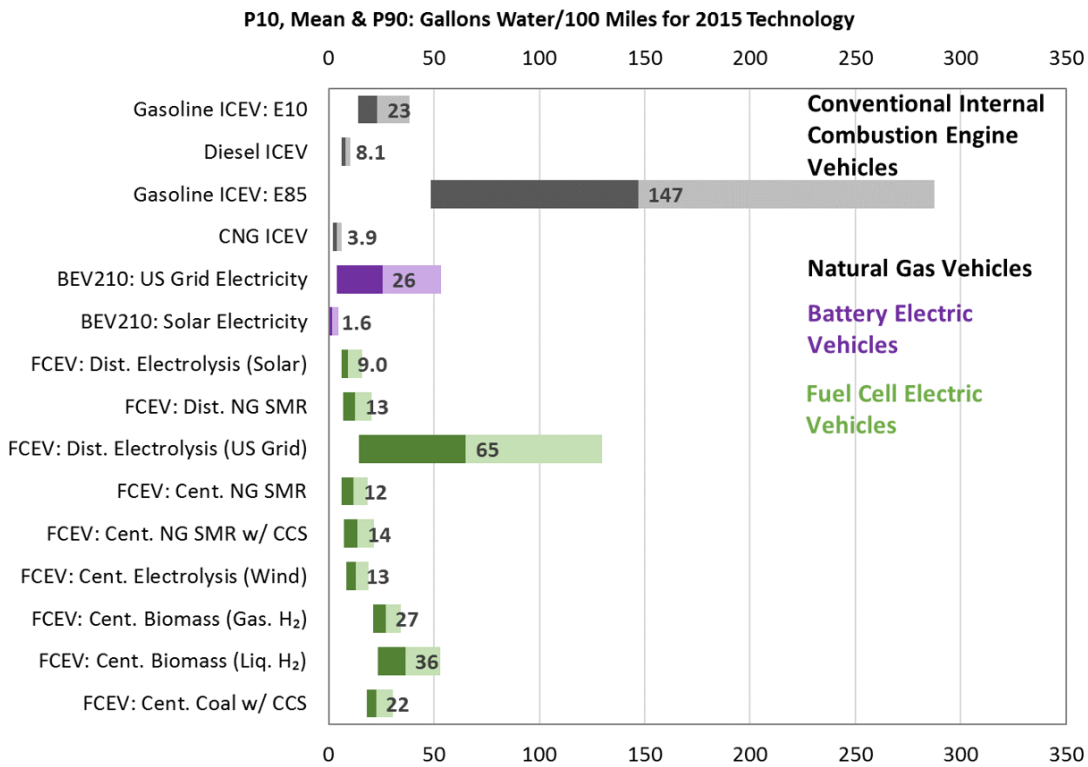

Source: ANL

E10 – fuel mixture with 90% gasoline and 10% ethanol; E85 – fuel mixture with 15% gasoline and 85% ethanol; CNG – compressed natural gas; BEV210 – battery electric vehicle with 210 mile electric-only range; Dist. – distributed; NG – natural gas; CCS – carbon capture and storage; Cent. – central; Gas. H2 – gaseous hydrogen; Liq. H2 – liquid hydrogen; w/ – with

FIGURE 6. Lifecycle water consumption per 100 miles driven

Resource Availability for Hydrogen Production

Over the long term, the widespread deployment of FCEVs will require hydrogen produced from a diverse array of low-carbon domestic energy resources, such as coal (with carbon capture and storage), nuclear, biomass, wind, and solar energy. This analysis focused on (1) estimating the hydrogen production required to meet potential future FCEV demand and (2) providing updated estimates of total hydrogen production potential from domestic energy resources. The analysis considered resource requirements for hydrogen in a future without significant FCEV market growth (i.e., from the U.S. Energy Information Administration's [EIA's] *Annual Energy Outlook* [AEO]) and with significant market growth (i.e., 50 million FCEVs deployed by 2040). The spatial resource availability was determined on a per-kilogram-of-hydrogen basis.

Figure 7 shows the updated comparison of current (2015) and future (2040) total hydrogen consumption for the AEO 2017 Reference Case. The ratio of projected 2040 consumption to additional resources needed to supply 50 million FCEVs is shown as a factor in parenthesis below each resource label. These numbers indicate how much more of a particular resource would be needed to fuel 50 million FCEVs. The percentage increases are relatively low for natural gas (5%), coal (18%), and biomass (48%), and highest for wind (87%) and solar (171%). These results will be published in a National Renewable Energy Laboratory report.

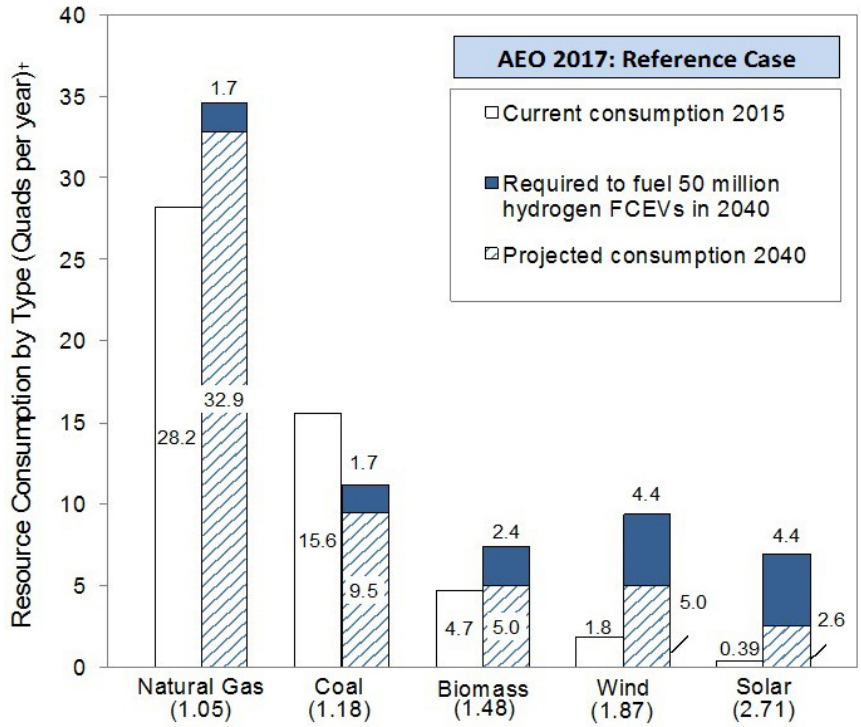

Source: National Renewable Energy Laboratory

FIGURE 7. Resource requirements for hydrogen production

Patents Resulting from DOE-Sponsored R&D

The commercial impact of FCTO funding continues to be analyzed by tracking the patents resulting from FCTO-funded R&D projects. As shown in Figure 8, the number of patents issued has continued to grow. Over 650 patents were awarded by 2016 as a result of research funded by FCTO in the areas of storage, production, delivery, and fuel cells. This work, completed by Pacific Northwest National Laboratory, will be highlighted in the 2016 Pathways to Commercial Success Report.

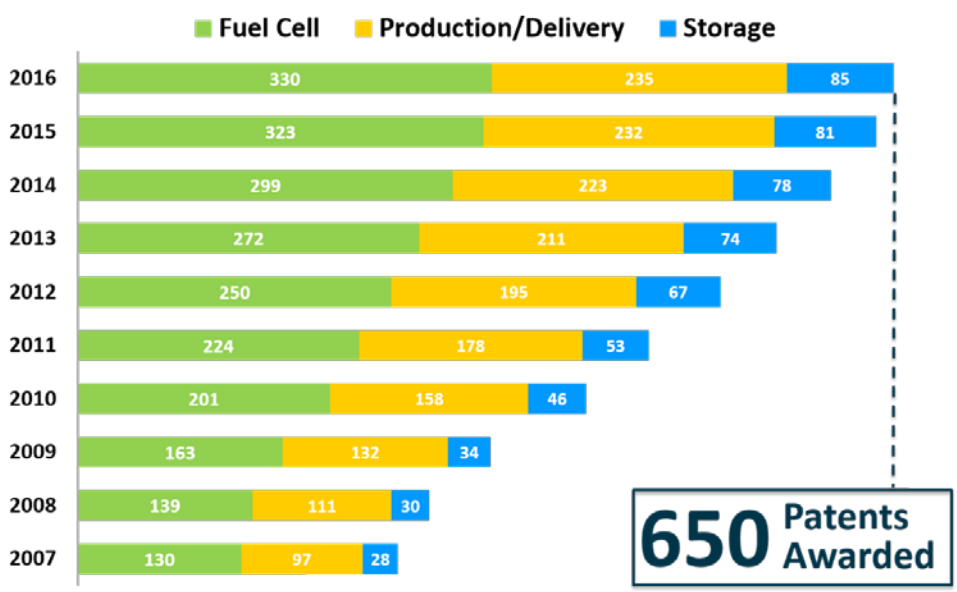

Figure 8. Cumulative number of patents awarded

BUDGET

The FY 2017 appropriation for the Systems Analysis sub-program was $3 million.

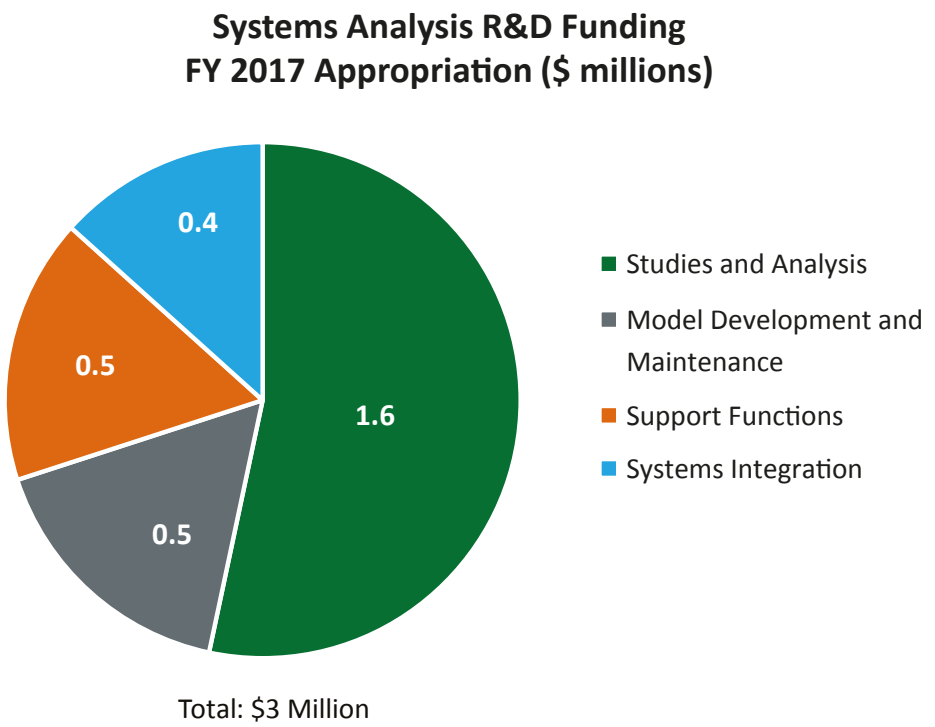

FIGURE 9. FY 2017 Systems Analysis appropriation

UPCOMING ACTIVITIES AND PLANS

Funding continues to be allocated to conduct analysis using the models developed by the sub-program. In particular, analysis projects are concentrated on:

- Market adoption of fuel cells
- Lifecycle analysis of criteria emissions and water use for hydrogen production technology pathways for light-duty vehicles
- Quantifying employment impacts of hydrogen and fuel cell technologies
- Calculating the cost of onboard hydrogen storage options
- Estimating GHG emissions and petroleum use in medium- and heavy-duty trucks based on various hydrogen pathways
- Estimating the hydrogen production (from diverse domestic energy resources such as natural gas, coal, uranium, biomass, wind, and solar) required to meet potential future FCEV demand
- Performing hydrogen fueling station business assessments
- Investigating hydrogen use as an energy carrier with applications across sectors (e.g., industrial, grid services, vehicles) supporting the H2@Scale initiative.

Future activities are subject to appropriations.

Fred Joseck
Systems Analysis Program Manager
Fuel Cell Technologies Office
Office of Energy Efficiency and Renewable Energy
U.S. Department of Energy
1000 Independence Ave., SW
Washington, DC 20585-0121
Phone: (202) 586-7932
Email: Fred.Joseck@ee.doe.gov

IX.1 Employment Impacts of Hydrogen and Fuel Cell Technologies

Marianne Mintz
Argonne National Laboratory
9700 S. Cass Ave.
Argonne, IL 60439
Phone: (630) 252-5627
Email: mmintz@anl.gov

DOE Manager: Fred Joseck
Phone: (202) 586-7932
Email: Fred.Joseck@ee.doe.gov

Subcontractor:
RCF Economic and Financial Consulting, Inc. (RCF)
Chicago, IL

Project Start Date: October 1, 2015
Project End Date: September 30, 2018

Overall Objectives

- Update 2008 DOE Report to Congress, *Effects of a Transition to a Hydrogen Economy on Employment in the United States* [1] to reflect current levels of technology advancement and anticipated fuel prices, economic activity and market success.
- Expand the 2008 Report by adding materials handling, backup power and other early market applications of fuel cells, and modeling the effects of market development between industries and regions.
- Estimate net impacts of hydrogen (H_2) and fuel cell (FC) development on national and regional employment, earnings and economic output under alternative scenarios.
- Identify implications of scenario results on work force development.

Fiscal Year (FY) 2017 Objectives

- Develop a reference scenario ("Core Multi-Market Scenario") focusing on development of light-duty vehicles (LDVs) and hydrogen fueling for each of five regions over 35 years (2015–2050).
- Adjust existing industry cost vectors and define new cost vectors to enable economic modeling of the impact of that scenario.
- Estimate the magnitude of total and regional impacts and identify industries most heavily impacted by H_2 and FC development in LDVs. Examine occupational composition of affected industries.

Technical Barriers

This project addresses the following technical barriers from the Systems Analysis section of the Fuel Cell Technologies Office (FCTO) Multi-Year Research, Development, and Demonstration Plan.

(A) Future Market Behavior

(B) Stove-piped/Siloed Analytical Capability

(C) Inconsistent Data, Assumptions and Guidelines

(D) Insufficient Suite of Models and Tools

Contribution to Achievement of DOE Systems Analysis Milestones

This project will contribute to achieving the following milestones for the Systems Analysis section of the Fuel Cell Technologies Office Multi-Year Research, Development, and Demonstration Plan.

- Milestones 2.3–2.6: Develop and maintain models and tools.
- Milestones 1.7, 1.10, and 1.14: Perform studies and analyses of job impacts.

FY 2017 Accomplishments

- Developed custom industries corresponding to FC stacks, FC systems, FC cars and FC light trucks at a level of detail to permit supply chain modeling for five regions (Western United States, zero emission vehicle (ZEV)/ Eastern United States, Central/Southern United States, Central/Industrial United States, and the rest of United States) from 2015 to 2050 in the Regional Economic Models, Inc. (REMI) Policy Insight model.
- Estimated the number and value of FC stacks, systems, cars and light trucks produced and sold by region under the Core Multi-Market Scenario and associated demands for hydrogen and retail fueling stations.
- Estimated gross impacts on regional employment by industry and occupation.

✧ ✧ ✧ ✧ ✧

INTRODUCTION

The project is analyzing economic impacts associated with the development of FCs and associated hydrogen infrastructure. Insights from this work will assist FCTO and its stakeholders in estimating employment and other economic impacts from DOE technology development and in

identifying FC markets and regions that are most likely to see economic gains from the advancement of these technologies. In earlier work, Argonne National Laboratory and RCF analyzed economic impacts associated with a large-scale transition to hydrogen and fuel cells. That work formed the basis for a 2008 DOE Report to Congress which is being updated and expanded in this effort.

APPROACH

FCs are being developed for a range of demands and duty cycles, from small portable devices to megawatt-scale, from steady-state to variable power output, and from continuous to quick-start backup operation. Each of these applications represents a unique market with different packaging/integration, installation, and operation and maintenance needs. Not only do these markets differ in size and anticipated growth, they also displace incumbent technologies with different production locations and supply chains. Thus, modeling the effects of H_2 and FC development requires an understanding of likely applications and their anticipated growth; the penetration of FCs into those markets and their associated H_2 fueling needs; the cost of FCs, H_2 and the existing technologies currently serving those markets; and supply chains for H_2 and FCs as well as incumbent technologies.

RESULTS

As the second year of a three-year project, FY 2017 efforts focused on data acquisition/enhancement to finalize scenario parameters and industry cost vectors. These efforts produced initial, preliminary estimates of employment associated with the production and distribution/sale of FC cars and light trucks for a Core Multi-Market Scenario.

Scenario Development and Data Enhancement

Several FCTO- and Vehicle Technologies Office (VTO)-supported tools and efforts were used to expand the Energy Information Administration's (EIA's) *Annual Energy Outlook* (AEO-2016) reference scenario for vehicle sales and energy prices, tailor it to the five regions shown in Figure 1, and add the anticipated cost and market performance of fuel cell technologies under a successful FCTO program. These tools include Autonomie (which provides estimates of vehicle and component costs over time); MA3T, ParaChoice and Lave-TRANS (which provide estimates of market shares for fuel cell electric vehicles [FCEVs] consistent with FCTO's analysis for the Government Performance and Results Act); and VISION (which translates regional estimates of FC and conventional vehicle sales into estimates of vehicle stocks and fuel use for each of the five regions). Other efforts that informed the scenario development process include findings from the H2USA Locations Roadmap Working Group and FCTO's Fuel Cell System Cost Analyses. Thus, the Core Multi-Market Scenario reflects key assumptions and methodologies not only from AEO-2016, but also from several related FCTO-affiliated tools and efforts.

Under the Core Multi-Market scenario, FC cars and light trucks represent 20% of LDV sales and nearly 10% of LDV stocks nationally in 2050. However, because of greater

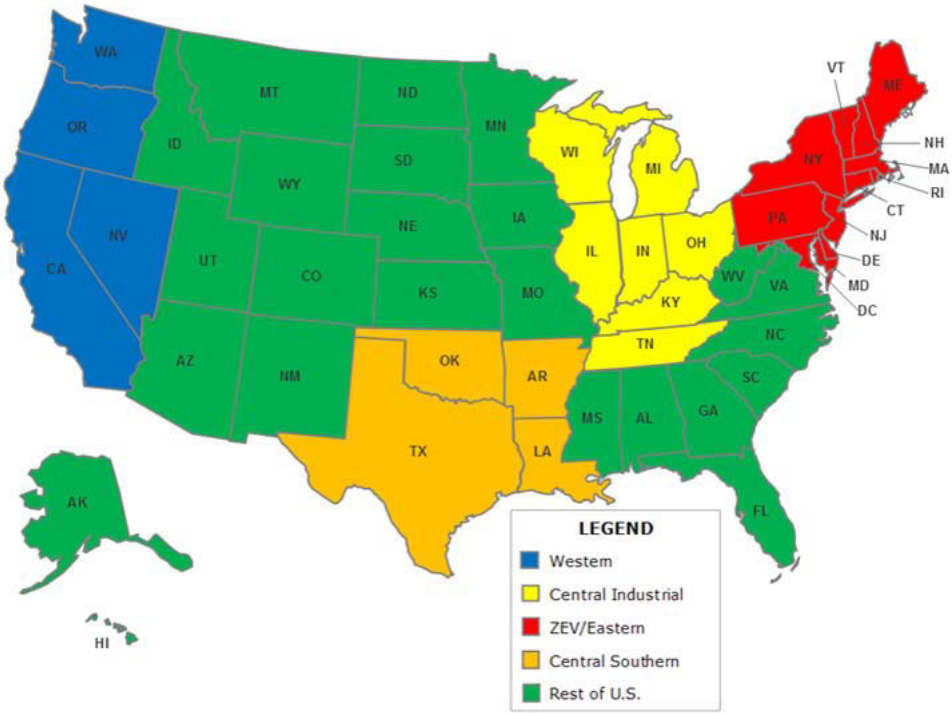

FIGURE 1. Economic analysis regions

ongoing support in the Western and ZEV/Eastern regions, FC cars and light trucks represent a much larger share (35%) of 2050 sales in those regions. Similarly, FCEVs account for 32% and 28% of LDV stocks, respectively, in Western and ZEV/Eastern regions in 2050.

Estimates and assumptions from the Core Multi-Market Scenario provided the basis for adjusting industrial sectors in the REMI[1] model and for creating new sectors to reflect adaptation within the U.S. economy to changing demand and supply chains. Four additional sectors were constructed (FC stack, FC system, FC car, FC light truck) using data from related industries, the U.S. National Input and Product Accounts and the U.S. Censuses of Manufacturing, Wholesale and Retail Trade, and Construction. Two variants of the core scenario were examined, a case in which FCEV production reflects the current split between domestic and foreign assembly of *all LDVs* sold in the U.S., and a case in which production reflects the current split between domestic and foreign assembly of *plug-in hybrid electric vehicles* sold in the United States.

Preliminary Results

Figure 2 shows total gross employment associated with the Core Multi-Market Scenario. Initially, growth is strongest in the Western region in response to ongoing efforts to achieve clean fuel targets. However, since the Core Multi-Market Scenario assumes that states achieve their deployment targets and that regions retain their historic shares of national LDV sales, ZEV/Eastern employment eventually exceeds FC-associated employment in the Western region (because while the two regions come to have comparable FCEV market shares, the ZEV/Eastern region has a larger population and thus higher LDV sales). Employment in other regions rises steadily over the forecast period, and total gross employment reaches approximately 260,000 in 2050.

Manufacturing employment (roughly 100,000 gross jobs in 2050) tends to be concentrated in states where manufacturing supply chains are most dense, generally in the Central Industrial region (Figure 3). The number of manufacturing jobs is very sensitive to domestic versus foreign assembly, with preliminary results varying from approximately 60,000 gross supply-chain jobs if FCEV assembly mirrors current U.S. LDV assembly shares to over 120,000 gross supply-chain jobs if the U.S. share mirrors current assembly patterns. Note that "manufacturing" jobs include not only direct employment in FC stack, system, and FCEV fabrication and assembly, but also "white collar" jobs and support service employment throughout the supply chain.

Unlike manufacturing, jobs associated with FC distribution and sales tend to be located in those regions where FCEV demand is greatest (Figure 4). By 2050 over 160,000 gross jobs in distribution/sales are associated with FC development. Most of these jobs are in retail sales. Note that FC "employment intensity" or jobs per 100,000 LDVs produced or sold declines over time in response to automation and other improvements in supply chain efficiency (Figure 5). Such improvements affect both FCs and conventional powertrain technologies.

[1] Regional Economic Models, Inc. (REMI) is an econometric model. In this application of the model, 160 standard industries and six custom industries (FC car, FC light truck, FC stack, FC system, H_2 production from fossil sources, and H_2 production from renewable sources) are represented for each of five individual regions, and changes between that representation and a base case are calculated. Since industries are modeled in terms of transactions, outputs may be associated with supply chains and product distribution. When summed across regions, the results are estimates of employment, earnings and occupational impacts for the entire United States.

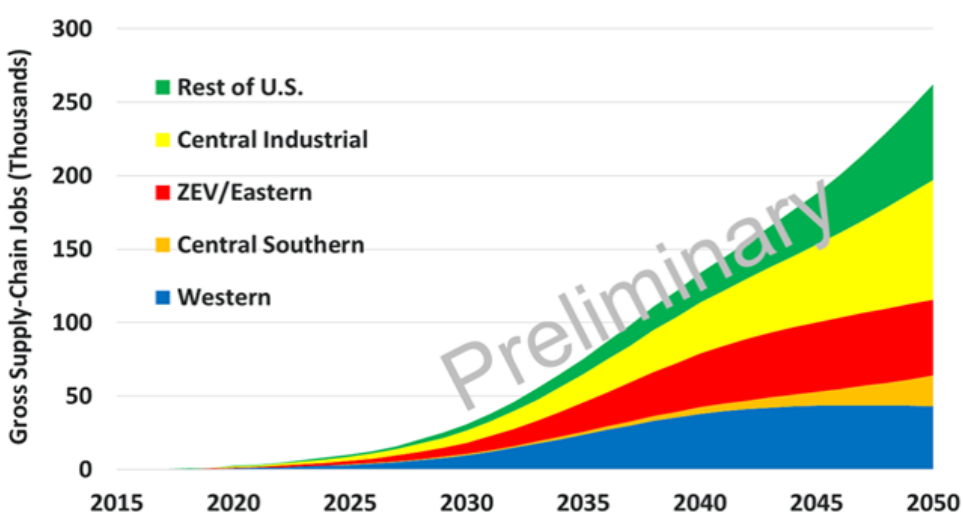

FIGURE 2. Gross manufacturing, distribution & sales jobs associated with FCEVs (Core Multi-Market Scenario)

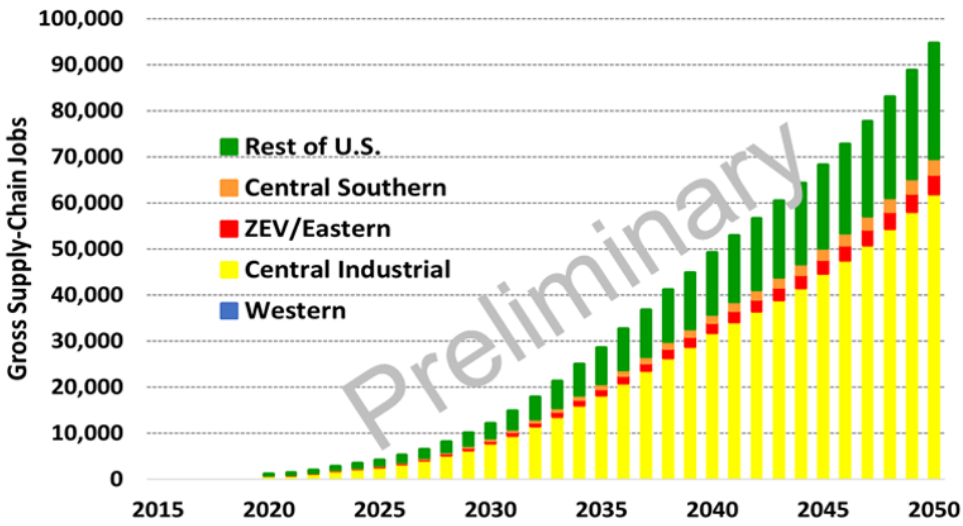

FIGURE 3. Gross manufacturing jobs associated with FCEVs (Core Multi-Market Scenario)

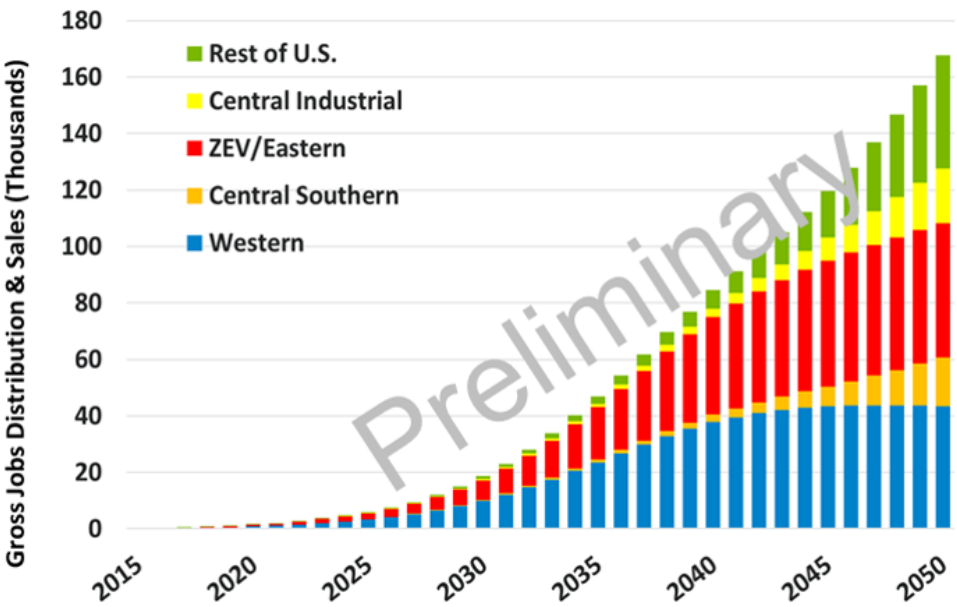

FIGURE 4. Gross distribution/sales jobs associated with FCEVs (Core Multi-Market Scenario)

CONCLUSIONS AND UPCOMING ACTIVITIES

This project is a multi-year effort to update DOE's 2008 Report to Congress, (*Effects of a Transition to a Hydrogen Economy on Employment in the United States*) in order to reflect current levels of technology advancement and anticipated fuel prices, economic activity, and market success. FY 2017 work focused on finalizing a reference scenario of FCEV deployment in five U.S. regions and generating initial estimates of gross employment under two manufacturing assumptions. Under this scenario (called the Core Multi-Market Scenario) approximately 100,000 jobs associated with manufacturing, and 160,000 jobs associated with distribution and sale of 3.7 million FCEV cars and light trucks were estimated nationally in 2050. Future work may include expanding the "core" scenario to include heavy-duty trucks and buses, and hydrogen production, distribution and sale to all FCEVs (light- and heavy-duty); and analyzing sensitivities and workforce development needs.

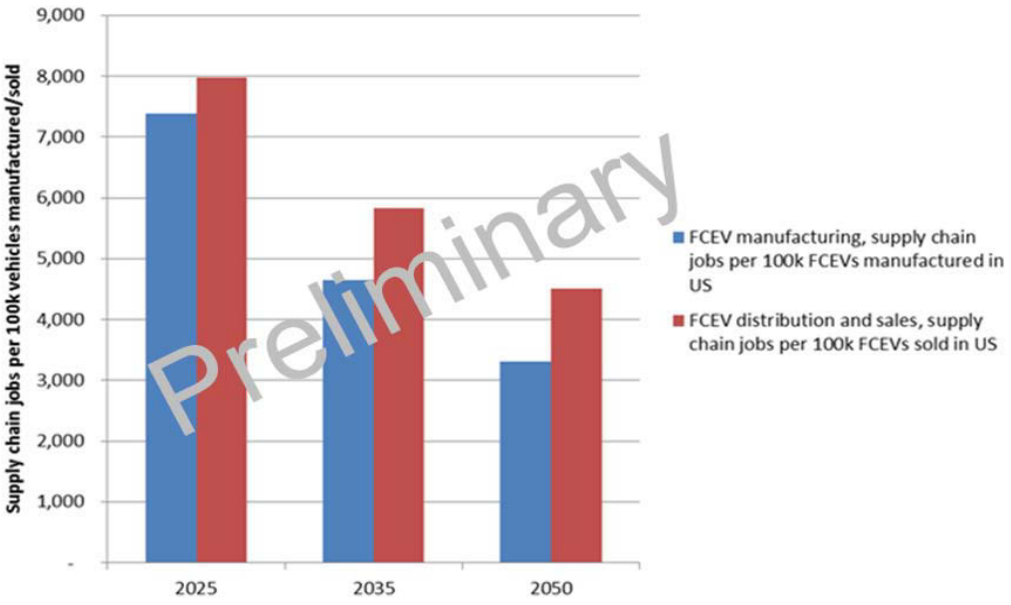

FIGURE 5. Gross jobs per 100,000 FCEVs produced or sold (Core Multi-Market Scenario)

REFERENCES

1. U.S. Department of Energy, 2008. *Effects of a Transition to a Hydrogen Economy on Employment in the United States: Report to Congress*, July.

IX.2 Regional Water Stress Analysis with Hydrogen Production at Scale

Amgad Elgowainy (Primary Contact), Uisung Lee, Hui Xu, Jeongwoo Han, and Michael Wang
Argonne National Laboratory
9700 South Cass Avenue
Argonne, IL 60439
Phone: (630) 252-3074
Email: aelgowainy@anl.gov

DOE Manager: Fred Joseck
Phone: (202) 586-7932
Email: Fred.Joseck@ee.doe.gov

Project Start Date: April 2013
Project End Date: Project continuation and direction determined annually by DOE

Overall Objectives

- Incorporate water consumption associated with hydrogen as a transportation fuel for use in fuel cell electric vehicles (FCEVs).
- Compare water consumption of hydrogen for use in FCEVs with other fuel or vehicle systems on a life cycle basis.
- Identify major contributors in the upstream supply chain to water consumption.
- Analyze the technology environmental impacts on regional water stress for hydrogen and fuel cell deployment scenarios.

Fiscal Year (FY) 2017 Objectives

- Estimate regional hydrogen demand and associated water consumption for large scale deployment of hydrogen FCEVs.
- Evaluate the fresh water supply and demand at a county level and generate a water index representing relative water scarcity for the conterminous United States.
- Perform regional water consumption impact analyses for hydrogen production at scale.

Technical Barriers

This project directly addresses Technical Barriers B, C, and D in the Systems Analysis section of the Fuel Cell Technologies Office Multi-Year Research, Development, and Demonstration Plan. These barriers are as follows.

(B) Stove-piped/Siloed Analytical Capability

(C) Inconsistent Data, Assumptions and Guidelines

(D) Insufficient Suite of Models and Tools

Contribution to Achievement of DOE Systems Analysis Milestones

This project will contribute to achievement of the following DOE milestones from the Systems Analysis section of the Fuel Cell Technologies Office Multi-Year Research, Development, and Demonstration Plan.

- Milestone 1.13: Complete environmental analysis of the technology environmental impacts for hydrogen and fuel cell scenarios and technology readiness. (4Q, 2015)
- Milestone 2.2: Annual model update and validation. (4Q, 2011 through 4Q, 2020)

FY 2017 Accomplishments

- Developed hydrogen production scenarios based on H2@Scale and National Renewable Energy Laboratory's resource analysis.
- Estimated regional hydrogen demand and associated water consumption for FCEVs by 2040.
- Evaluated county-level water index for regional water stress impact analysis.
- Performed water consumption impact analysis for the large-scale deployment scenarios of hydrogen FCEVs.

✧ ✧ ✧ ✧ ✧

INTRODUCTION

Hydrogen is a zero-carbon energy carrier that can be produced from various domestic feedstock sources. Hydrogen is also important for FCEVs and the processing and upgrading of other fuels. Fresh water is essential for various energy systems, including transportation fuel production, since those systems typically consume a significant amount of water. However, available fresh water resources vary greatly by region. Large scale deployment of energy production in water-stressed regions has the potential to deprive water required to sustain human activities and the environment, which may lead to negative environmental and social impacts. Thus, water stress analysis at a regional level is critical for a sustainable future of energy systems. Life-cycle impact analysis is a method that provides a consistent

accounting of fresh water consumption for the production of fuels along their supply chain.

The objective of this study is performing regional water consumption impact analysis for hydrogen production at scale using life-cycle water consumption of various hydrogen production pathways. In this study, the regional impact of hydrogen production at scale for FCEVs on water stress is evaluated based on the estimated water consumption for hydrogen demand and a newly developed regional water stress index at the county level. This study contributes information that can be used to guide sustainable water management decisions.

APPROACH

The project mainly consists of two parts; one is estimating regional hydrogen and water demand for hydrogen FCEVs by 2040, and the other is evaluating fresh water supply and demand at a county level to generate a water index that represents relative water scarcity locally across the United States. These together can be used to perform water stress impact analyses using life-cycle water consumption data. First, using Argonne's VISION model, a scenario for the number of hydrogen FCEVs that can be deployed by 2040 was developed, and the required hydrogen production to satisfy the FCEV stock was calculated at a county level. Regional hydrogen production pathways were generated based on resource availability (National Renewable Energy Laboratory's resource analysis). This provides an estimation of water consumption for hydrogen production at a county level by integrating the life cycle water consumption factors of various hydrogen production pathways [1] and the hydrogen demand at each county.

For water consumption impact analyses, fresh water supply and demand should be evaluated by region since water availability shows significant spatial variation, which leads to significantly different impacts on regional water stress, even for the same amount of water consumption across regions [2]. Thus, we evaluated fresh water supply and demand using measured runoff and human water use data provided by United States Geological Survey; then the water index representing water scarcity was calculated at a county level. This index was named AWARE-US, which quantitatively indicates available water remaining that can be used for other activities. Argonne evaluated the regional impact caused by the water consumption to meet the hydrogen demand for FCEVs by combining estimated water consumption for hydrogen production and the AWARE-US index. This study also evaluated the possibility of groundwater depletion by comparing groundwater recharge and human groundwater consumption. Where a human consumes more groundwater than recharge, it can be assumed that the region depletes stored groundwater, which is not a sustainable practice.

RESULTS

Figure 1 represents county-level water consumption for hydrogen production to support a deployment scenario of FCEVs by 2030, and shows significant regional water demand variation. There are many factors that influence the water consumption such as the number of deployed fuel cell vehicles, the employed hydrogen production technologies (e.g., electrolysis or steam methane reforming), and the upstream water consumption along hydrogen production supply chain. The most influential driver for the regional variation is the difference in the number of deployed FCEVs. The employed technologies for hydrogen production and the FCEVs' fuel economy do not notably change the regional variation trend. The results shows that western and eastern United States, where FCEVs may be more actively deployed, would require a significant amount of fresh water for hydrogen production that meets number of deployed vehicles.

Figure 2 shows the AWARE-US index calculated from measured fresh water supply and demand. AWARE-US ranges from 0.1 to 100, representing regional water scarcity relative to the U.S. consumption-weighted average (AWARE-US = 1). For example, when the index is 0.1, the regionally available remaining water is 10 times higher than the U.S. average, which means the region has abundant fresh water resources leading to less water stress. On the other hand, if the index value is 10, the region has only 10% of available water resource when compared to the U.S. average, and there would be significant competition over fresh water among various purposes in that region. The results shows that western U.S. counties have high index values, while most counties in the eastern United States have indices lower than the average. The west central U.S. counties have the highest index values mainly because they have low runoff (due to low precipitation with high evapotranspiration) and high water consumption (mostly for irrigation). This means any marginal increase in water demand in these regions magnifies its impact on water stress and may result in depletion of stored groundwater.

Since available fresh water resources vary by region significantly (Figure 2), water consumption for FCEVs in Figure 1 should be considered along with the balance of fresh water supply and demand, i.e., available water. For the regional water consumption impact analysis, water footprint for FCEVs in each county can be expressed in terms of equivalent water consumption at a reference flow by multiplying the volume of water consumption and the AWARE-US in the region where it is consumed. Figure 3 represents the impact of water consumption for FCEVs at a county level. The results showed that the western United States has much higher water consumption impact compared to the eastern United States. For example, using the FCEV deployment scenario generated by VISION, California consumes only 1.3 times the volume of fresh water consumed in New York in order to meet the hydrogen demand in their

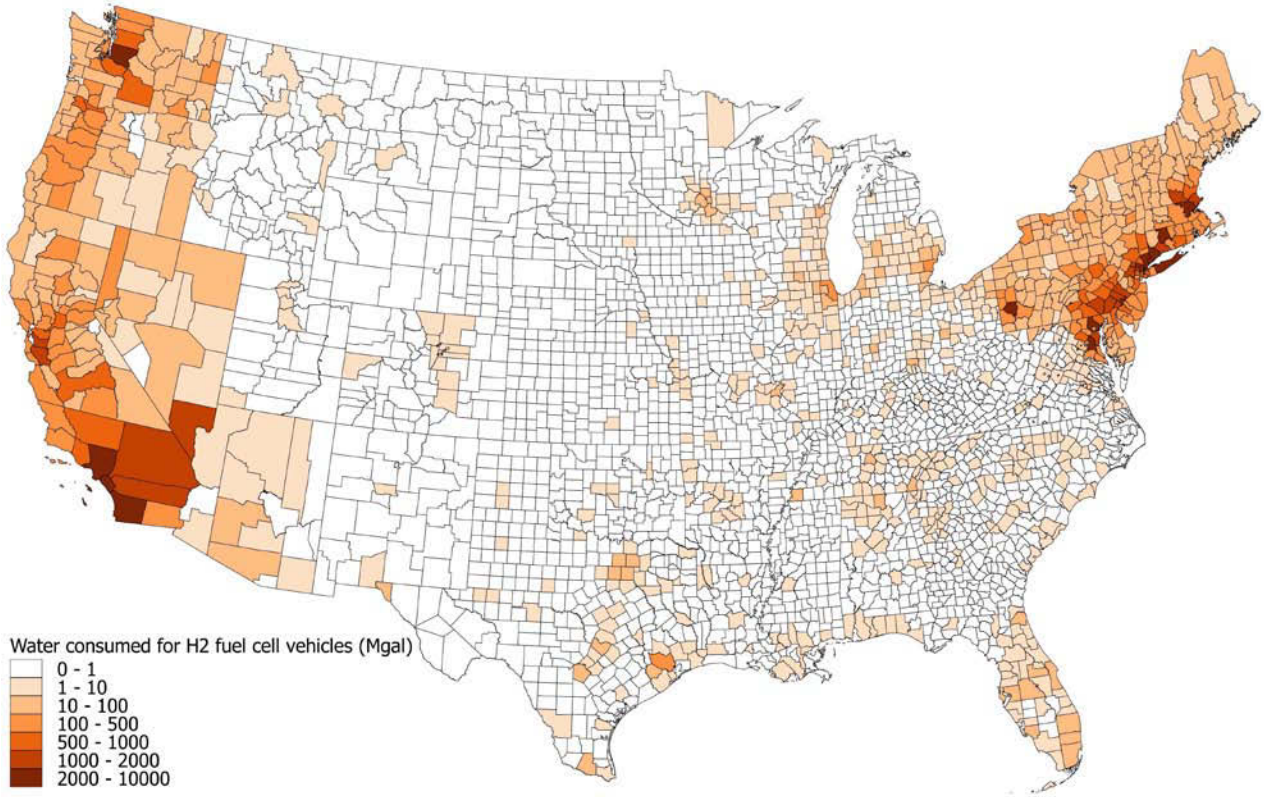

FIGURE 1. County-level water consumption to support hydrogen production for FCEVs by 2040

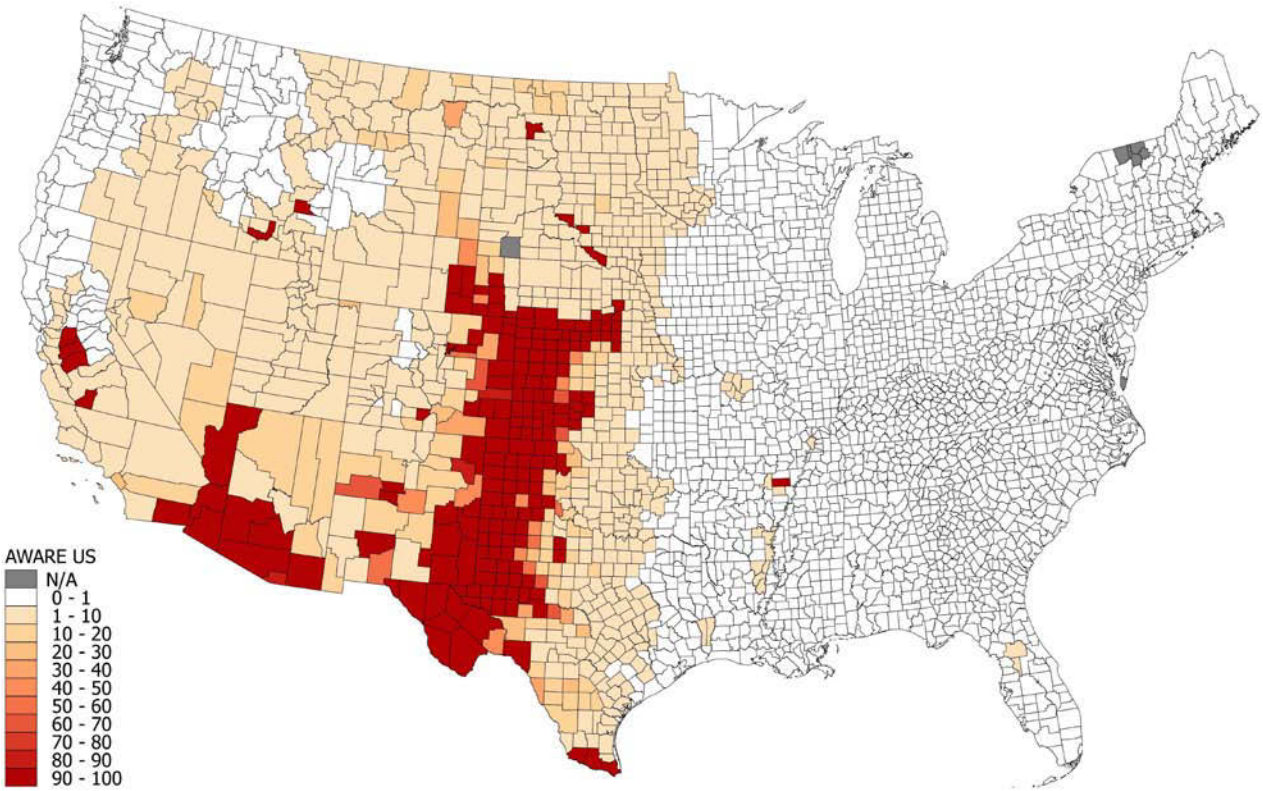

FIGURE 2. AWARE-US index range from 0.1 (water-abundant) to 100 (water-stressed)

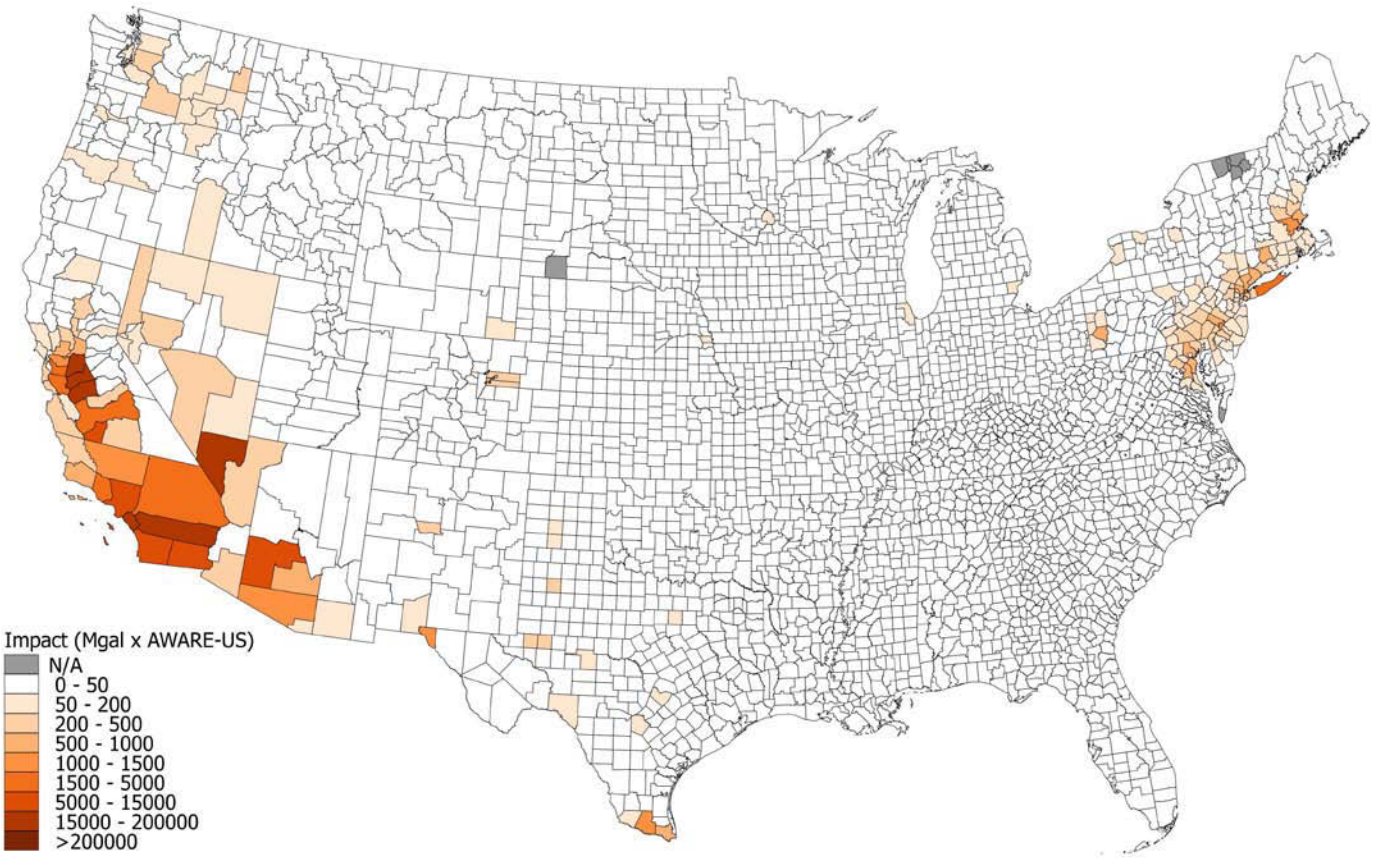

FIGURE 3. Regional water consumption impact analysis for hydrogen production for FCEVs by 2040 in the conterminous United States

respective states. However, the water consumption impact in California is 27 times higher compared to New York due to the higher AWARE-US (water stress index in California).

The red colored counties in Figure 4 indicate the regions where human groundwater consumption may exceed the groundwater recharge in the county. When compared with Figure 2, Figure 4 also shows that counties with AWARE-US of 100 deplete stored groundwater due to the insufficient surface water supply. Therefore, any additional fresh water demand for fuel production in these counties will likely incur further groundwater depletion. If groundwater is used to supply additional water demand in this region, it may lead to additional groundwater depletion problems.

CONCLUSIONS AND UPCOMING ACTIVITIES

This analysis focused on identifying the regional impact of water consumption for large scale deployment of hydrogen FCEVs. The results showed that significant regional variation exists for water consumption for FCEVs, and there is spatial variation in fresh water supply and demand between counties. Any marginal increase in water demand for fuel production in water-stressed regions will magnify the impact on water stress. This study provides a systematical approach to evaluating the sustainability of various energy systems in terms of water use and its impact on water stress in various regions in the United States. Further analysis is needed to address issues such as analyzing existing baseline fuels (non-marginal). Life-cycle water consumption inventory needs to be expanded further to include alternative hydrogen pathways with low water consumption.

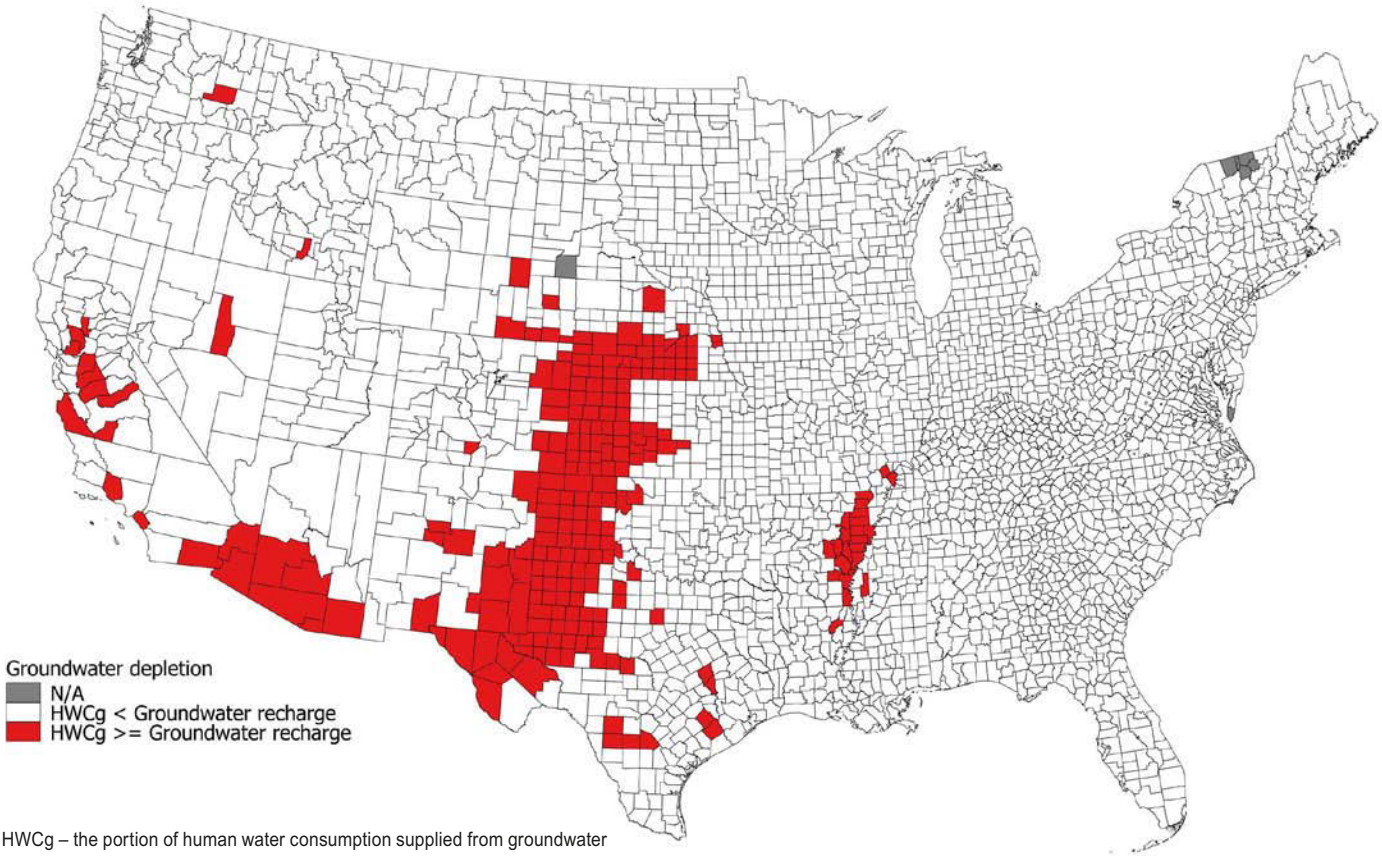

FIGURE 4. Groundwater depletion in the conterminous United States

FY 2017 PUBLICATIONS/PRESENTATIONS

1. Lee, Uisung, Jeongwoo Han, Amgad Elgowainy, and Michael Wang. 2017. "Regional Water Consumption for Hydro and Thermal Electricity Generation in the United States." Applied Energy. doi:10.1016/j.apenergy.2017.05.025.

REFERENCES

1. U.S. Department of Energy. 2016 Annual Progress Report, DOE Hydrogen and Fuel Cell Program. No. DOE/GO-102017-4891. Washington, D.C., 2016.

2. Boulay, A-M., Jane Bare, Lorenzo Benini, Markus Berger, Michael J. Lathuillière, Alessandro Manzardo, Manuele Margni et al. "The WULCA consensus characterization model for water scarcity footprints: Assessing impacts of water consumption based on available water remaining (AWARE)." *The International Journal of Life Cycle Assessment* (2017): 1–11.

IX.3 Cost Benefits Analysis of Technology Improvement in Light-Duty Fuel Cell Vehicles

A. Rousseau (Primary Contact), R. Vijayagopal
Argonne National Laboratory
9700 S. Cass Ave.
Lemont, IL 60439
Phone: (630) 252-7261
Email: arousseau@anl.gov

DOE Manager: Fred Joseck
Phone: (202) 586-7932
Email: Fred.Joseck@ee.doe.gov

Project Start Date: October 1, 2016
Project End Date: September 30, 2017

Overall Objective

Quantify the impact of system improvements on energy consumption and economic viability of fuel cell electric vehicles (FCEVs).

Fiscal Year (FY) 2017 Objectives

- Quantify the fuel savings to the consumer that are attributable to improvements in fuel cell peak efficiency, and increases in weight ratio of usable hydrogen from a tank.
- Determine the breakeven point up to which the technology improvements are justifiable to the consumer.

Technical Barriers

This project addresses the following technical barriers from the System Analysis section of the Fuel Cell Technologies Office (FCTO) Multi-Year Research, Development, and Demonstration Plan.

(A) Future Market Behavior

(C) Inconsistent Data, Assumptions, and Guidelines

(D) Insufficient Suite of Models and Tools

(E) Unplanned Studies and Analysis

Contribution to Achievement of DOE Systems Analysis Milestones

This project will contribute to achievement of the following DOE milestones from the Systems Analysis section of the FCTO Multi-Year Research, Development, and Demonstration Plan.

- Milestone 1.1: Complete an analysis of the hydrogen infrastructure and technical target progress for hydrogen fuel and vehicles. (2Q, 2011)
- Milestone 1.17: Complete analysis of program technology performance and cost status, and potential to enable use of fuel cells for a portfolio of commercial applications. (4Q, 2018)
- Milestone 2.2: Annual model update and validation. (4Q, 2011 through 4Q, 2020)

FY 2017 Accomplishments

- Evaluated the impact of FCTO funded technologies on vehicle fuel consumption for multiple vehicle classes and powertrains.
- Identified optimum technology levels where the fuel savings will offset the cost incurred in adopting a better technology.

✧ ✧ ✧ ✧ ✧

INTRODUCTION

FCEVs are commercially available in the United States and may achieve operational cost parity with conventional vehicles by 2025–2030 based on DOE's assumptions related to technology progress, market penetration, and production volumes. At present, fuel cells system peak efficiency reaches 60%, representing 85% of the "ultimate" target (70%) set by DOE. Future technology improvements, such as reduction of platinum group metals, are expected to reduce the cost in the long run. In the short term, various design choices are available with existing technologies to achieve tradeoffs between cost and efficiency. This study aims to evaluate various short-term design choices and quantify their impact on FCEV ownership and operational costs. The objective is to identify the optimum level of technology progress that creates sufficient savings to the consumer to justify the higher initial investment.

This analysis utilizes the results of a baseline scenario analysis study (BaSce) for fuel cell vehicles that quantified the fuel consumption benefits associated with achieving the DOE technology targets [1]. Although technology progress and cost reduction are expected to be achieved within the same time span, they are not usually accomplished through the same technology change. As fuel cell technology is currently focused on proton exchange membranes, the cost reduction is primarily achieved by reducing the quantity of platinum group metals needed as a catalyst. Reduction

in platinum loading could adversely impact efficieny. The design choices considered in this study either achieve improved efficiency or reduce weight with incremental increases in the initial component cost.

APPROACH

This study assumes that present-day FCEVs meet or exceed DOE targets for 2015 on parameters such as peak efficiency of the fuel cell and weight ratio of usable hydrogen in the storage system. These vehicles already provide an alternative fuel vehicle with lower petroleum use and emissions compared to conventional vehicles, so further technology improvements should aim to make these vehicles competitive in terms of ownership cost.

Ownership Cost Assumptions

The vehicle costs were separated into initial cost and operational cost. Additional factors such as maintenance costs, depreciation, and cost of financing are assumed to be comparable across technologies. Over the 5-year service time of the vehicle, the fuel savings will yield monetary benefits to the consumer. The total present value (TPV) of the fuel will show whether the initial investment in improved technology is justified monetarily or not. The details of the TPV calculation assumptions are leveraged from previous work [2]. The increase in initial cost and the overall savings can be converted to $/kW to determine the cost tolerance of the technology. An example of the analysis is illustrated in Figure 1.

RESULTS

The first step in this study was to understand how the various technology changes affect the fuel consumption of an FCEV, and the monetary impact over a 5-year ownership period. The following assumptions were considered:

- Vehicle usage is assumed to be 14,000 miles per year.
- Hydrogen is expected to cost $4/gge.
- A discount rate of 7% is assumed for the TPV calculations. This rate determines the present value of future cash flow. Based on this assumption, getting $107 one year from now is same as getting $100 today.

The default FCEV model from Autonomie [3] was used for this analysis. Although the impact on a hybrid vehicle and a plug-in hybrid vehicle with a 20-mile range (PHEV 20) were studied, since both powertrain show similar trends, we only show the results for the hybrid vehicle. We examine the impact of changes in vehicle usage and hydrogen cost later in this document.

Figure 2 shows the sensitivity of the TPV of fuel savings to the improvements in hydrogen storage and fuel cell efficiency. The efficiency term refers to the peak efficiency of the stack, usually at about 25% of the rated load. We computed the variation in operational efficiency as part of the simulation analysis. Achieving 70% fuel cell efficiency can save the consumer over $600 in fuel costs over the 5-year period. For hydrogen storage, the improvement in weight ratio results in modest fuel savings, and even a 60% improvement in the current ratio of H_2 to tank mass only results in approximately $100 worth of fuel savings. Therefore, the primary focus in storage technologies should be on reducing the cost of the components, even if doing so does not contribute to weight reduction. If the cost targets are achieved along with efficiency and weight ratio targets, the savings could be as high as $4,000 compared to present day FCEVs.

Note that the component cost savings are not equivalent to the difference in vehicle selling price. In this study, we assume that the manufacturers will pass on the manufacturing cost savings to the consumers. Consumers will experience fuel cost savings directly; the TPV of fuel cost savings is computed to compare the value of future savings against the initial investment needed for the technology improvement.

Hydrogen storage technology changes are expected to reduce the cost of the tank and will be economically more attractive than the present scenario. This study focuses on the various design choices available for fuel cell efficiency

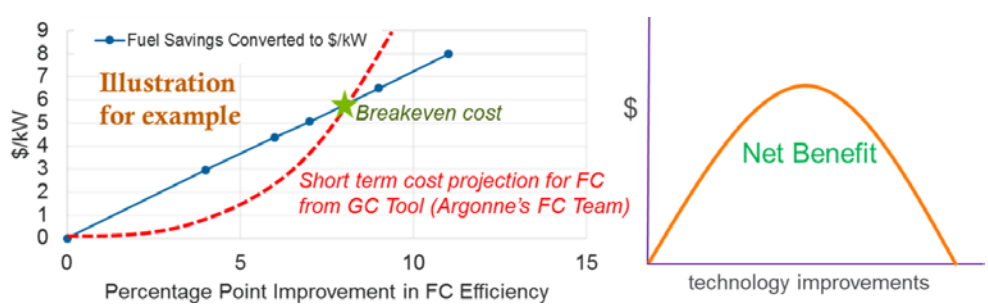

FC – fuel cell

FIGURE 1. Illustrated example for cost benefit analysis

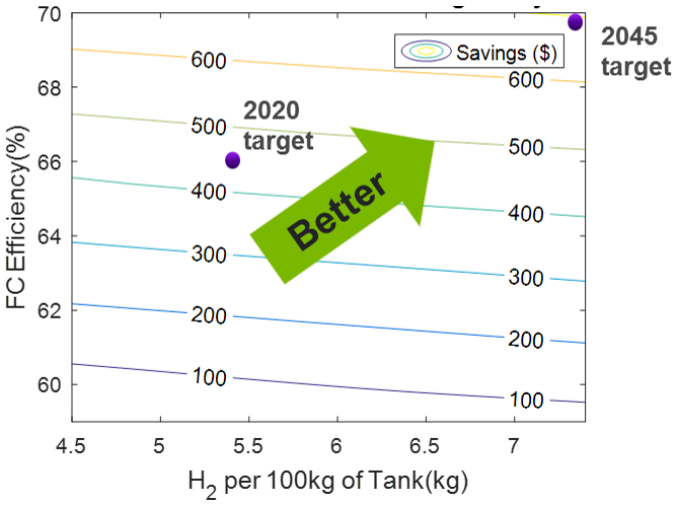

FIGURE 2. Sensitivity of TPV to improvements in H_2 storage and fuel cell efficiency

improvements. The savings due to efficiency improvement are fairly linear and proportional to the fuel cost. Figure 3 shows the TPV of fuel savings with improvement in efficiency.

Argonne's fuel cell experts developed multiple design choices representing today's technology. Figure 4 shows the tradeoffs between efficiency and cost for these choices. They are achieved by varying platinum loading as well as varying the parameters affecting the operating temperature and heat rejection from the stack. Table 1 summarizes the design choices from GC Tool.

The design choices are grouped based on their platinum loading. The second column in Table 1 shows the ratio of power output to the difference in operating and ambient temperature. Lower values for this ratio (resulting from higher temperature operation) are more efficient, but result in a higher manufacturing cost.

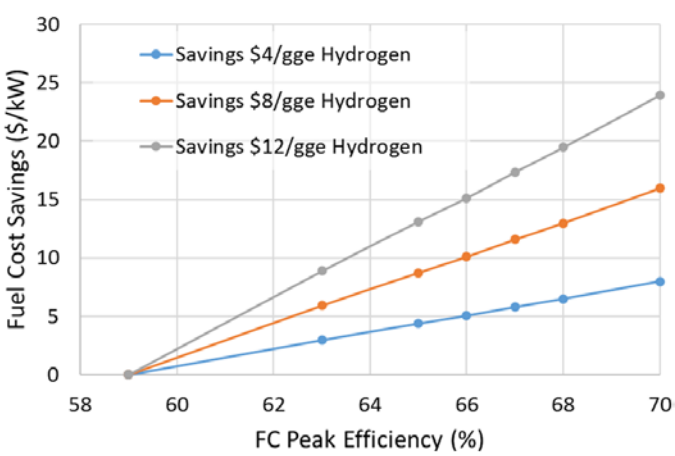

FIGURE 3. TPV of fuel savings with improvement in efficiency

TABLE 1. Design Choices Derived from GC Tool for Varying Platinum Loading and Thermal Considerations

Design Choices	Heat Rejection (kW/°C)	Platinum Loading (mg/cm^2)	Peak Efficiency (%)	Fuel Cell Cost ($/kW)
1a	1.0	0.1	61.7	56.9
1b	1.25	0.1	60.8	46.8
1c	1.45	0.1	60.5	44.9
1d	1.75	0.1	60.2	44.7
2a	1.0	0.2	62.9	58.8
2b	1.25	0.2	62.0	49.3
2c	1.45	0.2	61.7	47.2
2d	1.75	0.2	61.4	46.7
3a	1.0	0.4	64.1	68.6
3b	1.25	0.4	63.3	57.1
3c	1.45	0.4	62.9	53.9
3d	1.75	0.4	62.5	52.5

We assume that present fuel cells have a peak efficiency of 59% at a cost of $51.4/kW. This year, improvements have resulted in more efficient fuel cells, and some design choices achieve better efficiency at a lower cost compared to the baseline. Such lower-cost choices are obviously better than the present scenario; however, it is important to see which of these choices maximize the overall consumer savings. Combining the fuel savings TPV and the initial cost information quantifies the net savings associated with these design choices.

Figure 4 shows the cost and efficiency values from each design choice. A pareto front can be derived for the lower cost and higher efficiency choice, making some choices (1a, 2a) irrelevant, as lower-cost and higher-efficiency solutions are available.

Figure 5 shows the pareto front for the cost and efficiency tradeoff intersecting with the TPV of fuel savings associated with different fuel cost assumptions. This shows that at 63% peak efficiency at $54/kW is the limiting point beyond which the initial investment does not yield justifiable returns.

From the consumer's point of view, maximizing net savings is more important than achieving the highest possible efficiency. To understand the net savings, the difference between TPV of fuel savings and the incremental cost difference is examined in Figure 6. For three different fuel cost assumptions, we examine the consumer net savings.

Net savings is shown to depend on the hydrogen cost. At $4/gge, the most economical choice for the consumer is design choice 1d, which yields 60.2% peak efficiency at $44.7/kW. It is the least efficient choice available, but due to the reduction in initial cost of the fuel cell, net savings for the consumer is highest.

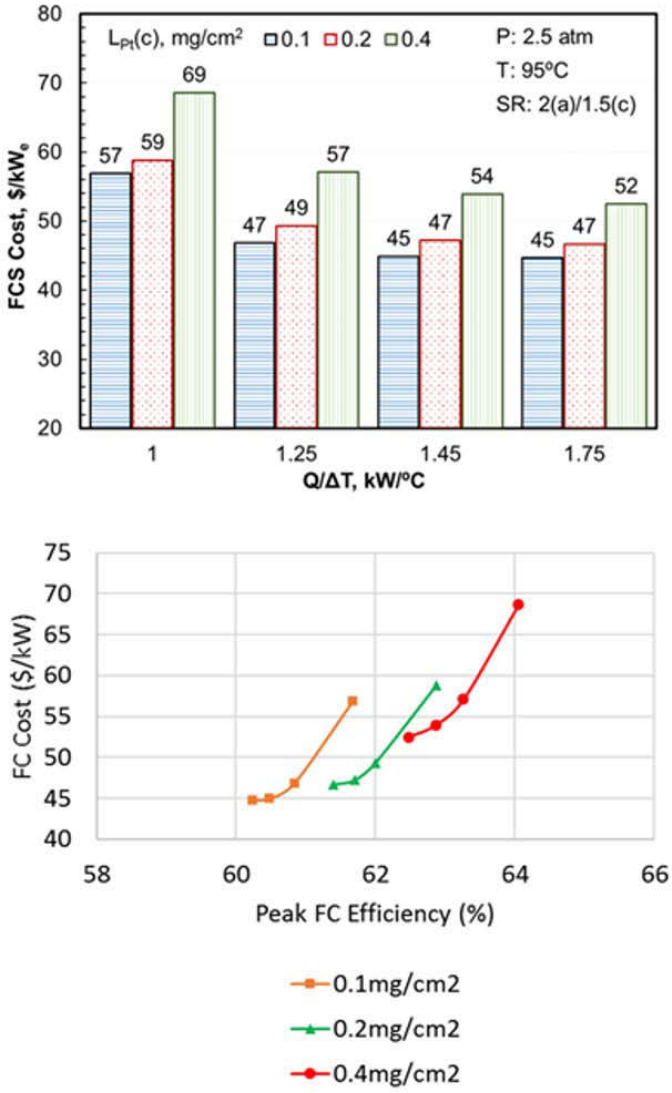

FCS – fuel cell system

FIGURE 4. Cost and efficiency impact of platinum loading and other design choices

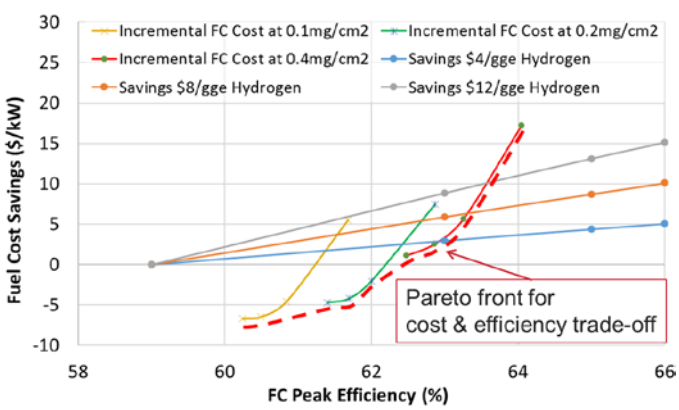

FIGURE 5. Comparing initial cost and the present value of future savings

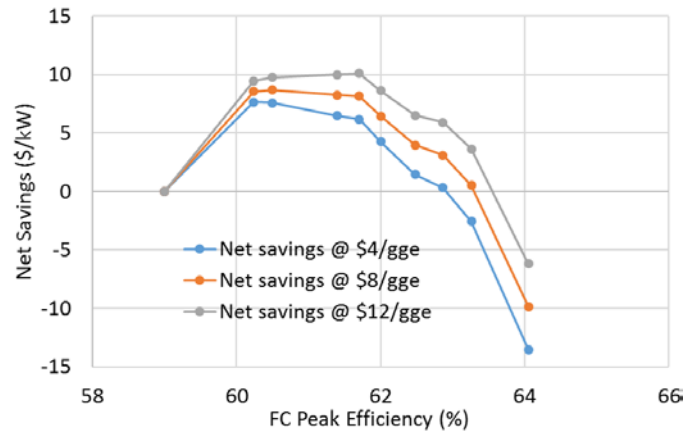

FIGURE 6. Net savings from design choices

For a higher fuel cost, say $12/gge, the cost of fuel saved offsets the initial investment and provides a 7% return on investment during the period of ownership. In this case, the maximum net benefit is design choice 2c, with a 61.7% peak efficiency and $47.2/kW. Note that many design choices yield net savings for the consumer, but the above-mentioned choices are the ones that maximize savings.

If the objective is to maximize efficiency while remaining economically viable, the design choice would be 3c. In this case, achieving 62.9% peak efficiency at a cost of $53.9/kW results in enough fuel savings to provide a 7% return on the investment made for efficiency improvements.

CONCLUSIONS AND UPCOMING ACTIVITIES

This study shows that for each analysis year, a technology level exists that maximizes benefits to the consumer. For the current technology choices, we identified the optimum design choices that maximize consumer savings. While fuel prices are uncertain, the trends associated with the net benefit of technology change are clearly understood.

Since the economic benefits are dependent on both the baseline and the future component technologies performance and cost, this study should be regularly updated when new information becomes available.

FY 2017 PUBLICATIONS/PRESENTATIONS

1. Vijayagopal, R., N. Kim, A. Rousseau, "Fuel Cell Powered Vehicles: An Analysis of How Technology Progress Affects the Technical and Economic Feasibility," Argonne Report ANL-17/07, May 2017.

2. Islam, E., A. Moawad, N. Kim, A. Rousseau, "Fuel Displacement and Cost Feasibility Study of Fuel Cell Vehicles Based on U.S. Department of Energy Targets," (paper accepted for presentation

at the 30th International Battery and Fuel Cell Electric Vehicle Symposium and Exposition [EVS 30], Stuttgart, Germany, October 2017).

REFERENCES

1. Moawad, A., N. Shidore, A. Rousseau, *Assessment of Vehicle Sizing, Energy Consumption and Cost through Large Scale Simulation of Advanced Vehicle Technologies*, ANL/ESD-15/28, report to the U.S. Department of Energy, March 2016.

2. A. Vyas, "Plug-in hybrid electric vehicles: How does one determine their potential for reducing U.S. oil dependence?" (paper presented at the 23rd International Battery and Fuel Cell Electric Vehicle Symposium and Exposition [EVS 23], Anaheim, California, December 2–5, 2007).

3. Autonomie, available from www.autonomie.net.

IX.4 Hydrogen Analysis with the Sandia ParaChoice Model

Rebecca S. Levinson (Primary Contact) and
Todd H. West
Sandia National Laboratories
P.O. Box 969
Livermore, CA 94551
Phone: (925) 294-2402
Email: rslevin@sandia.gov

DOE Manager: Fred Joseck
Phone: (202) 586-7932
Email: Fred.Joseck@ee.doe.gov

Project Start Date: October 1, 2014
Project End Date: Project continuation and direction determined annually by DOE

Overall Objectives

- Model the evolving market penetration potential of fuel cell electric vehicles (FCEVs) and hydrogen fuel.
- Assess the factors that influence the competition between FCEVs, conventional vehicles, and other alternative vehicle technologies such as battery electric vehicles.
- Assess the impacts of FCEV market penetration and hydrogen production pathways on greenhouse gas emissions and petroleum consumption.
- Provide context for the role of policy, technology development, infrastructure, and consumer behavior on the vehicle and fuel mix.

Fiscal Year (FY) 2017 Objectives

- Add additional detail to the fuel price sub-model of the ParaChoice model.
- Conduct scenario analyses to understand and provide context for the market penetration potential of FCEVs, hydrogen demand, costs, and production pathways.
- Complete sensitivity analysis, varying factors including station availability, fuel cost, efficiency, or technology cost.
- Conduct parametric analyses to understand sensitivities and tipping points driving FCEV sales, emissions, and hydrogen consumption and production.
- Analyze hydrogen prices and FCEV sales in response to various coal and natural gas futures.

Technical Barriers

This project addresses the following technical barriers from the Systems Analysis section of the Fuel Cell Technologies Office Multi-Year Research, Development, and Demonstration Plan.

(A) Future Market Behavior

(C) Inconsistent Data, Assumptions and Guidelines

(D) Insufficient Suite of Models and Tools

Contribution to Achievement of DOE Systems Analysis Milestones

This project will contribute to achievement of the following DOE milestones from the System's Analysis section of the Fuel Cell Technologies Office Multi-Year Research, Development, and Demonstration Plan.

- Milestone 1.1: Complete an analysis of the hydrogen infrastructure and technical target progress for hydrogen fuel and vehicles. (2Q, 2011)
- Milestone 1.12: Complete an analysis of the hydrogen infrastructure and technical target progress for technology readiness. (4Q, 2015)
- Milestone 1.13: Complete environmental analysis of the technology environmental impacts for hydrogen and fuel cell scenarios and technology readiness. (4Q, 2015)
- Milestone 1.19: Complete analysis of the potential for hydrogen, stationary fuel cells, fuel cell vehicles, and other fuel cell applications such as material handling equipment including resources, infrastructure and system effects resulting from the growth in hydrogen market shares in various economic sectors. (4Q, 2020)
- Milestone 2.2: Annual model update and validation. (4Q, 2011 through 4Q, 2020)

FY 2017 Accomplishments

- Updated the hydrogen production and pricing sub-model in ParaChoice vehicle simulation.
  - Incorporated new pricing and emissions data from the Macro-Systems Model.
  - Incorporated feedback from the Vehicle Technologies Office concerning obsolete distributed production pathways.
  - Incorporated smaller station size detail for lower demand, industrial hydrogen supply.

- Conducted scenario assessments of hydrogen production pathways, hydrogen price, FCEV sales, and fleet emissions in a baseline case and in cases with different coal and natural gas price futures.
- Performed parametric assessment of the response of hydrogen price and FCEV sales to coal and natural gas futures.
- Matched a simulated seeding of hydrogen station growth to the H_2USA Urban Scenario, and updated the ParaChoice simulation's initial hydrogen station data to present day values.
- Added modeling capability for parametric analysis of the market response of hydrogen infrastructure growth to FCEV sales.
- Performed parametric assessment of the impact of suppressed or stimulated hydrogen infrastructure growth in response to FCEV sales on FCEV sales.

✧ ✧ ✧ ✧ ✧

INTRODUCTION

In the coming decades, light-duty vehicle options and their supporting infrastructure must undergo significant transformations to achieve aggressive petroleum consumption reduction and lower greenhouse gas emissions. FCEVs, battery and hybrid electric vehicles, and biofuels are among the promising advanced technology options. This project examines the market penetration of FCEVs in a range of market segments, and in different energy, technology, and policy futures. Analyses are conducted in the context of varying hydrogen production and distribution pathways, as well as public infrastructure availability, fuel (gasoline, ethanol, hydrogen) and electricity costs, vehicle costs and fuel economies to better understand under what conditions, and for which market segments, FCEVs can best compete with battery electric and other alternative fuel vehicles.

APPROACH

The ParaChoice model simulates the dynamic interaction and evolution of the light-duty vehicle stock, fuel production, and energy supplies through 2050. At its core, ParaChoice is very simple, taking inputs for current vehicle price and vehicle price projections, fuel prices, etc., and asking a set of modeled consumers at each time step which powertrain vehicles are the least expensive options given their driving habits and the cost of inconvenience for finding alternative fueling stations or being stuck with a very short range vehicle with a long refueling time. The choice model structure is similar to that of Lin and Greene [1] and Struben and Sterman [2]. In implementation, we model the fuel sector internally capturing the feedback between fuel production pathways, refueling infrastructure, and the vehicle market. Additionally, the market is segmented by state, vehicle size, population density, driver intensity, dwelling type, and workplace charging ability to capture consumer and fuel production and price market niches.

In order to explore uncertainty, sensitivities to inputs, and trade spaces, we run the core model thousands of times with varying inputs. The model is designed to vary parameters of uncertain variables easily to facilitate these analyses. These parametric analyses provide insights that are not as easily accessible to individual scenario-focused studies.

RESULTS

In FY 2017, we updated the ParaChoice hydrogen price production sub-model using inputs from the Hydrogen Macro System Model [3] and AEO [4] to inform full-scale (50,000 kg/d) hydrogen production for various station sizes and commodity prices. *Hydrogen and Fuel Cells: The US Market Report* [5] was used to determine hydrogen prices for nascent hydrogen markets in the sub-model. With the updated model, we then analyzed the influence of uncertain commodity price futures on hydrogen fuel prices for vehicles. Sample results are show in Figure 1 for full-scale production in central production plants and dispensation at 1,500 kg/d stations. The two pathways shown are steam methane reformation of natural gas (SMR) and coal gasification with sequestration of carbon (COAL + SEQ). Three scenarios are shown for each production pathway, one showing the nominal AEO case, one showing a case where the price of the feedstock commodity (natural gas or coal) is twice as expensive as projected by 2050, and one where the feedstock commodity is half as expected as projected by 2050. One can conclude from the figure that, for nominal AEO projections, SMR is the preferred production pathway for hydrogen, leading to the least expensive fuel. However, uncertainties in the AEO projections may render coal gasification plus sequestration a more economically preferable production pathway, lowering the carbon footprint of hydrogen fuel. If delivery and dispensing technologies can be lowered, it will benefit both pathways equally.

Expanding on the trade between commodity prices and fuel prices, we show the full carbon and natural gas tradespace in Figure 2. Figure 2a shows the simulated national average hydrogen price in 2050 given consumer demand and in response to a range coal and natural gas prices. Figure 2b shows the corresponding 2050 FCEV sales. (For all parameters other than coal and natural gas prices, assumptions are held to ParaChoice's baselines, which reflect the Autonomie [6] low technology, low uncertainty case and correspondingly pessimistic policy and investment options.) Because hydrogen can be produced via multiple pathways, Hydrogen prices are robust to commodity prices, remaining

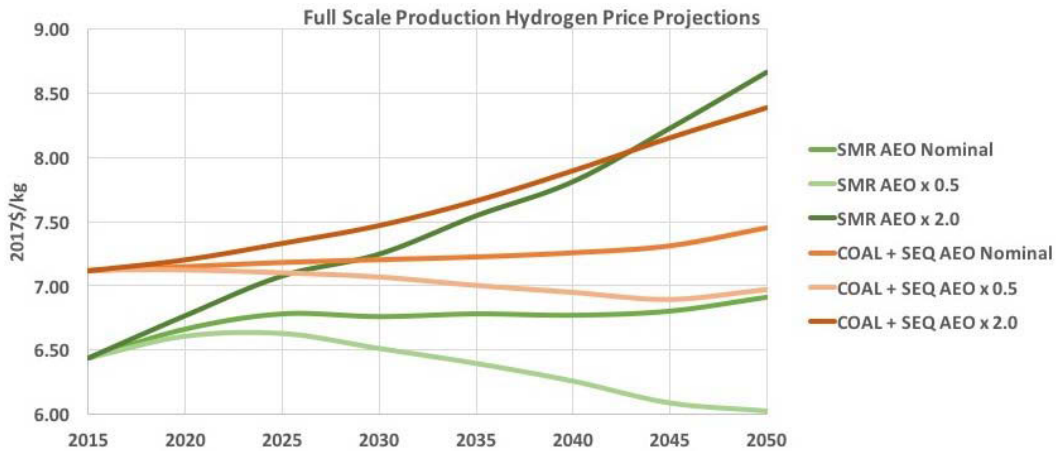

FIGURE 1. Hydrogen price projections under different production pathways and commodity price scenarios

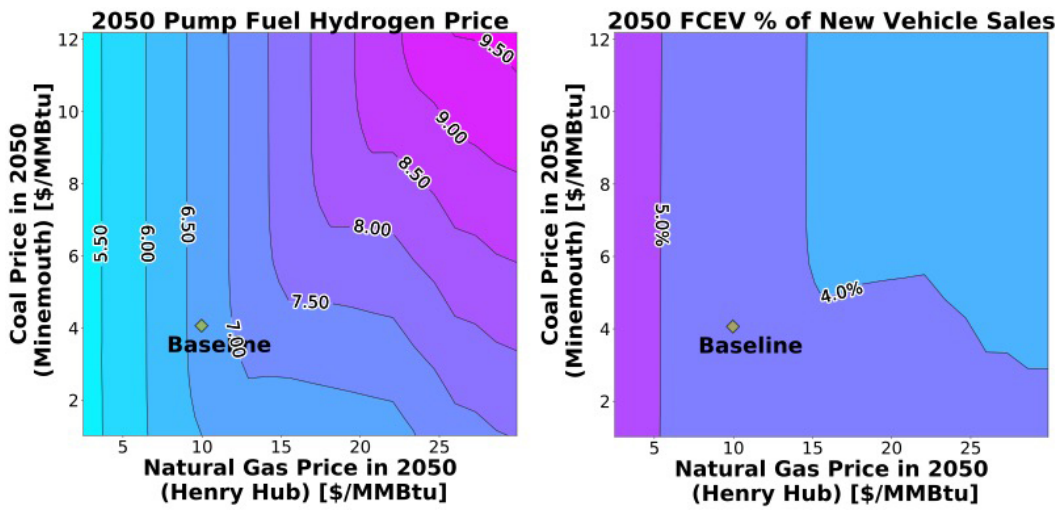

FIGURE 2. 2050 hydrogen prices (left) and FCEV sales (right) for tradespace of coal and natural gas prices

low even if either natural gas or coal prices are unexpectedly high. Only if both natural gas and coal prices are high will hydrogen prices rise substantially. The exception is for very extreme natural gas prices; since existing industrial hydrogen is produced via SMR, high natural gas prices raise industrial hydrogen prices for the early market, lowering demand. If hydrogen demand is insufficient, dedicated hydrogen production for FCEV use will not be built, and the reliance on expensive natural gas will continue, creating a negative feedback loop. FCEV sales largely follow the trend of hydrogen prices.

FCEV sales are subject to a wide range of drivers, which we explore in depth with the ParaChoice model. Technology price and efficiency uncertainties, energy price uncertainty, and modeling and behavioral assumptions such as consumer payback period and penalties all drive the future vehicle sales uncertainties shown in Figure 3. Monte Carlo uncertainty analysis can only constrain 2050 FCEV sales between 0.3% and 19% in 90% of scenarios; sales futures for FCEVs are highly uncertain. Scenarios with the greatest number of FCEV sales are ones with the lowest FCEV technology prices, the lowest logit choice exponent (consumer sensitivity to price), the lowest cost penalties (consumer sensitivity to infrastructure scarcity or range anxiety), the highest oil prices, the greatest FCEV efficiencies, the lowest conventional engine efficiencies, and the greatest hydrogen infrastructure growth rates. These results imply that the greatest gains to FCEV sales might be had for investments that lead to FCEV technology cost reduction or efficiency improvements, infrastructure expansion, or community education to reduce the perceived requirement for hydrogen infrastructure.

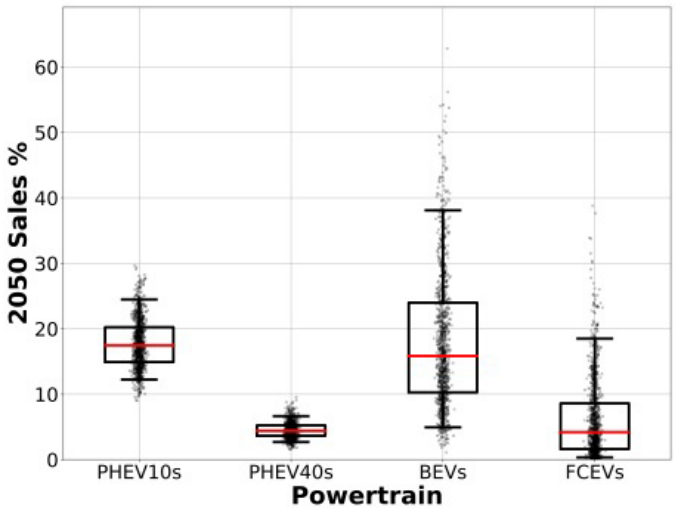

BEV – battery electric vehicle; PHEV – plug-in hybrid electric vehicle

FIGURE 3. Uncertainty in 2050 alternative energy vehicle sales. Shown are 1,024 scenarios (black dots) from a Monte Carlo analysis of technology, energy, behavior, and modeling parameters. Boxes show 25th/75th percentiles. Whiskers show 5th/95th percentiles. Red line shows median.

CONCLUSIONS AND UPCOMING ACTIVITIES

Fuel cell electric vehicles play a role in the future light duty vehicle mix, diversifying the fuel source and options to consumers. How large a role they can play is highly uncertain, but might be guided through directed technology investment. The hydrogen that fuels these vehicles may be produced via multiple pathways, and thus it is likely that hydrogen fuel prices can stay low through many uncertain commodity futures.

Future work for this project would include a write-up of our full results for the program office and participation in the multi-lab Baseline and Scenerio Analysis (BaSce) scenarios. Multi-lab scenario analysis in support of BaSce will continue into FY 2018.

FY 2017 PUBLICATIONS/PRESENTATIONS

1. Levinson, Rebecca S. et al., "Hydrogen Analysis with the Sandia ParaChoice Model." Presentation at the Annual Merit Review, June 2017.

2. Levinson, Rebecca S., Dawn K. Manley, and Todd H. West, "History v. Simulation: An analysis of the drivers of alternative energy vehicle sales." SAE Int. J. Alt. Power 5(2), 2016.

REFERENCES

1. Lin, Zhenhong and David L. Greene, "A Plug-In Hybrid Consumer Choice Model with Detailed Market Segmentation." Transportation Research Board 10-1698, 2010.

2. Struben, Jeroen and John D. Sterman, "Transition challenges for alternative fuel vehicle and transportation systems." Environment and Planning B: Planning and Design, 35:1070–1097, 2008.

3. U.S. Energy Information Administration. Annual Energy Outlook 2016: with Projections to 2040. U.S. Department of Energy, April 2016.

4. G. Bromaghim, K. Gibeault, J. Serfass, P. Serfass, E. Wagner, and the National Hydrogen Association. Hydrogen and Fuel Cells: The U.S. Market Report. Technical report, Technology Transition Corporation, March 2010. Prepared by the Technology Transition Corporation for the National hydrogen Association.

5. M. Ruth, M. Laffen, and T.A. Timbario. Hydrogen pathways: Cost, well-to-wheels energy use, and emissions for the current technology status of seven hydrogen production, delivery, and distribution scenarios. Technical Report NREL/TP-6A1-46612, National Renewable Energy Laboratory, September 2009.

6. A. Moawad, N. Kim, N. Shidore, and A. Rousseau. Assessment of Vehicle Sizing, Energy Consumption, and Cost through Large-Scale Simulation of Advanced Vehicle Technologies. Argonne National Laboratory, Argonne, IL, March 2016.

IX.5 Sustainability Analysis: Hydrogen Regional Sustainability (HyReS)

Marc Melaina (Primary Contact),
Elizabeth Connelly, Yuche Chen, Joshua Sperling
National Renewable Energy Laboratory (NREL)
15031 Denver West Parkway
Golden, CO 80401
Phone: (303) 275-3836
Email: Marc.Melaina@nrel.gov

DOE Manager: Fred Joseck
Phone: (202) 586-7932
Email: Fred.Joseck@ee.doe.gov

Project Start Date: October 1, 2015
Project End Date: September 30, 2018

Overall Objectives

- Develop a regional hydrogen sustainability analysis (HyReS) assessment framework that can be applied to hydrogen supply and fuel cell systems and is consistent with a broad range of existing sustainability assessment tools used by relevant stakeholders.
- Apply the framework as an enhancement to the existing suite of hydrogen systems analysis models developed for the U.S. Department of Energy's Fuel Cell Technologies Office (FCTO).
- Refine the framework to incorporate the latest developments in the field of sustainable development assessment, including recent data and analytic approaches, and to capture current issues relevant to key stakeholders.
- Implement the framework through a user interface that is accessible to target audiences, including private sector sustainability managers, industry stakeholders, government and non-government agencies, and potential investors.

Fiscal Year (FY) 2017 Objectives

- Review existing sustainable development frameworks in order to identify and select metrics to be included in the HyReS framework.
- Develop case studies to quantify environmental burdens for a select number of hydrogen supply chains and the fuel cell electric vehicle (FCEV) life cycle, consistent with the Greenhouse gases, Regulated Emissions, and Energy use in Transportation (GREET) model and Hydrogen Analysis (H2A) production models.
- Explore how regionalizing parameters in the hydrogen supply chain impact life cycle results.
- Benchmark hydrogen case study results against comparable vehicle–fuel systems, including conventional vehicles, hybrid electric vehicles (HEVs), and battery electric vehicles with 400-mile driving range using only electricity (BEV400s).

Technical Barriers

This project addresses the following technical barriers from the Systems Analysis section of the FCTO Multi-Year Research, Development, and Demonstration Plan.

(A) Future Market Behavior

(B) Stove-piped/Siloed Analytical Capability

(D) Insufficient Suite of Models and Tools

Contribution to Achievement of DOE Systems Analysis Milestones

This project will contribute to achievement of the following DOE milestones from the Systems Analysis section of the FCTO Multi-Year Research, Development, and Demonstration Plan.

- Milestone 1.19: Complete analysis of the potential for hydrogen, stationary fuel cells, fuel cell vehicles, and other fuel cell applications such as material handling equipment including resources, infrastructure and system effects resulting from the growth in hydrogen market shares in various economic sectors. (4Q, 2020)
- Milestone 2.2: Annual model update and validation. (4Q, 2011 through 4Q, 2020)

FY 2017 Accomplishments

- Of 63 sustainability indicators identified through literature review, twenty-two will be directly modeled in the HyReS framework, and an additional 26 will be related and potentially estimated using the HyReS framework. Fifteen of the identified indicators will not be addressed by the HyReS framework.
- Developed an analytic framework that integrates Argonne National Laboratory's GREET model and the National Renewable Energy Laboratory's Scenario Evaluation and Regionalization Analysis (SERA), Automotive Deployment Options Projection Tool (ADOPT), and Future Automotive Systems Technology Simulator (FASTSim) models, updating results to reflect current model capabilities (Milestone 2.2).

- Evaluated environmental impacts of four hydrogen supply pathways (two natural-gas-based and two renewable-based) for FCEVs. The impacts were evaluated at both national and regional levels based on state electricity generation mixes.
- Compared impacts from the four FCEV case study life cycles to the life cycle impacts from conventional gasoline vehicles, HEVs, and a BEV400.
- Example calculations monetized the social benefits from greenhouse gas (GHG) reductions, air pollution reductions, energy security benefits, and water use reductions for each vehicle–fuel system replacing one million conventional gasoline miles.
- Documented methods and results in an annual report for peer review.
- Presented methodology and preliminary results at two international conferences.

✧ ✧ ✧ ✧ ✧

INTRODUCTION

The Hydrogen Regional Sustainability (HyReS) project examines environmental burdens in a regional life cycle assessment approach that takes into account the economic and social aspects of hydrogen supply chains and FCEV production and operation. The HyReS framework enhances, extends, and complements the capabilities of a number of analytic models developed for the U.S. Department of Energy, including the GREET and SERA models [1,2]. The HyReS framework will also incorporate data and analytic capabilities from other models relevant to sustainability assessment, such as the Environmental Benefits Mapping and Analysis Program (BenMAP) and Co-Benefits Risk Assessment (COBRA) models developed by the U.S. Environmental Protection Agency (EPA) [3,4]. The integrated framework will address a number of sustainability metrics, such as greenhouse gas and criteria pollutant emissions, water usage, energy usage, and life cycle costs.

Progress to date has involved reviewing the sustainability literature to better understand how the HyReS framework can interface with and be useful to key stakeholders. The result is a set of proposed HyReS indicators. Analytic progress in developing the framework has focused on integrating environmental metrics from the GREET model, which have been used to develop four case studies for distinct hydrogen supply pathways. Integrating these case studies into the HyReS framework has highlighted the importance of assessing environmental impacts on a regional basis. Current analysis also provides example results of an approach to monetizing benefits (on a national scale) related to GHG emissions, air pollution, oil dependency, and water consumption.

APPROACH

In order to assess regional sustainability impacts of hydrogen supply to FCEVs, HyReS relies upon an analytical framework that integrates the following capabilities: hydrogen demand based upon a detailed geospatial vehicle stock model (SERA) [2]; optimized, least-cost hydrogen infrastructure supply chain networks (SERA) [1]; life cycle fuel and vehicle impacts based upon GREET [5]; market adoption of FCEVs based upon the ADOPT model [6]; and a health benefits mapping and analysis of criteria pollutant emissions using, for example, BenMAP or COBRA [3,4]. Figure 1 provides an overview of FCTO targets, the integrated HyReS analytic framework, and key sustainability metric categories.

To demonstrate the effect of regionalization on the life cycle environmental impacts of hydrogen supply, four pathways are analyzed first on a national basis and then on a state basis. Differences across states are based on the 2015 estimated state electricity mixes, provided by GREET. Transportation distances and process efficiencies are also varied to test the sensitivity of results. The baseline results (assuming U.S. average grid mix) are then benchmarked against other vehicle–fuel systems. For this benchmarking, the Future Automotive Systems Technology Simulator [7] is used to simulate an electric vehicle with a test cycle range of 400 miles, where the lower real-world driving range would be comparable to that of an FCEV.

RESULTS

The four hydrogen supply pathways considered in the preliminary case studies are gaseous hydrogen produced from natural gas and transported via heavy-duty truck ("GH2 from NG via Truck"), liquefied hydrogen produced from natural gas and transported via heavy-duty truck ("LH2 from NG via Truck"), gaseous hydrogen produced from poplar biomass transported via pipeline ("GH2 from Poplar via Pipeline"), and gaseous hydrogen produced from wind power and transported via pipeline ("GH2 from Wind via Pipeline"). For the baseline results the transportation distance, by either truck or pipeline, is 100 miles. Additionally, the baseline results are calculated assuming the U.S. average grid mix for electricity. Conversion efficiencies are, when necessary, altered from the GREET defaults to match those described in the Hydrogen Analysis (H2A) production models.

Figure 2 presents the baseline case study results for GHG emissions (g CO_2e/mi) and water usage (cm^3/mi) for each of the four pathways and for the vehicle cycle, hydrogen supply (well-to-pump), and vehicle operation (pump-to-wheels). The results indicate that the "LH2 from NG via Truck" pathway is associated with the highest life cycle GHG emissions. The difference in impacts from the two natural gas pathways is from the additional electricity for liquefaction. Compared

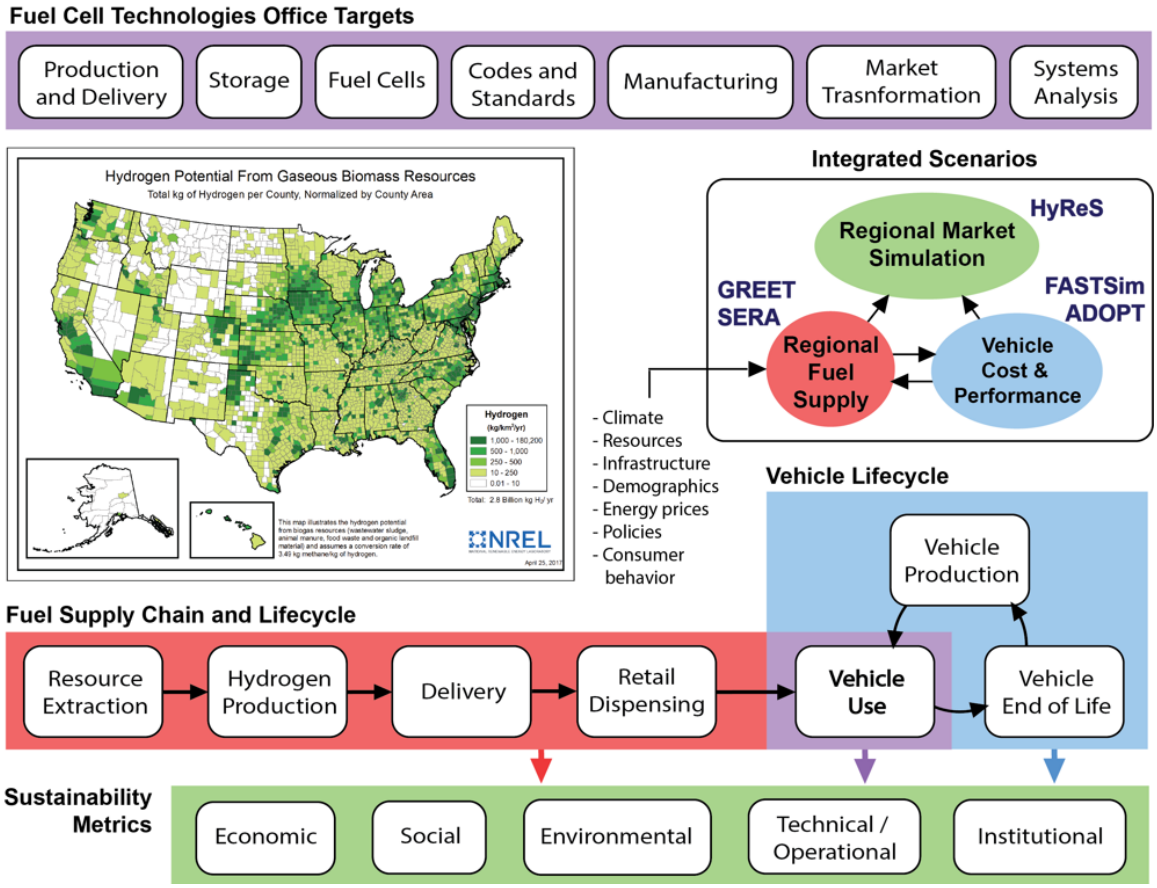

FIGURE 1. HyReS framework scope and sustainability metrics with respect to FCTO targets, fuel and vehicle life cycle stages, and regional integrated market assessment

to the natural gas pathways, the renewable-based pathways result in a 55–75% reduction in life cycle GHG emissions. On the other hand, the "GH2 from Poplar via Pipeline" pathway results in the highest life cycle water usage, where over 50% of the life cycle water usage is associated with the production of the poplar biomass.

Because the "LH2 from NG via Truck" pathway requires the most electricity, its life cycle GHG emissions are the most sensitive to the regional electricity mix. The baseline well-to-pump GHG emissions (based on the U.S. average grid mix) increase by up to 36% for this pathway. The grid mix associated with West Virginia has the highest GHG intensity due to the relatively high proportion of electricity from coal. In West Virginia, for example, results show that the FCEVs based on the "LH2 from NG via Truck" pathway produce up to 25% more life cycle GHG emissions than gasoline vehicles on a per-mile basis.

The baseline GHG results, shown in Figure 3, reveal that all four hydrogen supply pathways result in FCEVs with lower life cycle GHG emissions per mile than conventional gasoline vehicles. We compare these pathways also to HEVs and find that all but the "LH2 from NG via Truck" are less GHG-intensive. When comparing the "GH2 from Poplar via Pipeline" FCEV to a vehicle running on ethanol produced from poplar, results show that the FCEV produces 50% more GHG emissions over the life cycle. This difference is mostly due to the co-production of electricity during ethanol production, the displacement of which results in GHG credits for the ethanol life cycle. The default GREET assumptions include electricity co-generation for ethanol production, while the default biomass-to-hydrogen pathway does not include co-generation. The FCEV based on hydrogen from wind electrolysis is compared to an electric vehicle powered by wind with a range of 400 miles. In order to make such a comparison, it was necessary to simulate vehicle specifications for the battery electric vehicle (BEV400) and then make modifications to the GREET model accordingly. The results show that the BEV400 from wind has lower life cycle GHG emissions than the "GH2 from Wind via Pipeline" FCEV, because the electricity for transportation and distribution is assumed as the U.S. average grid mix as opposed to 100% renewable. Recent research [8,9] suggests that the GHG emissions of battery materials and manufacturing may actually be up to an order of magnitude higher than the GREET results. Figure 3 includes a symbol

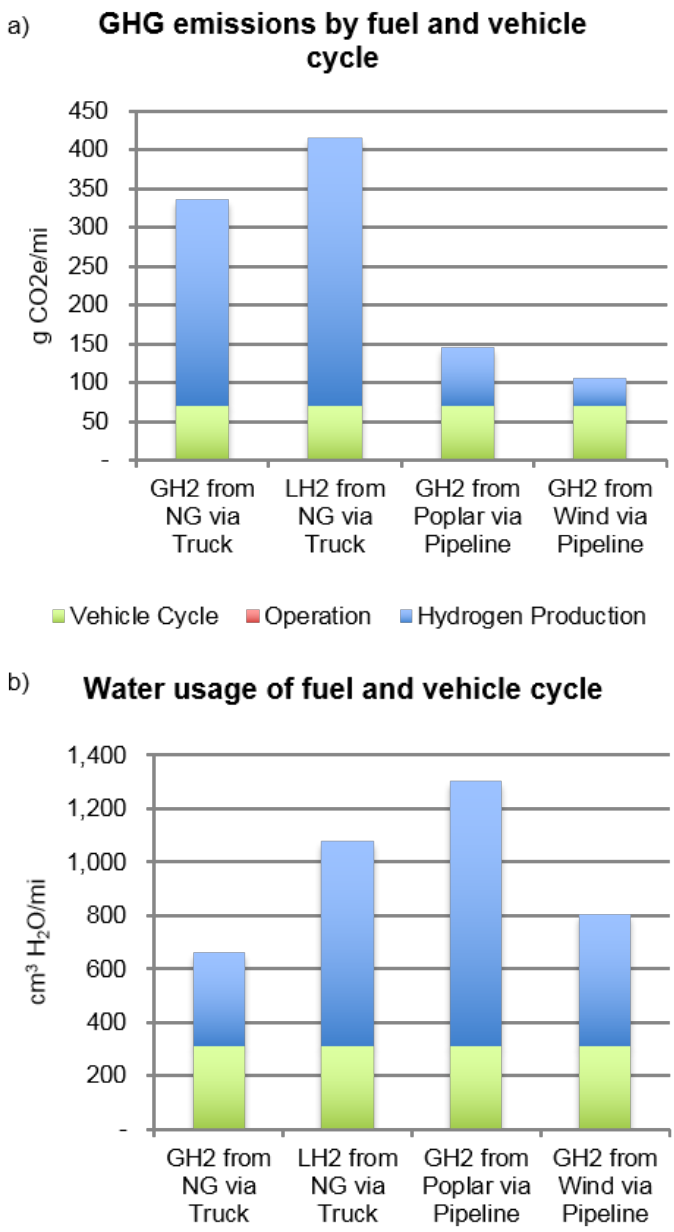

FIGURE 2. Life cycle (a) GHG emissions and (b) water usage associated with four hydrogen supply pathways for FCEVs

representing the life cycle emissions of a BEV400 (with electricity generated from wind) that uses the battery production cycle emissions from [9] in addition to the other GREET-based life cycle emissions. When the additional emissions from battery materials and manufacturing are taken into account, the FCEV from wind appears to be less GHG-intensive. These results will be revised according to future GREET model updates.

While the results presented in this report are limited to GHG emissions and water usage, other metrics from the GREET model are being integrated into the HyReS framework, such as petroleum and other fossil fuel consumption and criteria air pollution emissions. The HyReS framework is spatially and temporally explicit in assessing environmental impacts, allowing for location-based benefits to be calculated and monetized. For example, the COBRA model [4] can be used to monetize the costs and benefits associated with increases or decreases in local and regional criteria pollution emissions.

The social cost of GHGs [10], air pollution benefits from the COBRA model, energy security benefits [11], and water reduction benefits [12] are assessed as part of the HyReS framework. Figure 4 indicates the monetized benefit results for the four case study pathways in terms of dollars per one million conventional vehicle gasoline miles displaced. The baseline impacts (on a national scale) from each pathway are used for calculating these monetized benefits presented. The results show that the "GH2 from Wind via Pipeline" pathway accrues the highest benefits from displacing one million gasoline miles, with the highest level of benefits corresponding to reductions in criteria pollutant emissions.

CONCLUSIONS AND FUTURE WORK

The results from analyzing the environmental impacts of four hydrogen supply pathways reveal that FCEVs tend to have lower life cycle GHG emissions than conventional gasoline vehicles, in addition to lower criteria emissions, petroleum use, and water use. Monetizing the social benefits of these reductions results in up to $60,000 worth of benefits (from the "GH2 from Wind via Pipeline" pathway) associated with displacing one million gasoline miles. However, calculating results using state-based electricity mixes emphasizes the importance of spatially explicit analyses, with electricity mix being a major factor in determining whether FCEVs perform better or worse than conventional vehicles (i.e., result in a net positive or negative social benefit on a life cycle basis).

Future work includes expanding the framework beyond the case studies to incorporate analytic representations of all metrics associated with major hydrogen supply pathways and ensuring that regional hydrogen supply pathways are made consistent with the benchmark fuel pathways. Second, the framework will be applied to major supply chain components in a manner that allows for both project-specific evaluations (e.g., a particular hydrogen production facility or transmission pipeline) as well as general high-level assessments of geographically extensive supply networks (e.g., networked supply chains serving multiple demand centers in the Midwest). Third, additional work will ensure that HyReS is in alignment with goals and metrics in use by representative companies, government agencies, and other relevant stakeholders.

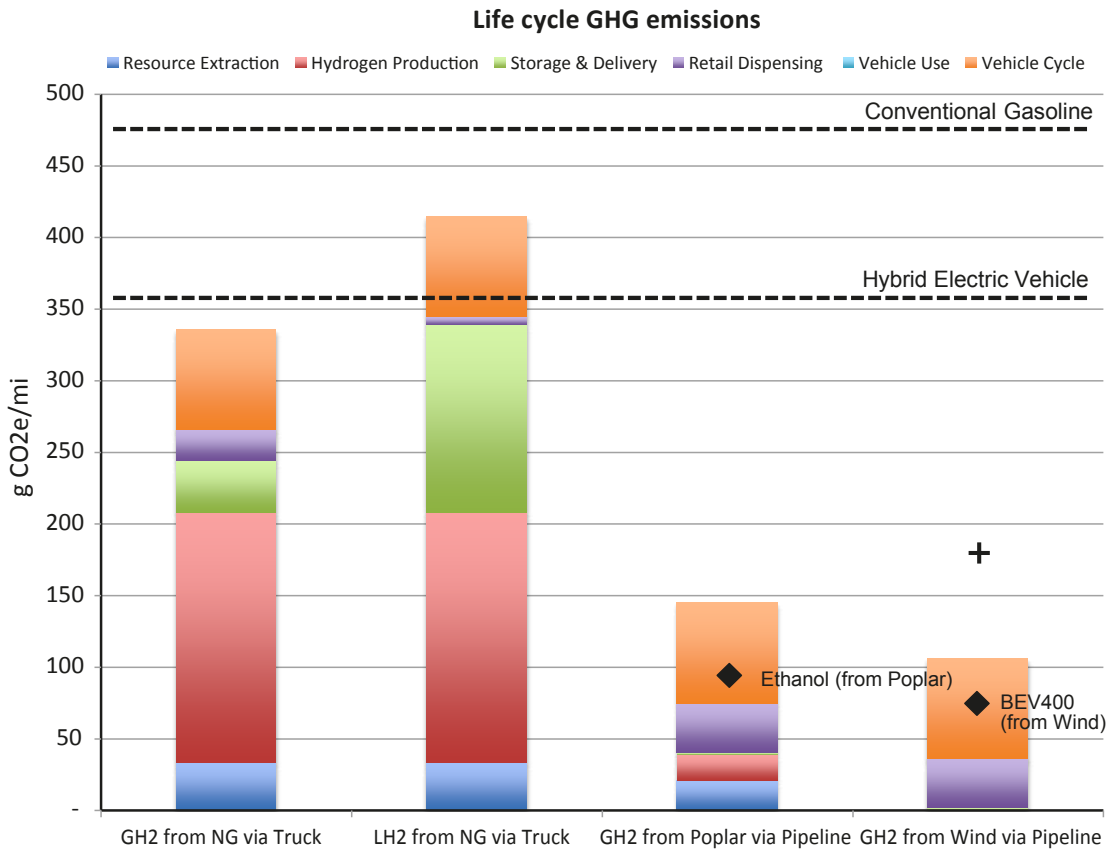

FIGURE 3. Baseline life cycle GHG-100 emissions per mile by stage of each hydrogen FCEV case study pathway, benchmarked against four reference vehicle–fuel systems: conventional gasoline vehicle, HEV, ethanol (from poplar) vehicle, and BEV400 from wind. The + represents the life cycle GHG emissions of a BEV400 using the per-kWh emissions from Kim et al. (2016).

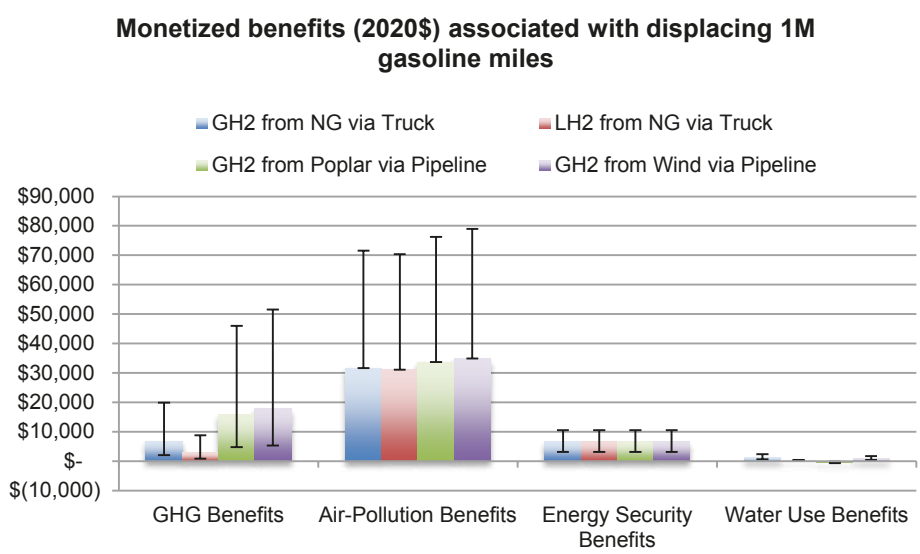

FIGURE 4. Monetized benefits associated with displacing one million gasoline miles with an FCEV fueled by one of the four hydrogen supply pathways

FY 2017 PUBLICATIONS/PRESENTATIONS

1. Connelly, E., Melaina, M., Lambert, J., and Linkov, I., "Resilience Analysis to Inform Priority-Setting." Presentation. Society for Risk Analysis Annual Meeting, San Diego, CA, December 11–15, 2016.

2. Connelly, E., Melaina, M., "Strategic Analysis of Transportation Policies." Poster Presentation. NREL Postdoc Career and Networking Fair, Golden, CO, February 23, 2017.

3. Connelly, E., Melaina, M., "Incorporating Resilience into Transportation Infrastructure Planning." Presentation. 2017 Joint Conference International Society for Industrial Ecology and International Symposium on Sustainable Systems and Technology, Chicago, IL, June 25–29, 2017.

4. Melaina, M., Connelly, E., Chen, Y., "Sustainability Analysis: Hydrogen Regional Sustainability (HyReS)." Presentation at the 2017 Annual Merit Review and Peer Evaluation Meeting, June 6, 2017, Washington, DC. Available from https://www.hydrogen.energy.gov/pdfs/review17/sa059_melaina_2017_o.pdf

5. Connelly, E., Melaina, M., Chen, Y., and Sperling, J., *Hydrogen Regional Sustainability (HyReS): Analytic Framework and Case Study Results.* Prepared for the U.S. Department of Energy's Fuel Cell Technologies Office. 2017. *Forthcoming.*

REFERENCES

1. Melaina, M. "SERA Scenarios of Early Market Fuel Cell Electric Vehicle Introductions: Modeling Framework, Regional Markets, and Station Clustering." NREL/PR-5400-64395. Presented at the 2015 ICEPAG Conference, Irvine, CA, March 23, 2015. Available online: http://www.nrel.gov/docs/fy15osti/64395.pdf

2. Bush, B., Melaina, M., Penev, M., Daniel, W., "SERA Scenarios of Early Market Fuel Cell Electric Vehicle Introductions," National Renewable Energy Laboratory, Technical Report NREL/TP-5400-56588, 2013. Available from http://www.nrel.gov/docs/fy13osti/56588.pdf

3. EPA. *Environmental Benefits Mapping and Analysis Program – Community Edition (BenMAP-CE).* U.S. Environmental Protection Agency, 2016. Available online: https://www.epa.gov/benmap

4. EPA. *Co-Benefits Risk Assessment (COBRA) Screening Model.* U.S. Environmental Protection Agency, 2015. Available online: https://www.epa.gov/statelocalclimate/co-benefits-risk-assessment-cobra-screening-model

5. Elgowainy, A., Dieffenthaler, D., Sokolov, V., Sabbisetti, R., Cooney, C., and Anjum, A. *The Greenhouse gases, Regulated Emissions, and Energy use in Transportation (GREET) Model (v1.3.0.13081).* [Software]. Argonne National Laboratory. 2013. Available from https://greet.es.anl.gov/

6. Brooker, A., Gonder, J., Lopp, S., and Ward, J., "ADOPT: A Historically Validated Light Duty Vehicle Consumer Choice Model," SAE Technical Paper 2015-01-0974. 2015. doi:10.4271/2015-01-0974.

7. Brooker, A., Gonder, J., Wang, L., Wood, E. et al., "FASTSim: A Model to Estimate Vehicle Efficiency, Cost and Performance," SAE Technical Paper 2015-01-0973. 2015. doi:10.4271/2015-01-0973.

8. Ellingsen, L.A.-W., Majeau-Bettez, G., Singh, B., Srivastava, A.K., Valøen, L.O., and Strømman, A.H. "Life Cycle Assessment of a Lithium-Ion Battery Vehicle Pack." *Journal of Industrial Ecology,* 18: 113–124. 2014. doi:10.1111/jiec.12072

9. Kim, H.C., Wallington, T.J., Arsenault, R., Bae, C., Ahn, S., and Lee, J. "Cradle-to-gate emissions from a commercial electric vehicle Li-ion battery: a comparative analysis." *Environmental science & technology*, 50(14), 7715–7722. 2016.

10. U.S. Government Interagency Working Group on Social Cost of Greenhouse Gases. "Technical Support Document: Technical Update of the Social Cost of Carbon for Regulatory Impact Analysis Under Executive Order 12866." 2016. Available online: https://www.epa.gov/sites/production/files/2016-12/documents/sc_co2_tsd_august_2016.pdf

11. EPA and NHTSA. "Light-Duty Vehicle Greenhouse Gas Emission Standards and Corporate Average Fuel Economy Standards; Final Rule." 2010. Available online: https://www.gpo.gov/fdsys/pkg/FR-2010-05-07/pdf/2010-8159.pdf

12. Ecolab and Trucost. *Water Risk Monetizer* [Software]. 2015. Available from https://www.waterriskmonetizer.com/

IX.6 Hydrogen Financial Analysis Scenario Tool (H2FAST) Updates with Analysis of 101st Station

Marc Melaina (Primary Contact) and Michael Penev
National Renewable Energy Laboratory
15013 Denver West Parkway
Golden, CO 80401-3305
Phone: (303) 275-3836
Email: Marc.Melaina@nrel.gov

DOE Manager: Fred Joseck
Phone: (202) 586-7932
Email: Fred.Joseck@ee.doe.gov

Project Start Date: September 2014
Project End Date: Project continuation and direction determined annually by DOE

Overall Objectives

- Provide convenient detailed hydrogen infrastructure financial analysis to facilitate investments in hydrogen refueling stations and improve policy-design decisions to support early hydrogen station and fuel cell electric vehicle (FCEV) market development.
- Inform multiple stakeholders (policy and government decision makers, station operators, equity investors, strategic investors, lenders).
- Enable transparent incentive analysis.
- Provide embedded investment risk analysis.

Fiscal Year (FY) 2017 Objectives

- Incorporate H2FAST into the Scenario Evaluation, Regionalization, and Analysis (SERA) model.
- Evaluate when hydrogen refueling stations in each state are projected to become profitable on average in national hydrogen deployment scenarios.
- Use H2FAST to evaluate real-world installations and identify key hydrogen cost factors.

Technical Barriers

This project addresses the following technical barriers from the Systems Analysis section of the Fuel Cell Technologies Office Multi-Year Research, Development, and Demonstration Plan.

(A) Future Market Behavior

(E) Unplanned Studies and Analysis

Contribution to Achievement of DOE Systems Analysis Milestones

This project will contribute to achievement of the following DOE milestones from the Systems Analysis section of the Fuel Cell Technologies Office Multi-Year Research, Development, and Demonstration Plan:

- Milestone 1.19: Complete analysis of the potential for hydrogen, stationary fuel cells, fuel cell vehicles, and other fuel cell applications such as material handling equipment including resources, infrastructure and system effects resulting from the growth in hydrogen market shares in various economic sectors. (4Q, 2020)
- Milestone 2.2: Annual model update and validation. (4Q, 2011 through 4Q, 2020)

FY 2017 Accomplishments

- Incorporated H2FAST into the SERA model.
- Showed that national scenarios have variable transition to un-incentivized financial profitability for different states.
- Used H2FAST to evaluate real-world installations.
- Demonstrated that early station operation demand charges are major cost factors.

✧ ✧ ✧ ✧ ✧

INTRODUCTION

Limited availability of hydrogen stations is a significant barrier to the successful commercialization of FCEVs. Investment risk is one of the factors that may inhibit the expansion of hydrogen stations in advance of widespread FCEV adoption. While the U.S. Department of Energy's Fuel Cell Technologies Office has supported extensive cost-estimation tools based on engineering principles and vetted by industry experts, these tools have been limited in their ability to explore finance options. This is a barrier to conveying the relevance of hydrogen station investment opportunities to key stakeholders and project partners through existing assessments of station costs and deployment.

Multiple studies have examined hydrogen infrastructure in terms of financial metrics. A 2008 National Academies study conveyed costs in terms of cash flows, highlighting the shortfall period—or "Valley of Death"—between when a company receives initial capital investment and when it

begins generating profit [1]. A 2013 Energy Independence Now report incorporated greater detail at the individual station level and examined policy support mechanisms [2]. A 2013 National Academies study examined cash flows in terms of private and social costs and compared a hydrogen scenario with success scenarios for other alternative fuels, with a study goal of examining light-duty-vehicle greenhouse gas emission reductions of 80% by 2050 [3]. The development of H2FAST builds on these previous studies, providing a rigorous framework and set of tools that can be used alongside or in conjunction with standard financial tools used in the private sector.

APPROACH

H2FAST provides a quick and convenient in-depth financial analysis for hydrogen refueling stations. It is meant to facilitate investments in hydrogen stations, improve policy design decisions to support early station and FCEV market development, and examine the market and financial implications of such support strategies. Intended users include policy and government decision makers, station operators, equity investors, strategic investors, and lenders. The H2FAST framework is based on the discounted-cash-flow framework originally implemented in the H2A suite of cost estimation models. This cash flow basis allows future capital costs, such as component replacements or station upgrades, to be treated consistently with upfront capital and annual operating costs. H2FAST extends the financial calculations to develop a much broader range of outputs than is contained in the H2A models. The financial calculations conform to generally accepted accounting principles and are compatible with analysis for International Financial Reporting Standards [4,5], and the format and terms used to convey financial results are consistent with standard reports used by private companies. H2FAST also can interface with many other models to provide enhanced analysis capabilities. Collaborative model development and use by a variety of public and private stakeholders helps ensure relevance to ongoing analytical needs.

H2FAST accepts user inputs including capital and maintenance costs, incentives, demand profile, feedstock use, retail hydrogen price, and various financial parameters. The model then provides users with detailed annual finance projections in the form of income statements, cash flow statements, and balance sheets; graphical presentation of financial performance parameters for numerous common metrics; life cycle cost breakdown for each analysis scenario; and common ratio analysis results such as debt/equity position, return on equity, and debt service coverage ratio. It also enables risk analysis based on user-defined input value upper- and lower-bounds.

RESULTS

H2FAST was integrated into the SERA model and used to evaluate the financial performance of hydrogen stations deployed to support urban hydrogen demand growth in the United States over the 2015–2050 timeframe. Financial performance drivers included station cost reduction (learning curves), the construction of larger stations over time (driven by higher demand per location), and accelerating utilization growth. H2FAST was used to estimate the crossover point when stations become financially profitable without incentives. Relevant local conditions were modeled, and net present value (NPV) was estimated for every projected station. Figure 1 shows example results for projected stations in Massachusetts. Although poorly performing stations (those with negative NPVs) exist throughout the analysis span, the average NPV rises over time and becomes positive in 2033. Average station NPV indicates when profits from high-performing stations can offset losses from other stations, and it may be a good indicator of the advent of self-sustaining infrastructure.

This approach was applied to analyze when each state achieves a positive average station NPV without incentives. Figure 2 shows the results. California and New York achieve a positive average NPV by 2029, and most other states follow over the next 20 years. However, eight states in the contiguous 48 still have negative average NPVs in 2049.

H2FAST was also used for detailed analysis of real-world hydrogen stations in California, showing the impact of electricity costs and use patterns on station economics. The U.S. Energy Information Administration reports California's average commercial blended electricity rate at 15.73¢/kWh. However, California stations use electricity at peak daily rate times (Figure 3) and incur substantial service and demand charges, resulting in electricity costs around 50¢/kWh. Figure 4 shows the electricity cost breakdown for stations in three California cities in 2016. Total electricity costs for these stations are 2.8–3.5 times higher than the California average, with the largest cost contribution from demand charges. Because maximum demand charges are incurred even at minimal station utilization, demand charges are most relevant for stations with low utilization. For this reason, demand charges should be treated as a fixed operating cost.

CONCLUSIONS AND UPCOMING ACTIVITIES

H2FAST continues to be an effective and flexible tool for analyzing the financial performance of hydrogen refueling stations. Subject to funding received, upcoming activities may include exploring national and regional station deployment scenarios in greater detail as well as integrating H2FAST further with SERA to account for hydrogen production scenarios and transitions to renewable hydrogen.

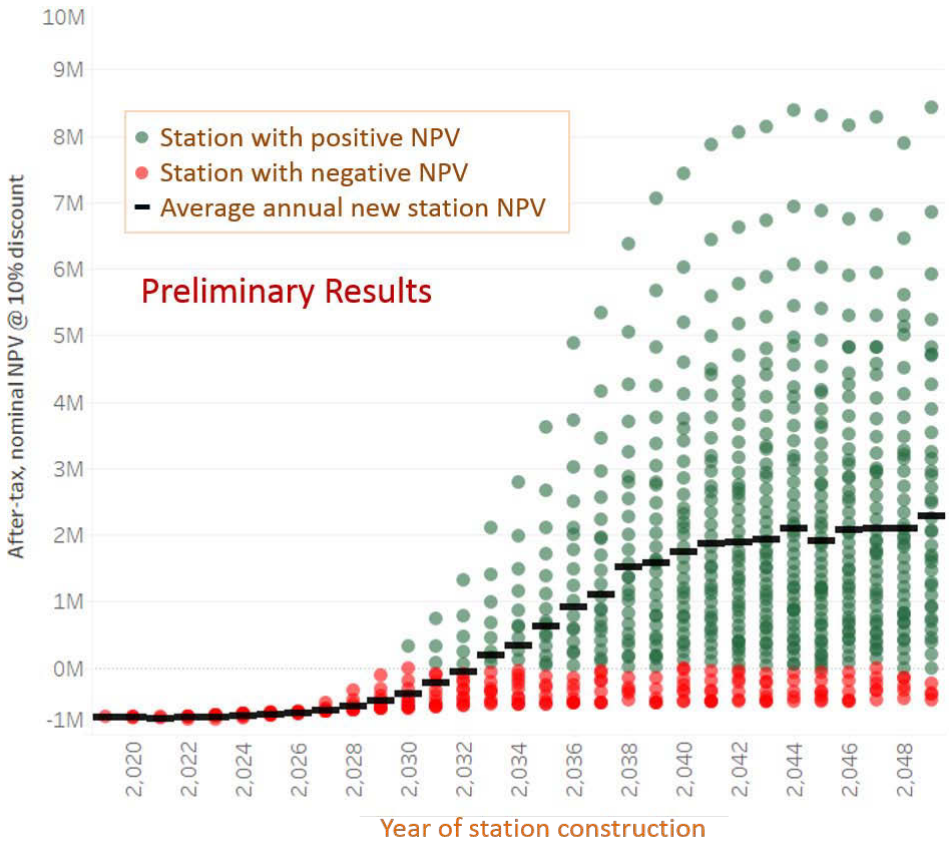

FIGURE 1. After-tax, nominal NPV at a 10% discount rate for simulated hydrogen refueling stations deployed in Massachusetts through 2049

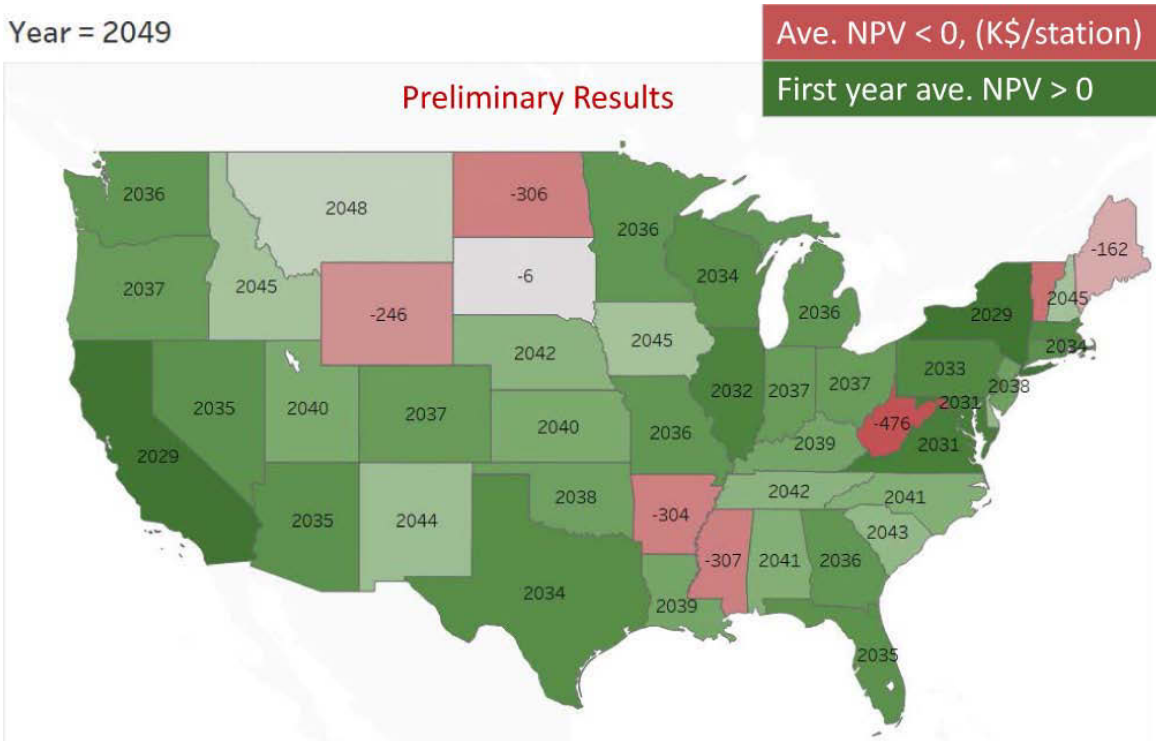

FIGURE 2. Projections of the years at which hydrogen refueling stations in each state achieve a positive NPV on average without incentives

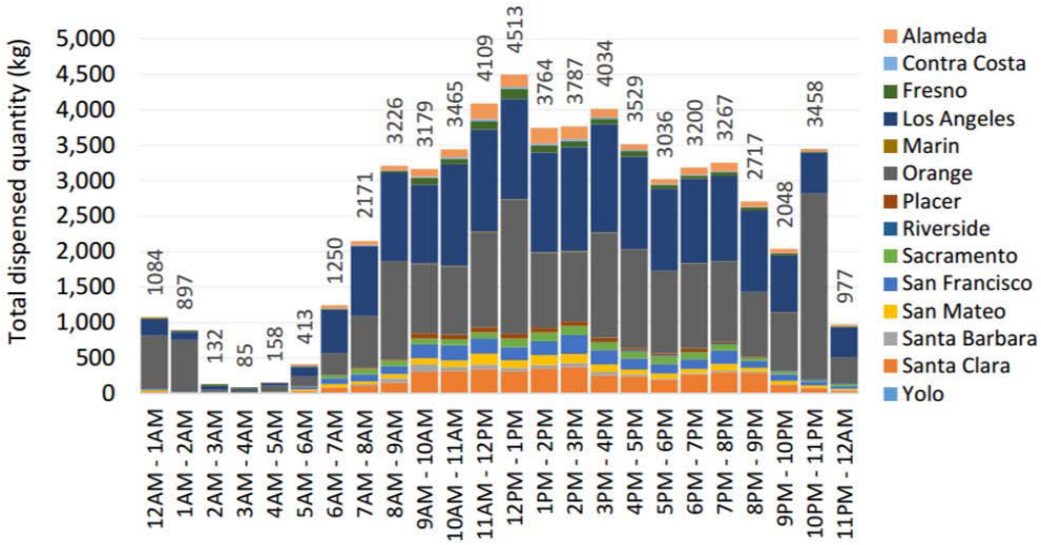

FIGURE 3. Total hydrogen dispensed by hour of day and California county; use profile from Baronas, et al. [6], rate structure from First Element Electricity [7]

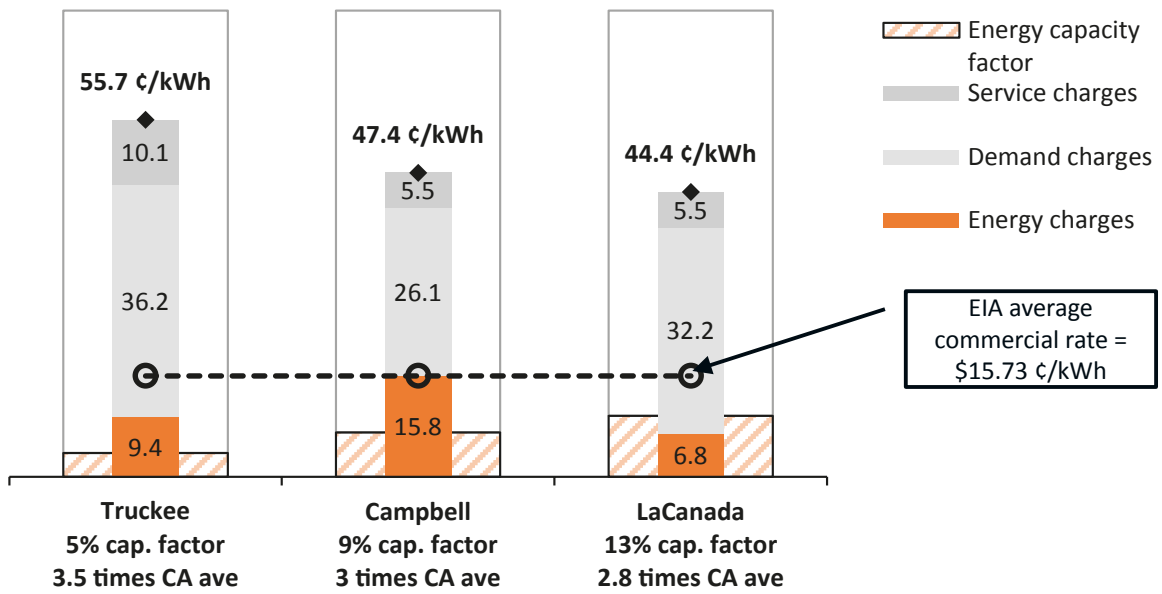

EIA – Energy Information Administration

FIGURE 4. Empirical electricity cost for hydrogen refueling stations operating in three California cities in 2016; utility bills from First Element Electricity [7]

The model could also be enhanced via features such as additional fixed operating costs (e.g., demand charges), more detailed demand ramp-up specifications, and the ability to provide custom feedstock and retail price profiles. Finally, ongoing maintenance and support could include supporting custom analysis and user-base requests and producing model updates as needed.

FY 2017 PUBLICATIONS/PRESENTATIONS

1. M. Melaina, and M. Penev, "Hydrogen Financial Analysis Scenario Tool (H2FAST)," presented to the H2USA Location Roadmap Working Group, 2017.

2. M. Penev, "Hydrogen Financial Analysis Scenario Tool (H2FAST) Model Summary and Demonstration," webinar, February 2017, https://energy.gov/eere/fuelcells/downloads/hydrogen-financial-analysis-scenario-tool-h2fast-model-summary-and.

REFERENCES

1. National Research Council, 2008, *Transitions to Alternative Transportation Technologies: A Focus on Hydrogen*, Washington, D.C.: National Academies Press.

2. T. Eckerle, and R. Garderet, 2013, *Hydrogen Network Investment Plan*, Energy Independence Now, http://www.einow.org/images/stories/factsheets/h2nip_full_paper_final.pdf.

3. National Research Council, 2013, *Transitions to Alternative Vehicles and Fuels*, Washington, D.C.: National Academies Press.

4. Federal Accounting Standards Advisory Board, 2014, *FASAB Handbook of Federal Accounting Standards and Other Pronouncements, as Amended*, Washington, DC: Federal Accounting Standards Advisory Board.

5. Investopedia, 2014, "Accounting (Fundamental Analysis) Terms," accessed December 2014, http://www.investopedia.com/categories/accounting.asp.

6. J. Baronas, and G. Achtelik, 2017, *Joint Agency Staff Report on Assembly Bill 8: 2016 Assessment of Time and Cost Needed to Attain 100 Hydrogen Refueling Stations in California*, California Energy Commission and California Air Resources Board, http://www.energy.ca.gov/2017publications/CEC-600-2017-002/CEC-600-2017-002.pdf.

7. First Element Electricity, 2017, electricity bills, with permission of Tim Brown, COO.

IX.7 Regional Supply of Hydrogen

Marc Melaina (Primary Contact) and Michael Penev
National Renewable Energy Laboratory
15013 Denver West Parkway
Golden, CO 80401-3305
Phone: (303) 275-3836
Email: Marc.Melaina@nrel.gov

DOE Manager: Fred Joseck
Phone: (202) 586-7932
Email: Fred.Joseck@ee.doe.gov

Project Start Date: October 2016
Project End Date: Project continuation and direction determined annually by DOE

Overall Objectives

- Evaluate existing hydrogen production capacity and hypothetical excess capacity.
- Forecast production capacity expansion requirements for growing fuel cell electric vehicle (FCEV) market demand.
- Simulate regional supply chain network dynamics.
- Incorporate market competition considerations.

Fiscal Year (FY) 2017 Objectives

- Assess current hydrogen production assets by capacity and type as well as current hydrogen and natural gas pipelines.
- Identify potentially constrained production regions.
- Develop modeling framework for semi-central production with spoke-hub distribution pipelines, with eventual transition to large-scale central renewable production.
- Complete preliminary cost estimates for spoke-hub pipeline distribution networks.

Technical Barriers

This project addresses the following technical barriers from the Systems Analysis section of the Fuel Cell Technologies Office Multi-Year Research, Development, and Demonstration Plan.

(A) Future Market Behavior

(E) Unplanned Studies and Analysis

Contribution to Achievement of DOE Systems Analysis Milestones

This project will contribute to achievement of the following DOE milestones from the Systems Analysis section of the Fuel Cell Technologies Office Multi-Year Research, Development, and Demonstration Plan.

- Milestone 1.19: Complete analysis of the potential for hydrogen, stationary fuel cells, fuel cell vehicles, and other fuel cell applications such as material handling equipment including resources, infrastructure and system effects resulting from the growth in hydrogen market shares in various economic sectors. (4Q, 2020)
- Milestone 2.2: Annual model update and validation. (4Q, 2011 through 4Q, 2020)

FY 2017 Accomplishments

- Assessed current hydrogen production assets by capacity and type as well as current hydrogen and natural gas pipelines.
- Identified the Northeast as a potentially constrained production region.
- Developed modeling framework for semi-central production with spoke-hub distribution pipelines, with eventual transition to large-scale central renewable production.
- Completed preliminary cost estimates for spoke-hub pipeline distribution networks.
- Completed initial simulation of regional supply chain network dynamics.

✧ ✧ ✧ ✧ ✧

INTRODUCTION

Numerous supply chain components will contribute to the regional availability and cost of hydrogen for fueling FCEVs. For this reason, comprehensively forecasting the near- and long-term development of hydrogen supply chains is critical for forecasting the regional and national growth of FCEV markets and supporting refueling infrastructure. For such analyses, the National Renewable Energy Laboratory uses its Scenario Evaluation, Regionalization, and Analysis (SERA) model. Work on this project accomplished in FY 2017 expands SERA's capabilities by accounting for current hydrogen production and distribution assets as well as producing a design for semi-central hydrogen production with spoke-hub distribution pipelines.

APPROACH

Additional hydrogen supply pathways and market-competition parameters are developed to extend the SERA modeling framework and forecast competitive retail price and hydrogen availability on a regional basis. SERA is used to develop optimized hydrogen supply networks in response to FCEV hydrogen demands. It accounts for the geography of energy resource availability, extraction and conversion costs, transmission and distribution costs, and retail station network costs. The modeling approach also accounts for a broad range of influences on the decision to invest in new hydrogen production capacity. These include internal rate of return, 5-year demand growth horizon, capacity function of demand growth rate, potential installations, market growth (internal and external FCEV market forecasts), investment risk reduction due to an emerging track record, and total cost of FCEV ownership including policy support. It bases market competition and resulting prices on the production/delivery cost of the second-nearest competitive source.

In FY 2017, this project used data from IHS Markit [1] and ABB [2] to assess current hydrogen production and distribution assets. This information is used to forecast when various regions would experience stress on their hydrogen supply infrastructure based on projected demand from FCEVs. A modeling framework for semi-central hydrogen production with spoke-hub distribution pipelines—with eventual transition to large-scale central renewable hydrogen production—is also developed, and cost information derived from the *Oil & Gas Journal* is applied to estimate hydrogen supply costs [3]. Parameters from Argonne National Laboratory's Hydrogen Delivery Scenario Analysis Model [4] and H2A Delivery Components Model [5] also inform the analysis.

RESULTS

The assessment of current hydrogen production and distribution assets is illustrated in Figure 1. Based on that information, Figure 2 projects the development of

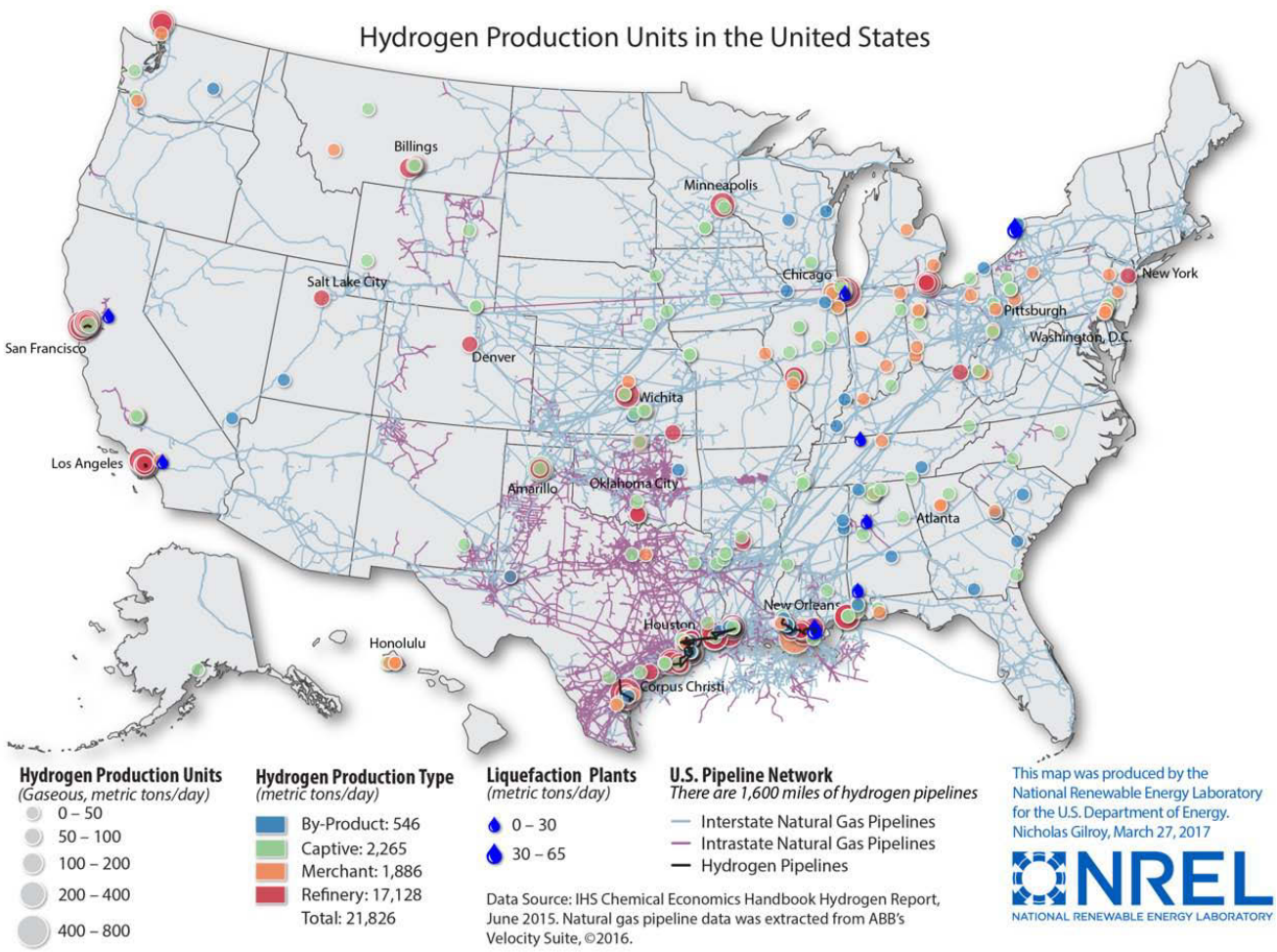

FIGURE 1. Existing U.S. hydrogen production units and hydrogen and natural gas pipelines

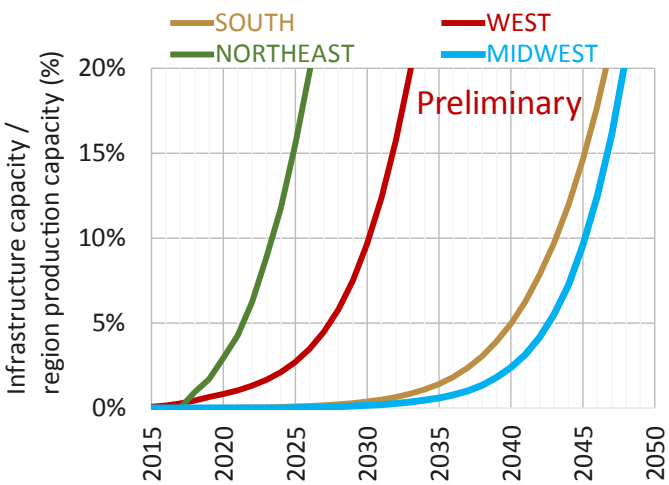

FIGURE 2. Projected regional development of infrastructure capacity as a percentage of total regional production capacity through 2050

infrastructure capacity as a percentage of total existing regional production capacity through 2050. Projected development for growing FCEV markets is based upon national scenarios developed in conjunction with H2USA. Because the Northeast's FCEV market and refueling station network is projected to develop relatively rapidly and its hydrogen production capacity is relatively low, it likely would be the first region to experience stresses in supply. The West, South, and Midwest—in that order—likely would experience stress on regional supply capacities next as their FCEV markets developed.

Figure 3 compares the modeling framework for semi-central hydrogen production with spoke-hub distribution pipelines with a traditional central production framework with long-distance pipeline distribution. In the traditional framework, each retail refueling station in a network would draw hydrogen directly from a pipeline connected to a large hydrogen production facility (Figure 3a). Compared with some other supply approaches, this approach simplifies retail station delivery, eliminates delivery truck emissions, reduces station storage requirements, and enables siting on small urban sites. However, it also requires a large upfront investment, presents high investor risk, and has a long demand ramp-up period (resulting in a poor return on investment). In addition, subsequent investments for network off-shoots may still be needed. Semi-central hydrogen production with spoke-hub distribution pipelines addresses these drawbacks by connecting stations in series to a smaller, scalable production plant (Figure 3b). This approach enables organic growth of the station network, which requires smaller incremental investments, reduces investment risk, provides quicker capital utilization ramp-up, allows for diverse

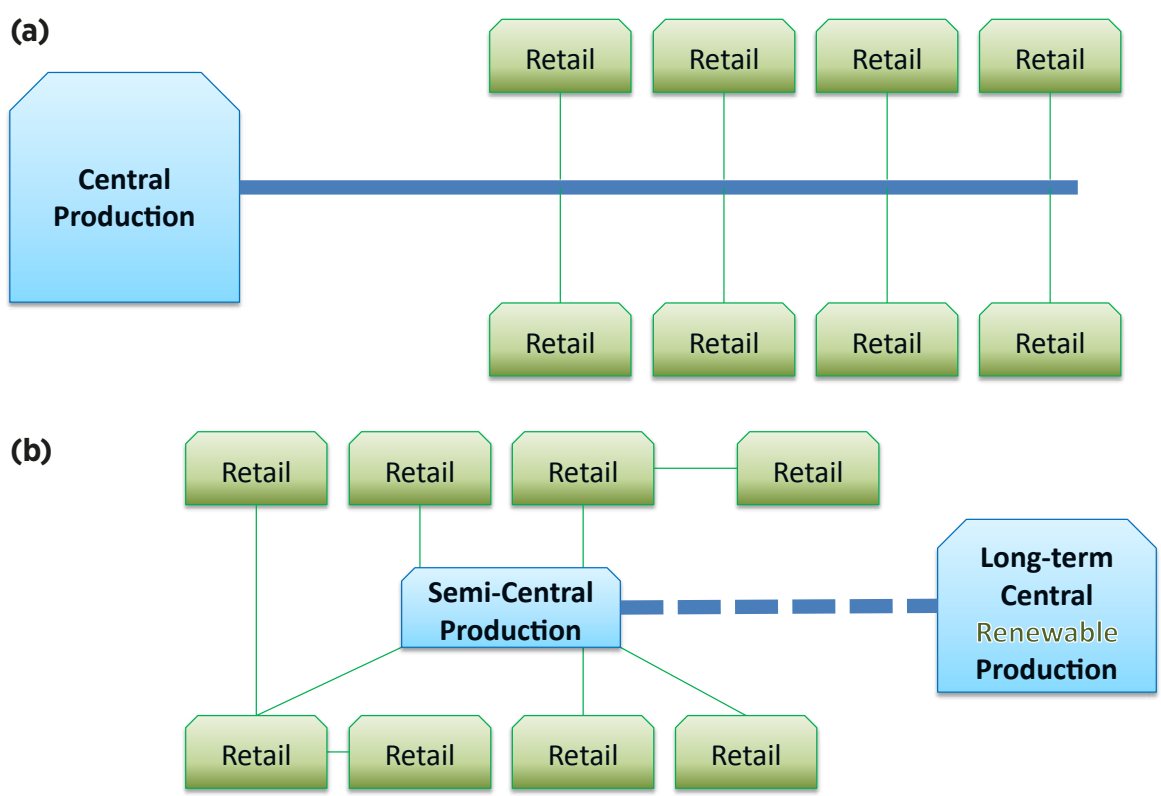

FIGURE 3. Schematics of central production with long-distance pipeline distribution (a) and semi-central production with spoke-hub distribution pipelines (b)

production strategies, and results in higher resilience and redundancy of supply. It also provides the opportunity to connect large centralized renewable production plants to the semi-central production nodes in the future.

Preliminary costs for the semi-central approach are benchmarked and compared with the costs of other hydrogen supply options. Figure 4 shows the resulting profited cost of hydrogen (in dollars per kilogram) for central steam methane reforming (SMR) with truck delivery, forecourt SMR (with hydrogen produced onsite at stations), low-pressure semi-central SMR with spoke-hub distribution pipelines, and dispensing-pressure semi-central SMR with spoke-hub distribution pipelines. Both semi-central approaches cost significantly less than the central approach. The low-pressure semi-central approach is slightly more expensive than the forecourt approach, although this gap narrows as more retail stations are added to the network. Dispensing-pressure semi-central SMR with spoke-hub distribution pipelines is the lowest-cost option in this analysis, and it becomes increasingly favorable as more retail stations are added to the network, demonstrating the effect of economies of scale. Centralizing compression can provide significant performance, siting, and economic benefits. A central compressor is much cheaper than many smaller compressors and enables improved compressor oversight and reliability. It greatly improves back-to-back fill capability. It also minimizes the retail footprint—because stations have no onsite storage, storage set-back distances, compressor, or maintenance access setbacks—so stations can be established on relatively small urban retail locations.

CONCLUSIONS AND UPCOMING ACTIVITIES

Extension of the SERA modeling framework has revealed potential regional hydrogen supply bottlenecks as well as the potential advantages of semi-central hydrogen production with spoke-hub distribution pipelines. Subject to funding received, upcoming activities may include continuing SERA updates based on evolving hydrogen production and delivery components, updating investment decision parameters and valuation metrics in response to stakeholder feedback, and integrating investment decision financial metrics with hydrogen sustainability indicators (the HyReS framework). In addition, activities could include accounting for the influence of additional market drivers and growth, such as power-to-gas with natural gas pipeline blending opportunities, promising near-term non-FCEV markets identified through H2@Scale, and Low Carbon Fuel Standard price signals in California.

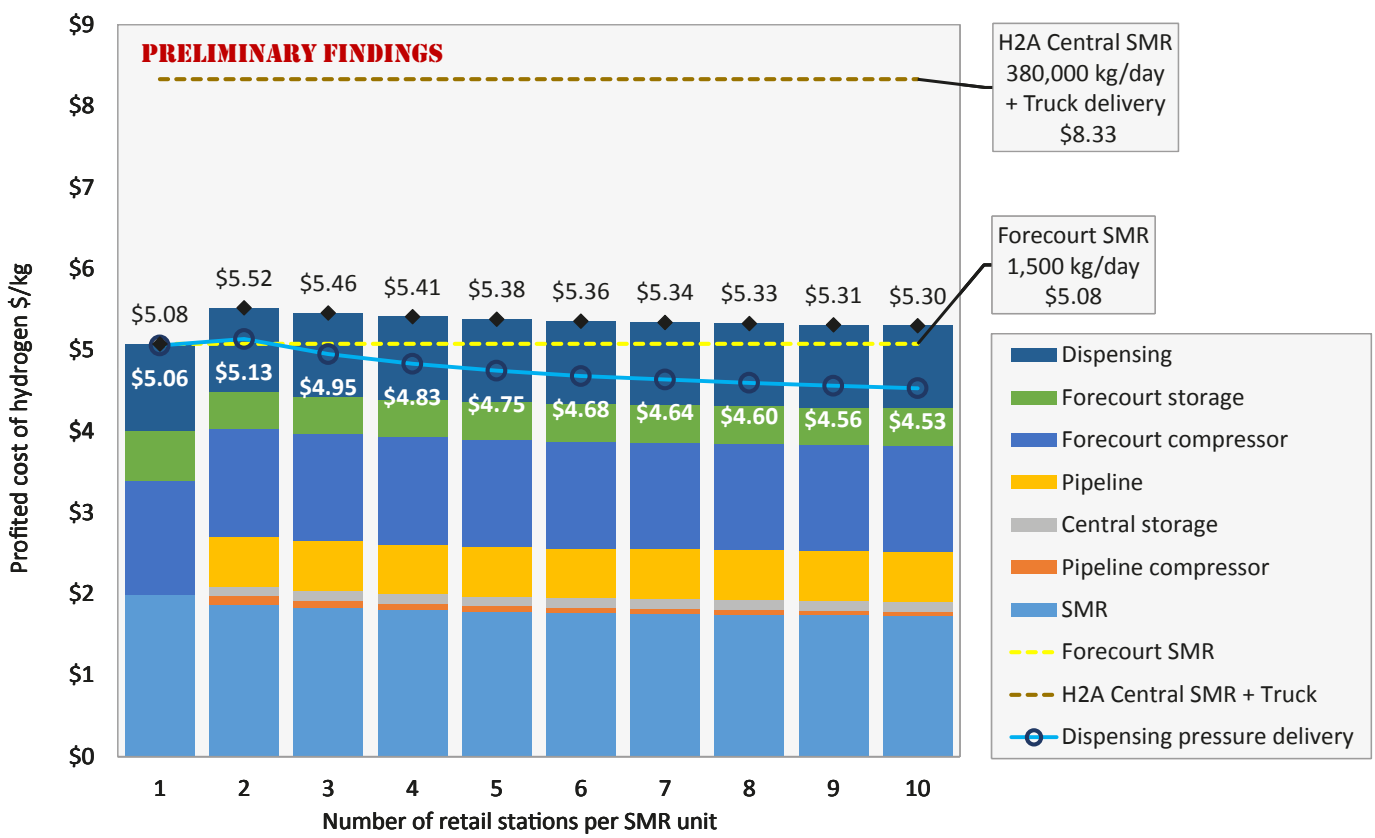

FIGURE 4. Profited cost of hydrogen estimates for various production/distribution approaches

REFERENCES

1. IHS Markit, 2015, *Chemical Economics Handbook: Hydrogen*, London: IHS Markit, https://www.ihs.com/products/hydrogen-chemical-economics-handbook.html.

2. ABB, 2016, *Velocity Suite*, accessed 2017, http://new.abb.com/enterprise-software/energy-portfolio-management/market-intelligence-services/velocity-suite.

3. *Oil & Gas Journal*, 2017, pipeline and compressor data, accessed 2017, http://www.ogj.com/index.html.

4. Argonne National Laboratory, 2017, *Hydrogen Delivery Scenario Analysis Model (HDSAM)*, accessed 2017, https://www.hydrogen.energy.gov/h2a_delivery.html.

5. Argonne National Laboratory, 2017, *H2A Delivery Components Model*, accessed 2017, https://www.hydrogen.energy.gov/h2a_delivery.html.

IX.8 Greenhouse Gas (GHG) Emissions and Petroleum Use Reduction of Medium- and Heavy-Duty Trucks

Amgad Elgowainy (Primary Contact),
Dong-Yeon (D-Y) Lee, and Michael Wang
Argonne National Laboratory
9700 S. Cass Ave.
Lemont, IL 60439
Phone: (630) 252-3074
Email: aelgowainy@anl.gov

DOE Manager: Fred Joseck
Phone: (202) 586-7932
Email: Fred.Joseck@ee.doe.gov

Project Start Date: October 2016
Project End Date: Project continuation and direction are determined annually by DOE

Overall Objectives

- Evaluate the potential benefits and trade-offs of hydrogen fuel cell electric vehicle (HFCEV) technology in comparison with conventional diesel internal combustion engine (ICE) for medium- and heavy-duty vehicle (MHDV) applications in terms of air emissions and petroleum use.
- Develop representative and up-to-date estimates of well-to-wheels (WTW) petroleum consumption and air emissions.
- Collaborate with vehicle manufacturers, modelers/analysts (national laboratories, universities, and consulting firms), and fleet operators and managers in the MHDV sector to acquire/review data and results.
- Inform DOE program managers and other stakeholders of the environmental benefits of medium- and heavy-duty hydrogen fuel cell vehicle applications to guide research, development, and demonstration decisions.

Fiscal Year (FY) 2017 Objectives

- Quantify WTW petroleum use and air emissions for medium- and heavy-duty HFCEVs.
- Reflect the diversity of MHDV sector by incorporating different vehicle types, weight classes, and vocations.
- Compare HFCEV technology to conventional diesel and other alternatives in terms of energy use and air emissions (GHGs and criteria air pollutants).
- Incorporate different hydrogen fuel production pathways into the WTW comparison.
- Accurately represent real-world vehicle operation characteristics and its impact on energy consumption and air emissions.
- Actively involve experts from industry (manufacturers and fleet managers) and academia/national laboratories (researchers and analysts) to ensure accuracy of data and results.

Technical Barriers

This project addresses the following technical barriers from the Systems Analysis section of the Fuel Cell Technologies Office Multi-Year Research, Development, and Demonstration Plan.

(C) Inconsistent Data, Assumptions and Guidelines

(D) Insufficient Suite of Models and Tools

Contribution to Achievement of DOE Systems Analysis Milestones

This project contributes to achievement of the following DOE milestones from the Systems Analysis section of the Fuel Cell Technologies Office Multi-Year Research, Development, and Demonstration Plan.

- Milestone 2.2: Annual model update and validation. (4Q, 2011 through 4Q, 2020)
- Milestone 3.1: Annual update of Analysis Portfolio. (4Q, 2011 through 4Q, 2020)

FY 2017 Accomplishments

- Developed representative fuel economy values for a variety of medium- and heavy-duty hydrogen fuel cell electric and diesel vehicle classes, based on the most recent heavy-duty vehicle fuel efficiency standards, and employing a high-fidelity advanced vehicle dynamic simulation software (Autonomie), supplemented with real-world idle fuel rates.
- Compared different fuel economy simulation models with different approaches and data sources.
- Expanded the Greenhouse gases, Regulated Emissions, and Energy use in Transportation (GREET®) model by adding HFCEV to the existing MHDV technology portfolio.

- Incorporated up-to-date air emissions factors for refineries and steam methane reforming (SMR) operations.
- Evaluated regional fuel economy variations for various types, weight classes, and vocations of medium- and heavy-duty hydrogen fuel cell electric and diesel vehicles.
- Assessed WTW petroleum use and air emissions reduction benefits by switching from conventional diesel ICE vehicles to HFCEVs, more than 90% for petroleum use, 20–50% for GHG emissions, and 25–70% for criteria air pollutants emissions can be reduced.
- Examined the impacts of different hydrogen production pathways (e.g., conventional central SMR, central solar electrolysis, and central biomass gasification) for the comparison of WTW petroleum consumption and air emissions of hydrogen fuel cell electric and baseline diesel vehicles.
- Analyzed the differences between gaseous and liquid hydrogen fuels for MHDVs in terms of WTW petroleum use and GHG emissions.

✧ ✧ ✧ ✧ ✧

INTRODUCTION

MHDVs, particularly trucks, are the second largest and fastest-growing petroleum consumers and GHG emitters in the U.S. transportation sector. The significance of MHDVs becomes even more important for local air quality management in some areas. For instance, in the South Coast of California (Los Angeles and Long Beach), MHDVs account for 40% of the total summer NO_x (a ground-level ozone precursor) emissions. Whether it's national or local, MHDVs can make a considerable contribution to reducing petroleum consumption, lowering GHG emissions, and improving air quality. To this end, HFCEVs can play an important role, as they create zero tail-pipe emissions and don't consume petroleum fuels. However, information is scarce as to how exactly hydrogen fuel cell MHDVs compare to other vehicle technologies and what the potential benefits are on a holistic life-cycle basis. The main goal of this project is to quantify and examine the WTW petroleum energy use and air emissions of hydrogen fuel cell MHDVs in comparison with conventional diesel ICE vehicles.

APPROACH

For a holistic and subjective analysis, a WTW analysis framework is adopted to quantify and examine life cycle petroleum use and air emissions of medium- and heavy-duty hydrogen fuel cell electric vehicles. More specifically, GREET MHDVs module was expanded to include HFCEV technology. GREET accounts for both direct (i.e., tail-pipe) and indirect (e.g., fuel production) lifecycle stages, providing well-to-wheels energy use and emissions results for different vehicle technologies and fuel pathways.

Real-world data for vehicle operation characteristics and fuel consumption were collected from several sources in industry and academia. When combined with real-world data, fuel economy estimates were developed from a high-fidelity vehicle dynamic simulation too (Autonomie). The fuel economy results were incorporated into GREET. Fuel economy (or fuel consumption) of HFCEVs is estimated based on the most recent heavy-duty vehicle fuel efficiency standards. The same method is used for conventional diesel for an apples-to-apples comparison. Based on real-world duty cycles for MHDVs and the high-resolution spatial and temporal data for meteorology and vehicle activity, variations in the life-cycle results were evaluated under different vehicle operating conditions, and in different locations and times. This detailed analysis helps develop representative regional and national average fuel economy values for incorporation into GREET.

RESULTS

Simulation results show that medium- and heavy-duty HFCEVs generally achieve 1.7 times better fuel economy (miles per diesel gallon equivalent) compared to conventional diesel vehicles. The fuel economy comparison varies by vehicle type and weight class, which have different duty cycles. For instance, the fuel economy benefit of HFCEVs over diesel ICE vehicle is larger for classes with high share of urban driving compared to classes that serve regional operation, which has a larger share of highway driving. For the early market medium- and heavy-duty HFCEVs, urban driving is a more appropriate reference operating condition. Also, fuel economy of HFCEVs tends to be more sensitive to climate conditions, compared to diesel vehicles. For example, waste heat from the internal combustion engine available is for miscellaneous thermal energy demand in diesel vehicles (e.g., cabin heating). Fuel economy estimates also vary by employed vehicle simulation model, but the comparison of different models reveals that Autonomie (the primary model used for this study) provides more accurate and consistent results that are comparable to surveyed fuel economy values obtained from actual operation. Developing representative fuel economy values and evaluating their sensitivity to various factors and parameters are crucial for fair and realistic comparison between HFCEVs and diesel vehicles.

The WTW results from the GREET model show that HFCEVs provide significant reduction in petroleum consumption (95–99%) compared to conventional diesel vehicles for all hydrogen production pathways (Figure 1). Additional reduction benefits can be found in terms of WTW GHG emissions (Figure 2). Compared to conventional diesel

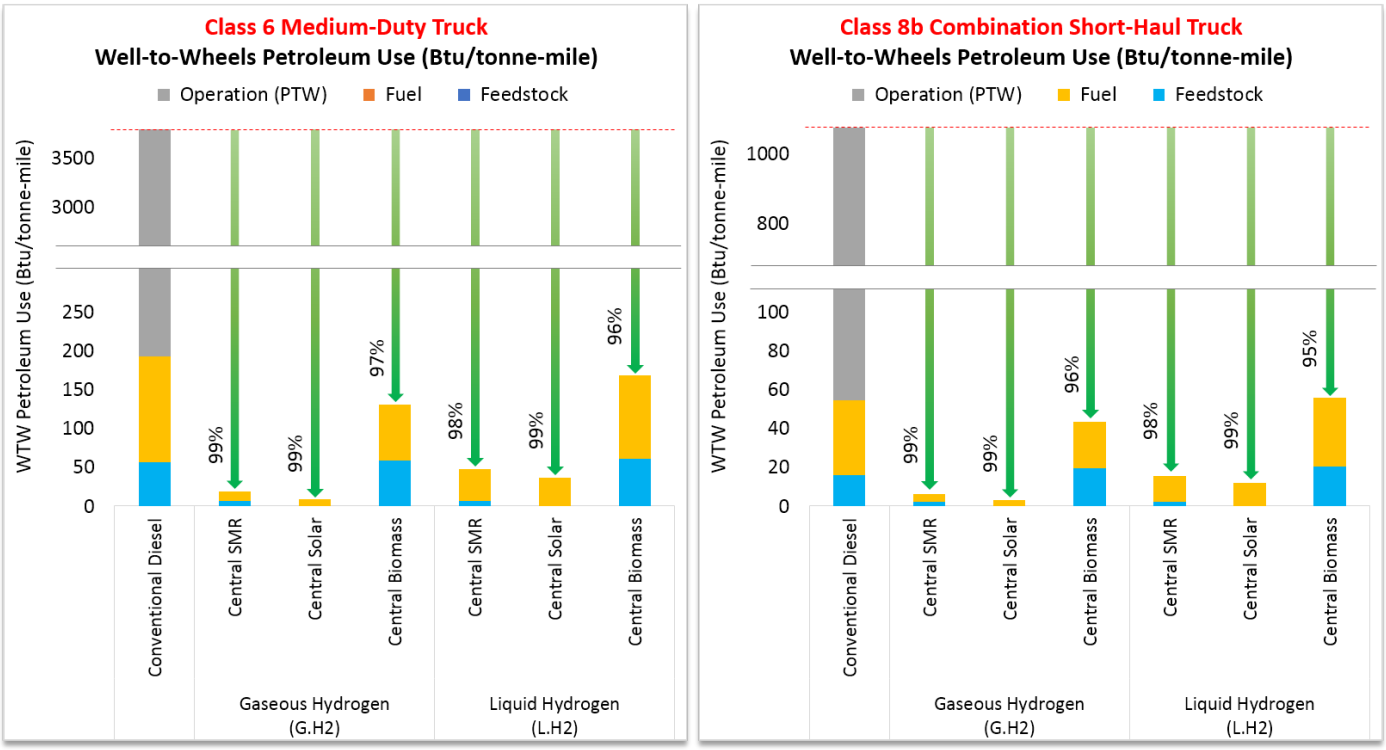

G.H2 – gaseous hydrogen; LH2 – liquid hydrogen; PTW – pump to wheels

FIGURE 1. WTW load-specific petroleum consumption: conventional diesel vs. HFCEVs (gaseous and liquid hydrogen fuel)–examples for medium-duty (left) and heavy-duty (right) trucks

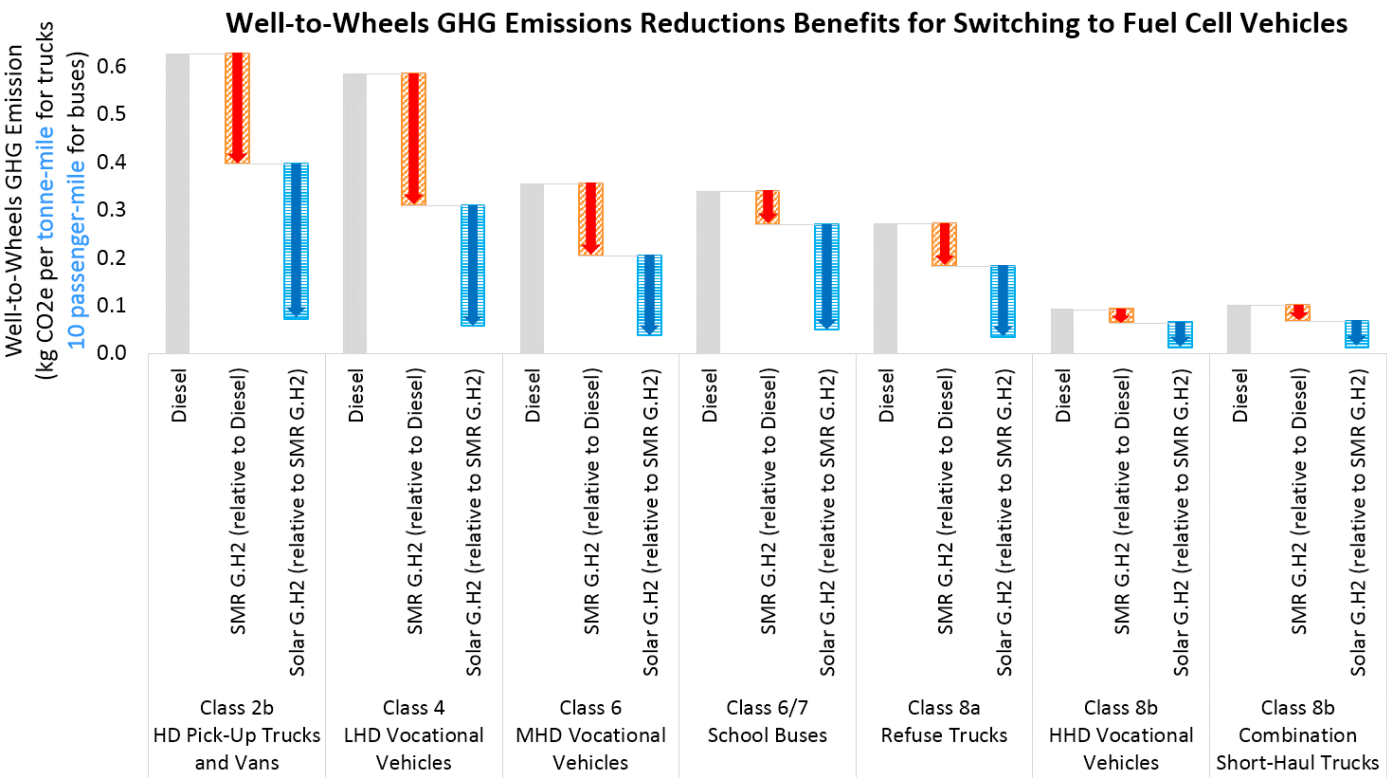

HD – heavy duty; LHD – light and heavy duty; MHD – medium and heavy duty; HHD - heavy and heavy duty

FIGURE 2. WTW load-specific GHG emissions for MHDVs–conventional diesel vs. hydrogen fuel cell

vehicles, HFCEVs using hydrogen fuel from central SMR generates 30% lower GHG emissions on a WTW basis, while the central solar electrolysis pathway provides about 90% emissions reduction. Regardless of vehicle types, weight classes, or vocations, HFCEVs provide significant reductions in WTW GHG emissions over conventional diesel counterparts (Figure 2). HFCEVs that use liquid hydrogen fuel along its supply chain achieve lower GHG emissions reduction benefits compared to gaseous hydrogen, mainly due to the high energy intensity of the hydrogen liquefaction process. HFCEVs also reduce criteria air pollutants emissions compared to conventional diesel trucks and buses. For example, relative to conventional diesel-powered heavy-duty combination short-haul trucks, HFCEVs can provide 70% lower NO_x and 25% lower PM2.5 emissions on a WTW basis (Figure 3). For other types of air pollutants (e.g., carbon monoxide, volatile organic compounds, etc.), 50–60% reductions are achieved. These WTW petroleum use and emissions information provide decision-makers and stakeholders a better understanding of the benefits and trade-offs of HFCEV technology for MHDV applications.

CONCLUSIONS AND UPCOMING ACTIVITIES

Medium- and heavy-duty HFCEVs provide large reductions of petroleum consumption and air emissions (GHG and criteria air pollutants). Although the exact magnitude may vary, the reductions benefits apply to all the MHDV types and vocations considered. For gaseous hydrogen fuel, the reductions of petroleum use and air emissions are robust across different pathways. Liquid hydrogen pathways tend to achieve lower reductions benefits compared to gaseous hydrogen pathways, mainly due to the energy intensity of the hydrogen liquefaction process. However, as the future of the electric grid relies on larger share of renewables, the benefits of liquid hydrogen pathways will also improve. Future work includes a detailed regional analysis, the inclusion of more diverse duty cycles, the harmonization of suite of models/approaches, and integrated sensitivity analysis. The methods and results will be published as a report, and the obtained HFCEV fuel economy values will be used to update the GREET model.

FY 2017 PUBLICATIONS/PRESENTATIONS

1. Lee, D.-Y., Elgowainy, A., and Wang, M. "Greenhouse Gas (GHG) Emissions and Petroleum Use Reduction of Medium-and Heavy-Duty Trucks." Presented at the DOE Hydrogen and Fuel Cells Program Annual Merit Review and Peer Evaluation Meeting, Washington, D.C., June 5–9, 2017.

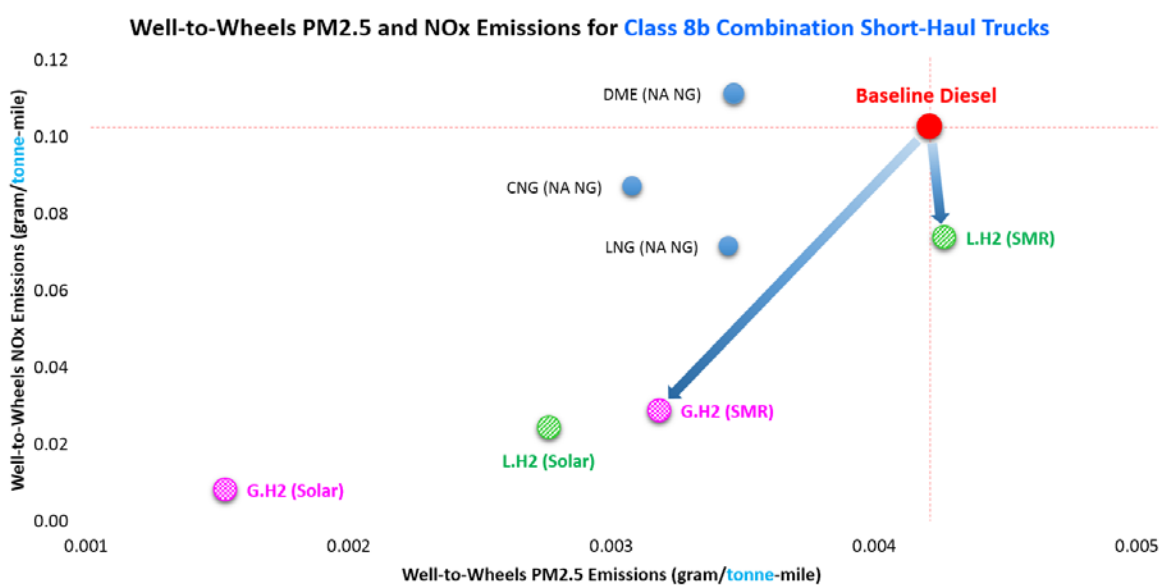

PM2.5 – Particulate matter with diameters of 2.5 micrometers or less; CNG – compressed natural gas; LNG – liquid natural gas; DME – dimethyl ether

FIGURE 3. WTW criteria air pollutants emissions comparison between hydrogen fuel cell and other fuel-vehicle technologies for heavy-duty combination short-haul truck

IX.9 Agent-Based Modeling of Consumer Behavior

Marianne Mintz
Argonne National Laboratory
9700 S. Cass Ave.
Argonne, IL 60439
Phone: (630) 252-5627
Email: mmintz@anl.gov

DOE Manager: Fred Joseck
Phone: (202) 586-7932
Email: Fred.Joseck@ee.doe.gov

Project Start Date: December 1, 2016
Project End Date: Subject to DOE

Overall Objectives

- Explore the role of consumer choice in the expansion and support of consumer-facing hydrogen fueling infrastructure.
- Understand how the system works rather than provide a single forecast of system development.
  - What role do consumer attitudes and behavioral characteristics play?
  - To what extent do social interactions influence purchasing behavior?
  - How do different offerings from original equipment manufacturers affect consumer adoption?
  - How sensitive and to what extent is growth affected by policy makers?
- Consider in a complex adaptive system the interactions between consumers of hydrogen fuel and fuel cell vehicles (FCVs), hydrogen fuel producers and suppliers, manufacturers of FCVs.

Fiscal Year (FY) 2017 Objectives

- Update zip code-level data on income, jobs, population density, etc.; augment it with national- and state-level data on fleet age, vehicle travel, etc.
- Expand spatial resolution from 1 mi square to 1/4 mi square zones.
- Expand study area to 100 mi x 60 mi and apportion it into a higher-resolution grid.
- Update "seed" data on existing FCVs and hydrogen fueling stations.
- Revise agent decision algorithms to reflect most recent behavioral research.

Technical Barriers

This project addresses the following technical barriers from the Systems Analysis section of the Fuel Cell Technologies Office Multi-Year Research, Development, and Demonstration Plan.

(A) Future Market Behavior

(B) Stove-piped/Siloed Analytical Capability

(C) Inconsistent Data, Assumptions and Guidelines

(D) Insufficient Suite of Models and Tools

Contribution to Achievement of DOE Systems Analysis Milestones

This project will contribute to achieving the following milestones for the Systems Analysis section of the Fuel Cell Technologies Office Multi-Year Research, Development, and Demonstration Plan.

- Milestones 2.3–2.6: Develop and maintain models and tools.

FY 2017 Accomplishments

- Upgraded model to 64-bit platform to enable more computationally demanding tasks (e.g., more agents, finer time scale, higher resolution space, more sophisticated algorithms).
- Completed spatial update and expansion. Expanded study area and spatial resolution to 1/4 mile square zones. Mapped zones to zip code-segmented data within study area.
- Acquired improved spatial data to seed the model with locations of existing FCVs and hydrogen fueling stations.
- Revised station characteristics to reflect tube-trailer delivery of gaseous hydrogen (in place of distributed hydrogen production as characterized in the earlier model). Began revising agent decision algorithms.

✧ ✧ ✧ ✧ ✧

INTRODUCTION

This project is updating and expanding an existing agent-based model that simulates the buildout of hydrogen fueling infrastructure in order to examine the effect of that buildout on FCV adoption. It relies on a complex adaptive systems framework and builds on earlier work by Argonne National Laboratory, Ford Motor Co., RCF Economic & Financial Consulting, and Synovate Motoresearch.

APPROACH

A complex adaptive systems framework is uniquely suited to examine the inter-relationship between supply and demand for new technologies like FCVs. Since vehicle adoption is affected by the availability (or lack) of fueling infrastructure, increases in the supply of that infrastructure may be expected to spur adoption which will produce further increases in infrastructure and, in turn, additional adoption. This "virtuous cycle" is the result of numerous decisions by individual agents who purchase vehicles, who invest in fueling stations, who manufacture vehicles, who develop policies to promote the technology, etc. For this application, the model simulates the behavior of consumer/driver agents living and working in a 60 x 100 mi study area roughly equivalent to the Los Angeles metropolitan area (Figure 1); investor agents who plan, develop and operate hydrogen fueling stations; original equipment manufacturer agents who produce and market vehicles; and government agents who enact policies affecting vehicle and infrastructure deployment.

RESULTS

For this new project, FY 2017 efforts focused on data acquisition to update and enhance the algorithms in the existing model and enhance spatial granularity, and coding to accomplish those updates and enhancements. Table 1 shows some of the parameters that were updated using new or revised data or findings from the literature.

Spatial Enhancement

In order to increase the model's geographic scope and resolution, each 1 mi square travel zone was split into sixteen 1/4 mile square zones, and mapped to zip codes and to locations of seed drivers and stations; the road network was expanded to add major arterials; and travel patterns were reconfigured to reflect more realistic trip routes. The updated, higher-resolution model now has more precise location information for seed drivers and stations, permitting investors to consider additional potential fueling locations and consumers to utilize them.

TABLE 1. Parameters updated or added to agent-based model in FY 2017

Parameter or Set of Parameters	Data Update (FY 2017)	Modeling/ Sensitivity (FY 2018)
Investor planning horizon	○	●
Fueling station capital & O&M cost	○	●
Station salvage value	○	
Station debt financing	○	●
Station capacity, delivery option[A]	○●	●
Augmenting station capacity	○●	●
H_2 price (production, tax, retail, etc.)	○●	●
FCV purchase price	○●	●
FCV tank capacity, mi/kg, etc.	○●	●
FCV age, VMT distribution	○	●
FCV driver VMT	○	●
FCV driver fueling preferences	○	
FCV driver worry	○	

○ = Updates with more recent, more complete, and/or more robust research/reports.
● = Updates with observed data.
A = New parameter added.
O&M – operation and maintenance
VMT – vehicle miles travelled

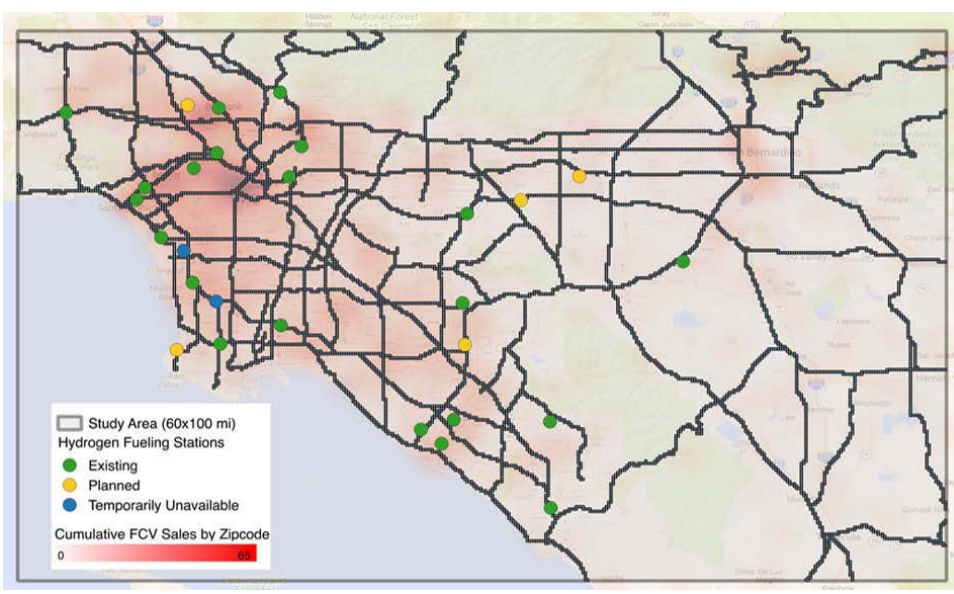

FIGURE 1. Study area

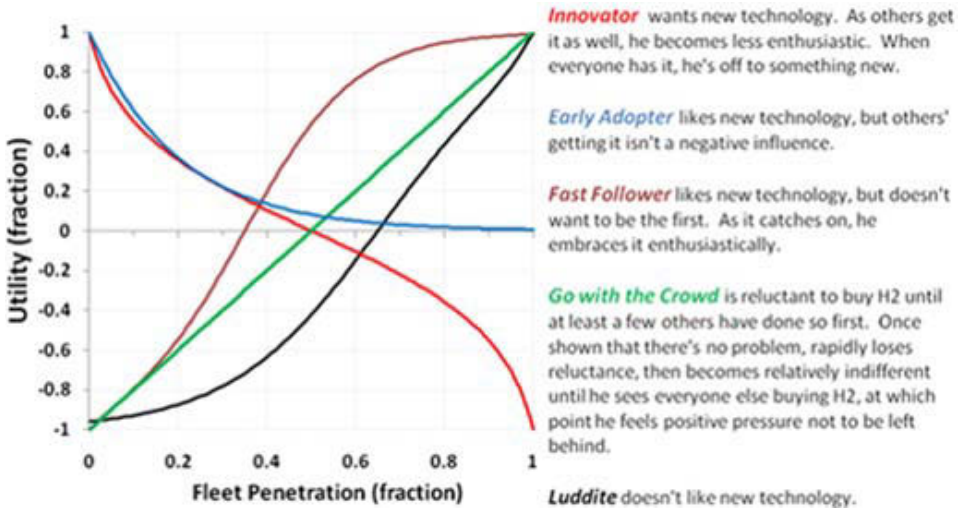

FIGURE 2. Consumer preferences for new technology and how those preferences influence adoption

Agent and Choice Representation

Along with spatial enhancement, FY 2017 efforts used new and improved research results to update the representation of hydrogen fueling stations and the behavior of the consumer, driver, investor, and original equipment manufacturer agents. While some of the parameters required for that update (see Table 1) are straightforward, others (e.g., driver worry, fueling preferences) involve complex relationships that can vary across populations or even within the same population over time. Given this heterogeneity, the model incorporates not only an initial distribution of preferences for new technology adoption (e.g., innovator, early adopter, fast follower, crowd follower, or Luddite, see Figure 2), but also memory and experience-based costs. The latter include the driver agent's most recent on-road experience or exposure, the rate of decay in operational memory of that recent experience or exposure, variations in personal preferences for when to refuel (remaining tank level), the extent of social influence on vehicle selection, etc.

Model Seeding

To initiate the simulation, a set of existing FCVs and hydrogen fueling stations (termed seeds) must be located within the study area. When the original, circa 2007, version of the model was developed, there were only a limited number of pre-commercial FCVs and hydrogen fueling stations. Thus seeding could not reflect a true market response. According to the California Fuel Cell Partnership, over 1,300 FCVs are on the road in California and 29 retail stations are in operation today. Most of the vehicles and 17 of the stations are in the Los Angeles metropolitan area. In addition to mapping the locations of these 17 retail stations, FCVs were mapped to analysis zones within the study area based on cumulative FCV sales by zip code.

CONCLUSIONS AND UPCOMING ACTIVITIES

This project is a two-year effort with FY 2017 activities focused primarily on refreshing and updating the circa 2007 model. In FY 2017, we expanded the model's geographic scope and resolution, augmented the types of stations represented, obtained new data to seed the model, and began work on integrating state-of-the-art consumer decision-science algorithms. Planned FY 2018 activities include representing different vehicle categories, allowing consumers to choose between different FCV types, and modeling additional methods of vehicle adoption (e.g., leases, rentals, fleets). However, in light of anticipated funding, work on FY 2018 planned activities is unlikely to occur.

FY 2017 PUBLICATIONS/PRESENTATIONS

Guo, W. Behavioral Modeling of the Adoption and Use of Fuel Cell Electric Vehicles, submitted to the 2017 Behavior, Energy and Climate Change Conference, ACEEE, Sacramento, CA, October 15–18, 2017.

IX.10 Life-Cycle Analysis of Air Pollutants Emission for Refinery and Hydrogen Production from SMR

Amgad Elgowainy (Primary Contact), Pingping Sun, Zifeng Lu, Jeongwoo Han, Michael Wang
Argonne National Laboratory
9700 S. Cass Ave.
Argonne, IL 60439
Phone: (630) 252-3074
Email: aelgowainy@anl.gov

DOE Manager: Fred Joseck
Phone: (202) 586-7932
Email: Fred.Joseck@ee.doe.gov

Subcontractor:
Eastern Research Group, Inc., Lexington, MA
(Troy Hawkins, Ben Morelli, Ben Young)

Project Start Date: October 2016
Project End Date: Project continuation and direction determined annually by DOE

Overall Objectives

- Develop criteria air pollutants emission factors (EF) (in g/MJ) for refinery products to serve as a baseline for comparison with alternative transportation fuels.
- Develop criteria air pollutants emission factors (in g/MJ) for hydrogen production via steam methane reforming (SMR) process.
- Assess the life cycle analysis emissions impact of hydrogen fuel cell vehicles (FCVs), relative to baseline petroleum fuels usage in internal combustion engine (ICE) vehicles.
- Develop emission factors associated with combustion of refinery fuels (e.g., refinery still gas, catalyst petroleum coke).
- Investigate refinery air pollutants emissions variations among regions.
- Incorporate updated criteria air pollutants emission factors in Greenhouse gases, Regulated Emissions, and Energy use in Transportation Model (GREET®) model.

Fiscal Year (FY) 2017 Objectives

- Collect and match U.S. refinery air pollutants emissions data with refinery operation data for individual refineries at facility and sub-facility (unit) levels.
- Develop methodologies to allocate individual refinery air pollutants emissions to individual refinery products (e.g., gasoline, diesel, etc.), and aggregate the results to Petroleum Administration for Defense Districts and national levels.
- Match U.S. standalone SMR air pollutants emissions data with hydrogen production data to derive emission factors, and aggregate the results to national level.
- Conduct life cycle analysis of criteria air pollutants emissions associated with petroleum fuels use in ICE vehicles and hydrogen use in FCVs.

Technical Barriers

This project addresses the following technical barriers from the Systems Analysis section of the Fuel Cell Technologies Office Multi-Year Research, Development, and Demonstration Plan.

(C) Inconsistent Data, Assumptions and Guidelines

(D) Insufficient Suite of Models and Tools

Contribution to Achievement of DOE's Systems Analysis Milestones

This project contributes to achievement of the following DOE milestones from the Systems Analysis section of the Fuel Cell Technologies Office Multi-Year Research, Development, and Demonstration Plan.

- Milestone 2.2: Annual model update and validation. (4Q, 2011 through 4Q, 2020)
- Milestone 3.1: Annual update of Analysis Portfolio. (4Q, 2011 through 4Q, 2020)

FY 2017 Accomplishments

- Collected refinery pollutants emissions data at various levels (unit level, facility level, and national level) and calculated emission factors.
- Conducted life cycle emissions analyses for petroleum fuels (gasoline, diesel, liquefied petroleum gas [LPG]) for updating the default values in GREET. Compared to previous GREET emissions estimates, the updated results show significant reduction in SOx (-20% to -42%), moderate reduction in NOx (-3% to -6%), and minor change (-2% to +3%) in other pollutant emissions (volatile organic compound [VOC], CO, particulate matters with emissions less than 10 µm [PM10] and less than 2.5 µm [PM2.5]).

- Conducted life cycle emissions analyses for hydrogen production via central SMR. Compared to previous emissions estimates in GREET 2016, the updated results are lower for most criteria pollutants emissions (-24% to -60%), with the exception of SOx which had +3% increase.
- Use of SMR hydrogen in FCVs can significantly reduce most criteria pollutant emissions when compared to gasoline ICE vehicles (Figure 1).

✧ ✧ ✧ ✧ ✧

INTRODUCTION

Under the Clean Air Act, criteria pollutants, nitrogen dioxide (NO_2), ozone (O_3), sulfur dioxide (SO_2), particulate matter (PM), carbon monoxide (CO), and lead (Pb) are regulated by the Environmental Protection Agency for protecting public health and welfare. In addition to these pollutants, emissions reduction of VOCs is also of interest as they react with NOx to form ozone under sunlight. Among the emission sources, transportation section is a major contributor, responsible for over 50% of NOx, over 30% of VOCs and over 20% of PM emissions of the total emissions inventory in the U.S. This stimulates efforts from both federal and local governments to promote low or zero emission vehicles to reduce air pollutions. The present study focuses on evaluating air pollutants, VOC, CO, nitrogen oxides (NOx), sulfur oxides (SOx), PM10, and PM2.5, associated with the production transportation fuels, to update the GREET model. This study evaluates pollutants emissions from a major industrial sector (petroleum refining and hydrogen production via SMR) using up-to-date emissions inventory data. Allocation methods are used to estimate emissions associated with each refinery product using refinery operation optimization linear programming model for individual refineries. This is particularly important since petroleum fuels (such as gasoline, diesel, and jet) serve as baseline fuels, against which the environmental impacts of alternative transportation fuels and vehicle technologies are compared.

APPROACH

The refinery and SMR facility emission information are collected from National Emission Inventory (NEI) database [1]. The NEI database is updated every three years. Thus, the most recent available datasets are from years 2011 and 2014, both of which are used in the present study. The refinery capacity information is obtained from Energy Information Administration RefCap database [2,3], while hydrogen capacity information is obtained from Pacific Northwest National Laboratory report [4]. The actual production of refinery facilities is estimated by applying Energy Information Administration reported Petroleum Administration for Defense Districts level utilization rate to RefCap capacity [5]. The hydrogen plant production is calculated by multiplying plant capacity with an assumed 80% utilization rate, as provided by industrial partners. Only standalone SMR facilities were investigated, while captive hydrogen production within refineries was excluded since SMR facilities within refineries often do not have clear boundaries in terms of material and energy flows, thus complicating the emissions allocation between refinery products and hydrogen. While the process of calculating emission factors (EFs) (in g/mmbtu hydrogen) for standalone SMRs is straightforward, the allocation of refinery facility emission to various refinery products requires detailed

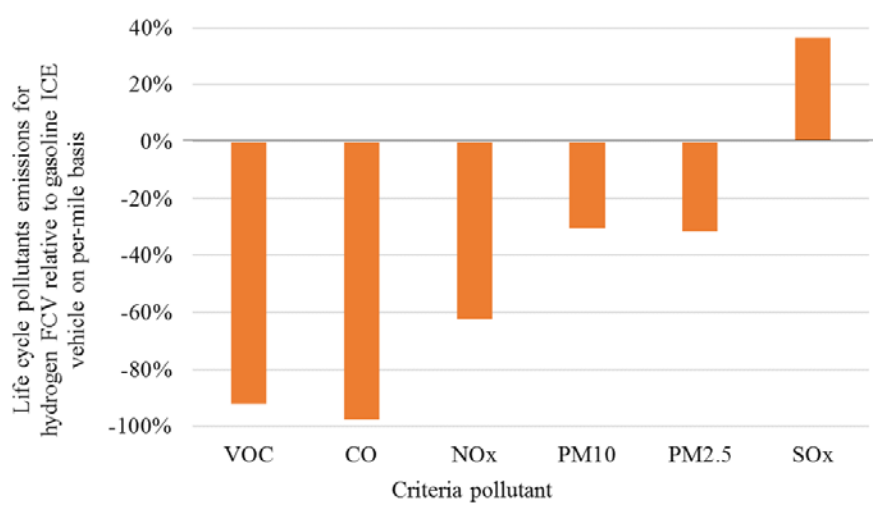

FIGURE 1. Life cycle pollutants emissions of hydrogen FCV relative to spark ignition gasoline vehicle

analysis of refinery energy and material flows at the process unit level, which is different for each refinery.

The allocation of refinery facility emissions to refinery products was guided by refinery operation simulations using a linear programming model. Each refinery has specific configuration, crude quality and products portfolio, and thus requires unique simulation of each refinery operation. Argonne developed a database of material and energy flows for a large number of U.S. refineries, representing 70% of total U.S. refining capacity [6]. Guided by the material and energy flow information in the database, the facility emissions are allocated to intermediate products from each process unit. The energy and emissions burden allocated to intermediate products are carried to the subsequent process units until the facility energy and emissions burdens are cascaded into the final refinery products [6]. The present study includes 14 refineries with 2011 emissions data and 21 refineries with 2014 emissions data. The number of these facilities were constrained by the proper matching of NEI emissions database and the Argonne refinery database.

RESULTS

Emission Factors for Central SMR Hydrogen Plant

The national weighted average pollutant emissions factors for SMR facilities are shown in Figure 2. The dataset includes 36 facilities from 2014 NEI database; the number of considered facilities were constrained by availability of standalone facility capacity/production data, which are often business confidential.

Comparing to previous estimates in GREET 2016, the updated results show much lower pollutants emission factors, except for SOx. The first and third quartiles of the emissions factors from various SMR facilities are displayed in Figure 2, indicating a large variation of emissions among these facilities.

Emission Factors for Refinery Products

Guided by the energy and material flows from individual refinery linear programming simulations, the refinery facility criteria pollutants emissions are allocated to refinery products, resulting in EFs per refinery products. Two sets of EFs, derived from emissions and productions in 2011 [1,2] and 2014 [1,3], respectively, were developed. The EFs from 2014 refinery emissions data are plotted in Figure 3 (the EFs from 2011 data were omitted for legibility of figure).

Figure 3 shows that among the many refinery products, gasoline and LPG carry higher emission burdens relative to the other refinery products, such as diesel and jet. This is consistent with the greenhouse gas emission and energy intensity trends for these products [6]. Gasoline and LPG fuels are produced via more energy intensive process units than diesel and jet. For each pollutant, the wide spread between first and third quartiles in Figure 3 indicate the large variations in criteria pollutants emissions among refineries. This is not surprising given the unique configuration and operation of each individual refinery. Table 1 shows the EFs of refinery products and hydrogen using 2011 and 2014 emissions data, and those from previous GREET 2016 estimates.

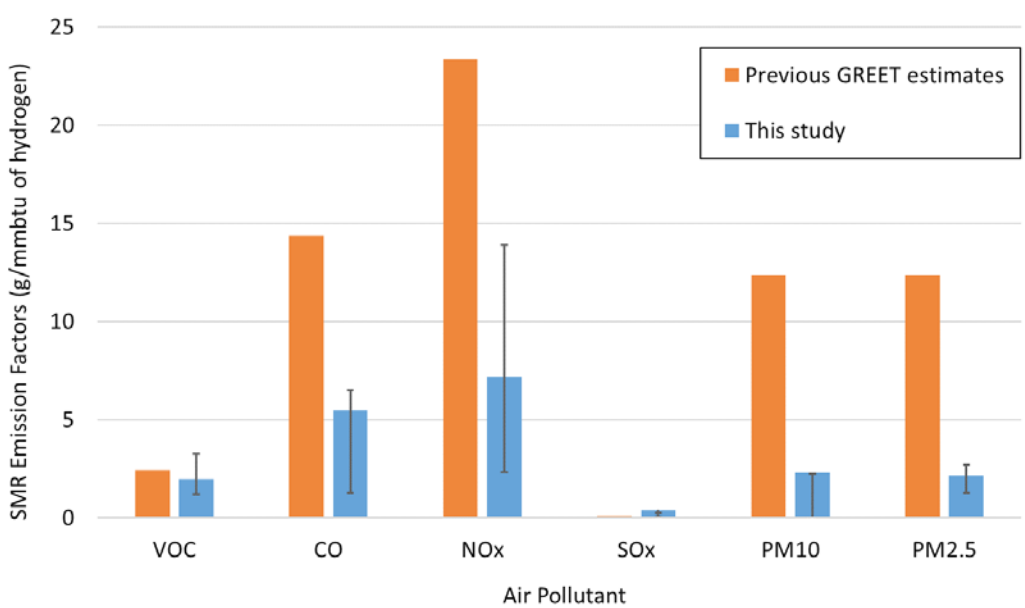

FIGURE 2. National average criteria pollutant emissions factors for SMR facilities

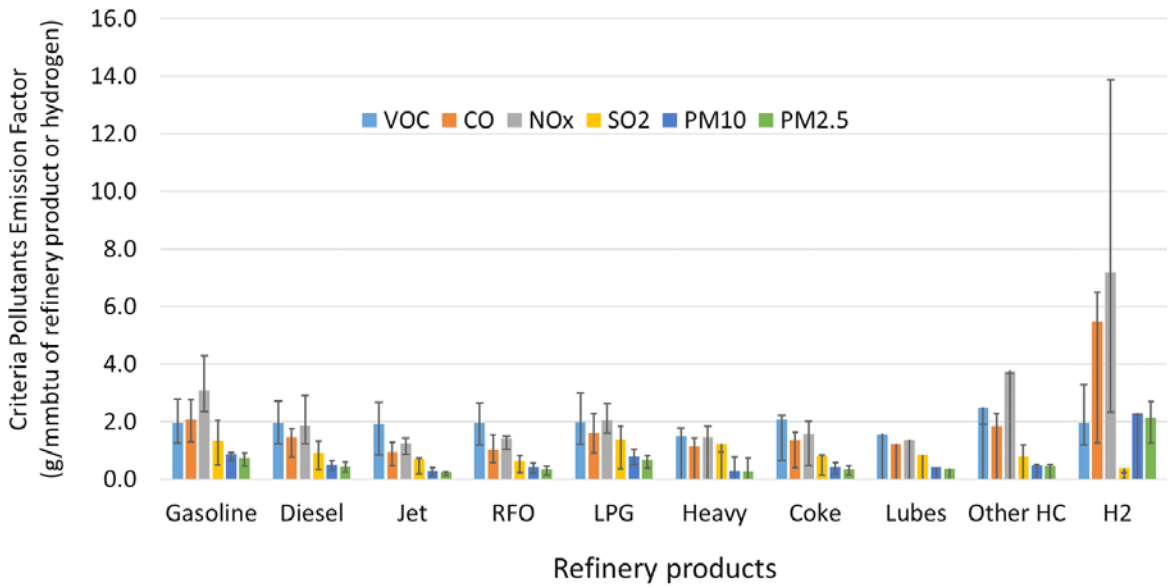

FIGURE 3. Refinery product-specific emission factors derived from NEI 2014 refinery emissions (error bars for each pollutant represent first and third quartiles)

TABLE 1. U.S. Refinery Criteria Pollutants Emission Factors for Refinery Products and Hydrogen (g/mmbtu)

	Data Source	Gasoline	Diesel	Jet	RFO	LPG	Heavy	Coke	Lubes	Other HC	H_2
VOC	GREET 2016	2.55	1.95	0.96	1.08	1.99	--	1.59	--	--	2.44
	2011	2.10	2.09	1.96	1.76	2.13	1.68	2.20	1.26	2.74	2.67
	2014	1.98	1.96	1.92	1.97	1.98	1.48	2.07	1.56	2.48	1.96
CO	GREET 2016	3.75	2.40	1.20	1.56	2.94	--	2.16	--	--	14.37
	2011	1.76	1.14	0.91	0.85	1.36	1.74	1.11	0.77	1.62	9.02
	2014	2.07	1.47	0.93	1.04	1.63	1.13	1.36	1.23	1.83	5.48
NOx	GREET 2016	7.47	4.24	1.99	3.18	6.73	--	3.57	--	--	23.34
	2011	2.76	1.65	0.97	1.20	1.85	1.38	1.41	0.99	3.21	7.97
	2014	3.08	1.86	1.26	1.42	2.04	1.47	1.58	1.35	3.74	7.18
SO2	GREET 2016	16.68	8.21	3.15	7.46	18.85	--	5.19	--	--	0.06
	2011	1.35	0.93	0.56	0.62	0.95	0.87	0.68	0.54	1.35	0.42
	2014	1.34	0.92	0.70	0.63	1.37	1.23	0.81	0.85	0.79	0.39
PM10	GREET 2016	0.70	0.48	0.24	0.29	0.54	--	0.42	--	--	12.38
	2011	1.10	0.65	0.41	0.47	0.94	0.81	0.53	0.46	0.71	2.85
	2014	0.87	0.50	0.30	0.42	0.79	0.29	0.42	0.41	0.48	2.30
PM2.5	GREET 2016	0.54	0.35	0.18	0.22	0.41	--	0.32	--	--	12.38
	2011	0.95	0.58	0.38	0.41	0.82	0.68	0.46	0.43	0.69	2.62
	2014	0.75	0.43	0.24	0.36	0.68	0.26	0.36	0.38	0.46	2.14

RFO – residual fuel oil; HC - hydrocarbon

Table 1 shows that the EFs derived from 2011 and 2014 refinery emission datasets are consistent. For most pollutants, the EFs from the present study are less than previous GREET 2016 estimates. In particular, the current emission factors for SOx are significantly lower compared to previous GREET 2016 estimates across all refinery products.

Comparison between Life Cycle Emissions of Refinery Fuels and Hydrogen on a Per-Mile Basis

A life cycle analysis was conducted for SMR-hydrogen use in FCV, gasoline use in spark ignition vehicle, diesel use in compression ignition direct injection vehicle-diesel, and spark ignition LPG vehicle. Fuel economy estimates for these four vehicle technologies are shown in Table 2.

TABLE 2. Fuel Economy of Various Fuel–Vehicle Technologies

	Fuel economy (mile/gge)
Gasoline ICE	26
Diesel ICE	31
LPG ICE	26
Hydrogen FCV	55

With the fuel economy estimates in Table 2, the life cycle criteria pollutants emissions can be estimated on per-mile. The comparison of life cycle criteria pollutants emissions for various fuel–vehicle technologies is provided in Table 3, which shows that hydrogen FCV has significantly lower per-mile WTW emissions for most pollutants except for SOx. The FCV does not have tailpipe emissions. The WTW SOx emissions is attributed to the emissions associated with electricity generation for hydrogen compression, which is required for both hydrogen delivery and refueling into FCVs. As the future grid electricity generation mix is projected to have reduced share of coal-based generation, the WTW SOx emissions for FCVs is expected to be proportionally reduced.

TABLE 3. Life Cycle Emissions for Various Fuel–Vehicle Technologies on Per-Energy Basis and Per-Mile Basis (Using 2014 Emissions Dataset)

(g/mmbtu basis)	VOC	CO	NOx	SOx	PM10	PM2.5
Gasoline ICE	84.7	645	65.3	21.3	8.89	4.58
Diesel ICE	42.3	796	67.0	14.4	8.58	4.42
LPG ICE	59.2	645	56.4	21.5	6.82	3.36
Hydrogen FCV	13.7	33.6	51.8	61.0	13.2	6.35
(g/mile basis)						
Gasoline ICE	0.364	2.78	0.281	0.091	0.038	0.020
Diesel ICE	0.152	2.86	0.240	0.051	0.031	0.016
LPG ICE	0.255	2.77	0.243	0.092	0.029	0.014
Hydrogen FCV	0.028	0.069	0.106	0.125	0.027	0.013

CONCLUSIONS AND UPCOMING ACTIVITIES

The national criteria pollutants emissions from refinery and SMR facilities have been investigated to derive emission factors for the refining of petroleum fuels and SMR-hydrogen. A methodology is developed to allocate refinery facility emissions to individual refinery products. Relative to previous GREET 2016 model estimates, the results from current study demonstrate significant reduction in most pollutants for these fuels. The future work will update the GREET 2017 model with emission factors from this analysis.

FY 2017 PUBLICATIONS/PRESENTATIONS

1. Pingping Sun, Amgad Elgowainy, Zifeng Lu, Jeongwoo Han, Michael Wang, Troy Hawkins, Ben Morelli, and Ben Young, "A Life Cycle Analysis of Refinery Fuel Products Air Emissions Using Refinery Emissions Inventory Data," International Emissions Inventory Conference, Baltimore, MD, August 14–18, 2017.

REFERENCES

1. National emission inventory, by United States Environmental Protection Agency, Accessed March 3rd, 2017. https://www.epa.gov/air-emissions-inventories/national-emissions-inventory-nei

2. U.S. Energy Information Administration refinery capacity report, Refinery Capacity Data by individual refinery as of January 1, 2011. https://www.eia.gov/petroleum/refinerycapacity/archive/2011/refcap2011.php

3. U.S. Energy Information Administration refinery capacity report, Refinery Capacity Data by individual refinery as of January 1, 2014. https://www.eia.gov/petroleum/refinerycapacity/archive/2014/refcap2014.php

4. Hydrogen tools (H2Tools) by Pacific Northwest National Laboratory, accessed March 24th, 2017. http://hydrogen.pnl.gov/hydrogen-data/hydrogen-production

5. Refinery capacity and utilization by U.S. Energy Information Administration. https://www.eia.gov/dnav/pet/pet_pnp_unc_dcu_nus_a.htm

6. Amgad Elgowainy, Jeongwoo Han, Hao Cai, Michael Wang, Grant S. Forman and Vincent B. DiVita, "Energy Efficiency and Greenhouse Gas Emission Intensity of Petroleum Products at U.S. Refineries," *Environmental Science & Technology* 48 (13) (2014): 7612–7624, accessed March 24th, 2017, DOI: 10.1021/es5010347

IX.11 Resource Availability for Hydrogen Production

Marc Melaina (Primary Contact), Michael Penev, Elizabeth Connelly, Donna Heimiller, and Anelia Milbrandt
National Renewable Energy Laboratory
15013 Denver West Parkway
Golden, CO 80401-3305
Phone: (303) 275-3836
Email: Marc.Melaina@nrel.gov

DOE Manager: Fred Joseck
Phone: (202) 586-7932
Email: Fred.Joseck@ee.doe.gov

Project Start Date: October 2016
Project End Date: Project continuation and direction determined annually by DOE.

Overall Objectives

- Estimate hydrogen production required for potential future fuel cell electric vehicle (FCEV) demand.
- Provide updated estimates of hydrogen production potential from a wide range of energy resources: natural gas, coal, uranium, biomass, wind, solar.
- Compare resource requirements for hydrogen to projected consumption in a future without significant FCEV market growth (from the U.S. Energy Information Administration's [EIA's] *Annual Energy Outlook* [AEO]) and with significant market growth (e.g., 50 million FCEVs deployed by 2040).
- Determine resource availability spatially and on a per-kilogram-of-hydrogen basis.

Fiscal Year (FY) 2017 Objectives

- Begin updating hydrogen production potential for natural gas, coal (with carbon capture and sequestration), nuclear, biomass (solid and gaseous), wind, and solar resources.
- Compare results with future 2040 consumption with and without significant growth in FCEV markets.
- Prepare results to be captured in final report and made available through HyDRA tool.

Technical Barriers

This project addresses the following technical barriers from the Systems Analysis section of the Fuel Cell Technologies Office Multi-Year Research, Development and Demonstration Plan.

(A) Future Market Behavior

(E) Unplanned Studies and Analysis

Contribution to Achievement of DOE Systems Analysis Milestones

This project will contribute to achievement of the following DOE milestones from the Systems Analysis section of the Fuel Cell Technologies Office Multi-Year Research, Development, and Demonstration Plan.

- Milestone 1.19: Complete analysis of the potential for hydrogen, stationary fuel cells, fuel cell vehicles, and other fuel cell applications such as material handling equipment including resources, infrastructure and system effects resulting from the growth in hydrogen market shares in various economic sectors. (4Q, 2020)

FY 2017 Accomplishments

- Began updating hydrogen production potential for natural gas, coal (with carbon capture and sequestration), nuclear, biomass (solid and gaseous), wind, and solar resources.
- Compared results with future 2040 consumption with and without significant growth in FCEV markets.
- Prepared results to be captured in final report and made available through HyDRA tool.

✧ ✧ ✧ ✧ ✧

INTRODUCTION

A successful, long-term strategy for FCEV deployment is to use hydrogen produced from a diverse array of low-carbon domestic energy resources, such as coal (with carbon capture and storage), nuclear, biomass, wind, and solar energy. Natural gas is considered a transitional energy feedstock, as well as a long-term, domestic, low-carbon option if converted to hydrogen in a large central plant with carbon capture and storage. Understanding the potential of multiple domestic, low-carbon energy resources to produce hydrogen is important for analyzing long-term scenarios with high FCEV deployment and a hydrogen infrastructure system that is robust, resilient, and economically competitive. To estimate these resource potentials, this study builds directly upon previous work [1], which in turn was based on previous estimates for hydrogen production potentials for wind,

solar, and biomass [2] and for coal, natural gas, nuclear, and hydro power [3]. These renewable resource potentials are based upon an updated and consistent calculation of technical potential, part of the National Renewable Energy Laboratory's (NREL's) ongoing work to compare technical potential consistently across renewable energy technologies [4].

APPROACH

A framework is established to draw comparisons across different resource estimate types. The approach relies upon the same basic analytic methods used in Melaine et al. [1]. Updates are made to key input parameters where new information or improved assumptions are available. Comparisons to projected consumption depend upon new EIA AEO cases [5]. Production efficiencies—the amount of resource required to produce a kilogram of hydrogen—are key input assumptions for estimating future resource requirements; improved future conversion rates would reduce reliance on any particular resource. Most values are based upon H2A production model conversion efficiencies. The uranium conversion rate is being updated in coordination with the H2@Scale team. The resource requirements are estimated through simple energy-balance calculations and do not account for future policies or market competition. A clear and consistent approach is used to characterize and compare different estimates of the availability of fossil and renewable energy resources. The economic potential estimates for renewables from Lopez et al. [4] will be updated to reflect improved resource potentials for biomass, wind, and solar. This analytical framework is used to estimate total potential to produce hydrogen from major energy resources. Each major resource is tested for its potential to supply 4–10 million metric tons of hydrogen per year, and these results are compared with expected consumption in 2040 without significant FCEV market share.

RESULTS

The updated total resources and hydrogen production potentials for fossil and nuclear fuels are shown in Table 1. These account for significantly increased proved and unproved reserves of natural gas as well as lower estimates for uranium resources and coal estimates, which have continued a downward trend over time. The conversion efficiency of coal-to-hydrogen has been updated [5] such that, despite a lower physical coal resource, the hydrogen production potential from coal has increased by about 50%. Table 2 shows the total resources and hydrogen production potentials for renewables. The technically recoverable resources (TRRs) for solar and biomass (high) have been

TABLE 1. Fossil and Nuclear Resource and Hydrogen Production Potentials

Resource	Resource Potential		Hydrogen Production Potential	
Fossil and Nuclear	Physical Resource	Quads	Hydrogen Potential (MMT)	Quads of Hydrogen
Natural Gas (EP)	340 trillion cubic feet	350	2,030	270
Natural Gas (TRR)	2,500 trillion cubic feet	2,500	14,700	2,000
Coal (EP)	250 billion short tons	5,100	29,500	4,000
Coal (TRR)	480 billion short tons	9,500	55,100	7,400
Uranium (EP)	200 million lb U_3O_8	300	900	100
Uranium (TRR)	400 million lb U_3O_8	600	2,100	300

EP = economic potential, MMT = million metric tons, TRR = technically recoverable resource

TABLE 2. Renewable Resource and Hydrogen Production Potentials

Resource	Resource Potential		Hydrogen Production Potential	
Renewable	Physical Resource	Quads/yr	Hydrogen Potential (MMT/yr)	Quads of Hydrogen/yr
Biomass (EP)	900 million tons eq.	15	60	8
Biomass (moderate)	400 million tons eq.	7	30	4
Biomass (high)	1,200 million tons eq.	19	80	10
Wind (EP)	2,000 TWh electricity	20	40	6
Wind (TRR)	50,000 TWh electricity	500	1,100	150
Solar (EP)	1,000 TWh electricity	10	20	3
Solar (TRR)	180,000 TWh electricity	1,800	4,000	500

EP = economic potential, MMT = million metric tons, TRR = technically recoverable resource. Biomass TRR is shown as a moderate to high range. Conversions to quads are on a higher-heating basis; EIA thermal equivalent of 9,760 Btu/kWh is used for wind and solar. Sums are rounded.

updated, while other values are the same as reported in previous work [1].

Figure 1 shows the updated comparison to current (2015) and future (2040) consumption for the AEO 2017 Reference Case [6]. The ratio of projected 2040 consumption and additional resource needed to supply 50 million FCEVs is shown as a factor in parenthesis below each resource label. The percentage increases are relatively low for natural gas (5%) and coal (18%), higher for nuclear (40%) and biomass (48%), and highest for wind (87%) and solar (171%). However, the updated increases for wind and solar are much lower than the 2013 results for wind (183%) and solar (780%) [1].

Figure 2 shows the updated comparison to current (2015) and future (2040) consumption for the AEO Low Oil and Gas Case [6]. This case includes limited domestic fossil resources and future consumption, resulting in greater reliance on nuclear, biomass, wind, and solar resources. The differences between these results and those from the Reference Case (Figure 1) suggest hydrogen production would likely be more diversified under the Low Oil and Gas Case market conditions. For example, the higher projected market success of wind and solar suggest increased viability of those sources for hydrogen production. At the same time, a larger increase in natural gas (7%) and coal (62%) resources is required to satisfy the demand from 50 million FCEVs, compared with the Reference Case.

Updated final resource assessment results will be provided in a final report and made available through HyDRA (https://maps.nrel.gov/hydra/). HyDRA is an online data-sharing and visualization tool, providing access to spatial data from a variety of studies. Figure 3 shows a screenshot of the enhanced HyDRA tool to be released later in FY 2017. The update includes new resource assessment data and enhanced end-user capabilities.

CONCLUSIONS AND UPCOMING ACTIVITIES

An improved understanding of U.S. resource potential for hydrogen production will help in analyzing long-term FCEV deployment scenarios. The forthcoming resource report is the main project deliverable. Subject to funding received, upcoming activities will include updating all renewable economic and technical potentials. Activities may also include using resource potential estimates as inputs to the Scenario Evaluation and Regionalization Analysis cost-optimization routine. Including spatial resource availability constraints will improve the realism of hydrogen supply chain cost estimates by generating more realistic depictions of production facility scales and locations as well as delivery distances between production facilities and demand centers (urban areas).

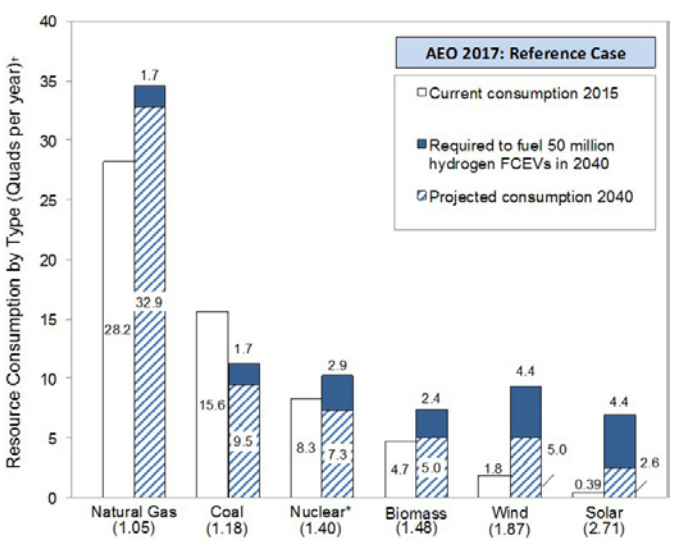

NOTE: Wind and solar resource requirements are calculated using a thermal equivalent value of 9,510 Btu per kWh, following the convention used by EIA (see [6], Table A17)

FIGURE 1. Updated comparison to current (2015) and future (2040) consumption for the AEO 2017 Reference Case (ratio of projected 2040 consumption and additional resource needed to supply 50 million FCEVs shown as a factor in parenthesis below each resource label), *nuclear values are for high-temperature electrolysis

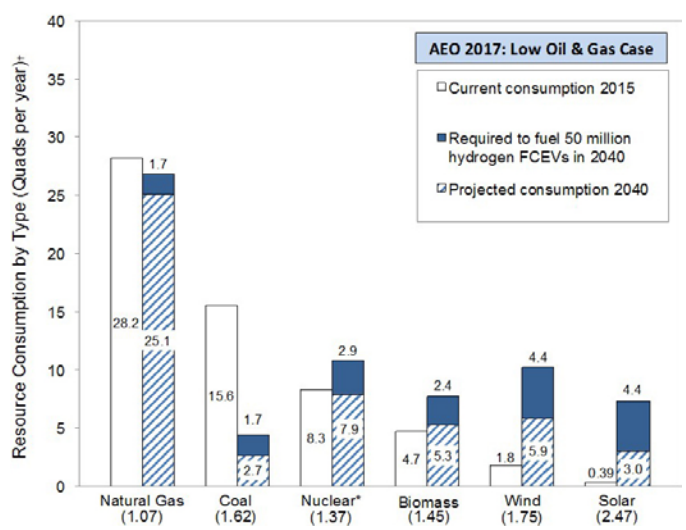

FIGURE 2. Updated comparison to current (2015) and future (2040) consumption for the AEO Low Oil and Gas Case (ratio of projected 2040 consumption and additional resource needed to supply 50 million FCEVs shown as a factor in parenthesis below each resource label), *nuclear values are for high-temperature electrolysis

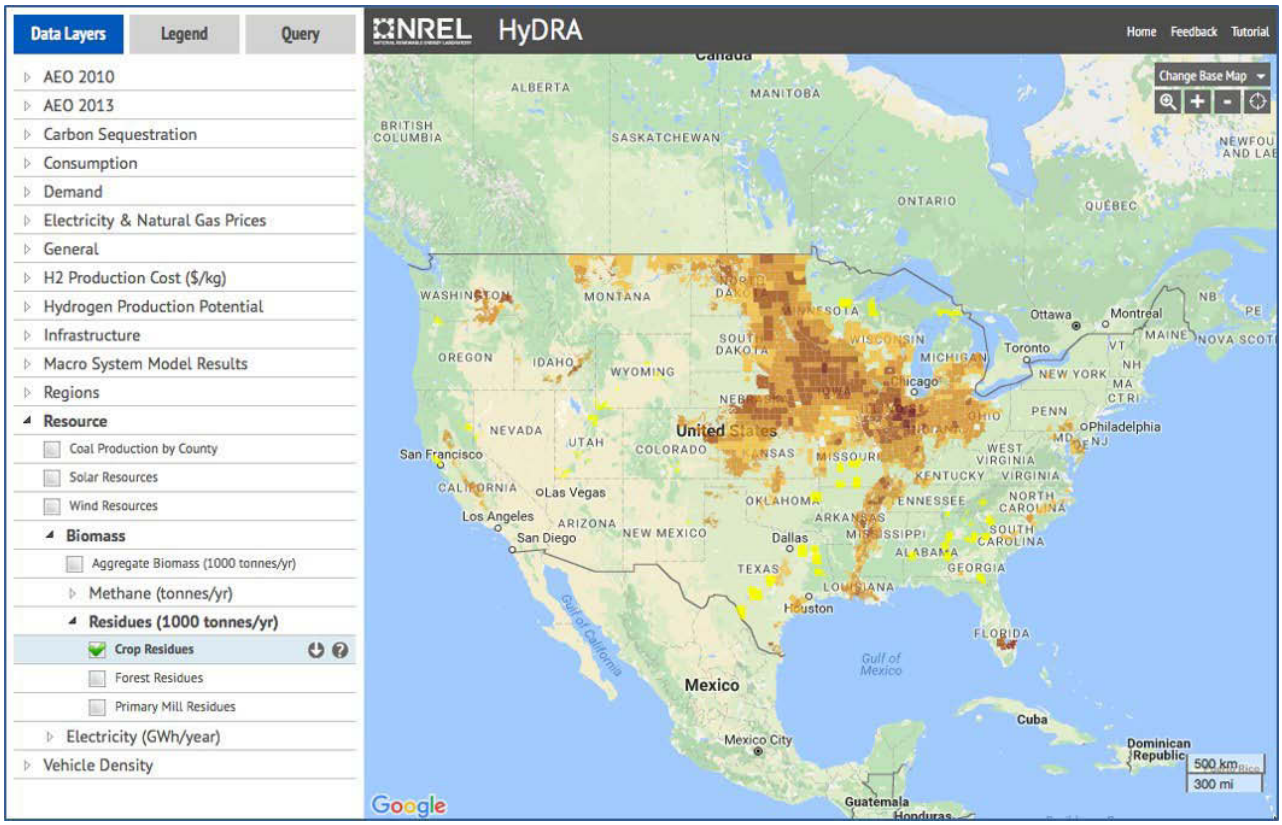

FIGURE 3. Screenshot of the enhanced HyDRA tool to be released later in FY 2017

REFERENCES

1. M. Melaina, M. Penev, and D. Heimiller, 2013, *Resource Assessment for Hydrogen Production: Hydrogen Production Potential from Fossil and Renewable Energy Resources*, NREL/TP-5400-55626, Golden, CO: National Renewable Energy Laboratory, http://www.nrel.gov/docs/fy13osti/55626.pdf.

2. A. Milbrandt and M. Mann, 2007, *Potential for Hydrogen Production from Key Renewable Resources in the United States*, NREL/TP-640-41134, Golden, CO: National Renewable Energy Laboratory, http://www.nrel.gov/docs/fy07osti/41134.pdf.

3. A. Milbrandt and M. Mann, 2009, *Hydrogen Resource Assessment: Hydrogen Potential from Coal, Natural Gas, Nuclear, and Hydro Power*, NREL/TP-560-42773, Golden, CO: National Renewable Energy Laboratory, http://www.nrel.gov/docs/fy09osti/42773.pdf.

4. A. Lopez, B. Roberts, D. Heimiller, N. Blair, and G. Porro, 2012, *U.S. Renewable Energy Technical Potentials: A GIS-Based Analysis*, NREL/TP-6A20-51946, Golden, CO: National Renewable Energy Laboratory, Golden, CO, http://www.nrel.gov/docs/fy12osti/51946.pdf.

5. M. Rutkowski, 2008, "Current (2005) Hydrogen from Coal with CO_2 Capture and Sequestration," H2A Version 2.1, https://www.hydrogen.energy.gov/h2a_prod_studies.html.

6. U.S. Energy Information Administration, 2017, *Annual Energy Outlook 2017*. Washington, D.C.: U.S. Energy Information Administration, http://www.eia.gov/forecasts/aeo/.

IX.12 Benefits Analysis of Multi-Fuel/Vehicle Platforms with a Focus on Hydrogen Fuel Cell Electric Vehicles

Thomas Stephens
Argonne National Laboratory
9700 South Cass Ave.
Lemont, IL 60439
Phone: (630) 252-2997
Email: tstephens@anl.gov

DOE Manager: Fred Joseck
Phone: (202) 586-7932
Email: Fred.Joseck@ee.doe.gov

Project Start Date: October 1, 2015
Project End Date: Project continuation and direction determined annually by DOE

Overall Objectives

- Estimate potential future benefits attributable to the Hydrogen and Fuel Cells Technologies Office (FCTO) program, including:
  - Petroleum use reduction
  - Greenhouse gas emissions reduction
  - Economic impacts

While considering synergies and interactions with the Vehicle Technologies Office (VTO) program.

- Examine the sensitivity of estimated benefits to input assumptions.

Fiscal Year (FY) 2017 Objectives

- Issue report documenting results and methods of the analysis of program benefits.
- Present results to FCTO and VTO analysts.
- Assess sensitivity of benefits estimates to assumptions about technology progress.

Technical Barriers

This project addresses the following technical barriers from the Systems Analysis section of the FCTO Multi-Year Research, Development, and Demonstration Plan.

(B) Stove-piped/Siloed Analytical Capability

(C) Inconsistent Data, Assumptions and Guidelines

Contribution to Achievement of DOE Systems Analysis Milestones

This project will contribute to achievement of the following DOE milestones from the Systems Analysis section of the FCTO Multi-Year Research, Development, and Demonstration Plan.

- Milestone 3.1: Annual update of Analysis Portfolio (4Q, 2011 through 4Q, 2020)

FY 2017 Accomplishments

- Produced estimates of petroleum use reduction attributable to hydrogen fuel cell vehicle and storage technologies ranging from 0.3 to 1.0 million barrels per day (MMbpd) by 2050, and a reduction in greenhouse gas emissions ranging from 59–148 million metric tons CO_2 equivalent by 2050.
- Estimated that successful achievement of FCTO research and development program goals and commercialization of FCTO technologies could lower the cost of fuel cell vehicle ownership, as measured by a levelized cost of driving metric to be competitive with conventional gasoline-powered vehicles by 2035.
- Documented these analysis methods and results in a technical report (Stephens et al., 2017 [1]).

✧ ✧ ✧ ✧ ✧

INTRODUCTION

Potential future benefits resulting from successful achievement and deployment of technologies being developed under the FCTO and VTO research and development programs were estimated out to the year 2050. These benefits include:

- Petroleum use reduction
- Greenhouse gas emissions reduction
- Economic impacts

These benefits are estimated under assumed future conditions, and the sensitivity of the estimates to these assumptions is being evaluated.

APPROACH

Scenarios were developed and analyzed to estimate benefits of successful development and deployment of

advanced vehicle technologies, comparing a case with completely successful deployment of FCTO and VTO technologies ("Program Success" case) to a future in which there is no contribution after FY 2017 by the FCTO or VTO to these technologies ("No Program" case). Benefits were disaggregated by individual program technology areas, which included the FCTO and VTO research and development programs.

RESULTS

Projections for the Program Success case indicate that by 2035, the average fuel economy of on-road, light-duty vehicle (LDV) stock could be 24% to 30% higher than in the No Program case[1]. The resulting petroleum savings in 2035 were estimated to be as high as 1.5 MMbpd, and reductions in greenhouse gas (GHG) emissions were estimated to be as high as 250 million metric tons of CO_2 equivalent per year. Such petroleum reductions result in significant reductions in fuel expenditure for light-duty vehicles, totaling $62–85 billion annually by 2035.

Figure 1 shows the projected petroleum consumption by LDVs (entire on-road stock) in years 2035 and 2050 under both the No Program and Program Success scenarios, with uncertainty bars showing the range of projected values. Projections were made using four different vehicle market penetration models. Savings for LDVs are shown in the plot on the left. Figure 1 also shows the range of projected cumulative petroleum savings since 2019 attributed to FCTO and VTO technology programs in the plot on the right.

FCTO and VTO technologies are projected to improve fuel economy by 35–62% for new LDVs sold in 2035, and by as much as 73% by 2050, relative to improvements in the absence of DOE funding. These increases, due in part to market penetration by fuel cell vehicles, are shown in Figure 2.

Projections of LDV adoption indicate that although advanced-technology vehicles may be somewhat more expensive to purchase, the fuel savings result in a net reduction of consumer cost. As shown in Figure 3, in 2035, projections of decreases in annual fuel expenditures for LDVs range from $62–85 billion, while the projected increase in new LDV expenditures in the same year ranges from $3–1 billion (both in 2015$). By 2050, annual fuel savings for LDVs reach $94–184 billion, while vehicle purchases are projected to be $27–$32 billion more expensive.

Benefits were disaggregated by individual program technology areas, which included the FCTO program and the VTO research and development programs of electrification, advanced combustion engines and lubricants, and materials technology. Benefits to medium-duty vehicles and HDVs were attributed to advanced combustion engines and lubricants, the program which funds most of the heavy-duty technologies. Ranges of projected petroleum savings and greenhouse gas reductions attributed to these programs are plotted in Table 1.

[1] The Program Success case represents a future in which FCTO (and VTO) R&D programs successfully reach all technology targets and these technologies are successfully commercialized. The No Progam case represents a future in which no further R&D investments are made by FCTO or VTO, and technological progress advances more slowly.

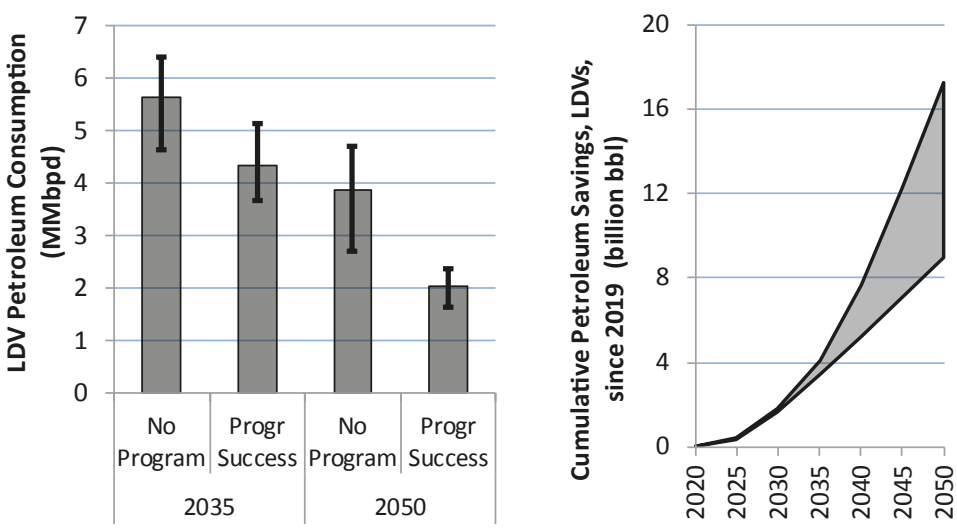

FIGURE 1. Projected on-road petroleum consumption by light-duty vehicles under the No Program and Program Success scenarios in 2035 and 2050 (left), and cumulative petroleum savings since 2019 attributed to FCTO and VTO technology programs (right). Projections made using four vehicle market penetration models.

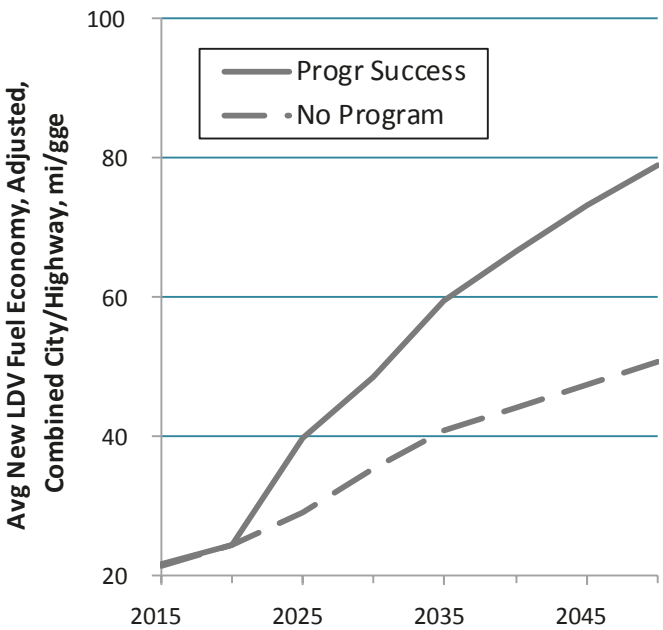

FIGURE 2. Projected fleet-averaged fuel economy (adjusted, combined city/highway) through 2050 for light-duty for Program Success and No Program scenarios. Harmonic average of four projections from different market penetration models).

CONCLUSIONS AND UPCOMING ACTIVITIES

A Program Success scenario and a No Program scenario were analyzed to estimate the combined benefits of successful FCTO and VTO technology programs. Projections for the Program Success case indicate that by 2035, the average fuel economy of on-road, LDV stock could be 24% to 30% higher than in the No Program case, and by 2050, the increase could be 39% to 68%. The resulting petroleum savings were estimated to be as high as 1.5 MMbpd in 2035 and up to 2.7 MMbpd in 2050, and reductions in GHG emissions were estimated to be as high as 250 million and 390 million metric tons of CO_2 equivalent per year in 2030 and 2050, respectively. Petroleum savings in 2035 and 2050 attributable to the FCTO program range from 0.11 MMbpd to 0.45 MMbpd in 2035 and from 0.35 MMbpd to 0.96 MMbpd in 2050. Projections of LDV adoption indicate that although advanced-technology vehicles may be somewhat more expensive to purchase, the fuel savings result in a net reduction of consumer cost. In 2035, reductions in annual fuel expenditures for LDVs are projected to range from $62–$85 billion, while the projected increase in new vehicle

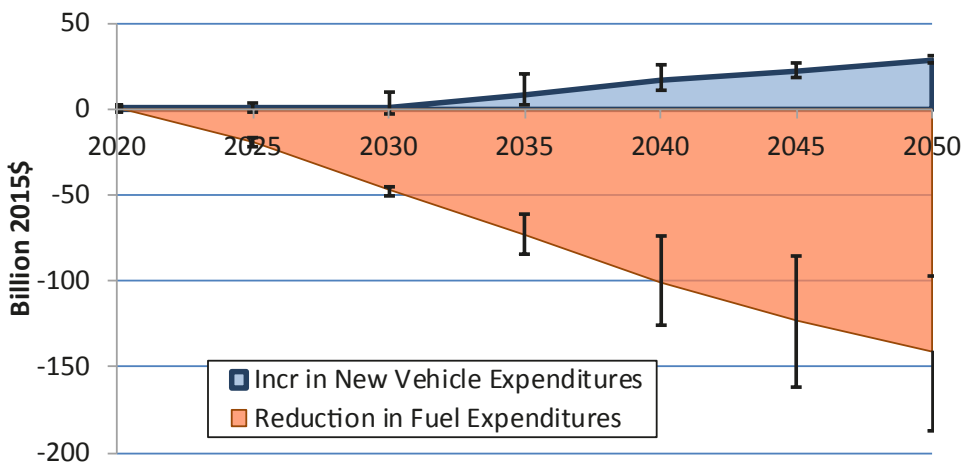

FIGURE 3. Differences in annual national consumer costs of vehicle purchases and fuel costs for on-road light-duty vehicles through 2050, between the No Program and Program Success scenarios. Increased expenditures shown as positive; decreased expenditures shown as negative.

TABLE 1. Projected Ranges of Petroleum Savings and Emissions Reductions in 2025, 2035, and 2050 by VTO and FCTO Technology Programs

Program Area	Petroleum savings (MMbpd)			Annual GHG reduction (million tons CO_2-eq)		
	2025	2035	2050	2025	2035	2050
Electrification	0.03–0.19	0.28–0.61	0.38–1.44	5–29	57–123	74–272
Combustion & Fuels	0.25–0.32	0.66–1.01	0.85–1.01	46–62	122–194	151–182
Materials	0.02–0.03	0.06–0.12	0.06–0.08	4–7	11–24	10–15
Hydrogen Fuel Cells	0.00–0.05	0.11–0.45	0.35–0.96	0–6	14–46	59–148

TABLE 2. Side Cases (Scenarios) to be Analyzed

Case	H_2 storage cost	Fuel Cell System cost	H_2 price	H_2 availability	Fuel Cell Vehicle configuration
H_2 price medium	Progr Success	Progr Success	Medium	Progr Success	Progr Success
H_2 storage cost accel	Accel	No Program	No Program	No Program	No Program
FC system cost accel	No Program	Accel	No Program	No Program	No Program
H_2 price, availability	No Program	No Program	Accel	Progr Success	No Program
All accel	Accel	Accel	Accel	Progr Success	Accel

expenditures in the same year ranges from $6–$21 billion (both in 2015$).

In addition to the two scenarios analyzed to provide estimated future program benefits, several side cases will be developed and analyzed (Table 2). The sensitivity of projected benefits to different input assumptions about hydrogen price, costs of fuel cell systems, and hydrogen storage will provide insight into which technology area might provide the most benefit if accelerated beyond FCTO program plans. It is recommended to include medium- and heavy-duty fuel cell vehicles to the scenarios to account for future benefits of FCTO technologies in these applications.

FY 2017 PUBLICATIONS/PRESENTATIONS

1. Stephens, T.S. *Benefits Analysis of Multi-Fuel/Vehicle Platforms with a Focus on Hydrogen Fuel Cell Electric Vehicles*. U.S. Department of Energy Hydrogen and Fuel Cells Program 2017 Annual Merit Review and Peer Evaluation Meeting, Washington, D.C., June, 2017, https://www.hydrogen.energy.gov/pdfs/review17/sa068_stephens_2017_o.pdf.

2. Stephens, T.S., A. Birky, and D, Gohlke. *Vehicle Technologies and Fuel Cell Technologies Office Research and Development Programs: Prospective Benefits Assessment Report for Fiscal Year 2018*. Argonne National Laboratory, Argonne, IL, in review.

REFERENCES

1. Stephens, T.S., A. Birky, and D, Gohlke. *Vehicle Technologies and Fuel Cell Technologies Office Research and Development Programs: Prospective Benefits Assessment Report for Fiscal Year 2018*. Argonne National Laboratory, Argonne, IL, in review.

X.0 Market Transformation Sub-Program Overview

INTRODUCTION

The purpose of the Market Transformation sub-program is to verify commercial readiness for domestically produced hydrogen and fuel cell systems. The Market Transformation sub-program conducts activities to evaluate the technical and economic viability of pre-commercial hydrogen and fuel cell systems in real-world operating environments. The results from these evaluations are used to provide feedback to research programs, U.S. industry manufacturers, and potential technology users. By supporting technology operations testing and use in key early market applications, this sub-program helps to identify and overcome technical and non-technical barriers to user adoption. These early market applications will also address other user acceptance factors (such as value propositions beyond incumbent technologies), resulting in further expansion of technology opportunities.

The Market Transformation sub-program aims to support research and development validation to enable more commercial successes such as those realized in material handling equipment (e.g., lift trucks) and emergency backup power applications. For example, Market Transformation has partnered on industry-led projects in applications like fuel cell powered airport ground support baggage tractors, fuel cell electric medium-duty hybrid trucks for cargo delivery applications, and a light-duty utility vehicle range extender. These projects are highly leveraged, with an average of more than half of the projects' funds provided by DOE's industry partners. Partners who provide resources and financial investment to these projects demonstrate their high level of interest to explore these applications and markets. This level of industry interest is very promising for the potential growth of the domestic fuel cell industry and related jobs. Market Transformation also partners with other federal agencies such as the U.S. Department of Transportation Maritime Administration on projects such as auxiliary power for ships in port and onboard ocean-going vessels.

GOAL

The sub-program's goal is to enable and accelerate expansion of hydrogen and fuel cell system use by lowering the life cycle costs of hydrogen and fuel cell power and by identifying and reducing the barriers impeding full technology commercialization.

OBJECTIVES

Specific objectives of the Market Transformation sub-program in Fiscal Year (FY) 2017 are:

- Test emerging approaches to grid management using renewable hydrogen.
- Advance the knowledge and expertise of distributed hydrogen fuel generation and dockside and shipboard fuel cell systems in partnership with the U.S. Army, the U.S. Navy, and civilian agencies such as the U.S. Department of Transportation's Maritime Administration.
- Continue industry-led demonstration projects on truck auxiliary power units, fuel cell cargo delivery vans, and aviation ground support applications through targeted testing and evaluation efforts.
- Identify lessons learned from demonstration projects, and complete technical-economic analyses to help identify the best early market applications for industry to commercialize.

FY 2017 TECHNOLOGY STATUS AND ACCOMPLISHMENTS

In FY 2017, the sub-program continued the collection and analysis of early-market project data. These data are being made available on an ongoing basis so that industry technology developers can:

- Assess the performance of integrated hydrogen and fuel cell systems;
- Determine the technical and economic viability of these applications; and
- Advance applications into production products.

Collaboration with other federal agencies continued. A workshop was held with U.S. Army organizations to determine the best technologies for producing hydrogen fuel at forward operating bases for tactical military

operations. Interagency collaborations also focused on pre-commercial applications such as maritime power through an interagency collaboration with the U.S. Department of Transportation's Maritime Administration and unmanned aerial vehicle testing with the U.S. Navy.

Fuel cells continue to enjoy growing success in material handling equipment and backup power applications. The sub-program's early market deployment efforts have successfully catalyzed a significant level of market activity in these areas. Material handling and backup power industrial orders are up 42%[1] and 9%,[2] respectively, from the cumulative total orders through 2016.

FY 2017 activities include the following.

- **Hydrogen Energy Storage Project:** This project supports the demonstration of a hydrogen energy storage system as a grid management tool. While hydrogen produced from the system could be used in a variety of value-added applications, the initial phase of the project will use the hydrogen for fuel cell buses operated by the County of Hawaii Mass Transportation Agency and the National Park Service. This year construction began, and initial operation is expected to begin in late 2017. (Naval Research Laboratory and the State of Hawaii)
- **Airport Ground Support Vehicles:** This project has a high potential to meet sub-program goals and enable expansion of fuel cells into additional airport applications such as shuttle buses. The initial design has been completed, and 15 units were assembled with the cargo tractors and tested in field operations. Failures in the stacks occurred, and root-cause analysis revealed that the stacks were not robust enough for the air cargo duty cycle. The stacks were redesigned, and new stacks replaced the original stacks. Units in the new fleet operations are showing positive results. (Plug Power)
- **Maritime Fuel Cell Generator Project:** Testing of a first-of-its-kind hydrogen fuel cell power generator for maritime applications was completed and results published. The system was designed to replace pier-side or onboard diesel generators for refrigerated containers used for ocean vessel operations. Initial operations testing at a pier-side site was completed with results confirming substantial energy efficiency improvements compared to diesel engines. Balance of plant components have been redesigned and replaced. A Phase 2 project is now being initiated. (Sandia National Laboratories)
- **Fuel Cell Hybrid Electric Medium-Duty Truck Project:** In this project, a design is being developed for a battery electric powertrain system hybridized with fuel cell power to improve drive performance and range on a medium-duty cargo truck. The project team completed a prototype design, and vehicle testing is being initiated. (FedEx Express)
- **Fuel Cell Auxiliary Power Unit Project:** This project will demonstrate a single-temperature fuel cell auxiliary power system for truck refrigeration units. Subsystems have been assembled, and an integrated system test was successful. The next step is to demonstrate the truck refrigeration unit for a continuous eight-hour operation. (Pacific Northwest National Laboratory)
- **Light-Duty Utility Vehicle Range Extender:** This project is developing a fuel cell range-extended, plug-in hybrid, light-duty utility vehicle. By adding a fuel cell and a few kilograms of hydrogen to a battery electric powertrain, the zero-emission driving range of the vehicle will be extended from ~100 mi up to as much as 250 mi before the batteries need to be recharged, which will greatly increase the commercial potential of these all-electric vehicles. Upon the successful validation of one initial prototype vehicle, US Hybrid will deploy a fleet of 19 additional vehicles for use by National Grid, a leading utility fleet owner and operator in the northeastern United States. The project scope also includes collection and validation of performance data and a complete economic assessment of the value proposition. (US Hybrid)
- **Commercial Acceleration Outreach and Analysis:** Efforts this past year focused on enabling the commercialization process for various industries and organizations, including forums for investors and infrastructure developers, training of state and municipal staff on safe and successful technology operations, and developing novel hydrogen and fuel cell technical-economic analyses. In collaboration with industry, investor outreach events were conducted in key early market regions of the country, bringing together private hydrogen refueling developers, fuel cell automotive manufacturers, and potential investors. To help the launch of fuel

[1] *Industry Deployed Fuel Cell Powered Lift Trucks*, Program Record (Hydrogen and Fuel Cells Program) 17003, U.S. Department of Energy, 2017. https://www.hydrogen.energy.gov/pdfs/17003_industry_deployed_fc_powered_lift_trucks.pdf
[2] *Industry Deployed Fuel Cell Backup Power (BuP)*, Program Record (Hydrogen and Fuel Cells Program) 17004, U.S. Department of Energy, 2017. https://www.hydrogen.energy.gov/pdfs/17004_industry_deployed_fc_bup.pdf

cell electric vehicles and hydrogen fueling infrastructure in the Northeast, meetings were conducted to educate state and city officials and municipal authorities in New Jersey, Rhode Island, Connecticut, and Massachusetts on station network locations and technical performance targets. To help accelerate the commercialization of various fuel cell technologies and overcome technology cost barriers, the sub-program supported various focused technical-economic analyses on topics such as ground support equipment, medium-duty vehicles, and auxiliary power systems for port power and refrigerated trucks.

BUDGET

The FY 2017 Market Transformation sub-program funding allocation totaled $1 million. These funds were used primarily to support data collection and analysis for continuing demonstration projects and to support projects selected from the H2@Scale cooperative research and development agreement (CRADA) call.

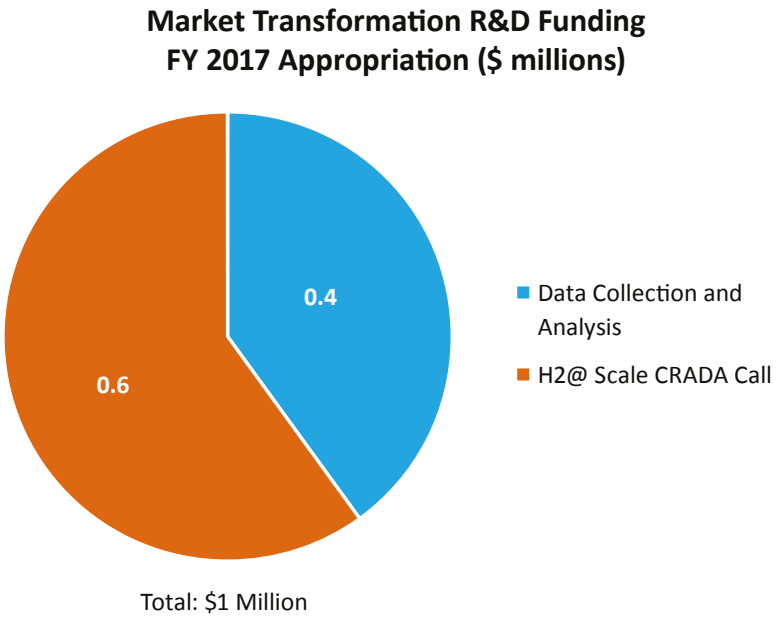

FIGURE 1. FY 2017 Appropriations

UPCOMING ACTIVITIES AND PLANS

In FY 2018, projects with funding remaining from previous fiscal year appropriations will continue. A major priority is alignment with the H2@Scale concept.

Future activities are subject to appropriations.

Pete Devlin
Market Transformation Project Manager
Fuel Cell Technologies Office
Office of Energy Efficiency and Renewable Energy
U.S. Department of Energy
1000 Independence Ave., SW
Washington, DC 20585-0121
Phone: (202) 586-4905
Email: Peter.Devlin@ee.doe.gov

X.1 Hydrogen Energy Systems as a Grid Management Tool

Richard (Rick) E. Rocheleau (Principal Investigator), Mitch Ewan (Primary Contact)
Hawaii Natural Energy Institute
School of Ocean and Earth Science and Technology
University of Hawaii at Manoa
1680 East-West Road, POST 109
Honolulu, HI 96822
Phone: (808) 956-2337; (808) 956-8346
Email: ewan@hawaii.edu; rochelea@hawaii.edu

DOE Manager: Peter Devlin
Phone: (202) 586-4905
Email: Peter.Devlin@ee.doe.gov

Technical Advisor: Karen Swider-Lyons
Naval Research Laboratory
Phone: (202) 404-3314
Email: karen.lyons@nrl.navy.mil

Contract Number: DE-EE0002811

Project Start Date: September 30, 2010
Project End Date: September 29, 2015

Overall Objectives

- Demonstrate the use of electrolyzers to mitigate the impacts of intermittent renewable energy by regulating grid frequency.
- Characterize performance/durability of commercially available electrolyzers under dynamic load conditions.
- Supply hydrogen to fuel cell shuttle buses operated by County of Hawaii Mass Transit Agency and Hawaii Volcanoes National Park (HAVO).
- Conduct performance/cost analysis to identify the benefits of an integrated system including grid ancillary services and off-grid revenue streams.
- Evaluate effect on reducing overall hydrogen costs offset by value-added revenue streams.

Fiscal Year (FY) 2017 Objectives

- Install site improvements and utilities at Natural Energy Laboratory Hawaii Authority (NELHA) to support the operation of the hydrogen system.
- Install, commission, and operate the hydrogen system at NELHA.
- Install a 350-bar hydrogen fuel dispenser at NELHA to fuel the County of Hawaii Mass Transit Agency fuel cell electric shuttle bus.
- Install a 350-bar hydrogen fuel dispenser at HAVO to fuel two HAVO shuttle buses.
- Develop a HAVO compressor boost system to extract up to 90% of the hydrogen from the hydrogen transport trailers and reduce hydrogen transport cost by 50%.

Technical Barriers

This project addresses the following technical barriers from the Market Transformation section of the Fuel Cell Technologies Office Multi-Year Research, Development, and Demonstration Plan.

(A) Inadequate standards and complex and expensive permitting procedures

(B) High hydrogen fuel infrastructure capital costs for polymer electrolyte membrane (PEM) fuel cell applications

(C) Inadequate private sector resources available for infrastructure development

(F) Inadequate user experience for many hydrogen and fuel cell applications

(G) Lack of knowledge regarding the use of hydrogen inhibits siting (e.g., indoor refueling)

(H) Utility and other key industry stakeholders lack awareness of potential renewable hydrogen storage application

Technical Targets

No specific technical targets have been set.

FY 2017 Accomplishments

- Obtained permits from the County of Hawaii for the installation of site infrastructure at NELHA.
- Commenced installation of site improvements and utilities at NELHA to support the operation of the hydrogen system.
- Delivered the hydrogen system equipment to the NELHA site.
- Completed the conversion of the County of Hawaii Mass Transit Agency bus.
- Completed the conversion of the HAVO buses, including installation of a novel environmental sensor system for the air filtration system to protect their fuel cells from high levels of air contamination experienced in the park.

- Executed a memorandum of agreement with HAVO for the siting and operation of the hydrogen system at HAVO.
- Completed the HAVO compressor boost system.
- Completed modifications to the three hydrogen transport trailers to interface with the HAVO hydrogen boost system.
- Commenced the development of a dynamic model of the hydrogen production system.

✧ ✧ ✧ ✧ ✧

INTRODUCTION

While solar and wind resources offer a major opportunity for supplying energy for electrical grid electricity production and delivery systems, their variability and intermittency can raise challenges for the cost-effective and high-reliability integration of these renewable sources on electrical grids. In Hawaii, the curtailment and grid management-related challenges experienced by these renewable sources are a challenge at today's level of generation capacity, and these costs will hinder the substantive additional penetration of electricity generation supplied by these renewable resources. Hydrogen production through electrolysis may provide an opportunity to mitigate curtailment and grid management costs by serving as a controllable load, allowing real-time control in response to changes in electricity production. The renewable hydrogen product can also create new and incremental revenue streams to the power producers through the sale of hydrogen products to customers outside of the electricity delivery system. Accordingly, hydrogen energy production at a utility scale offers the potential for increasing the levels of variable renewable energy that can be harnessed by the power producers or system operators.

APPROACH

This project evaluates the value proposition of using electrolyzers to both regulate the grid and use the product hydrogen for transportation applications. An electrolyzer system is being installed at NELHA on the Big Island. The electrolyzer will be ramped up and down to simulate frequency regulation. Data will be collected to analyze the optimum electrolyzer ramp rates and determine its durability and performance under dynamic operating conditions over time. The hydrogen produced by the system will be used to fuel three hydrogen-fueled buses. It is planned to deliver hydrogen to HAVO to support two HAVO buses. The third bus will be operated in Kailua-Kona. A schematic of the project concept is shown in Figure 1.

FIGURE 1. Hydrogen production and delivery system

RESULTS

This was the first hydrogen project evaluated by the County of Hawaii Planning Department. Several revisions to the NELHA infrastructure design were developed and reviewed by a third party hydrogen safety consultant (Boyd Hydrogen). The permitting package was approved in June 2017. Work was started on the site improvements, and the hydrogen system equipment was shipped and delivered to the site (Figures 2 and 3). In parallel, work was completed on the conversion of the three hydrogen buses, including installation of a novel fuel cell air filtration Environmental Sensor Array system designed to protect the two HAVO buses' fuel cells from high levels of volcanic sulfurous air contaminants experienced in the park. The delivery of hydrogen to HAVO will be accomplished via three hydrogen transport trailers using a drag-and-drop strategy. Using a cascade fill would result in the trailers being able to dispense only ~50% of their contents. Given the high cost of transportation, it was decided to develop a compressor system that could extract more hydrogen from the trailer. This was accomplished through the development of a compressor boost system (Figure 4), which will allow ~90% of the hydrogen to be dispensed, resulting in a reduction of hydrogen transport costs of ~50%. Work also started on the development of a hydrogen energy system simulation tool that includes models for different renewable power sources, the utility grid, electrolyzer, battery energy storage system, and system control algorithms. The overall structure has been developed in MATLAB and Simulink. A steady state model of a PEM electrolyzer has been created

FIGURE 2. NELHA site infrastructure

FIGURE 3. Delivery of hydrogen system equipment

and validated with measured data from the project Proton C30 electrolyzer. The electrolyzer steady state model has been implemented in the MATLAB and Simulink environment, where the dynamic characteristics and control of the electrolyzer system will be implemented.

CONCLUSIONS AND UPCOMING ACTIVITIES

This project has coordinated the efforts of a diverse group of stakeholders to provide a technology solution to facilitate integration of intermittent renewable energy sources on an electrical grid while producing hydrogen for transportation. The project has identified and provided valuable solutions to the many non-technical barriers associated with introducing hydrogen technology into a

FIGURE 4. Compressor boost system

community for the first time. Lessons learned from this project will make the way easier for projects that follow.

It is concluded that a hydrogen energy system is a valuable grid frequency management tool capable of controlling intermittent renewable sources of energy for grid frequency management applications. While the hydrogen energy system is not as fast as the battery energy storage system (BESS), the performance measured with the modified control system under different load demands is much closer to the BESS performance. However, our current thinking is that replicating the exact operational response time as the BESS cannot be achieved with an electrolyzer. The data shows that the electrolyzer can only be used for slower-acting changes (1 Hz to 0.5 Hz). A potential solution is to design an electrolyzer/BESS hybrid system and develop a modeling program to find the optimum mix of battery and electrolyzer to provide the maximum grid regulation services at minimum cost. Additional work is required to develop a control scheme that can manage power distribution between the electrolyzer and BESS.

While the U.S. Department of Energy participation in the project formally ended on September 30, 2015, the project is being continued using other funding. Future work involves the following:

- Completing installation, and operating hydrogen production systems and dispensing infrastructure at the NELHA site;
- Operating the 26-passenger fuel cell electric bus based at the NELHA site;
- Transporting hydrogen in hydrogen transport trailers from the NELHA production site to the HAVO dispenser to support the two HAVO buses;
- Collecting and analyzing hydrogen system and fuel cell electric vehicle bus performance data;
- Preparing performance reports and sharing it with project sponsors and industry; and
- Conducting outreach activities with the public to inform them about hydrogen technologies.

SPECIAL RECOGNITIONS & AWARDS/ PATENTS ISSUED

1. A utility patent application was submitted for the Environmental Sensor Array system.

FY 2017 PUBLICATIONS/PRESENTATIONS

1. Ewan, M., Rocheleau, R., Oral presentation at U.S. Department of Energy Annual Merit Review, "Hydrogen Energy Systems as a Grid Management Tool," Washington, DC, June 7, 2017.

2. Ewan, M., Oral presentation at the Natural Energy Laboratory Hawaii Authority "Conference on Energy Storage Trends and Opportunities," "Hydrogen Energy Systems as a Grid Management Tool," Kailua-Kona, HI, September 13, 2016.

ACKNOWLEDGEMENT

This project was funded by the U.S. DOE Fuel Cell Technologies Office with additional funding from the Office of Naval Research and the State of Hawaii.

X.2 Ground Support Equipment Demonstration

Jim Petrecky
Plug Power
968 Albany-Shaker Road
Latham, NY 12110
Phone: (518) 817-9124
Email: James_Petrecky@plugpower.com

DOE Managers:
Pete Devlin
Phone: (202) 586-4905
Email: Peter.Devlin@ee.doe.gov
James Alkire
Phone: (720) 356-1426
Email: James.Alkire@ee.doe.gov

Contract Number: DE-EE0006093

Project Start Date: January 2013
Project End Date: December 2017

Overall Objectives

- Create a hydrogen fuel cell-based solution for cargo tractors (airport vehicle) that is cost-competitive and more energy-efficient compared to incumbent internal combustion engine-powered alternatives.
- Enable airport end users to accomplish daily tasks with a hydrogen fuel cell solution while reducing consumption of gasoline and diesel fuels, reducing U.S. demand for petroleum.
- Demonstrate lower carbon emissions with fuel cells.
- Demonstrate a value proposition that shows decreased energy expenditures when compared to diesel-powered airport vehicles.

Additional program objectives are shown in Table 1.

Fiscal Year (FY) 2017 Objectives

- Second year of demonstration.
- Incorporate improvements to design and service.
- Vetting the value proposition.
  - Vetting the assumptions.
  - Diesel fuel consumption, idle time, and annual operating hours.
  - Diesel tractor maintenance, specifically starters, brakes, and oil changes.
  - Diesel maintenance interval.
  - Fuel cell maintenance.
- System and tractor improvements.
  - Optimizing efficiency (lower kWh usage per shift).
  - Optimizing regenerative braking (recover maximum energy).
- Run time with plug stack-based system.
  - Four seasons of operation, precipitation, temperature fluctuations, etc.
  - Long-term durability, effects of months of shock and vibration.
  - Expand the fleet to full 15 tractors (nine as of late April 2017).
  - Increased usage by FedEx operators (training required).
- Service: feedback from FedEx service technicians.
  - FedEx technicians performing preventative maintenance.
  - Integrate into FedEx standard operating procedure and management system.

TABLE 1. Program Objectives

DOE Project Objectives	Plug Power–FedEx Project Expectations
Reduce petroleum consumption	Each tractor uses ~2 gal/h. Total tractor run time of 15 tractors over 2 years will be upwards of **175,200 gallons of diesel fuel reduced**.
Reduce emissions at airports	At 9.8 kg CO_2 per gallon of diesel, there will be upwards of **1,717 metric tonnes of CO_2 eliminated at airports**.
Operate 10 h/day and 5,000+ h	Tractor operation occurs during two shifts: day (10 AM–2 PM) and night (10 PM–2 AM). The total clock day is 10 AM–2 AM (16 hours). **Actual tractor activity is 8 h/day. Total run time of 15 tractors over 2 years will be upwards of 87,600 fleet hours.**
Drawbar capacity 3,000 to 6,000 lb	The tractor will be able to tow 4 FedEx containers each weighing 40,000 lb. The corresponding **drawbar capacity of the fuel cell-powered tractor is 5,000 lb**.
Accelerated development of fuel cell-powered GSE	**Fleet of 15 80 V fuel cell systems in real world application gaining significant field experience while allowing a premier tractor end user to evaluate for larger deployments.**

Technical Barriers

This project addresses the following technical barriers from the Market Transformation section of the Fuel Cell Technologies Office Multi-Year Research, Development, and Demonstration Plan.

(B) High hydrogen fuel infrastructure capital costs for Polymer Electrolyte Membrane (PEM) fuel cell applications

(F) Inadequate user experience for many hydrogen and fuel cell applications

In addition, the project addresses the following specific technology barriers.

- Adapt GenDrive architecture to tractor voltage/power requirements.
- Weatherproof for outdoor application.

Technical Targets

- Power: capable of 5,000 lb drawbar capacity
- Availability: >80%
- Run time: >1 shift
- Reliability (mean time between failures): >100 h
- Speed rating: 10 mph
- Outdoor operation: no non-recoverable issues
- Hydrogen fills: 350 bar

FY 2017 Accomplishments

- Completed first year of demonstration.
- Decision to move away from third party stack (16 stack failures averaging 61 h life) and build a new design with Plug Power stacks for the second year of the demonstration.
  - Note: stack issues included hard failures requiring refurbishment, inability to start, and excessive purging.
- Incorporated design improvements into the new design to optimize serviceability.
- Summarized learning from Year 1.
  - Tractor handles application load.
  - Operating outdoor 24 hours per day, seven days per week is not a problem.
  - Weatherproofing strategy works well; no water ingress.
  - Air filtration protects the system from airport hydrocarbon emissions.
  - Tractor can operate worst route for full shift without needing to refuel.
  - Handful of components that had a drastic effect on reliability.
- First year evaluation.
  - Power: capable of 5,000 lb drawbar capacity – yes
  - Availability: >80% – no (initially 70% but dropped due to accelerating stack failures)
  - Run time: >1 shift – yes
  - Reliability (Mean time between failures): >100 h – no (98 h)
  - Speed rating: 10 mph – yes
  - Outdoor operation: no non-recoverable issues – yes
  - Hydrogen fills: 350 bar – yes
- System redesign with Plug Power stacks (Figure 1).
- Redesigned system completed and tested.

✧ ✧ ✧ ✧ ✧

INTRODUCTION

This project deploys 15 fuel cell-powered units for two years at FedEx Express's busiest airport. The project is planned for two phases. The first is a one year development phase where Plug Power develops, builds, and tests the 80 VDC (20 kW) fuel cell system for the cargo tractor application. The second is a two-year demonstration where a fleet of cargo tractors are integrated into Charlatte CT5E electric cargo tractors and deployed at the FedEx locations under real-world conditions. The fuel cell fleet is fueled by a GenFuel hydrogen compression, storage, and dispensing solution.

APPROACH

Plug Power designed an 80 VDC fuel cell system as a drop-in-place replacement of an electric Charlatte tractor (Figure 2).

Hydrogen is supplied to the tractors via GenFuel hydrogen infrastructure, which provides onsite hydrogen at 350 bar dispensed directly to the fuel cell in the tractor (Figure 3).

- Definition of requirements – complete
- Alpha prototype – complete
- Cargo tractor beta builds – complete
- Cargo tractor testing and certification – complete

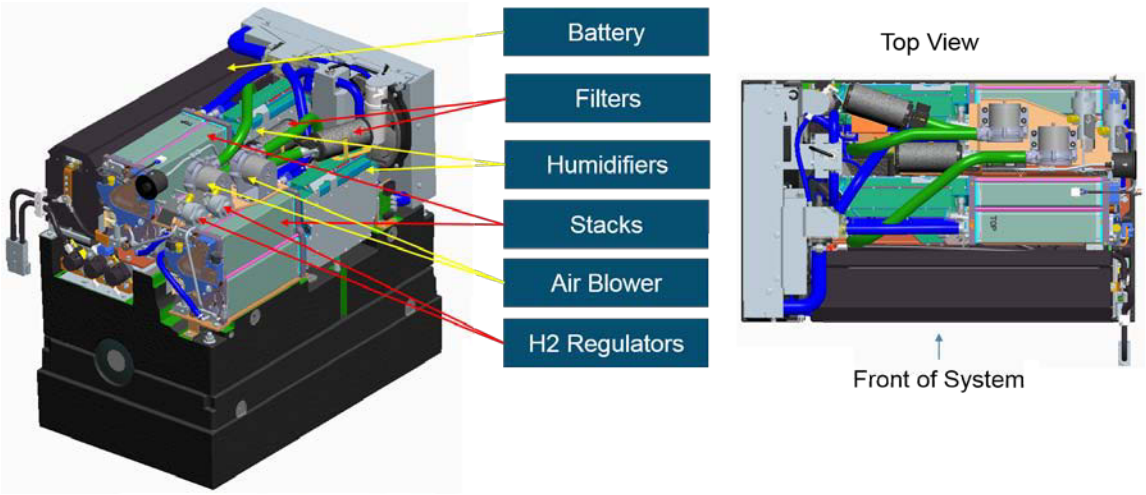

FIGURE 1. System redesign with Plug Power stacks

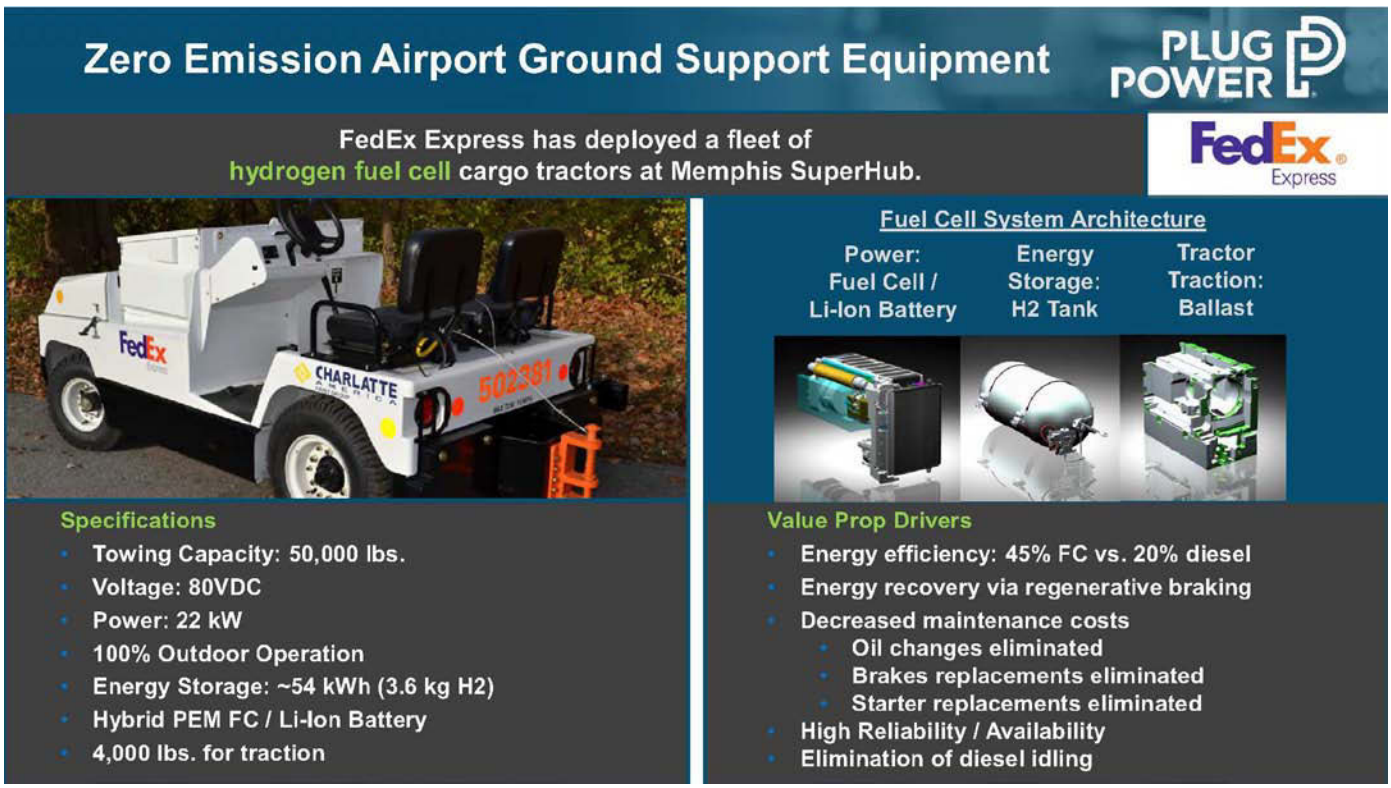

FIGURE 2. Fuel cell system as drop-in-place replacement of battery

- Site preparation – complete
- Commissioning – complete
- First year of demonstration – complete
- Assessment after Year 1 – complete
- Second year of demonstration – third quarter of 2016 to fourth quarter 2017
- Assessment after Year 2 – fourth quarter of 2017

RESULTS

The program delivered a tractor that meets the application requirements in terms of towing the required weight in an outdoor airport application even in the face of elevated hydrocarbon emissions. Stack lifetime has not been sufficient. The program has recovered with a system redesign using Plug Power stacks. The demonstration continues with

FIGURE 3. Liquid hydrogen station on airport ramp

design and service improvements in order to validate the changes made as a result of the learning in the first year.

CONCLUSION AND UPCOMING ACTIVITIES

The first year showed that fuel cells are technically viable for ground support equipment operations. The fuel cell stack is critical to demonstrate lifetime and economic viability. Upcoming activities include to continue the deployment of the redesigned fuel cell solution in the tractor fleet. Focus of the second year of demonstration is on system lifetime, reliability, and economic evaluation.

FY 2017 PUBLICATIONS/PRESENTATIONS

1. J. Petrecky, "MT011 Ground Support Equipment Demonstration," presented at the DOE Annual Merit Review, Washington, DC, June 7, 2017.

X.3 Maritime Fuel Cell Generator Project

Joe Pratt
Sandia National Laboratories
PO Box 969, MS-9052
Livermore, CA 94551
Phone: (925) 294-2133
Email: jwpratt@sandia.gov

DOE Manager: Pete Devlin
Phone: (202) 586-4905
Email: Peter.Devlin@ee.doe.gov

Subcontractor:
Hydrogenics, Mississauga, ON, Canada

Project Start Date: September 15, 2013
Project End Date: 2017

Overall Objectives

- Lower the technology risk of future port fuel cell deployments by providing performance data of hydrogen polymer electrolyte membrane fuel cell technology in this environment.
- Lower the investment risk by providing a validated economic assessment for this and future potential projects.
- Enable easier permitting and acceptance of hydrogen fuel cell technology in maritime applications by assisting the U.S. Coast Guard and American Bureau of Shipping develop hydrogen and fuel cell codes and standards.
- Engage potential adopters and end users of hydrogen fuel cells to enable more widespread acceptance of the technology.

Fiscal Year (FY) 2017 Objectives

- Lower technology risk and lower investment risk through technical performance analysis and economic analysis.
- Enable easier permitting and acceptance by continually engaging the U.S. Coast Guard and Class Societies (e.g., American Bureau of Shipping) on other projects, which proves usefulness of the Maritime Generator project in developing these standards and guidelines.
- Engage potential adopters such as numerous potential hosts for subsequent demonstration, teaching them about the technology and potential benefits.

Technical Barriers

This project addresses the following technical barriers from the Market Transformation section of the Fuel Cell Technologies Office Multi-Year Research, Development, and Demonstration Plan.

(A) Inadequate standards and complex and expensive permitting procedures

(E) A lack of flexible, simple, and proven financing mechanisms

(F) Inadequate user experience for many hydrogen and fuel cell applications

Technical Targets

No specific technical targets have been set.

FY 2017 Accomplishments

The data analysis and reporting was completed in FY 2017. This showed the following:

- During the demonstration period the generator ran for 278 h and produced 7,285 kWh of electricity. It had an average gross power output of 29.4 and reached 91 kW over a continuous 5-minute period. It was able to handle all electrical requirements of the reefer systems.
- Efficiency measurements illustrate the inherent higher part-load efficiency of fuel cell power systems compared to diesel generators, for example, up to a 30% efficiency gain at 30% load.
- Technical issues caused significant downtime with the inverter being the most frequent technical issue and the one causing the longest cumulative down time.
- Nontechnical issues also were responsible for limiting the run time of the unit, with availability of on-site labor the most frequent reason.
- The generator was filled with 428 kg of hydrogen during the demonstration period and all fills were smooth and trouble free.
- The marine environment had no effect on the condition of the stainless steel piping components during the 9-month demonstration period.
- Economic analysis shows that even with fuel cell costs reaching the DOE target of $50/kW, the capital cost of the generator system is projected to remain three times higher than today's comparable diesel generator due to the balance of plant, in particular the hydrogen storage tanks and the power conversion equipment.

- The economic analysis also shows that today's hydrogen prices make fuel to be a major operating expense and hinders the ability of today's fuel cell systems to achieve cost parity with today's diesel systems.

✧ ✧ ✧ ✧ ✧

INTRODUCTION

Fuel costs and emissions in maritime ports are an opportunity for transportation energy efficiency improvement and emissions reduction efforts. Ocean-going vessels, harbor craft, and cargo handling equipment are still major contributors to air pollution in and around ports. Diesel engine costs continually increase as tighter criteria pollutant regulations come into effect and will continue to do so with expected introduction of carbon emission regulations. Diesel fuel costs will also continue to rise as requirements for cleaner fuels are imposed. Both aspects will increase the cost of diesel-based power generation on the vessel and on shore.

Although fuel cells have been used in many successful applications, they have not been technically or commercially validated in the port environment. One opportunity to do so was identified in Honolulu Harbor at the Young Brothers Ltd. wharf. At this facility, barges sail regularly to and from neighbor islands and containerized diesel generators provide power for the reefers while on the dock and on the barge during transport, nearly always at part load. Due to inherent efficiency characteristics of fuel cells and diesel generators, switching to a hydrogen fuel cell power generator was found to have potential emissions and cost savings.

APPROACH

This project developed and demonstrated a nominally 100 kW, integrated fuel cell prototype for marine applications (Figure 1). This project brought together industry partners in this prototype development as a first step towards eventual commercialization of the technology. To be successful, the project incorporated interested industry and regulatory stakeholders: an end user, technology supplier and product integrator, and land- and maritime-based safety and code authorities. Project costs were shared by the primary stakeholders in the form of funds, in-kind contribution, and material and equipment either loaned or donated to the project. Co-funding was provided by the Department of Transportation, Maritime Administration's Maritime Environmental and Technical Assistance program.

The project had four phases:

1. Establishment and specification (September 2013–December 2013)
2. Detailed design and engineering (January 2014–March 2015)
3. Prototype fabrication/site construction (October 2014–June 2015)
4. Demonstration at Young Brothers and analysis (August 2015–June 2016)

RESULTS

From the period of August 2015 to June 2016 the generator was used by Young Brothers at their dock (Figure 2) on 52 different days for a total of 278 h. It averaged 29.4 kW (gross) during this period for a total energy generation output of 7,285 kWh and achieved a 5-minute continuous peak power of 91.3 kW (gross). As shown in Figure 3, its net energy efficiency ranged from 36% to 54% over the load range of 16% to 62%. By comparison, the net

FIGURE 1. The maritime fuel cell generator, with integrated hydrogen storage, PEM fuel cell power generation, and power inverter equipment can power up to 10 reefers with a total rated output of 100 kW at 240 VAC

FIGURE 2. The generator (blue) in the "Icehouse" area powering reefers (white)

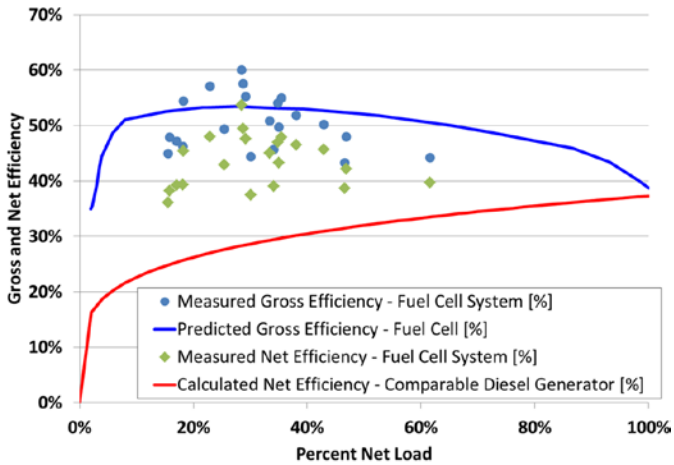

FIGURE 3. Comparison of measured fuel cell efficiencies with predicted fuel cell efficiency (blue line) and comparable diesel engine efficiency (red line). The measured gross efficiency compares well with the predicted fuel cell efficiency. The measured net efficiency of the fuel cell system shows a higher efficiency than the diesel generator at part load, and nearly 30 percentage points higher at the 30% net load point.

efficiency of a comparable diesel generator efficiency is from 25% to 34% in this same load range. Using no diesel fuel and producing zero emissions at the point of use, during the demonstration period the fuel cell generator displaced 865 gallons of diesel fuel, over 16 MT of CO_2 emissions, and avoided nearly 150 combined kilograms of criteria pollutants (NO_x, CO, hydrocarbons, particulate matter, and SO_x) as compared to an existing Young Brothers 350 kW Tier 3 diesel generator.

The deployment experienced numerous technical issues with the generator that limited its use. The primary technical issue during the deployment was an inconsistent startup which was attributed to a communication problem between the overall system controller, inverter, and fuel cell rack. This in turn led to problems with draining of the startup battery, and the overall result was many aborted attempted starts and non-use until the problem could be identified and fixed. The generator's fuel cells also experienced higher-than-anticipated consumption of deionized water, which was exacerbated by the high ambient temperature along with a small deionized water reservoir, causing the operators to have to fill the reservoir more than expected. The consumption was within specification of the fuel cells and not a serious issue, but nonetheless was an unanticipated inconvenience. The generator did not experience any safety-related events and did not exhibit any serious signs of wear or deterioration in the seaport environment. The technical lessons learned from the deployment will be used by the manufacturer to modify this generator for subsequent testing as well as to improve next generation products.

One objective of this deployment was to gather real-world experience with operating hydrogen fuel cell equipment. A flawlessly operating generator would likely have been integrated smoothly into the existing Young Brothers operations. However, the technical issues meant that time needed to be spent by Young Brothers staff to assist in troubleshooting and performing minor maintenance. Many times, Young Brothers staff was not available due to numerous other activities needed to maintain normal operation of the facility. The testing revealed that a dedicated operator would have been needed to maintain continuous operation of the generator because of its technical issues.

Figure 4 shows the results of an economic analysis of capital and operating costs of the hydrogen fuel cell generator were determined for three cases: (1) the deployment, (2) a notional deployment with full usage, and (3) a future deployment where fuel cell and hydrogen costs have come down. These were compared to that of a diesel generator at current costs of equipment and fuel. This presents a worst-case scenario for the fuel cell generator since expected stricter emissions regulations and increase fossil fuel costs are expected in the future (e.g., a doubling of today's diesel fuel cost in 10 yr), the result being continually higher diesel equipment and fuel costs as time goes on.

The analysis showed that even with fuel cell costs reaching the DOE target of $50/kW, the capital cost of the generator system is projected to remain three times higher than today's comparable diesel generator due to the balance of plant. Large portions of the balance of plant cost are the

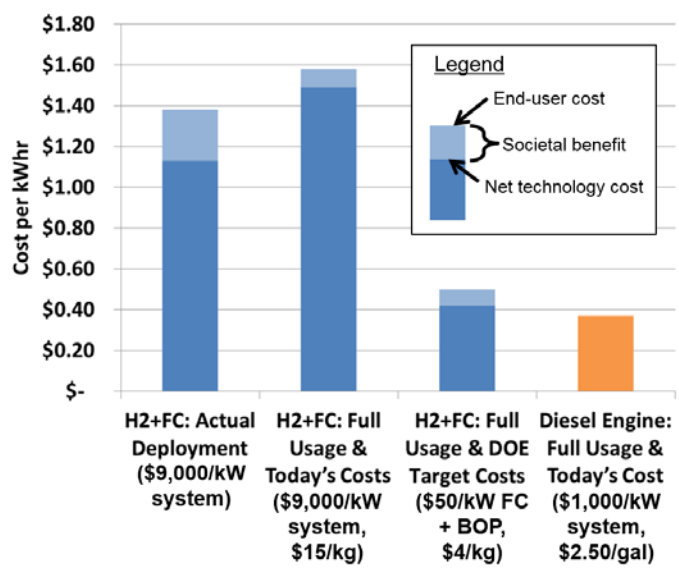

FIGURE 4. Summary economic evaluation of the 100 kW fuel cell generator for the deployment and projected full usage, with comparison to a notional 100 kW diesel generator. Today's highest cost factors are hydrogen fuel, hydrogen storage tanks, and power conditioning equipment.

power conditioning (inverter) and hydrogen storage tubes, where future cost reductions (to approximately 1/3 of today's costs) are necessary to enable competitiveness. The analysis also revealed that fuel is the major operating expense for these systems. While this demonstration enjoyed free fuel from the Hickam station, this will not be the case in true commercial adoption. Today's difference in hydrogen costs (high) and diesel costs (low) is expected to significantly decrease in the future as hydrogen costs decrease and diesel costs increase, but the current differential hinders the ability of today's fuel cell systems to achieve cost parity with today's diesel systems.

CONCLUSIONS AND UPCOMING ACTIVITIES

As the first validation of a self-contained hydrogen fuel cell generator at a port, this project showed that it is possible to reduce maritime-related emissions through the use of hydrogen fuel cells, and identified paths forward to more widespread adoption of the technology in the marine sector. This includes not only the use of a generator for reefer power but other applications as well. These include port equipment, electrical resiliency against grid outages, auxiliary power for vessels, and vessel propulsion power. Establishing hydrogen equipment usage at port also has the benefit of establishing a local hydrogen infrastructure hub that can be leveraged to provide hydrogen for regional transportation uses. Future usage of the generator by other hosts will continue to collect the information needed to completely assess the business case as well as provide opportunity for continued development of the technology.

The DOE–Maritime Administration–Sandia National Laboratories project leads are currently working to arrange a follow-on demonstration at a different partner following upgrade and refurbishment of generator features by the manufacturer. It is expected that this generator will continue to be demonstration by various partners in the future, displacing additional diesel generator emissions and breaking down market barriers to widespread hydrogen fuel cell technology deployment at each stop.

FY 2017 PUBLICATIONS/PRESENTATIONS

1. J.W. Pratt and S.H. Chan, "Maritime Fuel Cell Generator Project," Sandia National Laboratories Report #SAND2017-5751, May 2017. Available from: maritime.sandia.gov

2. J. Pratt, "Maritime Fuel Cell Generator Project," DOE Annual Merit Review, June 7, 2016, Washington, DC, Sandia National Laboratories presentation #SAND2017-3799 PE.

X.4 Demonstration of Fuel Cell Auxiliary Power Unit (APU) to Power Truck Refrigeration Units (TRUs) in Refrigerated Trucks

Kriston Brooks (Primary Contact)
Pacific Northwest National Laboratory
P.O. Box 999
Richland, WA 99352
Phone: (509) 372-4343
Email: kriston.brooks@pnnl.gov

DOE Manager: Pete Devlin
Phone: (202) 586-4905
Email: Peter.Devlin@ee.doe.gov

Subcontractors:
- Nuvera Fuel Cells, Billerica, MA
- Ballard Power Systems, Burnaby, BC, Canada

Project Start Date: June 1, 2012
Project End Date: September 30, 2018

Overall Objectives

- Demonstrate the viability of fuel cell-based transport refrigeration units (TRUs) for refrigerated Class 8 trailers.
- Assess the performance of the fuel cell-based TRUs by demonstrating these systems with 800–1,000 hours of commercial deliveries.
- Use the demonstration data and market assessment to develop a business case that will determine if lifecycle cost parity can be achieved with incumbent technologies.

Fiscal Year (FY) 2017 Objectives

- Direct subcontract teams led by Nuvera Fuel Cells and Ballard Power Systems as they each develop a fuel cell-based TRU for a refrigerated Class 8 trailer.
- Complete Phase I of the Ballard subcontract team development effort by producing a business case, a safety plan and a preliminary design.
- Complete Phase II of the Nuvera subcontract team development effort by performing an 8-hour integrated laboratory demonstration of the fuel cell system, power electronics, and TRU.

Technical Barriers

This project addresses the following technical barriers from the Market Transformation section of the Fuel Cell Technologies Office Multi-Year Research, Development, and Demonstration Plan.

(B) High hydrogen fuel infrastructure capital costs for Polymer Electrolyte Membrane (PEM) fuel cell applications

(C) Inadequate private sector resources available for infrastructure development

(E) A lack of flexible, simple, and proven financing mechanisms

(F) Inadequate user experience for many hydrogen and fuel cell applications

Technical Targets

This project directly addresses the Market Transformation sub-program targets described in Section 3.9.4 of the Fuel Cell Technologies Office Multi-Year Research, Development, and Demonstration Plan by developing a pathway for the introduction of fuel cell technologies into the transport refrigeration unit market. This niche market will increase hydrogen usage, reduce hydrogen cost, and further establish the hydrogen infrastructure at food distribution centers. The project involves the two primary U.S. TRU manufactures, Thermo King and Carrier Transicold. They will be actively involved in overcoming the logistical and other nontechnical challenges associated with implementing this new technology, resulting in a smoother adoption into the marketplace. The project involves demonstrations by two large potential customers, Walmart and WinCo Foods. These companies already use fuel cell-based lift trucks and as a result have experience with hydrogen infrastructure and safety issues. These demonstrations will provide valuable data on the performance of the technology in real-world operations and can be used to benchmark the benefits of the technologies. Both the TRU manufacturers and demonstrators will provide input into the business case to create a clear picture of the value proposition of this new technology.

FY 2017 Accomplishments

- Nuvera integrated the fuel cell system (stack and packaged balance of plant) and power electronics and tested it in a laboratory environment at low power in preparation for the real-world demonstration.
- Thermo King has identified WinCo as a new demonstration partner.
- Zen Clean Energy Solutions developed business case with assistance from Walmart, Carrier, and Ballard.

They developed a preliminary value proposition analysis to determine the tipping point between positive and negative net present values. This value proposition will help determine the conditions when lifecycle cost parity can be achieved with incumbent technologies.

- Ballard developed a preliminary system design and completed the Phase I go/no-go decision.

✧ ✧ ✧ ✧ ✧

INTRODUCTION

A TRU is a high-powered air conditioning system used in cooling cold goods during on-road transport. It is generally powered by a separate diesel engine. Replacing this diesel engine with a fuel cell will address recent state and federal environmental mandates to reduce emissions, address noise restrictions found in many urban areas, reduce system maintenance, and improve the overall energy efficiency of the system. The initial market for this application would be food distributions centers where vehicles return to a central facility for refueling and where fuel cell lift trucks have already been established. This market will further expand the hydrogen usage at these sites and increase fuel cell market penetration.

The purpose of this project is to perform two demonstrations of fuel cell-based TRUs using two separate fuel cell teams as shown in Table 1. These demonstrations will provide user experience for over-the-road fuel cell applications that will mitigate commercial risk in developing this new technology.

TABLE 1. Fuel Cell-Based TRU Demonstration Teams

Project Role	Nuvera Team	Ballard Team
Fuel Cell Supplier, System Integrator	Nuvera	Ballard
TRU Supplier	Thermo King	Carrier Transicold
Demonstration Partner	WinCo	Walmart

APPROACH

Each of the two demonstrations will be performed by a team consisting of a fuel cell system supplier and integrator, a TRU system manufacturer, and a demonstration site. Each demonstration will be 800 to 1,000 hours in duration and will consist of actual deliveries of cold goods. During the demonstration, data will be collected from the hydrogen refueling station, fuel cell system, TRU, and the trailer to allow an independent techno-economic analysis and a system evaluation relative to available DOE targets. These results will be used to develop a business case and commercialization plan that can be implemented at the conclusion of the demonstration.

In preparation for these demonstrations, a preliminary business case will be developed and safety and regulatory issues addressed. The system development will include appropriately sizing the fuel cell stack and hardening the system to be comparable in performance and robustness with the incumbent technology. These demonstrations may also require installation or augmentation of the on-site hydrogen infrastructure for refueling.

RESULTS

The Nuvera and Ballard team's progress with the fuel cell-based TRU demonstration projects are described below.

Nuvera Fuel Cell System Development. The Nuvera team completed packaging of the fuel cell system. It will be undermounted on a Class 8 trailer using the frame of an existing Thermo King SGSM 3000 diesel genset. The original components were removed and replaced with the fuel cell stack, balance of plant, and power electronics as shown in Figure 1. In addition to packaging the system hardware, the system controls, software and communication were finalized to allow integration with the Thermo King Precedent C-600 TRU. This particular TRU is a plug-in hybrid system that allows the use of either the diesel generated power or 480 VAC three-phase shore power during operations. As a result, the demonstration of this system requires that the fuel cell direct current (DC) power be converted to alternating current (AC) power to supply the TRU. The system also requires DC power boost convertors to supply DC power at other voltages for components such as the control system, sensors and the air compressor. The power conversions are one of the major challenges of this system integration.

The first integrated demonstration was performed at low power. It included an integrated test with the fuel cell and power electronics modules. The system included DC converters from 112 to 15 and 500 VDC. The DC/AC inverter and TRU were not included in this first integrated demonstration but 2.5 kW of power that would normally be used by the TRU was dissipated with resistors as surrogates. This first low power demonstration was successfully performed and results were as expected.

A follow-on demonstration included the DC/AC inverter and TRU at full power levels. Unfortunately, the fuel cell air compressor and the DC boost converter failed during the first 30 minutes of operation. The air compressor bearings failed and boost converter failed due to a software bug. These issues have been fixed and the diodes within the converter were replaced. To date, the required 8-hour integrated laboratory demonstration that will finalize the Phase II milestone has not been completed.

During this year, the original demonstration partner, H-E-B chose not to continue participation. As a result, Thermo King identified WinCo Foods in Modesto, CA as the new demonstration partner.

FIGURE 1. Photographs of the Nuvera packaged fuel cell system

Ballard Fuel Cell System Development. During FY 2017, the Ballard team completed their Phase I milestone. This milestone included a preliminary design, safety strategy, and market assessment. The preliminary design included system sizing, system balance of plant selection, packaging, and placement of the fuel cell system on the trailer. To perform the system sizing, Ballard and Walmart selected a demonstration site and used power usage and location data to size the fuel cell system and hydrogen tankage. Winter Haven, Florida, was the selected demonstration site to be a bounding case for Walmart distribution centers because of its high summer temperatures and humidity. Analysis of the data collected from 16 TRUs indicated that the Carrier electric hybrid TRUs required a peak power of 18 kW (see Figure 2). The highest hydrogen usage was 19 kg over the course of a 22-hour day, while 83% of the TRUs had less than 10 kg hydrogen consumption per day. Location data indicated that some of the trailers did not return to the distribution center of origin each day and as a result would require refrigeration longer than a single day. As a result of the disparity between the various trailer operations, Ballard and Walmart determined that 20 kg of hydrogen storage would be a reasonable for nearly all of the TRUs at this site.

In addition to system sizing, Ballard used the Winter Haven TRU data to determine if hybridization of the fuel cell is required. Based on the data provided, the system runs at maximum power for many hours and transients are relatively slow. As a result, hybridization would not benefit such a design, therefore batteries are required only for startup. During the design process, the best location of

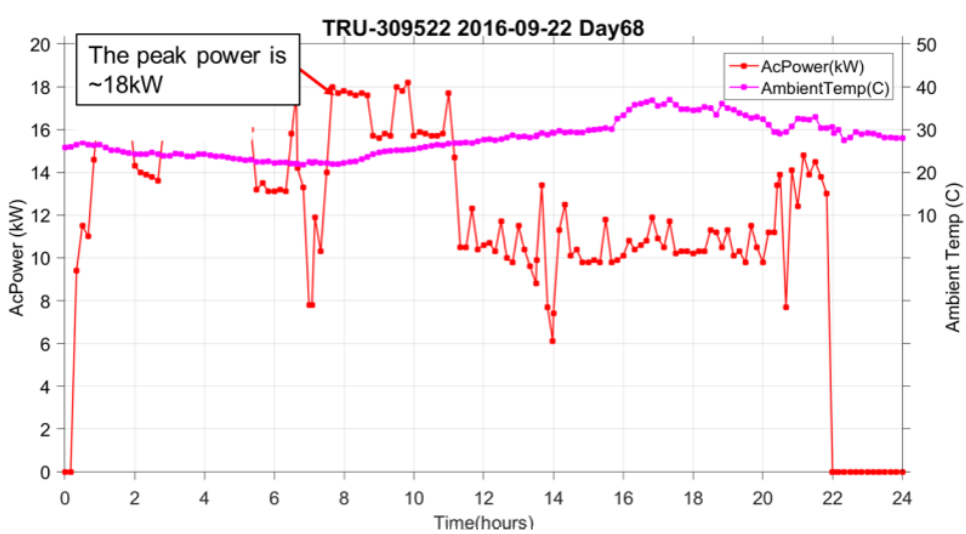

FIGURE 2. AC power required and ambient temperature for bounding TRU at the Winter Haven, Florida, Walmart Distribution Center

the fuel cell system and tankage was determined to be the bottom of the trailer. No other location could be found that would not impact tractor or trailer operations. Although space is available under the trailer, this location does require additional shielding to protect the system from on-road projectiles.

Ballard developed a safety strategy that incorporated input from applicable codes and standards and a Product Potential Hazard Analysis. A risk reduction plan was developed that recommended design approaches and features to mitigate the hazards identified.

Zen Clean Energy Solutions developed a market analysis for the Class 8 trailer TRU. This analysis identified three recent changes that may impact the business case favorably: (1) increased availability of hydrogen at distribution centers with the deployment of fuel cell forklifts; (2) availability of higher-efficiency, all-electric TRUs; and (3) reduction of fuel cell cost. The market analysis estimated the total cost of ownership comparing a diesel-based TRU with a "clean sheet design" fuel cell TRU over a 10-year lifecycle. In this analysis, the cost of fuel and capital cost of the system are the driving factors. Using a cost of $3.27/gallon for diesel fuel and $4.00/kg for hydrogen, the net present value (NPV) comparison of the two systems is -$25,000, or the fuel cell system costs are higher than the incumbent technology. Table 2 compares the NPV difference between a fuel cell and a diesel system. The green highlighted cells are where this difference is positive and the fuel cell system has economic benefits over the incumbent technology.

The fuel cell system capital cost has been estimated at nearly twice that of the diesel engine. It is not only the fuel cell itself that drives this increased cost, but also the tankage required for storage of 20 kg of hydrogen and the power electronics, including DC/DC and DC/AC conversion. These non-fuel cell items make up more than half of the total capital cost of the system (58%). As a result, additional cost reduction research should be done not only on the fuel cell but on the tanks and power electronics as well.

Another challenge identified with the fuel cell system is that it is much heavier than conventional technology. With the weight of the 20 kg hydrogen tanks, fuel cell system, and the shielding needed to protect the system on the undercarriage of the trailer, it is more than 1,000 lb greater than a typical TRU. Due to weight constraints on the Walmart trailers, this additional weight results in an equal amount of product that cannot be shipped. This loss of capacity was a significant concern for Walmart.

A final challenge is the expiration of the federal Business Energy Investment Tax Credit for fuel cells that expired in December 2016. This tax credit provided 30% tax credit to offset the cost of using a fuel cell option.

As a result of the negative estimated NPV lifecycle cost comparison to the diesel engine TRU, the loss of carrying capacity, and the less favorable federal incentives, the Ballard team (including Walmart and Carrier) decided to not continue the project into Phase II. This team will not build a fuel cell TRU nor perform their originally planned demonstration. Instead, they will write a final report and close out the subcontract.

CONCLUSIONS AND UPCOMING ACTIVITIES

The development and demonstration of a fuel cell auxiliary power system for Class 8 refrigerated trailers is a first step in expanding fuel cell use to TRUs. This demonstration will increase fuel cell market penetration and further break down technical and nontechnical barriers to hydrogen and fuel cell use.

During FY 2017 the Nuvera team packaged and tested the integrated fuel cell system in the laboratory at low power and attempted testing at high power. In FY 2018,

TABLE 2. Impact of Diesel and Hydrogen Fuel Costs on NPV Difference between Fuel Cell and Incumbent TRU Technology

		Hydrogen Cost ($/kg)						
		$ 2.00	$ 3.00	$ 4.00	$ 5.00	$ 6.00	$ 7.00	$ 8.00
Diesel Cost ($/gallon)	$ 2.00	$ (15,925)	$ (31,286)	$ (46,648)	$ (62,009)	$ (77,371)	$ (92,732)	$ (108,093)
	$ 3.00	$ 973	$ (14,389)	$ (29,750)	$ (45,112)	$ (60,473)	$ (75,834)	$ (91,196)
	$ 4.00	$ 17,870	$ 2,509	$ (12,853)	$ (28,214)	$ (43,575)	$ (58,937)	$ (74,298)
	$ 5.00	$ 34,768	$ 19,406	$ 4,045	$ (11,316)	$ (26,678)	$ (42,039)	$ (57,401)
	$ 6.00	$ 51,665	$ 36,304	$ 20,942	$ 5,581	$ (9,780)	$ (25,142)	$ (40,503)
	$ 7.00	$ 68,563	$ 53,201	$ 37,840	$ 22,479	$ 7,117	$ (8,244)	$ (23,606)
	$ 8.00	$ 85,460	$ 70,099	$ 54,738	$ 39,376	$ 24,015	$ 8,653	$ (6,708)
	$ 9.00	$ 102,358	$ 86,997	$ 71,635	$ 56,274	$ 40,912	$ 25,551	$ 10,189
	$ 10.00	$ 119,256	$ 103,894	$ 88,533	$ 73,171	$ 57,810	$ 42,448	$ 27,087

Nuvera will finalize Phase II by performing the 8-hour laboratory demonstration at high power with the fuel cell system integrated with the TRU. They will then upgrade the system for on-road operations by installing a stack cover and redesigned external enclosure for on-road projectiles. They will also improve component connections for the higher-than-anticipated levels of vibration. The Nuvera team can then move to Phase III where they will perform the on-road demonstration with WinCo as their new demonstration partner.

Work performed by the Ballard team this fiscal year includes the development of a preliminary design based on TRU data at the Walmart distribution center at Winter Haven, Florida, a safety plan, and a market assessment. The market assessment was not considered favorable enough for the Ballard team to continue into Phase II. As a result, the team will not develop the fuel cell system, integrate it with the TRU, or perform the demonstration. Instead, Ballard will complete its final reports and conclude this work in the upcoming months.

X.5 FedEx Express Hydrogen Fuel Cell Extended-Range Battery Electric Vehicles

Imran Ahmed
Federal Express Corporation
3690 Hacks Cross Rd.
Memphis, TN 38125
Phone: (901-434-5725)
Email: Imran.ahmed@fedex.com

DOE Manager: James Alkire
Phone: (720) 356-1426
Email: James.Alkire@ee.doe.gov

Contract Number: DE-EE0006522

Subcontractors:
- Workhorse Technologies Inc, Loveland, OH
- Plug Power Inc, Latham, NY

Project Start Date: October 15, 2015
Project End Date: October 10, 2019

Overall Objectives

- To convert an existing electric parcel delivery unit (PUD) into a zero emission extended range electric vehicle by utilizing hydrogen fuel cell technology.
- Understand, demonstrate, and deploy hydrogen fuel cell technologies in a real-world environment.

Fiscal Year (FY) 2017 Objectives

- Test and verify the performance of the fuel cell.
- Optimize, test and complete the integration between the fuel cell and the electric vehicle (EV).
- Determined the optimal hydrogen storage quantity and location.
- Complete the body manufacturing and installation.
- Optimize the power generation and charge strategy.

Technical Barriers

This project addresses the following technical barriers from the Market Transformation section of the Fuel Cell Technologies Office Multi-Year Research, Development, and Demonstration Plan [1].

(B) High hydrogen fuel infrastructure capital costs for Polymer Electrolyte Membrane (PEM) fuel cell applications

(D) Market uncertainty around the need for hydrogen infrastructure versus timeframe and volume of commercial fuel cell applications

(F) Inadequate user experience for many hydrogen and fuel cell applications

(J) Insufficient numbers of trained and experienced servicing personnel

(L) Lack of qualified technicians for maintenance

(M) Lack of certified service providing organizations for installation and maintenance

Technical Targets

- The target is to achieve a driving range of 150 miles.
- Operate a safe, reliable, and cost effective asset with zero tail pipe emissions.

FY 2017 Accomplishments

- Fuel cell fabrication
- Fuel cell validation and testing
- Computer aided design models finalized
- EV and fuel cell (FC) integration
- Bracketry design and production
- Power generation and charge strategy optimization
- Hydrogen tanks storage and location
- Body modification for hydrogen tank compartmentation
- Body design, manufacture and installation
- Dilution and vent testing
- Optimized thermal management
- Controller area network messaging and instrument cluster integration
- Final placement location site preparation
- Durability test preparation

✧ ✧ ✧ ✧ ✧

INTRODUCTION

The ability to reduce fuel consumption and emissions while delivering packages is an immense challenge, particularly with the available technology. This is further

complicated by the diversity of the different duty cycles utilized by the PUDs at FedEx. This has created enormous opportunities for an extended range, zero emission electric PUD.

As a part of this project, we will be converting 20 existing electric vehicles into hydrogen fuel cell powered extended range electric vehicles (eREV), in two different phases and budget periods (BPs).

Successful utilization of fuel cell technologies in real world environments will help foster a better understanding while providing the opportunity to identify and utilize additional duty cycles, eventually reducing costs by achieving economies of scale, while providing clean, safe, secure and affordable energy.

APPROACH

The first step was to find industry partners that had the experience, capabilities and the knowledge to collaborate with us in embarking on this project. As a result, we are collaborating with Workhorse, the EV manufacturer; Plug Power, the fuel cell manufacturer; and Morgan Olson, who is the body manufacturer for the eREV.

The project is divided into two separate phases/budget periods (BP1 and BP2). The first period concentrates on the conversion of just one asset. This will enable the project team to test, analyze and measure the performance. BP2 will only be launched if the first phase is considered successful and the team will utilize the lessons learned and implement those in the second phase.

We have made significant progress in BP1 and are close to launching the first eREV PUD. The identification of the ideal route and location for the first PUD was completed. The optimized charge strategy and power generation for the fuel cell was implemented. The fabrication, validation and testing of the fuel cells has successfully been completed. The various integration activities between the EV and FC is completed. The ideal hydrogen tank size, packaging and compartment locations are finalized and being utilized. The body for the PUD was installed on the electric chassis. The safety and venting testing has been initiated. Next, the eREV will be taken through a series of durability tests, before it is placed in active service.

The second phase is launched if the first phase is considered successful and will convert an additional 19 EVs into FC extended range electric PUDs.

RESULTS

This is an ongoing project but the desired results have been achieved. Our analysis of the drive cycle and overall FC performance enabled us to implement the best performance, power generation and charge strategy (Figures 1 and 2).

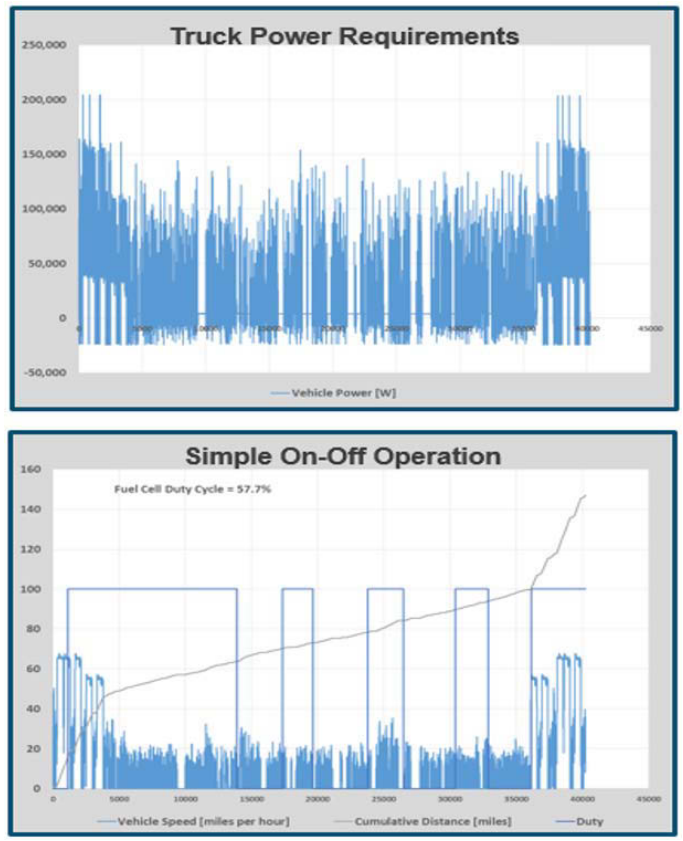

FIGURE 1. Simulated truck requirements

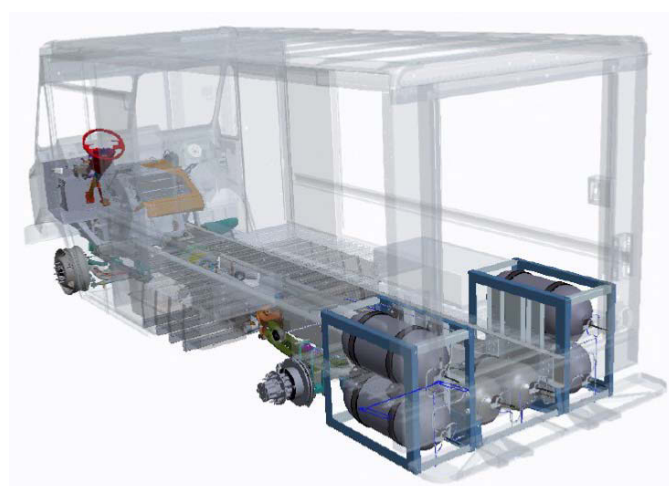

FIGURE 2. Simulated fuel cell duty cycle

The size, capacity and location of the hydrogen tanks in the PUD body were a big challenge and finding the right balance was critical. This was successfully accomplished, providing the eREV the desired range and overall performance (Figure 3).

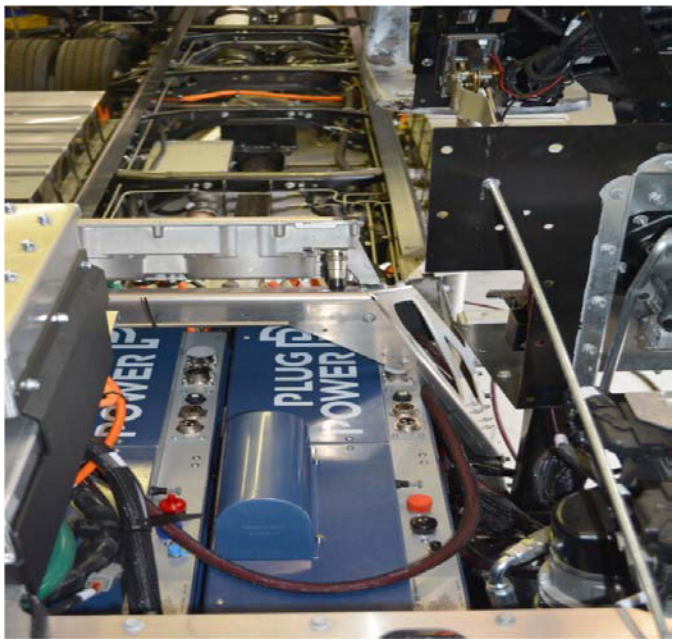

FIGURE 3. Illustration of H_2 tank compartment on the fuel cell eREV

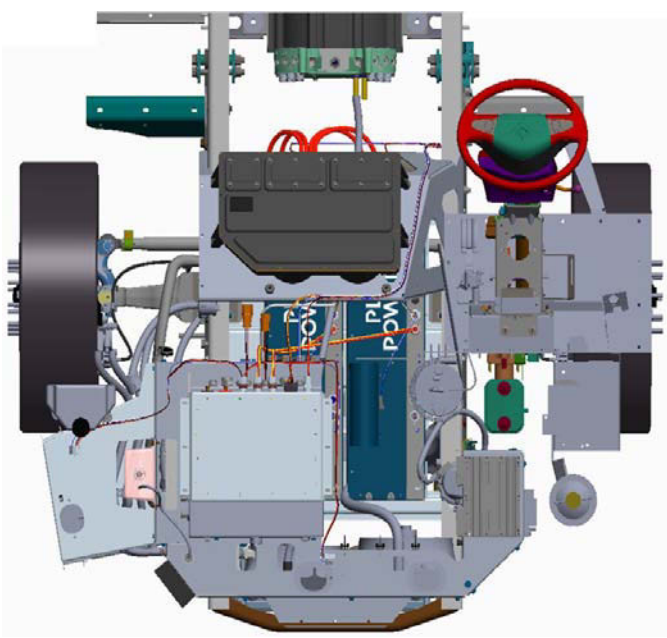

FIGURE 4. Fully integrated FCs in the EV

The integration between the FC and the EV chassis is complete, providing the project team a better understanding (Figure 4).

CONCLUSIONS AND UPCOMING ACTIVITIES

Based on the initial results, the fuel cell eREV PUD is proving to be a viable option, when looking at the overall emission reduction requirements. This will be further clarified as the first unit is put into service and actual data from real life utilization is collected and evaluated.

Since the project is split into two separate budget periods, the future direction is divided accordingly:

BP1

- Fuel system design
- Safety planning
- Design requirements
- Verify optimization analysis
- Communications and control strategies
- Leak detection and fuel isolation
- Integration of fuel cell into first truck
- Durability testing
- Commissioning
- Place into revenue service
- Validation
- Prepare for BP2

FY 2017 PUBLICATIONS/PRESENTATIONS

1. Imran Ahmed, "FedEx Express Hydrogen Fuel Cell Extended Range Battery Electric Vehicles," presented at the DOE Annual Merit Review, Washington, DC, June 5–9, 2017.

REFERENCES

1. Section 3.9 Market Transformation. (n.d.). Retrieved July 10, 2017, from http://energy.gov/eere/fuelcells/downloads/fuel-cell-technologies-office-multi-year-research-development-and-22

X.6 Northeast Demonstration and Deployment of FCRx200

Abas Goodarzi
US Hybrid
445 Maple Ave.
Torrance, CA 90503
Phone: (310) 212-1200
Email: abas@ushybrid.com

DOE Manager: James Alkire
Phone: (720) 356-1426
Email: James.Alkire@ee.doe.gov

Contract Number: DE-EE0007276

Project Start Date: September 1, 2016
Project End Date: February 28, 2022

Overall Objectives

- Design, develop, test, and demonstrate one fuel cell range extended plug-in hybrid utility vehicle (FCRx200) at the operator's site.
- Given a DOE "go" approval, deploy and operate a minimum of 20 FCRx200s for at least 5,000 hours per vehicle at the operator's site.
- Conduct an economic assessment, including a payback analysis cost per unit, and payback time concerning the use of hydrogen-fueled fuel cells for range extenders used in commercial operations.

Fiscal Year (FY) 2017 Objectives

- Complete fuel cell power plant design.
- Initiate final procurement of all system components.
- Develop vehicle model.
- Receive vehicle computer-aided design files and Controller Area Network data.
- Release vehicle system interface (mechanical, electrical, and communications).
- Electronic packaging of the integrated isolated direct current to direct current converter
- Balance of plant component design, packaging, and testing.
- Fuel cell engine controller.
- Fuel cell engine vehicle packaging.
- Hydrogen storage tanks selection and integration.
- Hydrogen fill interface.
- Hydrogen sensors and safety system.

Technical Barriers

This project addresses the following technical barriers from the Market Transformation section of the Fuel Cell Technologies Office Multi-Year Research, Development, and Demonstration Plan.

(A) Inadequate standards and complex and expensive permitting procedures

(B) High hydrogen fuel infrastructure capital costs for Polymer Electrolyte Membrane (PEM) fuel cell applications

(E) A lack of flexible, simple, and proven financing mechanisms

Technical Targets

This project directly addresses the Market Transformation program targets described in Section 3.9.4 of the Fuel Cell Technologies Office Multi-Year Research, Development, and Demonstration Plan. The FCRx200 features Nissan's lithium-ion battery, which is entirely housed under the cargo floor. This project meets United States customer duty cycles using proven Nissan LEAF battery technology in the FCRx200 and UTC derived proton exchange membrane fuel cell technology. The FCRx200's 24 kWh battery is similar to the Nissan LEAF's, but with a revised module layout for packaging requirements and with the addition of an active battery cooler to accommodate the higher quick charging and driving load demands expected in commercial usage. By more than doubling the range, the FCRx200 will be a deployment that can demonstrate fuel cell range extenders for battery-based electric vehicles in Class 1 vehicle platforms. It is an enabling technology that makes electric-powered cargo vehicles a viable solution for a wide range of applications, including passenger transportation services, light freight transport, and dispatch utility operations where electric drive transportation systems are beginning to be introduced commercially.

FY 2017 Accomplishments

- Developed model for powertrain optimization.
- Designed fuel cell auxiliary power unit and balance of plant.
- Finalized concept for cell stack assembly prototype and validated testing.
- Performed short stack performance testing.
- Defined the vehicle packaging boundaries.
- Tested the initial scaled isolated direct current-to-direct converter.

✧ ✧ ✧ ✧ ✧

INTRODUCTION

Although battery-electric vehicles emit zero tailpipe emissions and are less expensive to operate than conventional vehicles, the range of battery-electric vehicles is severally limited. Short driving range and charging time reduces the usefulness of these vehicles, especially for commercial use and/or long trips. Also, the use of heating, ventilation, and air conditioning will reduce the battery-electric vehicle range, making it not practical for cold climates. While some vehicles extend range through internal combustion engine-based generators, these decrease fuel efficiency and increase emissions. Alternatively, fuel cell generators can be used to extend range with zero emissions and reduce the need for charging. In the long-term, fuel cell electric systems may offer lower costs, shorter payback times, and a higher return of investments all the while providing additional benefits such as better performance. In this project, US Hybrid and other strategic project partners collaborate to build a fuel cell range extended plug-in hybrid utility vehicle and demonstrate it in real-world operation.

- US Hybrid: prime contractor
- Nissan North America: original equipment manufacturer partner
- Argonne National Laboratory: national laboratory partner
- National Grid: end user, fleet operator

APPROACH

US Hybrid is the prime contractor. It leads the design and development of the FCRx200. It is responsible for the design, development, and manufacturing of the fuel cell power plant range extender sub-system, fueling (storage and fill) and the integration of the vehicles. US Hybrid also leads the controls integration and battery hybridization work. US Hybrid is responsible for end user training and service and maintenance of the vehicles as they operate in the field.

RESULTS

US Hybrid began the process of developing the model for the powertrain optimization as well as designing the fuel cell auxiliary power unit and balance of plant. Fuel cell design iterations for flow field design, platform sizing, sealing, as well as axial loading structure were performed. An initial concept of the cell stack assembly for prototype and validation testing was finalized and the initial power plant packaging concept started. Fuel cell full-size test stand preparation was started to enable testing of the new system (Figure 1). A new load bank was installed to enable cell stack assembly voltage range and power limits, as well as fuel, air, and water test stand systems to provide required flows. US Hybrid also worked on the 3-D modeling component performance specifications as well as control constraints. A process and instrumentation diagram for the fuel cell power plant and thermal management system initial concept was released and components were added to 3-D model (Figure 2 and Figure 3).

FIGURE 1. Fuel cell stacks at test stand

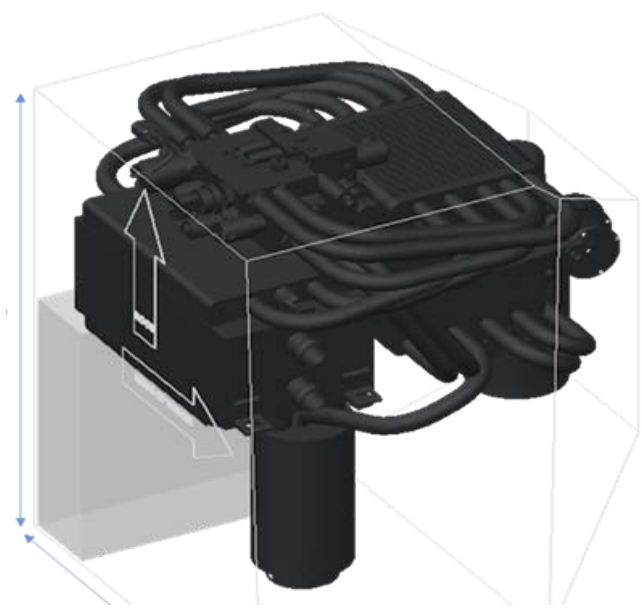

FIGURE 2. Fuel cell engine concept

FIGURE 3. Thermal management system

UPCOMING ACTIVITIES

The following work is proposed for FY 2018.

- Complete design and integration of prototype vehicle.
- Validate vehicle's performance.
- Demonstrate FCRx200 at operator's site.

XI.0 Small Business Innovation Research (SBIR) Fuel Cell Technologies Office New Projects Awarded in Fiscal Year (FY) 2017

The SBIR program provides small businesses with opportunities to participate in DOE research activities by exploring new and innovative approaches to achieve research and development (R&D) objectives. The funds set aside for SBIR projects are used to support an annual competition for Phase I awards of up to $225,000 each for about nine months to explore the feasibility of innovative concepts. Phase II R&D efforts further demonstrate the technologies to move them into the marketplace, and these awards are up to $1,500,000 over a two-year period. Small Business Technology Transfer projects include substantial (at least 30%) cooperative research collaboration between the small business and a non-profit research institution.

Table 1 lists the SBIR Phase I projects and Table 2 lists the SBIR Phase II projects awarded in FY 2017 related to the Hydrogen and Fuel Cells Program. Brief descriptions of each project follow the tables.

TABLE 1. FY 2017 SBIR Phase I Projects Related to the Hydrogen and Fuel Cells Program

Report Number[1]/Title		Company	City, State
V.A.15	Highly Robust Low PGM MEAs Based upon Composite Supports[2]	Forge Nano	Louisville, CO
V.A.14	Multi-Functional Catalyst Support[2]	pH Matter LLC	Columbus, OH
V.A.13	Development of Durable Active Supports for Low Platinum Group Metal Catalysts[2]	Pajarito Powder, LLC	Albuquerque, NM
V.A.12	Mesoporous Non-Carbon Catalyst Supports of PEMFC[2]	CertainTech Inc.	Sterling, VA
V.A.11	Development of Corrosion Resistant Carbon Support for Ultra-Low Platinum Group Metal Catalysts[2]	Greenway Energy, LLC	Aiken, SC
XI.1	Metal Hydride Material Development for High Efficiency and Low Cost Hydrogen Compressors[2]	Greenway Energy, LLC	Aiken, SC
XI.2	Over-Molded Plates for Reduced Cost and Mass PEM Fuel Cells	American Fuel Cell	Rochester, NY
XI.3	Emergency Hydrogen Refueler for Individual Consumer Fuel Cell Vehicles	Reactive Innovations, LLC	Westford, MA

TABLE 2. FY 2017 SBIR Phase II Projects Related to the Hydrogen and Fuel Cells Program

Report Number[1]/Title		Company	City, State
XI.4	Novel Hydrocarbon Ionomers for Durable Proton Exchange Membranes[2]	NanoSonic, Inc.	Pembroke, VA
II.B.7	New Approaches to Improved PEM Electrolyzer Ion Exchange Membranes[2]	Tetramer Technologies, LLC	Pendleton, SC
XI.5	Flexible Barrier Coatings for Harsh Environments[2]	GVD Corp.	Cambridge, MA
XI.6	Cryogenically Flexible, Low Permeability Thoraeus Rubber H_2 Dispenser Hose	NanoSonic, Inc.	Pembroke, VA
XI.7	Low Cost Alloys for Magnetocaloric Refrigeration	General Engineering & Research, LLC	San Diego, CA

[1] Section XI titles (e.g., projects with report number XI.1, XI.2, XI.3) do not have separate entries in the Annual Progress Report. A brief description of each SBIR project listed in Tables 1 and 2 can be found below.
[2] Funded under the Basic Energy Sciences (BES) Office.

PHASE I PROJECTS

V.A.15 Highly Robust Low PGM MEAs Based upon Composite Supports

Forge Nano
1172 Century Dr., #240
Louisville, CO 80027

This project will use a recently developed low-cost atomic layer deposition technique to apply ultra-thin conductive barrier coatings onto carbon particles to prepare drop-in-ready materials suitable for use in highly robust membrane electrode assemblies (MEAs), without sacrificing cost or performance, and while extending system durability. In addition, the high-throughput atomic layer deposition technology developed by PneumatiCoat is very low cost and may even lower the cost of the electrode by enabling further reductions in platinum group metal (PGM) catalyst loading. These attributes promise to facilitate use of the current inexpensive carbon material, yet solve the durability issues experienced today, which will further accelerate commercial adoption. This project will develop high-performance, highly durable supports for low-PGM fuel cells using low-cost techniques to achieve the 2020 targets for cost ($40/kW at the system level, $14/kW at the MEA level), start-up/shutdown durability (5,000 cycles), and less than 10% loss in power after 5,000 h.

V.A.14 Multi-Functional Catalyst Support

pH Matter LLC
1275 Kinnear Rd.
Columbus, OH 43212

The overall objective of the proposed project is to develop and demonstrate a multi-functional carbon support for polymer electrolyte membrane fuel cell cathodes that is engineered to improve stability/durability and lower Pt loading requirements. The approach will be based on nitrogen- and phosphorus-doped carbon with hydrophobicity treatments to improve MEA performance.

V.A.13 Development of Durable Active Supports for Low Platinum Group Metal Catalysts

Pajarito Powder, LLC
317 Commercial Street NE
Albuquerque, NM 87102

This project aims to develop a catalyst that will combine low cost through low platinum loading with high durability through increased corrosive-resistant support. The proposed technology will be based on decoration with PGM of carbon-based metal–nitrogen–carbon materials, which intrinsically have high activity towards oxygen reduction, called active supports.

V.A.12 Mesoporous Non-Carbon Catalyst Supports of PEMFC

CertainTech Inc.
20695 Settlers Point Place
Sterling, VA 20165

This project aims to develop a new catalyst support for polymer electrolyte membrane fuel cells (PEMFCs) that will dually benefit from the support of both materials synthesis and electrochemical evaluation aspects. CertainTech will use a nano-casting route to produce mesoporous boron carbide supports. The resultant product will have a very high specific surface area, well-ordered pore structures, and narrowly distributed pore sizes, all of which will aid the even dispersion of platinum for fuel cell applications. The catalytic properties of the Pt-impregnated boron carbide mesoporous support will also be studied.

V.A.11 Development of Corrosion Resistant Carbon Support for Ultra-Low Platinum Group Metal Catalysts

Greenway Energy, LLC
301 Gateway Dr., Suite 169
Aiken, SC 29083

Carbon is used as a support material for both anode and cathode catalysts in state-of-the-art PEM fuel cells. Carbon support is susceptible to corrosion under the cathode operating conditions such as presence of oxygen and water, low pH, and high potential at the cathode interface. Corrosion of state-of-the-art carbon supports is inevitable, which leads to platinum catalyst particle detachment from the support and subsequent poor performance. Hence, modifications to the carbon supports that make them more corrosion resistant are of great importance to achieve the DOE targets. Phase I of this project will focus on the synthesis of a corrosion resistant carbon (CRC) support and Pt/CRC and Pt-alloy/CRC catalysts. A commercially available carbon will be subjected to various treatments to tailor the physical properties such as the specific surface area, pore size distribution, and hydrophilicity/hydrophobicity without sacrificing the electronic conductivity. Surface functionalization using an inexpensive bifunctional additive helps achieve uniform catalyst particle distribution and enhances catalyst/support interaction, which is critical for PEM fuel cells operating under transient conditions.

XI.1 Metal Hydride Material Development for High Efficiency and Low Cost Hydrogen Compressors

Greenway Energy, LLC
301 Gateway Dr., Suite 169
Aiken, SC 29083

Phase I of this project was awarded in FY 2017 and involved thermodynamic and technoeconomic analyses to identify key performance characteristics that metal hydride materials must achieve to be viable in cost-competitive high-pressure (875 bar) hydrogen compression. The team additionally explored the potential for cantilever beams to enable high-throughput characterization of metal hydride properties and began development of machine learning models that may predict enthalpy and entropy of metal hydride alloys that work at specified temperatures and pressures.

XI.2 Over-Molded Plates for Reduced Cost and Mass PEM Fuel Cells

American Fuel Cell
1200 Ridgeway Ave., Suite 123
Rochester, NY 14615

Development of low-cost bipolar plates for use in PEM fuel cells is critical for large-scale deployment of clean fuel cell technology. The main goal of this project is development of a low-cost bipolar plate with reduced mass by utilizing a plastic frame in the non-active regions. The development will be constrained with a design for roll-to-roll manufacturing that reduces diffusion layer stiffness constraints with narrow flow channels. The Phase I effort will focus on demonstrating the validity of the underlying concepts through design in concert with fuel cell transport and injection molding experts. Additionally, various configurations and sequences of coating all layers of the fuel cell will be investigated using the flow field as the primary carrier. Ultimately, a unitized and fully bonded fuel cell with plastic headers will result.

XI.3 Emergency Hydrogen Refueler for Individual Consumer Fuel Cell Vehicles

Reactive Innovations, LLC
2 Park Drive, Unit 4
Westford, MA 01886

Reactive Innovations, LLC, is developing an emergency hydrogen refueler to be stored in the trunk of fuel cell powered vehicles. Especially in the early stage of commercial release of hydrogen fuel cell vehicles, the sparsity of hydrogen fueling stations is expected to lead to "range anxiety." This refueler will help lessen range anxiety that consumers feel by offering them assurance of reaching a fueling station. The system will contain a hydrogen-rich solid material, which reacts with water to produce hydrogen on demand. The system will be able to be safely stored within the vehicle, to be taken out and used when needed to provide sufficient hydrogen to reach the nearest hydrogen fueling station.

PHASE II PROJECTS

XI.4 Novel Hydrocarbon Ionomers for Durable Proton Exchange Membranes

NanoSonic, Inc.
158 Wheatland Drive
Pembroke, VA 24136-3645

The objective of this project is to develop and demonstrate high-temperature hydrocarbon-based membranes with the chemical, thermal, and mechanical properties necessary to qualify for the demanding environments within a fuel cell vehicle. The approach involves the synthesis of novel high-molecular-weight aromatic hydrocarbon membranes that possess polar moieties along the polymer backbone and pendant quaternary ammonium groups. During the Phase II project, a series of novel phosphoric-acid-imbibed poly (thioether benzonitrile) copolymers shall be evaluated per DOE's 2020 technical targets for membranes for transportation applications. Specifically, the synthesized polymers will be chemically tailored to contain the ideal balance of ion exchange capacities and ionically doped phosphoric acid to demonstrate safe and reliable energy generation. The ionomers will be down-selected, transitioned from a technology readiness level of 3 to 7, and presented to PEM fuel cell manufacturers and integrators with a detailed integration design plan and cost analysis. The fully integrated PEM fuel cell system will be demonstrated as compliant with DOE's 2020 technical targets for MEAs for transportation applications, positioning the PEM fuel cells as environmentally friendly alternatives to internal combustion engines.

II.B.7 New Approaches to Improved PEM Electrolyzer Ion Exchange Membranes

Tetramer Technologies, LLC
657 S. Mechanic Street
Pendleton, SC 29670

Tetramer Technologies, LLC, has developed a new membrane molecular architecture that has demonstrated equivalent or better performance compared to the current Nafion materials at 50% lower cost. These attributes directly address the high electrolyzer cost and performance issues. Key attributes of Tetramer's technology versus the current Nafion electrolyzer membranes are improved physical performance properties, 50% lower hydrogen permeability, and equal or higher conductivity. This technology will provide thinner membranes, which can lower costs and increase performance directly through decreased ionic resistance and indirectly through the reduction of the overall cell potential. Tetramer's membranes can also provide 50% less hydrogen crossover loss, thus improving the electrolyzer yield and lowering costs.

XI.5 Flexible Barrier Coatings for Harsh Environments

GVD Corp.
45 Spinelli Place
Cambridge, MA 02138

Phase II of this project was awarded in 2016, and the project was further selected for a Phase IIA award in FY 2017. This project has focused on the development of a multi-layer vapor deposition approach to deposit coatings on top of compressor seals. These coatings are meant to enhance the resistance of seals to friction and to mitigate hydrogen ingress, therein increasing reliability. Seals are a common point of failure for reciprocating compressors, and GVD aims to enable a seal life of at least 8,000 h. In Phase IIA, they will optimize the thicknesses of their seal coatings, along with the deposition process, and test coating performance in relevant environments.

XI.6 Cryogenically Flexible, Low Permeability Thoraeus Rubber H_2 Dispenser Hose

NanoSonic, Inc.
158 Wheatland Drive
Pembroke, VA 24136

In FY 2017, NanoSonic conducted R&D to develop a low-cost, reliable hydrogen dispensing hose under an SBIR Phase II award. Dispensing hoses today fall short of DOE reliability and cost targets and are manufactured outside of the United States. NanoSonic's prototype is being designed for resistance to hydrogen embrittlement, flexibility under the low temperatures (-40°C) and high pressures (875 bar) of hydrogen dispensing, durability under consistent customer use, and manufacturability at large scales in the United States. The hose utilizes a novel polymer that is wrapped in carbon fiber and is infused with a ceramer at the ends that enables the hose to tolerate high-strength crimps. Carbon fiber winding patterns for maximum hose strength have been developed from extensive modelling and experimental testing in Phase II. In FY 2017, NanoSonic was also selected for a Phase IIB award, wherein they will develop a hose fitting that would enable evaluation of the hose›s mechanical properties and would ultimately enable integration of the hose with a dispenser.

XI.7 Low Cost Alloys for Magnetocaloric Refrigeration

General Engineering & Research LLC
10459 Roselle St. Suite A
San Diego, CA 92121

Phase I of this project was awarded in FY 2016 and evaluated the cooling capacity of low-cost rare earth alloys to assess their potential for use in hydrogen liquefaction. The team identified and filed a patent on a novel class of alloys and also determined that micro- or nano-grained structuring can lower material synthesis times, thereby reducing cost. In FY 2017, the project was selected for a Phase II award, in which they optimized the structuring approach and tune the compositions of their patent-pending alloy class for specific temperature ranges of interest to hydrogen liquefaction.

XII. Acronyms, Abbreviations, and Definitions

~	Approximately
@	At
°C	Degrees Celsius
°F	Degrees Fahrenheit
Δ	Change, delta
$\Delta H°_{des}$	Desorption enthalpy
ΔK	Stress intensity factor
ΔP	Pressure drop, pressure change
≈	Equals approximately
>	Greater than
≥	Greater than or equal to
<	Less than
≤	Less than or equal to
µm	Micrometer(s), micron(s)
η	Viscosity
#	Number
Ω	Ohm(s)
Ω/cm^2	Ohm(s) per square centimeter
$\Omega\text{-}cm^2$	Ohm-square centimeter
%	Percent
®	Registered trademark
$	United States dollars
^{11}B-NMR	Nuclear magnetic resonance of boron with mass number 11
^{19}FNMR	Nuclear magnetic resonance of fluorine with mass number 19
1-D, 1D	One-dimensional
1Q	First quarter of the fiscal year
2-D, 2D	Two-dimensional
2Q	Second quarter of the fiscal year
3-D, 3D	Three-dimensional
3Q	Third quarter of the fiscal year
4D	Four-dimensional
4Q	Fourth quarter of the fiscal year
6PGDH	6-phosphogluconate dehydrogenase
9MeTTP+	tris(2,4,6-trimethylphenyl) phosphonium
9MeOTTP+	tris(2,4,6-trimethoxyphenyl) phosphonium
A	Ampere(s), amp(s)
A	Alkali
Å	Angstrom(s)
Abs	Absolute
AC	Activated carbon; Alternating current
A/cm^2	Amp(s) per square centimeter
AD	Adsorption; Adsorbent; Anode dew point; Atomically dispersed
ADF	Annular dark-field imaging
AE	Acceptability envelope; Acoustic emissions
Ae	Alkaline earth
AEM	Anion exchange membrane; Analytical electron microscopy
AEMFC	Anion exchange membrane fuel cell
AEO	Annual Energy Outlook
AF1	Autofrettage option 1
AF2	Autofrettage option 2
AFCB	American Fuel Cell Bus Project
Ag	Silver
A-h	Amp-hour(s)
AHJ	Authority having jurisdiction
AHMF	Advanced Hydrogen Mobile Fueler
AHP	Absorption heat pump
AK	Alkali
a.k.a.	Also known as
Al	Aluminum
Al*	Aluminum particles catalyzed with titanium
Al-AB	Aluminum-ammonia-borane
$AlCl_3$	Aluminum chloride
ALD	Atomic layer deposition
AlH_3	Aluminum hydride; Alane
Al_2O_3	Aluminum oxide
ALS	Advanced Light Source at Lawrence Berkeley National Laboratory
ALT	Accelerated life test
A/m^3	Amp(s) per cubic meter
AMBER	Advanced Materials Beamline for Energy Research at Advanced Light Source
AMBH	Ammine metal borohydride
AMFC	Anion exchange membrane fuel cell; Alkaline membrane fuel cell
AMR	U.S. Department of Energy Hydrogen and Fuel Cells Annual Merit Review; Active magnetic regenerator
ANL	Argonne National Laboratory
ANSI	American National Standards Institute
API	American Petroleum Institute
APS	Advanced Photon Source
APU	Auxiliary power unit

AP-XPS	Ambient pressure X-ray photoelectron spectroscopy
Ar	Argon
As	Arsenic
ASME	American Society of Mechanical Engineers
ASPEN	Modeling software, computer code for process analysis
ASR	Area-specific resistance; areal surface resistance
AST	Accelerated stress test; DOE Accelerated Stability Test
ASTM	ASTM International, originally known as the American Society for Testing and Materials
at%	Atomic percent
A&TM	Atomistic and thermodynamic modeling
atm	Atmosphere(s)
atmA	Atmosphere(s) pressure, absolute
ATM-PP	Benzyl trimethyl ammonium functionalized Diels-Alder poly(phenylene)
ATO	Antimony-doped tin oxide
ATP	Acceptance test procedure; Adenosine triphosphate; Advanced Technology Program
a.u.	Arbitrary units
Au	Gold
AuS	Gold sulfide
Avg	Average
AWARE-US	Available water resource in the United States
B	Boron
Ba	Barium
bara	Bar absolute
BaSce	Baseline and Scenario Analysis
$B_{25}B'_{75}$	General term to describe $AB_{0.25}B'_{0.75}O_y$, perovskite composition
BCV	Benzyl viologen-derived conjugate
Be	Beryllium
BES	Basic Energy Sciences office within the DOE Office of Science
BET	Brunauer–Emmett–Teller surface area analysis method
BETO	Bioenergy Technologies Office within the U.S. Department of Energy's Office of Energy Efficiency and Renewable Energy
BEV	Battery electric vehicle
Bi	Bismuth
BJH	Barrett, Joyner, and Halenda
BM	Base metal; Ball-milled, ball mill
BN	Boron–nitrogen
BNL	Brookhaven National Laboratory
^{11}B-NMR	Nuclear magnetic resonance of boron with mass number 11
BOC	Best of class
$B(OH)_3$	Boric acid
BOL, BoL	Beginning of life
BOP, BoP	Balance of plant
BOT	Beginning of test
BP	Budget Period; Bisphenol; Biphenyl
BP1	Budget Period 1
BP2	Budget Period 2
BP-Ar	Perfluoroalkylsulfonate polymer
BPV	Boiler and pressure vessel
BPVC	Boiler and Pressure Vessel Code
Br	Bromine
BTU, Btu	British thermal unit(s)
BV	Benzyl viologen
BY	Brewer's yeast
C	Carbon; Coulomb
C5	Five-carbon sugar
C6	Six-carbon sugar
ca.	About, approximately
Ca	Calcium
CAD	Computer-aided design; computer aided drawing
CaFCP	California Fuel Cell Partnership
cal	Calorie(s)
CalTech	California Institute of Technology
CAN	Controller area network
CARB	California Air Resources Board
CaS	Calcium sulfide
CBET	Division of Chemical, Bioengineering, Environmental, and Transport Systems
CBS	Casa Bonita strain; Complete basis set
cc	Cubic centimeter(s)
CCAT	Connecticut Center for Advanced Technology, Inc.
CcH_2	Cryo-compressed hydrogen
CCL	Cathode catalyst layer
CCM	Catalyst-coated membrane; Coordinate measuring machine
Cc/min, ccm	Cubic centimeter(s) per minute
CCSI	Continuous Codes and Standards Improvement
Cd	Cadmium

CD	Current density; Compact disk; Charge depleting; Cathode dewpoint
CDP	Composite data product
Ce	Cerium
CEC	California Energy Commission
CEMI	Clean Energy Manufacturing Initiative
CeO_2	Ceric oxide
CF	Carbon fiber
CFD	Computational fluid dynamics
cfm	Cubic feet per minute
cH_2	Compressed hydrogen gas
CH_4	Methane
CHEX	Cold heat exchanger
CHG	Compressed hydrogen gas
CHP	Combined heat and power
CI	Cathode interlayer
CIDI	Compression ignition direct injection
CIS	CuInSe (alloy of copper, indium, and selenium)
CKAN	Comprehensive Knowledge Archive Network
Cl	Chlorine
CL	Catalyst layer
cm	Centimeter(s)
cm^2	Square centimeter(s)
CMK3	Nanoporous carbon prepared with SBA-15
CMU	Carnegie Mellon University
CNF	Carbon nano-fiber
CNG	Compressed natural gas
CNGV	Compressed natural gas vehicle
CNT	Carbon nanotube
CNxPY	Doped carbon nano-structures
Co	Cobalt
CO	Carbon monoxide
CO_2	Carbon dioxide
COD	Chemical oxygen demand
CoE	Center of Excellence
COP	Cooefficient of performance
COPV	Composite overwrapped pressure vessel
cP	Centipoise
CP	Cross polarization
CPA	Coherent potential approximation
CPMAS	Cross polarization magic angle spinning
CPR^2	Cascading pressure receiver reactor
c.p.s.	Counts per second
CPU	Computer processing unit
CPV	Composite pressure vessel
Cr	Chromium
CRADA	Cooperative Research and Development Agreement
Cs	Cesium
C&S	Codes and standards
CSA	Canadian Standards Association
CSL	Corn steep liquor
CSM	Colorado School of Mines; Combined structure & material
CSU	California State University
CSULA	California State University, Los Angeles
CSV	Comma separated values
CT	Computed tomography
CTE	Coefficient of thermal expansion; Center for Transportation and the Environment
CTL	Cryogenics Test Laboratory
Cu	Copper
CU	University of Colorado
cu in.	Cubic inch(es)
cu. yd.	Cubic yard(s)
CV	Cyclic voltammatry; Cyclic voltammogram
CVD	Chemical vapor deposition
CVP	Cold vapor pressure
CWG	Catalysis Working Group
CZO	Ceria-zirconia
d	Day(s)
D_2	Deuterium
D-A	Dubinin-Astakhov
DAC	Direct air cooling; Data acquisition and control system
da/dN	Fatigue crack growth rate
DAE	Diels-Alder ether
DAPP	Diels-Alder poly(phenylene)
DAQ	Data acquisition
DARPA	Defense Advanced Research Projects Agency
DC	Direct current
DDCA	Durability descriptor calculation automation
Deg	Degree(s)
ΔG	Gibbs free energy of reaction
ΔH	Enthalpy of reaction; Enthalpy of hydrogenation
ΔK	Stress intensity factor
ΔP	Pressure drop; Pressure change
DFC®	Direct fuel cell
DFM	Design for manufacturing

DFMA®	Design for Manufacturing and Assembly
DFT	Density functional theory
DG	Distributed generation
DHLA	Dihydrolipoic acid
DI	Diaphorase; Direct injection; Deionized; De-ionized water
DMA	Dynamic mechanical analysis
DME	Dimethyl ether
DMEA	Dimethlethylamine
DMEAA	Dimethlethylamine alane
DMF	n, n-di-methyl formamide
DMFC	Direct methanol fuel cell
DMR	De-acetylation and mechanically refined
DMTA	Dynamic mechanical thermal analysis
DOD	U.S. Department of Defense
DOE	U.S. Department of Energy
DOT	U.S. Department of Transportation
DOT/NHTSA	U.S. Department of Transportation National Highway Traffic Safety Administration
DP	Dew point
DPMAS	Direct polarization magic angle spinning
D-R	Dubinov-Radushkevich
DRIFTS	Diffuse reflectance infrared Fourier transform spectroscopy
DSC	Differential scanning calorimetry
DSM™	Dimensionally stable membrane
DSM 1313	Deutsche Sammlung von Mikroorganismen 1313 strain of C. thermocellum
DSM-MC	Distance scaling method Monte Carlo
DSRC	Dedicated short-range wireless communication
e^-	Electron
E	Activation energy, kJ/mol; Potential
E85	Fuel blend consisting of 85% ethanol and 15% gasoline
E_a	Activation energy
EC	Electrochemical capacitance
ECA	Electrochemical surface area
ECS	Engineered carbon support
ECSA	Electrochemically active surface area; Electrochemical surface area
EDC	Energy distribution curve
EDPM	Ethylene propylenediamene
EDS	Energy dispersive X-ray spectroscopy; Energy dispersive spectrum
EDX	Energy dispersive X-ray
EELS	Electron energy loss spectroscopy
EENW	Emerald Energy NW, LLC
EF	Emission factor
e.g.	*Exempli gratia*: for example
EG	Ethylene glycol
EGR	Exhaust gas recirculation
eGRID	Emissions & Generation Resource Integrated Database
EH	Electrochemical hydrogen
EHC	Electrochemical hydrogen compressor; Ethylperhydrocarbazole
EIA	Energy Information Administration of the U.S. Department of Energy
EIS	Electrochemical impedance spectroscopy
EISA	Evaporation induced self assembly
EISF	Elastic incoherent structure factor
ELAT®	Registered trademark of De Nora North America, Inc., covers gas diffusion layers and gas diffusion electrodes
ENG	Expanded natural graphite
EOD	Electro-osmotic drag
EOL, EoL	End of life
EOS	Economies of scale
EOT	End of test
EP	Economic potential
EPA	U.S. Environmental Protection Agency
EPDM	Ethylene propylene diene monomer
EPIC	Energy Policy Institute of Chicago
EPMA	Electron probe micro analyzer
EPR	Electron paramagnetic resonance
EQCM	Electrochemical quartz crystal microbalance
eREV	Extended range electric vehicle
ESIF	Energy Systems Integration Facility
et al.	*Et Alii:* and others
ETC	Electron transport chain
etc.	*Et cetera*: and so on
ETFECS	Extended thin-film electrocatalyst structures
EU	European Union
eV	Electron volt(s)
EV	Electric vehicle
EVOH	Ethylene vinyl alcohol
EW	Equivalent weight
EXAFS	Extended X-ray absorption fine structure analysis
F	Fluorine; Faraday constant, the amount of electric charge in one mole of electrons (96,485.3383 coulomb/mole)
F_6PBI	Hexafluoro polybenzimidazole

FA	Formic acid
FC	Fuel cell
FCB	Fuel cell bus
FCE	FuelCell Energy
FCEB	Fuel cell electric bus
FCEV	Fuel cell electric vehicle
FCGR	Fatigue crack growth rate
FCHEA	Fuel Cell Hydrogen Energy Association
FCH JU	Fuel Cells and Hydrogen Joint Undertaking
FC-PAD	Fuel Cell Performance and Durability Consortium
FCPP	Fuel cell power plant
FCRx200	Fuel cell range extended plug-in hybrid utility vehicle
FCS	Fuel cell system
fct	Face-centered tetragonal
FCTO	Fuel Cell Technologies Office within the U.S. Department of Energy's Office of Energy Efficiency and Renewable Energy
FCTT	Fuel Cell Technical Team
FCV	Fuel cell vehicle
Fd	Ferredoxin
Fe	Iron
FE	Finite element; U.S. Department of Energy's Office of Fossil Energy
FEA	Finite element analysis
FER	Fluoride emission rate
FLUENT	Computer code for computational fluid dynamics
FMEA	Failure modes and effects analysis
^{19}FNMR	Nuclear magnetic resonance of fluorine with mass number 19
FOA	Funding opportunity announcement
FOM	Figure of merit
FPGA	Field-programmable gate array
ft	Feet
ft^2	Square feet
ft^3	Cubic feet
FTA	Federal Transit Administration of the U.S. Department of Transportation
FTATR	Fourier transform attenuated total reflection
FT-IR, FTIR	Fourier transform infrared
FY	Fiscal year
g	Gram; Acceleration of gravity
G	Graphite
G6P	Glucose 6-phosphate
G6PDH	Glucose 6-phosphate dehydrogenase
Ga	Gallium
gal	Gallon(s)
GB	Gigabyte(s)
GC	Glassy, or vitreous carbon; a pure carbon that is amorphous (non-crystalline)
g/cc	Gram(s) per cubic centimeter
GCMC	Grand Canonical Monte Carlo
GCMS	Gas chromatograph-mass spectroscopy
Gd	Gadolinium
GDE	Gas diffusion electrode
GDL	Gas diffusion layer
GDS	Galvanodynamic scan
Ge	Germanium
Gen	Generation
Gen 1, GEN I	First generation
Gen 2, GEN II	Second generation
Gen 3, GEN III	Third generation
GGE, gge	Gasoline gallon equivalent
GH_2	Gaseous hydrogen
GHG	Greenhouse gas
GISAXS	Grazing-incidence small-angle X-ray scattering; Grazing-incidence small-angle X-ray spectroscopy
GJ	Gigajoule(s)
g/kW	Gram(s) per kilowatt
GLWN	Westside Industrial Retention & Expansion Network
gm	Gram(s)
GM	General Motors
gm/d	Gram(s) per day
g/min	Gram(s) per minute
GNG	Go/no-go
GNR	Graphene nanoribbon
GPa	Gigapascal(s)
GPRA	Government Performance and Results Act
gps	Gram(s) per second
GrC	Graphetized carbon
GREET	Greenhouse gases, Regulated Emissions and Energy use in Transportation model
g/s	Gram(s) per second
GTI	Gas Technology Institute
GTR	Global Technical Regulation
GUI	Graphical user interface

GWe, GW_e	Gigawatt(s) electric
h	Hour(s)
H	Hydrogen
H+	Proton
H^-	Hydride
H_2	Diatomic hydrogen
H2@Scale	A concept that explores the potential for wide-scale hydrogen production and utilization in the United States
H2A	Hydrogen Analysis project sponsored by DOE
H2FAST	Hydrogen Financial Analysis Scenario Tool
H2I	Hawaii Hydrogen Initiative
H_2O	Water
H_2O_2	Hydrogen peroxide
H_2S	Hydrogen sulfide
H2SCOPE	Hydrogen Station Cost Optimization and Performance Evaluation
H_2SO_4	Sulfuric acid
H2USA	Hydrogen Technology Learning Centers (for California, Florida, and New York)
H2VGI	Hydrogen–vehicle–grid integration model
HAADF	High-angle annular dark field
HAADF-STEM	High-angle annular dark field scanning transmission electron microscopy
HA-FCG	Hydrogen accelerated fatigue crack growth
HAZ	Heat-affected zone
HAZOP	Hazards and Operational Safety Analysis
HC	Hydrocarbon; High concentration
HCD	High current density; Hydrogen contaminant detector
HCl	Hydrochloric acid
HDFCV	Heavy-duty fuel cell vehicle
HDPE	High-density polyethylene
HDSAM	Hydrogen Delivery Scenario Analysis Model
HDTT	Hydrogen Delivery Technical Team
He	Helium
HER	Hydrogen evolution reaction
HEX	Heat exchanger
Hf	Hafnium
HFCEV	Hydrogen fuel cell electric vehicle
HFR	High-frequency resistance
HFSF	High-flux solar furnace
HGV	Hydrogen gaseous vehicle
HHC	Hawaii Hydrogen Carriers
HHV	Higher heating value
HiPoD	High power density
HITRF	Hydrogen Infrastructure Testing and Research Facility
HKUST	1 Cu_3(1,3,5-benzenetricarboxylate)$_2$
HMPA	Hexamethylphosphoramide
HOR	Hydrogen oxidation reaction
HOV	High occupancy vehicle
hp	Horsepower
HP	High pressure
HPA	Heteropoly acid
HPC	High pressure cell; Highly porous carbon
hr	Hour(s)
HRL	Hughes Research Laboratory, HRL Laboratories, LLC
HRS	Hydrogen refueling stations
HRSAM	Hydrogen refueling station analysis model
HR-STEM	High resolution scanning transmission electron microscopy
HRT	Hydraulic retention time
HR-TEM	High resolution transmission electron microscopy
HSA	High surface area
HSAC	High surface area carbon
HSC	High surface area carbon
HSECoE	Hydrogen Storage Engineering Center of Excellence
HT	High throughput; High temperature; Heat-treatment/thermal annealing
HTAC	Hydrogen and Fuel Cell Technical Advisory Committee
HTPEM	High-temperature polymer electrolyte membrane
HTWS	High temperature water splitting
HVAC	Heating, ventilation and cooling
HX	Heat exchanger
HyMARC	Hydrogen Storage Materials Advanced Research Consortium
HyRAM	Hydrogen Risk Assessment Models
HyROC-1	pH Matter's down-selected proprietary catalyst with no Pt
HyS	Hybrid sulfur
HySCORE	Hydrogen Storage Characterization and Optimization Research Effort
HyStEP	Hydrogen Station Equipment Performance
HyVS	Hydrogen Vehicle Simulator
Hz	Hertz
i	Current density (mA/cm^2)

I2CNER	International Institute for Carbon-Neutral Energy Research
IACMI	Institute for Advanced Composite Manufacturing Innovation
I/C	Ionomer to carbon ratio; Ionomer to catalyst
ICE	Internal combustion engine
ICP	Inductively coupled plasma
ICP-MS, ICP/MS	Inductively coupled plasma mass spectrometry
ICP-OES	Inductively coupled plasma optical emission spectroscopy
iCVD	Initiated chemical vapor deposition
ID	Inside diameter
i.e.	*id est*: that is
IEA	International Energy Agency
IEC	International Electrotechnical Commission; Ion exchange capacity, milliequivalents of acid groups per gram of material
IEEE	Institute of Electrical and Electronics Engineers, Inc.
IL	Ionic liquid
IMM	Inverted metamorphic multijunction
In	Indium
In., in	Inch(es)
in^2	Square inch(es)
INL	Idaho National Laboratory
INTEGRATE	Integrated Network Testbed for Energy Grid Research and Technology Experimentation
IPA	Isopropyl alcohol
IR	Infrared
IR, iR	Internal resistance
Ir	Iridium
IrDA	Infrared Data Association
IRIG	Inter-Laboratory Research Integration Group
IRMOF	Isoreticular metal organic framework
ISO	International Organization for Standardization
ISO/TC197	International Standards Organization Technical Committee 197
IV, iV	Current-voltage
J	Joule(s)
JARI	Japan Automobile Research Institute
JMC	Japan Metals and Chemicals
JPL	Jet Propulsion Laboratory
JRC	Joint Research Centre
J-V, JV	Current density-voltage
K	Sievert's constant, ml/[cm^2-min-atm½]; Kelvin, absolute temperature; Potassium
kÅ	1,000 angstroms
kA/m^2	Kilo-ampere(s) per square meter
kb	Kilo-base pair, a unit of measurement used in genetics equal to 1,000 nucleotides
KBr	Potassium bromide
kcal	Kilocalorie(s)
kcal/mol	Kilocalorie(s) per mole
kg	Kilogram(s)
kg/d	Kilogram(s) per day
kg/hr	Kilogram(s) per hour
kg/m^3	Kilogram(s) per cubic meter
KH	Potassium hydride
kHz	Kilohertz
kJ	Kilojoule(s)
KJ300	Ketjen Black EC 300J, a high surface-area carbon support
kJ/mol	Kilojoule(s) per mole
km	Kilometer(s)
kMC	Kinetic Monte Carlo
KODTE	Knock-on displacement threshold energy
KOH	Potassium hydroxide
kPa	Kilopascal(s)
kph	Kilometer(s) per hour
ksi	1,000 pounds-force per square inch
kT/y	Kiloton(s) per year
kW	Kilowatt(s)
kWe, kW_e	Kilowatt(s) electric
kWh	Kilowatt-hour(s)
kWh/kg	Kilowatt-hour(s) per kilogram
kWh/L	Kilowatt-hour(s) per liter
kW/kg	Kilowatt(s) per kilogram
kWt	Kilowatt(s) thermal
L, l	Liter(s), length
La	Lanthanum
LAG	Liquid assisted grinding
LANL	Los Alamos National Laboratory
lb	Pound(s)
LBL	Lawrence Berkeley National Laboratory
lbmol	Pound-mole(s)
LBNL	Lawrence Berkeley National Laboratory
LCA	Life cycle assessment; Life-cycle analysis
LCD	Low current density
L/D	Length-to-diameter ratio
LDV	Light-duty vehicle

LEIS	Low-energy ion scattering
L/h, l/h	Liter(s) per hour
LH2, LH_2	Liquid hydrogen
LHV	Lower heating value
Li	Lithium
LiOH	Lithium hydroxide
LLC	Limited Liability Company
LLNL	Lawrence Livermore National Laboratory
L/min, l/min	Liter(s) per minute
LMRC	Linear motor reciprocating compressor
LP	Low pressure
LPG	Liquefied petroleum gas
LPM	Liter(s) per minute
LT	Low-temperature
m	Meter(s)
M	Mole(s), molar; Million
m^2	Square meter(s)
m^3	Cubic meter(s)
m^2/g	Square meter(s) per gram
m^2/s	Square meter(s) per second
µA	Microampere(s)
mA	Milliampere(s)
MA	Mass activity
$\mu A/cm^2$	Microampere(s) per square centimeter
mA/cm^2	Milliampere(s) per square centimeter
MAE	Modal acoustic emissions
MAS	Magic angle spinning
MAS ^{11}B-NMR	Magic angle spinning boron-11 nuclear magnetic resonance spectroscopy
MAS NMR	Magic angle spinning nuclear magnetic resonance
MASC	Multi-acid side chain
MATI	Modular adsorption tank insert
MAWP	Maximum allowable working pressure
MB	Megabyte(s)
mbar	Millibar
MBRC	Miles between roadcall
MC	Monte Carlo; Metal carbide
MCF	Mesostructured cellular foam
MCHL	Magnetocaloric hydrogen liquefier
µCHP	Micro-combined heat and power
MCM	Mobile crystalline material
MCP	Microchannel plate
MD	Molecular dynamics
m-dobdc^{4-}	4,6-Dioxido-1,3-benzenedicarboxylate
MDR	Manufacturer's design report
MEA	Membrane electrode assembly
MEC	Microbial electrolysis cell; Minimum explosive concentration
MFC	Microbial fuel cell; Mass flow controller
µg	Microgram(s)
mg	Milligram(s)
MGCLP	Multi-gas canonical linear programing
mg/cm^2	Milligram(s) per square centimeter
MH	Metal hydride
MHC	Metal hydride-based compressor
MHDV	Medium- and heavy-duty vehicle
MHz	Megahertz
mi	Mile(s)
mi/kg	Mile(s) per kilogram
mil	Millimeter(s)
min	Minute(s); Minimum
MJ	Megajoule(s)
mL, ml	Milliliter(s)
ML	Monolayer
MLI	Multi-layer vacuum insulation
MLS	Milestone
µm	Micrometer(s); micron(s)
µM	Micromolar
mM	Millimolar
mm	Millimeter(s)
mmol	Millimole(s)
µmol	Micromole(s)
MMT	Million metric tonne(s)
Mn	Manganese
MnO	Manganese oxide
mΩ	Milli-ohm(s)
MΩ	Mega-ohm(s)
$m\Omega/cm^2$	Milli-ohm(s) per square centimeter
$\mu\Omega\text{-}cm^2$	Micro-ohm(s) - square centimeter
Mo	Molybdenum
MOF	Metal-organic framework
mol	Mole(s)
MOL	Middle of life
mol%	Mole percent
mol/min	Mole(s) per minute
MoP	Molybdenum phosphide
MPa	Megapascal(s)
MPG, mpg	Mile(s) per gallon
mph	Mile(s) per hour

ms	Millisecond(s)
MSAC	Mid-range carbon support; Medium surface area carbon
MSC	Medium surface area carbon
mS/cm	Milli-Siemen(s) per centimeter
MSU	Montana State University
MT	Mass transfer
mtorr	Millitorr
MTPD	Metric tonne(s) per day
MTU	Michigan Technological University
µV	Microvolt(s)
mV	Millivolt(s)
mW	Milliwatt(s)
MW	Megawatt(s); Molecular weight
mW/cm^2	Milliwatt(s) per square centimeter
MWCNT	Multiple-wall carbon nanotube
MWe	Megawatt(s) electric
MWh	Megawatt-hour(s)
MYRDD, MYRD&DP	Multi-Year Research, Development, and Demonstration Plan
N	Nitrogen atom; Newton (unit of force)
N112	Nafion® 1100 equivalent weight, 2 millimeter thick membrane
Na	Sodium
NA	North American; Not applicable
NaCl	Sodium chloride
NAD	Nicotinamide adenine dinucleotide
NADH	(reduced) Nicotinamide adenine dinucleotide
NADP	Nicotinamide adenine dinucleotide phosphate
NADPH	Nicotinamide adeninine dinucleotide phosphate
Nafion®	Registered trademark of E.I. DuPont de Nemours
NASA	National Aeronautics and Space Administration
NAU	Northern Arizona University
Nb	Niobium
NBR	Nitrile butyl rubber
NC	Nanocrystals; Nano-carbon; Nanocomposite
N/cm^2	Newton(s) per square centimeter
NCMK3	CMK3 carbons containing nitrogen
NDA	Non-disclosure agreement
NDC	New delivery concept; Naphthalene-2,6-dicarboxylate
nDDB	n-Dodecyl benzene
NDE	Non-destructive examination
NDP	Neutron depth profiling
NDTE	Non-destructive testing and evaluation
NE	U.S. Department of Energy's Office of Nuclear Energy, Science and Technology
NEB	Nudged elastic band
NEF	n-Ethylformamide
NEI	National Emission Inventory
NETL	National Energy Technology Laboratory
NEU	Northeastern University
NEXAFS	Near edge X-ray absorption fine structure
NFCRC	National Fuel Cell Research Center
NFCTEC	National Fuel Cell Technology Evaluation Center, at National Renewable Energy Laboratory
NFPA	National Fire Protection Association
NG	Natural gas
NGO	Non-government organization
NGV	Natural gas vehicle
NH_3	Ammonia
NHFCCSCC	National Hydrogen and Fuel Cells Codes and Standards Coordinating Committee
Ni	Nickel
NIST	National Institute of Standards and Technology
nm	Nanometer(s)
nmol	Nanomole(s)
NMR	Nuclear magnetic resonance
NMSU	New Mexico State University
NNIF	NIST Neutron Imaging Facility
NNPC	Nitrogen-doped nanopourous carbons
NO_2	Nitric oxide
NOx, NO_x	Oxides of nitrogen
NP	Nanoparticle
NPC	Nanoporous carbon
NPTF	Nanoporous thin film
NPV	Net present value
NR211	Nafion® 211 membrane
NR212	Nafion® 212 membrane
NREL	National Renewable Energy Laboratory
NROR	NADPH rubredoxin oxidoreductase
NRVS	Nuclear resonance vibrational spectroscopy
NSF	National Science Foundation
NSTF	Nanostructured thin film
NT	Nanotube
NTCNA	Nissan Technical Center, North America
NUWC	Naval Underwater Warfare Center

NW	Nanowire
Ω	Ohm(s)
Ωcm^2	Ohm(s) - square centimeter
O	Oxygen
O_2	Diatomic oxygen
OCV	Open-circuit voltage
o.d., OD	Outer diameter
OEM	Original equipment manufacturer
OER	Oxygen evolution reaction
OFCC	Ohio Fuel Cell Coalition
O&M	Operation and maintenance
ORNL	Oak Ridge National Laboratory
ORR	Oxygen reduction reaction
P	Phosphorus; Pressure
Pa	Pascal(s)
PAA	Poly(acrylic acid)
PADD	Petroleum Administration for Defense District
PAN	Peroxyacetyl nitrate; Polyacrylonitrile
PANI	Polyaniline
PAN-MA	Polyacrylonitrile with methyl acrylate
PA/PBI	Phosphoric-acid-doped polybenzimidazole
Pb	Lead
PBI	Polybenzimidazole
PBPA-Br	Bromoalkyl-tethered aromatic polymer
PBS	Phosphate buffer solution
PCET	Proton-coupled electron transfer
PCI	Phase-change induced
PCT	Pressure-composition-temperature
Pd	Palladium
PD	Particle drain chamber; Pressure decay
PDOS	Partial density of state
PEC	Photoelectrochemical; Photoelectrocatalyst; Photoelectrochemical cell
PECVD	Plasma-enhanced chemical vapor deposition
PEEK	Polyether ether ketone
PEFC	Polymer electrolyte fuel cell; Proton exchange fuel cell
PEG	Polyethylene glycol
PEGS	Prototype electrostatic ground state
PEM	Proton exchange membrane; Polymer electrolyte membrane
PEMFC	Polymer electrolyte membrane fuel cell; Proton exchange membrane fuel cell
PET	Photosynthetic electron transport
PEV	Plug-in electric vehicle
PF	Perfluoro
PFD	Process flow diagram
PFIA	Perfluoroimide acid
PFICE	Perfluoro ionene chain extended
PFSA	Perfluorinated sulfonic acid, perfluorosulfonic acid, poly(fluorosulfonic acid)
PGM	Precious group metal; Platinum group metal
PHEV	Plug-in hybrid electric vehicle
P&ID	Piping and instrumentation diagram
PM	Particulate matter
PM_{10}	Particulate matter with diameter of 10 micrometers or less
$PM_{2.5}$	Particulate matter with diameter of 2.5 micrometers or less
PNNL	Pacific Northwest National Laboratory
ppb	Part(s) per billion
ppbv	Part(s) per billion by volume
PPC	Pajarito Powder
PPI	Plug Power, Inc.
ppm, PPM	Part(s) per million
PPO	Phenyl phosphine oxide
PRD	Pressure relief device
PRV	Pressure relief valve
PS	Particle source chamber; Photosystem
PSD	Particle size distribution; Pore size distribution
psi, PSI	Pound(s) per square inch
psia	Pound(s) per square inch absolute
PSU	Pennsylvania State University
Pt	Platinum
Pt/C	Platinum/carbon, carbon-supported platinum catalyst
PTFE	Teflon® – poly-tetrafluoroethylene
Pt-MC	Platinum metal carbide
Pt-TF	Platinum thin film
PTW	Pump to wheels
PV	Photovoltaic; Pressure vessel; Present value
PVD	Physical vapor deposition
PVP	Pressure vessel and piping
Q1, Q2, Q3, Q4	Quarters of the fiscal year
QD	Quantum dot
QE	Quantum efficiency
QENS	Quasielastic neutron scattering
QMC	Quantum Monte Carlo
R	Load ratio(s)
RAMAN	A spectroscopic technique

RBS	Rutherford back scattering
RCS	Regulations, codes and standards
R&D	Research and development
RDA	Rotating disk atomization
RD&D	Research, development, and demonstration
RDE	Rotating disk electrode
Re	Rhenium
RE	Rare earth metal
REMI	Regional Enconomic Models, Inc.
RF, rf	Radio frequency
RFO	Residual fuel oil
RGA	Residual gas analyzer (analysis)
rGO	Reduced graphene oxide
Rh	Rhodium
RH	Relative humidity
RHE	Reference hydrogen electrode; Reversible hydrogen electrode
ROI	Return on investment
RPI	Rensselaer Polytechnic Institute
rpm	Revolution(s) per minute
RPN	Risk priority number
RRDE	Rotating ring disc electrode
RT	Room temperature
Ru	Ruthenium
RWS	RijksWaterStaat
s	Second(s)
S	Siemen(s); Sulfur
SA	Strategic Analysis, Inc.
SAD	Selected area diffraction
SAE	SAE International, originally known as the Society of Automotive Engineers
SANS	Small angle neutron scattering
SAXS	Small angle X-ray scattering
SBA-15	Nanostructured silica template used for synthesis of carbons
SBIR	Small Business Innovation Research
Sc	Scandium
sccm, SCCM	Standard cubic centimeter(s) per minute
scfd	Standard cubic feet per day
SCFM	Standard cubic feet per minute
S/cm	Siemen(s) per centimeter
Se	Selenium
sec	Second(s)
SECA	Solid State Energy Conversion Alliance
SEF	Surface enhancement factor
SEM	Scanning electron microscopy; Scanning electron microscope; Secondary electron microscopy
SERA	Scenario Evaluation, Regionalization and Analysis
SERC	Schatz Energy Research Center
SFE	Stacking fault energy
SFR	Stagnation flow reactor
SGD	Spontaneous galvanic displacement; System gravimetric density
SHI	Soluble [FeNi]-hydrogenase 1
Si	Silicon
SI	Spark ignition; Sulfur-iodine cycle; Spectrum image
SIA	Structural Integrity Associates
Si-BH	Silicon-based borohydrides
SIU	Southern Illinois University
sL	Standard liter (0°C, 1 atm)
SLMA	Strontium- and manganese-doped $LaAlO_3$, general term to describe $Sr_xLa_{1-x}Mn_yAl_{1-y}O_3$ perovskite compositions
SLPH	Standard liter(s) per hour
SLPM; slpm	Standard liter(s) per minute
SMR	Steam methane reformer; Steam methane reforming
SMYS	Specified minimum yield strength
Sn	Tin
SNL	Sandia National Laboratories
SNLL	Sandia National Laboratory Livermore
SOA	State of the art
SOEC	Solid oxide electrolyzer cell
SOFC	Solid oxide fuel cell
SOPO	Statement of project objectives
SOTA	State of the art
SOW	Statement of work
SOx	Oxides of sulfur
S-PEEK	Sulfonated poly(ether ether ketone)
sq. in.	Square inch(es)
Sr	Strontium
SR	Stoichometric ratio
SS	Stainless steel
SSIM	4-lamp, 20 kW_{ele} solar simulator
SSM	Sacrificial support method
SSNMR	Solid-state nuclear magnetic resonance
S&T	Shell and tube
STCH	Solar thermochemical hydrogen

STD	Soon to demonstrate
STEB	Standard test evaluation bottle
STEM	Scanning transmission electron microscopy
STH	Solar-to-hydrogen
STP	Standard temperature and pressure
STTR	Small Business Technology Transfer
STWS	Solar thermal water splitting
STXM	Scanning transmission X-ray microscopy
SUNY	State University of New York
SU/SD	Start up and shut down
SUSD	Startup-shutdown
SwRI®	Southwest Research Institute®
sys/yr	Systems per year
T	Temperature
T, t	Ton, tonne
TAMU	Texas A&M University
TBD	To be determined
Te	Tellurium
TEA	Techno-economic analysis
TEM	Transmission electron microscopy
TG	Thermogravimetric
TGA	Thermal gravimetric analysis; Thermogravimetric analysis; Thermogravimetric analyzer
TGA-DSC	Thermogravimetric analysis-differential scanning calorimetry
THF	Tetrahydrofuran
Ti	Titanium
TiO_2	Titanium dioxide (anatase)
TIR	Technical information report
TKK	Tanaka Kikinzoku Kogyo K. K.
TM	Transition metal
TON	Turnover number
TOU	Time of use
TPD	Tonne(s) per day; Thermally programmed desorption; Temperature-programmed desorption
TPRD	Thermally-activated pressure relief device
TPV	Total present value; Through-plate voltage
TR	Thermal reduction chamber; Traditional reactor
TRL	Technology readiness level
TRR	Technically recoverable resource
TT/A	Technology transfer and agreement
TTN	Total turnover number
UALR	University of Arkansas at Little Rock
UAV	Unmanned aerial vehicle
UC	University of California
UCB	University of California, Berkeley
UCF	University of Central Florida
UCI	University of California, Irvine
UCLA	University of California, Los Angeles
UCONN	University of Connecticut
UGA	University of Georgia, Athens
UH	University of Hawaii
UHPR	Ultra-High-Pressure Reactor at Sandia National Laboratories
UM	University of Michigan
UNLV	University of Nevada, Las Vegas
UNM	University of New Mexico
UNM IMID	Blended imidazole-based material
UPL	Upper potential limit
UPS	United Parcel Service
UQTR	University of Québec, Trios Rivieres
U.S.	United States
USA	United States of America
USC	University of South Carolina; University of Southern California
USCAR	United States Council for Automotive Research, U.S. Cooperative Automotive Research
U.S. DRIVE	United States Driving Research and Innovation for Vehicle efficiency and Energy sustainability
UT	University of Tennessee
UTF	Ultrathin film
UTRC	United Technologies Research Center
UUV	Unmanned underwater vehicle
UV	Ultraviolet
V	Vanadium; Volt; Vulcan
VA	Vinyl acetate
VCC	Vapor compression cycle; Virginia Clean Cities at James Madison University
VDC	Volt(s) direct current
VOC	Volatile organic compound
VOC, Voc	Voltage open circuit
Vol., vol.	Volume
vol%	Volume percent
VP	Variable pressure
VT	Virginia Polytechnic Institute and State University (Virginia Tech)
W	Tungsten; Watt(s)

WaMM	Water management membrane
WAXS	Wide angle X-ray scattering
W/cm^2	Watt(s) per square centimeter
We, W_e	Watt(s) electric
WG	Working group
WG-12	Working Group 12
Wh	Watt-hour(s)
W-h/kg	Watt-hour(s) per kilogram
W-h/L, Wh/liter, Wh/L	Watt-hour(s) per liter
W/kg	Watt(s) per kilogram
W/L, W/l	Watt(s) per liter
W/m.K, W/mK	Watt(s) per meter-Kelvin (unit of thermal conductivity)
WS	Water splitting
WSU	Washington State University
wt	Weight
Wt	Watt(s) thermal
wt%, wt.%	Weight percent (percent by weight)
WTW	Well-to-wheels
XAFS	X-ray absorption fine structure
XANES	X-ray absorption near-edge spectroscopy
XAS	X-ray absorption spectroscopy
XCT, X-CT	X-ray computed tomography
XES	X-ray emission spectroscopy
XPS	X-ray photoelectron spectroscopy; X-ray photon spectroscopy; X-ray photoemission spectroscopy; X-ray photoluminescence spectroscopy
XRD	X-ray diffraction
XRF	X-ray fluorescence
Y	Yttrium
yr, YR	Year
YSZ	Yttria-stablized zirconia
ZEBA	Zero Emission Bay Area
ZEV	Zero emission vehicle
Zn	Zinc
ZnO	Zinc oxide
Zr	Zirconium

XIII. Primary Contacts Index

A

Aceves, Salvador . . . VII.B.5
Adzic, Radoslav . . . V.A.5
Ahluwalia, Rajesh . . . IV.A.1, V.E.4
Ahmed, Imran . . . X.5
Ahn, Channing . . . IV.C.7
Ainscough, Christopher . . . III.5, III.15
Allendorf, Mark . . . IV.C.1
Ardo, Shane . . . II.D.3
Autrey, Tom . . . IV.C.5
Ayers, Katherine . . . II.B.3, II.B.6

B

Barilo, Nick . . . VIII.6
Barnes, Ted . . . VII.B.3
Bigelow, Erik . . . IV.D.1
Borup, Rod . . . V.B.1
Bren, Kara . . . II.F.3
Broerman, Eugene . . . III.2
Brooks, Kriston . . . X.4
Buttner, William . . . VIII.7

C

Ceballos, Bianca . . . II.F.1
Chung, Mike . . . IV.C.8
Coppage-Gross, Jacob . . . V.A.12

D

Dameron, Arrelaine . . . V.A.15
De Castro, Emory . . . V.D.2
Denver, Jessie . . . VIII.11
Deutsch, Todd . . . II.D.1

E

Edgecombe, Brian . . . IV.D.2
Elangovan, S. (Elango) . . . II.B.8
Elgowainy, Amgad . . . III.9, IX.2, IX.8, IX.10
Eudy, Leslie . . . VII.A.2
Ewan, Mitch . . . X.1

F

Fabian, Tibor . . . IV.C.17
Fujita, Etsuko . . . II.F.6
Fullenkamp, Patrick . . . VI.4
Fultz, Brent . . . IV.C.14

G

Gaillard, Nicolas . . . II.D.2
Ganesan, Prabhu . . . V.A.11
Gennett, Thomas . . . IV.C.4
Ghezel-Ayagh, Hossein . . . VII.C.4
Goodarzi, Abas . . . X.6
Greenway, Scott . . . III.12

H

Hamdan, Monjid . . . III.11
Hanlin, Jason . . . VII.A.3
Harned, Alleyn . . . VI.3
Harrison, Kevin . . . III.7
Haug, Andrew . . . V.B.4
Hecht, Ethan . . . III.16, VIII.4
Herring, Andrew . . . V.C.2
Holladay, Jamie . . . III.6
Hovsapian, Rob . . . VII.C.3

J

Jacobson, David . . . V.E.1
James, Brian . . . II.A.1, IV.A.2, V.E.5
Jankowska, Joanna . . . II.F.2
Johnson, Terry . . . III.13

K

Kim, Yu Seung . . . V.C.6
Kimball, Brett . . . VI.5
Kongkanand, Anusorn . . . V.A.8
Kumaraguru, Swami . . . V.B.5
Kurtz, Jennifer . . . V.E.3, VII.A.1

L

LaFleur, Chris . . . VIII.10
Lalli, Jennifer . . . III.8
Levinson, Rebecca . . . IX.4
Liu, Di-Jia . . . IV.C.9
Liu, Hong . . . II.E.3
Long, Jeffrey . . . IV.C.6

M

Majzoub, E.H. . . . IV.C.10
Maness, Pin-Ching . . . II.E.1
Matter, Paul . . . V.A.10
Mayyas, Ahmad . . . VI.7

McDaniel, Anthony II.C.1
Melaina, Marc. IX.5, IX.6, IX.7, IX.11
Meneghelli, Barry. IV.D.4
Mintz, Marianne IX.1, IX.9
More, Karren V.B.2
Mukerjee, Sanjeev V.A.3
Mulder, David II.F.4, II.F.5
Muna, Alice VIII.5

O

O'Brien, James VII.D.2
Ocampo, Minette V.A.14
Odom, Sara VII.B.1
O'Shaughnessy, Shannan III.4

P

Pecharsky, Vitalij IV.C.13
Perry, Mike V.B.6
Peters, Michael II.B.1, VII.B.6
Petitpas, Guillaume III.10
Petrecky, Jim. X.2
Petri, Randy II.B.5
Pintauro, Peter V.B.7
Pivovar, Bryan V.A.6, V.C.7
Pollica, Darryl. III.14
Prakash, Amit III.3
Pratt, Joe X.3

Q

Quackenbush, Karen. VIII.8

R

Ramani, Vijay V.A.9
Rivkin, Carl VIII.1
Rockward, Tommy V.E.2, VIII.3
Ronevich, Joe III.1
Rousseau, A. IX.3
Ruth, Mark VII.D.1

S

San Marchi, Chris. IV.D.3, VIII.2
Saur, Genevieve VII.C.1
Saxena, Sam VII.C.2
Serov, Alexey V.A.2
Severa, Godwin IV.C.11
Siegel, Donald. IV.C.15
Simmons, Kevin VIII.9
Spendelow, Jacob V.A.16
Sprik, Sam VII.B.2
Stamenkovic, Vojislav V.A.4
Steinbach, Andrew V.A.7
Stephens, Thomas. IX.12

T

Terlip, Danny VII.B.4
Thornton, Matthew. IV.B.1

U

Ulsh, Michael VI.1
Urban, Jeffrey IV.C.3

V

Valente, Patrick. VI.2

W

Wagener, Earl II.B.7
Waldecker, James V.A.17
Wang, CH V.D.1
Weber, Adam V.B.3
Weimer, Alan II.C.2
Wood, Brandon. IV.C.2, IV.C.12

X

Xu, Hui II.B.2, II.B.4, V.C.4, V.D.3

Y

Yan, Yushan V.C.5
Yandrasits, Michael V.C.1
Yelvington, Paul VI.6
Yuh, Chao-Yi V.C.3

Z

Zelenay, Piotr V.A.1
Zhang, Y-H Percival II.E.2
Zidan, Ragaiy IV.B.2, IV.C.16
Zulevi, Barr. V.A.13

XIV. Hydrogen and Fuel Cells Program Contacts

Sunita Satyapal
Director
Fuel Cell Technologies Office
Office of Energy Efficiency and Renewable Energy
U.S. Department of Energy
Phone: (202) 586-2336
Email: Sunita.Satyapal@ee.doe.gov

Erika Gupta
Operations Supervisor
Fuel Cell Technologies Office
Office of Energy Efficiency and Renewable Energy
U.S. Department of Energy
Phone: (202) 586-3152
Email: Erika.Gupta@ee.doe.gov

John Vetrano
Materials Sciences and Engineering Division
Basic Energy Sciences Program
Office of Science
U.S. Department of Energy
Phone: (301) 903-5976
Email: John.Vetrano@science.doe.gov

Jai-Woh Kim
Advanced Combustion & Fuel Cells Program Manager
Office of Fossil Energy
U.S. Department of Energy
Phone: (301) 903-9448
Email: Jai-Woh.Kim@hq.doe.gov

Carl Sink
Office of Advanced Reactor Deployment
Office of Nuclear Energy
U.S. Department of Energy
Phone: (301) 903-5131
Email: Carl.Sink@nuclear.energy.gov

HYDROGEN PRODUCTION AND DELIVERY

Eric Miller
Hydrogen Production and Delivery Program Manager
Fuel Cell Technologies Office
Office of Energy Efficiency and Renewable Energy
U.S. Department of Energy
Phone: (202) 287-5829
Email: Eric.Miller@ee.doe.gov

HYDROGEN STORAGE

Ned Stetson
Hydrogen Storage Program Manager
Fuel Cell Technologies Office
Office of Energy Efficiency and Renewable Energy
U.S. Department of Energy
Phone: (202) 586-9995
Email: Ned.Stetson@ee.doe.gov

FUEL CELLS

Dimitrios Papageorgopoulos
Fuel Cells Program Manager
Fuel Cell Technologies Office
Office of Energy Efficiency and Renewable Energy
U.S. Department of Energy
Phone: (202) 586-5463
Email: Dimitrios.Papageorgopoulos@ee.doe.gov

MANUFACTURING R&D

Nancy L. Garland
Manufacturing R&D Project Manager
Fuel Cell Technologies Office
Office of Energy Efficiency and Renewable Energy
U.S. Department of Energy
Phone: (202) 586-5673
Email: Nancy.Garland@ee.doe.gov

TECHNOLOGY VALIDATION

Jason Marcinkoski
Technology Validation Project Manager
Fuel Cell Technologies Office
Office of Energy Efficiency and Renewable Energy
U.S. Department of Energy
Phone: (202) 586-7466
Email: Jason.Marcinkoski@ee.doe.gov

SAFETY, CODES & STANDARDS

Charles James, Jr.
Safety, Codes & Standards Project Manager
Fuel Cell Technologies Office
Office of Energy Efficiency and Renewable Energy
U.S. Department of Energy
Phone: (202) 287-6223
Email: Charles.James@ee.doe.gov

MARKET TRANSFORMATION

Pete Devlin
Market Transformation Project Manager
Fuel Cell Technologies Office
Office of Energy Efficiency and Renewable Energy
U.S. Department of Energy
Phone: (202) 586-4905
Email: Peter.Devlin@ee.doe.gov

SYSTEMS ANALYSIS

Fred Joseck
Systems Analysis Program Manager
Fuel Cell Technologies Office
Office of Energy Efficiency and Renewable Energy
U.S. Department of Energy
Phone: (202) 586-7932
Email: Fred.Joseck@ee.doe.gov

XV. Project Listings by State

Alabama

III.1 University of Alabama: Fatigue Performance of High-Strength Pipeline Steels and Their Welds in Hydrogen Gas Service

Arizona

II.C.1 Arizona State University: High Efficiency Solar Thermochemical Reactor for Hydrogen Production

Arkansas

V.B.6 University of Arkansas at Little Rock: High Performance Polymer Electrolyte Membrane Fuel Cell Electrode Structures

California

II.B.8 Palo Alto Research Center: Multi-Scale Ordered Cell Structure for Cost Effective Production of Hydrogen by HTWS

II.C.1 Sandia National Laboratories: High Efficiency Solar Thermochemical Reactor for Hydrogen Production

II.C.1 Stanford University: High Efficiency Solar Thermochemical Reactor for Hydrogen Production

II.D.2 Lawrence Livermore National Laboratory: Wide Bandgap Chalcopyrite Photoelectrodes for Direct Solar Water Splitting

II.D.2 Stanford University: Wide Bandgap Chalcopyrite Photoelectrodes for Direct Solar Water Splitting

II.D.3 California Institute of Technology: Tandem Particle-Slurry Batch Reactors for Solar Water Splitting

II.D.3 Lawrence Berkeley National Laboratory: Tandem Particle-Slurry Batch Reactors for Solar Water Splitting

II.D.3 University of California, Irvine: Tandem Particle-Slurry Batch Reactors for Solar Water Splitting

II.F.1 University of California, Irvine: Tailoring Hydrogen Evolution Reaction (HER) Catalysts for Operation at Specific pH Values

II.F.2 University of Southern California: Hybrid Perovskites and Non-Adiabatic Dynamics Simulations: Catching Realistic Aspects of the Charge Recombination Process

III.1 Sandia National Laboratories: Fatigue Performance of High-Strength Pipeline Steels and Their Welds in Hydrogen Gas Service

III.10 Lawrence Livermore National Laboratory: Liquid Hydrogen Infrastructure Analysis

III.13 Sandia National Laboratories: Metal Hydride Compression

III.16 Sandia National Laboratories: Reference Station Design, Phase II

III.3 Structural Integrity Associates, Inc.: Low Cost Hydrogen Storage at 875 bar Using Steel Liner and Steel Wire Wrap

IV.C.1 Sandia National Laboratories: HyMARC (Core): SNL Effort

IV.C.2 Lawrence Livermore National Laboratory: HyMARC (Core): LLNL Effort

IV.C.3 Lawrence Berkeley National Laboratory: HyMARC (Core): LBNL Effort

IV.C.6 Lawrence Berkeley National Laboratory: HyMARC (Support): LBNL Effort

IV.C.7 HRL Laboratories, LLC: HyMARC Seedling: Electrolyte Assisted Hydrogen Storage Reactions

IV.C.7 Liox Power, Inc.: HyMARC Seedling: Electrolyte Assisted Hydrogen Storage Reactions

IV.C.12 Lawrence Livermore National Laboratory: Improving the Kinetics and Thermodynamics of $Mg(BH_4)_2$ for Hydrogen Storage

IV.C.12 Sandia National Laboratories: Improving the Kinetics and Thermodynamics of $Mg(BH_4)_2$ for Hydrogen Storage

IV.C.14 California Institute of Technology: Design and Synthesis of Materials with High Capacities for Hydrogen Physisorption

IV.C.17 Ardica Technologies, Inc.: Low-Cost α-Alane for Hydrogen Storage

IV.C.17 SRI International: Low-Cost α-Alane for Hydrogen Storage

California (Continued)

IV.D.2 Materia, Inc.: Next Generation Hydrogen Storage Vessels Enabled by Carbon Fiber Infusion with a Low Viscosity, High Toughness Resin System

IV.D.2 Spencer Composites Corporation: Next Generation Hydrogen Storage Vessels Enabled by Carbon Fiber Infusion with a Low Viscosity, High Toughness Resin System

IV.D.3 Sandia National Laboratories: Development, Selection and Testing to Reduce Cost and Weight of Materials for BOP Components

V.A.4 Lawrence Berkeley National Laboratory: Tailored High-Performance Low-PGM Alloy Cathode Catalysts

V.B.1 Lawrence Berkeley National Laboratory: FC-PAD: Fuel Cell Performance and Durability Consortium

V.B.2 Lawrence Berkeley National Laboratory: FC-PAD: Components and Characterization

V.B.3 Lawrence Berkeley National Laboratory: FC-PAD: Electrode Layers and Optimization

V.B.4 Lawrence Berkeley National Laboratory: Novel Ionomers and Electrode Structures for Improved PEMFC Electrode Performance at Low PGM Loadings

V.C.7 Lawrence Berkeley National Laboratory: Advanced Ionomers and MEAs for Alkaline Membrane Fuel Cells

VI.1 Altergy: Fuel Cell Membrane Electrode Assembly Manufacturing R&D

VI.1 Lawrence Berkeley National Laboratory: Fuel Cell Membrane Electrode Assembly Manufacturing R&D

VI.2 National Fuel Cell Research Center: Clean Energy Supply Chain and Manufacturing Competitiveness Analysis for Hydrogen and Fuel Cell Technologies

VII.A.3 Hydrogenics USA: Fuel Cell Hybrid Electric Delivery Van Project

VII.B.1 Electricore, Inc.: Innovative Advanced Hydrogen Mobile Fueler

VII.B.1 Manta Consulting: Innovative Advanced Hydrogen Mobile Fueler

VII.B.1 Quong & Associates, Inc.: Innovative Advanced Hydrogen Mobile Fueler

VII.B.3 Linde Gas, LLC: Performance Evaluation of Delivered Hydrogen Fueling Stations

VII.B.4 Smart Chemistry: Hydrogen Component Validation

VII.B.5 Linde LLC: Liquid Hydrogen Pump Performance and Durability Testing

VII.B.5 Lawrence Livermore National Laboratory: Liquid Hydrogen Pump Performance and Durability Testing

VII.B.5 Spencer Composites Corporation: Liquid Hydrogen Pump Performance and Durability Testing

VII.C.2 Lawrence Berkeley National Laboratory: Integrated Systems Modeling of the Interactions between Stationary Hydrogen, Vehicles, and Grid Resources

VII.C.3 Humboldt State University: Dynamic Modeling and Validation of Electrolyzers in Real-Time Grid Simulation

VII.D.1 Lawrence Berkeley National Laboratory: H2@Scale Analysis

VIII.2 Sandia National Laboratories: R&D for Safety, Codes and Standards: Materials and Components Compatibility

VIII.3 Smart Chemistry: Hydrogen Fuel Quality

VIII.4 Sandia National Laboratories: R&D for Safety, Codes and Standards: Hydrogen Behavior

VIII.6 City of Santa Fe Springs: Hydrogen Safety Panel, Safety Knowledge Tools and First Responder Training Resources

VIII.6 Santa Monica Fire Department: Hydrogen Safety Panel, Safety Knowledge Tools and First Responder Training Resources

VIII.9 Sandia National Laboratories: Compatibility of Polymeric Materials Used in the Hydrogen Infrastructure

VIII.11 Business Council on Climate Change: Advancing Fuel Cell Electric Vehicles in San Francisco and Beyond

VIII.11 City and County of San Francisco: Advancing Fuel Cell Electric Vehicles in San Francisco and Beyond

VIII.11 Frontier Energy: Advancing Fuel Cell Electric Vehicles in San Francisco and Beyond

VIII.11 Newcomb Anderson McCormick: Advancing Fuel Cell Electric Vehicles in San Francisco and Beyond

IX.4 Sandia National Laboratories: Hydrogen Analysis with the Sandia ParaChoice Model

X.3 Sandia National Laboratories: Maritime Fuel Cell Generator Project

X.6 US Hybrid: Northeast Demonstration and Deployment of FCRx200

Colorado

II.A.1 National Renewable Energy Laboratory: Analysis of Advanced H_2 Production Pathways

II.B.1 National Renewable Energy Laboratory: Renewable Electrolysis Integrated Systems Development and Testing

II.B.1 Spectrum Automation Controls: Renewable Electrolysis Integrated Systems Development and Testing

II.B.2 National Renewable Energy Laboratory: High-Performance, Long-Lifetime Catalysts for Proton Exchange Membrane Electrolysis

II.C.1 Colorado School of Mines: High Efficiency Solar Thermochemical Reactor for Hydrogen Production

II.C.2 National Renewable Energy Laboratory: Flowing Particle Bed Solarthermal Redox Process to Split Water

II.C.2 University of Colorado Boulder: Flowing Particle Bed Solarthermal Redox Process to Split Water

II.D.1 National Renewable Energy Laboratory: High-Efficiency Tandem Absorbers for Economical Solar Hydrogen Production

II.D.2 National Renewable Energy Laboratory: Wide Bandgap Chalcopyrite Photoelectrodes for Direct Solar Water Splitting

II.E.1 National Renewable Energy Laboratory: Biomass to Hydrogen (B2H2)

II.F.4 National Renewable Energy Laboratory: Mechanistic Investigations on Hydrogen Catalysis by [FeFe]-Hydrogenase

II.F.5 National Renewable Energy Laboratory: Bioenergetics of Photosynthetic Energy Transduction: Control of Pathways through Redox Biochemistry

III.5 National Renewable Energy Laboratory: Improved Hydrogen Liquefaction through Heisenberg Vortex Separation of para- and ortho-hydrogen

III.7 National Renewable Energy Laboratory: 700 bar Hydrogen Dispenser Hose Reliability and Improvement

III.7 Spectrum Automation Controls: 700 bar Hydrogen Dispenser Hose Reliability and Improvement

III.8 National Renewable Energy Laboratory: Cryogenically Flexible, Low Permeability H_2 Delivery Hose

III.11 National Renewable Energy Laboratory: Electrochemical Compression

III.14 National Renewable Energy Laboratory: Advancing Hydrogen Dispenser Technology by Using Innovative Intelligent Networks

III.15 National Renewable Energy Laboratory: H2FIRST Consolidation

IV.B.1 National Renewable Energy Laboratory: Hydrogen Storage System Modeling: Public Access, Maintenance, and Enhancements

IV.C.4 National Renewable Energy Laboratory: HyMARC (Support): NREL Effort

IV.C.4 Thesis Corporation: HyMARC (Support): NREL Effort

IX.5 National Renewable Energy Laboratory: Sustainability Analysis: Hydrogen Regional Sustainability (HyReS)

IX.6 National Renewable Energy Laboratory: Hydrogen Financial Analysis Scenario Tool (H2FAST) Updates with Analysis of 101st Station

IX.7 National Renewable Energy Laboratory: Regional Supply of Hydrogen

IX.11 National Renewable Energy Laboratory: Resource Availability for Hydrogen Production

V.A.1 National Renewable Energy Laboratory: ElectroCat (Electrocatalysis Consortium)

V.A.6 ALD Nanosolutions: Extended Surface Electrocatalyst Development

V.A.6 Colorado School of Mines: Extended Surface Electrocatalyst Development

V.A.6 National Renewable Energy Laboratory: Extended Surface Electrocatalyst Development

V.A.6 University of Colorado Boulder: Extended Surface Electrocatalyst Development

V.A.8 National Renewable Energy Laboratory: Highly Accessible Catalysts for Durable High-Power Performance

V.A.10 National Renewable Energy Laboratory: Regenerative Fuel Cell System (SBIR Phase II)

V.A.15 Forge Nano: Highly Robust Low PGM MEAs Based upon Composite Supports (SBIR I)

V.B.1 National Renewable Energy Laboratory: FC-PAD: Fuel Cell Performance and Durability Consortium

V.B.2 National Renewable Energy Laboratory: FC-PAD: Components and Characterization

V.B.3 National Renewable Energy Laboratory: FC-PAD: Electrode Layers and Optimization

Colorado (Continued)

V.B.4 National Renewable Energy Laboratory: Novel Ionomers and Electrode Structures for Improved PEMFC Electrode Performance at Low PGM Loadings

V.C.2 Colorado School of Mines: Advanced Hybrid Membranes for Next Generation PEMFC Automotive Applications

V.C.2 National Renewable Energy Laboratory: Advanced Hybrid Membranes for Next Generation PEMFC Automotive Applications

V.C.5 National Renewable Energy Laboratory: Highly Stable Anion Exchange Membranes for High-Voltage Redox-Flow Batteries

V.C.7 Colorado School of Mines: Advanced Ionomers and MEAs for Alkaline Membrane Fuel Cells

V.C.7 National Renewable Energy Laboratory: Advanced Ionomers and MEAs for Alkaline Membrane Fuel Cells

V.D.3 National Renewable Energy Laboratory: Advanced Catalysts and Membrane Electrode Assemblies (MEAs) for Reversible Alkaline Membrane Fuel Cells

V.E.3 National Renewable Energy Laboratory: Fuel Cell Technology Status: Degradation

V.E.5 National Renewable Energy Laboratory: Fuel Cell Vehicle Cost Analysis

VI.1 Colorado School of Mines: Fuel Cell Membrane Electrode Assembly Manufacturing R&D

VI.1 National Renewable Energy Laboratory: Fuel Cell Membrane Electrode Assembly Manufacturing R&D

VI.2 National Renewable Energy Laboratory: Clean Energy Supply Chain and Manufacturing Competitiveness Analysis for Hydrogen and Fuel Cell Technologies

VI.6 National Renewable Energy Laboratory: In-line Quality Control of PEM Materials

VI.7 National Renewable Energy Laboratory: Manufacturing Competitiveness Analysis for Hydrogen Refueling Stations

VII.A.1 National Renewable Energy Laboratory: Fuel Cell Electric Vehicle Evaluation

VII.A.2 National Renewable Energy Laboratory: Technology Validation: Fuel Cell Bus Evaluations

VII.B.2 National Renewable Energy Laboratory: Hydrogen Station Data Collection and Analysis

VII.B.4 National Renewable Energy Laboratory: Hydrogen Component Validation

VII.B.4 Spectrum Automation Controls: Hydrogen Component Validation

VII.B.6 National Renewable Energy Laboratory: Hydrogen Meter Benchmark Testing

VII.B.6 Spectrum Automation Controls: Hydrogen Meter Benchmark Testing

VII.C.1 National Renewable Energy Laboratory: Optimal Stationary Fuel Cell Integration and Control (Energy Dispatch Controller)

VII.C.1 University of Colorado Boulder: Optimal Stationary Fuel Cell Integration and Control (Energy Dispatch Controller)

VII.C.2 National Renewable Energy Laboratory: Integrated Systems Modeling of the Interactions between Stationary Hydrogen, Vehicles, and Grid Resources

VII.C.3 National Renewable Energy Laboratory: Dynamic Modeling and Validation of Electrolyzers in Real-Time Grid Simulation

VII.D.1 National Renewable Energy Laboratory: H2@Scale Analysis

VIII.1 National Renewable Energy Laboratory: National Codes and Standards Development and Outreach

VIII.7 Bloomfield Automation: NREL Hydrogen Sensor Testing Laboratory

VIII.7 Element One: NREL Hydrogen Sensor Testing Laboratory

VIII.7 National Renewable Energy Laboratory: NREL Hydrogen Sensor Testing Laboratory

Connecticut

II.B.3 Proton OnSite: High Performance Platinum Group Metal Free Membrane Electrode Assemblies through Control of Interfacial Processes

II.B.5 FuelCell Energy, Inc.: Solid Oxide Based Electrolysis and Stack Technology with Ultra-High Electrolysis Current Density (>3 A/cm^2) and Efficiency

Connecticut (Continued)

- II.B.6 Proton OnSite: Economical Production of Hydrogen through Development of Novel, High Efficiency Electrocatalysts for Alkaline Membrane Electrolysis
- II.B.7 Proton OnSite: New Approaches to Improved PEM Electrolyzer Ion Exchange Membranes
- III.12 Sustainable Innovations, LLC: Hybrid Electrochemical Hydrogen/Metal Hydride Compressor
- V.A.15 Center for Clean Energy Engineering: Highly Robust Low PGM MEAs Based upon Composite Supports (SBIR I)
- V.A.3 eT2M: Innovative Non-PGM Catalysts for High-Temperature PEMFCs
- V.B.3 United Technologies Research Center: FC-PAD: Electrode Layers and Optimization
- V.B.6 United Technologies Research Center: High Performance Polymer Electrolyte Membrane Fuel Cell Electrode Structures
- V.C.3 FuelCell Energy, Inc.: Smart Matrix Development for Direct Carbonate Fuel Cell
- V.C.3 University of Connecticut: Smart Matrix Development for Direct Carbonate Fuel Cell
- VI.2 Connecticut Center for Advanced Technology: Clean Energy Supply Chain and Manufacturing Competitiveness Analysis for Hydrogen and Fuel Cell Technologies
- VII.C.4 FuelCell Energy, Inc.: Modular SOEC System for Efficient Hydrogen Production at High Current Density
- VIII.6 Proton OnSite: Hydrogen Safety Panel, Safety Knowledge Tools and First Responder Training Resources
- VIII.6 GWS Solutions of Tolland LLC: Hydrogen Safety Panel, Safety Knowledge Tools and First Responder Training Resources

Delaware

- V.A.6 University of Delaware: Extended Surface Electrocatalyst Development
- V.B.1 Ion Power Inc.: FC-PAD: Fuel Cell Performance and Durability Consortium
- V.B.1 University of Delaware: FC-PAD: Fuel Cell Performance and Durability Consortium
- V.B.2 Ion Power Inc.: FC-PAD: Components and Characterization
- V.B.6 Ion Power Inc.: High Performance Polymer Electrolyte Membrane Fuel Cell Electrode Structures
- V.C.5 University of Delaware: Highly Stable Anion Exchange Membranes for High-Voltage Redox-Flow Batteries

Florida

- IV.D.4 VENCORE Solutions and Services: Integrated Insulation System for Automotive Cryogenic Storage Tanks
- IV.D.4 Energy Florida: Integrated Insulation System for Automotive Cryogenic Storage Tanks
- IV.D.4 ITB Inc.: Integrated Insulation System for Automotive Cryogenic Storage Tanks
- IV.D.4 NASA: Integrated Insulation System for Automotive Cryogenic Storage Tanks
- VI.1 Mainstream Engineering: Fuel Cell Membrane Electrode Assembly Manufacturing R&D
- VI.6 Mainstream Engineering: In-line Quality Control of PEM Materials
- VII.C.3 Florida State University: Dynamic Modeling and Validation of Electrolyzers in Real-Time Grid Simulation
- VIII.6 Witte Engineered Gases: Hydrogen Safety Panel, Safety Knowledge Tools and First Responder Training Resources

Georgia

- II.B.6 Georgia Institute of Technology: Economical Production of Hydrogen through Development of Novel, High Efficiency Electrocatalysts for Alkaline Membrane Electrolysis
- II.E.2 University of Georgia: Sweet Hydrogen: High-Yield Production of Hydrogen from Biomass Sugars Catalyzed by in vitro Synthetic Biosystems
- IV.D.1 Center for Transportation and the Environment: Conformable Hydrogen Storage Coil Reservoir
- V.B.7 Georgia Institute of Technology: Fuel Cell Membrane Electrode Assemblies with Ultra-Low Pt Nanofiber Electrodes
- VI.1 Georgia Institute of Technology: Fuel Cell Membrane Electrode Assembly Manufacturing R&D

Georgia (Continued)

VI.6 Georgia Institute of Technology: In-line Quality Control of PEM Materials

VII.A.3 Center for Transportation and the Environment: Fuel Cell Hybrid Electric Delivery Van Project

VII.A.3 United Parcel Service: Fuel Cell Hybrid Electric Delivery Van Project

Hawaii

II.D.1 University of Hawaii: High-Efficiency Tandem Absorbers for Economical Solar Hydrogen Production

II.D.2 University of Hawaii: Wide Bandgap Chalcopyrite Photoelectrodes for Direct Solar Water Splitting

III.13 Hawaii Hydrogen Carriers LLC: Metal Hydride Compression

IV.C.5 University of Hawaii at Manoa: HyMARC (Support): PNNL Effort

IV.C.11 University of Hawaii at Manoa: HyMARC Seedling: Development of Magnesium Boride Etherates as Hydrogen Storage Materials

V.D.1 Hawaii Natural Energy Institute: Novel Structured Metal Bipolar Plates for Low Cost Manufacturing

X.1 Hawaii Natural Energy Institute: Hydrogen Energy Systems as a Grid Management Tool

Idaho

VII.C.2 Idaho National Laboratory: Integrated Systems Modeling of the Interactions between Stationary Hydrogen, Vehicles, and Grid Resources

VII.C.3 Idaho National Laboratory: Dynamic Modeling and Validation of Electrolyzers in Real-Time Grid Simulation

VII.D.2 Idaho National Laboratory: High Temperature Electrolysis Test Stand

Illinois

II.A.1 Argonne National Laboratory: Analysis of Advanced H_2 Production Pathways

III.9 Argonne National Laboratory: Hydrogen Refueling Analysis of Heavy-Duty Fuel Cell Vehicle Fleet

III.15 Argonne National Laboratory: H2FIRST Consolidation

IV.A.1 Argonne National Laboratory: System Analysis of Physical and Materials-Based Hydrogen Storage

IV.A.2 Argonne National Laboratory: Hydrogen Storage Cost Analysis

IV.C.9 Argonne National Laboratory: HyMARC Seedling: "Graphene-Wrapped" Complex Hydrides as High-Capacity, Regenerable Hydrogen Storage Materials

IV.C.9 Southern Illinois University: HyMARC Seedling: "Graphene-Wrapped" Complex Hydrides as High-Capacity, Regenerable Hydrogen Storage Materials

V.A.1 Argonne National Laboratory: ElectroCat (Electrocatalysis Consortium)

V.A.4 Argonne National Laboratory: Tailored High-Performance Low-PGM Alloy Cathode Catalysts

V.A.7 Argonne National Laboratory: Highly Active, Durable, and Ultra-Low PGM NSTF Thin Film ORR Catalysts and Supports

V.B.1 Argonne National Laboratory: FC-PAD: Fuel Cell Performance and Durability Consortium

V.B.2 Argonne National Laboratory: FC-PAD: Components and Characterization

V.B.3 Argonne National Laboratory: FC-PAD: Electrode Layers and Optimization

V.B.4 Argonne National Laboratory: Novel Ionomers and Electrode Structures for Improved PEMFC Electrode Performance at Low PGM Loadings

V.C.6 Argonne National Laboratory: Advanced Materials for Fully-Integrated MEAs in AEMFCs

V.E.4 Argonne National Laboratory: Performance and Durability of Advanced Automotive Fuel Cell Stacks and Systems with Dispersed Alloy Cathode Catalyst in Membrane Electrode Assemblies

V.E.5 Argonne National Laboratory: Fuel Cell Vehicle Cost Analysis

VII.B.3 Gas Technology Institute: Performance Evaluation of Delivered Hydrogen Fueling Stations

VII.D.1 Argonne National Laboratory: H2@Scale Analysis

VIII.6 UL: Hydrogen Safety Panel, Safety Knowledge Tools and First Responder Training Resources

Illinois (Continued)

IX.1 Argonne National Laboratory: Employment Impacts of Hydrogen and Fuel Cell Technologies

IX.1 RCF Economic and Financial Consulting, Inc.: Employment Impacts of Hydrogen and Fuel Cell Technologies

IX.2 Argonne National Laboratory: Regional Water Stress Analysis with Hydrogen Production at Scale

IX.3 Argonne National Laboratory: Cost Benefits Analysis of Technology Improvement in Light-Duty Fuel Cell Vehicles

IX.8 Argonne National Laboratory: Greenhouse Gas (GHG) Emissions and Petroleum Use Reduction of Medium- and Heavy-Duty Trucks

IX.9 Argonne National Laboratory: Agent-Based Modeling of Consumer Behavior

IX.10 Argonne National Laboratory: Life-Cycle Analysis of Air Pollutants Emission for Refinery and Hydrogen Production from SMR

IX.12 Argonne National Laboratory: Benefits Analysis of Multi-Fuel/Vehicle Platforms with a Focus on Hydrogen Fuel Cell Electric Vehicles

Indiana

IV.D.1 High Energy Coil Reservoirs, LLC: Conformable Hydrogen Storage Coil Reservoir

V.A.7 Purdue University: Highly Active, Durable, and Ultra-Low PGM NSTF Thin Film ORR Catalysts and Supports

Iowa

III.6 Ames Laboratory: Magnetocaloric Hydrogen Liquefaction

IV.C.13 Ames Laboratory: High-Capacity Hydrogen Storage Systems via Mechanochemistry

Maryland

III.1 National Institute of Standards and Technology: Fatigue Performance of High-Strength Pipeline Steels and Their Welds in Hydrogen Gas Service

IV.C.4 National Institute of Standards and Technology: HyMARC (Support): NREL Effort

V.A.7 Johns Hopkins University: Highly Active, Durable, and Ultra-Low PGM NSTF Thin Film ORR Catalysts and Supports

V.B.3 National Institute of Standards and Technology: FC-PAD: Electrode Layers and Optimization

V.E.1 National Institute of Standards and Technology: Neutron Imaging Study of the Water Transport in Operating Fuel Cells

VI.1 W.L. Gore & Associates: Fuel Cell Membrane Electrode Assembly Manufacturing R&D

Massachusetts

II.B.2 Giner, Inc.: High-Performance, Long-Lifetime Catalysts for Proton Exchange Membrane Electrolysis

II.B.3 Northeastern University: High Performance Platinum Group Metal Free Membrane Electrode Assemblies through Control of Interfacial Processes

II.B.4 Giner, Inc.: High Temperature Alkaline Water Electrolysis

III.4 GVD Corporation: Advanced Barrier Coatings for Harsh Environments

III.11 Giner, Inc.: Electrochemical Compression

III.14 Ivys Energy Solutions: Advancing Hydrogen Dispenser Technology by Using Innovative Intelligent Networks

IV.D.4 Aspen Aerogels: Integrated Insulation System for Automotive Cryogenic Storage Tanks

V.A.3 Advent Technologies, Inc.: Innovative Non-PGM Catalysts for High-Temperature PEMFCs

V.A.3 Northeastern University: Innovative Non-PGM Catalysts for High-Temperature PEMFCs

V.A.10 Giner, Inc.: Regenerative Fuel Cell System (SBIR Phase II)

V.A.13 Advent Technologies, Inc.: Development of Durable Active Supports for Low Platinum Group Metal Catalysts (SBIR I)

V.A.17 Northeastern University: Vapor Deposition Process for Engineering of Dispersed PEMFC ORR Pt/NbO_x/C Catalysts

Massachusetts (Continued)

V.B.3 Tufts University: FC-PAD: Electrode Layers and Optimization

V.B.4 Tufts University: Novel Ionomers and Electrode Structures for Improved PEMFC Electrode Performance at Low PGM Loadings

V.B.5 Giner, Inc.: Durable High-Power Membrane Electrode Assemblies with Low Pt Loading

V.C.4 Giner, Inc.: Ionomer Dispersion Impact on Fuel Cell and Electrolyzer Performance and Durability (SBIR Phase II TTO)

V.D.2 Advent Technologies, Inc.: Facilitated Direct Liquid Fuel Cells with High Temperature Membrane Electrode Assemblies

V.D.3 Giner, Inc.: Advanced Catalysts and Membrane Electrode Assemblies (MEAs) for Reversible Alkaline Membrane Fuel Cells

VI.1 Tufts University: Fuel Cell Membrane Electrode Assembly Manufacturing R&D

VIII.6 Firexplo: Hydrogen Safety Panel, Safety Knowledge Tools and First Responder Training Resources

IX.10 Eastern Research Group, Inc.: Life-Cycle Analysis of Air Pollutants Emission for Refinery and Hydrogen Production from SMR

X.4 Nuvera Fuel Cells: Demonstration of Fuel Cell Auxiliary Power Unit (APU) to Power Truck Refrigeration Units (TRUs) in Refrigerated Trucks

Michigan

IV.C.12 University of Michigan: Improving the Kinetics and Thermodynamics of $Mg(BH_4)_2$ for Hydrogen Storage

IV.C.15 Ford Motor Company: Hydrogen Adsorbents with High Volumetric Density: New Materials and System Projections

IV.C.15 University of Michigan: Hydrogen Adsorbents with High Volumetric Density: New Materials and System Projections

V.A.17 Ford Motor Company: Vapor Deposition Process for Engineering of Dispersed PEMFC ORR $Pt/NbO_x/C$ Catalysts

V.A.17 University of Michigan: Vapor Deposition Process for Engineering of Dispersed PEMFC ORR $Pt/NbO_x/C$ Catalysts

V.A.8 General Motors: Highly Accessible Catalysts for Durable High-Power Performance

V.A.9 Nissan Technical Center North America: Corrosion-Resistant Non-Carbon Electrocatalyst Supports for PEFCs

V.B.2 General Motors: FC-PAD: Components and Characterization

V.B.4 Michigan Technological University: Novel Ionomers and Electrode Structures for Improved PEMFC Electrode Performance at Low PGM Loadings

V.B.5 General Motors: Durable High-Power Membrane Electrode Assemblies with Low Pt Loading

V.B.7 Nissan Technical Center North America: Fuel Cell Membrane Electrode Assemblies with Ultra-Low Pt Nanofiber Electrodes

V.C.1 General Motors Fuel Cell Activities: New Fuel Cell Membranes with Improved Durability and Performance

V.C.2 Nissan Technical Center North America: Advanced Hybrid Membranes for Next Generation PEMFC Automotive Applications

VI.1 General Motors: Fuel Cell Membrane Electrode Assembly Manufacturing R&D

VIII.9 Ford Motor Company: Compatibility of Polymeric Materials Used in the Hydrogen Infrastructure

Minnesota

II.B.2 3M Company: High-Performance, Long-Lifetime Catalysts for Proton Exchange Membrane Electrolysis

V.A.7 3M Company: Highly Active, Durable, and Ultra-Low PGM NSTF Thin Film ORR Catalysts and Supports

V.A.8 3M Company: Highly Accessible Catalysts for Durable High-Power Performance

V.B.4 3M Company: Novel Ionomers and Electrode Structures for Improved PEMFC Electrode Performance at Low PGM Loadings

Minnesota (Continued)

V.B.7 3M Company: Fuel Cell Membrane Electrode Assemblies with Ultra-Low Pt Nanofiber Electrodes

V.C.1 3M Company: New Fuel Cell Membranes with Improved Durability and Performance

V.C.2 3M Company: Advanced Hybrid Membranes for Next Generation PEMFC Automotive Applications

V.C.7 3M Company: Advanced Ionomers and MEAs for Alkaline Membrane Fuel Cells

Missouri

II.B.6 Washington University in St. Louis: Economical Production of Hydrogen through Development of Novel, High Efficiency Electrocatalysts for Alkaline Membrane Electrolysis

IV.C.10 Saint Louis University: HyMARC Seedling: Fundamental Studies of Surface-Functionalized Mesoporous Carbons for Thermodynamic Stabilization and Reversibility of Metal Hydrides

IV.C.10 University of Missouri—St. Louis: HyMARC Seedling: Fundamental Studies of Surface-Functionalized Mesoporous Carbons for Thermodynamic Stabilization and Reversibility of Metal Hydrides

IV.C.10 Washington University in St. Louis: HyMARC Seedling: Fundamental Studies of Surface-Functionalized Mesoporous Carbons for Thermodynamic Stabilization and Reversibility of Metal Hydrides

IV.C.13 University of Missouri: High-Capacity Hydrogen Storage Systems via Mechanochemistry

V.A.9 Washington University in St. Louis: Corrosion-Resistant Non-Carbon Electrocatalyst Supports for PEFCs

VIII.6 Becht Engineering: Hydrogen Safety Panel, Safety Knowledge Tools and First Responder Training Resources

Montana

IV.D.2 Montana State University: Next Generation Hydrogen Storage Vessels Enabled by Carbon Fiber Infusion with a Low Viscosity, High Toughness Resin System

Nebraska

IV.D.4 Hexagon Lincoln: Integrated Insulation System for Automotive Cryogenic Storage Tanks

Nevada

II.D.1 University of Las Vegas: High-Efficiency Tandem Absorbers for Economical Solar Hydrogen Production

II.D.2 University of Las Vegas: Wide Bandgap Chalcopyrite Photoelectrodes for Direct Solar Water Splitting

New Hampshire

V.A.17 Exothermics, Inc.: Vapor Deposition Process for Engineering of Dispersed PEMFC ORR Pt/NbO_x/C Catalysts

New Jersey

V.D.1 TreadStone Technologies, Inc.: Novel Structured Metal Bipolar Plates for Low Cost Manufacturing

New Mexico

II.B.3 University of New Mexico: High Performance Platinum Group Metal Free Membrane Electrode Assemblies through Control of Interfacial Processes

II.B.6 Pajarito Powder, LLC: Economical Production of Hydrogen through Development of Novel, High Efficiency Electrocatalysts for Alkaline Membrane Electrolysis

V.A.1 Los Alamos National Laboratory: ElectroCat (Electrocatalysis Consortium)

V.A.2 EWII Fuel Cells LLC: Development of PGM-Free Catalysts for Hydrogen Oxidation Reaction in Alkaline Media

V.A.2 Los Alamos National Laboratory: Development of PGM-Free Catalysts for Hydrogen Oxidation Reaction in Alkaline Media

V.A.2 Pajarito Powder, LLC: Development of PGM-Free Catalysts for Hydrogen Oxidation Reaction in Alkaline Media

V.A.2 University of New Mexico: Development of PGM-Free Catalysts for Hydrogen Oxidation Reaction in Alkaline Media

V.A.3 Pajarito Powder, LLC: Innovative Non-PGM Catalysts for High-Temperature PEMFCs

New Mexico (Continued)

V.A.3 University of New Mexico: Innovative Non-PGM Catalysts for High-Temperature PEMFCs

V.A.4 Los Alamos National Laboratory: Tailored High-Performance Low-PGM Alloy Cathode Catalysts

V.A.5 Los Alamos National Laboratory: Platinum Monolayer Electrocatalysts

V.A.9 University of New Mexico: Corrosion-Resistant Non-Carbon Electrocatalyst Supports for PEFCs

V.A.13 Pajarito Powder, LLC: Development of Durable Active Supports for Low Platinum Group Metal Catalysts (SBIR I)

V.A.16 EWII Fuel Cells LLC: Advanced Electro-Catalysts through Crystallographic Enhancement

V.A.16 Los Alamos National Laboratory: Advanced Electro-Catalysts through Crystallographic Enhancement

V.A.17 EWII Fuel Cells, LLC: Vapor Deposition Process for Engineering of Dispersed PEMFC ORR Pt/NbO_x/C Catalysts

V.B.1 Los Alamos National Laboratory: FC-PAD: Fuel Cell Performance and Durability Consortium

V.B.2 EWII Fuel Cells, LLC: FC-PAD: Components and Characterization

V.B.2 Los Alamos National Laboratory: FC-PAD: Components and Characterization

V.B.3 Los Alamos National Laboratory: FC-PAD: Electrode Layers and Optimization

V.B.4 Los Alamos National Laboratory: Novel Ionomers and Electrode Structures for Improved PEMFC Electrode Performance at Low PGM Loadings

V.C.4 Los Alamos National Laboratory: Ionomer Dispersion Impact on Fuel Cell and Electrolyzer Performance and Durability (SBIR Phase II TTO)

V.C.6 Los Alamos National Laboratory: Advanced Materials for Fully-Integrated MEAs in AEMFCs

V.C.6 Sandia National Laboratories: Advanced Materials for Fully-Integrated MEAs in AEMFCs

V.D.2 Los Alamos National Laboratory: Facilitated Direct Liquid Fuel Cells with High Temperature Membrane Electrode Assemblies

V.E.2 Los Alamos National Laboratory: Technical Assistance to Developers

VIII.3 Los Alamos National Laboratory: Hydrogen Fuel Quality

VIII.5 Sandia National Laboratories: Hydrogen Quantitative Risk Assessment

VIII.10 Sandia National Laboratories: Enabling Hydrogen Infrastructure Through Science-Based Codes and Standards

New York

II.F.3 University of Rochester: Nano-bio Systems for Light-Driven Hydrogen Production

II.F.6 Brookhaven National Laboratory: Reversible Conversion between CO_2/H_2 and Formic Acid by Molecular Catalysts

III.11 Rensselaer Polytechnic Institute: Electrochemical Compression

V.A.5 Brookhaven National Laboratory: Platinum Monolayer Electrocatalysts

V.A.8 Cornell University: Highly Accessible Catalysts for Durable High-Power Performance

V.A.16 University at Buffalo: Advanced Electro-Catalysts through Crystallographic Enhancement

V.C.6 Rensselaer Polytechnic Institute: Advanced Materials for Fully-Integrated MEAs in AEMFCs

V.D.3 University at Buffalo: Advanced Catalysts and Membrane Electrode Assemblies (MEAs) for Reversible Alkaline Membrane Fuel Cells

VI.5 Automated Dynamics: Continuous Fiber Composite Electrofusion Coupler

VII.A.3 Unique Electric Solutions: Fuel Cell Hybrid Electric Delivery Van Project

X.2 Plug Power: Ground Support Equipment Demonstration

X.5 Plug Power: FedEx Express Hydrogen Fuel Cell Extended-Range Battery Electric Vehicles

Ohio

III.2 ACI Services: Hydrogen Compression Application of the Linear Motor Reciprocating Compressor (LMRC)

III.3 N & R Engineering: Low Cost Hydrogen Storage at 875 bar Using Steel Liner and Steel Wire Wrap

Ohio (Continued)

V.A.10 pH Matter LLC: Regenerative Fuel Cell System (SBIR Phase II)

V.A.14 pH Matter LLC: Multi-Functional Catalyst Support (SBIR I)

VI.2 DJW Technology, LLC: Clean Energy Supply Chain and Manufacturing Competitiveness Analysis for Hydrogen and Fuel Cell Technologies

VI.2 Ohio Fuel Cell Coalition: Clean Energy Supply Chain and Manufacturing Competitiveness Analysis for Hydrogen and Fuel Cell Technologies

VI.4 DJW Technology, LLC: U.S. Clean Energy Hydrogen and Fuel Cell Technologies: A Competiveness Analysis

VI.4 GLWN, Westside Industrial Retention & Expansion Network: U.S. Clean Energy Hydrogen and Fuel Cell Technologies: A Competiveness Analysis

X.5 Workhorse Technologies Inc.: FedEx Express Hydrogen Fuel Cell Extended-Range Battery Electric Vehicles

Oregon

II.E.3 Oregon State U.: Novel Hybrid Microbial Electrochemical System for Efficient Hydrogen Generation from Biomass

III.3 Hy-Performance Materials Testing, LLC: Low Cost Hydrogen Storage at 875 bar Using Steel Liner and Steel Wire Wrap

IV.D.3 Hy-Performance Materials Testing, LLC: Development, Selection and Testing to Reduce Cost and Weight of Materials for BOP Components

Pennsylvania

II.B.3 The Pennsylvania State University: High Performance Platinum Group Metal Free Membrane Electrode Assemblies through Control of Interfacial Processes

II.C.1 Bucknell University: High Efficiency Solar Thermochemical Reactor for Hydrogen Production

II.E.1 The Pennsylvania State University: Biomass to Hydrogen (B2H2)

III.3 C P Industries: Low Cost Hydrogen Storage at 875 bar Using Steel Liner and Steel Wire Wrap

III.8 LifeGuard Technologies: Cryogenically Flexible, Low Permeability H2 Delivery Hose

III.15 PDC Machines: H2FIRST Consolidation

IV.C.8 The Pennsylvania State University: HyMARC Seedling: Developing a Novel Hydrogen Sponge with Ideal Binding Energy and High Surface Area for Practical Hydrogen Storage

V.A.8 Carnegie Mellon University: Highly Accessible Catalysts for Durable High-Power Performance

V.A.8 Drexel University: Highly Accessible Catalysts for Durable High-Power Performance

V.A.16 University of Pennsylvania: Advanced Electro-Catalysts through Crystallographic Enhancement

VIII.3 SAE International: Hydrogen Fuel Quality

VIII.6 Air Products and Chemicals, Inc.: Hydrogen Safety Panel, Safety Knowledge Tools and First Responder Training Resources

Rhode Island

V.A.16 Brown University: Advanced Electro-Catalysts through Crystallographic Enhancement

South Carolina

II.B.7 Tetramer Technologies, LLC: New Approaches to Improved PEM Electrolyzer Ion Exchange Membranes

III.12 Greenway Energy, LLC: Hybrid Electrochemical Hydrogen/Metal Hydride Compressor

III.12 Savannah River National Laboratory: Hybrid Electrochemical Hydrogen/Metal Hydride Compressor

IV.B.1 Savannah River National Laboratory: Hydrogen Storage System Modeling: Public Access, Maintenance, and Enhancements

IV.B.2 Savannah River Consulting: Investigation of Solid State Hydrides for Autonomous Fuel Cell Vehicles

IV.B.2 Savannah River National Laboratory: Investigation of Solid State Hydrides for Autonomous Fuel Cell Vehicles

South Carolina (Continued)

IV.C.16 Savannah River Consulting: Electrochemical Reversible Formation of Alane

IV.C.16 Savannah River National Laboratory: Electrochemical Reversible Formation of Alane

IV.D.4 Savannah River National Laboratory: Integrated Insulation System for Automotive Cryogenic Storage Tanks

V.A.11 Greenway Energy, LLC: Development of Corrosion Resistant Carbon (CRC) Support for Ultra-Low Platinum Group Metal (PGM) Catalysts (SBIR Phase I)

V.A.11 Savannah River National Laboratory: Development of Corrosion Resistant Carbon (CRC) Support for Ultra-Low Platinum Group Metal (PGM) Catalysts (SBIR Phase I)

VI.5 Savannah River National Laboratory: Continuous Fiber Composite Electrofusion Coupler

Tennessee

III.1 Oak Ridge National Laboratory: Fatigue Performance of High-Strength Pipeline Steels and Their Welds in Hydrogen Gas Service

III.3 Oak Ridge National Laboratory: Low Cost Hydrogen Storage at 875 bar Using Steel Liner and Steel Wire Wrap

III.4 Oak Ridge National Laboratory: Advanced Barrier Coatings for Harsh Environments

III.13 Oak Ridge National Laboratory: Metal Hydride Compression

V.A.1 Oak Ridge National Laboratory: ElectroCat (Electrocatalysis Consortium)

V.A.4 Oak Ridge National Laboratory: Tailored High-Performance Low-PGM Alloy Cathode Catalysts

V.A.7 Oak Ridge National Laboratory: Highly Active, Durable, and Ultra-Low PGM NSTF Thin Film ORR Catalysts and Supports

V.B.1 Oak Ridge National Laboratory: FC-PAD: Fuel Cell Performance and Durability Consortium

V.B.2 Oak Ridge National Laboratory: FC-PAD: Components and Characterization

V.B.3 Oak Ridge National Laboratory: FC-PAD: Electrode Layers and Optimization

V.B.4 Oak Ridge National Laboratory: Novel Ionomers and Electrode Structures for Improved PEMFC Electrode Performance at Low PGM Loadings

V.B.7 Vanderbilt University: Fuel Cell Membrane Electrode Assemblies with Ultra-Low Pt Nanofiber Electrodes

V.C.1 Vanderbilt University: New Fuel Cell Membranes with Improved Durability and Performance

V.C.4 Oak Ridge National Laboratory: Ionomer Dispersion Impact on Fuel Cell and Electrolyzer Performance and Durability (SBIR Phase II TTO)

V.C.7 Oak Ridge National Laboratory: Advanced Ionomers and MEAs for Alkaline Membrane Fuel Cells

VIII.9 Oak Ridge National Laboratory: Compatibility of Polymeric Materials Used in the Hydrogen Infrastructure

X.5 Federal Express Corporation: FedEx Express Hydrogen Fuel Cell Extended-Range Battery Electric Vehicles

Texas

III.14 Air Liquide Advanced Technologies: Advancing Hydrogen Dispenser Technology by Using Innovative Intelligent Networks

III.2 Southwest Research Institute®: Hydrogen Compression Application of the Linear Motor Reciprocating Compressor (LMRC)

IV.D.1 The University of Texas at Austin: Conformable Hydrogen Storage Coil Reservoir

V.B.5 University of Texas at Austin: Durable High-Power Membrane Electrode Assemblies with Low Pt Loading

VII.A.3 University of Texas at Austin: Fuel Cell Hybrid Electric Delivery Van Project

VII.A.3 Valence Technology: Fuel Cell Hybrid Electric Delivery Van Project

VII.B.1 Air Liquide: Innovative Advanced Hydrogen Mobile Fueler

VI.5 NOV Fiberglass Systems: Continuous Fiber Composite Electrofusion Coupler

Utah

II.B.8 Ceramatec, Inc: Multi-Scale Ordered Cell Structure for Cost Effective Production of Hydrogen by HTWS

Virginia

- II.A.1 Strategic Analysis, Inc.: Analysis of Advanced H_2 Production Pathways
- II.B.8 Gaia Energy Research Institute LLC: Multi-Scale Ordered Cell Structure for Cost Effective Production of Hydrogen by HTWS
- II.E.2 Virginia Polytechnic Institute and State University: Sweet Hydrogen: High-Yield Production of Hydrogen from Biomass Sugars Catalyzed by in vitro Synthetic Biosystems
- III.3 WireTough Cylinders, LLC: Low Cost Hydrogen Storage at 875 bar Using Steel Liner and Steel Wire Wrap
- III.8 Cardinal Rubber & Seal: Cryogenically Flexible, Low Permeability H2 Delivery Hose
- III.8 Nanosonic, Inc.: Cryogenically Flexible, Low Permeability H2 Delivery Hose
- III.11 Gaia Energy Research Institute LLC: Electrochemical Compression
- IV.A.2 Strategic Analysis, Inc.: Hydrogen Storage Cost Analysis
- V.A.12 CertainTech Inc.: Mesoporous Non-Carbon Catalyst Supports of PEMFC (SBIR I)
- V.E.5 Strategic Analysis, Inc.: Fuel Cell Vehicle Cost Analysis
- VI.3 Birch Studio: Fuel Cell and Hydrogen Opportunity Center, www.hfcnexus.com (Hydrogen Fuel Cell Nexus)
- VI.3 Breakthrough Technologies Institute: Fuel Cell and Hydrogen Opportunity Center, www.hfcnexus.com (Hydrogen Fuel Cell Nexus)
- VI.3 Virginia Clean Cities at James Madison University: Fuel Cell and Hydrogen Opportunity Center, www.hfcnexus.com (Hydrogen Fuel Cell Nexus)
- VI.4 Strategic Analysis, Inc.: U.S. Clean Energy Hydrogen and Fuel Cell Technologies: A Competiveness Analysis

Washington

- III.3 MVP Co.: Low Cost Hydrogen Storage at 875 bar Using Steel Liner and Steel Wire Wrap
- III.6 Emerald Energy NW LLC: Magnetocaloric Hydrogen Liquefaction
- III.6 Pacific Northwest National Laboratory: Magnetocaloric Hydrogen Liquefaction
- IV.A.2 Pacific Northwest National Laboratory: Hydrogen Storage Cost Analysis
- IV.B.1 Pacific Northwest National Laboratory: Hydrogen Storage System Modeling: Public Access, Maintenance, and Enhancements
- IV.C.5 Pacific Northwest National Laboratory: HyMARC (Support): PNNL Effort
- VII.C.1 Washington State University: Optimal Stationary Fuel Cell Integration and Control (Energy Dispatch Controller)
- VII.D.1 Pacific Northwest National Laboratory: H2@Scale Analysis
- VIII.6 Pacific Northwest National Laboratory: Hydrogen Safety Panel, Safety Knowledge Tools and First Responder Training Resources
- VIII.9 Pacific Northwest National Laboratory: Compatibility of Polymeric Materials Used in the Hydrogen Infrastructure
- X.4 Pacific Northwest National Laboratory: Demonstration of Fuel Cell Auxiliary Power Unit (APU) to Power Truck Refrigeration Units (TRUs) in Refrigerated Trucks

Washington, D.C.

- III.1 National Institute of Standards and Technology: Fatigue Performance of High-Strength Pipeline Steels and Their Welds in Hydrogen Gas Service
- VIII.8 Fuel Cell & Hydrogen Energy Association: Fuel Cell & Hydrogen Energy Association Codes and Standards Support Alabama

FOREIGN COUNTRIES

Canada

II.B.5 Versa Power Systems Ltd.: Solid Oxide Based Electrolysis and Stack Technology with Ultra-High Electrolysis Current Density (>3 A/cm^2) and Efficiency

V.B.3 University of Alberta: FC-PAD: Electrode Layers and Optimization

VII.B.1 Hydrogen Technology & Energy Corporation: Innovative Advanced Hydrogen Mobile Fueler

VII.C.4 Versa Power Systems Ltd.: Modular SOEC System for Efficient Hydrogen Production at High Current Density

VIII.1 A.V. Tchouvelev & Associates, Inc.: National Codes and Standards Development and Outreach

VIII.6 CSA Group: Hydrogen Safety Panel, Safety Knowledge Tools and First Responder Training Resources

VIII.7 A.V. Tchouvelev & Associates, Inc.: NREL Hydrogen Sensor Testing Laboratory

X.3 Hydrogenics: Maritime Fuel Cell Generator Project

X.4 Ballard Power Systems: Demonstration of Fuel Cell Auxiliary Power Unit (APU) to Power Truck Refrigeration Units (TRUs) in Refrigerated Trucks

Finland

VIII.3 VTT: Hydrogen Fuel Quality

France

VIII.3 CEA-Liten: Hydrogen Fuel Quality

Germany

III.14 Rheonik GmBH: Advancing Hydrogen Dispenser Technology by Using Innovative Intelligent Networks

V.B.2 Umicore: FC-PAD: Components and Characterization

Japan

VIII.3 Japan Automotive Research Institute: Hydrogen Fuel Quality

Norway

V.B.3 Norwegian University Science and Technology: FC-PAD: Electrode Layers and Optimization

Poland

II.F.2 Institute of Physics, Polish Academy of Sciences: Hybrid Perovskites and Non-Adiabatic Dynamics Simulations: Catching Realistic Aspects of the Charge Recombination Process

Switzerland

VI.4 E4tech: U.S. Clean Energy Hydrogen and Fuel Cell Technologies: A Competiveness Analysis

VIII.3 International Organization for Standardization: Hydrogen Fuel Quality

XVI. Project Listings by Organization

3M Company

- II.B.2 High-Performance, Long-Lifetime Catalysts for Proton Exchange Membrane Electrolysis
- V.A.7 Highly Active, Durable, and Ultra-Low PGM NSTF Thin Film ORR Catalysts and Supports
- V.A.8 Highly Accessible Catalysts for Durable High-Power Performance
- V.B.4 Novel Ionomers and Electrode Structures for Improved PEMFC Electrode Performance at Low PGM Loadings
- V.B.7 Fuel Cell Membrane Electrode Assemblies with Ultra-Low Pt Nanofiber Electrodes
- V.C.1 New Fuel Cell Membranes with Improved Durability and Performance
- V.C.2 Advanced Hybrid Membranes for Next Generation PEMFC Automotive Applications
- V.C.7 Advanced Ionomers and MEAs for Alkaline Membrane Fuel Cells

ACI Services

- III.2 Hydrogen Compression Application of the Linear Motor Reciprocating Compressor (LMRC)

Advent Technologies Inc.

- V.A.3 Innovative Non-PGM Catalysts for High-Temperature PEMFCs
- V.A.13 Development of Durable Active Supports for Low Platinum Group Metal Catalysts (SBIR I)
- V.D.2 Facilitated Direct Liquid Fuel Cells with High Temperature Membrane Electrode Assemblies

Air Liquide

- III.14 Advancing Hydrogen Dispenser Technology by Using Innovative Intelligent Networks
- VII.B.1 Innovative Advanced Hydrogen Mobile Fueler

Air Products and Chemicals, Inc.

- VIII.6 Hydrogen Safety Panel, Safety Knowledge Tools and First Responder Training Resources

ALD Nanosolutions

- V.A.6 Extended Surface Electrocatalyst Development

Altergy

- VI.1 Fuel Cell Membrane Electrode Assembly Manufacturing R&D

Ames Laboratory

- III.6 Magnetocaloric Hydrogen Liquefaction
- IV.C.13 High-Capacity Hydrogen Storage Systems via Mechanochemistry

Ardica Technologies, Inc.

- IV.C.17 Low-Cost α-Alane for Hydrogen Storage

Argonne National Laboratory

- II.A.1 Analysis of Advanced H_2 Production Pathways
- III.9 Hydrogen Refueling Analysis of Heavy-Duty Fuel Cell Vehicle Fleet
- III.15 H2FIRST Consolidation
- IV.A.1 System Analysis of Physical and Materials-Based Hydrogen Storage
- IV.A.2 Hydrogen Storage Cost Analysis
- IV.C.9 HyMARC Seedling: "Graphene-Wrapped" Complex Hydrides as High-Capacity, Regenerable Hydrogen Storage Materials

Argonne National Laboratory (Continued)

V.A.1 ElectroCat (Electrocatalysis Consortium)
V.A.4 Tailored High-Performance Low-PGM Alloy Cathode Catalysts
V.A.7 Highly Active, Durable, and Ultra-Low PGM NSTF Thin Film ORR Catalysts and Supports
V.B.1 FC-PAD: Fuel Cell Performance and Durability Consortium
V.B.2 FC-PAD: Components and Characterization
V.B.3 FC-PAD: Electrode Layers and Optimization
V.B.4 Novel Ionomers and Electrode Structures for Improved PEMFC Electrode Performance at Low PGM Loadings
V.C.6 Advanced Materials for Fully-Integrated MEAs in AEMFCs
V.E.4 Performance and Durability of Advanced Automotive Fuel Cell Stacks and Systems with Dispersed Alloy Cathode Catalyst in Membrane Electrode Assemblies
V.E.5 Fuel Cell Vehicle Cost Analysis
VII.D.1 H2@Scale Analysis
IX.1 Employment Impacts of Hydrogen and Fuel Cell Technologies
IX.2 Regional Water Stress Analysis with Hydrogen Production at Scale
IX.3 Cost Benefits Analysis of Technology Improvement in Light-Duty Fuel Cell Vehicles
IX.8 Greenhouse Gas (GHG) Emissions and Petroleum Use Reduction of Medium- and Heavy-Duty Trucks
IX.9 Agent-Based Modeling of Consumer Behavior
IX.10 Life-Cycle Analysis of Air Pollutants Emission for Refinery and Hydrogen Production from SMR
IX.12 Benefits Analysis of Multi-Fuel/Vehicle Platforms with a Focus on Hydrogen Fuel Cell Electric Vehicles

Arizona State University

II.C.1 High Efficiency Solar Thermochemical Reactor for Hydrogen Production

Aspen Aerogels

IV.D.4 Integrated Insulation System for Automotive Cryogenic Storage Tanks

Automated Dynamics

VI.5 Continuous Fiber Composite Electrofusion Coupler

A.V. Tchouvelev & Associates, Inc.

VIII.1 National Codes and Standards Development and Outreach
VIII.7 NREL Hydrogen Sensor Testing Laboratory

Ballard Power Systems

X.4 Demonstration of Fuel Cell Auxiliary Power Unit (APU) to Power Truck Refrigeration Units (TRUs) in Refrigerated Trucks

Becht Engineering

VIII.6 Hydrogen Safety Panel, Safety Knowledge Tools and First Responder Training Resources

Birch Studio

VI.3 Fuel Cell and Hydrogen Opportunity Center, www.hfcnexus.com (Hydrogen Fuel Cell Nexus)

Bloomfield Automation

VIII.7 NREL Hydrogen Sensor Testing Laboratory

Breakthrough Technologies Institute

VI.3 Fuel Cell and Hydrogen Opportunity Center, www.hfcnexus.com (Hydrogen Fuel Cell Nexus)

Brookhaven National Laboratory

II.F.6 Reversible Conversion between CO_2/H_2 and Formic Acid by Molecular Catalysts

V.A.5 Platinum Monolayer Electrocatalysts

Brown University

V.A.16 Advanced Electro-Catalysts through Crystallographic Enhancement

Bucknell University

II.C.1 High Efficiency Solar Thermochemical Reactor for Hydrogen Production

Business Council on Climate Change

VIII.11 Advancing Fuel Cell Electric Vehicles in San Francisco and Beyond

California Institute of Technology

II.D.3 Tandem Particle-Slurry Batch Reactors for Solar Water Splitting

IV.C.14 Design and Synthesis of Materials with High Capacities for Hydrogen Physisorption

Cardinal Rubber & Seal

III.8 Cryogenically Flexible, Low Permeability H_2 Delivery Hose

Carnegie Mellon University

V.A.8 Highly Accessible Catalysts for Durable High-Power Performance

CEA-Liten

VIII.3 Hydrogen Fuel Quality

Center for Clean Energy Engineering

V.A.15 Highly Robust Low PGM MEAs Based upon Composite Supports (SBIR I)

Center for Transportation and the Environment

IV.D.1 Conformable Hydrogen Storage Coil Reservoir

VII.A.3 Fuel Cell Hybrid Electric Delivery Van Project

Ceramatec, Inc.

II.B.8 Multi-Scale Ordered Cell Structure for Cost Effective Production of Hydrogen by HTWS

CertainTech Inc.

V.A.12 Mesoporous Non-Carbon Catalyst Supports of PEMFC (SBIR I)

City and County of San Francisco

VIII.11 Advancing Fuel Cell Electric Vehicles in San Francisco and Beyond

City of Santa Fe Springs

VIII.6 Hydrogen Safety Panel, Safety Knowledge Tools and First Responder Training Resources

Colorado School of Mines

II.C.1 High Efficiency Solar Thermochemical Reactor for Hydrogen Production

V.A.6 Extended Surface Electrocatalyst Development

V.C.2 Advanced Hybrid Membranes for Next Generation PEMFC Automotive Applications

V.C.7 Advanced Ionomers and MEAs for Alkaline Membrane Fuel Cells

VI.1 Fuel Cell Membrane Electrode Assembly Manufacturing R&D

Connecticut Center for Advanced Technology

VI.2 Clean Energy Supply Chain and Manufacturing Competitiveness Analysis for Hydrogen and Fuel Cell Technologies

Cornell University

V.A.8 Highly Accessible Catalysts for Durable High-Power Performance

C P Industries

III.3 Low Cost Hydrogen Storage at 875 bar Using Steel Liner and Steel Wire Wrap

CSA Group

VIII.6 Hydrogen Safety Panel, Safety Knowledge Tools and First Responder Training Resources

DJW Technology, LLC

VI.2 Clean Energy Supply Chain and Manufacturing Competitiveness Analysis for Hydrogen and Fuel Cell Technologies

VI.4 U.S. Clean Energy Hydrogen and Fuel Cell Technologies: A Competiveness Analysis

Drexel University

V.A.8 Highly Accessible Catalysts for Durable High-Power Performance

E4tech

VI.4 U.S. Clean Energy Hydrogen and Fuel Cell Technologies: A Competiveness Analysis

Eastern Research Group, Inc.

IX.10 Life-Cycle Analysis of Air Pollutants Emission for Refinery and Hydrogen Production from SMR

Electricore, Inc.

VII.B.1 Innovative Advanced Hydrogen Mobile Fueler

Element One

VIII.7 NREL Hydrogen Sensor Testing Laboratory

Emerald Energy NW LLC

III.6 Magnetocaloric Hydrogen Liquefaction

Energy Florida

IV.D.4 Integrated Insulation System for Automotive Cryogenic Storage Tanks

eT2M

V.A.3 Innovative Non-PGM Catalysts for High-Temperature PEMFCs

EWII Fuel Cells LLC

V.A.2 Development of PGM-Free Catalysts for Hydrogen Oxidation Reaction in Alkaline Media

V.A.16 Advanced Electro-Catalysts through Crystallographic Enhancement

V.A.17 Vapor Deposition Process for Engineering of Dispersed PEMFC ORR Pt/NbO_x/C Catalysts

V.B.2 FC-PAD: Components and Characterization

Exothermics, Inc.

V.A.17 Vapor Deposition Process for Engineering of Dispersed PEMFC ORR Pt/NbO_x/C Catalysts

Federal Express Corporation

X.5 FedEx Express Hydrogen Fuel Cell Extended-Range Battery Electric Vehicles

Firexplo

VIII.6 Hydrogen Safety Panel, Safety Knowledge Tools and First Responder Training Resources

Florida State University

VII.C.3 Dynamic Modeling and Validation of Electrolyzers in Real-Time Grid Simulation

Ford Motor Company

IV.C.15 Hydrogen Adsorbents with High Volumetric Density: New Materials and System Projections

V.A.17 Vapor Deposition Process for Engineering of Dispersed PEMFC ORR Pt/NbO_x/C Catalysts

VIII.9 Compatibility of Polymeric Materials Used in the Hydrogen Infrastructure

Forge Nano

V.A.15 Highly Robust Low PGM MEAs Based upon Composite Supports (SBIR I)

Frontier Energy

VIII.11 Advancing Fuel Cell Electric Vehicles in San Francisco and Beyond

Fuel Cell & Hydrogen Energy Association

VIII.8 Fuel Cell & Hydrogen Energy Association Codes and Standards Support

FuelCell Energy, Inc.

II.B.5 Solid Oxide Based Electrolysis and Stack Technology with Ultra-High Electrolysis Current Density (>3 A/cm^2) and Efficiency

V.C.3 Smart Matrix Development for Direct Carbonate Fuel Cell

VII.C.4 Modular SOEC System for Efficient Hydrogen Production at High Current Density

Gaia Energy Research Institute LLC

II.B.8 Multi-Scale Ordered Cell Structure for Cost Effective Production of Hydrogen by HTWS

III.11 Electrochemical Compression

Gas Technology Institute

VII.B.3 Performance Evaluation of Delivered Hydrogen Fueling Stations

General Motors

V.A.8 Highly Accessible Catalysts for Durable High-Power Performance

V.B.2 FC-PAD: Components and Characterization

V.B.5 Durable High-Power Membrane Electrode Assemblies with Low Pt Loading

V.C.1 New Fuel Cell Membranes with Improved Durability and Performance

VI.1 Fuel Cell Membrane Electrode Assembly Manufacturing R&D

Georgia Institute of Technology

II.B.6 Economical Production of Hydrogen through Development of Novel, High Efficiency Electrocatalysts for Alkaline Membrane Electrolysis

V.B.7 Fuel Cell Membrane Electrode Assemblies with Ultra-Low Pt Nanofiber Electrodes

VI.1 Fuel Cell Membrane Electrode Assembly Manufacturing R&D

VI.6 In-line Quality Control of PEM Materials

Giner, Inc.

II.B.2 High-Performance, Long-Lifetime Catalysts for Proton Exchange Membrane Electrolysis
II.B.4 High Temperature Alkaline Water Electrolysis
III.11 Electrochemical Compression
V.A.10 Regenerative Fuel Cell System (SBIR Phase II)
V.B.5 Durable High-Power Membrane Electrode Assemblies with Low Pt Loading
V.C.4 Ionomer Dispersion Impact on Fuel Cell and Electrolyzer Performance and Durability (SBIR Phase II TTO)
V.D.3 Advanced Catalysts and Membrane Electrode Assemblies (MEAs) for Reversible Alkaline Membrane Fuel Cells

GLWN, Westside Industrial Retention & Expansion Network

VI.4 U.S. Clean Energy Hydrogen and Fuel Cell Technologies: A Competiveness Analysis

Greenway Energy, LLC

III.12 Hybrid Electrochemical Hydrogen/Metal Hydride Compressor
V.A.11 Development of Corrosion Resistant Carbon (CRC) Support for Ultra-Low Platinum Group Metal (PGM) Catalysts (SBIR Phase I)

GVD Corporation

III.4 Advanced Barrier Coatings for Harsh Environments

GWS Solutions of Tolland LLC

VIII.6 Hydrogen Safety Panel, Safety Knowledge Tools and First Responder Training Resources

Hawaii Hydrogen Carriers LLC

III.13 Metal Hydride Compression

Hawaii Natural Energy Institute

V.D.1 Novel Structured Metal Bipolar Plates for Low Cost Manufacturing
X.1 Hydrogen Energy Systems as a Grid Management Tool

Hexagon Lincoln

IV.D.4 Integrated Insulation System for Automotive Cryogenic Storage Tanks

High Energy Coil Reservoirs, LLC

IV.D.1 Conformable Hydrogen Storage Coil Reservoir

HRL Laboratories, LLC

IV.C.7 HyMARC Seedling: Electrolyte Assisted Hydrogen Storage Reactions

Humboldt State University

VII.C.3 Dynamic Modeling and Validation of Electrolyzers in Real-Time Grid Simulation

Hydrogen Technology & Energy Corporation

VII.B.1 Innovative Advanced Hydrogen Mobile Fueler

Hydrogenics

VII.A.3 Fuel Cell Hybrid Electric Delivery Van Project
X.3 Maritime Fuel Cell Generator Project

Hy-Performance Materials Testing, LLC

III.3 Low Cost Hydrogen Storage at 875 bar Using Steel Liner and Steel Wire Wrap
IV.D.3 Development, Selection and Testing to Reduce Cost and Weight of Materials for BOP Components

Idaho National Laboratory

VII.C.2 Integrated Systems Modeling of the Interactions between Stationary Hydrogen, Vehicles, and Grid Resources
VII.C.3 Dynamic Modeling and Validation of Electrolyzers in Real-Time Grid Simulation
VII.D.2 High Temperature Electrolysis Test Stand

Institute of Physics, Polish Academy of Sciences

II.F.2 Hybrid Perovskites and Non-Adiabatic Dynamics Simulations: Catching Realistic Aspects of the Charge Recombination Process

International Organization for Standardization

VIII.3 Hydrogen Fuel Quality

Ion Power Inc.

V.B.1 FC-PAD: Fuel Cell Performance and Durability Consortium
V.B.2 FC-PAD: Components and Characterization
V.B.6 High Performance Polymer Electrolyte Membrane Fuel Cell Electrode Structures

ITB Inc.

IV.D.4 Integrated Insulation System for Automotive Cryogenic Storage Tanks

Ivys Energy Solutions

III.14 Advancing Hydrogen Dispenser Technology by Using Innovative Intelligent Networks

Japan Automotive Research Institute

VIII.3 Hydrogen Fuel Quality

Johns Hopkins University

V.A.7 Highly Active, Durable, and Ultra-Low PGM NSTF Thin Film ORR Catalysts and Supports

Lawrence Berkeley National Laboratory

II.D.3 Tandem Particle-Slurry Batch Reactors for Solar Water Splitting
IV.C.3 HyMARC (Core): LBNL Effort
IV.C.6 HyMARC (Support): LBNL Effort
V.A.4 Tailored High-Performance Low-PGM Alloy Cathode Catalysts
V.B.1 FC-PAD: Fuel Cell Performance and Durability Consortium
V.B.2 FC-PAD: Components and Characterization
V.B.3 FC-PAD: Electrode Layers and Optimization
V.B.4 Novel Ionomers and Electrode Structures for Improved PEMFC Electrode Performance at Low PGM Loadings
V.C.7 Advanced Ionomers and MEAs for Alkaline Membrane Fuel Cells
VI.1 Fuel Cell Membrane Electrode Assembly Manufacturing R&D
VII.C.2 Integrated Systems Modeling of the Interactions between Stationary Hydrogen, Vehicles, and Grid Resources
VII.D.1 H2@Scale Analysis

Lawrence Livermore National Laboratory

II.D.2 Wide Bandgap Chalcopyrite Photoelectrodes for Direct Solar Water Splitting
III.10 Liquid Hydrogen Infrastructure Analysis
IV.C.2 HyMARC (Core): LLNL Effort
IV.C.12 Improving the Kinetics and Thermodynamics of $Mg(BH_4)_2$ for Hydrogen Storage
VII.B.5 Liquid Hydrogen Pump Performance and Durability Testing

LifeGuard Technologies

III.8 Cryogenically Flexible, Low Permeability H_2 Delivery Hose

Linde LLC

VII.B.3 Performance Evaluation of Delivered Hydrogen Fueling Stations
VII.B.5 Liquid Hydrogen Pump Performance and Durability Testing

Liox Power, Inc.

IV.C.7 HyMARC Seedling: Electrolyte Assisted Hydrogen Storage Reactions

Los Alamos National Laboratory

V.A.1 ElectroCat (Electrocatalysis Consortium)
V.A.2 Development of PGM-Free Catalysts for Hydrogen Oxidation Reaction in Alkaline Media
V.A.4 Tailored High-Performance Low-PGM Alloy Cathode Catalysts
V.A.5 Platinum Monolayer Electrocatalysts
V.A.16 Advanced Electro-Catalysts through Crystallographic Enhancement
V.B.1 FC-PAD: Fuel Cell Performance and Durability Consortium
V.B.2 FC-PAD: Components and Characterization
V.B.3 FC-PAD: Electrode Layers and Optimization
V.B.4 Novel Ionomers and Electrode Structures for Improved PEMFC Electrode Performance at Low PGM Loadings
V.C.4 Ionomer Dispersion Impact on Fuel Cell and Electrolyzer Performance and Durability (SBIR Phase II TTO)
V.C.6 Advanced Materials for Fully-Integrated MEAs in AEMFCs
V.D.2 Facilitated Direct Liquid Fuel Cells with High Temperature Membrane Electrode Assemblies
V.E.2 Technical Assistance to Developers
VIII.3 Hydrogen Fuel Quality

Mainstream Engineering

VI.1 Fuel Cell Membrane Electrode Assembly Manufacturing R&D
VI.6 In-line Quality Control of PEM Materials

Manta Consulting

VII.B.1 Innovative Advanced Hydrogen Mobile Fueler

Materia, Inc.

IV.D.2 Next Generation Hydrogen Storage Vessels Enabled by Carbon Fiber Infusion with a Low Viscosity, High Toughness Resin System

Michigan Technological University

V.B.4 Novel Ionomers and Electrode Structures for Improved PEMFC Electrode Performance at Low PGM Loadings

Montana State University

IV.D.2 Next Generation Hydrogen Storage Vessels Enabled by Carbon Fiber Infusion with a Low Viscosity, High Toughness Resin System

MVP Co.

III.3 Low Cost Hydrogen Storage at 875 bar Using Steel Liner and Steel Wire Wrap

N & R Engineering

III.3 Low Cost Hydrogen Storage at 875 bar Using Steel Liner and Steel Wire Wrap

Nanosonic, Inc.

III.8 Cryogenically Flexible, Low Permeability H_2 Delivery Hose

NASA

IV.D.4 Integrated Insulation System for Automotive Cryogenic Storage Tanks

National Fuel Cell Research Center

VI.2 Clean Energy Supply Chain and Manufacturing Competitiveness Analysis for Hydrogen and Fuel Cell Technologies

National Institute of Standards and Technology

III.1 Fatigue Performance of High-Strength Pipeline Steels and Their Welds in Hydrogen Gas Service
IV.C.4 HyMARC (Support): NREL Effort
V.B.3 FC-PAD: Electrode Layers and Optimization
V.E.1 Neutron Imaging Study of the Water Transport in Operating Fuel Cells

National Renewable Energy Laboratory

II.A.1 Analysis of Advanced H_2 Production Pathways
II.B.1 Renewable Electrolysis Integrated Systems Development and Testing
II.B.2 High-Performance, Long-Lifetime Catalysts for Proton Exchange Membrane Electrolysis
II.C.2 Flowing Particle Bed Solarthermal Redox Process to Split Water
II.D.1 High-Efficiency Tandem Absorbers for Economical Solar Hydrogen Production
II.D.2 Wide Bandgap Chalcopyrite Photoelectrodes for Direct Solar Water Splitting
II.E.1 Biomass to Hydrogen (B2H2)
II.F.4 Mechanistic Investigations on Hydrogen Catalysis by [FeFe]-Hydrogenase
II.F.5 Bioenergetics of Photosynthetic Energy Transduction: Control of Pathways through Redox Biochemistry
III.5 Improved Hydrogen Liquefaction through Heisenberg Vortex Separation of para- and ortho-hydrogen
III.7 700 bar Hydrogen Dispenser Hose Reliability and Improvement
III.8 Cryogenically Flexible, Low Permeability H_2 Delivery Hose
III.11 Electrochemical Compression
III.14 Advancing Hydrogen Dispenser Technology by Using Innovative Intelligent Networks
III.15 H2FIRST Consolidation
IV.B.1 Hydrogen Storage System Modeling: Public Access, Maintenance, and Enhancements
IV.C.4 HyMARC (Support): NREL Effort
V.A.1 ElectroCat (Electrocatalysis Consortium)
V.A.6 Extended Surface Electrocatalyst Development
V.A.8 Highly Accessible Catalysts for Durable High-Power Performance
V.A.10 Regenerative Fuel Cell System (SBIR Phase II)

National Renewable Energy Laboratory (Continued)

V.B.1 FC-PAD: Fuel Cell Performance and Durability Consortium
V.B.2 FC-PAD: Components and Characterization
V.B.3 FC-PAD: Electrode Layers and Optimization
V.B.4 Novel Ionomers and Electrode Structures for Improved PEMFC Electrode Performance at Low PGM Loadings
V.C.2 Advanced Hybrid Membranes for Next Generation PEMFC Automotive Applications
V.C.5 Highly Stable Anion Exchange Membranes for High-Voltage Redox-Flow Batteries
V.C.7 Advanced Ionomers and MEAs for Alkaline Membrane Fuel Cells
V.D.3 Advanced Catalysts and Membrane Electrode Assemblies (MEAs) for Reversible Alkaline Membrane Fuel Cells
V.E.3 Fuel Cell Technology Status: Degradation
V.E.5 Fuel Cell Vehicle Cost Analysis
VI.1 Fuel Cell Membrane Electrode Assembly Manufacturing R&D
VI.2 Clean Energy Supply Chain and Manufacturing Competitiveness Analysis for Hydrogen and Fuel Cell Technologies
VI.6 In-line Quality Control of PEM Materials
VI.7 Manufacturing Competitiveness Analysis for Hydrogen Refueling Stations
VII.A.1 Fuel Cell Electric Vehicle Evaluation
VII.A.2 Technology Validation: Fuel Cell Bus Evaluations
VII.B.2 Hydrogen Station Data Collection and Analysis
VII.B.4 Hydrogen Component Validation
VII.B.6 Hydrogen Meter Benchmark Testing
VII.C.1 Optimal Stationary Fuel Cell Integration and Control (Energy Dispatch Controller)
VII.C.2 Integrated Systems Modeling of the Interactions between Stationary Hydrogen, Vehicles, and Grid Resources
VII.C.3 Dynamic Modeling and Validation of Electrolyzers in Real-Time Grid Simulation
VII.D.1 H2@Scale Analysis
VIII.1 National Codes and Standards Development and Outreach
VIII.7 NREL Hydrogen Sensor Testing Laboratory
IX.5 Sustainability Analysis: Hydrogen Regional Sustainability (HyReS)
IX.6 Hydrogen Financial Analysis Scenario Tool (H2FAST) Updates with Analysis of 101st Station
IX.7 Regional Supply of Hydrogen
IX.11 Resource Availability for Hydrogen Production

Newcomb Anderson McCormick

VIII.11 Advancing Fuel Cell Electric Vehicles in San Francisco and Beyond

Nissan Technical Center North America

V.A.9 Corrosion-Resistant Non-Carbon Electrocatalyst Supports for PEFCs
V.B.7 Fuel Cell Membrane Electrode Assemblies with Ultra-Low Pt Nanofiber Electrodes
V.C.2 Advanced Hybrid Membranes for Next Generation PEMFC Automotive Applications

Northeastern University

II.B.3 High Performance Platinum Group Metal Free Membrane Electrode Assemblies through Control of Interfacial Processes
V.A.3 Innovative Non-PGM Catalysts for High-Temperature PEMFCs
V.A.17 Vapor Deposition Process for Engineering of Dispersed PEMFC ORR Pt/NbO_x/C Catalysts

Norwegian University Science and Technology

V.B.3 FC-PAD: Electrode Layers and Optimization

NOV Fiberglass Systems

VI.5 Continuous Fiber Composite Electrofusion Coupler

Nuvera Fuel Cells

X.4 Demonstration of Fuel Cell Auxiliary Power Unit (APU) to Power Truck Refrigeration Units (TRUs) in Refrigerated Trucks

Oak Ridge National Laboratory

III.1 Fatigue Performance of High-Strength Pipeline Steels and Their Welds in Hydrogen Gas Service
III.3 Low Cost Hydrogen Storage at 875 bar Using Steel Liner and Steel Wire Wrap
III.4 Advanced Barrier Coatings for Harsh Environments
III.13 Metal Hydride Compression
V.A.1 ElectroCat (Electrocatalysis Consortium)
V.A.4 Tailored High-Performance Low-PGM Alloy Cathode Catalysts
V.A.7 Highly Active, Durable, and Ultra-Low PGM NSTF Thin Film ORR Catalysts and Supports
V.B.1 FC-PAD: Fuel Cell Performance and Durability Consortium
V.B.2 FC-PAD: Components and Characterization
V.B.3 FC-PAD: Electrode Layers and Optimization
V.B.4 Novel Ionomers and Electrode Structures for Improved PEMFC Electrode Performance at Low PGM Loadings
V.C.4 Ionomer Dispersion Impact on Fuel Cell and Electrolyzer Performance and Durability (SBIR Phase II TTO)
V.C.7 Advanced Ionomers and MEAs for Alkaline Membrane Fuel Cells
VIII.9 Compatibility of Polymeric Materials Used in the Hydrogen Infrastructure

Ohio Fuel Cell Coalition

VI.2 Clean Energy Supply Chain and Manufacturing Competitiveness Analysis for Hydrogen and Fuel Cell Technologies

Oregon State University

II.E.3 Novel Hybrid Microbial Electrochemical System for Efficient Hydrogen Generation from Biomass

Pacific Northwest National Laboratory

III.6 Magnetocaloric Hydrogen Liquefaction
IV.A.2 Hydrogen Storage Cost Analysis
IV.B.1 Hydrogen Storage System Modeling: Public Access, Maintenance, and Enhancements
IV.C.5 HyMARC (Support): PNNL Effort
VII.D.1 H2@Scale Analysis
VIII.6 Hydrogen Safety Panel, Safety Knowledge Tools and First Responder Training Resources
VIII.9 Compatibility of Polymeric Materials Used in the Hydrogen Infrastructure
X.4 Demonstration of Fuel Cell Auxiliary Power Unit (APU) to Power Truck Refrigeration Units (TRUs) in Refrigerated Trucks

Pajarito Powder, LLC

II.B.6 Economical Production of Hydrogen through Development of Novel, High Efficiency Electrocatalysts for Alkaline Membrane Electrolysis
V.A.2 Development of PGM-Free Catalysts for Hydrogen Oxidation Reaction in Alkaline Media

Pajarito Powder, LLC (Continued)

V.A.3 Innovative Non-PGM Catalysts for High-Temperature PEMFCs

V.A.13 Development of Durable Active Supports for Low Platinum Group Metal Catalysts (SBIR I)

Palo Alto Research Center

II.B.8 Multi-Scale Ordered Cell Structure for Cost Effective Production of Hydrogen by HTWS

PDC Machines

III.15 H2FIRST Consolidation

pH Matter LLC

V.A.10 Regenerative Fuel Cell System (SBIR Phase II)

V.A.14 Multi-Functional Catalyst Support (SBIR I)

Plug Power

X.2 Ground Support Equipment Demonstration

X.5 FedEx Express Hydrogen Fuel Cell Extended-Range Battery Electric Vehicles

Proton OnSite

II.B.3 High Performance Platinum Group Metal Free Membrane Electrode Assemblies through Control of Interfacial Processes

II.B.6 Economical Production of Hydrogen through Development of Novel, High Efficiency Electrocatalysts for Alkaline Membrane Electrolysis

II.B.7 New Approaches to Improved PEM Electrolyzer Ion Exchange Membranes

VIII.6 Hydrogen Safety Panel, Safety Knowledge Tools and First Responder Training Resources

Purdue University

V.A.7 Highly Active, Durable, and Ultra-Low PGM NSTF Thin Film ORR Catalysts and Supports

Quong & Associates, Inc.

VII.B.1 Innovative Advanced Hydrogen Mobile Fueler

RCF Economic and Financial Consulting, Inc.

IX.1 Employment Impacts of Hydrogen and Fuel Cell Technologies

Rensselaer Polytechnic Institute

III.11 Electrochemical Compression

V.C.6 Advanced Materials for Fully-Integrated MEAs in AEMFCs

Rheonik GmBH

III.14 Advancing Hydrogen Dispenser Technology by Using Innovative Intelligent Networks

SAE International

VIII.3 Hydrogen Fuel Quality

Saint Louis University

IV.C.10 HyMARC Seedling: Fundamental Studies of Surface-Functionalized Mesoporous Carbons for Thermodynamic Stabilization and Reversibility of Metal Hydrides

Sandia National Laboratories

- II.C.1 High Efficiency Solar Thermochemical Reactor for Hydrogen Production
- III.1 Fatigue Performance of High-Strength Pipeline Steels and Their Welds in Hydrogen Gas Service
- III.13 Metal Hydride Compression
- III.16 Reference Station Design, Phase II
- IV.C.1 HyMARC (Core): SNL Effort
- IV.C.12 Improving the Kinetics and Thermodynamics of $Mg(BH_4)_2$ for Hydrogen Storage
- IV.D.3 Development, Selection and Testing to Reduce Cost and Weight of Materials for BOP Components
- V.C.6 Advanced Materials for Fully-Integrated MEAs in AEMFCs
- VIII.2 R&D for Safety, Codes and Standards: Materials and Components Compatibility
- VIII.4 R&D for Safety, Codes and Standards: Hydrogen Behavior
- VIII.5 Hydrogen Quantitative Risk Assessment
- VIII.9 Compatibility of Polymeric Materials Used in the Hydrogen Infrastructure
- VIII.10 Enabling Hydrogen Infrastructure Through Science-Based Codes and Standards
- IX.4 Hydrogen Analysis with the Sandia ParaChoice Model
- X.3 Maritime Fuel Cell Generator Project

Santa Monica Fire Department

- VIII.6 Hydrogen Safety Panel, Safety Knowledge Tools and First Responder Training Resources

Savannah River Consulting

- IV.B.2 Investigation of Solid State Hydrides for Autonomous Fuel Cell Vehicles
- IV.C.16 Electrochemical Reversible Formation of Alane

Savannah River National Laboratory

- III.12 Hybrid Electrochemical Hydrogen/Metal Hydride Compressor
- IV.B.1 Hydrogen Storage System Modeling: Public Access, Maintenance, and Enhancements
- IV.B.2 Investigation of Solid State Hydrides for Autonomous Fuel Cell Vehicles
- IV.C.16 Electrochemical Reversible Formation of Alane
- IV.D.4 Integrated Insulation System for Automotive Cryogenic Storage Tanks
- V.A.11 Development of Corrosion Resistant Carbon (CRC) Support for Ultra-Low Platinum Group Metal (PGM) Catalysts (SBIR Phase I)
- VI.5 Continuous Fiber Composite Electrofusion Coupler

Smart Chemistry

- VII.B.4 Hydrogen Component Validation
- VIII.3 Hydrogen Fuel Quality

Southern Illinois University

- IV.C.9 HyMARC Seedling: "Graphene-Wrapped" Complex Hydrides as High-Capacity, Regenerable Hydrogen Storage Materials

Southwest Research Institute®

- III.2 Hydrogen Compression Application of the Linear Motor Reciprocating Compressor (LMRC)

Spectrum Automation Controls

- II.B.1 Renewable Electrolysis Integrated Systems Development and Testing
- III.7 701 bar Hydrogen Dispenser Hose Reliability and Improvement

Spectrum Automation Controls (Continued)

VII.B.4 Hydrogen Component Validation

VII.B.6 Hydrogen Meter Benchmark Testing

Spencer Composites Corporation

IV.D.2 Next Generation Hydrogen Storage Vessels Enabled by Carbon Fiber Infusion with a Low Viscosity, High Toughness Resin System

VII.B.5 Liquid Hydrogen Pump Performance and Durability Testing

SRI International

IV.C.17 Low-Cost α-Alane for Hydrogen Storage

Stanford University

II.C.1 High Efficiency Solar Thermochemical Reactor for Hydrogen Production

II.D.2 Wide Bandgap Chalcopyrite Photoelectrodes for Direct Solar Water Splitting

State University of New York at Buffalo

V.A.16 Advanced Electro-Catalysts through Crystallographic Enhancement

V.D.3 Advanced Catalysts and Membrane Electrode Assemblies (MEAs) for Reversible Alkaline Membrane Fuel Cells

Strategic Analysis, Inc.

II.A.1 Analysis of Advanced H_2 Production Pathways

IV.A.2 Hydrogen Storage Cost Analysis

V.E.5 Fuel Cell Vehicle Cost Analysis

VI.4 U.S. Clean Energy Hydrogen and Fuel Cell Technologies: A Competiveness Analysis

Structural Integrity Associates, Inc.

III.3 Low Cost Hydrogen Storage at 875 bar Using Steel Liner and Steel Wire Wrap

Sustainable Innovations, LLC

III.12 Hybrid Electrochemical Hydrogen/Metal Hydride Compressor

Tetramer Technologies, LLC

II.B.7 New Approaches to Improved PEM Electrolyzer Ion Exchange Membranes

The Pennsylvania State University

II.B.3 High Performance Platinum Group Metal Free Membrane Electrode Assemblies through Control of Interfacial Processes

II.E.1 Biomass to Hydrogen (B2H2)

IV.C.8 HyMARC Seedling: Developing a Novel Hydrogen Sponge with Ideal Binding Energy and High Surface Area for Practical Hydrogen Storage

Thesis Corporation

IV.C.4 HyMARC (Support): NREL Effort

The University of Texas at Austin

IV.D.1 Conformable Hydrogen Storage Coil Reservoir

V.B.5 Durable High-Power Membrane Electrode Assemblies with Low Pt Loading

VII.A.3 Fuel Cell Hybrid Electric Delivery Van Project

TreadStone Technologies, Inc.

V.D.1 Novel Structured Metal Bipolar Plates for Low Cost Manufacturing

Tufts University

V.B.3 FC-PAD: Electrode Layers and Optimization

V.B.4 Novel Ionomers and Electrode Structures for Improved PEMFC Electrode Performance at Low PGM Loadings

VI.1 Fuel Cell Membrane Electrode Assembly Manufacturing R&D

UL

VIII.6 Hydrogen Safety Panel, Safety Knowledge Tools and First Responder Training Resources

Umicore

V.B.2 FC-PAD: Components and Characterization

Unique Electric Solutions

VII.A.3 Fuel Cell Hybrid Electric Delivery Van Project

United Parcel Service

VII.A.3 Fuel Cell Hybrid Electric Delivery Van Project

United Technologies Research Center

V.B.3 FC-PAD: Electrode Layers and Optimization

V.B.6 High Performance Polymer Electrolyte Membrane Fuel Cell Electrode Structures

University of Alabama

III.1 Fatigue Performance of High-Strength Pipeline Steels and Their Welds in Hydrogen Gas Service

University of Alberta

V.B.3 FC-PAD: Electrode Layers and Optimization

University of Arkansas at Little Rock

V.B.6 High Performance Polymer Electrolyte Membrane Fuel Cell Electrode Structures

University of California, Irvine

II.D.3 Tandem Particle-Slurry Batch Reactors for Solar Water Splitting

II.F.1 Tailoring Hydrogen Evolution Reaction (HER) Catalysts for Operation at Specific pH Values

University of Colorado Boulder

II.C.2 Flowing Particle Bed Solarthermal Redox Process to Split Water

V.A.6 Extended Surface Electrocatalyst Development

VII.C.1 Optimal Stationary Fuel Cell Integration and Control (Energy Dispatch Controller)

University of Connecticut

V.C.3 Smart Matrix Development for Direct Carbonate Fuel Cell

University of Delaware

V.A.6 Extended Surface Electrocatalyst Development

V.B.1 FC-PAD: Fuel Cell Performance and Durability Consortium

V.C.5 Highly Stable Anion Exchange Membranes for High-Voltage Redox-Flow Batteries

University of Georgia

II.E.2 Sweet Hydrogen: High-Yield Production of Hydrogen from Biomass Sugars Catalyzed by in vitro Synthetic Biosystems

University of Hawaii

II.D.1 High-Efficiency Tandem Absorbers for Economical Solar Hydrogen Production

II.D.2 Wide Bandgap Chalcopyrite Photoelectrodes for Direct Solar Water Splitting

University of Hawaii at Mānoa

IV.C.5 HyMARC (Support): PNNL Effort

IV.C.11 HyMARC Seedling: Development of Magnesium Boride Etherates as Hydrogen Storage Materials

University of Michigan

IV.C.12 Improving the Kinetics and Thermodynamics of $Mg(BH_4)_2$ for Hydrogen Storage

IV.C.15 Hydrogen Adsorbents with High Volumetric Density: New Materials and System Projections

V.A.17 Vapor Deposition Process for Engineering of Dispersed PEMFC ORR $Pt/NbO_x/C$ Catalysts

University of Missouri

IV.C.13 High-Capacity Hydrogen Storage Systems via Mechanochemistry

University of Missouri—St. Louis

IV.C.10 HyMARC Seedling: Fundamental Studies of Surface-Functionalized Mesoporous Carbons for Thermodynamic Stabilization and Reversibility of Metal Hydrides

University of Nevada, Las Vegas

II.D.1 High-Efficiency Tandem Absorbers for Economical Solar Hydrogen Production

II.D.2 Wide Bandgap Chalcopyrite Photoelectrodes for Direct Solar Water Splitting

University of New Mexico

II.B.3 High Performance Platinum Group Metal Free Membrane Electrode Assemblies through Control of Interfacial Processes

V.A.2 Development of PGM-Free Catalysts for Hydrogen Oxidation Reaction in Alkaline Media

V.A.3 Innovative Non-PGM Catalysts for High-Temperature PEMFCs

V.A.9 Corrosion-Resistant Non-Carbon Electrocatalyst Supports for PEFCs

University of Pennsylvania

V.A.16 Advanced Electro-Catalysts through Crystallographic Enhancement

University of Rochester

II.F.3 Nano-bio Systems for Light-Driven Hydrogen Production

University of Southern California

II.F.2 Hybrid Perovskites and Non-Adiabatic Dynamics Simulations: Catching Realistic Aspects of the Charge Recombination Process

US Hybrid

X.6 Northeast Demonstration and Deployment of FCRx200

Valence Technology

VII.A.3 Fuel Cell Hybrid Electric Delivery Van Project

Vanderbilt University

V.B.7 Fuel Cell Membrane Electrode Assemblies with Ultra-Low Pt Nanofiber Electrodes

V.C.1 New Fuel Cell Membranes with Improved Durability and Performance

VENCORE Solutions and Services

IV.D.4 Integrated Insulation System for Automotive Cryogenic Storage Tanks

Versa Power Systems

II.B.5 Solid Oxide Based Electrolysis and Stack Technology with Ultra-High Electrolysis Current Density (>3 A/cm^2) and Efficiency

VII.C.4 Modular SOEC System for Efficient Hydrogen Production at High Current Density

Virginia Clean Cities at James Madison University

VI.3 Fuel Cell and Hydrogen Opportunity Center, www.hfcnexus.com (Hydrogen Fuel Cell Nexus)

Virginia Polytechnic Institute and State University

II.E.2 Sweet Hydrogen: High-Yield Production of Hydrogen from Biomass Sugars Catalyzed by in vitro Synthetic Biosystems

VTT

VIII.3 Hydrogen Fuel Quality

Washington State University

VII.C.1 Optimal Stationary Fuel Cell Integration and Control (Energy Dispatch Controller)

Washington University in St. Louis

II.B.6 Economical Production of Hydrogen through Development of Novel, High Efficiency Electrocatalysts for Alkaline Membrane Electrolysis

IV.C.10 HyMARC Seedling: Fundamental Studies of Surface-Functionalized Mesoporous Carbons for Thermodynamic Stabilization and Reversibility of Metal Hydrides

V.A.9 Corrosion-Resistant Non-Carbon Electrocatalyst Supports for PEFCs

WireTough Cylinders, LLC

III.3 Low Cost Hydrogen Storage at 875 bar Using Steel Liner and Steel Wire Wrap

Witte Engineered Gases

VIII.6 Hydrogen Safety Panel, Safety Knowledge Tools and First Responder Training Resources

W.L. Gore & Associates

VI.1 Fuel Cell Membrane Electrode Assembly Manufacturing R&D

Workhorse Technologies Inc.

X.5 FedEx Express Hydrogen Fuel Cell Extended-Range Battery Electric Vehicles